nagra.

Technical Report 21-03

The PSI Chemical Thermodynamic Database 2020

April 2023

W. Hummel & T. Thoenen

National Cooperative
for the Disposal of
Radioactive Waste

Hardstrasse 73
5430 Wettingen
Switzerland
Tel. +41 56 437 11 11

nagra.ch

nagra.

Technical Report 21-03

The PSI Chemical Thermodynamic Database 2020

April 2023

W. Hummel[1] & T. Thoenen[1]

[1] PSI

National Cooperative
for the Disposal of
Radioactive Waste

Hardstrasse 73
5430 Wettingen
Switzerland
Tel. +41 56 437 11 11

nagra.ch

ISSN 1015-2636

Abstract

The PSI Chemical Thermodynamic Database 2020 (TDB 2020) was prepared for the next safety assessments related to the general licence application (*Rahmenbewilligungsgesuch* – RBG) in the framework of the Sectoral Plan for Deep Geological Repositories (*Sachplan Geologische Tiefenlager* – SGT) for the planned repositories for low- and intermediate-level (L/ILW) and high-level (HLW) radioactive waste in Switzerland.

The TDB 2020 is an update from the Paul Scherrer Institute (PSI)/Nagra TDB 12/07, published in 2014, and its predecessor Nagra/PSI TDB 01/01, published in 2002. The update was carried out over the period 2017 – 2020 and was completed in 2021 with the implementation of an electronic database for the GEMS geochemical speciation code.

For the preparation of the solubility and sorption databases for the RBG, the TDB had to be updated and existing gaps filled. The TDB 2020 contains data for all radionuclides to be considered in the safety assessment for the RBG, as well as a complete data set for corresponding pore water models and data for some important chemotoxic elements.

The TDB 2020 includes new reviews for the elements Ac, Ag, Cd, Cf, Cu, Hg, Ho, Pa, Pb, Po, Sm, Ti and Zn, and updates of previous data for Al, alkali (Li, Na, K) and alkaline earth elements (Mg, Ca, Sr, Ba, Ra), Am, Eu, Fe, Mn, Mo, Nb, Np, organic ligands, Pd, Pu, S, Se, silicates, Sn, Tc and U. Data for Ni, Th and Zr, included in PSI/Nagra TDB 12/07 based on NEA TDB reviews remain essentially unchanged.

The data evaluation procedures and the selection of values are documented in all steps to maximise traceability of the review process.

As in the review volumes of the Nuclear Energy Agency (NEA) and in PSI/Nagra TDB 12/07 and Nagra/PSI TDB 01/01, the specific ion interaction theory (SIT) was used to extrapolate experimental data to zero ionic strength. In this update, particular care has been taken to describe how the corresponding SIT coefficients were obtained, and the selected values are all tabulated.

For the application of SIT to environmental systems where salinity is governed by NaCl, an estimation method has been developed to fill the numerous gaps in the set of experimentally determined SIT coefficients in NaCl background media.

The TDB 2020 includes thermodynamic data for 53 elements, 1'034 aqueous species (and SIT ion interaction coefficients for all species), 358 solids and 8 gases.

Zusammenfassung

Die PSI Chemisch-thermodynamische Datenbank 2020 (TDB 2020) wurde für die nächsten Sicherheitsanalysen im Zusammenhang mit dem Rahmenbewilligungsgesuch (RBG) im Rahmen des Sachplans Geologische Tiefenlager (SGT) für die geplanten Tiefenlager zur dauerhaften Einlagerung von schwach- und mittelaktiven (SMA) sowie hochaktiven (HAA) radioaktiven Abfällen in der Schweiz erstellt.

Die TDB 2020 ist eine Aktualisierung der 2014 publizierten PSI/Nagra TDB 12/07 und ihres Vorgängers Nagra/PSI TDB 01/01 aus dem Jahr 2002. Die Aktualisierung erfolgte im Zeitraum 2017 – 2020 und wurde 2021 mit der Implementierung einer elektronischen Datenbank für den geochemischen Speziationscode GEMS abgeschlossen.

Für die Erstellung der Löslichkeits- und Sorptionsdatenbanken für das RBG musste die TDB aktualisiert, und bestehende Lücken mussten geschlossen werden. Die TDB 2020 enthält Daten für alle Radionuklide, die bei der Sicherheitsanalyse für das RBG zu berücksichtigen sind, sowie einen vollständigen Datensatz für entsprechende Porenwassermodelle und Daten für einige wichtige chemotoxische Elemente.

Die TDB 2020 enthält Evaluierungen für die neuen Elemente Ac, Ag, Cd, Cf, Cu, Hg, Ho, Pa, Pb, Po, Sm, Ti und Zn sowie Aktualisierungen früherer Daten für Al, Alkali- (Li, Na, K) und Erdalkalielemente (Mg, Ca, Sr, Ba, Ra), Am, Eu, Fe, Mn, Mo, Nb, Np, organische Liganden, Pd, Pu, S, Se, Silikate, Sn, Tc und U. Die Daten für Ni, Th und Zr, die in PSI/Nagra TDB 12/07 auf der Grundlage von NEA TDB-Reviews aufgenommen wurden, bleiben im Wesentlichen unverändert.

Die Datenbewertungsverfahren und die Auswahl der Werte werden in allen Schritten dokumentiert, um die Nachvollziehbarkeit des Evaluierungsprozesses zu maximieren.

Wie in den NEA-Büchern und in PSI/Nagra TDB 12/07 und Nagra/PSI TDB 01/01 wurde die spezifische Ionenwechselwirkungstheorie (SIT) verwendet, um experimentelle Daten auf die Ionenstärke Null zu extrapolieren. Bei der vorliegenden Aktualisierung wurde besonders sorgfältig beschrieben, wie die entsprechenden SIT-Koeffizienten ermittelt wurden, und die ausgewählten Werte sind alle tabellarisch aufgeführt.

Zur Anwendung der SIT auf die Modellierung von Umweltsystemen, bei denen NaCl die Salinität dominiert, wurde eine Schätzmethode entwickelt, um die zahlreichen Lücken in den experimentell bestimmten SIT-Koeffizienten für NaCl-Medien zu schließen.

Die TDB 2020 umfasst thermodynamische Daten für 53 Elemente, 1'034 wässrige Spezies (und SIT-Ionenwechselwirkungskoeffizienten für alle Spezies), 358 Feststoffe und 8 Gase.

Résumé

Dans le cadre du plan sectoriel suisse pour les dépôts en couches géologiques profondes des déchets radioactifs de faible et moyenne activité (DFMA) et de haute activité (DHA), la base de données thermodynamique chimique 2020 (TDB 2020) du PSI a été finalisée pour les prochaines évaluations de sûreté liées à la demande d'autorisation générale (Rahmenbewilligungsgesuch – RBG).

La TDB 2020 est une mise à jour de la PSI/Nagra TDB 12/07 et Nagra/PSI TDB 01/01, respectivement publiées en 2014 et 2002. La mise à jour a été réalisée sur la période 2017 - 2020 et s'est achevée en 2021 avec la mise en place d'une base de données électronique pour le code de spéciation géochimique GEMS.

Pour la préparation des bases de données de solubilité et de sorption nécessaires pour les évaluations de sûreté, la TDB a été complétée. Elle contient désormais les données pour tous les radionucléides et les différents modèles d'eau interstitielle à considérer. En plus, elle contient les données pour les éléments chimiotoxiques les plus importants.

La TDB 2020 comprend notamment de nouvelles évaluations pour les éléments Ac, Ag, Cd, Cf, Cu, Hg, Ho, Pa, Pb, Po, Sm, Ti et Zn, et des mises à jour pour Al, les éléments alcalins (Li, Na, K) et alcalino-terreux (Mg, Ca, Sr, Ba, Ra), Am, Eu, Fe, Mn, Mo, Nb, Np, les ligands organiques, Pd, Pu, S, Se, les silicates, Sn, Tc et U. Les données pour Ni, Th et Zr, incluses dans la TDB 12/07 sur la base des évaluations de la NEA TDB, restent globalement inchangées.

Les procédures d'évaluation des données et la sélection des valeurs sont documentées étape par étape, afin de maximiser la traçabilité du processus.

Comme dans les documents de la NEA, PSI/Nagra TDB 12/07 et Nagra/PSI TDB 01/01, la théorie de l'intéraction ionique spécifique (SIT) a été utilisée pour extrapoler les données expérimentales à une force ionique nulle. Dans cette nouvelle version de la base de données, la manière dont les coefficients SIT ont été obtenus a été détaillée. Les valeurs sélectionnées ont également toutes été présentées sous la forme de tableaux.

Pour l'application de la théorie SIT aux systèmes environnementaux où la salinité est régie par le chlorure de sodium, une méthode d'estimation a été développée pour combler le manque de données expérimentales.

La TDB 2020 comprend des données thermodynamiques pour 53 éléments, 1'034 espèces dissoutes (et des coefficients SIT pour toutes les espèces), 358 solides et 8 gaz.

Table of Contents

List of Tables

List of Figures

1 Introduction

1.1 Scope of the database

A high-quality Thermodynamic Data Base (TDB) is an essential prerequisite for defining pore water models and for preparing databases for solubility limits and radionuclide sorption in the framework of the *Sachplan Geologische Tiefenlager* (Sectoral Plan for Deep Geological Repositories – SGT) for the planned repositories for low- and intermediate-level (L/ILW) and high-level (HLW) radioactive waste in Switzerland. The current update from the PSI/Nagra Chemical Thermodynamic Database 12/07 (PSI/Nagra TDB 12/07, Thoenen et al. 2014) to the PSI Chemical Thermodynamic Database 2020 (TDB 2020) was prepared for the next safety assessments related to the general license application (in German "Rahmenbewilligungsgesuch" – RBG).

The TDB needed to be updated and existing gaps had to be filled for preparing the solubility and sorption databases for RBG. TDB 2020 comprises data for all radionuclides to be considered in the safety assessment for RBG, as well as a complete data set for related pore water models, and data for a some important chemotoxic elements.

Compared to the previous version (PSI/Nagra TDB 12/07), TDB 2020 includes reviews for the new elements Ac, Ag, Cd, Cf, Cu, Hg, Ho, Pa, Pb, Po, Sm, Ti and Zn, and updates of former data for Al, alkali (Li, Na, K) and alkaline earth elements (Mg, Ca, Sr, Ba, Ra), Eu, Fe, Mn, Mo, Nb, organic ligands, Pd, S, Se, silicates and Sn. New and updated data from the NEA TDB Second Update on the Chemical Thermodynamics of Uranium, Neptunium, Plutonium, Americium and Technetium (Grenthe et al. 2020) have been included in TDB 2020.

Data for Ni, Th and Zr, included in PSI/Nagra TDB 12/07 based on NEA TDB reviews, generally remain unchanged and are not discussed in the present report. Only some Ni – organic data (Section 18.3.2) and Ni and Th silicate data (Sections 25.4.2 and 25.4.7, respectively) were review in the present report.

Similar thermodynamic data bases tailored to the needs of their deep geological repository projects have been developed in Sweden by SKB (Duro et al. 2006), in Finland by Posiva (Grivé et al. 2008), in Japan by JAEA (Kitamura 2019), in Germany by GRS (Hagemann 2012, Hagemann et al. 2012) and by a national consortium (THEREDA, Moog et al. 2015), in France by Andra (ThermoChimie, Giffaut et al. 2014) and BRGM (Thermoddem, Blanc et al. 2012), and in the USA for the Yucca Mountain Project (Wolery & Jove-Colon 2004).

For a survey of eleven major compilations of equilibrium constants including those from authoritative groups such as CODATA, IUPAC, NIST, and NEA see Hummel et al. (2019).

1.2 Data quality and data categories

The Nagra TDB version 05/92 (Pearson & Berner 1991, Pearson et al. 1992) distinguished two types of data, "core data" and "supplemental data". The data for the aqueous species and minerals in the core subset were selected individually. In contrast, the supplemental data were selected (imported) in groups, each from one of several existing data sets, e.g., the HATCHES database, or the MINEQL-PSI and PHREEQE-PSI databases.

In the Nagra/PSI TDB 01/01 (Hummel et al. 2002) the classification of "core data" and "supplemental data" has been retained, although the supplemental data were selected individually (element by element), either taken from NEA TDB reviews or derived by in-house reviews.

Considering the ongoing NEA TDB review project, resulting in the publication of presently 14 volumes of "Chemical Thermodynamics", a series of IUPAC reviews on chemotoxic elements, and the efforts of the present authors concerning in-house reviews, the historic data categories have been redefined and extended. The PSI/Nagra TDB 12/07 (Thoenen et al. 2014) distinguished between three categories of data, i.e., **core data**, **recommended data**, and **supplemental data** (Fig. 1-1). In the present TDB 2020, these data categories were retained.

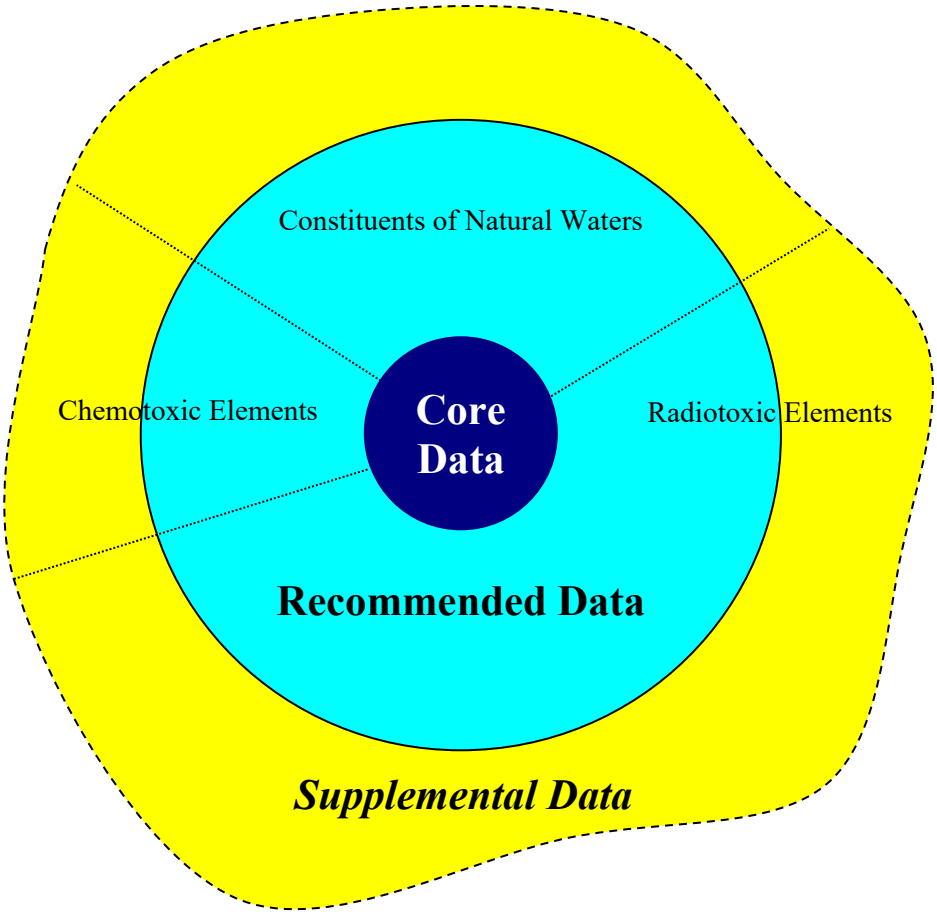

Fig. 1-1: Data types distinguished in the TDB 2020
For a detailed explanation see text.

Core Data: Well-characterised aqueous species, minerals and gases of elements involved in almost any type of speciation calculation. These data have been carefully selected and are widely accepted in different fields of application. The core data basically comprise the CODATA key values (Cox et al. 1989) and some other values of similar quality and with almost worldwide acceptance.

Recommended Data: Well-characterised aqueous species, minerals and gases of elements important in different fields of application. These fields are a modelling of ground and surface waters, b safety assessments of nuclear waste repositories and c pollution dynamics of chemotoxic substances. The boundaries of the three fields are fuzzy, e.g., strontium is a minor constituent of natural waters but also of interest as radiotoxic isotope ^{90}Sr, and the chemotoxic element mercury has also to be included in safety assessments of nuclear waste facilities as ^{194}Hg. The recommended data are of high quality and well established, but in contrast to the core data, which may not be revised in the foreseeable future, the recommended data originate from rather active fields of environmental sciences and may be revised and improved over time.

Supplemental Data: Supplemental aqueous species and minerals are less well characterised than those in the recommended data. They comprise uncertain data, not selected in the NEA TDB and other reviews but discussed there as suitable for scoping calculations and qualitative modelling. The numerical values either are accompanied by large ± uncertainties, or they are given as approximate (≈) or limiting (≤) values. Also, estimates are provided for important species where experimental data are missing or unreliable, particularly in cases where omission of such estimated constants would lead to obviously unacceptable results. These estimates are based on chemical analogues, linear free energy relationships, isocoulombic reactions or other estimation methods found reliable by the reviewers.

As a visual aid for identifying the different types of data in tables of numerical values,

- the **`core data`** will be printed in **`bold face`**,
- whereas the `recommended data` are shown in `normal face`,
- and the *`supplemental data`* are given in *`italics`*.

Uncertainties: All ± uncertainties given in this report refer to the 95% confidence level if not indicated otherwise.

1.3 Solid compounds included in the database

The data concerning solid compounds in TDB 2020 are restricted to pure phases. We envision to include data for solid solutions in future updates when there is an agreement on the use of solid solution models and, more importantly, when reliable thermodynamic data will become available for selected environmental systems. The current status of chemical thermodynamics of solid solutions is discussed by Bruno et al. (2007).

Solid compounds included in the TDB 2020 are supposed to attain thermodynamic equilibrium at conditions including surface environments as well as deep radioactive waste repository systems.

Hence, thermodynamic data derived for mineral phases at hydrothermal conditions (T > 300 °C and high pressure) are included only if there is convincing evidence that these phases may also reach equilibrium at ambient conditions, i.e., that solubility values calculated from these data are

found in concentration ranges not in contradiction with experimental data. The same criteria apply for thermodynamic data of solid phases solely derived from high temperature calorimetry. In any case of doubt from an application point of view, data from these sources are not included in TDB 2020.

A notable exception from these principles is the inclusion of some clay minerals in TDB 2020. However, as discussed in Section 25.4.3.2, the present authors have serious doubts that these clay minerals will ever attain thermodynamic equilibrium in surface and shallow depth environments, and consequently these data are classified as supplemental data.

Detailed discussion and inclusion of solid compounds are restricted in TDB 2020 to the so-called "sparingly soluble" solids. These are the important solids governing the chemistry of most ground and surface waters and determining the solubility limits of radionuclides. There is no exact numerical definition of "sparingly soluble". However, data for highly soluble salts leading to solutions of molar concentrations at saturation are generally not included in TDB 2020. This means that TDB 2020 is not suited to model the evolution of salt lakes or radioactive waste repositories situated in salt domes.

1.4 Thermodynamic quantities and equilibrium constants

Selected thermodynamic data for reactions refer to the reference temperature T° of 298.15 K (25 °C) and to the standard state, i.e., a pressure of 0.1 MPa (1 bar) and, for aqueous species, infinite dilution ($I = 0$). The reaction parameters include

$\log_{10}K°$	the equilibrium constant of the reaction, logarithmic	
$\Delta_r G_m°$	the standard molar Gibbs free energy of reaction	$(kJ \cdot mol^{-1})$
$\Delta_r H_m°$	the standard molar enthalpy of reaction	$(kJ \cdot mol^{-1})$
$\Delta_r S_m°$	the standard molar entropy of reaction	$(J \cdot K^{-1} \cdot mol^{-1})$
$\Delta_r C_{p,m}°$	the standard molar heat capacity of reaction	$(J \cdot K^{-1} \cdot mol^{-1})$

The equilibrium constant, $K°$, is related to $\Delta_r G_m°$ according to the following relation,

$$\Delta_r G_m° = - R \cdot T° \cdot \ln(10) \cdot \log_{10}K°$$

and the molar quantities $\Delta_r G_m°$, $\Delta_r H_m°$ and $\Delta_r S_m°$ are related according to the Gibbs-Helmholtz equation:

$$\Delta_r G_m° = \Delta_r H_m° - T° \cdot \Delta_r S_m°$$

Thermodynamic data of individual entities are tabulated using standard state properties of formation from the elements in their reference state,

$\Delta_f G_m°$	the standard molar Gibbs free energy of formation	($kJ \cdot mol^{-1}$)
$\Delta_f H_m°$	the standard molar enthalpy of formation	($kJ \cdot mol^{-1}$)
$\Delta_f S_m°$	the standard molar entropy of formation	($J \cdot K^{-1} \cdot mol^{-1}$)
$\Delta_f C_{p,m}°$	the standard molar heat capacity of formation	($J \cdot K^{-1} \cdot mol^{-1}$)

or the absolute quantities,

$S_m°$	the standard molar entropy	($J \cdot K^{-1} \cdot mol^{-1}$)
$C_{p,m}°$	the standard molar heat capacity	($J \cdot K^{-1} \cdot mol^{-1}$)

The properties of a reaction are calculated from the standard state properties of its reactants and products as follows:

$$\Delta_r X_m° = \Sigma\Delta_f X_m°(\text{products}) - \Sigma\Delta_f X_m°(\text{reactants})$$

where X represents the thermodynamic property.

The standard molar quantities $\Delta_f G_m°$, $\Delta_f H_m°$ and $\Delta_f S_m°$ are related according to the Gibbs-Helmholtz equation:

$$\Delta_f G_m° = \Delta_f H_m° - T° \cdot \Delta_f S_m°$$

For neutral species,

$$\Delta_f S_m° = S_m° - \Sigma S_m°(\text{elements})$$

$$\Delta_f C_{p,m}° = C_{p,m}° - \Sigma C_{p,m}°(\text{elements})$$

and for charged species,

$$\Delta_f S_m° = S_m° - \Sigma S_m°(\text{elements}) + (n/2)\, S_m°(H_2g)$$

$$\Delta_f C_{p,m}° = C_{p,m}° - \Sigma C_{p,m}°(\text{elements}) + (n/2)\, C_{p,m}°(H_2g)$$

in which n is the charge (Wagman et al. 1982, p. 2-22).

Note that the above equations for charged species are based on the formulation of redox equilibria in terms of H_2g and H^+, where all thermodynamic properties of H^+ are zero by definition. For example, the redox equilibrium $Cm(cr) + 3\ H^+ \rightleftharpoons Cm^{3+} + 3/2\ H_2g$ leads to $\Delta_f S_m°(Cm^{3+}) = S_m°(Cm^{3+}) - S_m°(Cm, cr) + (3/2)\, S_m°(H_2g)$.

Some gas data are given at 1 atm (0.101325 MPa) in their original sources. The entropy values of gases are sensitive to pressure and were converted from 1 atm to 1 bar using equations given by Wagman et al. (1982, p. 2-23):

$$S_m°(\text{bar}) - S_m°(\text{atm}) = R \cdot \ln(1.01325/1.0) = 0.1094\ \text{J} \cdot \text{K}^{-1} \cdot \text{mol}^{-1}$$

1.5 Medium effects

The selected thermodynamic data in our database refer to standard state conditions, i.e., infinite dilution ($I = 0$) for aqueous species. Equilibrium constants studied in the laboratory are usually determined in an ionic medium. However, there is no "standard" ionic medium, or ionic strength, preferred in experimental determinations of equilibrium constants. The historically most "popular" media were $NaClO_4$ and KNO_3 at high concentrations. Both are of no relevance for environmental modelling. Nowadays, also NaCl is used as ionic medium.

All experimental data have to be extrapolated to zero ionic strength as part of the data review procedure. Users of thermodynamic data given for standard state conditions must recalculate these data to the conditions present in the system under study. Ideally, the same method should be used for extrapolation of experimental data to $I = 0$ and subsequent recalculation to environmental conditions, but usually this is not the case.

Ionic solutions depart strongly from ideality, and this non-ideality is accounted for by the introduction of an activity coefficient γ_j relating concentration m_i of species j with its "thermodynamic concentration" or activity a_j

$$a_j = m_j \cdot \gamma_j$$

There are different semi-empirical methods for the estimation of activity coefficients. All these electrolyte models are based on microscopic physico-chemical descriptions of the interactions between dissolved ions, and sometimes the interactions between ions and solvent. The method of choice in this review is the Specific Ion interaction Theory (SIT), which is described in some detail in the following.

1.5.1 General SIT formalism

The discussion in this section is based on Appendix B in Grenthe et al. (2020), where additional details can be found.

The activity coefficient γ_j of an ion j with charge z_j in an aqueous solution of ionic strength I_m is given according to SIT by

$$\log_{10}\gamma_j = - z_j^2 D + \Sigma_k \varepsilon(j, k, I_m)\, m_k \qquad (1.1)$$

D is the Debye-Hückel term

$$D = \frac{A\sqrt{I_m}}{1 + 1.5\sqrt{I_m}}$$

where A, the Debye-Hückel limiting slope, is a constant depending on pressure and temperature (with a value of 0.509 $kg^{½} \cdot mol^{-½}$ at 298.15 K and 1 bar) and I_m, the molal ionic strength, is defined by

$$I_m = ½ \Sigma_i m_i z_i^2 \quad (1.2)$$

where the summation extends over all ions i present in the solution and m_i refers to the molal concentration of i.

In $\Sigma_k \varepsilon(j, k, I_m) m_k$ the summation extends over all species k in the solution, and $\varepsilon(j, k, I_m)$ is the specific ion interaction coefficient for ion j with species k. In general, $\varepsilon(j, k, I_m)$ depends only slightly on ionic strength. For this review, $\varepsilon(j, k)$ was assumed to be independent of ionic strength. In a few cases (e.g., see Section 23.3.4.1), this required to restrain the applicability of derived ion interaction parameters to a limited range of ionic strengths, where the assumption of independence of ionic strength remains valid. SIT assumes that there are no interactions between ions with the same charge sign, therefore $\varepsilon(cation_j, cation_k) = \varepsilon(anion_j, anion_k) = 0$. In general, there are also no specific ion interactions between cations or anions with neutral species and, therefore, $\varepsilon(cation_j, neutral\ species_k) = \varepsilon(anion_j, neutral\ species_k) = 0$. In some cases, however, experimental data suggest that there are interactions (albeit weak) between ions and neutral species, and therefore $\varepsilon(ion_j, neutral\ species_k) \neq 0$.

When calculating $\log_{10}\gamma_j$ of species j in the presence of a background electrolyte (e.g. the 1:1 salt NX) where the concentrations of N and X are much larger than those of all other solutes, the term $\Sigma_k \varepsilon(j, k, I_m) m_k$ in eq. (1.1) can be simplified, since in this case only the interactions between j with k = N or k = X contribute substantially to the sum, while all other interactions can be safely neglected. In addition, the ionic strength of a solution dominated by the 1:1 background electrolyte NX (where N is the cation and X the anion) can be approximated by $I_m \approx m_N = m_X >> m_k$, for k ≠ N or X, which is obvious from eq. (1.2). With these simplifications, eq. (1.1) can now be written as

$$\log_{10}\gamma_j = - z_j^2 D + \varepsilon(j, X) I_m \quad (1.3a)$$

for cations j

$$\log_{10}\gamma_j = - z_j^2 D + \varepsilon(j, N) I_m \quad (1.3b)$$

for anions j, and

$$\log_{10}\gamma_j = \varepsilon(j, N+X) I_m \quad (1.3c)$$

for neutral j.

Note that in eq. (1.3c) lies a hidden subtlety: If a neutral species interacts with the background electrolyte, it may interact with both the cation and the anion and eq. (1.3c) should be written as

$$\log_{10}\gamma_j = \varepsilon(j, N)\, m_N + \varepsilon(j, X)\, m_X$$

If $m_N = m_X = I_m$, then

$$\log_{10}\gamma_j = (\varepsilon(j, N) + \varepsilon(j, X))\, I_m$$

where $(\varepsilon(j, N) + \varepsilon(j, X))$ can be replaced with the shorthand $\varepsilon(j, N+X)$, since in such a case, interactions of the neutral species with cations cannot be distinguished from those with anions. If $\varepsilon(j, N+X)$ needs to be applied in situations where $m_N \neq m_X$, one may use the assumption that

$$\varepsilon(j, N) = \varepsilon(j, X) = ½\ \varepsilon(j, N+X)$$

As noted, e.g., by Grenthe et al. (2013), the specific ion interaction coefficients are not strictly constant. They may vary slightly as a function of ionic strength. The variation depends on the charge and is often negligible, as is usually the case for 1:1, 1:2, and 2:1 electrolytes for molalities lower than 3.5 mol · kg^{-1} (Grenthe et al. 2013). In order to cope with variations of ε with ionic strength, Ciavatta (1980) proposed the use of

$$\varepsilon = \varepsilon_1 + \varepsilon_2 \log_{10} I_m$$

in a footnote to a table without any further explanation or theoretical justification. He applied this expression in all cases where the uncertainties in the specific interaction coefficients exceeded ± 0.03 kg · mol^{-1}. This expression was used occasionally in NEA reviews and was systematically applied by Brown & Ekberg (2016), but Grenthe et al. (2020) remarked that "even if the value of ε calculated in this way describes the variation with ionic strength slightly better than a constant value, this equation has no theoretical basis; ε is a fitting parameter and the term $\varepsilon_2 \log_{10} I_m$ goes to minus infinity at the limiting value $I_m = 0$. This expression for the composition dependence of ε should be avoided, even though the term $\varepsilon \cdot m = (\varepsilon = \varepsilon_1 + \varepsilon_2 \log_{10} I_m) \cdot m$ (in the calculation of activity coefficients) is zero at $I_m = 0$. There may be cases where reviewers may still want to use $[\varepsilon = \varepsilon_1 + \varepsilon_2 \log_{10} I_m]$ to describe ionic strength variation of the interaction parameters, but the rationale behind this should then be described".

As an alternative, Grenthe et al. (2013), suggested the use of

$$\varepsilon = \varepsilon_1 + \varepsilon_{1.5}\, I_m^{1/2}$$

with the well-behaved property that $\varepsilon \rightarrow \varepsilon_1$ as $I_m \rightarrow 0$. This expression is the consequence of a virial expansion of the mean-activity coefficient $\gamma_\pm$ (in this case for a binary electrolyte with charge z_+ and z_-), see Grenthe et al. (1997), p. 347, truncated after the term with $I_m^{3/2}$ (the classical SIT equation is truncated one term earlier)

$$\log_{10}\gamma_\pm = -(A|z_+ z_-|I_m^{0.5})/(1 + 1.5\, I_m^{0.5}) + \varepsilon_1 I_m + \varepsilon_{1.5} I_m^{1.5}$$

where the last two terms can be written as $\varepsilon I_m = (\varepsilon_1 + \varepsilon_{1.5}\, I_m^{0.5}) I_m$. This alternative SIT equation is sporadically discussed in NEA reviews, but no coefficients were recommended so far.

In TDB 2020 none of these "extended" SIT equations was used, neither the $\varepsilon_2 \log_{10} I_m$ extension favoured by Brown & Ekberg (2016), nor the $\varepsilon_{1.5} I_m^{1/2}$ extension proposed by Grenthe et al. (2013). The main reason for not using any of these "extensions" is that in TDB 2020 a complete set of SIT coefficients is provided for use in speciation calculations (Tab. A-6). In order to get this self-consistent set of SIT coefficients it is necessary to do all SIT regression analyses with the same SIT equation. Brown & Ekberg (2016) decided to use the $\varepsilon_2 \log_{10} I_m$ extension in all their fits, but just ignoring this term usually leads to very bad approximations in the ionic strength range of interest. Hence, many of their data were re-fitted in this review with the "standard" SIT equation.

1.5.2 Derivation of equilibrium constants from experimental data at varying ionic strengths using activity coefficient corrections according to SIT

In order to illustrate the activity coefficient corrections using SIT, as performed by this review, we follow Grenthe et al. (2020) by considering the general complex formation reaction,

$$m\ M + q\ L + n\ H_2O(l) \rightleftharpoons M_mL_q(OH)_n + n\ H^+$$

where charges on M (a metal cation), L (an anionic ligand), and $M_mL_q(OH)_n$ have been omitted for better readability.

The formation constant of $M_mL_q(OH)_n$ at zero ionic strength, $\log_{10}{}^*\beta^\circ_{q,n,m}$, can be expressed in terms of the activities of the species taking part in the reaction:

$$\log_{10}{}^*\beta^\circ_{q,n,m} = \log_{10} a_{M_mL_q(OH)_n} + n \log_{10} a_{H^+} - m \log_{10} a_M - q \log_{10} a_L - n \log_{10} a_{H_2O(l)} \quad (1.4)$$

The activities of the solutes are given by

$$\log_{10} a_{M_mL_q(OH)_n} = \log_{10} \gamma_{M_mL_q(OH)_n} + \log_{10} m_{M_mL_q(OH)_n}$$

$$\log_{10} a_{H^+} = \log_{10} \gamma_{H^+} + \log_{10} m_{H^+}$$

$$\log_{10} a_M = \log_{10} \gamma_M + \log_{10} m_M$$

$$\log_{10} a_L = \log_{10} \gamma_L + \log_{10} m_L$$

Inserting these expressions for the activities into eq. (1.4) leads to

$$\log_{10}{}^*\beta^\circ_{q,n,m} = \log_{10} \gamma_{M_mL_q(OH)_n} + \log_{10} m_{M_mL_q(OH)_n} + n(\log_{10} \gamma_{H^+} + \log_{10} m_{H^+}) - m\ (\log_{10} \gamma_M + \log_{10} m_M) - q(\log_{10} \gamma_L + \log_{10} m_L) - n \log_{10} a_{H_2O(l)}$$

The conditional formation constant of $M_mL_q(OH)_n$, $\log_{10}{}^*\beta_{q,n,m}$, is given by the molalities of the solute species,

$$\log_{10}{}^*\beta_{q,n,m} = \log_{10} m_{M_mL_q(OH)_n} + n \log_{10} m_{H^+} - m \log_{10} m_M - q \log_{10} m_L \quad (1.5)$$

Therefore, $\log_{10}{}^{*}\beta_{q,n,m}$ is related to $\log_{10}{}^{*}\beta^{\circ}_{q,n,m}$ by

$$\log_{10}{}^{*}\beta_{q,n,m} = \log_{10}{}^{*}\beta^{\circ}_{q,n,m} + m \log_{10}\gamma_{M} + q \log_{10}\gamma_{L} + n \log_{10} a_{H_2O(l)} - \log_{10}\gamma_{M_mL_q(OH)_n} - n \log_{10}\gamma_{H^+} \quad (1.6)$$

The activity coefficients for the solute species follow from eqs. (1.1) and (1.3):

$$\log_{10}\gamma_{M} = -z_{M}^2 D + \varepsilon(M, X)\, I_m$$

$$\log_{10}\gamma_{L} = -z_{L}^2 D + \varepsilon(N, L)\, I_m$$

$$\log_{10}\gamma_{H^+} = -D + \varepsilon(H^+, X)\, I_m$$

$$\log_{10}\gamma_{M_mL_q(OH)_n} = -z^2_{M_mL_q(OH)_n} D + \varepsilon(M_mL_q(OH)_n, N \text{ or } X \text{ or } N{+}X)\, I_m$$

where

$$z^2_{M_mL_q(OH)_n} = (m\, z_M - q\, z_L - n)^2$$

Inserting these expressions for the activity coefficients into eq. (1.6) and rearranging leads to

$$\log_{10}{}^{*}\beta_{q,n,m} - \Delta z^2 D - n \log_{10} a_{H_2O(l)} = \log_{10}{}^{*}\beta^{\circ}_{q,n,m} - \Delta\varepsilon\, I_m \quad (1.7a)$$

with:

$$\Delta z^2 = (m\, z_M - q\, z_L - n)^2 + n - m\, z_M^2 - q\, z_L^2 \quad (1.7b)$$

$$D = \frac{0.509\sqrt{I_m}}{1+1.5\sqrt{I_m}} \text{ (at 298.15 K and 1 bar)} \quad (1.7c)$$

$$\Delta\varepsilon = \varepsilon\left(M_mL_q(OH)_n, N \text{ or } X \text{ or } N{+}X\right) + n\, \varepsilon(H^+, X) - q\, \varepsilon(N, L) - m\, \varepsilon(M, X) \quad (1.7d)$$

Eq. (1.7) serves to derive $\log_{10}{}^{*}\beta^{\circ}_{q,n,m}$ and $\Delta\varepsilon$ from experimental values of conditional stability constants $\log_{10}{}^{*}\beta^{\circ}_{q,n,m}$ at ionic strength I_m. Note that equilibria involving $H_2O(l)$ as reactant or product also require that the activity of water is known at the experimental conditions. Water activities can be calculated from osmotic coefficients of electrolyte mixtures (see Grenthe et al. 2020 for further details), or can be taken from tabulated data. For example, Lemire et al. (2013) tabulated the water activities for the most common ionic media at various concentration (see their Tab. B-1). For the purposes of this review, we fitted the water activity data for NaCl, $NaClO_4$, $NaNO_3$, and $LiClO_4$ tabulated by Lemire et al. (2013) at various concentrations c (molar scale) to the polynomial function $a_w c = 1 + a\, c + b\, c^2$. The resulting coefficients a and b are listed in Tab. 1-1.

Tab. 1-1: Polynomial coefficients for the water activity function $a_w c = 1 + a\ c + b\ c^2$

They are used to fit water activity data as a function of background electrolyte concentration (on the molar scale) for some electrolytes given in Tab. B-1 of Lemire et al. (2013).

Electrolyte	**a**	**b**
NaCl	-0.0303533	-0.00276723
$NaClO_4$	-0.0294804	-0.00316899
$NaNO_3$	-0.0304957	-0.000125847
$LiClO_4$	-0.0299656	-0.0092743

Since the specific ion interaction coefficients are only weakly dependent on I_m, $\Delta\varepsilon$ can be assumed to be constant, and eq. (1.7a) can then be interpreted as a linear function y = m x + b, where the experimental data (given by the left-hand side of the equation) corresponds to the dependent variable y, the ionic strength to the independent variable x, $-\Delta\varepsilon$ to the slope m and $\log_{10}{}^*\beta^\circ_{q,n,m}$ to the y-axis intercept b.

1.5.2.1 Conversion from molarity to molality

The discussion in this section is based on Section 2.2 in Grenthe et al. (2020). SIT, as used by NEA and by this review, is based on molal concentrations m (mol · kg^{-1}, abbreviated as m for molality). For this reason, molar concentrations c of solutes (mol · dm^{-3}, abbreviated as M for molarity) and conditional equilibrium constants $\log_{10}K_c$, (based on molar concentrations) have to be converted into molal concentrations m and conditional equilibrium constants $\log_{10}K_m$ (based on molal concentrations), respectively. Likewise, ionic strengths expressed in the molar scale, I_c (mol · dm^{-3}), must be converted into I_m in the molal scale (mol · kg^{-1}).

The molality of substance B, m_B, is defined as the number of moles of B, n_B, dissolved in the mass of pure solvent A (in most cases pure water), $mass_A$,

$$m_B = n_B / mass_A \tag{1.8}$$

The molarity of substance B, c_B, is defined as the number of moles of B, n_B, dissolved in the volume V of solution,

$$c_B = n_B / V \tag{1.9}$$

The density ρ of a solution of solute B in solvent A is given by the mass of the solution divided by its volume,

$$\rho = (n_B M_B + mass_A) / V$$

where M_B is the molar mass of solute B.

If the solution additionally contains n_I moles of an inert background electrolyte I of molar mass M_I, whose molarity c_I is given by

$$c_I = n_I / V \tag{1.10}$$

The density of the solution is given by

$$\rho = (n_B M_B + n_I M_I + mass_A) / V \tag{1.11}$$

From eqs. (1.8) to (1.11) then follows ξ, the conversion factor from molarity c_B to molality m_B of solute B,

$$\xi \equiv m_B / c_B = 1 / (\rho - c_B M_B - c_I M_I)$$

If the molarity c_B of solute B is small compared to the molarity c_I of the background electrolyte I, the conversion factor ξ can be approximated by

$$\xi \equiv m_B / c_B = 1 / (\rho - c_I M_I) \tag{1.12}$$

Thus, the conversion factor ξ can be calculated from the density ρ of the background electrolyte as a function of its molar concentration c_I and from its molar mass M_I.

Knowing ξ, the molarity c_B of solute B can be converted into its molality m_B according to

$$m_B = \xi c_B$$

Similarly, the molar ionic strength I_c can be converted into the molal ionic strength I_m according to

$$I_m = \xi I_c$$

In their Tab. II-5, Lemire et al. (2013) present conversion factors ξ for several electrolytes, based on densities given by Söhnel & Novotny (1985).

Söhnel & Novotny (1985) derived polynomial expressions for the densities ρ (in kg · m^{-3}, which is equivalent to g·cm^{-3}) of numerous electrolytes as a function of temperature t (in °C!) and concentration c (in mol · dm^{-3}). The general form of the polynomial is

$$\rho(c, t) = \rho_I(t) + A\ c + B\ c\ t + C\ c\ t^2 + D\ c^{3/2} + E\ c^{3/2}\ t + F\ c^{3/2}\ t^2 \tag{1.13}$$

where $\rho_I(t)$ is the density of pure liquid water as a function of temperature, given by the polynomial

$$\rho_I(t) = a + b\ t + c\ t^{3/2}$$

with a = 999.65, b = 0.20438, and c = -0.061744.

The polynomial coefficients derived by Söhnel & Novotny (1985) for several electrolytes used in this review are given in Tab. 1-2.

Tab. 1-2: Polynomial coefficients for the density function $\rho(c, t) = \rho_l(t) + A\ c + B\ c\ t + C\ c\ t^2 + D\ c^{3/2} + E\ c^{3/2}\ t + F\ c^{3/2}\ t^2$

These are used for several electrolytes in this review. Note that t is the temperature in °C. Resulting densities are in in $kg \cdot m^{-3}$, which is equivalent to $g \cdot cm^{-3}$. Coefficients are derived from Söhnel & Novotny (1985).

Electrolyte	**A**	**B**	**C**	**D**	**E**	**F**
NaCl	44.85	-0.09634	0.0006136	-2.712	0.01009	0
$NaClO_4$	84.62	-0.3788	0.003966	-3.025	0.09968	-0.001113
$NaNO_3$	62.98	-0.2382	0.00152	-4.138	0.06626	-0.0004208
$LiClO_4$	69.57	-0.328	0.002913	-3.409	0.1242	-0.001288

Conditional equilibrium constants expressed in terms of molar concentrations, $\log_{10}K_c$, need also to be converted into conditional equilibrium constants expressed in terms of molal concentrations, $\log_{10}K_m$. For a general equilibrium reaction $\Sigma_B\ \nu_B\ B = 0$ involving substances B with the stoichiometric coefficients ν_B (negative for reactants and positive for products) the conditional equilibrium constants are given by

$$\log_{10}K_c = \Sigma_B(\nu_B \log_{10}c_B)$$

for molar concentrations and by

$$\log_{10}K_m = \Sigma_B(\nu_B \log_{10}m_B)$$

for molal concentrations.

With $\xi = m_B / c_B$, or $\log_{10}\xi = (\log_{10}m_B - \log_{10}c_B)$ it follows from the last two equations that

$$\log_{10}K_m = \log_{10}K_c + \Sigma_B(\nu_B \log_{10}\xi)$$

which is equivalent to

$$\log_{10}K_m = \log_{10}K_c + \log_{10}\xi\ \Sigma_B\nu_B \qquad (1.14)$$

It is important to note that for conditional equilibrium constants the sums in the last four equations are extended over the solutes only, since the activity of water is not included in conditional constants (see eq. (1.5)), as well as the activities of solids and the partial pressures of gases. Thus, the stoichiometric coefficients of water, solids and gases are not included in the sum of stoichiometric coefficients $\Sigma_B\nu_B$ appearing in eq. (1.14).

1.5.2.2 Example for the approach

As an example, consider the formation of the complex $Ps(CO_3)(OH)_3^-$ of the hypothetical element Ps (Psium)

$$Ps^{4+} + CO_3^{2-} + 3\ H_2O(l) \rightleftharpoons Ps(CO_3)(OH)_3^- + 3\ H^+$$

According to eq. (1.7b)

$$\Delta z^2 = \left(z_{Ps(CO_3)(OH)_3^-}\right)^2 + 3\left(z_{H^+}\right)^2 - \left(z_{Ps^{4+}}\right)^2 - \left(z_{CO_3^{2-}}\right)^2 = -16$$

From eq. (1.7a) then follows

$$\log_{10}{}^*\beta + 16\,D - 3\log_{10} a_{H_2O(l)} = \log_{10}{}^*\beta^\circ - \Delta\varepsilon\, I_m$$

where the subscripts of the formation constants have been removed for the sake of simplicity. Given a set of experimental values for $\log_{10}{}^*\beta$ with uncertainties σ, determined over a range of ionic strengths, the following steps have to be taken to obtain $\log_{10}{}^*\beta^\circ$ and $\Delta\varepsilon$ from linear regression of the data.

1. **Conversion from molarity to molality:** The hypothetical experimental values for the conditional stability constants $\log_{10}{}^*\beta_c$ (with uncertainties σ at the 95% confidence level) at ionic strengths I_c (the background electrolyte is assumed to be NaCl with $I_c = c_{NaCl}$), see Tab. 1-3, are given on the molar scale. In order to apply the SIT formalism, $\log_{10}{}^*\beta_c$ and I_c have to be converted into the molal scale. For these conversions, $\xi = m_B / c_B$, the ratio of molality to molarity of substance B, needs to be known for the NaCl background electrolyte. ξ is calculated from eq. (1.12) where the density ρ of the NaCl solution as a function of molar concentration is calculated according to eq. (1.13) with the polynomial coefficients for NaCl as given in Tab. 1.2. The molar mass of NaCl used in eq. (1.12) is 58.443 g · mol^{-1}. ξ can be used directly to convert I_c into I_m. For the conversion of $\log_{10}{}^*\beta_c$ into $\log_{10}{}^*\beta_m$, eq. (1.14) is used, with $\Sigma_B \nu_B = 2$ for the reaction $Ps^{4+} + CO_3^{2-} + 3\ H_2O(l) \rightleftharpoons Ps(CO_3)(OH)_3^- + 3\ H^+$ (note that, as already pointed out before, the stoichiometric coefficient of $H_2O(l)$ is not included in this sum). ρ(NaCl) and ξ at the "experimental" ionic strengths I_c are given in Tab. 1-3, as well as the resulting values for I_m and $\log_{10}{}^*\beta_m$.

2. **Calculation of $\log_{10}{}^*\beta_m - \Delta z^2\, D - n \log_{10} a(H_2O)$:** For the reaction $Ps^{4+} + CO_3^{2-} + 3\ H_2O(l) \rightleftharpoons Ps(CO_3)(OH)_3^- + 3\ H^+$, Δz^2 is equal to -16. D is calculated from I_m according to eq. (1.7c), n is equal to -3, and $a(H_2O)$ is taken from tabulated data, e.g., by Lemire et al. (2013), or calculated, as in this case, from the function $a(H_2O) = 1 + a\ c + b\ c^2$, where c is the molar concentration of the background electrolyte NaCl (equivalent to I_c), and a and b are the corresponding coefficients taken from Tab. 1-1. The uncertainty of $\log_{10}{}^*\beta_m + 16\ D - 3 \log_{10} a(H_2O)$ is assumed to be equal to σ determined for $\log_{10}{}^*\beta_c$, neglecting uncertainties in D and $a(H_2O)$ and neglecting the effect on σ when $\log_{10}{}^*\beta_c$ is converted into $\log_{10}{}^*\beta_m$.

3. **Linear regression:** Now that $\log_{10}{}^*\beta_m + 16\,D - 3\,\log_{10}a(H_2O)$ with uncertainty σ is known at each experimental ionic strength I_m, a weighted linear regression of the data can be carried out. NEA selected a weighted linear regression procedure, described, e.g., by Grenthe et al. (2020) in their Section C.5, which was also adopted for this review. A peculiarity of their approach is that the uncertainties of $\log_{10}{}^*\beta_m - \Delta z^2\,D - n\,\log_{10}a(H_2O)$ are not only used for the weighting of the data but also for the calculation of the uncertainties of the intercept ($\log_{10}{}^*\beta^\circ$) and the slope ($-\Delta\varepsilon$). Thus, as pointed out by Grenthe et al. (2020), the uncertainties of intercept and slope do not depend on the dispersion of the data points around the regression line, but rather directly on the uncertainties of the data themselves. This has also the consequence that if the uncertainties of the datapoints represent the 95% confidence level, the uncertainties of intercept and slope will also do so.

The weighted linear regression of the hypothetical experimental data shown in Tab. 1-3 is carried out as follows:

The experimental data given in the form of $\log_{10}{}^*\beta_m + 16\,D - 3\,\log_{10}a_{H_2O(l)}$ are a linear function of the ionic strength I_m:

$$\log_{10}{}^*\beta_m + 16\,D - 3\,\log_{10}a_{H_2O(l)} = \log_{10}{}^*\beta_m^\circ - \Delta\varepsilon\,I_m \qquad (1.15)$$

This equation corresponds to the equation of a line in a plot of $\log_{10}{}^*\beta + 16\,D - 3\,\log_{10}a_{H_2O(l)}$ vs. I_m, which has the form y = m x + b, where

$y = \log_{10}{}^*\beta_m + 16\,D - 3\,\log_{10}a_{H_2O(l)}$ (experimental data)

$m = -\Delta\varepsilon$ (slope)

$x = I_m$ (experimental conditions)

$b = \log_{10}{}^*\beta_m^\circ$ (y-axis intercept)

For the linear regression, the following nomenclature is used (it is understood that the molal scale is used and the subscript m is dropped at the appropriate places in the equations used for the regression):

y_i: Experimental data point i at ionic strength I_i, with index i running from 1 to N

N: Number of experimental data points

i: Index of experimental data point y_i, running from 1 to N

σ_i: Uncertainty of experimental data point i

σ_b: Uncertainty of y-axis intercept b

σ_m: Uncertainty of slope m

Tab. 1-3: Hypothetical experimental data ($\log_{10}{}^*\beta_c$ at I_c) for the example

The data are for the complexation reaction $Ps^{4+} + CO_3^{2-} + 3\ H_2O(l) \rightleftharpoons Ps(CO_3)(OH)_3^- + 3\ H^+$ of the hypothetical element Ps (Psium) in NaCl solutions, and derived and auxiliary data used for the SIT regression discussed in the text and shown in Fig. 1-2.

I_c [mol · dm^{-3}]	$\log_{10}{}^*\beta_c$ [molar scale]	ρ(NaCl) [kg · dm^{-3}]	ξ [dm^{-3} · kg^{-1}]	I_m [mol · kg^{-1}]	$\log_{10}{}^*\beta_m$ [molal scale]	D	$a(H_2O)$	$\log_{10}{}^*\beta_m - \Delta z^2 D + n \log a(H_2O)$	σ
0.3	9.14 ± 0.10	1.0095	1.0081	0.302	9.15	0.1534	0.9906	11.61	0.10
0.5	8.72 ± 0.12	1.0176	1.0118	0.506	8.73	0.1752	0.9841	11.55	0.12
0.9	8.32 ± 0.05	1.0335	1.0195	0.918	8.34	0.2001	0.9704	11.58	0.05
1.2	8.08 ± 0.11	1.0452	1.0256	1.231	8.10	0.2120	0.9596	11.55	0.11
1.5	7.84 ± 0.08	1.0568	1.0319	1.548	7.87	0.2209	0.9482	11.47	0.08
1.8	7.69 ± 0.10	1.0682	1.0384	1.869	7.72	0.2281	0.9364	11.46	0.10
2.0	7.55 ± 0.14	1.0757	1.0429	2.086	7.59	0.2322	0.9282	11.40	0.14
2.4	7.38 ± 0.09	1.0907	1.0522	2.525	7.42	0.2390	0.9112	11.37	0.09
2.8	7.26 ± 0.06	1.1054	1.0618	2.973	7.31	0.2447	0.8933	11.37	0.06
3.0	7.16 ± 0.11	1.1127	1.0668	3.200	7.22	0.2472	0.8840	11.33	0.11
3.5	6.99 ± 0.13	1.1308	1.0796	3.779	7.06	0.2527	0.8599	11.30	0.13

With this nomenclature, eqs. (C.11) through (C.15) by Grenthe et al. (2020), used for the calculation of b = $\log_{10}{}^*\beta_m^\circ$ and m = -$\Delta\varepsilon$, can be written as follows:

$$b = \log_{10}{}^*\beta^\circ = \frac{1}{\Delta}\left(\sum_{i=1}^{N}\frac{I_i^2}{\sigma_i^2}\sum_{i=1}^{N}\frac{y_i}{\sigma_i^2} - \sum_{i=1}^{N}\frac{I_i}{\sigma_i^2}\sum_{i=1}^{N}\frac{I_i y_i}{\sigma_i^2}\right) \tag{1.16}$$

$$m = -\Delta\varepsilon = \frac{1}{\Delta}\left(\sum_{i=1}^{N}\frac{1}{\sigma_i^2}\sum_{i=1}^{N}\frac{I_i y_i}{\sigma_i^2} - \sum_{i=1}^{N}\frac{I_i}{\sigma_i^2}\sum_{i=1}^{N}\frac{y_i}{\sigma_i^2}\right) \tag{1.17}$$

$$\sigma_b = \sqrt{\frac{1}{\Delta}\sum_{i=1}^{N}\frac{I_i^2}{\sigma_i^2}} \tag{1.18}$$

$$\sigma_m = \sqrt{\frac{1}{\Delta}\sum_{i=1}^{N}\frac{1}{\sigma_i^2}} \tag{1.19}$$

where

$$\Delta = \sum_{i=1}^{N}\frac{1}{\sigma_i^2}\sum_{i=1}^{N}\frac{I_i^2}{\sigma_i^2} - \left(\sum_{i=1}^{N}\frac{I_i}{\sigma_i^2}\right)^2 \tag{1.20}$$

The weighted linear regression of $\log_{10}{}^*\beta_m + 16\ D - 3\ \log_{10}a(H_2O)$ vs. I_m for the data given in Tab. 1-3 using eqs. (1.16) - (1.20) leads to $\log_{10}{}^*\beta_m^\circ$(298.15 K) = (11.65 ± 0.05) and $\Delta\varepsilon$ = (0.10 ± 0.03), see Fig. 1-2. Note that $\Delta\varepsilon$ corresponds to the negative slope of the regression line.

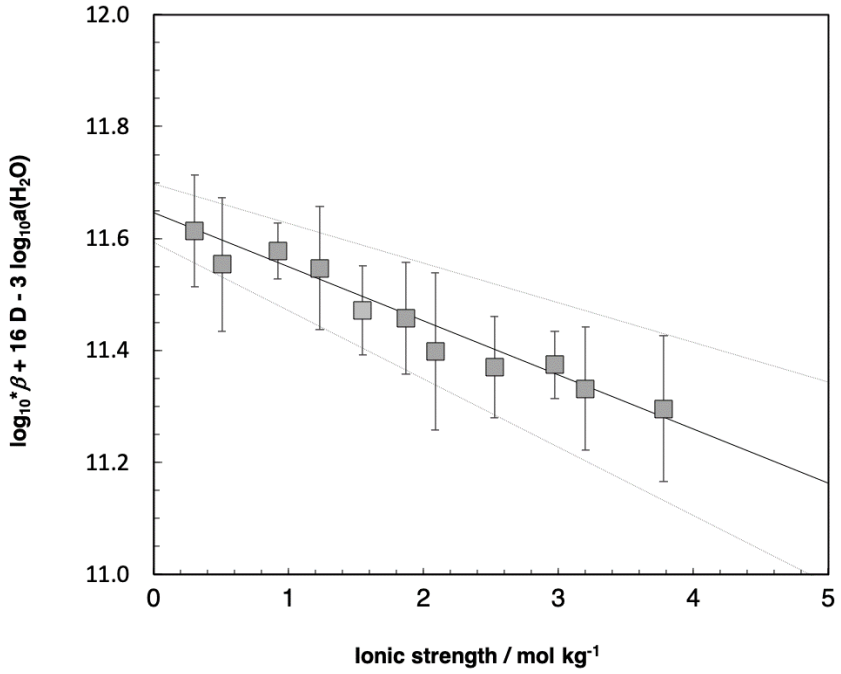

Fig. 1-2: SIT plot for the complexation reaction $Ps^{4+} + CO_3^{2-} + 3\ H_2O(l) \rightleftharpoons Ps(CO_3)(OH)_3^- + 3\ H^+$ of the hypothetical element Ps (Psium) based on the data given in Tab. 1-3

The solid line results from the linear regression of the data, where the negative slope corresponds to the SIT interaction coefficient $\Delta\varepsilon = (0.10 \pm 0.03)$ kg · mol^{-1}, and the y-axis intercept to the stability constant at zero ionic strength $\log_{10}{}^*\beta_m^\circ(298.15\ K) = (11.65 \pm 0.05)$. The dotted lines represent the associated uncertainty range extrapolated from zero ionic strength to higher ionic strengths.

1.5.3 Estimations of SIT parameters by charge considerations only

In the past, SIT was mainly used to extrapolate experimental values of equilibrium constants to zero ionic strength, as described above. If experimental data were not available, or not sufficiently reliable for SIT analyses, SIT interaction parameters sometimes were estimated in order to extrapolate experimental values to zero ionic strength.

The simplest and most often used estimation procedure is based on chemical analogy reasoning.

The similar ionic radii of the actinide series are often used to justify assumptions like $\varepsilon(UO_2^{2+},ClO_4^-) \approx \varepsilon(NpO_2^{2+},ClO_4^-) \approx \varepsilon(PuO_2^{2+},ClO_4^-)$. In this series, only $\varepsilon(UO_2^{2+},ClO_4^-)$ has been derived from mean activity data, and the values for NpO_2^{2+} and PuO_2^{2+} were assumed to be the same as for UO_2^{2+}.

The similar values for Na and K forms of SIT interaction coefficients are used as an argument for analogies like $\varepsilon(Mg(ox)_2^{2-},Na^+) \approx \varepsilon(Mg(ox)_2^{2-},K^+)$. Likewise, the similar values for Ca and Mg forms of SIT interaction coefficients may justify $\varepsilon(Mg(ox)_2^{2-},Na^+) \approx \varepsilon(Ca(ox)_2^{2-},Na^+)$. In these cases, only $\varepsilon(Mg(ox)_2^{2-},Na^+)$ has been derived from experimental values of equilibrium constants at different ionic strengths as described above.

Sometimes, only charge considerations serve as a plausibility argument, e.g., $\varepsilon(Np(SCN)_3^+,ClO_4^-) \approx \varepsilon(AmF_2^+,ClO_4^-)$. In this example the actinides do not have the same charge and the complexes have different stoichiometries, only the resulting charge of the complex is the same. All the above examples were taken from Appendix B in Rand et al. (2007).

There are no formal criteria for estimating SIT interaction parameters by chemical analogy. They are all based on expert judgement, mostly introduced ad hoc when the need arose in the review procedure.

However, when SIT is applied in environmental modelling, the formally correct implementation of SIT in a speciation code like GEMS is not sufficient. The remaining gaps in the SIT interaction coefficient matrix have to be filled with reasonably justified "default values" in all cases.

In the current version of our TDB, we decided to restrict the application of SIT to environmental systems where the salinity is governed by NaCl.

In addition, laboratory systems can be modelled for NaCl and $NaClO_4$ media. The nowadays rarely used background medium KNO_3 was not considered.

The method to estimate "default" SIT values was a thorough statistical analysis of all published SIT interaction coefficients for NaCl and $NaClO_4$ media.

SIT $\varepsilon(j,k)$ values were taken from Tab. B-4, B-5 and B-7 in Rand et al. (2007). Care was taken only to consider values which were obtained from experimental data and did not involve any estimates. If, e.g., $\Delta\varepsilon$ for the formation reaction of a specific product species is derived from experimental data, the ε-value for the product species can be calculated from $\Delta\varepsilon$ and the ε-values of the remaining species in the reaction. The resulting ε-value of the product species was only accepted if the ε-values of the remaining species in the reaction were not estimated (and did not depend themselves on estimated values, if they were derived from experimental $\Delta\varepsilon$ values). In this way, the whole chain of dependencies was checked for estimates.

For the statistical analysis, uncertainties of individual $\varepsilon(j,k)$ smaller than $\pm$ 0.05 were increased to $\pm$ 0.05.

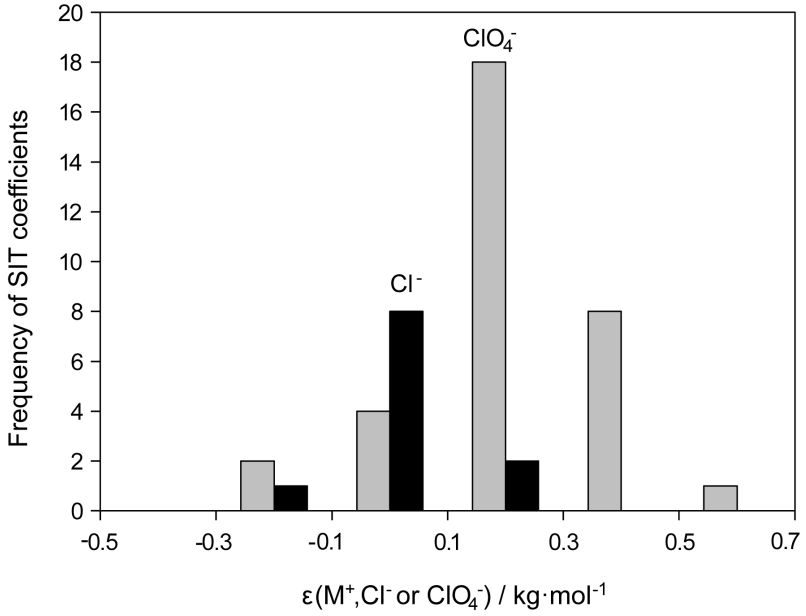

Fig. 1-3: Frequency of SIT interaction parameters $\varepsilon(M^+,Cl^-)$ (black bars) and $\varepsilon(M^+,ClO_4^-)$ (grey bars)

The histogram is produced with experimental data taken from Rand et al. (2007). Statistical analyses of these data resulted in $\varepsilon(M^+,Cl^-) = 0.02 \pm 0.08$ (unweighted mean) or 0.04 ± 0.02 (weighted mean); and $\varepsilon(M^+,ClO_4^-) = 0.22 \pm 0.07$ (unweighted mean) or 0.20 ± 0.01 (weighted mean).

Tab. 1-4: SIT interaction parameter estimations based on charge considerations only

For each charge type and medium the number of data used for statistical analysis, the unweighted mean, the weighted mean and the finally selected "default value" is given.

Charge	$\varepsilon(M^{n+},ClO_4^-)$				$\varepsilon(M^{n+},Cl^-)$			
	No.	Unweighted mean	Weighted mean	Selected	No.	Unweighted mean	Weighted mean	Selected
1	33	0.22 ± 0.07	0.22 ± 0.01	0.2	12	0.08 ± 0.16	0.05 ± 0.02	0.05
2	24	0.39 ± 0.08	0.33 ± 0.01	0.4	15	0.21 ± 0.10	0.16 ± 0.02	0.15
3	17	0.64 ± 0.08	0.57 ± 0.02	0.6	3	0.31 ± 0.03	0.27 ± 0.02	0.25
4	10	0.75 ± 0.17	0.82 ± 0.02	0.8	5	0.29 ± 0.23	0.29 ± 0.07	0.35
5	2	1.11 ± 0.20	1.23 ± 0.09	1.0	2	0.48 ± 0.16	0.46 ± 0.07	0.45

Tab. 1-5: SIT interaction parameter estimations based on charge considerations only

For each charge type the number of data used for statistical analysis, the unweighted mean, the weighted mean and the finally selected "default value" is given.

Charge	**ε(MX, NaCl or $NaClO_4$)**			
	No.	**Unweighted mean**	**Weighted mean**	**Selected**
0	11	-(0.01 ± 0.11)	0.03 ± 0.02	0.0
	ε(X^{n-}, Na^+)			
-1	38	-(0.03 ± 0.06)	-(0.03 ± 0.01)	-0.05
-2	21	-(0.10 ± 0.06)	-(0.10 ± 0.01)	-0.10
-3	8	-(0.10 ± 0.19)	-(0.15 ± 0.03)	-0.15
-4	4	-(0.1 ± 0.4)	-(0.18 ± 0.04)	-0.20

Tab. 1-6: SIT interaction parameter estimations based on charge considerations only

The results of linear regression analyses, based on weighted means given in Tabs. 1-4 and 1.5 and Fig. 1-4, and the finally selected "default values" are given.

SIT coefficient	**Linear regression of weighted mean values**			**Selected**	
	Charge range	**Constant**	**Slope**	**Constant**	**Slope**
ε(M^{n+},Cl^-)	1 … 5	0.02 ± 0.05	0.094 ± 0.029	0.00	0.10
ε(M^{n+},ClO_4^-)	0 … 4	0.01 ± 0.04	0.194 ± 0.008	0.00	0.20
ε(X^{n-},Na^+)	-1 … -4	0.01 ± 0.02	0.050 ± 0.011	0.00	0.05

The statistical analyses comprised the following procedures:

(1) Calculation of the unweighted mean, $< X> \pm t \cdot s / \sqrt{n}$, for each charge type and medium, where $< X> = \Sigma\varepsilon(j,k) / n$, $s = \sqrt{[\Sigma(\varepsilon(j,k) - < X>)^2 / (n - 1)]}$ is the standard deviation, n is the number of ε(j,k) values, and t is the Student t factor accounting for the number of data points used (for $n \rightarrow \infty$ t = 1.96). The uncertainty, $\pm t \cdot s / \sqrt{n}$, represents the dispersion of the data points at the 95% confidence level. Results are given in Tabs. 1-4 and 1-5, and in Figs. 1-3 and 1-4.

(2) Calculation of the weighted mean, $< X> \pm \sigma_{< X>}$, for each charge type and medium, where $< X> = \Sigma[\varepsilon(j,k) / \sigma(j,k)] / \Sigma[1 / \sigma(j,k)^2]$, $\sigma_{< X>} = \Sigma[1 / \Sigma\{1 / \sigma(j,k)^2\}]$ and σ(j,k) is the individual uncertainty assigned to each ε(j,k) value at the 95% confidence level (data taken from Rand et al. 2007). Hence, the uncertainty of the weighted mean, $\pm \sigma_{< X>}$, is based on the individual uncertainties σ(j,k) only, and is independent of the dispersion of the data points. Results are given in Tabs. 1-4 and 1-5, and in Figs. 1-3 and 1-4.

(3) Calculation of linear regressions based on the weighted means. Results are given in Tab. 1-6.

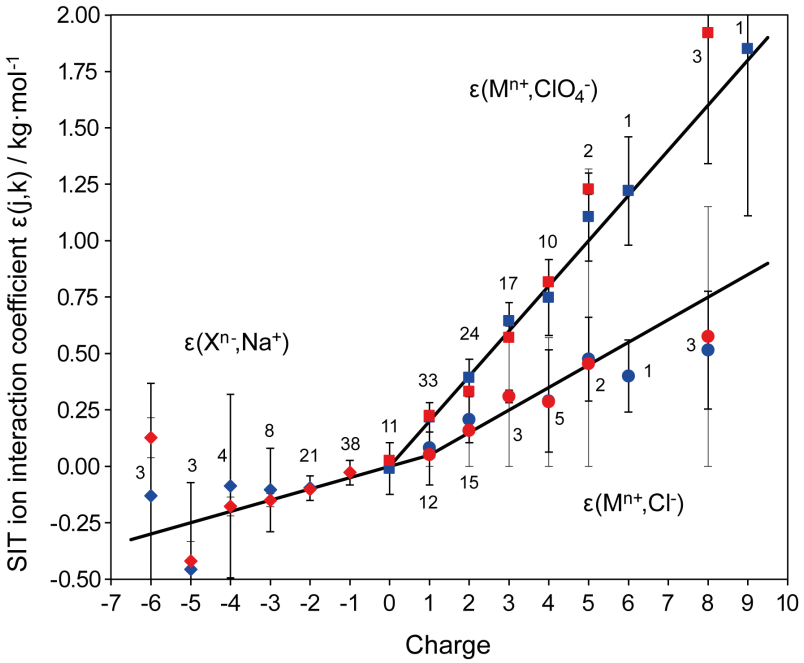

Fig. 1-4: Correlation of SIT interaction parameters with charge only

Blue symbols with error bars represent unweighted means where the uncertainty is based on the dispersion of the data points. Red symbols with error bars represent weighted means. The number of data points used to calculate the means are given in the figure. In the case of just one data point the estimated uncertainty of the SIT parameter is shown. Solid lines visualise the finally selected "default values" of SIT interaction parameters.

The finally selected "default values" given in Tabs. 1-4 – 1.6 and visualised in Fig. 1-4 are based on these statistical results. However, they are expert choices which were guided by the idea to provide numbers as simple as possible which are still compatible with the statistical results.

The recommended "default values" are summarised in Tab. 1-7 with estimated uncertainties. As uncertainty estimates in the charge range -3 to +3 the uncertainties of the unweighted means were taken (Tab. 1.4 and 1.5, rounded to one significant digit), i.e., the uncertainty estimate is based on the dispersion of the data points. Uncertainties outside this charge range are mere guesses following the uncertainty trends revealed in Fig. 1-4. The "default values" can also be calculated using the following equations:

$$\varepsilon(M^{n+},ClO_4^-) = \text{Charge} \times 0.2$$

$$\varepsilon(M^{n+},Cl^-) = -0.05 + \text{Charge} \times 0.1$$

$$\varepsilon(X^{n-},Na^+) = \text{Charge} \times 0.05$$

Tab. 1-7: SIT interaction parameter estimations based on charge considerations only

These values are recommended as "default values", i.e., in the absence of any specific SIT parameters.

Charge	$\varepsilon(M^{n+},ClO_4^-)$	$\varepsilon(M^{n+},Cl^-)$	$\varepsilon(MX,NaCl)$	$\varepsilon(X^{n-},Na^+)$	Uncertainty ±
9	1.8	0.85			0.7
8	1.6	0.75			0.5
7	1.4	0.65			0.4
6	1.2	0.55			0.3
5	1.0	0.45			0.2
4	0.8	0.35			0.1
3	0.6	0.25			0.1
2	0.4	0.15			0.1
1	0.2	0.05			0.1
0			0.0		0.1
-1				-0.05	0.1
-2				-0.10	0.1
-3				-0.15	0.2
-4				-0.20	0.3
-5				-0.25	0.4
-6				-0.30	0.5

1.6 Temperature effects

The present update includes temperature information related to $\log_{10}K$ values in different degrees of approximation, depending on the availability of calorimetric data or of $\log_{10}K$ data measured over a certain temperature range. This section discusses interrelations of temperature parameters and describes some approximations used for modelling temperature effects in TDB 2020.

1.6.1 Temperature dependence of equilibrium constants

The following equation is used, e.g., in PHREEQC and GEMS and has been adopted as the equation relating $\log_{10}K°$ values to temperature in TDB 2020.

$$\log_{10}K°\,(T) = A + B \cdot T + C / T + D \cdot \log_{10}(T) + E / T^2$$

In this equation, $\log_{10}K°(T)$ is the base 10 logarithm of the equilibrium constant K at the temperature T (K) at ionic strength zero and A, B, C, D and E are constants. The form of this equation results from choosing the equation of Maier & Kelley (1932) to express the variation of

the heat capacity at constant pressure, $C_{p,m}°$, with absolute temperature, T. The Maier-Kelley equation is written:

$$C_{p,m}°(T) = a + b \cdot T - c / T^2$$

The equation for $\Delta_r C_{p,m}°(T)$ is:

$$\Delta_r C_{p,m}°(T) = \Delta_r a + \Delta_r b \cdot T - \Delta_r c / T^2$$

The following equations show the relations between the temperature dependent equilibrium constant, $\log_{10} K°(T)$, and such other thermodynamic properties of reaction as $\Delta_r G_m°$, $\Delta_r H_m°$, $\Delta_r S_m°$, $\Delta_r C_{p,m}°$ and $\Delta_r a$, $\Delta_r b$ and $\Delta_r c$ of the heat capacity equation.

$$\Delta_r G_m°(T) = - R \cdot T \cdot \ln(10) \cdot \log_{10} K°(T)$$

$$\Delta_r G_m°(T) = - R \cdot \ln(10) \cdot (A \cdot T + B \cdot T^2 + C + D \cdot T \cdot \log_{10}(T) + E / T)$$

$$\Delta_r H_m°(T) = R \cdot T^2 \cdot \ln(10) \cdot (\partial \log_{10} K°(T) / \partial T)$$

$$\Delta_r H_m°(T) = R \cdot \ln(10) \cdot (B \cdot T^2 - C + D \cdot T / \ln(10) - 2 \cdot E / T)$$

$$\Delta_r S_m°(T) = - \partial \Delta_r G_m°(T) / \partial T$$

$$\Delta_r S_m°(T) = R \cdot \ln(10) \cdot (A + 2 \cdot B \cdot T + D / \ln(10) \cdot (1 + \ln(T)) - E / T^2)$$

$$\Delta_r C_{p,m}°(T) = \partial \Delta_r H_m°(T) / \partial T$$

$$\Delta_r C_{p,m}°(T) = R \cdot \ln(10) \cdot (2 \cdot B \cdot T + D / \ln(10) + 2 \cdot E / T^2)$$

$$\Delta_r a = R \cdot D$$

$$\Delta_r b = 2 \cdot R \cdot \ln(10) \cdot B$$

$$\Delta_r c = - 2 \cdot R \cdot \ln(10) \cdot E$$

If sufficient experimental data are available to define all five coefficients A through E, the values of the Gibbs energy, enthalpy, entropy, heat capacity, and all three coefficients *a* through *c* of the heat capacity expression, can be found using the above equations.

It is also necessary to be able to calculate values of the coefficients A through E of the $\log_{10} K°(T)$ equation from thermodynamic properties of a reaction. If the coefficients $\Delta_r a$, $\Delta_r b$ and $\Delta_r c$ of the heat capacity equation are available, the coefficients B, D and E are calculated according to:

$$E = - \Delta_r c / (2 \cdot R \cdot \ln(10))$$

$$D = \Delta_r a / R$$

$$B = \Delta_r b / (2 \cdot R \cdot \ln(10))$$

The coefficient C is calculated using $\Delta_r H_m$ ° at the reference temperature T°:

$$C = B \cdot T°^2 + D \cdot T° / \ln(10) - 2 \cdot E / T° - \Delta_r H_m °(T°) / (R \cdot \ln(10))$$

$$C = (\Delta_r b / 2 \cdot T°^2 + \Delta_r a \cdot T° + \Delta_r c / T° - \Delta_r H_m °(T°)) / (R \cdot \ln(10))$$

A is calculated from $\Delta_r S_m°$ at the reference temperature T°:

$$A = \Delta_r S_m°(T°) / (R \cdot \ln(10)) - 2 \cdot B \cdot T° - D / \ln(10) \cdot (1 + \ln(T°)) + E / T°^2$$

$$A = (\Delta_r S_m°(T°) - \Delta_r b \cdot T°^2 - \Delta_r a \cdot (1 + \ln(T°)) - \Delta_r c / (2 \cdot T°^2)) / (R \cdot \ln(10))$$

1.6.2 Constant heat capacity of reaction

If $\Delta_r C_{p,m}°$ is known only at the reference temperature T°, it is often assumed to be constant with temperature. In this case, $\Delta_r C_{p,m}° = \Delta_r a$ and $\Delta_r b = \Delta_r c = 0$, so that B = E = 0, and the expression for $\log_{10} K°(T)$ has the form:

$$\log_{10} K°(T) = A + C / T + D \cdot \log_{10}(T)$$

This equation is called the three-term approximation of temperature dependence. From the equations of Section 1.6.1 it follows that:

$$D = \Delta_r C_{p,m}° / R$$

$$C = (\Delta_r C_{p,m}° \cdot T° - \Delta_r H_m°(T°)) / (R \cdot \ln(10))$$

$$A = (\Delta_r S_m°(T°) - \Delta_r C_{p,m}° \cdot (1 + \ln(T°)) / (R \cdot \ln(10))$$

Considering the above expressions for the coefficients A and C, and the relation

$$\Delta_r H_m°(T°) - T° \cdot (\Delta_r S_m °(T°) = - R \cdot T° \cdot \ln(10) \cdot \log_{10} K°(T°)$$

the expression for $\log_{10} K°(T)$ becomes:

$$\log_{10} K°(T) = \log_{10} K°(T°) + \Delta_r H_m°(T°) / (R \cdot \ln(10)) \cdot (1 / T° - 1 / T) + \Delta_r C_{p,m}° / (R \cdot \ln(10)) \cdot (T° / T - 1 + \ln(T/ T°))$$

If $\Delta_r C_{p,m}°$ is not known and we can assume $\Delta_r C_{p,m}° = 0$ the equation simplifies to the integrated van't Hoff equation, as described in the following section.

1.6.3 Constant enthalpy of reaction

For most reactions, $\Delta_r C_{p,m}°$ is not known and it must be assumed that $\Delta_r H_m°$ is constant with temperature. In this case, B = D = E = 0, and the expression for $\log_{10} K°(T)$ has the form:

$$\log_{10} K°(T) = A + C / T$$

This equation is called the two-term approximation of temperature dependence. From the equations of Section 1.6.1 it follows that:

$$C = - \Delta_r H_m°(T°) / (R \cdot \ln(10))$$

$$A = \Delta_r S_m°(T°) / (R \cdot \ln(10))$$

$$\log_{10} K°(T) = \log_{10} K°(T°) + \Delta_r H_m°(T°) / (R \cdot \ln(10)) \cdot (1 / T° - 1 / T)$$

This is the integrated van't Hoff equation as used in many geochemical programmes.

1.7 Database contents

The contents of TDB 2020 are shown here as graphical summaries in the form of the periodic table of the elements.

First, the elements considered in TDB 2020 are shown (Fig. 1-5), then the aqueous species included in TDB 2020 are listed (Figs. 1-6 – 1-20), and finally the redox states of aqueous species considered in TDB 2020 are shown (Fig. 1-21).

TDB 2020 comprises elements for all dose-relevant radionuclides to be considered in the safety assessments related to the general license application (marked red in Fig. 1-5).

Furthermore, all important elements for ground and pore water definitions are included (marked blue in Fig. 1-5) and finally, some chemical toxic elements are also included in TDB 2020 (marked yellow in Fig. 1-5).

The oxidation states of the elements considered in TDB 2020 are graphically summarised in Fig. 1-21. The reasons to exclude some oxidation states for certain elements are discussed in the introductory sections of the individual elements' chapters.

Note that all radium aqueous complexation and interaction constants included in TDB 2020 were estimated via alkaline earth – ionic radii systematics (Section 4.5). The various formulae for calculating weighted or unweighted means and linear regressions of selected data discussed in Section 4.5.1 were only used in this chapter.

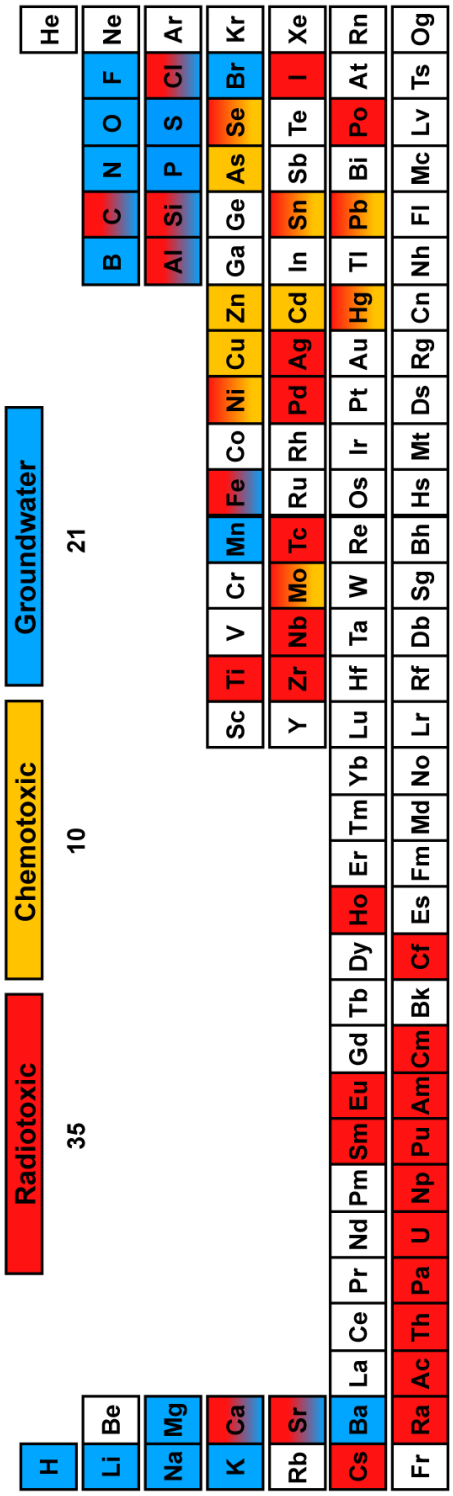

Fig. 1-5: Chemical elements considered in the PSI Chemical Thermodynamic Database 2020 (TDB 2020)

Some elements shown in two colours are chemotoxic and have radioactive isotopes occurring in the list of dose-relevant nuclides for radioactive waste disposal. Likewise, elements can be constituents of ground and pore waters and also occur in the list of radionuclides to be considered in the safety assessment.

Fig. 1-6: Aqueous hydroxide species included in TDB 2020

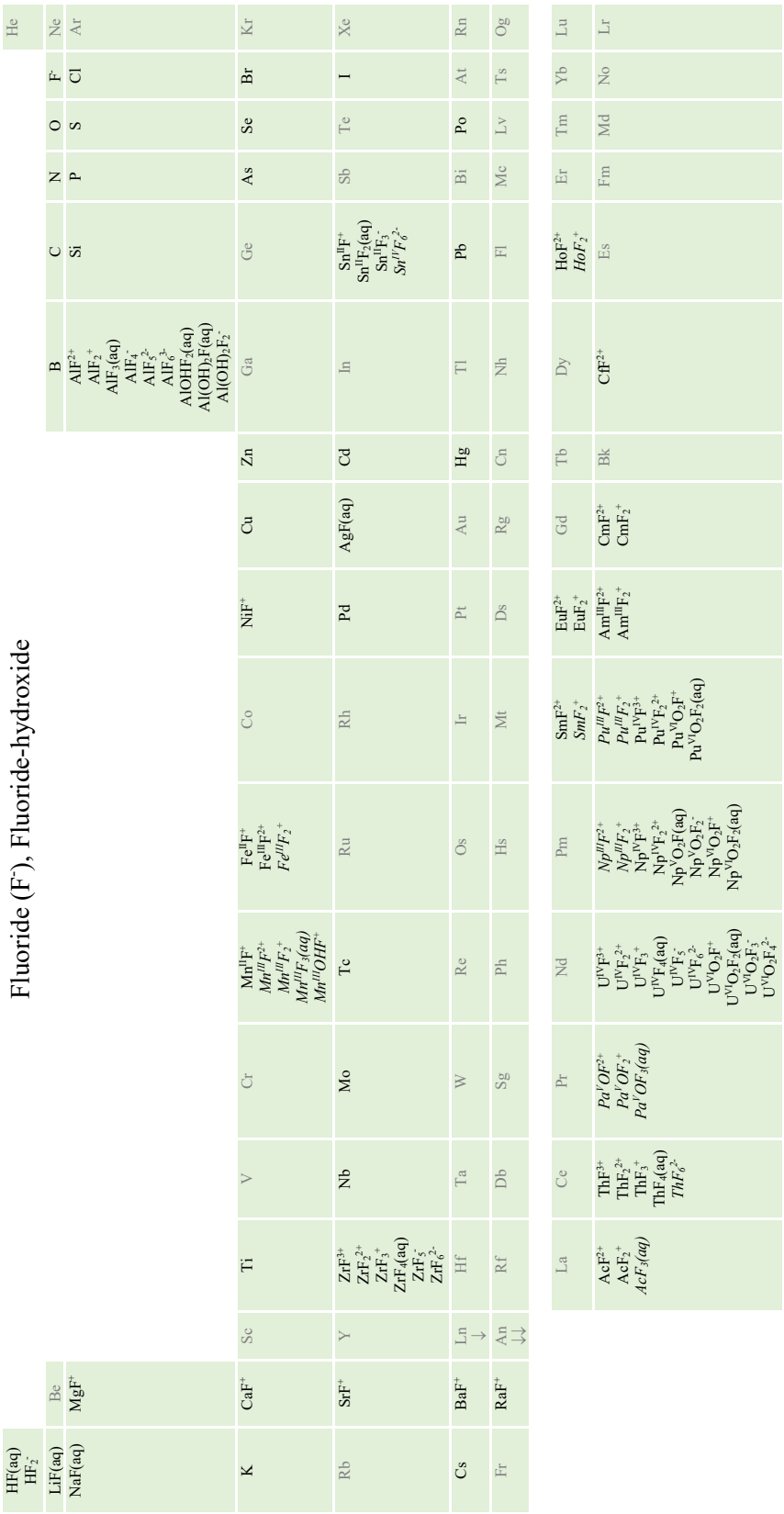

Fig. 1-7: Aqueous fluoride and fluoride-hydroxide species included in TDB 2020

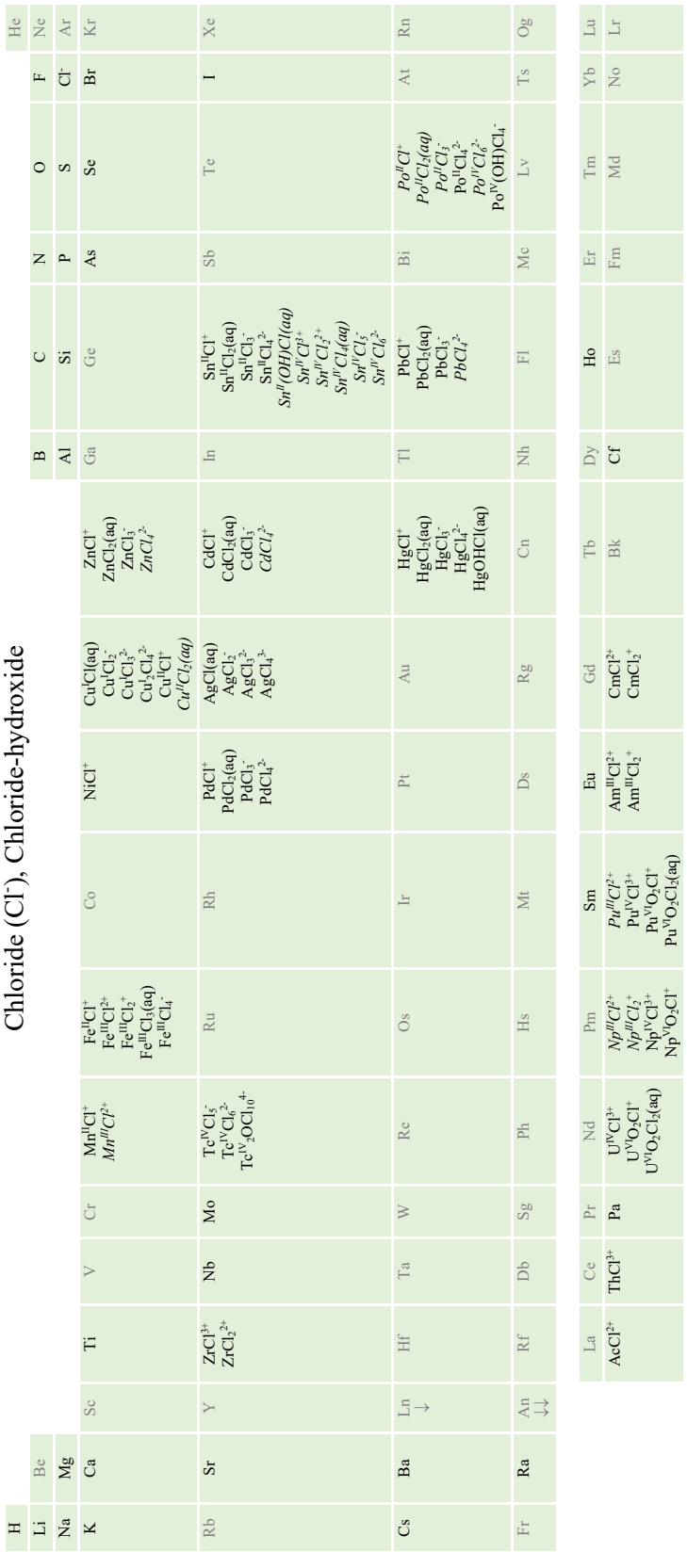

Fig. 1-8: Aqueous chloride and chloride-hydroxide species included in TDB 2020

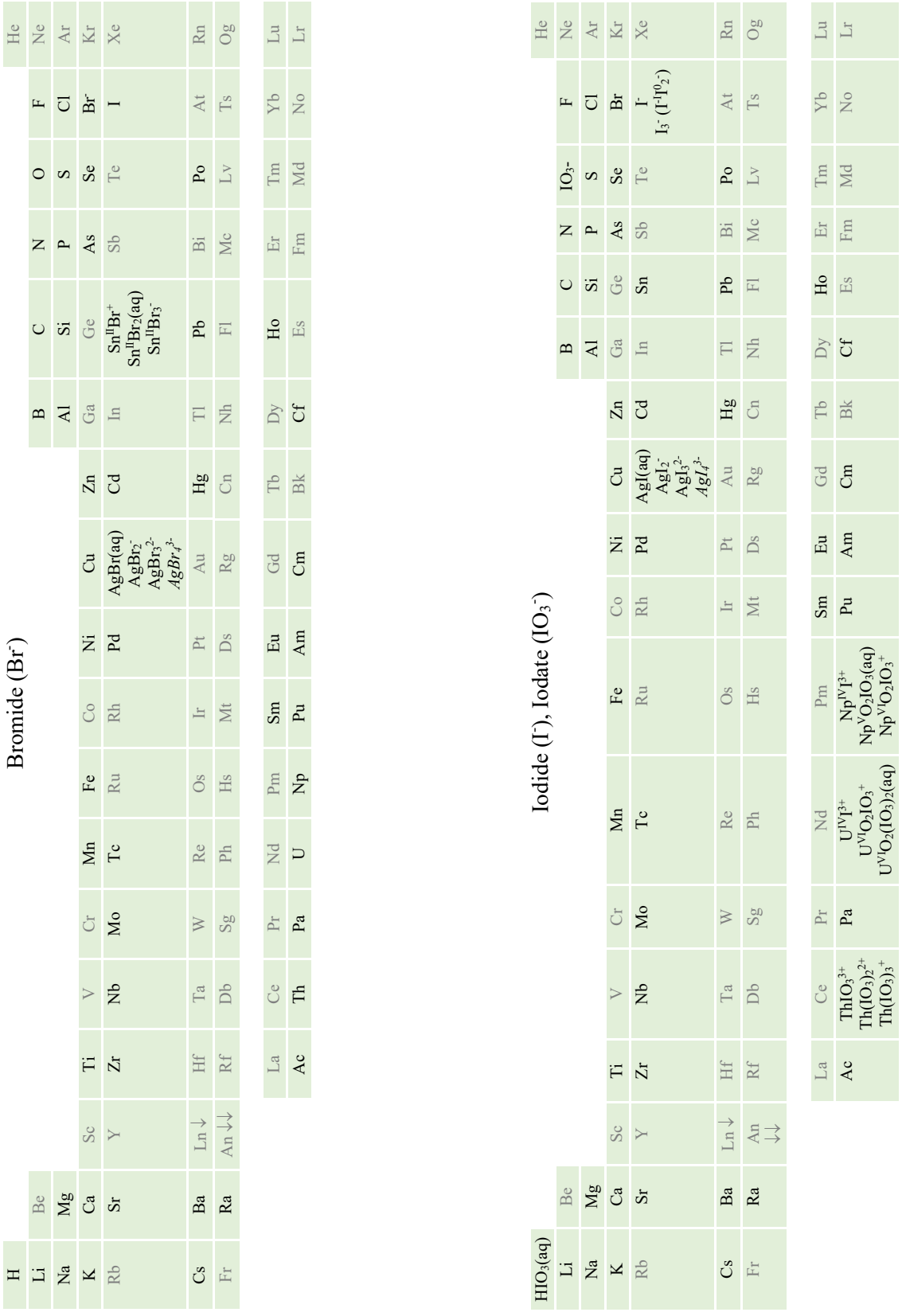

Fig. 1-9: Aqueous bromide, iodide and iodate species included in TDB 2020

Fig. 1-10: Aqueous sulphide, sulphate, bisulphate, sulphite and thiosulphate species included in TDB 2020

Fig. 1-11: Aqueous nitrate and ammine species included in TDB 2020

Fig. 1-12: Aqueous phosphate, pyrophosphate and arsenate species included in TDB 2020

Fig. 1-13: Aqueous carbonate, bicarbonate, carbonate-hydroxide, carbonate-fluoride and carbonate-chloride species included in TDB 2020

Fig. 1-14: Aqueous thiocyanate, selenocyanate and cyanide species included in TDB 2020

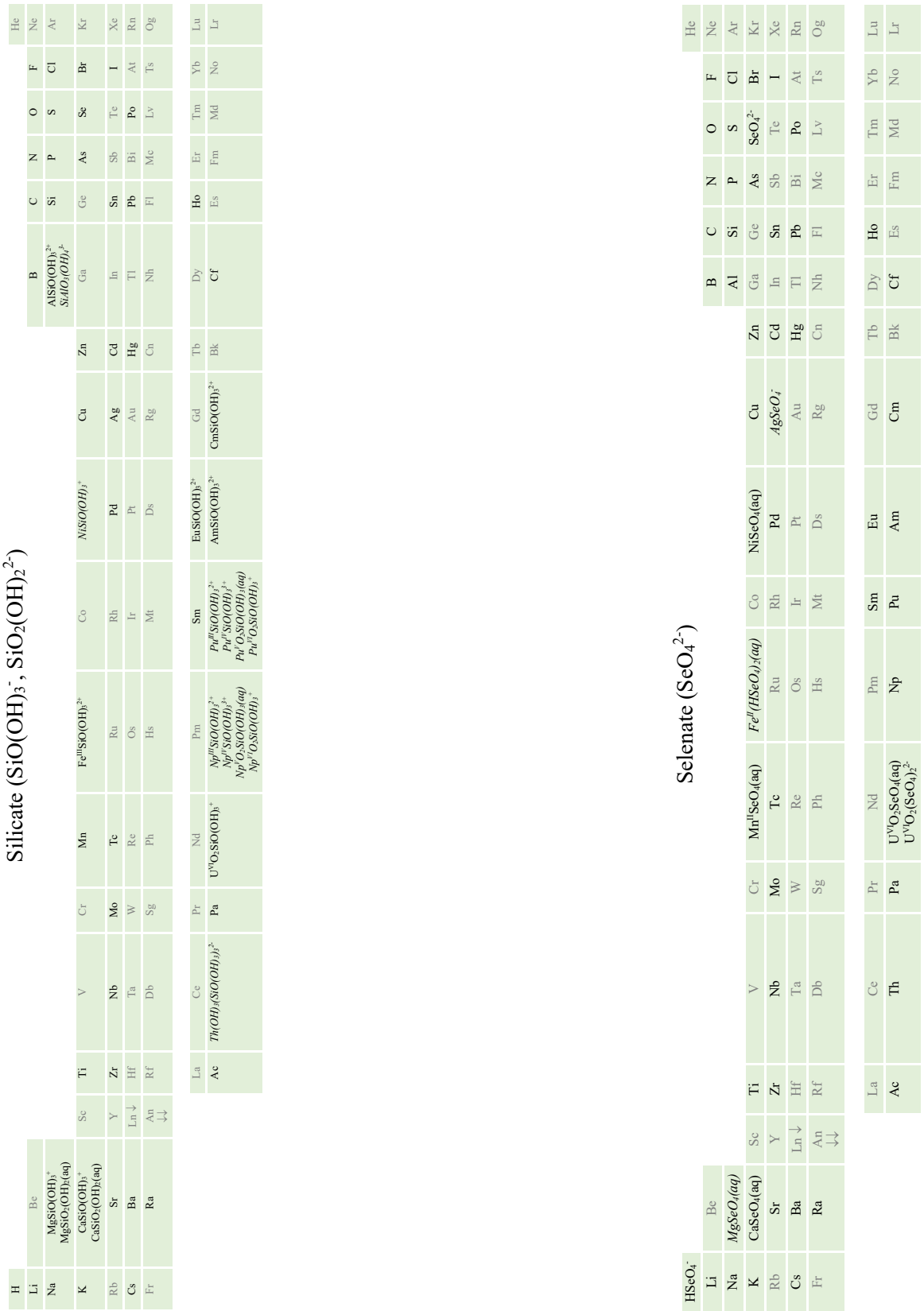

Fig. 1-15: Aqueous silicate and selenate species included in TDB 2020

Fig. 1-16: Aqueous selenite and selenide species included in TDB 2020

Fig. 1-17: Aqueous molybdate, Nb-polyanionic and polonide species included in TDB 2020

Isosaccharinate (isa^-)

Hisa(aq)*																			He
Li	Be											B	C	N	O	F	Ne		
Na	Mg											Al	Si	P	S	Cl	Ar		
K	$Ca(isa)^+$ $Ca(isa_{-H})aq$	Sc	Ti	V	Cr	Mn	Fe	Co	$Ni(isa)^+$	Cu	Zn	Ga	Ge	As	Se	Br	Kr		
Rb	Sr	Y	Zr	Nb	Mo	Tc	Ru	Rh	Pd	Ag	Cd	In	Sn	Sb	Te	I	Xe		
Cs	Ba	Ln ↓	Hf	Ta	W	Re	Os	Ir	Pt	Au	Hg	Tl	Pb	Bi	Po	At	Rn		
Fr	Ra	An ↓↓	Rf	Db	Sg	Ph	Hs	Mt	Ds	Rg	Cn	Nh	Fl	Mc	Lv	Ts	Og		

		La	Ce	Pr	Nd	Pm	Sm	Eu	Gd	Tb	Dy	Ho	Er	Tm	Yb	Lu			
		Ac	Th	Pa	$U^{VI}O_2isa^+$ $U^{VI}O_2(isa)_2(aq)$ $U^{VI}O_2(isa)_3^-$	$Np^{IV}(OH)_3(isa)(aq)$ $Np^{IV}(OH)_3(isa)_2^-$ $Np^{IV}(OH)_4(isa)^-$ $Np^{IV}(OH)_4(isa)_2^{2-}$	Pu	$Am^{III}(isa_{-3H})^+$	Cm	Bk	Cf	Es	Fm	Md	No	Lr			

Oxalate (ox^{2-})

Hox^- $H_2ox(aq)$																			He
Li	Be											B	C	N	O	F	Ne		
Na	$Mg(ox)(aq)$ $Mg(ox)_2^{2-}$											Al	Si	P	S	Cl	Ar		
K	$Ca(ox)(aq)$ $Ca(ox)_2^{2-}$	Sc	Ti	V	Cr	Mn	Fe	Co	$Ni(ox)(aq)$ $Ni(ox)_2^{2-}$	Cu	Zn	Ga	Ge	As	Se	Br	Kr		
Rb	Sr	Y	Zr	Nb	Mo	Tc	Ru	Rh	Pd	Ag	Cd	In	Sn	Sb	Te	I	Xe		
Cs	Ba	Ln ↓	Hf	Ta	W	Re	Os	Ir	Pt	Au	Hg	Tl	Pb	Bi	Po	At	Rn		
Fr	Ra	An ↓↓	Rf	Db	Sg	Ph	Hs	Mt	Ds	Rg	Cn	Nh	Fl	Mc	Lv	Ts	Og		

		La	Ce	Pr	Nd	Pm	Sm	Eu	Gd	Tb	Dy	Ho	Er	Tm	Yb	Lu			
		$Ac(ox)^+$ $Ac(ox)_2^-$	Th	Pa	$U^{IV}ox^{2+}$ $U^{IV}(ox)_2(aq)$ $U^{IV}(ox)_3^{2-}$ $U^{IV}(ox)_4^{4-}$ $U^{VI}O_2ox(aq)$ $U^{VI}O_2(ox)_2^{2-}$ $U^{VI}O_2(ox)_3^{4-}$	$Np^{IV}ox^{2+}$ $Np^{IV}(ox)_2(aq)$ $Np^{IV}(ox)_3^{2-}$ $Np^{V}O_2ox^-$ $Np^{V}O_2(ox)_2^{3-}$	$Pu^{III}ox^+$ $Pu^{III}(ox)_2^-$ $Pu^{III}(ox)_3^{3-}$ $Pu^{IV}(ox)^{2+}$ $Pu^{IV}(ox)_2(aq)$ $Pu^{IV}(ox)_3^{2-}$	$Am^{III}(ox)^+$ $Am^{III}(ox)_2^-$ $Am^{III}(ox)_3^{3-}$	Cm	Bk	Cf	Es	Fm	Md	No	Lr			

Fig. 1-18: Aqueous isosaccharinate and oxalate species included in TDB 2020

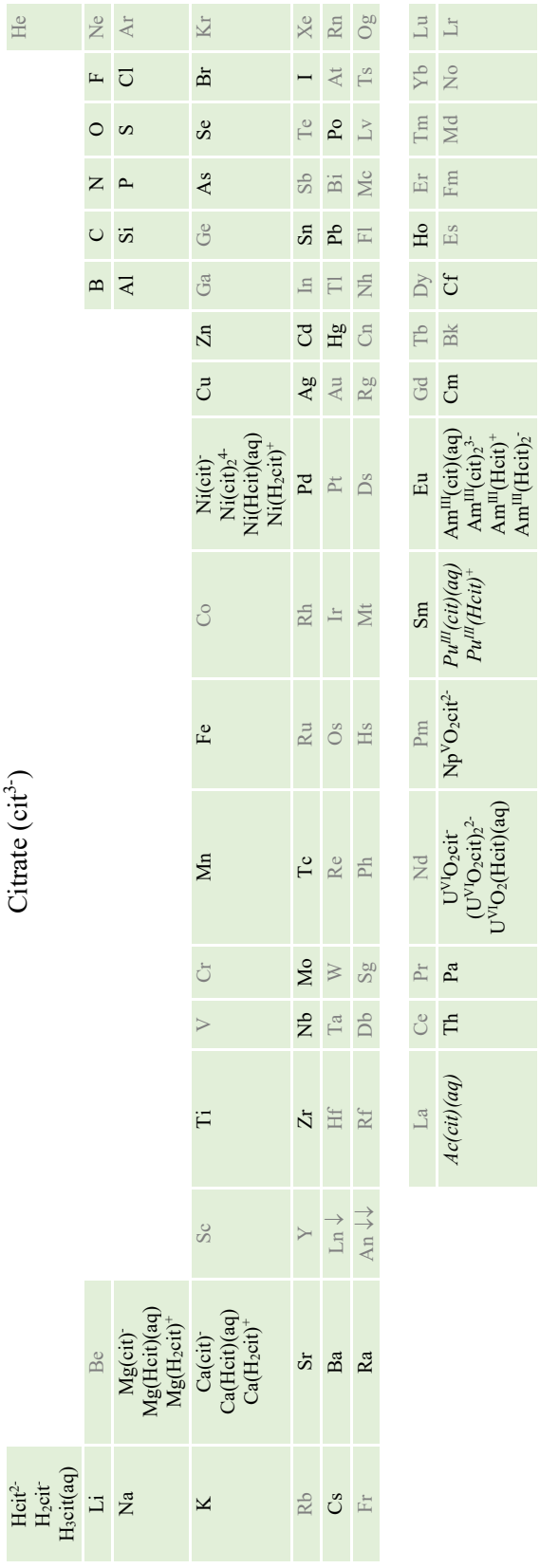

Fig. 1-19: Aqueous citrate species included in TDB 2020

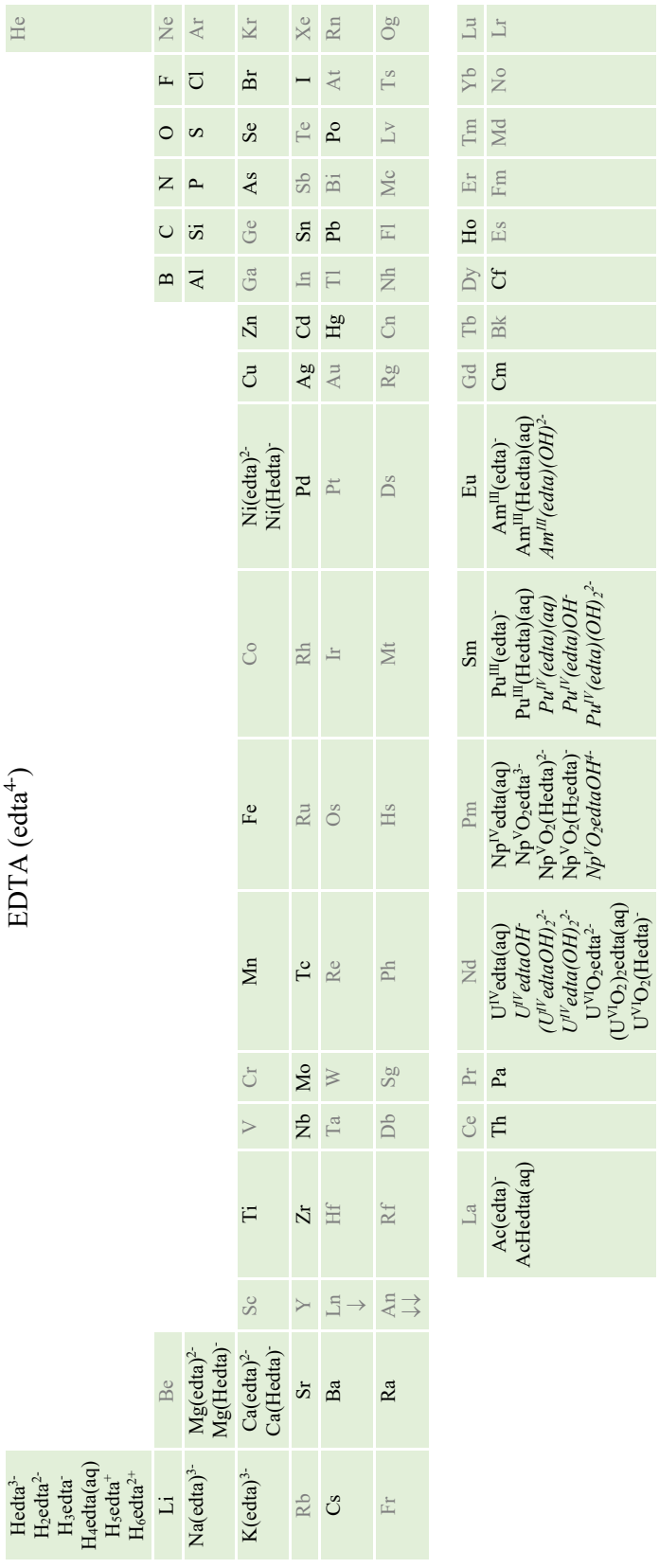

Fig. 1-20: Aqueous EDTA (ethylenediamine-tetraacetate) species included in TDB 2020

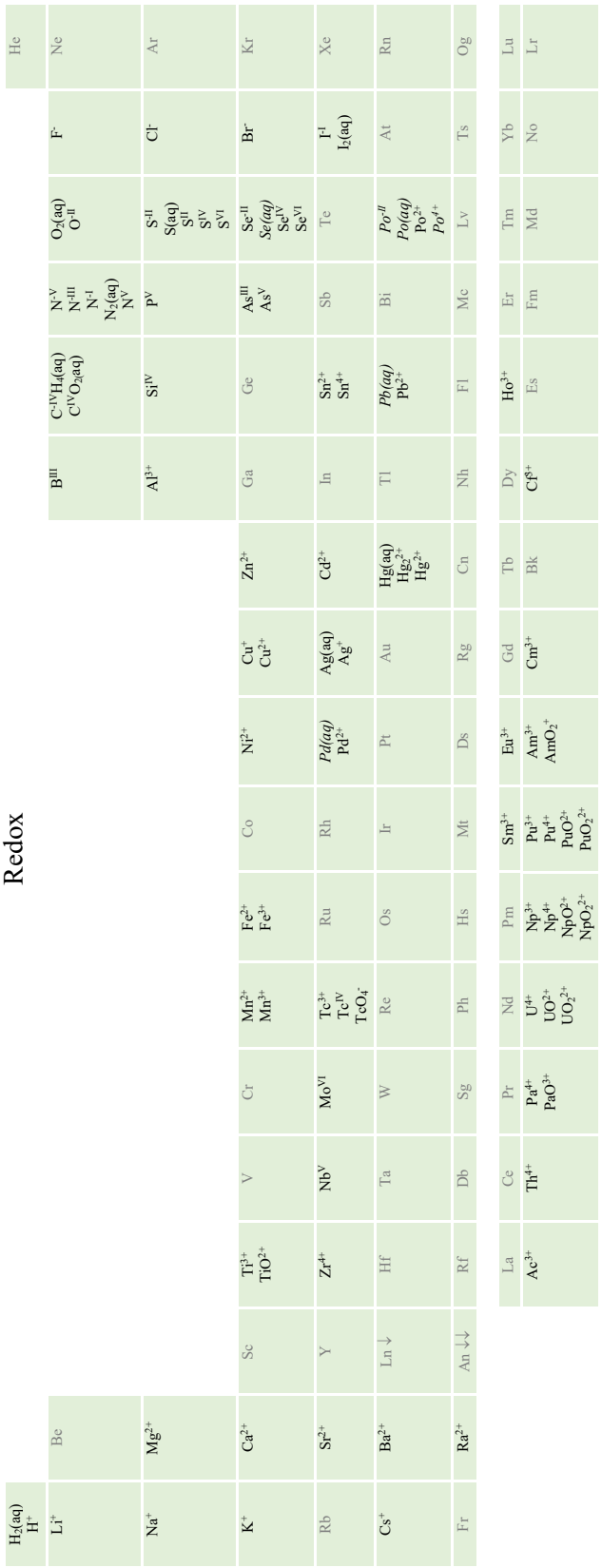

Fig. 1-21: Redox states of aqueous species considered in TDB 2020

1.8 References

Blanc, Ph., Lassin, A., Piantone, P., Azaroual, M., Jacquemet, N., Fabbri, A. & Gaucher, E.C. (2012): Thermoddem: A geochemical database focused on low temperature water/rock interactions and waste materials, Applied Geochemistry, 27, 2107-2116.

Brown, P.L. & Ekberg, C. (2016): Hydrolysis of Metal Ions. Vol. 2, Wiley-VCH, Weinheim.

Bruno, J., Bosbach, D., Kulik, D. & Navrotsky, A. (2007): Chemical Thermodynamics of Solid Solutions of Interest in Radioactive Waste Management – A State-of-the-Art-Report. Chemical Thermodynamics, Vol. 10. OECD Publications, Paris, 266 pp.

Ciavatta, L. (1980): The specific interaction theory in evaluating ionic equilibria. Annali di Chimica, 70, 551-567.

Cox, J.D., Wagman, D.D. & Medvedev, V.A. (1989): CODATA Key Values for Thermodynamics. Hemisphere, New York, 271 pp.

Duro, L., Grivé, M., Cera, E., Domènech, C. & Bruno, J. (2006): Update of a thermodynamic database for radionuclides to assist solubility limits calculation for performance assessment, SKB Technical Report TR-06-17, SKB, Sweden, 120 pp.

Giffaut, E., Grivé, M., Blanc, P., Vieillard, P., Colàs, E., Gailhanou, H., Gaboreau, S., Marty, N., Madé, B. & Duro, L. (2014): Andra thermodynamic database for performance assessment: ThermoChimie. Applied Geochemistry, 49, 225-236

Grenthe, I., Gaona, X., Plyasunov, A.V., Rao, L., Runde, W.H., Grambow, B., Konings, R.J.M., Smith, A.L. & Moore, E.E. (2020): Second Update on the Chemical Thermodynamics of Uranium, Neptunium, Plutonium, Americium and Technetium. Chemical Thermodynamics, Vol. 14. OECD Publications, Paris, France, 1503 p.

Grenthe, I., Mompean, F., Spahiu, K. & Wanner, H. (2013): TDB-2 Guidelines for the extrapolation to zero ionic strength (Version of 18 June 2013). OECD NEA, Data Bank, Issy-les-Moulineaux, France, 78 pp.

Grenthe, I., Plyasunov, A.V. & Spahiu, K. (1997): Estimations of medium effects on thermodynamic data. In: Grenthe, I. & Puigdomènech, I. (eds.): Modelling in Aquatic Chemistry. OECD NEA, Paris, France, 325-426.

Grivé, M., Montoya, V. & Duro, L. (2008): Assessment of the Concentration Limits for Radionuclides for Posiva, Posiva Oy Working Report 2007-103, Eurajoki. Finland, 102 pp.

Hagemann, S. (2012): Entwicklung eines thermodynamischen Modells für Zink, Blei und Cadmium in salinaren Lösungen, GRS-Report 219, GRS, Braunschweig, Germany, 494 pp.

Hagemann, S., Moog, H.C., Herbert, H.J. & Erich, A. (2012): Rückhaltung und thermodynamische Modellierung von Iod und Selen in hochsalinaren Lösungen – Gewinnung von Daten für Selenit, Selenat und Iodid für Belange der Langzeitsicherheitsanalyse des Nahfelds eines Endlagers für gefährliche Abfälle, GRS-Report 245, GRS, Braunschweig, Germany, 176 pp.

Hummel, W., Berner, U., Curti, E., Pearson, F.J. & Thoenen, T. (2002): Nagra/PSI Chemical Thermodynamic Data Base 01/01. Nagra Technical Report NTB 02-16 and Universal Publishers, Parkland, Florida, 565 pp.

Hummel, W., Filella, M. & Rowland, D. (2019): Where to find equilibrium constants? Science of the Total Environment, 692, 49-59.

Kitamura, A. (2019): Update of JAEA-TDB Update of thermodynamic data for zirconium and those for isosaccharinate, tentative selection of thermodynamic data for ternary M^{2+}-UO_2^{2+}-CO_3^{2-} system and integration with JAEA's thermodynamic database for geochemical calculations. JAEA-Data/Code 2018-018. JAEA, Japan, 116 pp.

Lemire, R.J., Berner, U., Musikas, C., Palmer, D.A., Taylor, P. & Tochiyama, O. (2013): Chemical Thermodynamics of Iron, Part 1. Chemical Thermodynamics, Vol. 13a. OECD Publications, Paris, France, 1082 pp.

Maier, C.G. & Kelley, K.K. (1932): An equation for the representation of high-temperature heat content data. Journal of the American Chemical Society, 54, 3243-3246.

Moog, H.C., Bok, F., Marquardt, C.M., Brendler, V. (2015): Disposal of nuclear waste in host rock formations featuring high-saline solutions – Implementation of a thermodynamic reference database (THEREDA). Applied Geochemistry, 55, 72-84.

Pearson, F.J. & Berner, U. (1991): Nagra Thermochemical Data Base I. Core Data. Nagra Technical Report NTB 91-17.

Pearson, F.J., Berner, U. & Hummel, W. (1992): Nagra Thermochemical Data Base II. Supplemental Data 05/92. Nagra Technical Report NTB 91-18.

Rand, M., Fuger, J., Grenthe, I., Neck, V. & Rai, D. (2007): Chemical Thermodynamics of Thorium. Chemical Thermodynamics, Vol. 11. OECD Nuclear Energy Agency, Paris, 900 pp.

Söhnel, O. & Novotný, P. (1985): Densities of aqueous solutions of inorganic substances. Elsevier, Amsterdam.

Thoenen, T., Hummel, W., Berner, U. & Curti, E. (2014): The PSI/Nagra Chemical Thermodynamic Database 12/07. Technical Report, PSI Bericht Nr. 14-04, Paul Scherrer Institut, Villigen, Switzerland, 416 pp.

Wagman, D.D., Evans, W.H., Parker, V.B., Schumm, R.H., Halow, I., Bailey, S.M., Churney, K.L. & Nuttall, R.L. (1982): The NBS tables of chemical thermodynamic properties: Selected values for inorganic and C1 and C2 organic substances in SI units. Journal of Physical and Chemical Reference Data, 11, Supplement No. 2, 1-392.

Wolery, T.J. & Jove-Colon, C.F. (2004): Qualification of Thermodynamic Data for Geochemical Modeling of Mineral-Water Interactions in Dilute Systems. ANL-WIS-GS-000003 REV 00, Bechtel SAIC Company, Las Vegas, Nevada, 212 pp.

2 Actinium

2.1 Introduction

The most important isotope of actinium is Ac-227, a member of the naturally occurring uranium-actinium ($4n + 3$) family of radioelements, with a moderately long half-life of 21.773 ± 0.003 years. Ac-227 contributes in dose-relevant quantities to the inventory of radioactive waste coming from nuclear power plants, which is the reason for inclusion of actinium into TDB 2020.

The only stable oxidation state of actinium in aqueous solution is Ac(III) (Kirby & Morss 2006). Experimental data on solubility and complexation of Ac(III) is scarce (Kirby & Morss 2006) and the Ac-O_{H2O} and Ac-Cl bond distances and coordination numbers in aqueous solution were not measured until 2016 (Ferrier et al. 2016, 2017).

The thermodynamic data included into TDB 2020 have been taken from

- Konings et al. (2006) and the literature discussed by Kirby & Morss (2006)
- the recent review of the hydrolysis of metal ions (Brown & Ekberg 2016)
- and own reviews of experimental data

The selected thermodynamic data for actinium compounds and complexes are presented in Tab. 2-1.

Ion interaction coefficients of actinium species were not available. We approximated these using analogous Am interaction coefficients derived in Hummel et al. (2005) and with the estimation method described in Section 1.5.3, which draws on a statistical analysis of published SIT ion interaction coefficients and which allows the estimation of missing coefficients for the interaction of cations with Cl^- and ClO_4^-, and for the interaction of anions with Na^+, from the charge of the cations or anions of interest.

The selected SIT ion interaction coefficients for actinium species are presented in Tab. 2-2.

2.2 Elemental actinium

Actinium metal, liquid and gas are not relevant under environmental conditions. Hence, the gas phase Acg and the liquid phase Ac(l) are not included in the data base. The absolute entropy and heat capacity of Ac(cr) are included as they are used for the calculation of certain thermodynamic reaction properties. The selected values have been taken from Konings et al. (2006):

$$S_m°(\text{Ac, cr, 298.15 K}) = (61.9 \pm 0.8)\ \text{J} \cdot \text{K}^{-1} \cdot \text{mol}^{-1}$$

$$C_{p,m}°(\text{Ac, cr, 298.15 K}) = (26 \pm 2)\ \text{J} \cdot \text{K}^{-1} \cdot \text{mol}^{-1}$$

2.3 Actinium(III)

2.3.1 Actinium(III) aqua ion

Actinium(III) exists as the Ac^{3+} cation in aqueous solutions. Ac^{3+} is the largest +3 cation known, as shown by the spectroscopic study of Ferrier et al. (2016, 2017) who found that 10.9 ± 0.5 water molecules are directly coordinated to the Ac(III) cation with an incredibly long Ac-O_{H2O} distance of 2.63 ± 0.01 Å.

The selected thermodynamic values for Ac^{3+} are taken from Konings et al. (2006):

$$\Delta_f H_m°(Ac^{3+}, 298.15\ K) = -(653 \pm 25)\ kJ \cdot mol^{-1}$$

$$S_m°(Ac^{3+}, 298.15\ K) = -(180 \pm 17)\ J \cdot K^{-1} \cdot mol^{-1}$$

The Gibbs energy of formation calculated from the above values, $S_m°$(Ac, cr, 298.15 K) (see Section 2.2) and the CODATA value $S_m°(H_2, g, 298.15\ K) = (130.680 \pm 0.003)\ J \cdot K^{-1} \cdot mol^{-1}$ (Grenthe et al. 1992) according to the Gibbs-Helmholtz equation:

$$\Delta_f G_m°(Ac^{3+}, 298.15\ K) = \Delta_f H_m°(Ac^{3+}, 298.15\ K) - T° \cdot \Delta_f S_m°(Ac^{3+}, 298.15\ K)$$

$$\Delta_f S_m°(Ac^{3+}, 298.15\ K) = S_m°(Ac^{3+}, 298.15\ K) - S_m°(Ac, cr, 298.15\ K) + (3/2)\ S_m°(H_2, g, 298.15\ K)$$

$$\Delta_f G_m°(Ac^{3+}, 298.15\ K) = -(639.3 \pm 25.5)\ kJ \cdot mol^{-1}$$

Using this value, the redox equilibrium

$$Ac(cr) \rightleftharpoons Ac^{3+} + 3e^-$$

is calculated as

$$\log_{10} K°(298.15\ K) = 112.0 \pm 4.5$$

2.3.2 Actinium(III) (hydr)oxide compounds and complexes

2.3.2.1 Actinium(III) hydroxide complexes

Brown & Ekberg (2016) state that there have been very few studies on the hydrolytic reactions of actinium(III). Three studies have reported data on stability constants of actinium hydrolysis species, with two reporting data for $AcOH^{2+}$ (Moutte & Guillaumont 1969, Zielińska & Bilewicz 2004) and one for $Ac(OH)_3(aq)$ (Kulikov et al. 1992).

Moutte & Guillaumont (1969) examined the complexation of Ac(III) and Cm(III) with citrate using solvent extraction and also determined the first hydrolysis constants of the two cations. For Ac(III), they obtained

$$Ac^{3+} + H_2O(l) \rightleftharpoons AcOH^{2+} + H^+$$

$$\log_{10}{}^*\beta_1 \text{ (298.15 K)} = -8.49$$

in 0.1 M perchlorate and 25 °C. Brown & Ekberg (2016) state that typically, these authors have obtained constants that are too stable, possibly because of difficulties encountered in using the solvent extraction technique for lanthanides and actinides, and consequently, their constant for $AcOH^{2+}$ is not accepted by Brown & Ekberg (2016). This review agrees with this decision, also the citrate data of Moutte & Guillaumont (1969) have not been accepted in this review (see Section 2.3.9).

Zielińska & Bilewicz (2004) used an ion exchange method to measure the stability constant for $AcOH^{2+}$. They utilised a medium of 1.0 M $NaClO_4$ at 25 °C and obtained a value of

$$\log_{10}{}^*\beta_1 \text{ (298.15 K)} = -9.4 \pm 0.1$$

Brown & Ekberg (2016) assumed that the correction to zero ionic strength is similar for $AcOH^{2+}$ as it was for $LaOH^{2+}$, and thus a stability constant of $AcOH^{2+}$ at zero ionic strength of

$$\log_{10}{}^*\beta_1^\circ \text{ (298.15 K)} = -9.3 \pm 0.2$$

has been calculated by Brown & Ekberg (2016) from the datum of Zielińska & Bilewicz (2004). The uncertainty has been estimated by Brown & Ekberg (2016).

This review estimated a $\Delta\varepsilon$ value for extrapolation of $\log_{10}{}^*\beta_1$ to zero ionic strength, using $\varepsilon(H^+, ClO_4^-) = (0.14 \pm 0.02)$ kg · mol^{-1} (Lemire et al. 2013), and using the estimation method (described in Section 1.5.3) for $\varepsilon(Ac^{3+}, ClO_4^-) = (0.6 \pm 0.1)$ kg · mol^{-1} and $\varepsilon(AcOH^{2+}, ClO_4^-) = (0.4 \pm 0.1)$ kg · mol^{-1} (Tab. 2-2)

$$\Delta\varepsilon\text{(estimated)} = -(0.06 \pm 0.14) \text{ kg} \cdot \text{mol}^{-1}$$

$$\log_{10}{}^*\beta_1^\circ \text{ (298.15 K)} = -8.6 \pm 0.2$$

This value is included in TDB 2020.

Kulikov et al. (1992) used an electromigration technique to determine the stability constant for $Ac(OH)_3(aq)$. They used a medium of 0.1 M perchlorate at 25 °C. They obtained

$$Ac^{3+} + 3\ H_2O(l) \rightleftharpoons Ac(OH)_3(aq) + 3\ H^+$$

$$\log_{10}{}^*\beta_3\ (298.15\ K) = -31.9 \pm 0.2$$

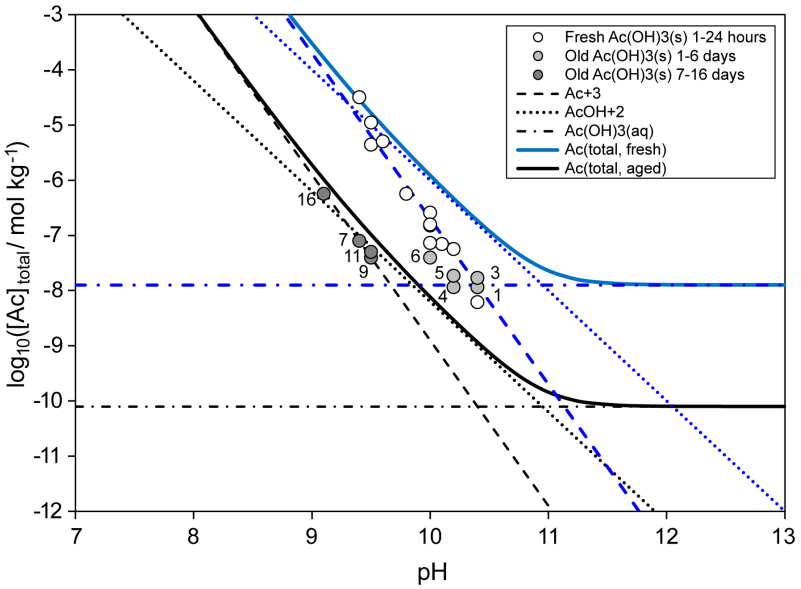

Fig. 2-1: Solubility of $Ac(OH)_3(s)$ as a function of pH

Lines are calculated using the stability constants selected in this review at $I = 0$. The solubility products of "fresh" and "aged" differ by about 2 orders of magnitude. Using these solubility products together with the selected hydrolysis constants, all calculated lines shift by about 2 orders of magnitude from Ac "fresh" (blue lines) to Ac "aged" (black lines). Symbols are experimental solubility data taken from Ziv & Shestakova (1965b), where the numbers represent the ageing time of the precipitate in days.

Brown & Ekberg (2016) state that this value appears consistent with that determined for $AcOH^{2+}$, as well as that determined for $Nd(OH)_3(aq)$, and is retained in their review.

This review agrees and estimated a $\Delta\varepsilon$ value for extrapolation of $\log_{10}{}^*\beta_3$ to zero ionic strength, using $\varepsilon(H^+, ClO_4^-) = (0.14 \pm 0.02)$ kg · mol^{-1} (Lemire et al. 2013), and using the estimation method (described in Section 1.5.3) for $\varepsilon(Ac^{3+}, ClO_4^-) = (0.6 \pm 0.1)$ kg · mol^{-1} and $\varepsilon(Ac(OH)_3(aq), NaClO_4) = (0.0 \pm 0.1)$ kg · mol^{-1} (Tab. 2-2)

$$\Delta\varepsilon(\text{estimated}) = -(0.18 \pm 0.14)\ \text{kg} \cdot \text{mol}^{-1}$$

$$\log_{10}{}^*\beta_3^\circ\ (298.15\ K) = -31.2 \pm 0.2$$

This value is included in TDB 2020.

2.3.2.2 Actinium(III) (hydr)oxide compounds

Brown & Ekberg (2016) report that there is only one study on the solubility of $Ac(OH)_3(s)$ (Ziv & Shestakova 1965b). These authors studied the solubility in a medium of 0.001 M NH_4NO_3 at 22 °C. They corrected for the activities of the ions in the solution and obtained solubility constants

$$Ac(OH)_3(s) + 3H^+ \rightleftharpoons Ac^{3+} + 3\ H_2O(l)$$

$$\log_{10}{}^*K_{s0}^\circ \text{ (fresh, 295.15 K)} = 23.3 \pm 0.2$$

$$\log_{10}{}^*K_{s0}^\circ \text{ (aged, 295.15 K)} = 21.1 \pm 0.2$$

with uncertainties assigned by this review. These values are included in TDB 2020.

$Log_{10}{}^*K_{s0}^\circ$ (fresh, 295.15 K) has been determined by Ziv & Shestakova (1965b) from freshly precipitated $Ac(OH)_3(s)$ where the time from precipitation varied from 1 – 24 hours.

By contrast, $\log_{10}{}^*K_{s0}^\circ$ (aged, 295.15 K) has been determined from "old" $Ac(OH)_3(s)$. Ziv & Shestakova (1965b) state that the ageing of actinium hydroxide ends in approximately a week and is accompanied by a decrease in its solubility product, which is evidently related to recrystallization of the precipitate.

The longest ageing time in the study of Ziv & Shestakova (1965b) was only 16 days, hence it is not known whether the α-radiation of actinium will over time destroy the crystalline structure of $Ac(OH)_3(s)$ and its solubility may increase again.

Fig. 2-1 shows that the stability constants selected by this review are compatible with the experimental solubility data of Ziv & Shestakova (1965b).

2.3.3 Actinium(III) fluoride complexes

Aziz & Lyle (1970) determined the complex formation of Ac(III) with fluoride in 0.5 M $NaClO_4$ at 25 °C by a liquid-liquid partition method at a fixed pH of 3.60 while varying the total fluoride concentration from $1.7 \cdot 10^{-4} – 4.0 \cdot 10^{-3}$ M. They interpreted their data in terms of three complexes

$$Ac^{3+} + F^- \rightleftharpoons AcF^{2+}$$

$$\beta_1 \text{ (298.15 K)} = 529 \pm 8$$

$$Ac^{3+} + 2F^- \rightleftharpoons AcF_2^+$$

$$\beta_2 \text{ (298.15 K)} = (1.67 \pm 0.09) \cdot 10^5$$

$$Ac^{3+} + 3F^- \rightleftharpoons AcF_3(aq)$$

$$\beta_3 \text{ (298.15 K)} = 0.8 \cdot 10^8$$

and remark that the β_3 value is likely to be "somewhat uncertain".

These values translate to

$\log_{10}\beta_1$ (298.15 K) = 2.72 ± 0.01

$\log_{10}\beta_2$ (298.15 K) = 5.22 ± 0.02

$\log_{10}\beta_3$ (298.15 K) = 7.9

Makarova et al. (1973) used an electromigration method to determine the complex formation of AcF^{2+} in 0.1 M $NaClO_4$ at (25 ± 0.5) °C at a fixed pH of 1.8 and a fixed NaF concentration of $4.25 \cdot 10^{-4}$ M. They obtained

β_1 (298.15 K) = 885

This value translates to

$\log_{10}\beta_1$ (298.15 K) = 2.95

This review estimated Δε values for extrapolation of $\log_{10}\beta_x$ to zero ionic strength, using ε(F^-, Na^+) = (0.02 ± 0.02) kg · mol^{-1} (Lemire et al. 2013), and using the estimation method (described in Section 1.5.3) for ε(Ac^{3+}, ClO_4^-) = (0.6 ± 0.1) kg · mol^{-1}, ε(AcF^{2+}, ClO_4^-) = (0.4 ± 0.1) kg · mol^{-1}, ε(AcF_2^+, ClO_4^-) = (0.2 ± 0.1) kg · mol^{-1} and ε(AcF_3(aq), $NaClO_4$) = (0.0 ± 0.1) kg · mol^{-1} (Tab. 2-2)

Δε(estimated) = -(0.22 ± 0.14) kg · mol^{-1}

Aziz & Lyle (1970)

$\log_{10}\beta_1°$ (298.15 K) = 3.65

Makarova et al. (1973)

$\log_{10}\beta_1°$ (298.15 K) = 3.58

Both values are almost identical and hence, the average

$\log_{10}\beta_1°$ (298.15 K) = 3.61 ± 0.20

with an uncertainty assigned by this review, is included in TDB 2020.

Δε(estimated) = -(0.44 ± 0.14) kg · mol^{-1}

Aziz & Lyle (1970)

$\log_{10}\beta_2°$ (298.15 K) = 6.73 ± 0.20

This value, with an uncertainty assigned by this review, is also included in TDB 2020.

$\Delta\varepsilon(\text{estimated}) = -(0.66 \pm 0.15)\ \text{kg} \cdot \text{mol}^{-1}$

Aziz & Lyle (1970)

$\log_{10}\beta_3^\circ (298.15\ \text{K}) \approx 9.75$

This value, classified as "somewhat uncertain", is included in TDB 2020 as supplemental datum.

2.3.4 Actinium(III) chloride complexes

Shahani et al. (1968) determined the complex formation of Ac(III) with chloride at 27 °C by a solvent extraction technique at a fixed $[H^+]$ concentration of 1.0 M and at unit ionic strength, which was kept constant while varying the ligand concentration by suitably adjusting the concentration of perchloric acid. They interpreted their data in terms of two complexes

$Ac^{3+} + Cl^- \rightleftharpoons AcCl^{2+}$

$\beta_1\ (300.15\ \text{K}) = 0.80 \pm 0.09$

$Ac^{3+} + 2Cl^- \rightleftharpoons AcCl_2^+$

$\beta_2\ (300.15\ \text{K}) = 0.24 \pm 0.08$

which translates to

$\log_{10}\beta_1\ (300.15\ \text{K}) = -0.10 \pm 0.05$

and

$\log_{10}\beta_2\ (300.15\ \text{K}) = -0.62 \pm 0.15$

While the first value might actually represent complex formation, the second value most probably reflects medium effects, as the concentration of $[Cl^-]$ was varied from 0.06 to 1.00 M, i.e., a complete exchange of ClO_4^- with Cl^-.

Sekine & Sakairi (1969) also used a solvent extraction technique to determine the complex formation of Ac(III) with chloride at 25 °C and pH 2 in 4 M $NaClO_4$. They report the values $\log_{10}\beta_1\ (298.15\ \text{K}) = -0.04$, $\log_{10}\beta_2\ (298.15\ \text{K}) = -1.04$, and $\log_{10}\beta_3\ (298.15\ \text{K}) = -1.26$.

No information is given by Sekine & Sakairi (1969) about the concentration range of Cl^- used in their solvent extraction experiments. Consequently, there is no way to properly address possible medium effects. However, considering the weak complex formation of Ac(III) with chloride, the reviewer decided that the $\log_{10}\beta_2$ and $\log_{10}\beta_3$ values most probably reflect medium effects, and they are not included in the data analysis.

Fukusawa et al. (1982) also used a solvent extraction technique to determine the complex formation of Ac(III) with chloride at about 20 °C and at a fixed $[H^+]$ concentration of 0.15 M in 3 M $LiClO_4$. They report the values β_1 (293.15 K) = 0.44 ± 0.02 and β_2 (293.15 K) = 0.31 ± 0.02, which translates to $\log_{10}\beta_1$ (293.15 K) = -0.36 ± 0.02 and $\log_{10}\beta_2$ (293.15 K) = -0.51 ± 0.03.

While the first value might actually represent complex formation, the second value most probably reflects medium effects, as the concentration of $[Cl^-]$ was varied from 0.01 to 3.0 M, i.e., a complete exchange of ClO_4^- with Cl^-.

This review estimated Δε values for extrapolation of $\log_{10}\beta_1$ to zero ionic strength, using ε(Cl^-, Na^+) = (0.03 ± 0.01) kg · mol^{-1} and ε(Cl^-, Li^+) = (0.10 ± 0.01) kg · mol^{-1} (Lemire et al. 2013), and using the estimation method (described in Section 1.5.3) for ε(Ac^{3+}, ClO_4^-) = (0.6 ± 0.1) kg · mol^{-1} and ε($AcCl^{2+}$, ClO_4^-) = (0.4 ± 0.1) kg · mol^{-1} (Tab. 2-2)

$$\Delta\varepsilon(NaClO_4, \text{estimated}) = -(0.23 \pm 0.14) \text{ kg} \cdot \text{mol}^{-1}$$

$$\Delta\varepsilon(LiClO_4, \text{estimated}) = -(0.30 \pm 0.14) \text{ kg} \cdot \text{mol}^{-1}$$

Shahani et al. (1968)

$\log_{10}\beta_1°$ (298.15 K) = 0.87

Sekine & Sakairi (1969)

$\log_{10}\beta_1°$ (298.15 K) = 0.30

Fukusawa et al. (1982)

$\log_{10}\beta_1°$ (298.15 K) = 0.03

The unweighted average

$\log_{10}\beta_1°$ (298.15 K) = 0.6 ± 0.5

is included in TDB 2020.

2.3.5 Actinium(III) phosphate complexes

Rao et al. (1970) studied the complex formation of Ac(III) and La(III) with phosphate by a solvent extraction method at pH 2 and 3, 25 ± 1 °C, and an ionic strength of 0.5 M which was maintained constant by varying the total phosphate concentration and suitably adjusting $HClO_4$ and NH_4ClO_4 concentrations. The total phosphate concentrations employed were in the range 0.15 – 0.01 M.

Rao et al. (1970) found that the best fit of their experimental data was obtained by assuming that only one complex is formed under the experimental conditions. The numerical results for Ac(III) and La(III) are the same within the experimental uncertainties. For Ac(III), Rao et al. (1970) report

$Ac^{3+} + H_2PO_4^- \rightleftharpoons AcH_2PO_4^{2+}$

$\beta_1 = 38.8 \pm 5$

which translates to

$\log_{10}\beta_1 = 1.59 \pm 0.06$

This review estimated a $\Delta\varepsilon$ value for extrapolation of $\log_{10}\beta_1$ to zero ionic strength, assuming $\varepsilon(H_2PO_4^-, NH_4^+) \approx \varepsilon(H_2PO_4^-, K^+) = -(0.14 \pm 0.04)$ kg · mol^{-1} (Lemire et al. 2013), and using the estimates according to Section 1.5.3 for $\varepsilon(Ac^{3+}, ClO_4^-) = (0.6 \pm 0.1)$ kg · mol^{-1} and $\varepsilon(AcH_2PO_4^{2+}, ClO_4^-) = (0.4 \pm 0.1)$ kg · mol^{-1} (Tab. 2-2)

$\Delta\varepsilon$(estimated) = $-(0.06 \pm 0.15)$ kg · mol^{-1}

$\log_{10}\beta_1^\circ$ (298.15 K) = 2.7 ± 0.2

where the uncertainty refers to 2σ. This value is included in TDB 2020.

2.3.6 Actinium(III) sulphate complexes

Shahani et al. (1968) determined the complex formation of Ac(III) with sulphate at 27 °C by a solvent extraction technique at a fixed $[H^+]$ concentration of 1.0 M but the ionic strength varied from 1.0 – 1.16 M. They interpreted their data in terms of two complexes

$Ac^{3+} + SO_4^{2-} \rightleftharpoons AcSO_4^+$

β_1 (300.15 K) = 15.9 ± 1.3

$Ac^{3+} + 2\ SO_4^{2-} \rightleftharpoons Ac(SO_4)_2^-$

β_2 (300.15 K) = 71.4 ± 7.3

which translates to

$\log_{10}\beta_1$ (300.15 K) = 1.20 ± 0.04

and

$\log_{10}\beta_2$ (300.15 K) = 1.85 ± 0.05

While the first value might actually represent complex formation, the second value most probably reflects medium effects, as the concentration of $[SO_4^{2-}]$ varied from 0.01 to 0.16 M, i.e., a significant exchange of ClO_4^- with SO_4^{2-}.

Sekine & Sakairi (1969) also used a solvent extraction technique to determine the complex formation of Ac(III) with sulphate at 25 °C and pH 3.0 – 3.5 in 1 M $NaClO_4$. They report the values $\log_{10}\beta_1$ (298.15 K) = 1.36 and $\log_{10}\beta_2$ (298.15 K) = 2.68.

No information is given by Sekine & Sakairi (1969) about the concentration range of SO_4^{2-} used in their solvent extraction experiments. Consequently, there is no way to properly address possible medium effects. However, considering that the stepwise stability constant $\log_{10}K_2 = 1.32$ for the equilibrium $AcSO_4^+ + SO_4^{2-} \rightleftharpoons Ac(SO_4)_2^-$ is virtually the same as $\log_{10}\beta_1 = 1.36$ (if real, $\log_{10}K_2$ should be significantly smaller than $\log_{10}\beta_1$) the reviewer decided that the $\log_{10}\beta_2$ value most probably reflects medium effects and is not included in the data analysis.

Aziz & Lyle (1970) determined the complex formation of Ac(III) with sulphate in 0.5 M $NaClO_4$ at 25 °C by a liquid-liquid partition method at pH 3.60 while varying the total sulphate concentration from $6 \cdot 10^{-3}$ – 0.12 M. They interpreted their data in terms of the complexes

β_1 (298.15 K) = 56.05 ± 0.54

β_2 (298.15 K) = 431.8 ± 8.4

which translates to

$\log_{10}\beta_1$ (298.15 K) = 1.75 ± 0.01

and

$\log_{10}\beta_2$ (298.15 K) = 2.64 ± 0.01

While the first value might actually represent complex formation, the second value most probably reflects medium effects, as the concentration of $[SO_4^{2-}]$ varied from 0.01 to 0.12 M, i.e., a significant exchange of ClO_4^- with SO_4^{2-}.

This review estimated a $\Delta\varepsilon$ value for extrapolation of $\log_{10}\beta_1$ to zero ionic strength, $\varepsilon(SO_4^{2-}, Na^+)$ = -(0.12 ± 0.06) kg · mol^{-1} (Lemire et al. 2013), and using the estimation method (described in Section 1.5.3) for $\varepsilon(Ac^{3+}, ClO_4^-)$ = (0.6 ± 0.1) kg · mol^{-1} and $\varepsilon(AcSO_4^+, ClO_4^-)$ = (0.2 ± 0.1) kg · mol^{-1} (Tab. 2-2)

$\Delta\varepsilon$(estimated) = -(0.28 ± 0.15) kg · mol^{-1}

Shahani et al. (1968)

$\log_{10}\beta_1°$ (300.15 K) = 3.35

Sekine & Sakairi (1969)

$\log_{10}\beta_1°$ (298.15 K) = 3.51

Aziz & Lyle (1970)

$\log_{10}\beta_1°$ (298.15 K) = 3.70

The unweighted average

$\log_{10}\beta_1°$ (298.15 K) = 3.5 ± 0.2

where the uncertainty refers to 2σ, is included in TDB 2020.

2.3.7 Actinium(III) thiocyanate complexes

Rao et al. (1968) determined the complex formation of Ac(III) and La(III) with thiocyanate at 27 °C by a solvent extraction technique. The ionic strength of the medium in presence of varying thiocyanate concentration was adjusted to 1.0 using $NaClO_4$ and sufficient $HClO_4$ to give a pH value of 2.0. They interpreted their data in terms of two complexes

$Ac^{3+} + SCN^- \rightleftharpoons AcSCN^{2+}$

β_1 (300.15 K) = 1.11 ± 0.07

$Ac^{3+} + 2\ SCN^- \rightleftharpoons Ac(SCN)_2^+$

β_2 (300.15 K) = 0.82 ± 0.08

which translates to

$\log_{10}\beta_1$ (300.15 K) = 0.045 ± 0.027

and

$\log_{10}\beta_2$ (300.15 K) = -0.09 ± 0.04

While the first value might actually represent complex formation, the second value most probably reflects medium effects, as the concentration of [SCN^-] was varied from 0.05 to 0.90 M, i.e., an almost complete exchange of ClO_4^- with SCN^-.

Sekine & Sakairi (1969) also used a solvent extraction technique to determine the complex formation of Ac(III) with thiocyanate at 25 °C and pH 3.0 – 3.5 in 5 M $NaClO_4$. They report the values $\log_{10}\beta_1$ (298.15 K) = -0.75 and $\log_{10}\beta_2$ (298.15 K) = -0.46.

No information is given by Sekine & Sakairi (1969) about the concentration range of SCN^- used in their solvent extraction experiments. Consequently, there is no way to properly address possible medium effects. However, considering the weak complex formation of Ac(III) with thiocyanate, the reviewer decided that the $\log_{10}\beta_2$ value most probably reflects medium effects and is not included in the data analysis.

This review estimated a $\Delta\varepsilon$ value for extrapolation of $\log_{10}\beta_1$ to zero ionic strength, using $\varepsilon(SCN^-, Na^+) = (0.05 \pm 0.01)$ kg · mol^{-1} (Lemire et al. 2013), and using the estimation method (described in Section 1.5.3) for $\varepsilon(Ac^{3+}, ClO_4^-) = (0.6 \pm 0.1)$ kg · mol^{-1} and $\varepsilon(AcSCN^{2+}, ClO_4^-) = (0.4 \pm 0.1)$ kg · mol^{-1} (Tab. 2-2)

$\Delta\varepsilon$(estimated) = -(0.25 ± 0.14) kg · mol^{-1}

Rao et al. (1968)

$\log_{10}\beta_1°$ (300.15 K) = 0.99 ± 0.15

Sekine & Sakairi (1969)

$\log_{10}\beta_1°$ (298.15 K) = -0.9 ± 0.9

The uncertainties of the above values are solely the consequence of extrapolating the values to zero ionic strength with the estimated $\Delta\varepsilon$. Extrapolating the value of Sekine & Sakairi (1969) from 6.58 mol/kg$_{H2O}$ ($LiClO_4$) to zero does not yield a meaningful result anymore. Hence, this review decided to consider only the value of Rao et al. (1968) with an increased uncertainty:

$log_{10}\beta_1°(298.15\ K) = 1.0 \pm 0.5$

This value is included in TDB 2020 as supplemental datum.

2.3.8 Actinium(III) oxalate compounds and complexes

2.3.8.1 Actinium(III) oxalate complexes

Sekine & Sakairi (1969) used a solvent extraction technique to determine the complex formation of Ac(III) with oxalate (ox) at 25 °C and pH 3.0 – 3.5 in 1 M $NaClO_4$. They report

$Ac^{3+} + ox^{2-} \rightleftharpoons Ac(ox)^+$

$\log_{10}\beta_1$ (298.15 K) = 3.56

$Ac^{3+} + 2\ ox^{2-} \rightleftharpoons Ac(ox)_2^-$

$\log_{10}\beta_2$ (298.15 K) = 6.16

Aziz & Lyle (1970) determined the complex formation of Ac(III) with sulphate in 0.5 M $NaClO_4$ at 25 °C by a liquid-liquid partition method at pH 3.60 while varying the total oxalate concentration from $2.2 \cdot 10^{-5}$ – $2.6 \cdot 10^{-4}$ M. They interpreted their data in terms of the complexes

β_1 (298.15 K) = $(2.96 \pm 0.09) \cdot 10^4$

β_2 (298.15 K) = $(9.99 \pm 0.72) \cdot 10^7$

which translates to

$\log_{10}\beta_1$ (298.15 K) = 4.47 ± 0.01

and

$\log_{10}\beta_2$ (298.15 K) = 8.00 ± 0.01

This review estimated Δε values for extrapolation of $\log_{10}\beta_x$ to zero ionic strength, using $\varepsilon(ox^{2-}, Na^+)$ = -(0.08 ± 0.01) kg · mol^{-1} (Hummel et al. 2005), assuming $\varepsilon(Ac(ox)^+, ClO_4^-) \approx \varepsilon(Am(ox)^+, ClO_4^-)$ = (0.08 ± 0.10) kg · mol^{-1} and $\varepsilon(Ac(ox)_2^-, Na^+) \approx \varepsilon(Ac(ox)_2^-, Na^+)$ = -(0.21 ± 0.08) kg · mol^{-1} (Hummel et al. 2005), and using the estimation method (described in Section 1.5.3) for $\varepsilon(Ac^{3+}, ClO_4^-)$ = (0.6 ± 0.1) kg · mol^{-1} (Tab. 2-2)

Δε(estimated) = -(0.44 ± 0.14) kg · mol^{-1}

Sekine & Sakairi (1969)

$\log_{10}\beta_1°$ (298.15 K) = 5.5

Aziz & Lyle (1970)

$\log_{10}\beta_1°$ (298.15 K) = 6.3

The unweighted average

$\log_{10}\beta_1°$ (298.15 K) = 5.9 ± 0.6

with an uncertainty assigned by this review, is included in TDB 2020.

Δε(estimated) = -(0.65 ± 0.13) kg · mol^{-1}

Sekine & Sakairi (1969)

$\log_{10}\beta_2°$ (298.15 K) = 8.7

Aziz & Lyle (1970)

$\log_{10}\beta_2°$ (298.15 K) = 10.5

The unweighted average

$\log_{10}\beta_2°$ (298.15 K) = 9.6 ± 1.2

with an uncertainty assigned by this review, is included in TDB 2020.

Note that Hummel et al. (2005) selected $\log_{10}\beta_1°$ (298.15 K) = 6.51 ± 0.15 for $Am^{3+} + ox^{2-} \rightleftharpoons Am(ox)^{+}$ and $\log_{10}\beta_2°$ (298.15 K) = 10.71 ± 0.20 for $Am^{3+} + 2\ ox^{2-} \rightleftharpoons Am(ox)_2^{-}$.

2.3.8.2 Actinium(III) oxalate compounds

Kirby & Morss (2006) discuss in their chapter about Ac(III) solubility that, besides $Ac(OH)_3(s)$ (see Section 2.3.2), $Ac_2(ox)_3(s)$ is the only other sparingly soluble Ac(III) compound whose solubility in aqueous solutions has been studied in some detail.

Ziv & Shestakova (1965a) determined the solubility of $Ac_2(ox)_3(s)$ in 0.01 M HNO_3 and in pure water and report

$$Ac_2(ox)_3(s) \rightleftharpoons 2\ Ac^{3+} + 3\ ox^{2-}$$

$$\log_{10}K_{sp}° \text{ (298.15 K)} = -25.7 \pm 0.6$$

where the uncertainty has been assigned in the present review considering the spread of results obtained by Ziv & Shestakova (1965a) under different experimental conditions and using different methods. This value is included in TDB 2020.

Note that combining the above selected solubility product with the complexation constants selected in Section 3.8.1, a minimum solubility of $[Ac]_{total} = 1.6 \cdot 10^{-5}$ M is calculated for $[ox^{2-}] = 2 \cdot 10^{-4}$ M in "pure water", i.e. $I = 0$. This is compatible with $[Ac]_{total} = 7 \cdot 10^{-6}$ M measured by Ziv & Shestakova (1965a) in pure water.

2.3.9 Actinium(III) citrate complexes

Moutte & Guillaumont (1969) determined the complexation of Ac(III) and Cm(III) with citrate (cit) by solvent extraction at 25 °C and pH 7 – 9. The ionic strength was adjusted to 0.1 M by $LiClO_4$ and Li_3cit. The concentration of citrate was always below $1.6 \cdot 10^{-2}$ M.

Moutte & Guillaumont (1969) interpreted their experimental data in terms of the complexes $Ac(OH)cit^{-}$, $Ac(OH)(cit)_2^{4-}$ and $Ac(OH)_2cit^{2-}$. However, it is unlikely that mixed Ac(III) – OH – citrate complexes form at pH < 10, considering the strong interaction of Ac(III) with citrate and the weak hydrolysis of Ac(III) (see Section 2.3.2). Moreover, similar complexes proposed for the Am(III) – citrate system by the same group have been rejected by Hummel et al. (2005). In summary, the results of Moutte & Guillaumont (1969) are not considered further in this review.

Kirby & Morss (2006) report data about Ac(III) cit complexation referring to a Chemical Abstracts citation (Makarova, T.P., Sinitsyna, G.S., Stepanov, A.V., Gritschenko, I.A., Shestakova, I.A. & Shestakov, B.I. (1974) Chem. Abs., 82, 176644). No related paper could be detected by the present review.

According to Kirby & Morss (2006), the complexation of Ac(III) with cit was determined at pH 2 – 3 and ionic strength 0.1 M, probably by the same electromigration method used by Makarova et al. (1972), leading to

$Ac^{3+} + cit^{3-} \rightleftharpoons Ac(cit)(aq)$

$\beta_1 = 9.55 \cdot 10^6$

which translates to

$\log_{10}\beta_1 = 6.98$

This review estimated a $\Delta\varepsilon$ value for extrapolation of $\log_{10}\beta_1$ to zero ionic strength, using $\varepsilon(cit^{3-}, Na^+) = -(0.08 \pm 0.03)$ kg · mol^{-1} (Hummel et al. 2005), assuming $\varepsilon(Ac(cit)(aq), NaClO_4) \approx \varepsilon(Am(cit)(aq), NaClO_4) = (0.00 \pm 0.05)$ kg · mol^{-1} (Hummel et al. 2005), and using the estimation method (described in Section 1.5.3) for $\varepsilon(Ac^{3+}, ClO_4^-) = (0.6 \pm 0.1)$ kg · mol^{-1} (Tab. 2-2)

$\Delta\varepsilon(\text{estimated}) = -(0.52 \pm 0.12)$ kg · mol^{-1}

$\log_{10}\beta_1°(298.15\ K) = 8.9 \pm 0.5$

with a large uncertainty is assumed by this review.

Considering that the above value is based on a single indirect reference without any details about the experimental methods, this value is included in TDB 2020 as supplemental datum.

Note that Hummel et al. (2005) selected $\log_{10}\beta_1°$ (298.15 K) = 8.55 ± 0.20 for $Am^{3+} + cit^{3-} \rightleftharpoons Am(cit)(aq)$.

2.3.10 Actinium(III) edta complexes

Makarova et al. (1972) determined the complex formation of Ac(III) with ethylenediaminetetraacetate (edta) by electromigration. They varied the pH of the solutions from 1 – 4 with a constant total concentration of edta ($5 \cdot 10^{-4}$ M) and varied the total concentration of edta from $5 \cdot 10^{-4} – 1 \cdot 10^{-3}$ M at a constant pH of 2.8. The ionic strength of the solutions was constant in all experiments and equal to 0.1 M. No information about the medium and temperature are given.

The experimental results lead Makarova et al. (1972) to the conclusion that the formation of a neutral hydrogen containing complex occurs in the region of pH < 2.7, whereas at higher pH the complex form $Ac(edta)^-$ dominates.

The stability constants of the complexes $Ac(edta)^-$ and AcHedta(aq), coexisting at pH < 2.7 were determined as

$Ac^{3+} + edta^{4-} \rightleftharpoons Ac(edta)^-$

$\beta_1 = (1.6 \pm 0.4) \cdot 10^{14}$

$Ac(edta)^- + H^+ \rightleftharpoons AcHedta(aq)$

$K = (2.8 \pm 2.0) \cdot 10^2$

which translates to

$$\log_{10}\beta_1 = 14.20 \pm 0.11$$

and

$$\log_{10}K = 2.4 \pm 0.4$$

Calculations according to the data obtained in the electromigration of actinium in solutions with a variable concentration of edta at pH = 2.8, where the dominant process is the formation of the complex $Ac(edta)^-$, lead to the value

$$K_1 = (2.44 \pm 0.7) \cdot 10^{14}$$

which translates to

$$\log_{10}\beta_1 = 14.39 \pm 0.13$$

This review estimated $\Delta\varepsilon$ values for extrapolation of $\log_{10}\beta_1$ and $\log_{10}K$ to zero ionic strength, using $\varepsilon(edta^{4-}, Na^+) = (0.32 \pm 0.14)$ kg · mol^{-1} (Hummel et al. 2005), assuming $\varepsilon(Ac(edta)^-, Na^+) \approx \varepsilon(Am(edta)^-, Na^+) = (0.01 \pm 0.16)$ kg · mol^{-1} (Hummel et al. 2005), and using the estimation method (described in Section 1.5.3) for $\varepsilon(Ac^{3+}, ClO_4^-) = (0.6 \pm 0.1)$ kg · mol^{-1} and $\varepsilon(AcHedta(aq), NaClO_4) = (0.00 \pm 0.10)$ kg · mol^{-1} (Tab. 2-2)

$$\Delta\varepsilon(\text{estimated}) = -(0.91 \pm 0.23) \text{ kg} \cdot \text{mol}^{-1}$$

$$\log_{10}\beta_1^\circ\ (298.15\ \text{K}) = 16.8 \pm 0.5$$

where $\log_{10}\beta_1^\circ$ is the average of both values given by Makarova et al. (1972), with a large uncertainty assumed by this review. This value is included in TDB 2020.

$$\Delta\varepsilon(\text{estimated}) = -(0.15 \pm 0.19) \text{ kg} \cdot \text{mol}^{-1}$$

$$\log_{10}K^\circ\ (298.15\ \text{K}) = 2.6 \pm 0.8$$

where the uncertainty refers to 2σ. This value is included in TDB 2020.

Note that Hummel et al. (2005) selected $\log_{10}\beta_1^\circ\ (298.15\ \text{K}) = 19.67 \pm 0.11$ for $Am^{3+} + edta^{4-} \rightleftharpoons Am(edta)^-$, and $\log_{10}K^\circ\ (298.15\ \text{K}) = 2.17 \pm 0.25$ for $Am(edta)^- + H^+ \rightleftharpoons AmHedta(aq)$.

2.4 Selected actinium data

Tab. 2-1: Selected actinium data

Supplemental data are in italics

Name	**$\Delta_f G_m°$** [kJ · mol^{-1}]	**$\Delta_f H_m°$** [kJ · mol^{-1}]	**$S_m°$** [J · K^{-1} · mol^{-1}]	**$C_{p,m}°$** [J · K^{-1} · mol^{-1}]	**Species**
Ac(cr)	0.0	0.0	61.9 ± 0.8	26 ± 2	Ac(cr)
Ac+3	-639.3 ± 25.5	-653 ± 25	-180 ± 17		Ac^{3+}

Name	**$\log_{10}\beta°$**	**$\Delta_r H_m°$** [kJ · mol^{-1}]	**Reaction**
AcOH+2	-8.6 ± 0.2	-	$Ac^{3+} + H_2O(l) \rightleftharpoons AcOH^{2+} + H^+$
Ac(OH)3(aq)	-31.2 ± 0.2	-	$Ac^{3+} + 3\ H_2O(l) \rightleftharpoons Ac(OH)_3(aq) + 3\ H^+$
AcF+2	3.61 ± 0.20	-	$Ac^{3+} + F^- \rightleftharpoons AcF^{2+}$
AcF2+	6.73 ± 0.20	-	$Ac^{3+} + 2F^- \rightleftharpoons AcF_2^+$
AcF3(aq)	*≈ 9.75*	-	*$Ac^{3+} + 3F^- \rightleftharpoons AcF_3(aq)$*
AcCl+2	0.6 ± 0.5	-	$Ac^{3+} + Cl^- \rightleftharpoons AcCl^{2+}$
AcH2PO4+2	2.7 ± 0.2	-	$Ac^{3+} + H_2PO_4^- \rightleftharpoons AcH_2PO_4^{2+}$
AcSO4+	3.5 ± 0.2	-	$Ac^{3+} + SO_4^{2-} \rightleftharpoons AcSO_4^+$
AcSCN+2	*1.0 ± 0.5*	-	*$Ac^{3+} + SCN^- \rightleftharpoons AcSCN^{2+}$*
Ac(ox)+	5.9 ± 0.6	-	$Ac^{3+} + ox^{2-} \rightleftharpoons Ac(ox)^+$
Ac(ox)2-	9.6 ± 1.2	-	$Ac^{3+} + 2\ ox^{2-} \rightleftharpoons Ac(ox)_2^-$
Ac(cit)(aq)	*8.9 ± 0.5*	-	*$Ac^{3+} + cit^{3-} \rightleftharpoons Ac(cit)(aq)$*
Ac(edta)-	16.8 ± 0.5	-	$Ac^{3+} + edta^{4-} \rightleftharpoons Ac(edta)^-$
AcHedta(aq)	2.6 ± 0.8	-	$Ac(edta)^- + H^+ \rightleftharpoons AcHedta(aq)$

Name	**$\log_{10}K_{s,0}°$**	**$\Delta_r H_m°$** [kJ · mol^{-1}]	**Reaction**
Ac(OH)3(fresh)	23.3 ± 0.2	-	$Ac(OH)_3(s) + 3\ H^+ \rightleftharpoons Ac^{3+} + 3\ H_2O(l)$
Ac(OH)3(aged)	21.1 ± 0.2	-	$Ac(OH)_3(s) + 3\ H^+ \rightleftharpoons Ac^{3+} + 3\ H_2O(l)$
Ac2(ox)3(s)	-25.7 ± 0.6	-	$Ac_2(ox)_3(s) \rightleftharpoons 2\ Ac^{3+} + 3\ ox^{2-}$

Tab. 2-2: Selected SIT ion interaction coefficients $\varepsilon_{j,k}$ [kg · mol^{-1}] for actinium species

Data in normal face are derived or estimated in this review. Data estimated according to charge correlations and taken from Tab. 1-7 are shaded. Supplemental data are in italics.

j k → ↓	**Cl^-** $\varepsilon_{j,k}$ [kg · mol^{-1}]	**ClO_4^-** $\varepsilon_{j,k}$ [kg · mol^{-1}]	**Na^+** $\varepsilon_{j,k}$ [kg · mol^{-1}]	**$Na^+ + Cl^-$** $\varepsilon_{j,k}$ [kg · mol^{-1}]	**$Na^+ + ClO_4^-$** $\varepsilon_{j,k}$ [kg · mol^{-1}]
Ac3+	0.6 ± 0.1 [a]	0.6 ± 0.1	0	0	0
AcOH+2	0.4 ± 0.1 [a]	0.4 ± 0.1	0	0	0
Ac(OH)3(aq)	0	0	0	0.0 ± 0.1	0.0 ± 0.1
AcF+2	0.4 ± 0.1 [a]	0.4 ± 0.1	0	0	0
AcF2+	0.2 ± 0.1 [a]	0.2 ± 0.1	0	0	0
AcF3(aq)	*0*	*0*	*0*	*0.0 ± 0.1*	*0.0 ± 0.1*
AcCl+2	0.4 ± 0.1 [a]	0.4 ± 0.1	0	0	0
AcH2PO4+2	0.4 ± 0.1 [a]	0.4 ± 0.1	0	0	0
AcSO4+	0.2 ± 0.1 [a]	0.2 ± 0.1	0	0	0
AcSCN+2	*0.4 ± 0.1* [a]	*0.4 ± 0.1*	*0*	*0*	*0*
Ac(ox)+	(0.08 ± 0.10) [a]	(0.08 ± 0.10) [b]	0	0	0
Ac(ox)2-	0	0	-(0.21 ± 0.08) [b]	0	0
Am(cit)(aq)	0	0	0	(0.00 ± 0.05) [a]	(0.00 ± 0.05) [b]
Ac(edta)-	0	0	(0.01 ± 0.16) [b]	0	0
AcHedta(aq)	0	0	0	0.0 ± 0.1	0.0 ± 0.1

[a] Assumed to be equal to the corresponding ion interaction coefficient with ClO_4^-.
[b] Assumed to be equal to the corresponding ion interaction coefficient with Am(III) (Hummel et al. 2005).

2.5 References

Aziz, A. & Lyle, S.J. (1970): Complexes of lanthanum and actinium with fluoride, oxalate and sulphate in aqueous solutions. J. Inorg. Nucl. Chem., 32, 1925-1932.

Brown, P.L. & Ekberg, C. (2016): Hydrolysis of Metal Ions. Wiley-VCH Verlag GmbH & Co. KGaA, Weinheim, Germany, 917 pp.

Ferrier, M.G., Batista, E.R., Berg, J.M., Birnbaum, E.R., Cross, J.N., Engle, J.W., La Pierre, H.S., Kozimor, S.A., Lezama Pacheco, J.S., Stein, B.W., Stieber, S.C.E. & Wilson, J.J. (2016): Spectroscopic and computational investigation of actinium coordination chemistry. Nature Communications, 7, 12312, doi: 10.1038/ncomms12312.

Ferrier, M.G., Stein, B.W., Batista, E.R., Berg, J.M., Birnbaum, E.R., Cross, Engle, J.W., John, K.D., Kozimor, S.A., Lezama Pacheco, J.S. & Redman, L.N. (2017): Synthesis and characterization of the actinium aquo ion. ACS Cent. Sci., 3, 176-185.

Fukusawa, T., Kawasuji, I., Mitsugashira, T., Satô, A. & Suzuki, S. (1982): Investigation on the complex formation of some lanthanoids(III) and actinoids(III) with chloride and bromide. Bulletin of the Chemical Society of Japan, 55, 726-729.

Grenthe, I., Fuger, J., Konings, R.J.M., Lemire, R.J., Muller, A.B., Nguyen-Trung, C. & Wanner, H. (1992): Chemical Thermodynamics of Uranium. Chemical Thermodynamics, Vol. 1. North-Holland, Amsterdam, 715 pp.

Hummel, W., Anderegg, G., Puigdomènech, I., Rao, L. & Tochiyama, O. (2005): Chemical Thermodynamics of Compounds and Complexes of U, Np, Pu, Am, Tc, Se, Ni and Zr with Selected Organic Ligands. Chemical Thermodynamics, Vol 9. North-Holland, Amsterdam, 1088 pp.

Kirby, H.W. & Morss, L.R. (2006): Actinium. *In:* Morss, L.R., Edelstein, N.M., Fuger, J. & Katz, J.J. (Eds.): The Chemistry of the Actinide and Transactinide Elements, Volume 1, 3$^{r\,d}$ Edition, Springer, The Netherlands, p. 18-51.

Konings, R.J.M., Morss, L.R. & Fuger, J. (2006): Thermodynamic Properties of Actinides and Actinide Compounds. *In:* Morss, L.R., Edelstein, N.M., Fuger, J. & Katz, J.J. (Eds.): The Chemistry of the Actinide and Transactinide Elements, Volume 4, 3$^{r\,d}$ Edition, Springer, The Netherlands, p. 2113-2224.

Kulikov, E.V., Novgorodov, A.F. & Schumann, D. (1992): Hydrolysis of ^{225}Actinium trace quantities. J. Radioanal. Nucl. Chem., Letters, 164, 103-108.

Lemire, R.J., Berner, U., Musikas, C., Palmer, D.A., Taylor, P. & Tochiyama, O. (2013): Chemical Thermodynamics of Iron, Part 1. Chemical Thermodynamics, Vol. 13a. OECD Publications, Paris, France, 1082 pp.

Makarova, T.P., Sinitsyna, G.S., Stepanov, A.V., Shestakova, I.A. & Shestakov, B.I. (1972): Complex formation of actinium I. Determination of the stability constants of ethylenediaminetetraacetate complexes of actinium and its separation from lanthanum in solutions of edta by the method of electromigration. Soviet Radiochemistry, 14, 555-557 (translated from: Radiokhimiya, 14 (1972), 538-541).

Makarova, T.P., Stepanov, A.V. & Shestakov, B.I. (1973): Electromigration investigation of the comparative stability of fluoro-complexes of the MF^{2+} type of certain rare-earth and actinide elements. Russian Journal of Inorganic Chemistry, 18, 783-785.

Moutte, A. & Guillaumont, R. (1969): Complexes citriques d'actinium et de curium. Revue de Chimie minérale, 6, 603-610.

Rao, V.R., Shahani, C.J. & Mathew, K.A. (1968): Chemistry of actinium – II Stability constants of thiocyanate complexes of actinium and lanthanum. Inorg. Nucl. Chem. Letters, 4, 655-659.

Rao, V.R., Shahani, C.J. & Rao, C.L. (1970): Studies on the phosphate complexes of actinium and lanthanum. Radiochim. Acta, 14, 31-34.

Sekine, T. & Sakairi, M. (1969): Studies of actinium(III) in various solutions. III. Actinium(III) complexes of oxalate, sulfate, chloride, and thiocyanate ions in perchlorate media. Bulletin of the Chemical Society of Japan, 42, 2712-2713.

Shahani, C.J., Mathew, K.A., Rao, C.L. & Ramaniah, M.V. (1968): Chemistry of actinium I. Stability constants of chloride, bromide, nitrate and sulphate complexes. Radiochim. Acta, 10, 165-167.

Zielińska, B. & Bilewicz, A. (2004): The hydrolysis of actinium. J. Radioanal. Nucl. Chem., 261, 195-198.

Ziv, D.M. & Shestakova, I.A. (1965a): Investigation of the solubility of certain actinium compounds I. Determination of the solubility of actinium oxalate. Soviet Radiochemistry, 7, 168-175 (translated from: Radiokhimiya, 7 (1965) 166-175).

Ziv, D.M. & Shestakova, I.A. (1965b): Investigation of the solubility of certain actinium compounds II. Determination of the solubility and estimation of the relative basicity of actinium hydroxide. Soviet Radiochemistry, 7, 176-186 (translated from: Radiokhimiya, 7 (1965), 175-187).

3 Alkali elements

Chemical thermodynamic data for ground and pore water models in our original database (Pearson & Berner 1991, Pearson et al. 1992) have been taken from the USGS review of data for major water-mineral reactions (Nordstrom et al. 1990) and basically have not been changed since then. The USGS summary of equilibrium constants and reaction enthalpies for aqueous association reactions and mineral solubilities has been compiled from the literature for common equilibria occurring in natural waters at 0 – 100 °C and 1 bar pressure. The species have been limited to those containing the metals Li, Na, K, Mg, Ca, Sr, Ba, Mn(II,III,IV), Fe(II,III) and Al, and the ligands OH^-, F^-, Cl^-, CO_3^{2-}, HCO_3^-, SO_4^{2-} and $Si(OH)_4(aq)$.

Meanwhile, new experimental data have been reported, as well as new reviews of the hydrolysis of metal ions (Brown & Ekberg 2016), which are considered in the present update of chemical thermodynamic data for ground and pore water models.

The thermodynamic data included in TDB 2020 have been taken from

- CODATA key values (Cox et al. 1989)
- the USGS review of data for major water-mineral reactions (Nordstrom et al. 1990)
- the recent review of the hydrolysis of metal ions (Brown & Ekberg 2016)
- and own reviews of experimental data

NEA (see, e.g., Grenthe et al. 1992, Lemire et al. 2013) used the specific ion interaction theory (SIT) for making ionic strength corrections to the experimental data, an approach which is also adopted for TDB 2020 (as has been for all its predecessors).

In many cases, the ion interaction coefficients for species under consideration here were not available. We approximated these with the estimation method described in Section 1.5.3, which draws on a statistical analysis of published SIT ion interaction coefficients and which allows the estimation of missing coefficients for the interaction of cations with Cl^- and ClO_4^-, and for the interaction of anions with Na^+, from the charge of the cations or anions of interest.

3.0 References

Brown, P.L. & Ekberg, C. (2016): Hydrolysis of Metal Ions. Wiley-VCH Verlag GmbH & Co. KGaA, Weinheim, Germany, 917 pp.

Cox, J.D., Wagman, D.D. & Medvedev, V.A. (1989): CODATA Key Values for Thermodynamics. Hemisphere Publishing, New York, 271 pp.

Grenthe, I., Fuger, J., Konings, R.J.M., Lemire, R.J., Muller, A.B., Nguyen-Trung, C. & Wanner, H. (1992): Chemical Thermodynamics of Uranium. Chemical Thermodynamics, Vol. 1. North-Holland, Amsterdam, 715 pp.

Lemire, R.J., Berner, U., Musikas, C., Palmer, D.A., Taylor, P. & Tochiyama, O. (2013): Chemical Thermodynamics of Iron, Part 1. Chemical Thermodynamics, Vol. 13a. OECD Publications, Paris, France, 1082 pp.

Nordstrom, D.K., Plummer, L.N., Langmuir, D., Busenberg, E., May, H.M., Jones, B.F. & Parkhurst, D.L. (1990): Revised Chemical Equilibrium Data for Major Water-Mineral Reactions and Their Limitations. In: Melchior, D.C., and Bassett, R.L. (eds.): Chemical Modeling of Aqueous Systems II. Washington, D.C., American Chemical Society, ACS Symposium Series 416, p. 398-413.

Pearson, F.J., Jr. & Berner, U. (1991): Nagra Thermochemical Data Base I. Core Data. Nagra Technical Report NTB 91-17.

Pearson, F.J., Jr., Berner, U. & Hummel W. (1992): Nagra Thermochemical Data Base II. Supplemental Data 05/92. Nagra Technical Report NTB 91-18.

3.1 Lithium

3.1.1 Elemental lithium

Lithium metal and gas are not relevant under environmental conditions. Hence, the gas phase Lig is not included in the data base. The absolute entropy and heat capacity of Li(cr) are included as they are used for the calculation of certain thermodynamic reaction properties.

The selected values for Li(cr) are taken from CODATA (Cox et al. 1989):

$$S_m°(\text{Li, cr, 298.15 K}) = (29.120 \pm 0.200)\ \text{J} \cdot \text{K}^{-1} \cdot \text{mol}^{-1}$$

$$C_{p,m}°(\text{Li, cr, 298.15 K}) = (24.860 \pm 0.200)\ \text{J} \cdot \text{K}^{-1} \cdot \text{mol}^{-1}$$

3.1.2 Lithium(I) aqua ion

Lithium(I) exists as the Li^+ cation in aqueous solutions. The selected thermodynamic values for Li^+ are taken from CODATA (Cox et al. 1989):

$$\Delta_f G_m°(Li^+, \text{298.15 K}) = -(292.918 \pm 0.109)\ \text{kJ} \cdot \text{mol}^{-1}$$

$$\Delta_f H_m°(Li^+, \text{298.15 K}) = -(278.470 \pm 0.080)\ \text{kJ} \cdot \text{mol}^{-1}$$

$$S_m°(Li^+, \text{298.15 K}) = (12.240 \pm 0.150)\ \text{J} \cdot \text{K}^{-1} \cdot \text{mol}^{-1}$$

Using the selected CODATA $\Delta_f G_m°(Li^+, \text{298.15 K})$, the redox equilibrium

$$\text{Li(cr)} \rightleftharpoons Li^+ + e^-$$

is calculated as

$$\log_{10} K°(\text{298.15 K}) = 51.32 \pm 0.02$$

Since this review does not consider the formation of lithium(I) chloride complexes (see Section 3.1.5), $\varepsilon(Li^+, Cl^-)$ is taken as selected by NEA (Grenthe et al. 1992, Lemire et al. 2013):

$$\varepsilon(Li^+, Cl^-) = (0.10 \pm 0.01)\ \text{kg} \cdot \text{mol}^{-1}$$

3.1.3 Lithium(I) (hydr)oxide compounds and complexes

3.1.3.1 Lithium(I) hydroxide complexes

Nordstrom et al. (1990) selected a $\log_{10}{}^{*}\beta_1°$ value and an estimate of $\Delta_r H_m°$ based on the values reported by Baes & Mesmer (1976) for the equilibrium:

$$Li^+ + OH^- \rightleftharpoons LiOH(aq)$$

$$\log_{10}\beta_1° \text{ (298.15 K)} = 0.36 \pm 0.06$$

$$\Delta_r H_m°(298.15 \text{ K}) = (0 \pm 13) \text{ kJ} \cdot \text{mol}^{-1}$$

This can be recalculated via the dissociation of water parameters (Grenthe et al. 1992) to

$$Li^+ + H_2O(l) \rightleftharpoons LiOH(aq) + H^+$$

$$\log_{10}{}^{*}\beta_1° \text{ (298.15 K)} = -13.64 \pm 0.06$$

$$\Delta_r H_m°(298.15 \text{ K}) = (56 \pm 13) \text{ kJ} \cdot \text{mol}^{-1}$$

Note that Nordstrom et al. (1990) erroneously took $\Delta_r H_m°(298.15 \text{ K}) = 0$ as the estimate for the reaction $Li^+ + H_2O(l) \rightleftharpoons LiOH(aq) + H^+$.

Brown & Ekberg (2016) report that there have been a number of studies of the hydrolysis of the Li(I) ion determining the association constant for LiOH(aq), using either conductivity or emf measurements. The data accepted by Brown & Ekberg (2016) across the temperature range of 5 – 350 °C clearly show a non-linear behaviour when plotted against the reciprocal temperature (Fig. 6-1 of Brown & Ekberg 2016). For the reaction

$$Li^+ + H_2O(l) \rightleftharpoons LiOH(aq) + H^+$$

Brown & Ekberg (2016) fitted the function

$$\log_{10}{}^{*}\beta_1° \text{ (T)} = 18.3 - 3889 / \text{T} - 3.35 \cdot \ln \text{T}$$

and obtained

$$\log_{10}{}^{*}\beta_1° \text{ (298.15 K)} = -13.84 \pm 0.14$$

$$\Delta_r H_m°(298.15 \text{ K}) = (55.3 \pm 3.7) \text{ kJ} \cdot \text{mol}^{-1}$$

$$\Delta_r C_{p,m}°(298.15 \text{ K}) = -(64.1 \pm 34.6) \text{ J} \cdot \text{K}^{-1} \cdot \text{mol}^{-1}$$

These values have been included in TDB 2020, as well as the estimate

$$\varepsilon(\text{LiOH(aq)}, \text{NaCl}) = (0.0 \pm 0.1)\ \text{kg} \cdot \text{mol}^{-1}.$$

The values reported by Brown & Ekberg (2016) are in good agreement with those of the older evaluation of Baes & Mesmer (1976), considering the assigned uncertainties by both authors.

3.1.3.2 Lithium(I) (hydr)oxide compounds

LiOH(s) is a highly soluble caustic base ("Ätzlithium") with a solubility of 113 g/L at 20 °C (gestis.itrust.de). The solid is hygroscopic. No solubility data have been considered for TDB 2020.

3.1.4 Lithium(I) fluoride compounds and complexes

3.1.4.1 Lithium(I) fluoride complexes

Chan et al. (1984) did measurements by fluoride ion-selective electrode potentiometry on the very weak monofluoride complexes LiF(aq), NaF(aq), KF(aq) and RbF(aq). They report for LiF(aq)

$$\text{Li}^+ + \text{F}^- \rightleftharpoons \text{LiF(aq)}$$

$$K_1^\circ\ (298.15\ \text{K}) = 1.7 \pm 0.2$$

$$\log_{10} K_1^\circ\ (298.15\ \text{K}) = 0.23 \pm 0.05$$

$$\Delta_r H_m(298.15\ \text{K}, 1\ \text{M}\ \text{NaClO}_4) = (6.0 \pm 0.6)\ \text{kJ} \cdot \text{mol}^{-1}$$

Chan et al. (1984) obtained K_1° by non-linear regression using an extended form of the Debye-Hückel equation from data measured at 0.02 to 1.0 M $NaClO_4$ at 25 °C and calculated $\Delta_r H_m$ by linear regression from data measured at 15, 25 and 35 °C at 1 M $NaClO_4$.

Using the data of Chan et al. (1984) measured at 0.02 to 1.0 M $NaClO_4$ at 25 °C with assigned uncertainties of ±0.2 $\log_{10}$-units for an SIT analysis (Fig. 3.1-1), this review obtained

$$\log_{10} K_1^\circ\ (298.15\ \text{K}) = 0.23 \pm 0.11$$

$$\Delta\varepsilon(\text{NaClO}_4) = 0.00 \pm 0.22$$

These are the same results for $\log_{10} K_1^\circ$ as reported by Chan et al. (1984) where the uncertainties now refer to 2σ.

Considering $\varepsilon(\text{Li}^+, \text{ClO}_4^-) = (0.15 \pm 0.01)\ \text{kg} \cdot \text{mol}^{-1}$ and $\varepsilon(\text{Na}^+, \text{F}^-) = (0.02 \pm 0.02)\ \text{kg} \cdot \text{mol}^{-1}$ (Grenthe et al. 1992) this review derives from the experimental Δε value

$$\varepsilon(\text{LiF(aq)}, \text{NaClO}_4) = (0.17 \pm 0.23)\ \text{kg} \cdot \text{mol}^{-1}.$$

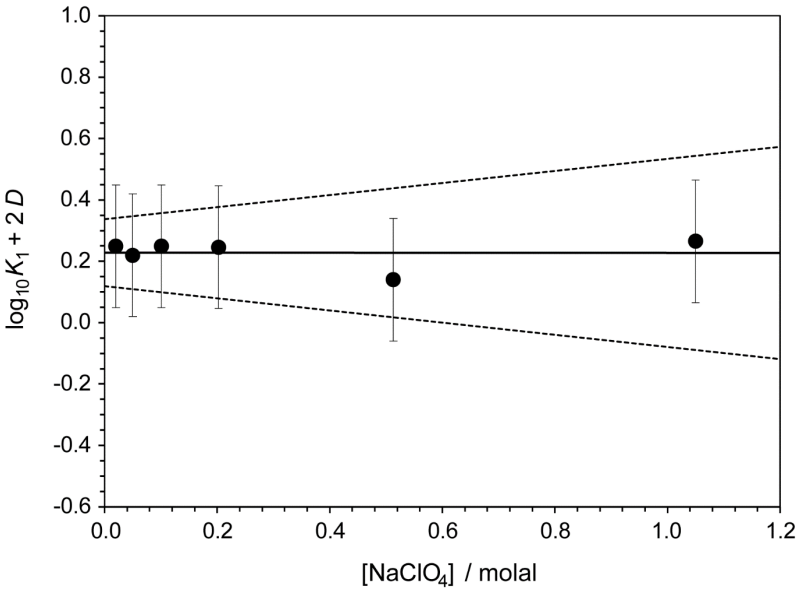

Fig. 3.1-1: Dependence of the equilibrium $Li^+ + F^- \rightleftharpoons LiF(aq)$ on ionic strength in $NaClO_4$ using the data of Chan et al. (1984)

The solid line is obtained using the derived SIT interaction coefficient and stability constant at zero ionic strength. Dotted lines represent the 95% uncertainty range extrapolated from I = 0 to higher $NaClO_4$ concentrations.

Within its uncertainty this value cannot be distinguished from zero, as expected, and thus it seems justified to include the estimate

$$\varepsilon(\text{LiF(aq)}, \text{NaCl}) = (0.0 \pm 0.1)\ \text{kg} \cdot \text{mol}^{-1}$$

in TDB 2020, together with $\log_{10}K_1°$ obtained from the SIT analysis.

A linear regression of the temperature data reported by Chan et al. (1984) yielded

$$\Delta_r H_m(298.15\ \text{K}, 1\ \text{M}\ \text{NaClO}_4) = (6.0 \pm 1.2)\ \text{kJ} \cdot \text{mol}^{-1}$$

in perfect agreement with the value reported by Chan et al. (1984), where the uncertainty now refers to 2σ. No attempt has been made to extrapolate this value to zero ionic strength, and it is included in TDB 2020 as an approximation of $\Delta_r H_m°$ (298.15 K).

3.1.4.2 Lithium(I) fluoride compounds

LiF(s) is a slightly soluble salt with a solubility of 1.3 g/L at 25 °C (gestis.itrust.de). It is found in nature as the extremely rare mineral griceite. No solubility data have been considered for TDB 2020.

3.1.5 Lithium(I) chloride compounds and complexes

3.1.5.1 Lithium(I) chloride complexes

This report does not consider the formation of weak lithium(I) chloride complexes but includes possible ion interactions into the SIT interaction coefficient $\varepsilon(Li^+, Cl^-)$, see below.

3.1.5.2 Lithium(I) chloride compounds

LiCl(cr) is a highly soluble salt with a solubility of 832 g/L at 20 °C (gestis.itrust.de). Its isopiestic properties have been measured up to 20 $mol \cdot kg_{H2O}^{-1}$ (Robinson & Stokes 1959). Hence, no solubility data, but the specific ion interaction coefficient selected by NEA (Grenthe et al. 1992, Lemire et al. 2013) is adopted for TDB 2020:

$$\varepsilon(Li^+, Cl^-) = (0.10 \pm 0.01)\ kg \cdot mol^{-1}$$

3.1.6 Lithium(I) carbonate compounds and complexes

3.1.6.1 Lithium(I) carbonate complexes

No thermodynamic data could be found by this review concerning the formation of aqueous lithium(I) carbonate complexes.

3.1.6.2 Lithium(I) carbonate compounds

$Li_2CO_3(s)$ is a soluble salt with a solubility of 13 g/L at 20 °C (gestis.itrust.de). It is found in nature as the rare mineral zabuyelite. No solubility data have been considered for TDB 2020.

3.1.7 Lithium(I) sulphate compounds and complexes

3.1.7.1 Lithium(I) sulphate complexes

Nordstrom et al. (1990) selected $\log_{10}K_1°$ reported by Smith & Martell (1976) for the complex

$$Li^+ + SO_4^{2-} \rightleftharpoons LiSO_4^-$$

$$\log_{10}K_1° (298.15\ K) = 0.64$$

As usual, Smith & Martell (1976) do not give any hint concerning their data selection; just seven references are listed referring to the system Li^+, Na^+, K^+ – SO_4^{2-}. Inspecting all these references, this review concludes that Smith & Martell (1976) refer to Righellato & Davies (1930) for their data selection. In addition, Smith & Martell (1976) give an enthalpy of reaction of zero, obviously based on the estimate of Austin & Mair (1962), which for unknown reasons was not selected by Nordstrom et al. (1990).

However, concerning the complex

$$Li^+ + SO_4^{2-} \rightleftharpoons LiSO_4^-$$

two somewhat discrepant results have been published. Righellato & Davies (1930) report

$$\log_{10}\beta_1^\circ\ (291.15\ K) = 0.64 \pm 0.05$$

from conductivity measurements at 18 °C, with its uncertainty estimated by this review based on the experimental data of Righellato & Davies (1930), whereas Daniele et al. (1982) report

$$\log_{10}\beta_1^\circ\ (310.15\ K) = 1.12 \pm 0.04$$

derived from potentiometric measurements at 37 °C and ionic strength 0.03 – 0.5 M, and extrapolated to I = 0 by Daniele et al. (1982) using a function similar to the SIT equation.

Austin & Mair (1962) conclude from their calorimetric measurements at 25 °C, concerning the standard enthalpy of formation of HSO_4^-, $LiSO_4^-$ and $NaSO_4^-$, that the results for the $LiSO_4^-$ complex indicate that the heat of formation of the $LiSO_4^-$ complex is zero or that there is no complex formation between lithium and sulphate ions. As the results of Righellato & Davies (1930) and Daniele et al. (1982) show that lithium forms a complex with sulphate, this review includes the result of Austin & Mair (1962)

$$\Delta_r H_m^\circ(298.15\ K) \approx 0\ kJ \cdot mol^{-1}$$

as supplemental datum in TDB 2020.

Considering the $\Delta_r H_m^\circ(298.15\ K)$ estimate of Austin & Mair (1962) this review concluded that $\log_{10}\beta_1^\circ$ does not change between 18 and 37 °C, and the values of Righellato & Davies (1930) and Daniele et al. (1982) should also be valid at 25 °C. The discrepancy of 0.5 $\log_{10}$-units in their results remains unclear as both experimental studies are considered reliable, and the values from the same authors for $NaSO_4^-$ agree within 0.03 $\log_{10}$-units (see Section 3.2.7.1), and their values for KSO_4^- agree within 0.05 $\log_{10}$-units with the overall fit of all data (see Section 3.3.7.1, Fig. 3.3-1). Hence, this review calculated the unweighted average of the discrepant data and assigned an uncertainty covering the range of expectation of both source data:

$$\log_{10}\beta_1^\circ\ (298.15\ K) = 0.9 \pm 0.3$$

This value has been included in TDB 2020, as well as the estimate

$$\varepsilon(LiSO_4^-, Na^+) = -(0.05 \pm 0.10)\ kg \cdot mol^{-1}.$$

3.1.7.2 Lithium(I) sulphate compounds

Li_2SO_4(s) is a highly soluble salt with a solubility of 340 g/L at 20 °C (gestis.itrust.de). It has not been found in nature as a mineral. No solubility data have been considered for TDB 2020.

3.1.8 Lithium(I) phosphate compounds and complexes

3.1.8.1 Lithium(I) phosphate complexes

Two studies, Smith & Alberty (1956) and Daniele et al. (1983), report stability constants for aqueous lithium phosphate complexes.

Tab. 3.1-1: Reported and accepted lithium phosphate complexation data

Temp. [°C]	Medium	$\log_{10}K$ reported [a]	I_m	$\log_{10}K_m$	Δε	$\log_{10}K°$ accepted [b]	Reference
$Li^+ + PO_4^{3-} \rightleftharpoons LiPO_4^{2-}$							
37	0.15 M Me_4NCl	0.95 ± 0.15	0.153	0.942	-0.6	1.8 ± 0.3	Daniele et al. (1983)
$Li^+ + HPO_4^{2-} \rightleftharpoons LiHPO_4^-$							
0	0.2 M Pr_4NCl	0.32 ± 0.06	0.210	0.300	-0.5	0.94 ± 0.20	Smith & Alberty (1956)
25	0.2 M Pr_4NCl	0.72 ± 0.04	0.210	0.694	-0.5	1.37 ± 0.20	Smith & Alberty (1956)
37	0.15 M Me_4NCl	0.79 ± 0.04	0.153	0.782	-0.5	1.29 ± 0.20	Daniele et al. (1983)
$Li^+ + H_2PO_4^- \rightleftharpoons LiH_2PO_4$(aq)							
37	0.3 M Me_4NCl	0.2 ± 0.2	0.311	0.185	-0.3	0.6 ± 0.4	Daniele et al. (1983)

[a] Data as reported in the cited publications or calculated by this review from the reported data, see text.
[b] 2σ uncertainties assigned or estimated by this review.

Smith & Alberty (1956) calculated from measurements with a glass electrode at 25 and 0 °C in 0.2 M Pr_4NCl (tetrapropylammonium chloride, $(CH_3CH_2CH_2)_4NCl$) the values K(25 °C) = 5.2 ± 0.5 (corresponding to $\log_{10}K$(25 °C) = 0.72 ± 0.04) and K(0 °C) = 2.1 ± 0.3 (corresponding to $\log_{10}K$(0 °C) = 0.32 ± 0.06) for the equilibrium $Li^+ + HPO_4^{2-} \rightleftharpoons LiHPO_4^-$. This review retained these values and obtained $\log_{10}K°$(25 °C) = 1.35 ± 0.20 and $\log_{10}K°$(0 °C) = 0.94 ± 0.20 by extrapolation to zero ionic strength using SIT with the estimate $\Delta\varepsilon(Pr_4NCl) \approx -0.5$ in analogy with $\Delta\varepsilon(Et_4NI) = -(0.51 \pm 0.15)$ obtained for $Na^+ + HPO_4^{2-} \rightleftharpoons NaHPO_4^-$ (see Section 3.2.8.1). The uncertainties have been estimated by this review.

Daniele et al. (1983) studied the complex formation between lithium and phosphate at 37 °C and 0.15 and 0.3 M Me_4NCl (tetramethylammonium chloride, $(CH_3)_4NCl$). They report the values $\log_{10}K$(0.15 M Me_4NCl) = 0.95 ± 0.15 for $Li^+ + PO_4^{2-} \rightleftharpoons LiPO_4^{2-}$, $\log_{10}K$(0.15 M Me_4NCl) = 0.79 ± 0.04 for $Li^+ + HPO_4^{2-} \rightleftharpoons LiHPO_4^-$ and $\log_{10}K$(0.3 M Me_4NCl) = 0.2 ± 0.2 for $Li^+ + H_2PO_4^- \rightleftharpoons LiH_2PO_4$(aq). This review retained these values and obtained for the above equilibria $\log_{10}K° = 1.8 \pm 0.3$, $\log_{10}K° = 1.29 \pm 0.20$ and $\log_{10}K° = 0.6 \pm 0.4$, respectively, by extrapolation to zero ionic strength using SIT with estimates for $\Delta\varepsilon(Me_4NCl)$ in analogy with $\Delta\varepsilon(Et_4NI)$ values derived from SIT regressions for sodium phosphate complexes (see Section 3.2.8.1). The uncertainties have been estimated by this review.

The accepted data of Tab. 3.1-1 have been used for a weighted linear regression of the $\log_{10}K°$ values for the equilibrium $Li^+ + HPO_4^{2-} \rightleftharpoons LiHPO_4^-$ versus the reciprocal of absolute temperature (Fig. 3.1-2), and this review obtained:

$Li^+ + HPO_4^{2-} \rightleftharpoons LiHPO_4^-$

$\log_{10}K°$ (298.15 K) = 1.28 ± 0.12

$\Delta_r H_m°$(298.15 K) = (20 ± 12) kJ · mol^{-1}

$\Delta_r C_{p,m}°$(298.15 K) = 0

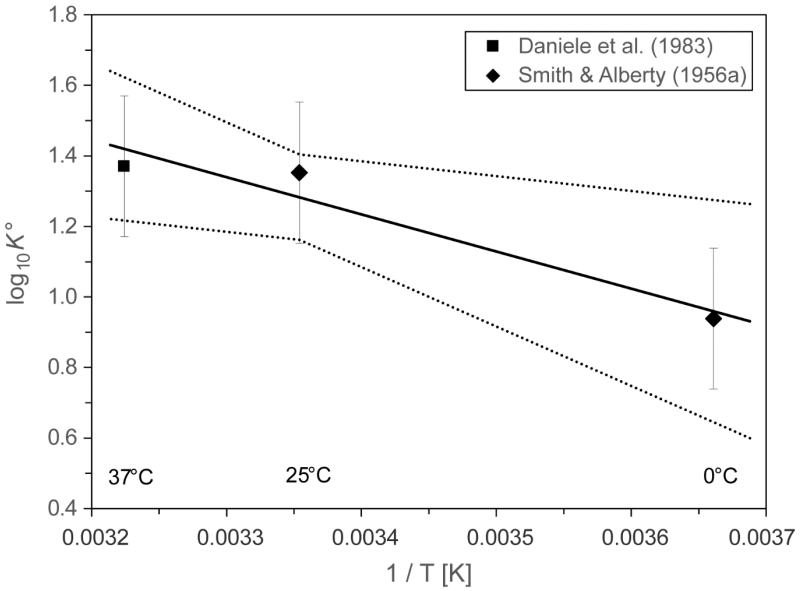

Fig. 3.1-2: The equilibrium constant $\log_{10}K°$ for $Li^+ + HPO_4^{2-} \rightleftharpoons LiHPO_4^-$ as function of reciprocal absolute temperature in the range 0 – 37 °C

Symbols: accepted $\log_{10}K°$ values taken from Tab. 3.1-1. Solid line: weighted linear regression. Dotted lines: lower and upper limits using $\log_{10}K°$ (298.15 K) = 1.28 ± 0.12 and $\Delta_r H_m°$ (298.15 K) = (20 ± 12) kJ · mol^{-1} and extrapolated to lower and higher temperatures.

In the cases of $Li^+ + H_2PO_4^- \rightleftharpoons LiH_2PO_4(aq)$ and $Li^+ + PO_4^{3-} \rightleftharpoons LiPO_4^{2--}$ there is only one data point for each at 37 °C (Tab. 3.1-1). This review selected these values as representative also for 25 °C:

$Li^+ + H_2PO_4^- \rightleftharpoons LiH_2PO_4(aq)$

$\log_{10}K°$ (298.15 K) = 0.6 ± 0.4

$Li^+ + PO_4^{3-} \rightleftharpoons LiPO_4^{2-}$

$\log_{10}K°$ (298.15 K) = 1.8 ± 0.3

These values are included in TDB 2020, together with the estimates

$\varepsilon(LiH_2PO_4(aq), NaCl) = (0.0 \pm 0.1)$ kg · mol^{-1}

$\varepsilon(LiHPO_4^-, Na^+) = -(0.05 \pm 0.10)$ kg · mol^{-1}

$\varepsilon(LiPO_4^{2-}, Na^+) = -(0.10 \pm 0.10)$ kg · mol^{-1}.

3.1.8.2 Lithium(I) phosphate compounds

Li_3PO_4(cr) is a slightly soluble salt with a solubility of 0.3 g/L at 20 °C (gestis.itrust.de). Li_3PO_4(cr) is found in nature as the extremely rare mineral lithiophosphate. Other extremely rare alkali phosphate minerals are nalipoite, $NaLi_2PO_4$(cr), and olympite, $LiNa_5(PO_4)_2$(cr). No detailed solubility studies for lithium phosphate compounds seem to have been published, and hence, no solubility data are included in TDB 2020.

3.1.9 Selected lithium data

Tab. 3.1-2: Selected lithium data

Core data are in bold face.

Name	**$\Delta_f G_m°$** [kJ · mol^{-1}]	**$\Delta_f H_m°$** [kJ · mol^{-1}]	**$S_m°$** [J · K^{-1} · mol^{-1}]	**$C_{p,m}°$** [J · K^{-1} · mol^{-1}]	**Species**
Li(cr)	0.0	0.0	**29.120 ± 0.200**	**24.860 ± 0.200**	Li(cr)
Li+	**-292.918 ± 0.109**	**-278.470 ± 0.080**	**12.240 ± 0.150**		Li^+

Name	**$\log_{10}\beta°$**	**$\Delta_r H_m°$** [kJ · mol^{-1}]	**$\Delta_r C_{p,m}°$** [J · K^{-1} · mol^{-1}]	**T-range** [°C]	**Reaction**
Li(cr)	51.32 ± 0.02	-278.47 ± 0.08	-		$Li(cr) \rightleftharpoons Li^+ + e^-$
LiOH(aq)	-13.84 ± 0.14	55.3 ± 3.7	-64.1 ± 34.6	5 – 350	$Li^+ + H_2O(l) \rightleftharpoons LiOH(aq) + H^+$
LiF(aq)	0.23 ± 0.11	6.0 ± 1.2	0	15 – 35	$Li^+ + F^- \rightleftharpoons LiF(aq)$
LiSO4-	0.9 ± 0.3	*≈ 0*	-		$Li^+ + SO_4^{2-} \rightleftharpoons LiSO_4^-$
LiPO4-2	1.8 ± 0.3	-	-		$Li^+ + PO_4^{3-} \rightleftharpoons LiPO_4^{2-}$
LiHPO4-	1.28 ± 0.12	20 ± 12	0	0 – 37	$Li^+ + HPO_4^{2-} \rightleftharpoons LiHPO_4^-$
LiH2PO4(aq)	0.6 ± 0.4	-	-		$Li^+ + H_2PO_4^- \rightleftharpoons LiH_2PO_4(aq)$

Tab. 3.1-3: Selected SIT ion interaction coefficients $\varepsilon_{j,k}$ [kg · mol^{-1}] for lithium species

Data in bold face are taken from Lemire et al. (2013). Data estimated according to charge correlations and taken from Tab. 1-7 are shaded.

j k → ↓	**Cl^-** $\varepsilon_{j,k}$ [kg · mol^{-1}]	**Na^+** $\varepsilon_{j,k}$ [kg · mol^{-1}]	**$Na^+ + Cl^-$** $\varepsilon_{j,k}$ [kg · mol^{-1}]
Li+	**0.10 ± 0.01**	0	0
LiOH(aq)	0	0	0.0 ± 0.1
LiF(aq)	0	0	0.0 ± 0.1
LiSO4-	0	-0.05 ± 0.10	0
LiPO4-2	0	-0.10 ± 0.10	0
LiHPO4-	0	-0.05 ± 0.10	0
LiH2PO4(aq)	0	0	0.0 ± 0.1

3.1.10 References

Austin, J.M. & Mair, A.D. (1962): The standard enthalpy of formation of complex sulfate ions in water. I. HSO_4^-, $LiSO_4^-$, $NaSO_4^-$. Journal of Physical Chemistry, 66, 519-521.

Baes, C.F. & Mesmer, R.E. (1976): The Hydrolysis of cations. Wiley, New York, 490 pp.

Brown, P.L. & Ekberg, C. (2016): Hydrolysis of Metal Ions. Wiley-VCH Verlag GmbH & Co. KGaA, Weinheim, Germany, 917 pp.

Chan, C.B., Tioh, N.H. & Hefter, G.T. (1984): Fluoride complexes of the alkali metal anions. Polyhedron, 3, 845-851.

Cox, J.D., Wagman, D.D. & Medvedev, V.A. (1989): CODATA Key Values for Thermodynamics. Hemisphere Publishing, New York, 271 pp.

Daniele, P.G., Grasso, M., Rigano, C., Sammartano, S. (1983): The formation of proton- and alkali metal complexes with ligands of biological interest in aqueous solution. Formation constants of H^+, Li^+, Na^+, K^+ – phosphate complexes and their dependence on ionic strength. Annali di Chimica, 73, 495-515.

Daniele, P.G., Rigano, C. & Sammartano, S. (1982): Studies on sulphate complexes. Part I. Potentiometric investigation of Li^+, Na^+, K^+, Rb^+ and Cs^+ complexes at 37 °C and $0.03 \leq I \leq 0.5$. Inorganica Chimica Acta, 63, 267-272.

Grenthe, I., Fuger, J., Konings, R.J.M., Lemire, R.J., Muller, A.B., Nguyen-Trung, C. & Wanner, H. (1992): Chemical Thermodynamics of Uranium. Chemical Thermodynamics, Vol. 1. North-Holland, Amsterdam, 715 pp.

Lemire, R.J., Berner, U., Musikas, C., Palmer, D.A., Taylor, P. & Tochiyama, O. (2013): Chemical Thermodynamics of Iron, Part 1. Chemical Thermodynamics, Vol. 13a. OECD Publications, Paris, France, 1082 pp.

Nordstrom, D.K., Plummer, L.N., Langmuir, D., Busenberg, E., May, H.M., Jones, B.F. & Parkhurst, D.L. (1990): Revised Chemical Equilibrium Data for Major Water-Mineral Reactions and Their Limitations. In: Melchior, D.C., and Bassett, R.L. (eds.): Chemical Modeling of Aqueous Systems II. Washington, D.C., American Chemical Society, ACS Symposium Series 416, p. 398-413.

Righellato, E.C. & Davies, C.W. (1930): The extent of dissociation of salts in water. Part II. Unibivalent salts. Trans. Faraday Soc., 26, 592-600.

Robinson, R.A. & Stokes, R.H. (1959): Electrolyte Solutions. Second Revised Edition. Academic Press, New York, 559 pp.

Smith, R.P. & Alberty, R.A. (1956): The apparent stability constants of ionic complexes of various adenosine phosphates with monovalent cations. J. Phys. Chem., 60, 180-184.

Smith, R.M. & Martell, A.E. (1976): Critical Stability Constants. Volume 4: Inorganic Complexes. Plenum Press, New York, 257 pp.

3.2 Sodium

3.2.1 Elemental sodium

Sodium metal and gas are not relevant under environmental conditions. Hence, the gas phase Nag is not included in the data base. The absolute entropy and heat capacity of Na(cr) are included as they are used for the calculation of certain thermodynamic reaction properties.

The selected values for Na(cr) are taken from CODATA (Cox et al. 1989):

$$S_m°(\text{Na, cr, 298.15 K}) = (51.300 \pm 0.200)\ \text{J} \cdot \text{K}^{-1} \cdot \text{mol}^{-1}$$

$$C_{p,m}°(\text{Na, cr, 298.15 K}) = (28.230 \pm 0.200)\ \text{J} \cdot \text{K}^{-1} \cdot \text{mol}^{-1}$$

3.2.2 Sodium(I) aqua ion

Sodium(I) exists as the Na^+ cation in aqueous solutions. The selected thermodynamic values for Na^+ are taken from CODATA (Cox et al. 1989):

$$\Delta_f G_m°(\text{Na}^+, \text{298.15 K}) = -(261.953 \pm 0.096)\ \text{kJ} \cdot \text{mol}^{-1}$$

$$\Delta_f H_m°(\text{Na}^+, \text{298.15 K}) = -(240.340 \pm 0.060)\ \text{kJ} \cdot \text{mol}^{-1}$$

$$S_m°(\text{Na}^+, \text{298.15 K}) = (58.450 \pm 0.150)\ \text{J} \cdot \text{K}^{-1} \cdot \text{mol}^{-1}$$

Using the selected CODATA $\Delta_f G_m°(Na^+, 298.15\ K)$, the redox equilibrium

$$\text{Na(cr)} \rightleftharpoons \text{Na}^+ + \text{e}^-$$

is calculated as

$$\log_{10} K°(\text{298.15 K}) = 45.89 \pm 0.02$$

Since this review does not consider the formation of sodium(I) chloride complexes (see Section 3.2.5), $\varepsilon(Na^+, Cl^-)$ is taken as selected by NEA (Grenthe et al. 1992, Lemire et al. 2013):

$$\varepsilon(\text{Na}^+, \text{Cl}^-) = (0.03 \pm 0.01)\ \text{kg} \cdot \text{mol}^{-1}$$

3.2.3 Sodium(I) (hydr)oxide compounds and complexes

3.2.3.1 Sodium(I) hydroxide complexes

Nordstrom et al. (1990) selected a $\log_{10}{}^{*}\beta_1°$ value and an estimate of $\Delta_r H_m°$ based on the values reported by Baes & Mesmer (1976) for the equilibrium:

$$Na^+ + OH^- \rightleftharpoons NaOH(aq)$$

$$\log_{10}\beta_1° \text{ (298.15 K)} = -0.18 \pm 0.25$$

$$\Delta_r H_m°(298.15 \text{ K}) = (0 \pm 13) \text{ kJ} \cdot \text{mol}^{-1}$$

This can be recalculated via the dissociation of water parameters (Grenthe et al. 1992) to

$$Na^+ + H_2O(l) \rightleftharpoons NaOH(aq) + H^+$$

$$\log_{10}{}^{*}\beta_1° \text{ (298.15 K)} = -14.18 \pm 0.25$$

$$\Delta_r H_m°(298.15 \text{ K}) = (56 \pm 13) \text{ kJ} \cdot \text{mol}^{-1}$$

Note that Nordstrom et al. (1990) erroneously took $\Delta_r H_m°(298.15 \text{ K}) = 0$ as the estimate for the reaction $Na^+ + H_2O(l) \rightleftharpoons NaOH(aq) + H^+$.

Brown & Ekberg (2016) report that there have been more studies on the hydrolysis of sodium(I) than there have been on lithium(I) even though the stability of NaOH(aq) is much less than that of LiOH(aq). The weak stability of the NaOH(aq) complex has led to a large scatter in the available data. Nevertheless, data have been acquired across the temperature range of 0 – 350 °C. Brown & Ekberg (2016) used a linear correlation between the stability constants and the reciprocal temperature and state that because of the large scatter in the available data, the fitting of a more complex equation to the data is not justified. They obtained

$$Na^+ + H_2O(l) \rightleftharpoons NaOH(aq) + H^+$$

$$\log_{10}{}^{*}\beta_1° \text{ (298.15 K)} = -14.4 \pm 0.2$$

$$\Delta_r H_m°(298.15 \text{ K}) = (51.9 \pm 1.8) \text{ kJ} \cdot \text{mol}^{-1}$$

$$\Delta C_{p,m}°(298.15 \text{ K}) = 0 \text{ J} \cdot \text{K}^{-1} \cdot \text{mol}^{-1}$$

These values have been included in TDB 2020, as well as the estimate

$$\varepsilon(\text{NaOH(aq), NaCl}) = (0.0 \pm 0.1) \text{ kg} \cdot \text{mol}^{-1}.$$

The values reported by Brown & Ekberg (2016) are in good agreement with those of the older evaluation of Baes & Mesmer (1976), considering the assigned uncertainties by both authors.

3.2.3.2 Sodium(I) (hydr)oxide compounds

NaOH(s) is a highly soluble caustic base ("caustic soda", "Ätznatron") with a solubility of 1'090 g/L at 20 °C (gestis.itrust.de). The solid is hygroscopic. Its isopiestic properties have been measured up to 29 mol · kg_{H2O}^{-1} (Robinson & Stokes 1959). Hence, no solubility data, but the specific ion interaction coefficient selected by NEA (Grenthe et al. 1992, Lemire et al. 2013) is adopted for TDB 2020:

$$\varepsilon(Na^+, OH^-) = (0.04 \pm 0.01)\ kg \cdot mol^{-1}$$

Note that the weak NaOH(aq) complex formation, discussed above, has not been considered in deriving the SIT coefficient $\varepsilon(Na^+, OH^-)$.

3.2.4 Sodium(I) fluoride compounds and complexes

3.2.4.1 Sodium(I) fluoride complexes

Nordstrom et al. (1990) selected a $\log_{10}\beta_1°$ value reported by Duer et al. (1972) for the complex

$$Na^+ + F^- \rightleftharpoons NaF(aq)$$

$$\log_{10}K_1° (298.15\ K) = -0.24$$

Duer et al. (1972) state that this value is their best guess, where a range of $\log_{10}K_1° = -0.54$ – +0.15 would be consistent with their conductivity measurements.

Chan et al. (1984) did measurements by fluoride ion-selective electrode potentiometry on the very weak monofluoride complexes LiF(aq), NaF(aq), KF(aq) and RbF(aq). They obtained

$$K_1° (298.15\ K) = 1.0 \pm 0.3$$

$$\log_{10}K_1° (298.15\ K) = 0.00 \pm 0.13$$

$$\Delta_r H_m(298.15\ K, 1\ M\ KNO_3) = (13 \pm 1)\ kJ \cdot mol^{-1}$$

where $K_1°$ was estimated graphically from data measured at 0.2, 0.5 and 1.0 M KNO_3 and $\Delta_r H_m$ was calculated by linear regression from data measured at 15, 25 and 35 °C at 1 M KNO_3.

Butler & Huston (1970) calculated from their potentiometric study of multicomponent activity coefficients an equilibrium constant for the formation of the $Na^+ – F^-$ ion pair in 1 mol · kg_{H2O} NaCl as $\log_{10}K_1$ (298.15 K, 1 m NaCl) = -0.79 ± 0.04.

Richardson & Holland (1979) report equilibrium constants for NaF(aq) derived from their solubility measurements of fluorite, CaF_2(s), at 200 and 260 °C in 1 M NaCl.

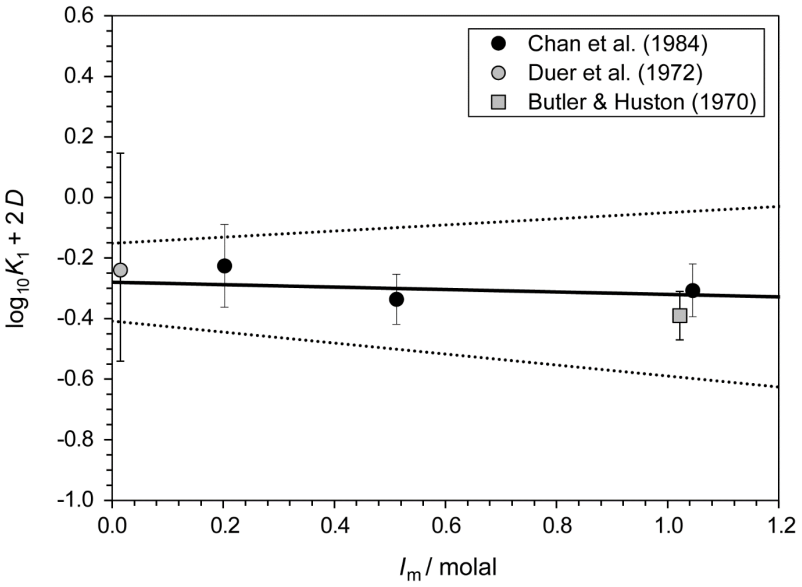

Fig. 3.2-1: Dependence of the equilibrium $Na^+ + F^- \rightleftharpoons NaF(aq)$ on ionic strength in KNO_3 using the data of Chan et al. (1984)

The solid line is obtained using the derived SIT interaction coefficient and stability constant at zero ionic strength. Dotted lines represent the 95% uncertainty range extrapolated from I = 0 to higher KNO_3 concentrations. The data of Duer et al. (1972) at very low ionic strength and Butler & Huston (1970) in 1 m NaCl are shown for comparison only.

Using the mentioned data of Chan et al. (1984) for an SIT analysis this review obtained (Fig. 3.2-1):

$$\log_{10}K_1° \text{ (298.15 K)} = -0.28 \pm 0.13$$

$$\Delta\varepsilon(KNO_3) = 0.04 \pm 0.17$$

Considering $\varepsilon(Na^+, NO_3^-) = -(0.04 \pm 0.03)$ kg · mol^{-1} and $\varepsilon(K^+, F^-) = (0.03 \pm 0.02)$ kg · mol^{-1} (Grenthe et al. 1992) this review derives from the experimental $\Delta\varepsilon$ value

$$\varepsilon(NaF(aq), KNO_3) = (0.03 \pm 0.18) \text{ kg} \cdot \text{mol}^{-1}.$$

Within its uncertainty this value cannot be distinguished from zero, as expected, and thus it seems justified to include the estimate

$$\varepsilon(NaF(aq), NaCl) = (0.0 \pm 0.1) \text{ kg} \cdot \text{mol}^{-1}$$

in TDB 2020, together with $\log_{10}K_1°$ obtained from the SIT analysis.

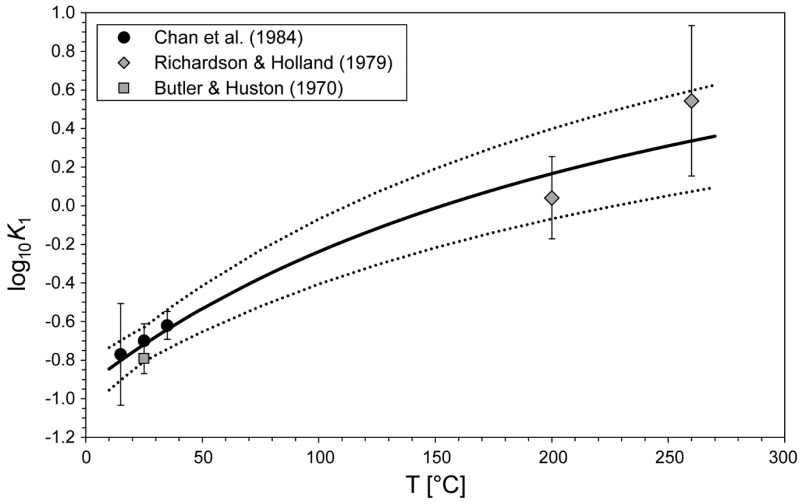

Fig. 3.2-2: The equilibrium constant $\log_{10}K_1$ for $Na^+ + F^- \rightleftharpoons NaF(aq)$ as function of temperature in the range 15 – 260 °C at I = 1 M

Solid line: Weighted linear regression of all data versus the reciprocal of the absolute temperature. Dotted lines: lower and upper limits using $\log_{10}K_1(298.15\ K) = -0.72 \pm 0.09$ and $\Delta_r H_m(298.15\ K) = (13.6 \pm 2.2)\ kJ \cdot mol^{-1}$ and extrapolated to lower and higher temperatures.

A weighted linear regression of the temperature data reported by Chan et al. (1984), Richardson & Holland (1979) and Butler & Huston (1970) versus the reciprocal of the absolute temperature yields (Fig. 3.2-2):

$$\Delta_r H_m(298.15\ K, 1\ M) = (13.6 \pm 2.2)\ kJ \cdot mol^{-1}$$

in good agreement with the value reported by Chan et al. (1984). No attempt has been made to extrapolate this value to zero ionic strength, and it is included in TDB 2020 as an approximation of $\Delta_r H_m°$ (298.15 K).

3.2.4.2 Sodium(I) fluoride compounds

NaF(cr) is a soluble salt with a solubility of 42.2 g/L at 20 °C (gestis.itrust.de). Its isopiestic properties have been measured up to 1 $mol \cdot kg_{H2O}^{-1}$ (Robinson & Stokes 1959). Hence, no solubility data, but the specific ion interaction coefficient selected by NEA (Grenthe et al. 1992, Lemire et al. 2013) is adopted for TDB 2020:

$$\varepsilon(Na^+, F^-) = (0.02 \pm 0.02)\ kg \cdot mol^{-1}$$

Note that the weak NaF(aq) complex formation, discussed above, has not been considered in deriving the SIT coefficient $\varepsilon(Na^+, F^-)$.

3.2.5 Sodium(I) chloride compounds and complexes

3.2.5.1 Sodium(I) chloride complexes

This report does not consider the formation of weak sodium(I) chloride complexes but includes possible ion interactions in the SIT interaction coefficient $\varepsilon(Na^+, Cl^-)$, see below.

3.2.5.2 Sodium(I) chloride compounds

NaCl(cr) is a highly soluble salt with a solubility of 358 g/L at 20 °C (gestis.itrust.de). Its isopiestic properties have been measured up to 6.4 $mol \cdot kg_{H2O}^{-1}$ (Robinson & Stokes 1959). Hence, no solubility data, but the specific ion interaction coefficient selected by NEA (Grenthe et al. 1992, Lemire et al. 2013) is adopted for TDB 2020:

$$\varepsilon(Na^+, Cl^-) = (0.03 \pm 0.01)\ kg \cdot mol^{-1}$$

3.2.6 Sodium(I) carbonate compounds and complexes

3.2.6.1 Sodium(I) carbonate complexes

Nordstrom et al. (1990) selected a $\log_{10}K°$ value reported by Garrels & Thompson (1962) for

$$Na^+ + HCO_3^- \rightleftharpoons NaHCO_3(aq)$$

$$\log_{10}K° (298.15\ K) = -0.25$$

and a $\log_{10}K_1°$ value reported by Garrels et al. (1961) for

$$Na^+ + CO_3^{2-} \rightleftharpoons NaCO_3^-$$

$$\log_{10}K_1° (298.15\ K) = 1.27 \pm 0.08$$

The same value is reported later by Garrels & Thompson (1962). In addition, Nordstrom et al. (1990) report a $\Delta_r H_m°$ value for $Na^+ + CO_3^{2-} \rightleftharpoons NaCO_3^-$ with the reference Garrels et al. (1961)

$$\Delta_r H_m°(298.15\ K) = 8.91\ kcal \cdot mol^{-1} = 37.3\ kJ \cdot mol^{-1}$$

However, the work of Garrels et al. (1961) and Garrels & Thompson (1962) is restricted to 25 °C and no temperature data are reported. Hence, the source of $\Delta_r H_m°$ reported by Nordstrom et al. (1990) remains unclear.

Recently, Stefánsson et al. (2013) published a potentiometric and spectrophotometric study of sodium bicarbonate and carbonate ion pairs to 200 °C. They report temperature functions derived from their own measurements as well as literature data for

$Na^+ + CO_3^{2-} \rightleftharpoons NaCO_3^-$

$\log_{10}K_1°\ (T) = 4.1659 – 941.150 / T$

$Na^+ + HCO_3^- \rightleftharpoons NaHCO_3(aq)$

$\log_{10}K°\ (T) = 1.8528 – 606.240 / T$

From these temperature functions this review calculated

$Na^+ + CO_3^{2-} \rightleftharpoons NaCO_3^-$

$\log_{10}K_1°\ (298.15\ K) = 1.01 \pm 0.20$

$\Delta_r H_m°(298.15\ K) = (18.0 \pm 4.0)\ kJ \cdot mol^{-1}$

$\Delta_r C_{p,m}°(298.15\ K) = 0\ J \cdot K^{-1} \cdot mol^{-1}$

$Na^+ + HCO_3^- \rightleftharpoons NaHCO_3(aq)$

$\log_{10}K°\ (298.15\ K) = -0.18 \pm 0.25$

$\Delta_r H_m°(298.15\ K) = (11.6 \pm 4.0)\ kJ \cdot mol^{-1}$

$\Delta_r C_{p,m}°(298.15\ K) = 0\ J \cdot K^{-1} \cdot mol^{-1}$

The uncertainties have been estimated by this review from regression analyses of the temperature data reported by Stefánsson et al. (2013).

These values are included in TDB 2020, as well as the estimates

$\varepsilon(NaCO_3^-, Na^+) = -(0.05 \pm 0.10)\ kg \cdot mol^{-1}$

$\varepsilon(NaHCO_3(aq), NaCl) = (0.0 \pm 0.1)\ kg \cdot mol^{-1}$.

3.2.6.2 Sodium(I) carbonate compounds

$Na_2CO_3(s)$ is a highly soluble salt with a solubility of 217 g/L at 20 °C (gestis.itrust.de). Its isopiestic properties have been measured up to 1.6 $mol \cdot kg_{H2O}^{-1}$ (Ciavatta 1980). Hence, no solubility data, but the specific ion interaction coefficients selected by NEA (Lemire et al. 2013) are adopted for TDB 2020:

$\varepsilon(Na^+, CO_3^{2-}) = -(0.08 \pm 0.03)\ kg \cdot mol^{-1}$

$\varepsilon(Na^+, HCO_3^-) = (0.00 \pm 0.02)\ kg \cdot mol^{-1}$

Note that the weak $NaCO_3^-$ and $NaHCO_3(aq)$ complex formation, discussed above, has not been considered in deriving the SIT coefficients $\varepsilon(Na^+, CO_3^{2-})$ and $\varepsilon(Na^+, HCO_3^-)$.

3.2.7 Sodium(I) sulphate compounds and complexes

3.2.7.1 Sodium(I) sulphate complexes

Nordstrom et al. (1990) selected a $\log_{10}\beta_1°$ value derived by Righellato & Davies (1930) from conductivity measurements at 18 °C, and a $\Delta_r H_m°$ value reported by Austin & Mair (1962), determined by calorimetric measurements at 25 °C, for the complex

$$Na^+ + SO_4^{2-} \rightleftharpoons NaSO_4^-$$

$$\log_{10}\beta_1° (291.15\ K) = 0.70$$

$$\Delta_r H_m°(298.15\ K) = (1.12 \pm 0.80)\ kcal \cdot mol^{-1} = (4.7 \pm 3.3)\ kJ \cdot mol^{-1}$$

In addition, Daniele et al. (1982) report

$$\log_{10}\beta_1° (310.15\ K) = 0.72 \pm 0.05$$

derived from potentiometric measurements at 37 °C and ionic strength 0.03 – 0.5 M, and extrapolated to I = 0 by Daniele et al. (1982) using a function similar to the SIT equation.

Using the $\Delta_r H_m°(298.15\ K)$ value of Austin & Mair (1962) this review extrapolated $\log_{10}\beta_1° (291.15\ K) = 0.70$ to $\log_{10}\beta_1° (298.15\ K) = 0.72 \pm 0.05$, with its uncertainty estimated by this review based on the experimental data of Righellato & Davies (1930), as well as the value $\log_{10}\beta_1° (310.15\ K) = 0.72 \pm 0.05$ of Daniele et al. (1982) to $\log_{10}\beta_1° (298.15\ K) = 0.69 \pm 0.05$.

Within their uncertainties both values are in good agreement and this review selected the average

$$\log_{10}\beta_1° (298.15\ K) = 0.71 \pm 0.05$$

This value has been included in TDB 2020, as well as

$$\Delta_r H_m°(298.15\ K) = (4.7 \pm 3.3)\ kJ \cdot mol^{-1}$$

and the estimate

$$\varepsilon(NaSO_4^-, Na^+) = -(0.05 \pm 0.10)\ kg \cdot mol^{-1}.$$

3.2.7.2 Sodium(I) sulphate compounds

Na_2SO_4(s) is a highly soluble salt with a solubility of 170 g/L at 20 °C (gestis.itrust.de). Its isopiestic properties have been measured up to 4 mol · kg_{H2O}^{-1} (Robinson & Stokes 1959). Hence, no solubility data, but the specific ion interaction coefficient selected by NEA (Grenthe et al. 1992, Lemire et al. 2013) is adopted for TDB 2020:

$$\varepsilon(Na^+, SO_4^{2-}) = -(0.12 \pm 0.06)\ kg \cdot mol^{-1}$$

Note that the weak $NaSO_4^-$ complex formation, discussed above, has not been considered in deriving the SIT coefficient $\varepsilon(Na^+, SO_4^{2-})$.

3.2.8 Sodium(I) phosphate compounds and complexes

3.2.8.1 Sodium(I) phosphate complexes

Four studies, Smith & Alberty (1956), Patel et al. (1974), Daniele et al. (1983) and Daniele et al. (1991), report stability constants for aqueous sodium phosphate complexes.

Smith & Alberty (1956) calculated from measurements with a glass electrode at 25 and 0 °C in 0.2 M Pr_4NCl (tetrapropylammonium chloride, $(CH_3CH_2CH_2)_4NCl$) the values K(25 °C) = 4.0 ± 0.4 (corresponding to $\log_{10}K$(25 °C) = 0.60 ± 0.04) and K(0 °C) = 1.2 ± 0.3 (corresponding to $\log_{10}K$(0 °C) = 0.08 ± 0.11) for the equilibrium $Na^+ + HPO_4^{2-} \rightleftharpoons NaHPO_4^-$. This review retained these values, included the value at 25 °C in an SIT analysis (Fig. 3.2-3) and used the resulting $\Delta\varepsilon$ value for extrapolating all data measured in tetraalkylammonium halide media (Tab. 3.2-1). The results are $\log_{10}K°$(298.15 K) = 1.02 ± 0.20 and $\log_{10}K°$(273.15 K) = 0.5 ± 0.4, with uncertainties estimated by this review.

Patel et al. (1974) determined the solubility of brushite, $CaHPO_4 \cdot 2H_2O$, in the quaternary system $Ca(OH)_2 – H_3PO_4 – NaCl – H_2O$ at 25 °C in the pH range 4.4 – 6.4. The ionic strengths, I, of the saturated solutions varied from 0.005 to 0.55 M, mainly due to the variation in NaCl concentrations. Satisfactory constancy in the solubility product was obtained when the ion activity coefficients, γ_i, were calculated with the extended Debye-Hückel equation, $\log_{10}\gamma_i = -A \cdot z_i^2 \cdot \sqrt{I} / (1 + B \cdot \alpha_i \cdot \sqrt{I}) + 0.0626 \cdot I$, and the formation of an ion pair $NaHPO_4^-$ was taken into account. Patel et al. (1974) report a statistically derived value for the stability constant of this ion pair as $K°$(298.15 K) = 7.0 ± 2.4 (corresponding to $\log_{10}K°$(298.15 K) = 0.85 ± 0.15). This review retained this value with an uncertainty increased to 2σ (Tab. 3.2-1).

Daniele et al. (1983) studied the complex formation between sodium and phosphate at 37 °C and 0.15 and 0.3 M Me_4NCl (tetramethylammonium chloride, $(CH_3)_4NCl$). They report the values $\log_{10}K$(0.15 M Me_4NCl) = 0.75 ± 0.15 for $Na^+ + PO_4^{3-} \rightleftharpoons NaPO_4^{2-}$, $\log_{10}K$(0.15 M Me_4NCl) = 0.65 ± 0.05 for $Na^+ + HPO_4^{2-} \rightleftharpoons NaHPO_4^-$ and $\log_{10}K$(0.3 M Me_4NCl) = 0.1 ± 0.2 for $Na^+ + H_2PO_4^- \rightleftharpoons NaH_2PO_4$(aq). This review retained these values and obtained for the above equilibria $\log_{10}K° = 1.4 \pm 0.3$, $\log_{10}K° = 1.08 \pm 0.20$ and $\log_{10}K° = 0.3 \pm 0.4$, respectively (Tab. 3.2-1), by extrapolation to zero ionic strength using SIT with $\Delta\varepsilon$ values obtained from SIT regressions for sodium phosphate complexes (Fig. 3.2-3). The uncertainties have been estimated by this review.

Daniele et al. (1991) studied the protonation constants of orthophosphate potentiometrically using a glass electrode in aqueous NaCl, KCl and tetraethylammonium iodide (Et_4NI, $(CH_3CH_2)_4NI$) solutions at an ionic strength range 0.04 – 1M in the temperature range 10 – 50 °C. The differences found in the protonation constants for different salt solutions are explained by a complex formation model. Daniele et al. (1991) report in their Tab. VII stability constants for the equilibria $Na^+ + PO_4^{3-} \rightleftharpoons NaPO_4^{2-}$, $Na^+ + HPO_4^{2-} \rightleftharpoons NaHPO_4^-$ and $Na^+ + H_2PO_4^- \rightleftharpoons NaH_2PO_4(aq)$ at 25 °C in 0.16, 0.64 and 1 M Et_4NI, and at 37 °C in 0.16 M Et_4NI (Tab. 3.2-1). The values at 25 °C have been used by this review for SIT analyses (Fig. 3.2-3) and the obtained $\Delta\varepsilon$ values were then used for extrapolating all data measured in tetraalkylammonium halide media to zero ionic strength. It has been assumed that $\Delta\varepsilon$ does not vary with temperature in the temperature range 0 – 37 °C (Tab. 3.2-1). The uncertainties have been estimated by this review.

Tab. 3.2-1: Reported and accepted sodium phosphate complexation data

Temp. [°C]	**Medium**	**$\log_{10}K$ reported** [a]	**I_m**	**$\log_{10}K_m$**	**$\Delta\varepsilon$**	**$\log_{10}K°$ accepted** [b]	**Reference**
$Na^+ + PO_4^{3-} \rightleftharpoons NaPO_4^{2-}$							
37	0.15 M Me_4NCl	0.75 ± 0.15	0.153	0.742	-0.62	1.4 ± 0.3	Daniele et al. (1983)
25	0.16 M Et_4NI	0.88	0.165	0.886	-0.62	1.53 ± 0.15	Daniele et al. (1991)
25	0.64 M Et_4NI	0.98	0.731	0.923	-0.62	1.61 ± 0.15	Daniele et al. (1991)
25	1.0 M Et_4NI	1.11	1.230	1.020	-0.62	1.53 ± 0.15	Daniele et al. (1991)
37	0.16 M Et_4NI	0.95	0.165	0.742	-0.62	1.62 ± 0.15	Daniele et al. (1991)
$Na^+ + HPO_4^{2-} \rightleftharpoons NaHPO_4^-$							
0	0.2 M Pr_4NCl	0.08 ± 0.11	0.210	0.057	-0.52	0.5 ± 0.4	Smith & Alberty (1956)
25	0.2 M Pr_4NCl	0.60 ± 0.04	0.210	0.580	-0.52	1.02 ± 0.20	Smith & Alberty (1956)
25	$\rightarrow 0$	0.85 ± 0.15	0	0.850		0.85 ± 0.30	Patel et al. (1974)
37	0.15 M Me_4NCl	0.65 ± 0.05	0.153	0.642	-0.52	1.08 ± 0.20	Daniele et al. (1983)
25	0.16 M Et_4NI	0.69	0.165	0.676	-0.52	1.10 ± 0.15	Daniele et al. (1991)
25	0.64 M Et_4NI	0.79	0.731	0.733	-0.52	1.12 ± 0.15	Daniele et al. (1991)
25	1.0 M Et_4NI	0.90	1.230	0.810	-0.52	1.02 ± 0.15	Daniele et al. (1991)
37	0.16 M Et_4NI	0.77	0.165	0.756	-0.52	1.20 ± 0.15	Daniele et al. (1991)
$Na^+ + H_2PO_4^- \rightleftharpoons NaH_2PO_4(aq)$							
37	0.3 M Me_4NCl	0.1 ± 0.2	0.311	0.085	-0.25	0.3 ± 0.4	Daniele et al. (1983)
25	0.16 M Et_4NI	0.09	0.165	0.076	-0.25	0.29 ± 0.15	Daniele et al. (1991)
25	0.64 M Et_4NI	0.17	0.731	0.113	-0.25	0.31 ± 0.15	Daniele et al. (1991)
25	1.0 M Et_4NI	0.26	1.230	0.170	-0.25	0.29 ± 0.15	Daniele et al. (1991)
37	0.16 M Et_4NI	0.22	0.165	0.206	-0.25	0.43 ± 0.15	Daniele et al. (1991)

[a] Data as reported in the cited publications or calculated by this review from the reported data, see text.
[b] 2σ uncertainties assigned or estimated by this review.

The results of the SIT analyses (Fig. 3.2-3) are:

$Na^+ + PO_4^{3-} \rightleftharpoons NaPO_4^{2-}$

$\log_{10}K°$ (298.15 K) = 1.56 ± 0.17

$\Delta\varepsilon$ = -(0.62 ± 0.20) kg · mol^{-1}

$Na^+ + HPO_4^{2-} \rightleftharpoons NaHPO_4^-$

$\log_{10}K°$ (298.15 K) = 1.06 ± 0.13

$\Delta\varepsilon$ = -(0.52 ± 0.17) kg · mol^{-1}

$Na^+ + H_2PO_4^- \rightleftharpoons NaH_2PO_4(aq)$

$\log_{10}K°$ (298.15 K) = 0.30 ± 0.17

$\Delta\varepsilon$ = -(0.25 ± 0.20) kg · mol^{-1}

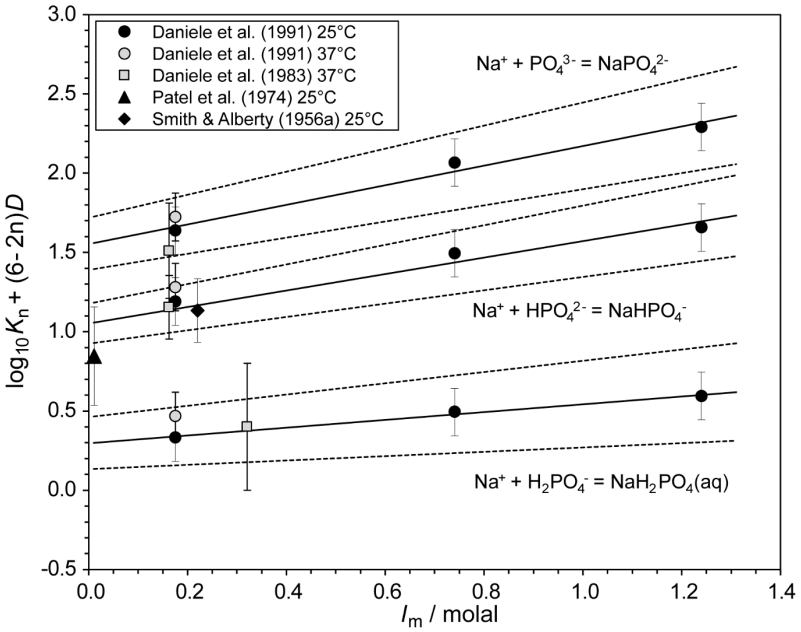

Fig. 3.2-3: Dependence of $\log_{10}K_n$ of the equilibria $Na^+ + H_nPO_4^{n-3} \rightleftharpoons NaH_nPO_4^{n-2}$ on ionic strength in tetraalkylammonium halide media

Data are taken from Tab. 3.2-1 with their "accepted" uncertainties. Data at 25 °C are used for the weighted linear regressions, while data at 37 °C are shown for comparison only. The solid lines are obtained using the derived SIT interaction coefficients and stability constants at zero ionic strength. Dotted lines represent the 95% uncertainty range extrapolated from I = 0 to higher concentrations.

Note that Daniele et al. (1991) extrapolated their values obtained for the above equilibria to zero ionic strength using their own, with respect to the SIT analysis (Fig. 3.2-3), non-linear extrapolation formula and report $\log_{10}K°$ (298.15 K) = 1.43 ± 0.03, $\log_{10}K°$ (298.15 K) = 1.07 ± 0.03 and $\log_{10}K°$ (298.15 K) = 0.28 ± 0.08, respectively. Their uncertainties refer to one standard deviation.

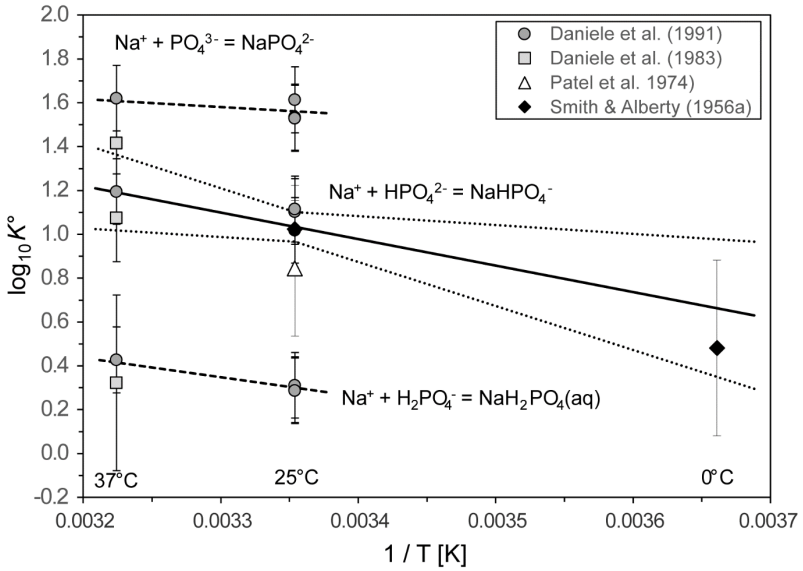

Fig. 3.2-4: The equilibrium constants $\log_{10}K°$ for the indicated equilibria as functions of reciprocal absolute temperature in the range 0 – 37 °C

Symbols: accepted $\log_{10}K°$ values taken from Tab. 3.2-1. Solid line: weighted linear regression. Dotted lines: lower and upper limits using $\log_{10}K°$ (298.15 K) = 1.03 ± 0.07 and $\Delta_r H_m°$ (298.15 K) = (23 ± 15) kJ · mol^{-1} and extrapolated to lower and higher temperatures. Dashed lines are calculated using $\Delta_r H_m°$(298.15 K) values as reported by Daniele et al. (1991).

The accepted data of Tab. 3.2-1 have been used for a weighted linear regression of the $\log_{10}K°$ values for the equilibrium $Na^+ + HPO_4^{2-} \rightleftharpoons NaHPO_4^-$ versus the reciprocal of absolute temperature (Fig. 3.2-4), and this review obtained:

$Na^+ + HPO_4^{2-} \rightleftharpoons NaHPO_4^-$

$\log_{10}K°$ (298.15 K) = 1.03 ± 0.07

$\Delta_r H_m°$(298.15 K) = (23 ± 15) kJ · mol^{-1}

$\Delta_r C_{p,m}°$(298.15 K) = 0

In the cases of $Na^+ + H_2PO_4^- \rightleftharpoons NaH_2PO_4(aq)$ and $Na^+ + PO_4^{3-} \rightleftharpoons NaPO_4^{2-}$ the results of the SIT analyses (Fig. 3.2-3) have been selected, together with $\Delta_r H_m°$(298.15 K) values reported by Daniele et al. (1991) (dashed lines in Fig. 3.2-4):

$Na^+ + H_2PO_4^- \rightleftharpoons NaH_2PO_4(aq)$

$\log_{10}K°$ (298.15 K) = 0.30 ± 0.17

$\Delta_r H_m°$(298.15 K) = (17 ± 8) kJ · mol^{-1}

$\Delta_r C_{p,m}°$(298.15 K) = 0

$Na^+ + PO_4^{3-} \rightleftharpoons NaPO_4^{2-}$

$\log_{10}K°$ (298.15 K) = 1.56 ± 0.17

$\Delta_r H_m°$(298.15 K) = (7 ± 8) kJ · mol^{-1}

$\Delta_r C_{p,m}°$(298.15 K) = 0

These values are included in TDB 2020, together with the estimates

$\varepsilon(NaH_2PO_4(aq), NaCl)$ = (0.0 ± 0.1) kg · mol^{-1}

$\varepsilon(NaHPO_4^-, Na^+)$ = -(0.05 ± 0.10) kg · mol^{-1}

$\varepsilon(NaPO_4^{2-}, Na^+)$ = -(0.10 ± 0.10) kg · mol^{-1}.

Note a potential inconsistency by using the stability constants for the complexes $NaH_2PO_4(aq)$, $NaHPO_4^-$ and $NaPO_4^{2-}$ derived here together with the SIT interaction coefficients $\varepsilon(Na^+, H_2PO_4^-)$, $\varepsilon(Na^+, HPO_4^{2-})$ and $\varepsilon(Na^+, PO_4^{3-})$: These SIT interaction coefficients have been derived from isopiestic measurements of sodium phosphate salts without considering complex formation. They are approximations only and as Lemire et al. (2013) remark in their Tab. B-5, these ion interaction coefficients can be described more accurately with an ionic strength dependent function, $\varepsilon = \varepsilon_1 + \varepsilon_2 \cdot \log_{10} I_m$, listed in their Tab. B-6. However, this or any other ionic strength dependent function, e.g., $\varepsilon = \varepsilon_1 + \varepsilon_2 \cdot \sqrt{I_m}$, are incompatible with the "standard" SIT formalism. A better approximation would be to use the $\log_{10}K°$ values, derived here from measurements in tetraalkylammonium-halide media, and to fit two SIT interaction coefficients to isopiestic data of the corresponding salt, e.g., considering $\log_{10}K°$ of the complex $NaHPO_4^-$ as a fixed value and $\varepsilon(Na^+, HPO_4^{2-})$ and $\varepsilon(Na^+, NaHPO_4^-)$ as fit parameters for isopiestic data of the salt Na_2HPO_4. Such re-evaluations of isopiestic data are outside the scope of the present review and are left as future tasks for the next generation of data evaluators.

3.2.8.2 Sodium(I) phosphate compounds

$Na_2HPO_4(cr)$ is a highly soluble salt with a solubility of 77 g/L at 20 °C. $Na_3PO_4(cr)$ and $NaH_2PO_4(cr)$ show at 20 °C even higher solubilities of 285 g/L and 850 g/L, respectively (gestis.itrust.de).

Nahpoite, $Na_2HPO_4(cr)$, dorfmanite, $Na_2HPO_4 \cdot 2H_2O(cr)$, and catalanoite, $Na_2HPO_4 \cdot 8H_2O(cr)$, have been found in nature as extremely rare minerals.

No solubility data for any of these highly soluble salts have been considered for TDB 2020.

3.2.9 Selected sodium data

Tab. 3.2-2: Selected sodium data

Core data are in bold face.

Name	**$\Delta_f G_m°$** [kJ · mol^{-1}]	**$\Delta_f H_m°$** [kJ · mol^{-1}]	**$S_m°$** [J · K^{-1} · mol^{-1}]	**$C_{p,m}°$** [J · K^{-1} · mol^{-1}]	**Species**
Na(cr)	**0.0**	0.0	**51.300 ± 0.200**	**28.230 ± 0.200**	Na(cr)
Na+	**-261.953 ± 0.096**	**-240.340 ± 0.060**	**58.450 ± 0.150**		Na^+

Name	**$\log_{10}\beta°$**	**$\Delta_r H_m°$** [kJ · mol^{-1}]	**$\Delta_r C_{p,m}°$** [J · K^{-1} · mol^{-1}]	**T-range** [°C]	**Reaction**
Na(cr)	45.89 ± 0.02	-240.34 ± 0.06	-		$Na(cr) \rightleftharpoons Na^+ + e^-$
NaOH(aq)	-14.4 ± 0.2	51.9 ± 1.8	0	0 – 350	$Na^+ + H_2O(l) \rightleftharpoons NaOH(aq) + H^+$
NaF(aq)	-0.28 ± 0.13	13.6 ± 2.2	0	15 – 260	$Na^+ + F^- \rightleftharpoons NaF(aq)$
NaCO3-	1.01 ± 0.20	18.0 ± 4.0	0	25 – 200	$Na^+ + CO_3^{2-} \rightleftharpoons NaCO_3^-$
NaHCO3(aq)	-0.18 ± 0.25	11.6 ± 4.0	0	25 – 200	$Na^+ + HCO_3^- \rightleftharpoons NaHCO_3(aq)$
NaSO4-	0.71 ± 0.05	4.7 ± 3.3	-		$Na^+ + SO_4^{2-} \rightleftharpoons NaSO_4^-$
NaPO4-2	1.56 ± 0.17	7 ± 8	0	25 – 37	$Na^+ + PO_4^{3-} \rightleftharpoons NaPO_4^{2-}$
NaHPO4-	1.03 ± 0.07	23 ± 15	0	0 – 37	$Na^+ + HPO_4^{2-} \rightleftharpoons NaHPO_4^-$
NaH2PO4(aq)	0.30 ± 0.17	17 ± 8	0	25 – 37	$Na^+ + H_2PO_4^- \rightleftharpoons NaH_2PO_4(aq)$

Tab. 3.2-3: Selected SIT ion interaction coefficients $\varepsilon_{j,k}$ [kg · mol^{-1}] for sodium species

Data in bold face are taken from Lemire et al. (2013). Data estimated according to charge correlations and taken from Tab. 1-7 are shaded.

j k → ↓	**Cl^-** $\varepsilon_{j,k}$ [kg · mol^{-1}]	**Na^+** $\varepsilon_{j,k}$ [kg · mol^{-1}]	**$Na^+ + Cl^-$** $\varepsilon_{j,k}$ [kg · mol^{-1}]
OH-	0	**0.04 ± 0.01**	0
F-	0	**0.02 ± 0.02**	0
Cl-	0	**0.03 ± 0.01**	0
HCO3-	0	**0.00 ± 0.02**	0
CO3-2	0	**-0.08 ± 0.05**	0
SO4-2	0	**-0.12 ± 0.06**	0
PO4-3	0	**-0.25 ± 0.03**	0
HPO4-2	0	**-0.15 ± 0.06**	0
H2PO4-	0	**-0.08 ± 0.04**	0
NaOH(aq)	0	0	0.0 ± 0.1
NaF(aq)	0	0	0.0 ± 0.1
NaHCO3(aq)	0	0	0.0 ± 0.1
NaCO3-	0	-0.05 ± 0.10	0
NaSO4-	0	-0.05 ± 0.10	0
NaPO4-2	0	-0.10 ± 0.10	0
NaHPO4-	0	-0.05 ± 0.10	0
NaH2PO4(aq)	0	0	0.0 ± 0.1

3.2.10 References

Austin, J.M. & Mair, A.D. (1962): The standard enthalpy of formation of complex sulfate ions in water. I. HSO_4^-, $LiSO_4^-$, $NaSO_4^-$. Journal of Physical Chemistry, 66, 519-521.

Baes, C.F. & Mesmer, R.E. (1976): The Hydrolysis of cations. Wiley, New York, 490 pp.

Brown, P.L. & Ekberg, C. (2016): Hydrolysis of Metal Ions. Wiley-VCH Verlag GmbH & Co. KGaA, Weinheim, Germany, 917 pp.

Butler, J.N. & Huston, R. (1970): Potentiometric studies of multicomponent activity coefficients using the lanthanum fluoride membrane electrode. Analytical Chemistry, 42,1308-1311.

Chan, C.B., Tioh, N.H. & Hefter, G.T. (1984): Fluoride complexes of the alkali metal anions. Polyhedron, 3, 845-851.

Ciavatta, L. (1980): The specific interaction theory in evaluating ionic equilibria. Annali di Chimica, 70, 551-567.

Cox, J.D., Wagman, D.D. & Medvedev, V.A. (1989): CODATA Key Values for Thermodynamics. Hemisphere Publishing, New York, 271 pp.

Daniele, P.G., De Robertis, A., De Stefano, C., Gianguzza, A. & Sammartano, S. (1991): Salt effects on the protonation of ortho-phosphate between 10 and 50 °C in aqueous solution. A complex formation model. J. Solution Chem., 20, 495-515.

Daniele, P.G., Grasso, M., Rigano, C. & Sammartano, S. (1983): The formation of proton- and alkali metal complexes with ligands of biological interest in aqueous solution. Formation constants of H^+, Li^+, Na^+, K^+ – phosphate complexes and their dependence on ionic strength. Annali di Chimica, 73, 495-515.

Daniele, P.G., Rigano, C. & Sammartano, S. (1982): Studies on sulphate complexes. Part I. Potentiometric investigation of Li^+, Na^+, K^+, Rb^+ and Cs^+ complexes at 37 °C and $0.03 \leq I \leq 0.5$. Inorganica Chimica Acta, 63, 267-272.

Duer, W.C., Robinson, R.A. & Bates, R.G. (1972): Molar conductivity of sodium fluoride in aqueous solution at 25 °C. J. Chem. Soc. Faraday Trans. I, 68, 716-722.

Garrels, R.M. & Thompson, M.E. (1962): A chemical model for sea water at 25 °C and one atmosphere total pressure. American Journal of Science, 260, 57-66.

Garrels, R.M., Thompson, M.E. & Siever, R. (1961): Control of carbonate solubility by carbonate complexes. American Journal of Science, 259, 24-45.

Grenthe, I., Fuger, J., Konings, R.J.M., Lemire, R.J., Muller, A.B., Nguyen-Trung, C. & Wanner, H. (1992): Chemical Thermodynamics of Uranium. Chemical Thermodynamics, Vol. 1. North-Holland, Amsterdam, 715 pp.

Lemire, R.J., Berner, U., Musikas, C., Palmer, D.A., Taylor, P. & Tochiyama, O. (2013): Chemical Thermodynamics of Iron, Part 1. Chemical Thermodynamics, Vol. 13a. OECD Publications, Paris, France, 1082 pp.

Nordstrom, D.K., Plummer, L.N., Langmuir, D., Busenberg, E., May, H.M., Jones, B.F. & Parkhurst, D.L. (1990): Revised Chemical Equilibrium Data for Major Water-Mineral Reactions and Their Limitations. In: Melchior, D.C., and Bassett, R.L. (eds.): Chemical Modeling of Aqueous Systems II. Washington, D.C., American Chemical Society, ACS Symposium Series 416, p. 398-413.

Patel, P.R., Gregory, T.M. & Brown, W.E. (1974): Solubility of $CaHPO_4 \cdot 2H_2O$ in the quaternary system $Ca(OH)_2 – H_3PO_4 – NaCl – H_2O$ at 25 °C. J. Res. Natl. Bur. Stand., 78A, 675-681.

Richardson, C.K. & Holland, H.D. (1979): The solubility of fluorite in hydrothermal solutions, an experimental study. Geochim. Cosmochim. Acta, 43, 1313-1325.

Righellato, E.C. & Davies, C.W. (1930): The extent of dissociation of salts in water. Part II. Uni-bivalent salts. Trans. Faraday Soc., 26, 592-600.

Robinson, R.A. & Stokes, R.H. (1959): Electrolyte Solutions. Second Revised Edition. Academic Press, New York, 559 pp.

Smith, R.P. & Alberty, R.A. (1956): The apparent stability constants of ionic complexes of various adenosine phosphates with monovalent cations. J. Phys. Chem., 60, 180-184.

Stefánsson, A., Bénézeth, P. & Schott, J. (2013): Carbonic acid ionization and the stability of sodium bicarbonate and carbonate ion pairs to 200 °C – A potentiometric and spectrophotometric study. Geochim. Cosmochim. Acta, 120, 600-611.

3.3 Potassium

3.3.1 Elemental potassium

Potassium metal and gas are not relevant under environmental conditions. Hence, the gas phase Kg is not included in the data base. The absolute entropy and heat capacity of K(cr) are included as they are used for the calculation of certain thermodynamic reaction properties.

The selected values for K(cr) are taken from CODATA (Cox et al. 1989):

$$S_m°(\text{K, cr, 298.15 K}) = (64.680 \pm 0.200)\ \text{J} \cdot \text{K}^{-1} \cdot \text{mol}^{-1}$$

$$C_{p,m}°(\text{K, cr, 298.15 K}) = (29.600 \pm 0.100)\ \text{J} \cdot \text{K}^{-1} \cdot \text{mol}^{-1}$$

3.3.2 Potassium(I) aqua ion

Potassium(I) exists as the K^+ cation in aqueous solutions. The selected thermodynamic values for K^+ are taken from CODATA (Cox et al. 1989):

$$\Delta_f G_m°(K^+, \text{298.15 K}) = -(282.510 \pm 0.116)\ \text{kJ} \cdot \text{mol}^{-1}$$

$$\Delta_f H_m°(K^+, \text{298.15 K}) = -(252.140 \pm 0.080)\ \text{kJ} \cdot \text{mol}^{-1}$$

$$S_m°(K^+, \text{298.15 K}) = (101.200 \pm 0.200)\ \text{J} \cdot \text{K}^{-1} \cdot \text{mol}^{-1}$$

Using the selected CODATA $\Delta_f G_m°(K^+, \text{298.15 K})$, the redox equilibrium

$$\text{K(cr)} \rightleftharpoons K^+ + e^-$$

is calculated as

$$\log_{10} K°(\text{298.15 K}) = 49.49 \pm 0.02$$

Since this review does not consider the formation of potassium chloride complexation (see Section 3.3.5), $\varepsilon(K^+, Cl^-)$ is taken as selected by NEA (Grenthe et al. 1992, Lemire et al. 2013):

$$\varepsilon(K^+, Cl^-) = (0.00 \pm 0.01)\ \text{kg} \cdot \text{mol}^{-1}$$

3.3.3 Potassium(I) (hydr)oxide compounds and complexes

3.3.3.1 Potassium(I) hydroxide complexes

Nordstrom et al. (1990) selected a $\log_{10}{}^{*}\beta_1°$ value reported by Baes & Mesmer (1976) for the equilibrium:

$$K^+ + H_2O(l) \rightleftharpoons KOH(aq) + H^+$$

$$\log_{10}{}^{*}\beta_1° \text{ (298.15 K)} = -14.46 \pm 0.4$$

Brown & Ekberg (2016) scrutinised all available data concerning the hydrolysis of potassium(I). They report that, as a function of the reciprocal temperature, the data are virtually linear below about 150 °C, and they obtained

$$K^+ + H_2O(l) \rightleftharpoons KOH(aq) + H^+$$

$$\log_{10}{}^{*}\beta_1° \text{ (298.15 K)} = -14.5 \pm 0.4$$

$$\Delta_r H_m° \text{(298.15 K)} = (59.0 \pm 1.9) \text{ kJ} \cdot \text{mol}^{-1}$$

$$\Delta_r C_{p,m}° \text{(298.15 K)} = 0 \text{ J} \cdot \text{K}^{-1} \cdot \text{mol}^{-1}$$

These values have been included in TDB 2020, as well as the estimate

$$\varepsilon(\text{KOH(aq), NaCl}) = (0.0 \pm 0.1) \text{ kg} \cdot \text{mol}^{-1}.$$

Brown & Ekberg (2016) state that it is not surprising that there is a large uncertainty for the stability constant. The value obtained at 25 °C is substantially outside the range of the majority of data used to derive the linear fit, and additionally there is some scatter in the available data, no doubt as a consequence of the very low stability of the complex.

Note that $\log_{10}{}^{*}\beta_1°$values reported by Brown & Ekberg (2016) are in excellent agreement with those of the older evaluation of Baes & Mesmer (1976).

3.3.3.2 Potassium(I) (hydr)oxide compounds

KOH(s) is a highly soluble caustic base ("caustic potash", "Ätzkali") with a solubility of 1'130 g/L at 20 °C (gestis.itrust.de). The solid is hygroscopic. No solubility data have been considered for TDB 2020.

3.3.4 Potassium(I) fluoride compounds and complexes

3.3.4.1 Potassium(I) fluoride complexes

Chan et al. (1984) tried to measure the equilibrium $K^+ + F^- \rightleftharpoons KF(aq)$ using fluoride ion-selective electrode potentiometry. They report $\log_{10}K$ (298.15 K) = -1.5 to -2.0 in 1 M $RbNO_3$ and $\log_{10}K$ (298.15 K) = -1.0 to -1.3 and 1 M $CsNO_3$. At lower concentrations of the nitrate media no effect could be detected, in contrast to the case of NaF(aq) (see Section 3.4.1).

Hence, this review concludes that the complex KF(aq) is exceedingly weak, if it "exists" at all, and no data have been included in TDB 2020.

3.3.4.2 Potassium(I) fluoride compounds

KF(s) is a highly soluble salt with a solubility of 485 g/L at 20 °C (gestis.itrust.de). It is found in nature as the rare mineral carobbiite. No solubility data have been considered for TDB 2020.

3.3.5 Potassium(I) chloride compounds and complexes

3.3.5.1 Potassium(I) chloride complexes

This report does not consider the formation of weak potassium chloride complexes but includes possible ion interactions in the SIT interaction coefficient $\varepsilon(K^+, Cl^-)$ (see below).

3.3.5.2 Potassium(I) chloride compounds

KCl(cr) is a highly soluble salt with a solubility of 347 g/L at 20 °C (gestis.itrust.de). It is found in nature as the mineral sylvine. Its isopiestic properties have been measured up to 4.5 $mol \cdot kg_{H2O}^{-1}$ (Robinson & Stokes 1959). Hence, no solubility data, but the specific ion interaction coefficient selected by NEA (Grenthe et al. 1992, Lemire et al. 2013) is adopted for TDB 2020:

$$\varepsilon(K^+, Cl^-) = (0.00 \pm 0.01)\ kg \cdot mol^{-1}$$

3.3.6 Potassium(I) carbonate compounds and complexes

3.3.6.1 Potassium(I) carbonate complexes

Wimberley et al. (1985) report measurements of sodium and potassium bicarbonate solutions with an ion-selective electrode system at 37 °C. They obtained

$$K^+ + HCO_3^- \rightleftharpoons KHCO_3(aq)$$

$$\log_{10}K° \text{ (310.15 K)} = -0.26$$

$$K^+ + CO_3^{2-} \rightleftharpoons KCO_3^-$$

$$\log_{10}K° \text{ (310.15 K)} = 1.03$$

The values reported by Wimberley et al. (1985) for the equilibria $Na^+ + HCO_3^- \rightleftharpoons NaHCO_3(aq)$, $\log_{10}K°$ (310.15 K) = -0.14, and $Na^+ + CO_3^{2-} \rightleftharpoons NaCO_3^-$, $\log_{10}K°$ (310.15 K) = 0.92, are in good agreement with the values of Stefánsson et al. (2013) selected by this review (see Section 3.2.6.1), $\log_{10}K°$ (310.15 K) = -0.10 ± 0.25 and $\log_{10}K_1°$ (310.15 K) = 1.13 ± 0.20, respectively.

However, no temperature data are available for the potassium carbonate and bicarbonate equilibria. This review estimated the temperature effects via the isocoulombic reactions

$$NaHCO_3(aq) + K^+ \rightleftharpoons KHCO_3(aq) + Na^+$$

$$NaCO_3^- + K^+ \rightleftharpoons KCO_3^- + Na^+$$

In both cases we assume that in the Gibbs-Helmholtz equation

$$\Delta_r G_m°\text{(iso, 298.15 K)} = \Delta_r H_m°\text{(iso, 298.15 K)} - T° \cdot \Delta_r S_m°\text{(iso, 298.15 K)}$$

the term $\Delta_r S_m°$(iso, 298.15 K) = 0 and hence, this so-called 1-term extrapolation results in

$$\Delta_r G_m°\text{(iso, T)} = \text{constant} = \Delta_r H_m°\text{(iso, 298.15 K)}$$

Using the selected $\log_{10}K°$ values for the potassium and sodium (see Section 3.2.6.1) equilibria results in

$$\Delta_r G_m°(\text{iso}, HCO_3^-) = \Delta_r G_m°(K^+ + HCO_3^- \rightleftharpoons KHCO_3(aq)) - \Delta_r G_m°(Na^+ + HCO_3^- \rightleftharpoons NaHCO_3(aq))$$

$$\Delta_r G_m°(\text{iso}, CO_3^{2-}) = \Delta_r G_m°(K^+ + CO_3^{2-} \rightleftharpoons KCO_3^-) - \Delta_r G_m°(Na^+ + CO_3^{2-} \rightleftharpoons NaCO_3^-)$$

which in turn are used to estimate $\Delta_r H_m°$ values of the potassium equilibria from the sodium data:

$$\Delta_r H_m°(K^+ + HCO_3^- \rightleftharpoons KHCO_3(aq)) = \Delta_r G_m°(iso, HCO_3^-) + \Delta_r H_m°(Na^+ + HCO_3^- \rightleftharpoons NaHCO_3(aq))$$

$$\Delta_r H_m°(K^+ + CO_3^{2-} \rightleftharpoons KCO_3^-) = \Delta_r G_m°(iso, CO_3^{2-}) + \Delta_r H_m°(Na^+ + CO_3^{2-} \rightleftharpoons NaCO_3^-)$$

As the potassium equilibria reported by Wimberley et al. (1985) have been obtained at 37 °C, an iterative procedure has been used to obtain internally consistent data for 25 °C:

$$K^+ + HCO_3^- \rightleftharpoons KHCO_3(aq)$$

$$log_{10}K°\ (298.15\ K) = -0.34 \pm 0.50$$

$$\Delta_r H_m°(298.15\ K) = (12.5 \pm 5.0)\ kJ \cdot mol^{-1}$$

$$K^+ + CO_3^{2-} \rightleftharpoons KCO_3^-$$

$$log_{10}K°\ (298.15\ K) = 0.90 \pm 0.50$$

$$\Delta_r H_m°(298.15\ K) = (18.6 \pm 5.0)\ kJ \cdot mol^{-1}$$

As no independent confirmation exists for the $\log_{10}K°$ values reported by Wimberley et al. (1985) and the temperature effects are estimated, these values are included in TDB 2020 as supplemental data, as well as the estimates

$$\varepsilon(KCO_3^-, Na^+) = -(0.05 \pm 0.10)\ kg \cdot mol^{-1}$$

$$\varepsilon(KHCO_3(aq), NaCl) = (0.0 \pm 0.1)\ kg \cdot mol^{-1}$$

3.3.6.2 Potassium(I) carbonate compounds

$K_2CO_3(s)$ is a highly soluble salt with a solubility of 1'120 g/L at 20 °C (gestis.itrust.de). It is the primary component of potash. The solid is deliquescent. No solubility data have been considered for TDB 2020.

3.3.7 Potassium(I) sulphate compounds and complexes

3.3.7.1 Potassium(I) sulphate complexes

Nordstrom et al. (1990) selected a $\log_{10}\beta_1°$ value reported by Truesdell & Hostetler (1968) and a $\Delta_r H_m°$ value communicated by Siebert & Christ (1976, unpublished estimation) for the complex

$$K^+ + SO_4^{2-} \rightleftharpoons KSO_4^-$$

$$\log_{10}K_1° \text{ (298.15 K)} = 0.85$$

$$\Delta_r H_m°(298.15 \text{ K}) = 2.25 \text{ kcal} \cdot \text{mol}^{-1} = 9.41 \text{ kJ} \cdot \text{mol}^{-1}$$

This review considered the data reported by Truesdell & Hostetler (1968) from emf measurements at 10, 25, 38 and 50 °C, the datum of Righellato & Davies (1930) from conductivity measurements at 18 °C, the datum of Quist et al. (1963) from conductivity measurements at 100 °C, and the datum of Daniele et al. (1982) from potentiometric measurements at 37 °C and ionic strength 0.03 – 0.5 M, extrapolated to $I = 0$, and obtained (Fig. 3.3-1):

$$K^+ + SO_4^{2-} \rightleftharpoons KSO_4^-$$

$$\log_{10}\beta_1° \text{ (298.15 K)} = 0.84 \pm 0.05$$

$$\Delta_r H_m°(298.15 \text{ K}) = (12.9 \pm 1.7) \text{ kJ} \cdot \text{mol}^{-1}$$

$$\Delta_r C_{p,m}°(298.15 \text{ K}) = 0 \text{ J} \cdot \text{K}^{-1} \cdot \text{mol}^{-1}$$

These values have been included in TDB 2020, as well as the estimate

$$\varepsilon(KSO_4^-, Na^+) = -(0.05 \pm 0.10) \text{ kg} \cdot \text{mol}^{-1}.$$

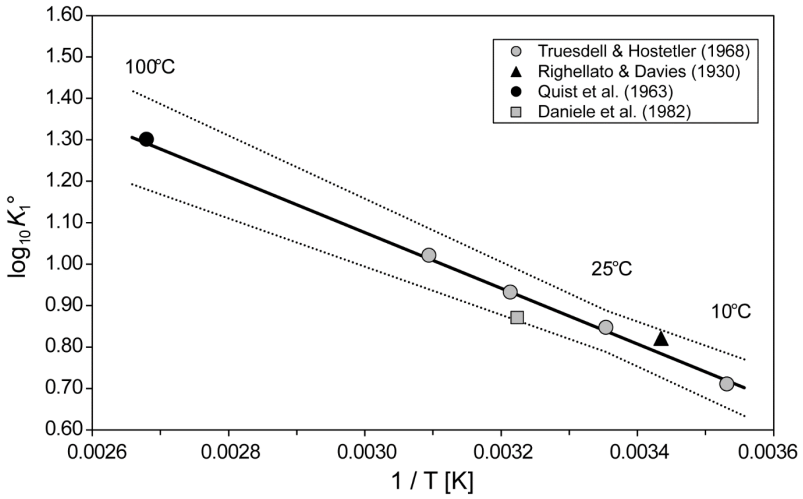

Fig. 3.3-1: The equilibrium constant $\log_{10}K_1°$ for $K^+ + SO_4^{2-} \rightleftharpoons KSO_4^-$ as function of temperature in the range 10 – 100 °C

Solid line: unweighted linear regression of all data. Dotted lines: lower and upper limits using $\log_{10}K_1(298.15\ K) = 0.84 \pm 0.05$ and $\Delta_r H_m(298.15\ K) = (12.9 \pm 1.7)\ kJ \cdot mol^{-1}$ and extrapolated to lower and higher temperatures.

3.3.7.2 Potassium(I) sulphate compounds

$K_2SO_4(s)$ is a highly soluble salt with a solubility of 111 g/L at 20 °C (gestis.itrust.de). It is found in nature as the rare mineral arcanite. No solubility data have been considered for TDB 2020.

3.3.8 Potassium(I) phosphate compounds and complexes

3.3.8.1 Potassium(I) phosphate complexes

Three studies, Smith & Alberty (1956), Daniele et al. (1983) and Daniele et al. (1991), report stability constants for aqueous potassium phosphate complexes.

Smith & Alberty (1956) calculated from measurements with a glass electrode at 25 and 0 °C in 0.2 M Pr_4NCl (tetrapropylammonium chloride, $(CH_3CH_2CH_2)_4NCl$) the values K(25 °C) = 3.1 ± 0.4 (corresponding to $\log_{10}K$(25 °C) = 0.49 ± 0.06) and K(0 °C) = 1.2 ± 0.3 (corresponding to $\log_{10}K$(0 °C) = 0.08 ± 0.11) for the equilibrium $K^+ + HPO_4^{2-} \rightleftharpoons KHPO_4^-$. This review retained these values, included the value at 25 °C in an SIT analysis (Fig. 3.3-2) and used the resulting Δε value for extrapolating all data measured in tetraalkylammonium halide media (Tab. 3.3-1). The results are $\log_{10}K°(298.15\ K) = 0.93 \pm 0.20$ and $\log_{10}K°(273.15\ K) = 0.5 \pm 0.4$, with uncertainties estimated by this review.

Daniele et al. (1983) studied the complex formation between potassium and phosphate at 25 and 37 °C and 0.15, 0.3 and 0.5 M Me_4NCl (tetramethylammonium chloride, $(CH_3)_4NCl$). They report the values $\log_{10}K$(25 °C, 0.5 M Me_4NCl) = 0.54 and $\log_{10}K$(37 °C, 0.15 M Me_4NCl) = 0.6 ± 0.2 for $K^+ + PO_4^{3-} \rightleftharpoons KPO_4^{2-}$, $\log_{10}K$(25 °C, 0.5 M Me_4NCl) = 0.36 and $\log_{10}K$(37 °C, 0.15 M Me_4NCl) = 0.48 ± 0.05 for $K^+ + HPO_4^{2-} \rightleftharpoons KHPO_4^-$ and $\log_{10}K$(25 °C, 0.5 M Me_4NCl) = 0.18 and $\log_{10}K$(37 °C, 0.3 M Me_4NCl) = -0.2 ± 0.3 for $K^+ + H_2PO_4^- \rightleftharpoons KH_2PO_4(aq)$. This review retained

these values, included the values at 25 °C in SIT analyses (Fig. 3.3-2) and used the resulting Δε value for extrapolating all data measured in tetraalkylammonium halide media (Tab. 3.3-1). The uncertainties have been estimated by this review.

Daniele et al. (1991) studied the protonation constants of orthophosphate potentiometrically using a glass electrode in aqueous NaCl, KCl and tetraethylammonium iodide (Et_4NI, $(CH_3CH_2)_4NI$) solutions at an ionic strength range 0.04 – 1M in the temperature range 10 – 50 °C. The differences found in the protonation constants for different salt solutions are explained by a complex formation model. Daniele et al. (1991) report in their Tab. VII stability constants for the equilibria $K^+ + PO_4^{3-} \rightleftharpoons KPO_4^{2-}$, $K^+ + HPO_4^{2-} \rightleftharpoons KHPO_4^-$ and $K^+ + H_2PO_4^- \rightleftharpoons KH_2PO_4(aq)$ at 25 °C in 0.16, 0.64 and 1 M Et_4NI, and at 37 °C in 0.16 M Et_4NI (Tab. 3.3-1). The values at 25 °C have been used by this review for SIT analyses (Fig. 3.3-2) and the obtained Δε values were then used for extrapolating all data measured in tetraalkylammonium halide media to zero ionic strength (Tab. 3.3-1). The uncertainties have been estimated by this review.

Tab. 3.3-1: Reported and accepted potassium phosphate complexation data

Temp. [°C]	**Medium**	**$\log_{10}K$ reported** [a]	**I_m**	**$\log_{10}K_m$**	**Δε**	**$\log_{10}K°$ accepted** [b]	**Reference**
$K^+ + PO_4^{3-} \rightleftharpoons KPO_4^{2-}$							
25	0.5 M Me_4NCl	0.54	0.530	0.515	-0.62	1.24 ± 0.30	Daniele et al. (1983)
37	0.15 M Me_4NCl	0.6 ± 0.2	0.153	0.592	-0.62	1.3 ± 0.4	Daniele et al. (1983)
25	0.16 M Et_4NI	0.81	0.165	0.796	-0.62	1.46 ± 0.15	Daniele et al. (1991)
25	0.64 M Et_4NI	0.91	0.731	0.853	-0.62	1.54 ± 0.15	Daniele et al. (1991)
25	1.0 M Et_4NI	1.03	1.230	0.940	-0.62	1.44 ± 0.15	Daniele et al. (1991)
37	0.16 M Et_4NI	0.85	0.165	0.836	-0.62	1.52 ± 0.15	Daniele et al. (1991)
$K^+ + HPO_4^{2-} \rightleftharpoons KHPO_4^-$							
0	0.2 M Pr_4NCl	0.08 ± 0.11	0.210	0.057	-0.43	0.5 ± 0.4	Smith & Alberty (1956)
25	0.2 M Pr_4NCl	0.49 ± 0.06	0.210	0.496	-0.43	0.93 ± 0.20	Smith & Alberty (1956)
25	0.5 M Me_4NCl	0.36	0.530	0.335	-0.43	0.82 ± 0.20	Daniele et al. (1983)
37	0.15 M Me_4NCl	0.48 ± 0.05	0.153	0.472	-0.43	0.92 ± 0.20	Daniele et al. (1983)
25	0.16 M Et_4NI	0.50	0.165	0.486	-0.43	0.93 ± 0.15	Daniele et al. (1991)
25	0.64 M Et_4NI	0.44	0.731	0.383	-0.43	0.83 ± 0.15	Daniele et al. (1991)
25	1.0 M Et_4NI	0.71	1.230	0.620	-0.43	0.94 ± 0.15	Daniele et al. (1991)
37	0.16 M Et_4NI	0.58	0.165	0.566	-0.43	1.02 ± 0.15	Daniele et al. (1991)
$K^+ + H_2PO_4^- \rightleftharpoons KH_2PO_4(aq)$							
25	0.5 M Me_4NCl	0.18	0.530	0.155	-0.24	0.4 ± 0.6	Daniele et al. (1983)
37	0.3 M Me_4NCl	-0.2 ± 0.3	0.311	-0.215	-0.24	0.0 ± 0.6	Daniele et al. (1983)
25	0.16 M Et_4NI	0.07	0.165	0.056	-0.24	0.27 ± 0.15	Daniele et al. (1991)
25	0.64 M Et_4NI	0.16	0.731	0.103	-0.24	0.31 ± 0.15	Daniele et al. (1991)
25	1.0 M Et_4NI	0.24	1.230	0.150	-0.24	0.27 ± 0.15	Daniele et al. (1991)
37	0.16 M Et_4NI	0.02	0.165	0.006	-0.24	0.23± 0.15	Daniele et al. (1991)

[a] Data as reported in the cited publications or calculated by this review from the reported data, see text.
[b] 2σ uncertainties assigned or estimated by this review.

The results of the SIT analyses (Fig. 3.3-2) are:

$K^+ + PO_4^{3-} \rightleftharpoons KPO_4^{2-}$

$\log_{10}K°$ (298.15 K) = 1.46 ± 0.16

$\Delta\varepsilon$ = -(0.63 ± 0.20) kg · mol^{-1}

$K^+ + HPO_4^{2-} \rightleftharpoons KHPO_4^-$

$\log_{10}K°$ (298.15 K) = 0.89 ± 0.13

$\Delta\varepsilon$ = -(0.43 ± 0.18) kg · mol^{-1}

$K^+ + H_2PO_4^- \rightleftharpoons KH_2PO_4(aq)$

$\log_{10}K°$ (298.15 K) = 0.29 ± 0.16

$\Delta\varepsilon$ = -(0.24 ± 0.20) kg · mol^{-1}

Note that Daniele et al. (1991) extrapolated their values obtained for the above equilibria to zero ionic strength using their own, with respect to the SIT analysis (Fig. 3.3-2), non-linear extrapolation formula and report $\log_{10}K°$ (298.15 K) = 1.47 ± 0.04, $\log_{10}K°$ (298.15 K) = 0.88 ± 0.04 and $\log_{10}K°$ (298.15 K) = 0.26 ± 0.10, respectively. Their uncertainties refer to one standard deviation.

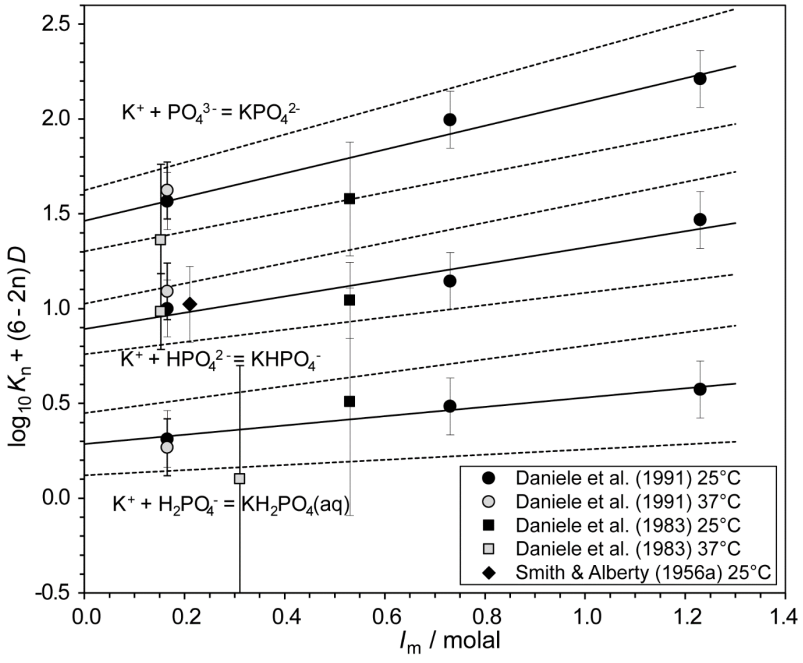

Fig. 3.3-2: Dependence of $\log_{10}K_n$ of the equilibria $K^+ + H_nPO_4^{n-3} \rightleftharpoons KH_nPO_4^{n-2}$ on ionic strength in tetraalkylammonium halide media

Data are taken from Tab. 3.3-1 with their "accepted" uncertainties. Data at 25 °C are used for the weighted linear regressions, while data at 37 °C are shown for comparison only. The solid lines are obtained using the derived SIT interaction coefficients and stability constants at zero ionic strength. Dotted lines represent the 95% uncertainty range extrapolated from I = 0 to higher concentrations.

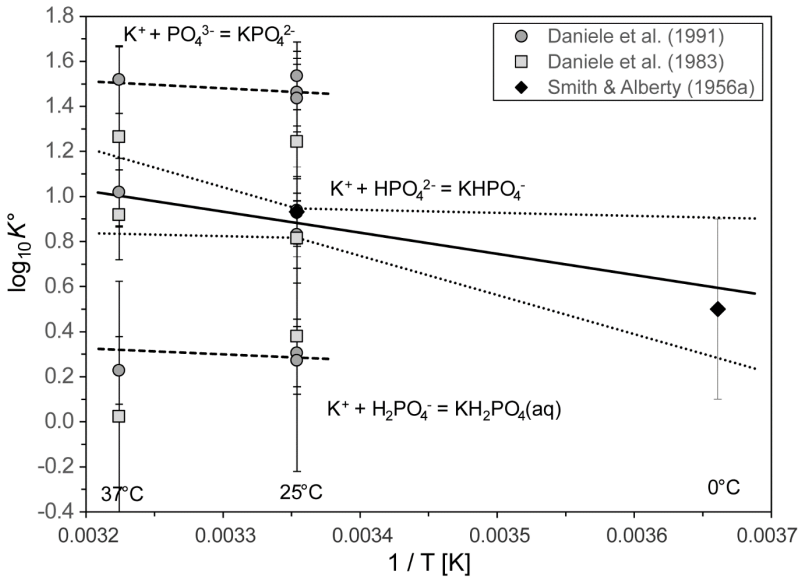

Fig. 3.3-3: The equilibrium constants $\log_{10}K°$ for the indicated equilibria as functions of reciprocal absolute temperature in the range 0 – 37 °C

Symbols: accepted $\log_{10}K°$ values taken from Tab. 3.3-1. Solid line: weighted linear regression. Dotted lines: lower and upper limits using $\log_{10}K°$ (298.15 K) = 0.88 ± 0.07 and $\Delta_r H_m°$ (298.15 K) = (18 ± 15) kJ · mol^{-1} and extrapolated to lower and higher temperatures. Dashed lines: using $\Delta_r H_m°$(298.15 K) values as reported by Daniele et al. (1991).

The accepted data of Tab. 3.3-1 have been used for a weighted linear regression of the $\log_{10}K°$ values for the equilibrium $K^+ + HPO_4^{2-} \rightleftharpoons KHPO_4^-$ versus the reciprocal of absolute temperature (Fig. 3.3-3), and this review obtained:

$K^+ + HPO_4^{2-} \rightleftharpoons KHPO_4^-$

$\log_{10}K°$ (298.15 K) = 0.88 ± 0.07

$\Delta_r H_m°$(298.15 K) = (18 ± 15) kJ · mol^{-1}

$\Delta_r C_{p,m}°$(298.15 K) = 0

In the cases of $K^+ + H_2PO_4^- \rightleftharpoons KH_2PO_4(aq)$ and $K^+ + PO_4^{3-} \rightleftharpoons KPO_4^{2-}$ the results of the SIT analyses (Fig. 3.3-2) have been selected, together with $\Delta_r H_m°$(298.15 K) values reported by Daniele et al. (1991) (dashed lines in Fig. 3.3-3):

$K^+ + H_2PO_4^- \rightleftharpoons KH_2PO_4(aq)$

$\log_{10}K°$ (298.15 K) = 0.29 ± 0.16

$\Delta_r H_m°$(298.15 K) = (5 ± 8) kJ · mol^{-1}

$\Delta_r C_{p,m}°$(298.15 K) = 0

$K^+ + PO_4^{3-} \rightleftharpoons KPO_4^{2-}$

$\log_{10}K°$ (298.15 K) = 1.46 ± 0.16

$\Delta_r H_m°$(298.15 K) = (6 ± 8) kJ · mol^{-1}

$\Delta_r C_{p,m}°$(298.15 K) = 0

These values are included in TDB 2020, together with the estimates

$\varepsilon(KH_2PO_4(aq), NaCl)$ = (0.0 ± 0.1) kg · mol^{-1}

$\varepsilon(KHPO_4^-, Na^+)$ = -(0.05 ± 0.10) kg · mol^{-1}

$\varepsilon(KPO_4^{2-}, Na^+)$ = -(0.10 ± 0.10) kg · mol^{-1}

3.3.8.2 Potassium(I) phosphate compounds

KH_2PO_4(cr) is a highly soluble salt with a solubility of 222 g/L at 20 °C. K_3PO_4(cr) and K_2HPO_4(cr) show even higher solubilities of 508 g/L at 25 °C and 1'600 g/L at 20 °C, respectively (gestis.itrust.de). $(K,NH_4)H_2PO_4$(cr) has been found in nature as the extremely rare mineral archerite. No solubility data for any of these highly soluble salts have been considered for TDB 2020.

3.3.9 Selected potassium data

Tab. 3.3-2: Selected potassium data

Core data are in bold face and supplemental data in italics.

Name	**$\Delta_f G_m°$** [kJ · mol^{-1}]	**$\Delta_f H_m°$** [kJ · mol^{-1}]	**$S_m°$** [J · K^{-1} · mol^{-1}]	**$C_{p,m}°$** [J · K^{-1} · mol^{-1}]	**Species**
K(cr)	0.0	0.0	**64.680 ± 0.200**	**29.600 ± 0.100**	K(cr)
K+	**-282.510 ± 0.116**	**-252.140 ± 0.080**	**101.200 ± 0.200**		K^+

Name	**$\log_{10}\beta°$**	**$\Delta_r H_m°$** [kJ · mol^{-1}]	**$\Delta_r C_{p,m}°$** [J · K^{-1} · mol^{-1}]	**T-range** [°C]	**Reaction**
K(cr)	45.89 ± 0.02	-252.14 ± 0.08	-		K(cr) ⇌ $K^+ + e^-$
KOH(aq)	-14.5 ± 0.4	59.0 ± 1.9	0	25 – 150	$K^+ + H_2O(l)$ ⇌ KOH(aq) + H^+
KCO3-	*0.90 ± 0.50*	*18.6 ± 5.0*	-		*$K^+ + CO_3^{2-}$ ⇌ KCO_3^-*
KHCO3(aq)	*-0.34 ± 0.50*	*12.5 ± 5.0*	-		*$K^+ + HCO_3^-$ ⇌ $KHCO_3(aq)$*
KSO4-	0.84 ± 0.05	12.9 ± 1.7	0	10 – 100	$K^+ + SO_4^{2-}$ ⇌ KSO_4^-
KPO4-2	1.46 ± 0.16	6 ± 8	0	25 – 37	$K^+ + PO_4^{3-}$ ⇌ KPO_4^{2-}
KHPO4-	0.88 ± 0.07	18 ± 15	0	0 – 37	$K^+ + HPO_4^{2-}$ ⇌ $KHPO_4^-$
KH2PO4(aq)	0.29 ± 0.16	5 ± 8	0	25 – 37	$K^+ + H_2PO_4^-$ ⇌ KH_2PO_4(aq)

Tab. 3.3-3: Selected SIT ion interaction coefficients $\varepsilon_{j,k}$ [kg · mol^{-1}] for potassium species

Data in bold face are taken from Lemire et al. (2013). Data estimated according to charge correlations and taken from Tab. 1-7 are shaded. Supplemental data are in italics.

j k → ↓	**Cl^-** $\varepsilon_{j,k}$ [kg · mol^{-1}]	**Na^+** $\varepsilon_{j,k}$ [kg · mol^{-1}]	**$Na^+ + Cl^-$** $\varepsilon_{j,k}$ [kg · mol^{-1}]
K+	**0.00 ± 0.01**	0	0
KOH(aq)	0	0	0.0 ± 0.1
KHCO3(aq)	*0*	*0*	*0.0 ± 0.1*
KCO3-	*0*	*-0.05 ± 0.10*	*0*
KSO4-	0	-0.05 ± 0.10	0
KPO4-2	0	-0.10 ± 0.10	0
KHPO4-	0	-0.05 ± 0.10	0
KH2PO4(aq)	0	0	0.0 ± 0.1

3.3.10 References

Baes, C.F. & Mesmer, R.E. (1976): The Hydrolysis of cations. Wiley, New York, 490 pp.

Brown, P.L. & Ekberg, C. (2016): Hydrolysis of Metal Ions. Wiley-VCH Verlag GmbH & Co. KGaA, Weinheim, Germany, 917 pp.

Chan, C.B., Tioh, N.H. & Hefter, G.T. (1984): Fluoride complexes of the alkali metal anions. Polyhedron, 3, 845-851.

Cox, J.D., Wagman, D.D. & Medvedev, V.A. (1989): CODATA Key Values for Thermodynamics. Hemisphere Publishing, New York, 271 pp.

Daniele, P.G., De Robertis, A., De Stefano, C., Gianguzza, A. & Sammartano, S. (1991): Salt effects on the protonation of ortho-phosphate between 10 and 50 °C in aqueous solution. A complex formation model. J. Solution Chem., 20, 495-515.

Daniele, P.G., Grasso, M., Rigano, C. & Sammartano, S. (1983): The formation of proton- and alkali metal complexes with ligands of biological interest in aqueous solution. Formation constants of H^+, Li^+, Na^+, K^+ – phosphate complexes and their dependence on ionic strength. Annali di Chimica, 73, 495-515.

Daniele, P.G., Rigano, C. & Sammartano, S. (1982): Studies on sulphate complexes. Part I. Potentiometric investigation of Li^+, Na^+, K^+, Rb^+ and Cs^+ complexes at 37 °C and $0.03 \leq I \leq 0.5$. Inorganica Chimica Acta, 63, 267-272.

Grenthe, I., Fuger, J., Konings, R.J.M., Lemire, R.J., Muller, A.B., Nguyen-Trung, C. & Wanner, H. (1992): Chemical Thermodynamics of Uranium. Chemical Thermodynamics, Vol. 1. North-Holland, Amsterdam, 715 pp.

Lemire, R.J., Berner, U., Musikas, C., Palmer, D.A., Taylor, P. & Tochiyama, O. (2013): Chemical Thermodynamics of Iron, Part 1. Chemical Thermodynamics, Vol. 13a. OECD Publications, Paris, France, 1082 pp.

Nordstrom, D.K., Plummer, L.N., Langmuir, D., Busenberg, E., May, H.M., Jones, B.F. & Parkhurst, D.L. (1990): Revised Chemical Equilibrium Data for Major Water-Mineral Reactions and Their Limitations. In: Melchior, D.C., and Bassett, R.L. (eds.): Chemical Modeling of Aqueous Systems II. Washington, D.C., American Chemical Society, ACS Symposium Series 416, p. 398-413.

Quist, A.S., Franck, E.U., Jolley, H.R. & Marshall, W.L. (1963): Electrical conductance measurements of aqueous solutions at high temperature and pressure. I. The conductances of potassium sulfate-water solutions from 25 to 800 °C and pressures up to 4000 bars. J. Phys. Chem., 67, 2453-2459.

Righellato, E.C. & Davies, C.W. (1930): The extent of dissociation of salts in water. Part II. Uni-bivalent salts. Trans. Faraday Soc., 26, 592-600.

Robinson, R.A. & Stokes, R.H. (1959): Electrolyte Solutions. Second Revised Edition. Academic Press, New York, 559 pp.

Smith, R.P. & Alberty, R.A. (1956): The apparent stability constants of ionic complexes of various adenosine phosphates with monovalent cations. J. Phys. Chem., 60, 180-184.

Stefánsson, A., Bénézeth, P. & Schott, J. (2013): Carbonic acid ionization and the stability of sodium bicarbonate and carbonate ion pairs to 200 °C – A potentiometric and spectrophotometric study. Geochim. Cosmochim. Acta, 120, 600-611.

Truesdell, A.H. & Hostetler, P.B. (1968): Dissociation constants of KSO_4^- from 10°-50 °C. Geochim. Cosmochim. Acta, 32, 1019-1022.

Wimberley, P.D., Siggard-Andersen, O., Fogh-Andersen, N. & Boink, A.B.T.J. (1985): Are sodium bicarbonate and potassium bicarbonate fully dissociated under physiological conditions? Scand. J. Clin. Lab. Invest., 45, 7-10.

4 Alkaline earth elements

Chemical thermodynamic data for ground and pore water models in our original data base (Pearson & Berner 1991, Pearson et al. 1992) have been taken from the USGS review of data for major water-mineral reactions (Nordstrom et al. 1990) and basically have not been changed since then. The USGS summary of equilibrium constants and reaction enthalpies for aqueous association reactions and mineral solubilities has been compiled from the literature for common equilibria occurring in natural waters at 0 – 100 °C and 1 bar pressure. The species have been limited to those containing the metals Li, Na, K, Mg, Ca, Sr, Ba, Mn(II,III,IV), Fe(II,III) and Al, and the ligands OH^-, F^-, Cl^-, CO_3^{2-}, HCO_3^-, SO_4^{2-} and $Si(OH)_4(aq)$.

The fission product Sr-90 with 28.79 ± 0.06 years half-life contributes in dose-relevant quantities to the inventory of radioactive waste. Hence, Sr is of double interest, as dose-relevant radionuclide and as ground and pore water component.

Meanwhile, new experimental data have been reported, as well as new reviews of the hydrolysis of metal ions (Brown & Ekberg 2016) and of the solubility of alkaline earth sulphate and carbonate phases (Brown et al. 2019), have been published, which are considered in the present update of chemical thermodynamic data for ground and pore water models.

The thermodynamic data included in the PSI TDB 2020 have been taken from

- CODATA key values (Cox et al. 1989)
- the USGS review of data for major water-mineral reactions (Nordstrom et al. 1990
- the recent review of the hydrolysis of metal ions (Brown & Ekberg 2016
- the recent review of the solubility of alkaline earth sulphate and carbonate phases (Brown et al. 2019)
- and own reviews of experimental data

NEA (see, e.g., Grenthe et al. 1992) used the specific ion interaction theory (SIT) for making ionic strength corrections to the experimental data, an approach which is also adopted for TDB 2020 (as has been for all its predecessors).

In many cases, the ion interaction coefficients for species under consideration here were not available. We approximated these with the estimation method described in Section 1.5.3, which draws on a statistical analysis of published SIT ion interaction coefficients, and which allows the estimation of missing coefficients for the interaction of cations with Cl^- and ClO_4^-, and for the interaction of anions with Na^+, from the charge of the cations or anions of interest.

4.0 References

Brown, P.L. & Ekberg, C. (2016): Hydrolysis of Metal Ions. Wiley-VCH Verlag GmbH & Co. KGaA, Weinheim, Germany, 917 pp.

Brown, P.L., Ekberg, C. & Matyskin, A.V. (2019): On the solubility of radium and other alkaline earth sulfate and carbonate phases at elevated temperature. Geochim. Cosmochim. Acta, 255, 88-104.

Cox, J.D., Wagman, D.D. & Medvedev, V.A. (1989): CODATA Key Values for Thermodynamics. Hemisphere Publishing, New York, 271 pp.

Grenthe, I., Fuger, J., Konings, R.J.M., Lemire, R.J., Muller, A.B., Nguyen-Trung, C. & Wanner, H. (1992): Chemical Thermodynamics of Uranium. Chemical Thermodynamics, Vol. 1. North-Holland, Amsterdam, 715 pp.

Nordstrom, D.K., Plummer, L.N., Langmuir, D., Busenberg, E., May, H.M., Jones, B.F. & Parkhurst, D.L. (1990): Revised Chemical Equilibrium Data for Major Water-Mineral Reactions and Their Limitations. In: Melchior, D.C., and Bassett, R.L. (eds.): Chemical Modeling of Aqueous Systems II. Washington, D.C., American Chemical Society, ACS Symposium Series 416, p. 398-413.

Pearson, F.J., Jr. & Berner, U. (1991): Nagra Thermochemical Data Base I. Core Data. Nagra Technical Report NTB 91-17.

Pearson, F.J., Jr., Berner, U. & Hummel W. (1992): Nagra Thermochemical Data Base II. Supplemental Data 05/92. Nagra Technical Report NTB 91-18.

4.1 Magnesium

4.1.1 Elemental magnesium

Magnesium metal and gas are not relevant under environmental conditions. Hence, the gas phase Mgg is not included in the data base. The absolute entropy and heat capacity of Mg(cr) are included as they are used for the calculation of certain thermodynamic reaction properties.

The selected values for Mg(cr) are taken from CODATA (Cox et al. 1989):

$S_m°$(Mg, cr, 298.15 K) = (32.670 ± 0.100) J · K^{-1} · mol^{-1}

$C_{p,m}°$(Mg, cr, 298.15 K) = (24.869 ± 0.020) J · K^{-1} · mol^{-1}

4.1.2 Magnesium(II) aqua ion

Magnesium(II) exists as the Mg^{2+} cation in aqueous solutions. The selected thermodynamic values for Mg^{2+} are taken from CODATA (Cox et al. 1989):

$\Delta_f G_m°(Mg^{2+}, 298.15\ K) = -(455.375 \pm 1.335)$ kJ · mol^{-1}

$\Delta_f H_m°(Mg^{2+}, 298.15\ K) = -(467.000 \pm 0.600)$ kJ · mol^{-1}

$S_m°(Mg^{2+}, 298.15\ K) = -(137.000 \pm 4.000)$ J · K^{-1} · mol^{-1}

Using the selected CODATA $\Delta_f G_m°(Mg^{2+}, 298.15\ K)$, the redox equilibrium

$$Mg(cr) \rightleftharpoons Mg^{2+} + 2\ e^-$$

is calculated as

$\log_{10} K°(298.15\ K) = 79.78 \pm 0.23$

Since this review does not consider the formation of magnesium chloride complexes, $\varepsilon(Mg^{2+}, Cl^-)$ is taken as selected by NEA (Grenthe et al. 1992, Lemire et al. 2013):

$\varepsilon(Mg^{2+}, Cl^-) = (0.19 \pm 0.02)$ kg · mol^{-1}

4.1.3 Magnesium(II) (hydr)oxide ompounds and complexes

4.1.3.1 Magnesium(II) hydroxide complexes

Nordstrom et al. (1990) selected a $\log_{10}{}^{*}\beta_1^\circ$ value from Baes & Mesmer (1976) for the complex

$$Mg^{2+} + H_2O(l) \rightleftharpoons MgOH^{+} + H^{+}$$

$$\log_{10}{}^{*}\beta_1^\circ\ (298.15\ K) = -11.44$$

Brown & Ekberg (2016) state that only a single monomeric hydrolysis species, $MgOH^{+}$, is known to form. They scrutinised all available hydrolysis data and report that the data have a linear relationship with the reciprocal temperature in the range 0 – 350 °C. They obtained

$$Mg^{2+} + H_2O(l) \rightleftharpoons MgOH^{+} + H^{+}$$

$$\log_{10}{}^{*}\beta_1^\circ\ (298.15\ K) = -11.70 \pm 0.04$$

$$\Delta_r H_m^\circ(298.15\ K) = (70.8 \pm 0.7)\ kJ \cdot mol^{-1}$$

$$\Delta_r C_{p,m}^\circ(298.15\ K) = 0\ J \cdot K^{-1} \cdot mol^{-1}$$

These values have been included in TDB 2020, as well as the estimate

$$\varepsilon(MgOH^{+}, Cl^{-}) = (0.05 \pm 0.10)\ kg \cdot mol^{-1}$$

4.1.3.2 Magnesium(II) (hydr)oxide compounds

Nordstrom et al. (1990) selected thermodynamic data from Baes & Mesmer (1976) for brucite

$$Mg(OH)_2(cr) + 2\ H^{+} \rightleftharpoons Mg^{2+} + 2\ H_2O(l)$$

$$\log_{10}{}^{*}K_{s0}^\circ\ (298.15\ K) = 16.84$$

$$\Delta_r H_m^\circ(298.15\ K) = -27.1\ kcal \cdot mol^{-1} = -113.4\ kJ \cdot mol^{-1}$$

Brown & Ekberg (2016) report that the solubility of brucite, $Mg(OH)_2(s)$, has been measured in a number of studies at temperatures ranging from 10 to 350 °C, and estimates of the constant at zero ionic strength across this temperature range have been obtained. Brown & Ekberg (2016) show that the values join smoothly across the whole temperature range, and the solubility constant has been found to be a linear function of the reciprocal temperature. They obtained

$Mg(OH)_2(cr) + 2\ H^+ \rightleftharpoons Mg^{2+} + 2\ H_2O(l)$

$\log_{10}{}^*K_{s0}°$ (298.15 K) = 17.11 ± 0.04

$\Delta_r H_m°$(298.15 K) = -(111.5 ± 0.7) kJ · mol^{-1}

$\Delta_r C_{p,m}°$(298.15 K) = 0 J · K^{-1} · mol^{-1}

These values have been included in TDB 2020.

4.1.4 Magnesium(II) fluoride compounds and complexes

4.1.4.1 Magnesium(II) fluoride complexes

Nordstrom et al. (1990) selected a $\log_{10K}\beta_1°$ value reported by Sillén et al. (1964) and a $\Delta_r H_m°$ value reported by Smith & Martell (1976) for the complex

$Mg^{2+} + F^- \rightleftharpoons MgF^+$

$\log_{10}K_1°$ (298.15 K) = 1.82

$\Delta_r H_m°$(298.15 K) = 3.2 kcal · mol^{-1} = 13.4 kJ · mol^{-1}

Since the publication of these data compilations, several new studies have been published concerning the MgF^+ complex formation, covering the temperature range 2 – 200 °C. Data obtained in 1 M $NaClO_4$ (Tanner et al. 1968, Bond & Hefter 1971), 1 M NaCl (Elgquist 1970, Richardson & Holland 1979, Bilal & Müller 1992) and 1 M $NaNO_3$ (Gamsjäger et al. 1969, Majer & Štulĭk 1982) join relatively smoothly across the whole temperature range (Fig. 4.1-1). An unweighted regression of all data resulted in $\log_{10}K_1$ (298.15 K, 1 M) = 1.33 ± 0.05

$\Delta_r H_m$ (298.15 K, 1 M) = (10.5 ± 1.0) kJ · mol^{-1}

$\Delta_r C_{p,m}$ (298.15 K, 1M) = -(30.5 ± 7.3) J · K^{-1} · mol^{-1}

Note that the data reported for 25 °C, and in 1 M $NaClO_4$ (Tanner et al. 1968, Bond & Hefter 1971), 1 M NaCl (Elgquist 1970, Bilal & Müller 1992) and 1 M $NaNO_3$ (Gamsjäger et al. 1969, Majer & Štulĭk 1982) are in the range $\log_{10}K_1$ (298.15 K, 1 M) = 1.27 – 1.38, with an unweighted average of $\log_{10}K_1$ (298.15 K, 1 M) = 1.32 ± 0.04.

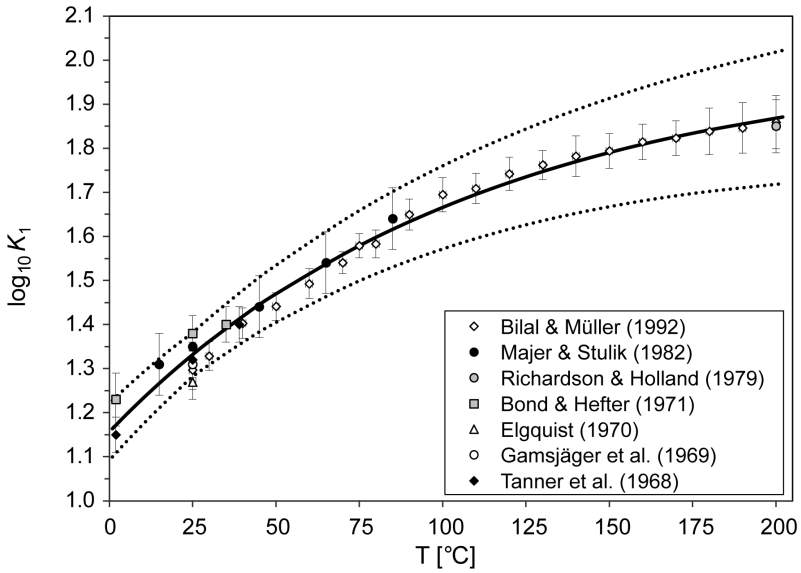

Fig. 4.1-1: The equilibrium constant $\log_{10}K_1$ for $Mg^{2+} + F^- \rightleftharpoons MgF^+$ as a function of temperature in the range 2 – 200 °C at 1 M ionic strength

Solid line: unweighted regression of all data. Dotted lines: lower and upper limits using $\log_{10}K$ (298.15 K) = 1.33 ± 0.05, $\Delta_r H_m$(298.15 K) = (10.5 ± 1.0) kJ · mol^{-1} and $\Delta_r C_{p,m}°$(298.15 K) = -(30.5 ± 7.3) J · K^{-1} · mol^{-1} and extrapolated to lower and higher temperatures.

No attempts have been made to extrapolate $\Delta_r H_m$ and $\Delta_r C_{p,m}$ to zero ionic strength, and they are included in TDB 2020 as an approximation of $\Delta_r H_m°$ (298.15 K) and $\Delta_r C_{p,m}°$ (298.15 K).

Using the data of Bilal & Müller (1992) and Elgquist (1970) in NaCl for an SIT analysis this review obtained (Fig. 4.1.2):

$$\log_{10}K_1° \text{ (298.15 K)} = 1.88 \pm 0.05$$

$$\Delta\varepsilon(\text{NaCl}) = -(0.23 \pm 0.06)$$

Considering $\varepsilon(Mg^{2+}, Cl^-)$ = (0.19 ± 0.02) kg · mol^{-1} and $\varepsilon(Na^+, F^-)$ = (0.02 ± 0.02) kg · mol^{-1} (Grenthe et al. 1992) this review derives from the experimental Δε value

$$\varepsilon(MgF^+, Cl^-) = -(0.02 \pm 0.06) \text{ kg} \cdot \text{mol}^{-1}$$

This value is included in TDB 2020, together with $\log_{10}K_1°$ obtained from the SIT analysis.

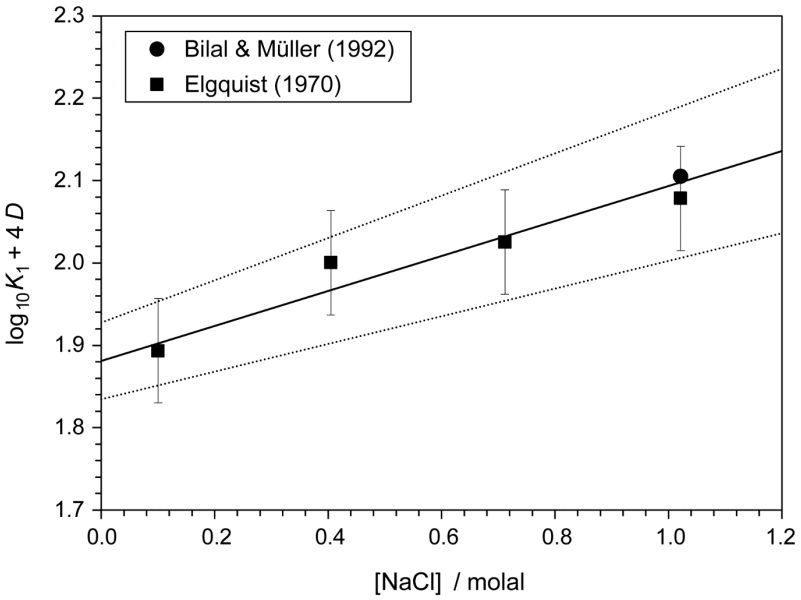

Fig. 4.1.2: Dependence of the equilibrium $Mg^{2+} + F^- \rightleftharpoons MgF^+$ on ionic strength in NaCl using the data of Bilal & Müller (1992) and Elgquist (1970)

The solid line is obtained using the derived SIT interaction coefficient and stability constant at zero ionic strength. Dotted lines represent the 95% uncertainty range extrapolated from I = 0 to higher NaCl concentrations.

4.1.4.2 Magnesium(II) fluoride compounds

MgF_2(cr) is found in nature as the rare mineral sellaite. For the solubility product

$$MgF_2(cr) \rightleftharpoons Mg^{2+} + 2\ F^-$$

$\log_{10}K_{s0}°$ (298.15 K) = -8.18 has been selected by Smith & Martell (1976). Later, this value has been revised to $\log_{10}K_{s0}°$ (298.15 K) = -8.13 ± 0.06 (Smith & Martell 1989). The data sources and the selection procedure of Smith & Martell (1976, 1989) remain unclear.

However, these values indicate that the solubility of sellaite, MgF_2(s), is significantly higher than that of fluorite, CaF_2(cr), $\log_{10}K_{s0}°$ (298.15 K) = -10.46 ± 0.09 (see Section 4.2.4.2). This is in accord with the observation that the concentration of dissolved fluoride, F^-, in environmental systems is usually governed by the precipitation of the ubiquitous mineral fluorite. Hence, sellaite, MgF_2(cr), is only formed under very special chemical conditions and does not play any role in common environmental systems.

No solubility data for MgF_2(cr) are included in TDB 2020.

4.1.5 Magnesium(II) chloride compounds and complexes

4.1.5.1 Magnesium(II) chloride complexes

This report does not consider the formation of weak magnesium chloride complexes but includes possible ion interactions in the SIT interaction coefficient $\varepsilon(Mg^{2+}, Cl^-)$ (see below).

4.1.5.2 Magnesium(II) chloride compounds

$MgCl_2(s)$ is a highly soluble salt with a solubility of 542 g/L at 20 °C (gestis.itrust.de). Its isopiestic properties have been measured up to 5 mol · kg_{H2O}^{-1} (Robinson & Stokes 1959). Hence, no solubility data, but the specific ion interaction coefficient selected by NEA (Grenthe et al. 1992, Lemire et al. 2013) is adopted for TDB 2020:

$$\varepsilon(Mg^{2+}, Cl^-) = (0.19 \pm 0.02)\ kg \cdot mol^{-1}$$

4.1.6 Magnesium(II) carbonate compounds and complexes

4.1.6.1 Magnesium(II) carbonate complexes

Nordstrom et al. (1990) selected thermodynamic data based on the $\log_{10}K_1°$ values for 10 to 90 °C reported by Siebert & Hostetler (1977b) for the complex

$$Mg^{2+} + CO_3^{2-} \rightleftharpoons MgCO_3(aq)$$

$$\log_{10}K_1° (298.15\ K) = 2.98$$

$$\Delta_r H_m°(298.15\ K) = 2.713\ kcal \cdot mol^{-1} = 11.35\ kJ \cdot mol^{-1}$$

$$\log_{10}K_1° (T) = 0.9910 - 0.0066 \cdot T$$

Note that the "simple" linear temperature function implies that $\Delta_r C_{p,m}°$ is a function of temperature.

In addition, Nordstrom et al. (1990) selected a $\log_{10}K°$ and a $\Delta_r H_m°$ value reported by Siebert & Hostetler (1977a) for the complex

$$Mg^{2+} + HCO_3^- \rightleftharpoons MgHCO_3^+$$

$$\log_{10}K° (298.15\ K) = 1.07$$

$$\Delta_r H_m°(298.15\ K) = 0.79\ kcal \cdot mol^{-1} = 3.31\ kJ \cdot mol^{-1}$$

$$\log_{10}K° (T) = -59.215 + 2537.455 / T + 20.92298 \cdot \log_{10}(T)$$

Note that the temperature function yields

$\Delta_r H_m°(298.15\ K) = 3.29\ kJ \cdot mol^{-1}$

$\Delta_r C_{p,m}°(298.15\ K) = 174.0\ J \cdot K^{-1} \cdot mol^{-1}$

The stability data of Siebert & Hostetler (1977b, 1977a) show a slight and strong curvature, respectively, when plotted versus the reciprocal absolute temperature. Hence this review fitted both data sets assuming $\Delta_r C_{p,m}°$ = constant and obtained (Figs. 4.1-3 and 4.1-4):

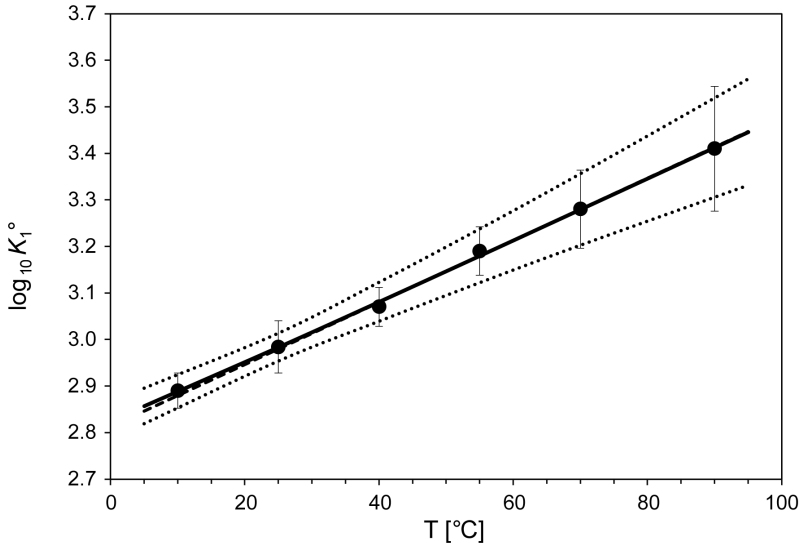

Fig. 4.1-3: The equilibrium constant log10K1° for Mg2+ + CO32- ⇌ MgCO3(aq) as a function of temperature in the range 10 – 90 °C as reported by Siebert & Hostetler (1977b)

Solid line: unweighted regression. Dotted lines: lower and upper limits using $\log_{10} K_1°$ (298.15 K) = 2.98 ± 0.03, $\Delta_r H_m°$(298.15 K) = (11.0 ± 1.1) kJ · mol^{-1} and $\Delta_r C_{p,m}°$(298.15 K) = (90 ± 44) J · K^{-1} · mol^{-1} and extrapolated to lower and higher temperatures. Dashed line: temperature function selected by Nordstrom et al. (1990), shown for comparison.

$Mg^{2+} + CO_3^{2-} \rightleftharpoons MgCO_3(aq)$

$\log_{10} K_1°$ (298.15 K) = 2.98 ± 0.03

$\Delta_r H_m°(298.15\ K) = (11.0 \pm 1.1)\ kJ \cdot mol^{-1}$

$\Delta_r C_{p,m}°(298.15\ K) = (90 \pm 44)\ J \cdot K^{-1} \cdot mol^{-1}$

$Mg^{2+} + HCO_3^- \rightleftharpoons MgHCO_3^+$

$\log_{10} K°$ (298.15 K) = 1.07 ± 0.03

$\Delta_r H_m°(298.15\ K) = (3.25 \pm 0.22)\ kJ \cdot mol^{-1}$

$\Delta C_{p,m}°(298.15\ K) = (175.7 \pm 8.8)\ J \cdot K^{-1} \cdot mol^{-1}$

Note that in both cases the stability constant and enthalpy values are in perfect and very good agreement, respectively, with the values selected by Nordstrom et al. (1990). In the case of $MgHCO_3^+$ also $\Delta_r C_{p,m}°$ is in very good agreement with the value selected by Nordstrom et al. (1990). The $\Delta_r C_{p,m}°$ value of $MgCO_3(aq)$ has a large uncertainty but is not zero.

These values are included in TDB 2020, as well as the estimates

$$\varepsilon(MgHCO_3^+, Cl^-) = (0.05 \pm 0.10)\ kg \cdot mol^{-1}$$

$$\varepsilon(MgCO_3(aq), NaCl) = (0.0 \pm 0.1)\ kg \cdot mol^{-1}$$

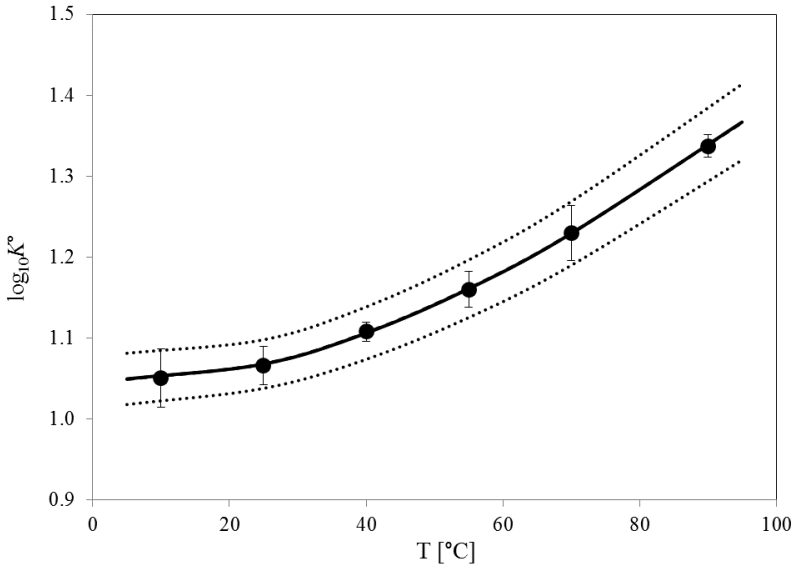

Fig. 4.1.4: The equilibrium constant $\log_{10}K°$ for $Mg^{2+} + HCO_3^- \rightleftharpoons MgHCO_3^+$ as a function of temperature in the range 10 – 90 °C as reported by Siebert & Hostetler (1977a)

Solid line: unweighted regression. Dotted lines: lower and upper limits using $\log_{10}K°$ (298.15 K) = 1.07 ± 0.03, $\Delta_r H_m°$(298.15 K) = (3.25 ± 0.22) kJ · mol^{-1} and $\Delta C_{p,m}°$(298.15 K) = (175.7 ± 8.8) J · K^{-1} · mol^{-1} and extrapolated to lower and higher temperatures. Dashed line (hardly visible below the solid line): temperature function selected by Nordstrom et al. (1990), shown for comparison.

4.1.6.2 Magnesium(II) carbonate compounds

Nordstrom et al. (1990) did not select any thermodynamic data for magnesite, $MgCO_3$(cr).

Hummel et al. (2002) discussed thermodynamic data reported by Königsberger et al. (1999) for synthetic and natural magnesite derived from solubility measurements at 25 and 50 °C:

$MgCO_3(s) \rightleftharpoons Ca^{2+} + CO_3^{2-}$

$\log_{10}K_{s0}°$ (natural magnesite, 298.15 K) = -8.915

$\Delta_r H_m°$(298.15 K) = -24.09 kJ · mol^{-1}

$\log_{10}K_{s0}°$ (synthetic magnesite, 298.15 K) = -8.288

$\Delta_r H_m°$(298.15 K) = -27.67 kJ · mol^{-1}

As Königsberger et al. (1999) did not comment on the discrepancy between both data sets, Hummel et al. (2002) included the data for synthetic magnesite in TDB 01/01 with the argument that a comparison with the solubility product for calcite (see Section 6.6.2) "reveals that natural magnesite is less soluble and synthetic magnesite more soluble than calcite. According to Fajan's rule, magnesite is expected to be more soluble than calcite … thus, the recommended value for synthetic magnesite is consistent with this empirical geochemical rule, quite in contrast to the rejected value for natural magnesite."

Brown et al. (2019) in their recent review of the solubility of alkaline earth sulphate and carbonate phases at elevated temperature recommend for the solubility of magnesite, $MgCO_3$(s)

$\log_{10}K_{s0}°$ (298.15 K) = -7.66 ± 0.34

$\Delta_r H_m°$(298.15 K) = -(35.9 ± 1.9) kJ · mol^{-1}

$\Delta_r C_{p,m}°$(298.15 K) = -(387.7 ± 9.6) J · K^{-1} · mol^{-1}

mainly determined from the data reported by Bénézeth et al. (2011) and valid for the temperature range 25 – 200 °C.

These values have been included in TDB 2020.

Note that the uncertainties in all thermodynamic parameters for magnesite are significantly larger than for any other alkaline earth carbonate phase (see Sections 4.2.6.2, 4.3.6.2 and 4.4.6.2), but even considering these large uncertainties, according to these data magnesite is significantly more soluble than calcite, as expected. The discrepancy to the data reported by Königsberger et al. (1999) remains unclear.

4.1.7 Magnesium(II) sulphate compounds and complexes

4.1.7.1 Magnesium(II) sulphate complexes

Nordstrom et al. (1990) based their selection of thermodynamic data on the values reported by Nair & Nancollas (1958), valid for the temperature range 0 – 45 °C, for the complex

$$Mg^{2+} + SO_4^{2-} \rightleftharpoons MgSO_4(aq)$$

$$\log_{10}\beta_1^\circ\,(298.15\ K) = 2.25 \pm 0.05$$

$$\Delta_r H_m^\circ(298.15\ K) = (20.3 \pm 2.0)\ kJ \cdot mol^{-1}$$

$$\Delta_r C_{p,m}^\circ(298.15\ K) = 0$$

The uncertainties have been estimated by this review.

These values have been included in TDB 2020, as well as the estimate

$$\varepsilon(MgSO_4(aq), NaCl) = (0.0 \pm 0.1)\ kg \cdot mol^{-1}$$

Note that Nordstrom et al. (1990) erroneously selected the value $\log_{10}\beta_1^\circ(298.15\ K) = 2.37$ for $MgSO_4(aq)$, given by Nair & Nancollas (1958) for $ZnSO_4(aq)$. In addition, the value $\Delta_r H_m^\circ(298.15\ K) = 4.55\ kcal \cdot mol^{-1}$, selected by Nordstrom et al. (1990) for $MgSO_4(aq)$ is somewhere in between the values $\Delta_r H_m^\circ(298.15\ K) = 4.84\ kcal \cdot mol^{-1}$ and $\Delta_r H_m^\circ(298.15\ K) = 4.01\ kcal \cdot mol^{-1}$, given by Nair & Nancollas (1958) for $MgSO_4(aq)$ and $ZnSO_4(aq)$, respectively.

4.1.7.2 Magnesium(II) sulphate compounds

$MgSO_4(s)$ is a highly soluble salt with a solubility of 300 g/L at 20 °C (gestis.itrust.de), whereas the heptahydrate, $MgSO_4 \cdot 7H_2O$, is even three times more soluble than the anhydrous form. Hence, no solubility data are included in TDB 2020 for these highly soluble salts.

4.1.8 Magnesium(II) phosphate compounds and complexes

4.1.8.1 Magnesium(II) phosphate complexes

The equilibrium constants of magnesium phosphate complexes have been determined by various methods in a considerable number of studies, published over the course of half a century by Greenwald et al. (1940), Tabor & Hastings (1943), Clarke et al. (1954), Smith & Alberty (1956), Taylor et al. (1963), Childs (1970), Frey & Stuehr (1972), Havel & Högfeldt (1974), Verbeeck et al. (1984), Ciavatta et al. (1994) and Saha et al. (1996) (see Tab. 4.1-1).

Greenwald et al. (1940) were the first to recognise that the pH of phosphate containing solutions was lowered by the addition of Mg^{2+} ions and concluded, from measurements with glass as well as with hydrogen gas electrodes in various NaCl and KCl media, that $MgHPO_4(aq)$ is the main

complex in solution. They report in their Tab. VI the value $\log_{10}K = 1.65 \pm 0.16$ (1σ) in 0.2 M KCl at 25 °C for the equilibrium $Mg^{2+} + HPO_4^{2-} \rightleftharpoons MgHPO_4(aq)$. This review obtained $\log_{10}K° = 2.72 \pm 0.32$ (2σ) by extrapolating the above value to zero ionic strength using SIT with $\varepsilon(Mg^{2+}, Cl^-) = (0.19 \pm 0.02)$, $\varepsilon(K^+, HPO_4^{2-}) = -(0.10 \pm 0.06)$ and the estimate $\varepsilon(MgHPO_4(aq), KCl) = (0.0 \pm 0.1)$.

Tabor & Hastings (1943) determined the stability constant of $MgHPO_4(aq)$ by conductivity measurements at 38 °C. For an ionic strength of 0.16 M NaCl they report $\log_{10}K = 1.62$, without an uncertainty estimate. This review obtained $\log_{10}K° = 2.65 \pm 0.30$ by extrapolating the above value to zero ionic strength using SIT with $\varepsilon(Mg^{2+}, Cl^-) = (0.19 \pm 0.02)$, $\varepsilon(Na^+, HPO_4^{2-}) = -(0.15 \pm 0.06)$ and the estimate $\varepsilon(MgHPO_4(aq), NaCl) = (0.0 \pm 0.1)$. The uncertainty has been estimated by this review considering the experimental data shown in Fig. 2 of Tabor & Hastings (1943) and their discussion of experimental and calculational procedures.

Clarke et al. (1954) used potentiometric measurements with a glass electrode to determine the stability constant of $MgHPO_4(aq)$ in KH_2PO_4 – $KNaHPO_4$ – $MgCl_2$ solutions of low concentrations (I = 0.01 – 0.08 M) in the temperature range 10 to 50 °C. Clarke et al. (1954) extrapolated their data by an SIT-like procedure to zero ionic strength and reported results for two sets of experiments. The values from these two sets differ by less than 0.03 $\log_{10}$ units, so this review retained the unweighted averages, $\log_{10}K°(10\ °C) = 2.61$, $\log_{10}K°(20\ °C) = 2.67$, $\log_{10}K°(30\ °C) = 2.75$, $\log_{10}K°(40\ °C) = 2.83$ and $\log_{10}K°(50\ °C) = 2.92$ and estimated their uncertainties as ± 0.2.

Smith & Alberty (1956) calculated from measurements with a glass electrode at 25 and 0 °C in 0.2 M Pr_4NCl (tetrapropylammonium chloride, $(CH_3CH_2CH_2)_4NCl$) the values $K(25\ °C) = 76 \pm 2$ (corresponding to $\log_{10}K(25\ °C) = 1.881 \pm 0.01$) and $K(0\ °C) = 32 \pm 2$ (corresponding to $\log_{10}K(0\ °C) = 1.505 \pm 0.03$) for the equilibrium $Mg^{2+} + HPO_4^{2-} \rightleftharpoons MgHPO_4(aq)$. This review retained these values and obtained $\log_{10}K°(25\ °C) = 2.89 \pm 0.20$ and $\log_{10}K°(0\ °C) = 2.48 \pm 0.20$ by extrapolation to zero ionic strength using SIT with the estimate $\Delta\varepsilon(Pr_4NCl) \approx -0.4$ in analogy with $\Delta\varepsilon(Et_4NI) = -(0.41 \pm 0.15)$ obtained for $Na^+ + HPO_4^{2-} \rightleftharpoons NaHPO_4^-$ (see Section 2.2.1). The uncertainties have been estimated by this review.

Taylor et al. (1963) measured the solubility of $MgHPO_4 \cdot 3H_2O$ (newberyite) at 25 °C in the pH range 5.2 – 7.8 in dilute solutions (I = 0.01 – 0.06 M). They extrapolated their data to zero ionic strength using the extended Debye-Hückel equation and fitted a dissociation constant $K°$ (25 °C) = 0.00124 for the complex $MgHPO_4(aq)$ in order to obtain a pH independent solubility product for $MgHPO_4 \cdot 3H_2O$. This review calculated $\log_{10}K°(25\ °C) = 2.91 \pm 0.30$ for the equilibrium $Mg^{2+} + HPO_4^{2-} \rightleftharpoons MgHPO_4(aq)$, where the uncertainty has been estimated considering the experimental data of Taylor et al. (1963) and their discussion of experimental and calculational procedures.

Childs (1970) report from a potentiometric study with a glass electrode at 37 °C in 0.15 M KNO_3 $\log_{10}K = 0.7 \pm 0.3$ for the equilibrium $Mg^{2+} + H_2PO_4^- \rightleftharpoons MgH_2PO_4^+$, $\log_{10}K = 1.8 \pm 0.1$ for the equilibrium $Mg^{2+} + HPO_4^{2-} \rightleftharpoons MgHPO_4(aq)$ and $\log_{10}K = 3.4 \pm 0.1$ for the equilibrium $Mg^{2+} + PO_4^{3-} \rightleftharpoons MgPO_4^-$. This review obtained $\log_{10}K° = 1.21 \pm 0.60$ (2σ), $\log_{10}K° = 2.81 \pm 0.20$ (2σ), $\log_{10}K° = 4.91 \pm 0.20$ (2σ), respectively, by extrapolating the above values to zero ionic strength using SIT with $\varepsilon(Mg^{2+}, NO_3^-) = (0.17 \pm 0.02)$, $\varepsilon(K^+, H_2PO_4^-) = -(0.14 \pm 0.06)$, $\varepsilon(K^+, HPO_4^{2-}) = -(0.10 \pm 0.06)$, $\varepsilon(K^+, PO_4^{3-}) = -(0.09 \pm 0.02)$ and the estimates $\varepsilon(MgH_2PO_4^+, NO_3^-) \approx \varepsilon(MgH_2PO_4^+, Cl^-) = (0.05 \pm 0.10)$, $\varepsilon(CaHPO_4(aq), KNO_3) = (0.0 \pm 0.1)$ and $\varepsilon(K^+, MgPO_4^-) \approx \varepsilon(Na^+, MgPO_4^-) = (0.05 \pm 0.10)$.

Frey & Stuehr (1972) did potentiometric titrations with a glass electrode at 15 °C in 0.1 M KNO_3 and report K(15 °C) = 60 (corresponding to $\log_{10}K$(15 °C) = 1.78), without error estimate, for the equilibrium $Mg^{2+} + HPO_4^{2-} \rightleftharpoons MgHPO_4(aq)$. This review obtained $\log_{10}K°$(15 °C) = 2.63 ± 0.60 by extrapolating the above value to zero ionic strength using SIT with $\varepsilon(Mg^{2+}, NO_3^-) = (0.17 \pm 0.02)$, $\varepsilon(K^+, HPO_4^{2-}) = -(0.10 \pm 0.06)$ and the estimate $\varepsilon(MgH_2PO_4^+, NO_3^-) \approx \varepsilon(MgH_2PO_4^+, Cl^-) = (0.05 \pm 0.10)$.

Havel & Högfeldt (1974) studied the formation between Mg^{2+} and HPO_4^{2-} in 3 M (Na,Mg)ClO_4 at 25 °C using glass and hydrogen electrodes in a cell with liquid junction. The experiments were carried out as emf titrations in the pH range 1 – 7. They report $\log_{10}K = 1.421 \pm 0.029$ for the equilibrium $Mg^{2+} + HPO_4^{2-} \rightleftharpoons MgHPO_4(aq)$ and $\log_{10}K = 6.438 \pm 0.048$ for the equilibrium $Mg^{2+} + H^+ + HPO_4^{2-} \rightleftharpoons MgH_2PO_4^+$. Combining the latter value with $\log_{10}K = 6.279 \pm 0.015$ for the equilibrium $H^+ + HPO_4^{2-} \rightleftharpoons H_2PO_4^-$ as determined by Havel & Högfeldt (1974) results in $\log_{10}K = 0.159 \pm 0.050$ for the equilibrium $Mg^{2+} + H_2PO_4^- \rightleftharpoons MgH_2PO_4^+$. Using SIT with $\varepsilon(Mg^{2+}, ClO_4^-) = (0.33 \pm 0.03)$, $\varepsilon(Na^+, H_2PO_4^-) = -(0.08 \pm 0.04)$, $\varepsilon(Na^+, HPO_4^{2-}) = -(0.15 \pm 0.06)$ and the estimates $\varepsilon(MgH_2PO_4^+, ClO_4^-) = (0.2 \pm 0.1)$ and $\varepsilon(MgHPO_4(aq), NaClO_4) = (0.0 \pm 0.1)$ this review obtained $\log_{10}K° = 2.72 \pm 0.42$ for the equilibrium $Mg^{2+} + HPO_4^{2-} \rightleftharpoons MgHPO_4(aq)$ and $\log_{10}K° = 0.92 \pm 0.43$ for $Mg^{2+} + H_2PO_4^- \rightleftharpoons MgH_2PO_4^+$. Note that the uncertainties are due to the uncertainties of the SIT coefficients and the large extrapolation from 3.5 m to zero.

Verbeeck et al. (1984) measured the solubility of $MgHPO_4 \cdot 3H_2O$ (newberyite) at 25 °C in the pH range 5.0 – 7.3 in dilute solutions (I = 0.01 – 0.07 M). They extrapolated their data to zero ionic strength using the Davies equation and fitted the association constants $K°$(25 °C) = 712 ± 23 for the complex $MgHPO_4(aq)$ and $K°$(25 °C) = 18.9 ± 1.7 for the complex $MgH_2PO_4^+$ in order to obtain a pH independent solubility product for $MgHPO_4 \cdot 3H_2O$. This review calculated $\log_{10}K°$(25 °C) = 2.85 ± 0.30 for the equilibrium $Mg^{2+} + HPO_4^{2-} \rightleftharpoons MgHPO_4(aq)$ and $\log_{10}K°$(25 °C) = 1.28 ± 0.30 for the equilibrium $Mg^{2+} + HPO_4^{2-} \rightleftharpoons MgHPO_4(aq)$, where the uncertainties have been estimated considering the experimental data of Verbeeck et al. (1984) and their discussion of experimental and calculational procedures.

Ciavatta et al. (1994) measured magnesium phosphate equilibria at 25 °C in 3 M $NaClO_4$ with a glass electrode in cells without liquid junction. They report $\log_{10}K = 0.16 \pm 0.05$ for the equilibrium $Mg^{2+} + H_2PO_4^- \rightleftharpoons MgH_2PO_4^+$ and $\log_{10}K = -3.17 \pm 0.03$ for the equilibrium $Mg^{2+} + 2\ H_2PO_4^- \rightleftharpoons MgHPO_4(aq) + H_3PO_4(aq)$. Combining the latter value with $\log_{10}K = 6.279 \pm 0.015$ for the equilibrium $H^+ + HPO_4^{2-} \rightleftharpoons H_2PO_4^-$ and $\log_{10}K = 8.158 \pm 0.035$ for the equilibrium $2\ H^+ + HPO_4^{2-} \rightleftharpoons H_3PO_4(aq)$, determined by Havel & Högfeldt (1974) under the same conditions, i.e., at 25 °C in 3 M $NaClO_4$, this review calculated $\log_{10}K = 1.23 \pm 0.05$ for the equilibrium $Mg^{2+} + HPO_4^{2-} \rightleftharpoons MgHPO_4(aq)$. Using SIT with the same interaction coefficients as above this review obtained $\log_{10}K° = 2.53 \pm 0.42$ for the equilibrium $Mg^{2+} + HPO_4^{2-} \rightleftharpoons MgHPO_4(aq)$ and $\log_{10}K° = 0.92 \pm 0.42$ for $Mg^{2+} + H_2PO_4^- \rightleftharpoons MgH_2PO_4^+$. Note that Ciavatta et al. (1994) report the values $\log_{10}K° = 2.85 \pm 0.2$ and 0.61 ± 0.2, respectively, from their SIT extrapolation probably using slightly different, but not reported, SIT interaction coefficients.

Saha et al. (1996) determined the stability constants of the 1:1 complexes formed between a series of divalent metal cations and hydrogen phosphate by potentiometric pH titration in aqueous solution at 25 °C in 0.1 M $NaNO_3$. For Mg^{2+} they report $\log_{10}K = 1.83 \pm 0.03$. Using SIT with $\varepsilon(Mg^{2+}, NO_3^-) = (0.17 \pm 0.01)$, $\varepsilon(Na^+, HPO_4^{2-}) = -(0.15 \pm 0.06)$ and the estimate $\varepsilon(MgHPO_4(aq), NaNO_3) = (0.0 \pm 0.1)$ this review obtained $\log_{10}K° = 2.70 \pm 0.20$ for the equilibrium $Mg^{2+} + HPO_4^{2-} \rightleftharpoons MgHPO_4(aq)$, with an uncertainty assigned by this review.

The accepted data of Tab. 4.1-1 have been used for a weighted linear regression of the $\log_{10}K°$ values for the equilibrium $Mg^{2+} + HPO_4^{2-} \rightleftharpoons MgHPO_4(aq)$ versus the reciprocal of absolute temperature (Fig. 4.1-5), and this review obtained:

$Mg^{2+} + HPO_4^{2-} \rightleftharpoons MgHPO_4(aq)$

$\log_{10}K°$ (298.15 K) = 2.73 ± 0.06

$\Delta_r H_m°$(298.15 K) = (13.3 ± 7.4) kJ · mol^{-1}

$\Delta_r C_{p,m}°$(298.15 K) = 0

The accepted data of Tab. 4.1-1 have been used for a weighted linear regression of the $\log_{10}K°$ values for the equilibrium $Mg^{2+} + HPO_4^{2-} \rightleftharpoons MgHPO_4(aq)$ versus the reciprocal of absolute temperature (Fig. 4.1-5), and this review obtained:

Tab. 4.1-1: Reported and accepted magnesium phosphate complexation data

Temp. [°C]	Medium	$\log_{10}K$ reported [a]	I_m	$\log_{10}K_m$	Δε	$\log_{10}K°$ accepted [b]	Reference
$Mg^{2+} + PO_4^{3-} \rightleftharpoons MgPO_4^-K^+ + PO_4^{3-} \rightleftharpoons KPO_4^{2-}$							
37	0.15 KNO_3	3.4 ± 0.1	0.151	3.396	-0.13	4.91 ± 0.20	Childs (1970)
$Mg^{2+} + HPO_4^{2-} \rightleftharpoons MgHPO_4(aq)K^+ + HPO_4^{2-} \rightleftharpoons KHPO_4^-$							
25	0.2 M KCl	1.65 ± 0.16	0.202	1.646	-0.09	2.72 ± 0.32	Greenwald et al. (1940)
38	0.16 M NaCl	1.62	0.161	1.617	-0.04	2.65 ± 0.30	Tabor & Hastings (1943)
10	dilute → 0	2.61	0	2.61		2.61 ± 0.20	Clarke et al. (1954)
20	dilute → 0	2.67	0	2.67		2.67 ± 0.20	Clarke et al. (1954)
30	dilute → 0	2.75	0	2.75		2.75 ± 0.20	Clarke et al. (1954)
40	dilute → 0	2.83	0	2.83		2.83 ± 0.20	Clarke et al. (1954)
50	dilute → 0	2.92	0	2.92		2.92 ± 0.20	Clarke et al. (1954)
0	0.2 M Pr_4NCl	1.505 ± 0.03	0.201	1.502	-0.4	2.48 ± 0.20	Smith & Alberty (1956)
25	0.2 M Pr_4NCl	1.881 ± 0.01	0.201	1.878	-0.4	2.89 ± 0.20	Smith & Alberty (1956)
25	dilute → 0	2.91	0	2.91		2.91 ± 0.30	Taylor et al. (1963)
37	0.15 M KNO_3	1.8 ± 0.1	0.151	1.796	-0.07	2.81 ± 0.20	Childs (1970)
15	0.1 M KNO_3	1.78	0.101	1.775	-0.07	2.63 ± 0.20	Frey & Stuehr (1972)
25	3 M $NaClO_4$	1.42 ± 0.03	3.503	1.354	-0.18	2.72 ± 0.42	Havel & Högfeldt (1974)
25	dilute → 0	2.85 ± 0.01	0	2.85		2.85 ± 0.30	Verbeeck et al. (1984)
25	3 M $NaClO_4$	1.23 ± 0.05	3.503	1.163	-0.18	2.53 ± 0.42	Ciavatta et al. (1994)
25	0.1 M $NaNO_3$	1.83 ± 0.03	0.101	1.828	-0.02	2.70 ± 0.20	Saha et al. (1996)
$Mg^{2+} + H_2PO_4^- \rightleftharpoons MgH_2PO_4^+K^+ + H_2PO_4^- \rightleftharpoons KH_2PO_4(aq)$							
37	0.15 KNO_3	0.7 ± 0.3	0.151	0.696	0.02	1.21 ± 0.60	Childs (1970)
25	3 M $NaClO_4$	0.16 ± 0.05	3.503	0.093	-0.05	0.92 ± 0.43	Havel & Högfeldt (1974)
25	dilute → 0	1.28 ± 0.04	0	1.28		1.28 ± 0.30	Verbeeck et al. (1984)
25	3 M $NaClO_4$	0.16 ± 0.05	3.503	0.093	-0.05	0.92 ± 0.43	Ciavatta et al. (1994)

[a] Data as reported in the cited publications or calculated by this review from the reported data, see text.
[b] 2σ uncertainties assigned or estimated by this review.

$Mg^{2+} + HPO_4^{2-} \rightleftharpoons MgHPO_4(aq)$

$\log_{10}K°\ (298.15\ K) = 2.73 \pm 0.06$

$\Delta_r H_m°(298.15\ K) = (13.3 \pm 7.4)\ kJ \cdot mol^{-1}$

$\Delta_r C_{p,m}°(298.15\ K) = 0$

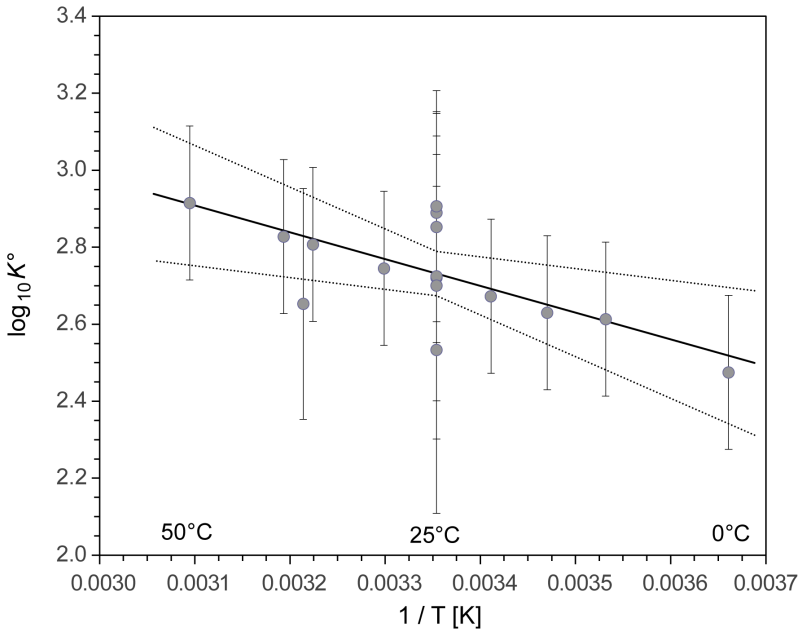

Fig. 4.1-5: The equilibrium constant $\log_{10}K°$ for $Mg^{2+} + HPO_4^{2-} \rightleftharpoons MgHPO_4(aq)$ as a function of reciprocal absolute temperature in the range 0 – 50 °C

Symbols: accepted $\log_{10}K°$ values taken from Tab. 4.1-1. Solid line: weighted linear regression. Dotted lines: lower and upper limits using $\log_{10}K°$ (298.15 K) = 2.73 ± 0.06 and $\Delta_r H_m°$ (298.15 K) = (13.3 ± 7.4) kJ · mol^{-1} and extrapolated to lower and higher temperatures.

In the case of $Mg^{2+} + H_2PO_4^- \rightleftharpoons MgH_2PO_4^+$, no temperature effect can be deduced from three data points at 25 °C and one value with a large uncertainty at 37 °C (Tab. 4.1-1), and hence, a weighted mean has been calculated from these few data:

$$Mg^{2+} + H_2PO_4^- \rightleftharpoons MgH_2PO_4^+$$

$$\log_{10}K° \text{ (298.15 K)} = 1.11 \pm 0.20$$

In the case of $Mg^{2+} + PO_4^{3-} \rightleftharpoons MgPO_4^-$, there is only one data point at 37 °C (Tab. 4.1-1). This review selected this value, with an increased uncertainty, as representative also for 25 °C:

$$Mg^{2+} + PO_4^{3-} \rightleftharpoons MgPO_4^-$$

$$\log_{10}K° \text{ (298.15 K)} = 4.9 \pm 0.5$$

These values are included in TDB 2020, together with the estimates

$$\varepsilon(MgH_2PO_4^+, Cl^-) = (0.05 \pm 0.10) \text{ kg} \cdot \text{mol}^{-1}$$

$$\varepsilon(MgHPO_4(aq), NaCl) = (0.0 \pm 0.1) \text{ kg} \cdot \text{mol}^{-1}$$

$$\varepsilon(MgPO_4^-, Na^+) = -(0.05 \pm 0.10) \text{ kg} \cdot \text{mol}^{-1}$$

4.1.8.2 Magnesium(II) phosphate compounds

Lothenbach et al. (2019) built a consistent thermodynamic database for magnesium phosphate hydrates based on solubility measurements for newberyite, phosphorröslerite, $MgKPO_4 \cdot H_2O$, K-struvite, $Mg_2KH(PO_4)_2 \cdot 15H_2O$, farringtonite ($Mg_3(PO_4)_2$), $Mg_3(PO_4)_2 \cdot 4H_2O$, bobierrite and cattite, carried out at different temperatures, and a critical review of existing thermodynamic data and solubility measurements from the literature (Tab. 4.1-2).

Tab. 4.1-2: Magnesium phosphate hydrate data considered by Lothenbach et al. (2019)

Compound	**Experimental data**	**Literature data**	$S_m°$, $C_{p,m}°$
	Temperature range [°C]		
K-struvite $MgKPO_4 \cdot 6H_2O$	5 – 50	10 – 36	Luff &Reed (1980), used for isocoulombic reactions ↓
Newberyite $MgHPO_4 \cdot 3H_2O$	5 – 50	5 – 80	Isocoulombic $\Delta_r s_m° = \Delta_r c_{p,m}° = 0$
Phosphorröslerite $MgHPO_4 \cdot 7H_2O$	20	5, 12	Isocoulombic $\Delta_r s_m° = \Delta_r c_{p,m}° = 0$
$MgKPO_4 \cdot H_2O$	40, 50		Isocoulombic $\Delta_r s_m° = \Delta_r c_{p,m}° = 0$
$Mg_2KH(PO_4)_2 \cdot 15H_2O$	5, 20		Isocoulombic $\Delta_r s_m° = \Delta_r c_{p,m}° = 0$
Farringtonite $Mg_3(PO_4)_2$		25	Oeting & mcdonald (1963), used for isocoulombic reactions ↓
Bobierrite $Mg_3(PO_4)_2 \cdot 8H_2O$	20 – 90	20 – 75	Isocoulombic $\Delta_r s_m° = \Delta_r c_{p,m}° = 0$
Cattite $Mg_3(PO_4)_2 \cdot 22H_2O$	5 – 40	5 – 25	Isocoulombic $\Delta_r s_m° = \Delta_r c_{p,m}° = 0$
$Mg_3(PO_4)_2 \cdot 4H_2O$ (MO4)	20 – 80	38, 85	$S_m°$ fitted, isocoulombic $\Delta_r C_{p,m}° = 0$

Lothenbach et al. (2019) selected data for $S_m°$ and $C_{p,m}°$ from the calorimetric studies of Luff & Reed (1980) and Oeting & McDonald (1963).

Luff &Reed (1980) measured the low-temperature heat capacity of $MgKPO_4 \cdot 6H_2O$ (K-struvite) by adiabatic calorimetry over the temperature range 10 – 316 K, fitted a smoothed curve to their data and obtained $C_{p,m}°(298.15\ K) = 77.62\ cal \cdot K^{-1} \cdot mol^{-1}$ ($324.8\ J \cdot K^{-1} \cdot mol^{-1}$) and $S_m°(298.15\ K) = 83.67\ cal \cdot K^{-1} \cdot mol^{-1}$ ($350.1\ J \cdot K^{-1} \cdot mol^{-1}$). The maximum deviation of the observed heat capacities from the smoothed values is $\pm 0.4\ J \cdot K^{-1} \cdot mol^{-1}$. No such calorimetric data are available for the related compounds $MgHPO_4 \cdot 3H_2O$ (newberyite), $MgHPO_4 \cdot 7H_2O$ (phosphorröslerite), $MgKPO_4 \cdot H_2O$ and $Mg_2KH(PO_4)_2 \cdot 15H_2O$. Hence, Lothenbach et al. (2019) estimated $S_m°$ and $C_{p,m}°$ values for these compounds via isocoulombic reactions assuming $\Delta_r S_m° = \Delta_r C_{p,m}° = 0$.

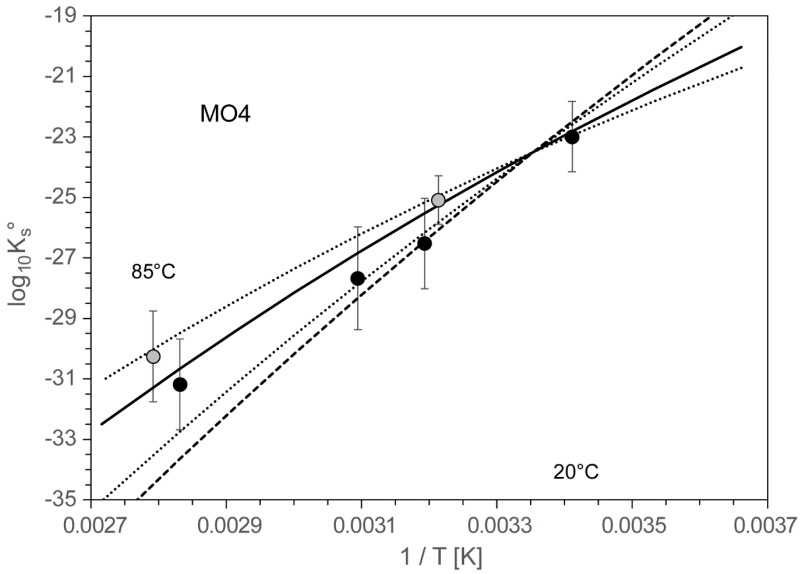

Fig. 4.1-6: The equilibrium constants $\log_{10}K_s°$ for $Mg_3(PO_4)_2 \cdot 4H_2O$ (MO4) (Tab. 4.1-2) as a function of reciprocal absolute temperature in the range 20 – 85 °C

Black symbols: $\log_{10}K_s°$ measured by Lothenbach et al. (2019), grey symbols: literature data evaluated by Lothenbach et al. (2019). Solid line: calculated using $\log_{10}K_s°$(298.15 K), $\Delta_rH_m°$(298.15 K) and $\Delta_rC_{p,m}°$(298.15 K) from Tab. 4.1-3. Dotted lines: lower and upper limits using $S_m°$(298.15 K) = 650 ± 200 J · K^{-1} · mol^{-1}. Dashed line: $S_m°$(298.15 K) = 339 J · K^{-1} · mol^{-1} estimated from farringtonite.

Oeting & McDonald (1963) measured the low-temperature heat capacity of $Mg_3(PO_4)_2$ (farringtonite) by adiabatic calorimetry over the temperature range 17 – 320 K, fitted a smoothed curve to their data and obtained $C_{p,m}°$(298.15 K) = 51.02 cal · K^{-1} · mol^{-1} (213.5 J · K^{-1} · mol^{-1}) and $S_m°$(298.15 K) = 45.22 ± 0.15 cal · K^{-1} · mol^{-1} (189.2 ± 0.6 J · K^{-1} · mol^{-1}). No such calorimetric data are available for the related compounds $Mg_3(PO_4)_2 \cdot 4H_2O$, $Mg_3(PO_4)_2 \cdot 8H_2O$ (bobierrite) and $Mg_3(PO_4)_2 \cdot 22H_2O$ (cattite). Hence, Lothenbach et al. (2019) estimated $S_m°$ and $C_{p,m}°$ values for these compounds via isocoulombic reactions assuming $\Delta_rS_m° = \Delta_rC_{p,m}° = 0$. Only in the case of $Mg_3(PO_4)_2 \cdot 4H_2O$ (MO4) the estimated entropy value (339 J · K^{-1} · mol^{-1}) did not well describe the decrease in solubility with temperature and Lothenbach et al. (2019) fitted a value of $S_m°$(298.15 K) = 650 ± 200 J · K^{-1} · mol^{-1}) (Fig. 4.1-6).

Tab. 4.1-3: Thermodynamic data for magnesium phosphate hydrate

Data are reported by Lothenbach et al. (2019) (bold face) and calculated therefrom by this review (normal face).

Name	**$\log_{10}K_s°$**	**$\Delta_f H_m°$** [kJ · mol^{-1}]	**$\Delta_r H_m°$** [kJ · mol^{-1}]	**$C_{p,m}°$** [J · K^{-1} · mol^{-1}]	**$\Delta_r C_{p,m}°$** [J · K^{-1} · mol^{-1}]	**Reaction**
K^+		**-252.14**		**8.39**		
Mg^{2+}		**-465.93**		**-21.66**		
H_2O(l)		**-285.88**		**75.36**		
PO_4^{3-}		**-1'277.79**		**-518.92**		
Newberyite	**-17.93 ± 0.23**	**-2'600.6**	-0.8	**182.6**	-497	$MgHPO_4 \cdot 3H_2O \rightleftharpoons Mg^{2+} + H^+ + PO_4^{3-} + 3\ H_2O$(l)
Phosphorröslerite	**-17.01 ± 0.25**	**-3'772.8**	27.9	**342.8**	-356	$MgHPO_4 \cdot 7H_2O \rightleftharpoons Mg^{2+} + H^+ + PO_4^{3-} + 7\ H_2O$(l)
K-struvite	**-10.96 ± 0.31**	**-3'717.3**	6.2	**324.8**	-405	$MgKPO_4 \cdot 6H_2O \rightleftharpoons Mg^{2+} + K^+ + PO_4^{3-} + 6\ H_2O$(l)
$MgKPO_4 \cdot H_2O$	**-10.95 ± 1.50**	**-2'245.8**	-35.9	**124.6**	-581	$MgKPO_4 \cdot H_2O \rightleftharpoons Mg^{2+} + K^+ + PO_4^{3-} + H_2O$(l)
$Mg_2KH(PO_4)_2 \cdot 15H_2O$	**-28.67 ± 0.60**	**-8'086.7**	58.9	**747.8**	-690	$Mg_2KH(PO_4)_2 \cdot 15H_2O \rightleftharpoons 2\ Mg^{2+} + K^+ + H^+ + 2\ PO_4^{3-} + 15\ H_2O$(l)
Farringtonite	**-22.41 ± 0.30**	**-3'769.1**	-184.3	**213.5**	-1'316	$Mg_3(PO_4)_2 \rightleftharpoons 3\ Mg^{2+} + 2\ PO_4^{3-}$
$Mg_3(PO_4)_2 \cdot 4H_2O$	**-23.50 ± 1.80**	**-4'864.9**	-232.0	**373.6**	-1'175	$Mg_3(PO_4)_2 \cdot 4H_2O \rightleftharpoons 3\ Mg^{2+} + 2\ PO_4^{3-} + 4\ H_2O$(l)
Bobierrite	**-25.30 ± 1.00**	**-6'056.5**	-183.9	**533.8**	-1'034	$Mg_3(PO_4)_2 \cdot 8H_2O \rightleftharpoons 3\ Mg^{2+} + 2\ PO_4^{3-} + 8\ H_2O$(l)
Cattite	**-23.03 ± 0.56**	**-10'265.1**	22.4	**1'003.6**	-449	$Mg_3(PO_4)_2 \cdot 22H_2O \rightleftharpoons 3\ Mg^{2+} + 2\ PO_4^{3-} + 22\ H_2O$(l)

Thermodynamic modelling was carried out by Lothenbach et al. (2019) using GEMS. Thermodynamic data for aqueous species, as well as for many solids, were taken from the GEMS-PSI thermodynamic database. The stability constants of the formation reactions (from aqueous master species) of aqueous species and solids given in the original PSI/Nagra thermodynamic database (Thoenen et al. 2014) were included in the GEMS-PSI thermodynamic database and combined with the standard molar Gibbs energies of master species from the slop98.dat database for SUPCRT (Johnson et al. 1992). For aqueous species, this dataset includes the parameters for the HKF (Helgeson-Kirkham-Flower) equation of state which is used to calculate temperature and pressure corrections up to 1'000 °C and 5 kbar.

This means that only $\log_{10}K$ values used by Lothenbach et al. (2019) are identical with those given by Thoenen et al. (2014), e.g., the deprotonation constants of phosphoric and pyrophosphoric acid, but $\Delta_f G_m°$, $\Delta_f H_m°$, $S_m°$ and $C_{p,m}°$ are different because they were made consistent with the slop98.dat database. Therefore, this review calculated $\Delta_r H_m°$ and $\Delta_r C_{p,m}°$ from the $\Delta_f H_m°$ and $C_{p,m}°$ values given by Lothenbach et al. (2019) (Tab. 4.1-3). For a certain solubility reaction, the data triple $\log_{10}K_s°$, $\Delta_r H_m°$ and $\Delta_r C_{p,m}°$ results in an identical description of the solubility versus temperature as the triple $\log_{10}K_s°$, $\Delta_f H_m°$ and $C_{p,m}°$, but is independent of $\Delta_f H_m°$ and $C_{p,m}°$ chosen for K^+, Mg^{2+}, H_2O(l) and PO_4^{3-}.

Uncertainty estimates are given for $\log_{10}K_s°$ values by Lothenbach et al. (2019) but not for $\Delta_f H_m°$ and $C_{p,m}°$ and none have been estimated for the calculated $\Delta_r H_m°$ and $\Delta_r C_{p,m}°$ by this review. However, as can be seen in Figs. 4.1-7 and 4.1-8, the ± of $\log_{10}K_s°$(298.15 K) represent a reasonable uncertainty estimate for the entire temperature region covered by experimental data.

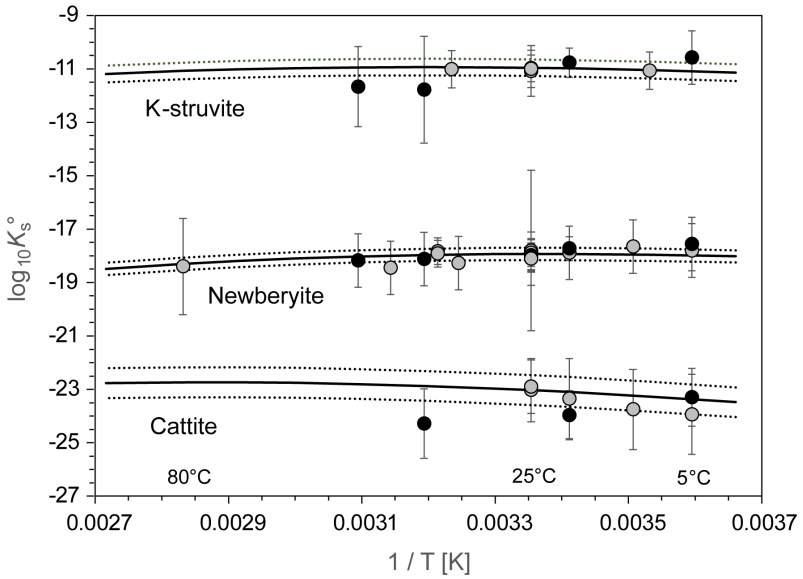

Fig. 4.1-7: The equilibrium constants $\log_{10}K_s°$ for K-struvite, newberyite and cattite (Tab. 4.1-2) as a function of reciprocal absolute temperature in the range 5 – 80 °C

Black symbols: $\log_{10}K_s°$ measured by Lothenbach et al. (2019), grey symbols: literature data evaluated by Lothenbach et al. (2019). Solid line: calculated using $\log_{10}K_s°$(298.15 K), $\Delta_r H_m°$(298.15 K) and $\Delta_r C_{p,m}°$(298.15 K) from Tab. 4.1-3. Dotted lines: lower and upper limits using ± of $\log_{10}K_s°$(298.15 K) (Tab. 4.1-3).

As Lothenbach et al. (2019) remark, the PSI/Nagra thermodynamic database (Thoenen et al. 2014) contains data for the deprotonation of phosphoric acid and pyrophosphoric acid but no data to account for the complex formation of alkali and alkaline earth ions with aqueous phosphate species. Thus, the aqueous data were complemented by Lothenbach et al. (2019) with data for aqueous phosphate complexes taken from the literature. This unfortunate situation is remedied now by this review, but the question arises whether this leads to significant inconsistencies with the dataset derived by Lothenbach et al. (2019).

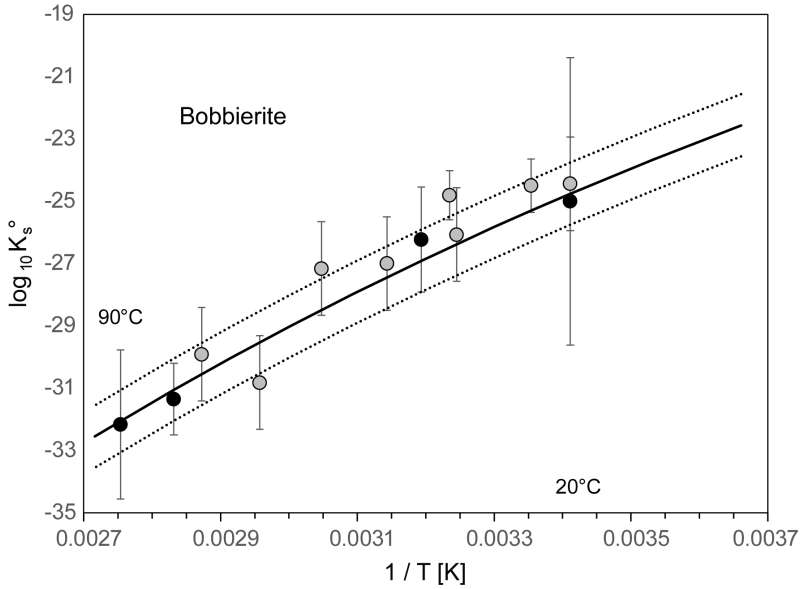

Fig. 4.1-8: The equilibrium constants $\log_{10}K_s°$ for bobbierite (Tab. 4.1-2) as a function of reciprocal absolute temperature in the range 20 – 90 °C

Black symbols: $\log_{10}K_s°$ measured by Lothenbach et al. (2019), grey symbols: literature data evaluated by Lothenbach et al. (2019). Solid line: calculated using $\log_{10}K_s°$(298.15 K), $\Delta_rH_m°$(298.15 K) and $\Delta_rC_{p,m}°$(298.15 K) from Tab. 4.1-3. Dotted lines: lower and upper limits using ± of $\log_{10}K_s°$(298.15 K) (Tab. 4.1-3).

Lothenbach et al. (2019) took $\log_{10}K° = 1.05$ for $K^+ + HPO_4^{2-} \rightleftharpoons KHPO_4^-$ from Turner et al. (1981), while this review selected $\log_{10}K°$ (298.15 K) = 0.88 ± 0.07 (see Section 2.3.1). Turner et al. (1981) cite Smith & Martell (1976) as the source of the value $\log_{10}K = 0.49$ ($I = 0.2$). In general, it is difficult to trace back a "critically selected value" of Smith & Martell (1976) as they report all references related to a certain equilibrium but do not disclose how they obtained their selected value from these references. However, this case is simple, the source is Smith & Alberty (1956), the only publication available in 1976 (see Tab. 3.3-1). This review extrapolated the value of Smith & Alberty (1956) to zero ionic strength, $\log_{10}K° = 0.93$, using SIT with $\Delta\varepsilon = -0.43$, valid for tetraalkylammonium halide media. Turner et al. (1981) used an extrapolation formula similar to SIT with a parameter C = -0.02, equivalent to $\Delta\varepsilon$, and valid for NaCl media. This is the best they could do in 1981. A difference of about 0.2 $\log_{10}$ units in the selected stability constant of $KHPO_4^-$ by Lothenbach et al. (2019) and this review is not expected to lead to significant inconsistencies.

Lothenbach et al. (2019) cite Babić-Ivančić et al. (2006) as the source of their selected data for aqueous sodium and magnesium phosphate complexes. Babić-Ivančić et al. (2006) report a list of "equilibrium constants (I = 0) used in calculations" in their Tab. 1 without references and state in the text that they have used the Davies equation to account for ionic strength effects.

The case of $\log_{10}K° = 0.85$ for $Na^+ + HPO_4^{2-} \rightleftharpoons NaHPO_4^-$, as reported by Babić-Ivančić et al. (2006), is easy to resolve, and Lothenbach et al. (2019) correctly cite Patel et al. (1974) as the source of this value (see Tab. 3.2-1). This review selected $\log_{10}K°$ (298.15 K) = 1.06 ± 0.13, (see Section 2.2.1). Again, we see a difference of about 0.2 $\log_{10}$ units in the selected stability constant of $NaHPO_4^-$ by Lothenbach et al. (2019) and this review, but in the opposite direction than in the case of $KHPO_4^-$. This difference is also not expected to lead to significant inconsistencies.

The case of $\log_{10}K°$ = 4.920 for $Mg^{2+} + PO_4^{3-} \rightleftharpoons MgPO_4^-$, as reported by Babić-Ivančić et al. (2006), is also easy to resolve, as Childs (1970) is the only publication reporting a value for this equilibrium (see Tab. 4.1-1), and this review also selected $\log_{10}K°$ (298.15 K) = 4.9 ± 0.5 but with an increased uncertainty (see preceding Section).

Also $\log_{10}K°$ = 1.207 for $Mg^{2+} + H_2PO_4^- \rightleftharpoons MgH_2PO_4^+$, as reported by Babić-Ivančić et al. (2006), most probably has been taken from Childs (1970) (Tab. 4.1-1). This review selected $\log_{10}K°$ (298.15 K) = 1.11 ± 0.20, so no consistency problem here with a difference of less than 0.1 $\log_{10}$ units.

Surprisingly, Babić-Ivančić et al. (2006) did not consequently select $\log_{10}K°$ = 2.81 for $Mg^{2+} + HPO_4^{2-} \rightleftharpoons MgHPO_4(aq)$ from Childs (1970) (Tab. 4.1-1) but list a value $\log_{10}K°$ = 2.428. Lothenbach et al. (2019) claim that this value has been experimentally determined by Babić-Ivančić et al. (2006), but not the slightest hint on any experimental determination can be found in the publication of Babić-Ivančić et al. (2006). Hence, the source of this value, which is lower than all values reported in the literature for all temperatures studied (see Tab. 4.1-1), remains a mystery. Unfortunately, Lothenbach et al. (2019) have chosen this erratic value, 0.3 $\log_{10}$ units, or ½ $K°$, lower than $\log_{10}K°$ (298.15 K) = 2.73 ± 0.06 selected by this review (see preceding Section). Moreover, Lothenbach et al. (2019) state in their discussion of solubility products for newberyite that, as in the older papers the formation of $MgHPO_4(aq)$ was neglected or a stronger formation constant of $\log_{10}K°$ (298.15 K) = 2.88 was used, all solubility data were recalculated as far as possible. This may lead to small inconsistencies, but no effort was made by this review to re-recalculate these data, and the $\log_{10}K_s°$, $\Delta_r H_m°$ and $\Delta_r C_{p,m}°$ values as listed in Tab. 4.1-3 have been included in TDB 2020.

4.1.9 Selected magnesium data

Tab. 4.1-4: Selected magnesium data

Core data are in bold face.

Name	**$\Delta_f G_m°$** [kJ · mol^{-1}]	**$\Delta_f H_m°$** [kJ · mol^{-1}]	**$S_m°$** [J · K^{-1} · mol^{-1}]	**$C_{p,m}°$** [J · K^{-1} · mol^{-1}]	**Species**
Mg(cr)	0.0	0.0	**32.670 ± 0.100**	**24.869 ± 0.020**	Mg(cr)
Mg+2	**-455.375 ± 1.335**	**-467.000 ± 0.600**	**-137.000 ± 4.000**		Mg^{2+}

Name	**$\log_{10}\beta°$**	**$\Delta_r H_m°$** [kJ · mol^{-1}]	**$\Delta_r C_{p,m}°$** [J · K^{-1} · mol^{-1}]	**T-range** [°C]	**Reaction**
MgOH+	-11.70 ± 0.04	70.8 ± 0.7	0	0 – 350	$Mg^{2+} + H_2O(l) \rightleftharpoons MgOH^+ + H^+$
MgF+	1.88 ± 0.05	10.5 ± 1.0	-30.5 ± 7.3	2 – 200	$Mg^{2+} + F^- \rightleftharpoons MgF^+$
MgCO3(aq)	2.98 ± 0.03	11.0 ± 1.1	90 ± 44	10 – 90	$Mg^{2+} + CO_3^{2-} \rightleftharpoons MgCO_3(aq)$
MgHCO3+	1.07 ± 0.03	3.25 ± 0.22	175.7 ± 8.8	10 – 90	$Mg^{2+} + HCO_3^- \rightleftharpoons MgHCO_3^+$
MgSO4(aq)	2.25 ± 0.05	20.3 ± 2.0	0	0 – 45	$Mg^{2+} + SO_4^{2-} \rightleftharpoons MgSO_4(aq)$
MgPO4-	4.9 ± 0.5	-	-		$Mg^{2+} + PO_4^{3-} \rightleftharpoons MgPO_4^-$
MgHPO4(aq)	2.73 ± 0.06	13.3 ± 7.4	0	0 – 50	$Mg^{2+} + HPO_4^{2-} \rightleftharpoons MgHPO_4(aq)$
MgH2PO4+	1.11 ± 0.20	-	-		$Mg^{2+} + H_2PO_4^- \rightleftharpoons MgH_2PO_4^+$
Mg(cr)	79.78 ± 0.23	-467.0 ± 0.6	-		$Mg(cr) \rightleftharpoons Mg^{2+} + 2\ e^-$
Brucite	17.11 ± 0.04	-111.5 ± 0.7	0	10 – 350	$Mg(OH)_2(s) + 2\ H^+ \rightleftharpoons Mg^{2+} + 2\ H_2O(l)$
Magnesite	-7.66 ± 0.34	-35.9 ± 1.9	-387.7 ± 9.6	25 – 200	$MgCO_3(s) \rightleftharpoons Mg^{2+} + CO_3^2$
Newberyite	-17.93 ± 0.23	-0.8	-497	5 – 80	$MgHPO_4 \cdot 3H_2O \rightleftharpoons Mg^{2+} + H^+ + PO_4^{3-} + 3\ H_2O(l)$
Phosphorröslerite	-17.01 ± 0.25	-27.9	-356	5 – 20	$MgHPO_4 \cdot 7H_2O \rightleftharpoons Mg^{2+} + H^+ + PO_4^{3-} + 7\ H_2O(l)$
K-struvite	-10.96 ± 0.31	6.2	-405	5 – 50	$MgKPO_4 \cdot 6H_2O \rightleftharpoons Mg^{2+} + K^+ + PO_4^{3-} + 6\ H_2O(l)$
$MgKPO_4 \cdot H_2O$	-10.95 ± 1.50	-35.9	-581	40 – 50	$MgKPO_4 \cdot H_2O \rightleftharpoons Mg^{2+} + K^+ + PO_4^{3-} + H_2O(l)$
$Mg_2KH(PO_4)_2 \cdot 15H_2O$	-28.67 ± 0.60	58.9	-690	5 – 20	$Mg_2KH(PO_4)_2 \cdot 15H_2O \rightleftharpoons 2\ Mg^{2+} + K^+ + H^+ + 2\ PO_4^{3-} + 15\ H_2O(l)$
Farringtonite	-22.41 ± 0.30	-184.3	-1'316	25	$Mg_3(PO_4)_2 \rightleftharpoons 3\ Mg^{2+} + 2\ PO_4^{3-}$

Tab. 4.1-4: Cont.

Name	**$\log_{10}\beta°$**	**$\Delta_r H_m°$** [kJ · mol^{-1}]	**$\Delta_r C_{p,m}°$** [J · K^{-1} · mol^{-1}]	**T-range** [°C]	**Reaction**
Bobierrite	-25.30 ± 1.00	-183.9	-1'034	20 – 90	$Mg_3(PO_4)_2 \cdot 8H_2O \rightleftharpoons 3\ Mg^{2+} + 2\ PO_4^{3-} + 8\ H_2O(l)$
Cattite	-23.03 ± 0.56	22.4	-449	5 – 40	$Mg_3(PO_4)_2 \cdot 22H_2O \rightleftharpoons 3Mg^{2+} + 2PO_4^{3-} + 22H_2O(l)$

Tab. 4.1-5: Selected SIT ion interaction coefficients $\varepsilon_{j,k}$ [kg · mol^{-1}] for magnesium species

Data in bold face are taken from Lemire et al. (2013). Data in normal face are derived in this review. Data estimated according to charge correlations and taken from Tab. 1-7 are shaded.

j k → ↓	**Cl^-** $\varepsilon_{j,k}$ [kg · mol^{-1}]	**Na^+** $\varepsilon_{j,k}$ [kg · mol^{-1}]	**$Na^+ + Cl^-$** $\varepsilon_{j,k}$ [kg · mol^{-1}]
Mg+2	**0.19 ± 0.02**	0	0
MgOH+	0.05 ± 0.10	0	0
MgF+	-0.02 ± 0.06	0	0
MgHCO3+	0.05 ± 0.10	0	0
MgCO3(aq)	0	0	0.0 ± 0.1
MgSO4(aq)	0	0	0.0 ± 0.1
MgPO4-	0	-0.05 ± 0.10	0
MgHPO4(aq)	0	0	0.0 ± 0.1
MgH2PO4+	0.05 ± 0.10	0	0

4.1.10 References

Babić-Ivančić, V., Kontrec, J., Brečević, L. & Kralj, D. (2006): Kinetics of struvite to newberyite transformation in the precipitation system $MgCl_2$-$NH_4H_2PO_4$-NaOH-H_2O. Water Research, 40, 3447-3455.

Baes, C.F. & Mesmer, R.E. (1976): The Hydrolysis of cations. Wiley, New York, 490 pp.

Bénézeth, P., Saldi, G.D., Dandurand, J.-L. & Schott, J. (2011): Experimental determination of the solubility product of magnesite at 50 to 200 °C. Chem. Geol., 286, 21-31.

Bilal, B.A. & Müller, E. (1992): Potentiometric study of magnesium fluoro complexes in aqueous solutions up to 473 K and 1 kbar. Zeitschrift für Naturforschung, 47a, 1034-1038.

Bond, A.M. & Hefter, G. (1971): Use of the fluoride ion-selective electrode for the detection of weak fluoride complexes. J. Inorg. Nucl. Chem., 33, 429-434.

Brown, P.L. & Ekberg, C. (2016): Hydrolysis of Metal Ions. Wiley-VCH Verlag GmbH & Co. KGaA, Weinheim, Germany, 917 pp.

Brown, P.L., Ekberg, C. & Matyskin, A.V. (2019): On the solubility of radium and other alkaline earth sulfate and carbonate phases at elevated temperature. Geochim. Cosmochim. Acta, 255, 88-104.

Childs, C.W. (1970): A potentiometric study of equilibria in aqueous divalent metal orthophosphate solutions. Inorg. Chem., 9, 2465-2469.

Clarke, H.B., Cusworth, D.C. & Datta, S.P. (1954): Thermodynamic quantities for the dissociation equilibria of biologically important compounds. 3. The dissociations of the magnesium salts of phosphoric acid, glucose 1-phosphoric acid and glycerol 2-phosphoric acid. Biochem. J., 58, 146-154.

Ciavatta, L., Iuliano, M. & Porto, R. (1994): Complex formation equilibria in magnesium orthophosphate aqueous solutions. Annali di Chimica, 84, 95-112.

Cox, J.D., Wagman, D.D. & Medvedev, V.A. (1989): CODATA Key Values for Thermodynamics. Hemisphere Publishing, New York, 271 pp.

Elgquist, B. (1970): Determination of the stability constants of MgF^+ and CaF^+ using a fluoride ion selective electrode. J. Inorg. Nucl. Chem., 32, 937-944.

Frey, C.M. & Stuehr, J.E. (1972): Interaction of divalent metal ions with inorganic and nucleoside phosphates. I. Thermodynamics. J. Amer. Chem. Soc., 94, 8898-8904.

Gamsjäger, H., Schindler, P. & Kleinert, B. (1969): Potentiometrische Untersuchung der Komplexbildung im System Mg^{2+} – F^- – H_2O. Chimia, 23, 229-230.

Greenwald, I., Redish, J. & Kibrick, A.C. (1940): The dissociation of calcium and magnesium phosphates. J. Biol. Chem., 135, 65-76.

Grenthe, I., Fuger, J., Konings, R.J.M., Lemire, R.J., Muller, A.B., Nguyen-Trung, C. & Wanner, H. (1992): Chemical Thermodynamics of Uranium. Chemical Thermodynamics, Vol. 1. North-Holland, Amsterdam, 715 pp.

Havel, J. & Högfeldt, E. (1974): On some phosphate equilibria. V. The system magnesium-phosphoric acid in 3M (Na, Mg) ClO_4. Chemica Scripta, 5, 164-169.

Hummel, W., Berner, U., Curti, E., Pearson, F.J. & Thoenen, T. (2002): Nagra/PSI Chemical Thermodynamic Data Base 01/01. Nagra Technical Report NTB 02-16 and Universal Publishers, Parkland, Florida, 565 pp.

Königsberger, E., Königsberger, L.-C. & Gamsjäger, H. (1999): Low-temperature thermodynamic model for the system Na_2CO_3-$MgCO_3$-$CaCO_3$-H_2O. Geochim. Cosmochim. Acta, 63, 3105-3119.

Lemire, R.J., Berner, U., Musikas, C., Palmer, D.A., Taylor, P. & Tochiyama, O. (2013): Chemical Thermodynamics of Iron, Part 1. Chemical Thermodynamics, Vol. 13a. OECD Publications, Paris, France, 1082 pp.

Lothenbach, B., Xu, B. & Winnefeld, F. (2019): Thermodynamic data for magnesium (potassium) phosphates. Applied Geochemistry, 111, 104450.

Luff, B.B & Reed, R.B. (1980): Thermodynamic properties of magnesium potassium orthophosphate hexahydrate. J. Chem. Eng. Data, 25, 310-312.

Majer, V. & Štulĭk, K. (1982): A study of the stability of alkaline-earth metal complexes with fluoride and chloride ions at various temperatures by potentiometry with ion-selective electrodes. Talanta, 29, 145-148.

Nair, V.S.K. & Nancollas, G.H. (1958): Thermodynamics of ion association. Part IV. Magnesium and zinc sulphates. J. Chem. Soc., 3706-3710.

Nordstrom, D.K., Plummer, L.N., Langmuir, D., Busenberg, E., May, H.M., Jones, B.F. & Parkhurst, D.L. (1990): Revised Chemical Equilibrium Data for Major Water-Mineral Reactions and Their Limitations. In: Melchior, D.C., and Bassett, R.L. (eds.): Chemical Modeling of Aqueous Systems II. Washington, D.C., American Chemical Society, ACS Symposium Series 416, p. 398-413.

Oeting, F.L. & McDonald, R.A. (1963): The thermodynamic properties of magnesium orthophosphate and magnesium pyrophosphate. J. Phys. Chem., 67, 2737-2743.

Richardson, C.K. & Holland, H.D. (1979): The solubility of fluorite in hydrothermal solutions, an experimental study. Geochim. Cosmochim. Acta, 43, 1313-1325.

Robinson, R.A. & Stokes, R.H. (1959): Electrolyte Solutions. Second Revised Edition. Academic Press, New York, 559 pp.

Saha, A., Saha, N., Ji, L., Zhao, J., Gregáň, F., Sajadi, S.A., Song, B. & Sigel, H. (1996): Stability of metal ion complexes formed with methyl phosphate and hydrogen phosphate. Journal of Biological Inorganic Chemistry, 1, 231-238.

Siebert, R.M. & Hostetler, P.B. (1977a): The stability of the magnesium bicarbonate ion pair from 10° to 90 °C. American Journal of Science, 277, 697-715.

Siebert, R.M. & Hostetler, P.B. (1977b): The stability of the magnesium carbonate ion pair from 10° to 90 °C. American Journal of Science, 277, 716-734.

Sillén, L.G., Martell, A.E. & Smith, R.M. (1964): Stability Constants of Metal-Ion Complexes. Special Publication no. 17. Chemical Society, London, UK.

Smith, R.P. & Alberty, R.A. (1956a): The apparent stability constants of ionic complexes of various adenosine phosphates with monovalent cations. J. Phys. Chem., 60, 180-184.

Smith, R.P. & Alberty, R.A. (1956b): The apparent stability constants of ionic complexes of various adenosine phosphates with divalent cations. J. Phys. Chem., 78, 2376-2380.

Smith, R.M. & Martell, A.E. (1976): Critical Stability Constants. Volume 4: Inorganic Complexes. Plenum Press, New York, 257 pp.

Smith, R.M. & Martell, A.E. (1989): Critical Stability Constants. Volume 6: Second Supplement. Plenum Press, New York, 643 pp.

Tabor, H. & Hastings, A.B. (1943): The ionization constant of secondary magnesium phosphate. J. Biol. Chem., 148, 627-632.

Tanner, S.P., Walker, J.B. & Choppin, G.R. (1968): Thermodynamic parameters of the alkaline earth monofluorides. J. Inorg. Nucl. Chem., 30, 2067-2070.

Taylor, A.W., Frazier, A.W., Gurney, E.L. & Smith, J.P. (1963): Solubility products of di- and trimagnesium phosphates and the dissociation of magnesium phosphate solutions. Trans. Farad. Soc., 59, 1585-1589.

Thoenen, T., Hummel, W., Berner, U. & Curti, E. (2014): The PSI/Nagra Chemical Thermodynamic Database 12/07. Technical Report, PSI Bericht Nr. 14-04, Paul Scherrer Institut, Villigen, Switzerland, 416 pp.

Turner, D., Whitfield, M. & Dickson, A. (1981): The equilibrium speciation of dissolved components in freshwater and sea water at 25 °C and 1 atm pressure. Geochim. Cosmochim. Acta, 45, 855-881.

Verbeeck, R.M.H., De Bruyne, P.A.M., Driessens, F.C.M & Verbeek, F. (1984): Solubility of magnesium hydrogen phosphate trihydrate and ion-pair formation in the system $Mg(OH)_2$-H_3PO_4-H_2O at 25 °C. Inorg. Chem., 23, 1922-1926.

4.2 Calcium

4.2.1 Elemental calcium

Calcium metal and gas are not relevant under environmental conditions. Hence, the gas phase Cag is not included in the data base. The absolute entropy and heat capacity of Ca(cr) are included as they are used for the calculation of certain thermodynamic reaction properties.

The selected values for Ca(cr) are taken from CODATA (Cox et al. 1989):

$$S_m°(\text{Ca, cr, 298.15 K}) = (41.590 \pm 0.400)\ \text{J} \cdot \text{K}^{-1} \cdot \text{mol}^{-1}$$

$$C_{p,m}°(\text{Ca, cr, 298.15 K}) = (25.929 \pm 0.300)\ \text{J} \cdot \text{K}^{-1} \cdot \text{mol}^{-1}$$

4.2.2 Calcium(II) aqua ion

Calcium(II) exists as the Ca^{2+} cation in aqueous solutions. The selected thermodynamic values for Ca^{2+} are taken from CODATA (Cox et al. 1989):

$$\Delta_f G_m°(Ca^{2+}, \text{298.15 K}) = -(552.806 \pm 1.050)\ \text{kJ} \cdot \text{mol}^{-1}$$

$$\Delta_f H_m°(Ca^{2+}, \text{298.15 K}) = -(543.000 \pm 1.000)\ \text{kJ} \cdot \text{mol}^{-1}$$

$$S_m°(Ca^{2+}, \text{298.15 K}) = -(56.200 \pm 1.000)\ \text{J} \cdot \text{K}^{-1} \cdot \text{mol}^{-1}$$

Using the selected CODATA $\Delta_f G_m°(Ca^{2+}, \text{298.15 K})$, the redox equilibrium

$$Ca(cr) \rightleftharpoons Ca^{2+} + 2\ e^-$$

is calculated as

$$\log_{10} K°(\text{298.15 K}) = 96.85 \pm 0.18$$

Since this review does not consider the formation of calcium chloride complexation, $\varepsilon(Ca^{2+}, Cl^-)$ is taken as selected by NEA (Grenthe et al. 1992, Lemire et al. 2013):

$$\varepsilon(Ca^{2+}, Cl^-) = (0.14 \pm 0.01)\ \text{kg} \cdot \text{mol}^{-1}$$

4.2.3 Calcium(II) (hydr)oxide compounds and complexes

Brown & Ekberg (2016) state that the hydrolytic reactions of calcium have been the subject of a substantial number of investigations because of the importance of lime in the cement industry. The hydrolysis of the calcium(II) ion occurs at high pH, and portlandite, $Ca(OH)_2(s)$, is sparingly soluble. There are many studies that have investigated the solubility of portlandite using a vast range of experimental conditions (ionic medium, strength and temperature). In such studies, however, it is necessary to determine both the solubility constant and the stability of $CaOH^+$ simultaneously. This has rarely been done, requiring that the data in such studies be re-evaluated to obtain both constants.

4.2.3.1 Calcium(II) hydroxide complexes

Nordstrom et al. (1990) selected a $\log_{10}{}^*\beta_1°$ value for

$$Ca^{2+} + H_2O(l) \rightleftharpoons CaOH^+ + H^+$$

$$\log_{10}{}^*\beta_1° \text{ (298.15 K)} = -12.78$$

with the remark "CODATA compatible, in good agreement with Baes & Mesmer (1976)". Baes & Mesmer (1976) actually selected

$$\log_{10}{}^*\beta_1° \text{ (298.15 K)} = -12.85$$

Brown & Ekberg (2016) state that the data reported, or recalculated in their review, for the first hydrolysis constant of calcium, $CaOH^+$, cover the range of temperature from 0 – 150 °C, above which the stability of $CaOH^+$ becomes relatively weak. The studies considered by Brown & Ekberg (2016) have used a variety of techniques including solubility, potentiometry, kinetic measurements, emf measurements and calorimetry. The stability constant data at zero ionic strength join relatively smoothly when plotted against the reciprocal of absolute temperature. Brown & Ekberg (2016) fitted a non-linear function and obtained

$$Ca^{2+} + H_2O(l) \rightleftharpoons CaOH^+ + H^+$$

$$\log_{10}{}^*\beta_1° \text{ (298.15 K)} = -12.57 \pm 0.03$$

$$\Delta_r H_m° \text{(298.15 K)} = (53.9 \pm 1.4) \text{ kJ} \cdot \text{mol}^{-1}$$

$$\Delta_r C_{p,m}° \text{(298.15 K)} = -(446.8 \pm 39.3) \text{ J} \cdot \text{K}^{-1} \cdot \text{mol}^{-1}$$

These values have been included in TDB 2020, as well as the estimate

$$\varepsilon(CaOH^+, Cl^-) = (0.05 \pm 0.10) \text{ kg} \cdot \text{mol}^{-1}$$

4.2.3.2 Calcium(II) (hydr)oxide compounds

Nordstrom et al. (1990) selected thermodynamic data for portlandite, $Ca(OH)_2(cr)$, from Baes & Mesmer (1976)

$$Ca(OH)_2(cr) + 2\ H^+ \rightleftharpoons Ca^{2+} + 2\ H_2O(l)$$

$$\log_{10}{}^*K_{s0}^\circ\ (298.15\ K) = 22.8$$

$$\Delta_r H_m^\circ(298.15\ K) = -31.0\ kcal \cdot mol^{-1} = -129.7\ kJ \cdot mol^{-1}$$

Brown & Ekberg (2016) report that the solubility of portlandite, $Ca(OH)_2(s)$, has been studied over a period of greater than 100 years. Nevertheless, there is very good agreement between the data from all of the studies (both before and after re-evaluation). The studies have investigated the solubility in a wide variety of ionic media and over a large range of temperature (0 – 350 °C). Brown & Ekberg (2016) show that the values at zero ionic strength join smoothly across the whole temperature range, and the solubility constant has been found to be a slightly non-linear function of the reciprocal temperature, which leads to

$$Ca(OH)_2(cr) + 2\ H^+ \rightleftharpoons Ca^{2+} + 2\ H_2O(l)$$

$$\log_{10}{}^*K_{s0}^\circ\ (298.15\ K) = 22.75 \pm 0.02$$

$$\Delta_r H_m^\circ(298.15\ K) = -(122.8 \pm 0.6)\ kJ \cdot mol^{-1}$$

$$\Delta_r C_{p,m}^\circ(298.15\ K) = (104.5 \pm 6.5)\ J \cdot K^{-1} \cdot mol^{-1}$$

These values have been included in TDB 2020.

4.2.4 Calcium(II) fluoride compounds and complexes

4.2.4.1 Calcium(II) fluoride complexes

Nordstrom et al. (1990) selected a $\log_{10}K_1^\circ$ and a $\Delta_r H_m^\circ$ value reported by Nordstrom & Jenne (1977) for the complex

$$Ca^{2+} + F^- \rightleftharpoons CaF^+$$

$$\log_{10}K_1^\circ\ (298.15\ K) = 0.94$$

$$\Delta_r H_m^\circ(298.15\ K) = 4.12\ kcal \cdot mol^{-1} = 17.24\ kJ \cdot mol^{-1}$$

The data sources of Nordstrom & Jenne (1977) are the experimental results of Tanner et al. (1968), Elgquist (1970) and Bond & Hefter (1971) covering the temperature range 2 – 40 °C.

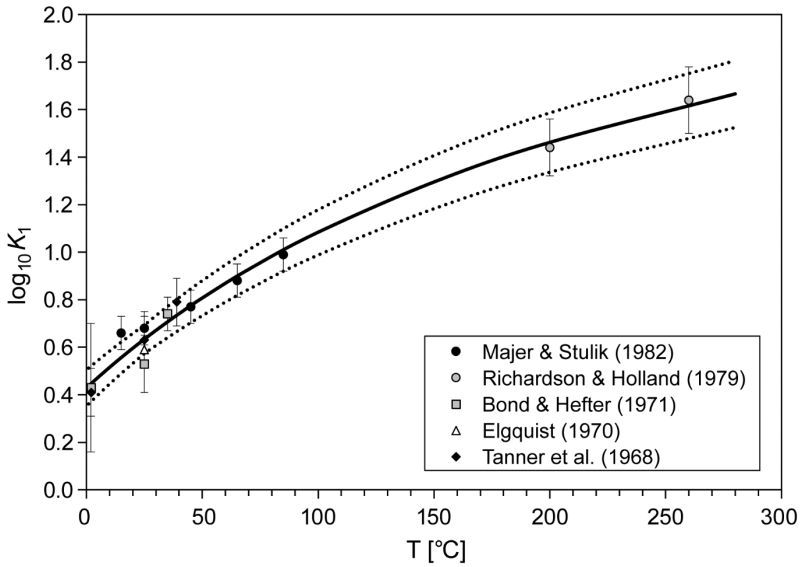

Fig. 4.2-1: The equilibrium constant $\log_{10}K_1$ for $Ca^{2+} + F^- \rightleftharpoons CaF^+$ as a function of temperature in the range 2 – 260 °C at 1 M ionic strength

Solid line: unweighted regression of all data. Dotted lines: lower and upper limits using $\log_{10}K$ (298.15 K) = 0.63 ± 0.06 and $\Delta_r H_m$(298.15 K) = (12.8 ± 1.0) kJ · mol^{-1} and extrapolated to lower and higher temperatures.

Since the publication of the Nordstrom & Jenne (1977) data compilation, new studies have been published concerning the CaF^+ complex formation, covering the temperature range 2 – 260 °C. Data obtained in 1 M $NaClO_4$ (Tanner et al. 1968, Bond & Hefter 1971), 1 M NaCl (Elgquist 1970, Richardson & Holland 1979) and 1 M $NaNO_3$ (Majer & Štulīk 1982) join relatively smoothly across the whole temperature range (Fig. 4.2-1). An unweighted regression of all data resulted in

$\log_{10}K_1$ (298.15 K, 1 M) = 0.63 ± 0.06

$\Delta_r H_m$ (298.15 K, 1 M) = (12.8 ± 1.0) kJ · mol^{-1}

$\Delta_r C_{p,m}$ (298.15 K, 1M) = 0 J · K^{-1} · mol^{-1}

Note that the data reported for 25 °C, and in 1 M $NaClO_4$ (Tanner et al. 1968, Bond & Hefter 1971), 1 M NaCl (Elgquist 1970) and 1 M $NaNO_3$ (Majer & Štulīk 1982) are in the range $\log_{10}\beta_1$ (298.15 K, 1 M) = 0.53 – 0.68, with an unweighted average of $\log_{10}\beta_1$ (298.15 K, 1 M) = 0.61 ± 0.10.

No attempt has been made to extrapolate $\Delta_r H_m$ to zero ionic strength, which is included in TDB 2020 as an approximation of $\Delta_r H_m°$ (298.15 K).

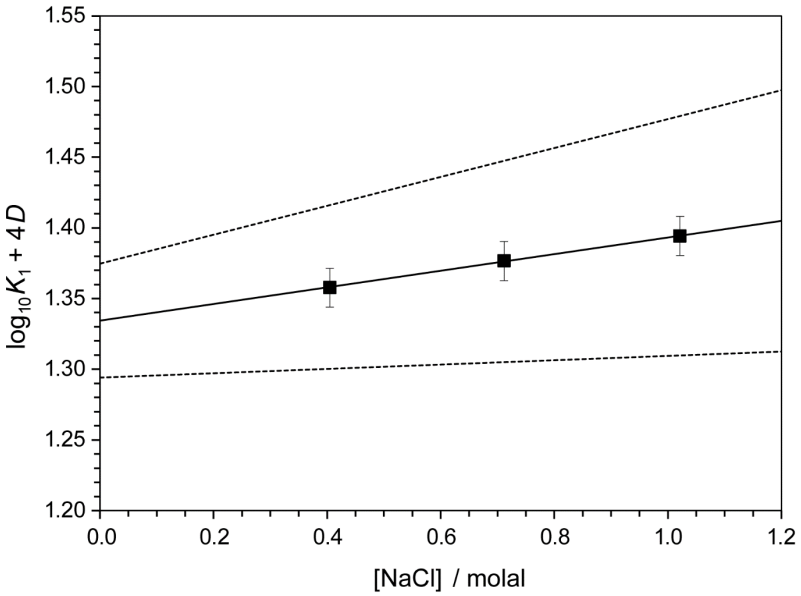

Fig. 4.2-2: Dependence of the equilibrium $Ca^{2+} + F^- \rightleftharpoons CaF^+$ on ionic strength in NaCl using the data of Elgquist (1970)

The solid line is obtained using the derived SIT interaction coefficient and stability constant at zero ionic strength. Dotted lines represent the 95% uncertainty range extrapolated from I = 0 to higher NaCl concentrations.

Using the data of Elgquist (1970) in NaCl for an SIT analysis this review obtained (Fig. 4.2-2):

$\log_{10}K_1°$ (298.15 K) = 1.33 ± 0.04

$\Delta\varepsilon$(NaCl) = -(0.06 ± 0.05)

Considering $\varepsilon(Ca^{2+}, Cl^-)$ = (0.14 ± 0.01) kg · mol^{-1} and $\varepsilon(Na^+, F^-)$ = (0.02 ± 0.02) kg · mol^{-1} (Grenthe et al. 1992) this review derives from the experimental $\Delta\varepsilon$ value

$\varepsilon(CaF^+, Cl^-)$ = (0.10 ± 0.06) kg · mol^{-1}.

This value is included in TDB 2020, together with $\log_{10}K_1°$ obtained from the SIT analysis.

4.2.4.2 Calcium(II) fluoride compounds

Nordstrom et al. (1990) selected a $\log_{10}K_s°$ and a $\Delta_rH_m°$ value as well as a temperature function for the solubility of fluorite

$CaF_2(cr) \rightleftharpoons Ca^{2+} + 2\ F^-$

$\log_{10}K_s°$ (298.15 K) = -10.6

$\Delta_r H_m°(298.15\ K) = 4.69\ kcal \cdot mol^{-1} = 19.62\ kJ \cdot mol^{-1}$

$\log_{10} K_s° (T) = 66.348 - 4298.2 / T - 25.271 \cdot \log_{10}(T)$

which allows to calculate

$\Delta_r C_{p,m}°(298.15\ K) = -210\ J \cdot K^{-1} \cdot mol^{-1}$

with the remark "based on Nordstrom & Jenne (1977) but forced to go through $\log_{10} K_s° = -10.6$ at 298.15 K to be in agreement with the solubility data of Macaskill & Bates (1977) and Brown & Roberson (1977)".

Note that Macaskill & Bates (1977) report $\log_{10} K_s°$ (298.15 K) = -10.51 and Brown & Roberson (1977) report $\log_{10} K_{s0}°$ (298.15 K) = -10.58 ± 0.17 while the value originally derived by Nordstrom & Jenne (1977) is $\log_{10} K_s°$ (298.15 K) = -10.96. The temperature function of Nordstrom & Jenne (1977) has been derived from solubility data at room temperature, calorimetric data and, at that time, the only available solubility data measured at elevated temperatures by Strübel (1965) (dot-dashed line in Fig. 4.2-3). As it seems, "forced to go through $\log_{10} K_s° = -10.6$ at 298.15 K" just means shifting the temperature function of Nordstrom & Jenne (1977) by a constant value of +0.36 log-units by Nordstrom et al. (1990) (dashed line in Fig. 4.2-3).

Hummel et al. (2002) remark "the mineral fluorite, CaF_2(cr), is common in aqueous systems, and may influence ground-water chemistry. In spite of the ubiquity and simple chemistry of this mineral, values for its thermodynamic properties differ widely. Values given by CODATA, Nordstrom et al. (1990, Tab. I) and other data bases differ by as much as 0.55 in $\log_{10} K_s°$. Hence, fluorite is included as supplemental data only, and reaction data for this mineral are taken from Nordstrom et al. (1990)".

This review considered the solubility data of Garand & Mucci (2004) at 25 °C, Zhang et al. (2017) at 30 and 50 °C, Richardson & Holland (1979) at 100, 200 and 260 °C, and Strübel (1965) at > 70 °C. It seems that due to the short equilibration times the solubility experiments of Strübel (1965) did not reach equilibrium at temperatures below 70 °C. These data have not been used.

The value $\log_{10} K_s°$ (298.15 K) = -10.51 of Macaskill & Bates (1977), extrapolated from measurements at 1 m KCl to zero ionic strength by an undefined extrapolation procedure, has not been considered by this review, although it is numerically identical to the value obtained by Garand & Mucci (2004).

Brown & Roberson (1977) measured the solubility products of two samples of natural fluorite, at very low (0.0007 M) to low (0.1 M) ionic strengths resulting from impurities in the samples. The authors tried many different variants of extrapolation to zero ionic strength and finally reported $\log_{10} K_{s0}°$ (298.15 K) = -10.58 ± 0.17 as their "more correct value" derived from one sample, while the values derived from the second sample are always +0.2 log-units or more at variance. Also, these values have not been considered in this review.

All data shown in Fig. 4.2-3 join relatively smoothly across the whole temperature range. An unweighted regression of all data resulted in

$CaF_2(cr) \rightleftharpoons Ca^{2+} + 2\ F^-$

$\log_{10}K_s°\ (298.15\ K) = -10.46 \pm 0.09$

$\Delta_r H_m°(298.15\ K) = (7.8 \pm 1.9)\ kJ \cdot mol^{-1}$

$\Delta_r C_{p,m}°(298.15\ K) = -(170 \pm 15)\ J \cdot K^{-1} \cdot mol^{-1}$

These values have been included in TDB 2020.

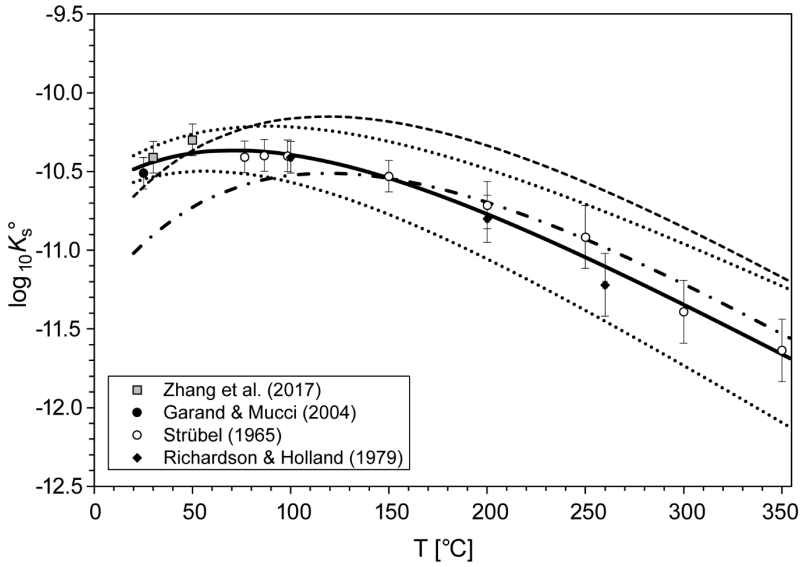

Fig. 4.2-3: The solubility product $\log_{10}K_s°$ for $CaF_2(s) \rightleftharpoons Ca^{2+} + 2\ F^-$, fluorite, as a function of temperature in the range 25 – 350 °C

Solid line: unweighted regression of all data. Dotted lines: lower and upper limits using $\log_{10}K_s°$ (298.15 K) = -10.46 ± 0.09, $\Delta_r H_m°$(298.15 K) = (7.8 ± 1.9) kJ · mol^{-1} and $\Delta C_{p,m}°$(298.15 K) = -(170 ± 15) J · K^{-1} · mol^{-1} and extrapolated to higher temperatures. Dashed line: temperature function selected by Nordstrom et al. (1990); dot-dashed line: temperature function derived by Nordstrom & Jenne (1977); both shown for comparison.

Note that the value $\log_{10}K_{s0}°$ (298.15 K) = -10.46 ± 0.09, obtained by this review, is in good agreement with the value $\log_{10}K_{s0}°$ (298.15 K) = -10.41 selected by Smith & Martell (1976), as well as with their "revised" value $\log_{10}K_{s0}°$ (298.15 K) = -10.50 ± 0.05 (Smith & Martell 1989). As the data sources and the selection procedure of Smith & Martell (1976, 1989) remain unclear, this agreement could be a coincidence.

4.2.5 Calcium(II) chloride compounds and complexes

4.2.5.1 Calcium(II) chloride complexes

This report does not consider the formation of weak calcium(II) chloride complexes, but includes possible ion interactions in the SIT interaction coefficient $\varepsilon(Ca^{2+}, Cl^-)$, see below.

4.2.5.2 Calcium(II) chloride compounds

$CaCl_2(s)$ is a highly soluble salt with a solubility of 740 g/L at 20 °C (gestis.itrust.de). Its isopiestic properties have been measured up to 6 $mol \cdot kg_{H2O}^{-1}$ (Robinson & Stokes 1959). Hence, no solubility data, but the specific ion interaction coefficient selected by NEA (Grenthe et al. 1992, Lemire et al. 2013) is adopted for TDB 2020:

$$\varepsilon(Ca^{2+}, Cl^-) = (0.14 \pm 0.01)\ kg \cdot mol^{-1}$$

4.2.6 Calcium(II) carbonate compounds and complexes

4.2.6.1 Calcium(II) carbonate complexes

Nordstrom et al. (1990) selected thermodynamic data reported by Plummer & Busenberg (1982) for the complexes

$$Ca^{2+} + CO_3^{2-} \rightleftharpoons CaCO_3(aq)$$

$$\log_{10}K_1^\circ\ (298.15\ K) = 3.224$$

$$\Delta_r H_m^\circ(298.15\ K) = 3.545\ kcal \cdot mol^{-1} = 14.83\ kJ \cdot mol^{-1}$$

$$\log_{10}K_1^\circ\ (T) = -1228.732 - 0.299444 \cdot T + 35512.75 / T + 485.818 \cdot \log_{10}(T)$$

$$Ca^{2+} + HCO_3^- \rightleftharpoons CaHCO_3^+$$

$$\log_{10}K^\circ\ (298.15\ K) = 1.106$$

$$\Delta_r H_m^\circ(298.15\ K) = 2.69\ kcal \cdot mol^{-1} = 11.25\ kJ \cdot mol^{-1}$$

$$\log_{10}K^\circ\ (T) = 1209.120 + 0.31294 \cdot T - 34765.05 / T - 478.782 \cdot \log_{10}(T)$$

Note that in both cases the reported temperature functions imply temperature dependent $\Delta_r C_{p,m}^\circ$ values. This might be an effect of over-fitting the experimental data.

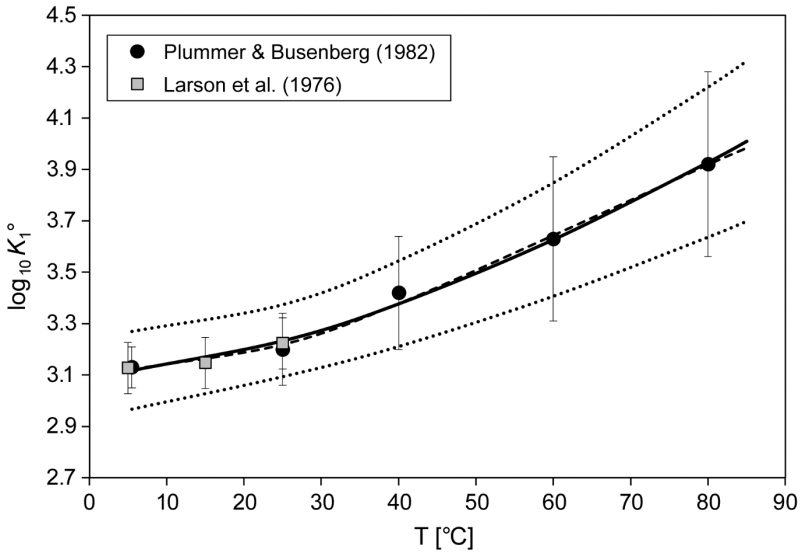

Fig. 4.2-4: The equilibrium constant $\log_{10}K_1°$ for $Ca^{2+} + CO_3^{2-} \rightleftharpoons CaCO_3(aq)$ as a function of temperature in the range 5 – 80 °C

Solid line: unweighted regression. Dotted lines: lower and upper limits using $\log_{10}K_1°$ (298.15 K) = 3.23 ± 0.14, $\Delta_r H_m°$(298.15 K) = (13.9 ± 2.2) kJ · mol^{-1} and $\Delta_r C_{p,m}°$(298.15 K) = (447 ± 130) J · K^{-1} · mol^{-1} and extrapolated to lower and higher temperatures. Dashed line: temperature function selected by Plummer & Busenberg (1982), shown for comparison.

Hence, this review re-fitted the experimental data reported by Plummer & Busenberg (1982), together with data reported by Larson et al. (1976) for $CaCO_3(aq)$, with the assumption $\Delta_r C_{p,m}°(T)$ = constant for $CaCO_3(aq)$, as in this case a plot of $\log_{10}K_1°$ versus the reciprocal of the absolute temperature showed a significant curvature. The results are (Fig. 4.2.4):

$Ca^{2+} + CO_3^{2-} \rightleftharpoons CaCO_3(aq)$

$\log_{10}K_1°$ (298.15 K) = 3.23 ± 0.14

$\Delta_r H_m°$(298.15 K) = (13.9 ± 2.2) kJ · mol^{-1}

$\Delta_r C_{p,m}°$(298.15 K) = (447 ± 130) J · K^{-1} · mol^{-1}

These values are included in TDB 2020.

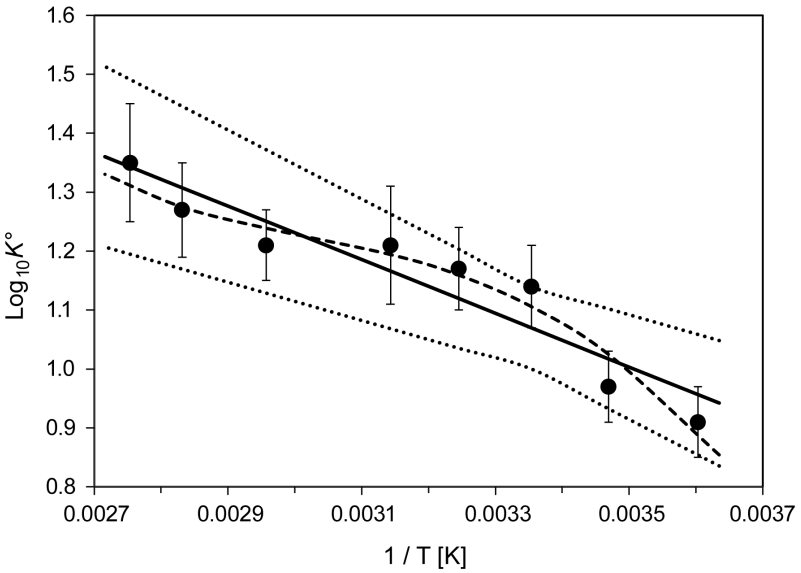

Fig. 4.2-5: The equilibrium constant $\log_{10}K°$ for $Ca^{2+} + HCO_3^- \rightleftharpoons CaHCO_3^+$ as a function of reciprocal absolute temperature in the range 5 – 80 °C

Solid line: unweighted linear regression. Dotted lines: lower and upper limits using $\log_{10}K°$ (298.15 K) = 1.07 ± 0.07 and $\Delta_r H_m°$(298.15 K) = (8.7 ± 2.5) kJ · mol^{-1} and extrapolated to lower and higher temperatures. Dashed line: temperature function selected by Plummer & Busenberg (1982), shown for comparison.

In the case of $CaHCO_3^+$ a plot of $\log_{10}K°$ values versus the reciprocal of the absolute temperature shows (Fig. 4.2-5) that Plummer & Busenberg (1982) obviously fitted a bizarre temperature function to their somewhat scattered experimental data. This review concluded that only a linear regression, implying $\Delta_r C_{p,m}° = 0$, is an adequate treatment of these scattered data and obtained:

$$Ca^{2+} + HCO_3^- \rightleftharpoons CaHCO_3^+$$

$$\log_{10}K° \text{ (298.15 K)} = 1.07 \pm 0.07$$

$$\Delta_r H_m°\text{(298.15 K)} = (8.7 \pm 2.5) \text{ kJ} \cdot \text{mol}^{-1}$$

$$\Delta_r C_{p,m}°\text{(298.15 K)} = 0 \text{ J} \cdot \text{K}^{-1} \cdot \text{mol}^{-1}$$

These values are included in TDB 2020 as well as the estimates

$$\varepsilon(CaHCO_3^+, Cl^-) = (0.05 \pm 0.10) \text{ kg} \cdot \text{mol}^{-1}$$

$$\varepsilon(CaCO_3(aq), NaCl) = (0.0 \pm 0.1) \text{ kg} \cdot \text{mol}^{-1}$$

4.2.6.2 Calcium(II) carbonate compounds

CaCO3(cr), calcite, aragonite, vaterite

Nordstrom et al. (1990) selected thermodynamic data reported by Plummer & Busenberg (1982) for calcite and aragonite, valid in the temperature range 0 – 90 °C:

$CaCO_3(calcite) \rightleftharpoons Ca^{2+} + CO_3^{2-}$

$\log_{10}K_s° \text{ (298.15 K)} = -8.480$

$\Delta_rH_m°(298.15\text{ K}) = -2.297\text{ kcal} \cdot \text{mol}^{-1} = -9.611\text{ kJ} \cdot \text{mol}^{-1}$

$\log_{10}K_{s0}° \text{ (T)} = -171.9065 - 0.077993 \cdot T + 2839.319 / T + 71.595 \cdot \log_{10}(T)$

$CaCO_3(aragonite) \rightleftharpoons Ca^{2+} + CO_3^{2-}$

$\log_{10}K_s° \text{ (298.15 K)} = -8.336$

$\Delta_rH_m°(298.15\text{ K}) = -2.589\text{ kcal} \cdot \text{mol}^{-1} = -10.832\text{ kJ} \cdot \text{mol}^{-1}$

$\log_{10}K_{s0}° \text{ (T)} = -171.9773 - 0.077993 \cdot T + 2903.293 / T + 71.595 \cdot \log_{10}(T)$

Note that in both cases the reported temperature functions imply temperature dependent $\Delta_rC_{p,m}°$ values. This might be an effect of over-fitting the experimental data.

Hence, this review re-fitted the experimental data reported by Plummer & Busenberg (1982), with the assumption $\Delta_rC_{p,m}°$ = constant for all $CaCO_3$(s) phases, calcite, aragonite and vaterite and obtained (Fig. 4.2-6):

$CaCO_3(calcite) \rightleftharpoons Ca^{2+} + CO_3^{2-}$

$\log_{10}K_s° \text{ (298.15 K)} = -8.47 \pm 0.04$

$\Delta_rH_m°(298.15\text{ K}) = -(9.7 \pm 0.6)\text{ kJ} \cdot \text{mol}^{-1}$

$\Delta_rC_{p,m}°(298.15\text{ K}) = -(357 \pm 31)\text{ J} \cdot \text{K}^{-1} \cdot \text{mol}^{-1}$

$CaCO_3(aragonite) \rightleftharpoons Ca^{2+} + CO_3^{2-}$

$\log_{10}K_s° \text{ (298.15 K)} = -8.32 \pm 0.05$

$\Delta_rH_m°(298.15\text{ K}) = -(10.9 \pm 0.3)\text{ kJ} \cdot \text{mol}^{-1}$

$\Delta_rC_{p,m}°(298.15\text{ K}) = -(366 \pm 19)\text{ J} \cdot \text{K}^{-1} \cdot \text{mol}^{-1}$

$CaCO_3(vaterite) \rightleftharpoons Ca^{2+} + CO_3^{2-}$

$\log_{10}K_s° \text{ (298.15 K)} = -7.91 \pm 0.05$

$\Delta_rH_m°(298.15\text{ K}) = -(15.4 \pm 0.8)\text{ kJ} \cdot \text{mol}^{-1}$

$\Delta_rC_{p,m}°(298.15\text{ K}) = -(321 \pm 36)\text{ J} \cdot \text{K}^{-1} \cdot \text{mol}^{-1}$

Note that in all cases the maximum difference in $\log_{10}K_{s0}°$ values calculated from the temperature functions given by Plummer & Busenberg (1982) and the parameters obtained by this review is ±0.02 $\log_{10}$-units.

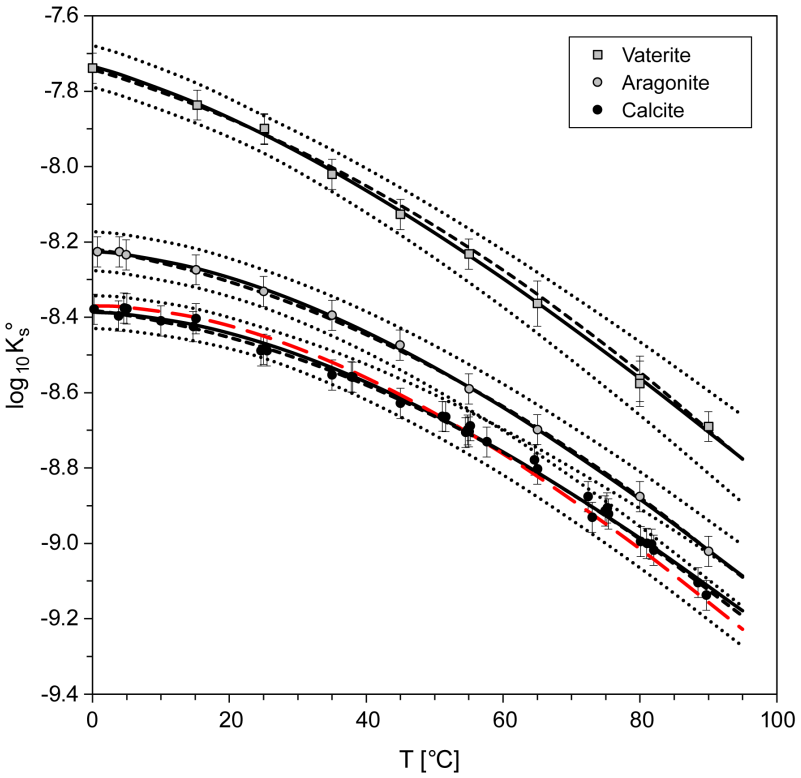

Fig. 4.2-6: The equilibrium constant $\log_{10}K_s°$ for $CaCO_3(s) \rightleftharpoons Ca^{2+} + CO_3^{2-}$, calcite, aragonite and vaterite, as a function of temperature in the range 0 – 90 °C

Solid line: unweighted regression of all data reported by Plummer & Busenberg (1982). Dotted lines: lower and upper limits using $\log_{10}K_s°$ (298.15 K), $\Delta_r H_m°$(298.15 K) and $\Delta_r C_{p,m}°$(298.15 K) values given in the text, and extrapolated to higher temperatures. Dashed lines: temperature functions selected by Plummer & Busenberg (1982), shown for comparison. Large dashed (red) line: temperature function selected by Brown et al. (2019) for calcite, shown for comparison.

Brown et al. (2019) in their recent review of the solubility of alkaline earth sulphate and carbonate phases at elevated temperature recommend for the solubility of calcite, $CaCO_3(s)$

$$\log_{10}K_{s0}° \text{ (298.15 K)} = -8.45 \pm 0.07$$

$$\Delta_r H_m°(298.15\text{ K}) = -(10.2 \pm 0.4)\text{ kJ} \cdot \text{mol}^{-1}$$

$$\Delta_r C_{p,m}°(298.15\text{ K}) = -(404.0 \pm 2.6)\text{ J} \cdot \text{K}^{-1} \cdot \text{mol}^{-1}$$

determined from a large and very consistent data set and valid for the temperature range 0 – 250 °C.

These values for calcite have been included in TDB 2020, together with the values for aragonite and vaterite obtained by this review from the Plummer & Busenberg (1982) data.

$CaMg(CO_3)_2$(cr), dolomite

Nordstrom et al. (1990) selected thermodynamic data for dolomite(ordered) reported by Robie et al. (1979), and for dolomite(disordered) reported by Helgeson et al. (1978), using in both cases ion values from Wagman et al. (1982) for calculating $\log_{10}K_{s0}°$ and $\Delta_r H_m°$ values:

$CaMg(CO_3)_2$(dolomite, ordered) $\rightleftharpoons Ca^{2+} + Mg^{2+} + 2\ CO_3^{2-}$

$\log_{10}K_{s0}°$ (298.15 K) = -17.09

$\Delta_r H_m°$(298.15 K) = -9.436 kcal · mol^{-1} = -39.48 kJ · mol^{-1}

$CaMg(CO_3)_2$(dolomite, disordered) $\rightleftharpoons Ca^{2+} + Mg^{2+} + 2\ CO_3^{2-}$

$\log_{10}K_{s0}°$ (298.15 K) = -16.54

$\Delta_r H_m°$(298.15 K) = -11.09 kcal · mol^{-1} = -46.40 kJ · mol^{-1}

Robie et al. (1979) list

$\Delta_f G_m°(CaMg(CO_3)_2, \text{dolomite}, 298.15\ K) = -(2161.672 \pm 1.670)$ kJ · mol^{-1}

$\Delta_f H_m°(CaMg(CO_3)_2, \text{dolomite}, 298.15\ K) = -(2324.480 \pm 1.469)$ kJ · mol^{-1}

$S_m°(CaMg(CO_3)_2, \text{dolomite}, 298.15\ K) = (155.18 \pm 0.29)$ J · K^{-1} · mol^{-1}.

with the reference "Robie, R.A. & Hemingway, B.S. (1977) unpublished data" for $\Delta_f G_m°$ and $\Delta_f H_m°$, and Stout & Robie (1963) for $S_m°$.

Stout & Robie (1963) report low-temperature heat capacity measurements from 11 to 300 K from which the entropy of dolomite is calculated. The samples used were naturally occurring glass-clear crystals from Binntal, Switzerland. Stout & Robie (1963) obtained

$S_m°(CaMg(CO_3)_2, \text{cr}, 298.15\ K) = (37.09 \pm 0.10)$ cal · K^{-1} · mol^{-1} = (155.18 ± 0.42) J · K^{-1} · mol^{-1}

$C_{p,m}°(CaMg(CO_3)_2, \text{cr}, 298.15\ K) = (37.65 \pm 0.10)$ cal · K^{-1} · mol^{-1} = (157.53 ± 0.42) J · K^{-1} · mol^{-1}

Later, in their revised and enlarged report, Robie & Hemingway (1995) list

$\Delta_f G_m°(CaMg(CO_3)_2, \text{dolomite}, 298.15\ K) = -(2161.3 \pm 1.7)$ kJ · mol^{-1}

$\Delta_f H_m°(CaMg(CO_3)_2, \text{dolomite}, 298.15\ K) = -(2324.5 \pm 1.5)$ kJ · mol^{-1}

$S_m°(CaMg(CO_3)_2, \text{dolomite}, 298.15\ K) = (155.2 \pm 0.3)$ J · K^{-1} · mol^{-1}.

with the same reference for $S_m°$ (Stout & Robie 1963) but with the new reference Hemingway & Robie (1994) for $\Delta_f G_m°$ and $\Delta_f H_m°$.

Hemingway & Robie (1994) state that dolomite "is an ordered double salt having a widespread geologic distribution. It is the most important phase involved in the Ca-Mg geochemistry of sea water and surface waters, and it is a common participant in the thermal metamorphism of siliceous carbonate rocks. A knowledge of the Gibbs energy of formation of dolomite is important for modelling many geologic problems".

Hemingway & Robie (1994) continue: "Robie et al. (1979) provided a value for the enthalpy of formation of dolomite and listed the source as unpublished data. Their result has been used as a thermodynamic reference value or has been compared to results derived from phase equilibrium reactions by Holland & Powell (1990) and Berman (1988). Good agreement was found in both studies. However, the basis for their value has not been documented in the literature. In this study we present the calorimetric data supporting the value selected by Robie et al. (1979)".

The enthalpy of formation, $\Delta_f H_m°$, of dolomite has been determined by Hemingway & Robie (1994) using hydrochloric acid solution chemistry. The dolomite sample was taken from a large, water-clear, single crystal from Binntal, Switzerland. Actually, a sample from the same location and with the same quality has been used by Stout & Robie (1963) for their low temperature heat capacity measurements. For the reaction

$$CaO(cr) + MgO(cr) + 2\ CO_2g \rightleftharpoons CaMg(CO_3)_2(cr)$$

Hemingway & Robie (1994) obtained $\Delta_r H_m° = -(300.94 \pm 0.49)$ kJ · mol^{-1}.

Using the CODATA values $\Delta_f H_m°(CaO, cr, 298.15\ K) = -(634.92 \pm 0.90)$ kJ · mol^{-1}, $\Delta_f H_m°(MgO, cr, 298.15\ K) = -(634.92 \pm 0.30)$ kJ · mol^{-1} and $\Delta_f H_m°(CO_2, g, 298.15\ K) = -(393.51 \pm 0.13)$ kJ · mol^{-1} (Cox et al. 1989) this review calculated

$$\Delta_f H_m°(CaMg(CO_3)_2, cr, 298.15\ K) = -(2324.48 \pm 1.08)\ kJ \cdot mol^{-1}$$

in perfect agreement with the value given by Robie et al. (1979), and Hemingway & Robie (1994) $\Delta_f H_m°(CaMg(CO_3)_2, cr, 298.15\ K) = -(2324.5 \pm 1.1)$ kJ · mol^{-1}.

Using the CODATA values $S_m°(Ca, cr, 298.15\ K) = (32.67 \pm 0.10)$ J · K^{-1} · mol^{-1}, $S_m°(Mg, cr, 298.15\ K) = (41.59 \pm 0.40)$ J · K^{-1} · mol^{-1}, $S_m°(C, cr, 298.15\ K) = (7.74 \pm 0.10)$ J · K^{-1} · mol^{-1}, $S_m°(O_2, g, 298.15\ K) = (205.152 \pm 0.005)$ J · K^{-1} · mol^{-1} (Cox et al. 1989), and $S_m°(CaMg(CO_3)_2, cr, 298.15\ K) = (155.18 \pm 0.42)$ J · K^{-1} · mol^{-1} (Stout & Robie 1963) this review calculated

$$Ca(cr) + Mg(cr) + 2\ C(cr) + 3\ O_2g \rightleftharpoons CaMg(CO_3)_2(cr)$$

$$\Delta_f S_m°(CaMg(CO_3)_2, cr, 298.15\ K) = -(546.02 \pm 0.60)\ J \cdot K^{-1} \cdot mol^{-1}.$$

According to the Gibbs-Helmholtz equation this review further calculated

$$\Delta_f G_m°(CaMg(CO_3)_2, cr, 298.15\ K) = \Delta_f H_m°(CaMg(CO_3)_2, cr, 298.15\ K)$$
$$- T° \cdot \Delta_f S_m°(CaMg(CO_3)_2, cr, 298.15\ K)$$

$$\Delta_f G_m°(CaMg(CO_3)_2, cr, 298.15\ K) = -(2161.69 \pm 1.10)\ kJ \cdot mol^{-1}$$

in perfect agreement with the value given by Robie et al. (1979), and Hemingway & Robie (1994) $\Delta_f G_m°(CaMg(CO_3)_2$, dolomite, 298.15 K) = -(2161.7 ± 1.1) kJ · mol^{-1}. Hence, the values

$\Delta_f G_m°(CaMg(CO_3)_2$, cr, 298.15 K) = -(2161.69 ± 1.10) kJ · mol^{-1}.

$\Delta_f H_m°(CaMg(CO_3)_2$, cr, 298.15 K) = -(2324.48 ± 1.08) kJ · mol^{-1}

$S_m°(CaMg(CO_3)_2$, cr, 298.15 K) = (155.18 ± 0.42) J · K^{-1} · mol^{-1}

$C_{p,m}°(CaMg(CO_3)_2$, cr, 298.15 K) = (157.53 ± 0.42) J · K^{-1} · mol^{-1}

are included in TDB 2020.

Using CODATA (Cox et al. 1989) values for Ca^{2+}, Mg^{2+} and CO_3^{2-}, a "solubility product" and reaction enthalpy of dolomite can be calculated:

$CaMg(CO_3)_2(cr) \rightleftharpoons Ca^{2+} + Mg^{2+} + 2\ CO_3^{2-}$

$\log_{10} K_{s0}°$ (298.15 K) = -17.12 ± 0.37

$\Delta_r H_m°$(298.15 K) = -(36.0 ± 1.6) kJ · mol^{-1}

Helgeson et al. (1978) list

$\Delta_f G_m°(CaMg(CO_3)_2$, (ordered) dolomite, 298.15 K) = -517.980 kcal · mol^{-1} = -2'167.23 kJ · mol^{-1}

$\Delta_f H_m°(CaMg(CO_3)_2$, (ordered) dolomite, 298.15 K) = -556.851 kcal · mol^{-1} = -2'329.86 kJ · mol^{-1}

$\Delta_f G_m°(CaMg(CO_3)_2$, disordered dolomite, 298.15 K) = -515.873 kcal · mol^{-1} = -2'158.41 kJ · mol^{-1}

$\Delta_f H_m°(CaMg(CO_3)_2$, disordered dolomite, 298.15 K) = -553.924 kcal · mol^{-1} = -2'317.62 kJ · mol^{-1}

As discussed by Helgeson et al. (1978), the order/disorder in dolomite is a function of temperature, and the temperature above which dolomite is completely disordered has been assumed to be 1200 °C in the model of Helgeson et al. (1978). Below 1'200 °C the dolomite structure becomes more and more ordered and below about 200 °C ordered dolomite is the thermodynamically stable phase.

As TDB 2020 is not intended for modelling hydrothermal systems at high temperatures, thermodynamic data for disordered dolomite have not been retained.

The values of Helgeson et al. (1978) for ordered dolomite are both about 5.5 kJ · mol^{-1} more negative than the values derived by Robie & Hemingway (1994).

Last but not least some final remarks concerning the "The Dolomite Problem":

Until now all attempts failed to precipitate dolomite at room temperature without "little helpers".

An impressive document about such unsuccessful efforts is the publication of Land (1998), where the author reports that dolomite failed to precipitate despite more than 1000-fold oversaturation (IAP approximately $10^{-13.8}$) from dilute solution (ionic strength = 0.025) at 25 °C after 32 years.

The present author remembers from his days as a student in Tübingen, Germany, that Friedrich Lippmann also unsuccessfully tried for years to precipitate dolomite, in a 300 L plastic barrel. The duration and exact conditions of his experiment are unknown as Lippmann never published his failure.

The lowest temperature reported for a successful dolomite synthesis in the laboratory so far is 60 °C (Usdowski 1989). The author reacted aragonite with solutions saturated with respect to $CaCl_2$ and $MgCl_2$ in parallel runs of different Ca^{2+}/Mg^{2+} ratios. With increasing ratios magnesite, dolomite, and dolomite + calcite precipitated. The reactions went to completion after a period of seven years.

And the quest for solving "the dolomite problem" goes on: Do microbes mediate dolomite precipitation (McKenzie & Vasconcelos 2009)? Does this advocated new "bandwagon", namely "microbial dolomitisation", perhaps via surface chemistry (carboxyl groups, Roberts et al. 2013), allow for precipitation of dolomite at low temperature? As Land (1998) concludes, only time will tell whether or not this new paradigm will lead us closer to solution of "the dolomite problem", or whether the "microbial dolomite" bandwagon, like other bandwagons before it ("mixing-zone dolomite", "low-SO_4 dolomite") will lie upended, wheels still slowly spinning, along the side of this long and frustrating road which we trust must have an end.

4.2.7 Calcium(II) sulphate compounds and complexes

4.2.7.1 Calcium(II) sulphate complexes

Nordstrom et al. (1990) selected thermodynamic data reported by Bell & George (1953), valid for the temperature range 0 – 40 °C, for the complex

$$Ca^{2+} + SO_4^{2-} \rightleftharpoons CaSO_4(aq)$$

$$\log_{10}\beta_1^\circ\ (298.15\ K) = 2.31 \pm 0.04$$

$$\Delta_r H_m^\circ(298.15\ K) = (6.9 \pm 1.7)\ kJ \cdot mol^{-1}$$

$$\Delta_r C_{p,m}^\circ(298.15\ K) = 0$$

The 1σ uncertainties given by Bell & George (1953) have been increased to 2σ by this review.

These values have been included in TDB 2020, as well as the estimate

$$\varepsilon(CaSO_4(aq), NaCl) = (0.0 \pm 0.1)\ kg \cdot mol^{-1}$$

4.2.7.2 Calcium(II) sulphate compounds

Nordstrom et al. (1990) calculated thermodynamic data for gypsum, $CaSO_4 \cdot 2H_2O$(cr), and anhydrite, $CaSO_4$(cr), from the temperature functions

$$\log_{10}K_{s0}(\text{gypsum}) = 68.2401 - 3221.51/\,T - 25.0627 \cdot \log_{10}T$$

$$\log_{10}K_{s0}(\text{anhydrite}) = 197.52 - 8669.8 / T - 69.835 \cdot \log_{10}T$$

as reported by Langmuir & Melchior (1985), which results in:

$CaSO_4 \cdot 2H_2O(\text{gypsum}) \rightleftharpoons Ca^{2+} + SO_4^{2-} + 2\ H_2O(l)$

$\log_{10}K_{s0}°\ (298.15\ K) = -4.58$

$\Delta_r H_m°(298.15\ K) = -0.456\ kJ \cdot mol^{-1}$

$\Delta_r C_{p,m}°(298.15\ K) = -208.4\ J \cdot K^{-1} \cdot mol^{-1}$

$CaSO_4(\text{anhydrite}) \rightleftharpoons Ca^{2+} + SO_4^{2-}$

$\log_{10}K_{s0}°\ (298.15\ K) = -4.36$

$\Delta_r H_m°(298.15\ K) = -7.15\ kJ \cdot mol^{-1}$

$\Delta_r C_{p,m}°(298.15\ K) = -580.6\ J \cdot K^{-1} \cdot mol^{-1}$

Nordstrom et al. (1990) remark that the gypsum data of Langmuir & Melchior (1985) is refitted from Blount & Dickson (1973), valid for the temperature range 25 – 90 °C and is in excellent agreement with the highly precise data of Lilley & Briggs (1976).

Brown et al. (2019) in their recent review of the solubility of alkaline earth sulphate and carbonate phases at elevated temperature recommend for the solubility of anhydrite, $CaSO_4$(cr)

$\log_{10}K_{s0}°\ (298.15\ K) = -4.21 \pm 0.17$

$\Delta_r H_m°(298.15\ K) = -(17.7 \pm 1.0)\ kJ \cdot mol^{-1}$

$\Delta_r C_{p,m}°(298.15\ K) = -(396.9 \pm 2.9)\ J \cdot K^{-1} \cdot mol^{-1}$

determined from various data sets, including Blount & Dickson (1973), as well as more recent experimental data, and valid for the temperature range 0 – 350 °C.

These values have been included in TDB 2020, together with the values reported by Langmuir & Melchior (1985) for gypsum, $CaSO_4 \cdot 2H_2O$(cr):

$$\log_{10}K_{s0}^\circ\ (298.15\ K) = -4.58 \pm 0.05$$

$$\Delta_r H_m^\circ(298.15\ K) = -(0.46 \pm 0.04)\ kJ \cdot mol^{-1}$$

$$\Delta_r C_{p,m}^\circ(298.15\ K) = -(208.4 \pm 3.0)\ J \cdot K^{-1} \cdot mol^{-1}$$

where the uncertainties have been estimated in this review.

At 25 °C, the solubility of anhydrite is higher than that of gypsum and thus, gypsum is the thermodynamically stable phase at 25 °C. However, with increasing temperature, the solubility of anhydrite approaches that of gypsum, and above a certain temperature anhydrite becomes the thermodynamically stable phase. As discussed by Langmuir & Melchior (1985), this phase transition temperature is somewhat uncertain, a best guess is 58 ± 2 °C. Langmuir & Melchior (1985) fitted their temperature function for anhydrite such that the calculated phase transition temperature, using their temperature functions for anhydrite and gypsum, is exactly 58.0 °C. Using the revised data of Brown et al. (2019) together with the retained data for gypsum of Langmuir & Melchior (1985), the calculated phase transition temperature is 59.5 °C, well within the best guess of 58 ± 2 °C.

4.2.8 Calcium(II) phosphate compounds and complexes

4.2.8.1 Calcium(II) phosphate complexes

The equilibrium constants of calcium phosphate complexes have been determined by various methods in a considerable number of studies, published over the course of half a century by Greenwald et al. (1940), Davies & Hoyle (1953), Gosselin & Coghlan (1953), Smith & Alberty (1956), Bjerrum (1958), Greenwald (1963), Moreno et al. (1966), Chughtai et al. (1968), Childs (1970), Gregory et al. (1970), McDowell et al. (1971), Tung et al. (1988), Ciavatta et al. (1991) and Saha et al. (1996) (Tab. 4.2-1).

Tab. 4.2-1: Reported and accepted calcium phosphate complexation data

Temp. [°C]	Medium	$\log_{10}K$ reported [a]	I_m	$\log_{10}K_m$	$\Delta\varepsilon$	$\log_{10}K^\circ$ accepted [b]	Reference
$Ca^{2+} + PO_4^{3-} \rightleftharpoons CaPO_4^-$							
18	dilute	6.48 ± 0.15	0	6.48		6.48 ± 0.30	Greenwald (1963)
25	dilute	6.45 ± 0.02	0	6.45		6.45 ± 0.20	Chughtai et al. (1968)
37	dilute	6.54 ± 0.03	0	6.54		6.54 ± 0.20	Chughtai et al. (1968)
25	dilute → 0	6.41	0	6.41		6.41 ± 0.20	Tung et al. (1988)
37	dilute → 0	6.41	0	6.41		6.41 ± 0.20	Tung et al. (1988)
45	dilute → 0	6.41	0	6.41		6.41 ± 0.20	Tung et al. (1988)
$Ca^{2+} + HPO_4^{2-} \rightleftharpoons CaHPO_4$(aq)							
25	0.2 M KCl	1.50 ± 0.17	0.202	1.496	-0.04	2.58 ± 0.34	Greenwald et al. (1940)
25	dilute → 0	2.70	0	2.70		2.70 ± 0.20	Davies & Hoyle (1953)

Tab. 4.2-1: Cont.

Temp. [°C]	Medium	$\log_{10}K$ reported [a]	I_m	$\log_{10}K_m$	$\Delta\varepsilon$	$\log_{10}K°$ accepted [b]	Reference
37	0.15 M NaCl	1.86	0.151	1.858	0.01	2.88 ± 0.30	Gosselin & Coghlan (1953)
0	0.2 M Pr_4NCl	1.36 ± 0.04	0.201	1.359	-0.4	2.33 ± 0.20	Smith & Alberty (1956)
25	0.2 M Pr_4NCl	1.70 ± 0.02	0.201	1.696	-0.4	2.71 ± 0.20	Smith & Alberty (1956)
18	dilute	2.63 ± 0.15	0	2.63		2.63 ± 0.30	Greenwald (1963)
37.5	dilute → 0	2.77 ± 0.01	0	2.77		2.77 ± 0.20	Moreno et al. (1966)
25	dilute	2.739 ± 0.002	0	2.74		2.74 ± 0.20	Chughtai et al. (1968)
37	dilute	2.833 ± 0.002	0	2.83		2.83 ± 0.20	Chughtai et al. (1968)
37	0.15 M KNO_3	1.3 ± 0.2	0.151	1.296	0.08	2.33 ± 0.40	Childs (1970)
5	dilute → 0	2.65 ± 0.05	0	2.65		2.65 ± 0.20	Gregory et al. (1970)
15	dilute → 0	2.43 ± 0.07	0	2.43		2.43 ± 0.20	Gregory et al. (1970)
25	dilute → 0	2.41 ± 0.06	0	2.41		2.41 ± 0.20	Gregory et al. (1970)
37.5	dilute → 0	2.60 ± 0.08	0	2.60		2.60 ± 0.25	Gregory et al. (1970)
5	dilute → 0	2.38 ± 0.05	0	2.38		2.38 ± 0.20	McDowell et al. (1971)
15	dilute → 0	2.28 ± 0.05	0	2.28		2.28 ± 0.20	McDowell et al. (1971)
25	dilute → 0	2.58 ± 0.05	0	2.58		2.58 ± 0.20	McDowell et al. (1971)
37	dilute → 0	2.59 ± 0.10	0	2.59		2.59 ± 0.30	McDowell et al. (1971)
25	dilute → 0	2.42	0	2.42		2.42 ± 0.20	Tung et al. (1988)
37	dilute → 0	2.55	0	2.55		2.55 ± 0.20	Tung et al. (1988)
45	dilute → 0	2.70	0	2.70		2.70 ± 0.20	Tung et al. (1988)
25	3 M $NaClO_4$	1.42 ± 0.03	3.503	1.353	-0.12	2.93 ± 0.42	Ciavatta et al. (1991)
25	0.1 M $NaNO_3$	1.64 ± 0.02	0.101	1.638	0.13	2.53 ± 0.20	Saha et al. (1996)
$Ca^{2+} + H_2PO_4^- \rightleftharpoons CaH_2PO_4^+$							
25	dilute → 0	1.08	0	1.08		1.08 ± 0.30	Davies & Hoyle (1953)
37.5	dilute → 0	0.87 ± 0.01	0	0.87		0.87 ± 0.30	Moreno et al. (1966)
25	dilute	1.41 ± 0.03	0	1.41		1.41 ± 0.30	Chughtai et al. (1968)
37	dilute	1.50 ± 0.02	0	1.50		1.50 ± 0.30	Chughtai et al. (1968)
37	0.15 M KNO_3	0.6 ± 0.3	0.151	0.596	0.17	1.13 ± 0.60	Childs (1970)
5	dilute → 0	1.00 ± 0.07	0	1.00		1.00 ± 0.40	Gregory et al. (1970)
15	dilute → 0	0.82 ± 0.08	0	0.82		0.82 ± 0.40	Gregory et al. (1970)
25	dilute → 0	0.71 ± 0.09	0	0.71		0.71 ± 0.40	Gregory et al. (1970)
37.5	dilute → 0	0.65 ± 0.14	0	0.65		0.65 ± 0.60	Gregory et al. (1970)
5	dilute → 0	0.70 ± 0.09	0	0.70		0.70 ± 0.40	McDowell et al. (1971)
15	dilute → 0	1.00 ± 0.04	0	1.00		1.00 ± 0.30	McDowell et al. (1971)
25	dilute → 0	1.00 ± 0.04	0	1.00		1.00 ± 0.30	McDowell et al. (1971)
37	dilute → 0	1.04 ± 0.04	0	1.04		1.04 ± 0.30	McDowell et al. (1971)
25	dilute → 0	0.93	0	0.93		0.93 ± 0.20	Tung et al. (1988)
37	dilute → 0	0.85	0	0.85		0.85 ± 0.20	Tung et al. (1988)
45	dilute → 0	0.75	0	0.75		0.75 ± 0.20	Tung et al. (1988)

[a] Data as reported in the cited publications or calculated by this review from the reported data, see text.
[b] Extrapolated to $I = 0$ by this review, see text, and 2σ uncertainties assigned or estimated by this review.

Greenwald et al. (1940) were the first to recognise that the pH of phosphate containing solutions was lowered by the addition of Ca^{2+} ions and concluded, from measurements with glass as well as with hydrogen gas electrodes in various NaCl and KCl media, that $CaHPO_4(aq)$ is the main complex in solution. They report in their Tab. VI the value $\log_{10}K = 1.50 \pm 0.17$ (1σ) in 0.2 M KCl at 25 °C for the equilibrium $Ca^{2+} + HPO_4^{2-} \rightleftharpoons CaHPO_4(aq)$. This review obtained $\log_{10}K° = 2.58 \pm 0.34$ (2σ) by extrapolating the above value to zero ionic strength using SIT with $\varepsilon(Ca^{2+}, Cl^-) = (0.14 \pm 0.01)$, $\varepsilon(K^+, HPO_4^{2-}) = -(0.10 \pm 0.06)$ and the estimate $\varepsilon(CaHPO_4(aq), KCl) = (0.0 \pm 0.1)$.

Davies & Hoyle (1953) measured colorimetrically the solubility of calcium iodate in phosphate buffers as a function of pH and assumed, in addition to $CaHPO_4(aq)$, the species $CaH_2PO_4^+$. Davies & Hoyle (1953) worked with dilute solutions of ionic strengths ranging from 0.05 to 0.09 M and applied what is nowadays known as the "Davies equation" to obtain stability constants at zero ionic strength. They report in their Tab. I the values $K° = 0.0024$, 0.0020 and 0.0016 for the equilibrium $CaHPO_4(aq) \rightleftharpoons Ca^{2+} + HPO_4^{2-}$, and $K° = 0.087$, 0.084 and 0.080 for the equilibrium $CaH_2PO_4^+ \rightleftharpoons Ca^{2+} + H_2PO_4^-$. Davies & Hoyle (1953) conclude that "the dissociation constants derived show some variation, which may be due to traces of $CaPO_4^-$ and $KHPO_4^-$ for which we were unable to allow; corrections for these two species would act in opposition, however, so we think the mean values 0.084 and 0.0020 are the most reliable at present available". This review retained these mean values, $\log_{10}K° = 2.70 \pm 0.20$ for the equilibrium $Ca^{2+} + HPO_4^{2-} \rightleftharpoons CaHPO_4(aq)$ and $\log_{10}K° = 1.08 \pm 0.30$ for the equilibrium $Ca^{2+} + H_2PO_4^- \rightleftharpoons CaH_2PO_4^+$ with uncertainties assigned by this review.

Gosselin & Coghlan (1953) employed a cation-exchange resin to measure the equilibrium of Ca-45 in the presence and absence of phosphate, and report in their Tab. I the value $\log_{10}K = 1.79$ in 0.15 M NaCl at pH 7.4 and 37 °C for the equilibrium $Ca^{2+} + HPO_4^{2-} \rightleftharpoons CaHPO_4(aq)$. This value has been calculated with the assumption that all dissolved phosphate is HPO_4^{2-}. In their discussion Gosselin & Coghlan (1953) conclude that at pH 7.4 only 85% of the dissolved phosphate is HPO_4^{2-} and thus, the corrected value becomes $\log_{10}K = 1.86$. This review retained this value and obtained $\log_{10}K° = 2.88 \pm 0.20$ by extrapolation to zero ionic strength using SIT with $\varepsilon(Ca^{2+}, Cl^-) = (0.14 \pm 0.01)$, $\varepsilon(Na^+, HPO_4^{2-}) = -(0.15 \pm 0.06)$ and the estimate $\varepsilon(CaHPO_4(aq), NaCl) = (0.0 \pm 0.1)$. The uncertainty has been estimated by this review.

Smith & Alberty (1956) calculated from measurements with a glass electrode at 25 and 0 °C in 0.2 M Pr_4NCl (tetrapropylammonium chloride, $(CH_3CH_2CH_2)_4NCl$) the values K(25 °C) = 50 ± 2 (corresponding to $\log_{10}K$(25 °C) = 1.70 ± 0.02) and K(0 °C) = 23 ± 2 (corresponding to $\log_{10}K$(0 °C) = 1.36 ± 0.04) for the equilibrium $Ca^{2+} + HPO_4^{2-} \rightleftharpoons CaHPO_4(aq)$. This review retained these values and obtained $\log_{10}K°$(25 °C) = 2.71 ± 0.20 and $\log_{10}K°$(0 °C) = 2.33 ± 0.20 by extrapolation to zero ionic strength using SIT with the estimate $\Delta\varepsilon(Pr_4NCl) \approx -0.4$ in analogy with $\Delta\varepsilon(Et_4NI) = -(0.41 \pm 0.15)$ obtained for $Na^+ + HPO_4^{2-} \rightleftharpoons NaHPO_4^-$ (see Section 2.2.1). The uncertainties have been estimated by this review.

Bjerrum (1958) reported pH measurements of experiments in which he mixed very dilute solutions of phosphoric acid and calcium hydroxide at 18 °C, where the ionic strengths ranged from 0.0014 to 0.0040 M and the measured pH from 5.9 – 8.0. Bjerrum (1958) tried to interpret the data considering two cases, first assuming that only the 1:1 complex $CaPO_4^-$ is formed and second, that only the 1:2 complexes $Ca(HPO_4)_2^{2-}$, $Ca(HPO_4)(PO_4)^{3-}$ and $Ca(PO_4)_2^{4-}$ are formed. In both cases he could not determine constant values for any of the equilibrium constants.

Greenwald (1963) states that Bjerrum (1958) "was unable to decide between the formation of a complex in which P : Ca = 1 and another in which it would be 2. Probably, this was due to his insistence that $CaHPO_4$ and $Ca(H_2PO_4)(HPO_4)^-$ must be strong acids, with pK ≈ 2. Our

assumption that the complex was $CaHPO_4$ was applied to Bjerrum's data. It was found that the values for the negative logarithm of the instability constant increased with increasing pH. Calculations of the instability constant were made, assuming that pK' for the hydrogen ion dissociation of $CaHPO_4$ was 8.0, 8.5, and 9.0. The most consistent values were obtained with pK' = 8.5. These are given in Tab. I." This review calculated from 16 values of Tab. I in Greenwald (1963), ranging from 2.36 to 2.96, the unweighted mean $\log_{10}K° = 2.63 \pm 0.15$ for the equilibrium $Ca^{2+} + HPO_4^{2-} \rightleftharpoons CaHPO_4(aq)$. Taking this value, accepting $\log_{10}K° = -8.5$ for the equilibrium $CaHPO_4(aq) \rightleftharpoons CaPO_4^- + H^+$, and using the selected value $\log_{10}K° = -12.35$ for the equilibrium $HPO_4^{2-} \rightleftharpoons PO_4^{3-} + H^+$, this review calculated $\log_{10}K° = 6.48 \pm 0.15$ for the equilibrium $Ca^{2+} + PO_4^{3-} \rightleftharpoons CaPO_4^-$.

Moreno et al. (1966) measured the solubility of dicalcium[1] phosphate dihydrate (DCPD), $CaHPO_4 \cdot 2H_2O$, in dilute phosphoric acid solutions in the pH range 3.5 – 6.8 at 37.5 °C. In order to account for the pH dependence of the measured solubilities Moreno et al. (1966) considered the complexes $CaHPO_4(aq)$ and $CaH_2PO_4^+$, and report in their Tab. 2 the values $K° = 588 \pm 0.09$ (1σ) for the equilibrium $Ca^{2+} + HPO_4^{2-} \rightleftharpoons CaHPO_4(aq)$ and $K° = 7.49 \pm 0.11$ (1σ) for the equilibrium $Ca^{2+} + H_2PO_4^- \rightleftharpoons CaH_2PO_4^+$, having used the extended Debye-Hückel equation for extrapolating data obtained in the ionic strength range 0.003 to 0.126 to zero ionic strength. This review calculated from the above values $\log_{10}K° = 2.77 \pm 0.01$ and $\log_{10}K° = 0.87 \pm 0.01$, respectively.

The same authors in a subsequent paper (Gregory et al. 1970) extended their solubility measurements of $CaHPO_4 \cdot 2H_2O$ to the temperature range 5 – 37.5 °C. For extrapolating their data to zero ionic strength Gregory et al. (1970) used both the extended Debye-Hückel equation and the Davies equation and report in their Tab. 12 for the equilibrium $Ca^{2+} + HPO_4^{2-} \rightleftharpoons CaHPO_4(aq)$ $K°(5\ °C) = 446 \pm 54$, $K°(15\ °C) = 272 \pm 35$, $K°(25\ °C) = 255 \pm 35$ and $K°(37.5\ °C) = 401 \pm 71$, obtained with the extended Debye-Hückel equation, and $K°(5\ °C) = 479 \pm 57$, $K°(15\ °C) = 283 \pm 36$, $K°(25\ °C) = 264 \pm 36$ and $K°(37.5\ °C) = 431 \pm 74$, obtained with the Davies equation, and for the equilibrium $Ca^{2+} + H_2PO_4^- \rightleftharpoons CaH_2PO_4^+$ $K°(5\ °C) = 10.1 \pm 1.7$, $K°(15\ °C) = 6.62 \pm 1.23$, $K°(25\ °C) = 5.10 \pm 1.03$ and $K°(37.5\ °C) = 4.51 \pm 1.44$, obtained with the extended Debye-Hückel equation, and $K°(5\ °C) = 9.69 \pm 1.83$, $K°(15\ °C) = 5.23 \pm 1.29$, $K°(25\ °C) = 3.67 \pm 0.98$ and $K°(37.5\ °C) = 3.28 \pm 1.48$, obtained with the Davies equation. Gregory et al. (1970) preferred the values obtained with the extended Debye-Hückel equation for further calculations of thermodynamic quantities and hence, this review retained these values, transformed to $\log_{10}$ units (Tab. 4.2-1)

Chughtai et al. (1968) used potentiometric measurements with a glass electrode to determine the association constants for the formation of the complexes $CaH_2PO_4^+$, $CaHPO_4(aq)$ and $CaPO_4^-$ in solutions of calcium phosphate at very low concentrations at 25.0 and 37.0 °C. They report $K(25\ °C) = 25.6 \pm 1.7$ and $K(37\ °C) = 31.9 \pm 1.6$ for the equilibrium $Ca^{2+} + H_2PO_4^- \rightleftharpoons CaH_2PO_4^+$, $K(25\ °C) = 548 \pm 2.8$ and $K(37\ °C) = 681 \pm 2.8$ for the equilibrium $Ca^{2+} + HPO_4^{2-} \rightleftharpoons CaHPO_4(aq)$, and $K(25\ °C) = (2.90 \pm 0.1) \cdot 10^6$ and $K(37\ °C) = (3.46 \pm 0.2) \cdot 10^6$ for the equilibrium $Ca^{2+} + PO_4^{3-} \rightleftharpoons CaPO_4^-$. This review retained these values, transformed to $\log_{10}$ units (Tab. 4.2-1).

[1] "Dicalcium" refers to the valency of Ca^{2+} and not to the moles of Ca in the formula.

Childs (1970) reported from a potentiometric study with a glass electrode at 37 °C in 0.15 M KNO_3 $\log_{10}K = 0.6 \pm 0.3$ for the equilibrium $Ca^{2+} + H_2PO_4^- \rightleftharpoons CaH_2PO_4^+$ and $\log_{10}K = 1.3 \pm 0.2$ for the equilibrium $Ca^{2+} + HPO_4^{2-} \rightleftharpoons CaHPO_4(aq)$. This review obtained $\log_{10}K° = 1.13 \pm 0.60$ (2σ) and $\log_{10}K° = 2.33 \pm 0.40$ (2σ), respectively, by extrapolating the above values to zero ionic strength using SIT with $\varepsilon(Ca^{2+}, NO_3^-) = (0.02 \pm 0.01)$), $\varepsilon(K^+, H_2PO_4^-) = -(0.14 \pm 0.06)$, $\varepsilon(K^+, HPO_4^{2-}) = -(0.10 \pm 0.06)$ and the estimates $\varepsilon(CaH_2PO_4^+, NO_3^-) \approx \varepsilon(CaH_2PO_4^+, Cl^-) = (0.05 \pm 0.10)$ and $\varepsilon(CaHPO_4(aq), KNO_3) = (0.0 \pm 0.1)$.

McDowell et al. (1971) measured the solubility of anhydrous calcium hydrogen phosphate, $CaHPO_4(cr)$, in dilute phosphoric acid solutions in the pH range 3.3 – 7.8 in the temperature range 5 – 37 °C. For extrapolating their data to zero ionic strength McDowell et al. (1971) used both the extended Debye-Hückel equation and the Davies equation and report in their Tab. III for the equilibrium $Ca^{2+} + HPO_4^{2-} \rightleftharpoons CaHPO_4(aq)$ $K°(5\ °C) = 220 \pm 30$, $K°(15\ °C) = 170 \pm 30$, $K°(25\ °C) = 360 \pm 40$ and $K°(37\ °C) = 360 \pm 70$, obtained with the extended Debye-Hückel equation, and $K°(5\ °C) = 240 \pm 30$, $K°(15\ °C) = 190 \pm 20$, $K°(25\ °C) = 380 \pm 40$ and $K°(37\ °C) = 390 \pm 90$, obtained with the Davies equation, and for the equilibrium $Ca^{2+} + H_2PO_4^- \rightleftharpoons CaH_2PO_4^+$ $K°(5\ °C) = 6 \pm 1$, $K°(15\ °C) = 11 \pm 1$, $K°(25\ °C) = 11 \pm 1$ and $K°(37\ °C) = 12 \pm 1$, obtained with the extended Debye-Hückel equation, and $K°(5\ °C) = 5 \pm 1$, $K°(15\ °C) = 10 \pm 1$, $K°(25\ °C) = 10 \pm 1$ and $K°(37\ °C) = 11 \pm 1$, obtained with the Davies equation. McDowell et al. (1971) preferred the values obtained with the Davies equation for further calculations of thermodynamic quantities and hence, this review retained these values, transformed to $\log_{10}$ units (Tab. 4.2-1).

Tung et al. (1988) measured the solubility of octacalcium phosphate, $Ca_8H_2(PO_4)_6 \cdot 5H_2O$, in dilute phosphoric acid solutions in the pH range 3.2 – 6.4 in the temperature range 25 – 45 °C. For extrapolating their data to zero ionic strength Tung et al. (1988) used both the extended Debye-Hückel equation and the Davies equation, which gave the same result, and report in their Tab. 13 $K°(25\ °C) = 8.48$, $K°(37\ °C) = 7.01$ and $K°(45\ °C) = 5.57$ for the equilibrium $Ca^{2+} + H_2PO_4^- \rightleftharpoons CaH_2PO_4^+$, $K°(25\ °C) = 264$, $K°(37\ °C) = 355$ and $K°(45\ °C) = 503$ for the equilibrium $Ca^{2+} + HPO_4^{2-} \rightleftharpoons CaHPO_4(aq)$, and a constant value $K = 2.9 \cdot 10^6$ at all temperatures for the equilibrium $Ca^{2+} + PO_4^{3-} \rightleftharpoons CaPO_4^-$. This review retained these values, transformed to $\log_{10}$ units, and with uncertainties assigned by this review (Tab. 4.2-1).

Ciavatta et al. (1991) measured calcium phosphate equilibria at 25 °C in 3 M $NaClO_4$ with a glass electrode in cells with no liquid junction potential. They report $\log_{10}K = -2.98 \pm 0.02$ for the equilibrium $Ca^{2+} + 2\ H_2PO_4^- \rightleftharpoons CaHPO_4(aq) + H_3PO_4(aq)$. Combining this value with $\log_{10}K = 6.279 \pm 0.015$ for the equilibrium $H^+ + HPO_4^{2-} \rightleftharpoons H_2PO_4^-$ and $\log_{10}K = 8.158 \pm 0.035$ for the equilibrium $2\ H^+ + HPO_4^{2-} \rightleftharpoons H_3PO_4(aq)$, determined by Havel & Högfeldt (1974) under the same conditions, i.e., at 25 °C in 3 M $NaClO_4$, this review calculated $\log_{10}K = 1.42 \pm 0.04$ for the equilibrium $Ca^{2+} + HPO_4^{2-} \rightleftharpoons CaHPO_4(aq)$. Using SIT with $\varepsilon(Ca^{2+}, ClO_4^-) = (0.27 \pm 0.03)$, $\varepsilon(Na^+, HPO_4^{2-}) = -(0.15 \pm 0.06)$ and the estimate $\varepsilon(CaHPO_4(aq), NaClO_4) = (0.0 \pm 0.1)$ this review obtained $\log_{10}K° = 2.93 \pm 0.42$ for the equilibrium $Mg^{2+} + HPO_4^{2-} \rightleftharpoons MgHPO_4(aq)$. Note that Ciavatta et al. (1994) report the value $\log_{10}K° = 2.54 \pm 0.05$, claiming to have carried out a SIT extrapolation with $\varepsilon(Ca^{2+}, ClO_4^-) = 0.27$, $\varepsilon(Na^+, HPO_4^{2-}) = -0.16$ and the estimate $\varepsilon(CaHPO_4(aq), NaClO_4) = 0.055$. However, using these SIT interaction coefficients, this review calculated $\log_{10}K° = 3.16$ for the equilibrium $Mg^{2+} + HPO_4^{2-} \rightleftharpoons MgHPO_4(aq)$. Hence, it remains unclear how Ciavatta et al. (1994) obtained the value $\log_{10}K° = 2.54$, largely differing from the result obtained by this review.

Saha et al. (1996) determined the stability constants of the 1:1 complexes formed between a series of divalent metal cations and hydrogen phosphate by potentiometric pH titration in aqueous solution at 25 °C in 0.1 M $NaNO_3$. For Ca^{2+} they report $\log_{10}K = 1.64 \pm 0.02$. Using SIT with $\varepsilon(Ca^{2+}, NO_3^-) = (0.02 \pm 0.01)$, $\varepsilon(Na^+, HPO_4^{2-}) = -(0.15 \pm 0.06)$ and the estimate $\varepsilon(CaHPO_4(aq), NaNO_3) = (0.0 \pm 0.1)$ this review obtained $\log_{10}K° = 2.53 \pm 0.20$ for the equilibrium $Ca^{2+} + HPO_4^{2-} \rightleftharpoons CaHPO_4(aq)$, with an uncertainty assigned by this review.

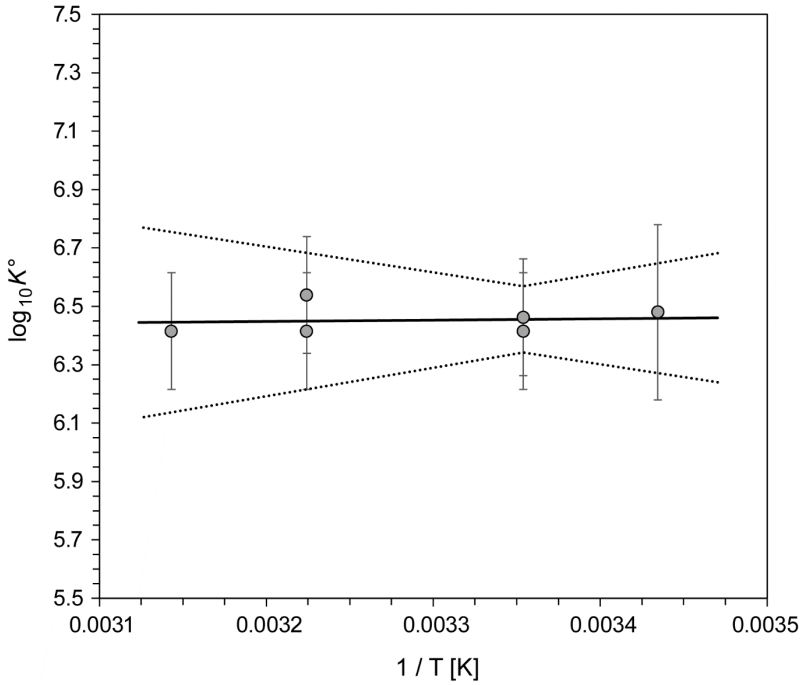

Fig. 4.2-7: The equilibrium constant $\log_{10}K°$ for $Ca^{2+} + PO_4^{3-} \rightleftharpoons CaPO_4^-$ as a function of reciprocal absolute temperature in the range 18 – 45 °C

Symbols: accepted $\log_{10}K°$ values taken from Tab. 4.2-1. Solid line: weighted linear regression. Dotted lines: lower and upper limits using $\log_{10}K°$ (298.15 K) = 6.46 ± 0.11 and $\Delta_rH_m°$ (298.15 K) = -(1 ± 18) kJ · mol^{-1} and extrapolated to lower and higher temperatures.

The accepted data of Tab. 4.2-1 have been used for weighted linear regressions of the $\log_{10}K°$ values versus the reciprocal of absolute temperature (Figs. 4.2-7 – 4.2-9). While the stability constants are fairly well established by these regression analyses, the obtained $\Delta_rH_m°$ values should be considered as approximate values only because of the small experimentally explored temperature intervals and the substantial scatter in $\log_{10}K°$ values, resulting in large uncertainties:

$Ca^{2+} + PO_4^{3-} \rightleftharpoons CaPO_4^-$

$\log_{10}K°$ (298.15 K) = 6.46 ± 0.11

$\Delta_rH_m°$(298.15 K) = -(1 ± 18) kJ · mol^{-1}

$\Delta_rC_{p,m}°$(298.15 K) = 0

$Ca^{2+} + HPO_4^{2-} \rightleftharpoons CaHPO_4(aq)$

$\log_{10}K°$ (298.15 K) = 2.58 ± 0.05

$\Delta_rH_m°$(298.15 K) = (13.1 ± 6.3) kJ · mol^{-1}

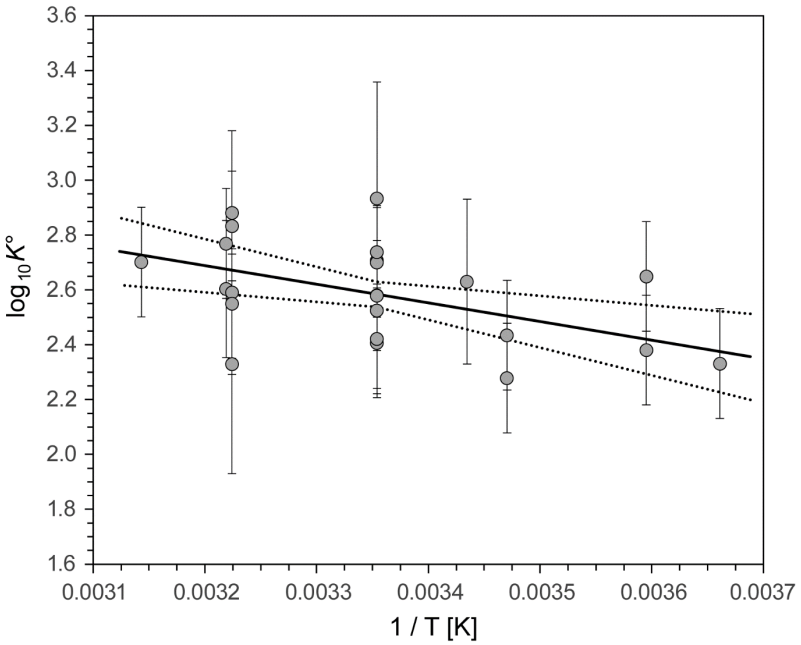

Fig. 4.2-8: The equilibrium constant $\log_{10}K°$ for $Ca^{2+} + HPO_4^{2-} \rightleftharpoons CaHPO_4(aq)$ as a function of reciprocal absolute temperature in the range 0 – 45 °C

Symbols: accepted $\log_{10}K°$ values taken from Tab. 4.2-1. Solid line: weighted linear regression. Dotted lines: lower and upper limits using $\log_{10}K°$ (298.15 K) = 2.58 ± 0.05 and $\Delta_r H_m°$ (298.15 K) = (13.1 ± 6.3) kJ · mol^{-1} and extrapolated to lower and higher temperatures.

$\Delta_r C_{p,m}°(298.15\ K) = 0$

$Ca^{2+} + H_2PO_4^- \rightleftharpoons CaH_2PO_4^+$

$\log_{10}K°\ (298.15\ K) = 0.99 \pm 0.09$

$\Delta_r H_m°(298.15\ K) = (3 \pm 13)\ kJ \cdot mol^{-1}$

$\Delta_r C_{p,m}°(298.15\ K) = 0$

These values are included in TDB 2020, together with the estimates

$\varepsilon(CaPO_4^-, Na^+) = -(0.05 \pm 0.10)\ kg \cdot mol^{-1}$

$\varepsilon(CaHPO_4(aq), NaCl) = (0.0 \pm 0.1)\ kg \cdot mol^{-1}$

$\varepsilon(CaH_2PO_4^+, Cl^-) = (0.05 \pm 0.10)\ kg \cdot mol^{-1}$

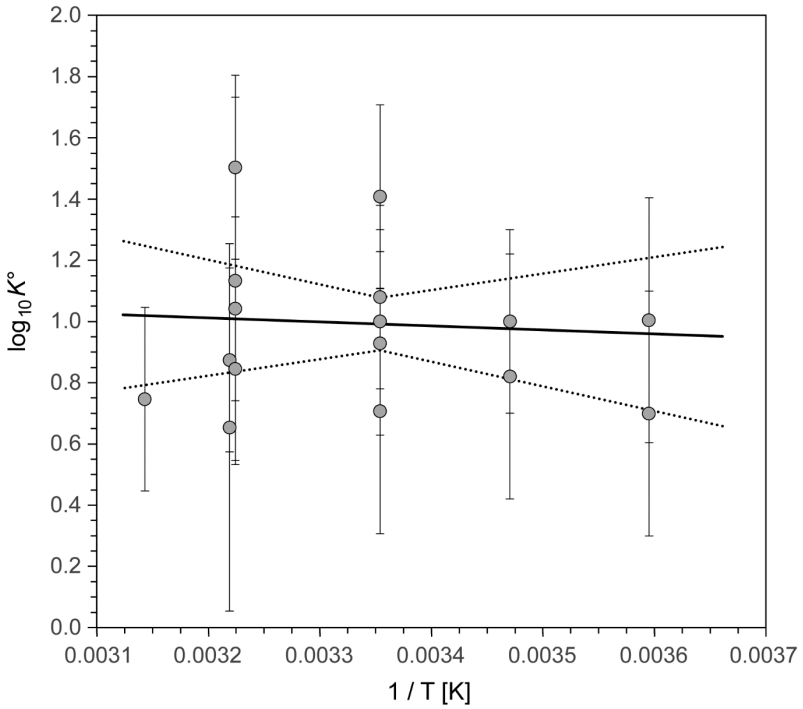

Fig. 4.2-9: The equilibrium constant $\log_{10}K°$ for $Ca^{2+} + H_2PO_4^- \rightleftharpoons CaH_2PO_4^+$ as a function of reciprocal absolute temperature in the range 5 – 45 °C

Symbols: accepted $\log_{10}K°$ values taken from Tab. 4.2-1. Solid line: weighted linear regression. Dotted lines: lower and upper limits using $\log_{10}K°$ (298.15 K) = 0.99 ± 0.09 and $\Delta_r H_m°$ (298.15 K) = (3 ± 13) kJ · mol^{-1} and extrapolated to lower and higher temperatures.

4.2.8.2 Calcium(II) phosphate compounds

As the principal concentrator of phosphorus in the earth's crust apatite is of great industrial importance and of great interest to geochemists. Depending on the predominance of fluorine, chlorine or hydroxyl, the mineral is called fluorapatite, $Ca_5(PO_4)_3F(s)$, chlorapatite, $Ca_5(PO_4)_3Cl(s)$, or hydroxyapatite (also called hydroxylapatite), $Ca_5(PO_4)_3OH(s)$. Fluorapatite is the most abundant of the three variants. Pure hydroxyapatites have been found, but pure chlorapatites are not known in nature, only chlorine-bearing hydroxyapatites (Valyashko et al. 1968). This review could not find any experimental investigations of the solubility of chlorapatite, and the information on the behaviour of fluorapatite in water is very limited. There are more data on the solubility of hydroxyapatite (Tab. 4.2-2)

Valyashko et al. (1968) state that hydroxyapatite gives well-defined powder photographs and when dissolved in water at high temperature yields solutions with the correct stoichiometric composition. Hence, Valyashko et al. (1968) conclude that "OH-apatite (and Cl-apatite and F-apatite), being a compound of constant composition, dissolves congruently in water. Using the thermodynamic data for the three varieties of apatite and their component ions, it is possible to calculate the solubility of apatites in water at different temperatures."

There are other calcium phosphate compounds, which, in addition to the apatites, are mainly of interest in studies of tooth and bone material. Hence, many studies have been done at 37 °C. Some of these phosphate compounds have been found as minerals in nature, such as monetite, $CaHPO_4$(cr), also called "dicalcium phosphate anhydrous" DCPA; brushite, $CaHPO_4 \cdot 2H_2O$(cr), also called "dicalcium phosphate dihydrate" DCPD; and tuite, β-$Ca_3(PO_4)_2$(cr), called "tricalcium phosphate" TCP. The metastable phase "octacalcium phosphate" OCP, $Ca_8(HPO_4)_2(PO4)_4 \cdot 5H_2O$, is not known as a mineral.

Tab. 4.2-2: Reported and accepted calcium phosphate solubility data

Temp. [°C]	**Medium**	**$\log_{10}K_s°$ reported** [a]	**$\log_{10}K_s°$ accepted** [b]	**Reference**
$Ca_5(PO_4)_3OH(cr) \rightleftharpoons 5\ Ca^{2+} + 3\ PO_4^{3-} + OH^-$				
25	dilute → 0	-57.75	-58.4 ± 0.7	Clark (1955)
25		-56.85		Lindsay & Moreno (1960)
25	dilute → 0	-57.43 ± 0.06	(-57.27 ± 0.42)	Moreno et al. (1968)
25	dilute → 0	-54.60 ± 0.07	(-54.49 ± 0.27)	Moreno et al. (1968)
25	dilute → 0	-58.3	-58.2 ± 0.9	Wier et al. (1971)
25	dilute → 0	-58.20 ± 0.15	-58.19 ± 0.47	Avnimelech et al. (1973)
25	dilute → 0	-58.37 to -58.12	-58.19 ± 0.23	Chuong (1973)
5	dilute → 0	-58.491 ± 0.044	-57.84 ± 0.29	McDowell et al. (1977)
15	dilute → 0	-58.535 ± 0.033	-58.11 ± 0.28	McDowell et al. (1977)
25	dilute → 0	-58.517 ± 0.036	-58.40 ± 0.36	McDowell et al. (1977)
37	dilute → 0	-58.629 ± 0.049	-58.74 ± 0.22	McDowell et al. (1977)
25	dilute → 0	-58.539 ± 0.023	-58.46 ± 0.36	Verbeek et al. (1980)
25	dilute → 0	-56.02 ± 0.38		Jaynes et al. (1999)
$Ca_5(PO_4)_3F(cr) \rightleftharpoons 5\ Ca^{2+} + 3\ PO_4^{3-} + F^-$				
25	0.8 – 5.0 m Ca + P → 0	-60.43 ± 0.03	-60.4 ± 1.0	Farr & Elmore (1962)
25	dilute → 0	-59.6	-59.6 ± 0.2	McCann (1968)
34	dilute → 0	-60.07 ± 0.07	-60.07 ± 0.20	McCann (1968)
45	dilute → 0	-60.3	-60.3 ± 0.2	McCann (1968)
25	dilute → 0	-58.13		Jaynes et al. (1999)
$CaHPO_4(cr) \rightleftharpoons Ca^{2+} + HPO_4^{2-}$				
5	dilute → 0	-6.706 ± 0.007	-6.66 ± 0.06	McDowell et al. (1971)
15	dilute → 0	-6.785 ± 0.003	-6.75 ± 0.08	McDowell et al. (1971)
25	dilute → 0	-6.900 ± 0.007	-6.86 ± 0.05	McDowell et al. (1971)
37	dilute → 0	-7.036 ± 0.009	-6.99 ± 0.05	McDowell et al. (1971)
25	dilute → 0	-6.60 ± 0.01		Jaynes et al. (1999)
$CaHPO_4 \cdot 2H_2O \rightleftharpoons Ca^{2+} + HPO_4^{2-} + 2\ H_2O(l)$				
25	0.165 M KCl	-6.57	-6.60 ± 0.15	Strates et al. (1957)
25	dilute → 0	-6.56	-6.59 ± 0.08	Moreno et al. (1960a)
37.5	dilute → 0	-6.66	-6.63 ± 0.02	Moreno et al. (1966)
5	dilute → 0	-6.63	-6.55 ± 0.05	Gregory et al. (1970)
15	dilute → 0	-6.60	-6.59 ± 0.03	Gregory et al. (1970)

Tab. 4.2-2: Cont.

Temp. [°C]	Medium	$\log_{10}K_s°$ reported [a]	$\log_{10}K_s°$ accepted [b]	Reference
25	dilute → 0	-6.59	-6.58 ± 0.07	Gregory et al. (1970)
37.5	dilute → 0	-6.62	-6.62 ± 0.02	Gregory et al. (1970)
37	dilute → 0	-6.646	-6.65 ± 0.10	Madsen (1970)
25	NaCl	-6.60 ± 0.02	-6.60 ± 0.02	Patel et al. (1974)
β-$Ca_3(PO_4)_2$				
5	dilute → 0	-29.01 ± 0.03	-28.60 ± 0.24	Gregory et al. (1974)
15	dilute → 0	-28.77 ± 0.02	-28.57 ± 0.21	Gregory et al. (1974)
25	dilute → 0	-28.92 ± 0.02	-28.90 ± 0.20	Gregory et al. (1974)
37.5	dilute → 0	-29.55 ± 0.02	-29.67 ± 0.14	Gregory et al. (1974)
25	dilute → 0	-30.74		Jaynes et al. (1999)
$CaK_3H(PO_4)_2$				
20	dilute → 0	-22.4 ± 0.8	-22.4 ± 0.8	Xu et al. (2020)
$Ca_4H(PO_4)_3 \cdot 3H_2O(s) \rightleftharpoons 4\ Ca^{2+} + 3\ PO_4^{3-} + H^+ + 2.5\ H_2O(l)$				
25	dilute → 0	-46.9	-47.0 ± 1.0	Moreno et al. (1960b)
37	dilute → 0	-48.34 ± 0.10	-48.3 ± 0.5	Madsen (1970)
37	KNO_3	-49.3 ± 0.2	-49.07 ± 0.72	Shyu et al. (1983)
25	KNO_3	-49.6 ± 0.2	-48.75 ± 0.52	Heughebaert & Nancollas (1985)
45	KNO_3	-49.8 ± 0.3	-48.71 ± 0.94	Heughebaert & Nancollas (1985)
4	dilute → 0	-48.3 ± 0.2	-48.3 ± 0.4	Tung et al. (1988)
4.8	dilute → 0	-48.3 ± 0.2	-48.3 ± 0.4	Tung et al. (1988)
6.0	dilute → 0	-48.2	-48.2 ± 0.4	Tung et al. (1988)
18	dilute → 0	-48.3	-48.3 ± 0.4	Tung et al. (1988)
23.5	dilute → 0	-48.4 ± 0.1	-48.4 ± 0.4	Tung et al. (1988)
37	dilute → 0	-48.7 ± 0.2	-48.7 ± 0.4	Tung et al. (1988)

[a] Data as reported in the cited publications or calculated by this review from the reported data, see text.
[b] Recalculated and/or extrapolated to $I = 0$ by this review, see text, and 2σ uncertainties assigned or estimated by this review.

As Nancollas (1984) reports, in discussions of the precipitation of calcium phosphates, the phase which forms is usually loosely referred to as hydroxyapatite, the thermodynamically stable form. However, most calcium phosphate solutions in which precipitation experiments are made are initially supersaturated with respect to other calcium phosphate phases, such as tricalcium phosphate, TCP, octacalcium phosphate, OCP, and dicalcium phosphate dihydrate, DCPD.

As Dorozhkin (2011) discusses, $Ca_3(PO_4)_2$, TCP, cannot be precipitated from aqueous solutions, and the only calcium phosphate compound which becomes less soluble than hydroxyapatite is $CaHPO_4 \cdot 2H_2O$, DCPD, however only at pH < 4 and at a concentration of dissolved calcium and phosphate above 0.01 mol/L.

$Ca_5(PO_4)_3OH$(cr), OH-apatite

Clark (1955) was the first who obtained a constant solubility product of hydroxyapatite. As Clark (1955) reports, the solid phase calcium phosphates used for the solubility measurements were prepared by reacting dilute solutions of $Ca(OH)_2$ and H_3PO_4 at different temperatures for varying periods of time while N_2 (CO_2 free) was passed through the systems. Following reactions at elevated temperatures, the flasks containing the suspensions were placed in a water bath at 25 °C for 96 hours and the pH was measured with a glass electrode in the presence of N_2. The suspensions were filtered rapidly, and the phosphate and calcium determinations were made on the filtrates. The activities of the ions were estimated by means of the Debye-Hückel equation. From 27 oversaturation experiments, where the precipitates before had reacted at 90 °C for 120 hours, and from 7 undersaturation experiments, where some of these precipitates had been redispersed in water, Clark (1955) obtained $\log_{10}K_s° = -115.5$ for $Ca_{10}(PO_4)_6(OH)_2$(cr) ⇌ 10 Ca^{2+} + 6 PO_4^{3-} + 2OH^- ($\log_{10}K_s° = -57.75$ for $Ca_5(PO_4)_3OH$(cr) ⇌ 5 Ca^{2+} + 3 PO_4^{3-} + OH^-). Note that this value has been used by Valyashko et al. (1968) in their evaluation of thermochemical data for apatites (see discussion below). Clark (1955) did not consider calcium phosphate complexes and he does not state which phosphoric acid dissociation data he has used. As all experimental data are reported in Tab. I and II of Clark (1955), this review re-evaluated the solubility product of $Ca_5(PO_4)_3OH$(cr) using SIT with $\Delta\varepsilon = 0$ (I = 0.0001 to 0.007 M), phosphoric acid and dissociation data as included in TDB 2020 and complexation data of $CaPO_4^-$, $CaHPO_4$(cr) and $CaH_2PO_4^+$ as selected by this review, and obtained $\log_{10}K_s° = -58.4 \pm 0.7$ for $Ca_5(PO_4)_3OH$(cr) ⇌ 5 Ca^{2+} + 3 PO_4^{3-} + OH^-.

Lindsay & Moreno (1960) calculated a solubility diagram for phosphate compounds in soils at 25 °C from literature data. For hydroxyapatite, $Ca_{10}(PO_4)_6(OH)_2$(cr), they give $\log_{10}K = -113.7$, calculated from a thermochemical data compilation. This value of uncertain origin has not been retained by this review.

Moreno et al. (1968) prepared two portions of a synthetic hydroxyapatite, $Ca_5(PO_4)_3OH$(cr), fully characterised by X-ray, infrared, petrographic and chemical analyses, by heating them at 1'000 °C for 6 days in room atmosphere and in the presence of one bar water vapour. Solubility isotherms for these two samples, air heated and steam heated, were determined at 25 °C in the pH range 5.0 – 7.4 by equilibrating the solids with dilute H_3PO_4 solutions. Moreno et al. (1968) report that both samples dissolved stoichiometrically. Moreno et al. (1968) calculated solubility products using the extended Debye-Hückel equation and including data for the complexes $CaHPO_4$(cr) and $CaH_2PO_4^+$ taken from Moreno et al. (1966) (see preceding Section). They obtained $K_s° = (3.7_3 \pm 0.5) \cdot 10^{-58}$ ($\log_{10}K_s° = -57.43 \pm 0.06$) for the steam heated sample, and $K_s° = (2.5_1 \pm 0.4) \cdot 10^{-55}$ ($\log_{10}K_s° = -54.60 \pm 0.07$) for the air heated sample. As all experimental data are reported in Tab. 1 and 2 of Moreno et al. (1968), this review re-evaluated the solubility product of $Ca_5(PO_4)_3OH$(cr) using SIT with $\Delta\varepsilon = 0$ (I = 0.0003 to 0.0095 M), phosphoric acid dissociation data as included in TDB 2020 and complexation data of $CaPO_4^-$, $CaHPO_4$(cr) and $CaH_2PO_4^+$ as selected by this review, and obtained $\log_{10}K_s° = -57.27 \pm 0.42$ (steam heated) and $\log_{10}K_s° = -54.49 \pm 0.27$ (air heated) for $Ca_5(PO_4)_3OH$(cr) ⇌ 5 Ca^{2+} + 3 PO_4^{3-} + OH^-.

Moreno et al. (1968) tried to rationalise the large discrepancy of almost three orders of magnitude in the solubility products by a possible dehydration effect in the air heated sample. However, the solubility product of the steam heated sample is also significantly at variance with most other results discussed here (see Tab. 4.2-2). Both samples had been washed with distilled water only after heat treatment, while Verbeek et al. (1980) washed their steam heated samples with dilute phosphoric acid solutions and obtained solubility products in line with other studies (see Tab. 4.2-2 and discussion below). It seems that treatment with distilled water only does not remove surface layers of the steam heated sample which leads to spurious solubility effects.

Hence, this review did not consider the results of Moreno et al. (1968) in the final data analysis for hydroxyapatite.

Wier et al. (1971) studied the solubility of commercially available synthetic hydroxyapatite at 25 °C in five series of experiments lasting from 14 to 120 days. For a sixth series, the synthetic hydroxyapatite was heated in a steam autoclave for 50 days at a temperature of 120 °C, and the subsequent solubility experiments at 25 °C lasted 28 days. Solubility experiments were made with the aid of Plexiglas dialysis cells fitted with a cellulose acetate dialysing membrane. The solid was placed on one side of the membrane, solution was added to both sides, and solution was removed for analysis from the side containing no solid. In all experiments Wier et al. (1971) observed substantial scatter in the resulting solubility constants of about two orders of magnitude. In the first five series of experiments Wier et al. (1971) report that no systematic effect could be seen except an insignificantly higher solubility for experiments with the highest solid to liquid ratio of 1 g/L, while for the sixth series Wier et al. (1971) report a significantly lower mean solubility product for experiments done with 0.01g solid/L than found for experiments with 0.1 g/L. McDowell et al. (1977) discuss the effect of selective permeability of cellulose membranes and conclude that the different solubility constants obtained for two solid to liquid ratios indicate that these equilibrations had not reached saturation. Hence, this review accepted only the results of the experiments with 120 days equilibration time. For these experiments Wier et al. (1971) report $\log_{10}K_s° = -116.6$ for $Ca_{10}(PO_4)_6(OH)_2(cr) \rightleftharpoons 10\ Ca^{2+} + 6\ PO_4^{3-} + 2OH^-$, translating to $\log_{10}K_s° = -58.3$ for $Ca_5(PO_4)_3OH(cr) \rightleftharpoons 5\ Ca^{2+} + 3\ PO_4^{3-} + OH^-$. As all experimental data are reported in Tab. 1 of Wier et al. (1971), this review re-evaluated the solubility product of $Ca_5(PO_4)_3OH(cr)$ using SIT with $\Delta\varepsilon = 0$ (I = 0.001 to 0.021 M), phosphoric acid dissociation data as included in TDB 2020 and complexation data of $CaPO_4^-$, $CaHPO_4(cr)$ and $CaH_2PO_4^+$ as selected by this review, and obtained $\log_{10}K_s° = -58.2 \pm 0.9$.

Avnimelech et al. (1973) measured the solubility of freshly prepared hydroxyapatite at 25 °C by equilibration with dilute phosphoric acid solutions in the pH range 4.8 – 6.9. Avnimelech et al. (1973) report $K_s° = (6.3 \pm 2.1) \cdot 10^{-59}$ ($\log_{10}K_s° = -58.20 \pm 0.15$). As all experimental data are reported in Tab. 1 of Avnimelech et al. (1973), this review re-evaluated the solubility product of $Ca_5(PO_4)_3OH(cr)$ using SIT with $\Delta\varepsilon = 0$ (I = 0.0002 to 0.007 M), phosphoric acid dissociation data as included in TDB 2020 and complexation data of $CaPO_4^-$, $CaHPO_4(cr)$ and $CaH_2PO_4^+$ as selected by this review, and obtained $\log_{10}K_s° = -58.19 \pm 0.47$.

Chuong (1973) investigated the solubility of hydroxyapatite in the quaternary system $Ca(OH)_2$-H_3PO_4-H_2O-HCl at 25 °C in the pH range 4.8 – 6.0, and reports in his Tab. $K_s° = 4.22 \cdot 10^{-59}$ to $7.66 \cdot 10^{-59}$ ($\log_{10}K_s° = -58.37$ to -58.12). As all experimental data are reported in the Tab. of Chuong (1973), this review re-evaluated the solubility product of $Ca_5(PO_4)_3OH(cr)$ using SIT with $\Delta\varepsilon = 0$ (I = 0.002 to 0.026 M), phosphoric acid dissociation data as included in TDB 2020 and complexation data of $CaPO_4^-$, $CaHPO_4(cr)$ and $CaH_2PO_4^+$ as selected by this review, and obtained $\log_{10}K_s° = -58.19 \pm 0.23$.

McDowell et al. (1977) prepared hydroxyapatite by titrating a boiling aqueous suspension of $Ca(OH)_2$ with 0.5 M H_3PO_4. The solid was characterised by chemical analysis, the optical microscope and IR spectroscopy. A series of equilibration experiments with dilute H_3PO_4 solutions was done at 5, 15, 25 and 37 °C in the pH range 3.7 – 6.7. McDowell et al. (1977) calculated solubility products using the extended Debye-Hückel equation and including data for the complexes $CaHPO_4(cr)$ and $CaH_2PO_4^+$ taken from Gregory et al. (1970). They report $\log_{10}K_s°(5\ °C) = -58.491 \pm 0.044$, $\log_{10}K_s°(15\ °C) = -58.535 \pm 0.033$, $\log_{10}K_s°(25\ °C) = -58.517 \pm 0.036$ and $\log_{10}K_s°(37\ °C) = -58.629 \pm 0.049$. However, the complexation data of Gregory et al. (1970) are slightly at variance with those selected by this review, especially at temperatures below

25 °C (see preceding Section). As all experimental data are reported in Tab. 1 – 4 of McDowell et al. (1977), this review re-evaluated the solubility product of $Ca_5(PO_4)_3OH$(cr) using SIT with $\Delta\varepsilon = 0$ (I = 0.0003 to 0.11 M), phosphoric acid and water dissociation data as included in TDB 2020 and complexation data of $CaPO_4^-$, $CaHPO_4$(cr) and $CaH_2PO_4^+$ as selected by this review, and obtained $\log_{10}K_s°$(5 °C) = -57.84 ± 0.29, $\log_{10}K_s°$(15 °C) = -58.11 ± 0.28, $\log_{10}K_s°$(25 °C) = -58.40 ± 0.36 and $\log_{10}K_s°$(37 °C) = -58.74 ± 0.22.

McDowell et al. (1977) in addition evaluated published solubility data at 25 °C and concluded that the best value for the solubility product is $\log_{10}K_s°$ (298.15 K) = -58.33 ± 0.24. This value is cited by Nancollas (1984) but without the uncertainty estimate.

Verbeek et al. (1980) determined the solubilities of synthetic calcium hydroxyapatites, prepared by different procedures, in the ternary system $Ca(OH)_2$-H_3PO_4-H_2O at 25 °C in the pH range 4.8 – 6.0 by equilibration in dilute H_3PO_4 solutions. Hydroxyapatite prepared by solid state reaction of $CaCO_3$ and $CaHPO_4$, as well as precipitated hydroxyapatite, both heated at 1200 °C in water vapour atmosphere, showed no constant $K_s°$ values (series A and B in Tab. 1 of Verbeek et al. 1980). After being washed with a dilute phosphoric acid solution at boiling temperature, these samples equilibrate to a common solubility product of $K_s° = (2.89 \pm 0.15) \cdot 10^{-59}$ ($\log_{10}K_s° = -58.539 \pm 0.023$) (series C, D and E in Tab. 1 of Verbeek et al. 1980). As all experimental data are reported in Tab. 1 of Verbeek et al. (1980), this review re-evaluated the solubility product of $Ca_5(PO_4)_3OH$(cr) using SIT with $\Delta\varepsilon = 0$ (I = 0.0005 to 0.0090 M), phosphoric acid dissociation data as included in TDB 2020 and complexation data of $CaPO_4^-$, $CaHPO_4$(aq) and $CaH_2PO_4^+$ as selected by this review, and obtained $\log_{10}K_s°$(25 °C) = -58.46 ± 0.36.

Jaynes et al. (1999) state that "most phosphate mineral solubility data in use were measured more than 20 yr ago when instrumentation and methods were generally less sophisticated. The objective of this study was to measure calcium phosphate mineral solubilities using modern analytical equipment and techniques. Natural and synthetic Ca phosphate minerals (< 50 μm) were equilibrated in water and dilute HCl for 6 mo with continuous agitation. X-ray diffraction (XRD) was used to identify compositions before and after equilibration. Filtered (< 0.2 μm) solution aliquots were analysed for pH and chemistry. Chemical compositions were determined using inductively coupled plasma spectroscopy (ICP). Aqueous carbonates were determined from alkalinity titrations after phosphate alkalinity corrections. The chemical speciation model 'Soilchem' was used to calculate free ion concentrations and ionic strengths. Ion activity products (IAPs) were determined from free ion concentrations and single ion activity coefficients."

After this proud announcement, Jaynes et al. (1999) report in their Tab. 2 a "Measured Log IAP" of -56.02 ± 0.38 for hydroxyapatite, a value more than two orders of magnitude higher than most results discussed here (Tab. 4.2-2). Jaynes et al. (1999) do not report any numerical analytical results, no measured pH values, just a plot with huge symbols of Ca and P concentrations versus time, and a plot of log IAP versus time, where the symbols have the size of 2 $\log_{10}$-units. Further, no details of their calculations are disclosed, and it remains unclear if they considered Ca phosphate complexes. No re-calculation or re-evaluation whatsoever is possible. It seems that the message of this publication is "we used modern analytical equipment and techniques and here is the final number, take it or leave it". This review decided to leave it.

Liu et al. (2014) measured the effect of "excess" phosphate on the solubility of hydroxyapatite by "solid titration". Solid titration seems to be used exclusively by a group associated with its inventor, Brian W. Darvell, one of the corresponding authors of this publication. "In essence, the method depends on determining, by a laser-scattering detector, the point at which no further solid may dissolve, or at which a new precipitate forms, using small increments of solid that must

dissolve completely before a further increment is added" (Liu et al. 2014). The solubilities determined by solid titration are orders of magnitude lower than the "conventional solubility" (see Fig. 5 in Liu et al. 2014), In the latter case, according to Liu et al. (2014), "the calculated solubility in such a system depends critically on the solution speciation – complexes and ion pairs – and a simplistic approach is doomed … unlike the absolute determination by solid titration of a physical endpoint". Whatever in the complex dissolution – precipitation processes of micrometre to nanometre particles during "solid titration" is observed, it seems unlikely that this is related to the thermodynamic equilibrium of a macroscopic solid and an aqueous solution. Hence, the discussion of phenomena described by Liu et al. (2014) has not been further considered by this review.

The weighted mean of the solubility constants of Clark (1955), Wier et al. (1971), Avnimelech et al. (1973), Chuong (1973), McDowell et al. (1977) and Verbeek et al. (1980) at 25 °C, as re-calculated and accepted by this review (Tab. 4.2-2), is selected:

$$Ca_5(PO_4)_3OH(cr) \rightleftharpoons 5\ Ca^{2+} + 3\ PO_4^{3-} + OH^-$$

$$\log_{10}K_s^\circ\ (298.15\ K) = -58.29 \pm 0.15$$

Note that this value and its 2σ uncertainty are in excellent agreement with the value -58.33 ± 0.24 recommended by McDowell et al. (1977).

$Ca_5(PO_4)_3F(cr)$, F-apatite

Farr et al. (1962) determined phase equilibria in the system CaO – P_2O_5 – HF – H_2O at 25 and 50 °C for the region represented by liquid phases containing 4 – 35% P_2O_5, 0.7 – 5.5% CaO and less than 0.07% F. The stable solids in equilibrium with the saturated solutions were $CaF_2(cr)$ and $Ca_5(PO_4)_3F(cr)$ or $CaF_2(cr)$ and $Ca(H_2PO_4)_2{\cdot}H_2O$. The invariant points representing solutions saturated with all three compounds were located at both temperatures. Measurements on the saturated solutions included pH, density and vapour pressure.

Farr & Elmore (1962) used the experimental data of Farr et al. (1962), saturated at 25 °C with both $Ca_5(PO_4)_3F(cr)$ and $CaF_2(cr)$, for estimating the activities of $H_2O(l)$, $H_3PO_4(aq)$, $H_2PO_4^-$ and Ca^{2+}, and the activity solubility product of fluorapatite in the pH range 0.81 to 1.76 at ionic strengths 0.8 – 5.0 m calcium phosphate. Farr & Elmore (1962) obtained $K_s^\circ = (1.4 \pm 0.2) \cdot 10^{-121}$ ($\log_{10}K_s^\circ = -120.85 \pm 0.06$) for $Ca_{10}(PO_4)_6F_2(cr) \rightleftharpoons 10\ Ca^{2+} + 6\ PO_4^{3-} + 2\ F^-$, translating to $\log_{10}K_s^\circ = -60.43 \pm 0.03$ for $Ca_5(PO_4)_3F(cr) \rightleftharpoons 5\ Ca^{2+} + 3\ PO_4^{3-} + F^-$. Note that this value has been used by Valyashko et al. (1968) in their evaluation of thermochemical data for apatites (see discussion below).

The solubility product of fluorapatite obtained from solutions saturated with both $Ca_5(PO_4)_3F(cr)$ and $CaF_2(cr)$, depends on the chosen solubility product for $CaF_2(cr)$. Farr & Elmore (1962) used $\log_{10}K_s^\circ = -9.79$, calculated from tabulated thermochemical data, which is at variance with the value -10.46 selected by this review (Section 4.2.4.2). Farr & Elmore (1962) did not consider any calcium fluoride or phosphate complexes. The ionic medium consisted of varying amounts of calcium phosphate and in their activity estimation procedures Farr & Elmore (1962) had to use different modified Debye-Hückel equations to describe the activity coefficients of Ca^{2+} and $H_2PO_4^-$ in these widely varying concentrations of "self-medium". These factors add considerable uncertainty to the seemingly very precise solubility product of Farr & Elmore (1962), which is retained by this review as $\log_{10}K_s^\circ = -60.4 \pm 1.0$ but with a substantially increased uncertainty.

McCann (1968) measured the solubility of fluorite, CaF_2(cr), and fluorapatite, $Ca_5(PO_4)_3F$(cr), in dilute phosphoric acid solutions under various conditions and found that the obtained solubility product was not significantly affected by variation of crystal size, solid to solution ratios, or ionic strength, and was constant from pH 4.5 – 6.4. McCann (1968) reports K_s°(34 °C) = (3.58 ± 0.18) · 10^{-11} ($\log_{10}K_s$°(34 °C) = -10.446 ± 0.022) for CaF_2(cr) ⇌ Ca^{2+} + 2 F^-, and K_s°(34 °C) = (8.6 ± 1.3) · 10^{-61} ($\log_{10}K_s$°(34 °C) = -60.07 ± 0.07) for $Ca_5(PO_4)_3F$(cr) ⇌ 5 Ca^{2+} + 3 PO_4^{3-} + F^-. In addition, McCann (1968) reports for fluorapatite $\log_{10}K_s$°(25 °C) = -59.6 and $\log_{10}K_s$°(45 °C) = -60.3.

McCann (1968) used phosphoric acid dissociation constants which do not differ more than ± 0.02 $\log_{10}$-units at 25, 34 and 45 °C from the data included in TDB 2020. McCann (1968) considered CaF^+ complexation and used the complexation constants of Moreno et al. (1966) for the complexes $CaHPO_4$(aq) and $CaH_2PO_4^+$, which differ from those selected in this review by +0.12 and -0.12 $\log_{10}$-units (see Tab. 4.2-1). However, at pH around 5 the concentrations of both complexes are of the same order of magnitude in the experiments of McCann (1968), and the effect of the small variations in the stability constants cancels out. Furthermore, the obtained solubility constant for CaF_2(cr), $\log_{10}K_s$°(34 °C) = -10.446 ± 0.022, is in excellent agreement with $\log_{10}K_s$°(34 °C) = -10.42 ± 0.10 selected for TDB 2020 (Section 4.2.4.2). In summary, the solubility products reported by McCann (1968) are retained by this review with an assigned uncertainty of ± 0.2 $\log_{10}$-units (see Tab. 4.2-2).

Jaynes et al. (1999) report in their Tab. 2 a value -58.13 for fluorapatite with the remark "Calculated log IAP from 25 mmol L^{-1} HCl addition, 6-mo equilibration sample only". Jaynes et al. (1999) do not report any numerical analytical results, no measured pH values, just a plot with huge symbols of Ca, P and F concentrations versus time, and plots of log IAP versus time and HCl concentration (their Fig. 8), where the symbols have the size of 2 $\log_{10}$-units. These plots show that after 6 months equilibration time the calculated ion activity products (IAP) decreased from about -46 to about -58 with increasing HCl added. Vice versa, the calculated IAP increased with increasing equilibration time from about -62 to about -58 in the experiment with 25 mmol HCl added. As Jaynes et al. (1999) conclude "fluorapatite equilibrium was evidently not achieved", and hence, the values of Jaynes et al. (1999) have not been considered further by this review.

The weighted mean of the solubility constants of Farr & Elmore (1962) and McCann (1968) at 25 °C, as accepted by this review (Tab. 4.2-2), is selected:

$$Ca_5(PO_4)_3F(cr) \rightleftharpoons 5\ Ca^{2+} + 3\ PO_4^{3-} + F^-$$

$$\log_{10}K_s^\circ\ (298.15\ K) = -59.63 \pm 0.20$$

Apatites: synthesis

The group of the late I. L. Khodakovskiy published in 1968 a synthesis of thermodynamic data for hydroxy-, fluor- and chlorapatite (Valyashko et al. 1968). They accepted measured low-temperature heat capacity and entropy data of hydroxyapatite (Egan et al. 1951a) and fluorapatite (Egan et al. 1951b) and estimated the heat capacity and entropy of chlorapatite. Using the entropy of hydroxyapatite (Egan et al. 1951a) and the solubility product of Clark (1955), combined with entropy and enthalpy of formation data for aqueous species (in their Tab. 3), they calculated the enthalpy of formation of hydroxyapatite. Likewise, using the entropy of fluorapatite (Egan et al. 1951b) and the solubility product of Farr & Elmore (1962), they calculated the

enthalpy of formation of fluorapatite. The enthalpy of formation of chlorapatite has been taken from Gottschal (1958). Note that the entropy and heat capacity values reported in Tab. 2 and 3 of Valyashko et al. (1968) refer to cal and not to kcal, as erroneously written in their table headers.

Valyashko et al. (1968) then explain that the solubility constants of the apatites for different temperatures were calculated from the equation

$$\log_{10}K_s°(T) = -A^* / T + B^* - C^* \cdot T$$

derived on the assumption that

$$\Delta_r C_{p,m}°(T°) = -2 \cdot \ln(10) \cdot R \cdot T° \cdot C^*$$

where R is the gas constant and T° = 298.15 K. Valyashko et al. (1968) state that, as shown by one of the authors (Khodakovskiy), this assumption is justified for solution reactions of sparingly soluble substances over a broad range of temperatures up to 350 °C. The coefficients A*, B* and C* are related to the standard thermodynamic functions by

$$A^* = \Delta_r H_m°(T°) / (\ln(10) \cdot R) + C^* \cdot T°$$

$$B^* = \Delta_r S_m°(T°) / (\ln(10) \cdot R) + 2 \cdot C^* \cdot T°$$

$$C^* = -\Delta_r C_{p,m}°(T°) / (2 \cdot \ln(10) \cdot R \cdot T°)$$

Note that Valyashko et al. (1968) always write T even if they mean T° in their equations, and it needed some trial-and-error calculation efforts by this review until the numerical $\log_{10}K_s°(T)$ values reported in Tab. 4 of Valyashko et al. (1968) could exactly be reproduced using the above correctly labelled equations.

The temperature function of Valyashko et al. (1968) is at variance with the type of function used in TDB 2020

$$\log_{10}K_s°(T) = A + C / T + D \cdot \log_{10}(T)$$

where the coefficients A, C and D are related to the standard thermodynamic functions by

$$A = \Delta_r S_m°(T°) / (\ln(10) \cdot R) + D \cdot (1 + \ln(T°)) / \ln(10)$$

$$C = -\Delta_r H_m°(T°) / (\ln(10) \cdot R) + D / \ln(10)$$

$$D = \Delta_r C_{p,m}°(T°) / R$$

Combining and rearranging the above equations gives

$$\log_{10}K_s°(T) = -\Delta_r H_m°(T°) / (\ln(10) \cdot R \cdot T) + \Delta_r S_m°(T°) / (\ln(10) \cdot R) +$$

$$\Delta_r C_{p,m}°(T°) / (\ln(10) \cdot R) \cdot (-1 + T° / T + \ln(T / T°))$$

while combining and rearranging the equations of Valyashko et al. (1968) gives

$$\log_{10}K_s°(T) = -\Delta_r H_m°(T°) / (\ln(10) \cdot R \cdot T) + \Delta_r S_m°(T°) / (\ln(10) \cdot R) + \Delta_r C_{p,m}°(T°) / (\ln(10) \cdot R) \cdot (-1 + T° / (2 \cdot T) + T / (2 \cdot T°))$$

The difference between the two temperature functions is the temperature variation of the heat capacity term, i.e. -1 + T° / T + ln(T / T°) versus -1 + T° / (2 · T) + T / (2 · T°). At 25 °C both functions are 0, and between 0 °C and 50 °C the difference in the calculated apatite solubility constants does not exceed 0.01 $\log_{10}$-units. At 100 °C the difference is about 0.2 $\log_{10}$-units, increasing to 0.7 at 150 °C and approaching 7 orders of magnitude at 350 °C.

This review follows the approach of Valyashko et al. (1968), i.e., deriving constant enthalpy and heat capacity terms for the apatites, but recommends using the temperature function of TDB 2020 for calculations in the temperature range 0 – 100 °C.

Egan et al. (1951a) measured heat capacities of hydroxyapatite, $Ca_{10}(PO_4)_6(OH)_2$(cr), for temperatures from 13.18 to 298.15 K and used a Debye extrapolation between 0 and 13.18 K. The derived entropy is reported as $S_m°$(298.15 K) = 186.6 ± 0.2 cal · K^{-1} · mol^{-1} (780.7 ± 0.8 J · K^{-1} · mol^{-1}) and the heat capacity is $C_{p,m}°$(298.15 K) = 184.07 cal · K^{-1} · mol^{-1} (770.15 J · K^{-1} · mol^{-1}). This review selected $S_m°$(298.15 K) = 390.4 ± 0.5 J · K^{-1} · mol^{-1} and $C_{p,m}°$(298.15 K) = 385.1 ± 0.5 J · K^{-1} · mol^{-1} for $Ca_5(PO_4)_3OH$(cr).

Egan et al. (1951b) measured heat capacities of fluorapatite, $Ca_{10}(PO_4)_6F_2$(cr), for temperatures from 13.32 to 298.15 K and used a Debye extrapolation between 0 and 13.32 K. The derived entropy is reported as $S_m°$(298.15 K) = 185.5 ± 0.2 cal · K^{-1} · mol^{-1} (776.1 ± 0.8 J · K^{-1} · mol^{-1}) and the heat capacity is $C_{p,m}°$(298.15 K) = 179.73 cal · K^{-1} · mol^{-1} (751.99 J · K^{-1} · mol^{-1}. This review selected $S_m°$(298.15 K) = 388.1 ± 0.5 J · K^{-1} · mol^{-1} and $C_{p,m}°$(298.15 K) = 376.0 ± 0.5 J · K^{-1} · mol^{-1} for $Ca_5(PO_4)_3F$(cr).

Valyashko et al. (1968) report for chlorapatite, $Ca_{10}(PO_4)_6Cl_2$(cr), an estimated entropy $S_m°$(298.15 K) = 190.2 cal · K^{-1} · mol^{-1} (795.8 J · K^{-1} · mol^{-1}) and an estimated heat capacity of $C_{p,m}°$(298.15 K) = 181.15 cal · K^{-1} · mol^{-1} (757.93 J · K^{-1} · mol^{-1} with a footnote to their Tab. 2 "calculated by the method of Karapet'yants", with a reference to a "Nauka" report not available to this review. This review selected $S_m°$(298.15 K) = 397.9 ± 1.0 J · K^{-1} · mol^{-1} and $C_{p,m}°$(298.15 K) = 379.0 ± 1.0 J · K^{-1} · mol^{-1} for $Ca_5(PO_4)_3Cl$(cr).

For calculating $\Delta_r C_{p,m}°$(298.15 K) and $\Delta_r S_m°$(298.15 K) values for the reaction $Ca_5(PO_4)_3X$(cr) ⇌ 5 Ca^{2+} + 3 PO_4^{3-} + X^- (X = OH, F, Cl) this review used the above selected values together with entropy and heat capacity values for the aqueous species taken from CODATA (Cox et al. 1989): $S_m°$(Ca^{2+}, 298.15 K) = -56.2 ± 1.0 J · K^{-1} · mol^{-1}, $S_m°$(OH^-, 298.15 K) = -10.9 ± 0.2 J · K^{-1} · mol^{-1}, $S_m°$(F^-, 298.15 K) = -13.8 ± 0.8 J · K^{-1} · mol^{-1}, $S_m°$(Cl^-, 298.15 K) = 56.6 ± 0.2 J · K^{-1} · mol^{-1}; from Grenthe et al. (1992): $S_m°$(PO_4^{3-}, 298.15 K) = -220.97 ± 12.85 J · K^{-1} · mol^{-1}; from Wagman et al. (1982): $C_{p,m}°$(OH^-, 298.15 K) = -148.5 J · K^{-1} · mol^{-1}, $C_{p,m}°$(F^-, 298.15 K) = -106.7 J · K^{-1} · mol^{-1}, $C_{p,m}°$(Cl^-, 298.15 K) = -136.4 J · K^{-1} · mol^{-1}; and from Valyashko et al. (1968): $C_{p,m}°$(Ca^{2+}, 298.15 K) = 1.7 cal · K^{-1} · mol^{-1} (7.1 J · K^{-1} · mol^{-1}) and $C_{p,m}°$(PO_4^{3-}, 298.15 K) = -114.7 cal · K^{-1} · mol^{-1} (-479.9 J · K^{-1} · mol^{-1}). Referring to the latter quantity, a footnote to Tab. 3 in Valyashko et al. (1968) states that $C_{p,m}°$(PO_4^{3-}, 298.15 K) "was calculated by means of an empirical equation, derived by I.L. Khodakovskiy, which relates partial molar heat capacities and entropies of anions of oxygen acids".

The major uncertainty in calculating $\Delta_r C_{p,m}°$(298.15 K) and $\Delta_r S_m°$(298.15 K) values is related to PO_4^{3-}. $S_m°(PO_4^{3-}$, 298.15 K) is derived from experimental data and associated with an uncertainty of ±13 J · K^{-1} · mol^{-1}, and $C_{p,m}°(PO_4^{3-}$, 298.15 K) is an estimated quantity. Hence, this review assigned uncertainties of ±50 J · K^{-1} · mol^{-1} to $\Delta_r C_{p,m}°$(298.15 K) and $\Delta_r S_m°$(298.15 K) of hydroxy- and fluorapatite, and an uncertainty of ±100 J · K^{-1} · mol^{-1} to $\Delta_r C_{p,m}°$(298.15 K) and $\Delta_r S_m°$(298.15 K) of chlorapatite, as in this case also $S_m°$(298.15 K) and $C_{p,m}°$(298.15 K) of the solid are estimates:

$Ca_5(PO_4)_3OH(cr) \rightleftharpoons 5\ Ca^{2+} + 3\ PO_4^{3-} + OH^-$

$\Delta_r S_m°(298.15\ K) = -(1'345 \pm 50)\ J \cdot K^{-1} \cdot mol^{-1}$

$\Delta_r C_{p,m}°(298.15\ K) = -(1'938 \pm 50)\ J \cdot K^{-1} \cdot mol^{-1}$

$Ca_5(PO_4)_3F(cr) \rightleftharpoons 5\ Ca^{2+} + 3\ PO_4^{3-} + F^-$

$\Delta_r S_m°(298.15\ K) = -(1'346 \pm 50)\ J \cdot K^{-1} \cdot mol^{-1}$

$\Delta_r C_{p,m}°(298.15\ K) = -(1'887 \pm 50)\ J \cdot K^{-1} \cdot mol^{-1}$

$Ca_5(PO_4)_3Cl(cr) \rightleftharpoons 5\ Ca^{2+} + 3\ PO_4^{3-} + Cl^-$

$\Delta_r S_m°(298.15\ K) = -(1'285 \pm 100)\ J \cdot K^{-1} \cdot mol^{-1}$

$\Delta_r C_{p,m}°(298.15\ K) = -(1'920 \pm 100)\ J \cdot K^{-1} \cdot mol^{-1}$

Using the selected $\Delta_r S_m°$(298.15 K) and $\log_{10} K_s°$(298.15 K) values this review calculated

$Ca_5(PO_4)_3OH(cr) \rightleftharpoons 5\ Ca^{2+} + 3\ PO_4^{3-} + OH^-$

$\Delta_r H_m°(298.15\ K) = -(68 \pm 15)\ kJ \cdot mol^{-1}$

$Ca_5(PO_4)_3F(cr) \rightleftharpoons 5\ Ca^{2+} + 3\ PO_4^{3-} + F^-$

$\Delta_r H_m°(298.15\ K) = -(61 \pm 15)\ kJ \cdot mol^{-1}$

There are no experimental solubility data reported in the literature for chlorapatite and hence, $\log_{10} K_s°$(298.15 K) has to be estimated using the above selected $\Delta_r S_m°$(298.15 K) value and an experimentally determined enthalpy.

Cruz et al. (2005) determined the standard molar enthalpies of formation of crystalline hydroxy-, chlor-, and bromapatite and critically assessed the results of previously published data. They report $\Delta_f H_m°(Ca_{10}(PO_4)_6(OH)_2$, cr, 298.15 K) = -(13'430 ± 80) kJ · mol^{-1} and $\Delta_f H_m°(Ca_{10}(PO_4)_6Cl_2$, cr, 298.15 K) = -(13'231 ± 82) kJ · mol^{-1}, obtained under the same experimental conditions (dilute HCl solutions). As Cruz et al. (2005) explain, the large errors that affect these values based on the reaction with dilute HCl solutions are mainly due to the uncertainty of ±8 kJ · mol^{-1} associated with $\Delta_f H_m°(CaCl_2$, cr).

Using the values of Cruz et al. (2005) for the solids and together with standard molar enthalpies of formation values for the aqueous species taken from CODATA (Cox et al. 1989): $\Delta_f H_m°(Ca^{2+}, 298.15\ K) = -543.0 \pm 1.0\ J \cdot K^{-1} \cdot mol^{-1}$, $\Delta_f H_m°(OH^-, 298.15\ K) = -230.015 \pm 0.040\ J \cdot K^{-1} \cdot mol^{-1}$, $\Delta_f H_m°(Cl^-, 298.15\ K) = -167.08 \pm 0.10\ J \cdot K^{-1} \cdot mol^{-1}$; and from Grenthe et al. (1992): $\Delta_f H_m°(PO_4^{3-}, 298.15\ K) = -1284.4 \pm 4.1\ J \cdot K^{-1} \cdot mol^{-1}$; this review calculated $\Delta_r H_m°(298.15\ K) = -(83 \pm 40)\ kJ \cdot mol^{-1}$ for $Ca_5(PO_4)_3OH(cr) \rightleftharpoons 5\ Ca^{2+} + 3\ PO_4^{3-} + OH^-$ and

$$Ca_5(PO_4)_3Cl(cr) \rightleftharpoons 5\ Ca^{2+} + 3\ PO_4^{3-} + Cl^-$$

$$\Delta_r H_m°(298.15\ K) = -(120 \pm 41)\ kJ \cdot mol^{-1}$$

Note that the value $\Delta_r H_m°(298.15\ K) = -(83 \pm 40)\ kJ \cdot mol^{-1}$ calculated from the experimental results of Cruz et al. (2005) for $Ca_5(PO_4)_3OH(cr) \rightleftharpoons 5\ Ca^{2+} + 3\ PO_4^{3-} + OH^-$ is in reasonable agreement with $\Delta_r H_m°(298.15\ K) = -(68 \pm 15)\ kJ \cdot mol^{-1}$ obtained by this review from the selected $\Delta_r S_m°(298.15\ K)$ and $\log_{10} K_s°(298.15\ K)$ values. This gives some confidence in the $\log_{10} K_s°(298.15\ K)$ value estimated for $Ca_5(PO_4)_3Cl(cr) \rightleftharpoons 5\ Ca^{2+} + 3\ PO_4^{3-} + Cl^-$ using $\Delta_r H_m°(298.15\ K) = -(120 \pm 41)\ kJ \cdot mol^{-1}$ and $\Delta_r S_m°(298.15\ K) = -(1'285.2 \pm 100)\ J \cdot K^{-1} \cdot mol^{-1}$:

$$Ca_5(PO_4)_3Cl(cr) \rightleftharpoons 5\ Ca^{2+} + 3\ PO_4^{3-} + Cl^-$$

$$\log_{10} K_s°\ (298.15\ K) = -46 \pm 5$$

The uncertainty of the above $\log_{10} K_s°(298.15\ K)$ value has been adjusted to a value such that calculating $\Delta_r H_m°(298.15\ K)$ from $\log_{10} K_s°(298.15\ K)$ and $\Delta_r S_m°(298.15\ K)$ results in $\pm 41\ kJ \cdot mol^{-1}$, thus avoiding cumulative error propagation effects.

The estimated solubility of chlorapatite is significantly higher than the solubilities of hydroxy- and fluorapatite, in agreement with the observation that pure chlorapatites are not known in nature, only chlorine-bearing hydroxyapatites (Valyashko et al. 1968).

In summary, the following values have been finally included in TDB 2020:

$$Ca_5(PO_4)_3OH(cr) \rightleftharpoons 5\ Ca^{2+} + 3\ PO_4^{3-} + OH^-$$

$$\log_{10} K_s°\ (298.15\ K) = -58.29 \pm 0.15$$

$$\Delta_r H_m°(298.15\ K) = -(68 \pm 15)\ kJ \cdot mol^{-1}$$

$$\Delta_r C_{p,m}°(298.15\ K) = -(1938 \pm 50)\ J \cdot K^{-1} \cdot mol^{-1}$$

$$Ca_5(PO_4)_3F(cr) \rightleftharpoons 5\ Ca^{2+} + 3\ PO_4^{3-} + F^-$$

$$\log_{10} K_s°\ (298.15\ K) = -59.63 \pm 0.20$$

$$\Delta_r H_m°(298.15\ K) = -(61 \pm 15)\ kJ \cdot mol^{-1}$$

$$\Delta_r C_{p,m}°(298.15\ K) = -(1'887 \pm 50)\ J \cdot K^{-1} \cdot mol^{-1}$$

$Ca_5(PO_4)_3Cl(cr) \rightleftharpoons 5\ Ca^{2+} + 3\ PO_4^{3-} + Cl^-$

$\log_{10}K_s°\ (298.15\ K) = -46 \pm 5$

$\Delta_r H_m°(298.15\ K) = -(120 \pm 41)\ kJ \cdot mol^{-1}$

$\Delta_r C_{p,m}°(298.15\ K) = -(1'920 \pm 100)\ J \cdot K^{-1} \cdot mol^{-1}$

As can be seen in Fig. 4.2-10, the experimental solubility data at other temperatures than 25 °C of McDowell et al. (1971) for hydroxyapatite and McCann (1968) for fluorapatite, which have not been used in the derivation of the temperature functions of the apatites, are in good agreement with the calculated solubilities (lines in Fig. 4.2-10).

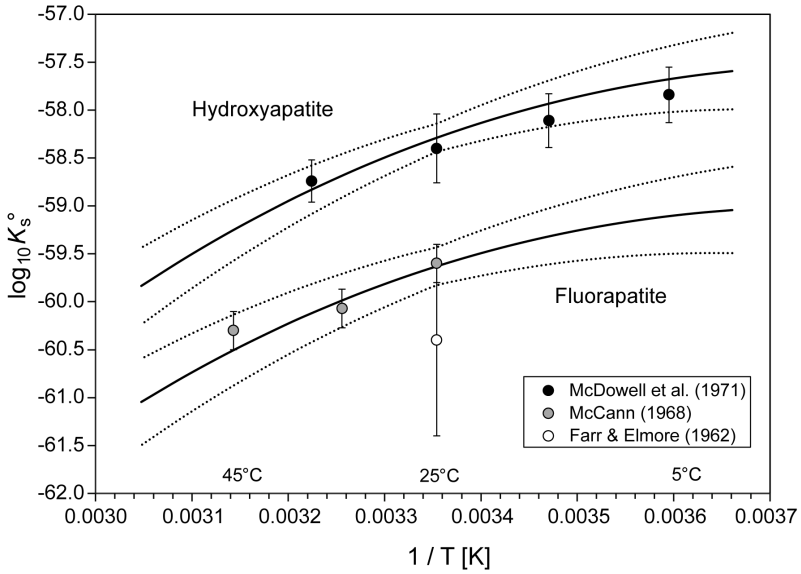

Fig. 4.2-10: The equilibrium constants $\log_{10}K_s°$ for hydroxyapatite, $Ca_5(PO_4)_3OH(cr) \rightleftharpoons 5\ Ca^{2+} + 3\ PO_4^{3-} + OH^-$, and fluorapatite, $Ca_5(PO_4)_3F(cr) \rightleftharpoons 5\ Ca^{2+} + 3\ PO_4^{3-} + F^-$, as a function of temperature in the range 5 – 45 °C

Solid lines: obtained from $\log_{10}K_s°(298.15\ K)$, $S_m°(298.15\ K)$ and $C_{p,m}°(298.15\ K)$ values as described in the text. Dotted lines: lower and upper limits using $\log_{10}K_s°(298.15\ K)$, $\Delta_r H_m°(298.15\ K)$ and $\Delta_r C_{p,m}°(298.15\ K)$ as given in the text and extrapolated to lower and higher temperatures.

$CaHPO_4$(cr), monetite

Lindsay & Moreno (1960) calculated a solubility diagram for phosphate compounds in soils at 25 °C from literature data. For "dicalcium phosphate anhydrous", $CaHPO_4$(cr), they report $\log_{10}K_s = -6.66$, taken from an older compilation report not available to this review. This value of uncertain origin has not been retained by this review.

McDowell et al. (1971) measured the solubility of $CaHPO_4$(cr) in dilute phosphoric acid solutions in the pH range 3.3 – 7.8 in the temperature range 5 – 37 °C. For extrapolating their data to zero ionic strength McDowell et al. (1971) used both the extended Debye-Hückel equation and the Davies equation and fitted simultaneously the solubility product of $CaHPO_4$(cr) as well as the complexation constants for $CaHPO_4$(aq) and $CaH_2PO_4^+$. The latter complexation constants have

been included in the data evaluation by this review, but the final results are slightly different than the values reported by McDowell et al. (1971) (see preceding Section). As all experimental data are reported in Tab. I and II of McDowell et al. (1971), this review re-evaluated the solubility product of $CaHPO_4$(cr) using SIT with $\Delta\varepsilon = 0$ (I = 0.002 to 0.16), phosphoric acid dissociation data as included in TDB 2020 and complexation data of $CaPO_4^-$, $CaHPO_4$(cr) and $CaH_2PO_4^+$ as selected by this review. The results of this re-evaluation are for the equilibrium $CaHPO_4$(cr) ⇌ $Ca^{2+} + HPO_4^{2-}$ $\log_{10}K_s°$(5 °C) = -6.66 ± 0.06, $\log_{10}K_s°$(15 °C) = -6.75 ± 0.08, $\log_{10}K_s°$(25 °C) = - .86 ± 0.05 and $\log_{10}K_s°$(37 °C) = -6.99 ± 0.05. These values are all only 0.04 $\log_{10}$-units higher than the values reported by McDowell et al. (1971).

Jaynes et al. (1999) report in their Tab. 2 identical "Measured Log IAP" of -6.60 ± 0.01 for monetite, $CaHPO_4$(cr), and for brushite, $CaHPO_4 \cdot 2H_2O$. However, only the value for monetite, $CaHPO_4$(cr), is obtained from experimental data, but because this value is very close to published solubility products for brushite, $CaHPO_4 \cdot 2H_2O$ (see Tab. 4.2-2), Jaynes et al. (1999) conclude that "data collected in this study indicate that monetite and brushite solubilities are identical" and put identical numbers in their table of "Measured Log IAP". Jaynes et al. (1999) do not report any numerical analytical results, no measured pH values, just a plot with huge symbols of Ca and P concentrations versus time, and a plot of log IAP versus time. Further, no details of their calculations are disclosed, and it remains unclear if they considered Ca phosphate complexes. No re-calculation or re-evaluation whatsoever is possible. Hence, the solubility product for monetite reported by Jaynes et al. (1999), and their unsubstantiated claim of identical solubilities of monetite and brushite, have not been considered further by this review.

Egan & Wakefield (1964a) measured the low-temperature heat capacity of $CaHPO_4$(cr) in the temperature range 10 to 310 K, and report $C_{p,m}°$(298.15 K) = 26.30 cal · K^{-1} · mol^{-1} (110.04 J · K^{-1} · mol^{-1}). Combining this value with $C_{p,m}°(Ca^{2+}$, 298.15 K) = 1.7 cal · K^{-1} · mol^{-1} (7.1 J · K^{-1} · mol^{-1}) (Valyashko et al. 1968) and $C_{p,m}°(HPO_4^{2-}$, 298.15 K) = -242.50 J · K^{-1} · mol^{-1} (Lothenbach et al. 2019) this review calculated $\Delta_r C_{p,m}°$(298.15 K) = -(345 ± 20) J · K^{-1} · mol^{-1} for $CaHPO_4$(cr) ⇌ $Ca^{2+} + HPO_4^{2-}$. The major uncertainty in calculating $\Delta_r C_{p,m}°$(298.15 K) is related to HPO_4^{2-}.

An unweighted regression of the data of McDowell et al. (1971), as accepted by this review (Tab. 4.2-2), resulted in $\log_{10}K_s°$ (298.15 K) = -6.86 ± 0.05, $\Delta_r H_m°$(298.15 K) = -(18.6 ± 1.3) kJ · mol^{-1}, and $\Delta_r C_{p,m}°$(298.15 K) = -(307 ± 200) J · K^{-1} · mol^{-1} (Fig. 4.2-11). The obtained $\Delta_r C_{p,m}°$(298.15 K) value is close to one calculated from the data of Egan & Wakefield (1964a) but shows a very high statistical uncertainty. Hence, $\Delta_r C_{p,m}°$(298.15 K) = -345 J · K^{-1} · mol^{-1} has been used as a fixed value in a second unweighted regression analysis, resulting in $\log_{10}K_s°$ (298.15 K) = -6.86 ± 0.02 and $\Delta_r H_m°$(298.15 K) = -(18.8 ± 0.7) kJ · mol^{-1}. These values have been included in TDB 2020:

$CaHPO_4$(cr) ⇌ $Ca^{2+} + HPO_4^{2-}$

$\log_{10}K_s°$ (298.15 K) = -6.86 ± 0.02

$\Delta_r H_m°$(298.15 K) = -(18.8 ± 0.7) kJ · mol^{-1}

$\Delta_r C_{p,m}°$(298.15 K) = -(345 ± 20) J · K^{-1} · mol^{-1}

$CaHPO_4 \cdot 2H_2O$, brushite

Strates et al. (1957) measured the solubility of $CaHPO_4 \cdot 2H_2O$ in dilute phosphoric acid solutions in the pH range 5.9 – 6.6 at 25 °C in 0.165 M KCl. Their results from precipitation and dissolution experiments are consistent and Strates et al. (1957) report $\log_{10}K_s°(25\ °C) = -6.57$ for $CaHPO_4 \cdot 2H_2O \rightleftharpoons Ca^{2+} + HPO_4^{2-} + 2\ H_2O(l)$. Strates et al. (1957) used $\log_{10}K°(25\ °C) = 7.19$ for the protonation of $H_2PO_4^-$, in fair agreement with 7.212 ± 0.013 selected in TDB 2020, and the activities $\gamma(Ca^{2+}) = 0.36$, $\gamma(HPO_4^{2-}) = 0.23$ and $\gamma(H_2PO_4^-) = 0.62$, also in fair agreement with the values 0.323, 0.295 and 0.705, respectively, calculated by this review for 0.165 M KCl medium using SIT. Strates et al. (1957) used maleic acid as pH buffer and considered the formation of a calcium maleate complex in their calculations but not the formation of calcium phosphate complexes. This review calculated that including the complexation data of $CaPO_4^-$, $CaHPO_4(aq)$ and $CaH_2PO_4^+$ as selected by this review, changes the solubility product by -0.03 $\log_{10}$ units and thus, the value $\log_{10}K_s°(25\ °C) = -6.60 \pm 0.15$ is retained, with an uncertainty assigned by this review.

Moreno et al. (1960a) established the metastable solubility isotherm of "dicalcium phosphate dihydrate (DCPD)", $CaHPO_4 \cdot 2H_2O$, in the pH range 5.9 – 6.6 at 25 °C by a leaching solutions of dilute phosphoric acid through columns of DCPD, and b by shaking suspensions of DCPD in dilute phosphoric acid solutions containing also NaCl. The results are consistent and Moreno et al. (1960a) obtained from the analytical results given in their Tab. 2 and 3 $\log_{10}K_s°(25\ °C) = -6.56$ using the extended Debye-Hückel equation. Moreno et al. (1960a) did not consider calcium phosphate complexation and hence, this review re-evaluated the solubility product of $CaHPO_4 \cdot 2H_2O$ using SIT with $\Delta\varepsilon = 0$ (I = 0.003 to 0.15), phosphoric acid dissociation data as included in TDB 2020 and complexation data of $CaPO_4^-$, $CaHPO_4(aq)$ and $CaH_2PO_4^+$ as selected by this review, and obtained $\log_{10}K_s°(25\ °C) = -6.59 \pm 0.08$.

Moreno et al. (1966) measured the solubility of $CaHPO_4 \cdot 2H_2O$, in dilute phosphoric acid solutions in the pH range 3.5 – 6.8 at 37.5 °C. In order to account for the pH dependence of the measured solubilities Moreno et al. (1966) considered the complexes $CaHPO_4(aq)$ and $CaH_2PO_4^+$, and report $\log_{10}K_s°(37.5\ °C) = -6.66$. Their calcium complexation constants have been included in the data evaluation by this review, but the final results are slightly different than the values reported by Moreno et al. (1966) (see preceding section). As all experimental data are reported in Tab. 1 of Moreno et al. (1966), this review re-evaluated the solubility product of $CaHPO_4 \cdot 2H_2O$ using SIT with $\Delta\varepsilon = 0$ (I = 0.003 to 0.14), phosphoric acid dissociation data as included in TDB 2020 and complexation data of $CaPO_4^-$, $CaHPO_4(cr)$ and $CaH_2PO_4^+$ as selected by this review. The result of this re-evaluation for the equilibrium $CaHPO_4 \cdot 2H_2O \rightleftharpoons Ca^{2+} + HPO_4^{2-} + 2\ H_2O(l)$ is $\log_{10}K_s°(37.5\ °C) = -6.63 \pm 0.02$.

The same authors in a subsequent paper (Gregory et al. 1970) extended their solubility measurements of $CaHPO_4 \cdot 2H_2O$ to the temperature range 5 – 37.5 °C. Gregory et al. (1970) evaluated the complexation constants for $CaHPO_4(aq)$ and $CaH_2PO_4^+$ at all temperatures and report $\log_{10}K_s°(5\ °C) = -6.63$, $\log_{10}K_s°(15\ °C) = -6.60$, $\log_{10}K_s°(25\ °C) = -6.59$ and $\log_{10}K_s°(37.5\ °C) = -6.62$. Their calcium complexation constants have been included in the data evaluation by this review, but the final results are slightly different than the values reported by Gregory et al. (1970) (see preceding Section). As all experimental data are reported in Tab. 2 – 5 of Gregory et al. (1970), this review re-evaluated the solubility product of $CaHPO_4(cr)$ using SIT with $\Delta\varepsilon = 0$ (I = 0.003 to 0.15), phosphoric acid dissociation data as included in TDB 2020 and complexation data of $CaPO_4^-$, $CaHPO_4(cr)$ and $CaH_2PO_4^+$ as selected by this review. The results of this re-evaluation for the equilibrium $CaHPO_4 \cdot 2H_2O \rightleftharpoons Ca^{2+} + HPO_4^{2-} + 2\ H_2O(l)$ are $\log_{10}K_s°(5\ °C) = -6.55 \pm 0.05$, $\log_{10}K_s°(15\ °C) = -6.59 \pm 0.03$, $\log_{10}K_s°(25\ °C) = -6.58 \pm 0.07$, $\log_{10}K_s°(37.5\ °C) = -6.62 \pm 0.02$.

Madsen (1970) reports that "approximate solubility products of the most important calcium phosphates were determined by Bjerrum and coworkers" and presented by Bjerrum at a conference in 1936. The solubility product for $CaHPO_4 \cdot 2H_2O$, $\log_{10}K_s°(37\ °C) = -6.62$, has been extrapolated to zero ionic strength using the Debye-Hückel limiting law. Madsen (1970) further states that the solubility product of $CaHPO_4(s)$ has "recently been redetermined in this laboratory" and reports $\log_{10}K_s°(37\ °C) = -6.646$, also extrapolated to zero ionic strength using the Debye-Hückel limiting law and being the mean of 17 determinations with pH ranging from 5.5 – 7.5, with a standard deviation of ±0.014. This review retains this value, but with increased uncertainty of ±0.10, as Madsen (1970) did not consider calcium phosphate complexes in his data evaluation, but also no experimental data are reported which would allow recalculation.

Patel et al. (1974) determined the solubility of brushite, $CaHPO_4 \cdot 2H_2O$, in the quaternary system $Ca(OH)_2 – H_3PO_4 – NaCl – H_2O$ at 25 °C in the pH range 4.4 – 6.4. The ionic strengths, I, of the saturated solutions varied from 0.005 to 0.55 M, mainly due to the variation in NaCl concentrations. Satisfactory constancy in the solubility product was obtained when the ion activity coefficients, γ_i, were calculated with the extended Debye-Hückel equation, $\log_{10}\gamma_i = -A \cdot z_i^2 \cdot \sqrt{I} / (1 + B \cdot \alpha_i \cdot \sqrt{I}) + 0.0626 \cdot I$, and the formation of an ion pair $NaHPO_4^-$ was taken into account. The result of the statistical analysis of Patel et al. (1974) is $\log_{10}K_s°(25\ °C) = -6.60 \pm 0.02$.

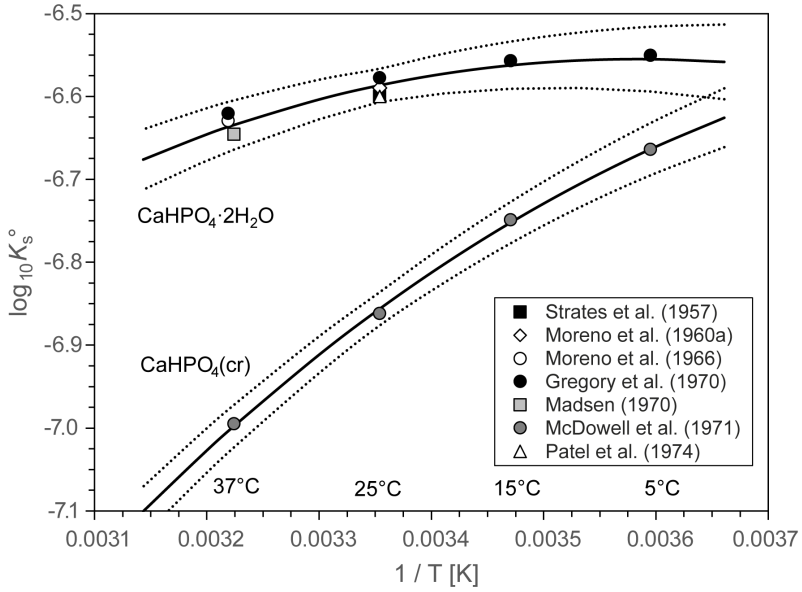

Fig. 4.2-11: The equilibrium constants $\log_{10}K_s°$ for $CaHPO_4 \cdot 2H_2O(cr) \rightleftharpoons Ca^{2+} + HPO_4^{2-} + 2\ H_2O(l)$ and $CaHPO_4(cr) \rightleftharpoons Ca^{2+} + HPO_4^{2-}$ as a function of temperature in the range 5 – 37 °C

Solid lines: unweighted least squares fits of all data shown as symbols (Tab. 4.2-2) as described in the text. Dotted lines: lower and upper limits using $\log_{10}K_s°(298.15\ K)$, $\Delta_r H_m°(298.15\ K)$ and $\Delta_r C_{p,m}°(298.15\ K)$ as given in the text and extrapolated to lower and higher temperatures.

Egan & Wakefield (1964b) measured the low-temperature heat capacity of $CaHPO_4 \cdot 2H_2O(cr)$ in the temperature range 10 to 310 K, and report $C_{p,m}°(298.15\ K) = 47.10\ cal \cdot K^{-1} \cdot mol^{-1}$ ($197.07\ J \cdot K^{-1} \cdot mol^{-1}$). Combining this value with $C_{p,m}°(Ca^{2+}, 298.15\ K) = 1.7\ cal \cdot K^{-1} \cdot mol^{-1}$ ($7.1\ J \cdot K^{-1} \cdot mol^{-1}$) (Valyashko et al. 1968), $C_{p,m}°(HPO_4^{2-}, 298.15\ K) = -242.50\ J \cdot K^{-1} \cdot mol^{-1}$ (Lothenbach et al. 2019) and the CODATA value $C_{p,m}°(H_2O, l, 298.15\ K) = (75.351 \pm 0.080)\ J \cdot K^{-1} \cdot mol^{-1}$

(Cox et al. 1989), this review calculated $\Delta_r C_{p,m}°(298.15\ K) = -(282 \pm 20)\ J \cdot K^{-1} \cdot mol^{-1}$ for $CaHPO_4 \cdot 2H_2O \rightleftharpoons Ca^{2+} + HPO_4^{2-} + 2\ H_2O(l)$. The major uncertainty in calculating $\Delta_r C_{p,m}°(298.15\ K)$ is related to HPO_4^{2-}.

An unweighted regression of the re-evaluated and accepted data (Tab. 4.2-2) of Strates et al. (1957), Moreno et al. (1960a), Moreno et al. (1966), Gregory et al. (1970) Patel et al. (1974) resulted in $\log_{10} K_s°\ (298.15\ K) = -6.59 \pm 0.05$, $\Delta_r H_m°(298.15\ K) = -(5.1 \pm 1.5)\ kJ \cdot mol^{-1}$, and $\Delta_r C_{p,m}°(298.15\ K) = -(167 \pm 220)\ J \cdot K^{-1} \cdot mol^{-1}$ (Fig. 4.2-11). The obtained $\Delta_r C_{p,m}°(298.15\ K)$ value is, within its very high statistical uncertainty, not in contradiction to that calculated from the data of Egan & Wakefield (1964b). Hence, $\Delta_r C_{p,m}°(298.15\ K) = -282\ J \cdot K^{-1} \cdot mol^{-1}$ has been used as a fixed value in a second unweighted regression analysis, resulting in $\log_{10} K_s°\ (298.15\ K) = -6.59 \pm 0.02$ and $\Delta_r H_m°(298.15\ K) = -(5.4 \pm 1.3)\ kJ \cdot mol^{-1}$. These values have been included in TDB 2020:

$CaHPO_4 \cdot 2H_2O(cr) \rightleftharpoons Ca^{2+} + HPO_4^{2-} + 2\ H_2O(l)$

$\log_{10} K_s°\ (298.15\ K) = -6.59 \pm 0.02$

$\Delta_r H_m°(298.15\ K) = -(5.4 \pm 1.3)\ kJ \cdot mol^{-1}$

$\Delta_r C_{p,m}°(298.15\ K) = -(282 \pm 20)\ J \cdot K^{-1} \cdot mol^{-1}$

β-$Ca_3(PO_4)_2$, tuite

In the literature, β-$Ca_3(PO_4)_2$(cr) is often related to the mineral whitlockite. However, the IMA (International Mineralogical Association) approved mineral name whitlockite actually refers to $Ca_9Mg(PO_4)_6(HPO_4)$(cr), belonging to the trigonal crystal system with space group R3c. By contrast, a mineral with the composition $Ca_3(PO_4)_2$(cr) has the 2001 IMA approved name tuite, also belonging to the trigonal crystal system but with space group $R\bar{3}m$. Both minerals belong to the "whitlockite group" which comprises other trigonal Ca phosphate minerals like strontiowhitlockite, $Sr_9Mg(PO_4)_6(HPO_4)$(cr) and merrillite, $Ca_9NaMg(PO_4)_7$(cr) (www.mindat.org).

Gregory et al. (1974) report that solubility isotherms of beta-tricalcium phosphate, β-$Ca_3(PO_4)_2$, prepared by heating mixtures of $CaCO_3$ and $CaHPO_4$ above 800 °C, were determined in the ternary system $Ca(OH)_2 – H_3PO_4 – H_2O$ at 5, 15, 25, and 37 °C in the pH range 6.0 – 7.5 by equilibration with dilute H_3PO_4 solutions. Gregory et al. (1974) evaluated the complexation constants for $CaHPO_4$(aq) and $CaH_2PO_4^+$ at all temperatures. Their calcium complexation constants have been included in the data evaluation by this review (see Tab. 4.2-1), but the final results are slightly different than the values reported by Gregory et al. (1974) (see preceding Section). As all experimental data are reported in Tab. 1 – 4 of Gregory et al. (1974), this review re-evaluated the solubility product of $Ca_3(PO_4)_2$(cr) using SIT with $\Delta\varepsilon = 0$ ($I = 0.0007 – 0.006$), phosphoric acid dissociation data as included in TDB 2020 and complexation data of $CaPO_4^-$, $CaHPO_4$(cr) and $CaH_2PO_4^+$ as selected by this review. The results of this re-evaluation for the equilibrium $Ca_3(PO_4)_2$(cr) $\rightleftharpoons 3\ Ca^{2+} + 2\ PO_4^{3-}$ are $\log_{10} K_s°(5\ °C) = -28.60 \pm 0.24$, $\log_{10} K_s°(15\ °C) = -28.57 \pm 0.21$, $\log_{10} K_s°(25\ °C) = -28.90 \pm 0.20$, and $\log_{10} K_s°(37.5\ °C) = -29.67 \pm 0.14$.

Jaynes et al. (1999) report in their Tab. 2 "Measured Log IAP" of -30.74 ± 0.08 for β-$Ca_3(PO_4)_2$. This value is almost two orders of magnitude at variance with the value reported by Gregory et al. (1974). Jaynes et al. (1999) do not report any numerical analytical results, no measured pH values, just a plot with huge symbols of Ca and P concentrations versus time, and a plot of log IAP versus HCl concentrations (their Fig. 3). Further, no details of their calculations are disclosed, and it remains unclear if they considered Ca phosphate complexes. No re-calculation or re-evaluation whatsoever is possible. Hence, the solubility product for β-$Ca_3(PO_4)_2$ reported by Jaynes et al. (1999), has not been considered further by this review.

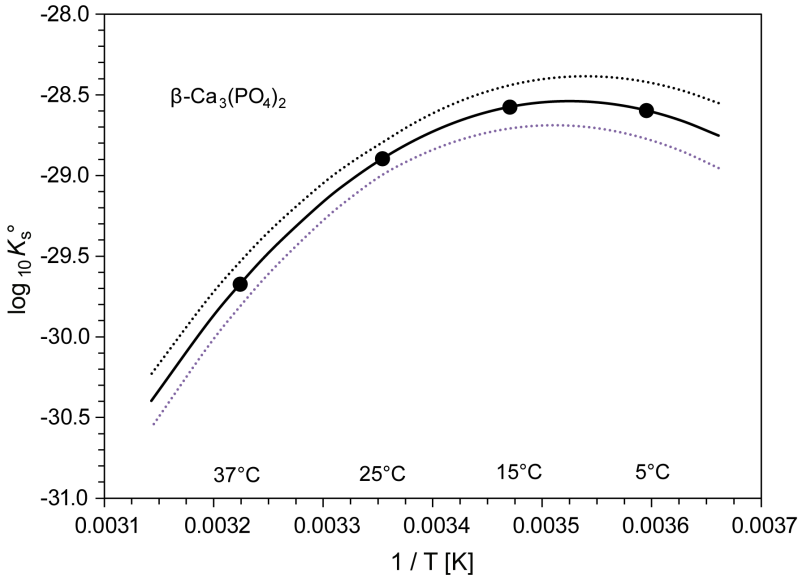

Fig. 4.2-12: The equilibrium constant $\log_{10}K_s°$ for $Ca_3(PO_4)_2(cr) \rightleftharpoons 3\ Ca^{2+} + 2\ PO_4^{3-}$ as a function of temperature in the range 5 – 37 °C

Solid line: unweighted least squares fit of data shown as symbols (Tab. 4.2-2). Dotted lines: lower and upper limits using $\log_{10}K_s°(298.15\ K) = -28.90 \pm 0.10$, $\Delta_r H_m°(298.15\ K) = -(81.2 \pm 5.0)\ kJ \cdot mol^{-1}$ and $\Delta_r C_{p,m}°(298.15\ K) = -(5'620 \pm 100)\ J \cdot K^{-1} \cdot mol^{-1}$ and extrapolated to lower and higher temperatures.

An unweighted regression of the data of Gregory et al. (1974) as re-calculated and accepted by this review (Tab. 4.2-2), resulted in (Fig. 4.2-12):

$Ca_3(PO_4)_2(cr) \rightleftharpoons 3\ Ca^{2+} + 2\ PO_4^{3-}$

$\log_{10}K_s°\ (298.15\ K) = -28.90 \pm 0.10$

$\Delta_r H_m°(298.15\ K) = -(81.2 \pm 5.0)\ kJ \cdot mol^{-1}$

$\Delta_r C_{p,m}°(298.15\ K) = -(5620 \pm 100)\ J \cdot K^{-1} \cdot mol^{-1}$

These values have been included in TDB 2020.

$CaK_3H(PO_4)_2$

Xu et al. (2020) determined the solubility of $CaK_3H(PO_4)_2$(cr) by two oversaturation experiments at 20 °C with 7 weeks equilibration time. Xu et al. (2020) report X-ray diffraction patterns (their Fig. A) which indicate that they obtained a crystalline product. The solubility was calculated based on the measured concentrations of Ca, K, phosphate and the pH values using the thermodynamic software GEMS and auxiliary data as detailed in Lothenbach et al. (2019). The obtained solubility product for $CaHK_3(PO_4)_2$(cr) ⇌ Ca^{2+} + H^+ + 3 K^+ + 2 PO_4^{3-} equals $\log_{10}K_s°$ (293.15 K) = -22.4 ± 0.8. As the study of Xu et al. (2020) is part of a larger study and database development on the properties of magnesium potassium phosphate cements (Lothenbach et al. 2019), see also Section 2.4.2, this value is used as approximation for 25 °C and included in TDB 2020:

$CaHK_3(PO_4)_2$(cr) ⇌ Ca^{2+} + H^+ + 3 K^+ + 2 PO_4^{3-}

$\log_{10}K_s°$ (298.15 K) = -22.4 ± 0.8

$Ca_4H(PO_4)_3 \cdot 2.5H_2O$

Octacalcium phosphate (OCP, $Ca_8(HPO_4)_2(PO4)_4 \cdot 5H_2O$) seems to occur in soils as a metastable phase (Moreno et al. 1960b) and is proving to be an important intermediary in the formation of tooth and bone material and various pathological calcifications (Tung et al. 1988). Solubility measurements of such a metastable phase are difficult and the reported results show some scatter. Although the name "octacalcium phosphate" (in the older literature also "oct**o**calcium phosphate") is used, the stoichiometry used in the literature mainly refers to $Ca_4H(PO4)_3 \cdot 2.5H_2O$.

Moreno et al. (1960b) investigated the hydrolysis of $CaHPO_4{\cdot}2H_2O$ in dilute phosphoric acid solutions and in water at 25 °C in the absence of CO_2. Octacalcium phosphate, $Ca_4H(PO4)_3 \cdot 2.5H_2O$, was found to precipitate when the pH of the solution was higher than 6.38. The extent of hydrolysis was larger the higher the initial pH of the solution. The solution composition followed the metastable solubility for $CaHPO_4{\cdot}2H_2O$ until a singular point between $Ca_4H(PO4)_3{\cdot}2.5H_2O$ and $CaHPO_4{\cdot}2H_2O$ was reached. At this point the solution had a pH of 6.38. The solubility product of octacalcium phosphate was calculated by Moreno et al. (1960b) to be $K_s°$(25 °C) = $1.25 \cdot 10^{-47}$ ($\log_{10}K°$(25 °C) = -46.90). This value has been re-calculated by Tung et al. (1988), including the complexes $CaHPO_4$(aq) and $CaH_2PO_4^+$, $\log_{10}K°$(25 °C) = -46.97. Considering that this value depends on the solubility isotherm of $CaHPO_4{\cdot}2H_2O$ and extrapolation procedures, this review retains the latter value but assigns an uncertainty of ± 1.0.

Madsen (1970) reports that "approximate solubility products of the most important calcium phosphates were determined by Bjerrum and coworkers" and presented by Bjerrum at a conference in 1936. The solubility products for $Ca_4H(PO_4)_3 \cdot 2.5H_2O$(s) + 2 H^+ ⇌ 4 Ca^{2+} + 3 HPO_4^{2-} + 2.5 H_2O(l), $\log_{10}K_s°$(37 °C) = -10.7 (equilibration from supersaturated solution) and $\log_{10}K_s°$(37 °C) = -12.1 (equilibration from unsaturated solution), have been extrapolated to zero ionic strength using the Debye-Hückel limiting law. Madsen (1970) further states that the solubility product of $Ca_4H(PO_4)_3 \cdot 3H_2O$(s) has "recently been redetermined in this laboratory" and reports $\log_{10}K_s°$(37 °C) = -11.59, also extrapolated to zero ionic strength using the Debye-Hückel limiting law. Madsen (1970) explains that this value was determined by extrapolation to infinite time of data from the hydrolysis of $CaHPO_4{\cdot}2H_2O$ in pure water and has a probable error of about ±0.1. Using the HPO_4^{2-} dissociation data included in TDB 2020, $\log_{10}K°$(37 °C) = -12.25, this review calculated $\log_{10}K_s°$(37 °C) = -48.34 ± 0.10 for the equilibrium $Ca_4H(PO_4)_3 \cdot 2.5H_2O$(s)

$\rightleftharpoons$ 4 Ca^{2+} + 3 PO_4^{3-} + H^+ + 2.5 H_2O(l). This review retains the latter value, but with increased uncertainty of ±0.5, as Madsen (1970) did not consider calcium phosphate complexes in his data evaluation, but also no experimental data are reported which would allow recalculation.

Shyu et al. (1983) determined the solubility of octacalcium phosphate, $Ca_4H(PO_4)_3 \cdot 2.5H_2O$, in the system $Ca(OH)_2$ – H_3PO_4 – KNO_3 – H_2O at 37 °C in experiments involving a range of hydrodynamics, ionic strength, and equilibration time. Shyu et al. (1983) obtained $\log_{10}K_s°$ = -49.3 ± 0.2 for three different solid preparations by considering activity coefficients and ion-pair corrections. Shyu et al. (1983) used the complexation constants of Chughtai et al. (1968) which are at the high end of the variability discussed by this review (see Tab. 4.2-1). As all experimental data are reported in the table of Shyu et al. (1983), this review re-evaluated the solubility product of $Ca_4H(PO_4)_3 \cdot 2.5H_2O$(s) using SIT with $\Delta\varepsilon = 0$ (I = 0.003 – 0.16), phosphoric acid dissociation data as included in TDB 2020 and complexation data of $CaPO_4^-$, $CaHPO_4$(cr) and $CaH_2PO_4^+$ as selected by this review, and obtained $\log_{10}K°$(37.5 °C) = -49.08 ± 0.72.

Heughebaert & Nancollas (1985) continued the work of Shyu et al. (1983), exploring the same system with the same methods at 25 and 45 °C, allowing both growth and dissolution experiments over a range of ionic strength to come to equilibrium. Heughebaert & Nancollas (1985) obtained $\log_{10}K_s°$(25 °C) = -49.6 ± 0.2 and $\log_{10}K_s°$(45 °C) = -49.8 ± 0.3. As all experimental data are reported in Tab. II and III of Heughebaert & Nancollas (1985), this review re-evaluated the solubility product of $Ca_4H(PO_4)_3 \cdot 2.5H_2O$(s) using SIT with $\Delta\varepsilon = 0$ (I = 0.004 – 0.10), phosphoric acid dissociation data as included in TDB 2020 and complexation data of $CaPO_4^-$, $CaHPO_4$(cr) and $CaH_2PO_4^+$ as selected by this review, and obtained $\log_{10}K_s°$(25 °C) = -48.75 ± 0.52 and $\log_{10}K_s°$(45 °C) = -48.71 ± 0.94.

Tung et al. (1988) measured the solubility of octacalcium phosphate, $Ca_8H_2(PO_4)_6 \cdot 5H_2O$, in dilute phosphoric acid solutions in the pH range 3.2 – 6.4 in the temperature range 4 – 37 °C. For extrapolating their data to zero ionic strength Tung et al. (1988) used both the extended Debye-Hückel equation and the Davies equation, which gave the same results, and also determined values for the complexes $CaHPO_4$(aq) and $CaH_2PO_4^+$ which are in good ($CaHPO_4$(aq)) to fair ($CaH_2PO_4^+$) agreement with the values selected by this review (see preceding Section). Tung et al. (1988) report $\log_{10}K_s°$(4 °C) = -48.3 ± 0.2, $\log_{10}K_s°$(4.8 °C) = -48.3 ± 0.2, $\log_{10}K_s°$(6.0 °C) = -48.2, $\log_{10}K_s°$(18 °C) = -48.3, $\log_{10}K_s°$(23.5 °C) = 48.4 ± 0.1 and $\log_{10}K_s°$(37 °C) = -48.7 ± 0.2. These values are retained by this review with increased uncertainties of ± 0.4.

A weighted regression analysis of the data of Moreno et al. (1960b), Madsen (1970), Shyu et al. (1983), Heughebaert & Nancollas (1985) and Tung et al. (1988) as re-calculated and accepted by this review (Tab. 4.2-2), resulted in (Fig. 4.2-13):

$$Ca_4H(PO_4)_3 \cdot 2.5H_2O(s) \rightleftharpoons 4\ Ca^{2+} + 3\ PO_4^{3-} + H^+ + 2.5\ H_2O(l)$$

$$\log_{10}K_s° (298.15\ K) = -48.48 \pm 0.16$$

$$\Delta_r H_m°(298.15\ K) = -(21 \pm 19)\ kJ \cdot mol^{-1}$$

$$\Delta_r C_{p,m}°(298.15\ K) = 0\ J \cdot K^{-1} \cdot mol^{-1}$$

These values have been included in TDB 2020.

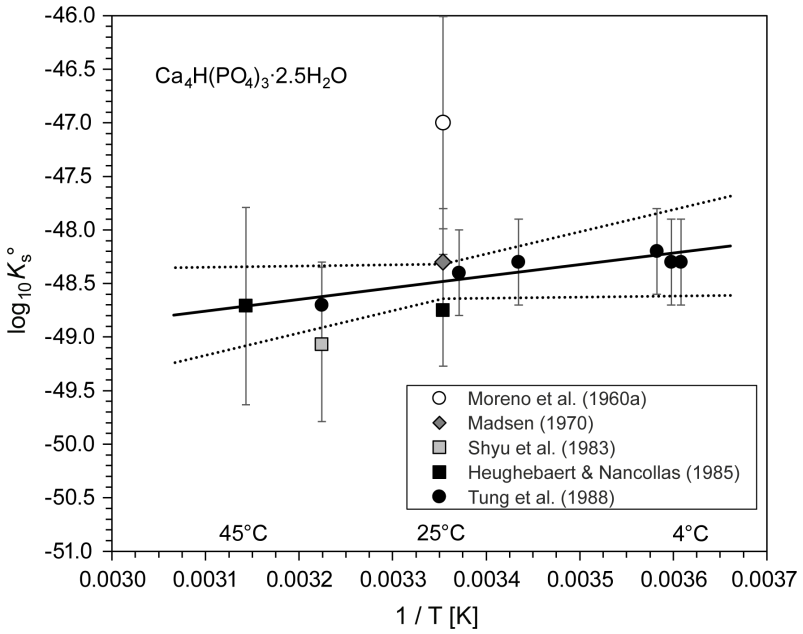

Fig. 4.2-13: The equilibrium constant $\log_{10}K_s°$ for $Ca_4H(PO_4)_3 \cdot 2.5H_2O(s) \rightleftharpoons 4\ Ca^{2+} + 3\ PO_4^{3-} + H^+ + 2.5\ H_2O(l)$ as a function of temperature in the range 4 – 45 °C

Solid line: weighted least squares fit of all data shown as symbols (Tab. 4.2-2). Dotted lines: lower and upper limits using $\log_{10}K_s°(298.15\ K) = -48.48 \pm 0.16$ and $\Delta_r H_m°(298.15\ K) = -(21 \pm 19)\ kJ \cdot mol^{-1}$ and extrapolated to lower and higher temperatures.

4.2.9 Selected calcium data

Tab. 4.2-3: Selected calcium data

Core data are in bold face.

Name	**$\Delta_f G_m°$** [kJ · mol^{-1}]	**$\Delta_f H_m°$** [kJ · mol^{-1}]	**$S_m°$** [J · K^{-1} · mol^{-1}]	**$C_{p,m}°$** [J · K^{-1} · mol^{-1}]	**Species**
Ca(cr)	**0.0**	**0.0**	**41.590 ± 0.400**	**25.929 ± 0.300**	Ca(cr)
Ca+2	**-552.806 ± 1.050**	**-543.000 ± 1.000**	**-56.200 ± 1.000**		Ca^{2+}
Dolomite	**-2'161.69 ± 1.10**	**-2'324.48 ± 1.08**	**155.18 ± 0.42**	**157.53 ± 0.42**	$CaMg(CO_3)_2$(cr)

Name	**$\log_{10}\beta°$**	**$\Delta_r H_m°$** [kJ · mol^{-1}]	**$\Delta_r C_{p,m}°$** [J · K^{-1} · mol^{-1}]	**T-range** [°C]	**Reaction**
CaOH+	-12.57 ± 0.03	53.9 ± 1.4	-446.8 ± 39.3	0 – 150	$Ca^{2+} + H_2O(l) \rightleftharpoons CaOH^+ + H^+$
CaF+	1.33 ± 0.04	12.8 ± 1.0	0	2 – 260	$Ca^{2+} + F^- \rightleftharpoons CaF^+$
CaCO3(aq)	3.23 ± 0.14	13.9 ± 2.2	447 ± 130	5 – 80	$Ca^{2+} + CO_3^{2-} \rightleftharpoons CaCO_3(aq)$
CaHCO3+	1.07 ± 0.07	8.7 ± 2.5	0	5 – 80	$Ca^{2+} + HCO_3^- \rightleftharpoons CaHCO_3^+$
CaSO4(aq)	2.31 ± 0.04	6.9 ± 1.7	0	0 – 40	$Ca^{2+} + SO_4^{2-} \rightleftharpoons CaSO_4(aq)$
CaPO4-	6.46 ± 0.11	-1 ± 18	0	18 – 45	$Ca^{2+} + PO_4^{3-} \rightleftharpoons CaPO_4^-$
CaHPO4(aq)	2.58 ± 0.05	13.1 ± 6.3	0	0 – 45	$Ca^{2+} + HPO_4^{2-} \rightleftharpoons CaHPO_4(aq)$
CaH2PO4+	0.99 ± 0.09	3 ± 13	0	5 – 45	$Ca^{2+} + H_2PO_4^- \rightleftharpoons CaH_2PO_4^+$
Ca(cr)	96.85 ± 0.18	-543.0 ± 1.0	-		$Ca(cr) \rightleftharpoons Ca^{2+} + 2\ e^-$
Portlandite	22.75 ± 0.02	-122.8 ± 0.6	104.5 ± 6.5	0 – 350	$Ca(OH)_2(cr) + 2\ H^+ \rightleftharpoons Ca^{2+} + 2\ H_2O(l)$
Fluorite	-10.46 ± 0.09	7.8 ± 1.9	-170 ± 15	25 – 350	$CaF_2(cr) \rightleftharpoons Ca^{2+} + 2\ F^-$
Calcite	-8.45 ± 0.07	-10.2 ± 0.4	-404.0 ± 2.6	0 – 250	$CaCO_3(calcite) \rightleftharpoons Ca^{2+} + CO_3^{2-}$
Aragonite	-8.32 ± 0.05	-10.9 ± 0.3	-366 ± 19	0 – 90	$CaCO_3(aragonite) \rightleftharpoons Ca^{2+} + CO_3^{2-}$
Vaterite	-7.91 ± 0.05	-15.4 ± 0.8	-321 ± 36	0 – 90	$CaCO_3(vaterite) \rightleftharpoons Ca^{2+} + CO_3^{2-}$
Dolomite	-17.12 ± 0.37	-36.0 ± 1.6	-	-	$CaMg(CO_3)_2(cr) \rightleftharpoons Ca^{2+} + Mg^{2+} + 2\ CO_3^{2-}$
Anhydrite	-4.21 ± 0.17	-17.7 ± 1.0	-396.9 ± 2.9	0 – 350	$CaSO_4(cr) \rightleftharpoons Ca^{2+} + SO_4^{2-}$
Gypsum	-4.58 ± 0.05	-0.46 ± 0.04	-208.4 ± 3.0	25 – 90	$CaSO_4{\cdot}2H_2O(cr) \rightleftharpoons Ca^{2+} + SO_4^{2-} + 2\ H_2O(l)$

Tab. 4.2-3: Cont.

Name	**$\log_{10}\beta°$**	**$\Delta_r H_m°$** [kJ · mol^{-1}]	**$\Delta_r C_{p,m}°$** [J · K^{-1} · mol^{-1}]	**T-range** [°C]	**Reaction**
OH-apatite	-58.29 ± 0.15	-68 ± 15	-1938 ± 50	5 – 37	$Ca_5(PO_4)_3OH(cr) \rightleftharpoons 5\ Ca^{2+} + 3\ PO_4^{3-} + OH^-$
F-apatite	-59.63 ± 0.20	-61 ± 15	-1'887 ± 50	25 – 45	$Ca_5(PO_4)_3F(cr) \rightleftharpoons 5\ Ca^{2+} + 3\ PO_4^{3-} + F^-$
Cl-apatite	-46 ± 5	-120 ± 41	-1'920 ± 100	25	$Ca_5(PO_4)_3Cl(cr) \rightleftharpoons 5\ Ca^{2+} + 3\ PO_4^{3-} + Cl^-$
Monetite	-6.86 ± 0.02	-18.8 ± 0.7	-345 ± 20	5 – 37	$CaHPO_4(cr) \rightleftharpoons Ca^{2+} + HPO_4^{2-}$
Brushite	-6.59 ± 0.02	-5.4 ± 1.3	-282 ± 20	5 – 37	$CaHPO_4{\cdot}2H_2O(cr) \rightleftharpoons Ca^{2+} + HPO_4^{2-} + 2\ H_2O(l)$
Tuite	-28.90 ± 0.10	-81.2 ± 5.0	-5'620 ± 100	5 – 37	$Ca_3(PO_4)_2(cr) \rightleftharpoons 3\ Ca^{2+} + 2\ PO_4^{3-}$
CaHK3(PO4)2	-22.4 ± 0.8	-	-		$CaHK_3(PO_4)_2(cr) \rightleftharpoons Ca^{2+} + H^+ + 3\ K^+ + 2\ PO_4^{3-}$
Ca4H(PO4) 3 · 2.5H2O	-48.48 ± 0.16	-21 ± 19	0	4 – 45	$Ca_4H(PO_4)_3 \cdot 2.5H_2O\ (s) \rightleftharpoons 4\ Ca^{2+} + 3\ PO_4^{3-} + H^+ + 2.5\ H_2O(l)$

Tab. 4.2-4: Selected SIT ion interaction coefficients $\varepsilon_{j,k}$ [kg · mol^{-1}] magnesium species

Data in bold face are taken from Lemire et al. (2013). Data in normal face are derived in this review. Data estimated according to charge correlations and taken from Tab. 1-7 are shaded.

j k → ↓	**Cl^-** $\varepsilon_{j,k}$ [kg · mol^{-1}]	**Na^+** $\varepsilon_{j,k}$ [kg · mol^{-1}]	**$Na^+ + Cl^-$** $\varepsilon_{j,k}$ [kg · mol^{-1}]
Ca^{2+}	**0.14 ± 0.01**	0	0
$CaOH^+$	0.05 ± 0.10	0	0
CaF^+	0.10 ± 0.06	0	0
$CaHCO_3^+$	0.05 ± 0.10	0	0
$CaCO_3(aq)$	0	0	0.0 ± 0.1
$CaSO_4(aq)$	0	0	0.0 ± 0.1
$CaPO_4^-$	0	-0.05 ± 0.10	0
$CaHPO_4(aq)$	0	0	0.0 ± 0.1
$CaH_2PO_4^+$	0.05 ± 0.10	0	0

4.2.10 References

Avnimelech, Y., Moreno, E.C. & Brown, W.E. (1973): Solubility and surface properties of finely divided hydroxyapatite. J. Res. Natl. Bur. Stand., 77A, 149-155.

Baes, C.F. & Mesmer, R.E. (1976): The Hydrolysis of cations. Wiley, New York, 490 pp.

Bell, R.P. & George, J.H.B. (1953): The incomplete dissociation of some thallous and calcium salts at different temperatures. Trans. Faraday Soc., 49, 619-627.

Berman, R.G. (1988): Internally-consistent thermodynamic data for minerals in the system Na_2O-K_2O-CaO-MgO-FeO-Fe_2O_3-Al_2O_3-SiO_2-TiO_2-H_2O-CO_2. Journal of Petrology, 29, 445-522.

Bjerrum, N. (1958): Calciumorthophosphate II. Komplexbildung in Lösungen von Calcium- und Phosphat-Ionen. Matematisk-fysiske Meddelelser udgivet af Det Kongelige Danske Videnskabernes Selskab (Mat. Fys. Medd. Dan. Vid. Selsk.), 31, nr. 7, 69-79.

Blount, C.W. & Dickson, F.W. (1973): Gypsum–anhydrite equilibria in systems $CaSO_4$ – H_2O and $CaSO_4$ – NaCl – H_2O. American Mineralogist, 58, 323-331.

Bond, A.M. & Hefter, G. (1971): Use of the fluoride ion-selective electrode for the detection of weak fluoride complexes. J. Inorg. Nucl. Chem., 33, 429-434.

Brown, P.L. & Ekberg, C. (2016): Hydrolysis of Metal Ions. Wiley-VCH Verlag GmbH & Co. KGaA, Weinheim, Germany, 917 pp.

Brown, P.L., Ekberg, C. & Matyskin, A.V. (2019): On the solubility of radium and other alkaline earth sulfate and carbonate phases at elevated temperature. Geochim. Cosmochim. Acta, 255, 88-104.

Brown, D.E. & Roberson, C.E. (1977): Solubility of natural fluorite at 25 °C. Journal of Research of the U.S. Geological Survey, 5, 509-517.

Childs, C.W. (1970): A potentiometric study of equilibria in aqueous divalent metal orthophosphate solutions. Inorg. Chem., 9, 2465-2469.

Chughtai, A., Marshall, R. & Nancollas, G.H. (1968): Complexes in calcium phosphate solutions. J. Phys. Chem., 72, 208-211.

Chuong, R. (1973): Experimental study of surface and lattice effects on the solubility of hydroxyapatite. Journal of Dental Research, 52, 911-914.

Clark, J.S. (1955): Solubility criteria for the existence of hydroxyapatite. Canadian Journal of Chemistry, 33, 1696-1700.

Ciavatta, L., Iuliano, M. & Porto, R. (1991): Complex formation equilibria in calcium phosphate solutions. Annali di Chimica, 81, 243-258.

Cox, J.D., Wagman, D.D. & Medvedev, V.A. (1989): CODATA Key Values for Thermodynamics. Hemisphere Publishing, New York, 271 pp.

Cruz, F.J.A.L., Minas da Piedade, M.E. & Calado, J.C.G. (2005): Standard molar enthalpies of formation of hydroxy-, chlor-, and bromapatite. J. Chem. Thermodynamics, 37, 1061-1070.

Davies, C.W. & Hoyle, B.E. (1953): The interaction of calcium ions with some phosphate and citrate buffers. J. Chem. Soc., 4134-4136.

Dorozhkin, S.V. (2011): Calcium orthophosphates: Occurrence, properties, biomineralization, pathological calcification and biomimetic applications. Biomatter, 1, 121-164.

Egan, E.P. & Wakefield, Z.T. (1964a): Low-temperature heat capacity and entropy of anhydrous dicalcium phosphate, 10° to 310 °K. Journal of Chemical and Engineering Data, 9, 541-544.

Egan, E.P. & Wakefield, Z.T. (1964b): Low-temperature heat capacity and entropy of dicalcium phosphate dihydrate, 10° to 310 °K. Journal of Chemical and Engineering Data, 9, 544-545.

Egan, E.P., Wakefield, Z.T. & Elmore, K.L. (1951a): Low-temperature heat capacity and entropy of hydroxyapatite. J. Am. Chem. Soc., 73, 5579-5580.

Egan, E.P., Wakefield, Z.T. & Elmore, K.L. (1951b): Thermodynamic properties of fluorapatite, 15 to 1'600 °K. J. Am. Chem. Soc., 73, 5581-5582.

Elgquist, B. (1970): Determination of the stability constants of MgF^+ and CaF^+ using a fluoride ion selective electrode. J. Inorg. Nucl. Chem., 32, 937-944.

Farr, T.D. & Elmore, K.L. (1962): System CaO-P_2O_5-HF-H_2O: Thermodynamic properties. J. Phys. Chem., 66, 315-318.

Farr, T.D., Tarbutton, G. & Lewis, H.T. (1962): System CaO–P_2O_5–HF–H_2O: Equilibrium at 25 and 50°. J. Phys. Chem., 66, 318-321.

Garand, A. & Mucci, A. (2004): The solubility of fluorite as a function of ionic strength and solution composition at 25 °C and 1 atm total pressure. Marine Geochemistry, 91, 27-35.

Gosselin, R.E. & Coghlan, E.R. (1953): The stability of complexes between calcium and orthophosphate, polymeric phosphate, and phytate. Arch. Biochem. Biophys., 45, 301-311.

Gottschal, A.I. (1958): Heats of formation of hydroxy-, fluor- and chlorapatites. Journal of the South African Chemical Institute, 11, 45-52 (as cited by Cruz et al. 2005).

Greenwald, I. (1963): The instability constant and hydrogen ion dissociation of calcium hydrogen phosphate. J. Phys. Chem., 67, 2853-2854.

Greenwald, I., Redish, J. & Kibrick, A.C. (1940): The dissociation of calcium and magnesium phosphates. J. Biol. Chem., 135, 65-76.

Gregory, T.M., Moreno, E.C. & Brown, W.E. (1970): Solubility of $CaHPO_4 \cdot 2H_2O$ in the system $Ca(OH)_2$ – H_3PO_4 – H_2O at 5, 15, 25, and 37.5 °C. J. Res. Natl. Bur. Stand., 74A, 461-475.

Gregory, T.M., Moreno, E.C., Patel, J.M. & Brown, W.E. (1974): Solubility of β-$Ca_3(PO_4)_2$ in the system $Ca(OH)_2$ – H_3PO_4 – H_2O at 5, 15, 25, and 37 °C. J. Res. Natl. Bur. Stand., 78A, 667-674.

Grenthe, I., Fuger, J., Konings, R.J.M., Lemire, R.J., Muller, A.B., Nguyen-Trung, C. & Wanner, H. (1992): Chemical Thermodynamics of Uranium. Chemical Thermodynamics, Vol. 1. North-Holland, Amsterdam, 715 pp.

Helgeson, H.C., Delany, J.M., Nesbitt, H.W. & Bird, D.K. (1978): Summary and critique of the thermodynamic properties of rock-forming minerals. American Journal of Science, 278-A, 1-229.

Hemingway, B.S. & Robie, R.A. (1994): Enthalpy and Gibbs energy of formation of dolomite, CaMg(CO3)2, at 298.15 K from HCl solution calorimetry. United States Geological Survey Open-file Report 94-575, 12 pp.

Heughebaert, J.C. & Nancollas, G.H. (1985): Solubility of octacalcium phosphate at 25 and 45 °C in the system $Ca(OH)_2 – H_3PO_4 – KNO_3 – H_2O$. J. Chem. Eng. Data, 30, 279-281.

Holland, T.J.B. & Powell, R. (1990): An enlarged and updated internally consistent thermodynamic dataset with uncertainties and correlations: The system K_2O-Na_2O-CaO-MgO-MnO-FeO-Fe_2O_3-Al_2O_3-TiO_2-SiO_2-C-H_2-O_2. Journal of Metamorphic Petrology, 8, 89-124.

Hummel, W., Berner, U., Curti, E., Pearson, F.J. & Thoenen, T. (2002): Nagra/PSI Chemical Thermodynamic Data Base 01/01. Nagra Technical Report NTB 02-16 and Universal Publishers, Parkland, Florida, 565 pp.

Jaynes, W.F., Moore, P.A. & Miller. D.M. (1999): Solubility and ion activity products of calcium phosphate minerals. J. Environ. Qual., 28, 530-536.

Land, L.D. (1998): Failure to precipitate dolomite at 25 °C from dilute solution despite 1000-fold oversaturation after 32 years. Aquatic Geochemistry, 4, 361-368.

Langmuir, D. & Melchior, D. (1985): The geochemistry of Ca, Sr, Ba and Ra sulfates in some deep brines from the Palo Duro Basin, Texas. Geochim. Cosmochim. Acta, 49, 2423-2432.

Larson, T.E., Sollo, F.W., Jr. & McGurk, F.F. (1976): Complexes affecting the solubility of calcium carbonate in water – Phase II. UILU-WRC-76-0108. University of Illinois, Urbana.

Lemire, R.J., Berner, U., Musikas, C., Palmer, D.A., Taylor, P. & Tochiyama, O. (2013): Chemical Thermodynamics of Iron, Part 1. Chemical Thermodynamics, Vol. 13a. OECD Publications, Paris, France, 1082 pp.

Lilley, T.H. & Briggs, C.C. (1976): Activity coefficients of calcium sulphate in water at 25 °C. Proc. Royal Society London, A 349, 355-368.

Lindsay, W.L. & Moreno, E.C. (1960): Phosphate phase equilibria in soils. Soil Science Society of America Journal, 24, 177-182.

Liu, Q., Chen, Z., Pan, H. & Darvell, B.W. (2014): The effect of excess phosphate on the solubility of hydroxyapatite. Ceramics International, 40, 2751-2761.

Lothenbach, B., Xu, B. & Winnefeld, F. (2019): Thermodynamic data for magnesium (potassium) phosphates. Applied Geochemistry, 111, 104450.

Macaskill, J.B. & Bates, R.G. (1977): Solubility product constant of calcium fluoride. Journal of Physical Chemistry, 81, 496-498.

Madsen, H.E.L. (1970): Ionic concentrations in calcium phosphate solutions I. Solutions saturated with respect to brushite or tetracalcium monohydrogen phosphate at 37 °C. Acta Chemica Scandinavica, 24, 1671-1676.

Majer, V. & Štulĭk, K. (1982): A study of the stability of alkaline-earth metal complexes with fluoride and chloride ions at various temperatures by potentiometry with ion-selective electrodes. Talanta, 29, 145-148.

McCann, H.G. (1968): The solubility of fluorapatite and its relationship to that of calcium fluoride. Arch. oral Biol., 13, 987-1001.

McDowell, H., Brown, W.E. & Sutter, J.R. (1971): Solubility study of calcium hydrogen phosphate. Ion-pair formation. Inorg. Chem., 10, 1638-1643.

McDowell, H., Gregory, T.M. & Brown, W.E. (1977): Solubility of $Ca_5(PO_4)_3OH$ in the System $Ca(OH)_2$-H_3PO_4-H_2O at 5, 15, 25, and 37 °C. Institute for Materials Research, National Bureau of Standards, Washington, C.C. 20234.

McKenzie, J.A. & Vasconcelos, C. (2009): Dolomite Mountains and the origin of the dolomite rock of which they mainly consist: historical developments and new perspectives. Sedimentology, 56, 205-219.

Moreno, E.C., Gregory, T.M. & Brown, W.E. (1966): Solubility of $CaHPO_4 \cdot 2H_2O$ and formation of ion pairs in the system $Ca(OH)_2 – H_3PO_4 – H_2O$ at 37.5 °C. J. Res. Natl. Bur. Stand., 70A, 545-552.

Moreno, E.C., Gregory, T.M. & Brown, W.E. (1968): Preparation and solubility of hydroxyapatite. J. Res. Natl. Bur. Stand., 72A, 773-782.

Moreno, E.C., Gregory, T.M. & Osborn, G. (1960a): Solubility of dicalcium phosphate dihydrate in aqueous systems. Soil Science Society of America Journal.

Moreno, E.C., Gregory, T.M. & Osborn, G. (1960b): Solubility of dicalcium phosphate dihydrate in aqueous solutions and solubility of octocalcium phosphate. Soil Science Society of America Journal, 24, 99-102.

Nancollas, G.H. (1984): The nucleation and growth of phosphate minerals. In: Nriagu, J.O. & Moore, P.B. (eds.) Phosphate Minerals, Springer-Verlag, Berlin, p. 137-154.

Nordstrom, D.K. & Jenne, A.E. (1977): Fluorite solubility equilibria in selected geothermal waters. Geochim. Cosmochim. Acta, 41, 175-188.

Nordstrom, D.K., Plummer, L.N., Langmuir, D., Busenberg, E., May, H.M., Jones, B.F. & Parkhurst, D.L. (1990): Revised Chemical Equilibrium Data for Major Water-Mineral Reactions and Their Limitations. In: Melchior, D.C., and Bassett, R.L. (eds.): Chemical Modeling of Aqueous Systems II. Washington, D.C., American Chemical Society, ACS Symposium Series 416, p. 398-413.

Patel, P.R., Gregory, T.M. & Brown, W.E. (1974): Solubility of $CaHPO_4 \cdot 2H_2O$ in the quaternary system $Ca(OH)_2 – H_3PO_4 – NaCl – H_2O$ at 25 °C. J. Res. Natl. Bur. Stand., 78A, 675-681.

Plummer, L.N. & Busenberg, E. (1982): The solubilities of calcite, aragonite and vaterite in CO_2-H_2O solutions between 0 and 90 °C, and an evaluation of the aqueous model for the system $CaCO_3$-CO_2-H_2O. Geochim. Cosmochim. Acta, 46, 1011-1040.

Richardson, C.K. & Holland, H.D. (1979): The solubility of fluorite in hydrothermal solutions, an experimental study. Geochim. Cosmochim. Acta, 43, 1313-1325.

Roberts, J.A., Kenward, P.A., Fowle, D.A., Goldstein. R.H., González, L.A. & Moore, D.S. (2013): Surface chemistry allows for abiotic precipitation of dolomite at low temperature. PNAS, 110, 14540-14545.

Robie, R.A. & Hemingway, B.S. (1995): Thermodynamic Properties of Minerals and Related Substances at 298.15 K and 1 Bar (10^5 Pascals) Pressure and at Higher Temperatures. United States Geological Survey Bulletin, 2131, 470 pp.

Robie, R.A., Hemingway, B.S. & Fisher, J.R. (1979): Thermodynamic Properties of Minerals and Related Substances at 298.15 K and 1 Bar (10^5 Pascals) Pressure and at Higher Temperatures. United States Geological Survey Bulletin, 1452, Reprinted with corrections, 464 pp.

Robinson, R.A. & Stokes, R.H. (1959): Electrolyte Solutions. Second Revised Edition. Academic Press, New York, 559 pp.

Saha, A., Saha, N., Ji, L., Zhao, J., Gregáň, F., Sajadi, S.A., Song, B. & Sigel, H. (1996): Stability of metal ion complexes formed with methyl phosphate and hydrogen phosphate. Journal of Biological Inorganic Chemistry, 1, 231-238.

Shyu, L.J., Perez, L., Zawacki, S.J., Heughebaert, J.C. & Nancollas, G.H. (1983): The solubility of octacalcium phosphate at 37 °C in the system $Ca(OH)_2 – H_3PO_4 – KNO_3 – H_2O$. Journal of Dental Research, 62, 398-400.

Smith, R.P. & Alberty, R.A. (1956): The apparent stability constants of ionic complexes of various adenosine phosphates with divalent cations. J. Phys. Chem., 78, 2376-2380.

Smith, R.M. & Martell, A.E. (1976): Critical Stability Constants. Volume 4: Inorganic Complexes. Plenum Press, New York, 257 pp.

Smith, R.M. & Martell, A.E. (1989): Critical Stability Constants. Volume 6: Second Supplement. Plenum Press, New York, 643 pp.

Stout, J.W. & Robie, R.A. (1963): Heat capacity from 11 to 300°K, entropy, and heat of formation of dolomite. Journal of Physical Chemistry, 67, 2248-2252.

Strates, B.S., Neuman, W.F: & Levinskas, G.J. (1957): The solubility of bone mineral. II. Precipitation of near-neutral solutions of calcium and phosphate. J. Am. Chem. Soc., 61, 279-282.

Strübel, G. (1965): Quantitative Untersuchungen über die hydrothermale Löslichkeit von Flußspat (CaF_2). Neues Jahrbuch für Mineralogie Monatshefte, 3, 83-95.

Tanner, S.P., Walker, J.B. & Choppin, G.R. (1968): Thermodynamic parameters of the alkaline earth monofluorides. J. Inorg. Nucl. Chem., 30, 2067-2070.

Tung, M.S., Eidelman, N., Sieck, B. & Brown, W.E. (1988): Octacalcium phosphate solubility product from 4 to 37 °C. J. Res. Natl. Bur. Stand., 93, 613-624.

Usdowski, E. (1989): Synthesis of dolomite and magnesite at 60 °C in the system Ca^{2+}-Mg^{2+}-CO_3^{2-}-Cl_2^{2-}-H_2O. Naturwissenschaften, 76, 374-375.

Valyashko, V.M., Kogaro, L.N. & Khodakovskiy, I.L. (1968): Stability of fluorapatite, chlorapatite and hydroxyapatite in aqueous solutions at different temperatures. Geochemistry International, 5, 21-30

Verbeek, R.M.H., Steyaer, H., Thun, H.P. & Verbeek, F. (1980): Solubility of synthetic calcium hydroxyapatites. J. Chem. Soc. Farad. Trans., 76, 209-219.

Wagman, D.D., Evans, W.H., Parker, V.B., Schumm, R.H., Halow, I., Bailey, S.M., Churney, K.L. & Nuttall, R.L. (1982): The NBS tables of chemical thermodynamic properties: Selected values for inorganic and C1 and C2 organic substances in SI units. Journal of Physical and Chemical Reference Data, 11, Supplement No. 2, 1-392.

Wier, D.R., Chien, S.H. & Black, C.A. (1971): Solubility of hydroxyapatite. Soil Science, 111, 107-112.

Xu, B., Lothenbach, B. & Winnefeld, F. (2020): Influence of wollastonite on hydration and properties of magnesium potassium phosphate cements. Cement and Concrete Research, 131, 106012.

Zhang, W., Zhou, L., Tang, H., Li, H., Song, W. & Xie, G. (2017): The solubility of fluorite in Na-K-Cl solutions at temperatures up to 260 °C and ionic strengths up to 4 mol/kg H_2O. Applied Geochemistry, 82, 79-88.

4.3 Strontium

4.3.1 Elemental strontium

Strontium metal is not relevant under environmental conditions. However, the absolute entropy of Sr(cr) is used for the calculation of certain thermodynamic reaction properties.

The selected value for Sr(cr) is taken from Grenthe et al. (1992):

$$S_m°(\text{Sr, cr, 298.15 K}) = (55.700 \pm 0.210)\ \text{J} \cdot \text{K}^{-1} \cdot \text{mol}^{-1}$$

4.3.2 Strontium(II) aqua ion

Strontium(II) exists as the Sr^{2+} cation in aqueous solutions. The selected thermodynamic values for Sr^{2+} are taken from Grenthe et al. (1992):

$$\Delta_f G_m°(Sr^{2+}, 298.15\ \text{K}) = -(563.864 \pm 0.781)\ \text{kJ} \cdot \text{mol}^{-1}$$

$$\Delta_f H_m°(Sr^{2+}, 298.15\ \text{K}) = -(550.900 \pm 0.500)\ \text{kJ} \cdot \text{mol}^{-1}$$

$$S_m°(Sr^{2+}, 298.15\ \text{K}) = -(31.500 \pm 2.000)\ \text{J} \cdot \text{K}^{-1} \cdot \text{mol}^{-1}$$

Using the selected $\Delta_f G_m°(Sr^{2+}, 298.15\ \text{K})$, the redox equilibrium

$$\text{Sr(cr)} \rightleftharpoons Sr^{2+} + 2\ e^-$$

is calculated as

$$\log_{10} K°(298.15\ \text{K}) = 98.78 \pm 0.14$$

Since this review does not consider the formation of strontium chloride complexes, $\varepsilon(Sr^{2+}, Cl^-)$ is taken as evaluated in this review (see Section 4.3.5.2):

$$\varepsilon(Sr^{2+}, Cl^-) = (0.12 \pm 0.01)\ \text{kg} \cdot \text{mol}^{-1}$$

4.3.3 Strontium(II) (hydr)oxide compounds and complexes

4.3.3.1 Strontium(II) hydroxide complexes

Nordstrom et al. (1990) selected a $\log_{10}{}^{*}\beta_1°$ value from Baes & Mesmer (1976) for the complex

$$Sr^{2+} + H_2O(l) \rightleftharpoons SrOH^{+} + H^{+}$$

$$\log_{10}{}^{*}\beta_1° \text{ (298.15 K)} = -13.29$$

Brown & Ekberg (2016) state that the hydrolysis of strontium(II) is weak and occurs in quite alkaline pH solutions, and only the species $SrOH^{+}$ has been detected. They continue that there are few studies that have determined the stability constant for $SrOH^{+}$, and the majority of these studies corrected their own, or earlier, data to zero ionic strength. The data were acquired across the relatively small temperature interval of 5 – 45 °C, but there is relatively good agreement between the data obtained. Brown & Ekberg (2016) show that the data have a linear relationship with the reciprocal of temperature and obtained

$$Sr^{2+} + H_2O(l) \rightleftharpoons SrOH^{+} + H^{+}$$

$$\log_{10}{}^{*}\beta_1° \text{ (298.15 K)} = -13.15 \pm 0.05$$

$$\Delta_r H_m° \text{(298.15 K)} = (61.6 \pm 10.5) \text{ kJ} \cdot \text{mol}^{-1}$$

$$\Delta_r C_{p,m}° \text{(298.15 K)} = 0 \text{ J} \cdot \text{K}^{-1} \cdot \text{mol}^{-1}$$

These values have been included in TDB 2020, as well as the estimate

$$\varepsilon(SrOH^{+}, Cl^{-}) = (0.05 \pm 0.10) \text{ kg} \cdot \text{mol}^{-1}$$

4.3.3.2 Strontium(II) (hydr)oxide compounds

$Sr(OH)_2(s)$ is soluble in water with a solubility of 20 g/L at 20 °C (gestis.itrust.de), and it has not been found as a mineral in nature. Hence, no thermodynamic data for $Sr(OH)_2(s)$ are included in TDB 2020.

4.3.4 Strontium(II) fluoride compounds and complexes

4.3.4.1 Strontium(II) fluoride complexes

Three studies have been published concerning the SrF^+ complex formation, covering the temperature range 2 – 85 °C. Data obtained in 1 M $NaClO_4$ (Tanner et al. 1968, Bond & Hefter 1971) and 1 M $NaNO_3$ (Majer & Štulík 1982) show a more or less consistent temperature behaviour (Fig. 4.3-1). An unweighted regression of all data resulted in

$$\log_{10}K_1 \text{ (298.15 K, 1 M)} = 0.16 \pm 0.10$$

$$\Delta_r H_m \text{ (298.15 K, 1 M)} = (10.9 \pm 3.7) \text{ kJ} \cdot \text{mol}^{-1}$$

$$\Delta_r C_{p,m} \text{ (298.15 K, 1M)} = 0 \text{ J} \cdot \text{K}^{-1} \cdot \text{mol}^{-1}$$

Note that the data reported for 25 °C, in 1 M $NaClO_4$ (Tanner et al. 1968, Bond & Hefter 1971) and 1 M $NaNO_3$ (Majer & Štulík 1982), are in the range $\log_{10}\beta_1$ (298.15 K, 1 M) = 0.11 – 0.15, with an unweighted average of $\log_{10}K_1$ (298.15 K, 1 M) = 0.13 ± 0.04.

No attempt has been made to extrapolate $\Delta_r H_m$ to zero ionic strength, which is included in TDB 2020 as an approximation of $\Delta_r H_m°$ (298.15 K).

Considering $\varepsilon(Sr^{2+}, ClO_4^-) = (0.22 \pm 0.01)$ kg · mol^{-1} (see Section 4.3.5.2) and $\varepsilon(Na^+, F^-) = (0.02 \pm 0.02)$ kg · mol^{-1} (Grenthe et al. 1992), and the estimate $\varepsilon(SrF^+, ClO_4^-) = (0.2 \pm 0.1)$ kg · mol^{-1}, this review calculated $\Delta\varepsilon(NaClO_4) = -(0.04 \pm 0.11)$ kg · mol^{-1}. Using this $\Delta\varepsilon$ value, $\log_{10}K_1$ (298.15 K, 1 M) = 0.16 ± 0.10 has been extrapolated to zero ionic strength:

$$Sr^{2+} + F^- \rightleftharpoons SrF^+$$

$$\log_{10}K_1° \text{ (298.15 K)} = 0.92 \pm 0.15$$

This datum is included in TDB 2020, as well as the estimate

$$\varepsilon(SrF^+, Cl^-) = (0.05 \pm 0.10) \text{ kg} \cdot \text{mol}^{-1}$$

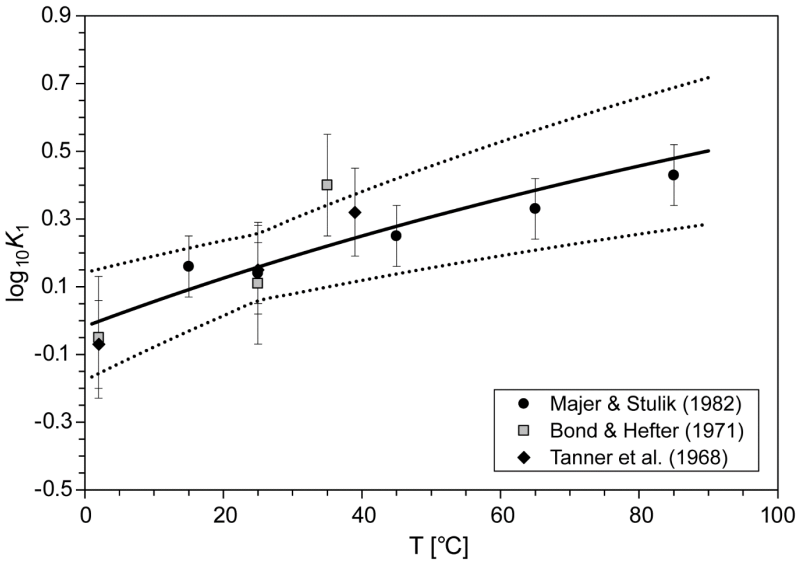

Fig. 4.3-1: The equilibrium constant $\log_{10}K_1$ for $Sr^{2+} + F^- \rightleftharpoons SrF^+$ as a function of temperature in the range 2 – 85 °C at 1 M ionic strength

Solid line: unweighted regression of all data. Dotted lines: lower and upper limits using $\log_{10}K$ (298.15 K) = 0.16 ± 0.10 and $\Delta_r H_m$(298.15 K) = (10.9 ± 3.7) kJ · mol^{-1} and extrapolated to lower and higher temperatures.

4.3.4.2 Strontium(II) fluoride compounds

SrF_2(cr) has been found as the very rare mineral strontifluorite. For the solubility product

$$SrF_2(cr) \rightleftharpoons Sr^{2+} + 2\ F^-$$

$\log_{10}K_s°$ (298.15 K) = -8.54 has been selected by Smith & Martell (1976). Later, this value has been revised to $\log_{10}K_s°$ (298.15 K) = -8.58 ± 0.04 (Smith & Martell 1989). The data sources and the selection procedure of Smith & Martell (1976, 1989) remain unclear.

However, these values indicated that the solubility of strontifluorite, SrF_2(cr), is significantly higher than that of fluorite, CaF_2(cr), $\log_{10}K_s°$ (298.15 K) = -10.46 ± 0.09 (see Section 6.4.2). This is in accord with the observation that the concentration of dissolved fluoride, F^-, in environmental systems is usually governed by the precipitation of the ubiquitous mineral fluorite. Hence, strontifluorite, SrF_2(cr), is only formed under very special chemical conditions and does not play any role in common environmental systems.

No solubility data for SrF_2(cr) are included in TDB 2020.

4.3.5 Strontium(II) chloride compounds and complexes

4.3.5.1 Strontium(II) chloride complexes

This report does not consider the formation of weak strontium chloride complexes but includes possible ion interactions in the SIT interaction coefficient $\varepsilon(Sr^{2+}, Cl^-)$ (see below).

4.3.5.2 Strontium(II) chloride compounds

$SrCl_2$(s) is a highly soluble salt with a solubility of 1'062 g/L at 0 °C and 2'058 g/L at 40 °C (gestis.itrust.de). Its isopiestic properties have been measured up to 4 mol · kg_{H2O}^{-1} (Robinson & Stokes 1959). However, no specific ion interaction coefficient $\varepsilon(Sr^{2+}, Cl^-)$ has ever been selected by NEA (Grenthe et al. 1992, Lemire et al. 2013), simply because Ciavatta (1980), the source of the $\varepsilon(Mg^{2+}, Cl^-)$, $\varepsilon(Ca^{2+}, Cl^-)$ and $\varepsilon(Ba^{2+}, Cl^-)$ values selected by NEA, for unknown reasons did not include Sr in his list of SIT interaction coefficients. Hence, this review evaluated from mean activity data reported by Robinson & Stokes (1959)

$$\varepsilon(Sr^{2+}, Cl^-) = (0.12 \pm 0.01)\ kg \cdot mol^{-1}$$

as well as

$$\varepsilon(Sr^{2+}, ClO_4^-) = (0.22 \pm 0.01)\ kg \cdot mol^{-1}$$

Scharge (2016) derived from literature data binary Pitzer coefficients for the system SrCl – H_2O and ternary Pitzer coefficients for the systems SrCl – NaCl – H_2O, SrCl – KCl – H_2O, SrCl – $CaCl_2$ – H_2O and SrCl – $MgCl_2$ – H_2O and based on these Pitzer coefficients a solubility product for the highly soluble salt $SrCl_2 \cdot 6H_2O$(cr). None of these data have been considered in TDB 2020.

4.3.6 Strontium(II) carbonate compounds and complexes

4.3.6.1 Strontium(II) carbonate complexes

Nordstrom et al. (1990) selected thermodynamic data reported by Busenberg et al. (1984) for the complexes

$$Sr^{2+} + CO_3^{2-} \rightleftharpoons SrCO_3(aq)$$

$$\log_{10}K_1^\circ\ (298.15\ K) = 2.81$$

$$\Delta_r H_m^\circ(298.15\ K) = 5.22\ kcal \cdot mol^{-1} = 21.84\ kJ \cdot mol^{-1}$$

$$\log_{10}K_1^\circ\ (T) = -1.019 + 0.012826 \cdot T$$

$Sr^{2+} + HCO_3^- \rightleftharpoons SrHCO_3^+$

$\log_{10}K°$ (298.15 K) = 1.18

$\Delta_r H_m°$(298.15 K) = 6.05 kcal · mol^{-1} = 25.31 kJ · mol^{-1}

$\log_{10}K°$ (T) = -3.248 + 0.014867 · T

Note that in both cases the reported temperature functions imply temperature dependent $\Delta C_{p,m}°$ values. Hence, the seemingly simple linear temperature function actually might be an over-fitting of the experimental data. This review re-fitted the experimental data reported by Busenberg et al. (1984), with the assumption $\Delta_r C_{p,m}°$ = constant for $SrCO_3$(aq) and $SrHCO_3^+$, as in both cases a plot of stability constants versus the reciprocal of the absolute temperature indicated a significant curvature. The results are (Figs. 4.3-2 and 4.3-3):

$Sr^{2+} + CO_3^{2-} \rightleftharpoons SrCO_3$(aq)

$\log_{10}K_1°$ (298.15 K) = 2.79 ± 0.05

$\Delta_r H_m°$(298.15 K) = (20.6 ± 1.9) kJ · mol^{-1}

$\Delta_r C_{p,m}°$(298.15 K) = (241 ± 100) J · K^{-1} · mol^{-1}

$Sr^{2+} + HCO_3^- \rightleftharpoons SrHCO_3^+$

$\log_{10}K°$ (298.15 K) = 1.18 ± 0.04

$\Delta_r H_m°$(298.15 K) = (25.0 ± 1.5) kJ · mol^{-1}

$\Delta_r C_{p,m}°$(298.15 K) = (226 ± 90) J · K^{-1} · mol^{-1}

These values are included in TDB 2020, as well as the estimates

$\varepsilon(SrHCO_3^+, Cl^-)$ = (0.05 ± 0.10) kg · mol^{-1}

$\varepsilon(SrCO_3$(aq), NaCl) = (0.0 ± 0.1) kg · mol^{-1}

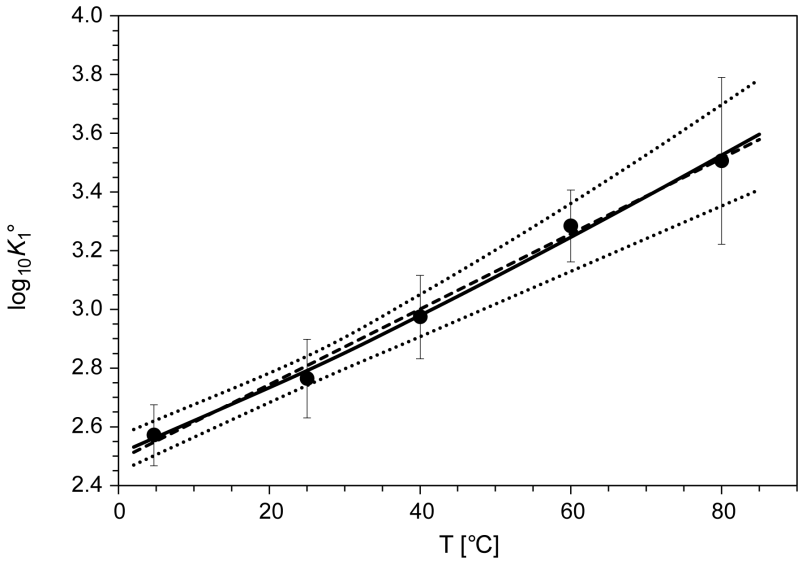

Fig. 4.3-2: The equilibrium constant $\log_{10}K_1°$ for $Sr^{2+} + CO_3^{2-} \rightleftharpoons SrCO_3(aq)$ as a function of temperature in the range 5 – 80 °C

Solid line: unweighted regression. Dotted lines: lower and upper limits using $\log_{10}K_1°$ (298.15 K) = 2.79 ± 0.05, $\Delta_r H_m°$(298.15 K) = (20.6 ± 1.9) kJ · mol^{-1} and $\Delta_r C_{p,m}°$(298.15 K) = (241 ± 100) J · K^{-1} · mol^{-1} and extrapolated to lower and higher temperatures. Dashed line: temperature function selected by Busenberg et al. (1984), shown for comparison.

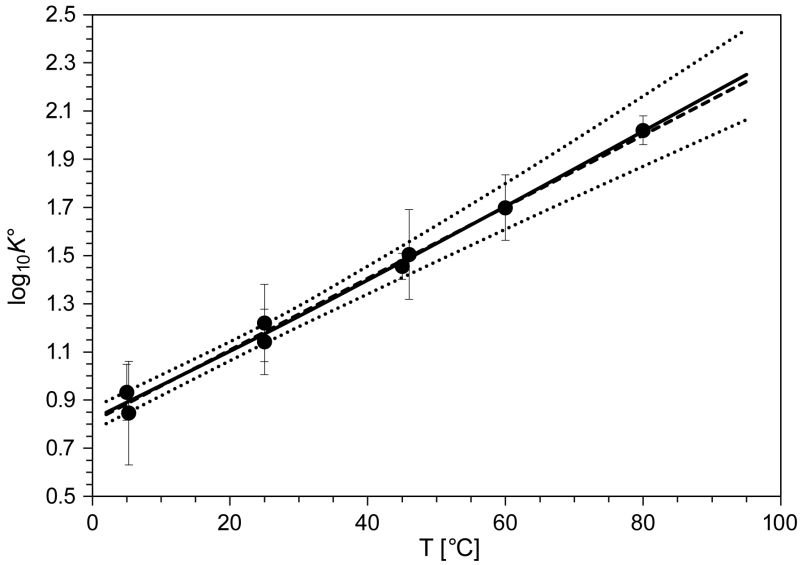

Fig. 4.3-3: The equilibrium constant $\log_{10}K°$ for $Sr^{2+} + HCO_3^- \rightleftharpoons SrHCO_3^+$ as a function of temperature in the range 5 – 80 °C

Solid line: unweighted regression. Dotted lines: lower and upper limits using $\log_{10}K°$ (298.15 K) = 1.18 ± 0.04, $\Delta_r H_m°$(298.15 K) = (25.0 ± 1.5) kJ · mol^{-1} and $\Delta_r C_{p,m}°$(298.15 K) = (226 ± 90) J · K^{-1} · mol^{-1} and extrapolated to lower and higher temperatures. Dashed line: temperature function selected by Busenberg et al. (1984), shown for comparison.

4.3.6.2 Strontium(II) carbonate compounds

Nordstrom et al. (1990) selected thermodynamic data reported by Busenberg et al. (1984) for strontianite, $SrCO_3$(cr), valid in the temperature range 0 – 90 °C:

$$SrCO_3(strontianite) \rightleftharpoons Sr^{2+} + CO_3^{2-}$$

$$\log_{10}K_s^\circ\ (298.15\ K) = -9.271$$

$$\Delta_r H_m^\circ(298.15\ K) = -0.40\ kcal \cdot mol^{-1} = -1.67\ kJ \cdot mol^{-1}$$

$$\log_{10}K_{s0}^\circ\ (T) = 155.0305 - 7239.594 / T - 56.58638 \cdot \log_{10}(T)$$

Note that the reported temperature functions implies $\Delta_r C_{p,m}^\circ$ = constant. This review re-fitted the experimental data reported by Busenberg et al. (1984), together with data reported by Townley et al. (1937) at 25 and 40 °C, and obtained (Fig. 4.3-4):

$$\log_{10}K_s^\circ\ (298.15\ K) = -9.27 \pm 0.03$$

$$\Delta_r H_m^\circ(298.15\ K) = -(1.6 \pm 0.6)\ kJ \cdot mol^{-1}$$

$$\Delta_r C_{p,m}^\circ(298.15\ K) = -(471 \pm 28)\ J \cdot K^{-1} \cdot mol^{-1}$$

These values are included in TDB 2020.

Brown et al. (2019), in their recent review of the solubility of alkaline earth sulphate and carbonate phases at elevated temperatures, recommend for the solubility of strontianite, $SrCO_3$(s)

$$\log_{10}K_{s0}^\circ\ (298.15\ K) = -9.27 \pm 0.10$$

$$\Delta_r H_m^\circ(298.15\ K) = -(2.7 \pm 0.6)\ kJ \cdot mol^{-1}$$

$$\Delta_r C_{p,m}^\circ(298.15\ K) = -(412.6 \pm 3.8)\ J \cdot K^{-1} \cdot mol^{-1}$$

Brown et al. (2019) used the same data as the present review (Busenberg et al. 1984 and Townley et al. 1937) and obtained an identical $\log_{10}K_{s0}^\circ$ (298.15 K) value but slightly different $\Delta_r H_m^\circ$(298.15 K) and $\Delta_r C_{p,m}^\circ$(298.15 K) values. Why their fit below 15 °C deviates from the experimental data (Fig 4.3.4) remains unclear.

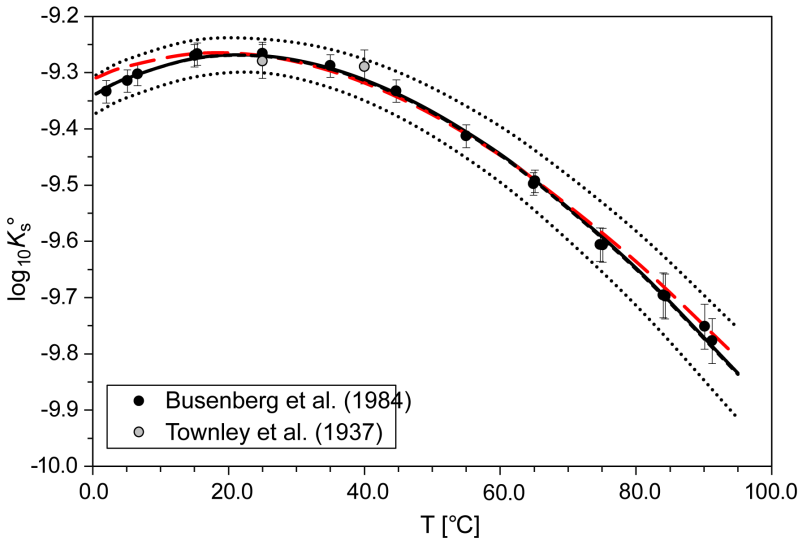

Fig. 4.3-4: The equilibrium constant $\log_{10}K_s°$ for $SrCO_3(s) \rightleftharpoons Sr^{2+} + CO_3^{2-}$, strontianite, as a function of temperature in the range 0 – 90 °C

Solid line: unweighted regression of all data. Dotted lines: lower and upper limits using $\log_{10}K_{s0}°$ (298.15 K) = -9.27 ± 0.03, $\Delta_rH_m°$(298.15 K) = -(1.6 ± 0.6) kJ · mol^{-1} and $\Delta_rC_{p,m}°$(298.15 K) = -(471 ± 28) J · K^{-1} · mol^{-1}, and extrapolated to higher temperatures. Dashed line (hardly visible): temperature function selected by Busenberg et al. (1984), shown for comparison. Large dashed (red) line: temperature function selected by Brown et al. (2019), shown for comparison.

4.3.7 Strontium(II) sulphate compounds and complexes

4.3.7.1 Strontium(II) sulphate complexes

Nordstrom et al. (1990) selected thermodynamic data reported by Reardon (1983), determined at 25 °C by a conductimetric and an ion-exchange approach. The latter technique was also applied at 10, 40 and 60 °C. Reardon (1983) obtained for the complex

$$Sr^{2+} + SO_4^{2-} \rightleftharpoons SrSO_4(aq)$$

$$\log_{10}K_1° \text{ (298.15 K)} = 2.29 \pm 0.04$$

$$\Delta_rH_m°\text{(298.15 K)} = (8.7 \pm 2.0) \text{ kJ} \cdot \text{mol}^{-1}$$

$$\Delta_rC_{p,m}°\text{(298.15 K)} = 0$$

These values have been included in TDB 2020, as well as the estimate

$$\varepsilon(SrSO_4(aq), NaCl) = (0.0 \pm 0.1) \text{ kg} \cdot \text{mol}^{-1}.$$

4.3.7.2 Strontium(II) sulphate compounds

Nordstrom et al. (1990) selected thermodynamic data reported by Reardon & Armstrong (1987) for celestite, $SrSO_4$(cr), valid in the temperature range 10 to 90 °C:

$SrSO_4$(celestite) ⇌ $Sr^{2+} + SO_4^{2-}$

$\log_{10}K_s°$ (298.15 K) = -6.63

$\Delta_r H_m°$(298.15 K) = -1.037 kcal · mol^{-1} = -4.34 kJ · mol^{-1}

$\log_{10}K_{s0}$(celesite) =
14805.9622 + 2.4660924 · T – 756968.533 / T + 40553604 / T^2 – 48.595 · $\log_{10}$T

Note that the reported temperature function implies that $\Delta_r C_{p,m}°$ is a function of temperature, which indicates over-fitting the experimental data.

Brown et al. (2019) in their recent review of the solubility of alkaline earth sulphate and carbonate phases at elevated temperature recommend for the solubility of celestite, $SrSO_4$(cr)

$\log_{10}K_s°$ (298.15 K) = -6.58 ± 0.10

$\Delta_r H_m°$(298.15 K) = -(1.3 ± 0.6) kJ · mol^{-1}

$\Delta_r C_{p,m}°$(298.15 K) = -(413.5 ± 2.9) J · K^{-1} · mol^{-1}

determined from various data sets, also considering by Reardon & Armstrong (1987), as well as more recent experimental data, and valid for the temperature range 0 – 300 °C.

These values have been included in TDB 2020.

Scharge (2016) derived from literature data binary and ternary Pitzer coefficients for the systems $SrSO_4$ – H_2O and $SrSO_4$ – Na_2SO_4 – H_2O and derived a solubility product for $SrSO_4$(celestite) of $\log_{10}K_s°$ = -6.55, which is in excellent agreement with the value selected in TDB 2020.

4.3.8 Strontium(II) phosphate compounds and complexes

4.3.8.1 Strontium(II) phosphate complexes

Three studies, Smith & Alberty (1956), Gnepf et al. (1962) and Saha et al. (1996), report stability constants for aqueous strontium phosphate complexes (Tab. 4.3-1).

Smith & Alberty (1956) calculated from measurements with a glass electrode at 25 and 0 °C in 0.2 M Pr_4NCl (tetrapropylammonium chloride, $(CH_3CH_2CH_2)_4NCl$) the values K(25 °C) = 33 ± 2 (corresponding to $\log_{10}K$(25 °C) = 1.519 ± 0.026) and K(0 °C) = 18 ± 2 (corresponding to $\log_{10}K$(0 °C) = 1.255 ± 0.048) for the equilibrium $Sr^{2+} + HPO_4^{2-} \rightleftharpoons SrHPO_4(aq)$. This review retained these values and obtained $\log_{10}K°$(25 °C) = 2.53 ± 0.20 and $\log_{10}K°$(0 °C) = 2.23 ± 0.20 by extrapolation to zero ionic strength using SIT with the estimate $\Delta\varepsilon(Pr_4NCl) \approx -0.4$ in analogy with $\Delta\varepsilon(Et_4NI) = -(0.41 \pm 0.15)$ obtained for $Na^+ + HPO_4^{2-} \rightleftharpoons NaHPO_4^-$ (see Section 2.2.1). The uncertainties have been estimated by this review.

Gnepf et al. (1962) used a cation-exchange resin to measure the equilibrium of Sr-89 spiked solutions in the presence and absence of phosphate at 20 °C in 0.15 M NaCl at pH 2.6, 4.6, 7.0 and 8.9. They report the values $\log_{10}K = 4.2$ for the equilibrium $Sr^{2+} + PO_4^{3-} \rightleftharpoons SrPO_4^-$, $\log_{10}K = 1.2$ for $Sr^{2+} + HPO_4^{2-} \rightleftharpoons SrHPO_4(aq)$ and $\log_{10}K = 0.2 – 0.3$ for $Sr^{2+} + H_2PO_4^- \rightleftharpoons SrH_2PO_4^+$. These values have been calculated by Gnepf et al. (1962) using literature values for the phosphoric acid dissociation constants determined in 0.1 M KNO_3. This review used for the phosphoric acid dissociation constants $\log_{10}K°(298.15)$ and $\Delta_rH_m°(298.15\ K)$ values of TDB 2020, calculated $\log_{10}K°(293.15)$ values therefrom and extrapolated the obtained values to 0.1 M NaCl using SIT. The re-fitted values for the above equilibria, $\log_{10}K = 4.12$, $\log_{10}K = 1.2$ and $\log_{10}K = 0.2$, respectively, are only in the first case slightly different from those reported by Gnepf et al. (1962). These values have been extrapolated to zero ionic strength using SIT with $\varepsilon(Na^+, PO_4^{3-}) = -(0.25 \pm 0.03)$, $\varepsilon(Na^+, HPO_4^{2-}) = -(0.15 \pm 0.06)$, $\varepsilon(Na^+, H_2PO_4^-) = -(0.08 \pm 0.04)$, $\varepsilon(Sr^{2+}, Cl^-) = (0.12 \pm 0.02)$ (Section 4.2.4.2), and the estimates $\varepsilon(Na^+, SrPO_4^-) = -(0.05 \pm 0.10)$, $\varepsilon(CaHPO_4(aq), NaCl) = (0.0 \pm 0.1)$ and $\varepsilon(SrH_2PO_4^+, Cl^-) = (0.05 \pm 0.10)$ and given in Tab. 4.3-1. The uncertainties have been estimated by this review.

Tab. 4.3-1: Reported and accepted strontium phosphate complexation data

Temp. [°C]	Medium	$\log_{10}K$ reported [a]	I_m	$\log_{10}K_m$	$\Delta\varepsilon$	$\log_{10}K°$ accepted [b]	Reference
$Sr^{2+} + PO_4^{3-} \rightleftharpoons SrPO_4^-$							
20	0.15 M NaCl	4.12	0.151	4.118	0.08	5.62 ± 0.20	Gnepf et al. (1962)
$Sr^{2+} + HPO_4^{2-} \rightleftharpoons SrHPO_4(aq)$							
0	0.2 M Pr_4NCl	1.255 ± 0.048	0.201	1.252	-0.4	2.23 ± 0.20	Smith & Alberty (1956)
25	0.2 M Pr_4NCl	1.519 ± 0.026	0.201	1.516	-0.4	2.53 ± 0.20	Smith & Alberty (1956)
20	0.15 M NaCl	1.2	0.151	1.198	0.03	2.19 ± 0.20	Gnepf et al. (1962)
25	0.1 M $NaNO_3$	1.38 ± 0.02	0.101	1.378	0.20	2.27 ± 0.20	Saha et al. (1996)
$Sr^{2+} + H_2PO_4^- \rightleftharpoons SrH_2PO_4^+$							
20	0.15 M NaCl	0.2	0.151	0.198	0.01	0.69 ± 0.20	Gnepf et al. (1962)

[a] Data as reported in the cited publications or calculated by this review from the reported data, see text.
[b] Extrapolated to $I = 0$ by this review, see text, and 2σ uncertainties assigned or estimated by this review.

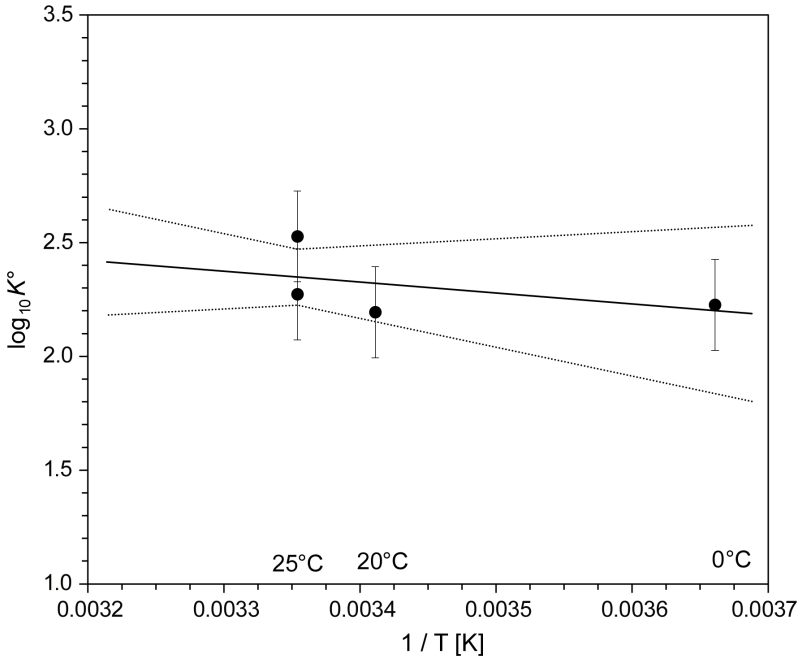

Fig. 4.3-5: The equilibrium constant $\log_{10}K°$ for $Sr^{2+} + HPO_4^{2-} \rightleftharpoons SrHPO_4(aq)$ as a function of reciprocal absolute temperature in the range 0 – 25 °C

Symbols: accepted $\log_{10}K°$ values taken from Tab 4.3.1. Solid line: weighted linear regression. Dotted lines: lower and upper limits using $\log_{10}K°$ (298.15 K) = 2.35 ± 0.12 and $\Delta_r H_m°$ (298.15 K) = (9 ± 15) kJ · mol^{-1} and extrapolated to lower and higher temperatures.

Saha et al. (1996) determined the stability constants of the 1:1 complexes formed between a series of divalent metal cations and hydrogen phosphate by potentiometric pH titration in aqueous solution at 25 °C in 0.1 M $NaNO_3$. For Sr^{2+} they report $\log_{10}K$ = 1.38 ± 0.02. Using SIT with $\varepsilon(Sr^{2+}, NO_3^-)$ = -(0.05 ± 0.02), $\varepsilon(Na^+, HPO_4^{2-})$ = -(0.15 ± 0.06) and the estimate $\varepsilon(SrHPO_4(aq), NaNO_3)$ = (0.0 ± 0.1) this review obtained $\log_{10}K°$ = 2.27 ± 0.20 for the equilibrium $Sr^{2+} + HPO_4^{2-} \rightleftharpoons SrHPO_4(aq)$, with an uncertainty assigned by this review.

The accepted data of Tab. 4.3-1 have been used for weighted linear regressions of the $\log_{10}K°$ values for the equilibrium $Sr^{2+} + HPO_4^{2-} \rightleftharpoons SrHPO_4(aq)$ versus the reciprocal of absolute temperature (Fig. 4.3-5). While the stability constant is fairly well established by this regression analysis, the obtained $\Delta_r H_m°$ value should be considered as approximate value only:

$Sr^{2+} + HPO_4^{2-} \rightleftharpoons SrHPO_4(aq)$

$\log_{10}K°$ (298.15 K) = 2.35 ± 0.12

$\Delta_r H_m°$(298.15 K) = (9 ± 15) kJ · mol^{-1}

$\Delta_r C_{p,m}°$(298.15 K) = 0

In the cases of $Sr^{2+} + PO_4^{3-} \rightleftharpoons SrPO_4^-$ and $Sr^{2+} + H_2PO_4^- \rightleftharpoons SrH_2PO_4^+$ there is only one data point for each equilibrium (Tab. 4.3-1):

$Sr^{2+} + PO_4^{3-} \rightleftharpoons SrPO_4^-$

$\log_{10}K°$ (298.15 K) = 5.62 ± 0.20

$Sr^{2+} + H_2PO_4^- \rightleftharpoons SrH_2PO_4^+$

$\log_{10}K°$ (298.15 K) = 0.69 ± 0.20

These values are included in TDB 2020, together with the estimates

$\varepsilon(SrH_2PO_4^+, Cl^-) = (0.05 \pm 0.10)$ kg · mol^{-1}

$\varepsilon(SrHPO_4(aq), NaCl) = (0.0 \pm 0.1)$ kg · mol^{-1}

$\varepsilon(SrPO_4^-, Na^+) = -(0.05 \pm 0.10)$ kg · mol^{-1}

4.3.8.2 Strontium(II) phosphate compounds

Extremely rare strontium phosphate minerals are nastrophite, $NaSrPO_4 \cdot 9H_2O$, stronadelphite, $Sr_5(PO_4)_3F$, fluorstrophite, $SrCaSr_3(PO_4)_3F$, fluorcaphite, $SrCaCa_3(PO_4)_3F$ (the latter three belonging to the apatite supergroup) and strontiowhitlockite, $Sr_9Mg(PO_4)_6(HPO_4)$ (www.mindat.org). No solubility data are known for these compounds.

Three studies, Holt et al. (1954), Frere (1962) and Aia et al. (1964), report solubility product constants for $SrHPO_4$(cr), and only the study by Holt et al. (1954) reports a solubility product constant for $Sr_3(PO_4)_2$(s) (Tab. 4.3-2). Aia et al. (1964) report that SrHPO4(cr) exists as two crystallographically different modifications, α-$SrHPO_4$(cr) and β-$SrHPO_4$(cr), where β-$SrHPO_4$(cr) is the thermodynamically stable phase in the temperature range 25 – 90 °C.

Holt et al. (1954) explored the titration curve of phosphoric acid with $Sr(OH)_2$ solutions at 38 °C to determine the regions in which stable precipitates formed. Two points on the curve were then selected for further study, the appropriate quantities of acid and base mixed together and shaken continuously at 38 °C for periods varying from one to six weeks, at the end of which time the precipitate was separated, the solution analysed for pH, phosphorus and strontium. Holt et al. (1954) identified $SrHPO_4$(cr) by chemical analysis and optical microscopy, showing that the phase is definitely crystalline, being transparent prismatic to acicular crystals belonging to the triclinic or possibly monoclinic systems, but definitely not orthorhombic. Holt et al. (1954) were not aware of the two modifications of $SrHPO_4$(cr), but probably report the properties of the thermodynamically stable β-$SrHPO_4$(cr). The phase $Sr_3(PO_4)_2$(s) seemed to be completely amorphous, although no X-ray analysis was made.

Holt et al. (1954) report $\log K_s°$(38 °C) = -7.06 for $SrHPO_4$(cr) and $\log K_s°$(38 °C) = -27.8 for $Sr(PO_4)_2$(s). For their data analysis Holt et al. (1954) used the Debye-Hückel limiting law with the phosphate protonation constants $\log K_1° = 2.11$, $\log K_2° = 7.15$, $\log K_3° = 12.66$. Especially $\log K_3°$ is at variance with the value 12.35 included in TDB 2020, and the use of the Debye-Hückel limiting law seems inappropriate at ionic strengths ranging from 0.002 to 0.012 M. Hence, this review reanalysed the data of Holt et al. (1954) using SIT (assuming $\Delta\varepsilon = 0$) with the phosphate

protonation constants of TDB 2020 and the strontium phosphate complexes selected by this review (see preceding section). Unweighted means of the results obtained from the two variable time experiments (Tab. IV of Holt et al. 1954), excluding the first value for the shortest time of 7 days, are logK_s°(38 °C) = -7.01 ± 0.34 (2σ) for $SrHPO_4(cr) = Sr^{2+} + HPO_4^{2-}$, and log$K_s$°(38 °C) = -28.82 ± 0.38 (2σ) for $Sr_3(PO_4)_2(s) = 3\ Sr^{2+} + 2\ PO_4^{3-}$.

Tab. 4.3-2: Reported and accepted strontium phosphate solubility data

Temp. [°C]	**Medium**	**$\log_{10}K_s$° reported** [a]	**$\log_{10}K_s$° accepted** [b]	**Reference**
β-$SrHPO_4(cr) \rightleftharpoons Sr^{2+} + HPO_4^{2}$				
38	dilute → 0	-7.06	-7.01 ± 0.34	Holt et al. (1954)
25	dilute → 0	-6.38	-6.5 ± 0.7	Frere (1962)
25	dilute → 0	-6.97 ± 0.04	-6.93 ± 0.11	Aia et al. (1964)
37	dilute → 0	-7.12 ± 0.04	-7.06 ± 0.10	Aia et al. (1964)
50	dilute → 0	-7.39	-7.13 ± 0.17	Aia et al. (1964)
70	dilute → 0	-7.76 ± 0.02	-7.53 ± 0.20	Aia et al. (1964)
90	dilute → 0	-8.09 ± 0.06	-7.74 ± 0.18	Aia et al. (1964)
$Sr_3(PO_4)_2$				
38	dilute → 0	-27.8	-28.82 ± 0.38	Holt et al. (1954)

[a] Data as reported in the cited publications or calculated by this review from the reported data, see text.
[b] Recalculated and/or extrapolated to I = 0 by this review, see text, and 2σ uncertainties assigned or estimated by this review.

Frere (1962) determined the strontium phosphate precipitates formed by mixing different amounts of very dilute $Sr(OH)_2$ and H_3PO_4 solutions at 25 °C. He prepared a solubility diagram from the analysis of the supernatant in equilibrium with the precipitate. From the experiments where X-ray diffraction patterns indicated the formation of $SrHPO_4$(cr), Frere (1962) estimated K_s°(25 °C) to be about $4.2 \cdot 10^{-7}$ (logK_s°(25 °C) = -6.38). Note that Frere (1962) does not report whether the X-ray diffraction patterns were those of α-$SrHPO_4$(cr) and β-$SrHPO_4$(cr), but probably report the solubility of the thermodynamically stable β-$SrHPO_4$(cr). However, he obtained from the data in his solubility diagram (Fig. 1 of Frere 1962) a slope of 1.16 ± 0.37 while the theoretical slope should be 1.00 for $SrHPO_4$(cr). Frere (1962) used the Debye-Hückel limiting law for extrapolating his data to zero ionic strength and did not consider Sr phosphate complexes. As all experimental data are reported in Tab. 1 of Frere (1962), this review reanalysed the data of Frere (1962) using SIT with Δε = 0 (I = 0.0001 to 0.023 M) with the phosphate protonation constants of TDB 2020 and the strontium phosphate complexes selected by this review (see preceding section). The results are logK_s°(25 °C) = -6.5 ± 0.7 and a slope of 1.01 ± 0.22 for the solubility diagram.

Aia et al. (1964) determined the solubility products of α-$SrHPO_4$(cr) and β-$SrHPO_4$(cr) in dilute H_3PO_4 solutions at 25, 37, 50, 70 and 90 °C by adding an excess of either α- or β-$SrHPO_4$(cr) to their dilute H_3PO_4 solutions and allowing equilibration times from 2 – 25 days, until a constant pH was obtained. The precipitate remaining after equilibration was examined by X-ray diffraction and identified as either α- or β-$SrHPO_4$(cr). Aia et al. (1964) report that in the experiments at 25, 37 and 50 °C, the starting solid remained unchanged crystallographically with one exception at 50 °C. However, several of the samples which started as α-$SrHPO_4$(cr) recrystallised at 70 and 90 °C to large well-developed crystals of β-$SrHPO_4$(cr) during the course of the experiment. In no instance did β-$SrHPO_4$(cr) change to α-$SrHPO_4$(cr). The obvious conclusion to be drawn from

these results is that β-$SrHPO_4$(cr) is more stable, i.e., less soluble in water at all temperatures studied. The recrystallisation of α-$SrHPO_4$(cr) to β-$SrHPO_4$(cr) was favoured by higher temperatures and lower pH.

Aia et al. (1964) used a variant of the extended Debye-Hückel equation to extrapolate their data to zero ionic strength and conclude from their results that "ions such as $SrH_2PO_4^-$ (sic!) are apparently not formed". They report logK_s°(25 °C) = -6.97 ± 0.04, logK_s°(37 °C) = -7.12 ± 0.04, logK_s°(50 °C) = -7.39, logK_s°(70 °C) = -7.76 ± 0.02 and logK_s°(90 °C) = -8.09 ± 0.06 for β-$SrHPO_4$(cr), and logK_s°(37 °C) = -7.00, logK_s°(50 °C) = -7.17 ± 0.04, logK_s°(70 °C) = -7.69 and logK_s°(90 °C) = -7.98 ± 0.03 for α-$SrHPO_4$(cr). As all experimental data are reported in Tab. I of Aia et al. (1964), this review reanalysed the data of Aia et al. (1964) using SIT with Δε = 0 (I = 0.002 to 0.23 M) with the phosphate protonation constants of TDB 2020 and the strontium phosphate complexes selected by this review (see preceding Section). The results are logK_s°(25 °C) = -6.93 ± 0.11, logK_s°(37 °C) = -7.07 ± 0.08, logK_s°(50 °C) = -7.32 ± 0.15, logK_s°(70 °C) = -7.61 ± 0.09 and logK_s°(90 °C) = -7.81 ± 0.10 for β-$SrHPO_4$(cr), and logK_s°(37 °C) = -6.96, logK_s°(50 °C) = -7.11 ± 0.07, logK_s°(70 °C) = -7.44 and logK_s°(90 °C) = -7.66 ± 0.10 for α-$SrHPO_4$(cr).

This reanalysis corroborates now on a statistical 2σ level the conclusion of Aia et al. (1964) that β-$SrHPO_4$(cr) is the thermodynamically stable phase in water at all temperatures studied. Hence, the metastable phase α-$SrHPO_4$(cr) has not been included in TDB 2020.

A weighted regression of the reanalysed and accepted data of Holt et al. (1954), Frere (1962) and Aia et al. (1964) (Tab. 4.3-2) yields logK_s°(298.15 K) = -6.89 ± 0.07, $\Delta_r H_m$°(298.15 K) = -(29.9 ± 3.9) kJ · mol^{-1} and a statistically insignificant $\Delta_r C_{p,m}$°(298.15 K) value. Aia et al. (1964) in a similar data analysis obtained $\Delta_r H_m$°(298.15 K) = -7.91 cal · mol^{-1} (-33.1 kJ · mol^{-1}). However, assuming that the heat capacities of $CaHPO_4$(cr) and β-$SrHPO_4$(cr) are very similar and using $\Delta_r C_{p,m}$°(298.15 K) = -345 J · K^{-1} · mol^{-1} as fixed value in the data analysis, the weighted regression of the data of Holt et al. (1954), Frere (1962) and Aia et al. (1964) results in logK_s°(298.15 K) = -6.94 ± 0.07, $\Delta_r H_m$°(298.15 K) = -(19.3 ± 3.9) kJ · mol^{-1} (Fig. 4.3-6). Now, the $\Delta_r H_m$°(298.15 K) values of $CaHPO_4$(cr) and β-$SrHPO_4$(cr) are in excellent agreement, corroborating the assumption of very similar temperature behaviour of the two phases.

Finally, the following data have been included in TDB 2020, where the uncertainty of $\Delta_r C_{p,m}$°(298.15 K) has been increased to ±50 J · K^{-1} · mol^{-1}:

β-$SrHPO_4$(cr) ⇌ Sr^{2+} + HPO_4^{2-}

$\log_{10} K_s$° (298.15 K) = -6.94 ± 0.07

$\Delta_r H_m$°(298.15 K) = -(19.3 ± 3.9) kJ · mol^{-1}

$\Delta_r C_{p,m}$°(298.15 K) = -(345 ± 50) J · K^{-1} · mol^{-1}

No temperature data are available for $Sr_3(PO_4)_2$(s) and hence, the reanalysed datum of Holt et al. (1954), valid for 38 °C, has been used as approximation for 25 °C and also included in TDB 2020:

$$Sr_3(PO_4)_2(s) \rightleftharpoons 3\ Sr^{2+} + 2\ PO_4^{3-}$$

$$\log_{10}K_s^\circ\ (298.15\ K) = -28.8 \pm 0.4$$

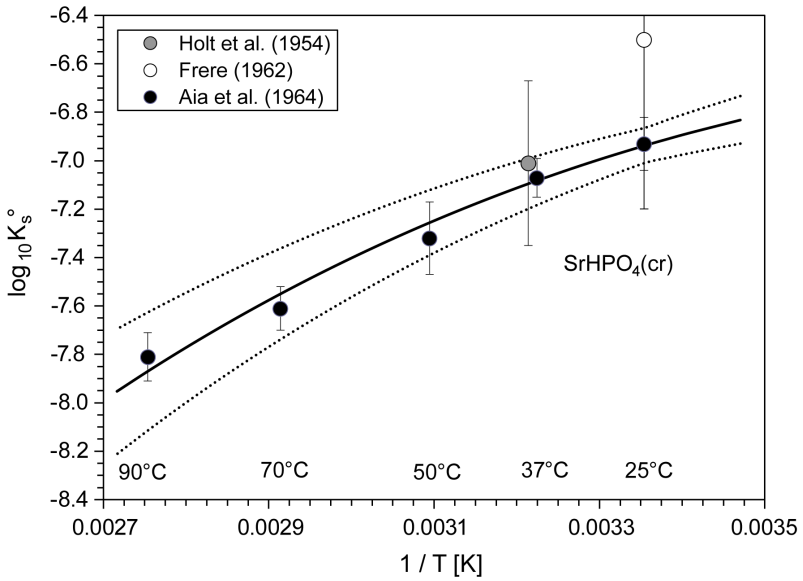

Fig. 4.3-6: The equilibrium constant $\log_{10}K_s^\circ$ for β-$SrHPO_4$(cr) ⇌ $Sr^{2+} + HPO_4^{2-}$ as a function of temperature in the range 25 – 90 °C

Solid line: weighted least squares fit of all data shown as symbols (Tab. 4.3-2). Dotted lines: lower and upper limits using $\log_{10}K_s^\circ(298.15\ K) = -6.94 \pm 0.07$, $\Delta_r H_m^\circ(298.15\ K) = -(19.3 \pm 3.9)$ kJ · mol^{-1} $\Delta_r C_{p,m}^\circ(298.15\ K) = -(345 \pm 50)$ J · K^{-1} · mol^{-1} and extrapolated to lower and higher temperatures.

4.3.9 Selected strontium data

Tab. 4.3-3: Selected strontium data

Name	**$\Delta_f G_m°$** [kJ · mol^{-1}]	**$\Delta_f H_m°$** [kJ · mol^{-1}]	**$S_m°$** [J · K^{-1} · mol^{-1}]	**$C_{p,m}°$** [J · K^{-1} · mol^{-1}]	**Species**
Sr(cr)	0.0	0.0	55.700 ± 0.210		Sr(cr)
Sr+2	-563.864 ± 0.781	-550.900 ± 0.500	-31.500 ± 2.000		Sr^{2+}

Name	**$\log_{10}\beta°$**	**$\Delta_r H_m°$** [kJ · mol^{-1}]	**$\Delta_r C_{p,m}°$** [J · K^{-1} · mol^{-1}]	**T-range** [°C]	**Reaction**
SrOH+	-13.15 ± 0.05	61.6 ± 10.5	0	5– 45	$Sr^{2+} + H_2O(l) \rightleftharpoons SrOH^+ + H^+$
SrF+	0.92 ± 0.15	10.9 ± 3.7	0	2 – 85	$Sr^{2+} + F^- \rightleftharpoons SrF^+$
SrCO3(aq)	2.79 ± 0.05	20.6 ± 1.9	241 ± 100	5 – 80	$Sr^{2+} + CO_3^{2-} \rightleftharpoons SrCO_3(aq)$
SrHCO3+	1.18 ± 0.04	25.0 ± 1.5	226 ± 90	5 – 80	$Sr^{2+} + HCO_3^- \rightleftharpoons SrHCO_3^+$
SrSO4(aq)	2.29 ± 0.04	8.7 ± 2.0	0	10 – 60	$Sr^{2+} + SO_4^{2-} \rightleftharpoons SrSO_4(aq)$
SrPO4-	5.62 ± 0.20	-	-		$Sr^{2+} + PO_4^{3-} \rightleftharpoons SrPO_4^-$
SrHPO4(aq)	2.35 ± 0.12	9 ± 15	0	0 – 25	$Sr^{2+} + HPO_4^{2-} \rightleftharpoons SrHPO_4(aq)$
SrH2PO4+	0.69 ± 0.20	-	-		$Sr^{2+} + H_2PO_4^- \rightleftharpoons SrH_2PO_4^+$
Sr(cr)	98.78 ± 0.14	-550.9 ± 0.5	-		$Sr(cr) \rightleftharpoons Sr^{2+} + 2\ e^-$
Strontianite	-9.27 ± 0.03	-1.6 ± 0.6	-471 ± 28	0 – 90	$SrCO_3(cr) \rightleftharpoons Sr^{2+} + CO_3^{2-}$
Celestite	-6.58 ± 0.10	-1.3 ± 0.6	-413.5 ± 2.9	0 – 300	$SrSO_4(cr) \rightleftharpoons Sr^{2+} + SO_4^{2-}$
β-SrHPO4	-6.94 ± 0.07	-19.3 ± 3.9	-345 ± 50	25 – 90	$SrHPO_4(cr) = Sr^{2+} + HPO_4^{2-}$
Sr3(PO4)2	-28.8 ± 0.4	-	-		$Sr_3(PO_4)_2(s) = 3\ Sr^{2+} + 2\ PO_4^{3-}$

Tab. 4.3-4: Selected SIT ion interaction coefficients $\varepsilon_{j,k}$ [kg · mol^{-1}] for strontium species

Data in normal face are derived in this review. Data estimated according to charge correlations and taken from Tab. 1-7 are shaded.

j k → ↓	**Cl^-** $\varepsilon_{j,k}$ [kg · mol^{-1}]	**Na^+** $\varepsilon_{j,k}$ [kg · mol^{-1}]	**$Na^+ + Cl^-$** $\varepsilon_{j,k}$ [kg · mol^{-1}]
Sr+2	0.12 ± 0.01	0	0
SrOH+	0.05 ± 0.10	0	0
SrF+	0.05 ± 0.10	0	0
SrHCO3+	0.05 ± 0.10	0	0
SrCO3(aq)	0	0	0.0 ± 0.1
SrSO4(aq)	0	0	0.0 ± 0.1
SrPO4-	0	-0.05 ± 0.10	0
SrHPO4(aq)	0	0	0.0 ± 0.1
SrH2PO4+	0.05 ± 0.10	0	0

4.3.10 References

Aia, M.A., Mathers, J.E. & Mooney, R.W. (1964): Thermodynamic solubility products of α- and β-$SrHPO_4$ from 25° to 90 °C. J. Chem. Eng. Data, 9, 333-338.

Baes, C.F. & Mesmer, R.E. (1976): The Hydrolysis of cations. Wiley, New York, 490 pp.

Bond, A.M. & Hefter, G. (1971): Use of the fluoride ion-selective electrode for the detection of weak fluoride complexes. J. Inorg. Nucl. Chem., 33, 429-434.

Brown, P.L. & Ekberg, C. (2016): Hydrolysis of Metal Ions. Wiley-VCH Verlag GmbH & Co. KGaA, Weinheim, Germany, 917 pp.

Brown, P.L., Ekberg, C. & Matyskin, A.V. (2019): On the solubility of radium and other alkaline earth sulfate and carbonate phases at elevated temperature. Geochim. Cosmochim. Acta, 255, 88-104.

Busenberg, E., Plummer, L.N. & Parker. V.B. (1984): The solubility of strontianite ($SrCO_3$) in CO_2-H_2O solutions between 2 and 91 °C, the association constants of $SrHCO_3^+$(aq) and $SrCO_3^0$(aq) between 5 and 80 °C, and an evaluation of the thermodynamic properties of Sr^{2+}(aq) and $SrCO_3$(cr) at 25 °C and 1 atm total pressure. Geochim. Cosmochim. Acta, 48, 2021-2035.

Ciavatta, L. (1980): The specific interaction theory in evaluating ionic equilibria. Annali di Chimica, 70, 551-567.

Frere, M.H. (1962): The solubility of some strontium phosphates. Soil Science Society of America Journal, 26, 49-51.

Gnepf, H., Gübeli, O & Schwarzenbach, G. (1962): Stabilitätskonstanten mononuclearer Phosphatokomplexe des Strontiums. Helvetica Chimica Acta, 45, 1171-1183.

Grenthe, I., Fuger, J., Konings, R.J.M., Lemire, R.J., Muller, A.B., Nguyen-Trung, C. & Wanner, H. (1992): Chemical Thermodynamics of Uranium. Chemical Thermodynamics, Vol. 1. North-Holland, Amsterdam, 715 pp.

Holt, L.E., Pierce, J.A. & Kajdi, C.N. (1954): The solubility of the phosphates of strontium, barium, and magnesium and their relation to the problem of calcification. J. Coll. Sci., 9, 409-426.

Majer, V. & Štulīk, K. (1982): A study of the stability of alkaline-earth metal complexes with fluoride and chloride ions at various temperatures by potentiometry with ion-selective electrodes. Talanta, 29, 145-148.

Nordstrom, D.K., Plummer, L.N., Langmuir, D., Busenberg, E., May, H.M., Jones, B.F. & Parkhurst, D.L. (1990): Revised Chemical Equilibrium Data for Major Water-Mineral Reactions and Their Limitations. In: Melchior, D.C., and Bassett, R.L. (eds.): Chemical Modeling of Aqueous Systems II. Washington, D.C., American Chemical Society, ACS Symposium Series 416, p. 398-413.

Reardon, E.J. (1983): Determination of $SrSO_4^0$ ion pair formation using conductometric and ion exchange techniques. Geochim. Cosmochim. Acta, 47, 1917-1922.

Reardon, E.J. & Armstrong, D.K. (1987): Celestite ($SrSO_4(s)$) solubility in water, seawater and NaCl solution. Geochim. Cosmochim. Acta, 51, 63-72.

Robinson, R.A. & Stokes, R.H. (1959): Electrolyte Solutions. Second Revised Edition. Academic Press, New York, 559 pp.

Saha, A., Saha, N., Ji, L., Zhao, J., Gregáň, F., Sajadi, S.A., Song, B. & Sigel, H. (1996): Stability of metal ion complexes formed with methyl phosphate and hydrogen phosphate. Journal of Biological Inorganic Chemistry, 1, 231-238.

Scharge, T. (2016): Thermodynamic model for the systems Sr – Na, K, Mg, Ca – Cl, SO_4 –H_2O at 298.15 K, THEREDA Technical Paper (Revision 1.0 as of 2016-09-26), accessible (after registration) from https://www.thereda.de/de/dokumente/technical-paper-test-calculations/releases

Smith, R.P. & Alberty, R.A. (1956): The apparent stability constants of ionic complexes of various adenosine phosphates with divalent cations. J. Phys. Chem., 78, 2376-2380.

Smith, R.M. & Martell, A.E. (1976): Critical Stability Constants. Volume 4: Inorganic Complexes. Plenum Press, New York, 257 pp.

Smith, R.M. & Martell, A.E. (1989): Critical Stability Constants. Volume 6: Second Supplement. Plenum Press, New York, 643 pp.

Tanner, S.P., Walker, J.B. & Choppin, G.R. (1968): Thermodynamic parameters of the alkaline earth monofluorides. J. Inorg. Nucl. Chem., 30, 2067-2070.

Townley, R.W., Whitney, W.B. & Felsing, W.A. (1937): The solubilities of barium and strontium carbonates in aqueous solutions of some alkali chlorides. Journal of the American Chemical Society, 59, 631-633.

4.4 Barium

4.4.1 Elemental barium

Barium metal is not relevant under environmental conditions. However, the absolute entropy of Ba(cr) is used for the calculation of certain thermodynamic reaction properties.

The selected value for Ba(cr) is taken from Grenthe et al. (1992):

$$S_m°(\text{Ba, cr, 298.15 K}) = (62.420 \pm 0.840)\ \text{J} \cdot \text{K}^{-1} \cdot \text{mol}^{-1}$$

4.4.2 Barium(II) aqua ion

Barium(II) exists as the Ba^{2+} cation in aqueous solutions. The selected thermodynamic values for Ba^{2+} are taken from Grenthe et al. (1992):

$$\Delta_f G_m°(Ba^{2+}, 298.15\ \text{K}) = -(557.656 \pm 2.582)\ \text{kJ} \cdot \text{mol}^{-1}$$

$$\Delta_f H_m°(Ba^{2+}, 298.15\ \text{K}) = -(534.800 \pm 2.500)\ \text{kJ} \cdot \text{mol}^{-1}$$

$$S_m°(Ba^{2+}, 298.15\ \text{K}) = (8.400 \pm 2.000)\ \text{J} \cdot \text{K}^{-1} \cdot \text{mol}^{-1}$$

Using the selected $\Delta_f G_m°(Ba^{2+}, 298.15\ \text{K})$, the redox equilibrium

$$\text{Ba(cr)} \rightleftharpoons Ba^{2+} + 2\ e^-$$

is calculated as

$$\log_{10} K°(298.15\ \text{K}) = 97.70 \pm 0.45$$

Since this review does not consider the formation of barium chloride complexes, $\varepsilon(Ba^{2+}, Cl^-)$ is taken as selected by NEA (Grenthe et al. 1992, Lemire et al. 2013):

$$\varepsilon(Ba^{2+}, Cl^-) = (0.07 \pm 0.01)\ \text{kg} \cdot \text{mol}^{-1}$$

4.4.3 Barium(II) (hydr)oxide compounds and complexes

4.4.3.1 Barium(II) hydroxide complexes

Nordstrom et al. (1990) selected a $\log_{10}{}^{*}\beta_1^\circ$ value from Baes & Mesmer (1976) for the complex

$$Ba^{2+} + H_2O(l) \rightleftharpoons BaOH^+ + H^+$$

$$\log_{10}{}^{*}\beta_1^\circ\ (298.15\ K) = -13.47$$

Brown & Ekberg (2016) state that the hydrolysis of barium(II) is even weaker than that of strontium(II) and also occurs in quite alkaline pH solutions, and similarly, only the species $BaOH^+$ has been detected. They continue that there are few more available data in the literature where the stability constant for $BaOH^+$ has been determined, compared to those for $SrOH^+$, but like strontium the majority of these studies corrected their own, or earlier, data to zero ionic strength. As with strontium, the data were acquired across the temperature interval of 5 – 45 °C, but, again, there is relatively good agreement between the data obtained. Brown & Ekberg (2016) show that the data have a linear relationship with the reciprocal of temperature and obtained

$$Ba^{2+} + H_2O(l) \rightleftharpoons BaOH^+ + H^+$$

$$\log_{10}{}^{*}\beta_1^\circ\ (298.15\ K) = -13.32 \pm 0.07$$

$$\Delta_r H_m^\circ(298.15\ K) = (60.9 \pm 10.5)\ kJ \cdot mol^{-1}$$

$$\Delta_r C_{p,m}^\circ(298.15\ K) = 0\ J \cdot K^{-1} \cdot mol^{-1}$$

These values have been included in TDB 2020, as well as the estimate

$$\varepsilon(BaOH^+, Cl^-) = (0.05 \pm 0.10)\ kg \cdot mol^{-1}$$

4.4.3.2 Barium(II) (hydr)oxide compounds

$Ba(OH)_2(s)$ is soluble in water with a solubility of 72 g/L at 20 °C (gestis.itrust.de), and it has not been found as a mineral in nature. Hence, no thermodynamic data for $Ba(OH)_2(s)$ are included in TDB 2020.

4.4.4 Barium(II) fluoride compounds and complexes

4.4.4.1 Barium(II) fluoride complexes

Three studies have been published concerning the BaF^+ complex formation, covering the temperature range 2 – 85 °C. Data obtained in 1 M $NaClO_4$ (Tanner et al. 1968, Bond & Hefter 1971) and 1 M $NaNO_3$ (Majer & Štulík 1982) show a more or less consistent temperature behaviour (Fig. 4.4-1). An unweighted regression of all data resulted in

$\log_{10}K_1$ (298.15 K, 1 M) = -0.16 ± 0.18

$\Delta_r H_m$ (298.15 K, 1 M) = (11.7 ± 3.4) kJ · mol^{-1}

$\Delta_r C_{p,m}$ (298.15 K, 1M) = 0 J · K^{-1} · mol^{-1}

Note that the data reported for 25 °C, in 1 M $NaClO_4$ (Tanner et al. 1968, Bond & Hefter 1972) and 1 M $NaNO_3$ (Majer & Štulík 1982), are in the range $\log_{10}\beta_1$ (298.15 K, 1 M) = -0.22 to -0.15, with an unweighted average of $\log_{10}K_1$ (298.15 K, 1 M) = -0.19 ± 0.05.

No attempt has been made to extrapolate $\Delta_r H_m$ to zero ionic strength, which is included in TDB 2020 as an approximation of $\Delta_r H_m°$ (298.15 K).

Considering $\varepsilon(Ba^{2+}, ClO_4^-)$ = (0.15 ± 0.02) kg · mol^{-1} and $\varepsilon(Na^+, F^-)$ = (0.02 ± 0.02) kg · mol^{-1} (Grenthe et al. 1992), and the estimate $\varepsilon(BaF^+, ClO_4^-)$ = (0.2 ± 0.1) kg · mol^{-1}, this review calculated $\Delta\varepsilon(NaClO_4)$ = (0.03 ± 0.10) kg · mol^{-1}. Using this $\Delta\varepsilon$ value, the value $\log_{10}K_1$ (298.15 K, 1 M) = -0.16 ± 0.18 has been extrapolated to zero ionic strength:

$Ba^{2+} + F^- \rightleftharpoons BaF^+$

$\log_{10}K_1°$ (298.15 K) = 0.67 ± 0.21

This datum is included in TDB 2020, as well as the estimate

$\varepsilon(BaF^+, Cl^-)$ = (0.05 ± 0.10) kg · mol^{-1}

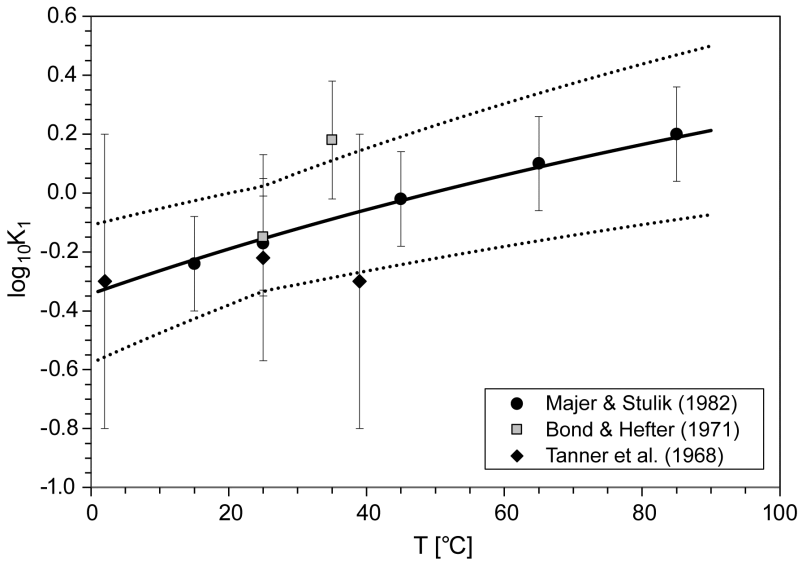

Fig. 4.4-1: The equilibrium constant $\log_{10}K_1$ for $Ba^{2+} + F^- \rightleftharpoons BaF^+$ as a function of temperature in the range 2 – 85 °C at 1 M ionic strength

Solid line: unweighted regression of all data. Dotted lines: lower and upper limits using $\log_{10}K$ (298.15 K) = -0.16 ± 0.18 and $\Delta_r H_m$(298.15 K) = (11.7 ± 3.4) kJ · mol^{-1} and extrapolated to lower and higher temperatures.

4.4.4.2 Barium(II) fluoride compounds

BaF_2(cr) has been found as the very rare mineral frankdicksonite. For the solubility product

$$BaF_2(cr) \rightleftharpoons Ba^{2+} + 2\ F^-$$

$\log_{10}K_s°$ (298.15 K) = -5.76 has been selected by Smith & Martell (1976). Later, this value has been revised to $\log_{10}K_s°$ (298.15 K) = -5.82 ± 0.06 (Smith & Martell 1989). The data sources and the selection procedure of Smith & Martell (1976, 1989) remain unclear.

However, these values indicate that the solubility of frankdicksonite, BaF_2(cr), is significantly higher than that of fluorite, CaF_2(cr), $\log_{10}K_s°$ (298.15 K) = -10.46 ± 0.09 (see Section 4.2.4.2). This is in accord with the observation that the concentration of dissolved fluoride, F^-, in environmental systems is usually governed by the precipitation of the ubiquitous mineral fluorite. Hence, frankdicksonite, BaF_2(cr), is only formed under very special chemical conditions and does not play any role in common environmental systems.

No solubility data for BaF_2(cr) are included in TDB 2020.

4.4.5 Barium(II) chloride compounds and complexes

4.4.5.1 Barium(II) chloride complexes

This report does not consider the formation of weak barium chloride complexes but includes possible ion interactions in the SIT interaction coefficient $\varepsilon(Ba^{2+}, Cl^-)$ (see below).

4.4.5.2 Barium(II) chloride compounds

$BaCl_2(s)$ is a highly soluble salt with a solubility of 375 g/L at 20 °C (gestis.itrust.de). Its isopiestic properties have been measured up to 1.8 $mol \cdot kg_{H2O}^{-1}$ (Robinson & Stokes 1959). Hence, no solubility data, but the specific ion interaction coefficient selected by NEA (Grenthe et al. 1992, Lemire et al. 2013) is adopted for TDB 2020:

$$\varepsilon(Ba^{2+}, Cl^-) = (0.07 \pm 0.01)\ kg \cdot mol^{-1}$$

4.4.6 Barium(II) carbonate compounds and complexes

4.4.6.1 Barium(II) carbonate complexes

Nordstrom et al. (1990) selected thermodynamic data reported by Busenberg & Plummer (1986) for the complexes

$$Ba^{2+} + CO_3^{2-} \rightleftharpoons BaCO_3(aq)$$

$$\log_{10}K_1^\circ\ (298.15\ K) = 2.71$$

$$\Delta_r H_m^\circ(298.15\ K) = 3.55\ kcal \cdot mol^{-1} = 14.85\ kJ \cdot mol^{-1}$$

$$\log_{10}K_1^\circ\ (T) = 0.113 + 0.008721 \cdot T$$

$$Ba^{2+} + HCO_3^- \rightleftharpoons BaHCO_3^+$$

$$\log_{10}K^\circ\ (298.15\ K) = 0.982$$

$$\Delta_r H_m^\circ(298.15\ K) = 5.56\ kcal \cdot mol^{-1} = 23.26\ kJ \cdot mol^{-1}$$

$$\log_{10}K^\circ\ (T) = -3.0938 + 0.013669 \cdot T$$

Note that in both cases the reported temperature functions imply temperature dependent $\Delta_r C_{p,m}^\circ$ values. Hence, the seemingly simple linear temperature function actually might be an over-fitting of the experimental data. This review re-fitted the experimental data reported by Busenberg & Plummer (1986), with the assumption $\Delta_r C_{p,m}^\circ$ = constant, as in both cases a plot of stability constants versus the reciprocal of the absolute temperature indicated a significant curvature. The results are (Figs. 4.4-2 and 4.4-3):

$Ba^{2+} + CO_3^{2-} \rightleftharpoons BaCO_3(aq)$

$\log_{10}K_1°$ (298.15 K) = 2.68 ± 0.05

$\Delta_r H_m°$(298.15 K) = (12.6 ± 1.0) kJ · mol^{-1}

$\Delta_r C_{p,m}°$(298.15 K) = (286 ± 53) J · K^{-1} · mol^{-1}

$Ba^{2+} + HCO_3^- \rightleftharpoons BaHCO_3^+$

$\log_{10}K°$ (298.15 K) = 0.99 ± 0.05

$\Delta_r H_m°$(298.15 K) = (22.0 ± 2.8) kJ · mol^{-1}

$\Delta_r C_{p,m}°$(298.15 K) = (266 ± 13) J · K^{-1} · mol^{-1}

These values are included in TDB 2020, as well as the estimates

$\varepsilon(BaHCO_3^+, Cl^-)$ = (0.05 ± 0.10) kg · mol^{-1}

$\varepsilon(BaCO_3(aq), NaCl)$ = (0.0 ± 0.1) kg · mol^{-1}

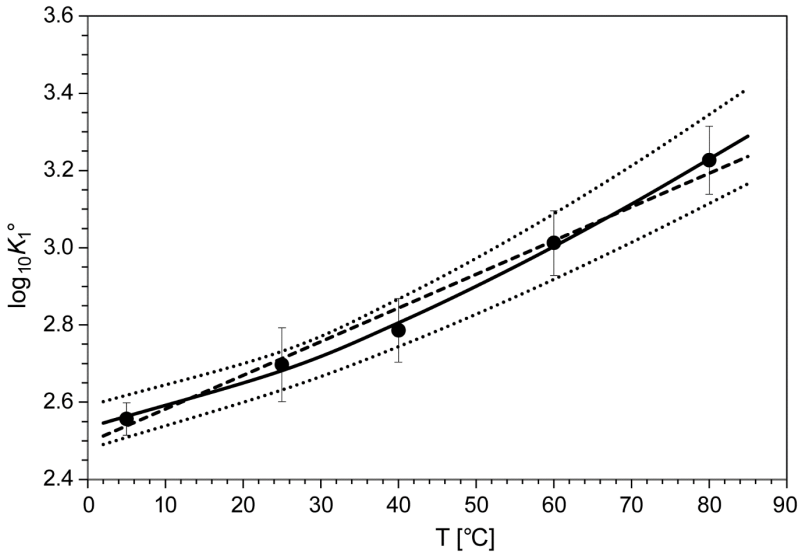

Fig. 4.4-2: The equilibrium constant $\log_{10}K_1°$ for $Ba^{2+} + CO_3^{2-} \rightleftharpoons BaCO_3(aq)$ as a function of temperature in the range 5 – 80 °C

Solid line: unweighted regression. Dotted lines: lower and upper limits using $\log_{10}K_1°$ (298.15 K) = 2.68 ± 0.05, $\Delta_r H_m°$(298.15 K) = (12.6 ± 1.0) kJ · mol^{-1} and $\Delta_r C_{p,m}°$(298.15 K) = (286 ± 53) J · K^{-1} · mol^{-1} and extrapolated to lower and higher temperatures. Dashed line: temperature function selected by Busenberg & Plummer (1986), shown for comparison.

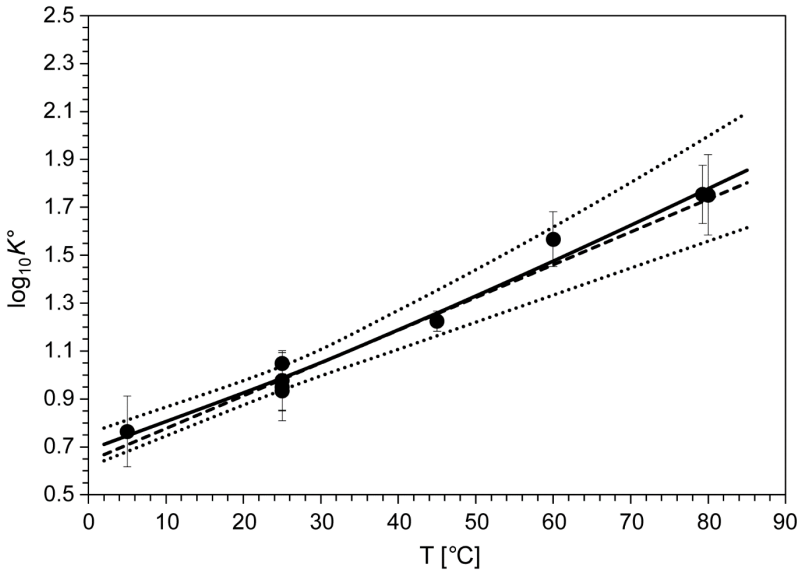

Fig. 4.4-3: The equilibrium constant $\log_{10}K°$ for $Ba^{2+} + HCO_3^- \rightleftharpoons BaHCO_3^+$ as a function of temperature in the range 5 – 80 °C

Solid line: unweighted regression. Dotted lines: lower and upper limits using $\log_{10}K°$ (298.15 K) = 0.99 ± 0.05, $\Delta_r H_m°$(298.15 K) = (22.0 ± 2.8) kJ · mol^{-1} and $\Delta_r C_{p,m}°$(298.15 K) = (266 ± 13) J · K^{-1} · mol^{-1} and extrapolated to lower and higher temperatures. Dashed line: temperature function selected by Busenberg & Plummer (1986), shown for comparison.

4.4.6.2 Barium(II) carbonate compounds

Nordstrom et al. (1990) selected thermodynamic data reported by Busenberg & Plummer (1986) for witherite, $BaCO_3$(cr), valid in the temperature range 0 – 90 °C:

$BaCO_3$(witherite) ⇌ $Ba^{2+} + CO_3^{2-}$

$\log_{10}K_{s0}°$ (298.15 K) = -8.562

$\Delta_r H_m°$(298.15 K) = 0.703 kcal · mol^{-1} = 2.94 kJ · mol^{-1}

$\log_{10}K_{s0}°$ (T) = 607.642 + 0.121098 · T – 20011.25 / T – 236.4948 · $\log_{10}$(T)

Note that the reported temperature function implies a temperature dependent $\Delta C_{p,m}°$ value. This might be an effect of over-fitting the experimental data. Hence, this review re-fitted the experimental data reported by Busenberg & Plummer (1986) with the assumption $\Delta C_{p,m}°$(298.15 K) = constant and obtained (Fig. 4.4-4):

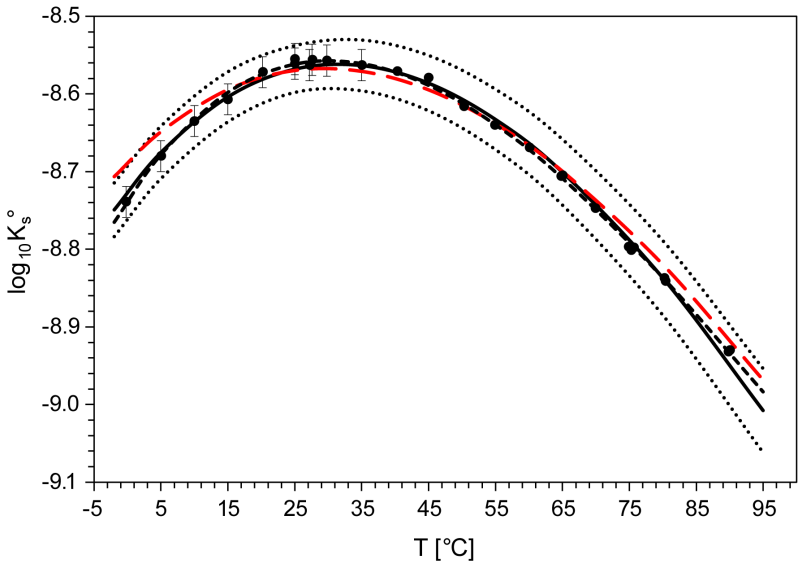

Fig. 4.4-4: The equilibrium constant $\log_{10}K_s°$ for $BaCO_3(s) \rightleftharpoons Ba^{2+} + CO_3^{2-}$, witherite, as a function of temperature in the range 0 – 90 °C

Solid line: unweighted regression of all data. Dotted lines: lower and upper limits using $\log_{10}K_{s0}°$ (298.15 K) = -8.57 ± 0.03, $\Delta_rH_m°$(298.15 K) = (3.3 ± 0.4) kJ · mol^{-1} and $\Delta_rC_{p,m}°$(298.15 K) = -(508 ± 10) J · K^{-1} · mol^{-1}, and extrapolated to higher temperatures. Dashed line: temperature function selected by Busenberg & Plummer (1986), shown for comparison. Large dashed (red) line: temperature function selected by Brown et al. (2019), shown for comparison.

$\log_{10}K_{s0}°$ (298.15 K) = -8.57 ± 0.03

$\Delta_rH_m°$(298.15 K) = (3.3 ± 0.4) kJ · mol^{-1}

$\Delta_rC_{p,m}°$(298.15 K) = -(508 ± 10) J · K^{-1} · mol^{-1}

These values are included in TDB 2020.

Brown et al. (2019) in their recent review of the solubility of alkaline earth sulphate and carbonate phases at elevated temperature recommend for the solubility of witherite, $BaCO_3(s)$

$\log_{10}K_{s0}°$ (298.15 K) = -8.57 ± 0.10

$\Delta_rH_m°$(298.15 K) = (1.9 ± 0.6) kJ · mol^{-1}

$\Delta_rC_{p,m}°$(298.15 K) = -(426.0 ± 3.8) J · K^{-1} · mol^{-1}

Brown et al. (2019) also used the data set of Busenberg & Plummer (1986), and a few more experimental data at 9, 16, 18 and 25 °C, all very consistent with the data of Busenberg & Plummer (1986), and obtained an identical $\log_{10}K_{s0}°$ (298.15 K) value but a slightly different $\Delta_rH_m°$(298.15 K) value and a very different $\Delta_rC_{p,m}°$(298.15 K) value. Why their fit below 15 °C deviates significantly from the experimental data (Fig. 4.4-4) remains unclear.

4.4.7 Barium(II) sulphate compounds and complexes

4.4.7.1 Barium(II) sulphate complexes

Nordstrom et al. (1990) selected $\log_{10}K_1°$ reported by Smith & Martell (1976) for the complex

$$Ba^{2+} + SO_4^{2-} \rightleftharpoons BaSO_4(aq)$$

$$\log_{10}K_1° \text{ (298.15 K)} = 2.7$$

As usual, Smith & Martell (1976) do not give any hint concerning their data selection; just eight references are listed referring to the system $Ba^{2+} – SO_4^{2-}$.

Inspecting all of these references, this review found that Rosseinsky (1958) stated "since calcium and barium sulphate show some similarity, *K*, the dissociation constant of barium sulphate, was assumed to be within the former group, and was taken as 0.0045 ± 0.0010, from the values at 25 °C of 0.0043 for copper sulphate, and 0.0049 for calcium sulphate".

This results in $\log_{10}K_1°$ (298.15 K) = 2.35 ± 0.01 for $Ba^{2+} + SO_4^{2-} \rightleftharpoons BaSO_4(aq)$.

Note that Rosseinsky (1958) took the value $\log_{10}K_1°$ (298.15 K) = 2.31 for $CaSO_4(aq)$ from Bell & George (1953), the same source as selected by this review (see Section 4.2.7.1).

In addition, Lieser (1965) determined from his radiochemical measurements of the solubility of $BaSO_4(s)$ and $SrSO_4(s)$ the dissociation constant of $BaSO_4(aq)$ as $K_1°$ (298.15 K) ≈ $5 \cdot 10^{-3}$.

This results in $\log_{10}K_1°$ (298.15 K) ≈ 2.3 for $Ba^{2+} + SO_4^{2-} \rightleftharpoons BaSO_4(aq)$.

Later, Smith & Martell (1989) revised their value to

$$\log_{10}K_1° \text{ (298.15 K)} = 2.2 \pm 0.1$$

with a single reference to Hanna et al. (1971). However, the only barium data discussed by Hanna et al. (1971), with $\log_{10}K_1° = 2.1$, refer to barium dithionate, $BaS_2O_6(aq)$, and not to $BaSO_4(aq)$.

It seems that Smith, for his update in 1989, revisited his old papers and found that they report 2.3 and not 2.7, and mistook the value 2.1 from Hanna et al. (1971) as a new value for $BaSO_4(aq)$, and finally reported the average of the old, corrected, value and the new, erroneous, value as 2.2 ± 0.1. However, these are just guesses by this review.

Felmy et al. (1990) measured the solubility of barite, $BaSO_4(cr)$, and celestite, $SrSO_4(cr)$, in Na_2SO_4 medium and interpreted their experimental data either in terms of the Pitzer ion interaction model or in terms of an ion association model. Their solubility products, evaluated with the Pitzer model, $\log_{10}K_{s0}°$ (298.15 K) = -6.62 ± 0.02 for celestite, and $\log_{10}K_{s0}°$ (298.15 K) = -10.05 ± 0.05 for barite, are in good agreement with the values recommended by Brown et al. (2019) and selected in this review, $\log_{10}K_s°$ (298.15 K) = -6.58 ± 0.10 for celestite, and $\log_{10}K_s°$ (298.15 K) = -9.96 ± 0.07 for barite.

For deriving stability constants for $SrSO_4(aq)$ and $BaSO_4(aq)$ Felmy et al. (1990) state that "in the ion association model, all interaction parameters involving the ion association species are set to zero and the nonideal specific-ion-interaction effects in the aqueous solution free energy are accounted for by including standard chemical potentials for ion association species". This approach is at variance from an extended Debye-Hückel approach or the SIT approach because of the unique Pitzer variant of the Debye-Hückel term and the "standard chemical potentials for ion association species" are still Pitzer parameters.

Felmy et al. (1990) report $\log_{10}K_1°$ (298.15 K) = 1.86 ± 0.03 for $SrSO_4(aq)$ and $\log_{10}K_1°$ (298.15 K) = 2.72 ± 0.09 for $BaSO_4(aq)$. The value for $SrSO_4(aq)$ is inconsistent with the value $\log_{10}K_1°$ (298.15 K) = 2.29 ± 0.04 selected in this review (see Section 6.7.1) and hence, the value for $BaSO_4(aq)$ reported by Felmy et al. (1990), about one order of magnitude stronger than their $SrSO_4(aq)$ value, is not considered in this review.

Monnin (1999) describes a model of barite and celestite solubilities in the Na-K-Ca-Mg-Ba-Sr-Cl-SO_4-H_2O system to 200 °C and to 1 kbar. With this model, Monnin (1999) re-interpreted experimental solubility data of barite reported by Jiang (1996) for the temperature range 0 – 80 °C and obtained stability constants for $BaSO_4(aq)$. Within this review the data given in Fig. 4 of Monnin (1999) have been digitised and re-fitted, yielding results in perfect agreement with Monnin (1999) but with increased uncertainties (Fig. 4.4-5):

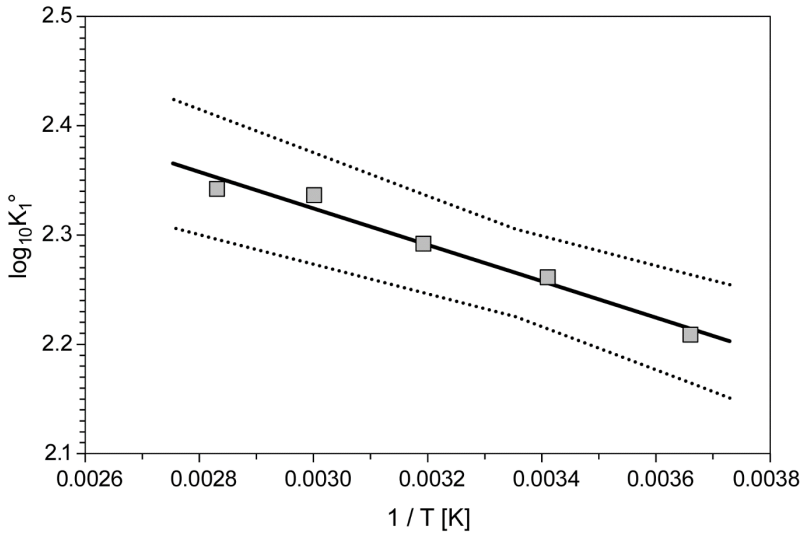

Fig. 4.4-5: The equilibrium constant $\log_{10}K_1°$ for $Ba^{2+} + SO_4^{2-} \rightleftharpoons BaSO_4(aq)$ as a function of reciprocal absolute temperature in the range 0 – 80 °C

Solid line: unweighted linear regression of data given by Monnin (1999). Dotted lines: lower and upper limits using $\log_{10}K_1°$ (298.15 K) = 2.27 ± 0.04 and $\Delta_r H_m°$(298.15 K) = (3.2 ± 0.6) kJ · mol^{-1} and extrapolated to lower and higher temperatures.

$Ba^{2+} + SO_4^{2-} \rightleftharpoons BaSO_4(aq)$

$\log_{10}K_1°$ (298.15 K) = 2.27 ± 0.04

$\Delta_r H_m°$(298.15 K) = (3.2 ± 0.6) kJ · mol^{-1}

Brown et al. (2019) state, concerning their evaluation of the solubility product of $BaSO_4$(cr) (see Section 4.4.7.2), "the experimental data of Blount (1977) are utilised in the present assessment and the equation utilised by Monnin (1999) gives solubility data, utilising an equation identical to that used herein, that are in close agreement with those derived in the present study".

Hence, the above values have been included in TDB 2020, as well as the estimate

$$\varepsilon(BaSO_4(aq), NaCl) = (0.0 \pm 0.1)\ kg \cdot mol^{-1}.$$

Recently, Djamali et al. (2016) reported a model for the solubility of barite to high temperatures and high pressures. With this model they re-interpreted the data of Jiang (1996) for deriving $BaSO_4$(aq) equilibrium constants and fitted them to a temperature function:

$$\log_{10}K_1^\circ\ (T) = a_1 + a_2 \cdot T + a_3 \cdot T^2 + a_4 / (a_5 - T)^2$$

This five-term temperature function is not considered by this review.

4.4.7.2 Barium(II) sulphate compounds

Nordstrom et al. (1990) selected thermodynamic data reported by Langmuir & Melchior (1985), who in turn based their selection of data for barite, $BaSO_4$(s), on Blount (1977):

$$BaSO_4(barite) \rightleftharpoons Ba^{2+} + SO_4^{2-}$$

$$\log_{10}K_{s0}^\circ\ (298.15\ K) = -9.97$$

$$\Delta_r H_m^\circ(298.15\ K) = 6.35\ kcal \cdot mol^{-1} = 26.6\ kJ \cdot mol^{-1}$$

$$\log_{10}K_{s0}(barite) = 136.035 - 7680.41/\ T - 48.595 \cdot \log_{10}T$$

The data are valid in the temperature range 20 to 280 °C and the temperature function implies

$$\Delta_r C_{p,m}^\circ(298.15\ K) = -404\ J \cdot K^{-1} \cdot mol^{-1}$$

Brown et al. (2019) in their recent review of the solubility of alkaline earth sulphate and carbonate phases at elevated temperature recommend for the solubility of barite, $BaSO_4$(s)

$$\log_{10}K_{s0}^\circ\ (298.15\ K) = -9.96 \pm 0.07$$

$$\Delta_r H_m^\circ(298.15\ K) = (26.1 \pm 0.4)\ kJ \cdot mol^{-1}$$

$$\Delta_r C_{p,m}^\circ(298.15\ K) = -(422.5 \pm 2.9)\ J \cdot K^{-1} \cdot mol^{-1}$$

determined from various data sets, also considering the results of Blount (1977), as well as more recent experimental data, and valid for the temperature range 0 – 300 °C.

These values have been included in TDB 2020.

4.4.8 Barium(II) phosphate compounds and complexes

4.4.8.1 Barium(II) phosphate complexes

Saha et al. (1996) determined the stability constants of the 1:1 complexes formed between a series of divalent metal cations and hydrogen phosphate by potentiometric pH titration in aqueous solution at 25 °C in 0.1 M $NaNO_3$. For Ba^{2+} they report $\log_{10}K = 1.38 \pm 0.02$. Using SIT with $\varepsilon(Na^+, HPO_4^{2-}) = -(0.15 \pm 0.06)$ and the estimates $\varepsilon(Ba^{2+}, NO_3^-) \approx \varepsilon(Sr^{2+}, NO_3^-) = -(0.05 \pm 0.02)$ and $\varepsilon(SrHPO_4(aq), NaNO_3) = (0.0 \pm 0.1)$ this review obtained $\log_{10}K° = 2.25 \pm 0.20$ for the equilibrium $Ba^{2+} + HPO_4^{2-} \rightleftharpoons BaHPO_4(aq)$, with an uncertainty assigned by this review.

No other publications concerning Ba phosphate complexes could be found by this review.

This review used the selected $\log_{10}K°$ values of Mg^{2+}, Ca^{2+} and Sr^{2+} and plotted them versus their effective ionic radii in 8-fold coordination (Shannon 1976). The $\log_{10}K°$ values indicate a negative linear correlation versus their effective ionic radii (Fig. 4.4.6).

The result of an unweighted linear regression of $\log_{10}K°$ values for $M^{2+} + HPO_4^{2-} \rightleftharpoons MHPO_4(aq)$ is $\log_{10}K°$ (M = Ba) = 2.23 ± 0.20. This value is in perfect agreement with the experimental value $\log_{10}K° = 2.25 \pm 0.20$ of Saha et al. (1996), which corroborates the validity of the estimation procedure.

The result of an unweighted linear regression of $\log_{10}K°$ values for $M^{2+} + H_2PO_4^- \rightleftharpoons MH_2PO_4^+$ is $\log_{10}K°$ (M = Ba) = 0.6 ± 0.3.

In the case of $M^{2+} + PO_4^{3-} \rightleftharpoons MPO_4^-$, $\log_{10}K°$ (M = Mg) is a clear outlier. This value is based on only one experimental study (see Tab. 4.1-1), but it is unlikely that its stability constant is in error by several orders of magnitude. One may speculate that $MgPO_4^-$ has another cation to ligand coordination than $CaPO_4^-$ and $SrPO_4^-$, but no information is available. This review decided to use only $\log_{10}K°$ (M = Ca) and $\log_{10}K°$ (M = Sr) for an extrapolation and obtained $\log_{10}K°$ (M = Ba) = 4.7 ± 0.3. The uncertainty is an estimate considering the increasing uncertainties from Ca (±0.11) to Sr (±0.20).

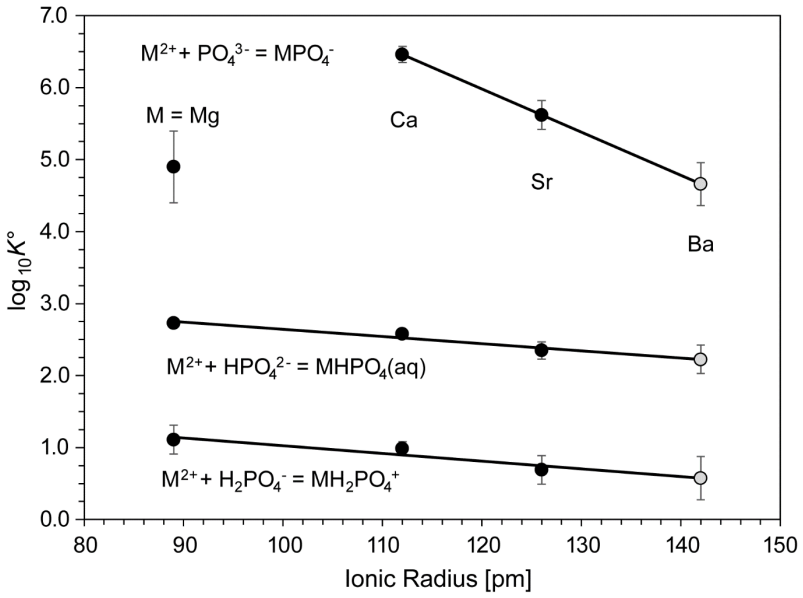

Fig. 4.4.6: The equilibrium constants $\log_{10}K°$ of the indicated equilibria as a function of effective ionic radius

Solid lines: unweighted regressions of data selected by this review (black circles). Grey circles: $\log_{10}K°$ (298.15 K) for Ba calculated from the linear regressions.

In summary, the following values are included in TDB 2020:

$Ba^{2+} + PO_4^{3-} \rightleftharpoons BaPO_4^-$

$\log_{10}K°$ (298.15 K) = 4.7 ± 0.3

$Ba^{2+} + HPO_4^{2-} \rightleftharpoons BaHPO_4(aq)$

$\log_{10}K°$ (298.15 K) = 2.25 ± 0.20

$Ba^{2+} + H_2PO_4^- \rightleftharpoons BaH_2PO_4^+$

$\log_{10}K°$ (298.15 K) = 0.6 ± 0.3

together with the estimates

$\varepsilon(BaH_2PO_4^+, Cl^-) = (0.05 \pm 0.10)$ kg · mol^{-1}

$\varepsilon(BaHPO_4(aq), NaCl) = (0.0 \pm 0.1)$ kg · mol^{-1}

$\varepsilon(BaPO_4^-, Na^+) = -(0.05 \pm 0.10)$ kg · mol^{-1}

4.4.8.2 Barium(II) phosphate compounds

Alforsite, $Ba_5(PO_4)_3Cl$, has been found in nature as very rare mineral. It is the barium analogue to chlorapatite, $Ca_5(PO_4)_3Cl$. Another extremely rare barium phosphate mineral is nabaphite, $NaBaPO_4 \cdot 9H_2O$ (www.mindat.org). No solubility data are known for these compounds.

Only one study by Holt et al. (1954) reports solubility product constants for $BaHPO_4$(cr) and $Ba_3(PO_4)_2$(s).

Holt et al. (1954) explored the titration curve of phosphoric acid with $Ba(OH)_2$ solutions at 38 °C to determine the regions in which stable precipitates formed. Appropriate quantities of acid and base were mixed together and shaken continuously at 38 °C for 12 days, then the precipitate was separated, the solution analysed for pH, phosphorus and barium. Holt et al. (1954) found $BaHPO_4$(cr) to be "grossly crystalline", while the phase $Ba_3(PO_4)_2$(s) seemed to be amorphous, although no X-ray analysis was made.

Holt et al. (1954) report $\log K_s°$(38 °C) = -7.19 for $BaHPO_4$(cr) and $\log K_s$(38 °C) = -29.34 at I = 0.0008 M for $Ba_3(PO_4)_2$(s). For their data analysis Holt et al. (1954) used the Debye-Hückel limiting law with the phosphate protonation constants $\log K_1° = 2.11$, $\log K_2° = 7.15$, $\log K_3° = 12.66$. Especially $\log K_3°$ is at variance with the value 12.35 included in TDB 2020, and the use of the Debye-Hückel limiting law seems inappropriate at ionic strengths ranging from 0.002 to 0.013 M. Hence, this review reanalysed the data of Holt et al. (1954) using SIT (assuming $\Delta\varepsilon$ = 0) with the phosphate protonation constants of TDB 2020 and the barium phosphate complexes selected by this review (see preceding section). Unweighted means of the results obtained from the phosphoric acid titration experiments reported in Tab. II of Holt et al. (1954), are $\log K_s°$ (38 °C) = -7.19 ± 0.25 (2σ) for $BaHPO_4$(cr) = $Ba^{2+} + HPO_4^{2-}$, using the first nine values of Tab. II, and $\log K_s°$ (38 °C) = -28.99 ± 0.50 (2σ) for $Ba_3(PO_4)_2$(s) = $3\ Ba^{2+} + 2\ PO_4^{3-}$, using the last four values of Tab. II.

No temperature data are available for these compounds and hence, this review takes the above values as approximations for 25 °C and included them in TDB 2020:

$BaHPO_4$(cr) ⇌ $Ba^{2+} + HPO_4^{2-}$

$\log_{10} K_s°$ (298.15 K) = -7.2 ± 0.3

$Ba_3(PO_4)_2$(s) ⇌ $3\ Ba^{2+} + 2\ PO_4^{3-}$

$\log_{10} K_s°$ (298.15 K) = -29.0 ± 0.5

4.4.9 Selected barium data

Tab. 4.4-1: Selected barium data

Name	**$\Delta_f G_m°$** [kJ · mol^{-1}]	**$\Delta_f H_m°$** [kJ · mol^{-1}]	**$S_m°$** [J · K^{-1} · mol^{-1}]	**$C_{p,m}°$** [J · K^{-1} · mol^{-1}]	**Species**
Ba(cr)	0.0	0.0	62.420 ± 0.840		Ba(cr)
Ba+2	-557.656 ± 2.582	-534.800 ± 2.500	8.400 ± 2.000		Ba^{2+}

Name	**$\log_{10}\beta°$**	**$\Delta_r H_m°$** [kJ · mol^{-1}]	**$\Delta_r C_{p,m}°$** [J · K^{-1} · mol^{-1}]	**T-range** [°C]	**Reaction**
BaOH+	-13.32 ± 0.07	60.9 ± 10.5	0	5– 45	$Ba^{2+} + H_2O(l) \rightleftharpoons BaOH^+ + H^+$
BaF+	0.67 ± 0.21	11.7 ± 3.4	0	2 – 85	$Ba^{2+} + F^- \rightleftharpoons BaF^+$
BaCO3(aq)	2.68 ± 0.05	12.6 ± 1.0	286 ± 53	5 – 80	$Ba^{2+} + CO_3^{2-} \rightleftharpoons BaCO_3(aq)$
BaHCO3+	0.99 ± 0.05	22.0 ± 2.8	266 ± 13	5 – 80	$Ba^{2+} + HCO_3^- \rightleftharpoons BaHCO_3^+$
BaSO4(aq)	2.27 ± 0.04	3.2 ± 0.6	0	0 – 80	$Ba^{2+} + SO_4^{2-} \rightleftharpoons BaSO_4(aq)$
BaPO4-	4.7 ± 0.3	-	-		$Ba^{2+} + PO_4^{3-} \rightleftharpoons BaPO_4^-$
BaHPO4(aq)	2.25 ± 0.20	-	-		$Ba^{2+} + HPO_4^{2-} \rightleftharpoons BaHPO_4(aq)$
BaH2PO4+	0.6 ± 0.3	-	-		$Ba^{2+} + H_2PO_4^- \rightleftharpoons BaH_2PO_4^+$
Ba(cr)	97.70 ± 0.45	-534.8 ± 2.5	-		$Ba(cr) \rightleftharpoons Ba^{2+} + 2\ e^-$
Witherite	-8.57 ± 0.03	3.3 ± 0.4	-508 ± 10	0 – 95	$BaCO_3(cr) \rightleftharpoons Ba^{2+} + CO_3^{2-}$
Barite	-9.96 ± 0.07	26.1 ± 0.4	-422.5 ± 2.9	0 – 300	$BaSO_4(cr) \rightleftharpoons Ba^{2+} + SO_4^{2-}$
BaHPO4	-7.2 ± 0.3	-	-		$BaHPO_4(cr) \rightleftharpoons Ba^{2+} + HPO_4^{2-}$
Ba3(PO4)2	-29.0 ± 0.5	-	-		$Ba_3(PO_4)_2(s) \rightleftharpoons 3\ Ba^{2+} + 2\ PO_4^{3-}$

Tab. 4.4-2: Selected SIT ion interaction coefficients $\varepsilon_{j,k}$ [kg · mol^{-1}] for barium species

Data in bold face are taken from Lemire et al. (2013). Data estimated according to charge correlations and taken from Tab. 1-7 are shaded.

j k → ↓	**Cl^-** $\varepsilon_{j,k}$ [kg · mol^{-1}]	**Na^+** $\varepsilon_{j,k}$ [kg · mol^{-1}]	**$Na^+ + Cl^-$** $\varepsilon_{j,k}$ [kg · mol^{-1}]
Ba+2	**0.07 ± 0.01**	0	0
BaOH+	0.05 ± 0.10	0	0
BaF+	0.05 ± 0.10	0	0
BaHCO3+	0.05 ± 0.10	0	0
BaCO3(aq)	0	0	0.0 ± 0.1
BaSO4(aq)	0	0	0.0 ± 0.1
BaPO4-	0	-0.05 ± 0.10	0
BaHPO4(aq)	0	0	0.0 ± 0.1
BaH2PO4+	0.05 ± 0.10	0	0

4.4.10 References

Baes, C.F. & Mesmer, R.E. (1976): The Hydrolysis of cations. Wiley, New York, 490 pp.

Blount, C.W. (1977): Barite solubilities and thermodynamic quantities up to 300 °C and 1'400 bars. American Mineralogist, 62, 942-957.

Bond, A.M. & Hefter, G. (1972): A study of the weak fluoride complexes of the divalent first row transition metal ions with a fluoride ion-selective electrode. J. Inorg. Nucl. Chem., 34, 603607.

Brown, P.L. & Ekberg, C. (2016): Hydrolysis of Metal Ions. Wiley-VCH Verlag GmbH & Co. KGaA, Weinheim, Germany, 917 pp.

Brown, P.L., Ekberg, C. & Matyskin, A.V. (2019): On the solubility of radium and other alkaline earth sulfate and carbonate phases at elevated temperature. Geochim. Cosmochim. Acta, 255, 88-104.

Busenberg, E. & Plummer, L.N. (1986): The solubility of $BaCO_3$(cr) (witherite) in CO_2-H_2O solutions between 0 and 90 °C, evaluation of the association constants of $BaHCO_3^+$(aq) and $BaCO_3^0$(aq) between 5 and 80 °C, and a preliminary evaluation of the thermodynamic properties of Ba^{2+}(aq). Geochim. Cosmochim. Acta, 50, 2225-2233.

Djamali, E., Chapman, W.G. & Cox, K.R. (2016): A systematic investigation of thermodynamic properties of aqueous barium sulfate up to high temperatures and high pressures. Journal of Chemical & Engineering Data, 61, 3585-3594.

Felmy, A.R., Rai, D. & Amonette, J.E. (1990): The solubility of barite and celestite in sodium sulfate: Evaluation of thermodynamic data. Journal of Solution Chemistry, 19, 175-185.

Grenthe, I., Fuger, J., Konings, R.J.M., Lemire, R.J., Muller, A.B., Nguyen-Trung, C. & Wanner, H. (1992): Chemical Thermodynamics of Uranium. Chemical Thermodynamics, Vol. 1. North-Holland, Amsterdam, 715 pp.

Hanna, E.M., Pethybridge, A.D. & Prue, J.E. (1971): Ion association and the analysis of precise conductimetric data. Electrochimica Acta, 16, 677-686.

Holt, L.E., Pierce, J.A. & Kajdi, C.N. (1954): The solubility of the phosphates of strontium, barium, and magnesium and their relation to the problem of calcification. J. Coll. Sci., 9, 409-426.

Jiang, C. (1996): Solubility and solubility constant of barium sulfate in aqueous sodium sulfate solution between 0 and 80 °C. Journal of Solution Chemistry, 25, 105-111.

Lieser, K.H. (1965): Radiochemische Messung der Löslichkeit von Erdalkalisulfaten in Wasser und in Natriumsulfatlösungen. Zeitschrift für anorganische und allgemeine Chemie, 335, 225-231.

Majer, V. & Štulīk, K. (1982): A study of the stability of alkaline-earth metal complexes with fluoride and chloride ions at various temperatures by potentiometry with ion-selective electrodes. Talanta, 29, 145-148.

Monnin, C. (1999): A thermodynamic model for the solubility of barite and celestite in electrolyte solutions and seawater to 200 °C and to 1 bar. Chemical Geology, 153, 187-209.

Nordstrom, D.K., Plummer, L.N., Langmuir, D., Busenberg, E., May, H.M., Jones, B.F. & Parkhurst, D.L. (1990): Revised Chemical Equilibrium Data for Major Water-Mineral Reactions and Their Limitations. In: Melchior, D.C., and Bassett, R.L. (eds.): Chemical Modeling of Aqueous Systems II. Washington, D.C., American Chemical Society, ACS Symposium Series 416, p. 398-413.

Robinson, R.A. & Stokes, R.H. (1959): Electrolyte Solutions. Second Revised Edition. Academic Press, New York, 559 pp.

Saha, A., Saha, N., Ji, L., Zhao, J., Gregáň, F., Sajadi, S.A., Song, B. & Sigel, H. (1996): Stability of metal ion complexes formed with methyl phosphate and hydrogen phosphate. Journal of Biological Inorganic Chemistry, 1, 231-238.

Shannon, R.D. (1976): Revised effective ionic radii and systematic studies of interatomic distances in halides and chalcogenides. Acta Crystallographica A, 32, 751-767.

Smith, R.M. & Martell, A.E. (1976): Critical Stability Constants. Volume 4: Inorganic Complexes. Plenum Press, New York, 257 pp.

Smith, R.M. & Martell, A.E. (1989): Critical Stability Constants. Volume 6: Second Supplement. Plenum Press, New York, 643 pp.

Tanner, S.P., Walker, J.B. & Choppin, G.R. (1968): Thermodynamic parameters of the alkaline earth monofluorides. J. Inorg. Nucl. Chem., 30, 2067-2070.

4.5 Radium

4.5.1 Introduction

Radium isotopes are constantly produced in all actinide decay chains. The longest-lived isotope of radium is Ra-226, a member of the naturally occurring uranium-238 ($4n + 2$) family of radioelements, with a half-life of 1'600 ± 7 years. Ra-226 contributes in dose-relevant quantities to the inventory of radioactive waste coming from nuclear power plants, which was the reason for inclusion of radium into Nagra/PSI TDB 01/01 (Hummel et al. 2002).

The thermodynamic properties of radium included in the Nagra/PSI TDB 01/01 were all taken from Langmuir & Riese (1985). Due to a lack of experimental investigations, all data were based on estimates only, with the notable exception of the solubility product for $RaSO_4$(cr).

Meanwhile, new reviews of the hydrolysis of metal ions (Brown & Ekberg 2016) and of the solubility of alkaline earth sulphate and carbonate phases (Brown et al. 2019) have been published, which are considered in the present update of radium data. In addition, this review provides new estimates for aqueous radium species based on data for Mg, Ca, Sr and Ba selected by this review.

Data estimation can be done by calculating weighted or unweighted means and linear regressions of selected data. In all NEA TDB books, Appendix C (see, e.g., Grenthe et al. 1992), weighted mean and weighted linear regression (for SIT analysis) are discussed and recommended, based on the formulae given by Bevington (1969). The estimated standard errors (s) of unweighted means, i.e., $y_{mean} = \Sigma y_i / N$ where N is the number of data,

$$\sigma_{dispersion} \cong s = \sqrt{ [1 / (N - 1) \cdot \Sigma (y_i - y_{mean})^2] }$$

and unweighted linear regressions $y = a + b \cdot x$

$$\sigma_{dispersion} \cong s = \sqrt{ [1 / (N - 2) \cdot \Sigma (y_i - a - b \cdot x_i)^2] }$$

solely depend on the dispersion of the data. By contrast, uncertainties derived from weighted means and linear regressions depend on the uncertainties (σ_i) associated with the data but not on their dispersion

$$\sigma_{weights} = \sqrt{ [1 / \Sigma (1 / \sigma_i^2)] }$$

Bevington (1969) discusses a third option (p. 73): "It often happens that the relative values of the σ_i are known, but the absolute magnitudes are not. … In such a case the *relative* values of $\sigma_i' \cong \sigma_i$ should be included as weighting factors in the determination of the mean and its uncertainty, and the *absolute* magnitudes of the σ_i can be estimated from the dispersion of the data points around the mean". This leads to the average uncertainty of the data, used for calculating the weighted mean,

$$\sigma_{average} \cong s = \sqrt{ \{ N \cdot \Sigma [(1 / \sigma_i'^2) \cdot (y_i - y_{mean})^2] / [(N - 1) \cdot \Sigma (1 / \sigma_i'^2)] \} }$$

or likewise to the average uncertainty of the data, used for calculating a weighted linear regression

$$\sigma_{average} \cong s = \sqrt{\{ N \cdot \Sigma [(1 / \sigma_i'^2) \cdot (y_i - a - b\, x_i)^2] / [(N - 2) \cdot \Sigma (1 / \sigma_i'^2)] \}}$$

All these variants have been explored in this review for estimating values and their uncertainties for aqueous radium species.

The thermodynamic data included in TDB 2020 have been taken from

- the recent review of the hydrolysis of metal ions (Brown & Ekberg 2016)
- the recent review of the solubility of alkaline earth sulphate and carbonate phases (Brown et al. 2019)
- and own estimates for aqueous radium species

The selected thermodynamic data are presented in Tab. 4.5-1.

NEA (see, e.g., Grenthe et al. 1992) used the specific ion interaction theory (SIT) for making ionic strength corrections to the experimental data, an approach which is also adopted for TDB 2020 (as has been for all its predecessors). Ion interaction coefficients for aqueous radium species were not available. We approximated these with the estimation method described in Section 1.5.3, which draws on a statistical analysis of published SIT ion interaction coefficients and which allows the estimation of missing coefficients for the interaction of cations with Cl^-, and for the interaction of anions with Na^+, from the charge of the cations or anions of interest.

The selected SIT ion interaction coefficients are presented in Tab. 4.5-2.

4.5.2 Elemental radium

Radium metal is not relevant under environmental conditions. However, the absolute entropy of Ra(cr) is used for the calculation of certain thermodynamic reaction properties.

Brown & Ekberg (2016) report in their Tab. 7-27 for Ra(s) a value $S_m^\circ = (54 \pm 5)\ J \cdot K^{-1} \cdot mol^{-1}$ with the remark "accepted uncertainty estimated in this work" and the reference Bard et al. (1985). Bard et al. (1985) in turn cite Wagman et al. (1982) as the source of their value. However, the value $54\ J \cdot K^{-1} \cdot mol^{-1}$ is given by Wagman et al. (1982) for the entropy of the Ra^{2+} cation (see Section 3) while for Ra(cr) Wagman et al. (1982) selected $71\ J \cdot K^{-1} \cdot mol^{-1}$. This review selected the value of Wagman et al. (1982) and retained the uncertainty estimate of Brown & Ekberg (2016):

$$S_m^\circ(Ra, cr, 298.15\ K) = (71 \pm 5)\ J \cdot K^{-1} \cdot mol^{-1}$$

4.5.3 Radium(II) aqua ion

Radium(II) exists as the Ra^{2+} cation in aqueous solutions.

Brown & Ekberg (2016) report in their Tab. 7-27 for Ra^{2+} the values $\Delta_f G_m° = -(561.5 \pm 2.0)$ kJ · mol^{-1} and $\Delta_f H_m° = -(527.6 \pm 2.0)$ kJ · mol^{-1} with the remark "accepted uncertainty estimated in this work" and the reference Bard et al. (1985). Bard et al. (1985) in turn cite Wagman et al. (1982) as the source of their values. Brown & Ekberg (2016) do not report an $S_m°$ value for Ra^{2+} but as discussed in Section 2, the value $S_m° = (54 \pm 5)$ J · K^{-1} · mol^{-1} given by Brown & Ekberg (2016) actually is the value selected by Wagman et al. (1982) for Ra^{2+}, with an uncertainty estimated by Brown & Ekberg (2016). Hence, this review selected thermodynamic values for Ra^{2+} as given by Wagman et al. (1982) with uncertainty estimates for $S_m°$ and $\Delta_f H_m°$ from Brown & Ekberg (2016), while the uncertainty of $\Delta_f G_m°(Ra^{2+}, 298.15\ K)$ was calculated by this review from the uncertainties of $\Delta_f H_m°(Ra^{2+}, 298.15\ K)$, $S_m°(Ra^{2+}, 298.15\ K)$ and $S_m°$(Ra, cr, 298.15 K) by error propagation:

$$\Delta_f G_m°(Ra^{2+}, 298.15\ K) = -(561.5 \pm 2.9)\ kJ \cdot mol^{-1}$$

$$\Delta_f H_m°(Ra^{2+}, 298.15\ K) = -(527.6 \pm 2.0)\ kJ \cdot mol^{-1}$$

$$S_m°(Ra^{2+}, 298.15\ K) = (54 \pm 5)\ J \cdot K^{-1} \cdot mol^{-1}$$

Using the selected $\Delta_f G_m°(Ra^{2+}, 298.15\ K)$ and $\Delta_f H_m°(Ra^{2+}, 298.15\ K)$, the redox equilibrium

$$Ra(cr) \rightleftharpoons Ra^{2+} + 2\ e^-$$

is calculated as

$$\log_{10} K°(298.15\ K) = 98.40 \pm 0.51$$

$$\Delta_r H_m°(298.15\ K) = -(527.6 \pm 2.0)\ kJ \cdot mol^{-1}$$

Since this review does not consider the formation of radium chloride complexes, $\varepsilon(Ra^{2+}, Cl^-)$ has been estimated by this review (see Section 4.5.6.1) as:

$$\varepsilon(Ra^{2+}, Cl^-) = (0.06 \pm 0.02)\ kg \cdot mol^{-1}$$

4.5.4 Radium(II) (hydr)oxide compounds and complexes

4.5.4.1 Radium(II) hydroxide complexes

Langmuir & Riese (1985) plotted the formation constants ($\log_{10}\beta_1°$ values) for $CaOH^+$, $SrOH^+$ and $BaOH^+$ by Baes & Mesmer (1981) against the effective ionic radii of Ca^{2+}, Sr^{2+}, Ba^{2+} and Ra^{2+} in 8-fold coordination. From the observed trend they estimated the formation constant of

$$Ra^{2+} + OH^- \rightleftharpoons RaOH^+$$

$$\log_{10}\beta_1° \text{ (298.15 K)} = 0.5$$

The enthalpy of reaction was taken to be

$$\Delta_r H_m° \text{(298.15 K)} = 1.1 \text{ kcal} \cdot \text{mol}^{-1} = 4.6 \text{ kJ} \cdot \text{mol}^{-1}$$

Brown & Ekberg (2016) accepted the estimates of Langmuir & Riese (1985) and re-calculated them to

$$Ra^{2+} + H_2O(l) \rightleftharpoons RaOH^+ + H^+$$

$$\log_{10}{}^*\beta_1° \text{ (298.15 K)} = -13.49 \pm 0.20$$

$$\Delta_r H_m° \text{(298.15 K)} = (60.4 \pm 2.0) \text{ kJ} \cdot \text{mol}^{-1}$$

The uncertainties have been assigned by Brown & Ekberg (2016).

This review used the $\log_{10}{}^*\beta_1°$ and $\Delta_r H_m°$ values of Mg^{2+}, Ca^{2+}, Sr^{2+} and Ba^{2+} (Section 4.4.2) and plotted them versus their effective ionic radii in 8-fold coordination (Shannon 1976).

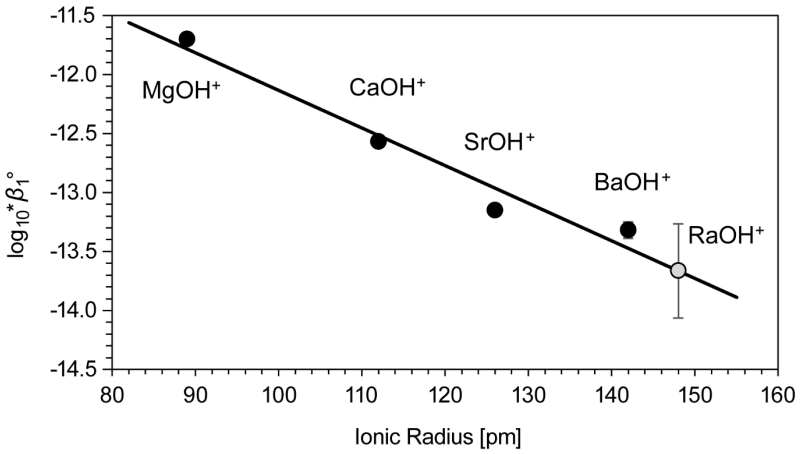

Fig. 4.5-1: The equilibrium constant $\log_{10}{}^{*}\beta_1°$ for $M^{2+} + H_2O(l) \rightleftharpoons MOH^+ + H^+$ as a function of effective ionic radius

Solid line: unweighted regression of all selected data (black circles). Grey circle: $\log_{10}{}^{*}\beta_1°$ (298.15 K) = -13.7 ± 0.4 calculated from the linear regression for $Ra^{2+} + H_2O(l) \rightleftharpoons RaOH^+ + H^+$.

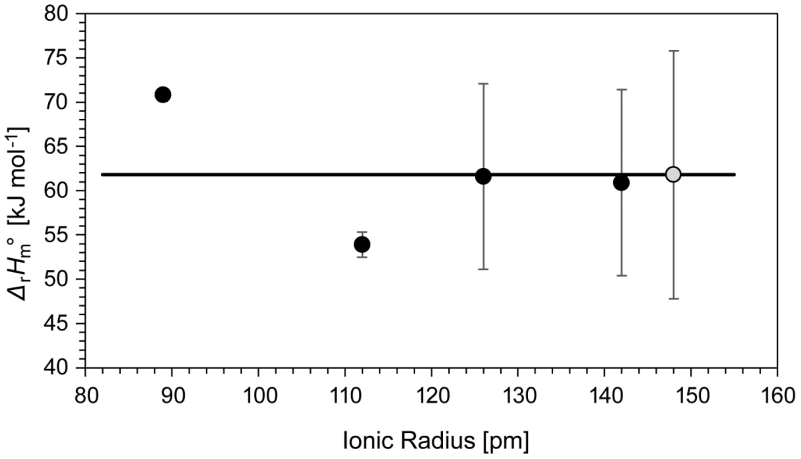

Fig. 4.5-2: Reaction enthalpy $\Delta_r H_m°$ for $M^{2+} + H_2O(l) \rightleftharpoons MOH^+ + H^+$ as a function of effective ionic radius

Solid line: unweighted mean of all selected data (black circles). Grey circle: $\Delta_r H_m°(298.15\ K) = (62 \pm 14)\ kJ \cdot mol^{-1}$ for $Ra^{2+} + H_2O(l) \rightleftharpoons RaOH^+ + H^+$.

The $\log_{10}{}^{*}\beta_1°$ values indicate a negative linear correlation versus the effective ionic radii (Fig. 4.5-1). The results of an unweighted linear regression are $\log_{10}{}^{*}\beta_1°$ ($RaOH^+$) = -13.66 with $2\sigma_{dispersion}$ = 0.37. A weighted linear regression results in $\log_{10}{}^{*}\beta_1°$ ($RaOH^+$) = -13.77 with $\sigma_{weights}$ = 0.02 and $2\sigma_{average}$ = 0.27. The results of the regression analyses are governed by the dispersion of the data and hence, the results of the unweighted linear regression have been selected by this review.

$Ra^{2+} + H_2O(l) \rightleftharpoons RaOH^+ + H^+$

$\log_{10}{}^{*}\beta_1°$ (298.15 K) = -13.7 ± 0.4

The $\Delta_r H_m°$ values do not show any correlation with their effective ionic radii (Fig. 4.5-2) and hence, their means have been calculated. The unweighted mean is $\Delta_r H_m°$ ($RaOH^+$) = 61.8 with $2\sigma_{dispersion}$ = 13.8. The weighted mean is $\Delta_r H_m°$ ($RaOH^+$) = 67.3 with $\sigma_{weights}$ = 0.6 and $2\sigma_{average}$ = 15.6. This is an extreme case as the Mg and Ca values are associated with very low uncertainties (i.e., very high weights) but show large dispersion, whereas the Sr and Ba values have very high uncertainties (i.e., very low weights) but show almost no dispersion. Consequently, the weighted mean is close to the Mg value whereas $2\sigma_{average}$ is mainly determined by the very large dispersion of the Mg and Ca values, and the Sr and Ba values do not play any role. In conclusion, this review decided to select the unweighted mean

$$\Delta_r H_m°(298.15\ K) = (62 \pm 14)\ kJ \cdot mol^{-1}$$

These values have been included in TDB 2020, as well as the estimate

$$\varepsilon(RaOH^+, Cl^-) = (0.05 \pm 0.10)\ kg \cdot mol^{-1}.$$

4.5.4.2 Radium(II) (hydr)oxide compounds

Radium hydroxide is the most soluble of the alkaline earth hydroxides and more basic than barium hydroxide (Kirby & Salutsky 1964). No thermodynamic data for $Ra(OH)_2(s)$ are available and because of its high solubility no attempt has been made to estimate thermodynamic data.

4.5.5 Radium(II) fluoride compounds and complexes

4.5.5.1 Radium(II) fluoride complexes

No estimates of thermodynamic data for RaF^+ seem to have ever been published. This review used the $\log_{10}K_1°$ and $\Delta_r H_m$ values of Mg^{2+}, Ca^{2+}, Sr^{2+} and Ba^{2+} (Section 4.4.4.2) and plotted them versus their effective ionic radii in eight-fold coordination (Shannon 1976).

The $\log_{10}K_1°$ values indicate a negative linear correlation versus their effective ionic radii (Fig. 4.5-3). The results of an unweighted linear regression are $\log_{10}K_1°$ (RaF^+) = 0.48 with $2\sigma_{dispersion}$ = 0.13. A weighted linear regression results in $\log_{10}K_1°$ (RaF^+) = 0.46 with $\sigma_{weights}$ = 0.03 and $2\sigma_{average}$ = 0.05. The $\log_{10}K_1°$ values obtained by weighted and unweighted regression analyses are the same within their uncertainties. The results of the unweighted linear regression with the higher uncertainty have been selected by this review.

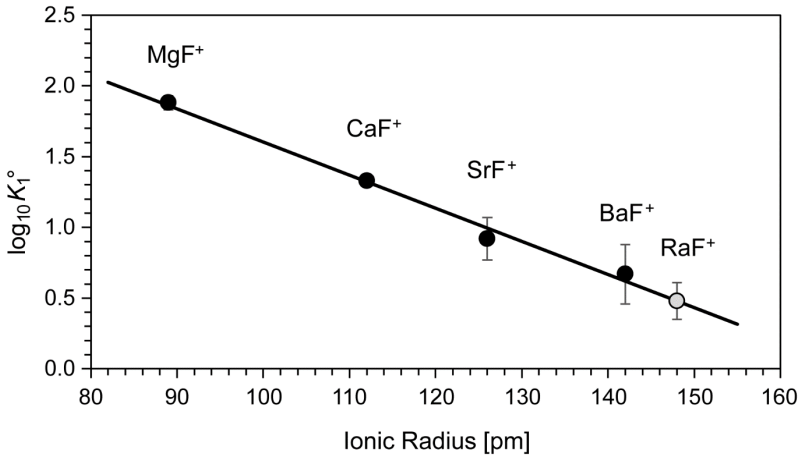

Fig. 4.5-3: The equilibrium constant $\log_{10}K_1°$ for $M^{2+} + F^- \rightleftharpoons MF^+$ as a function of effective ionic radius

Solid line: unweighted regression of all selected data (black circles). Grey circle: $\log_{10}K_1°$ (298.15 K) = 0.48 ± 0.13 calculated from the linear regression for $Ra^{2+} + F^- \rightleftharpoons RaF^+$.

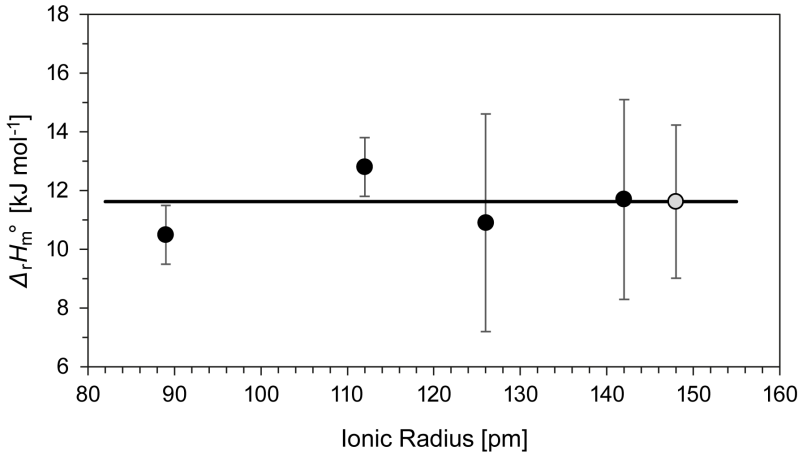

Fig. 4.5-4: Reaction enthalpy $\Delta_rH_m°$ for $M^{2+} + F^- \rightleftharpoons MF^+$ as a function of effective ionic radius

Solid line: weighted mean of all selected data (black circles). Grey circle: $\Delta_rH_m°(298.15\ K) = (11.6 \pm 2.6)\ kJ \cdot mol^{-1}$ for $Ra^{2+} + F^- \rightleftharpoons RaF^+$.

$Ra^{2+} + F^- \rightleftharpoons RaF^+$

$\log_{10}K_1°$ (298.15 K) = 0.48 ± 0.13

This value has been included in TDB 2020.

The $\Delta_r H_m$ values do not show any correlation with the effective ionic radii (Fig. 4.5-4) and hence, their means have been calculated. The unweighted mean is $\Delta_r H_m$ (RaF^+) = 11.5 with $2\sigma_{dispersion}$ = 2.0. The weighted mean is $\Delta_r H_m$ (RaF^+) = 11.6 with $\sigma_{weights}$ = 0.7 and $2\sigma_{average}$ = 2.6. The weighted and unweighted means of $\Delta_r H_m$ are the same within their uncertainties. The weighted mean with the higher uncertainty has been selected by this review

$$\Delta_r H_m \text{ (298.15 K, 1 M)} = (11.6 \pm 2.6) \text{ kJ} \cdot \text{mol}^{-1}$$

No attempt has been made to extrapolate $\Delta_r H_m$ to zero ionic strength; it is considered as an approximation of $\Delta_r H_m°$ (298.15 K).

This value has been included in TDB 2020, as well as the estimate

$$\varepsilon(RaF^+, Cl^-) = (0.05 \pm 0.10) \text{ kg} \cdot \text{mol}^{-1}.$$

4.5.5.2 Radium(II) fluoride compounds

RaF_2(cr) might be slightly soluble, similar to BaF_2(cr), but no quantitative data could be found by this review.

Nevertheless, the same argument as for BaF_2(cr) (Section 4.2.4.2) applies for RaF_2(cr), namely that the concentration of dissolved fluoride, F^-, in environmental systems is usually governed by the precipitation of the ubiquitous mineral fluorite. Hence, RaF_2(cr), may only be formed under very special chemical conditions and does not play any role in common environmental systems.

No attempt has been made to estimate a solubility constant for RaF_2(cr).

4.5.6 Radium(II) chloride compounds and complexes

4.5.6.1 Radium(II) chloride complexes

Langmuir & Riese (1985) estimated $\log_{10} K_1°$ for

$$Ra^{2+} + Cl^- \rightleftharpoons RaCl^+$$

by using the Fuoss equation (Fuoss 1958), an electrostatic model for calculating formation constants of ion pairs:

$$\log_{10} K_1° \text{ (298.15 K)} = -0.10$$

The Fuoss equation was also used to estimate $\Delta_r S_m°$ (298.15 K) which then leads to

$$\Delta_r H_m°(298.15\ K) = 0.50\ kcal \cdot mol^{-1} = 2.1\ kJ \cdot mol^{-1}$$

using the Gibbs-Helmholtz equation with $\Delta_r G_m°(298.15\ K)$ calculated from $\log_{10} K_1°$ (298.15 K).

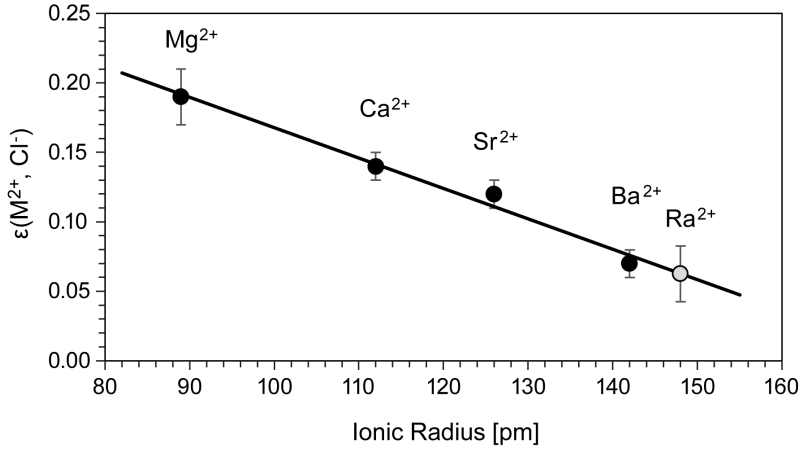

Fig. 4.5-5: SIT interaction coefficients $\varepsilon(M^{2+}, Cl^-)$ as a function of effective ionic radius

Solid line: linear regression of all selected data (black circles). Grey circle: $\varepsilon(Ra^{2+}, Cl^-) = (0.06 \pm 0.02)\ kg \cdot mol^{-1}$ calculated from the linear regression. The value estimated from charge considerations alone would be $\varepsilon(M^{2+}, Cl^-) = 0.15 \pm 0.10$ (Tab. 1-7). The uncertainty range covers all values shown in the figure.

This report does not consider the formation of weak alkaline earth chloride complexes but includes possible ion interactions in their SIT interaction coefficients. There are no isopiestic or any other experimental data concerning $RaCl_2 \cdot 2H_2O$ which could be used to derive a value for $\varepsilon(Ra^{2+}, Cl^-)$. This review used the $\varepsilon(M^{2+}, Cl^-)$ values for $M^{2+} = Mg^{2+}$, Ca^{2+}, Sr^{2+} and Ba^{2+} selected in Sections 4.1 – 4.4 and plotted them versus their effective ionic radii in 8-fold coordination (Shannon 1976). The $\varepsilon(M^{2+}, Cl^-)$ values indicate a negative linear correlation versus their effective ionic radii (Fig. 4.5-5). The results of an unweighted linear regression are $\varepsilon(Ra^{2+}, Cl^-) = 0.063$ with $2\sigma_{dispersion} = 0.016$. A weighted linear regression results in $\varepsilon(Ra^{2+}, Cl^-) = 0.062$ with $\sigma_{weights} = 0.006$ and $2\sigma_{average} = 0.017$. Hence, the weighted and the unweighted linear regressions give the same results and this review selected

$$\varepsilon(Ra^{2+}, Cl^-) = (0.06 \pm 0.02)\ kg \cdot mol^{-1}$$

4.5.6.2 Radium(II) chloride compounds

Radium chloride is a colourless and spontaneously luminous compound which gradually becomes yellowish as it ages. When crystallised from aqueous solution the compound forms a dihydrate, $RaCl_2 \cdot 2H_2O$, which is isomorphous with $BaCl_2 \cdot 2H_2O$. The solubility of radium chloride is 245 g per 1 kg of water (Kirby & Salutsky 1964).

No solubility data for this highly soluble salt are included in TDB 2020.

4.5.7 Radium(II) carbonate compounds and complexes

4.5.7.1 Radium(II) carbonate complexes

Langmuir & Riese (1985) estimated a formation constant for $BaCO_3(aq)$ using the oxalate method (linear relation between $\log_{10}K_1°$ values of 1:1 carbonate and 1:1 oxalate complexes for various cations) by Langmuir (1979). Linear extrapolation of the $\log_{10}K_1°$ values for $BaCO_3(aq)$ (estimated above) and $SrCO_3(aq)$ (Plummer 1983, oral communication) plotted against the effective ionic radii of Sr^{2+}, Ba^{2+} and Ra^{2+} in 8-fold coordination resulted in

$$Ra^{2+} + CO_3^{2-} \rightleftharpoons RaCO_3(aq)$$

$$\log_{10}K_1° (298.15\ K) = 2.5$$

The Fuoss equation was used to estimate $\Delta_r S_m^{\circ}(298.15\ K)$ which then led to

$$\Delta_r H_m°(298.15\ K) = 1.07\ kcal \cdot mol^{-1} = 4.48\ kJ \cdot mol^{-1}$$

No estimate of thermodynamic data for $RaHCO_3^+$ seems to have been published.

This review used the $\log_{10}K_1°$ and $\Delta_r H_m°$ values of Mg^{2+}, Ca^{2+}, Sr^{2+} and Ba^{2+} (Section 4.4.4.2) and plotted them versus their effective ionic radii in 8-fold coordination (Shannon 1976).

The $\log_{10}K_1°$ values for the reaction $M^{2+} + CO_3^{2-} \rightleftharpoons MCO_3(aq)$ indicate a negative linear correlation versus the effective ionic radii, however, with the $CaCO_3(aq)$ value as an "outlier" associated with a large uncertainty compared with the other data (Fig. 4.5-6). A weighted linear regression of all data results in $\log_{10}K_1°$ ($RaCO_3(aq)$) = 2.67 with $\sigma_{weights}$ = 0.02 and $2\sigma_{average}$ = 0.09. The results of an unweighted linear regression, excluding the $CaCO_3(aq)$ value, are $\log_{10}K_1°$ ($RaCO_3(aq)$) = 2.66 with $2\sigma_{dispersion}$ = 0.03. This review decided to select the results of the weighted linear regression

$$Ra^{2+} + CO_3^{2-} \rightleftharpoons RaCO_3(aq)$$

$$\log_{10}K_1° (298.15\ K) = 2.67 \pm 0.09$$

The $\Delta_r H_m°$ values do not show any clear correlation with their effective ionic radii (Fig. 4.5-7) and hence, their means have been calculated. The unweighted mean is $\Delta_r H_m°$ ($RaHCO_3^+$) = 14.5 with $2\sigma_{dispersion}$ = 8.4. The weighted mean is $\Delta_r H_m°$ ($RaHCO_3^+$) = 13.1 with $\sigma_{weights}$ = 0.7 and $2\sigma_{average}$ = 6.7. The weighted and unweighted means of $\Delta_r H_m°$ are the same within their uncertainties. The weighted mean has been selected by this review

$$\Delta_r H_m°(298.15\ K) = (13 \pm 7)\ kJ \cdot mol^{-1}$$

This value has been included in TDB 2020, as well as the estimate

$$\varepsilon(RaCO_3(aq), NaCl) = (0.0 \pm 0.1)\ kg \cdot mol^{-1}.$$

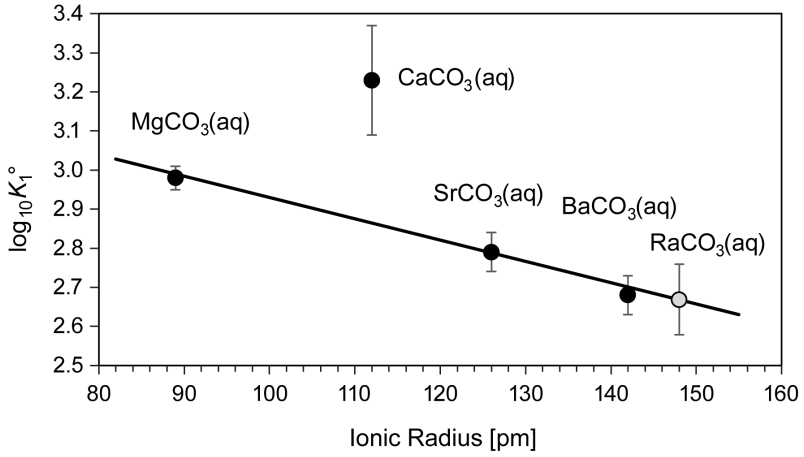

Fig. 4.5-6: The equilibrium constant $\log_{10}K_1°$ for $M^{2+} + CO_3^{2-} \rightleftharpoons MCO_3(aq)$ as a function of effective ionic radius

Solid line: weighted regression of all selected data (black circles). Grey circle: $\log_{10}K_1°$ (298.15 K) = 2.67 ± 0.09 calculated from the linear regression for $Ra^{2+} + CO_3^{2-} \rightleftharpoons RaCO_3(aq)$.

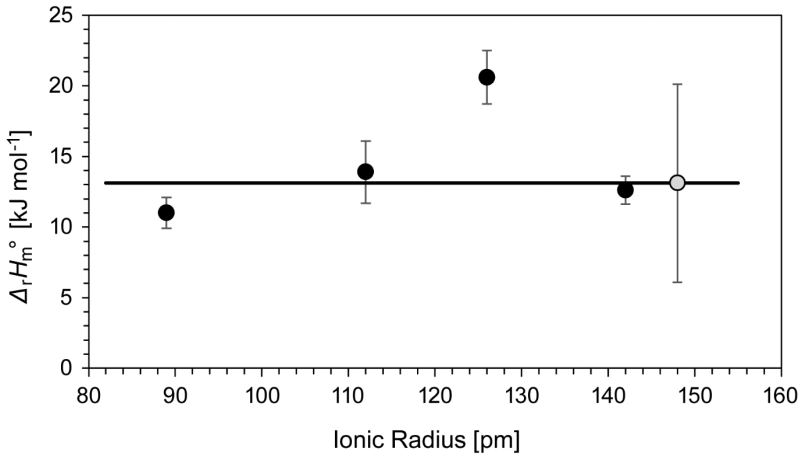

Fig. 4.5-7: Reaction enthalpy $\Delta_r H_m°$ for $M^{2+} + CO_3^{2-} \rightleftharpoons MaCO_3(aq)$ as a function of effective ionic radius

Solid line: unweighted mean of all selected data (black circles). Grey circle: $\Delta_r H_m°(298.15\ K) = (13 \pm 7)\ kJ \cdot mol^{-1}$ for $Ra^{2+} + CO_3^{2-} \rightleftharpoons RaCO_3(aq)$.

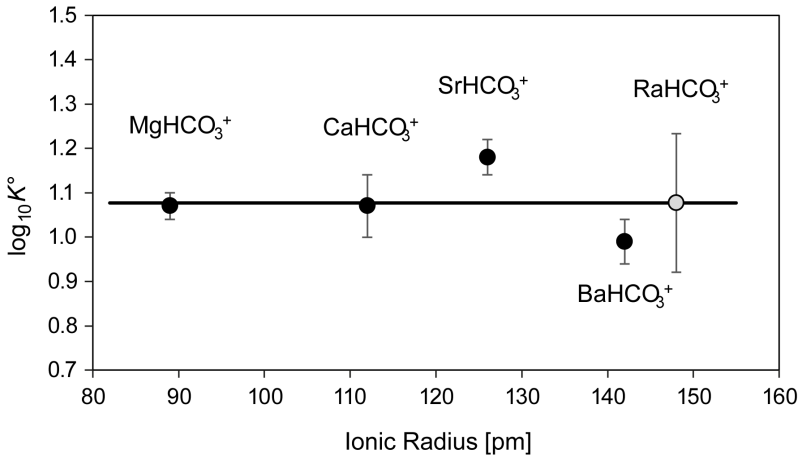

Fig. 4.5-8: The equilibrium constant $\log_{10} K°$ for $M^{2+} + HCO_3^- \rightleftharpoons MHCO_3^+$ as a function of effective ionic radius

Solid line: unweighted mean of all selected data (black circles). Grey circle: $\log_{10} K°$ (298.15 K) = 1.08 ± 0.16 for $Ra^{2+} + HCO_3^- \rightleftharpoons RaHCO_3^+$.

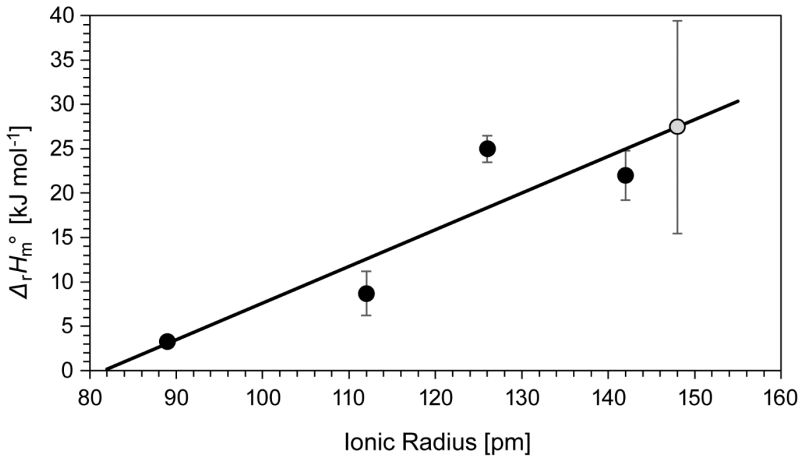

Fig. 4.5-9: Reaction enthalpy $\Delta_r H_m°$ for $M^{2+} + HCO_3^- \rightleftharpoons MHCO_3^+$ as a function of effective ionic radius

Solid line: unweighted regression of all selected data (black circles). Grey circle: $\Delta_r H_m°(298.15\ K) = (27 \pm 12)$ kJ · mol^{-1} calculated from the linear regression for $Ra^{2+} + HCO_3^- \rightleftharpoons RaHCO_3^+$.

The $\log_{10}K°$ values for the reaction $M^{2+} + HCO_3^- \rightleftharpoons MHCO_3^+$ do not show any correlation with the effective ionic radii (Fig. 4.5-8) and hence, their means have been calculated. The unweighted mean is $\log_{10}K°$ ($RaHCO_3^+$) = 1.08 with $2\sigma_{dispersion}$ = 0.16. The weighted mean is $\log_{10}K°$ ($RaHCO_3^+$) = 1.09 with $\sigma_{weights}$ = 0.02 and $2\sigma_{average}$ = 0.15. The weighted and unweighted means are the same within their uncertainties. The unweighted mean with the slightly larger uncertainty has been selected by this review

$$Ra^{2+} + HCO_3^- \rightleftharpoons RaHCO_3^+$$

$$\log_{10}K°\ (298.15\ K) = 1.08 \pm 0.16$$

This value is included in TDB 2020.

The $\Delta_r H_m°$ values indicate a positive linear correlation versus the effective ionic radii (Fig. 4.5-9). The results of an unweighted linear regression are $\Delta_r H_m°$ ($RaHCO_3^+$) = 27.4 with $2\sigma_{dispersion}$ = 11.7. A weighted linear regression results in $\Delta_r H_m°$ ($RaHCO_3^+$) = 31.6 with $\sigma_{weights}$ = 0.22 and $2\sigma_{average}$ = 2.6. The correlation of the $\Delta_r H_m°$ values is dominated by their dispersion and even $2\sigma_{average}$ does not account for the scatter of the data. Hence, the results of the unweighted linear regression have been selected by this review

$$\Delta_r H_m°(298.15\ K) = (27 \pm 12)\ kJ \cdot mol^{-1}$$

This value is included in TDB 2020, as well as the estimate

$$\varepsilon(RaHCO_3^+, Cl^-) = (0.05 \pm 0.10)\ kg \cdot mol^{-1}$$

4.5.7.2 Radium(II) carbonate compounds

Langmuir & Riese (1985) plotted the solubility product constants for strontianite, $SrCO_3$(cr), (Busenberg et al. 1984), and witherite, $BaCO_3$(cr), (calculated from Gibbs free energy data given by Wagman et al. 1982), against the effective ionic radii of Sr^{2+}, Ba^{2+} and Ra^{2+} in eight-fold coordination and obtained an estimate of $\log_{10}K_{s0}°$ for

$$RaCO_3(cr) \rightleftharpoons Ra^{2+} + CO_3^{2-}$$

$$\log_{10}K_{s0}° \text{ (298.15 K)} = -8.3$$

from an extrapolation of the linear trend.

$S_m°(RaCO_3, cr)$ was estimated and used to calculate

$$\Delta_r H_m°(298.15\text{ K}) = 2.8\text{ kcal} \cdot \text{mol}^{-1} = 11.7\text{ kJ} \cdot \text{mol}^{-1}$$

Note that in their Tab. 2, Langmuir & Riese (1985) gave the wrong sign for this value.

Brown et al. (2019) in their recent review of the solubility of alkaline earth sulphate and carbonate phases at elevated temperature recommend for the solubility of $RaCO_3$(cr)

$$\log_{10}K_{s0}° \text{ (298.15 K)} = -7.57 \pm 0.70$$

$$\Delta_r H_m°(298.15\text{ K}) = (3.4 \pm 1.0)\text{ kJ} \cdot \text{mol}^{-1}$$

$$\Delta_r C_{p,m}°(298.15\text{ K}) = -(430.8 \pm 5.0)\text{ J} \cdot \text{K}^{-1} \cdot \text{mol}^{-1}$$

These values are included in TDB 2020.

The uncertainty of $\log_{10}K_{s0}°$ has been derived by this review from the uncertainties given by Brown et al. (2019) for $\Delta_f G_m°(Ra^{2+}, 298.15\text{ K})$, $\Delta_f G_m°(CO_3^{2-}, 298.15\text{ K})$ and $\Delta_f G_m°(RaCO_3, cr, 298.15\text{ K})$, assuming that Brown et al. (2019) calculated the uncertainty of $\Delta_f G_m°(RaCO_3, cr, 298.15\text{ K})$ from $\Delta_f G_m°(Ra^{2+}, 298.15\text{ K})$, $\Delta_f G_m°(CO_3^{2-}, 298.15\text{ K})$ and $\Delta_r G_m°(RaCO_3(cr) \rightleftharpoons Ra^{2+} + CO_3^{2-}, 298.15\text{ K})$ by error propagation.

Brown et al. (2019) did not use the single experimentally derived solubility constant for radium carbonate by Matyskin (2016), actually a co-author of Brown et al. (2019), but derived $\Delta_r C_{p,m}°(298.15\text{ K})$ from a correlation of heat capacity values versus ionic radii of the other alkaline earth carbonate phases. This $\Delta_r C_{p,m}°(298.15\text{ K})$ value in turn was used by Brown et al. (2019) to derive the reaction entropy, $\Delta_r S_m°$ (298.15K), from a correlation of reaction entropy values versus heat capacity values of the other alkaline earth carbonate phases.

Brown et al. (2019) comment their obtained results as follows: "The $\log_{10}K_s$ value determined for 25 °C is -7.57 which is in quite good agreement with the value determined by Matyskin (2106) ($\log_{10}K_s = -7.7 \pm 0.6$). More recently, in our laboratory, the solubility of this phase was measured from undersaturation experiments and a $\log_{10}K_s$ value of -7.5 ± 0.2 was determined, in much better agreement with the solubility derived in this study".

4.5.8 Radium(II) sulphate compounds and complexes

4.5.8.1 Radium(II) sulphate complexes

Langmuir & Riese (1985) estimated $\log_{10}K_1°$ and $\Delta_r S_m°$ for the reaction

$$Ra^{2+} + SO_4^{2-} \rightleftharpoons RaSO_4(aq)$$

by using the Fuoss equation. They obtained

$$\log_{10}K_1° (298.15\ K) = 2.75$$

and calculated $\Delta_r H_m°$ from $\Delta_r S_m°$

$$\Delta_r H_m°(298.15\ K) = 1.3\ kcal \cdot mol^{-1} = 5.4\ kJ \cdot mol^{-1}$$

This review used the $\log_{10}K_1°$ and $\Delta_r H_m°$ values of Mg^{2+}, Ca^{2+}, Sr^{2+} and Ba^{2+} (Section 4.4.4.2) and plotted them versus their effective ionic radii in eight-fold coordination (Shannon 1976).

The $\log_{10}K_1°$ values do not show any correlation with the effective ionic radii (Fig. 4.5-10) and hence, their means have been calculated. The unweighted mean is $\log_{10}K_1°$ ($RaSO_4(aq)$) = 2.28 with $2\sigma_{dispersion} = 0.05$. The weighted mean is $\log_{10}K_1°$ ($RaSO_4(aq)$) = 2.28 with $\sigma_{weights} = 0.02$ and $2\sigma_{average} = 0.05$. The weighted and unweighted means are numerically identical and have been selected by this review

$$Ra^{2+} + SO_4^{2-} \rightleftharpoons RaSO_4(aq)$$

$$\log_{10}K_1° (298.15\ K) = 2.28 \pm 0.05$$

This value is included in TDB 2020.

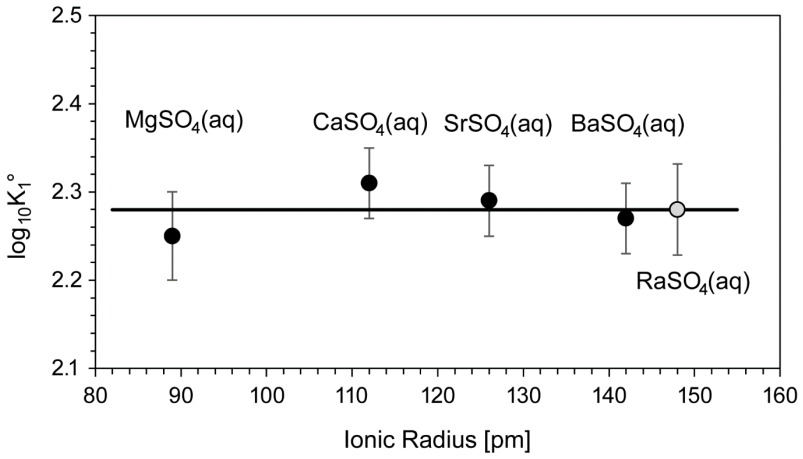

Fig. 4.5-10: The equilibrium constant $\log_{10}K_1°$ for $M^{2+} + SO_4^{2-} \rightleftharpoons MSO_4(aq)$ as a function of effective ionic radius

Solid line: mean of all selected data (black circles). Grey circle: $\log_{10}K_1°$ (298.15 K) = 2.28 ± 0.05 for $Ra^{2+} + SO_4^{2-} \rightleftharpoons RaSO_4(aq)$.

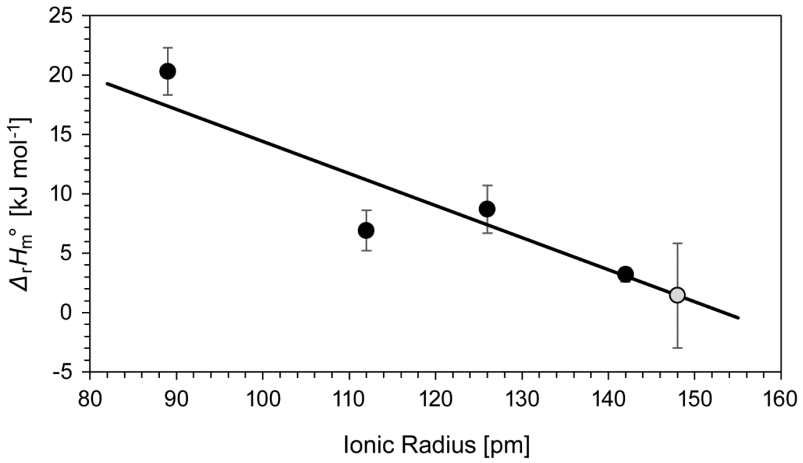

Fig. 4.5-11: Reaction enthalpy $\Delta_rH_m°$ for $M^{2+} + SO_4^{2-} \rightleftharpoons MSO_4(aq)$ as a function of effective ionic radius

Solid line: weighted regression of all selected data (black circles). Grey circle: $\Delta_rH_m°(298.15\ K) = (1.4 \pm 4.4)\ kJ \cdot mol^{-1}$ calculated from the linear regression for $Ra^{2+} + SO_4^{2-} \rightleftharpoons RaSO_4(aq)$.

The $\Delta_rH_m°$ values indicate a negative linear correlation versus the effective ionic radii (Fig. 4.5-11). The results of an unweighted linear regression are $\Delta_rH_m°$ ($RaSO_4(aq)$) = 0.6 with $2\sigma_{dispersion}$ = 7.4. A weighted linear regression results in $\Delta_rH_m°$ ($RaSO_4(aq)$) = 1.4 with $\sigma_{weights}$ = 0.5 and $2\sigma_{average}$ = 4.4. The $\Delta_rH_m°$ values obtained by weighted and unweighted regression analyses are the same within their uncertainties. The results of the weighted linear regression have been selected by this review

$$\Delta_rH_m°(298.15\ K) = (1.4 \pm 4.4)\ kJ \cdot mol^{-1}$$

This value is included in TDB 2020, as well as the estimate

$$\varepsilon(RaSO_4(aq), NaCl) = (0.0 \pm 0.1)\ kg \cdot mol^{-1}$$

4.5.8.2 Radium(II) sulphate compounds

Nikitin & Tolmatscheff (1933) measured the solubility of $RaSO_4$(cr) at 20 °C in pure water and in Na_2SO_4 solutions. Their experimental data were used by Langmuir & Riese (1985) to extract the solubility product constant

$$RaSO_4(cr) \rightleftharpoons Ra^{2+} + SO_4^{2-}$$

$$\log_{10}K_{s0}^\circ\ (298.15\ K) = -10.26$$

The corresponding enthalpy of reaction

$$\Delta_r H_m^\circ(298.15\ K) = 9.4\ kcal \cdot mol^{-1} = 39.3\ kJ \cdot mol^{-1}$$

was estimated by Langmuir & Riese (1985) through extrapolation of a linear plot of the dissociation enthalpies for celestine, $SrSO_4$(cr), and barite, $BaSO_4$(cr), against the effective ionic radii of the cations in eight-fold coordination.

Note that in their Tab. 2, Langmuir & Riese (1985) gave the wrong sign for this value.

Brown et al. (2019) in their recent review of the solubility of alkaline earth sulphate and carbonate phases at elevated temperature also considered the solubility of $RaSO_4$(cr) measured at 20 °C by Nikitin & Tolmatscheff (1933) and new solubility data measured in the temperature range 10 – 70 °C by Hedström (2013), and finally recommend for the solubility of $RaSO_4$(cr)

$$\log_{10}K_{s0}^\circ\ (298.15\ K) = -10.26 \pm 0.30$$

$$\Delta_r H_m^\circ(298.15\ K) = (38.8 \pm 1.0)\ kJ \cdot mol^{-1}$$

$$\Delta_r C_{p,m}^\circ(298.15\ K) = -(428.3 \pm 3.8)\ J \cdot K^{-1} \cdot mol^{-1}$$

These values have been included in TDB 2020.

The uncertainty of $\log_{10}K_{s0}^\circ$ has been derived by this review from the uncertainties given by Brown et al. (2019) for $\Delta_f G_m^\circ(Ra^{2+}, 298.15\ K)$, $\Delta_f G_m^\circ(SO_4^{2-}, 298.15\ K)$ and $\Delta_f G_m^\circ(RaSO_4, cr, 298.15\ K)$, assuming that Brown et al. (2019) calculated the uncertainty of $\Delta_f G_m^\circ(RaSO_4, cr, 298.15\ K)$ from $\Delta_f G_m^\circ(Ra^{2+}, 298.15\ K)$, $\Delta_f G_m^\circ(SO_4^{2-}, 298.15\ K)$ and $\Delta_r G_m^\circ(RaSO_4(cr) \rightleftharpoons Ra^{2+} + SO_4^{2-}, 298.15\ K)$ by error propagation.

4.5.9 Selected radium data

Tab. 4.5-1: Selected radium data

Name	TDB 01/01			TDB 2020				Species
	$\Delta_f G_m°$ [kJ · mol^{-1}]	$\Delta_f H_m°$ [kJ · mol^{-1}]	$S_m°$ [J · K^{-1} · mol^{-1}]	$\Delta_f G_m°$ [kJ · mol^{-1}]	$\Delta_f H_m°$ [kJ · mol^{-1}]	$S_m°$ [J · K^{-1} · mol^{-1}]	$C_{p,m}°$ [J · K^{-1} · mol^{-1}]	
Ra(cr)	0.0	0.0	71	0.0	0.0	71 ± 5		Ra(cr)
Ra+2	-561.5	-527.6	54	-561.5 ± 2.9	-527.6 ± 2.0	54 ± 5		Ra^{2+}

Name	TBD 01/01		TBD 2020				Reaction
	$\log_{10}\beta°$	$\Delta_r H_m°$ [kJ · mol^{-1}]	$\log_{10}\beta°$	$\Delta_r H_m°$ [kJ · mol^{-1}]	$\Delta_r C_{p,m}°$ [J · K^{-1} · mol^{-1}]	T-range [°C]	
RaOH+	-13.5	60.4	-13.7 ± 0.4	62 ± 14	-		$Ra^{2+} + H_2O(l) \rightleftharpoons RaOH^+ + H^+$
RaF+	-	-	0.48 ± 0.13	11.6 ± 2.6	-		$Ra^{2+} + F^- \rightleftharpoons RaF^+$
RaCl+	-0.10	2.1	-	-	-		$Ra^{2+} + Cl^- \rightleftharpoons RaCl^+$
RaCO3(aq)	2.5	4.48	2.67 ± 0.09	13 ± 7	-		$Ra^{2+} + CO_3^{2-} \rightleftharpoons RaCO_3(aq)$
RaHCO3+	-	-	1.08 ± 0.16	27 ± 12	-		$Ra^{2+} + HCO_3^- \rightleftharpoons RaHCO_3^+$
RaSO4(aq)	2.75	5.4	2.28 ± 0.05	1.4 ± 4.4	-		$Ra^{2+} + SO_4^{2-} \rightleftharpoons RaSO_4(aq)$
Ra(cr)	-	-	98.40 ± 0.51	-527.6 ± 2.0	-		$Ra(cr) \rightleftharpoons Ra^{2+} + 2\ e^-$
RaCO3(cr)	-8.3	11.7	-7.57 ± 0.70	3.4 ± 1.0	-430.8 ± 5.0	25	$RaCO_3(cr) \rightleftharpoons Ra^{2+} + CO_3^{2-}$
RaSO4(cr)	-10.26	39.3	-10.26 ± 0.30	38.8 ± 1.0	-428.3 ± 3.8	10 – 70	$RaSO_4(cr) \rightleftharpoons Ra^{2+} + SO_4^{2-}$

Tab. 4.5-2: Selected SIT ion interaction coefficients $\varepsilon_{j,k}$ [kg · mol^{-1}] for radium species

Data in normal face are estimated in this review. Data estimated according to charge correlations and taken from Tab. 1-7 are shaded.

j k → ↓	Cl^- $\varepsilon_{j,k}$ [kg · mol^{-1}]	Na^+ $\varepsilon_{j,k}$ [kg · mol^{-1}]	$Na^+ + Cl^-$ $\varepsilon_{j,k}$ [kg · mol^{-1}]
Ra+2	0.06 ± 0.02	0	0
RaOH+	0.05 ± 0.10	0	0
RaF+	0.05 ± 0.10	0	0
RaHCO3+	0.05 ± 0.10	0	0
RaCO3(aq)	0	0	0.0 ± 0.1
RaSO4(aq)	0	0	0.0 ± 0.1

4.5.10 References

Baes, C.F., Jr. & Mesmer, R.E. (1981): The thermodynamics of cation hydrolysis. American Journal of Science, 281, 935-962.

Bard, A.J., Parsons, R. & Jordan, J. (1985): Standard Potentials in aqueous Solution. Marcel Dekker, Inc., New York, 834 pp.

Bevington, P.R. (1969): Data Reduction and Error Analysis for the Physical Sciences. McGraw-Hill, New York, 336 pp.

Brown, P.L. & Ekberg, C. (2016): Hydrolysis of Metal Ions. Wiley-VCH Verlag GmbH & Co. KGaA, Weinheim, Germany, 917 pp.

Brown, P.L., Ekberg, C. & Matyskin, A.V. (2019): On the solubility of radium and other alkaline earth sulfate and carbonate phases at elevated temperature. Geochimica et Cosmochimica Acta, 255, 88-104.

Busenberg, E., Plummer, L.N. & Parker, V.B. (1984): The solubility of strontianite ($SrCO_3$) in CO_2–H_2O solutions between 2 and 91 °C, the association constants of $SrHCO_3^+$(aq) and $SrCO_3$°(aq) between 5 and 80 °C, and an evaluation of the thermodynamic properties of Sr^{2+}(aq) and $SrCO_3$(cr) at 25 °C and 1 atm total pressure. Geochimica et Cosmochimica Acta, 48, 2021-2035.

Fuoss, R.D. (1958): Ionic association III. The equilibrium between ion pairs and free ions. Journal of the American Chemical Society, 80, 5059-5061.

Grenthe, I., Fuger, J., Konings, R.J.M., Lemire, R.J., Muller, A.B., Nguyen-Trung, C. & Wanner, H. (1992): Chemical Thermodynamics of Uranium. Chemical Thermodynamics, Vol. 1. North-Holland, Amsterdam, 715 pp.

Hedström, H. (2013): Radium sulfate and its co-precipitation with barium and radium. PhD dissertation. Chalmers University of Technology, Göteborg, Sweden (as cited by Brown et al. 2019).

Hummel, W., Berner, U., Curti, E., Pearson, F.J. & Thoenen, T. (2002): Nagra/PSI Chemical Thermodynamic Data Base 01/01. Nagra Technical Report NTB 02-16 and Universal Publishers, Parkland, Florida, 565 pp.

Kirby, H.W. & Salutsky M.L. (1964): The Radiochemistry of Radium. National Academy of Sciences – National Research Council, Nuclear Science Series, NAS-NS 3057, U.S. Atomic Energy Commission, 205 pp.

Langmuir, D. (1979): Techniques of estimating thermodynamic properties for some aqueous complexes of geochemical interest. In: Jenne, E.A. (ed.): Chemical Modeling in Aqueous Systems, American Chemical Society Symposium Series, 93, 353-387.

Langmuir, D. & Riese, A.C. (1985): The thermodynamic properties of radium. Geochimica et Cosmochimica Acta, 49, 1593-1601.

Matyskin, A.V. (2016): On the solubility of radium sulfate and carbonate. Licentiate dissertation. Chalmers University of Technology, Göteborg, Sweden, 49 pp.

Nikitin, B. & Tolmatscheff, P. (1933): Ein Beitrag zur Gültigkeit des Massenwirkungsgesetzes II. Quantitative Bestimmung der Löslichkeit des Radiumsulfates in Natriumsulfatlösungen und in Wasser. Zeitschrift für Physikalische Chemie, A167, 260-272.

Shannon, R.D. (1976): Revised effective ionic radii and systematic studies of interatomic distances in halides and chalcogenides. Acta Crystallographica A, 32, 751-767.

Wagman, D.D., Evans, W.H., Parker, V.B., Schumm, R.H., Halow, I., Bailey, S.M., Churney, K.L. & Nuttall, R.L. (1982): The NBS tables of chemical thermodynamic properties: Selected values for inorganic and C1 and C2 organic substances in SI units. Journal of Physical and Chemical Reference Data, 11, Supplement No. 2, 1-392.

5 Aluminium

5.1 Introduction

Aluminium is an important component in ground and pore waters. In addition, a long-lived radioactive isotope of aluminium, Al-26 with $(7.17 \pm 0.24) \cdot 10^5$ years half-life, is produced in spallation induced neutron sources (e.g., SINQ at PSI) and contributes in dose-relevant quantities to the inventory of radioactive waste coming from research facilities like PSI. Hence, Al is of double interest, as a radionuclide to be considered in the safety assessment and as a ground and pore water component.

Chemical thermodynamic data for ground and pore water models in our original data base (Pearson & Berner 1991, Pearson et al. 1992) have been taken from the USGS review of data for major water-mineral reactions (Nordstrom et al. 1990). Since then, aluminium data have been updated only once (Hummel et al. 2002). Meanwhile, new experimental data have been reported, as well as new reviews of the hydrolysis of metal ions (Brown & Ekberg 2016), which are considered in the present update.

The thermodynamic data of aluminium included in TDB 2020 have been taken from

- CODATA key values (Cox et al. 1989)
- the USGS review of data for major water-mineral reactions (Nordstrom et al. 1990)
- the recent review of the hydrolysis of metal ions (Brown & Ekberg 2016)
- and own reviews of experimental data

The selected thermodynamic data are presented in Tab. 5-2.

NEA (see, e.g., Grenthe et al. 1992) used the specific ion interaction theory (SIT) for making ionic strength corrections to the experimental data, an approach which is also adopted for TDB 2020 (as has been for all its predecessors).

In many cases, the ion interaction coefficients for species under consideration here were not available. We approximated these with the estimation method described in Section 1.5.3, which draws on a statistical analysis of published SIT ion interaction coefficients and which allows the estimation of missing coefficients for the interaction of cations with Cl^- and ClO_4^-, and for the interaction of anions with Na^+, from the charge of the cations or anions of interest.

The selected SIT ion interaction coefficients are presented in Tab. 5-3.

5.2 Elemental aluminium

Aluminium metal is unstable in contact with water and thus, it is not relevant under environmental conditions. Hence, the gas phase Alg is not included in the data base. The absolute entropy and heat capacity of Al(cr) are included as they are used for the calculation of certain thermodynamic reaction properties.

The selected values for Al(cr) are taken from CODATA (Cox et al. 1989):

$S_m°$(Al, cr, 298.15 K) = (28.300 ± 0.100) J · K^{-1} · mol^{-1}

$C_{p,m}°$(Al, cr, 298.15 K) = (24.200 ± 0.070) J · K^{-1} · mol^{-1}

5.3 Aluminium(III) aqua ion

Aluminium(III) exists as the Al^{3+} cation in aqueous solutions. The selected thermodynamic values for Al^{3+} in the Nagra Thermochemical Data Base 05/92 (Pearson & Berner 1991, Pearson et al. 1992) were taken from Wagman et al. (1982):

$\Delta_f G_m°(Al^{3+}, 298.15\ K) = -491.5\ kJ \cdot mol^{-1}$

$\Delta_f H_m°(Al^{3+}, 298.15\ K) = -538.4\ kJ \cdot mol^{-1}$

From the revised aluminium hydrolysis reaction data included in the Nagra/PSI Thermochemical Data Base 01/01 (see Section 5.4.1) Hummel et al. (2002) calculated:

$\Delta_f G_m°(Al^{3+}, 298.15\ K) = -487.740\ kJ \cdot mol^{-1}$

$\Delta_f H_m°(Al^{3+}, 298.15\ K) = -538.424\ kJ \cdot mol^{-1}$

$S_m°(Al^{3+}, 298.15\ K) = -337.71\ J \cdot K^{-1} \cdot mol^{-1}$

$C_{p,m}°(Al^{3+}, 298.15\ K) = -133.07\ J \cdot K^{-1} \cdot mol^{-1}$

Brown & Ekberg (2016) selected thermochemical properties of Al^{3+} as derived by Bénézeth et al. (2001) from their solubility measurements of boehmite (see Section 5.4.2):

$\Delta_f G_m°(Al^{3+}, 298.15\ K) = -(487.2 \pm 2.3)\ kJ \cdot mol^{-1}$

$\Delta_f H_m°(Al^{3+}, 298.15\ K) = -(539.4 \pm 2.7)\ kJ \cdot mol^{-1}$

$S_m°(Al^{3+}, 298.15\ K) = -(342.8 \pm 5.0)\ J \cdot K^{-1} \cdot mol^{-1}$

$C_{p,m}°$(Al, cr, 298.15 K) = -(96 ± 30) J · K^{-1} · mol^{-1}

These values have been included in TDB 2020.

However, this review changed $S_m°(Al^{3+}, 298.15\ K) = -(342.4 \pm 5.0)\ J \cdot K^{-1} \cdot mol^{-1}$ as reported by Bénézeth et al. (2001) and accepted by Brown & Ekberg (2016) to $S_m°(Al^{3+}, 298.15\ K) = -(342.8 \pm 5.0)\ J \cdot K^{-1} \cdot mol^{-1}$ in order to achieve internal consistency of all selected thermochemical values for Al(cr) and Al^{3+}.

Using the selected $\Delta_f G_m°(Al^{3+}, 298.15\ K)$, the redox equilibrium

$$Al(cr) \rightleftharpoons Al^{3+} + 3\ e^-$$

is calculated as

$$\log_{10} K°(298.15\ K) = 85.35 \pm 0.40$$

Since this review does not consider the formation of aluminium chloride complexes, $\varepsilon(Al^{3+}, Cl^-)$ is taken as selected by NEA (Grenthe et al. 1992, Lemire et al. 2013):

$$\varepsilon(Al^{3+}, Cl^-) = (0.33 \pm 0.02)\ kg \cdot mol^{-1}$$

5.4 Aluminium(III) (hydr)oxide compounds and complexes

Aluminium occurs naturally as Al^{3+}. In aqueous solution it hydrolyses to form a series of species of the form $Al(OH)_n^{3-n}$ with n ranging from 0 – 4. The solubility of aluminium oxides and hydroxides is minimal at near-neutral pH values and becomes higher with both increasing and decreasing pH. This indicates that the most stable aqueous species are Al^{3+} and its hydrolysis products with n = 1 and 4. In addition, at higher aluminium concentrations in the acidic region polymeric aluminium hydrolysis products may form.

Values of the stability constants of aluminium hydrolysis products are derived from measurements of the solubilities of aluminium solids at various pH values. From such measurements over a range of temperatures, values for the thermodynamic properties ($\Delta_r G_m°$, $\Delta_r H_m°$, $\Delta_r S_m°$and $\Delta_r C_{p,m}°$) of the hydrolysis reactions can be determined. If the solid used in the dissolution experiment is well characterised and has known thermodynamic properties of formation, the thermodynamic properties of Al^{3+} and its hydrolysis products can also be determined.

5.4.1 Aluminium(III) hydroxide complexes

The stability constants for aluminium hydrolysis products that were included in the Nagra Thermochemical Data Base 05/92 (Pearson & Berner 1991, Pearson et al. 1992) were taken from a compilation of data by Nordstrom et al. (1990) for use in geochemical modelling. These values were taken, in turn, from a review of aqueous aluminium data by Nordstrom & May (1996):

$Al^{3+} + H_2O(l) \rightleftharpoons AlOH^{2+} + H^+$

$\log_{10}{}^*\beta_1^\circ$ (298.15 K) = -5.00

$\Delta_r H_m^\circ$(298.15 K) = 48.08 kJ · mol^{-1}

$\Delta_r C_{p,m}^\circ$(298.15 K) = 119.1 J · K^{-1} · mol^{-1}

$Al^{3+} + 2\ H_2O(l) \rightleftharpoons Al(OH)_2{}^+ + 2\ H^+$

$\log_{10}{}^*\beta_2^\circ$ (298.15 K) = -10.11

$\Delta_r H_m^\circ$(298.15 K) = 112.57 kJ · mol^{-1}

$\Delta_r C_{p,m}^\circ$(298.15 K) = -225.5 J · K^{-1} · mol^{-1}

$Al^{3+} + 3\ H_2O(l) \rightleftharpoons Al(OH)_3(aq) + 3\ H^+$

$\log_{10}{}^*\beta_3^\circ$ (298.15 K) = -16.94

$\Delta_r H_m^\circ$(298.15 K) = 166.9 kJ · mol^{-1}

$\Delta_r C_{p,m}^\circ$(298.15 K) = -611.9 J · K^{-1} · mol^{-1}

$Al^{3+} + 4\ H_2O(l) \rightleftharpoons Al(OH)_4{}^- + 4\ H^+$

$\log_{10}{}^*\beta_4^\circ$ (298.15 K) = -22.67

$\Delta_r H_m^\circ$(298.15 K) = 177.0 kJ · mol^{-1}

$\Delta_r C_{p,m}^\circ$(298.15 K) = -123.6 J · K^{-1} · mol^{-1}

Since 1990, a number of new experimental studies on aluminium hydroxide solubility and aluminium speciation have been published, as well as several exhaustive reviews of aluminium chemistry in aqueous solution. Hence, the data in the Nagra/PSI database have been revised by Hummel et al. (2002) according to the following considerations:

Pokrovskii & Helgeson (1995) and Shock et al. (1997) have performed exhaustive reviews of the chemistry of aluminium in aqueous solutions over wide ranges of temperature and pressure. Both reviews conclude that the experimental data on the reaction:

$Al(OH)_3(cr) + OH^- \rightleftharpoons Al(OH)_4{}^-$

obtained at Oak Ridge National Laboratory (ORNL) (Wesolowski 1992) are particularly reliable. From the standard thermodynamic properties of this reaction and selected data on the properties of formation of OH^- and the solid used in the experiment, Pokrovskii & Helgeson (1995) and Shock et al. (1997) calculate values for the properties of formation of $Al(OH)_4{}^-$.

Pokrovskii & Helgeson (1995) also accept ORNL data (Palmer & Wesolowski 1992, 1993), together with similar results from other studies, for the reaction

$$Al(OH)_3(cr) + 3\ H^+ \rightleftharpoons Al^{3+} + 3\ H_2O(l)$$

From the standard thermodynamic properties of this reaction and selected data on the properties of formation of H_2O, H^+, and the solid used in the experiment, they calculate values for the properties of formation of Al^{3+}.

The reaction properties of the aluminium hydroxide aqueous species extracted by Pokrovskii & Helgeson (1995) from the data of the ORNL group and other authors have been chosen as the aluminium hydrolysis reaction data included in the Nagra/PSI Thermochemical Data Base 01/01 (Hummel et al. 2002):

$$Al^{3+} + H_2O(l) \rightleftharpoons AlOH^{2+} + H^+$$

$\log_{10}{}^*\beta_1^\circ$ (298.15 K) = -4.957

$\Delta_r H_m^\circ$(298.15 K) = 49.798 kJ · mol^{-1}

$\Delta_r C_{p,m}^\circ$(298.15 K) = 127.194 J · K^{-1} · mol^{-1}

$$Al^{3+} + 2\ H_2O(l) \rightleftharpoons Al(OH)_2{}^+ + 2\ H^+$$

$\log_{10}{}^*\beta_2^\circ$ (298.15 K) = -10.594

$\Delta_r H_m^\circ$(298.15 K) = 98.282 kJ · mol^{-1}

$\Delta_r C_{p,m}^\circ$(298.15 K) = 134.306 J · K^{-1} · mol^{-1}

$$Al^{3+} + 3\ H_2O(l) \rightleftharpoons Al(OH)_3(aq) + 3\ H^+$$

$\log_{10}{}^*\beta_3^\circ$ (298.15 K) = -16.432

$\Delta_r H_m^\circ$(298.15 K) = 144.704 kJ · mol^{-1}

$\Delta_r C_{p,m}^\circ$(298.15 K) = 155.645 J · K^{-1} · mol^{-1}

$$Al^{3+} + 4\ H_2O(l) \rightleftharpoons Al(OH)_4{}^- + 4\ H^+$$

$\log_{10}{}^*\beta_4^\circ$ (298.15 K) = -22.879

$\Delta_r H_m^\circ$(298.15 K) = 180.899 kJ · mol^{-1}

$\Delta_r C_{p,m}^\circ$(298.15 K) = -57.321 J · K^{-1} · mol^{-1}

These reaction data and selected standard thermodynamic data for gibbsite, $Al(OH)_3$(cr), and H_2O, Al(cr), H_2g and O_2g, were then used to develop a consistent set of standard thermodynamic properties for Al^{3+} (see Section 5.3).

Brown & Ekberg (2016) scrutinised the above-mentioned studies, as well as older studies and the most recent ORNL data concerning aluminium hydrolysis (Bénézeth et al. 2001, Palmer et al. (2001) and obtained the following parameters

$Al^{3+} + H_2O(l) \rightleftharpoons AlOH^{2+} + H^+$

$\log_{10}{}^*\beta_1°$ (298.15 K) = -4.98 ± 0.02

$\Delta_r H_m°$(298.15 K) = (56.0 ± 0.5) kJ · mol^{-1}

$\Delta_r C_{p,m}°$(298.15 K) = 0 J · K^{-1} · mol^{-1}

$Al^{3+} + 2\ H_2O(l) \rightleftharpoons Al(OH)_2{}^+ + 2\ H^+$

$\log_{10}{}^*\beta_2°$ (298.15 K) = -10.63 ± 0.02

$\Delta_r H_m°$(298.15 K) = (110.8 ± 0.8) kJ · mol^{-1}

$\Delta_r C_{p,m}°$(298.15 K) = 0 J · K^{-1} · mol^{-1}

$Al^{3+} + 3\ H_2O(l) \rightleftharpoons Al(OH)_3(aq) + 3\ H^+$

$\log_{10}{}^*\beta_3°$ (298.15 K) = -15.99 ± 0.23

$\Delta_r H_m°$(298.15 K) = (135.2 ± 2.1) kJ · mol^{-1}

$\Delta_r C_{p,m}°$(298.15 K) = 0 J · K^{-1} · mol^{-1}

$Al^{3+} + 4\ H_2O(l) \rightleftharpoons Al(OH)_4{}^- + 4\ H^+$

$\log_{10}{}^*\beta_4°$ (298.15 K) = -22.91 ± 0.10

$\Delta_r H_m°$(298.15 K) = (190.4 ± 2.5) kJ · mol^{-1}

$\Delta_r C_{p,m}°$(298.15 K) = -(182 ± 27) J · K^{-1} · mol^{-1}

Brown & Ekberg (2016) observed that the stability constants reported for $AlOH^{2+}$, $Al(OH)_2{}^+$ and $Al(OH)_3(aq)$ vary linearly with respect to the inverse of absolute temperature across the temperature range 0 – 300 °C, whereas the data for $Al(OH)_4{}^-$ in the same temperature range are curvilinear. Hence, in the latter case $\Delta_r C_{p,m}°$(298.15 K) is non-zero whereas it is zero in all other cases.

These values have been included in TDB 2020, together with the estimates

$\varepsilon(AlOH^{2+}, Cl^-) = (0.15 \pm 0.10)$ kg · mol^{-1}

$\varepsilon(Al(OH)_2{}^+, Cl^-) = (0.05 \pm 0.10)$ kg · mol^{-1}

$\varepsilon(Al(OH)_3(aq), NaCl) = (0.0 \pm 0.1)$ kg · mol^{-1}

$\varepsilon(Al(OH)_4{}^-, Na^+) = -(0.05 \pm 0.10)$ kg · mol^{-1}.

In addition, Brown & Ekberg (2016) fitted temperature data for polymeric aluminium hydrolysis species, reported for 1.0 mol · kg^{-1} KCl in the temperature range 25 – 150 °C and obtained

$2\ Al^{3+} + 2\ H_2O(l) \rightleftharpoons Al_2(OH)_2{}^{4+} + 2\ H^+$

$\Delta_r H_m°$(298.15 K) = (83.6 ± 4.9) kJ · mol^{-1}

$\Delta_r C_{p,m}°$(298.15 K) = 0 J · K^{-1} · mol^{-1}

$3\ Al^{3+} + 4\ H_2O(l) \rightleftharpoons Al_3(OH)_4^{5+} + 4\ H^+$

$\Delta_r H_m°(298.15\ K) = (146.3 \pm 4.5)\ kJ \cdot mol^{-1}$

$\Delta_r C_{p,m}°(298.15\ K) = 0\ J \cdot K^{-1} \cdot mol^{-1}$

$13\ Al^{3+} + 32\ H_2O(l) \rightleftharpoons Al_{13}(OH)_{32}^{7+} + 32\ H^+$

$\Delta_r H_m°(298.15\ K) = (1255.8 \pm 9.7)\ kJ \cdot mol^{-1}$

$\Delta_r C_{p,m}°(298.15\ K) = 0\ J \cdot K^{-1} \cdot mol^{-1}$

In all cases Brown & Ekberg (2016) observed that the reported stability constants vary linearly with respect to the inverse of absolute temperature and hence $\Delta C_{p,m}°(298.15\ K)$ is zero. The enthalpy is retained for zero ionic strength since it is assumed that the relevant value will be within the uncertainty of that determined for 1.0 $mol \cdot kg^{-1}$ KCl.

These values have been included in TDB 2020.

Brown & Ekberg (2016) extrapolated stability constants reported for $Al_2(OH)_2^{4+}$ and $Al_{13}(OH)_{32}^{7+}$ at 25 °C in NaCl and KCl media to zero ionic strength by linear SIT analyses and obtained

$2\ Al^{3+} + 2\ H_2O(l) \rightleftharpoons Al_2(OH)_2^{4+} + 2\ H^+$

$\log_{10}{}^*\beta_{22}°\ (298.15\ K) = -7.62 \pm 0.11$

$\Delta\varepsilon(Na,KCl) = -(0.06 \pm 0.07)\ kg \cdot mol^{-1}$

$13\ Al^{3+} + 32\ H_2O(l) \rightleftharpoons Al_{13}(OH)_{32}^{7+} + 32\ H^+$

$\log_{10}{}^*\beta_{13,32}°\ (298.15\ K) = -100.03 \pm 0.09$

$\Delta\varepsilon(Na,KCl) = (0.76 \pm 0.07)\ kg \cdot mol^{-1}$

These values have been included in TDB 2020.

Using $\varepsilon(Al^{3+}, Cl^-) = (0.33 \pm 0.02)\ kg \cdot mol^{-1}$, and $\varepsilon(H^+, Cl^-) = (0.12 \pm 0.01)\ kg \cdot mol^{-1}$ this review calculated from the above $\Delta\varepsilon(Na,KCl)$ values

$\varepsilon(Al_2(OH)_2^{4+}, Cl^-) = (0.36 \pm 0.08)\ kg \cdot mol^{-1}$

$\varepsilon(Al_{13}(OH)_{32}^{7+}, Cl^-) = (1.21 \pm 0.08)\ kg \cdot mol^{-1}$

These values have been included in TDB 2020.

In addition, Brown & Ekberg (2016) extrapolated stability constants reported for $Al_3(OH)_4^{5+}$ at 25 °C in LiCl, NaCl and KCl media to zero ionic strength by a non-linear SIT analysis and obtained

$$3\ Al^{3+} + 4\ H_2O(l) \rightleftharpoons Al_3(OH)_4^{5+} + 4\ H^+$$

$$\log_{10}{}^*\beta_{34}^\circ\ (298.15\ K) = -14.06 \pm 0.22$$

$$\Delta\varepsilon_1(Li,Na,KCl) = -(0.3 \pm 0.3)\ kg \cdot mol^{-1}$$

$$\Delta\varepsilon_2(Li,Na,KCl) = (0.5 \pm 0.6)\ kg \cdot mol^{-1}$$

The present review repeated the extrapolation procedure by a linear SIT analysis (Fig. 5-1), using the same values with the same assigned uncertainties as selected by Brown & Ekberg (2016), and obtained

$$\log_{10}{}^*\beta_{34}^\circ\ (298.15\ K) = -13.90 \pm 0.12$$

$$\Delta\varepsilon(Li,Na,KCl) = (0.00 \pm 0.06)$$

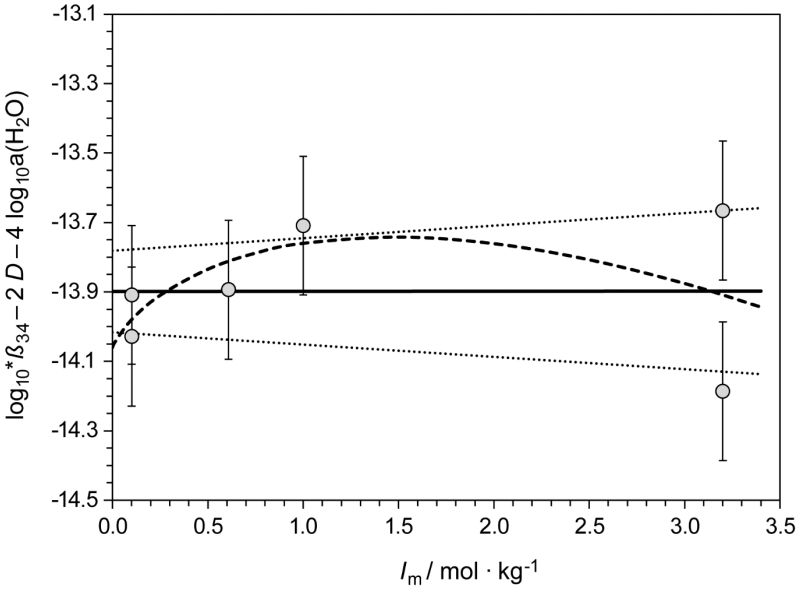

Fig. 5-1: Dependence of the equilibrium $3Al^{3+} + 4H_2O(l) \rightleftharpoons Al_3(OH)_4^{5+} + 4H^+$ on ionic strength in (Li,Na,K)Cl using the data selected by Brown & Ekberg (2016, Tab. 13-15)

The solid line is obtained using the derived SIT interaction coefficient and stability constant at zero ionic strength. Dotted lines represent the 95% uncertainty range extrapolated from I = 0 to higher (Li,Na,K)Cl concentrations. The dashed line represents the non-linear SIT extrapolation reported by Brown & Ekberg (2016).

Using $\varepsilon(Al^{3+}, Cl^-) = (0.33 \pm 0.02)$ kg · mol^{-1}, and $\varepsilon(H^+, Cl^-) = (0.12 \pm 0.01)$ kg · mol^{-1} this review calculated from the $\Delta\varepsilon$(Li,Na,KCl) value

$$\varepsilon(Al_3(OH)_4^{5+}, Cl^-) = (0.51 \pm 0.07)$$

These values have been included in TDB 2020.

Note that the non-linear SIT curve reported by Brown & Ekberg (2016) is within the uncertainty limits of the linear SIT extrapolation, except the value at zero ionic strength (Fig. 5-1).

5.4.2 Aluminium(III) (hydr)oxide compounds

The stability constants for $Al(OH)_3$(s) that were included in the Nagra Thermochemical Data Base 05/92 (Pearson & Berner 1991, Pearson et al. 1992) were taken from a compilation of data by Nordstrom et al. (1990) for use in geochemical modelling:

$$Al(OH)_3(\text{gibbsite, crystalline}) + 3\ H^+ \rightleftharpoons Al^{3+} + 3\ H_2O(l)$$

$$\log_{10}{}^*K_{s0}^\circ\ (298.15\ K) = 8.11$$

$$\Delta_r H_m^\circ(298.15\ K) = -22.8\ \text{kcal} \cdot \text{mol}^{-1} = -95.4\ \text{kJ} \cdot \text{mol}^{-1}$$

$$Al(OH)_3(\text{gibbsite, microcrystalline}) + 3\ H^+ \rightleftharpoons Al^{3+} + 3\ H_2O(l)$$

$$\log_{10}{}^*K_{s0}^\circ\ (298.15\ K) = 9.35$$

$$\Delta_r H_m^\circ(298.15\ K) = -24.5\ \text{kcal} \cdot \text{mol}^{-1} = -102.5\ \text{kJ} \cdot \text{mol}^{-1}$$

$$Al(OH)_3(\text{amorphous}) + 3\ H^+ \rightleftharpoons Al^{3+} + 3\ H_2O(l)$$

$$\log_{10}{}^*K_{s0}^\circ\ (298.15\ K) = 10.80$$

$$\Delta_r H_m^\circ(298.15\ K) = -26.5\ \text{kcal} \cdot \text{mol}^{-1} = -110.9\ \text{kJ} \cdot \text{mol}^{-1}$$

In their above-mentioned revision of aluminium hydroxide solubility and aluminium speciation data for Nagra/PSI Thermochemical Data Base 01/01, Hummel et al. (2002) only retained data for $Al(OH)_3$(gibbsite, crystalline) and selected

$$Al(OH)_3(cr) + 3\ H^+ \rightleftharpoons Al^{3+} + 3\ H_2O(l)$$

$$\log_{10}{}^*K_{s0}^\circ\ (298.15\ K) = 7.756$$

$$\Delta_r H_m^\circ(298.15\ K) = -102.784\ \text{kJ} \cdot \text{mol}^{-1}$$

$$\Delta_r C_{p,m}^\circ(298.15\ K) = 1.255\ \text{J} \cdot \text{K}^{-1} \cdot \text{mol}^{-1}$$

Brown & Ekberg (2016) state that solubility data for gibbsite, $Al(OH)_3$(s), at zero ionic strength have been reported over the temperature range of 0 – 100 °C, and that the data available indicate that the solubility is a linear function of the reciprocal of absolute temperature over the temperature range for which data are available. Brown & Ekberg (2016) thus obtained

$Al(OH)_3(cr) + 3\ H^+ \rightleftharpoons Al^{3+} + 3\ H_2O(l)$

$\log_{10}{}^*K_{s0}°\ (298.15\ K) = 7.75 \pm 0.08$

$\Delta_r H_m°(298.15\ K) = -(104.3 \pm 2.3)\ kJ \cdot mol^{-1}$

$\Delta_r C_{p,m}°(298.15\ K) = 0\ J \cdot K^{-1} \cdot mol^{-1}$

These values have been included in TDB 2020.

Note that $\log_{10}{}^*K_{s0}°$ and $\Delta_r H_m°(298.15\ K)$ obtained by Brown & Ekberg (2016) are, within their assigned uncertainties, in excellent agreement with the data selected by Hummel et al. (2002).

Brown & Ekberg (2016) further state that "boehmite (γ-AlOOH(cr)) becomes the stable solid oxyhydroxide phase of aluminium at a temperature of around 100 °C. However, solubility data at zero ionic strength are available to lower temperatures (on the basis of the reported temperature dependence of the solubility). As was the case with gibbsite, the solubility constants of boehmite are a linear function of the reciprocal of absolute temperature." Brown & Ekberg (2016) obtained

$AlOOH(cr) + 3\ H^+ \rightleftharpoons Al^{3+} + 2\ H_2O(l)$

$\log_{10}{}^*K_{s0}°\ (298.15\ K) = 7.69 \pm 0.15$

$\Delta_r H_m°(298.15\ K) = -(119.8 \pm 1.1)\ kJ \cdot mol^{-1}$

$\Delta_r C_{p,m}°(298.15\ K) = 0\ J \cdot K^{-1} \cdot mol^{-1}$

However, a comparison of the $\log_{10}{}^*K_{s0}°$ (298.15 K) values for gibbsite and boehmite suggests that boehmite is the less soluble and thus the thermodynamically stable phase at 25 °C. Moreover, the temperature function derived by Brown & Ekberg (2016) for boehmite suggests that gibbsite is stable only at T < 19 °C, in contradiction to their own statement that boehmite becomes the stable phase at around 100 °C. Palmer et al. (2001) corroborate the latter statement: "In fact, gibbsite is known (Wesolowski 1992, Palmer & Wesolowski 1992) not to convert to boehmite even after several months at temperatures < 80 °C, whereas conversion readily occurs at higher temperatures (Wesolowski 1992)".

In fact, no experimental determination of boehmite solubility is known below 70 °C (Fig. 5-2).

Palmer et al. (2001) fitted a temperature function to experimental boehmite solubility data in the temperature range 100 – 290 °C. Values derived from this temperature function are cited by Bénézeth et al. (2001) from 25 to 300 °C in 25 °C steps, where the values calculated for 75, 50 and 25 °C are extrapolations. Brown & Ekberg (2016) combined these calculated and extrapolated values with the experimental data shown in Fig. 5-2 but excluding the data of Verdes et al. (1992) at 90 and 70 °C in order to fit their temperature function for boehmite solubility.

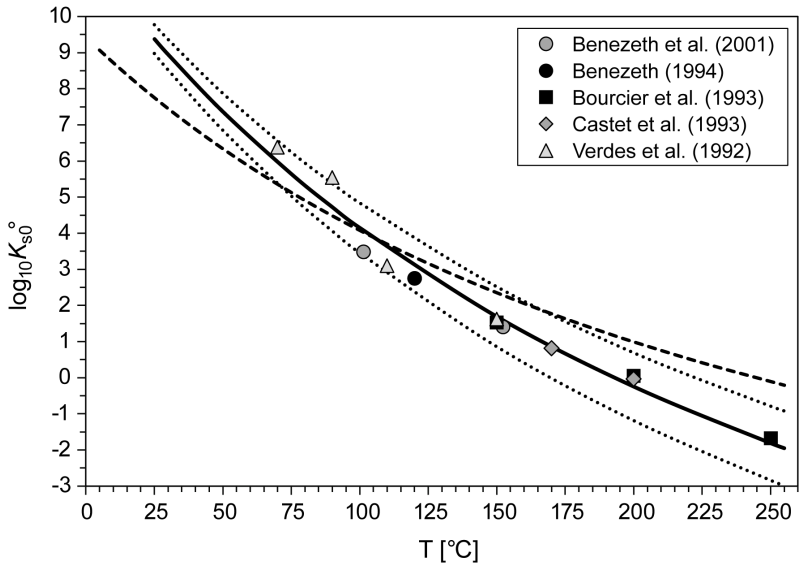

Fig. 5-2: The solubility product $\log_{10}{}^{*}K_s°$ for AlOOH(cr) + 3 H^+ ⇌ Al^{3+} + 2 H_2O(l), boehmite, as a function of temperature in the range 25 – 250 °C

Solid line: unweighted regression of all data. Dotted lines: lower and upper limits using $\log_{10}{}^{*}K_{s0}°$ (298.15 K) = 9.4 ± 0.4 and $\Delta_r H_m°$(298.15 K) = -(148.5 ± 8.3) kJ · mol^{-1} and extrapolated to higher temperatures. Dashed line: temperature function of gibbsite, $Al(OH)_3$(cr), reported by Brown & Ekberg (2016) and selected by this review, shown for comparison.

This review re-fitted all experimental data shown in Fig. 5-2 (Verdes et al. 1992, Castet et al. 1993, Bourcier et al. 1993, Bénézeth 1994, Bénézeth et al. 2001) but excluding the extrapolated values from Palmer et al. (2001), and obtained:

AlOOH(s) + 3 H^+ ⇌ Al^{3+} + 2 H_2O(l)

$\log_{10}{}^{*}K_{s0}°$ (298.15 K) = 9.4 ± 0.4

$\Delta_r H_m°$(298.15 K) = -(148.5 ± 8.3) kJ · mol^{-1}

$\Delta_r C_{p,m}°$(298.15 K) = 0 J · K^{-1} · mol^{-1}

These values have been included in TDB 2020.

Note that the selected temperature functions of boehmite and gibbsite now cross at 100 °C (Fig. 5-2), in agreement with experimental findings.

5.5 Aluminium(III) fluoride compounds and complexes

5.5.1 Aluminium(III) fluoride complexes

Thermodynamic data on Al fluoride complexation have been reported by Brosset & Orring (1943), Baumann (1969), Agarwal & Moreno (1971), Katorina et al. (1982), Yuchi et al. (1987), and Walker et al. (1971).

The first study on this topic by Brosset & Orring (1943) obtained ñ, the average number of fluoride ions bound per aluminium(III) ion, as a function of fluoride ion concentration, i.e., ñ = f (log[F^-]), in 0.53M KNO_3 and NH_4NO_3 at 25 °C. In KNO_3 the range of ñ was 0.49 to 3.29; in NH_4NO_3 the range of ñ was 2.23 to 4.65. In the calculation of $\log_{10}K_n$ values Brosset & Orring (1943) used six points from the smoothed curve ñ = f (log[F^-]), ignoring the small systematic differences of data obtained in different media. It is obvious that with a maximum observed value ñ = 4.65, the value of $\log_{10}K_6$ is a very uncertain quantity.

King & Gallagher (1959) re-evaluated the experimental data of Brosset & Orring (1943) by a more elaborate graphical method. King & Gallagher (1959) also concluded that the data of Brosset & Orring (1943) indicated that different sets of $\log_{10}K_n$ values are appropriate for each of the two media, KNO_3 and NH_4NO_3.

Baumann (1969) used a fluoride-sensitive electrode to study the aluminium fluoride complexation in 0.5, 0.3, 0.1 and 0.01M NH_4NO_3 at 25 °C. The range of ñ, the average number of fluoride ions bound per aluminium(III) ion, was 0.5 – 3.8 and thus, the experimental data was not sufficient to define $\log_{10}K_5$ and $\log_{10}K_6$ experimentally.

Agarwal & Moreno (1971) used the same type of fluoride-sensitive electrode as Baumann (1969) to study the aluminium fluoride complexation in 0.5, 0.3, 0.1 and 0.05M KNO_3 at 25 and 37 °C. Formation constants were calculated by different methods, and the authors reported that best results had been obtained by applying a generalised non-linear least squares fit. However, the values reported for $\log_{10}K_4$ can only be considered as approximate, as the range of experimentally determined values for ñ extends only to about 2.8.

Katorina et al. (1982) used the fluoride-sensitive electrode to study the aluminium fluoride complexation in 1.0, 0.5, and 0.2M NH_4NO_3 at 25 °C in the pH range 2 – 5. The authors claim that no ionic strength effect has been observed and fitted all experimental data to a common formation curve. This result is somewhat surprising, at least $\log_{10}K_1$, and to a lesser extent $\log_{10}K_2$, are expected to exhibit a measurable dependence on ionic strength. However, a close examination of the numerical data reported by Katorina et al. (1982) revealed that their results are not in contradiction with our expectations. Measurements in 1.0M NH_4NO_3 cover the range $1.6 < ñ < 5.4$, in 0.5M NH_4NO_3 it is $1.0 < ñ < 3.8$, and in 0.2M NH_4NO_3 $0.7 < ñ < 3.7$. Hence, the values of $\log_{10}K_6$ and $\log_{10}K_5$ are experimentally defined only in 1.0M NH_4NO_3 solutions. In the range $1.6 < ñ < 3.7$ all data series overlap, and for $ñ > 2$ we indeed found no variation with ionic strength. This means that common values of $\log_{10}K_4$ and $\log_{10}K_3$ may represent the experimental data. But towards the "lower end" of the 1.0M data a significant shift commences which may be represented by an increase of $\log_{10}K_2$ by at least 0.1 with respect to the 0.5 and 0.2M data. Finally, the value of $\log_{10}K_1$ is experimentally defined only in 0.2M NH_4NO_3 solutions.

Yuchi et al. (1987) used the fluoride-sensitive electrode to study trivalent metal fluoride complexation in 0.1M KNO_3 at 25 °C. No experimental data for the aluminium fluoride system are reported in this paper (e.g., in Fig. 1 of Yuchi et al. (1987) the caption reads "data for

aluminum and yttrium complexes are omitted for clarity"). However, comparing the other data ranges with the reported uncertainties of the respective formation constants, the value reported for $\log_{10}K_4$ can only be considered as approximate.

Walker et al. (1971) studied the first Al fluoride complexation step by potentiometry in 1.0M $NaClO_4$ at 25 °C. They also report an enthalpy of reaction value obtained calorimetrically under the same conditions.

These data, summarised in Tab. 5-1, have been extrapolated to zero ionic strength using SIT. Approximate data, given in parentheses in Tab. 5-1, and values at I < 0.1M have been excluded from the regression analyses. No systematic differences have been found for data referring to KNO_3 or NH_4NO_3 media (Fig. 5-3). The $\log_{10}K_1$ value of Walker et al. (1971) referring to 1.0M $NaClO_4$ has not been included in the regression analysis. Surprisingly, it agrees perfectly with the extrapolated regression line calculated with $\log_{10}K_1$ data in KNO_3 and NH_4NO_3 media (Fig. 5-3)

Tab. 5-1: Experimental $\log_{10}K_n$ data compiled for the equilibria $AlF_{n-1}^{(4-n)} + F^- \rightleftharpoons AlF_n^{(3-n)}$

Methods: pot = potentiometry, calc = re-evaluation of Brosset & Orring (1943) data, ise = ion selective electrode

Method	**Temp.** [°C]	**Medium**	***I*** [M]	**logK_1**	**logK_2**	**logK_3**	**logK_4**	**logK_5**	**logK_6**	**Reference**
pot	25	KNO_3	0.53	6.13	5.02	3.85	2.74	1.63	(0.47)	Brosset & Orring (1943)
calc	25	KNO_3	0.53	6.16	5.05	3.91	2.71	(1.46)		King & Gallagher (1959)
		NH_4NO_3	0.53			3.57	2.64	1.46	(0.04)	
ise	25	NH_4NO_3	0.5	6.08	4.93	3.69	2.50			Baumann (1969)
			0.3	6.29	4.97	3.73	2.50			
			0.1	6.40	5.19	3.91	2.42			
			0.01	6.65	5.44	3.92	2.38			
ise	25	NH_4NO_3	0.5	6.14	5.09	3.93	(3.68)			Agarwal & Moreno (1971)
			0.2	6.32	5.16	3.85	(3.30)			
			0.1	6.45	5.21	3.79	(3.18)			
			0.05	6.51	5.29	3.76	(3.05)			
	37		0.5	6.29	5.09	3.84	(3.43)			
			0.2	6.39	5.17	3.86	(3.38)			
			0.1	6.49	5.24	3.86	(3.38)			
			0.05	6.71	5.26	3.92	(3.29)			
ise	25	NH_4NO_3	1.0		4.8	3.6	2.6	1. 6	0.9	Katorina et al. (1982)
			0.5		4.98	3.72	2.67			
			0.2	6.40	4.98	3.72	2.67			
ise	25	KNO_3	0.1	6.40	5.24	3.86	(2.7)			Yuchi et al. (1987)
pot	25	$NaClO_4$	1.0	6.09						Walker et al. (1971)

The results are

$AlF_{n-1}^{(4-n)} + F^- \rightleftharpoons AlF_n^{(3-n)}$

$\log_{10}K_1°$ (n = 1, 298.15 K)	= 7.08 ± 0.07	$\Delta\varepsilon(1)$ = -(0.23 ± 0.21)
$\log_{10}K_2°$ (n = 2, 298.15 K)	= 5.65 ± 0.08	$\Delta\varepsilon(2)$ = -(0.04 ± 0.17)
$\log_{10}K_3°$ (n = 3, 298.15 K)	= 4.05 ± 0.11	$\Delta\varepsilon(3)$ = -(0.09 ± 0.22)
$\log_{10}K_4°$ (n = 4, 298.15 K)	= 2.51 ± 0.14	$\Delta\varepsilon(4)$ = -(0.19 ± 0.25)
$\log_{10}K_5°$ (n = 5, 298.15 K)	= 1.0 ± 0.2	
$\log_{10}K_6°$ (n = 6, 298.15 K)	= 0 ± 0.3	

These $\log_{10}K_n°$ values have been included in TDB 2020.

The $\Delta\varepsilon(n)$ values cannot be used directly, as they refer to $(K,NH_4)NO_3$ media. However, using $\varepsilon(Al^{3+}, Cl^-)$ = (0.33 ± 0.02) kg · mol^{-1} and $\varepsilon(Na^+, F^-)$ = (0.02 ± 0.02) kg · mol^{-1}, and the estimates $\varepsilon(AlF^{2+}, Cl^-)$ = (0.15 ± 0.10) kg · mol^{-1}, $\varepsilon(AlF_2^+, Cl^-)$ = (0.05 ± 0.10) kg · mol^{-1}, $\varepsilon(AlF_3(aq), NaCl)$ = (0.0 ± 0.1) kg · mol^{-1}, $\varepsilon(AlF_4^-, Na^+)$ = -(0.05 ± 0.10) kg · mol^{-1}, $\varepsilon(AlF_5^{2-}, Na^+)$ = -(0.10 ± 0.10) kg · mol^{-1} and $\varepsilon(AlF_6^{3-}, Na^+)$ = -(0.15 ± 0.10) kg · mol^{-1}, this review calculated

$\Delta\varepsilon(1, NaCl)$ = -(0.20 ± 0.10)

$\Delta\varepsilon(2, NaCl)$ = -(0.12 ± 0.14)

$\Delta\varepsilon(3, NaCl)$ = -(0.07 ± 0.14)

$\Delta\varepsilon(4,5,6\ NaCl)$ = -(0.07 ± 0.14)

Within their assigned uncertainties, these values are in good agreement with the experimental $\Delta\varepsilon(n, (K,NH_4)NO_3)$ values and hence, the use of the above-mentioned estimates seems reasonable.

Note that the values for $\log_{10}K_5°$ and $\log_{10}K_6°$ are estimates based on two and one data point, respectively, and the observed trend for the other stepwise stability constants (Fig. 5-3). Anyhow, AlF_5^{2-} and AlF_6^{3-} are negligible for any natural water.

In their thermodynamic data selection for aluminium species, Tagirov & Schott (2001) considered only the data of Baumann (1969). Nevertheless, the data selected by Tagirov & Schott (2001), $\log_{10}K_1°$(298.15 K) = 6.98, $\log_{10}K_2°$(298.15 K) = 5.62, $\log_{10}K_3°$(298.15 K) = 4.05 and $\log_{10}K_4°$(298.15 K) = 2.38, are in good to excellent agreement with the data derived by the SIT analyses in this review.

The fluoride complexation constants evaluated by Nordstrom & May (1996) and selected by Nordstrom et al. (1990) are in good agreement with the values selected in this review within their assigned uncertainties:

$$Al^{3+} + n\ F^- \rightleftharpoons AlF_n^{(3-n)}$$

	This review	Nordstrom et al. (1990)
$\log_{10}\beta_1^\circ$ (n = 1, 298.15 K) =	7.08 ± 0.07	7.0
$\log_{10}\beta_2^\circ$ (n = 2, 298.15 K) =	12.73 ± 0.11	12.7
$\log_{10}\beta_3^\circ$ (n = 3, 298.15 K) =	16.78 ± 0.15	16.8
$\log_{10}\beta_4^\circ$ (n = 4, 298.15 K) =	19.29 ± 0.21	19.4
$\log_{10}\beta_5^\circ$ (n = 5, 298.15 K) =	20.29 ± 0.3	20.6
$\log_{10}\beta_6^\circ$ (n = 6, 298.15 K) =	20.29 ± 0.4	20.6

Values for the enthalpy of reaction are taken from the careful calorimetric study of Latimer & Jolly (1953). They measured $\Delta_r H_m$ values at ionic strengths from 0.06 to 0.2. They did not mention any significant variation with ionic strength and thus, we assumed that their results are also valid at I = 0. Uncertainties are assigned according to the estimates given by Latimer & Jolly (1953).

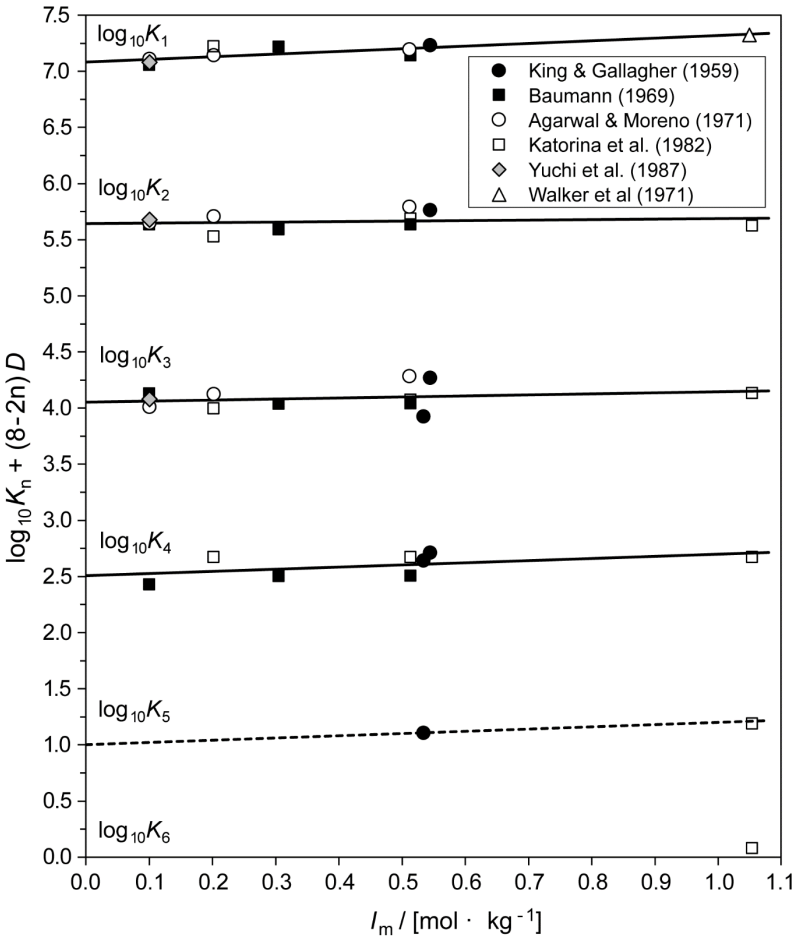

Fig. 5-3: Extrapolation to zero ionic strength of experimental data for the formation of $AlF_n^{(3-n)}$ using SIT

The data are taken from Tab. 5-1. Approximate data, given in parentheses in Tab. 5-1, and values at I < 0.1 M have been excluded from the regression analyses.

$$AlF_{n-1}^{(4-n)} + F^- \rightleftharpoons AlF_n^{(3-n)}$$

$\Delta_r H_m°$ (n = 1, 298.15 K) = (1.15 ± 0.05) kcal · mol^{-1} = (4.81 ± 0.2) kJ · mol^{-1}

$\Delta_r H_m°$ (n = 2, 298.15 K) = (0.78 ± 0.10) kcal · mol^{-1} = (3.26 ± 0.4) kJ · mol^{-1}

$\Delta_r H_m°$ (n = 3, 298.15 K) = (0.19 ± 0.10) kcal · mol^{-1} = (0.79 ± 0.4) kJ · mol^{-1}

$\Delta_r H_m°$ (n = 4, 298.15 K) = (0.28 ± 0.10) kcal · mol^{-1} = (1.17 ± 0.4) kJ · mol^{-1}

$\Delta_r H_m°$ (n = 5, 298.15 K) = -(0.75 ± 0.10) kcal · mol^{-1} = -(3.14 ± 0.4) kJ · mol^{-1}

$\Delta_r H_m°$ (n = 6, 298.15 K) = -(1.55 ± 0.20) kcal · mol^{-1} = -(6.5 ± 0.8) kJ · mol^{-1}

These values have been included in TDB 2020.

The enthalpy data reported by Nordstrom et al. (1990) and Nordstrom & May (1996) were also taken from Latimer & Jolly (1953). Note however, that their first five $\Delta_r H_m°$ values refer to the overall reaction $\log_{10}\beta_n°$ whereas the last one erroneously seems to refer to $\log_{10}K_6°$.

In their thermodynamic data selection for aluminium species, Tagirov & Schott (2001) calculated HKF equations of state parameters from published correlations. In the temperature range 25 – 70 °C their calculated temperature effects correspond to $\Delta_r H_m°$ (n = 1, 298.15 K) = 3.4 kJ · mol^{-1}, $\Delta_r H_m°$ (n = 2, 298.15 K) = 3.3 kJ · mol^{-1}, $\Delta_r H_m°$ (n = 3, 298.15 K) = 3.1 kJ · mol^{-1} and $\Delta_r H_m°$ (n = 4, 298.15 K) = 2.6 kJ · mol^{-1}, in fair agreement with the calorimetric data selected by this review.

Tóth et al. (1985), Couturier (1986), Tagirov & Schott (2001) and Tagirov et al. (2002a, 2002b) report the formation of mixed Al fluoride hydroxide complexes.

Tóth et al. (1985) varied in their potentiometric experiments the ionic medium from 0.5M KNO_3 to 0.05M KNO_3 + 0.45M total fluoride at constant total Al concentration at 25 ± 0.2 °C and interpreted the observed pH change (at pH 11) as the formation of $Al(OH)_3F^-$.

Couturier (1986) reports from potentiometric measurements in 0.1M KNO_3 at 25, 37.5 and 50 °C the formation of the species $AlOHF^+$ and $AlOHF_2$(aq) in "weakly acidic" solutions (pH 5) and the formation of $Al(OH)_3F^-$ in "weakly basic" solutions (pH 9.4 – 10.4).

The stability constants reported by Tóth et al. (1985) and Couturier (1986) for $Al(OH)_3F^-$

$$Al(OH)_4^- + F^- \rightleftharpoons Al(OH)_3F^- + OH^-$$

$\log_{10}K$ (0.5M KNO_3, 298.15 K) = -2.20 ± 0.13 Tóth et al. (1985)

$\log_{10}K$ (0.1M KNO_3, 298.15 K) = -3.73 ± 0.09 Couturier (1986)

differ by 1.5 log-units. This difference is not due to different concentrations of the KNO_3 medium, because the ionic strength effect of this isocoulombic reaction is expected to be vanishingly small.

Tagirov et al. (2002a) measured the solubility of gibbsite (at 44.5 °C) and boehmite (from 90 to 300 °C) as a function of NaF concentration in near-neutral to alkaline solutions (pH 6 – 8). The marked increase of gibbsite and boehmite solubility in the presence of fluorine is explained by the formation of $Al(OH)_2F_2^-$ according to

$$Al(OH)_4^- + 2\ F^- \rightleftharpoons Al(OH)_2F_2^- + 2\ OH^-$$

By regression analyses of the data reported by Tagirov et al. (2002) this review obtained (Fig. 5-4):

$\log_{10}K°$ (298.15 K) = -7.26 ± 0.15

$\Delta_r H_m°$(298.15 K) = (75.2 ± 2.8) kJ · mol^{-1}

$\Delta_r C_{p,m}°$(298.15 K) = -(216 ± 22) J · K^{-1} · mol^{-1}

In perfect agreement with the values $\log_{10}K°$ (298.15 K) = -7.26 and $\Delta_r H_m°$(298.15 K) = 75.28 kJ · mol^{-1} reported by Tagirov et al. (2002a) but without error estimate.

These values have been included in TDB 2020, together with the estimate

$$\varepsilon(Al(OH)_2F_2^-, Na^+) = -(0.05 \pm 0.10)\ kg \cdot mol^{-1}$$

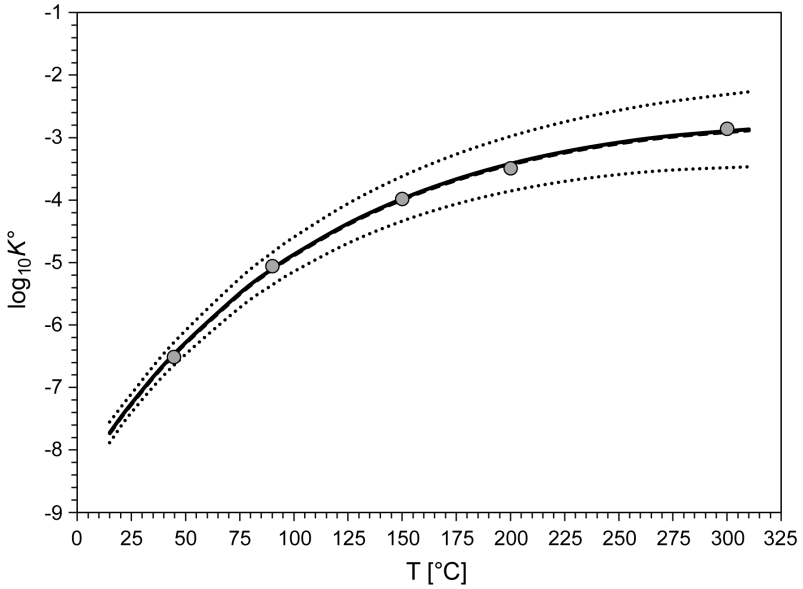

Fig. 5-4: The stability constant $\log_{10}K°$ for $Al(OH)_4^- + 2F^- \rightleftharpoons Al(OH)_2F_2^- + 2OH^-$ as a function of temperature in the range 45 – 300 °C

Solid line: unweighted regression of data reported by Tagirov et al. (2002a). Dotted lines: lower and upper limits using parameters given in the text and extrapolated to higher temperatures. Dashed line (hardly visible): temperature function reported by Tagirov et al. (2002a), shown for comparison.

Tagirov et al. (2002a) also tried alternative models to interpret their data, the formation of $Al(OH)_3F^-$ alone or the formation of both $Al(OH)_2F_2^-$ and $Al(OH)_3F^-$, and discuss the data of Couturier (1986). Tagirov et al. (2002a) conclude that "as the formation of $Al(OH)_3F^-$ is not certain, even at low temperatures we prefer to assume that $Al(OH)_2F_2^-$ was the only Al – F complex formed at all temperatures of this study". This review agrees with the conclusions of Tagirov et al. (2002a) and does not include any thermodynamic data for $Al(OH)_3F^-$ in TDB 2020.

Tagirov & Schott (2001) include in their aluminium speciation model two additional mixed Al fluoride hydroxide complexes, $Al(OH)_2F(aq)$ and $AlOHF_2(aq)$, whose stability constants were mainly calculated from corundum, $Al_2O_3(cr)$, solubility data in the temperature range 300 – 600 °C (Tagirov et al. 2002b).

Tagirov & Schott (2001) state that speciation calculations show that $Al(OH)_2F(aq)$ is the most important mixed Al fluoride hydroxide complex below 300 °C. However, experimental data for neutral Al-O-H-F mixed species are available only for higher temperatures (except for the potentiometric measurements of Couturier (1986) which unfortunately do not match the solubility data). Therefore, to minimize extrapolation errors and to check the aluminium speciation model built up in their study, Tagirov & Schott (2001) performed a series of gibbsite solubility measurements in HF solutions at 72 °C and the value of the apparent Gibbs free energy of $Al(OH)_2F(aq)$ calculated at 72 °C was included into their fit.

This review re-fitted the values reported for 25, 50, 100, 150, 200, 250 and 300 °C in Tab. B2 of Tagirov & Schott (2001) to a temperature function with constant $\Delta_r C_{p,m}°$(298.15 K):

$Al(OH)_4^- + HF(aq) \rightleftharpoons Al(OH)_2F(aq) + OH^- + H_2O(l)$

$\log_{10}K°$ (298.15 K) = 1.41 ± 0.15

$\Delta_r H_m°$(298.15 K) = -(14.7 ± 3.0) kJ · mol^{-1}

$\Delta_r C_{p,m}°$(298.15 K) = -(201 ± 27) J · K^{-1} · mol^{-1}

$Al(OH)_4^- + 2\ HF(aq) \rightleftharpoons AlOHF_2(aq) + OH^- + 2\ H_2O(l)$

$\log_{10}K°$ (298.15 K) = 2.63 ± 0.15

$\Delta_r H_m°$(298.15 K) = -(8.4 ± 2.9) kJ · mol^{-1}

$\Delta_r C_{p,m}°$(298.15 K) = -(192 ± 27) J · K^{-1} · mol^{-1}

Note that the maximum deviation of $\log_{10}K°$ derived from the above parameters compared with the original data in Tab. B2 of Tagirov & Schott (2001) does not exceed ± 0.04 log-units.

These values have been included in TDB 2020, together with the estimates

$\varepsilon(Al(OH)_2F(aq), NaCl) = (0.0 \pm 0.1)$ kg · mol^{-1}

$\varepsilon(AlOHF_2(aq), NaCl) = (0.0 \pm 0.1)$ kg · mol^{-1}

Couturier (1986) reports for $AlOH^{2+} + 2\ F^- \rightleftharpoons AlOHF_2(aq)$ the value $\log_{10}K$ (0.1 M KNO_3, 298.15 K) = 10.36 which is, extrapolated to zero ionic strength, $\log_{10}K°$ (298.15 K) = 11.0. Transforming the value reported by Tagirov & Schott (2001) for $AlOHF_2(aq)$ to the same equilibrium yields $\log_{10}K°$ (298.15 K) = 5.1, about six orders of magnitude at variance with the value of Couturier (1986). Hence, the values of Couturier (1986) for $AlOHF_2(aq)$ and $AlOHF^+$ are not retained by this review.

5.5.2 Aluminium(III) fluoride compounds

$AlF_3(s)$ is a soluble salt with a solubility of 5.59 g/L at 25 °C (gestis.itrust.de). Aside from anhydrous $AlF_3(s)$, a number of hydrates are known, $AlF_3 \cdot xH_2O(s)$ with x = 1, 3, 6 and 9. None of them has been found in nature as a mineral. They are of no relevance for environmental modelling and hence, no data have been included in TDB 2020.

Thermodynamic data are available for the mineral cryolite (Na_3AlF_6) (Nordstrom et al. 1990):

$Na_3AlF_6(s) \Leftrightarrow 3\ Na^+ + Al^{3+} + 6\ F^-$

$\log_{10}K_{s,0}°$ (cryolite, cr, 298.15 K) = -33.84

$\Delta_r H_m°$(cryolite, cr, 298.15 K) = 9.09 kcal · mol^{-1} = 38.03 kJ · mol^{-1}

However, as discussed by Hummel et al. (2002), cryolite may be of relevance only in extreme water compositions, characterised by high fluoride concentrations (above 10^{-3} mol · kg^{-1}), and the absence of fluorite, CaF_2(s). Hence, no data have been included in TDB 2020.

5.6 Aluminium(III) chloride compounds and complexes

5.6.1 Aluminium(III) chloride complexes

Aluminium chloride complexes are expected to be weak and it probably would be difficult to distinguish between complex formation and changes in the activity coefficients of the solutes.

In fact, Palmer et al. (2001) did not see any need to include aluminium chloride complexes in their solubility model of boehmite, AlOOH(s), based on their experimental solubility data up to 5 mol · kg^{-1} NaCl and up to 290 °C.

Hence, no experimental data on aluminium chloride complexation are available.

5.6.2 Aluminium(III) chloride compounds

$AlCl_3$(s), with a solubility of 450 g/L at 20 °C (gestis.itrust.de), and $AlCl_3 \cdot 6H_2O$ are highly soluble salts. Their isopiestic properties have been measured up to 2 mol · kg_{H2O}^{-1} (Robinson & Stokes 1959). Hence, no solubility data, but the specific ion interaction coefficient selected by NEA (Grenthe et al. 1992, Lemire et al. 2013) is adopted for TDB 2020:

$$\varepsilon(Al^{3+}, Cl^-) = (0.33 \pm 0.02) \text{ kg} \cdot \text{mol}^{-1}$$

5.7 Aluminium(III) carbonate compounds and complexes

No values for aluminium – carbonate complexes can be found in thermodynamic data compilations.

Nordstrom & May (1996) report that the only experimental study known to them can be interpreted by assuming the formation of polymeric aluminium – hydroxide – carbonate (and bicarbonate) species. Nordstrom & May (1996) conclude that the high pCO_2 and the difficulty of interpreting these results indicate that aluminium and carbonate or bicarbonate ions have very weak interactions that can be neglected for most natural waters.

$Al_2(CO_3)_3$(s) belongs to the class of "non-existing compounds".

However, aluminium – carbonate – hydroxide minerals are known ("basic aluminium carbonates"), for example the rare mineral dawsonite, $NaAlCO_3(OH)_2$(s). Bénézeth et al. (2007) report solubility measurements of dawsonite in the temperature range 50 – 200 °C and obtained:

$NaAlCO_3(OH)_2(cr) + 2\ H_2O(l) \rightleftharpoons Al(OH)_4^- + HCO_3^- + Na^+ + H^+$

$\Delta_r G_m°(298.15\ K) = 102.1\ kJ \cdot mol^{-1} \rightarrow \log_{10} K_{s4}°\ (298.15\ K) = -17.89$

$\Delta_r H_m°(298.15\ K) = 97.0\ kJ \cdot mol^{-1}$

$\Delta_r C_{p,m}°(298.15\ K) = -185.5\ J \cdot K^{-1} \cdot mol^{-1}$

Bénézeth et al. (2007) first calculated $\Delta_r C_{p,m}°(298.15\ K)$ from $C_{p,m}°$(dawsonite, cr, 298.15 K) = 142.6 ± 0.3 $J \cdot K^{-1} \cdot mol^{-1}$, measured by Ferrante et al. (1976), and the heat capacities of the aqueous species in the above equilibrium. Then, they made a constrained regression analysis of their solubility data and obtained $\Delta_r G_m°$ (298.15 K) and $\Delta_r H_m°(298.15\ K)$. Bénézeth et al. (2007) state that "the three parameters obtained from this regression allowed us to calculate the thermodynamic properties of dawsonite, providing refinements of the values derived by Ferrante et al. (1976) from calorimetric measurements".

Using the data

$Al^{3+} + 4\ H_2O(l) \rightleftharpoons Al(OH)_4^- + 4\ H^+$

$\log_{10}{}^*\beta_4°\ (298.15\ K) = -22.91 \pm 0.10$

$\Delta_r H_m°(298.15\ K) = (190.4 \pm 2.5)\ kJ \cdot mol^{-1}$

$\Delta_r C_{p,m}°(298.15\ K) = -(182 \pm 27)\ J \cdot K^{-1} \cdot mol^{-1}$

selected in this review (see Section 10.3.1) this review obtained

$NaAlCO_3(OH)_2(cr) + 3\ H^+ \rightleftharpoons Al^{3+} + HCO_3^- + Na^+ + 2\ H_2O(l)$

$\log_{10} K_{s0}°(298.15\ K) = 5.02 \pm 0.3$

$\Delta_r H_m°(298.15\ K) = -(93.4 \pm 7)\ kJ \cdot mol^{-1}$

$\Delta_r C_{p,m}°(298.15\ K) = -(3.5 \pm 30)\ J \cdot K^{-1} \cdot mol^{-1}$

These values are included in TDB 2020 as supplemental data.

The reasons for classifying the dawsonite data as "supplemental" are some doubts on the formation of dawsonite according to the above equilibria. Bénézeth et al. (2007) state that experimental dawsonite dissolution occurs via an incongruent pathway, favouring bayerite formation at temperatures ≤ 100 °C and boehmite formation at higher temperatures. Bayerite is the metastable (more soluble) form of $Al(OH)_3$(s), while gibbsite is the thermodynamically stable form at T ≤ 100 °C. Bénézeth et al. (2007) further state that their predominance diagrams suggest that dawsonite can be stable at alkaline down to slightly acidic pH values whereas silica-containing minerals will impose tight constraints on its formation. On the other hand, whereas dawsonite is by no means a common mineral, it is found in a number of localities. Bénézeth et al. (2007) conclude that these facts may imply that, in addition to simple thermodynamic considerations, nucleation and other kinetic processes may impose limitations on dawsonite precipitation.

The most important aluminium – carbonate – hydroxide mineral is hydrotalcite, $Mg_6Al_2(OH)_{16}CO_3 \cdot 4H_2O$(s). Its nickel analogue is takovite, $Ni_6Al_2(OH)_{16}CO_3 \cdot 4H_2O$(s).

Hydrotalcite and takovite are two endmembers of a vast group of solid-solutions called "layered double hydroxides". These solid-solution systems are important in cementitious waste forms and they are explored more generally in studies concerning the immobilisation of hazardous waste. No parameters characterising these solid-solution systems are included in TDB 2020.

5.8 Aluminium(III) sulphate compounds and complexes

5.8.1 Aluminium(III) sulphate complexes

Nordstrom et al. (1990) selected data for aluminium sulphate complexes which they claim to have taken from Nordstrom & May (1996):

$Al^{3+} + SO_4^{2-} \rightleftharpoons AlSO_4^+$

$\log_{10}\beta_1°$ (298.15 K) = 3.02

$\Delta_r H_m°$(298.15 K) = 2.15 kcal · mol^{-1} = 9.00 kJ · mol^{-1}

$Al^{3+} + 2\ SO_4^{2-} \rightleftharpoons Al(SO_4)_2^-$

$\log_{10}\beta_2°$ (298.15 K) = 4.92

$\Delta_r H_m°$(298.15 K) = 2.84 kcal · mol^{-1} = 11.88 kJ · mol^{-1}

Although the complexation of aluminium with sulphate is significantly weaker than with fluoride, it is strong enough to have an effect on potentiometric, conductance and spectroscopic measurements of aluminium sulphate solutions. However, evaluation of published data for aluminium sulphate stability constants revealed largely discrepant values (Nordstrom & May 1996, Ridley et al. 1999).

Nordstrom & May (1996) considered five published $\log_{10}\beta_1°$ (298.15 K) values which show a bimodal distribution suggesting that the value should be close to either 3.2 or 3.8. They selected the midpoint value, $\log_{10}\beta_1°$ (298.15 K) = 3.5 ± 0.5, "with an uncertainty that covers the range of better literature values". Nordstrom & May (1996) found only two measurements of $\log_{10}\beta_2°$ (298.15 K) that gave nearly identical values and state that the determinations of both values were not of high quality and need confirmation. They propose $\log_{10}\beta_2°$ (298.15 K) = 5.0 ± 0.5, which "should be adequate for most purposes of chemical modelling".

Nordstrom & May (1996) did not discuss any temperature data. So, what is the origin of the data selected by Nordstrom et al. (1990)?

Izatt et al. (1969) report calorimetrically determined $\log_{10}K°$ and $\Delta_r H_m°$ values for $Al^{3+} + SO_4^{2-} \rightleftharpoons AlSO_4^+$, $\log_{10}K_1°$ (298.15 K) = 3.01 ± 0.08 and $\Delta_r H_m°$(298.15 K) = 2.29 ± 0.08 kcal · mol^{-1}, and for $AlSO_4^+ + SO_4^{2-} \rightleftharpoons Al(SO_4)_2^-$, $\log_{10}K_2°$ (298.15 K) = 1.89 ± 0.10 and $\Delta_r H_m°$(298.15 K) = 0.78 ± 0.2 kcal · mol^{-1}. These values are close but not identical to the ones selected by Nordstrom et al. (1990). Hence, the source of the data given by Nordstrom et al. (1990) remains unclear.

This review considered results from the potentiometric studies of Nishide & Tsuchiya (1965) at 25 °C and Matsushima et al. (1988) in the temperature range 25 – 125 °C and the potentiometric and solubility study of Ridley et al. (1999) who measured aluminium sulphate complexation in 0.1, 0.2 and 1.0m NaCl media from 50 to 125 °C. By regression analyses of these data (Fig. 5-5) this review obtained:

$Al^{3+} + SO_4^{2-} \rightleftharpoons AlSO_4^+$

$\log_{10}K_1°$ (298.15 K) = 3.56 ± 0.20

$\Delta_r H_m°$(298.15 K) = -(10.7 ± 5.0) kJ · mol^{-1}

$\Delta_r C_{p,m}°$(298.15 K) = (1'180 ± 200) J · K^{-1} · mol^{-1}

$AlSO_4^+ + SO_4^{2-} \rightleftharpoons Al(SO_4)_2^-$

$\log_{10}K_2°$ (298.15 K) = 1.89 ± 0.20

$\Delta_r H_m°$(298.15 K) = -(12.8 ± 5.0) kJ · mol^{-1}

$\Delta_r C_{p,m}°$(298.15 K) = (1'100 ± 200) J · K^{-1} · mol^{-1}

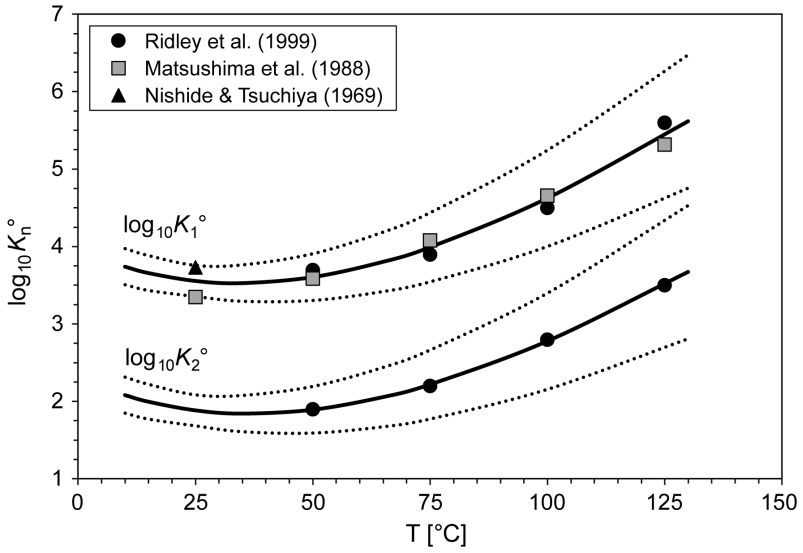

Fig. 5-5: The equilibrium constants $\log_{10}K_n°$ for $Al(SO_4)_{n-1}^{(5-2n)} + SO_4^{2-} \rightleftharpoons Al(SO_4)_n^{(3-2n)}$ as a function of temperature in the range 25 – 125 °C

Solid lines: unweighted regressions. Dotted lines: lower and upper limits using parameters given in the text and extrapolated to lower and higher temperatures.

These values are included in TDB 2020.

Using the $\log_{10}K_1$(323.15 K) data reported by Ridley et al. (1999) at 50 °C, a SIT analysis was performed, using A = 0.534 $kg^{-½} \cdot mol^{-½}$ in the Debye-Hückel term. The results are (Fig. 5-6):

$\log_{10}K_1°$ (323.15 K) = 3.69 ± 0.10

$\Delta\varepsilon$(NaCl) = -(0.16 ± 0.19)

Note that the $\log_{10}K_1°$ (323.15 K) value obtained by the SIT analysis is in perfect agreement with $\log_{10}K_1°$ (323.15 K) = 3.7 ± 0.4 reported by Ridley et al. (1999).

Using $\varepsilon(Al^{3+}, Cl^-)$ = (0.33 ± 0.02) kg · mol^{-1}, and $\varepsilon(Na^+, SO_4^{2-})$ = -(0.12 ± 0.05) kg · mol^{-1} this review calculated from the $\Delta\varepsilon$(NaCl) value, assuming that the temperature effects between 25 and 50 °C are within the assigned uncertainty:

$\varepsilon(AlSO_4^+, Cl^-)$ = (0.05 ± 0.20)

This value is included in TDB 2020.

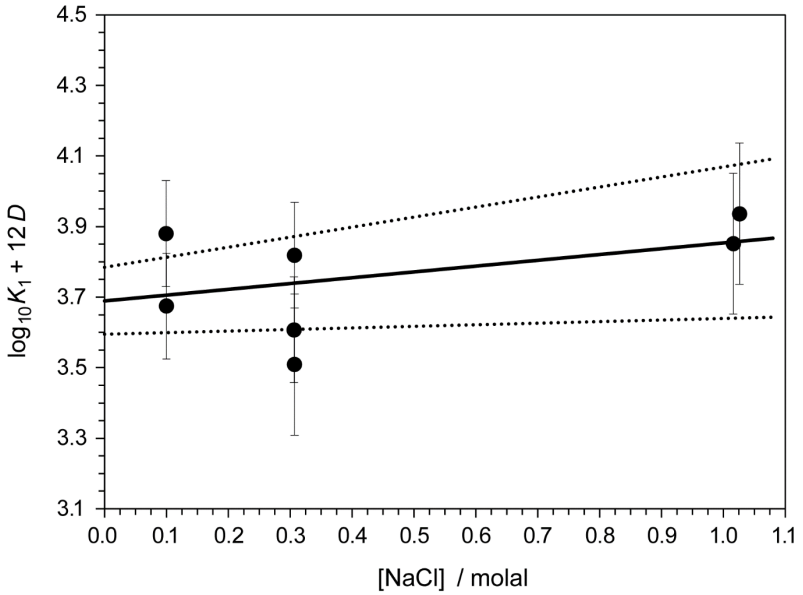

Fig. 5-6: Dependence of the equilibrium $Al^{3+} + SO_4^{2-} \rightleftharpoons AlSO_4^+$ on ionic strength in NaCl using the data reported by Ridley et al. (1999) at 50 °C

The solid line is obtained using the derived SIT interaction coefficient and stability constant at zero ionic strength. Dotted lines represent the 95% uncertainty range extrapolated from I = 0 to higher NaCl concentrations.

There are too few $\log_{10}K_2$(323.15 K) data reported by Ridley et al. (1999) at 50 °C for a SIT analysis and thus, the estimate

$\varepsilon(Al(SO_4)_2^-, Na^+)$ = -(0.05 ± 0.10) kg · mol^{-1}

is included in TDB 2020.

5.8.2 Aluminium(III) sulphate compounds

$Al_2(SO_4)_3(s)$, with a solubility of 360 g/L at 20 °C (gestis.itrust.de), and $Al_2(SO_4)_3 \cdot 18H_2O(s)$ are hygroscopic, highly soluble salts. They are of no relevance for environmental modelling.

Thermodynamic data are available for the rare mineral alunite, $KAl_3(SO_4)_2(OH)_6(s)$ (Nordstrom et al. 1990):

$$KAl_3(SO_4)_2(OH)_6(s) + 6\ H^+ \rightleftharpoons K^+ + 3\ Al^{3+} + 2\ SO_4^{2-} + 6\ H_2O(l)$$

$\log_{10}{}^*K_{s0}^\circ$ (alunite, cr, 298.15 K) = -1.4

$\Delta_r H_m^\circ$(Alunite, cr, 298.15 K) = -50.25 kcal $\cdot$ mol^{-1} = -210.25 kJ $\cdot$ mol^{-1}

The solubility constant of $KAl_3(SO_4)_2(OH)_6(s)$ indicates that alunite is a highly soluble salt. Combining its solubility constant with the hydrolysis constants of aluminium selected by this review (see Section 5.4.1), and assuming constant K^+ and SO_4^{2-} concentrations, reveals that the minimum solubility of alunite is expected at pH 5, with increasing solubility at lower and higher pH values. Hence, alunite may be of relevance only in acidic mine waters characterised by high concentrations of sulphuric acid.

Following our philosophy of ballast discharge, we decided not to include alunite in TDB 2020.

5.9 Selected aluminium data

Tab. 5-2: Selected aluminium data

Core data are in bold face.

Name	**$\Delta_f G_m°$** [kJ · mol^{-1}]	**$\Delta_f H_m°$** [kJ · mol^{-1}]	**$S_m°$** [J · K^{-1} · mol^{-1}]	**$C_{p,m}°$** [J · K^{-1} · mol^{-1}]	**Species**
Al(cr)	0.0	0.0	**28.300 ± 0.100**	**24.200 ± 0.070**	Al(cr)
Al+3	-487.2 ± 2.3	-539.4 ± 2.7	-342.8 ± 5.0	-96 ± 30	Al^{3+}

Name	**$\log_{10}\beta°$**	**$\Delta_r H_m°$** [kJ · mol^{-1}]	**$\Delta_r C_{p,m}°$** [J · K^{-1} · mol^{-1}]	**T-range** [°C]	**Reaction**
AlOH+2	-4.98 ± 0.02	56.0 ± 0.5	0	0 – 300	$Al^{3+} + H_2O(l) \rightleftharpoons AlOH^{2+} + H^+$
Al(OH)2+	-10.63 ± 0.02	110.8 ± 0.8	0	0 – 300	$Al^{3+} + 2\ H_2O(l) \rightleftharpoons Al(OH)_2^+ + 2\ H^+$
Al(OH)3(aq)	-15.99 ± 0.23	135.2 ± 2.1	0	25 – 300	$Al^{3+} + 3\ H_2O(l) \rightleftharpoons Al(OH)_3(aq) + 3\ H^+$
Al(OH)4-	-22.91 ± 0.10	190.4 ± 2.5	-182 ± 27	0 – 300	$Al^{3+} + 4\ H_2O(l) \rightleftharpoons Al(OH)_4^- + 4\ H^+$
Al2(OH)2+4	-7.62 ± 0.11	83.6 ± 4.9	0	25 – 150	$2\ Al^{3+} + 2\ H_2O(l) \rightleftharpoons Al_2(OH)_2^{4+} + 2\ H^+$
Al3(OH)4+5	-13.90 ± 0.12	146.3 ± 4.5	0	25 – 125	$3\ Al^{3+} + 4\ H_2O(l) \rightleftharpoons Al_3(OH)_4^{5+} + 4\ H^+$
Al13(OH)32+7	-100.03 ± 0.09	1255.8 ± 9.7	0	30 – 150	$13Al^{3+} + 32H_2O(l) \rightleftharpoons Al_{13}(OH)_{32}^{7+} + 32H^+$
AlF+2	7.08 ± 0.07	4.81 ± 0.2	-		$Al^{3+} + F^- \rightleftharpoons AlF^{2+}$
AlF2+	5.65 ± 0.08	3.26 ± 0.4	-		$AlF^{2+} + F^- \rightleftharpoons AlF_2^+$
AlF3(aq)	4.05 ± 0.11	0.79 ± 0.4	-		$AlF_2^+ + F^- \rightleftharpoons AlF_3(aq)$
AlF4-	2.51 ± 0.14	1.17 ± 0.4	-		$AlF_3(aq) + F^- \rightleftharpoons AlF_4^-$
AlF5-2	1.0 ± 0.2	-3.14 ± 0.4	-		$AlF_4^- + F^- \rightleftharpoons AlF_5^{2-}$
AlF6-3	0 ± 0.3	-6.5 ± 0.8	-		$AlF_5^{2-} + F^- \rightleftharpoons AlF_6^{3-}$
AlOHF2(aq)	2.63 ± 0.15	-8.4 ± 2.9	-192 ± 27	25 – 300	$Al(OH)_4^- + 2\ HF(aq) \rightleftharpoons AlOHF_2(aq) + OH^- + 2\ H_2O(l)$
Al(OH)2F(aq)	1.41 ± 0.15	-14.7 ± 3.0	-201 ± 27	25 – 300	$Al(OH)_4^- + HF(aq) \rightleftharpoons Al(OH)_2F(aq) + OH^- + H_2O(l)$
Al(OH)2F2-	-7.26 ± 0.15	75.2 ± 2.8	-216 ± 22	25 – 300	$Al(OH)_4^- + 2\ F^- \rightleftharpoons Al(OH)_2F_2^- + 2\ OH^-$
AlSO4+	3.56 ± 0.20	-10.7 ± 5.0	1'180 ± 200	25 – 125	$Al^{3+} + SO_4^{2-} \rightleftharpoons AlSO_4^+$
Al(SO4)2-	1.89 ± 0.20	-12.8 ± 5.0	1'100 ± 200	25 – 125	$AlSO4^+ + SO_4^{2-} \rightleftharpoons Al(SO_4)_2^-$
Al(cr)	85.35 ± 0.40	-539.4 ± 2.7	-		$Al(cr) \rightleftharpoons Al^{3+} + 3\ e^-$
Gibbsite	7.75 ± 0.08	-104.3 ± 2.3	0	0 – 100	$Al(OH)_3(cr) + 3\ H^+ \rightleftharpoons Al^{3+} + 3\ H_2O(l)$

Tab. 5-2: Cont.

Name	**$\log_{10}\beta°$**	**$\Delta_r H_m°$** [kJ · mol^{-1}]	**$\Delta_r C_{p,m}°$** [J · K^{-1} · mol^{-1}]	**T-range** [°C]	**Reaction**
Boehmite	9.4 ± 0.4	-148.5 ± 8.3	0	70 – 250	AlOOH(cr) + 3 H^+ ⇌ Al^{3+} + 2 H_2O(l)
Dawsonite	*5.02 ± 0.3*	*-93.4 ± 7*	*-3.5 ± 30*	*50 – 200*	*$NaAlCO_3(OH)_2(cr)$ + 3 H^+ ⇌ Al^{3+} + HCO_3^- + Na^+ + 2 $H_2O(l)$*

Tab. 5-3: Selected SIT ion interaction coefficients $\varepsilon_{j,k}$ [kg · mol^{-1}] for aluminium species

Data in bold face are taken from Lemire et al. (2013). Data in normal face are derived in this review. Data estimated according to charge correlations and taken from Tab. 1-7 are shaded.

j k → ↓	**Cl^-** $\varepsilon_{j,k}$ [kg · mol^{-1}]	**Na^+** $\varepsilon_{j,k}$ [kg · mol^{-1}]	**$Na^+ + Cl^-$** $\varepsilon_{j,k}$ [kg · mol^{-1}]
Al+3	**0.33 ± 0.02**	0	0
AlOH+2	0.15 ± 0.10	0	0
Al(OH)2+	0.05 ± 0.10	0	0
Al(OH)3(aq)	0	0	0.0 ± 0.1
Al(OH)4-	0	-0.05 ± 0.10	0
Al2(OH)2+4	0.36 ± 0.08	0	0
Al3(OH)4+5	0.51 ± 0.07	0	0
Al13(OH)32+7	1.21 ± 0.08	0	0
AlF+2	0.15 ± 0.10	0	0
AlF2+	0.05 ± 0.10	0	0
AlF3(aq)	0	0	0.0 ± 0.1
AlF4-	0	-0.05 ± 0.10	0
AlF5-2	0	-0.10 ± 0.10	0
AlF6-3	0	-0.15 ± 0.10	0
AlOHF2(aq)	0	0	0.0 ± 0.1
Al(OH)2F(aq)	0	0	0.0 ± 0.1
Al(OH)2F-2	0	-0.05 ± 0.10	0
AlSO4+	0.05 ± 0.20	0	0
Al(SO4)2-	0	-0.05 ± 0.10	0

5.10 References

Agarwal, R.P. & Moreno, E.C. (1971): Stability constants of aluminium fluoride complexes. Talanta, 18, 873-880.

Baumann, E.W. (1969): Determination of stability constants of hydrogen and aluminum fluorides with a fluoride-selective electrode. J. Inorg. Nucl. Chem., 31, 3155-3162.

Bénézeth, P. (1994): Etude expérimentale de la spéciation de l'aluminium at du gallium avec l'ion acétate en solution aqueuse. Thèse de l'Université Paul-Sabatier, Toulouse, (as cited by Bénézeth et al. 2001).

Bénézeth, P., Palmer, D.A., Anovitz, L.M. & Horita, J. (2007): Dawsonite synthesis and reevalution of its thermodynamic properties from solubility measurements: Implication for mineral trapping of CO_2. Geochim. Cosmochim. Acta, 71, 4438-4455.

Bénézeth, P., Palmer, D.A. & Wesolowski. D.J. (2001): Aqueous high temperature solubility studies. II. The solubility of boehmite at 0.03 m ionic strength as a function of temperature and pH as determined by in situ measurements. Geochim. Cosmochim. Acta, 65, 2097-2111.

Bourcier, W.L., Knauss, K.G. & Jackson, J.J. (1993): Aluminum hydrolysis constants to 250 °C from boehmite solubility measurements. Geochim. Cosmochim. Acta, 57, 747-762.

Brosset, C. & Orring, J. (1943): Studies on the consecutive formation of aluminium fluoride complexes. Svensk Kemisk Tidskrift, 55, 101-116.

Brown, P.L. & Ekberg, C. (2016): Hydrolysis of Metal Ions. Wiley-VCH Verlag GmbH & Co. KGaA, Weinheim, Germany, 917 pp.

Castet, S., Dandurand, J.-L., Schott, J. & Gout, R. (1993): Boehmite solubility and aqueous aluminium speciation in hydrothermal solutions (90 – 350 °C): Experimental study and modeling. Geochim. Cosmochim. Acta, 57, 4869-4884.

Couturier, Y. (1986): Contribution à l'étude des complexes mixtes de l'aluminium(III) avec les ions fluorure et hydroxyde. Bulletin de la Société Chimique de France, 171-177.

Cox, J.D., Wagman, D.D. & Medvedev, V.A. (1989): CODATA Key Values for Thermodynamics. Hemisphere Publishing, New York, 271 pp.

Ferrante, M.J., Stuve, J.M. & Richardson, D.W. (1976): Thermodynamic data for synthetic dawsonite. U.S. Bureau of Mines Report Investigation 8129, Washington D.C., 13pp. (as cited by Bénézeth et al. 2007).

Grenthe, I., Fuger, J., Konings, R.J.M., Lemire, R.J., Muller, A.B., Nguyen-Trung, C. & Wanner, H. (1992): Chemical Thermodynamics of Uranium. Chemical Thermodynamics, Vol. 1. North-Holland, Amsterdam, 715 pp.

Hummel, W., Berner, U., Curti, E., Pearson, F.J. & Thoenen, T. (2002): Nagra/PSI Chemical Thermodynamic Data Base 01/01. Nagra Technical Report NTB 02-16 and Universal Publishers, Parkland, Florida, 565 pp.

Izatt, R.M., Eatough, D., Christensen, J.J & Bartholomew, C.H. (1969): Calorimetrically determined log *K*, $\Delta H°$, and $\Delta S°$ values for the interaction of sulphate ion with several bi- and ter-valent metal ions. Journal of the Chemical Society A, 47-53.

Katorina, O.V., Masalovich, V.M. & Korobitsyn, A. S. (1982): Stability constants of aluminium fluoro-complexes. Russian Journal of Inorganic Chemistry, 27, 1566-1567.

King, E.L. & Gallagher, P.K. (1959): The thermodynamics of aluminum(III) fluoride complex ion reactions. The graphical evaluation of equilibrium quotients from ñ([x]). Journal of Physical Chemistry, 63, 1073-1076.

Latimer, W.M. & Jolly, W.L. (1953): Heats and entropies of successive steps in the formation of AlF_6^{---}. J. Amer. Chem. Soc., 75, 1548-1550.

Lemire, R.J., Berner, U., Musikas, C., Palmer, D.A., Taylor, P. & Tochiyama, O. (2013): Chemical Thermodynamics of Iron, Part 1. Chemical Thermodynamics, Vol. 13a. OECD Publications, Paris, France, 1082 pp.

Matsushima, Y., Matsunaga, A., Sakai, K. & Okuwaki, A. (1988): Potentiometric studies on sulfato complex of aluminium(III) in aqueous solution at elevated temperatures. Bulletin of the Chemical Society of Japan, 61, 4259-4263.

Nishide, T. & Tsuchiya, R. (1965): The formation of $Al^{3+} – SO_4^{2-}$ ion-pair in an aqueous solution of potassium aluminum alum. Bulletin of the Chemical Society of Japan, 38, 1398-1400.

Nordstrom, D.K. & May, H.M. (1996): Aqueous Equilibrium Data for Mononuclear Aluminium Species. In: Sposito, G. (ed.): The Environmental Chemistry of Aluminium. CRC Press, Lewis Publishers, Boca Raton, USA, 39-80.

Nordstrom, D.K., Plummer, L.N., Langmuir, D., Busenberg, E., May, H.M., Jones, B.F. & Parkhurst, D.L. (1990): Revised Chemical Equilibrium Data for Major Water-Mineral Reactions and Their Limitations. In: Melchior, D.C., and Bassett, R.L. (eds.): Chemical Modeling of Aqueous Systems II. Washington, D.C., American Chemical Society, ACS Symposium Series 416, p. 398-413.

Palmer, D.A., Bénézeth, P. & Wesolowski. D.J. (2001): Aqueous high temperature solubility studies. I. The solubility of boehmite as a function of ionic strength (to 5 molal, NaCl), temperature (100-290 °C), and pH as determined by in situ measurements. Geochim. Cosmochim. Acta, 65, 2081-2095.

Palmer, D.A. & Wesolowski, D.J. (1992): Aluminum speciation and equilibria in aqueous solution: II. The solubility of gibbsite in acidic sodium chloride solutions from 30 to 70 °C. Geochimica et Cosmochimica Acta, 56, 1093-1111.

Palmer, D.A. & Wesolowski, D.J. (1993): Aluminum speciation and equilibria in aqueous solution: III. Potentiometric determination of the first hydrolysis constant of aluminum(III) in sodium chloride solutions to 125 °C. Geochimica et Cosmochimica Acta, 57, 2929-2938.

Pearson, F.J., Jr. & Berner, U. (1991): Nagra Thermochemical Data Base I. Core Data. Nagra Technical Report NTB 91-17.

Pearson, F.J., Jr., Berner, U. & Hummel W. (1992): Nagra Thermochemical Data Base II. Supplemental Data 05/92. Nagra Technical Report NTB 91-18.

Pokrovskii, V.A. & Helgeson, H.C. (1995): Thermodynamic properties of aqueous species and the solubilities of minerals at high pressures and temperatures: The system Al_2O_3 - H_2O – NaCl. American Journal of Science, 295, 1255-1342.

Ridley, M.K., Wesolowski, D.J., Palmer, D.A. & Kettler, R.M. (1999): Association quotients of aluminium sulphate complexes in NaCl media from 50 to 125 °C: Results of a potentiometric and solubility study. Geochim. Cosmochim. Acta, 63, 459-472.

Robinson, R.A. & Stokes, R.H. (1959): Electrolyte Solutions. Second Revised Edition. Academic Press, New York, 559 pp.

Shock, E.L., Sassani, D.C., Willis, M. & Sverjensky, D.A. (1997): Inorganic species in geologic fluids: Correlations among standard molal thermodynamic properties of aqueous ions and hydroxide complexes. Geochimica et Cosmochimica Acta, 61, 907-950.

Tagirov, B. & Schott, J. (2001): Aluminum speciation in crustal fluids revisited. Geochimica et Cosmochimica Acta, 65, 3965-3992.

Tagirov, B., Schott, J. & Harrichoury, J.-C. (2002a): Experimental study of aluminium–fluoride complexation in near-neutral and alkaline solutions to 300 °C. Chemical Geology, 184, 310-310.

Tagirov, B., Schott, J., Harrichoury, J.-C. & Salvi, S. (2002b): Experimental study of aluminium speciation in fluoride–rich supercritical fluids. Geochimica et Cosmochimica Acta, 66, 2013-2024.

Tóth, I., Zékány, L. & Brücher, E. (1985): Comparative study of hydroxo-fluoro and hydroxo-sulphido mixed ligand complexes of aluminium(III) and gallium(III). Polyhedron, 4, 279-283.

Verdes, G., Gout, R. & Castet, S. (1992): Thermodynamic properties of the aluminate ion and of bayerite, boehmite, diaspore and gibbsite. European Journal of Mineralogy, 4, 767-792.

Wagman, D.D., Evans, W.H., Parker, V.B., Schumm, R.H., Halow, I., Bailey, S.M., Churney, K.L. & Nuttall, R.L. (1982): The NBS tables of chemical thermodynamic properties: Selected values for inorganic and C1 and C2 organic substances in SI units. Journal of Physical and Chemical Reference Data, 11, Supplement No. 2, 1-392.

Walker, J.B., Twine, C.R. & Choppin, G.R. (1971): Thermodynamic parameters of fluoride complexes of group IIIA ions. J. Inorg. Nucl. Chem., 33, 1813-1817.

Wells, C.F. & Davies, G. (1967): A spectroscopic investigation of the aquomanganese(III) ion in perchlorate media. Journal of the Chemical Society A, 1858-1861.

Wesolowski, D.J. (1992): Aluminum speciation and equilibria in aqueous solution: I. The solubility of gibbsite in the system Na-K-Cl-OH-$Al(OH)_4$ from 0 to 100 °C. Geochimica et Cosmochimica Acta, 56, 1065-1091.

Yuchi, A., Hotta, H., Wada, H. & Nakagawa, G. (1987): Mixed ligand complexes of trivalent metal ions with an amine-*n*-polycarboxylate and fluoride. Bull. Chem. Soc. Japan, 60, 1379-1382.

6 Americium

In a late state of the review work for TDB 2020 the NEA TDB Second Update on the Chemical Thermodynamics of Uranium, Neptunium, Plutonium, Americium and Technetium (Grenthe et al. 2020) became available to the reviewers. In the following, only changes with respect to previous TDB versions are shortly discussed. For a detailed discussion of the previous americium chemical thermodynamic data the reader is referred to Thoenen et al. (2014) and Hummel et al. (2002).

Note that Guillaumont et al. (2003) and Grenthe et al. (2020) used experimental data on Cm(III) in order to evaluate the thermodynamic data of Am(III) complexes. They have mainly used spectroscopic data for Cm(III) to select equilibrium constants for Am(III).

6.1 Elemental americium

From a review of low temperature heat capacity measurements Grenthe et al. (2020) selected

$$C_{p,m}°(\text{Am, cr, 298.15 K}) = (25.5 \pm 1.5)\ \text{J} \cdot \text{K}^{-1} \cdot \text{mol}^{-1}$$

This value has been included in TDB 2020.

6.2 Americium oxygen and hydrogen compounds and complexes

Equilibrium constants for the formation of three monomeric Am(III) hydrolysis species were first selected by Silva et al. (1995), and later updated by Guillaumont et al. (2003). Similar hydrolysis reactions have been proposed for both Am(III) and Cm(III). No new experimental hydrolysis data for Am(III) have been published and Grenthe et al. (2020) retain the thermodynamic constants selected by Guillaumont et al. (2003).

Rabung et al. (2008) used time-resolved laser fluorescence spectroscopy (TRLFS) to study Cm(III) solutions in 0.1 – 3.5 M $CaCl_2$ at pH 10.8 – 11.9 and identified ternary Ca-Cm(III)-OH complexes. They reported standard formation constants and ion interaction coefficients for $CaCm(OH)_3^{2+}$, $Ca_2Cm(OH)_4^{3+}$ and $Ca_3Cm(OH)_6^{3+}$ that were included as supplemental data in TDB Version 12/07. Grenthe et al. (2020) discuss the study of Rabung et al. (2008) but report their data "for information only". Hence, these values are retained in TDB 2020 as supplemental data.

6.3 Americium halogen complexes

Grenthe et al. (2020) report that there are no new studies of the thermodynamics of the Am(III)-fluoride system since the previous review. However, Skerencak et al. (2010) studied the complex formation of Cm(III) with fluoride by TRLFS across the temperature range 20 – 90 °C in 0.10 m $NaClO_4$ solution. The stepwise equilibrium constants for CmF^{2+} and CmF_2^{+} were extrapolated to $I = 0$ using SIT and the values obtained at 25 °C agree within the reported uncertainties with the values selected by Guillaumont et al. (2003). The selection by Guillaumont et al. (2003) was based on data reported for both Am(III) and Cm(III) in four independent experimental studies and has been retained by Grenthe et al. (2020).

The values of $\Delta_r H_m°$ for

$Cm^{3+} + F^- \rightleftharpoons CmF^{2+}$

$\Delta_r H_m° = (12.1 \pm 2.2)$ kJ · mol^{-1}

$CmF^{2+} + F^- \rightleftharpoons CmF_2^+$

$\Delta_r H_m° = (33.0 \pm 14.3)$ kJ · mol^{-1}

were calculated by Skerencak et al. (2010) from the temperature-dependence of the equilibrium constants. The stepwise stability constants show a linear correlation with the reciprocal temperature, i.e., the assumption $\Delta_r C_{p,m}° = 0$ is justified in the temperature range 20 – 90 °C (Fig. 6-1).

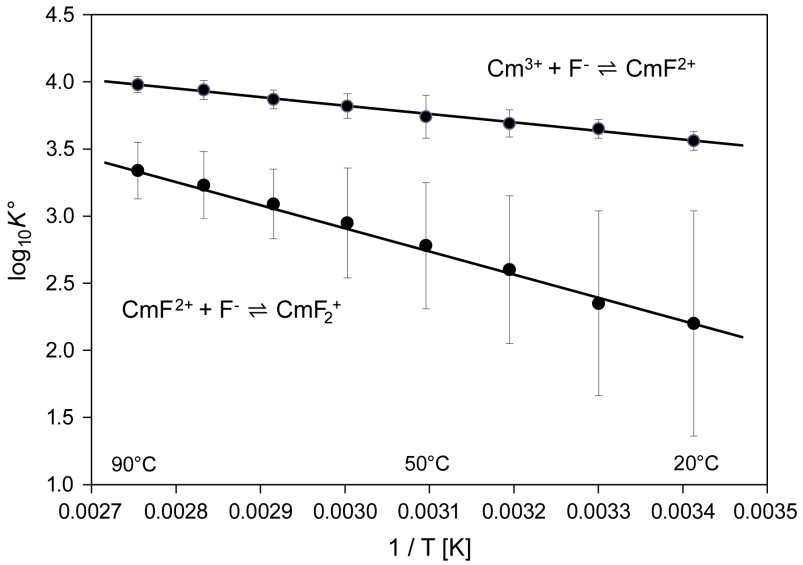

Fig. 6-1: The equilibrium constants $\log_{10}K°$ for $Cm^{3+} + F^- \rightleftharpoons CmF^{2+}$ and $CmF^{2+} + F^- \rightleftharpoons CmF_2^+$ as a function of reciprocal absolute temperature in the range 20 – 90 °C

Symbols: $\log_{10}K°$ values taken from Skerencak et al. (2010). Solid lines: calculated using $\log_{10}K_1°$ (298.15 K) = 3.60 ± 0.07, $\Delta_r H_m°$ (298.15 K) = (12.1 ± 2.2) kJ · mol^{-1} and $\log_{10}K_2°$ (298.15 K) = 2.3 ± 0.7, $\Delta_r H_m°$ (298.15 K) = (33.0 ± 14.3) kJ · mol^{-1}, respectively, as given by Skerencak et al. (2010).

The enthalpy data reported by Skerencak et al. (2010) for CmF^{2+} and CmF_2^+ are accepted by Grenthe et al. (2020) as estimates for the corresponding Am(III) complexes and they select:

$$Am^{3+} + F^- \rightleftharpoons AmF^{2+}$$

$$\Delta_r H_m^\circ = (12.1 \pm 2.2)\ kJ \cdot mol^{-1}$$

$$Am^{3+} + 2\ F^- \rightleftharpoons AmF_2^+$$

$$\Delta_r H_m^\circ = (45.1 \pm 14.5)\ kJ \cdot mol^{-1}$$

These values have been included in TDB 2020.

Skerencak-Frech et al. (2014) studied the Cm(III) chloride complexation at 50 – 200 °C by spectroscopy at chloride molality ranging from 0.5 – 4.0 m. In addition, they also studied the structure of Am(III) chloride complexes using EXAFS. Skerencak-Frech et al. (2014) note a strong increase in the stability of the chloride complexes with increasing temperature and that $CmCl_2^+$ is always the predominant complex and the only one for which an equilibrium constant can be obtained. By using SIT, the conditional equilibrium constants at the different ionic strengths were used by Skerencak-Frech et al. (2014) to obtain the equilibrium constant at zero ionic strength. From the temperature dependence of $\log_{10}\beta_2^\circ$ in the temperature range 100 – 200 °C, Skerencak-Frech et al. (2014) obtained:

$$Cm^{3+} + 2\ Cl^- \rightleftharpoons CmCl_2^+$$

$$\log_{10}\beta_2^\circ = -(0.81 \pm 0.35)$$

$$\Delta_r H_m^\circ = (54.9 \pm 4.5)\ kJ \cdot mol^{-1}$$

$$\Delta_r C_{p,m}^\circ = (40 \pm 10)\ J \cdot K^{-1} \cdot mol^{-1}$$

Grenthe et al. (2020) selected these values as reported by Skerencak-Frech et al. (2014), and used these data also for the Am(III)-chloride system. Note that the selected value for $\Delta_r C_{p,m}^\circ$ (Tab. 12-8 of Grenthe et al. 2020) for formal reasons is not included in their Tab. 6-2: Selected thermodynamic data for reactions involving americium compounds and complexes.

The temperature dependence of the experimental data of Skerencak-Frech et al. (2014) can be described even better by assuming $\Delta_r C_{p,m}^\circ = 0$ (dashed line in Fig. 6-2) than by using the reported value $\Delta_r C_{p,m}^\circ = (40 \pm 10)\ J \cdot K^{-1} \cdot mol^{-1}$ (solid line in Fig. 6-2). Hence, this review accepts the values for $\log_{10}\beta_2^\circ$ and $\Delta_r H_m^\circ$ as reported by Skerencak-Frech et al. (2014) and selected by Grenthe et al. (2020), but selects $\Delta_r C_{p,m}^\circ = 0$.

Grenthe et al. (2020) considered the uncertainty of $\log_{10}\beta_1^\circ$, estimated by Guillaumont et al. (2003), as too low and selected ± 0.35, given for $\log_{10}\beta_2^\circ$ by Skerencak-Frech et al. (2014), also for $\log_{10}\beta_1^\circ$. This enlarged uncertainty has been included in TDB 2020.

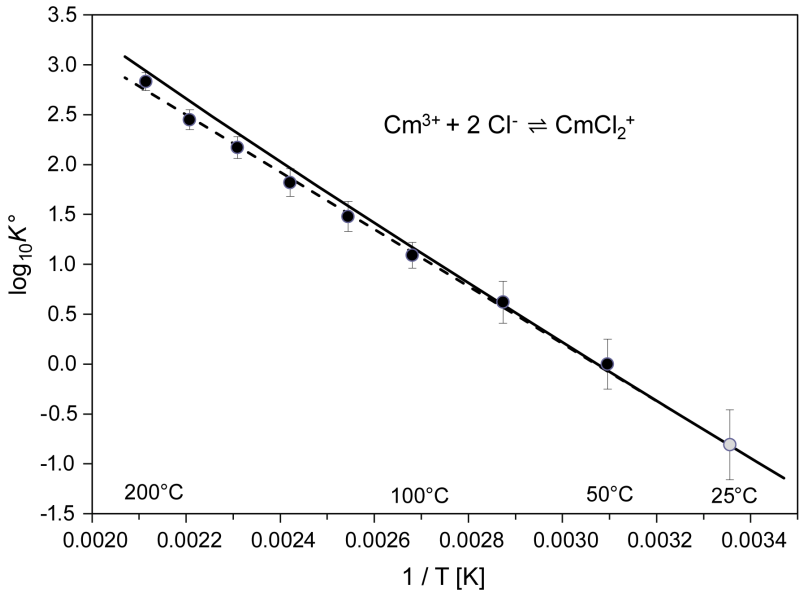

Fig. 6-2: The equilibrium constants $\log_{10}\beta_2°$ for $Cm^{3+} + 2Cl^- \rightleftharpoons CmCl_2^+$ as a function of reciprocal absolute temperature in the range 25 – 200 °C

Black symbols: Experimental data from Skerencak-Frech et al. (2014). Grey symbol: Value extrapolated by Skerencak-Frech et al. (2014). Solid line: calculated using $\log_{10}\beta_2° = -(0.80 \pm 0.35)$, $\Delta_r H_m° = (54.9 \pm 4.5)$ kJ · mol^{-1} and $\Delta_r C_{p,m}° = (40 \pm 10)$ J · K^{-1} · mol^{-1} as given by Skerencak-Frech et al. (2014). Dashed line: assuming $\Delta_r C_{p,m}° = 0$.

6.4 Americium sulphate complexes

Grenthe et al. (2020) considered equilibrium constants for the formation of Eu(III) (Vercouter et al. 2005) and Cm(III) (Skerencak et al. 2013) sulphate complexes determined from electro-spray mass spectroscopy and fluorescence spectroscopy. The Cm(III) studies have been made over the temperature range 25 – 200 °C and these data have been used by Skerencak et al. (2013) to obtain equilibrium constants, molar enthalpies and heat capacities of reaction.

Grenthe et al. (2020) state that they "have no basis to prefer one set of equilibrium constants to the other among the published data and have selected the average of the equilibrium constants for formation of $AmSO_4^+$ and $Am(SO_4)_2^-$, $\log_{10}\beta_1° = (3.50 \pm 0.30)$ and $\log_{10}\beta_2° = (5.0 \pm 1.0)$, respectively; both these values and their estimated uncertainty differ from previously selected values".

It is not entirely clear what average of what published data has been calculated by Grenthe et al. (2020), but re-calculations by this review indicate that Grenthe et al. (2020) calculated the weighted average of the Eu(III) data of Vercouter et al. (2005) and the Cm(III) of Skerencak et al. (2013), and assigned uncertainties such that the new values also cover the range of expectation of the previously selected values of Silva et al. (1995) and Guillaumont et al. (2003).

Grenthe et al. (2020) continue that they selected also the values of $\Delta_r H_m°$ and $\Delta_r C_{p,m}°$ reported by Skerencak et al. (2013) (their Tab. 12-9), noting that the heat capacity term becomes relevant only above 100 °C:

$Am^{3+} + SO_4^{2-} \rightleftharpoons AmSO_4^+$

$\log_{10}\beta_1° = (3.50 \pm 0.30)$

$\Delta_r H_m° = (40 \pm 4)$ kJ · mol^{-1}

$\Delta_r C_{p,m}° = (280 \pm 12)$ J · K^{-1} · mol^{-1}

$Am^{3+} + 2\ SO_4^{2-} \rightleftharpoons Am(SO_4)_2^-$

$\log_{10}\beta_2° = (5.0 \pm 1.0)$

$\Delta_r H_m° = (70 \pm 7)$ kJ · mol^{-1}

$\Delta_r C_{p,m}° = (430 \pm 19)$ J · K^{-1} · mol^{-1}

Note that the selected $\Delta_r C_{p,m}°$ values (Tab. 12-9 of Grenthe et al. 2020) for formal reasons are not included in their Tab. 6-2: Selected thermodynamic data for reactions involving americium compounds and complexes.

Furthermore, these $\Delta_r C_{p,m}°$ values cannot be used in speciation calculations as no $C_{p,m}°$ value is known for Am^{3+}, and consequently, no $C_{p,m}°$ values for $AmSO_4^+$ and $Am(SO_4)_2^-$ have been calculated by Grenthe et al. (2020). Hence, this review accepts the values for $\log_{10}\beta_n°$ and $\Delta_r H_m°$ as selected by Grenthe et al. (2020), but selects $\Delta_r C_{p,m}° = 0$, valid for the temperature range 25 – 100 °C (Fig. 6-3).

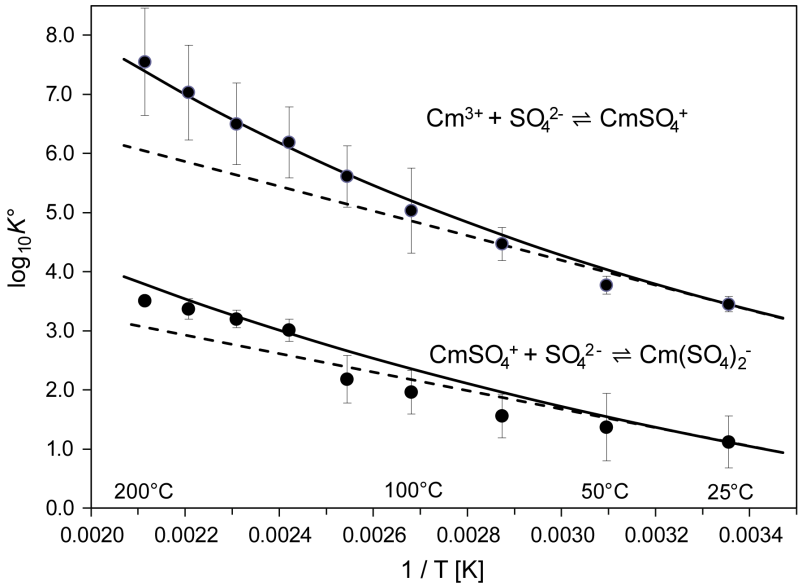

Fig. 6-3: The equilibrium constants $\log_{10}K°$ for $Cm^{3+} + SO_4^{2-} \rightleftharpoons CmSO_4^+$ and $CmSO_4^+ + SO_4^{2-} \rightleftharpoons Cm(SO_4)_2^-$ as a function of reciprocal absolute temperature in the range 25 – 200 °C

Symbols: $\log_{10}K°$ values taken from Skerencak et al. (2013). Solid lines: calculated using $\log_{10}K_1°$ (298.15 K) = 3.45 ± 0.13, $\Delta_r H_m°$ (298.15 K) = (40 ± 4) kJ · mol^{-1}, $\Delta_r C_{p,m}°$ = (280 ± 12) J · K^{-1} · mol^{-1} and $\log_{10}K_2°$ (298.15 K) = 1.12 ± 0.44, $\Delta_r H_m°$ (298.15 K) = (30 ± 6) kJ · mol^{-1}, $\Delta_r C_{p,m}°$ = (150 ± 15) J · K^{-1} · mol^{-1}, respectively, as given by Skerencak et al. (2013). Dashed lines: assuming $\Delta_r C_{p,m}° = 0$.

6.5 Americium nitrate and phosphate complexes

6.5.1 Americium nitrate complexes

Grenthe et al. (2020) discuss three new studies exploring the stability of the complexes $AmNO_3^{2+}$ and $CmNO_3^{2+}$ in the temperature ranges 10 – 85 °C, 5 – 85 °C and 5 – 200 °C, and finally select the thermodynamic data reported by Skerencak et al. (2009) for $CmNO_3^{2+}$ in the temperature range 5 – 200 °C as the more accurate ones because they cover a larger temperature range. Furthermore, Grenthe et al. (2020) find strong evidence for the formation of $Cm(NO_3)_2^{+}$ and also select the thermodynamic data reported by Skerencak et al. (2009):

$Cm^{3+} + NO_3^- \rightleftharpoons CmNO_3^{2+}$

$\log_{10}K_1° = (1.28 \pm 0.05)$

$\Delta_r H_m° = (1.8 \pm 1.0)\ kJ \cdot mol^{-1}$

$\Delta_r C_{p,m}° = (170 \pm 20)\ J \cdot K^{-1} \cdot mol^{-1}$

$CmNO_3^{2+} + NO_3^- \rightleftharpoons Cm(NO_3)_2^{+}$

$\log_{10}K_2° = -(0.40 \pm 0.10)$

$\Delta_r H_m° = (9.0 \pm 2.0)\ kJ \cdot mol^{-1}$

$\Delta_r C_{p,m}° = (80 \pm 30)\ J \cdot K^{-1} \cdot mol^{-1}$

Grenthe et al. (2020) used these data also for the Am(III)-nitrate system. Note that the selected $\Delta_r C_{p,m}°$ values (Tab. 12-12 of Grenthe et al. 2020) for formal reasons are not included in their Tab. 6-2: Selected thermodynamic data for reactions involving americium compounds and complexes.

Furthermore, these $\Delta_r C_{p,m}°$ values cannot be used in speciation calculations as no $C_{p,m}°$ value is known for Am^{3+}, and consequently, no $C_{p,m}°$ values for $AmNO_3^{2+}$ and $Am(NO_3)_2^{+}$ have been calculated by Grenthe et al. (2020).

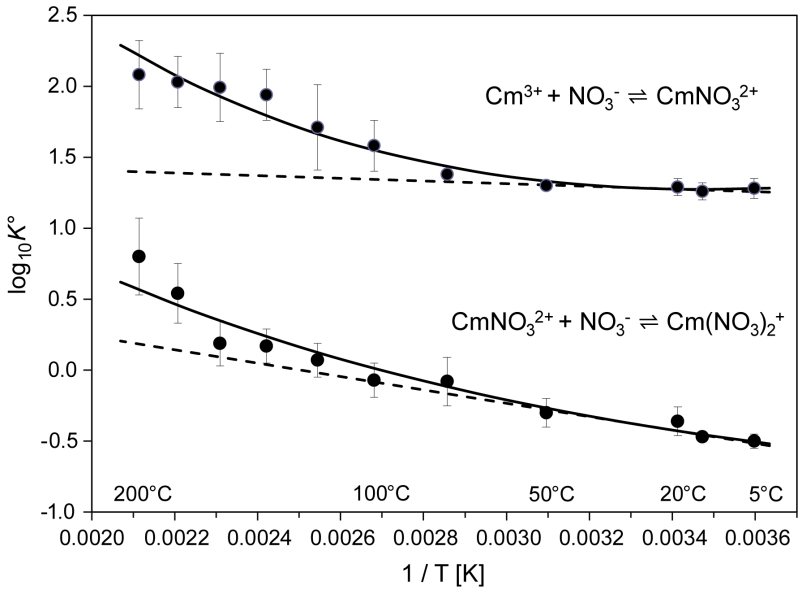

Fig. 6-4: The equilibrium constants $\log_{10}K°$ for $Cm^{3+} + NO_3^- \rightleftharpoons CmNO_3^{2+}$ and $CmNO_3^{2+} + NO_3^- \rightleftharpoons Cm(NO_3)_2^+$ as a function of reciprocal absolute temperature in the range 5 – 200 °C

Symbols: $\log_{10}K°$ values taken from Skerencak et al. (2009). Solid lines: calculated using $\log_{10}K_1°$ (298.15 K) = 1.28 ± 0.05, $\Delta_rH_m°$ (298.15 K) = (1.8 ± 1.0) kJ · mol^{-1}, $\Delta_rC_{p,m}°$ = (170 ± 20) J · K^{-1} · mol^{-1} and $\log_{10}K_2°$ (298.15 K) = -0.40 ± 0.10, $\Delta_rH_m°$ (298.15 K) = (9.0 ± 2.0) kJ · mol^{-1}, $\Delta_rC_{p,m}°$ = (80 ± 30) J · K^{-1} · mol^{-1}, respectively, as given by Skerencak et al. (2009). Dashed lines: assuming $\Delta_rC_{p,m}° = 0$.

Hence, this review accepts the values for $\log_{10}\beta_n°$ and $\Delta_rH_m°$ as selected by Grenthe et al. (2020) in their Tab. 6-2, but selects $\Delta_rC_{p,m}° = 0$, valid for the temperature range 5 – 80 °C (Fig. 6-4):

$Am^{3+} + NO_3^- \rightleftharpoons AmNO_3^{2+}$

$\log_{10}\beta_1° = (1.28 \pm 0.05)$

$\Delta_rH_m° = (1.8 \pm 1.0)$ kJ · mol^{-1}

$Am^{3+} + 2\ NO_3^- \rightleftharpoons Am(NO_3)_2^+$

$\log_{10}\beta_2° = (0.88 \pm 0.11)$

$\Delta_rH_m° = (10.8 \pm 2.2)$ kJ · mol^{-1}

These values have been included in TDB 2020, together with SIT estimates (Tab. 6-2) for $Am(NO_3)_2^+$ based on charge correlations (see Section 1.5.3).

6.5.2 Americium phosphate complexes

Grenthe et al. (2020) report that there is only one new experimental study on the interaction of Cm(III) with phosphate published since the previous reviews. Moll et al. (2011) investigated the Cm(III) phosphate complex formation in 0.1 M $NaClO_4$ solution using TRLFS at room temperature. This sensitive probe makes it possible to use small Cm(III) concentrations and thereby to avoid precipitation of insoluble Cm(III)-phosphate phases. Moll et al. (2011) report the formation of two complexes, $CmH_2PO_4^{2+}$ and $CmHPO_4^{+}$. Grenthe et al. (2020) consider

$$Cm^{3+} + H_2PO_4^{-} \rightleftharpoons CmH_2PO_4^{2+}$$

$$\log_{10}K^\circ = (2.46 \pm 0.13)$$

and state that this value is consistent within the rather large uncertainty ranges with the one selected in previous reviews, $\log_{10}K^\circ = (3.00 \pm 0.50)$, but the value reported by Moll et al. (2011) is based on a method that gives direct and more accurate information on the speciation in the system and for this reason Grenthe et al. (2020) select $\log_{10}K^\circ = (2.46 \pm 0.13)$**,** assuming that this value is a good approximation for the corresponding Am(III) complex.

This value has been included in TDB 2020.

Because of the large discrepancy in the reported constants and the possibility of precipitation of a Cm(III)-phosphate solid phase, Grenthe et al. (2020) do not select a value for the formation of the complex $CmHPO_4^{+}$, and the equilibrium constant reported by Moll et al. (2011) is given for information only:

$$Cm^{3+} + HPO_4^{2-} \rightleftharpoons CmHPO_4^{+}$$

$$\log_{10}K^\circ = (6.2 \pm 0.8)$$

This value has been included in TDB 2020 as supplemental datum, together with SIT estimates (Tab. 6.3) based on charge correlations (see Section 1.5.3).

6.6 Americium carbonate and silicate compounds and complexes

6.6.1 Americium carbonate compounds and complexes

After a somewhat opaque discussion, Grenthe et al. (2020) retain the equilibrium constant $\log_{10}\beta_3^\circ = (15.0 \pm 0.5)$, selected by Guillaumont et al. (2003) for $Am(CO_3)_3^{3-}$, but with a decreased uncertainty (instead of ± 1.0). This decreased uncertainty has been included in TDB 2020.

6.6.2 Americium silicate compounds and complexes

Americium silicate compounds and complexes are discussed in Section 25.5.

6.7 Selected americium data

Tab. 6-1: Selected americium data

All data included in TDB 2020 are taken from Silva et al. (1995), Guillaumont et al. (2003) and Grenthe et al. (2020), except where marked with an asterisk (*). The latter data were taken unchanged from Thoenen et al. (2014). Supplemental data are given in italics. New or changed data with respect to TDB Version 12/07 (Thoenen et al. 2014) are shaded.

Name	Redox	TDB Version 12/07				TDB 2020				
		$\Delta_f G_m°$ [kJ · mol^{-1}]	$\Delta_f H_m°$ [kJ · mol^{-1}]	$S_m°$ [J · K^{-1} · mol^{-1}]	$C_{p,m}°$ [J · K^{-1} · mol^{-1}]	$\Delta_f G_m°$ [kJ · mol^{-1}]	$\Delta_f H_m°$ [kJ · mol^{-1}]	$S_m°$ [J · K^{-1} · mol^{-1}]	$C_{p,m}°$ [J · K^{-1} · mol^{-1}]	Species
Am(cr)	0	0	0	55.4 ± 2.0	-	0	0	55.4 ± 2.0	25.5 ± 1.5	Am(cr)
Am+3	III	-598.7 ± 4.8	-616.7 ± 1.5	-201 ± 15	-	-598.7 ± 4.8	-616.7 ± 1.5	-201 ± 15	-	Am^{3+}
AmO2+	V	(-732.4 ± 6.3)*	-804.3 ± 5.4	(-45.9 ± 10.7)*	-	(-732.4 ± 6.3)*	-804.3 ± 5.4	(-45.9 ± 10.7)*	-	AmO_2^+

Name	Redox	TBD Version 12/07		TBD 2020				
		$\log_{10}\beta°$	$\Delta_r H_m°$ [kJ · mol^{-1}]	$\log_{10}\beta°$	$\Delta_r H_m°$ [kJ · mol^{-1}]	$\Delta_r C_{p,m}°$ [J · K^{-1} · mol^{-1}]	T-range [°C]	Reaction
AmO2+	III/V	(-59.7 ± 1.4)*	384.1 ± 5.2	(-59.7 ± 1.4)*	384.1 ± 5.2	-		$Am^{3+} + 2\ H_2O(l) \rightleftharpoons AmO_2^+ + 4\ H^+ + 2\ e^-$
AmO2OH(aq)	V	(-11.3 ± 0.7) [c]	-	(-11.3 ± 0.7) [c]	-	-		$AmO_2^+ + H_2O(l) \rightleftharpoons AmO_2OH(aq) + H^+$
AmO2(OH)2-	V	(-23.6 ± 0.5) [c]	-	(-23.6 ± 0.5) [c]	-	-		$AmO_2^+ + 2\ H_2O(l) \rightleftharpoons AmO_2(OH)_2^- + 2\ H^+$
AmO2CO3-	V	5.1 ± 0.5	-	5.1 ± 0.5	-	-		$AmO_2^+ + CO_3^{2-} \rightleftharpoons AmO_2CO_3^-$
AmO2(CO3)2-3	V	6.7 ± 0.8	-	6.7 ± 0.8	-	-		$AmO_2^+ + 2\ CO_3^{2-} \rightleftharpoons AmO_2(CO_3)_2^{3-}$
AmO2(CO3)3-5	V	5.1 ± 1.0	-	5.1 ± 1.0	-	-		$AmO_2^+ + 3\ CO_3^{2-} \rightleftharpoons AmO_2(CO_3)_3^{5-}$
AmOH+2	III	(-7.2 ± 0.5) [a]	-	(-7.2 ± 0.5) [a]	-	-		$Am^{3+} + H_2O(l) \rightleftharpoons AmOH^{2+} + H^+$
Am(OH)2+	III	(-15.1 ± 0.7) [a]	-	(-15.1 ± 0.7) [a]	-	-		$Am^{3+} + 2\ H_2O(l) \rightleftharpoons Am(OH)_2^+ + 2\ H^+$
Am(OH)3(aq)	III	(-26.2 ± 0.5) [a]	-	(-26.2 ± 0.5) [a]	-	-		$Am^{3+} + 3\ H_2O(l) \rightleftharpoons Am(OH)_3(aq) + 3\ H^+$
CaAm(OH)3+2	III	*(-26.3 ± 0.5)* [*,b]	-	*(-26.3 ± 0.5)* [b]	-	-		*$Ca^{2+} + Am^{3+} + 3\ H_2O(l) \rightleftharpoons CaAm(OH)_3^{2+} + 3\ H^+$*
Ca2Am(OH)4+3	III	*(-37.2 ± 0.6)* [*,b]	-	*(-37.2 ± 0.6)* [b]	-	-		*$2\ Ca^{2+} + Am^{3+} + 4\ H_2O(l) \rightleftharpoons Ca_2Am(OH)_4^{3+} + 4\ H^+$*
Ca3Am(OH)6+3	III	*(-60.7 ± 0.5)* [*,b]	-	*(-60.7 ± 0.5)* [b]	-	-		*$3\ Ca^{2+} + Am^{3+} + 6\ H_2O(l) \rightleftharpoons Ca_3Am(OH)_6^{3+} + 6\ H^+$*
AmF+2	III	(3.4 ± 0.3) [a]	-	(3.4 ± 0.3) [a]	(12.1 ± 2.2) [b]	0	20 – 90	$Am^{3+} + F^- \rightleftharpoons AmF^{2+}$
AmF2+	III	5.8 ± 0.2	-	5.8 ± 0.2	(45.1 ± 14.5) [b]	0	20 – 90	$Am^{3+} + 2\ F^- \rightleftharpoons AmF_2^+$
AmCl+2	III	(0.24 ± 0.03) [a]	-	(0.24 ± 0.35) [a]	-	-		$Am^{3+} + Cl^- \rightleftharpoons AmCl^{2+}$
AmCl2+	III	(-0.74 ± 0.05) [a]	-	(-0.81 ± 0.35) [b]	(54.9 ± 4.5) [b]	0	25 – 200	$Am^{3+} + 2\ Cl^- \rightleftharpoons AmCl_2^+$
AmSO4+	III	(3.30 ± 0.15) [b]	-	(3.50 ± 0.30) [d]	(40 ± 4) [b]	0	25 - 100	$Am^{3+} + SO_4^{2-} \rightleftharpoons AmSO_4^+$
Am(SO4)2-	III	(3.70 ± 0.15) [b]	-	(5.0 ± 1.0) [d]	(70 ± 7) [b]	0	25 - 100	$Am^{3+} + 2\ SO_4^{2-} \rightleftharpoons Am(SO_4)_2^-$

Tab. 6-1: Cont.

Name	Redox	TBD Version 12/07		TBD 2020				
		$\log_{10}\beta°$	$\Delta_r H_m°$ [kJ · mol^{-1}]	$\log_{10}\beta°$	$\Delta_r H_m°$ [kJ · mol^{-1}]	$\Delta_r C_{p,m}°$ [J · K^{-1} · mol^{-1}]	T-range [°C]	Reaction
AmNO3+2	III	1.33 ± 0.20	-	(1.28 ± 0.05) [b]	(1.8 ± 1.0) [b]	0	5 – 80	$Am^{3+} + NO_3^- \rightleftharpoons AmNO_3^{2+}$
Am(NO3)2+	III	-	-	(0.88 ± 0.11) [b]	(10.8 ± 2.2) [b]	0	5 – 80	$Am^{3+} + 2\ NO_3^- \rightleftharpoons Am(NO_3)_2^+$
AmH2PO4+2	III	3.0 ± 0.5	-	(2.46 ± 0.13) [b]	-	-		$Am^{3+} + H_2PO_4^- \rightleftharpoons AmH_2PO_4^{2+}$
$AmHPO_4^+$	III	-	-	*(6.2 ± 0.8)* [b]	-	-		*$Am^{3+} + HPO_4^{2-} \rightleftharpoons AmHPO_4^+$*
AmCO3+	III	(8.0 ± 0.4) [a]	-	(8.0 ± 0.4) [a]	-	-		$Am^{3+} + CO_3^{2-} \rightleftharpoons AmCO_3^+$
Am(CO3)2-	III	(12.9 ± 0.4) [a]	-	(12.9 ± 0.4) [a]	-	-		$Am^{3+} + 2\ CO_3^{2-} \rightleftharpoons Am(CO_3)_2^-$
Am(CO3)3-3	III	(15.0 ± 1.0) [a]	-	(15.0 ± 0.5) [a]	-	-		$Am^{3+} + 3\ CO_3^{2-} \rightleftharpoons Am(CO_3)_3^{3-}$
AmHCO3+2	III	(3.1 ± 0.3) [b]	-	(3.1 ± 0.3) [b]	-	-		$Am^{3+} + HCO_3^- \rightleftharpoons AmHCO_3^{2+}$
AmSCN+2	III	1.3 ± 0.3	-	1.3 ± 0.3	-	-		$Am^{3+} + SCN^- \rightleftharpoons AmSCN^{2+}$

[a] Formation constant is based on combined Am and Cm data
[b] Constant is based on Cm data only
[c] Recommended by Guillaumont et al. (2003) as reasonable estimate
[d] Formation constant is based on combined Eu and Cm data

Name	Redox	TBD Version 12/07		TBD 2020		
		$\log_{10}K_{s,0}°$	$\Delta_r H_m°$ [kJ · mol^{-1}]	$\log_{10}K_{s,0}°$	$\Delta_r H_m°$ [kJ · mol^{-1}]	Reaction
AmO2OH(am)	V	5.3 ± 0.5	-	5.3 ± 0.5	-	$AmO_2OH(am) + H^+ \rightleftharpoons AmO_2^+ + H_2O(l)$
NaAmO2CO3(s)	V	-10.9 ± 0.4	-	-10.9 ± 0.4	-	$NaAmO_2CO_3(s) \rightleftharpoons Na^+ + AmO_2^+ + CO_3^{2-}$
Am(OH)3(cr)	III	15.6 ± 0.6	-	15.6 ± 0.6	-	$Am(OH)_3(cr) + 3\ H^+ \rightleftharpoons Am^{3+} + 3\ H_2O(l)$
Am(OH)3(am)	III	16.9 ± 0.8	-	16.9 ± 0.8	-	$Am(OH)_3(am) + 3\ H^+ \rightleftharpoons Am^{3+} + 3\ H_2O(l)$
AmOHCO3:0.5H2O(cr)	III	-22.4 ± 0.5	-	-22.4 ± 0.5	-	$AmOHCO_3 \cdot 0.5\ H_2O(cr) \rightleftharpoons Am^{3+} + OH^- + CO_3^{2-} + 0.5\ H_2O(l)$
AmOHCO3(am, hyd)	III	-20.2 ± 1.0	-	-20.2 ± 1.0	-	$AmOHCO_3(am, hyd) \rightleftharpoons Am^{3+} + OH^- + CO_3^{2-}$
Am(CO3)1.5(am, hyd) [a]	III	-16.7 ± 1.1	-	-16.7 ± 1.1	-	$0.5\ Am_2(CO_3)_3(am, hyd) \rightleftharpoons Am^{3+} + 1.5\ CO_3^{2-}$
NaAm(CO3)2:5H2O(cr)	III	-21.0 ± 0.5	-	-21.0 ± 0.5	-	$NaAm(CO_3)_2 \cdot 5H_2O(cr) \rightleftharpoons Na^+ + Am^{3+} + 2\ CO_3^{2-} + 5\ H_2O(l)$

[a] This phase is referred to as Am(CO3)1.5(cr) in TDB Version 01/01, and as $Am_2(CO_3)_3 \cdot xH_2O$ (am) by Guillaumont et al. (2003).

Tab. 6-2: Selected SIT ion interaction coefficients $\varepsilon_{j,k}$ [kg · mol^{-1}] for americium species

The data included in TDB 2020 are taken from Silva et al. (1995), Guillaumont et al. (2003) and Grenthe et al. (2020) unless indicated otherwise. Own data estimates based on charge correlations (see Section 1.5.3) are shaded.

j k → ↓	**Cl^-** $\varepsilon_{j,k}$ [kg · mol^{-1}]	**ClO_4^-** $\varepsilon_{j,k}$ [kg · mol^{-1}]	**NO_3^-** $\varepsilon_{j,k}$ [kg · mol^{-1}]	**Li^+** $\varepsilon_{j,k}$ [kg · mol^{-1}]	**Na^+** $\varepsilon_{j,k}$ [kg · mol^{-1}]	**K^+** $\varepsilon_{j,k}$ [kg · mol^{-1}]
Am+3	0.23 ± 0.02	0.49 ± 0.03	-	0	0	0
AmO2+	(0.09 ± 0.05) [a,b]	(0.25 ± 0.05) [b,e]	-	0	0	0
AmO2OH(aq)	0	0	0	0	0	0
AmO2(OH)2-	0	0	0	-	(-0.01 ± 0.07) [b,e]	-
AmO2CO3-	0	0	0	-	(-0.18 ± 0.15) [b,e]	-
AmO2(CO3)2-3	0	0	0	-	(-0.33 ± 0.17) [b,e]	-
AmO2(CO3)3-5	0	0	0	-	(-0.53 ± 0.19) [b,e]	(-0.22 ± 0.03) [b,e]
AmOH+2	-0.04 ± 0.07	(0.39 ± 0.10) [f]	-	0	0	0
Am(OH)2+	-0.27 ± 0.20	(0.17 ± 0.10) [f]	-	0	0	0
Am(OH)3(aq)	0	0	0	0	0	0
CaAm(OH)3+2	*(0.05 ± 0.04)* [c]	*0.4 ± 0.1*	-	*0*	*0*	*0*
Ca2Am(OH)4+3	*(0.29 ± 0.07)* [c]	*0.6 ± 0.1*	-	*0*	*0*	*0*
Ca3Am(OH)6+3	*(0.00 ± 0.06)* [c]	*0.6 ± 0.1*	-	*0*	*0*	*0*
AmF+2	0.15 ± 0.10	(0.39 ± 0.10) [f]	-	0	0	0
AmF2+	0.05 ± 0.10	(0.17 ± 0.10) [f]	-	0	0	0
AmCl+2	0.15 ± 0.10	(0.39 ± 0.10) [f]	-	0	0	0
AmCl2+	0.05 ± 0.10	(0.17 ± 0.10) [f,g]	-	0	0	0
AmSO4+	0.05 ± 0.10	0.22 ± 0.08	-	0	0	0
Am(SO4)2-	0	0	0	-	-0.05 ± 0.05	-
AmNO3+2	0.15 ± 0.10	(0.39 ± 0.10) [f]	-	0	0	0
Am(NO3)2+	0.05 ± 0.10	0.2 ± 0.1	-	0	0	0
AmH2PO4+2	0.15 ± 0.10	(0.39 ± 0.10) [f]	-	0	0	0
AmHPO4+	*0.05 ± 0.10*	*0.2 ± 0.1*	-	*0*	*0*	*0*
AmCO3+	0.01 ± 0.05	(0.17 ± 0.10) [f]	-	0	0	0
Am(CO3)2-	0	0	0	-	-0.14 ± 0.06	-
Am(CO3)3-3	0	0	0	-	-0.23 ± 0.07	-
AmHCO3+2	(0.16 ± 0.10) [a,d,f]	0.4 ± 0.1	-	0	0	0
AmSCN+2	0.15 ± 0.10	(0.39 ± 0.10) [f]	-	0	0	0

[a] Value discussed by Guillaumont et al. (2003) but not listed in their Tab. B-4
[b] Value taken from analogous Np(V) species or complex
[c] Value taken from analogous Cm(III) complex (Rabung et al. 2008)
[d] Value taken from analogous Cm(III) complex
[e] Thoenen et al. (2014)
[f] Increased error
[g] Value selected by Silva et al. (1995) but omitted in all further NEA-reviews

6.8 References

Grenthe, I., Gaona, X., Plyasunov, A.V., Rao, L., Runde, W.H., Grambow, B., Konings, R.J.M., Smith, A.L. & Moore, E.E. (2020): Second Update on the Chemical Thermodynamics of Uranium, Neptunium, Plutonium, Americium and Technetium. Chemical Thermodynamics, Vol. 14. OECD Publications, Paris, France, 1503 pp.

Guillaumont, R., Fanghänel, T., Fuger, J., Grenthe, I., Neck, V., Palmer, D.A. & Rand, M.H. (2003): Update on the Chemical Thermodynamics of Uranium, Neptunium, Plutonium, Americium and Technetium. Chemical Thermodynamics, Vol. 5. Elsevier, Amsterdam, 919 pp.

Hummel, W., Berner, U., Curti, E., Pearson, F.J. & Thoenen, T. (2002): Nagra/PSI Chemical Thermodynamic Data Base 01/01. Nagra Technical Report NTB 02-16.

Moll, H., Brendler, V. & Bernhard, G. (2011): Aqueous curium(III) phosphate species characterized by time-resolved laser-induced fluorescence spectroscopy. Radiochim. Acta, 99, 775-782.

Rabung, T., Altmaier, M., Neck, V. & Fanghänel, T. (2008): A TRLFS study of Cm(III) hydroxide complexes in alkaline $CaCl_2$ solutions. Radiochim. Acta, 96, 551-559.

Silva, R.J., Bidoglio, G., Rand, M.H., Robouch, P.B., Wanner, H. & Puigdomènech, I. (1995): Chemical Thermodynamics of Americium. Chemical Thermodynamics, Vol. 2. Elsevier, Amsterdam, 374 pp.

Skerencak, A., Panak, P.J. & Fanghänel, T. (2013): Complexation and thermodynamics of Cm(III) at high temperatures: the formation of $[Cm(SO_4)_n]^{3-2n}$ (n = 1, 2, 3) complexes at T = 25 to 200 °C. Dalton Trans., 42, 542-549.

Skerencak, A., Panak, P.J., Hauser, W., Neck, V., Klenze, R., Lindqvist-Reis, P. & Fanghänel, T. (2009): TRLFS study on the complexation of Cm(III) with nitrate in the temperature range from 5 to 200 °C. Radiochim. Acta, 97, 385-393.

Skerencak, A., Panak, P.J., Neck, V., Trumm, M., Schimmelpfennig, B., Lindqvist-Reis, P., Klenze, R. & Fanghänel, T. (2010): Complexation of Cm(III) with fluoride in aqueous solution in the temperature range from 20 to 90 °C. A joint TRLFS and quantum chemical study. J. Phys. Chem. B, 114, 15626-15634.

Skerencak-Frech, A., Fröhlich, D.R., Rothe, J., Dardenne, K. & Panak, P.J. (2014): Combined time-resolved laser fluorescence spectroscopy and extended X-ray absorption fine structure spectroscopy study on the complexation of trivalent actinides with chloride at T = 25 – 200 °C. Inorg. Chem., 53, 1062-1069.

Thoenen, T., Hummel, W., Berner, U. & Curti, E. (2014): The PSI/Nagra Chemical Thermodynamic Database 12/07. Technical Report, PSI Bericht Nr. 14-04, Paul Scherrer Institut, Villigen, Switzerland, 416 pp.

Vercouter, T., Amekraz, B., Moulin, C., Giffaut, E. & Vitorge, P. (2005): Sulfate complexation of trivalent lanthanides probed by nanoelectrospray mass spectrometry and time-resolved laser-induced luminescence. Inorg. Chem., 44, (2005), 7570-7581.

7 Cadmium

7.1 Introduction

Many cadmium compounds and complexes are toxic and thus, cadmium is an environmentally significant heavy metal. Cadmium is included in assessments of human health issues arising from the potential release of chemotoxic substances from a geological disposal facility for radioactive waste (Wilson et al. 2011). This fact triggered the inclusion of cadmium into the PSI Chemical Thermodynamic Database 2020 (PSI TDB 2020).

The only stable oxidation state of cadmium in aqueous solution is Cd(II).

The thermodynamic data included into the PSI TDB 2020 have been taken from

- CODATA key values (Cox et al. 1989)
- an IUPAC review of Cd^{2+} + OH^-, Cl^-, CO_3^{2-}, SO_4^{2-} and PO_4^{3-} aqueous systems (Powell et al. 2011)
- the recent review of the hydrolysis of metal ions (Brown & Ekberg 2016)
- and own reviews of experimental data concerning the CdS(s) – H_2S – water system

The selected thermodynamic data for cadmium compounds and complexes are presented in Tab. 7-1.

Hagemann (2012) provides Pitzer coefficients and solubility products of highly soluble Cd chloride and sulphate salts derived from own experimental data in highly saline solutions. None of these data are included in TDB 2020.

IUPAC, as well as NEA (see, e.g., Grenthe et al. 1992) used the specific ion interaction theory (SIT) for making ionic strength corrections to the experimental data, an approach which is also adopted for TDB 2020 (as has been for all its predecessors). Powell et al. (2011) only evaluated experiments in perchlorate media and explicitly considered the formation of cadmium chloride complexes. Therefore, ion interaction coefficients ε for cationic cadmium species with Cl^- are missing. They can be approximated by the corresponding interaction coefficients with ClO_4^-. Thus, e.g., $\varepsilon(Cd^{2+}, Cl^-) \approx \varepsilon(Cd^{2+}, ClO_4^-) = (0.23 \pm 0.04)$ kg · mol^{-1}.

In some cases, the ion interaction coefficients of cadmium species were not available. We approximated these with the estimation method described in Section 1.5.3, which draws on a statistical analysis of published SIT ion interaction coefficients and which allows the estimation of missing coefficients for the interaction of cations with Cl^- and ClO_4^-, and for the interaction of anions with Na^+, from the charge of the cations or anions of interest.

The selected SIT ion interaction coefficients for cadmium species are presented in Tab. 7-2.

7.2 Elemental cadmium

Cadmium metal and gas are not relevant under environmental conditions. Hence, the gas phase Cdg is not included in the data base. The absolute entropy and heat capacity of Cd(cr) are included as they are used for the calculation of certain thermodynamic reaction properties.

The selected values for Cd(cr) are taken from CODATA (Cox et al. 1989):

$$S_m°(\text{Cd, cr, 298.15 K}) = (51.800 \pm 0.150)\ \text{J} \cdot \text{K}^{-1} \cdot \text{mol}^{-1}$$

$$C_{p,m}°(\text{Cd, cr, 298.15 K}) = (26.020 \pm 0.040)\ \text{J} \cdot \text{K}^{-1} \cdot \text{mol}^{-1}$$

7.3 Cadmium(II)

7.3.1 Cadmium(II) aqua ion

Cadmium(II) exists as the Cd^{2+} cation in aqueous solutions. The selected thermodynamic values for Cd^{2+} are taken from CODATA (Cox et al. 1989):

$$\Delta_f G_m°(Cd^{2+}, \text{298.15 K}) = -(77.733 \pm 0.750)\ \text{kJ} \cdot \text{mol}^{-1}$$

$$\Delta_f H_m°(Cd^{2+}, \text{298.15 K}) = -(75.920 \pm 0.600)\ \text{kJ} \cdot \text{mol}^{-1}$$

$$S_m°(Cd^{2+}, \text{298.15 K}) = -(72.800 \pm 1.500)\ \text{J} \cdot \text{K}^{-1} \cdot \text{mol}^{-1}$$

Using the selected CODATA $\Delta_f G_m°(Cd^{2+}, \text{298.15 K})$, the redox equilibrium

$$Cd(cr) \rightleftharpoons Cd^{2+} + 2e^-$$

is calculated as

$$\log_{10} K°(\text{298.15 K}) = 13.82 \pm 0.13$$

7.3.2 Cadmium(II) (hydr)oxide compounds and complexes

7.3.2.1 Cadmium(II) hydroxide complexes

$CdOH^+$

For the formation of the first mononuclear hydrolysis species of cadmium(II)

$$Cd^{2+} + H_2O(l) \rightleftharpoons CdOH^+ + H^+$$

Powell et al. (2011) select the recommended value

$$\log_{10}{}^*\beta_1^\circ\ (298.15\ K) = -9.80 \pm 0.10$$

derived from a weighted linear SIT regression analysis with $\Delta\varepsilon = -(0.05 \pm 0.04)$ kg · mol^{-1}. These values are included in TDB 2020.

Brown & Ekberg (2016) repeated the SIT regression analysis with the same data and the same assigned uncertainties as Powell et al. (2011) and report (almost) numerically identical results: $\log_{10}{}^*\beta_1^\circ\ (298.15\ K) = -9.81 \pm 0.10$ and $\Delta\varepsilon = -(0.05 \pm 0.04)$ kg · mol^{-1}.

Using $\Delta\varepsilon$ and the reported values $\varepsilon(Cd^{2+}, ClO_4^-) = (0.23 \pm 0.04)$ kg · mol^{-1} (see Section 6.3.2.2) and $\varepsilon(H^+, ClO_4^-) = (0.14 \pm 0.02)$ kg · mol^{-1} (Lemire et al. 2013) this review calculated the new value

$$\varepsilon(CdOH^+, ClO_4^-) = (0.04 \pm 0.06)\ kg \cdot mol^{-1}$$

and estimated

$$\varepsilon(CdOH^+, Cl^-) \approx \varepsilon(CdOH^+, ClO_4^-) = (0.04 \pm 0.06)\ kg \cdot mol^{-1}$$

These values are included in TDB 2020.

Based on a calorimetric study at 25 °C in 3 M $LiClO_4$ Powell et al. (2011) selected

$$\Delta_r H_m^\circ(298.15\ K) = (54.8 \pm 2.0)\ kJ \cdot mol^{-1}$$

as a provisional value with an assigned uncertainty ± 2 kJ · mol^{-1}. Brown & Ekberg (2016) retained this selection in their review.

This value is included in TDB 2020 as supplemental datum.

$Cd(OH)_2(aq)$

For the formation of the second mononuclear hydrolysis species of cadmium(II)

$$Cd^{2+} + 2OH^- \rightleftharpoons Cd(OH)_2(aq)$$

Powell et al. (2011) select the recommended value

$$\log_{10}\beta_2^\circ\ (298.15\ K) = 7.81 \pm 0.13$$

derived from a weighted linear SIT regression analysis with $\Delta\varepsilon = -(0.32 \pm 0.02)\ kg \cdot mol^{-1}$.

Brown & Ekberg (2016) considered the same data as Powell et al. (2011) to derive $\log_{10}\beta_2^\circ$ (298.15 K) = 7.4 ± 0.4 from an extended SIT regression analysis with the parameters $\Delta\varepsilon_1 = -(0.7 \pm 0.3)\ kg \cdot mol^{-1}$ and $\Delta\varepsilon_2 = (0.4 \pm 0.3)\ kg \cdot mol^{-1}$. As we cannot mix the "linear SIT" with the "extended SIT" in practical applications this review decided to retain the values of Powell et al. (2009) for our TDB.

Using $\Delta\varepsilon = -(0.32 \pm 0.02)\ kg \cdot mol^{-1}$ and the reported values $\varepsilon(Cd^{2+}, ClO_4^-) = (0.23 \pm 0.04)\ kg \cdot mol^{-1}$ (see Section 6.3.2.2) and $\varepsilon(Na^+, OH^-) = (0.04 \pm 0.01)\ kg \cdot mol^{-1}$ (Tab. 7-2) this review calculated the new value

$$\varepsilon(Cd(OH)_2(aq), Na^+, ClO_4^-) = -(0.01 \pm 0.04)\ kg \cdot mol^{-1}$$

and estimated

$$\varepsilon(Cd(OH)_2(aq), Na^+, Cl^-) \approx \varepsilon(Cd(OH)_2(aq), Na^+, ClO_4^-) = -(0.01 \pm 0.04)\ kg \cdot mol^{-1}$$

These values are included in TDB 2020.

Note that Powell et al. (2011) report $\varepsilon(Cd(OH)_2(aq), Na^+, ClO_4^-) = -(0.02 \pm 0.03)\ kg \cdot mol^{-1}$.

From $\log_{10}\beta_2^\circ$ and the ionisation of water we get

$$Cd^{2+} + 2H_2O(l) \rightleftharpoons Cd(OH)_2(aq) + 2H^+$$

$$\log_{10}{}^*\beta_2^\circ\ (298.15\ K) = -20.19 \pm 0.13$$

This value is included in TDB 2020.

$Cd(OH)_3^-$

Powell et al. (2011) report that data for the formation of $Cd(OH)_3^-$, or the derivation thereof, have been reported in only two publications. In both cases, the reported stability constant ($\log_{10}{}^*\beta_3°$) appears to be too positive compared with the $\log_{10}{}^*\beta_2°$ and $\log_{10}{}^*\beta_4°$values derived by Powell et al. (2011). Accordingly, neither of the derived values for $Cd(OH)_3^-$ has been accepted by Powell et al. (2011) but they concluded that, on the basis of the hydrolysis constants selected for the other three monomeric hydroxo species, the third hydrolysis constant lies in the range $-33 > \log_{10}{}^*\beta_3° > -34$.

$$\log_{10}{}^*\beta_3°\,(298.15\ K) = -33.5 \pm 0.5$$

is thus assigned as indicative for the formation of $Cd(OH)_3^-$ by Powell et al. (2011). This value is included in TDB 2020 as supplemental datum, as well as the estimate

$$\varepsilon(Na^+, Cd(OH)_3^-) = -(0.05 \pm 0.10)\ kg \cdot mol^{-1}$$

$Cd(OH)_4^{2-}$

For the formation of the fourth mononuclear hydrolysis species of cadmium(II)

$$Cd^{2+} + 4OH^- \rightleftharpoons Cd(OH)_4^{2-}$$

Powell et al. (2011) select the provisional value

$$\log_{10}\beta_4° \text{ (298.15 K)} = 8.73 \pm 0.15$$

derived from a weighted linear SIT regression analysis with $\Delta\varepsilon = -(0.19 \pm 0.02)$ kg · mol^{-1}.

Brown & Ekberg (2016) repeated the SIT regression analysis with the same data and the same assigned uncertainties as Powell et al. (2011) and report numerically identical results: $\log_{10}\beta_1°$ (298.15 K) = 8.73 ± 0.15 and $\Delta\varepsilon = -(0.19 \pm 0.02)$ kg · mol^{-1}.

Using $\Delta\varepsilon$ and the reported values $\varepsilon(Cd^{2+}, ClO_4^-) = (0.23 \pm 0.04)$ kg · mol^{-1} (see Section 6.3.2.2) and $\varepsilon(Na^+, OH^-) = (0.04 \pm 0.01)$ kg · mol^{-1} (Tab. 7-2) this review calculated the new value

$$\varepsilon(Na^+, Cd(OH)_4^{2-}) = (0.20 \pm 0.05)\ kg \cdot mol^{-1}.$$

From $\log_{10}\beta_4°$ and the ionisation of water we get

$$Cd^{2+} + 4H_2O(l) \rightleftharpoons Cd(OH)_4^{2-} + 4H^+$$

$$\log_{10}{}^*\beta_4° \text{ (298.15 K)} = -47.28 \pm 0.15$$

These values are included in TDB 2020.

Cd_2OH^{3+}

For the formation of the dimeric hydrolysis species of cadmium(II)

$$2Cd^{2+} + H_2O(l) \rightleftharpoons Cd_2OH^{3+} + H^+$$

Powell et al. (2011) select the recommended value

$$\log_{10}{}^*\beta_{2,1}^\circ\ (298.15\ K) = -8.73 \pm 0.01$$

derived from a weighted linear SIT regression analysis with $\Delta\varepsilon = (0.242 \pm 0.004)\ kg \cdot mol^{-1}$.

Brown & Ekberg (2016) repeated the SIT regression analysis with the same data as Powell et al. (2011) but with increased (and probably more realistic) assigned uncertainties and report

$$\log_{10}{}^*\beta_{2,1}^\circ\ (298.15\ K) = -8.74 \pm 0.10$$

$$\Delta\varepsilon = (0.24 \pm 0.04)\ kg \cdot mol^{-1}$$

These values are included in TDB 2020.

Using $\Delta\varepsilon$ and the reported values $\varepsilon(Cd^{2+}, ClO_4^-) = (0.23 \pm 0.04)\ kg \cdot mol^{-1}$ (see Section 7.3.2.2) and $\varepsilon(H^+, ClO_4^-) = (0.14 \pm 0.02)\ kg \cdot mol^{-1}$ (Tab. 7-2) this review calculated the new value

$$\varepsilon(Cd_2OH^{3+}, ClO_4^-) = (0.56 \pm 0.07)\ kg \cdot mol^{-1}.$$

and estimated

$$\varepsilon(Cd_2OH^{3+}, Cl^-) \approx \varepsilon(Cd_2OH^{3+}, ClO_4^-) = (0.56 \pm 0.07)\ kg \cdot mol^{-1}$$

These values are included in TDB 2020.

Based on a calorimetric study at 25 °C in 3 M $LiClO_4$ Powell et al. (2011) selected

$$\Delta_r H_m^\circ (298.15\ K) = (45.6 \pm 2.0)\ kJ \cdot mol^{-1}$$

as a provisional value with an assigned uncertainty $\pm 2\ kJ \cdot mol^{-1}$. Brown & Ekberg (2016) retained this selection in their review.

This value is included in TDB 2020 as supplemental datum.

$Cd_4(OH)_4^{4+}$

Powell et al. (2011) state that there is only one value reported for the formation of $Cd_4(OH)_4^{4+}$. This species is only likely to form at elevated concentrations of cadmium, and therefore is unlikely to be important in the environment. Pending further studies, no data were selected for this species, neither by Powell et al. (2011) nor by Brown & Ekberg (2016).

7.3.2.2 Cadmium(II) (hydr)oxide compounds

$Cd(OH)_2(s)$

Powell et al. (2011) report that there have been few reliable studies on the solubility of cadmium hydroxide, $Cd(OH)_2(s)$,

$$Cd(OH)_2(s) \rightleftharpoons Cd^{2+} + 2OH^-$$

Three of these values were determined in dilute solutions and the fourth in 3 M $NaClO_4$. Using these data in a weighted linear SIT regression analysis Powell et al. (2011) obtained

$$\log_{10}K_{s0}^\circ\ (298.15\ K) = -14.28 \pm 0.12$$

$$\Delta\varepsilon = (0.31 \pm 0.04)\ kg \cdot mol^{-1}$$

Brown & Ekberg (2016) repeated the SIT regression analysis with the same data but an increased uncertainty for the 3 M $NaClO_4$ datum and report (almost) numerically identical results: $\log_{10}K_{s0}^\circ$ (298.15 K) = -14.28 ± 0.12 and $\Delta\varepsilon = (0.32 \pm 0.07)\ kg \cdot mol^{-1}$.

Using $\Delta\varepsilon = (0.31 \pm 0.04)\ kg \cdot mol^{-1}$ and the reported value $\varepsilon(Na^+, OH^-) = (0.04 \pm 0.01)\ kg \cdot mol^{-1}$ (Tab. 7-2), Powell et al. (2011) calculated and recommended the new value

$$\varepsilon(Cd^{2+}, ClO_4^-) = (0.23 \pm 0.04)\ kg \cdot mol^{-1}$$

This review estimated

$$\varepsilon(Cd^{2+}, Cl^-) \approx \varepsilon(Cd^{2+}, ClO_4^-) = (0.23 \pm 0.04)\ kg \cdot mol^{-1}$$

These values are included in TDB 2020.

From $\log_{10}K_{s0}^\circ$ and the ionisation of water we get

$$Cd(OH)_2(s) + 2H^+ \rightleftharpoons Cd^{2+} + 2H_2O(l)$$

$$\log_{10}{}^*K_{s0}^\circ\ (298.15\ K) = 13.72 \pm 0.12$$

This value is included in TDB 2020.

Powell et al. (2011) report that two enthalpy values for the reaction

$$Cd(OH)_2(s) \rightleftharpoons Cd^{2+} + 2OH^-$$

have been reported, one determined at 25 °C in 8.76 M $HClO_4$ and one at 25 °C and zero ionic strength. From these values Powell et al. (2011) accepted a provisional value $\Delta_r H_m°(298.15\ K) = -(94.6 \pm 2.0)\ kJ \cdot mol^{-1}$. Brown & Ekberg (2016) accepted the same value but with increased uncertainty:

$$\Delta_r H_m°(298.15\ K) = -(94.6 \pm 5.0)\ kJ \cdot mol^{-1}$$

Using $\Delta_f H_m°(H_2O, l, 298.15\ K) = -(285.830 \pm 0.400)\ kJ \cdot mol^{-1}$ and $\Delta_f H_m°(OH^-, 298.15\ K) = -(230.015 \pm 0.400)\ kJ \cdot mol^{-1}$ from CODATA (Cox et al. 1989) this review calculated

$$Cd(OH)_2(s) + 2H^+ \rightleftharpoons Cd^{2+} + 2H_2O(l)$$

$$\textit{Δ}_r H_m°\textit{(298.15 K) = -(206.2 ± 5.0) kJ · mol}^{-1}$$

This value is included in TDB 2020 as supplemental datum.

CdO(cr)

Note that there are CODATA key values (Cox et al. 1989) for CdO(cr):

$$\Delta_f G_m°(CdO, cr, 298.15\ K) = -(228.661 \pm 0.602)\ kJ \cdot mol^{-1}$$

$$\Delta_f H_m°(CdO, cr, 298.15\ K) = -(258.350 \pm 0.400)\ kJ \cdot mol^{-1}$$

$$S_m°(CdO, cr, 298.15\ K) = (54.800 \pm 1.500)\ J \cdot K^{-1} \cdot mol^{-1}$$

Using $\Delta_f G_m°(CdO, cr, 298.15\ K)$, $\Delta_f G_m°(Cd^{2+}, 298.15\ K)$ (see Section 7.3.1) and $\Delta_f G_m°(H_2O, l, 298.15\ K) = -(237.140 \pm 0.041)\ kJ \cdot mol^{-1}$ (Cox et al. 1989), this review calculated

$$CdO(cr) + 2H^+ \rightleftharpoons Cd^{2+} + H_2O(l)$$

$$\log_{10}{}^*K_{s0}°\ (298.15\ K) = 15.10 \pm 0.17$$

According to this result, CdO(cr) is more than 20 times more soluble than $Cd(OH)_2(s)$ at 25 °C.

Hence, CdO(cr) is unstable in environmental aqueous solutions with respect to $Cd(OH)_2(s)$ and thus no data for CdO(cr) are included in TDB 2020.

7.3.3 Cadmium(II) chloride compounds and complexes

7.3.3.1 Cadmium(II) chloride complexes

Cadmium(II) forms three consecutive chloride complexes in aqueous solution

$$Cd^{2+} + Cl^- \rightleftharpoons CdCl^+$$

$$Cd^{2+} + 2Cl^- \rightleftharpoons CdCl_2(aq)$$

$$Cd^{2+} + 3Cl^- \rightleftharpoons CdCl_3^-$$

each with a well-characterised stability constant. The stability constant of the tetrachloride complex

$$Cd^{2+} + 4Cl^- \rightleftharpoons CdCl_4^{2-}$$

is less certain.

For the first three complexes Powell et al. (2011) recommend stability constants and SIT interaction parameters, derived from weighted linear SIT regression analyses of stability constants in $NaClO_4$ media. For $CdCl^+$ and $CdCl_2(aq)$ Powell et al. (2011) used published reaction enthalpy constants measured calorimetrically at different $NaClO_4$ and $LiClO_4$ concentrations for weighted linear SIT regression analyses of reaction enthalpies and obtained $\Delta_r H_m°$ and $\Delta\varepsilon_L$ values:

$\log_{10}\beta_1°$ (298.15 K) = 1.98 ± 0.06
$\Delta\varepsilon$ = -(0.14 ± 0.02) kg · mol^{-1}
$\Delta_r H_m°$(298.15 K) = (3.3 ± 0.6) kJ · mol^{-1}
$\Delta\varepsilon_L$ = (0.6 ± 0.3) · 10^{-3} kg · K^{-1} · mol^{-1}

$\log_{10}\beta_2°$ (298.15 K) = 2.64 ± 0.09
$\Delta\varepsilon$ = -(0.27 ± 0.03) kg · mol^{-1}
$\Delta_r H_m°$(298.15 K) = (7.9 ± 1.4) kJ · mol^{-1}
$\Delta\varepsilon_L$ = (2.1 ± 0.6) · 10^{-3} kg · K^{-1} · mol^{-1}

$\log_{10}\beta_3°$ (298.15 K) = 2.30 ± 0.21
$\Delta\varepsilon$ = -(0.40 ± 0.07) kg · mol^{-1}

These values have been included in TDB 2020.

The $\Delta\varepsilon$ values derived by Powell et al. (2011), together with the reported values $\varepsilon(Cd^{2+}, ClO_4^-)$ = (0.23 ± 0.04) kg · mol^{-1} and $\varepsilon(Cl^-, Na^+)$ = (0.03 ± 0.01) kg · mol^{-1} (Lemire et al. 2013) were used to calculate the new values

$\varepsilon(CdCl^+, ClO_4^-) = (0.12 \pm 0.05)$ kg · mol^{-1}

$\varepsilon(CdCl_2(aq), NaClO_4) = (0.02 \pm 0.05)$ kg · mol^{-1}

$\varepsilon(Na^+, CdCl_3^-) = -(0.08 \pm 0.08)$ kg · mol^{-1}.

as well as the estimates

$\varepsilon(CdCl^+, Cl^-) \approx \varepsilon(CdCl^+, ClO_4^-) = (0.12 \pm 0.05)$ kg · mol^{-1}

$\varepsilon(CdCl_2(aq), NaCl) \approx \varepsilon(CdCl_2(aq), NaClO_4) = (0.02 \pm 0.05)$ kg · mol^{-1}

Powell et al. (2011) state that on the basis of emf measurements and calorimetric measurements there is some evidence for the existence of $CdCl_4^{2-}$ at ionic strengths ≥ 3 M, but the reported formation constants are limited in number and differ significantly in magnitude. Powell et al. (2011) conclude that if the 1:4 complex does exist then it is extremely weak. They further state that Smith & Martell (1976) proposed

$log_{10}\beta_4°(298.15\ K) = 1.7$

although it was not revealed on what basis this value was selected. Considering that the selected values of Smith & Martell (1976) for the other chloride complexes, i.e. $\log_{10}\beta_1°$ (298.15 K) = 1.98 ± 0.03, $\log_{10}\beta_2°$ (298.15 K) = 2.6 ± 0.1 and $\log_{10}\beta_3°$ (298.15 K) = 2.4 ± 0.1, agree well with the values derived by Powell et al. (2011), the above value is included in TDB 2020 as supplemental datum, as well as the estimate

$\varepsilon(Na^+, CdCl_4^{2-}) = -(0.10 \pm 0.10)$ kg · mol^{-1}

7.3.3.2 Cadmium(II) chloride compounds

Cadmium chloride, $CdCl_2$(s), is a hygroscopic solid that is highly soluble in water. Also known are the highly soluble compounds $CdCl_2 \cdot H_2O$ and $CdCl_2 \cdot 5H_2O$.

No thermodynamic data of any of these highly soluble salts are included in TDB 2020.

7.3.4 Cadmium(II) carbonate compounds and complexes

7.3.4.1 Cadmium(II) carbonate complexes

Powell et al. (2011) state that the equilibria for the homogeneous system $Cd^{2+} + H^{+} + CO_3^{2-}$ have not been studied extensively. Concerning the equilibrium

$$Cd^{2+} + CO_3^{2-} \rightleftharpoons CdCO_3(aq)$$

Powell et al. (2011) scrutinised four publications and obtained the provisional value

$$\log_{10}K_1^\circ\ (298.15\ K) = 4.4 \pm 0.2$$

This value is included in TDB 2020, as well as the estimate

$$\varepsilon(CdCO_3(aq), NaCl) \approx \varepsilon(CdCO_3(aq), NaClO_4) = (0.0 \pm 0.1)\ kg \cdot mol^{-1}$$

Powell et al. (2011) state that the formation constant for the reaction

$$Cd^{2+} + 2CO_3^{2-} \rightleftharpoons Cd(CO_3)_2^{2-}$$

is very poorly defined by the available experimental data and report

$$log_{10}\beta_2^\circ = 6.2$$

derived from a single study at an unspecified temperature. Powell et al. (2011) do not recommend this value, but it is included in TDB 2020 as supplemental datum, as well as the estimate

$$\varepsilon(Na^{+}, Cd(CO_3)_2^{2-}) = -(0.10 \pm 0.10)\ kg \cdot mol^{-1}$$

Powell et al. (2011) state that there is considerable uncertainty in the equilibrium constant for the formation of $CdHCO_3^{+}$

$$Cd^{2+} + HCO_3^{-} \rightleftharpoons CdHCO_3^{+}$$

From a single measurement in 3.5 $mol \cdot kg^{-1}$ $NaClO_4$ Powell et al. (2011) derived

$$\log_{10}K\ (298.15\ K) = 0.84 \pm 0.1$$

Using the reported values $\varepsilon(Cd^{2+}, ClO_4^-) = (0.23 \pm 0.04)$ kg · mol^{-1}, $\varepsilon(Na^+, HCO_3^-) = (0.00 \pm 0.02)$ kg · mol^{-1} and the estimated value $\varepsilon(CdHCO_3^+, ClO_4^-) = (0.2 \pm 0.1)$ kg · mol^{-1} (Tab. 7-2) this review calculated $\Delta\varepsilon = -(0.03 \pm 0.11)$ kg · mol^{-1} for extrapolation of the above value to zero ionic strength:

$$\log_{10}K° \text{ (298.15 K)} = 1.7 \pm 0.4$$

As Powell et al. (2011) did not include the constant derived at 3.5 mol · kg^{-1} $NaClO_4$ in their list of selected values, not even as "provisional" or "indicative", the above $\log_{10}K°$ value is included in TDB 2020 as supplemental datum, as well as the estimate

$$\varepsilon(CdHCO_3^+, Cl^-) \approx \varepsilon(CdHCO_3^+, ClO_4^-) = (0.2 \pm 0.1) \text{ kg} \cdot \text{mol}^{-1}$$

7.3.4.2 Cadmium(II) carbonate compounds

The solubility of $CdCO_3$(s) (otavite) according to the reaction

$$CdCO_3(s) + 2H^+ \rightleftharpoons Cd^{2+} + H_2O(l) + CO_2g$$

has been determined at 25 °C for the ionic strengths 0.15 to 5.35 mol · kg^{-1} $NaClO_4$. Powell et al. (2011) derived from a weighted linear SIT regression analysis the recommended values

$$\log_{10}{}^*K_{s0}° \text{ (298.15 K)} = 6.08 \pm 0.03$$

$$\Delta\varepsilon = (0.058 \pm 0.009) \text{ kg} \cdot \text{mol}^{-1}$$

Note that $\Delta\varepsilon$, together with $\varepsilon(H^+, ClO_4^-) = (0.14 \pm 0.02)$ kg · mol^{-1} (Tab. 7-2), leads to $\varepsilon(Cd^{2+}, ClO_4^-) = (0.34 \pm 0.03)$ kg · mol^{-1}, in contrast to $\varepsilon(Cd^{2+}, ClO_4^-) = (0.23 \pm 0.04)$ kg · mol^{-1} derived from $Cd(OH)_2$(s) solubility data (see Section 7.3.2.2). There is no discussion by Powell et al. (2011) why they preferred the latter value and did not recommend the value derived from $CdCO_3$(s) solubility data.

Powell et al. (2011) report that investigation of the temperature dependence of $CdCO_3$(s) solubility over a temperature range between 25 °C and 75 °C indicated that ${}^*K_{s0}$ is constant within experimental error. Hence, they conclude that the reaction enthalpy of the above reaction is approximately zero

$$\Delta_r H_m°(298.15 \text{ K}) \approx 0 \text{ kJ} \cdot \text{mol}^{-1}$$

Using $\Delta_f H_m°(H_2O, l, 298.15 \text{ K}) = -(285.830 \pm 0.400)$ kJ · mol^{-1}, $\Delta_f H_m°(CO_2, g, 298.15 \text{ K}) = -(393.510 \pm 0.130)$ kJ · mol^{-1} and $\Delta_f H_m°(CO_3^{2-}, 298.15 \text{ K}) = -(675.230 \pm 0.250)$ kJ · mol^{-1} from CODATA (Cox et al. 1989), this review calculated for the reaction $CdCO_3(s) \rightleftharpoons Cd^{2+} + CO_3^{2-}$:

$$\Delta_r H_m°(298.15 \text{ K}) \approx 8 \text{ kJ} \cdot \text{mol}^{-1}$$

This value is included in TDB 2020 as supplemental datum.

Using CODATA key values (Cox et al. 1989), Powell et al. (2011) calculated for the reaction

$$CdCO_3(s) \rightleftharpoons Cd^{2+} + CO_3^{2-}$$

the recommended value

$$\log_{10}K_{s0}^\circ\ (298.15\ K) = -12.06 \pm 0.04$$

This value is included in TDB 2020.

7.3.5 Cadmium(II) phosphate compounds and complexes

7.3.5.1 Cadmium(II) phosphate complexes

Powell et al. (2011) found very few papers reporting equilibrium constants for the water-soluble phosphate complexes of Cd(II). They state that the available data at 25 °C allow the assignment of only two provisional values for $CdHPO_4(aq)$ and $CdH_2PO_4^+$, in the first case at $I = 0.101$ M and in the second case at $I = 3$ M $NaClO_4$. This review estimated $\Delta\varepsilon$ values, using ε(j,k) values taken from Lemire et al. (2013), for extrapolation of the data to zero ionic strength.

$$Cd^{2+} + HPO_4^{2-} \rightleftharpoons CdHPO_4(aq)$$

$$\log_{10}K_1\ (298.15\ K) = 2.85 \pm 0.20$$

$$\Delta\varepsilon(\text{estimated}) = -(0.08 \pm 0.12)\ kg \cdot mol^{-1}$$

$$\log_{10}K_1^\circ\ (298.15\ K) = 3.72 \pm 0.20$$

$$Cd^{2+} + H_2PO_4^- \rightleftharpoons CdH_2PO_4^+$$

$$\log_{10}K_1\ (298.15\ K) = 0.76 \pm 0.20$$

$$\Delta\varepsilon(\text{estimated}) = (0.05 \pm 0.11)\ kg \cdot mol^{-1}$$

$$\log_{10}K_1^\circ\ (298.15\ K) = 1.9 \pm 0.4$$

These values are included in TDB 2020, as well as the estimates

$$\varepsilon(CdHPO_4(aq), NaCl) \approx \varepsilon(CdHPO_4(aq), NaClO_4) = (0.0 \pm 0.1)\ kg \cdot mol^{-1}$$

$$\varepsilon(CdH_2PO_4^+, Cl^-) \approx \varepsilon(CdH_2PO_4^+, ClO_4^-) = (0.2 \pm 0.1)\ kg \cdot mol^{-1}$$

7.3.5.2 Cadmium(II) phosphate compounds

Powell et al. (2011) state that the formation of insoluble phosphates is one of the most effective methods for cadmium immobilisation in soils. However, only one value is reported for

$$Cd_3(PO_4)_2(s) \rightleftharpoons 3\ Cd^{2+} + 2\ PO_4^{3-}$$

$$log_{10}K_{s0} = -36.9 \pm 0.4$$

derived from the solubility at 20 °C in media of low but varying ionic strength. Powell et al. (2011) conclude that because complex formation between Cd^{2+} and PO_4^{3-} was not taken into account, the reported constant can be considered only as a rough estimate.

This review agrees with that judgment and includes the value in TDB 2020 as supplemental datum.

Powell et al. (2011) further state that the solubility constants reported for $Cd_5H_2(PO_4)_4 \cdot H_2O(s)$

$$Cd_5H_2(PO_4)_4 \cdot 4H_2O(s) + 2\ H^+ \rightleftharpoons 5\ Cd^{2+} + 4\ HPO_4^{2-} + 4\ H_2O(l)$$

are in poor agreement: $\log_{10}{}^*K_s = -30.9 \pm 0.3$ ($I = 0.0$, 37 °C) and $\log_{10}{}^*K_s = -25.4 \pm 0.3$ ($I = 3.0$ M $NaClO_4$, 25 °C); even after considering the contribution of the Debye-Hückel term $\Delta z^2 D$ in which $\Delta z^2 = 34$. However, this is just half of the truth. This review extrapolated the latter value to zero ionic strength considering the recalculation of $\log_{10}{}^*K_s$ from molar to molal scale, considering the activity of water and using an estimated value $\Delta\varepsilon = (0.27 \pm 0.15)$ kg · mol^{-1}, derived from ε(j,k) values listed in Tab. 7-2, and obtained $\log_{10}{}^*K_s° = -32.6 \pm 0.6$. An unweighted average of this value and the value reported for $I = 0.0$ and 37 °C yields

$$log_{10}{}^*K_s° = -31.8 \pm 1.0$$

This value is included in TDB 2020 as supplemental datum.

7.3.6 Cadmium(II) sulphate compounds and complexes

7.3.6.1 Cadmium(II) sulphate complexes

Powell et al. (2011) state that the stability constants for the formation of Cd^{2+} - sulphate complexes in homogenous solution are relatively poorly characterised, except at very low ionic strengths (infinite dilution). This is surprising because the required measurements should be relatively straightforward, and the constants are of potential importance in natural water systems.

For the formation of $CdSO_4(aq)$

$$Cd^{2+} + SO_4^{2-} \rightleftharpoons CdSO_4(aq)$$

is the only significant equilibrium between Cd^{2+} and SO_4^{2-} relevant to typical natural water conditions. At low concentrations (ionic strengths) stability constants were determined mostly by conductivity measurements. Powell et al. (2011) provide a weighted average of accepted values:

$$\log_{10}K_1° \text{ (298.15 K)} = 2.36 \pm 0.04$$

This value is recommended by Powell et al. (2011) and included in TDB 2020.

Powell et al. (2011) also did a SIT regression of accepted values for both $NaClO_4$ and $LiClO_4$ media which yielded $\log_{10}K_1° \text{ (298.15 K)} = 2.41 \pm 0.07$, which is consistent with (but less accurate than) the recommended value discussed above. The derived value

$$\Delta\varepsilon = -(0.09 \pm 0.02) \text{ kg} \cdot \text{mol}^{-1}$$

can be regarded as provisional. Using the values $\varepsilon(Cd^{2+}, ClO_4^-) = (0.23 \pm 0.04)$ kg · mol^{-1} and $\varepsilon(Na^+, SO_4^{2-}) = -(0.12 \pm 0.06)$ kg · mol^{-1} (Tab. 7-2) this review calculated the new value

$$\varepsilon(CdSO_4(aq), NaClO_4) = (0.02 \pm 0.07) \text{ kg} \cdot \text{mol}^{-1}.$$

and estimated

$$\varepsilon(CdSO_4(aq), NaCl) \approx \varepsilon(CdSO_4(aq), NaClO_4) = (0.02 \pm 0.07) \text{ kg} \cdot \text{mol}^{-1}$$

Powell et al. (2011) report that the enthalpy change for the formation of CdSO4(aq) has been extensively studied using a range of different approaches. At infinite dilution ($I = 0$) Powell et al. (2011) give an unweighted average value from six accepted reaction enthalpy values

$$\Delta_r H_m° \text{ (298.15 K)} = 8.3 \pm 0.5 \text{ kJ} \cdot \text{mol}^{-1}$$

which is recommended. This value is included in TDB 2020.

Powell et al. (2011) did a SIT regression of the combined reaction enthalpy data for $NaClO_4$ and $LiClO_4$ media which yielded $\Delta_r H_m° \text{ (298.15 K)} = 9.2 \pm 1.9$ kJ · mol^{-1} and $\Delta\varepsilon_L = (1.8 \pm 1.2) \cdot 10^{-3}$ kg · K^{-1} · mol^{-1}, with the former being consistent with (but less precise than) the above recommended value.

Powell et al. (2011) state that, pending further investigations, all published $\log_{10}\beta_2$ values for

$$Cd^{2+} + 2SO_4^{2-} \rightleftharpoons Cd(SO_4)_2^{2-}$$

should be considered as indicative only. Powell et al. (2011) did a SIT regression of the combined data for $NaClO_4$ and $LiClO_4$ media which yielded the indicative values

$\log_{10}\beta_2°$ (298.15 K) = 3.32 ± 0.15

$\Delta\varepsilon$ = (0.11 ± 0.05) kg · mol^{-1}

Using the values $\varepsilon(Cd^{2+}, ClO_4^-)$ = (0.23 ± 0.04) kg · mol^{-1} and $\varepsilon(Na^+, SO_4^{2-})$ = -(0.12 ± 0.06) kg · mol^{-1} (Tab. 7-2) this review calculated the new value

$\varepsilon(Na^+, Cd(SO_4)_2^{2-})$ = (0.10 ± 0.11) kg · mol^{-1}

These values are included in TDB 2020.

Powell et al. (2011) state that the enthalpy values listed in their Tab. A-2-15 have been assigned rather large uncertainties and should be regarded as indicative only. None of these values is included in their list of selected values. Hence, the value listed in their Tab. A-2-15 for I = 0

$\Delta_r H_m°(298.15\ K) = 5.7 \pm 2.5\ kJ \cdot mol^{-1}$

is included in TDB 2020 as supplemental datum.

7.3.6.2 Cadmium(II) sulphate compounds

Powell et al. (2011) report that under conditions typically encountered in the natural environment, the equilibrium form of solid cadmium(II) sulphate is the monohydrate, $CdSO_4 \cdot H_2O$(s). The solubility of this salt is high (> 3 mol ·kg^{-1} in water at 25 °C) and increases rapidly with temperature. Therefore, it will not influence Cd(II) speciation in natural waters.

Note that there are CODATA key values (Cox et al. 1989) for $CdSO_4 \cdot 8/3H_2O$(cr):

$\Delta_f G_m°(CdSO_4 \cdot 8/3H_2O, cr, 298.15\ K)$ = -(1464.959 ± 0.810) kJ · mol^{-1}

$\Delta_f H_m°(CdSO_4 \cdot 8/3H_2O, cr, 298.15\ K)$ = -(1'720.300 ± 0.800) kJ · mol^{-1}

$S_m°(CdSO_4 \cdot 8/3H_2O, cr, 298.15\ K)$ = (229.650 ± 0.400) J · K^{-1} · mol^{-1}

Using $\Delta_f G_m°(CdSO_4 \cdot 8/3H_2O, cr, 298.15\ K)$, $\Delta_f G_m°(Cd^{2+}, 298.15\ K)$ (see Section 7.3.1), and $\Delta_f G_m°(H_2O, l, 298.15\ K)$ = -(237.140 ± 0.041) kJ · mol^{-1} and $\Delta_f G_m°(SO_4^{2-}, 298.15\ K)$ = -(744.004 ± 0.418) kJ · mol^{-1} (Cox et al. 1989), this review calculated

$CdSO_4 \cdot 8/3H_2O(cr) \rightleftharpoons Cd^{2+} + SO_4^{2-} + 8/3\ H_2O(l)$

$\log_{10}K_{s0}°$ (298.15 K) = -1.90 ± 0.21

Combining this constant with the constant for $Cd^{2+} + SO_4^{2-} \rightleftharpoons CdSO_4(aq)$ (see Section 7.3.6.1) we obtain

$$CdSO_4 \cdot 8/3H_2O(cr) \rightleftharpoons CdSO_4(aq) + 8/3\ H_2O(l)$$

$$\log_{10}K_{s1}^\circ\ (298.15\ K) = 0.46 \pm 0.21$$

This translates into a solubility $[Cd]_{total} = 2.9\ mol \cdot kg^{-1}$ in solutions with $[SO_4]_{total} > 0.044\ mol \cdot kg^{-1}$, where $CdSO_4(aq)$ predominates (see Fig. 4 of Powell et al. 2011).

In solutions with $[SO_4]_{total} < 0.044\ mol \cdot kg^{-1}$ a solubility of $[Cd]_{total} > 2.9\ mol \cdot kg^{-1}$ results according to the equilibrium $CdSO_4 \cdot 8/3H_2O(cr) \rightleftharpoons Cd^{2+} + SO_4^{2-} + 8/3\ H_2O(l)$.

This is in agreement with the statements of Powell et al. (2011) about the solubility of the monohydrate, $CdSO_4 \cdot H_2O(s)$, and hence the CODATA key values for $CdSO_4 \cdot 8/3H_2O(cr)$ are not included in TDB 2020.

7.3.7 Cadmium(II) sulphide compounds and complexes

7.3.7.1 Cadmium(II) sulphide compounds

Kraft et al. (1966) report from careful emf-measurements and thermal data the solubility constant for the reaction

$$CdS(s) + 2H^+ \rightleftharpoons Cd^{2+} + H_2Sg$$

$$\log_{10}K_{ps0}^\circ(298.15\ K) = -6.1 \pm 0.3$$

at 25 °C and zero ionic strength. Kraft et al. (1966) precipitated CdS(s) by bubbling H_2Sg through oxygen-free acidic, neutral and basic solutions containing 0.01 M $CdSO_4$. They compared X-ray diffraction (Debye – Scherrer) photographs of the three CdS(s) precipitates with well-crystalline commercial CdS(cr) (Merck, ultrapure). All photographs showed only lines of the cubic phase β-CdS (hawleyite) and the hexagonal phase α-CdS (greenockite). The diffraction lines were very sharp for CdS(cr) and broad for all CdS(s) precipitates.

Using $\log_{10}K^\circ\ (298.15\ K) = -8.01 \pm 0.17$ for $H_2Sg \rightleftharpoons H^+ + HS^-$ (Hummel et al. 2002) this review obtains from the above value:

$$CdS(s) + H^+ \rightleftharpoons Cd^{2+} + HS^-$$

$$\log_{10}K_{s0}^\circ\ (CdS, s, 298.15\ K) = -14.1 \pm 0.3$$

This value is included in TDB 2020.

Wang & Tessier (1999) precipitated CdS(s) in a N_2-filled glovebag by mixing 0.15 M $Cd(NO_3)_2$ solutions with 0.2 M Na_2S solutions or 0.6 M thioacetamide solutions and report $\log_{10}K_{s0}°$ (298.15 K) = -14.15 ± 0.06 and $\log_{10}K_{s0}°$ (298.15 K) = -14.40 ± 0.06, respectively. Within their uncertainties, these values agree well with the above selected value from Kraft et al. (1966).

Wang & Tessier (1999) compared the X-ray diffraction pattern of a commercial high-purity crystalline CdS(cr) (Aldrich) with those of their precipitates and found that the pattern for CdS(cr) comprised all the peaks of greenockite (α-CdS) as well as those of hawleyite (β-CdS), while the X-ray diffraction patterns of the precipitates exhibited broader peaks of lower intensity, indicating less ordered solids.

For the commercial high-purity crystalline CdS(cr) Wang & Tessier (1999) report

$$\log_{10}K_{s0}°\ (\text{CdS, cr, 298.15 K}) = -14.82 \pm 0.03$$

Daskalakis & Helz (1992) synthesised CdS(cr) from pure Cd shavings and a slight excess of sulphur in thick-walled silica tubes. The tubes were heated at 270 °C for 3 days and then at 600 °C for 1 week, yielding an orange powder. After being ground in acetone, the solid was sealed in new quartz tubes and heated to 600 °C for 1 week. Subsequent annealing at 900 °C for 1 week gave dark orange aggregates of crystals 10-100 μm in diameter. The X-ray diffraction spectrum was identical with greenockite (α-CdS).

Daskalakis & Helz (1992) report $\log_{10}K_{s0}°$ (CdS, cr, 298.15 K) = -14.36 ± 0.26 at 25 °C and zero ionic strength. However, Wang & Tessier (1999) recalculated the $\log_{10}K_{s0}°$ from the experimental data given by Daskalakis & Helz (1992) using the equilibrium constants reported in their paper and obtained $\log_{10}K_{s0}°$ (CdS, cr, 298.15 K) = -14.92 ± 0.19. The discrepancy is probably a consequence of an error made in the calculation of Daskalakis & Helz (1992). Within their uncertainties, this recalculated value of CdS(cr) agrees well with the value determined by Wang & Tessier (1999).

The difference in the solubility constants for CdS(cr) and CdS(s) is less than one order of magnitude and as it is more probable that the solubility of Cd in the presence of sulphide in environmental systems is governed by a precipitate, and not by well-crystalline CdS(cr), the solubility constant for CdS(s) is included in TDB 2020.

Note that Ste-Marie et al. (1964) report a much higher solubility constant, $\log_{10}K_{s0}$ (CdS, am, 298.15 K) = -12.28, determined by a radiochemical method at 25 °C in 1 M $NaClO_4$ from an uncharacterised precipitate. The only information given by Ste-Marie et al. (1964) is that the following reagents were added to pure oxygen-free water to obtain the desired concentrations of cadmium: 0.01 M $CdSO_4$, 0.021 M Na_2S, buffer solutions 0.001 – 0.1 M. They probably produced an amorphous solid. The solubility constant of this uncharacterised amorphous solid is not considered in TDB 2020. However, the variation of CdS(am) solubility with pH, as reported by Ste-Marie et al. (1964), can be reproduced very well with the cadmium(II) sulphide complexes selected by this review (Fig. 7-1, see Section 7.3.7.2).

7.3.7.2 Cadmium(II) sulphide complexes

Rickard & Luther (2006) and Rickard (2012) stated that: cadmium(II) is classed firmly as a soft metal ion. It is therefore expected that Cd(II) will have a significant sulphide chemistry. Cd(II) is also a toxic metal and thus its sulphide chemistry has some environmental interest. In view of this, it is surprising how little is known about Cd sulphide complexes. None have ever been observed and all evidence stems from curve fitting of solubility data or voltammetric titrations. Little other evidence for their composition or structure has been reported.

From voltammetric titrations of Cd(II) versus S(-II) stability constants for the species $CdHS^+$ and $Cd(HS)_2(aq)$ were proposed (Rickard & Luther 2006, Rickard 2012), clearly insufficient to explain the solubility of CdS(s) as a function of pH and sulphide concentration. We are left with few studies where the solubility of CdS(s) in the Cd – H_2S – H_2O system has been studied with the aim to obtain values for aqueous cadmium sulphide complexes.

Wang & Tessier (1999) reported the most extensive series of solubility measurements, using two CdS(s) precipitates and a commercial crystalline product CdS(cr) (see Section 7.3.7.1), at 25 °C and I = 0.01 – 0.06 M, and varying the total dissolved sulphide concentration, $[S]_{total}$, from 0.05 to 0.0006 M over a pH range 4 – 8.5. A fit of all their solubility data resulted in

$$Cd^{2+} + HS^- \rightleftharpoons CdHS^+$$

$$\log_{10}\beta_1^\circ \text{ (298.15 K)} = 7.38 \pm 0.68$$

$$Cd^{2+} + 2\ HS^- \rightleftharpoons Cd(HS)_2(aq)$$

$$\log_{10}\beta_2^\circ \text{ (298.15 K)} = 14.43 \pm 0.01$$

$$Cd^{2+} + 3\ HS^- \rightleftharpoons Cd(HS)_3^-$$

$$\log_{10}\beta_3^\circ \text{ (298.15 K)} = 16.26 \pm 0.58$$

$$Cd^{2+} + 4\ HS^- \rightleftharpoons Cd(HS)_4^{2-}$$

$$\log_{10}\beta_4^\circ \text{ (298.15 K)} = 18.43 \pm 0.05$$

According to this speciation model, the calculated solubility of CdS(s) will drop to extremely low values at pH > 9.

Daskalakis & Helz (1992) reported a less extensive series of solubility measurements, using a crystalline product, CdS(cr) (see Section 7.3.7.1), at 25 °C and I = 0.05 – 0.20 M, and varying the total dissolved sulphide concentration, $[S]_{total}$, from 0.1 – 0.05 M over a pH range 6 – 9. They fitted their solubility data with the same speciation model as Wang & Tessier (1999), i.e. considering $CdHS^+$, $Cd(HS)_2(aq)$, $Cd(HS)_3^-$ and $Cd(HS)_4^{2-}$, but in addition including $CdOHS^-$ to fit their data points at pH 9. This latter species causes an increase of the calculated CdS(s) solubility above pH 9 and is rejected by Wang & Tessier (1999). It is also at variance with the data of Ste-Marie et al. (1964) who found a constant CdS(s) solubility above pH 9 (Fig. 7-1).

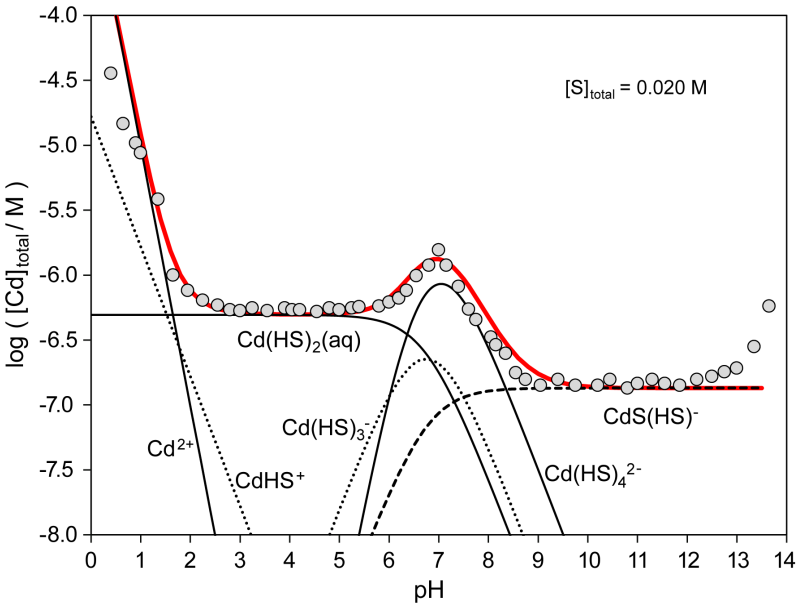

Fig. 7-1: Solubility of CdS(am) in 1 M $NaClO_4$ as a function of pH at 0.02 M total dissolved sulphide concentration, $[S]_{total}$

Symbols: experimental data of Ste-Marie et al. (1964). Thick solid line: calculated total dissolved concentration of cadmium, $[Cd]_{total}$. Thin solid, dashed and dotted lines: calculated concentrations of the indicated species, using $\log_{10}K_{s0}°$ (CdS, am, 298.15 K) = -12.1 together with the selected values (Tab. 7-1), all extrapolated to I = 1 M $NaClO_4$ using estimated SIT coefficients (Tab. 7-2).

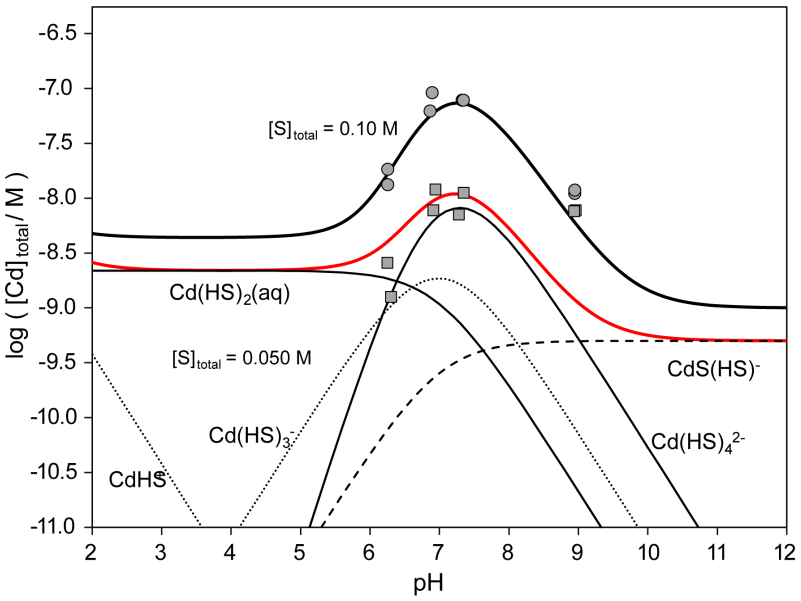

Fig. 7-2: Solubility of CdS(cr) in water as a function of pH at different total dissolved sulphide concentrations, $[S]_{total}$

Different symbols: experimental data of Daskalakis & Helz (1992). Thick solid lines: calculated total dissolved concentration of cadmium, $[Cd]_{total}$. Thin solid, dashed and dotted lines: calculated concentrations of the indicated species, using $\log_{10}K_{s0}°$ (CdS, cr, 298.15 K) = -14.8 together with the selected values (Tab. 7-1).

Ste-Marie et al. (1964) report a single series of solubility measurements, using an uncharacterised precipitate, probably an amorphous solid, CdS(am) (see Section 7.3.7.1), at 1 M $NaClO_4$ and a the total dissolved sulphide concentration, $[S]_{total}$ = 0.021 M over a pH range 0.5 – 13.5 (Fig. 7-1). They fitted their solubility data with the same speciation model as Wang & Tessier (1999), i.e. considering $CdHS^+$, $Cd(HS)_2(aq)$, $Cd(HS)_3^-$ and $Cd(HS)_4^{2-}$, but in addition including $CdOH^+$ to fit their data points above pH 9. However, they used a stability constant for $CdOH^+$, which is 14orders of magnitude higher than the established value (see Section 7.3.2.1). This has to be rejected.

Considering all experimental solubility data reported by Ste-Marie et al. (1964), Daskalakis & Helz (1992) and Wang & Tessier (1999) this review proposes

$$Cd^{2+} + 2\ HS^- \rightleftharpoons CdS(HS)^- + H^+$$

$$\log_{10}K^\circ\ (298.15\ K) = 6.8 \pm 0.2$$

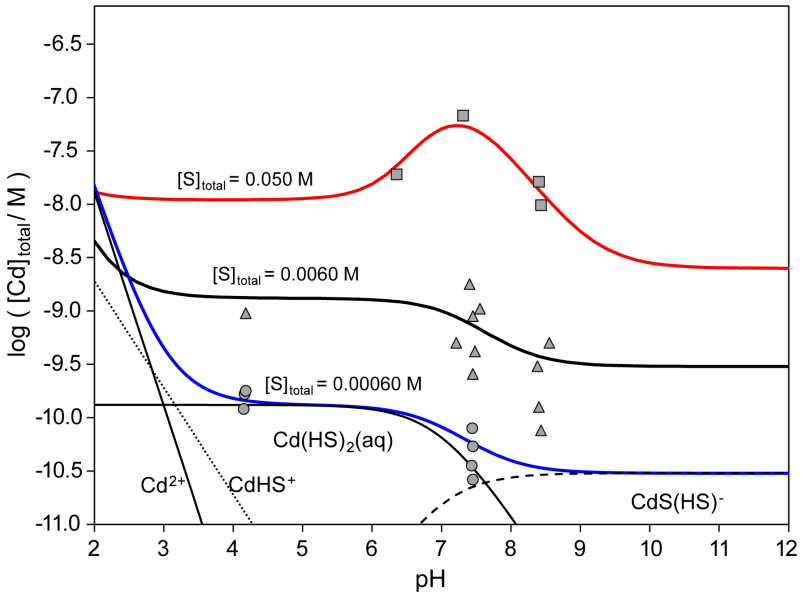

Fig. 7-3: Solubility of CdS(s) in water as a function of pH at different total dissolved sulphide concentrations, $[S]_{total}$

Different symbols: experimental data of Wang & Tessier (1999). Thick solid lines: calculated total dissolved concentration of cadmium, $[Cd]_{total}$. Thin solid, dashed and dotted lines: calculated concentrations of the indicated species, using $\log_{10}K_{s0}^\circ$ (CdS, s, 298.15 K) = -14.1 together with the selected values (Tab. 7-1).

and takes the values from Wang & Tessier (1999), but with an increased uncertainty for $\log_{10}\beta_2^\circ$

$$Cd^{2+} + HS^- \rightleftharpoons CdHS^+$$

$$\log_{10}\beta_1^\circ\ (298.15\ K) = 7.4 \pm 0.7$$

$$Cd^{2+} + 2\ HS^- \rightleftharpoons Cd(HS)_2(aq)$$

$$\log_{10}\beta_2^\circ\ (298.15\ K) = 14.43 \pm 0.05$$

$Cd^{2+} + 3\ HS^- \rightleftharpoons Cd(HS)_3^-$

$\log_{10}\beta_3^\circ$ (298.15 K) = 16.3 ± 0.6

$Cd^{2+} + 4\ HS^- \rightleftharpoons Cd(HS)_4^{2-}$

$\log_{10}\beta_4^\circ$ (298.15 K) = 18.43 ± 0.05

to describe the solubility of cadmium sulphide. These values are included in TDB 2020, as well as the estimates

$\varepsilon(CdHS^+, Cl^-) \approx \varepsilon(CdHS^+, ClO_4^-) = (0.2 \pm 0.1)$ kg · mol^{-1}

$\varepsilon(Cd(HS)_2(aq), NaCl) \approx \varepsilon(Cd(HS)_2(aq), NaClO_4) = (0.0 \pm 0.1)$ kg · mol^{-1}

$\varepsilon(Na^+, Cd(HS)_3^-) = -(0.05 \pm 0.10)$ kg · mol^{-1}

$\varepsilon(Na^+, Cd(HS)_4^{2-}) = -(0.10 \pm 0.10)$ kg · mol^{-1}

$\varepsilon(Na^+, CdS(HS)^-) = -(0.05 \pm 0.10)$ kg · mol^{-1}

Taking $\log_{10}K_{s0}^\circ$ (CdS, am, 298.15 K) = -12.1 together with the above selected values, all extrapolated to I = 1 M $NaClO_4$ using estimated SIT coefficients (Tab. 7-2), yields a very good fit of the data reported by Ste-Marie et al. (1964) (Fig. 7-1).

Likewise, using $\log_{10}K_{s0}^\circ$ (CdS, cr, 298.15 K) = -14.8 together with the above selected values, also yields a very good fit of the data reported by Daskalakis & Helz (1992) (Fig. 7-2). Note that in both cases $CdHS^+$ and $Cd(HS)_3^-$ remain minor species, reflected in the large uncertainty in the fit of Wang & Tessier (1999), whereas the "peak" in cadmium sulphide solubility around pH 7 is mainly explained by $Cd(HS)_4^{2-}$.

Finally, using $\log_{10}K_{s0}^\circ$ (CdS, s, 298.15 K) = -14.1 together with the above selected values, again yields a very good fit of the data reported by Wang & Tessier (1999) (Fig. 7-3). Note that the "peak" in solubility around pH 7, mainly explained by $Cd(HS)_4^2$, only appears in solutions of $[S]_{total} \geq 0.05$ M, while at concentrations $[S]_{total} \leq 0.006$ M the two species $Cd(HS)_2(aq)$ and $CdS(HS)^-$ describe the CdS(s) solubility behaviour.

This means that for environmental systems, with total dissolved sulphide concentrations in the millimolar region, the CdS(s) solubility is characterised in the pH range 4 – 7 by

$CdS(s) + H_2S(aq) \rightleftharpoons Cd(HS)_2(aq)$

$\log_{10}K_{s2}^\circ$ (298.15 K) = -6.7 ± 0.3

and in the pH range 8 – 13 by

$CdS(s) + HS^- \rightleftharpoons CdS(HS)^-$

$\log_{10}K_s^\circ$ (298.15 K) = -7.3 ± 0.4

i.e. two horizontal solubility regions with respect to pH with a decrease of about a factor of 4 in solubility from the acidic to the basic region. As both reactions are isocoulombic, this factor does not depend on ionic strength.

This slight decrease in CdS(s) solubility with increasing pH is corroborated by the findings of Van Hövell tot Westerflier et al. (1987) who determined by radiochemical methods the solubility of cadmium sulphide particles (mean particle diameter about 0.3 μm) at very low but unspecified $[S]_{total}$ concentrations. Using dialysis and ultracentrifugation as particle separation procedure, they found in the pH range 5 – 13 a decrease in cadmium sulphide solubility of about a factor of 3 – 4 by a scatter in the data points in the same range.

7.3.8 Selected cadmium data

Tab. 7-1: Selected cadmium data

Core data are in bold face and supplemental data in italics.

Name	**$\Delta_f G_m°$** [kJ · mol^{-1}]	**$\Delta_f H_m°$** [kJ · mol^{-1}]	**$S_m°$** [J · K^{-1} · mol^{-1}]	**$C_{p,m}°$** [J · K^{-1} · mol^{-1}]	**Species**
Cd(cr)	0.0	0.0	**51.800 ± 0.150**	**26.020 ± 0.040**	Cd(cr)
Cd+2	**-77.733 ± 0.750**	**-75.920 ± 0.600**	**-72.800 ± 1.500**		Cd^{2+}

Name	**$\log_{10}\beta°$**	**Δε** [kJ · mol^{-1}]	**$\Delta_r H_m°$** [J · K^{-1} · mol^{-1}]	**T-range** [°C]	**Reaction**
CdOH+	-9.80 ± 0.10	-0.05 ± 0.04	*54.8 ± 2.0*	25	$Cd^{2+} + H_2O(l) \rightleftharpoons CdOH^+ + H^+$
Cd(OH)2(aq)	-20.19 ± 0.13	-0.32 ± 0.02 [a]	-		$Cd^{2+} + 2\ H_2O(l) \rightleftharpoons Cd(OH)_2(aq) + 2\ H^+$
Cd(OH)3-	*-33.5 ± 0.5*		-		*$Cd^{2+} + 3\ H_2O(l) \rightleftharpoons Cd(OH)_3^- + 3\ H^+$*
Cd(OH)4-2	-47.28 ± 0.15	-0.19± 0.02 [b]	-		$Cd^{2+} + 4\ H_2O(l) \rightleftharpoons Cd(OH)_4^{2-} + 4\ H^+$
Cd2OH+3	-8.74 ± 0.10	0.24 ± 0.04	*45.6 ± 2.0*	25	$2\ Cd^{2+} + H_2O(l) \rightleftharpoons Cd_2OH^{3+} + H^+$
CdCl+	1.98 ± 0.06	-0.14 ± 0.02	3.3 ± 0.6	25	$Cd^{2+} + Cl^- \rightleftharpoons CdCl^+$
CdCl2(aq)	2.64 ± 0.09	-0.27 ± 0.03	7.9 ± 1.4	25	$Cd^{2+} + 2\ Cl^- \rightleftharpoons CdCl_2(aq)$
CdCl3-	2.30 ± 0.21	-0.40 ± 0.07	-		$Cd^{2+} + 3\ Cl^- \rightleftharpoons CdCl_3^-$
CdCl4-2	*1.7*		-		*$Cd^{2+} + 4\ Cl^- \rightleftharpoons CdCl_4^{2-}$*
CdCO3(aq)	4.4 ± 0.2		-		$Cd^{2+} + CO_3^{2-} \rightleftharpoons CdCO_3(aq)$
Cd(CO3)2-2	*≈ 6.2*		-		*$Cd^{2+} + 2\ CO_3^{2-} \rightleftharpoons Cd(CO_3)_2^{2-}$*
CdHCO3+	*1.7 ± 0.4*		-		*$Cd^{2+} + HCO_3^- \rightleftharpoons CdHCO_3^+$*
CdHPO4(aq)	3.72 ± 0.20		-		$Cd^{2+} + HPO_4^{2-} \rightleftharpoons CdHPO_4(aq)$
CdH2PO4+	1.9 ± 0.4		-		$Cd^{2+} + H_2PO_4^- \rightleftharpoons CdH_2PO_4^+$
CdSO4(aq)	2.36 ± 0.04	-0.09 ± 0.02	8.3 ± 0.5	25	$Cd^{2+} + SO_4^{2-} \rightleftharpoons CdSO_4(aq)$

Tab. 7-1: Cont.

Name	**$\log_{10}\beta°$**	**$\Delta\varepsilon$** [kJ · mol^{-1}]	**$\Delta_r H_m°$** [J · K^{-1} · mol^{-1}]	**T-range** [°C]	**Reaction**
Cd(SO4)2-2	3.32 ± 0.15	0.11 ± 0.05	*5.7 ± 2.5*	25	$Cd^{2+} + 2\ SO_4^{2-} \rightleftharpoons Cd(SO_4)_2^{2-}$
CdHS+	7.4 ± 0.7		-		$Cd^{2+} + HS^- \Leftrightarrow CdHS^+$
Cd(HS)2(aq)	14.43 ± 0.05		-		$Cd^{2+} + 2\ HS^- \rightleftharpoons Cd(HS)_2(aq)$
Cd(HS)3-	16.3 ± 0.6		-		$Cd^{2+} + 3\ HS^- \rightleftharpoons Cd(HS)_3^-$
Cd(HS)4-2	18.43 ± 0.05		-		$Cd^{2+} + 4\ HS^- \rightleftharpoons Cd(HS)_4^{2-}$
CdS(HS)-	6.8 ± 0.2		-		$Cd^{2+} + 2\ HS^- \rightleftharpoons CdS(HS)^- + H^+$

Tab. 7-1: Cont.

Name	**$\log_{10}K_{s,0}°$**	**$\Delta_r H_m°$** [kJ · mol^{-1}]	**T-range** [°C]	**Reaction**
$Cd(OH)_2$(s)	13.72 ± 0.12	*206.2± 5.0*	25	$Cd(OH)_2(s) + 2H^+ \rightleftharpoons Cd^{2+} + 2H_2O(l)$
Otavite	-12.06 ± 0.04	*≈ 8*	*5 – 75*	$CdCO_3(s) \rightleftharpoons Cd^{2+} + CO_3^{2-}$
Cd3(PO4)2(s)	*-36.9 ± 0.4*	-		*$Cd_3(PO_4)_2(s) \rightleftharpoons 3\ Cd^{2+} + 2\ PO_4^{3-}$*
Cd5H2(PO4)4 · 4H2O(s)	*-31.8 ± 1.0*	-		*$Cd_5H_2(PO_4)_4 \cdot 4H_2O(s) + 2H^+ \rightleftharpoons 5Cd^{2+} + 4HPO_4^{2-} + 4H_2O(l)$*
CdS(s)	-14.1 ± 0.3	-		$CdS(s) + H^+ \rightleftharpoons Cd^{2+} + HS^-$

[a] The reported Δε value refers to the reaction $Cd^{2+} + 2\ OH^- \rightleftharpoons Cd(OH)_2(aq)$.
[b] The reported Δε value refers to the reaction $Cd^{2+} + 4\ OH^- \rightleftharpoons Cd(OH)_4^{2-}$.

Tab. 7-2: Selected SIT ion interaction coefficients $\varepsilon_{j,k}$ [kg · mol^{-1}] for auxiliary and cadmium species

Data in normal face are derived or estimated in this review. Data estimated according to charge correlations and taken from Tab. 1-7 are shaded. Supplemental data are in italics.

j k → ↓	**Cl^-** $\varepsilon_{j,k}$ [kg · mol^{-1}]	**ClO_4^-** $\varepsilon_{j,k}$ [kg · mol^{-1}]	**Na^+** $\varepsilon_{j,k}$ [kg · mol^{-1}]	**$Na^+ + Cl^-$** $\varepsilon_{j,k}$ [kg · mol^{-1}]	**$Na^+ + ClO_4^-$** $\varepsilon_{j,k}$ [kg · mol^{-1}]
H_2S(aq)	0	0	0	(0.055 ± 0.004) [b]	(0.055 ± 0.004) [c]
HS^-	0	0	(0.08 ± 0.01) [b]	0	0
Cd^{2+}	(0.23 ± 0.04) [a]	0.23 ± 0.04	0	0	0
$CdOH^+$	(0.04 ± 0.06) [a]	0.04 ± 0.06	0	0	0
$Cd(OH)_2$(aq)	0	0	0	(-0.01 ± 0.04) [a]	-0.01 ± 0.04
$Cd(OH)_3^-$	*0*	*0*	*-0.05 ± 0.10*	*0*	*0*
$Cd(OH)_4^{2-}$	0	0	0.20 ± 0.05	0	0
Cd_2OH^{3+}	(0.56 ± 0.07) [a]	0.56 ± 0.07	0	0	0
$CdCl^+$	(0.12 ± 0.05) [a]	0.12 ± 0.05	0	0	0
$CdCl_2$(aq)	0	0	0	(0.02 ± 0.05) [a]	0.02 ± 0.05
$CdCl_3^-$	0	0	-0.08 ± 0.08	0	0
$CdCl_4^{2-}$	*0*	*0*	*-0.10 ± 0.10*	*0*	*0*
$CdCO_3$(aq)	0	0	0	0.0 ± 0.1	0.0 ± 0.1
$Cd(CO3)_2^{2-}$	*0*	*0*	*-0.10 ± 0.10*	*0*	*0*
$CdHCO_3^+$	*0.2 ± 0.1* [a]	*0.2 ± 0.1*	*0*	*0*	*0*
$CdHPO_4$(aq)	0	0	0	0.0 ± 0.1	0.0 ± 0.1
$CdH_2PO_4^+$	0.2 ± 0.1 [a]	0.2 ± 0.1	0	0	0
$CdSO_4$(aq)	0	0	0	(0.02 ± 0.07) [a]	0.02 ± 0.07
$Cd(SO_4)_2^{2-}$	0	0	0.10 ± 0.11	0	0
$CdHS^+$	0.2 ± 0.1 [a]	0.2 ± 0.1	0	0	0
$Cd(HS)_2$(aq)	0	0	0	0.0 ± 0.1	0.0 ± 0.1
$Cd(HS)_3^-$	0	0	-0.05 ± 0.10	0	0
$Cd(HS)_4^{2-}$	0	0	-0.10 ± 0.10	0	0
$CdS(HS)^-$	0	0	-0.05 ± 0.10	0	0

[a] Assumed to be equal to the corresponding ion interaction coefficient with ClO_4^-, see Section 7.1 for explanation.
[b] Hummel et al. (2002)
[c] Assumed to be equal to the corresponding ion interaction coefficient with NaCl.

7.4 References

Brown, P.L. & Ekberg, C. (2016): Hydrolysis of Metal Ions. Wiley-VCH Verlag GmbH & Co. KGaA, Weinheim, Germany, 917 pp.

Cox, J.D., Wagman, D.D. & Medvedev, V.A. (1989): CODATA Key Values for Thermodynamics. New York, Hemisphere Publishing, 271 pp.

Daskalakis, K.D. & Helz, G.R. (1992): Solubility of cadmium sulfide (greenockite) in sulfidic waters at 25 °C. Environ. Sci. Technol., 26, 2462-2468.

Grenthe, I., Fuger, J., Konings, R.J.M., Lemire, R.J., Muller, A.B., Nguyen-Trung, C. & Wanner, H. (1992): Chemical Thermodynamics of Uranium. Chemical Thermodynamics, Vol. 1. North-Holland, Amsterdam, 715 pp.

Hagemann, S. (2012): Entwicklung eines thermodynamischen Modells für Zink, Blei und Cadmium in salinaren Lösungen, GRS-Report 219, GRS, Braunschweig, Germany, 494 pp.

Hummel, W., Berner, U., Curti, E., Pearson, F.J. & Thoenen, T. (2002): Nagra/PSI Chemical Thermodynamic Data Base 01/01. Nagra Technical Report NTB 02-16 and Universal Publishers, Parkland, Florida, 565 pp.

Kraft, W., Gamsjäger H. & Schwarz-Bergkampf, E. (1966): Löslichkeitskonstanten und Freie Bildungsenthalpien von Metallsulfiden, 3. Mitt.: ${}^{*}K_{ps0}$ von α-CdS (Greenockit). Monatshefte für Chemie, 97, 1134-1141.

Lemire, R.J., Berner, U., Musikas, C., Palmer, D.A., Taylor, P. & Tochiyama, O. (2013): Chemical Thermodynamics of Iron, Part 1. Chemical Thermodynamics, Vol. 13a. OECD Publications, Paris, France, 1082 pp.

Powell, K.J., Brown, P.L., Byrne, R.H., Gajda, T., Hefter, G., Leuz, A.-K., Sjöberg, S. & Wanner, H. (2011): Chemical speciation of environmentally significant metals with inorganic ligands. Part 4: The Cd^{2+} + OH^-, Cl^-, CO_3^{2-}, SO_4^{2-}, and PO_4^{3-} systems. Pure Appl. Chem., 83, 1163-1214.

Rickard, D. & Luther III, G.W. (2006): Metal sulfide complexes and clusters. Reviews in Mineralogy & Geochemistry, 61, 421-504.

Rickard, D. (2012): Aqueous metal-sulfide chemistry: Complexes, clusters and nanoparticles. Developments in Sedimentology, 65, 121-194.

Smith, R.M. & Martell, A.E. (1976): Critical Stability Constants. Volume 4: Inorganic Complexes. Plenum Press, New York, 257 pp.

Ste-Marie, J., Torma, A.E. & Gübeli, A.O. (1964): The stability of thiocomplexes and solubility products of metal sulphides I. Cadmium sulphide. Canadian Journal of Chemistry, 42, 662-668.

Van Hövell tot Westerflier, S.W.F.M., Kolar, Z., Binsma, J.J.M., Stein, H.N. & Vandecasteele, C. (1987): Solubility of particulate cadmium sulphide at pH = 1 – 14: A radiotracer study. Journal of Radioanalytical and Nuclear Chemistry, Articles, 111, 305-317.

Wang, F. & Tessier, A. (1999): Cadmium complexation with bisulfide. Environ. Sci. Technol., 33, 4270-4277.

Wilson, J.C., Thorne, M.C., Towler, G. & Norris, S. (2011): Illustrative assessment of human health issues arising from the potential release of chemotoxic substances from a generic geological disposal facility for radioactive waste. Journal of Radiological Protection, 31, 411-430.

8 Californium

8.1 Introduction

Californium isotopes are produced in nuclear reactors by repeated neutron capture / β^- decay nuclear reactions. Cf-249 and Cf-251 with long half-lives of 351 ± 2 and 898 ± 44 years, respectively, contribute in dose-relevant quantities to the inventory of radioactive waste coming from nuclear power plants, which is the reason for inclusion of californium into the PSI Chemical Thermodynamic Database 2020 (PSI TDB 2020).

As discussed by Haire (2006), several reduction potentials for californium have been derived from both experimental data and from systematic calculations. The calculated Cf(IV)/Cf(III) couple of 3.2 V is in accord with the inability to obtain Cf(IV) in most aqueous media. This value for californium can be compared to the Am(IV)/Am(III) couple of 2.2 – 2.5 V, and the Cm(IV)/Cm(III) couple of 3.1 – 3.5 V. It is difficult to maintain Am(IV) and essentially not feasible to produce Cm(IV) in most aqueous solutions. Hence, the only stable oxidation state of californium in aqueous solution considered in this review is Cf(III).

The thermodynamic data included into the PSI TDB 2020 have been taken from

- Konings et al. (2006) and the literature discussed by Haire (2006)
- the recent review of the hydrolysis of metal ions (Brown & Ekberg 2016)
- and own reviews of experimental data

The selected thermodynamic data for californium complexes are presented in Tab. 8-1.

Ion interaction coefficients of californium species were not available. We approximated these with the estimation method described in Section 1.5.3, which draws on a statistical analysis of published SIT ion interaction coefficients and which allows the estimation of missing coefficients for the interaction of cations with Cl^- and ClO_4^-, and for the interaction of anions with Na^+, from the charge of the cations or anions of interest.

The selected SIT ion interaction coefficients for californium species are presented in Tab. 8-2.

8.2 Elemental californium

Californium metal, liquid and gas are not relevant under environmental conditions. Hence, the gas phase Cfg and the liquid phase Cf(l) are not included in the data base. The absolute entropy of Cf(cr) is included as it is used for the calculation of certain thermodynamic reaction properties. The selected value has been taken from Konings et al. (2006):

$$S_m°(\text{Cf, cr, 298.15 K}) = (81 \pm 5)\ \text{J} \cdot \text{K}^{-1} \cdot \text{mol}^{-1}$$

8.3 Californium(III)

8.3.1 Californium(III) aqua ion

Californium(III) exists as the Cf^{3+} cation in aqueous solutions. The selected thermodynamic values for Cf^{3+} are taken from Konings et al. (2006):

$$\Delta_f H_m°(Cf^{3+}, 298.15\ K) = -(577 \pm 5)\ kJ \cdot mol^{-1}$$

$$S_m°(Cf^{3+}, 298.15\ K) = -(197 \pm 17)\ J \cdot K^{-1} \cdot mol^{-1}$$

The Gibbs energy of formation is calculated from the above values, $S_m°$(Cf, cr, 298.15 K) (see Section 8.2) and the CODATA value $S_m°(H_2, g, 298.15\ K) = (130.680 \pm 0.003)\ J \cdot K^{-1} \cdot mol^{-1}$ (Grenthe et al. 1992) according to the Gibbs-Helmholtz equation

$$\Delta_f G_m°(Cf^{3+}, 298.15\ K) = \Delta_f H_m°(Cf^{3+}, 298.15\ K) - T° \cdot \Delta_f S_m°(Cf^{3+}, 298.15\ K)$$

$$\Delta_f S_m°(Cf^{3+}, 298.15\ K) = S_m°(Cf^{3+}, 298.15\ K) - S_m°(Cf, cr, 298.15\ K) + (3/2)\ S_m°(H_2, g, 298.15\ K)$$

$$\Delta_f G_m°(Cf^{3+}, 298.15\ K) = -(552.6 \pm 7.3)\ kJ \cdot mol^{-1}$$

These values are included in TDB 2020 as well as the estimates

$$\varepsilon(Cf^{3+}, ClO_4^-) = (0.6 \pm 0.1)\ kg \cdot mol^{-1}$$

$$\varepsilon(Cf^{3+}, Cl^-) = (0.25 \pm 0.10)\ kg \cdot mol^{-1}$$

Using $\Delta_f G_m°(Cf^{3+}, 298.15\ K)$ the redox equilibrium

$$Cf(cr) + 3H^+ \rightleftharpoons Cf^{3+} + 1.5H_2g$$

or

$$Cf(cr) \rightleftharpoons Cf^{3+} + 3e^-$$

is calculated as

$$\log_{10}K°(298.15\ K) = 96.8 \pm 1.3$$

8.3.2 Californium(III) (hydr)oxide compounds and complexes

8.3.2.1 Californium(III) hydroxide complexes

Desiré et al. (1969) determined stability constants for the species $AnOH^{2+}$ for the actinides americium(III), curium(III), berkelium(III) and californium(III), using a solvent extraction technique with thenoyltrifluoroacetone (TTA) in benzene at (23 ± 1) °C in 0.1 M (H,Li)ClO_4. They obtained

$$An^{3+} + H_2O(l) \rightleftharpoons AnOH^{2+} + H^+$$

$\log_{10}\beta_1$ (An = Am, 296.15 K) = -5.92

$\log_{10}\beta_1$ (An = Cm, 296.15 K) = -5.92

$\log_{10}\beta_1$ (An = Bk, 296.15 K) = -5.66

$\log_{10}\beta_1$ (An = Cf, 296.15 K) = -5.62

Hussonnois et al. (1973) determined stability constants for the species $AnOH^{2+}$ for the actinides americium(III), curium(III), californium(III) and einsteinium(III) using the same experimental technique under the same conditions as Desiré et al. (1969). They obtained

$\log_{10}\beta_1$ (An = Am, 296.15 K) = -5.30

$\log_{10}\beta_1$ (An = Cm, 296.15 K) = -5.40

$\log_{10}\beta_1$ (An = Cf, 296.15 K) = -5.05

$\log_{10}\beta_1$ (An = Es, 296.15 K) = -5.14

In both studies the stability constants obtained for Am and Cm are either identical (Desiré et al. 1969) or very close (Hussonnois et al. 1973), in accord with many later studies (Guillaumont et al. 2003). The stability constant obtained for Cf is in both studies about 0.3 log-units (or two times) larger than that reported for Am and Cm, not unexpected considering the actinide contraction (the same effect as the lanthanide contraction, i.e., the decrease of the ionic radius with increasing proton number).

However, the stability constants obtained for americium(III) and curium(III) by Desiré et al. (1969) and Hussonnois et al. (1973) are two orders of magnitude larger than other similar data available in the literature studies (Guillaumont et al. 2003). As Brown & Ekberg (2016) discuss, the hydrolysis constants of the lanthanide(III) and actinide(III) ions are very difficult to obtain using solvent extraction due to problems associated with attainment of maximum extraction into the solvent phase in the narrow band of pH between the onset of hydrolysis reactions and the precipitation of solid hydroxide phases. Consequently, the data of Desiré et al. (1969) are not retained in the review of Brown & Ekberg (2016). The paper of Hussonnois et al. (1973) is not mentioned by Brown & Ekberg (2016).

This review agrees with the conclusion of Brown & Ekberg (2016) and none of the above values is included in TDB 2020.

8.3.2.2 Californium(III) (hydr)oxide compounds

As discussed by Guillaumont et al. (2003) in their Appendix A, Morss & Williams (1994) determined the enthalpy of solution of $Am(OH)_3$(cr) in 6 M HCl and calculated the standard molar enthalpy, standard molar Gibbs energy, and solubility constant for crystalline Am(III) hydroxide. As their calculated solubility constant was considerably lower than those derived from solubility measurements, Morss & Williams (1994) proposed for

$$An(OH)_3(s) \rightleftharpoons An^{3+} + OH^-$$

a "working value" of

$$\log_{10}K_{s0}^\circ \text{ (An = Am, 295.15 K)} = -27.5 \pm 2$$

for a less crystalline $Am(OH)_3$(s), typical for a hydroxide in contact with an aqueous solution. Applying a correlation of the relative basicity of actinide and lanthanide hydroxides as a function of ionic size, Morss & Williams (1994) propose further "working values" for

$$\log_{10}K_{s0}^\circ \text{ (An = Cm, 295.15 K)} = -28.0 \pm 2$$

$$\log_{10}K_{s0}^\circ \text{ (An = Bk, 295.15 K)} = -28.5 \pm 2$$

$$\log_{10}K_{s0}^\circ \text{ (An = Cf, 295.15 K)} = -29.0 \pm 2$$

These values translate to

$$An(OH)_3(s) + 3H^+ \rightleftharpoons An^{3+} + 3H_2O(l)$$

$$\log_{10}{}^*K_{s0}^\circ \text{ (An = Am, 295.15 K)} = 14.5 \pm 2$$

$$\log_{10}{}^*K_{s0}^\circ \text{ (An = Cm, 295.15 K)} = 14.0 \pm 2$$

$$\log_{10}{}^*K_{s0}^\circ \text{ (An = Bk, 295.15 K)} = 13.5 \pm 2$$

$$\log_{10}{}^*K_{s0}^\circ \text{ (An = Cf, 295.15 K)} = 13.0 \pm 2$$

Brown & Ekberg (2016) retain the latter two values in their review "but with the reduced uncertainty of 1.0 log units".

Considering that Guillaumont et al. (2003) select in their review of experimental data$\log_{10}{}^*K_{s0}^\circ$ (An = Am, cr, 295.15 K) = 15.6 ± 0.6

$$\log_{10}{}^*K_{s0}^\circ \text{ (An = Am, am, 295.15 K)} = 16.9 \pm 0.8$$

for crystalline and amorphous americium hydroxide, respectively, the "working value" of Morss & Williams (1994) still is orders of magnitude too low for representing "a less crystalline $Am(OH)_3(s)$, typical for a hydroxide in contact with an aqueous solution", even with respect to the large uncertainty of 2 log units assigned to their estimate.

Consequently, the estimate for $Cf(OH)_3(s)$ most probably also would underestimate the solubility of experimentally determined amorphous californium hydroxide by orders of magnitude if this would have been measured.

Furthermore, including an estimated solubility product into the database without Cf hydrolysis species inevitably would lead to grossly wrong modelling results concerning the solubility of californium in environmental systems.

Hence, the estimated solubility product is not included in TDB 2020.

8.3.3 Californium(III) fluoride complexes

Choppin & Unrein (1976) determined the complex formation of some trivalent actinide elements with fluoride in 1.0 M $NaClO_4$ at 25 °C by a solvent extraction method at a fixed pH of 2.7. In the investigated range of ligand concentration, Choppin & Unrein (1976) only found the existence of AnF^{2+}, and calculated the following values

$$An^{3+} + F^- \rightleftharpoons AnF^{2+}$$

$\log_{10}\beta_1$ (An = Am, 298.15 K) = 2.49 ± 0.02

$\log_{10}\beta_1$ (An = Cm, 298.15 K) = 2.61 ± 0.02

$\log_{10}\beta_1$ (An = Bk, 298.15 K) = 2.89 ± 0.02

$\log_{10}\beta_1$ (An = Cf, 298.15 K) = 3.03 ± 0.04

Choppin & Unrein (1976) in addition did measurements at 10, 40 and 55 °C and their results are

$\log_{10}\beta_1$ (An = Cf, 283.15 K) = 2.93 ± 0.02

$\log_{10}\beta_1$ (An = Cf, 313.15 K) = 3.13 ± 0.04

$\log_{10}\beta_1$ (An = Cf, 228.15 K) = 3.23 ± 0.04

The uncertainties given by Choppin & Unrein (1976) represent 1σ.

This review applied the van't Hoff relation to the Cf equilibrium constants obtained by Choppin & Unrein (1976), with 2σ uncertainties to represent the 95% confidence level, and obtained (Fig. 8-1)

$\log_{10}\beta_1$ (An = Cf, 298.15 K) = $3.03_5 \pm 0.04$

$\Delta_r H_m(298.15\ K) = (11.8 \pm 1.6)\ kJ \cdot mol^{-1}$

No attempt has been made to extrapolate the enthalpy value to zero ionic strength, and this value obtained at 1.0 M $NaClO_4$ is included in TDB 2020 as supplemental datum.

Considering $\varepsilon(Na^+, F^-) = (0.02 \pm 0.02)$ kg · mol^{-1} (Lemire et al. 2013) and using the estimation method (described in Section 1.5.3) $\varepsilon(An^{3+}, ClO_4^-) = (0.6 \pm 0.1)$ kg · mol^{-1}, and $\varepsilon(AnF^{2+}, ClO_4^-) = (0.4 \pm 0.1)$ kg · mol^{-1}, (Tab. 8-2), the values of Choppin & Unrein (1976) have been extrapolated to I = 0

$\Delta\varepsilon = -(0.22 \pm 0.14)$ kg · mol^{-1}

$\log_{10}\beta_1°$ (An = Am, 298.15 K) = 3.47 ± 0.15

$\log_{10}\beta_1°$ (An = Cf, 298.15 K) = 4.01 ± 0.16

Considering that Silva et al. (1995) selected for Am(III), based on the data of Choppin & Unrein (1976) and a second data source,

$\log_{10}\beta_1°$ (An = Am, 298.15 K) = 3.4 ± 0.4

this review decided to apply the same uncertainty estimate for Cf(III) and the value

$\log_{10}\beta_1°$ (An = Cf, 298.15 K) = 4.0 ± 0.4

is included in TDB 2020 as well as the estimates

$\varepsilon(CfF^{2+}, ClO_4^-) = (0.4 \pm 0.1)$ kg · mol^{-1}

$\varepsilon(CfF^{2+}, Cl^-) = (0.15 \pm 0.10)$ kg · mol^{-1}

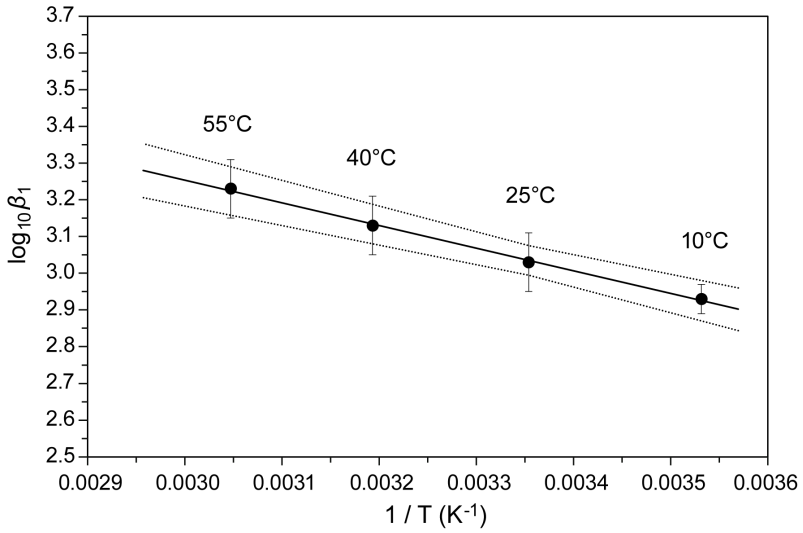

Fig. 8-1: The equilibrium constant $\log_{10}\beta_1$ for $Cf^{3+} + F^- \rightleftharpoons CfF^{2+}$ at 1.0 M $NaClO_4$ as a function of temperature in the range 10 – 55 °C.

Solid line: unweighted linear regression using the data of Choppin & Unrein (1976). Dotted lines: lower and upper limits using $\log_{10}\beta_1(298.15\ K) = 3.03_5 \pm 0.04$ and $\Delta_r H_m(298.15\ K) = (11.8 \pm 1.6)\ kJ \cdot mol^{-1}$ and extrapolated to lower and higher temperatures.

8.3.4 Californium(III) sulphate complexes

De Carvalho & Choppin (1967a) determined the complex formation of some trivalent lanthanide and actinide elements with sulphate in 2.0 M $NaClO_4$ at (25.0 ± 0.1) °C by a solvent extraction method at a fixed pH of 3.0 while varying the total sulphate concentrations from 0.03 to 0.33 M. They interpreted their data in terms of the complexes

$An^{3+} + SO_4^{2-} \rightleftharpoons AnSO_4^+$

β_1 (An = Am, 298.15 K) = 27 ± 4

β_1 (An = Cm, 298.15 K) = 22 ± 4

β_1 (An = Cf, 298.15 K) = 23 ± 3

$An^{3+} + 2SO_4^{2-} \rightleftharpoons An(SO_4)_2^-$

β_2 (An = Am, 298.15 K) = 71 ± 19

β_2 (An = Cm, 298.15 K) = 73 ± 18

β_2 (An = Cf, 298.15 K) = 117 ± 28

De Carvalho & Choppin (1967b) in addition did measurements at 0, 40 and 55 °C and their results are

β_1 (An = Cf, 273.15 K) = 11 ± 2

β_1 (An = Cf, 313.15 K) = 31 ± 4

β_1 (An = Cf, 228.15 K) = 42 ± 7

β_2 (An = Cf, 273.15 K) = 56 ± 13

β_2 (An = Cf, 313.15 K) = 123 ± 25

β_2 (An = Cf, 228.15 K) = 220 ± 57

The uncertainties given by De Carvalho & Choppin (1967a, 1967b) represent 2σ.

This review applied the Van't Hoff relation to the Cf equilibrium constants β_1 obtained by De Carvalho & Choppin (1967a, 1967b) and obtained (Fig. 8-2).

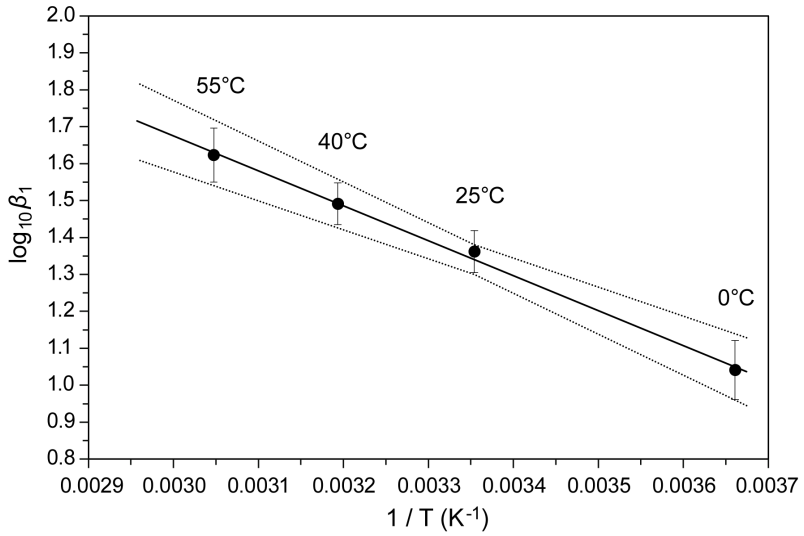

Fig. 8-2: The equilibrium constant $\log_{10}\beta_1$ for $Cf^{3+} + SO_4^{2-} \rightleftharpoons CfSO_4^+$ at 2.0 M $NaClO_4$ as a function of temperature in the range 0 – 55 °C

Solid line: unweighted linear regression using the data of De Carvalho & Choppin (1967b). Dotted lines: lower and upper limits using $\log_{10}\beta_1(298.15\ K) = 1.34 \pm 0.04$ and $\Delta_r H_m(298.15\ K) = (18.1 \pm 3.1)\ kJ \cdot mol^{-1}$ and extrapolated to lower and higher temperatures.

$\log_{10}\beta_1$ (An = Cf, 298.15 K) = 1.34 ± 0.04

$\Delta_r H_m(298.15\ K) = (18.1 \pm 3.1)\ kJ \cdot mol^{-1}$

Carvalho & Choppin (1967b) report a value of $\Delta_r H_m(298.15\ K) = 18.8\ kJ \cdot mol^{-1}$, without providing an uncertainty estimate.

Note that the stepwise stability constants K_2, calculated from β_1 and β_2 for

$CfSO_4^+ + SO_4^{2-} \rightleftharpoons Cf(SO_4)_2^-$

K_2 (An = Cf, 273.15 K) = 5.1 ± 1.5

K_2 (An = Cf, 298.15 K) = 5.1 ± 1.4

K_2 (An = Cf, 313.15 K) = 4.0 ± 1.0

K_2 (An = Cf, 228.15 K) = 5.2 ± 1.7

do not show any temperature dependence, and no enthalpy value for K_2 or β_2 is given in Carvalho & Choppin (1967b).

Considering $\varepsilon(Na^+, SO_4^{2-}) = -(0.12 \pm 0.06)\ kg \cdot mol^{-1}$ (Lemire et al. 2013) and using the estimation method (described in Section 1.5.3) for $\varepsilon(An^{3+}, ClO_4^-) = (0.6 \pm 0.1)\ kg \cdot mol^{-1}$, $\varepsilon(AnSO_4^+, ClO_4^-) = (0.2 \pm 0.1)\ kg \cdot mol^{-1}$, and $\varepsilon(Na^+, An(SO_4)_2^-) = -(0.05 \pm 0.1)\ kg \cdot mol^{-1}$, the values of De Carvalho & Choppin (1967a) have been extrapolated to I = 0

$\Delta\varepsilon = -(0.28 \pm 0.15)\ kg \cdot mol^{-1}$

$\log_{10}\beta_1^\circ$ (An = Am, 298.15 K) = 3.58 ± 0.23

$\log_{10}\beta_1^\circ$ (An = Cf, 298.15 K) = 3.51 ± 0.22

$\Delta\varepsilon = -(0.41 \pm 0.16)\ kg \cdot mol^{-1}$

$\log_{10}\beta_1^\circ$ (An = Am, 298.15 K) = 4.61 ± 0.33

$\log_{10}\beta_1^\circ$ (An = Cf, 298.15 K) = 4.87 ± 0.32

McDowell & Coleman (1972) performed solvent extraction experiments to investigate the sulphate complexes with trivalent transplutonium elements. The experimental data were interpreted assuming the formation of $An(SO_4)_n^{(3-2n)}$ (n = 1,2,3). Activity coefficient effects over the ligand concentration range examined (up to 0.5 M) were estimated by a Debye-Hückel expression. The stability constants at zero ionic strength, as obtained by McDowell & Coleman (1972), are

$\log_{10}\beta_1^\circ$ (An = Am, 298.15 K) = 3.78 ± 0.11

$\log_{10}\beta_1^\circ$ (An = Cm, 298.15 K) = 3.88 ± 0.09

$\log_{10}\beta_1^\circ$ (An = Cf, 298.15 K) = 3.73 ± 0.11

$\log_{10}\beta_2^\circ$ (An = Am, 298.15 K) = 5.64 ± 0.10

$\log_{10}\beta_2^\circ$ (An = Cm, 298.15 K) = 5.70 ± 0.09

$\log_{10}\beta_2°$ (An = Cf, 298.15 K) = 5.58 ± 0.11

$\log_{10}\beta_3°$ (An = Am, 298.15 K) = 5.29 ± 0.05

$\log_{10}\beta_3°$ (An = Cm, 298.15 K) = 5.15 ± 0.05

$\log_{10}\beta_3°$ (An = Cf, 298.15 K) = 5.09 ± 0.05

Silva et al. (1995) discuss in their Appendix A the Am data of McDowell & Coleman (1972) as follows: "As low concentrations of H_2SO_4 – Na_2SO_4 were used, the Debye-Hückel relation was appropriately applied. The stability constants $\log_{10}\beta_1°$ and $\log_{10}\beta_2°$ … are in good agreement with the values extrapolated by this review … using the specific ion interaction equations of Appendix B. Further experimental work is necessary to confirm the presences of $Am(SO_4)_3^{3-}$. The value of $\log_{10}\beta_3°$ is therefore not selected by this review."

Silva et al. (1995) finally selected

$\log_{10}\beta_1°$ (An = Am, 298.15 K) = 3.85 ± 0.03

$\log_{10}\beta_2°$ (An = Am, 298.15 K) = 5.4 ± 0.7

In their NEA update volume, Guillaumont et al. (2003) state that there are no new experimental data on the sulphate complexation of Am(III) since the previous review (Silva et al. 1995) was published. However, there are more recent investigations of sulphate complexes of Cm(III) by using Time-Resolved Laser Fluorescence Spectroscopy (TRLFS). The spectroscopically determined $\log_{10}\beta_1$ values in NaCl are about 0.6 log units lower than the literature data for Am(III) and Cm(III) in $NaClO_4$ and NH_4ClO_4 media of comparable ionic strength and the $\log_{10}\beta_2$ values are 1.5 – 2 orders of magnitude smaller. The large discrepancies in the data from the two groups of methods, i.e., solvent extraction and spectroscopy, are far beyond the experimental uncertainties of the two types of methods and are typical for systems where weak complexes are formed.

The experimental techniques based on two-phase equilibria such as ion exchange and solvent extraction are in these cases unable to distinguish between ion-ion interaction and inner-sphere complexation. The replacement of large parts of the background electrolyte by the ligand causes changes in the activity coefficients, which are misinterpreted as complex formation. The same can hold for activity changes caused by the formation of outer-sphere complexes or ion pairs. In the solvent extraction studies of De Carvalho & Choppin (1967a) and McDowell & Coleman (1972) analogous experiments with both Am(III) and Cm(III) gave very similar equilibrium constants for the two actinides (see above) indicating that discrepancies between spectroscopic results for Cm(III) and non-spectroscopic methods for Am(III) are primarily not a result of chemical differences, but rather that the two types of experiments measure different phenomena. Hence, the review by Guillaumont et al. (2003) based the selection of equilibrium constants for aqueous sulphate complexes on the spectroscopically determined Cm(III) data rather than on those from other sources, and selected common Am(III)/Cm(III) values:

$\log_{10}\beta_1°$ (An = Am/Cm, 298.15 K) = 3.30 ± 0.15

$\log_{10}\beta_2°$ (An = Am/Cm, 298.15 K) = 3.70 ± 0.15

In the light of the above discussion by Guillaumont et al. (2003), this review decided not to include any value for $\log_{10}\beta_2°$ (An = Cf, 298.15 K) in TDB 2020, but to consider the average of the values given by De Carvalho & Choppin (1967a) and McDowell & Coleman (1972), extrapolated to I = 0 in this review,

$$Cf^{3+} + SO_4^{2-} \rightleftharpoons CfSO_4^+$$

$$\log_{10}\beta_1°(298.15\ K) = 3.6 \pm 0.4$$

as a rough estimate, with increased uncertainty. This value is included in TDB 2020 as supplemental datum as well as the estimates

$$\varepsilon(CfSO_4^+, ClO_4^-) = (0.2 \pm 0.1)\ kg \cdot mol^{-1}$$

$$\varepsilon(CfSO_4^+, Cl^-) = (0.05 \pm 0.10)\ kg \cdot mol^{-1}$$

No attempt has been made to extrapolate the enthalpy value (Fig. 8-2) to zero ionic strength, and the value obtained at 2.0 M $NaClO_4$

$$\Delta_r H_m(298.15\ K) = (18.1 \pm 3.1)\ kJ \cdot mol^{-1}$$

is also included in TDB 2020 as supplemental datum.

8.3.5 Californium(III) thiocyanate complexes

Choppin & Ketels (1965) determined the complex formation of some trivalent lanthanide and actinide elements with thiocyanate in 1.0 M $NaClO_4$ at 25 °C by a solvent extraction method at a fixed pH of 2.00. They interpreted their data in terms of the complex

$$An^{3+} + SCN^- \rightleftharpoons AnSCN^{2+}$$

β_1 (An = Am, 298.15 K) = 3.19 ± 0.10

β_1 (An = Cm, 298.15 K) = 2.70 ± 0.19

β_1 (An = Cf, 298.15 K) = 3.06 ± 0.18

The uncertainties given by Choppin & Ketels (1965) represent 1σ.

Hence, within a 2σ confidence interval the above values do not show any significant variation.

For Am and Cm Choppin & Ketels (1965) also reported β_2 values, but no β_2 value is given for Cf. No comment on this omission can be found in the text of Choppin & Ketels (1965).

Harmon et al. (1972) also used a solvent extraction method to examine the formation of actinide thiocyanate complexes under the same conditions as Choppin & Ketels (1965), i.e., in 1.0 M $NaClO_4$ at 25 °C and at a fixed pH of 2.00. They obtained

β_1 (An = Am, 298.15 K) = 2.29 ± 0.15

β_1 (An = Cm, 298.15 K) = 2.84 ± 0.19

β_1 (An = Bk, 298.15 K) = 3.11 ± 0.22

β_1 (An = Cf, 298.15 K) = 3.71 ± 0.20

β_1 (An = Es, 298.15 K) = 3.62 ± 0.22

In addition, they interpreted their data in terms of the complexes

$An^{3+} + 2\ SCN^- \rightleftharpoons An(SCN)_2^+$

β_2 (An = Am, 298.15 K) = 1.09 ± 0.49

β_2 (An = Cm, 298.15 K) = 0.86 ± 0.62

β_2 (An = Bk, 298.15 K) = 0.31 ± 0.74

β_2 (An = Cf, 298.15 K) = 0.28 ± 0.65

β_2 (An = Es, 298.15 K) = 0.04 ± 0.74

$An^{3+} + 3\ SCN^- \rightleftharpoons An(SCN)_3(aq)$

β_3 (An = Am, 298.15 K) = 0.70 ± 0.37

β_3 (An = Cm, 298.15 K) = 0.84 ± 0.47

β_3 (An = Bk, 298.15 K) = 2.34 ± 0.56

β_3 (An = Cf, 298.15 K) = 2.65 ± 0.50

β_3 (An = Es, 298.15 K) = 2.94 ± 0.54

The uncertainties given by Harmon et al. (1972) also represent 1σ.

Hence, within a 2σ confidence interval, the β_1 values seem to indicate slightly increasing stability of the $AnSCN^{2+}$ complex with increasing proton number.

On the other hand, the β_2 values seem to be pure error absorbers in the data fitting procedure, as all these values cannot be distinguished from zero from a statistical point of view. This can also be seen in Tab. 2 of Harmon et al. (1972) where they show the sum of the squared deviations for the curve fitting procedure. They tried three different variants, β_1,β_2 model, β_1,β_3 model, and β_1,β_2,β_3 model. While the sums comparing the β_1,β_3 model with the β_1,β_2,β_3 model slightly decrease in the case of Am by including β_2, the differences get smaller for Cm, Bk and Cf and vanish for Es.

The β_3 values again seem to indicate increasing stability of the $An(SCN)_3(aq)$ complex with increasing proton number. However, a speciation model where the $An(SCN)_2^+$ complex virtually does not exist while the $An(SCN)_3(aq)$ complex is fairly strong does not make sense from the viewpoint of coordination chemistry. In addition, inspecting Fig. 5 of Harmon et al. (1972), showing experimental data for Am(III) and Cf(III), it can be seen that a good fit of the data in the

[SCN^-] concentration range 0.05 – 0.4 M can be achieved by considering only $AnSCN^{2+}$. In the [SCN^-] concentration range 0.5 – 1.0 M the $An(SCN)_3(aq)$ complex is needed, but there the $NaClO_4$ medium is largely to completely exchanged with NaSCN, and the β_3 values may just represent medium effects.

In summary, the β_2 and β_3 values of Harmon et al. (1972) are not considered in this review.

This review estimated a $\Delta\varepsilon$ value for extrapolation of $\log_{10}\beta_1$ to zero ionic strength, using $\varepsilon(SCN^-, Na^+) = (0.05 \pm 0.01)$ kg · mol^{-1} (Lemire et al. 2013), and using the estimates according to Section 1.5.3 for $\varepsilon(Cf^{3+}, ClO_4^-) = (0.6 \pm 0.1)$ kg · mol^{-1} and $\varepsilon(CfSCN^{2+}, ClO_4^-) = (0.4 \pm 0.1)$ kg · mol^{-1} (Tab. 8-2)

$$Cf^{3+} + SCN^- \rightleftharpoons CfSCN^{2+}$$

$$\Delta\varepsilon(\text{estimated}) = -(0.25 \pm 0.14) \text{ kg} \cdot \text{mol}^{-1}$$

Choppin & Ketels (1965)

$$\log_{10}\beta_1^\circ\ (298.15 \text{ K}) = 1.44 \pm 0.15$$

Harmon et al. (1972)

$$\log_{10}\beta_1^\circ\ (298.15 \text{ K}) = 1.52 \pm 0.15$$

The average of these two values with an increased uncertainty is:

$$\log_{10}\beta_1^\circ\ (298.15 \text{ K}) = 1.5 \pm 0.3$$

This value is included in TDB 2020 as well as the estimates

$$\varepsilon(CfSCN^{2+}, ClO_4^-) = (0.4 \pm 0.1) \text{ kg} \cdot \text{mol}^{-1}$$

$$\varepsilon(CfSCN^{2+}, Cl^-) = (0.15 \pm 0.10) \text{ kg} \cdot \text{mol}^{-1}$$

Note that Silva et al. (1995) selected for Am(III):

$$Am^{3+} + SCN^- \rightleftharpoons AmSCN^{2+}$$

$$\log_{10}\beta_1^\circ\ (298.15 \text{ K}) = 1.3 \pm 0.3$$

8.4 Summary and conclusions

Thermodynamic data for californium have mainly been obtained in experimental studies comprising the transplutonium elements americium, curium, berkelium, californium and sometimes even einsteinium.

Generally, the differences in the stability constants obtained for these transplutonium elements are small, from insignificant, as in the cases of sulphate and thiocyanate complexation, to 0.3 log units, or a factor of 2 in β_1, for the first hydrolysis constant, to a maximum of 0.5 log units, or a factor of 3 in β_1, for the first fluoride stability constants.

If these differences are statistically significant at all, they are in accord with the expectations considering the actinide contraction, the same effect as the lanthanide contraction, i.e., the decrease of the ionic radius with increasing proton number, which leads to slightly increasing complex stability for Cf(III) with respect to Am(III) and Cm(III).

However, thermodynamic data for Cf(III) are very scarce and no solubility data at all are available (Tab. 8-1).

Considering that Guillaumont et al. (2003) decided to evaluate experimental Am(III) and Cm(III) data together and to select common Am(III)/Cm(III) stability constants, and further considering the small to insignificant difference to the few available Cf(III) data, this review recommends to use modelling results obtained for Am(III)/Cm(III) as a proxy for Cf(III).

8.5 Selected californium data

Tab. 8-1: Selected californium data

Supplemental data are in italics.

Name	**$\Delta_f G_m°$** [kJ · mol^{-1}]	**$\Delta_f H_m°$** [kJ · mol^{-1}]	**$S_m°$** [J · K^{-1} · mol^{-1}]	**$C_{p,m}°$** [J · K^{-1} · mol^{-1}]	**Species**
Cf(cr)	0.0	0.0	81 ± 5	-	Cf(cr)
Cf+3	-552.6 ± 7.3	-577 ± 5	-197 ± 17	-	Cf^{3+}

Name	**$\log_{10} K_{s,0}°$**	**$\Delta_r H_m°$** [kJ · mol^{-1}]	**T-range** [°C]	**Reaction**
CfF+2	4.0 ± 0.4	*11.8 ± 1.6*	10 – 55	$Cf^{3+} + F^- \rightleftharpoons CfF^{2+}$
CfSO4+	*3.6 ± 0.4*	*18.1 ± 3.1*	*0 – 55*	$Cf^{3+} + SO_4^{2-} \rightleftharpoons CfSO_4^+$
CfSCN+2	1.5 ± 0.3	-		$Cf^{3+} + SCN^- \rightleftharpoons CfSCN^{2+}$

Tab. 8-2: Selected SIT ion interaction coefficients εj,k [kg · mol-1] for californium species

Data in bold face are taken from Lemire et al. (2013). Data estimated according to charge correlations and taken from Tab. 1-7 are shaded. Supplemental data are in italics.

j k → ↓	**Cl^-** $\varepsilon_{j,k}$ [kg · mol^{-1}]	**ClO_4^-** $\varepsilon_{j,k}$ [kg · mol^{-1}]	**Na^+** $\varepsilon_{j,k}$ [kg · mol^{-1}]	**$Na^+ + Cl^-$** $\varepsilon_{j,k}$ [kg · mol^{-1}]	**$Na^+ + ClO_4^-$** $\varepsilon_{j,k}$ [kg · mol^{-1}]
Cf +3	0.25 ± 0.1	0.6 ± 0.1	0	0	0
CfF+2	0.15 ± 0.1	0.4 ± 0.1	0	0	0
CfSO4+	*0.05 ± 0.1*	*0.2 ± 0.1*	*0*	*0*	*0*
CfSCN+2	0.15 ± 0.1	0.4 ± 0.1	0	0	0

8.6 References

Brown, P.L. & Ekberg, C. (2016): Hydrolysis of Metal Ions. Wiley-VCH Verlag GmbH & Co. KGaA, Weinheim, Germany, 917 pp.

Choppin, G.R. & Ketels, J. (1965): Thiocyanate complexes of some trivalent lanthanide and actinide elements. J. Inorg. Nucl. Chem., 27, 1335-1339.

Choppin, G.R. & Unrein, P.J. (1976): Thermodynamic study of actinide fluoride complexation. *In:* Müller, W. & Lindner, R. (Eds.): Transplutonium 1975. 4th International Transplutonium Element Symposium. Proceedings of the Symposium at Baden-Baden September 13-17, 1975, North-Holland, Amsterdam, pp. 97-107.

De Carvalho, R.G. & Choppin, G.R. (1967a): Lanthanide and actinide sulfate complexes – I Determination of stability constants. J. Inorg. Nucl. Chem., 29, 725-735.

De Carvalho, R.G. & Choppin, G.R. (1967b): Lanthanide and actinide sulfate complexes – II Determination of stability constants. J. Inorg. Nucl. Chem., 29, 737-743.

Désiré, B., Hussonnois, M. & Guillaumont, R. (1969): Détermination de la première constante d'hydrolyse de l'americium, du curium, du berkelium et du californium. C.R. Acad. Sc. Paris, Série C, 269, 448-451.

Grenthe, I., Fuger, J., Konings, R.J.M., Lemire, R.J., Muller, A.B., Nguyen-Trung, C. & Wanner, H. (1992): Chemical Thermodynamics of Uranium. Chemical Thermodynamics, Vol. 1. North-Holland, Amsterdam, 715 pp.

Guillaumont, R., Fanghänel, T., Fuger, J., Grenthe, I., Neck, V., Palmer, D.A. & Rand, M.H. (2003): Update on the Chemical Thermodynamics of Uranium, Neptunium, Plutonium, Americium and Technetium. Chemical Thermodynamics, Vol. 5. Elsevier, Amsterdam, 919 pp.

Hussonnois, M., Hubert, S., Brillard, L. & Guillaumont, R. (1973): Détermination de la première constante d'hydrolyse de l'einsteinium. Radiochem. Radioanal. Letters, 15, 47-56.

Haire, R.G. (2006): Californium. *In:* Morss, L.R., Edelstein, N.M., Fuger, J. & Katz, J.J. (Eds.): The Chemistry of the Actinide and Transactinide Elements, Volume 3, 3$^{r\,d}$ Edition, Springer, The Netherlands, p. 1499-1576.

Harmon, H.D., Peterson, J.R., McDowell, W.J. & Coleman, C.F. (1972): The tetrad effect: The thiocyanate complex stability constants of some trivalent actinides. J. Inorg. Nucl. Chem., 34, 1381-1397.

Konings, R.J.M., Morss, L.R. & Fuger, J. (2006): Thermodynamic Properties of Actinides and Actinide Compounds. *In:* Morss, L.R., Edelstein, N.M., Fuger, J. & Katz, J.J. (Eds.): The Chemistry of the Actinide and Transactinide Elements, Volume 4, 3$^{r\,d}$ Edition, Springer, The Netherlands, p. 2113-2224.

Lemire, R.J., Berner, U., Musikas, C., Palmer, D.A., Taylor, P. & Tochiyama, O. (2013): Chemical Thermodynamics of Iron, Part 1. Chemical Thermodynamics, Vol. 13a. OECD Publications, Paris, France, 1082 pp.

McDowell, W.J. & Coleman, C.F. (1972): The sulfate complexes of some trivalent transplutonium actinides and europium. J. Inorg. Nucl. Chem., 34, 2837-2850.

Morss, L.R. & Williams, C.W. (1994): Synthesis of crystalline americium hydroxide, $Am(OH)_3$, and determination of its enthalpy of formation; estimation of the solubility-product constants of actinide(III) hydroxides. Radiochim. Acta, 66/67, 89-93.

Silva, R.J., Bidoglio, G., Rand, M.H., Robouch, P., Wanner, H. & Puigdomenech, I. (1995): Chemical Thermodynamics of Americium. Chemical Thermodynamics, Vol. 2. Elsevier, Amsterdam, 374 pp.

9 Copper

9.1 Introduction

Thermodynamic data for copper were not included in the PSI/Nagra Chemical Thermodynamic Database 12/07 (TDB 12/07, Thoenen et al. 2014) and its predecessors. Since Nagra is considering copper-coated canister concepts as an alternative to the carbon steel canister (Diomidis et al. 2017), it is appropriate to include copper in TDB 2020.

In a series of reviews devoted to the chemical speciation of environmentally significant metals with inorganic ligands, IUPAC (Powell et al. 2007) reviewed thermodynamic data for Cu(II) which provided the basis for the present data selection. Own reviews were made to evaluate thermodynamic data for Cu(I). The Cu (I) systems, however, even such simple ones as Cu(I) chloride, are much less well known than the corresponding Cu(II) systems, because Cu(I) solutions tend to disproportionate into Cu(II) and metallic copper, and are also very sensitive to oxidation in air (Ahrland & Rawsthorne 1970).

The selected thermodynamic data for Cu(I) and Cu(II) compounds and complexes are presented in Tab. 9-3.

IUPAC, as well as NEA (see, e.g., Grenthe et al. 1992) used the specific ion interaction theory (SIT) for making ionic strength corrections to the experimental data, an approach which is also adopted for TDB 2020 (as has been for all its predecessors). Powell et al. (2007) only evaluated experiments in perchlorate media and explicitly considered the formation of copper chloride complexes. Therefore, ion interaction coefficients ε for cationic copper species with Cl^- are missing. They can be approximated by the corresponding interaction coefficients with ClO_4^-. Thus, e.g., $\varepsilon(CuOH^+, Cl^-) \approx \varepsilon(CuOH^+, ClO_4^-) = -(0.15 \pm 0.08)$ kg · mol^{-1}. If equilibrium constants of reactions with copper species are determined in solutions with chloride salts as background electrolytes (see Section 9.6.1 for an example), the equilibrium constants must be corrected for the formation of copper chloride complexes. The ion interaction coefficients for cationic copper species with Cl^- can then be approximated by the corresponding interaction coefficients with ClO_4^-. Likewise, if ion interaction coefficients for cationic Fe species with Cl^- are not known, they can be estimated by equating them to the corresponding interaction coefficients with ClO_4^-.

In a few cases, the ion interaction coefficients of anionic copper species with Na^+ were not available. We approximated these with the estimation method described in Section 1.5.3, which draws on a statistical analysis of published SIT ion interaction coefficients, and which allows the estimation of missing coefficients for the interaction of cations with Cl^- and ClO_4^-, and for the interaction of anions with Na^+, from the charge of the cations or anions of interest. Powell et al. (2007) reported $\Delta\varepsilon$ values for the formation reactions of copper species. The corresponding ion interaction coefficients for the individual species (compiled in Tabs. 9-4 and 9-5) were calculated from $\Delta\varepsilon$ by using the SIT coefficients listed in Tab. 9-6. If not explicitly written otherwise, the specific ion interaction coefficients ε for neutral species with the background electrolyte are assumed to be equal to zero.

9.2 Cu(cr), Cu^+, and Cu^{2+}

Powell et al. (2007) did not select any data for elemental Cu(cr) and the simple aqueous copper ions Cu^+ and Cu^{2+}. For TDB 2020 we adopt the following CODATA key values (Cox et al. 1989) for Cu(cr) and Cu^{2+}, as selected by NEA (Grenthe et al. 1992)[2]:

$\Delta_f G_m°(Cu, cr, 298.15\ K) = \Delta_f H_m°(Cu, cr, 298.15\ K) = 0.0\ kJ \cdot mol^{-1}$ [3]

$S_m°(Cu, cr, 298.15\ K) = (33.15 \pm 0.08)\ J \cdot K^{-1} \cdot mol^{-1}$

$C_{p,m}°(Cu, cr, 298.15\ K) = (24.44 \pm 0.05)\ J \cdot K^{-1} \cdot mol^{-1}$

$\Delta_f G_m°(Cu^{2+}, 298.15\ K) = (65.04 \pm 1.56)\ kJ \cdot mol^{-1}$

$\Delta_f H_m°(Cu^{2+}, 298.15\ K) = (64.9 \pm 1.0)\ kJ \cdot mol^{-1}$

$S_m°(Cu^{2+}, 298.15\ K) = -(98 \pm 4)\ J \cdot K^{-1} \cdot mol^{-1}$

From these values follow the selected reaction properties for the Cu(cr)/Cu^{2+} redox equilibrium

$$Cu(cr) \rightleftharpoons Cu^{2+} + 2\ e^-$$

$\log_{10} K_{s,0}°(298.15\ K) = -11.39 \pm 0.27$

$\Delta_r H_m°(298.15\ K) = (64.9 \pm 1.0)\ kJ \cdot mol^{-1}$

The specific ion interaction coefficients selected by NEA (Grenthe et al. 1992, Lemire et al. 2013), also adopted for TDB 2020,

$\varepsilon(Cu^{2+}, ClO_4^-) = (0.32 \pm 0.02)\ kg \cdot mol^{-1}$

$\varepsilon(Cu^{2+}, NO_3^-) = (0.11 \pm 0.01)\ kg \cdot mol^{-1}$

were determined by Ciavatta (1980) from isopiestic mean activity coefficient data.

Note that $\varepsilon(Cu^{2+}, Cl^-) = (0.08 \pm 0.01)\ kg \cdot mol^{-1}$ determined by Ciavatta (1980) from isopiestic mean activity coefficient data should not be used with the copper data selected in this report since Ciavatta (1980) did not explicitly consider the formation of copper chloride complexes and therefore any possible effects of copper chloride complexation are included in $\varepsilon(Cu^{2+}, Cl^-)$. Since this report explicitly considers the formation of copper chloride complexation, $\varepsilon(Cu^{2+}, Cl^-)$ must be approximated by using the corresponding ion interaction coefficient with perchlorate:

$\varepsilon(Cu^{2+}, Cl^-) \approx \varepsilon(Cu^{2+}, ClO_4^-) = (0.32 \pm 0.02)\ kg \cdot mol^{-1}$

Neither CODATA nor NEA selected any values for Cu^+.

---

[2] Note that Grenthe et al. (1992) did not select any value for $C_{p,m}°$(Cu, cr, 298.15 K), the corresponding CODATA value was selected by Silva et al. (1995).

[3] By definition.

Wang et al. (1997) reviewed several experimental determinations of the disproportionation reaction

$$2\ Cu^{+} \rightleftharpoons Cu^{2+} + Cu(cr)$$

in perchlorate media at 25 °C and selected data from 5 studies with perchlorate molalities between 0.52 and 8.02. Their linear SIT fit, using the value for $\varepsilon(Cu^{2+}, ClO_4^-)$ given above, resulted in

$$\log_{10}K°(298.15\ K) = (5.76 \pm 0.06)$$

$$\varepsilon(Cu^{+}, ClO_4^-) = (0.11 \pm 0.01)\ kg \cdot mol^{-1}$$

From this $\log_{10}K°(298.15\ K)$ and $\Delta_f G_m°(Cu^{2+}, 298.15\ K)$ selected above then follows

$$\Delta_f G_m°(Cu^{+}, 298.15\ K) = (48.96 \pm 0.80)\ kJ \cdot mol^{-1}$$

which is included in TDB 2020, as well as $\varepsilon(Cu^{+}, ClO_4^-)$ and the estimated

$$\varepsilon(Cu^{+}, Cl^-) \approx \varepsilon(Cu^{+}, ClO_4^-) = (0.11 \pm 0.01)\ kg \cdot mol^{-1}$$

The equilibrium constant for the Cu^{2+}/Cu^{+} redox equilibrium

$$Cu^{2+} + e^- \rightleftharpoons Cu^{+}$$

can be calculated from the selected $\Delta_f G_m°(Cu^{2+}, 298.15\ K)$ and $\Delta_f G_m°(Cu^{+}, 298.15\ K)$. Therefore,

$$\log_{10}K°(298.15\ K) = (2.82 \pm 0.31)$$

This value is also included in TDB 2020.

9.3 Oxygen and hydrogen compounds and complexes

9.3.1 Cu(I) hydroxo complexes

Palmer (2011) measured the solubility of Cu_2O(cuprite) in aqueous solutions at low ionic strengths as a function of pH (3 – 13) and temperature (19.5 – 350 °C) using a low-temperature flow-through apparatus, a high-temperature flow-through apparatus, and a batch reactor apparatus. Metallic copper beads were placed at the inlet regions of the flow-through reactors and added to the solid charge of the batch reactor to ensure that the Cu(I) redox state was preserved. The synthetic cuprous oxide (cuprite) was carefully analysed before and after the experiments with X-ray diffraction (XRD) and scanning electron microscopy, demonstrating that cuprite was the solubility limiting solid throughout all experiments, with the exception of one particular loading of the flow-through apparatus, where the data points collected near the minimum of the solubility curve were characterized by solubilities about an order of magnitude lower than the other data points. These lower solubilities were consistent with the formation of a thin coating of CuO(cr) on Cu_2O(cuprite), but Palmer (2011) was not able to provide a reason for the formation and persistence of this coating (which was apparently too thin to be detected by the subsequent XRD analysis). These data points were consequently excluded from the data analysis.

The dominant Cu(I) species were found to be Cu^+ and $Cu(OH)_2^-$. CuOH(aq) was only found to be of any importance below 100 °C in a narrow pH range at the solubility minimum. Thus, Palmer (2011) interpreted the solubility of cuprite in terms of the following reactions

$$0.5\ Cu_2O(\text{cuprite}) + H^+ \rightleftharpoons Cu^+ + 0.5\ H_2O(l) \quad (3.1)$$

$$0.5\ Cu_2O(\text{cuprite}) + 0.5\ H_2O(l) \rightleftharpoons CuOH(aq) \quad (3.2)$$

$$0.5\ Cu_2O(\text{cuprite}) + 1.5\ H_2O(l) \rightleftharpoons Cu(OH)_2^- + H^+ \quad (3.3)$$

He obtained $\log_{10}{}^*K_{s,0}^\circ(3.1)$, $\log_{10}K_{s,1}^\circ(3.2)$, and $\log_{10}{}^*K_{s,2}^\circ(3.3)$ at each experimental temperature from the solubility vs. pH data and used various 2-, 3- and 4-term functions to represent the solubility constants $\log_{10}{}^*K_{s,0}^\circ(3.1)$ (2-term: constant, $1/T$; 4-term: constant, $1/T$, $\ln T$, T) and $\log_{10}{}^*K_{s,2}^\circ(3.3)$ (3-term: constant, $1/T$, T; 4-term: constant, $1/T$, $\ln T$, T) as a function of temperature. The experimental data by Palmer (2011) were reanalysed by Brown & Ekberg (2016).

9.3.1.1 CuOH(aq)

Brown & Ekberg (2016) accepted the experimental data by Palmer (2011). They combined the values of $\log_{10}K_{s,0}^\circ(3.1)$ and $\log_{10}K_{s,1}^\circ(3.2)$ at each experimental temperature (25, 50, 75 and 100 °C) to obtain $\log_{10}{}^*\beta_1^\circ$ for

$$Cu^+ + H_2O(l) \rightleftharpoons CuOH(aq) + H^+$$

and increased the uncertainties to ± 0.20 if those calculated from the uncertainties by Palmer (2011) were lower. Palmer (2011) did not attempt to fit a temperature function to the data for CuOH(aq). Brown & Ekberg (2016), however, used a 3-term function to describe the dependence of $\log_{10}{}^*\beta_1^\circ$ on temperature and obtained

$$\log_{10}{}^*\beta_1^\circ(T) = 296.3 - 15'374/T - 44.3 \ln T$$

Thus,

$$\log_{10}{}^*\beta_1^\circ(298.15\ \mathrm{K}) = -(7.85 \pm 0.41)$$

From $\log_{10}{}^*\beta_1^\circ(T)$, Brown & Ekberg (2016) also obtained[4]

$$\Delta_r H_m^\circ(298.15\ \mathrm{K}) = (41.3 \pm 4.4)\ \mathrm{kJ \cdot mol^{-1}}$$

and

$$\Delta_r C_{p,m}^\circ(298.15\ \mathrm{K}) = -(848 \pm 123)\ \mathrm{J \cdot K^{-1} \cdot mol^{-1}}$$

These values of $\log_{10}{}^*\beta_1^\circ(298.15\ \mathrm{K})$, $\Delta_r H_m^\circ(298.15\ \mathrm{K})$, and $\Delta_r C_{p,m}^\circ(298.15\ \mathrm{K})$ for the formation reaction of CuOH(aq) derived by Brown & Ekberg (2016) from the data by Palmer (2011) are included in TDB 2020, as well as

$$\varepsilon(\mathrm{CuOH(aq)}, \mathrm{NaClO_4}) = \varepsilon(\mathrm{CuOH(aq)}, \mathrm{NaCl}) = 0$$

9.3.1.2 $Cu(OH)_2$

As in the case of CuOH(aq), Brown & Ekberg (2016) accepted the experimental data by Palmer (2011). They combined the values of $\log_{10}K_{s,0}^\circ(3.1)$ and $\log_{10}K_{s,2}^\circ(3.3)$ at each experimental temperature (25, 50, 51.8, 75, 100, 200, 250, 300, and 350 °C) to obtain $\log_{10}{}^*\beta_2^\circ$ for

$$Cu^+ + 2\ H_2O(l) \rightleftharpoons Cu(OH)_2^- + 2\ H^+$$

increasing the uncertainties to ± 0.20 if those calculated from the uncertainties by Palmer (2011) were lower. Again, Brown & Ekberg (2016) preferred a 3-term function to describe the dependence of $\log_{10}{}^*\beta_2^\circ$ on temperature and obtained

$$\log_{10}{}^*\beta_2^\circ(T) = 89.11 - 7529/T - 14.48 \ln T$$

---

[4] The 3-term function $\log_{10}K^\circ(T) = a + b/T + c \ln T$ is equivalent to
$\log_{10}K^\circ(T) = \log_{10}K^\circ(T_0) - \left(\frac{1}{T} - \frac{1}{T_0}\right)\frac{\Delta_r H_m^\circ(T_0)}{R \ln(10)} - \left(1 - \frac{T_0}{T} + \ln\frac{T_0}{T}\right)\frac{\Delta_r C_{p,m}^\circ(T_0)}{R \ln(10)}$,
and $\log_{10}K^\circ(298.15\ \mathrm{K})$, $\Delta_r H_m^\circ(298.15\ \mathrm{K})$, and $\Delta_r C_{p,m}^\circ(298.15\ \mathrm{K})$ can be easily calculated from a, b, c, and $T_0 = 298.15$ K, see Hummel et al. (2002).

From this temperature function Brown & Ekberg (2016) derived

$$\log_{10}{}^*\beta_2^\circ(298.15\ \mathrm{K}) = -(18.64 \pm 0.60)$$

$$\Delta_r H_m^\circ(298.15\ \mathrm{K}) = (61 \pm 12)\ \mathrm{kJ \cdot mol^{-1}}$$

$$\Delta_r C_{p,m}^\circ(298.15\ \mathrm{K}) = -(277 \pm 98)\ \mathrm{J \cdot K^{-1} \cdot mol^{-1}}$$

These values are included in TDB 2020, as well as the ion interaction coefficient

$$\varepsilon(\mathrm{Cu(OH)_2^-}, \mathrm{Na^+}) \approx -(0.05 \pm 0.10)\ \mathrm{kg \cdot mol^{-1}}$$

estimated according to Tab. 1-7.

9.3.2 Cu(II) hydroxo complexes

According to Powell et al. (2007) the identification and quantification of the mononuclear $Cu(OH)_n^{(2-n)+}$ complexes with n = 1 and 2 is difficult, since even modest total concentrations of Cu(II) lead to the formation of di- and trinuclear complexes. In addition, measurements are complicated by the formation of possibly metastable colloidal suspensions of "Cu(II)-hydroxide". Therefore, Powell et al. (2007) only considered studies of the formation of $CuOH^+$ and $Cu(OH)_2(aq)$ that were carried out at millimolar total copper concentrations. The determination of the formation constants for $Cu(OH)_3^-$ and $Cu(OH)_4^{2-}$ was mainly based on solubility measurements in alkaline solutions while the formation constants for $CuOH^+$ and $Cu(OH)_2(aq)$ and the stoichiometries and formation constants for the polynuclear species Cu_2OH^{3+}, $Cu_2(OH)_2^{2+}$, and $Cu_3(OH)_4^{2+}$ were determined from potentiometric titrations.

9.3.2.1 $CuOH^+$

Powell et al. (2007) relied on two studies that determined the stability constant of the reaction

$$\mathrm{Cu^{2+} + H_2O(l) \rightleftharpoons CuOH^+ + H^+}$$

using cell potential measurements with a copper sensitive electrode in combination with pH measurements with a glass electrode. SIT analysis of three data points at $NaClO_4$ molalities of 0.050, 0.70, and 3.503 $\mathrm{mol \cdot kg^{-1}}$ resulted in

$$\log_{10}{}^*K_1^\circ(298.15\ \mathrm{K}) = -(7.95 \pm 0.16)$$

$$\Delta\varepsilon = -(0.33 \pm 0.08)\ \mathrm{kg \cdot mol^{-1}}$$

From this $\Delta\varepsilon$ and the ε values listed in Tab. 9-6 for the other species taking part in the formation reaction follows

$$\varepsilon(\mathrm{CuOH^+}, \mathrm{ClO_4^-}) = -(0.15 \pm 0.08)\ \mathrm{kg \cdot mol^{-1}}$$

We estimated the ion interaction parameter with Cl^- as

$$\varepsilon(CuOH^+, Cl^-) \approx \varepsilon(CuOH^+, ClO_4^-) = -(0.15 \pm 0.08)\ kg \cdot mol^{-1}$$

All these data for $CuOH^+$ are included in TDB 2020.

Brown & Ekberg (2016) reviewed experimental determinations of the stability constant of $CuOH^+$ as a function of temperature. They accepted values at 18 and 25 °C from two sources, and values at 100, 150, 200, 250, 300, and 350 °C from a third source (for references see Brown & Ekberg 2016). Their 3-term fit to the data resulted in

$$\log_{10}{}^*\beta_1^\circ(T) = -348.8 + 12256/T + 52.67 \ln T$$

From this temperature function Brown & Ekberg (2016) obtained

$$\log_{10}{}^*\beta_1^\circ(298.15\ K) = -(7.64 \pm 0.17)$$

which is in reasonable agreement with the value selected by Powell et al. (2007) and included in TDB 2020, and

$$\Delta_r H_m^\circ(298.15\ K) = (66.0 \pm 2.8)\ kJ \cdot mol^{-1}$$

$$\Delta_r C_{p,m}^\circ(298.15\ K) = (1'008 \pm 23)\ J \cdot K^{-1} \cdot mol^{-1}$$

The latter two values are also included in TDB 2020.

9.3.2.2 $Cu(OH)_2(aq)$

Two studies using copper ion sensitive electrodes were considered by Powell et al. (2007) that investigated the reaction

$$Cu^{2+} + 2\ H_2O(l) \rightleftharpoons Cu(OH)_2(aq) + 2\ H^+$$

using cell potential measurements with a copper sensitive electrode in combination with pH measurements with a glass electrode. Three data points were selected, covering $NaClO_4$ molalities up to 0.70 $mol \cdot kg^{-1}$, and the SIT analysis resulted in

$$\log_{10}{}^*\beta_2^\circ(298.15\ K) = -(16.2 \pm 0.2)$$

$$\Delta\varepsilon = (0.14 \pm 0.36)\ kg \cdot mol^{-1}$$

From this $\Delta\varepsilon$ and the ε values listed in Tab. 9-6 for the other species taking part in the formation reaction follows

$$\varepsilon(Cu(OH)_2, NaClO_4) = (0.18 \pm 0.36)\ kg \cdot mol^{-1}$$

Powell et al. (2007) remarked that this value[5] is high for an uncharged complex but has a large error, which includes zero in its range. All these data for $Cu(OH)_2(aq)$ are included in TDB 2020.

Brown & Ekberg (2016) reviewed experimental determinations of the stability constant of $Cu(OH)_2(aq)$ as a function of temperature. They accepted four values at 25 °C from four different studies, and values at 25, 50, 100, 150, 200, 250, 300, and 350 °C from a fifth study (for references see Brown & Ekberg (2016). Their 3-term fit to the data resulted in

$$\log_{10}{}^*\beta_2^\circ(T) = -411.3 + 13'591/T + 61.33\ \ln T$$

From this temperature function Brown & Ekberg (2016) obtained

$$\log_{10}{}^*\beta_2^\circ(298.15\ K) = -(16.24 \pm 0.03)$$

which is in excellent agreement with the value selected by Powell et al. (2007) and included in TDB 2020, and

$$\Delta_r H_m^\circ(298.15\ K) = (89.9 \pm 0.7)\ kJ \cdot mol^{-1}$$

$$\Delta_r C_{p,m}^\circ(298.15\ K) = (1'174 \pm 6)\ J \cdot K^{-1} \cdot mol^{-1}$$

The latter two values are also included in TDB 2020.

9.3.2.3 $Cu(OH)_3^-$ and $Cu(OH)_4^{2-}$

The formation of $Cu(OH)_3^-$ and $Cu(OH)_4^{2-}$ was studied with solubility experiments involving CuO(tenorite). Both species form in alkaline environments: $Cu(OH)_3^-$ is the predominant species at pH between 10 and 13, while $Cu(OH)_4^{2-}$ becomes predominant at pH above 13.

Powell et al. (2007) accepted the results of a solubility study of CuO(tenorite) by McDowell & Johnston (1936) which were re-evaluated by Plyasunova et al. (1997) using SIT, resulting in

$$CuO(tenorite) + H_2O(l) + OH^- \rightleftharpoons Cu(OH)_3^-$$

$$\log_{10}K_{s,3}^\circ(298.15\ K) = -(4.96 \pm 0.05)$$

---

[5] Note that Powell et al. (2007) reported a value of $(0.14 \pm 0.36)\ kg \cdot mol^{-1}$. The reason for this is that in the text they rounded $\Delta\varepsilon(Cu^{2+} + 2\ H_2O(l) \rightleftharpoons Cu(OH)_2(aq) + 2\ H^+) = (0.14 \pm 0.36)\ kg \cdot mol^{-1}$ to $(0.1 \pm 0.3)\ kg \cdot mol^{-1}$, and then most likely used $(0.1 \pm 0.36)\ kg \cdot mol^{-1}$ for calculating $\varepsilon(Cu(OH)_2, NaClO_4) = (0.14 \pm 0.36)\ kg \cdot mol^{-1}$.

and

$$CuO(tenorite) + H_2O(l) + 2\ OH^- \rightleftharpoons Cu(OH)_4^{2-}$$

$$\log_{10}K_{s,4}°(298.15\ K) = -(4.10 \pm 0.15)$$

with

$$\varepsilon(Cu(OH)_3^-, K^+) = (0.40 \pm 0.02)\ kg \cdot mol^{-1}$$

$$\varepsilon(Cu(OH)_4^{2-}, K^+) = (0.29 \pm 0.05)\ kg \cdot mol^{-1}$$

Combining both tenorite dissolution reactions and their solubility constants leads to

$$Cu(OH)_3^- + OH^- \rightleftharpoons Cu(OH)_4^{2-}$$

$$\log_{10}K_4°(298.15\ K) = (0.86 \pm 0.16)$$

For the tenorite solubility reaction

$$CuO(tenorite) + H_2O(l) \rightleftharpoons Cu^{2+} + 2\ OH^-$$

the solubility product selected by Powell et al. (2007) is (see Section 9.3.4)

$$\log_{10}K_{s,0}°(298.15\ K) = -(20.36 \pm 0.06)$$

Combining this $\log_{10}K_{s,0}°(298.15\ K)$ with $\log_{10}K_{s,3}°(298.15\ K)$ results in

$$\log_{10}\beta_3°(298.15\ K) = (15.40 \pm 0.08)$$

for the reaction

$$Cu^{2+} + 3\ OH^- \rightleftharpoons Cu(OH)_3^-$$

and combining $\log_{10}\beta_3°(298.15\ K)$ with $\log_{10}K_4°(298.15\ K)$ results in

$$\log_{10}\beta_4°(298.15\ K) = (16.26 \pm 0.24)$$

for the reaction

$$Cu^{2+} + 4\ OH^- \rightleftharpoons Cu(OH)_4^{2-}$$

Finally, Powell et al. (2007) formulated the latter two reactions in terms of H^+ instead of OH^- and recalculated the corresponding formation constants using the dissociation constant of water. Thus,

$$Cu^{2+} + 3\ H_2O(l) \rightleftharpoons Cu(OH)_3^- + 3\ H^+$$

$$\log_{10}{}^*\beta_3^\circ(298.15\ K) = -(26.60 \pm 0.09)$$

$$Cu^{2+} + 4\ H_2O(l) \rightleftharpoons Cu(OH)_4^{2-} + 4\ H^+$$

$$\log_{10}{}^*\beta_4^\circ(298.15\ K) = -(39.74 \pm 0.18)$$

Powell et al. (2007) adopted $\Delta\varepsilon$ values for these two reactions from Plyasunova et al. (1997), thus

$$\Delta\varepsilon(Cu^{2+} + 3\ H_2O(l) \rightleftharpoons Cu(OH)_3^- + 3\ H^+) = (0.50 \pm 0.06)\ kg \cdot mol^{-1}$$

and

$$\Delta\varepsilon(Cu^{2+} + 4\ H_2O(l) \rightleftharpoons Cu(OH)_4^{2-} + 4\ H^+) = (0.43 \pm 0.05)\ kg \cdot mol^{-1}$$

From these $\Delta\varepsilon$ values and the ε values listed in Tab. 9-6 for the other species taking part in the formation reactions follow

$$\varepsilon(Cu(OH)_3^-, Na^+) = (0.40 \pm 0.09)\ kg \cdot mol^{-1}$$

$$\varepsilon(Cu(OH)_4^{2-}, Na^+) = (0.19 \pm 0.10)\ kg \cdot mol^{-1}$$

Powell et al. (2007) considered $\log_{10}{}^*K_1^\circ(298.15\ K)$, $\log_{10}{}^*\beta_2^\circ(298.15\ K)$, $\log_{10}{}^*\beta_3^\circ(298.15\ K)$, and $\log_{10}{}^*\beta_4^\circ(298.15\ K)$ as "Recommended" but remarked that "they exhibit some worrying features". In particular, Powell et al. (2007) noted that the stepwise constants $\log_{10}K_n^\circ$ show a normal sequence of declining values with increasing n, however, the difference $\log_{10}K_2^\circ - \log_{10}K_1^\circ = -0.27$ is unreasonably small, while the differences between $\log_{10}K_2^\circ = 5.78$, $\log_{10}K_3^\circ = 3.57$, and $\log_{10}K_4^\circ = 0.86$ are large, as to be expected.

The values for $\log_{10}{}^*\beta_3^\circ(298.15\ K)$, $\log_{10}{}^*\beta_4^\circ(298.15\ K)$, $\Delta\varepsilon(Cu^{2+} + 3\ H_2O(l) \rightleftharpoons Cu(OH)_3^- + 3\ H^+)$, $\Delta\varepsilon(Cu^{2+} + 4\ H_2O(l) \rightleftharpoons Cu(OH)_4^{2-} + 4\ H^+)$, $\varepsilon(Cu(OH)_3^-, K^+)$, $\varepsilon(Cu(OH)_3^-, Na^+)$, $\varepsilon(Cu(OH)_4^{2-}, K^+)$, and $\varepsilon(Cu(OH)_4^{2-}, Na^+)$ were all recommended by Powell et al. (2007) (or derived from values recommended by them), and are all included in TDB 2020.

Brown & Ekberg (2016) reviewed experimental determinations of the stability constant of $Cu(OH)_4^{2-}$ as a function of temperature. They accepted four values at 25 °C from four different studies, two values at 50 and 75 °C from a fifth study and values at 25, 50, 100, 150, 200, 250, and 300 °C from a sixth study (for references see Brown & Ekberg (2016). Their 3-term fit to the data resulted in

$$\log_{10}{}^*\beta_4^\circ(T) = -312.6 + 4727/T + 45.11\ \ln T$$

From this temperature function Brown & Ekberg (2016) obtained

$$\log_{10}{}^*\beta_4^\circ(298.15\ \mathrm{K}) = -(39.70 \pm 0.19)$$

which is in excellent agreement with the value selected by Powell et al. (2007) and included in TDB 2020, and

$$\Delta_r H_m^\circ(298.15\ \mathrm{K}) = (167.0 \pm 5.7)\ \mathrm{kJ \cdot mol^{-1}}$$

$$\Delta_r C_{p,m}^\circ(298.15\ \mathrm{K}) = (864 \pm 57)\ \mathrm{J \cdot K^{-1} \cdot mol^{-1}}$$

The latter two values are also included in TDB 2020.

9.3.2.4 Cu_2OH^{3+}, $Cu_2(OH)_2^{2+}$, and $Cu_3(OH)_4^{2+}$

According to Powell et al. (2007), $Cu_2(OH)_2^{2+}$ is the predominant polynuclear complex in slightly acidic solutions at moderate (millimolar) Cu(II) total concentrations. In contrast, Cu_2OH^{3+} appears to form only at high total Cu(II) concentrations (0.3 – 0.9 mol · dm^{-3}) at pH ≤ 3.5, and still only to less than 1%. The trinuclear complex, $Cu_3(OH)_4^{2+}$, finally, appears in measurable amounts only in solutions supersaturated with respect to CuO(s) and $Cu(OH)_2$(s).

Concerning the formation of Cu_2OH^{3+}, Powell et al. (2007) accepted the results of three studies performed in $NaClO_4$. A SIT analysis of seven measurements at perchlorate molalities between 0.101 to 3.503 mol · kg^{-1} resulted in

$$2\ Cu^{2+} + H_2O(l) \rightleftharpoons Cu_2OH^{3+} + H^+$$

$$\log_{10}{}^*\beta_{2,1}^\circ(298.15\ \mathrm{K}) = -(6.40 \pm 0.12)$$

$$\Delta\varepsilon = (0.04 \pm 0.04)\ \mathrm{kg \cdot mol^{-1}}$$

Powell et al. (2007) accepted these results only as "Provisional" since the data were not well represented by the linear SIT fit. Three values at 3.503 mol · kg^{-1} $NaClO_4$, where the accuracy should be highest, show large discrepancies, while the values at lower molality from a single study are clearly discordant to the trend imposed by the SIT analysis. These "Provisional" data for Cu_2OH^{3+} are included in TDB 2020 as supplemental data, as well as

$$\varepsilon(Cu_2OH^{3+}, ClO_4^-) = (0.54 \pm 0.06^6)\ \mathrm{kg \cdot mol^{-1}}$$

calculated from this $\Delta\varepsilon$ and the ε values listed in Tab. 9-6 for the other species taking part in the formation reaction, and

$$\varepsilon(Cu_2OH^{3+}, Cl^-) \approx (Cu_2OH^{3+}, ClO_4^-) = (0.54 \pm 0.06)\ \mathrm{kg \cdot mol^{-1}}$$

---

6 The uncertainty reported by Powell et al. (2007) is ± 0.05 kg · mol^{-1}.

Four studies dealing with the formation of $Cu_2(OH)_2^{2+}$

$$2\ Cu^{2+} + 2\ H_2O(l) \rightleftharpoons Cu_2(OH)_2^{2+} + 2\ H^+$$

were accepted by Powell et al. (2007). An SIT analysis of eight data points covering $NaClO_4$ concentrations from 0.101 to 3.503 mol · kg^{-1} resulted in

$$\log_{10}{}^*\beta_{2,2}^\circ(298.15\ K) = -(10.43 \pm 0.07)$$

$$\Delta\varepsilon = -(0.07 \pm 0.04)\ kg \cdot mol^{-1}$$

From this $\Delta\varepsilon$ value and the ε values listed in Tab. 9-6 for the other species taking part in the formation reactions follows

$$\varepsilon(Cu_2(OH)_2^{2+}, ClO_4^-) = (0.29 \pm 0.12^7)\ kg \cdot mol^{-1}$$

and thus the estimate

$$\varepsilon(Cu_2(OH)_2^{2+}, Cl^-) \approx \varepsilon(Cu_2(OH)_2^{2+}, ClO_4^-) = (0.29 \pm 0.12)\ kg \cdot mol^{-1}$$

All these values for $Cu_2(OH)_2^{2+}$ are included in TDB 2020.

Brown & Ekberg (2016) reviewed experimental determinations of the stability constant of $Cu_2(OH)_2^{2+}$ as a function of temperature. They accepted a value at 18 °C from one study, three values at 25 °C from three additional studies, values at 10, 25 and 45 °C from a fifth study and values at 15, 20, 25, 30, 36, and 42 °C from a sixth study (for references see Brown & Ekberg (2016). Their 2-term fit to the data resulted in

$$\log_{10}{}^*\beta_{22}^\circ(T) = 1.96 - 3730/T$$

From this temperature function Brown & Ekberg (2016) obtained

$$\log_{10}{}^*\beta_{22}^\circ(298.15\ K) = -(10.55 \pm 0.02)$$

which is in reasonable agreement with the value selected by Powell et al. (2007) and included in TDB 2020, and

$$\Delta_r H_m^\circ(298.15\ K) = (71.4 \pm 5.0)\ kJ \cdot mol^{-1}$$

$$\Delta_r C_{p,m}^\circ(298.15\ K) = 0$$

The latter two values are also included in TDB 2020.

---

7 The uncertainty according to our own calculations is ± 0.07 kg · mol^{-1}, we adopt the higher value by Powell et al. (2007).

For the trimeric complex $Cu_3(OH)_4^{2+}$ (observed at pH around 6 and high total Cu(II) concentrations) with the formation reaction

$$3\ Cu^{2+} + 4\ H_2O(l) \rightleftharpoons Cu_3(OH)_4^{2+} + 4\ H^+$$

only two studies with limited data (two data points at 0.101 mol · kg^{-1} $NaClO_4$ and KNO_3, resp.) were available to Powell et al. (2007). Since an SIT analysis was not possible with these data alone, Powell et al. (2007) assumed that the ionic strength dependence of the formation of the trimer is identical to that of the dimer $Cu_2(OH)_2^{2+}$ and thus used

$$\Delta\varepsilon = -(0.07 \pm 0.04)\ kg \cdot mol^{-1}$$

for the SIT analysis, which led to their "Provisional" value

$$log_{10}{}^*\beta_{2,2}°(298.15\ K) = -(21.1 \pm 0.2)$$

These data for $Cu_3(OH)_4^{2+}$ are included in TDB 2020 as supplemental data, as well as

$$\varepsilon(Cu_3(OH)_4^{2+}, ClO_4^-) = (0.33 \pm 0.11)\ kg \cdot mol^{-1}$$

calculated from $\Delta\varepsilon$ and the ε values listed in Tab. 9-6 for the other species taking part in the formation reaction, and the estimate

$$\varepsilon(Cu_3(OH)_4^{2+}, Cl^-) \approx \varepsilon(Cu_3(OH)_4^{2+}, ClO_4^-) = (0.33 \pm 0.11)\ kg \cdot mol^{-1}$$

9.3.3 Solid Cu(I) oxides and hydroxides

9.3.3.1 Solubility of Cu_2O(cuprite)

As discussed above, Palmer (2011) determined the solubility of Cu_2O(cuprite) as a function of pH and temperature. In the acid region, the solubility can be expressed by

$$0.5\ Cu_2O(cuprite) + H^+ \rightleftharpoons Cu^+ + 0.5\ H_2O(l)$$

Palmer (2011) measured the solubility at 19.5, 25, 50, 51.8, 75, 100, 150, 200, 250, 300, and 350 °C and used a 2-term (constant, 1/T) and a 4-term (constant, 1/T, ln$T$, T) equation to express $\log_{10}{}^*K_{s,0}°$(3.1) as a function of temperature. As is the case with CuOH(aq) and $Cu(OH)_2^-$, Brown & Ekberg (2016) accepted the data provided by Palmer (2011), but increased the uncertainties to ± 0.20. They used a 2-term function to fit the data, resulting in

$$\log_{10}{}^*K_{s,0}°(T) = 1.26 - 451/T$$

From this temperature function Brown & Ekberg (2016) derived

$\log_{10}{}^{*}K_{s,0}^{\circ}(298.15\ \mathrm{K}) = -(0.25 \pm 0.12)$

$\Delta_r H_m^{\circ}(298.15\ \mathrm{K}) = (8.6 \pm 1.9)\ \mathrm{kJ \cdot mol^{-1}}$

$\Delta_r C_{p,m}^{\circ}(298.15\ \mathrm{K}) = 0$

These data are included in TDB 2020.

9.3.4 Solid Cu(II) oxides and hydroxides

9.3.4.1 Solubility of CuO(tenorite) and $Cu(OH)_2$(s)

According to Powell et al. (2007) there are two phases commonly formed in Cu(II)-OH^- solutions, namely CuO(tenorite) and $Cu(OH)_2$(s). Under ambient conditions, CuO(tenorite) is the more stable and thus less soluble phase, while $Cu(OH)_2$(s) refers to a less well defined, metastable species. Powell et al. (2007) accepted experimental data by Feitknecht & Schindler (1963) and Schindler et al. (1965) on the solubility of these two phases. Powell et al. (2007) corrected the experimental data for the reactions

$\mathrm{CuO(tenorite) + 2\ H^+ \rightleftharpoons Cu^{2+} + H_2O(l)}$

$\mathrm{Cu(OH)_2(s) + 2\ H^+ \rightleftharpoons Cu^{2+} + H_2O(l)}$

to zero ionic strength by using

$\Delta\varepsilon = (0.04 \pm 0.06)\ \mathrm{kg \cdot mol^{-1}}$

which they calculated from $\varepsilon(Cu^{2+}, ClO_4^-) = (0.32 \pm 0.02)\ \mathrm{kg \cdot mol^{-1}}$ and $\varepsilon(H^+, ClO_4^-) = (0.14 \pm 0.02)\ \mathrm{kg \cdot mol^{-1}}$ under the assumption that ε(solid phase, $NaClO_4$) = 0. They obtained

$\log_{10}{}^{*}K_{s,0}^{\circ}(\mathrm{CuO, tenorite}, 298.15\ \mathrm{K}) = (7.64 \pm 0.06)$

$\log_{10}{}^{*}K_{s,0}^{\circ}(\mathrm{Cu(OH)_2, s}, 298.15\ \mathrm{K}) = (8.67 \pm 0.05)$

These data for CuO(tenorite) and $Cu(OH)_2$(s) are included in TDB 2020.

Brown & Ekberg (2016) reviewed solubility data for tenorite and accepted data at zero ionic strength and 25 °C from 4 publications and data at zero ionic strength in the temperature range 25 to 350 °C from one publication (see Brown & Ekberg 2016 for references). Their 3-term fit to the solubility data resulted in

$\log_{10}{}^{*}K_{s,0}^{\circ}(\mathrm{CuO, tenorite}, T) = 407.9 - 15'076/T - 61.38 \ln T$

from which they derived $\log_{10}{}^{*}K_{s,0}°$(CuO, tenorite, 298.15 K) = (7.63 ± 0.05), which is in excellent agreement with the value selected by Powell et al. (2007), and

$\Delta_r H_m°$(CuO, tenorite, 298.15 K) = -(61.7 ± 1.5) kJ·mol^{-1}

$\Delta_r C_{p,m}°$(CuO, tenorite, 298.15 K) = -(1'175 ± 13) J · K^{-1} · mol^{-1}

The latter two values are also included in TDB 2020.

9.4 Chloride compounds and complexes

9.4.1 Cu(I) chloride complexes

The complexation of Cu(I) with chloride has been studied, e.g., by Ahrland & Rawsthorne (1970), Hikita et al. (1973), Fritz (1980, 1984), and Xiao et al. (1998). The main conclusion of these studies is that $CuCl_2^-$ and $CuCl_3^{2-}$ are the predominant species within a wide range of chloride concentrations below 5 M (Ahrland & Rawsthorne 1970, Fritz 1980), while $Cu_2Cl_4^{2-}$ and triply charged complexes (represented by $Cu_3Cl_6^{3-}$) appear to become important at higher chloride concentrations. There are indications that CuCl(aq) may be formed at chloride concentrations < 0.01 M (Ahrland & Rawsthorne 1970).

Ahrland & Rawsthorne (1970) studied the formation of Cu(I) chloride complexes at 25 °C at a constant ionic strength of 5 M (4.9 M $NaClO_4$ electrolyte at an acidity of 0.1 M $HClO_4$) using solubility, CuCl(s), and potentiometric methods. They reported conditional formation constants for the first three mononuclear complexes CuCl(aq), $CuCl_2^-$, and $CuCl_3^{2-}$, and obtained evidence for the formation of a polynuclear species with a charge of -2, which they represented as $Cu_2Cl_4^{2-}$.

Hikita et al. (1973) measured the solubility of CuCl(s) in mixed HCl/$HClO_4$ solutions at ionic strengths of 0.5, 1.0, 2.0, 3.5, 5.0, and 6.5 M, at 15, 25, and 35 °C. They interpreted their solubility data in terms of $CuCl_2^-$, $CuCl_3^{2-}$, and $CuCl_4^{3-}$ and determined formation constants of these species from CuCl(s) as a function of temperature and nominal ionic strength. According to Fritz (1980), Hikita et al. (1973) were able to fit their data to only about 10%, and their constants are only very approximate.

For this reason, Fritz (1980) reinterpreted the data, introducing the Pitzer formalism to derive activity coefficients. In his analysis, he needed CuCl(aq), $CuCl_2^-$, $CuCl_3^{2-}$, $Cu_2Cl_4^{2-}$, and triply charged complexes (represented by $Cu_3Cl_6^{3-}$) to account for the solubility data over the entire experimental range. In order to calculate stability constants for the complexes from their formation constants from CuCl(s), Fritz (1980) selected a solubility product $K_{s,0}°$(298.15 K) = 2.0 × 10^{-7}, or $\log_{10}K_{s,0}°$(298.15 K) = -6.7, from a range of tabulated values between 1.2 × 10^{-7} and 2.3 × 10^{-7}, without giving any sources for these numbers. Thus, he obtained $\log_{10}\beta_2°$(298.15 K) = 5.48, $\log_{10}\beta_3°$(298.15 K) = 4.81 $\log_{10}\beta_{42}°$(298.15 K) = 10.32. We include these data in TDB 2020 by assigning uncertainties that reflect the range of values the solubility constant was chosen from:

$Cu^+ + 2\ Cl^- \rightleftharpoons CuCl_2^-$

$\log_{10}\beta_2°$(298.15 K) = 5.48 ± 0.25

$Cu^+ + 3\ Cl^- \rightleftharpoons CuCl_3^{2-}$

$\log_{10}\beta_3°(298.15\ K) = 4.81 \pm 0.25$

$2\ Cu^{+} + 4\ Cl^{-} \rightleftharpoons Cu_2Cl_4^{2-}$

$\log_{10}\beta_{42}°(298.15\ K) = 10.32 \pm 0.50$

Xiao et al. (1998) studied the formation of Cu(I) complexes in vapor-saturated hydrothermal HCl/NaCl solutions at 40 to 300 °C. For temperatures up to 150 °C, they used CuCl(s) as solid reactant and at higher temperatures Cu(s). Total chloride concentrations varied from 0.01 to 1 mol · kg^{-1}, and pH from 0 – 3.5. Copper or copper chloride dissolved mainly as CuCl(aq), $CuCl_2^{-}$, and $CuCl_3^{2-}$. For these species, Xiao et al. (1998) obtained the following stability constants: $\log_{10}K_1°$(CuCl, aq, 298.15 K) = 3.30, $\log_{10}\beta_2°(CuCl_2^{-}, 298.15\ K) = 5.57$, and $\log_{10}\beta_3°(298.15\ K) = 4.86$. The latter two are close to those determined by Fritz (1980), thus it is reasonable to also include $\log_{10}K_1°$(CuCl, aq, 298.15 K), by assigning an uncertainty of similar magnitude to the uncertainties chosen for $CuCl_2^{-}$ and $CuCl_3^{2-}$ above:

$Cu^{+} + Cl^{-} \rightleftharpoons CuCl(aq)$

$\log_{10}K_1°(298.15\ K) = 3.30 \pm 0.25$

For inclusion in TDB 2020, we estimated ion interaction coefficients using the method described in Section 1.5.3:

$\varepsilon(CuCl_2^{-}, Na^{+}) \approx -(0.05 \pm 0.10)\ kg \cdot mol^{-1}$

$\varepsilon(CuCl_3^{2-}, Na^{+}) \approx -(0.10 \pm 0.10)\ kg \cdot mol^{-1}$

$\varepsilon(Cu_2Cl_4^{2-}, Na^{+}) \approx -(0.10 \pm 0.10)\ kg \cdot mol^{-1}$

9.4.2 Cu(II) chloride complexes

Cu(II) is generally thought to form four chloride complexes in aqueous solution, $CuCl_n^{(2-n)}$ with n = 1-4. Powell et al. (2007) mentioned that the formation of these complexes has been mainly investigated by UV-vis spectrometry and that the different electronic absorption bands are strongly overlapping, requiring simultaneous determination of the formation constants and absorptivities, leading to correlation problems in the data. Furthermore, since $CuCl^{+}$ and $CuCl_2$(aq) are weak and $CuCl_3^{-}$ and $CuCl_4^{2-}$ extremely weak complexes, they form only at high chloride concentrations. Reliable stability constants can therefore only be measured in solutions with high concentrations of background electrolyte. Powell et al. (2007) warned, however, that high ionic strength media do not guarantee constant activity coefficients, especially in cases where the replacement of the background anion (usually ClO_4^{-}) by chloride is significant.

9.4.2.1 $CuCl^{+}$

Powell et al. (2007) accepted data from eight publications concerning the reaction

$Cu^{2+} + Cl^{-} \rightleftharpoons CuCl^{+}$

An SIT analysis of eight data points with $NaClO_4$ molalities ranging from 1.051 to 6.584 mol · kg^{-1} resulted in

$$\log_{10}\beta_1°(298.15\ K) = (0.83 \pm 0.09)$$

$$\Delta\varepsilon = -(0.05 \pm 0.02)\ kg \cdot mol^{-1}$$

From this $\Delta\varepsilon$ and the ε values listed in Tab. 9-6 for the other species taking part in the formation reaction follows

$$\varepsilon(CuCl^+, ClO_4^-) = (0.30 \pm 0.05^{8})\ kg \cdot mol^{-1}$$

and the estimate

$$\varepsilon(CuCl^+, Cl^-) \approx \varepsilon(CuCl^+, ClO_4^-) = (0.30 \pm 0.05)\ kg \cdot mol^{-1}$$

These data for $CuCl^+$ are all included in TDB 2020.

9.4.2.2 $CuCl_2$(aq)

Six studies concerning the formation of $CuCl_2$(aq)

$$Cu^{2+} + 2\ Cl^- \rightleftharpoons CuCl_2(aq)$$

were accepted by Powell et al. (2007). Since $CuCl_2$(aq) is weaker than $CuCl^+$, reliable data could only be obtained at ionic strengths of more than 3 mol · dm^{-3}. However, a reliable extrapolation to zero ionic strength can only be achieved if data at lower ionic strength is included. For this reason, Powell et al. (2007) carried out their SIT analysis of five measurements in $NaClO_4$ solutions with molalities ranging from 3.503 to 6.584 mol · kg^{-1} by including an additional measurement obtained in 1.051 mol · kg^{-1} $HClO_4$ and obtained

$$\log_{10}\beta_2°(298.15\ K) = (0.6 \pm 0.3)$$

$$\Delta\varepsilon = -(0.10 \pm 0.06)\ kg \cdot mol^{-1}$$

which they accepted as "Provisional".

From $\Delta\varepsilon$ and the ε values listed in Tab. 9-6 for the other species taking part in the formation reaction follows

$$\varepsilon(CuCl_2, NaClO_4) = (0.28 \pm 0.07)\ kg \cdot mol^{-1}$$

---

8 The uncertainty according to our own calculations is ± 0.03 kg · mol^{-1}, we adopt the higher value by Powell et al. (2007).

All these data for $CuCl_2$(aq) are included in TDB 2020 as supplemental data.

9.4.2.3 $CuCl_3^-$ and $CuCl_4^{2-}$

Powell et al. (2007) did not recommend any data for the higher complexes since the few reported formation constants refer to very high ionic strengths and differ considerably.

9.4.3 Solid Cu(I) chlorides

The solubility of CuCl(nantokite) was measured by Liu et al. (2008) in supercritical water, however no data applicable to 25 °C were derived.

As discussed above in Section 9.4.1, Fritz (1980) selected a solubility product $K_{s,0}°(298.15\ K) = 2.0 \times 10^{-7}$, or $\log_{10}K_{s,0}°(298.15\ K) = -6.7$ for CuCl(s), from a range of tabulated values between 1.2×10^{-7}, $\log_{10}K_{s,0}°(298.15\ K) = -6.9$, and 2.3×10^{-7}, $\log_{10}K_{s,0}°(298.15\ K) = -6.6$, in order to calculate stability constants for Cu(I) chloride complexes from their formation constants from CuCl(s). Even though Fritz (1980) did not report any sources for the solubility products, and the quality of these values may be questionable, we include his selected one

$$\log_{10}K_{s,0}°(298.15\ K) = -6.7 \pm 0.2$$

for

$$CuCl(s) \rightleftharpoons Cu^+ + Cl^-$$

in TDB 2020, assigning an uncertainty to cover the range of the tabulated values. One has to bear in mind, that this solubility product only makes sense in combination with the stability constants of the Cu(I) chloride complexes $CuCl_2^-$, $CuCl_3^{2-}$, $Cu_2Cl_4^{2-}$ discussed in Section 9.4.1.

9.4.4 Solid Cu(II) chlorides

$CuCl_2$(tolbachite) is hygroscopic and unstable in air, converting into $CuCl_2{\cdot}2H_2O$(eriochalcite). Both minerals are very soluble and therefore not considered for TDB 2020.

9.5 Carbonate compounds and complexes

9.5.1 Cu(I) carbonate complexes

There appear to be no data on Cu(I) carbonate complexes.

9.5.2 Cu(II) carbonate complexes

As stated in Powell et al. (2007), Cu(II) carbonate complexes dominate the hydroxide complexes over a wide range of solution compositions unless the fugacity of CO_2g is significantly lower than atmospheric levels.

9.5.2.1 $CuCO_3$(aq)

Powell et al. (2007) accepted data from three publications reporting formation constants for the reaction

$$Cu^{2+} + CO_3^{2-} \rightleftharpoons CuCO_3(aq)$$

An SIT analysis of four stability constants measured in solutions with $NaClO_4$ molalities between 0.022 and 1.051 mol · kg^{-1}, and two constants already corrected to zero ionic strength resulted in

$$\log_{10}K_1°(298.15\ K) = (6.75 \pm 0.03)$$

$$\Delta\varepsilon = -(0.18 \pm 0.04)\ kg \cdot mol^{-1}$$

Noting that CO_3^{2-} forms ion pairs to significant extents with Na^+, Mg^{2+}, and Ca^{2+} in natural waters, Powell et al. (2007) chose to express the formation of $CuCO_3$(aq) in terms of HCO_3^- which forms only weak ion pairs with said cations. For this purpose, they derived formation constants for

$$Cu^{2+} + HCO_3^- \rightleftharpoons CuCO_3(aq) + H^+$$

from the experimental data mentioned above with the equilibrium constants for the reaction $CO_3^{2-} + H^+ \rightleftharpoons HCO_3^-$ that were used in the original publications. Their SIT analysis resulted in

$$\log_{10}K°(298.15\ K) = -(3.56 \pm 0.03)$$

$$\Delta\varepsilon = -(0.19 \pm 0.04)\ kg \cdot mol^{-1}$$

From this $\Delta\varepsilon$ and the ε values listed in Tab. 9-6 for the other species taking part in the formation reaction follows

$$\varepsilon(CuCO_3, NaClO_4) = -(0.01 \pm 0.10\ ^{9})\ kg \cdot mol^{-1}\ ^{10}$$

The last three values are included in TDB 2020.

---

9 The uncertainty according to our own calculations is ± 0.05 kg · mol^{-1}, we adopt the higher value by Powell et al. (2007).

10 Note that from $\Delta\varepsilon = -(0.18 \pm 0.04)$ kg · mol^{-1} for $Cu^{2+} + CO_3^{2-} \rightleftharpoons CuCO_3$(aq) follows $\varepsilon(CuCO_3, NaClO_4) = (0.06 \pm 0.05)$ kg · mol^{-1}, within the uncertainty of $\varepsilon(CuCO_3, NaClO_4) = -(0.01 \pm 0.10)$ kg · mol^{-1}.

9.5.2.2 $Cu(CO_3)_2^{2-}$

Formation constants for

$$Cu^{2+} + 2\ CO_3^{2-} \rightleftharpoons Cu(CO_3)_2^{2-}$$

were accepted by Powell et al. (2007) from two publications. Four constants were measured in solutions with $NaClO_4$ molalities between 0.022 and 1.051 mol · kg^{-1}, and one constant was already corrected to zero ionic strength. Powell et al. (2007) obtained from their SIT analysis

$$\log_{10}\beta_2°(298.15\ K) = (10.3 \pm 0.1)$$

$$\Delta\varepsilon = (0.3 \pm 0.2)\ kg \cdot mol^{-1}$$

Using an analogous procedure as discussed in Section 9.5.2.1 for $CuCO_3(aq)$, Powell et al. (2007) reformulated the formation of $Cu(CO_3)_2^{2-}$ in terms of HCO_3^- and obtained

$$Cu^{2+} + 2\ HCO_3^- \rightleftharpoons Cu(CO_3)_2^{2-} + 2\ H^+$$

$$\log_{10}{}^*K°(298.15\ K) = -(10.3 \pm 0.1)$$

$$\Delta\varepsilon = (0.3 \pm 0.2)\ kg \cdot mol^{-1}$$

From this $\Delta\varepsilon$ and the ε values listed in Tab. 9-6 for the other species taking part in the formation reaction follows

$$\varepsilon(Cu(CO_3)_2^{2-}, Na^+) = (0.34 \pm 0.21)\ kg \cdot mol^{-1}\ ^{11}$$

The last three values are included in TDB 2020.

9.5.2.3 $CuHCO_3^+$

For $CuHO_3^+$, Powell et al. (2007) accepted 4 stability constants from a single study measured at $NaClO_4$ molalities between 0.022 and 1.051 mol · kg^{-1}. From an SIT analysis they obtained

$$Cu^{2+} + HCO_3^- \rightleftharpoons CuHCO_3^+$$

$$\log_{10}K°(298.15\ K) = (1.84 \pm 0.10)$$

$$\Delta\varepsilon = (0.14 \pm 0.15)\ kg \cdot mol^{-1}$$

---

11 Note that from $\Delta\varepsilon = (0.3 \pm 0.2)\ kg \cdot mol^{-1}$ for $Cu^{2+} + 2\ CO_3^{2-} \rightleftharpoons Cu(CO_3)_2^{2-}$ follows $\varepsilon(Cu(CO_3)_2^{2-}, Na^+) = (0.46 \pm 0.21)\ kg \cdot mol^{-1}$, within the uncertainty of $\varepsilon(Cu(CO_3)_2^{2-}, Na^+) = (0.34 \pm 0.21)\ kg \cdot mol^{-1}$.

From this $\Delta\varepsilon$ and the ε values listed in Tab. 9-6 for the other species taking part in the formation reaction follows

$$\varepsilon(CuHCO_3^+, ClO_4^-) = (0.46 \pm 0.15)\ kg \cdot mol^{-1}$$

and therefore also the estimate

$$\varepsilon(CuHCO_3^+, Cl^-) \approx \varepsilon(CuHCO_3^+, ClO_4^-) = (0.46 \pm 0.15)\ kg \cdot mol^{-1}$$

These data are included in TDB 2020.

9.5.2.4 $Cu(CO_3)OH^-$

Powell et al. (2007) reported a single conditional stability constant for the reaction $CuCO_3(aq) + H_2O(l) \rightleftharpoons Cu(CO_3)OH^- + H^+$, $\log_{10}K$(298.15 K, 0.72 mol · kg^{-1} $NaClO_4$) = -9.27. They considered this value as indicative only but noted that this ternary complex could become significant in marine and alkaline systems. They combined the conditional constant with $\log_{10}K_w$(298.15 K, 0.72 mol · kg^{-1} $NaClO_4$) = -13.73 to obtain the conditional constant $\log_{10}K$(298.15 K, 0.72 mol · kg^{-1} $NaClO_4$) = (4.46 ± 0.30) for the reaction $CuCO_3(aq) + OH^- \rightleftharpoons Cu(CO_3)OH^-$. Since this reaction is isocoulombic, it can be assumed that it depends only minimally on ionic strength, such that $\Delta\varepsilon \approx 0$ and therefore $\log_{10}K°$(298.15 K) = (4.46 ± 0.30). Finally, Powell et al. (2007) combined this reaction with $Cu^{2+} + CO_3^{2-} \rightleftharpoons CuCO_3(aq)$ to obtain

$$Cu^{2+} + CO_3^{2-} + OH^- \rightleftharpoons Cu(CO_3)OH^-$$

with

$$\log_{10}K°(298.15\ K) = (11.21 \pm 0.30)$$

They assumed that $\Delta\varepsilon$ for this reaction has the same value as $\Delta\varepsilon$ for $Cu^{2+} + CO_3^{2-} \rightleftharpoons CuCO_3(aq)$. Thus

$$\Delta\varepsilon = -(0.18 \pm 0.04)\ kg \cdot mol^{-1}$$

From this $\Delta\varepsilon$ and the ε values listed in Tab. 9-6 for the other species taking part in the formation reaction follows

$$\varepsilon(Cu(CO_3)OH^-, Na^+) = (0.10 \pm 0.05)\ kg \cdot mol^{-1}$$

These data are included in TDB 2020 as supplemental data.

9.5.3 Solid Cu(I) carbonates

There appear to be no data on Cu(I) carbonate solids.

9.5.4 Solid Cu(II) carbonates

9.5.4.1 Solubility of $Cu_2CO_3(OH)_2$(malachite)

Powell et al. (2017) considered two solubility studies of malachite that reported solubility constants for the reaction

$$Cu_2CO_3(OH)_2(malachite) \rightleftharpoons 2\ Cu^{2+} + CO_3^{2-} + 2\ OH^-$$

The solubility constants were determined by Schindler et al. (1968) and Symes & Kester (1984) in 0.2 and 0.72 mol · dm^{-3} $NaClO_4$, respectively. Powell et al. (2017) deemed the measurement made at the lower ionic strength as more reliable and accepted the solubility constant, corrected by Schindler et al. (1968) to zero ionic strength,

$$log_{10}K_{s,0}°(298.15\ K) = -(33.16 \pm 0.08)$$

as "Provisional". Powell et al. (2007) extrapolated this value to 0.72 mol · dm^{-3} $NaClO_4$ by using

$$\Delta\varepsilon = 0.64\ kg \cdot mol^{-1}$$

calculated from $\varepsilon(Cu^{2+}, ClO_4^-) = (0.32 \pm 0.02)$ kg · mol^{-1}, $\varepsilon(CO_3^{2-}, Na^+) = -(0.08 \pm 0.03)$ kg · mol^{-1}, $\varepsilon(OH^-, Na^+) = (0.04 \pm 0.01)$ kg · mol^{-1}, and assuming that ε(malachite, $NaClO_4$) = 0. They obtained $\log_{10}K_{s,0}$(298.15 K, 0.72 mol · dm^{-3} $NaClO_4$) = -31.9 which is in reasonable agreement with the value $\log_{10}K_{s,0}$(298.15 K, 0.72 mol · dm^{-3} $NaClO_4$) = -(31.2 ± 0.1)[12] reported by Symes & Kester (1984).

Preis & Gamsjäger (2002) determined the solubility constant for the reaction $Cu_2CO_3(OH)_2$(malachite) + 4 H^+ ⇌ 2 Cu^{2+} + CO_2g + 3 H_2O(l) as a function of ionic strength (1.0 – 3.0 mol · kg^{-1} $HClO_4/NaClO_4$). From the solubility constant corrected by Preis & Gamsjäger (2002) to zero ionic strength using SIT, Powell et al. (2007) derived a value for $\Delta_f G_m°$(malachite, 298.15 K) which they used to calculate $\log_{10}K_{s,0}°$(298.15 K) = -(33.49 ± 0.22) for the reaction studied by Schindler et al. (1968). This value is in agreement with $\log_{10}K_{s,0}°$(298.15 K) = -(33.16 ± 0.08) determined by the latter authors.

The solubility constant by Schindler et al. (1968) and the corresponding $\Delta\varepsilon$ derived by Powell et al. (2007) are included in TDB 2020 as supplemental data.

---

[12] Including corrections for a the formation of $NaCO_3^-$ and b the activity coefficient of OH^-.

9.5.4.2 Solubility of $Cu_3(CO_3)_2(OH)_2$(azurite)

The solubility constant for

$$Cu_3(CO_3)_2(OH)_2(azurite) \rightleftharpoons 3\ Cu^{2+} + 2\ CO_3^{2-} + 2\ OH^-$$

determined by Schindler et al. (1968) in 0.2 mol · dm^{-3} $NaClO_4$ was corrected to zero ionic strength by Powell et al. (2007) by using

$$\Delta\varepsilon = 0.88\ kg \cdot mol^{-1}$$

which they calculated from $\varepsilon(Cu^{2+}, ClO_4^-) = (0.32 \pm 0.02)$ kg · mol^{-1}, $\varepsilon(CO_3^{2-}, Na^+) = -(0.08 \pm 0.03)$ kg · mol^{-1}, $\varepsilon(OH^-, Na^+) = (0.04 \pm 0.01)$ kg · mol^{-1}, and the assumed ε(azurite, $NaClO_4$) = 0. Thus, they arrived at

$$log_{10}K_{s,0}°(298.15\ K) = -(44.9 \pm 0.2)$$

and accepted this value as "Provisional". This solubility product and the corresponding $\Delta\varepsilon$ are both included in TDB 2020 as supplemental data.

Preis & Gamsjäger (2002) determined the solubility constant for the reaction $Cu_3(CO_3)_2(OH)_2$(azurite) + 6 $H^+ \rightleftharpoons$ 3 Cu^{2+} + 2 CO_2g + 4 H_2O(l) as a function of ionic strength (1.0 – 3.0 mol · kg^{-1} $HClO_4/NaClO_4$). As in the case of malachite discussed above, Powell et al. (2007) derived a value for $\Delta_f G_m°$(azurite, 298.15 K) which they used to calculate $\log_{10}K_{s,0}°$(298.15 K) = -(45.42 ± 0.35) for the reaction studied by Schindler et al. (1968). This value is in reasonable agreement with $\log_{10}K_{s,0}°$(298.15 K) = -(44.9 ± 0.2) determined by the latter authors and accepted by Powell et al. (2007).

9.6 Sulphur compounds and complexes

9.6.1 Sulphide compounds and complexes

Rickard & Luther (2006) and Rickard (2012) presented extensive reviews on the chemistry of aqueous metal-sulphide complexes and clusters. Concerning copper, they noted that Cu(I) and Cu(II) have contrasting properties which influences complexation with sulphide. Cu(II) shows typical borderline hard-soft behaviour, whereas Cu(I) is a soft, B-class metal with a particular attraction for sulphides. As cited by Rickard & Luther (2006), Luther et al. (2002) demonstrated this difference with an electron paramagnetic resonance study of the reaction between aqueous Cu(II) and S(-II), showing that Cu(I) was produced in solution before the formation of the CuS precipitate. Thus, according to Rickard & Luther (2006), Cu in complexes with the soft base S(-II) is the soft Cu(I) while Cu complexed with hard H_2O in the aquo ion is the relatively hard Cu(II). Also, it appears that in most sulphide minerals Cu is present as Cu(I), this has been shown, e.g., for covellite, CuS, by van der Laan et al. (1992) using Cu 2*p* X-ray absorption spectroscopy.

Rickard & Luther (2006) and Rickard (2012) discussed several problems associated with the determination of copper sulphide complexes:

The solubilities of copper sulphides have been explained in numerous studies with various copper sulphide complexes. Simple curve fitting, however, does not give a unique solution and independent evidence for the proposed complexes is required, but is often not available. Several copper sulphide complexes with unusual coordination or conformation have been proposed on the basis of X-ray structural analyses of precipitated salts. It is, however, not possible to extrapolate the structure of the moiety in the solid to structure and stoichiometry of the species in solution without independent evidence.

Another major problem is the definition of the stoichiometry and structure of the investigated solid precipitated at low temperatures. Several copper sulphide phases may be formed with compositions varying between CuS and CuS_2, and the nature of the precipitate may change with time (see Rickard 2012 for references), such that the solubility may change with time and steady-state measurements may not reflect the initial composition of the precipitate.

A whole zoo of different copper sulphide and polysulphide complexes has been proposed. Rickard & Luther (2006) and Rickard (2012) mentioned the following (see these authors for references and details): $Cu(HS)^+$, $Cu(HS)_2(aq)$, CuS(aq), $Cu_3S_3(aq)$, $Cu_2S_3^{2-}$, $Cu_4S_6^{2-}$, $Cu(HS)_2^-$, $Cu_2S(HS)_2^{2-}$, CuHS(aq), $Cu(HS)_3^{2-}$, $Cu_3S_4H_2^{2-}$, $Cu_2S(HS)_2^{2-}$, $Cu_4S_4H_2^{2-}$, $Cu_2S_2(HS)_3^{3-}$, $Cu_2(S_3)(S_4)^{2-}$, $Cu(S_9)(S_{10})^{3-}$, multinuclear Cu complexes, $Cu_3(S_4)_3^{3-}$, $Cu_3(S_6)_3^{3-}$, $Cu_6(S_5)(S_4)_3^{2-}$, $Cu_4(S_5)_3^{2-}$, $Cu_4(S_4)(S_5)_2^{2-}$, $Cu_4(S_4)_2(S_5)^{2-}$, $[Cu(S_4)]_2(aq)$, $[Cu(S_5)]_2(aq)$, $Cu(S_4)_2^{3-}$, and $Cu(S_5)(S_4)^{3-}$.

Rickard (2012) ended his review on copper sulphides with the remark that "the confusing situation with regard to Cu-sulphide complexes is likely not to be resolved for some time". In light of this disillusioning comment one can expect that the copper sulphide data selected for TDB 2020 and discussed in the following sections may not stand the test of time.

Note that we have deliberately left out polysulphide complexes in our selection, since they are not expected to be of any long-term importance under repository conditions.

9.6.1.1 Cu(I) sulphide complexes

Rickard & Luther (2006) and Rickard (2012) recommended stability constants for CuHS(aq) and $Cu(HS)_2^-$ based on experimental data by Zhang & Millero (1994), Al-Farawati & van den Berg (1999) and Mountain & Seward (1999), and a stability constant for $Cu_2S(HS)_2^{2-}$ based on experimental data by Mountain & Seward (1999). Since Zhang & Millero (1994) and Al-Farawati & van den Berg (1999) carried out their experiments in seawater, we relied on the data by Mountain & Seward (1999) for our selection.

Mountain & Seward (1999) measured the solubility of Cu_2S(chalcocite) at 22 °C and pH between 4 and 11.5 in aqueous sulphide solutions using a flow through column to determine equilibrium between solid and aqueous solution. In total 46 experiments were carried out resulting in a dataset comprising 750 analyses of total copper, total sulphur and pH. The experimental results were explained by the formation of CuHS(aq), $Cu(HS)_2^-$, and $Cu_2S(HS)_2^{2-}$. It was found that CuHS(aq) is the dominant complex at low sulphide concentrations (< 0.001 mol $\cdot$ kg^{-1}) and low pH, $Cu(HS)_2^-$ predominates at near-neutral pH and intermediate to high sulphide concentrations (> 0.001 mol $\cdot$ kg^{-1}), while $Cu_2S(HS)_2^{2-}$ becomes important at alkaline pH values and high sulphur concentrations.

Based on the solubility product for chalcocite

$$Cu_2S(\text{chalcocite}) + H^+ \rightleftharpoons 2\ Cu^+ + HS^-$$

$$\log_{10}{}^*K_{s,0}^\circ(298.15\ K) = -(34.62 \pm 0.13)$$

calculated from $\Delta_f G_m^\circ(Cu_2S, 298.15\ K)$ measured by Potter (1977) at low temperature by electrochemical methods and $\Delta_f G_m^\circ(Cu^+, 298.15\ K)$ and $\Delta_f G_m^\circ(HS^-, 298.15\ K)$ from Wagman et al. (1982), Mountain & Seward (1999) derived the following stability constants from their experimental data:

$$Cu^+ + 2\ HS^- \rightleftharpoons Cu(HS)_2^-$$

$$\log^*\beta_2^\circ(298.15\ K) = (17.18 \pm 0.13)$$

$$2\ Cu^+ + 3\ HS^- \rightleftharpoons Cu_2S(HS)_2^{2-} + H^+$$

$$\log^*\beta^\circ(298.15\ K) = (29.87 \pm 0.13)$$

These data are included in TDB 2020, as well as the ion interaction coefficients

$$\varepsilon(Cu(HS)_2^-, Na^+) = -(0.05 \pm 0.10)\ kg \cdot mol^{-1}$$

$$\varepsilon(Cu_2S(HS)_2^{2-}, Na^+) = -(0.10 \pm 0.10)\ kg \cdot mol^{-1}$$

derived by using the estimation method described in Section 1.5.3.

The stability of CuHS(aq), expected to occur only at low pH, could not be determined by Mountain & Seward (1999), since at low pH the copper concentration was near or below the detection limit. Because Cu should behave similarly as its congeners Ag and Au in Group 11, and AgHS(aq) and AuHS(aq) are the dominant bisulphide species for Ag and Au at low pH, it can be assumed that CuHS(aq) may also appear at low pH. There is an approximately linear relation between stability constants at room temperature of Ag(I) and Cu(I) complexes, $M_2S(HS)_2^{2-}$, $M(HS)_2^-$, and ML and ML_2 with various ligands (L = Cl^-, Br^-, I^-, SO_3^{2-}, $S_2O_3^{2-}$, CN^-, and NH_3). The linear regression line among the stability constants of these complexes was used by Mountain & Seward (1999) to derive

$$Cu^+ + HS^- \rightleftharpoons CuHS(aq)$$

$$\log^*K_1^\circ(298.15\ K) \approx 13$$

from the known stability constant $\log^*K_1^\circ(298.15\ K) = 13.5$ of AgHS(aq). This estimate is included in TDB 2020 as supplemental datum.

Mountain & Seward (2003) performed additional experiments between 35 and 90 °C at pH 6.5 – 7.5 in order to determine the temperature dependence of the $Cu(HS)_2^-$ complex. The quality of the data was sufficient to resolve 0.1 log unit changes in the formation constant of the complex from chalcocite. Analysis of the experimental data resulted in

$$\Delta_r H_m°(Cu^+ + 2\ HS^- \rightleftharpoons Cu(HS)_2^-, 298.15\ K) = -(102 \pm 7)\ kJ{\cdot}mol^{-1}$$

$$\Delta_r C_{p,m}°(Cu^+ + 2\ HS^- \rightleftharpoons Cu(HS)_2^-, 298.15\ K) = (800 \pm 300)\ J \cdot K^{-1} \cdot mol^{-1}$$

These data are included in TDB 2020.

9.6.1.2 Cu(II) sulphide complexes

Rickard & Luther (2006) and Rickard (2012) reported stability constants for $CuHS^+$, CuS(aq), $Cu(HS)_2(aq)$, and $Cu_2S_3^{2-}$ (see Tab. 9-1). All constants were measured in undiluted seawater and can therefore not be extrapolated to zero ionic strength, with the exception of those by Al-Farawati & van den Berg (1999) who did measurements of the stability constants for $CuHS^+$ and $Cu(HS)_2(aq)$ in pure (35‰ salinity) and diluted (21 and 14‰ salinity) seawater. These data could in principle be extrapolated to zero ionic strength, as was done by Hummel et al. (2002) for the stability constants of $NiHS^+$ and $Ni(HS)_2(aq)$ also determined by Al-Farawati & van den Berg (1999), but the linearity of the SIT regressions for $CuHS^+$ and $Cu(HS)_2(aq)$ is not convincing (see Fig. 9-1). In addition, both conditional constants determined by Al-Farawati & van den Berg (1999) in undiluted seawater are in marked disagreement with those determined by Zhang & Millero (1994) and Luther et al. (1996) for $CuHS^+$, and by Zhang & Millero (1994) for $Cu(HS)_2(aq)$, see Tab. 9-1. At the time being, it is not possible to recommend reliable data for Cu(II) sulphide complexes and none are included in TDB 2020.

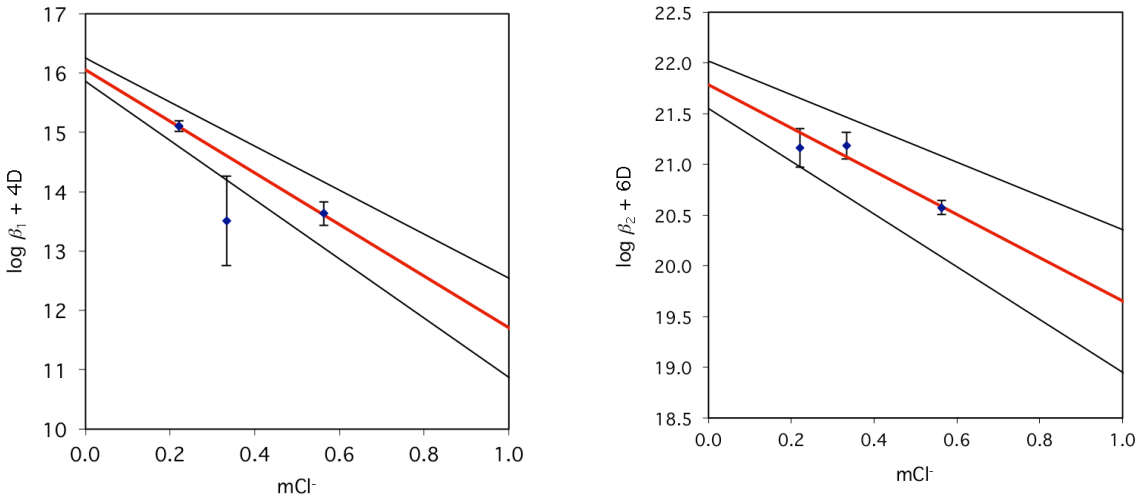

Fig. 9-1: SIT regression for the reactions $Cu^{2+} + HS^- \rightleftharpoons CuHS^+$ (left) and $Cu^{2+} + 2\ HS^- \rightleftharpoons Cu(HS)_2(aq)$ (right).

Stability constants measured by Al-Farawati & van den Berg (1999) in pure (35‰ salinity) and diluted (21 and 14‰ salinity) seawater.

Tab. 9-1: Stability data for Cu(II) sulphide complexes as reported by Rickard & Luther (2006) and Rickard (2012)

All constants were measured in seawater.

Species	**$Log_{10}K$**	**Ionic strength**	**Method**	**Reference**
$CuHS^+$	11.52	0.7	Ligand competition	Al-Farawati & van den Berg (1999)
	7.0	0.7	Sulphide titration	Zhang & Millero (1994)
	5.98	0.7	Sulphide titration	Luther et al. (1996)
CuS(aq)	11.2	0.7	Sulphide titration	Luther et al. (1996)
$Cu(HS)_2(aq)$	18.02	0.7	Ligand competition	Al-Farawati & van den Berg (1999)
	13.0	0.7	Sulphide titration	Zhang & Millero (1994)
$Cu_2S_3^{2-}$	11.68	0.7	Sulphide titration	Luther et al. (1996)
	38.29	0.7	Sulphide titration	Luther et al. (1996)

9.6.1.3 Solid Cu(I) sulphides

For the solubility of Cu_2S(chalcocite) see Section 9.6.1.1.

9.6.1.4 Solid Cu(II) sulphides

Shea & Helz (1989) determined the solubility of CuS(covellite) and a poorly crystalline phase ($Cu_{1.18}S$) at 25 °C in aqueous solution. Chelating agents were used ($DCTA^{4-}$, trans 1-2 diamino-cyclohexyltetraacetic acid, in the case of covellite) to enhance the solubility, which was measured at various HS^- and $HDCTA^{3-}$ concentrations at pH 8.2 and I = 0.2, 0.70, and 1.0 M NaCl. The equilibrium constant of the reaction

$$CuS(covellite) + HDCTA^{3-} \rightleftharpoons CuDCTA^{2-} + HS^-$$

was determined from the measured solubilities and combined with the measured equilibrium constants for

$$CuDCTA^{2-} + 2\ H^+ \rightleftharpoons Cu^{2+} + H_2DCTA^{2-}$$

$$H_2DCTA^{2-} \rightleftharpoons H^+ + HDCTA^{3-}$$

to get the solubility product for

$$CuS(covellite) + H^+ \rightleftharpoons Cu^{2+} + HS^-$$

$$\log_{10}{}^*K_{s,0}°(298.15\ K) = -(22.27 \pm 0.30)$$

Shea & Helz (1989) used the Davies equation for the extrapolation of the solubility products to zero ionic strength and did not explicitly account for the formation of copper chloride complexes. In order to be consistent with all other data selected for TDB 2020, we reanalysed the data by correcting the solubility products determined by Shea & Helz (1989) for the formation of Cu(II) chloride complexes and by using SIT to extrapolate the solubility products to zero ionic strength. In order to use SIT, NaCl concentrations and conditional solubility products were converted from the molar to the molal concentration scale (see Grenthe & Puigdomènech 1997) using ρ-values (ρ = (molal concentration) / (molar concentration)) for NaCl solutions calculated from a polynomial fit to ρ-values for NaCl tabulated by Grenthe & Puigdomènech (1997). Note that these conversions have practically no effect (see Tab. 9-2), due to the relatively low ionic strengths. Corrections for the formation of CuCl(aq) and $CuCl_2^-$ were made by using the following equation (see Hummel et al. 2005, Section V.4)

$$K_{s,0}{}^{corr} = K_{s,0} / (1 + \beta_1 [Cl^-] + \beta_2 [Cl^-]^2)$$

where $K_{s,0}{}^{corr}$ is the conditional solubility constant corrected for the formation of CuCl(aq) and $CuCl_2^-$, $K_{s,0}$ the experimentally determined conditional solubility constant, β_1 the conditional stability constant of CuCl(aq), β_2 the conditional stability constant of $CuCl_2^-$, and $[Cl^-]$ the molality of chloride. β_1 and β_2 were extrapolated from zero ionic strength, where $\log_{10}\beta_1°(298.15\ K) = (0.83 \pm 0.09)$ and $\log_{10}\beta_2°(298.15\ K) = (0.6 \pm 0.3)$, using SIT with $\Delta\varepsilon = -(0.05 \pm 0.02)\ kg \cdot mol^{-1}$ and $\Delta\varepsilon = -(0.10 \pm 0.06)\ kg \cdot mol^{-1}$, respectively.

Standard linear SIT regression (see Fig. 9-2) of the data in Tab. 9-2 resulted in

$$\log_{10}{}^*K_{s,0}°(298.15\ K) = -(22.05 \pm 0.16)$$

with

$$\Delta\varepsilon = (0.10 \pm 0.19)\ kg \cdot mol^{-1}$$

These values are included in TDB 2020. Note that this $\Delta\varepsilon$ can be calculated independently from $\varepsilon(H^+, Cl^-) = (0.12 \pm 0.01)\ kg \cdot mol^{-1}$ selected by NEA (Lemire et al. 2013), $\varepsilon(Cu^{2+}, Cl^-) \approx \varepsilon(Cu^{2+}, ClO_4^-) = (0.32 \pm 0.02)\ kg \cdot mol^{-1}$, see Section 9.2, and $\varepsilon(HS^-, Na^+) = (0.08 \pm 0.02)\ kg \cdot mol^{-1}$ selected by Hummel et al. (2002). The result $\Delta\varepsilon = (0.28 \pm 0.02)\ kg \cdot mol^{-1}$ is in reasonable agreement with the value calculated above.

Tab. 9-2: Selected solubility constants, $\log_{10}{}^{*}K_{s,0}{}^{corr.}$, for the reaction CuS(covellite) + H^+ ⇌ Cu^{2+} + HS^- and auxiliary data

Original data by Shea & Helz (1989) are shaded and data used in the SIT regression (Fig. 9-2) are shown in bold. See text for discussion.

NaCl [a] [mol · dm^{-3}]	**NaCl** [b] [mol · kg^{-1}]	**$\log_{10}{}^{*}K_{s,0}$** [a] [mol · dm^{-3}]	**$\log_{10}{}^{*}K_{s,0}$** [b] [mol · kg^{-1}]	**$\log_{10}\beta_1$ (CuCl, aq)** [c] [mol^{-1} · kg]	**$\log_{10}\beta_2$ ($CuCl_2^-$)** [d] [mol^{-2} · kg^2]	**$\log_{10}{}^{*}K_{s,0}{}^{corr.}$** [e] [mol · kg^{-1}]
0.20	**0.20**	-21.39 ± 0.13	-21.39 ± 0.13	0.29	-0.20	**-21.54 ± 0.13**
0.70	**0.71**	-20.96 ± 0.14	-20.95 ± 0.15	0.11	-0.47	**-21.27± 0.15**
0.70	**0.71**	-21.13 ± 0.16	-21.12 ± 0.17	0.11	-0.47	**-21.44 ± 0.17**
0.70	**0.71**	-21.03 ± 0.16	-21.02 ± 0.17	0.11	-0.47	**-21.34 ± 0.17**
1.00	**1.02**	-20.89 ± 0.16	-20.88 ± 0.17	0.063	-0.52	**-21.28 ± 0.17**
1.00	**1.02**	-20.92 ± 0.15	-20.91 ± 0.16	0.063	-0.52	**-21.31 ± 0.16**
1.00	**1.02**	-21.01 ± 0.15	-21.00 ± 0.16	0.063	-0.52	**-21.40 ± 0.16**
1.00	**1.02**	-20.95 ± 0.14	-20.94 ± 0.15	0.063	-0.52	**-21.34 ± 0.15**
1.00	**1.02**	-20.99 ± 0.16	-20.98 ± 0.17	0.063	-0.52	**-21.38 ± 0.17**

[a] Original data by Shea & Helz (1989) in the molarity scale
[b] Converted from the molarity to the molality scale
[c] Extrapolated from zero ionic strength, $\log_{10}\beta_1°$(298.15 K) = (0.83 ± 0.09), using SIT with $\Delta\varepsilon$ = -(0.05 ± 0.02) kg · mol^{-1}
[d] Extrapolated from zero ionic strength, $\log_{10}\beta_2°$(298.15 K) = (0.6 ± 0.3), using SIT with $\Delta\varepsilon$ = -(0.10 ± 0.06) kg · mol^{-1}
[e] Corrected for the formation of CuCl(aq) and$CuCl_2^-$

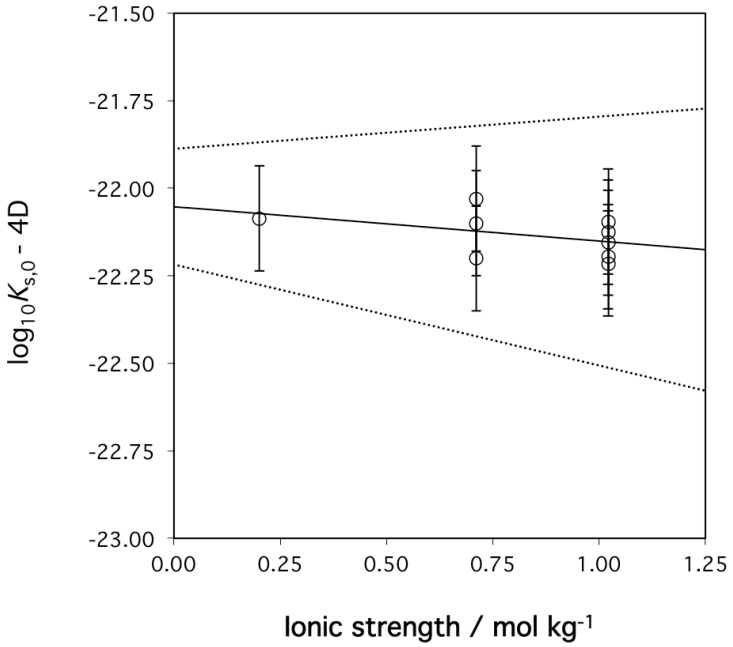

Fig. 9-2: SIT regression for the reaction CuS(covellite) + H^+ ⇌ Cu^{2+} + HS^-

Original data measured in NaCl by Shea & Helz (1989), see Tab. 9-2.

Although we did select the solubility product for covellite by Shea & Helz (1989), there is a big caveat associated with its inclusion in TDB 2020. It is derived from the careful measurements by Shea & Helz (1989) in the system Cu(II)-H_2S-H_4DCTA-H_2O. In this system, any Cu-HS^- complexes cannot compete with the overwhelmingly strong $CuDCTA^{2-}$ complex such that they cannot have any measurable effect on the solubility of covellite. Thus, the solubility product determined by Shea & Helz (1989) at pH = 8 is a "pure" solubility product that leads to solubilities which are too low, if the formation of Cu(II)-HS^- complexes is not considered. As discussed in Section 9.6.1.4, we were not able to include such complexes in TDB 2020, since the available experimental data for $CuHS^+$ and $Cu(HS)_2$(aq) are extremely divergent. Therefore, if in any calculation with TDB 2020 covellite turns out as solubility limiting, the actual solubility could be much higher (even by orders of magnitude!) and the result cannot be trusted. In such a case the modeler has a problem which we cannot resolve at the time being. But at least she is warned that there is a problem with this specific calculation due to insufficient experimental data.

In addition to the solubility of covellite, Shea & Helz (1989) also measured the solubility of a poorly crystalline precipitate, $Cu_{1.18}S$(precipitate), produced by mixing Cu^{2+} and HS^- solutions. Its solubility turned out to be about three orders of magnitude greater than that of covellite. However, this precipitate is not stable and recrystallizes to covellite when brought in contact with polysulphide ions. For this reason, no data for $Cu_{1.18}S$(precipitate) are included in TDB 2020.

9.6.2 Sulphate compounds and complexes

9.6.2.1 Cu(I) sulphate complexes

There appear to be no data on Cu(I) sulphate complexes.

9.6.2.2 Cu(II) sulphate complexes

Powell et al. (2007) presented a detailed discussion on the problems associated with deriving equilibrium constants for complex formation between polyvalent ions, such as Cu^{2+} and SO_4^{2-}. The gist of their discussion can be summarized as follows: The association between Cu^{2+} and SO_4^{2-} is relatively weak, and due to the high charges on the ions, it depends strongly on ionic strength. At present, there is no theoretically rigorous method to disentangle weak complexation and activity coefficient effects and drawing a line between both is rather arbitrary (see also the discussion by Hummel et al. 2005, Section V.4.). In extended Debye-Hückel treatments (SIT is a simple example of this) this is reflected in the strong correlation between the stability constant $K°$ and the ion size (or distance of closest approach) parameter $å$ (or a_j in SIT, assumed to be constant[13]) in the activity coefficient expression. Another problem addressed by Powell et al. (2007), see also Powell et al. (2005), is associated with ion pair formation involving strongly hydrated anions such as SO_4^{2-}. Because of their relatively high charge/radius ratios they tend to keep their solvent sheaths when interacting with cations, leading to different types of ion pairs: a 2SIP (double solvent separated or "outer sphere" ion pair) where the primary solvent sheaths of both ions remain largely intact b SIP (solvent shared or "bridged" ion pair, c CIP (contact or "inner sphere" ion pairs). Spectroscopic methods generally can detect CIPs, but cannot distinguish

[13] The Debye-Hückel term in the SIT formulation is $D = (A\sqrt{I_m})/(1 + Ba_j\sqrt{I_m})$, where A and B are temperature and pressure dependent parameters and a_j is an ion size parameter ("distance of closest approach") for the hydrated ion j. At 298.15 K, $Ba_j = 1.5$ for all ions.

between free hydrated ions, SIPs and 2SIPs. Therefore, such methods measure the equilibrium {free hydrated ions + 2SIP + SIP ⇌ CIP}. Potentiometric and conductivity measurements, in contrast, cannot distinguish between different hydration states of a species and measure the equilibrium{free hydrated ions ⇌ 2SIP + SIP + CIP}.

For this reason, Powell et al. (2007) relied on high-quality conductivity measurements to derive a stability constant for the reaction

$$Cu^{2+} + SO_4^{2-} \rightleftharpoons CuSO_4(aq)$$

They accepted 14 values for the stability constant of the reaction, leading to their "Recommended"

$$\log_{10}K_1°(298.15\ K) = (2.35 \pm 0.05)$$

which is included in TDB 2020.

Powell et al. (2007) also considered measurements of the stability constant of $CuSO_4(aq)$ based on UV-vis spectrometry in $NaClO_4$ and $LiClO_4$ media. An SIT analysis of stability constants measured in $LiClO_4$ (15 measurements, 0.202 to 4.906 mol · kg^{-1} $LiClO_4$) resulted in $\log_{10}K_1°(298.15\ K) = (2.30 \pm 0.10)$, in agreement with the "Recommended" value, and in $\Delta\varepsilon = -(0.08 \pm 0.04)$ kg · mol^{-1}. Analysis of the $NaClO_4$ data (23 measurements, 0.041 to 6.584 mol · kg^{-1} $NaClO_4$) gave $\log_{10}K_1°(298.15\ K) = (2.19 \pm 0.07)$ and $\Delta\varepsilon = -(0.10 \pm 0.03)$ kg · mol^{-1}, only in modest agreement with the "Recommended" $\log_{10}K_1°(298.15\ K)$. The regression plot shows a significant deviation of the data from linearity at lower ionic strength. This was interpreted by Powell et al. (2007) as a result of strong Na^+-SO_4^{2-} interactions, which are underestimated when using $Ba_j = 1.5$ in the SIT relationship. Therefore, they carried out another SIT regression for the $NaClO_4$ data, this time using Ba_j as an additional fit parameter, giving $\log_{10}K_1°(298.15\ K) = (2.36 \pm 0.07)$, $\Delta\varepsilon = -(0.16 \pm 0.07)$ kg · mol^{-1}, and $Ba_j = 1.15$. A similar regression with the $LiClO_4$ data gave $\log_{10}K_1°(298.15\ K) = (2.34 \pm 0.09)$, $\Delta\varepsilon = -(0.09 \pm 0.04)$ kg · mol^{-1}, and $Ba_j = 1.40$. Both stability constants are in excellent agreement with the "Recommended" value. However, these values for $\Delta\varepsilon$ cannot be used to calculate $\varepsilon(CuSO_4, NaClO_4)$ or $\varepsilon(CuSO_4, LiClO_4)$, since the available ion interaction coefficients for all other species were calculated for $Ba_j = 1.5$. Therefore, Powell et al. (2007) performed a last SIT regression with the $NaClO_4$ data, keeping the stability constant $\log_{10}K_1°(298.15\ K)$ fixed at the "Recommended" value of 2.35 ± 0.05, and keeping Ba_j fixed at 1.5. This lead to

$$\Delta\varepsilon = -(0.05 \pm 0.02)$$

which was accepted by Powell et al. (2007) as "Provisional" value and is included in TDB 2020. From this $\Delta\varepsilon$ and the ε values listed in Tab. 9-6 for the other species taking part in the formation reaction follows

$$\varepsilon(CuSO_4, NaClO_4) = (0.15 \pm 0.07)$$

which is also included in TDB 2020.

Powell et al. (2007) accepted 15 measurements of the enthalpy of reaction, $\Delta_r H_m°(298.15\ K)$, for $Cu^{2+} + SO_4^{2-} \rightleftharpoons CuSO_4(aq)$, based on various calorimetric techniques and on the variation of the stability constant as a function of temperature. Averaging of the accepted data resulted in the "Recommended" value

$$\Delta_r H_m°(298.15\ K) = (7.3 \pm 1.5)\ kJ \cdot mol^{-1}$$

which is also included in TDB 2020.

A number of publications reported the formation of higher order $Cu(SO_4)_n^{2(1-n)+}$ species with n = 2 and 3. Powell et al. (2007) rejected these data, because the observed effects might rather be due to changes in activity coefficients, since significant replacement of ClO_4^- by SO_4^{2-} occurs at the high constant ionic strengths maintained during experimentation. By analogy with Cl^- and CO_3^{2-} discussed above, Powell et al. (2007) suggested that a comparatively weak complex $Cu(SO_4)_2^{2-}$ might be formed.

9.6.2.3 Solid Cu(I) sulphates

The synthesis and stability of $Cu_2SO_4(s)$ was investigated by Vo Van & Habashi (1972). It is not possible to crystallize $Cu_2SO_4(s)$ from aqueous solutions. Synthesized $Cu_2SO_4(s)$ is fairly stable in dry air at room temperature, but decomposes rapidly in the presence of moisture. In water, it disproportionates into Cu(s) and $CuSO_4(aq)$. $Cu_2SO_4(s)$ is not considered in TDB 2020.

9.6.2.4 Solid Cu(II) sulphates

Powell et al. (2007) presented only a short discussion of Cu(II) sulphate solids. They stated that under most environmental conditions, $CuSO_4 \cdot 5H_2O$(chalcanthite) is the equilibrium form. Since this salt has a high solubility ($> 2\ mol \cdot dm^{-3}$, increasing rapidly with temperature) it is not expected to precipitate in common natural waters. Powell et al. (2007) noted that there are a number of "basic" sulphates, such as $Cu_3(OH)_4SO_4$(antlerite) and $Cu_4(OH)_6SO_4$(brochantite), that are sparingly soluble in basic media and may become important under such conditions. However, these solids were not considered in their review. According to Pollard et al. (1992), the paragenetic sequence chalcanthite – antlerite – brochanthite – tenorite is observed in the oxidized zone of the copper sulphide bearing orebody at Chuquicamata (Atacama desert, Chile) with increasing distance from the primary sulphide source, due to decreasing sulphate concentration and increasing pH. Pollard et al. (1992) presented stability field diagrams for these minerals. At 25 °C, pH > 6, and activities of $SO_4^{2-} < 10^{-2}$, tenorite appears to be more stable than the sulphate minerals.

9.7 Phosphorus compounds and complexes

9.7.1 Cu(I) phosphate complexes

Ciavatta et al. (1993b) investigated the formation of Cu(I) phosphate complexes at 25 °C in 3 M ($NaClO_4$, NaH_2PO_4) media coulometrically by measuring the displacement of the equilibrium $Cu^{2+} + Cu(s) \rightleftharpoons 2\ Cu^{+}$ as a function of phosphate concentration and acidity. The phosphate concentrations varied from 0.1 – 3 M and the copper concentrations were $\geq 2 \times 10^{-3}$ M. At the high acidities of the experiments, the equilibria were interpreted in terms of $CuH_2PO_4(aq)$, $Cu(H_2PO_4)_2^-$, and $Cu(H_2PO_4)(HPO_4)^{2-}$. Ciavatta et al. (1993b) corrected the conditional formation constants using estimated interaction coefficients for the complex species by applying empirical rules (Ciavatta 1990) and tabulated (Ciavatta 1980) interaction coefficients for the other species. Ciavatta et al. (1993b) did not give enough information to reproduce their procedure, but we assume that they used the following estimated interaction coefficients:

$$\varepsilon(CuH_2PO_4, NaClO_4) \approx 0$$ [14]

$$\varepsilon(Cu(H_2PO_4)_2^-, Na^+) \approx -0.04\ kg \cdot mol^{-1}$$ [15]

$$\varepsilon(Cu(H_2PO_4)(HPO4)^{2-}, Na^+) \approx -0.06\ kg \cdot mol^{-1}$$ [16]

They arrived at the following stability constants:

$$Cu^+ + H_2PO_4^- \rightleftharpoons CuH_2PO_4(aq)$$
$$\log_{10}K_1°(298.15) = (0.87 \pm 0.3)$$

$$Cu^+ + 2\ H_2PO_4^- \rightleftharpoons Cu(H_2PO_4)_2^-$$
$$\log_{10}\beta_2°(298.15) = (1.8 \pm 0.2)$$

$$Cu^+ + 2\ H_2PO_4^- \rightleftharpoons Cu(H_2PO_4)(HPO4)^{2-} + H^+$$
$$\log_{10}{}^*\beta_2°(298.15) = -(3.0 \pm 0.2)$$

The estimated interaction coefficients and the stability constants for these Cu(I) phosphate complexes are included in TDB 2020 as supplemental data, because the stability constants were based by Ciavatta et al. (1993b) on estimates for the interaction coefficients of the phosphate complexes and because their extrapolation procedure with SIT could not be reproduced by us.

---

[14] $\varepsilon(CuH_2PO_4, NaClO_4) \approx ½\ \varepsilon(Cu^+, ClO_4^-) + ½\ \varepsilon(H_2PO_4^-, Na^+) = ½\ (0.11) + ½\ (-0.11)\ kg \cdot mol^{-1} = 0$

[15] $\varepsilon(Cu(H_2PO_4)_2^-, Na^+) \approx ⅓\ [\varepsilon(Cu^+, ClO_4^-) + 2\ \varepsilon(H_2PO_4^-, Na^+)] = ⅓\ [0.11 + 2\ (-0.11)]\ kg \cdot mol^{-1} = -0.037\ kg \cdot mol^{-1}$

[16] $\varepsilon(Cu(H_2PO_4)(HPO4)^{2-}, Na^+) \approx ⅓\ [\varepsilon(Cu^+, ClO_4^-) + \varepsilon(H_2PO_4^-, Na^+) + \varepsilon(HPO_4^{2-}, Na^+)] = ⅓\ [0.11 - 0.11 - 0.19]\ kg \cdot mol^{-1} = -0.063\ kg \cdot mol^{-1}$

9.7.2 Cu(II) phosphate complexes

The number of data for Cu(II) phosphate complexes is very limited. Powell et al. (2007) discussed data for the rather weak complexes $CuH_2PO_4^+$ and $Cu(H_2PO_4)_2(aq)$, both formed in acidic solution ($2 \leq pH \leq 5$), and $CuHPO_4(aq)$ and $Cu(HPO_4)_2^{2-}$, both formed in the range $5 \leq pH \leq 6$. They did not select any data for $CuH_2PO_4^+$, $Cu(H_2PO_4)_2(aq)$, and $Cu(HPO_4)_2^{2-}$ as "Recommended" or "Provisional". For the formation of $CuHPO_4(aq)$ according to the reaction $Cu^{2+} + HPO_4^{2-} \rightleftharpoons CuHPO_4(aq)$, Powell et al. (2007) accepted two measurements in 0.10 mol · dm^{-3} $NaNO_3$ and $NaClO_4$ and accepted

$$\log_{10}K_1(298.15\ \text{K}, I_c = 0.10\ \text{mol} \cdot \text{dm}^{-3}) = (3.25 \pm 0.20)$$

as "Recommended". They estimated

$$\Delta\varepsilon \approx -(0.17 \pm 0.06)\ \text{kg} \cdot \text{mol}^{-1}$$

by using $\varepsilon(Cu^{2+}, ClO_4^-) = (0.32 \pm 0.02)$ kg · mol^{-1}, $\varepsilon(HPO4_2^-, Na^+) = -(0.15 \pm 0.06)$ kg · mol^{-1}, and assuming that $\varepsilon(CuHPO_4, NaClO_4) = 0$ and used this value to correct $\log_{10}K_1(298.15\ \text{K}, I_c = 0.10\ \text{mol} \cdot \text{dm}^{-3})$ to zero ionic strength. Thus,

$$Cu^{2+} + HPO_4^{2-} \rightleftharpoons CuHPO_4(aq)$$

$$\log_{10}K_1°(298.15\ \text{K}) = (4.11 \pm 0.30)$$

This value, as well as the estimated $\Delta\varepsilon \approx -(0.17 \pm 0.06)$ kg · mol^{-1} and $\varepsilon(CuHPO_4, NaClO_4) = 0$ are included in TDB 2020.

Ciavatta et al. (1993a) determined the formation constants of Cu(II) complexes at 25 °C in 3 M ($NaClO_4$, NaH_2PO_4) media using potentiometric titrations with a copper amalgam half-cell and with a glass electrode. Copper concentrations were lower than 5×10^{-3} M and phosphate concentrations varied between 0.015 and 3 M. Experimental results were interpreted in terms of $CuH_2PO_4^+$, $Cu(H_2PO_4)_2(aq)$, $Cu(H_2PO_4)(HPO_4)^-$, and $Cu(HPO_4)_2^{2-}$. Models including $CuHPO_4(aq)$ and/or $CuPO_4^-$ were also tried but including these complexes did not improve the fits to the data sufficiently to prove their presence. As in the case of the Cu(I) phosphate complexes discussed in the preceding Section, Ciavatta et al. (1993a) corrected the conditional formation constants using estimated interaction coefficients for the complex species by applying empirical rules (Ciavatta 1990) and tabulated (Ciavatta 1980) interaction coefficients for the other species. Ciavatta et al. (1993a) did not give enough information to reproduce their procedure, but we assume that they used the following estimated interaction coefficients:

$\varepsilon(CuH_2PO_4^+, ClO_4^-) \approx 0.10\ kg \cdot mol^{-1}$ [17]

$\varepsilon(Cu(H_2PO_4)_2, NaClO_4) \approx 0.03\ kg \cdot mol^{-1}$ [18]

$\varepsilon(Cu(H_2PO_4)(HPO4)^-, Na^+) \approx 0.007\ kg \cdot mol^{-1}$ [19]

$\varepsilon(Cu(HPO_4)_2^{2-}, Na^+) \approx -0.02\ kg \cdot mol^{-1}$ [20]

With these estimates, they obtained

$Cu^{2+} + H_2PO_4^- \rightleftharpoons CuH_2PO_4^+$

$\log_{10}K_1°(298.15) = (1.14 \pm 0.15)$

$Cu^{2+} + 2\ H_2PO_4^- \rightleftharpoons Cu(H_2PO_4)_2(aq)$

$\log_{10}\beta_2°(298.15) = (1.9 \pm 0.2)$

$Cu^{2+} + H_2PO_4^- + HPO_4^{2-} \rightleftharpoons Cu(H_2PO_4)(HPO_4)^-$

$\log_{10}K°(298.15) = (5.4 \pm 0.2)$

$Cu^{2+} + 2\ HPO_4^{2-} \rightleftharpoons Cu(HPO_4)_2^{2-}$

$\log_{10}K°(298.15) = (7.4 \pm 0.2)$

The estimated interaction coefficients and the stability constants for these Cu(II) phosphate complexes are included in TDB 2020 as supplemental data, because the stability constants were based by Ciavatta et al. (1993a) on estimates for the interaction coefficients of the phosphate complexes and because their extrapolation procedure with SIT could not be reproduced by us. The estimated

$\varepsilon(CuH_2PO_4^+, Cl^-) \approx \varepsilon(CuH_2PO_4^+, ClO_4^-) \approx 0.10\ kg \cdot mol^{-1}$

where $\varepsilon(CuH_2PO_4^+, ClO_4^-)$ itself was estimated (see above) is also included in TDB 2020 as supplemental datum.

---

[17] $\varepsilon(CuH_2PO_4^+, ClO_4^-) \approx ½\ \varepsilon(Cu^{2+}, ClO_4^-) + ½\ \varepsilon(H_2PO_4^-, Na^+) = ½\ (0.32) + ½\ (-0.11)\ kg \cdot mol^{-1} = 0.105\ kg \cdot mol^{-1}$

[18] $\varepsilon(Cu(H_2PO_4)_2, NaClO_4) \approx ⅓\ [\varepsilon(Cu^{2+}, ClO_4^-) + 2\ \varepsilon(H_2PO_4^-, Na^+)] = ⅓\ [0.32 + 2\ (-0.11)]\ kg \cdot mol^{-1} = 0.033\ kg \cdot mol^{-1}$

[19] $\varepsilon(Cu(H_2PO_4)(HPO_4)^-, Na^+) \approx ⅓\ [\varepsilon(Cu^{2+}, ClO_4^-) + \varepsilon(H_2PO_4^-, Na^+) + \varepsilon(HPO_4^{2-}, Na^+)] = ⅓\ [0.32 - 0.11 - 0.19]\ kg \cdot mol^{-1} = 0.0067\ kg \cdot mol^{-1}$

[20] $\varepsilon(Cu(HPO_4)_2^{2-}, Na^+) \approx ⅓\ [\varepsilon(Cu^{2+}, ClO_4^-) + 2\ \varepsilon(HPO_4^{2-}, Na^+)] = ⅓\ [0.32 + 2\ (-0.19)]\ kg \cdot mol^{-1} = -0.02\ kg \cdot mol^{-1}$

9.7.3 Solid Cu(I) phosphates

There appear to be no data on Cu(I) phosphate solids.

9.7.4 Solid Cu(II) phosphates

Powell et al. (2017) reported one measurement for the solubility product of $Cu_3(PO_4)_2(s)$ but did not accept it, since no account was taken of the complex formation between Cu^{2+} and HPO_4^{2-}.

9.8 Tab. of selected data

Tab. 9-3: Selected copper data (1 bar, 298.15 K) for TDB 2020

All data are taken from Powell et al. (2007) with the exception of those marked with an asterisk (*) and CODATA values, which are bold. Supplemental data are in italics. T-range refers to the experimental range of temperatures at which equilibrium constants, $\Delta_r H_m°$ and $\Delta_r C_{p,m}°$ were determined. Quality indicators by Powell et al. (2007): R = Recommended, P = Provisional.

Name	**Redox**	**$\Delta_f G_m°$** [kJ · mol^{-1}]	**$\Delta_f H_m°$** [kJ · mol^{-1}]	**$S_m°$** [J · K^{-1} · mol^{-1}]	**$C_{p,m}°$** [J · K^{-1} · mol^{-1}]	**Species**
Cu(cr)	0	**0.0**	**0.0**	**33.15 ± 0.08**	**24.44 ± 0.05**	Cu(cr)
Cu+	I	(48.96 ± 0.80)*	-	-	-	Cu^+
Cu+2	II	**(65.04 ± 1.56)** [a]	**64.9 ± 1.0**	**-98 ± 4**	-	Cu^{2+}

[a] Calculated using $\Delta_f G_m° = \Delta_f H_m° - T \sum S_m°$

Name	**Redox**	**$\log_{10}\beta°$**	**$\Delta\varepsilon$** [kg · mol^{-1}]	**$\Delta_r H_m°$** [kJ · mol^{-1}]	**$\Delta_r C_{p,m}°$** [J · K^{-1} · mol^{-1}]	**T-range** [°C]	**Reaction**	**Quality**
CuOH+	II	-7.95 ± 0.16	-0.33 ± 0.08	(66.0 ± 2.8)*	(1'008 ± 23)*	18 – 350	$Cu^{2+} + H_2O(l) \rightleftharpoons CuOH^+ + H^+$	R
Cu(OH)2(aq)	II	-16.2 ± 0.2	0.14 ± 0.36	(89.9 ± 0.7)*	(1'174 ± 6)*	25 – 350	$Cu^{2+} + 2\ H_2O(l) \rightleftharpoons Cu(OH)_2(aq) + 2\ H^+$	R
Cu(OH)3-	II	-26.60 ± 0.09	0.50 ± 0.06	-	-	-	$Cu^{2+} + 3\ H_2O(l) \rightleftharpoons Cu(OH)_3^- + 3\ H^+$	R
Cu(OH)4-2	II	-39.74 ± 0.18	0.43 ± 0.05	(167.0 ± 5.7)*	(864 ± 57) *	25 – 300	$Cu^{2+} + 4\ H_2O(l) \rightleftharpoons Cu(OH)_4^{2-} + 4H^+$	R [a]
Cu2OH+3	*II*	*-6.40 ± 0.12*	*0.04 ± 0.04*	-	-	-	*$2\ Cu^{2+} + H_2O(l) \rightleftharpoons Cu_2OH^{3+} + H^+$*	*P*
Cu2(OH)2+2	II	-10.43 ± 0.07	-0.07 ± 0.04	(71.4 ± 5.0) *	0*	15 – 45	$2\ Cu^{2+} + 2\ H_2O(l) \rightleftharpoons Cu_2(OH)_2^{2+} + 2\ H^+$	R
Cu3(OH)4+2	*II*	*-21.1 ± 0.2*	*-0.07 ± 0.04*	-	-	-	*$3\ Cu^{2+} + 4\ H_2O(l) \rightleftharpoons Cu_3(OH)_4^{2+} + 4\ H^+$*	*P*
CuCl+	II	0.83 ± 0.09	-0.05 ± 0.02	-	-	-	$Cu^{2+} + Cl^- \rightleftharpoons CuCl^+$	R
CuCl2(aq)	*II*	*0.6 ± 0.3*	*-0.10 ± 0.06*	-	-	-	*$Cu^{2+} + 2\ Cl^- \rightleftharpoons CuCl_2(aq)$*	*P*
CuCO3(aq)	II	-3.56 ± 0.03	-0.19 ± 0.04	-	-	-	$Cu^{2+} + HCO_3^- \rightleftharpoons CuCO_3(aq) + H^+$	R
Cu(CO3)2-2	II	-10.3 ± 0.1	0.3 ± 0.2	-	-	-	$Cu^{2+} + 2\ HCO_3^- \rightleftharpoons Cu(CO_3)_2^{2-} + 2\ H^+$	R
CuHCO3+	II	1.84 ± 0.10	0.14 ± 0.15	-	-	-	$Cu^{2+} + HCO_3^- \rightleftharpoons CuHCO_3^+$	R
Cu(CO3)OH-	*II*	*11.21 ± 0.3*	*-0.18 ± 0.04*	-	-	-	*$Cu^{2+} + CO_3^{2-} + OH^- \rightleftharpoons Cu(CO_3)OH^-$*	- [b]

Tab. 9-3: Cont.

Name	Redox	$\log_{10}\beta°$	$\Delta\varepsilon$ [kg · mol^{-1}]	$\Delta_r H_m°$ [kJ · mol^{-1}]	$\Delta_r C_{p,m}°$ [J · K^{-1} · mol^{-1}]	T-range [°C]	Reaction	Quality
CuSO4(aq)	II	2.35 ± 0.05	(-0.05 ± 0.02) [c]	7.3 ± 1.5	-	25	$Cu^{2+} + SO_4^{2-} \rightleftharpoons CuSO_4(aq)$	R
CuHPO4(aq)	II	4.11 ± 0.30	(-0.17 ± 0.06) [d]	-	-	-	$Cu^{2+} + HPO_4^{2-} \rightleftharpoons CuHPO_4(aq)$	P
CuH2PO4+	*II*	*(1.14 ± 0.15)*[*]	-	-	-	-	*$Cu^{2+} + H_2PO_4^- \rightleftharpoons CuH_2PO_4^+$*	-
Cu(H2PO4)2	*II*	*(1.9 ± 0.2)*[*]	-	-	-	-	*$Cu^{2+} + 2\ H_2PO_4^- \rightleftharpoons Cu(H_2PO_4)_2\ (aq)$*	-
Cu(H2PO4) (HPO4)-	*II*	*(5.4 ± 0.2*[*]	-	-	-	-	*$Cu^{2+} + H_2PO_4^- + HPO_4^{2-} \rightleftharpoons Cu(H_2PO_4)(HPO_4)^-$*	-
Cu(HPO4)2-2	*II*	*(7.4 ± 0.2)*[*]	-	-	-	-	*$Cu^{2+} + 2\ HPO_4^{2-} \rightleftharpoons Cu(HPO_4)_2^{2-}$*	-
Cu+	II/I	(2.82 ± 0.31)[*]	-	-	-	-	$Cu^{2+} + e^- \rightleftharpoons Cu^+$	-
CuOH(aq)	I	(-7.85 ± 0.41)[*]	-	(41.3 ± 4.4) [*]	(-848 ± 123) [*]	25 – 100	$Cu^+ + H_2O(l) \rightleftharpoons CuOH(aq) + H^+$	-
Cu(OH)2-	I	(-18.64 ± 0.60)[*]	-	(61 ± 12) [*]	(-277 ± 98) [*]	25 – 350	$Cu^+ + 2\ H_2O(l) \rightleftharpoons Cu(OH)_2^- + 2\ H^+$	-
CuCl(aq)	I	(3.30 ± 0.25)[*]	-	-	-	-	$Cu^+ + Cl^- \rightleftharpoons CuCl(aq)$	-
CuCl2-	I	(5.48 ± 0.25)[*]	-	-	-	-	$Cu^+ + 2\ Cl^- \rightleftharpoons CuCl_2^-$	-
CuCl3-2	I	(4.81 ± 0.25)[*]	-	-	-	-	$Cu^+ + 3\ Cl^- \rightleftharpoons CuCl_3^{2-}$	-
Cu2Cl4-2	I	(10.32 ± 0.50)[*]	-	-	-	-	$2\ Cu^+ + 4\ Cl^- \rightleftharpoons Cu_2Cl_4^{2-}$	-
CuHS(aq)	*I*	*13*[*]	-	-	-	-	*$Cu^+ + HS^- \rightleftharpoons CuHS(aq)$*	-
Cu(HS)2-	I	(17.18 ± 0.13)[*]	-	(-102 ± 7) [*]	(800 ± 300)[*]	22 – 90	$Cu^+ + 2\ HS^- \rightleftharpoons Cu(HS)_2^-$	-
Cu2S(HS)2-2	I	(29.87 ± 0.13)[*]	-	-	-	-	$2\ Cu^+ + 3\ HS^- \rightleftharpoons Cu_2S(HS)_2^{2-} + H^+$	-
CuH2PO4 (aq)	*I*	*(0.87 ± 0.3)*[*]	-	-	-	-	*$Cu^+ + H_2PO_4^- \rightleftharpoons CuH_2PO_4(aq)$*	-
Cu(H2PO4)2-	*I*	*(1.8 ± 0.2)* [*]	-	-	-	-	*$Cu^+ + 2\ H_2PO_4^- \rightleftharpoons Cu(H_2PO_4)_2^-$*	-
Cu(H2PO4) (HPO4)-2	*I*	*(-3.0 ± 0.2)* [*]	-	-	-	-	*$Cu^+ + 2\ H_2PO_4^- \rightleftharpoons Cu(H_2PO_4)(HPO4)^{2-} + H^+$*	-

[a] Note that in their Tab. 1, Powell et al. (2007) list the data as "Provisional", although in the text on p. 905 they refer to them as "Recommended"

[b] Data were reported by Powell et al. (2007) as indication only and are neither "Recommended" nor "Provisional"

[c] Accepted by Powell et al. (2007) as "Provisional"

[d] Estimated by using $\varepsilon(Cu^{2+}, ClO_4^-) = (0.32 \pm 0.02)$ kg · mol^{-1}, $\varepsilon(HPO4_2^-, Na^+) = -(0.15 \pm 0.06)$ kg · mol^{-1}, and assuming that $\varepsilon(CuHPO_4, NaClO_4) = 0$

Name	**Redox**	**$\log_{10}K_{s,0}°$**	**$\Delta\varepsilon$** [kg · mol^{-1}]	**$\Delta_r H_m°$** [kJ · mol^{-1}]	**$\Delta_r C_{p,m}°$** [J · K^{-1} · mol^{-1}]	**T-range** [°C]	**Reaction**	**Quality**
Cu(cr)	0/II	(-11.39 ± 0.27)*	-	(64.9 ± 1.0) *	-	-	Cu(cr) ⇌ Cu^{2+} + 2 e^-	-
CuO(tenorite)	II	7.64 ± 0.06	(0.04 ± 0.06) [a]	(-61.7 ± 1.5) *	(-1'175 ± 13)*	25 – 350	CuO(cr) + 2 H^+ ⇌ Cu^{2+} + H_2O(l)	R
Cu(OH)2(s)	II	8.67 ± 0.05	(0.04 ± 0.06) [a]	-	-	-	$Cu(OH)_2$(s) + 2 H^+ ⇌ Cu^{2+} + 2 H_2O(l)	R
Cu2CO3(OH)2 (malachite)	*II*	*-33.16 ± 0.08*	*0.64* [b]	-	-	-	*$Cu_2CO_3(OH)_2$ (cr) ⇌ 2 Cu^2 + CO_3^{2-} + 2 OH^-*	*P*
Cu3(CO3)2(OH)2(azurite)	*II*	*-44.9 ± 0.2*	*0.88* [b]	-	-	-	*$Cu_3(CO_3)_2(OH)_2$ (cr) ⇌ 3 Cu^{2+} + 2 CO_3^{2-} + 2 OH^-*	*P*
CuS(covellite) [c]	II	(-22.05 ± 0.16)* [c]	(-0.10 ± 0.19)* [c]	-	-	-	CuS(cr) + H^+ ⇌ Cu^{2+} + HS^-	-
Cu2O(cuprite)	I	(-0.25 ± 0.12)*	-	(8.6 ± 1.9)*	0*	20 – 350	0.5 Cu_2O(cr) + H^+ ⇌ Cu^+ + 0.5 H_2O(l)	-
CuCl(s)	I	(-6.7 ± 0.2)*	-	-	-	-	CuCl(s) ⇌ Cu^+ + Cl^-	-
Cu2S (chalcocite)	I	(-34.62 ± 0.13)*	-	-	-	-	Cu_2S(cr) + H^+ ⇌ 2 Cu^+ + HS^-	-

[a] Calculated by Powell et al (2007) using $\varepsilon(Cu^{2+}, ClO_4^-)$ = (0.32 ± 0.02) kg · mol^{-1}, $\varepsilon(H^+, ClO_4^-)$= (0.14 ± 0.02) kg · mol^{-1}, and assuming that ε(solid phase, $NaClO_4$) = 0.

[b] Calculated by Powell et al (2007) using $\varepsilon(Cu^{2+}, ClO_4^-)$ = (0.32 ± 0.02) kg · mol^{-1}, $\varepsilon(CO_3^{2-}, Na^+)$= -(0.08 ± 0.03) kg · mol^{-1}, $\varepsilon(OH^-, Na^+)$ = (0.04 ± 0.01) kg · mol^{-1}, and assuming that ε(solid phase, $NaClO_4$) = 0.

[c] **Warning:** Although the solubility product of covellite is a selected value, it cannot be used to calculate the solubility of Cu in sulphide systems, because, due to extremely divergent experimental data, no formation constants of Cu-sulphide complexes could be included in TDB 2020. If in any geochemical calculation covellite turns out to be solubility limiting, the resulting solubility of Cu is a minimal value and could be much higher, even by orders of magnitude. See Section 6.1.4 for a discussion.

Tab. 9-4: SIT ion interaction coefficients $\varepsilon_{j,k}$ [kg · mol^{-1}] with copper species selected for TDB 2020

All data are calculated from $\Delta\varepsilon$ values selected by Powell et al. (2007), see Tab. 9-3, unless indicated otherwise. Data estimated according to charge correlations and taken from Tab. 1-7 are shaded. Supplemental data are in italics.

Redox	**j k →** ↓	**Cl^-** $\varepsilon_{j,k}$ [kg · mol^{-1}]	**ClO_4^-** $\varepsilon_{j,k}$ [kg · mol^{-1}]	**NO_3^-** $\varepsilon_{j,k}$ [kg · mol^{-1}]	**Li^+** $\varepsilon_{j,k}$ [kg · mol^{-1}]	**Na^+** $\varepsilon_{j,k}$ [kg · mol^{-1}]	**K^+** $\varepsilon_{j,k}$ [kg · mol^{-1}]
II	Cu+2	(0.32 ± 0.02) [a]	(0.32 ± 0.02) [b]	(0.11 ± 0.01) [b]	0	0	0
II	CuOH+	(-0.15 ± 0.08) [a]	-0.15 ± 0.08	-	0	0	0
II	Cu(OH)3-	0	0	0	-	0.40 ± 0.09	(0.40 ± 0.02) [c]
II	Cu(OH)4-2	0	0	0	-	0.19 ± 0.10	(0.29 ± 0.05) [c]
II	*Cu2OH+3*	*(0.54 ± 0.06)* [a]	*0.54 ± 0.06*	-	*0*	*0*	*0*
II	Cu2(OH)2+2	(0.29 ± 0.12) [a]	0.29 ± 0.12	-	0	0	0
II	*Cu3(OH)4+2*	*(0.33 ± 0.11)* [a]	*0.33 ± 0.11*	-	*0*	*0*	*0*
II	CuCl+	(0.30 ± 0.05) [a]	0.30 ± 0.05	-	0	0	0
II	Cu(CO3)2-2	0	0	0	-	0.34 ± 0.21	-
II	CuHCO3+	(0.46 ± 0.15) [a]	0.46 ± 0.15	-	0	0	0
II	*Cu(CO3)OH-*	*0*	*0*	*0*	-	*0.10 ± 0.05*	-
II	*CuH2PO4+*	*0.10* [a]	*0.10* [d]	-	*0*	*0*	*0*
II	*Cu(H2PO4)(HPO4)-*	*0*	*0*	*0*	-	*0.007* [d]	-
II	*Cu(HPO4)2-2*	*0*	*0*	*0*	-	*-0.02* [d]	-
I	Cu+	(0.11 ± 0.01) [a]	0.11 ± 0.01	-	0	0	0
I	Cu(OH)2-	0	0	0	-	-0.05 ± 0.10	-
I	CuCl2-	0	0	0	-	-0.05 ± 0.10	-
I	CuCl3-2	0	0	0	-	-0.10 ± 0.10	-
I	Cu2Cl4-2	0	0	0	-	-0.10 ± 0.10	-
I	Cu(HS)2-	0	0	0	-	-0.05 ± 0.10	-
I	Cu2S(HS)2-2	0	0	0	-	-0.10 ± 0.10	-
I	*Cu(H2PO4)2-*	*0*	*0*	*0*	-	*-0.04* [d]	-
I	*Cu(H2PO4)(HPO4)-2*	*0*	*0*	*0*	-	*-0.06* [d]	-

[a] Assumed to be equal to the corresponding ion interaction coefficient with ClO_4^-, see Section 9.1 for explanation
[b] Selected NEA value (Lemire et al. 2013)
[c] Value adopted by Powell et al. (2007) from Plyasunova et al. (1997)
[d] This work, estimated according to Ciavatta (1990)

Tab. 9-5: SIT ion interaction coefficients $\varepsilon_{j,k}$ [kg · mol^{-1}] with neutral copper species selected for TDB 2020

All data are calculated from $\Delta\varepsilon$ values selected by Powell et al. (2007), see Tab. 9-4, unless indicated otherwise. Supplemental data are in italics.

Redox	**j k →** ↓	**$Na^+ + Cl^-$** $\varepsilon_{j,k}$ [kg · mol^{-1}]	**$Na^+ + ClO_4^-$** $\varepsilon_{j,k}$ [kg · mol^{-1}]
II	Cu(OH)2(aq)	(0.18 ± 0.36) [a]	(0.18 ± 0.36) [b]
II	*CuCl2(aq)*	*(0.28 ± 0.07)* [a]	*0.28 ± 0.07*
II	CuCO3(aq)	(-0.01 ± 0.10) [a]	-0.01 ± 0.10
II	CuSO4(aq)	(0.15 ± 0.07) [a]	0.15 ± 0.07
II	CuHPO4(aq)	0 [a]	0 [c]
II	*Cu(H2PO4)2(aq)*	*0.03* [a]	*0.03* [d]
I	CuOH(aq)	0 [a]	0 [e]
I	CuCl(aq)	0 [a]	0 [e]
I	CuHS(aq)	0 [a]	0 [e]
I	*CuH2PO4(aq)*	*0* [a]	*0* [d]

[a] Assumed to be equal to the corresponding ion interaction coefficient with ClO_4^-, see Section 9.1 for explanation
[b] Powell et al. (2007) reported (0.14 ± 0.36) kg · mol^{-1}, see Section 9.3.2.2 for discussion
[c] Set to zero by Powell et al. (2007)
[d] This work, estimated according to Ciavatta (1990)
[e] Set to zero (this work)

Tab. 9-6: SIT ion interaction coefficients $\varepsilon_{j,k}$ [kg · mol^{-1}] (from Lemire et al. 2013, unless indicated otherwise) used for deriving $\varepsilon_{j,k}$ for copper species

See Tabs. 9.4 and 9.5 from the $\Delta\varepsilon$ values selected by Powell et al. (2007).

j k → ↓	**ClO_4^-** $\varepsilon_{j,k}$ [kg · mol^{-1}]	**Na^+** $\varepsilon_{j,k}$ [kg · mol^{-1}]
0.32 ± 0.02	0	(0.18 ± 0.36) [b]
0.14 ± 0.02	0	*0.28 ± 0.07*
0	0.04 ± 0.01	
0	0.03 ± 0.01	
0	(0.08 ± 0.01) [a]	
0	-0.08 ± 0.03	
0	0.00 ± 0.02	
0	-0.12 ± 0.06	
0	-0.15 ± 0.06	

[a] Hummel et al. (2002)

9.9 References

Ahrland, S. & Rawsthorne, J. (1970): The stability of metal halide complexes in aqueous solution VII. The chloride complexes of copper(I). Acta Chemica Scandinavica, 24, 157-172.

Al-Farawati, R. & van den Berg, C.M.G. (1999): Metal-sulfide complexation in seawater. Marine Chemistry, 63, 331-352.

Brown, P.L. & Ekberg, C. (2016): Hydrolysis of Metal Ions. Vol. 2, Wiley-VCH, Weinheim.

Ciavatta, L. (1980): The specific interaction theory in evaluating ionic equilibria. Annali di Chimica, 70, 551-567.

Ciavatta, L. (1990): The specific interaction theory in equilibrium analysis. Some empirical rules for estimating interaction coefficients of metal ion complexes. Annali di Chimica, 80, 255-263.

Ciavatta, L., Iuliano, M. & Porto, R. (1993a): Complex formation equilibria in copper(II) orthophosphate solutions. Annali di Chimica, 83, 19-38.

Ciavatta, L., Iuliano, M. & Porto, R. (1993b): Complex formation between copper(I) phosphate ions. Annali di Chimica, 83, 39-51.

Cox, J.D., Wagman, D.D. & Medvedev, V.A. (1989): CODATA Key Values for Thermodynamics. Hemisphere, New York, 271 pp.

Diomidis, N., Johnson, L.H., Bastid, P. & Allen, C. (2017): Design development of a copper-coated canister for the disposal of spent fuel in a deep geological repository in Opalinus Clay. Corrosion Engineering, Science and Technology, 52(sup1), 31-39.

Feitknecht, W. & Schindler, P. (1963): Löslichkeitskonstanten von Metalloxiden, -hydroxiden und -hydroxidsalzen in wässerigen Lösungen. Pure and Applied Chemistry 6, 130-199.

Fritz, J.J. (1984): Heats of solution of cuprous chloride in aqueous HCl-$HClO_4$ mixtures. Journal of Solution Chemistry, 13, 369-382.

Fritz, J.J. (1980): Chloride complexes of copper(I) in aqueous solution. Journal of Physical Chemistry, 84, 2241-2246.

Grenthe, I. & Puigdomènech, I. (1997): Symbols, standards, and conventions. In: Grenthe, I. & Puigdomènech, I. (eds.): Modelling in Aquatic Chemistry. OECD NEA, Paris, 35-67.

Grenthe, I., Fuger, J., Konings, R.J.M., Lemire, R.J., Muller, A.B., Nguyen-Trung, C. & Wanner, H. (1992): Chemical Thermodynamics of Uranium. Chemical Thermodynamics, Vol. 1., North-Holland, Amsterdam, 715 pp.

Hikita, H., Ishikawa, H. & Esaka, N. (1973): Solubility and equilibrium of copper(I) chloride in hydrochloric acid solutions. Nippon Kagaku Kaishi, Vol. 1973, 13-18, (text in Japanese, title, abstract, figures and tables in English).

Hummel, W., Anderegg G., Puigdomènech, I., Rao, L. & Tochiyama, O. (2005): Chemical Thermodynamics of Compounds and Complexes of U, Np, Pu, Am, Tc, Se, Ni and Zr with Selected Organic Ligands. Chemical Thermodynamics Series, Vol. 9, OECD NEA, Paris, 1088 pp.

Hummel, W., Berner, U., Curti, E., Pearson, F.J. & Thoenen, T. (2002): Nagra/PSI Chemical Thermodynamic Data Base 01/01. Nagra Technical Report NTB 02-16 and Universal Publishers, Parkland, Florida, 565 pp.

Lemire, R.J., Berner, U., Musikas, C., Palmer, D.A., Taylor, P. & Tochiyama, O. (2013): Chemical Thermodynamics of Iron, Part 1. Chemical Thermodynamics, Vol. 13a, OECD Publications, Paris, France, 1082 pp.

Liu, W., Brugger, J., Etschmann, B., Testemale, D. & Hazemann, J.-L. (2008): The solubility of nantokite (CuCl(s)) and Cu speciation in low-density fluids near the critical isochore: An in-situ XAS study. Geochimica et Cosmochimica Acta, 72, 4094-4106.

Luther III, G.W., Rickard, D.T., Theberge, S. & Olroyd, A. (1996): Determination of metal (bi)sulfide stability constants of Mn^{2+}, Fe^{2+}, Co^{2+}, Ni^{2+}, Cu^{2+}, and Zn^{2+} by voltammetric methods. Environmental Science and Technology, 30, 671-679.

Luther III, G.W., Theberge, S.M., Rozan, T.F., Rickard, D., Rowlands, C.C. & Oldroyd, A. (2002): Aqueous copper sulfide clusters as intermediates during copper sulfide formation. Environmental Science and Technology, 36, 394-402.

McDowell, L.A. & Johnston, H.L. (1936): The solubility of cupric oxide in alkali and the second dissociation constant of cupric acid. The analysis of very small amounts of copper. Journal of the American Chemical Society, 58, 2009-2014.

Mountain, B.W. & Seward, T.M. (1999): The hydrosulphide/sulphide complexes of copper(I): Experimental determination of stoichiometry and stability at 22 °C and reassessment of high temperature data. Geochimica et Cosmochimica Acta, 63, 11-29.

Mountain, B.W. & Seward, T.M. (2003): Hydrosulfide/sulfide complexes of copper(I): Experimental confirmation of the stoichiometry and stability of $Cu(HS)_2^-$ to elevated temperatures. Geochimica et Cosmochimica Acta, 67, 3005-3014.

Palmer, D.A. (2011): Solubility measurements of crystalline Cu_2O in aqueous solution as a function of temperature and pH. Journal of Solution Chemistry, 40, 1067-1093.

Plyasunova, N.V., Wang, M., Zhang, Y. & Muhammed, M. (1997): Critical evaluation of thermodynamics of complex formation of metal ions in aqueous solutions II. Hydrolysis and hydroxo-complexes of Cu^{2+} at 298.15 K. Hydrometallurgy, 45, 37-51.

Pollard, A.M., Thomas, R.G. & Williams, P.A. (1992): The stabilities of antlerite and $Cu_3SO_4(OH)_4.2H_2O$: their formation and relationships to other copper (II) sulfate minerals. Mineralogical Magazine 56, 359-365.

Potter, R. (1977): An electrochemical investigation of the system copper-sulfur. Economic Geology, 72, 1524-1542.

Powell, K.J., Brown, P.L., Byrne, R.H., Gajda, T., Hefter, G., Sjöberg, S. & Wanner, H. (2005): Chemical speciation of environmentally significant metals with inorganic ligands. Part 1: The Hg^{2+}-OH^-, Cl^-, CO_3^{2-}, SO_4^{2-}, and PO_4^{3-} aqueous systems (IUPAC Technical Report). Pure and Applied Chemistry, 77, 739-800.

Powell, K.J., Brown, P.L., Byrne, R.H., Gajda, T., Hefter, G., Sjöberg, S. & Wanner, H. (2007): Chemical speciation of environmentally significant metals with inorganic ligands. Part 2: The Cu^{2+}-OH^-, Cl^-, CO_3^{2-}, SO_4^{2-}, and PO_4^{3-} systems (IUPAC Technical Report). Pure and Applied Chemistry, 79, 895-950.

Preis, W. & Gamsjäger, H. (2002): Solid–solute phase equilibria in aqueous solution. XVI. Thermodynamic properties of malachite and azurite – predominance diagrams for the system Cu^{2+}–H_2O–CO_2. The Journal of Chemical Thermodynamics, 34, 631-650.

Rickard, D. (2012): Aqueous metal-sulfide chemistry: Complexes, clusters and nanoparticles. Developments in Sedimentology, 65, 121-194.

Rickard, D. & Luther III, G.W. (2006): Metal sulfide complexes and clusters. Reviews in Mineralogy & Geochemistry, 61, 421-504.

Schindler, P., Althaus, H., Hofer, F. & Minder, W. (1965): Löslichkeitsprodukte von Metalloxiden und -hydroxiden. 10. Mitteilung. Löslichkeitsprodukte von Zinkoxid, Kupferhydroxid und Kupferoxid in Abhängigkeit von Teilchengrösse und molarer Oberfläche. Ein Beitrag zur Thermodynamik von Grenzflächen fest-flüssig. Helvetica Chimica Acta, 48, 1204-1215.

Schindler, P., Reinert, M. & Gamsjäger, H. (1968): Zur Thermodynamik der Metallcarbonate. 2. Mitteilung. Löslichkeitskonstanten und Freie Bildungsenthalpien von $Cu_2(OH)_2CO_3$ (Malachit) und $Cu_3(OH)_2(CO_3)_2$ (Azurit) bei 25 °C. Helvetica Chimica Acta, 51, 1845-1856.

Shea, D. & Helz, G.R. (1988): The solubility of copper in sulfidic waters: Sulfide and polysulfide complexes in equilibrium with covellite. Geochimica et Cosmochimica Acta, 52, 1815-1825.

Shea, D. & Helz, G.R. (1989): Solubility product constants of covellite and a poorly crystalline copper sulfide precipitate at 298 K. Geochimica et Cosmochimica Acta, 53, 229-236.

Silva, R.J., Bidoglio, G., Rand, M.H., Robouch, P.B., Wanner, H. & Puigdomènech, I. (1995): Chemical Thermodynamics of Americium. Chemical Thermodynamics, Vol. 2, North-Holland, Amsterdam, 374 pp.

Symes, J.L. & Kester, D.R. (1984): Thermodynamic stability studies of the basic copper carbonate mineral, malachite. Geochimica et Cosmochimica Acta, 48, 2219-2229.

Thoenen, T., Hummel, W., Berner, U. & Curti, E. (2014): The PSI/Nagra Chemical Thermodynamic Database 12/07. PSI Bericht Nr. 14-04, Paul Scherrer Institut, Villigen PSI.

van der Laan, G., Pattrick, R.A.D., Henderson, C.M.B. & Vaughan, D.J. (1992): Oxidation-state variations in copper minerals studied with Cu 2*p* X-ray absorption spectroscopy. Journal of Physics and Chemistry of Solids, 53, 1185-1190.

Vo Van, K. & Habashi, F. (1972): Identification and thermal stability of copper(I) sulfate. Canadian Journal of Chemistry, 50, 3872-3875.

Wagman, D.D., Evans, W.H., Parker, V.B., Schumm, R.H., Halow, I., Bailey, S.M., Churney, K.L. & Nuttall, R.L. (1982): The NBS tables of chemical thermodynamic properties: Selected values for inorganic and C1 and C2 organic substances in SI units. Journal of Physical and Chemical Reference Data, 11, Supplement No. 2, 1-392.

Wang, M., Zhang, Y. & Muhammed, M. (1997): Critical evaluation of thermodynamics of complex formation of metal ions in aqueous solutions III. The system Cu(I,II) - Cl^- - e at 298.15 K. Hydrometallurgy, 45, 53-72.

Xiao, Z., Gammons, C.H. & Williams-Jones, A.E. (1998): Experimental study of copper(I) chloride complexing in hydrothermal solutions at 40 to 300 °C and saturated water vapor pressure. Geochimica et Cosmochimica Acta, 62, 2949-2964.

Zhang, J.-Z. & Millero, F.J. (1994): Investigation of metal sulfide complexes in sea water using cathodic stripping square wave voltammetry. Analytica Chimica Acta, 284, 497-504.

10 Curium

We have not systematically reviewed thermodynamic data of curium solids or aqueous species. However, as mentioned in Chapter 6 on americium, Guillaumont et al. (2003) and Grenthe et al. (2020) used the chemical analogy between Am(III) and Cm(III) and included experimental data for Cm(III) in the evaluation of thermodynamic data for aqueous Am(III) complexes because spectroscopic data for Cm(III) are often more accurate and more abundant than other experimental data for Am(III). This similarity can also be used vice versa, and we have therefore included in our database formation constants of aqueous Cm(III) complexes by adopting the selected formation constants of the corresponding Am(III) complexes.

10.1 Selected curium data

Tab. 10-1: Selected curium data

All data included in TDB 2020 are taken from the corresponding data for americium selected by Silva et al. (1995), Guillaumont et al. (2003) and Grenthe et al. (2020), except where marked with an asterisk (*). The latter data were taken unchanged from Thoenen et al. (2014). Supplemental data are given in italics. New or changed data with respect to TDB Version 12/07 (Thoenen et al. 2014) are shaded.

Name	Redox	TDB Version 12/07				TDB 2020				
		$\Delta_f G_m°$ [kJ · mol^{-1}]	$\Delta_f H_m°$ [kJ · mol^{-1}]	$S_m°$ [J · K^{-1} · mol^{-1}]	$C_{p,m}°$ [J · K^{-1} · mol^{-1}]	$\Delta_f G_m°$ [kJ · mol^{-1}]	$\Delta_f H_m°$ [kJ · mol^{-1}]	$S_m°$ [J · K^{-1} · mol^{-1}]	$C_{p,m}°$ [J · K^{-1} · mol^{-1}]	Species
Cm(cr)	0	0	0	(70.8 ± 3.0) *	-	0	0	(70.8 ± 3.0) *	-	Cm(cr)
Cm+3	III	(-595.4 ± 6.8) *	(-615.0 ± 6.0) *	(-191 ± 10) *	-	(-595.4 ± 6.8) *	(-615.0 ± 6.0) *	(-191 ± 10) *	-	Cm^{3+}

Name	Redox	TBD Version 12/07		TBD 2020				
		$\log_{10}\beta°$	$\Delta_r H_m°$ [kJ · mol^{-1}]	$\log_{10}\beta°$	$\Delta_r H_m°$ [kJ · mol^{-1}]	$\Delta_r C_{p,m}°$ [J · K^{-1} · mol^{-1}]	T-range [°C]	Reaction
CmOH+2	III	(-7.2 ± 0.5) [a]	-	(-7.2 ± 0.5) [a]	-			$Cm^{3+} + H_2O(l) \rightleftharpoons CmOH^{2+} + H^+$
Cm(OH)2+	III	(-15.1 ± 0.7) [a]	-	(-15.1 ± 0.7) [a]	-			$Cm^{3+} + 2\ H_2O(l) \rightleftharpoons Cm(OH)_2^+ + 2\ H^+$
Cm(OH)3(aq)	III	(-26.2 ± 0.5) [a]	-	(-26.2 ± 0.5) [a]	-			$Cm^{3+} + 3\ H_2O(l) \rightleftharpoons Cm(OH)_3(aq) + 3\ H^+$
CaCm(OH)3+2	III	*(-26.3 ± 0.5)* *, [b]	-	*(-26.3 ± 0.5)* [b]				*$Ca^{2+} + Cm^{3+} + 3\ H_2O(l) \rightleftharpoons CaCm(OH)_3^{2+} + 3\ H^+$*
Ca2Cm(OH)4+3	III	*(-37.2 ± 0.6)* *, [b]	-	*(-37.2 ± 0.6)* [b]				*$2Ca^{2+} + Cm^{3+} + 4\ H_2O(l) \rightleftharpoons Ca_2Cm(OH)_4^{3+} + 4\ H^+$*
Ca3Cm(OH)6+3	III	*(-60.7 ± 0.5)* *, [b]	-	*(-60.7 ± 0.5)* [b]				*$3Ca^{2+} + Cm^{3+} + 6\ H_2O(l) \rightleftharpoons Ca_3Cm(OH)_6^{3+} + 6\ H^+$*
CmF+2	III	(3.4 ± 0.3) [a]	-	(3.4 ± 0.3) [a]	(12.1 ± 2.2) [b]	0	20 – 90	$Cm^{3+} + F^- \rightleftharpoons CmF^{2+}$
CmF2+	III	(5.8 ± 0.2) [c]	-	5.8 ± 0.2	(45.1 ± 14.5) [b]	0	20 – 90	$Cm^{3+} + 2\ F^- \rightleftharpoons CmF_2^+$
CmCl+2	III	(0.24 ± 0.03) [a]	-	(0.24 ± 0.35) [a]	-	-		$Cm^{3+} + Cl^- \rightleftharpoons CmCl^{2+}$
CmCl2+	III	(-0.74 ± 0.05) [a]	-	(-0.81 ± 0.35) [b]	(54.9 ± 4.5) [b]	0	25 – 200	$Cm^{3+} + 2\ Cl^- \rightleftharpoons CmCl_2^+$
CmSO4+	III	(3.30 ± 0.15) [b]	-	(3.50 ± 0.30) [d]	(40 ± 4) [b]	0	25 - 100	$Cm^{3+} + SO_4^{2-} \rightleftharpoons CmSO_4^+$
Cm(SO4)2-	III	(3.70 ± 0.15) [b]	-	(5.0 ± 1.0) [d]	(70 ± 7) [b]	0	25 - 100	$Cm^{3+} + 2\ SO_4^{2-} \rightleftharpoons Cm(SO_4)_2^-$
CmNO3+2	III	(1.33 ± 0.20) [c]	-	(1.28 ± 0.05) [b]	(1.8 ± 1.0) [b]	0	5 – 80	$Cm^{3+} + NO_3^- \rightleftharpoons CmNO_3^{2+}$
Cm(NO3)2+	III	-	-	(0.88 ± 0.11) [b]	(10.8 ± 2.2) [b]	0	5 – 80	$Cm^{3+} + 2\ NO_3^- \rightleftharpoons Cm(NO_3)_2^+$
CmH2PO4+2	III	(3.0 ± 0.5) [c]	-	(2.46 ± 0.13) [b]	-			$Cm^{3+} + H_2PO_4^- \rightleftharpoons CmH_2PO_4^{2+}$
$CmHPO_4^+$	III	-	-	*(6.2 ± 0.8)* [b]	-	-		*$Cm^{3+} + HPO_4^{2-} \rightleftharpoons CmHPO_4^+$*
CmCO3+	III	(8.0 ± 0.4) [a]	-	(8.0 ± 0.4) [a]	-			$Cm^{3+} + CO_3^{2-} \rightleftharpoons CmCO_3^+$
Cm(CO3)2-	III	(12.9 ± 0.4) [a]	-	(12.9 ± 0.4) [a]	-			$Cm^{3+} + 2\ CO_3^{2-} \rightleftharpoons Cm(CO_3)_2^-$
Cm(CO3)3-3	III	(15.0 ± 1.0) [a]	-	(15.0 ± 0.5) [a]	-			$Cm^{3+} + 3\ CO_3^{2-} \rightleftharpoons Cm(CO_3)_3^{3-}$

Tab. 10-1: Cont.

Name	Redox	TBD Version 12/07		TBD 2020				
		$\log_{10}\beta°$	$\Delta_r H_m°$ [kJ · mol^{-1}]	$\log_{10}\beta°$	$\Delta_r H_m°$ [kJ · mol^{-1}]	$\Delta_r C_{p,m}°$ [J · K^{-1} · mol^{-1}]	T-range [°C]	Reaction
CmHCO3+2	III	(3.1 ± 0.3) [b]	-	(3.1 ± 0.3) [b]	-			$Cm^{3+} + HCO_3^- \rightleftharpoons CmHCO_3^{2+}$
CmSCN+2	III	(1.3 ± 0.3) [c]		(1.3 ± 0.3) [c]				$Cm^{3+} + SCN^- \rightleftharpoons CmSCN^{2+}$

[a] Formation constant is based on combined Am and Cm data.
[b] Constant is based on Cm data only.
[c] Recommended by Guillaumont et al. (2003) as reasonable estimate.
[d] Formation constant is based on combined Eu and Cm data.

Name	Redox	TBD Version 12/07		TBD 2020		
		$\log_{10}K_{s,0}°$	$\Delta_r H_m°$ [kJ · mol^{-1}]	$\log_{10}K_{s,0}°$	$\Delta_r H_m°$ [kJ · mol^{-1}]	Reaction
Cm(OH)3(am, coll)	III	*(17.2 ± 0.4)* [*]	-	*(17.2 ± 0.4)* [*]	-	*$Cm(OH)_3$(am, coll) + 3 $H^+ \rightleftharpoons Cm^{3+}$ + 3 H_2O(l)*

Tab. 10-2: Selected SIT ion interaction coefficients $\varepsilon_{j,k}$ [kg · mol^{-1}] for curium species

The data included in TDB Version 12/07 are taken from the corresponding data for americium selected by Silva et al. (1995), Guillaumont et al. (2003) and Grenthe et al. (2020) unless indicated otherwise. Own data estimates based on charge correlations (see Section 1.5.3) are shaded. Supplemental data are in italics.

j k → ↓	Cl^- $\varepsilon_{j,k}$	ClO_4^- $\varepsilon_{j,k}$	NO_3^- $\varepsilon_{j,k}$	Li^+ $\varepsilon_{j,k}$	Na^+ $\varepsilon_{j,k}$	K^+ $\varepsilon_{j,k}$
Cm+3	0.23 ± 0.02	0.49 ± 0.03	-	0	0	0
CmOH+2	-0.04 ± 0.07	(0.39 ± 0.10) [a]	-	0	0	0
Cm(OH)2+	-0.27 ± 0.20	(0.17 ± 0.10) [a]	-	0	0	0
Cm(OH)3(aq)	0	0	0	0	0	0
CaCm(OH)3+2	*(0.05 ± 0.04)* [b]	*0.4 ± 0.1*	-	*0*	*0*	*0*
Ca2Cm(OH)4+3	*(0.29 ± 0.07)* [b]	*0.6 ± 0.1*	-	*0*	*0*	*0*
Ca3Cm(OH)6+3	*(0.00 ± 0.06)* [b]	*0.6 ± 0.1*	-	*0*	*0*	*0*
CmF+2	0.15 ± 0.10	(0.39 ± 0.10) [a]	-	0	0	0
CmF2+	0.05 ± 0.10	(0.17 ± 0.10) [a]	-	0	0	0
CmCl+2	0.15 ± 0.10	(0.39 ± 0.10) [a]	-	0	0	0
CmCl2+	0.05 ± 0.10	(0.17 ± 0.10) [a,c]	-	0	0	0
CmSO4+	0.05 ± 0.10	0.22 ± 0.08	-	0	0	0
Cm(SO4)2-	0	0	0	-	-0.05 ± 0.05	-
CmNO3+2	0.15 ± 0.10	(0.39 ± 0.10) [a]	-	0	0	0
Cm(NO3)2+	0.05 ± 0.10	0.2 ± 0.1	-	0	0	0
CmH2PO4+2	0.15 ± 0.10	(0.39 ± 0.10) [a]	-	0	0	0
CmHPO4+	*0.05 ± 0.10*	*0.2 ± 0.1*	-	*0*	*0*	*0*

Tab. 10-2: Cont.

j k → ↓	Cl^- $\varepsilon_{j,k}$	ClO_4^- $\varepsilon_{j,k}$	NO_3^- $\varepsilon_{j,k}$	Li^+ $\varepsilon_{j,k}$	Na^+ $\varepsilon_{j,k}$	K^+ $\varepsilon_{j,k}$
CmCO3+	0.01 ± 0.05	(0.17 ± 0.10) [a]	-	0	0	0
Cm(CO3)2-	0	0	0	-	-0.14 ± 0.06	-
Cm(CO3)3-3	0	0	0	-	-0.23 ± 0.07	-
CmHCO3+2	(0.16 ± 0.10) [a,d,e]	0.4 ± 0.1	-	0	0	0
CmSCN+2	0.15 ± 0.10	(0.39 ± 0.10) [a]	-	0	0	0

[a] Increased error
[b] Value taken from Cm(III) data by Rabung et al. (2008)
[c] Value selected by Silva et al. (1995) but omitted in all further NEA-reviews
[d] Value originally from Cm(III) data
[e] Value discussed by Guillaumont et al. (2003) but not listed in their Tab. B-4

10.2 References

Grenthe, I., Gaona, X., Plyasunov, A.V., Rao, L., Runde, W.H., Grambow, B., Konings, R.J.M., Smith, A.L. & Moore, E.E. (2020): Second Update on the Chemical Thermodynamics of Uranium, Neptunium, Plutonium, Americium and Technetium. Chemical Thermodynamics, Vol. 14. OECD Publications, Paris, France, 1503 pp.

Guillaumont, R., Fanghänel, T., Fuger, J., Grenthe, I., Neck, V., Palmer, D.A. & Rand, M.H. (2003): Update on the Chemical Thermodynamics of Uranium, Neptunium, Plutonium, Americium and Technetium. Chemical Thermodynamics, Vol. 5. Elsevier, Amsterdam, 919 pp.

Rabung, T., Altmaier, M., Neck, V. & Fanghänel, T. (2008): A TRLFS study of Cm(III) hydroxide complexes in alkaline $CaCl_2$ solutions. Radiochim. Acta, 96, 551-559.

Silva, R.J., Bidoglio, G., Rand, M.H., Robouch, P.B., Wanner, H. & Puigdomènech, I. (1995): Chemical Thermodynamics of Americium. Chemical Thermodynamics, Vol. 2. Elsevier, Amsterdam, 374 pp.

Thoenen, T., Hummel, W., Berner, U. & Curti, E. (2014): The PSI/Nagra Chemical Thermodynamic Database 12/07. Technical Report, PSI Bericht Nr. 14-04, Paul Scherrer Institut, Villigen, Switzerland, 416 pp.

11 Iron

11.1 Introduction

The chemical thermodynamic data for iron selected by Pearson et al. (1992) for their Nagra Thermochemical Data Base 05/92 (TDB 05/92) were taken from Wagman et al. (1982) (properties of formation of the master species Fe^{2+}) and from Nordstrom et al. (1990) (inorganic complexes of iron and iron solids). Since Pearson et al. (1992) did not discuss the data they adopted from Nordstrom et al. (1990), we provide short discussions regarding the ultimate sources of the data. The iron data by Pearson et al. (1992) were adopted without any change by Hummel et al. (2002) for the Nagra/PSI Chemical Thermodynamic Data Base 01/01 (TDB 01/01). The organic complexes of iron selected by Pearson et al. (1992), however, were not included. In addition to the iron solids inherited from TDB 05/92, Hummel et al. (2002) also selected data for hematite, magnetite, pyrite, and troilite. All data concerning iron selected by Hummel et al. (2002) were also accepted by Thoenen et al. (2014) for the PSI/Nagra Chemical Thermodynamic Data Base 12/07 (TDB 12/07) and no new data were evaluated in anticipation of OECD NEA's review "Chemical Thermodynamics of Iron, Part 1" (Lemire et al. 2013) and "Chemical Thermodynamics of Iron, Part 2" (Lemire et al. 2020) which unfortunately both appeared after the cut-off date for inclusion into TDB 12/07.

Lemire et al. (2013) reviewed data for the metal, simple ions, and aqueous complexes with hydroxide, chloride, sulphide, sulphate, and carbonate. In addition, they also reviewed data for solid oxides, hydroxides, halides, sulphates, carbonates and simple silicates. Lemire et al. (2020) reviewed data for aqueous complexes with halides other than chloride, as well as data for sulphide solids, solid solutions of the oxides and sulphides, solid and aqueous solution species with selenium, tellurium, sulphite, nitrate, phosphate, and arsenate, and complexes with thiocyanate and cyanate.

These reviews are the basis of our iron update for the PSI Chemical Thermodynamic Database 2020 (TDB 2020), but we also took advantage of the review of the hydrolysis of metal ions by Brown & Ekberg (2016). Since the review by Lemire et al. (2020) was published at a very late stage of our update procedure, we refer to it only if data, both recommended by Lemire et al. (2013) and included in TDB 2020, were changed or if data were selected for compounds and complexes that were not considered by Lemire et al. (2013).

Note that not all values recommended by Lemire et al. (2013) and Lemire et al. (2020) were considered for our database since the NEA reviews (unlike our database) are not restricted to data relevant for radioactive waste management or even environmental modelling in general. We tried to exclude from our database all phases and complexes which most probably will never be relevant in low-temperature and low-salinity environmental systems. The excluded data are listed in Tab. 11.8-1 and the selected data in Tab. 11.8-2.

The notation of formulae and symbols used in this text follows the NEA recommendations.

11.1.1 SIT

NEA chose the specific ion interaction theory (SIT) for the extrapolation of experimental data to zero ionic strength, see, e.g., Grenthe et al. (1997), an approach which is also adopted for TDB 2020 (as has been for all its predecessors). When referring to ion interaction coefficients recommended by NEA, we took those from Tab. B.3 in Lemire et al. (2013). Lemire et al. (2013) explicitly considered the formation of weak chloride complexes with ferric (+3 oxidation state) iron[21]. If equilibrium constants of reactions with ferric iron species are determined in solutions with chloride salts as background electrolytes, the equilibrium constants must be corrected for the formation of these ferric iron chloride complexes. The ion interaction coefficients for cationic Fe(III) species with Cl^- can then be approximated by the corresponding interaction coefficients with ClO_4^- (see Hummel et al. 2005, Chapter V.4.). Likewise, if ion interaction coefficients for cationic Fe(III) species with Cl^- are not known, they can be approximated by equating them to the corresponding interaction coefficients with ClO_4^-.

Due to a lack of experimental data, several ion interaction coefficients for cationic Fe species with ClO_4^- and for anionic Fe species with Na^+ are unknown. We filled these gaps by applying the estimation method described in Section 1.5.3, which is based on a statistical analysis of published SIT ion interaction coefficients, and which allows the estimation of such coefficients for the interaction of cations with Cl^- and ClO_4^-, and for the interaction of anions with Na^+ from the charge of the considered cations or anions.

Ion interaction coefficients of neutral iron species with background electrolytes were assumed to be zero.

The ion interaction coefficients for iron species selected for TDB 2020 are listed in Tab. 11.8-3.

In several cases, Lemire et al. (2013) deviated from the standard practice of using a weighted linear regression (termed SIT_1) for deriving the stability constant and $\Delta\varepsilon$ from experimental conditional constant and ionic strength data and used a non-linear regression (termed SIT_2) where the specific ion interaction coefficient ε is not a constant but a function of the logarithm of the ionic strength:

$$\varepsilon = \varepsilon_1 + \varepsilon_2 \log_{10} I_m$$

This variable specific ion interaction coefficient was introduced by Ciavatta (1980) in a footnote to a table without any further explanation or theoretical justification. Grenthe et al. (2020) remarked that "even if the value of ε calculated in this way describes the variation with ionic strength slightly better than a constant value, this equation has no theoretical basis; ε is a fitting parameter and the term $\varepsilon_2 \log_{10} I_m$ goes to minus infinity at the limiting value $I_m = 0$. This expression for the composition dependence of ε should be avoided, even though the term $\varepsilon \cdot m = (\varepsilon = \varepsilon_1 + \varepsilon_2 \log_{10} I_m) \cdot m$ (in the calculation of activity coefficients) is zero at $I_m = 0$. There may be cases where reviewers may still want to use $[\varepsilon = \varepsilon_1 + \varepsilon_2 \log_{10} I_m]$ to describe ionic strength variation of the interaction parameters, but the rationale behind this should then be described". For these reasons, we preferred to include in TDB 2020 only ion interaction coefficients based on SIT_1.

---

[21] Lemire et al. (2013) also considered the formation of weak chloride complexes with ferrous (+2 oxidation state) iron, but these complexes are too weak to have any influence and can be neglected for all practical purposes.

A typical example of SIT_2 used by Lemire et al. (2013) is the evaluation of experimental data for the Fe^{3+}/Fe^{2+} redox couple

$$Fe^{2+} + H^+ \rightleftharpoons Fe^{3+} + 0.5\ H_2g$$

as discussed in Section 11.3.3 below. They used both SIT_1 and SIT_2 for evaluating $E°(Fe^{3+}/Fe^{2+})$, or equivalently $\log_{10}{}^*K°(298.15\ K)$, and $\Delta\varepsilon$ for this reaction in perchlorate media and obtained from SIT_1

$$\log_{10}{}^*K°(298.15\ K) = -(13.105 \pm 0.007)$$

$$\Delta\varepsilon = -(0.36 \pm 0.02)\ kg \cdot mol^{-1}$$

$$\varepsilon(Fe^{3+}, ClO_4^-) = (0.73 \pm 0.04)\ kg \cdot mol^{-1}$$

and from SIT_2

$$\log_{10}{}^*K°(298.15\ K) = -(13.051 \pm 0.160)$$

$$\Delta\varepsilon = -((0.41 \pm 0.03) - (0.41 \pm 0.05)\ \log_{10}I_m)\ kg \cdot mol^{-1}$$

$$\varepsilon(Fe^{3+}, ClO_4^-) = ((0.78 \pm 0.05) - (0.41 \pm 0.05)\ \log_{10}I_m)\ kg \cdot mol^{-1}$$

Lemire et al. (2013) selected the latter values based on SIT_2. However, while $\log_{10}{}^*K°(298.15\ K) = -(13.051 \pm 0.160)$ based on SIT_2 appears in their Tab. III-2 of selected thermodynamic data for reactions involving iron compounds and complexes, it is $\varepsilon(Fe^{3+}, ClO_4^-) = (0.73 \pm 0.04)\ kg \cdot mol^{-1}$ based on SIT_1 that appears in their Tab. B-4 of selected specific ion interaction coefficients. This inconsistency is not the only case: whenever thermodynamic properties of reactions or of compounds and complexes were selected based on SIT_2, they appear in Tab. III-1 and III-2 of selected thermodynamic data, the simultaneously derived ion interaction coefficients based on SIT_2 are also selected, but they are neither listed in Tab. B-4 and B-5 of selected specific ion interaction coefficients nor in Tab. B-6, which specifically lists ion interaction coefficients derived with SIT_2. Instead, Tab. B-4 and B-5 tacitly contain the corresponding ion interaction coefficients based on SIT_1. We did not attempt to resolve these inconsistencies and, in all cases, selected the ion interaction coefficients derived with SIT_1. Incidentally, in the case of the first hydrolysis constant for the reaction

$$Fe^{3+} + H_2O(l) \rightleftharpoons FeOH^{2+} + H^+$$

Lemire et al. (2013) showed a viable procedure for combining $\log_{10}{}^*\beta_1°(298.15\ K)$ obtained from SIT_2 with $\Delta\varepsilon$ obtained from a linear SIT_1 fit. A plot of all accepted experimental values for $\log_{10}{}^*\beta_1 - \log_{10}a_{water} + 4\ D$ vs. I_m clearly shows that $\Delta\varepsilon$ is not a linear function of I_m as required by the conventional linear SIT_1 fit. In order "to reconcile the $\Delta\varepsilon$ to be recommended for this equilibrium with those of other systems where they are generally independent of I_m albeit over restricted ranges" Lemire et al. (2013) derived $\log_{10}{}^*\beta_1°(298.15\ K)$ and $\Delta\varepsilon$ in two steps. First, they used the non-linear SIT_2 fit to obtain $\log_{10}{}^*\beta_1°(298.15\ K)$ with the reasoning that this "should yield a more accurate value of $\log_{10}{}^*\beta_{1,1}°$, which is more important than obtaining the most accurate ion interaction parameter for the equilibrium". They then used a forced linear SIT_1 fit to determine

$\Delta\varepsilon$, with $\log_{10}{}^{*}\beta_1°$(298.15 K) fixed at the value obtained in the first step. This procedure is probably in many cases sufficient for describing the dependence of conditional stability constants as a function of ionic strength at low values of ionic strength. We followed this procedure in the case of $FeOH^{2+}$ (see Section 11.4.1.3.1), $Fe(OH)_2^{+}$ (see Section 11.4.1.3.2), and $Fe_2(OH)_2^{4+}$ (see Section 11.4.1.3.5).

11.1.2 Re-evaluation or optimization procedure used by Lemire et al. (2013)

The iron review by Lemire et al. (2013) was the first NEA-review using an optimization procedure for "post-processing" selected thermodynamic data. According to Lemire et al. (2013) "the experimentally determined values of thermodynamic quantities for many iron species are linked […] After completion of the initial assessments for iron compounds and species in the previous sections, re-examination is necessary to try to ensure that the values from different thermodynamic cycles are consistent. For example, the value of $\Delta_f H_m°(Fe^{2+})$ is related not only to the heats of solution of FeCl(cr), $FeBr_2$(cr), $FeSO_4 \cdot 7H_2O$(cr), and the heats of formation of these solids, but also, among many other quantities, to the solubility and entropy for $FeCO_3$(cr). Re-evaluation is done as part of the selection process to determine final database values. Inconsistencies within each cycle must be resolved, usually by changing the value and increasing the uncertainty for one or more reactions or formation quantities."

Tab. 11.1-1: Input experimental quantities for the optimisation procedure

$\Delta_{red}G°(Fe^{2+})$	$\Delta_{ox}H°(Fe^{2+})$	
$\Delta_{red}G°(Fe^{3+})$		$\Delta_{red}S°(Fe^{3+})$
	$\Delta_{ox}H°$(Fe, α)	
	$\Delta_f H_m°(FeCl_2$, cr)	$S_m°(FeCl_2$, cr)
	$\Delta_{sln}H_m°(FeCl_2$, cr)	
$\Delta_{sln}G_m°(FeCl_2 \cdot 4H_2O$, cr)		
$\Delta_{dehyd}G_m°(FeCl_2 \cdot 4H_2O$, cr)		
	$\Delta_f H_m°(FeCl_3$, cr)	
	$\Delta_{sln}H_m°(FeCl_3$, cr)	
	$\Delta_f H_m°(FeBr_2$, cr)	
	$\Delta_{sln}H_m°(FeBr_2$, cr)	
	$\Delta_f H_m°(FeBr_3$, cr)	
	$\Delta_{sln}H_m°(FeBr_3$, cr)	
	$\Delta_f H(FeSO_4 \cdot 7H_2O$, cr)	$S_m°(FeSO_4 \cdot 7H_2O$, cr)
$\Delta_{sln}G(FeSO_4 \cdot 7H_2O$, cr)	$\Delta_{sln}H(FeSO_4 \cdot 7H_2O$, cr)	
$\Delta_{sln}G(FeCO_3$, cr)	$\Delta_{decomp}H(FeCO_3$, cr)	$S_m°(FeCO_3$, cr)

Based on the experimental quantities listed in Tab. 11.1-1, the auxiliary values for species listed in Tab. 11.1-2, and the fixed assessed values for $S_m°$(Fe, α) and $\Delta_f H_m°(Fe_2O_3$, α), Lemire et al. (2013) optimised the assessed and selected values for species and solids listed in Tab. 11.1-3.

For this purpose, Lemire et al. (2013) took advantage of a computer code that uses a weighted least-squares procedure for the optimisation process.

Lemire et al. (2013) explained the procedure as follows: "When several experimental results for a key quantity were found to differ by more than the assessed uncertainties, the optimization program was used with each of the values and its uncertainty. After the optimization, in some cases it was clear that certain experimental results were inconsistent, and their assessed uncertainties were increased, or in a few cases a reassessment of an experimental paper was done, and if necessary, the results were rejected. The optimization resulted in "best" values and uncertainties, and these are used in the final iron database."

They used two optimisation cycles to derive the final values for inclusion in the iron database.

Tab. 11.1-2: Input auxiliary quantities for the optimisation procedure

$\Delta_f G_m°(Cl^-)$	$\Delta_f H_m°(Cl^-)$	
$\Delta_f G_m°(Br^-)$	$\Delta_f H_m°(Br^-)$	
$\Delta_f G_m°(SO_4^{2-})$	$\Delta_f H_m°(SO_4^{2-})$	
$\Delta_f G_m°(CO_2, aq)$	$\Delta_f H_m°(CO_2, aq)$	
	$\Delta_f H_m°(H_2O_2, aq)$	
$\Delta_f G_m°(H_2O, l)$	$\Delta_f H_m°(H_2O, l)$	
		$S_m°(S, cr)$
		$S_m°(C, cr)$
		$S_m°(Cl_2, g)$
		$S_m°(O_2, g)$
		$S_m°(H_2, g)$

Tab. 11.1-3: Optimised quantities from the optimisation procedure

$\Delta_f G_m°(Fe^{2+})$	$\Delta_f H_m°(Fe^{2+})$	
$\Delta_f G_m°(Fe^{3+})$	$\Delta_f H_m°(Fe^{3+})$	
	$\Delta_f H_m°(FeCl_2, cr)$	$S_m°(FeCl_2, cr)$
$\Delta_f G_m°(FeCl_2 \cdot 4H_2O, cr)$		
	$\Delta_f H_m°(FeCl_3, cr)$	
	$\Delta_f H_m°(FeBr_2, cr)$	
	$\Delta_f H_m°(FeBr_3, cr)$	
	$\Delta_f H_m°(FeSO_4 \cdot 7H_2O, cr)$	$S_m°(FeSO_4 \cdot 7H_2O, cr)$
	$\Delta_f H_m°(FeCO_3, cr)$	$S_m°(FeCO_3, cr)$

11.2 Elemental Iron

Elemental iron is unstable in contact with water, but thermodynamic data may still be useful when modelling iron corrosion processes. The data for metallic iron selected in TDB 01/01 and TDB 12/07, $S_m°$(Fe, α, 298.15 K) = 27.28 J · K^{-1} · mol^{-1} and $C_{p,m}°$(Fe, α, 298.15 K) = 25.10 J · K^{-1} · mol^{-1}, were taken from the compilation by Wagman et al. (1982). For TDB 2020, we accept the data selected by Lemire et al. (2013):

$S_m°$(Fe, α, 298.15 K) = (27.085 ± 0.160) J · K^{-1} · mol^{-1}

$C_{p,m}°$(Fe, α, 298.15 K) = (25.084 ± 0.500) J · K^{-1} · mol^{-1}

11.3 Iron aquo ions

11.3.1 Data in TDB 05/92, TDB 01/01 and TDB 12/07

The thermodynamic data for the iron aquo ions Fe^{2+} and Fe^{3+} selected in TDB 01/01 and TDB 12/07 were all adopted from TDB 05/92 (Pearson et al. 1992). For Fe^{2+}, Pearson et al. (1992) selected

$\Delta_f G_m°(Fe^{2+}, 298.15\ K) = -78.90\ kJ \cdot mol^{-1}$

$\Delta_f H_m°(Fe^{2+}, 298.15\ K) = -89.1\ kJ \cdot mol^{-1}$

$S_m°(Fe^{2+}, 298.15\ K) = -137.7\ J \cdot K^{-1} \cdot mol^{-1}$

from the compilation by Wagman et al. (1982). From $\Delta_f G_m°(Fe^{2+}, 298.15\ K)$, $\Delta_f H_m°(Fe^{2+}, 298.15\ K)$, and $\Delta_f G_m°$(Fe, α, 298.15 K) = $\Delta_f H_m°$(Fe, α, 298.15 K) = 0 then follow

$Fe(\alpha) \rightleftharpoons Fe^{2+} + 2\ e^-$

$\log_{10} K_{s,0}°(298.15\ K) = 13.82$

$\Delta_r H_m°(298.15\ K) = 89.1\ kJ \cdot mol^{-1}$

For the redox reaction

$Fe^{2+} \rightleftharpoons Fe^{3+} + e^-$

Pearson et al. (1992) relied on Nordstrom et al. (1990) who selected

$\log_{10} K°(298.15\ K) = -13.02$

based on the standard electrode potentials measured by Whittemore & Langmuir (1972), and

$\Delta_r H_m°(298.15\ K) = 40.5\ kJ \cdot mol^{-1}$

based on a personal communication by V. Parker. From these two values and $\Delta_f G_m°(Fe^{2+}, 298.15\ K)$ and $\Delta_f H_m°(Fe^{2+}, 298.15\ K)$ then follow

$\Delta_f G_m°(Fe^{3+}, 298.15\ K) = -4.581\ kJ \cdot mol^{-1}$

$\Delta_f H_m°(Fe^{3+}, 298.15\ K) = -48.6\ kJ \cdot mol^{-1}$

All thermodynamic data for the iron aquo ions Fe^{2+} and Fe^{3+} selected in TDB 12/07 are superseded by the data discussed and selected below.

11.3.2 Fe^{2+}

Evaluating E° for the $Fe^{2+}/Fe(0)$ redox couple, Lemire at al. (2013) remarked that potential-difference measurements in electrochemical cells (consisting of a reference half-cell and another half-cell with a metallic iron electrode immersed in an Fe(II) salt electrolyte) have the disadvantage that, in acidic solutions, there is extensive interference with the $H^+/H_2(0)$ couple, shifting the measured E° towards the higher $H^+/H_2(0)$ potential. The presence of hydrogen in the iron electrode may shift E° towards more negative values. For these reasons, Lemire et al. (2013) favoured electrochemical kinetics measurements that make it possible to find conditions for which the redox reaction of the couple of interest, $Fe^{2+}/Fe(0)$, is faster than the reaction of the interfering $H^+/H_2(0)$ couple. Consequently, they relied on the electrochemical kinetics measurements by Hurlen (1960) for obtaining E° of the $Fe^{2+}/Fe(0)$ redox couple with the reduction reaction

$Fe^{2+} + H_2g \rightleftharpoons Fe(\alpha) + 2\ H^+$

Lemire et al. (2013) used the SIT formalism for correcting the experimental data to zero ionic strength and obtained[22]

$E_0°(298.15\ K) = -(0.4745 \pm 0.0088)\ V$

which corresponds to

$\Delta_r G_m°(298.15\ K) = (91.56 \pm 1.70)\ kJ \cdot mol^{-1}$

by virtue of $\Delta_r G_m° = n\ F\ E_0°$ (with $n = 2$ and $F = 96485.309\ J \cdot V^{-1} \cdot mol^{-1}$).

From $\Delta_f G_m°(H_2, g, 298.15\ K) = \Delta_f G_m°(Fe, \alpha, 298.15\ K) = \Delta_f G_m°(H^+, 298.15\ K) = 0$ then follows

$\Delta_f G_m°(Fe^{2+}, 298.15\ K) = -(91.56 \pm 1.70)\ kJ \cdot mol^{-1}$

---

[22] Lemire et al. (2013) did not explain how they arrived at this value from the three values given in their Table VI-3.

As $\Delta_r G_m°(298.15\ K)$ was used in the optimization procedure (see Section 11.1.2), which lead to the optimized value (90.72 ± 0.64) kJ · mol^{-1}, Lemire et al. (2013) selected the optimised

$$\Delta_r G_m°(298.15\ K) = (90.72 \pm 0.64)\ kJ \cdot mol^{-1}$$

and

$$\Delta_f G_m°(Fe^{2+}, 298.15\ K) = -(90.72 \pm 0.64)\ kJ \cdot mol^{-1}$$

and the resulting

$$\log_{10}{}^*K°(298.15\ K) = -(15.89 \pm 0.11)$$

These data are also included in our database, as well as

$$\Delta_f H_m°(Fe^{2+}, 298.15\ K) = -(90.29 \pm 0.52)\ kJ \cdot mol^{-1}$$

which also resulted from the optimization procedure by Lemire et al. (2013).

By virtue of G = H - T S, $\Delta_f S_m°(Fe^{2+}, 298.15\ K)$ can be calculated from $\Delta_f G_m°(Fe^{2+}, 298.15\ K)$ and $\Delta_f H_m°(Fe^{2+}, 298.15\ K)$, while $S_m°(Fe^{2+}, 298.15\ K)$ follows from the expression $\Delta_f S_m°(Fe^{2+}, 298.15\ K) = S_m°(Fe^{2+}, 298.15\ K) - S_m°(Fe, \alpha, 298.15\ K) + S_m°(H_2,g, 298.15\ K)$[23]. Using their recommended data for Fe^{2+} and Fe(α), as well as $S_m°(H_2, g, 298.15\ K)$ = (130.680 ± 0.003) J · K^{-1} · mol^{-1}, Lemire et al. (2013) obtained

$$S_m°(Fe^{2+}, 298.15\ K) = -(102.17 \pm 2.78)\ J \cdot K^{-1} \cdot mol^{-1}$$

which is also included in TDB 2020.

Lemire et al. (2013) derived their selected

$$C_{p,m}°(Fe^{2+}, 298.15\ K) = -(23^{24} \pm 10)\ J \cdot K^{-1} \cdot mol^{-1}$$

from apparent molar heat capacity measurements by Hovey (1988) for $Fe(ClO_4)_2$ in aqueous $HClO_4$ solutions between 10 and 50 °C. This value is also included in our database.

---

[23] According to Wagman et al. (1982), the standard molar entropy of formation from the elements of a charged species $\Delta_f S_m°$ can be calculated from $\Delta_f S_m° = S_m° - \Sigma S_m°(\text{elements}) + (n/2)\ S_m°(H_2, g)$, where n is the charge. In the case of Fe^{2+} this follows from the reaction Fe(α) + 2 H^+ ⇌ Fe^{2+} + H_2g.

[24] Note that on p.112 in Lemire et al. (2013) the value for $C_{p,m}°(Fe^{2+}, 298.15\ K)$ is reported as -(25 ± 10) J · K^{-1} · mol^{-1}.

The selected ion interaction coefficient

$$\varepsilon(Fe^{2+}, Cl^-) = (0.17 \pm 0.01)\ kg \cdot mol^{-1}$$

was calculated by Lemire et al. (2013) from a SIT analysis[25] of osmotic coefficient data from four isopiestic studies of Fe(II) chloride solutions up to 5.5 mol · kg^{-1} and a separate analysis of relative vapor pressure measurements of Fe(II) chloride solutions reported in one of these studies.

There are no experimental data that allow to derive $\varepsilon(Fe^{2+}, ClO_4^-)$. Therefore, Lemire et al. (2013) took recourse to an estimate. The NEA-selected ion interaction coefficients of the divalent first-row transition metals Zn, Cu, Ni, Co, and Mg with ClO_4^- vary between 0.32 and 0.37, and those for Cu, Ni, Co, Mn, and Mg with Cl^- between 0.08 and 0.19. Considering that their selected $\varepsilon(Fe^{2+}, Cl^-) = (0.17 \pm 0.01)$ kg · mol^{-1} is equal to the NEA-selected $\varepsilon(Ni^{2+}, Cl^-) = (0.17 \pm 0.02)$ kg · mol^{-1}, they adopted the NEA-selected $\varepsilon(Ni^{2+}, ClO_4^-) = (0.37 \pm 0.03)$ kg · mol^{-1} and, increasing the uncertainty, selected

$$\varepsilon(Fe^{2+}, ClO_4^-) = (0.37 \pm 0.04)\ kg \cdot mol^{-1}$$

Both ion interaction coefficients are included in our database.

11.3.3 Fe^{3+}

According to Lemire et al. (2013), the Fe^{3+}/Fe^{2+} redox couple is reversible at inert solid electrodes and the measured potential differences are well suited to determine reliable values for $E°(Fe^{3+}/Fe^{2+})$ and its variation with temperature. This is reflected in the good agreement between the values for $E°(Fe^{3+}/Fe^{2+})$ determined with cell measurements since 1934 (all values within ± 2 mV from $E° = 0.770$ V). Lemire et al. (2013) analysed data according to the SIT method from five experimental studies carried out in perchlorate ($HClO_4$, $NaClO_4$) media (Schumb et al. 1937, Connick & McVey 1951, Magnusson & Huizenga 1953, Whittemore & Langmuir 1972, Tagirov et al. 2000). They remarked on p. 95 that[26] "it was not possible to fit a single curve of the form $E^‡ + (5D)(RT\ln(10)/F) = f(m_{ClO_4^-})$ to all the perchloric-acid-medium data points (for 298 K) from all five papers", see their Fig. VI-2 (p. 95). Further (on p. 95), Lemire et al. (2013) noted that "the two almost identical points for a total perchlorate molality of 0.0571 mol · kg^{-1} [1972WHI/LAN] are well off the line established by the values from the rest of the experimental studies (see Fig. VI-2). For these points the concentration of iron (II + III) is not negligible with respect to the ionic strength. However, the junction-potential problem is different from that in the study of Schumb *et al*. [1937SCH/SHE] as discussed below because of the use of a silver/silver chloride reference electrode with saturated KCl as the internal solution. The Whittemore and Langmuir results have not been used in our final determination of $E_0°$ by the SIT treatment". Schumb et al. (1937) measured the (Fe^{3+}/Fe^{2+}) potential difference at a series of four $HClO_4$ concentrations (0.02586, 0.05212, 0.1046, and 0.2726 mol · kg^{-1}). In an SIT-plot, $(E^‡ + (5D)(RT\ln(10)/F)$ vs.

---

[25] A peculiarity of this SIT analysis of osmotic data is the simultaneous retrieval of $\varepsilon(Fe^{2+}, Cl^-)$, $\varepsilon(FeCl^+, Cl^-)$, and $\log_{10}\beta_1°(FeCl^+, 298.15\ K)$. However, only $\varepsilon(Fe^{2+}, Cl^-)$ was declared as a selected value.

[26] $E^‡$ in the following citation is defined by $E^‡ = E°' + (RT/F)\ln\gamma_{H^+}$ such that in the equation $E^‡ + 5D(RT\ln(10)/F) = E° - (RT\ln(10)/F)\,\Delta\varepsilon\, m_{ClO_4^-}$, $\Delta\varepsilon$ is equal to $\varepsilon(Fe^{2+}, ClO_4^-) - \varepsilon(Fe^{3+}, ClO_4^-)$.

$m_{ClO_4^-}$, the experimental data lie on four distinct lines (one for each $HClO_4$ concentration) with different curvatures. Lemire et al. (2013) stated that "the systematic problem is probably due to substantial junction potentials generated by the more concentrated iron solutions in which iron (II + III) is responsible for a non-negligible part of the ionic strength" and that "it is possible to limit the junction-potential deviations by selecting from the Schumb et al. data only the measured potential values for solutions having higher $HClO_4$/Fe ratios". Thus, Lemire et al. (2013) eliminated all the data points for which the $HClO_4$/Fe ratios were lower than 10, and additionally eliminated two data points gathered in mixed $NaClO_4$-$HClO_4$ media. They remarked that "this selection was effective, in that all the remaining points fall on a common curve". They then performed an SIT analysis using four different fitting functions, the standard linear SIT fit, a two term fit involving a logarithmic ionic strength term ($\varepsilon = \varepsilon_1 + \varepsilon_2 \log_{10} I_m$, introduced by Ciavatta 1980), and a 2$^{n\,d}$ and 3$^{r\,d}$ degree polynomial. Lemire et al. (2013) only reported the results of the first two fits, since the 2$^{n\,d}$ and 3$^{r\,d}$ degree polynomial fits reproduced the data well within the range of the experimental ionic strengths but deviated unreasonably outside the range. The two term fit with the logarithmic ionic strength term (designated as SIT_2) resulted in a better fit to the data than the standard linear fit (designated as SIT_1). Therefore, Lemire et al. (2013) recommended the results of the SIT_2 fit as best values for $E_0°$ and $\Delta\varepsilon = \varepsilon(Fe^{2+}, ClO_4^-) - \varepsilon(Fe^{3+}, ClO_4^-)$, but also reported the results of SIT_1, as the linear fit is the standard fitting procedure in the NEA TDB Project. The results of the fits were:

$$E_0° = (0.7753 \pm 0.0004)\ \text{V} \qquad (SIT_1)$$

$$\Delta\varepsilon = -(0.36 \pm 0.02)\ \text{kg} \cdot \text{mol}^{-1} \qquad (SIT_1)$$

$$E_0° = (0.772 \pm 0.002)\ \text{V} \qquad (SIT_2)$$

$$\Delta\varepsilon = -((0.41 \pm 0.03) - (0.41 \pm 0.05) \log_{10} I_m)\ \text{kg} \cdot \text{mol}^{-1} \qquad (SIT_2)$$

for the reaction

$$Fe^{2+} + H^+ \rightleftharpoons Fe^{3+} + 0.5\ H_2g$$

Lemire et al. (2013) derived their selected

$$\log_{10}{}^*K°(298.15\ \text{K}) = -(13.051 \pm 0.160) \qquad (SIT_2)$$

from $E_0°(SIT_2)$[27]. Using $\varepsilon(Fe^{2+}, ClO_4^-) = (0.37 \pm 0.04)\ \text{kg} \cdot \text{mol}^{-1}$ (see Section 11.3.2) with $\Delta\varepsilon(SIT_2)$ results in the selected

$$\varepsilon(Fe^{3+}, ClO_4^-) = ((0.78 \pm 0.05) - (0.41 \pm 0.05) \log_{10} I_m)\ \text{kg} \cdot \text{mol}^{-1} \qquad (SIT_2)$$

[27] Lemire et al. (2013) used $E_0°(SIT_2)$ to calculate $\Delta_r G_m°(298.15\ \text{K}) = (74.49 \pm 0.193)\ \text{kJ} \cdot \text{mol}^{-1}$, which after the optimization procedure received a larger uncertainty, such that $\Delta_r G_m°(298.15\ \text{K}) = (74.49 \pm 0.913)\ \text{kJ} \cdot \text{mol}^{-1}$, which then led to $\log_{10}{}^*K°(298.15\ \text{K}) = -(13.051 \pm 0.160)$.

Corresponding calculations for values derived with SIT_1 result in

$$\log_{10}{}^*K°(298.15\ \text{K}) = -(13.105 \pm 0.007) \qquad (SIT_1)$$

and

$$\varepsilon(Fe^{3+}, ClO_4^-) = (0.73 \pm 0.04)\ \text{kg} \cdot \text{mol}^{-1} \qquad (SIT_1)$$

For the determination of $\varepsilon(Fe^{3+}, Cl^-)$, Lemire et al. (2013) relied on the Fe^{3+}/Fe^{2+} potential difference measurements in a HCl medium by Popoff & Kunz (1929). For the SIT analysis, they considered the hydrolysis of Fe^{3+} (formation of $FeOH^{2+}$) and the formation of chloride complexes ($FeCl^{2+}$ and $FeCl_2^+$ for Fe^{3+}, and $FeCl^+$ for Fe^{2+}). Since the formation constant $\log_{10}\beta_1°(FeCl^+, 298.15\ \text{K})$ is not very well known[28], Lemire et al. (2013) considered two cases with different stabilities. In the first case, calculations were done with $\log_{10}\beta_1°(FeCl^+, 298.15\ \text{K}) = -(1.0 \pm 0.8)$, see Section 11.5.1.3.2, and $\Delta\varepsilon = -(0.12 \pm 0.02)\ \text{kg} \cdot \text{mol}^{-1}$, calculated from $\varepsilon(FeCl^+, Cl^-) = (0.17 \pm 0.01)\ \text{kg} \cdot \text{mol}^{-1}$, see Section 11.5.1.3.2[29], $\varepsilon(Fe^{2+}, Cl^-) = (0.17 \pm 0.01)\ \text{kg} \cdot \text{mol}^{-1}$, see Section 11.3.2, and the NEA-selected $\varepsilon(H^+, Cl^-) = (0.12 \pm 0.01)\ \text{kg} \cdot \text{mol}^{-1}$. In the second case, calculations were done with $\log_{10}\beta_1°(FeCl^+, 298.15\ \text{K}) = -0.11$ and $\Delta\varepsilon = -0.173\ \text{kg} \cdot \text{mol}^{-1}$; both values were chosen such that $FeCl^+$ becomes more stable. SIT analyses were carried out both with the linear (SIT_1) and the non-linear (SIT_2) formulation. With SIT_1, both cases resulted in the same value

$$\varepsilon(Fe^{3+}, Cl^-) = (0.76 \pm 0.03)\ \text{kg} \cdot \text{mol}^{-1} \qquad (SIT_1)$$

which was selected by Lemire et al. (2013) and shows that Fe(II) chloride complexes have no effect at all. Comparing this value with $\varepsilon(Fe^{3+}, ClO_4^-) = (0.73 \pm 0.04)\ \text{kg} \cdot \text{mol}^{-1}$ obtained above is an indication that the approximation $\varepsilon(Fe^{3+}, Cl^-) \approx \varepsilon(Fe^{3+}, ClO_4^-)$ is reasonable if Fe(III) chloride complexes are considered explicitly (see discussion in Section 11.1.1). This is one of the few examples (at least to our knowledge) where this approximation could be tested (for another example see Section 11.5.1.4.2).

For SIT_2, Lemire et al. (2013) selected the result from the first case (without explaining this choice)

$$\varepsilon(Fe^{3+}, Cl^-) = ((0.84 \pm 0.04) - (0.59 \pm 0.06)\ \log_{10} I_m)\ \text{kg} \cdot \text{mol}^{-1} \qquad (SIT_2)$$

---

[28] Lemire et al. (2013) did not select any value for $\log_{10}\beta_1°(FeCl^+, 298.15\ \text{K})$ but suggested the value $-(1.0 \pm 0.8)$ in order to "provide some assistance to modellers who must select a constant due to the specifics of their speciation code", see Section 12.5.1.3.2.

[29] Note that on p. 123 and p. 245, Lemire et al. (2013) reported $\varepsilon(FeCl^+, Cl^-) = (0.16 \pm 0.01)\ \text{kg·mol}^{-1}$.

At this place, it is perhaps useful to present diagrams of $\varepsilon(Fe^{3+}, Cl^-)$ and $\varepsilon(Fe^{3+}, ClO_4^-)$ as functions of ionic strength (Fig. 11.3-1) and to compare the epsilons obtained with SIT_1 and SIT_2. While the epsilons determined with SIT_1 are independent of ionic strength, $\varepsilon(Fe^{3+}, Cl^-)$ and $\varepsilon(Fe^{3+}, ClO_4^-)$ determined with SIT_2 increase with decreasing ionic strength and, due to the logarithmic term, approach infinity as the ionic strength approaches zero. As discussed in Section 12.1.1, SIT_2 has no theoretical justification and even though the term $\varepsilon \cdot m = (\varepsilon = \varepsilon_1 + \varepsilon_2 \log_{10} I_m) \cdot m$ (in the calculation of activity coefficients with SIT_2) is zero at $I_m = 0$ (Grenthe et al. 2020), we prefer specific ion interaction coefficients derived with SIT_1 over those derived with SIT_2.

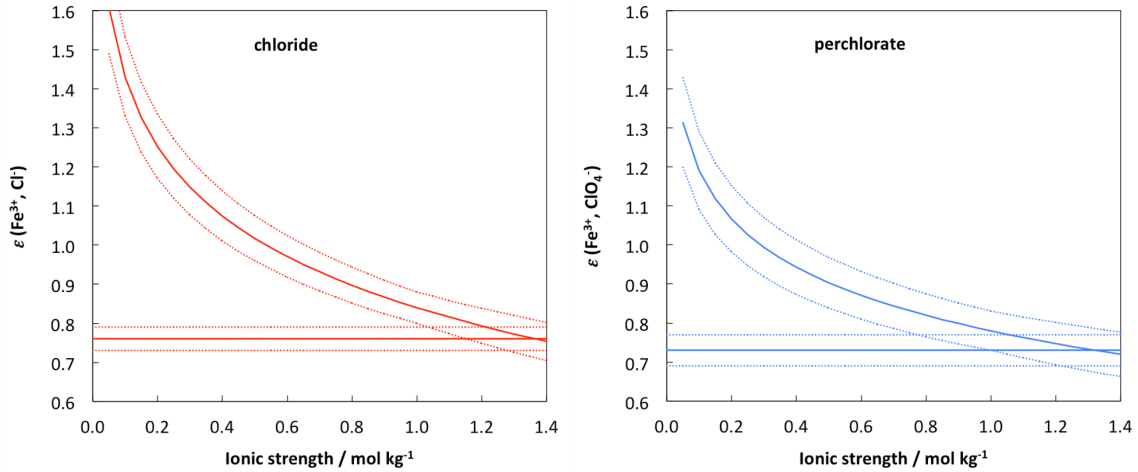

Fig. 11.3-1: Specific ion interaction coefficients for Fe^{3+} with Cl^- (left) and for Fe^{3+} with ClO_4^- (right) according to SIT_1 (straight lines) and SIT_2 (curved lines)

Calculated with data selected by Lemire et al. (2013), see text for discussion. Dotted lines: 95% uncertainty range.

Lemire et al. (2013) also determined $\Delta_r S_m°(298.15\ K) = (117.7 \pm 8.6)\ J \cdot K^{-1} \cdot mol^{-1}$ from an SIT_2 fit to $E_0°$ data in perchlorate media as a function of temperature (5 – 35 °C).

After optimization, this resulted in the selected

$$\Delta_r S_m°(298.15\ K) = (114.9 \pm 4.8)\ J \cdot K^{-1} \cdot mol^{-1} \qquad (SIT_2)$$

Combining this with

$$\Delta_r G_m°(298.15\ K) = (74.494 \pm 0.913)\ kJ \cdot mol^{-1} \qquad (SIT_2)$$

derived from $E_0°(SIT_2)$ and optimised, results in

$$\Delta_r H_m°(298.15\ K) = (40.238 \pm 1.699)\ kJ \cdot mol^{-1} \qquad (SIT_2)$$

From these and the selected $\Delta_f G_m°(Fe^{2+}, 298.15\ K)$ and $\Delta_f H_m°(Fe^{2+}, 298.15\ K)$ (see Section 11.3.2), then follow the selected

$$\Delta_f G_m°(Fe^{3+}, 298.15\ K) = -(16.23 \pm 0.65)\ kJ \cdot mol^{-1} \quad (SIT_2)$$

$$\Delta_f H_m°(Fe^{3+}, 298.15\ K) = -(50.06 \pm 0.97)\ kJ \cdot mol^{-1} \quad (SIT_2)$$

By virtue of G = H - T S, $\Delta_f S_m°(Fe^{3+}, 298.15\ K)$ can be calculated from $\Delta_f G_m°(Fe^{3+}, 298.15\ K)$ and $\Delta_f H_m°(Fe^{3+}, 298.15\ K)$, while $S_m°(Fe^{3+}, 298.15\ K)$ follows from the expression $\Delta_f S_m°(Fe^{3+}, 298.15\ K) = S_m°(Fe^{3+}, 298.15\ K) - S_m°(Fe, \alpha, 298.15\ K) + 1.5\ S_m°(H_2, g, 298.15\ K)$[30].

Using their recommended data for Fe^{2+} and Fe(α), as well as $S_m°(H_2, g, 298.15\ K) = (130.680 \pm 0.003)\ J \cdot K^{-1} \cdot mol^{-1}$, Lemire et al. (2013) obtained

$$S_m°(Fe^{3+}, 298.15\ K) = -(282.40 \pm 3.93)\ J \cdot K^{-1} \cdot mol^{-1}$$

Lemire et al. (2013) derived their selected

$$C_{p,m}°(Fe^{3+}, 298.15\ K) = -(108 \pm 20)\ J \cdot K^{-1} \cdot mol^{-1}$$

from apparent molar heat capacity measurements by Hovey (1988) for $Fe(ClO_4)_3$ in aqueous $HClO_4$ solutions between 10 and 50 °C.

For our database, we have accepted $\Delta_f G_m°(Fe^{3+}, 298.15\ K) = -(16.23 \pm 0.65)\ kJ \cdot mol^{-1}$, $\Delta_f H_m°(Fe^{3+}, 298.15\ K) = -(50.06 \pm 0.97)\ kJ \cdot mol^{-1}$ and $S_m°(Fe^{3+}, 298.15\ K) = -(282.40 \pm 3.93)\ J \cdot K^{-1} \cdot mol^{-1}$ selected by Lemire et al. (2013) based on SIT_2, the selected values for $\varepsilon(Fe^{3+}, ClO_4^-) = (0.73 \pm 0.04)\ kg \cdot mol^{-1}$ and $\varepsilon(Fe^{3+}, Cl^-) = (0.76 \pm 0.03)\ kg \cdot mol^{-1}$ based on SIT_1, and the selected value for $C_{p,m}°(Fe^{3+}, 298.15\ K) = -(108 \pm 20)\ J \cdot K^{-1} \cdot mol^{-}$.

---

[30] According to Wagman et al. (1982), the standard molar entropy of formation from the elements of a charged species $\Delta_f S_m°$ can be calculated from $\Delta_f S_m° = S_m° - \Sigma S_m°(elements) + (n/2)\ S_m°(H_2, g)$, where n is the charge. In the case of Fe^{3+} this follows from the reaction $Fe(\alpha) + 3\ H^+ \rightleftharpoons Fe^{3+} + 1.5\ H_2 g$.

11.4 Iron oxygen and hydrogen compounds and complexes

11.4.1 Aqueous iron hydroxo complexes

11.4.1.1 Data in TDB 05/92, TDB 01/01 and TDB 12/07

The thermodynamic data for the iron hydroxo complexes selected in TDB 01/01 and TDB 12/07 were all adopted from TDB 05/92 (Pearson et al. 1992). Pearson et al. (1992) took all thermodynamic data for ferrous ($FeOH^+$) and ferric hydroxo complexes ($FeOH^{2+}$, $Fe(OH)_2^+$, $Fe(OH)_3(aq)$, $Fe(OH)_4^-$, $Fe_2(OH)_2^{4+}$, $Fe_3(OH)_4^{5+}$) from Nordstrom et al. (1990) who themselves obtained the data from Baes & Mesmer (1976), except for $\Delta_r H_m°(Fe(OH)_2^+, 298.15\ K)$, $\Delta_r H_m°(Fe(OH)_3, aq, 298.15\ K)$, and $\Delta_r H_m°(Fe(OH)_4^-, 298.15\ K)$, which they estimated by combining $\Delta_r G_m°$ and entropies estimated from correlation plots (no details given). For $\log_{10}{}^*\beta_{3,1}°(298.15\ K)$ Nordstrom et al. (1990) selected the value determined by Kester et al. (1975) and corrected it to $I = 0$ (without explaining how this was done).

Thus, the following data were included in TDB 01/01 and TDB 12/07:

$Fe^{2+} + H_2O(l) \rightleftharpoons FeOH^+ + H^+$

$\log_{10}{}^*\beta_{1,1}°(298.15\ K) = -9.5$

$\Delta_r H_{m,1,1}°(298.15\ K) = 55.2\ kJ \cdot mol^{-1}$

$Fe^{3+} + H_2O(l) \rightleftharpoons FeOH^{2+} + H^+$

$\log_{10}{}^*\beta_{1,1}°(298.15\ K) = -2.19$

$\Delta_r H_{m,1,1}°(298.15\ K) = 43.5\ kJ \cdot mol^{-1}$

$Fe^{3+} + 2\ H_2O(l) \rightleftharpoons Fe(OH)_2^+ + 2\ H^+$

$\log_{10}{}^*\beta_{2,1}°(298.15\ K) = -5.67$

$\Delta_r H_{m,2,1}°(298.15\ K) = 71.5\ kJ \cdot mol^{-1}$

$Fe^{3+} + 3\ H_2O(l) \rightleftharpoons Fe(OH)_3(aq) + 3\ H^+$

$\log_{10}{}^*\beta_{3,1}°(298.15\ K) = -12.56$

$\Delta_r H_{m,3,1}°(298.15\ K) = 104\ kJ \cdot mol^{-1}$

$Fe^{3+} + 4\ H_2O(l) \rightleftharpoons Fe(OH)_4^- + 4\ H^+$

$\log_{10}{}^*\beta_{4,1}°(298.15\ K) = -21.6$

$\Delta_r H_{m,4,1}°(298.15\ K) = 133\ kJ \cdot mol^{-1}$

$2\ Fe^{3+} + 2\ H_2O(l) \rightleftharpoons Fe_2(OH)_2^{4+} + 2\ H^+$

$\log_{10}{}^*\beta_{2,2}°(298.15\ K) = -2.95$

$\Delta_r H_{m,2,2}°(298.15\ K) = 56.5\ kJ \cdot mol^{-1}$

$3\ Fe^{3+} + 4\ H_2O(l) \rightleftharpoons Fe_3(OH)_4^{5+} + 4\ H^+$

$\log_{10}{}^*\beta_{4,3}°(298.15\ K) = -6.3$

$\Delta_r H_{m,4,3}°(298.15\ K) = 59.8\ kJ \cdot mol^{-1}$

All these data (with the exception of those for $Fe_3(OH)_4^{5+}$) are superseded by the data selected in the following sections.

11.4.1.2 Aqueous iron(II) hydroxo complexes

11.4.1.2.1 Data reported by Lemire et al. (2013)

$FeOH^+$: According to Lemire et al. (2013), the predominant hydrolysis equilibrium that could be studied by "classic homogeneous studies" is the first hydrolysis constant $\log_{10}{}^*\beta_1°(298{,}15\ K)$ for

$Fe^{2+} + H_2O(l) \rightleftharpoons FeOH^+ + H^+$

Lemire et al. (2013) accepted data from two studies using potentiometry and the glass electrode in dilute HCl and NaCl (I_m from 0.0097 to 0.12 $kg \cdot mol^{-1}$) and corrected the data to zero ionic strength using only the Debye-Hückel correction and selected $\log_{10}{}^*\beta_1°(298{,}15\ K) = -(9.1 \pm 0.4)$. Apart from stating that "the disparity between the various values simply highlights the experimental difficulties of this system" and that "given the sparse and scattered nature of these data, there can be no estimate of the $\varepsilon(FeOH^+, X^-)$ value at this time" Lemire et al. (2013) did not discuss explicitly why experimental data reported in six other investigations were not accepted.

Lemire et al. (2013) also reviewed the results of reductive solubility studies of magnetite in dilute systems (with no background electrolyte) at various temperatures and used the generalized equation

$\log_{10}{}^*K_{s,x}°(T) = a + b/T + c\ \log_{10}T$

for fitting the data with standard least-squares methods.

First solubility constant of magnetite: For the first solubility constant of magnetite

$1/3\ Fe_3O_4(magnetite) + 2\ H^+ + 1/3\ H_2g \rightleftharpoons Fe^{2+} + 4/3\ H_2O(l)$

Lemire et al. (2013) tried four different fits to the experimental data by Sweeton & Baes (1970) and Tremaine & LeBlanc (1980) in the temperature range 25 to 300 °C:

Fit 1: Assuming that $\Delta_r C_{p,m}°(298.15\ K)$ = constant, with no other constraints

Fit 2: Assuming that $\Delta_r C_{p,m}°(298.15\ K) = 0$, with no other constraints

Fit 3: Assuming that $S_m°(Fe^{2+}, 298.15\ K) = -101.01\ J \cdot K^{-1} \cdot mol^{-1}$, a value selected in an initial phase of the NEA-review and later superseded by $-(102.18 \pm 2.78)\ J \cdot K^{-1} \cdot mol^{-1}$, and that $\Delta_r C_{p,m}°(298.15\ K) = 0$

Fit 4: Assuming that, as in Fit 3, $S_m°(Fe^{2+}, 298.15\ K) = -101.01\ J \cdot K^{-1} \cdot mol^{-1}$, and that $C_{p,m}°(Fe^{2+}, 298.15\ K) = -22\ J \cdot K^{-1} \cdot mol^{-1}$, a value selected in an initial phase of the NEA-review and later superseded by $-(23 \pm 10)\ J \cdot K^{-1} \cdot mol^{-1}$. Note that, as discussed below, it is very likely that Lemire et al. (2013) inadvertently held $\Delta_r C_{p,m}°(298.15\ K)$ constant at $-22\ J \cdot K^{-1} \cdot mol^{-1}$, and not $C_{p,m}°(Fe^{2+}, 298.15\ K)$

Lemire et al. (2013) "adopted" the most constrained Fit 4 and used the resulting a, b and c parameters of the fit to calculate the reaction properties $\Delta_r G_m°(298.15)$, $\Delta_r H_m°(298.15)$, $\Delta_r S_m°(298.15)$, and $\Delta_r C_{p,m}°(298.15\ K)$[31]. Curiously, they then used these reaction properties in combination with $\Delta_f G_m°$(magnetite, 298.15), $\Delta_f H_m°$(magnetite, 298.15), $S_m°$(magnetite, 298.15), and $C_{p,m}°$(magnetite, 298.15 K) (values that they derived later in their review from calorimetric data) and the corresponding data for H_2g and $H_2O(l)$ to calculate $\Delta_f G_m°(Fe^{2+}, 298.15)$, $\Delta_f H_m°(Fe^{2+}, 298.15)$, $S_m°(Fe^{2+}, 298.15)$, and $C_{p,m}°(Fe^{2+}, 298.15\ K)$. It would have been more obvious to us to calculate the thermodynamic properties of magnetite from the reaction data and the already selected data for Fe^{2+}. Finally, they compared the data derived for Fe^{2+} with those reported by Parker & Khodakowskii (1995) and Wagman et al. (1982) without further discussion and without comparison with their own data earlier selected for Fe^{2+}.

It also appears that Fit 4 by Lemire et al. (2013) contains an error. While they claim that they had fixed $C_{p,m}°(Fe^{2+}, 298.15\ K)$ to the value of $-22\ J \cdot K^{-1} \cdot mol^{-1}$, it seems that they erroneously fixed $\Delta_r C_{p,m}°(298.15\ K)$ to this value. We deduce this from their Tab. VII-3, where they listed the a, b, and c parameters of the fits, and from their Tab. VII-4, where they listed the resulting thermodynamic properties of Fe^{2+}. In Tab. VII-3 the c parameters for Fit 2 and Fit 3 are equal to zero, which means that $\Delta_r C_{p,m}°(298.15\ K)$ is also equal to zero. In Tab. VII-4 they list $C_{p,m}°(Fe^{2+}, 298.15\ K)$ for the different fits. For Fit 4, $C_{p,m}°(Fe^{2+}, 298.15\ K) = -22\ J \cdot K^{-1} \cdot mol^{-1}$, for Fit 2 and Fit 3, however, $C_{p,m}°(Fe^{2+}, 298.15\ K) = 0$. This is a strong indication that Lemire et al. (2013) actually fixed $\Delta_r C_{p,m}°(298.15\ K)$ to a constant or zero value and not $C_{p,m}°(Fe^{2+}, 298.15\ K)$ and that the values reported in Tab. VII-4 for $C_{p,m}°(Fe^{2+}, 298.15\ K)$ are actually values for $\Delta_r C_{p,m}°(298.15\ K)$.

Therefore, $\log_{10}{}^*K_{s,0}°(298.15\ K) = (11.5 \pm 0.2)$ and all other reaction properties calculated by Lemire et al. (2013) from the a, b, and c parameters derived from Fit 4 are based on the incorrect assumption that $\Delta_r C_{p,m}°(298.15\ K) = -22\ J \cdot K^{-1} \cdot mol^{-1}$.

Second solubility constant of magnetite: For the second solubility constant of magnetite

$$1/3\ Fe_3O_4(\text{magnetite}) + H^+ + 1/3\ H_2g \rightleftharpoons FeOH^+ + 1/3\ H_2O(l)$$

Lemire et al. (2013) also accepted the experimental data by Sweeton & Baes (1970) and Tremaine & LeBlanc (1980) in the temperature range 25 to 300 °C and used 3 types of fits:

---

[31] For a discussion of the relationship between a, b, and c and $\Delta_r G_m°(298.15)$ or $\log_{10}K°$, $\Delta_r H_m°(298.15)$ or $\Delta_r S_m°(298.15)$, and $\Delta_r C_{p,m}°(298.15\ K)$ see HUMMEL et al. (2002), Section 12.2.3.

Fit 1: Assuming that $\Delta_r C_{p,m}°(298.15\ K) = 0$, with no other constraints.

Fit 2: Fixing $\log_{10}{}^*K_{s,1}°(298.15\ K) = 3.20$, such that combining it with $\log_{10}{}^*K_{s,0}°(298.15\ K) = 12.3$, obtained from Fit 3, as discussed above, results in $\log_{10}{}^*\beta_1°(298.15\ K) = -9.1$, the value selected by Lemire et al. (2013), see above, and assuming that $\Delta_r C_{p,m}°(298.15\ K) = 0$.

Fit 3: Fixing $\log_{10}{}^*K_{s,1}°(298.15\ K) = 3.36$, such that combining it with $\log_{10}{}^*K_{s,0}°(298.15\ K) = 12.5$, obtained from the flawed (see above) Fit 4 for the first solubility constant, results in $\log_{10}{}^*\beta_1°(298.15\ K) = -9.1$, the value selected by Lemire et al. (2013), see above, and assuming that $\Delta_r C_{p,m}°(298.15\ K) = 0$.

Lemire et al. (2013) "preferred" Fit 3 (based on the flawed Fit 4 for the first solubility constant), derived from it the "proposed" quantities $\Delta_f G_m°(FeOH^+, 298.15)$, $\Delta_f H_m°(FeOH^+, 298.15)$, and $S_m°(FeOH^+, 298.15)$ and compared them with those reported by Wagman et al. (1982). Since Fit 4 for the first solubility constant is flawed and Fit 3 for the second solubility constant depends on it, all data derived from the respective Fit 3 inherit the flaws from the respective Fit 4.

Third solubility constant of magnetite: For the third solubility constant of magnetite

$$1/3\ Fe_3O_4(magnetite) + 1/3\ H_2g + 2/3\ H_2O(l) \rightleftharpoons Fe(OH)_2(aq)$$

Lemire et al. (2013) accepted the solubility data by Sweeton & Baes (1970) and Tremaine & LeBlanc (1980) in the temperature range 25 to 300 °C and carried out a weighted, but unrestrained, linear fit to the data, using the equation $\log_{10}{}^*K_{s,2}°(T) = a + b/T$. From the fit with a = -(6.700 ± 0.911) and b = -(786.38 ± 412.73), they derived $\log_{10}{}^*K_{s,2}°(298.15) = -(8.7 \pm 1.1)$, as well as the quantities $\Delta_f G_m°(Fe(OH)_2, aq, 298.15)$, $\Delta_f H_m°(Fe(OH)_2, aq, 298.15)$, and $S_m°(Fe(OH)_2, aq, 298.15)$. However, either the values for a and b reported by Lemire et al. (2013) are incorrect, or their value for $\log_{10}{}^*K_{s,2}°(298.15)$, since we calculated $\log_{10}{}^*K_{s,2}°(298.15) = -9.34$ from the same a and b parameters. Combining their $\log_{10}{}^*K_{s,2}°(298.15) = -(8.7 \pm 1.1)$ with their preferred value $\log_{10}{}^*K_{s,0}°(298.15\ K) = (12.5 \pm 0.2)$, Lemire et al. (2013) obtained $\log_{10}{}^*\beta_2°(298.15\ K) = -(21.2 \pm 1.1)$.

Fourth solubility constant of magnetite: For the fourth solubility constant of magnetite

$$1/3\ Fe_3O_4(magnetite) + 1/3\ H_2g + 5/3\ H_2O(l) \rightleftharpoons Fe(OH)_3^- + H+$$

Lemire et al. (2013) accepted solubility data by Kanert et al. (1976) and Tremaine & LeBlanc (1980) in the temperature range 100 to 300 °C and explicitly excluded the data by Sweeton & Baes (1970), "due to the unrecognized and dominant presence of iron(III) in aqueous solution in their experiments". From the weighted linear fit to the data, Lemire et al. (2013) derived, in addition to $\Delta_f G_m°(Fe(OH)_3^-, 298.15)$, $\Delta_f H_m°(Fe(OH)_3^-, 298.15)$, and $S_m°(Fe(OH)_3^-, 298.15)$, $\log_{10}{}^*K_{s,3}°(298.15) = -(21.84 \pm 0.12)$. Combining this value with their preferred $\log_{10}{}^*K_{s,0}°(298.15\ K) = (12.5 \pm 0.2)$, Lemire et al. (2013) obtained $\log_{10}{}^*\beta_3°(298.15\ K) = -(34.3 \pm 0.2)$.

11.4.1.2.2 Data selected by Lemire et al. (2013)

From all the data by Lemire et al. (2013) discussed in the previous section, they only selected $\log_{10}{}^{*}\beta_1°(298{,}15\ \mathrm{K}) = -(9.1 \pm 0.4)$ based on two investigations studying the formation of $FeOH^+$ in aqueous solution using potentiometry and the glass electrode.

Although they described in detail, how they derived thermodynamic data for $Fe(OH)_2(aq)$ and $Fe(OH)_3^-$ from reductive solubility studies, Lemire et al. (2013) selected none of these, without giving any explanations and not even stating that they could be used for scoping calculations. Since, as discussed above, some of their "preferred" fits to the experimental data are flawed, we completely neglected their Fe(II) hydrolysis data, whether selected or not. Instead, we relied on the corresponding data recommended by Brown & Ekberg (2016) discussed in the following sections.

11.4.1.2.3 $FeOH^+$

Brown & Ekberg (2016) accepted stability constants for $FeOH^+$ from the solubility study of magnetite by Sweeton & Baes (1970) in the range 25 to 300 °C and from the potentiostatic (pH-stat) study by Morozumi & Posey (1967), as cited by Brown & Ekberg (2016), in the range 25 to 75 °C, as well as four stability constants at 25 °C from four other studies. The accepted stability constants for the reaction

$$Fe^{2+} + H_2O(l) \rightleftharpoons FeOH^+ + H^+$$

are linear in $1/T$, and Brown & Ekberg (2016) obtained

$$\log_{10}{}^{*}\beta_1°(T) = 0.136 - 2851/T$$

leading to

$$\log_{10}{}^{*}\beta_1°(298.15\ \mathrm{K}) = -(9.43 \pm 0.10)$$

$$\Delta_r H_m°(298.15\ \mathrm{K}) = (54.6 \pm 0.9)\ \mathrm{kJ \cdot mol^{-1}}$$

$$\Delta_r C_{p,m}°(298.15\ \mathrm{K}) = 0$$

which are all included in TDB 2020. The stability constant determined by Brown & Ekberg (2016) is more negative than $\log_{10}{}^{*}\beta_1°(298.15\ \mathrm{K}) = -(9.1 \pm 0.4)$ selected by Lemire et al. (2013) but lies within its uncertainty limits.

Since the stability constants accepted by Brown & Ekberg (2016) were determined in experiments with no background electrolytes, specific ion interaction coefficients for $FeOH^+$ must be estimated. From the estimation method described in Section 1.5.3 follows

$$\varepsilon(FeOH^+, ClO_4^-) \approx (0.2 \pm 0.1)\ \mathrm{kg \cdot mol^{-1}}$$

and

$\varepsilon(FeOH^+, Cl^-) \approx (0.05 \pm 0.10)$ kg · mol^{-1}

Both of these values are included in TDB 2020.

11.4.1.2.4 $Fe(OH)_2(aq)$

Brown & Ekberg (2016) accepted stability constant data for

$$Fe^{2+} + 2\ H_2O(l) \rightleftharpoons Fe(OH)_2(aq) + 2\ H^+$$

from the magnetite solubility experiments by Sweeton & Baes (1970) and Ziemniak et al. (1995) in the temperature range 25 to 300 °C and a constant at 25 °C by Millero & Hawke (1992). From their linear fit to the data

$$\log_{10}{}^*\beta_2^\circ(T) = -0.291 - 6030/T$$

Brown & Ekberg (2016) obtained

$\log_{10}{}^*\beta_2^\circ(298.15\ K) = (-20.52 \pm 0.08)$

$\Delta_r H_m^\circ(298.15\ K) = (115.4 \pm 1.0)$ kJ · mol^{-1}

$\Delta_r C_{p,m}^\circ(298.15\ K) = 0$

which are all included in TDB 2020, as well as

$\varepsilon(Fe(OH)_2(aq), NaCl) = \varepsilon(Fe(OH)_2(aq), NaClO_4) \approx (0.0 \pm 0.1)$ kg · mol^{-1}

estimated according to Tab. 1-7.

11.4.1.2.5 $Fe(OH)_3^-$

For the reaction

$$Fe^{2+} + 3\ H_2O(l) \rightleftharpoons Fe(OH)_3^- + 3\ H^+$$

Brown & Ekberg (2016) accepted stability constants from the magnetite solubility studies by Kanert et al. (1976), Tremaine & LeBlanc (1980), and Ziemniak et al. (1995) in the temperature range 25 to 300 °C. As Lemire et al. (2013), they did not accept the stability constants determined by Sweeton & Baes (1970) because of the possibility that the experimental results were influenced

by the presence of a ferric hydrolysis species. As was the case for $FeOH^+$ and $Fe(OH)_2(aq)$, the accepted data are well represented by a linear function in $1/T$. Brown & Ekberg (2016) obtained

$$\log_{10}{}^*\beta_3°(T) = -8.10 - 7330/T$$

and consequently

$$\log_{10}{}^*\beta_3°(298.15\ \mathrm{K}) = (-32.68 \pm 0.15)$$

$$\Delta_r H_m°(298.15\ \mathrm{K}) = (140.3 \pm 2.2)\ \mathrm{kJ \cdot mol^{-1}}$$

$$\Delta_r C_{p,m}°(298.15\ \mathrm{K}) = 0$$

These data are all included in TDB 2020.

The stability constants accepted by Brown & Ekberg (2016) were determined in experiments with no background electrolytes, thus specific ion interaction coefficients for $Fe(OH)_3^-$ must be estimated. From the estimation method described in Section 1.5.3 follows

$$\varepsilon(Fe(OH)_3^-, Na^+) \approx (-0.05 \pm 0.10)\ \mathrm{kg \cdot mol^{-1}}$$

This value is included in TDB 2020.

11.4.1.2.6 Comparison between selected Fe(II) hydroxo complexes by Lemire et al. (2013) and TDB 2020

As discussed in Section 11.4.1.2.2, Lemire et al. (2013) decided not to select any data for the higher hydroxo complexes $Fe(OH)_2(aq)$ and $Fe(OH)_3^-$. This has unfortunate consequences, e.g., for the reductive solubility of magnetite (dissolution into ferrous iron species) as a function of pH (see Fig. 11.4-1). The data selected by Lemire et al. (2013) lead to a linear decrease of Fe solubility at pH > 10, while the data included in TDB 2020 result in a solubility minimum at pH around 11.5. Thus, at a pH of 13, the data by Lemire et al. (2013) underestimate the solubility by two orders of magnitude.

Tab. 11.4-1: Comparison of data for magnetite and Fe(II) hydroxo complexes selected by Lemire et al. (2013) and TDB 2020

Based on the data selected by Brown & Ekberg (2016)

Name	**Reaction**	**$\log_{10}K°$ Lemire et al. (2013)**	**$\log_{10}K°$ TDB 2020**
Fe3O4(magnetite)	$1/3\ Fe_3O_4(cr) + 2\ H^+ + 1/3\ H_2g \rightleftharpoons Fe^{2+} + 4/3\ H_2O(l)$	12.15 ± 0.15	11.77 ± 0.22
FeOH+	$Fe^{2+} + H_2O(l) \rightleftharpoons FeOH^+ + H^+$	-9.1 ± 0.4	-9.43 ± 0.10
Fe(OH)2(aq)	$Fe^{2+} + 2\ H_2O(l) \rightleftharpoons Fe(OH)_2(aq) + 2\ H^+$	-	-20.52 ± 0.08
Fe(OH)3-	$Fe^{2+} + 3\ H_2O(l) \rightleftharpoons Fe(OH)_3^- + 3\ H^+$	-	-32.68 ± 0.15

11.4.1.3 Aqueous iron(III) hydroxo complexes

Lemire et al. (2013) selected data for the Fe(III) hydroxo complexes $FeOH^{2+}$ and $Fe(OH)_2^+$, and for the dimer $Fe_2(OH)_2^{4+}$, but chose to abstain from selecting data for $Fe(OH)_3(aq)$ and $Fe(OH)_4^-$. Neglecting the latter species has grave consequences for calculating Fe(III) solubilities at pH > 8, leading to severe underestimations (see Section 11.4.1.3.7). For this reason we relied on Brown & Ekberg (2016) who selected a set of data including $Fe(OH)_3(aq)$ and $Fe(OH)_4^-$.

11.4.1.3.1 $FeOH^{2+}$

Brown & Ekberg (2016) accepted stability constant data for $FeOH^{2+}$ as a function of temperature at zero ionic strength from 10 different studies spanning the temperature range between 18 and 300 °C. The accepted data for the reaction

$$Fe^{3+} + H_2O(l) \rightleftharpoons FeOH^{2+} + H^+$$

could be well reproduced by Brown & Ekberg (2016) with the linear function.

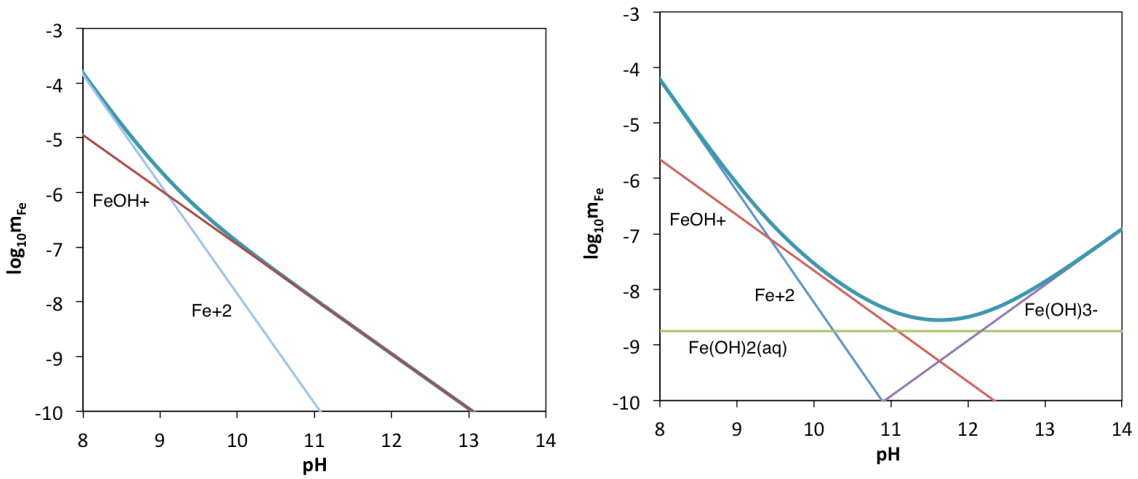

Fig. 11.4-1: Reductive solubility (dissolution into Fe(II) species) of magnetite (Fe_3O_4) at a H_2g pressure of 1 bar

calculated with data selected by Lemire et al. (2013) (left), and calculated with data selected for TDB 2020, based on Brown & Ekberg (2016) (right), see Tab. 11.4-1. The decision by Lemire et al. (2013) to abstain from selecting data for $Fe(OH)_2(aq)$ and $Fe(OH)_3^-$ leads to an underestimation of the solubility of magnetite at pH > 12.5.

$\log_{10}{}^{*}\beta_{1,1}°(T) = 5.393 - 2263/T$

from which they derived

$\log_{10}{}^{*}\beta_{1,1}°(298.15\ \text{K}) = -(2.20 \pm 0.02)$

$\Delta_r H_{m,1,1}°(298.15\ \text{K}) = (43.3 \pm 0.6)\ \text{kJ} \cdot \text{mol}^{-1}$

$\Delta_r C_{p,m}°(298.15\ \text{K}) = 0$

These data are included in TDB 2020.

Lemire et al. (2013) selected $\log_{10}{}^{*}\beta_{1,1}°(298.15\ \text{K}) = -(2.15 \pm 0.03)$[32], which compares well with our selection.

Brown & Ekberg (2016) also compiled an extensive set of stability constant data for $FeOH^{2+}$ measured in $NaClO_4$ background electrolytes at 25 °C and ionic strengths up to 6 mol · dm^{-3} or 8.45 mol · kg^{-1}. They accepted data from 22 studies and used a constrained non-linear SIT analysis with a fixed $\log_{10}{}^{*}\beta_{1,1}°(298.15\ \text{K}) = -(2.20 \pm 0.02)$ to derive $\Delta\varepsilon_1(FeOH^{2+}, ClO_4^-) = -(0.24 \pm 0.01)\ \text{kg} \cdot \text{mol}^{-1}$ and $\Delta\varepsilon_2(FeOH^{2+}, ClO_4^-) = (0.18 \pm 0.01)\ \text{kg} \cdot \text{mol}^{-1}$.

For TDB 2020 we preferred to carry out a linear SIT analysis using data limited to $I_m \leq 1.05\ \text{mol} \cdot \text{kg}^{-1}$ (see Tab. 11.4-2) with the constraint of $\log_{10}{}^{*}\beta_{1,1}°(298.15\ \text{K}) = -2.20$, see Fig. 11.4-2.

[32] See p. 147 in Lemire et al. (2013), in their Table III-2 on p. 48, however, the uncertainty is reported as ± 0.07.

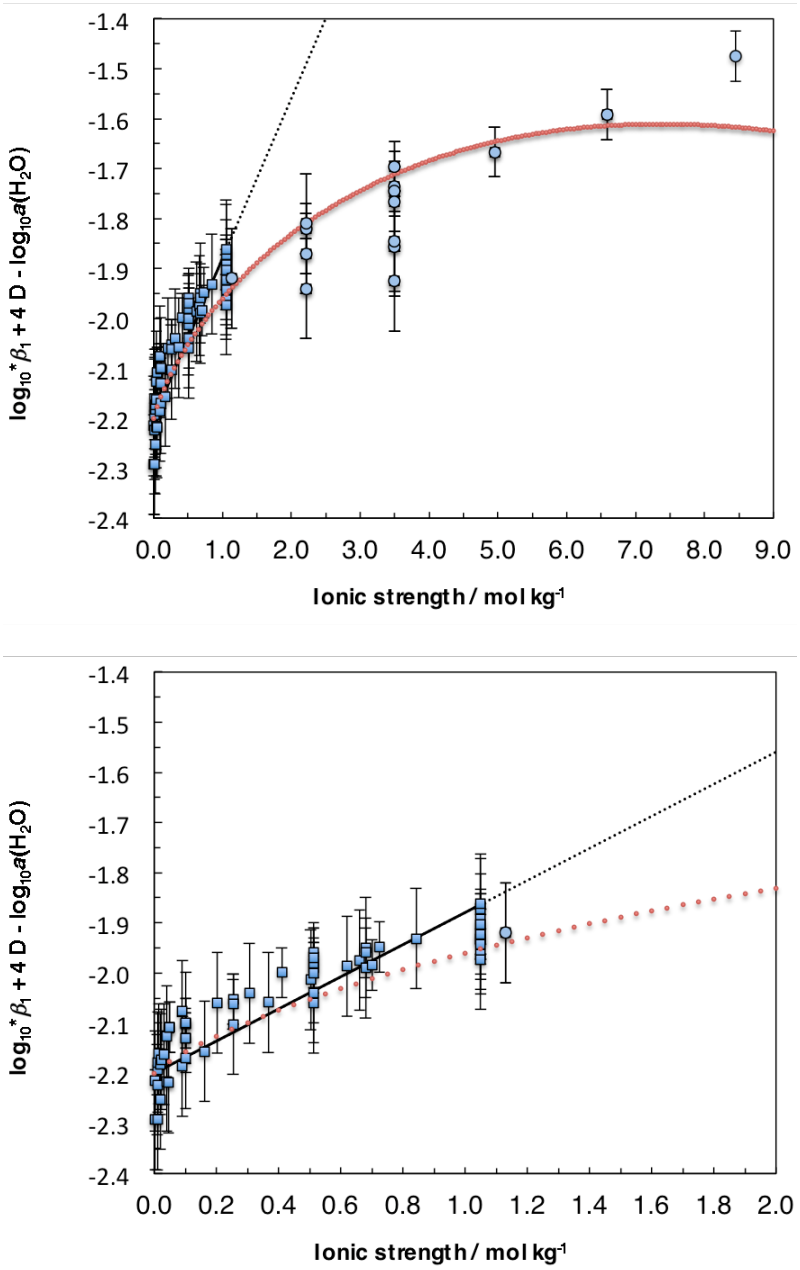

Fig. 11.4-2: SIT analyses for the reaction $Fe^{3+} + H_2O(l) \rightleftharpoons FeOH^{2+} + H^+$ in $NaClO_4$

(Top) Full range of experimental ionic strengths, (bottom) lower end of range of experimental ionic strengths. Squares indicate data that we used for the constrained linear SIT fit (solid black line within the fitting range $I_m \leq 1.05$ mol · kg^{-1}, dotted black line at higher ionic strengths), see Tab. 11.4-2. Constraint: $\log_{10}{}^*\beta_{1,1}°(298.15\ K) = -2.20$. Circles indicate additional data that were used by Brown & Ekberg (2016) for their non-linear SIT fit (dotted red curve).

Tab. 11.4-2: Subset of experimental data reported and accepted by Brown & Ekberg (2016)

Data are used for the constrained linear SIT fit shown in Fig. 11.4-2.
Constraint: $\log_{10}{}^{*}\beta_{1,1}°(298.15\ \mathrm{K}) = -2.20$

I_m [mol · kg^{-1}]	$\log_{10}{}^{*}\beta_{1,1}$ reported	$\log_{10}{}^{*}\beta_{1,1}$ accepted	Original references, as cited by Brown & Ekberg (2016)
0.0025	-2.31	-2.31 ± 0.10	Bray & Hershey (1934)
0.004	-2.41 ± 0.01	-2.41 ± 0.10	Turner & Miles (1957)
0.01	-2.47 ± 0.01	-2.47 ± 0.10	Turner & Miles (1957)
0.01	-2.40	-2.40 ± 0.10	Bray & Hershey (1934)
0.01	-2.37 ± 0.04	-2.37 ± 0.05	Byrne et al. (2000)
0.012	-2.37	-2.37 ± 0.10	Milburn (1957)
0.0147	-2.37	-2.37 ± 0.10	Milburn & Vosburgh (1955)
0.02	-2.49 ± 0.01	-2.49 ± 0.10	Turner & Miles (1957)
0.02	-2.42 ± 0.03	-2.42 ± 0.10	Zotov & Kotova (1979)
0.022	-2.42	-2.42 ± 0.10	Milburn (1957)
0.032	-2.45	-2.45 ± 0.10	Milburn (1957)
0.04	-2.44	-2.44 ± 0.10	Milburn & Vosburgh (1955)
0.04	-2.53	-2.53 ± 0.10	Bray & Hershey (1934)
0.046	-2.55	-2.55 ± 0.10	Olson & Simonson (1949)
0.05	-2.45 ± 0.02	-2.45 ± 0.05	Byrne et al. (2000)
0.05	-2.45 ± 0.04	-2.45 ± 0.05	Zotov & Kotova (1979)
0.091	-2.50	-2.50 ± 0.10	Milburn & Vosburgh (1955)
0.091	-2.61	-2.61 ± 0.10	Bray & Hershey (1934)
0.101	-2.54 ± 0.02	-2.54 ± 0.05	Stefánsson (2007)
0.101	-2.57 ± 0.04	-2.57 ± 0.05	Stefánsson (2007)
0.101	-2.54 ± 0.04	-2.54 ± 0.05	Byrne et al. (2000)
0.101	-2.61	-2.61 ± 0.10	Sapieszko et al. (1977)
0.101	-2.57 ± 0.05	-2.57 ± 0.05	Zotov & Kotova (1979)
0.102	-2.54	-2.54 ± 0.10	Milburn & Vosburgh (1955)
0.162	-2.67	-2.67 ± 0.10	Bray & Hershey (1934)
0.203	-2.62	-2.61 ± 0.10	Milburn & Vosburgh (1955)
0.254	-2.65 ± 0.02	-2.64 ± 0.05	Byrne et al. (2000)
0.254	-2.70	-2.69 ± 0.10	Bray & Hershey (1934)
0.254	-2.66	-2.65 ± 0.05	Behar & Stein (1969)
0.306	-2.67	-2.66 ± 0.10	Milburn & Vosburgh (1955)
0.367	-2.72	-2.71 ± 0.10	Bray & Hershey (1934)
0.41	-2.68 ± 0.02	-2.67 ± 0.05	Byrne et al. (2000)

Tab. 11.4-2: Cont.

I_m [mol · kg^{-1}]	$\log_{10}{}^{*}\beta_{1,1}$ reported	$\log_{10}{}^{*}\beta_{1,1}$ accepted	Original references, as cited by Brown & Ekberg (2016)
0.503	-2.73	-2.72 ± 0.10	Bray & Hershey (1934)
0.513	-2.70 ± 0.02	-2.70 ± 0.05	Salvatore & Vasca (1990)
0.513	-2.70 ± 0.01	-2.69 ± 0.05	Stefánsson (2007)
0.513	-2.68 ± 0.03	-2.67 ± 0.05	Stefánsson (2007)
0.513	-2.76	-2.75 ± 0.10	Sapieszko et al. (1977)
0.513	-2.72	-2.71 ± 0.10	Connick et al. (1956)
0.513	-2.78	-2.77 ± 0.10	Wilson & Taube (1952)
0.513	-2.69 ± 0.06	-2.68 ± 0.06	Zotov & Kotova (1979)
0.62	-2.74	-2.73 ± 0.10	Milburn & Vosburgh (1955)
0.661	-2.74	-2.73 ± 0.10	Bray & Hershey (1934)
0.68	-2.71	-2.71 ± 0.10	Byrne & Kester (1976)
0.68	-2.72 ± 0.02	-2.72 ± 0.05	Byrne & Kester (1978)
0.68	-2.75	-2.75 ± 0.10	Soli & Byrne (1996)
0.7	-2.75 ± 0.01	-2.75 ± 0.05	Byrne & Thompson (1997)
0.725	-2.74 ± 0.02	-2.72 ± 0.05	Byrne et al. (2000)
0.842	-2.75	-2.73 ± 0.10	Bray & Hershey (1934)
1.05	-2.8 ± 0.02	-2.80 ± 0.05	Salvatore & Vasca (1990)
1.05	-2.77 ± 0.03	-2.75 ± 0.05	Stefánsson (2007)
1.05	-2.75 ± 0.02	-2.73 ± 0.05	Stefánsson (2007)
1.05	-2.79	-2.77 ± 0.10	Milburn (1957)
1.05	-2.79 ± 0.02	-2.77 ± 0.05	Byrne et al. (2000)
1.05	-2.80	-2.78 ± 0.10	Milburn & Vosburgh (1955)
1.05	-2.73 ± 0.006	-2.71 ± 0.10	Khoe et al. (1986)
1.05	-2.76 ± 0.04	-2.76 ± 0.05	Nikolskii et al. (1971)
1.05	-2.83	-2.81 ± 0.10	Sapieszko et al. (1977)
1.05	-2.72 ± 0.04	-2.70 ± 0.10	Lente & Fábián (1998)
1.05	-2.76	-2.74 ± 0.10	Bray & Hershey (1934)

We did this as follows: According to SIT, conditional stability constants $\log_{10}{}^{*}\beta_{1,1}(298.15\ K)$ for the reaction

$$Fe^{3+} + H_2O(l) \rightleftharpoons FeOH^{2+} + H^{+}$$

can be extrapolated to zero ionic strength using the following equation (see, e.g., Grenthe et al. 1997)

$$\log_{10}{}^{*}\beta_{1,1}(298.15\ K) + 4\ D - \log_{10}a(H_2O) = \log_{10}{}^{*}\beta_{1,1}°(298.15\ K) - \Delta\varepsilon\ I_m$$

where

$$D = 0.509\ \sqrt{I_m}\ /(1 + 1.5\ \sqrt{I_m})$$

and

$$\Delta\varepsilon = \varepsilon(FeOH^{2+}, ClO_4^{-}) + \varepsilon(H^{+}, ClO_4^{-}) - \varepsilon(Fe^{3+}, ClO_4^{-})$$

For a constrained fit with a fixed value for $\log_{10}{}^{*}\beta_{1,1}°(298.15\ K)$, $\Delta\varepsilon$ is the only unknown and rearranging the SIT expression leads to

$$\Delta\varepsilon = -1/I_m\ [\log_{10}{}^{*}\beta_{1,1}(298.15\ K) - \log_{10}{}^{*}\beta_{1,1}°(298.15\ K) + 4\ D - \log_{10}a(H_2O)]$$

Experimental data needed are I_m and $\log_{10}{}^{*}\beta_{1,1}(298.15\ K)$, while the activity of water as a function of the molality m of the $NaClO_4$ background electrolyte at 25 °C can be calculated from

$$a(H_2O) = 1 + a_1\ m + a_2\ m^2$$

with

$$a_1 = -(0.03216 \pm 0.00012)\ kg \cdot mol^{-1}$$

$$a_2 = -(3.007 \pm 0.166) \cdot 10^{-4}\ kg^2 \cdot mol^{-2}$$

see Brown & Ekberg (2016), p. 25.

From the $\Delta\varepsilon$ values calculated with the data listed in Tab. 11.4-2 we obtained the weighted mean

$$\Delta\varepsilon = -(0.32 \pm 0.02)\ kg \cdot mol^{-1}$$

From this value and the selected $\varepsilon(Fe^{3+}, ClO_4^{-}) = (0.73 \pm 0.04)\ kg \cdot mol^{-1}$ and $\varepsilon(H^{+}, ClO_4^{-}) = (0.14 \pm 0.02)\ kg \cdot mol^{-1}$ follows

$\varepsilon(FeOH^{2+}, ClO_4^-) = (0.27 \pm 0.05)$ kg · mol^{-1}

In order to be consistent with the explicit consideration of iron(III) chloride complexes (see Section 11.1.1), $\varepsilon(FeOH^{2+}, Cl^-)$ is approximated by $\varepsilon(FeOH^{2+}, ClO_4^-)$, thus

$\varepsilon(FeOH^{2+}, Cl^-) \approx \varepsilon(FeOH^{2+}, ClO_4^-) \approx (0.27 \pm 0.05)$ kg · mol^{-1}

Both of these values are included in TDB 2020. One has to keep in mind, however, that they should only be used if $I_m \leq 1.05$, but this covers the application range that TDB 2020 is designed for.

11.4.1.3.2 $Fe(OH)_2^+$

The second hydrolysis constant for

$Fe^{3+} + 2\ H_2O(l) \rightleftharpoons Fe(OH)_2^+ + 2\ H^+$

is much less well studied than the first one due to the presence of the dimer and the onset of precipitation of generally fine grained amorphous iron(III) hydroxide phases (Lemire et al. 2013). Brown & Ekberg (2016) accepted three stability constants for $Fe(OH)_2^+$ that were determined for zero ionic strength by Daniele et al. (1994), Diakonov (1995), and Stefánsson (2007). Brown & Ekberg (2016) selected the average of the three values

$\log_{10}{}^*\beta_{2,1}°(298.15\ K) = -(5.71 \pm 0.10)$

which is also adopted for TDB 2020. Lemire et al. (2013) selected $\log_{10}{}^*\beta_{2,1}°(298.15\ K) = -(4.8 \pm 0.4)$ which is considerably larger. This discrepancy reflects the lack of high-quality data for $Fe(OH)_2^+$ which, according to Lemire et al. (2013), is a "minor species, which only becomes significant at pH values where colloids are readily formed".

Brown & Ekberg (2016) also reviewed stability constant data obtained in $NaClO_4$ solutions at 25 °C. They accepted 6 constants from 3 studies covering a range of ionic strengths from 0.101 to 3.50 mol · kg^{-1}. Using a constrained non-linear SIT analysis with a fixed $\log_{10}{}^*\beta_{2,1}°(298.15\ K) = -(5.71 \pm 0.10)$, they obtained $\Delta\varepsilon_1 = -(0.04 \pm 0.02)$ kg · mol^{-1} and $\Delta\varepsilon_2 = (0.18 \pm 0.04)$ kg · mol^{-1}.

As in the case of $FeOH^{2+}$, we preferred a constrained linear SIT analysis using data limited to $I_m \leq 1.05$ mol · kg^{-1} (see Tab. 11.4-3 and Fig. 11.4-3) with the constraint of $\log_{10}{}^*\beta_{2,1}°(298.15\ K) = -5.71$. Following the procedure explained for $FeOH^{2+}$ in Section 11.4.1.3.1, we calculated values for

$\Delta\varepsilon = -1/I_m\ [\log_{10}{}^*\beta_{2,1}(298.15\ K) - \log_{10}{}^*\beta_{2,1}°(298.15\ K) + 6\ D - 2\ \log_{10}a(H_2O)]$

from the experimental data listed in Tab. 11.4-3 and obtained the weighted mean

$\Delta\varepsilon = -(0.02 \pm 0.08)$ kg · mol^{-1}

From this value and the selected $\varepsilon(Fe^{3+}, ClO_4^-) = (0.73 \pm 0.04)$ kg · mol^{-1} and $\varepsilon(H^+, ClO_4^-) = (0.14 \pm 0.02)$ kg · mol^{-1} follows

$$\varepsilon(Fe(OH)_2^+, ClO_4^-) = (0.43 \pm 0.10) \text{ kg} \cdot \text{mol}^{-1}$$

In order to be consistent with the explicit consideration of iron(III) chloride complexes (see Section 11.1.1), $\varepsilon(Fe(OH)_2^+, Cl^-)$ is approximated by $\varepsilon(Fe(OH)_2^+, ClO_4^-)$, thus.

Tab. 11.4-3: Subset of experimental data reported and accepted by Brown & Ekberg (2016)

Data are used for the constrained linear SIT fit shown in Fig. 11.4-3.
Constraint: $\log_{10}{}^*\beta_{2,1}°(298.15\text{ K}) = -5.71$.

I_m [mol · kg^{-1}]	$\log_{10}{}^*\beta_{2,1}$ reported	$\log_{10}{}^*\beta_{2,1}$ accepted	Original references, as cited by Brown & Ekberg (2016)
0.101	-6.34 ± 0.13	-6.33 ± 0.13	Stefánsson (2007)
0.513	-6.80 ± 0.03	-6.78 ± 0.1	Stefánsson (2007)
0.513	-6.8 ± 0.5	-6.78 ± 0.2	Perera & Hefter (2003)
1.05	-6.98 ± 0.02	-6.94 ± 0.1	Stefánsson (2007)
1.05	-7.0 ± 0.3	-6.96 ± 0.2	Perera & Hefter (2003)

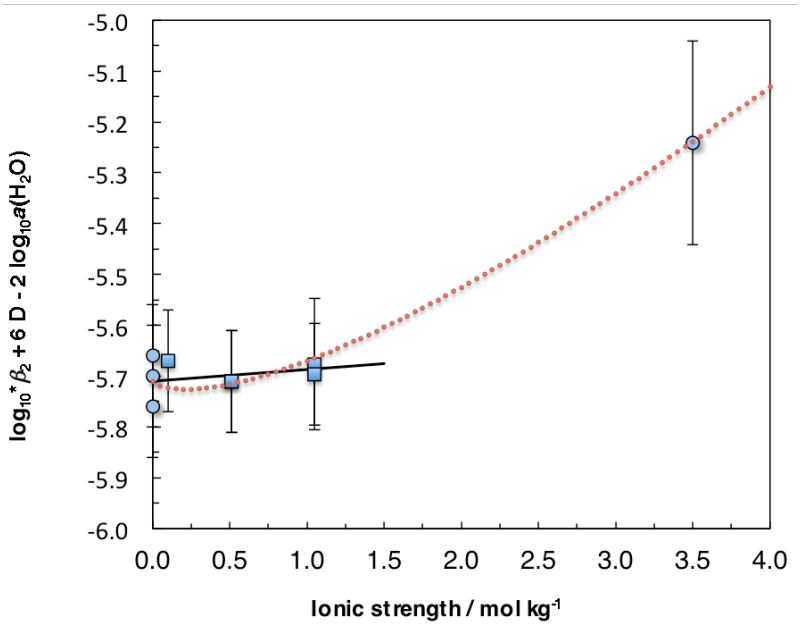

Fig. 11.4-3: SIT analysis for the reaction $Fe^{3+} + 2\ H_2O(l) \rightleftharpoons Fe(OH)_2^+ + 2\ H^+$ in $NaClO_4$

Squares indicate data that we used for the constrained linear SIT fit, see Tab. 11.4-3, (solid black line). Circles indicate additional data that were used by Brown & Ekberg (2016) for their constrained non-linear SIT fit (dotted red curve). The data at zero ionic strength were used to determine $\log_{10}{}^*\beta_{2,1}°(298.15\text{ K}) = -5.71$ for the constrained fit.

$\varepsilon(Fe(OH)_2^+, Cl^-) \approx \varepsilon(Fe(OH)_2^+, ClO_4^-) \approx (0.43 \pm 0.10)$ kg · mol^{-1}

Both of these values are included in TDB 2020. One has to keep in mind, however, that they should only be used if $I_m \leq 1.05$, but this covers the application range that TDB 2020 is designed for.

11.4.1.3.3 $Fe(OH)_3(aq)$

Brown & Ekberg (2016) accepted stability constants for the reaction

$$Fe^{3+} + 3\ H_2O(l) \rightleftharpoons Fe(OH)_3(aq) + 3\ H^+$$

from the studies on the oxidative solubility of magnetite by Tremaine & LeBlanc (1980) and Ziemniak et al. (1995) at zero ionic strength in the temperature range from 25 to 300 °C as well as a constant at zero ionic strength and 25 °C determined by Diakonov (1995). Brown & Ekberg (2016) described the accepted data with a non-linear function of temperature

$$\log_{10}{}^*\beta_{3,1}^\circ(T) = 66.0 - 9987/T - 7.86 \ln T$$

from which they derived

$$\log_{10}{}^*\beta_{3,1}^\circ(298.15\ K) = -(12.26 \pm 0.26)$$

$$\Delta_r H_m^\circ(298.15\ K) = (146.3 \pm 4.8)\ kJ{\cdot}mol^{-1}$$

$$\Delta_r C_{p,m}^\circ(298.15\ K) = -(150 \pm 43)\ J \cdot K^{-1} \cdot mol^{-1}$$

These data are included in TDB 2020, as well as

$$\varepsilon(Fe(OH)_3(aq), NaCl) = \varepsilon(Fe(OH)_3(aq), NaClO_4) \approx (0.0 \pm 0.1)\ kg \cdot mol^{-1}$$

estimated according to Tab. 1-7.

11.4.1.3.4 $Fe(OH)_4^-$

For the reaction

$$Fe^{3+} + 4\ H_2O(l) \rightleftharpoons Fe(OH)_4^- + 4\ H^+$$

Brown & Ekberg (2016) accepted stability constants from the studies on the oxidative solubility of magnetite by Tremaine & LeBlanc (1980) and Ziemniak et al. (1995) at zero ionic strength in the temperature range from 25 to 300 °C. The linear relationship

$$\log_{10}{}^*\beta_{4,1}^\circ(T) = 4.12 - 7669/T$$

reproduces the stability constant of $Fe(OH)_4^-$ as a function of temperature from which Brown & Ekberg (2016) derived

$$\log_{10}{}^*\beta_{4,1}°(298.15\ K) = -(21.60 \pm 0.23)$$

$$\Delta_r H_m°(298.15\ K) = (146.8 \pm 1.8\ kJ \cdot mol^{-1}$$

$$\Delta_r C_{p,m}°(298.15\ K) = 0$$

These values are included in TDB 2020.

In the absence of data for ion interaction coefficients, we estimated $\varepsilon(Fe(OH)_4^-, Na^+)$ estimated according to Tab. 1-7. Thus

$$\varepsilon(Fe(OH)_4^-, Na^+) \approx -(0.05 \pm 0.10)\ kg \cdot mol^{-1}$$

which is also included in TDB 2020.

11.4.1.3.5 $Fe_2(OH)_2^{4+}$

According to Brown & Ekberg (2016) there is a large amount of stability constant data available for the reaction

$$2\ Fe^{3+} + 2\ H_2O(l) \rightleftharpoons Fe_2(OH)_2^{4+} + 2\ H^+$$

in $NaClO_4$ media at 25 °C. They state that the agreement between the different data is generally good but becomes poorer with increasing ionic strength. They accepted data from 7 studies covering the range of ionic strengths from 0.101 to 3.50 $mol \cdot kg^{-1}$. From a non-linear SIT analysis of the accepted data they obtained

$$\log_{10}{}^*\beta_{2,2}°(298.15\ K) = -(2.91 \pm 0.07)$$

with $\Delta\varepsilon_1 = -(0.17 \pm 0.09)\ kg \cdot mol^{-1}$ and $\Delta\varepsilon_2 = (0.17 \pm 0.13)\ kg \cdot mol^{-1}$. We include this stability constant in TDB 2020, but for deriving an ion interaction coefficient for $Fe_2(OH)_2^{4+}$, we carried out a constrained linear SIT analysis using data limited to $I_m \leq 1.05\ mol \cdot kg^{-1}$ (see Tab. 11.4-4 and Fig. 11.4-4) with the constraint of $\log_{10}{}^*\beta_{2,2}°(298.15\ K) = -2.91$. Following the procedure explained for $FeOH^{2+}$ in Section 11.4.1.3.1, we calculated values for

$$\Delta\varepsilon = -1/I_m\ [\log_{10}{}^*\beta_{2,2} - \log_{10}{}^*\beta_{2,2}° - 2\ \log_{10} a(H_2O)]$$

from the experimental data listed in Tab. 11.4-4 and obtained the weighted mean

$$\Delta\varepsilon = -(0.18 \pm 0.05)\ kg \cdot mol^{-1}$$

Tab. 11.4-4: Subset of experimental data reported and accepted by Brown & Ekberg (2016)

Data are used for the constrained linear SIT fit shown in Fig. 11.4-4.
Constraint: $\log_{10}{}^{*}\beta_{2,2}°(298.15\ \mathrm{K}) = -2.91$

I_m [mol · kg^{-1}]	$\log_{10}{}^{*}\beta_{2,2}$ reported	$\log_{10}{}^{*}\beta_{2,2}$ accepted	Original references, as cited by Brown & Ekberg (2016)
0.101	-2.92 ± 0.01	-2.92 ± 0.10	Stefánsson (2007)
0.102	-2.85	-2.85 ± 0.10	Milburn & Vosburgh (1955)
0.203	-2.83	-2.82 ± 0.10	Milburn & Vosburgh (1955)
0.306	-2.82	-2.81 ± 0.10	Milburn & Vosburgh (1955)
0.513	-2.90 ± 0.01	-2.89 ± 0.10	Stefánsson (2007)
0.513	-2.84 ± 0.02	-2.84 ± 0.10	Salvatore & Vasca (1990)
0.62	-2.77	-2.76 ± 0.10	Milburn & Vosburgh (1955)
1.05	-2.74	-2.72 ± 0.10	Milburn & Vosburgh (1955)
1.05	-2.83 ± 0.02	-2.83 ± 0.10	Salvatore & Vasca (1990)
1.05	-2.89 ± 0.01	-2.87 ± 0.10	Stefánsson (2007)
1.05	-2.71	-2.69 ± 0.10	Milburn (1957)

Using this value together with the selected $\varepsilon(Fe^{3+}, ClO_4^-) = (0.73 \pm 0.04)$ kg · mol^{-1} and $\varepsilon(H^+, ClO_4^-) = (0.14 \pm 0.02)$ kg · mol^{-1} leads to

$$\varepsilon(Fe_2(OH)_2^{4+}, ClO_4^-) = (1.00 \pm 0.10)\ \mathrm{kg \cdot mol^{-1}}$$

In order to be consistent with the explicit consideration of iron(III) chloride complexes (see Section 11.1.1), we approximated $\varepsilon(Fe_2(OH)_2^{4+}, Cl^-)$ by $\varepsilon(Fe_2(OH)_2^{4+}, ClO_4^-)$. Thus

$$\varepsilon(Fe_2(OH)_2^{4+}, Cl^-) \approx \varepsilon(Fe_2(OH)_2^{4+}, ClO_4^-) \approx (1.00 \pm 0.10)\ \mathrm{kg \cdot mol^{-1}}$$

Both of these values are included in TDB 2020. They should only be used if $I_m \leq 1.05$, but this covers the application range that TDB 2020 is designed for.

Brown & Ekberg (2016) also considered a small number of stability constant data (8 constants from 6 papers) measured in 1.0 M $NaClO_4$ in the temperature range from 18 to 32 °C. From a linear fit to the data plotted versus 1/T, they obtained

$$\Delta_r H_m(298.15\ \mathrm{K}, 1.0\ \mathrm{M\ NaClO_4}) = (30.1 \pm 9.5)\ \mathrm{kJ \cdot mol^{-1}}$$

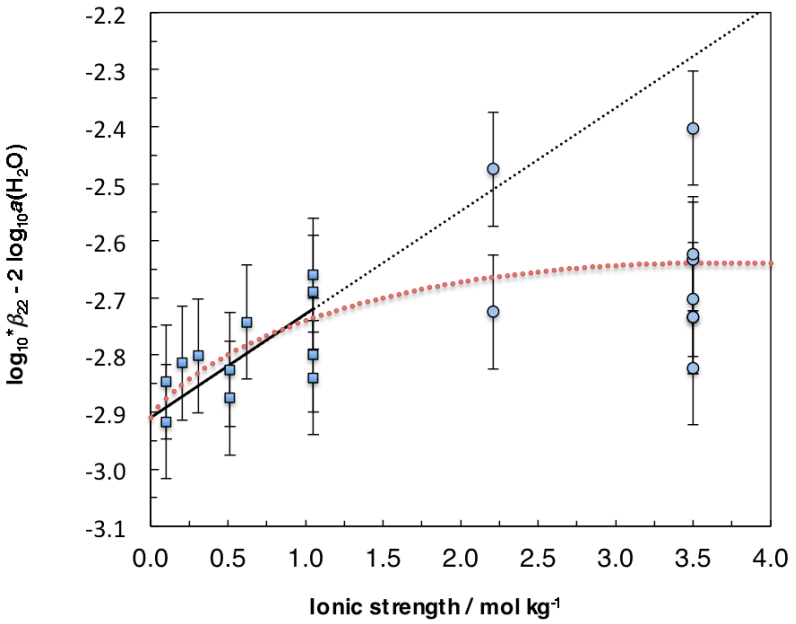

Fig. 11.4-4: SIT analysis for the reaction 2 Fe^{3+} + 2 H_2O(l) ⇌ $Fe_2(OH)_2^{4+}$ + 2 H^+ in $NaClO_4$

Squares indicate data that we used for the constrained linear SIT fit (solid black line within the fitting range, dotted black line at higher ionic strengths), see Tab. 11.4-4. Constraint: $\log_{10}{}^*\beta_{2,2}°(298.15\ K) = -2.91$. Circles indicate additional data that were used by Brown & Ekberg (2016) for their non-linear SIT fit (dotted red curve).

Brown & Ekberg (2016) argue that $\Delta_r H_m°(298.15\ K)$ would be within the 95% uncertainty limits of the value determined in 1.0 M $NaClO_4$. It is therefore reasonable to assume that

$$\Delta_r H_m°(298.15\ K) = (30.1 \pm 9.5)\ kJ \cdot mol^{-1}$$

This value is included in TDB 2020 as well as

$$\Delta_r C_{p,m}°(298.15\ K) = 0$$

11.4.1.3.6 $Fe_3(OH)_4^{5+}$

Lemire et al. (2013) did not select any data for the trimer $Fe_3(OH)_4^{5+}$. Brown & Ekberg (2016) selected the stability constant determined by Baes & Mesmer (1976). Since

$$\log_{10}{}^*\beta_{4,3}°(298.15\ K) = -6.3$$

and

$$\Delta_r H_{m,4,3}°(298.15\ K) = 59.8\ kJ \cdot mol^{-1}$$

selected in TDB 12/07 for

$$3\ Fe^{3+} + 4\ H_2O(l) \rightleftharpoons Fe_3(OH)_4^{5+} + 4\ H^+$$

were also taken from Baes & Mesmer (1976), they are retained in TDB 2020.

In the absence of data for ion interaction coefficients, we estimated $\varepsilon(Fe_3(OH)_4^{5+}, ClO_4^-)$ estimated according to Tab. 1-7. In order to be consistent with the explicit consideration of iron(III) chloride complexes (see Section 11.1.1), $\varepsilon(Fe_3(OH)_4^{5+}, Cl^-)$ is approximated by $\varepsilon(Fe_3(OH)_4^{5+}, ClO_4^-)$:

$$\varepsilon(Fe_3(OH)_4^{5+}, Cl^-) \approx \varepsilon(Fe_3(OH)_4^{5+}, ClO_4^-) \approx (1.0 \pm 0.2)\ kg \cdot mol^{-1}$$

Both values are included in TDB 2020.

11.4.1.3.7 Comparison between selected Fe(III) hydroxo complexes by Lemire et al. (2013) and TDB 2020

Lemire et al. (2013) decided to abstain from selecting data for $Fe(OH)_3(aq)$ and $Fe(OH)_4^-$. This has serious consequences for calculated Fe(III) solubilities. Consider the solubility of goethite (α–FeOOH) as a function of pH (see Fig. 11.4-5): The hydrolysis data selected by Lemire et al. (2013) lead to a linear decrease of Fe solubility at pH > 4, while the data included in TDB 2020 result in a solubility minimum at pH around 8. Up to this solubility minimum, solubilities calculated with both data sets are comparable, at higher pH, the calculated solubilities diverge and the data by Lemire et al. (2013) lead to absurdly low solubilities at pH values expected for cement systems (pH ≥ 12.5).

Tab. 11.4-5: Comparison of data for goethite and Fe(III) hydroxo complexes selected by Lemire et al. (2013) and TDB 2020

Based on the data selected by Brown & Ekberg (2016)

Name	**Reaction**	**$\log_{10}K°$ Lemire et al. (2013)**	**$\log_{10}K°$ TDB 2020**
α-FeOOH(goethite)	$FeOOH(cr) + 3\ H^+ \rightleftharpoons Fe^{3+} + 2\ H_2O(l)$	0.17 ± 0.37	0.33 ± 0.10
FeOH+2	$Fe^{3+} + H_2O(l) \rightleftharpoons FeOH^{2+} + H^+$	-2.15 ± 0.03	-2.20 ± 0.02
Fe(OH)2+	$Fe^{3+} + 2\ H_2O(l) \rightleftharpoons Fe(OH)_2^+ + 2\ H^+$	-4.8 ± 0.4	-5.71 ± 0.10
Fe(OH)3(aq)	$Fe^{3+} + 3\ H_2O(l) \rightleftharpoons Fe(OH)_3(aq) + 3\ H^+$	-	-12.26 ± 0.26
Fe(OH)4-	$Fe^{3+} + 4\ H_2O(l) \rightleftharpoons Fe(OH)_4^- + 4\ H^+$	-	-21.60 ± 0.23
Fe2(OH)2+4	$2\ Fe^{3+} + 2\ H_2O(l) \rightleftharpoons Fe_2(OH)_2^{4+} + 2\ H^+$	-2.82 ± 0.07	-2.91 ± 0.07
Fe3(OH)4+5	$3\ Fe^{3+} + 4\ H_2O(l) \rightleftharpoons Fe_3(OH)_4^{5+} + 4\ H^+$	-	-6.3

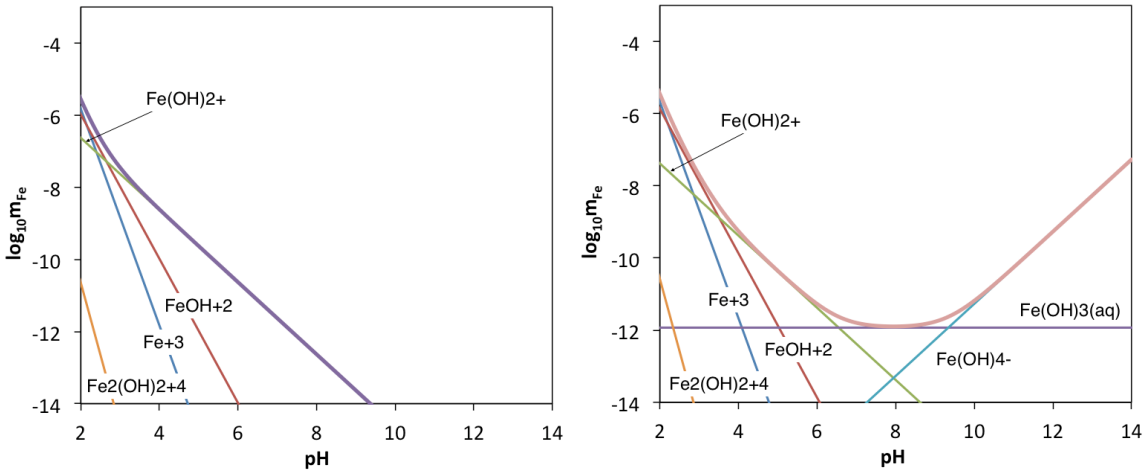

Fig. 11.4-5: Solubility of goethite (α-FeOOH), calculated with data selected by Lemire et al. (2013) (left), and calculated with data selected for TDB 2020, based on Brown & Ekberg (2016) (right)

See Tab. 11.4-5

The decision by Lemire et al. (2013) to abstain from selecting data for $Fe(OH)_3(aq)$ and $Fe(OH)_4^-$ leads to an underestimation of the solubility of goethite at pH > 8, with absurdly low solubilities at pH values expected for cement systems (pH ≥ 12.5).

11.4.2 Iron oxide and oxyhydroxide solids

11.4.2.1 Data in TDB 05/92, TDB 01/01 and TDB 12/07

All data selections discussed in this section are superseded by those discussed in the following Sections 11.4.2.2 – 11.4.2.8.

Magnetite: The solubility constant of magnetite (Fe_3O_4) selected by Hummel et al. (2002) for TDB 01/01 and retained in TDB 12/07 was based on solubility measurements by Sweeton & Baes (1970) in dilute aqueous solutions saturated with H_2g at temperatures between 50 and 300 °C. The measurements were made in an experimental setup that streamed a continuous flow of aqueous solution (ranging in composition from 0.4 mmol · kg^{-1} KOH to 0.1 mmol · kg^{-1} HCl) over a bed of synthetic magnetite. Equilibrium was therefore attained from undersaturation. The extracted solution was then analysed for iron. Chemical and X-ray analyses before and after the experiments revealed no compositional or structural changes in magnetite. For the interpretation of the experimental results Fe^{2+}, $Fe(OH)^+$, $Fe(OH)_2(aq)$, and $Fe(OH)_3^-$ were considered as iron species in equilibrium with magnetite according to

$$1/3\ Fe_3O_4(\text{magnetite}) + (2\text{-}b)\ H^+ + 1/3\ H_2g \rightleftharpoons Fe(OH)_b^{(2-b)+} + (4/3\text{-}b)\ H_2O(l)$$

with b = 0 for Fe^{2+}, b =1 for $Fe(OH)^+$, b = 2 for $Fe(OH)_2(aq)$, and b = 3 for $Fe(OH)_3^-$. Ferric iron was neglected because data from the literature suggested that the proportion of dissolved iron in the ferric state is negligible at pH values below 9 and rather small above. Temperature dependent

equilibrium constants of the above-mentioned reaction for each species were then fit to the experimental data. The best fits were obtained by including all four ferrous iron species. Thus, in the case of

$$1/3\ Fe_3O_4(\text{magnetite}) + 2\ H^+ + 1/3\ H_2g \rightleftharpoons Fe^{2+} + 4/3\ H_2O(l)$$

the following expression was found for the equilibrium constant (in units of calories)

$$R \ln {}^*Ks,0°(T) = \frac{26876}{T} + 9.81\ (\ln T - 1) - 81.21$$

from which follows (with R = 1.9872 cal · mol^{-1} · K^{-1})

$$\log_{10} {}^*K_{s,0}°(298.15\ K) = 11.02$$

This reaction can be tripled and reformulated as

$$Fe_3O_4(\text{magnetite}) + 8\ H^+ + 2\ e^- \rightleftharpoons 3\ Fe^{2+} + 4\ H_2O(l)$$

by adding

$$2\ H^+ + 2\ e^- \rightleftharpoons H_2g$$

with $\log_{10} K°(298.15\ K) = 0$. Therefore

$$\log_{10} {}^*K_{s,0}°(298.15\ K) = 36.06$$

Finally, adding

$$2\ Fe^{2+} \rightleftharpoons 2\ Fe^{3+} + 2\ e^-$$

With

$$\log_{10} K°(298.15\ K) = -26.04$$

(see Section 11.3.1) results in

$$Fe_3O_4(\text{magnetite}) + 8\ H^+ \rightleftharpoons Fe^{2+} + 2\ Fe^{3+} + 4\ H_2O(l)$$

$$\log_{10} {}^*K°(298.15\ K) = 10.02$$

This value was included in TDB 01/01 and TDB 12/07 (magnetite was not included in TDB 05/92).

Hematite: The solubility constant for hematite (Fe_2O_3) selected by Hummel et al. (2002) for TDB 01/01 and retained in TDB 12/07 (hematite was not included in TDB 05/92) was based on Diakonov et al. (1999) who measured the solubility of well-crystallized natural and synthetic hematite in NaOH-NaCl solutions (0.007 - 2.0 m NaOH) at 60, 110, 150, 200, 250 and 300 °C at saturated water vapor pressure and under excess oxygen in the pH range from 9.3 – 13.1. Duration of experiments was up to 208 days at 60 °C and between 4 and 82 days at higher temperatures. Equilibrium was attained from undersaturation. The reversibility of equilibrium was checked at 60 °C with a precipitation experiment that produced the same final iron concentrations as the dissolution experiments. XRD analyses made before and after the experiments confirmed that no changes in the solid phase took place during the experiments. No differences in measured aqueous iron concentrations were observed between experiments with synthetic and natural hematites. For the interpretation of the experimental results, $Fe(OH)_4^-$ was the only iron(III) species considered which is reasonable for the pH-range of these experiments. The dissolution of hematite was therefore described by

$$Fe_2O_3(\text{hematite}) + 5\ H_2O(l) \rightleftharpoons 2\ Fe(OH)_4^- + 2\ H^+$$

Assuming unit activity for water and hematite, the dissociation constant ${}^*K_{s,41}°$ was calculated for each experiment from the measured molalities of Fe and the calculated pH, using activity coefficients of charged species calculated according to the equation proposed by Helgeson et al. (1981) for concentrated NaCl solutions. These dissociation constants were then extrapolated to 25 °C by fitting them to the Helgeson-Kirkham-Flowers (HKF) equation of state by Helgeson et al. (1981), resulting in

$$\log_{10}{}^*K_{s,4,1}°(298.15\ K) = -\ 42.08$$

Using

$$Fe^{3+} + 4\ H_2O(l) \rightleftharpoons Fe(OH)_4^- + 4\ H^+$$

with

$$\log_{10}{}^*\beta_{4,1}°(298.15\ K) = -21.6$$

(see Section 11.4.1.1) leads to

$$Fe_2O_3(\text{hematite}) + 6\ H^+ \rightleftharpoons 2\ Fe^{3+} + 3\ H_2O(l)$$

with

$$\log_{10}{}^*K_{s,0}°(298.15\ K) = 1.12$$

which was included in TDB 01/01 and TDB 12/07.

Ferrihydrite: The solubility constants for amorphous and microcrystalline ferrihydrite selected by Nordstrom et al. (1990)

$$Fe(OH)_3(am) + 3\ H^+ \rightleftharpoons Fe^{3+} + 3\ H_2O(l)$$

$$\log_{10}{}^*K_{s,0}^\circ = 5.0$$

$$Fe(OH)_3(mic) + 3\ H^+ \rightleftharpoons Fe^{3+} + 3\ H_2O(l)$$

$$\log_{10}{}^*K_{s,0}^\circ = 3.0$$

were based on the range of values reported by Langmuir & Whittemore (1971), Schwertmann & Taylor (1977), and Norvell & Lindsay (1982). Pearson et al. (1992) adopted these values for TDB 05/92[33] which were retained in TDB 01/01 and TDB 12/07.

Goethite: For the solubility constant of goethite(FeOOH), Pearson et al. (1992) chose

$$FeOOH(goethite) + 3\ H^+ \rightleftharpoons Fe^{3+} + 2\ H_2O(l)$$

$$\log_{10}{}^*K_{s,0}^\circ(298.15\ K) = -1$$

a value selected by Nordstrom et al. (1990) based on the solubility study by Langmuir & Whittemore (1971). This value was selected for TDB 05/02, TDB 01/01, and TDB 12/07.

11.4.2.2 "White rust" ($Fe(OH)_2$)

According to Lemire et al. (2013), "white rust" forms as a gelatinous precipitate by mixing solutions of $FeCl_2$ or $FeSO_4$ with alkaline hydroxides. Ziemniak et al. (1995) interpreted the results of solubility measurements of magnetite under reducing and alkaline conditions below 83 °C (at an initial hydrogen gas pressure of 0.3 atm at 25 °C) by postulating a solubility limiting surface film of $Fe(OH)_2(s)$. Lemire et al. (2013) discussed several solubility and equilibrium-potential measurements, but did not select any data. They remarked that most solubility products were obtained from fresh precipitates and are therefore upper limits and concluded that, in order for $Fe(OH)_2(s)$ to have a stability field in the chemical system Fe-O-H, $\Delta_r G_m^\circ(298.15\ K)$ must be negative for the reaction

$$Fe_3O_4(cr) + Fe(cr) + 4\ H_2O(l) \rightleftharpoons 4\ Fe(OH)_2(s)$$

and therefore $\Delta_f G_m^\circ(Fe(OH)_2, s, 298.15\ K) < -(490.3 \pm 0.4)\ kJ \cdot mol^{-1}$.

Brown & Ekberg (2016) evaluated essentially the same data as Lemire et al. (2013) and selected $\Delta_f G_m^\circ(Fe(OH)_2, s, 298.15\ K) = -(495 \pm 5)\ kJ \cdot mol^{-1}$. This value is accepted for TDB 2020 but is classified as supplemental because of the uncertainties due to the in general poor characterization

---

[33] Note that the $\log_{10}{}^*K_{s,0}^\circ$ values for amorphous and microcrystalline ferrihydrite were confounded by Nordstrom et al. (1990) and consequently also by Pearson et al. (1992). This error was corrected in TDB 01/01 and TDB 12/07.

of the precipitated solids. Combining this value with $\Delta_f G_m°(Fe^{2+}, 298.15\ K) = -(90.72 \pm 0.64)$ kJ·mol^{-1} and the NEA-selected $\Delta_f G_m°(H_2O, l, 298.15\ K) = -(237.140 \pm 0.041)$ kJ·mol^{-1} leads to

$$\Delta_r G_m°(298.15\ K) = -(70.00 \pm 5.04)\ kJ{\cdot}mol^{-1}$$

or

$$log_{10}{}^{*}K_{s,0}°(298.15\ K) = (12.26 \pm 0.88)$$

for the reaction

$$Fe(OH)_2(s) + 2H^{+} \rightleftharpoons Fe^{2+} + 2\ H_2O(l)$$

According to Génin et al. (1998), $Fe(OH)_2$(s) has a brucite-like layer structure and oxidation in the presence of anionic species at pH > 6 involves the formation of intermediate Fe(II)-Fe(III) compounds called "green rusts", as the partial oxidation of Fe(II) to Fe(III) leads to a charge surplus in the brucite-like layers which is compensated by the insertion of anions, such as Cl^{-}, SO_4^{2-}, and CO_3^{2-} (accompanied by water molecules) in the interlayers. This leads to the formation of "chloride green rust one" (see Section 11.5.2.2.1), "sulphate green rust two" (see Section 11.6.2.3.6), and "carbonate green rust one" (see Section 11.7.1.3.3).

11.4.2.3 Magnetite (α-Fe_3O_4)

As discussed in Section 11.4.1.2 the solubility of magnetite has been used to derive stability constants for the iron(II) hydroxo complexes in addition to the solubility constant of magnetite itself. Brown & Ekberg (2016) evaluated solubility data for the reaction

$$1/3\ Fe_3O_4(\text{magnetite}) + 2\ H^{+} + 1/3\ H_2g \rightleftharpoons Fe^{2+} + 4/3\ H_2O(l)$$

and accepted the data by Sweeton & Baes (1970), Ziemniak et al. (1995), and Tremaine & LeBlanc (1980), spanning the temperature range from 25 to 300 °C. Brown & Ekberg (2016) described the temperature dependence of the solubility constant with the 3-term equation

$$\log_{10}{}^{*}K_{s,0}°(T) = -33.7904 + 6380/T + 4.24014\ \ln T$$

See Fig. 11.4-6, from which they derived.

$$\log_{10}{}^{*}K_{s,0}°(298.15\ K) = (11.77 \pm 0.22)$$

$$\Delta_r H_m°(298.15\ K) = -(97.9 \pm 4.7)\ kJ{\cdot}mol^{-1}$$

$$\Delta_r C_{p,m}°(298.15\ K) = (81 \pm 42)\ J \cdot K^{-1} \cdot mol^{-1}$$

From this value for $\Delta_r C_{p,m}°(298.15\ K)$ and the selected $C_{p,m}°(H_2, g, 298.15\ K) = -28.836\ J \cdot K^{1} \cdot mol^{-1}$, $C_{p,m}°(Fe^{2+}, 298.15\ K) = -23 J \cdot K^{1} \cdot mol^{-1}$ and $C_{p,m}°(H_2O, l, 298.15\ K) = 75.351\ J \cdot K^{1} \cdot mol^{-1}$ follows that $C_{p,m}°$(magnetite, 298.15 K) = -39.4 J · K^{1} · mol^{-1}. A negative heat

capacity value for a solid is unreasonable. Assuming $\Delta_r C_{p,m}°$(298.15 K) = 0 would lead to a positive heat capacity value for magnetite (203.6 J · K^1 · mol^{-1}). As can be seen from Fig. 11.4-6, the line of $\log_{10}{}^{*}K_{s,0}°$(298.15 K) vs. 1/T only slightly curved (black line in the figure, suggesting that a linear fit, which implies that $\Delta_r C_{p,m}°$(298.15 K) = 0, is also compatible with the experimental data. Such a linear fit is shown in Fig. 11.4-6 a as red line. From the fit follow $\log_{10}{}^{*}K_{s,0}°$(298.15 K) = (11.65 ± 0.57) and $\Delta_r H_m°$(298.15 K) = -(89.4 ± 3.4) kJ·mol^{-1}. In order to remain consistent with the stability constants for the Fe(II) hydroxo complexes derived by Brown & Ekberg (2016) from magnetite solubility data (see Sections 11.4.1.2.3 – 11.4.1.2.5), we accepted $\log_{10}{}^{*}K_{s,0}°$(298.15 K) = (11.77 ± 0.22) obtained by these authors from the 3-term fit, but selected $\Delta_r H_m°$(298.15 K) = -(89.4 ± 3.4) kJ·mol^{-1} from our 2-term fit. This combination of thermodynamic data is also compatible with the experimental data, as can be seen from the green line in the bottom figure of Fig. 11.4-6.

Thus, for inclusion in TDB 2020, we selected

$\log_{10}{}^{*}K_{s,0}°$(298.15 K) = (11.77 ± 0.22)

$\Delta_r H_m°$(298.15 K) = -(89.4 ± 3.4) kJ·mol^{-1}

$\Delta_r C_{p,m}°$(298.15 K) = 0

Although Lemire et al. (2013) discussed solubility studies of magnetite (see Sections 11.4.1.2.1 and 11.4.1.2.2), they did not select any data derived from these. In the case of magnetite, they selected $\Delta_f H_m°$(magnetite, 298.15 K) = -(1'115.78 ± 1.60) kJ·mol^{-1}, $S_m°$(magnetite, 298.15 K) = (145.89 ± 0.30) J · K^{-1} · mol^{-1}, and $C_{p,m}°$(magnetite, 298.15 K) = (150.78 ± 1.25) J · K^{-1} · mol^{-1} from calorimetric studies. From $\Delta_f H_m°$(magnetite, 298.15 K), $S_m°$(magnetite, 298.15 K) and other NEA-selected data, $S_m°$(O_2, g, 298.15 K) = (205.152 ± 0.005) J·K^{-1}·mol^{-1}, $S_m°$(H_2, g, 298.15 K) = (130.68 ± 0.003) J·K^{-1}·mol^{-1}, and $S_m°$(Fe, cr, 298.15 K) = (27.085 ± 0.160) J·K^{-1}·mol^{-1}, they obtained $\Delta_f G_m°$(magnetite, 298.15 K) = -(1'012.719 ± 1.609) kJ·mol^{-1}. From this value and the selected $\Delta_f G_m°$(Fe^{2+}, 298.15 K) = (-90.72 ± 0.64) kJ·mol^{-1} and $\Delta_f G_m°$(H_2O, l, 298.15 K) = -(237.140 ± 0.041) kJ·mol^{-1} follows $\Delta_r G_m°$(298.15 K) kJ·mol^{-1} = -(69.33 ± 0.84) for the above mentioned solubility reaction of magnetite, which corresponds to $\log_{10}{}^{*}K_{s,0}°$(298.15 K) = (12.15 ± 0.15).

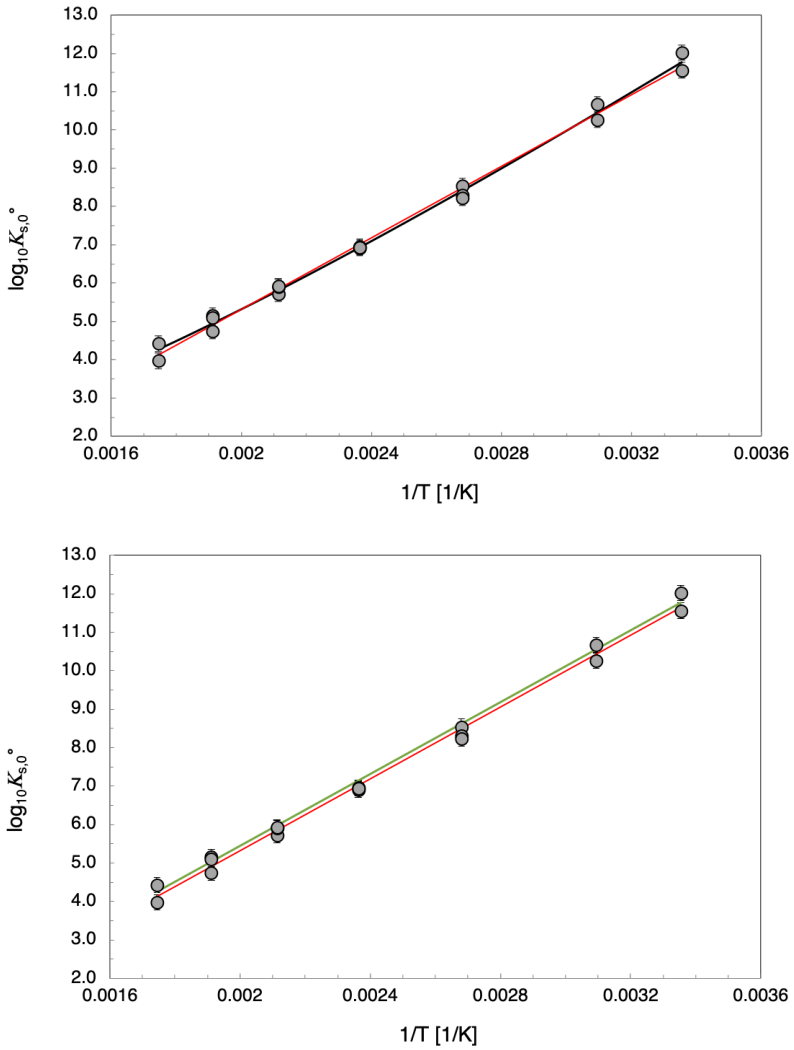

Fig. 11.4-6: Solubility of magnetite, 1/3 Fe_3O_4(magnetite) + 2 H^+ + 1/3 H_2g ⇌ Fe^{2+} + 4/3 H_2O(l), as a function of temperature

Experimental data by Sweeton & Baes (1970), Ziemniak et al. (1995), and Tremaine & LeBlanc (1980), as reported by Brown & Ekberg (2016). (Top) Black curve: 3-term fit by Brown & Ekberg (2016), red line: 2-term fit (this work). (Bottom) Red line: 2-term fit (this work), green line: calculated from selected data for TDB 2020. See text for discussion.

11.4.2.4 Hematite (α-Fe_2O_3)

Diakonov et al. (1999) carried out solubility experiments with hematite under basic conditions in the temperature range 25 to 300 °C and reported values for $\log_{10}{}^*K_{s,4}°(T)$ of the reaction

$$½\ Fe_2O_3(\text{hematite}) + 5/2\ H_2O(l) \rightleftharpoons Fe(OH)_4^- + H^+$$

In addition, they reviewed and compiled similar data from other authors obtained from temperatures between 20 and 300 °C.

Brown & Ekberg (2016) accepted these data and combined the $\log_{10}{}^*K_{s,4}°(T)$ values with those for $\log_{10}{}^*\beta_4°(T)$ that they calculated from their own $\log_{10}{}^*\beta_4°$ temperature function (see Section 11.4.1.3.4) to obtain values of $\log_{10}{}^*K_{s,0}°(T)$ for the solubility reaction

$$½\ Fe_2O_3(\text{hematite}) + 3\ H^+ \rightleftharpoons Fe^{3+} + 3/2\ H_2O(l)$$

They described the data with the linear temperature function

$$\log_{10}{}^*K_{s,0}°(T) = -11.61 + 3568/T$$

from which follows

$$\log_{10}{}^*K_{s,0}°(298.15\ K) = (0.36 \pm 0.40)$$

$$\Delta_r H_m°(298.15\ K) = -(68.3 \pm 1.9)\ kJ{\cdot}mol^{-1}$$

$$\Delta_r C_{p,m}°(298.15\ K) = 0$$

These data for hematite are included in TDB 2020 and are preferred over those selected by Lemire et al. (2013) who relied entirely on calorimetric data for their selected values $\Delta_f H_m°$(hematite, 298.15 K) = -(826.29 ± 2.63) kJ·mol^{-1}, $S_m°$(hematite, 298.15 K) = (87.40 ± 0.16) J·K^{-1}·mol^{-1}, and $C_{p,m}°$(hematite, 298.15 K) = (103.93 ± 0.17) J·K^{-1}·mol^{-1}, deriving $\Delta_f G_m°$(hematite, 298.15 K) = -(744.448 ± 2.632) kJ·mol^{-1} from $\Delta_f H_m°$(hematite, 298.15 K), $S_m°$(hematite, 298.15 K), $S_m°$(O_2, g, 298.15 K) = (205.152 ± 0.005) J·K^{-1}·mol^{-1}, and $S_m°$(Fe, cr, 298.15 K) = (27.085 ± 0.160) J·K^{-1}·mol^{-1}.

From $\Delta_f G_m°$(hematite, 298.15 K) = -(744.448 ± 2.632) kJ·mol^{-1}, $\Delta_f G_m°(Fe^{3+}$, 298.15 K) = -(16.23 ± 0.65) kJ·mol^{-1}, and $\Delta_f G_m°(H_2O$, l, 298.15) = -(237.140 ± 0.041) kJ·mol^{-1}, all selected by Lemire et al. (2013), follows $\log_{10}{}^*K_{s,0}°(298.15\ K)$ = -(0.05 ± 0.26), which leads to smaller solubility values than the solubility product selected for TDB 2020 (but the uncertainties overlap).

11.4.2.5 Maghemite (γ-Fe_2O_3)

Lemire et al. (2013) reported the results of a study by Taylor & Owen (1997) who investigated the solubilities of powders of hematite and maghemite in aqueous HNO_3 and estimated a difference in the solubility products of these phases. Lemire et al. (2013) recalculated this difference using SIT and obtained $\log_{10}{}^*K_{s,0}°$(maghemite, s, 298.15 K) - $\log_{10}{}^*K_{s,0}°$(hematite, s, 298.15 K) = (1.25 ± 0.46). Brown & Ekberg (2016) accepted this difference and combined it with their selected $\log_{10}{}^*K_{s,0}°$(hematite, s, 298.15 K) = (0.36 ± 0.40), see the preceding section, and obtained

$$\log_{10}{}^*K_{s,0}°(298.15\ K) = (1.61 \pm 0.61)$$

for the dissolution reaction

$$½\ Fe_2O_3(\text{maghemite}) + 3\ H^+ \rightleftharpoons Fe^{3+} + 3/2\ H_2O(l)$$

which is included in TDB 2020.

Note that Lemire et al. (2013) did not follow this approach but relied on calorimetric data for their selection of $\Delta_f H_m°$(maghemite, 298.15 K) = -(807.990 ± 3.023) kJ·mol^{-1}, $S_m°$(maghemite, 298.15 K) = (93.04 ± 0.40) J·K^{-1}·mol^{-1}, and $C_{p,m}°$(maghemite, 298.15 K) = (104.69 ± 0.35) J·K^{-1}·mol^{-1}. They calculated $\Delta_f G_m°$(maghemite, 298.15 K) = -(727.830 ± 3.027) kJ·mol^{-1} from their selected values for $\Delta_f H_m°$(maghemite, 298.15 K), $S_m°$(maghemite, 298.15 K), $S_m°$(O_2, g, 298.15 K) = (205.152 ± 0.005) J·K^{-1}·mol^{-1}, and $S_m°$(Fe, cr, 298.15 K) = (27.085 ± 0.160) J·K^{-1}·mol^{-1}. From $\Delta_f G_m°$(maghemite, 298.15 K) = -(727.830 ± 3.027) kJ·mol^{-1}, $\Delta_f G_m°$(Fe^{3+}, 298.15 K) = -(16.23 ± 0.65) kJ·mol^{-1}, and $\Delta_f G_m°$(H_2O, l, 298.15) = -(237.140 ± 0.041) kJ·mol^{-1}, all selected by Lemire et al. (2013), follows $\log_{10}{}^*K_{s,0}°$(298.15 K) = (1.41 ± 0.29), which leads to smaller solubility values than the solubility product selected for TDB 2020 (but the uncertainties overlap).

11.4.2.6 Goethite (α-FeOOH)

Lemire et al. (2013) derived their selected thermodynamic data for goethite from calorimetric data although they also discussed some solubility experiments. For TDB 2020 we chose to follow Brown & Ekberg (2016) who accepted solubility constants from Diakonov et al. (1994) in the range 25 to 300 °C. Brown & Ekberg (2016) combined the $\log_{10}{}^*K_{s,4}°(T)$ values, as calculated by Diakonov et al. (1999) from data by Diakonov et al. (1994), with those for $\log_{10}{}^*\beta_4°(T)$ that they calculated from their own $\log_{10}{}^*\beta_4°$ temperature function (see Section 11.4.1.3.4) to obtain values of $\log_{10}{}^*K_{s,0}°(T)$ for the solubility reaction

$$FeOOH(goethite) + 3\ H^+ \rightleftharpoons Fe^{3+} + 2\ H_2O(l)$$

In addition, they also accepted data for $\log_{10}{}^*K_{s,0}°$(298.15) from two other studies and used a linear fit to obtain the temperature function

$$\log_{10}{}^*K_{s,0}°(T) = -11.14 + 3421/T$$

which leads to

$$\log_{10}{}^*K_{s,0}°(298.15\ K) = (0.33 \pm 0.10)$$

$$\Delta_r H_m°(298.15\ K) = -(65.5 \pm 2.3)\ kJ·mol^{-1}$$

$$\Delta_r C_{p,m}°(298.15\ K) = 0$$

These data are included in TDB 2020.

As mentioned, Lemire et al. (2013) relied on calorimetric data for selecting $\Delta_f H_m°$(goethite, 298.15 K) = -(560.46 ± 1.99) kJ·mol^{-1}, $S_m°$(goethite, 298.15 K) = (59.70 ± 0.50) J·K^{-1}·mol^{-1}, and $C_{p,m}°$(goethite, 298.15 K) = (74.36 ± 0.42) J·K^{-1}·mol^{-1}. They calculated $\Delta_f G_m°$(goethite, 298.15 K) = -(489.537 ± 1.996) kJ·mol^{-1} from their selected values for $\Delta_f H_m°$(goethite, 298.15 K), $S_m°$(goethite, 298.15 K), $S_m°$(O_2, g, 298.15 K) = (205.152 ± 0.005) J·K^{-1}·mol^{-1}, $S_m°$(H_2, g, 298.15 K) = (130.68 ± 0.003) J·K^{-1}·mol^{-1}, and $S_m°$(Fe, cr, 298.15 K) = (27.085 ± 0.160) J·K^{-1}·mol^{-1}.

From $\Delta_f G_m°$(goethite, 298.15 K) = -(489.537 ± 1.996) kJ·mol^{-1}, $\Delta_f G_m°(Fe^{3+}$, 298.15 K) = -(16.23 ± 0.65) kJ·mol^{-1}, and $\Delta_f G_m°(H_2O$, l, 298.15) = -(237.140 ± 0.041) kJ·mol^{-1}, all selected by Lemire et al. (2013), follows $\log_{10}{}^*K_{s,0}°$(298.15 K) = (0.17 ± 0.37), which leads to smaller solubility values than the solubility product of goethite selected for TDB 2020 (but the uncertainties overlap).

Note that compared to our selected $\log_{10}{}^*K_{s,0}°$(298.15 K) = (0.36 ± 0.40) for hematite, goethite with $\log_{10}{}^*K_{s,0}°$(298.15 K) = (0.33 ± 0.10) is slightly less soluble. However, both solubility products have large uncertainties and thus either one could be more stable.

11.4.2.7 Lepidocrocite (γ-FeOOH)

According to Lemire et al. (2013), there appear to be no reasonable solubility data for lepidocrocite, as the "evaluation of various solubility and equilibrium potential studies is hampered by uncertainties with ample characterization (both phase identity and surface area estimates), aqueous speciation, and activity". Therefore, they reviewed calorimetric data and selected $\Delta_f H_m°$(lepidocrocite, 298.15 K) = -(549.2 ± 2.0) kJ·mol^{-1}, $S_m°$(lepidocrocite, 298.15 K) = (65.08 ± 0.46) J·K^{-1}·mol^{-1}, and $C_{p,m}°$(lepidocrocite, 298.15 K) = (69.14 ± 0.56) J·K^{-1}·mol^{-1}. From the selected $\Delta_f H_m°$(lepidocrocite, 298.15 K), $S_m°$(lepidocrocite, 298.15 K), $S_m°(O_2$, g, 298.15 K) = (205.152 ± 0.005) J·K^{-1}·mol^{-1}, $S_m°(H_2$, g, 298.15 K) = (130.68 ± 0.003) J·K^{-1}·mol^{-1}, and $S_m°$(Fe, cr, 298.15 K) = (27.085 ± 0.160) J·K^{-1}·mol^{-1} follows $\Delta_f G_m°$(lepidocrocite, 298.15 K) = -(479.881 ± 2.005) kJ·mol^{-1}.

Using this value together with the selected $\Delta_f G_m°(Fe^{3+}$, 298.15 K) = -(16.23 ± 0.65) kJ·mol^{-1} and $\Delta_f G_m°(H_2O$, l, 298.15 K) = -(237.140 ± 0.041) kJ·mol^{-1} leads to $\Delta_r G_m°$(298.15 K) = -(10.63 ± 2.11) or

$$\log_{10}{}^*K_{s,0}°(298.15\ K) = (1.86 \pm 0.37)$$

for the reaction

$$FeOOH(lepidocrocite) + 3\ H^+ \rightleftharpoons Fe^{3+} + 2\ H_2O(l)$$

From $\Delta_f H_m°$(lepidocrocite, 298.15 K) selected by Lemire et al. (2013), and $\Delta_f H_m°(Fe^{3+}$, 298.15 K) = -(50.06 ± 0.97) kJ·mol^{-1} and $\Delta_f H_m°(H_2O$, l, 298.15 K) = -(285.83 ± 0.04) kJ·mol^{-1}, also selected by Lemire et al. (2013), follows

$$\Delta_r H_m°(298.15\ K) = -(72.5 \pm 2.2)\ kJ·mol^{-1}$$

Both $\log_{10}{}^*K_{s,0}°$(298.15 K) and $\Delta_r H_m°$(298.15 K) are included in TDB 2020.

11.4.2.8 2-line ferrihydrite ($Fe(OH)_3$)

According to Lemire et al. (2013) and references cited therein, the substance once referred to as colloidal or amorphous $Fe(OH)_3$ is characterized by diagnostic X-ray diffraction patterns with extremely broad peaks and is commonly classified as 2-line or 6-line ferrihydrite, based on the number of distinguishable bands (2-line) or lines (6-line) in X-ray diffraction patterns.

Stefánsson (2007) measured the solubility of 2-line ferrihydrite in 0.01 M ($NaClO_4$) at 25 °C in the pH range between about 3 and 11. Although these authors did not provide any raw data, Lemire et al. (2013) derived the following solubility constants from a total Fe(III) concentration vs. pH_c plot by Stefánsson (2007): $\log_{10}{}^{*}K_{s,0}°$(298.15 K) = 3.5, $\log_{10}{}^{*}K_{s,1}°$(298.15 K) = 1.3, $\log_{10}{}^{*}K_{s,2}°$(298.15 K) = -2.3, $\log_{10}{}^{*}K_{s,3}°$(298.15 K) ≤ -10.8, and $\log_{10}{}^{*}K_{s,4}°$(298.15 K) = -18.2. Lemire et al. (2013) did not select any data for 2-line ferrihydrite but reported an enthalpy of formation "to facilitate calculations". We follow Brown & Ekberg (2016), who selected

$$\log_{10}{}^{*}K_{s,0}°(298.15\ \text{K}) = (3.50 \pm 0.40)$$

for

$$Fe(OH)_3(\text{2-line ferrihydrite}) + 3\ H^+ \rightleftharpoons Fe^{3+} + 3\ H_2O(l)$$

based on Stefánsson (2007) and include this solubility product in TDB 2020.

11.4.2.9 Other iron oxide and oxyhydroxide solids

Wüstite ($Fe_{0.932}O$): Lemire et al. (2013) selected $\Delta_f G_m°$(298.15 K), $\Delta_f H_m°$(298.15 K), $S_m°$(298.15 K), $C_{p,m}°$(298.15 K), and $C_{p,m}°(T, 298.15\text{-}1'000\ \text{K})$ for $Fe_{0.932}O$(wüstite) based on calorimetric measurements. According to Lemire et al. (2013), wüstite is unstable with respect to Fe(cr) and Fe_3O_4(magnetite) at temperatures below 840 K and is rarely found in nature (e.g., in fusion crusts of meteorites or in natural coke). For these reasons, wüstite is not included in TDB 2020.

β-Fe_2O_3(cr): According to Lemire et al. (2013), synthetic β-Fe_2O_3(cr) is the Fe-endmember of the bixbyite solid solution, $(Mn,Fe)_2O_3$. Apparently, there are no thermodynamic data known for this phase.

δ-Fe_2O_3(cr): Lemire et al. (2013) mention that δ-Fe_2O_3(cr) is not a valid phase and is actually δ–FeOOH(cr) misidentified as a form of Fe_2O_3(cr).

ε-Fe_2O_3(cr): For this rare and metastable form of Fe_2O_3, which does not occur in nature as a mineral but has biogenic origins in an iron storage substance in plants, Lemire et al. (2013) reported a value for $\Delta_f H_m°$(298.15 K) but did not select it.

β-FeOOH(akaganéite): Akaganéite is an iron corrosion product but is also formed in natural environments. Natural occurrences are rare, however, due to the specific environmental requirements for its formation, such as hyper-chlorinated, acidic and oxidizing conditions, as well as large concentrations of dissolved ferrous and chloride ions (Font et al. 2017). Lemire et al. (2013) reported values for $\Delta_f H_m°$(298.15 K), $S_m°$(298.15 K), and $C_{p,m}°$(298.15 K), but didn't select any of these data.

Lemire et al. (2020) discussed calorimetric data for an akaganéite with a specific composition, β-$FeOOH{\cdot}0.652H_2O{\cdot}0.0096HCl$(cr), and selected values for $S_m°$(298.15 K), and $C_{p,m}°$(298.15 K). Since these data are not sufficient for calculating chemical equilibria, they are not included in TDB 2020.

δ-FeOOH(feroxyhyte): Feroxyhyte is found in oceanic iron-manganese nodules and in gley soils (Chukhrov et al. 1977). Lemire et al. (2013) discussed structural properties but did not report any thermodynamic data.

$Fe(OH)_3$(bernalite): Bernalite is a very rare mineral. Lemire et al. (2013) discussed compositional and structural properties. No thermodynamic data are known.

"Ferrosic Hydroxides", $Fe_3(OH)_8$(s) and $Fe_4(OH)_{10}$(s): No thermodynamic data are discussed for these phases as Lemire et al. (2013) deem their existence, suggested in a solubility study and favoured by soil scientists, as doubtful in the light of recent work on hydroxycarbonate green rust.

High-pressure Fe-O-H phases: Lemire et al. (2013) discussed the stability fields in terms of pressure and temperature of several high-pressure phases but did not report any thermodynamic data.

11.4.2.10 Iron oxide spinel-type endmembers and solid solutions

Lemire et al. (2020) devoted a chapter to the discussion of endmembers and solid solutions of Fe-spinels belonging to the Fe-Ni-Cr-O system, i.e. to magnetite (α-Fe_3O_4), maghemite (γ-Fe_2O_3), trevorite ($NiFe_2O_4$), chromite ($FeCr_2O_4$), and their known binary solid solutions. For the endmembers magnetite and maghemite, Lemire et al. (2020) did not selected any new data, while trevorite and chromite had not been discussed by Lemire et al. (2013). Lemire et al. (2020) considered trevorite and chromite because they are important constituents of corrosion films on stainless-steel surfaces, notably in cooling circuits of nuclear reactors.

$NiFe_2O_4$(trevorite): Lemire et al. (2020) selected calorimetrically determined values of $\Delta_f H_m°$(298.15 K), $S_m°$(298.15 K), and $C_{p,m}°$(298.15 K) for trevorite. This mineral can be rarely found in terrestrial natural environments and is more commonly found in meteorites (O'Driscoll et al. 2014). It is not known to form at ambient conditions, and it is very unlikely that this mineral may control the solubilities of Fe or Ni in the range of applications that TDB 2020 is designed for. For this reason, these data are not included in TDB 2020.

$FeCr_2O_4$(chromite): Lemire et al. (2020) selected calorimetric data, $S_m°$(298.15 K), and $C_{p,m}°$(298.15 K), for chromite. Since Cr is not included in TDB 2020, these data were not considered for TDB 2020.

Magnetite-maghemite solid solution: Lemire et al. (2020) reported enthalpies of formation of two specific magnetite-hematite solid solutions, $Fe_{2.900}O_4$(cr), with a magnetite mole fraction of 0.700 ± 0.030, and $Fe_{2.964}O_4$(cr), with a magnetite mole fraction of 0.892 ± 0.030, as well as mixing parameters for a Margules expression of ΔH^{mix}.

Magnetite-trevorite solid solution: Lemire et al. (2020) discussed the distribution of Ni^{2+}, Fe^{2+}, and Fe^{3+} on the tetrahedral and octahedral sites of the spinel structure and reported Gibbs energies of mixing, but stated that there are no data for the latter at temperatures below 1'200 K.

Magnetite-chromite solid solution: According to Lemire et al. (2020), magnetite has an inverse spinel structure at ambient temperatures, while chromite has a normal spinel structure at all temperatures. Therefore, solid solution of these two endmembers is limited, and Lemire et al. (2020) stated that it is reasonable to assume a complete miscibility gap between magnetite and chromite at ambient temperatures.

11.5 Group 17 halogen compounds and complexes

11.5.1 Aqueous iron halide complexes

Lemire et al. (2013) only considered Fe(II) fluoride, Fe(II) chloride, and Fe(III) chloride complexes (the review of other iron halide complexes being foreseen for the second iron

11.5.1.1 Aqueous iron(II) fluoride complexes

11.5.1.1.1 Data in TDB 05/92, TDB 01/01 and TDB 12/07

For

$$Fe^{2+} + F^- \rightleftharpoons FeF^+$$

Nordstrom et al. (1990) estimated

$$\log_{10}\beta_1^\circ(298.15\ K) = 1$$

from a measurement of 0.83 at $I = 1$ M (no reference given) and the tendency for divalent fluorides to have $\log_{10}\beta_1^\circ \approx 1$. This estimate was selected by Pearson et al. (1992) for TDB 05/92 and was retained in TDB 01/01 and TDB 12/07.

11.5.1.1.2 FeF^+

According to Lemire et al. (2013) there are only two quantitative investigations of the formation of FeF^+ in aqueous solution. Both are based on potentiometry with a fluoride-sensitive electrode, one was carried out in 1.0 M $NaClO_4$ and the other in 0.05 M tetraethylammonium perchlorate, Et_4NClO_4. Lemire et al. (2013) extrapolated both conditional constants to zero ionic strength and obtained 1.58 ± 0.07 for the $NaClO_4$ medium and 1.82 ± 0.11 or 1.83 ± 0.11 for the Et_4NClO_4 medium, the latter two values calculated with the extremes of the estimated interval -0.3 to

0.0 kg · mol^{-1} for $\varepsilon(Et_4N^+, F^-)$. As the values for the $NaClO_4$ and the Et_4NClO_4 medium have no overlapping uncertainties, Lemire et al. (2013) used the NEA-procedure for averaging two discrepant data points and obtained

$$Fe^{2+} + F^- \rightleftharpoons FeF^+$$

$$\log_{10}\beta_1^\circ(298.15\ K) = (1.7 \pm 0.2)$$

(using either of the values for the Et_4NClO_4 medium leads to the same result when rounding it to two significant figures). For the extrapolation to zero ionic strength of the conditional constant in $NaClO_4$, Lemire et al. (2013) needed an estimate for $\Delta\varepsilon = \varepsilon(FeF^+, ClO_4^-) - \varepsilon(Fe^{2+}, ClO_4^-) - \varepsilon(F^-, Na^+)$ and assumed it by analogy to be equal to the corresponding value for the Ni-system reported by Gamsjäger et al. (2005) as $-(0.049 \pm 0.060)$ kg · mol^{-1}. From this value and $\varepsilon(Fe^{2+}, ClO_4^-) = (0.37 \pm 0.04)$ and $\varepsilon(F^-, Na^+) = (0.02 \pm 0.02)$ then follows that

$$\varepsilon(FeF^+, ClO_4^-) \approx (0.34 \pm 0.07) \text{ kg} \cdot \text{mol}^{-1}$$

For the specific ion interaction coefficient with chloride, we obtained

$$\varepsilon(FeF^+, Cl^-) \approx (0.05 \pm 0.10) \text{ kg} \cdot \text{mol}^{-1}$$

from the estimation method described in Section 1.5.3.

These data for FeF^+ are all included in our database.

11.5.1.1.3 $FeF_2(aq)$ and FeF_3^-

Lemire et al. (2013) discussed the results of a single study claiming the existence of the higher-order Fe(II) fluoride complexes, $FeF_2(aq)$ and FeF_3^- but did not accept them as reliable.

11.5.1.2 Aqueous iron(III) fluoride complexes

11.5.1.2.1 Data in TDB 05/92, TDB 01/01 and TDB 12/07

The thermodynamic data selected by Pearson et al. (1992) for TDB 05/92 (retained in TDB 01/01 and TDB 12/07) for FeF^{2+}, FeF_2^+, and $FeF_3(aq)$

$$Fe^{3+} + F^- \rightleftharpoons FeF^{2+}$$

$$\log_{10}\beta_1^\circ(298.15 \text{ K}) = 6.2$$

$$\Delta_r H_m^\circ(298.15 \text{ K}) = 11.3 \text{ kJ} \cdot \text{mol}^{-1}$$

$$Fe^{3+} + 2\ F^- \rightleftharpoons FeF_2^+$$

$$\log_{10}\beta_2^\circ(298.15 \text{ K}) = 10.8$$

$$\Delta_r H_m^\circ(298.15 \text{ K}) = 20.1 \text{ kJ} \cdot \text{mol}^{-1}$$

$$Fe^{3+} + 3\ F^- \rightleftharpoons FeF_3(aq)$$

$$\log_{10}\beta_3^\circ(298.15 \text{ K}) = 14.0$$

$$\Delta_r H_m^\circ(298.15 \text{ K}) = 22.6 \text{ kJ} \cdot \text{mol}^{-1}$$

were all taken from Nordstrom et al. (1990). These authors obtained the data from Nordstrom & Jenne (1977), who referred to an unpublished manuscript by Hogfeldt & Sillén (1966) that reported data selected from the compilation by Sillén & Martell (1964), which we could not trace back to the original references.

11.5.1.2.2 FeF^{2+}

At the outset of their analysis of published experimental data on the formation of FeF^{2+}, Lemire et al. (2020) remarked that there is virtually no data at $I_c < 0.5$ mol · dm^{-3}, where the dependence of $\varepsilon(FeF^{2+}, X^-)$ on ionic strength is most pronounced, making the extrapolation to zero ionic strength difficult. Lemire et al. (2020) selected data obtained in $NaClO_4$, $HClO_4$ and mixed $NaClO_4/HClO_4$ media and derived a value for $\log_{10}\beta_1°$(298.15 K) using SIT with the following expression

$$\log_{10}\beta_1° - \{\varepsilon(FeF^{2+}, ClO_4^-) - \varepsilon(Fe^{3+}, ClO_4^-)\}m_{ClO4-} = \log_{10}\beta_1 + 6\ D - \{\varepsilon(F^-, Na^+)m_{Na+} - \varepsilon(F^-, H^+)m_{H+}\}$$

where they designated $\{\varepsilon(FeF^{2+}, ClO_4^-) - \varepsilon(Fe^{3+}, ClO_4^-)\}$ as $\Delta\varepsilon'$. They obtained $\log_{10}\beta_1°$(298.15 K) = (5.99 ± 0.28) and $\Delta\varepsilon'$ = -(0.45 ± 0.44) kg · mol^{-1} from which follows $\varepsilon(FeF^{2+}, ClO_4^-)$ = (0.28 ± 0.5) kg · mol^{-1}, which they compared with the selected $\varepsilon(FeCl^{2+}, ClO_4^-)$ = (0.63 ± 0.05) kg · mol^{-1} and $\varepsilon(FeOH^{2+}, ClO_4^-)$ = (0.46 ± 0.05) kg · mol^{-1} by Lemire et al. (2013)[34]. In mistrust of $\varepsilon(FeF^{2+}, ClO_4^-)$ = (0.28 ± 0.5) kg · mol^{-1} that they obtained from the regressed $\Delta\varepsilon'$, Lemire et al. (2020) assumed that $\Delta\varepsilon' = \{\varepsilon(FeF^{2+}, ClO_4^-) - \varepsilon(Fe^{3+}, ClO_4^-)\} \approx \{\varepsilon(FeOH^{2+}, ClO_4^-) - \varepsilon(Fe^{3+}, ClO_4^-)\}$ = -(0.27 ± 0.07) kg · mol^{-1} and obtained $\log_{10}\beta_1°$(298.15 K) = (6.10 ± 0.09) from the same data (without giving further explanations). Finally, Lemire et al. (2020) carried out a regression with the assumed $\Delta\varepsilon'$ = -(0.27 ± 0.07) kg · mol^{-1} considering only formation constants determined in $HClO_4/NaClO_4$ media[35], which resulted in their selected

$$Fe^{3+} + F^- \rightleftharpoons FeF^{2+}$$

$$\log_{10}\beta_1°(298.15\ K) = (6.09 \pm 0.04)$$

This value is also included in TDB 2020. From $\Delta\varepsilon' = \{\varepsilon(FeF^{2+}, ClO_4^-) - \varepsilon(Fe^{3+}, ClO_4^-)\} \approx$ -(0.27 ± 0.07) kg · mol^{-1} and the selected $\varepsilon(Fe^{3+}, ClO_4^-)$ = (0.73 ± 0.07) kg · mol^{-1} then follows

$$\varepsilon(FeF^{2+}, ClO_4^-) = (0.46 \pm 0.08)\ kg \cdot mol^{-1}$$

which is included in TDB 2020 as well as the estimate (see Section 11.1.1)

$$\varepsilon(FeF^{2+}, Cl^-) \approx \varepsilon(FeF^{2+}, ClO_4^-) = (0.46 \pm 0.08)\ kg \cdot mol^{-1}$$

---

[34] Note that we selected $\varepsilon(FeOH^{2+}, ClO_4^-)$ = (0.27 ± 0.05) kg · mol^{-1}, see Section 12.4.1.3.1.

[35] From the explanations given by Lemire et al. (2020) it is not entirely clear how this regression differs from that where they obtained $\log_{10}\beta_1°$(298.15 K) = (6.10 ± 0.09).

Lemire et al (2020) also selected

$$\Delta_r H_m°(298.15\ K) = (12.8 \pm 7.4)\ kJ \cdot mol^{-1}$$

However, no information was given on how this value was derived. Since in their Tab. VIII-2 of formation constants for FeF_n^{3-n} complexes cited in the literature, $\log_{10}\beta_1°$ values for FeF^{2+} in perchlorate media can be found for temperatures from 273.15 up to 308.15 K (corresponding to 0 – 35 °C) we assume that Lemire et al. (2020) obtained $\Delta_r H_m°(298.15\ K)$ from a van't Hoff plot. This value is also included in TDB 2020 and consequently also

$$\Delta_r C_{p,m}°(298.15\ K) = 0$$

11.5.1.2.3 FeF_2^+

Lemire et al. (2020) reported several experimental determinations of $\log_{10}\beta_2(298.15\ K)$ for the formation of FeF_2^+ in $HClO_4/NaClO_4$ media. The corresponding SIT equation

$$\log_{10}\beta_2° - \{\varepsilon(FeF_2^+, ClO_4^-) - \varepsilon(Fe^{3+}, ClO_4^-)\}m_{ClO4-} = \log_{10}\beta_2 + 10\ D -$$

$$2\ \{\varepsilon(F^-, Na^+)m_{Na+} - \varepsilon(F^-, H^+)m_{H+}\}$$

where $\{\varepsilon(FeF_2^+, ClO_4^-) - \varepsilon(Fe^{3+}, ClO_4^-)\} = \Delta\varepsilon'$, was used by Lemire et al. (2020) for an unweighted linear regression, resulting in $\log_{10}\beta_2°(298.15\ K) = (9.96 \pm 0.33)$ and $\Delta\varepsilon' = -(1.32 \pm 0.54)$. From $\Delta\varepsilon'$ and the selected $\varepsilon(Fe^{3+}, ClO_4^-) = (0.73 \pm 0.07)\ kg \cdot mol^{-1}$ follows (after rounding) $\varepsilon(FeF_2^+, ClO_4^-) = -(0.6 \pm 0.5)\ kg \cdot mol^{-1}$. Lemire et al. (2020) considered this value as "totally unrealistic". For this reason, they performed "a regression of all the $\log_{10}\beta_{m,2}$ values in Tab. VIII-2 at the various temperatures with the exception of that from [1961YAL], which proved to be an extreme outlier, and assuming that $\Delta_r H_m°$(VIII.7) and $\Delta\varepsilon'$ are independent of temperature" but gave no further details on the regression procedure. They obtained

$$Fe^{3+} + 2\ F^- \rightleftharpoons FeF_2^+$$

$$\log_{10}\beta_2°(298.15\ K) = (10.41 \pm 0.33)$$

$$\Delta_r H_m°(298.15\ K) = (22 \pm 14)\ kJ \cdot mol^{-1}$$

with $\Delta\varepsilon' = -(0.64 \pm 0.31)\ kg \cdot mol^{-1}$, which leads (after rounding) to

$$\varepsilon(FeF_2^+, ClO_4^-) = (0.1 \pm 0.3)\ kg \cdot mol^{-1}$$

Lemire et al. (2020) remarked that "based on this value alone, the results of this second regression are to be preferred", but tacitly selected neither of them. For scoping calculations, the results of the second regression are included in TDB 2020, together with the estimated

$$\varepsilon(FeF_2^+, Cl^-) \approx \varepsilon(FeF_2^+, ClO_4^-) = (0.1 \pm 0.3)\ kg \cdot mol^{-1}$$

(see Section 11.1.1). In analogy to FeF^+, we assume that temperatures at which the complexation constants included in the second regression were determined are in the range of 0 – 35 °C. Since $\Delta_r H_m°$ was assumed to be independent of temperature, it follows that

$$\Delta_r C_{p,m}°(298.15\ K) = 0$$

which is also included in TDB 2020.

11.5.1.2.4 $FeF_3(aq)$

Lemire et al. (2020) did not select any data for $FeF_3(aq)$ noting that "the scatter in the formation constants for higher-order fluoridoiron(III) complexes is such that it is unreasonable to attempt to treat these values further at this time, while also acknowledging that high fluoride concentrations were generally employed to allow speciation calculations to be made". For this reason, the supplemental data selected for $FeF_3(aq)$ in TDB 12/07 is not retained in TDB 2020. Furthermore, these data could not be traced back to their original reference.

11.5.1.3 Aqueous iron(II) chloride complexes

11.5.1.3.1 Data in TDB 05/92, TDB 01/01 and TDB 12/07

Pearson et al. (1992) selected

$$Fe^{2+} + Cl^- \rightleftharpoons FeCl^+$$

$$\log_{10}\beta_1°(298.15\ K) = 0.14$$

for TDB 05/92 (retained in TDB 01/01 and TDB 12/07). This value was taken from Nordstrom et al. (1990) who adopted it from Davison (1979). The latter author derived his stability constant from an experimental value by Po & Sutin (1968) who studied the kinetics of the oxidation of iron(II) by hydrogen peroxide in mixtures of perchloric and hydrochloric acid at I = 1 M. The dependence of the rate constant on the chloride concentration was assumed by Po & Sutin (1968) to be due to the formation of iron chloride complexes that react faster with hydrogen peroxide than the free iron aquo ion. From an analysis of the rate constant as a function of chloride concentration, Po & Sutin (1968) determined a value of $(0.5 \pm 0.3)\ M^{-1}$ for the conditional stability constant at I = 1 M but noting that "other interpretations of the variation of the rate constants with the chloride ion concentrations are also consistent with the data, and we therefore do not attach much significance to this estimate of K_1" and that the real value was probably smaller. Davison (1979) extrapolated the conditional constant to I = 0, assuming that the activity coefficients of $FeCl^+$ and Cl^- cancel, and using $\gamma(Fe^{2+}) = 0.36$ calculated from the mean activity coefficients for $FeCl_2$ and KCl by Robinson & Stokes (1965), assuming that $\gamma(K^+) = \gamma(Cl^-) = \gamma(KCl)$.

The formation constant for $FeCl^+$ is replaced by the constant discussed in the following section.

11.5.1.3.2 $FeCl^+$

Lemire et al. (2013) found only two experimental studies dealing with the formation of the very weak $FeCl^+$ complex that varied the chloride concentrations in the solutions sufficiently to enable the application of SIT for the extrapolation to zero ionic strength. One study used UV-spectrophotometry at temperatures from 25 °C up to 200 °C with HCl solutions up to 3.3 kg · mol^{-1}, the other used isopiestic methods to determine osmotic coefficients for the system $FeCl_2$-H_2O at 25 °C. Extrapolation with SIT of the spectrophotometric data resulted in $\log_{10}K°(298.15\ K) = -(0.11 \pm 0.03)$. A re-evaluation of the isopiestic data using a non-linear least-squares fit to determine $\log_{10}\beta_1°$, $\varepsilon(FeCl^+, Cl^-)$, and $\varepsilon(Fe^{2+}, Cl^-)$ resulted in $\log_{10}\beta_1°(298.15\ K) = -(2.5 \pm 0.15)$, $\varepsilon(FeCl^+, Cl^-) = (0.16 \pm 0.01)$ kg · mol^{-1}, and $\varepsilon(Fe^{2+}, Cl^-) = (0.17 \pm 0.01)$ kg · mol^{-1}. Lemire et al. (2013) noted, that the osmotic data could be equally well interpreted without assuming the formation of the very weak complex. The formation constants from the two studies differ by nearly two orders of magnitude and there are no obvious criteria for preferring one value over the other. Therefore, Lemire et al. (2013) did not select any formation constant for $FeCl^+$. In order to "provide some assistance to modelers who must select a constant due to the specifics of their speciation code", they suggested the use of

$$Fe^{2+} + Cl^- \rightleftharpoons FeCl^+$$

$$\log_{10}\beta_1°(298.15\ K) = -(1.0 \pm 0.8)$$

with

$$\varepsilon(FeCl^+, Cl^-) = (0.16 \pm 0.01)\ kg \cdot mol^{-1}$$

Since there is no information concerning the interaction coefficient of $FeCl^+$ with ClO_4^-, we estimated

$$\varepsilon(FeCl^+, ClO_4^-) = (0.2 \pm 0.1)\ kg \cdot mol^{-1}$$

estimated according to Tab. 1-7.

Lemire et al. (2013) derived an enthalpy of reaction for the formation of $FeCl^+$ by performing a linear 1/T fit to experimental data (recalculated to zero ionic strength) determined by two studies in the temperature range 25 °C – 200 °C and 10 °C – 100 °C, respectively. They obtained the selected[36] value

$$\Delta_r H_m°(FeCl^+, 298.15\ K) = (21.55 \pm 1.77)\ kJ \cdot mol^{-1}$$

From the linear 1/T fit also follows

$$\Delta_r C_{p,m}°(298.15\ K) = 0$$

---

[36] $\Delta_r H_m°(FeCl^+, 298.15\ K)$ was selected by Lemire et al. (2013) despite the non-selection of $\log_{10}\beta_1°(298.15\ K)$ and $\varepsilon(FeCl^+, Cl^-) = (0.16 \pm 0.01)$ kg · mol^{-1}.

although Lemire et al. (2013) did not select this value explicitly. All these data for $FeCl^+$ are included in our database as supplemental data.

11.5.1.3.3 $FeCl_2$(aq)

Lemire et al. (2013) reviewed several experimental investigations dealing with the formation of $FeCl_2$(aq) and concluded that the available data clearly indicate that substantially high chloride concentrations and/or elevated temperatures are required for the formation of $FeCl_2$(aq). Therefore, they did not recommend any data.

11.5.1.4 Aqueous iron(III) chloride complexes

According to Lemire et al. (2013) the Fe(III) chloride system is well studied and various aqueous Fe(III) chloride complexes have been claimed to exist:

$Fe^{3+} \cdot 6H_2O \cdot Cl^-$ or $FeCl^{2+}_{(out)}$: Corresponds to an octahedral outer-sphere ion pair with 6 water molecules in the first coordination sphere.

$FeCl^{2+} \cdot 5H_2O$ or $FeCl^{2+}_{(in)}$: Corresponds to an inner-sphere complex with 5 water molecules and 1 chloride anion in the first coordination sphere.

$FeCl_2^+ \cdot 4H_2O$ or $FeCl_2^+$: Corresponds to an inner-sphere complex with 4 water molecules and 2 chloride anions in the first coordination sphere.

$FeCl_3 \cdot 3H_2O$ or $FeCl_3$(aq): Corresponds to an inner-sphere complex with 3 water molecules and 3 chloride anions in the first coordination sphere.

$FeCl_4^- \cdot 2H_2O$ or $FeCl_4^-$: Corresponds to an inner-sphere complex with 2 water molecules and 4 chloride anions in the first coordination sphere.

$FeClOH^+ \cdot 4H_2O$ or $FeClOH^+$: Corresponds to an inner-sphere complex with 4 water molecules, one deprotonated water molecule and 1 chloride anion in the first coordination sphere.

Like Fe(II) chloride complexes, Fe(III) chloride complexes are weak and relatively high chloride concentrations are needed to observe $FeCl^{2+}$, and even higher ones to observe the higher-order complexes $FeCl_2^+$, $FeCl_3$(aq), and $FeCl_4^-$. There are also indications that the stabilities of the higher-order complexes increase with temperature. Lemire et al. (2013) recommended thermodynamic data for $FeCl^{2+}$ (choosing as complex only $FeCl^{2+}_{(in)}$ by noting that outer-sphere interactions are accounted for by the SIT formalism), $FeCl_2^+$, $FeCl_3$(aq), and $FeCl_4^-$.

11.5.1.4.1 Aqueous iron(III) chloride complexes

Pearson et al. (1992) (TDB 05/92) included the following data from Nordstrom et al. (1990) which were retained in TDB 01/01 and TDB 12/07:

$Fe^{3+} + Cl^- \rightleftharpoons FeCl^{2+}$

$\log_{10}\beta_1°(298.15\ K) = 1.48$

$\Delta_r H_m°(298.15\ K) = 23.4\ kJ \cdot mol^{-1}$

$Fe^{3+} + 2\ Cl^- \rightleftharpoons FeCl_2^+$

$\log_{10}\beta_2°(298.15\ K) = 2.13$

$Fe^{3+} + 3\ Cl^- \rightleftharpoons FeCl_3(aq)$

$\log_{10}\beta_3°(298.15\ K) = 1.13$

Nordstrom et al. (1990) selected the data for $FeCl^{2+}$ and $FeCl_2^+$ from the compilation by Smith & Martell (1976) and $\log_{10}\beta_3°(298.15\ K)$ for $FeCl_3(aq)$ from the compilation by Yatsimirskii & Vasil'ev (1960) who obtained it from the spectroscopic study by Rabinovitch & Stockmayer (1942). As discussed below, all these data for Fe(III) chloride complexes are replaced by data from Lemire et al. (2013).

11.5.1.4.2 $FeCl^{2+}_{(in)}$, $FeCl^{2+}_{(out)}$, and $FeClOH^+$

$FeCl^{2+}_{(in)}$ and $FeCl^{2+}_{(out)}$ or $FeCl^{2+}$: The 1:1 Fe(III) chloride complexes, $FeCl^{2+}_{(in)}$ and $FeCl^{2+}_{(out)}$, are rather weak. The existence of distinct inner- and outer-sphere complexes was demonstrated for the first time by the kinetic pressure-jump method (Wendt & Strehlow 1962). Lemire et al. (2013) analysed several studies that determined the stability of the 1:1 complex as a function of ionic strength using mainly spectrophotometry and, in a few cases, potentiometry. They concluded that the formation constants determined in these experiments are most probably those of the inner-sphere complex and that the effect of the outer-sphere complex would be reflected in the ionic strength effects. Lemire et al. (2013) grouped the data according to the background electrolytes used in the experiments and performed three different SIT analyses, one for $HClO_4$-$NaClO_4$ mixtures, one for HCl-$HClO_4$-$NaClO_4$ mixtures, and one for pure $HClO_4$.

The results of the three linear SIT fits were quite consistent, with $\log_{10}\beta_1°(298.15\ K) = (1.51 \pm 0.07)$ for $HClO_4$-$NaClO_4$ mixtures, $\log_{10}\beta_1°(298.15\ K) = (1.53 \pm 0.04)$ for HCl-$HClO_4$-$NaClO_4$ mixtures, and $\log_{10}\beta_1°(298.15\ K) = (1.52 \pm 0.06)$ for $HClO_4$. Based on these results, Lemire et al. (2013) selected

$Fe^{3+} + Cl^- \rightleftharpoons FeCl^{2+}$

$\log_{10}\beta_1°(298.15\ K) = (1.52 \pm 0.10)$

which is included in our database and is in excellent agreement with the value of 1.48 selected by Nordstrom et al. (1990) and included in TDB 01/01, see Section 11.5.1.4.1.

Lemire et al. (2013) derived $\varepsilon(FeCl^{2+}, ClO_4^-)$ from $\Delta\varepsilon = -(0.22 \pm 0.02)$ kg · mol^{-1} obtained from the SIT fit to the measurements in $HClO_4$. From $\varepsilon(FeCl^{2+}, ClO_4^-) = \varepsilon(Fe^{3+}, ClO_4^-) + \varepsilon(Cl^-, H^+) + \Delta\varepsilon$ and $\varepsilon(Cl^-, H^+) = (0.12 \pm 0.01)$ kg · mol^{-1} together with the SIT_1 value $\varepsilon(Fe^{3+}, ClO_4^-) = (0.73 \pm 0.04)$, see Section 11.3.3, then follows

$$\varepsilon(FeCl^{2+}, ClO_4^-) = (0.63 \pm 0.05) \text{ kg} \cdot \text{mol}^{-1}$$

which is also included in TDB 2020. With the SIT_2 value $\varepsilon(Fe^{3+}, ClO_4^-) = ((0.78 \pm 0.05)-(0.41 \pm 0.05) \log_{10} I_m)$ kg · mol^{-1}, see Section 11.3.3, the resulting expression is $\varepsilon(FeCl^{2+}\ ClO_4^-) = ((0.68 \pm 0.05)-(0.41 \pm 0.05) \log_{10} I_m)$ kg · mol^{-1}. As discussed in Section 11.1.1, we do not advocate the use of SIT_2 and thus the SIT_2 value for $\varepsilon(Fe^{3+}, ClO_4^-)$ is not included in our database. Lemire et al. (2013) also derived SIT_1 and SIT_2 values for $\varepsilon(FeCl^{2+}, ClO_4^-)$ from the experimental data in $HClO_4$-$NaClO_4$ and in HCl-$HClO_4$-$NaClO_4$ mixtures, but the results are practically identical to those derived from pure $HClO_4$[37].

Lemire et al. (2013) derived a value for $\varepsilon(FeCl^{2+}, Cl^-)$ from the potentiometric data in aqueous HCl solutions by Tagirov et al. (2000). From their linear SIT fit, Lemire et al. (2013) obtained $\Delta\varepsilon = -(0.237 \pm 0.014)$ kg · mol^{-1}. With $\varepsilon(Cl^-, H^+) = (0.12 \pm 0.01)$ kg · mol^{-1} and $\varepsilon(Fe^{3+}, Cl^-) = (0.76 \pm 0.03)$, see Section 11.3.3, this results in

$$\varepsilon(FeCl^{2+}, Cl^-) = (0.64 \pm 0.06) \text{ kg} \cdot \text{mol}^{-1}$$

which is included in TDB 2020[38]. Note that $\varepsilon(FeCl^{2+}, ClO_4^-)$ and $\varepsilon(FeCl^{2+}, Cl^-)$ are almost identical. This is another example of the similarity between ion interaction coefficients of a ferric species with Cl^- and ClO_4^-, if Fe(III) chloride complexes are considered explicitly (see Section 11.3.3 for the first example).

Lemire et al. (2013) selected

$$\Delta_r H_m°(298.15 \text{ K}) = (22.48 \pm 4.60)^{39} \text{ kJ} \cdot \text{mol}^{-1}$$

as determined by Tagirov et al. (2000) from formation constants measured with potentiometry at temperatures between 20.8 and 90 °C and additional data from another study. This value is also included in TDB 2020 and is in excellent agreement with the value of 23.4 kJ · mol^{-1} selected by Nordstrom et al. (1990) and included in TDB 01/01, see Section 11.5.1.4.1. Note that the selected $\log_{10}\beta_1°(298.15 \text{ K})$ and $\Delta_r H_m°(298.15 \text{ K})$ can be used for a linear (in $1/T$) van't Hoff extrapolation of $\log_{10}\beta_1°$ to temperatures up to about 65 °C (see Fig. 11.5-1), even though Tagirov et al. (2000)

---

[37] $HClO_4$-$NaClO_4$: $\varepsilon(FeCl^{2+}, ClO_4^-, SIT_1) = (0.62 \pm 0.05)$ kg · mol^{-1},
$\varepsilon(FeCl^{2+}, ClO_4^-, SIT_2) = ((0.67 \pm 0.05) - (0.41 \pm 0.05) \log_{10} I_m)$ kg · mol^{-1}
HCl-$HClO_4$-$NaClO_4$: $\varepsilon(FeCl^{2+}, ClO_4^-, SIT_1) = (0.63 \pm 0.05)$ kg · mol^{-1},
$\varepsilon(FeCl^{2+}, ClO_4^-, SIT_2) = ((0.68 \pm 0.05) - (0.41 \pm 0.05) \log_{10} I_m)$ kg · mol^{-1}

[38] Lemire et al. (2013) also derived an expression for $\varepsilon(FeCl^{2+}, Cl^-)$ by using $\varepsilon(Fe^{3+}, Cl^-, SIT_2)$ and obtained $\varepsilon(FeCl^{2+}, Cl^-, SIT_2) = ((0.72 \pm 0.06) - (0.55 \pm 0.05) \log_{10} I_m)$ kg · mol^{-1}. 0.55 in this expression should probably be replaced by 0.59, since Lemire et al. (2013) reported $\varepsilon(Fe^{3+}, Cl^-, SIT_2) = ((0.84 \pm 0.04) - (0.59 \pm 0.05) \log_{10} I_m)$ kg · mol$^-$.

[39] As reported by Lemire et al. (2013) in their Table III-2 (p. 49), the value in the text is (22.5 ± 4.6) kJ · mol^{-1} (p. 269).

used a non-linear fit to describe the experimental data (from which it follows that $\Delta_r H_m°$ is not constant with temperature and that $\Delta_r C_{p,m}°$ is not equal to zero and also varies with temperature):

$$\log_{10}\beta_1°(T) = 0.018\ T + 420.12/T - 5.23$$

This temperature function and the van't Hoff approximation are compared in Fig. 11.5-1.

If the van't Hoff approximation is used (as selected in TDB 2020), it follows that

$$\Delta_r C_{p,m}°(298.15\ \text{K}) \approx 0$$

over the restricted temperature range.

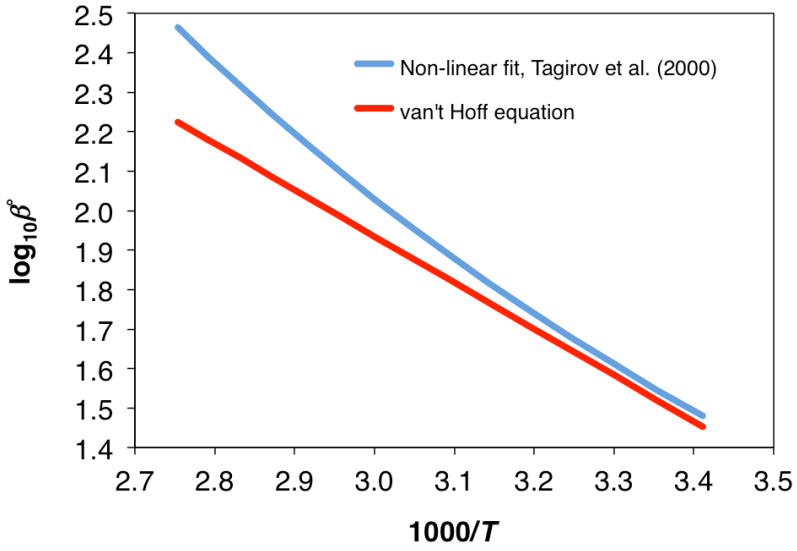

Fig. 11.5-1: Stability constant $\log_{10}\beta_1°$ for $FeCl^{2+}$ as a function of 1/T

Non-linear fit to experimental data by Tagirov et al. (2000) in blue, and linear van't Hoff approximation using $\Delta_r H_m°(298.15\ \text{K})$ and $\log_{10}\beta_1°(298.15\ \text{K})$ selected by Lemire et al. (2013) and included in TDB 2020 in red. Experimental range from 20 °C (1'000/T = 3.41) to 90 °C (1'000/T = 2.75). The non-linear fit to experimental data overlaps with the upper uncertainty boundary of $\log_{10}\beta_1°(298.15\ \text{K}) = (1.52 \pm 0.10)$ selected by Lemire et al. (2013) up to about 65 °C (1'000/T = 2.96).

$FeClOH^+$: Lemire et al. (2013) discussed two experimental studies dealing with the stability of $FeClOH^+$. They did not recommend any data but noted that with the proposed stability constant determined with spectrophotometry, the concentration of $FeClOH^+$ reaches a maximum at pH around 3.5 and rather high chloride concentrations (2 m), but does not contribute to more than 3% of the total* Fe(III) species.

11.5.1.4.3 $FeCl_2^+$

Lemire et al. (2013) considered nine experimental studies devoted to the formation of $FeCl_2^+$. An SIT analysis of data from all nine studies led to erratic fits. Removing the data from three of the studies resulted in an SIT fit that was more satisfactory and Lemire et al. (2013) selected

$$FeCl^{2+} + Cl^- \rightleftharpoons FeCl_2^+$$

$$\log_{10}K_2°(298.15\ K) = (0.7 \pm 0.2)$$

which is also accepted for our database. Since the experiments were performed in mixed $HClO_4/NaClO_4$ media, Lemire et al. (2013) plotted $\log_{10}K_{2m} + 4D - \varepsilon(Cl^-, Na^+)\ m(Na^+) - \varepsilon(Cl^-, H^+)\ m(H^+)$ against $m(ClO_4^-)$ for the SIT fit, with $\varepsilon(Cl^-, Na^+) = (0.03 \pm 0.01)$ kg · mol^{-1} and $\varepsilon(Cl^-, H^+) = (0.12 \pm 0.01)$ kg · mol^{-1}, and obtained from the slope

$$\Delta'\varepsilon = \varepsilon(FeCl_2^+, ClO_4^-) - \varepsilon(FeCl^{2+}, ClO_4^-) = -(0.11 \pm 0.04)\ kg \cdot mol^{-1}$$

With $\varepsilon(FeCl^{2+}, ClO_4^-, SIT_1) = (0.63 \pm 0.05)$ kg · mol^{-1} one gets

$$\varepsilon(FeCl_2^+, ClO_4^-) = (0.52 \pm 0.05)\ kg \cdot mol^{-1}$$

which is also included in our database[40] as well as the estimate (see Section 11.1.1)

$$\varepsilon(FeCl_2^+, Cl^-) \approx \varepsilon(FeCl_2^+, ClO_4^-) = (0.52 \pm 0.05)\ kg \cdot mol^{-1}$$

For inclusion in our database, we reformulated the formation reaction for $FeCl_2^+$ to

$$Fe^{3+} + 2\ Cl^- \rightleftharpoons FeCl_2^+$$

and used $\log_{10}K_2°(298.15\ K)$ with the selected value for $\log_{10}\beta_1°(298.15\ K)$ to obtain

$$\log_{10}\beta_2°(298.15\ K) = (2.2 \pm 0.2)$$

which is in excellent agreement with the value of 2.13 selected by Nordstrom et al. (1990) and included in TDB 01/01, see Section 11.5.1.4.1.

---

[40] Lemire et al. (2013) also derived an expression for $\varepsilon(FeCl_2^+, ClO_4^-)$ by using $\varepsilon(FeCl^{2+}, ClO_4^-, SIT_2)$ and obtained $\varepsilon(FeCl_2^+, ClO_4^-, SIT_2) = ((0.57 \pm 0.05)-(0.41 \pm 0.05)\ \log_{10}I_m)$ kg · mol^{-1}.

11.5.1.4.4 $FeCl_3(aq)$

Experimental data on the formation of $FeCl_3(aq)$ is very limited and spread over various background media. For this reason, Lemire et al. (2013) were not able to apply the SIT formalism and instead averaged the formation constants from three experimental studies, leading to the selected

$$FeCl_2^+ + Cl^- \rightleftharpoons FeCl_3(aq)$$

$$\log_{10}K_3°(298.15\ K) = -(1.2 \pm 0.2)$$

For inclusion in our database, we reformulated this formation reaction to

$$Fe^{3+} + 3\ Cl^- \rightleftharpoons FeCl_3(aq)$$

and used $\log_{10}K_3°(298.15\ K)$ with the selected value for $\log_{10}\beta_2°(298.15\ K)$ to obtain

$$\log_{10}\beta_3°(298.15\ K) = (1.0 \pm 0.3)$$

which is in excellent agreement with the value of 1.13 selected by Nordstrom et al. (1990) and included in TDB 01/01, see Section 11.5.1.4.1. We estimated

$$\varepsilon(FeCl_3(aq), NaCl) = \varepsilon(FeCl_3(aq), NaClO_4) \approx (0.0 \pm 0.1)\ kg \cdot mol^{-1}$$

according to Tab. 1-7 and included these values in TDB 2020.

11.5.1.4.5 $FeCl_4^-$

As in the case of $FeCl_3(aq)$, experimental data on the formation of $FeCl_4^-$ is limited and an SIT analysis could not be carried out by Lemire et al. (2013). Instead, they averaged the results of three experimental studies and selected

$$FeCl_3(aq) + Cl^- \rightleftharpoons FeCl_4^-$$

$$\log_{10}K_4°(298.15\ K) = -(2.0 \pm 0.7)$$

For inclusion in TDB 2020, we reformulated this formation reaction to

$$Fe^{3+} + 4\ Cl^- \rightleftharpoons FeCl_4^-$$

and used $\log_{10}K_4°(298.15\ K)$ with the selected value for $\log_{10}\beta_3°(298.15\ K)$ to obtain

$$\log_{10}\beta_4°(298.15\ K) = -(1.0 \pm 0.8)$$

We estimated

$$\varepsilon(FeCl_4^-, Na^+) \approx -(0.05 \pm 0.10) \text{ kg} \cdot \text{mol}^{-1}$$

according to Tab. 1-7.

11.5.2 Iron halide compounds

11.5.2.1 Iron fluoride compounds

Lemire et al. (2013) reviewed heat capacity, entropy and enthalpy of formation measurements for FeF_2(cr) and selected a heat capacity function $C_{p,m}°$(250-675 K), and values for $C_{p,m}°$(298.15 K), $S_m°$(298.15 K), $\Delta_f H_m°$(298.15 K), and $\Delta_f G_m°$(298.15 K), the latter of which was calculated using $\Delta_f G_m° = \Delta_f H_m° - \sum T\, S_m°$. For FeF_3(cr), they reviewed heat capacity and enthalpy of formation measurements and selected values for $C_{p,m}°$(298.15 K) and $\Delta_f H_m°$(298.15 K).

Both FeF_2(cr) and FeF_3(cr) do not appear as minerals in nature and are "slightly soluble" in water. The solubility product $K_{s,0}° = 2.36 \cdot 10^{-6}$ ($\log_{10} K_{s,0}° = -5.63$) reported by Haynes (2017) for FeF_2(cr) results in a solubility of $1.6 \cdot 10^{-2}$ mol FeF_2 per 1 kg of pure water. Combining $\Delta_f G_m°(FeF_2,cr, 298.15\text{ K}) = -669.499$ kJ · mol^{-1} selected by Lemire et al. (2013) with $\Delta_f G_m°(Fe^{2+}, 298.15\text{ K}) = -90.719$ kJ · mol^{-1} and $\Delta_f G_m°(F^-, 298.15\text{ K}) = -281.523$ kJ · mol^{-1} leads to $\Delta_r G_m°(298.15\text{ K}) = 15.73$ kJ · mol^{-1} or $\log_{10} K_{s,0}° = -2.76$. With this value, the solubility of FeF_2(cr) in pure water amounts to $4.1 \cdot 10^{-1}$ mol FeF_2 per 1 kg of pure water. According to Haynes (2017), the solubility of FeF_3(cr) is 59.2 g or 0.52 mol per 1 kg of pure water (with a gram formula weight 112.84). In any case, the solubilities of FeF_2(cr) and FeF_3(cr) are high enough, that the chances of their precipitation in natural ground- or porewater environments are nearly nil, since the presence of Ca in solution would lead to a massive oversaturation of fluorite, CaF_2(cr). For this reason, FeF_2(cr) and FeF_3(cr) are not included in our database.

In addition to FeF_2(cr) and FeF_3(cr), Lemire et al. (2013) also considered iron fluoride hydrates. They mention a tetrahydrate and an octahydrate of FeF_2 for which no thermodynamic data are known and two polymorphs of FeF_3-trihydrate for which they did not select any thermodynamic data.

11.5.2.2 Iron chloride, oxychloride, hydroxychloride and perchlorate compounds

Lemire et al. (2013) reviewed and selected thermodynamic data for $FeCl_2$(cr), $FeCl_2 \cdot H_2O$(cr), $FeCl_2 \cdot 2H_2O$(cr), and $FeCl_2 \cdot 4H_2O$(cr), as well as for $FeCl_3$(cr), $FeCl_3 \cdot 2H_2O$(cr), $FeCl_3 \cdot 2.5H_2O$(cr), $FeCl_3 \cdot 3.5H_2O$(cr), and $FeCl_3 \cdot 6H_2O$(cr). These solids are all soluble in water and hygroscopic or even deliquescent and are not relevant for low salinity ground- or porewater systems. They are therefore not included in our database.

Lemire et al. (2013) also discussed and selected thermodynamic data for FeOCl(cr). This solid is not a mineral and decomposes at room temperature in the presence of moist air into $Fe(OH)_3$(cr) and Fe_2Cl_6(cr), according to Stirnemann (1925), or into $Fe_3O_4Cl{\cdot}nH_2O$(cr), according to Schäfer (1951). In contact with water, FeOCl(cr) decomposes pseudomorphically into FeOOH(cr) (Goldsztaub 1935). For these reasons, it is very improbable that FeOCl(cr) plays any role in natural ground- or porewater systems and is not included in our database.

Hydrated perchlorate salts of Fe(II) and Fe(III) are very soluble, > 2 mol · L^{-1} (Lemire et al. 2013). Lemire et al. (2013) discussed solubility experiments on $Fe(ClO_4)_2{\cdot}nH_2O$(cr), with n = (2, 4, 5, 6), and on $Fe(ClO_4)_3{\cdot}nH_2O$(cr), with n = (6, 9, 10), but selected no thermodynamic data.

11.5.2.2.1 "Chloride green rust one"

Green rusts are intermediate Fe(II)-Fe(III) compounds consisting of brucite-like $Fe(OH)_2$ layers where the charge surplus created by the partial oxidation of ferrous to ferric iron is compensated by anions inserted (together with water molecules) into the interlayer. Two structural types of green rust can be distinguished: Green rust one (GR1) contains spherical or planar anions in the interlayer, such as F^-, Cl^-, CO_3^{2-}, CH_3COOH^- (acetate) or $C_2O_4^{2-}$ (oxalate), while green rust two (GR2) is intercalated with tetrahedral anions, such as SO_4^{2-} and SeO_4^{2-} (Mills et al. 2012). Chloride GR1 is found in chloride-containing aqueous environments as an intermediate corrosion product of steels before the final formation of end products such as goethite, lepidocrocite or magnetite (Refait & Génin 1993). Refait & Génin (1993) prepared chloride GR1 by oxidation of ferrous hydroxide precipitates obtained by mixing aqueous solutions of NaOH and $FeCl_2$. Precipitates were characterized by X-ray diffraction and Mössbauer spectroscopy was used to determine the Fe^{2+}/Fe^{3+} ratio. The chemical composition of chloride GR1 was found to be $(Fe^{III})(Fe^{II})_3(OH)_8Cl{\cdot}nH_2O$(s). The electrode potentials measured by Refait & Génin (1993) during the oxidation reaction

$$4\ Fe(OH)_2(s) + Cl^- + H^+ + n\ H_2O(l) \rightleftharpoons (Fe^{III})(Fe^{II})_3(OH)_8Cl{\cdot}nH_2O(s) + ½\ H_2g$$

were corrected by Lemire et al. (2013) to zero ionic strength using SIT, resulting in an average value of E_0 = -(0.552 ± 0.012) V vs. the standard hydrogen electrode and leading to $\Delta_r G_m°$(298.15 K) = -(53.2 ± 2.0) kJ · mol^{-1}, with an increased uncertainty. Lemire et al. (2013) did not select this value (without explanation), but we accept the corresponding

$$log_{10}{}^*K°(298.15\ K) = (9.32 \pm 0.35)$$

as supplemental datum (as there remain uncertainties with respect to the grain size and crystallinity of the precipitates and the number of structural waters in the formula unit). For inclusion in TDB 2020 we used $log_{10}{}^*K_{s,0}°(298.15\ K) = (12.26 \pm 0.88)$ for $Fe(OH)_2(s) + 2H^+ \rightleftharpoons Fe^{2+} + 2\ H_2O(l)$ (see Section 11.4.2.2) to obtain

$$(Fe^{III})(Fe^{II})_3(OH)_8Cl{\cdot}nH_2O(s) + 7\ H^+ + ½\ H_2g \rightleftharpoons 4\ Fe^{2+} + Cl^- + (n+8)\ H_2O(l)$$

$$log_{10}{}^*K_{s,0}°(298.15\ K) = (39.7 \pm 3.5)$$

Other green rusts are "sulphate green rust two" (see Section 11.6.2.3.6), and "carbonate green rust one" (see Section 11.7.1.3.3). "White rust" was discussed in Section 11.4.2.2.

11.5.2.2.2 β-$Fe_2Cl(OH)_3$(cr), Fe-hibbingite

Nemer et al. (2011) investigated the solubility of β-$Fe_2Cl(OH)_3$(cr), the Fe-endmember of hibbingite, in NaCl and Na_2SO_4 brines. Based on this study, Lemire et al. (2020) selected

$$Fe_2Cl(OH)_3(cr) + 3\ H^+ \rightleftharpoons 2\ Fe^{2+} + Cl^- + 3\ H_2O(l)$$

$$\log_{10}{}^*K_{s,0}^\circ(298.15\ K) = (17.2 \pm 0.2)$$

β-$Fe_2Cl(OH)_3$(cr) is stable in the presence of anoxic chloride-rich brines (Nemer et al. 2011) and is therefore probably not relevant for the main application range of TDB 2020. However, β-$Fe_2Cl(OH)_3$(cr) can be expected to be a likely corrosion product of low-carbon steel interacting with chloride-rich anoxic brines (Nemer et al. 2011). For this reason, the solubility product of β-$Fe_2Cl(OH)_3$(cr) is included in TDB 2020.

11.5.2.3 Iron bromide compounds

Lemire et al. (2013) selected thermodynamic data for $FeBr_2$(cr) and $FeBr_3$(cr). Since both solids are soluble in water and hygroscopic (Perry 2011) and do not occur in nature as minerals, they are not relevant for low salinity ground- or porewater systems and they are not included in our database.

Lemire et al. (2013) also mentioned a solubility study concerning $FeBr_2 \cdot nH_2O$(cr), with n = (2, 4, 6, 9), but did not select any thermodynamic data.

11.5.2.4 Iron iodide compounds

The thermodynamic data selected by Lemire et al. (2013) for FeI_2(cr) are not included in our database, since FeI_2(cr) is soluble in water and very hygroscopic (Perry 2011) and does not occur in nature as a mineral.

11.6 Group 16 and 15 compounds and complexes

11.6.1 Iron sulphides

11.6.1.1 Aqueous iron(II) sulphide complexes

Lemire et al. (2013) discussed various aqueous iron(II) sulphide complexes, some of which were derived from the interpretation of solubility data of FeS(mackinawite), which forms as a black precipitate when Fe(II)-solutions are mixed at room temperature with sulphide solutions. The precipitate consists of nanoparticulate mackinawite. As seen in Fig. 11.6-1 to Fig. 11.6-4, the solubility of mackinawite decreases with pH under acidic conditions and becomes constant under more basic conditions (pH > 6). The slope of the solubility curve under acidic conditions is well constrained and very close to -2, which is compatible with the dissolution reaction

$$FeS(mackinawite) + 2\ H^+ \rightleftharpoons Fe^{2+} + H_2 \quad S(aq)$$

Lemire et al. (2013) accepted 5 equilibrium constants for this reaction from 5 different experimental studies and determined a weighted arithmetic mean of 3.79 ± 0.16. They assigned a larger uncertainty to this mean and selected

$$\log_{10}{}^{*}K_{s,0}°(298.15\ K) = (3.8 \pm 0.4)$$

which is also accepted for our database.

The solubility in the plateau region at higher pH is less well constrained. The experimental data by Mehra (1968), see Fig. 11.6-3, and Rickard (2006), see Fig. 11.6-1, indicate that the solubility in the plateau region is independent of the sulphide concentration. For the plateau region, Rickard (2006) suggested the pH-independent reaction

$$FeS(mackinawite) \rightleftharpoons FeS(cluster)$$

where FeS(cluster) is a monomeric representation of the aqueous cluster complex Fe_xS_x, whose presence was inferred by Rickard (2006) from voltammetry.

In contrast to the findings by Rickard (2006), the experimental data by Davison et al. (1999) suggest a dependence of the solubility from the partial pressure of H_2Sg, see Fig. 11.6-2, which they explained with the existence of the neutral complex $Fe(HS)_2(aq)$, leading to the pH-independent mackinawite solubility reaction $FeS(mackinawite) + H_2S(aq) \rightleftharpoons Fe(HS)_2(aq)$.

Lemire et al. (2013) discussed data from the literature for various Fe(II) sulphide complexes: $FeS(aq)$, $FeHS^+$, $Fe(HS)_2(aq)$, $FeSHS^-$, $Fe_2(HS)^{3+}$, and $Fe_3(HS)^{5+}$. They concluded that no good evidence was given for the existence of any of these complexes.

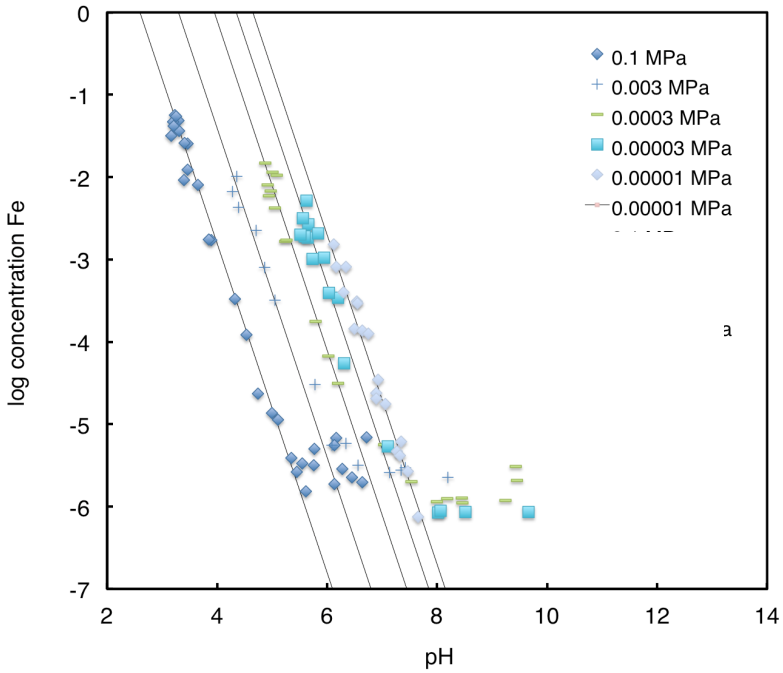

Fig. 11.6-1: Solubility of mackinawite as a function of pH and several partial pressures of H_2Sg

With indicative slopes of -2 (fitted to the data by eye), corresponding to the reaction FeS(mackinawite) + 2 H^+ ⇌ Fe^{2+} + H_2 S(aq) in the acid region. Experimental data by Rickard (2006).

With respect to the discrepant solubility behaviour at higher pH reported by Davison et al. (1999) and Rickard (2006), Lemire et al. (2013) made the following comment: "[T]wo seemingly very reliable papers report quite different solubility behaviour at higher pH values, and the reviewer cannot discern a reason for the difference. The difference in the crystallinity or in the surface condition, formation of a very small amount of surface FeS solid other than mackinawite, or differences in the rates of precipitation and dissolution at higher pH values may affect the solubility. The speciation of the soluble iron sulphide can be discussed only after reproducible and reliable solubility data in this pH region are obtained. So far, this review cannot recommend any speciation or formation constant in this pH region".

It is obvious from Fig. 11.6-1 to Fig. 11.6-4, that neglecting iron-sulphide complexes in geochemical models invariably leads to absurdly small Fe-solubilities at pH > 6. For practical calculation purposes, therefore, a pragmatic approach is required. Based on Fig. 11.6-4, which is a compilation of all experimental data by Mehra (1968), Davison et al. (1999), and Rickard (2006), we decided to express the solubility of mackinawite in the pH-independent region according to the reaction

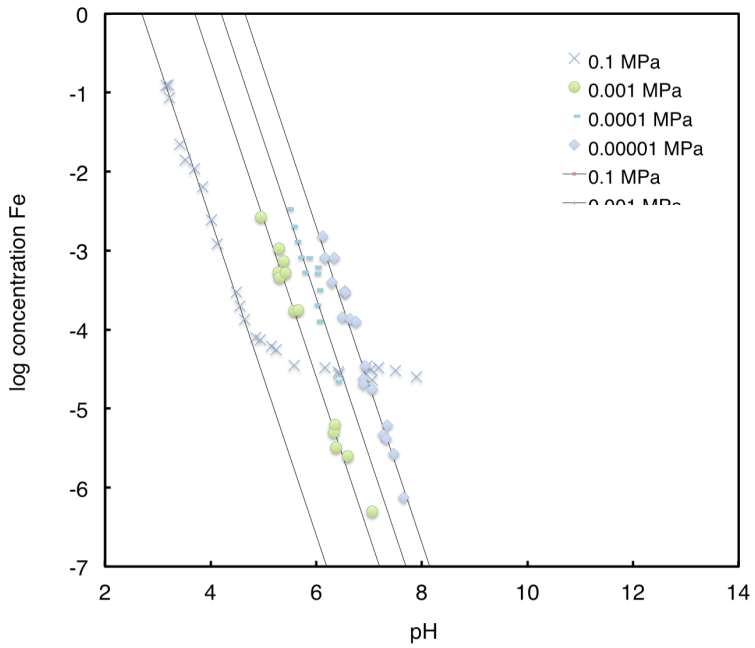

Fig. 11.6-2: Solubility of mackinawite as a function of pH and several partial pressures of H_2Sg

With indicative slopes of -2 (fitted to the data by eye), corresponding to the reaction FeS(mackinawite) + 2 H^+ ⇌ Fe^{2+} + H_2 S(aq) in the acid region. Experimental data by Davison et al. (1999).

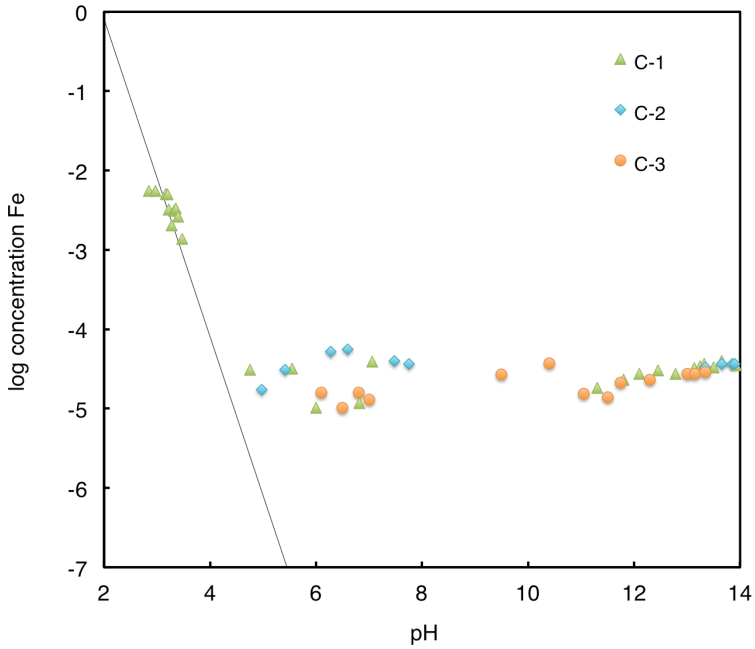

Fig. 11.6-3: Solubility of mackinawite as a function of pH and several total sulphide concentrations

With an indicative slope of -2 (fitted to the data by eye), corresponding to the reaction FeS(mackinawite) + 2 H^+ ⇌ Fe^{2+} + H_2 S(aq) in the acid region. Experimental data by Mehra (1968). C-1: pS_{tot} between 1.31 and 1.61, C-2: pS_{tot} between 1.03 and 1.18, C-3: pS_{tot} between 1.62 and 1.76.

$$FeS(mackinawite) \rightleftharpoons Fe\ \ S(aq)$$

with the solubility constant

$$log_{10}K_{s,1}°(298.15\ K) = -(5 \pm 1)$$

This value with its uncertainty covers the largest part of the experimental data points in the pH-independent region (all high-solubility data points are included, see Fig. 11.6-4) and belongs in our database to the supplemental data. We justify the choice of FeS(aq) as relevant Fe-sulphide species by noting that the explicit purpose of the experimental study by Rickard (2006) was to investigate the pH-independent region and to decide whether the solubility was dependent on the sulphide concentration, with $Fe(HS)_2(aq)$ as dominant species, or not. The experimental data by Rickard (2006) strongly suggest that the solubility is indeed independent of the sulphide concentration and the choice of an FeS-cluster, represented as FeS(aq), is the simplest one possible.

The experimental data by Mehra (1968), not mentioned by Lemire et al. (2013), at pH > 5 support the assumption that the solubility of mackinawite is independent of pH and sulphide concentration. In addition, his data show that the plateau of constant Fe-concentration extends almost up to pH = 14, a strong indication that no other Fe-sulphide species become dominant under very basic conditions.

For inclusion in our database, we combined FeS(mackinawite) + 2 H^+ ⇌ Fe^{2+} + H_2S(aq), $\log_{10}{}^*K_{s,0}°$(298.15 K) = (3.8 ± 0.4), with $FeS(mackinawite) \rightleftharpoons FeS(aq)$, $log_{10}K_{s,1}°(298.15\ K) = -(5 \pm 1)$, leading to

$$Fe^{2+} + H_2S(aq) \rightleftharpoons FeS(aq) + 2\ H^+$$

$$log_{10}{}^*K°(298.15\ K) = -(8.8 \pm 1.1)$$

and estimated

$$\varepsilon(FeS(aq), NaCl) = \varepsilon(FeS(aq), NaClO_4) \approx (0.0 \pm 0.1)\ kg \cdot mol^{-1}$$

estimated according to Tab. 1-7.

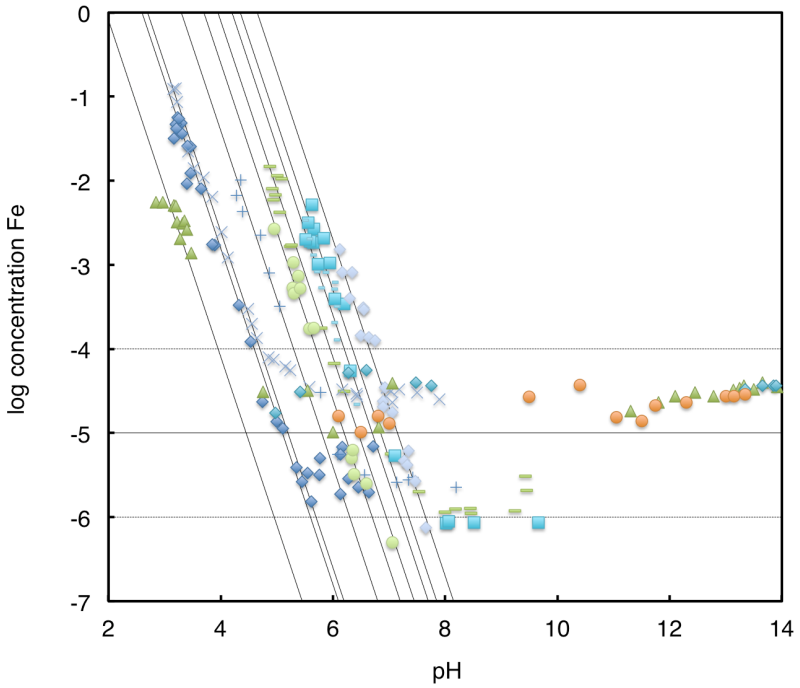

Fig. 11.6-4: Solubility of mackinawite as a function of pH and several partial pressures of H_2Sg or total sulphide concentrations

With indicative slopes of -2 (fitted to the data by eye), corresponding to the reaction FeS(mackinawite) + 2 H^+ ⇌ Fe^{2+} + H_2 S(aq). The solid horizontal line corresponds to the reaction FeS(mackinawite) ⇌ FeS(aq), with $\log_{10}K_{s,1}°$(298.15 K) = -5. The dotted horizontal lines represent the uncertainty ± 1. Combined experimental data by Mehra (1968), Davison et al. (1999), and Rickard (2006) from Figs. 11.6.3, 11.6.2, and 11.6.1, respectively.

11.6.1.2 Iron sulphide solids

TDB 12/07 contains solubility products for FeS_2(pyrite) and FeS(troilite). Except mackinawite (discussed in the preceding section) Lemire et al. (2013) did not consider any iron sulphide solids while Lemire et al. (2020) reviewed the thermodynamic properties of minerals of the pyrrhotite group, and selected data for troilite (stoichiometric or near-stoichiometric, hexagonal FeS), 5C pyrrhotite (nominally Fe_9S_{10} or $Fe_{9/10}S$), 6C pyrrhotite (nominally $Fe_{11}S_{12}$ or $Fe_{11/12}S$), and 4C pyrrhotite (compositions near $Fe_{0.875}S$, nominally Fe_7S_8 of $Fe_{7/8}S$). In addition, Lemire et al. (2020) also selected data for pyrite (cubic FeS_2), greigite (cubic Fe_3S_4), and marcasite (orthorhombic FeS_2).

11.6.1.2.1 Data in TDB 05/92, TDB 01/01 and TDB 12/07

Pyrite: The low solubility of FeS_2(pyrite) makes the direct measurement of the solubility constant rather difficult. In a review on the solubility of iron sulphides in synthetic and natural waters at ambient temperature Davison (1991) rejected the solubility measurements on pyrite by Olshanskii & Ivanenko (1958) and Tewari et al. (1978). According to Davison (1991), the data presented by Olshanskii & Ivanenko (1958) are suspect because there was no systematic dependence of aqueous iron on pH and it is doubtful whether the measurements were made at equilibrium. Similarly, the aqueous iron concentrations measured by Tewari et al. (1978) did not vary with pH

and were so close to the background iron concentration that there appeared to be no discernible interaction with pyrite. Therefore, Davison (1991) concluded that the solubility product of pyrite has to be calculated from free energies of formation. Hummel et al. (2002) calculated the Gibbs free energy of reaction for

$$FeS_2(\text{pyrite}) + 2\ H^+ + 2\ e^- \rightleftharpoons Fe^{2+} + 2\ HS^-$$

from $\Delta_f G_m°$(pyrite, 298.15 K) = -160.1 kJ · mol^{-1} (Robie & Hemingway 1995), $\Delta_f G_m°(Fe^{2+}$, 298.15 K) = -78.90 kJ · mol^{-1} (Pearson et al. 1992, see Section 3.1), and $\Delta_f G_m°(HS^-$, 298.15 K) = 12.243 kJ · mol^{-1} (see Section 5.19 in Hummel et al. 2002), resulting in $\Delta_r G_m°$(298.15 K) = 105.7 kJ · mol^{-1} which corresponds to

$$\log_{10}{}^*K_{s,0}°(298.15\ \text{K}) = -18.5$$

In the absence of reliable solubility data, Hummel et al. (2002) included this value in TDB 01/01 (retained in TDB 12/07). Pyrite was not included in TDB 05/92.

Troilite: FeS(troilite) is the polymorph of stoichiometric FeS(cr) stable below 140 °C. A common constituent of meteorites, troilite is only occasionally found in terrestrial environments, usually together with low-temperature hexagonal pyrrhotite, $Fe_{1-x}S$(cr) (Craig & Scott 1974). All of the solubility data for troilite reviewed by Davison (1991) were approached from undersaturation. The data by Tewari & Campbell (1976) and Tewari et al. (1978) for two different samples of natural troilite produce a good straight line in a plot of $\log_{10}[Fe^{2+}]$ versus pH. Using these data, Davison (1991) calculated

$$\log_{10}{}^*K_{s,0}°(298.15\ \text{K}) = -(5.31 \pm 0.20)$$

for

$$FeS(\text{troilite}) + H^+ \rightleftharpoons Fe^{2+} + HS^-$$

Hummel et al. (2002) selected this value for TDB 01/01 (retained in TDB 12/07) but warned that troilite (just like pyrrhotite) may not be the relevant iron sulphide in low-temperature aquatic environments. Troilite was not included in TDB 05/92.

11.6.1.2.2 Mackinawite (FeS)

Mackinawite: As discussed in Section 11.6.1.1, Lemire et al. (2013) selected

$$\log_{10}{}^*K_{s,0}°(298.15\ \text{K}) = (3.8 \pm 0.4)$$

for the reaction

$$FeS(\text{mackinawite}) + 2\ H^+ \rightleftharpoons Fe^{2+} + H_2\quad S(aq)$$

which is included in TDB 2020.

11.6.1.2.3 Pyrrhotite group

According to Lemire et al. (2020) and references therein, five phases in the pyrrhotite group appear to be stable near ambient temperature, $Fe_{1.000}S$ (2C, troilite), $Fe_{11/12}S$ (6C pyrrhotite), $Fe_{10/11}S$ (11C pyrrhotite), $Fe_{9/10}S$ (5C pyrrhotite), and $Fe_{7/8}S$ (4C pyrrhotite). Since Lemire et al. (2020) derived their selected data ($\Delta_f H_m°$, $S_m°$, and $C_{p,m}°$) from calorimetric measurements and calculated $\Delta_f G_m°$ from $\Delta_f H_m°$ and $S_m°$, reaction properties had to be calculated from these. In the case of the non-stoichiometric pyrrhotites, there are several possibilities for expressing solubility reactions, depending on the way how oxidation numbers are assigned. Thus, the solubility of a general non-stoichiometric pyrrhotite with the composition $Fe_{1-x}S$ can be written, e.g., as

$$Fe_{1-x}S(cr) + 2(1-x)\ H^+ \rightleftharpoons (1-x)\ Fe^{2+} + (1-x)\ H_2S(aq) + x\ S(cr)$$

where S in pyrrhotite is assumed to be in different oxidation states, -II and 0, such that the pyrrhotite formula is $Fe^{II}_{1-x}S^{-II}_{1-x}S^{0}_{x}(cr)$ or as

$$Fe_{1-x}S(cr) + 2\ H^+ \rightleftharpoons (1-3x)\ Fe^{2+} + (2x)\ Fe^{3+} + H_2S(aq)$$

where Fe in pyrrhotite is assumed to be in different oxidation states, II and III, such that the pyrrhotite formula is $Fe^{II}_{1-3x}Fe^{III}_{2x}S^{-II}(cr)$. From a thermodynamic point of view, both types of reaction are equivalent.

Troilite (stoichiometric or near-stoichiometric, hexagonal $Fe_{1.000}S$): According to Lemire et al. (2020) and references therein, troilite is a rare mineral, which is limited to strongly reducing conditions. It is often associated with meteorites and can also be found on the lunar surface (see also Section 11.6.1.2.1).

Based on calorimetric data, Lemire et al. (2020) selected for $Fe_{1.000}S$(troilite)

$$C_{p,m}°(\text{troilite, cr, 298.15 K}) = (50.61 \pm 0.17)\ J \cdot K^{-1} \cdot mol^{-1}$$

$$S_m°(\text{troilite, cr, 298.15 K}) = (60.31 \pm 0.22)\ J \cdot K^{-1} \cdot mol^{-1}$$

$$\Delta_f H_m°(\text{troilite, cr, 298.15 K}) = -(100.91 \pm 2.00)\ kJ \cdot mol^{-1}$$

$$\Delta_f G_m°(\text{troilite, cr, 298.15 K}) = -(101.259 \pm 2.002)\ kJ \cdot mol^{-1}$$

The solubility product $\log_{10}{}^{*}K_{s,0}°(298.15\ K)$ for

$$FeS(cr) + 2\ H^+ \rightleftharpoons Fe^{2+} + H_2S(aq)$$

can be calculated from $\Delta_f G_m°$(troilite, cr, 298.15 K), and the selected $\Delta_f G_m°(Fe^{2+}$, 298.15 K) = -(90.72 ± 0.64) kJ · mol^{-1} and $\Delta_f G_m°(H_2S$, aq, 298.15 K) = -(27.648 ± 2.115) kJ · mol^{-1}, resulting in $\Delta_r G_m°$(298.15 K) = -(17.109 ± 2.98) kJ · mol^{-1} or

$$\log_{10}{}^{*}K_{s,0}°(298.15\ K) = (3.00 \pm 0.52)$$

and $\Delta_r H_m°$(298.15 K) from $\Delta_f H_m°$(troilite, cr, 298.15 K), and the selected $\Delta_f H_m°(Fe^{2+}$, 298.15 K) = -(90.29 ± 0.52) kJ · mol^{-1} and $\Delta_f H_m°(H_2S$, aq, 298.15 K) = -(38.6 ± 1.5) kJ · mol^{-1}, resulting in

$$\Delta_r H_m°(298.15\ K) = -(27.98 \pm 2.55)\ kJ \cdot mol^{-1}$$

These values are included in TDB 2020.

Note that the calculated solubility of troilite is a bit lower than the solubility of nanoparticulate mackinawite (see Section 11.6.1.1) which makes sense, considering that troilite is the stable phase below 140 °C.

5C pyrrhotite (nominally Fe_9S_{10} or $Fe_{9/10}S$): For 5C pyrrhotite Lemire et al. (2020) considered calorimetric data and selected

$$C_{p,m}°(\text{5C pyrrhotite, cr, 298.15 K}) = (51.14 \pm 0.30)\ J \cdot K^{-1} \cdot mol^{-1}$$

$$S_m°(\text{5C pyrrhotite, cr, 298.15 K}) = (63.15 \pm 0.25)\ J \cdot K^{-1} \cdot mol^{-1}$$

$$\Delta_f H_m°(\text{5C pyrrhotite, cr, 298.15 K}) = -(95.89 \pm 2.23)\ kJ \cdot mol^{-1}$$

$$\Delta_f G_m°(\text{5C pyrrhotite, cr, 298.15 K}) = -(97.893 \pm 2.232)\ kJ \cdot mol^{-1}$$

The solubility product $\log_{10}{}^{*}K_{s,0}°$(298.15 K) for the reaction

$$Fe_{0.9}S(cr) + 2\ H^+ \rightleftharpoons 0.7\ Fe^{2+} + 0.2\ Fe^{3+} + H_2S(aq)$$

can be calculated from $\Delta_f G_m°$(5C pyrrhotite, cr, 298.15 K), and the selected $\Delta_f G_m°(Fe^{2+}$, 298.15 K) = -(90.72 ± 0.64) kJ · mol^{-1}, $\Delta_f G_m°(Fe^{3+}$, 298.15 K) = -(16.23 ± 0.65) kJ · mol^{-1}, and $\Delta_f G_m°(H_2S$, aq, 298.15 K) = -(27.648 ± 2.115) kJ · mol^{-1}, resulting in $\Delta_r G_m°$(298.15 K) = (3.495 ± 3.110) kJ · mol^{-1} or

$$\log_{10}{}^{*}K_{s,0}°(298.15\ K) = -(0.61 \pm 0.54)$$

and $\Delta_r H_m°$(298.15 K) from $\Delta_f H_m°$(5C pyrrhotite, cr, 298.15 K), and the selected $\Delta_f H_m°(Fe^{2+}$, 298.15 K) = -(90.29 ± 0.52) kJ · mol^{-1}, $\Delta_f H_m°(Fe^{3+}$, 298.15 K) = -(50.06 ± 0.97) kJ · mol^{-1}, and $\Delta_f H_m°(H_2S$, aq, 298.15 K) = -(38.6 ± 1.5) kJ · mol^{-1}, resulting in

$$\Delta_r H_m°(298.15\ K) = -(15.93 \pm 2.72)\ kJ \cdot mol^{-1}$$

These values are included in TDB 2020.

6C pyrrhotite (nominally $Fe_{11}S_{12}$ or $Fe_{11/12}S$): Lemire et al. (2020) selected only a value for $\Delta_f H_m°$(298.15 K). Since this is not sufficient for equilibrium calculations, no data for 6C pyrrhotite are included in TDB 2020.

4C pyrrhotite (compositions near $Fe_{0.875}S$, nominally Fe_7S_8 of $Fe_{7/8}S$): Lemire et al. (2020) considered calorimetric data for 4C pyrrhotite and selected

$C_{p,m}°$(4C pyrrhotite, cr, 298.15 K) = (49.88 ± 0.35) J · K^{-1} · mol^{-1}

$S_m°$(4C pyrrhotite, cr, 298.15 K) = (60.70 ± 0.34) J · K^{-1} · mol^{-1}

$\Delta_f H_m°$(4C pyrrhotite, cr, 298.15 K) = -(95.53 ± 2.00) kJ · mol^{-1}

$\Delta_f G_m°$(4C pyrrhotite, cr, 298.15 K) = -(97.005 ± 2.003) kJ · mol^{-1}

The solubility product $\log_{10}{}^{*}K_{s,0}°$(298.15 K) for the reaction

$$Fe_{0.875}S(cr) + 2\ H^+ \rightleftharpoons 0.625\ Fe^{2+} + 0.250\ Fe^{3+} + H_2S(aq)$$

can be calculated from $\Delta_f G_m°$(4C pyrrhotite, cr, 298.15 K), and the selected $\Delta_f G_m°(Fe^{2+}$, 298.15 K) = -(90.72 ± 0.64) kJ · mol^{-1}, $\Delta_f G_m°(Fe^{3+}$, 298.15 K) = -(16.23 ± 0.65) kJ · mol^{-1}, and $\Delta_f G_m°(H_2S$, aq, 298.15 K) = -(27.648 ± 2.115) kJ · mol^{-1}, resulting in $\Delta_r G_m°$(298.15 K) = (8.60 ± 2.94) kJ · mol^{-1} or

$\log_{10}{}^{*}K_{s,0}°$(298.15 K) = -(1.51 ± 0.52)

and $\Delta_r H_m°$(298.15 K) from $\Delta_f H_m°$(4C pyrrhotite, cr, 298.15 K), and the selected $\Delta_f H_m°(Fe^{2+}$, 298.15 K) = -(90.29 ± 0.52) kJ · mol^{-1}, $\Delta_f H_m°(Fe^{3+}$, 298.15 K) = -(50.06 ± 0.97) kJ · mol^{-1}, and $\Delta_f H_m°(H_2S$, aq, 298.15 K) = -(38.6 ± 1.5) kJ · mol^{-1}, resulting in

$\Delta_r H_m°$(298.15 K) = -(12.02 ± 2.53) kJ · mol^{-1}

These values are included in TDB 2020.

11.6.1.2.4 Pyrite (cubic FeS_2)

Lemire et al. (2020) reviewed calorimetric data for pyrite and selected

$C_{p,m}°$(pyrite, cr, 298.15 K) = (62.27 ± 0.20) J · K^{-1} · mol^{-1}

$S_m°$(pyrite, cr, 298.15 K) = (52.92 ± 0.14) J · K^{-1} · mol^{-1}

$\Delta_f H_m°$(pyrite, cr, 298.15 K) = -(173.63 ± 2.36) kJ · mol^{-1}

$\Delta_f G_m°$(pyrite, cr, 298.15 K) = -(162.219 ± 2.361) kJ · mol^{-1}

The solubility product $\log_{10}{}^{*}K_{s,0}°$(298.15 K) for the reaction

$$FeS_2(\text{pyrite}) + 4\ H^+ + 2\ e^- \rightleftharpoons Fe^{2+} + 2\ H_2S(aq)$$

can be calculated from $\Delta_f G_m°$(pyrite, cr, 298.15 K), and the selected $\Delta_f G_m°(Fe^{2+}$, 298.15 K) = -(90.72 ± 0.64) kJ · mol^{-1} and $\Delta_f G_m°(H_2S$, aq, 298.15 K) = -(27.648 ± 2.115) kJ · mol^{-1}, resulting in $\Delta_r G_m°$(298.15 K) = (16.203 ± 4.886) kJ · mol^{-1} or

$$\log_{10}{}^{*}K_{s,0}°(298.15\ K) = = -(2.84 \pm 0.86)$$

and $\Delta_r H_m°$(298.15 K) from $\Delta_f H_m°$(pyrite, cr, 298.15 K), and the selected $\Delta_f H_m°(Fe^{2+}$, 298.15 K) = -(90.29 ± 0.52) kJ · mol^{-1} and $\Delta_f H_m°(H_2S$, aq, 298.15 K) = -(38.6 ± 1.5) kJ · mol^{-1}, resulting in

$$\Delta_r H_m°(298.15\ K) = (6.14 \pm 3.85)\ kJ \cdot mol^{-1}$$

These values are included in TDB 2020.

11.6.1.2.5 Marcasite (orthorhombic FeS_2)

Based on calorimetric data for marcasite, Lemire et al. (2020) selected

$$C_{p,m}°(\text{marcasite, cr, 298.15 K}) = (62.66 \pm 0.40)\ J \cdot K^{-1} \cdot mol^{-1}$$

$$S_m°(\text{marcasite, cr, 298.15 K}) = (53.92 \pm 0.41)\ J \cdot K^{-1} \cdot mol^{-1}$$

$$\Delta_f H_m°(\text{marcasite, cr, 298.15 K}) = -(169.43 \pm 2.38^{41})\ kJ \cdot mol^{-1}$$

$$\Delta_f G_m°(\text{marcasite, cr, 298.15 K}) = -(158.317 \pm 2.442)\ kJ \cdot mol^{-1}$$

The solubility product $\log_{10}{}^{*}K_{s,0}°$(298.15 K) for the reaction

$$FeS_2(\text{marcasite}) + 4\ H^+ + 2\ e^- \rightleftharpoons Fe^{2+} + 2\ H_2S(aq)$$

can be calculated from $\Delta_f G_m°$(marcasite, cr, 298.15 K), and the selected $\Delta_f G_m°(Fe^{2+}$, 298.15 K) = -(90.72 ± 0.64) kJ · mol^{-1} and $\Delta_f G_m°(H_2S$, aq, 298.15 K) = -(27.648 ± 2.115) kJ · mol^{-1}, resulting in $\Delta_r G_m°$(298.15 K) = (12.30 ± 4.93) kJ · mol^{-1} or

$$\log_{10}{}^{*}K_{s,0}°(298.15\ K) = -(2.16 \pm 0.86)$$

---

41 An uncertainty of ± 2.438 kJ · mol^{-1} is reported by Lemire et al. (2020) in their Table III-1, however, on p. 183 they reported a value of ± 2.38 kJ · mol^{-1}. From the discussion on p. 183 follows that the latter value is most likely correct.

and $\Delta_r H_m°$(298.15 K) from $\Delta_f H_m°$(marcasite, cr, 298.15 K), and the selected $\Delta_f H_m°(Fe^{2+}$, 298.15 K) = -(90.29 ± 0.52) kJ · mol^{-1} and $\Delta_f H_m°(H_2S$, aq, 298.15 K) = -(38.6 ± 1.5) kJ · mol^{-1}, resulting in

$$\Delta_r H_m°(298.15\ K) = (1.94 \pm 3.86)\ kJ \cdot mol^{-1}$$

These values are included in TDB 2020.

The calculated solubility of marcasite is a bit higher than the calculated solubility of pyrite, which makes sense as pyrite is considered to be the stable phase.

11.6.1.2.6 Greigite (cubic Fe_3S_4)

Berner (1967) measured the solubility of synthetic greigite and interpreted his data in terms of the metastable solubility equilibrium

$$Fe_3S_4(cr) \rightleftharpoons 3\ Fe^{2+} + 3\ S^{2-} + S(cr)$$

Rickard & Luther (2007) re-interpreted these measurements by using the following alternative formulation of the solubility reaction

$$Fe_3S_4(cr) + 3\ H^+ \rightleftharpoons 3\ Fe^{2+} + 3\ HS^{2-} + S(cr)$$

Obtaining

$$\log_{10}{}^*K_{s,0}°(298.15\ K) = -12.84$$

Lemire et al. (2020) accepted this value and included a 2 σ value of 0.75, based on the variation of the data by Berner (1967). Using the selected $\Delta_f G_m°(Fe^{2+}$, 298.15 K) = -(90.72 ± 0.64) kJ · mol-^{1} and $\Delta_f G_m°(HS^-$, 298.15 K) = (12.243 ± 2.115) kJ · mol^{-1}, they derived $\Delta_f G_m°(Fe_3S_4$, cr, 298.15 K) = -(308.7 ± 7.9) kJ · mol^{-1}, which they rounded to their selected

$$\Delta_f G_m°(Fe_3S_4, cr, 298.15\ K) = -(309 \pm 8)\ kJ \cdot mol^{-1}$$

From this value and the selected $\Delta_f G_m°(Fe^{2+}$, 298.15 K), $\Delta_f G_m°(Fe^{3+}$, 298.15 K) = -(16.23 ± 0.65) kJ · mol^{-1}, and $\Delta_f G_m°(H_2S$, aq, 298.15 K) = -(27.648 ± 2.115) kJ · mol^{-1} then follows

$$Fe_3S_4(cr) + 8\ H^+ \rightleftharpoons Fe^{2+} + 2\ Fe^{3+} + 4\ H_2S(aq)$$

$$\log_{10}{}^*K_{s,0}°(298.15\ K) = -(13.18 \pm 2.31)$$

which is included in TDB 2020.

11.6.2 Iron sulphates

11.6.2.1 Aqueous iron(II) sulphate complexes

Sulphate complexes with Fe^{2+} are weak. The PSI/Nagra TDB 12/07 included thermodynamic data for $FeSO_4(aq)$ and $FeHSO_4^+$. In addition to these complexes, Lemire et al. (2013) also discussed data for $Fe(SO_4)_2^{2-}$.

11.6.2.1.1 Data in TDB 05/92, TDB 01/01 and TDB 12/07

The data for $FeSO_4(aq)$ and $FeHSO_4^+$ included in TDB 05/92, TDB 01/01 and TDB 12/07 were taken by Pearson et al. (1992) from Nordstrom et al. (1990), who selected

$$Fe^{2+} + SO_4^{2-} \rightleftharpoons FeSO_4(aq)$$

$$\log_{10}K°(298.15\ K) = 2.25$$

$$\Delta_r H_m°(298.15\ K) = 13.5\ kJ \cdot mol^{-1}$$

Nordstrom et al. (1990) did not indicate where their data for this reaction was taken from but stated that the $\log_{10}K°$ value is in good agreement with Smith & Martell (1976), Siebert & Christ (unpublished data on Fuoss fitting of stability constant data, 1976), and Stipp (unpublished M.S. thesis, 1983). The enthalpy was derived with the Fuoss fitting method of Siebert & Christ (1976), but Nordstrom et al. (1990) gave no details on the procedure.

The stability constant for $FeHSO_4^+$

$$Fe^{2+} + HSO_4^- \rightleftharpoons FeHSO_4^+$$

$$\log_{10}K°(298.15\ K) = 1.08$$

selected by Nordstrom et al. (1990) was estimated by Mattigod & Sposito (1977). For TDB 05/92, Pearson et al. (1992) reformulated the reaction in terms of SO_4^{2-} and recalculated the stability constant using $\log_{10}{}^*K°(298.15\ K) = 1.988$ for $SO_4^{2-} + H^+ \rightleftharpoons HSO_4^-$, resulting in

$$Fe^{2+} + SO_4^{2-} + H^+ \rightleftharpoons FeHSO_4^+$$

$$\log_{10}{}^*K°(298.15\ K) = 3.068$$

In TDB 2020, the data for $FeSO_4(aq)$ are superseded by the data discussed below, whereas the formation constant for $FeHSO_4^+$ is retained, but relegated to the set of supplemental data.

11.6.2.1.2 FeSO4(aq)

Lemire et al. (2013) considered experimental data from 8 studies using conductometry, spectrophotometry, reaction rate measurements, cation exchange, calorimetry, isopiestic measurements, and electrochemical potential measurements. They re-evaluated the conductivity measurements by Kubota et al. (1988) in dilute aqueous Fe(II) sulphate solutions (10^{-4} – 10^{-3} molar) at temperatures between 10 and 35 °C and selected

$$Fe^{2+} + SO_4^{2-} \rightleftharpoons FeSO_4(aq)$$

$$\log_{10}K°(298.15\ K) = (2.44 \pm 0.03)$$

$$\Delta_r H_m°(298.15\ K) = (8.4 \pm 6.2)\ kJ \cdot mol^{-1}$$

based on their re-evaluation and a linear regression of $\log_{10}K°(T)$ vs. (1/298.15 - 1/T), which also implies that

$$\Delta_r C_{p,m}°(298.15\ K) \approx 0$$

over the limited temperature range.

These values are also added to our database as well as

$$\varepsilon(FeSO_4(aq), NaCl) = \varepsilon(FeSO_4(aq), NaClO_4) \approx (0.0 \pm 0.1)\ kg \cdot mol^{-1}$$

estimated according to Tab. 1-7.

11.6.2.1.3 Fe(SO4)22-

Ciavatta et al. (2002) investigated the stability constants of Fe(II) sulphate complexes by measuring the competition of H^+ and Fe^{2+} ions for the sulphate ion at 25 °C in a 3 M $NaClO_4$ solution using a glass electrode. For $Fe(SO_4)_2^{2-}$ they obtained $\log_{10}\beta_2(298.15\ K, 3\ M\ NaClO_4) = (0.87 \pm 0.05)$, which they extrapolated to zero ionic strength by using SIT (using slightly different ion interaction coefficients than recommended by NEA). This resulted in $\log_{10}\beta_2°(298.15\ K) = (2.5 \pm 0.2)$.

Lemire et al. (2013) accepted the value for $\log_{10}\beta_2(298.15\ K, 3\ M\ NaClO_4)$ but chose to redo the extrapolation to zero ionic strength. By using the calculation scheme shown in Tab. 11.6-1, they had to take recourse to several estimates for ion interaction coefficients and to several approximate values for ion concentrations (estimates and approximate values are shaded in Tab. 11.6-1), see p. 321 in Lemire et al. (2013) for details.

Tab. 11.6-1: Calculation scheme used by Lemire et al. (2013) for extrapolating the value for $\log_{10}\beta_2(Fe(SO_4)_2^{2-}$, 298.15 K, 3 M $NaClO_4$) by Ciavatta et al. (2002) to zero ionic strength

Estimated ion interaction coefficients and approximated ion concentrations (see p. 312 in Lemire et al. 2013 for details) are indicated by shading.

$\log_{10}\beta_2°$ =	$\log_{10}\beta_2$	= (0.73 ± 0.05)
	+ 8 D	= (2.018 ± 0.074)
	+ $\varepsilon(Na^+, Fe(SO_4)_2^{2-})$ $m(Na^+)$	≈ -(0.35 ± 0.35)
	- $\varepsilon(Fe^{2+}, ClO_4^-)$ $m(ClO_4^-)$	= -(1.12 ± 0.16)
	- 2 $\varepsilon(Na^+, SO_4^{2-})$ $m(Na^+)$	= (0.73 ± 0.04)
	- $\varepsilon(Fe^{2+}, Fe(SO_4)_2^{2-})$ ($m(Fe^{2+})$ - $m(Fe(SO_4)_2^{2-})$)	≈ -(0.01 ± 0.01)
	- $\varepsilon(Fe^{2+}, SO_4^{2-})$ (2 $m(Fe^{2+})$ + $m(SO_4^{2-})$)	≈ (0.045 ± 0.015)
	- $\varepsilon(Fe^{2+}, HSO_4^-)$ $m(HSO_4^-)$	≈ (0.02 ± 0.02)
	- 2 $\varepsilon(H+, SO_4^{2-})$ $m(H^+)$	≈ (0.006 ± 0.001)
$\log_{10}\beta_2°$ =		(2.0 ± 0.4)

They obtained $\log_{10}\beta_2°(298.15\ K) = (2.0 \pm 0.4)$ but remarked that "Too many corrections with too many assumptions and estimates are involved in this correction to zero ionic strength, and therefore no value is selected in the present review for the formation constant of the 2:1 complex". Inspection of Tab. 11.6-1, however, shows that, with the exception of the estimated $\varepsilon(Na^+, Fe(SO_4)_2^{2-})$, estimates and approximations have only a small influence on the final result. We therefore decided to include

$$Fe^{2+} + 2\ SO_4^{2-} \rightleftharpoons Fe(SO_4)_2^{2-}$$

$$\log_{10}\beta_2°(298.15\ K) = (2.0 \pm 0.4)$$

as supplemental data in TDB 2020, as well as the ion interaction coefficient

$$\varepsilon(Fe(SO_4)_2^{2-}, Na^+) \approx -(0.10 \pm 0.10)\ kg \cdot mol^{-1}$$

as estimated according to Tab. 1-7.

11.6.2.1.4 $FeHSO_4^+$

Lemire et al. (2013) reported on two experimental studies concerning the formation of $FeHSO_4^+$, one at $I < 2.2$ m and the other at $I \approx 5.5$ m but considered the data to be insufficient for extrapolation to zero ionic strength and made no recommendation.

We decided to retain

$$Fe^{2+} + SO_4^{2-} + H^+ \rightleftharpoons FeHSO_4^+$$

$$log_{10}{}^*K°(298.15\ K) = 3.068$$

from the PSI/Nagra TDB 12/07. Since this formation constant is based on an estimate (see Section 11.6.2.2.1) we reassigned it to the supplemental dataset.

For inclusion in TDB 2020 we estimated

$$\varepsilon(FeHSO_4^+, Cl^-) \approx (0.05 \pm 0.10)\ kg \cdot mol^{-1}$$

and

$$\varepsilon(FeHSO_4^+, ClO_4^-) \approx (0.2 \pm 0.1)\ kg \cdot mol^{-1}$$

estimated according to Tab. 1-7.

11.6.2.2 Aqueous iron(III) sulphate complexes

According to Lemire et al. (2013) the speciation of Fe(III) in sulphate solutions is not firmly established. The best known and most stable species is $FeSO_4^+$. The existence of other species is unclear (with the exception $Fe(SO_4)_2^-$ and $FeHSO_4^{2+}$) and their stability constants indicate that in most solutions their concentrations would be low.

The PSI/Nagra TDB 12/07 included thermodynamic data for $FeSO_4^+$, $Fe(SO_4)_2^-$, and $FeHSO_4^{2+}$.

11.6.2.2.1 Data in TDB 05/92, TDB 01/01 and TDB 12/07

The data for $FeSO_4^+$, $Fe(SO_4)_2^-$, and $FeHSO_4^{2+}$ included in TDB 05/92, TDB 01/01 and TDB 12/07 were taken by Pearson et al. (1992) from Nordstrom et al. (1990) who selected for $FeSO_4^+$ and $Fe(SO_4)_2^-$

$$Fe^{3+} + SO_4^{2-} \rightleftharpoons FeSO_4^+$$

$$\log_{10}K_{1,1}°(298.15\ K) = 4.04$$

$$\Delta_r H_{m,1,1}°(298.15\ K) = 16.4\ kJ \cdot mol^{-1}$$

$Fe^{3+} + 2\ SO_4^{2-} \rightleftharpoons Fe(SO_4)_2^-$

$\log_{10}K_{2,1}°(298.15\ K) = 5.38$

$\Delta_r H_{m,2,1}°(298.15\ K) = 19.2\ kJ \cdot mol^{-1}$

Nordstrom et al. (1990) did not explain where they obtained their values for $\log_{10}K_{1,1}°$ and $\log_{10}K_{2,1}°$, but stated that they were in good agreement with Smith & Martell (1976), Siebert & Christ (unpublished data on Fuoss fitting of stability constant data, 1976), and Stipp (unpublished M.S. thesis, 1983). $\Delta_r H_{m,1,1}°(298.15\ K)$ was derived by Nordstrom et al. (1990) from the Fuoss fitting method of Siebert & Christ (1976), but they gave no details on the procedure. Nordstrom et al. (1990) assumed $\Delta_r H_{m,2,1}°(298.15\ K)$ to be equal to that of $Al(SO_4)_2^-$. However, they reported $\Delta_r H_{m,2,1}°(Al(SO_4)_2^-, 298.15\ K) = 2.84\ kcal \cdot mol^{-1}$, as opposed to $\Delta_r H_{m,2,1}°(Fe(SO_4)_2^-, 298.15\ K) = 4.60\ kcal \cdot mol^{-1}$.

The stability constant for $FeHSO_4^{2+}$

$Fe^{3+} + HSO_4^- \rightleftharpoons FeHSO_4^{2+}$

$\log_{10}K°(298.15\ K) = 2.48$

selected by Nordstrom et al. (1990) was estimated by Mattigod & Sposito (1977). For TDB 05/92, Pearson et al. (1992) reformulated the reaction in terms of SO_4^{2-} and recalculated the stability constant using $\log_{10}{}^*K°(298.15\ K) = 1.988$ for $SO_4^{2-} + H^+ \rightleftharpoons HSO_4^-$, resulting in

$Fe^{3+} + SO_4^{2-} + H^+ \rightleftharpoons FeHSO_4^{2+}$

$\log_{10}{}^*K°(298.15\ K) = 4.468$

All these data are superseded in TDB 2020 by those discussed in the following sections.

11.6.2.2.2 $FeSO_4^+$

Lemire et al. (2013) accepted formation constants for $FeSO_4^+$ from nine studies in mixed media ($HClO_4/NaClO_4$, $HClO_4/H_2SO_4$, $NaClO_4/H_2SO_4$), that used spectrophotometry (five studies), potentiometry (two studies), spectrophotometry combined with ion exchange (one study), and kinetic methods (one study), covering a range of ionic strengths from about 0.07 to 3.5 $mol \cdot kg^{-1}$. From their SIT-analysis (neglecting differences in the major cations H^+ or Na^+ in the experimental solutions), Lemire et al. (2013) obtained and selected

$Fe^{3+} + SO_4^{2-} \rightleftharpoons FeSO_4^+$

$\log_{10}K_{1,1}°(298.15\ K) = 4.25 \pm 0.10$

$\Delta\varepsilon = -(0.19 \pm 0.06)\ kg \cdot mol^{-1}$

From $\Delta\varepsilon$ follows

$$\varepsilon(FeSO_4^+, ClO_4^-) = (0.4 \pm 0.1)\ kg \cdot mol^{-1}$$

by using the NEA-recommended $\varepsilon(Fe^{3+}, ClO_4^-) = (0.73 \pm 0.05)\ kg \cdot mol^{-1}$ and $\varepsilon(Na^+, SO_4^{2-}) = -(0.12 \pm 0.06)\ kg \cdot mol^{-1}$. The value for $\varepsilon(FeSO_4^+, ClO_4^-)$ served for the estimate

$$\varepsilon(FeSO_4^+, Cl^-) \approx \varepsilon(FeSO_4^+, ClO_4^-) = (0.4 \pm 0.1)\ kg \cdot mol^{-1}$$

(see Section 11.1.1).

All these data for $FeSO_4^+$ are included in TDB 2020.

11.6.2.2.3 $Fe(SO_4)_2^-$ and $FeSO_4(HSO_4)(aq)$

$Fe(SO_4)_2^-$: There are very few studies on the formation constant of $Fe(SO_4)_2^-$. In their analysis, Lemire et al. (2013) considered one potentiometric study where the formation constant was measured over a range of ionic strengths (I_m from 0.253 to 3.5 $mol \cdot kg^{-1}$), an ion exchange study at $I_c = 1\ mol \cdot l^{-1}$, and two potentiometric and a combined potentiometric/spectrophotometric study at $I_c = 3\ mol \cdot l^{-1}$. Based on an SIT analysis with a weighted linear fit, Lemire et al. (2013) obtained

$$FeSO_4^+ + SO_4^{2-} \rightleftharpoons Fe(SO_4)_2^-$$

$$\log_{10}K_2°(298.15\ K) = 1.97 \pm 0.13$$

$$\Delta\varepsilon = -(0.057 \pm 0.055)\ kg \cdot mol^{-1}$$

These values were recommended by Lemire et al. (2013), but the authors remarked that the data were limited, the data points widely scattered, and the linearity of the function poor (r = 0.52). Despite these caveats, we concur with this recommendation and include these data in TDB 2020. Using $\varepsilon(FeSO_4^+, ClO_4^-) = (0.42 \pm 0.12)$, $\varepsilon(SO_4^{2-}, Na^+) = -(0.12 \pm 0.06)$ with the recommended value for $\Delta\varepsilon$, Lemire et al. (2013) calculated

$$\varepsilon(Fe(SO_4)_2^-, Na^+) = (0.24 \pm 0.14)\ kg \cdot mol^{-1}$$

which is also included in TDB 2020.

$FeSO_4(HSO_4)(aq)$: Lemire et al. (2013) discussed two studies concerning the stability constant for $FeSO_4(HSO_4)(aq)$. Conditional constants ($\log_{10}K$) for the reaction $Fe^{3+} + SO_4^{2-} + HSO_4^- \rightleftharpoons FeSO_4(HSO_4)(aq)$ turned out to be 2.6 and 6. Lemire et al. (2013) considered these values to be too disparate (even in light of the different ionic strengths of the respective experimental solutions) and did not make any recommendations. $FeSO_4(HSO_4)(aq)$ is only to be expected under very acid conditions, which are well outside the application range of our database. For this reason, no data for $FeSO_4(HSO_4)(aq)$ are included in our database, not even as supplemental data.

11.6.2.2.4 $FeHSO_4^{2+}$

$FeHSO_4^{2+}$ is a very weak complex and only a limited number of experimental results on its formation constant could be considered by Lemire et al. (2013). An SIT-analysis of three formation constants[42] resulted in

$$Fe^{3+} + HSO_4^- \rightleftharpoons FeHSO_4^{2+}$$

$$log_{10}K_1°(298.15\ K) = (1.73 \pm 0.76)$$

$$\Delta\varepsilon = -(0.14 \pm 0.12)\ kg \cdot mol^{-1}$$

with

$$\varepsilon(FeHSO_4^{2+}, ClO_4^-) = (0.58 \pm 0.13)\ kg \cdot mol^{-1}$$

following from $\Delta\varepsilon$ and the NEA-selected $\varepsilon(Fe^{3+}, ClO_4^-) = (0.73 \pm 0.05)$ kg · mol^{-1} and $\varepsilon(Na^+, HSO_4^-) = -(0.01 \pm 0.02)$ kg · mol^{-1}.

Since the number of measurements for the formation constant of $FeHSO_4^{2+}$ is very limited and the linear fit to the data statistically unreliable (r = -0.32 for the weighted linear fit), Lemire et al. (2013) did not recommend these data. They are, however, included in our database as supplemental data for scoping calculations, as well as the estimate

$$\varepsilon(FeHSO_4^{2+}, Cl^-) \approx \varepsilon(FeHSO_4^{2+}, ClO_4^-) = (0.58 \pm 0.13)\ kg \cdot mol^{-1}$$

(see Section 11.1.1).

11.6.2.2.5 Other Fe(III) sulphate complexes

$Fe(SO_4)_3^{3-}$: According to Lemire et al. (2013), potentiometric data have indicated that at higher sulphate concentrations, complex species in addition to $FeSO_4^+$ and $Fe(SO_4)^{2-}$ are formed, which could be $Fe(SO_4)_3^{3-}$ or a ternary Fe(III) hydroxide sulphate complex.

Ternary Fe(III) hydroxide sulphate complexes: Lemire et al. (2013) reported on studies indicating that ternary Fe(III) hydroxide sulphate complexes, such as $Fe(OH)_2SO_4^-$, $Fe_2(OH)_2(SO_4)^{2+}$, $Fe_2(OH)_2(SO_4)_2$(aq), and $Fe_3(OH)_4(SO_4)^{3+}$, may exist. However, they did not recommend any data for these complexes.

Ternary Fe(III) thiocyanate sulphate complexes: Investigations of the competition between thiocyanate and sulphate for Fe(III) have indicated that sulphate does not simply replace thiocyanate in Fe(III) thiocyanate complexes, but may rather form ternary complexes such as $Fe(SO_4)(SCN)$(aq) or (probably) $Fe(SO_4)_2(SCN)^{2-}$. Lemire et al. (2013) did not recommend any thermodynamic data for such complexes.

---

[42] Note that in the legend to their Figure IX-5, Lemire et al. (2013) list four references for four data points, but only three data points are shown in the figure.

11.6.2.3 Iron sulphate compounds

11.6.2.3.1 Data in TDB 05/92, TDB 01/01 and TDB 12/07

The solubility constant and the corresponding standard heat of reaction for melanterite ($FeSO_4 \cdot 7H_2O$) was adopted by Pearson et al. (1992) for TDB 05/92 (retained in TDB 01/01 and 12/07) from Nordstrom et al. (1990) whose selected values for

$$FeSO_4 \cdot 7H_2O(\text{melanterite}) \rightleftharpoons Fe^{2+} + SO_4^{2-} + 7\ H_2O(l)$$

were based on an evaluation by Reardon & Beckie (1987) of several experimental solubility studies of melanterite. Reardon & Beckie (1987) made a detailed analysis of experimental activity coefficient, heat capacity and mineral solubility data in the $FeSO_4$-H_2SO_4-H_2O system using the Pitzer formalism to determine the temperature dependencies of the ion interaction coefficients necessary for describing this chemical system. Using the resulting Pitzer parameters, Reardon & Beckie (1987) calculated solubility constants for melanterite from solubility data measured at temperatures between 0 and 55 °C. The solubility constants were then fit with the following equation

$$\log_{10}K_{s,0}°(T, 0 – 55\ °C) = 1.447 - 0.004153\ T - 214949\ T^{-2}$$

leading to

$$\log_{10}K_{s,0}°(298.15\ K) = -2.209$$

the value selected by Nordstrom et al. (1990). Apparently, Nordstrom et al. (1990) then used the van't Hoff equation for deriving

$$\Delta_r H_m°(298.15\ K) = 20.5\ kJ \cdot mol^{-1}$$

Melanterite is not included in TDB 2020, since it is soluble in water and occurs mainly as secondary oxidation product of sulphide minerals in the near-surface environment as an efflorescence or as a product of volcanic fumaroles.

11.6.2.3.2 Ferrous sulphates

Lemire et al. (2013) selected thermodynamic data for the acidic ferrous sulphates $FeSO_4$(cr), $FeSO_4 \cdot H_2O$(cr) (szomolnokite), $FeSO_4 \cdot 4H_2O$(cr) (rozenite), and $FeSO_4 \cdot 7H_2O$(cr) (melanterite). For $FeSO_4$(cr), Lemire et al. (2013) selected only a value for $C_{p,m}°(298.15\ K)$. For this reason, $FeSO_4$(cr) is not included in our database. The hydrous sulphates szomolnokite, rozenite, and melanterite are all secondary oxidation products of sulphide minerals, occur as efflorescences and are soluble in water. They are therefore not included in our database.

Lemire et al. (2013) also selected $\Delta_f H_m°$(298.15 K) for $(NH_4)_2Fe(SO_4)_2 \cdot 6H_2O$(cr), a rare mineral (mohrite) and a common chemical reagent (Mohr's salt). Due to its large solubility, it is not included in our database, and knowing only $\Delta_f H_m°$ is not sufficient for equilibrium calculations anyway.

11.6.2.3.3 Ferric sulphates

Lemire et al. (2013) selected thermodynamic data for the ferric sulphates $Fe_2(SO_4)_3$(cr) (mikasaite) and $Fe_2(SO_4)_3 \cdot 5H_2O$(cr). Both solids are not included in our database: Mikasaite is hygroscopic and soluble in water, and for $Fe_2(SO_4)_3 \cdot 5H_2O$(cr) there is only a value for $\Delta_f H_m°$(298.15 K).

Lemire et al. (2020) selected values for $\Delta_f H_m°$(298.15 K) for $Fe_2(SO_4)_3 \cdot 7.53H_2O$(cr) and $Fe_2(SO_4)_3 \cdot 9H_2O$(cr). Since this is not sufficient for equilibrium calculations, these solids are not included in TDB 2020.

11.6.2.3.4 Ferric hydroxy-sulphates

Lemire et al. (2013) selected thermodynamic data for the efflorescent salts $Fe_{4.78}(SO_4)_6(OH)_{2.34}(H_2O)_{20.71}$(cr) (ferricopiapite) and $(H_3O)_{1.34}Fe(SO_4)_{2.17}(H_2O)_{3.06}$(cr) (rhomboclase), which form in surficial acid mine drainage environments at very low pH. Only values for $\Delta_f H_m°$(298.15 K) were given by Lemire et al. (2013) and these minerals are therefore not included in our database.

Based on calorimetric measurements, Lemire et al. (2013) selected $\Delta_f H_m°$(298.15 K) and $S_m°$(298.15 K) for hydronium jarosite, $(H_3O)_{0.91}Fe_{2.91}(SO_4)_2(OH)_{5.64}(H_2O)_{0.18}$(cr), and a derived value of $\Delta_f H_m°$(298.15 K) for an idealized composition, $(H_3O)Fe_3(SO_4)_2(OH)_6$(cr).

According to Dutrizac & Jambor (2000), the essential requirement for the formation of jarosite-group minerals is an acidic (pH < 3) environment, once removed from such an environment, however, they decompose readily, typically into goethite, FeO(OH)(cr). For this reason, the data selected by Lemire et al. (2013) for jarosite are not included in our database.

11.6.2.3.5 Ferric oxy-hydroxy-sulphates

Lemire et al. (2013) selected thermodynamic data for two compositions of schwertmannite, $FeO(SO_4)_{0.157}(OH)_{0.686}(H_2O)_{0.972}$(cr) and $FeO(SO_4)_{0.168}(OH)_{0.664}(H_2O)_{1.226}$(cr). This mineral forms in surficial acid mine drainage environments at pH below 4.5 (Bigham et al. 1996). Since only values for $\Delta_f H_m°$(298.15 K) were given by Lemire et al. (2013), schwertmannite is not included in our database.

11.6.2.3.6 "Sulphate green rust two"

Sulphate green rust two (sulphate GR2) is an intermediate Fe(II)-Fe(III) compound consisting of brucite-like $Fe(OH)_2$ layers where the excess charge created by the partial oxidation of ferrous to ferric iron is compensated by sulphate anions inserted (together with water molecules) into the interlayer. Génin et al. (1998) mention the observation (see reference therein) that sulphate GR2 was observed as corrosion product under the fouling crust covering sheet piles at the lowest anoxic

level of tide at the harbour of Boulogne sur Mer. Refait et al. (1999) prepared sulphate GR2 by oxidation of ferrous hydroxide precipitates obtained by mixing aqueous solutions of melanterite ($FeSO_4 \cdot 7H_2O$) with NaOH solutions. Based on the electrochemical data by Refait et al. (1999), Lemire et al. (2013) reported $\Delta_r G_m°(298.15\ K) = -(105 \pm 2)\ kJ \cdot mol^{-1}$ for the oxidation reaction

$$6\ Fe(OH)_2(s) + SO_4^{2-} + 2\ H^+ + n\ H_2O(l) \rightleftharpoons (Fe^{III})_2(Fe^{II})_4(OH)_{12}SO_4 \cdot nH_2O(s) + H_2g$$

but did not select this value (without explanation). We accept the corresponding

$$log_{10}{}^*K°(298.15\ K) = (18.40 \pm 0.35)$$

as supplemental datum (as there remain uncertainties with respect to the grain size and crystallinity of the precipitates and the number of structural waters in the formula unit). For inclusion in TDB 2020 we used $log_{10}{}^*K_{s,0}°(298.15\ K) = (12.26 \pm 0.88)$ for $Fe(OH)_2(s) + 2H^+ \rightleftharpoons Fe^{2+} + 2\ H_2O(l)$ (see Section 11.4.2.2) to obtain

$$(Fe^{III})_2(Fe^{II})_4(OH)_{12}SO_4 \cdot nH_2O(s) + 10\ H^+ + H_2g \rightleftharpoons 6\ Fe^{2+} + SO_4^{2-} + (n+12)\ H_2O(l)$$

$$log_{10}{}^*K°(298.15\ K) = (55.2 \pm 5.3)$$

Other green rusts are "chloride green rust one" (see Section 11.5.2.2.1) and "carbonate green rust one" (see Section 11.7.1.3.3). "White rust" was discussed in Section 11.4.2.2

11.6.3 Selenium compounds and complexes

11.6.3.1 Iron selenide compounds and complexes

There seems to be no information on any iron selenide complexes, as neither Olin et al. (2005) nor Lemire et al. (2020) made any mention of these.

Apparently, there are also no solubility data on iron selenide solids, therefore, Lemire et al. (2020) only selected calorimetric data for $FeSe_{1.95}$(cr, β), $Fe_{1.042}Se$(cr), Fe_7Se_8(cr, α), Fe_3Se_4(cr, γ), and $FeSe_2$(cr). Lemire et al. (2020) only selected $C_{p,m}°(298.15\ K)$ and $S_m°(298.15\ K)$ for $FeSe_{1.95}$(cr), which is not sufficient for equilibrium calculations; this solid is therefore not further discussed.

Before discussing the selected thermodynamic data for these solids, it is important to recognize that including iron selenide solids in geochemical calculations, even though there are no data for aqueous iron selenide complexes, may lead to severely underestimated solubilities! If any iron selenide solid turns out to be solubility limiting, the resulting solubility of Se is a minimal value and could be much higher, even by orders of magnitude.

11.6.3.1.1 $Fe_{1.042}Se$(cr, β)

$Fe_{1.042}Se$(cr, β) is trigonal, and structurally probably analogous to mackinawite. This phase is sometimes referred to as selenium deficient, $FeSe_{1-y}$, or as iron rich, $Fe_{1+x}Se$. Lemire et al. (2020) chose the latter version. Based on calorimetric data they selected

$$C_{p,m}°(Fe_{1.042}Se, \beta, 298.15\ K) = (57.1 \pm 0.7)\ J \cdot K^{-1} \cdot mol^{-1}$$

$$S_m°(Fe_{1.042}Se, \beta, 298.15\ K) = (72.1 \pm 0.8)\ J \cdot K^{-1} \cdot mol^{-1}$$

$$\Delta_f H_m°(Fe_{1.042}Se, \beta, 298.15\ K) = -(74.7 \pm 4.0)\ kJ \cdot mol^{-1}$$

$$\Delta_f G_m°(Fe_{1.042}Se, \beta, 298.15\ K) = -(75.233 \pm 4.009)\ kJ \cdot mol^{-1}$$

The solubility product $\log_{10}{}^{*}K_{s,0}°(298.15\ K)$ for the reaction

$$Fe_{1.042}Se(cr) + 2\ H^{+} \rightleftharpoons 1.042\ Fe^{2+} + H_2Se(aq) + 0.084\ e^{-}$$

can be calculated from $\Delta_f G_m°(Fe_{1.042}Se, \beta, 298.15\ K)$, and the selected $\Delta_f G_m°(Fe^{2+}, 298.15\ K) = -(90.72 \pm 0.64)\ kJ \cdot mol^{-1}$ and $\Delta_f G_m°(H_2Se, aq, 298.15\ K) = (21.5 \pm 2.0)\ kJ \cdot mol^{-1}$, resulting in $\Delta_r G_m°(298.15\ K) = (2.203 \pm 4.53)\ kJ \cdot mol^{-1}$ or

$$\log_{10}{}^{*}K_{s,0}°(298.15\ K) = -(0.39 \pm 0.79)$$

and $\Delta_r H_m°(298.15\ K)$ from $\Delta_f H_m°(Fe_{1.042}Se, \beta, 298.15\ K)$, and the selected $\Delta_f H_m°(Fe^{2+}, 298.15\ K) = -(90.29 \pm 0.52)\ kJ \cdot mol^{-1}$ and $\Delta_f H_m°(H_2Se, aq, 298.15\ K) = (14.3 \pm 2.0)\ kJ \cdot mol^{-1}$, resulting in

$$\Delta_r H_m°(298.15\ K) = -(5.08 \pm 4.50)\ kJ \cdot mol^{-1}$$

These values are included in TDB 2020.

11.6.3.1.2 Fe_7Se_8(cr, α) or $Fe_{0.875}Se$(cr, α)

Fe_7Se_8(cr, α) cannot be found in nature as a mineral. Based on calorimetric data, Lemire et al. (2020) selected

$$C_{p,m}°(Fe_7Se_8, \alpha, 298.15\ K) = (442.1 \pm 4.0)\ J \cdot K^{-1} \cdot mol^{-1}$$

$$S_m°(Fe_7Se_8, \alpha, 298.15\ K) = (613.8 \pm 5.0)\ J \cdot K^{-1} \cdot mol^{-1}$$

$$\Delta_f H_m°(Fe_7Se_8, \alpha, 298.15\ K) = -(521 \pm 39)\ kJ \cdot mol^{-1}$$

$$\Delta_f G_m°(Fe_7Se_8, \alpha, 298.15\ K) = -(547.084 \pm 39.038)\ kJ \cdot mol^{-1}$$

Expressing Fe_7Se_8(cr, α) as $Fe_{0.875}Se$(cr, α), the solubility reaction can be written as

$$Fe_{0.875}Se(cr, \alpha) + 2\ H^+ \rightleftharpoons 0.625\ Fe^{2+} + 0.25\ Fe^{3+} + H_2Se(aq)$$

From $\Delta_f G_m°(Fe_7Se_8, \alpha, 298.15\ K)/8$ and the selected $\Delta_f G_m°(Fe^{2+}, 298.15\ K) = -(90.72 \pm 0.64)$ kJ · mol^{-1}, $\Delta_f G_m°(Fe^{3+}, 298.15\ K) = -(16.23 \pm 0.65)$ kJ · mol^{-1}, and $\Delta_f G_m°(H_2Se, aq, 298.15\ K) = (21.5 \pm 2.0)$ kJ · mol^{-1} then follows $\Delta_r G_m°(298.15\ K) = (29.128 \pm 5.291)$ kJ · mol^{-1} or

$$\log_{10}{}^*K_{s,0}°(298.15\ K) = -(5.10 \pm 0.93)$$

and from $\Delta_f H_m°(Fe_7Se_8, \alpha, 298.15\ K)/8$, the selected $\Delta_f H_m°(Fe^{2+}, 298.15\ K) = -(90.29 \pm 0.52)$ kJ · mol^{-1}, $\Delta_f H_m°(Fe^{3+}, 298.15\ K) = -(50.06 \pm 0.97)$ kJ · mol^{-1} and $\Delta_f H_m°(H_2Se, aq, 298.15\ K) = (14.3 \pm 2.0)$ kJ · mol^{-1}

$$\Delta_r H_m°(298.15\ K) = (10.48 \pm 5.28)\ kJ \cdot mol^{-1}$$

which are included in TDB 2020.

11.6.3.1.3 Fe_3Se_4(cr, γ)

Fe_3Se_4(cr, γ) cannot be found in nature as a mineral. Lemire et al. (2020) reviewed calorimetric data and selected

$$C_{p,m}°(Fe_3Se_4, \gamma, 298.15\ K) = (220.1 \pm 2.0)\ J \cdot K^{-1} \cdot mol^{-1}$$

$$S_m°(Fe_3Se_4, \gamma, 298.15\ K) = (279.8 \pm 3.0)\ J \cdot K^{-1} \cdot mol^{-1}$$

$$\Delta_f H_m°(Fe_3Se_4, \gamma, 298.15\ K) = -(248 \pm 20)\ kJ \cdot mol^{-1}$$

$$\Delta_f G_m°(Fe_3Se_4, \gamma, 298.15\ K) = -(257.000 \pm 20.024)\ kJ \cdot mol^{-1}$$

The solubility product $\log_{10}{}^*K_{s,0}°(298.15\ K)$ for the reaction

$$Fe_3Se_4(cr, \gamma) + 8\ H^+ \rightleftharpoons Fe^{2+} + 2\ Fe^{3+} + 4\ H_2Se(aq)$$

can be calculated from $\Delta_f G_m°(Fe_3Se_4, \gamma, 298.15\ K)$ and the selected $\Delta_f G_m°(Fe^{2+}, 298.15\ K) = -(90.72 \pm 0.64)$ kJ · mol^{-1}, $\Delta_f G_m°(Fe^{3+}, 298.15\ K) = -(16.23 \pm 0.65)$ kJ · mol^{-1}, and $\Delta_f G_m°(H_2Se, aq, 298.15\ K) = (21.5 \pm 2.0)$ kJ · mol^{-1}, resulting in $\Delta_r G_m°(298.15\ K) = (219.82 \pm 21.61)$ kJ · mol^{-1} or

$$\log_{10}{}^*K_{s,0}°(298.15\ K) = -(38.51 \pm 3.79)$$

and $\Delta_r H_m°$(298.15 K) from $\Delta_f H_m°(Fe_3Se_4, \gamma, 298.15\ K)$, the selected $\Delta_f H_m°(Fe^{2+}, 298.15\ K) = -(90.29 \pm 0.52)$ kJ · mol^{-1}, $\Delta_f H_m°(Fe^{3+}, 298.15\ K) = -(50.06 \pm 0.97)$ kJ · mol^{-1}, and $\Delta_f H_m°(H_2Se, aq, 298.15\ K) = (14.3 \pm 2.0)$ kJ · mol^{-1}, resulting in

$$\Delta_r H_m°(298.15\ K) = (114.8 \pm 21.6)\ kJ \cdot mol^{-1}$$

which are included in TDB 2020.

11.6.3.1.4 $FeSe_2$(cr)

$FeSe_2$(cr) is found in nature as ferroselite, the marcasite-type polymorph of $FeSe_2$(cr), and, much rarer, as dzharkenite, the pyrite-type polymorph.

Based on calorimetric data for $FeSe_2$(cr) (ferroselite-structured), Lemire et al. (2020) selected

$$C_{p,m}°(FeSe_2, cr, 298.15\ K) = (70.6 \pm 2.0)\ J \cdot K^{-1} \cdot mol^{-1}$$

$$S_m°(FeSe_2, cr, 298.15\ K) = (83.5 \pm 2.0)\ J \cdot K^{-1} \cdot mol^{-1}$$

$$\Delta_f H_m°(FeSe_2, cr, 298.15\ K) = -(120 \pm 9)\ kJ \cdot mol^{-1}$$

$$\Delta_f G_m°(FeSe_2, cr, 298.15\ K) = -(111.722 \pm 9.022)\ kJ \cdot mol^{-1}$$

The solubility product $\log_{10}{}^{*}K_{s,0}°$(298.15 K) for the reaction

$$FeSe_2(cr) + 4\ H^+ + 2\ e^- \rightleftharpoons Fe^{2+} + 2\ H_2Se(aq)$$

can be calculated from $\Delta_f G_m°(FeSe_2, cr, 298.15\ K)$, and the selected $\Delta_f G_m°(Fe^{2+}, 298.15\ K) = -(90.72 \pm 0.64)$ kJ · mol^{-1} and $\Delta_f G_m°(H_2Se, aq, 298.15\ K) = (21.5 \pm 2.0)$ kJ · mol^{-1}, resulting in $\Delta_r G_m°(298.15\ K) = (64.00 \pm 9.89)$ kJ · mol^{-1} or

$$\log_{10}{}^{*}K_{s,0}°(298.15\ K) = -(11.21 \pm 1.73)$$

and $\Delta_r H_m°$(298.15 K) from $\Delta_f H_m°(\ FeSe_2, cr, 298.15\ K)$, and the selected $\Delta_f H_m°(Fe^{2+}, 298.15\ K) = -(90.29 \pm 0.52)$ kJ · mol^{-1} and $\Delta_f H_m°(H_2Se, aq, 298.15\ K) = (14.3 \pm 2.0)$ kJ · mol^{-1}, resulting in

$$\Delta_r H_m°(298.15\ K) = (58.31 \pm 9.86)\ kJ \cdot mol^{-1}$$

These values are included in TDB 2020.

11.6.3.2 Iron selenite compounds and complexes

11.6.3.2.1 Iron(II) selenite compounds and complexes

The potentiometric titration study by Torres et al. (2010) was the only one found by Lemire et al. (2020) which deals with the complexation of iron(II) with selenite. Torres et al. (2010) carried out their potentiometric titrations in 0.15 M $NaClO_4$ at 293.15 K and reported

$\log_{10}{}^{*}K_{c,1,1}(I_c = 1.50\ M, 293.15\ K, Fe^{2+} + H^{+} + SeO_3^{2-} \rightleftharpoons FeHSeO_3^{+}) = (11.42 \pm 0.06)$

$\log_{10}{}^{*}\beta_{c,3,2}(I_c = 1.50\ M, 293.15\ K, Fe^{2+} + 3\ H^{+} + 2\ SeO_3^{2-} \rightleftharpoons FeH_3(SeO_3)_2^{+}) = (24.65 \pm 0.06)$

Lemire et al. (2020) converted these equilibria and their constants in the molar scale into simple complexation equilibria in the molal scale (I_m = 1.51 m), based on an SIT treatment of the selenite protonation constants derived by Torres et al. (2010) and obtained

$\log_{10}K_m(I_m = 1.51\ m, 293.15\ K, Fe^{2+} + HSeO_3^{-} \rightleftharpoons FeHSeO_3^{+}) = (3.68 \pm 0.06)$

$\log_{10}\beta_m(I_m = 1.51\ m, 293.15\ K, Fe^{2+} + HSeO_3^{-} + H_2SeO_3(aq) \rightleftharpoons FeHSeO_3(H_2SeO_3)^{+}) = (7.00 \pm 0.07)$

However, these data were not selected by Lemire et al. (2020), because Torres et al. (2010) did not provide primary experimental data, did not present their criteria for selecting the speciation, and derived selenite protonation constants at variance with those adopted in the NEA database project. Despite these grave shortcomings, we included these data in TDB 2020 for scoping calculations (neglecting that they refer to I_m = 1.51 m and 293.15 K). Thus, after rounding and increasing the uncertainties

$Fe^{2+} + HSeO_3^{-} \rightleftharpoons FeHSeO_3^{+}$

$\log_{10}K°(298.15\ K), = (3.7 \pm 1.0)$

$Fe^{2+} + HSeO_3^{-} + H_2SeO_3(aq) \rightleftharpoons FeHSeO_3(H_2SeO_3)^{+}$

$\log_{10}\beta°(298.15\ K) = (7.0 \pm 1.0)$

are included in TDB 2020 as supplemental data. Since ion interaction coefficients for these species are not known, we estimated them according to Tab. 1-7 and obtained

$\varepsilon(FeHSeO_3^{+}, Cl^{-}) \approx (0.05 \pm 0.10)\ kg \cdot mol^{-1}$

$\varepsilon(FeHSeO_3^{+}, ClO_4^{-}) \approx (0.2 \pm 0.1)\ kg \cdot mol^{-1}$

$\varepsilon(FeHSeO_3(H_2SeO_3)^{+}, Cl^{-}) \approx (0.05 \pm 0.10)\ kg \cdot mol^{-1}$

$\varepsilon(FeHSeO_3(H_2SeO_3)^{+}, ClO_4^{-}) \approx (0.2 \pm 0.1)\ kg \cdot mol^{-1}$

These interaction coefficients are also included in TDB 2020 as supplemental data.

There appear to be no data on Fe(II) selenite solids.

11.6.3.2.2 Iron(III) selenite compounds and complexes

There are only limited thermodynamic data available for the iron(III) selenite system. Based on the solubility study by Rai et al. (1995) under acidic conditions, Olin et al. (2005) selected

$$Fe_2(SeO_3)_3 \cdot 6H_2O(cr) \rightleftharpoons 2\ Fe^{3+} + 3\ SeO_3^{2-} + 6\ H_2O(l)$$

$$\log_{10}K_{s,0}°(298.15\ K) = -(41.58 \pm 0.11)$$

$$Fe^{3+} + SeO_3^{2-} \rightleftharpoons FeSeO_3^{+}$$

$$\log_{10}\beta°(298.15\ K) = (11.15 \pm 0.11)$$

which they adopted from Rai et al. (1995) without any recalculations (even though these authors used auxiliary data not consistent with those of the NEA database project). Thoenen et al. (2014) included the value for $\log_{10}\beta°(298.15\ K)$ in TDB 12/07, but did not include the value for $\log_{10}K_{s,0}°(298.15\ K)$. Lemire et al. (2020) reanalysed the data by Rai et al. (1995) using auxiliary data consistent with the NEA TDB values and obtained (considering the solid as a trihydrate)

$$Fe_2(SeO_3)_3 \cdot 3H_2O(cr) + 6\ H^{+} \rightleftharpoons 2\ Fe^{3+} + 3\ H_2SeO_3(aq) + 3\ H_2O(l)$$

$$\log_{10}{}^{*}K_s°(298.15\ K) = -(11.3 \pm 0.6)$$

$$Fe^{3+} + H_2SeO_3(aq) \rightleftharpoons FeSeO_3^{+} + 2\ H^{+}$$

$$\log_{10}{}^{*}\beta°(298.15\ K) = (0.9 \pm 0.5)$$

These values are included in TDB 2020.

Since Lemire et al. (2020) did not provide any ion interaction coefficients for the complex, we estimated them according to Tab. 1-7, see also Section 11.1.1, and included

$$\varepsilon(FeSeO_3^{+}, Cl^{-}) \approx \varepsilon(FeSeO_3^{+}, ClO_4^{-}) \approx (0.2 \pm 0.1)\ kg \cdot mol^{-1}$$

in TDB 2020.

11.6.3.3 Iron selenate compounds and complexes

11.6.3.3.1 Iron(II) selenate compounds and complexes

For iron(II) selenate complexation, Lemire et al. (2020) reviewed the study by Torres et al. (2010), already mentioned in Section 11.6.3.2.1 on iron(II) selenites. From their potentiometric titrations in 0.15 M $NaClO_4$ at 293.15 K, Torres et al. (2010) derived

$\log_{10}{}^{*}\beta_c(I_c = 1.50\ M, 293.15\ K, Fe^{2+} + 2\ H^{+} + 2\ SeO_4^{2-} \rightleftharpoons Fe(HSeO_4)_2(aq)) = (9.69 \pm 0.04)$

which was converted by Lemire et al. (2020), as in the case of the iron(II) selenite complexes, into

$\log_{10}\beta_m(I_m = 1.51\ m, 293.15\ K, Fe^{2+} + 2\ HSeO_4^{-} \rightleftharpoons Fe(HSeO_4)_2(aq)) = (5.67 \pm 0.08)$

but was also not selected for the reasons discussed in Section 11.6.3.2.1. Despite these shortcomings we accepted the rounded complexation constant with increased uncertainty

$Fe^{2+} + 2\ HSeO_4^{-} \rightleftharpoons Fe(HSeO_4)_2(aq)$

$\log_{10}\beta°(298.15\ K) = (5.7 \pm 1.0)$

together with the estimated (according to Tab. 1-7)

$\varepsilon(Fe(HSeO_4)_2\ (aq), NaCl) = \varepsilon(Fe(HSeO_4)_2\ (aq), NaClO_4) \approx (0.0 \pm 0.1)\ kg \cdot mol^{-1}$

for inclusion in TDB 2020 as supplemental data for scoping calculations.

11.6.3.3.2 Iron(III) selenate compounds and complexes

There appears to be no literature on iron(III) selenate complexation. Lemire et al. (2020) mentioned three studies reporting the preparation of a "green rust two" selenate compound, analogous to the "sulphate green rust two" (see Section 11.6.2.3.6). However, the "selenate green rust two" is metastable and the Se(VI) is reduced, first to Se(IV), and then to Se(0) or $FeSe_2$(cr). Lemire et al. (2020) did not select any thermodynamic quantities for this solid.

11.6.4 Nitrogen compounds and complexes

11.6.4.1 Iron(II) nitrate compounds and complexes

According to Lemire et al. (2020) there is no evidence in the literature for the formation of iron(II) nitrate complexes.

Values for $\varepsilon(Fe^{2+}, NO_3^{-})$ are also not known, due to the lack of osmotic coefficient data for iron(II) nitrate solutions which are instable to oxidation over extended periods of time. Therefore, Lemire et al. (2020) estimated a value based on a linear correlation of known $\varepsilon(M^{2+}, NO_3^{-})$ values (derived from osmotic-coefficient data) with the reciprocal of mean ion-water distances for six H_2O in the first solvation shell. From this correlation, Lemire et al. (2020) obtained the estimate

$\varepsilon(Fe^{2+}, NO_3^{-}) = (0.14 \pm 0.03)\ kg \cdot mol^{-1}$

which is very similar to the interaction coefficients of other first-row transition element metal ions, such as Ni^{2+}, Co^{2+}, and Zn^{2+}, which have similar ionic radii (Lemire et al. 2020). Lemire et al. (2020) did not select this value (no reasons given), but it appears to be very reasonable and is therefore included in TDB 2020.

The iron(II) nitrate solids, $Fe(NO_3)_2$(cr) and its hexa- and nonahydrates $Fe(NO_3)_2 \cdot 6H_2O$(cr) and $Fe(NO_3)_2 \cdot 9H_2O$(cr), are very soluble in water and no thermodynamic data were selected by Lemire et al. (2020).

11.6.4.2 Iron(III) nitrate compounds and complexes

According to Lemire et al. (2020), several experimental studies claimed the formation of $FeNO_3^{2+}$ in aqueous solution, but so far, no definitive evidence has been presented. Lemire et al. (2020) suggested to treat Fe(III) nitrate solutions as strong electrolyte up to moderate concentrations of 2 mol $\cdot$ dm^{-3}.

Since there are no osmotic coefficient data for $Fe(NO_3)_3$ solutions, Lemire et al. (2020) resorted to such data for $Al(NO_3)_3$ and $Cr(NO_3)_3$ as proxies and obtained

$$\varepsilon(Fe^{3+}, NO_3^-) = (0.26 \pm 0.08)\ kg \cdot mol^{-1}$$

as a "tentative value" (for $I_m \leq 6$) which they did not select. It is, however, included in TDB 2020.

Solid iron(III) nitrate occurs as the nonahydrate $Fe(NO_3)_3 \cdot 9H_2O$(cr) and possibly also as the hexahydrate $Fe(NO_3)_3 \cdot 6H_2O$(cr), they are very soluble in water and no thermodynamic data were selected by Lemire et al. (2020). There appears to be no unambiguous evidence for the formation of lower hydrates or of anhydrous $Fe(NO_3)_3$(cr).

Lemire et al. (2020) also discussed several iron(III) hydroxide nitrate solids, such as $Fe(OH)_2NO_2$(s), $FeO(OH)_{1-x}(NO_3)_x$(cr) (x = 0.2 – 0.3), $Fe(OH)(NO_3)_2 \cdot yH_2O$(s) (y = 2.0 – 2.2), $Fe_4(OH)_{11}NO_3$(cr), and $Fe_4(OH)_{11}NO_3 \cdot 2H_2O$(cr), but no reliable thermodynamic data are available for any of these.

11.6.5 Phosphorous compounds and complexes

Lemire et al. (2020) reviewed and selected thermodynamic data for aqueous iron(II) phosphate complexes and for iron(II) and iron(III) phosphorous solids. Aqueous iron(II) polyphosphate complexes and iron(III) monophosphate, diphosphate, phosphite and hypophosphite complexes were also reviewed, but Lemire et al. (2020) did not select any data.

11.6.5.1 Aqueous iron(II) phosphate complexes

Lemire et al. (2020) reviewed experimental data on the formation of $FeHPO_4$(aq) and $FeH_2PO_4^+$ and selected

$$Fe^{2+} + HPO_4^{2-} \rightleftharpoons FeHPO_4(aq)$$

$$\log_{10}K°(298.15\ K) = (3.6 \pm 1.0)$$

$Fe^{2+} + H_2PO_4^- \rightleftharpoons FeH_2PO_4^+$

$\log_{10}K°(298.15\ K) = (2.7 \pm 1.0)$

These data are included in TDB 2020. Since Lemire et al. (2020) did not select any specific ion interaction coefficients for these species, we estimated

$\varepsilon(FeHPO_4(aq), NaCl) = \varepsilon(FeHPO_4(aq), NaClO_4) \approx (0.0 \pm 0.1)\ kg \cdot mol^{-1}$

$\varepsilon(FeH_2PO_4^+, Cl^-) \approx (0.05 \pm 0.10)\ kg \cdot mol^{-1}$

$\varepsilon(FeH_2PO_4^+, ClO_4^-) \approx (0.2 \pm 0.1)\ kg \cdot mol^{-1}$

according to Tab. 1-7. These values are also included in TDB 2020.

Lemire et al. (2020) also reviewed several experimental studies on the formation of the iron(II) polyphosphate complexes $FeP_2O_7^{2-}$, $FeHP_2O_7^-$, $Fe(H_xP_2O_7)_3^{(6-2x)-}$, $FeP_3O_{10}^{3-}$, $FeHP_3O_{10}^{2-}$, $FeH_2P_3O_{10}^-$, $FeH_3P_3O_{10}(aq)$, $FeP_3O_9^-$, and $FeHP_3O_9(aq)$ but did not recommend any data.

11.6.5.2 Iron(II) phosphate compounds

Lemire et al. (2020) reviewed several experimental studies on the solubility of vivianite, $Fe_3(PO_4)_2 \cdot 8H_2O(cr)$, and selected the following solubility product

$Fe_3(PO_4)_2 \cdot 8H_2O(vivianite) + 2\ H^+ \rightleftharpoons 3\ Fe^{2+} + 2\ HPO_4^{2-} + 8\ H_2O(l)$

$\log_{10}K_s°(298.15\ K) = -(11.3 \pm 0.4)$

which is included in TDB 2020.

Lemire et al. (2020) also selected calorimetrically determined values of $C_{p,m}°(298.15\ K)$ and $S_m°(298.15\ K)$ for $Fe_2P_2O_7(cr)$. Since these data are not sufficient for equilibrium calculations, they are not included in TDB 2020.

11.6.5.3 Aqueous iron(III) phosphorous complexes

Lemire et al. (2020) remarked that despite a large number of experimental investigations, there is still a considerable uncertainty with respect to the stoichiometry and stability of the major aqueous iron(III) phosphorous complexes. They discussed experimental data concerning the monophosphate complexes $FeH_3PO_4^{3+}$, $FeH_2PO_4^{2+}$, $FeHPO_4^+$, $FePO_4(aq)$, $Fe(OH)PO_4^-$, $FeH(H_2PO_4)_2^{2+}$, $Fe(H_2PO_4)_2^+$, $Fe(PO_4)_2^{3-}$, $Fe(HPO_4)_2^-$, $Fe(HPO_4)(H_2PO_4)(aq)$, $FeH(H_2PO_4)_3^+$, $Fe(H_2PO_4)_3(aq)$, $Fe(H_2PO_4)_4^-$, $Fe_2HPO_4^{4+}$, $Fe_3H(PO_4)_2^{4+}$, $Fe_3H_2(PO_4)_3^{2+}$, $Fe_3H_4(PO_4)_3^{4+}$, $Fe_3H_6(PO_4)_4^{3+}$, $Fe_3H_9(PO_4)_5^{3+}$, $Fe_3H_8(PO_4)_5^{2+}$, $Fe_3H_9(PO_4)_6(aq)$, $Fe(OH)_3(HPO_4)^{2-}$, $Fe(OH)_4(HPO_4)^{3-}$, and $Fe(OH)_3(H_2PO_4)^-$, the diphosphate complexes $Fe(HP_2O_7)_2^{3-}$, $Fe(H_2P_2O_7)_2^-$, $Fe(H_3P_2O_7)_2^+$, $FeH_3P_2O_7^{2+}$, $FeH_2P_2O_7^+$, $Fe_2P_2O_7^{2+}$, $FeH_2P_3O_{10}(aq)$, and $Fe(HP_3O_{10})_2^{5-}$, the phosphite complexes $FeH_2PO_3^{2+}$, and $Fe(H_2PO_3)_2^+$, and the hypophosphite complexes $FeH_2PO_2^{2+}$, $Fe(H_2PO_2)_2^+$, and $Fe(H_2PO_2)_3(aq)$. Lemire et al. (2020) did not select data for any of these complexes.

11.6.5.4 Iron(III) and mixed iron(II/III) phosphorous compounds

Lemire et al. (2020) selected calorimetrically determined values of $C_{p,m}°$(298.15 K) and $S_m°$(298.15 K) for the following iron(III) or iron (II/III) phosphorous solids: $Fe(PO_3)_3$(cr, monoclinic), $Fe(PO_3)_3 \cdot 0.128H_2O$(cr, monoclinic), $FePO_4 \cdot 2H_2O$(cr, orthorhombic), Fe_3PO_7(cr), $Fe_4(P_2O_7)_3$(cr), and $Fe^{II}Fe^{III}_2(P_2O_7)_2$(cr). Since values for heat capacities and entropies alone are insufficient for equilibrium calculations, they are not included in TDB 2020.

Calorimetric data selected by Lemire et al. (2020) for the anhydrous, trigonal Fe(III) phosphate $FePO_4$(rodolicoite) are discussed in the next section.

Lemire et al. (2020) also reviewed the solubility of $FePO_4 \cdot 2H_2O$(s), whose crystalline form corresponds to the mineral strengite, but did not recommend any data. Their conclusions with respect to the quality of the reviewed solubility data are discussed in the next section.

11.6.5.5 Selected iron(III) data for scoping calculations

Lemire et al. (2020) reviewed several solubility studies of iron(III) phosphate solids, namely $FePO_4$(am), $FePO_4 \cdot 2H_2O$(cr), $FePO_4 \cdot 2H_2O$("strengite"), $Fe(H_2PO_4)(HPO_4) \cdot xH_2O$(s), and $Fe(HPO_4)_{1.5}$(s), but noted that the reported solubility products are in general inconsistent, because they refer in many cases to ill-defined, amorphous or metastable solids, or because, in the light of the numerous proposed Fe(III) phosphorous complexes, complexation was not properly accounted for. They also pointed out that studies referring to orthorhombic strengite may actually have dealt with the possibly more stable monoclinic "metastrengite II". After an extensive discussion of several solubility studies of $FePO_4 \cdot 2H_2O$(s) and various speciation schemes for Fe(III) phosphorous complexes, Lemire et al. (2020) came to the conclusion that the results of the solubility studies can be explained reasonably well with a range of values for the equilibrium constants of the following reactions (where complex formation is expressed by $Fe^{3+} + q\ H_3PO_4(aq) \rightleftharpoons FeH_{-p}(H_3PO_4)_q^{3-p} + p\ H^+$ with $\log_{10}\beta_{p,q}°$):

$$FePO_4 \cdot 2H_2O(s) + 2\ H^+ \rightleftharpoons Fe^{3+} + H_2PO_4^- + 2\ H_2O(l)$$

$$Fe^{3+} + H_3PO_4(aq) \rightleftharpoons FePO_4(aq) + 3\ H^+$$

$$Fe^{3+} + 3\ H_3PO_4(aq) \rightleftharpoons FeH_6(PO_4)_3(aq) + 3\ H^+$$

where $\log_{10}K_s°$(298.15 K) varies from -9.1 to -7.1, $\log_{10}\beta_{3,1}°$(298.15 K) from 1.7 to -0.3, and $\log_{10}\beta_{3,3}°$(298.15 K) from 4.5 – 2.5. However, Lemire et al. (2020) also stated that it "is clear that other complexes exist and probably contribute to the total solubility. Thus the complicated speciation in low ionic-strength solutions containing low concentrations of iron(III) and an excess of phosphate (> 0.02 m) remains unresolved. […] there also is no reason to assume that the structures of such complexes are those of the simple formulae used here. In the present review no values are selected for the formation constants of iron(III) complexes with phosphate or for the solubility product of FePO4 · 2H2O(cr)."

Despite these uncertainties with respect to solubility and complex formation, this set of reactions with the averaged values

$$log_{10}K_s°(298.15\ K) = -(8.1 \pm 1.0)$$

$$log_{10}\beta_{3,1}°(298.15\ K) = (0.7 \pm 1.0)$$

$$log_{10}\beta_{3,3}°(298.15\ K) = (3.5 \pm 1.0)$$

where each uncertainty covers the complete range of values suggested by Lemire et al. (2020), are included in TDB 2020 as supplemental data, serving as placeholders for scoping calculations.

Missing specific ion interaction coefficients were estimated according to Tab. 1-7

$$\varepsilon(FePO_4(aq), NaCl) = \varepsilon(FePO_4(aq), NaClO_4) \approx (0.0 \pm 0.1)\ kg \cdot mol^{-1}$$

$$\varepsilon(FeH_6(PO_4)_3(aq), NaCl) = \varepsilon(FeH_6(PO_4)_3\ (aq), NaClO_4) \approx (0.0 \pm 0.1)\ kg \cdot mol^{-1}$$

and are also included in TDB 2020 as supplemental data. Note that $FeH_6(PO_4)_3$(aq) is equivalent to $Fe(H_2PO_4)_3$(aq).

For the anhydrous, trigonal Fe(III) phosphate $FePO_4$(rodolicoite), Lemire et al. (2020) reviewed calorimetric data and selected

$$C_{p,m}°(\text{rodolicoite, cr, 298.15 K}) = (101.96 \pm 1.12)\ J \cdot K^{-1} \cdot mol^{-1}$$

$$S_m°(\text{rodolicoite, cr, 298.15 K}) = (122.21 \pm 1.34)\ J \cdot K^{-1} \cdot mol^{-1}$$

$$\Delta_f H_m°(\text{rodolicoite, cr, 298.15 K}) = -(1'267.56 \pm 1.35)\ kJ \cdot mol^{-1}$$

$$\Delta_f G_m°(\text{rodolicoite, cr, 298.15 K}) = -(1'161.338 \pm 1.411)\ kJ \cdot mol^{-1}$$

The solubility product $\log_{10}{}^{*}K_{s,0}°(298.15\ K)$ for the reaction

$$FePO_4(\text{rodolicoite}) + 2\ H^+ \rightleftharpoons Fe^{3+} + H_2PO_4^-$$

can be calculated from $\Delta_f G_m°$(rodolicoite, cr, 298.15 K), and the selected $\Delta_f G_m°(Fe^{3+}, 298.15\ K) = -(16.23 \pm 0.65)\ kJ \cdot mol^{-1}$, and $\Delta_f G_m°(H_2PO_4^-, 298.15\ K) = -(1'137.152 \pm 1.567)\ kJ \cdot mol^{-1}$, resulting in $\Delta_r G_m°(298.15\ K) = (7.956 \pm 2.207)\ kJ \cdot mol^{-1}$ or $\log_{10}K_{s,0}°(298.15\ K) = -(1.39 \pm 0.39)$ and $\Delta_r H_m°(298.15\ K)$ from $\Delta_f H_m°$(rodolicoite, cr, 298.15 K), and the selected $\Delta_f H_m°(Fe^{3+}, 298.15\ K) = -(50.06 \pm 0.97)\ kJ \cdot mol^{-1}$ and $\Delta_f H_m°(H_2PO_4^-, 298.15\ K) = -(1'267.56 \pm 1.35)\ kJ \cdot mol^{-1}$, resulting in $\Delta_r H_m°(298.15\ K) = -(85.1 \pm 2.2)\ kJ \cdot mol^{-1}$.

These data for rodolicoite may supplement scoping calculations with FePO4 · 2H2O(s) and therefore

$$FePO_4(rodolicoite) + 2\ H^+ \rightleftharpoons Fe^{3+} + H_2PO_4^-$$

$$log_{10}K_{s,0}°(298.15\ K) = -(1.39 \pm 0.39)$$

$$\Delta_r H_m°(298.15\ K) = -(85.1 \pm 2.2)\ kJ \cdot mol^{-1}$$

are also included in TDB 2020 as supplemental data. Note, however, that the calculated solubility of rodolicoite is orders of magnitude higher than that of $FePO_4 \cdot 2H_2O$(s).

11.6.6 Arsenic compounds and complexes

11.6.6.1 Iron(II) arsenate compounds and complexes

Lemire et al. (2020) discussed the Fe(II) arsenate complexes $FeAsO_4^-$, $FeHAsO_4$(aq), and FeH2AsO4+ and the mineral polymorphs symplesite and parasymplesite, Fe3(AsO4)2 · 8H2O(cr), but did not select any data.

11.6.6.2 Iron(III) arsenate compounds and complexes

Lemire et al. (2020) discussed the Fe(III) arsenate complexes FeAsO4(aq), FeHAsO4+, FeH2AsO42+ but did not select any data. For the arsenate solids FeAsO4(cr), FeAsO4 · 2H2O(scorodite), FeAsO4 · 2H2O(parascorodite), and FeAsO4 · 3.5H2O(kankite) they selected calorimetric data and for Fe4(AsO4)4 · 3H2O(cr) a solubility product based on solubility measurements.

The data for these solids are not included in TDB 2020, since it is not conceivable that they may play any role in the application range of TDB 2020.

11.7 Group 14 compounds and complexes

11.7.1 Carbon compounds and complexes

11.7.1.1 Aqueous iron(II) carbonate complexes

11.7.1.1.1 Data in TDB 05/92, TDB 01/01 and TDB 12/07

For the stability constants of $FeCO_3(aq)$ and $FeHCO_3^+$, Pearson et al. (1992) relied on the values reported by Nordstrom et al. (1990). The latter authors estimated the stability constant for $FeCO_3(aq)$ according to Langmuir (1979), who presented a linear correlation between stability constants for carbonate and oxalate complexes of divalent metals, $MCO_3(aq)$ and $MC_2O_4(aq)$

$$\log_{10}K°(MCO_3, aq, 298.15\ K) = 1.11\ \log_{10}K°(MC_2O_4, aq, 298.15\ K)$$

For the calculation of $\log_{10}K°(MC_2O_4, aq, 298.15\ K)$, Langmuir (1979) suggested the use of a semi-empirical relationship by Yatsimirskii & Vasil'ev (1960)

$$\log_{10}K°(MC_2O_4, aq, 298.15\ K) = 2.5 + 0.47\ B$$

where B is 2.0 for Mg^{2+}, 3.0 for Mn^{2+}, 4.0 for Fe^{2+}, 4.8 for Co^{2+}, 5.2 for Zn^{2+}, 6.0 for Ni^{2+}, and 8.5 for Cu^{2+}. Using these two relationships for Fe^{2+}, one obtains $\log_{10}K°(FeC_2O_4, aq, 298.15\ K) = 4.38$ and $\log_{10}K°(FeCO_3, aq, 298.15\ K) = 4.86$.

Unfortunately, Nordstrom et al. (1990) mistook $\log_{10}K°(FeC_2O_4, aq, 298.15\ K)$ for $\log_{10}K°(FeCO_3, aq, 298.15\ K)$ and selected the incorrect

$$\log_{10}K°(298.15\ K) = 4.38$$

for

$$Fe^{2+} + CO_3^{2-} \rightleftharpoons FeCO_3(aq)$$

For TDB 05/92, Pearson et al. (1992) accepted this incorrect value and, using $HCO_3^- \rightleftharpoons CO_3^{2-} + H^+$ with $\log_{10}{}^*K°(298.15\ K) = -10.329$, selected

$$Fe^{2+} + HCO_3^- \rightleftharpoons FeCO_3(aq) + H^+$$

$$\log_{10}{}^*K°(298.15\ K) = -5.949$$

This value was retained in TDB 01/01 and TDB 12/07.

Nordstrom et al. (1990) selected

$$Fe^{2+} + HCO_3^- \rightleftharpoons FeHCO_3^+$$

$$\log_{10}K°(298.15\ K) = 2$$

referring to Fouillac & Criaud (1984) who took this value from Serebrennikov (1977) who listed it as a "rough estimate from I.L. Khodakovskiy". This estimate, selected by Pearson et al. (1992) for TDB 05/92, was retained in TDB 01/01 and TDB 12/07.

All these data are not retained in TDB 2020 and are replaced by data presented in the following sections.

11.7.1.1.2 $FeHCO_3^+$

Lemire et al. (2013) discussed 4 experimental studies concerned with the formation of the Fe(II) bicarbonate complex. In two of the studies, it was impossible to determine its formation constant, and in the other two studies the inclusion of $FeHCO_3^+$ in the data analysis led to poorer fits. Lemire et al. (2013) concluded that there is no strong evidence for the formation of this complex (it is at best very weak) and did not select any formation constant. We agree with this evaluation, therefore the constant selected for TDB 05/92, TDB 01/01 and TDB 12/07 discussed in the previous section is not included in TDB 2020.

11.7.1.1.3 $FeCO_3(aq)$ and $Fe(CO_3)_2^{2-}$

According to Lemire et al. (2013), the solubility study of Bruno et al. (1992b) is the only one that quantitatively describes the formation of $FeCO_3(aq)$ and $Fe(CO_3)_2^{2-}$. These authors investigated the solubility of hydrothermally produced $FeCO_3$(siderite) at 25 °C in 1.0 M $NaClO_4$ (1.0515 m) and pH in the range from 6 – 9 and interpreted it in terms of the formation of $FeCO_3(aq)$ and $Fe(CO_3)_2^{2-}$, assuming that these are the only Fe(II) species. Lemire et al. (2013) reanalysed the experimental data by also taking into account Fe^{2+} and obtained

$$FeCO_3(siderite) + 2\ H^+ \rightleftharpoons Fe^{2+} + CO_2g + H_2O(l) \qquad (11.7.1)$$

$$\log_{10}{}^*K_{p,s,0}((11.7.1), 298.15\ K, 1.0515\ m\ NaClO_4) = (7.52 \pm 0.05)$$

$$FeCO_3(siderite) \rightleftharpoons FeCO_3(aq) \qquad (11.7.2)$$

$$\log_{10}K_{p,s,1}((11.7.2), 298.15\ K, 1.0515\ m\ NaClO_4) = -(5.41 \pm 0.04)$$

$$FeCO_3(siderite) + H_2O(l) + CO_2g \rightleftharpoons Fe(CO_3)_2^{2-} + 2\ H^+ \qquad (11.7.3)$$

$$\log_{10}{}^*K_{p,s,2}((11.7.3), 298.15\ K, 1.0515\ m\ NaClO_4) = -(20.82 \pm 0.06)$$

They extrapolated $\log_{10}{}^*K_{p,s,0}((11.7.1), 298.15\ K, 1.0515\ m\ NaClO_4)$ to zero ionic strength by applying the standard SIT procedure, using, $\varepsilon(H^+, ClO_4^-) = (0.14 \pm 0.02)\ kg \cdot mol^{-1}$, $\varepsilon(Fe^{2+}, ClO_4^-) = (0.37 \pm 0.04)\ kg \cdot mol^{-1}$, and $a(H_2O) = 0.966$. Thus,

$$\log_{10}{}^*K_{p,s,0}°((11.7.1), 298.15\ K) = (7.19 \pm 0.05)$$

which corresponds to $\Delta_r G_m°((11.7.1), 298.15\ K) = -(41.04 \pm 0.29)\ kJ \cdot mol^{-1}$. In the Appendix A (p. 723) Lemire et al. (2013) made the remark that "because there was no confirmation that the nature of the solid did not change as a function of the hydrogen ion concentration … the uncertainty in $\log_{10}{}^{*}K_{s,0}$(A.143) for the author's sample of $FeCO_3$(s) is more realistically estimated as ± 0.15"[43]. However, in the main text (p. 362) the uncertainty of $\log_{10}{}^{*}K_{p,s,0}°((7.1), 298.15\ K)$ is still given as ± 0.05 and the corresponding unchanged uncertainty of ± 0.29 for $\Delta_r G_m°((7.1), 298.15\ K)$ was used by Lemire et al. (2013) in further calculations.

Since $FeCO_3$(siderite) ⇌ $FeCO_3$(aq) is an isocoulombic reaction, it does, to a first approximation, not depend on ionic strength. Therefore,

$$\log_{10}K_{p,s,1}°((7.2), 298.15\ K) = -(5.41 \pm 0.04)$$

or $\Delta_r G_m°((7.2), 298.15\ K) = (30.88 \pm 0.90)\ kJ \cdot mol^{-1}$ (uncertainty increased by Lemire et al. 2013, from ± 0.23 to ± 0.90 to account for the "uncertainty in the consistency of the nature of the solid", which corresponds to an uncertainty for $\log_{10}K_{p,s,1}°((7.2), 298.15\ K)$ of ± 0.16).

Finally, Lemire et al. (2013) extrapolated $\log_{10}{}^{*}K_{p,s,2}((7.3), 298.15\ K, 1.0515\ m\ NaClO_4)$ to zero ionic strength with $\varepsilon(H^+, ClO_4^-) = (0.14 \pm 0.02)\ kg \cdot mol^{-1}$, $a(H_2O) = 0.966$, and $\varepsilon(Fe(CO_3)_2^{2-}, Na^+) \approx -(0.05 \pm 0.05)\ kg \cdot mol^{-1}$.

The latter value was estimated by analogy with $\varepsilon(CO_3^{2-}, Na^+) = -(0.08 \pm 0.03)\ kg \cdot mol^{-1}$ and $\varepsilon(UO_2(CO_3)_2^{2-}, Na^+) = -(0.02 \pm 0.09)\ kg \cdot mol^{-1}$. With this estimate

$$\log_{10}{}^{*}K_{p,s,2}°((7.3), 298.15\ K) = -(21.80 \pm 0.12)$$

or $\Delta_r G_m°((7.3), 298.15\ K) = (124.44 \pm 0.90)\ kJ \cdot mol^{-1}$ (uncertainty increased by Lemire et al. 2013, from ± 0.68 to ± 0.90 for the reason mentioned above, which corresponds to an uncertainty for $\log_{10}{}^{*}K_{p,s,2}°((7.3), 298.15\ K)$ of ± 0.16).

Lemire et al. (2013) recommended

$$\log_{10}K_{p,s,1}°((7.2), 298.15\ K) = -(5.41 \pm 0.16)$$

and

$$\log_{10}{}^{*}K_{p,s,2}°((7.3), 298.15\ K) = -(21.80 \pm 0.16)$$

which are both listed in Tab. III-2 (Lemire et al. 2013, p. 50), in contrast to $\log_{10}{}^{*}K_{p,s,0}°(298.15\ K)$, which is not listed.

---

[43] The increased uncertainty ± 0.15 for $\log_{10}{}^{*}K_{p,s,0}°((12.7.1), 298.15\ K)$ corresponds to ± 0.86 for $\Delta_r G_m°((12.7.1), 298.15\ K)$.

Lemire et al. (2013) then went on to calculate $\Delta_f G_m°(FeCO_3, aq, 298.15\ K)$ from

$$\Delta_f G_m°(FeCO_3, aq, 298.15\ K) = \Delta_f G_m°(Fe^{2+}, 298.15\ K) + \Delta_f G_m°(CO_2, g, 298.15\ K)$$

$$+ \Delta_f G_m°(H_2O, l, 298.15\ K) + \Delta_r G_m°((11.7.2), 298.15\ K)$$

$$- \Delta_r G_m°((11.7.1), 298.15\ K)$$

and $\Delta_f G_m°(Fe(CO_3)_2^{2-}, aq, 298.15\ K)$ from

$$\Delta_f G_m°(Fe(CO_3)_2^{2-}, aq, 298.15\ K) = \Delta_f G_m°(Fe^{2+}, 298.15\ K) + 2\ \Delta_f G_m°(CO_2, g, 298.15\ K)$$

$$+ 2\ \Delta_f G_m°(H_2O, l, 298.15\ K) + \Delta_r G_m°((11.7.3), 298.15\ K)$$

$$- \Delta_r G_m°((11.7.1), 298.15\ K)$$

Note that both $\Delta_f G_m°(FeCO_3, aq, 298.15\ K)$ and $\Delta_f G_m°(Fe(CO_3)_2^{2-}, aq, 298.15\ K)$ depend on $\Delta_r G_m°((11.7.1), 298.15\ K)$, and thus on $\log_{10}{}^{*}K_{p,s,0}°((11.7.1), 298.15\ K)$.

With $\Delta_r G_m°((11.7.1), 298.15\ K) = -(41.04 \pm 0.29)\ kJ \cdot mol^{-1}$, $\Delta_r G_m°((11.7.2), 298.15\ K) = (30.88 \pm 0.90)\ kJ \cdot mol^{-1}$, $\Delta_r G_m°((11.7.3), 298.15\ K) = (124.44 \pm 0.90)\ kJ \cdot mol^{-1}$, $\Delta_f G_m°(Fe^{2+}, 298.15\ K) = -(90.72 \pm 0.64)\ kJ \cdot mol^{-1}$, $\Delta_f G_m°(CO_2, g, 298.15\ K) = (-394.373 \pm 0.133)\ kJ \cdot mol^{-1}$, and $\Delta_f G_m°(H_2O, l, 298.15\ K) = -(237.140 \pm 0.041)\ kJ \cdot mol^{-1}$, Lemire et al. (2013) obtained $\Delta_f G_m°(FeCO_3, aq, 298.15\ K) = -(648.68 \pm 1.29)\ kJ \cdot mol^{-1}$ and $\Delta_f G_m°(Fe(CO_3)_2^{2-}, aq, 298.15\ K) = -(1'186.67 \pm 1.30)\ kJ \cdot mol^{-1}$.

Doing the same calculations with the same data[44] we obtained different values: $-(650.31 \pm 1.41)\ kJ \cdot mol^{-1}$ instead of $-(648.68 \pm 1.29)\ kJ \cdot mol^{-1}$ for $\Delta_f G_m°(FeCO_3, aq, 298.15\ K)$, and $-(1'188.31 \pm 1.43)\ kJ \cdot mol^{-1}$ instead of $-(1'186.67 \pm 1.30)\ kJ \cdot mol^{-1}$ for $\Delta_f G_m°(Fe(CO_3)_2^{2-}, 298.15\ K)$. We used these values for further calculations, as well as $\Delta_f G_m°(FeCO_3, siderite, 298.15\ K) = -(681.19 \pm 1.08)\ kJ \cdot mol^{-1}$, which follows from

$$\Delta_f G_m°(FeCO_3, siderite, 298.15\ K) = \Delta_f G_m°(Fe^{2+}, 298.15\ K) + \Delta_f G_m°(CO_2, g, 298.15\ K)$$

$$+ \Delta_f G_m°(H_2O, l, 298.15\ K) - \Delta_r G_m°((11.7.1), 298.15\ K)$$

In summary, the experimental data by Bruno et al. (1992b) as reanalysed by Lemire et al. (2013) can be represented by

$$\log_{10}{}^{*}K_{p,s,0}°((11.7.1), 298.15\ K) = (7.19 \pm 0.15)$$

$$\log_{10}K_{p,s,1}°((11.7.2), 298.15\ K) = -(5.41 \pm 0.16)$$

$$\log_{10}{}^{*}K_{p,s,2}°((11.7.3), 298.15\ K) = -(21.80 \pm 0.16)$$

---

[44] Note that we used the increased uncertainty of ± 0.86 for $\Delta_r G_m°((12.7.1), 298.15\ K)$, corresponding to the uncertainty of ± 0.15 for $\log_{10}{}^{*}K_{p,s,0}°(298.15\ K)$ proposed by Lemire et al. (2013).

Eqs. (11.7.1), (11.7.2), and (11.7.3) can be converted into

$$FeCO_3(siderite) + H^+ \rightleftharpoons Fe^{2+} + HCO_3^- \quad (11.7.4)$$

$$Fe^{2+} + HCO_3^- \rightleftharpoons FeCO_3(aq) + H^+ \quad (11.7.5)$$

$$Fe^{2+} + 2\ HCO_3^- \rightleftharpoons Fe(CO_3)_2^{2-} + 2\ H^+ \quad (11.7.6)$$

Using our values for $\Delta_f G_m°(FeCO_3, siderite, 298.15\ K)$, $\Delta_f G_m°(FeCO_3, aq, 298.15\ K)$, and $\Delta_f G_m°(Fe(CO_3)_2^{2-}, aq, 298.15\ K)$ discussed above and $\Delta_f G_m°(HCO_3^-, 298.15\ K) = -(586.845 \pm 0.251)\ kJ \cdot mol^{-1}$ leads to

$$\Delta_r G_m°((11.7.4), 298.15\ K) = (3.63 \pm 1.28)\ kJ \cdot mol^{-1}$$

$$\Delta_r G_m°((11.7.5), 298.15\ K) = (27.25 \pm 1.57)\ kJ \cdot mol^{-1}$$

$$\Delta_r G_m°((11.7.6), 298.15\ K) = (76.10 \pm 1.64)\ kJ \cdot mol^{-1}$$

which is equivalent to

$$\log_{10}{}^*K_{s,0}°((11.7.4), 298.15\ K) = -(0.64 \pm 0.22)$$

$$\log_{10}{}^*\beta_1°((11.7.5), 298.15\ K) = -(4.77 \pm 0.27)$$

$$\log_{10}{}^*\beta_2°((11.7.6), 298.15\ K) = -(13.33 \pm 0.29)$$

The values for $\log_{10}{}^*\beta_1°((11.7.5), 298.15\ K)$ and $\log_{10}{}^*\beta_2°((11.7.6), 298.15\ K)$ are included in TDB 2020, as well as

$$\varepsilon(FeCO_3(aq), NaCl) = \varepsilon(FeCO_3(aq), NaClO_4) \approx (0.0 \pm 0.1)\ kg \cdot mol^{-1}$$

and

$$\varepsilon(Fe(CO_3)_2^{2-}, Na^+) \approx -(0.05 \pm 0.05)\ kg \cdot mol^{-1}$$

estimated according to Tab. 1-7.

The selected thermodynamic data for $FeCO_3$(siderite) are discussed in Section 11.7.1.3.2.

11.7.1.2 Aqueous iron(III) carbonate complexes

11.7.1.2.1 Data in TDB 05/92, TDB 01/01 and TDB 12/07

No data for Fe(III) carbonate complexes were included in TDB 05/92. During the update procedure for TDB 01/01 this lack of stability constants of Fe(III) carbonate complexes was regarded as a serious deficiency in the database, and therefore, the work of Bruno et al. (1992a) on the solubility of hematite in aqueous $NaHCO_3$ solutions was carefully reviewed with the aim of including their results in TDB 01/01.

Unfortunately, the findings of Bruno et al. (1992a) were disguised by gross computational errors and some inconsistencies in the treatment of the experimental data that, in turn, concealed an unresolved ambiguity in the experiments (see Hummel 2000 for a detailed discussion).

The stability constants of the complexes as reported by Bruno et al. (1992a) are such small numbers that Fe(III) carbonate complexes are predicted to be completely negligible in any aqueous system. A detailed re-examination by Hummel (2000) of the reported experimental data revealed that these small numbers resulted from computational errors of 19 orders of magnitude. However, using the correctly derived constants and assuming solubility equilibrium with hematite lead to the stunning picture of carbonate complexes dominating the entire aqueous chemistry of ferric iron, thus contradicting all experimental evidence of Fe(III) solubility at high pH. The conclusion was that the solubility controlling solid phase in the experiments of Bruno et al. (1992a) was not the initial hematite but most probably some freshly precipitated ferrihydrite (Hummel 2000).

Bruno & Duro (2000) agreed with the general conclusions of Hummel (2000) and stated that "all the inconclusive issues of this particular work - identification of the controlling solid phase and the existence and stability of the mixed Fe(III) hydroxo-carbonato complexes - are now part of an ongoing Ph.D. thesis"[45].

Thus, no equilibrium constants were recommended for TDB 01/01. However, for exploring the possible effects of Fe(III) carbonate complexation in modelling exercises the following estimate was reported

$$Fe^{3+} + 2\ CO_3^{2-} \rightleftharpoons Fe(CO_3)_2^-$$

$$20 \le \log_{10}\beta_2^\circ \le 22$$

This range of stability was estimated on the basis of the experimental data by Bruno et al. (1992a) by assuming $Fe(OH)_3$(am) or $Fe(OH)_3$(mic), respectively, as the solubility controlling phase. For a detailed discussion see Hummel (2000).

[45] The mentioned Ph.D. thesis is that of Grivé (2005).

11.7.1.2.2 $FeCO_3OH(aq)$ and $Fe(CO_3)_3^{3-}$

In light of the deficiencies of the solubility study by Bruno et al. (1992a) discussed in the previous section, Grivé (2005) undertook a similar study on the solubility of hematite and ferrihydrite and interpreted the solubility in terms of the formation of $FeCO_3OH(aq)$ and $Fe(CO_3)_3^{3-}$. According to Lemire et al. (2013), the solubility data for ferrihydrite, $Fe(OH)_3(s)$, gave the best evidence for the formation of these complexes, but Lemire et al. (2013) also remarked that the solubility product obtained from the experimental data for ferrihydrite "is probably more in line with a poorly crystalline goethite (α-FeOOH) or lepidocrocite (γ-FeOOH) than a true ferrihydrite specimen". The solubility of ferrihydrite was measured by Grivé (2005) in 0.5 M $NaClO_4$ at 25 °C under CO_2g partial pressures of 0.97, 0.297, and 0.01 atm. Fe(III) concentrations between pH 4 and 7 were constant, suggesting the dominance of the neutral complex $FeCO_3OH(aq)$, while solubility increased strongly at pH greater than 7 with a slope compatible with $Fe(CO_3)_3^{3-}$. Although Lemire et al. (2013) stated that "the stability of a soluble neutral species, $FeCO_3OH(aq)$, in equilibrium with ferrihydrite or hematite is highly improbable, because it would require 1 or 3 water molecules to fulfil the coordination number of 4 or 6 for iron. As there is a strong tendency for OH^- to act as a bridging ligand, it is unlikely that $FeCO_3OH(aq)$ prefers water to complete its coordination sphere. Also the apparent extended region of stability of $Fe(OH)CO_3(aq)$ from a pH value of approximately 4.5 to a pH value of approximately 7 [...] is puzzling. It would seem to require a stabilizing effect such as bridging, yet the solubility dependence on p_{CO_2} does not fit with a predominantly polymeric iron(III) species". These problems notwithstanding, Lemire et al. (2013) concluded that the data by Grivé (2005) are probably the best available. They recalculated the values for the formation constants from the original data and applied the standard SIT procedure to extrapolate the constants to zero ionic strength, using $\varepsilon(Fe^{3+}, ClO_4^-) = (0.73 \pm 0.04)$ kg · mol^{-1}, $\varepsilon(H^+, ClO_4^-) = (0.14 \pm 0.02)$ kg · mol^{-1}, and $\varepsilon(CO_3^{2-}, Na^+) = -(0.08 \pm 0.03)$ kg · mol^{-1}, and assuming $\varepsilon(Fe(CO_3)_3^{3-}, Na^+)$ to be equal to $\varepsilon(Am(CO_3)_3^{3-}, Na^+) = -(0.23 \pm 0.07)$ kg · mol^{-1} and the interaction coefficient for the neutral $Fe(OH)CO_3(aq)$ to be zero with any cation or anion. In this way, Lemire et al. (2013) obtained

$$Fe^{3+} + CO_3^{2-} + H_2O(l) \rightleftharpoons Fe(OH)CO_3(aq) + H^+$$

$$\log_{10}{}^*\beta_{111}°(298.15\ K) = (10.7 \pm 2.0)$$

and

$$Fe^{3+} + 3\ CO_3^{2-} \rightleftharpoons Fe(CO_3)_3^{3-}$$

$$\log_{10}{}^*\beta_{103}°(298.15\ K) = (24.0 \pm 2.0)$$

The uncertainties were substantially increased because the statistical uncertainties of the data treatment were thought to be too small in comparison with the uncertainties pointed out above. These data are included in TDB 2020, as well as

$$\varepsilon(Fe(CO_3)_3^{3-}, Na^+) \approx -(0.23 \pm 0.07)\ kg \cdot mol^{-1}$$

estimated above and

$\varepsilon(Fe(OH)CO_3(aq), NaCl) = \varepsilon(Fe(OH)CO_3(aq), NaClO_4) \approx (0.0 \pm 0.1)$ kg · mol^{-1}

estimated according to Tab. 1-7.

Grivé et al. (2014) also reanalysed the data by Grivé (2005); their formation constants $\log_{10}{}^{*}\beta_{111}°(298.15\ K) = (10.76 \pm 0.38)$ and $\log_{10}{}^{*}\beta_{103}°(298.15\ K) = (24.24 \pm 0.42)$ are very similar to those recommended by Lemire et al. (2013), although with much smaller uncertainties.

11.7.1.3 Iron carbonate compounds

11.7.1.3.1 Data in TDB 05/92, TDB 01/01 and TDB 12/07

The thermodynamic data for crystalline and precipitated siderite ($FeCO_3$) selected by Pearson et al. (1992) originate from Nordstrom et al. (1990), who selected

$FeCO_3(siderite) \rightleftharpoons Fe^{2+} + CO_3^{2-}$

$\log_{10}K_{s,0}°(298.15\ K) = -10.89$

$\Delta_rH_m°(298.15\ K) = -10.4$ kJ · mol^{-1}

The latter authors recalculated the $\log_{10}K_{s,0}(303\ K)$ determined by Smith (1918) using their own data for aqueous species at 30 °C and adjusted the obtained value to 25 °C using $\Delta_rH_m°(298.15\ K)$ calculated from the standard enthalpies of formation for the ions from Wagman et al. (1982) and for the solid from Robie et al. (1984).

Similarly, Nordstrom et al. (1990) recalculated the solubility constant determined by Singer & Stumm (1970) at 25 °C and obtained

$FeCO_3(pr) \rightleftharpoons Fe^{2+} + CO_3^{2-}$

$\log_{10}K_{s,0}°(298.15\ K) = -10.45$

For TDB 05/92, Pearson et al. (1992) reformulated both reaction equilibria in terms of HCO_3^-, by using $HCO_3^- \rightleftharpoons CO_3^{2-} + H^+$ with $\log_{10}{}^{*}K°(298.15\ K) = -10.329$ and $\Delta_rH_m°(298.15\ K) = 14.901$ kJ · mol^{-1}. Thus,

$FeCO_3(cr) + H^+ \rightleftharpoons Fe^{2+} + HCO_3^-$

$\log_{10}{}^{*}K_{s,0}°(298.15\ K) = -0.5612$

$\Delta_rH_m°(298.15\ K) = -25.28$ kJ · mol^{-1}

$FeCO_3(pr) + H^+ \rightleftharpoons Fe^{2+} + HCO_3^-$

$\log_{10}{}^{*}K_{s,0}°(298.15\ K) = -0.1211$

These data were retained in TDB 01/01 and TDB 12/07.

11.7.1.3.2 Siderite ($FeCO_3$)

The solubility of $FeCO_3$(siderite) in terms of Fe^{2+} can be expressed in several ways:

$$FeCO_3(siderite) + 2\ H^+ \rightleftharpoons Fe^{2+} + CO_2g + H_2O(l) \quad (11.7.1)$$

$$FeCO_3(siderite) + H^+ \rightleftharpoons Fe^{2+} + HCO_3^- \quad (11.7.4)$$

$$FeCO_3(siderite) \rightleftharpoons Fe^{2+} + CO_3^{2-} \quad (11.7.7)$$

The corresponding solubility constants for siderite from the experimental solubility determinations by Bruno et al. (1992b) used for the determination of the selected formation constants of $FeCO_3(aq)$ and $Fe(CO_3)_2^{2-}$ in Section 11.7.1.1.3 are

$$\log_{10}{}^*K_{p,s,0}°((11.7.1), 298.15\ K) = (7.19 \pm 0.15)$$

$$\log_{10}{}^*K_{s,0}°((11.7.4), 298.15\ K) = -(0.64 \pm 0.22)$$

$$\log_{10}K_{s,0}°((11.7.7), 298.15\ K) = -(10.96 \pm 0.23)$$

Lemire et al. (2013) discussed several other solubility studies for siderite (see Tab. 11.7-1) and noted that there is a difference of a about half an order of magnitude in solubility between solids prepared by precipitation at room temperature (more soluble) and solids synthesized at higher temperatures or heated after precipitation at room temperature (less soluble). Since Lemire et al. (2013) also considered calorimetric data for siderite, they only evaluated solubility data from heat-treated siderites. They accepted solubility product values $\log_{10}{}^*K_{p,s,0}((11.7.1))$ by Smith (1918) (30 °C), Reiterer et al. (1981) (50 °C), Bruno et al. (1992b) (25 °C), and Greenberg & Tomson (1992) (25 °C - 94 °C). An unweighted linear regression of the data as a function of temperature resulted in $\log_{10}{}^*K_{p,s,0}°((11.7.1), 298.15\ K) = (7.42 \pm 0.25)$, equivalent to $\Delta_rG_m°((11.7.1), 298.15\ K) = -(42.4 \pm 1.4)\ kJ \cdot mol^{-1}$, and $\Delta_rH_m°((11.7.1), 298.15\ K) = -(5.96 \pm 3.08)\ kJ \cdot mol^{-1}$. Lemire et al. (2013) accepted the value for $\Delta_rG_m°((11.7.1), 298.15\ K)$ and used it in the optimization procedure (see below).

Tab. 11.7-1: Experimentally determined solubility products of $FeCO_3$(siderite) at 25 °C

$\log_{10}K_{s,0}°$	Reference	Comments
-10.40	Bardy & Péré (1976), as cited by Lemire et al. (2013)	
-10.43[46]	Jensen et al. (2002)	Wet crystals[47]
-10.45	Nordstrom et al. (1990) based on experimental data by Singer & Stumm (1970)	TDB 12/07, precipitate
-10.55	Langmuir (1969), as cited by Lemire et al. (2013)	

[46] This value was erroneously reported as -11.43 by Lemire et al. (2013) on p. 368.

[47] Jensen et al. (2002) produced siderite from supersaturation. One part of the precipitated material was then dried at 105 °C ("dried crystals") and subsequently resuspended in solution to determine the solubility from undersaturation, while the other part ("wet crystals") was directly resuspended.

Tab. 11.7-11 cont.

$\log_{10}K_{s,0}°$	Reference	Comments
-10.77	Greenberg & Tomson (1992)	
-10.89	Nordstrom et al. (1990) based on experimental data by Smith (1918) at 30 °C	TDB 12/07, crystalline
-10.90	Bénézeth et al. (2009)	TDB 2020
-10.90	Silva et al. (2002)	
-10.96	Bruno et al. (1992b), recalculated by Lemire et al. (2013)	
-11.03	Jensen et al. (2002)	Dried crystals[48]
-11.03	Ptacek & Blowes (1994), as cited by Bénézeth et al. (2009)	
-11.06	Ptacek & Reardon (1992), as cited by Lemire et al. (2013)	

Lemire et al. (2013) also reviewed calorimetric data. They accepted the differential scanning calorimetry and adiabatic calorimetry results by Robie et al. (1984) on natural siderite and derived an expression for $C_{p,m}°$ as a function of temperature valid between 230 and 500 K:

$$C_{p,m}°(FeCO_3, \text{siderite, 230-500 K})/(J \cdot K^{-1} \cdot mol^{-1}) = 52.390 + 125.798 \times 10^{-3}(T/K)$$

$$- 4.004 \times 10^{5}(T/K)^{-2} + 0.3308 \times 10^{-4}(T/K)^{2}$$

From this function then follows the value selected by Lemire et al. (2013)

$$C_{p,m}°(FeCO_3, \text{siderite, 298.15 K}) = (82.45 \pm 2.00)\ J \cdot K^{-1} \cdot mol^{-1}$$

For the entropy they accepted the value by Robie et al. (1984), $S_m°(FeCO_3, \text{siderite, 298.15 K}) = (95.47 \pm 1.00)\ J \cdot K^{-1} \cdot mol^{-1}$ with an increased uncertainty and used it in the optimization procedure (see below). Finally, for the reaction

$$FeCO_3(\text{siderite}) + ¼\ O_2g \rightleftharpoons ½\ Fe_2O_3a + CO_2g \qquad (11.7.8)$$

Lemire et al. (2013) accepted $\Delta_r H_m°((11.7.8), 298.15\ K) = -(56.14 \pm 2.30)\ kJ \cdot mol^{-1}$ from drop calorimetry by Chai & Navrotsky (1994).

Finally, Lemire et al. (2013) used $\Delta_r G_m°((11.7.1), 298.15\ K) = -(42.4 \pm 1.1^{49})\ kJ \cdot mol^{-1}$, $S_m°(FeCO_3, \text{siderite, 298.15 K}) = (95.47 \pm 1.00)\ J \cdot K^{-1} \cdot mol^{-1}$, and $\Delta_r H_m°((11.7.8), 298.15\ K) = -(56.14 \pm 2.30)\ kJ \cdot mol^{-1}$ as part of the input for the optimization procedure. After two optimization cycles, the final optimized values for siderite were

[48] ditto

[49] In their discussion on p. 369 of the experimental solubility data, Lemire et al. (2013) reported an uncertainty of ± 1.4 kJ · mol^{-1}, while in their Table XI-1 on p. 388 of the input quantities for their optimization procedure, they assigned an uncertainty of ± 1.1 kJ · mol^{-1}.

$$\Delta_f H_m°(FeCO_3, \text{siderite}, 298.15\ K) = -(752.61 \pm 0.90)\ kJ \cdot mol^{-1}$$

and

$$S_m°(FeCO_3, \text{siderite}, 298.15\ K) = (95.54 \pm 0.65)\ J \cdot K^{-1} \cdot mol^{-1}$$

which Lemire et al. (2013) selected together with $C_{p,m}°(FeCO_3$, siderite, 298.15 K) and the temperature function $C_{p,m}°(FeCO_3$, siderite, 230-500 K) discussed above. From the selected $\Delta_f H_m°(FeCO_3$, siderite, 298.15 K) and $S_m°(FeCO_3$, siderite, 298.15 K) together with corresponding NEA-values for Fe^{2+} and CO_3^{2-}[50] follows $\Delta_r G_m°((11.7.7), 298.15\ K) = (60.94 \pm 1.18)\ kJ \cdot mol^{-1}$ and therefore $\log_{10} K_{s,0}°((11.7.7), 298.15\ K) = -(10.68 \pm 0.21)$.

For TDB 2020 we decided to select thermodynamic data for siderite that were derived from the solubility experiments by Bénézeth et al. (2009), which were published after the editorial deadline of the NEA iron review and could only be acknowledged by Lemire et al. (2013) in a footnote.

Bénézeth et al. (2009) measured the solubility of natural siderite in aqueous NaCl solutions ($0.1\ mol \cdot kg^{-1}$) from 25 to 250 °C using a hydrogen-electrode concentration cell providing the means of continuous measurement of hydrogen ion molalities. Fe(II) was determined by spectrophotometry.

Six experimental runs were made: (1) from 99.4 down to 26.5 °C, (2) from 198.8 down to 73.9 °C, (3) from 26.4 up to 98.2 °C, (4) at 251.5 °C, (5) from 149.1 up to 198.0 °C, and (6) at 25.3 °C. Since the solubility of siderite decreases with increasing temperature, the experimental series with increasing temperature (3 and 5) approached equilibrium from supersaturation, while, conversely, the series with decreasing temperature (1 and 2) approached equilibrium from undersaturation. As shown in Fig. 11.7-1 the solubilities determined by Greenberg & Tomson (1992) between 25 and 94 °C are higher, as equilibrium was only approached from supersaturation. The solubilities measured by Braun (1991) between 30 to 80 °C are lower than those measured by Bénézeth et al. (2009) and deviate considerably at temperatures above 40 °C. The data by Braun (1991) were not accepted by Lemire et al. (2013), since the solid was not characterized either before or after the measurements, the partial pressure of CO_2g was not measured, and no attempt was made to determine the presence of Fe(III).

Bénézeth et al. (2009) fitted their experimental data with the following 4-term temperature function:

$$\log_{10} K_{s,0}°((11.7.7), T) = a + b\ T + c\ T^{-1} + d \log_{10}(T)$$

which (owing to $\Delta_r G$ = - RT lnK) is equivalent to

$$\Delta_r G_m°((11.7.7), T) = -R \ln(10)\ \{a\ T + b\ T^2 + c + d\ T \log_{10}(T)\}$$

---

[50] $\Delta_f H_m°(Fe^{2+}$, 298.15 K) = -(90.29 ± 0.52) kJ · mol^{-1}, see Section 12.3.2, $S_m°(Fe^{2+}$, 298.15 K) = -(102.17 ± 2.78) J · K^{-1} · mol^{-1}, see Table 12.8.2, $\Delta_f H_m°(CO_3^{2-}$, 298.15 K) = -(675.23 ± 0.25) kJ · mol^{-1}, and $S_m°(CO_3^{2-}$, 298.15 K) = -(50 ± 1) J · K^{-1} · mol^{-1}.

From the Gibbs-Helmholtz equation[51] then follows

$$\Delta_r H_m°((11.7.7), T) = R \ln(10) \{b\ T^2 - c + d\ T/\ln(10)\}$$

and from $\left(\frac{\partial H}{\partial T}\right)_p = C_p$

$$\Delta_r C_{p,m}°((11.7.7), T) = R \ln(10) \{2\ b\ T + d/\ln(10)\}$$

The regression by Bénézeth et al. (2009) resulted in the coefficients a = 175.568, b = 0.0139, c = -6738.483, and d = -67.898. Inserting these coefficients into the respective temperature functions (with R = 8.314517 J · K^{-1} · mol^{-1}) leads to

$$\log_{10} K_{s,0}°((11.7.7), 298.15) = -10.90$$

$$\Delta_r H_m°((11.7.7), 298.15\ K) = -15.654\ kJ \cdot mol^{-1}$$

$$\Delta_r C_{p,m}°((11.7.7), 298.15\ K) = -405.855\ J \cdot K^{-1} \cdot mol^{-1}$$

These data are included in TDB 2020.

[51] Gibbs-Helmholtz equation: $\left(\frac{\partial}{\partial T}\left(\frac{G}{T}\right)\right)_p = -\frac{H}{T^2}$

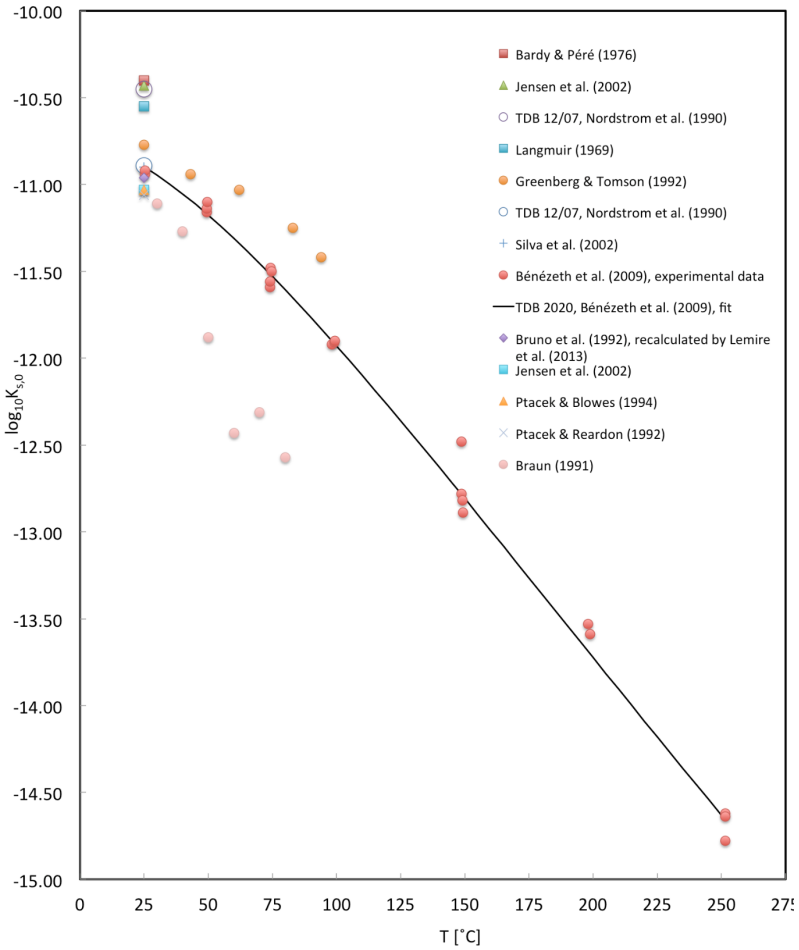

Fig. 11.7-1: Solubility of siderite as a function of temperature

Shown are the experimentally determined solubility products for the reaction $FeCO_3$(siderite) ⇌ Fe^{2+} + CO_3^{2-} by various authors, as well as the experimental data by Bénézeth et al. (2009) with their 4-term fit.

The selected value of -10.90 for $\log_{10}K_{s,0}°$((11.7.7), 298.15) is close to that in TDB 07/12 (-10.89), but smaller (just barely outside the lower uncertainty limit) than $\log_{10}K_{s,0}°$((11.7.7), 298.15 K) = -(10.68 ± 0.21) calculated from the values selected by Lemire et al. (2013) for $\Delta_f H_m°$($FeCO_3$, siderite, 298.15 K) and $S_m°$($FeCO_3$, siderite, 298.15 K).

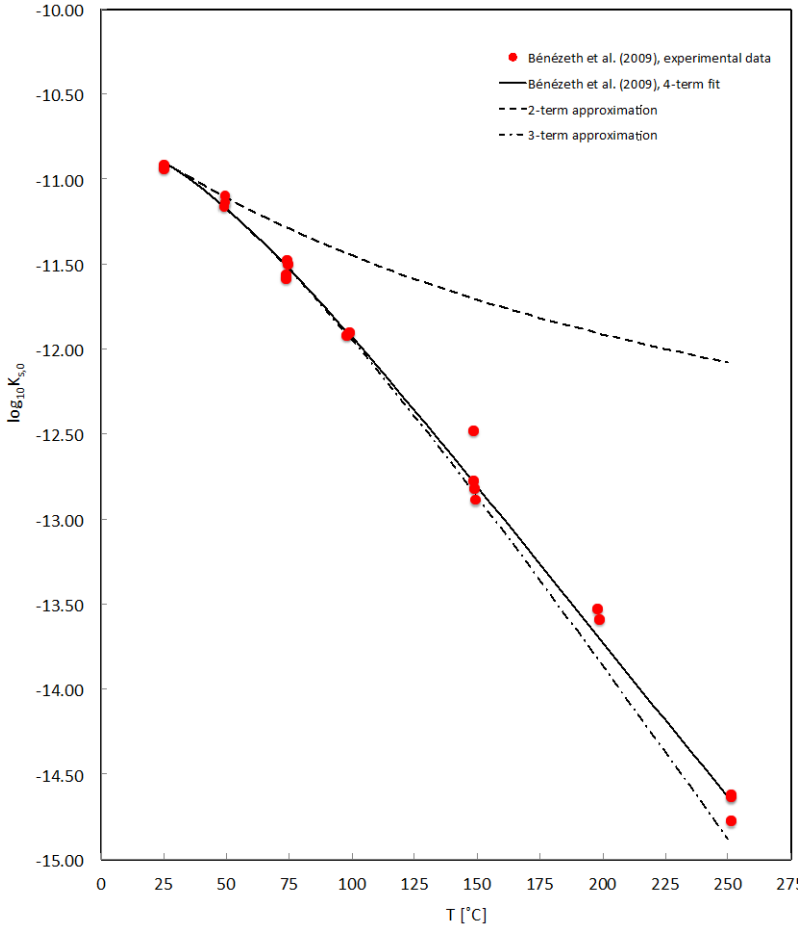

Fig. 11.7-2: Solubility of siderite as a function of temperature

Shown are the experimentally determined solubility products for the reaction $FeCO_3$(siderite) ⇌ Fe^{2+} + CO_3^{2-} by Bénézeth et al. (2009) and the 4-term fit to the data. The 3-term approximation using $\log_{10}K_{s,0}°(298.15)$, $\Delta_rH_m°(298.15\ K)$, and $\Delta_rC_{p,m}°(298.15\ K)$ is practically indistinguishable from the 4-term fit up to about 100 °C and deviates at 250 °C by only 0.25 log units. The 2-term approximation (or van't Hoff equation) is clearly inadequate, a deviation of 0.25 log units is already reached at about 75 °C.

The solubility product $\log_{10}K_{s,0}°((11.7.7), 298.15)$ can be extrapolated to higher temperatures using the values for $\log_{10}K_{s,0}°((11.7.7), 298.15)$, $\Delta_rH_m°((11.7.7), 298.15\ K)$, and $\Delta_rC_{p,m}°((11.7.7), 298.15\ K)$ in the following, so called 3-term approximation (see, e.g., Puigdomenech et al. 1997)

$$\log_{10}K^\circ(T) = \log_{10}K^\circ(T_0) - \left(\frac{1}{T} - \frac{1}{T_0}\right)\frac{\Delta_r H_m^\circ(T_0)}{R\ln(10)} - \left(1 - \frac{T_0}{T} + \ln\frac{T_0}{T}\right)\frac{\Delta_r C_{p,m}^\circ(T_0)}{R\ln(10)}$$

where T_0 = 298.15 K. This approximation is practically indistinguishable from the 4-term fit up to about 100 °C and deviates at 250 °C by only 0.25 log units (see Fig. 11.7-2). The 2-term approximation (or van't Hoff equation)

$$\log_{10}\mathrm{K}^\circ(T) = \log_{10}K^\circ(T_0) - \left(\frac{1}{T} - \frac{1}{T_0}\right)\frac{\Delta_\mathrm{r}H^\circ_\mathrm{m}(T_0)}{\mathrm{R}\ln(10)}$$

using only $\log_{10}K_{s,0}$°((11.7.7), 298.15) and $\Delta_\mathrm{r}H_\mathrm{m}$°((11.7.7), 298.15 K) is much less suited for extrapolation, a deviation of 0.25 log units is already reached at about 75 °C. A much better 2-term approximation can be expected from an isocoulombic reaction generated by combining the solubility reaction of siderite with that of, e.g., calcite.

11.7.1.3.3 "Carbonate green rust one"

Carbonate green rust one (carbonate GR1) is an intermediate Fe(II)-Fe(III) compound consisting of brucite-like $Fe(OH)_2$ layers where the excess charge created by the partial oxidation of ferrous to ferric iron is compensated by carbonate anions inserted (together with water molecules) into the interlayer. Carbonate GR1 was observed as corrosion product of iron in water pipes, see Drissi et al. (1995) and references therein.

Drissi et al. (1995) prepared precipitates of carbonate GR1 by mixing aqueous solutions of melanterite ($FeSO_4{\cdot}7H_2O$) with NaOH solutions and adding carbonate as Na_2CO_3 solutions. Precipitates were characterized by X-ray diffraction and Mössbauer spectroscopy was used to determine the Fe^{2+}/Fe^{3+} ratio. The chemical composition of carbonate GR1 was found to be $(Fe^{III})_2(Fe^{II})_4(OH)_{12}CO_3{\cdot}nH_2O(s)$. Thermodynamic data for carbonate GR1 were obtained by Drissi et al. (1995) by monitoring electrode potentials during the oxidation process according to

$$6\ Fe(OH)_2(s) + CO_3^{2-} + 2\ H^+ + n\ H_2O(l) \rightleftharpoons (Fe^{III})_2(Fe^{II})_4(OH)_{12}CO_3{\cdot}nH_2O(s) + H_2g$$

Lemire et al. (2013) corrected the reported potentials to zero ionic strength using SIT and obtained an average value of E_0 = -0.625 V vs. the standard hydrogen electrode, or $\Delta_\mathrm{r}G_\mathrm{m}$°(298.15 K) = -(121 ± 2) kJ · mol^{-1} with an estimated uncertainty. Lemire et al. (2013) did not select this value (without explanation), but we accept the corresponding

$$log_{10}{}^*K^\circ(298.15\ K) = (21.20 \pm 0.35)$$

as supplemental datum (as there remain uncertainties with respect to the grain size and crystallinity of the precipitates and the number of structural waters in the formula unit). For inclusion in TDB 2020 we used $log_{10}{}^*K_{s,0}^\circ(298.15\ K) = (12.26 \pm 0.88)$ for $Fe(OH)_2(s) + 2H^+ \rightleftharpoons Fe^{2+} + 2\ H_2O(l)$ (see Section 11.4.2.2) to obtain

$$(Fe^{III})_2(Fe^{II})_4(OH)_{12}CO_3{\cdot}nH_2O(s) + 10\ H^+ + H_2g \rightleftharpoons 6\ Fe^{2+} + CO_3^{2-} + (n+12)\ H_2O(l)$$

$$log_{10}{}^*K^\circ(298.15\ K) = (52.4 \pm 5.3)$$

Other green rusts are "chloride green rust one" (see Section 11.5.2.2.1) and "sulphate green rust two" (see Section 11.6.2.3.6). "White rust" was discussed in Section 11.4.2.2.

11.7.1.4 Cyanide compounds and complexes

Lemire et al. (2020) reviewed thermodynamic data for aqueous iron hexacyanide complexes and their potassium salts from a wide range of experiments. They carried out a weighted least-squares fitting process – similar to that of Lemire et al. (2013), see Section 11.1.2 – in order to generate a self-consistent set of selected values for the thermodynamic quantities of $Fe(CN)_6^{4-}$ and $Fe(CN)_6^{3-}$ and their potassium salts. Note that the only linkage between this self-consistent set of enthalpies and Gibbs free energies of reaction and that by Lemire et al. (2013) for other iron species is through the value of $\Delta_r H_m°(298.15\ K) = -(358.86 \pm 0.33)\ kJ \cdot mol^{-1}$ for the reaction

$$Fe^{2+} + 6\ CN^- \rightleftharpoons Fe(CN)_6^{4-}$$

We will not discuss the optimization procedure by Lemire et al. (2020) any further, details can be found in their Section X.1.1.3.

11.7.1.4.1 Aqueous iron(II) cyanide complexes

Since experimental investigations of iron(II) cyanide complexes have been focussed almost entirely on the strongly bound $Fe(CN)_6^{4-}$, Lemire et al (2020) only considered thermodynamic data for this complex. From their least-squares optimization calculations, they obtained and selected

$$\Delta_f G_m°(Fe(CN)_6^{4-}, 298.15\ K) = (680.226 \pm 21.26)\ kJ \cdot mol^{-1}$$

$$\Delta_f H_m°(Fe(CN)_6^{4-}, 298.15\ K) = (434.945 \pm 21.255)\ kJ \cdot mol^{-1}$$

These values can be used to derive $\Delta_r G_m°(298.15\ K)$ and $\Delta_r H_m°(298.15\ K)$ for the reaction

$$Fe^{2+} + 6\ CN^- \rightleftharpoons Fe(CN)_6^{4-}$$

by combining them with the selected $\Delta_f G_m°(Fe^{2+}, 298.15\ K) = -(90.72 \pm 0.64)\ kJ \cdot mol^{-1}$ and $\Delta_f G_m°(CN^-, 298.15\ K) = (166.939 \pm 2.519)\ kJ \cdot mol^{-1}$, and with the selected $\Delta_f H_m°(Fe^{2+}, 298.15\ K) = -(90.29 \pm 0.52)\ kJ \cdot mol^{-1}$ and $\Delta_f H_m°(CN^-, 298.15\ K) = (147.35 \pm 3.541)\ kJ \cdot mol^{-1}$, respectively. This results in $\Delta_r G_m°(298.15\ K) = -(230.69 \pm 26.09)$, which corresponds to

$$\log_{10}\beta_6°(298.15\ K) = (40.41 \pm 4.57)$$

and in

$$\Delta_r H_m°(298.15\ K) = -(358.9 \pm 30.1)\ kJ \cdot mol^{-1}$$

respectively. These values are included in TDB 2020. Lemire et al. (2020) did not provide any specific ion interaction coefficients, therefore, we estimated for TDB 2020

$$\varepsilon(Fe(CN)_6^{4-}, Na^+) \approx -(0.20 \pm 0.30)\ kg \cdot mol^{-1}$$

estimated according to Tab. 1-7

Protonation of $Fe(CN)_6^{4-}$ results in $HFe(CN)_6^{3-}$ and further protonation to $H_2Fe(CN)_6^{2-}$. Lemire et al. (2020) selected the following data for the first protonation

$$Fe(CN)_6^{4-} + H^+ \rightleftharpoons HFe(CN)_6^{3-}$$

$$\log_{10}\beta_{6,1}°(298.15\ K) = (4.28 \pm 0.10)$$

$$\Delta_r H_m°(298.15\ K) = (2.1 \pm 3.0)\ kJ \cdot mol^{-1}$$

and for the second protonation

$$HFe(CN)_6^{3-} + H^+ \rightleftharpoons H_2Fe(CN)_6^{2-}$$

$$\log_{10}\beta_{6,2}°(298.15\ K) = (2.4 \pm 0.3)$$

These values are included in TDB 2020, as well as the following ion interaction coefficients that we estimated according to Tab. 1-7

$$\varepsilon(HFe(CN)_6^{3-}, Na^+) \approx -(0.15 \pm 0.20)\ kg \cdot mol^{-1}$$

$$\varepsilon(H_2Fe(CN)_6^{2-}, Na^+) \approx -(0.10 \pm 0.10)\ kg \cdot mol^{-1}$$

For the association of potassium ions with $Fe(CN)_6^{3-}$ according to the reaction

$$Fe(CN)_6^{4-} + K^+ \rightleftharpoons KFe(CN)_6^{3-}$$

Lemire et al. (2020) selected

$$\log_{10}K°(298.15\ K) = (2.35 \pm 0.05)$$

$$\Delta_r H_m°(298.15\ K) = (3.6 \pm 1.0)\ kJ \cdot mol^{-1}$$

These values are included in TDB 2020. Since Lemire et al. (2020) did not provide any specific ion interaction coefficients, we estimated for TDB 2020

$$\varepsilon(KFe(CN)_6^{3-}, Na^+) \approx -(0.15 \pm 0.20)\ kg \cdot mol^{-1}$$

according to Tab. 1-7.

11.7.1.4.2 Iron(II) cyanide compounds

The iron(II) cyanide compounds $K_4Fe(CN)_6(cr)$ and $K_4Fe(CN)_6(cr) \cdot 3H_2O(cr)$ are soluble in water. For both solids, Lemire et al. (2020) selected calorimetrically determined heat capacity and entropy values, as well as enthalpy of solution values. For the trihydrate they also selected a Gibbs

free energy of solution from a solubility experiment and enthalpies and Gibbs free energies of dehydration. From these data, Lemire et al. (2020) also calculated solubility products for both solids. Since these are very soluble, the thermodynamic values selected by Lemire et al. (2020) are not included in TDB 2020.

11.7.1.4.3 Aqueous iron (III) cyanide complexes

In their discussion of aqueous iron(III) cyanide complexes, Lemire et al. (2020) state that there are surprisingly few thermodynamic data for the formation of $Fe(CN)_n^{3-n}$ complexes, with the exception of data for $Fe(CN)_6^{3-}$, which is a very strong complex. Lemire et al. (2020) only selected data for this complex, although there are indications for the existence of complexes with n = 1-3 from a spectrophotometric study. Based on their least-squares optimization calculations, Lemire et al. (2020) selected

$$\Delta_f G_m°(Fe(CN)_6^{3-}, 298.15\ K) = (714.921 \pm 25)\ kJ \cdot mol^{-1}$$

$$\Delta_f H_m°(Fe(CN)_6^{3-}, 298.15\ K) = (547.185 \pm 25)\ kJ \cdot mol^{-1}$$

Note that we estimated these uncertainties, as Lemire et al. (2020) did not assess uncertainties for these values "because of approximations needed to generate a self-consistent set of values for iron cyanido species and the large uncertainty in $\Delta_f H_m°(Fe(CN)_6^{4-}$". These values can be used to derive $\Delta_r G_m°(298.15\ K)$ and $\Delta_r H_m°(298.15\ K)$ for the reaction

$$Fe^{3+} + 6\ CN^- \rightleftharpoons Fe(CN)_6^{3-}$$

by combining them with the selected $\Delta_f G_m°(Fe^{3+}, 298.15\ K) = -(16.23 \pm 0.65)\ kJ \cdot mol^{-1}$ and $\Delta_f G_m°(CN^-, 298.15\ K) = (166.939 \pm 2.519)\ kJ \cdot mol^{-1}$, and with the selected $\Delta_f H_m°(Fe^{3+}, 298.15\ K) = -(50.06 \pm 0.97)\ kJ \cdot mol^{-1}$and $\Delta_f H_m°(CN^-, 298.15\ K) = (147.35 \pm 3.541)\ kJ \cdot mol^{-1}$, respectively. This leads to $\Delta_r G_m°(298.15\ K) = -(270.48 \pm 29.22)$, which is equivalent to

$$\log_{10}\beta_6°(298.15\ K) = (47.39 \pm 5.12)$$

and to

$$\Delta_r H_m°(298.15\ K) = -(286.9 \pm 32.8)$$

respectively. These values are included in TDB 2020.

Many studies have been devoted to the reduction of $Fe(CN)_6^{3-}$ to $Fe(CN)_6^{4-}$. For the reaction

$$Fe(CN)_6^{4-} + H^+ \rightleftharpoons Fe(CN)_6^{3-} + 0.5\ H_2g$$

Lemire et al. (2020) selected

$$\log_{10}K°(298.15\ K) = -(6.078 \pm 0.178)$$

$\Delta_r H_m°(298.15\ K) = (112.240 \pm 0.656)\ kJ \cdot mol^{-1}$

We did not include this reaction in TDB 2020, since it is a linear combination of reactions already included in TDB 2020:

$Fe(CN)_6^{4-} \rightleftharpoons Fe^{2+} + 6\ CN^-$ (see Section 11.7.1.4.1)

$Fe^{3+} + 6\ CN^- \rightleftharpoons Fe(CN)_6^{3-}$ (see above)

$Fe^{2+} + H^+ \rightleftharpoons Fe^{3+} + 0.5\ H_2g$ (see Section 11.3.3)

Note, however, that the reduction reaction provided input for the least-squares optimization calculations by Lemire et al. (2020).

As reported by Lemire et al. (2020), $Fe(CN)_6^{3-}$ is essentially unprotonated in solutions with a pH value > 1 and these authors did not select any value for the protonation constant.

For the association of potassium ions with $Fe(CN)_6^{3-}$ according to the reaction

$Fe(CN)_6^{3-} + K^+ \rightleftharpoons KFe(CN)_6^{2-}$

Lemire et al. (2020) selected

$\log_{10}K°(298.15\ K) = (1.46 \pm 0.05)$

$\Delta_r H_m°(298.15\ K) = (2.1 \pm 1.3)\ kJ \cdot mol^{-1}$

These values are included in TDB 2020. Since Lemire et al. (2020) did not provide any specific ion interaction coefficients, we estimated for TDB 2020

$\varepsilon(Fe(CN)_6^{3-}, Na^+) \approx -(0.15 \pm 0.20)\ kg \cdot mol^{-1}$

and

$\varepsilon(KFe(CN)_6^{2-}, Na^+) \approx -(0.10 \pm 0.10)\ kg \cdot mol^{-1}$

according to Tab. 1-7.

11.7.1.4.4 Iron (III) cyanide compounds

The iron(III) cyanide compound $K_3Fe(CN)_6$(cr) is soluble in water. Lemire et al. (2020) selected calorimetrically determined heat capacity and entropy values, a Gibbs free energy of solution from solubility measurements (from which they calculated a solubility product) and a calorimetrically determined enthalpy of solution. Since $K_3Fe(CN)_6$(cr) is very soluble, the thermodynamic values selected by Lemire et al. (2020) are not included in TDB 2020.

11.7.1.5 Aqueous iron(III) thiocyanate complexes

There appear to be no data on iron thiocyanate solids and on iron(II) thiocyanate complexes, therefore, Lemire et al. (2020) only considered iron(III) thiocyanate complexes. They found formation constants for all six $Fe(SCN)_n^{3-n}$ complexes (with n = 1-6) but noted that for complexes with n > 2 the thiocyanate concentration needed for their formation in the experiments exceeded about 20 % of the ionic strength. In the absence of supporting spectroscopic data, the derived values for higher-order-complex formation constants are rather ambiguous. For this reason, Lemire et al. (2020) only selected formation constants for $FeSCN^{2+}$ and $Fe(SCN)_2^+$. From an SIT treatment of conditional formation constants for the 1:1 complex determined in $HClO_4$ and/or $NaClO_4$ solutions they obtained the selected

$$Fe^{3+} + SCN^- \rightleftharpoons FeSCN^{2+}$$

$$\log_{10}\beta_1°(298.15\ K) = (3.06 \pm 0.05)$$

$$\varepsilon(FeSCN^{2+}, ClO_4^-) = (0.49 \pm 0.05)\ kg \cdot mol^{-1}$$

which are included in TDB 2020. The value for $\log_{10}\beta_1°(298.15\ K)$ is in very good agreement with $\log_{10}\beta_1°(298.15\ K) = (3.07 \pm 0.02)$ determined in predominantly HNO_3 solutions. The corresponding

$$\varepsilon(FeSCN^{2+}, NO_3^-) = (0.13 \pm 0.04)\ kg \cdot mol^{-1}$$

selected by Lemire et al. (2020) is also included in TDB 2020, as well as the estimate

$$\varepsilon(FeSCN^{2+}, Cl^-) \approx \varepsilon(FeSCN^{2+}, ClO_4^-) = (0.49 \pm 0.05)\ kg \cdot mol^{-1}$$

(see Section 11.1.1). For the 1:2 complex, the formation constant data gathered in $NaClO_4$-$HClO_4$-NaSCN solutions showed a considerable scatter. An SIT regression for

$$FeSCN^{2+} + SCN^- \rightleftharpoons Fe(SCN)_2^+$$

resulted in $\log_{10}K_2°(298.15\ K) = (1.88 \pm 0.53)$ with $\Delta\varepsilon = -(0.24 \pm 0.34)\ kg \cdot mol^{-1}$. However, Lemire et al. (2020) did not select these values since the linear regression was strongly biased by an experimental value at the highest ionic strength (2.21 m). Instead, they selected a simple average of the conditional constants:

$$\log_{10}K_2°(298.15\ K) = (2.23 \pm 0.50)$$

This value is included in TDB 2020, as well as

$$\varepsilon(Fe(SCN)_2^+, ClO_4^-) = (0.2 \pm 0.1)\ kg \cdot mol^{-1}$$

estimated according to Tab. 1-7 and

$\varepsilon(Fe(SCN)_2^+, Cl^-) \approx \varepsilon(Fe(SCN)_2^+, ClO_4^-) = (0.2 \pm 0.1)$ kg · mol^{-1}

(see Section 11.1.1).

11.7.2 Iron silicate compounds and complexes

11.7.2.1 Data in TDB 05/92, TDB 01/01 and TDB 12/07

No iron silicate complexes were considered in TDB 05/92. For TDB 01/01, Hummel et al. (2002) evaluated four studies reporting experimental data on Fe(III) silicate complexation. The experimental methods used were absorbance measurements with a spectrophotometer at $I = 0.1$ M (Weber & Stumm 1965, Porter & Weber 1971), spectrophotometric analyses at $I = 0.1$ M and polarography at $I = 0.15$ M (Olson & O'Melia 1973), and determination of amorphous silica solubility in acidified ferric nitrate solutions at $I < 0.08$ M (Reardon 1979). For the reaction

$$Fe^{3+} + SiO(OH)_3^- \rightleftharpoons FeSiO(OH)_3^{2+}$$

the following stability constants were derived for zero ionic strength: $\log_{10}K° = 10.0$ (Weber & Stumm 1965), 9.5 (Porter & Weber 1971), 9.6 and 9.8 from spectrophotometric and polarographic data, respectively (Olson & O'Melia 1973), and 9.8 from silica solubility data (Reardon 1979). These constants are in close agreement and an unweighted mean is

$$\log_{10}K° = (9.7 \pm 0.3)$$

which was included in TDB 01/01 and retained in TDB 12/07.

Note that all the studies mentioned above have been carried out at pH < 4. No conclusions can be drawn from these investigations whether bidentate Fe(III) complexes with $SiO_2(OH)_2^{2-}$ form at high pH in analogy with Ca and Mg complexation, or whether a complex of the stoichiometry $Fe(OH)_nSiO(OH)_3^{2-n}$ dominates in neutral and alkaline groundwater in analogy with Al.

11.7.2.2 Iron silicate complexes

Lemire et al. (2013) did not consider any aqueous iron silicate complexes, whose discussion they deferred to the second volume of the NEA-review on iron. Lemire et al. (2020) discussed the studies on the formation of $FeSiO(OH)_3^{2+}$ by Weber & Stumm (1965), Porter & Weber (1971), Olson & O'Melia (1973), Reardon (1979), and Patten & Byrne (2017). Based on a weighted average of $\log_{10}{}^*K_1°$(28.15 K) values for

$$Fe^{3+} + Si(OH)_4(aq) \rightleftharpoons FeSiO(OH)_3^{2+} + H^+$$

by Reardon (1979) and Patten & Byrne (2017), Lemire et al. (2020) obtained $\log_{10}{}^*K_1°(298.15\ K)$ = -(0.08 ± 0.15), which they did not select but reported for "informational purposes only". By virtue of $\log_{10}{}^*K°(298.15\ K)$ = -(9.81± 0.02) for $Si(OH)_4(aq) \rightleftharpoons SiO(OH)_3^{2-} + H^+$ (see Section 25.3.2), this value corresponds to $\log_{10}{}^*K_1°(298.15\ K)$ = (9.73 ± 0.15) for the reaction

$$Fe^{3+} + SiO(OH)_3^- \rightleftharpoons FeSiO(OH)_3^{2+}$$

which is very similar to $\log_{10}{}^*K_1°(298.15\ K)$ = (9.69 ± 0.06) selected for TDB 2020 (see Section 25.4.4).

11.7.2.3 Iron silicate compounds

Lemire et al. (2013) discussed a number of iron silicate minerals and selected thermodynamic data based on calorimetry for seven of them, all of which are not included in our database: Fayalite (α-Fe_2SiO_4), ahrensite (γ-Fe_2SiO_4), ferrosilite ($FeSiO_3$(ortho)), clinoferrosilite ($FeSiO_3$(clino)), deerite ($((Fe^{2+})_{4.87}(Fe^{3+})_{2.76}Mn_{1.07}Mg_{0.15}Ti_{0.15}O_3)(Si_{5.94}Al_{0.03}Ti_{0.03}O_{17})$(cr)), and two compositional varieties of grunerite, namely

$$((Fe^{2+})_{5.38}(Fe^{3+})_{0.66}Mn_{0.08}Mg_{0.80}Ca_{0.05})(Si_8O_{22})((OH)_{1.37}Cl_{0.03}O_{0.60})(cr)$$

and

$$((Fe^{2+})_{5.2766}(Fe^{3+})_{0.1200}Mn_{0.0825}Mg_{1.5209})(Si_{7.9163}Al_{0.0837}O_{22.0363})(OH)_{1.9637}(cr)$$

With the exception of fayalite (α-Fe_2SiO_4), Lemire et al. (2013) provided only heat capacity or entropy data, which is insufficient for the purposes of geochemical equilibrium modelling. In addition, all of these minerals are not expected to be in equilibrium with low-temperature (T < 200 °C) aqueous solutions. Fayalite is an olivine-group mineral, which is an important constituent of Earth's mantle. According to Rasmussen et al. (1998) a "low-temperature" formation of fayalite took place during hydrothermal alteration of a Permian volcanogenic, massive magnetite-sulphide seafloor deposit at a temperature of about 300 °C. Ahrensite forms from fayalite at high pressures and its first natural occurrence was reported by Ma et al. (2016) as a shock-metamorphic mineral from the Tissint meteorite. Ferrosilite and clinoferrosilite belong to the orthopyroxene and clinopyroxene groups, resp., and are found in many igneous and metamorphic rocks. Deerite is a metamorphic mineral restricted to blueschist facies rocks, which are commonly formed at pressures equivalent to burial depths in excess of 15 km and temperatures between 200 and 500 °C (high-pressure/low-temperature metamorphism). Grunerite, finally, belongs to the amphibole group and is found in high-grade metamorphic iron formations.

No new data were selected by Lemire et al. (2020), except for an entropy value for ahrensite (γ-Fe_2SiO_4).

11.8 Selected iron data

Tab. 11.8-1: Iron bearing solids for which NEA selected thermodynamic data (Lemire et al. 2013, Lemire et al. 2020, Tab. III-1 and III-2) but are not included in TDB 2020

See text for explanations. All aqueous species for which Lemire et al. (2013) and Lemire et al. (2020) selected thermodynamic data are also included in TDB 2020.

Solids	$Fe_{0.932}O(cr)$ [a], β-$FeOOH{\cdot}0.652H_2O{\cdot}0.0096HCl(cr)$ [b], $FeF_2(cr)$ [a], $FeF_3(cr)$ [b], $FeCl_2(cr)$ [a,c], $FeCl_2{\cdot}H_2O(cr)$ [a,c], $FeCl_2 \cdot 2H_2O(cr)$ [a,c], $FeCl_2{\cdot}4H_2O(cr)$ [a,c], $FeCl_3(cr)$ [a], $FeCl_3{\cdot}2H_2O(cr)$ [b], $FeCl_3 \cdot 2.5H_2O(cr)$ [b], $FeCl_3{\cdot}3.5H_2O(cr)$ [b], $FeCl_3 \cdot 6H_2O(cr)$ [b], $FeOCl(cr)$ [a,d], $FeBr_2(cr)$ [a], $FeBr_3(cr)$ [a], $FeI_2(cr)$ [a], $Fe_{11}S_{12}$(cr, 6C pyrrhotite) [b], $FeSO_4(cr)$ [b], $FeSO_4{\cdot}H_2O(cr)$ [a,c], $FeSO_4{\cdot}4H_2O(cr)$ [a,c], $FeSO_4{\cdot}7H_2O(cr)$ [a,c], $(NH_4)_2Fe(SO_4)_2{\cdot}6H_2O(cr)$ [b], $Fe_2(SO_4)_3(cr)$ [a], $Fe_2(SO_4)_3{\cdot}5H_2O(cr)$ [b], $Fe_2(SO_4)_3 \cdot 7.53H_2O(cr)$ [b], $Fe_2(SO_4)_3 \cdot 9H_2O(cr)$ [b], $Fe_{4.78}(SO_4)_6(OH)_{2.34}(H_2O)_{20.71}(cr)$ [b], $(H_3O)_{0.91}Fe_{2.91}(SO_4)_2(OH)_{5.64}(H_2O)_{0.18}(cr)$ [a], $(H_3O)_{1.34}Fe(SO_4)_{2.17}(H_2O)_{3.06}(cr)$ [b], $(H_3O)Fe_3(SO_4)_2(OH)_6(cr)$ [b], $FeO(SO_4)_{0.157}(OH)_{0.686}(H_2O)_{0.972}(cr)$ [b], $FeO(SO_4)_{0.168}(OH)_{0.664}(H_2O)_{1.226}(cr)$ [b], $FeSe_{1.95}(cr)$ [b], $Fe_{1.111}Te$(cr,β) [a], $FeTe_2$(cr,ε) [b], $Fe_2TeO_6(cr)$ [b], $Fe_2P_2O_7(cr)$ [b], $Fe(PO_3)_3$(cr, monoclinic) [b], $Fe(PO_3)_3 \cdot 0.128H_2O$(cr, monoclinic) [b], $FePO_4{\cdot}2H_2O$(cr, orthorhombic) [b], $Fe_3PO_7(cr)$ [b], $Fe_4(P_2O_7)_3(cr)$ [b], $F_3(P_2O_7)_2(cr)$ [b], $FeAsO_4(cr)$ [b], $FeAsO_4{\cdot}2H_2O$(scorodite) [a], $FeAsO_4{\cdot}2H_2O$(parascorodite) [b], and $FeAsO_4{\cdot}3.5H_2O$(kankite) [a], $Fe_4(AsO_4)_4 \cdot 3H_2O(cr)$ [a,c], $FeSiO_3$(clino) [b], $FeSiO_3$(ortho) [b], α-Fe_2SiO_4 [a], γ-Fe_2SiO_4 [b], $((Fe^{2+})_{4.87}(Fe^{3+})_{2.76}Mn_{1.07}Mg_{0.15}Ti_{0.15}O_3)(Si_{5.94}Al_{0.03}Ti_{0.03}O_{17})(cr)$ [b], $((Fe^{2+})_{5.38}(Fe^{3+})_{0.66}Mn_{0.08}Mg_{0.80}Ca_{0.05})(Si_8O_{22})((OH)_{1.37}Cl_{0.03}O_{0.60})(cr)$ [b], $((Fe^{2+})_{5.2766}(Fe^{3+})_{0.1200}Mn_{0.0825}Mg_{1.5209})(Si_{7.9163}Al_{0.0837}O_{22.0363})(OH)_{1.9637}(cr)$ [b] $FeCr_2O_4(cr)$ [b], $NiFe_2O_4(cr)$ [a], $K_4Fe(CN)_6 \cdot 3H_2O(cr)$ [a,c], $K_4Fe(CN)_6(cr)$ [a,c], $K_3Fe(CN)_6(cr)$ [a,c]

[a] Single species data including $\Delta_f G_m°$
[b] Single species data excluding $\Delta_f G_m°$
[c] Reaction data including $\log_{10} K°$
[d] Reaction data excluding $\log_{10} K°$

Tab. 11.8-2: Selected iron data (1 bar, 298.15 K) for TDB 2020

All data are taken from Lemire et al. (2013) and Lemire et al. (2020) with the exception of those marked with an asterisk (*). Supplemental data are in italics. New or changed data with respect to TDB Version 12/07 (Thoenen et al. 2014) are shaded. T-range refers to the experimental range of temperatures at which equilibrium constants, $\Delta_r H_m°$ and $\Delta_r C_{p,m}°$ were determined.

Name	Redox	TDB Version 12/07				TDB 2020				
		$\Delta_f G_m°$ [kJ · mol^{-1}]	$\Delta_f H_m°$ [kJ · mol^{-1}]	$S_m°$ [J · K^{-1} · mol^{-1}]	$C_{p,m}°$ [J · K^{-1} · mol^{-1}]	$\Delta_f G_m°$ [kJ · mol^{-1}]	$\Delta_f H_m°$ [kJ · mol^{-1}]	$S_m°$ [J · K^{-1} · mol^{-1}]	$C_{p,m}°$ [J · K^{-1} · mol^{-1}]	Species
Fe(α)	0	0.0	0.0	27.28	25.10	0.0	0.0	27.085 ± 0.160	25.084 ± 0.500	Fe(α)
Fe+2	II	-78.90	-89.1	-137.7	-	(-90.72 ± 0.64) [b]	-90.29 ± 0.52	(-102.17 ± 2.78) [a]	-23 ± 10	Fe^{2+}
Fe+3	III	-4.581	-48.6	-	-	(-16.23 ± 0.65) [b]	(-50.06 ± 0.97) [b]	(-282.40 ± 3.93) [b]	-108 ± 20	Fe^{3+}

[a] Calculated using $\Delta_f G_m° = \Delta_f H_m° - T \sum S_m°$.
[b] Calculated from reaction data.

Name	Redox	TDB Version 12/07		TDB 2020				
		$\log_{10}\beta°$	$\Delta_r H_m°$ [kJ · mol^{-1}]	$\log_{10}\beta°$	$\Delta_r H_m°$ [kJ · mol^{-1}]	$\Delta_r C_{p,m}°$ [J · K^{-1} · mol^{-1}]	T-range [°C]	Reaction
FeOH+	II	-9.5	55.2	(-9.43 ± 0.10) *	(54.6 ± 0.9) *	0 *	25 – 300	$Fe^{2+} + H_2O(l) \rightleftharpoons FeOH^+ + H^+$
Fe(OH)2(aq)	II	-	-	(-20.52 ± 0.08) *	(115.4 ± 1.0) *	0 *	25 – 300	$Fe^{2+} + 2\ H_2O(l) \rightleftharpoons Fe(OH)_2(aq) + 2\ H^+$
Fe(OH)3-	II	-	-	(-32.68 ± 0.15) *	(140.3 ± 2.2) *	0 *	25 – 300	$Fe^{2+} + 3\ H_2O(l) \rightleftharpoons Fe(OH)_3^- + 3\ H^+$
FeF+	II	1	-	1.7 ± 0.2	-	-	-	$Fe^{2+} + F^- \rightleftharpoons FeF^+$
FeCl+	II	0.14	-	*(-1.0 ± 0.8)* *	*21.55 ± 1.77*	*0* [j]	*10 – 200*	*$Fe^{2+} + Cl^- \rightleftharpoons FeCl^+$*
FeS(aq)	*II*	-	-	*(-8.8 ± 1.1)* *	-	-	-	*$Fe^{2+} + H_2S(aq) \rightleftharpoons FeS(aq) + 2\ H^+$*
FeSO4(aq)	II	2.25	13.5	2.44 ± 0.03	8.4 ± 6.2	0 [j]	10 – 35	$Fe^{2+} + SO_4^{2-} \rightleftharpoons FeSO_4(aq)$
Fe(SO4)2-2	*II*	-	-	*(2.0 ± 0.4)* *		-	-	*$Fe^{2+} + 2\ SO_4^{2-} \rightleftharpoons Fe(SO_4)_2^{2-}$*
FeHSO4+	II	3.068	-	*3.068* *	-	-	-	*$Fe^{2+} + SO_4^{2-} + H^+ \rightleftharpoons FeHSO_4^+$*
FeHSeO3+	*II*	-	-	*3.7 ± 1.05*	-	-	-	*$Fe^{2+} + HSeO_3^- \rightleftharpoons FeHSeO_3^+$*
FeHSeO3(H2SeO3)+	*II*	-	-	*7.0 ± 1.0*	-	-	-	*$Fe^{2+} + HSeO_3^- + H_2SeO_3(aq) \rightleftharpoons FeHSeO_3(H_2SeO_3)^+$*
Fe(HSeO4)2(aq)	*II*	-	-	*5.7 ± 1.0*	-	-	-	*$Fe^{2+} + 2\ HSeO_4^- \rightleftharpoons Fe(HSeO_4)_2(aq)$*
FeHPO4(aq)	II	-	-	3.6 ± 1.0	-	-	-	$Fe^{2+} + HPO_4^{2-} \rightleftharpoons FeHPO_4(aq)$
FeH2PO4+	II	-	-	2.7 ± 1.0	-	-	-	$Fe^{2+} + H_2PO_4^- \rightleftharpoons FeH_2PO_4^+$
FeCO3(aq)	II	-5.949	-	(-4.77 ± 0.27) [g]	-	-	-	$Fe^{2+} + HCO_3^- \rightleftharpoons FeCO_3(aq) + H^+$
Fe(CO3)2-2	II	-	-	(-13.33 ± 0.29) [h]	-	-	-	$Fe^{2+} + 2\ HCO_3^- \rightleftharpoons Fe(CO_3)_2^{2-} + 2\ H^+$
FeHCO3+	II	2	-	-	-	-	-	$Fe^{2+} + HCO_3^- \rightleftharpoons FeHCO_3^+$
Fe(CN)6-4	II	-	-	40.41 ± 4.57	-358.9 ± 30.1	-	25	$Fe^{2+} + 6\ CN^- \rightleftharpoons Fe(CN)_6^{4-}$

Tab. 11.8-2: Cont.

Name	Redox	TDB Version 12/07		TDB 2020				
		$\log_{10}\beta°$	$\Delta_r H_m°$ [kJ · mol^{-1}]	$\log_{10}\beta°$	$\Delta_r H_m°$ [kJ · mol^{-1}]	$\Delta_r C_{p,m}°$ [J · K^{-1} · mol^{-1}]	T-range [°C]	Reaction
HFe(CN)6-3	II	-	-	4.28 ± 0.10	2.1 ± 3.0	-	25	$Fe(CN)_6^{4-} + H^+ \rightleftharpoons HFe(CN)_6^{3-}$
H2Fe(CN)6-2	II	-	-	2.4 ± 0.3	-	-	-	$HFe(CN)_6^{3-} + H^+ \rightleftharpoons H_2Fe(CN)_6^{2-}$
KFe(CN)6-3	II	-	-	2.35 ± 0.05	3.6 ± 1.0	-	25	$Fe(CN)_6^{4-} + K^+ \rightleftharpoons KFe(CN)_6^{3-}$
Fe^{3+}	II/III	-13.02	40.5	(-13.051 ± 0.160) [b]	(40.238 ± 1.699) [a]	-	25	$Fe^{2+} + H^+ \rightleftharpoons Fe^{3+} + 0.5\ H_2$ [g]
FeOH+2	III	-2.19	43.5	(-2.20 ± 0.02) *	(43.3 ± 0.6) *	(0) *	18 – 300	$Fe^{3+} + H_2O(l) \rightleftharpoons FeOH^{2+} + H^+$
Fe(OH)2+	III	-5.67	71.5	(-5.71 ± 0.10) *	-	-	-	$Fe^{3+} + 2\ H_2O(l) \rightleftharpoons Fe(OH)_2^+ + 2\ H^+$
Fe(OH)3(aq)	III	-12.56	104	(-12.26 ± 0.26) *	(146.3 ± 4.8) *	(-150 ± 43) *	25 – 300	$Fe^{3+} + 3\ H_2O(l) \rightleftharpoons Fe(OH)_3(aq) + 3\ H^+$
Fe(OH)4-	III	-21.6	133	(-21.60 ± 0.23) *	(146.8 ± 1.8) *	(0) *	25 – 300	$Fe^{3+} + 4\ H_2O(l) \rightleftharpoons Fe(OH)_4^- + 4\ H^+$
Fe2(OH)2+4	III	-2.95	56.5	(-2.91 ± 0.07) *	(30.1 ± 9.5) *	(0) *	18 – 32	$2\ Fe^{3+} + 2\ H_2O(l) \rightleftharpoons Fe_2(OH)_2^{4+} + 2\ H^+$
Fe3(OH)4+5	III	-6.3	59.8	(-6.3) *	(59.8) *	-	25	$3\ Fe^{3+} + 4\ H_2O(l) \rightleftharpoons Fe_3(OH)_4^{5+} + 4\ H^+$
FeF+2	III	6.2	11.3	6.09 ± 0.04	12.8 ± 7.4	(0) *	0 – 35	$Fe^{3+} + F^- \rightleftharpoons FeF^{2+}$
FeF2+	*III*	*10.8*	*20.1*	*(10.41 ± 0.33)* [m]	*(22 ± 14)* [m]	*(0)* *	0 – 35	*$Fe^{3+} + 2\ F^- \rightleftharpoons FeF_2^+$*
FeF3(aq)	*III*	14.0	22.6	-	-	-	-	*$Fe^{3+} + 3\ F^- \rightleftharpoons FeF_3(aq)$*
FeCl+2	III	1.48	23.4	1.52 ± 0.10	22.48 ± 4.60	≈ 0 *,k	20 – 65 (l)	$Fe^{3+} + Cl^- \rightleftharpoons FeCl^{2+}$
FeCl2+	III	2.13	-	(2.2 ± 0.2) [c]	-	-	-	$Fe^{3+} + 2\ Cl^- \rightleftharpoons FeCl_2^+$
FeCl3(aq)	III	1.13	-	(1.0 ± 0.3) [d]	-	-	-	$Fe^{3+} + 3\ Cl^- \rightleftharpoons FeCl_3(aq)$
FeCl4-	III	-	-	(-1.0 ± 0.8) [e]	-	-	-	$Fe^{3+} + 4\ Cl^- \rightleftharpoons FeCl_4^-$
FeSO4+	III	4.04	16.4	4.25 ± 0.10	-	-	-	$Fe^{3+} + SO_4^{2-} \rightleftharpoons FeSO_4^+$
Fe(SO4)2-	III	5.38	19.2	(6.22 ± 0.16) [f]	-	-	-	$Fe^{3+} + 2\ SO_4^{2-} \rightleftharpoons Fe(SO_4)_2^-$
FeHSO4+2	III	2.480 [i]	-	*1.73 ± 0.76*	-	-	-	*$Fe^{3+} + HSO_4^- \rightleftharpoons FeHSO_4^{2+}$*
FeSeO3+	III	11.15 ± 0.11	-	-	-	-	-	$Fe^{3+} + SeO_3^{2-} \rightleftharpoons FeSeO_3^+$
FeSeO3+	III	-	-	0.9 ± 0.5	-	-	-	$Fe^{3+} + H_2SeO_3(aq) \rightleftharpoons FeSeO_3^+ + 2\ H^+$
FePO4(aq)	*III*	-	-	*(0.7 ± 1.0)* [m]	-	-	-	*$Fe^{3+} + H_3PO_4(aq) \rightleftharpoons FePO_4(aq) + 3\ H^+$*
Fe(H2PO4)3 (aq)	*III*	-	-	*(3.5 ± 1.0)* [m]	-	-	-	*$Fe^{3+} + 3\ H_3PO_4(aq) \rightleftharpoons Fe(H_2PO_4)_3(aq) + 3\ H^+$*

Tab. 11.8-2: Cont.

Name	Redox	TDB Version 12/07		TDB 2020				
		$\log_{10}\beta°$	$\Delta_r H_m°$ [kJ · mol^{-1}]	$\log_{10}\beta°$	$\Delta_r H_m°$ [kJ · mol^{-1}]	$\Delta_r C_{p,m}°$ [J · K^{-1} · mol^{-1}]	T-range [°C]	Reaction
Fe(CO3)3-3	III	-	-	24.0 ± 2.0	-	-	-	$Fe^{3+} + 3\ CO_3^{2-} \rightleftharpoons Fe(CO_3)_3^{3-}$
Fe(OH)CO3(aq)	III	-	-	10.7 ± 2.0	-	-	-	$Fe^{3+} + CO_3^{2-} + H_2O(l) \rightleftharpoons Fe(OH)CO_3(aq) + H^+$
Fe(CN)6-3	III	-	-	47.39 ± 5.12	-286.9 ± 32.8	-	25	$Fe^{3+} + 6\ CN^- \rightleftharpoons Fe(CN)_6^{3-}$
KFe(CN)6-2	III	-	-	1.46 ± 0.05	2.1 ± 1.3	-	25	$Fe(CN)_6^{3-} + K^+ \rightleftharpoons KFe(CN)_6^{2-}$
FeSCN+2	III	-	-	3.06 ± 0.05	-	-	-	$Fe^{3+} + SCN^- \rightleftharpoons FeSCN^{2+}$
Fe(SCN)2+	III	-	-	2.23 ± 0.50	-	-	-	$FeSCN^{2+} + SCN^- \rightleftharpoons Fe(SCN)_2^+$

[a] Calculated using $\Delta_r G_m° = \Delta_r H_m° - T\Delta_r S_m°$.
[b] Calculated from $\Delta_r G_m°$.
[c] Calculated from $FeCl^{2+} + Cl^- \rightleftharpoons FeCl_2^+$, for which $\log_{10}K_2° = (0.7 \pm 0.2)$.
[d] Calculated from $FeCl_2^+ + Cl^- \rightleftharpoons FeCl_3(aq)$, for which $\log_{10}K_3° = (-1.2 \pm 0.2)$.
[e] Calculated from $FeCl_3(aq) + Cl^- \rightleftharpoons FeCl_4^-$, for which $\log_{10}K_4° = (-2.0 \pm 0.7)$.
[f] Calculated from $FeSO_4^+ + SO_4^{2-} \rightleftharpoons Fe(SO_4)_2^-$, for which $\log_{10}K_2° = (1.97 \pm 0.13)$.
[g] Discrepancies with Lemire et al. (2013), see text for discussion.
[h] Discrepancies with Lemire et al. (2013), see text for discussion.
[i] Recalculated from $Fe^{3+} + SO_4^{2-} + H^+ \rightleftharpoons FeHSO_4^{2+}$, for which $\log_{10}K° = 4.468$, and $SO_4^{2-} + H^+ \rightleftharpoons HSO_4^-$, for which $\log_{10}K° = 1.988$.
[j] Not explicitly selected by Lemire et al. (2013), but implicit in the extraction of $\Delta_r H_m°$ from a linear $\log_{10}\beta°$ vs. $1/T$ plot.
[k] The van't Hoff equation can be used for approximate extrapolation of $\log_{10}\beta°$ to temperatures up to about 65 °C, even though it follows from the experimental data that $\Delta_r H_m°$ is not constant with temperature and that $\Delta_r C_{p,m}°$ is not equal to zero and varies with temperature.
[l] Temperature range where van't Hoff equation can be used (experimental data was derived within 20 to 90 °C).
[m] Reported, but not selected, by Lemire et al. (2020).

Name	TDB Version 12/07		TDB 2020				
	$\log_{10}K_{s,0}°$	$\Delta_r H_m°$ [kJ · mol^{-1}]	$\log_{10}K_{s,0}°$	$\Delta_r H_m°$ [kJ · mol^{-1}]	$\Delta_r C_{p,m}$ [J · K^{-1} · mol^{-1}]	T-range [°C]	Reaction
Fe(α)	13.82	-89.1	15.89 ± 0.11	-	-	-	$Fe(cr) + 2\ H^+ \rightleftharpoons Fe^{2+} + H_2g$
Fe(OH)2(s) "white rust"	-	-	*(12.26 ± 0.88)* [*]	-	-	-	*$Fe(OH)_2(s) + 2H^+ \rightleftharpoons Fe^{2+} + 2\ H_2O(l)$*
Fe4(OH)8Cl:nH2O(s) "chloride green rust one"	-	-	*(39.7 ± 3.5)* [*]	-	-	-	*$Fe_4(OH)_8Cl{\cdot}nH_2O(s) + 7\ H^+ + ½\ H_2g \rightleftharpoons 4\ Fe^{2+} + Cl^- + (n+8)\ H_2O(l)$*
β-$Fe_2Cl(OH)_3$(Fe-hibbingite)	-	-	17.2 ± 0.2	-	-	-	$Fe_2Cl(OH)_3(cr) + 3\ H^+ \rightleftharpoons 2\ Fe^{2+} + Cl^- + 3\ H_2O(l)$
FeS(mackinawite)	-	-	3.8 ± 0.4	-	-	-	$FeS(cr) + 2\ H^+ \rightleftharpoons Fe^{2+} + H_2S(aq)$
FeS(troilite)	1.68 ± 0.26 [a]	-	3.00 ± 0.52	-27.98 ± 2.55	-	25	$FeS(cr) + 2\ H^+ \rightleftharpoons Fe^{2+} + H_2S(aq)$
Fe0.9S(5C pyrrhotite)	-	-	-0.61 ± 0.54	-15.93 ± 2.72	-	25	$Fe_{0.9}S(cr) + 2\ H^+ \rightleftharpoons 0.7\ Fe^{2+} + 0.2\ Fe^{3+} + H_2S(aq)$
Fe0.875S(4C pyrrhotite)			-1.51 ± 0.52	-12.02 ± 2.53	-	25	$Fe_{0.875}S(cr) + 2\ H^+ \rightleftharpoons 0.625\ Fe^{2+} + 0.250\ Fe^{3+} + H_2S(aq)$
FeS2(pyrite)	-4.52 [b]	-	-2.84 ± 0.86	6.14 ± 3.85	-	25	$FeS_2(cr) + 4\ H^+ + 2\ e^- \rightleftharpoons Fe^{2+} + 2\ H_2S(aq)$

Tab. 11.8-2: Cont.

FeS2(marcasite)	-	-	-2.16± 0.86	1.94 ± 3.86	-	25	$FeS_2(cr) + 4\ H^+ + 2\ e^- \rightleftharpoons Fe^{2+} + 2\ H_2S(aq)$
Fe3S4(greigite)	-	-	-13.18 ± 2.31	-	-	-	$Fe_3S_4(cr) + 8\ H^+ \rightleftharpoons Fe^{2+} + 2\ Fe^{3+} + 4\ H_2S(aq)$
FeSO4:7H2O(melanterite)	-2.209	20.5	- [c]	- [c]	-	-	$FeSO_4{\cdot}7H_2O(cr) \rightleftharpoons Fe^{2+} + SO_4^{2-} + 7\ H_2O(l)$
Fe6(OH)12SO4:nH2O(s) "sulphate green rust two"	-	-	*(55.2 ± 5.3)* [*]	-	-	-	*$Fe_6(OH)_{12}SO_4{\cdot}nH_2O(s) + 10\ H^+ + H_2g \rightleftharpoons 6\ Fe^{2+} + SO_4^{2-} + (n+12)\ H_2O(l)$*
Fe1.042Se(cr) [d]	-	-	(-0.39 ± 0.79) [d]	-5.08 ± 4.5	-	25	$Fe_{1.042}Se(cr) + 2\ H^+ \rightleftharpoons 1.042\ Fe^{2+} + H_2Se(aq) + 0.084\ e^-$
Fe0.875Se(cr) [d]	-	-	(-5.10 ± 0.93) [d]	10.48 ± 5.28	-	25	$Fe_{0.875}Se(cr,) + 2H^+ \rightleftharpoons 0.625\ Fe^{2+} + 0.25\ Fe^{3+} + H_2Se(aq)$
γ-Fe3Se4(cr) [d]	-	-	(-38.51 ± 3.79) [d]	114.8 ± 21.6	-	25	$Fe_3Se_4(cr) + 8\ H^+ \rightleftharpoons Fe^{2+} + 2\ Fe^{3+} + 4\ H_2Se(aq)$
FeSe2(ferroselite) [d]	-	-	(-11.21 ± 1.73) [d]	58.31 ± 9.86	-	25	$FeSe_2(cr) + 4\ H^+ + 2\ e^- \rightleftharpoons Fe^{2+} + 2\ H_2Se(aq)$
Fe2(SeO3)3:3H2O(cr)	-	-	-11.3 ± 0.6	-	-	-	$Fe_2(SeO_3)_3 \cdot 3H_2O(cr) + 6\ H^+ \rightleftharpoons 2\ Fe^{3+} + 3\ H_2SeO_3(aq) + 3\ H_2O(l)$
Fe3(PO4)2:8H2O(vivianite)	-	-	-11.3 ± 0.4	-	-	-	$Fe_3(PO_4)_2{\cdot}8H_2O(cr) + 2H^+ \rightleftharpoons 3Fe^{2+} + 2HPO_4^{2-} + 8H_2O(l)$
FeCO3(siderite) [e]	-0.5612	-25.28	-	-	-	-	$FeCO_3(cr) + H^+ \rightleftharpoons Fe^{2+} + HCO_3^-$
FeCO3(siderite)	-10.89 [f]	-10.38 [f]	-10.90 [*]	-15.654 [*]	-405.855 [*]	25 – 250	$FeCO_3(cr) \rightleftharpoons Fe^{2+} + CO_3^{2-}$
FeCO3(pr)	-0.1211	-14.901	-	-	-	-	$FeCO_3(pr) + H^+ \rightleftharpoons Fe^{2+} + HCO_3^-$
Fe6(OH)12CO3:nH2O(s) "carbonate green rust one"	-	-	*(52.4 ± 5.3)* [*]	-	-	-	*$Fe_6(OH)_{12}CO_3{\cdot}nH_2O(s) + 10\ H^+ + H_2g \rightleftharpoons 6\ Fe^{2+} + CO_3^{2-} + (n+12)\ H_2O(l)$*
Fe3O4(magnetite) [g]	10.02	-	-	-	-	-	$Fe_3O_4(cr) + 8\ H^+ \rightleftharpoons Fe^{2+} + 2\ Fe^{3+} + 4\ H_2O(l)$
Fe3O4(magnetite)	12.02 [h]	-	(11.77 ± 0.22) [*]	(-89.4 ± 3.4) [*]	0 [*]	25 – 300	$1/3\ Fe_3O_4(cr) + 2\ H^+ + 1/3\ H_2g \rightleftharpoons Fe^{2+} + 4/3\ H_2O(l)$
α-Fe2O3(hematite)	0.56 [i]	-	(0.36 ± 0.40) [*]	(-68.3 ± 1.9) [*]	0 [*]	20 – 300	$½\ Fe_2O_3(cr) + 3\ H+ \rightleftharpoons Fe^{3+} + 1.5\ H_2O(l)$
γ-Fe2O3(maghemite)	-	-	(1.61 ± 0.61) [*]	-	-	-	$½\ Fe_2O_3(cr) + 3\ H+ \rightleftharpoons Fe^{3+} + 1.5\ H_2O(l)$
α-FeOOH(goethite)	-1	-	(0.33 ± 0.10) [*]	(-65.5 ± 2.3) [*]	0 [*]	25 – 300	$FeOOH(cr) + 3\ H^+ \rightleftharpoons Fe^{3+} + 2\ H_2O(l)$
γ-FeOOH(lepidocrocite)	-	-	1.86 ± 0.37	-72.5 ± 2.2	-	25	$FeOOH(cr) + 3\ H^+ \rightleftharpoons Fe^{3+} + 2\ H_2O(l)$

Tab. 11.8-2: Cont.

Name	TDB Version 12/07		TDB 2020				
	$\log_{10}K_{s,0}°$	$\Delta_r H_m°$ [kJ · mol^{-1}]	$\log_{10}K_{s,0}°$	$\Delta_r H_m°$ [kJ · mol^{-1}]	$\Delta_r C_{p,m}$ [J · K^{-1} · mol^{-1}]	T-range [°C]	Reaction
Fe(OH)3(am)	5	-	-	-	-	-	$Fe(OH)_3$(am) + 3 $H^+ \rightleftharpoons Fe^{3+}$ + 3 H_2O(l)
Fe(OH)3(mic)	3	-	-	-	-	-	$Fe(OH)_3$(mic) + 3 $H^+ \rightleftharpoons Fe^{3+}$ + 3 H_2O(l)
Fe(OH)3(2-line ferrihydrite)	-	-	(3.50 ± 0.40) *	-	-	-	$Fe(OH)_3$(mic) + 3 $H^+ \rightleftharpoons Fe^{3+}$ + 3 H_2O(l)
FePO4:2H2O(s)	-	-	*-8.1 ± 1.0*	-	-	-	*$FePO_4 \cdot 2H_2O$(s) + 2 $H^+ \rightleftharpoons Fe^{3+}$ + $H_2PO_4^-$ + 2 H_2O(l)*
FePO4(rodolicoite)	-	-	*-1.39 ± 0.39*	*-85.1 ± 2.2*	-	*25*	*$FePO_4$(cr) + 2 $H^+ \rightleftharpoons Fe^{3+}$ + $H_2PO_4^-$*

[a] Calculated from $\log_{10}K_{s,0}° = -(5.31 \pm 0.20)$ for FeS(troilite) + $H^+ \rightleftharpoons Fe^{2+}$ + HS^- and $\log_{10}K° = (6.99 \pm 0.17)$ for $HS^- + H^+ \rightleftharpoons H_2S$(aq).
[b] Calculated from $\log_{10}K_{s,0}° = -(18.5)$ for FeS_2(pyrite) + 2 H^+ + 2 $e^- \rightleftharpoons Fe^{2+}$ + 2 HS^- and $\log_{10}K° = (6.99 \pm 0.17)$ for $HS^- + H^+ \rightleftharpoons H_2S$(aq).
[c] Lemire et al. (2013) selected values for $\log_{10}K_{s,0}°$ and $\Delta_r H_m°$, but due to its high solubility, melanterite was removed from our database.
[d] **Warning:** Although the solubility product of this iron selenide is a selected value, it cannot be used to calculate the solubility of Se, because the formation constants of Fe-selenide complexes are not known. If in any geochemical calculation this iron selenide should turn out to be solubility limiting, the resulting solubility of Se is only a minimal value and could be much higher, even by orders of magnitude. See Section 11.6.3.1.
[e] The dissolution reaction of siderite in TDB 12/07, expressed in terms of HCO_3^-, is reformulated for TDB 2020 in terms of CO_3^{2-}.
[f] Recalculated with data from TDB 12/07.
[g] The dissolution reaction of magnetite in TDB 12/07, expressed in terms of Fe^{2+} and Fe^{3+}, is reformulated for TDB 2020 in terms of Fe^{2+} only.
[h] Calculated with data from TDB 12/07.
[i] Calculated from the original value of 1.12 for the doubled reaction.

Tab. 11.8-3: Selected SIT ion interaction coefficients $\varepsilon_{j,k}$ [kg · mol^{-1}] for iron species

All data included in TDB 2020 are taken from Lemire et al. (2013) and Lemire et al. (2020) unless indicated otherwise. Data estimated according to charge correlations and taken from Tab. 1-7 are shaded. Supplemental data are in italics.

J k → ↓	Cl^- $\varepsilon_{j,k}$ [kg · mol^{-1}]	ClO_4^- $\varepsilon_{j,k}$ [kg · mol^{-1}]	NO_3^- $\varepsilon_{j,k}$ [kg · mol^{-1}]	Li^+ $\varepsilon_{j,k}$ [kg · mol^{-1}]	Na^+ $\varepsilon_{j,k}$ [kg · mol^{-1}]	K^+ $\varepsilon_{j,k}$ [kg · mol^{-1}]
Fe+2	0.17 ± 0.01	0.37 ± 0.04	0.14 ± 0.03 [a e]	0	0	0
FeOH+	0.05 ± 0.10	0.2 ± 0.1	-	0	0	0
Fe(OH)3-	0	0	0	-	-0.05 ± 0.10	-
FeF+	0.05 ± 0.10	0.34 ± 0.07	-	0	0	0
FeCl+	*0.16 ± 0.01*	*0.2 ± 0.1*	-	*0*	*0*	*0*
Fe(SO4)2-2	*0*	*0*	*0*	-	*-0.10 ± 0.10*	-
FeHSO4+	*0.05 ± 0.10*	*0.2 ± 0.1*	-	*0*	*0*	*0*
FeHSeO3+	*0.05 ± 0.10*	*0.2 ± 0.1*	-	*0*	*0*	*0*
FeHSeO3(H2SeO3)+	*0.05 ± 0.10*	*0.2 ± 0.1*	-	*0*	*0*	*0*
FeH2PO4+	0.05 ± 0.10	0.2 ± 0.1	-	0	0	0
Fe(CO3)2-2	0	0	0	-	-0.05 ± 0.05	-
Fe(CN)6-4	0	0	0	-	-0.20 ± 0.30	-
HFe(CN)6-3	0	0	0	-	-0.15 ± 0.20	-
H2Fe(CN)6-2	0	0	0	-	-0.10 ± 0.10	-
KFe(CN)6-3	0	0	0	-	-0.15 ± 0.20	-

Tab. 11.8-3: Cont.

J k → ↓	**Cl^-** $\varepsilon_{j,k}$ [kg · mol^{-1}]	**ClO_4^-** $\varepsilon_{j,k}$ [kg · mol^{-1}]	**NO_3^-** $\varepsilon_{j,k}$ [kg · mol^{-1}]	**Li^+** $\varepsilon_{j,k}$ [kg · mol^{-1}]	**Na^+** $\varepsilon_{j,k}$ [kg · mol^{-1}]	**K^+** $\varepsilon_{j,k}$ [kg · mol^{-1}]
Fe+3	0.76 ± 0.03	0.73 ± 0.04	0.26 ± 0.08 [a e]	0	0	0
FeOH+2	(0.27 ± 0.05) [b d]	(0.27 ± 0.05) [c d]	-	0	0	0
Fe(OH)2+	(0.43 ± 0.10) [b d]	(0.43 ± 0.10) [c d]	-	0	0	0
Fe(OH)4-	0	0	0	-	-0.05 ± 0.10	-
Fe2(OH)2+4	(1.00 ± 0.10) [b d]	(1.00 ± 0.10) [c d]	-	0	0	0
Fe3(OH)4+5	(1.0 ± 0.2) [b]	1.0 ± 0.2	-	0	0	0
FeF+2	(0.46 ± 0.08) [b]	0.46 ± 0.08 [c]	-	0	0	0
FeF2+	*(0.1 ± 0.3)* [b]	*(0.1 ± 0.3)* [a]	-	*0*	*0*	*0*
FeCl+2	0.64 ± 0.06	0.63 ± 0.05	-	0	0	0
FeCl2+	(0.52 ± 0.05) [b]	0.52 ± 0.05	-	0	0	0
FeCl4-	0	0	0	-	-0.05 ± 0.10	-
FeSO4+	(0.4 ± 0.1) [b]	0.4 ± 0.1	-	0	0	0
Fe(SO4)2-	0	0	0	-	0.24 ± 0.14	-
FeHSO4+2	*(0.58 ± 0.13)* [b]	*0.58 ± 0.13*	-	*0*	*0*	*0*
FeSeO3+	(0.2 ± 0.1) [b]	0.2 ± 0.1	-	0	0	0
Fe(CO3)3-3	0	0	0	-	-0.23 ± 0.07	-
Fe(CN)6-3	0	0	0	-	-0.15 ± 0.20	-
KFe(CN)6-2	0	0	0	-	-0.10 ± 0.10	-
FeSCN+2	0.49 ± 0.05 [b]	0.49 ± 0.05 [e]	0.13 ± 0.04 [e]	0	0	0
Fe(SCN)2+	(0.2 ± 0.1) [b]	0.2 ± 0.1	-	0	0	0

[a] Estimated (but not selected) by Lemire et al. (2020)
[b] Assumed to be equal to the corresponding ion interaction coefficient with ClO_4^-, see Section 11.1.1 for explanation
[c] This work
[d] Restricted to $I_m \leq 1.05$ mol · kg^{-1}, see Section 11.4.1.3.1
[e] Lemire et al. (2020)

Tab. 11.8-4: SIT ion interaction coefficients $\varepsilon_{j,k}$ [kg · mol^{-1}] with neutral iron species selected for TDB 2020

All data included in TDB 2020 are taken from Lemire et al. (2013) and Lemire et al. (2020) unless indicated otherwise. Data estimated according to charge correlations and taken from Tab. 1-7 are shaded. Supplemental data are in italics.

Redox	**j k →** ↓	**$Na^+ + Cl^-$** $\varepsilon_{j,k}$ [kg · mol^{-1}]	**$Na^+ + ClO_4^-$** $\varepsilon_{j,k}$ [kg · mol^{-1}]
II	Fe(OH)2(aq)	0.0 ± 0.1	0.0 ± 0.1
II	*FeS(aq)*	*0.0 ± 0.1*	*0.0 ± 0.1*
II	FeSO4(aq)	0.0 ± 0.1	0.0 ± 0.1
II	*Fe(HSeO4)2(aq)*	*0.0 ± 0.1*	*0.0 ± 0.1*
II	FeHPO4(aq)	0.0 ± 0.1	0.0 ± 0.1
II	FeCO3(aq)	0.0 ± 0.1	0.0 ± 0.1
III	Fe(OH)3(aq)	0.0 ± 0.1	0.0 ± 0.1
III	FeCl3(aq)	0.0 ± 0.1	0.0 ± 0.1
III	*FePO4(aq)*	*0.0 ± 0.1*	*0.0 ± 0.1*
III	*Fe(H2PO4)3(aq)*	*0.0 ± 0.1*	*0.0 ± 0.1*
III	Fe(OH)CO3(aq)	0.0 ± 0.1	0.0 ± 0.1

11.9 References

Baes, C.F., Jr. & Mesmer, R.E. (1976): The Hydrolysis of Cations. Wiley-Interscience, New York. 489 pp.

Bardy, J. & Péré, C. (1976): Détermination expérimentale du coefficient de solubilité du carbonate ferreux en milieu aqueux. Tribune de CEBEDEAU, 29, 75-81 (as cited by Lemire et al. 2013).

Behar, B. & Stein, G. (1969): A spectroscopic study of hydrolysis and dimerization in aqueous ferric solutions. Israel Journal of Chemistry, 7, 827-830 (as cited by Brown & Ekberg 2016).

Bénézeth, P., Dandurand, J.L. & Harrichoury, J.C. (2009): Solubility product of siderite ($FeCO_3$) as a function of temperature (25-250 °C). Chemical Geology, 265, 3-12.

Berner, R.A. (1967): Thermodynamic stability of sedimentary iron sulfides. American Journal of Science, 265, 773-785

Bigham, J.M, Schwertmann, U., Carlson, L. & Murad, E. (1996): Schwertmannite and the chemical modeling of iron in acid sulfate waters. Geochimica et Cosmochimica Acta, 60, 2111-2121.

Braun, R. D. (1991): Solubility of iron(II) carbonate at temperatures between 30 and 80˚. Talanta, 38, 205-211.

Bray, W.C. & Hershey, A.V. (1934): The hydrolysis of ferric ion. The standard potential of the ferric-ferrous electrode at 25 °C. The equilibrium $Fe^{+++} + Cl^{-} = FeCl^{++}$. Journal of the American Chemical Society, 56, 1889-1893 (as cited by Brown & Ekberg 2016).

Brown, P.L. & Ekberg, C. (2016): Hydrolysis of Metal Ions. Vol. 2, Wiley-VCH, Weinheim.

Bruno, J. & Duro, L. (2000): Reply to W. Hummel's comment on and correction to "On the influence of carbonate in mineral dissolution: 1. The thermodynamics and kinetics of hematite dissolution in bicarbonate solutions at T = 25 °C" by J. Bruno, W. Stumm, P. Wersin, and F. Brandberg. Geochimica et Cosmochimica Acta, 64, 2173-2176.

Bruno, J., Stumm, W., Wersin, P. & Brandberg, F. (1992a): On the influence of carbonate in mineral dissolution: I. The thermodynamics and kinetics of hematite dissolution in bicarbonate solutions at T = 25 °C. Geochimica et Cosmochimica Acta, 56, 1139-1147.

Bruno, J., Wersin, P. & Stumm, W. (1992b): On the influence of carbonate in mineral dissolution: II. The solubility of $FeCO_3$(s) at 25 °C and 1 atm total pressure. Geochimica et Cosmochimica Acta, 56, 1149-1155.

Byrne, R.H. & Kester, D.R. (1976): A potentiometric study of ferric ion complexes in synthetic media and seawater. Marine Chemistry, 4, 275-287 (as cited by Brown & Ekberg 2016).

Byrne, R.H. & Kester, D.R. (1978): Ultraviolet spectroscopic study of ferric hydroxide complexation. Journal of Solution Chemistry, 7, 373-383 (as cited by Brown & Ekberg 2016).

Byrne, R.H. & Thompson, S.W. (1997): Ferric borate formation in aqueous solution. Journal of Solution Chemistry, 26, 729-734 (as cited by Brown & Ekberg 2016).

Byrne, R.H., Luo, Y.-R. & Young, R.W. (2000): Iron hydrolysis and solubility revisited: observations and comments on iron hydrolysis characterisations. Marine Chemistry, 70, 23-35 (as cited by Brown & Ekberg 2016).

Chai, L. & Navrotsky, A. (1994): Enthalpy of formation of siderite and its application in phase equilibrium calculation. American Mineralogist, 79, 921-929.

Chukhrov, F.V., Zvyagin, B.B., Gorshkov, A.I., Yermilova, L.P., Korovushkin, V.V., Rudnitskaya, Y.S. & Yakubovskaya, N.Y. (1977): Feroxyhyte, a new modification of FeOOH. International Geology Review, 19, 873-890.

Ciavatta, L. (1980): The specific interaction theory in evaluating ionic equilibria. Annali di Chimica, 70, 551-567.

Ciavatta, L., de Tommaso, G. & Iuliano, M. (2002): Stability constants of iron(II) sulfate complexes. Annali di Chimica, 92, 513-520.

Connick, R.E. & McVey, W.H. (1951): Oxidation potentials of the Pu(III)-Pu(IV) and Fe(II)-Fe(III) couples in perchloric acid solution – Heat content and entropy changes. Journal of the American Chemical Society, 73, 1798-1804.

Connick, R.E., Hepler, L.G., Hugus, Z.Z., Kury, J.W., Latimer, W.M. & Tsao, M.-S. (1956): The complexing of iron(III) by fluoride ions in aqueous solution: free energies, heats and entropies. Journal of the American Chemical Society, 78, 1827-1829 (as cited by Brown & Ekberg 2016).

Craig, J.R. & Scott, S.D. (1974): Sulfide phase equilibria. In: Ribbe, P.H. (ed.): Sulfide Mineralogy. Reviews in Mineralogy, Vol. 1, Mineralogical Society of America, CS1–CS110.

Daniele, P.G., Rigano, C., Sammartano, S. & Zelano, V. (1994): Ionic strength dependence of formation constants – XVIII. The hydrolysis of iron(III) in aqueous KNO_3 solutions. Talanta, 41, 1577-1582.

Davison, W. (1979): Soluble inorganic ferrous complexes in natural waters. Geochimica et Cosmochimica Acta, 43, 1693-1696.

Davison, W. (1991): The solubility of iron sulphides in synthetic and natural waters at ambient temperature. Aquatic Sciences, 53, 309-329.

Davison, W., Phillips, N. & Tabner, B.J. (1999): Soluble iron sulfide species in natural waters: Reappraisal of their stoichiometry and stability constants. Aquatic Science, 61, 23-43.

Diakonov, I.I. (1995): Etude expérimentale de la complexation de l'aluminium avec l'ion sodium et de la speciation du gallium et du fer(III) dans les solutions naturalles. PhD thesis. Université Toulouse III Paul Sabatier, Toulouse, France (as cited by Brown & Ekberg 2016).

Diakonov, I.I., Khodakovskiy, I., Schott, J. & Sergeeva, E. (1994): Thermodynamic properties of iron oxides and hydroxides. I. Surface and bulk thermodynamic properties of goethite (α-FeOOH) up to 500 K. European Journal of Mineralogy, 6, 967-983.

Diakonov, I.I., Schott, J., Martin, F., Harrichourry, J.-C. & Escalier, J. (1999): Iron(III) solubility and speciation in aqueous solutions. Experimental study and modeling: Part 1. Hematite solubility from 60 to 300 °C in NaOH-NaCl solutions and thermodynamic properties of $Fe(OH)_4^-$(aq). Geochimica et Cosmochimica Acta, 63, 2247-2261.

Drissi, S.H., Refait, P., Abdelmoula, M. & Génin, J.-M.R. (1995): The preparation and thermodynamic properties of Fe(II)-Fe(III) hydroxide-carbonate (green rust 1); Pourbaix diagram of iron in carbonate-containing aqueous media. Corrosion Science, 37, 2025-2041.

Dutrizac, J.E. & Jambor, J.L. (2000): Jarosites and their application in hydrometallurgy. In: Alpers, C.N, Jambor, J.L & Nordstrom, D.K (eds.): Sulfate Minerals–Crystallography, Geochemistry and Environmental Significance. Reviews in Mineralogy & Geochemistry, 40, 405-452.

Font, E., Carlut, J., Rémazeilles, C., Mather, T.A., Nédélec, A., Mirão, J. & Casale S. (2017): End-Cretaceous akaganéite as a mineral marker of Deccan volcanism in the sedimentary record. Scientific Reports, 7(11453), 1-10.

Fouillac, C. & Criaud, A. (1984): Carbonate and bicarbonate trace metal complexes: Critical reevaluation of stability constants. Geochemical Journal, 18, 297-303.

Génin, J.-M.R., Bourrié, G., Trolard, F., Abdelmoula, M., Jaffrezic, A., Refait, P., Maître, V., Humbert, B. & Herbillon, A. (1998a): Thermodynamic equilibria in aqueous suspensions of synthetic and natural Fe(II)−Fe(III) green rusts: occurrences of the mineral in hydromorphic soils. Environmental Science & Technology, 32, 1058-1068.

Goldsztaub, M.S. (1935): Étude de quelques dérivés de l'oxyde ferrique (FeO.OH, FeO^2Na, FeOCl); détermination de leurs structures. Bulletin de la Société Française de Minéralogie, 58, 6-76.

Greenberg, J., & Tomson, M. (1992): Precipitation and dissolution kinetics and equilibria of aqueous ferrous carbonate vs temperature. Applied Geochemistry, 7, 185-190.

Grenthe, I., Gaona, X., Plyasunov, A.V., Rao, L., Runde, W.H., Grambow, B., Konings, R.J.M., Smith, A.L. & Moore, E.E. (2020): Second Update on the Chemical Thermodynamics of Uranium, Neptunium, Plutonium, Americium and Technetium. Chemical Thermodynamics, Vol. 14. OECD Publications, Paris, France, 1503 pp.

Grenthe, I., Plyasunov, A.V. & Spahiu, K. (1997): Estimations of medium effects on thermodynamic data. In: Grenthe, I., Puigdomènech, I. (eds.): Modelling in Aquatic Chemistry. OECD NEA, Paris, France, 325-426.

Grivé, M. (2005): The linkage between uranium, iron and carbon cycling, processes at interfaces: Evidences from combined solution chemical and spectroscopic studies. Ph.D. thesis. Universitat Politècnica de Catalunya (as cited by Lemire et al. 2013).

Grivé, M., Duro, L. & Bruno, J. (2014): Fe(III) mobilisation by carbonate in low temperature environments: Study of the solubility of ferrihydrite in carbonate media and the formation of Fe(III) carbonate complexes. Applied Geochemistry, 49, 57-67.

Haynes, W.M. (ed.) (2017): CRC Handbook of Chemistry and Physics, 97th edition (internet version 2017). CRC Press/Taylor & Francis, Boca Raton, FL.

Helgeson, H.C., Kirkham, D.H. & Flowers, G.C. (1981): Theoretical prediction of the thermodynamic behavior of aqueous electrolytes at high pressures and temperatures: IV. Calculation of activity coefficients, osmotic coefficients, and apparent molal and standard and relative partial molal properties to 600 °C and 5 kbar. American Journal of Science, 281, 1249-1516

Hogfeldt, E. & Sillén, L.G. (1966): Unpublished manuscript.

Hovey, J.K. (1988): Thermodynamics of aqueous solutions. Ph.D. thesis, University of Alberta, Edmonton, AB, Canada, 569 pp (as cited by Lemire et al. 2013).

Hummel, W. (2000): Comment on "On the influence of carbonate in mineral dissolution: 1. The thermodynamics and kinetics of hematite dissolution in bicarbonate solutions at T = 25 °C" by J. Bruno, W. Stumm, P. Wersin, and F. Brandberg. Geochimica et Cosmochimica Acta, 64, 2167-2171.

Hummel, W., Anderegg G., Puigdomènech, I., Rao, L. & Tochiyama, O. (2005): Chemical Thermodynamics of Compounds and Complexes of U, Np, Pu, Am, Tc, Se, Ni and Zr with Selected Organic Ligands. Chemical Thermodynamics Series, Vol. 9, OECD NEA, Paris, 1088 pp.

Hummel, W., Berner, U., Curti, E., Pearson, F.J. & Thoenen, T. (2002): Nagra/PSI Chemical Thermodynamic Data Base 01/01. Nagra NTB 02-16. Also published by Universal Publishers/upublish.com, Parkland, USA, 565 pp.

Hurlen, T. (1960): Electrochemical behaviour of iron. Acta Chemica Scandinavica, 14, 1533-1554.

Jensen, D.L., Boddum, J.K., Tjell, J.C. & Christensen, T.H. (2002): The solubility of rhodochrosite ($MnCO_3$) and siderite ($FeCO_3$) in anaerobic aquatic systems. Applied Geochemistry, 17, 503-511.

Kanert, G.A., Gray, G.W. & Baldwin, W.G. (1976): The solubility of magnetite in basic solutions at elevated temperatures. Atomic Energy of Canada Limited Report, AECL-5528, 11 pp.

Kester, D.R., Byrne, R.H., Jr. & Liang Y.-J. (1975): Redox reactions and solution complexes of iron in marine systems. In: Church, T.M. (ed.): Marine Chemistry in the Coastal Environment, ACS Symposium Series, Vol. 18, American Chemical Society, Washington, DC, 56-79.

Khoe, G., Brown, P.L., Sylva, R.N. & Robins, R.G. (1986): The hydrolysis of metal ions. Part 9. Iron(III) in perchlorate, nitrate and chloride media (1 mol dm^{-3}). Journal of the Chemical Society, Dalton Transactions, 1901-1906 (as cited by Brown & Ekberg 2016).

Kubota, E., Mochizuki, Y. & Yokoi, M. (1988): Conductivity of iron(II) sulfate in aqueous solution at various temperatures. Bulletin of the Chemical Society of Japan, 61, 3723-3724.

Langmuir, D. (1969): The Gibbs free energies of substances in the system $Fe\text{-}O_2\text{-}H_2O\text{-}CO_2$ at 25 °C. U.S. Geological Survey Professional Paper, 650-B, B180–B184 (as cited by Lemire et al. 2013).

Langmuir, D. (1979): Techniques of estimating thermodynamic properties for some aqueous complexes of geochemical interest. In: Jenne, E.A. (ed.): Chemical Modeling in Aqueous Systems, ACS Symposium Series, Vol. 93, American Chemical Society, Washington DC, 353-387.

Langmuir, D. & Whittemore, D.O. (1971): Variations in the stability of precipitated ferric oxyhydroxides. In: Hem, J.D. (ed.): Nonequilibrium Systems in Natural Water Chemistry, Advances in Chemistry Series, Vol. 106, American Chemical Society, Washington DC, 209-234.

Lemire, R.J., Berner, U., Musikas, C., Palmer, D.A., Taylor, P. & Tochiyama, O. (2013): Chemical Thermodynamics of Iron, Part 1. Chemical Thermodynamics, Vol. 13a. OECD Publications, Paris, France, 1082 pp.

Lemire, R.J., Palmer, D.A., Schlenz, H. & Taylor, P. (2020): Chemical Thermodynamics of Iron, Part 2. Chemical Thermodynamics, Vol. 13b. OECD Publications, Paris, France, 882 pp.

Lente, G. & Fábián, I. (1998): The early phase of the iron(III)-sulfite reaction. Formation of a novel iron(III)-sulfito complex. Inorganic Chemistry, 37, 4204-4209 (as cited by Brown & Ekberg 2016).

Ma, C., Tschauner, O., Beckett, J. R., Liu, Y., Rossman, G. R., Sinogeikin, S. V., Smith J. S. & Taylor, L. A. (2016): Ahrensite, γ-Fe_2SiO_4 , a new shock-metamorphic mineral from the Tissint meteorite: Implications for the Tissint shock event on Mars. Geochimica et Cosmochimica Acta, 184, 240-256.

Magnusson, L.B. & Huizenga, J.R. (1953): Stabilities of +4 and +5 oxidation states of the actinide elements - the Np(IV) - Np(V) couple in perchloric acid solution. Journal of the American Chemical Society, 75, 2242-2246.

Mattigod, S.V. & Sposito, G. (1977): Estimated association constants for some complexes of trace metals with inorganic ligands. Soil Science Society of America Journal, 41, 1092-1097.

Mehra, M.C. (1968): Studies on the stabilities of some metal selenite, sulphide, and selenide complexes in solution. Ph.D. thesis, Laval University, Quebec.

Milburn, R.M. (1957): A spectrophotometric study of the hydrolysis of iron(III) ion. III. Heats and entropies of hydrolysis. Journal of the American Chemical Society, 79, 537-540 (as cited by Brown & Ekberg 2016).

Milburn, R.M. & Vosburgh, W.C. (1955): A spectrophotometric study of the hydrolysis of iron(III) ion. II. Polynuclear species 1. Journal of the American Chemical Society, 77, 1352-1355 (as cited by Brown & Ekberg 2016).

Millero, F.J. & Hawke, D.J. (1992): Ionic interactions of divalent metals in natural waters. Marine Chemistry, 40, 19-48.

Mills, S.J., Christy, A.G., Génin, J.-M.R., Kameda, T. & Colombo, F. (2012): Nomenclature of the hydrotalcite supergroup: natural layered double hydroxides. Mineralogical Magazine, 76, 1289-1336.

Nemer, M.B., Xiong, Y., Ismail, A.E. & Jang, J.-H. (2011): Solubility of $Fe_2(OH)_3Cl$ (pure-iron end-member of hibbingite) in NaCl and Na_2SO_4 brines. Chemical Geology, 280, 26-32.

Nikolskii, B.P., Palchevskii, V.V., Pendin, A.A., Tkatschuk, E.C., Isaeva, S.N. & Jakubov, C.M. (1971): Study of Fe(III) hydrolysis by ion exchange method. Doklady Akademii Nauk SSSR, 196, 609-612 (as cited by Brown & Ekberg 2016).

Nordstrom, D.K. & Jenne, E.A. (1977): Fluorite solubility equilibria in selected geothermal waters. Geochimica et Cosmochimica Acta, 41, 175-188.

Nordstrom, D.K., Plummer, L.N., Langmuir, D., Busenberg, E., May, H.M., Jones, B.F. & Parkhurst, D.L. (1990): Revised Chemical Equilibrium Data for Major Water-Mineral Reactions and Their Limitations. In: Melchior, D.C., and Bassett, R.L. (eds.): Chemical Modeling of Aqueous Systems II. Washington, D.C., American Chemical Society, ACS Symposium Series 416, p. 398-413.

Norvell, W.A. & Lindsay, W.L. (1982): Estimation of the concentration of Fe^{3+} and the $(Fe^{3+})(OH^-)^3$ ion product from equilibria of EDTA in soil. Soil Science Society of America Journal, 46, 710-715.

O'Driscoll, B., Clay, P.L., Cawthorn, R.G., Lenaz, D., Adetunji, J. & Kronz A. (2014): Trevorite: Ni-rich spinel formed by metasomatism and desulfurization processes at Bon Accord, South Africa? Mineralogical Magazine, 78, 145-163.

Olin, Å., Noläng, G., Osadchii, E., Öhman, L.-O. & Rosén, E. (2005): Chemical Thermodynamics of Selenium. Chemical Thermodynamics, Vol. 7. Elsevier, Amsterdam, 851 pp.

Olshanskii, Y.I. & Ivanenko, V.V. (1958): Mechanism of mass transfer in the formation of hydrothermal deposits of sulphides. Tr. Inst. Geol. rudn. Mestorosh., 16, 14-46 (as cited by Davison 1991).

Olson, A.R. & Simonson, T.R. (1949): The hydrolysis of ferric ion. Journal of Chemical Physics, 17, 1322-1325 (as cited by Brown & Ekberg 2016).

Olson, L.L. & O'Melia, C.R. (1973): The interaction of Fe(III) with $Si(OH)_4$. Journal of Inorganic and Nuclear Chemistry, 35, 1977-1985.

Parker, V.B. & Khodakovskii, I.L. (1995): Thermodynamic properties of the aqueous ions (2+ and 3+) of iron and the key compounds of iron. Journal of Physical and Chemical Reference Data, 24, 1699-1745.

Patten, J.T. & Byrne, R.H. (2017): Assessment of Fe(III) and Eu(III) complexation by silicate in aqueous solutions. Geochimimica et Cosmochimica Acta, 202, 361-373.

Pearson, F.J., Jr., Berner, U. & Hummel W. (1992): Nagra Thermochemical Data Base II. Supplemental Data 05/92. Nagra Technical Report NTB 91-18.

Perera, W.N. & Hefter, G. (2003): Mononuclear cyano- and hydroxo-complexes of iron(III). Inorganic Chemistry, 42, 5917-5923 (as cited by Brown & Ekberg 2016).

Perry, D.L. (2011): Handbook of Inorganic Compounds, $2^{n\ d}$ edition. CRC Press/Taylor & Francis, Boca Raton, FL.

Po, H.N. & Sutin, N. (1968): The stability constant of the monochloro complex of iron(II). Inorganic Chemistry, 7, 621-624 (as cited by Davison 1979).

Popoff, S. & Kunz, A. H. (1929): Oxidation-reduction potentials. I. The ferric-ferrous electrode. Journal of the American Chemical Society, 51, 382-394 (as cited by Lemire et al. 2013).

Porter, R.A. & Weber, W.J. (1971): The interaction of silicic acid with iron(III) and uranyl ions in dilute aqueous solution. Journal of Inorganic and Nuclear Chemistry, 33, 2443-2449.

Ptacek, C.J. & Blowes, D.W. (1994): Influence of siderite on the pore-water chemistry of inactive mine-tailings impoundments. In: Alpers, C.N. & Blowes, D.W. (Eds.): Environmental Geochemistry of Sulfide Oxidation. American Chemical Society, Washington, DC, 172-189 (as cited by Bénézeth et al. 2009).

Ptacek, C.J. & Reardon, E.J., (1992): Solubility of siderite ($FeCO_3$) in concentrated NaCl and Na_2SO_4 solutions at 25 °C. Water-Rock Interaction: Proceedings of the 7th International Symposium on Water-Rock Interaction, WRI-7, Park City, Utah, 181-183 (as cited by Lemire et al. 2013).

Puigdomenech, I., Plyasunov, A.V., Rard, J.A. & Grenthe, I. (1997): Temperature corrections to thermodynamic data and enthalpy calculations. In: Puigdomenech, I. & Grenthe, I. (eds.): Modelling in Aquatic Chemistry. NEA OECD, Paris, 427-493.

Rabinovitch, E. & Stockmayer, W.H. (1942): Association of ferric ions with chloride, bromide and hydroxyl ions (a spectroscopic study). Journal of the American Chemical Society, 64, 335-347.

Rai, D., Felmy, A.R. & Moore, D.A. (1995): The solubility product of crystalline ferric selenite hexahydrate and the complexation constant of $FeSeO_3^+$. Journal of Solution Chemistry, 24, 735-752.

Rasmussen, M. G., Evans, B. W. & Kuehner, S. M. (1998): Low-temperature fayalite, greenalite, and minnesotaite from the Overlook gold deposit, Washington; phase relations in the system FeO-SiO_2-H_2O. The Canadian Mineralogist, 36, 147-162.

Reardon, E.J. (1979): Complexing of silica by iron(III) in natural waters. Chemical Geology, 25, 339-345.

Reardon, E.J. & Beckie, R.D. (1987): Modelling chemical equilibria of acid mine-drainage: The $FeSO_4$-H_2SO_4-H_2O system. Geochimica et Cosmochimica Acta, 51, 2355-2368.

Refait, P. & Génin, J.-M.R. (1993): The oxidation of ferrous hydroxide in chloride-containing aqueous media and Pourbaix diagrams of green rust one. Corrosion Science 34, 797-819.

Refait, P., Bon, C., Simon, L., Bourrié, G., Trolard, F., Bessière, J. & Génin J.-M.R. (1999): Chemical composition and Gibbs standard free energy of formation of Fe(II)-Fe(III) hydroxysulphate green rust and Fe(II) hydroxide. Clay Minerals, 34, 499-510.

Reiterer, F., Johannes, W. & Gamsjäger, H. (1981): Semimicro determination of solubility constants: Copper(II) carbonate and iron(II) carbonate. Mikrochimica Acta, 75, 63-72.

Rickard, D. (2006): The solubility of FeS. Geochimica et Cosmochimica Acta, 70, 5779-5789.

Rickard, D. & Luther, G.W., III (2007): Chemistry of iron sulfides. Chemical Reviews, 107, 514-562

Robie, R.A. & Hemingway, B.S. (1995): Thermodynamic properties of minerals and related substances at 298.15 K and 1 bar (10^5 Pascals) pressure and at higher temperatures. United States Geological Survey Bulletin, 2131, 453.

Robie, R.A., Haselton, H.T, Jr., & Hemingway, B.S. (1984): Heat capacities and entropies of rhodochrosite ($MnCO_3$) and siderite ($FeCO_3$) between 5 and 600 K. American Mineralogist, 69, 349-357.

Robinson, R.A. & Stokes, R.H. (1965): Electrolyte Solutions, 2nd ed., Butterworths.

Salvatore, F. & Vasca, E. (1990): Formation constants of $FeOH^{2+}$, $Fe(OH)_2^{+}$ and $Fe_2(OH)_2^{4+}$ at zero ionic strength. Annali di Chimica, 80, 515-521 (as cited by Brown & Ekberg 2016).

Sapieszko, R.S., Patel, R.C. & Matijević, E. (1977): Ferric hydrous oxide sols. 2. Thermodynamics of aqueous hydroxo and sulfate ferric complexes. Journal of Physical Chemistry, 81, 1061-1068 (as cited by Brown & Ekberg 2016).

Schäfer, H. (1951): Untersuchungen am System Fe_2O_3–$FeCl_3$–H_2O–HCl. VII) Über den hydrolytischen Abbau des Eisenoxychlorids unter der Einwirkung von feuchter Luft bei Raumtemperatur. Zeitschrift für anorganische und allgemeine Chemie, 264, 249-254.

Schumb, W.C., Sherrill, M.S. & Sweetser, S.B. (1937): The measurement of the molal ferric-ferrous electrode potential. Journal of the American Chemical Society, 59, 2360-2365 (as cited by Lemire et al. 2013).

Schwertmann, U. & Taylor, R.M. (1977): Iron oxides. In: Dixon, J.B. & Weed, S.B. (eds.): Minerals in Soil Environments. Soil Science Society of America, Madison, Wisconsin, 145-180 (as cited by Nordstrom et al. 1990).

Sillén, L.G. & Martell A.E. (1964): Stability Constants of Metal-Ion Complexes. Chemical Society (London) Special Publication No. 17, 754 pp (as cited by Nordstrom & Jenne 1977).

Silva, C.A., Liu, X. & Millero, F.J. (2002): Solubility of siderite ($FeCO_3$) in NaCl solutions. Journal of Solution Chemistry, 31, 97-108.

Singer, P.C. & Stumm, W. (1970): The solubility of ferrous iron in carbonate-bearing waters. Journal (American Water Works Association), 62, 198-202.

Smith R.M. & Martell A.E. (1976): Critical stability constants: Vol. 4, Inorganic complexes. Plenum Press, New York, 257 pp.

Smith, H.J. (1918): On equilibrium in the system: Ferrous carbonate, carbon dioxide and water. Journal of the American Chemical Society, 40, 879-883.

Soli, A.L. & Byrne, R.H. (1996): The hydrolysis and fluoride complexation behaviour of Fe(III) at 25 °C and 0.68 molal ionic strength. Journal of Solution Chemistry, 25, 773-785 (as cited by Brown & Ekberg 2016).

Stefánsson, A. (2007): Iron(III) hydrolysis and solubility at 25 °C. Environmental Science & Technology, 41, 6117-6123.

Stirnemann, E. (1925): Das System Eisenchlorid-Wasser bei höherer Temperatur. Neues Jahrbuch für Mineralogie, Geologie und Paläontologie, Beilageband, Abteilung A, Mineralogie, Petrographie, 52, 334-377.

Sweeton, F.H. & Baes, C.F., Jr. (1970): The solubility of magnetite and hydrolysis of ferrous ion in aqueous solutions at elevated temperatures. Journal of Chemical Thermodynamics, 2, 479-500.

Tagirov, B. R., Diakonov, I. I., Devina, O. A. & Zotov, A. V. (2000): Standard ferric-ferrous potential and stability of $FeCl^{2+}$ to 90 °C. Thermodynamic properties of Fe^{3+}(aq) and ferric-chloride species. Chemical Geology, 162, 193-219.

Taylor, P. & Owen, D. G., (1997): Comparison of the solubilities of synthetic hematite (α-Fe_2O_3) and maghemite (γ-Fe_2O_3). Report AECL-11668, Atomic Energy Canada Ltd., 16 pp.

Tewari, P.H. & Campbell, A.B. (1976): Dissolution of iron sulphide (troilite) in aqueous sulphuric acid. Journal of Physical Chemistry, 80, 1844-1848 (as cited by Davison 1991).

Tewari, P.H., Wallace, G. & Campbell, A.B. (1978): The solubility of iron sulphides and their role in mass transport in Girdler-Sulphide heavy water plants. Report AECL-5960, Atomic Energy Canada Ltd., 34 pp (as cited by Davison 1991).

Thoenen, T., Hummel, W., Berner, U. & Curti, E. (2014): The PSI/Nagra Chemical Thermodynamic Database 12/07. Technical Report, PSI Bericht Nr. 14-04, Paul Scherrer Institut, Villigen, Switzerland, 416 pp.

Torres, J., Pintos, V., Domínguez, S., Kremer, C. & Kremer, E. (2010): Selenite and selenate speciation in natural waters: interaction with divalent metal ions. Journal of Solution Chemistry, 39, 1-10.

Tremaine, P.R. & LeBlanc J.C. (1980): The solubility of magnetite and the hydrolysis and oxidation of Fe^{2+} in water to 300 °C. Journal of Solution Chemistry, 9, 415-442.

Turner, R.C. & Miles, K.E. (1957): The ultraviolet absorption spectra of the ferric ion and its first hydrolysis product in aqueous solutions. Canadian Journal of Chemistry, 35, 1002-1009 (as cited by Brown & Ekberg 2016).

Wagman, D.D., Evans, W.H., Parker, V.B., Schumm, R.H., Halow, I., Bailey, S.M., Churney, K.L. & Nuttall, R.L. (1982): The NBS tables of chemical thermodynamic properties: Selected values for inorganic and C1 and C2 organic substances in SI units. Journal of Physical and Chemical Reference Data, 11, Supplement No. 2, 1-392.

Weber, W.J. & Stumm, W. (1965): Formation of a silicato-iron(III) complex in dilute aqueous solution. Journal of Inorganic and Nuclear Chemistry, 27, 237-239.

Wendt, H. & Strehlow, H. (1962): Schnelle Ionenreaktionen in Lösungen. II. Die Bildung einiger einfacher Komplexe des Eisen-III-ions. Zeitschrift für Elektrochemie, 66, 228-234.

Whittemore, D.O. & Langmuir, D. (1972): Standard electrode potential of $Fe^{3+} + e^{-} = Fe^{2+}$ from 5-35 °C. Journal of Chemical and Engineering Data, 17, 288-290.

Wilson, A.S. & Taube, H. (1952): The affinities of chromic ion and gallium ion for fluoride ion. Journal of the American Chemical Society, 74, 3509-3512 (as cited by Brown & Ekberg 2016).

Yatsimirskii, K.B. & Vasil'ev, V.P. (1960): Instability Constants of Complex Compounds. Pergamon Press, Oxford, 220 pp.

Ziemniak, S.E., Jones, M.E. & Combs, K.E.S. (1995): Magnetite solubility and phase stability in alkaline media at elevated temperatures. Journal of Solution Chemistry, 24, 837-877.

Zotov, A.V. & Kotova, Z.Y. (1979): Spectrophotometric determination of the first hydrolysis constant of Fe^{3+} at 25 to 80 °C. Geokhimiya, 285-290 (as cited by Brown & Ekberg 2016).

12 Lead

12.1 Introduction

Metallic lead and many lead compounds and complexes are toxic and thus, lead is an environmentally significant heavy metal. In addition, long-lived radioactive isotopes, Pb-202 and Pb-205 with $(5.3 \pm 0.2)\cdot 10^4$ and $(1.53 \pm 0.07)\cdot 10^7$ years half-life, respectively, are produced in spallation induced neutron sources (e.g., SINQ at PSI) and contribute in dose-relevant quantities to the inventory of radioactive waste coming from research facilities like PSI. The latter fact triggered the inclusion of lead into the PSI Chemical Thermodynamic Database 2020 (PSI TDB 2020), besides its relevance as a chemically toxic substance.

In aqueous solution, lead occurs in three oxidation states: Pb(0), Pb(II), the dominant form under most conditions, and Pb(IV).

Eh-pH diagrams indicate that Pb(IV) is stable in aqueous solution only as the mixed Pb(II)/Pb(IV) oxide mineral minium, Pb_3O_4(s), and as plattnerite, PbO_2(s); these exist to appreciable extents only under very oxidising conditions, at near-neutral to strongly basic pH (Brookins 1988). Brown & Ekberg (2016) report that very few data are available for Pb(IV) hydrolysis and the solubility of PbO_2(s) in alkaline media. From these scarce data they assess a stability constant for $Pb(OH)_6^{2-}$. None of these values for Pb(IV) compounds and complexes is included in TDB 2020.

The thermodynamic data included into the PSI TDB 2020 have been taken from

- CODATA key values (Cox et al. 1989)
- an IUPAC review of Pb^{2+} + OH^-, Cl^-, CO_3^{2-}, SO_4^{2-} and PO_4^{3-} aqueous systems (Powell et al. 2009)
- the recent review of the hydrolysis of metal ions (Brown & Ekberg 2016)
- a JNC review (Lothenbach et al. 1999) and own reviews of experimental data concerning the PbS(s) – H_2S – water system

The selected thermodynamic data for lead compounds and complexes are presented in Tab. 12-1.

Hagemann (2012) provides complexation constants of Pb hydrolysis and carbonate species from own experimental data in highly saline solutions. All these species are also considered in TDB 2020 and their selected values are in good agreement with the data of Hagemann (2012). Hagemann (2012) also reports solubility products for PbO (red, litharge), PbO (yellow, massicot), PbClOH (laurionite), $PbCO_3$ (cerussite) and $Pb_2(CO_3)Cl_2$ (phosgenite). These solid compounds are also considered in TDB 2020 and their selected values are in good agreement with the data of Hagemann (2012). In addition, Hagemann (2012) provides solubility products of more soluble Pb hydroxide, chloride, sulphate, and carbonate salts which are not included in TDB 2020.

IUPAC, as well as NEA (see, e.g., Grenthe et al. 1992) used the specific ion interaction theory (SIT) for making ionic strength corrections to the experimental data, an approach which is also adopted for TDB 2020 (as has been for all its predecessors). Powell et al. (2009) only evaluated experiments in perchlorate media and explicitly considered the formation of lead chloride complexes. Therefore, ion interaction coefficients ε for cationic lead species with Cl^- are missing. They can be approximated by the corresponding interaction coefficients with ClO_4^-. Thus, e.g., $\varepsilon(PbOH^+, Cl^-) \approx \varepsilon(PbOH^+, ClO_4^-) = -(0.05 \pm 0.05)$ kg · mol^{-1}.

In some cases, the ion interaction coefficients of lead species were not available. We approximated these with the estimation method described in Section 1.5.3, which draws on a statistical analysis of published SIT ion interaction coefficients, and which allows the estimation of missing coefficients for the interaction of cations with Cl^- and ClO_4^-, and for the interaction of anions with Na^+, from the charge of the cations or anions of interest.

The selected SIT ion interaction coefficients for lead species are presented in Tab. 12-2.

12.2 Lead(0)

12.2.1 Elemental lead

Elemental lead has, in the absence of sulphide, a considerable stability field in the Eh – pH range of water (e.g., Brookins 1988) and hence, metallic lead, Pb(cr), is an environmentally important substance under reducing conditions. On the other hand, the gas phase Pbg is not important in aqueous systems and is not included in TDB 2020.

The selected values for Pb(cr) are taken from CODATA (Cox et al. 1989):

$$S_m°(\text{Pb, cr, 298.15 K}) = (64.800 \pm 0.30)\ \text{J} \cdot \text{K}^{-1} \cdot \text{mol}^{-1}$$

$$C_{p,m}°(\text{Pb, cr, 298.15 K}) = (26.650 \pm 0.10)\ \text{J} \cdot \text{K}^{-1} \cdot \text{mol}^{-1}$$

12.2.2 Lead(0) solubility

While the solubility of metallic mercury in water

$$\text{Hg(l)} \rightleftharpoons \text{Hg(aq)}$$

$$\log_{10}K°(\text{298.15 K}) = -6.53 \pm 0.03$$

is well known (see Section 14.2.2), to the present knowledge of the reviewer, nothing has ever been published concerning the solubility of metallic lead

$$Pb(cr) \rightleftharpoons Pb(aq)$$

although, as already mentioned in Section 12.1, elemental lead has, in the absence of sulphide, a considerable stability field in the Eh – pH range of water. However, in the course our review of experimental data concerning the PbS(s) – H_2S – water system, an alternative speciation model was tested involving the above equilibrium (see Section 12.3.7.2). The hypothesis that Pb(aq) is mainly responsible for the measured PbS(s) solubility data was found to be a valid alternative to a speciation model comprising the complexes $Pb(HS)_2(aq)$ and $PbS(HS)^-$. As a result of this model testing exercise the rough estimate

$log_{10}K°(298.15\ K \approx -7.3$

is included in TDB 2020 as supplemental datum.

Note that using both, $Pb(HS)_2(aq)$ and $PbS(HS)^-$ **and** Pb(aq) in geochemical modelling may lead to inconsistent results in sulphide containing systems. Calculations in this case should be done either with $Pb(HS)_2(aq)$ and $PbS(HS)^-$ **or** with Pb(aq).

12.3 Lead(II)

12.3.1 Lead(II) aqua ion

Lead(II) exists as the Pb^{2+} cation in aqueous solutions. The selected thermodynamic values for Pb^{2+} are taken from CODATA (Cox et al. 1989):

$\Delta_f G_m°(Pb^{2+}, 298.15\ K) = -(24.238 \pm 0.399)\ kJ \cdot mol^{-1}$

$\Delta_f H_m°(Pb^{2+}, 298.15\ K) = (0.920 \pm 0.25)\ kJ \cdot mol^{-1}$

$S_m°(Pb^{2+}, 298.15\ K) = (18.500 \pm 1.0)\ J \cdot K^{-1} \cdot mol^{-1}$

Using the selected CODATA $\Delta_f G_m°(Pb^{2+}, 298.15\ K)$, the redox equilibrium

$Pb(cr) \rightleftharpoons Pb^{2+} + 2e^-$

is calculated as

$\log_{10}K°(298.15\ K) = 4.25 \pm 0.07$

12.3.2 Lead(II) (hydr)oxide compounds and complexes

12.3.2.1 Lead(II) hydroxide complexes

For the formation of the first mononuclear hydrolysis species of lead(II)

$Pb^{2+} + H_2O(l) \rightleftharpoons PbOH^+ + H^+$

Powell et al. (2009) select the recommended value

$\log_{10}{}^*K_1°\ (298.15\ K) = -7.46 \pm 0.06$

derived from a weighted linear SIT regression analysis with $\Delta\varepsilon = -(0.06 \pm 0.04)$ kg · mol^{-1}. Using the reported values $\varepsilon(Pb^{2+}, ClO_4^-) = (0.15 \pm 0.02)$ kg · mol^{-1} and $\varepsilon(H^+, ClO_4^-) = (0.14 \pm 0.02)$ kg · mol^{-1} (Lemire et al. 2013) this review calculated the new value

$$\varepsilon(PbOH^+, ClO_4^-) = -(0.05 \pm 0.05) \text{ kg} \cdot \text{mol}^{-1}.$$

and estimated

$$\varepsilon(PbOH^+, Cl^-) \approx \varepsilon(PbOH^+, ClO_4^-) = -(0.05 \pm 0.05) \text{ kg} \cdot \text{mol}^{-1}$$

Brown & Ekberg (2016) scrutinised data measured at different temperatures and reported for zero ionic strength. Their accepted data set indicates that the stability constant is a linear function of the reciprocal absolute temperature in the range 15 to 300 °C. From their temperature function they derive $\log_{10}{}^*K_1°$ (298.15 K) = -7.49 ± 0.13, in excellent agreement with the value recommended by Powell et al. (2009), and

$$\Delta_r H_m°(298.15 \text{ K}) = (56.0 \pm 1.5) \text{ kJ} \cdot \text{mol}^{-1}$$

$$\Delta_r C_{p,m}°(298.15 \text{ K}) = 0$$

which are included in TDB 2020.

For the formation of the second mononuclear hydrolysis species of lead(II)

$$Pb^{2+} + 2H_2O(l) \rightleftharpoons Pb(OH)_2(aq) + 2H^+$$

Powell et al. (2009) select the recommended value

$$\log_{10}{}^*\beta_2° \text{ (298.15 K)} = -16.94 \pm 0.09$$

derived from a weighted linear SIT regression analysis of a rather limited data set with $\Delta\varepsilon = -0.13 \pm 0.04)$ kg · mol^{-1}. Using the reported values $\varepsilon(Pb^{2+}, ClO_4^-) = (0.15 \pm 0.02)$ kg · mol^{-1} and $\varepsilon(H^+, ClO_4^-) = (0.14 \pm 0.02)$ kg · mol^{-1} (Tab. 12-2) this review calculated the new value

$$\varepsilon(Pb(OH)_2, NaClO_4) = -(0.26 \pm 0.05) \text{ kg} \cdot \text{mol}^{-1}.$$

and estimated

$$\varepsilon(Pb(OH)_2, NaCl) \approx \varepsilon(Pb(OH)_2, NaClO_4) = -(0.26 \pm 0.05) \text{ kg} \cdot \text{mol}^{-1}$$

Brown & Ekberg (2016) scrutinised data measured at different temperatures and reported for zero ionic strength. Their accepted data set indicates that the stability constant is a linear function of the reciprocal absolute temperature in the range 25 to 260 °C. From their temperature function they derive $\log_{10}{}^{*}\beta_2^\circ$ (298.15 K) = -16.99 ± 0.06, in excellent agreement with the value recommended by Powell et al. (2009), and

$$\Delta_r H_m^\circ(298.15\ \mathrm{K}) = (90.0 \pm 0.9)\ \mathrm{kJ \cdot mol^{-1}}$$

$$\Delta_r C_{p,m}^\circ(298.15\ \mathrm{K}) = 0$$

which are included in TDB 2020.

For the formation of the third mononuclear hydrolysis species of lead(II)

$$Pb^{2+} + 3H_2O(l) \rightleftharpoons Pb(OH)_3^- + 3H^+$$

Powell et al. (2009) select the recommended value

$$\log_{10}{}^{*}\beta_3^\circ\ (298.15\ \mathrm{K}) = -28.03 \pm 0.06$$

derived from a weighted linear SIT regression analysis with $\Delta\varepsilon = (0.26 \pm 0.05)\ \mathrm{kg \cdot mol^{-1}}$. Using the reported values $\varepsilon(Pb^{2+}, ClO_4^-) = (0.15 \pm 0.02)\ \mathrm{kg \cdot mol^{-1}}$ and $\varepsilon(H^+, ClO_4^-) = (0.14 \pm 0.02)\ \mathrm{kg \cdot mol^{-1}}$ (Lemire et al. 2013) this review calculated the new value

$$\varepsilon(Na^+, Pb(OH)_3^-) = -(0.01 \pm 0.06)\ \mathrm{kg \cdot mol^{-1}}$$

Brown & Ekberg (2016) scrutinised data measured at different temperatures and reported for zero ionic strength. Their accepted data set indicates that the stability constant is a non-linear function of the reciprocal absolute temperature in the range 20 to 260 °C and, as such, a non-zero but constant heat capacity change has been assumed. From their temperature function they derive $\log_{10}{}^{*}\beta_3^\circ$ (298.15 K) = -27.94 ± 0.21, in good agreement with the value recommended by Powell et al. (2009), and

$$\Delta_r H_m^\circ(298.15\ \mathrm{K}) = (135.8 \pm 3.0)\ \mathrm{kJ \cdot mol^{-1}}$$

$$\Delta C_{p,m}^\circ(298.15\ \mathrm{K}) = (251 \pm 36)\ \mathrm{J \cdot K^{-1} \cdot mol^{-1}}$$

which are included in TDB 2020.

Powell et al. (2009) state that stability constant data have been reported for the species $Pb(OH)_4^{2-}$ and $Pb(OH)_6^{4-}$ at pH > 13. There is no spectroscopic or polarographic evidence for the existence of the latter species, and stability constant values for $Pb(OH)_4^{2-}$ are considered doubtful. None of these species is included in our data base.

For the formation of the dimeric hydrolysis species of lead(II)

$$2Pb^{2+} + H_2O(l) \rightleftharpoons Pb_2OH^{3+} + H^+$$

Powell et al. (2009) solely derived a provisional value from a SIT regression analysis in nitrate media. Brown & Ekberg (2016) derived a very similar constant for nitrate media, stating that most of the experimental data refer to 18 °C. Brown & Ekberg (2016) further report that data from perchlorate media (at 25 °C) are only available at two ionic strengths. Their selected value

$$\log_{10}{}^*\beta_{2,1}^\circ \text{ (298.15 K)} = -6.73 \pm 0.31$$

was derived from a "two-point" weighted linear SIT regression analysis with $\Delta\varepsilon = (0.18 \pm 0.09)$ kg · mol^{-1}. Using the reported values $\varepsilon(Pb^{2+}, ClO_4^-) = (0.15 \pm 0.02)$ kg · mol^{-1} and $\varepsilon(H^+, ClO_4^-) = (0.14 \pm 0.02)$ kg mol^{-1} (Tab. 12-2) this review calculated the new value

$$\varepsilon(Pb_2OH^{3+}, ClO_4^-) = (0.34 \pm 0.10) \text{ kg} \cdot \text{mol}^{-1}$$

and estimated

$$\varepsilon(Pb_2OH^{3+}, Cl^-) \approx \varepsilon(Pb_2OH^{3+}, ClO_4^-) = (0.34 \pm 0.10) \text{ kg} \cdot \text{mol}^{-1}$$

This species only forms to a relatively small percentage at elevated Pb(II) concentrations and is unlikely to be an important species in the environment. Nevertheless, it is included in TDB 2020.

For the formation of the trimeric hydrolysis species of lead(II)

$$3Pb^{2+} + 4H_2O(l) \rightleftharpoons Pb_3(OH)_4{}^{2+} + 4H^+$$

Powell et al. (2009) select the recommended value

$$\log_{10}{}^*\beta_{3,4}^\circ \text{ (298.15 K)} = -23.01 \pm 0.07$$

derived from a weighted linear SIT regression analysis in perchlorate media with $\Delta\varepsilon = -(0.39 \pm 0.03)$ kg · mol^{-1}. Using the reported values $\varepsilon(Pb^{2+}, ClO_4^-) = (0.15 \pm 0.02)$ kg · mol^{-1} and $\varepsilon(H^+, ClO_4^-) = (0.14 \pm 0.02)$ kg · mol^{-1} (Tab. 12-2) this review calculated the new value

$$\varepsilon(Pb_3(OH)_4{}^{2+}, ClO_4^-) = -(0.50 \pm 0.06) \text{ kg} \cdot \text{mol}^{-1}$$

and estimated

$$\varepsilon(Pb_3(OH)_4{}^{2+}, Cl^-) \approx \varepsilon(Pb_3(OH)_4{}^{2+}, ClO_4^-) = -(0.50 \pm 0.06) \text{ kg} \cdot \text{mol}^{-1}$$

Brown & Ekberg (2016) considered the same data as Powell et al. (2009) in perchlorate media but decided first to derive $\log_{10}{}^{*}\beta_{3,4}°$ (298.15 K) = -23.46 ± 0.10 from two data points in nitrate media and then used this value to fit the extended SIT parameters $\Delta\varepsilon_1$ = -(1.60 ± 0.10) kg · mol^{-1} and $\Delta\varepsilon_2$ = (1.93 ± 0.19) kg · mol^{-1} to the perchlorate media. As we cannot mix the "linear SIT" with the "extended SIT" in practical applications and the $\log_{10}{}^{*}\beta_{3,4}°$ value derived by Brown & Ekberg (2016) is in fair agreement with Powell et al. (2009) this review decided to include the values of Powell et al. (2009) in TDB 2020.

For the formation of the tetrameric hydrolysis species of lead(II)

$$4Pb^{2+} + 4H_2O(l) \rightleftharpoons Pb_4(OH)_4{}^{4+} + 4H^+$$

Powell et al. (2009) select the recommended value

$$\log_{10}{}^{*}\beta_{4,4}° \text{ (298.15 K)} = -20.57 \pm 0.06$$

derived from a weighted linear SIT regression analysis in perchlorate media with $\Delta\varepsilon$ = -(0.19 ± 0.02) kg · mol^{-1}. Using the reported values $\varepsilon(Pb^{2+}, ClO_4^-)$ = (0.15 ± 0.02) kg · mol^{-1} and $\varepsilon(H^+, ClO_4^-)$ = (0.14 ± 0.02) kg · mol^{-1} (Tab. 12-2) this review calculated the new value

$$\varepsilon(Pb_4(OH)_4{}^{4+}, ClO_4^-) = -(0.15 \pm 0.06) \text{ kg} \cdot \text{mol}^{-1}$$

and estimated

$$\varepsilon(Pb_4(OH)_4{}^{4+}, Cl^-) \approx \varepsilon(Pb_4(OH)_4{}^{4+}, ClO_4^-) = -(0.15 \pm 0.06) \text{ kg} \cdot \text{mol}^{-1}$$

Brown & Ekberg (2016) considered the same data as Powell et al. (2009) in perchlorate media to derive $\log_{10}{}^{*}\beta_{4,4}°$ (298.15 K) = -20.71 ± 0.18 from an extended SIT regression analysis with the parameters $\Delta\varepsilon_1$ = -(0.39 ± 0.24) kg · mol^{-1} and $\Delta\varepsilon_2$ = (0.27 ± 0.38) kg · mol^{-1}. As we cannot mix the "linear SIT" with the "extended SIT" in practical applications and the $\log_{10}{}^{*}\beta_{4,4}°$ value derived by Brown & Ekberg (2016) is in good agreement with Powell et al. (2009) this review decided to include the values of Powell et al. (2009) in our TDB.

For the formation of the hexameric hydrolysis species of lead(II)

$$6Pb^{2+} + 8H_2O(l) \rightleftharpoons Pb_6(OH)_8{}^{4+} + 8H^+$$

Powell et al. (2009) select the recommended value

$$\log_{10}{}^{*}\beta_{6,8}° \text{ (298.15 K)} = -42.89 \pm 0.07$$

derived from a weighted linear SIT regression analysis in perchlorate media with $\Delta\varepsilon = -(0.41 \pm 0.02)$ kg · mol^{-1}. Using the reported values $\varepsilon(Pb^{2+}, ClO_4^-) = (0.15 \pm 0.02)$ kg · mol^{-1} and $\varepsilon(H^+, ClO_4^-) = (0.14 \pm 0.03)$ kg · mol^{-1} (Lemire et al. 2013) this review calculated the new value

$$\varepsilon(Pb_6(OH)_8^{4+}, ClO_4^-) = -(0.63 \pm 0.08) \text{ kg} \cdot \text{mol}^{-1}$$

and estimated

$$\varepsilon(Pb_6(OH)_8^{4+}, Cl^-) \approx \varepsilon(Pb_6(OH)_8^{4+}, ClO_4^-) = -(0.63 \pm 0.08) \text{ kg} \cdot \text{mol}^{-1}$$

Brown & Ekberg (2016) considered the same data as Powell et al. (2009) in perchlorate media to derive $\log_{10}{}^*\beta_{6,8}^\circ$ (298.15 K) = -43.27 ± 0.47 from an extended SIT regression analysis with the parameters $\Delta\varepsilon_1 = -(1.1 \pm 0.7)$ kg · mol^{-1} and $\Delta\varepsilon_2 = (1.0 \pm 1.1)$ kg · mol^{-1}. As we cannot mix the "linear SIT" with the "extended SIT" in practical applications and the $\log_{10}{}^*\beta_{4,4}^\circ$ value derived by Brown & Ekberg (2016) is in fair agreement with Powell et al. (2009) this review decided to include the values of Powell et al. (2009) in our TDB.

Brown & Ekberg (2016) state that for the majority of the lead(II) polymeric hydrolysis species, enthalpy data are available from more than one source. The average of these values has been retained and an uncertainty assigned to span the range in the values and their respective assigned uncertainties:

$$\Delta_r H_m^\circ(Pb_3(OH)_4^{2+}, 298.15 \text{ K}) = (111.4 \pm 5.6) \text{ kJ} \cdot \text{mol}^{-1}$$

$$\Delta_r H_m^\circ(Pb_4(OH)_4^{4+}, 298.15 \text{ K}) = (85.0 \pm 2.0) \text{ kJ} \cdot \text{mol}^{-1}$$

$$\Delta_r H_m^\circ(Pb_6(OH)_8^{4+}, 298.15 \text{ K}) = (210.9 \pm 7.1) \text{ kJ} \cdot \text{mol}^{-1}$$

These values have been included in TDB 2020.

12.3.2.2 Lead(II) oxide compounds

Solubility product data have been reported for the dissolution reactions of red (litharge, tetragonal) and yellow (massicot, orthorhombic) lead oxide, PbO(s). The majority of these data were determined in dilute solutions and were corrected by the original authors to zero ionic strength. For the reaction

$$PbO(s) \text{ (red or yellow)} + 2H^+ \rightleftharpoons Pb^{2+} + H_2O(l)$$

Powell et al. (2009) recommend

$$\log_{10}{}^*K_{s0}^\circ \text{ (red, 298.15 K)} = 12.62 \pm 0.07$$

$$\log_{10}{}^*K_{s0}^\circ \text{ (yellow, 298.15 K)} = 12.90 \pm 0.08$$

These values, showing that litharge (red PbO(s)) is slightly less soluble than massicot (yellow PbO(s)), have been included in our TDB.

The value for massicot (PbO(s), yellow) given by Powell et al. (2009) is retained by Brown & Ekberg (2016). For litharge (PbO(s), red) Brown & Ekberg (2016) fitted a linear function of the reciprocal of absolute temperature to data in the temperature range 20 to 350 °C. From this relationship they determined the solubility constant $\log_{10}{}^{*}K_{s0}°$ (red, 298.15 K) = 12.64 ± 0.04, which is in excellent agreement with the value of Powell et al. (2009). The enthalpy derived from the temperature function is

$$\Delta_r H_m°(\text{red, } 298.15 \text{ K}) = -(66.1 \pm 0.7) \text{ kJ} \cdot \text{mol}^{-1}$$

$$\Delta_r C_{p,m}°(298.15 \text{ K}) = 0$$

These values have been included in TDB 2020.

Powell et al. (2009) state that based on published values it appears that hydrated lead oxide, $Pb(OH)_2(s)$, is less soluble than either red or yellow PbO(s). This is unexpected as hydrated compounds are normally more soluble than analogous anhydrous ones. Further, there is a large degree of scatter in the published values. Powell et al. (2009) conclude that the solid phase used in the solubility studies was not pure "$Pb(OH)_2(s)$", which does not appear to exist. For this reason, they did not provide a solubility constant for $Pb(OH)_2(s)$.

12.3.3 Lead(II) chloride compounds and complexes

12.3.3.1 Lead(II) chloride complexes

Lead(II) appears to form up to four consecutive chloride complexes in aqueous solution:

$$Pb^{2+} + Cl^- \rightleftharpoons PbCl^+$$

$$Pb^{2+} + 2Cl^- \rightleftharpoons PbCl_2(aq)$$

$$Pb^{2+} + 3Cl^- \rightleftharpoons PbCl_3^-$$

$$Pb^{2+} + 4Cl^- \rightleftharpoons PbCl_4^{2-}$$

For the first three complexes Powell et al. (2009) recommend stability constants and SIT interaction parameters, derived from weighted linear SIT regression analyses of data in $NaClO_4$ media. In addition, they give provisional enthalpy values determined from the temperature dependence of stability constants in $NaClO_4$ media in the temperature range 15 to 50 °C. They are judged "provisional" because the stability constants at 25 °C in this temperature study are in fair (but only fair) agreement with those recommended by Powell et al. (2009).

$\log_{10}K_1°$ (298.15 K) = 1.50 ± 0.03

$\Delta_r H_m°$(298.15 K) = (10.3 ± 1.5) kJ · mol^{-1}

$\Delta_r C_{p,m}°$(298.15 K) = 0

$\Delta\varepsilon$ = -(0.14 ± 0.01) kg · mol^{-1}

$\log_{10}\beta_2°$ (298.15 K) = 2.10 ± 0.05

$\Delta_r H_m°$(298.15 K) = (17.0 ± 0.6) kJ · mol^{-1}

$\Delta_r C_{p,m}°$(298.15 K) = 0

$\Delta\varepsilon$ = -(0.26 ± 0.02) kg · mol^{-1}

$\log_{10}\beta_3°$ (298.15 K) = 2.00 ± 0.10

$\Delta_r H_m°$(298.15 K) = (14.7 ± 1.0) kJ · mol^{-1}

$\Delta_r C_{p,m}°$(298.15 K) = 0

$\Delta\varepsilon$ = -(0.32 ± 0.03) kg · mol^{-1}

These values have been included in TDB 2020.

The $\Delta\varepsilon$ values derived by Powell et al. (2009), together with the reported values $\varepsilon(Pb^{2+}, ClO_4^-)$ = (0.15 ± 0.02) kg · mol^{-1} and $\varepsilon(Cl^-, Na^+)$ = (0.03 ± 0.01) kg · mol^{-1} (Lemire et al. 2013) were used to calculate the new values

$\varepsilon(PbCl^+, ClO_4^-)$ = (0.04 ± 0.02) kg · mol^{-1}

$\varepsilon(PbCl_2(aq), NaClO_4)$ = -(0.05 ± 0.03) kg · mol^{-1}

$\varepsilon(Na^+, PbCl_3^-)$ = -(0.08 ± 0.04) kg · mol^{-1}

as well as the estimates

$\varepsilon(PbCl^+, Cl^-) \approx \varepsilon(PbCl^+, ClO_4^-)$ = (0.04 ± 0.02) kg · mol^{-1}

$\varepsilon(PbCl_2(aq), NaCl) \approx \varepsilon(PbCl_2(aq), NaClO_4)$ = -(0.05 ± 0.03) kg · mol^{-1}

A detailed UV-spectrometric analysis of the Pb^{2+} – Cl^- system in NaCl media (0.001 to 3.22 mol · kg^{-1}) and at temperatures from 25 to 300 °C (Seward 1984) suggested the existence of $PbCl_4^{2-}$ between 25 and 150 °C at high chloride concentrations. Seward (1984) reports $\log_{10}\beta_4°$ (298.15 K) = 1.46 ± 0.05 (uncertainty given as 1σ) and considered the value derived for 150 °C only as a rough estimate. Seward (1984) derived temperature functions and thermodynamic parameters for $PbCl^+$, $PbCl_2$(aq) and $PbCl_3^-$ but not for $PbCl_4^{2-}$. Taking the three $\log_{10}\beta_4°$ values given by Seward (1984) for 25, 50 and 100 °C this review calculated a rough estimate $\Delta_r H_m°(298.15\ K) = (14 \pm 5)$ kJ · mol^{-1}.

Powell et al. (2009) cite the $\log_{10}\beta_4°$ value of Seward (1984), mention evidence for the existence of $PbCl_4^{2-}$ on the basis of UV-spectrometric and emf measurements reported in three other papers, but also mention two papers where the authors could not detect $PbCl_4^{2-}$ in solutions with chloride concentrations up to 2 mol kg^{-1} or $[Cl^-]/[Pb^{2+}]$ ratios up to 70'000, respectively. Powell et al. (2009) conclude in the text (their Section 6.2.2): "These conflicting results imply that at present not even an indicative value for the formation of $PbCl_4^{2-}$ is possible" while they state in the abstract: "the available value being considered as 'indicative' only". Despite these conflicting conclusions of Powell et al. (2009), the values

$$log_{10}\beta_4°(298.15\ K) = 1.46 \pm 0.10$$

$$\Delta_r H_m°(298.15\ K) = (14 \pm 5)\ kJ \cdot mol^{-1}$$

have been included in TDB 2020 as "supplemental data".

No polynuclear complexes have been reported in aqueous solution.

12.3.3.2 Lead(II) chloride compounds

Powell et al. (2009) state that "The solubility of $PbCl_2$(s) is comparatively high ($\log_{10}K_{s0}° \approx -4.75$), and therefore $PbCl_2$(s) would not influence the speciation of Pb(II) in natural fresh or saline waters. However, the solubility of laurionite, PbClOH(s) is much lower ($\log_{10}K_{s0}° \approx -13.27$), and this phase might affect the speciation of Pb(II) in heavily polluted saline water systems". None of these values is selected by Powell et al. (2009) but this review decided to include the solubility of laurionite

$$PbClOH(s) \rightleftharpoons Pb^{2+} + Cl^- + OH^-$$

$$log_{10}K_{s0}°(298.15\ K) \approx -13.27$$

in TDB 2020 as "supplemental data".

12.3.4 Lead(II) carbonate compounds and complexes

12.3.4.1 Lead(II) carbonate complexes

Powell et al. (2009) state that an accurate estimate of the value for $\log_{10}K_1°$ for reaction

$$Pb^{2+} + CO_3^{2-} \rightleftharpoons PbCO_3(aq)$$

is not possible on the basis of available data, since each of their "accepted" values for $\log_{10}K_1$ is poorly defined. Nevertheless, a SIT regression analysis (not shown in Powell et al. 2009) lead to the following approximate values:

$$\log_{10}K_1° \text{ (298.15 K)} = 6.4_5 \pm 0.7$$

$$\Delta\varepsilon = -(0.6 \pm 1.2) \text{ kg} \cdot \text{mol}^{-1}$$

Powell et al. (2009) consider the value of $\log_{10}K_1° = 6.4_5 \pm 0.7$ to be an underestimate and classify it as "indicative" only. This value is included in TDB 2020.

The $\Delta\varepsilon$ value is too poorly defined for deriving a new value for $\varepsilon(PbCO_3(aq), NaClO_4)$ therefrom. It is recommended to use the estimated values for $\varepsilon(PbCO_3(aq), NaClO_4)$ and $\varepsilon(PbCO_3(aq), NaCl)$ given in Tab. 12-2.

For the formation of $Pb(CO_3)_2^{2-}$ according to the reaction

$$Pb^{2+} + 2CO_3^{2-} \rightleftharpoons Pb(CO_3)_2^{2-}$$

Powell et al. (2009) select the provisional value

$$\log_{10}\beta_2° \text{ (298.15 K)} = 10.13 \pm 0.24$$

derived from a weighted linear SIT regression analysis with $\Delta\varepsilon = -(0.19 \pm 0.10)$ kg · mol^{-1}. Using the reported values $\varepsilon(Pb^{2+}, ClO_4^-) = (0.15 \pm 0.02)$ kg · mol^{-1} and $\varepsilon(Na^+, CO_3^{2-}) = -(0.08 \pm 0.05)$ kg · mol^{-1} (Lemire et al. 2013) this review calculated the new value

$$\varepsilon(Na^+, Pb(CO_3)_2^{2-}) = -(0.20 \pm 0.12) \text{ kg} \cdot \text{mol}^{-1}$$

Powell et al. (2009) report a provisional stability constant from a single study for reaction

$$Pb^{2+} + HCO_3^- \rightleftharpoons PbHCO_3^+$$

in 3.5 mol kg^{-1} $NaClO_4$ as

$$\log_{10}K\ (298.15\ K) = 1.86 \pm 0.1$$

Using the reported values $\varepsilon(Pb^{2+}, ClO_4^-) = (0.15 \pm 0.02)$ kg · mol^{-1} and $\varepsilon(Na^+, HCO_3^-) = (0.00 \pm 0.02)$ kg · mol^{-1} (Lemire et al. 2013), and the estimated value $\varepsilon(PbHCO_3^+, ClO_4^-) = (0.2 \pm 0.1)$ kg · mol^{-1} (Tab. 12-2) this review calculated $\Delta\varepsilon = (0.05 \pm 0.10)$ kg · mol^{-1} for extrapolation of the above value to zero ionic strength:

$$\log_{10}K^\circ\ (298.15\ K) = 3.0 \pm 0.4$$

This value is included in TDB 2020.

For the formation of the ternary complexes $Pb(CO_3)OH^-$ and $Pb(CO_3)Cl^-$, which are expected to be important in natural fresh and saline waters, Powell et al. (2009) found one and no reported stability constants, respectively. Hence, they used statistical predictions to estimate stability constants for the reactions

$$Pb^{2+} + CO_3^{2-} + OH^- \rightleftharpoons Pb(CO_3)OH^-$$

$$\log_{10}K^\circ\ (298.15\ K) = 10.9 \pm 0.2$$

$$Pb^{2+} + CO_3^{2-} + Cl^- \rightleftharpoons Pb(CO_3)Cl^-$$

$$\log_{10}K^\circ\ (298.15\ K) = 6.47 \pm 0.16$$

These values have been included in TDB 2020 as "supplemental data".

A singly study reported stability constants for the polynuclear carbonato species $Pb_2CO_3^{2+}$ and $Pb_3CO_3^{4+}$. Powell et al. (2009) discussed their possible significance and concluded that neither polynuclear species is likely to be significant for environmentally relevant concentrations of lead.

12.3.4.2 Lead(II) carbonate compounds

The solubility of $PbCO_3$(s) (cerussite) is determined by the average of the solubility constants reported by two studies (Powell et al. 2009) for the reaction

$$PbCO_3(s) \rightleftharpoons Pb^{2+} + CO_3^{2-}$$

which lead to the recommended value

$$\log_{10}K_{s0}^\circ = -13.18 \pm 0.07$$

The solubility of $Pb_2(CO_3)Cl_2$(s) (phosgenite) is also determined by the average of the solubility constants reported by two studies (Powell et al. 2009) for the reaction

$$0.5\ Pb_2(CO_3)Cl_2(s) \rightleftharpoons Pb^{2+} + 0.5\ CO_3^{2-} + Cl^-$$

which lead to the recommended value

$$\log_{10}K_{s0}° = -9.93 \pm 0.08$$

12.3.5 Lead(II) phosphate compounds and complexes

12.3.5.1 Lead(II) phosphate complexes

Powell et al. (2009) found that only three papers report equilibrium constants for the water-soluble phosphate complexes of Pb(II). The formation of the protonated complexes $PbH_2PO_4^+$, $PbHPO_4$(aq) and $Pb(HPO_4)_2^{2-}$ in acidic solution has been proposed. All reported data refer to 0.1 mol kg^{-1} $NaClO_4$. This review estimated $\Delta\varepsilon$ values, using ε(j,k) values taken from Lemire et al. (2013), for extrapolation of the data to zero ionic strength.

$$Pb^{2+} + HPO_4^{2-} \rightleftharpoons PbHPO_4(aq)$$

$$\log_{10}K_1 = 3.3 \pm 0.2$$

$$\Delta\varepsilon(\text{estimated}) = (0.00 \pm 0.12)\ kg \cdot mol^{-1}$$

$$\log_{10}K_1° (298.15\ K) = 4.2 \pm 0.2$$

$$Pb^{2+} + 2\ HPO_4^{2-} \rightleftharpoons Pb(HPO_4)_2^{2-}$$

$$\log_{10}\beta_2 = \approx 5.6$$

$$\Delta\varepsilon(\text{estimated}) = (0.05 \pm 0.13)\ kg \cdot mol^{-1}$$

$$\log_{10}\beta_2° (298.15\ K) = \approx 6.5$$

$$Pb^{2+} + H_2PO_4^- \rightleftharpoons PbH_2PO_4^+$$

$$\log_{10}K_1 = \approx 2.4$$

$$\Delta\varepsilon(\text{estimated}) = (0.10 \pm 0.11)\ kg \cdot mol^{-1}$$

$$\log_{10}K_1° (298.15\ K) = \approx 2.8$$

For the first reaction the reported stability constants are in acceptable agreement and hence, Powell et al. (2009) assigned the selected value as a provisional value. This value is included in TDB 2020.

The stability constant values for the formation of the latter two phosphate complexes can only be considered as indicative and hence, these two values have been included in TDB 2020 as "supplemental data".

12.3.5.2 Lead(II) phosphate compounds

Powell et al. (2009) state that the least soluble Pb(II) minerals in aerobic soils are the lead phosphates, especially the pyromorphites ($Pb_5(PO_4)_3X$, with X = F^-, Cl^-, Br^-, or OH^-). Thus, the concentration of phosphate in soil solutions may control the solubility and bioavailability of lead. Despite this significance, few studies report the determination of solubility constants for lead phosphates. Only one author determined a comprehensive dataset and the solubility constants for the following reactions were accepted by Powell et al. (2009) as provisional:

$PbHPO_4(s) \rightleftharpoons Pb^{2+} + HPO_4^{2-}$

$\log_{10}K_{s0}°$ (298.15 K) = -11.4 ± 0.3

$Pb_3(PO_4)_2(s) \rightleftharpoons 3\ Pb^{2+} + 2\ PO_4^{3-}$

$\log_{10}K_{s0}°$ (298.15 K) = -44.4 ± 1.0

These values are included in TDB 2020.

Chloropyromorphite, $Pb_5(PO_4)_3Cl(s)$, has fundamental importance among the lead phosphate solids because the phosphate-induced immobilisation strategies for lead are based on its low solubility. Powell et al. (2009) state that the two available K_{s0} values for chloropyromorphite

$Pb_5(PO_4)_3Cl(s) \rightleftharpoons 5\ Pb^{2+} + 3\ PO_4^{3-} + Cl^-$

show only moderate agreement, and hence the value given in their Tab. A-2-15

$log_{10}K_{s0}°(298.15\ K) = -84.4 \pm 2.0$

has been included in TDB 2020 as "supplemental data".

12.3.6 Lead(II) sulphate compounds and complexes

12.3.6.1 Lead(II) sulphate complexes

For the formation of $PbSO_4(aq)$ according to the reaction

$$Pb^{2+} + SO_4^{2-} \rightleftharpoons PbSO_4(aq)$$

Powell et al. (2009) select the recommended value

$$\log_{10}K_1\ (298.15\ K) = 2.72 \pm 0.05$$

derived from a weighted linear SIT regression analysis of their accepted data for $NaClO_4$ media with $\Delta\varepsilon = (0.02 \pm 0.03)$ kg · mol^{-1}. Using the reported values $\varepsilon(Pb^{2+}, ClO_4^-) = (0.15 \pm 0.02)$ kg · mol^{-1} and $\varepsilon(Na^+, SO_4^{2-}) = -(0.12 \pm 0.06)$ kg · mol^{-1} (Lemire et al. 2013) this review calculated the new value

$$\varepsilon(PbSO_4(aq), NaClO_4) = (0.05 \pm 0.07)\ kg \cdot mol^{-1}$$

and estimated

$$\varepsilon(PbSO_4(aq), NaCl) \approx \varepsilon(PbSO_4(aq), NaClO_4) = (0.05 \pm 0.07)\ kg \cdot mol^{-1}$$

Powell et al. (2009) state that the existence of $Pb(SO_4)_2^{2-}$ is controversial: some papers have presented evidence for its formation, whereas others have argued the opposite. The available stability constants for equilibrium

$$Pb^{2+} + 2SO_4^{2-} \rightleftharpoons Pb(SO_4)_2^{2-}$$

are shown in their Tab. A-2-10. Powell et al. (2009) further state that a SIT analysis did not show consistency among these reported values, thus no value is recommended. This review used the "accepted" data given in Tab. A-2-10 of Powell et al. (2009) with increased assigned uncertainties of ± 0.6 for a weighted linear SIT regression analysis (Fig. 12-1). The results are

$$\log_{10}\beta_2^\circ\ (298.15\ K) = 3.1_5 \pm 0.5$$

$$\Delta\varepsilon = -(0.02 \pm 0.19)\ kg \cdot mol^{-1}$$

Using the reported values $\varepsilon(Pb^{2+}, ClO_4^-) = (0.15 \pm 0.02)$ kg · mol^{-1} and $\varepsilon(Na^+, SO_4^{2-}) = -(0.12 \pm 0.06)$ kg · mol^{-1} (Tab. 12-2) this review calculated the new value

$$\varepsilon(Na^+, Pb(SO_4)_2^{2-}) = -(0.11 \pm 0.20)\ kg \cdot mol^{-1}$$

These values have been included in TDB 2020 as "supplemental data".

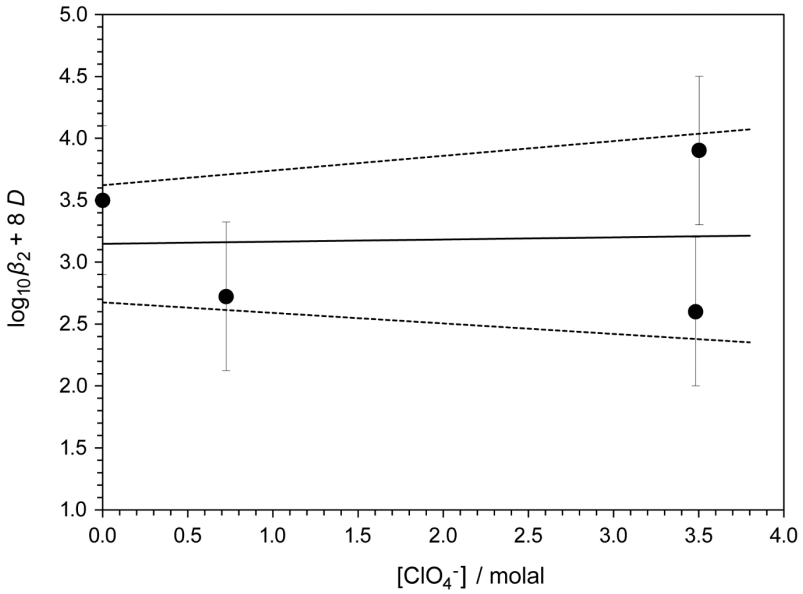

Fig. 12-1: Dependence of $\log_{10}\beta_2$ of $Pb(SO_4)_2^{2-}$ on ionic strength in perchlorate media

The solid line is obtained using the derived SIT interaction coefficient and stability constant at zero ionic strength. The dotted lines represent the 95% uncertainty range extrapolated from zero ionic strength to higher perchlorate concentrations. Data taken from Tab. A-2-10 of Powell et al. (2009) with increased assigned uncertainties of ± 0.6.

Powell et al. (2009) state that no direct calorimetric studies have been reported for the above equilibrium reactions. They give the estimated reaction enthalpy values $\Delta_r H_m°_1 = 9.2 \pm 0.5$ kJ · mol^{-1} and $\Delta_r H_m°_2 = 18.4 \pm 1.0$ kJ · mol^{-1} from solubility measurements in 3 mol dm^{-3} $LiClO_4$ at 25 °C. These values should be regarded as indicative only and hence, they have been included in our TDB as "supplemental data".

12.3.6.2 Lead(II) sulphate compounds

Powell et al. (2009) report that at infinite dilution, most of the available data for the solubility of anglesite, PbSO4(s), all obtained by direct solubility measurements, are in excellent agreement. Thus, for the equilibrium

$$PbSO_4(s) \rightleftharpoons Pb^{2+} + SO_4^{2-}$$

Powell et al. (2009) recommend the unweighted average of six experimental studies at 25 °C:

$$\log_{10}K_{s0}° \text{ (298.15 K)} = -7.80 \pm 0.05$$

Powell et al. (2009) state that the solubility of PbSO4(s) as a function of temperature is moderately well known and that the most recent analysis of these data gives

$$\Delta_r H_m°(298.15 \text{ K}) = (13 \pm 1) \text{ kJ} \cdot \text{mol}^{-1}$$

This number should be regarded as indicative only.

CODATA (Cox et al. 1989) recommend

$$\Delta_f G_m°(PbSO_4, cr, 298.15\ K) = -(813.036 \pm 0.447)\ kJ \cdot mol^{-1}$$

Together with the recommended values $\Delta_f G_m°(Pb^{2+}, 298.15\ K) = -(24.238 \pm 0.399)\ kJ \cdot mol^{-1}$ and $\Delta_f G_m°(SO_4^{2-}, 298.15\ K) = -(744.004 \pm 0.418)\ kJ \cdot mol^{-1}$ this results in

$$\Delta_r G_m°(PbSO_4(cr) \rightleftharpoons Pb^{2+} + SO_4^{2-}, 298.15\ K) = (44.794 \pm 0.73)\ kJ \cdot mol^{-1}$$

and

$$\log_{10} K_{s0}°\ (298.15\ K) = -7.85 \pm 0.13$$

Within their 95% uncertainty ranges the CODATA and IUPAC values agree well and thus, the CODATA value is retained in this review.

Furthermore, CODATA (Cox et al. 1989) recommend

$$\Delta_f H_m°(PbSO_4, cr, 298.15\ K) = -(919.97 \pm 0.4)\ kJ \cdot mol^{-1}$$

Together with the recommended values $\Delta_f H_m°(Pb^{2+}, 298.15\ K) = (0.92 \pm 0.25)\ kJ \cdot mol^{-1}$ and $\Delta_f H_m°(SO_4^{2-}, 298.15\ K) = -(909.34 \pm 0.4)\ kJ \cdot mol^{-1}$ this results in

$$\Delta_r H_m°(PbSO_4(cr) \rightleftharpoons Pb^{2+} + SO_4^{2-}, 298.15\ K) = (11.55 \pm 0.62)\ kJ \cdot mol^{-1}$$

Within their 95% uncertainty ranges the CODATA and IUPAC values agree reasonably well, and as the IUPAC value is regarded as indicative only the CODATA value is retained in this review.

12.3.7 Lead(II) sulphide compounds and complexes

12.3.7.1 Galena (PbS)

Lothenbach et al. (1999) stated that PbS(s), galena, has a very low solubility and often controls lead solubility in reducing environments. However, data reported in the literature for the equilibrium

$$PbS(s) + H^+ \rightleftharpoons Pb^{2+} + HS^-$$

are mainly based on calculations from ΔS and ΔH values measured at high temperature. For example, Hemley (1953) reported that "in this study an activity product of 2.63×10^{-30} is used, as calculated from the thermodynamic data of Kelley". The reference cited by Hemley (1953) contains "Data on theoretical metallurgy", published 1937, and the calculated activity product refers to the equilibrium $PbS(s) \rightleftharpoons Pb^{2+} + S^{2-}$.

Experimentally determined values are scarce. Lothenbach et al. (1999) found papers from three authors (their Tab. 6-28): Kivalo & Ringbom (1956), Shamsuddin (1977) and Uhler & Helz (1984).

Lothenbach et al. (1999) stated that Kivalo & Ringbom (1956) tried to determine the Pb^{2+} concentration directly via competitive complex formation with chloride ions (in 0.8 – 1.1 M HCl). This method, however, is prone to errors as the complex formation with chloride is much weaker than the complex formation of Pb^{2+} with HS^-.

Shamsuddin (1977) used liquid metal solution calorimetry and electrochemical measurements. The emf measurements in the temperature range 360 – 425 °C resulted in a relationship of $\Delta_r G_m°$ versus T for the reaction Pb(l) + S(l) ⇌ PbS(s).

Lothenbach et al. (1999) did not consider further the results of Kivalo & Ringbom (1956) and Shamsuddin (1977). This review agrees with that decision.

The solubility product of galena was determined more precisely by Uhler & Helz (1984) who stated that "because the stability of lead-bisulfide complexes have not been measured independently of galena's solubility, we completely eliminated these complexes as significant dissolved lead species by adding ethylenediaminetetraacetic acid (EDTA). … The solubility product is written in terms of HS^-, rather than S^{2-} because it is now clear that the controversial second ionization constant of H_2S is in fact so small as to preclude its accurate measurement at room temperature." Hence, by competitive complex formation of Pb with EDTA Uhler & Helz (1984) obtained at 25 °C and I = 0.16 (NaCl):

$$\log_{10}{}^*K_s\ (298.15\ K) = -11.79 \pm 0.05$$

where the given uncertainty most probably refers to 1 σ. Uhler & Helz (1984) extrapolated this value to zero ionic strength by a combination of extrapolating the above value using the Davies equation and two additional solubility experiments performed at lower ionic strength (data shown in their Fig. 4 only) and reported a median value from both methods as

$\log_{10}{}^{*}K_s°$ (298.15 K) = -12.25 ± 0.17

This review extrapolated the value obtained at I = 0.16 (NaCl) to zero ionic strength using the SIT equation, with $\Delta\varepsilon = 0.11 \pm 0.02$ kg · mol^{-1} calculated from the known values $\varepsilon(Pb^{2+}, Cl^-) \approx \varepsilon(Pb^{2+}, ClO_4^-) = 0.15 \pm 0.02$, $\varepsilon(H^+, Cl^-) = 0.12 \pm 0.01$ kg · mol^{-1} and $\varepsilon(HS^-, Na^+) = 0.08 \pm 0.01$ kg · mol^{-1} (Tab. 12-2), and obtained

$\log_{10}{}^{*}K_s°$ (298.15 K) = -12.28 ± 0.10

(uncertainty 2σ) in excellent agreement with the value reported by Uhler & Helz (1984). This value is included in TDB 2020.

12.3.7.2 Lead(II) sulphide complexes

Rickard & Luther (2006) and Rickard (2012) stated that "lead forms the well-known isometric sulphide phase PbS, galena, which is renowned for its insolubility. In fact, in sulphide solutions, Pb displays enhanced solubility over that expected for aqueous Pb^{2+} and a series of sulphide complexes have been assigned. None of these has actually been observed and all are theoretical constructs. Both $PbHS^+$ and $Pb(HS)_2$(aq) have been assumed by a number of authors … Earlier suggestions … that higher complexes, such as $Pb(HS)_3^-$, might contribute to the total PbS solubility have not been followed up."

Rickard & Luther (2006) and Rickard (2012) mentioned only one more recent study by Rozan et al. (2003) who used pseudovoltammetry to evaluate the actual Pb complexation occurring in natural water samples of varying oxygen and sulphide concentration. Rozan et al. (2003) stated that "one possible explanation for the observed complexation is the existence of lead sulfide clusters". By contrast, Rickard & Luther (2006) stated that "Rozan et al. (2003) used mole ratio titration methodology and showed that only a 1:1 complex formed. However, the Pb complexes were not protonated based on acid-base titrations." Nevertheless, in their Tab. 25 Rickard & Luther (2006) not only included a stability constant (at I = 0.7 M) for PbS(aq) but also for $PbHS^+$ with reference to Rozan et al. (2003), the latter complex in clear contradiction to their above statement, and also their footnote to Tab. 25, that the species is not protonated. These values of unclear origin are not considered further in this review.

We are left with few studies where the solubility of galena in the Pb – H_2S – H_2O system has been studied with the aim to obtain values for aqueous lead sulphide complexes.

The first, and still most reliable, study has been published by Hemley (1953) who measured the concentration of dissolved lead in the presence of galena at 25 °C and I = 0.1 M (NaCl) in the pH range 1 – 8 and 0.10 and 0.19 M total dissolved sulphide. Hemley (1953) interpreted his results (Fig. 12-2) in terms of the formation of $Pb(HS)_2$(aq) and $Pb(HS)_3^-$.

Anderson (1962) applied similar experimental procedures as Hemley (1953) to determine the concentration of dissolved lead in the presence of galena. The values found by Anderson (1962) at 30 °C and H_2S saturation in the pH range 2 – 8 are, within the analytical uncertainty, almost identical to those of Hemley (1953) (Fig. 12-2). Anderson (1962) reported that the solution at pH 4.6 contained 0.11 M NaCl and the solution at pH 7.9 contained 0.20 M NaCl.

Anderson (1962) also measured solubilities at elevated temperatures, keeping the solutions saturated with H_2S and the pH constant at about 2.8. The slight variations found in the temperature range 30 – 90 °C are small, at the verge of insignificance compared with the scatter of data points.

Nriagu (1971) reported the solubility of PbS in 1.0 m and 3.0 m NaCl – HCl – H_2O solutions saturated with H_2S at 90 °C and pH 2.0 – 6.7. The solubilities measured by Nriagu (1971) are about two orders of magnitude higher than the values reported by Hemley (1953) and Anderson (1962).

Hamann & Anderson (1978) stated that their "study of the solubility of galena in slightly acidic to strongly alkaline, chloride and reduced sulfur-rich brines at 25 °C and 90 °C was undertaken to confirm and gain further information on the stoichiometries and stabilities of the PbS-reduced sulfur complexes determined by Nriagu (1971) and to resolve the discrepancy between his data and those of Hemley (1953) and Anderson (1962)". The authors conclude that their "results are in general agreement with those of Hemley (1953) and Anderson (1962) but not with those of Nriagu (1971). No straightforward explanation can be given for the difference between Nriagu's results and those in this study since solution conditions were nearly identical and similar analytical method was used".

The lead concentrations reported by Hamann & Anderson (1978) are in the range of a few tens of ppb and no significant variation with pH in the range 3 – 13 was found. It is tempting to use e.g. the value 9 ± 2 ppb at 25 °C and pH 9.7 (Tab. 1 in Hamann & Anderson 1978), translating into $\log[Pb]_{total} = -7.36 \pm 0.10$ mol · L^{-1}, which would fit perfectly to the dotted and dot – dashed lines in Fig. 12-2. However, the data reported by Hamann & Anderson (1978) show a large scatter and "the reproducibility of the lead values was poor, indicating either that fine particles were getting past the filter or that the analytical method was not sufficiently precise at this level. (The method was chosen in the expectation that Nriagu's (1971) much higher lead values would be found)". Hence, no clear conclusions can be drawn from the data reported by Hamann & Anderson (1978)

Giordano & Barnes (1979) measured galena solubility in the temperature range 30 – 300 °C in 0 – 2.85 m NaHS solutions at H_2S pressures of 0.8 – 75 atm. Giordano & Barnes (1979) interpreted their experimental results at $T < 200$ °C in terms of the complexes $Pb(HS)_2(aq)$ and $Pb(HS)_3^-$. At 30 °C, the obtained stability constants are in excellent agreement with the results of Hemley (1953) and Anderson (1962). At 90 °C the stability constants of Giordano & Barnes (1979) for $Pb(HS)_2(aq)$ and $Pb(HS)_3^-$ are one and three orders of magnitude lower, respectively, than the results obtained from the data of Nriagu (1971). Hence, the study of Nriagu (1971) is not considered further in this review.

Finally, Barrett & Anderson (1982, 1988) studied the solubility of galena in NaCl brines. Barrett & Anderson (1982) determined galena solubility at 27, 60, 80 and 95 °C in 1, 2 and 3 m NaCl at pH < 2.5. Barrett & Anderson (1988) extended their former study on galena solubility, at the same temperatures but 3, 4 and 5 m NaCl at pH < 2. As TDB 2020 is not intended for modelling brines, the studies of Barrett & Anderson (1982, 1988) have not been considered in this review.

We are left with the experimental values of Hemley (1953) and Anderson (1962) and the supporting information by Giordano & Barnes (1979).

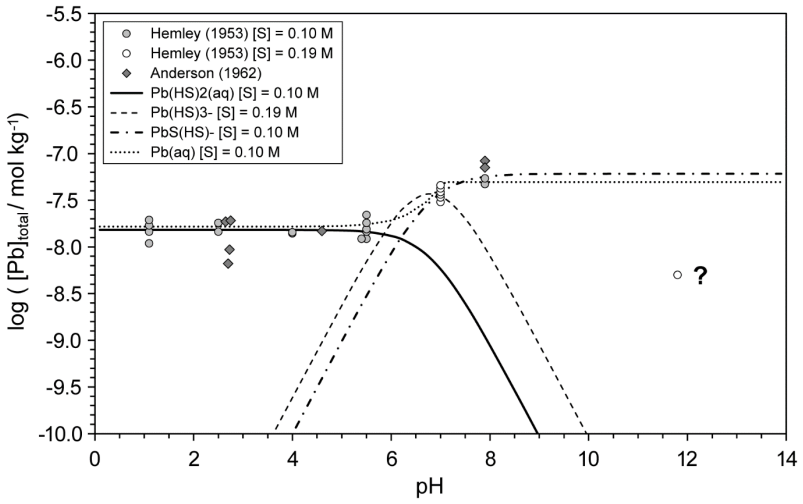

Fig. 12-2: Solubility of PbS(s) in water as a function of pH at different total dissolved sulphide concentrations, $[S]_{total}$

Different symbols: experimental data of Hemley (1953) and Anderson (1962)
Solid line: calculated concentration of the species $Pb(HS)_2(aq)$, for $[S]_{total} = 0.010$ M
Dashed line: calculated concentration of the species $Pb(HS)_3^-$, for $[S]_{total} = 0.019$ M
Dot – dashed line: calculated concentration of the species $PbS(HS)^-$, for $[S]_{total} = 0.010$ M. Dotted line: calculated concentration of the species Pb(aq), for $[S]_{total} = 0.010$ M and 0.05 bar H_2g pressure

$Pb(HS)_2(aq)$

In the pH range 1 – 6 Hemley (1953), Anderson (1962) and Giordano & Barnes (1979) interpreted their data in terms of the equilibrium

$$PbS(s) + H_2S(aq) \rightleftharpoons Pb(HS)_2(aq)$$

A re-evaluation of experimental solubility data at pH < 6 given by Hemley (1953) and Anderson (1962) (Fig. 12-2) in this review gives (solid line in Fig. 12-2)

$$\log_{10}K_s\ (298.15\ K) = \log_{10}K_s°(298.15\ K) = -6.8$$

Assuming that $\varepsilon(Pb(HS)_2(aq), NaCl) = 0.055 \pm 0.10$ kg · mol^{-1} ≈ $\varepsilon(H_2S(aq), NaCl) = 0.055 \pm 0.004$ kg · mol^{-1} (Tab. 12-2) this isocoulombic reaction is not ionic strength dependent and hence, $\log_{10}K_s = \log_{10}K_s°$.

Note that Giordano & Barnes (1979) report $\log_{10}K_{s,gas}°(303.15\ K) = -7.8 \pm 0.2$ for the equilibrium $PbS(s) + H_2Sg \rightleftharpoons Pb(HS)_2(aq)$. Using $\log_{10}K°(298.15\ K) = 1.02 \pm 0.38$ for the equilibrium $H_2S(aq) \rightleftharpoons H_2Sg$ (Hummel et al. 2002) we get

$$\log_{10}K_s°(303.15\ K) = -6.8 \pm 0.4$$

in perfect agreement with the value obtained from experimental data of Hemley (1953) and Anderson (1962).

Using $\log_{10}{}^{*}K°(298.15\ K) = 6.99 \pm 0.17$ for the equilibrium $HS^- + H^+ \rightleftharpoons H_2S(aq)$ (Hummel et al. 2002) we get

$$PbS(s) + HS^- + H^+ \rightleftharpoons Pb(HS)_2(aq)$$

$$\log_{10}K_s°(298.15\ K) = 0.2$$

and finally, using the above selected solubility product (see Section 12.3.7.1), we arrive at

$$Pb^{2+} + 2\ HS^- \rightleftharpoons Pb(HS)_2(aq)$$

$$\log_{10}\beta_2°(298.15\ K) \approx 12.5$$

This value is included as supplemental datum in TDB 2020. Why this constant is classified as supplemental datum is discussed below.

$Pb(HS)_3^-$?

In the range $6 < pH < 8$ Hemley (1953), Anderson (1962) and Giordano & Barnes (1979) interpreted their data in terms of the equilibrium

$$PbS(s) + 2\ HS^- + H^+ \rightleftharpoons Pb(HS)_3^-$$

A re-evaluation of experimental solubility data at pH 7 given by Hemley (1953) (Fig. 12-2) in this review gives (dashed line in Fig. 12-2)

$$\log_{10}K_s\ (298.15\ K) = 1.4$$

Note that according to Lothenbach et al. (1999) (see their Tab. 6-27), Hemley (1953) reported a value of 1.43 and Giordano & Barnes (1979) reported a value of 1.41, in perfect agreement with the above re-evaluation.

Nevertheless, the above complex and its associated stability constant are rejected by the present review. First, the experimental data of Hemley (1953) and Anderson (1962) at pH 7.9 (Fig. 12-2) do not agree with the predicted decrease of galena solubility with increasing pH above 7 (dashed line in Fig. 12-2). But the more serious deficiency of a galena solubility model comprising the complexes $Pb(HS)_2(aq)$ and $Pb(HS)_3^-$ is that the calculated solubility will decrease with increasing pH in the alkaline region to absurdly low values, e.g., at pH 12 to about 10^{-12} mol · kg^{-1} $[Pb]_{total}$.

$PbS(HS)^-$

Although Hemley (1953) put a big question mark on his measured galena solubility at pH 11.8 concerning the reliability of this value (Fig. 12-2) and the results of Hamann & Anderson (1978), suggesting a roughly pH independent galena solubility, are doubtful, there is no indication that galena solubility would reach extremely low values in alkaline solutions. On the other hand, a strong increase of solubility with increasing pH, as observed in the chemically similar mercury (II) – sulphide system (see Section 14.4.7), can be ruled out for galena.

Hence, for the time being it seems to be appropriate to assume galena solubility being pH independent at pH > 8. Recurring to the mentioned chemically similar mercury (II) – sulphide system we assume that the complex $Pb(HS)_2(aq)$ may deprotonate to form the complex $PbS(HS)^-$. The latter complex leads to pH independent galena solubility at pH > 8 according to the equilibrium

$$PbS(s) + HS^- \rightleftharpoons PbS(HS)^-$$

A re-evaluation of experimental solubility data at pH 7 and 7.9 given by Hemley (1953) and Anderson (1962) (Fig. 12-2) in this review gives (dot – dashed line in Fig. 12-2)

$$\log_{10}K_s\ (298.15\ K) = \log_{10}K_s°(298.15\ K) = -6.2$$

Assuming that $\varepsilon(PbS(HS)^-, Na^+) = 0.08 \pm 0.10\ kg \cdot mol^{-1} \approx \varepsilon(HS^-, Na^+) = 0.08 \pm 0.01\ kg \cdot mol^{-1}$ (Tab. 12-2) this isocoulombic reaction is not ionic strength dependent and hence, $\log_{10}K_s = \log_{10}K_s°$.

Using the above selected solubility product (see Section 12.3.7.1), we arrive at

$$Pb^{2+} + 2\ HS^- \rightleftharpoons PbS(HS)^- + H^+$$

$$\log_{10}\beta_2°(298.15\ K) \approx 6.1$$

This value is included as supplemental datum in TDB 2020. Why this constant is classified as supplemental datum is discussed below.

Pb(aq) ?

A speciation model comprising the complexes $Pb(HS)_2(aq)$ and $PbS(HS)^-$ reproduces the experimental galena solubility data (Fig.12.2). However, the question remains whether the galena solubility remains constant with decreasing pH, down to pH 1, and does not increase due to the species $PbHS^+$ and finally Pb^{2+} which may predominate in very acidic conditions.

In the chemically similar mercury (II) – sulphide system it was shown (see Section 14.4.7) that a possible solution to this riddle involves the consideration of Hg(aq) in the speciation model. A similar solubility equilibrium between PbS(s) and Pb(aq) can be formulated as

$$PbS(s) + H_2g \rightleftharpoons Pb(aq) + H_2S(aq)$$

with its stability constant $\log_{10}K_{H2}$. If this equilibrium predominates, the measured galena solubility is pH independent at constant partial pressure of hydrogen. However, to the present knowledge of the reviewer there is no published information at all about the solubility of metallic lead

$$Pb(cr) \rightleftharpoons Pb(aq)$$

The respective stability constant $\log_{10}K_{aq}$ is missing and we cannot simply calculate $\log_{10}K_{H2}$ of the above equilibrium as it was done for the analogous mercury (II) – sulphide case. In order to test the above hypothesis, nevertheless, the problem has to be re-formulated so that it can be explored whether for reasonable partial pressures of hydrogen a fit to the experimental data (Fig. 12-2) results, which in turn results in a "not unreasonable" Pb(aq) solubility.

First, we calculate for

$$PbS(s) + 2\ H^+ \rightleftharpoons Pb^{2+} + H_2S(aq)$$

$$\log_{10}{}^*K_{sol}\ (298.15\ K,\ I = 0.1\ M\ NaCl) = -5.07$$

using $\log_{10}{}^*K_s$ (298.15 K, I = 0.1 M NaCl) = -11.86 extrapolated from the selected solubility product $\log_{10}{}^*K_s°$ (298.15 K) = -12.28 (see Section 12.3.7.1) and $\log_{10}{}^*K$ ($HS^- + H^+ \rightleftharpoons H_2S(aq)$, 298.15 K, I = 0.1 M NaCl) = 6.79 extrapolated from the selected $\log_{10}{}^*K_s°$ ($HS^- + H^+ \rightleftharpoons H_2S(aq)$, 298.15 K) = 6.99 (Hummel et al. 2002).

Then, we calculate

$$Pb^{2+} + 2e^- \rightleftharpoons Pb(cr)$$

$$\log_{10}K_{redox}(298.15\ K,\ I = 0.1\ M\ NaCl) = -4.89$$

extrapolated from the selected $\log_{10}K°_{redox}(298.15\ K) = -4.25$ (see Section 12.3.1).

Considering that

$$H_2g \rightleftharpoons 2\ e^- + 2\ H^+$$

is $\log_{10}K = 0$ (per definition), we arrive at the equations:

$$\log_{10}K_{H2} = \log_{10}{}^*K_{sol} + \log_{10}K_{aq} - \log_{10}K_{redox}$$

$$\log_{10}K_{H2} = \log[Pb]_{total} + \log[H_2S(aq)] - \log P_{H2}$$

which by combination results in:

$$\log_{10}K_{aq} = \log_{10}K_{redox} - \log_{10}{}^*K_{sol} + \log[Pb]_{total} + \log[H_2S(aq)] - \log P_{H2}$$

Assuming that the total dissolved lead, $[Pb]_{total}$, actually is Pb(aq), and calculating $[H_2S(aq)]$ from the total dissolved sulphide, $\log_{10}K_{aq}$ can be calculated as a function of $\log P_{H2}$, the assumed partial pressure of hydrogen.

For P_{H2} = 0.05 bar this review calculated $\log_{10}K_{aq}$ = -7.3, or a solubility of Pb(aq) = $5 \cdot 10^{-8}$ mol · kg^{-1} in the presence of metallic lead.

These values are "not unreasonable". In the chemically similar mercury (II) – sulphide system (see Section 14.4.7) a partial pressure of hydrogen P_{H2} = 0.13 ± 0.04 bar resulted from a fit of experimental HgS(s) solubility data and $\log_{10}K_{aq}$ = -6.52 ± 0.03 as determined from experimental Hg(l) solubility data.

But most important, the above parameters fit all the experimental galena solubility data (dotted line in Fig. 12-2), leading to constant values in the acid region, increasing at pH > 6 until the solubility of Pb(aq) in the presence of metallic lead is reached, leading to constant values at pH > 7.

Hence, the hypothesis that Pb(aq) is mainly responsible for the measured galena solubility data is a valid alternative to the above discussed speciation model comprising the complexes $Pb(HS)_2(aq)$ and $PbS(HS)^-$.

For the time being there is no possibility to discern the two models, and thus the constants for $Pb(HS)_2(aq)$, $PbS(HS)^-$ and Pb(aq) are all included as supplemental data in TDB 2020 to remind the user that there is an unresolved ambiguity. Dedicated experiments are needed to finally resolve this question

Note that using both, $Pb(HS)_2(aq)$ and $PbS(HS)^-$ **and** Pb(aq) in geochemical modelling may lead to inconsistent results in sulphide containing systems. Calculations in this case should be done either with $Pb(HS)_2(aq)$ and $PbS(HS)^-$ **or** with Pb(aq).

12.4 Selected lead data

Tab. 12-1: Selected lead data

Core data are in bold face and supplemental data in italics.

Name	**$\Delta_f G_m°$** [kJ · mol^{-1}]	**$\Delta_f H_m°$** [kJ · mol^{-1}]	**$S_m°$** [J · K^{-1} · mol^{-1}]	**$C_{p,m}°$** [J · K^{-1} · mol^{-1}]	**Species**
Pb(cr)	0.0	0.0	**64.800 ± 0.30**	**26.650 ± 0.10**	Pb(cr)
Pb+2	**-24.238 ± 0.399**	**0.920 ± 0.25**	**18.500 ± 1.0**		Pb^{2+}
$PbSO_4$(cr)	**-813.036 ± 0.447**	**-919.970 ± 0.40**	**148.500 ± 0.60**		$PbSO_4$(cr)

Name	**$\log_{10}\beta°$**	**$\Delta\varepsilon$** [kg · mol^{-1}]	**$\Delta_r H_m°$** [kJ · mol^{-1}]	**$\Delta_r C_{p,m}°$** [J · K^{-} mol^{-1}]	**T-range** [°C]	**Reaction**
Pb(aq) [a]	*≈ -7.3*		-	-		*Pb(cr) ⇌ Pb(aq)*
PbOH+	-7.46 ± 0.06	-0.06 ± 0.04	56.0 ± 1.5	0	15 – 300	$Pb^{2+} + H_2O(l) \rightleftharpoons PbOH^+ + H^+$
Pb(OH)2(aq)	-16.94 ± 0.09	-0.13 ± 0.04	90.0 ± 0.9	0	25 – 260	$Pb^{2+} + 2\ H_2O(l) \rightleftharpoons Pb(OH)_2(aq) + 2\ H^+$
Pb(OH)3-	-28.03 ± 0.06	0.26 ± 0.05	135.8 ± 3.0	251 ± 36	20 – 260	$Pb^{2+} + 3\ H_2O(l) \rightleftharpoons Pb(OH)_3^- + 3\ H^+$
Pb2OH+3	-6.73 ± 0.31	0.18 ± 0.09	-	-		$2\ Pb^{2+} + H_2O(l) \rightleftharpoons Pb_2OH^{3+} + H^+$
Pb3(OH)4+2	-23.01 ± 0.07	-0.39 ± 0.03	111.4 ± 5.6	-		$3\ Pb^{2+} + 4\ H_2O(l) \rightleftharpoons Pb_3(OH)_4^{2+} + 4\ H^+$
Pb4(OH)4+4	-20.57 ± 0.06	-0.19 ± 0.02	85.0 ± 2.0	-		$4\ Pb^{2+} + 4\ H_2O(l) \rightleftharpoons Pb_4(OH)_4^{4+} + 4\ H^+$
Pb6(OH)8+4	-42.89 ± 0.07	-0.41 ± 0.03	210.9 ± 7.1	-		$6\ Pb^{2+} + 8\ H_2O(l) \rightleftharpoons Pb_6(OH)_8^{4+} + 8\ H^+$
PbCl+	1.50 ± 0.03	-0.14 ± 0.01	10.3 ± 1.5	0	15 – 50	$Pb^{2+} + Cl^- \rightleftharpoons PbCl^+$
PbCl2(aq)	2.10 ± 0.05	-0.26 ± 0.02	17.0 ± 0.6	0	15 – 50	$Pb^{2+} + 2\ Cl^- \rightleftharpoons PbCl_2(aq)$
PbCl3-	2.00 ± 0.10	-0.32 ± 0.03	14.7 ± 1.0	0	15 – 50	$Pb^{2+} + 3\ Cl^- \rightleftharpoons PbCl_3^-$
PbCl4-2	*1.46 ± 0.10*		*14 ± 5*	-		*$Pb^{2+} + 4\ Cl^- \rightleftharpoons PbCl_4^{2-}$*
PbCO3(aq)	6.4_5 ± 0.7	(-0.6 ± 1.2)	-	-		$Pb^{2+} + CO_3^{2-} \rightleftharpoons PbCO_3(aq)$
Pb(CO3)2-2	10.13 ± 0.24	-0.19 ± 0.10	-	-		$Pb^{2+} + 2\ CO_3^{2-} \rightleftharpoons Pb(CO_3)_2^{2-}$
PbHCO3+	3.0 ± 0.4		-	-		$Pb^{2+} + HCO_3^- \rightleftharpoons PbHCO_3^+$
Pb(CO3)OH-	*10.9 ± 0.2*		-	-		*$Pb^{2+} + CO_3^{2-} + OH^- \rightleftharpoons Pb(CO_3)OH^-$*
Pb(CO3)Cl-	*6.47 ± 0.16*		-	-		*$Pb^{2+} + CO_3^{2-} + Cl^- \rightleftharpoons Pb(CO_3)Cl^-$*
PbHPO4(aq)	4.2 ± 0.2		-	-		$Pb^{2+} + HPO_4^{2-} \rightleftharpoons PbHPO_4(aq)$
Pb(HPO4)2-2	*≈ 6.5*		-	-		*$Pb^{2+} + 2\ HPO_4^{2-} \rightleftharpoons Pb(HPO_4)_2^{2-}$*
PbH2PO4+	*≈ 2.8*		-	-		*$Pb^{2+} + H_2PO_4^- \rightleftharpoons PbH_2PO_4^+$*
PbSO4(aq)	2.72 ± 0.05	0.02 ± 0.03	*9.2 ± 0.5*	-		$Pb^{2+} + SO_4^{2-} \rightleftharpoons PbSO_4(aq)$
Pb(SO4)2-2	*3.1_5 ± 0.5*	*-0.02 ± 0.19*	*18.4 ± 1.0*	-		*$Pb^{2+} + 2\ SO_4^{2-} \rightleftharpoons Pb(SO_4)_2^{2-}$*

Tab. 12-1: Cont.

Name	**$\log_{10}\beta°$**	**$\Delta\varepsilon$** [kg · mol^{-1}]	**$\Delta_r H_m°$** [kJ · mol^{-1}]	**$\Delta_r C_{p,m}°$** [J · K^{-} mol^{-1}]	**T-range** [°C]	**Reaction**
Pb(HS)2(aq) [a]	*≈ 12.5*		-	-		*Pb^{2+} + 2 HS^- ⇌ $Pb(HS)_2(aq)$*
PbS(HS)- [a]	*≈ 6.1*		-	-		*Pb^{2+} + 2 HS^- ⇔ $PbS(HS)^-$ + H^+*

a Note that using both, $Pb(HS)_2$(aq) and $PbS(HS)^-$ **and** Pb(aq) in geochemical modelling may lead to inconsistent results in sulphide containing systems. Calculations in this case should be done either with $Pb(HS)_2$(aq) and $PbS(HS)^-$ **or** with Pb(aq).

Name	**$\log_{10}K_{s,0}°$**	**$\Delta_r H_m°$** [kJ · mol^{-1}]	**$\Delta_r C_{p,m}°$** [J · K^{-1} · mol^{-1}]	**T-range** [°C]	**Reaction**
PbO(s)(red)	12.62 ± 0.07	-66.1 ± 0.7	0	20 – 350	PbO(s)(red) + 2 H^+ ⇌ Pb^{2+} + H_2O(l)
PbO(s)(yellow)	12.90 ± 0.08	-	-		PbO(s)(yellow) + 2 H^+ ⇌ Pb^{2+} + H_2O(l)
PbClOH(s)	*≈ -13.27*	-	-		*PbClOH(s) ⇌ Pb^{2+} + Cl^- + OH^-*
PbCO3(s)	-13.18 ± 0.07	-	-		$PbCO_3$(s) ⇌ Pb^{2+} + CO_3^{2-}
Pb2(CO3)Cl2(s)	-9.93 ± 0.08	-	-		0.5 $Pb_2(CO_3)Cl_2$(s) ⇌ Pb^{2+} + 0.5 CO_3^{2-} + Cl^-
PbHPO4(s)	-11.4 ± 0.3	-	-		PbHPO4(s) ⇌ Pb^{2+} + HPO_4^{2-}
Pb3(PO4)2(s)	-44.4 ± 1.0	-	-		$Pb_3(PO4)_2$(s) ⇌ 3 Pb^{2+} + 2 PO_4^{3-}
$Pb_5(PO_4)_3Cl$(s)	*-84.4 ± 2.0*	-	-		*$Pb_5(PO_4)_3Cl$(s) ⇌ 5 Pb^{2+} + 3 PO_4^{3-} + Cl^-*
PbS(s)	-12.28 ± 0.10	-	-		PbS(s) + H^+ ⇌ Pb^{2+} + HS^-

Tab. 12-2: Selected SIT ion interaction coefficients $\varepsilon_{j,k}$ [kg · mol^{-1}] for lead species

Data in bold face are taken from Lemire et al. (2013). Data in normal face are derived or estimated in this review. Data estimated according to charge correlations and taken from Tab. 1-7 are shaded. Supplemental data are in italics.

j k → ↓	**Cl^-** $\varepsilon_{j,k}$ [kg · mol^{-1}]	**ClO_4^-** $\varepsilon_{j,k}$ [kg · mol^{-1}]	**Na^+** $\varepsilon_{j,k}$ [kg · mol^{-1}]	**$Na^+ + Cl^-$** $\varepsilon_{j,k}$ [kg · mol^{-1}]	**$Na^+ + ClO_4^-$** $\varepsilon_{j,k}$ [kg · mol^{-1}]
H2S(aq)	0	0	0	(0.055 ± 0.004) [b]	(0.055 ± 0.004) [c]
HS-	0	0	(0.08 ± 0.01) [b]	0	0
Pb(aq)	0	0	0	0.0 ± 0.1	0.0 ± 0.1
Pb+2	(0.15 ± 0.02) [a]	**0.15 ± 0.02**	0	0	0
PbOH+	(-0.05 ± 0.05) [a]	-0.05 ± 0.05	0	0	0
Pb(OH)2(aq)	0	0	0	(-0.26 ± 0.05) [a]	-0.26 ± 0.05
Pb(OH)3-	0	0	-0.01 ± 0.06	0	0
Pb2OH+3	(0.34 ± 0.10) [a]	0.34 ± 0.10	0	0	0
Pb3(OH)4+2	(-0.50 ± 0.06) [a]	-0.50 ± 0.06	0	0	0
Pb4(OH)4+4	(-0.15 ± 0.06) [a]	-0.15 ± 0.06	0	0	0
Pb6(OH)8+4	(-0.63 ± 0.08) [a]	-0.63 ± 0.08	0	0	0
PbCl+	(0.04 ± 0.02) [a]	0.04 ± 0.02	0	0	0
PbCl2(aq)	0	0	0	(-0.05 ± 0.03) [a]	-0.05 ± 0.03
PbCl3-	0	0	-0.08 ± 0.04	0	0
PbCl4-2	*0*	*0*	*-0.10 ± 0.10*	*0*	*0*
PbCO3(aq)	0	0	0	0.0 ± 0.1	0.0 ± 0.1
Pb(CO3)2-2	0	0	-0.20 ± 0.12	0	0
PbHCO3+	0.2 ± 0.1 [a]	0.2 ± 0.1	0	0	0
Pb(CO3)OH-	*0*	*0*	*-0.05 ± 0.10*	*0*	*0*
Pb(CO3)Cl-	*0*	*0*	*-0.05 ± 0.10*	*0*	*0*
PbHPO4(aq)	0	0	0	0.0 ± 0.1	0.0 ± 0.1
Pb(HPO4)2-2	*0*	*0*	*-0.10 ± 0.10*	*0*	*0*
PbH2PO4+	*0.2 ± 0.1* [a]	*0.2 ± 0.1*	*0*	*0*	*0*
PbSO4(aq)	0	0	0	(0.05 ± 0.07) [a]	0.05 ± 0.07
Pb(SO4)2-2	*0*	*0*	*-0.11 ± 0.20*	*0*	*0*
Pb(HS)2(aq)	*0*	*0*	*0*	*(0.055 ± 0.10)* [d]	*(0.055 ± 0.10)* [d]
PbS(HS)-	*0*	*0*	*(0.08 ± 0.10)* [e]	*0*	*0*

[a] Assumed to be equal to the corresponding ion interaction coefficient with ClO_4^-, see Section 12.1 for explanation
[b] Hummel et al. (2002)
[c] Assumed to be equal to the corresponding ion interaction coefficient with NaCl.
[d] Assumed to be equal to the corresponding ion interaction coefficient of H_2S(aq), with increased uncertainty.
[e] Assumed to be equal to the corresponding ion interaction coefficient of HS^-, with increased uncertainty.

12.5 References

Anderson, G.M. (1962): The solubility of PbS in H_2S-water solutions. Economic Geology, 57, 809-828.

Barrett, T.J. & Anderson, G.M. (1982): The solubility of sphalerite and galena in NaCl brines. Economic Geology, 77, 1923-1933.

Barrett, T.J. & Anderson, G.M. (1988): The solubility of sphalerite and galena in 1-5 m NaCl solutions to 300 °C. Geochim. Cosmochim. Acta, 52, 813-820.

Brookins, D.G. (1988): Eh-pH Diagrams for Geochemistry. Springer-Verlag Berlin Heidelberg, Germany, 184 pp.

Brown, P.L. & Ekberg, C. (2016): Hydrolysis of Metal Ions. Wiley-VCH Verlag GmbH & Co. KGaA, Weinheim, Germany, 917 pp.

Cox, J.D., Wagman, D.D., Medvedev, V.A. (1989): CODATA Key Values for Thermodynamics. New York, Hemisphere Publishing, 271 pp.

Giordano, T.H. & Barnes. H.L. (1979): Ore solution chemistry VI. PbS solubility in bisulfide solution to 300 °C. Economic Geology, 74, 1637-1646.

Grenthe, I., Fuger, J., Konings, R.J.M., Lemire, R.J., Muller, A.B., Nguyen-Trung, C. & Wanner, H. (1992): Chemical Thermodynamics of Uranium. Chemical Thermodynamics, Vol. 1. North-Holland, Amsterdam, 715 pp.

Hagemann, S. (2012): Entwicklung eines thermodynamischen Modells für Zink, Blei und Cadmium in salinaren Lösungen, GRS-Report 219, GRS, Braunschweig, Germany, 494 pp.

Hamann, R.J. & Anderson, G.M. (1978): Solubility of galena in sulfur-rich NaCl solutions. Economic Geology, 73, 96-100.

Hemley, J.J. (1953): A study of lead sulfide solubility and its relation to ore deposition. Economic Geology, 48, 113-138.

Hummel, W., Berner, U., Curti, E., Pearson, F.J. & Thoenen, T. (2002): Nagra/PSI Chemical Thermodynamic Data Base 01/01. Nagra Technical Report NTB 02-16 and Universal Publishers, Parkland, Florida, 565 pp.

Kivalo, P. & Ringbom, A. (1956): Polarographic determination of the solubility products of the sulfides of lead and cadmium. Suomen Kemistilethi, 29, 109-112.

Lemire, R.J., Berner, U., Musikas, C., Palmer, D.A., Taylor, P. & Tochiyama, O. (2013): Chemical Thermodynamics of Iron, Part 1. Chemical Thermodynamics, Vol. 13a. OECD Publications, Paris, France, 1082 pp.

Lothenbach, B., Ochs, M., Wanner, H. & Yui, M. (1999): Thermodynamic Data for the Speciation and Solubility of Pb, Pd, Sn, Sb, Nb and Bi in Aqueous Solution. JNC TN8400 99-011, Japan Nuclear Cycle Development Institute (JNC), Japan, 340 pp.

Nriagu, J.O. (1971): Studies in the system PbS-NaCl-H_2S-H_2O: Stability of lead (II) thiocomplexes at 90 °C. Chemical Geology, 8, 299-310.

Powell, K.J., Brown, P.L., Byrne, R.H., Gajda, T., Hefter, G., Leuz, A.-K., Sjöberg, S. & Wanner, H. (2009): Chemical speciation of environmentally significant metals with inorganic ligands. Part 3: The Hg^{2+} + OH^-, Cl^-, CO_3^{2-}, SO_4^{2-}, and PO_4^{3-} systems. Pure Appl. Chem., 81, 2425-2476.

Rickard, D. & Luther III, G.W. (2006): Metal sulfide complexes and clusters. Reviews in Mineralogy & Geochemistry, 61, 421-504.

Rickard, D. (2012): Aqueous metal-sulfide chemistry: Complexes, clusters and nanoparticles. Developments in Sedimentology, 65, 121-194.

Rozan, T.F., Luther III, G.W., Ridge, D. & Robinson, S. (2003): Determination of Pb complexation in oxic and sulfidic waters using pseudovoltammetry. Environ. Sci. Technol., 37, 3845 – 3852.

Shamsuddin (1977): Thermodynamic studies on lead sulphide. Metallurgical Transactions B, 8B, 349-352.

Seward, T.M. (1984): The formation of lead(II) chloride complexes to 300 °C: A spectrophotometric study. Geochim. Cosmochim. Acta, 48, 121-134.

Uhler, A.D. & Helz, G.R. (1984): Solubility product of galena at 298°K: A possible explanation for apparent supersaturation in nature. Geochim. Cosmochim. Acta, 48, 1155-1160.

13 Manganese

13.1 Introduction

Chemical thermodynamic data for ground and pore water models in our original data base (Pearson & Berner 1991, Pearson et al. 1992) have been taken from the USGS review of data for major water-mineral reactions (Nordstrom et al. 1990) and basically have not been changed since then. Meanwhile, new experimental data have been reported, as well as new reviews of the hydrolysis of metal ions (Brown & Ekberg 2016), which are considered in the present update of chemical thermodynamic data for manganese.

The thermodynamic data included in TDB 2020 have been taken from

- the USGS review of data for major water-mineral reactions (Nordstrom et al. 1990)
- the recent review of the hydrolysis of metal ions (Brown & Ekberg 2016)
- and own reviews of experimental data

The selected thermodynamic data are presented in Tab. 13-1

NEA (see, e.g., Grenthe et al. 1992) used the specific ion interaction theory (SIT) for making ionic strength corrections to the experimental data, an approach which is also adopted for TDB 2020 (as has been for all its predecessors). In the case of manganese, the thermodynamic model explicitly considered the formation of manganese chloride complexes. Therefore, ion interaction coefficients ε for cationic manganese species with Cl^- should be approximated by the corresponding interaction coefficients with ClO_4^-, e.g., $\varepsilon(MnF^+, Cl^-) \approx \varepsilon(MnF^+, ClO_4^-) = (0.23 \pm 0.09)$ kg · mol^{-1}.

In many cases, the ion interaction coefficients for species under consideration here were not available. We approximated these with the estimation method described in Section 1.5.3, which draws on a statistical analysis of published SIT ion interaction coefficients, and which allows the estimation of missing coefficients for the interaction of cations with Cl^- and ClO_4^-, and for the interaction of anions with Na^+, from the charge of the cations or anions of interest.

The selected SIT ion interaction coefficients are presented in Tab. 13-2.

13.2 Elemental manganese

Manganese metal is unstable in contact with water and thus, it is not relevant under environmental conditions. However, the absolute entropy of Mn(cr) is used for the calculation of certain thermodynamic reaction properties.

The selected $S_m°$ value for Mn(α) is taken from Brown & Ekberg (2016), who cite Robie & Hemingway (1995), whose reported $S_m°$ value is identical with that given (without error estimate) by Wagman et al. (1982):

$$S_m°(\text{Mn}, \alpha, 298.15\ \text{K}) = (32.01 \pm 0.08)\ \text{J} \cdot \text{K}^{-1} \cdot \text{mol}^{-1}$$

13.3 Manganese(II) aqua ion

Manganese(II) exists as the Mn^{2+} cation in aqueous solutions. The selected thermodynamic values for Mn^{2+} are taken from Brown & Ekberg (2016), who cite Robie & Hemingway (1995), whose reported values are identical with those given (without error estimates) by Wagman et al. (1982):

$$\Delta_f G_m°(Mn^{2+}, 298.15\ K) = -(228.27 \pm 0.58)\ kJ \cdot mol^{-1}$$

$$\Delta_f H_m°(Mn^{2+}, 298.15\ K) = -(220.8 \pm 0.5)\ kJ \cdot mol^{-1}$$

$$S_m°(Mn^{2+}, 298.15\ K) = -(73.6 \pm 1.0)\ J \cdot K^{-1} \cdot mol^{-1}$$

Note that $\Delta_f G_m°(Mn^{2+}, 298.15\ K) = -(228.1 \pm 0.5)\ kJ \cdot mol^{-1}$ given by Brown & Ekberg (2016), has been recalculated by this review to $\Delta_f G_m°(Mn^{2+}, 298.15\ K) = -(228.27 \pm 0.58)\ kJ \cdot mol^{-1}$ for internal consistency with the selected values for $S_m°(Mn, \alpha, 298.15\ K)$, $S_m°(Mn^{2+}, 298.15\ K)$ and $\Delta_f H_m°(Mn^{2+}, 298.15\ K)$.

Using the selected $\Delta_f G_m°(Mn^{2+}, 298.15\ K)$, the redox equilibrium

$$Mn(cr) \rightleftharpoons Mn^{2+} + 2\ e^-$$

is calculated as

$$\log_{10} K°(298.15\ K) = 39.99 \pm 0.09$$

in agreement with the value given by Robie & Hemingway (1995).

The specific ion interaction coefficient selected by NEA (Grenthe et al. 1992, Lemire et al. 2013), for $\varepsilon(Mn^{2+}, Cl^-)$ is

$$\varepsilon(Mn^{2+}, Cl^-) = (0.13 \pm 0.01)\ kg \cdot mol^{-1}$$

Since this report explicitly considers the formation of manganese(II) chloride complexation, $\varepsilon(Mn^{2+}, Cl^-)$ must be approximated by using the corresponding ion interaction coefficient with perchlorate. However, no value for $\varepsilon(Mn^{2+}, ClO_4^-)$ has been selected by NEA (Grenthe et al. 1992, Lemire et al. 2013). This review took the mean activity data evaluated by Goldberg (1979) for $Mn(ClO_4)_2$, as well as for $MnCl_2$, and obtained (Fig. 13-1)

$$\varepsilon(Mn^{2+}, ClO_4^-) = (0.38 \pm 0.02)\ kg \cdot mol^{-1}$$

Note that $\varepsilon(Mn^{2+}, Cl^-)$ obtained by this review from the data evaluated by Goldberg (1979) is in perfect agreement with the value selected by NEA (Grenthe et al. 1992, Lemire et al. 2013).

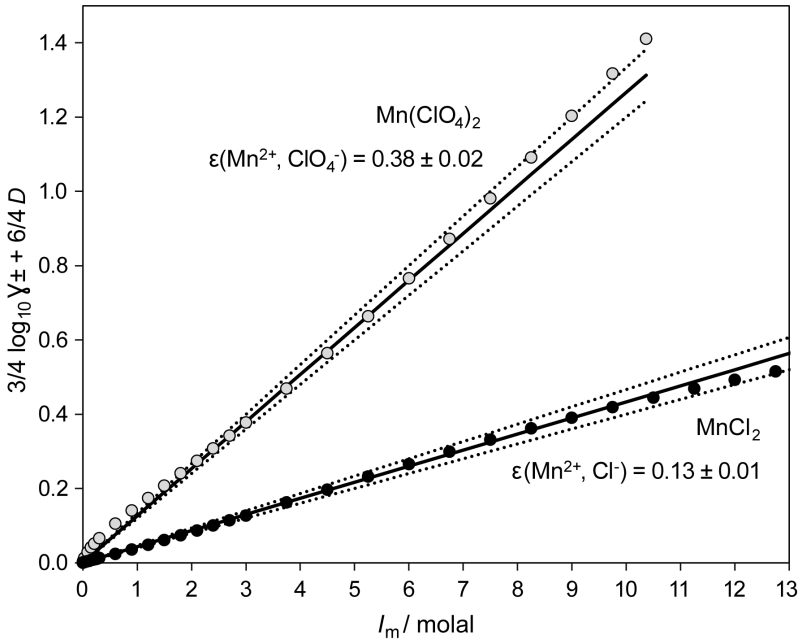

Fig. 13-1: The SIT correlation $3/4 \log_{10}\gamma\pm + 6/4\ D = \varepsilon(Mn^{2+}, X^-) \cdot I_m$

Where I_m, is the ionic strength in [mol · kg_{H2O}^{-1}], X^- is Cl^- or ClO_4^-, D is the SIT Debye-Hückel term with A = 0.5091, (lines), and γ± are the mean activity coefficients of $MnCl_2$ or $Mn(ClO_4)_2$ taken from Goldberg (1979) (circles).

13.4 Manganese(II) (hydr)oxide compounds and complexes

13.4.1 Manganese(II) hydroxide complexes

Nordstrom et al. (1990) selected $\log_{10}{}^*\beta_1°$ and $\Delta_r H_m°$ values from Baes & Mesmer (1976), who in turn took these values from Perrin (1962):

$$Mn^{2+} + H_2O(l) \rightleftharpoons MnOH^+ + H^+$$

$$\log_{10}{}^*\beta_1° \text{ (298.15 K)} = -10.59$$

$$\Delta_r H_m° \text{(298.15 K)} = 14.4 \text{ kcal} \cdot \text{mol}^{-1} = 60.2 \text{ kJ} \cdot \text{mol}^{-1}$$

Brown & Ekberg (2016) state that manganese(II) hydrolyses at the highest pH of the divalent first series transition metals, and report that stability constants for $MnOH^+$ have been experimentally measured by Perrin (1962) across the temperature range of 15 – 42 °C. More recently, data have been estimated to 300 °C in two studies. Analysing all these data Brown & Ekberg (2016) obtained

$$Mn^{2+} + H_2O(l) \rightleftharpoons MnOH^+ + H^+$$

$$\log_{10}{}^*\beta_1° \text{ (298.15 K)} = -10.58 \pm 0.04$$

$\Delta_r H_m°(298.15\ K) = (57.3 \pm 1.1)\ kJ \cdot mol^{-1}$

$\Delta_r C_{p,m}°(298.15\ K) = 0\ J \cdot K^{-1} \cdot mol^{-1}$

These values have been included in TDB 2020, as well as the estimate

$\varepsilon(MnOH^+, Cl^-) \approx \varepsilon(MnOH^+, ClO_4^-) = (0.2 \pm 0.1)\ kg \cdot mol^{-1}$

Note that $\log_{10}{}^*\beta_1°$ is in excellent agreement with the value reported by Perrin (1962), $\log_{10}{}^*\beta_1°$ (298.15 K) = -10.59 ± 0.04, while $\Delta_r H_m°$ is somewhat less positive than $\Delta_r H_m°(298.15\ K)$ = 60.2 kJ · mol^{-1}, derived solely from the data of Perrin (1962).

Note further that Perrin (1962) also studied the formation of $MnOH^+$ as a function of ionic strength in KNO_3 medium. However, SIT coefficients related to NO_3^- are not included in TDB 2020.

Brown & Ekberg (2016) further report that stability constants for $Mn(OH)_2(aq)$, $Mn(OH)_3^-$ and $Mn(OH)_4^{2-}$ have been estimated to 300 °C in two studies. Analysing these data Brown & Ekberg (2016) obtained

$Mn^{2+} + 2\ H_2O(l) \rightleftharpoons Mn(OH)_2(aq) + 2\ H^+$

$\log_{10}{}^*\beta_2°(298.15\ K) = -22.18 \pm 0.20$

$\Delta_r H_m°(298.15\ K) = (117.4 \pm 2.6)\ kJ \cdot mol^{-1}$

$\Delta_r C_{p,m}°(298.15\ K) = 0\ J \cdot K^{-1} \cdot mol^{-1}$

$Mn^{2+} + 3\ H_2O(l) \rightleftharpoons Mn(OH)_3^- + 3\ H^+$

$\log_{10}{}^*\beta_3°(298.15\ K) = -34.34 \pm 0.45$

$\Delta_r H_m°(298.15\ K) = (171.9 \pm 3.1)\ kJ \cdot mol^{-1}$

$\Delta_r C_{p,m}°(298.15\ K) = 0\ J \cdot K^{-1} \cdot mol^{-1}$

$Mn^{2+} + 4\ H_2O(l) \rightleftharpoons Mn(OH)_4^{2-} + 4\ H^+$

$\log_{10}{}^*\beta_4°(298.15\ K) = -48.28 \pm 0.40$

$\Delta_r H_m°(298.15\ K) = (256.4 \pm 5.2)\ kJ \cdot mol^{-1}$

$\Delta_r C_{p,m}°(298.15\ K) = 0\ J \cdot K^{-1} \cdot mol^{-1}$

These estimated values have been included in TDB 2020 as supplemental data, as well as the estimates

$\varepsilon(Mn(OH)_2(aq), NaCl) \approx \varepsilon(Mn(OH)_2(aq), NaClO_4) = (0.0 \pm 0.1)\ kg \cdot mol^{-1}$

$\varepsilon(Mn(OH)_3^-, Na^+) = -(0.05 \pm 0.10)\ kg \cdot mol^{-1}$

$\varepsilon(Mn(OH)_4^{2-}, Na^+) = -(0.10 \pm 0.10)\ kg \cdot mol^{-1}$

13.4.2 Manganese(II) (hydr)oxide compounds

MnO(cr), manganosite

Brown & Ekberg (2016) report that Robie & Hemingway (1995) provide thermochemical data for manganosite, MnO(cr). These values are identical with those given (without error estimate) by Wagman et al. (1982):

$\Delta_f G_m°(MnO, cr, 298.15\ K) = -(362.90 \pm 0.50)\ kJ \cdot mol^{-1}$

$\Delta_f H_m°(MnO, cr, 298.15\ K) = -(385.22 \pm 0.50)\ kJ \cdot mol^{-1}$

$S_m°(MnO, cr, 298.15\ K) = (59.71 \pm 0.40)\ J \cdot K^{-1} \cdot mol^{-1}$

These values have been included in TDB 2020.

Using $\Delta_f G_m°(MnO, cr, 298.15\ K)$, $\Delta_f H_m°(MnO, cr, 298.15\ K)$ and $\Delta_f G_m°(Mn^{2+}, 298.15\ K)$, $\Delta_f H_m°(Mn^{2+}, 298.15\ K)$ (see Section 8.2) and the CODATA values $\Delta_f G_m°(H_2O, l, 298.15\ K) = -(237.140 \pm 0.041)\ kJ \cdot mol^{-1}$, $\Delta_f H_m°(H_2O, l, 298.15\ K) = -(285.83 \pm 0.04)\ kJ \cdot mol^{-1}$ (Grenthe et al. 1992), a "solubility product" and a reaction enthalpy can be calculated:

$MnO(cr) + 2\ H^+ \rightleftharpoons Mn^{2+} + H_2O(l)$

$\log_{10}{}^*K_{s0}°\ (298.15\ K) = 17.93 \pm 0.12$

$\Delta_r H_m°\ (298.15\ K) = -(121.4 \pm 0.7)\ kJ \cdot mol^{-1}$

Brown & Ekberg (2016) calculated $\log_{10}{}^*K_s°\ (298.15\ K) = 17.94 \pm 0.12$, using their own value $\Delta_f G_m°(H_2O, l, 298.15\ K) = -(237.17 \pm 0.04)\ kJ \cdot mol^{-1}$.

$Mn(OH)_2$(cr), pyrochroite

Nordstrom et al. (1990) selected a $\log_{10}{}^*K_{s0}°$ value from Baes & Mesmer (1976) for $Mn(OH)_2$(cr), pyrochroite:

$Mn(OH)_2(cr) + 2\ H^+ \rightleftharpoons Mn^{2+} + 2\ H_2O(l)$

$\log_{10}{}^*K_{s0}°\ (298.15\ K) = -15.2$

Brown & Ekberg (2016) report that there have been a number of determinations of the solubility of pyrochroite, $Mn(OH)_2$(cr), all of which are in good agreement. One datum has been obtained at 22 °C, whereas all of the other values relate to 25 °C. Brown & Ekberg (2016) averaged the 25 °C data and obtained

$$Mn(OH)_2(cr) + 2\ H^+ \rightleftharpoons Mn^{2+} + 2\ H_2O(l)$$

$$\log_{10}{}^*K_{s0}^\circ\ (298.15\ K) = 15.19 \pm 0.10$$

This value has been included in TDB 2020.

Brown & Ekberg (2016) state that the solubility constant for the hydroxide is unexpected since it shows that it is much less soluble than the oxide. This indicates that $Mn(OH)_2(cr)$ is the stable phase at 25 °C.

However, no temperature data are available for the solubility of pyrochroite, $Mn(OH)_2(cr)$. This review estimated the temperature effect first via the isocoulombic reaction with brucite, $Mg(OH)_2(cr)$

$$Mg(OH)_2(cr) + Mn^{2+} \rightleftharpoons Mn(OH)_2(cr) + Mg^{2+}$$

We assume that in the Gibbs-Helmholtz equation

$$\Delta_r G_m^\circ(iso, 298.15\ K) = \Delta_r H_m^\circ(iso, 298.15\ K) - T^\circ \cdot \Delta_r S_m^\circ(iso, 298.15\ K)$$

the term $\Delta_r S_m^\circ(iso, 298.15\ K) = 0$ and hence, this so-called 1-term extrapolation results in

$$\Delta_r G_m^\circ(iso, T) = \Delta_r G_m^\circ(iso, 298.15\ K) = constant = \Delta_r H_m^\circ(iso, 298.15\ K)$$

Using the selected $\log_{10}{}^*K_{s0}^\circ$ (298.15 K) values for brucite, $Mg(OH)_2(cr)$ (see Section 5.3.2) and pyrochroite, $Mn(OH)_2(cr)$, results in

$$\Delta_r G_m^\circ(iso, 298.15\ K) = \Delta_r G_m^\circ(Mg(OH)_2(cr), 298.15\ K) - \Delta_r G_m^\circ(Mn(OH)_2(cr), 298.15\ K)$$

$$\Delta_r G_m^\circ(iso, 298.15\ K) = -10.96 \pm 0.61)\ kJ \cdot mol^{-1}$$

which in turn is used to estimate the $\Delta_r H_m^\circ$ value for pyrochroite, $Mn(OH)_2(cr)$ as

$$Mn(OH)_2(cr) + 2\ H^+ \rightleftharpoons Mn^{2+} + 2\ H_2O(l)$$

$$\Delta_r H_m^\circ(Mn(OH)_2(cr), 298.15\ K) = \Delta_r G_m^\circ(iso, 298.15\ K) + \Delta_r H_m^\circ(Mg(OH)_2(cr), 298.15\ K)$$

$$\Delta_r H_m^\circ\ (Mn(OH)_2(cr), 298.15\ K) = -(122.5 \pm 0.9)\ kJ \cdot mol^{-1}$$

Alternatively, we can assume that in the above isocoulombic reaction with brucite

$$\log_{10}{}^*K_{s0}^\circ\ (iso, T) = \log_{10}{}^*K_{s0}^\circ\ (iso, 298.15\ K) = const$$

another 1-term extrapolation which results in

$\Delta_r H_m°(Mn(OH)_2(cr), 298.15\ K) = \Delta_r H_m°(Mg(OH)_2(cr), 298.15\ K) = -(111.5 \pm 0.7)\ kJ \cdot mol^{-1}$

Another isocoulombic reaction can be formulated with manganosite, MnO(cr)

$MnO(cr) + H_2O(l) \rightleftharpoons Mn(OH)_2(cr)$

leading either, via $\Delta_r G_m°(iso, T) = constant$, to

$\Delta_r G_m°(iso, 298.15\ K) = -15.64 \pm 0.89)\ kJ \cdot mol^{-1}$

$\Delta_r H_m°\ (Mn(OH)_2(cr), 298.15\ K) = -(137 \pm 1.1)\ kJ \cdot mol^{-1}$

or, via $\log_{10}{}^*K_{s0}°$ (iso, T) = const, to

$\Delta_r H_m°\ (Mn(OH)_2(cr), 298.15\ K) = -(121.4 \pm 0.7)\ kJ \cdot mol^{-1}$

As there is no clear preference to any of these 1-term extrapolations, this review calculated an unweighted average of the four values:

$Mn(OH)_2(cr) + 2\ H^+ \rightleftharpoons Mn^{2+} + 2\ H_2O(l)$

$\Delta_r H_m°\ (298.15\ K) = -(123 \pm 17)\ kJ \cdot mol^{-1}$

This value has been included in TDB 2020 as supplemental datum.

13.5 Manganese(II) fluoride compounds and complexes

13.5.1 Manganese(II) fluoride complexes

Nordstrom et al. (1990) selected

$Mn^{2+} + F^- \rightleftharpoons MnF^+$

$\log_{10} K_1°\ (298.15\ K) = 0.84$

with the reference Wagman et al. (1982). As there is no documentation concerning their data evaluation, the source of the Wagman et al. (1982) value remains unclear.

This review identified a number of studies concerning manganese(II) fluoride complexation, Ciavatta & Grimaldi (1965), Bond (1971), Bond & Hefter (1972) and Kul'vinova et al. (1976), all at 25 °C and in $NaClO_4$ medium, and Solomon et al. (1983) at 25 °C in 0.05 M tetraethylammonium fluoride.

Using the data in $NaClO_4$ for an SIT analysis this review obtained (Fig. 13-2):

$$\log_{10}K_1° \text{ (298.15 K)} = 1.35 \pm 0.18$$

$$\Delta\varepsilon(NaClO_4) = -(0.17 \pm 0.08)$$

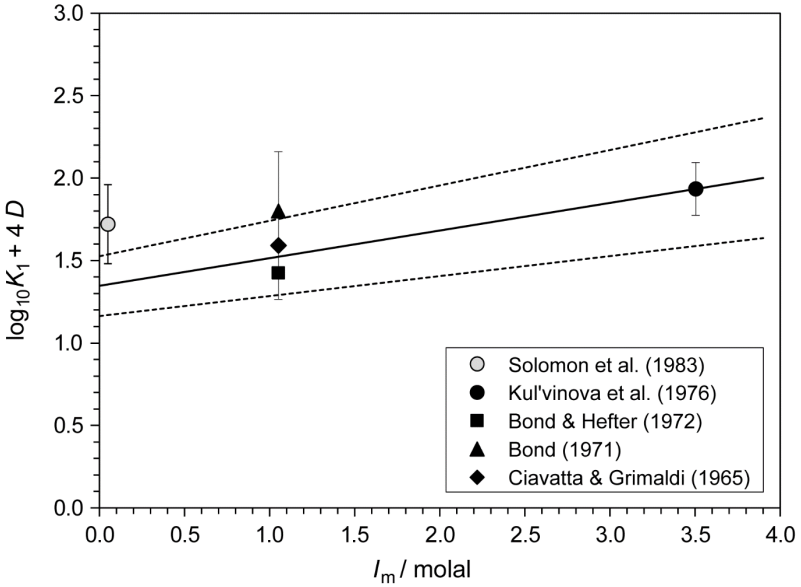

Fig. 13-2: Dependence of the equilibrium $Mn^{2+} + F^- \rightleftharpoons MnF^+$ on ionic strength

Using the data obtained in $NaClO_4$ (black symbols). The solid line is obtained using the derived SIT interaction coefficient and stability constant at zero ionic strength. Dotted lines represent the 95% uncertainty range extrapolated from I = 0 to higher $NaClO_4$ concentrations. The data of Solomon et al. (1983) in tetraethylammonium fluoride are shown for comparison only.

Considering $\varepsilon(Mn^{2+}, ClO_4^-) = (0.38 \pm 0.02)$ kg · mol^{-1} and $\varepsilon(Na^+, F^-) = (0.02 \pm 0.02)$ kg · mol^{-1} (Grenthe et al. 1992) this review derived from the experimental $\Delta\varepsilon$ value

$$\varepsilon(MnF^+, ClO_4^-) = (0.23 \pm 0.09) \text{ kg} \cdot \text{mol}^{-1}$$

This value is included in TDB 2020, together with $\log_{10}K_1°$ obtained from the SIT analysis.

Kul'vinova et al. (1976) report a calorimetrically determined enthalpy of reaction

$$\Delta_r H_m°(298.15 \text{ K}) = (15.1 \pm 1.6) \text{ kJ} \cdot \text{mol}^{-1}$$

This value has been included in TDB 2020, with the original uncertainty doubled to 2σ.

13.5.2 Manganese(II) fluoride compounds

MnF_2(cr) is a pale pink crystalline solid with a solubility of about 1 g/L. It is synthetized by treating $MnCO_3$(cr) with hydrofluoric acid. It has not been found as a mineral.

No thermodynamic data for MnF_2(cr) are included in TDB 2020.

13.6 Manganese(II) chloride compounds and complexes

13.6.1 Manganese(II) chloride complexes

Nordstrom et al. (1990) selected

$$Mn^{2+} + Cl^- \rightleftharpoons MnCl^+$$

$$\log_{10}\beta_1^\circ\ (298.15\ K) = 0.61$$

$$Mn^{2+} + 2\ Cl^- \rightleftharpoons MnCl_2(aq)$$

$$\log_{10}\beta_2^\circ\ (298.15\ K) = 0.25$$

$$Mn^{2+} + 3\ Cl^- \rightleftharpoons MnCl_3^-$$

$$\log_{10}\beta_3^\circ\ (298.15\ K) = -0.31$$

with the reference Wagman et al. (1982). As there is no documentation concerning their data evaluation, the source of the Wagman et al. (1982) values cannot be traced back to any experimental study. Probably the data originate from Morris & Short (1961), the only study postulating the existence of $MnCl^+$, $MnCl_2$(aq) and $MnCl_3^-$, based on measurements by a cation-exchange method. Morris & Short (1961) report $\log_{10}\beta_1$ (293.15 K) = 0.59, $\log_{10}\beta_2$ (293.15 K) = 0.25, and $\log_{10}\beta_3$ (293.15 K) = -0.36, valid for 20 °C and 0.691 M perchloric acid.

Actually, a considerable number of studies has been published since the publication of Morris & Short (1961), most of them for the temperature range 20 – 25 °C (Masterton & Berka 1966, McCain & Myers 1968, Hutchinson & Higginson 1973, Bixler & Larson 1974, Libuś & Tiałowska 1975, Carpenter 1983), at 25 and 50 °C (Ashurst 1976), 50 – 170 °C (Wheat & Carpenter 1988), 25 – 200 °C (Gammons & Seward 1996) and 25 – 300 °C (Suleimenov & Seward 2000), as shown in Fig. 13-3.

Note that Gammons & Seward (1996) fitted their experimental data to a linear temperature function, resulting in $\log_{10}K_1^\circ$ (298.15 K) = -0.6 ± 0.5, and show in their Fig. 11 only data supporting this linear behaviour (McCain & Myers 1968, Libuś & Tiałowska 1975, Ashurst 1976, Carpenter 1983, Wheat & Carpenter 1988). This review used the original, non-smoothed data of Gammons & Seward (1996), obtained by two alternate sets of data for HCl ion pairing (Fig. 13-3).

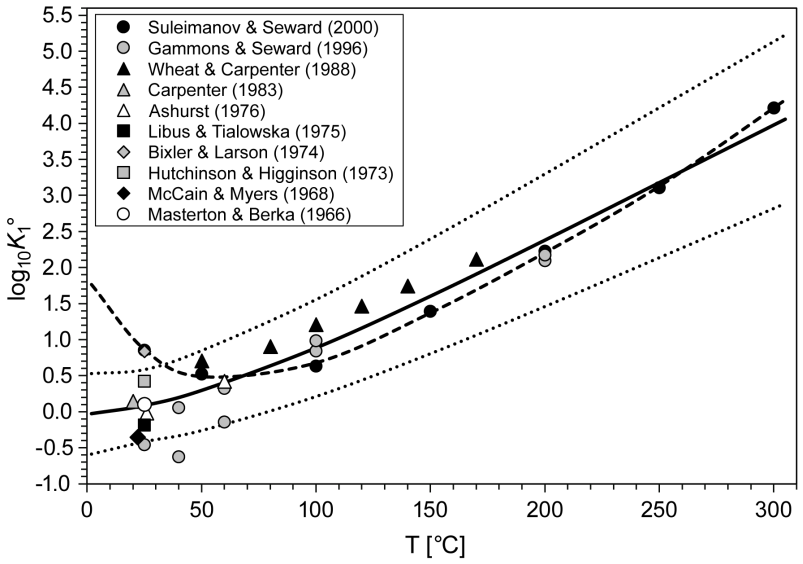

Fig. 13-3: The equilibrium constant $\log_{10}K_1°$ for $Mn^{2+} + Cl^- \rightleftharpoons MnCl^+$ as a function of temperature in the range 20 – 300 °C

Solid line: unweighted regression of all data. Dotted lines: lower and upper limits using $\log_{10}K_1°$ (298.15 K) = 0.1 ± 0.5, $\Delta_r H_m°$(298.15 K) = (11.5 ± 3.4) kJ · mol^{-1} and $\Delta_r C_{p,m}°$(298.15 K) = (323 ± 40) J · K^{-1} · mol^{-1}, and extrapolated to lower and higher temperatures. Dashed line: temperature function selected by Suleimenov & Seward (2000), shown for comparison.

By contrast, Suleimenov & Seward (2000) fitted their experimental data to a highly non-linear temperature function, resulting in $\log_{10}K_1°$ (298.15 K) = 0.85 ± 0.08, and show in their Fig. 9 only data supporting this non-linear behaviour (Morris & Short 1961, Bixler & Larson 1974, Wheat & Carpenter 1988). Note that their non-linear temperature functions predicts a strong increase of $MnCl^+$ complex stability at temperatures below 25 °C (dashed line in Fig. 13-3).

This review decided to use all data shown in Fig. 13-3 for an unweighted regression assuming $\Delta C_{p,m}°$ = const and obtained

$$Mn^{2+} + Cl^- \rightleftharpoons MnCl^+$$

$$\log_{10}K_1° \text{ (298.15 K)} = 0.1 \pm 0.5$$

$$\Delta_r H_m°\text{(298.15 K)} = (11.5 \pm 3.5) \text{ kJ} \cdot \text{mol}^{-1}$$

$$\Delta C_{p,m}°\text{(298.15 K)} = (323 \pm 40) \text{ J} \cdot \text{K}^{-1} \cdot \text{mol}^{-1}$$

These values have been included in TDB 2020.

The average of all data in the temperature range 20 – 25 °C is $\log_{10}K_1°$ (298.15 K) = 0.15 ± 0.47, in good agreement with the value obtained from the overall regression analysis.

There is one data set, Libuś & Tiałowska (1975), measured at 25 °C in different concentrations of $Mn(ClO_4)_2$. These data have been used for an SIT analysis (Fig. 13-4)

$\log_{10}K_1°$ (298.15 K) = -0.19 ± 0.13

$\Delta\varepsilon(NaClO_4)$ = -(0.11 ± 0.02)

Note that the $\log_{10}K_1°$(298.15 K) value obtained by the SIT analysis (Fig. 13-4) is in good agreement with the value obtained from the unweighted regression of temperature data (Fig. 13-3).

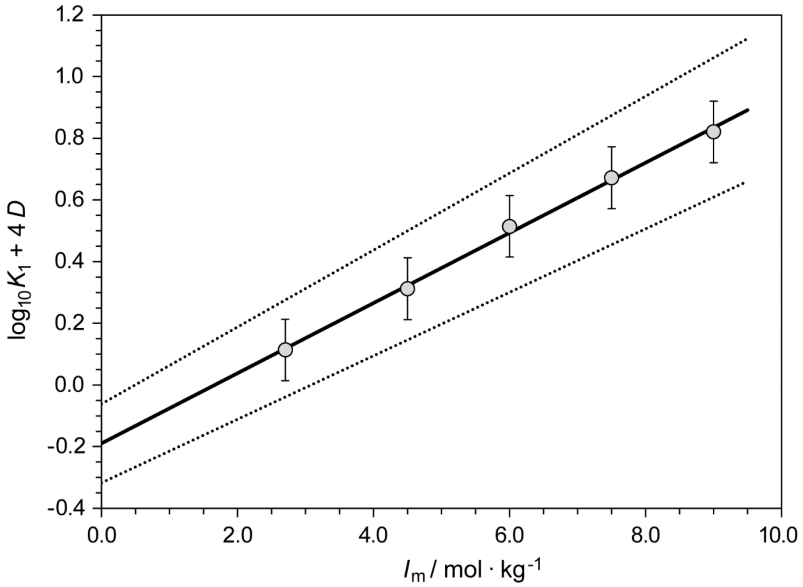

Fig. 13-4: Dependence of the equilibrium $Mn^{2+} + Cl^- \rightleftharpoons MnCl^+$ on ionic strength

Using the data of Libuś & Tiałowska (1975) obtained in $Mn(ClO_4)_2$ medium. The solid line is obtained using the derived SIT interaction coefficient and stability constant at zero ionic strength. Dotted lines represent the 95% uncertainty range extrapolated from I = 0 to higher $Mn(ClO_4)_2$ concentrations.

Considering $\varepsilon(Mn^{2+}, ClO_4^-)$ = (0.38 ± 0.02) kg · mol^{-1} and $\varepsilon(Mn^{2+}, Cl^-)$ = (0.13 ± 0.02) kg · mol^{-1} this review derived from the experimental Δε value

$\varepsilon(MnCl^+, ClO_4^-)$ = (0.40 ± 0.03) kg · mol^{-1}

This value is included in TDB 2020.

Note that Gamsjäger et al. (2005) discuss the analogous Ni data of Libuś & Tiałowska (1975) as follows: "The data in Libuś & Tiałowska (1975) are free of significant medium effects. And this is the only data set where the systematic errors can be assumed identical for each point. Therefore, these data were used to determine the ion interaction coefficient between $NiCl^+$ and ClO_4^-, although the applied ionic strength (I_m = 3 – 9 m) is well above of the recommended range for the SIT analysis". Gamsjäger et al. (2005) continue that there is some uncertainty in the calculation

of $\varepsilon(NiCl^+, ClO_4^-)$ because generally $\varepsilon(Ni^{2+}, Cl^-)$ should be replaced by $\varepsilon(Ni^{2+}, ClO_4^-)$ when chloride complexation is considered explicitly in the model. But in this case $\varepsilon(Ni^{2+}, Cl^-)$ should be used for the interaction of Cl^- with Ni^{2+} because otherwise the "value of $\varepsilon(NiCl^+, ClO_4^-)$ is too high, taking into account the relatively accurate value for $\varepsilon(NiF^+, ClO_4^-)$". Exactly the same argumentation applies to the case of $\varepsilon(MnCl^+, ClO_4^-)$ and $\varepsilon(MnF^+, ClO_4^-)$.

13.6.2 Manganese(II) chloride compounds

$MnCl_2(s)$ has been found as the very rare mineral scacchite, its type locality being Mt Vesuvius, Naples, Italy. $MnCl_2(s)$ is a highly soluble salt with a solubility of 723 g/L at 25 °C (gestis.itrust.de). Besides the anhydrous form a dihydrate, $MnCl_2 \cdot 2H_2O$, with a solubility of 1'200 g/L at 20 °C (gestis.itrust.de), and a tetrahydrate, $MnCl_2 \cdot 4H_2O$, with a solubility of 1'980 g/L at 20 °C (gestis.itrust.de) are also known.

No thermodynamic data for these highly soluble salts are included in TDB 2020.

The isopiestic properties of $MnCl_2$ have been measured up to 7.7 mol $\cdot$ kg_{H2O}^{-1} (Goldberg 1979), see Section 13.3.

13.7 Manganese(II) carbonate compounds and complexes

13.7.1 Manganese(II) carbonate complexes

Nordstrom et al. (1990) selected a $\log_{10}K_1°$value given by Palmer & van Eldik (1983) for

$$Mn^{2+} + CO_3^{2-} \rightleftharpoons MnCO_3(aq)$$

$$\log_{10}K_1° \text{ (298.15 K)} = 4.90$$

Palmer & van Eldik (1983) in turn cite Zirino & Yamamoto (1972) as the source of this value. However, Zirino & Yamamoto (1972) report (mainly estimated) values for copper, zinc, cadmium and lead carbonate complexes, but no data at all for manganese. Hence, the source of the above value remains unclear.

Experimental data concerning $MnCO_3(aq)$ complex formation have been obtained by Néher-Neumann (1994) from solubility measurements of crystalline $MnCO_3(cr)$ in the pH range 3.0 – 6.1 at (25.0 ± 0.3) °C in 3 M $NaClO_4$ (see Section 13.7.2). Néher-Neumann (1994) obtained

$$Mn^{2+} + CO_3^{2-} \rightleftharpoons MnCO_3(aq)$$

$$\log_{10}K_1 \text{ (3 M } NaClO_4\text{, 298.15 K)} = 3.72 \pm 0.03$$

Extrapolating this value to zero ionic strength via SIT, using $\varepsilon(Mn^{2+}, ClO_4^-) = (0.38 \pm 0.02)$ kg · mol^{-1} (see Section 9.2), $\varepsilon(Na^+, CO_3^{2-}) = -(0.08 \pm 0.06)$ kg · mol^{-1} (Lemire et al. 2013), and the estimate $\varepsilon(MnCO_3(aq), NaClO_4) = (0.0 \pm 0.1)$ kg · mol^{-1}, this review obtained

$$\log_{10}K_1^\circ\ (298.15\ K) = 4.60 \pm 0.17$$

This value has been included in TDB 2020.

Note that the extrapolation reported by Néher-Neumann (1994) should not be considered, as SIT was used on the molar scale (mol · dm^{-3}) and not on the molal scale (mol · kg$_{H2O}^{-1}$).

No reliable temperature data are available for $MnCO_3(aq)$ or any other carbonate complexes of the first-row transition elements. Hence, this review estimated the temperature effect first via the isocoulombic reaction with $MgCO_3(aq)$

$$MgCO_3(aq) + Mn^{2+} \rightleftharpoons MnCO_3(aq) + Mg^{2+}$$

We assume that in the Gibbs-Helmholtz equation

$$\Delta_r G_m^\circ(iso, 298.15\ K) = \Delta_r H_m^\circ(iso, 298.15\ K) - T^\circ \cdot \Delta_r S_m^\circ(iso, 298.15\ K)$$

the term $\Delta_r S_m^\circ(iso, 298.15\ K) = 0$ and hence, this so-called 1-term extrapolation results in

$$\Delta_r G_m^\circ(iso, T) = \Delta_r G_m^\circ(iso, 298.15\ K) = constant = \Delta_r H_m^\circ(iso, 298.15\ K)$$

Using the selected $\log_{10}K_1^\circ$ (298.15 K) values for $MgCO_3(aq)$ (see Section 5.3.2) and $MnCO_3(aq)$ results in

$$\Delta_r G_m^\circ(iso, 298.15\ K) = \Delta_r G_m^\circ(MgCO_3(aq), 298.15\ K) - \Delta_r G_m^\circ(MnCO_3(aq), 298.15\ K)$$

$$\Delta_r G_m^\circ(iso, 298.15\ K) = 9.2 \pm 1.0)\ kJ \cdot mol^{-1}$$

which in turn is used to estimate the $\Delta_r H_m^\circ$ value for $MnCO_3(aq)$ as

$$Mn^{2+} + CO_3^{2-} \rightleftharpoons MnCO_3(aq)$$

$$\Delta_r H_m^\circ(MnCO_3(aq), 298.15\ K) = \Delta_r G_m^\circ(iso, 298.15\ K) + \Delta_r H_m^\circ(MgCO_3(aq), 298.15\ K)$$

$$\Delta_r H_m^\circ\ (MnCO_3(aq), 298.15\ K) = (20.2 \pm 1.5)\ kJ \cdot mol^{-1}$$

Alternatively, we can assume that in the above isocoulombic reaction with brucite

$$\log_{10}{}^*K_{s0}^\circ\ (iso, T) = \log_{10}{}^*K_{s0}^\circ\ (iso, 298.15\ K) = const$$

another 1-term extrapolation which results in

$$\Delta_r H_m°(MnCO_3(aq), 298.15\ K) = \Delta_r H_m°(MgCO_3(aq), 298.15\ K) = (11.0 \pm 1.1)\ kJ \cdot mol^{-1}$$

As there is no clear preference to any of these 1-term extrapolations, this review calculated an unweighted average of the two values:

$$Mn^{2+} + CO_3^{2-} \rightleftharpoons MnCO_3(aq)$$

$$\Delta_r H_m°(298.15\ K) = (16 \pm 6)\ kJ \cdot mol^{-1}$$

This value has been included in TDB 2020 as supplemental datum.

Nordstrom et al. (1990) selected a $\log_{10}K°$value given in the compilation of Morgan (1967) for:

$$Mn^{2+} + HCO_3^- \rightleftharpoons MnHCO_3^+$$

$$\log_{10}K°\ (298.15\ K) = 1.95$$

Note that later Morgan (2005) critically selected the values of Lesht & Bauman (1978). This review used the data of Lesht & Bauman (1978) for an unweighted regression (Fig. 13.5) assuming $\Delta_r C_{p,m}° = const$ and obtained

$$Mn^{2+} + HCO_3^- \rightleftharpoons MnHCO_3^+$$

$$\log_{10}K°\ (298.15\ K) = 1.27 \pm 0.05$$

$$\Delta_r H_m°(298.15\ K) = (4.2 \pm 1.4)\ kJ \cdot mol^{-1}$$

$$\Delta_r C_{p,m}°(298.15\ K) = (231 \pm 90)\ J \cdot K^{-1} \cdot mol^{-1}$$

These values have been included in TDB 2020, as well as the estimate

$$\varepsilon(MnHCO_3^+, Cl^-) \approx \varepsilon(MnHCO_3^+, ClO_4^-) = (0.2 \pm 0.1)\ kg \cdot mol^{-1}.$$

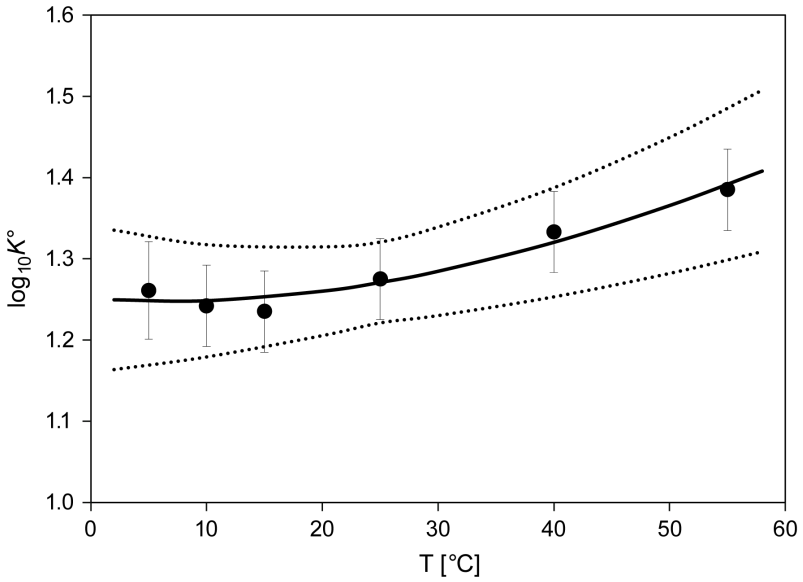

Fig. 13.5: The equilibrium constant $\log_{10}K°$ for $Mn^{2+} + HCO_3^- \rightleftharpoons MnHCO_3^+$ as a function of temperature in the range 5 – 55 °C

Solid line: unweighted regression of data reported by Lesht & Bauman (1978). Dotted lines: lower and upper limits using $\log_{10}K°$ (298.15 K) = 1.27 ± 0.05, $\Delta_r H_m°$(298.15 K) = (4.2 ± 1.4) kJ · mol^{-1} and $\Delta_r C_{p,m}°$(298.15 K) = (231 ± 90) J · K^{-1} · mol$^-$, and extrapolated to lower and higher temperatures.

13.7.2 Manganese(II) carbonate compounds

Nordstrom et al. (1990) selected from thermodynamic data reported by Garrels et al. (1960) for rhodochrosite, $MnCO_3$(s),

$$MnCO_3(s) \rightleftharpoons Mn^{2+} + CO_3^{2-}$$

$\log_{10}K_{s0}°$ (rhodochrosite, crystalline, 298.15 K) = -11.13

$\log_{10}K_{s0}°$ (rhodochrosite, precipitated, 298.15 K) = -10.39

and derived from thermodynamic data reported by Robie et al. (1984)

$\Delta_r H_m°$(rhodochrosite, crystalline, 298.15 K) = -1.43 kcal · mol^{-1} = -5.98 kJ · mol^{-1}

Grauer (1999) discussed the data of Garrels et al. (1960), Gamsjäger et al. (1970), Reiterer (1980) and others, and concluded that only the solubility data of Reiterer (1980), obtained at 50 °C for hydrothermally produced crystalline rhodochrosite, and the measurements of Gamsjäger et al. (1970) for fine-grained $MnCO_3$(s) appear reliable. Grauer (1999) finally recommends

$\log_{10}K_{s0}°$ (rhodochrosite, crystalline, 298.15 K) = -11.0 ± 0.2

$\log_{10}K_{s0}°$ (rhodochrosite, precipitated, 298.15 K) = -10.5 ± 0.2

but only as provisional values.

Robie et al. (1984) measured the heat capacity of natural, very pure, rhodochrosite between 5 and 550 K by combined cryogenic-adiabatic and differential scanning calorimetry. From their measurements they obtained

$C_{p,m}°(MnCO_3, cr, 298.15\ K) = (80.62 \pm 0.10)\ J \cdot K^{-1} \cdot mol^{-1}$

$S_m°(MnCO_3, cr, 298.15\ K) = (98.03 \pm 0.10)\ J \cdot K^{-1} \cdot mol^{-1}$

and finally calculated

$\Delta_f H_m°\ (MnCO_3, cr, 298.15\ K) = -(891.91 \pm 0.52)\ kJ \cdot mol^{-1}$

$\Delta_f G_m°(MnCO_3, cr, 298.15\ K) = -(818.13 \pm 0.55)\ kJ \cdot mol^{-1}$

Using $\Delta_f G_m°(MnCO_3, cr, 298.15\ K)$ together with $\Delta_f G_m°(Mn^{2+}, 298.15\ K) = -(228.27 \pm 0.58)\ kJ \cdot mol^{-1}$ (see Section 8.2) and $\Delta_f G_m°(CO_3^{2-}, 298.15\ K) = -(527.90 \pm 0.39)\ kJ \cdot mol^{-1}$ (Grenthe et al. 1992) this review calculated

$\log_{10}K_{s0}°\ (298.15\ K) = -10.85 \pm 0.16$

Likewise, using $\Delta_f H_m°(MnCO_3, cr, 298.15\ K)$ together with $\Delta_f H_m°(Mn^{2+}, 298.15\ K) = -(220.8 \pm 0.5)\ kJ \cdot mol^{-1}$ (see Section 8.2) and $\Delta_f H_m°(CO_3^{2-}, 298.15\ K) = -(675.23 \pm 0.25)\ kJ \cdot mol^{-1}$ (Grenthe et al. 1992) this review calculated

$\Delta_f H_m°\ (98.15\ K) = -(4.1 \pm 0.8)\ kJ \cdot mol^{-1}$

Néher-Neumann (1994) determined the solubility product of crystalline $MnCO_3$(cr) in the pH range 3.0 – 6.1 at (25.0 ± 0.3) °C in 3 M $NaClO_4$ as

$\log_{10}K_{s0}\ (3\ M\ NaClO_4, 298.15\ K) = -9.78 \pm 0.04$

Extrapolating this value to zero ionic strength via SIT, using $\varepsilon(Mn^{2+}, ClO_4^-) = (0.38 \pm 0.02)\ kg \cdot mol^{-1}$ (see Section 9.2) and $\varepsilon(Na^+, CO_3^{2-}) = -(0.08 \pm 0.06)\ kg \cdot mol^{-1}$ (Lemire et al. 2013), this review obtained

$\log_{10}K_{s0}°\ (298.15\ K) = -10.80 \pm 0.17$

in excellent agreement with the value calculated from the thermochemical data of Robie et al. (1984), and in good agreement with the provisional value recommended by Grauer (1999) for crystalline rhodochrosite.

Hence, the values of Robie et al. (1984) for rhodochrosite have been included in TDB 2020.

13.8 Manganese(II) sulphate compounds and complexes

13.8.1 Manganese(II) sulphate complexes

Nordstrom et al. (1990) selected thermodynamic data from Nair & Nancollas (1959), valid for the temperature range 0 – 45 °C, for the complex

$$Mn^{2+} + SO_4^{2-} \rightleftharpoons MnSO_4(aq)$$

$$\log_{10}K_1^\circ\ (298.15\ K) = 2.25$$

$$\Delta_r H_m^\circ(298.15\ K) = 3.37\ kcal \cdot mol^{-1} = 14.1\ kJ \cdot mol^{-1}$$

This review also considered the experimental data of Nair & Nancollas (1959), determined by emf measurements in the range 0 – 45 °C, and data reported by Wheat & Carpenter (1988), obtained from electron spin resonance (ESR) spectra of the manganese(II) ion in the temperature range 25 – 170 °C. As can be seen in Fig. 13.6, the two data sets join smoothly in the temperature range 25 – 50 °C, and an overall least-squares fit of all data yielded

$$Mn^{2+} + SO_4^{2-} \rightleftharpoons MnSO_4(aq)$$

$$\log_{10}K^\circ\ (298.15\ K) = 2.23 \pm 0.05$$

$$\Delta_r H_m^\circ(298.15\ K) = (12.7 \pm 1.1)\ kJ \cdot mol^{-1}$$

$$\Delta_r C_{p,m}^\circ(298.15\ K) = (180 \pm 23)\ J \cdot K^{-1} \cdot mol^{-1}$$

These values have been included in TDB 2020, as well as the estimate

$$\varepsilon(MnSO_4(aq), NaCl) = (0.0 \pm 0.1)\ kg \cdot mol^{-1}$$

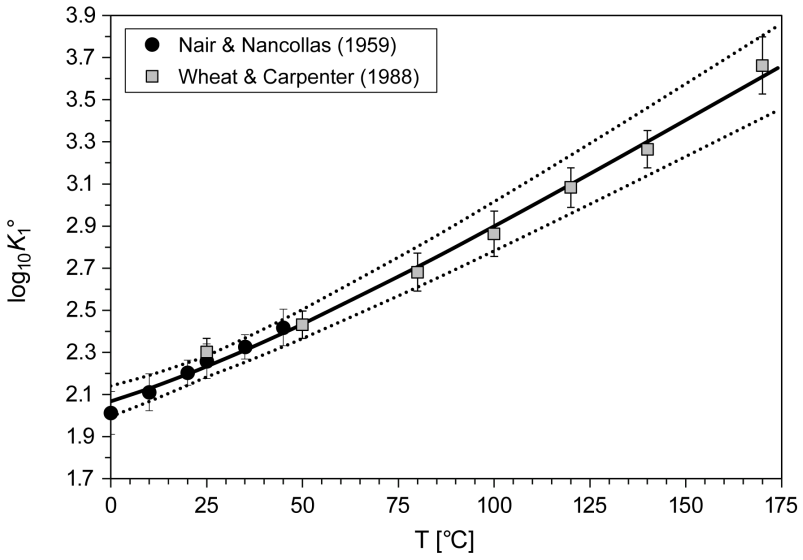

Fig. 13.6: The equilibrium constant $\log_{10}K_1°$ for $Mn^{2+} + SO_4^{2-} \rightleftharpoons MnSO_4(aq)$ as a function of temperature in the range 0 – 170 °C

Solid line: unweighted regression. Dotted lines: lower and upper limits using $\log_{10}K_1°$ (298.15 K) = 2.23 ± 0.05, $\Delta_r H_m°$(298.15 K) = (12.7 ± 1.1) kJ · mol^{-1} and $\Delta_r C_{p,m}°$(298.15 K) = (180 ± 23) J · K^{-1} · mol^{-1} and extrapolated to lower and higher temperatures.

13.8.2 Manganese(II) sulphate compounds

Manganese(II) sulphate usually refers to the inorganic compound with the formula $MnSO_4 \cdot H_2O$. This pale pink deliquescent solid, with a solubility of 762 g/L at 20 °C (gestis.itrust.de), is a commercially significant manganese(II) salt.

No thermodynamic data for this highly soluble salt are included in TDB 2020.

13.9 Manganese(III) aqua ion

Bard et al. (1985) report that the Mn(II) state is generally the most stable state in aqueous solution, while Mn(III) species are strongly oxidising in acidic solution and tend to disproportionate to Mn(II) and Mn(IV) species. In alkaline solution one finds the stable Mn(III) compound Mn_2O_3(s) as well as the oxyhydroxide MnOOH(s). However, the Mn^{3+} ion has been studied in very strongly acidic solutions where the disproportionation is less favourable.

Brown & Ekberg (2016) accepted the values estimated by Bard et al. (1985):

$$\Delta_f G_m°(Mn^{3+}, 298.15\ K) = -(83.0 \pm 0.5)\ kJ \cdot mol^{-1}$$

$$\Delta_f H_m°(Mn^{3+}, 298.15\ K) = -(113 \pm 2)\ kJ \cdot mol^{-1}$$

with uncertainties estimated by Brown & Ekberg (2016).

Using the selected $\Delta_f G_m°(Mn^{3+}, 298.15\ K)$, the redox equilibrium

$$Mn(cr) \rightleftharpoons Mn^{3+} + 3\ e^-$$

is calculated as

$$\log_{10}K°(298.15\ K) = 14.54 \pm 0.09$$

Combining this value with the redox equilibrium for Mn(II) (see Section 8.2) we obtain

$$Mn^{2+} \rightleftharpoons Mn^{3+} + e^-$$

$$\log_{10}K°(298.15\ K) = -25.42 \pm 0.12$$

$$\Delta_r H_m° (298.15\ K) = (107.8 \pm 2.1)\ kJ \cdot mol^{-1} = (25.8 \pm 0.5)\ kcal \cdot mol^{-1}$$

Nordstrom et al. (1990) give $\log_{10}K°(298.15\ K) = -25.51$ and $\Delta_r H_m°(298.15\ K) = 25.8\ kcal \cdot mol^{-1}$ "based on Wagman et al. (1982) in agreement with Bard et al. (1985)". The reason for the small difference of 0.1 log-units in $\log_{10}K°(298.15\ K)$ remains unclear.

Since this report explicitly considers the formation of manganese(III) chloride complexation, $\varepsilon(Mn^{3+}, Cl^-)$ must be approximated by using the corresponding ion interaction coefficient with perchlorate. However, as no value for $\varepsilon(Mn^{3+}, ClO_4^-)$ is available, this review decided to use the estimate (according to charge correlations and taken from Tab. 1-7)

$$\varepsilon(Mn^{3+}, ClO_4^-) = (0.6 \pm 0.1)\ kg \cdot mol^{-1}$$

13.10 Manganese(III) (hydr)oxide compounds and complexes

13.10.1 Manganese(III) hydroxide complexes

Brown & Ekberg (2016) state that hydrolysis data for manganese(III) have only been obtained for the first monomeric species, $MnOH^{2+}$ and that there is no indication whether higher monomeric species form, actually ignoring the results of Biedermann & Palombari (1978) whose results for $MnOH^{2+}$ they probably included in their SIT analysis (Fig. 11.38 of Brown & Ekberg 2016), although only a "reported" but no "accepted" stability constant from Biedermann & Palombari (1978) can be found in Tab. 11.23 of Brown & Ekberg (2016).

Brown & Ekberg (2016) found few data for the stability constant of $MnOH^{2+}$ at 25 °C as a function of ionic strength in $HClO_4$ media. Each of the available values has been determined at quite high concentrations of $HClO_4$, ranging from 3.0 – 5.6 mol L^{-1}. Doing a normal SIT analysis Brown & Ekberg (2016) obtained

$Mn^{3+} + H_2O(l) \rightleftharpoons MnOH^{2+} + H^+$

$\log_{10}{}^*\beta_1^\circ$ (298.15 K) = 0.75 ± 0.18

$\Delta\varepsilon$ = -(0.08 ± 0.04) kg · mol^{-1}

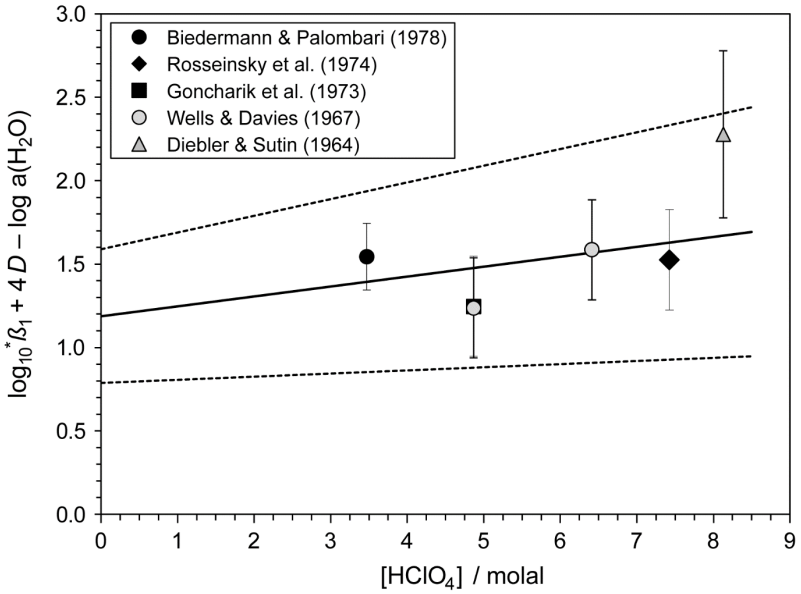

Fig. 13-7: Dependence of the equilibrium $Mn^{3+} + H_2O(l) \rightleftharpoons MnOH^{2+} + H^+$ on ionic strength in $HClO_4$ using all data

The solid line is obtained using the derived SIT interaction coefficient and stability constant at zero ionic strength. Dotted lines represent the 95% uncertainty range extrapolated from I = 0 to higher $HClO_4$ concentrations.

However, it is not obvious which values from their Tab. 11.23 Brown & Ekberg (2016) ultimately used for their SIT analysis. This review repeated the SIT analysis, taking all data of Tab. 11.23 in Brown & Ekberg (2016) reported for 23 and 25 °C (Diebler & Sutin 1964, Wells & Davies 1967, Goncharik et al. 1973, Rosseinsky et al. 1974, Biedermann & Palombari 1978), and obtained (Fig. 13-7):

$\log_{10}{}^*\beta_1^\circ$ (298.15 K) = 1.2 ± 0.4

$\Delta\varepsilon$ = -(0.06 ± 0.07) kg · mol^{-1}

Considering $\varepsilon(Mn^{3+}, ClO_4^-)$ = (0.6 ± 0.1) kg · mol^{-1} and $\varepsilon(H^+, ClO_4^-)$ = (0.14 ± 0.02) kg · mol^{-1} this review derived from the experimental $\Delta\varepsilon$ value

$\varepsilon(MnOH^{2+}, ClO_4^-)$ = (0.40 ± 0.13) kg · mol^{-1}

These values have been included in TDB 2020.

Brown & Ekberg (2016) state that the formation $MnOH^{2+}$ has been studied by three groups using 4.0 mol L^{-1} $HClO_4$ across the combined temperature range of 1.2 – 34.5 °C. The stability constants obtained are in quite good agreement and demonstrate that they vary linearly with respect to the inverse of absolute temperature. Assuming that the difference between the enthalpy of reaction for 4.0 mol L^{-1} $HClO_4$ is within the uncertainty of that for zero ionic strength, Brown & Ekberg (2016) obtained

$$\Delta_r H_m°(298.15\ K) = (22.9 \pm 5.5)\ kJ \cdot mol^{-1}$$

$$\Delta C_{p,m}°(298.15\ K) = 0\ J \cdot K^{-1} \cdot mol^{-1}$$

These values have been included in TDB 2020.

Biedermann & Palombari (1978) report a stability constant for $Mn(OH)_2^+$ at 25 °C in 3.0 mol L^{-1} (H,Li)ClO_4:

$$Mn^{3+} + 2\ H_2O(l) \rightleftharpoons Mn(OH)_2^+ + 2\ H^+$$

$$log_{10}{}^*\beta_2\ (298.15\ K) = 0.1 \pm 0.1$$

This value has been extrapolated to zero ion strength via SIT, considering $\varepsilon(H^+, ClO_4^-) = (0.14 \pm 0.02)\ kg \cdot mol^{-1}$, and the estimates $\varepsilon(Mn^{3+}, ClO_4^-) = (0.6 \pm 0.1)\ kg \cdot mol^{-1}$ and $\varepsilon(Mn(OH)_2^+, ClO_4^-) = (0.2 \pm 0.1)\ kg \cdot mol^{-1}$:

$$log_{10}{}^*\beta_2°\ (298.15\ K) = 1.5 \pm 0.5$$

This value has been included in TDB 2020 as supplemental datum.

It is classified as supplemental datum because there is no independent confirmation of the results reported by Biedermann & Palombari (1978), and the extrapolation from high ionic strength to zero, using estimated SIT interaction coefficients, introduces considerable uncertainty to the final value.

No temperature data are available for $Mn(OH)_2^+$, and no suitable isocoulombic reaction could be identified which would allow an estimate.

13.10.2 Manganese(III) (hydr)oxide compounds

Mn_2O_3(cr), bixbyite

Brown & Ekberg (2016) report that Robie & Hemingway (1995) provide thermochemical data for bixbyite, Mn_2O_3(cr), the oxide phase of manganese(III):

$\Delta_f G_m°(Mn_2O_3, cr, 298.15\ K) = -(882.1 \pm 1.0)\ kJ \cdot mol^{-1}$

$\Delta_f H_m°(Mn_2O_3, cr, 298.15\ K) = -(959.0 \pm 1.0)\ kJ \cdot mol^{-1}$

$S_m°(Mn_2O_3, cr, 298.15\ K) = (113.7 \pm 0.2)\ J \cdot K^{-1} \cdot mol^{-1}$

Using $\Delta_f G_m°(Mn_2O_3, cr, 298.15\ K)$, $\Delta_f H_m°(Mn_2O_3, cr, 298.15\ K)$ and $\Delta_f G_m°(Mn^{3+}, 298.15\ K)$, $\Delta_f H_m°(Mn^{3+}, 298.15\ K)$ and the CODATA values $\Delta_f G_m°(H_2O, l, 298.15\ K) = -(237.140 \pm 0.041)\ kJ \cdot mol^{-1}$, $\Delta_f H_m°(H_2O, l, 298.15\ K) = -(285.83 \pm 0.04)\ kJ \cdot mol^{-1}$ (Grenthe et al. 1992), a "solubility product" can be calculated:

$1/2\ Mn_2O_3(cr) + 3\ H^+ \rightleftharpoons Mn^{3+} + 3/2\ H_2O(l)$

$\log_{10}{}^*K_{s0}°\ (298.15\ K) = -0.41 \pm 0.30$

$\Delta_r H_m°\ (298.15\ K) = -(62.2 \pm 2.1)\ kJ \cdot mol^{-1}$

Brown & Ekberg (2016) calculated $\log_{10}{}^*K_s°\ (298.15\ K) = -0.40 \pm 0.30$, using their own value $\Delta_f G_m°(H_2O, l, 298.15\ K) = -(237.17 \pm 0.04)\ kJ \cdot mol^{-1}$.

Using $\Delta_f G_m°(Mn^{2+}, 298.15\ K)$, $\Delta_f H_m°(Mn^{2+}, 298.15\ K)$ (see Section 8.2) an alternative "solubility product" can be calculated from the same thermochemical data as

$1/2\ Mn_2O_3(cr) + 3\ H^+ + e^- \rightleftharpoons Mn^{2+} + 3/2\ H_2O(l)$

$\log_{10}{}^*K_s°\ (298.15\ K) = 25.01 \pm 0.30$

$\Delta_r H_m°\ (298.15\ K) = -(170.0 \pm 1.1)\ kJ \cdot mol^{-1}$

MnOOH(cr), manganite

Brown & Ekberg (2016) report that from an earlier work of Bricker (1965), Parc et al. (1989) determined a stability constant for the formation of manganite, MnOOH(cr):

$MnOOH(cr) + 2\ H^+ \rightleftharpoons Mn^{2+} + 3/2\ H_2O(l) + 1/4\ O_2g$

$\log_{10}{}^*K_s°\ (298.15\ K) = 4.57$

From this value Brown & Ekberg (2016) derived

$$MnOOH(cr) + 3\ H^+ \rightleftharpoons Mn^{3+} + 2\ H_2O(l)$$

$$\log_{10}{}^*K_{s0}^\circ\ (298.15\ K) = -0.08 \pm 0.30$$

Combining $\log_{10}{}^*K_s^\circ\ (298.15\ K) = 4.57$ with the reaction

$$1/4\ O_2g + H^+ + e^- \rightleftharpoons 1/2\ H_2O(l)$$

$$\log_{10}K^\circ\ (298.15\ K) = 20.772 \pm 0.007$$

yields an alternative "solubility product"

$$MnOOH(cr) + 3\ H^+ + e^- \rightleftharpoons Mn^{2+} + 2\ H_2O(l)$$

$$\log_{10}{}^*K_s^\circ\ (298.15\ K) = 25.34 \pm 0.30$$

Nordstrom et al. (1990) give the same value, $\log_{10}{}^*K_s^\circ(298.15\ K) = 25.34$, without error estimate, claiming Wagman et al. (1982) as their reference. However, Wagman et al. (1982) do not provide any data for MnOOH(cr). Nordstrom et al. (1990) perhaps have used the same data source as Brown & Ekberg (2016).

As Brown & Ekberg (2016) remark "as can be seen, the solubility constant for this phase, manganite, is consistent with that found for bixbyite, Mn_2O_3(cr), being slightly more soluble than the oxide phase as would be expected". However, the difference of 0.3 log-units is within the assigned uncertainties.

However, no temperature data are available for the solubility of manganite, MnOOH(cr). This review estimated the temperature effect first via the isocoulombic reaction with goethite, FeOOH(cr)

$$FeOOH(cr) + Mn^{3+} \rightleftharpoons MnOOH(cr) + Fe^{3+}$$

We assume that in the Gibbs-Helmholtz equation

$$\Delta_r G_m^\circ(iso, 298.15\ K) = \Delta_r H_m^\circ(iso, 298.15\ K) - T^\circ \cdot \Delta_r S_m^\circ(iso, 298.15\ K)$$

the term $\Delta_r S_m^\circ(iso, 298.15\ K) = 0$ and hence, this so-called 1-term extrapolation results in

$$\Delta_r G_m^\circ(iso, T) = constant = \Delta_r G_m^\circ(iso, 298.15\ K) = \Delta_r H_m^\circ(iso, 298.15\ K)$$

Using the selected $\log_{10}{}^{*}K_{s0}°$ (298.15 K) = 0.33 ± 0.10 for goethite, FeOOH(cr) + 3 H^+ ⇌ Fe^{3+} + 2 H_2O(l) (see Section 12.4.2.6) and $\log_{10}{}^{*}K_{s0}°$ (298.15 K) = -0.08 ± 0.30 for manganite, MnOOH(cr) + 3 H^+ ⇌ Mn^{3+} + 2 H_2O(l), results in

$$\Delta_r G_m°(\text{iso, 298.15 K}) = \Delta_r G_m°(\text{FeOOH(cr), 298.15 K}) - \Delta_r G_m°(\text{MnOOH(cr), 298.15 K})$$

$$\Delta_r G_m°(\text{iso, 298.15 K}) = -2.34 \pm 1.81)\ \text{kJ} \cdot \text{mol}^{-1}$$

which in turn is used to estimate the $\Delta_r H_m°$ value for manganite, MnOOH(s) as

$$\text{MnOOH(s)} + 3\ H^+ \rightleftharpoons Mn^{3+} + 2\ H_2O(l)$$

$$\Delta_r H_m°(\text{MnOOH(cr), 298.15 K}) = \Delta_r G_m°(\text{iso, 298.15 K}) + \Delta_r H_m°(\text{FeOOH(cr), 298.15 K})$$

$$\Delta_r H_m°\ (\text{MnOOH(cr), 298.15 K}) = -(67.8 \pm 2.9)\ \text{kJ} \cdot \text{mol}^{-1}$$

Alternatively, we can assume that in the above isocoulombic reaction with goethite

$$\log_{10}{}^{*}K_{s0}°\ (\text{iso, T}) = \log_{10}{}^{*}K_{s0}°\ (\text{iso, 298.15 K}) = \text{const}$$

another 1-term extrapolation which results in

$$\Delta_r H_m°(\text{MnOOH(cr), 298.15 K}) = \Delta_r H_m°(\text{MnOOH(cr), 298.15 K}) = -(65.5 \pm 2.3)\ \text{kJ} \cdot \text{mol}^{-1}$$

Another isocoulombic reaction can be formulated with bixbyite, Mn_2O_3(cr)

$$1/2\ Mn_2O_3(cr) + 1/2\ H_2O(l) \rightleftharpoons \text{MnOOH(cr)}$$

leading either, via $\Delta_r G_m°$(iso, T) = constant, to

$$\Delta_r G_m°(\text{iso, 298.15 K}) = (1.88 \pm 2.42)\ \text{kJ} \cdot \text{mol}^{-1}$$

$$\Delta_r H_m°\ (\text{MnOOH(cr), 298.15 K}) = -(60.3 \pm 3.2)\ \text{kJ} \cdot \text{mol}^{-1}$$

or, via $\log_{10}{}^{*}K_{s0}°$ (iso, T) = const, to

$$\Delta_r H_m°\ (\text{MnOOH(cr), 298.15 K}) = -(62.2 \pm 2.1)\ \text{kJ} \cdot \text{mol}^{-1}$$

As there is no clear preference to any of these 1-term extrapolations, this review calculated an unweighted average of the four values:

$$\textit{MnOOH(cr)} + 3\ H^+ \rightleftharpoons \textit{Mn}^{3+} + 2\ \textit{H}_2\textit{O(l)}$$

$$\Delta_r H_m°\ (298.15\ \text{K}) = -(64.0 \pm 5.3)\ \text{kJ} \cdot \text{mol}^{-1}$$

This value has been included in TDB 2020 as supplemental datum.

Mn_3O_4(cr), hausmannite

Brown & Ekberg (2016) report that Robie & Hemingway (1995) provide thermochemical data for the mixed manganese(II/III) phase hausmannite, Mn_3O_4(cr):

$\Delta_f G_m°(Mn_3O_4, cr, 298.15\ K) = -(1'282.5 \pm 1.4)\ kJ \cdot mol^{-1}$

$\Delta_f H_m°(Mn_3O_4, cr, 298.15\ K) = -(13'84.5 \pm 1.5)\ kJ \cdot mol^{-1}$

$S_m°(Mn_3O_4, cr, 298.15\ K) = (164.1 \pm 0.2)\ J \cdot K^{-1} \cdot mol^{-1}$

These values have been included in TDB 2020.

Using $\Delta_f G_m°(Mn_3O_4, cr, 298.15\ K)$, $\Delta_f H_m°(Mn_3O_4, cr, 298.15\ K)$ and $\Delta_f G_m°(Mn^{2+}, 298.15\ K)$, $\Delta_f H_m°(Mn^{2+}, 298.15\ K)$ (see Section 8.2) and the CODATA values $\Delta_f G_m°(H_2O, l, 298.15\ K) = -(237.140 \pm 0.041)\ kJ \cdot mol^{-1}$, $\Delta_f H_m°(H_2O, l, 298.15\ K) = -(285.83 \pm 0.04)\ kJ \cdot mol^{-1}$ (Grenthe et al. 1992), a "solubility product" can be calculated:

$1/3\ Mn_3O_4(cr) + 2\ H^+ + 1/3\ H_2g \rightleftharpoons Mn^{2+} + 4/3\ H_2O(l)$

$\log_{10}{}^*K_s°\ (298.15\ K) = 20.46 \pm 0.26$

$\Delta_r H_m°\ (298.15\ K) = -(140 \pm 1.6)\ kJ \cdot mol^{-1}$

Brown & Ekberg (2016) calculated $\log_{10}{}^*K_s°\ (298.15\ K) = -(6.6 \pm 0.3)$. The huge difference of 27 orders of magnitude of their value compared with the present calculation cannot be.

An alternative "solubility product" can be calculated from the same thermochemical data as

$Mn_3O_4(cr) + 8\ H^+ + 2\ e^- \rightleftharpoons 3\ Mn^{2+} + 4\ H_2O(l)$

$\log_{10}{}^*K_s°\ (298.15\ K) = 61.38 \pm 0.26$

$\Delta_r H_m°\ (298.15\ K) = -(421.1 \pm 1.6)\ kJ \cdot mol^{-1} = -(100.64 \pm 0.38)\ kcal \cdot mol^{-1}$

Nordstrom et al. (1990) give $\log_{10}{}^*K_s°(298.15\ K) = 61.03$ and $\Delta_r H_m°(298.15\ K) = -100.64\ kcal \cdot mol^{-1}$, having used in their calculations the same thermochemical data for Mn_3O_4(cr) and Mn^{2+} as selected here. While their $\Delta_r H_m°(298.15\ K)$ is identical to the one calculated here, the reason for the small difference of 0.35 log-units in $\log_{10}{}^*K_s°(298.15\ K)$ remains unclear.

13.11 Manganese(III) fluoride complexes

Ciavatta et al. (1981) studied the formation of Mn(III) fluoride complexes at 25 °C and in the ionic medium 3 M (H,Li)ClO_4 by measuring the redox potential of the couple Mn^{3+} – Mn^{2+} as a function of the concentration of HF and $HClO_4$. They interpreted their results in terms of

$Mn^{3+} + HF(aq) \rightleftharpoons MnF^{2+} + H^+$

$\log_{10}\beta_{01}$ (298.15 K) = 2.6 ± 0.2

$Mn^{3+} + 2\ HF(aq) \rightleftharpoons MnF_2^{+} + 2\ H^+$

$\log_{10}\beta_{02}$ (298.15 K) = 4.42 ± 0.15

$Mn^{3+} + 3\ HF(aq) \rightleftharpoons MnF_3(aq) + 3\ H^+$

$\log_{10}\beta_{03}$ (298.15 K) = 4.95 ± 0.25

$Mn^{3+} + HF(aq) + H_2O(l) \rightleftharpoons MnOHF^{+} + 2\ H^+$

$\log_{10}\beta_{11}$ (298.15 K) = 2.9 ± 0.2

These values have been extrapolated to zero ion strength via SIT, considering $\varepsilon(H^+, ClO_4^-)$ = (0.14 ± 0.02) kg · mol^{-1}, and the estimates $\varepsilon(Mn^{3+}, ClO_4^-)$ = (0.6 ± 0.1) kg · mol^{-1}, $\varepsilon(MnF^{2+}, ClO_4^-)$ = (0.4 ± 0.1) kg · mol^{-1}, $\varepsilon(MnF_2^{+}, ClO_4^-)$ = (0.2 ± 0.1) kg · mol^{-1}, $\varepsilon(MnOHF^{+}, ClO_4^-)$ = (0.2 ± 0.1) kg · mol^{-1}, and $\varepsilon(MnF_3(aq), (H,Li)ClO_4)$ = (0.0 ± 0.1) kg · mol^{-1}:

$\log_{10}\beta_{01}°$ (298.15 K) = 3.4 ± 0.5

$\log_{10}\beta_{02}°$ (298.15 K) = 5.5 ± 0.5

$\log_{10}\beta_{03}°$ (298.15 K) = 5.8 ± 0.6

$\log_{10}\beta_{11}°$ (298.15 K) = 4.1 ± 0.5

Using $\log_{10}K°$ (298.15 K) = 3.18 ± 0.02 for $H^+ + F^- = HF(aq)$ (Lemire et al. 2013) these values have been transformed into

$Mn^{3+} + F^- \rightleftharpoons MnF^{2+}$

$\log_{10}\beta_1°$ (298.15 K) = 6.6 ± 0.5

$Mn^{3+} + 2\ F^- \rightleftharpoons MnF_2^{+}$

$\log_{10}\beta_2°$ (298.15 K) = 11.9 ± 0.5

$Mn^{3+} + 3\ F^- \rightleftharpoons MnF_3(aq)$

$\log_{10}\beta_3°$ (298.15 K) = 15.3 ± 0.6

$Mn^{3+} + F^- + H_2O(l) \rightleftharpoons MnOHF^{+} + H^+$

$\log_{10}{}^*\beta_{11}°$ (298.15 K) = 7.3 ± 0.5

These values have been included in TDB 2020 as supplemental data.

They are classified as supplemental data because there is no independent confirmation of the results reported by Ciavatta et al. (1981), and the extrapolation from high ionic strength to zero, using estimated SIT interaction coefficients, introduces considerable uncertainty to the final values.

No temperature data are available for the above equilibria.

However, as the stepwise stability constants

$$log_{10}K_1° \ (MnF^{2+}, 298.15\ K) = 6.6 \pm 0.5$$

$$log_{10}K_2° \ (MnF_2^{+}, 298.15\ K) = 5.3 \pm 0.5$$

$$log_{10}K_3° \ (MnF_3(aq), 298.15\ K) = 3.5 \pm 0.6$$

are in the same order of magnitude as the values selected by this review for aluminium (see Section 5.5.1)

$$\log_{10}K_1° \ (AlF^{2+}, 298.15\ K) = 7.08 \pm 0.07$$

$$\log_{10}K_2° \ (AlF_2^{+}, 298.15\ K) = 5.65 \pm 0.08$$

$$\log_{10}K_3° \ (AlF_3(aq), 298.15\ K) = 4.05 \pm 0.11$$

this review considered the isocoulombic reactions

$$AlF^{2+} + Mn^{3+} \rightleftharpoons MnF^{2+} + Al^{3+}$$

$$AlF_2^{+} + Mn^{3+} \rightleftharpoons MnF_2^{+} + Al^{3+}$$

$$AlF_3(aq) + Mn^{3+} \rightleftharpoons MnF_3(aq) + Al^{3+}$$

and assumed that in the above isocoulombic reactions

$$\log_{10}K_n° \ (iso, T) = \log_{10}K_n° \ (iso, 298.15\ K) = const$$

a 1-term extrapolation which results in

$$\Delta_r H_m°(MnF^{2+}, 298.15\ K) = \Delta_r H_m°(AlF^{2+}, 298.15\ K) = (4.81 \pm 0.2)\ kJ \cdot mol^{-1}$$

$$\Delta_r H_m°(MnF_2^{+}, 298.15\ K) = \Delta_r H_m°(AlF_2^{+}, 298.15\ K) = (3.26 \pm 0.4)\ kJ \cdot mol^{-1}$$

$$\Delta_r H_m°(MnF_3(aq), 298.15\ K) = \Delta_r H_m°(AlF_3(aq), 298.15\ K) = (0.79 \pm 0.4)\ kJ \cdot mol^{-1}$$

Hence, the following estimated values, with increased uncertainties, have been included in TDB 2020 as supplemental data:

$$Mn^{3+} + F^- \rightleftharpoons MnF^{2+}$$

$$\Delta_r H_m°(298.15\ K) = (4.8 \pm 1.0)\ kJ \cdot mol^{-1}$$

$$Mn^{3+} + 2\ F^- \rightleftharpoons MnF_2^+$$

$$\Delta_r H_m°(298.15\ K) = (8.1 \pm 1.0)\ kJ \cdot mol^{-1}$$

$$Mn^{3+} + 3\ F^- \rightleftharpoons MnF_3(aq)$$

$$\Delta_r H_m°(298.15\ K) = (8.9 \pm 1.0)\ kJ \cdot mol^{-1}$$

No suitable isocoulombic reaction could be identified for $MnOHF^+$ which would allow an estimate.

13.12 Manganese(III) chloride complexes

Rosseinsky et al. (1974) studied the formation of $MnCl^{2+}$ by spectrophotometry at ionic strength 3.26 M $HClO_4$ and obtained

$$Mn^{3+} + Cl^- \rightleftharpoons MnCl^{2+}$$

$$\log_{10}\beta_1\ (3.26\ M\ HClO_4, 298.15\ K) = 1.12 \pm 0.03$$

As their value for the formation of $MnOH^{2+}$, studied by voltammetry and potentiometry in 5.6 M $HClO_4$, is in good agreement with results from other studies (see Section 9.10.1), this review accepts the results obtained by Rosseinsky et al. (1974) for $MnCl^{2+}$.

The value valid for 3.26 M $HClO_4$ has been extrapolated to zero ion strength via SIT, considering $\varepsilon(H^+, Cl^-) = (0.12 \pm 0.01)$ kg · mol^{-1}, and the estimates $\varepsilon(Mn^{3+}, ClO_4^-) = (0.6 \pm 0.1)$ kg · mol^{-1} and $\varepsilon(MnCl^{2+}, ClO_4^-) = (0.4 \pm 0.1)$ kg · mol^{-1}:

$$Mn^{3+} + Cl^- \rightleftharpoons MnCl^{2+}$$

$$log_{10}\beta_1° (298.15\ K) = 0.8 \pm 0.5$$

This value has been included in TDB 2020 as supplemental datum.

It is classified as supplemental datum because there is no independent confirmation of the results reported by Rosseinsky et al. (1974), and the extrapolation from high ionic strength to zero, using estimated SIT interaction coefficients, introduces considerable uncertainty to the final value.

No temperature data are available for $MnCl^{2+}$.

However, as the stability constant selected by this review (see Section 12.5.1.4.2) for $Fe^{III}Cl^{2+}$

$$\log_{10}\beta_1^\circ\ (FeCl^{2+}, 298.15\ K) = 1.52 \pm 0.10$$

is in the same order of magnitude as $MnCl^{2+}$ this review considered the isocoulombic reaction

$$FeCl^{2+} + Mn^{3+} \rightleftharpoons MnCl^{2+} + Fe^{3+}$$

and assumed for the isocoulombic reaction

$$\log_{10}K^\circ\ (iso, T) = \log_{10}K^\circ\ (iso, 298.15\ K) = const$$

a 1-term extrapolation which results in

$$\Delta_r H_m^\circ(MnCl^{2+}, 298.15\ K) = \Delta_r H_m^\circ(FeCl^{2+}, 298.15\ K) = (22.48 \pm 4.60)\ kJ \cdot mol^{-1}$$

Hence, the following estimated value, with increased uncertainties, has been included in TDB 2020 as supplemental datum:

$$Mn^{3+} + Cl^- \rightleftharpoons MnCl^{2+}$$

$$\Delta_r H_m^\circ(298.15\ K) = (22.5 \pm 10)\ kJ \cdot mol^{-1}$$

13.13 Manganese(IV)

Bard et al. (1985) report that Mn(IV) is found in the oxide MnO_2(cr), the sulphate $Mn(SO_4)_2$(s), the fluoride MnF_4(s) and in certain complex halides. However, only the oxide is stable in contact with water, and that is due mainly to its insolubility. In fact, the redox potential manganese(II/IV) has been determined in various experimental set-ups but always including MnO_2(cr).

MnO_2(cr), pyrolusite

Brown & Ekberg (2016) report that Robie & Hemingway (1995) provide thermochemical data for pyrolusite, MnO_2(cr):

$$\Delta_f G_m^\circ(MnO_2, cr, 298.15\ K) = -(465.0 \pm 0.7)\ kJ \cdot mol^{-1}$$

$$\Delta_f H_m^\circ(MnO_2, cr, 298.15\ K) = -(520.0 \pm 0.7)\ kJ \cdot mol^{-1}$$

$$S_m^\circ(MnO_2, cr, 298.15\ K) = (52.8 \pm 0.1)\ J \cdot K^{-1} \cdot mol^{-1}$$

These values have been included in TDB 2020.

Using $\Delta_f G_m°(MnO_2, cr, 298.15\ K)$, $\Delta_f H_m°(MnO_2, cr, 298.15\ K)$ and $\Delta_f G_m°(Mn^{2+}, 298.15\ K)$, $\Delta_f H_m°(Mn^{2+}, 298.15\ K)$ (see Section 8.2) and the CODATA values $\Delta_f G_m°(H_2O, l, 298.15\ K) = -(237.140 \pm 0.041)\ kJ \cdot mol^{-1}$, $\Delta_f H_m°(H_2O, l, 298.15\ K) = -(285.83 \pm 0.04)\ kJ \cdot mol^{-1}$ (Grenthe et al. 1992), a "solubility product" can be calculated:

$$MnO_2(cr) + 2\ H^+ \rightleftharpoons Mn^{2+} + H_2O(l) + 0.5\ O_2g$$

$$\log_{10}{}^*K_s° (298.15\ K) = 0.04 \pm 0.15$$

$$\Delta_r H_m° (298.15\ K) = (13.4 \pm 0.9)\ kJ \cdot mol^{-1}$$

Brown & Ekberg (2016) calculated $\log_{10}{}^*K_s° (298.15\ K) = 0.05 \pm 0.15$, using their own value $\Delta_f G_m°(H_2O, l, 298.15\ K) = -(237.17 \pm 0.04)\ kJ \cdot mol^{-1}$. An alternative "solubility product" can be calculated from the same thermochemical data as

$$MnO_2(cr) + 4\ H^+ + 2\ e^- \rightleftharpoons Mn^{2+} + 2\ H_2O(l)$$

$$\log_{10}{}^*K_s° (298.15\ K) = 41.59 \pm 0.15$$

$$\Delta_r H_m° (298.15\ K) = -(272.4 \pm 0.9)\ kJ \cdot mol^{-1} = -(65.11 \pm 0.21)\ kcal \cdot mol^{-1}$$

Nordstrom et al. (1990) give $\log_{10}{}^*K_s°(298.15\ K) = 41.38$ and $\Delta_r H_m°(298.15\ K) = -65.11\ kcal \cdot mol^{-1}$, having used in their calculations the same thermochemical data for $MnO_2(cr)$ and Mn^{2+} as selected here but $\Delta_f G_m°(H_2O, l, 298.15\ K) = -237.129\ kJ \cdot mol^{-1}$ from Wagman et al. (1982). Using the latter $\Delta_f G_m°(H_2O, l, 298.15\ K)$ this review calculated $\log_{10}{}^*K_s° (298.15\ K) = 41.58 \pm 0.15$. Hence, the reason for the small difference of 0.2 log-units in $\log_{10}{}^*K_s°(298.15\ K)$ remains unclear.

13.14 Selected manganese data

Tab. 13-1: Selected manganese data

Supplemental data are in italics.

Name	**Redox**	**$\Delta_f G_m°$** [kJ · mol^{-1}]	**$\Delta_f H_m°$** [kJ · mol^{-1}]	**$S_m°$** [J · K^{-1} · mol^{-1}]	**Species**
Mn(cr)	0	0.0	0.0	32.01 ± 0.08	Mn(cr)
Mn+2	II	-228.27 ± 0.58	-220.8 ± 0.5	-73.6 ± 1.0	Mn^{2+}
Manganosite	II	-362.90 ± 0.50	-385.22 ± 0.50	59.71 ± 0.40	MnO(cr)
Rhodochrosite	II	-818.13 ± 0.55	-891.91 ± 0.52	98.03 ± 0.10	$MnCO_3$(cr)
Mn+3	III	-83.0 ± 0.5	-113 ± 2		Mn^{3+}
Bixbyite	III	-882.1 ± 1.0	-959.0 ± 1.0	113.7 ± 0.2	Mn_2O_3(cr)
Hausmannite	II/III	-1'282.5 ± 1.4	-1'384.5 ± 1.5	164.1 ± 0.2	Mn_3O_4(cr)
Pyrolusite	IV	-465.0 ± 0.7	-520.0 ± 0.7	52.8 ± 0.1	MnO_2(cr)

Name	**Redox**	**$\log_{10}\beta°$**	**$\Delta_r H_m°$** [kJ · mol^{-1}]	**$\Delta_r C_{p,m}°$** [J · K^{-1} · mol^{-1}]	**T-range** [°C]	**Reaction**
MnOH+	II	-10.58 ± 0.04	57.3 ± 1.1	0	15 – 300	$Mn^{2+} + H_2O(l) \rightleftharpoons MnOH^+ + H^+$
Mn(OH)2(aq)	*II*	*-22.18 ± 0.20*	*117.4 ± 2.6*	*0*	*15 – 300*	*$Mn^{2+} + 2H_2O(l) \rightleftharpoons Mn(OH)_2(aq) + 2H^+$*
Mn(OH)3-	*II*	*-34.34 ± 0.45*	*171.9 ± 3.1*	*0*	*15 – 300*	*$Mn^{2+} + 3H_2O(l) \rightleftharpoons Mn(OH)_3^- + 3H^+$*
Mn(OH)4-2	*II*	*-48.28 ± 0.40*	*256.4 ± 5.2*	*0*	*15 – 300*	*$Mn^{2+} + 4H_2O(l) \rightleftharpoons Mn(OH)_4^{2-} + 4H^+$*
MnF+	II	1.35 ± 0.18	15.1 ± 1.6	-		$Mn^{2+} + F^- \rightleftharpoons MnF^+$
MnCl+	II	0.1 ± 0.5	11.5 ± 3.5	323 ± 40	20 – 300	$Mn^{2+} + Cl^- \rightleftharpoons MnCl^+$
MnCO3(aq)	II	4.60 ± 0.17	*16 ± 6*	-		$Mn^{2+} + CO_3^{2-} \rightleftharpoons MnCO_3(aq)$
MnHCO3+	II	1.27 ± 0.05	4.2 ± 1.4	231 ± 90	5 – 55	$Mn^{2+} + HCO_3^- \rightleftharpoons MnHCO_3^+$
MnSO4(aq)	II	2.23 ± 0.05	12.7 ± 1.1	180 ± 23	0 – 170	$Mn^{2+} + SO_4^{2-} \rightleftharpoons MnSO_4(aq)$
Mn+3	II/III	-25.42 ± 0.12	107.8 ± 2.1	-		$Mn^{2+} \rightleftharpoons Mn^{3+} + e^-$
MnOH+2	III	1.2 ± 0.4	22.9 ± 5.5	0	1 – 35	$Mn^{3+} + H_2O(l) \rightleftharpoons MnOH^{2+} + H^+$
Mn(OH)2+	*III*	*1.5 ± 0.5*	-	-		*$Mn^{3+} + 2H_2O(l) \rightleftharpoons Mn(OH)_2^+ + 2H^+$*
MnF+2	*III*	*6.6 ± 0.5*	*4.8 ± 1.0*	-		*$Mn^{3+} + F^- \rightleftharpoons MnF^{2+}$*
MnF2+	*III*	*11.9 ± 0.5*	*8.1 ± 1.0*	-		*$Mn^{3+} + 2\,F^- \rightleftharpoons MnF_2^+$*
MnF3(aq)	*III*	*15.3 ± 0.6*	*8.9 ± 1.0*	-		*$Mn^{3+} + 3\,F^- \rightleftharpoons MnF_3(aq)$*
MnOHF+	*III*	*7.3 ± 0.5*	-	-		*$Mn^{3+} + F^- + H_2O(l) \rightleftharpoons MnOHF^+ + H^+$*
MnCl+2	*III*	*0.8 ± 0.5*	*22.5 ± 10*	-		*$Mn^{3+} + Cl^- \rightleftharpoons MnCl^{2+}$*

Tab. 13-1: Cont.

Name	**Redox**	**$\log_{10}K_{s,0}°$**	**$\Delta_r H_m°$** [kJ · mol^{-1}]	$\Delta_r C_{p,m}°$ [J · K^{-1} · mol^{-1}]	**T-range** [°C]	**Reaction**
Mn(cr)/II	0/II	39.99 ± 0.09	-220.8 ± 0.5			$Mn(cr) \rightleftharpoons Mn^{2+} + 2\ e^-$
Mn(cr)/III	0/III	14.54 ± 0.09	-113 ± 2			$Mn(cr) \rightleftharpoons Mn^{3+} + 3\ e^-$
Manganosite	II	17.93 ± 0.12	-121.4 ± 0.7			$MnO(cr) + 2\ H^+ \rightleftharpoons Mn^{2+} + H_2O(l)$
Pyrochroite	II	15.19 ± 0.10	*-123 ± 17*			$Mn(OH)_2(cr) + 2\ H^+ \rightleftharpoons Mn^{2+} + 2\ H_2O(l)$
Rhodochrosite	II	-10.85 ± 0.16	-4.1 ± 0.8			$MnCO_3(s) \rightleftharpoons Mn^{2+} + CO_3^{2}$
Bixbyite	III	-0.41 ± 0.30	-62.2 ± 2.1			$1/2\ Mn_2O_3(cr) + 3\ H^+ \rightleftharpoons Mn^{3+} + 3/2\ H_2O(l)$
Manganite	III	-0.08 ± 0.30	*-64.0 ± 5.3*			$MnOOH(cr) + 3\ H^+ \rightleftharpoons Mn^{3+} + 2\ H_2O(l)$
Hausmannite	II/III	61.38 ± 0.26	-421.1 ± 1.6			$Mn_3O_4(cr) + 8H^+ + 2e^- \rightleftharpoons 3\ Mn^{2+} + 4H_2O(l)$
Pyrolusite	IV	41.59 ± 0.15	-272.4 ± 0.9			$MnO_2(cr) + 4\ H^+ + 2\ e^- \rightleftharpoons Mn^{2+} + 2\ H_2O(l)$

Tab. 13-2: Selected SIT ion interaction coefficients $\varepsilon_{j,k}$ [kg · mol^{-1}] for manganese species

Data in normal face are derived or estimated in this review. Data estimated according to charge correlations and taken from Tab. 1-7 are shaded. Supplemental data are in italics.

j k → ↓	**Cl^-** $\varepsilon_{j,k}$ [kg · mol^{-1}]	**ClO_4^-** $\varepsilon_{j,k}$ [kg · mol^{-1}]	**Na^+** $\varepsilon_{j,k}$ [kg · mol^{-1}]	**$Na^+ + Cl^-$** $\varepsilon_{j,k}$ [kg · mol^{-1}]	**$Na^+ + ClO_4^-$** $\varepsilon_{j,k}$ [kg · mol^{-1}]
Mn+2	(0.38 ± 0.02) [a]	0.38 ± 0.02	0	0	0
MnOH+	0.2 ± 0.1	0.2 ± 0.1	0	0	0
Mn(OH)2(aq)	*0*	*0*	*0*	*0.0 ± 0.1*	*0.0 ± 0.1*
Mn(OH)3-	*0*	*0*	*-0.05 ± 0.10*	*0*	*0*
Mn(OH)4-2	*0*	*0*	*-0.10 ± 0.10*	*0*	*0*
MnF+	(0.23 ± 0.09) [a]	0.23 ± 0.09	0	0	0
MnCl+	(0.40 ± 0.03) [a]	0.40 ± 0.03	0	0	0
MnCO3(aq)	0	0	0	0.0 ± 0.1	0.0 ± 0.1
MnHCO3+	0.2 ± 0.1	0.2 ± 0.1	0	0	0
MnSO4(aq)	0	0	0	0.0 ± 0.1	0.0 ± 0.1
Mn+3	0.6 ± 0.1	0.6 ± 0.1	0	0	0
MnOH+2	(0.40 ± 0.13) [a]	0.40 ± 0.13	0	0	0
Mn(OH)2+	*0.2 ± 0.1*	*0.2 ± 0.1*	*0*	*0*	*0*
MnF+2	*0.4 ± 0.1*	*0.4 ± 0.1*	*0*	*0*	*0*
MnF2+	*0.2 ± 0.1*	*0.2 ± 0.1*	*0*	*0*	*0*
MnF3(aq)	*0*	*0*	*0*	*0.0 ± 0.1*	*0.0 ± 0.1*
MnOHF+	*0.2 ± 0.1*	*0.2 ± 0.1*	*0*	*0*	*0*
MnCl+2	*0.4 ± 0.1*	*0.4 ± 0.1*	*0*	*0*	*0*

[a] Assumed to be equal to the corresponding ion interaction coefficient with ClO_4^-, see Section 13.1 for explanation.

13.15 References

Ashurst, K.G. (1976): The thermodynamics of the formation of chlorocomplexes of iron(III), cobalt(III), iron(II), manganese(II) and copper(II) in perchlorate medium. Nat. Inst. Metallurgy, S. Africa, Rept. 1820 (as cited by Gammons & Seward 1996).

Baes, C.F. & Mesmer, R.E. (1976): The Hydrolysis of cations. Wiley, New York, 490 pp.

Bard, A.J., Parsons, R. & Jordan, J. (1985): Standard Potentials in aqueous Solution. Marcel Dekker, Inc., New York, 834 pp.

Biedermann, G. & Palombari, R. (1978): On the hydrolysis of the manganese(III) ion. Acta Chemica Scandinavica A, 32, 381-390.

Bixler, J.W. & Larson, T.M. (1974): Ion association studies using a chloride ion selective electrode. J. Inorg. Nucl. Chem., 36, 224-226.

Bond, A.M. (1971): Correlation of heterogeneous charge-transfer rate constants and homogeneous rate constants for removal of coordinated water in the ac and dc polarographic study of some irreversibly reduced complex ions in aqueous solution. Journal of Physical Chemistry, 75, 2640-2649.

Bond, A.M. & Hefter, G. (1972): A study of the weak fluoride complexes of the divalent first row transition metal ions with a fluoride ion-selective electrode. J. Inorg. Nucl. Chem., 34, 603-607.

Bricker, O. (1965): Some stability relations in the system $Mn\text{-}O_2\text{-}H_2O$ at 25 °C and one atmosphere total pressure. American Mineralogist, 50, 1296-1354.

Brown, P.L. & Ekberg, C. (2016): Hydrolysis of Metal Ions. Wiley-VCH Verlag GmbH & Co. KGaA, Weinheim, Germany, 917 pp.

Carpenter, R. (1983): Quantitative electron spin resonance (ESR) determinations of forms and total amounts of Mn in aqueous environmental samples. Geochim. Cosmochim. Acta, 47, 875-885.

Ciavatta, L. & Grimaldi, M. (1965): On the complex formation between manganese (II) and fluoride ions. J. Inorg. Nucl. Chem., 27, 2019-2025.

Ciavatta, L., De Capua, R. & Palombari, R. (1981): On the formation of Mn(III) fluoride complexes in aqueous 3 M $(Li^+, H^+)ClO_4^-$. J. Inorg. Nucl. Chem., 43, 1305-1309.

Diebler, H. & Sutin, N. (1964): The kinetics of some oxidation-reduction reactions involving manganese(III). Journal of Physical Chemistry, 68, 174-180.

Gammons, C.H. & Seward, T.M. (1996): Stability of manganese(II) chloride complexes from 25 to 300 °C. Geochim. Cosmochim. Acta, 60, 4295-4311.

Gamsjäger, H., Bugajski, J., Gajda, T., Lemire, R.J. & Preis, W. (2005): Chemical Thermodynamics of Nickel. Chemical Thermodynamics, Vol. 6. Elsevier, Amsterdam, 617 pp.

Gamsjäger, H., Kraft, W. & Schindler, P. (1970): Zur Thermodynamik der Metallcarbonate 4. Potentiometrische Untersuchungen am System Mn^{2+} – CO_3 – H_2O. Helvetica Chimica Acta, 53, 290-299.

Garrels, R.M., Thompson, M.E. & Siever, R. (1960): Stability of some carbonates at 25 °C and one atmosphere total pressure. American Journal of Science, 258, 402-418.

Goldberg, R.N. (1979): Evaluated activity and osmotic coefficients for aqueous solutions: Bi-univalent compounds of lead, copper, manganese, and uranium. Journal of Physical and Chemical Reference Data, 8, 1005-1050.

Goncharik, V.P., Tikhonova, L.P. & Yatsimirskii, K.B. (1973): State of manganese(III) in solutions of perchloric and sulfuric acids. Russian Journal of Inorganic Chemistry, 18, 658-662.

Grenthe, I., Fuger, J., Konings, R.J.M., Lemire, R.J., Muller, A.B., Nguyen-Trung, C. & Wanner, H. (1992): Chemical Thermodynamics of Uranium. Chemical Thermodynamics, Vol. 1. North-Holland, Amsterdam, 715 pp.

Grauer, R. (1999): Solubility Products of M(II) – Carbonates. PSI Bericht Nr. 99-04 (edited and translated by U. Berner), Paul Scherrer Institut, Villigen PSI, Switzerland, 24 pp.

Hutchinson, M.H. & Higginson, C.E. (1973): Stability constants for association between bivalent cations and some univalent anions. Journal of the Chemical Society, Dalton Transactions, 12, 1247-1253.

Kul'vinova, L.A., Blokhin, V.V. & Mironov, V.E. (1976): Thermodynamic properties of certain transition metal fluoride complexes in aqueous salt solutions. Russian Journal of Physical Chemistry, 50, 773-774 (translated from Zhurnal Fizicheskoi Khimii, 50, 1287-1288).

Lemire, R.J., Berner, U., Musikas, C., Palmer, D.A., Taylor, P. & Tochiyama, O. (2013): Chemical Thermodynamics of Iron, Part 1. Chemical Thermodynamics, Vol. 13a. OECD Publications, Paris, France, 1082 pp.

Lesht, D. & Bauman, J.E., Jr. (1978): Thermodynamics of the manganese(II) bicarbonate system. Inorganic Chemistry, 17, 3332-3334.

Libuś, Z. & Tiałowska, H. (1975): Stability and nature of complexes of the type MCl^+ in aqueous solution (M = Mn, Co, Ni and Zn). Journal of Solution Chemistry, 4, 1011-1022.

McCain, D.C. & Myers, R.J. (1968): Electron paramagnetic resonance studies of complex ion formation between Mn^{2+} and F^-, Cl^-, Br^-, I^- or SO_4^{2-}. Journal of Physical Chemistry, 72, 4115-4122.

Masterton, W.L. & Berka, L.H. (1966): Evaluation of ion-pair dissociation constants from osmotic coefficients. Journal of Physical Chemistry, 70, 1924-1929.

Morgan, J.J. (1967): Chemical equilibria and kinetic properties oh manganese in natural waters. In: Faust, S.D. & Hunter, J.V. (eds.): Principles and Applications of Water Chemistry, Wiley, New York, p. 561-624.

Morgan, J.J. (2005): Kinetics of reaction between O_2 and Mn(II) species in aqueous solutions. Geochimica et Cosmochimica Acta, 69, 35-48.

Morris, D.F.C. & Short, E.L. (1961): Manganese(II) chloride complexes. Part I. Stability constants. Journal of the Chemical Society, 5148-5153.

Nair, V.S.K. & Nancollas, G.H. (1958): Thermodynamics of ion association. Part VI. Some transition-metal sulphates. J. Chem. Soc., 3706-3710.

Néher-Neumann, E. (1994): Studies on metal carbonate equilibria 26. The hydrogen carbonate complex of manganese(II) in acid solutions and a 3 M (Na)ClO_4 ionic medium at 25 °C. Determination of the solubility product of $MnCO_3$(s). Acta Chemica Scandinavica, 48, 393-398.

Nordstrom, D.K., Plummer, L.N., Langmuir, D., Busenberg, E., May, H.M., Jones, B.F. & Parkhurst, D.L. (1990): Revised Chemical Equilibrium Data for Major Water-Mineral Reactions and Their Limitations. In: Melchior, D.C., and Bassett, R.L. (eds.): Chemical Modeling of Aqueous Systems II. Washington, D.C., American Chemical Society, ACS Symposium Series 416, p. 398-413.

Palmer, D.A. & van Eldik, R. (1983): The chemistry of metal carbonato and carbon dioxide complexes. Chemical Reviews, 83, 651-731.

Parc, S., Nahon, D. Tardy, Y. & Vieillard, P. (1989): Estimated solubility products and fields of stability for cryptomelane, nsutite, birnessite and lithiophorite based on natural lateritic weathering sequences. American Mineralogist, 74, 466-475.

Pearson, F.J., Jr. & Berner, U. (1991): Nagra Thermochemical Data Base I. Core Data. Nagra Technical Report NTB 91-17.

Pearson, F.J., Jr., Berner, U. & Hummel W. (1992): Nagra Thermochemical Data Base II. Supplemental Data 05/92. Nagra Technical Report NTB 91-18.

Perrin, D.D. (1962): The hydrolysis of manganese(II) ion. J. Chem. Soc. 2197-2200.

Reiterer, F. (1980): Löslichkeitskonstanten und Freie Bildungsenthalpien neutraler Übergangsmetallcarbonate. Thesis, Montanuniversität Leoben (as cited by Grauer 1999).

Robie, R.A., Haselton, H.T., Jr. & Hemingway. B.S. (1984): Heat capacities and entropies of rhodochrosite ($MnCO_3$) and siderite ($FeCO_3$) between 5 and 600 K. American Mineralogist, 69, 349-357.

Robie, R.A. & Hemingway, B.S. (1995): Thermodynamic Properties of Minerals and Related Substances at 298.15 K and 1 Bar (10^5 Pascals) Pressure and at Higher Temperatures. United States Geological Survey Bulletin, 2131, 470 pp.

Rosseinsky, D.R., Nicol, M.J., Kite, K. & Hill, R.J. (1974): Manganese(III) and its hydroxo- and chloro-complexes in aqueous perchloric acid: comparison with similar transition-metal(III) complexes. Transactions of the Faraday Society, 70, 2232-2238.

Solomon, L.R., Bond, A.M., Bixler, J.W., Hallenbeck, D.R. & Logsdon, K.M. (1983): Stability of monofluoride complexes of the Irving-Williams series acceptors in methanol. Inorganic Chemistry, 22 1644-1648.

Suleimenov, O.M. & Seward, T.M. (2000): Spectrophotometric measurements of metal complex formation at high temperatures: the stability of Mn(II) chloride species. Chemical Geology, 167, 177-192.

Wagman, D.D., Evans, W.H., Parker, V.B., Schumm, R.H., Halow, I., Bailey, S.M., Churney, K.L. & Nuttall, R.L. (1982): The NBS tables of chemical thermodynamic properties: Selected values for inorganic and C1 and C2 organic substances in SI units. Journal of Physical and Chemical Reference Data, 11, Supplement No. 2, 1-392.

Wells, C.F. & Davies, G. (1967): A spectroscopic investigation of the aquomanganese(III) ion in perchlorate media. Journal of the Chemical Society A, 1858-1861.

Wheat, C.G. & Carpenter, R. (1988): $MnCl^+$ and $MnSO_4$ association constants to 170 °C. Journal of Solution Chemistry, 17, 467-480.

Zirino, A, & Yamamoto, S. (1972): A pH-dependent model for the chemical speciation of copper, zinc, cadmium, and lead in seawater. Limnol. Oceanogr., 17, 661-671.

14 Mercury

14.1 Introduction

Metallic mercury and many mercury compounds and complexes are toxic and thus, mercury is an environmentally significant heavy metal. In addition, a long-lived radioactive isotope, Hg-194 with 440 ± 80 years half-life, is produced in spallation induced neutron sources (e.g., SINQ at PSI) and contributes in dose-relevant quantities to the inventory of radioactive waste coming from research facilities like PSI. The latter fact triggered the inclusion of mercury into the PSI Chemical Thermodynamic Database 2020 (TDB 2020), besides its relevance as a chemically toxic substance.

The thermodynamic data included into TDB 2020 have been taken from

- CODATA key values (Cox et al. 1989)
- an IUPAC review of solubility data in the Hg(I) chloride – water system (Marcus 1980)
- a review of the solubility of mercury and some sparingly soluble mercury salts in water and aqueous electrolyte systems (Clever et al. 1985)
- an IUPAC review of the Hg^{2+} – Cl^-, OH^-, CO_3^{2-}, SO_4^{2-} and PO_4^{3-} aqueous systems (Powell et al. 2005)
- the recent review of the hydrolysis of metal ions (Brown & Ekberg 2016)
- and own reviews of experimental data concerning the HgS(s) – H_2S – water system

The selected thermodynamic data for mercury compounds and complexes are presented in Tab. 14-1.

IUPAC, as well as NEA (see, e.g., Grenthe et al. 1992) used the specific ion interaction theory (SIT) for making ionic strength corrections to the experimental data, an approach which is also adopted for TDB 2020 (as has been for all its predecessors). Powell et al. (2005) only evaluated experiments in perchlorate media and explicitly considered the formation of mercury chloride complexes. Therefore, ion interaction coefficients ε for cationic mercury species with Cl^- are missing. They can be approximated by the corresponding interaction coefficients with ClO_4^-. Thus, e.g., $\varepsilon(HgOH^+, Cl^-) \approx \varepsilon(HgOH^+, ClO_4^-) = (0.06 \pm 0.05)$ kg · mol^{-1}.

In some cases, the ion interaction coefficients of mercury species were not available. We approximated these with the estimation method described in Section 1.5.3, which draws on a statistical analysis of published SIT ion interaction coefficients, and which allows the estimation of missing coefficients for the interaction of cations with Cl^- and ClO_4^-, and for the interaction of anions with Na^+, from the charge of the cations or anions of interest.

The selected SIT ion interaction coefficients for mercury species are presented in Tab. 14-2.

14.2 Mercury(0)

14.2.1 Elemental mercury

Elemental mercury is liquid under environmental conditions (melting point: -38.83 °C, boiling point: 356.7 °C).

Mercury is not the only element which is liquid in the temperature range 10 – 40 °C, other elements are bromine (melting point: -7.2 °C, boiling point: 58.8 °C), gallium (melting point: 29.77 °C), rubidium, caesium, and francium (melting points: 39.3, 28.5 and 27 °C, respectively). However, bromine is thermodynamically stable in environmental aquatic systems as the Br^- anion, gallium as Ga(III), like Al(III), and the alkali metals as the Rb^+, Cs^+ and Fr^+ cations, and thus, their elemental states are formal reference states only with respect to thermodynamic equilibria in aquatic systems.

By contrast, elemental mercury has a large stability field in the Eh – pH range of water (e.g., Brookins 1988) and hence, liquid mercury, Hg(l), is an environmentally important substance. Likewise, the gas phase Hgg is included in the data base for estimates of mercury concentrations in soil vapour and air.

The selected values for Hg(l) and Hgg are taken from CODATA (Cox et al. 1989):

$$S_m°(\text{Hg, l, 298.15 K}) = (75.90 \pm 0.12)\ \text{J} \cdot \text{K}^{-1} \cdot \text{mol}^{-1}$$

$$\Delta_f G_m°(\text{Hg, g, 298.15 K}) = (31.842 \pm 0.054)\ \text{kJ} \cdot \text{mol}^{-1}$$

$$\Delta_f H_m°(\text{Hg, g, 298.15 K}) = (61.380 \pm 0.040)\ \text{kJ} \cdot \text{mol}^{-1}$$

$$S_m°(\text{Hg, g, 298.15 K}) = (174.971 \pm 0.005)\ \text{J} \cdot \text{K}^{-1} \cdot \text{mol}^{-1}$$

$$C_{p,m}°(\text{Hg, g, 298.15 K}) = (20.786 \pm 0.001)\ \text{J} \cdot \text{K}^{-1} \cdot \text{mol}^{-1}$$

14.2.2 Mercury(0) solubility

Mercury dissolved in air-free water is monoatomic and unionized with the zero-valent mercury atom in the spherically symmetric $^1S_0$ ground state (Clever et al. 1985).

The solubility of metallic mercury in water has been measured by a variety of experimental techniques and the published results have been critically reviewed by Clever et al. (1985). Their recommended value of the solubility of mercury in water is $(3.03 \pm 0.12) \cdot 10^{-7}$ mol · kg^{-1} at 298.15 K. This value is the average of five published experimental values measured at 25 °C and an additional value interpolated from two measured data at 20 °C and 30 °C. Recalculations by the present author using the values given in Tab. 3 of Clever et al. (1985) confirmed the above numbers and showed that the uncertainty refers to 1σ. For the equilibrium

$$\text{Hg(l)} \rightleftharpoons \text{Hg(aq)}$$

this transforms into

$$\log_{10}K°(298.15\ \text{K}) = -6.52 \pm 0.03$$

Clever et al. (1985) have fitted 36 solubility values, marked "*" in their Tab. 3, by a three-parameter function to obtain smoothed values of Hg(aq) solubility as a function of temperature. The present author used the same solubility values in the temperature range 0 – 90 °C for a linear regression with the integrated Van't Hoff equation

$$\log_{10}K°(T) = \log_{10}K°(T°) + \Delta_r H_m°(T°) / (R \cdot \ln(10)) \cdot (1 / T° - 1 / T)$$

with T° = 298.15 K and R = 8.31451 J · K^{-1} · mol^{-1}. The results (Fig. 14-1) are:

$$\log_{10}K°(298.15\ \text{K}) = -6.53 \pm 0.03$$

$$\Delta_r H_m°(298.15\ \text{K}) = (23.0 \pm 2.2)\ \text{kJ} \cdot \text{mol}^{-1}$$

The $\log_{10}K°$ value derived from a larger data set in the temperature range 0 – 90 °C (Fig. 14-1) agrees very well with the recommended value of Clever et al. (1985) derived from six data close to 25 °C. Hence, the consistent $\log_{10}K°$ and $\Delta_r H_m°$ values resulting from the linear regression with the integrated van't Hoff equation are selected in this review (Tab. 14-1).

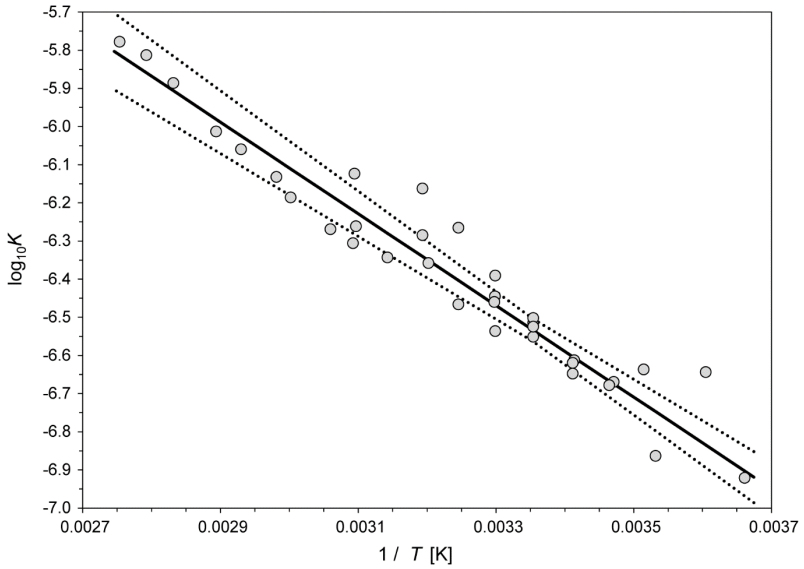

Fig. 14-1: Temperature dependence of Hg(l) ⇌ Hg(aq)

Data (circles) taken from Clever et al. (1985), values marked "*" in their Tab. 3. Solid line: linear regression with the integrated van't Hoff equation. Dotted lines: 95% uncertainty range extrapolated from 25 °C to higher and lower temperatures.

The specific ion interaction coefficients for Hg(aq) are estimated to be zero (Section 1.5.3):

$$\varepsilon(\text{Hg(aq)}, \text{NaCl}) = \varepsilon(\text{Hg(aq)}, \text{NaClO}_4) = (0.0 \pm 0.1)\ \text{kg} \cdot \text{mol}^{-1}$$

14.3 Mercury(I)

14.3.1 Mercury(I) aqua ion

Mercury(I) exists in aqueous solutions as a di-ion, Hg_2^{2+}, composed of two singly charged ions. The selected thermodynamic values for Hg_2^{2+} are taken from CODATA (Cox et al. 1989):

$$\Delta_f G_m^\circ(Hg_2^{2+}, 298.15\ \text{K}) = (153.567 \pm 0.56)\ \text{kJ} \cdot \text{mol}^{-1}$$

$$\Delta_f H_m^\circ(Hg_2^{2+}, 298.15\ \text{K}) = (166.870 \pm 0.50)\ \text{kJ} \cdot \text{mol}^{-1}$$

$$S_m^\circ(Hg_2^{2+}, 298.15\ \text{K}) = (65.740 \pm 0.80)\ \text{J} \cdot \text{K}^{-1} \cdot \text{mol}^{-1}$$

The specific ion interaction coefficient selected by NEA (Grenthe et al. 1992, Lemire et al. 2013), is also adopted for TDB 2020:

$$\varepsilon(Hg_2^{2+}, ClO_4^-) = (0.09 \pm 0.02)\ \text{kg} \cdot \text{mol}^{-1}$$

Since this report explicitly considers the formation of mercury chloride complexation, although no mercury (I) chloride complexes are formed in measurable quantities (see Section 14.3.3), $\varepsilon(Hg_2^{2+}, Cl^-)$ must be approximated by using the corresponding ion interaction coefficient with perchlorate:

$$\varepsilon(Hg_2^{2+}, Cl^-) \approx \varepsilon(Hg_2^{2+}, ClO_4^-) = (0.09 \pm 0.02)\ \text{kg} \cdot \text{mol}^{-1}$$

14.3.2 Mercury(I) hydroxide complexes

The hydrolysis of mercury(I) is discussed by Brown & Ekberg (2016). For the equilibrium:

$$Hg_2^{2+} + H_2O(l) \rightleftharpoons Hg_2OH^+ + H^+$$

they mention three sources of experimental data (with quoted remarks): Forsling et al. (1959) "$\log^*\beta_1 = -5.0 \pm 0.3$ from measurements conducted in 0.5 mol l^{-1} $NaClO_4$ and at 25 °C", Hietanen & Högfeldt (1976) "obtained $\log^*\beta_1 = -4.88 \pm 0.07$ from a study conducted at the same temperature but a higher ionic strength (3.0 mol l^{-1} $NaClO_4$)", and Newberry (1936) "found that the constant varied as a function of the concentration of mercurous perchlorate used … at the lowest concentration used (ionic strength = 0.019 mol l^{-1}; temperature not given), the stability

constant obtained was $\log^{*}\beta_1 = -4.59$". Brown & Ekberg (2016) further state "these data have been utilised with the extended specific ion interaction theory to determine the stability constant at zero ionic strength". The results are given as

$$\log_{10}{}^{*}\beta_1^{\circ} = -4.45 \pm 0.10,\ \Delta\varepsilon_1 = 0.21 \pm 0.10\ \text{kg} \cdot \text{mol}^{-1},\ \Delta\varepsilon_2 = -(0.48 \pm 0.10)\ \text{kg} \cdot \text{mol}^{-1}$$

without any further discussion, without providing a table of experimental values and without showing an SIT plot, in contrast to their discussion of mercury(II) hydrolysis data.

In modelling applications, results obtained by the "extended SIT" with $\Delta\varepsilon_1$ and $\Delta\varepsilon_2$ cannot be mixed with the "linear SIT" with only one $\Delta\varepsilon$ as used in TDB 2020. Furthermore, fitting three data points by a three-parameter function seems a bit odd and thus, the present author scrutinized the above-mentioned papers and re-fitted the data (Fig. 14-2).

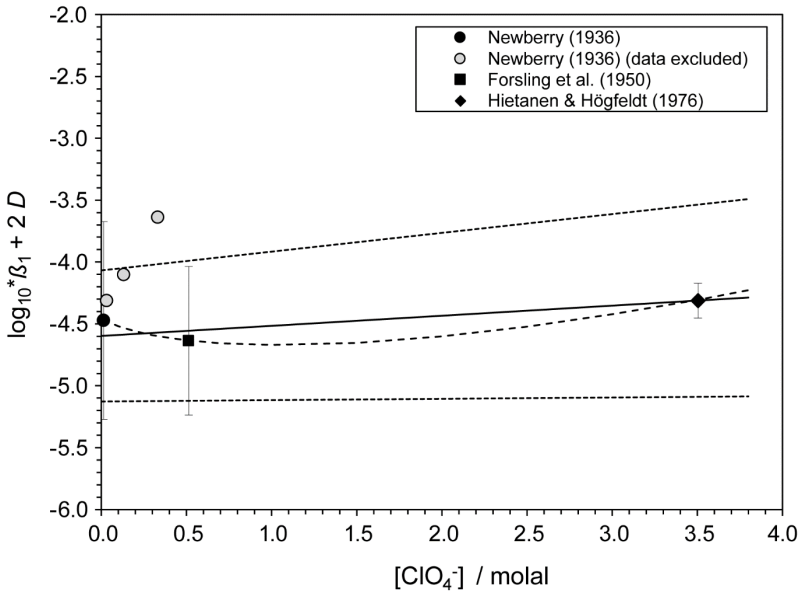

Fig. 14-2: Dependence of $\log_{10}{}^{*}\beta_1$ of Hg_2OH^{+} on ionic strength in perchlorate media

The solid line is obtained using the derived SIT interaction coefficient and stability constant at zero ionic strength. The dotted lines represent the 95% uncertainty range extrapolated from zero ionic strength to higher perchlorate concentrations. The dashed curve represents the three-parameter fit of Brown & Ekberg (2016).

The data selection of Brown & Ekberg (2016) is reasonable. The study of Hietanen & Högfeldt (1976) is the most reliable one, while Forsling et al. (1959) provide "an estimate" with a larger uncertainty. In both cases the reported 1σ uncertainty has been increased to 2σ for the present SIT regression analysis. Hietanen & Högfeldt (1976) found that above 0.01 M of Hg(I) the species $(Hg_2)_2OH^{3+}$ predominates. Newberry (1936) did measurements in the concentration range 0.0065 – 0.162 M of Hg(I) but did not consider $(Hg_2)_2OH^{3+}$ in the data analysis. Hence, only the stability constant derived from experimental data measured at the lowest Hg(I) concentration (0.0065 M) is included in the SIT analysis, but with a large, estimated uncertainty of ± 0.8.

The new results are

$$\log_{10}{}^{*}\beta_1^\circ = -4.6 \pm 0.5$$

$$\Delta\varepsilon = -(0.08 \pm 0.16)\ \text{kg} \cdot \text{mol}^{-1}$$

Using $\varepsilon(Hg_2^{2+}, ClO_4^-) = 0.09 \pm 0.02\ \text{kg} \cdot \text{mol}^{-1}$ and $\varepsilon(H^+, ClO_4^-) = 0.14 \pm 0.02\ \text{kg} \cdot \text{mol}^{-1}$ a new value

$$\varepsilon(Hg_2OH^+, ClO_4^-) = -(0.13 \pm 0.16)\ \text{kg} \cdot \text{mol}^{-1}$$

is derived. Since this report explicitly considers the formation of mercury chloride complexation, although no mercury (I) chloride complexes are formed in measurable quantities (see Section 14.3.3), $\varepsilon(Hg_2OH^+, Cl^-)$ must be approximated by using the corresponding ion interaction coefficient with perchlorate:

$$\varepsilon(Hg_2OH^+, Cl^-) \approx \varepsilon(Hg_2OH^+, ClO_4^-) = -(0.13 \pm 0.16)\ \text{kg} \cdot \text{mol}^{-1}$$

14.3.3 Mercury(I) chloride compounds and complexes

The compound $Hg_2Cl_2(s)$ is sparingly soluble. It is known as "calomel", which is also found as a rare mineral in nature.

Numerous solubility, e.m.f. and standard electrode potential measurements have been published, and these data have been compiled and evaluated by Marcus (1980) within the scope of the "IUPAC Solubility Data Project". Marcus (1980) states that "mercury (I) chloride dissolves in water, forming the following species: $Hg(OH)_2(aq)$, $HgCl_2(aq)$, $HgOH^+$, $HgCl^+$, Hg_2^{2+} and Hg_2OH^+, in addition to H^+ and Cl^-. In excess chloride solutions it dissolves to give, mainly, $HgCl_3^-$ and $HgCl_4^{2-}$." Note that no mercury (I) chloride complexes are formed in measurable quantities.

Marcus (1980) reports the total aqueous solubility of mercury (I) chloride at 25 °C as

$$c_{Hg} = (8.4 \pm 1.0) \times 10^{-6}\ \text{mol} \cdot \text{dm}^{-3}$$

For the solubility product

$$Hg_2Cl_2(s) \rightleftharpoons Hg_2^{2+} + 2\ Cl^-$$

Marcus (1980) gives for the range 5 – 45 °C the temperature function

$$\log_{10}K^\circ(298.15\ \text{K}) = -(17.844 \pm 0.05) + (0.0622 \pm 0.0002)\Delta T - (3.0 \pm 0.2) \times 10^{-4}\ (\Delta T)^2$$

where ΔT = T/K 298.15. The first term on the right-hand side represents the value at 25 °C. The selected thermodynamic values of Marcus (1980) for the solubility product are:

$$\Delta_r G_m°(298.15\ K) = (101.86 \pm 0.10)\ kJ \cdot mol^{-1}$$

$$\Delta_r H_m°(298.15\ K) = (98.08 \pm 0.18)\ kJ \cdot mol^{-1}$$

$$\Delta_r S_m°(298.15\ K) = -(12.7 \pm 0.9)\ J \cdot K^{-1} \cdot mol^{-1}$$

Note that the CODATA values $\Delta_f G_m°$, $\Delta_f H_m°$ and $S_m°$ given for $Hg_2Cl_2(s)$, Hg_2^{2+} (Tab. 14-1) and Cl^- (Cox et al. 1989) lead to numerically identical values for $\Delta_r G_m°$, $\Delta_r H_m°$ and $\Delta_r S_m°$ as given by Marcus (1980). The derivation of CODATA values is not traceable to any experimental data due to the complete lack of documentation. However, the mentioned numerical identity suggests that the CODATA team used the data compiled and evaluated by Marcus (1980) in their overall (and generally opaque) data optimisation procedure.

14.4 Mercury(II)

14.4.1 Mercury(II) aqua ion

Mercury(II) exists as the Hg^{2+} cation in aqueous solutions. The selected thermodynamic values for Hg^{2+} are taken from CODATA (Cox et al. 1989):

$$\Delta_f G_m°(Hg^{2+}, 298.15\ K) = (164.667 \pm 0.31)\ kJ \cdot mol^{-1}$$

$$\Delta_f H_m°(Hg^{2+}, 298.15\ K) = (170.210 \pm 0.20)\ kJ \cdot mol^{-1}$$

$$S_m°(Hg^{2+}, 298.15\ K) = -(36.190 \pm 0.80)\ J \cdot K^{-1} \cdot mol^{-1}$$

The specific ion interaction coefficient selected by NEA (Grenthe et al. 1992, Lemire et al. 2013), is also adopted for TDB 2020:

$$\varepsilon(Hg^{2+}, ClO_4^-) = (0.34 \pm 0.03)\ kg \cdot mol^{-1}$$

Since this report explicitly considers the formation of mercury chloride complexation, $\varepsilon(Hg^{2+}, Cl^-)$ must be approximated by using the corresponding ion interaction coefficient with perchlorate:

$$\varepsilon(Hg^{2+}, Cl^-) \approx \varepsilon(Hg^{2+}, ClO_4^-) = (0.34 \pm 0.03)\ kg \cdot mol^{-1}$$

Using the selected CODATA $\Delta_f G_m°(Hg^{2+}, 298.15\ K)$, the redox equilibrium

$$Hg^{2+} + 2e^- \rightleftharpoons Hg(l)$$

is calculated as

$$\log_{10}K°(298.15\ \text{K}) = 28.85 \pm 0.05$$

Using the selected value $\log_{10}K°(\text{Hg(l)} \rightleftharpoons \text{Hg(aq)}, 298.15\ \text{K}) = -6.53 \pm 0.03$, see Section 14.2.2, the redox equilibrium of aqueous species

$$Hg^{2+} + 2e^- \rightleftharpoons Hg(aq)$$

is calculated as

$$\log_{10}K°(298.15\ \text{K}) = 22.32 \pm 0.06$$

14.4.2 Mercury(II) (hydr)oxide compounds and complexes

14.4.2.1 Mercury(II) hydroxide complexes

For the formation of the first mononuclear hydrolysis species of mercury(II)

$$Hg^{2+} + H_2O(l) \rightleftharpoons HgOH^+ + H^+$$

Powell et al. (2005) select the recommended value

$$\log_{10}{}^*K_1°\ (298.15\ \text{K}) = -3.40 \pm 0.08$$

derived from a weighted linear SIT regression analysis with $\Delta\varepsilon = -(0.14 \pm 0.03)\ \text{kg} \cdot \text{mol}^{-1}$, leading to the selected SIT interaction parameter

$$\varepsilon(HgOH^+, ClO_4^-) = (0.06 \pm 0.05)\ \text{kg} \cdot \text{mol}^{-1}$$

and the estimated

$$\varepsilon(HgOH^+, Cl^-) \approx \varepsilon(HgOH^+, ClO_4^-) = (0.06 \pm 0.05)\ \text{kg} \cdot \text{mol}^{-1}$$

Brown & Ekberg (2016) report identical values based on a weighted linear SIT regression analysis using the same experimental data set as Powell et al. (2005).

For the formation of the second mononuclear hydrolysis species of mercury(II)

$$Hg^{2+} + 2H_2O(l) \rightleftharpoons Hg(OH)_2(aq) + 2H^+$$

Powell et al. (2005) select the recommended value

$$\log_{10}{}^{*}\beta_2^\circ\ (298.15\ \text{K}) = -5.98 \pm 0.06$$

derived from a weighted linear SIT regression analysis with $\Delta\varepsilon = -(0.14 \pm 0.02)\ \text{kg} \cdot \text{mol}^{-1}$, leading to the selected SIT interaction parameter

$$\varepsilon(\text{Hg(OH)}_2, \text{NaClO}_4) = -(0.08 \pm 0.05)\ \text{kg} \cdot \text{mol}^{-1}$$

and the estimated

$$\varepsilon(\text{Hg(OH)}_2, \text{NaCl}) \approx \varepsilon(\text{Hg(OH)}_2, \text{NaClO}_4) = -(0.08 \pm 0.05)\ \text{kg} \cdot \text{mol}^{-1}$$

Note that Brown & Ekberg (2016) report marginally different values, $\log_{10}{}^{*}\beta_2^\circ\ (298.15\ \text{K}) = -5.96 \pm 0.08$ and $\Delta\varepsilon = -(0.13 \pm 0.03)\ \text{kg} \cdot \text{mol}^{-1}$, based on a weighted linear SIT regression analysis using the same experimental data set as Powell et al. (2005) but with increased assigned uncertainties for some of the experimental data. The present author decided to retain the recommended values of the IUPAC review (Powell et al. 2005).

Powell et al. (2005) recommend an enthalpy change for the above hydrolysis reaction:

$$\Delta_r H_m^\circ(298.15\ \text{K}) = (51.5 \pm 1.8)\ \text{kJ} \cdot \text{mol}^{-1}$$

This value is derived from their selected values $\Delta_r H_m^\circ(\text{HgO(s)} + \text{H}_2\text{O} \rightleftharpoons \text{Hg(OH)}_2\text{(aq)}, 298.15\ \text{K}) = (26.2 \pm 1.8)\ \text{kJ} \cdot \text{mol}^{-1}$ and $\Delta_r H_m^\circ(\text{HgO(s)} + 2\text{H}^+ \rightleftharpoons \text{Hg}^{2+} + \text{H}_2\text{O(l)}, 298.15\ \text{K}) = -(25.3 \pm 0.2)\ \text{kJ} \cdot \text{mol}^{-1}$. As discussed in Section 4.2.2, using CODATA values, a slightly different value for $\Delta_r H_m^\circ(\text{HgO(s)} + 2\text{H}^+ \rightleftharpoons \text{Hg}^{2+} + \text{H}_2\text{O(l)}, 298.15\ \text{K}) = -(24.83 \pm 0.24)\ \text{kJ} \cdot \text{mol}^{-1}$ is calculated. As the CODATA values are selected in this review, the above value is thus slightly changed for internal consistency:

$$\Delta_r H_m^\circ(298.15\ \text{K}) = (51.0 \pm 1.8)\ \text{kJ} \cdot \text{mol}^{-1}$$

Powell et al. (2005) state: "Reliable stability constant data have been reported for the formation of Hg(OH)_3^-, $\text{Hg}_2\text{OH}^{3+}$ and $\text{Hg}_2\text{(OH)}_2^{2+}$. However, there are insufficient data for a SIT analysis." Hence, for the third mononuclear hydrolysis species of mercury(II)

$$\text{Hg}^{2+} + 3\text{H}_2\text{O(l)} \rightleftharpoons \text{Hg(OH)}_3^- + 3\text{H}^+$$

Powell et al. (2005) give a provisional value

$$\log_{10}{}^{*}\beta_3^\circ\ (298.15\ \text{K}) = -21.1 \pm 0.3$$

This value is selected in the present review, together with an estimated SIT interaction coefficient (Section 1.5.3)

$$\varepsilon(Hg(OH)_3^-,Na^+) = -(0.05 \pm 0.10)\ kg \cdot mol^{-1}$$

This species will form only in highly alkaline solutions (pH > 13).

The species Hg_2OH^{3+} and $Hg_2(OH)_2^{2+}$ will form only at relatively high Hg(II) concentrations (ca. 0.005 mol dm^{-3}) and acid conditions (pH < 5); they are unlikely to be environmentally important and thus not included in our TDB.

14.4.2.2 Mercury(II) oxide compounds

HgO(s) exists in three forms, two orthorhombic (red and yellow) and one hexagonal. The orthorhombic form is stable at 25 °C. The mineral montroydite (orthorhombic, red) is very rarely found. The three forms have similar standard solubility products. Hence, Powell et al. (2005) recommend for

$$HgO(s) + 2H^+ \rightleftharpoons Hg^{2+} + H_2O(l)$$

a single value

$$\log_{10}{}^*K_{s0}^\circ\ (298.15\ K) = 2.37 \pm 0.08$$

together with

$$\Delta_r H_m^\circ(298.15\ K) = -(25.3 \pm 0.2)\ kJ \cdot mol^{-1}$$

Brown & Ekberg (2016) retain the solubility product of Powell et al. (2005) in their review. However, they did not notice that this solubility product was derived by Powell et al. (2005) from the equilibrium constant of the reaction $HgO(s) + H_2O(l) \rightleftharpoons Hg(OH)_2(aq)$ and their recommended value for $Hg^{2+} + 2H_2O(l) \rightleftharpoons Hg(OH)_2(aq) + 2H^+$. As mentioned above, the latter equilibrium was evaluated marginally differently by Brown & Ekberg (2016) and hence, their solubility product should have been adjusted to $\log_{10}{}^*K_{s0}^\circ\ (298.15\ K) = 2.35 \pm 0.09$.

CODATA (Cox et al. 1989) recommend

$$\Delta_f G_m^\circ(HgO, montroydite, red, 298.15\ K) = -(58.523 \pm 0.15)\ kJ \cdot mol^{-1}$$

Together with the recommended values $\Delta_f G_m^\circ(Hg^{2+}, 298.15\ K) = (153.567 \pm 0.56)\ kJ \cdot mol^{-1}$ and $\Delta_f G_m^\circ(H_2O, l, 298.15\ K) = -(237.14 \pm 0.04)\ kJ \cdot mol^{-1}$ this results in

$$\Delta_r G_m^\circ(HgO(s) + 2H^+ \rightleftharpoons Hg^{2+} + H_2O(l), 298.15\ K) = -(13.95 \pm 0.35)\ kJ \cdot mol^{-1}$$

and

$\log_{10}{}^{*}K_{s0}°$ (298.15 K) = 2.44 ± 0.06

Within their 95% uncertainty ranges the CODATA and IUPAC values agree well and thus, the CODATA value is preferred in this review.

Furthermore, CODATA (Cox et al. 1989) recommend

$\Delta_f H_m°$(HgO, montroydite, red, 298.15 K) = -(90.79 ± 0.12) kJ · mol^{-1}

Together with the recommended values $\Delta_f H_m°(Hg^{2+}, 298.15\ K) = (170.210 \pm 0.20)$ kJ · mol^{-1} and $\Delta_f H_m°(H_2O, l, 298.15\ K) = -(285.83 \pm 0.04)$ kJ · mol^{-1} this results in

$\Delta_r H_m°(HgO(s) + 2H^+ \rightleftharpoons Hg^{2+} + H_2O(l), 298.15\ K) = -(24.83 \pm 0.24)$ kJ · mol^{-1}

Within their 95% uncertainty ranges the CODATA and IUPAC values agree reasonably well and thus, the CODATA value is preferred in this review.

14.4.3 Mercury(II) chloride compounds and complexes

14.4.3.1 Mercury(II) chloride complexes

Mercury(II) forms very stable chloro complexes, and the 1:1 and 1:2 chloro complexes of Hg(II) are among the most stable of metal-chloro complexes known in chemical thermodynamics. For the equilibria

$Hg^{2+} + Cl^- \rightleftharpoons HgCl^+$

$Hg^{2+} + 2Cl^- \rightleftharpoons HgCl_2(aq)$

$HgCl_2(aq) + Cl^- \rightleftharpoons HgCl_3^-$

$HgCl_3^- + Cl^- \rightleftharpoons HgCl_4^{2-}$

Powell et al. (2005) recommend

$\log_{10}K_1°$ (298.15 K) = 7.31 ± 0.04

$\Delta_r H_m°(298.15\ K) = -(21.3 \pm 0.7)$ kJ · mol^{-1}

$\Delta\varepsilon = -(0.22 \pm 0.04)$ kg · mol^{-1}

$\log_{10}\beta_2°$ (298.15 K) = 14.00 ± 0.07

$\Delta_r H_m°(298.15\ K) = -(49.1 \pm 1.0)$ kJ · mol^{-1}

$\Delta\varepsilon = -(0.39 \pm 0.03)$ kg · mol^{-1}

$\log_{10}K_3°$ (298.15 K) = $0.92_5 \pm 0.09$

$\Delta_r H_m°$(298.15 K) = (0.5 ± 2.5) kJ · mol^{-1}

$\Delta\varepsilon$ = (0.01 ± 0.05) kg · mol^{-1}

$\log_{10}K_4°$ (298.15 K) = 0.61 ± 0.12

$\Delta_r H_m°$(298.15 K) = -(10.5 ± 2.5) kJ · mol^{-1}

$\Delta\varepsilon$ = (0.00 ± 0.06) kg · mol^{-1}

and these values have been included in our TDB.

The $\Delta\varepsilon$ values derived by Powell et al. (2005) from weighted linear SIT regression analyses are used, together with the reported values $\varepsilon(Hg^{2+}, ClO_4^-)$ = (0.34 ± 0.03) kg · mol^{-1} and $\varepsilon(Cl^-, Na^+)$ = (0.03 ± 0.01) kg · mol^{-1} (Lemire et al. 2013) to calculate the new values

$\varepsilon(HgCl^+, ClO_4^-)$ = (0.15 ± 0.05) kg · mol^{-1}

$\varepsilon(HgCl_2(aq), NaClO_4)$ = (0.01 ± 0.04) kg · mol^{-1}

$\varepsilon(Na^+, HgCl_3^-)$ = (0.05 ± 0.06) kg · mol^{-1}

$\varepsilon(Na^+, HgCl_4^{2-})$ = (0.08 ± 0.09) kg · mol^{-1}

As well as the estimated values

$\varepsilon(HgCl^+, Cl^-) \approx \varepsilon(HgCl^+, ClO_4^-)$ = (0.15 ± 0.05) kg · mol^{-1}

$\varepsilon(HgCl_2(aq), NaCl) \approx \varepsilon(HgCl_2(aq), NaClO_4)$ = (0.01 ± 0.04) kg · mol^{-1}

Powell et al. (2005) state that the formation of Hg(II) chloro complexes higher than 1:4 has not been observed in aqueous solution, and there is no evidence for polynuclear Hg(II) – Cl^- complexes. It is thus inferred that the binary Hg(II) chloride system in acidic aqueous solution is fully characterized by the complexes $HgCl^+$, $HgCl_2(aq)$, $HgCl_3^-$, and $HgCl_4^{2-}$.

Powell et al. (2005) report evidence for the formation of HgOHCl(aq) in solution at pH 3 – 9 and $\log_{10}[Cl^-]$ in the range -1 to -7. Because of the scarcity of experimental data, extrapolation of the stability constants to zero ionic strength by SIT regression analysis was not possible. Hence, Powell et al. (2005) estimated the value

$\varepsilon(HgOHCl, NaClO_4)$ = -(0.01 ± 0.09) kg mol^{-1}

and derived for reaction

$Hg^{2+} + Cl^- + H_2O(l) \rightleftharpoons HgOHCl(aq) + H^+$

$\log_{10}{}^*\beta°$ (298.15 K) = 4.27 ± 0.35

These values are included in TDB 2020 as well as the estimated

$$\varepsilon(HgOHCl, NaCl) \approx \varepsilon(HgOHCl, NaClO_4) = -(0.01 \pm 0.09)\ kg \cdot mol^{-1}$$

The temperature dependence of the above reaction is unknown.

14.4.3.2 Mercury(II) chloride compounds

Solid $HgCl_2$ is very soluble in water. Reported values for the solubility at 25 °C range from 0.263 to 0.266 mol dm^{-3} (Powell et al. 2005). Because of its high solubility, $HgCl_2(s)$ would not influence the speciation of mercury in natural fresh or saline waters.

14.4.4 Mercury(II) carbonate compounds and complexes

14.4.4.1 Mercury(II) carbonate complexes

Powell et al. (2005) report few studies of aqueous Hg(II) interactions with carbonate. Extrapolation to zero ionic strength was not possible and hence, they derived isocoulombic reactions which should have minimal dependence on ionic strength. Consequently, the isocoulombic equilibrium constants have been used as recommended values appropriate to I_m = 0 mol · kg^{-1}, 25 °C, and 1 bar total pressure:

$$Hg(OH)_2(aq) + CO_2g + H^+ \rightleftharpoons HgHCO_3^+ + H_2O(l)$$

$$\log_{10}{}^*K^\circ\ (298.15\ K) = 3.63 \pm 0.10$$

$$Hg(OH)_2(aq) + CO_2g \rightleftharpoons HgCO_3(aq) + H_2O(l)$$

$$\log_{10}K^\circ\ (298.15\ K) = -0.70 \pm 0.20$$

$$Hg(OH)_2(aq) + HCO_3^- \rightleftharpoons HgOHCO_3^- + H_2O(l)$$

$$\log_{10}K^\circ\ (298.15\ K) = 0.98 \pm 0.10$$

and these values have been included in TDB 2020 together with the estimated SIT interaction coefficients

$$\varepsilon(HgHCO_3^+, Cl^-) \approx \varepsilon(HgHCO_3^+, ClO_4^-) = (0.2 \pm 0.1)\ kg \cdot mol^{-1}$$

$$\varepsilon(HgCO_3(aq), NaCl) \approx \varepsilon(HgCO_3(aq), NaClO_4) = (0.0 \pm 0.1)\ kg \cdot mol^{-1}$$

$$\varepsilon(Na^+, Hg(OH)CO_3^-) = -(0.05 \pm 0.10)\ kg \cdot mol^{-1}$$

14.4.4.2 Mercury(II) carbonate compounds

Powell et al. (2005) state: $Hg(OH)_2(aq)$ is dominant relative to Hg(II)-carbonate species over a wide range of pH and CO_2 partial pressure. Therefore, it is useful to consider the solubility of $HgCO_3 \cdot 2HgO(s)$ in terms of aqueous $Hg(OH)_2$ concentrations:

$$HgCO_3 \cdot 2HgO(s) + 3\ H_2O(l) \rightleftharpoons 3Hg(OH)_2(aq) + CO_2g$$

$$\log_{10}K_s = -11.27 \pm 0.35$$

Powell et al. (2005) further state: The provisional standard solubility product for I_c = 3.0 mol · dm^{-3} $NaClO_4$ indicates that the concentration of aqueous $Hg(OH)_2$ in equilibrium with $HgCO_3 \cdot 2HgO(s)$ will exceed 175 µmol · dm^{-3} even at a CO_2 partial pressure of one atmosphere. Thus, it is unlikely that $HgCO_3 \cdot 2HgO(s)$ will set bounds on the concentration of Hg(II) in natural waters. A SIT analysis was not possible.

However, the above isocoulombic reaction should have minimal dependence on ionic strength, and consequently, the isocoulombic equilibrium constant has been included in our TDB as appropriate to I_m = 0 mol · kg^{-1}, 25 °C, and 1 bar total pressure (Tab. 14-1).

14.4.5 Mercury(II) phosphate compounds and complexes

14.4.5.1 Mercury(II) phosphate complexes

Powell et al. (2005) state that there are a limited number of data for phosphate complexes at I_c = 3.0 mol · dm^{-3} $NaClO_4$ only. A SIT analysis is not possible; their selected data are neither "Recommended" nor "Provisional". This review estimated Δε values, using ε(j,k) values taken from Lemire et al. (2013), for extrapolation of the selected data to zero ionic strength. These extrapolated data are included in TDB 2020 as "supplemental data":

$$Hg^{2+} + HPO_4^{2-} \rightleftharpoons HgHPO_4(aq)$$

$$\log_{10}K = 8.8 \pm 0.2$$

$$\Delta\varepsilon(estimated) = (0.06 \pm 0.12)\ kg \cdot mol^{-1}$$

$$\log_{10}K°(298.15\ K) = 10.9 \pm 0.6$$

$$Hg^{2+} + HPO_4^{2-} \rightleftharpoons HgPO_4^{-} + H^{+}$$

$$\log_{10}{}^{*}K = 3.25 \pm 0.2$$

$$\Delta\varepsilon(estimated) = (0.15 \pm 0.12)\ kg \cdot mol^{-1}$$

$$\log_{10}{}^{*}K°(298.15\ K) = 5.3 \pm 0.6$$

together with the estimated SIT interaction coefficients

$$\varepsilon(HgHPO_4(aq), NaCl) \approx \varepsilon(HgHPO_4(aq), NaClO_4) = (0.0 \pm 0.1)\ kg \cdot mol^{-1}$$

$$\varepsilon(Na^+, HgPO_4^-) = -(0.05 \pm 0.10)\ kg \cdot mol^{-1}$$

14.4.5.2 Mercury(II) phosphate compounds

Powell et al. (2005) state that there are a limited number of solubility data for phosphate compounds at I_c = 3.0 mol · dm^{-3} $NaClO_4$ only. A SIT analysis is not possible; their selected data are neither "Recommended" nor "Provisional. This review estimated Δε values, using ε(j,k) values listed in Tab. 14-2, for extrapolation of the selected data to zero ionic strength. These extrapolated data are included in our TDB as "supplemental data":

$$Hg_3(PO_4)_2(s) + 2\ H^+ \rightleftharpoons 3\ Hg^{2+} + 2\ HPO_4^{2-}$$

$$log_{10}{}^*K_s\ (298.15\ K) = -24.6 \pm 0.6$$

$$\Delta\varepsilon(estimated) = -(0.31 \pm 0.10)\ kg \cdot mol^{-1}$$

$$log_{10}{}^*K_s^\circ\ (298.15\ K) = -30.0 \pm 0.9$$

$$(HgOH)_3PO_4(s) + 4\ H^+ \rightleftharpoons 3\ Hg^{2+} + HPO_4^{2-} + 3\ H_2O(l)$$

$$log_{10}{}^*K_s\ (298.15\ K) = -9.4 \pm 0.8$$

$$\Delta\varepsilon(estimated) = -(0.44 \pm 0.08)\ kg \cdot mol^{-1}$$

$$log_{10}{}^*K_s^\circ\ (298.15\ K) = -14.0 \pm 1.1$$

$$HgHPO_4(s) \rightleftharpoons Hg^{2+} + HPO_4^{2-}$$

$$log_{10}K_s\ (298.15\ K) = -13.1 \pm 0.1$$

$$\Delta\varepsilon(estimated) = -(0.06 \pm 0.06)\ kg \cdot mol^{-1}$$

$$log_{10}{}^*K_s^\circ\ (298.15\ K) = -15.2 \pm 0.3$$

Powell et al. (2005) state that i these solid phases form as a function of pH when the total concentrations of Hg^{2+} and phosphate are sufficiently high, (ii) $HgHPO_4$(s) is likely to be the least soluble phase at environmental pH, and (iii) it will form from equimolar solution when the concentration of Hg^{2+} is > 40 μmol dm^{-3}.

14.4.6 Mercury(II) sulphate compounds and complexes

14.4.6.1 Mercury(II) sulphate complexes

Powell et al. (2005) state that only three papers report quantitative measurements for the Hg^{2+} – H^+ – SO_4^{2-} system, all at similar I_c, so a SIT analysis is not possible. Their selected data, neither of which is "Recommended", refer to I_c = 0.5 mol dm^{-3} ($NaClO_4$). The reported value for K_1 must be regarded as "Provisional", while the reported value of β_2 is considered doubtful. This review estimated Δε values, using ε(j,k) values listed in Tab. 14-2, for extrapolation of the selected data to zero ionic strength.

$Hg^{2+} + SO_4^{2-} \rightleftharpoons HgSO_4(aq)$

$\log_{10}K_1$ (298.15 K) = 1.4 ± 0.1

$\Delta\varepsilon$(estimated) = (0.03 ± 0.12) kg · mol^{-1}

$\log_{10}K_1°$ (298.15 K) = 2.8 ± 0.2

$Hg^{2+} + 2\ SO_4^{2-} \rightleftharpoons Hg(SO_4)_2^{2-}$

$\log_{10}\beta_2$ (298.15 K) = 2.4

$\Delta\varepsilon$(estimated) = (0.05 ± 0.13) kg · mol^{-1}

$\log_{10}\beta_2°$ (298.15 K) = 3.8

The $\log_{10}K_1°$ and $\log_{10}\beta_2°$ values are included in TDB 2020 (although $\log_{10}\beta_2°$ as "supplemental data" only) together with the estimated SIT interaction coefficients

$\varepsilon(HgSO_4(aq), NaCl) \approx \varepsilon(HgSO_4(aq), NaClO_4)$ = (0.0 ± 0.1) kg · mol^{-1}

$\varepsilon(Na^+, Hg(SO_4)_2^{2-})$ = -(0.10 ± 0.10) kg · mol^{-1}

14.4.6.2 Mercury(II) sulphate compounds

Solid mercury(II) sulphate and several "basic salts" have been prepared in the laboratory. The only "basic salt" occurring naturally is schuetteite, $HgSO_4{\cdot}2HgO$ (or $Hg_3O_2SO_4$).

Parks & Nordstrom (1979) conclude that $HgSO_4$(cr) is unlikely to be found in nature, first, because it is unstable with respect to schuetteite except under unrealistically high SO_4^{2-} and H^+ activities and, second, because it is so soluble ($\log_{10}K_s$ = -2.8).

Parks & Nordstrom (1979) further conclude that the formation of schuetteite requires acid, oxidising conditions which might be expected in or near oxidising sulphide ore deposits, mine dumps, or smelter waste dumps. The solubility of schuetteite is high relative to that of the common rock forming minerals and heavy metal sulphides, i.e., a minimum of about $10^{-4.5}$ molar or roughly 10 mg Hg per litre.

None of these solids is included in TDB 2020.

14.4.7 Mercury(II) sulphide compounds and complexes

Rickard & Luther (2006) and Rickard (2012) presented extensive reviews on the chemistry of aqueous metal-sulphide complexes and clusters. Concerning mercury, they reported that addition of S(-II) to aqueous Hg^{2+} produces black mercuric sulphide, HgS, which is similar to metacinnabar, which has a ZnS structure. Metacinnabar is unstable with respect to red, rhombohedral HgS or cinnabar, at temperatures lower than 344 °C, and the transformation is kinetically rapid.

Several Hg – sulphide complexes have been proposed. The first group stems from the original work of Schwarzenbach & Widmer (1963), which is based on the Ph.D. thesis of Widmer (1962), who measured the solubility of HgS in 1M KCl at 20 °C by radiochemical methods and showed that $Hg(HS)_2(aq)$, $HgS(HS)^-$ and HgS_2^{2-} fit the titration curves. Schwarzenbach and Widmer used the black HgS precipitate and therefore were probably examining metacinnabar solubility.

However, decades later Paquette & Helz (1997) investigated the solubilities of red cinnabar (HgS) and of cinnabar + elemental sulphur (S^0). They used the Schwarzenbach & Widmer (1963) model parameters for the analysis of their S^0 undersaturated data and concluded: "The absence of a systematic offset suggests that Schwarzenbach and Widmer's "black HgS" may in fact have been cinnabar, presumably an S-rich, non-stoichiometric variant having a diminished reflectivity for red light. However, this conclusion is tentative."

Hence, either Paquette & Helz (1997) are right or the difference in solubility of cinnabar and metacinnabar is within the uncertainty of experimental solubility data. For the time being we use the common term HgS(s) for all solids studied in the works cited here.

Several years after Widmer's pioneering work, Mehra (1968) used similar experimental methods in his extensive solubility studies of metal selenites, sulphides and selenides in 1M $NaClO_4$ at 25 °C. Most results of his Ph.D. thesis have never been published in journals, and hence the study of HgS solubility went unnoticed until the present author re-discovered the Ph.D. thesis, almost half a century after its publication.

Mehra (1968) fitted his HgS(s) solubility data with the species Hg(HS)OH(aq), $Hg(HS)_2OH^-$, $Hg(HS)_2(OH)_2^{2-}$. While the species $Hg(HS)_2OH^-$ and $Hg(HS)_2(OH)_2^{2-}$ are formally identical to Schwarzenbach and Widmer's model species $HgS(HS)^-$ and HgS_2^{2-}, respectively, the species Hg(HS)OH(aq) could also be written as HgS(aq).

Zhang & Millero (1994) used cathodic stripping square wave voltammetry to detect H_2S in sea water over a wide range of concentrations (nM to mM). The addition of metal ions to the solutions was found to depress the signal. This depression was attributed to the formation of the metal sulphide complexes MHS^+ and $M(HS)_2(aq)$. The complex $Hg(HS)_2(aq)$ was already proposed by Schwarzenbach & Widmer (1963) to explain their solubility data at pH < 5. By contrast, a strong complex $HgHS^+$ would cause an increase of dissolved Hg concentration with decreasing pH in the acid region. Such an increase has been detected neither by Schwarzenbach & Widmer (1963) nor by Mehra (1968), not even at pH 0 (Fig. 14-3). Hence, if the complex $HgHS^+$ exists at all it is so weak that it has no influence on the Hg – sulphur speciation in the presence of HgS(s).

Paquette & Helz (1997) and Jay et al. (2000) showed that the solubility of cinnabar was increased in the presence of elemental sulphur and proposed a series of Hg – polysulphide complexes. Paquette & Helz (1997) proposed $Hg(S_n)HS^-$ and Jay et al. (2000) proposed $Hg(S_n)_2^{2-}$ in the presence of elemental sulphur and $Hg(S_n)OH^-$ at lower sulphide concentrations and high pH.

As geochemical systems comprising elemental sulphur are outside the scope of TDB 2020, Hg – polysulphide complexes will not be further discussed here, and we are left with the solubility studies of Schwarzenbach & Widmer (1963) and Mehra (1968) (Fig. 14-3).

Rickard & Luther (2006) and Rickard (2012) stated that there is very limited spectroscopic information on Hg – sulphide complexes: A Raman study demonstrated that HgS_2^{2-} was the likely composition in alkali sulphide solutions. An EXAFS study demonstrated that Hg was in two-coordination with S in alkaline sulphide solutions, which "is not inconsistent with" the result of the Raman study.

HgS_2^{2-}

Therefore, the systematic increase of Hg solubility at pH > 8 most likely is due to the formation of HgS_2^{2-} according to the equilibrium

$$HgS(s) + HS^- \rightleftharpoons HgS_2^{2-} + H^+$$

A re-evaluation of the experimental solubility data at pH > 8.7 given by Schwarzenbach & Widmer (1963) and Widmer (1962) in this review gives

$$\log_{10}{}^*K_s\ (298.15\ K) = -13.58 \pm 0.04$$

in perfect agreement with the value -13.58 reported by Schwarzenbach & Widmer (1963). This value was extrapolated to zero ionic strength by using $\varepsilon(H^+, Cl^-) = 0.12 \pm 0.01$ kg · mol^{-1} (Tab. 14-2) and assuming that $\varepsilon(HS^-, K^+) \approx \varepsilon(HS^-, Na^+) = 0.08 \pm 0.01$ kg · mol^{-1} (Tab. 14-2) and $\varepsilon(HgS_2^{2-}, K^+) \approx \varepsilon(HgS_2^{2-}, Na^+) = 0.10 \pm 0.10$ kg · mol^{-1} (Tab. 14-2), resulting in

$$\log_{10}{}^*K_s^\circ\ (298.15\ K) = -14.46 \pm 0.11$$

The above equilibrium implies an increase in Hg solubility with increasing total dissolved sulphide concentration. As Schwarzenbach & Widmer (1963) did measurements at a single sulphide concentration only, they could not prove this effect. However, Mehra (1968) did measurements at three different total sulphide concentration ranges and his data clearly show a systematic increase of Hg solubility in the expected order of magnitude (Fig. 14-3).

$HgS(HS)^-$

In the range 6 < pH < 8 Schwarzenbach & Widmer (1963) explained the observed "bump" in the measured Hg solubility by the formation of $HgS(HS)^-$. At pH > 7 HS^- is the dominating dissolved sulphide species and the solubility equilibrium can be written as

$$HgS(s) + HS^- \rightleftharpoons HgS(HS)^-$$

A re-evaluation of experimental solubility data in the range 7 < pH < 8 given by Schwarzenbach & Widmer (1963) and Widmer (1962) in this review gives

$$\log_{10}K_s\ (298.15\ K) = -5.26 \pm 0.04$$

in excellent agreement with the value -5.28 reported by Schwarzenbach & Widmer (1963). Assuming that $\varepsilon(HgS(HS)^-, K^+) \approx \varepsilon(HgS(HS)^-, Na^+) = 0.08 \pm 0.10\ kg \cdot mol^{-1} \approx \varepsilon(HS^-, K^+) \approx \varepsilon(HS^-, Na^+) = 0.08 \pm 0.01\ kg \cdot mol^{-1}$ (Tab. 14-2) this isocoulombic reaction is not ionic strength dependent. However, the recalculation from the molar to the molal concentration scale has a minute effect:

$$\log_{10}K_s^\circ\ (298.15\ K) = -5.27 \pm 0.11$$

At pH > 7 the Hg solubility depends little to none on pH. At pH < 7 $H_2S(aq)$ is the dominating dissolved sulphide species and the solubility equilibrium can be written as

$$HgS(s) + H_2S(aq) \rightleftharpoons HgS(HS)^- + H^+$$

and an increase of the Hg solubility with pH is observed. Again, the above equilibria imply a systematic increase in Hg solubility with increasing total dissolved sulphide concentration, which is shown clearly in the expected order of magnitude in the combined Schwarzenbach & Widmer (1963) and Mehra (1968) data (Fig. 14-3).

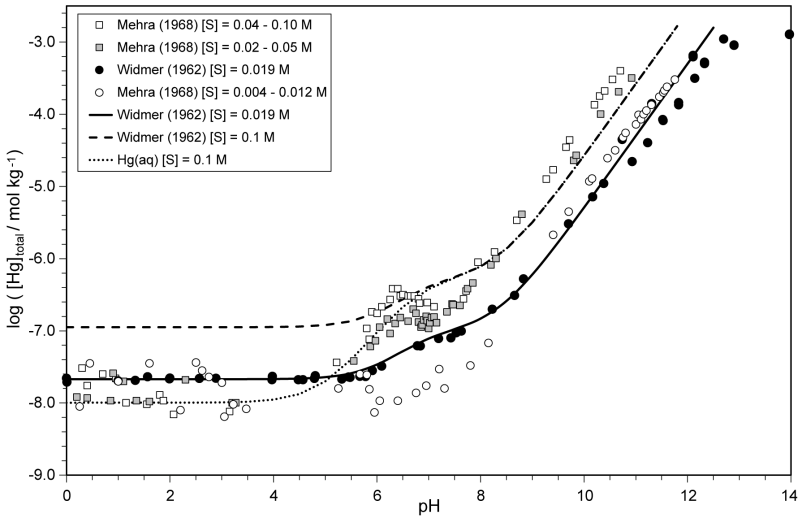

Fig. 14-3: Solubility of HgS(s) in water as a function of pH at different total dissolved sulphide concentrations, $[S]_{total}$

Different symbols: experimental data of Widmer (1962) and Mehra (1968). Solid line: solubility model according to Widmer (1962) comprising the species $Hg(HS)_2(aq)$, $HgS(HS)^-$ and HgS_2^{2-}, for $[S]_{total}$ = 0.019 M. Dashed line: the same solubility model for $[S]_{total}$ = 0.1 M. Dotted line: the species Hg(aq) replaces the species $Hg(HS)_2(aq)$ in the solubility model; calculations done for 1 bar H_2g pressure.

$Hg(HS)_2(aq)$?

The situation at pH < 6 is less clear. Schwarzenbach & Widmer (1963) did not observe any pH dependence of the measured Hg solubility and attributed this to the formation of $Hg(HS)_2(aq)$, according to the equilibrium

$$HgS(s) + H_2S(aq) \rightleftharpoons Hg(HS)_2(aq)$$

A re-evaluation of experimental solubility data at pH < 7 given by Schwarzenbach & Widmer (1963) and Widmer (1962) in this review gives

$$\log_{10}K_s\ (298.15\ K) = -5.95 \pm 0.01$$

in excellent agreement with the value -5.97 reported by Schwarzenbach & Widmer (1963). Assuming that $\varepsilon(Hg(HS)_2(aq), KCl) \approx \varepsilon(Hg(HS)_2(aq), NaCl) = 0.055 \pm 0.10\ kg \cdot mol^{-1} \approx \varepsilon(H_2S(aq), KCl) \approx \varepsilon(H_2S(aq), NaCl) = 0.055 \pm 0.004\ kg \cdot mol^{-1}$ (Tab. 14-2) this isocoulombic reaction is not ionic strength dependent. However, the recalculation from the molar to the molal concentration scale has a minute effect:

$$\log_{10}K_s^\circ(298.15\ K) = -5.96 \pm 0.10$$

From a coordination chemistry point of view, this choice makes sense: Hg(II) usually forms strong two-coordinated complexes and thus, it is not unlikely that with increasing pH first $Hg(HS)_2(aq)$ is formed, then one of the HS^- ligands is deprotonated and $HgS(HS)^-$ predominates, and finally the second HS^- ligand is deprotonated to result in HgS_2^{2-}.

However, the above choice of $Hg(HS)_2(aq)$ again implies an increase in Hg solubility with increasing total dissolved sulphide concentration at pH < 6. Mehra (1968) found the same pH independent Hg solubility at pH < 6 as Schwarzenbach & Widmer (1963), with an increased scatter of the experimental data, but no increase (or decrease) of Hg solubility as a function of total dissolved sulphide concentration (Fig. 14-3). Mehra (1968) interpreted his findings in terms of

$$HgS(s) + H_2O(l) \rightleftharpoons Hg(HS)OH(aq)$$

which is formally equivalent to

$$HgS(s) \rightleftharpoons HgS(aq)$$

The mixed Hg(II) – HS^- – OH^- complex, if formed at all, is highly unlikely to predominate in the acid region from pH 6 down to pH 0. And the formally equivalent one coordinated complex HgS(aq) is probably unstable in aqueous solutions according to quantum mechanical computations (Rickard & Luther 2006).

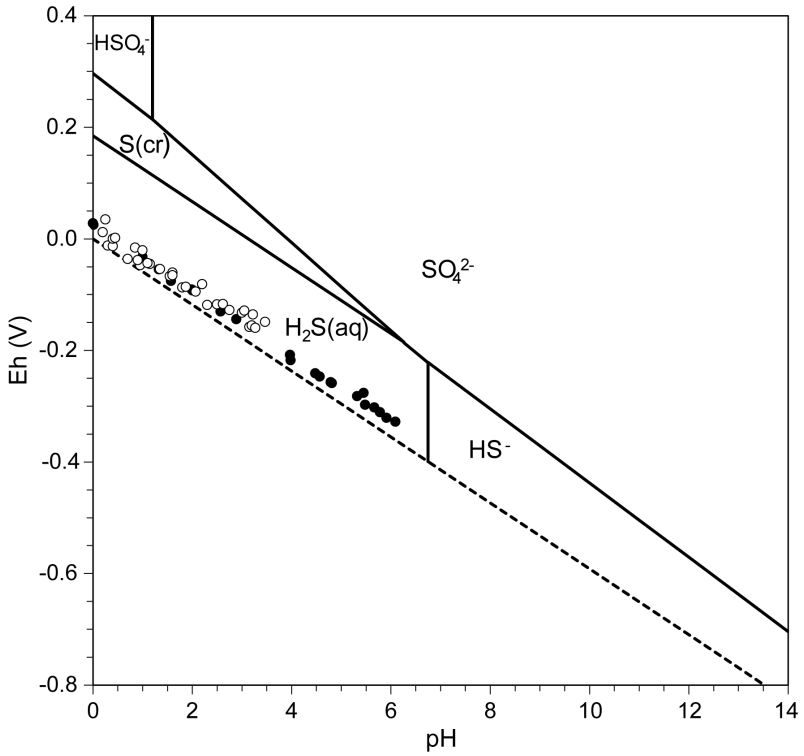

Fig. 14-4: Eh – pH diagram for part of the S – O – H system at 1 M $NaClO_4$ and $[S]_{total}$ = 0.02 M

The dashed line represents the lower stability limit of water where P_{H2} = 1 bar. Symbols: Experimental HgS(s) solubility data assuming Hg(aq) as the predominating aqueous mercury species (see text). White symbols: Mehra (1968), black symbols: Schwarzenbach & Widmer (1963).

Hg(aq) ?

A possible solution to this riddle involves the consideration of Hg(aq) in the speciation model. A solubility equilibrium between HgS(s) and Hg(aq) can be formulated as

$$HgS(s) + H_2g \rightleftharpoons Hg(aq) + H_2S(aq)$$

If this equilibrium predominates, the measured Hg solubility is pH independent at constant partial pressure of hydrogen. In order to test whether the hypothesis works that Hg(aq) could have been the predominating species in the studies of Schwarzenbach & Widmer (1963) and Mehra (1968) at pH < 6, the partial pressure of hydrogen, P_{H2}, has been calculated for each experimental datum (Fig. 14-4).

The basic equilibria for these calculations are

$$H_2g \rightleftharpoons 2\ e^- + 2\ H^+$$

with $\log_{10}K(H_2g) = 0$ (per definition),

$$Hg^{2+} + 2e^- \rightleftharpoons Hg(aq)$$

with $\log_{10}K°(298.15\ K) = 22.32 \pm 0.06$, as discussed in Section 4.1, extrapolated to 1M KCl using $\varepsilon(Hg^{2+}, Cl^-) = 0.34 \pm 0.03$ kg · mol^{-1} (Tab. 14-2) and assuming $\varepsilon(Hg(aq), KCl) \approx \varepsilon(Hg(aq), NaCl) = 0.0 \pm 0.1$ kg · mol^{-1} (Tab. 14-2), leading to

$$\log_{10}K(1M\ KCl, 298.15\ K) = 21.44 \pm 0.12$$

and the solubility product

$$HgS(s) + 2\ H^+ \rightleftharpoons Hg^{2+} + H_2S(aq)$$

A re-evaluation of the experimental data given by Schwarzenbach & Widmer (1963) and Widmer (1962) in this review gives

$$\log_{10}{}^*K_s\ (298.15\ K) = -29.93 \pm 0.06$$

in perfect agreement with the value -29.93 reported by Schwarzenbach & Widmer (1963). This value was extrapolated to zero ionic strength by using $\varepsilon(H^+, Cl^-) = 0.12 \pm 0.01$ kg · mol^{-1} and $\varepsilon(Hg^{2+}, Cl^-) = 0.34 \pm 0.03$ kg · mol^{-1} (Tab. 14-2) and assuming $\varepsilon(H_2S(aq), KCl) \approx \varepsilon(H_2S(aq), NaCl) = 0.055 \pm 0.004$ kg · mol^{-1} (Tab. 14-2), resulting in

$$\log_{10}{}^*K_s°\ (298.15\ K) = -29.78 \pm 0.07$$

Combining $\log_{10}K(H_2g) = 0$, $\log_{10}K(1M\ KCl, 298.15\ K) = 21.44 \pm 0.12$ and $\log_{10}{}^*K_s\ (298.15\ K) = -29.93 \pm 0.06$ results in

$$\log_{10}K_s\ (298.15\ K) = -8.49 \pm 0.12 \text{ for}$$

$$HgS(s) + H_2g \rightleftharpoons Hg(aq) + H_2S(aq)$$

At pH < 6 total dissolved sulphur is $H_2S(aq)$, $[H_2S(aq)] = [S]_{total}$, and we assume that the total dissolved mercury is Hg(aq), $[Hg]_{total} = [Hg(aq)]$.

In Fig. 14-4 $[Hg]_{total}$ and $[S]_{total}$ values for individual measurements from Schwarzenbach & Widmer (1963) and Mehra (1968) were used to calculate $[H_2g]$, and Eh values have been calculated therefrom for the given pH values.

Taking $[S]_{total} = 0.019$ M and the average total dissolved mercury as $[Hg]_{total} = 2.14 \cdot 10^{-8}$ M from Schwarzenbach & Widmer (1963) we get $[H_2g]$, or the average partial pressure of hydrogen

$$P_{H2} = 0.13 \pm 0.04 \text{ bar}$$

These results suggest that Hg(aq) could have been the dominating dissolved mercury species at pH < 6 in the experiments of Schwarzenbach & Widmer (1963) and Mehra (1968).

Note that the above equilibrium predicts that at constant partial hydrogen pressure the total dissolved mercury concentration decreases with increasing $H_2S(aq)$ concentration, in contrast to an increase if $Hg(HS)_2(aq)$ would be the dominating mercury species (Fig. 14-3). However, P_{H2} was neither controlled nor measured in the above-mentioned experiments, and it is not unreasonable that P_{H2} increases with increasing dissolved sulphide concentration, leading to roughly constant Hg(aq) concentrations. Dedicated experiments are needed to finally resolve this question.

However, there are further indications that Hg(aq) is the predominating species in the discussed system.

Zhang & Millero (1994) reported a value for the formation of $Hg(HS)_2(aq)$, based on their cathodic stripping square wave voltammetry experiments in sea water (0.7 M), which is more than ten(!) orders of magnitude lower than the value derived by Schwarzenbach & Widmer (1963).

Shikina et al. (1981) measured the solubility of HgS(s) at pH 1 – 4 and 90 and 150 °C and reported for the equilibrium

$$HgS(s) + H_2S(aq) \rightleftharpoons Hg(HS)_2(aq)$$

the values $\log_{10}K_s°(363.15\ K) = -5.31 \pm 0.12$ and $\log_{10}K_s°(423.15\ K) = -4.63 \pm 0.10$.

Note, that the difference between the value $\log_{10}K_s°(298.15\ K) = -5.96 \pm 0.10$ derived from the Schwarzenbach & Widmer (1963) data and $\log_{10}K_s°(363.15\ K) = -5.31 \pm 0.12$ reported by Shikina et al. (1981) is 0.65 log units, very close to the difference in Hg(aq) solubility of 0.75 log units for the same temperature interval (Fig. 14-1). Hence, the increase in mercury solubility with temperature observed by Shikina et al. (1981) could mainly be due to the increase of Hg(aq) solubility with temperature.

In conclusion, the following stability constants, derived from the above discussed equilibria, are included in TDB 2020 (Tab. 14-1):

$$HgS(s) + H^+ \rightleftharpoons Hg^{2+} + HS^-$$

$$\log_{10}{}^*K_s°\ (298.15\ K) = -36.77 \pm 0.18$$

$$Hg^{2+} + 2\ HS^- \rightleftharpoons HgS_2^{2-} + 2\ H^+$$

$$\log_{10}K°\ (298.15\ K) = 22.3 \pm 0.2$$

$$Hg^{2+} + 2\ HS^- \rightleftharpoons HgS(HS)^- + H^+$$

$$\log_{10}K°\ (298.15\ K) = 31.5 \pm 0.2$$

$$Hg^{2+} + 2\ HS^- \rightleftharpoons Hg(HS)_2(aq)$$

$$\log_{10}K°\ (298.15\ K) < 37.8$$

The last value represents an upper limit of a probably much lower stability constant, due to the predominance of Hg(aq) in the experiments as discussed above. This value is included in TDB 2020 as supplemental datum.

14.5 Selected mercury data

Tab. 14-1: Selected mercury data

Core data are in bold face and supplemental data in italics.

Name	**$\Delta_f G_m°$** [kJ · mol^{-1}]	**$\Delta_f H_m°$** [kJ · mol^{-1}]	**$S_m°$** [J · K^{-1} · mol^{-1}]	**$C_{p,m}°$** [J · K^{-1} · mol^{-1}]	**Species**
Hg(l)	0.0	0.0	**75.900 ± 0.12**		Hg(l)
Hgg	**31.842 ± 0.054**	**61.380 ± 0.040**	**174.971 ±0.005**	**20.786 ± 0.001**	Hgg
Hg2+2	**153.567 ± 0.56**	**166.870 ± 0.50**	**65.740 ± 0.80**		Hg_2^{2+}
Hg2Cl2(cr)	**-210.725 ± 0.47**	**-265.370 ± 0.40**	**191.600 ± 0.80**		Hg_2Cl_2(cr)
Hg+2	**164.667 ± 0.31**	**170.210 ± 0.20**	**-36.190 ± 0.80**		Hg^{2+}
HgO(cr)	**-58.523 ± 0.15**	**-90.790 ± 0.12**	**70.250 ± 0.30**		HgO(montroydite, red)

Name	**$\log_{10}\beta°$**	**$\Delta\varepsilon$** [kg · mol^{-1}]	**$\Delta_r H_m°$** [kJ · mol^{-1}]	**$\Delta_r C_{p,m}°$** [J · K^{-1} · mol^{-1}]	**T-range** [°C]	**Reaction**
Hg(aq)	-6.53 ± 0.03		23.0 ± 2.2	0	0 – 90	$Hg(l) \rightleftharpoons Hg(aq)$
Hg2OH+	-4.6 ± 0.5	-0.08 ± 0.16	-			$Hg_2^{2+} + H_2O(l) \rightleftharpoons Hg_2OH^+ + H^+$
HgOH+	-3.40 ± 0.08	-0.14 ± 0.03	-			$Hg^{2+} + H_2O(l) \rightleftharpoons HgOH^+ + H^+$
Hg(OH)2(aq)	-5.98 ± 0.06	-0.14 ± 0.02	51.0 ± 1.8			$Hg^{2+} + 2\ H_2O(l) \rightleftharpoons Hg(OH)_2(aq) + 2\ H^+$
Hg(OH)3-	-21.1 ± 0.3		-			$Hg^{2+} + 3\ H_2O(l) \rightleftharpoons Hg(OH)_3^- + 3\ H^+$
HgCl+	7.31 ± 0.04	-0.22 ± 0.04	-21.3 ± 0.7			$Hg^{2+} + Cl^- \rightleftharpoons HgCl^+$
HgCl2(aq)	14.00 ± 0.07	-0.39 ± 0.03	-49.1 ± 1.0			$Hg^{2+} + 2\ Cl^- \rightleftharpoons HgCl_2(aq)$
HgCl3-	0.925 ± 0.09	0.01 ± 0.05	0.5 ± 2.5			$HgCl_2(aq) + Cl^- \rightleftharpoons HgCl_3^-$
HgCl4-2	0.61 ± 0.12	0.00 ± 0.06	-10.5 ± 2.5			$HgCl_3^- + Cl^- \rightleftharpoons HgCl_4^{2-}$
HgOHCl(aq)	4.27 ± 0.35		-			$Hg^{2+} + Cl^- + H_2O(l) \rightleftharpoons HgOHCl(aq) + H^+$
HgCO3(aq)	-0.70 ± 0.20		-			$Hg(OH)_2(aq) + CO_2g \rightleftharpoons HgCO_3(aq) + H_2O(l)$
HgOHCO3-	0.98 ± 0.10		-			$Hg(OH)_2(aq) + HCO_3^- \rightleftharpoons HgOHCO_3^- + H_2O(l)$
HgHCO3+	3.63 ± 0.10		-			$Hg(OH)_2(aq) + CO_2g + H^+ \rightleftharpoons HgHCO_3^+ + H_2O(l)$
HgHPO4(aq)	*10.9 ± 0.6*		-			*$Hg^{2+} + HPO_4^{2-} \rightleftharpoons HgHPO_4(aq)$*
HgPO4-	*5.3 ± 0.6*		-			*$Hg^{2+} + HPO_4^{2-} \rightleftharpoons HgPO_4^- + H^+$*
HgSO4(aq)	2.8 ± 0.2		-			$Hg^{2+} + SO_4^{2-} \rightleftharpoons HgSO_4(aq)$
Hg(SO4)2-2	*3.8*		-			*$Hg^{2+} + 2\ SO_4^{2-} \rightleftharpoons Hg(SO_4)_2^{2-}$*
Hg(HS)2(aq)	< 37.8		-			*$Hg^{2+} + 2\ HS^- \rightleftharpoons Hg(HS)_2(aq)$*
HgS(HS)-	31.5 ± 0.2		-			$Hg^{2+} + 2\ HS^- \rightleftharpoons HgS(HS)^- + H^+$
HgS2-2	22.3 ± 0.2		-			$Hg^{2+} + 2\ HS^- \Leftrightarrow HgS_2^{2-} + 2\ H^+$

Tab. 14-1: Cont.

Name	**$\log_{10}K_{s,0}°$**	**$\Delta_r H_m°$** [kJ · mol^{-1}]	**Reaction**
HgCO3.2HgO(s)	-11.27 ± 0.35	-	$HgCO_3 \cdot 2HgO(s) + 3\ H_2O(l) \rightleftharpoons 3\ Hg(OH)_2(aq) + CO_2g$
Hg3(PO4)2(s)	*-30.0 ± 0.9*	-	*$Hg_3(PO_4)_2(s) + 2\ H^+ \rightleftharpoons 3\ Hg^{2+} + 2\ HPO_4^{2-}$*
(HgOH)3PO4(s)	*-14.0 ± 1.1*	-	*$(HgOH)3PO4(s) + 4\ H^+ \rightleftharpoons 3\ Hg^{2+} + HPO_4^{2-} + 3\ H_2O(l)$*
HgHPO4(s)	*-15.2 ± 0.3*	-	*$HgHPO4(s) \rightleftharpoons Hg^{2+} + HPO_4^{2-}$*
HgS(s)	-36.77 ± 0.18	-	$HgS(s) + H^+ \rightleftharpoons Hg^{2+} + HS^-$

Tab. 14-2: Selected SIT ion interaction coefficients $\varepsilon_{j,k}$ [kg · mol^{-1}] for mercury species

Data in bold face are taken from Lemire et al. (2013). Data in normal face are derived or estimated in this review. Data estimated according to charge correlations and taken from Tab. 1-7 are shaded. Supplemental data are in italics.

j k → ↓	**Cl^-** $\varepsilon_{j,k}$ [kg · mol^{-1}]	**ClO_4^-** $\varepsilon_{j,k}$ [kg · mol^{-1}]	**Na^+** $\varepsilon_{j,k}$ [kg · mol^{-1}]	**$Na^+ + Cl^-$** $\varepsilon_{j,k}$ [kg · mol^{-1}]	**$Na^+ + ClO_4^-$** $\varepsilon_{j,k}$ [kg · mol^{-1}]
H2S(aq)	0	0	0	(0.055 ± 0.004) [a]	(0.055 ± 0.004) [c]
HS-	0	0	(0.08 ± 0.01) [a]	0	0
Hg(aq)	0	0	0	0.0 ± 0.1	0.0 ± 0.1
Hg2+2	(0.09 ± 0.02) [b]	**0.09 ± 0.02**	0	0	0
Hg2OH+	(-0.13 ± 0.16) [b]	-0.13 ± 0.16	0	0	0
Hg+2	(0.34 ± 0.03) [b]	**0.34 ± 0.03**	0	0	0
HgOH+	(0.06 ± 0.05) [b]	0.06 ± 0.05	0	0	0
Hg(OH)2(aq)	0	0	0	(-0.08 ± 0.05) [b]	-0.08 ± 0.05
Hg(OH)3-	0	0	-0.05 ± 0.10	0	0
HgCl+	(0.15 ± 0.05) [b]	0.15 ± 0.05	0	0	0
HgCl2(aq)	0	0	0	(0.01 ± 0.04) [b]	0.01 ± 0.04
HgCl3-	0	0	0.05 ± 0.06	0	0
HgCl4-2	0	0	0.08 ± 0.09	0	0
HgOHCl(aq)	0	0	0	(-0.01 ± 0.09) [b]	-0.01 ± 0.09
HgCO3(aq)	0	0	0	0.0 ± 0.1	0.0 ± 0.1
HgOHCO3-	0	0	-0.05 ± 0.10	0	0
HgHCO3+	0.2 ± 0.1	0.2 ± 0.1	0	0	0
HgHPO4(aq)	*0*	*0*	*0*	*0.0 ± 0.1*	*0.0 ± 0.1*
HgPO4-	*0*	*0*	*-0.05 ± 0.10*	0	*0*
HgSO4(aq)	0	0	0	0.0 ± 0.1	0.0 ± 0.1
Hg(SO4)2-2	*0*	*0*	*-0.10 ± 0.10*	*0*	*0*
Hg(HS)2(aq)	*0*	*0*	*0*	*(0.055 ± 0.10)* [d]	*(0.055 ± 0.10)* [d]

Tab. 14-2: Cont.

j k → ↓	**Cl^-** $\varepsilon_{j,k}$ [kg · mol^{-1}]	**ClO_4^-** $\varepsilon_{j,k}$ [kg · mol^{-1}]	**Na^+** $\varepsilon_{j,k}$ [kg · mol^{-1}]	**$Na^+ + Cl^-$** $\varepsilon_{j,k}$ [kg · mol^{-1}]	**$Na^+ + ClO_4^-$** $\varepsilon_{j,k}$ [kg · mol^{-1}]
HgS(HS)-	0	0	(0.08 ± 0.10) [e]	0	0
HgS2-2	0	0	-0.10 ± 0.10	0	0

[a] Section 1.5.3
[b] Assumed to be equal to the corresponding ion interaction coefficient with ClO_4^-, see Section 14.1 for explanation.
[c] Assumed to be equal to the corresponding ion interaction coefficient with NaCl.
[d] Assumed to be equal to the corresponding ion interaction coefficient of H_2S(aq), with increased uncertainty.
[e] Assumed to be equal to the corresponding ion interaction coefficient of HS^-, with increased uncertainty.

14.6 References

Brookins, D.G. (1988): Eh-pH Diagrams for Geochemistry. Springer-Verlag Berlin Heidelberg, Germany, 184 pp.

Brown, P.L. & Ekberg, C. (2016): Hydrolysis of Metal Ions. Wiley-VCH Verlag GmbH & Co. KGaA, Weinheim, Germany, 917 pp.

Clever, H.L., Johnson, S.A. & Derrick, M.E. (1985): The Solubility of Mercury and Some Sparingly Soluble Mercury Salts in Water and Aqueous Electrolyte Solutions. J. Phys. Chem. Ref. Data, 14, 631-680.

Cox, J.D., Wagman, D.D. & Medvedev, V.A. (1989): CODATA Key Values for Thermodynamics. New York, Hemisphere Publishing, 271 pp.

Grenthe, I., Fuger, J., Konings, R.J.M., Lemire, R.J., Muller, A.B., Nguyen-Trung, C. & Wanner, H. (1992): Chemical Thermodynamics of Uranium. Chemical Thermodynamics, Vol. 1. North-Holland, Amsterdam, 715 pp.

Forsling, W., Hietanen, S. & Sillén, L.G. (1959): Studies on the hydrolysis of metal ions. 3. The hydrolysis of the mercury(I) ion, Hg_2^{2+}. Acta Chem. Scand., 6, 901-909.

Hietanen, S. & Högfeldt, E. (1976): On the hydrolysis of Hg(I)-perchlorate in 3 M (Na)ClO_4. Chem. Scr., 10, 41-44.

Hummel, W., Berner, U., Curti, E., Pearson, F.J. & Thoenen, T. (2002): Nagra/PSI Chemical Thermodynamic Data Base 01/01. Nagra Technical Report NTB 02-16 and Universal Publishers, Parkland, Florida, 565 pp.

Jay, J.A., Morel, F.M.M. & Hemond, H.F. (2000): Mercury speciation in the presence of polysulfides. Environ. Sci. Technol., 34, 2196-2200.

Lemire, R.J., Berner, U., Musikas, C., Palmer, D.A., Taylor, P. & Tochiyama, O. (2013): Chemical Thermodynamics of Iron, Part 1. Chemical Thermodynamics, Vol. 13a. OECD Publications, Paris, France, 1082 pp.

Marcus, Y. (1980): Compilation and Evaluation of Solubility Data in the Mercury(I) Chloride-Water System. J. Phys. Chem. Ref. Data, 9, 1307-1329.

Mehra, M.C. (1968): Studies on the stabilities of some metal selenite, sulphide, and selenide complexes in solution. Ph.D. thesis, Laval University, Quebec, 191 pp.

Newberry, E. (1936): Some physico-chemical properties of mercurous perchlorate solutions. Trans. Electrochem. Soc. 69, 611-628.

Paquette, K.E. & Helz, G.R. (1997): Inorganic speciation of mercury in sulfidic waters: The importance of zero-valent sulfur. Environ. Sci. Technol., 31, 2148-2153.

Parks, G.A. & Nordstrom, D.K. (1979): Estimated Free Energies of Formation, Water Solubilities, and Stability Fields for Schuetteite ($Hg_3O_2SO_4$) and Corderoite ($Hg_3S_2Cl_2$) at 298 K. In: Jenne, E.A. (ed.): Chemical Modeling in Aqueous Systems. Washington, D.C., American Chemical Society, ACS Symposium Series 93, 339-352.

Powell, K.J., Brown, P.L., Byrne, R.H., Gajda, T., Hefter, G., Sjöberg, S. & Wanner, H. (2005): Chemical Speciation of Environmentally Significant Heavy Metals with Inorganic Ligands. Part 1: The Hg^{2+} – Cl^-, OH^-, CO_3^{2-}, SO_4^{2-}, and PO_4^{3-} Aqueous Systems. Pure Appl. Chem., 77, 739-800.

Rickard, D. & Luther III, G.W. (2006): Metal sulfide complexes and clusters. Reviews in Mineralogy & Geochemistry, 61, 421-504.

Rickard, D. (2012): Aqueous metal-sulfide chemistry: Complexes, clusters and nanoparticles. Developments in Sedimentology, 65, 121-194.

Schwarzenbach, G. & Widmer, M. (1963): Die Löslichkeit von Metallsulfiden I. Schwarzes Quecksilbersulfid. Helvetica Chimica Acta, 46, 2613-2628.

Shikina, N.D., Zotov, A.V. & Khodakovskii, I.L. (1981): An experimental investigation of the equilibria in the α-HgS-H_2S-H_2O system at 90 and 150 °C. Geochemistry International, 18, 109-117 (translated from Geokhimiya 4, 496-503, 1981).

Widmer, M. (1962): Über die Löslichkeit des schwarzen Quecksilbersulfids und Silbersulfids. Ph.D. thesis, ETH Zurich, Zürich, Switzerland, 104 pp.

Zhang, J.-Z. & Millero, F.J. (1994): Investigation of metal sulphide complexes in sea water using cathodic stripping square wave voltammetry. Analytica Chimica Acta, 284, 497-504.

15 Molybdenum

15.1 Introduction

Molybdenum is toxic especially if it is dissolved as aqueous molybdate species and thus, molybdenum is an environmentally significant heavy metal. In addition, a long-lived radioactive isotope, Mo-93 with $(4.0 \pm 0.8) \cdot 10^3$ years half-life, is produced by neutron activation of stable Mo-92 in nuclear power plants and contributes in dose-relevant quantities to the inventory of radioactive waste.

The latter fact triggered the inclusion of molybdenum already in our original data base (Pearson et al. 1992). However, only one aqueous species (MoO_4^{2-}) and three solids (Mo(cr), MoO_2(cr) and MoO_3(cr)) were included, and the molybdenum data have never been updated so far.

An NEA TDB review of molybdenum commenced in 2009 and the original plan was to include the results of this NEA review in TDB 2020. Unfortunately, the NEA molybdenum review is currently (spring 2020) still not available, and it is even unclear whether it will ever be finished.

However, the late first chairman of the NEA molybdenum review, Prof. Heinz Gamsjäger, published some important results of this review concerning Mo(cr), MoO_4^{2-}, $CaMoO_4$(cr) and MoO_3(cr) (Gamsjäger 2013, Gamsjäger & Morishita 2015). In addition, a recent review by Dadze et al. (2018) provides additional results for $HMoO_4^-$, H_2MoO_4(aq), MoO_3(cr) and $CaMoO_4$(cr) based on and consistent with the results reported by Gamsjäger (2013) and Gamsjäger & Morishita (2015). Furthermore, the experimental and modelling studies of Essington (1990) and Felmy et al. (1992) provide data which allow to estimate an equilibrium constant for $CaMoO_4$(aq)

The molybdenum data have been updated by this review based on the above-mentioned publications.

15.2 Elemental molybdenum

Molybdenum metal is not relevant under environmental conditions, but the absolute entropy of Mo(cr) is included in TDB 2020 as it is used for the calculation of certain thermodynamic reaction properties.

The selected value for Mo(cr) is taken from Gamsjäger & Morishita (2015):

$$S_m°(\text{Mo, cr, 298.15 K}) = (28.581 \pm 0.050)\ \text{J} \cdot \text{K}^{-1} \cdot \text{mol}^{-1}$$

Gamsjäger & Morishita (2015) state that $S_m°$(Mo, cr, 298.15 K) "has been compiled and evaluated recently" and quote as source of this value "OECD NEA Mo review project, to be published". Note that $S_m°$(Mo, cr, 298.15 K) = 28.66 J · K^{-1} · mol^{-1}, reported by Wagman et al. (1982) without error estimates, and originally selected by Pearson et al. (1992), is slightly outside the uncertainty range of the new (provisional) NEA value.

15.3 Molybdenum(IV)

Dadze et al. (2018) state in their review that in aqueous solutions, the species of molybdenum in the +VI oxidation state are most important. Even under strongly reducing conditions the molybdate ion, MoO_4^{2-}, and its protonated forms coexist with MoO_2(cr) (the mineral tugarinovite) with no Mo(V) and Mo(IV) aqueous species detected.

15.3.1 Molybdenum(IV) oxide

The thermochemical data for tugarinovite, MoO_2(cr), selected by this review have been taken from Robie et al. (1979):

$\Delta_f G_m°(MoO_2, cr, 298.15\ K) = -(533.053 \pm 2.510)\ kJ \cdot mol^{-1}$

$\Delta_f H_m°(MoO_2, cr, 298.15\ K) = -(587.850 \pm 2.090)\ kJ \cdot mol^{-1}$

$S_m°(MoO_2, cr, 298.15\ K) = (50.02 \pm 0.30)\ J \cdot K^{-1} \cdot mol^{-1}$

Note that $\Delta_f G_m°(MoO_2, cr, 298.15\ K) = -533.01\ kJ \cdot mol^{-1}$ and $\Delta_f H_m°(MoO_2, cr, 298.15\ K) = -88.94\ kJ \cdot mol^{-1}$, reported by Wagman et al. (1982) without error estimates, and originally selected by Pearson et al. (1992), are well within the uncertainty range of the values given by Robie et al. (1979).

Using the above selected thermochemical data together with the data for MoO_4^{2-} (see Section 15.4.1) and the CODATA values for H_2O(l), $\Delta_f G_m°(H_2O, l, 298.15\ K) = -(237.140 \pm 0.041)\ kJ \cdot mol^{-1}$ and $\Delta_f H_m°(H_2O, l, 298.15\ K) = -(285.830 \pm 0.040)\ kJ \cdot mol^{-1}$ (Cox et al. 1989), this review calculated

$MoO_2(cr) + 2\ H_2O(l) \rightleftharpoons MoO_4^{2-} + 4\ H^+ + 2\ e^-$

$\log_{10}{}^*K_{s,0}°\ (298.15\ K) = -29.92 \pm 0.47$

$\Delta_r H_m°(298.15\ K) = (162.70 \pm 2.25)\ kJ \cdot mol^{-1}$

These values have also been included in TDB 2020.

15.4 Molybdenum(VI)

15.4.1 Molybdate ion

Molybdenum(VI) exists as the MoO_4^{2-} oxyanion in aqueous solutions. The selected thermodynamic values for MoO_4^{2-} are taken from Gamsjäger & Morishita (2015):

$\Delta_f G_m°(MoO_4^{2-}, 298.15\ K) = -(836.542 \pm 0.881)\ kJ \cdot mol^{-1}$

$\Delta_f H_m°(MoO_4^{2-}, 298.15\ K) = -(996.807 \pm 0.826)\ kJ \cdot mol^{-1}$

$S_m°(MoO_4^{2-}, 298.15\ K) = (32.03 \pm 4.05)\ J \cdot K^{-1} \cdot mol^{-1}$

Gamsjäger & Morishita (2015) discuss in their review in detail the evaluation and final selection of the above values from experimental data and state that thermodynamic properties selected in their work for MoO_4^{2-} "will finally go in the OECD NEA Thermochemical Database (TDB) review on the inorganic compounds and aqueous complexes of molybdenum".

The values $\Delta_f G_m°(MoO_4^{2-}, 298.15\ K) = -836.3\ kJ \cdot mol^{-1}$, $\Delta_f H_m°(MoO_4^{2-}, 298.15\ K) = -997.9\ kJ \cdot mol^{-1}$ and $S_m°(MoO_4^{2-}, 298.15\ K) = 27.2\ J \cdot K^{-1} \cdot mol^{-1}$ reported by Wagman et al. (1982) without error estimates, have originally been selected by Pearson et al. (1992). While the value of $\Delta_f G_m°$ is well within the uncertainty range of the new value given by Gamsjäger & Morishita (2015), the $\Delta_f H_m°$ and $S_m°$ values are clearly outside the 95% uncertainty range of the new values given by Gamsjäger & Morishita (2015).

Using the above selected thermochemical data together with the CODATA values for $H_2O(l)$, $\Delta_f G_m°(H_2O, l, 298.15\ K) = -(237.140 \pm 0.041)\ kJ \cdot mol^{-1}$ and $\Delta_f H_m°(H_2O, l, 298.15\ K) = -(285.830 \pm 0.040)\ kJ \cdot mol^{-1}$ (Cox et al. 1989), this review calculated

$Mo(cr) + 4\ H_2O(l) \rightleftharpoons MoO_4^{2-} + 8\ H^+ + 6\ e^-$

$\log_{10} K°\ (298.15\ K) = -19.62 \pm 0.15$

$\Delta_r H_m°(298.15\ K) = (146.51 \pm 0.83\ kJ \cdot mol^{-1}$

These values have also been included in TDB 2020.

15.4.2 Molybdate hydrolysis

Dadze et al. (2018) evaluated literature data for the reaction

$$H^+ + MoO_4^{2-} \rightleftharpoons HMoO_4^-$$

in different media, i.e., $NaClO_4$ (3 values), NaCl (11 values) and $NaNO_3$ (1 value), at ionic strength 0.1 – 3.0 M and 25 °C, by a constrained SIT analysis, leading to a common $\log_{10}K°$ (298.15 K) value by explicitly including $\varepsilon(H^+, ClO_4^-)$, $\varepsilon(H^+, Cl^-)$ and $\varepsilon(H^+, NO_3^-)$ in the analytical function. Dadze et al. (2018) obtained from their SIT analysis

$$\log_{10}K° \text{ (298.15 K)} = 4.10 \pm 0.05 \text{ (2}\sigma\text{)}$$

$$\varepsilon(Na^+, MoO_4^{2-}) - \varepsilon(Na^+, HMoO_4^-) = 0.09 \pm 0.03 \text{ (2}\sigma\text{)}$$

Using their $\log_{10}K°$(298.15 K) Dadze et al. (2018) calculated $\Delta_rG_m°$(298.15 K) = -(23.40 ± 0.29) kJ · mol^{-1}, and combining this value with the selected Gibbs energy of formation of MoO_4^{2-} (see Section 15.4.1) they obtained

$$\Delta_fG_m°(HMoO_4^-, 298.15 \text{ K}) = -(859.94 \pm 0.93) \text{ kJ} \cdot \text{mol}^{-1}$$

Experimental $\log_{10}K°$ data in the temperature range 16 – 250 °C have been recast by Dadze et al. (2018) to the isocoulombic reaction

$$MoO_4^{2-} + HSO_4^- \rightleftharpoons SO_4^{2-} + HMoO_4^-$$

by combining them with the second ionisation constant of H_2SO_4, $H^+ + SO_4^{2-} \rightleftharpoons HSO_4^-$, and they found a linear relation of these recast data on 1 / T. Dadze et al. (2018) obtained

$$\Delta_rH_m°(298.15 \text{ K}) = -(6.77 \pm 1.71) \text{ kJ} \cdot \text{mol}^{-1} \text{ (2}\sigma\text{)}$$

$$\Delta_rC_{p,m}°(298.15 \text{ K}) = 0 \text{ J} \cdot \text{K}^{-1} \cdot \text{mol}^{-1}$$

Combining $\Delta_rH_m°$(298.15 K) with the enthalpies of formation of MoO_4^{2-} (see Section 15.4.1), SO_4^{2-} and HSO_4^-, Dadze et al. (2018) obtained

$$H^+ + MoO_4^{2-} \rightleftharpoons HMoO_4^-$$

$$\Delta_rH_m°(298.15 \text{ K}) = (15.67 \pm 1.98) \text{ kJ} \cdot \text{mol}^{-1}$$

and

$$\Delta_fH_m°(HMoO_4^-, 298.15 \text{ K}) = -(981.14 \pm 2.18) \text{ kJ} \cdot \text{mol}^{-1}$$

Using the Gibbs-Helmholtz relation, Dadze et al. (2018) calculated $\Delta_f S_m°(298.15\ K) = -(406.51 \pm 7.95)\ J \cdot K^{-1} \cdot mol^{-1}$, and in combination with the entropies for the elements, i.e., Mo(cr) (see Section 15.2), O_2g and H_2g (Cox et al. 1989), they obtained

$$S_m°(HMoO_4^-, 298.15\ K) = (163.1 \pm 7.9)\ J \cdot K^{-1} \cdot mol^{-1}$$

Dadze et al. (2018) estimated $C_{p,m}°(HMoO_4^-, 298.15\ K) = 44\ J \cdot K^{-1} \cdot mol^-$, considered the above-mentioned data in the temperature range 16 – 250 °C, evaluated experimental solubility data for the reaction $MoO_3(cr) + OH^- \rightleftharpoons HMoO_4^-$ in the temperature range 290 – 350 °C, and finally obtained 5-term temperature functions for both reactions $MoO_3(cr) + OH^- \rightleftharpoons HMoO_4^-$ and $H^+ + MoO_4^{2-} \rightleftharpoons HMoO_4^-$ (Fig. 15-1).

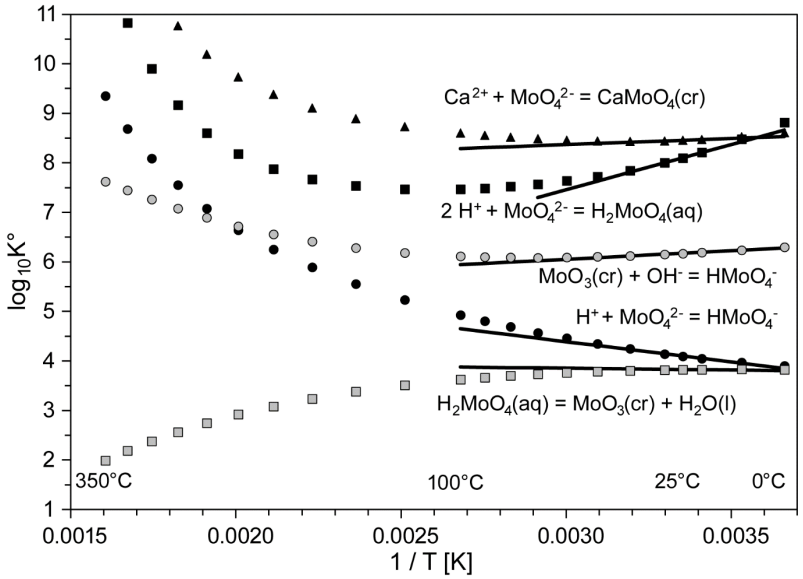

Fig. 15-1: Equilibrium constants of various reactions recommended by Dadze et al. (2018) (symbols) and approximations assuming $\Delta_r C_{p,m}°(298.15\ K) = 0$ (lines)

However, describing hydrothermal molybdenum systems up to 350 °C is outside the scope of TDB 2020, and assuming $\Delta_r C_{p,m}°(298.15\ K) = 0\ J \cdot K^{-1} \cdot mol^{-1}$ for the reaction $H^+ + MoO_4^{2-} \rightleftharpoons HMoO_4^-$ allows a good approximation of $\log_{10}K°$ values in the temperature range 0 – 100 °C (Fig. 5-1), with a maximum deviation of 0.28 $\log_{10}$-units at 100 °C. Thus, the values

$$H^+ + MoO_4^{2-} \rightleftharpoons HMoO_4^-$$

$$\log_{10}K°\ (298.15\ K) = 4.10 \pm 0.05$$

$$\Delta_r H_m°(298.15\ K) = (15.67 \pm 1.98)\ kJ \cdot mol^{-1}$$

$$\Delta_r C_{p,m}°(298.15\ K) = 0\ J \cdot K^{-1} \cdot mol^{-1}$$

and

$\Delta_f G_m°(HMoO_4^-, 298.15\ K) = -(859.94 \pm 0.93)\ kJ \cdot mol^{-1}$

$\Delta_f H_m°(HMoO_4^-, 298.15\ K) = -(981.14 \pm 2.18)\ kJ \cdot mol^{-1}$

$S_m°(HMoO_4^-, 298.15\ K) = (163.1 \pm 7.9)\ J \cdot K^{-1} \cdot mol^{-1}$

have been included in TDB 2020.

Dadze et al. (2018) evaluated literature data for the reaction

$2\ H^+ + MoO_4^{2-} \rightleftharpoons H_2MoO_4(aq)$

in $NaClO_4$ (3 values) and NaCl (11 values) at ionic strength 0.1 – 3.0 M and 25 °C. Dadze et al. (2018) correctly argue that "data obtained in $NaClO_4$ and NaCl media have to be treated separately, because the SIT coefficients of interaction between $H_2MoO_4(aq)$ and ions of an ionic medium are expected to be different in NaCl and $NaClO_4$ solutions". The results of their separate SIT analyses are

$\log_{10}K°\ (298.15\ K) = 8.12 \pm 0.08\ (2\sigma)$ (NaCl medium)

$\Delta\varepsilon(NaCl) = -(0.36 \pm 0.10)\ kg \cdot mol^{-1}\ (2\sigma)$

$\log_{10}K°\ (298.15\ K) = 8.05$ (no uncertainty estimates are possible) ($NaClO_4$)

$\Delta\varepsilon(NaClO_4) = -0.24\ kg \cdot mol^{-1}$ (no uncertainty estimates are possible)

Dadze et al. (2018) concluded that both values of $\log_{10}K°$ are in good agreement and they accepted the value

$\log_{10}K°\ (298.15\ K) = 8.1 \pm 0.1$

Using their $\log_{10}K°(298.15\ K)$ Dadze et al. (2018) calculated $\Delta_r G_m°(298.15\ K) = -(46.23 \pm 0.57)\ kJ \cdot mol^{-1}$, and combining this value with the selected Gibbs energy of formation of MoO_4^{2-} (see Section 15.4.1) they obtained

$\Delta_f G_m°(H_2MoO_4(aq), 298.15\ K) = -(882.78 \pm 1.05)\ kJ \cdot mol^{-1}$

Dadze et al. (2018) obtained, based on a data set in the temperature range 50 – 200 °C, and the evaluation of experimental solubility data in the temperature range 290 – 350 °C, $\Delta_r H_m°(298.15\ K) = -(1.4 \pm 5.0)\ kJ \cdot mol^{-1}$ for the reaction $MoO_3(cr) + H_2O(l) \rightleftharpoons H_2MoO_4(aq)$, as well as a 3-term temperature function (Fig. 5-1).

Combining $\Delta_r H_m°(298.15\ K)$ with the enthalpies of formation of $MoO_3(cr)$ (see Section 15.4.3) and $H_2O(l)$ (Cox et al. 1989) Dadze et al. (2018) calculated

$\Delta_f H_m°(H_2MoO_4(aq), 298.15\ K) = -(1'031.83 \pm 5.03)\ kJ \cdot mol^{-1}$

and, combining this result with the enthalpy of formation MoO_4^{2-} (see Section 15.4.1),

$2\ H^+ + MoO_4^{2-} \rightleftharpoons H_2MoO_4(aq)$

$\Delta_r H_m°(298.15\ K) = -(35.02 \pm 5.10)\ kJ \cdot mol^{-1}$

Using the Gibbs-Helmholtz relation in combination with the entropies for the elements, i.e., Mo(cr) (see Section 15.2) and O_2g (Cox et al. 1989) Dadze et al. (2018) calculated

$S_m°(H_2MoO_4(aq), 298.15\ K) = (69.64 \pm 17.2)\ J \cdot K^{-1} \cdot mol^{-1}$

Dadze et al. (2018) finally provide a 5-term temperature function for the reaction $2\ H^+ + MoO_4^{2-} \rightleftharpoons H_2MoO_4(aq)$ (Fig. 5-1).

However, describing hydrothermal molybdenum systems up to 350 °C is outside the scope of TDB 2020, and assuming $\Delta_r C_{p,m}°(298.15\ K) = 0\ J \cdot K^{-1} \cdot mol^{-1}$ for the reaction $2\ H^+ + MoO_4^{2-} \rightleftharpoons H_2MoO_4(aq)$ allows a good approximation of $\log_{10}K°$ values in the temperature range 0 – 70 °C (Fig. 5-1), with a maximum deviation of 0.27 $\log_{10}$-units at 70 °C. Thus, the values

$2\ H^+ + MoO_4^{2-} \rightleftharpoons H_2MoO_4(aq)$

$\log_{10}K°\ (298.15\ K) = 8.1 \pm 0.1$

$\Delta_r H_m°(298.15\ K) = -(35.02 \pm 5.10)\ kJ \cdot mol^{-1}$

$\Delta_r C_{p,m}°(298.15\ K) = 0\ J \cdot K^{-1} \cdot mol^{-1}$

and

$\Delta_f G_m°(H_2MoO_4(aq), 298.15\ K) = -(882.78 \pm 1.05)\ kJ \cdot mol^{-1}$

$\Delta_f H_m°(H_2MoO_4(aq), 298.15\ K) = -(1'031.83 \pm 5.03)\ kJ \cdot mol^{-1}$

$S_m°(H_2MoO_4(aq), 298.15\ K) = (69.64 \pm 17.2)\ J \cdot K^{-1} \cdot mol^{-1}$

have been included in TDB 2020.

Dadze et al. (2018) did not try to further evaluate their SIT coefficients. This review accepted the estimate (Hummel 2009)

$\varepsilon(H_2MoO_4(aq), NaCl) = \varepsilon(H_2MoO_4(aq), NaClO_4) = (0.0 \pm 0.1)\ kg \cdot mol^{-1}$

and using $\varepsilon(H^+, ClO_4^-)$ and $\varepsilon(H^+, Cl^-)$ (Tab. 15-2) calculated $\varepsilon(Na^+, MoO_4^{2-}) = (0.12 \pm 0.10)$ kg · mol^{-1} and $\varepsilon(Na^+, MoO_4^{2-}) = -0.04$ kg · mol^{-1} from $\Delta\varepsilon$(NaCl) and $\Delta\varepsilon(NaClO_4)$, respectively. Considering the scatter of experimental data in the SIT analyses (Fig. 5 of Dadze et al. 2018) the unweighted mean, with the uncertainty of $\Delta\varepsilon$(NaCl), is selected:

$$\varepsilon(Na^+, MoO_4^{2-}) = (0.04 \pm 0.10) \text{ kg} \cdot \text{mol}^{-1}$$

Combining this value with $\varepsilon(Na^+, MoO_4^{2-}) - \varepsilon(Na^+, HMoO_4^-) = 0.09 \pm 0.03$ (see above)

$$\varepsilon(Na^+, HMoO_4^-) = -(0.05 \pm 0.10) \text{ kg} \cdot \text{mol}^{-1}$$

is calculated. These values are included in TDB 2020.

15.4.3 Molybdenum(VI) oxide

The thermochemical data for molybdite, MoO_3(cr), selected by this review have been taken from Dadze et al. (2018):

$$\Delta_f G_m^\circ(MoO_3, \text{cr}, 298.15 \text{ K}) = -(667.49 \pm 0.52) \text{ kJ} \cdot \text{mol}^{-1}$$

$$\Delta_f H_m^\circ(MoO_3, \text{cr}, 298.15 \text{ K}) = -(744.60 \pm 0.50) \text{ kJ} \cdot \text{mol}^{-1}$$

$$S_m^\circ(MoO_3, \text{cr}, 298.15 \text{ K}) = (77.66 \pm 0.50) \text{ J} \cdot \text{K}^{-1} \cdot \text{mol}^{-1}$$

Note that $\Delta_f G_m^\circ(MoO_2, \text{cr}, 298.15 \text{ K}) = -667.97$ kJ · mol^{-1} and $\Delta_f H_m^\circ(MoO_2, \text{cr}, 298.15 \text{ K}) = -745.09$ kJ · mol^{-1}, reported by Wagman et al. (1982) without error estimates, and originally selected by Pearson et al. (1992), are barely within the uncertainty range of the values selected by this review.

Gamsjäger & Morishita (2015) report in their Tab. 14 (List of auxiliary data and references) $\Delta_f H_m^\circ(MoO_3, \text{cr}, 298.15 \text{ K}) = -(744.982 \pm 0.592)$ kJ · mol^{-1} and write "the value for $\Delta_f H_m^\circ(MoO_3$, cr, 298.15 K) has been compiled and evaluated recently" with the quote "OECD NEA Mo review project, to be published". However, for reasons of internal consistency the value selected by Dadze et al. (2018) has been included in TDB 2020.

Using the above selected thermochemical data together with the data for MoO_4^{2-} (see Section 15.4.1) and the CODATA values for H_2O(l), $\Delta_f G_m^\circ(H_2O, \text{l}, 298.15 \text{ K}) = -(237.140 \pm 0.041)$ kJ · mol^{-1} and $\Delta_f H_m^\circ(H_2O, \text{l}, 298.15 \text{ K}) = -(285.830 \pm 0.040)$ kJ · mol^{-1} (Cox et al. 1989), this review calculated

$$MoO_3(\text{cr}) + H_2O(\text{l}) \rightleftharpoons MoO_4^{2-} + 2\ H^+$$

$$\log_{10}{}^*K_{s0}^\circ\ (298.15 \text{ K}) = -11.93 \pm 0.18$$

$$\Delta_r H_m^\circ(298.15 \text{ K}) = (33.62 \pm 0.97) \text{ kJ} \cdot \text{mol}^{-1}$$

These values have also been included in TDB 2020.

15.4.4 Calcium molybdate compounds and complexes

15.4.4.1 Calcium molybdate compounds

The thermochemical data for powellite, $CaMoO_4$(cr), selected by this review have been taken from Gamsjäger & Morishita (2015):

$\Delta_f G_m°(CaMoO_4, cr, 298.15\ K) = -(1437.621 \pm 1.113)\ kJ \cdot mol^{-1}$

$\Delta_f H_m°(CaMoO_4, cr, 298.15\ K) = -(1'544.593 \pm 1.045)\ kJ \cdot mol^{-1}$

$S_m°(CaMoO_4, cr, 298.15\ K) = (121.69 \pm 1.22)\ J \cdot K^{-1} \cdot mol^{-1}$

Gamsjäger & Morishita (2015) state that thermodynamic properties for $CaMoO_4$(cr), based on the review of Gamsjäger (2013), and selected in their work, "will finally go in the OECD NEA Thermochemical Database (TDB) review on the inorganic compounds and aqueous complexes of molybdenum".

Using the above selected thermochemical data together with the data for MoO_4^{2-} (see Section 15.4.1) and the CODATA values for Ca^{2+}, $\Delta_f G_m°(Ca^{2+}, 298.15\ K) = -(552.806 \pm 1.050)\ kJ \cdot mol^{-1}$ and $\Delta_f H_m°(Ca^{2+}, 298.15\ K) = -(543.000 \pm 1.000)\ kJ \cdot mol^{-1}$ (Cox et al. 1989), this review calculated

$CaMoO_4(cr) \rightleftharpoons Ca^{2+} + MoO_4^{2-}$

$\log_{10} K_{s0}°\ (298.15\ K) = -8.46 \pm 0.31$

$\Delta_r H_m°(298.15\ K) = (4.79 \pm 1.66)\ kJ \cdot mol^{-1}$

These values have also been included in TDB 2020.

Dadze et al. (2018) state that the above solubility product is in excellent agreement with the value $\log_{10} K_{s0}°\ (298.15\ K) = -8.5 \pm 0.2$ based on a long-term (132 – 242 days) study of the solubility of large (1 – 3 mm) crystals of synthetic calcium molybdate conducted by Zhidikova & Khodakovsky (1971). Other studies, e.g., Essington (1990) and Felmy et al. (1992), see also the review by Gamsjäger (2013), report somewhat larger values, presumably due to smaller particle sizes of the solid phase, typically precipitated from aqueous solutions at room temperature.

Dadze et al. (2018) measured the solubility of powellite, $CaMoO_4$(cr), in NaCl solutions at 300 °C. Based on their own experimental data, using the thermochemical data selected by Gamsjäger & Morishita (2015) as reference values for 25 °C, and considering two published solubility studies in the temperature range 25 – 300 °C, Dadze et al. (2018) fitted a 5-term temperature function for the solubility product of $CaMoO_4$(cr) (Fig. 5-11).

However, describing hydrothermal molybdenum systems up to 350 °C is outside the scope of TDB 2020, and assuming $\Delta_r C_{p,m}°(298.15\ K) = 0\ J \cdot K^{-1} \cdot mol^{-1}$ for the reaction $CaMoO_4(cr) \rightleftharpoons Ca^{2+} + MoO_4^{2-}$ allows a good approximation of $\log_{10}K_{s0}°$ values in the temperature range 0 – 100 °C (Fig. 5-1), with a maximum deviation of 0.31 $\log_{10}$-units at 100 °C.

15.4.4.2 Calcium molybdate complexes

Essington (1990) measured the solubility of powellite, $CaMoO_4(cr)$, in deionised-distilled water and in 0.01, 0.05 and 0.10 M KNO_3 solutions at 25 °C, and interpreted his solubility data in terms of an ion association model including the species $CaNO_3^+$, $Ca(NO_3)_2(aq)$, $CaMoO_4(aq)$, $KNO_3(aq)$ and $KMoO_4^-$. Essington (1990) reports as results of his fitting procedure $\log_{10}K°$ (298.15 K) = 3.09 for $Ca^{2+} + MoO_4^{2-} \rightleftharpoons CaMoO_4(aq)$ and $\log_{10}K°$ (298.15 K) = 1.29 for $K^+ + MoO_4^{2-} \rightleftharpoons KMoO_4^-$. The $\log_{10}K°$ values are given without error estimate.

Felmy et al. (1992) measured the solubility of powellite, $CaMoO_4(cr)$, at ≈28 °C in aqueous Na_2MoO_4, $CaCl_2$ and $Ca(NO_3)_2$ solutions ranging in concentrations from $1 \cdot 10^{-4}$ M to 1.0 M. Felmy et al. (1992) modelled their solubility data in terms of the Pitzer ion interaction model, including the Pitzer parameters $\beta^{(0)}$ and $\beta^{(1)}$ for the systems $Ca^{2+} – Cl^-$ and $Ca^{2+} – NO_3^-$, and $\beta^{(0)}$, $\beta^{(1)}$ and $\beta^{(2)}$ for $Ca^{2+} – MoO_4^{2-}$.

Felmy et al. (1992) state that "on the subject of ion pair formation, it must be emphasised that these experimental data cannot be explained by assuming only a $CaMoO_4(aq)$ species without the inclusion of other $Ca^{2+} – MoO_4^{2-}$ ion-interaction parameters. Although our data can be adequately explained by retaining $\beta^{(0)}$ and $\beta^{(1)}$ for $Ca^{2+} – MoO_4^{2-}$ and replacing $\beta^{(2)}$ for $Ca^{2+} – MoO_4^{2-}$ with $CaMoO_4(aq)$ ($\log_{10}K°$ formation of 2.02, similar to proposed values for $CaSO_4(aq)$ of 2.31), there is no advantage of this model over the model that uses only ion-interaction parameters".

As TDB 2020 uses SIT, a specific ion interaction model somewhere in between a pure ion association model and the Pitzer ion interaction model, this review decided to select a value in between the values proposed by Essington (1990) and Felmy et al. (1992)

$$Ca^{2+} + MoO_4^{2-} \rightleftharpoons CaMoO_4(aq)$$

$$\log_{10}K°\ (298.15\ K) = 2.5 \pm 0.5$$

together with the estimate (Hummel 2009)

$$\varepsilon(CaMoO_4(aq), NaCl) = \varepsilon(CaMoO_4(aq), NaClO_4) = (0.0 \pm 0.1)\ kg \cdot mol^{-1}$$

Concerning their experimental solubility data of powellite, $CaMoO_4(cr)$, at 300 °C Dadze et al. (2018) state that "the species $CaMoO_4(aq)$ was not included in the modelling as its very small contribution cannot be determined from our solubility data". A very small temperature effect for $CaMoO_4(aq)$ is compatible with $\Delta_r H_m°(298.15\ K) = (6.9 \pm 1.7)\ kJ \cdot mol^{-1}$ selected for $CaSO_4(aq)$ (see Section 4.2.7.1). Hence the guess

$$Ca^{2+} + MoO_4^{2-} \rightleftharpoons CaMoO_4(aq)$$

$$\Delta_r H_m°(298.15\ K) = \approx 7\ kJ \cdot mol^{-1}$$

is included in TDB 2020 as supplemental datum.

15.5 Selected molybdenum data

Tab. 15-1: Selected molybdenum data

Supplemental data are in italics.

Name	**Redox**	**$\Delta_f G_m°$** [kJ · mol^{-1}]	**$\Delta_f H_m°$** [kJ · mol^{-1}]	**$S_m°$** [J · K^{-1} · mol^{-1}]	**Species**
Mo(cr)	0	0.0	0.0	28.581 ± 0.050	Mo(cr)
Tugarinovite	IV	-533.053 ± 2.510	-587.850 ± 2.090	50.02 ± 0.30	MoO_2(cr)
MoO4-2	VI	-836.542 ± 0.881	-996.807 ± 0.826	32.03 ± 4.05	MoO_4^{2-}
HMoO4-	VI	-859.94 ± 0.93	-981.14 ± 2.18	163.1 ± 7.9	$HMoO_4^-$
H2MoO4(aq)	VI	-882.78 ± 1.05	-1'031.83± 5.03	69.64 ± 17.2	H_2MoO_4(aq)
Molybdite	VI	-667.49 ± 0.52	-744.60 ± 0.50	77.66 ± 0.50	MoO_3(cr)
Powellite	VI	-1'437.621 ± 1.113	-1'544.593 ± 1.045	121.69 ± 1.22	$CaMoO_4$(cr)

Name	**Redox**	**$\log_{10}\beta°$**	**$\Delta_r H_m°$** [kJ · mol^{-1}]	**$\Delta_r C_{p,m}°$** [J · K^{-1} · mol^{-1}]	**T-range** [°C]	**Reaction**
MoO4-2	VI	-19.62 ± 0.15	146.51 ± 0.83	-		Mo(cr) + 4 H_2O(l) ⇌ MoO_4^{2-} + 8 H^+ + 6 e^-
HMoO4-	VI	4.10 ± 0.05	15.67 ± 1.98	0	0 – 100	H^+ + MoO_4^{2-} ⇌ $HMoO_4^-$
H2MoO4(aq)	VI	8.1 ± 0.1	-35.02 ± 5.10	0	0 – 70	2 H^+ + MoO_4^{2-} ⇌ H_2MoO_4(aq)
CaMoO4(aq)	VI	2.5 ± 0.5	*≈ 7*	-		Ca^{2+} + MoO_4^{2-} ⇌ $CaMoO_4$(aq)

Name	**Redox**	**$\log_{10}K_{s,0}°$**	**$\Delta_r H_m°$** [kJ · mol^{-1}]	**$\Delta_r C_{p,m}°$** [J · K^{-1} · mol^{-1}]	**T-range** [°C]	**Reaction**
Tugarinovite	IV	-29.92 ± 0.47	162.70 ± 2.25	-		MoO_2(cr) + 2 H_2O(l) ⇌ MoO_4^{2-} + 4 H^+ + 2 e^-
Molybdite	VI	-11.93 ± 0.18	33.62 ± 0.97	-		MoO_3(cr) + H_2O(l) ⇌ MoO_4^{2-} + 2 H^+
Powellite	VI	-8.46 ± 0.31	4.79 ± 1.66	0	0 – 100	$CaMoO_4$(cr) ⇌ Ca^{2+} + MoO_4^{2-}

Tab. 15-2: Selected SIT ion interaction coefficients $\varepsilon_{j,k}$ [kg · mol^{-1}] for molybdenum species

Data in bold face are taken from Lemire et al. (2013). Data in normal face are derived in this review. Data estimated according to charge correlations and taken from Tab. 1-7 are shaded.

J k → ↓	**Cl^-** $\varepsilon_{j,k}$ [kg · mol^{-1}]	**ClO_4^-** $\varepsilon_{j,k}$ [kg · mol^{-1}]	**Na^+** $\varepsilon_{j,k}$ [kg · mol^{-1}]	**$Na^+ + Cl^-$** $\varepsilon_{j,k}$ [kg · mol^{-1}]	**$Na^+ + ClO_4^-$** $\varepsilon_{j,k}$ [kg · mol^{-1}]
MoO4-2	0	0	0.04 ± 0.10	0	0
HMoO4-	0	0	-0.05 ± 0.10	0	0
H2MoO4(aq)	0	0	0	0.0 ± 0.1	0.0 ± 0.1
CaMoO4(aq)	0	0	0	0.0 ± 0.1	0.0 ± 0.1

15.6 References

Cox, J.D., Wagman, D.D. & Medvedev, V.A. (1989): CODATA Key Values for Thermodynamics. Hemisphere Publishing, New York, 271 pp.

Dadze, T.P., Kashirtseva, G.A., Novikov, M.P. & Plyasunov, A.V. (2018): Solubility of calcium molybdate in aqueous solutions at 573 K and thermodynamics of monomer hydrolysis of Mo(VI) at elevated temperatures. Monatshefte für Chemie, 149, 261-282.

Essington, M.E. (1990): Calcium molybdate solubility in spent oil shale and a preliminary evaluation of the association constants for the formation of $CaMoO_4^0$(aq), $KMoO_4^-$(aq), and $NaMoO_4^-$(aq). Environ. Sci. Technol., 24, 214-220.

Felmy, A.R., Rai, D. & Mason, M.J. (1992): The solubility of CaMoO4(cr) and an aqueous thermodynamic model for Ca^{2+}-MoO_4^{2-}-ion-interactions. J. Solution Chem., 21, 525-532.

Gamsjäger, H. (2013): Solubility phenomena in science and education: Experiments, thermodynamic analyses, and theoretical aspects. Pure Appl. Chem., 85, 2059-2076.

Gamsjäger, H. & Morishita, M. (2015): Thermodynamic properties of molybdate ion: reaction cycles and experiments. Pure Appl. Chem., 87, 461-476.

Lemire, R.J., Berner, U., Musikas, C., Palmer, D.A., Taylor, P. & Tochiyama, O. (2013): Chemical Thermodynamics of Iron, Part 1. Chemical Thermodynamics, Vol. 13a. OECD Publications, Paris, France, 1082 pp.

Pearson, F.J., Jr., Berner, U. & Hummel W. (1992): Nagra Thermochemical Data Base II. Supplemental Data 05/92. Nagra Technical Report NTB 91-18.

Robie, R.A., Hemingway, B.S. & Fisher, J.R. (1979): Thermodynamic Properties of Minerals and Related Substances at 298.15 K and 1 Bar (10^5 Pascals) Pressure and at Higher Temperatures. United States Geological Survey Bulletin, 1452, Reprinted with corrections, 464 pp.

Wagman, D.D., Evans, W.H., Parker, V.B., Schumm, R.H., Halow, I., Bailey, S.M., Churney, K.L. & Nuttall, R.L. (1982): The NBS tables of chemical thermodynamic properties: Selected values for inorganic and C1 and C2 organic substances in SI units. Journal of Physical and Chemical Reference Data, 11, Supplement No. 2, 1-392.

Zhidikova, A.P. & Khodakovsky, I.L (1971) Geokhimiya, 4, 427 (in Russian, as cited by Dadze et al. 2018).

16 Neptunium

In a late state of the review work for TDB 2020 the NEA TDB Second Update on the Chemical Thermodynamics of Uranium, Neptunium, Plutonium, Americium and Technetium (Grenthe et al. 2020) became available to the reviewers. In the following, only changes with respect to previous TDB versions are shortly discussed. For a detailed discussion of the previous neptunium chemical thermodynamic data the reader is referred to Thoenen et al. (2014) and Hummel et al. (2002).

16.1 Neptunium oxygen and hydrogen compounds and complexes

Based on an empirical correlation of actinide hydrolysis constants with the effective charge of the actinide cation, Gaona et al. (2012) estimated

$$NpO_2^{2+} + 2\ H_2O(l) \rightleftharpoons NpO_2(OH)_2(aq) + 2\ H^+$$

$$log_{10}{}^*\beta_2^\circ = -12.2$$

Grenthe et al. (2020) state that this value must be taken only as indicative because of the large uncertainties associated with the estimation method used. However, the estimated value is in excellent agreement with the equilibrium constant $\log_{10}\beta_2^\circ = -(12.15 \pm 0.07)$ for the analogous U(VI) species, $NpO_2(OH)_2(aq)$ (see Tab. 31-2). Nevertheless, Grenthe et al. (2020) do not select the estimate and "the value is given for information only".

This value is included in TDB 2020 as supplemental datum.

Grenthe et al. (2020) report that several new experimental (Gaona et al. 2013) and (semi)empirical modelling studies have provided thermodynamic quantities for the species $NpO_2(OH)_3^-$ and $NpO_2(OH)_4^{2-}$. Gaona et al. (2013) studied the solubility of Np(VI) in alkaline solutions from low to high concentration of NaCl. Based on this solubility study, Grenthe et al. (2020) selected the following equilibrium constants and SIT interaction coefficients

$$NpO_2^{2+} + 3\ H_2O(l) \rightleftharpoons NpO_2(OH)_3^- + 3\ H^+$$

$$\log_{10}{}^*\beta_3^\circ = -(21.2 \pm 1.1)$$

$$\varepsilon(NpO_2(OH)_3^-, Na^+) = -(0.20 \pm 0.02)\ kg \cdot mol^{-1}$$

$$NpO_2^{2+} + 4\ H_2O(l) \rightleftharpoons NpO_2(OH)_4^{2-} + 4\ H^+$$

$$\log_{10}{}^*\beta_4^\circ = -(33.0 \pm 1.1)$$

$$\varepsilon\ (NpO_2(OH)_4^{2-}, Na^+) = -(0.12 \pm 0.04)\ kg \cdot mol^{-1}$$

and state that the large uncertainties reported in Gaona et al. (2013) for $\log_{10}{}^*\beta_3^\circ$ and $\log_{10}{}^*\beta_4^\circ$ are due to the large uncertainty associated with $\log_{10}{}^*K_{s,0}^\circ(Na_2Np_2O_7 \cdot xH_2O, cr)$ (see below).

These values have been included in TDB 2020.

Solubility experiments of Np(IV) and Pu(IV) in alkaline $CaCl_2$ solutions (Fellhauer et al. 2010), see below), have been extended to Np(V) (Fellhauer et al. 2016a, 2016b). Fellhauer et al. (2016b) describe the concentrations of Np(V) in solution as function of pH and $CaCl_2$ and the characterisation of the solid phase and solution species by several analytical methods. These results are used by Fellhauer et al. (2016a) to develop thermodynamic data for the Np(V) hydrolysis in $CaCl_2$ solution. The increasing Np(V) solubility at pH > 10.5 in combination with EXAFS data is interpreted by the formation of two ternary Np(V) hydroxo complexes, $Ca[NpO_2(OH)_2]^+$ and $Ca_3[NpO_2(OH)_5]^{2+}$. Based on this comprehensive solubility dataset and the detailed characterisation of the solid equilibrium phases, Grenthe et al. (2020) selected the following equilibrium constants and SIT interaction coefficients

$$NpO_2^+ + Ca^{2+} + 2\ H_2O(l) \rightleftharpoons CaNpO_2(OH)_2^+ + 2\ H^+$$

$$\log_{10}{}^*\beta^\circ = -(20.6 \pm 0.2)$$

$$\varepsilon(CaNpO_2(OH)_2^+, Cl^-) = -(0.07 \pm 0.08)\ kg \cdot mol^{-1}$$

$$NpO_2^+ + 3\ Ca^{2+} + 5\ H_2O(l) \rightleftharpoons Ca_3NpO_2(OH)_5^{2+} + 5\ H^+$$

$$\log_{10}{}^*\beta^\circ = -(54.8 \pm 0.3)$$

$$\varepsilon(Ca_3NpO_2(OH)_5^{2+}, Cl^-) = -(0.20 \pm 0.11)\ kg \cdot mol^{-1}$$

These values have been included in TDB 2020.

Grenthe et al. (2020) remark that the stability constants of the ternary Ca-Np(V)-OH aqueous complexes reported by Fellhauer et al. (2016a, 2016b) can be evaluated based on the species predominant in solution, and this evaluation indicates that in the pH-range where $NpO_2(OH)_2^-$ prevails (pH above 11), the ternary complex $CaNpO_2(OH)_2^+$ becomes predominant at $[Ca^{2+}] > 10^{-3}$ M. These ternary species of Np(V) are accordingly expected to play a predominant role in cementitious systems, where strongly alkaline conditions and millimolar concentrations of Ca (up to 20 mM) are given.

Grenthe et al. (2020) report that Fellhauer et al. (2010) investigated the formation of ternary Ca-Np(IV)-OH aqueous complexes in concentrated alkaline $CaCl_2$ solutions. These complexes are characterised by many OH-groups in the first coordination sphere of the actinide, whose charge is compensated by a number of Ca^{2+} ions in the second coordination shell. The inner-sphere character of these complexes was confirmed by EXAFS for Th(IV). Based on their solubility data and the analogy with Th(IV), Fellhauer et al. (2010) reported the following data for the formation of the complex $Ca_4[Np(OH)_8]^{4+}$:

$$4\ Ca^{2+} + Np^{4+} + 8\ H_2O(l) \rightleftharpoons Ca_4Np(OH)_8^{4+} + 8\ H^+$$

$$\log_{10}{}^*\beta^\circ = -(56.1 \pm 0.8)$$

$$\varepsilon(Ca_4Np(OH)_8^{4+}, Cl^-) = \varepsilon(Ca_4Th(OH)_8^{4+}, Cl^-) = -(0.01 \pm 0.10)\ kg \cdot mol^{-1}$$

Grenthe et al. (2020) further remark that Fellhauer et al. (2010) observed the formation of this species only in $[CaCl_2] \geq 2.0$ M ($I \geq 6.0$ M), that is at concentrations beyond the applicability of SIT. Consequently, Grenthe et al. (2020) provided these values "for information only". A more accurate description of this system is achieved with the Pitzer model also reported by Fellhauer et al. (2010), but this is out of the scope of the NEA review.

Hence, these values have been included in TDB 2020 as supplemental data.

Only one Np(VI) hydrated oxide ($NpO_3 \cdot H_2O$, cr) was selected in the previous NEA TDB reviews by Lemire et al. (2001) and Guillaumont et al. (2003). Although acknowledging the quality of the solubility data the selection was based on, the review by Lemire et al. (2001) cast some doubts on the structure of the solid phase. Grenthe et al. (2020) reviewed a study ignored by Lemire et al. (2001) and Guillaumont et al. (2003), which provides insight into the structure of the solid phase under discussion, and selected $NpO_2(OH)_2 \cdot H_2O$(cr, hex) as the solid investigated in the solubility study, while retaining the equilibrium constant selected by Lemire et al. (2001).

Experimental solubility data of Np(V) oxides and hydroxides were reviewed by Lemire et al. (2001) and Guillaumont et al. (2003) and thermodynamic solubility products were selected for fresh and aged NpO_2OH(am), i.e., for NpO_2OH(am, fr) and NpO_2OH(am, ag). A new solubility study of Petrov et al. (2017) explored the solubility of NpO_2OH(am) in dilute and concentrated NaCl-NaOH solutions. Solubility data in 0.1 M NaCl are in good agreement with previous solubility studies in dilute $NaClO_4$ systems, but Petrov et al. (2017) did not observe ageing of the initial NpO_2OH(am), while their spectroscopic data provide independent information on the reported hydrolysis constants and solubility product. Grenthe et al. (2020) conclude that the recent spectroscopic data provide sufficient support to retain the value selected by Lemire et al. (2001) and Guillaumont et al. (2003) for the fresh solid phase, now named NpO_2OH(am), and to disregard NpO_2OH(am, ag).

16.2 Neptunium halogen compounds and complexes

Grenthe et al. (2020) report that new studies on the fluoride complex formation of neptunium in aqueous solution are only available for Np(V). The thermodynamic equilibrium constants for NpO_2F(aq) reported in the literature vary but are consistent within their large uncertainty ranges. The new equilibrium constants reported in three studies fall within the range of previously reported values. Including the new data, Grenthe et al. (2020) calculated an unweighted average. Only two new studies, both in 1.0 M $NaClO_4$, report the complex $NpO_2F_2^-$, and Grenthe et al. (2020) selected the weighted average value, while the extrapolation to zero ionic strength used $\varepsilon(NpO_2(OH)_2^-, Na^+) = -(0.01 \pm 0.07)$ kg · mol^{-1} as proxy for $\varepsilon(NpO_2F_2^-, Na^+)$:

$$NpO_2^+ + F^- \rightleftharpoons NpO_2F(aq)$$

$$\log_{10}\beta_1^\circ = (1.4 \pm 0.3)$$

$$NpO_2^+ + 2\ F^- \rightleftharpoons NpO_2F_2^-$$

$$\log_{10}\beta_2^\circ = (1.9 \pm 0.4)$$

$$\varepsilon(NpO_2F_2^-, Na^+) = \varepsilon(NpO_2(OH)_2^-, Na^+) = -(0.01 \pm 0.07)\ \text{kg} \cdot \text{mol}^{-1}$$

These values have been included in TDB 2020.

16.3 Neptunium sulphate compounds and complexes

Np(V) forms weak complexes with sulphate. The previous NEA TDB reviews by Lemire et al. (2001) and Guillaumont et al. (2003) only selected an equilibrium constant for the complex $NpO_2SO_4^-$, $\log_{10}\beta_1° = (0.44 \pm 0.27)$. Grenthe et al. (2020) found four new experimental studies reporting thermodynamic data for the system Np(V)-sulphate. From an SIT plot of all data considered reliable, Grenthe et al. (2020) selected:

$$NpO_2^+ + SO_4^{2-} \rightleftharpoons NpO_2SO_4^-$$

$$\log_{10}\beta_1° = (1.3 \pm 0.2)$$

$$\varepsilon(NpO_2SO_4^-, Na^+) = (0.07 \pm 0.13)\ kg \cdot mol^{-1}$$

Furthermore, Grenthe et al. (2020) selected an enthalpy of reaction based on the same source as Lemire et al. (2001) but extrapolated to zero ionic strength:

$$\Delta_r H_m° = (22.0 \pm 7.0)\ kJ \cdot mol^{-1}$$

All these values have been included in TDB 2020.

16.4 Neptunium nitrate and phosphate compounds and complexes

16.4.1 Neptunium nitrate complexes

Data selected by Guillaumont et al. (2003) for $NpNO_3^{3+}$ are retained by Grenthe et al. (2020), but no other data have been selected concerning neptunium nitrate compounds and complexes.

16.4.2 Neptunium phosphate complexes

There are no new thermodynamic data on aqueous Np(VI)-phosphate complexes, and the data selected by Guillaumont et al. (2003) are retained by Grenthe et al. (2020).

Only one aqueous Np(V)-phosphate complex ($NpO_2HPO_4^-$) was selected by Lemire et al. (2001) and Guillaumont et al. (2003), although based on the available experimental evidence, the formation of other complexes with $H_2PO_4^-$ and PO_4^{3-} ligands was suggested. Two new experimental studies reporting thermodynamic data for the system Np(V)-phosphate have been published since then. As Grenthe et al. (2020) report, these studies focused on experiments in weakly acidic to near-neutral solutions and report the formation of $NpO_2H_2PO_4(aq)$ and $NpO_2HPO_4^-$. For $NpO_2H_2PO_4(aq)$ Grenthe et al. (2020) selected the unweighted average of two new values after extrapolation to $I = 0$

$$NpO_2^+ + H_2PO_4^- \rightleftharpoons NpO_2H_2PO_4(aq)$$

$$\log_{10}\beta_1° = (1.4 \pm 0.2)$$

This value is included in TDB 2020.

Grenthe et al. (2020) accepted four studies reporting data in 0.1 and 1.0 M $NaClO_4$, extrapolated them to $I = 0$ using SIT, and found that the calculated equilibrium constant is in excellent agreement with the selection by Lemire et al. (2001) which has been retained. In addition, equilibrium constants measured at 25 – 55 °C in 1.0 M $NaClO_4$ have been used to determine the enthalpy of reaction, assuming $\Delta_r C_{p,m}^\circ = 0$. The resulting $\Delta_r H_m^\circ$ has been extrapolated to $I = 0$:

$$NpO_2^+ + HPO_4^{2-} \rightleftharpoons NpO_2HPO_4^-$$

$$\log_{10}\beta_1^\circ = (2.95 \pm 0.10)$$

$$\varepsilon(NpO_2HPO_4^-, Na^+) = -(0.05 \pm 0.11)\ kg \cdot mol^{-1}$$

$$\Delta_r H_m^\circ = -(11 \pm 11)\ kJ \cdot mol^{-1}$$

These values have been included in TDB 2020.

16.5 Neptunium carbonate and silicate compounds and complexes

16.5.1 Neptunium carbonate compounds and complexes

The previous NEA TDB selection of thermodynamic data for the complexes $NpO_2CO_3(aq)$ and $NpO_2(CO_3)_2^{2-}$ by Lemire et al. (2001) relied on a single solubility study conducted in 3.0 M $NaClO_4$ by Vitorge & Capdevila (1998). Both the original source and the NEA TDB review highlighted the limitations of this selection due to the restricted set of solubility measurements available, in addition thermodynamic equilibrium was not achieved in several of the investigated samples. Grenthe et al. (2020) report that the solubility study of Kato et al. (1998) provides a significantly larger dataset for the thermodynamics of $NpO_2CO_3(aq)$. Because of the more comprehensive and accurate dataset Grenthe et al. (2020) selected the equilibrium constant determined by Kato et al. (1998):

$$NpO_2^{2+} + CO_3^{2-} \rightleftharpoons NpO_2CO_3(aq)$$

$$\log_{10}\beta_1^\circ = (9.86 \pm 0.10)$$

This value is included in TDB 2020.

Grenthe et al. (2020) state that the large stability assigned by Lemire et al. (2001) to $NpO_2(CO_3)_2^{2-}$ is not consistent with the experimental results of Kato et al. (1998). Indeed, $NpO_2CO_3(cr)$ solubility data reported in 0.1 M $NaClO_4$ by the latter authors can be explained with the predominance of NpO_2^{2+} at $\log_{10}[CO_3^{2-}] \leq -9$, $NpO_2CO_3(aq)$ between $-9 < \log_{10}[CO_3^{2-}] \leq -5.5$ and $NpO_2(CO_3)_3^{4-}$ at $\log_{10}[CO_3^{2-}] \geq -5.5$. Based on these experimental observations, the complex $NpO_2(CO_3)_2^{2-}$ is expected to have a minor importance on the aqueous chemistry of the Np(VI)-CO_3 system. The upper limit proposed by Kato et al. (1998),

$NpO_2^{2+} + 2\ CO_3^{2-} \rightleftharpoons NpO_2(CO_3)_2^{2-}$

$log_{10}\beta_2° = \leq 15.0$

is not selected by Grenthe et al. (2020) and is reported "for information only". Hence, this value is included in TDB 2020 as supplemental datum.

For the thermodynamic description of the Np(VI) carbonate limiting complex $NpO_2(CO_3)_3^{4-}$ Lemire et al. (2001) took into account three experimental sources, reporting data for the Np(V) / Np(VI) redox equilibrium, and selected $\log_{10}\beta_3° = (19.37 \pm 0.19)$. Kato et al. (1998) derived from their solubility study $\log_{10}\beta_3° = (20.35 \pm 0.09)$, which is approximately one $\log_{10}$-unit larger than the selection of Lemire et al. (2001). Grenthe et al. (2020) took both data sources into account and selected their unweighted average, with the uncertainty equal to the maximum deviation from the mean:

$NpO_2^{2+} + 3\ CO_3^{2-} \rightleftharpoons NpO_2(CO_3)_3^{4-}$

$\log_{10}\beta_3° = (19.9 \pm 0.5)$

This value is included in TDB 2020.

There are no new experimental studies providing thermodynamic data for $(NpO_2)_3(CO_3)_6^{6-}$, and the selection of Lemire et al. (2001) is retained by Grenthe et al. (2020). However, as Lemire et al. (2001) selected $\log_{10}K° = -(8.27 \pm 1.45)$ for the equilibrium $3\ NpO_2(CO_3)_3^{4-} \rightleftharpoons (NpO_2)_3(CO_3)_6^{6-} + 3\ CO_3^{2-}$, the value $\log_{10}\beta_{6,3}° = (49.84 \pm 1.56)$ for $3\ NpO_2^{2+} + 6\ CO_3^{2-} \rightleftharpoons (NpO_2)_3(CO_3)_6^{6-}$ included in TDB Version 12/07 has to be recalculated taking into account the new selected value $\log_{10}\beta_3° = (19.9 \pm 0.5)$ for $NpO_2^{2+} + 3\ CO_3^{2-} \rightleftharpoons NpO_2(CO_3)_3^{4-}$:

$3\ NpO_2^{2+} + 6\ CO_3^{2-} \rightleftharpoons (NpO_2)_3(CO_3)_6^{6-}$

$\log_{10}\beta_{6,3}° = (51.43 \pm 1.69)$

This value is included in TDB 2020.

Likewise, only one mixed Np(VI) hydroxide-carbonate complex, $(NpO_2)_2CO_3(OH)_3^-$, was selected by Lemire et al. (2001). The equilibrium constant for $2\ NpO_2(CO_3)_3^{4-} + 7\ H^+ \rightleftharpoons (NpO_2)_2CO_3(OH)_3^- + 5\ CO_2g + 2\ H_2O(l)$ is retained by Grenthe et al. (2020). However, the value $\log_{10}K° = -(2.87 \pm 1.64)$ for $2\ NpO_2^{2+} + CO_3^{2-} + 3\ H_2O(l) \rightleftharpoons (NpO_2)_2CO_3(OH)_3^- + 3\ H^+$ included in TDB Version 12/07 has to be recalculated taking into account the new selected value $\log_{10}\beta_3° = (19.9 \pm 0.5)$ for $NpO_2^{2+} + 3\ CO_3^{2-} \rightleftharpoons NpO_2(CO_3)_3^{4-}$:

$2\ NpO_2^{2+} + CO_3^{2-} + 3\ H_2O(l) \rightleftharpoons (NpO_2)_2CO_3(OH)_3^- + 3\ H^+$

$\log_{10}K° = -(1.81 \pm 1.66)$

This value is included in TDB 2020.

Gaona et al. (2012) corrected to $I = 0$ the conditional equilibrium constants for the mixed Np(V) hydroxide-carbonate complexes $NpO_2CO_3OH^{2-}$ and $NpO_2CO_3(OH)_2^{3-}$ reported by Neck et al. (1997) in 3.0 M $NaClO_4$. Gaona et al. (2012) used estimated SIT ion interaction parameters as given in Tab. 16-2 to derive

$$NpO_2^+ + CO_3^{2-} + H_2O(l) \rightleftharpoons NpO_2CO_3OH^{2-} + H^+$$
$$log_{10}{}^*K° = -(7.0 \pm 0.3)$$

$$NpO_2^+ + CO_3^{2-} + 2\ H_2O(l) \rightleftharpoons NpO_2CO_3(OH)_2^{3-} + 2\ H^+$$
$$log_{10}{}^*K° = -(20.34 \pm 0.15)$$

These data are not selected by Grenthe et al. (2020) and are reported "for information only". Hence, these values are included in TDB 2020 as supplemental data.

The binary carbonate complexes of Np(IV) were discussed by Lemire et al. (2001) and the selected values are retained by Grenthe et al. (2020). New experimental and modelling studies published after Guillaumont et al. (2003) and focusing on the pH-range 9 – 13 support the formation of ternary Np(IV)-OH-CO_3 complexes. Grenthe et al. (2020) report that Np(IV) solubility in carbonate media within $8 < pH < 11$ is clearly enhanced compared to carbonate-free solutions. A strong pH-dependency of the solubility is observed in this pH-region, which is ascribed by Kitamura & Kohara (2004) to the formation of $Np(OH)_2CO_3^{2-}$. The pH-independent behaviour of the solubility observed in solutions with $pH > 11$ is attributed by Kitamura & Kohara (2004) to the predominance of $Np(OH)_4CO_3^{2-}$. Grenthe et al. (2020) do not select any thermodynamic data for the ternary system Np(IV)-OH-CO_3, but state that the series of publications by Kitamura and Kohara are considered as the most comprehensive ones for this system, and the thermodynamic data and activity models derived by Kitamura & Kohara (2004) (and recalculated by Grenthe et al. 2020) are reported "for information only":

$$Np(OH)_4(am) + 2\ HCO_3^{2-} \rightleftharpoons Np(OH)_2(CO_3)_2^{2-} + 2\ H_2O(l)$$
$$log_{10}K° = -(2.9 \pm 0.2)$$
$$\varepsilon(Np(OH)_2(CO_3)_2^{2-}, Na^+) = -(0.3 \pm 0.2)\ kg \cdot mol^{-1}$$

$$Np(OH)_4(am) + CO_3^{2-} \rightleftharpoons Np(OH)_4CO_3^{2-}$$
$$log_{10}K° = -(6.2 \pm 0.2)$$
$$\varepsilon(Np(OH)_4CO_3^{2-}, Na^+) = (0.0 \pm 0.3)\ kg \cdot mol^{-1}$$

Assuming that $Np(OH)_4(am)$ is $NpO_2(am)(hyd)$ (Tab. 16-1) this review calculated

$$Np^{4+} + 2\ H_2O(l) + 2\ HCO_3^- \rightleftharpoons Np(OH)_2(CO_3)_2^{2-} + 4\ H^+$$
$$log_{10}{}^*K° = -(2.2 \pm 0.5)$$

$$Np^{4+} + 4\ H_2O(l) + CO_3^{2-} \rightleftharpoons Np(OH)_4CO_3^{2-} + 4\ H^+$$
$$log_{10}{}^*K° = -(5.5 \pm 0.5)$$

These values are included in TDB 2020 as supplemental data, together with their SIT ion interaction coefficients. Consequently, the equilibrium constant for $NpCO_3(OH)_3^-$, included as an estimate in TDB Version 12/07 (Thoenen et al. 2014), is not retained in TDB 2020.

Grenthe et al. (2020) discuss three solubility studies concerning Np(VI) carbonate and state that the most comprehensive study by Kato et al. (1998) shows that NpO_2CO_3 was a crystalline phase, while the solid phase was not characterised in the study of Vitorge & Capdevila (1998). Grenthe et al. (2020) selected the unweighted average of all available data, which is virtually the same as the value reported by Kato et al. (1998), with an associated uncertainty covering all reported values:

$$NpO_2CO_3(cr) \rightleftharpoons NpO_2^{2+} + CO_3^{2-}$$

$$\log_{10}K_{s,0}^\circ = -(14.83 \pm 0.23)$$

This value is included in TDB 2020.

Grenthe et al. (2020) state that there are no new experimental studies providing thermodynamic data for $(NH_4)_4NpO_2(CO_3)_3(s)$ and $K_4NpO_2(CO_3)_3(s)$, and the selections by Lemire et al. (2001) for the equilibrium reactions $(NH_4)_4NpO_2(CO_3)_3(s) \rightleftharpoons 4\ NH_4^+ + NpO_2(CO_3)_3^{4-}$ and $K_4NpO_2(CO_3)_3(s) \rightleftharpoons 4\ K^+ + NpO_2(CO_3)_3^{4-}$ are retained by Grenthe et al. (2020). However, the values included in TDB Version 12/07 have to be recalculated taking into account the new selected value $\log_{10}\beta_3^\circ = (19.9 \pm 0.5)$ for $NpO_2^{2+} + 3\ CO_3^{2-} \rightleftharpoons NpO_2(CO_3)_3^{4-}$:

$$(NH_4)_4NpO_2(CO_3)_3(s) \rightleftharpoons 4\ NH_4^+ + NpO_2^{2+} + 3\ CO_3^{2-}$$

$$\log_{10}K_{s,0}^\circ = -(27.34 \pm 0.58)$$

$$K_4NpO_2(CO_3)_3(s) \rightleftharpoons 4\ K^+ + NpO_2^{2+} + 3\ CO_3^{2-}$$

$$\log_{10}K_{s,0}^\circ = -(26.93 \pm 1.00)$$

These values have been included in TDB 2020.

16.5.2 Neptunium silicate compounds and complexes

Neptunium silicate compounds and complexes are discussed in Section 25.9.

16.6 Neptunium alkaline-earth compounds

Grenthe et al. (2020) report that three new Ca^{2+}-containing Np(V) hydroxide solid phases have been identified at different pH and $CaCl_2$ concentrations. Fellhauer et al. (2016b) describe experimental observations, including the concentrations of Np(V) as function of pH and $CaCl_2$ and the characterisation of solid phase and solution species by a number of analytical methods. These results are used by Fellhauer et al. (2016a) to determine thermodynamic data for the Np(V) hydrolysis in $CaCl_2$ solutions. The Np(V) solubility data are described using different solid equilibrium phases and with the solution species NpO_2^+ and two ternary Np(V) hydroxo complexes, $Ca[NpO_2(OH)_2]^+$ and $Ca_3[NpO_2(OH)_5]^{2+}$ (see Section 16.1). The solid phase $NpO_2OH(am)$ is found to be unstable in $CaCl_2$ solutions at pH > 8.5 and transforms to $CaNpO_2(OH)_{2.6}Cl_{0.4} \cdot 2H_2O(cr)$ in 2 M $CaCl_2$ at pH = 11. At $CaCl_2$ concentrations below 2 M and pH < 10.5, this solid converts into a reddish ternary hydrated solid phase, $Ca_{0.5}NpO_2(OH)_2 \cdot 1.3H_2O(cr)$. The anhydrous form, $Ca_{0.5}NpO_2(OH)_2(cr)$, is found in 4.5 M $CaCl_2$ at pH = 11.6.

Grenthe et al. (2020) select the following solubility product reported by Fellhauer et al. (2016a)

$$Ca_{0.5}NpO_2(OH)_2 \cdot 1.3H_2O(cr) + 2\ H^+ \rightleftharpoons NpO_2^+ + 0.5\ Ca^{2+} + 3.3\ H_2O(l)$$

$$\log_{10}{}^*K_{s,0}^\circ = (12.30 \pm 0.07)$$

and remark that this solid phase might control the solubility of Np(V) in alkaline solutions containing Ca such as in cementitious systems or salt brines.

This value is included in TDB 2020.

Grenthe et al. (2020) further mention the solubility product reported by Fellhauer et al. (2016a)

$$CaNpO_2(OH)_{2.6}Cl_{0.4} \cdot 2H_2O(cr) + 2.6\ H^+ \rightleftharpoons NpO_2^+ + Ca^{2+} + 4.6\ H_2O(l) + 0.4\ Cl^-$$

$$\log_{10}{}^*K_{s,0}^\circ = (19.90 \pm 0.10)$$

but do not select it. Hence, this value is included in TDB 2020 as supplemental datum.

16.7 Neptunium alkali compounds

Gaona et al. (2013) investigated the solubility of $Na_2Np_2O_7 \cdot xH_2O(l)$ in dilute to concentrated alkaline NaCl solutions and determined $\log_{10}{}^*K_{s,0}^\circ$ of this phase considering the transformation of $Na_2Np_2O_7 \cdot xH_2O(l)$ into $NpO_2(OH)_2 \cdot H_2O(cr)$ observed within pH ≈ 7.5 and 8.5 in 0.1 M NaCl. The equilibrium between both solid phases is only dependent on the pH and Na^+ concentration, but is independent of the aqueous speciation of Np. Gaona et al. (2013) used $\log_{10}{}^*K_{s,0}^\circ$ for $NpO_2(OH)_2 \cdot H_2O(cr)$ as reported by Lemire et al. (2001) (Tab. 16-1) and obtained

$$0.5\ Na_2Np_2O_7 \cdot xH_2O(l) + 3\ H^+ \rightleftharpoons Na+ + NpO_2^{2+} + (1.5 + 0.5x)\ H_2O(l)$$

$$\log_{10}{}^*K_{s,0}^\circ = (12.6 \pm 1.1)$$

The very large uncertainty assigned by Gaona et al. (2013) accounts for the uncertainty in the determination of the pH at which the solid phase transformation takes place. Grenthe et al. (2020) selected this value but remark that it needs to be refined in the future by using independent experimental observations on the formation of $NpO_2(OH)_3^-$ and $NpO_2(OH)_4^{2-}$ under alkaline conditions. Grenthe et al. (2020) do not select a $\Delta_f G_m°$ value for $Na_2Np_2O_7 \cdot xH_2O(l)$ because of the uncertainties affecting *x*. This non-selection would cause problems for GEMS calculations. However, as mentioned in the Appendix A entry for the Gaona et al. (2013) paper, $x \leq 0.1$ and hence, this review assigns the maximum hydration value $x = 0.1$ and includes this in TDB 2020.

16.8 Selected neptunium data

Tab. 16-1: Selected neptunium data

All data included in TDB 2020 are taken from Lemire et al. (2001), Guillaumont et al. (2003) and Grenthe et al. (2020) with the exception of those marked with an asterisk (*). The latter data were taken unchanged from Thoenen et al. (2014). Supplemental data are in italics. New or changed data with respect to TDB Version 12/07 (Thoenen et al. 2014) are shaded.

Name	Redox	TDB Version 12/07				TDB 2020				
		$\Delta_f G_m°$ [kJ · mol^{-1}]	$\Delta_f H_m°$ [kJ · mol^{-1}]	$S_m°$ [J · K^{-1} · mol^{-1}]	$C_{p,m}°$ [J · K^{-1} · mol^{-1}]	$\Delta_f G_m°$ [kJ · mol^{-1}]	$\Delta_f H_m°$ [kJ · mol^{-1}]	$S_m°$ [J · K^{-1} · mol^{-1}]	$C_{p,m}°$ [J · K^{-1} · mol^{-1}]	Species
Np(cr)	0	0.0	0.0	50.46 ± 0.80	29.62 ± 0.80	0.0	0.0	50.46 ± 0.80	29.62 ± 0.80	Np(cr)
Np+3	III	-512.9 ± 5.7	-527.2 ± 2.1	-193.6 ± 20.3	-	-512.9 ± 5.7	-527.2 ± 2.1	-193.6 ± 20.3	-	Np^{3+}
Np+4	IV	-491.8 ± 5.6	-556.0 ± 4.2	-426.4 ± 12.4	-	-491.8 ± 5.6	-556.0 ± 4.2	-426.4 ± 12.4	-	Np^{4+}
NpO2+	V	-907.8 ± 5.6	-978.2 ± 4.6	-45.9 ± 10.7	-4 ± 25	-907.8 ± 5.6	-978.2 ± 4.6	-45.9 ± 10.7	-4 ± 25	NpO_2^+
NpO2+2	VI	-795.9 ± 5.6	-860.7 ± 4.7	-92.4 ± 10.5	-	-795.9 ± 5.6	-860.7 ± 4.7	-92.4 ± 10.5	-	NpO_2^{2+}

Name	Redox	TDB Version 12/07		TDB 2020				Reaction
		$\log_{10}\beta°$	$\Delta_r H_m°$ [kJ · mol^{-1}]	$\log_{10}\beta°$	$\Delta_r H_m°$ [kJ · mol^{-1}]	$\Delta_r C_{p,m}°$ [J · K^{-1} · mol^{-1}]	T-range [°C]	
NpO2OH+	VI	-5.1 ± 0.4	-	-5.1 ± 0.4	-	-		$NpO_2^{2+} + H_2O(l) \rightleftharpoons NpO_2OH^+ + H^+$
NpO2(OH)2(aq)	VI	-	-	*-12.2*	-	-		*$NpO_2^{2+} + 2\ H_2O(l) \rightleftharpoons NpO_2(OH)_2(aq) + 2\ H^+$*
NpO2(OH)3-	VI	*(≤-20)* *	-	-21.2 ± 1.1	-	-		$NpO_2^{2+} + 3\ H_2O(l) \rightleftharpoons NpO_2(OH)_3^- + 3\ H^+$
NpO2(OH)4-2	VI	*(≤-32)* *	-	-33.0 ± 1.1	-	-		$NpO_2^{2+} + 4\ H_2O(l) \rightleftharpoons NpO_2(OH)_4^{2-} + 4\ H^+$
(NpO2)2(OH)2+2	VI	-6.27 ± 0.21	-	-6.27 ± 0.21	-	-		$2\ NpO_2^{2+} + 2\ H_2O(l) \rightleftharpoons (NpO_2)_2(OH)_2^{2+} + 2\ H^+$
(NpO2)3(OH)5+	VI	-17.12 ± 0.22	-	-17.12 ± 0.22	-	-		$3\ NpO_2^{2+} + 5\ H_2O(l) \rightleftharpoons (NpO_2)_3(OH)_5^+ + 5\ H^+$
NpO2F+	VI	4.57 ± 0.07	-	4.57 ± 0.07	-	-		$NpO_2^{2+} + F^- \rightleftharpoons NpO_2F^+$
NpO2F2(aq)	VI	7.60 ± 0.08	-	7.60 ± 0.08	-	-		$NpO_2^{2+} + 2\ F^- \rightleftharpoons NpO_2F_2(aq)$
NpO2Cl+	VI	0.40 ± 0.17	-	0.40 ± 0.17	-	-		$NpO_2^{2+} + Cl^- \rightleftharpoons NpO_2Cl^+$
NpO2IO3+	VI	1.2 ± 0.3	-	1.2 ± 0.3	-	-		$NpO_2^{2+} + IO_3^- \rightleftharpoons NpO_2IO_3^+$
NpO2SO4(aq)	VI	3.28 ± 0.06	16.7 ± 0.5	3.28 ± 0.06	16.7 ± 0.5	-		$NpO_2^{2+} + SO_4^{2-} \rightleftharpoons NpO_2SO_4(aq)$
NpO2(SO4)2-2	VI	4.70 ± 0.10	26.0 ± 1.2	4.70 ± 0.10	26.0 ± 1.2	-		$NpO_2^{2+} + 2\ SO_4^{2-} \rightleftharpoons NpO_2(SO_4)_2^{2-}$
NpO2H2PO4+	VI	3.32 ± 0.50	-	3.32 ± 0.50	-	-		$NpO_2^{2+} + H_2PO_4^- \rightleftharpoons NpO_2H_2PO_4^+$
NpO2HPO4(aq)	VI	6.2 ± 0.7	-	6.2 ± 0.7	-	-		$NpO_2^{2+} + HPO_4^{2-} \rightleftharpoons NpO_2HPO_4(aq)$
NpO2(HPO4)2-2	VI	9.5 ± 1.0	-	9.5 ± 1.0	-	-		$NpO_2^{2+} + 2\ HPO_4^{2-} \rightleftharpoons NpO_2(HPO_4)_2^{2-}$
NpO2CO3(aq)	VI	9.32 ± 0.61	-	9.86 ± 0.10	-	-		$NpO_2^{2+} + CO_3^{2-} \rightleftharpoons NpO_2CO_3(aq)$
NpO2(CO3)2-2	VI	16.52 ± 0.73	-	*≤ 15.0*	-	-		*$NpO_2^{2+} + 2\ CO_3^{2-} \rightleftharpoons NpO_2(CO_3)_2^{2-}$*

Tab. 16-1: Cont.

Name	Redox	TDB Version 12/07		TDB 2020				Reaction
		$\log_{10}\beta°$	$\Delta_r H_m°$ [kJ · mol^{-1}]	$\log_{10}\beta°$	$\Delta_r H_m°$ [kJ · mol^{-1}]	$\Delta_r C_{p,m}°$ [J · K^{-1} · mol^{-1}]	T-range [°C]	
NpO2(CO3)3-4	VI	19.37 ± 0.19	-41.9 ± 4.1	19.9 ± 0.5	-41.9 ± 4.1	-		$NpO_2^{2+} + 3\ CO_3^{2-} \rightleftharpoons NpO_2(CO_3)_3^{4-}$
(NpO2)3(CO3)6-6	VI	49.84 ± 1.56	-	51.43 ± 1.69	-	-		$3\ NpO_2^{2+} + 6\ CO_3^{2-} \rightleftharpoons (NpO_2)_3(CO_3)_6^{6-}$
(NpO2)2CO3(OH)3-	VI	-2.87 ± 1.64	-	-1.81 ± 1.66	-	-		$2NpO_2^{2+} + CO_3^{2-} + 3H_2O(l) \rightleftharpoons (NpO_2)_2CO_3(OH)_3^- + 3H^+$
(UO2)2NpO2(CO3)6-6	VI	53.59 ± 2.70	-	53.59 ± 2.70	-	-		$2\ UO_2^{2+} + NpO_2^{2+} + 6\ CO_3^{2-} \rightleftharpoons (UO_2)_2NpO_2(CO_3)_6^{6-}$
NpO2+	VI/V	19.59 ± 0.07	-	19.59 ± 0.07	-	-		$NpO_2^{2+} + e^- \rightleftharpoons NpO_2^+$
NpO2OH(aq)	V	-11.3 ± 0.7	$S_m°$ 25 ± 60	-11.3 ± 0.7	$S_m°$ 25 ± 60	-		$NpO_2^+ + H_2O(l) \rightleftharpoons NpO_2OH(aq) + H^+$
NpO2(OH)2-	V	-23.6 ± 0.5	$S_m°$ 40 ± 100	-23.6 ± 0.5	$S_m°$ 40 ± 100	-		$NpO_2^+ + 2\ H_2O(l) \rightleftharpoons NpO_2(OH)_2^- + 2\ H^+$
CaNpO2(OH)2+	V	-	-	-20.6 ± 0.2	-	-		$NpO_2^+ + Ca^{2+} + 2\ H_2O(l) \rightleftharpoons CaNpO_2(OH)_2^+ + 2\ H^+$
Ca3NpO2(OH)5+2	V	-	-	-54.8 ± 0.3	-	-		$NpO_2^+ + 3\ Ca^{2+} + 5\ H_2O(l) \rightleftharpoons Ca_3NpO_2(OH)_5^{2+} + 5\ H^+$
NpO2F(aq)	V	1.2 ± 0.3	-	1.4 ± 0.3	-	-		$NpO_2^+ + F^- \rightleftharpoons NpO_2F(aq)$
NpO2F2-	V	-	-	1.9 ± 0.4	-	-		$NpO_2^+ + 2\ F^- \rightleftharpoons NpO_2F_2^-$
NpO2IO3(aq)	V	0.5 ± 0.3	-	0.5 ± 0.3	-	-		$NpO_2^+ + IO_3^- \rightleftharpoons NpO_2IO_3(aq)$
NpO2SO4-	V	0.44 ± 0.27	23.2 ± 7.2	1.3 ± 0.2	22.0 ± 7.0	-		$NpO_2^+ + SO_4^{2-} \rightleftharpoons NpO_2SO_4^-$
NpO2H2PO4(aq)	V	-	-	1.4 ± 0.2	-	-		$NpO_2^+ + H_2PO_4^- \rightleftharpoons NpO_2H_2PO_4(aq)$
NpO2HPO4-	V	2.95 ± 0.10	-	2.95 ± 0.10	-11 ± 11	0	25 – 55	$NpO_2^+ + HPO_4^{2-} \rightleftharpoons NpO_2HPO_4^-$
NpO2CO3-	V	4.96 ± 0.06	-	4.96 ± 0.06	-	-		$NpO_2^+ + CO_3^{2-} \rightleftharpoons NpO_2CO_3^-$
NpO2(CO3)2-3	V	6.53 ± 0.10	-	6.53 ± 0.10	-	-		$NpO_2^+ + 2\ CO_3^{2-} \rightleftharpoons NpO_2(CO_3)_2^{3-}$
NpO2(CO3)3-5	V	5.50 ± 0.15	-13.3 ± 5.1	5.50 ± 0.15	-13.3 ± 5.1	-		$NpO_2^+ + 3\ CO_3^{2-} \rightleftharpoons NpO_2(CO_3)_3^{5-}$
NpO2CO3OH-2	V	-	-	*-7.0 ± 0.3*	-	-		*$NpO_2^+ + CO_3^{2-} + H_2O(l) \rightleftharpoons NpO_2CO_3OH^{2-} + H^+$*
NpO2CO3(OH)2-3	V	-	-	*-20.34 ± 0.15*	-	-		*$NpO_2^+ + CO_3^{2-} + 2\ H_2O(l) \rightleftharpoons NpO_2CO_3(OH)_2^{3-} + 2\ H^+$*
NpO2(CO3)2OH-4	V	-5.30 ± 1.17	-	-5.30 ± 1.17	-	-		$NpO_2^+ + 2\ CO_3^{2-} + H_2O(l) \rightleftharpoons NpO_2(CO_3)_2OH^{4-} + H^+$

Tab. 16-1: Cont.

Name	Redox	TDB Version 12/07		TDB 2020				Reaction
		$\log_{10}\beta°$	$\Delta_r H_m°$ [kJ · mol^{-1}]	$\log_{10}\beta°$	$\Delta_r H_m°$ [kJ · mol^{-1}]	$\Delta_r C_{p,m}°$ [J · K^{-1} · mol^{-1}]	T-range [°C]	
NpO2SCN(aq)	V	*(0.08 ± 0.30)* [a]	-	*(0.08 ± 0.30)* [a]	-	-		*$NpO_2^+ + SCN^- \rightleftharpoons NpO_2SCN(aq)$*
Np+4	VI/IV	29.80 ± 0.14	-	29.80 ± 0.14	-	-		$NpO_2^{2+} + 4\ H^+ + 2\ e^- \rightleftharpoons Np^{4+} + 2\ H_2O(l)$
NpOH+3	IV	0.55 ± 0.20	-	0.55 ± 0.20	-	-		$Np^{4+} + H_2O(l) \rightleftharpoons NpOH^{3+} + H^+$
Np(OH)2+2	IV	0.35 ± 0.30	-	0.35 ± 0.30	-	-		$Np^{4+} + 2\ H_2O(l) \rightleftharpoons Np(OH)_2^{2+} + 2\ H^+$
Np(OH)3+	IV	*(-2.8 ± 1.0)* *	-	*(-2.8 ± 1.0)* *	-	-		*$Np^{4+} + 3\ H_2O(l) \rightleftharpoons Np(OH)_3^+ + 3\ H^+$*
Np(OH)4(aq)	IV	-8.3 ± 1.1	-	-8.3 ± 1.1	-	-		$Np^{4+} + 4\ H_2O(l) \rightleftharpoons Np(OH)_4(aq) + 4\ H^+$
Ca4Np(OH)8+4	IV	-	-	*-56.1 ± 0.8*	-	-		*$4\ Ca^{2+} + Np^{4+} + 8\ H_2O(l) \rightleftharpoons Ca_4Np(OH)_8^{4+} + 8\ H^+$*
NpF+3	IV	8.96 ± 0.14	1.5 ± 2.0	8.96 ± 0.14	1.5 ± 2.0	-		$Np^{4+} + F^- \rightleftharpoons NpF^{3+}$
NpF2+2	IV	15.7 ± 0.3	-	15.7 ± 0.3	-	-		$Np^{4+} + 2\ F^- \rightleftharpoons NpF_2^{2+}$
NpCl+3	IV	1.5 ± 0.3	-	1.5 ± 0.3	-	-		$Np^{4+} + Cl^- \rightleftharpoons NpCl^{3+}$
NpI+3	IV	1.5 ± 0.4	-	1.5 ± 0.4	-	-		$Np^{4+} + I^- \rightleftharpoons NpI^{3+}$
NpSO4+2	IV	6.85 ± 0.16	29.8 ± 8.9	6.85 ± 0.16	29.8 ± 8.9	-		$Np^{4+} + SO_4^{2-} \rightleftharpoons NpSO_4^{2+}$
Np(SO4)2(aq)	IV	11.05 ± 0.27	55.4 ± 3.9	11.05 ± 0.27	55.4 ± 3.9	-		$Np^{4+} + 2\ SO_4^{2-} \rightleftharpoons Np(SO_4)_2(aq)$
NpNO3+3	IV	1.90 ± 0.15	-	1.90 ± 0.15	-	-		$Np^{4+} + NO_3^- \rightleftharpoons NpNO_3^{3+}$
Np(CO3)4-4	IV	(38.9 ± 0.5) *	-	(38.9 ± 0.5) *	-	-		$Np^{4+} + 4\ CO_3^{2-} \rightleftharpoons Np(CO_3)_4^{4-}$
Np(CO3)5-6	IV	(37.8 ± 0.6) *	-	(37.8 ± 0.6) *	-	-		$Np^{4+} + 5\ CO_3^{2-} \rightleftharpoons Np(CO_3)_5^{6-}$
Np(OH)2(CO3)2-2	IV	-	-	*-2.2 ± 0.5*	-	-		*$Np^{4+} + 2\ H_2O(l) + 2\ HCO_3^- \rightleftharpoons Np(OH)_2(CO_3)_2^{2-} + 4\ H^+$*
NpCO3(OH)3-	IV	*(2)* *	-	-	-	-		*$Np^{4+} + CO_3^{2-} + 3\ H_2O(l) \rightleftharpoons NpCO_3(OH)_3^- + 3\ H^+$*
Np(OH)4CO3-2	IV	-	-	*-5.5 ± 0.5*	-	-		*$Np^{4+} + 4\ H_2O(l) + CO_3^{2-} \rightleftharpoons Np(OH)_4CO_3^{2-} + 4\ H^+$*
NpSCN+3	IV	3.0 ± 0.3	-7 ± 3	3.0 ± 0.3	-7 ± 3	-		$Np^{4+} + SCN^- \rightleftharpoons NpSCN^{3+}$
Np(SCN)2+2	IV	4.1 ± 0.5	-9 ± 9	4.1 ± 0.5	-9 ± 9	-		$Np^{4+} + 2\ SCN^- \rightleftharpoons Np(SCN)_2^{2+}$
Np(SCN)3+	IV	4.8 ± 0.5	-13 ± 9	4.8 ± 0.5	-13 ± 9	-		$Np^{4+} + 3\ SCN^- \rightleftharpoons Np(SCN)_3^+$
Np+3	VI/III	33.50 ± 0.23	-	33.50 ± 0.23	-	-		$NpO_2^{2+} + 4\ H^+ + 3\ e^- \rightleftharpoons Np^{3+} + 2\ H_2O(l)$
NpOH+2	III	-6.8 ± 0.3	-	-6.8 ± 0.3	-	-		$Np^{3+} + H_2O(l) \rightleftharpoons NpOH^{2+} + H^+$

Tab. 16-1: Cont.

Name	Redox	TDB Version 12/07		TDB 2020				Reaction
		$\log_{10}\beta°$	$\Delta_r H_m°$ [kJ · mol^{-1}]	$\log_{10}\beta°$	$\Delta_r H_m°$ [kJ · mol^{-1}]	$\Delta_r C_{p,m}°$ [J · K^{-1} · mol^{-1}]	T-range [°C]	
Np(OH)2+	III	*(-14.7)* [*]	-	*(-14.7)* [*]	-	-		$Np^{3+} + 2\ H_2O(l) \rightleftharpoons Np(OH)_2^{+} + 2\ H^{+}$
Np(OH)3(aq)	III	*(-25.8)* [*]	-	*(-25.8)* [*]	-	-		$Np^{3+} + 3\ H_2O(l) \rightleftharpoons Np(OH)_3(aq) + 3\ H^{+}$
NpF+2	III	*(3.4)* [*]	-	*(3.4)* [*]	-	-		$Np^{3+} + F^{-} \rightleftharpoons NpF^{2+}$
NpF2+	III	*(5.8)* [*]	-	*(5.8)* [*]	-	-		$Np^{3+} + 2\ F^{-} \rightleftharpoons NpF_2^{+}$
NpCl+2	III	*(0.24)* [*]	-	*(0.24)* [*]	-	-		$Np^{3+} + Cl^{-} \rightleftharpoons NpCl^{2+}$
NpCl2+	III	*(-0.74)* [*]	-	*(-0.74)* [*]	-	-		$Np^{3+} + 2\ Cl^{-} \rightleftharpoons NpCl_2^{+}$
NpSO4+	III	*(3.3)* [*]	-	*(3.3)* [*]	-	-		$Np^{3+} + SO_4^{2-} \rightleftharpoons NpSO_4^{+}$
Np(SO4)2-	III	*(3.7)* [*]	-	*(3.7)* [*]	-	-		$Np^{3+} + 2\ SO_4^{2-} \rightleftharpoons Np(SO_4)_2^{-}$
NpCO3+	III	*(8.0)* [*]	-	*(8.0)* [*]	-	-		$Np^{3+} + CO_3^{2-} \rightleftharpoons NpCO_3^{+}$
Np(CO3)2-	III	*(12.9)* [*]	-	*(12.9)* [*]	-	-		$Np^{3+} + 2\ CO_3^{2-} \rightleftharpoons Np(CO_3)_2^{-}$
Np(CO3)3-3	III	*(15.0)* [*]	-	*(15.0)* [*]	-	-		$Np^{3+} + 3\ CO_3^{2-} \rightleftharpoons Np(CO_3)_3^{3-}$

[a] Value given by Lemire et al. (2001) as a guideline only.

Name	Redox	TDB Version 12/07			TDB 2020		
		$\log_{10}K_{s,0}°$	$\Delta_r H_m°$ [kJ · mol^{-1}]	Name	$\log_{10}K_{s,0}°$	$\Delta_r H_m°$ [kJ · mol^{-1}]	Reaction
NpO3:H2O(cr)	VI	5.47 ± 0.40	-	NpO2(OH)2:H2O (cr, hex)	5.47 ± 0.40	-	$NpO_2(OH)_2 \cdot H_2O$(cr, hex) + $2H^{+} \rightleftharpoons NpO_2^{2+} + 3H_2O$(l)
NpO2CO3(s)	VI	-14.60 ± 0.47	-	NpO2CO3(cr)	-14.83 ± 0.23	-	$NpO_2CO_3(cr) \rightleftharpoons NpO_2^{2+} + CO_3^{2-}$
K4NpO2(CO3)3(s)	VI	-26.40 ± 0.90	-	K4NpO2(CO3)3 (s)	-26.93 ± 1.00	-	$K_4NpO_2(CO_3)_3(s) \rightleftharpoons 4\ K^{+} + NpO_2^{2+} + 3\ CO_3^{2-}$
(NH4)4NpO2(CO3)3 (s)	VI	-26.81 ± 0.35	-	(NH4)4NpO2 (CO3)3(s)	-27.34 ± 0.58	-	$(NH_4)_4NpO_2(CO_3)_3$ (s) $\rightleftharpoons 4\ NH_4^{+} + NpO_2^{2+} + 3\ CO_3^{2-}$
	V			Na2Np2O7:0.1H2O(cr)	12.6 ± 1.1	-	$0.5Na_2Np_2O_7{\cdot}0.1H_2O$(cr) + $3H^{+} \rightleftharpoons$ Na+ + NpO_2^{2+}+ $1.55H_2O$(l)
NpO2OH(am)(fr)	V	5.3 ± 0.2	-41.1 ± 3.0	NpO2OH(am)	5.3 ± 0.2	-41.1 ± 3.0	$NpO_2OH(am) + H^{+} \rightleftharpoons NpO_2^{+} + H_2O$(l)
NpO2OH(am)(ag)	V	4.7 ± 0.5	-41.1 ± 3.0	-	-	-	NpO_2OH(am, ag) + $H^{+} \rightleftharpoons NpO_2^{+} + H_2O$(l)
	V			Ca0.5NpO2(OH)2:1.3H2O(cr)	12.30 ± 0.07	-	$Ca_{0.5}NpO_2(OH)_2 \cdot 1.3H_2O$(cr) + $2H^{+} \rightleftharpoons NpO_2^{+} + 0.5Ca^{2+} + 3.3\ H_2O$(l)
	V			*CaNpO2(OH)2.6Cl0.4:2H2O(cr)*	*19.90 ± 0.10*		*$CaNpO_2(OH)_{2.6}Cl_{0.4} \cdot 2H_2O$(cr) + $2.6H^{+} \rightleftharpoons NpO_2^{+} + Ca^{2+} + 4.6H_2O$(l) + $0.4Cl^{-}$*

Tab. 16-1: Cont.

Name	Redox	TDB Version 12/07			TDB 2020		
		$\log_{10}K_{s,0}°$	$\Delta_r H_m°$ [kJ · mol^{-1}]	Name	$\log_{10}K_{s,0}°$	$\Delta_r H_m°$ [kJ · mol^{-1}]	Reaction
NaNpO2CO3:3.5H2O (cr)	V	-11.0 ± 0.24	-	NaNpO2CO3:3.5 H2O(cr)	-11.0 ± 0.24	-	$NaNpO_2CO_3 \cdot 3.5H_2O(cr) \rightleftharpoons Na^+ + NpO_2^+ + CO_3^{2-} + 3.5\ H_2O(l)$
Na3NpO2(CO3)2(cr)	V	-14.22 ± 0.50	-	Na3NpO2(CO3)2 (cr)	-14.22 ± 0.50	-	$Na_3NpO_2(CO_3)_2(cr) \rightleftharpoons 3\ Na^+ + NpO_2^+ + 2\ CO_3^{2-}$
KNpO2CO3(s)	V	-13.15 ± 0.19	-	KNpO2CO3(s)	-13.15 ± 0.19	-	$KNpO_2CO_3(s) \rightleftharpoons K^+ + NpO_2^+ + CO_3^{2-}$
K3NpO2(CO3)2(s)	V	-15.46 ± 0.16	-	K3NpO2(CO3)2 (s)	-15.46 ± 0.16	-	$K_3NpO_2(CO_3)_2(s) \rightleftharpoons 3\ K^+ + NpO_2^+ + 2\ CO_3^{2-}$
NpO2(am)(hyd)	IV	-0.7 ± 0.5	-	NpO2(am)(hyd)	-0.7 ± 0.5	-	$NpO_2(am, hyd) + 4\ H^+ \rightleftharpoons Np^{4+} + 2\ H_2O(l)$

Tab. 16-2: Selected SIT ion interaction coefficients $\varepsilon_{j,k}$ [kg · mol^{-1}] for neptunium species

All data included in TDB Version 12/07 are taken from Lemire et al. (2001), Guillaumont et al. (2003) and Grenthe et al. (2020) unless indicated otherwise. Own data estimates based on charge correlations (see Section 1.5.3) are shaded. Supplemental data are in italics.

j k → ↓	**Cl^-** $\varepsilon_{j,k}$ [kg · mol^{-1}]	**ClO_4^-** $\varepsilon_{j,k}$ [kg · mol^{-1}]	**NO_3^-** $\varepsilon_{j,k}$ [kg · mol^{-1}]	**Li^+** $\varepsilon_{j,k}$ [kg · mol^{-1}]	**Na^+** $\varepsilon_{j,k}$ [kg · mol^{-1}]	**K^+** $\varepsilon_{j,k}$ [kg · mol^{-1}]
NpO2+2	0.15 ± 0.10	0.46 ± 0.05	-	0	0	0
NpO2OH+	0.05 ± 0.10	-0.06 ± 0.40	-	0	0	0
NpO2(OH)2(aq)	0	0	0	0	0	0
NpO2(OH)3-	0	0	0	-	-0.20 ± 0.02	-
NpO2(OH)4-2	0	0	0	-	-0.12 ± 0.04	-
(NpO2)2(OH)2+2	0.15 ± 0.10	0.57 ± 0.10	-	0	0	0
(NpO2)3(OH)5+	0.05 ± 0.10	0.45 ± 0.20	-	0	0	0
NpO2F+	0.05 ± 0.10	0.29 ± 0.12	-	0	0	0
NpO2F2(aq)	0	0	0	0	0	0
NpO2Cl+	0.05 ± 0.10	0.50 ± 0.14	-	0	0	0
NpO2IO3+	0.05 ± 0.10	0.33 ± 0.04	-	0	0	0
NpO2SO4(aq)	0	0	0	0	0	0
NpO2(SO4)2-2	0	0	0	-	-0.10 ± 0.10	-
NpO2H2PO4+	0.05 ± 0.10	0.2 ± 0.10	-	0	0	0
NpO2HPO4(aq)	0	0	0	0	0	0
NpO2(HPO4)2-2	0	0	0	-	-0.1 ± 0.1	-
NpO2CO3(aq)	0	0	0	0	0	0
NpO2(CO3)2-2	*0*	*0*	*0*	-	*-0.02 ± 0.14*	-
NpO2(CO3)3-4	0	0	0	-	-0.40 ± 0.19	-0.62 ± 0.42
(NpO2)3(CO3)6-6	0	0	0	-	-0.46 ± 0.73	-
(NpO2)2CO3(OH)3-	0	0	0	-	0.00 ± 0.05	-
(UO2)2NpO2(CO3)6-6	0	0	0	-	0.09 ± 0.71	-
NpO2+	0.09 ± 0.05	0.25 ± 0.05	-	0	0	0
NpO2(OH(aq))	0	0	0	0	0	0
NpO2(OH)2-	0	0	0	-	-0.01 ± 0.07	-
CaNpO2(OH)2+	-0.07 ± 0.08	0.2 ± 0.10	-	0	0	0
Ca3NpO2(OH)5+2	-0.20 ± 0.11	0.4 ± 0.10	-	0	0	0
NpO2F(aq)	0	0	0	0	0	0
NpO2F2-	0	0	0	-	-0.01 ± 0.07	-
NpO2IO3(aq)	0	0	0	0	0	0
NpO2SO4-	0	0	0	-	0.07 ± 0.13	-
NpO2H2PO4(aq)	0	0	0	0	0	0
NpO2HPO4-	0	0	0	-	-0.05 ± 0.11	-
NpO2CO3-	0	0	0	-	-0.18 ± 0.15	-

Tab. 16-2: Cont.

j k → ↓	**Cl^-** $\varepsilon_{j,k}$ [kg · mol^{-1}]	**ClO_4^-** $\varepsilon_{j,k}$ [kg · mol^{-1}]	**NO_3^-** $\varepsilon_{j,k}$ [kg · mol^{-1}]	**Li^+** $\varepsilon_{j,k}$ [kg · mol^{-1}]	**Na^+** $\varepsilon_{j,k}$ [kg · mol^{-1}]	**K^+** $\varepsilon_{j,k}$ [kg · mol^{-1}]
NpO2(CO3)2-3	0	0	0	-	-0.33 ± 0.17	-
NpO2(CO3)3-5	0	0	0	-	-0.53 ± 0.19	-0.22 ± 0.03
NpO2CO3OH-2	*0*	*0*	*0*	*0*	*-0.10 ± 0.10*	*0*
NpO2CO3(OH)2-3	*0*	*0*	*0*	*0*	*-0.15 ± 0.10*	*0*
NpO2(CO3)2OH-4	0	0	0	-	-0.40 ± 0.19	-
NpO2SCN(aq)	*0*	*0*	*0*	*0*	*0*	*0*
Np+4	0.35 ± 0.10	0.84 ± 0.06	-	0	0	0
NpOH+3	0.25 ± 0.10	0.50 ± 0.05	-	0	0	0
Np(OH)2+2	0.15 ± 0.10	0.4 ± 0.1	-	0	0	0
Np(OH)3+	*0.05 ± 0.10*	*0.2 ± 0.1*	-	*0*	*0*	*0*
Np(OH)4(aq)	0	0	0	0	0	0
Ca4Np(OH)8+4	*-0.01 ± 0.10*	*0.8 ± 0.1*	-	*0*	*0*	*0*
NpF+3	0.25 ± 0.10	0.58 ± 0.07	-	0	0	0
NpF2+2	0.15 ± 0.10	0.38 ± 0.17	-	0	0	0
NpCl+3	0.25 ± 0.10	(0.81 ± 0.19) [a]	-	0	0	0
NpI+3	0.25 ± 0.10	(0.88 ± 0.26) [b]	-	0	0	0
NpSO4+2	0.15 ± 0.10	(0.50 ± 0.11) [c]	-	0	0	0
Np(SO4)2(aq)	0	0	0	0	0	0
NpNO3+3	0.25 ± 0.10	0.6 ± 0.1	-	0	0	0
Np(CO3)4-4	0	0	0	-	-0.20 ± 0.30	-
Np(CO3)5-6	0	0	0	-	-0.30 ± 0.50	-0.73 ± 0.68
Np(OH)2(CO3)2-2	*0*	*0*	*0*	-	*-0.3 ± 0.2*	-
Np(OH)4CO3-2	*0*	*0*	*0*	-	*0.0 ± 0.3*	-
NpSCN+3	0.25 ± 0.10	0.76 ± 0.12	-	0	0	0
Np(SCN)2+2	0.15 ± 0.10	0.38 ± 0.20	-	0	0	0
Np(SCN)3+	0.05 ± 0.10	0.17 ± 0.04	-	0	0	0
Np+3	0.25 ± 0.10	0.49 ± 0.05	-	0	0	0
NpOH+2	0.15 ± 0.10	0.4 ± 0.1	-	0	0	0
Np(OH)2+	*0.05 ± 0.10*	*0.2 ± 0.1*	-	*0*	*0*	*0*
Np(OH)3(aq)	*0*	*0*	*0*	*0*	*0*	*0*
NpF+2	*0.15 ± 0.10*	*0.4 ± 0.1*	-	*0*	*0*	*0*
NpF2+	*0.05 ± 0.10*	*0.2 ± 0.1*	-	*0*	*0*	*0*
NpCl+2	*0.15 ± 0.10*	*0.4 ± 0.1*	-	*0*	*0*	*0*
NpCl2+	*0.05 ± 0.10*	*0.2 ± 0.1*	-	*0*	*0*	*0*
NpSO4+	*0.05 ± 0.10*	*0.2 ± 0.1*	-	*0*	*0*	*0*
Np(SO4)2-	*0*	*0*	*0*	-	*-0.05 ± 0.10*	-

Tab. 16-2: Cont.

j k → ↓	**Cl^-** $\varepsilon_{j,k}$ [kg · mol^{-1}]	**ClO_4^-** $\varepsilon_{j,k}$ [kg · mol^{-1}]	**NO_3^-** $\varepsilon_{j,k}$ [kg · mol^{-1}]	**Li^+** $\varepsilon_{j,k}$ [kg · mol^{-1}]	**Na^+** $\varepsilon_{j,k}$ [kg · mol^{-1}]	**K^+** $\varepsilon_{j,k}$ [kg · mol^{-1}]
NpCO3+	*(0.01 ± 0.05)* [d]	*(0.17 ± 0.10)* [d]	-	*0*	*0*	*0*
Np(CO3)2-	*0*	*0*	*0*	-	*-(0.14 ± 0.06)* [d]	-
Np(CO3)3-3	*0*	*0*	*0*	-	*-(0.23 ± 0.07)* [d]	-

[a] Typographical error in Guillaumont et al. (2003) and in all following NEA-reviews: Uncertainty given as ± 0.09 instead of ± 0.19 kg · mol^{-1}.

[b] Recalculated by using $\varepsilon(I^-, H^+)$ from Hummel et al. (2005) instead of the assumption $\varepsilon(I^-, H^+) \approx \varepsilon(I^-, Na^+)$ by Lemire et al. (2001).

[c] The original value by Lemire et al. (2001), (0.48 ± 0.11) kg · mol^{-1}, is slightly incorrect.

[d] Estimated by adopting values from the corresponding Am(III) carbonate complexes, see Chapter 6.

16.9 References

Fellhauer, D., Altmaier, M., Gaona, X., Lützenkirchen, J. & Fanghänel, T. (2016a): Np(V)solubility, speciation and solid phase formation in alkaline $CaCl_2$ solutions. Part II: thermodynamics and implications for source term estimations of nuclear waste disposal. Radiochim. Acta, 104, 381-398.

Fellhauer, D., Neck, V., Altmaier, M., Lützenkirchen, J. & Fanghänel, T. (2010): Solubility of tetravalent actinides in alkaline $CaCl_2$ solutions and formation of $Ca_4[An(OH)_8]^{4+}$ complexes: A study of Np(IV) and Pu(IV) under reducing conditions and the systematic trend in the An(IV) series. Radiochim. Acta, 98, 541-548.

Fellhauer, D., Rothe, J., Altmaier, M., Neck, V., Runke, J., Wiss, T. & Fanghänel, T. (2016b): Np(V) solubility, speciation and solid phase formation in alkaline $CaCl_2$ solutions. Part I: experimental results. Radiochim. Acta, 104, 355-380.

Gaona, X., Fellhauer, D. & Altmaier, M. (2013): Thermodynamic description of Np(VI) solubility, hydrolysis, and redox behavior in dilute to concentrated alkaline NaCl solutions. Pure Appl. Chem., 85, 2027-2049.

Gaona, X., Tits, J., Dardenne, K., Liu, X., Rothe, J., Denecke, M.A., Wieland, E. & Altmaier, M. (2012): Spectroscopic investigations of Np(V/VI) redox speciation in hyperalkaline TMA-(OH, Cl) solutions. Radiochim. Acta, 100, 759-770.

Grenthe, I., Gaona, X., Plyasunov, A.V., Rao, L., Runde, W.H., Grambow, B., Konings, R.J.M., Smith, A.L. & Moore, E.E. (2020): Second Update on the Chemical Thermodynamics of Uranium, Neptunium, Plutonium, Americium and Technetium. Chemical Thermodynamics, Vol. 14. OECD Publications, Paris, France, 1503 pp.

Guillaumont, R., Fanghänel, T., Fuger, J., Grenthe, I., Neck, V., Palmer, D.A. & Rand, M.H. (2003): Update on the Chemical Thermodynamics of Uranium, Neptunium, Plutonium, Americium and Technetium. Chemical Thermodynamics, Vol. 5. Elsevier, Amsterdam, 919 pp.

Hummel, W., Anderegg, G., Puigdomènech, I., Rao, L. & Tochiyama, O. (2005): Chemical Thermodynamics of Compounds and Complexes of U, Np, Pu, Am, Tc, Se, Ni and Zr with Selected Organic Ligands. Chemical Thermodynamics, Vol. 9, Elsevier, Amsterdam, 1088 pp.

Hummel, W., Berner, U., Curti, E., Pearson, F.J. & Thoenen, T. (2002): Nagra/PSI Chemical Thermodynamic Data Base 01/01. Nagra Technical Report NTB 02-16. Also published by Universal Publishers/uPublish.com, Parkland, Florida, USA.

Kato, Y., Kimura, T., Yoshida, Z. & Nitani, N. (1998): Carbonate complexation of neptunyl(VI) ion. Radiochim. Acta, 82, 63-68.

Kitamura, A. & Kohara, Y. (2004): Carbonate complexation of neptunium(IV) in highly basic solutions. Radiochim. Acta, 92, 583-588.

Lemire, R. J., Fuger, J., Nitsche, H., Potter, P.E., Rand, M.H., Rydberg, J., Spahiu, K., Sullivan, J.C., Ullman, W.J., Vitorge, P. & Wanner, H. (2001): Chemical Thermodynamics of Neptunium and Plutonium. Chemical Thermodynamics, Vol. 4. Elsevier, Amsterdam, 845 pp.

Neck, V., Fanghänel, T., & Kim, J.I. (1997): Mixed hydroxo-carbonate complexes of neptunium(V). Radiochim. Acta, 77, 167-175.

Petrov, V.G., Fellhauer, D., Gaona, X., Dardenne, K., Rothe, J., Kalmykov, S.N. & Altmaier, M. (2017): Solubility and hydrolysis of Np(V) in dilute to concentrated alkaline NaCl solutions: formation of Na- Np(V)-OH solid phases at 22 °C. Radiochim. Acta, 105, 1-20.

Thoenen, T., Hummel, W., Berner, U. & Curti, E. (2014): The PSI/Nagra Chemical Thermodynamic Database 12/07. Technical Report, PSI Bericht Nr. 14-04, Paul Scherrer Institut, Villigen, Switzerland, 416 pp.

Vitorge, P. & Capdevila, H. (1998): Np(V) et Np(VI) en solution aqueuse bicarbonate/carbonate. CEA, Tech. Rep. CEA-R-5793.

17 Niobium

17.1 Introduction

There are three dose relevant Nb radionuclides for the planned Swiss repositories for radioactive waste (see Hummel 2018):

- ^{91}Nb with a half-life of 680 ± 130 years is a spallation product, which is, e.g., produced in solid Nb targets at the CERN Facility ISOLDE, designed to produce radioactive ion beams.
- ^{93m}Nb with a half-life of 16.13 ± 0.13 years is a fission product.
- ^{94}Nb with a half-life of (20.0 ± 2.4) × 10^3 years is a neutron activation product produced in structural materials of nuclear power plants.

Reliable thermodynamic data for Nb are scarce: The Nagra Thermochemical Data Base 05/92 (TDB 05/92, Pearson et al. 1992) contained only data for NbO_3^-, $Nb(OH)_4^+$, $Nb(OH)_5$(aq), Nb(cr), NbO_2(cr) and Nb_2O_5(cr), which were adopted without any change by the Nagra/PSI Chemical Thermodynamic Data Base 01/01 (TDB 01/01, Hummel et al. 2002) and the PSI/Nagra Chemical Thermodynamic Database 12/07 (TDB 12/07, Thoenen et al. 2014).

Wood (2005) explained the dearth of thermodynamic data for aqueous Nb species with the low solubility of Nb oxides in acidic solutions and the formation of polynuclear complexes in alkaline solutions, both impeding the quantitative study of Nb complexes.

Niobium has oxidation states ranging from -I to +V and +VII (Udupa et al. 1985), but only Nb(V) forms aqueous species (Lothenbach et al. 1999). For this reason, we omit the identifier (V) for the oxidation state of aqueous Nb in the following discussions. Since Nb^{5+} has a high charge and a relatively small ionic radius (0.64 Å for octahedral coordination, Shannon 1976) it qualifies as a Pearson hard acid, thus bonding preferably by electrostatic forces and forming strong complexes with strong, hard ligands such as O^{2-}, OH^-, and F^-, and somewhat weaker ones with weak, hard ligands such as carbonate, sulphate, and phosphate (Wood 2005). Complexes with borderline (e.g., Cl^-) or soft ligands (e.g., HS^-) can be expected to be considerably weaker (Wood 2005).

Lothenbach et al. (1999) and Wood (2005) reviewed the thermodynamic data and the aqueous geochemistry of Nb. These reviews served as a starting point for the present update report.
The data selected for TDB 2020 are listed in Tab. 17.9-1.

The notation of formulae and symbols used in this text largely follows the NEA recommendations.

17.1.1 Data in TDB 12/07

All data for Nb selected by Pearson et al. (1992) in TDB 05/92 were based on the NBS Tables of Chemical Thermodynamic Properties by Wagman et al. (1982). Pearson et al. (1992) used the following $\Delta_f G_m°$ values by Wagman et al. (1982) for calculating stability constants for $Nb(OH)_4^+$ and $Nb(OH)_5(aq)$, and solubility products for $Nb_2O_5(cr)$, designated by Wagman et al. (1982) as "high temperature form", and $NbO_2(cr)$:

$\Delta_f G_m°(NbO_3^-, 298.15\ K)$[52] $\approx \Delta_f G_m(NbO_3^-, 298.15\ K, I_m = 1\ mol \cdot kg^{-1}) = -932.1\ kJ \cdot mol^{-1}$

$\Delta_f G_m°(Nb(OH)_4^+, 298.15\ K) \approx \Delta_f G_m(Nb(OH)_4^+, 298.15\ K, I_m = 1\ mol \cdot kg^{-1}) =$
$-1'208.6\ kJ \cdot mol^{-1}$

$\Delta_f G_m°(Nb(OH)_5, aq, 298.15\ K) \approx \Delta_f G_m(Nb(OH)_5, aq, 298.15\ K, I_m = 1\ mol \cdot kg^{-1}) =$
$-1448.3\ kJ \cdot mol^{-1}$

$\Delta_f G_m°(Nb_2O_5, cr, 298.15\ K) = -1'766.0\ kJ \cdot mol^{-1}$

$\Delta_f G_m°(NbO_2, cr, 298.15\ K) = -740.5\ kJ \cdot mol^{-1}$

Note that $\Delta_f G_m$ selected by Wagman et al. (1982) for the aqueous species NbO_3^-, $Nb(OH)_4^+$, and $Nb(OH)_5(aq)$ are valid at $I_m = 1\ mol \cdot kg^{-1}$, but Pearson et al. (1992) did not mention this and did not attempt to recalculate these values to zero ionic strength.

From the $\Delta_f G_m°$ values reported above and $\Delta_f G_m°(H_2O, l, 298.15\ K) = -237.14\ kJ \cdot mol^{-1}$, Pearson et al. (1992) calculated and selected

$NbO_3^- + 2\ H^+ + H_2O(l) \rightleftharpoons Nb(OH)_4^+$

$\log_{10}\beta°(298.15\ K) = 6.896$

$NbO_3^- + H^+ + 2\ H_2O(l) \rightleftharpoons Nb(OH)_5(aq)$

$\log_{10}\beta°(298.15\ K) = 7.344$

$Nb_2O_5(cr) + H_2O(l) \rightleftharpoons 2\ NbO_3^- + 2\ H^+$

$\log_{10}K_{s,0}°(298.15\ K) = 24.341$

$NbO_2(cr) + H_2O(l) \rightleftharpoons NbO_3^- + 2\ H^+ + e^-$

$\log_{10}K_{s,0}°(298.15\ K) = 7.978$

---

[52] Note that NbO_3^- is equivalent to $Nb(OH)_6^-$, see Section 17.4.1.

In addition, Pearson et al. (1992) also selected

$S_m°$(Nb, cr, 298.15 K) = (36.40) J · K^{-1} · mol^{-1}

$C_{p,m}°$(Nb, cr, 298.15 K) = (24.60) J · K^{-1} · mol^{-1}

by Wagman et al. (1982).

17.1.2 Other reviews

In their review of thermodynamic data for Nb, Lothenbach et al. (1999) discussed the hydrolysis of Nb (including monomeric niobate and polymeric hexaniobate species), the solubility of precipitated niobium pentoxide, Nb_2O_5(pr), redox equilibria between Nb_2O_5(cr), Nb(cr), NbO(cr), and NbO_2(cr), and the formation of Nb fluoride complexes. They selected only

$$Nb(OH)_5(aq) + H_2O(l) \rightleftharpoons Nb(OH)_6^- + H^+$$

$$\log_{10}{}^*K_6°(298.15\ K) = -6.6$$

and (as a tentative value)

$$Nb_2O_5(pr) \rightleftharpoons 2\ Nb(OH)_5(aq) + 5\ H_2O(l)$$

$$\log_{10}{}^*K_{s,6}°(298.15\ K) = -16$$

(see Section 17.4.3) Wood (2005) reviewed the aqueous geochemistry of Nb. He compiled stability constants for the hydrolysis of Nb (including monomeric niobate, and polymeric tetra-, hexa-, and dodecaniobate) and for Nb fluoride complexes. Wood (2005) found only one study on the formation of Nb carbonate or bicarbonate complexes, but neither stoichiometries nor stability constants were determined. No stability constants were found by Wood (2005) for phosphate complexes, and he considered the reported stability constants for sulphate species to be questionable. He also reported on several studies on chloride complexes, but, again, no stability constants were measured. Finally, he discussed the solubilities of Nb_2O_5(pr) and the minerals columbite, $(Fe^{II}, Mn, Mg)Nb_2O_6$(cr), and pyrochlore, $(Na,Ca)_2Nb_2O_6(O,OH,F)$(cr), and concluded that, save for Nb_2O_5(pr), no solubility products are known.

17.1.3 SIT

NEA chose the specific ion interaction theory (SIT) for the extrapolation of experimental data to zero ionic strength, see, e.g., Grenthe et al. (1997), an approach which is also adopted for TDB 2020 (as has been for all its predecessors). When referring to ion interaction coefficients recommended by NEA, we took those from Tab. B.3 in Lemire et al. (2013).

Due to a lack of experimental data, many ion interaction coefficients for cationic Nb species with ClO_4^- and Cl^-, and for anionic Nb species with Na^+ are unknown. We filled these gaps by applying the estimation method described in Section 1.5.3, which is based on a statistical analysis of published SIT ion interaction coefficients, and which allows the estimation of such coefficients for the interaction of cations with Cl^- and ClO_4^-, and for the interaction of anions with Na^+ from

the charge of the considered cations or anions. Ion interaction coefficients of neutral niobium species with background electrolytes were assumed to be zero.

The ion interaction coefficients for niobium species selected for TDB 2020 are listed in Tab. 17.9-2.

17.2 Elemental niobium

CODATA (Cox et al. 1989) did not provide any data for Nb. According to the NBS Tables by Wagman et al. (1982)

$$S_m°(\text{Nb, cr, 298.15 K}) = (36.40)\ \text{J} \cdot \text{K}^{-1} \cdot \text{mol}^{-1}$$

and

$$C_{p,m}°(\text{Nb, cr, 298.15 K}) = (24.60)\ \text{J} \cdot \text{K}^{-1} \cdot \text{mol}^{-1}$$

The NIST-JANAF Tables by Chase (1998) reported slightly different values: $S_m°$(Nb, cr, 298.15 K) = (36.464) J · K^{-1} · mol^{-1} and $C_{p,m}°$(Nb, cr, 298.15 K) = (24.694) J · K^{-1} · mol^{-1}. Lacking objective criteria to prefer one set of data over the other, we retain the data by Wagman et al. (1982) for TDB 2020.

Elemental niobium does not occur as a mineral. For the calculation of certain reaction properties of niobium species, however, the selected values for $S_m°$(Nb, cr, 298.15 K) and $C_{p,m}°$(Nb, cr, 298.15 K) are useful.

17.3 Niobium aquo ions

Nb5+, like other HFSE (high field strength elements: Ti, Zr, Hf, Nb and Ta, all with a charge to ionic radius ratio Z/r > 2,) has a strong tendency to hydrolyse and even at pH as low as 0, no unhydrolyzed Nb species can be found. The least hydrolysed Nb species found in solubility experiments with Nb_2O_5(cr) is $Nb(OH)_4^+$ which is therefore selected as master species for Nb in TDB 2020 (in contrast to TDB 12/07 and precursors, where $Nb(OH)_6^-$, "disguised" as NbO_3^-, served as master species).

$\Delta_f G_m°(Nb(OH)_4^+, 298.15\ K)$ is based on

$$0.5\ Nb_2O_5(cr) + 1.5\ H_2O(l) + H^+ \rightleftharpoons Nb(OH)_4^+$$

$$\log_{10}{}^*K_s°(298.15\ K) = -(7.47 \pm 0.08)$$

as derived from the experimental data by Peiffert et al. (2010), see Section 17.4.1. From this value and $\Delta_f G_m°(H_2O, l, 298.15\ K) = -(237.140 \pm 0.041)$ kJ · mol^{-1}, selected by NEA (Lemire et al. 2013), and assuming that $\Delta_f G_m°(Nb_2O_5, cr, 298.15\ K) = -1'766.0$ kJ · mol^{-1} recommended by Wagman et al. (1982) also applies to B-Nb_2O_5(cr) used in the experiments by Peiffert et al. (2010), then follows the selected

$\Delta_f G_m°(Nb(OH)_4^+, 298.15\ K) = -1'196\ kJ \cdot mol^{-1}$

Likewise, the selected

$\Delta_f H_m°(Nb(OH)_4^+, 298.15\ K) = -1'375\ kJ \cdot mol^{-1}$

was calculated from $\Delta_r H_m(4.1, 298.15\ K, 1\ m\ NaClO_4) = (3 \pm 4)$ kJ · mol^{-1} determined by Peiffert et al. (2010) for the above solubility equilibrium, see Section 17.4.1, and from $\Delta_f H_m°(H_2O, l, 298.15\ K) = -(285.83 \pm 0.04)$ kJ · mol^{-1} selected by NEA (Lemire et al. 2013), and $\Delta_f H_m°(Nb_2O_5, cr, 298.15\ K) = -1'899.5$ kJ · mol^{-1} by Wagman et al. (1982). Since $\Delta_r H_m(4.1, 298.15\ K, 1\ m\ NaClO_4)$ is included in TDB 2020 only as supplemental datum, $\Delta_f H_m°(Nb(OH)_4^-, 298.15\ K)$ is only included as supplemental datum as well.

From $\Delta_f G_m°(Nb(OH)_4^+, aq, 298.15\ K)$, $\Delta_f H_m°(Nb(OH)_4^+, 298.15\ K)$ and the Gibbs-Helmholtz equation $\Delta_f G_m° = \Delta_f H_m° - T\ \Delta_f S_m°$ then follows $\Delta_f S_m°(Nb(OH)_4^+, 298.15\ K) = -600.37\ J \cdot K^{-1} \cdot mol^{-1}$. Using

$$S_m°(Nb(OH)_4^+, 298.15\ K) = \Delta_f S_m°(Nb(OH)_4^+, 298.15\ K) + S_m°(Nb, cr, 298.15\ K) +$$

$$2\ S_m°(O_2, g, 298.15\ K) + 1.5\ S_m°(H_2, g, 298.15\ K) + S_m°(H^+)$$

with $\Delta_f S_m°(Nb(OH)_4^+, 298.15\ K)$, the selected $S_m°(Nb, cr, 298.15\ K)$, as well as $S_m°(O_2, g, 298.15\ K) = (205.152 \pm 0.005)\ J \cdot K^{-1} \cdot mol^{-1}$ and $S_m°(H_2, g, 298.15\ K) = (130.680 \pm 0.003)\ J \cdot K^{-1} \cdot mol^{-1}$ selected by NEA (Lemire et al. 2013) results in the selected

$S_m°(Nb(OH)_4^+, 298.15\ K) = 42.4\ J \cdot K^{-1} \cdot mol^{-1}$

Since this value is based on supplemental data, it is also considered as supplemental datum in TDB 2020.

Finally, $\Delta_r C_{p,m}°(4.1, 298.15\ K) \approx \Delta_r C_{p,m}(4.1, 298.15\ K, 1\ m\ NaClO_4) = 0$, as determined by Peiffert et al. (2010), see Section 17.4.1, can be used, together with $C_{p,m}°(Nb_2O_5, cr, 298.15\ K) = 132.09\ J \cdot K^{-1} \cdot mol^{-1}$ (Wagman et al. 1982) and $C_{p,m}°(H_2O, l, 298.15\ K) = 75.351 \pm 0.080\ J \cdot K^{-1} \cdot mol^{-1}$ (NEA, Lemire et al. 2013) to derive

$C_{p,m}°(Nb(OH)_4^+, 298.15\ K) = 179\ J \cdot K^{-1} \cdot mol^{-1}$

which is included in TDB 2020 as supplemental datum.

17.4 Nb oxygen and hydrogen compounds and complexes

17.4.1 Aqueous Nb hydroxo complexes

The stoichiometry of aqueous niobium hydroxide complexes is not well understood. There are several ways, e.g., how the neutral Nb-hydroxo complex is expressed in the literature, either as $Nb(OH)_5(aq)$, $NbO(OH)_3(aq)$, or $NbO_2(OH)(aq)$, with decreasing numbers of H_2O in the formulae. All three formulations are thermodynamically equivalent as chemical experiments (such as solubility measurements) can generally not distinguish between aqueous species with different amounts of H_2O in the stoichiometric formula and the stability constants of formation reactions of complexes with such different stoichiometries are identical. Therefore, if two stoichiometric formulations of an aqueous species differ by n H_2O, their Gibbs free energies of formation differ by n $\Delta_f G_m°(H_2O, l, 298.15\ K)$.

Babko et al. (1963) measured the solubility of freshly precipitated $Nb_2O_5(pr)$ at 18 – 20 °C in $(H,K)NO_3$ media in the pH range 0 – 9.73 and reported stepwise conditional stability constants for $Nb(OH)_5(aq)$ and $Nb(OH)_6^-$ (see Section 17.4.3 and Tab. 17.4-3).

Peiffert et al. (2010) studied the solubility of crystalline B-$Nb_2O_5(cr)$[53] at 25 °C in 0.1, 0.3, 0.5, 1.0, and 6.0 mol · kg^{-1} $NaClO_4$ and additionally at 10, 50, and 70 °C in 1.0 mol · kg^{-1} $NaClO_4$, all in the pH range 1-9. Crystalline B-$Nb_2O_5(cr)$ was produced by heating reagent-grade Nb_2O_5 up to 1'000 °C at atmospheric pressure for ten hours. XRD-powder patterns of recovered solids after equilibration confirmed that in the pH range 1-9 no other solid was formed. The solubility data were interpreted in terms of the formation of $Nb(OH)_4^+$, $Nb(OH)_5(aq)$, $Nb(OH)_6^-$, and $Nb(OH)_7^{2-}$, resulting in a set of conditional solubility constants for reactions of the form

$$0.5\ Nb_2O_5(cr) + 0.5(2n - 5)\ H_2O(l) \rightleftharpoons Nb(OH)_n^{5-n} + (n-5)H^+$$

with n = 4, 5, 6, and 7. Since only limited data points were available for $Nb(OH)_7^{2-}$ (e.g., the fits to the data did not converge at the lowest ionic strength, when $Nb(OH)_7^{2-}$ was included), Peiffert et al. (2010) also reported alternative fits where $Nb(OH)_7^{2-}$ was excluded. The conditional solubility constants (including $Nb(OH)_7^{2-}$) at various temperatures and ionic strengths are listed in Tab. 17.4-1. Two methods were used by Peiffert et al. (2010) for deriving thermodynamic data from these conditional constants. The first approach applied an empirical fit to the conditional constants as a function of ionic strength and temperature, including appropriate Debye-Hückel terms. The second approach involved an SIT analysis of the ionic strength dependence of the conditional solubility constants for the data sets at 25 °C and 0.1, 0.3, 0.5, 1.0, and 6.0 mol · kg^{-1} $NaClO_4$, while the temperature dependence of the conditional solubility constants was derived from the data sets at 10, 25, 50, and 70 °C and 1.0 mol · kg^{-1} $NaClO_4$. According to Peiffert et al. (2010), the resulting solubility products from both approaches were consistent within the combined 2 σ uncertainties. They noted, however, that the derived SIT parameters for $Nb(OH)_5(aq)$, $Nb(OH)_6^-$, and $Nb(OH)_7^{2-}$, were "well outside the limits of accepted values for these charge types". For unknown reasons, Peiffert et al. (2010) did not include the data at I_m = 6.0 mol · kg^{-1} in their SIT analyses. We repeated the SIT analyses but included the data at I_m = 6.0 mol · kg^{-1}. In addition, we doubled the uncertainties of the conditional solubility constants

[53] B-$Nb_2O_5(cr)$ is one of a number of modifications of niobium pentoxide. B-$Nb_2O_5(cr)$ forms characteristic plate-like ("blättrig") crystals (Schäfer et al. 1966) and is a high-temperature modification.

(see Tab. 17.4-1) to account for the somewhat scattered data. The SIT fits are shown in Figs. 17.4-1 – 17.4-4. The resulting thermodynamic parameters are

$$0.5\ Nb_2O_5(cr) + 1.5\ H_2O(l) + H^+ \rightleftharpoons Nb(OH)_4^+ \quad (4.1)$$

$$\log_{10}{}^*K_s°(4.1, 298.15\ K) = -(7.47 \pm 0.08)$$

$$\Delta\varepsilon\,(4.1) = (0.07 \pm 0.04)\ kg \cdot mol^{-1}$$

$$0.5\ Nb_2O_5(cr) + 2.5\ H_2O(l) \rightleftharpoons Nb(OH)_5(aq) \quad (4.2)$$

$$\log_{10}{}^*K_s°(4.2, 298.15\ K) = -(9.36 \pm 0.09)$$

$$\Delta\varepsilon\,(4.2) = -(0.07 \pm 0.02)\ kg \cdot mol^{-1}$$

$$0.5\ Nb_2O_5(cr) + 3.5\ H_2O(l) \rightleftharpoons Nb(OH)_6^- + H^+ \quad (4.3)$$

$$\log_{10}{}^*K_s°(4.3, 298.15\ K) = -(14.16 \pm 0.11)$$

$$\Delta\varepsilon\,(4.3) = (1.61 \pm 0.26)\ kg \cdot mol^{-1}$$

$$0.5\ Nb_2O_5(cr) + 4.5\ H_2O(l) \rightleftharpoons Nb(OH)_7^{2-} + 2\ H^+ \quad (4.4)$$

$$\log_{10}{}^*K_s°(4.4, 298.15\ K) = -(23.56 \pm 0.33)$$

$$\Delta\varepsilon\,(4.4) = (2.26 \pm 0.64)\ kg \cdot mol^{-1}$$

Tab. 17.4-2 gives a comparison of these parameters with those obtained by Peiffert et al. (2010). We suspect that Peiffert et al. (2010) got the signs of their $\Delta\varepsilon$ values wrong. Fig. 17.4-1 shows a comparison of the SIT fits to the data for $0.5\ Nb_2O_5(cr) + 1.5\ H_2O(l) + H^+ \rightleftharpoons Nb(OH)_4^+$ with and without consideration of the data at $I_m = 6.0\ mol \cdot kg^{-1}$. A similar comparison is shown in Fig. 17.4-2 for $0.5\ Nb_2O_5(cr) + 2.5\ H_2O(l) \rightleftharpoons Nb(OH)_5(aq)$. It appears reasonable to include the data at $I_m = 6.0\ mol \cdot kg^{-1}$. The following discussion is based on the results of our SIT analyses.

Combining the values for $\Delta\varepsilon$ with $\varepsilon(H^+, ClO_4^-) = (0.14 \pm 0.02)\ kg \cdot mol^{-1}$ selected by NEA (Lemire et al. 2013) leads to

$$\varepsilon(Nb(OH)_4^+, ClO_4^-) = (0.21 \pm 0.04)\ kg \cdot mol^{-1}$$

$$\varepsilon(Nb(OH)_5(aq), NaClO_4(aq)) = -(0.07 \pm 0.02)\ kg \cdot mol^{-1}$$

$$\varepsilon(Nb(OH)_6^-, Na^+) = (1.57 \pm 0.26)\ kg \cdot mol^{-1}$$

$$\varepsilon(Nb(OH)_7^{2-}, Na^+) = (1.98 \pm 0.64)\ kg \cdot mol^{-1}$$

These values are included in TDB 2020, as well as

$$\varepsilon(Nb(OH)_4^+, Cl^-) = (0.05 \pm 0.10)\ kg \cdot mol^{-1}$$

estimated according to the method described in Section 1.5.3.

It is very obvious that the values for $\varepsilon(Nb(OH)_6^-, Na^+)$ and $\varepsilon(Nb(OH)_7^{2-}, Na^+)$ are beyond good and evil. For this reason, they are only considered as supplemental data.

The overall stability constants for $Nb(OH)_5(aq)$, $Nb(OH)_6^-$, and $Nb(OH)_7^{2-}$ can be obtained by subtracting $\log_{10}{}^*K_s°(4.1, 298.15\ K)$ from $\log_{10}{}^*K_s°(4.2, 298.15\ K)$, $\log_{10}{}^*K_s°(4.3, 298.15\ K)$, and $\log_{10}{}^*K_s°(4.4, 298.15\ K)$, respectively. The resulting stability constants

$$Nb(OH)_4^+ + H_2O(l) \rightleftharpoons Nb(OH)_5(aq) + H^+ \quad (4.5)$$

$$\log_{10}{}^*K°(4.5, 298.15\ K) = -(1.89 \pm 0.12)$$

$$Nb(OH)_4^+ + 2\ H_2O(l) \rightleftharpoons Nb(OH)_6^- + 2\ H^+ \quad (4.6)$$

$$\log_{10}\beta°(4.6, 298.15\ K) = -(6.69 \pm 0.14)$$

$$Nb(OH)_4^+ + 3\ H_2O(l) \rightleftharpoons Nb(OH)_7^{2-} + 3\ H^+ \quad (4.7)$$

$$\log_{10}\beta°(4.7, 298.15\ K) = -(16.09 \pm 0.34)$$

are included in TDB 2020.

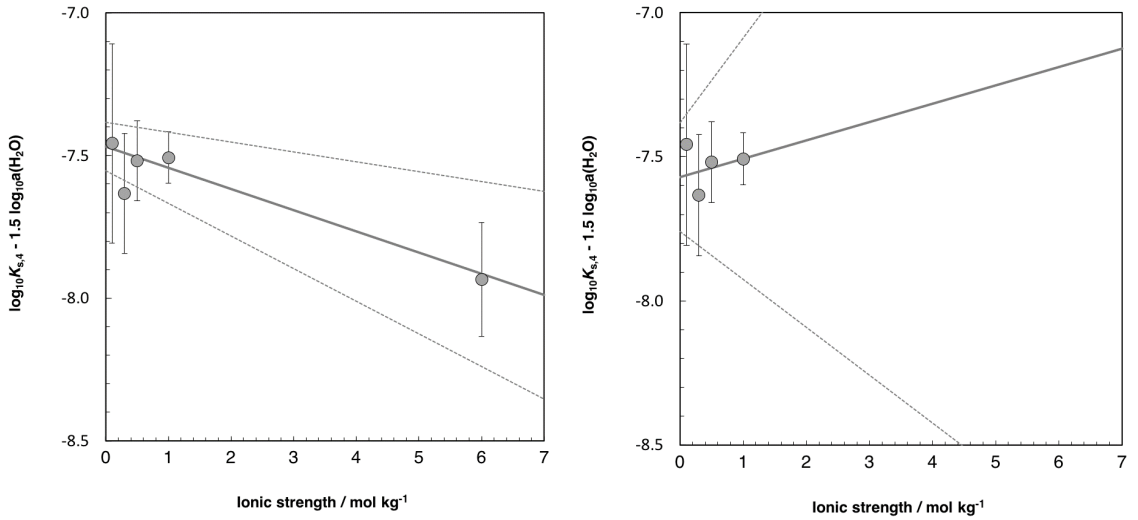

Fig. 17.4-1: SIT analyses of the equilibrium $0.5\ Nb_2O_5(cr) + 1.5\ H_2O(l) + H^+ \rightleftharpoons Nb(OH)_4^+$ in $NaClO_4$ at 25 °C

Using all data (left) and discarding the value at $I_m = 6\ mol \cdot kg^{-1}$ (right). The solid lines are obtained from the linear fits by using the derived SIT interaction coefficients ($\Delta\varepsilon$) and the derived stability constants at zero ionic strength. The dotted lines represent the 95% uncertainty ranges extrapolated from $I = 0$ to higher ionic strengths. Data by Peiffert et al. (2010), see Tab. 17.4-1.

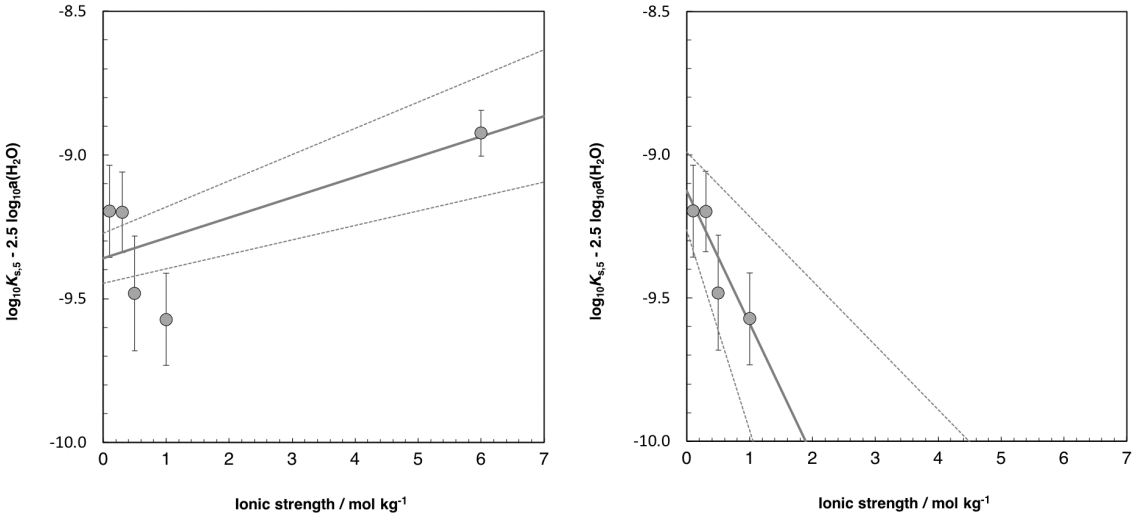

Fig. 17.4-2: SIT analyses of the equilibrium 0.5 Nb_2O_5(cr) + 2.5 H_2O(l) ⇌ $Nb(OH)_5$(aq) in $NaClO_4$ at 25 °C

Using all data (left) and discarding the value at I_m = 6 mol · kg^{-1} (right). The solid lines are obtained from the linear fits by using the derived SIT interaction coefficients ($\Delta\varepsilon$) and the derived stability constants at zero ionic strength. The dotted lines represent the 95% uncertainty ranges extrapolated from I = 0 to higher ionic strengths. Data by Peiffert et al. (2010), see Tab. 17.4-1.

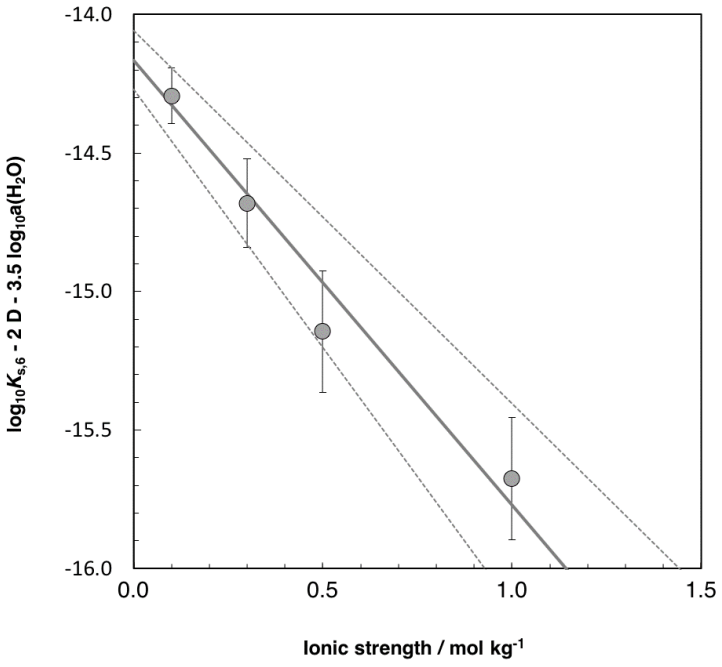

Fig. 17.4-3: SIT analysis of the equilibrium 0.5 Nb_2O_5(cr) + 3.5 H_2O(l) ⇌ $Nb(OH)_6^-$ + H^+ in $NaClO_4$ at 25 °C

The solid line is obtained from the linear fit by using the derived SIT interaction coefficient ($\Delta\varepsilon$) and the derived stability constant at zero ionic strength. The dotted lines represent the 95% uncertainty range extrapolated from I = 0 to higher ionic strengths. Data by Peiffert et al. (2010), see Tab. 17.4-1.

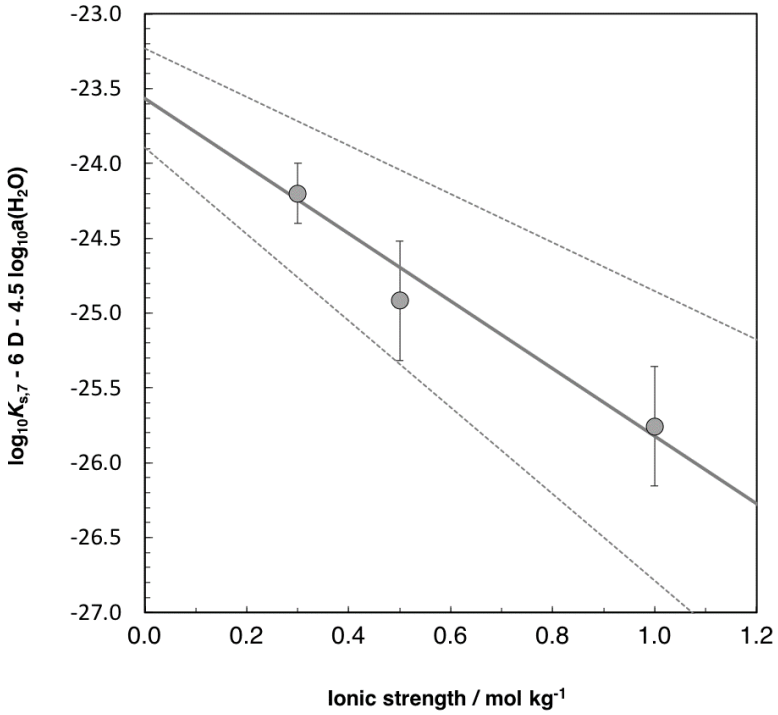

Fig. 17.4-4: SIT analysis of the equilibrium 0.5 Nb_2O_5(cr) + 4.5 H_2O(l) ⇌ $Nb(OH)_7^{2-}$ + 2 H^+ in $NaClO_4$ at 25 °

The solid line is obtained from the linear fit by using the derived SIT interaction coefficient ($\Delta\varepsilon$) and the derived stability constant at zero ionic strength. The dotted lines represent the 95% uncertainty range extrapolated from I = 0 to higher ionic strengths. Data by Peiffert et al. (2010), see Tab. 17.4-1.

Guillaumont et al. (1970) made a series of solvent extraction measurements of Nb solutions at 25 °C, covering a pH range from 1 – 9 in 0.1 and 3.0 M $LiClO_4$. Results were shown in two figures, but no numbers were given except a conditional stability constant for the reaction NbO_2^+ + H_2O(l) ⇌ NbO_2OH(aq) + H^+, which is equivalent to the reaction $Nb(OH)_4^+$ + H_2O(l) ⇌ Nb(OH)5(aq) + H^+. According to Peiffert et al. (2010), $\log_{10}{}^*K_{5,6}$(298.15 K, 0.101 mol · kg - 1 $LiClO_4$) = -3.2 by Guillaumont et al. (1970) is in poor agreement with $\log_{10}{}^*K_{5,6}$(298.15 K, 0.101 mol · kg - 1 $NaClO_4$) = -(1.7 ± 0.2) by Peiffert et al. (2010). The reason for this discrepancy is not known.

Peiffert et al. (2010) also measured the solubility of B-Nb_2O_5(cr) in 1 m $NaClO_4$ at 10, 25, 50, and 70 °C. From the experimental data they derived the conditional solubility constants $\log_{10}{}^*K_s(T)$ for reactions (4.1) to (4.4) at each of these temperatures. From linear fits to $\log_{10}{}^*K_s(T)$ vs. $1/T$, they obtained $\log_{10}{}^*K_s$(298.15 K, 1 m $NaClO_4$) and the corresponding $\Delta_r H_m$(298.15 K, 1 m $NaClO_4$).

They obtained

$\Delta_r H_m(4.1, 298.15\ K, 1\ m\ NaClO_4) = (3 \pm 4)\ kJ \cdot mol^{-1}$

$\Delta_r H_m(4.2, 298.15\ K, 1\ m\ NaClO_4) = (12 \pm 2)\ kJ \cdot mol^{-1}$

$\Delta_r H_m(4.3, 298.15\ K, 1\ m\ NaClO_4) = (29 \pm 8)\ kJ \cdot mol^{-1}$

$\Delta_r H_m(4.4, 298.15\ K, 1\ m\ NaClO_4) = (66 \pm 21)\ kJ \cdot mol^{-1}$

As a consequence of the linear fits, the corresponding isobaric heat capacities of reaction are equal to zero: $\Delta_r C_{p,m}(4.1, 298.15\ K, 1\ m\ NaClO_4) = \Delta_r C_{p,m}(4.2, 298.15\ K, 1\ m\ NaClO_4) = \Delta_r C_{p,m}(4.3, 298.15\ K, 1\ m\ NaClO_4) = \Delta_r C_{p,m}(4.3, 298.15\ K, 1\ m\ NaClO_4) = 0$. From the reaction enthalpies follow the reaction enthalpies of the overall formation reactions of the niobate hydroxide complexes

$\Delta_r H_m^\circ(4.5, 298.15\ K) \approx \Delta_r H(4.5, 298.15\ K, 1\ m\ NaClO_4) = (9 \pm 4)\ kJ \cdot mol^{-1}$

$\Delta_r H_m^\circ(4.6, 298.15\ K) \approx \Delta_r H_m(4.6, 298.15\ K, 1\ m\ NaClO_4) = (26 \pm 9)\ kJ \cdot mol^{-1}$

$\Delta_r H_m^\circ(4.7, 298.15\ K) \approx \Delta_r H_m(4.7, 298.15\ K, 1\ m\ NaClO_4) = (63 \pm 22)\ kJ \cdot mol^{-1}$

Since no efforts were made to extrapolate these reaction enthalpies to zero ionic strength, they are used as estimates and are included in TDB 2020 only as supplemental data, as well as the corresponding isobaric heat capacities of reaction

$\Delta_r C_{p,m}^\circ(4.5, 298.15\ K) = \Delta_r C_{p,m}^\circ(4.6, 298.15\ K) = \Delta_r C_{p,m}^\circ(4.7, 298.15\ K) = 0$

Tab. 17.4-1: Experimental solubility constants for B-Nb_2O_5(cr) determined by Peiffert et al. (2010)

Increased uncertainties are shown in bold.

Reaction	**$\log_{10}K$ reported**	**$\log_{10}K$ accepted**	***T*** [°C]	***I*** [m]	**Medium**	**Method**
0.5 Nb_2O_5(cr) + 1.5 H_2O(l) + H^+ ⇌ $Nb(OH)_4^+$	-7.46 ± 0.35	-7.46 ± 0.35	25	0.1	$NaClO_4$	sol.
	-7.64 ± 0.21	-7.64 ± 0.21		0.3		
	-7.53± 0.14	-7.53± 0.14		0.5		
	-7.44 ± 0.06	-7.44 ± 0.06	10	1.0		
	-7.53 ± 0.09	-7.53 ± 0.09	25			
	-7.42 ± 0.11	-7.42 ± 0.11	50			
	-7.24 ± 0.18	-7.24 ± 0.18	70			
	-8.16 ± 0.05	-8.16 ± **0.20**	25	6.0		
0.5 Nb_2O_5(cr) + 2.5 H_2O(l) ⇌ $Nb(OH)_5$(aq)	-9.20 ± 0.08	-9.20 ± **0.16**	25	0.1		
	-9.21 ± 0.07	-9.21 ± **0.14**		0.3		
	-9.50 ± 0.10	-9.50 ± **0.20**		0.5		
	-9.68 ± 0.06	-9.68 ± 0.06	10	1.0		
	-9.61 ± 0.08	-9.61 ± **0.16**	25			
	-9.38 ± 0.08	-9.38 ± 0.08	50			
	-9.31 ± 0.08	-9.31 ± 0.08	70			
	-9.30 ± 0.04	-9.30 ± **0.08**	25	6.0		
0.5 Nb_2O_5(cr) + 3.5 H_2O(l) ⇌ $Nb(OH)_6^-$ + H^+	-14.08 ± 0.05	-14.08 ± **0.10**	25	0.1		
	-14.39 ± 0.08	-14.39 ± **0.16**		0.3		
	-14.82 ± 0.11	-14.82 ± **0.22**		0.5		
	-16.03 ± 0.11	-16.03 ± 0.11	10	1.0		
	-15.33 ± 0.11	-15.33 ± **0.22**	25			
	-15.40 ± 0.21	-15.40 ± 0.21	50			
	-14.92 ± 0.12	-14.92 ± 0.12	70			
0.5 Nb_2O_5(cr) + 4.5 H_2O(l) ⇌ $Nb(OH)_7^{2-}$ + 2 H^+	-23.3 ± 0.2	-23.3 ± 0.2	25	0.3		
	-23.9 ± 0.4	-23.9 ± 0.4		0.5		
	-24.8 ± 0.2	-24.8 ± 0.2	10	1.0		
	-24.6 ± 0.4	-24.6 ± 0.4	25			
	-22.8 ± 0.1	-22.8 ± 0.1	50			
	-23.0 ± 0.1	-23.0 ± 0.1	70			

Tab. 17.4-2: SIT fitting parameters determined by Peiffert et al. (2010) and this work using the data at 25 °C in Tab. 17.4-1.

Note that Peiffert et al. (2010) excluded the data at I_m = 6.0 mol · kg^{-1}.

Reaction	**$\log_{10}K_s°$ Peiffert et al. 2010**	**$\log_{10}K_s°$ this work**	**$\Delta\varepsilon$** [kg · mol^{-1}] **Peiffert et al. 2010**	**$\Delta\varepsilon$** [kg · mol^{-1}] **this work**
0.5 Nb_2O_5(cr) + 1.5 H_2O(l) + H^+ ⇌ $Nb(OH)_4^+$	-7.57 ± 0.14	-7.47 ± 0.08	0.1 ± 0.2	0.07 ± 0.04
0.5 Nb_2O_5(cr) + 2.5 H_2O(l) ⇌ $Nb(OH)_5$(aq)	-9.13 ± 0.15	-9.36 ± 0.09	-0.5 ± 0.3	-0.07 ± 0.02
0.5 Nb_2O_5(cr) + 3.5 H_2O(l) ⇌ $Nb(OH)_6^-$ + H^+	-14.16 ± 0.14	-14.16 ± 0.11	-1.6 ± 0.3	1.61 ± 0.26
0.5 Nb_2O_5(cr) + 4.5 H_2O(l) ⇌ $Nb(OH)_7^{2-}$ + 2 H^+	-23.6 ± 0.4	-23.56 ± 0.33	-2.3 ± 0.8	2.26 ± 0.64
			ε [kg · mol^{-1}] **Peiffert et al. 2010**	**ε** [kg · mol^{-1}] **this work**
$\varepsilon(Nb(OH)_4^+, ClO_4^-)$			0.1 ± 0.2	0.21 ± 0.04
$\varepsilon(Nb(OH)_5$(aq), $NaClO_4$(aq))			-0.5 ± 0.3	-0.07 ± 0.02
$\varepsilon(Nb(OH)_6^-, Na^+)$			-1.6 ± 0.3	*1.57 ± 0.26*
$\varepsilon(Nb(OH)_7^{2-}, Na^+)$			-2.7 ± 0.8	*1.98 ± 0.64*

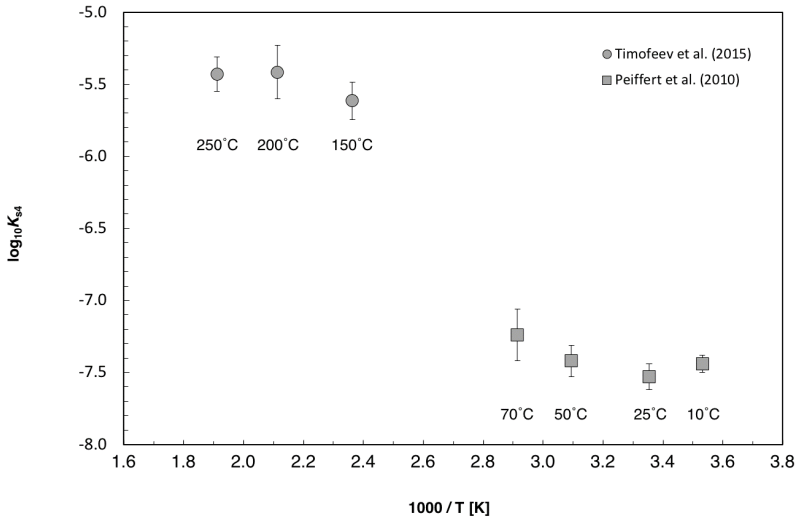

Fig. 17.4-5: Logarithm of the equilibrium constants for the reaction 0.5 Nb_2O_5(cr) + 1.5 H_2O(l) + H^+ ⇌ $Nb(OH)_4^+$ as a function of reciprocal temperature

Data by Peiffert et al. (2010), with original uncertainties, and Timofeev et al. (2015).

Timofeev et al. (2015) determined the solubility of synthetic Nb_2O_5(cr) in HF solutions (10^{-2} – 10^{-5} m) at 150, 200, and 250 °C, at saturated vapor pressure and under acidic conditions (pH < 3.5). They concluded from their experiments that at low HF concentrations Nb is dissolved as $Nb(OH)_4^+$ in significant amounts even at 150 °C but that much larger amounts of Nb are dissolved at HF concentrations > 10^{-3} m in the form of $NbF_2(OH)_3$(aq). From their experimental data, Timofeev et al. (2015) derived solubility constants for the reactions Nb_2O_5(cr) + 4 HF(aq) +

$H_2O(aq) \rightleftharpoons 2\ Nb(OH)_3F_2(aq)$ (see Section 17.5) and $Nb_2O_5(cr) + 3\ H_2O(aq) + 2\ H^+ \rightleftharpoons 2\ Nb(OH)_4^+$. Comparing the solubility constants for the latter reaction, -11.23 ± 0.26 at 150 °C, -10.83 ± 0.37 at 200 °C, and -10.86 ± 0.24 with those derived by Peiffert et al. (2010) at lower temperatures, see Fig. 17.4-5, clearly shows that both datasets are not compatible. We could not resolve this discrepancy. Since we used the experimental data by Peiffert et al. (2010) primarily for extracting stability constants among the aqueous Nb-hydroxide species and the solubility of crystalline Nb_2O_5 is of less concern, we did not consider the data by Timofeev et al. (2015).

17.4.2 Polynuclear aqueous Nb oxo/hydroxo species

According to Wood (2005) polynuclear hydrolysed Nb species are better studied than their mononuclear counterparts and there is broad agreement with respect to the existence and importance of hexaniobate species, i.e., $Nb_6O_{19}^{8-}$, $HNb_6O_{19}^{7-}$, $H_2Nb_6O_{19}^{6-}$, and $H_3Nb_6O_{19}^{5-}$. A few studies have also put forth the existence of tetraniobates and dodecaniobates.

17.4.2.1 Tetraniobates

Goiffon et al. (1973) used UV-absorption spectroscopy to study niobates and polyniobates in 1 M KCl at 25 °C and pH 8 – 15. The hexaniobates $Nb_6O_{19}^{8-}$, $HNb_6O_{19}^{7-}$, $H_2Nb_6O_{19}^{6-}$, $H_3Nb_6O_{19}^{5-}$ were found to be present at pH < 13.97 (see Tab. 17.4-3 for the measured equilibrium constants). At 13.97 < pH < 14.47 there is an equilibrium between $Nb_6O_{19}^{8-}$ and the tetraniobate $Nb_4O_{12}(OH)_4^{8-}$, at still higher pH > 14.47, this tetraniobate was found to transform into $NbO_2(OH)_4^{3-}$ (at Nb concentrations < 1.56×10^{-4} normal) which itself was transformed into $Nb_4O_{16}^{12-}$ at higher concentrations of Nb. Since these tetraniobates (see Tab. 17.4-3 for the measured equilibrium constants) are only stable at extremely high pH, well above the application range of TDB 2020, they are not included in TDB 2020.

17.4.2.2 Hexaniobates

Lindqvist (1953) observed by X-ray crystallography that $Na_{14}Nb_{12}O_{37}{\cdot}32H_2O(cr)$ contains the hexaniobate anion $Nb_6O_{19}^{8-}$ with an octahedral arrangement of the six Nb atoms. Since $Nb_6O_{19}^{8-}$ has no obvious relation to the formula $Na_{14}Nb_{12}O_{37}{\cdot}32H_2O$, Lindqvist (1953) argued that two water molecules must provide oxygen atoms to the hexaniobate anion such that the formula should rather be written as $Na_{14}H_2Nb_{12}O_{38}{\cdot}30H_2O$. Note that in the formula $Na_{14}H_2Nb_{12}O_{38}{\cdot}30H_2O$ one water is missing compared to $Na_{14}Nb_{12}O_{37}{\cdot}32H_2O$. However, no reason was given by Lindqvist (1953) for this discrepancy, and we cannot resolve this issue. Alkaline polyniobate salts such as $Na_{14}H_2Nb_{12}O_{38}{\cdot}30H_2O(cr)$ or $K_{14}H_2Nb_{12}O_{38}{\cdot}30H_2O(cr)$ are quite soluble and lead to very basic solutions with pH > 12 (Wood 2005), see also the solubility experiments on $Na_7HNb_6O_{19}{\cdot}15H_2O(cr)$ by Deblonde et al. (2015) discussed in Section 17.4.3. Hexaniobate anions have also been found in aqueous solution and were identified as $Nb_6O_{19}^{8-}$ and its protonated forms $HNb_6O_{19}^{7-}$, $H_2Nb_6O_{19}^{6-}$, and $H_3Nb_6O_{19}^{5-}$.

Based on potentiometry in 3 M KCl at 25 °Cl, Neumann (1964) determined the first and second protonation constant of the hexaniobate anion $Nb_6O_{19}^{8-}$ (see Tab. 17.4-3).

Spinner (1968) used potentiometry at 25 °C in 0.1, 0.5, 2.0, and 3.0 M KCl to determine the first three protonation constants of the hexaniobate anion (see Tab. 17.4-3).

This was also done by Etxebarria et al. (1994) at 25 °C, but only in 3.0 M KCl (see Tab. 17.4-3).

We accepted all the conditional stability constants reported by these authors with increased uncertainties (see Tab. 17.4-3) and used these data for the SIT analyses shown in Figs. 17.4-6 – 17.4-8 which resulted in

$$Nb_6O_{19}^{8-} + H^+ \rightleftharpoons HNb_6O_{19}^{7-}$$

$$\log_{10}\beta_{6,1}°(298.15\ K) = (14.0 \pm 0.4)$$

$$\Delta\varepsilon = -(0.99 \pm 0.15)\ kg \cdot mol^{-1}$$

$$Nb_6O_{19}^{8-} + 2\ H^+ \rightleftharpoons H_2Nb_6O_{19}^{6-}$$

$$\log_{10}\beta_{6,2}°(298.15\ K) = (27.0 \pm 0.4)$$

$$\Delta\varepsilon = -(1.34 \pm 0.15)\ kg \cdot mol^{-1}$$

$$Nb_6O_{19}^{8-} + 3\ H^+ \rightleftharpoons H_3Nb_6O_{19}^{5-}$$

$$\log_{10}\beta_{6,3}°(298.15\ K,) = (38.6 \pm 0.5)$$

$$\Delta\varepsilon = -(1.50 \pm 0.23)\ kg \cdot mol^{-1}$$

We included these formation constants in TDB 2020, but only as supplemental data. The reason for this is not that the data are of doubtful quality but rather that the thermodynamic link between hexaniobate species and niobate species is very weak. In fact, there appear to be no measured formation constants of hexaniobate species from niobate species. The only such relation we are aware of is a re-interpretation by Etxebarria et al. (1994) of the solubility data reported by Babko et al. (1963) for freshly precipitated Nb_2O_5(pr), see also Section 17.4.3. The solubility increase with increasing pH was interpreted by Babko et al. (1963) as a consequence of the formation of NbO_3^- (or, equivalently, $Nb(OH)_6^-$). Etxebarria et al. (1994) did not agree with this interpretation and proposed the formation of the hexaniobate species $H_3Nb_6O_{19}^{5-}$ leading to

$$6\ Nb(OH)_5(aq) \rightleftharpoons H_3Nb_6O_{19}^{5-} + 5\ H^+ + 11\ H_2O(l)$$

$$\log_{10}{}^*K(298.15\ K,\ I = 1\ M\ KNO_3) = -14.46 \pm 0.30$$

We extrapolated this equilibrium constant to $I = 0$ using SIT (neglecting the very small differences between molal concentrations, used in SIT, and the molar concentrations of the experimental data), according to which

$$\log_{10}K° = \log_{10}K - 30\ D + \Delta\varepsilon\, I + 11\ \log_{10}a(H_2O)$$

where $D = 0.509\ I^{½} / (1 + 1.5\ I^{½}) = 0.204$ for $I = 1$ M. $\Delta\varepsilon\, I$ and the last term containing the activity of water are small compared to 30 D and can be safely neglected. Thus,

$$6\ Nb(OH)_5(aq) \rightleftharpoons H_3Nb_6O_{19}^{5-} + 5\ H^+ + 11\ H_2O(l)$$

$$\log_{10}{}^*K°(298.15\ K) = -(20.6 \pm 0.8)$$

which is included in TDB 2020 as supplemental datum with an estimated uncertainty.

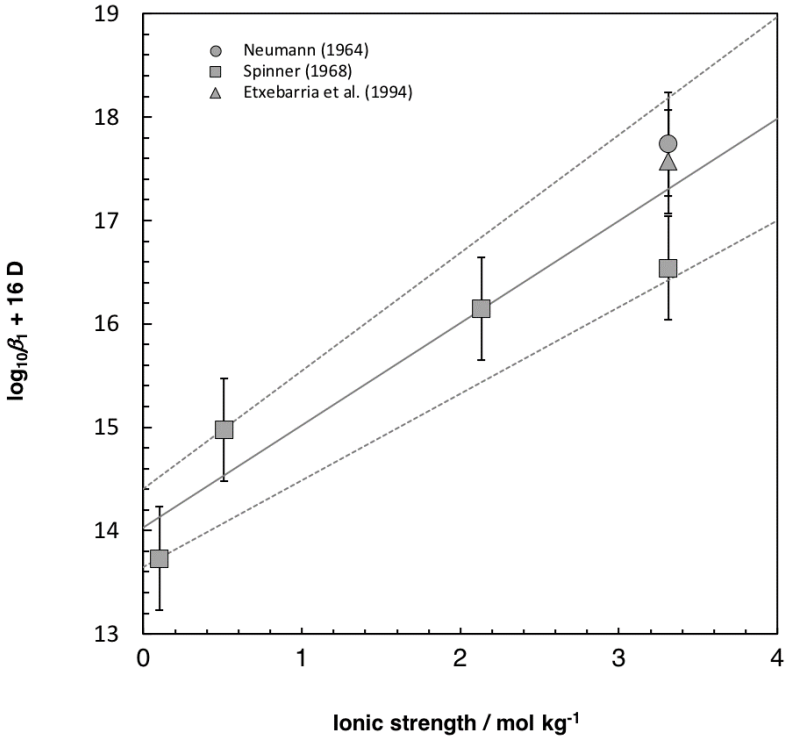

Fig. 17.4-6: SIT analysis of the equilibrium $Nb_6O_{19}^{8-} + H^+ \rightleftharpoons HNb_6O_{19}^{7-}$ in KCl media at 25 °C

The solid line is obtained from the linear fit by using the derived SIT interaction coefficient ($\Delta\varepsilon$) and the derived stability constant at zero ionic strength. The dotted lines represent the 95% uncertainty range extrapolated from $I = 0$ to higher ionic strengths. The data by Neumann (1964), Spinner (1968) and Etxebarria et al. (1994) are listed in Tab. 17.4-3.

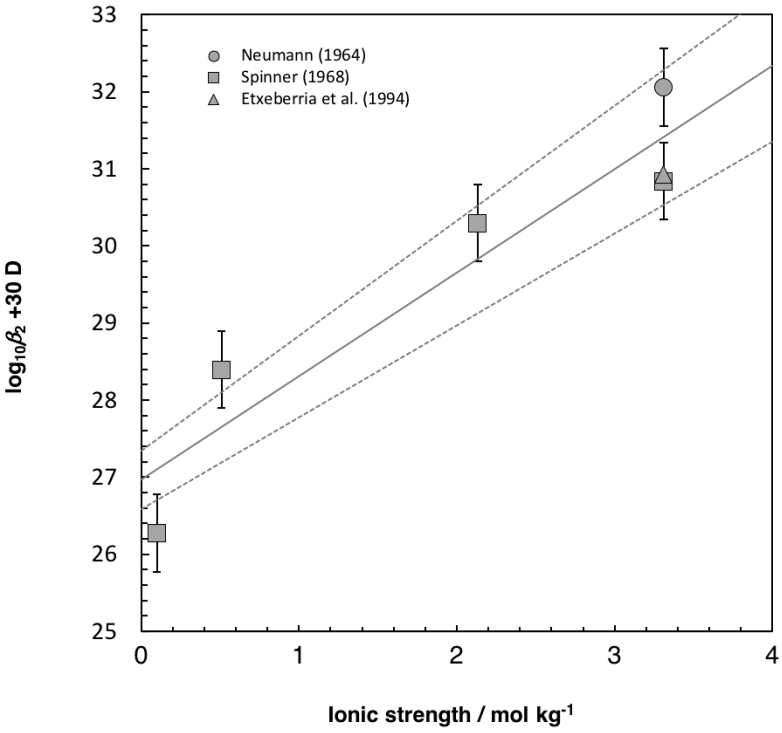

Fig. 17.4-7: SIT analysis of the equilibrium $Nb_6O_{19}^{8-} + 2\ H^+ \rightleftharpoons H_2Nb_6O_{19}^{6-}$ in KCl media at 25 °C

The solid line is obtained from the linear fit by using the derived SIT interaction coefficient ($\Delta\varepsilon$) and the derived stability constant at zero ionic strength. The dotted lines represent the 95% uncertainty range extrapolated from $I = 0$ to higher ionic strengths. The data by Neumann (1964), Spinner (1968) and Etxebarria et al. (1994) are listed in Tab. 17.4-3.

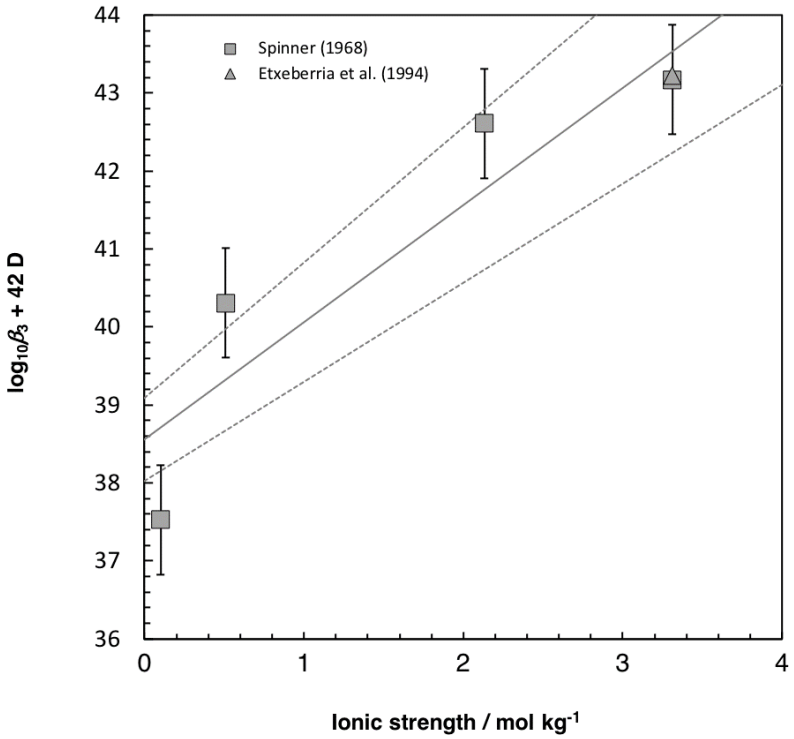

Fig. 17.4-8: SIT analysis of the equilibrium $Nb_6O_{19}^{8-} + 3\ H^+ \rightleftharpoons H_3Nb_6O_{19}^{5-}$ in KCl media at 25 °C

The solid line is obtained from the linear fit by using the derived SIT interaction coefficient ($\Delta\varepsilon$) and the derived stability constant at zero ionic strength. The dotted lines represent the 95% uncertainty range extrapolated from $I = 0$ to higher ionic strengths. The data by Spinner (1968) and Etxebarria et al. (1994) are listed in Tab. 17.4-3.

Due to a lack of experimental data in sodium media, we estimated

$\varepsilon(Nb_6O_{19}^{8-}, Na^+) \approx (0.40 \pm 0.70)$ kg · mol^{-1}

$\varepsilon(HNb_6O_{19}^{7-}, Na^+) \approx (0.35 \pm 0.60)$ kg · mol^{-1}

$\varepsilon(H_2Nb_6O_{19}^{6-}, Na^+) \approx (0.30 \pm 0.50)$ kg · mol^{-1}

$\varepsilon(H_3Nb_6O_{19}^{5-}, Na^+) \approx (0.25 \pm 0.40)$ kg · mol^{-1}

using the estimation method described in Section 1.5.3.

17.4.2.3 Dodecaniobates

In addition to the hexaniobates discussed above, Spinner (1968) also proposed the formation of the dodecaniobates $H_3Nb_{12}O_{36}^{9-}$, $H_4Nb_{12}O_{36}^{8-}$, $H_5Nb_{12}O_{36}^{7-}$, and $H_6Nb_{12}O_{36}^{6-}$ at pH below 9, reporting equilibrium constants among the first three of them (see Tab. 4.3).

Rozantsev et al. (2000) used pH-titrations and spectrophotometry in the ultraviolet region to study the polycondensation of Nb in solutions of varying acidity and alkalinity. Measurements were made at 25 °C in 1 M KCl at total Nb concentration between 0.5×10^{-4} and 2.0×10^{-4} mol/l. The absorption spectra were interpreted in terms of $H_2Nb_{12}O_{36}^{10-}$, $H_7Nb_{12}O_{36}^{5-}$, $H_9Nb_{12}O_{36}^{3-}$, $H_{10}Nb_{12}O_{36}^{2-}$ which gave the best fits to the data. Rozantsev et al. (2000) derived formation constants of these dodecaniobates from the hexaniobate $H_3Nb_6O_{19}^{5-}$ and an equilibrium constant between $Nb_6O_{19}^{8-}$ and $H_2Nb_{12}O_{36}^{10-}$ (see Tab.17. 4.3).

Noting that the dodecaniobate species proposed by Spinner (1968), on the one hand, and by Rozantsev et al. (2000), on the other hand, are perfectly complementary or, to put it less euphemistically, completely disagreeing by forming two disjoint sets, we were not at all tempted to include any of these dodecaniobate anions into TDB 2020.

17.4.3 Nb oxide and hydroxide solids

Nb and Ta, which are chemically very similar, do not occur as native metals in nature but are mainly found in oxides, such as columbite, $(Fe,Mn)(Nb,Ta)_2O_6$(cr), and pyrochlore, $(Na,Ca)_2Nb_2O_6(O,OH,F)$(cr), which are the main ore minerals mined for Nb. Nb also substitutes for major ions in many other minerals, although mainly at low concentrations.

Nb_2O_5(s) is not found in nature but can be experimentally precipitated at room temperature and circumneutral pH (see below). Nb_2O_5(pr) is hydrous and amorphous and is also referred to as "niobic acid". It is more soluble than the anhydrous, crystalline forms, but can still be considered as sparingly soluble (Babko et al. 1963).

At high pH, other solids seem to limit the solubility of Nb, in Ca-dominated systems a Ca-Nb-oxide, most likely $CaNb_4O_{11}\cdot 8H_2O$(cr) (Talerico et al. 2004), and in Na-dominated systems a Na-hexaniobate phase, $Na_7HNb_6O_{19}\cdot 15H_2O$(cr) (Deblonde et al. 2015).

NbO_2(cr)

Although NbO_2(cr) can be synthesized, it does not occur in nature as a mineral and is not expected to play any role in limiting the solubility of Nb in aqueous solution at ambient conditions. For this reason, the data selected for NbO_2(cr) in TDB 12/07 and precursors (see Section 17.1.1) are not included in TDB 2020.

$Nb_2O_5\cdot nH_2O$(pr) and Nb_2O_5(cr)

Babko et al. (1963) measured the solubility of freshly precipitated Nb_2O_5(pr) at 18 – 20 °C in the pH range 0 – 9.73 (see Fig. 17.4-10) The precipitate was prepared by adding HNO_3 to an alkaline solution (leading to a pH between 4 and 5) of $KNbO_3$, but neither composition nor structure of the precipitate were determined. The final pH values were obtained by adding suitable amounts of HNO_3 or KOH, and KNO_3 was added as needed to keep the ionic strength constant at $I = 1$ M. The concentration of Nb was measured photometrically from the reaction with xylenol orange. In

the pH range 0-7, the concentration of Nb remained constant at 1.4×10^{-5} M which was interpreted by Babko et al. (1963) in terms of the formation of $Nb(OH)_5(aq)$. From this solubility value follows

$$Nb_2O_5(pr) + 5\ H_2O(l) \rightleftharpoons 2\ Nb(OH)_5(aq)$$

$$\log_{10}{}^{*}K_{s,5}(298.15\ K, I = 1\ M) = 9.7$$

Lothenbach et al. (1999) suspected that the constant concentration rather corresponds to a detection limit and that the real concentrations are probably lower. At pH > 7, the solubility increases with increasing pH, according to Babko et al. (1963) due to the formation of NbO_3^- [54], represented by the reaction

$$Nb(OH)_5(aq) \rightleftharpoons NbO_3^- + H^+ + 2\ H_2O(l)$$

$$\log_{10}{}^{*}K(298.15\ K, I = 1\ M) = -7.4$$

which is equivalent to

$$Nb(OH)_5(aq) + H_2O(l) \rightleftharpoons Nb(OH)_6^- + H^+$$

with the same value for the conditional stability constant

$$\log_{10}{}^{*}K_6(298.15\ K, I = 1\ M) = -7.4$$

Etxebarria et al. (1994) did not agree with this interpretation of the experimental data by Babko et al. (1963) and proposed the formation of a protonated hexaniobate species (either one of $HNb_6O_{19}^{7-}$, $H_2Nb_6O_{19}^{6-}$, or $H_3Nb_6O_{19}^{5-}$) instead of NbO_3^- or $Nb(OH)_6^-$.The best fit to the data was obtained with $H_3Nb_6O_{19}^{5-}$, leading to

$$6\ Nb(OH)_5(aq) \rightleftharpoons H_3Nb_6O_{19}^{5-} + 5\ H^+ + 11\ H_2O(l)$$

$$\log_{10}{}^{*}K(298.15\ K, I = 1\ M) = -14.46 \pm 0.30$$

---

[54] This species is equivalent to $Nb(OH)_6^-$, see Section 17.4.1.

Tab. 17.4-3: Experimental formation constants for niobium hydroxo complexes

sol.: solubility, s.e.: solvent extraction, sp.: spectrophotometry, calc.: calculation, ext.: extrapolation, pot.: potentiometry)

Reaction	$\log_{10}K$ reported	$\log_{10}K$ accepted	T [°C]	I [M]	Medium	Method	Reference
Niobates							
$Nb(OH)_4^+ H_2O(l) \rightleftharpoons Nb(OH)5(aq) + H^+$ [a]	-3.22		25	0.1	$(H,Li)ClO_4$	s.e.	Guillaumont et al. (1970)
	-0.6		18 – 20	1	KNO_3	sol.	Babko et al. (1963)
$Nb(OH)_5(aq) + H_2O(l) \rightleftharpoons Nb(OH)_6^- + H^+$ [b]	-7.4		18 – 20	1	KNO_3	sol.	Babko et al. (1963)
	-6.6		25	0.1	NaCl	sol.	Lothenbach et al. (1999), based on Yajima et al. (1992) and Yajima (1994)
	> -6.322		25	0.1	NaCl	sol.	Kitamura et al. (2010), based on Yajima et al. (1992) and Yajima (1994)
Niobate to tetraniobate							
$4\ Nb(OH)_8^{3-} \rightleftharpoons Nb_4O_{16}^{12-} + 16\ H_2O(l)$ [c]	8.78 ± 0.48		25	1.0	KCl	sp.	Goiffon et al. (1973)
Tetraniobates							
$Nb_4O_{16}^{12-} + 4\ H_2O(l) \rightleftharpoons Nb_4O_{12}(OH)_4^{8-} + 4\ OH^-$	3.18 ± 0.50		25	1.0	KCl	sp.	Goiffon et al. (1973)
Tetraniobate to hexaniobate							
$3\ Nb_4O_{12}(OH)_4^{8-} \rightleftharpoons 2\ Nb_6O_{19}^{8-} + 8\ OH^- + 2\ H_2O(l)$	0.60 ± 0.06		25	1.0	KCl	sp.	Goiffon et al. (1973)
Niobate to hexaniobate							
$6\ Nb(OH)_5(aq) \rightleftharpoons Nb_6O_{19}^{8-} + 8\ H^+ + 11\ H_2O(l)$	-47.04		20	1	KNO_3	calc.	Etxebarria et al. (1994)
$6\ Nb(OH)_5(aq) \rightleftharpoons HNb_6O_{19}^{7-} + 7\ H^+ + 11\ H_2O(l)$	-33.49		20	1	KNO_3	calc.	Etxebarria et al. (1994)
$6\ Nb(OH)_5(aq) \rightleftharpoons H_2Nb_6O_{19}^{6-} + 6\ H^+ + 11\ H_2O(l)$	-24.06		20	1	KNO_3	calc.	Etxebarria et al. (1994)
$6\ Nb(OH)_5(aq) \rightleftharpoons H_3Nb_6O_{19}^{5-} + 5\ H^+ + 11\ H_2O(l)$	-14.46		20	1	KNO_3	calc.	Etxebarria et al. (1994)
Hexaniobates							
$Nb_6O_{19}^{8-} + H^+ \rightleftharpoons HNb_6O_{19}^{7-}$	11.9 ± 0.1		25	inf. dil.	KCl	ext.	Spinner (1968)
	16.11 ± 0.14		25	inf. dil.	KCl	ext.	Etxebarria et al. (1994)
	11.98 ± 0.10	11.98 ± 0.50	25	0.1	KCl	pot.	Spinner (1968)
	12.17 ±0.10	12.17 ±0.50	25	0.5	KCl	pot.	Spinner (1968)
	12.44 ± 0.10	12.44 ± 0.50	25	2.0	KCl	pot.	Spinner (1968)
	12.60 ± 0.10	12.60 ± 0.50	25	3.0	KCl	pot.	Spinner (1968)
	13.8 ± 0.2	13.8 ± 0.5	25	3	KCl	pot.	Neumann (1964)
	13.63 ± 0.04	13.63 ± 0.50	25	3.0	KCl	pot.	Etxebarria et al. (1994)

Tab. 17.4-3: Cont.

Reaction	$\log_{10}K$ reported	$\log_{10}K$ accepted	T [°C]	I [M]	Medium	Method	Reference
$Nb_6O_{19}^{8-} + 2\ H^+ \rightleftharpoons H_2Nb_6O_{19}^{6-}$	22.9 ± 0.1		25	inf. dil.	KCl	ext.	Spinner (1968)
	27.97 ± 0.13		25	inf. dil.	KCl	ext.	Etxebarria et al. (1994)
	22.99 ± 0.11	22.99 ± 0.50	25	0.1	KCl	pot.	Spinner (1968)
	23.14 ± 0.11	23.14 ± 0.50	25	0.5	KCl	pot.	Spinner (1968)
	23.35 ± 0.11	23.35 ± 0.50	25	2.0	KCl	pot.	Spinner (1968)
	23.46 ± 0.11	23.46 ± 0.50	25	3.0	KCl	pot.	Spinner (1968)
	24.68 ± 0.21	24.68 ± 0.50	25	3	KCl	pot.	Neumann (1964)
	23.55 ± 0.04	23.55 ± 0.50	25	3.0	KCl	pot.	Etxebarria et al. (1994)
$Nb_6O_{19}^{8-} + 3\ H^+ \rightleftharpoons H_3Nb_6O_{19}^{5-}$	32.9 ± 0.1		25	inf. dil.	KCl	ext.	Spinner (1968)
	39.91 ± 0.18		25	inf. dil.	KCl	ext.	Etxebarria et al. (1994)
	32.93 ± 0.11	32.93 ± 0.70	25	0.1	KCl	pot.	Spinner (1968)
	32.95 ± 0.11	32.95 ± 0.70	25	0.5	KCl	pot.	Spinner (1968)
	32.89 ± 0.11	32.89 ± 0.70	25	2.0	KCl	pot.	Spinner (1968)
	32.85 ± 0.11	32.85 ± 0.70	25	3.0	KCl	pot.	Spinner (1968)
	32.90 ± 0.07	32.90 ± 0.70	25	3.0	KCl	pot.	Etxebarria et al. (1994)
Niobate and tetraniobate to dodecaniobate							
$NbO_6^{7-} + 19/6\ H_2O(l) \rightleftharpoons 1/12\ H_2Nb_{12}O_{36}^{10-} + 37/6\ OH^-$	-35.80		25	1	KCl	pot./sp.	Rozantsev et al. (2000)
$Nb_4O_{16}^{12-} + 14/3\ H_2O(l) \rightleftharpoons 1/3\ H_2Nb_{12}O_{36}^{10-} + 26/3\ OH^-$	-5.08		25	1	KCl	pot./sp.	Rozantsev et al. (2000)
Hexaniobate to dodecaniobate							
$Nb_6O_{19}^{8-} + 2\ H_2O(l) \rightleftharpoons 1/2\ H_2Nb_{12}O_{36}^{10-} + 3\ OH^-$	-17.10		25	1	KCl	pot./sp.	Rozantsev et al. (2000)
$2\ H_3Nb_6O_{19}^{5-} \rightleftharpoons H_2Nb_{12}O_{36}^{10-} + 2\ H_2O(l)$	23.46		25	1	KCl	pot./sp.	Rozantsev et al. (2000)
$2\ H_3Nb_6O_{19}^{5-} + 5\ H^+ \rightleftharpoons H_7Nb_{12}O_{36}^{5-} + 2\ H_2O(l)$	61.03		25	1	KCl	pot./sp.	Rozantsev et al. (2000)
$2\ H_3Nb_6O_{19}^{5-} + 7\ H^+ \rightleftharpoons H_9Nb_{12}O_{36}^{3-} + 2\ H_2O(l)$	66.84		25	1	KCl	pot./sp.	Rozantsev et al. (2000)
$2\ H_3Nb_6O_{19}^{5-} + 8\ H^+ \rightleftharpoons H_{10}Nb_{12}O_{36}^{2-} + 2\ H_2O(l)$	78.03		25	1	KCl	pot./sp.	Rozantsev et al. (2000)
Dodecaniobates							
$H_3Nb_{12}O_{36}^{9-} + H^+ \rightleftharpoons H_4Nb_{12}O_{36}^{8-}$	7.83		25	1.0	KCl	pot.	Spinner (1968)
$H_4Nb_{12}O_{36}^{8-} + H^+ \rightleftharpoons H_5Nb_{12}O_{36}^{7-}$	6.34		25	1.0	KCl	pot.	Spinner (1968)

[a] Original formulation by Guillaumont et al. (1970): $NbO_2^+ + H_2O(l) \rightleftharpoons NbO_2OH(aq) + H^+$
[b] Original formulation by Babko et al. (1963): $Nb(OH)_5(aq) \rightleftharpoons NbO_3^- + H^+ + 2\ H_2O(l)$
[c] Original formulation by Goiffon et al. (1973): $4\ NbO_2(OH)_4^{3-} \rightleftharpoons Nb_4O_{16}^{12-} + 8\ H_2O(l)$

Babko et al. (1963) also measured the solubility of Nb_2O_5(pr) in concentrated nitric acid (1-6 M, with pH decreasing from 0 to -0.78) and observed an increase of the solubility with decreasing pH, which they explained by the formation of $Nb(OH)_4^+$

$$Nb(OH)_5(aq) \rightleftharpoons Nb(OH)_4^+ + OH^-$$

$$\log_{10}K(298.15\ K, I = 1\ M) = -14.6$$

which can also be written as

$$Nb(OH)_4^+ + H_2O(l) \rightleftharpoons Nb(OH)_5(aq) + H^+$$

$$\log_{10}K_5(298.15\ K, I = 1\ M) = -0.6$$

Yajima et al. (1992) and Yajima (1994) investigated the solubility of Nb in aqueous solution at ambient temperature as a function of pH. As we did not have access to these publications, the following discussion is based on Kitamura et al. (2010) who carried out a re-evaluation of the data presented by these authors. Lothenbach et al. (1999), see below, did also discuss the data by Yajima et al. (1992) and Yajima (1994). These authors carried out their batch experiments under anoxic conditions at an ionic strength of 0.1 M (adjusted with NaCl) and measured the solubilities both from under- and oversaturation after 7 – 28 days. In the oversaturation experiments, initial Nb concentrations were 10^{-2} M and the precipitates were analysed by X-ray diffractometry. In the first series of experiments (Yajima et al. 1992), the concentration of dissolved Nb was measured with inductively coupled plasma optical emission spectroscopy (ICP-OES), and in the second series (Yajima 1994) with inductively-coupled plasma mass spectroscopy (ICP-MS). The experimental results are shown in Fig. 17.4-9. Since the detection limit of ICP-OES (around 5×10^{-8} M) is higher than that of ICP-MS (around 10^{-8} M), Kitamura et al. (2010) neglected the data by (Yajima et al. 1992) at pH < 7 in their re-evaluation and considered the values by (Yajima 1994) around 10^{-8} M as maximum values. Kitamura et al. (2010) interpreted the data in terms of the following reactions:

$$Nb_2O_5(pr) + 7\ H_2O(l) \rightleftharpoons 2\ Nb(OH)_6^- + 2\ H^+$$

$$Nb(OH)_5(aq) + H_2O(l) \rightleftharpoons Nb(OH)_6^- + H^+$$

They used least-squares fitting to the data at pH < 11 and obtained the conditional constants $\log_{10}{}^*K_{s,6}(298.15\ K) = -(28.486 \pm 0.455)$ and $\log_{10}{}^*K_{5,6}(298.15\ K) > -6.322$. Using SIT, they extrapolated these constants to zero ionic strength[55] and obtained

$$\log_{10}{}^*K_{s,6}°(298.15\ K) = -(28.913 \pm 0.507)$$

and

[55] They used the NEA-selected $\varepsilon(H^+, Cl^-) = (0.12 \pm 0.01)\ kg \cdot mol^{-1}$ and estimated $\varepsilon(Nb(OH)_6^-, Na^+) = -(0.07 \pm 0.11)\ kg \cdot mol^{-1}$ as the average of the NEA-selected $\varepsilon(SiO(OH)_3^-, Na^+)$, $\varepsilon(Si_2O_2(OH)_5^-, Na^+)$, $\varepsilon(B(OH)_4^-, Na^+)$, $\varepsilon(NpO_2(OH)_2^-, Na^+)$, and $\varepsilon(UO_2(OH)_3^-, Na^+)$, all pertaining to hydrolysis species with a net charge of -1.

$\log_{10}{}^{*}K_{5,6}°(298.15\ K) > -6.535$[56]

These values lead to

$Nb_2O_5(pr) + 5\ H_2O(l) \rightleftharpoons 2\ Nb(OH)_5(aq)$

$\log_{10}{}^{*}K_{s,5}°(298.15\ K) < -15.842$

Lothenbach et al. (1999) based their only selected thermodynamic data for Nb on the experimental data presented by Yajima et al. (1992) and Yajima (1994) (see Fig. 17.4-9). From the observed maximum solubility of 1×10^{-8} M for $Nb_2O_5(pr)$ at pH < 6 in 0.1 M NaCl by Yajima (1994), Lothenbach et al. (1999) derived $\log_{10}{}^{*}K_{s,5}(298.15\ K) < -16$ and selected

$\log_{10}{}^{*}K_{s,5}°(298.15\ K) = -16$

as a tentative value. From the data at higher pH, Yajima et al. (1992) and Yajima (1994) obtained

$\log_{10}{}^{*}K_{s,6}°(298.15\ K) = -29.2$

(using the Davies equation for the extrapolation of the experimental data to zero ionic strength)

for the reaction

$Nb_2O_5(pr) + 7\ H_2O(l) \rightleftharpoons 2\ Nb(OH)_6^- + 2\ H^+$

Combining $\log_{10}{}^{*}K_{s,5}°(298.15\ K)$ and $\log_{10}{}^{*}K_{s,6}°(298.15\ K)$, Lothenbach et al. (1999) arrived at their selected

$Nb(OH)_5(aq) + H_2O(l) \rightleftharpoons Nb(OH)_6^- + H^+$

$\log_{10}{}^{*}K_{5,6}°(298.15\ K) = -6.6$

which is, not surprisingly, practically equal to the value obtained by Kitamura et al. (2010).

---

[56] Kitamura reported $\log_{10}{}^{*}K_6°(298.15\ K) > -6.758$ which is obviously incorrect. This can be seen from the following consideration: $\log_{10}{}^{*}K_{s,5}°$ for the reaction $Nb_2O_5(pr) + 5\ H_2O(l) \rightleftharpoons 2\ Nb(OH)_5(aq)$ is equal to $\log_{10}{}^{*}K_{s,6}° - 2\ \log_{10}{}^{*}K_{5,6}°$. From SIT follows that $\log_{10}{}^{*}K_{s,6}° = \log_{10}{}^{*}K_{s,6} - 4D + 2\ \Delta\varepsilon\ I_m$ and $\log_{10}{}^{*}K_{5,6}° = \log_{10}{}^{*}K_{5,6} - 2D + \Delta\varepsilon\ I_m$. In both cases $\Delta\varepsilon = \varepsilon(Nb(OH)_6^-, Na^+) + \varepsilon(H+, Cl^-)$, if it is assumed that the SIT coefficient for the neutral $Nb(OH)_5(aq)$ is equal to zero. From these SIT-equations then follows $\log_{10}{}^{*}K_{5,6}° = \log_{10}{}^{*}K_{s,6} - 2\ \log_{10}{}^{*}K_{5,6}$. Thus $\log_{10}{}^{*}K_{s,6}° - 2\ \log_{10}{}^{*}K_{5,6}°$ and $\log_{10}{}^{*}K_{s,6} - 2\ \log_{10}{}^{*}K_{5,6}$ must result in the same value, which is not true if $\log_{10}{}^{*}K_6°(298.15\ K) > -6.758$ is used.

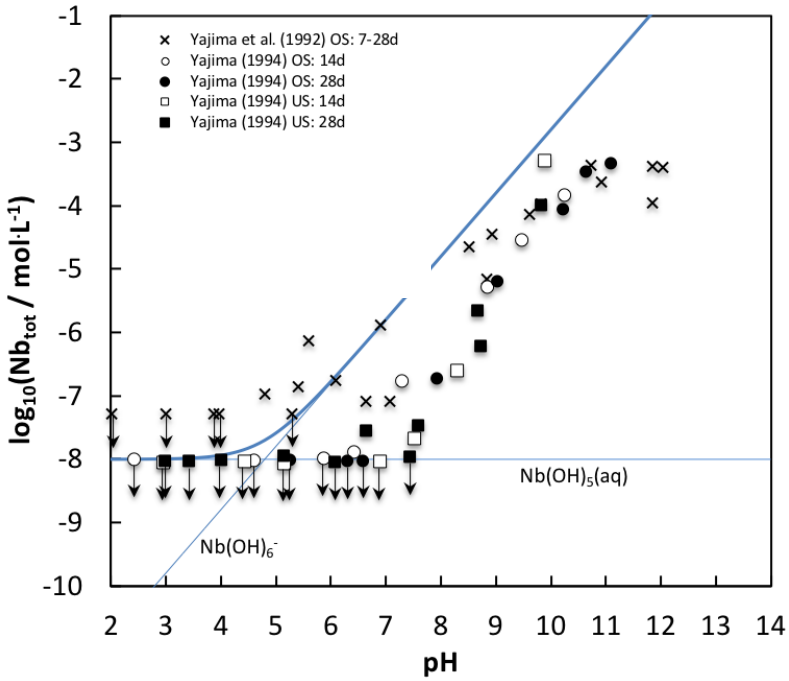

Fig. 17.4-9: Solubility of Nb_2O_5(pr) as a function of pH as determined by Yajima et al. (1992) and Yajima (1994) in 0.1 M NaCl

Arrows indicate the detection limits. OS: experiments from oversaturation, US: experiments from undersaturation, d: days of equilibration. The concentrations of $Nb(OH)_5$(aq) and $Nb(OH)_6^-$ shown as blue lines were calculated with the data selected for TDB 2020 which provide an upper solubility limit at pH > 6 (see text for discussion).

Kulmala & Hakanen (1993) studied the solubility of Nb_2O_5(pr) from oversaturation by adding $NbCl_5$ to NaOH solutions. Precipitates were not analysed for composition and ionic strength was not held constant. Concentrations of Nb increased as pH increased from 7 – 11 but decreased above pH 11 (see Fig. 17.4-10). No efforts were made by Kulmala & Hakanen (1993) to explain the decrease above pH 11 nor did they try to extract thermodynamic data from the experimental results.

Peiffer et al. (2010) used solubility measurements on B-Nb_2O_5(cr) to determine the stability constants for Nb hydroxide complexes as discussed in Section 17.4.1. Although Peiffer et al. (2010) reported an extensive experimental data set, which we accepted for the derivation of stability constants for the niobate species $Nb(OH)_5$(aq), $Nb(OH)_6^-$, and $Nb(OH)_7^{2-}$, we did not include any of the solubility products for B-Nb_2O_5(cr) written in terms of either one of $Nb(OH)_4^+$, $Nb(OH)_5$(aq), $Nb(OH)_6^-$, or $Nb(OH)_7^{2-}$. The reason for this decision is that it is unlikely that B-Nb_2O_5(cr), a high-temperature modification, precipitates under surficial conditions and may thus control the solubility of Nb in a repository environment (the solubility data by Peiffer et al. 2010 were obtained from undersaturation). It is more realistic to assume that the solubility limiting solid is an amorphous, hydrated precipitate, as formed in the experiments by Babko et al. (1963), Yajima et al. (1992), Yajima (1994), Kulmala & Hakanen (1993), or Deblonde et al. (2015).

For TDB 2020, we accept the solubility data on amorphous and hydrated Nb_2O_5(pr) by Yajima et al. (1992) and Yajima (1994) since the solubility data were obtained from both over- and undersaturation. As discussed above, Kitamura et al. (2010) derived

$$Nb_2O_5(pr) + 5\ H_2O(l) \rightleftharpoons 2\ Nb(OH)_5(aq)$$

$$\log_{10}{}^{*}K_{s,5}°(298.15\ K) < -15.842$$

from the data by Yajima et al. (1992) and Yajima (1994). For inclusion in TDB 2020, we have rounded this value to -16.0 and assigned an estimated uncertainty of ± 0.5. Hence

$$\log_{10}{}^{*}K_{s,5}°(298.15\ K) = -(16.0 \pm 0.5)$$

is included in TDB 2020. From $\log_{10}{}^{*}K_5°(Nb(OH)_4^+ + H_2O(l) \rightleftharpoons Nb(OH)_5(aq) + H^+, 298.15\ K) = -(1.89 \pm 0.12)$ and $\log_{10}{}^{*}K_5°(Nb(OH)_4^+ + 2\ H_2O(l) \rightleftharpoons Nb(OH)_6^- + 2\ H^+, 298.15\ K) = -(6.69 \pm 0.14)$ selected for TDB 2020 (see Section 17.4.1) follows $\log_{10}{}^{*}K_{5,6}°(298.15\ K) = -(4.80 \pm 0.18)$ which is substantially larger than the values derived by Lothenbach et al. (1999) and Kitamura et al. (2010) from the data by Yajima et al. (1992) and Yajima (1994). As seen in Fig. 17.4-9, the solubility of Nb_2O_5(pr) calculated from the selected data for TDB 2020 provides an upper limit to the experimental data by Yajima et al. (1992) and Yajima (1994) at pH > 6.

Ca-Nb-oxide phase

Talerico et al. (2004) investigated the solubility of Nb in solutions representing typical compositions (in terms of pH and Ca concentration) of cement-equilibrated systems. The solutions were prepared by dissolving suitable amounts of NaOH and $Ca(ClO_4)_2$ in CO_2-free bi-distilled water under argon atmosphere to reach the required pH (9.5 – 13.2) and the required Ca concentrations (0.1 – 20 millimolal, portlandite undersaturation). $NaClO_4$ was added to keep the ionic strength constant at about 0.2 M. Added amounts of $NbCl_5$ resulted in Nb concentrations between 5×10^{-7} and 10^{-5} M at the lower end of the pH range and between 10^{-9} and 2×10^{-5} M at the upper end, and in the precipitation of a solid Ca-Nb-oxide phase. Based on X-ray diffraction measurements, Talerico et al. (2004) considered $CaNb_4O_{11}{\cdot}8H_2O$ as the most likely composition. This corresponds to the mineral hochelagaite (Jambor et al. 1986). In general, the dissolved Nb concentrations decreased both with increasing pH and increasing Ca concentration. Due to the missing information on Nb hydrolysis and the resulting uncertainties with respect to Nb speciation, Talerico et al. (2004) were not able to derive a solubility product from the solubility data and derived the following empirical relationship instead:

$$[Nb]_{dissolved} = 1.4643\ e^{-1.3402\ pH}\ [Ca]^{-0.8922}/10^{2.6766}$$

In the absence of reliable information on Nb hydrolysis and speciation at pH > 9, this relationship can be used for estimating the solubility of Nb in cement systems. The results by Talerico et al. (2004) are in line with the experimental data by Kulmala & Hakanen (1993) who observed that the solubility of Nb in cement-equilibrated groundwaters (undersaturation experiments with Nb_2O_5(s), pH around 12.8) was orders of magnitude lower than at the corresponding pH in their experiments in NaOH solutions discussed above (on the order of 10^{-8} – 10^{-9} M vs. about 10^{-3} M).

$Na_7HNb_6O_{19}\cdot 15H_2O$(cr)

Deblonde et al. (2015) measured the solubility of $Nb_2O_5\cdot nH_2O$(am) at 25 °C and alkaline conditions (pH 6.5 – 12) from undersaturation at constant ionic strength (0.12 M $NaCl/Na_2CO_3/NaOH$). Nb concentrations were measured with ICP-OES. The solubility data are shown in Fig. 17.4-10. Raman spectra of $Nb_2O_5\cdot nH_2O$(am) equilibrated for 56 days with solutions at 25 °C and I = 0.12 M with pH ranging from 7.0 – 11.9 revealed that the amorphous and hydrated Nb_2O_5 is gradually transformed into a hexaniobate salt with increasing pH (where the conversion starts at a pH as low as 8). The Raman spectrum of a sample of $Nb_2O_5\cdot nH_2O$(am) equilibrated for several days with 1 molar NaOH was identical to the spectrum of pure $Na_7HNb_6O_{19}\cdot 15H_2O$(cr) and the XRD diffraction pattern of the equilibrated sample confirmed this conversion. Analysis of the Raman spectra at I = 0.12 M and pH 11.9 suggested the formation of a mixture of $Na_7HNb_6O_{19}\cdot 15H_2O$(cr) with another hexaniobate phase that may be $Na_{8-x}H_xNb_6O_{19}\cdot nH_2O$(cr) (x > 1). Therefore, Deblonde et al. (2015) carried out solubility experiments with $Na_7HNb_6O_{19}\cdot 15H_2O$(cr) from undersaturation at 25 °C and pH = 11.8 in NaCl solutions as a function of the Na^+ concentration (initial concentrations varied from 0 – 5.46×10^{-2} M and final concentrations from 4.47×10^{-2} M to 5.95×10^{-2} M). The ionic strength was not held constant and varied from 0.09 to 0.18 M at equilibrium (or steady state). With increasing Na concentration, the solubility of Nb decreased from 3.86×10^{-2} M to 4.08×10^{-2} M. Since alkali ions can form ion pairs with hexaniobate, Deblonde et al. (2015) considered the potential formation of ion pairs between Na^+ and $HNb_6O_{19}^{7-}$ in their least squares fit of the experimental data. The best fit, however, was obtained when no formation of ion pairs was assumed and Deblonde et al. (2015) obtained

$$Na_7HNb_6O_{19}\cdot 15H_2O(cr) \rightleftharpoons 7\ Na^+ + HNb_6O_{19}^{7-} + 15\ H_2O(l)$$

$$log_{10}K_{s,0}(298.15\ K) = -11.6$$

Since this solubility product was derived from data at variable ionic strengths and there is no straightforward way to extrapolate the data to I = 0 , we include this conditional solubility product as supplemental datum in TDB 2020.

Hexaniobate anions form ion pairs with the alkali metal ions and the strength of ion pairs increases with the alkali ion radius according to the series Li = Na < K < Rb = Cs (Antonio et al. 2009).

Therefore, ion pairs of $HNb_6O_{19}^{7-}$ with K^+ can be expected to be stronger than those with Na^+ and the formation of $K_8Nb_6O_{19}$(aq) and $K_{10}Nb_6O_{19}^{2+}$ was actually observed by Antonio et al. (2009). This incited Deblonde et al. (2015) to carry out additional solubility experiments with $Na_7HNb_6O_{19}\cdot 15H_2O$(cr) in KCl solutions and, indeed, the solubility increased considerably.

XRD analyses of the solids that were in contact for 25 days with the KCl solutions did not show any changes, suggesting that the increase in solubility is actually due to the ion pair formation of K^+ with hexaniobate oxyanions. However, Deblonde et al. (2015) did not quantify these observations.

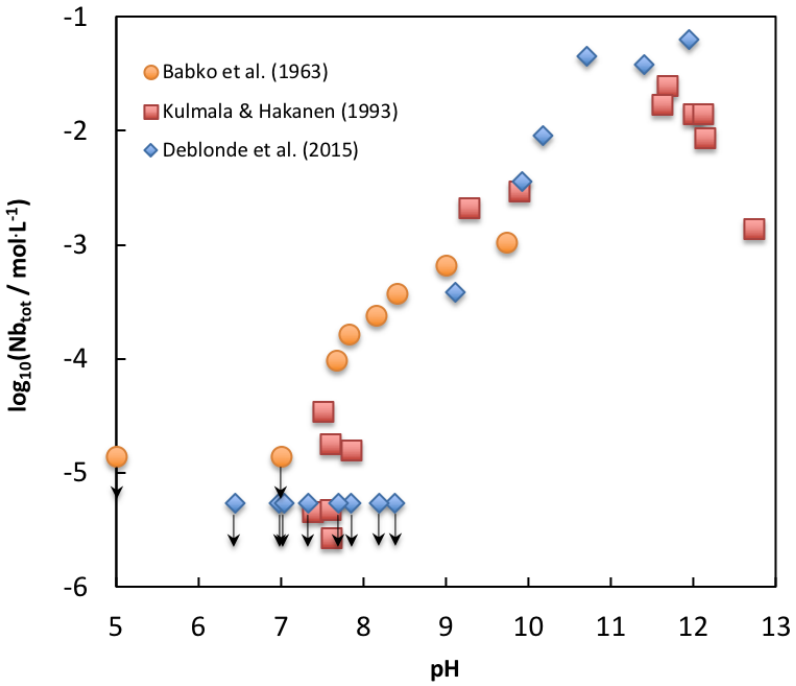

Fig. 17.4-10: Solubility of $Nb_2O_5 \cdot nH_2O$(am) as a function of pH

As determined by Babko et al. (1963) in 1 M HNO_3/KOH/KNO_3, Kulmala & Hakanen (1993) in NaOH solutions of variable ionic strength, and Deblonde et al. (2015) in 0.12 M NaCl/Na_2CO_3/NaOH. Arrows indicate the detection limits. The solubilities measured by Babko et al. (1963) at the detection limit in the pH range 0 to < 5 are not shown.

Columbite-tantalite

Due to the great chemical similarity of Nb and Ta, these elements form a solid solution (Fe,Mn)(Nb,Ta)$_2O_6$(cr) called columbite if the Nb content is higher and tantalite if the Ta content is higher. It is often referred to as coltan. Columbite and tantalite are of hydrothermal origin and are almost exclusively found in granites and pegmatites. It is therefore very unlikely that columbite plays any role in limiting the solubility of Nb in low temperature environments.

Zaraisky et al. (2010) measured the solubility of columbite-tantalite (Nb_2O_5: 59 wt.-%, Ta_2O_5: 18 wt.-%) in fluoride (HF, NaF, and KF), carbonate ($NaHCO_3$) and chloride (HCl) solutions from 300 to 550 °C and 50 to 100 MPa. At 400 °C and 100 MPa, the solubility of Nb in HF increases from between 10^{-6} and $10^{-5.5}$ m in 10^{-2} m HF up to 10^{-3} – 10^{-2} m in 1.0 m HF. The solubility of Nb is always highest in 1.0 m HF, and generally decreases successively in the order 2.0 m KF, 1.0 m $NaHCO_3$, 1.0 m NaF and 1.0 m HCl (although the order behind HF may change as a function of temperature and pressure). At 300 °C and 50 MPa, e.g., the solubilities of Nb are $10^{-1.49}$ m in 1.0 m HF, $10^{-3.50}$ m in 2.0 m KF, $10^{-5.01}$ in 1.0 m $NaHCO_3$, and $10^{-5.20}$ m in 1.0 m NaF (solubilities were not measured in HCl under these conditions). Zaraisky et al. (2010) concluded that Nb can be mobilized hydrothermally by concentrated fluoride solutions (mainly as HF and, less effectively, as KF), while hydrothermal carbonate and chloride solutions are much less effective. This result is in line with the expected behaviour of the ligands according to the Pearson hardness scale (see Section 17.1).

Pyrochlore group

The pyrochlore minerals are chemically very diverse. They have the general formula (Lumpkin & Ewing 1995): $A_{2-m}B_2X_{6-w}Y_{1-n}{\cdot}pH_2O$ where A = Na, Ca, Mn, Fe^{2+}, Sr, Sb, Cs, Ba, REE, Pb, Bi, Th, and U; B = Nb, Ta, Ti, Al, Fe^{3+}, Zr, Sn, and W; X = O and OH; and Y = O, OH, and F. The A, X, and Y sites can accommodate vacancies (m = 0-1.7, w = 0-0.7, n = 0-1).

Pyrochlore s. str., $(Na,Ca)_2Nb_2O_6(O,OH,F)$(cr) occurs mainly in carbonatites (igneous rocks that contain more than 50 wt.-% primary carbonate minerals). As in the case of columbite, the high temperatures required for the formation of pyrochlore make it very unlikely that pyrochlore limits the solubility of Nb in low temperature environments. There appear to be no published solubility products for endmember minerals of the pyrochlore group that could serve for quantitative geochemical modelling (Wood 2005).

17.5 Nb fluoride complexes

There are several spectroscopic studies that identified the stoichiometry of Nb-fluoride complexes. The discussion of these is based on the review by Wood (2005). $NbOF_5^{2-}$ was found with Raman and infrared spectroscopy in 1 – 35% solutions of HF, and NbF_6^- in 25 to 50% solutions (Keller 1963). No NbF_7^{2-} was identified in these experiments. Griffith & Wickins (1967) also found $NbOF_5^{2-}$ by Raman and infrared spectroscopy in 5 molar HF solutions. Raman spectroscopy was used by Tsikaeva et al. (1989) to study Nb fluoride complexes in solutions containing HF and NH_4F or alkali fluorides. NbF_6^- and $NbOF_5^{2-}$ were found simultaneously in solution and the proportion of $NbOF_5^{2-}$ increased upon addition of NH_4F or alkali fluorides. Wood (2005) concluded from these spectroscopic studies that, since $NbOF_5^{2-}$ and NbF_6^- were identified in solutions of high HF and/or NH_4F solutions unlikely to be found in natural environments, it is doubtful that these species are relevant for natural waters.

According to Lothenbach et al. (1999) and Wood (2005), there are only few measurements of stability constants of Nb fluoride complexes.

Lothenbach et al. (1999) reported a conditional stability constant for the reaction $NbOF_2^+ + F^- \rightleftharpoons NbOF_3(aq)$, and the stepwise conditional stability constants for $NbOF_4^-$, $NbOF_5^{2-}$, $NbOF_6^{3-}$, NbF_7^{2-}, NbF_8^{3-}, and NbF_9^{4-} (see Tab. 17.5-1). These were taken from the potentiometric study by Land & Osborne (1972) carried out with a fluoride selective ion electrode at 25 °C in 0.5 M $(Na,H)ClO_4$ at $-\log_{10}[H^+] < 1$ and free fluoride concentrations between $3 \times 10^{-5} – 1 \times 10^{-3}$ M. In addition, Lothenbach et al. (1999) also reported a conditional stability constant for the reaction $NbOF_4^- + F^- \rightleftharpoons NbOF_5^{2-}$ determined by Neumann (1970) in 3 M KCl (see Tab. 17.5-1). Total Nb concentrations were 0.01 and 0.02 molar and the fluoride concentrations varied between 0.06 and 0.40 molar. Lothenbach et al. (1999) did not select any of these data but gave no reasons for this decision.

Tab. 17.5-1: Experimental formation constants for niobium fluoride and hydroxofluoride complexes

For convenience, the stoichiometries with the maximum number of OH^- are additionally indicated, if in the original reactions the stoichiometries with smaller amounts of H_2O were used (e.g., $NbOF_2^+$ and $Nb(OH)_2F^{2+}$ differ by one H_2O, the former stoichiometry is written with the minimum number of H_2O and the latter with the maximum number of OH^-).

Reaction	**$\log_{10}K$**	***T*** [°C]	***I*** [M]	**Medium**	**Method**	**Reference**
$NbOF_2^+ + F^- \rightleftharpoons NbOF_3(aq)$ $Nb(OH)_2F_2^+ + F^- \rightleftharpoons Nb(OH)_2F_3(aq)$	3.78	25	0.50	$(Na,H)ClO_4$	pot.	Land & Osborne (1972)
$NbOF_3(aq) + F^- \rightleftharpoons NbOF_4^-$ $Nb(OH)_2F_3(aq) + F^- \rightleftharpoons Nb(OH)_2F_4^-$	4.30	25	0.50	$(Na,H)ClO_4$	pot.	Land & Osborne (1972)
$NbOF_4^- + F^- \rightleftharpoons NbOF_5^{2-}$ $Nb(OH)_2F_4^- + F^- \rightleftharpoons Nb(OH)_2F_5^{2-}$	2.51 ± 0.03	25	3	KCl	pot.	Neumann (1970)
	4.51	25	0.50	$(Na,H)ClO_4$	pot.	Land & Osborne (1972)
$NbOF_5^{2-} + F^- \rightleftharpoons NbOF_6^{3-}$ $Nb(OH)_2F_5^{2-} + F^- \rightleftharpoons Nb(OH)_2F_6^{3-}$	4.67	25	0.50	$(Na,H)ClO_4$	pot.	Land & Osborne (1972)
$NbOF_6^{3-} + F^- + 2\ H^+ \rightleftharpoons NbF_7^{2-} + H_2O(l)$ $Nb(OH)_2F_6^{3-} + F^- + 2\ H^+ \rightleftharpoons NbF_7^{2-} + 2\ H_2O(l)$	11.41	25	0.50	$(Na,H)ClO_4$	pot.	Land & Osborne (1972)
$NbF_7^{2-} + F^- \rightleftharpoons NbF_8^{3-}$	3.08	25	0.50	$(Na,H)ClO_4$	pot.	Land & Osborne (1972)
$NbF_8^{3-} + F^- \rightleftharpoons NbF_9^{4-}$	4.0	25	0.50	$(Na,H)ClO_4$	pot.	Land & Osborne (1972)
		25	3	KCl	pot.	Neumann (1970)
$Nb(OH)_n^{5-n} + HF(aq) \rightleftharpoons Nb(OH)_{n-1}F^{5-n} + H_2O(l)$	2.13	25	0.96	HNO_3	pot.	Hammer (1979)
	2.01	25	2.88	HNO_3	pot.	Hammer (1979)
	2.06	35	0.96	HNO_3	pot.	Hammer (1979)
	1.96	35	2.88	HNO_3	pot.	Hammer (1979)
	1.79	45	0.96	HNO_3	pot.	Hammer (1979)
$Nb(OH)_n^{5-n} + 2\ HF(aq) \rightleftharpoons Nb(OH)_{n-2}F_2^{5-n} + 2\ H_2O(l)$	4.00	25	0.96	HNO_3	pot.	Hammer (1979)
	4.23	25	2.88	HNO_3	pot.	Hammer (1979)
	3.30	35	0.96	HNO_3	pot.	Hammer (1979)
	3.04	35	2.88	HNO_3	pot.	Hammer (1979)
	3.40	45	0.96	HNO_3	pot.	Hammer (1979)

Tab. 17.5-1: Cont.

For convenience, the stoichiometries with the maximum number of OH^- are additionally indicated, if in the original reactions the stoichiometries with smaller amounts of H_2O were used (e.g., $NbOF_2^+$ and $Nb(OH)_2F^{2+}$ differ by one H_2O, the former stoichiometry is written with the minimum number of H_2O and the latter with the maximum number of OH^-).

Reaction	$\log_{10}K$	T [°C]	I [M]	Medium	Method	Reference
$Nb(OH)_n^{5-n} + 3\ HF(aq) \rightleftharpoons Nb(OH)_{n-3}F_3^{5-n} + 3\ H_2O(l)$	5.86	25	0.96	HNO_3	pot.	Hammer (1979)
	5.81	25	2.88	HNO_3	pot.	Hammer (1979)
	5.30	35	0.96	HNO_3	pot.	Hammer (1979)
	5.3	35	2.88	HNO_3	pot.	Hammer (1979)
	5.40	45	0.96	HNO_3	pot.	Hammer (1979)
$Nb(OH)_n^{5-n} + 4\ HF(aq) \rightleftharpoons Nb(OH)_{n-4}F_4^{5-n} + 4\ H_2O(l)$	8.66	25	0.96	HNO_3	pot.	Hammer (1979)
	8.66	25	2.88	HNO_3	pot.	Hammer (1979)
	8.57	35	0.96	HNO_3	pot.	Hammer (1979)
	8.47	35	2.88	HNO_3	pot.	Hammer (1979)
	8.41	45	0.96	HNO_3	pot.	Hammer (1979)
$Nb_2O_5(cr) + 4\ HF(aq) + H_2O(aq) \rightleftharpoons 2\ Nb(OH)_3F_2(aq)$	-3.84 ± 0.20	150		HF	sol.	Timofeev et al. (2015)
	-4.04 ± 0.22	200		HF	sol.	Timofeev et al. (2015)
	-5.08 ± 0.42	250		HF	sol.	Timofeev et al. (2015)

Wood (2005) argued that, even though the fluoride concentrations in the experiments by Neumann (1970) were lower than in the Raman studies, they are still considerably higher than those to be expected in hydrothermal fluids (and, incidentally, also much higher than in, e.g., Opalinus clay porewaters where the solubility of fluoride is limited by fluorite, CaF_2, at about 10^{-4} m) and that it is probable that, at lower fluoride concentrations, Nb-fluoride complexes become stable that have fewer fluoride ligands than $NbOF_4^-$ and $NbOF_5^{2}$. Wood (2005) also discussed the conditional stability constants for ternary complexes of the type $Nb(OH)_{n-m}F_m^{5-n}$ determined by Hammer (1979), see Tab. 17.5-1. Hammer (1979) used potentiometry to determine these constants at 25, 35 and 45 °C and in 0.96 and 2.88 M HNO_3 solutions but was unable to determine the number of hydroxide ligands from the experimental data, making it very difficult to use the corresponding stability constants in geochemical calculations. Wood (2005) remarked that it is unclear whether the initial Nb-hydroxide species or the ternary Nb-hydroxyfluoride complexes are mono- or polynuclear.

Timofeev et al. (2015) determined the solubility of synthetic Nb_2O_5(cr) in HF solutions (10^{-2} – 10^{-5} m) at 150, 200, and 250 °C, at saturated vapor pressure and under acidic conditions (pH < 3.5). They concluded from their experiments that at low HF concentrations Nb is dissolved as $Nb(OH)_4^+$ in significant amounts even at 150 °C but that much larger amounts of Nb are dissolved at HF concentrations > 10^{-3} m in the form of $NbF_2(OH)_3$(aq). From their experimental data, Timofeev et al. (2015) derived solubility constants for the reactions Nb_2O_5(cr) + 4 HF(aq) + H_2O(aq) ⇌ 2 $Nb(OH)_3F_2$(aq) (see Tab. 17.5-1) and Nb_2O_5(cr) + 2 H^+ + 3 H_2O(aq) ⇌ 2 $Nb(OH)_4^+$ (see Section 4.1).

Considering the available experimental data for Nb-fluoride and Nb-hydroxyfluoride complexes, we conclude that (apart from experimental shortcomings already discussed) none of the reported equilibrium constants can be selected. All experiments were conducted under very acid conditions far removed from the expected application range of TDB 2020 (pH > 6) and it is not clear whether the reported Nb-fluoride and Nb-hydroxyfluoride complexes are of any importance under neutral to alkaline conditions. Besides, the fluoride concentrations were generally larger than those expected in Ca-bearing ground- and porewaters, where the solubility of fluoride is controlled by fluorite.

17.6 Nb chloride complexes

None of the studies on the formation of Nb chloride complexes discussed by Wood (2005) reported any stability constants. Huffman et al. (1951) observed that in strong HCl solutions Nb is retained in anion exchange resins. This implies the formation of chloride or hydroxychloride complexes with ligand numbers sufficiently large to result in anionic complexes. Spectrophotometric investigations by Kanzelmeyer et al. (1956) of Nb (5.68×10^{-5} M) at 25 °C in high ionic strength (10.5 M) solutions – LiCl and HCl mixtures for varying the hydrogen ion concentrations at constant chloride concentration, and HCl and $HClO_4$ mixtures for varying chloride concentrations at constant hydrogen ion concentration – suggested the formation of three chloride species: $Nb(OH)_2Cl_4^-$ at high chloride and high hydrogen ion concentrations, $Nb(OH)Cl_3^+$ at extremely high hydrogen and low chloride ion concentrations and $Nb(OH)_2Cl_3$(aq) at approximately equal hydrogen and chloride ion concentrations. Kanzelmeyer et al. (1956) also observed the formation of colloids – probably of the type $Nb(OH)_2Cl_3$(aq) – upon lowering the hydrogen ion concentration below about 2 molar at high chloride concentrations. Griffith & Wickins (1967) proposed the formation of $NbOCl_5^{2-}$ based on Raman spectroscopy of niobium pentoxide dissolved in concentrated HCl. Davies & Long (1968) also used Raman spectroscopy to examine a saturated solution of NEt_4NbCl_6 in acetonitrile and niobium pentachloride dissolved in saturated HCl. They interpreted the Raman spectrum of the NEt_4NbCl_6 solution in terms of $NbCl_6^-$, but were not able to distinguish between $NbCl_6^-$ and $NbOCl_5^{2-}$ in the Nb_2O_5 solution. Finally, Pershina (1998) carried out relativistic molecular orbital calculations of the electronic structure of Nb, Ta, Db[57] (element 105, dubnium) and Pa and of their complexes $M(OH)_2Cl_4^-$, $MOCl_4^-$, $MOCl_5^{2-}$, and MCl_6^- in HCl. According to these calculations, the complexes are formed with increasing HCl concentration in the order $M(OH)_2Cl_4^- \rightarrow MOCl_4^- \rightarrow MCl_6^-$.

---

[57] After the discovery of Element 105 (first preparation in 1968 by a Russian team at the Joint Institute for Nuclear Research in Dubna and in 1970 by an American team at the Lawrence Berkeley Laboratory of the University of California, there was a controversy over the naming. The Joint Institute for Nuclear Research in Dubna suggested the name nielsbohrium (Ns), while the University of California, Berkeley, proposed the name hahnium (Ha). In 1994, IUPAC suggested the name joliotium (Jo) and finally named it dubnium (Db) in 1997. Pershina (1998) used the name Ha.

In all the reported experimental studies, extremely high HCl concentrations were required for the study of Nb chloride complexes. We agree with Wood (2005) that under geologically reasonable conditions, chloride as a borderline ligand can probably not compete with strong, hard ligands such as O^{2-} and OH^-.

17.7 Nb sulphate and phosphate complexes

Wood (2005) found two studies concerned with Nb sulphate complexes. Pevsner & Sheka (1968) studied the formation of Nb hydrosulphate complexes in the Nb-$HClO_4$-$(NH_4)_2SO_4$-H_2O system using ion-electromigration and spectrophotometry at room temperature. They identified a complex with an Nb:SO_4^{2-} ratio equal to 1 but an unknown number of hydroxides: $Nb(OH)_mSO_4^{3-m}$. The experiments were carried out at a constant hydrogen ion concentration of 0.93 M, a niobium concentration of 2.43×10^{-4} M, and ammonium sulphate concentrations varying between 0.083 and 0.999 M. From an average of 7 experiments Pevsner & Sheka (1968) obtained

$$Nb(OH)_m^{5-m} + SO_4^{2-} \rightleftharpoons Nb(OH)_mSO_4^{3-m}$$

$$\log\beta\,(298.15\ K) = 0.48$$

It is obvious from the conditional constant that this complex is very weak. On this account, and also because the composition of the complex with respect to hydroxide is uncertain, the conditional constant was determined at high acidity and is an average of measurements at variable ionic strengths, this complex is not included in TDB 2020.

Based on potentiometric measurements in sulfuric acid solutions (1 – 8 M H_2SO_4) at 70 °C and Nb concentrations varying from 1×10^{-2} – 5×10^{-5} M, Ivanenko et al. (1996) proposed the formation of various polynuclear Nb sulphate complexes:

- 1M H_2SO_4: $NbO(OH)_2SO_4^-$, $[NbO(OH)_2SO_4^-]_2$, and $[NbO(OH)_2SO_4^-]_3$
- 2-3 M H_2SO_4: $NbOSO_4^+$, $[NbOSO_4^+]_2$, and $[NbOSO_4^+]_3$
- 4-6 M H_2SO_4: $NbO(SO_4)_2^-$, $[NbO(SO_4)_2^-]_2$, $[NbOSO_4^+]_2$, and $[NbOSO_4^+]_3$

Ivanenko et al. (1996) reported stability constants for these complexes, but we agree with Wood (2005) that it is unclear how the stoichiometries and the stability constants were determined and that it is also unclear to which reactions the reported stability constants refer to. Wood (2005) concluded that the relevance of these species, apparently stable only in concentrated sulfuric acid solutions, to natural processes is questionable. For these reasons, they are not included in TDB 2020.

No information on Nb phosphate complexes was found by Wood (2005).

17.8 Nb carbonate complexes

According to Wood (2005), there appears to be almost no information on complex formation between Nb and carbonate or bicarbonate and only a single study by Aleksandrov (1967) was found. There is, however, a reference in Aleksandrov (1967) to a Russian article[58] on the solubility of niobium hydroxide in K_2CO_3 solutions at 100 °C that also suggests the formation of Nb carbonate complexes. Motivated by the fact that Nb is predominantly found in carbonatites (intrusive or extrusive igneous rocks containing more than 50 wt.-% carbonate minerals), Aleksandrov (1967) investigated the solubility of hydrated niobium pentoxide, $Nb_2O_5 \cdot nH_2O(s)$, with n varying between 2 and 3, in $KHCO_3$/KCl and K_2CO_3/KCl solutions under hydrothermal conditions at temperatures from 50 to 450 °C and pressures from 500 to 1'000 $kg \cdot cm^{-2}$ (1 $kg \cdot cm^{-2}$ = 0.98 bar = 0.098 MPa). He observed an increase in the concentration of aqueous Nb in equilibrium with the solid as the carbonate or bicarbonate concentrations were increased (at temperatures between 150 and 450 °C), which he interpreted as a consequence of the formation of Nb carbonate or bicarbonate complexes. However, he reported neither compositions, nor stability constants of the complexes.

Recently, Korzhinskaya et al. (2017) studied the solubility of pyrochlore (composition: Na_2O 7.61 wt.-%, CaO 14.28 wt.-%, Nb_2O_5 71.61 wt.-%, Ta_2O_5 < 1 wt.-%, F 5.18 wt.-%, TiO_2 0.83 wt.-%) and Nb_2O_5(cr) in NaF-Na_2CO_3 solutions at 300 to 550 °C and 50 to 100 MPa. At 550 °C and 100 MPa, the solubility of pyrochlore increased from Nb concentrations of about 10^{-7} to about 10^{-4} m as the concentration of Na_2CO_3 rose from 0.01 to 2 m. Under the same conditions the solubility of Nb_2O_5(cr) remained nearly constant in the range of about 10^{-6} to about $10^{-5.5}$ m. The influence of pressure and temperature conditions on the solubilities of both pyrochlore and Nb_2O_5(cr) turned out to be nearly insignificant. Korzhinskaya et al. (2017) made no mention of the potential formation of Nb carbonate complexes and did not attempt any thermodynamic analysis of the experimental results.

Given the few experimental data accessible to him, Wood (2005) considered it doubtful that carbonates or bicarbonates were able to compete effectively with O^{2-} and OH^- for Nb.

---

[58] Govorov, L.N., Minayev, N.A. & Stunzhas, A.A. (1963): K Geokhimii Niobiya (On the geochemistry of niobium). Soobshch. Dal'nevost. fil. SO Akad. Nauk SSSR, No. 21 (as cited by Aleksandrov 1967). We were not able to get hold of this publication.

17.9 Selected niobium data

Tab. 17.9-1: Selected niobium data (1 bar, 298.15 K) for TDB 2020

New or changed data with respect to TDB Version 12/07 (Thoenen et al. 2014) are shaded.

Name	Redox	TDB Version 12/07				TDB 2020				
		$\Delta_f G_m°$ [kJ · mol^{-1}]	$\Delta_f H_m°$ [kJ · mol^{-1}]	$S_m°$ [J · K^{-1} · mol^{-1}]	$C_{p,m}°$ [J · K^{-1} · mol^{-1}]	$\Delta_f G_m°$ [kJ · mol^{-1}]	$\Delta_f H_m°$ [kJ · mol^{-1}]	$S_m°$ [J · K^{-1} · mol^{-1}]	$C_{p,m}°$ [J · K^{-1} · mol^{-1}]	Species
Nb(cr)	0	0.0	0.0	36.40	24.60	0.0	0.0	36.40	24.60	Nb(cr)
Nb(OH)4+ [a]	V	-	-	-	-	-1'196	*-1'375*	*42.4*	*179*	$Nb(OH)_4^+$

[a] The primary master species selected in TDB 12/07 was NbO_3^- (equivalent to $Nb(OH)_6^-$), with $\Delta_f G_m°(NbO_3^-, 298.15\ K) = -932.1$ kJ · mol^{-1}, valid for $I_m = 1$ mol · kg^{-1}
[b] $I_m = 1$ mol · kg^{-1}, see Wagman et al. (1982) and discussion in Section 17.1.1

Name	Redox	TDB Version 12/07		TDB 2020				
		$\log_{10}\beta°$	$\Delta_r H_m°$ [kJ · mol^{-1}]	$\log_{10}\beta°$	$\Delta_r H_m°$ [kJ · mol^{-1}]	$\Delta_r C_{p,m}°$ [J · K^{-1} · mol^{-1}]	T-range [°C]	Reaction
Nb(OH)5(aq)	V	1.448 [a b]	-	-1.89 ± 0.12	*9 ± 4*	*0*	10 – 70	$Nb(OH)_4^+ + H_2O(l) \rightleftharpoons Nb(OH)_5(aq) + H^+$
Nb(OH)6-	V	-6.896 [a,c]	-	-6.69 ± 0.14	*26 ± 9*	*0*	10 – 70	$Nb(OH)_4^+ + 2\ H_2O(l) \rightleftharpoons Nb(OH)_6^- + 2\ H^+$
Nb(OH)7-2	V	-	-	-16.09 ± 0.34	*63 ± 22*	*0*	10 – 70	$Nb(OH)_4^+ + 3\ H_2O(l) \rightleftharpoons Nb(OH)_7^{2-} + 3\ H^+$
H3Nb6O19-5	V	-	-	*-20.6 ± 0.8*	-	-	-	*$6\ Nb(OH)_5(aq) \rightleftharpoons H_3Nb_6O_{19}^{5-} + 5\ H^+ + 11\ H_2O(l)$*
Nb6O19-8	V	-	-	*-38.6 ± 0.5*	-	-	-	*$H_3Nb_6O_{19}^{5-} \rightleftharpoons Nb_6O_{19}^{8-} + 3\ H^+$*
HNb6O19-7	V	-	-	*14.0 ± 0.4*	-	-	-	*$Nb_6O_{19}^{8-} + H^+ \rightleftharpoons HNb_6O_{19}^{7-}$*
H2Nb6O19-6	V	-	-	*27.0 ± 0.4*	-	-	-	*$Nb_6O_{19}^{8-} + 2\ H^+ \rightleftharpoons H_2Nb_6O_{19}^{6-}$*

[a] Calculated from $\Delta_f G_m°$.
[b] Calculated from $\log_{10}\beta° = 6.896$ for $NbO_3^- + 2\ H^+ + H_2O(l) \rightleftharpoons Nb(OH)_4^+$ and $\log_{10}\beta° = 7.344$ for the original reaction $NbO_3^- + H^+ + 2\ H_2O(l) \rightleftharpoons Nb(OH)_5(aq)$, which itself was calculated from the values for $\Delta_f G_m°(NbO_3^-)$ and $\Delta_f G_m°(Nb(OH)_5, aq)$ selected by Wagman et al. (1982), both valid for $I_m = 1$ mol · kg^{-1}, see discussion in Section 17.1.1.
[c] Original reaction: $NbO_3^- + 2\ H^+ + H_2O(l) \rightleftharpoons Nb(OH)_4^+$.

Name	Redox	TDB Version 12/07		TDB 2020		
		$\log_{10}K_{s,0}°$	$\Delta_r H_m°$ [kJ · mol^{-1}]	$\log_{10}K_{s,0}°$	$\Delta_r H_m°$ [kJ · mol^{-1}]	Reaction
NbO2(cr)	IV	7.978 [a b]	-	-		$NbO_2(cr) + H_2O(l) \rightleftharpoons NbO_3^- + 2\ H^+ + e^-$
Nb2O5(cr)	V	24.341 [a b]	-	-		$Nb_2O_5(cr) + H_2O(l) \rightleftharpoons 2\ NbO_3^- + 2\ H^+$
Nb2O5(pr)	V	-	-	-16.0 ± 0.5		$Nb_2O_5(pr) + 5\ H_2O(l) \rightleftharpoons 2\ Nb(OH)_5(aq)$
Na7HNb6O19: 15H2O(cr)	V	-	-	*-11.6*		*$Na_7HNb_6O_{19}{\cdot}15H_2O(cr) \rightleftharpoons 7\ Na^+ + HNb_6O_{19}^{7-} + 15\ H_2O(l)$*

[a] Calculated from $\Delta_f G_m°$.
[b] Ionic strength = 1 mol · kg^{-1} for $\Delta_f G_m°(NbO_3^-)$, see (Wagman et al. 1982) and discussion in Section 17.1.1.

Tab. 17.9-2: Selected SIT ion interaction coefficients $\varepsilon_{j,k}$ [kg · mol^{-1}] for niobium species.

Data estimated according to charge correlations and taken from Tab. 1-7 are shaded. Supplemental data are in italics.

j k → ↓	**Cl^-** $\varepsilon_{j,k}$ [kg · mol^{-1}]	**ClO_4^-** $\varepsilon_{j,k}$ [kg · mol^{-1}]	**Na^+** $\varepsilon_{j,k}$ [kg · mol^{-1}]	**$Na^+ + Cl^-$** $\varepsilon_{j,k}$ [kg · mol^{-1}]
Nb(OH)4+	0.05 ± 0.10	0.21 ± 0.04	0	-
Nb(OH)5(aq)	-	-	-	-0.07 ± 0.02
Nb(OH)6-	-	-	*1.57 ± 0.26*	-
Nb(OH)7-2	-	-	*1.98 ± 0.64*	-
Nb6O19-8	-	-	*0.40 ± 0.70*	-
HNb6O19-7	-	-	*0.35 ± 0.60*	-
H2Nb6O19-6	-	-	*0.30 ± 0.50*	-
H3Nb6O19-5	-	-	*0.25 ± 0.40*	-

17.10 References

Aleksandrov, I.V. (1967): Niobium in the carbonate solutions and some considerations on the migration of rare elements under hydrothermal conditions. Geochemistry International, 4, 558-566.

Antonio, M.R., Nyman, M. & Anderson, T.M. (2009): Direct observation of contact ion-pair formation in aqueous solution. Angewandte Chemie International Edition, 48, 6136-6140.

Babko, A.K., Lukachina, V.V. & Nabivanets, B.I. (1963): Solubility and acid-base properties of tantalum and niobium hydroxides. Russian Journal of Inorganic Chemistry, 957-961.

Chase, M.W., Jr. (1998): NIST-JANAF Thermochemical Tab., Fourth Edition, Part I, Al-Co. Journal of Physical and Chemical Reference Data, Monograph 9, 1-1961.

Cox, J.D., Wagman, D.D. & Medvedev, V.A. (1989): CODATA Key Values for Thermodynamics. New York, Hemisphere, 271p.

Davies, J.E.D. & Long, D.A. (1968): The vibrational spectra of titanium tetrachloride-hydrochloric acid and titanium tetrachloride–tri-n-butyl phosphate systems and the hexachloro-anions of zirconium(IV), hafnium(IV), niobium(V), and tantalum(V). Journal of the Chemical Society, A, 2560-2564.

Deblonde, G.J.P., Chagnes, A., Bélair, S. & Cote, G. (2015): Solubility of niobium(V) and tantalum(V) under mild alkaline conditions. Hydrometallurgy, 156, 99-106.

Etxebarria, N., Fernández, L.A. & Madariaga, J.M. (1994): On the hydrolysis of niobium(V) and tantalum(V) in 3 mol dm^{-3} KCl at 25 °C. Part 1. Construction of a thermodynamic model for Nb^{V}. Journal of the Chemical Society, Dalton Transactions, 20, 3055-3059.

Govorov, L.N., Minayev, N.A. & Stunzhas, A.A. (1963): K Geokhimii Niobiya (On the geochemistry of niobium). Soobshch. Dal'nevost. fil. SO Akad. Nauk SSSR, No. 21 (as cited by Aleksandrov 1967). We were not able to get hold of this publication.

Goiffon, A., Granger, R., Bockel, C. & Spinner, B. (1973): Étude des équilibres dans les solutions alcalines du niobium V. Revue de Chimie minérale, 10, 487-502.

Grenthe, I., Plyasunov, A.V. & Spahiu, K. (1997): Estimations of medium effects on thermodynamic data. In: Grenthe, I. & Puigdomènech, I. (eds.): Modelling in Aquatic Chemistry. OECD NEA, Paris, France, 325-426.

Griffith, W.P. & Wickins, T.D. (1967): Raman studies on species in aqueous solutions. Part II. Oxy-species of metals of Groups VIA, VA, and IVA. Journal of the Chemical Society, A, 675-679.

Guillaumont, R., Franck, J.C. & Muxart, R. (1970): Contribution à l étude de l'hydrolyse du niobium. Radiochemical and Radioanalytical Letters, 4, 73-79.

Hammer, R.R. (1979): A Determination of the Stability Constants of a Number of Metal Fluoride Complexes and Their Rates of Formation. USDOE Report, Idaho Chemical Processing Plant, EXXON Nuclear Idaho Company, ENICO 1004 (as cited by Wood 2005).

Huffman, E.H., Iddings, G.M. & Lilly, R.C. (1951): Anion exchange of zirconium, hafnium, niobium and tantalum in hydrochloric acid solutions. Journal of the American Chemical Society, 73, 4474-4475.

Hummel, W. (2018): Radioactive waste inventories for geochemists. PSI Internal Report, TM-44-18-03, Paul Scherrer Institut, Villigen, Switzerland, 55 pp.

Hummel, W., Berner, U., Curti, E., Pearson, F.J. & Thoenen, T. (2002): Nagra/PSI Chemical Thermodynamic Data Base 01/01. Nagra NTB 02-16. Also published by Universal Publishers/upublish.com, Parkland, USA, 565 pp.

Ivanenko, V.I., Kadyrova, G.I. & Kravtsov, V.I. (1996): Niobium (V) polynuclear complexes in sulfuric acid solutions. Russian Journal of Applied Chemistry, 69, 13-16.

Jambor, J.L., Sabina, A.P., Roberts, A.C., Bonardi, M., Owens D.R. & Sturman, B.D. (1986): Hochelagaite, a new calcium-niobium oxide mineral from Montreal, Quebec. Canadian Mineralogist, 24, 449-453.

Kanzelmeyer, J.H., Ryan, J. & Freund, H. (1956): The Nature of niobium(V) in hydrochloric acid solution. Journal of the American Chemical Society, 78, 3020-3023.

Keller, O.L., Jr. (1963): Identification of complex ions of niobium(V) in hydrofluoric acid solutions by Raman and infrared spectroscopy. Inorganic Chemistry, 2, 783-787.

Kitamura, A., Fujiwara, K., Doi, R., Yoshida,Y., Mihara, M., Terashima, M. & Yui, M. (2010): JAEA Thermodynamic Database for Performance Assessment of Geological Disposal of High-Level Radioactive and TRU-Wastes. Report JAEA-Data/Code 2009-024, Japan Atomic Energy Agency, 84 pp.

Korzhinskaya, V.S., Kotova, N.P. & Shapovalov, Y.B. (2017): Experimental study of natural pyrochlore and niobium oxide solubility in alkaline hydrothermal solutions. Doklady Earth Sciences, 475, 793-796.

Kulmala, S. & Hakanen, M. (1993): The solubility of Zr, Nb and Ni in groundwater and concrete water, and sorption on crushed rock and cement. Report YJT-93-21, Nuclear Waste Commission of Finnish Nuclear Power Companies, Helsinki, Finland.

Land, J.E. & Osborne, C.V. (1972): The formation constants of the niobium fluoride system. Journal of the Less Common Metals, 29, 147-153.

Lemire, R.J., Berner, U., Musikas, C., Palmer, D.A., Taylor, P. & Tochiyama, O. (2013): Chemical Thermodynamics of Iron, Part 1. Chemical Thermodynamics, Vol. 13a. OECD Publications, Paris, France, 1082 pp.

Lindqvist, I. (1953): The structure of the hexaniobate ion in $7Na_2O{\cdot}6Nb_2O_5 \cdot 32H_2O$. Arkiv för Kemi, 5, 247-250.

Lothenbach, B., Ochs, M., Wanner, H. & Yui, M. (1999): Thermodynamic Data for the Speciation and Solubility of Pd, Pb, Sn, Sb, Nb and Bi in Aqueous Solution. Japan Nuclear Cycle Development Institute (JNC), TN8400 99-011.

Lumpkin, G.R. & Ewing, R.C. (1995): Geochemical alteration of pyrochlore group minerals: Pyrochlore subgroup. American Mineralogist, 80, 732-743.

Neumann, G. (1964) On the hydrolysis of niobates in 3 M K(Cl) medium. Acta Chemica Scandinavica, 18, 278-280.

Neumann, G. (1970): A potentiometric study of the system Nb(V)-OH^--F^- in 3 M K(Cl) medium. Arkiv för Kemi, 32, 229-247.

Pearson, F.J., Jr., Berner, U. & Hummel, W. (1992): Nagra Thermochemical Data Base II. Supplemental Data 05/92. Nagra Technical Report NTB 91-18.

Peiffert, C., Nguyen-Trung C., Palmer, D.A., Laval, J.P. & Giffaut E. (2010): Solubility of B-Nb_2O_5 and the hydrolysis of niobium(V) in aqueous solution as a function of temperature and ionic strength. Journal of Solution Chemistry, 39, 197-218.

Pershina, V. (1998): Solution chemistry of element 105 Part II: Hydrolysis and complex formation of Nb, Ta, Ha and Pa in HCl solutions. Radiochimica Acta, 80, 75-84.

Pevsner, T.V. & Sheka, I.A. (1968): Reaction of niobium and tantalum with sulphate ions in solution. Russian Journal of Inorganic Chemistry, 13, 1381-1384.

Rozantsev, G.M., Dotsenko, O.I. & Taradina, G.V. (2000): Mathematical modeling and analysis of equilibria in solutions of Nb(V). Russian Journal of Coordination Chemistry, 26, 247-253.

Schäfer, H., Gruehn, R. & Schulte, F. (1966): The Modifications of niobium pentoxide. Angewandte Chemie International Edition, 5, 40-52.

Shannon, R.D. (1976): Revised effective ionic radii and systematic studies of interatomic distances in halides and chalcogenides. Acta Crystallographica, Section A, 32, 751-767.

Spinner, B. (1968): Étude quantitative de l'hydrolyse des niobates de potassium. Revue de Chimie minérale, 5, 839-868.

Talerico, C., Ochs, M. & Giffaut, E. (2004): Solubility of niobium(V) under cementitious conditions: Importance of Ca-niobate. Materials Research Society Symposium Proceedings, 824, CC8.31.1-CC8.31.6.

Thoenen, T., Hummel, W., Berner, U. & Curti, E. (2014): The PSI/Nagra Chemical Thermodynamic Database 12/07. Technical Report, PSI Bericht Nr. 14-04, Paul Scherrer Institut, Villigen, Switzerland, 416 pp.

Timofeev, A., Migdisov, A.A. & Williams-Jones, A.E. (2015): An experimental study of the solubility and speciation of niobium in fluoride-bearing aqueous solutions at elevated temperature. Geochimica et Cosmochimica Acta, 158, 103-111.

Tsikaeva, D.V., Agulyanskii, A.I., Balabanov, Yu.I., Kuznetsov, V.Ya. & Kalinnikov, V.T. (1989): Complexation of niobium(V) in hydrofluoric acid solutions in the presence of fluorides of alkali metals and ammonium. Russian Journal of Inorganic Chemistry, 34, 1740-1744.

Udupa, H.V.K., Venkatesan, V.K. & Krishnan, M. (1985): Niobium and tantalum. In: Bard, A.J., Parsons, R. & Jordan, J. (eds.): Standard Potentials in Aqueous Solution. Marcel Dekker, Basel, 526-537.

Wagman, D.D., Evans, W.H., Parker, V.B., Schumm, R.H., Halow, I., Bailey, S.M., Churney, K.L. & Nuttall, R.L. (1982): The NBS tables of chemical thermodynamic properties: Selected values for inorganic and C1 and C2 organic substances in SI units. Journal of Physical and Chemical Reference Data, 11, Supplement No. 2, 1-392.

Wood, S.A. (2005): The aqueous geochemistry of zirconium, hafnium, niobium, and tantalum. In: Linnen, R.L. & Samson, I.M. (eds.): Rare-element geochemistry and mineral deposits. Geological Association of Canada, GAC Short Course Notes, 17, 217-268.

Yajima, T. (1994): Solubility measurements of uranium and niobium, Report of Yayoi Kenkyukai, UTNL-R 0331, University of Tokyo, pp. 127-144 [in Japanese] (as cited by Kitamura et al. 2010).

Yajima, T., Tobita, S. & Ueta, S. (1992): Solubility measurements of niobium in the system Nb-O-H under CO_2-free condition, presented at 1992 Fall Meeting of Atomic Energy Society of Japan, F33, p. 341 [in Japanese] (as cited by Kitamura et al. 2010).

Zaraisky, G.P., Korzhinskaya, V. & Kotova, N. (2010): Experimental studies of Ta_2O_5 and columbite-tantalite solubility in fluoride solutions from 300 to 550 °C and 50 to 100 MPa. Mineralogy and Petrology, 99, 287-300.

18 Organic ligands

18.1 Introduction

Many organic substances yield anions that form aqueous complexes with metallic cations. Such substances may be naturally present in ground and pore waters or may be part of the radioactive waste inventory. There exists an enormous number of organic compounds which can form complexes in aqueous solutions, and hence, in some data bases a plethora of organic ligands is included.

For the original Nagra TDB 05/92 (Pearson et al. 1992) we had adopted a different approach. Rather than trying to assemble data on many organic ligands, Hummel (1991) had chosen four compounds that are typical of large classes of complexing ligands. These ligands are two carboxylic acids, oxalic (ox) and citric (cit) acid, and two polyaminepolycarboxylic acids, nitrilotriacetic (nta) and ethylenediaminetetraacetic (edta) acid.

Equilibrium constants for protonation and metal complexation data for ox, cit, nta and edta had been compiled by Hummel (1991) from other data bases, and a few data were estimated using chemical systematics and correlation procedures. These data were included in Nagra TDB 05/92.

A similar approach has been adopted by NEA in its TDB phase II organics review project which commenced in 1998. Hence, for the update from Nagra TDB 05/92 (Pearson et al. 1992) to Nagra/PSI TDB 01/01 (Hummel et al. 2002) we decided to remove all data referring to organic ligands and to wait for the completion of the NEA TDB review. Now, this "organics" section of TDB 2020 is based on the published NEA TDB review (Hummel et al. 2005a).

As discussed by Hummel et al. (2007), in the beginning of the NEA TDB organics review project it was decided that the evaluation of organic ligands should be limited to oxalate, citrate, ethylenediaminetetraacetate (edta) and α-isosaccharinate (isa). From the viewpoint of importance for radioactive waste problems this set of ligands is very well posed.

Oxalate is, with respect to its complexation strength, the major product of radiolytic degradation of bitumen, sometimes used for waste conditioning (Van Loon & Kopajtic 1991), and ion exchange resins used in decontamination procedures (Van Loon & Hummel 1999). In addition, oxalate is one of the strongest organic complexing ligands in nature (besides humic substances).

Citrate and edta are used in decontamination processes and thus, they become part of the radioactive waste inventory.

In terms of complexation strength, oxalate, citrate and edta cover a wide range of complex stability, and as mentioned above, they may be used in model calculations as representatives of dicarboxylic acids (oxalate), hydroxy-polycarboxylic acids (citrate) and polyamino-polycarboxylic acids (edta).

Finally, from the viewpoint of complexation strength, isa is the most important product of alkaline degradation of cellulose in cement pore waters (Van Loon & Glaus 1997). Thus, isa is of major concern in many performance assessments of planned radioactive waste repositories.

Regarding the availability of experimental data, the situation is less clear. In the case of oxalate, citrate and edta a large body of experimental studies has been published and the NEA organics

review (Hummel et al. 2005a) provides, based on the critical discussion of several hundreds of publications, a considerable set of selected thermodynamic values.

However, in the case of isa the number of experimental studies is very limited and, despite of the importance of isa for performance assessments, only a few thermodynamic values could be selected. The critical review of experimental studies concerning isa mainly is a status report pointing out gaps in our knowledge and further research needs (Hummel et al. 2005a).

As the task of the NEA organics review was to complement the other reviews of the NEA TDB project, which are restricted to inorganic compounds and complexes of actinides, fission and activation products, a natural choice of elements comprises U, Np, Pu, Am, Tc, Ni, Se and Zr.

Note that the review of Zr data was not completed in terms of selected values by Hummel et al. (2005a) since at the time of the organics review Zr hydrolysis was still under review by another team. Hence, no preliminary Zr data are included in TDB 2020.

However, the NEA organics review could not be restricted to these elements as it aimed at a thermodynamic data set useful for practical application. In addition to the above-mentioned actinides, fission, and activation products the review also considered the major constituents of ground and surface waters which may interact with the selected organic ligands, i.e., H, Na, K, Mg and Ca. Any geochemical model including organic ligands should consider these competing interactions and therefore, the NEA organics review provides a selected consistent set of these auxiliary constants.

In the realm of metal – organic complexes a plethora of experimental studies is found in the literature dealing with mixed complexes, i.e., complexes containing a common metal ion and two or more different ligands. In the NEA organics review mixed complexes, in general, were considered if they contain combinations of oxalate, citrate, edta and isa with or without additional inorganic ligands.

From the viewpoint of application by far the most important class of mixed complexes are ternary metal – hydroxide – organic ligand complexes. These hydrolysed organic complexes may predominate in alkaline ground and surface waters and in high pH cement pore waters and thus, they are important in assessing the influence of organic ligands on element complexation in cementitious repositories. The relevant literature about such complexes is discussed in the NEA organics review, but only in a few cases reliable thermodynamic constants could be selected (Hummel et al. 2005a).

Also, of importance in many ground and surface waters would be the class of metal – carbonate – organic ligand complexes. However, the NEA organics review could only state the almost complete lack of such data.

In the following sections the results of the NEA organics review (Hummel et al. 2005a) are summarised in qualitative terms from the viewpoint of their application in environmental modelling studies (Tab. 18-1 – 18-3).

Thermodynamic data of solid compounds could be selected for Ca oxalate, citrate and isa, as well as for U(VI) oxalate. However, although the matrix of possible metal cation – organic ligand compounds is almost empty (Tab. 18-1) no serious gaps must be reported from the viewpoint of environmental modelling studies.

Tab. 18-1: Summary of solid compounds with selected organic ligands

	ox^{2-}	**cit^{3-}**	**$edta^{4-}$**	**isa^{-}**
H^+	**α-H_2ox, β-H_2ox, $H_2ox \cdot 2H_2O$**	**$H_3cit(cr)$, $H_3cit \cdot H_2O$**	**$H_4edta(cr)$**	
Na^+	sol		sol	sol
K^+	sol	sol	sol	
Mg^{2+}	$Mg(ox) \cdot 2H_2O$	sol	sol	
Ca^{2+}	**$Ca(ox) \cdot H_2O$** **$Ca(ox) \cdot 2H_2O$** **$Ca(ox) \cdot 3H_2O$**	**$Ca_3(cit)_2 \cdot 4H_2O$**	sol	**$Ca(isa)_2(cr)$**
Se				
Ni^{2+}	$Ni(ox) \cdot 2H_2O$		sol	
Tc	**???**			
U^{3+}	-	-	-	-
Np^{3+}	-			
Pu^{3+}	$Pu_2(ox)_3 \cdot 10H_2O$			
Am^{3+}	*$Am_2(ox)_3 \cdot nH_2O$*			
U^{4+}	$U(ox)_2 \cdot 6H_2O$		sol	sol
Np^{4+}	$Np(ox)_2 \cdot 6H_2O$			sol
Pu^{4+}	$Pu(ox)_2 \cdot 6H_2O$			sol
Am^{4+}	-			
UO_2^+	-			
NpO_2^+	sol			
PuO_2^+	sol		-	
AmO_2^+	-		-	
UO_2^{2+}	**$UO_2ox \cdot 3H_2O$**		sol	
NpO_2^{2+}	-	-	-	
PuO_2^{2+}	- *$PuO_2ox \cdot 3H_2O$*	-	-	
AmO_2^{2+}	-	-	-	

Formula in **bold face** indicates a compound for which the NEA organic review selected thermodynamic constants. Compounds in normal face were not selected in the NEA review. However, the available data can be used for scoping calculations and as guidelines for data estimation procedures.

- Indicate that no thermodynamic data, or no reliable data are available, but the potentially forming compound, *shown in italics,* is highly unstable due to redox effects of the ligand and hence, it is of no importance in performance assessment.

"sol" Indicates a highly soluble salt, but no thermodynamic data are available.

Empty cells Indicate that no solubility data are available, but the potentially forming compounds are probably highly soluble and thus, they might not be of importance for PA.

??? Indicates a gap of knowledge in the database probably relevant for performance assessment; the potentially forming compound is given in *italics*.

Tab. 18-2: Summary of aqueous complexes with selected organic ligands for auxiliary data, fission and activation products

	ox^{2-}	**cit^{3-}**	**$edta^{4-}$**	**isa^{-}**
H^+	**Hox^-** **$H_2ox(aq)$**	**$Hcit^{2-}$** **H_2cit^-** **$H_3cit(aq)$**	**$Hedta^{3-}$,** **H_2edta^{2-}** **H_3edta^-** **$H_4edta(aq)$** **H_5edta^+** **H_6edta^{2+}**	**$Hisa(aq)$**
Na^+	**$\varepsilon(Na^+, ox^{2-})$**	**$\varepsilon(Na^+, cit^{3-})$**	**$Na(edta)^{3-}$**	$\varepsilon(Na^+, isa^-)$
K^+	**$\varepsilon(K^+, ox^{2-})$**	**$\varepsilon(K^+, cit^{3-})$**	**$Kedta^{3-}$**	$\varepsilon(K^+, isa^-)$
Mg^{2+}	**$Mg(ox)(aq)$** **$Mg(ox)_2^{2-}$**	**$Mg(cit)^-$** **$Mg(Hcit)(aq)$** **$Mg(H_2cit)^+$**	**$Mg(edta)^{2-}$** **$Mg(Hedta)^-$**	Ca(II) – isa
Ca^{2+}	**$Ca(ox)(aq)$** **$Ca(ox)_2^{2-}$**	**$Ca(cit)^-$** **$Ca(Hcit)(aq)$** **$Ca(H_2cit)^+$**	**$Ca(edta)^{2-}$** **$Ca(Hedta)^-$**	**$Ca(isa)^+$** **$Ca(isa_{-H})(aq)$**
Se				
Ni^{2+}	**$Ni(ox)(aq)$** **$Ni(ox)_2^{2-}$**	**$Ni(cit)^-$** **$Ni(cit)_2^{4-}$** **$Ni(Hcit)(aq)$** **$Ni(H_2cit)^+$**	**$Ni(edta)^{2-}$** **$Ni(Hedta)^-$**	$Ni(isa)^+$
Tc	**???**	**???**	**???** *$TcO(OH)edta^{3-}$*	**???**

Complexes in **bold face** indicate species for which the NEA organic review selected thermodynamic constants.
The term **$\varepsilon(M^+, X^{n-})$** in **bold face** indicates that the NEA organics review did not select an aqueous complex but describes the interaction solely by SIT ion interaction parameters.
Complexes in normal face were not selected in the NEA review. However, the available data can be used for scoping calculations and as guidelines for data estimation procedures.
Empty cells indicate that no data are available, but the potentially forming complexes probably are not important for performance assessment.
??? indicate gaps in the database relevant for performance assessment; the type of missing information or proposed complexes are given in *italics*.

Tab. 18-3: Summary of actinide aqueous complexes with selected organic ligands

	ox^{2-}	**cit^{3-}**	**$edta^{4-}$**	**isa^{-}**
U^{3+}	-	-	-	-
Np^{3+}	-	**???**	Pu(III) – edta Am(III) – edta	**???**
Pu^{3+}	$Pu(ox)^{+}$, $Pu(ox)_2^{-}$ $Pu(ox)_3^{3-}$	Pu(cit)(aq) $Pu(Hcit)^{+}$	**Pu(edta)** **Pu(Hedta)(aq)**	Am(III)/Eu(III) – isa
Am^{3+}	**$Am(ox)^{+}$** **$Am(ox)_2^{-}$** **$Am(ox)_3^{3-}$**	**Am(cit)(aq)** **$Am(cit)_2^{2-}$** **$Am(Hcit)^{+}$** **$Am(Hcit)_2^{-}$**	**$Am(edta)^{-}$** **Am(Hedta)(aq)** $Am(edta)(OH)^{2-}$	$Am(isa_{-3H})^{-}$
U^{4+}	Uox^{2+}, $U(ox)_2$(aq) $U(ox)_3^{2-}$, $U(ox)_4^{4-}$ **???** *U – ox – OH*	**???**	**Uedta(aq)** $UedtaOH^{-}$ $(UedtaOH)_2^{2-}$ $Uedta(OH)_2^{2-}$	**???** *$U(OH)_4isa^{-}$*
Np^{4+}	$Np(ox)^{2+}$ $Np(ox)_2$(aq) $Np(ox)_3^{2-}$ **???** *Np – ox – OH*	**???**	**Np(edta)(aq)** U(IV) – edta - OH	$Np(OH)_3isa$(aq) $Np(OH)_3(isa)_2^{-}$ $Np(OH)_4isa^{-}$ $Np(OH)_4(isa)_2^{2-}$
Pu^{4+}	$Pu(ox)^{2+}$, $Pu(ox)_2$(aq) $Pu(ox)_3^{2-}$ **???** *Pu – ox – OH*	**???**	Pu(edta)(aq) $Pu(edta)OH^{-}$ $Pu(edta)(OH)_2^{2-}$	**???** *$Pu(isa_{-4H})^{-}$* *$Pu(isa_{-2H})_2^{2-}$*
Am^{4+}	-			
UO_2^{+}	-			
NpO_2^{+}	**NpO_2ox^{-}** **$NpO_2(ox)_2^{3-}$**	**NpO_2cit^{2-}**	**NpO_2edta^{3-}** **$NpO_2(Hedta)^{2-}$** **$NpO_2(H_2edta)^{-}$** $NpO_2edtaOH^{4-}$	**???**
PuO_2^{+}	- *PuO_2ox^{-}, $PuO_2(ox)_2^{3-}$*	-	- *PuO_2edta^{3-},* *$PuO_2(Hedta)^{2-}$*	
AmO_2^{+}	- *AmO_2ox^{-}, $AmO_2(ox)_2^{3-}$*		- *$AmO_2(Hedta)^{2-}$*	
UO_2^{2+}	**UO_2ox(aq)** **$UO_2(ox)_2^{2-}$** **$UO_2(ox)_3^{4-}$**	**UO_2cit^{-}** **$(UO_2)_2(cit)_2^{2-}$** **UO_2(Hcit)(aq)**	**UO_2edta^{2-}** **$(UO_2)_2$edta(aq)** **$UO_2(Hedta)^{-}$**	UO_2isa^{+},$UO_2(isa)_2$(aq) , $UO_2(isa)_3^{-}$, **???***UO_2^{2+}– isa – OH*
NpO_2^{2+}	- *NpO_2ox(aq),$NpO_2(ox)_2^{2-}$*	-	-	
PuO_2^{2+}	- *PuO_2ox(aq),$PuO_2(ox)_2^{2-}$*	- *PuO_2cit^{-},* *$PuO_2(cit)_2^{4-}$*	- *PuO_2edta^{2},* *$PuO_2(Hedta)$* *$PuO_2(H_2edta)(aq)$*	
AmO_2^{2+}	-	-	-	

Complexes in **bold face** indicate species for which the NEA organic review selected thermodynamic constants. Complexes in normal face were not selected in the NEA review. However, the available data can be used for scoping calculations and as guidelines for data estimation procedures.

- indicate that no thermodynamic data, or no reliable data are available, but the potentially forming complexes, *shown in italics,* are highly unstable due to redox effects of the ligands and hence, they are of no importance in performance assessment.

Empty cells indicate that no data are available, but the potentially forming complexes may be unstable due to redox effects of the ligands.

??? indicate gaps in the database relevant for performance assessment; the type of missing information or proposed complexes are given in *italics*.

The compounds formed by citrate, edta and isa are generally highly soluble salts. Some of the actinide – oxalate compounds have low solubilities, but in environmental studies the concentration of oxalate in solution can be assumed to be limited by Ca oxalate precipitation, and the formation of actinide – oxalate compounds is unlikely as long as the dissolved actinides do not exceed trace level concentrations.

As a result of the NEA TDB organics review (Hummel et al. 2005a), a number of reliable values could be selected for aqueous complexes of oxalate, citrate and edta with the major competing elements H, Na, K, Mg, Ca and the activation product Ni (Tab. 18-2), as well as with actinides in their most common redox states, i.e., with Am(III), Np(V) and U(VI) (Tab. 18-3). In the cases of Pu(III), U(IV) and Np(IV) only data for edta complexes could be selected (Tab. 18-3).

For isa selected values could only be derived for Ca and H (Tab. 18-2).

The organic ligands considered in the NEA TDB organics review (Hummel et al. 2005a) not only form strong complexes with actinides, but they also influence the redox state of the actinides in aqueous solutions. Hence, two kinds of gaps in the matrix of possible actinide – organic ligand complexes were encountered (Tab. 18-3):

(1) Missing or unreliable thermodynamic data because the actinide in solution is oxidised or reduced in the presence of the organic ligand and thus, the actinide – organic complexes formed in that unstable redox state are short-lived species only. These unstable redox states in the presence of organics are: U(III), U(V), Pu(V), Am(V), Np(VI), Pu(VI) and Am(VI). These gaps in the database are of no importance from the viewpoint of environmental modelling studies or performance assessments for radioactive waste disposal.

(2) Missing or unreliable data in stable and important redox states. These gaps mainly concern aqueous complexes of oxalate, citrate and isa with the tetravalent actinides U(IV), Np(IV) and Pu(IV). Furthermore, for the systems Np(V) – isa in general and U(VI) – isa in alkaline solutions Hummel et al. (2005a) could not find any data. These are the real gaps from the viewpoint of environmental modelling studies or performance assessments for radioactive waste disposal.

A few data selected by Hummel et al. (2005a) have not been included in TDB 2020 (Tab. 18-4).

The numerical values derived from the NEA organics review (Hummel et al. 2005a) and included in TDB 2020 are given in Tab. 18.5-1 – 18.5-7.

NEA (see, e.g., Hummel et al. 2005a) used the specific ion interaction theory (SIT) for making ionic strength corrections to the experimental data, an approach which is also adopted for TDB 2020 (as has been for all its predecessors). In many cases, the ion interaction coefficients for species under consideration here were not available. We approximated these with the estimation method described in Section 1.5.3, which draws on a statistical analysis of published SIT ion interaction coefficients, and which allows the estimation of missing coefficients for the interaction of cations with Cl^- and ClO_4^-, and for the interaction of anions with Na^+, from the charge of the cations or anions of interest.

The selected SIT ion interaction coefficients are presented in Tab. 18-6. Note that SIT interaction coefficients with K^+ are given only for ligands, as in some cases (ox, cit) no complex formation with K^+ is included in the speciation model (see Section 18.2.2).

18.2 Auxiliary data

Most of the data selected in the NEA organics review (Hummel et al. 2005a) are equilibrium constants, i.e., protonation constants of the ligands, formation constants of metal – ligand complexes, and solubility constants of metal – organic compounds.

However, an internally consistent and widely applicable thermochemical data base should comprise not only equilibrium constants for reaction data but also thermodynamic parameters for compounds and complexes such as the standard molar Gibbs energies of formation. In order to derive the latter quantities from the selected equilibrium constants the standard molar Gibbs energies of formation of the ligand anions are needed, *i.e.* the quantities $\Delta_f G_m°(ox^{2-}, 298.15\ K)$, $\Delta_f G_m°(cit^{3-}, 298.15\ K)$, $\Delta_f G_m°(edta^{4-}, 298.15\ K)$ and $\Delta_f G_m°(isa^{-}, 298.15\ K)$ are prerequisites for internally consistent calculations of standard molar Gibbs energies of formation for all compounds and aqueous complexes where only reaction data were selected in the review procedure.

The derivation of the standard molar Gibbs energies of formation for the key species ox^{2-}, cit^{3-}, $edta^{4-}$ and isa^{-} proved to be far from trivial and has not been successful in all cases (Hummel et al. 2005a).

In the case of oxalate, the derivation of $\Delta_f G_m°(ox^{2-}, 298.15\ K)$ turned into a veritable Odyssey in experimental thermodynamic data space, while in the case of citrate, the derivation of $\Delta_f G_m°(cit^{3-}, 298.15\ K)$ was a somewhat more straightforward procedure.

In the case of edta, no value of $\Delta_f G_m°(edta^{4-}, 298.15\ K)$ could be obtained because there is no solid containing this ligand, or its acid, for which the entropy is available. Furthermore, there are no satisfactory methods to estimate this property.

No data at all are available for isa.

The NEA selected values (Hummel et al. 2005a) for the key species ox^{2-}, cit^{3-} and $edta^{4-}$ are

$$\Delta_f G_m°(ox^{2-}, 298.15\ K) = -(680.134 \pm 1.830)\ kJ \cdot mol^{-1}$$

$$\Delta_f H_m°(ox^{2-}, 298.15\ K) = -(830.660 \pm 1.592)\ kJ \cdot mol^{-1}$$

$$S_m°(ox^{2-}, 298.15\ K) = (47.597 \pm 3.020)\ J \cdot K^{-1} \cdot mol^{-1}$$

$$\Delta_f G_m°(cit^{3-}, 298.15\ K) = -(1'162.258 \pm 2.014)\ kJ \cdot mol^{-1}$$

$$\Delta_f H_m°(cit^{3-}, 298.15\ K) = -(1'519.920 \pm 2.070)\ kJ \cdot mol^{-1}$$

$$S_m°(cit^{3-}, 298.15\ K) = (75.587 \pm 1.855)\ J \cdot K^{-1} \cdot mol^{-1}$$

$$\Delta_f H_m°(edta^{4-}, 298.15\ K) = -(1'704.800 \pm 3.751)\ kJ \cdot mol^{-1}$$

These values have been included in TDB 2020.

For building an operational database of Gibbs energies, arbitrary values for $\Delta_f G_m°(edta^{4-}, 298.15\ K)$ and $\Delta_f G_m°(isa^{-}, 298.15\ K)$ have been assumed and included in TDB 2020:

$$\Delta_f G_m°(edta^{4-}, 298.15\ K) = 0.0\ kJ \cdot mol^{-1}$$

$$\Delta_f G_m°(isa^{-}, 298.15\ K) = 0.0\ kJ \cdot mol^{-1}$$

Within the scope of providing basic auxiliary data for the organic ligands the NEA organics review selected thermodynamic constants for some compounds formed by the acids, i.e., α-H_2ox, β-H_2ox, $H_2ox \cdot 2H_2O(cr)$, $H_3cit(cr)$, $H_3cit \cdot H_2O(cr)$ and $H_4edta(cr)$ (Tab. 18-1).

The solid formed at equilibrium in the system oxalic acid – water is the dihydrate, $H_2ox \cdot 2H_2O(cr)$. Its solubility in pure water at 25 °C is 1.3 $mol \cdot kg^{-1}$. At temperatures below 36 °C the solid formed at equilibrium in the system citric acid – water is the monohydrate, $H_3cit \cdot H_2O(cr)$. Above this temperature $H_3cit(cr)$ is formed instead. At 25 °C the solubility of $H_3cit \cdot H_2O(cr)$ in pure water is 8.45 $mol \cdot kg^{-1}$. In summary, the solids α-H_2ox and β-H_2ox are unstable in water, whereas $H_2ox \cdot 2H_2O(cr)$, $H_3cit(cr)$ and $H_3cit \cdot H_2O(cr)$ are highly soluble, and thus, none of these compounds is included in TDB 2020 (Tab. 18-3).

In contrast to these compounds, the minimum solubility of $H_4edta(cr)$ in aqueous solutions is below millimolar, and its NEA selected solubility constant, reaction enthalpy (obtained from calorimetric data), as well as the NEA selected SIT interaction parameter $\varepsilon(H_4edta(aq), MX)$ obtained from a SIT analysis of solubility data, have been included in TDB 2020:

$$H_4edta(cr) \rightleftharpoons H_4edta(aq)$$

$$\log_{10}K° (298.15\ K) = -3.80 \pm 0.19$$

$$\Delta_r H_m°(298.15\ K) = 29 \pm 3\ kJ \cdot mol^{-1}$$

$$\varepsilon(H_4edta(aq), NaCl) = \varepsilon(H_4edta(aq), NaClO_4) = -(0.29 \pm 0.14)\ kg \cdot mol^{-1}$$

18.2.1 Protonation constants of the organic ligands

The protonation constants of oxalate, citrate and edta are the best-established values of the NEA organics review (Hummel et al. 2005a) due to the large number of published experimental data that could be used in the data analysis procedures.

As a novel approach, data measured in different electrolyte media were fitted by a constrained multi-dimensional SIT least squares procedure, resulting in a common value at zero ionic strength consistent with all reliable experimental data (Hummel et al. 2005b). This was not only done for $\log_{10}K$ data but, also for the first time, for $\Delta_r H_m$ data describing the temperature effects of the protonation constants as a function of electrolyte concentration in terms of SIT interaction coefficients for enthalpies.

In the case of oxalate its two carboxyl groups can be protonated resulting in the species Hox^- and $H_2ox(aq)$. The following data, selected by Hummel et al. (2005a), have been included in TDB 2020:

$ox^{2-} + H^+ \rightleftharpoons Hox^-$

$\log_{10}K_1° (298.15\ K) = 4.25 \pm 0.01$

$\Delta_r H_m°(298.15\ K) = 7.3 \pm 0.1\ kJ \cdot mol^{-1}$

$Hox^- + H^+ \rightleftharpoons H_2ox(aq)$

$\log_{10}K_2° (298.15\ K) = 1.40 \pm 0.03$

$\Delta_r H_m°(298.15\ K) = 3.3 \pm 0.5\ kJ \cdot mol^{-1}$

$\varepsilon(Na^+, ox^{2-}) = -(0.08 \pm 0.01)\ kg \cdot mol^{-1}$

$\varepsilon(Na^+, Hox^-) = -(0.07 \pm 0.01)\ kg \cdot mol^{-1}$

$\varepsilon(K^+, ox^{2-}) = (0.07 \pm 0.08)\ kg \cdot mol^{-1}$

$\varepsilon(K^+, Hox^-) = -(0.01 \pm 0.08)\ kg \cdot mol^{-1}$

$\varepsilon(H_2ox(aq), NaCl) = \varepsilon(H_2ox(aq), NaClO_4) = (0.00 \pm 0.01)\ kg \cdot mol^{-1}$

Note that the latter value is a basic assumption of the review by Hummel et al. (2005a) who write: "It is expected that the value of $\varepsilon(H_2ox(aq), MX)$ will be small. In this review the approximation is made that $\varepsilon(H_2ox(aq), MX) = (0.00 \pm 0.01)\ kg \cdot mol^{-1}$. This approximation is corroborated by emf measurements (Larson & Tomsicek 1941) from which the authors concluded that the activity coefficient of the undissociated oxalic acid does not change in value over an ionic range of 0.02 to 0.33M".

Citrate has three carboxyl groups resulting in the protonated species $Hcit^{2-}$, H_2cit^- and $H_3cit(aq)$. The following data, selected by Hummel et al. (2005a), have been included in TDB 2020:

$cit^{3-} + H^+ \rightleftharpoons Hcit^{2-}$

$\log_{10}K_1° (298.15\ K) = 6.36 \pm 0.02$

$\Delta_r H_m°(298.15\ K) = (3.3 \pm 0.3)\ kJ \cdot mol^{-1}$

$\Delta_r C_{p,m}°(298.15\ K) = (222 \pm 14)\ J \cdot K^{-1} \cdot mol^{-1}$

$Hcit^{2-} + H^+ \rightleftharpoons H_2cit^-$

$\log_{10}K_2° (298.15\ K) = 4.78 \pm 0.01$

$\Delta_r H_m°(298.15\ K) = -(2.4 \pm 0.3)\ kJ \cdot mol^{-1}$

$\Delta_r C_{p,m}°(298.15\ K) = (167 \pm 8)\ J \cdot K^{-1} \cdot mol^{-1}$

$H_2cit^- + H^+ \rightleftharpoons H_3cit(aq)$

$\log_{10}K_3° (298.15\ K) = 3.13 \pm 0.01$

$\Delta_r H_m°(298.15\ K) = -(4.5 \pm 0.3)\ kJ \cdot mol^{-1}$

$\Delta_r C_{p,m}°(298.15\ K) = (116 \pm 6)\ J \cdot K^{-1} \cdot mol^{-1}$

$\varepsilon(Na^+, cit^{3-}) = -(0.076 \pm 0.030)\ kg \cdot mol^{-1}$

$\varepsilon(Na^+, Hcit^{2-}) = -(0.04 \pm 0.01)\ kg \cdot mol^{-1}$

$\varepsilon(Na^+, H_2cit^-) = -(0.05 \pm 0.01)\ kg \cdot mol^{-1}$

$\varepsilon(K^+, cit^{3-}) = (0.02 \pm 0.02)\ kg \cdot mol^{-1}$

$\varepsilon(K^+, Hcit^{2-}) = -(0.01 \pm 0.02)\ kg \cdot mol^{-1}$

$\varepsilon(K^+, H_2cit^-) = -(0.04 \pm 0.01)\ kg \cdot mol^{-1}$

$\varepsilon(H_3cit(aq), NaCl) = \varepsilon(H_3cit(aq), NaClO_4) = (0.00 \pm 0.01)\ kg \cdot mol^{-1}$

Note that the latter value is a basic assumption of the review by Hummel et al. (2005a) who write: "It is expected that the value of $\varepsilon(H_3cit(aq), MX)$ will be small. In this review the approximation is made that $\varepsilon(H_3cit(aq), MX) = (0.00 \pm 0.01)\ kg \cdot mol^{-1}$".

The hydroxyl group of citrates has been found to dissociate only at high pH-values (> 12) which may be schematically written as

$$cit^{3-} \rightleftharpoons H_{-1}cit^{4-} + H^+$$

The equilibrium constant for this reaction has been reported in a few papers, but no value is recommended in the NEA review as it is expected to be smaller than the dissociation constant of H_2O, i.e., $\log_{10}K° < -14$. Because of this $H_{-1}cit^{4-}$ cannot be used as a component when calculating equilibrium constants, although experimental data indicate a very large inductive effect on the dissociation constant of the OH-group in cit^{3-} upon coordination to metal ions. Such reactions have to be formulated, for example, as

$$Ni(cit)^- \rightleftharpoons Ni(H_{-1}cit)^{2-} + H^+$$

When dissolved in water H_4edta forms a double zwitterion which may act both as an acid releasing up to four protons, and as a base accepting up to two H^+ ions. Hence, six protonated species of edta have to be considered in speciation calculations, i.e., $Hedta^{3-}$, H_2edta^{2-}, H_3edta^-, $H_4edta(aq)$, H_5edta^+ and H_6edta^{2+}. The following data, selected by Hummel et al. (2005a), have been included in TDB 2020:

$$edta^{4-} + H^+ \rightleftharpoons Hedta^{3-}$$

$\log_{10}K_1°\ (298.15\ K) = 11.24 \pm 0.03$

$\Delta_r H_m°(298.15\ K) = -(19.8 \pm 0.5)\ kJ \cdot mol^{-1}$

$Hedta^{3-} + H^+ \rightleftharpoons H_2edta^{2-}$

$\log_{10}K_2°$ (298.15 K) = 6.80 ± 0.02

$\Delta_r H_m°$(298.15 K) = -(15.2 ± 0.4) kJ · mol^{-1}

$H_2edta^{2-} + H^+ \rightleftharpoons H_3edta^-$

$\log_{10}K_3°$ (298.15 K) = 3.15 ± 0.02

$\Delta_r H_m°$(298.15 K) = (7.1 ± 0.4) kJ · mol^{-1}

$H_3edta^- + H^+ \rightleftharpoons H_4edta(aq)$

$\log_{10}K_4°$ (298.15 K) = 2.23 ± 0.05

$\Delta_r H_m°$(298.15 K) = (1.9 ± 1.5) kJ · mol^{-1}

$H_4edta(aq) + H^+ \rightleftharpoons H_5edta^+$

$\log_{10}K_5°$ (298.15 K) = 1.3 ± 0.1

$H_5edta^+ + H^+ \rightleftharpoons H_6edta^{2+}$

$\log_{10}K_6°$ (298.15 K) = -0.5 ± 0.2

$\varepsilon(Na^+, edta^{4-})$ = (0.32 ± 0.14) kg · mol^{-1}

$\varepsilon(Na^+, Hedta^{3-})$ = -(0.10 ± 0.14) kg · mol^{-1}

$\varepsilon(Na^+, H_2edta^{2-})$ = -(0.37 ± 0.14) kg · mol^{-1}

$\varepsilon(Na^+, H_3edta^-)$ = -(0.33 ± 0.14) kg · mol^{-1}

$\varepsilon(K^+, edta^{4-})$ = (1.07 ± 0.19) kg · mol^{-1}

$\varepsilon(K^+, Hedta^{3-})$ = (0.31 ± 0.18) kg · mol^{-1}

$\varepsilon(K^+, H_2edta^{2-})$ = -(0.17 ± 0.18) kg · mol^{-1}

$\varepsilon(K^+, H_3edta^-)$ = -(0.14 ± 0.17) kg · mol^{-1}

$\varepsilon(H_5edta^+, Cl^-) = \varepsilon(H_5edta^+, ClO_4^-)$ = -(0.23 ± 0.15) kg · mol^{-1}

$\varepsilon(H_6edta^{2+}, Cl^-) = \varepsilon(H_6edta^{2+}, ClO_4^-)$ = -(0.20 ± 0.16) kg · mol^{-1}

Note that the large uncertainties in the SIT interaction parameters listed above are due to the large uncertainty of the basic parameter $\varepsilon(H_4edta(aq), MX)$ = -(0.29 ± 0.14) kg · mol^{-1} (see Section 18.2) used to calculate these parameters from experimental Δε values with much smaller uncertainties in the range of 0.01 – 0.06 (Hummel et al. 2005a).

Isosaccharinic acid has one carboxyl group which can deprotonate in a pH range comparable to other carboxylic acids. However, the protonation reaction

$$isa^- + H^+ \rightleftharpoons Hisa(aq)$$

is coupled with the lactonisation (formation of a ring structure by dehydration) of isa

$$Hisa(aq) \rightleftharpoons isa_L(aq) + H_2O$$

Most experimental techniques do not allow to distinguish between Hisa(aq) and $isa_L(aq)$, and a "composite" protonation constant is determined according to the reaction

$$isa^- + H^+ \rightleftharpoons Hisa(aq)^*$$

where $[Hisa(aq)^*] = [Hisa(aq)] + [isa_L(aq)]$.

The composite constant for isa is similar to that for carbonic acid where $HCO_3^- + H^+ \rightleftharpoons H_2CO_3(aq)$ and $H_2CO_3(aq) \rightleftharpoons CO_2(aq) + H_2O$ are coupled and generally a composite constant for the reaction $HCO_3^- + H^+ \rightleftharpoons H_2CO_3(aq)^*$ is used where $[H_2CO_3(aq)^*] = [H_2CO_3(aq)] + [CO_2(aq)]$.

Hummel et al. (2005a) selected

$$isa^- + H^+ \rightleftharpoons Hisa(aq)^*$$

$$\log_{10}K^\circ\ (298.15\ K) = 4.0 \pm 0.5$$

This value has been included in TDB 2020, together with the estimates

$$\varepsilon(K^+, isa^-) \approx \varepsilon(Na^+, isa^-) = -(0.05 \pm 0.10)\ kg \cdot mol^{-1}$$

$$\varepsilon(Hisa(aq)^*, NaCl) = \varepsilon(Hisa(aq)^*, NaClO_4) = (0.00 \pm 0.10)\ kg \cdot mol^{-1}$$

18.2.2 Alkali metal compounds and complexes

Solubility data are available for compounds $Na_2ox(cr)$, $NaHox \cdot H_2O(cr)$, $K_2ox \cdot H_2O(cr)$, $KHox(cr)$ and $KH_3(ox)_2 \cdot 2H_2O(cr)$. However, these compounds are highly soluble salts and no thermodynamic data have been selected by Hummel et al. (2005a).

As discussed by Hummel et al. (2005a) the complexes $Na(ox)^-$ and Kox^- sometimes have been included in speciation models to account for experimentally determined variations in different ionic media. However, Hummel et al. (2005a) successfully modelled oxalate protonation data using SIT with the interaction parameters $\varepsilon(Na^+, ox^{2-})$ and $\varepsilon(K^+, ox^{2-})$ without considering a complex $Na(ox)^-$ or Kox^- in the speciation model. Likewise, calcium oxalate solubility data can be modelled successfully (see Section 18.2.3) applying SIT with the interaction parameters $\varepsilon(Na^+, ox^{2-})$ and $\varepsilon(K^+, ox^{2-})$ without considering a complex $Na(ox)^-$ or Kox^- in the speciation model. Hence, no data are selected (nor needed) for the complexes $Na(ox)^-$ and Kox^-.

As discussed by Hummel et al. (2005a) the solubility of alkali citrate compounds is quite high, for example the reported solubility for $KH_2cit(cr)$ in water at 25 °C is 0.94 M. No thermodynamic data have been selected by Hummel et al. (2005a) for this highly soluble salt.

Equilibrium constants for the formation of citrate complexes with either Na^+ or K^+ are reported in several studies but, as discussed by Hummel et al. (2005a), most of these studies included the complexes in speciation models to account for experimentally determined variations in different ionic media, as in the case of oxalate, while two studies used ion-selective electrodes. Hummel et al. (2005a) conclude that, although there is some evidence suggesting the formation of citrate complexes with Na^+ and K^+, there are many uncertainties concerning their stoichiometry and stability, and the complexes, if formed, are weak ($K \leq 10$ kg · mol^{-1}). Interactions between alkali-metal ions and citrate at 25 °C are instead treated as specific ion interaction effects included in the SIT coefficients.

Na and K edta compounds are highly soluble salts, where $Na_2H_2edta \cdot 2H_2O(cr)$ is the most common commercial product, but other forms like $Na_4edta \cdot 5H_2O(cr)$ and $K_2H_2edta \cdot 2H_2O(cr)$ are also available. No thermodynamic data have been selected by Hummel et al. (2005a) for these highly soluble salts.

It was found early that the protonation constants of $edta^{4-}$ depend on the nature of the background electrolyte. Especially, the first protonation constant was found to be substantially lower in Na^+ solutions as compared with K^+ media. This was ascribed to the formation of sodium complexes, and Schwarzenbach & Ackermann (1947) determined the stability of the Na^+ and Li^+ complexes with $edta^{4-}$ in 0.1 M KCl media. Since then, several studies have reported equilibrium constants for the formation of edta complexes with Na^+ and K^+. Hummel et al. (2005a) evaluated data for the formation of $Na(edta)^{3-}$ and $Kedta^{3-}$ in tetraalkylammonium media by SIT regressions, as well as enthalpy data for $Na(edta)^{3-}$, and selected

$$Na^+ + edta^{4-} \rightleftharpoons Na(edta)^{3-}$$

$$\log_{10}K^\circ\ (298.15\ K) = 2.8 \pm 0.2$$

$$\Delta_r H_m^\circ(298.15\ K) = -(4 \pm 3)\ kJ \cdot mol^{-1}$$

$$K^+ + edta^{4-} \rightleftharpoons Kedta^{3-}$$

$$\log_{10}K^\circ\ (298.15\ K) = 1.8 \pm 0.3$$

This value has been included in TDB 2020, together with the estimates

$$\varepsilon(Na^+, Na(edta)^{3-}) = -(0.15 \pm 0.10)\ kg \cdot mol^{-1}$$

$$\varepsilon(Na^+, Kedta^{3-}) = -(0.15 \pm 0.10)\ kg \cdot mol^{-1}$$

No thermodynamic data on alkali metal isa compounds or complexes have been identified by Hummel et al. (2005a).

However, the solubilities of alkali isa compounds seem to be rather high. For example, Hummel et al. (2005a) report that the structure of $Na(isa) \cdot H_2O(cr)$ was determined, and its solubility measured as 1.7 – 1.9 M in the pH range 4.5 – 10.

Alkali metal isa complexes, if formed, are expected to be weak. Interactions between alkali-metal ions and isa may instead be treated as specific ion interaction effects included in the estimated SIT coefficients $\varepsilon(K^+, isa^-) \approx \varepsilon(Na^+, isa^-) = -(0.05 \pm 0.10)$ kg · mol^{-1}.

18.2.3 Calcium and magnesium compounds and complexes

Calcium oxalate forms three different hydrates at ambient conditions, $Ca(ox)\cdot H_2O(cr)$, $Ca(ox)\cdot 2H_2O(cr)$ and $Ca(ox)\cdot 3H_2O(cr)$. The monohydrate, $Ca(ox)\cdot H_2O(cr)$, is found in nature as the mineral whewellite and the dihydrate, $Ca(ox)\cdot 2H_2O(cr)$, occurs in nature as the mineral weddelite. A rather good and consistent set of published solubility data in the temperature range 15 – 50 °C has been evaluated by Hummel et al. (2005a) and they selected

$Ca(ox)\cdot H_2O(cr) \rightleftharpoons Ca^{2+} + ox^{2-} + H_2O(l)$

$\log_{10}K_{s,0}°$ (298.15 K) = -(8.73 ± 0.06)

$\Delta_r H_m°$(298.15 K) = 21.5 ± 0.5 kJ · mol^{-1}

$\Delta_r C_{p.m}°$(298.15 K) = 0 J · K^{-1} · mol^{-1}

$Ca(ox)\cdot 2H_2O(cr) \rightleftharpoons Ca^{2+} + ox^{2-} + 2\ H_2O(l)$

$\log_{10}K_{s,0}°$ (298.15 K) = -(8.30 ± 0.06)

$\Delta_r H_m°$(298.15 K) = 25.2 ± 1.1 kJ · mol^{-1}

$\Delta_r C_{p.m}°$(298.15 K) = 0 J · K^{-1} · mol^{-1}

$Ca(ox)\cdot 3H_2O(cr) \rightleftharpoons Ca^{2+} + ox^{2-} + 3\ H_2O(l)$

$\log_{10}K_{s,0}°$ (298.15 K) = -(8.19 ± 0.04)

$\Delta_r H_m°$(298.15 K) = 29.7 ± 1.3 kJ · mol^{-1}

$\Delta_r C_{p.m}°$(298.15 K) = 0 J · K^{-1} · mol^{-1}

These values have been included in TDB 2020.

Magnesium oxalate dihydrate, $Mg(ox)\cdot 2H_2O(cr)$, is the magnesium oxalate compound forming at ambient conditions. It is found in nature as the mineral glushinskite. A number of studies reporting solubility data for $Mg(ox)\cdot 2H_2O(cr)$ have been scrutinised by Hummel et al. (2005a) who identified slow dissolution and even slower precipitation kinetics as a general problem affecting all these solubility studies. Hummel et al. (2005a) concluded that for scoping calculations in modelling exercises related to radioactive waste disposal a value

$Mg(ox)\cdot 2H_2O(cr) \rightleftharpoons Mg^{2+} + ox^{2-} + 2\ H_2O(l)$

$\log_{10}K_{s,0}°(298.15\ K) = -(6.4 \pm 0.2)$

could be used, encompassing the available literature data, but this value is not recommended.

Hence, this value has been included in TDB 2020 as supplemental datum.

The equilibrium data for complex formation in Mg and Ca oxalate systems have been scrutinised by Hummel et al. (2005a) who state that the stabilities of Mg oxalate 1:1 and 1:2 complexes are in a range suitable for direct determination by alkalimetric titration. Based on SIT analyses of data measured in NaCl media and evaluating other data Hummel et al. (2005a) selected

$Mg^{2+} + ox^{2-} \rightleftharpoons Mg(ox)(aq)$

$\log_{10}\beta_1° \text{ (298.15 K)} = 3.56 \pm 0.04$

$Mg^{2+} + 2\ ox^{2-} \rightleftharpoons Mg(ox)_2^{2-}$

$\log_{10}\beta_2° \text{ (298.15 K)} = 5.17 \pm 0.08$

$\varepsilon(Mg(ox)(aq), NaCl) = (0.00 \pm 0.03)\ kg \cdot mol^{-1}$

$\varepsilon(Na^+, Mg(ox)_2^{2-}) = -(0.15 \pm 0.03)\ kg \cdot mol^{-1}$

These values have been included in TDB 2020.

Hummel et al. (2005a) state that the experimental determination of the formation of calcium oxalate complexes is severely hampered by the low solubility of $Ca(ox)\cdot H_2O(cr)$, and consequently only a few results reported in the literature could be accepted. The finally selected values are

$Ca^{2+} + ox^{2-} \rightleftharpoons Ca(ox)(aq)$

$\log_{10}\beta_1° \text{ (298.15 K)} = 3.19 \pm 0.06$

$Ca^{2+} + 2\ ox^{2-} \rightleftharpoons Ca(ox)_2^{2-}$

$\log_{10}\beta_2° \text{ (298.15 K)} = 4.02 \pm 0.19$

Furthermore, Hummel et al. (2005a) estimated

$\varepsilon(Ca(ox)(aq), NaCl) \approx \varepsilon(Mg(ox)(aq), NaCl) = (0.00 \pm 0.03)\ kg \cdot mol^{-1}$

$\varepsilon(Na^+, Ca(ox)_2^{2-}) \approx \varepsilon(Na^+, Mg(ox)_2^{2-}) = -(0.15 \pm 0.03)\ kg \cdot mol^{-1}$

These values have been included in TDB 2020.

The existence of the protonated species $Ca(Hox)^+$ and $Ca(Hox)_2(aq)$ has been postulated in a single study, but as discussed by Hummel et al. (2005a), the experiments are inconclusive and have been rejected by Hummel et al. (2005a).

Few experimental studies concerning $Mg_3(cit)_2 \cdot nH_2O(cr)$, n = 9 – 15, indicate that these compounds are fairly soluble, and no thermodynamic data have been derived by Hummel et al. (2005a) from these solubility studies.

By contrast, the compound $Ca_3(cit)_2 \cdot 4H_2O(cr)$ is orders of magnitude less soluble than the Mg citrate compounds, and Hummel et al. (2005a) selected a constant for the solubility of Ca^{2+} citrate at 25 °C

$$Ca_3(cit)_2 \cdot 4H_2O(cr) \rightleftharpoons 3\ Ca^{2+} + 2\ cit^{3-} + 4\ H_2O(l)$$

$$\log_{10}K_{s,0}^\circ\ (298.15\ K) = -(17.90 \pm 0.10)$$

This value has been included in TDB 2020.

Hummel et al. (2005a) found an appreciable number of experimental equilibrium data in the literature on the complex formation of Mg^{2+} and Ca^{2+} with citrate. Most of these experimental equilibrium constants were obtained by potentiometric titration, mainly at 25 °C, some at 37 °C. Only in the case of $Ca(cit)^-$ experimental data in the temperature range 18 – 45 °C allowed to derive a reaction enthalpy value. Hummel et al. (2005a) selected

$$Ca^{2+} + cit^{3-} \rightleftharpoons Ca(cit)^-$$

$$\log_{10}\beta_1^\circ\ (298.15\ K) = 4.80 \pm 0.03$$

$$\Delta_r H_m^\circ(298.15\ K) = 0 \pm 6\ kJ \cdot mol^{-1}$$

$$\Delta_r C_{p.m}^\circ(298.15\ K) = 0\ J \cdot K^{-1} \cdot mol^{-1}$$

$$Ca^{2+} + Hcit^{2-} \rightleftharpoons Ca(Hcit)(aq)$$

$$\log_{10}\beta_1^\circ\ (298.15\ K) = 2.92 \pm 0.07$$

$$Ca^{2+} + H_2cit^- \rightleftharpoons Ca(H_2cit)^+$$

$$\log_{10}\beta_1^\circ\ (298.15\ K) = 1.53 \pm 0.16$$

$$Mg^{2+} + cit^{3-} \rightleftharpoons Mg(cit)^-$$

$$\log_{10}\beta_1^\circ\ (298.15\ K) = 4.81 \pm 0.03$$

$$Mg^{2+} + Hcit^{2-} \rightleftharpoons Mg(Hcit)(aq)$$

$$\log_{10}\beta_1^\circ\ (298.15\ K) = 2.60 \pm 0.07$$

$$Mg^{2+} + H_2cit^- \rightleftharpoons Mg(H_2cit)^+$$

$$\log_{10}\beta_1^\circ\ (298.15\ K) = 1.31 \pm 0.16$$

$$\varepsilon(Mg(Hcit)(aq), NaCl) = (0.02 \pm 0.05)\ kg \cdot mol^{-1}$$

$$\varepsilon(Na^+, Mg(cit)^-) = (0.03 \pm 0.03)\ kg \cdot mol^{-1}$$

These values have been included in TDB 2020, together with the estimates

$\varepsilon(Ca(H_2cit)^+, Cl^-) = \varepsilon(Mg(H_2cit)^+, Cl^-) = (0.05 \pm 0.10)$ kg · mol^{-1}

$\varepsilon(Ca(Hcit)(aq), NaCl) \approx \varepsilon(Mg(Hcit)(aq), NaCl) = (0.02 \pm 0.05)$ kg · mol^{-1}

$\varepsilon(Na^+, Ca(cit)^-) \approx \varepsilon(Na^+, Mg(cit)^-) = (0.03 \pm 0.03)$ kg · mol^{-1}

Many edta compounds containing magnesium and calcium have been reported in the literature. Hummel et al. (2005a) list 16 compounds whose stoichiometry has been confirmed by elemental analysis. Solubility measurements in H_2O have been reported for several of these compounds, ranging from about 0.001 M for $Mg(H_2edta)\cdot 6H_2O$, about 0.01 M for $Ca(H_2edta)\cdot 2H_2O$ and $Mg_2edta\cdot 9H_2O$, about 0.04 M for $Ca_2edta\cdot 7H_2O$, to about 2 M for $Na_2Mg(edta)\cdot 4H_2O$ and $Na_2Ca(edta)\cdot 2H_2O$. Hummel et al. (2005a) conclude that "in qualitative terms, an overall consistent picture emerges from these solubility data. However, it is outside the scope of this review to develop a quantitative thermodynamic model for these rather soluble Mg and Ca edta compounds".

Complex formation in Ca and Mg edta systems have been studied by several investigators. The stabilities of the Ca and Mg edta 1:1 complexes are of an order of magnitude that allows the direct investigation of their equilibria. Hummel et al. (2005a) scrutinised all these data, and in the case of $Mg(edta)^{2-}$ and Mg(Hedta) measurements in NaCl media at different concentrations allowed to derive SIT interaction coefficients. In addition, enthalpy data for equilibria with $Ca(edta)^{2-}$ and $Mg(edta)^{2-}$ are available. Hummel et al. (2005a) selected

$Ca^{2+} + edta^{4-} \rightleftharpoons Ca(edta)^{2-}$

$\log_{10}K_1° (298.15\ K) = 12.69 \pm 0.06$

$\Delta_r H_m°(298.15\ K) = -(22.2 \pm 0.4)$ kJ · mol^{-1}

$Ca(edta)^{2-} + H^+ \rightleftharpoons Ca(Hedta)^-$

$\log_{10}K° (298.15\ K) = 3.54 \pm 0.09$

$Mg^{2+} + edta^{4-} \rightleftharpoons Mg(edta)^{2-}$

$\log_{10}K_1° (298.15\ K) = 10.90 \pm 0.10$

$\Delta_r H_m°(298.15\ K) = (19.8 \pm 0.4)$ kJ · mol^{-1}

$Mg(edta)^{2-} + H^+ \rightleftharpoons Mg(Hedta)^-$

$\log_{10}K° (298.15\ K) = 4.5 \pm 0.2$

$\varepsilon(Na^+, Mg(edta)^{2-}) = -(0.01 \pm 0.15)$ kg · mol^{-1}

$\varepsilon(Na^+, Mg(Hedta)^-) = (0.11 \pm 0.20)$ kg · mol^{-1}

These values have been included in TDB 2020, together with the estimates

$\varepsilon(Na^+, Ca(edta)^{2-}) \approx \varepsilon(Na^+, Mg(edta)^{2-}) = -(0.01 \pm 0.15)$ kg · mol^{-1}

$\varepsilon(Na^+, Ca(Hedta)^-) \approx \varepsilon(Na^+, Mg(Hedta)^-) = (0.11 \pm 0.20)$ kg · mol^{-1}

The crystal and molecular structure of calcium α-isosaccharinate, $Ca(isa)_2(cr)$ has been determined, and its solubility has been investigated, together with Ca isa complex formation. However, except for calcium, no thermodynamic data on the isa compounds or complexes with alkaline earth metals were identified in the literature by Hummel et al. (2005a). Evaluating the available data Hummel et al. (2005a) selected

$Ca(isa)_2(cr) \rightleftharpoons Ca^{2+} + 2\ isa^-$

$\log_{10}K_{s,0}°$ (298.15 K) = -(6.4 ± 0.2)

$Ca^{2+} + isa^- \rightleftharpoons Ca(isa)^+$

$\log_{10}K_1°$ (298.15 K) = 1.7 ± 0.3

$Ca^{2+} + isa^- \rightleftharpoons Ca(isa_{-H})(aq) + H^+$

$\log_{10}K°$ (298.15 K) = -(10.4 ± 0.5)

These values have been included in TDB 2020, together with the estimates

$\varepsilon(Ca(isa)^+, Cl^-) = (0.05 \pm 0.10)$ kg · mol^{-1}

$\varepsilon(Ca(isa_{-H})(aq), NaCl) = \varepsilon(Ca(isa_{-H})(aq), NaClO_4) = (0.0 \pm 0.1)$ kg · mol^{-1}

Note that combining the above two complexation reactions would result in the reaction

$Ca(isa)^+ \rightleftharpoons Ca(isa_{-H})(aq) + H^+$

$\log_{10}K°$ (298.15 K) = -12.1

This reaction represents the deprotonation of a hydroxyl group in $Ca(isa)^+$ at pH ≥ 12.

18.3 Compounds and complexes of fission and activation products

18.3.1 Selenium compounds and complexes

According to Hummel et al. (2005a) qualitative information has been published concerning the formation of the compound SeOox, and crystal structure data are available for mixed U(VI) selenate oxalates. A dubious study reports indications for the formation of an aqueous oxalate – selenite complex.

No thermodynamic data are available for any of these compounds and complexes, and no information about thermodynamic properties could be found for the selenium citrate, edta and isa systems.

There is no indication for the precipitation of sparingly soluble selenium compounds or the formation of strong aqueous selenium complexes with oxalate, citrate, edta and isa and hence, the lack of thermodynamic data is no gap in a database for performance assessment studies.

18.3.2 Nickel compounds and complexes

The nickel oxalate solid that precipitates from aqueous solution is nickel oxalate dihydrate, $Ni(ox)\cdot 2H_2O(cr)$. Scrutinising the available solubility data Hummel et al. (2005a) could only estimate an upper limit for the solubility product

$$Ni(ox)\cdot 2H_2O(cr) \rightleftharpoons Ni^{2+} + ox^{2-} + 2\ H_2O$$

$$log_{10}K_{s,0}^{\circ}(298.15\ K) \leq 9.96$$

This value is not recommended by Hummel et al. (2005a) but included in TDB 2020 as supplemental datum.

Data for the formation of $Ni(ox)(aq)$ and $Ni(ox)_2^{2-}$ have been evaluated by Hummel et al. (2005a). Measurements in NaCl media allowed to derive SIT interaction coefficients. Enthalpy data could be derived from calorimetric studies. Hummel et al. (2005a) finally selected

$$Ni^{2+} + ox^{2-} \rightleftharpoons Ni(ox)(aq)$$

$$\log_{10}\beta_1^{\circ}\ (298.15\ K) = 5.19 \pm 0.04$$

$$\Delta_r H_m^{\circ}(298.15\ K) = (0.0 \pm 0.3)\ kJ \cdot mol^{-1}$$

$$Ni^{2+} + 2\ ox^{2-} \rightleftharpoons Ni(ox)_2^{2-}$$

$$\log_{10}\beta_2^{\circ}\ (298.15\ K) = 7.64 \pm 0.07$$

$$\Delta_r H_m^{\circ}(298.15\ K) = -(7.8 \pm 0.3)\ kJ \cdot mol^{-1}$$

$$\varepsilon(Ni(ox)(aq), NaCl) = -(0.07 \pm 0.03)\ kg \cdot mol^{-1}$$

$$\varepsilon(Na^{+}, Ni(ox)_2^{2-}) = -(0.26 \pm 0.03)\ kg \cdot mol^{-1}$$

These values have been included in TDB 2020.

The complex $Ni(ox)_3^{4-}$ is formed only at high oxalate concentrations, perhaps at $[ox]_{tot} > 0.1$ M, and no complexation constant could be recommended by Hummel et al. (2005a).

The protonated complex $Ni(Hox)^+$ has been postulated from electromigration data, but these studies are considered unreliable by Hummel et al. (2005a).

No thermodynamic data for Ni citrate compounds could be identified by Hummel et al. (2005a).

Hummel et al. (2005a) state that potentiometric titrations were used in most studies concerning Ni citrate aqueous complexes, and the formation of $Ni(H_2cit)^+$, Ni(Hcit)(aq) and $Ni(cit)^-$ in the lower pH region is commonly accepted in the literature. When the ratio of citrate to nickel is higher, the formation of $Ni(cit)_2^{4-}$ can be detected. Hummel et al. (2005a) conclude that there is no well-grounded argument about the speciation, that is, no examinations have been done for the speciation other than the potentiometric titration at certain fixed concentrations of Ni^{2+} and citrate. Hummel et al. (2005a) could not judge the exact species but finally selected

$Ni^{2+} + H_2cit^- \rightleftharpoons Ni(H_2cit)^+$

$\log_{10}K°$ (298.15 K) = 2.05 ± 0.25

$Ni^{2+} + Hcit^{2-} \rightleftharpoons Ni(Hcit)(aq)$

$\log_{10}K°$ (298.15 K) = 4.16 ± 0.10

$Ni^{2+} + cit^{3-} \rightleftharpoons Ni(cit)^-$

$\log_{10}\beta_1°$ (298.15 K) = 6.76 ± 0.08

$Ni^{2+} + 2\ cit^{3-} \rightleftharpoons Ni(cit)_2^{4-}$

$\log_{10}\beta_2°$ (298.15 K) = 8.5 ± 0.4

$\varepsilon(Ni(H_2cit)^+, ClO_4^-) = (0.12 \pm 0.5)$ kg · mol^{-1}

$\varepsilon(Ni(Hcit)(aq), NaClO_4) = -(0.07 \pm 0.5)$ kg · mol^{-1}

$\varepsilon(Na^+, Ni(cit)^-) = (0.22 \pm 0.5)$ kg · mol^{-1}

These values have been included in TDB 2020, together with the estimates

$\varepsilon(Ni(H_2cit)^+, Cl^-) \approx \varepsilon(Ni(H_2cit)^+, ClO_4^-) = (0.12 \pm 0.5)$ kg · mol^{-1}

$\varepsilon(Ni(Hcit)(aq), NaCl) \approx \varepsilon(Ni(Hcit)(aq), NaClO_4) = -(0.07 \pm 0.5)$ kg · mol^{-1}

$\varepsilon(Na^+, Ni(cit)_2^{4-}) = -(0.20 \pm 0.10)$ kg · mol^{-1}

Numerous nickel containing edta compounds have been reported in the literature (Hummel et al. 2005a). Solubility measurements in H_2O have been reported for few of these compounds, ranging from 0.13 M for $Ni_2edta \cdot 6H_2O$ and $MgNi(edta) \cdot 6H_2O$, to 0.7 M for $Ni_2edta \cdot 6H_2O$, and 0.8 M for $Na_2Ni(edta) \cdot 2H_2O$. Hummel et al. (2005a) did not develop quantitative thermodynamic models for these highly soluble Ni edta compounds.

Hummel et al. (2005a) report that complex formation in Ni(II) – edta systems has been studied by several investigators, and in qualitative terms the data reveal that in aqueous solution edta may form the following species with Ni^{2+}: $Ni(H_2edta)(aq)$, $Ni(Hedta)^-$, $Ni(edta)^{2-}$, $Ni(edta)OH^{3-}$ and other ternary complexes with Ni(edta)X, where X is a second ligand.

Hummel et al. (2005a) discussed all available papers and finally accepted complexation constants only for $Ni(Hedta)^-$ and $Ni(edta)^{2-}$, all measured in 0.1 M KNO_3 and 0.1 M KCl media, and calorimetric enthalpy data for $Ni(edta)^{2-}$. Hummel et al. (2005a) finally selected

$$Ni^{2+} + edta^{4-} \rightleftharpoons Ni(edta)^{2-}$$

$$\log_{10}K_1^\circ\ (298.15\ K) = 20.54 \pm 0.13$$

$$\Delta_r H_m^\circ(298.15\ K) = -(26.1 \pm 0.4)\ kJ \cdot mol^{-1}$$

$$Ni(edta)^{2-} + H^+ \rightleftharpoons Ni(Hedta)^-$$

$$\log_{10}K^\circ\ (298.15\ K) = 3.66 \pm 0.16$$

These values have been included in TDB 2020.

Hummel et al. (2005a) report that only one study concerns the heat involved in the reaction $Ni(edta)^{2-} + H^+ \rightleftharpoons Ni(Hedta)^-$, $\Delta_r H_m(0.1\ M\ KNO_3, 298.15\ K) = -(7.5 \pm 1.3)\ kJ \cdot mol^{-1}$, and state that the result seems to be reasonable and it has been used for temperature corrections in their review. However, based on a single determination only, no value can be recommended by Hummel et al. (2005a). Therefore, the value

$$Ni(edta)^{2-} + H^+ \rightleftharpoons Ni(Hedta)^-$$

$$\Delta_r H_m(298.15\ K) = -(7.5 \pm 1.3)\ kJ \cdot mol^{-1}$$

has been included in TDB 2020 as supplemental datum, together with the estimates

$$\varepsilon(Na^+, Ni(edta)^{2-}) = -(0.10 \pm 0.10)\ kg \cdot mol^{-1}$$

$$\varepsilon(Na^+, Ni(Hedta)^-) = -(0.05 \pm 0.10)\ kg \cdot mol^{-1}$$

Hummel et al. (2005a) state that the species $Ni(edta)OH^{3-}$ is present in solutions of pH > 12 and only a few papers report quantitative data concerning its stability. The reported stability constants vary by 1.5 log-units and Hummel et al. (2005a) conclude that all these studies suffer from various shortcomings, and no value can be recommended.

Hummel et al. (2005a) report that stability constants of Ni(II) – isa complexes have been determined by different experimental methods. However, due to the scarcity and difference in the stability constants and the varying of uncertain ionic strength in the experiments, no value for Ni(II) – isa complexes is selected by Hummel et al. (2005a) who state that nevertheless, the values reported in the literature may serve as a guideline for Ni – isa complexation around neutral pH. Hence, this review decided to include the value

$$Ni^{2+} + isa^{-} \rightleftharpoons Ni(isa)^{+}$$

$$log_{10}K_1^{\circ}(298.15\ K) \approx 2.4$$

in TDB 2020 as supplemental datum, together with the estimate

$$\varepsilon(Ni(isa)^{+}, Cl^{-}) \approx \varepsilon(Ni(isa)^{+}, ClO_4^{-}) = (0.2 \pm 0.1)\ kg \cdot mol^{-1}$$

18.3.3 Technetium compounds and complexes

Hummel et al. (2005a) summarise that there is very little information in the literature concerning the compounds and aqueous complexes of technetium, and no thermodynamic data has been published. A few solid phases containing technetium and oxalate have been synthesised and characterised but there is no information available on the thermodynamic stability of these compounds. Some qualitative information about the interaction between technetium and oxalate in aqueous solutions has also been published. None of these publications report data that may be used to obtain thermodynamic information for the technetium – oxalate system in aqueous solutions.

Despite the various oxidation states of technetium, only a limited number of papers, all published by the same author, dealing with the complex formation of Tc(IV) with citrate, could be found by Hummel et al. (2005a). The stoichiometries of the species formed are not well established and no thermodynamic data are reported.

Hummel et al. (2005a) report that the structure of a Tc(IV) complex salt of edta, $H_4(TcO)_2(edta)_2 \cdot 5H_2O$, has been determined. However, no chemical thermodynamic data are available for this compound.

Hummel et al. (2005a) scrutinised two studies, by the same authors, which report data on the complex formation between Tc(IV) and edta. In the pH range 1 – 2.5 the results of experiments by cation exchange and electrophoresis were interpreted by assuming the presence of TcO^{2+} at pH 1, reacting to $TcO(OH)^{+}$ and $TcO(OH)_2(aq)$ at higher pH, and the concomitant formation of $TcO(OH)edta^{3-}$. The unexpectedly high value of $\log_{10}K_1 = 19.1$ for the reaction $TcO(OH)^{+} + edta^{4-} \rightleftharpoons TcO(OH)edta^{3-}$ differs considerably from the value evaluated by Hummel et al. (2005a) for NpO_2^{+} ($\log_{10}K_1 = 9.23 \pm 0.13$, see Section 18.4.2.3). After discussing several shortcomings of the above-mentioned studies, Hummel et al. (2005a) conclude that the reported equilibrium data need confirmation, and no equilibrium constant has been selected.

No thermodynamic data on technetium isa compounds or complexes could be identified in the literature by Hummel et al. (2005a).

18.4 Actinide compounds and complexes

In the following sections the results of the NEA organics review (Hummel et al. 2005a) concerning actinide compounds and aqueous complexes are summarised from the viewpoint of their application in environmental modelling. Note that this summary is largely based on the discussion in Hummel et al. (2007).

18.4.1 Actinide compounds with organic ligands

The detailed discussion of organic compounds has been restricted in the NEA organics review (Hummel et al. 2005a) to the so-called "sparingly soluble" solids which may be of importance in environmental modelling studies. These are mainly metal oxalates, which were evaluated in some detail, whereas the generally rather soluble citrate, edta and isa compounds (Tab. 18-1) are discussed in qualitative terms.

In the field of actinide compounds with oxalate the only value selected by Hummel et al. (2005a) refers to the U(VI) – oxalate system, $UO_2ox \cdot 3H_2O$, where the solubility constants show a linear behaviour versus the reciprocal of absolute temperature in the range 0 – 100 °C:

$$UO_2ox \cdot 3H_2O(cr) \rightleftharpoons UO_2ox(aq) + 3\ H_2O$$

$$\log_{10}K_s^\circ\ (298.15\ K) = -(1.8 \pm 0.27)$$

$$\Delta_r H_m^\circ(298.15\ K) = 20.2 \pm 3.5\ kJ \cdot mol^{-1}$$

$$\Delta_r C_{p,m}^\circ(298.15\ K) = 0\ J \cdot K^{-1} \cdot mol^{-1}$$

These values have been included in TDB 2020.

For the tetravalent actinides U(IV), Np(IV) and Pu(IV), thermodynamic data are reported for solids of the type $An(ox)_2 \cdot 6H_2O(cr)$ but no data were selected in the NEA review (Hummel et al. 2005a). However, the available data can be used for scoping calculations and as guidelines for data estimation procedures. Note that the experimental solubility constants cover the temperature range 25 – 90 °C.

$$U(ox)_2 \cdot 6H_2O(cr) \rightleftharpoons U(ox)_2(aq) + 6\ H_2O$$

$$\log_{10}K_s^\circ\ (298.15\ K) = -(4.82 \pm 0.20)$$

$$\Delta_r H_m^\circ(298.15\ K) = 10.4 \pm 1.0\ kJ \cdot mol^{-1}$$

$$\Delta_r C_{p,m}^\circ(298.15\ K) = 513 \pm 41\ J \cdot K^{-1} \cdot mol^{-1}$$

$$Np(ox)_2 \cdot 6H_2O(cr) + 4H^+ \rightleftharpoons Np^{4+} + 2\ H_2ox(aq) + 6\ H_2O$$

$$\log_{10}K_s^\circ\ (298.15\ K) = -(12.7 \pm 1.0)$$

$$Pu(ox)_2 \cdot 6H_2O(cr) \rightleftharpoons Pu(ox)_2(aq) + 6\ H_2O$$

$$log_{10}K_s°(298.15\ K) = -(4.6 \pm 0.2)$$

These values have been included in TDB 2020 as supplemental data.

Note that the values for $U(ox)_2 \cdot 6H_2O(cr)$ are taken directly from Hummel et al. (2005a), while the $log_{10}K_s°$ for $Np(ox)_2 \cdot 6H_2O(cr)$ is the average of two values given by Hummel et al. (2005a) in their Tab. VI-46, and the $log_{10}K_s°$ for $Pu(ox)_2 \cdot 6H_2O(cr)$ is taken from Tab. VI-55 of Hummel et al. (2005a) with an uncertainty assigned by this review.

For Pu(III) – oxalate, $Pu_2(ox)_3 \cdot 10H_2O(cr)$, no data were selected in the NEA review (Hummel et al. 2005a). However, the available data can be used for scoping calculations and as guidelines for data estimation procedures:

$$Pu_2(ox)_3 \cdot 10H_2O(cr) + 6\ H^+ \rightleftharpoons 2\ Pu^{3+} + 3\ H_2ox(aq) + 10\ H_2O$$

$$log_{10}K_s°(298.15\ K) \approx -7.5$$

This value has been included in TDB 2020 as supplemental datum.

By contrast, the data for $Am_2(ox)_3 \cdot nH_2O$ are contradicting and inconclusive (Hummel et al. 2005a) and represent the only gap in the database with respect to actinide compounds relevant for environmental modelling.

From the viewpoint of model application in performance assessments the most important solid is calcium oxalate because the possible precipitation of this solid in many ground and surface waters can limit the concentration of dissolved oxalate to rather low levels.

18.4.2 Actinide aqueous complexes with organic ligands

18.4.2.1 Trivalent actinides

In aqueous media, americium exists as the trivalent ion except under strongly oxidising conditions, where the penta- and hexavalent *trans*-dioxo americyl cations, AmO_2^+ and AmO_2^{2+}, are formed (Silva et al. 1995). Thus, a sufficient number of experimental studies could be reviewed and thermodynamic data could be selected (Hummel et al. 2005a) for Am(III) oxalate, citrate and edta complexes (Tab. 18-2).

A consistent picture emerges concerning the simple complexes. Whereas in the case of oxalate data have been selected for $Am(ox)^+$, $Am(ox)_2^-$ and $Am(ox)_3^{3-}$, citrate may form Am(cit)(aq) and $Am(cit)_2^{2-}$ complexes, but edta forms only $Am(edta)^-$, reflecting the increasing size and denticity of the ligands from bidentate (oxalate) to tridentate (citrate) to hexadentate (edta). Additional ligands may coordinate with Am(III) but the interactions are expected to be weak for steric reasons. Hummel et al. (2005a) finally selected

$Am^{3+} + ox^{2-} \rightleftharpoons Am(ox)^{+}$

$\log_{10}\beta_1°$ (298.15 K) = 6.51 ± 0.15

$Am^{3+} + 2\ ox^{2-} \rightleftharpoons Am(ox)_2^{-}$

$\log_{10}\beta_2°$ (298.15 K) = 10.71 ± 0.20

$Am^{3+} + 3\ ox^{2-} \rightleftharpoons Am(ox)_3^{3-}$

$\log_{10}\beta_3°$ (298.15 K) = 13.0 ± 1.0

$Am^{3+} + cit^{3-} \rightleftharpoons Am(cit)(aq)$

$\log_{10}\beta_1°$ (298.15 K) = 8.55 ± 0.20

$Am^{3+} + 2\ cit^{3-} \rightleftharpoons Am(cit)_2^{3-}$

$\log_{10}\beta_2°$ (298.15 K) = 13.9 ± 1.0

$Am^{3+} + edta^{4-} \rightleftharpoons Am(edta)^{-}$

$\log_{10}\beta_1°$ (298.15 K) = 19.67 ± 0.11

$\Delta_r H_m°$(298.15 K) = -(10.6 ± 2.0) kJ · mol^{-1}

$\varepsilon(Am(ox)^{+}, Cl^{-}) = \varepsilon(Am(ox)^{+}, ClO_4^{-})$ = (0.08 ± 0.05) kg · mol^{-1}

$\varepsilon(Na^{+}, Am(ox)_2^{-})$ = -(0.21 ± 0.08) kg · mol^{-1}

$\varepsilon(Na^{+}, Am(ox)_3^{3-})$ = -(0.23 ± 0.10) kg · mol^{-1}

ε(Am(cit)(aq), NaCl) = (0.00 ± 0.05) kg · mol^{-1}

$\varepsilon(Na^{+}, Am(edta)^{-})$ = (0.01 ± 0.16) kg · mol^{-1}

These values have been included in TDB 2020, together with the estimate

$\varepsilon(Na^{+}, Am(cit)_2^{3-})$ = -(0.15 ± 0.10) kg · mol^{-1}

The data also reveal a consistent pattern for protonated complexes. The complexes Am(Hedta)(aq), $Am(Hcit)^{+}$ and $Am(Hcit)_2^{-}$ are important species in acidic solutions. Although complexes with Hox^{-} may be possible, their stabilities are expected to be much smaller than those with ox^{2-}. The few experimental data concerning protonated Am(III) oxalate complexes have been considered inconclusive in the organics review. Hummel et al. (2005a) selected

$Am^{3+} + Hcit^{2-} \rightleftharpoons Am(Hcit)^{+}$

$\log_{10}\beta_1°$ (298.15 K) = 6.5 ± 1.0

$Am^{3+} + 2\ Hcit^{2-} \rightleftharpoons Am(Hcit)_2^-$

$\log_{10}\beta_2° (298.15\ K) = 10.8 \pm 1.0$

$Am(edta)^- + H^+ \rightleftharpoons Am(Hedta)(aq)$

$\log_{10}K° (298.15\ K) = 2.17 \pm 0.25$

These values have been included in TDB 2020, together with the estimates

$\varepsilon(Am(Hcit)^+, Cl^-) \approx \varepsilon(Am(Hcit)^+, ClO_4^-) = (0.2 \pm 0.1)\ kg \cdot mol^{-1}$

$\varepsilon(Na^+, Am(Hcit)_2^-) = -(0.05 \pm 0.10)\ kg \cdot mol^{-1}$

$\varepsilon(Am(Hedta)(aq), NaCl) \approx \varepsilon(Am(Hedta)(aq), NaClO_4) = (0.0 \pm 0.1)\ kg \cdot mol^{-1}$

The selected values for Am(III) oxalate, citrate and edta complexes describe well the respective speciation in acidic and neutral to slightly alkaline solutions. However, in alkaline solutions mixed hydroxo complexes may also form.

In the case of edta, a single study proposed the complex $Am(edta)(OH)^{2-}$. Although the data interpretation and the derived constant are not unreasonable, Hummel et al. (2005a) did not select a value based on a single study of uncertain accuracy.

This review used the value $\log_{10}K$ (0.1 M KNO_3, 298.15 K) = 19.98 ± 0.07 listed in Tab. VII-40 of Hummel et al. (2005a) for the reaction $Am^{3+} + edta^{4-} + OH^- \rightleftharpoons Am(edta)OH^{2-}$, increased its uncertainty to ±0.14 (2σ), combined this value with $\log_{10}K$ (0.1 M KNO_3, 298.15 K) = 17.08 ± 0.13 for the reaction $Am^{3+} + edta^{4-} \rightleftharpoons Am(edta)^-$, calculated from the selected $\log_{10}K°$ value and extrapolated the result, $\log_{10}K$ (0.1 M KNO_3, 298.15 K) = 2.90 ± 0.19 to zero ionic strength

$Am(edta)^- + OH^- \rightleftharpoons Am(edta)OH^{2-}$

$\log_{10}K° (298.15\ K) = 2.66 \pm 0.19$

This value is included in TDB 2020 as supplemental datum, together with the estimate

$\varepsilon(Na^+, Am(edta)OH^{2-}) = -(0.10 \pm 0.10)\ kg \cdot mol^{-1}$

For citrate mixed hydroxo complexes have also been proposed, but the data were considered as unreliable by the organics review. No information about mixed hydroxo complexes with oxalate could be found in the literature. However, one may infer from the analogous Am(III) – carbonate system, where no evidence for the formation of ternary hydroxide – carbonate complexes was found (Guillaumont et al. 2003), that they are always minor species if they form at all.

For isa the complex $Am(isa_{-3H})^-$ has been proposed to form in alkaline solutions. The subscript -3H indicates the assumption that three protons dissociated from the alcoholic OH groups of isa^- to form the Am(III) – isa complex in alkaline solutions. This stoichiometry is ambiguous, and the available experimental data may be more appropriately represented by the following reaction:

$$Am(OH)_3(aq) + isa^- \Leftrightarrow Am(OH)_{3-x}(isa_{-x\mathrm{H}})^- + x\ H_2O(l)$$

No value has been selected for these complexes by Hummel et al. (2005a). Nevertheless, the reported stability constant is of value by providing "first estimates" of Am(III) isa complexation in alkaline solutions in the absence of more reliable data. Hence, this review decided to include the value

$$Am^{3+} + isa^- \rightleftharpoons Am(isa_{-3H})^- + 3\ H^+$$

$$log_{10}K°(298.15\ K) = 22.2 \pm 1.0$$

in TDB 2020 as supplemental datum, together with the estimate

$$\varepsilon(Na^+, Am(isa_{-3H})^-) = -(0.05 \pm 0.10)\ kg \cdot mol^{-1}$$

In the case of Pu(III) only equilibrium constants for the edta complexes $Pu(edta)^-$ and Pu(Hedta)(aq) could be selected (Peretrukhin et al. 1970):

$$Pu^{3+} + edta^{4-} \rightleftharpoons Pu(edta)^-$$

$$\log_{10}\beta_1° (298.15\ K) = 20.18 \pm 0.37$$

$$\Delta_r H_m°(298.15\ K) = -(8.7 \pm 1.2)\ kJ \cdot mol^{-1}$$

$$Pu(edta)^- + H^+ \rightleftharpoons Pu(Hedta)(aq)$$

$$\log_{10}K° (298.15\ K) = 1.84 \pm 0.26$$

These values have been included in TDB 2020, together with the estimates

$$\varepsilon(Na^+, Pu(edta)^-) \approx \varepsilon(Na^+, Am(edta)^-) = (0.01 \pm 0.16)\ kg \cdot mol^{-1}$$

$$\varepsilon(Pu(Hedta)(aq), NaCl) = \varepsilon(Pu(Hedta)(aq), NaClO_4) = (0.0 \pm 0.1)\ kg \cdot mol^{-1}$$

These values are consistent with the corresponding Am(III) – edta complexes. No data for the Pu(III) – edta system in alkaline solutions could be identified.

The data published in only one paper for the Pu(III) – citrate system are not considered reliable enough by Hummel et al. (2005a) to derive selected values. However, the values reported for Pu(cit)(aq) and $Pu(Hcit)^+$ may be used as guidelines for scoping calculations and data estimation procedures.

This review used the values $\log_{10}\beta_1$ (0.1 M KCl, 294.15 K) = 6.71 ± 0.25 and $\log_{10}K$ (0.1 M KCl, 294.15 K) = 4.82 ± 0.27 listed in Tab. VII-28 of Hummel et al. (2005a) for the reactions $Pu^{3+} + cit^{3-} \rightleftharpoons Pu(cit)(aq)$ and $Pu^{3+} + Hcit^{2-} \rightleftharpoons Pu(Hcit)^+$, respectively, and extrapolated them to zero ionic strength

$Pu^{3+} + cit^{3-} \rightleftharpoons Pu(cit)(aq)$

$log_{10}\beta_1^\circ(298.15\ K) \approx 8.7$

$Pu^{3+} + Hcit^{2-} \rightleftharpoons Pu(Hcit)^{+}$

$log_{10}K^\circ(298.15\ K) \approx 6.1$

These values are included in TDB 2020 as supplemental data, together with the estimates

$\varepsilon(Pu(cit)(aq), NaCl) = \varepsilon(Pu(cit)(aq), NaClO_4) = (0.0 \pm 0.1)\ kg \cdot mol^{-1}$

$\varepsilon(Pu(Hcit)^{+}, Cl^{-}) = (0.05 \pm 0.10)\ kg \cdot mol^{-1}$

Several Pu(III) – oxalate complexes have been proposed in the literature. No values could be selected by Hummel et al. (2005a), but approximate values of equilibrium constants for $Pu(ox)^{+}$, $Pu(ox)_2^{-}$ and $Pu(ox)_3^{3-}$ are provided for qualitative modelling:

$Pu^{3+} + ox^{2-} \rightleftharpoons Pu(ox)^{+}$

$log_{10}\beta_1^\circ(298.15\ K) \approx 8.5$

$Pu^{3+} + 2\ ox^{2-} \rightleftharpoons Pu(ox)_2^{-}$

$log_{10}\beta_2^\circ(298.15\ K) \approx 12.7$

$Pu^{3+} + 3\ ox^{2-} \rightleftharpoons Pu(ox)_3^{3-}$

$log_{10}\beta_3^\circ(298.15\ K) \approx 12.1$

These values are included in TDB 2020 as supplemental data, together with the estimates

$\varepsilon(Pu(ox)^{+}, Cl^{-}) = (0.05 \pm 0.10)\ kg \cdot mol^{-1}$

$\varepsilon(Na^{+}, Pu(ox)_2^{-}) = -(0.05 \pm 0.10)\ kg \cdot mol^{-1}$

$\varepsilon(Na^{+}, Pu(ox)_3^{3-}) = -(0.15 \pm 0.10)\ kg \cdot mol^{-1}$

No data for the Pu(III) – isa system could be found. The discussion of the Am(III) – isa and Eu(III) – isa system in the organics review may serve as guideline for qualitative modelling.

Only one experimental study of the Np(III) – edta system could be identified. However, the reported details about the measurements are too poor in order to base a selection on this single study. For environmental modelling studies, the data selected for Pu(III) – edta and Am(III) – edta might be considered as guidelines for data estimation procedures concerning Np(III) – edta complexes.

There is no evidence in the literature on the formation of Np(III) – oxalate complexes in aqueous solutions. However, Np(III) is oxidised by oxalate (Mefod'eva & Gel'man 1971) and hence, the lack of data on unstable complexes is of no consequence for modelling of environmental systems.

No information about the Np(III) – citrate and the Np(III) – isa system could be found in the literature. As it is not clear whether citrate and isa oxidise Np(III), as oxalate does, or may form stable complexes, as edta does, this lack of information may represent a real gap in the database.

No experimentally determined thermodynamic data could be identified in the organics review for U(III) oxalates, citrates, edta and isa. However, U(III) is unstable in aqueous solution and is thermodynamically capable of being oxidised to U(IV) by many anions (Peretrukhin et al. 1970). For example, it was observed (Peretrukhin et al. 1970) that U(III) was almost instantaneously oxidised to U(IV) by ammonium oxalate, while oxalate was reduced to glyoxylic acid (OCHCOOH). Also, when edta is added to a U(III) acetate solution the strongly complexing ligand edta does not stabilise the trivalent state of uranium but accelerates its oxidation which indicates that edta plays the role of an oxidising agent with respect to U(III) (Peretrukhin et al. 1970). Hence, the lack of thermodynamic data for unstable U(III) complexes with organic ligands does not represent a gap in the database.

18.4.2.2 Tetravalent actinides

The tetravalent oxidation state of actinides is difficult to explore with respect to aqueous complexation. The very strong hydrolysis of U(IV), Np(IV) and Pu(IV) and the tendency of colloid formation in An(IV) aqueous solutions pose serious obstacles for experimental investigations.

Although colloid formation can be of importance in the environmental behaviour of An(IV) aqueous solutions, a general discussion of the colloidal properties of tetravalent actinides solutions was outside the scope of the NEA organics review. Colloid formation has been considered in the review of experimental data only with respect to its influence on the quality of thermodynamic data.

A few binary aqueous U(IV), Np(IV) and Pu(IV) oxalate complexes are reported in the literature (Tab. 18-2). Their stability constants are usually determined in conjunction with solubility measurements for solid An(IV) oxalates, which are associated with various shortcomings as discussed in detail by Hummel et al. (2005a). Hence, in spite of the qualitative self-consistency and the apparent reasonableness of the reported stability constants, no thermodynamic data for the complexes shown in Tab. 18-2 are recommended by Hummel et al. (2005a). Nevertheless, the data may serve as qualitative guidelines in modelling exercises.

$$U^{4+} + ox^{2-} \rightleftharpoons Uox^{2+}$$

$$\log_{10}K^\circ(298.15\ K) \approx 11$$

$$Uox^{2+} + ox^{2-} \rightleftharpoons U(ox)_2(aq)$$

$$\log_{10}K^\circ(298.15\ K) \approx 8$$

$$U(ox)_2(aq) + ox^{2-} \rightleftharpoons U(ox)_3^{2-}$$

$$\log_{10}K^\circ(298.15\ K) \approx 5$$

$$U(ox)_3^{2-} + ox^{2-} \rightleftharpoons U(ox)_4^{4-}$$

$$\log_{10}K^\circ(298.15\ K) \approx 3$$

$Np^{4+} + H_2ox(aq) \rightleftharpoons Np(ox)^{2+} + 2\ H^+$

$log_{10}{}^*\beta_1^\circ\ (298.15\ K) \approx 6.5$

$Np^{4+} + 2\ H_2ox(aq) \rightleftharpoons Np(ox)_2(aq) + 4\ H^+$

$log_{10}{}^*\beta_2^\circ\ (298.15\ K) \approx 7.5$

$Np^{4+} + 3\ H_2ox(aq) \rightleftharpoons Np(ox)_3^{2-} + 6\ H^+$

$log_{10}{}^*\beta_3^\circ\ (298.15\ K) \approx 8$

$Pu^{4+} + H_2ox(aq) \rightleftharpoons Pu(ox)^{2+} + 2\ H^+$

$log_{10}{}^*\beta_1^\circ\ (298.15\ K) \approx 7.3$

$Pu(ox)^{2+} + H_2ox(aq) \rightleftharpoons Pu(ox)_2(aq) + 2\ H^+$

$log_{10}{}^*K^\circ\ (298.15\ K) \approx 3.3$

$Pu(ox)_2(aq) + H_2ox(aq) \rightleftharpoons Pu(ox)_3^{2-} + 2\ H^+$

$log_{10}{}^*K^\circ\ (298.15\ K) \approx 0.3$

These values are included in TDB 2020 as supplemental data, together with the estimates

$\varepsilon(Pu(ox)^{2+}, Cl^-) = \varepsilon(Np(ox)^{2+}, Cl^-) = \varepsilon(Uox^{2+}, Cl^-) \approx \varepsilon(Uox^{2+}, ClO_4^-) = (0.4 \pm 0.1)\ kg \cdot mol^{-1}$

$\varepsilon(Pu(ox)_2(aq), NaCl) = \varepsilon(Np(ox)_2(aq), NaCl) = \varepsilon(U(ox)_2(aq), NaCl) = (0.0 \pm 0.1)\ kg \cdot mol^{-1}$

$\varepsilon(Pu(ox)_2(aq), NaClO_4) = \varepsilon(Np(ox)_2(aq), NaClO_4) = \varepsilon(U(ox)_2(aq), NaClO_4) = (0.0 \pm 0.1)\ kg \cdot mol^{-1}$

$\varepsilon(Na^+, Pu(ox)_3^{2-}) = \varepsilon(Na^+, Np(ox)_3^{2-}) = \varepsilon(Na^+, U(ox)_3^{2-}) = -(0.10 \pm 0.10)\ kg \cdot mol^{-1}$

$\varepsilon(Na^+, U(ox)_4^{4-}) = -(0.20 \pm 0.10)\ kg \cdot mol^{-1}$

The mentioned solubility measurements of An(IV) oxalates have been carried out in acidic solutions in order to minimise problems with the very strong hydrolysis. A ternary complex, $U(ox)_2(OH)_2^{2-}$, was assumed to form when $U(ox)_2 \cdot 6H_2O(cr)$ was dissolved in solutions of ammonium bicarbonate, but no stability constant was determined (Hummel et al. 2005a). Generally, the behaviour of U(IV), Np(IV) and Pu(IV) oxalates in neutral and alkaline solutions is unexplored and the missing stability constants for ternary An(IV) – ox – OH complexes represent serious gaps in the database.

The situation is even worse in the case of U(IV), Np(IV) and Pu(IV) citrates. Either no data at all could be identified, as in the case of Np(IV) citrates, or the few published data for the U(IV) and Pu(IV) citrate systems are ambiguous with respect to the stoichiometry and stability of the formed complexes. Although the limited information for An(IV) citrates suggests very strong complex formation, the ambiguous data cannot be used for scoping calculations (Hummel et al. 2005a).

In the system U(IV) – edta thermodynamic data for the complex Uedta(aq) could be selected by Hummel et al. (2005a):

$U^{4+} + edta^{4-} \rightleftharpoons Uedta(aq)$

$\log_{10}\beta_1^\circ$ (298.15 K) = 29.5 ± 0.2

$\varepsilon(Uedta(aq), NaCl) \approx \varepsilon(Uedta(aq), NaClO_4) = -(0.19 \pm 0.19)$ kg · mol^{-1}

These values are included in TDB 2020.

The hydrolysis of Uedta(aq) occurs already in acidic medium at pH > 3 with formation of $UedtaOH^-$ and of the dimeric species $(UedtaOH)_2^{2-}$. In addition, the formation of $Uedta(OH)_2^{2-}$ has been reported at pH > 7. Although no values could be selected by Hummel et al. (2005a) for U(IV) edta hydrolysis species, the data given in their Tab. VIII-30 may serve as qualitative guidelines in modelling exercises:

$Uedta(aq) + OH^- \rightleftharpoons UedtaOH^-$

$\log_{10}K^\circ (298.15\ K) \approx 9.1$

$2\ UedtaOH^- \rightleftharpoons (UedtaOH)_2^{2-}$

$\log_{10}K^\circ (298.15\ K) \approx 2.7$

$UedtaOH^- + OH^- \rightleftharpoons Uedta(OH)_2^{2-}$

$\log_{10}K^\circ (298.15\ K) \approx 5.9$

These values are included in TDB 2020 as supplemental data, together with the estimates

$\varepsilon(Na^+, UedtaOH^-) = -(0.05 \pm 0.10)$ kg · mol^{-1}

$\varepsilon(Na^+, (UedtaOH)_2^{2-}) = -(0.10 \pm 0.10)$ kg · mol^{-1}

$\varepsilon(Na^+, Uedta(OH)_2^{2-}) = -(0.10 \pm 0.10)$ kg · mol^{-1}

Furthermore, thermodynamic data for the complex Np(edta)(aq) could be selected by Hummel et al. (2005a) which is consistent with the Uedta(aq) data:

$Np^{4+} + edta^{4-} \rightleftharpoons Np(edta)(aq)$

$\log_{10}\beta_1^\circ$ (298.15 K) = 31.2 ± 0.6

$\varepsilon(Np(edta)(aq), NaCl) \approx \varepsilon(Np(edta)(aq), NaClO_4) \approx \varepsilon(Uedta(aq), NaClO_4) =$
$-(0.19 \pm 0.19)$ kg · mol^{-1}

These values are included in TDB 2020.

The Np(IV) – edta – OH system has not been explored experimentally, but data for the analogous U(IV) – edta – OH mixed complexes can be used as qualitative guidelines.

In the case of Pu(IV) – edta a paper of Boukhalfa et al. (2004) became available to Hummel et al. (2005a) only in the final stage of preparation of their review. Hummel et al. (2005a) state in a footnote that the reported species and their stability constants are consistent with the U(IV) and Np(IV) – edta data and the experimental procedures seem to be reliable, but the results need to be re-evaluated using NEA auxiliary constants and the SIT approach before an eventual data selection can be made.

This review took the value $\log_{10}\beta_1$ (1.0 M $NaClO_4$, 298.15 K) = 26.44 ± 0.20 given by Boukhalfa et al. (2004) for the reaction Pu^{4+} + $edta^{4-}$ ⇌ Pu(edta)(aq), assigned an uncertainty of ± 1.0 to this value to account for possible changes in a future re-evaluation, and extrapolated this value to zero ionic strength using ε(Pu^{4+}, ClO_4^-) = (0.82 ± 0.04) kg · mol^{-1}, ε(Na^+, $edta^{4-}$) = (0.32 ± 0.14) kg · mol^{-1} and ε(Pu(edta)(aq), $NaClO_4$) ≈ ε(Uedta(aq), $NaClO_4$) = -(0.19 ± 0.19) kg · mol^{-1}:

$$Pu^{4+} + edta^{4-} \rightleftharpoons Pu(edta)(aq)$$

$$\log_{10}\beta_1^\circ (298.15\ K) = 31.6 \pm 1.0$$

This value is included in TDB 2020 as supplemental datum.

Boukhalfa et al. (2004) report $\log_{10}K$ (0.1 M KNO_3, 298.15 K) = -4.49 and -6.66 for the reactions Pu(edta)(aq) + H_2O(l) ⇌ Pu(edta)OH^- + H^+ and Pu(edta)OH^- + H_2O(l) ⇌ Pu(edta)$(OH)_2^{2-}$ + H^+, respectively. Combining these values with $\log_{10}K$ (0.1 M KNO_3, 298.15 K) = 13.79 for H^+ + OH^- ⇌ H_2O(l) and extrapolating the results to zero ionic strength this review obtained

$$Pu(edta)(aq) + OH^- \rightleftharpoons Pu(edta)OH^-$$

$$\log_{10}K^\circ (298.15\ K) \approx 9.3$$

$$Pu(edta)OH^- + OH^- \rightleftharpoons Pu(edta)(OH)_2^{2-}$$

$$\log_{10}K^\circ (298.15\ K) \approx 6.9$$

These values are included in TDB 2020 as supplemental data, together with the estimates

$$\varepsilon(Na^+, Pu(edta)OH^-) = -(0.05 \pm 0.10)\ kg \cdot mol^{-1}$$

$$\varepsilon(Na^+, Pu(edta)(OH)_2^{2-}) = -(0.10 \pm 0.10)\ kg \cdot mol^{-1}$$

For the U(IV), Np(IV) and Pu(IV) – isa systems the few reported studies qualitatively agree that isa forms very strong complexes with these tetravalent actinides in alkaline solutions. However, the proposed number and stoichiometry of formed complexes widely disagree (Tab. 18-2). The most detailed study has been published for the Np(IV) – isa system, but due to the uncertainties in oxidation state analysis, the scarcity of data and the uncertainty in defining the reaction stoichiometries, no thermodynamic values have been selected by Hummel et al. (2005a). However, the results give an indication of the order of magnitude of Np(IV) – isa complexation and the reported values may be used for scoping calculations. They may also serve as guidelines for estimating U(IV) and Pu(IV) – isa complexation effects:

$Np^{4+} + 3\ OH^- + isa^- \rightleftharpoons Np(OH)_3(isa)(aq)$

$log_{10}K°(298.15\ K) \approx 43.5$

$Np(OH)_3(isa)(aq) + isa^- \rightleftharpoons Np(OH)_3(isa)_2^-$

$log_{10}K°(298.15\ K) \approx 2.1$

$Np^{4+} + 4\ OH^- + isa^- \rightleftharpoons Np(OH)_4(isa)^-$

$log_{10}K°(298.15\ K) \approx 50.1$

$Np(OH)_4(isa)^- + isa^- \rightleftharpoons Np(OH)_4(isa)_2^{2-}$

$log_{10}K°(298.15\ K) \approx 1.9$

These values are included in TDB 2020 as supplemental data, together with the estimates

$\varepsilon(Np(OH)_3(isa)(aq), NaCl) = \varepsilon(Np(OH)_3(isa)(aq), NaClO_4) = (0.0 \pm 0.1)\ kg \cdot mol^{-1}$

$\varepsilon(Na^+, Np(OH)_3(isa)_2^-) = -(0.05 \pm 0.10)\ kg \cdot mol^{-1}$

$\varepsilon(Na^+, Np(OH)_4(isa)^-) = -(0.05 \pm 0.10)\ kg \cdot mol^{-1}$

$\varepsilon(Na^+, Np(OH)_4(isa)_2^{2-}) = -(0.10 \pm 0.10)\ kg \cdot mol^{-1}$

Tetravalent americium is unstable in non-complexing solutions and is reduced spontaneously to its more stable III oxidation state (Runde & Schulz 2006). Am(IV) complexes can be obtained in the presence of high concentrations of strongly complexing agents such as carbonate (Silva et al. 1995). A thermodynamic constant was selected for the complex $Am^{IV}(CO_3)_5^{6-}$ by the NEA americium review (Silva et al. 1995) based on experimental data of Bourges et al. (1983). In the latter study, Am(IV) was prepared electrochemically by anodic oxidation in sodium bicarbonate-carbonate medium 1.2 M < $[HCO_3^- + CO_3^{2-}]$ < 2.3 M in the pH range from 9.5 – 10. The Am(IV) solutions were "stable for ~ 12 h in the best conditions" (Bourges et al. 1983). No study about the interaction of Am(IV) with oxalate, citrate, edta or isa could be found in the literature, except that Am(IV) is mentioned as reaction intermediate in the reduction of Am(VI) by oxalic acid (Shilov (1985), see Section 18.4.2.4). However, this lack of experimental data probably is of no importance for environmental modelling studies, as we might infer from the Am(IV) – carbonate system that Am(IV) in the presence of oxalate, citrate, edta or isa will be slowly reduced to Am(III).

18.4.2.3 Pentavalent actinides

Hummel et al. (2005a) report that oxalate complexes of U(V) were identified only as reaction intermediates in the reduction of U(VI). No experimental stability constants of aqueous U(V) oxalate complexes were identified in the literature. No information about U(V) citrate, edta or isa complexes could be found. There is no indication that U(V) could be stabilised by complexing ligands, and hence, the lack of thermodynamic data for unstable U(V) complexes with organic ligands does not represent a gap in the database.

Np(V) is the most common redox state of neptunium, reflected by a large body of experimental studies, which allowed Hummel et al. (2005a) to select thermodynamic constants for Np(V) oxalate, citrate and edta complexes.

In the Np(V) – oxalate system values for the complexes NpO_2ox^- and $NpO_2(ox)_2^{3-}$ have been selected:

$NpO_2^+ + ox^{2-} \rightleftharpoons NpO_2ox^-$

$\log_{10}\beta_1° (298.15\ K) = 3.9 \pm 0.1$

$NpO_2^+ + 2\ ox^{2-} \rightleftharpoons NpO_2(ox)_2^{3-}$

$\log_{10}\beta_1° (298.15\ K) = 5.8 \pm 0.2$

$\varepsilon(Na^+, NpO_2ox^-) = -(0.4 \pm 0.1)\ kg \cdot mol^{-1}$

$\varepsilon(Na^+, NpO_2(ox)_2^{3-}) = -(0.3 \pm 0.2)\ kg \cdot mol^{-1}$

These values are included in TDB 2020.

There is no evidence for the formation of higher complexes. A postulated protonated complex, $NpO_2Hox(aq)$, has been rejected by Hummel et al. (2005a) after re-analysis of a comprehensive experimental data set. On the other hand, although there were clear indications for the formation of mixed Np(V) – OH^- – ox^{2-} complexes at pH > 9, the sparse experimental data in the alkaline region do not allow to resolve ambiguities with respect to their stoichiometry.

A literature search by the organic review on the thermodynamics of neptunium – citrate systems revealed only information concerning the aqueous complexes of Np(V). Because of the small formal charge of Np(V) and the steric hindrance due to the linear dioxo structure O-Np-O, NpO_2^+ forms only one-to-one complexes with citrate. A value for the complex NpO_2cit^{2-} has been selected:

$NpO_2^+ + cit^{3-} \rightleftharpoons NpO_2cit^{2-}$

$\log_{10}\beta_1° (298.15\ K) = 3.68 \pm 0.05$

$\varepsilon(Na^+, NpO_2cit^{2-}) = -(0.06 \pm 0.03)\ kg \cdot mol^{-1}$

These values are included in TDB 2020.

Although the formation of a weak $NpO_2(Hcit)^-$ complex is probable, the thermodynamic data reported are not reliable enough to be accepted. The formation of $NpO_2(cit)(OH)^{3-}$ at pH > 9 has been claimed, the data are considered inconclusive by Hummel et al. (2005a).

The complexation of Np(V) with edta has been studied extensively, and Hummel et al. (2005a) could select thermodynamic values for NpO_2edta^{3-}, $NpO_2(Hedta)^{2-}$ and $NpO_2(H_2edta)^{-}$:

$NpO_2^+ + edta^{4-} \rightleftharpoons NpO_2edta^{3-}$

$\log_{10}K°$ (298.15 K) = 9.23 ± 0.13

$NpO_2^+ + Hedta^{3-} \rightleftharpoons NpO_2(Hedta)^{2-}$

$\log_{10}K°$ (298.15 K) = 5.82 ± 0.11

$NpO_2^+ + H_2edta^{2-} \rightleftharpoons NpO_2(H_2edta)^{-}$

$\log_{10}K°$ (298.15 K) = 4.47 ± 0.14

$\varepsilon(Na^+, NpO_2edta^{3-}) = (0.20 \pm 0.16)$ kg · mol^{-1}

$\varepsilon(Na^+, NpO_2(Hedta)^{2-}) = (0.07 \pm 0.16)$ kg · mol^{-1}

$\varepsilon(Na^+, NpO_2(H_2edta)^{-}) = -(0.18 \pm 0.16)$ kg · mol^{-1}

These values are included in TDB 2020.

A single value reported for the species $NpO_2edtaOH^{4-}$, $\log_{10}*K$ (0.1 M $NaClO_4$, 298.15 K) = -11.51 ± 0.08, has not yet been confirmed by any other study. Although the reported stability constant does not look unreasonable, indicating the formation of this species at pH > 11, the value is not selected by Hummel et al. (2005a), but it may serve as qualitative guidelines in modelling exercises. Hence this review extrapolated the above value to zero ionic strength:

$NpO_2edta^{3-} + H_2O(l) \rightleftharpoons NpO_2edtaOH^{4-} + H^+$

$\log_{10}*K°(298.15\ K) \approx -12.4$

This value has been included in TDB 2020 as supplemental datum, together with the estimate

$\varepsilon(Na^+, NpO_2edtaOH^{4-}) \approx \varepsilon(Na^+, edta^{4-}) = (0.32 \pm 0.14)$ kg · mol^{-1}

No information has been found for the Np(V) – isa system. As we may infer from the above discussion that Np(V) – isa complexes might be stable with respect to redox effects, and as there is no chemical analogue for this system, the lack of data represents a gap in the database.

Stability constants have been reported for Pu(V) oxalate and edta complexes (see Tab. 18-2). However, Pu(V) disproportionates strongly in oxalate solution (Ermolaev et al. 1967) and forms Pu(IV) and Pu(VI) oxalate complexes. The Pu(VI) oxalate complex was observed to be slowly reduced to a Pu(IV) oxalate complex without the build-up of a Pu(V) oxalate complex (Reed et al. 1998). Furthermore, Pu(VI) is reduced by edta to Pu(V) and finally to Pu(IV) (Reed et al. 1998). Hence, no reliable stability constants are available for Pu(V) oxalate and edta complexes, and no values are selected in the organics review for these systems. No data could be found for

the Pu(V) citrate and isa systems. However, there is no need to estimate values for highly unstable Pu(V) organic complexes, except perhaps for short term laboratory studies involving the kinetics of Pu(V) disproportionation and reduction in the presence of organic ligands.

Am(V) in oxalate and edta solutions slowly changes into the trivalent state. The rate of reduction of 1 mM solution of Am(V) at 25 °C is similar in both cases, i.e. 2 – 3% per hour in 0.05M edta (Nikolaevskii et al. 1974), and about 2% in 0.1 M oxalate (Shilov et al. 1974, Zubarev & Krot 1982). Stability constants were proposed in the literature for the complexes AmO_2ox^-, $AmO_2(ox)_2^{3-}$, and $AmO_2(Hedta)^{2-}$. Qualitatively, AmO_2^+ forms oxalate and edta complexes with similar stabilities as NpO_2^+ complexes, but no values were selected in the organics review because of various shortcomings in the experimental procedures. However, considering the instability of Am(V) in the presence of oxalate and edta, their values may only be of importance in short term laboratory studies. They are of no importance in any long-term environmental modelling study.

No information about Am(V) – citrate and – isa systems could be found, but we may infer that citrate and isa have similar reducing effects on Am(V) as oxalate and edta, as higher oxidation states of americium are generally reduced by organic complexing agents (Runde & Schulz 2006).

18.4.2.4 Hexavalent actinides

The U(VI) – oxalate, citrate and edta systems have been studied extensively, and in all cases Hummel et al. (2005a) could select thermodynamic values for several complexes (Tab. 18-2). In the case of oxalate only data for the mononuclear species $UO_2ox(aq)$, $UO_2(ox)_2^{2-}$ and $UO_2(ox)_3^{4-}$ were selected,

$$UO_2^{2+} + ox^{2-} \rightleftharpoons UO_2ox(aq)$$

$$\log_{10}\beta_1^\circ\ (298.15\ K) = 7.13 \pm 0.16$$

$$\Delta_r H_m^\circ(298.15\ K) = 25.4 \pm 18.4\ kJ \cdot mol^{-1}$$

$$UO_2^{2+} + 2\ ox^{2-} \rightleftharpoons UO_2(ox)_2^{2-}$$

$$\log_{10}\beta_2^\circ\ (298.15\ K) = 11.65 \pm 0.15$$

$$UO_2^{2+} + 3\ ox^{2-} \rightleftharpoons UO_2(ox)_3^{4-}$$

$$\log_{10}\beta_3^\circ\ (298.15\ K) = 13.8 \pm 1.5$$

$$\varepsilon(UO_2ox(aq), NaCl) = \varepsilon(UO_2ox(aq), NaClO_4) = -(0.05 \pm 0.06)\ kg \cdot mol^{-1}$$

$$\varepsilon(Na^+, UO_2(ox)_2^{2-}) = -(0.18 \pm 0.07)\ kg \cdot mol^{-1}$$

$$\varepsilon(Na^+, UO_2(ox)_3^{4-}) = -(0.01 \pm 0.11)\ kg \cdot mol^{-1}$$

These values are included in TDB 2020.

The existence of the protonated U(VI) oxalate complexes that were assumed to have formed in some experiments, $UO_2(Hox)^+$, $UO_2(Hox)_2(aq)$ and $UO_2(H_2ox)^{2+}$, is still open for debate. These species, difficult to identify by physical methods, were usually postulated to improve the fitting of potentiometric or spectrophotometric data. If they form, it is most likely that they occur in

strongly acidic solutions. Taking into consideration of the contradictory information in the literature on the presence of these complexes, stability constants reported in the literature were not accepted by Hummel et al. (2005a).

A few dinuclear U(VI) oxalate complexes were assumed to exist in solutions, i.e. $(UO_2)_2(ox)_3^{2-}$ and $(UO_2)_2(ox)_5^{6-}$. The inclusion of such species in models to interpret experimental data only slightly improved the overall fit, as they remained minor species (< 5%) under the chosen experimental conditions. More studies are needed to confirm the presence of such complexes in solution and to obtain reliable stability constants.

A variety of ternary U(VI) oxalate complexes were assumed to exist in solution. However, thermodynamic data for such complexes are rare. Among the reported ternary complexes, the U(VI) – hydroxide – oxalate complexes are of some importance in predicting the chemical behaviour of U(VI) in pH neutral environments. Using the reported data on the U(VI) – hydroxide – oxalate complexes for scoping calculations Hummel et al. (2005a) show that these ternary species could amount to 20 – 30% of the total U(VI) in the pH regions between 6 and 8. However, the stoichiometry of the formed complexes is ambiguous and further studies are needed to obtain reliable data on this system. None of the complexes is accepted by Hummel et al. (2005a).

In the citrate and edta systems, besides data for the mononuclear complexes UO_2cit^- and UO_2edta^{2-}, also data for dinuclear species, $(UO_2)_2(cit)_2^{2-}$ and $(UO_2)_2$edta(aq), and complexes with protonated ligands, UO_2(Hcit)(aq) and $UO_2(Hedta)^-$, were selected by Hummel et al. (2005a).

$UO_2^{2+} + cit^{3-} \rightleftharpoons UO_2cit^-$

$\log_{10}\beta_1^\circ$ (298.15 K) = 8.96 ± 0.17

$2\ UO_2^{2+} + 2\ cit^{3-} \rightleftharpoons (UO_2cit)_2^{2-}$

$\log_{10}K^\circ$ (298.15 K) = 21.3 ± 0.5

$UO_2^{2+} + Hcit^{2-} \rightleftharpoons UO_2(Hcit)(aq)$

$\log_{10}K^\circ$ (298.15 K) = 5.0 ± 1.0

$UO_2^{2+} + edta^{4-} \rightleftharpoons UO_2edta^{2-}$

$\log_{10}\beta_1^\circ$ (298.15 K) = 13.7 ± 0.2

$2\ UO_2^{2+} + edta^{4-} \rightleftharpoons (UO_2)_2edta(aq)$

$\log_{10}K^\circ$ (298.15 K) = 20.6 ± 0.4

$UO_2^{2+} + Hedta^{3-} \rightleftharpoons UO_2(Hedta)^-$

$\log_{10}K^\circ$ (298.15 K) = 8.37 ± 0.10

$\varepsilon(Na^+, UO_2cit^-) = -(0.11 \pm 0.09)$ kg · mol^{-1}

$\varepsilon(Na^+, UO_2edta^{2-}) = -(0.22 \pm 0.18)$ kg · mol^{-1}

$\varepsilon(UO_2(Hedta)^-) = -(0.18 \pm 0.16)$ kg · mol^{-1}

These values are included in TDB 2020 as supplemental data, together with the estimates

$\varepsilon(Na^+, (UO_2cit)_2^{2-}) = -(0.10 \pm 0.10)$ kg · mol^{-1}

$\varepsilon(UO_2(Hcit)(aq), NaCl) = \varepsilon(UO_2(Hcit)(aq), NaClO_4) = (0.0 \pm 0.1)$ kg · mol^{-1}

$\varepsilon((UO_2)_2edta(aq), NaCl) = \varepsilon((UO_2)_2edta(aq), NaClO_4) = (0.0 \pm 0.1)$ kg · mol^{-1}

A similar situation as in the U(VI) – oxalate system is found in the U(VI) – citrate system: Although the reported observations suggest the formation of U(VI) complexes with $H_{-1}cit^{4-}$ (deprotonation of the alcoholic hydroxyl group of citrate) or of mixed hydroxide – citrate complexes in the pH regions between 6 and 8, the available data are insufficient, and no conclusions can be drawn.

Note that from sterical considerations the complex UO_2edta^{2-} might actually be the ternary complex $UO_2(Hedta)OH^{2-}$, forming above pH 5 from $UO_2(Hedta)^-$ by the dissociation of a proton from a coordinated water molecule.

A variety of polynuclear U(VI) – edta species, including ternary U(VI) – hydroxide – edta complexes, have been suggested in the literature. No values for polymeric U(VI) edta other than $(UO_2)_2edta(aq)$ are selected by Hummel et al. (2005a), but as long as systems are modelled where edta is in excess with respect to uranium, these complexes are not of importance.

A complexation study of isa with U(VI) in acidic solutions at 25.0 °C and I = 1.0 M $NaClO_4$ by potentiometry and calorimetry could be interpreted in terms of the complexes UO_2isa^+, $UO_2(isa)_2(aq)$ and $UO_2(isa)_3^-$. Hummel et al. (2005a) state that although the reported stability constants appear reasonable, more studies are needed to confirm them. The values may be used for scoping calculations, but they only describe the U(VI) – isa system in acidic solutions. In alkaline solutions other complexes of the type $UO_2(OH)_x(isa_{-yH})^{1-x-y}$ may dominate the U(VI) – isa system.

This review extrapolated the values given in Tab. IX-7 of Hummel et al. (2005a) to zero ionic strength using $\varepsilon(UO_2^{2+}, ClO_4^-) = (0.46 \pm 0.03)$ kg · mol^{-1} (Lemire et al. 2013) and the estimates $\varepsilon(Na^+, isa^-) = -(0.05 \pm 0.10)$ kg · mol^{-1}, $\varepsilon(UO_2isa^+, ClO_4^-) = (0.2 \pm 0.1)$ kg · mol^{-1}, $\varepsilon(UO_2(isa)_2(aq), NaClO_4) = (0.0 \pm 0.1)$ kg · mol^{-1}, and $(Na^+, UO_2(isa)_3^-) = -(0.05 \pm 0.10)$ kg · mol^{-1}:

$UO_2^{2+} + isa^- \rightleftharpoons UO_2isa^+$

$log_{10}\beta_1° \ (298.15\ K) = 3.5 \pm 0.2$

$\Delta_r H_m \ (298.15\ K) = -(1.0 \pm 1.0)\ kJ \cdot mol^{-1}$

$UO_2^{2+} + 2\ isa^- \rightleftharpoons UO_2(isa)_2(aq)$

$log_{10}\beta_2° \ (298.15\ K) = 6.2 \pm 0.2$

$\Delta_r H_m \ (298.15\ K) = (1.4 \pm 1.8)\ kJ \cdot mol^{-1}$

$UO_2^{2+} + 3\ isa^- \rightleftharpoons UO_2(isa)_3^-$

$log_{10}\beta_3^\circ\ (298.15\ K) = 8.0 \pm 0.2$

$\Delta_r H_m\ (298.15\ K) = -(6.2 \pm 3.0)\ kJ \cdot mol^{-1}$

These values are included in TDB 2020 as supplemental data.

Note that this review made no attempt to extrapolate the enthalpy values given for 1.0 M $NaClO_4$ to zero ionic strength.

The reduction of Np(VI) and Pu(VI) by oxalate, citrate and edta has been investigated in low ionic strength media and brines (Reed et al. 1998). At low ionic strength Np(VI) was rapidly reduced to form Np(V) organic complexes, whereas Pu(VI) was predominantly reduced to Pu(IV). The presence of organic complexants also led to the rapid reduction of Np(VI) and Pu(VI) in brines, except in cases where carbonate and hydrolytic complexes predominated.

Hence, it is no surprise that no thermodynamic data have been found by Hummel et al. (2005a) for Np(VI) citrate, edta and isa complexes, and solely approximate values for Np(VI) oxalate complex formation are reported. However, these values are only of qualitative significance for laboratory studies. For any application modelling the long-term behaviour of neptunium, e.g., for nuclear waste disposal, the unstable Np(VI) oxalate complexes and the lack of experimental data for the Np(VI) citrate, edta and isa systems are of no importance, and there is no need to estimate values for highly unstable Np(VI) organic complexes.

Pu(VI) complexes with oxalate, citrate and edta have been proposed in the literature (see Tab. 18-2). However, none of these proposals have been considered reliable and no thermodynamic values are selected by Hummel et al. (2005a). Considering the instability of Pu(VI) organic solutions, this non-selection has no consequences for environmental modelling studies.

Powerful oxidants oxidise Am(III) and Am(V) to Am(VI), which forms the linear *trans*-dioxo americyl cation AmO_2^{2+} (Runde & Schulz 2006). In solutions with excess oxalic acid, Am(VI) was found to be rapidly reduced by oxalate to Am(IV), which disproportionates into Am(III) and Am(V) (Shilov 1985). Also, the simultaneous formation of Am(V) and Am(III) was observed in solutions of edta, citrate and tartrate, although not all the reactions proceeded rapidly, and the yield of Am(III) depended on the pH (Shilov 1985). No information is available for Am(VI) – isa interaction, but we may infer that isa has the same reducing effect on Am(VI) as citrate and tartrate. No thermodynamic data are available for these highly unstable Am(VI) complexes.

Tab. 18-4: Organic data selected by NEA (Hummel et al. 2005a) but not included in TDB 2020

For explanations see text.

Gases	-
Solids	α-H_2ox, β-H_2ox, $H_2ox \cdot 2H_2O$(cr), H_3cit(cr), $H_3cit \cdot H_2O$(cr)
Aqueous species	-

18.5 Selected organic data

Tab. 18.5-1: Selected organic data (ligands, H, Na, K)

Name	TDB 05/92	TDB 2020				Species
	$\Delta_f G_m°$ [kJ · mol^{-1}]	$\Delta_f G_m°$ [kJ · mol^{-1}]	$\Delta_f H_m°$ [kJ · mol^{-1}]	$S_m°$ [J · K^{-1} · mol^{-1}]	$C_{p,m}°$ [J · K^{-1} · mol^{-1}]	
ox-2	0.0 [a]	-680.134 ± 1.830	-830.660 ± 1.592	47.597 ± 3.020		ox^{2-}
cit-3	0.0 [a]	-1'162.258 ± 2.014	-1'519.920 ± 2.070	75.587 ± 1.855		cit^{3-}
edta-4	0.0 [a]	0.0 [a]	-1'704.800 ± 3.751			$edta^{4-}$
H3isa- [2)]	-	0.0 [a]				H_3isa^{-} [2)]

Name	TDB 05/92	TDB 2020				Reaction
	$\log_{10}\beta°$	$\log_{10}\beta°$	$\Delta_r H_m°$ [kJ · mol^{-1}]	$\Delta_r C_{p,m}°$ [J · K^{-1} · mol^{-1}]	T-range [°C]	
Hox-	4.266	4.25 ± 0.01	7.3 ± 0.1			$ox^{2-} + H^+ \rightleftharpoons Hox^-$
H2ox(aq)	1.252	1.40 ± 0.03	3.3 ± 0.5			$Hox^- + H^+ \rightleftharpoons H_2ox(aq)$
Hcit-2	6.396	6.36 ± 0.02	3.3 ± 0.3	222 ± 14	5 – 120	$cit^{3-} + H^+ \rightleftharpoons Hcit^{2-}$
H2cit-	4.761	4.78 ± 0.01	-2.4 ± 0.3	167 ± 8	5 – 120	$Hcit^{2-} + H^+ \rightleftharpoons H_2cit^-$
H3cit(aq)	3.128	3.13 ± 0.01	-4.5 ± 0.3	116 ± 6	5 – 120	$H_2cit^- + H^+ \rightleftharpoons H_3cit(aq)$
Hedta-3	11.014	11.24 ± 0.03	-19.8 ± 0.5			$edta^{4-} + H^+ \rightleftharpoons Hedta^{3-}$
H2edta-2	6.320	6.80 ± 0.02	-15.2 ± 0.4			$Hedta^{3-} + H^+ \rightleftharpoons H_2edta^{2-}$
H3edta-	3.106	3.15 ± 0.02	7.1 ± 0.4			$H_2edta^{2-} + H^+ \rightleftharpoons H_3edta^-$
H4edta(aq)	2.16	2.23 ± 0.05	1.9 ± 1.5			$H_3edta^- + H^+ \rightleftharpoons H_4edta(aq)$
H5edta+	1.5	1.3 ± 0.1				$H_4edta(aq) + H^+ \rightleftharpoons H_5edta^+$
H6edta+2	-0.2	-0.5 ± 0.2				$H_5edta^+ + H^+ \rightleftharpoons H_6edta^{2+}$
H4isa(aq) [*,b]	-	4.0 ± 0.5				$H_3isa^- + H^+ \rightleftharpoons H_4isa(aq)$ [*,a]
Na(ox)-	1.0	-				$Na+ + ox^{2-} \rightleftharpoons Na(ox)^-$
Na(cit)-2	1.34	-				$Na+ + cit^{3-} \rightleftharpoons Na(cit)^{2-}$
Na(edta)-3	2.7	2.8 ± 0.2	-4 ± 3			$Na+ + edta^{4-} \rightleftharpoons Na(edta)^{3-}$
Kox-	0.9	-				$K+ + ox^{2-} \rightleftharpoons Kox^-$
Kcit-2	1.22	-				$K+ + cit^{3-} \rightleftharpoons Kcit^{2-}$
Kedta-3	1.6	1.8 ± 0.3				$K+ + edta^{4-} \rightleftharpoons Kedta^{3-}$

Name	TDB 05/92		TDB 2020		Reaction
	$\log_{10}K_{s,0}°$	$\log_{10}K_{s,0}°$	$\Delta_r H_m°$ [kJ · mol^{-1}]	$\Delta_r C_{p,m}°$ [J · K^{-1} · mol^{-1}]	
H4edta(cr)	-	-3.80 ± 0.19	29 ± 3		$H_4edta(cr) \rightleftharpoons H_4edta(aq)$

[a] Assumed arbitrary value.
[b] Note that in this table isa^- has formally been replaced everywhere by H_3isa^- because speciation codes cannot cope with formulae like $Ca(isa_{-H})(aq)$ or $Am(isa_{-3H})^-$. H_3 in H_3isa^- can be interpreted as formally representing H of three hydroxyl groups of isosaccharinate.

Tab. 18.5-2: Selected organic data (Mg, Ca). Supplemental data are in italics.

Name	TDB 05/92	TDB 2020				Reaction
	$\log_{10}\beta°$	$\log_{10}\beta°$	$\Delta_r H_m°$ [kJ · mol^{-1}]	$\Delta_r C_{p,m}°$ [J · K^{-1} · mol^{-1}]	T-range [°C]	
Mg(ox)(aq)	3.42	3.56 ± 0.04				$Mg^{2+} + ox^{2-} \rightleftharpoons Mg(ox)(aq)$
Mg(ox)2-2	5.08	5.17 ± 0.08				$Mg^{2+} + 2\ ox^{2-} \rightleftharpoons Mg(ox)_2^{2-}$
Mg(cit)-	4.84	4.81 ± 0.03				$Mg^{2+} + cit^{3-} \rightleftharpoons Mg(cit)^-$
Mg(Hcit)(aq)	2.60	2.60 ± 0.07				$Mg^{2+} + Hcit^{2-} \rightleftharpoons Mg(Hcit)(aq)$
Mg(H2cit)+	1.14	1.31 ± 0.16				$Mg^{2+} + H_2cit^- \rightleftharpoons Mg(H_2cit)^+$
Mg(edta)-2	10.5	10.90 ± 0.10	19.8 ± 0.4			$Mg^{2+} + edta^{4-} \rightleftharpoons Mg(edta)^{2-}$
Mg(Hedta)-	3.8	4.5 ± 0.2				$Mg(edta)^{2-} + H^+ \rightleftharpoons Mg(Hedta)^-$
Ca(ox)(aq)	3.19	3.19 ± 0.06				$Ca^{2+} + ox^{2-} \rightleftharpoons Ca(ox)(aq)$
Ca(ox)2-2	0.61	4.02 ± 0.19				$Ca^{2+} + 2\ ox^{2-} \rightleftharpoons Ca(ox)_2^{2-}$
Ca(Hox)+	1.84	-				$Ca^{2+} + Hox^- \rightleftharpoons Ca(Hox)^+$
Ca(Hox)2(aq)	0.52	-				$Ca(Hox)+ + Hox^- \rightleftharpoons Ca(Hox)_2(aq)$
Ca(cit)-	4.85	4.80 ± 0.03	0 ± 6	0	18 – 45	$Ca^{2+} + cit^{3-} \rightleftharpoons Ca(cit)^-$
Ca(Hcit)(aq)	2.93	2.92 ± 0.07				$Ca^{2+} + Hcit^{2-} \rightleftharpoons Ca(Hcit)(aq)$
Ca(H2cit)+	1.44	1.53 ± 0.16				$Ca^{2+} + H_2cit^- \rightleftharpoons Ca(H_2cit)^+$
Ca(edta)-2	12.3	12.69 ± 0.06	-22.2 ± 0.4			$Ca^{2+} + edta^{4-} \rightleftharpoons Ca(edta)^{2-}$
Ca(Hedta)-	4.9	3.54 ± 0.09				$Ca(edta)^{2-} + H^+ \rightleftharpoons Ca(Hedta)^-$
Ca(H3isa)+ [a]	-	1.7 ± 0.3				$Ca^{2+} + H_3isa^- \rightleftharpoons Ca(H_3isa)^+$ [a]
Ca(H2isa)(aq) [a]	-	-10.4 ± 0.5				$Ca^{2+} + H_3isa^- \rightleftharpoons Ca(H_2isa)(aq) + H^+$ [a]

Name	TDB 05/92	TDB 2020				Reaction
	$\log_{10}K_{s,0}°$	$\log_{10}K_{s,0}°$	$\Delta_r H_m°$ [kJ · mol^{-1}]	$\Delta_r C_{p,m}°$ [J · K^{-1} · mol^{-1}]	T-range [°C]	
Glushinskite	-	*-6.4 ± 0.2*				*$Mg(ox)\cdot 2H_2O(cr) \rightleftharpoons Mg^{2+} + ox^{2-} + 2\ H_2O$*
Whewellite	-8.78	-8.73 ± 0.06	21.5 ± 0.5	0	15 – 50	$Ca(ox)\cdot H_2O(cr) \rightleftharpoons Ca^{2+} + ox^{2-} + H_2O$
Weddelite	-	-8.30 ± 0.06	25.2 ± 1.1	0	15 – 50	$Ca(ox)\cdot 2H_2O(cr) \rightleftharpoons Ca^{2+} + ox^{2-} + 2\ H_2O$
Ca(ox)·3H2O(cr)	-8.32	-8.19 ± 0.04	29.7 ± 1.3	0	15 – 50	$Ca(ox)\cdot 3H_2O(cr) \rightleftharpoons Ca^{2+} + ox^{2-} + 3\ H_2O$
Ca3(cit)2 · 4H2O(cr)	-	-17.90 ± 0.10				$Ca_3(cit)_2 \cdot 4H_2O(cr) \rightleftharpoons 3\ Ca^{2+} + 2\ cit^{3-} + 4\ H_2O$
Ca(H3isa)2(cr) [a]	-	-6.4 ± 0.2				$Ca(H_3isa)_2(cr) \rightleftharpoons Ca^{2+} + 2\ H_3isa^-$ [a]

[a] Note that in this table isa^- has formally been replaced everywhere by H_3isa^- because speciation codes cannot cope with formulae like $Ca(isa_{-H})(aq)$ or $Am(isa_{-3H})^-$. H_3 in H_3isa^- can be interpreted as formally representing H of three hydroxyl groups of isosaccharinate.

Tab. 18.5-3: Selected organic data (Ni)

Supplemental data are in italics.

Name	**TDB 05/92**	**TDB 2020**			**Reaction**
	$\log_{10}\beta°$	$\log_{10}\beta°$	$\Delta_r H_m°$ [kJ · mol^{-1}]	$\Delta_r C_{p,m}°$ [J · K^{-1} · mol^{-1}]	
Ni(ox)(aq)	5.13	5.19 ± 0.04	0.0 ± 0.3		$Ni^{2+} + ox^{2-} \rightleftharpoons Ni(ox)(aq)$
Ni(ox)2-2	8.72	7.64 ± 0.07	-7.8 ± 0.3		$Ni^{2+} + 2\ ox^{2-} \rightleftharpoons Ni(ox)_2^{2-}$
Ni(cit)-	6.5	6.76 ± 0.08			$Ni^{2+} + cit^{3-} \rightleftharpoons Ni(cit)^-$
Ni(cit)2-4	8.7	8.5 ± 0.4			$Ni^{2+} + 2\ cit^{3-} \rightleftharpoons Ni(cit)_2^{4-}$
Ni(Hcit)(aq)	4.1	4.16 ± 0.10			$Ni^{2+} + Hcit^{2-} \rightleftharpoons Ni(Hcit)(aq)$
Ni(H2cit)+	2.2	2.05 ± 0.25			$Ni^{2+} + H_2cit^- \rightleftharpoons Ni(H_2cit)^+$
Ni(edta)-2	20.1	20.54 ± 0.13	-26.1 ± 0.4		$Ni^{2+} + edta^{4-} \rightleftharpoons Ni(edta)^{2-}$
Ni(Hedta)-	3.5	3.66 ± 0.16	*-7.5 ± 1.3*		$Ni(edta)^{2-} + H^+ \rightleftharpoons Ni(Hedta)^-$
NiOHedta-	-12.5	-	-		$Ni(edta)^{2-} + H_2O \rightleftharpoons NiOHedta^- + H^+$
Ni(H3isa)+ [a]	-	*≈ 2.4*			*$Ni^{2+} + H_3isa^- \rightleftharpoons Ni(H_3isa)^+$* [a]

Name	**TDB 05/92**	**TDB 2020**			**Reaction**
	$\log_{10}K_{s,0}°$	$\log_{10}K_{s,0}°$	$\Delta_r H_m°$ [kJ · mol^{-1}]	$\Delta_r C_{p,m}°$ [J · K^{-1} · mol^{-1}]	
Ni(ox)·2H2O(cr)	-	*≤ 9.96*			*$Ni(ox)\cdot 2H_2O(cr) \rightleftharpoons Ni^{2+} + ox^{2-} + 2\ H_2O$*

[a] Note that in this table isa$^-$ has formally been replaced everywhere by H_3isa$^-$ because speciation codes cannot cope with formulae like Ca(isa$_{-H}$)(aq) or Am(isa$_{-3H}$)$^-$. H_3 in H_3isa$^-$ can be interpreted as formally representing H of three hydroxyl groups of isosaccharinate.

Tab. 18.5-4: Selected organic data (U)

Supplemental data are in italics.

Name	TDB 05/92	TDB 2020			Reaction
	$\log_{10}\beta°$	$\log_{10}\beta°$	$\Delta_r H_m°$ [kJ · mol^{-1}]	$\Delta_r C_{p,m}°$ [J · K^{-1} · mol^{-1}]	
Uox+2	11.1	*≈ 11*			*U^{4+} + ox^{2-} ⇌ Uox^{2+}*
U(ox)2(aq)	-	*≈ 8*			*Uox^{2+} + ox^{2-} ⇌ $U(ox)_2(aq)$*
U(ox)3-2	-	*≈ 5*			*$U(ox)_2(aq)$ + ox^{2-} ⇌ $U(ox)_3^{2-}$*
U(ox)4-4	-	*≈ 3*			*$U(ox)_3^{2-}$ + ox^{2-} ⇌ $U(ox)_4^{4-}$*
Ucit+	15.8	-			U^{4+} + cit^{3-} ⇌ $Ucit^{+}$
U(cit)22-	24.7	-			U^{4+} + 2 cit^{3-} ⇌ $U(cit)_2^{2-}$
Uedta(aq)	29.1	29.5 ± 0.2			U^{4+} + $edta^{4-}$ ⇌ Uedta(aq)
UedtaOH-	9.1	*≈ 9.1*			*Uedta(aq) + OH^- ⇌ $UedtaOH^-$*
(UedtaOH)2-2	2.7	*≈ 2.7*			*2 $UedtaOH^-$ ⇌ $(UedtaOH)_2^{2-}$*
Uedta(OH)2-2	-	*≈ 5.9*			*$UedtaOH^-$ + OH^- ⇌ $Uedta(OH)_2^{2-}$*
UO2ox(aq)	7.0	7.13 ± 0.16	25.4 ± 18.4		UO_2^{2+} + ox^{2-} ⇌ UO_2ox(aq)
UO2(ox)2-2	11.2	11.65 ± 0.15			UO_2^{2+} + 2 ox^{2-} ⇌ $UO_2(ox)_2^{2-}$
UO2(ox)3-4	-	13.8 ± 1.5			UO_2^{2+} + 3 ox^{2-} ⇌ $UO_2(ox)_3^{4-}$
UO2cit-	8.7	8.96 ± 0.17			UO_2^{2+} + cit^{3-} ⇌ UO_2cit^-
(UO2cit)2-2	21.18	21.3 ± 0.5			2 UO_2^{2+} + 2 cit^{3-} ⇌ $(UO_2cit)_2^{2-}$
UO2(Hcit)(aq)	-	5.0 ± 1.0			UO_2^{2+} + $Hcit^{2-}$ ⇌ UO_2(Hcit)(aq)
UO2edta-2	13.1	13.7 ± 0.2			UO_2^{2+} + $edta^{4-}$ ⇌ UO_2edta^{2-}
(UO2)2edta(aq)	20.3	20.6 ± 0.4			2 UO_2^{2+} + $edta^{4-}$ ⇌ $(UO_2)_2$edta(aq)
UO2(Hedta)-	8.19	8.37 ± 0.10			UO_2^{2+} + $Hedta^{3-}$ ⇌ $UO_2(Hedta)^-$
(UO2)2edtaOH-	13.9	-	-		$2UO_2^{2+}$ + $edta^{4-}$ + H_2O ⇌ $(UO_2)_2edtaOH^-$ + H^+
(UO2)2edta(OH)22-	28.7	-	-		$2UO_2^{2+}$ + $edta^{4-}$ + $2H_2O$ ⇌ $(UO_2)_2edta(OH)_2^{2-}$ + $2H^+$
UO2(H3isa)+ [a]	-	*3.5 ± 0.2*	*-1.0 ± 1.0*		*UO_2^{2+} + H_3isa^- ⇌ $UO_2(H_3isa)^+$* [a)]
UO2(H3isa)2(aq) [a]	-	*6.2 ± 0.2*	*1.4 ± 1.8*		*UO_2^{2+} + 2 H_3isa^- ⇌ $UO_2(H_3isa)_2(aq)$* [a]
UO2(H3isa)3- [a]	-	*8.0 ± 0.2*	*-6.2 ± 3.0*		*UO_2^{2+} + 3 H_3isa^- ⇌ $UO_2(H_3isa)_3$* [a)]

Name	TDB 05/92	TDB 2020				Reaction
	$\log_{10}K_{s,0}°$	$\log_{10}K_{s,0}°$	$\Delta_r H_m°$ [kJ · mol^{-1}]	$\Delta_r C_{p,m}°$ [J · K^{-1} · mol^{-1}]	T-range [°C]	
U(ox)2 · 6H2O(cr)	-	*-4.82 ± 0.20*	*10.4 ± 1.0*	*513 ± 41*	*25 – 90*	*$U(ox)_2$ · 6H_2O(cr) ⇌ $U(ox)_2$(aq) + 6 H_2O*
UO2ox·3H2O(cr)	-	-1.8 ± 0.27	20.2 ± 3.5	0	0 – 100	UO_2ox · 3H_2O(cr) ⇌ UO_2ox(aq) + 3 H_2O

[a] Note that in this table isa^- has formally been replaced everywhere by H_3isa^- because speciation codes cannot cope with formulae like Ca(isa_{-H})(aq) or Am(isa_{-3H})$^+$. H_3 in H_3isa^- can be interpreted as formally representing H of three hydroxyl groups of isosaccharinate.

Tab. 18.5-5: Selected organic data (Np)

Supplemental data are in italics

Name	TDB 05/92	TDB 2020			Reaction
	$\log_{10}\beta°$	$\log_{10}\beta°$	$\Delta_r H_m°$ [kJ · mol^{-1}]	$\Delta_r C_{p,m}°$ [J · K^{-1} · mol^{-1}]	
Np(ox)+2	6.3	*≈ 6.5*			*Np^{4+} + $H_2ox(aq)$ ⇌ $Np(ox)^{2+}$ + 2 H^+*
Np(ox)2(aq)	-	*≈ 7.5*			*Np^{4+} + 2 $H_2ox(aq)$ ⇌ $Np(ox)_2(aq)$ + 4 H^+*
Np(ox)3-2	-	*≈ 8*			*Np^{4+} + 3 $H_2ox(aq)$ ⇌ $Np(ox)_3^{2-}$ + 6 H^+*
Np(cit)+	16	-			Np4+ + cit^{3-} ⇌ $Np(cit)^+$
Np(edta)(aq)	29.3	31.2 ± 0.6			Np^{4+} + $edta^{4-}$ ⇌ Np(edta)(aq)
Np(OH)3(H3isa)(aq) [a]	-	*≈ 43.5*			*Np^{4+} + 3 OH^- + H_3isa^- ⇌ $Np(OH)_3(H_3isa)(aq)$* [1)]
Np(OH)3(H3isa)2- [a]	-	*≈ 2.1*			*$Np(OH)_3(isa)(aq)$ + H_3isa^- ⇌ $Np(OH)_3(H_3isa)_2^-$* [1)]
Np(OH)4(H3isa)- [a]	-	*≈ 50.1*			*Np^{4+} + 4 OH^- + H_3isa^- ⇌ $Np(OH)_4(H_3isa)^-$* [1)]
Np(OH)4(H3isa)2-2 [a]	-	*≈ 1.9*			*$Np(OH)_4(isa)^-$ + H_3isa^- ⇌ $Np(OH)_4(H_3isa)_2^{2-}$* [1)]
NpO2ox-	4.38	3.9 ± 0.1			NpO_2^+ + ox^{2-} ⇌ NpO_2ox^-
NpO2(ox)2-3	7.36	5.8 ± 0.2			NpO_2^+ + 2 ox^{2-} ⇌ $NpO_2(ox)_2^{3-}$
NpO2Hox(aq)	7.14	-			NpO_2^+ + H^+ + ox^{2-} ⇌ $NpO_2Hox(aq)$
NpO2cit-2	5.5	3.68 ± 0.05			NpO_2^+ + cit^{3-} ⇌ NpO_2cit^{2-}
NpO2Hcit-	9.51	-			NpO_2^+ + H^+ + cit^{3-} ⇌ NpO_2Hcit^-
NpO2edta-3	8.2	9.23 ± 0.13			NpO_2^+ + $edta^{4-}$ ⇌ NpO_2edta^{3-}
NpO2(Hedta)-2	5.9	5.82 ± 0.11			NpO_2^+ + $Hedta^{3-}$ ⇌ $NpO_2(Hedta)^{2-}$
NpO2(H2edta)-	-	4.47 ± 0.14			NpO_2^+ + H_2edta^{2-} ⇌ $NpO_2(H_2edta)^-$
NpO2edtaOH-4	-12.4	*≈ -12.4*			*NpO_2edta^{3-} + $H_2O(l)$ ⇌ $NpO_2edtaOH^{4-}$ + H^+*
NpO2ox(aq)	7.1	-			NpO_2^{2+} + ox^{2-} ⇌ $NpO_2ox(aq)$
NpO2(ox)2-2	11.2	-			NpO_2^{2+} + 2 ox^{2-} ⇌ $NpO_2(ox)_2^{2-}$
NpO2cit-	10	-			NpO_2^{2+} + cit^{3-} ⇌ NpO_2cit^-
NpO2edta-2	15	-			NpO_2^{2+} + $edta^{4-}$ ⇌ NpO_2edta^{2-}

Name	TDB 05/92	TDB 2020			Reaction
	$\log_{10}K_{s,0}°$	$\log_{10}K_{s,0}°$	$\Delta_r H_m°$ [kJ · mol^{-1}]	$\Delta_r C_{p,m}°$ [J · K^{-1} · mol^{-1}]	
Np(ox)2 · 6H2O(cr)	-	*-12.7 ± 1.0*			*$Np(ox)_2 \cdot 6H_2O(cr)$ + 4H^+ ⇌ Np^{4+} + 2 $H_2ox(aq)$ + 6 H_2O*

[a] Note that in this table isa^- has formally been replaced everywhere by H_3isa^- because speciation codes cannot cope with formulae like $Ca(isa_{-H})(aq)$ or $Am(isa_{-3H})^+$. H_3 in H_3isa^- can be interpreted as formally representing H of three hydroxyl groups of isosaccharinate.

Tab. 18.5-6: Selected organic data (Pu)

Supplemental data are in italics.

Name	TDB 05/92	TDB 2020			Reaction
	$\log_{10}\beta°$	$\log_{10}\beta°$	$\Delta_r H_m°$ [kJ · mol^{-1}]	$\Delta_r C_{p,m}°$ [J · K^{-1} · mol^{-1}]	
Pu(ox)+	6.5	*≈ 8.5*			*$Pu^{3+} + ox^{2-} \rightleftharpoons Pu(ox)^{+}$*
Pu(ox)2-	-	*≈ 12.7*			*$Pu^{3+} + 2\ ox^{2-} \rightleftharpoons Pu(ox)_2^{-}$*
Pu(ox)3-3	-	*≈ 12.1*			*$Pu^{3+} + 3\ ox^{2-} \rightleftharpoons Pu(ox)_3^{3-}$*
Pu(cit)(aq)	*9.5*	*≈ 8.7*			*$Pu^{3+} + cit^{3-} \rightleftharpoons Pu(cit)(aq)$*
Pu(Hcit)+	-	*≈ 6.1*			*$Pu^{3+} + Hcit^{2-} \rightleftharpoons Pu(Hcit)^{+}$*
Pu(edta)-	20.64	20.18 ± 0.37	-8.7 ± 1.2		$Pu^{3+} + edta^{4-} \rightleftharpoons Pu(edta)^{-}$
Pu(Hedta)(aq)	1.96	1.84 ± 0.26			$Pu(edta)^{-} + H^{+} \rightleftharpoons Pu(Hedta)(aq)$
Pu(ox)+2	5.4	*≈ 7.3*			*$Pu^{4+} + H_2ox(aq) \rightleftharpoons Pu(ox)^{2+} + 2\ H^{+}$*
Pu(ox)2(aq)	3.7	*≈ 3.3*			*$Pu(ox)^{2+} + H_2ox(aq) \rightleftharpoons Pu(ox)_2(aq) + 2\ H^{+}$*
Pu(ox)3-2	1.0	*≈ 0.3*			*$Pu(ox)_2(aq) + H_2ox(aq) \rightleftharpoons Pu(ox)_3^{2-} + 2\ H^{+}$*
Pu(cit)+	16.9	-			$Pu^{4+} + cit^{3-} \rightleftharpoons Pu(cit)^{+}$
Pu(cit)2-2	28.5	-			$Pu^{4+} + 2\ cit^{3-} \rightleftharpoons Pu(cit)_2^{2-}$
Pu(edta)(aq)	30.1	*31.6 ± 1.0*			*$Pu^{4+} + edta^{4-} \rightleftharpoons Pu(edta)(aq)$*
Pu(edta)OH-	-	*≈ 9.3*			*$Pu(edta)(aq) + OH^{-} \rightleftharpoons Pu(edta)OH^{-}$*
Pu(edta)(OH)2-2	-	*≈ 6.9*			*$Pu(edta)OH^{-} + OH^{-} \rightleftharpoons Pu(edta)(OH)_2^{2-}$*
PuO2ox-	4.30	-			$PuO_2^{+} + ox^{2-} \rightleftharpoons PuO_2ox^{-}$
PuO2(ox)2-3	6.70	-			$PuO_2^{+} + 2\ ox^{2-} \rightleftharpoons PuO_2(ox)_2^{3-}$
PuO2Hox(aq)	6.80	-			$PuO_2^{+} + H^{+} + ox^{2-} \rightleftharpoons PuO_2Hox(aq)$
PuO2cit-2	5.5	-			$PuO_2^{+} + cit^{3-} \rightleftharpoons PuO_2cit^{2-}$
PuO2edta-3	10.9	-			$PuO_2^{+} + edta^{4-} \rightleftharpoons PuO_2edta^{3-}$
PuO2Hedta-2	16.44	-			$PuO_2^{+} + H^{+} + edta^{4-} \rightleftharpoons PuO_2Hedta^{2-}$
PuO2ox(aq)	7	-			$PuO_2^{2+} + ox^{2-} \rightleftharpoons PuO_2ox(aq)$
PuO2(ox)2-2	10.57	-			$PuO_2^{2+} + 2\ ox^{2-} \rightleftharpoons PuO_2(ox)_2^{2-}$
PuO2cit-	10.6	-			$PuO_2^{2+} + cit^{3-} \rightleftharpoons PuO_2cit^{-}$
PuO2(cit)2-4	15.5	-			$PuO_2^{2+} + 2\ cit^{3-} \rightleftharpoons PuO_2(cit)_2^{4-}$
PuO2edta-2	17.71	-			$PuO_2^{2+} + edta^{4-} \rightleftharpoons PuO_2edta^{2-}$

Name	TDB 05/92	TDB 2020			Reaction
	$\log_{10}K_{s,0}°$	$\log_{10}K_{s,0}°$	$\Delta_r H_m°$ [kJ · mol^{-1}]	$\Delta_r C_{p,m}°$ [J · K^{-1} · mol^{-1}]	
Pu2(ox)3 · 10H2O(cr)	-	*≈ -7.5*			*$Pu_2(ox)_3 \cdot 10H_2O(cr) + 6H^{+} \rightleftharpoons 2Pu^{3+} + 3H_2ox(aq) + 10H_2O$*
Pu(ox)2 · 6H2O(cr)	-	*-4.6 ± 0.2*			*$Pu(ox)_2 \cdot 6H_2O(cr) \rightleftharpoons Pu(ox)_2(aq) + 6\ H_2O$*

Tab. 18.5-7: Selected organic data (Am)

Supplemental data are in italics.

Name	**TDB 05/92**	**TDB 2020**			**Reaction**
	$\log_{10}\beta°$	**$\log_{10}\beta°$**	**$\Delta_r H_m°$** [kJ · mol^{-1}]	**$\Delta_r C_{p,m}°$** [J · K^{-1} · mol^{-1}]	
Am(ox)+	6.51	6.51 ± 0.15			$Am^{3+} + ox^{2-} \rightleftharpoons Am(ox)^{+}$
Am(ox)2-	10.53	10.71 ± 0.20			$Am^{3+} + 2\ ox^{2-} \rightleftharpoons Am(ox)_2^{-}$
Am(ox)3-3	12.8	13.0 ± 1.0			$Am^{3+} + 3\ ox^{2-} \rightleftharpoons Am(ox)_3^{3-}$
Am(cit)(aq)	9.63	8.55 ± 0.20			$Am^{3+} + cit^{3-} \rightleftharpoons Am(cit)(aq)$
Am(cit)2-3	12.8	13.9 ± 1.0			$Am^{3+} + 2\ cit^{3-} \rightleftharpoons Am(cit)_2^{3-}$
Am(Hcit)+	6.1	6.5 ± 1.0			$Am^{3+} + Hcit^{2-} \rightleftharpoons Am(Hcit)^{+}$
Am(Hcit)2-	-	10.8 ± 1.0			$Am^{3+} + 2\ Hcit^{2-} \rightleftharpoons Am(Hcit)_2^{-}$
AmH(cit)2-2	18.5	-			$Am^{3+} + H^{+} + 2\ cit^{3-} \rightleftharpoons AmH(cit)_2^{2-}$
Am(edta)-	20.3	19.67 ± 0.11	-10.6 ± 2.0		$Am^{3+} + edta^{4-} \rightleftharpoons Am(edta)^{-}$
Am(edta)2-5	24.2	-			$Am^{3+} + 2\ edta^{4-} \rightleftharpoons Am(edta)_2^{5-}$
Am(Hedta)(aq)	2.3	2.17 ± 0.25			$Am(edta)^{-} + H^{+} \rightleftharpoons Am(Hedta)(aq)$
Am(edta)OH-2	*2.0*	*2.66 ± 0.19*			*$Am(edta)^{-} + OH^{-} \rightleftharpoons Am(edta)OH^{2-}$*
Am(isa)- [a]	-	*22.2 ± 1.0*			*$Am^{3+} + H_3isa^{-} \rightleftharpoons Am(isa)^{-} + 3\ H^{+}$* [1)]

[a] Note that in this table isa^{-} has formally been replaced everywhere by H_3isa^{-} because speciation codes cannot cope with formulae like $Ca(isa_{-H})(aq)$ or $Am(isa_{-3H})^{-}$. H_3 in H_3isa^{-} can be interpreted as formally representing H of three hydroxyl groups of isosaccharinate.

Tab. 18-6: Selected SIT ion interaction coefficients $\varepsilon_{j,k}$ [kg · mol^{-1}] for organic species

Data in normal face are taken from Hummel et al. (2005a). Data estimated according to charge correlations and taken from Tab. 1-7 are shaded. Supplemental data are in italics.

j k → ↓	**Cl^-** $\varepsilon_{j,k}$ [kg · mol^{-1}]	**ClO_4^-** $\varepsilon_{j,k}$ [kg · mol^{-1}]	**Na^+** $\varepsilon_{j,k}$ [kg · mol^{-1}]	**K^+** $\varepsilon_{j,k}$ [kg · mol^{-1}]	**$Na^+ + Cl^-$** $\varepsilon_{j,k}$ [kg · mol^{-1}]	**$Na^+ + ClO_4^-$** $\varepsilon_{j,k}$ [kg · mol^{-1}]
ox-2	0	0	-0.08 ± 0.01	0.07 ± 0.08	0	0
Hox-	0	0	-0.07 ± 0.01	-0.01 ± 0.08	0	0
H2ox(aq)	0	0	0	0	0.00 ± 0.01	0.00 ± 0.01
cit-3	0	0	-0.076 ± 0.030	0.02 ± 0.02	0	0
Hcit-2	0	0	-0.04 ± 0.02	-0.01 ± 0.02	0	0
H2cit-	0	0	-0.05 ± 0.01	-0.04 ± 0.01	0	0
H3cit(aq)	0	0	0	0	0.00 ± 0.01	0.00 ± 0.01
edta-4	0	0	0.32 ± 0.14	1.07 ± 0.19	0	0
Hedta-3	0	0	-0.10 ± 0.14	0.31 ± 0.18	0	0
H2edta-2	0	0	-0.37 ± 0.14	-0.17 ± 0.18	0	0
H3edta-	0	0	-0.33 ± 0.14	-0.14 ± 0.17	0	0
H4edta(aq)	0	0	0	0	-0.29 ± 0.14	-0.29 ± 0.14
H5edta+	-0.23 ± 0.15	-0.23 ± 0.15	0	0	0	0
H6edta+2	-0.20 ± 0.16	-0.20 ± 0.16	0	0	0	0
H3isa- [d]	0	0	-0.05 ± 0.10	-0.05 ± 0.10 [a]	0	0
H4isa(aq) [*,d]	0	0	0	0	0.0 ± 0.1	0.0 ± 0.1
Na(edta)-3	0	0	-0.15 ± 0.10		0	0
Kedta-3	0	0	-0.15 ± 0.10		0	0
Mg(ox)(aq)	0	0	0		0.00 ± 0.03	
Mg(ox)2-2	0	0	-0.15 ± 0.03		0	0
Ca(ox)(aq)	0	0	0		0.00 ± 0.03 [b]	
Ca(ox)2-2	0	0	-0.15 ± 0.03 [b]		0	0
Mg(cit)-	0	0	0.03 ± 0.03		0	0
Mg(Hcit)(aq)	0	0	0		0.02 ± 0.05	
Mg(H2cit)+	0.05 ± 0.10		0		0	0
Ca(cit)-	0	0	0.03 ± 0.03 [b]		0	0
Ca(Hcit)(aq)	0	0	0		0.02 ± 0.05 [b]	
Ca(H2cit)+	0.05 ± 0.10		0		0	0
Mg(edta)2-	0	0	-0.01 ± 0.15		0	0
Mg(Hedta)-	0	0	0.11 ± 0.20		0	0
Ca(edta)2-	0	0	-0.01 ± 0.15 [b]		0	0
Ca(Hedta)-	0	0	0.11 ± 0.20 [b]		0	0
Ca(H3isa)+ [d]	0.05 ± 0.10		0		0	0
Ca(H2isa)(aq) [d]	0	0	0		0.0 ± 0.1	0.0 ± 0.1
Ni(ox)(aq)	0	0	0		-0.07 ± 0.03	
Ni(ox)2-2	0	0	-0.26 ± 0.03		0	0

Tab. 18-6: Selected SIT ion interaction coefficients $\varepsilon_{j,k}$ [kg · mol^{-1}] for organic species

j k → ↓	**Cl^-** $\varepsilon_{j,k}$ [kg · mol^{-1}]	**ClO_4^-** $\varepsilon_{j,k}$ [kg · mol^{-1}]	**Na^+** $\varepsilon_{j,k}$ [kg · mol^{-1}]	**K^+** $\varepsilon_{j,k}$ [kg · mol^{-1}]	**$Na^+ + Cl^-$** $\varepsilon_{j,k}$ [kg · mol^{-1}]	**$Na^+ + ClO_4^-$** $\varepsilon_{j,k}$ [kg · mol^{-1}]
Ni(H2cit)+	0.12 ± 0.5 [c]	0.12 ± 0.5	0		0	0
Ni(Hcit)(aq)	0	0	0		-0.07 ± 0.5 [c]	-0.07 ± 0.5
Ni(cit)-	0	0	0.22 ± 0.5		0	0
Ni(cit)2-4	0	0	-0.20 ± 0.10		0	0
Ni(Hedta)-	0	0	-0.05 ± 0.10		0	0
Ni(edta)2-	0	0	-0.10 ± 0.10		0	0
Ni(H3isa)+ [d]	0.2 ± 0.1 [c]	0.2 ± 0.1	0		0	0
Uox+2	*0.4 ± 0.1* [c]	*0.4 ± 0.1*	*0*		*0*	*0*
U(ox)2(aq)	*0*	*0*	*0*		*0.0 ± 0.1*	*0.0 ± 0.1*
U(ox)3-2	*0*	*0*	*-0.10 ± 0.10*		*0*	*0*
U(ox)4-4	*0*	*0*	*-0.20 ± 0.10*		*0*	*0*
Uedta(aq)	0	0	0		-0.19 ± 0.19 [c]	-0.19 ± 0.19
UedtaOH-	*0*	*0*	*-0.05 ± 0.10*		*0*	*0*
(UedtaOH)2-2	*0*	*0*	*-0.10 ± 0.10*		*0*	*0*
Uedta(OH)2-2	*0*	*0*	*-0.10 ± 0.10*		*0*	*0*
UO2ox(aq)	0	0	0		-0.05 ± 0.06 [c]	-0.05 ± 0.06
UO2(ox)2-2	0	0	-0.18 ± 0.07		0	0
UO2(ox)3-4	0	0	-0.01 ± 0.11		0	0
UO2cit-	0	0	-0.11 ± 0.09		0	0
(UO2cit)2-2	0	0	-0.10 ± 0.10		0	0
UO2(Hcit)(aq)	0	0	0		0.0 ± 0.1	0.0 ± 0.1
UO2edta2-	0	0	-0.22 ± 0.18		0	0
(UO2)2edta(aq)	0	0	0		0.0 ± 0.1	0.0 ± 0.1
UO2(Hedta)-	0	0	-0.18 ± 0.16		0	0
UO2(H3isa)+ [d]	*0.2 ± 0.1* [c]	*0.2 ± 0.1*	*0*		*0*	*0*
UO2(H3isa)2(aq) [d]	*0*	*0*	*0*		*0.0 ± 0.1*	*0.0 ± 0.1*
UO2(H3isa)3- [d]	*0*	*0*	*-0.05 ± 0.10*		*0*	*0*
Np(ox)+2	*0.4 ± 0.1* [c]	*0.4 ± 0.1*	*0*		*0*	*0*
Np(ox)2(aq)	*0*	*0*	*0*		*0.0 ± 0.1*	*0.0 ± 0.1*
Np(ox)3-2	*0*	*0*	*-0.10 ± 0.10*		*0*	*0*
Np(edta)(aq)	0	0	0		-0.19 ± 0.19 [c]	-0.19 ± 0.19
Np(OH)3(H3isa)(aq) [d]	*0*	*0*	*0*		*0.0 ± 0.1*	*0.0 ± 0.1*
Np(OH)3(H3isa)2- [d]	*0*	*0*	*-0.05 ± 0.10*		*0*	*0*
Np(OH)4(H3isa)- [d]	*0*	*0*	*-0.05 ± 0.10*		*0*	*0*
Np(OH)4(H3isa)2-2 [d]	*0*	*0*	*-0.10 ± 0.10*		*0*	*0*
NpO2ox-	0	0	-0.4 ± 0.1		0	0
NpO2(ox)2-3	0	0	-0.3 ± 0.2		0	0
NpO2cit-2	0	0	-0.06 ± 0.03		0	0

Tab. 18-6: Cont.

j k → ↓	**Cl^-** $\varepsilon_{j,k}$ [kg · mol^{-1}]	**ClO_4^-** $\varepsilon_{j,k}$ [kg · mol^{-1}]	**Na^+** $\varepsilon_{j,k}$ [kg · mol^{-1}]	**K^+** $\varepsilon_{j,k}$ [kg · mol^{-1}]	**$Na^+ + Cl^-$** $\varepsilon_{j,k}$ [kg · mol^{-1}]	**$Na^+ + ClO_4^-$** $\varepsilon_{j,k}$ [kg · mol^{-1}]
NpO2(H2edta)-	0	0	-0.18 ± 0.16		0	0
NpO2(Hedta)-2	0	0	0.07 ± 0.16		0	0
NpO2edta-3	0	0	0.20 ± 0.16		0	0
NpO2edtaOH-4	*0*	*0*	*0.32 ± 0.14*		*0*	*0*
Pu(ox)+	*0.05 ± 0.10*		*0*		0	0
Pu(ox)2-	*0*	*0*	*-0.05 ± 0.10*		*0*	*0*
Pu(ox)3-3	*0*	*0*	*-0.15 ± 0.10*		*0*	*0*
Pu(cit)(aq)	*0*	*0*	*0*		*0.0 ± 0.1*	*0.0 ± 0.1*
Pu(Hcit)+	*0.05 ± 0.10*		*0*		*0*	*0*
Pu(edta)-	0	0	0.01 ± 0.16		0	0
Pu(Hedta)(aq)	0	0	0		0.0 ± 0.1	0.0 ± 0.1
Pu(ox)2+	*0.4 ± 0.1* [c]	*0.4 ± 0.1*	*0*		*0*	*0*
Pu(ox)2(aq)	*0*	*0*	*0*		*0.0 ± 0.1*	*0.0 ± 0.1*
Pu(ox)3-2	*0*	*0*	*-0.10 ± 0.10*		*0*	*0*
Pu(edta)(aq)	0	0	*0*		*-0.19 ± 0.19* [c]	*-0.19 ± 0.19*
Pu(edta)OH-	*0*	*0*	*-0.05 ± 0.10*		*0*	*0*
Pu(edta)(OH)2-2	*0*	*0*	*-0.10 ± 0.10*		*0*	*0*
Am(ox)+	0.08 ± 0.05	0.08 ± 0.05	0		0	0
Am(ox)2-	0	0	-0.21 ± 0.08		0	0
Am(ox)3-3	0	0	-0.23 ± 0.10		0	0
Am(cit)(aq)	0	0	0		0.00 ± 0.05	
Am(cit)2-3	0	0	-0.15 ± 0.10		0	0
Am(Hcit)+	0.2 ± 0.1 [c]	0.2 ± 0.1	0		0	0
Am(Hcit)2-	0	0	-0.05 ± 0.10		0	0
Am(edta)-	0	0	0.01 ± 0.16		0	0
Am(Hedta)(aq)	0	0	0		0.0 ± 0.1	0.0 ± 0.1
Am(edta)OH-2	*0*	*0*	*-0.10 ± 0.10*		*0*	*0*
Am(isa)- [d]	*0*	*0*	*-0.05 ± 0.10*		*0*	*0*

[a] Assumed to be equal to the corresponding ion interaction coefficient with Na.
[b] Assumed to be equal to the corresponding ion interaction coefficient with Mg.
[c] Assumed to be equal to the corresponding ion interaction coefficient with ClO_4^-.
[d] Note that in this table isa^- has formally been replaced everywhere by H_3isa^- because speciation codes cannot cope with formulae like $Ca(isa_{-H})(aq)$ or $Am(isa_{-3H})^-$. H_3 in H_3isa^- can be interpreted as formally representing H of three hydroxyl groups of isosaccharinate.

18.6 References

Boukhalfa, H., Reilly, S.D., Smith, W.H. & Neu, M.P. (2004): EDTA and mixed-ligand complexes of tetravalent and trivalent plutonium. Inorg. Chem., 43, 5816-5823.

Bourges, J.Y., Guillaume, B., Koehly, G., Hobart, D.E. & Peterson, J.R. (1983): Coexistence of americium in four oxidation states in sodium carbonate – sodium bicarbonate medium. Inorg. Chem., 22, 1179-1184.

Ermolaev, N.P., Krot, N.N. & Gel'man, A.D. (1967): Disproportionation of plutonium(V) in oxalate solutions. Sov. Radiochem., 9, 169-176.

Guillaumont, R., Fanghänel, T., Fuger, J., Grenthe, I., Neck, V., Palmer, D.A. & Rand, M.H. (2003): Update on the Chemical Thermodynamics of Uranium, Neptunium, Plutonium, Americium and Technetium. Chemical Thermodynamics, Vol. 5, Elsevier, Amsterdam, The Netherlands, 919 pp.

Hummel, W. (1991): Thermodynamic Data Base for Organic Ligands. PSI Internal Report TM-41-91-43, Paul Scherrer Institut, Villigen, Switzerland, 52 pp.

Hummel, W., Anderegg, G., Puigdomènech, I., Rao, L. & Tochiyama, O. (2005a): Chemical Thermodynamics of Compounds and Complexes of U, Np, Pu, Am, Tc, Se, Ni and Zr with Selected Organic Ligands. Chemical Thermodynamics, Vol. 9, Elsevier, Amsterdam, The Netherlands, 1088 pp.

Hummel, W., Anderegg, G., Puigdomènech, I., Rao, L., Tochiyama, O. (2005b): The OECD/NEA TDB review of selected organic ligands. Radiochim. Acta 93, 719-725.

Hummel, W., Berner, U., Curti, E., Pearson, F.J. & Thoenen, T. (2002): Nagra/PSI Chemical Thermodynamic Data Base 01/01. Nagra Technical Report NTB 02-16. Also published by Universal Publishers/uPublish.com, Parkland, Florida, USA.

Hummel, W., Puigdomènech, I., Rao, L. & Tochiyama, O. (2007): Thermodynamic data of compounds and complexes of U, Np, Pu and Am with selected organic ligands. C. R. Chimie, 10, 948-958.

Larson, W.D. & Tomsicek, W.J. (1941): The activity coefficients of the undissociated part of weak acids. II. Oxalic acid. J. Am. Chem. Soc., 63, 3329-3331.

Mefod'eva, M.P. & Gel'man, A.D. (1971): Production of solid compounds of neptunium(III) from aqueous solutions. Sov. Radiochem., 13, 613-618.

Nikolaevskii, V.B., Shilov, V.P. & Krot, N.N. (1974): Complex compounds of pentavalent americium in solutions of ethylenediaminetetraacetic and diethylenetriaminepentaacetic acids. Sov. Radiochem., 16, 57-61.

Pearson, F.J., Berner, U. & Hummel, W. (1992): Nagra Thermochemical Data Base II. Supplemental Data 05/92. Nagra Technical Report NTB 91-18.

Peretrukhin, V.F., Krot, N.N. & Gel'man, A.D. (1970): Influence of anions on the kinetics of the spontaneous oxidation of trivalent uranium in aqueous solution. Sov. Radiochem., 12, 85-88.

Reed, D.T., Wygmans, D.G., Aase, S.B. & Banaszak, J.E. (1998): Reduction of Np(VI) and Pu(VI) by organic chelating agents. Radiochim. Acta, 82, 109-114.

Runde, W.H. & Schulz, W.W. (2006): Americium, in: L.R. Morss, N.M. Edelstein, J. Fuger, J.J. Katz (Eds.), The Chemistry of the Actinides and Transactinide Elements, Springer, Dordrecht, The Netherlands, p.1265-1395.

Schwarzenbach, G. & Ackermann, H. (1947): Komplexone V. Die Äthylendiamin-tetraessigsäure. Helv. Chim. Acta, 30, 1798-1804.

Shilov, V.P. (1985): Mechanism of the interaction of Am(VI) and $H_2C_2O_4$ in aqueous acid solutions. Sov. Radiochem., 27, 540-543.

Shilov, V.P., Nikolaevskii, V.B. & Krot, N.N. (1974): Complex formation by americium(V) with oxalate ions. Russ. J. Inorg. Chem., 19, 254-257.

Silva, R.J., Bidoglio, G., Rand, M.H., Robouch, P.B., Wanner, H. & Puigdomènech, I. (1995): Chemical Thermodynamics of Americium, Chemical Thermodynamics, Vol. 2, Elsevier, Amsterdam, The Netherlands, 374 pp.

Van Loon, L.R. & Glaus, M.A. (1997): Review of the kinetics of alkaline degradation of cellulose in view of its relevance for safety assessment of radioactive waste repositories. J. Environ. Polymer Degradation 5, 97-109.

Van Loon, L.R. & Hummel, W. (1999): Radiolytic and chemical degradation of strong acidic ion-exchange resins: Study of the ligands formed. Nucl. Technol. 128, 359-371.

Van Loon, L.R. & Kopajtic, Z. (1991): Complexation of Cu^{2+}, Ni^{2+} and UO_2^{2+} by radiolytic degradation products of bitumen. Radiochim. Acta 54, 193-199.

Zubarev, V.G. & Krot, N.N. (1982): Separation of americium(V) oxalate compound from solution. Sov. Radiochem., 24, 264-267.

19 Palladium

19.1 Introduction

A long-lived radioactive isotope of palladium, Pd-107 with $(6.5 \pm 0.3) \cdot 10^6$ years half-life, is a major fission product of Pu-239 fission with thermal neutrons and a less abundant but still important fission product of U-235, and thus contributes in dose-relevant quantities to the inventory of radioactive waste. This fact triggered the inclusion of palladium already into our original data base (Pearson et al. 1992). A first update of the thermodynamic data for palladium has been carried out for the PSI/Nagra Chemical Thermodynamic Database 12/07 (TDB 12/07, Thoenen et al. 2014). This is the second update of the thermodynamic data for palladium for the PSI Chemical Thermodynamic Database 2020 (PSI TDB 2020).

In aqueous solution, palladium occurs in two oxidation states: Pd(0) and Pd(II).

Thermodynamic data referring to the Pd(0) – Pd(II) system, especially involving palladium oxide and hydroxide solids, are controversial, and a new interpretation of the available experimental data is presented by this review.

The selected thermodynamic data for palladium compounds and complexes are presented in Tab. 19-2.

NEA (see, e.g., Grenthe et al. 1992) used the specific ion interaction theory (SIT) for making ionic strength corrections to the experimental data, an approach which is also adopted for TDB 2020 (as has been for all its predecessors). In the case of palladium, the thermodynamic model explicitly considered the formation of palladium chloride complexes. Therefore, ion interaction coefficients ε for cationic palladium species with Cl^- should be approximated by the corresponding interaction coefficients with ClO_4^-.

In most cases, the ion interaction coefficients of palladium species were not available. We approximated these with the estimation method described in Section 1.5.3, which draws on a statistical analysis of published SIT ion interaction coefficients, and which allows the estimation of missing coefficients for the interaction of cations with Cl^- and ClO_4^-, and for the interaction of anions with Na^+, from the charge of the cations or anions of interest.

The selected SIT ion interaction coefficients for palladium species are presented in Tab. 19-3.

19.2 Palladium(0)

19.2.1 Elemental palladium

As a member of the platinum group elements, palladium occurs in nature mainly in elemental form or as inter-metallic compounds. Elemental palladium has a large stability field in the Eh – pH range of water (e.g., Brookins 1988) and thus, Pd(cr) is an environmentally important substance under reducing to mildly oxidising conditions. Hence, elemental palladium is an important solid for modelling studies concerning solubility and complexation of palladium.

No CODATA values (Cox et al. 1989) have been published for palladium.

Brown & Ekberg (2016) report an entropy value for elemental palladium, $S_m°$ = (37.71 ± 0.05) J · K^{-1} · mol^{-1}, with a reference to the compilation of Bard et al. (1985) and the remark "accepted uncertainty estimated in this work". The $S_m°$ value reported by Bard et al. (1985) in turn has been taken from the review of Furukawa et al. (1974).

Furukawa et al. (1974) actually report $S_m°$ = 9.013 cal · K^{-1} · mol^{-1} = 37.71 J · K^{-1} · mol^{-1} and $C_{p,m}°$ = 6.188 cal · K^{-1} · mol^{-1} = 25.89 J · K^{-1} · mol^{-1} as their recommended thermodynamic properties of Pd(cr).

Wagman et al. (1982) report $S_m°$ = 37.57 J · K^{-1} · mol^{-1} and $C_{p,m}°$ = 25.98 J · K^{-1} · mol^{-1} without error estimates. However, as the data selection process of the NBS Tables is not documented, the source of these values cannot be traced back to any experimental studies.

Sassani & Shock (1998) report $S_m°$ = 9.04 cal · K^{-1} · mol^{-1} = 37.82 J · K^{-1} · mol^{-1} and $C_{p,m}°$ = 6.06 cal · K^{-1} · mol^{-1} = 25.36 J · K^{-1} · mol^{-1}, without error estimates but with a reference to the review of Hultgren et al. (1973) for $S_m°$, and the remark "least-squares fit of data in Hultgren et al. (1973) to Eqn. 1" for $C_{p,m}°$.

Eqn. 1 of Sassani & Shock (1998) is $C_{p,m}(T) = a + bT + cT^{-2}$, and the $C_{p,m}$ data tabulated in Hultgren et al. (1973) refer to 1 – 298.15 K as "low-temperature data" and 298.15 – 1'800 K as "high-temperature data". It is unclear which data range Sassani & Shock (1998) used for their least-squares fit, but according to their focus on high-temperature data, they may have used the 298.15 – 1'800 K data. However, the value $C_{p,m}°$(298.15 K) = 6.06 cal · K^{-1} · mol^{-1} reported by Sassani & Shock (1998) could not be verified by this review: a least-squares fit of the 298.15 – 1'800 K data resulted in $C_{p,m}°$(298.15 K) = 6.25 cal · K^{-1} · mol^{-1}.

Hultgren et al. (1973) actually report $S_m°$(298.15 K) = (9.04 ± 0.05) cal · K^{-1} · mol^{-1} = (37.82 ± 0.21) J · K^{-1} · mol^{-1} and $C_{p,m}°$(298.15 K) = 6.21 cal · K^{-1} · mol^{-1} = 25.98 J · K^{-1} · mol^{-1} as their recommended thermodynamic properties of Pd(cr). The uncertainty estimate given by Hultgren et al. (1973) for $S_m°$ probably refers to 1σ.

The values reported by Hultgren et al. (1973) and Furukawa et al. (1974) for $S_m°$ and $C_{p,m}°$ vary by only 0.1 J · K^{-1} · mol^{-1}. This is no surprise as Hultgren et al. (1973) and Furukawa et al. (1974) basically reviewed the same published experimental data. Furukawa et al. (1974) show that the deviations of the heat-capacity data of the literature on palladium from their selected value in the range 30 to 300 K are about ±1% (Fig. 4 of Furukawa et al. 1974).

This review decided to accept the unweighted means of the $S_m°$ and $C_{p,m}°$ values recommended by Hultgren et al. (1973) and Furukawa et al. (1974), with uncertainties assigned by this review:

$S_m°$ (Pd, cr, 298.15 K) = (37.8 ± 0.4) J · K^{-1} · mol^{-1}

$C_{p,m}°$ (Pd, cr, 298.15 K) = (25.9 ± 0.3) J · K^{-1} · mol^{-1}

19.2.2 Palladium(0) solubility

While the solubility of metallic mercury in water has been measured with high precision and

$$Hg(l) \rightleftharpoons Hg(aq)$$

$$\log_{10}K°(298.15\ K) = -6.53 \pm 0.03$$

is well known (Section 14.2.2), to the present knowledge of the reviewer, no study has ever been published explicitly referring to the solubility of metallic palladium.

However, Wood (1991) and Azaroual et al. (2001) measured the solubility of metallic platinum. In both studies, no statistically significant pH dependence of the measured total concentration of dissolved platinum can be seen over the entire range from acidic to strongly basic conditions (Fig. 19-1). This is a strong indication that they really measured the equilibrium Pt(cr) ⇌ Pt(aq).

While the supersaturation experiments of Wood (1991) and the experiments with platinum powder of Azaroual et al. (2001) result in measured total dissolved platinum in the range of 10^{-6} – 10^{-8} mol · kg^{-1}, the experiments of Azaroual et al. (2001) with platinum wire from undersaturation result in measured total dissolved platinum in the range of 10^{-9} – 10^{-10} mol · kg^{-1} (Fig. 19-1). Only the latter data may represent the "true" solubility of platinum, while in the experiments from supersaturation and by using powder rather persistent colloidal or nanoparticles may have been generated.

Oda et al. (1996) report solubility experiments with palladium. They started from supersaturation by precipitating $Pd(OH)_2$(am) and observed with increasing time not only a decrease in their measured concentration of total dissolved palladium (Fig. 19-1), but also the increasing formation of Pd(cr), clearly visible in their XRD data. Oda et al. (1996) actually would have measured the solubility of Pd(cr) but unfortunately the detection limit of their analytical method to measure dissolved palladium was about 10^{-9} mol · kg^{-1}.

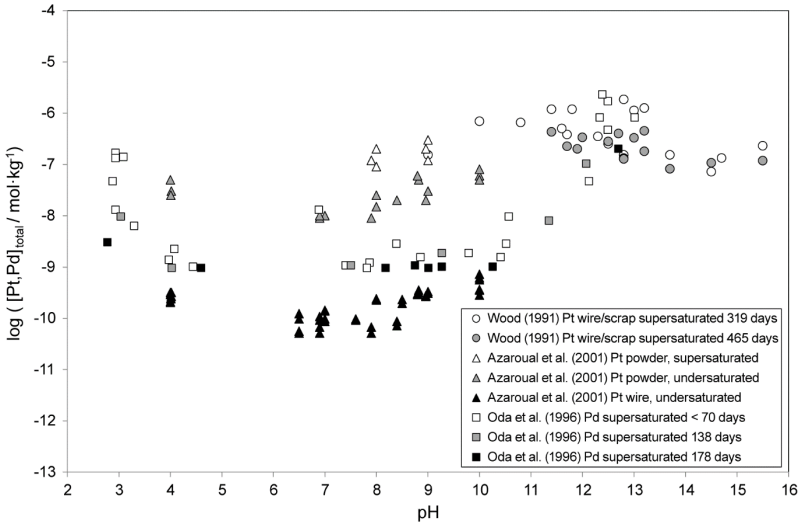

Fig. 19-1: Solubility of platinum and palladium metal as a function of pH

This review assumes that the solubility of palladium metal is like platinum metal and estimates, based on the solubility data of Azaroual et al. (2001) for platinum wire from undersaturation:

$$Pd(cr) \rightleftharpoons Pd(aq)$$

$$log_{10}K°(298.15\ K) = -9.5 \pm 0.5$$

This value is included in TDB 2020 as supplemental datum.

19.3 Palladium(II)

19.3.1 Palladium(II) aqua ion

The thermodynamics of the free ion Pd^{2+} has been evaluated by Sassani & Shock (1998). They estimated the absolute entropy of Pd^{2+} as $S_m°$ = -21.1 cal · K^{-1} · mol^{-1} = -88.28 J · K^{-1} · mol^{-1}, derived the Gibbs energy of formation as $\Delta_f G_m°$ = 42'200 cal · mol^{-1} = 176.56 kJ · mol^{-1} from the standard potential Pd^{2+}/Pd(s) as recommended by Izatt et al. (1967), and finally calculated $\Delta_f H_m°$ = 42'540 cal · mol^{-1} = 177.99 kJ · mol^{-1} from $S_m°$ and $\Delta_f G_m°$.

However, the value $log_{10}K°$ (298.15 K) = 30.9 of Izatt et al. (1967) (see Tab. 19-1) has been criticised by Lothenbach et al. (1999) who preferred the value $log_{10}K$ (298.15 K) = 33.4 (see Tab. 19-1) measured by Tempelton et al. (1943) in concentrated $HClO_4$. Lothenbach et al. (1999) extrapolated the value of Tempelton et al. (1943) to zero ionic strength with an estimated SIT coefficient $\varepsilon(Pd^{2+}, ClO_4^-) \approx 0.3$ and obtained $log_{10}K°$ (298.15 K) = 32.86, a value two orders at variance compared with the value recommended by Izatt et al. (1967).

In view of these discrepancies this review decided to re-evaluate the standard potential of the Pd^{2+} / Pd(cr) couple considering all available published data.

Experimental data for the redox potential of the half cell

$$Pd^{2+} + 2\ e^- \rightleftharpoons Pd(cr)$$

are compiled in Tab. 19-1.

Note that the careful and reliable measurements of Tempelton et al. (1943) have been carried out in 4.02 molal $HClO_4$, and not in 4.02 molar solutions as assumed by Lothenbach et al. (1999) (f in Tempelton et al. (1943) means "formula weights per kilogram water").

The redox potential given by Izatt et al. (1967) has been measured at low ionic strength and extrapolated by the authors to zero ionic strength using an extended Debye-Hückel expression. No data and no experimental details are reported by Izatt et al. (1967), and for this reason this review agrees with Lothenbach et al. (1999) that the Pd^{2+}/Pd(s) redox potential should not be based on this value, although it is compatible with the value selected by this review (see Fig. 19-2). However, the same group published additional data about this topic, measured in 3.94 m $HClO_4$ in the temperature range 10 to 40 °C (Izatt et al. 1970).

Tab. 19-1: Experimental data compiled for the redox pair Pd^{2+}/Pd(cr), according to the equilibrium $Pd^{2+} + 2\ e^- \rightleftharpoons Pd(cr)$

Methods: pot = potentiometry, vlt = voltammetry. Uncertainty estimates are based on statements in the papers, they should represent 95% of the statistical uncertainty.

Method	**Temp** [°C]	**Medium**	I_m [molal]	**Formal potential** E [V]	**$\log_{10}K$**	**Reference**
pot	25	$HClO_4$	4.02	0.987 ± 0.007	33.4 ± 0.4	Tempelton et al. (1943)
pot	25	$I \rightarrow 0$		0.915 ± 0.010	30.9 ± 0.6	Izatt et al. (1967)
pot	25	$HClO_4$	1.06	0.920 ± 0.006	31.1 ± 0.4	Levanda et al. (1968)
			2.22	0.924 ± 0.006	31.2 ± 0.4	
			3.46	0.952 ± 0.006	32.2 ± 0.4	
			4.87	0.996 ± 0.006	33.7 ± 0.4	
pot	10	$HClO_4$	3.94	0.978 ± 0.004	34.8 ± 0.4	Izatt et al. (1970)
	15			0.979 ± 0.010	34.2 ± 0.6	
	20			0.975 ± 0.010	33.5 ± 0.6	
	25			0.979 ± 0.010	33.1 ± 0.6	
	30			0.978 ± 0.006	32.5 ± 0.4	
	35			0.972 ± 0.010	31.8 ± 0.6	
	40			0.960 ± 0.008	30.9 ± 0.6	
vlt	25	$I \rightarrow 0$		0.91 ± 0.06	30.8 ± 2.0	Jackson & Pantony (1971)

The study by Levanda et al. (1968) using the same methods as the other groups, but varying the background electrolyte from 1.06 to 4.87 m $HClO_4$, allows an extrapolation to zero ionic strength by regression analysis. The most "recent" publication known to us is the study of Jackson & Pantony (1971) using polarography. The measurements have been carried out in 0.2 M $HClO_4$ and the results are given at zero ionic strength (i.e., extrapolated by the authors using a not specified version of the Debye-Hückel formalism). The redox potential reported by Jackson & Pantony (1971) is associated with a rather large uncertainty. It is compatible with the value selected by this review (see Fig. 19-2).

Using the data of Tempelton et al. (1943), Levanda et al. (1968) and Izatt et al. (1970) for an SIT analysis (Fig. 19-2), this review obtained

$$Pd^{2+} + 2\ e^- \rightleftharpoons Pd(cr)$$

$$\log_{10}K^\circ\ (298.15\ K) = 30.73 \pm 0.45$$

$$-\Delta\varepsilon = \varepsilon(Pd^{2+}, ClO_4^-) = 0.82 \pm 0.13$$

These values have been included in TDB 2020.

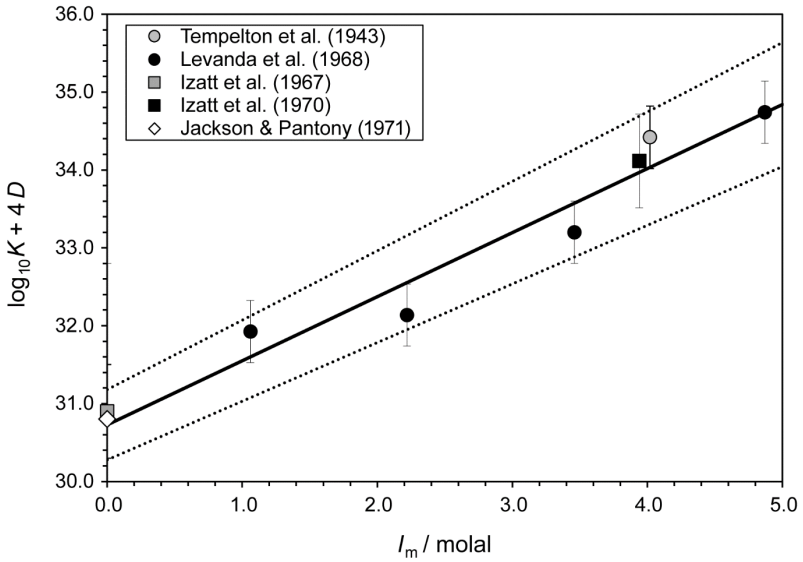

Fig. 19-2: Dependence of the equilibrium $Pd^{2+} + 2\ e^- \rightleftharpoons Pd(cr)$ on ionic strength in $HClO_4$

The solid line is obtained using the derived SIT interaction coefficient $\Delta\varepsilon = -0.81 \pm 0.11$ and the stability constant at zero ionic strength $\log_{10}K° = 30.79 \pm 0.36$. Dotted lines represent the 95% uncertainty range extrapolated from $I = 0$ to higher $HClO_4$ concentrations. The values at $I = 0$ have not been included in the SIT analysis.

Note that this reaction corresponds to the reaction $Pd^{2+} + H_2g \rightleftharpoons Pd(cr) + 2H^+$ where H^+ represents the cation in the standard hydrogen electrode, as all E(V) data in Tab. 19-1 are given as formal potentials with reference to the standard hydrogen electrode. Hence, H^+ is already in standard conditions and its activity coefficient must not be included in the expression for extrapolation to $I = 0$.

As can be seen in Fig. 19-2, an overall consistent picture emerges although the data of Izatt et al. (1967) and of Jackson & Pantony (1971) at zero ionic strength have not been included in the regression analysis.

Taking $\log_{10}K°$ from the SIT analysis we obtain

$$\Delta_f G_m° (Pd^{2+}, aq, 298.15\ K) = (175.4 \pm 2.6)\ kJ \cdot mol^{-1}$$

Using the estimated entropy from Sassani & Shock (1998)

$$S_m° (Pd^{2+}, aq, 298.15\ K) = -(88.3 \pm 0.3)\ J \cdot K^{-1} \cdot mol^{-1}$$

and the value $S_m°(Pd, cr, 298.15\ K) = (37.8 \pm 0.4)\ J \cdot K^{-1} \cdot mol^{-1}$, selected by this review (see Section 19.2.1), we obtain for the enthalpy of formation:

$$\Delta_f H_m° (Pd^{2+}, aq, 298.15\ K) = (176.8 \pm 2.6)\ kJ \cdot mol^{-1}$$

These values have been included in TDB 2020.

The temperature dependence of the Pd^{2+}/Pd(cr) redox potential has been measured by Izatt et al. (1970) in 3.94 m $HClO_4$ in the temperature range 10 to 40 °C (Tab. 19-1). Unweighted least squares fit of these data results in (Fig. 19-3):

$\log_{10}K$ (298.15 K, 3.94 m $HClO_4$) = 33.1 ± 0.2

$\Delta_r H_m$ (298.15 K, 3.94 m $HClO_4$) = -(214 ± 16) kJ · mol^{-1}

$\Delta_r C_{p,m}$ (298.15 K, 3.94 m $HClO_4$) = -(4.4 ± 3.5) kJ · mol^{-1}

Note that $\log_{10}K$ (298.15 K, 3.94 m $HClO_4$) = 33.1 ± 0.2 is in good agreement with the value selected by this review from the SIT analysis and extrapolated back to 3.94 m $HClO_4$, i.e.

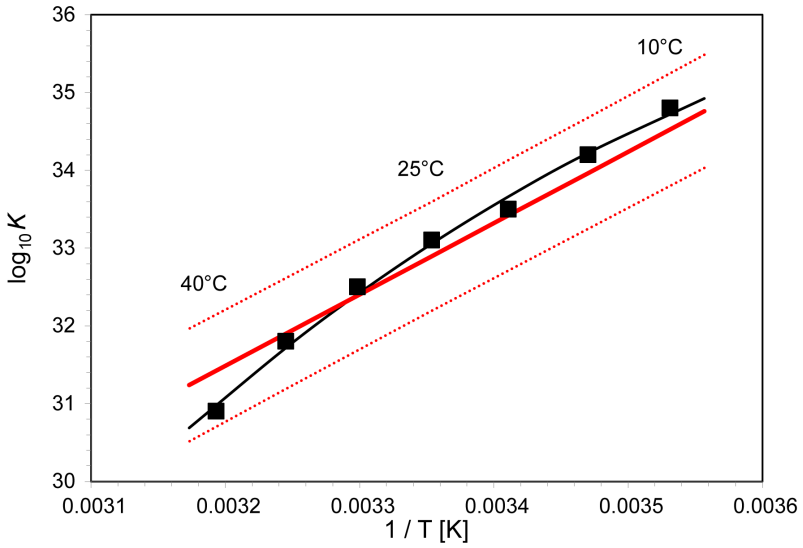

Fig. 19-3: Plot of $\log_{10}K$ versus reciprocal temperature for the reaction $Pd^{2+} + 2\ e^- \rightleftharpoons Pd(cr)$

The experimental data in 3.94 m $HClO_4$ have been taken from Izatt et al. (1970) (see Tab. 19-1). The curve represents a least squares fit of the experimental data assuming $\Delta_r C_{p,m}$ = const. The straight red lines have been calculated using $\log_{10}K°$ and $\Delta_r H_m°$ as selected in this review, extrapolated to 3.94 m $HClO_4$.

$\log_{10}K$ (298.15 K, 3.94 m $HClO_4$) = 32.9 ± 0.7

Extrapolating $\Delta_f H_m°$ (Pd^{2+}, aq, 298.15 K) = (176.8 ± 2.6) kJ · mol^{-1}, selected above, to 3.94 m $HClO_4$ can be achieved using the SIT model (see equation (IX.72) on page 412 of Grenthe et al. 1997) with an interaction coefficient $\varepsilon_L(Pd^{2+}, ClO_4) \approx \varepsilon_L(Mg^{2+}, Cl^-) = -1.2 \cdot 10^{-3}$ kg · K^{-1} · mol^{-1} (note that ε_L is the temperature derivative of the usual SIT ε). This results in

$\Delta_r H_m$ (298.15 K, 3.94 m $HClO_4$) = $-\Delta_f H_m$ = -(175.5 ± 2.6) kJ · mol^{-1}

Taking this value and $\log_{10}K$ (298.15 K, 3.94 m $HClO_4$) = 32.9 ± 0.7, the experimentally determined temperature dependence can be reproduced excellently in the temperature range 10 to 35 °C by the van't Hoff approximation, i.e., $\Delta_r C_{p,m} = 0$ (thick red line in Fig. 19-3). Whether the deviation of the measurement at 40 °C from a straight line is real or an artefact remains unclear.

19.3.2 Palladium(II) (hydr)oxide compounds and complexes

Polotnyanko & Khodakovskii (2013) report that the PdO – H_2O system contains two (meta)stable compounds, PdO(cr) and $Pd(OH)_2$(am). A compound $Pd(OH)_2$(cr) has not been synthesised yet. Freshly precipitated palladium(II) hydroxide has a light-yellow colour; dark brown $Pd(OH)_2$(am), forming during ageing, very slowly dissolves in concentrated perchloric acid during boiling.

Glemser & Peuschel (1955) report that in the presence of oxygen Pd(cr) is oxidised to PdO(cr) at 600 °C. In solutions which contain Pd(II), an amorphous, yellow-brown palladium-oxide-hydrate precipitates, PdO·H_2O(am) or $Pd(OH)_2$(am). In the absence of water, $Pd(OH)_2$(am) dehydrates to PdO(cr) above 90 °C, while in the presence of water above 100 °C, a PdO(s) solid with disturbed lattice is produced, indicating the incorporation of H_2O in the lattice (Glemser & Peuschel 1955).

PdO(cr) is reported to have been found in nature as an ochreous coating on palladian gold (porpezite) from Brazil and has been named palladinite. The IMA (International Mineralogical Association) status of this mineral is: approved, 'grandfathered' (first described prior to 1959), questionable (https://www.mindat.org/min-10660.html, accessed 26.1.2021).

19.3.2.1 Palladium(II) oxide

The temperature dependence of the heat capacity of palladium oxide, PdO(cr), has been studied for the first time in an adiabatic vacuum calorimeter in the range of 6.48 – 328.86 K by Smirnova et al. (2010) and Khodakovskii et al. (2011). Analytical-grade dark brown fine-grained powder of Russian production was used as samples. The correspondence of the structure of the studied phase to synthetic palladinite and the chemical homogeneity of the samples were confirmed by XRD and by analytical electron microscopy on a scanning electron microscope (Khodakovskii et al. 2011). The authors derive from their experimental calorimetric data

$\Delta_f G_m°$ (PdO, cr, 298.15 K) = -(82.68 ± 0.35) kJ · mol^{-1}

$\Delta_f H_m°$ (PdO, cr, 298.15 K) = -(112.69 ± 0.32) kJ · mol^{-1}

$S_m°$ (PdO, cr, 298.15 K) = (39.58 ± 0.15) J · K^{-1} · mol^{-1}

$C_{p,m}°$ (PdO, cr, 298.15 K) = (38.61 ± 0.10) J · K^{-1} · mol^{-1}

These values have been included in TDB 2020.

Koroleva et al. (2012) used the same samples of PdO(cr) as Smirnova et al. (2010) and Khodakovskii et al. (2011) to determine the solubility of crystalline palladium oxide (palladinite) in water and aqueous solutions of perchloric acid up to 2 mol · kg^{-1}. Concentrated $HClO_4$ solution was diluted by distilled water to prepare a set of solutions with concentrations from 2 – 0.05 m. The solid phase and solution were placed into cone glass flasks with ground stoppers and plastic

flasks and hermetically sealed. The experiments lasted for 18 months. The Pd concentrations in all samples were always several times higher than its detection limit by the analytical technique (Koroleva et al. 2012).

Using $\Delta_f G_m°$ (PdO, cr, 298.15 K) = -(82.68 ± 0.35) kJ · mol^{-1} (Smirnova et al. 2010), $\Delta_f G_m°$ (Pd^{2+}, aq, 298.15 K) = (175.4 ± 2.6) kJ · mol^{-1} (derived by this review, see Section 19.3.1) and $\Delta_f G_m°$ (H_2O, l, 298.15 K) = -(237.140 ± 0.040) kJ · mol^{-1} (Cox et al. 1989), this review calculates for the reaction

$$PdO(cr) + 2\ H^+ \rightleftharpoons Pd^{2+} + 2\ H_2O(l)$$

$$\Delta_r G_m° \text{ (298.15 K)} = (20.94 \pm 2.62) \text{ kJ} \cdot \text{mol}^{-1}$$

$$\log_{10} K_{s,0}° \text{ (298.15 K)} = -3.67 \pm 0.46$$

The latter value has also been included in TDB 2020.

Note that the solubility of PdO(cr) calculated from Gibbs free energies selected by this review at pH < = 2 is about one order of magnitude higher than the measured aqueous Pd concentrations of Koroleva et al. (2012) (dashed red line in Fig. 19-4).

This significant discrepancy seems to clearly indicate that Koroleva et al. (2012) did not measure the solubility of the solid PdO(cr) used in the calorimetric measurements. As discussed below, we assume that PdO(cr) reacted in the solubility experiments to a reduced form, and Koroleva et al. (2012) actually measured the solubility of metallic palladium, Pd(cr).

However, the group of the late Khodakovskii did not consider this interpretation of their data but tried to solve the problem otherwise, as described in the following.

Polotnyanko & Khodakovskii (2013) in turn used the solubility data of Koroleva et al. (2012) to assess $\Delta_f G_m°$ (Pd^{2+}, aq, 298.15 K). Polotnyanko & Khodakovskii (2013) state that "using the Gibbs free energy $\Delta_r G_m°$ (298.15 K) = (28.48 ± 1.7) kJ · mol^{-1} for reaction

$$PdO(cr) + 2\ H^+ \rightleftharpoons Pd^{2+} + 2\ H_2O(l)$$

calculated from data on palladium oxide solubility (Koroleva et al. 2012), the value $\Delta_f G_m°$ (PdO, cr, 298.15 K) = -(82.68 ± 0.35) kJ · mol^{-1} (Smirnova et al. 2010) as well as $\Delta_f G_m°$ (H_2O, l, 298.15 K) = -(237.140 ± 0.040) kJ · mol^{-1} (Cox et al. 1989), we obtain $\Delta_f G_m°$ (Pd^{2+}, aq, 298.15 K) = 182.9 ± 1.7) kJ · mol^{-1}. The latter value significantly differs (by 6 kJ · mol^{-1}) from those that are presented in fundamental thermodynamic reference books and based on experimentally measured palladium electrode potential".

Comparing the value of Polotnyanko & Khodakovskii (2013) with the one derived by this review, $\Delta_f G_m°$ (Pd^{2+}, aq, 298.15 K) = (175.4 ± 2.6) kJ · mol^{-1} (see Section 19.3.1), the difference is even a bit larger (7.5 kJ · mol^{-1}).

Polotnyanko & Khodakovskii (2013) conclude that "to reveal the reasons of revealed inconsistency, it is required to analyse in detail literature data on the Cl – Pd(aq) system allowing independent calculations of $\Delta_f G_m°$ (Pd^{2+}, aq, 298.15 K)".

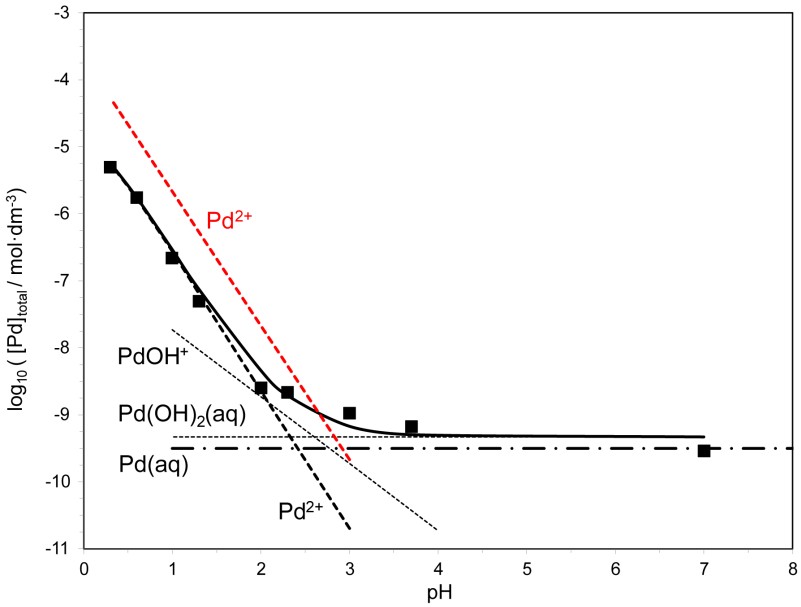

Fig. 19-4: Solubility of palladium as a function of pH

Symbols: experimental data of Koroleva et al. (2012), using PdO(cr) as starting material. Straight lines: supposed aqueous palladium species (see text). Solid line: total palladium solubility assuming only Pd(II) aqueous species in equilibrium with Pd(cr). Dashed red line: Solubility of PdO(cr) calculated from Gibbs free energies selected by this review.

However, from their literature review of Pd chloride complexes Polotnyanko & Khodakovskii (2014) obtained $\Delta_f G_m°$ (Pd^{2+}, aq, 298.15 K) = 190.1 ± 1.4) kJ · mol^{-1}, a value even another 7 kJ · mol^{-1} at variance from their value obtained from PdO(cr) solubility, and 14.6 kJ · mol^{-1} higher than the value selected by this review. This latter, even bigger inconsistency remained uncommented by Polotnyanko & Khodakovskii (2014).

Koroleva et al. (2012) used PdO(cr) as starting material, but was PdO(cr) still the solubility determining solid phase at the end of their long-term solubility experiments?

The theoretical redox potential of the equilibrium Pd(cr) + H_2O(l) ⇌ PdO(cr) + H_2g is $\Delta_r G_m°$ = $\Delta_f G_m°$ (PdO, cr, 298.15 K) – $\Delta_f G_m°$ (H_2O, l, 298.15 K) = -(154.46 ± 0.35) kJ · mol^{-1}, which in turn is $\log_{10} K°$ (298.15 K) = -27.06 ± 0.06. This value is equivalent to the hydrogen partial pressure, or the fugacity, *f*, of the redox couple PdO(cr)/Pd(cr): $\log_{10} f_{H2} = \log_{10} K° = -27.06 \pm 0.06$. For pH 7 this translates to Eh = 0.39 V, with respect to the standard hydrogen electrode (SHE).

The theoretical redox potential of "pure water" can be calculated from the equilibrium H_2g + ½ O_2g ⇌ H_2O(l) with $\Delta_r G_m° = \Delta_f G_m°$ (H_2O, l, 298.15 K) = -(237.14 ± 0.041) kJ · mol^{-1}, which in turn is $\log_{10} K°$ (298.15 K) = 41.545 ± 0.007. From this value, the hydrogen partial pressure, or the fugacity, *f*, of "pure water" is calculated as $\log_{10} f_{H2} = (-2 \cdot \log_{10} K° - \log_{10}(1/2)) / 3 = -27.60 \pm 0.10$. For pH 7 this translates to Eh = 0.40 V (SHE). This value is almost identical to the redox potential PdO(cr)/Pd(cr).

However, the measured redox potentials of distilled and degassed water, Eh = 0.2 V (SHE) at pH 7.0 and 7.6, respectively (Kazdobin et al. 2009), are still lower than this theoretical value of "pure water". The fugacities, *f*, of distilled water and degassed water are calculated as $\log_{10} f_{H2} = -20.8$ and -22.0, respectively. Therefore, distilled and degassed pure water can reduce PdO(cr) to Pd(cr).

Hence, this review assumes that the experimental data of Koroleva et al. (2012) at pH < = 2 actually refer to the equilibrium

$$Pd(cr) + 2\ H^+ \rightleftharpoons Pd^{2+} + H_2g$$

Using $\Delta_f G_m^\circ$ (Pd^{2+}, aq, 298.15 K) = (175.4 ± 2.6) kJ · mol^{-1}, as selected by this review (see Section 19.3.1), a perfect fit of data of Koroleva et al. (2012) at pH < = 2 was obtained for $\log_{10} f_{H2} = -26$ (dashed black line in Fig. 19-4).

The data of Koroleva et al. (2012) at pH > 2 have been fitted assuming a constant value of $\log_{10} f_{H2} = -26$ for the equilibria $Pd(cr) + H_2O(l) + H^+ \rightleftharpoons PdOH^+ + H_2g$ and $Pd(cr) + 2\ H_2O(l) \rightleftharpoons Pd(OH)_2(aq) + H_2g$. The best fit was obtained for (dotted lines in Fig. 19-4):

$$Pd^{2+} + H_2O(l) \rightleftharpoons PdOH^+ + H^+$$

$$\log_{10}{}^*\beta_1^\circ\ (298.15\ K) = -2$$

$$Pd^{2+} + 2\ H_2O(l) \rightleftharpoons Pd(OH)_2(aq) + 2\ H^+$$

$$\log_{10}{}^*\beta_2^\circ\ (298.15\ K) = -4.6$$

These values have been included in TDB 2020 as supplemental data.

The species $PdOH^+$ could not be confirmed in the fits of the solubility data of van Middlesworth & Wood (1999) (see Section 19.3.2.2).

Concerning the data of Koroleva et al. (2012) the species $Pd(OH)_2(aq)$ is speculative. At pH > 3 the solubility could also be explained by the equilibrium Pd(cr) = Pd(aq) (dot-dashed line in Fig. 19-4).

However, the value $\log_{10}{}^*\beta_2^\circ$ (298.15 K) = -4.6 explains the pH independent solubility data of van Middlesworth & Wood (1999) (Figs. 19-6 and 19-9).

19.3.2.2 Palladium(II) hydroxide

Nabivanets & Kalabina (1970) measured a constant Pd(II) concentration of $4 \cdot 10^{-6}$ M between pH 3 and 11 in 0.1M perchlorate media for freshly precipitated $Pd(OH)_2(precip)$, corresponding to log*K* = -5.4 for the reaction $Pd(OH)_2(precip) \rightleftharpoons Pd(OH)_2(aq)$. They did not indicate any detection limit but Lothenbach et al. (1999) and Rai et al. (2012) suspect that the measured minimum Pd(II) concentration reflects the detection limit of the analytical method used by Nabivanets & Kalabina (1970). Hence, the results of Nabivanets & Kalabina (1970) have not been considered further by this review.

Wood (1991) determined the solubility of palladium in the pH range 8 – 15.5 using Pd shot as starting material. Wood (1991) reports that "all preparation and handling of solutions were performed in a glovebox under a N_2 (reduced O_2) atmosphere. The solutions were transferred to 250-mL capacity high density polyethylene or polypropylene bottles along with a few grams of Pt wire and Pd shot. Once sealed, the bottles were shaken vigorously and placed in a constant-temperature water bath. To hasten the approach to equilibrium, the water bath was taken to 85 °C for 18 days and then lowered gradually to 25 °C. No attempt was made to bracket the solubilities from undersaturated conditions".

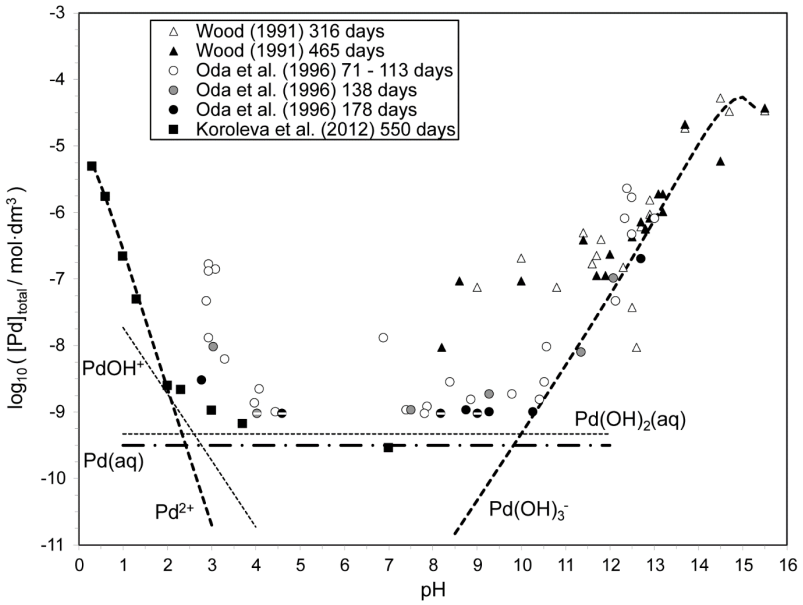

Fig. 19-5: Solubility of palladium as a function of pH

Symbols: experimental data of Koroleva et al. (2012), using PdO(cr) as starting material, Wood (1991), using Pd metal as starting material, and Oda et al. (1996), where Pd(cr) was formed during the solubility experiments. Lines: supposed aqueous palladium species (see text).

The solubility values determined by Wood (1991) in the pH range 8 – 12 from oversaturation might be orders of magnitude too high. Note the large scatter of data in Fig. 19-5 and the similarity to the effects seen by Oda et al. (1996), who also started from oversaturation with $Pd(OH)_2$(am) (Figs. 19-1 and 19-5). In addition, the platinum solubility of Wood (1991) shows the same effect (Fig. 19-1).

However, the data of Wood (1991) at pH > 12 may indicate the presence of $Pd(OH)_3^-$ as solubility determining species. Hence, the data of Wood (1991) at pH > 12 have been fitted assuming a constant value of $\log_{10}f_{H2} = -28$ for the equilibrium Pd(cr) + 3 H_2O(l) ⇌ $Pd(OH)_3^-$ + H^+ + H_2g. The value $\log_{10}f_{H2} = -28$ is close to the theoretical redox potential of "pure water" ($\log_{10}f_{H2} = -27.60 \pm 0.10$, see Section 19.3.2.1) and results in a good fit of the data of van Middlesworth & Wood (1999) (see below, Fig. 19-6). Using the estimate $\varepsilon(Pd(OH)_3^-, Na^+) = -0.05 \pm 0.10$ kg · mol^{-1} the best fit was obtained for (dashed line in Fig. 19-5):

$Pd^{2+} + 3\ H_2O(l) \rightleftharpoons Pd(OH)_3^- + 3\ H^+$

$log_{10}{}^*\beta_3^\circ\ (298.15\ K) = -16.6$

This value has been included in TDB 2020 as supplemental datum.

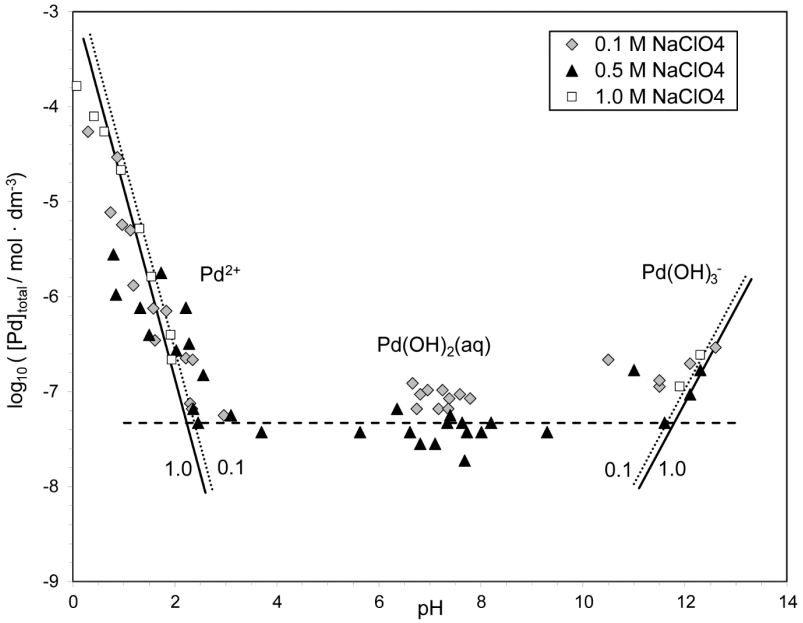

Fig. 19-6: Solubility of palladium as a function of pH

Symbols: experimental solubility data of van Middlesworth & Wood (1999) in $NaClO_4$ at 25 °C using $Pd(OH)_2$(am) as starting material. Straight lines: supposed aqueous palladium species (see text).

Note that the curvature of the dashed line in Fig. 19-5 at pH > 14 is an ionic strength effect.

Van Middlesworth & Wood (1999) measured the solubility of palladium, using amorphous $Pd(OH)_2$(am) as starting material, in $NaClO_4$ over a wide range of parameters ($0 \le pH \le 12$, 0.1 m $\le [NaClO_4] \le$ 1.0 m, 25 °C ≤ Temp ≤ 70 °C). As can be seen in Fig. 19-6, a synopsis of all experimental data of van Middlesworth & Wood (1999) in $NaClO_4$ at 25 °C shows a quite consistent overall pattern.

The data of van Middlesworth & Wood (1999) in $NaClO_4$ at 25 °C can be modelled simply by using the same hydrogen fugacity as for the data of Wood (1991), $\log_{10}f_{H2} = -28$, and the same parameters as for the data of Wood (1991) and Koroleva et al. (2012), i.e., $\log_{10}{}^*\beta_2^\circ$ (298.15 K) = -4.6 and $\log_{10}{}^*\beta_3^\circ$ (298.15 K) = 16.6 (lines in Fig. 19-6). The ionic strength effect on Pd^{2+} and $Pd(OH)_3^-$ is negligible (solid and dotted lines in Fig. 19-6).

From a statistical point of view, the existence of $PdOH^+$ cannot be confirmed by fitting the data of van Middlesworth & Wood (1999), as Rai et al. (2012) concluded from their modelling exercise using the same experimental data.

Considering all the above discussed solubility studies, where at the end always Pd(cr) seems to have been the solubility controlling solid, irrespective whether PdO(cr), $Pd(OH)_2$(am) or Pd(cr)

was the starting material, this review concludes that no solubility experiments have been done yet under sufficiently oxidising conditions to ensure that PdO(cr) or $Pd(OH)_2$(am) is the solubility limiting solid phase. Consequently, the solubility of PdO(cr) is calculated from calorimetric data, and no $\log_{10}K_{s,0}°$ value can be derived for $Pd(OH)_2$(am) from the available experimental solubility data.

19.3.3 Palladium(II) chloride complexes

Data for palladium chloride complexes are abundant. The most reliable studies of Pd(II) chloride complexes are the spectrophotometric investigations by Levanda (1968) in 1 – 4 M $LiClO_4$, Elding (1972) in 1 M $HClO_4$, and Boily & Seward (2005) in the temperature range 5 – 125 °C.

A re-evaluation of the extensive temperature data set published by Boily & Seward (2005) by this review resulted in (Fig. 19-7):

$Pd^{2+} + Cl^- \rightleftharpoons PdCl^+$

$\log_{10}K_1°$ (298.15 K) = 5.02 ± 0.04

$\Delta_r H_m°$(298.15 K) = -(18.6 ± 0.8) kJ · mol^{-1}

$\Delta_r C_{p,m}°$(298.15 K) = (121 ± 21) J · K^{-1} · mol^{-1}

$PdCl^+ + Cl^- \rightleftharpoons PdCl_2$(aq)

$\log_{10}K_2°$ (298.15 K) = 3.45 ± 0.06

$\Delta_r H_m°$(298.15 K) = -(10.9 ± 1.2) kJ · mol^{-1}

$\Delta_r C_{p,m}°$(298.15 K) = (124 ± 32) J · K^{-1} · mol^{-1}

$PdCl_2$(aq) + $Cl^- \rightleftharpoons PdCl_3^-$

$\log_{10}K_3°$ (298.15 K) = 2.10 ± 0.06

$\Delta_r H_m°$(298.15 K) = -(3.5 ± 1.1) kJ · mol^{-1}

$\Delta_r C_{p,m}°$(298.15 K) = (30 ± 32) J · K^{-1} · mol^{-1}

$PdCl_3^- + Cl^- \rightleftharpoons PdCl_4^{2-}$

$\log_{10}K_4°$ (298.15 K) = 0.88 ± 0.09

$\Delta_r H_m°$(298.15 K) = -(13.6 ± 1.9) kJ · mol^{-1}

$\Delta_r C_{p,m}°$(298.15 K) = (113 ± 52) J · K^{-1} · mol^{-1}

These values have been included in TDB 2020.

The stepwise stability constant $\log_{10}K_4$ has been investigated by Levanda (1968) in 1 – 4M $LiClO_4$ and Elding (1972) in 1 M $HClO_4$. Using these data for an SIT analysis results in (Fig. 19-8).

$\log_{10}K_4°$ (298.15 K) = 0.85 ± 0.09

$\Delta\varepsilon(H,LiClO_4)$ = -0.11 ± 0.03

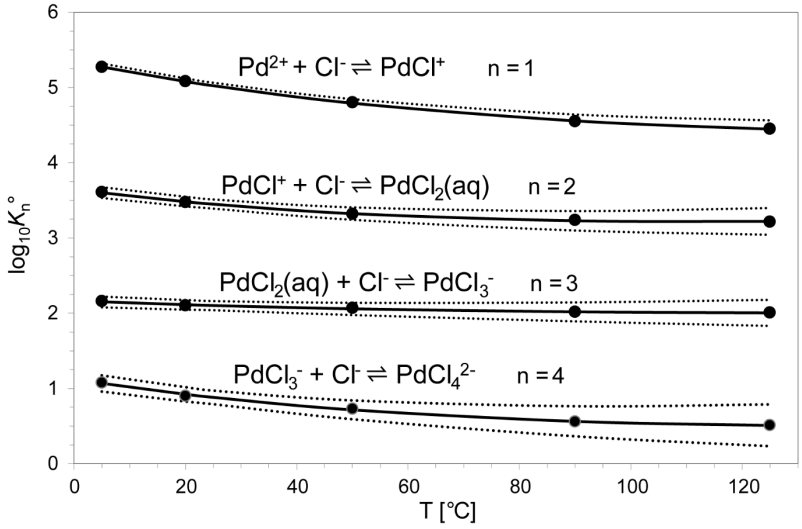

Fig. 19-7: The stepwise equilibrium constants $\log_{10}K_n°$ for $PdCl_{n-1}^{3-n} + Cl^- \rightleftharpoons PdCl_n^{2-n}$ as function of temperature in the range 5 – 125 °C.

Symbols: experimental data of Boily & Seward (2005). Solid line: unweighted regression of experimental data. Dotted lines: lower and upper limits using $\log_{10}K_i°$ (298.15 K), $\Delta_rH_m°$(298.15 K) and $\Delta_rC_{p,m}°$(298.15 K) values given in the text, and extrapolated to lower and higher temperatures.

The $\log_{10}K_4°$ value obtained from the SIT analysis is in excellent agreement with the result of the temperature study by Boily & Seward (2005).

Assuming that $\Delta\varepsilon(H,LiClO_4) \approx \Delta\varepsilon(NaClO_4)$ and using $\varepsilon(Na^+, Cl^-) = 0.03 \pm 0.01$ kg · mol^{-1} (Lemire et al. 2013) and the estimate $\varepsilon(PdCl_4^{2-}, Na^+) = -0.10 \pm 0.10$ kg · mol^{-1} this review calculated

$\varepsilon(PdCl_3^-, Na^+) = -0.02 \pm 0.10$ kg · mol^{-1}

a value in good agreement with the expected value for a singly charged anionic species.

This value has been included in TDB 2020.

Rai et al. (2012) modelled the solubility data of van Middlesworth & Wood (1999) obtained in 0.1 – 1.0 M KCl solutions assuming that $Pd(OH)_2$(am) is the solubility controlling solid phase. However, to fit the solubility data in KCl, Rai et al. (2012) had to assume $\log_{10}K_4°$ (298.15 K) = 2.12 for $PdCl_3^- + Cl^- \rightleftharpoons PdCl_4^{2-}$, a value more than one order of magnitude higher than the well-established value derived from all reliable studies (see above).

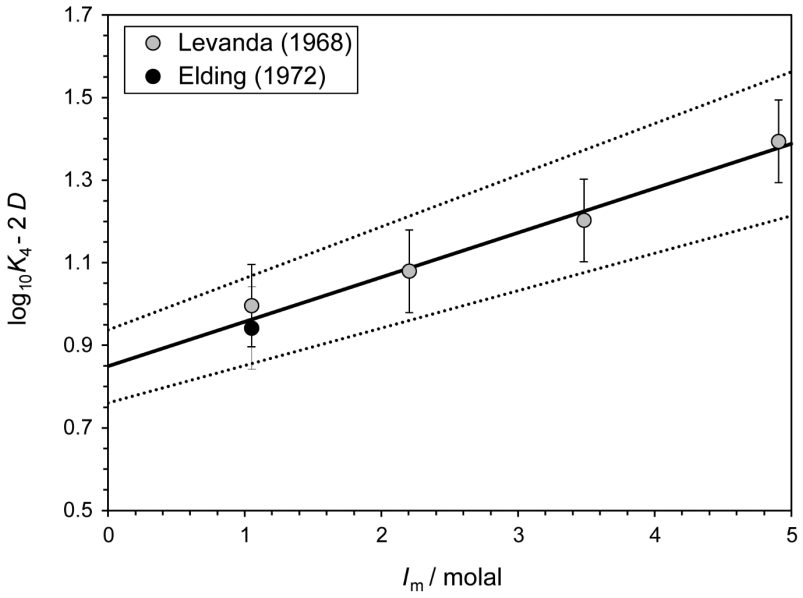

Fig. 19-8: Dependence of the equilibrium $PdCl_3^- + Cl^- \rightleftharpoons PdCl_4^{2-}$ on ionic strength in $LiClO_4$ (Levanda 1968) and $HClO_4$ (Elding 1972)

The solid line is obtained using the derived SIT interaction coefficient $\Delta\varepsilon = -0.11 \pm 0.03$ and the stability constant at zero ionic strength, $\log_{10}K_4°$ (298.15 K) = 0.85 ± 0.09. Dotted lines represent the 95% uncertainty range extrapolated from I = 0 to higher ClO_4^- concentrations.

By contrast, this review assumed that Pd(cr) was the solubility limiting solid phase not only in the $NaClO_4$ experiments (see Section 19.3.2.2, Fig. 19-6) but also in the KCl solubility data set of van Middlesworth & Wood (1999). A consistent and satisfactory representation of all data in KCl media has been obtained (Fig. 19-9) by assuming a hydrogen fugacity of $\log_{10}f_{H2} = -28.3$ and using the above selected stability constants for palladium(II) chloride complexes, as well as the values obtained by this review for $Pd(OH)_2(aq)$ and $Pd(OH)_3^-$. Note that according the equilibria

$$Pd(cr) + 2\ H_2O(l) \rightleftharpoons Pd(OH)_2(aq) + H_2g$$

$$Pd(cr) + 3\ H_2O(l) \rightleftharpoons Pd(OH)_3^- + H^+ + H_2g$$

the assumed decrease of the hydrogen fugacity by 0.3 log-units for the KCl data with respect to the $NaClO_4$ data accounts for the concomitant increase in $Pd(OH)_2(aq)$ and $Pd(OH)_3^-$ concentrations of the same 0.3 log-units.

Finally, this review agrees with the conclusion of Rai et al. (2012) that the experimental data of van Middlesworth & Wood (1999) in KCl media do not corroborate the existence of mixed Pd – Cl – OH complexes.

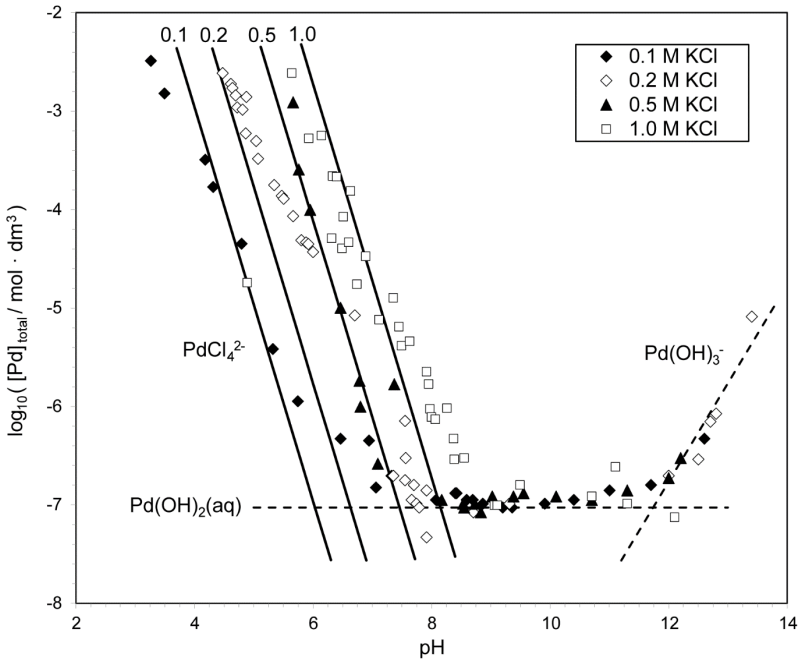

Fig. 19-9: Solubility of palladium as a function of pH in KCl media

Symbols: experimental solubility data of van Middlesworth & Wood (1999) in 0.1 – 1.0 M KCl at 25 °C using $Pd(OH)_2$(am) as starting material. Solid lines: $PdCl_4^{2-}$ calculated using stability constants selected by this review. Dashed lines: supposed aqueous palladium species as selected by this review (see text).

19.3.4 Palladium(II) sulphate complexes

An aqueous palladium sulphate complex has been reported by Jackson & Pantony (1971). Their polarographic study of the system Pd(II) sulphate - Pd(cr) in 0.2 M $HClO_4$ has been interpreted in terms of the equilibrium

$$Pd^{2+} + 2\ SO_4^{2-} \rightleftharpoons Pd(SO_4)_2^{2-}$$

$$\log_{10}\beta_2 = 3.16 \pm 0.15$$

This value is the source of the number found in Pearson et al. (1992), extrapolated to zero ionic strength using the Davies equation with a parameter 0.3, $\log_{10}\beta_2^\circ = 4.16$. However, the small uncertainty given in Jackson & Pantony (1971) is misleading. The authors themselves state that "the result is tentative, but no previous value appears to have been reported for the complex". In the same paper Jackson & Pantony (1971) report a Pd^{2+}/Pd(s) redox potential with a very large uncertainty, although, by chance, the number fits nicely in the overall picture (see Fig. 19-2 and Tab. 19-1). In addition, Jackson & Pantony (1971) studied Pd(II) chloride complexation by the same method as used in their Pd(II) sulphate work and reported stability constants more than two orders (!) of magnitude lower than all other studies, e.g., Elding (1972).

We conclude that the stability constant reported by Jackson & Pantony (1971) is very uncertain, to say the least. No other study about aqueous palladium sulphate complexation is known to us. Thus, we decided not to consider this value in TDB 2020.

19.3.5 Palladium(II) ammonia complexes

Aqueous nickel amine complexes are very stable, and they can be relevant for modelling work concerning the degradation products of anion exchange resins in a repository (Van Loon & Hummel 1999). Rasmussen & Jørgensen (1968) determined the consecutive formation constants of all four amino complexes of Pd(II) using visible absorption spectroscopy. This study is reliable and can be recommended (Lothenbach et al. 1999). Due to the isocoulombic equilibria, and assuming $\Delta\varepsilon = 0$ (Lothenbach et al. 1999) the ionic strength dependence will be very small, and the constants reported by Rasmussen & Jørgensen (1968) for 1M $NaClO_4$ are thus recommended at any ionic strength with an uncertainty of ±0.2 (Lothenbach et al. 1999):

$$Pd^{2+} + n\ NH_3(aq) \rightleftharpoons Pd(NH_3)_n^{2+}$$

$$\log_{10}\beta_1^\circ\ (298.15\ K) = 9.6 \pm 0.2$$

$$\log_{10}\beta_2^\circ\ (298.15\ K) = 18.5 \pm 0.2$$

$$\log_{10}\beta_3^\circ\ (298.15\ K) = 26.0 \pm 0.2$$

$$\log_{10}\beta_4^\circ\ (298.15\ K) = 32.8 \pm 0.2$$

It is very likely that mixed ammonia hydroxo complexes are formed in the Pd(II) - H_2O - NH_3 system. A palladium-ammonia-dihydroxo compound, $Pd(NH_3)_2(OH)_2(s)$, named Palladamin, is known since the middle of the 19th century (Müller 1853, Gmelin 1942). However, no thermodynamic data, neither for solid compounds nor for aqueous complexes have been reported. For a detailed discussion and estimates of maximum stabilities of such mixed complexes see Van Loon & Hummel (1999).

19.3.6 Palladium(II) carbonate compounds and complexes

No thermodynamic data have been reported concerning palladium carbonate compounds and complexes.

It has been argued by Lothenbach et al. (1999) "that carbonate complexes of Pd(II) may simply not form at all because of the enormous competition by hydroxide". On the other hand, mixed palladium carbonate compounds have been reported (Gmelin 1942). For example, the above mentioned Palladamin (see Section 19.3.5) is stable only in a CO_2-free atmosphere. Its solution, as well as the crystalline solid, takes up CO_2 rapidly, forming $Pd(NH_3)_2CO_3(s)$. It is remarkable in this context that to our present knowledge, the formation of pure palladium carbonate compounds has never been observed, neither in nature nor in the laboratory. The formation of mixed complexes with hard anions like carbonate, however, seems to be facilitated when at least two Pd bonds are occupied by ammonia or chloride. The long list of mixed compounds of this type described in Gmelin (1942) corroborates this general observation.

19.4 Selected palladium data

Tab. 19-2: Selected palladium data

Supplemental data are in italics.

Name	**$\Delta_f G_m°$** [kJ · mol^{-1}]	**$\Delta_f H_m°$** [kJ · mol^{-1}]	**$S_m°$** [J · K^{-1} · mol^{-1}]	**$C_{p,m}°$** [J · K^{-1} · mol^{-1}]	**Species**
Pd(cr)	0.0	0.0	37.8 ± 0.4	25.9 ± 0.3	Pd(cr)
Pd+2	175.4 ± 2.6	176.8 ± 2.6	-88.3 ± 0.3		Pd^{2+}
Palladinite	-82.68 ± 0.35	-112.69 ± 0.32	39.58 ± 0.15	38.61 ± 0.10	PdO(cr)

Name	**$\log_{10}\beta°$**	**$\Delta\varepsilon$** [kg · mol^{-1}]	**$\Delta_r H_m°$** [kJ · mol^{-1}]	**$\Delta_r C_{p,m}°$** [J · K^{-1} · mol^{-1}]	**T-range** [°C]	**Reaction**
Pd(aq)	*-9.5 ± 0.5*					*Pd(cr) ⇌ Pd(aq)*
Pd+2	-30.73 ± 0.45	0.82 ± 0.13	176.8 ± 2.6	0	10 – 35	$Pd(cr) \rightleftharpoons Pd^{2+} + 2\ e^-$
PdOH+	*-2*					*$Pd^{2+} + H_2O(l) \rightleftharpoons PdOH^+ + H^+$*
Pd(OH)2(aq)	*-4.6*					*$Pd^{2+} + 2H_2O(l) \rightleftharpoons Pd(OH)_2(aq) + 2H^+$*
Pd(OH)3-	*-16.6*					*$Pd^{2+} + 3H_2O(l) \rightleftharpoons Pd(OH)_3^- + 3H^+$*
PdCl+	5.02 ± 0.04		-18.6 ± 0.8	121 ± 21	5 – 125	$Pd^{2+} + Cl^- \rightleftharpoons PdCl^+$
PdCl2(aq)	3.45 ± 0.06		-10.9 ± 1.2	124 ± 32	5 – 125	$PdCl^+ + Cl^- \rightleftharpoons PdCl_2(aq)$
PdCl3-	2.10 ± 0.06		-3.5 ± 1.1	30 ± 32	5 – 125	$PdCl_2(aq) + Cl^- \rightleftharpoons PdCl_3^-$
PdCl4-2	0.88 ± 0.09	-0.11 ± 0.03	-13.6 ± 1.9	113 ± 52	5 – 125	$PdCl_3^- + Cl^- \rightleftharpoons PdCl_4^{2-}$
PdNH3+2	9.6 ± 0.2					$Pd^{2+} + NH_3(aq) \rightleftharpoons PdNH_3^{2+}$
Pd(NH3)2+2	18.5 ± 0.2					$Pd^{2+} + 2\ NH_3(aq) \rightleftharpoons Pd(NH_3)_2^{2+}$
Pd(NH3)3+2	26.0 ± 0.2					$Pd^{2+} + 3\ NH_3(aq) \rightleftharpoons Pd(NH_3)_3^{2+}$
Pd(NH3)4+2	32.8 ± 0.2					$Pd^{2+} + 4\ NH_3(aq) \rightleftharpoons Pd(NH_3)_4^{2+}$

Name	**$\log_{10}K_{s,0}°$**	**$\Delta_r H_m°$** [kJ · mol^{-1}]	**$\Delta_r C_{p,m}°$** [J · K^{-1} · mol^{-1}]	**Reaction**
Palladinite	-3.67 ± 0.46	-	-	$PdO(cr) + 2\ H^+ \rightleftharpoons Pd^{2+} + H_2O(l)$

Tab. 19-3: Selected SIT ion interaction coefficients $\varepsilon_{j,k}$ [kg · mol^{-1}] for palladium species

Data in normal face are derived or estimated in this review. Data estimated according to charge correlations and taken from Tab. 1-7 are shaded. Supplemental data are in italics.

j k → ↓	**Cl^-** $\varepsilon_{j,k}$ [kg · mol^{-1}]	**ClO_4^-** $\varepsilon_{j,k}$ [kg · mol^{-1}]	**Na^+** $\varepsilon_{j,k}$ [kg · mol^{-1}]	**$Na^+ + Cl^-$** $\varepsilon_{j,k}$ [kg · mol^{-1}]	**$Na^+ + ClO_4^-$** $\varepsilon_{j,k}$ [kg · mol^{-1}]
Pd(aq)	*0*	*0*	*0*	*0.0 ± 0.1*	*0.0 ± 0.1*
Pd+2	(0.82 ± 0.13) [a]	0.82 ± 0.13	0	0	0
PdOH+	*0.20 ± 0.10* [a]	*0.20 ± 0.10*	*0*	*0*	*0*
Pd(OH)2(aq)	*0*	*0*	*0*	*0.0 ± 0.1*	*0.0 ± 0.1*
Pd(OH)3-	*0*	*0*	*-0.05 ± 0.10*	*0*	*0*
PdCl+	0.20 ± 0.10 [a]	0.20 ± 0.10	0	0	0
PdCl2(aq)	0	0	0	0.0 ± 0.1	0.0 ± 0.1
PdCl3-	0	0	-0.02 ± 0.10	0	0
PdCl4-2	0	0	-0.10 ± 0.10	0	0
PdNH3+2	(0.82 ± 0.13) [a]	0.82 ± 0.13	0	0	0
Pd(NH3)2+2	(0.82 ± 0.13) [a]	0.82 ± 0.13	0	0	0
Pd(NH3)3+2	(0.82 ± 0.13) [a]	0.82 ± 0.13	0	0	0
Pd(NH3)4+2	(0.82 ± 0.13) [a]	0.82 ± 0.13	0	0	0

[a] Assumed to be equal to the corresponding ion interaction coefficient with ClO_4^-, see Section 19.1 for explanation.

19.5 References

Azaroual, M., Romand, B., Freyssinet, P. & Disnar, J.-R. (2001): Solubility of platinum in aqueous solutions at 25 °C and pHs 4 to 10 under oxidizing conditions. Geochim. Cosmochim. Acta, 65, 4453-4466.

Bard, A.J., Parsons, R. & Jordan, J. (1985): Standard Potentials in Aqueous Solution. Marcel Dekker, New York, 834 pp.

Boily, J.-F. & Seward, T.M. (2005): Palladium(II) chloride complexation: Spectrophotometric investigation in aqueous solutions from 5 to 125 °C and theoretical insight into Pd-Cl and Pd-OH_2 interactions. Geochim. Cosmochim. Acta, 69, 3773-2789.

Brookins, D.G. (1988): Eh-pH Diagrams for Geochemistry. Springer-Verlag Berlin Heidelberg, Germany, 184 pp.

Brown, P.L. & Ekberg, C. (2016): Hydrolysis of Metal Ions. Wiley-VCH Verlag GmbH & Co. KGaA, Weinheim, Germany, 917 pp.

Cox, J.D., Wagman, D.D., Medvedev, V.A. (1989): CODATA Key Values for Thermodynamics. New York, Hemisphere Publishing, 271 pp.

Elding, L.I. (1972): Palladium(II) Halide Complexes. I. Stabilities and Spectra of palladium(II) Chloro and Bromo Aqua Complexes. Inorganica Chimica Acta, 6, 647-651.

Furukawa, G.T., Reilly, M.L. & Gallagher, J.S. (1974): Critical analysis of heat-capacity data and evaluation of thermodynamic properties of ruthenium, rhodium, palladium, iridium, and platinum from 0 to 300 K. A survey of the literature data on osmium. Journal of Physical and Chemical Reference Data, 3, 163-209.

Glemser, O. & Peuschel, G. (1955): Beitrag zur Kenntnis des Systems PdO/H_2O. Zeitschrift für anorganische und allgemeine Chemie, 281, 44-53.

Gmelin, L. (1942): Gmelins Handbuch der Anorganischen Chemie, Palladium. Lieferung 2, System-Nummer 65, Verlag Chemie GmbH, Weinheim/ Bergstrasse (Photomechanischer Nachdruck 1968).

Grenthe, I., Fuger, J., Konings, R.J.M., Lemire, R.J., Muller, A.B., Nguyen-Trung, C. & Wanner, H. (1992): Chemical Thermodynamics of Uranium. Chemical Thermodynamics, Vol. 1. Elsevier, Amsterdam, 715 pp.

Grenthe, I., Plyasunov, A.V. & Spahiu, K. (1997): Estimation of Medium Effects on Thermodynamic Data. In: Grenthe, I., Puigdomènech, I. (eds.): Modelling in Aquatic Chemistry, OECD Nuclear Energy Agency, Paris, p.325-426.

Hultgren, R., Desai, P.D., Hawkins, D.T., Gleiser, M., Kelley, K.K. & Wagman, D.D. (1973): Selected Values of the Thermodynamic Properties of the Elements. American Society for Metal, Metals Park, Ohio, 636 pp.

Izatt, R.M., Eatough, D. & Christensen, J.J. (1967): A Study of Pd^{2+} (aq) Hydrolysis. Hydrolysis Constants and the Standard Potential for the Pd, Pd^{2+} Couple. Journal of the Chemical Society, A, 1301-1304.

Izatt, R.M., Eatough, D., Morgan, C.E. & Christensen, J.J. (1970): Half Cell Potential of the Pd,Pd^{2+} Couple in 3.94-molal Perchloric Acid and the Entropy of Pd^{2+} (aq). Journal of the Chemical Society, Section A, 2514-2515.

Jackson, E. & Pantony, D.A. (1971): Investigations in platinum metal group electrochemistry: II The Pd(II)-Pd° reduction. Journal of Applied Electrochemistry, 1, 283-291.

Kazdobin, K.A., Pershina, E.D., Kokhanenko, E.V. & Duma, V.Yu. (2009): Electrochemical behavior of diluted aqueous electrolytes containing oxygen after superimposition of mechanical effects. Journal of Water Chemistry and Technology, 31, 177-185 (Translated from: Khimiya I Tekhnologiya Vody, 31, 308-322).

Khodakovskii, I.L., Smirnova, N.N, Bykova, T.A., Polotnyanko, N.A., Kristavchuk, N.D., Shikina, N.D., Karimova, O.V., Mokhov, A.V. & Volchenkova, V.A. (2011): High-temperature heat capacity of palladinite PdOc. Geochemistry International, 49, 525-530 (Translated from: Geokhimiya, 49, 550-555).

Koroleva, L.A., Shikina, N.D., Kolodina, P.G., Zotov, A.V., Tagirov, B.R., Shvarov, Yu.V., Volchenkova, V.A. & Shazzo, Yu.K. (2012): Experimental study of Pd hydrolysis in aqueous solutions at 25-70 °C. Geochemistry International, 50, 853-859 (Translated from: Geokhimiya, 50, 949-956).

Lemire, R.J., Berner, U., Musikas, C., Palmer, D.A., Taylor, P. & Tochiyama, O. (2013): Chemical Thermodynamics of Iron, Part 1. Chemical Thermodynamics, Vol. 13a. OECD Publications, Paris, France, 1082 pp.

Levanda, O.G. (1968): Influence of Ionic Strength on the Stability Constant of the Tetrachloropalladate(II) Ion in Water. Russian Journal of Inorganic Chemistry, 13, 1707-1708.

Levanda, O.G., Moiseev, I.I. & Vargaftik, M.N. (1968): Potentiometric investigation of complexing between palladium(II) and chloride ions. Bulletin of the Academy of Sciences of the USSR 17 2237-2239 (translated from: Izvestiya Akademii Nauk USSR, Seriya Khimicheskaya 2368-2370).

Lothenbach, B., Ochs, M., Wanner, H. & Yui, M. (1999): Thermodynamic Data for the Speciation and Solubility of Pd, Pb, Sn, Sb, Nb and Bi in Aqueous Solution. LNC TN8400 99-011, Japan Nuclear Cycle Development Institute, Ibaraki, Japan.

Müller, H. (1853): Ueber die Palladamine. Liebigs Annalen der Chemie, 86**,** 341-368.

Nabivanets, B.I. & Kalabina, L.V. (1970): State of Palladium(II) in Perchlorate Solutions. Russian Journal of Inorganic Chemistry, 15, 818-821.

Oda, C., Yoshikawa, H. & Yui, M. (1996): Effects of aging on the solubility of palladium. Material Research society Symposium Proceedings, 412, 881-887.

Polotnyanko, N.A. & Khodakovskii, I.L. (2013): Thermodynamic properties of compounds in the PdO–H_2O system at 25 °C. Geochemistry International, 51, 912-916 (Translated from: Geokhimiya, 51, 1012-1020).

Polotnyanko, N.A. & Khodakovskii, I.L. (2014): Thermodynamic properties of Pd chloride complexes and the Pd^{2+} (aq) ion in aqueous solutions. Geochemistry International, 52, 46-56 (Translated from: Geokhimiya, 52, 52-63).

Pearson, F.J., Berner, U. & Hummel, W. (1992): Nagra Thermochemical Data Base II. Supplemental Data 05/92. Nagra Technical Report NTB 91-18.

Rai, D., Yui, M. & Kitamura, A. (2012): Thermodynamic model for amorphous $Pd(OH)_2$ solubility in the aqueous $Na^+ – K^+ – H^+ – OH^- – Cl^- – ClO_4^- – H_2O$ system at 25 °C: a critical review. Journal of Solution Chemistry, 41, 1965-1985.

Rasmussen, L. & Jørgensen, C.K. (1968): Palladium(II) Complexes I. Spectra and Formation Constants of Ammonia and Ethylenediamine Complexes. Acta Chemica Scandinavica, 22, 2313-2323.

Sassani, D.C. & Shock, E.L. (1998): Solubility and transport of platinum-group elements in supercritical fluids: Summary and estimates of thermodynamic properties for ruthenium, rhodium, palladium, and platinum solids, aqueous ions, and complexes to 1000 °C and 5 kbar. Geochim. Cosmochim. Acta, 62, 2643-2671.

Smirnova, N.N, Bykova, T.A., Polotnyanko, N.A., Shikina, N.D. & Khodakovskii, I.L. (2010): Low-temperature heat capacity and standard entropy of PdO(cr.). Russian Journal of Physical Chemistry a, 84, 1851-1855 (Translated from: Zhurnal Fizicheskoi Khimii, 84, 2030-2035).

Templeton, D.H., Watt, G.W. & Garner, C.S. (1943): The Formal Electrode Potentials of Palladium in Aqueous Hydrochloric and Perchloric Acid Solutions. Stability of Chloropalladite Ion. Journal of the American Chemical Society, 65, 1608-1612.

Thoenen, T., Hummel, W., Berner, U. & Curti, E. (2014): The PSI/Nagra Chemical Thermodynamic Database 12/07. Technical Report, PSI Bericht Nr. 14-04, Paul Scherrer Institut, Villigen, Switzerland, 416 pp.

Van Loon, L.R. & Hummel, W. (1999): The Degradation of Strong Basic Anion Exchange Resins and Mixed Bed Ion Exchange Resins. Effect of Degradation Products on Radionuclide Speciation. Nuclear Technol., 128, 388-401.

van Middlesworth, J.M. & Wood, S.A. (1999): The stability of palladium(II) hydroxide and hydroxy-chloride complexes: An experimental solubility study at 25-85 °C and 1 bar. Geochim. Cosmochim. Acta, 63, 1751-1765.

Wagman, D.D., Evans, W.H., Parker, V.B., Schumm, R.H., Halow, I., Bailey, S.M., Churney, K.L. & Nuttall, R.L. (1982): The NBS tables of chemical thermodynamic properties. Selected values for inorganic and C1 and C2 organic substances in SI units. Journal of Physical and Chemical Reference Data, 11, Supplement No. 2, 1-392.

Wood, S. (1991): Experimental determination of the hydrolysis constants of Pt^{2+} and Pd^{2+} at 25 °C from solubility of Pt and Pd in aqueous hydroxide solutions. Geochim. Cosmochim. Acta, 55, 1759-1767.

20 Plutonium

In a late state of the review work for TDB 2020 the NEA TDB Second Update on the Chemical Thermodynamics of Uranium, Neptunium, Plutonium, Americium and Technetium (Grenthe et al. 2020) became available to the reviewers. In the following, only changes with respect to previous TDB versions are shortly discussed. For a detailed discussion of the previous plutonium chemical thermodynamic data the reader is referred to Thoenen et al. (2014) and Hummel et al. (2002).

20.1 Plutonium aquo ions

Rand et al. (2008) selected $\varepsilon(Pu^{4+}, Cl^-) = (0.37 \pm 0.05)$ kg · mol^{-1} as derived by Neck et al. (2006). Grenthe et al. (2020) discuss this selection and conclude that "the value $\varepsilon(Pu^{4+}, Cl^-) = (0.37 \pm 0.10)$ kg · mol^{-1} (with uncertainty increased by this review) can be used in speciation models where chloride complexes have been excluded". The increased uncertainty is included in TDB 2020.

20.2 Plutonium oxygen and hydrogen compounds and complexes

The hydrolysis of Pu(VI) has been studied in detail and both structural information and thermodynamic data are available for the complexes PuO_2OH^+, $PuO_2(OH)_2(aq)$ and $(PuO_2)_2(OH)_2^{2+}$. Thermodynamic data for these complexes were selected by Lemire et al. (2001) and retained by Guillaumont et al. (2003) and Grenthe et al. (2020). However, Grenthe et al. (2020) acknowledged the relevance of $PuO_2(OH)_3^-$ based on the studies by Reilly & Neu (2006) and Cho et al. (2010) and selected the hydrolysis constant reported by Cho et al. (2010) with an increased uncertainty to consider the difference to the estimate by Reilly & Neu (2006):

$$PuO_2^{2+} + 3\ H_2O(l) \rightleftharpoons PuO_2(OH)_3^- + 3\ H^+$$

$$\log_{10}{}^*\beta_3^\circ = -(24.0 \pm 1.6)$$

This value has been included in TDB 2020 together with an SIT estimate (Tab. 20-2) based on charge correlations (see Section 1.5.3).

Grenthe et al. (2020) further state that the value $\Delta_r H_m^\circ(PuO_2^{2+} + H_2O(l) \rightleftharpoons PuO_2OH^+ + H^+) = (35.0 \pm 3.4)$ kJ · mol^{-1} reported by Rao et al. (2011) agrees reasonably well with the selected data in the NEA TDB $\Delta_r H_m^\circ(PuO_2^{2+} + H_2O(l) \rightleftharpoons PuO_2OH^+ + H^+) = (28 \pm 15)$ kJ · mol^{-1}, which is retained, while

$$2\ PuO_2^{2+} + 2\ H_2O(l) \rightleftharpoons (PuO_2)_2(OH)_2^{2+} + 2\ H^+$$

$$\Delta_r H_m^\circ = (65.4 \pm 1.0)\ kJ \cdot mol^{-1}$$

also reported by Rao et al. (2011) is provided by Grenthe et al. (2020) for information only.

This value has been included in TDB 2020 as supplemental datum.

There are only few studies on the hydrolysis of Pu(V) due to the difficulties to maintain the +V oxidation state in near neutral and alkaline conditions. Grenthe et al. (2020) state that no new experimental studies on the hydrolysis of Pu(V) have been published since the last reviews and they retained the previously selected upper estimate for the equilibrium constant for the formation of $PuO_2OH(aq)$.

Grenthe et al. (2020) retain the Pu(IV) hydrolysis constants selected by Guillaumont et al. (2003) who in turn adopted the values proposed in the review by Neck & Kim (2001). However, Thoenen et al. (2014) discuss the experimental study of Yun et al. (2007), accept their conclusion that the hydrolysis constants given by Neck & Kim (2001) are overestimated, and select the values given by Yun et al. (2007) for TDB Version 12/07 (Tab. 6-2). Grenthe et al. (2020) also discuss the experimental study of Yun et al. (2007), do not find any serious flaws, but finally state that the data of Yun et al. (2007) do not follow the expected trend for UOH^{3+} – $NpOH^{3+}$ – $PuOH^{3+}$ data. This seems to be a weak argument and thus, this review retains the values of Yun et al. (2007) in TDB 2020 as selected by Thoenen et al. (2014).

New experimental data on the solubility of $An(OH)_4(am)$ with An = Np and Pu in alkaline solutions containing $CaCl_2$ have been reported by Altmaier et al. (2008) and Fellhauer et al. (2010). In analogy to the behaviour of Th(IV), the increase in solubility at high pH and increasing $CaCl_2$ concentration is explained with the formation of the previously unknown ternary solution complex $Ca_4[Pu(OH)_8]^{4+}$. The authors adopted the analogous Th(IV) speciation model and the corresponding SIT ion interaction parameters. Altmaier et al. (2008) derived using SIT:

$$4\ Ca^{2+} + Pu^{4+} + 8\ H_2O(l) \rightleftharpoons Ca_4Pu(OH)_8^{4+} + 8\ H^+$$

$$log_{10}{}^*\beta^\circ = -(55.7 \pm 0.7)$$

$$\varepsilon(Ca_4Pu(OH)_8^{4+}, Cl^-) = \varepsilon(Ca_4Th(OH)_8^{4+}, Cl^-) = -(0.01 \pm 0.10)\ kg \cdot mol^{-1}$$

These values had been included in TDB Version 12/07 as supplemental data.

Fellhauer et al. (2010), also using SIT, later revised the stability constant to

$$log_{10}{}^*\beta^\circ = -(56.2 \pm 0.6)$$

This revised value has been included in TDB 2020 as supplemental datum.

Grenthe et al. (2020) actually discuss these studies twice, in their Sections 11.2.1.3 and 11.2.2.2.3.2, and conclude that "this data is compromised by the fact that the value $\varepsilon(Ca_4Th(OH)_8^{4+}, Cl^-)$ was obtained outside the validity range of the SIT and therefore cannot be accepted. A better approach to model these very high-ionic strength data is the Pitzer formalism. This review has not selected the thermodynamic equilibrium constants calculated by Fellhauer et al. (2010) with the Pitzer formalism, and these data are included for information only", i.e., $log_{10}{}^*\beta^\circ = -(57.0 \pm 0.6)$.

Trivalent plutonium is known to be stable in aqueous systems from highly reducing acidic to near-neutral conditions. The presence of any oxidant or complexing agent that forms strong complexes with Pu(IV) can stimulate the oxidation of Pu(III) to Pu(IV). The hydrolysis of Pu(III) has been extensively reviewed by Lemire et al. (2001), and they selected $log_{10}{}^*\beta_1^\circ = -(6.9 \pm 0.3)$.

In a new experimental study, Cho et al. (2016) used a spectrophotometric-coulometric titration to investigate the hydrolysis of Pu(III), and used laser-induced breakdown detection (LIBD) to verify the absence of colloids or the formation of a solid phase at pH < 6.3. Grenthe et al. (2020) acknowledge the uncertainties in the study by Cho et al. (2016) but consider the combination of absorbance spectroscopy and LIBD measurements to identify formation of particles and solids as a more reliable method of exploration than those used in previous studies. Grenthe et al. (2020) accept the value reported by Cho et al. (2016) with an increased uncertainty to consider the data scattering and select the hydrolysis constant:

$$Pu^{3+} + H_2O(l) \rightleftharpoons PuOH^{2+} + H^+$$

$$\log_{10}{}^{*}\beta_1^\circ = -(6.18 \pm 0.50)$$

This value has been included in TDB 2020.

Grenthe et al. (2020) further remark that "it is to note that this value has been selected in combination with the thermodynamic solubility product, $\log_{10}{}^{*}K_{s,0}^\circ(Pu(OH)_3, am) = (14.58 \pm 0.75)$ (see Section 11.2.2.2.4), and both data need to be used together in order to predict Pu(III) solubility data at up to about pH < 8.5".

Experimental data on the solubility of Pu(VI) hydroxide has been discussed by Lemire et al. (2001) and they selected a thermodynamic equilibrium constant $\log_{10}{}^{*}K_{s,0}^\circ(PuO_2(OH)_2{\cdot}H_2O, cr) = (5.5 \pm 1.0)$. Lemire et al. (2001) assumed $PuO_2(OH)_2{\cdot}H_2O(cr)$ to be the solubility-controlling solid phase in all solubility studies they had evaluated. However, as discussed by Grenthe et al. (2020), none of the reported solubility studies have properly characterised the solubility-limiting solid phases. Assuming the presence of the Pu(VI) hydroxide monohydrate in all reported solubility studies is highly speculative and degrees of crystallinity and hydration may vary due to different experimental conditions. In the absence of any solid phase characterisation, the solid phase could be $PuO_2(OH)_2$(am, hyd) or a more crystalline phase such as $PuO_2(OH)_2 \cdot nH_2O$(cr) with a variable number n of crystal waters. The differences in the thermodynamic properties of solid phases can be significant when exposed to high-energetic alpha-particles and radiation damage causes degradation of crystallinity. Consequentially, the assignment of solid Pu(VI) hydroxides as amorphous or crystalline phases is complicated and only of nominal value for estimating Gibbs free energies.

Grenthe et al. (2020) disagree with the acceptance criteria used for the original data and the selected value in Lemire et al. (2001). Consequently, Grenthe et al. (2020) re-evaluated the old data, considered a new solubility study, and select a revised average value for $PuO_2(OH)_2$(am, hyd):

$$PuO_2(OH)_2(am, hyd) + 2\ H^+ \rightleftharpoons PuO_2^{2+} + 2\ H_2O(l)$$

$$\log_{10}{}^{*}K_{s,0}^\circ = (5.17 \pm 0.65)$$

This value has been included in TDB 2020.

Lemire et al. (2001) reviewed experimental solubility data of Pu(III) hydroxide and selected the thermodynamic solubility product for a crystalline phase $Pu(OH)_3$(cr), $\log_{10}{}^{*}K_{s,0}^{\circ} = (15.8 \pm 1.5)$. As Grenthe et al. (2020) remark, this value is solely derived from the solubility study by Felmy et al. (1989), and it should be noted that the crystallinity of the solid equilibrium phase is uncertain because no Bragg reflections were observed in the X-ray diffraction spectra. Thus, the selected thermodynamic data should rather be assigned to an amorphous phase, $Pu(OH)_3$(am).

Recently, Cho et al. (2016) studied the Pu(III) hydrolysis and solubility under reducing conditions. As Grenthe et al. (2020) discuss, Cho et al. (2016) found the blue amorphous solid phase, assumed to be $Pu(OH)_3$(am), to be stable over the duration of the experiment, based on the unchanged X-ray diffraction pattern after three weeks. However, this argument is meaningless as the diffraction data do not show any distinct Bragg reflections, which is typical of a highly amorphous precipitate. Any transition of amorphous solid phases would not be detected using this analytical technique. From coulometric titrations and spectroscopic data, Cho et al. (2016) report $\log_{10}{}^{*}K_{s,0}^{\circ} = (14.58 \pm 0.50)$. This value is quite different from $\log_{10}{}^{*}K_{s,0}^{\circ} = (15.8 \pm 1.5)$ accepted by Lemire et al. (2001), although it is within the uncertainty range of their selected value. Grenthe et al. (2020) argue that this difference might be due to the disregard of Pu(III) hydrolysis in the solubility study of Felmy et al. (1989), which was carried out at pH > 6 where Pu(III) hydrolysis should not be neglected, and select the value reported by Cho et al. (2016) with increased uncertainty:

$$Pu(OH)_3(am) + 3\ H^+ \rightleftharpoons Pu^{3+} + 3\ H_2O(l)$$

$$\log_{10}{}^{*}K_{s,0}^{\circ} = (14.58 \pm 0.75)$$

This value has been included in TDB 2020.

20.3 Plutonium sulphate complexes

No thermodynamic data for aqueous plutonium(V) sulphates have been selected by Lemire et al. (2001) and Guillaumont et al. (2003) because of the lack of experimental studies. Since then, Topin et al. (2009a) investigated the complex formation of Pu(V) by capillary electrophoresis experiments in $NaClO_4/Na_2SO_4$ at room temperature. The changes of the electrophoretic mobility of the Pu(V) species with increasing sulphate concentration was interpreted with the formation of a 1:1 Pu(V) sulphate complex. Despite the concerns about the experimental shortcomings and data analysis, Grenthe et al. (2020) accept the data reported by Topin et al. (2009a), based on the agreement with the new selected value for $NpO_2SO_4^-$, $\log_{10}\beta_1^{\circ} = (1.3 \pm 0.2)$ (see Section 16.3), and select:

$$PuO_2^+ + SO_4^{2-} \rightleftharpoons PuO_2SO_4^-$$

$$\log_{10}\beta_1^{\circ} = (1.26 \pm 0.12)$$

This value has been included in TDB 2020, together with the estimate

$$\varepsilon(PuO_2SO_4^-, Na^+) = \varepsilon(NpO_2SO_4^-, Na^+) = (0.07 \pm 0.13)\ kg \cdot mol^{-1}$$

20.4 Plutonium phosphate compounds and complexes

No thermodynamic data for Pu(VI) phosphate compounds and complexes have been selected by Lemire et al. (2001) and Guillaumont et al. (2003). Rai et al. (2005) report solubility data of Pu(VI) in phosphate-containing solutions with $(PuO_2)_3(PO_4)_2 \cdot 4H_2O(s)$ as the designated solubility-controlling phase. Rai et al. (2005) assigned the composition of the solid phase in analogy to the corresponding U(VI) phase, although the absence of any peaks in the X-ray diffraction data of the solid Pu phosphate show that the phase is amorphous and EXAFS data show differences in the coordination modes between the U and Pu solid phosphate phase. However, the very similar solubility data of U(VI) and Pu(VI) at pH ≤ 4 support the assignment of the solid phase. Due to the consistency with the corresponding U(VI) data, Grenthe et al. (2020) select:

$$(PuO_2)_3(PO_4)_2 \cdot 4H_2O(am) \rightleftharpoons 3\ PuO_2^{2+} + 2\ PO_4^{3-} + 4H_2O(l)$$

$$\log_{10}{}^{*}K_{s,0}^{\circ} = -(48.97 \pm 0.69)$$

This value has been included in TDB 2020.

Rai et al. (2005) also report thermodynamic equilibrium constants for several Pu(VI) phosphate complexes. Grenthe et al. (2020) state that the Pu(VI) solubilities predicted based on this set of Pu(VI) phosphate complexes fit very well the experimental solubility data in 0.001 m NaH_2PO_4 up to pH ~ 9. However, in 0.01 m NaH_2PO_4 the speciation model agrees with experimental data at pH > 6.5 but does not match well the data at the lower solubility observed at pH < 6.5. The two solubility ranges in 0.01 m NaH_2PO_4 suggest that different solid phases are present in the experiments. Based on these inconsistencies and the uncertainties of the selected species, Grenthe et al. (2020) do not select any of the equilibrium constants for Pu(VI) phosphate solution species reported by Rai et al. (2005). However, just including a solubility product without the aqueous complexes derived from the same solubility data will inevitably lead to wrong results in model calculations. Therefore, the aqueous complexes reported by Rai et al. (2005) and given in Tab. 11-23 in Grenthe et al. (2020) have been included in TDB 2020 as supplemental data

$$PuO_2^{2+} + PO_4^{3-} \rightleftharpoons PuO_2PO_4^{-}$$

$$\log_{10}\beta_1^{\circ} = (11.76 \pm 0.70)$$

$$PuO_2^{2+} + HPO_4^{2-} \rightleftharpoons PuO_2HPO_4(aq)$$

$$\log_{10}\beta_1^{\circ} = 7.24$$

$$PuO_2^{2+} + H_2PO_4^{-} \rightleftharpoons PuO_2H_2PO_4^{+}$$

$$\log_{10}\beta_1^{\circ} = 3.26$$

$$PuO_2^{2+} + 2\ H_2PO_4^{-} \rightleftharpoons PuO_2(H_2PO_4)_2(aq)$$

$$\log_{10}\beta_2^{\circ} = 4.92$$

together with SIT estimates (Tab. 6.3) based on charge correlations (see Section 1.5.3).

Lemire et al. (2001) discussed the only solubility study available from Moskvin (1971) and selected $\log_{10}K_{s,0}^{\circ} = -(24.6 \pm 0.8)$ for $PuPO_4$(cr, hyd) after reinterpreting the original data.

A new solubility study of $PuPO_4$(cr, hyd) in NaH_2PO_4 solutions was reported by Rai et al. (2010). As Grenthe et al. (2020) discuss, $PuPO_4$(cr, hyd) was identified as solid phase in coexistence with a less crystalline $PuPO_4$(am, hyd) phase. Due to the mixed crystallinity of the solid phase, Grenthe et al. (2020) assign the value $\log_{10}K_{s,0}° = -(24.28 \pm 0.35)$ reported by Rai et al. (2010) to the amorphous $PuPO_4$(am, hyd) phase.

Combining the $\log_{10}K_{s,0}°$ values reported by Rai et al. (2010) and the previously selected TDB value, Grenthe et al. (2020) select:

$$PuPO_4(am, hyd) \rightleftharpoons Pu^{3+} + PO_4^{3-}$$

$$\log_{10}K_{s,0}° = -(24.44 \pm 0.55)$$

This value has been included in TDB 2020.

No thermodynamic values have been selected by Lemire et al. (2001) and Guillaumont et al. (2003) for Pu(III) phosphate complexes. In their solubility study Rai et al. (2010) assumed the interactions of phosphate with Pu(III) to be very weak based on the solubility behaviour of Pu across the pH range of 1-12, which in this respect is different from its chemical analogue Nd(III). Rai et al. (2010) modelled the measured Pu as function of NaH_2PO_4 concentration, assuming the formation of $PuH_2PO_4^{2+}$ under these conditions. The equilibrium constant reported by Rai et al. (2010) has been selected by Grenthe et al. (2020):

$$Pu^{3+} + H_2PO_4^- \rightleftharpoons PuH_2PO_4^{2+}$$

$$\log_{10}\beta_1° = (2.2 \pm 0.6)$$

This value has been included in TDB 2020 together with SIT estimates (Tab. 6.3) based on charge correlations (see Section 1.5.3).

20.5 Plutonium carbonate and silicate compounds and complexes

20.5.1 Plutonium carbonate compounds and complexes

The carbonate complex formation of Pu(VI) has been studied in detail and both structural information and thermodynamic data are available for the complexes PuO_2CO_3(aq), $PuO_2(CO_3)_2^{2-}$, and $PuO_2(CO_3)_3^{4-}$. Thermodynamic data for these complexes were selected by Lemire et al. (2001) and revised by Guillaumont et al. (2003).

Grenthe et al. (2020) state that thermodynamic data have also been selected by Lemire et al. (2001) for the trimeric Pu(VI) carbonate complex, $(PuO_2)_3(CO_3)_6^{6-}$. However, the equilibrium constant for the Pu(VI) trimer complex was not selected by Guillaumont et al. (2003), claiming the lack of sufficient data compared to the analogous U(VI) or Np(VI) trimeric carbonate complex. There is experimental evidence (mainly by NMR and UV-vis-NIR absorption spectroscopy) that the Pu(VI) carbonate trimer exists, but its stability field is much more restricted compared to the analogue U(VI) or Np(VI) carbonate trimers. Since Guillaumont et al. (2003) did not provide any further detailed justification for not selecting the trimeric Pu(VI) carbonate

species and in analogy to the U(VI) and Np(VI) system, Grenthe et al. (2020) retain the thermodynamic equilibrium constant selected by Lemire et al. (2001):

$$3\ PuO_2^{2+} + 6\ CO_3^{2-} \rightleftharpoons (PuO_2)_3(CO_3)_6^{6-}$$

$$\log_{10}\beta_{3,6}\ (3.0\ M\ NaClO_4) = (51.0 \pm 2.5)$$

Note that Grenthe et al. (2020) selected this value without extrapolation to $I = 0$.

As the Debye-Hückel term cancels in the above equilibrium an extrapolation to $I = 0$ solely depends on the chosen SIT interaction coefficients. This review first transformed the above stability constant from the molar to the molal scale, i.e. $\log_{10}\beta_{3,6}\ (3.0\ M\ NaClO_4) = (51.0 \pm 2.5) \rightarrow \log_{10}\beta_{3,6}\ (3.5\ m\ NaClO_4) = (50.46 \pm 2.50)$, and then used $\varepsilon(PuO_2^{2+}, ClO_4^-) = (0.46 \pm 0.05)\ kg \cdot mol^{-1}$, $\varepsilon(Na^+, CO_3^{2-}) = -(0.08 \pm 0.03)\ kg \cdot mol^{-1}$ and $\varepsilon(Na^+, (UO_2)_3(CO_3)_6^{6-}) = (0.37 \pm 0.11)\ kg \cdot mol^{-1}$ to extrapolate the molal constant to zero ionic strength by adding $\Delta\varepsilon \cdot I_m = -1.86$:

$$3\ PuO_2^{2+} + 6\ CO_3^{2-} \rightleftharpoons (PuO_2)_3(CO_3)_6^{6-}$$

$$\log_{10}\beta_{3,6}^\circ = (48.6 \pm 2.5)$$

$$\varepsilon(Na^+, (PuO_2)_3(CO_3)_6^{6-}) = \varepsilon(Na^+, (UO_2)_3(CO_3)_6^{6-}) = (0.37 \pm 0.11)\ kg \cdot mol^{-1}$$

These values have been included in TDB 2020.

Grenthe et al. (2020) also retain the thermodynamic constant for the mixed actinyl complex, $(UO_2)_2PuO_2(CO_3)_3^{6--}$, reported by Lemire et al. (2001) but neglected by Guillaumont et al. (2003). Note that this constant had been included in TDB Version 12/07 and is retained in TDB 2020.

The Pu(V) carbonate system has been discussed by Lemire et al. (2001) and thermodynamic data were selected for the complexes $PuO_2CO_3^-$ and $PuO_2(CO_3)_3^{5-}$. No thermodynamic data were added by Guillaumont et al. (2003). While the equilibrium constant for the formation of $PuO_2CO_3^-$ is based on experimental spectroscopic data reported by Bennett et al. (1992), Lemire et al. (2001) calculated the equilibrium constant for the limiting Pu(V) complex in carbonate, $PuO_2(CO_3)_3^{5-}$, from the recommended thermodynamic data for the formation of the Pu(VI) complex $PuO_2(CO_3)_3^{4-}$and the recommended potential for the Pu(VI)/Pu(V) redox couple in acid solution. Grenthe et al. (2020) reject the calculated value for $PuO_2(CO_3)_3^{5-}$.

The formation of Np(V) and Pu(V) carbonate complexes has been studied by Topin et al. (2009b) by measuring variations in the electrophoretic mobility of the different solution species as function of pH and carbonate concentration. Grenthe et al. (2020) report that the study by Topin et al. (2009b) provides the first set of equilibrium constants for the three major Pu(V) carbonate species in aqueous solution, and despite the concerns regarding the data analysis by Topin et al. (2009b), Grenthe et al. (2020) select the average of the two experimental data for $PuO_2CO_3^-$ reported by Bennett et al. (1992) and Topin et al. (2009b) and select the data in Topin et al. (2009b) for $PuO_2(CO_3)_2^{3-}$ and $PuO_2(CO_3)_3^{5-}$ with increased uncertainties:

$PuO_2^+ + CO_3^{2-} \rightleftharpoons PuO_2CO_3^-$

$\log_{10}\beta_1° = (5.03 \pm 0.12)$

$PuO_2^+ + 2\ CO_3^{2-} \rightleftharpoons PuO_2(CO_3)_2^{3-}$

$\log_{10}\beta_2° = (6.34 \pm 0.20)$

$PuO_2^+ + 3\ CO_3^{2-} \rightleftharpoons PuO_2(CO_3)_3^{5-}$

$\log_{10}\beta_3° = (5.61 \pm 0.24)$

These values have been included in TDB 2020 together with SIT estimates (Tab. 20-2) based on charge correlations (see Section 1.5)

Reilly et al. (2007) reported the solubility of PuO_2CO_3(cr) in 0.1 – 5.6 m NaCl and 5.6 m $NaClO_4$ solutions. The authors monitored spectroscopically the dissolution equilibrium and used the absorbance features characteristic for Pu(V) and Pu(VI) species to determine solution speciation. Grenthe et al. (2020) selected the solubility product reported by Reilly et al. (2007) with increased uncertainty

$PuO_2CO_3(cr) \rightleftharpoons PuO_2^{2+} + CO_3^{2-}$

$\log_{10}K_{s,0}° = -(4.82 \pm 0.12)$

This value has been included in TDB 2020.

In addition, Grenthe et al. (2020) derived from an SIT plot of conditional solubility products reported by Reilly et al. (2007) the ion interaction parameter

$\varepsilon(PuO_2^{2+}, Cl^-) = (0.19 \pm 0.09)\ kg \cdot mol^{-1}$

which for unknown reasons has not been included in "Tab. B-6: Ion interaction coefficients" of Grenthe et al. (2020). Nevertheless, this value is included in TDB 2020.

20.5.2 Plutonium silicate compounds and complexes

Plutonium silicate compounds and complexes are discussed in Section 25.9.

20.6 Selected plutonium data

Tab. 20-1: Selected plutonium data

All data included in TDB 2020 are taken from Lemire et al. (2001), Guillaumont et al. (2003) and Grenthe et al. (2020) except where marked with an asterisk (*). The latter data were taken unchanged from Thoenen et al. (2014). Supplemental data are in italics. New or changed data with respect to TDB Version 12/07 (Thoenen et al. 2014) are shaded.

Name	Redox	TDB Version 12/07				TDB 2020				
		$\Delta_f G_m°$ [kJ · mol^{-1}]	$\Delta_f H_m°$ [kJ · mol^{-1}]	$S_m°$ [J · K^{-1} · mol^{-1}]	$C_{p,m}°$ [J · K^{-1} · mol^{-1}]	$\Delta_f G_m°$ [kJ · mol^{-1}]	$\Delta_f H_m°$ [kJ · mol^{-1}]	$S_m°$ [J · K^{-1} · mol^{-1}]	$C_{p,m}°$ [J · K^{-1} · mol^{-1}]	Species
Pu(cr)	0	0.0	0.0	54.46 ± 0.80	31.49 ± 0.40	0.0	0.0	54.46 ± 0.80	31.49 ± 0.40	Pu(cr, α)
Pu+3	III	-579.0 ± 2.7	-591.8 ± 2.0	-184.5 ± 6.2	-	-579.0 ± 2.7	-591.8 ± 2.0	-184.5 ± 6.2	-	Pu^{3+}
Pu+4	IV	-478.0 ± 2.7	-539.9 ± 3.1	-414.5 ± 10.2	-	-478.0 ± 2.7	-539.9 ± 3.1	-414.5 ± 10.2	-	Pu^{4+}
PuO2	V	-852.6 ± 2.9	-910.1 ± 8.9	1 ± 30	-	-852.6 ± 2.9	-910.1 ± 8.9	1 ± 30	-	PuO_2^+
PuO2+2	VI	-762.4 ± 2.8	-822.0 ± 6.6	-71.2 ± 22.1	-	-762.4 ± 2.8	-822.0 ± 6.6	-71.2 ± 22.1	-	PuO_2^{2+}

Name	Redox	TDB Version 12/07		TDB 2020		
		$\log_{10}\beta°$	$\Delta_r H_m°$ [kJ · mol^{-1}]	$\log_{10}\beta°$	$\Delta_r H_m°$ [kJ · mol^{-1}]	Reaction
PuO2OH+	VI	-5.5 ± 0.5	28 ± 15	-5.5 ± 0.5	28 ± 15	$PuO_2^{2+} + H_2O(l) \rightleftharpoons PuO_2OH^+ + H^+$
PuO2(OH)2(aq)	VI	-13.2 ± (1.5) *	-	-13.2 ± 1.5	-	$PuO_2^{2+} + 2\ H_2O(l) \rightleftharpoons PuO_2(OH)_2(aq) + 2\ H^+$
PuO2(OH)3-	VI	-	-	-24.0 ± 1.6	-	$PuO_2^{2+} + 3\ H_2O(l) \rightleftharpoons PuO_2(OH)_3^- + 3\ H^+$
(PuO2)2(OH)2+2	VI	-7.5 ± (1.0) *	-	-7.5 ± 1.0	*65.4 ± 1.0*	$2\ PuO_2^{2+} + 2\ H_2O(l) \rightleftharpoons (PuO_2)_2(OH)_2^{2+} + 2\ H^+$
PuO2F+	VI	4.56 ± 0.20	-	4.56 ± 0.20	-	$PuO_2^{2+} + F^- \rightleftharpoons PuO_2F^+$
PuO2F2(aq)	VI	7.25 ± 0.45	-	7.25 ± 0.45	-	$PuO_2^{2+} + 2\ F^- \rightleftharpoons PuO_2F_2(aq)$
PuO2Cl+	VI	0.23 ± 0.03	-	0.23 ± 0.03	-	$PuO_2^{2+} + Cl^- \rightleftharpoons PuO_2Cl^+$
PuO2Cl2	VI	-1.15 ± 0.30	-	-1.15 ± 0.30	-	$PuO_2^{2+} + 2\ Cl^- \rightleftharpoons PuO_2Cl_2(aq)$
PuO2SO4(aq)	VI	3.38 ± 0.20	16.1 ± 0.6	3.38 ± 0.20	16.1 ± 0.6	$PuO_2^{2+} + SO_4^{2-} \rightleftharpoons PuO_2SO_4(aq)$
PuO2(SO4)2-2	VI	4.4 ± 0.2	43 ± 9	4.4 ± 0.2	43 ± 9	$PuO_2^{2+} + 2\ SO_4^{2-} \rightleftharpoons PuO_2(SO_4)_2^{2-}$
PuO2PO4-	VI	-	-	*11.76 ± 0.70*	-	*$PuO_2^{2+} + PO_4^{3-} \rightleftharpoons PuO_2PO_4^-$*
PuO2HPO4(aq)	VI	-	-	*7.24*	-	*$PuO_2^{2+} + HPO_4^{2-} \rightleftharpoons PuO_2HPO_4(aq)$*
PuO2H2PO4+	VI	-	-	*3.26*	-	*$PuO_2^{2+} + H_2PO_4^- \rightleftharpoons PuO_2H_2PO_4^+$*
PuO2(H2PO4)2(aq)	VI	-	-	*4.92*	-	*$PuO_2^{2+} + 2\ H_2PO_4^- \rightleftharpoons PuO_2(H_2PO_4)_2(aq)$*
PuO2CO3(aq)	VI	9.5 ± 0.5	-	9.5 ± 0.5	-	$PuO_2^{2+} + CO_3^{2-} \rightleftharpoons PuO_2CO_3(aq)$
PuO2(CO3)2-2	VI	14.7 ± 0.5	-27 ± 4	14.7 ± 0.5	-27 ± 4	$PuO_2^{2+} + 2\ CO_3^{2-} \rightleftharpoons PuO_2(CO_3)_2^{2-}$
PuO2(CO3)3-4	VI	18.0 ± 0.5	-38.6 ± 2.0	18.0 ± 0.5	-38.6 ± 2.0	$PuO_2^{2+} + 3\ CO_3^{2-} \rightleftharpoons PuO_2(CO_3)_3^{4-}$
(PuO2)3(CO3)6-6	VI	-	-	48.6 ± 2.5	-	$3\ PuO_2^{2+} + 6\ CO_3^{2-} \rightleftharpoons (PuO_2)_3(CO_3)_6^{6-}$

Tab. 20-1: Cont.

Name	Redox	TDB Version 12/07		TDB 2020		
		$\log_{10}\beta°$	$\Delta_r H_m°$ [kJ · mol^{-1}]	$\log_{10}\beta°$	$\Delta_r H_m°$ [kJ · mol^{-1}]	Reaction
(UO2)2PuO2(CO3)6-6	VI	(53.5 ± 1.4) [a]	-	(53.5 ± 1.4) [a]	-	$2UO_2^{2+} + PuO_2^{2+} + 6\,CO_3^{2-} \rightleftharpoons (UO_2)_2PuO_2(CO_3)_3^{6-}$
PuO2+	VI/V	15.82 ± 0.09	-	15.82 ± 0.09	-	$PuO_2^{2+} + e^- \rightleftharpoons PuO_2^+$
PuO2OH(aq)	V	≤ -9.73	-	≤ -9.73	-	$PuO_2^+ + H_2O(l) \rightleftharpoons PuO_2OH(aq) + H^+$
PuO2SO4-	V	-	-	1.26 ± 0.12	-	$PuO_2^+ + SO_4^{2-} \rightleftharpoons PuO_2SO_4^-$
PuO2CO3-	V	5.12 ± 0.14	-	5.03 ± 0.12	-	$PuO_2^+ + CO_3^{2-} \rightleftharpoons PuO_2CO_3^-$
PuO2(CO3)2-3	V	-	-	6.34 ± 0.20	-	$PuO_2^+ + 2\,CO_3^{2-} \rightleftharpoons PuO_2(CO_3)_2^{3-}$
PuO2(CO3)3-5	V	5.03 ± 0.92	-19.11 ± 8.50	5.61 ± 0.24	-19.11 ± 8.50	$PuO_2^+ + 3\,CO_3^{2-} \rightleftharpoons PuO_2(CO_3)_3^{5-}$
Pu+4	VI/IV	33.28 ± 0.15	-	33.28 ± 0.15	-	$PuO_2^{2+} + 4\,H^+ + 2\,e^- \rightleftharpoons Pu^{4+} + 2\,H_2O(l)$
PuOH+3	IV	(0.0 ± 0.2) *	-	(0.0 ± 0.2) *	-	$Pu^{4+} + H_2O(l) \rightleftharpoons PuOH^{3+} + H^+$
Pu(OH)2+2	IV	(-1.2 ± 0.6) *	-	(-1.2 ± 0.6) *	-	$Pu^{4+} + 2\,H_2O(l) \rightleftharpoons Pu(OH)_2^{2+} + 2\,H^+$
Pu(OH)3+	IV	(-3.1 ± 0.9) *	-	(-3.1 ± 0.9) *	-	$Pu^{4+} + 3\,H_2O(l) \rightleftharpoons Pu(OH)_3^+ + 3\,H^+$
Pu(OH)4(aq)	IV	(-9.3 ± 0.5) *	-	(-9.3 ± 0.5) *	-	$Pu^{4+} + 4\,H_2O(l) \rightleftharpoons Pu(OH)_4(aq) + 4\,H^+$
Ca4Pu(OH)8+4	IV	*(-55.7 ± 0.7)* *	-	*-(56.2 ± 0.6)* *	-	*$4\,Ca^{2+} + Pu^{4+} + 8\,H_2O(l) \rightleftharpoons Ca_4Pu(OH)_8^{4+} + 8\,H^+$*
PuF+3	IV	8.84 ± 0.10	9.1 ± 2.2	8.84 ± 0.10	9.1 ± 2.2	$Pu^{4+} + F^- \rightleftharpoons PuF^{3+}$
PuF2+2	IV	15.7 ± 0.2	11 ± 5	15.7 ± 0.2	11 ± 5	$Pu^{4+} + 2\,F^- \rightleftharpoons PuF_2^{2+}$
PuCl+3	IV	1.8 ± 0.3	-	1.8 ± 0.3	-	$Pu^{4+} + Cl^- \rightleftharpoons PuCl^{3+}$
PuSO4+2	IV	6.89 ± 0.23	-	6.89 ± 0.23	-	$Pu^{4+} + SO_4^{2-} \rightleftharpoons PuSO_4^{2+}$
Pu(SO4)2(aq)	IV	11.14 ± 0.34	-	11.14 ± 0.34	-	$Pu^{4+} + 2\,SO_4^{2-} \rightleftharpoons Pu(SO_4)_2(aq)$
PuNO3+3	IV	1.95 ± 0.15	-	1.95 ± 0.15	-	$Pu^{4+} + NO_3^- \rightleftharpoons PuNO_3^{3+}$
PuH3PO4+4	IV	2.4 ± 0.3	-	2.4 ± 0.3	-	$Pu^{4+} + H_3PO_4(aq) \rightleftharpoons PuH_3PO_4^{4+}$
Pu(CO3)4-4	IV	37.0 ± 1.1	-	37.0 ± 1.1	-	$Pu^{4+} + 4\,CO_3^{2-} \rightleftharpoons Pu(CO_3)_4^{4-}$
Pu(CO3)5-6	IV	35.65 ± 1.13	-	35.65 ± 1.13	-	$Pu^{4+} + 5\,CO_3^{2-} \rightleftharpoons Pu(CO_3)_5^{6-}$
PuCO3(OH)3-	IV	*(6)* *	-	*(6)* *	-	*$Pu^{4+} + CO_3^{2-} + 3\,H_2O(l) \rightleftharpoons PuCO_3(OH)_3^- + 3\,H^+$*
Pu+3	VI/III	50.97 ± 0.15	-	50.97 ± 0.15	-	$PuO_2^{2+} + 4\,H^+ + 3\,e^- \rightleftharpoons Pu^{3+} + 2\,H_2O(l)$
PuOH+2	III	-6.9 ± 0.3	-	-6.18 ± 0.50	-	$Pu^{3+} + H_2O(l) \rightleftharpoons PuOH^{2+} + H^+$
Pu(OH)2+	III	*(-14.8)* *	-	*(-14.8)* *	-	*$Pu^{3+} + 2\,H_2O(l) \rightleftharpoons Pu(OH)_2^+ + 2\,H^+$*
Pu(OH)3(aq)	III	*(-25.9)* *	-	*(-25.9)* *	-	*$Pu^{3+} + 3\,H_2O(l) \rightleftharpoons Pu(OH)_3(aq) + 3\,H^+$*
PuF+2	III	*(3.4)* *	-	*(3.4)* *	-	*$Pu^{3+} + F^- \rightleftharpoons PuF^{2+}$*
PuF2+	III	*(5.8)* *	-	*(5.8)* *	-	*$Pu^{3+} + 2\,F^- \rightleftharpoons PuF_2^+$*
PuCl+2	III	*(1.2 ± 0.2)* *	-	*(1.2 ± 0.2)* *	-	*$Pu^{3+} + Cl^- \rightleftharpoons PuCl^{2+}$*

Tab. 20-1: Cont.

Name	Redox	TDB Version 12/07		TDB 2020		
		$\log_{10}\beta°$	$\Delta_r H_m°$ [kJ · mol^{-1}]	$\log_{10}\beta°$	$\Delta_r H_m°$ [kJ · mol^{-1}]	Reaction
PuSO4+	III	3.9 ± 0.6	17.2 ± 2.3	3.9 ± 0.6	17.2 ± 2.3	$Pu^{3+} + SO_4^{2-} \rightleftharpoons PuSO_4^+$
Pu(SO4)2-	III	5.7 ± 0.8	12 ± 16	5.7 ± 0.8	12 ± 16	$Pu^{3+} + 2\ SO_4^{2-} \rightleftharpoons Pu(SO_4)_2^-$
PuH2PO4+2	III	-	-	2.2 ± 0.6	-	$Pu^{3+} + H_2PO_4^- \rightleftharpoons PuH_2PO_4^{2+}$
PuCO3+	III	*(8.0)* [*]	-	*(8.0)* [*]	-	$Pu^{3+} + CO_3^{2-} \rightleftharpoons PuCO_3^+$
Pu(CO3)2-	III	*(12.9)* [*]	-	*(12.9)* [*]	-	$Pu^{3+} + 2\ CO_3^{2-} \rightleftharpoons Pu(CO_3)_2^-$
Pu(CO3)3-3	III	*(15.0)* [*]	-	*(15.0)* [*]	-	$Pu^{3+} + 3\ CO_3^{2-} \rightleftharpoons Pu(CO_3)_3^{3-}$
PuSCN+2	III	1.3 ± 4		1.3 ± 4		$Pu^{3+} + SCN^- \rightleftharpoons PuSCN^{2+}$

[a] Note that in Thoenen (2012) and in the electronic versions of TDB 12/07 for PHREEQC and GEMS-PSI, the value was by mistake not updated.
[b] Note that in the electronic versions of TDB 01/01for PHREEQC and GEMS-PSI the value was erroneously entered as 5.00.

Name	Redox	TDB Version 12/07		TDB 2020			
		$\log_{10}K_{s,0}°$	$\Delta_r H_m°$ [kJ · mol^{-1}]	Name	$\log_{10}K_{s,0}°$	$\Delta_r H_m°$ [kJ · mol^{-1}]	Reaction
PuO2(OH)2:H2O(cr)	VI	5.5 ± 1.0	-	PuO2(OH)2 (am,hyd)	5.17 ± 0.65	-	$PuO_2(OH)_2$(am, hyd) + 2 $H^+ \rightleftharpoons PuO_2^{2+}$ + 2 H_2O(l)
	VI			(PuO2)3 (PO4)2:4H2O (am)	-48.97 ± 0.69	-	$(PuO_2)_3(PO_4)_2 \cdot 4H_2O$(am) $\rightleftharpoons 3PuO_2^{2+} + 2PO_4^{3-} + 4H_2O$(l)
PuO2CO3(s)	VI	-14.65 ± 0.47	-	PuO2CO3 (cr)	-14.82 ± 0.12	-	PuO_2CO_3(cr) $\rightleftharpoons PuO_2^{2+} + CO_3^{2-}$
PuO2OH(am)	V	5.0 ± 0.5	-	PuO2OH (am)	5.0 ± 0.5	-	PuO_2OH(am) + $H^+ \rightleftharpoons PuO_2^+ + H_2O$(l)
PuO2(hyd,ag) [a]	IV	-2.33 ± 0.52	-	PuO2 (am,hyd)	-2.33 ± 0.52	-	PuO_2(am, hyd) + 4 $H^+ \rightleftharpoons Pu^{4+}$ + 2 H_2O(l)
PuO2(coll, hyd)	IV	*(-8.3 ± 1.0)* [*]	-	*PuO2 (coll, hyd)*	*-8.3 ± 1.0*	-	*PuO_2(am, hyd) ⇌ PuO_2(coll, hyd)*
Pu(HPO4)2(am,hyd)	IV	-30.45 ± 0.51	-	Pu(HPO4)2 (am,hyd)	-30.45 ± 0.51	-	$Pu(HPO_4)_2$(am, hyd) $\rightleftharpoons Pu^{4+}$ + 2 HPO_4^{2-}
Pu(OH)3(cr)	III	15.8 ± 1.5	-	Pu(OH)3 (am)	14.58 ± 0.75	-	$Pu(OH)_3$(am) + 3 $H^+ \rightleftharpoons Pu^{3+}$ + 3 H_2O(l)
PuPO4(s,hyd)	III	-24.6 ± 0.8	-	PuPO4 (am,hyd)	-24.44 ± 0.55	-	$PuPO_4$(am, hyd) ⇌ $Pu^{3+} + PO_4^{3-}$

[a] Referred to as PuO_2(am, hydr.) by Guillaumont et al. (2003).

Tab. 20-2: Selected SIT ion interaction coefficients $\varepsilon_{j,k}$ [kg · mol^{-1}] for plutonium species

Data included in TDB 2020 are taken from Lemire et al. (2001), Guillaumont et al. (2003) and Grenthe et al. (2020) unless indicated otherwise. Own data estimates based on charge correlations (see Section 1.5.3) are shaded. Supplemental data are in italics.

j k → ↓	**Cl^-** $\varepsilon_{j,k}$	**ClO_4^-** $\varepsilon_{j,k}$	**NO_3^-** $\varepsilon_{j,k}$	**Li^+** $\varepsilon_{j,k}$	**Na^+** $\varepsilon_{j,k}$	**K^+** $\varepsilon_{j,k}$
PuO2+2	0.19 ± 0.09	0.46 ± 0.05	-	0	0	0
PuO2OH+	0.05 ± 0.10	0.2 ± 0.1	-	0	0	0
PuO2(OH)2(aq)	0	0	0	0	0	0
PuO2(OH)3-	0	0	0	-	-0.05 ± 0.10	-
(PuO2)2(OH)2+2	0.15 ± 0.10	0.4 ± 0.1	-	0	0	0
PuO2F+	0.05 ± 0.10	0.29 ± 0.11	-	0	0	0
PuO2F2(aq)	0	0	0	0	0	0
PuO2Cl+	(0.36 ± 0.06) [a]	0.50 ± 0.09	-	0	0	0
PuO2Cl2(aq)	0	0	0	0	0	0
PuO2SO4(aq)	0	0	0	0	0	0
PuO2(SO4)2-2	0	0	0	-	-0.10 ± 0.10	-
PuO2PO4-	0	0	0	-	-0.05 ± 0.10	-
PuO2HPO4(aq)	0	0	0	0	0	0
PuO2H2PO4+	0.05 ± 0.10	0.2 ± 0.1	-	0	0	0
PuO2(H2PO4)2	0	0	0	0	0	0
PuO2CO3(aq)	0	0	0	0	0	0
PuO2(CO3)2-2	0	0	0	-	-0.10 ± 0.10	-
PuO2(CO3)3-4	0	0	0	-	-0.20 ± 0.30	-
(PuO2)3(CO3)6-6	0	0	0	-	(0.37 ± 0.11) [b]	-
(UO2)2PuO2(CO3)6-6	0	0	0	-	(0.37 ± 0.11) [b]	-
PuO2+	0.05 ± 0.10	0.24 ± 0.05	-	0	0	0
PuO2OH(aq)	0	0	0	0	0	0
PuO2SO4-	0	0	0	-	0.07 ± 0.13	-
PuO2CO3-	0	0	0	-	-0.18 ± 0.18	-
PuO2(CO3)2-3	0	0	0	-	-0.15 ± 0.20	
PuO2(CO3)3-5	0	0	0	-	-0.25 ± 0.40	-
Pu+4	0.37 ± 0.10	0.82 ± 0.07	-	0	0	0
PuOH+3	(0.2 ± 0.1) [d]	0.50 ± 0.05	-	0	0	0
Pu(OH)2+2	(0.1 ± 0.1) [d]	0.4 ± 0.1	-	0	0	0
Pu(OH)3+	(0.05 ± 0.10) [d]	0.2 ± 0.1	-	0	0	0
Pu(OH)4(aq)	0	0	0	0	0	0
Ca4Pu(OH)8+4	*(-0.01 ± 0.10)* [e]	*(0.21 ± 0.17)* [f]	-	*0*	*0*	*0*
PuF+3	0.25 ± 0.10	0.56 ± 0.11	-	0	0	0
PuF2+2	0.15 ± 0.10	0.36 ± 0.17	-	0	0	0

Tab. 20-2: Cont.

j k → ↓	Cl^- $\varepsilon_{j,k}$	ClO_4^- $\varepsilon_{j,k}$	NO_3^- $\varepsilon_{j,k}$	Li^+ $\varepsilon_{j,k}$	Na^+ $\varepsilon_{j,k}$	K^+ $\varepsilon_{j,k}$
PuCl+3	(0.85 ± 0.09) [g]	0.85 ± 0.09	-	0	0	0
PuSO4+2	0.15 ± 0.10	(0.36 ± 0.14) [h]	-	0	0	0
Pu(SO4)2(aq)	0	0	0	0	0	0
PuNO3+3	0.25 ± 0.10	(0.70 ± 0.09) [h]	-	0	0	0
PuH3PO4+4	0.35 ± 0.10	0.8 ± 0.1	-	0	0	0
Pu(CO3)4-4	0	0	0	-	-0.20 ± 0.30	-
Pu(CO3)5-6	0	0	0	-	-0.30 ± 0.50	-
PuCO3(OH)3-	*0*	*0*	*0*	-	*-0.05 ± 0.10*	-
Pu+3	(0.23 ± 0.02) [c]	0.49 ± 0.05	-	0	0	0
PuOH+2	0.15 ± 0.10	(0.39 ± 0.04) [i]	-	0	0	0
Pu(OH)2+	*0.05 ± 0.10*	*0.2 ± 0.1*	-	*0*	*0*	*0*
Pu(OH)3(aq)	*0*	*0*	*0*	*0*	*0*	*0*
PuF+2	*0.15 ± 0.10*	*0.4 ± 0.1*	-	*0*	*0*	*0*
PuF2+	*0.05 ± 0.10*	*0.2 ± 0.1*	-	*0*	*0*	*0*
PuCl+2	*(0.39 ± 0.16)* [j]	*0.39 ± 0.16*	-	*0*	*0*	*0*
PuSO4+	0.05 ± 0.10	0.2 ± 0.1	-	0	0	0
Pu(SO4)2-	0	0	0	-	-0.05 ± 0.10	-
PuH2PO4+2	0.15 ± 0.10	0.4 ± 0.1	-	0	0	0
PuCO3+	*0.05 ± 0.10*	*0.2 ± 0.1*	-	*0*	*0*	*0*
Pu(CO3)2-	*0*	*0*	*0*	-	*-0.10 ± 0.10*	-
Pu(CO3)3-3	*0*	*0*	*0*	-	*-0.15 ± 0.20*	-
PuSCN+2	0.15 ± 0.10	0.39 ± 0.04	-	0	0	0

[a] Thoenen et al. (2014), to be used in combination with $\varepsilon(PuO_2^{2+}, Cl^-) = \varepsilon(PuO_2^{2+}, ClO_4^-) = (0.46 \pm 0.05)$ kg · mol^{-1}

[b] Estimated to be equal to $\varepsilon((UO_2)_3(CO_3)_6^{6-}, Na^+)$.

[d] Neck & Kim (2001)

[e] Altmaier et al. (2008), same coefficient as for the corresponding Th-complex.

[f] Thoenen et al. (2014), same coefficient as for the corresponding Th-complex.

[g] Thoenen et al. (2014), to be used in combination with $\varepsilon(Pu^{4+}, Cl^-) = \varepsilon(Pu^{4+}, ClO_4^-) = (0.82 \pm 0.07)$ kg · mol^{-1}

[h] Thoenen et al. (2014).

[i] Value estimated and used by Lemire et al. (2001) but not listed in their Tab. B.3 of selected ion interaction coefficients.

[j] Thoenen et al. (2014), to be used in combination with $\varepsilon(Pu^{3+}, Cl^-) = \varepsilon(Pu^{3+}, ClO_4^-) = (0.49 \pm 0.05)$ kg·

20.7 References

Altmaier, M., Neck, V. & Fanghänel, T. (2008): Solubility of Zr(IV), Th(IV) and Pu(IV) hydrous oxides in $CaCl_2$ solutions and the formation of ternary Ca-M(IV)-OH complexes. Radiochim. Acta, 96, 541-550.

Bennett, D.A., Hoffman, D.C., Nitsche, H., Russo, R.E., Torres, R.A., Baisden, P.A., Andrews, J.E., Palmer, C.E.A. & Silva, R.J. (1992): Hydrolysis and carbonate complexation of dioxoplutonium(V). Radiochim. Acta, 56, 15-19.

Cho, H.-R., Jung, E.-C., Park, K.K., Song, K. & Yun, J.-I. (2010): Effect of reduction on the stability of Pu(VI) hydrolysis species. Radiochim. Acta, 98, 555-561.

Cho, H.-R., Youn, Y.-S., Jung, E.-C. & Cha, W. (2016): Hydrolysis of trivalent plutonium and solubility of $Pu(OH)_3$(am) under electrolytic reducing conditions. Dalton Trans., 45, 19449-19457.

Fellhauer, D., Neck, V., Altmaier, M., Lützenkirchen, J. & Fanghänel, T. (2010): Solubility of tetravalent actinides in alkaline $CaCl_2$ solutions and formation of $Ca_4[An(OH)_8]^{4+}$ complexes: A study of Np(IV) and Pu(IV) under reducing conditions and the systematic trend in the An(IV) series. Radiochim. Acta, 98, 541-548.

Felmy, A.R., Rai, D., Schramke, J.A. & Ryan, J.L. (1989): The solubility of plutonium hydroxide in dilute solution and in high-ionic-strength chloride brines. Radiochim. Acta, 48, 29-35.

Grenthe, I., Gaona, X., Plyasunov, A.V., Rao, L., Runde, W.H., Grambow, B., Konings, R.J.M., Smith, A.L. & Moore, E.E. (2020): Second Update on the Chemical Thermodynamics of Uranium, Neptunium, Plutonium, Americium and Technetium. Chemical Thermodynamics, Vol. 14. OECD Publications, Paris, France, 1503p p.

Guillaumont, R., Fanghänel, T., Fuger, J., Grenthe, I., Neck, V., Palmer, D.A. & Rand, M.H. (2003): Update on the Chemical Thermodynamics of Uranium, Neptunium, Plutonium, Americium and Technetium. Chemical Thermodynamics, Vol. 5. Elsevier, Amsterdam, 919 pp.

Hummel, W., Berner, U., Curti, E., Pearson, F.J. & Thoenen, T. (2002): Nagra/PSI Chemical Thermodynamic Data Base 01/01. Nagra Technical Report NTB 02-16. Also published by Universal Publishers/uPublish.com, Parkland, Florida, USA.

Lemire, R. J., Fuger, J., Nitsche, H., Potter, P.E., Rand, M.H., Rydberg, J., Spahiu, K., Sullivan, J.C., Ullman, W.J., Vitorge, P. & Wanner, H. (2001): Chemical Thermodynamics of Neptunium and Plutonium. Chemical Thermodynamics, Vol. 4. Elsevier, Amsterdam, 845 pp.

Moskvin, A.I. (1971): Complex formation by neptunium(IV) and plutonium(IV) in nitrate solutions. Russ. J. Inorg. Chem., 16, 3, 405-408.

Neck, V., Altmaier, M. & Fanghänel, T. (2006): Ion interaction (SIT) coefficients for the Th^{4+} ion and trace activity coefficients in $NaClO_4$, $NaNO_3$ and NaCl solution determined by solvent extraction with TBP. Radiochim. Acta, 94, 501-507.

Neck, V. & Kim, J.I. (2001): Solubility and hydrolysis of tetravalent actinides. Radiochim. Acta, 89, 1-16.

Rai, D., Moore, D.A., Felmy, A.R. & Rosso, K.M. (2010): $PuPO_4$(cr, hyd) solubility product and Pu^{3+} complexes with phosphate and ethylenediaminetetraacetic acid. Journal of Solution Chemistry, 39, 778- 807.

Rai, D., Xia, Y., Rao, L., Hess, N.J., Felmy, A.R., Moore, D.A., McCready, D. E. (2005): Solubility of $(UO_2)_3(PO_4)_2 \cdot 4H_2O$ in H^+-Na^+-OH^--$H_2PO_4^-$-HPO_4^{2-}-PO_4^{3-}-H_2O and its comparison to the analogous PuO_2^{2+} system. J. Solution Chem., 34, 469-498.

Rand, M.H., Fuger, J., Grenthe, I., Neck, V. & Rai, D. (2007): Chemical Thermodynamics of Thorium. Chemical Thermodynamics, Vol. 11. OECD Publications, Paris, France, 900 p.

Rao, L., Tian, G., Di Bernardo, P. & Zanonato, P. (2011): Hydrolysis of plutonium(VI) at variable temperatures (283-343 K). Chem. Eur. J., 17, 10985-10993.

Reilly, S.D. & Neu, M.P. (2006): Pu(VI) hydrolysis: further evidence for a dimeric plutonyl hydroxide and contrasts with U(VI) chemistry. Inorg. Chem., 45, 1839-1846.

Reilly, S.D., Runde, W. & Neu, M.P. (2007): Solubility of plutonium(VI) carbonate in saline solutions. Geochim. Cosmochim. Acta, 71, 2672-2679.

Thoenen, T. (2012): The PSI/Nagra Chemical Thermodynamic Data Base 12/07: Compilation of updated and new data with respect to the Nagra/PSI Chemical Thermodynamic Data Base 01/01. PSI Technical Report TM-44-12-06. Paul Scherrer Institut, Villigen, Switzerland, 35 pp.

Thoenen, T., Hummel, W., Berner, U. & Curti, E. (2014): The PSI/Nagra Chemical Thermodynamic Database 12/07. Technical Report, PSI Bericht Nr. 14-04, Paul Scherrer Institut, Villigen, Switzerland, 416 pp.

Topin, S., Aupiais, J., Baglan, N., Vercouter, T., Vitorge, P. & Moisy, P. (2009a): Trace metal speciation by capillary electrophoresis hyphenated to inductively coupled plasma mass spectrometry: sulfate and chloride complexes of Np(V) and Pu(V). Anal. Chem., 81, 5354-5363.

Topin, S., Aupiais, J. & Moisy, P. (2009b): Direct determination of plutonium(V) and neptunium(V) complexation by carbonate ligand with CE-ICP-sector field MS. Electrophoresis, 30, 1747-1755.

Yun, J.-I., Cho, H.-R., Neck, V., Altmaier, M., Seibert, A., Marquardt, C. M., Walther, C. & Fanghänel, T. (2007): Investigation of the hydrolysis of plutonium(IV) by a combination of spectroscopy and redox potential measurements. Radiochim. Acta, 95, 89-95.

21 Polonium

21.1 Introduction

Several short-lived polonium isotopes are part of the actinide decay chains and as such, they occur in nature. Most of these isotopes have half-lives of less than a second, only Po-218 (3 minutes) and Po-210 (138 days) exhibit longer half-lives. In addition, the longest-lived polonium isotope, Po-209 with 102 ± 5 years half-life, is produced in spallation induced neutron sources (e.g. SINQ at PSI) and contributes in dose-relevant quantities to the inventory of radioactive waste coming from research facilities like PSI. The latter fact triggered the inclusion of polonium into the PSI Chemical Thermodynamic Database 2020 (TDB 2020).

The thermodynamic data included into the TDB 2020 are based on the PhD thesis of Brown (2001) and own reviews of the literature. Because of the paucity of reported experimental data, many of the thermodynamic data presented by Brown (2001) have been derived theoretically using linear free energy relationships.

Brown (2001) stated that it has been somewhat surprising to find from the literature survey that most of the experimental work to determine the characteristics and properties of polonium was conducted prior to 1960. One would assume that advances in technology would make such studies easier to pursue and yet our knowledge of the chemistry of polonium, as compared with other elements, is scanty. Nevertheless, it has been possible, through a critical evaluation of the data scattered in the literature, to elucidate the basics of the chemical properties of the element and present this as a thermochemical database.

The chemistry of polonium is complex. Valencies of –II, II and IV are comparatively well known and have been established by characterisation of polonides and a hydride (-II), the halides (II) and the dioxide (IV). There is evidence for a VI state. There is no conclusive evidence for the III state characteristic of many bismuth compounds.

Brown (2001) concluded that polonium has chemical characteristics of both, lead and tellurium, depending on conditions. In a pure water system, under acidic conditions, its behaviour is like that of lead because of its ability to form the divalent cation, Po^{2+}. Under basic conditions, however, its chemistry is like that of tellurium (and selenium) with aqueous species dominant for these elements in this region (Fig. 21-1).

Based on the present review, it should be noted in addition that Po(IV) has chemical characteristics of the tetravalent actinides Th(IV) and U(IV).

Following the general quality criteria of TDB 2020 almost all of the selected thermodynamic data of polonium should have been classified as "supplemental data". However, to discern data which have been obtained from at least one decent experimental study, and data which have been estimated by some sort of linear free energy relationship or mere chemical analogy and hand-waving arguments, only the latter ones are included in TDB 2020 as supplemental data.

The selected thermodynamic data for polonium compounds and complexes are presented in Tab. 21-2.

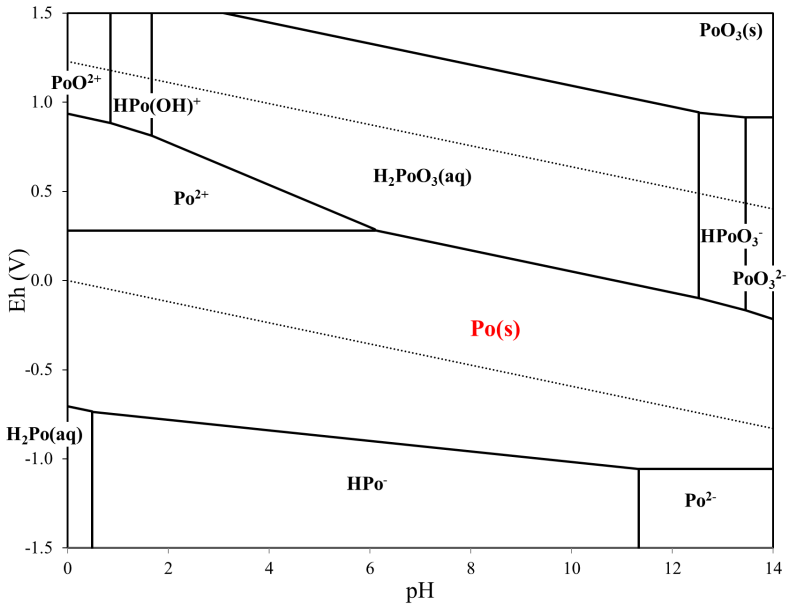

Fig. 21-1: Eh – pH diagram for the polonium water system according to thermodynamic data reported by Brown (2001).

Solid lines: $[Po]_{total} = 10^{-12}$ M, dashed lines: $[Po]_{total} = 10^{-24}$ M, dotted lines: stability region of water.

NEA (see, e.g., Grenthe et al. 1992) used the specific ion interaction theory (SIT) for making ionic strength corrections to the experimental data, an approach which is also adopted for TDB 2020 (as has been for all its predecessors). Brown (2001) and the present reviewer evaluated some experiments in KOH or sulphuric acid media using SIT but no interaction coefficients for NaCl or $NaClO_4$ media could be derived from these systems. Only in one case, SIT interaction coefficients for perchlorate media could be derived (see Section 21.5.6.1). In all other cases we approximated missing data with the estimation method described in Section 1.5.3, which draws on a statistical analysis of published SIT ion interaction coefficients, and which allows the estimation of missing coefficients for the interaction of cations with Cl^- and ClO_4^-, and for the interaction of anions with Na^+, from the charge of the cations or anions of interest.

As chloride complexation with polonium is considered explicitly in this review, ion interaction coefficients ε for cationic polonium species with Cl^- are approximated by the corresponding interaction coefficients with ClO_4^-. Thus, e.g., $\varepsilon(PoOH_3^+, Cl^-) \approx \varepsilon(PoOH_3^+, ClO_4^-) = 0.2 \pm 0.1$ kg · mol^{-1}.

The selected SIT ion interaction coefficients for polonium species are presented in Tab. 21-3.

21.2 Polonium(0)

21.2.1 Elemental polonium

Elemental polonium is reported to be metallic and resembles lead and bismuth in its physical properties, while chemically it is similar to the sulphur group elements, selenium and tellurium. X-ray diffraction studies have indicated that the metal exists in at least two crystalline forms: "high temperature" β-polonium with a simple rhombohedral lattice and "low temperature" α-polonium with a simple cubic lattice. The phase transformation occurs at about 75 °C. The melting point of polonium has been given as 254 °C (Brown 2001).

Polonium metal is the standard state for polonium and, by definition, both the Gibbs free energy of formation, $\Delta_f G_m°$, and the heat of formation, $\Delta_f H_m°$, values are 0.0 kJ · mol^{-1}. For the entropy of polonium metal Brown (2001) selected:

$$S_m°(\text{Po, s, 298.15 K}) = 62.8 \text{ J} \cdot \text{K}^{-1} \cdot \text{mol}^{-1}$$

This value is included in TDB 2020.

Elemental polonium has a large stability field in the Eh – pH range of water (Fig. 21-1) and hence, metallic polonium, Po(cr), could be an environmentally important substance under reducing conditions, although more probably the aqueous species Po(aq) might predominate in the trace concentration range of polonium (see Section 21.2.2).

On the other hand, the gas phases Pog and Po_2g, for which thermodynamic data have been reported, are not important in aqueous systems and are not included in the data base.

21.2.2 Polonium(0) solubility

Inspecting the polonium water system as presented by Brown (2001) the most striking feature of the Eh – pH diagram is the huge stability field of metallic polonium, Po(s), in the anoxic part of the stability region of water (Fig. 21-1). Under reducing conditions, the solubility of polonium is predicted to be absurdly low: A calculation assuming a total polonium concentration of 10^{-24} M, equivalent to about one atom of polonium in one litre of water, still results in a large stability field of Po(s) (dashed lines in Fig. 21-1). For a partial pressure of 1 bar H_2g, the solubility of polonium is predicted to be about 10^{-23} M at pH 12.5 and about 10^{-29} M at pH 7. The latter value corresponds to one atom of polonium in 100 m^3 of water.

These totally unrealistic solubility numbers are the consequence of ignoring the possibility that elemental polonium may dissolve as zero valent Po(aq):

$$Po(s) \rightleftharpoons Po(aq)$$

This possibility has never been discussed in the literature and no experimental data are available.

However, several solubilities of zero valent elements are known or have been estimated.

The solubility of elemental mercury is well known, $\log_{10}K°$(Hg(aq), 298.15 K) = -6.53 ± 0.03 (see Section 14.2.2). Likewise, the solubility of metallic silver has been reported as $\log_{10}K°$(Ag(aq)) = -6.5 ± 0.5 (see Section 26.2.2). The solubility of metallic lead has been estimated as $\log_{10}K°$(Pb(aq), 298.15 K) ≈ -7.3 (see Section 12.2.2).

Looking at elements in the same group of the Periodic Tab. of the elements, the solubility of elemental sulphur is well known, $\log_{10}K°$(S(aq), 298.15 K) = -6.65 ± 0.03 (see Section 27.3), while the solubility of elemental selenium is still unknown. Only rough estimate can be derived from preliminary experimental data, $\log_{10}K°$(Se(aq), 298.15 K) = -6 ± 1 (see Section 24.3). Nothing is known about the solubility of elemental tellurium.

Considering these solubility data, and recalling that elemental polonium resembles lead in its physical properties, while chemically it is similar to the sulphur group elements, the present review guesses:

$$\log_{10}K°(Po(aq), 298.15\ K) \approx -7$$

Note that this value is included as supplemental datum in TDB 2020 with the caveat to remind the modeller that there is an unresolved problem when Po(aq) pops up as the dominating species in a modelling result.

21.3 Polonium(-II)

21.3.1 Hydrogen polonide - polonide system

No thermodynamic data exist for the hydrogen polonide – polonide system.

Brown (2001) used the observation that a linear relationship often exists between the $\Delta_f H_m°$ of a particular type of species in a single group of the Periodic Tab. and the logarithm of the atomic number (log A) comprising the species. Following this methodology, a similar relationship may also exist between $\Delta_f G_m°$ and log A. Since $E°$ is directly proportional to $\Delta_f G_m°$ for the H_2X/X and X^{2-}/X couples, where X is S, Se, Te or Po, a plot of $E°$ versus log A may show a similar correlation.

Plots of log A of the respective chalcogen versus $E°$ for the H_2X/X and X^{2-}/X oxidation couples of S, Se and Te showed excellent correlations. The oxidation potentials determined by Brown (2001) for polonium from these linear relationships are -1.07 and -1.42 V for the $H_2Po(aq)/Po(s)$ and Po^{2-}/ Po(s) couples, respectively. From the estimated oxidation potentials, Brown (2001) calculated

$$\Delta_f G_m°(H_2Po, aq, 298.15\ K) = (206.5)\ kJ \cdot mol^{-1}$$

$$\Delta_f G_m°(Po^{2-}, 298.15\ K) = (274.0)\ kJ \cdot mol^{-1}$$

These values are included as supplemental data in TDB 2020.

The $\Delta_f G_m°$ value of HPo^- can be calculated in a similar manner to that for the $\Delta_f G_m°$ values of $H_2Po(aq)$ and Po^{2-} using the $\Delta_f G_m°$ values of HX^- for S, Se and Te. From a plot of log A versus $\Delta_f G_m°$ Brown (2001) calculated

$$\Delta_f G_m°(HPo^{2-}, 298.15\ K) = (209.3)\ kJ \cdot mol^{-1}$$

This value is included as supplemental datum in TDB 2020.

Using the estimated $\Delta_f G_m°$ values of $H_2Po(aq)$, HPo^- and Po^{2-}, $\log_{10}K°$ for the following equilibria are calculated:

$$H_2Po(aq) \rightleftharpoons HPo^- + H^+$$

$$\log_{10}K°(298.15\ K) = -0.49$$

$$HPo^- \rightleftharpoons Po^{2-} + H^+$$

$$\log_{10}K°(298.15\ K) = -11.33$$

These values are included as supplemental data in TDB 2020.

21.3.2 Metal polonides

Brown (2001) reported that a number of metal polonides have been prepared and analysed using X-ray diffraction, including those with Pb, Hg, Ca, Zn, Na, Pt, Ni, Ag and Be.

Of these metals, solubility data exist for the sulphides, selenides and tellurides of Pb, Hg, Zn, Ni and Ag only. Brown (2001) showed that a relationship exists between their solubility products and the dissociation constant of the respective hydrogen chalcogenide (HX^-). From the lines of best fit for each metal and the selected stability constant for HPo^- Brown (2001) obtained the following $\log_{10}K_{s0}$ values for metal polonides: -55.2 (PbPo(s)), -76.8 (HgPo(s)), -37.7 (ZnPo(s)) and -46.1 (NiPo(s)). The fit for Ag was not significant.

It is not clear whether any of these metal polonides has a thermodynamic stability region within the stability bounds of water (Fig. 21-1) under any chemical condition. However, if such a stability region exists, just including into the TDB solubility products, $\log_{10}K_{s0}$, for the reaction

$$MePo(s) \rightleftharpoons Me^{2+} + Po^{2-}$$

where Me is Pb, Hg, Zn or Ni, would inevitably lead to erroneous calculated polonium concentrations as we do not have any vague idea about aqueous metal polonide complexes. Therefore, these estimated metal polonide solubility products have not been included in TDB 2020.

21.4 Polonium(II)

21.4.1 Polonium(II) aqua ion

Brown (2001) considered measurements of the potential of the cathodic reduction of polonium to the metal

$$Po^{2+} + 2e^- \rightleftharpoons Po(s)$$

and calculated from the reported values 0.65, 0.6 and 0.68 V the mean $E°$ value of 0.643 V, equivalent to $\log_{10}K° = 21.74$, which in turn was used to calculate

$$\Delta_f G_m°(Po^{2+}, 298.15\ K) = (124.1)\ kJ \cdot mol^{-1}$$

This value is included in TDB 2020.

21.4.2 Polonium(II) (hydr)oxide compounds and complexes

21.4.2.1 Polonium(II) hydroxide complexes

Brown & Ekberg (2016) state that "polonium is known to form a number of oxidation states including Po^{2+}. Brown (2001) showed that the stability region (Eh – pH) of polonium(II) was quite narrow, occurring in a region that does not exceed a pH of 6 and is bounded by polonium metal at lower Eh and polonium(IV) at higher Eh. The hydrolytic properties of polonium(II) are expected to be similar to those of lead(II). As a consequence, polonium(II) is not expected to hydrolyse until a pH higher than 6, in a region where it is not expected to be stable. It is not expected, therefore, that polonium(II) hydrolysis species would exist and none have been reported."

21.4.2.2 Polonium(II) oxide compounds

Brown (2001) reported that monoxide, PoO(s), is produced by the spontaneous decomposition of polonium sulphite, $PoSO_3(s)$, or selenite, $PoSeO_3(s)$. The corresponding hydrated oxide or hydroxide forms as a dark brown precipitate on the addition of alkali to solutions of the dihalides in acid. It is rapidly oxidised to the IV state.

No thermodynamic data are available, and none have been estimated for these unstable compounds.

21.4.3 Polonium(II) halide compounds and complexes

21.4.3.1 Polonium(II) halide complexes

Brown (2001) evaluated for the reaction

$$PoCl_4^{2-} + 2e^- \rightleftharpoons Po(s) + 4Cl^-$$

a single study reporting oxidation potentials E measured in 1 – 4 M HCl. Taking these E values and correcting to zero ionic strength using SIT, Brown (2001) determined $E° = 0.420 \pm 0.005$ V, equivalent to $\log_{10}K° = 14.20$. Using this $E°$ and $\Delta_f G_m°(Cl^-, 298.15\ K) = -131.0\ kJ \cdot mol^{-1}$, Brown (2001) calculated $\Delta_f G_m°(PoCl_4^{2-}, 298.15\ K) = -(443.0)\ kJ \cdot mol^{-1}$. Using the CODATA value $\Delta_f G_m°(Cl^-, 298.15\ K) = -131.217\ kJ \cdot mol^{-1}$ (Cox et al. 1989), this review calculated

$$\Delta_f G_m°(PoCl_4^{2-}, 298.15\ K) = -(443.9)\ kJ \cdot mol^{-1}$$

This value is included in TDB 2020.

In turn, use of this $\Delta_f G_m°$ value and the $\Delta_f G_m°$ values for Po^{2+} (see Section 21.4.1) and Cl^- (see above) gives:

$$Po^{2+} + 4Cl^- \rightleftharpoons PoCl_4^{2-}$$
$$\log_{10}\beta_4° (298.15\ K) = 7.55$$

This value is also included in TDB 2020.

Note that the calculated $\log_{10}\beta_4°$ value does not depend on the $\Delta_f G_m°(Cl^-, 298.15\ K)$ value used as it cancels in the above two-step procedure.

Brown (2001) used linear free energy relationships between $MCl_n^{(z-n)+}$ and $MCl_{n-1}^{(z-n+1)+}$ species for the averaged stability constant data for various metal chloride species obtained from the literature to determine the corresponding polonium values.

In a stepwise procedure Brown (2001) used the above determined $\log_{10}\beta_4°$ value of $PoCl_4^{2-}$ and the results of a MCl_4 – MCl_3 plot to estimate $\log_{10}\beta_3°$ of $PoCl_3^-$, then used this estimated value and the results of a MCl_3 – MCl_2 plot to estimate $\log_{10}\beta_2°$ of $PoCl_2(aq)$, and finally the latter estimate and the results of a MCl_2 – MCl plot to estimate $\log_{10}\beta_1°$ of $PoCl^+$:

$$Po^{2+} + 3Cl^- \rightleftharpoons PoCl_3^-$$
$$\log_{10}\beta_3° (298.15\ K) = 7.02$$
$$Po^{2+} + 2Cl^- \rightleftharpoons PoCl_2(aq)$$
$$\log_{10}\beta_2° (298.15\ K) = 6.13$$

$Po^{2+} + Cl^- \rightleftharpoons PoCl^+$

$log_{10}\beta_1^\circ\ (298.15\ K) = 3.75$

These values are included as supplemental data in TDB 2020.

No thermodynamic data are available or have been estimated for other Po(II) halide complexes.

21.4.3.2 Polonium(II) halide compounds

Brown (2001) reported that dark, ruby-red polonium dichloride, $PoCl_2(s)$, is formed by the reduction of the solid tetrachloride, $PoCl_4(s)$ with sulphur dioxide at 25 °C. The solid is hygroscopic and mildly volatile. $PoCl_2(s)$ dissolves readily in dilute hydrochloric acid to form a pink solution that readily oxidises.

Brown (2001) reported further that polonium dibromide, $PoBr_2(s)$, is a purple-brown solid, formed by the reduction of the solid tetrabromide, $PoBr_4(s)$, with sulphur dioxide at 25 °C. The reduction, however, is incomplete. By analogy to the dichloride the solid is hygroscopic and somewhat volatile. $PoBr_2(s)$ is soluble in dilute hydrobromic acid, forming a purple solution that readily oxidises to the tetravalent state.

Finally, Brown (2001) reported that polonium tetraiodide, $PoI_4(s)$, is the only polonium iodide known. This means that $PoI_2(s)$ has never been prepared.

Brown (2001) stated that it has been shown that a correlation exists between $\Delta_f H_m^\circ$ and $\Delta_f G_m^\circ$, and therefore, it follows that a similar relationship will exist between $\Delta_f S_m^\circ$ and $\Delta_f G_m^\circ$. Hence, Brown (2001) used the relationship between $\Delta_f S_m^\circ$ and $\Delta_f G_m^\circ$ for the polonium species Po(s), Pog, Po_2g and $PoO_2(s)$ together with a value $S_m^\circ(PoCl_2, s, 298.15\ K) = 130\ J \cdot K^{-1} \cdot mol^{-1}$ reported in the literature, from which first $\Delta_f S_m^\circ(PoCl_2, s, 298.15\ K) = -155.8\ J \cdot K^{-1} \cdot mol^{-1}$ is obtained and then, via the line of best fit, $\Delta_f G_m^\circ(PoCl_2, s,, 298.15\ K) = -130.9\ kJ \cdot mol^{-1}$ is calculated.

In analogy, from a value $S_m^\circ(PoBr_2, s, 298.15\ K) = 155\ J \cdot K^{-1} \cdot mol^{-1}$ reported in the literature, first $\Delta_f S_m^\circ(PoBr_2, s, 298.15\ K) = -60.0\ J \cdot K^{-1} \cdot mol^{-1}$ is obtained and then, via the line of best fit, Brown (2001) calculated $\Delta_f G_m^\circ(PoBr_2, s, 298.15\ K) = -50.4\ kJ \cdot mol^{-1}$.

For $PoI_2(s)$, which has never been prepared and no data whatsoever exist, Brown (2001) used an empirical relationship between $\Delta_f H_m^\circ$ of solid halides and the corresponding gas-phase halide ions. Using $\Delta_f H_m^\circ$ values for $PoCl_2(s)$ and $PoBr_2(s)$ calculated from $\Delta_f G_m^\circ$ and $\Delta_f S_m^\circ$ estimated above, and $\Delta_f H_m^\circ$ of Cl^-g, Br^-g and I^-g taken from the literature, Brown (2001) calculated $\Delta_f H_m^\circ(PoI_2, s, 298.15\ K) = 76.3\ kJ \cdot mol^{-1}$. Using this value and the results of the relationship between $\Delta_f G_m^\circ$ and $\Delta_f H_m^\circ$ for the polonium species Po(s), Pog, Po_2g and $PoO_2(s)$, the value $\Delta_f G_m^\circ(PoI_2, s, 298.15\ K) = 56.7\ kJ \cdot mol^{-1}$ is obtained.

The estimated $\Delta_f G_m^\circ$ values for the highly soluble solids $PoCl_2(s)$ and $PoBr_2(s)$, and the hypothetical solid $PoI_2(s)$, have not been included in TDB 2020.

21.4.4 Polonium(II) sulphate compounds and complexes

21.4.4.1 Polonium(II) sulphate complexes

Brown (2001) reported a measurement of the cathodic deposition of divalent polonium in 0.25 M H_2SO_4 which resulted in an $E°$ of 0.63 V for reaction

$$PoSO_4(aq) + 2e^- \rightleftharpoons Po(s) + SO_4^{2-}$$

Correction of this $E°$ to zero ionic strength using the Davies equation results in an $E°$ of 0.61 V, equivalent to $\log_{10}K° = 20.62$. From this corrected $E°$ and $\Delta_fG_m°(SO_4^{2-}, 298.15\ K) = -(743.9)\ kJ \cdot mol^{-1}$ Brown (2001) calculated $\Delta_fG_m°(PoSO_4, aq, 298.15\ K) = -(626.2)\ kJ \cdot mol^{-1}$. Using the CODATA value $\Delta_fG_m°(SO_4^{2-}, 298.15\ K) = -744.004\ kJ \cdot mol^{-1}$ (Cox et al. 1989) this review calculated

$$\Delta_fG_m°(PoSO_4, aq, 298.15\ K) = -(626.3)\ kJ \cdot mol^{-1}$$

This value is included in TDB 2020.

Use of this $\Delta_fG_m°$ and $\Delta_fG_m°(Po^{2+}, 298.15\ K) = (124.1)\ kJ \cdot mol^{-1}$, see Section 21.4.1, gives

$$Po^{2+} + SO_4^{2-} \rightleftharpoons PoSO_4(aq)$$

$$\log_{10}K°(298.15\ K) = 1.12$$

Thus, the complexation of Po^{2+} by sulphate is weak. Note that the calculated $\log_{10}K°$ value does not depend on the $\Delta_fG_m°(SO_4^{2-}, 298.15\ K)$ value used as it cancels in the above two-step procedure.

This value is also included in TDB 2020.

21.4.4.2 Polonium(II) sulphate compounds

Brown (2001) reported an experiment where polonium was precipitated using $BaSO_4(s)$ as a carrier. Brown (2001) recalculated the experimental data using $\log_{10}K_{sp}°(298.15\ K) = -9.95$ for $BaSO_4(s)$ and obtained

$$PoSO_4(s) \rightleftharpoons Po^{2+} + SO_4^{2-}$$

$$\log_{10}K_{sp}°(298.15\ K) = -8.89$$

Note that Hummel et al. (2002) selected $\log_{10}K_{sp}°(298.15\ K) = -9.97$ for $BaSO_4(s)$ and thus the above value has been changed to

$$\log_{10}K_{sp}°(298.15\ K) = -8.91$$

This value is included in TDB 2020.

21.4.5 Polonium(II) sulphide compounds and complexes

Brown (2001) discussed a single experimental study where the black precipitate that formed when H_2S was passed through aqueous solutions of polonium dichloride or tetrachloride was found to be PoS(s). The solubility product of PoS(s) was determined by precipitating the compound from solutions of varying HCl concentration, which had been saturated with H_2S.

The equilibrium sulphide concentrations present in the original solutions were recalculated by Brown (2001) using more recent auxiliary data, i.e. 3.38 $g \cdot L^{-1}$ for the solubility of H_2S in water at 25 °C and $\Delta_f G_m°(S^{2-}, 298.15\ K) = (91.9)\ kJ \cdot mol^{-1}$. Using these values and the Po^{2+} and H^+ concentrations given in the original experimental study, Brown (2001) obtained

$$PoS(s) \rightleftharpoons Po^{2+} + S^{2-}$$

$$\log_{10}K_{sp}°(298.15\ K) = -27.26$$

This solubility product of polonium(II) sulphide should be re-evaluated in terms of the reaction

$$PoS(s) + 2H^+ \rightleftharpoons Po^{2+} + H_2S(aq)$$

as $\Delta_f G_m°(S^{2-}, 298.15\ K)$ is a highly uncertain number for a virtual aqueous species which actually does not exist in measurable quantities in aqueous solutions.

However, as all speciation calculations including Po(II) and sulphide will inevitably lead to erroneous results except for rather acidic conditions, as no information about aqueous Po(II) sulphide complexes is available, the reported solubility product was neither re-evaluated in this review, nor has the reported value been included in TDB 2020.

21.5 Polonium(IV)

21.5.1 Polonium(IV) aqua ion

In the older literature there is no agreement about the actual form of the Po(IV) aqua ion, some authors assumed Po^{4+} while others preferred PoO^{2+}. Brown (2001) decided, without any discussion, that the Po(IV) aqua ion is PoO^{2+}, and consequently used this form of the ion in all reactions where the polonium(IV) aqua ion presumably is involved.

Unfortunately, this was the wrong decision. Ayala et al. (2010) showed in their ab initio molecular dynamics studies that the Po(IV) aqua ion resembles Th(IV) and U(IV). First, the aqua ion itself is a tetravalent cation with 8 – 9 coordinated water molecules i.e. $Po(H_2O)_8^{4+}$ to $Po(H_2O)_9^{4+}$. Second, Po(IV) in aqueous solutions shows a strong tendency toward hydrolysis with a decrease in coordination numbers. Ayala et al. (2010) found that $Po(H_2O)_4(OH)_2^{2+}$ and $Po(H_2O)_3(OH)_3^{+}$ have both a coordination number of six, and that under their simulation conditions there is not a unique predominant species in solution but rather an equilibrium between both species. Finally, $Po(OH)_4(aq)$ is found to have a coordination number of four.

Hence, the species Po^{4+}, $PoOH^{3+}$, $Po(OH)_2^{2+}$, $Po(OH)_3^{+}$, $Po(OH)_4(aq)$ and $Po(OH)_6^{2-}$ were used in this review, and the original reactions given by Brown (2001) were re-written (and re-evaluated) where necessary. The value $\Delta_f G_m°(PoO^{2+}, 298.15\ K) = (67.4)\ kJ \cdot mol^{-1}$, reported by Brown (2001), is rejected by this review.

The Gibbs energy of formation of Po^{4+} is very poorly defined via the reaction

$$PoO_2(s) + 4H^+ \rightleftharpoons Po^{4+} + 2H_2O(l)$$

$$log_{10}K_{s,0}° \approx 1.0$$

$$\Delta_r G_m°(298.15\ K) \approx -5.7\ kJ \cdot mol^{-1}$$

involving several estimates of stepwise hydrolysis constants (see Section 21.5.2.1), and the assumption that the solid $PoO_2(s)$ investigated in the solubility studies (see Section 21.5.2.1) is the same as the one discussed in Section 5.2.2 and hence, $\Delta_f G_m°(PoO_2, s, 298.15\ K) = -(192.1)\ kJ \cdot mol^{-1}$ can be used. Considering $\Delta_f G_m°(H^+, 298.15\ K) = 0$, by definition, and using the CODATA value $\Delta_f G_m°(H_2O, l, 298.15\ K) = -(237.140)\ kJ \cdot mol^{-1}$ (Cox et al. 1989) this review calculated

$$\Delta_f G_m°(Po^{4+}, 298.15\ K) \approx 276.5\ kJ \cdot mol^{-1}$$

This value is included in TDB 2020 as supplemental datum.

21.5.2 Polonium(IV) (hydr)oxide compounds and complexes

21.5.2.1 Polonium(IV) hydroxide complexes

Brown (2001) started the derivation of Po(IV) hydroxide complexes with the statement that the solubility of PoO_2(s) in water can be described by the following reaction

$$PoO_2(s) + H_2O(l) \rightleftharpoons H_2PoO_3(aq)$$

Brown (2001) reported that Bagnall et al. (1955) quote a solubility of PoO_2(s) of 0.075 mg L^{-1} in either water or excess alkali. From this value Brown (2001) evaluated the solubility of PoO_2(s) and derived an equilibrium constant $K° = 3.57 \cdot 10^{-7}$.

The complete text of Bagnall et al. (1955) to this "quote" reads as follows: "Addition of ammonia or sodium hydroxide solution to solutions in dilute hydrochloric acid precipitates a buff to pale-brown flocculent solid (solubility 76 μg of ^{210}Po per litre of water or excess of alkali). When the suspension is boiled, the precipitate becomes crystalline and yellow-brown and the solubility in excess of potassium hydroxide increases to 12 mg of ^{210}Po per litre. The precipitate, which is probably a hydrated oxide, appears to be feebly amphoteric and is being further investigated."

These poorly defined solubility values are not further considered by this review.

Brown (2001) further reported that Bagnall & Freeman (1957) measured the solubility of polonium dioxide in KOH at 22 °C (data in Bagnall 1957). A plot of the logarithm of polonium solubility (Fig. 3-4) has a slope of 2 and therefore, the reaction can be described by equation

$$PoO_2(s) + 2OH^- \rightleftharpoons PoO_3^{2-} + H_2O(l)$$

A value of -4.43 for the logarithm of the equilibrium constant has been derived for the reaction using the specific ion interaction theory (Fig. 3-5)".

Note that the book Bagnall (1957) was not available to the reviewer and hence, Fig. 3-4 of Brown (2001) has been digitised to extract the experimental data (Fig. 21-2). The result for the above equilibrium, which is equivalent to

$$PoO_2(s) + 2H_2O(l) + 2OH^- \rightleftharpoons Po(OH)_6^{2-}$$

is $\log_{10}K_{s,6} = -4.12 \pm 0.05$. Bagnall & Freeman (1957) reported $K_{s,6} = (8.2 \pm 0.4) \times 10^{-5}$ which gives $\log_{10}K_{s,6} = -4.09 \pm 0.04$ (uncertainty 2σ). In both cases activity corrections were not applied.

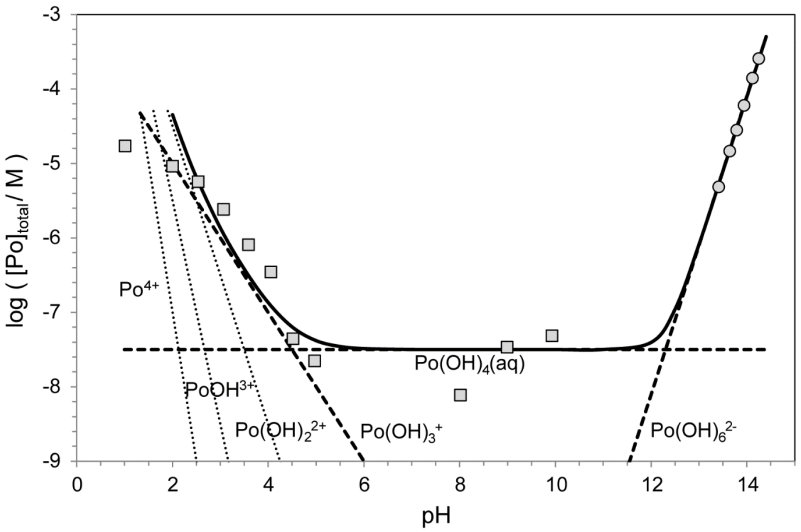

Fig. 21-2: Solubility of PoO_2(s) and concentration of Po^{4+} and Po(IV) hydrolysis species as a function of pH

Symbols: experimental solubility data of Treiman (1953) (squares) and Bagnall (1957) as cited by Brown (2001) (circles). Solid line: calculated solubility of PoO_2(s). Dashed lines: calculated concentrations of Po(IV) hydrolysis species as derived from experimental data. Dotted lines: concentrations of Po(IV) species estimated by this review.

This exercise shows that the data presented by Brown (2001) are correct and hence, her result using SIT to extrapolate the data to zero ionic strength has been accepted

$$\log_{10} K_{s,6}^\circ = -4.43 \pm 0.05$$

with the uncertainty assigned by this review. Note that no SIT interaction coefficients have been reported by Brown (2001) from her linear SIT regression in KOH medium, and none have been evaluated by this review.

For the equilibrium

$$PoO_2(s) + 4H_2O(l) \rightleftharpoons Po(OH)_6^{2-} + 2H^+$$

we finally obtain

$$\log_{10} {}^*K_{s,6}^\circ = -32.43 \pm 0.05$$

This value is included in TDB 2020.

Brown (2001) estimated a stability constant for the complex $HPoO_3^-$, equivalent to $Po(OH)_5^-$, by fitting something "in between" the data of Bagnall & Freeman (1957) for $H_2PoO_3^{2-}$, equivalent to $Po(OH)_6^{2-}$, and the solubility value $K^\circ = 3.57 \cdot 10^{-7}$ of Bagnall et al. (1955) for H_2PoO_3(aq), which has been rejected by this review. As we do not have experimental data in the pH region where $Po(OH)_5^-$ probably could predominate (Fig. 21-2), this review did not try to estimate a stability value for $Po(OH)_5^-$.

Brown (2001) did not consider the solubility study of Treiman (1953) who measured the solubility of polonium hydroxide, or hydrated oxide, $PoO_2 \cdot H_2O(s)$, in the pH range 1 – 10 in dilute solutions (Fig. 21-2). Treiman (1953) stated that "essentially, the procedure is the precipitation of polonium hydroxide in the presence of glass wool, followed by filtration of the solution through a fritted-glass filter funnel. Apparently, glass wool is an effective adsorbent for colloidal polonium hydroxide and/or for any radio-colloids which may be suspended in solution since the glass wool method proved very valuable in recovery operations" (Treiman & Treiman 1952).

This review used the data reported by Treiman (1953) (Fig. 21-2) to derive

$$PoO_2(s) + 2H_2O(l) \rightleftharpoons Po(OH)_4(aq)$$
$$\log_{10}K_{s,4}^\circ = \log_{10}K_{s,4} = -7.5$$

$$PoO_2(s) + H_2O(l) + H^+ \rightleftharpoons Po(OH)_3^+$$
$$\log_{10}{}^*K_{s,3}^\circ = \log_{10}{}^*K_{s,3} = -3.0$$

Note that in both cases the isocoulombic reactions are not ionic strength dependent and hence, $\log_{10}K_s = \log_{10}K_s^\circ$.

These values are included in TDB 2020.

Based on the above results and considering the general hydrolysis behaviour of tetravalent cations like Th^{4+} and U^{4+}, this review estimated (Fig. 21-2)

$$PoO_2(s) + 2H^+ \rightleftharpoons Po(OH)_2^{2+}$$
$$log_{10}{}^*K_{s,2}^\circ \approx -0.5$$

$$PoO_2(s) + 3H^+ \rightleftharpoons PoOH^{3+} + H_2O(l)$$
$$log_{10}{}^*K_{s,1}^\circ \approx 0.5$$

$$PoO_2(s) + 4H^+ \rightleftharpoons Po^{4+} + 2H_2O(l)$$
$$log_{10}{}^*K_{s,0}^\circ \approx 1.0$$

These values are included in TDB 2020 as supplemental data.

The above selected values can be transformed into the hydrolysis constants

$$Po^{4+} + H_2O(l) \rightleftharpoons PoOH^{3+} + H^+$$
$$log_{10}{}^*K_1^\circ = log_{10}{}^*\beta_1^\circ \approx -0.5$$

$$PoOH^{3+} + H_2O(l) \rightleftharpoons Po(OH)_2^{2+} + H^+$$
$$log_{10}{}^*K_2^\circ \approx -1.0$$

$$Po(OH)_2^{2+} + H_2O(l) \rightleftharpoons Po(OH)_3^+ + H^+$$
$$log_{10}{}^*K_3^\circ \approx -2.5$$

$Po(OH)_3^+ + H_2O(l) \rightleftharpoons Po(OH)_4(aq) + H^+$

$log_{10}{}^*K_4° \approx -4.5$

$Po^{4+} + 2H_2O(l) \rightleftharpoons Po(OH)_2^{2+} + 2H^+$

$log_{10}{}^*\beta_2° \approx -1.5$

$Po^{4+} + 3H_2O(l) \rightleftharpoons Po(OH)_3^+ + 3H^+$

$log_{10}{}^*\beta_3° \approx -4.0$

$Po^{4+} + 4H_2O(l) \rightleftharpoons Po(OH)_4(aq) + 4H^+$

$log_{10}{}^*\beta_4° \approx -8.5$

Note that the Po(IV) hydrolysis constants derived and estimated in this review are rather close to the U(IV) hydrolysis constants recently selected by NEA (Grenthe et al. 2020):

	$log_{10}{}^*K_1°$	$log_{10}{}^*K_2°$	$log_{10}{}^*K_3°$	$log_{10}{}^*K_4°$
U(IV) NEA	-0.54 ± 0.06	-1.4 ± 0.2	-3.3 ± 0.4	-4.8 ± 1.4
Po(IV) this review	*-0.5*	*-1.0*	*-2.5*	*-4.5*

Besides the solubility studies discussed here a number of solvent extraction and ion-exchange studies have been published concerning the hydrolysis of Po(IV): Koch & Schmidt (1963), Starik et al. (1964), Ampelogova (1975), Hataye et al. (1981a, 1981b), Suganuma et al. (1983).

Two of these studies, Starik et al. (1964) and Hataye et al. (1981a), have been cited by Brown (2001) for establishing stability constants for her postulated species PoO^{2+}, $PoO(OH)^+$ and $PoO(OH)_2$. These species are not considered further in this review.

In the earliest of these studies Koch & Schmidt (1963) obtained, by cation-exchange measurements in the pH range 2.5 – 4.5, hydrolysis constants $log_{10}{}^*\beta_3$ and $log_{10}{}^*\beta_4$ for the species $Po(OH)_3^+$ $Po(OH)_4(aq)$ dominating in this pH range (Fig. 21-2). These stability constants are in fair agreement with the ones selected in this review from solubility data.

Starik et al. (1964) obtained, by solvent extraction experiments in the pH range 1.0 – 2.1, hydrolysis constants for all four hydrolysis species. While $log_{10}{}^*\beta_1$ and $log_{10}{}^*\beta_2$ support the estimates made in this review, and $log_{10}{}^*\beta_3$ is in excellent agreement with the results of Koch & Schmidt (1963), $log_{10}{}^*\beta_4$ is rather low.

This was later corrected by Ampelogova (1975), also using solvent extraction but in an extended pH range 0.5 – 2.9. However, $log_{10}{}^*\beta_3$ and $log_{10}{}^*\beta_4$ are reported as approximate values only.

Considering the unresolved problem of extrapolating these values to a common ionic strength, and further considering the experimental difficulties described in the above cited papers, we observe a fair overall consistency of the results of Koch & Schmidt (1963), Starik et al. (1964) and Ampelogova (1975) with the results derived and estimated from solubility data in this review:

Po(IV) hydrolysis		$log_{10}{}^{*}\beta_1$	$log_{10}{}^{*}\beta_2$	$log_{10}{}^{*}\beta_3$	$log_{10}{}^{*}\beta_4$
This review	Solubility dilute solutions	-0.5	-1.5	-4.0	-8.5
Koch & Schmidt (1963)	Ion-exchange variable $(H,Na)ClO_4$			-3.4	-8.2
Starik et al. (1964)	Solvent extraction 0.1 M $(Na,H)ClO_4$	-1.1	-2.2	-3.1	-4.8
Ampelogova (1975)	Solvent extraction 1 M $NaClO_4$	-0.48	-2.74	-5.6	-9

Hataye et al. (1981a, 1981b) also reported the results of solvent extraction studies, in 1 M $(H,Na)ClO_4$ (Hataye et al. 1981a) and in 1 M $(H,Na)NO_3$ solutions (Hataye et al. 1981b).

In their first study Hataye et al. (1981a) obtained $\log_{10}{}^{*}K_4 = -1.1$. As this value refers to the isocoulombic reaction $Po(OH)_3^+ + H_2O(l) \rightleftharpoons Po(OH)_4(aq) + H^+$, it can be directly compared with the value $\log_{10}{}^{*}K_4^\circ \approx -4.5$ obtained from solubility data in this review (Fig. 21-2), which is at variance by more than three orders of magnitude. According to Hataye et al. (1981a) an increase in $PoO_2(s)$ solubility should be observed at pH < 1, in clear contradiction to pH 4.5 actually observed (Fig. 21-2).

In their companion study Hataye et al. (1981b) obtained $\log_{10}{}^{*}K_4 = -2.23$, higher than in their first study, but still more than two orders of magnitude at variance with the solubility data. In addition, they reported $\log_{10}{}^{*}K = -2.69$ for the equilibrium $Po(OH)_2^{2+} + 2H_2O(l) \rightleftharpoons Po(OH)_4(aq) + 2H^+$, which leads to $\log_{10}{}^{*}K_3 = -0.46$ for the equilibrium $Po(OH)_2^{2+} + H_2O(l) \rightleftharpoons Po(OH)_3^+ + H^+$, again two orders of magnitude at variance with the value estimated in this review.

Finally, Suganuma et al. (1983) reported a cation-exchange study of the hydrolysis of Po(IV) in 1 M $(H,Na)ClO_4$ at pH 1 where they found that trace concentrations of Po(IV) may exist in the mean chemical form of $Po(OH)_{3.43}^{0.53+}$. No thermodynamic data were obtained in this study.

Because of the obvious contradictions with solubility data and the ion-exchange and solvent extraction studies of Koch & Schmidt (1963), Starik et al. (1964), Ampelogova (1975), the results of Hataye et al. (1981a, 1981b) and Suganuma et al. (1983) have not been considered further in this review.

21.5.2.2 Polonium(IV) oxide compounds

Brown (2001) reported that the E° value for reaction

$$PoO_2(s) + 4H^+ + 4e^- \rightleftharpoons Po(s) + 2H_2O(l)$$

has been quoted as 0.74, 0.742 and 0.73 V. The average value is 0.731 V, equivalent to $\log_{10}K^\circ = 49.43$, which lead Brown (2001) to the calculated value $\Delta_f G_m^\circ(PoO_2, s, 298.15\ K) = -(192.2)\ kJ \cdot mol^{-1}$, using $\Delta_f G_m^\circ(H_2O, l, 298.15\ K) = -(237.2)\ kJ \cdot mol^{-1}$. Using the CODATA value $\Delta_f G_m^\circ(H_2O, l, 298.15\ K) = -(237.140)\ kJ \cdot mol^{-1}$ (Cox et al. 1989), this review calculated

$\Delta_f G_m°(PoO_2, s, 298.15\ K) = -(192.1)\ kJ \cdot mol^{-1}$

This value is included in TDB 2020.

21.5.3 Polonium(IV) halide compounds and complexes

21.5.3.1 Polonium(IV) halide complexes

Brown (2001) reported for the reaction

$$PoCl_6^{2-} + 2e^- \rightleftharpoons PoCl_4^{2-} + 2Cl^-$$

measured electrode potentials of 0.717 and 0.702 V in 1.0 and 1.5 M HCl, respectively, at 25 °C, 0.72 V in 1 M HCl at 22 °C, and 0.582 V in 4.7 M HCl at room temperature. From these values, and using SIT, a plot of ionic strength against $E - 118.4D$ resulted in a straight line with an intercept $E°$ = (0.775 ± 0.002) V, equivalent to $\log_{10}K°$ = 26.20. Using this $E°$ value and $\Delta_f G_m°(PoCl_4^{2-}, 298.15\ K) = -(443.0)\ kJ \cdot mol^{-1}$ (see Section 21.4.3.1) and $\Delta_f G_m°(Cl^-, 298.15\ K) = -(131.0)\ kJ \cdot mol^{-1}$, Brown (2001) calculated

$\Delta_f G_m°(PoCl_6^{2-}, 298.15\ K) = -(554.0)\ kJ \cdot mol^{-1}$

Note that $\Delta_f G_m°(PoCl_4^{2-}, 298.15\ K)$ has been changed in this review to $-(443.9)\ kJ \cdot mol^{-1}$ because of using the CODATA value $\Delta_f G_m°(Cl^-, 298.15\ K) = -131.217\ kJ \cdot mol^{-1}$ (Cox et al. 1989) (see Section 21.4.3.1). Using these values, this review calculated

$\Delta_f G_m°(PoCl_6^{2-}, 298.15\ K) = -(555.3)\ kJ \cdot mol^{-1}$

This value is included in TDB 2020.

Using $\Delta_f G_m°(PoCl_6^{2-}, 298.15\ K) = -(554.0)\ kJ \cdot mol^{-1}$, and $\Delta_f G_m°(PoO^{2+}, 298.15\ K) = (67.4)\ kJ \cdot mol^{-1}$, (see Section 21.5.1), $\Delta_f G_m°(H_2O, l, 298.15\ K) = -(237.2)\ kJ \cdot mol^{-1}$ and $\Delta_f G_m°(Cl^-, 298.15\ K) = -(131.0)\ kJ \cdot mol^{-1}$, Brown (2001) calculated

$$PoO^{2+} + 2H^+ + 6Cl^- \rightleftharpoons PoCl_6^{2-} + H_2O(l)$$

$$\log_{10}K°(298.15\ K) = 12.7$$

Reformulating the above equation in terms of the Po(IV) aqua ion chosen in this review, and using $\Delta_f G_m°(PoCl_6^{2-}, 298.15\ K) = -555.3\ kJ \cdot mol^{-1}$ and $\Delta_f G_m°(Po^{4+}, 298.15\ K) \approx 276.5\ kJ \cdot mol^{-1}$, derived in this review (see Section 21.5.1), and the CODATA value $\Delta_f G_m°(Cl^-, 298.15\ K) = -131.217\ kJ \cdot mol^{-1}$ (Cox et al. 1989), this review calculated

$$Po^{4+} + 6Cl^- \rightleftharpoons PoCl_6^{2-}$$

$$\Delta_r G_m°(298.15\ K) \approx -44.5\ kJ \cdot mol^{-1}$$

$log_{10}K°(298.15\ K) \approx 7.8$

This value has been included in TDB 2020 as supplemental datum.

Brown (2001) scrutinised absorption spectroscopy studies of polonium complex formation in hydrochloric acid. At high concentrations of hydrochloric acid (HCl > 2 M), the polonium species existing in solution is $PoCl_6^{2-}$. In dilute acid, the data can be interpreted according to equation

$$PoCl_6^{2-} + H_2O(l) \rightleftharpoons Po(OH)Cl_4^- + H^+ + 2Cl^-$$

$$\log_{10}K°(298.15\ K) = -2.16$$

This value is included in TDB 2020.

Brown (2001) reported results from a solvent extraction study exploring the hydrolysis of polonium(IV) in chloride solutions (Suganuma & Hataye 1981). According to Brown (2001), the experimental data in the acidic region (0 < pH < 4) were interpreted with the species $PoCl_6^{2-}$, $Po(OH)Cl_4^-$ and $PoOCl_4^{2-}$. As the pH is further increased (4 < pH < 5), the solvent extraction data are consistent with the following two reactions:

$$PoOCl_4^{2-} + 2H_2O(l) \rightleftharpoons PoO(OH)_2(aq) + 2H^+ + 4Cl^-$$

$$\log_{10}{}^*K\ (298.15\ K) = -8.7$$

$$\log_{10}{}^*K°(298.15\ K) = -8.9$$

$$PoO(OH)Cl_2^- + H_2O(l) \rightleftharpoons PoO(OH)_2(aq) + H^+ + 2Cl^-$$

$$\log_{10}{}^*K\ (298.15\ K) = -4.6$$

$$\log_{10}{}^*K°(298.15\ K) = -4.8$$

The $\log_{10}{}^*K$ values were determined in 1.0 M (H,Na)Cl. Brown (2001) extrapolated these values to zero ionic strength, $\log_{10}{}^*K°$, using the Davies equation.

Note that the above equilibria, as actually proposed by Suganuma & Hataye (1981), are

$$Po(OH)_2Cl_n^{2-n} + H_2O(l) \rightleftharpoons Po(OH)_4(aq) + 2H^+ + nCl^-$$

$$\log_{10}{}^*K\ (298.15\ K) = -8.7$$

$$Po(OH)_3Cl_n^{1-n} + H_2O(l) \rightleftharpoons Po(OH)_4(aq) + H^+ + nCl^-$$

$$\log_{10}{}^*K\ (298.15\ K) = -4.6$$

and that Suganuma & Hataye (1981) stated that "unfortunately, the chemical species of polonium dissolved in 1.0 M (H,Na)Cl solutions could not be decided thoroughly in this experiment". Brown (2001) just took one stoichiometry out of several possibilities offered by Suganuma & Hataye (1981) without any discussion.

No effort has been made in this review to unravel the stoichiometries of the ternary Po(IV) – chloride – hydroxide complexes probably compatible with the experimental data of Suganuma & Hataye (1981). Furthermore, as discussed in Section 5.2.1, the Po(IV) hydrolysis constants obtained by the same group of researchers using the same experimental methods (Hataye et al. 1981a, 1981b and Suganuma et al. 1983) are incompatible with solubility data and all other publications, and have not been considered in this review. Hence, the data reported by Suganuma & Hataye (1981) and Brown (2001) have also not been considered further in this review.

Brown (2001) reported a solubility study of $PoI_4(s)$ in hydroiodic acid. In concentrated HI the measurements were interpreted in terms of

$$PoI_4(s) + 2I^- \rightleftharpoons PoI_6^{2-}$$
$$\log_{10}K°(298.15\ K) = -2.23$$

while measurements at low acid concentration ([HI] < 0.02 M) were interpreted in terms of

$$PoI_4(s) + I^- \rightleftharpoons PoI_5^-$$
$$\log_{10}K°(298.15\ K) = -4.17$$

These results show that PoI_6^{2-} and PoI_5^- will be formed only at iodide concentrations far outside the iodide concentration range expected in environmental systems. Hence, these data have not been included in TDB 2020.

21.5.3.2 Polonium(IV) halide compounds

Brown (2001) reported that polonium tetrachloride, $PoCl_4(s)$, is hygroscopic and readily hydrolysed to a white solid of variable composition, which is possibly a mixture of a basic chloride and a hydroxide or hydrated oxide. Polonium tetrabromide, $PoBr_4(s)$, is also hygroscopic and easily hydrolysed, yielding a white solid of indefinite composition, presumably a basic bromide. Polonium tetraiodide, $PoI_4(s)$, is the only iodide known. It is slowly hydrolysed to a white solid of indefinite composition in water.

Even though all these polonium tetrahalide salts are highly soluble and unstable in water, Brown (2001) made an effort to estimate thermodynamic data for these solids via linear free energy relationships.

Brown (2001) state that for metal ions possessing an inert pair of electrons, namely, In^+, Tl^+, Sn^{2+}, Pb^{2+}, Sb^{3+}, Bi^{3+}, Te^{4+} and Po^{4+}, both the $\Delta_f G_m°$ and $\Delta_f H_m°$ values of the metal halides in the same group of the Periodic Tab. are similar. For example, the $\Delta_f G_m°$ and $\Delta_f H_m°$ values of $SnBr_2(s)$ are -248.9 and -266.1 kJ · mol^{-1}, respectively, which are like those for $PbBr_2(s)$, namely, -260.4 and -277.0 kJ · mol^{-1}. A plot of $\Delta_f G_m°$ values for the MX_b species In^+, Sn^{2+}, Sb^{3+} and Te^{4+} (for these ions, n, the principal quantum number, equals five and X is Cl, Br or I) against the respective values for the MX_b species of Tl^+, Pb^{2+}, Bi^{3+} and Po^{4+} (n = 6) is linear. Similarly, a plot of $\Delta_f H_m°$ is also linear.

Brown (2001) used such linear free energy relationships which allowed thermodynamic data for the PoX_b species to be determined from the corresponding data for tellurium. Brown (2001) estimated

$\Delta_f G_m°(PoCl_4, s, 298.15\ K) = -(242.7)\ kJ \cdot mol^{-1}$

$\Delta_f G_m°(PoBr_4, s, 298.15\ K) = -(153.4)\ kJ \cdot mol^{-1}$

$\Delta_f G_m°(PoI_4, s, 298.15\ K) = -(49.4)\ kJ \cdot mol^{-1}$.

Brown (2001) used $\Delta_f G_m°(PoCl_4, s, 298.15\ K) = -(242.7)\ kJ \cdot mol^{-1}$, $\Delta_f G_m°(PoCl_6^{2-}, 298.15\ K) = -(554.0)\ kJ \cdot mol^{-1}$ (see Section 21.5.3.1) and $\Delta_f G_m°(Cl^-, 298.15\ K) = -(131.0)\ kJ \cdot mol^{-1}$ to calculate

$PoCl_4(s) + 2Cl^- \rightleftharpoons PoCl_6^{2-}$

$\log_{10} K°(298.15\ K) = 8.63$

which shows that $PoCl_4(s)$ will be soluble in hydrochloric acid.

Likewise, Brown (2001) used $\Delta_f G_m°(PoCl_4, s, 298.15\ K) = -(242.7)\ kJ \cdot mol^{-1}$, $\Delta_f G_m°(PoOCl_4^{2-}, 298.15\ K) = -(493.1)\ kJ \cdot mol^{-1}$ (see Section 21.5.3.1) and $\Delta_f G_m°(H_2O, l, 298.15\ K) = -(237.2)\ kJ \cdot mol^{-1}$ to calculate

$PoCl_4(s) + 2H_2O(l) \rightleftharpoons PoOCl_4^{2-} + 2H^+$

$\log_{10} K°(298.15\ K) = 2.31$

which shows that $PoCl_4(s)$ will be soluble in water.

None of these values has been included in TDB 2020 because, as already mentioned, these salts are unstable in water and decompose into some indefinite products.

21.5.4 Polonium(IV) sulphate compounds and complexes

21.5.4.1 Polonium(IV) sulphate complexes

Brown (2001) reported a solvent extraction study where the complexation of polonium(IV) by sulphate has been investigated (Ampelogova 1973). The results were interpreted by Brown (2001) in terms of the following reactions:

$PoO^{2+} + SO_4^{2-} \rightleftharpoons PoOSO_4(aq)$

$\log_{10}\beta_1\ (298.15\ K) = 1.46$

$\log_{10}\beta_1°(298.15\ K) = 2.56$

$PoO^{2+} + 2SO_4^{2-} \rightleftharpoons PoO(SO_4)_2^{2-}$

$\log_{10}\beta_2\ (298.15\ K) = 3.40$

$\log_{10}\beta_2°(298.15\ K) = 4.50$

The stability constants $\log_{10}\beta$ refer to 2 M H(ClO_4,HSO_4). Brown (2001) corrected these stability constants to zero ionic strength, $\log_{10}\beta°$, based on the difference between data for other divalent metal ions in perchlorate media (at the same ionic strength) and those at zero ionic strength.

There are several shortcomings with this interpretation. First, the polonium aqua ion in this study is not PoO^{2+} but Po^{4+}. Second, the sulphate anion present in this study is not SO_4^{2-} but HSO_4^-. Third, the data should be extrapolated to zero ionic strength by a well-defined method. A re-interpretation of the data reported in Ampelogova (1973) in this review results in:

$Po^{4+} + HSO_4^- \rightleftharpoons PoSO_4^{2+} + H^+$

$\log_{10}{}^*\beta_1$ (298.15 K) = -0.10 ± 0.22

$\log_{10}{}^*\beta_1°$(298.15 K) = 3.26 ± 0.6

$Po^{4+} + 2HSO_4^- \rightleftharpoons Po(SO_4)_2(aq) + 2H^+$

$\log_{10}{}^*\beta_2$ (298.15 K) = 0.26 ± 0.30

$\log_{10}{}^*\beta_2°$(298.15 K) = 5.10 ± 0.7

The $\log_{10}{}^*\beta_1$ and $\log_{10}{}^*\beta_2$ values are derived from Ampelogova (1973), K_1 and K_2 in her Tab. 4, and the 1σ uncertainties given in her Tab. 4 were increased to 2σ in the present review.

The $\log_{10}{}^*\beta_1°$ and $\log_{10}{}^*\beta_2°$ values have been extrapolated in this review using SIT with $\Delta\varepsilon(HClO_4)$ = -(0.25 ± 0.17) and -(0.50 ± 0.20), respectively, using $\varepsilon(H^+, ClO_4^-)$ = 0.14 ± 0.02 and the estimated SIT interaction coefficients $\varepsilon(Po^{4+}, ClO_4^-)$ = 0.8 ± 0.1, $\varepsilon(PoSO_4^{2+}, ClO_4^-)$ = 0.4 ± 0.1 and $\varepsilon(Po(SO_4)_2(aq), HClO_4) = \varepsilon(Po(SO_4)_2(aq), NaClO_4)$ = 0.0 ± 0.1 (estimate according to Tab. 1-7), as well as $\varepsilon(H^+, HSO_4^-)$ = -(0.01 ± 0.10) ≈ $\varepsilon(Na^+, HSO_4^-)$ = -(0.01 ± 0.02) (Tab. 21-3).

Using $\log_{10}K°(SO_4^{2-} + H^+ \rightleftharpoons HSO_4^-, 298.15K)$ = 1.98 ± 0.05 the above values are recalculated to

$Po^{4+} + SO_4^{2-} \rightleftharpoons PoSO_4^{2+}$

$\log_{10}\beta_1°$(298.15 K) = 5.2 ± 0.6

$Po^{4+} + 2SO_4^{2-} \rightleftharpoons Po(SO_4)_2(aq)$

$\log_{10}\beta_2°$(298.15 K) = 9.1 ± 0.7

These values are included in TDB 2020.

Note that the stability constants selected by NEA for Th(IV) – sulphate complexes, $\log_{10}\beta_1°$(298.15 K) = 6.17 ± 0.32 and $\log_{10}\beta_2°$(298.15 K) = 9.69 ± 0.27, are very similar to the ones selected here for Po(IV) – sulphate complexes.

Also, the stability constants selected by NEA (Grenthe et al. 1992) for U(IV) – sulphate complexes, $\log_{10}\beta_1°$(298.15 K) = 6.58 ± 0.19 and $\log_{10}\beta_2°$(298.15 K) = 10.51 ± 0.20, are comparable with the ones selected here for Po(IV) – sulphate complexes.

Especially, the stepwise stability constant of the equilibrium

$PoSO_4^{2+} + SO_4^{2-} \rightleftharpoons Po(SO_4)_2(aq)$

$\log_{10}K_2°(298.15\ K) = 3.9 \pm 0.9$

is in excellent agreement with the values derived for U(IV) – sulphate, $\log_{10}K_2°(298.15\ K) = 3.93 \pm 0.26$, and Th(IV) – sulphate, $\log_{10}K_2°(298.15\ K) = 3.5 \pm 0.4$.

From a solubility study of polonium disulphate (Bagnall & Freeman 1956) (see Section 21.5.4.2) Brown (2001) derived from three measured solubility values at different sulphuric acid concentrations

$PoO(SO_4)_2^{2-} + SO_4^{2-} \rightleftharpoons PoO(SO_4)_3^{4-}$

$\log_{10}K_3°(298.15\ K) = 1.22$

As discussed in Section 5.4.1, this equilibrium and the derived constant are rejected by the present review, and based on a re-evaluation of the experimental solubility data of Bagnall & Freeman (1956) a lower limit for the equilibrium

$Po(SO_4)_2(aq) + SO_4^{2-} \rightleftharpoons Po(SO_4)_3^{2-}$

$\log_{10}K_3°(298.15\ K) > 2.2$

has been estimated. This value is included in TDB 2020 as supplemental datum.

Note that from the stability constants selected by NEA for Th(IV) – sulphate complexes, $\log_{10}\beta_2°(298.15\ K) = 9.69 \pm 0.27$ and $\log_{10}\beta_3°(298.15\ K) = 10.75 \pm 0.08$, a value

$\log_{10}K_3°(Th, 298.15\ K) = 1.06 \pm 0.28$

follows, not incompatible with the one estimated here for Po(IV) – sulphate complexes.

21.5.4.2 Polonium(IV) sulphate compounds

Brown (2001) reported experimental data from a solubility study of the basic sulphate, $2PoO_2 \cdot SO_3(s)$ or $(PoO)_2OSO_4(s)$, in various concentrations of sulphuric acid (Bagnall & Freeman 1956). A plot of the logarithm of the acid concentration versus the logarithm of the solubility exhibits a slope of 0.54 ± 0.03 (Fig. 21-3). According to Brown (2001) this indicates that one mole of acid will solubilise two moles of polonium. The reaction has therefore been written as (Brown 2001)

$(PoO)_2OSO_4(s) + H_2SO_4(aq) \rightleftharpoons 2PoOSO_4(aq) + H_2O(l)$

$\log_{10}K°(298.15\ K) = -9.48$

Since the above reaction involves uncharged species only (isocoulombic reaction), the ionic strength dependence of $\log_{10}K$ is negligible, and $\log_{10}K°$ is the average of the measured $\log_{10}K$ values.

There are two principal shortcomings with the proposed chemical equilibrium. First, the dominating sulphate species in this system is not H_2SO_4(aq) but HSO_4^-. Second, the Po(IV) – sulphate complex is not $PoOSO_4$(aq) but $PoSO_4^{2+}$, or perhaps $Po(SO_4)_3^{2-}$, as involved in the equilibrium with $Po(SO_4)_2 \cdot H_2O$(s) as discussed below. In the first case an equilibrium

$$(PoO)_2OSO_4(s) + HSO_4^- + 5H^+ \rightleftharpoons 2PoSO_4^{2+} + 3H_2O(l)$$

could be formulated, meeting the criterion that "one mole of acid will solubilise two moles of polonium". In the second case, assuming $Po(SO_4)_3^{2-}$ as the dominating complex, no formulation can be found meeting the above criterion.

However, there is no need to scrutinise this case further, as Bagnall & Freeman (1956) stated that "the basic sulphate appears to be metastable since the solubility curve of the disulphate can be extended to regions of lower acid concentration by diluting the acid in contact with solid polonium disulphate to concentrations at which the basic sulphate is normally formed; further, seeding the aqueous phase in contact with the basic sulphate with small crystals of the disulphate decreases the solubility to a marked degree".

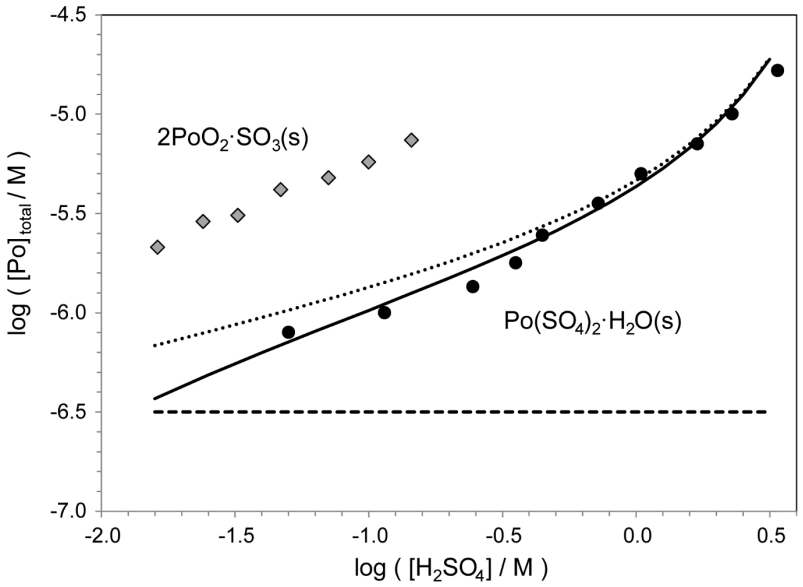

Fig. 21-3: Solubility of $2PoO_2 \cdot SO_3$(s) (diamonds) and $Po(SO_4)_2 \cdot H_2O$(s) (circles) as reported by Bagnall & Freeman (1956)

Solid line: calculated concentration of $Po(SO_4)_3^{2-}$ according to the equilibrium $Po(SO_4)_2 \cdot H_2O(s) + HSO_4^- \rightleftharpoons Po(SO_4)_3^{2-} + H^+ + H_2O(l)$. Dashed line: calculated maximum concentration of $Po(SO_4)_2$(aq) according to the equilibrium $Po(SO_4)_2 \cdot H_2O(s) \rightleftharpoons Po(SO_4)_2(aq) + H_2O(l)$ still compatible with solubility data (circles). Dotted line: Calculated solubility of $Po(SO_4)_2 \cdot H_2O$(s) considering $Po(SO_4)_3^{2-}$ and the estimated $Po(SO_4)_2$(aq).

Hence, the metastable solid $2PoO_2 \cdot SO_3$(s) (Fig. 21-3) has not been considered further in this review.

Brown (2001) reported further experimental data from the same solubility study (Bagnall & Freeman 1956) of polonium disulphate, $Po(SO_4)_2 \cdot H_2O(s)$, in various concentrations of sulphuric acid (Fig. 21-3). While three experimental measurements in the lowest concentration range 0.05 to 0.25 M H_2SO_4 were used by Brown (2001) to derive a stepwise stability constant for $PoO(SO_4)_3^{4-}$ (see Section 21.5.4.1), solubility data in the range 0.25 to 3.25 M H_2SO_4 were used to fit a stability constant for the reaction

$$Po(SO_4)_2 \cdot H_2O(s) + SO_4^{2-} \rightleftharpoons PoO(SO_4)_3^{4-} + 2H^+$$

$$\log_{10}K°(298.15\ K) = -3.5 \pm 0.2$$

by SIT regression analysis of the experimental data in H_2SO_4 medium. Note that the SIT plot presented by Brown (2001) (Fig. 3-20) shows a strong curvature.

Again, there are two principal shortcomings with the proposed chemical equilibrium. First, the dominating sulphate species in this system is not SO_4^{2-} but HSO_4^-. Second, the Po(IV) – sulphate complex is not $PoO(SO_4)_3^{4-}$ but $Po(SO_4)_3^{2-}$. This review thus re-formulated the above equilibrium:

$$Po(SO_4)_2 \cdot H_2O(s) + HSO_4^- \rightleftharpoons Po(SO_4)_3^{2-} + H^+ + H_2O(l)$$

$$\log_{10}{}^*K_{s,3}°(298.15\ K) = -6.33 \pm 0.04$$

$$\Delta\varepsilon = -0.16 \pm 0.03$$

Note that now the experimental data in the SIT regression analysis (Fig. 21-4) do not show any significant curvature. An uncertainty of ± 0.1 has been assigned to all experimental data, leading to the rather low uncertainties of the derived parameters $\log_{10}K°(298.15\ K)$ and $\Delta\varepsilon$. As the terms $\varepsilon(HSO_4^-, H^+) = \varepsilon(H^+, HSO_4^-)$ cancel we have

$$\Delta\varepsilon = \varepsilon(Po(SO_4)_3^{2-}, H^+) = -0.16 \pm 0.03$$

Although this value is compatible with the estimated value $\varepsilon(Po(SO_4)_3^{2-}, Na^+) = -0.10 \pm 0.10$, $\varepsilon(Po(SO_4)_3^{2-}, H^+)$ is not used as an approximation for $\varepsilon(Po(SO_4)_3^{2-}, Na^+)$, as all other know values involving H^+ are positive (e.g. $\varepsilon(H^+, ClO_4^-) = 0.14 \pm 0.02$, $\varepsilon(H^+, Cl^-) = 0.12 \pm 0.0$, $\varepsilon(H^+, NO_3^-) = 0.07 \pm 0.01$).

Brown (2001) derived by some unclear procedure from the three measured solubility values at the lowest sulphuric acid concentrations the equilibrium

$$PoO(SO_4)_2^{2-} + SO_4^{2-} \rightleftharpoons PoO(SO_4)_3^{4-}$$

$$\log_{10}K_3°(298.15\ K) = 1.22$$

This equilibrium and the derived constant are rejected by the present review.

As can be seen in Fig. 21-3, the entire experimental concentration range is dominated by the species $Po(SO_4)_3^{2-}$ (solid line in Fig. 21-3), and the reviewer could not find any possibility to directly determine a stability constant for the equilibrium

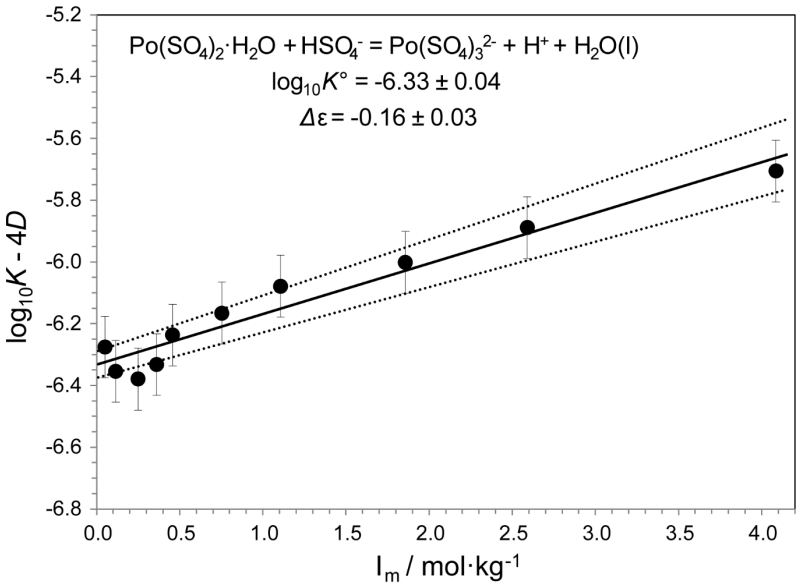

Fig. 21-4: Dependence of $\log_{10}K$ of $Po(SO_4)_3^{2-}$ on ionic strength in sulphuric acid media.

The solid line is obtained using the derived SIT interaction coefficient and stability constant at zero ionic strength. The dotted lines represent the 95% uncertainty range extrapolated from zero ionic strength to higher sulphuric acid concentrations. Data taken from Bagnall & Freeman (1956) with assigned uncertainties of ± 0.1.

$$Po(SO_4)_2\cdot H_2O(s) \rightleftharpoons Po(SO_4)_2(aq) + H_2O(l)$$

For this isocoulombic reaction only an upper limit can be estimated (dashed line in Fig. 21-3)

$$\log_{10}K_{s,2}°(298.15\ K) < -6.5$$

which leads to a total calculated solubility for $Po(SO_4)_2\cdot H_2O(s)$ (dotted line in Fig. 21-3) still compatible, within the experimental uncertainty, with the data of Bagnall & Freeman (1956).

From this upper limit, and $\log_{10}{}^{*}K_{s,3}°(298.15\ K) = -6.33 \pm 0.04$, the lower limit

$$Po(SO_4)_2(aq) + HSO_4^- \rightleftharpoons Po(SO_4)_3^{2-} + H^+$$

$$\log_{10}{}^{*}K_3°(298.15\ K) > 0.17$$

can be estimated. Considering $\log_{10}{}^{*}K°(298.15\ K) = -1.98 \pm 0.05$ for $HSO_4^- \rightleftharpoons SO_4^{2-} + H^+$, finally the lower limit

$$Po(SO_4)_2(aq) + SO_4^{2-} \rightleftharpoons Po(SO_4)_3^{2-}$$

$$\log_{10}K_3°(298.15\ K) > 2.2$$

has been estimated. This value is included in TDB 2020 as supplemental datum.

21.5.5 Polonium(IV) selenate compounds and complexes

21.5.5.1 Polonium(IV) selenate complexes

Brown (2001) estimated stability constants for polonium(IV) selenate complexes from the equivalent polonium(IV) sulphate complexes (see Section 21.5.4.1) using the unified theory of metal ion complexation (Brown & Sylva 1987):

$PoO^{2+} + SeO_4^{2-} \rightleftharpoons PoOSeO_4(aq)$

$\log_{10}\beta_1°(298.15\ K) = 2.43$

$PoO^{2+} + 2SeO_4^{2-} \rightleftharpoons PoO(SeO_4)_2^{2-}$

$\log_{10}\beta_2°(298.15\ K) = 3.78$

The stoichiometries and stability constants of the polonium(IV) sulphate complexes have been revised substantially in this review (see Section 21.5.4.1) and no effort has been made to re-estimate the above polonium(IV) selenate equilibria and stability constants. Thus, they are not included in TDB 2020.

21.5.5.2 Polonium(IV) selenate compounds

Brown (2001) reported experimental data from a solubility study of the basic selenate, $2PoO2 \cdot SeO_3(s)$ or $(PoO)_2OSeO_4(s)$, in various concentrations of selenic acid (Bagnall & Freeman 1956). A plot of the logarithm of the acid concentration versus the logarithm of the solubility exhibits a slope of 0.61 ± 0.02 at low selenic acid concentrations (≤ 0.56 M) and a slope of 1.61 ± 0.07 at high selenic acid concentrations (≥ 0.8 M). Brown (2001) interpreted these regions in terms of the reactions

$(PoO)_2OSeO_4(s) + H_2SeO_4(aq) \rightleftharpoons 2PoOSeO_4(aq) + H_2O(l)$

$\log_{10}K°(298.15\ K) = -9.97$

$(PoO)_2OSeO_4(s) + 3H_2SeO_4(aq) \rightleftharpoons 2PoO(SeO_4)_2^{2-} + H_2O(l) + 4H^+$

$\log_{10}K°(298.15\ K) = -7.8 \pm 0.3$

These equilibria and the derived constants are rejected by the present review.

The experimental data evaluated by Brown (2001) are part of the study by Bagnall & Freeman (1956) comprising the basic sulphate, $2PoO_2 \cdot SO_3(s)$, and the disulphate, $Po(SO_4)_2 \cdot H_2O(s)$, already discussed in Section 5.4.2. The experimental data for $2PoO_2 \cdot SeO_3(s)$ are in between the two sulphate solids and show a similar curvature as $Po(SO_4)_2 \cdot H_2O(s)$ (Bagnall & Freeman 1956). The data for $2PoO_2 \cdot SeO_3(s)$ thus could be re-evaluated as has been done for $Po(SO_4)_2 \cdot H_2O(s)$ in this review. However, as the selenate concentrations in natural systems will probably never be high enough for the basic polonium selenate to precipitate, no effort has been made in this review to repeat the sulphate evaluation procedure for selenate.

21.5.6 Polonium(IV) nitrate compounds and complexes

21.5.6.1 Polonium(IV) nitrate complexes

Brown (2001) reported a solvent extraction study where the complexation of polonium(IV) by nitrate has been investigated (Ampelogova 1973). The results were interpreted by Brown (2001) in terms of the following reactions:

$PoO^{2+} + NO_3^- \rightleftharpoons PoONO_3^+$

$\log_{10}\beta_1°(298.15\ K) = 1.29$

$PoO^{2+} + 2NO_3^- \rightleftharpoons PoO(NO_3)_2(aq)$

$\log_{10}\beta_2°(298.15\ K) = 2.31$

$PoO^{2+} + 3NO_3^- \rightleftharpoons PoO(NO_3)_3^-$

$\log_{10}\beta_3°(298.15\ K) = 2.33$

Brown (2001) corrected the stability constants reported by Ampelogova (1973) for 1.0 and 1.5 M $H(ClO_4,NO_3)$ to zero ionic strength using the Davies equation.

However, there are some ambiguities with this interpretation. First, the polonium aqua ion in this study is not PoO^{2+} but Po^{4+}. Second, the actual stoichiometry of the above reactions is ambiguous according to Ampelogova (1973). Third, the Davies equation is not appropriate for extrapolating data from 1.0 and 1.5 M $H(ClO_4,NO_3)$ to zero ionic strength.

Hence, the data reported in Ampelogova (1973) were re-interpreted in this review.

Ampelogova (1973) stated that the nitric acid concentration in her study was varied over a narrow range (from 0.1 – 1.2 M) since at low solution acidity (less than 1 M) there is hydrolysis of polonium, while with an HNO_3 concentration ≥ 1.5 M there may be appreciable disproportionation of Po(IV). The investigations were carried out using solutions with the composition $HClO_4 + HNO_3 = 1.0$ and 1.5 M. The hypothetical complex formation reaction was:

$$Po(OH)_x^{(4-x)+} + n\ NO_3^- \rightleftharpoons Po(OH)_x(NO_3)_n^{(4-x-n)+}$$

where x = 0 – 2. The stability constants obtained by Ampelogova (1973, Tab. 2) are

$\beta_1 = 3.6 \pm 1$, $\beta_2 = 14 \pm 1.5$ and $\beta_3 = 20 \pm 3$ for 1.0 M $H(ClO_4,NO_3)$, and

$\beta_1 = 3.4 \pm 0.5$, $\beta_2 = 12 \pm 1.7$ and $\beta_3 = 20 \pm 4$ for 1.5 M $H(ClO_4,NO_3)$

Assuming that the uncertainties given by Ampelogova (1973) refer to 1σ, this review increased them to 2σ, which results in:

$\log_{10}\beta_1 = 0.56 \pm 0.3$, $\log_{10}\beta_2 = 1.15 \pm 0.10$ and $\log_{10}\beta_3 = 1.30 \pm 0.13$ for 1.0 M $H(ClO_4,NO_3)$ and

$\log_{10}\beta_1 = 0.53 \pm 0.13$, $\log_{10}\beta_2 = 1.08 \pm 0.13$ and $\log_{10}\beta_3 = 1.30 \pm 0.18$ for 1.5 M $H(ClO_4,NO_3)$

There is no way to determine the appropriate stoichiometry from the experimental ion exchange data of Ampelogova (1973). Hence, in this review two variants were calculated, for x = 2 and x = 0. The values obtained at 1.0 and 1.5 M $H(ClO_4,NO_3)$ were treated according to the SIT formalism, although just using two data points for a "linear regression" results in large uncertainties.

The results of SIT regression analyses for x = 2 are:

$Po(OH)_2^{2+} + NO_3^- \rightleftharpoons Po(OH)_2NO_3^+$

$\log_{10}\beta_1°(298.15\ K) = 1.3 \pm 0.9$

$\Delta\varepsilon = -0.05 \pm 0.6\ kg \cdot mol^{-1}$

$Po(OH)_2^{2+} + 2NO_3^- \rightleftharpoons Po(OH)_2(NO_3)_2(aq)$

$\log_{10}\beta_2°(298.15\ K) = 2.3 \pm 0.4$

$\Delta\varepsilon = -0.02 \pm 0.3\ kg \cdot mol^{-1}$

$Po(OH)_2^{2+} + 3NO_3^- \rightleftharpoons Po(OH)_2(NO_3)_3^-$

$\log_{10}\beta_3°(298.15\ K) = 2.3 \pm 0.5$

$\Delta\varepsilon = -0.13 \pm 0.4\ kg \cdot mol^{-1}$

Using $\varepsilon(NO_3^-, H^+) = 0.07 \pm 0.01\ kg \cdot mol^{-1}$ and the estimated value $\varepsilon(Po(OH)_2^{2+}, ClO_4^-) = 0.4 \pm 0.1\ kg \cdot mol^{-1}$ (estimate according to Tab. 1-7), this review calculated

$\varepsilon(Po(OH)_2NO_3^+, ClO_4^-) = 0.4 \pm 0.6\ kg \cdot mol^{-1}$

$\varepsilon(Po(OH)_2(NO_3)_2(aq), HClO_4) = 0.5 \pm 0.3\ kg \cdot mol^{-1}$

$\varepsilon(Po(OH)_2(NO_3)_3^-, H^+) = 0.5 \pm 0.4\ kg \cdot mol^{-1}$

The results of SIT regression analyses for x = 0 are:

$Po^{4+} + NO_3^- \rightleftharpoons PoNO_3^{3+}$

$\log_{10}\beta_1°(298.15\ K) = 2.0 \pm 0.9$

$\Delta\varepsilon = -0.17 \pm 0.6\ kg \cdot mol^{-1}$

$Po^{4+} + 2NO_3^- \rightleftharpoons Po(NO_3)_2^{2+}$

$\log_{10}\beta_2°(298.15\ K) = 3.7 \pm 0.4$

$\Delta\varepsilon = -0.26 \pm 0.3\ kg \cdot mol^{-1}$

$Po^{4+} + 3NO_3^- \rightleftharpoons Po(NO_3)_3^+$

$\log_{10}\beta_3°(298.15\ K) = 4.4 \pm 0.5$

$\Delta\varepsilon = -0.49 \pm 0.4\ kg \cdot mol^{-1}$

Using $\varepsilon(NO_3^-, H^+) = 0.07 \pm 0.01\ kg \cdot mol^{-1}$ and the estimated value $\varepsilon(Po^{4+}, ClO_4^-) = 0.8 \pm 0.1\ kg \cdot mol^{-1}$ (estimate according to Tab. 1-7), this review calculated

$\varepsilon(PoNO_3^{3+}, ClO_4^-) = 0.7 \pm 0.6\ kg \cdot mol^{-1}$

$\varepsilon(Po(NO_3)_2^{2+}, ClO_4^-) = 0.7 \pm 0.3\ kg \cdot mol^{-1}$

$\varepsilon(Po(NO_3)_3^+, ClO_4^-) = 0.5 \pm 0.4\ kg \cdot mol^{-1}$

Considering the strong acidic conditions of 1.0 and 1.5 M $H(ClO_4,NO_3)$ in the experimental study of Ampelogova (1973), and the hydrolysis constants evaluated and estimated by this review (Fig. 21-2), the case x = 0 seems to be more realistic.

Hence, the latter set of values for x = 0 is included in TDB 2020.

21.5.6.2 Polonium(IV) nitrate compounds

Brown (2001) used experimental data from a solubility study of polonium(IV) nitrate and stated that according to Bagnall et al. (1958) the most likely structure of this nitrate compound was $(PoO)_2(NO_3)_3OH(s)$. Brown (2001) reported that a plot of the logarithm of the acid concentration versus the logarithm of the solubility exhibits a slope of 1.58 ± 0.09. This indicates that three moles of acid will solubilise two moles of polonium and is consistent with both, the proposed structure and the polonium(IV) nitrate complexes assumed by Brown (2001) (see Section 21.5.6.1):

$(PoO)_2(NO_3)_3OH(s) + 3HNO_3(aq) \rightleftharpoons 2PoO(NO_3)_3^- + H_2O(l) + 2H^+$

$\log_{10}K°(298.15\ K) = -6.5 \pm 0.3$

Note that the SIT plot presented by Brown (2001) exhibits a strong curvature.

The obtained stability constant is not included in TDB 2020 because this review does not agree with the above statements of Brown (2001).

First of all, the "most likely structure" of Bagnall et al. (1958) refers to their "compound A", a white crystalline product with a ratio NO_3^- : Po = 1.5 : 1 which could be dried under vacuum at room temperature with only slight decomposition. However, "compound A is readily decomposed by water". This is certainly not the polonium nitrate compound present in the solubility study evaluated by Brown (2001).

Second, the six experimental solubility values presented by Brown (2001) as a plot of the logarithm of the acid concentration versus the logarithm of the solubility show a significant curvature. The three data points at low nitric acid concentration show a slope of 2.0 while the three data points at high nitric acid concentration follow a slope of 1.2. Hence, the data cannot be described by a single reaction which may also be the reason of the strong curvature of the SIT plot presented by Brown (2001). Probably two solids of unknown composition are involved and/or changes in the aqueous speciation.

No re-evaluation of the solubility data has been tried in the present review because, last but not least, the solubility of the undefined compound(s) is rather high, ranging from 0.00015 M Po at 1 M HNO_3 to 0.005 M Po at 10 M HNO_3.

21.5.7 Polonium(IV) cyanide compounds and complexes

21.5.7.1 Polonium(IV) cyanide complexes

Brown (2001) estimated the stability constant

$$PoO^{2+} + 2H^{+} + 6CN^{-} \rightleftharpoons PoCN_6^{2-} + H_2O(l)$$

$$\log_{10}K°(298.15\ K) = 49.8$$

from the previously determined value $\log_{10}K°(298.15\ K) = 12.7$ for $PoCl_6^{2-}$ (see Section 21.5.3.1) and a linear free energy relationship between stability constants for metal chloride and metal cyanide species.

There is no experimental indication that a species $PoCN_6^{2-}$ exists. Actually, the only known aqueous species with CN^- in 6-fold coordination are the hexacyanoferrates, $Fe^{II}(CN)_6^{4-}$ and $Fe^{III}(CN)_6^{3-}$. All other known metal cyanide complexes have a maximum coordination of four (Hummel 2004).

In addition, inspecting the data used by Brown (2001) to establish a linear free energy relationship between metal chloride and metal cyanide complexes reveals strong inconsistencies: The value quoted for $Ni(CN)_4^{2-}$, $\log_{10}K° = 22$, actually is 30.2 ± 0.3 (Hummel 2004), the value for $Pd(CN)_4^{2-}$, $\log_{10}K° = 42.4$, is the lower limit of a large uncertainty range 42 … 63 (Hummel 2004), while the rather well-known values for $Cd(CN)_n^{(2-n)}$, n = 1 – 4, are not mentioned at all.

In summary, the estimated value for the hypothetical species $PoCN_6^{2-}$ is not included in TDB 2020.

21.5.7.2 Polonium(IV) cyanide compounds

Brown (2001) reported experimental data from a solubility study of polonium(IV) cyanide in 0.02 – 1.5 M KCN. The lower part of the investigated KCN concentration range, a linear fit of three values measured at 0.02, 0.03 and 0.05 M KCN, were interpreted by Brown (2001) in terms of the following reaction:

$$2PoO(CN)_2(s) + 2CN^- \rightleftharpoons PoO_2(s) + Po(CN)_6^{2-}$$

$$\log_{10}K°(298.15\ K) = -3.9 \pm 0.1$$

The measured solubility values in the range 0.05 – 1.5 M KCN were interpreted by Brown (2001) in terms of this reaction:

$$2PoO(CN)_2(s) + 2CN^- + OH^- \rightleftharpoons HPoO_3^- + Po(CN)_6^{2-}$$

$$\log_{10}K°(298.15\ K) = -8.86$$

The $\log_{10}K°$ value actually has been calculated from $\Delta_f G_m°$ values for $HPoO_3^-$, $Po(CN)_6^{2-}$, $PoO(CN)_2(s)$, CN^- and OH^-. The values are estimates for hypothetical species ($HPoO_3^-$ and $Po(CN)_6^{2-}$) and a solid of highly uncertain stoichiometry ($PoO(CN)_2(s)$) which is characterised as "a white crystalline solid, presumably a polonium cyanide, (which) is formed by treating solid polonium hydroxide or tetrachloride with aqueous hydrocyanic acid" (Brown 2001).

In addition, concentrated KCN solutions are not important in environmental aqueous systems.

In summary, the above values are not included in TDB 2020.

21.5.8 Metal polonites

Brown (2001) estimated the solubility product of silver polonite

$$Ag_2PoO_3(s) \rightleftharpoons 2Ag^+ + PoO_3^{2-}$$

$$\log_{10}K_{sp}°(298.15\ K) = -24.4$$

from a plot of $\log_{10}K°(HXO_3^-)$ versus $\log_{10}K_{sp}°(Ag_2XO_3(s))$, where X is S, Se or Te.

Including into the TDB just this solubility product, $\log_{10}K_{sp}$, would inevitably lead to erroneous calculated polonium concentrations as we do not have any vague idea about aqueous silver polonite complexes. Therefore, this estimated datum has not been included in TDB 2020.

21.6 Polonium(VI)

Brown (2001) reported that "the trioxide is thought to be formed on the tracer scale by anodic deposition of polonium from acidic media, though it has not been fully characterised. Fusion of polonium dioxide with a mixture of potassium hydroxide and chlorate yields a bluish coloured dioxide, which is more soluble in water than the dioxide alone and may well contain polonate(VI)".

Despite this vague evidence of the existence of PoO_3(s), Brown (2001) stated that in acid solution, PoO_3(s) reacts to form PoO_2(s) according to the following equation:

$$PoO_3(s) + 2H^+ + 2e^- \rightleftharpoons PoO_2(s) + H_2O(l)$$

Brown (2001) used the value of 1.509 V for the $E°$ of the PoO_3(s)/PoO_2(s) couple reported in the literature, $\Delta_f G_m°(PoO_2, s, 298.15\ K) = -(192.2)\ kJ \cdot mol^{-1}$ and $\Delta_f G_m°(H_2O, l, 298.15\ K) = -(237.2)\ kJ \cdot mol^{-1}$ to calculate $\Delta_f G_m°(PoO_3, s, 298.15\ K) = -(138.2)\ kJ \cdot mol^{-1}$.

For the reaction

$$PoO_3(s) + 2e^- \rightleftharpoons PoO_3^{2-}$$

Brown (2001) calculated an $E°$ value of 0.550 V using the above obtained $\Delta_f G_m°(PoO_3, s, 298.15\ K) = -(138.2)\ kJ \cdot mol^{-1}$ and $\Delta_f G_m°(PoO_3^{2-}, 298.15\ K) = -(244.3)\ kJ \cdot mol^{-1}$ and stated that this value is in excellent agreement with that of 0.55 V reported in the literature.

According to Fig. 21-1, calculated with data selected by Brown (2001), the stability field of PoO_3(s) is far outside the stability range of water and hence, PoO_3(s) is unimportant in any environmental aqueous system. Considering this fact and the vague evidence of its existence, PoO_3(s) is not included in TDB 2020.

Tab. 21-1: Polonium data selected by Brown (2001) but not included in TDB 2020

For explanations see text.

Gases	Pog, Po_2g
Solids	PbPo(s), HgPo(s), ZnPo(s), NiPo(s), $PoCl_2$(s), $PoBr_2$(s), PoI_2(s), PoS(s), $PoCl_4$(s), $PoBr_4$(s), PoI_4(s), $(PoO)_2OSO_4$(s), $(PoO)_2OSeO_4$(s), $(PoO)_2(NO_3)_3OH$(s), $PoO(CN)_2$(s), Ag_2PoO_3(s), PoO_3(s)
Aqueous species	PoO^{2+}, $PoO(OH)^+$, $PoO(OH)_2$(aq), H_2PoO_3(aq), $HPoO_3^-$, PoO_3^{2-}, $PoOCl_4^{2-}$, $PoO(OH)Cl_2^-$, PoI_6^{2-}, PoI_5^-, $PoOSO_4$(aq), $PoO(SO_4)_2^{2-}$, $PoO(SO_4)_3^{4-}$, $PoOSeO_4$(aq), $PoO(SeO_4)_2^{2-}$, $PoONO_3^+$, $PoO(NO_3)_2$(aq), $PoO(NO_3)_3^-$, $PoCN_6^{2-}$

21.7 Selected polonium data

Tab. 21-2: Selected polonium data

Supplemental data are in italics.

Name	**Redox**	**$\Delta_f G_m°$** [kJ · mol^{-1}]	**$\Delta_f H_m°$** [kJ · mol^{-1}]	**$S_m°$** [J · K^{-1} · mol^{-1}]	**Species**
Po(s)	0	0.0	0.0	62.8	Po(s)
H2Po(aq)	-II	*206.5*	-	-	*$H_2Po(aq)$*
HPo-	-II	*209.3*	-	-	*HPo^-*
Po-2	-II	*274.0*	-	-	*Po^{2-}*
Po+2	II	124.1	-	-	Po^{2+}
PoCl4-2	II	-443.9	-	-	$PoCl_4^{2-}$
PoSO4(aq)	II	-626.3	-	-	$PoSO_4$(aq)
PoO2(s)	IV	-192.1	-	-	PoO_2(s)
Po+4	IV	*≈ 276.5*	-	-	*Po^{4+}*
PoCl6-2	IV	-555.3	-	-	$PoCl_6^{2-}$

Name	**Redox**	**$\log_{10}\beta°$**	**$\Delta_r H_m°$** [kJ · mol^{-1}]	**Reaction**
Po(aq)	0	*≈ -7*	-	*$Po(s) \rightleftharpoons Po(aq)$*
HPo-	-II	*-0.49* [a]	-	*$H_2Po(aq) \rightleftharpoons HPo^- + H^+$*
Po-2	-II	*-11.33* [a]	-	*$HPo^- \rightleftharpoons Po^{2-} + H^+$*
PoCl4-2	II	7.55 [b]	-	$Po^{2+} + 4\ Cl^- \rightleftharpoons PoCl_4^{2-}$
PoCl3-	II	*7.02* [c]	-	*$Po^{2+} + 3\ Cl^- \rightleftharpoons PoCl_3^-$*
PoCl2(aq)	II	*6.13* [c]	-	*$Po^{2+} + 2\ Cl^- \rightleftharpoons PoCl_2(aq)$*
PoCl+	II	*3.75* [c]	-	*$Po^{2+} + Cl^- \rightleftharpoons PoCl^+$*
PoSO4(aq)	II	1.12 [b]	-	$Po^{2+} + SO_4^{2-} \rightleftharpoons PoSO_4$(aq)
Po(OH)6-2	IV	-32.43 ± 0.05	-	PoO_2(s) + 4H_2O(l) ⇌ $Po(OH)_6^{2-}$ + 2H^+
Po(OH)4(aq)	IV	-7.5	-	PoO_2(s) + 2H_2O(l) ⇌ $Po(OH)_4$(aq)
Po(OH)3+	IV	-3.0	-	PoO_2(s) + H_2O(l) + H^+ ⇌ $Po(OH)_3^+$
Po(OH)2+2	IV	*-0.5*	-	*$PoO_2(s) + 2H^+ \rightleftharpoons Po(OH)_2^{2+}$*
PoOH+3	IV	*0.5*	-	*$PoO_2(s) + 3H^+ \rightleftharpoons PoOH^{3+} + H_2O(l)$*
Po+4	IV	*1.0*	-	*$PoO_2(s) + 4H^+ \rightleftharpoons Po^{4+} + 2H_2O(l)$*
PoCl6-2	IV	*7.8* [b]	-	*$Po^{4+} + 6Cl^- \rightleftharpoons PoCl_6^{2-}$*
Po(OH)Cl4-	IV	-2.16	-	$PoCl_6^{2-}$ + H_2O(l) ⇌ $Po(OH)Cl_4^-$ + H^+ + 2Cl^-
PoSO4+2	IV	5.2 ± 0.6	-	$Po^{4+} + SO_4^{2-} \rightleftharpoons PoSO_4^{2+}$
Po(SO4)2(aq)	IV	9.1 ± 0.7	-	$Po^{4+} + 2SO_4^{2-} \rightleftharpoons Po(SO_4)_2$(aq)
Po(SO4)3-2	IV	*> 2.2*	-	*$Po(SO_4)_2(aq) + SO_4^{2-} \rightleftharpoons Po(SO_4)_3^{2-}$*
PoNO3+3	IV	2.0 ± 0.9	-	$Po^{4+} + NO_3^- \rightleftharpoons PoNO_3^{3+}$

Tab. 21-2: Selected polonium data

Name	**Redox**	**$\log_{10}\beta°$**	**$\Delta_r H_m°$** [kJ · mol^{-1}]	**Reaction**
Po(NO3)2+2	IV	3.7 ± 0.4	-	$Po^{4+} + 2NO_3^- \rightleftharpoons Po(NO_3)_2^{2+}$
Po(NO3)3+	IV	4.4 ± 0.5	-	$Po^{4+} + 3NO_3^- \rightleftharpoons Po(NO_3)_3^+$

Name	**$\log_{10}K_{s,0}°$**	**$\Delta_r H_m°$** [kJ · mol^{-1}]	**Reaction**
PoSO4(s)	-8.91	-	$PoSO_4(s) \rightleftharpoons Po^{2+} + SO_4^{2-}$
Po(SO4)2·H2O(s)	-6.33 ± 0.04	-	$Po(SO_4)_2 \cdot H_2O(s) + HSO_4^- \rightleftharpoons Po(SO_4)_3^{2-} + H^+ + H_2O(l)$

[a] Calculated from estimated $\Delta_f G_m°$ values.
[b] Calculated from $\Delta_f G_m°$ values.
[c] Estimated via linear free energy relationships.

Tab. 21-3: Selected SIT ion interaction coefficients $\varepsilon_{j,k}$ [kg · mol^{-1}] for polonium species

Data in bold face are taken from Grenthe et al. (1992). Data in normal face are derived or estimated in this review. Data estimated according to charge correlations and taken from Tab. 1-7 are shaded. Supplemental data are in italics.

j k → ↓	**Cl^-** $\varepsilon_{j,k}$ [kg · mol^{-1}]	**ClO_4^-** $\varepsilon_{j,k}$ [kg · mol^{-1}]	**Na^+** $\varepsilon_{j,k}$ [kg · mol^{-1}]	**$Na^+ + Cl^-$** $\varepsilon_{j,k}$ [kg · mol^{-1}]	**$Na^+ + ClO_4^-$** $\varepsilon_{j,k}$ [kg · mol^{-1}]
H+	**0.12 ± 0.01**	**0.14 ± 0.02**	0	0	0
HSO4-	0	0	**-0.01 ± 0.02**	0	0
Po(aq)	*0*	*0*	*0*	*0.0 ± 0.1*	*0.0 ± 0.1*
H2Po(aq)	*0*	*0*	*0*	*0.0 ± 0.1*	*0.0 ± 0.1*
HPo-	*0*	*0*	*-0.05 ± 0.10*	*0*	*0*
Po-2	*0*	*0*	*-0.10 ± 0.10*	*0*	*0*
Po+2	0.4 ± 0.1	0.4 ± 0.1	0	0	0
PoCl4-2	0	0	*-0.10 ± 0.10*	0	0
PoCl-2	*0*	*0*	*-0.05 ± 0.10*	*0*	*0*
PoCl2(aq)	*0*	*0*	*0*	*0.0 ± 0.1*	*0.0 ± 0.1*
PoCl+	*0.2 ± 0.1*	*0.2 ± 0.1*	*0*	*0*	*0*
PoSO4(aq)	0	0	0	0.0 ± 0.1	0.0 ± 0.1
Po(OH)6-2	0	0	*-0.10 ± 0.10*	0	0
Po(OH)4(aq)	*0*	*0*	0	0.0 ± 0.1	0.0 ± 0.1
Po(OH)3+	0.2 ± 0.1	0.2 ± 0.1	0	0	0
Po(OH)2+2	*0.4 ± 0.1*	*0.4 ± 0.1*	*0*	*0*	*0*
PoOH+3	*0.6 ± 0.1*	*0.6 ± 0.1*	*0*	*0*	*0*
Po4+	*0.8 ± 0.1*	*0.8 ± 0.1*	*0*	*0*	*0*
PoCl6-2	*0*	*0*	*-0.10 ± 0.10*	*0*	*0*
Po(OH)Cl4-	0	0	*-0.05 ± 0.10*	*0*	*0*
PoSO4+2	0.4 ± 0.1	0.4 ± 0.1	*0*	*0*	*0*
Po(SO4)2(aq)	0	0	0	0.0 ± 0.1	0.0 ± 0.1
Po(SO4)3-2	*0*	*0*	*-0.10 ± 0.10*	*0*	*0*
PoNO3+3	0.7 ± 0.6	0.7 ± 0.6	*0*	*0*	*0*
Po(NO3)2+2	0.7 ± 0.3	0.7 ± 0.3	*0*	*0*	*0*
Po(NO3)3+	0.5 ± 0.4	0.5 ± 0.4	*0*	*0*	*0*

21.8 References

Ampelogova, N.I. (1973): Investigation of complex formation of polonium by an ion exchange method. Soviet Radiochemistry 15, 823-829 (Translated from: Radiokhimiya (15) 1973, 813-820).

Ampelogova, N.I. (1975): Hydrolysis of polonium in perchlorate. Soviet Radiochemistry 17, 69-65 (Translated from: Radiokhimiya (17) 1975, 68-75).

Ayala, R., Spezia, R., Vuilleumier, R., Martinez, J.M., Pappalardo, R.R. & Marcos, E.S. (2010): An ab initio molecular dynamics study on the hydrolysis of the Po(IV) aquaion in water. J. Phys. Chem. B, 114, 12866-12874.

Bagnall, K.W (1957): The chemistry of the Rare Radioelements. Butterworths Scientific Publications. London (as cited by Brown (2001).

Bagnall, K.W., D'Eye, R.W.M. & Freeman, J.H. (1955): The polonium halides. Part I. Polonium chlorides. Journal of the Chemical Society, 2320-2326.

Bagnall, K.W. & Freeman, J.H. (1956): The sulphates and selenate of polonium. Journal of the Chemical Society, 4579-4582.

Bagnall, K.W. & Freeman, J.H. (1957): Solubility of some polonium compounds. Journal of the Chemical Society, 2161-2163.

Bagnall, K.W., Robertson, D.S. & Stewart, M.A.A. (1958): The polonium nitrates. Journal of the Chemical Society, 3633-3636.

Brown, S.A. (2001): The aqueous chemistry of polonium and its relationship to mineral processing streams. PhD Thesis, University of Western Sydney, Australia, 169p.

Brown, P.L. & Ekberg, C. (2016): Hydrolysis of Metal Ions. Wiley-VCH Verlag GmbH & Co. KGaA, Weinheim, Germany, 917p.

Brown, P.L. & Sylva, R.N. (1987): Unified Theory of Metal Ion Complex Formation Constants. Australian Atomic Energy Commission, AAEC/E656.

Cox, J.D., Wagman, D.D. & Medvedev, V.A. (1989): CODATA Key Values for Thermodynamics. New York, Hemisphere Publishing, 271p.

Grenthe, I., Fuger, J., Konings, R.J.M., Lemire, R.J., Muller, A.B., Nguyen-Trung, C. & Wanner, H. (1992): Chemical Thermodynamics of Uranium. Chemical Thermodynamics, Vol. 1. North-Holland, Amsterdam, 715 pp.

Grenthe, I., Gaona, X., Plyasunov, A.V., Rao, L., Runde, W.H., Grambow, B., Konings, R.J.M., Smith, A.L., Moore, E.E. (2020): Second Update on the Chemical Thermodynamics of Uranium, Neptunium, Plutonium, Americium and Technetium. Chemical Thermodynamics, Vol. 14. OECD Publications, Paris, France, 1503 p.

Hataye, I., Suganuma, H., Sakata, M. & Nagame, Y. (1981a): Solvent extraction study on the hydrolysis of tracer concentration of polonium(IV) in perchlorate solutions. J. inor. nucl. Chem., 43, 2101-2104.

Hataye, I., Suganuma, H. & Sakata, M. (1981b): Solvent extraction study on the hydrolysis of tracer concentration of polonium(IV) in nitrate solutions. J. inor. nucl. Chem., 43, 2575-2577.

Hummel, W. (2004): The influence of cyanide complexation on the speciation and stability of radionuclides in a geological repository. Environmental Geology 45, 633-646.

Hummel, W., Berner, U., Curti, E., Pearson, F.J. & Thoenen, T. (2002): Nagra/PSI Chemical Thermodynamic Data Base 01/01. Nagra Technical Report NTB 02-16 and Universal Publishers, Parkland, Florida, 565 pp.

Koch, H. & Schmidt, H. (1963): Die Bestimmung der Hydrolysekonstanten in wäßrigen Lösungen nach der Ionenaustauschermethode. Zeitschrift für Naturforschung, 18b, 936-940.

Starik, I.E., Ampelogova, N.I. & Kuznetsov, B.S. (1964): Hydrolysis of polonium in perchloric acid solutions. Soviet Radiochemistry, 6, 501-506 (Translated from: Radiokhimiya (6) 1964, 519-524).

Suganuma, H. & Hataye, I. (1981): Solvent extraction study on the hydrolysis of tracer concentrations of Po(IV) in chloride solutions. J. inor. nucl. Chem., 43, 2511-2515.

Suganuma, H., Hataye, I. & Takashima, Y. (1983): A cation-exchange study of the hydrolysis of tracer concentrations of polonium(IV). Bull. Chem. Soc. Jpn., 56, 1080-1083.

Treiman, L.H. (1953): The solubility product of polonium hydroxide. Los Alamos Scientific Laboratory Report LAMS-1549, 6 p.

Treiman, L.H. & Treiman, M.W. (1952): Purification of polonium by the glass wool adsorption of colloidal polonium hydroxide. Los Alamos Scientific Laboratory Report LA-140, 9 p.

22 Protactinium

22.1 Introduction

The most important isotope of protactinium is Pa-231, a member of the naturally occurring uranium-protactinium ($4n + 3$) family of radioelements, with a long half-life of $(32.76 \pm 0.11) \cdot 10^4$ years. Pa-231contributes in dose-relevant quantities to the inventory of radioactive waste coming from nuclear power plants, which is the reason for inclusion of protactinium into the PSI Chemical Thermodynamic Database 2020 (TDB 2020).

Myasoedov et al. (2006) report that two oxidation states, Pa(IV) and Pa(V), have been definitely established in aqueous solution, but all attempts to demonstrate the existence of Pa(III) in solution have led to negative or inconclusive results. Both Pa(IV) and Pa(V) show strong tendencies to hydrolyse in the absence of complexing agents and most studies of the ionic species of Pa in aqueous solution have therefore been carried out at tracer level. Furthermore, the instability of Pa(IV) toward re-oxidation has made it difficult to obtain reproducible data on this oxidation state, so that little quantitative information is available about the aqueous chemistry of Pa(IV).

As Di Giandomenico et al. (2007) confirm, in aqueous solution as well as in the solid state, the most stable oxidation state of Pa is (V). But unlike the other actinides(V) (U, Np, Pu, Am), that form a trans-dioxo cation AnO_2^+ with two short An-O bonds, Pa(V) complexes in aqueous solution possess at most one single oxo-bond, depending on the nature of the ligand (Le Naour et al. 2005).

In the absence of strong complexing agents, such as F^- and certain organic reagents, the aqueous complexes of Pa(V) are all oxo- or hydroxo-complexes. The relative complexing tendencies of inorganic anions with respect to Pa(V) are (Myasoedov et al. 2006):

$$F^- > OH^- > SO_4^{2-} > Cl^- > Br^- > I^- > NO_3^- \geq ClO_4^-$$

The thermodynamic data included into the PSI TDB 2020 have been taken from

- Konings et al. (2006) and the literature discussed by Myasoedov et al. (2006)
- the recent review of the hydrolysis of metal ions (Brown & Ekberg 2016)
- and own reviews of experimental data

The selected thermodynamic data for protactinium compounds and complexes are presented in Tab. 22-1.

In cases where ion interaction coefficients of protactinium species were not available, we approximated these with the estimation method described in Section 1.5.3, which draws on a statistical analysis of published SIT ion interaction coefficients and which allows the estimation of missing coefficients for the interaction of cations with Cl^- and ClO_4^-, and for the interaction of anions with Na^+, from the charge of the cations or anions of interest.

The selected SIT ion interaction coefficients for protactinium species are presented in Tab. 22-2.

22.2 Elemental protactinium

Protactinium metal, liquid and gas are not relevant under environmental conditions. Hence, the gas phase Pag and the liquid phase Pa(l) are not included in the data base. The absolute entropy and heat capacity of Pa(cr) are included as they are used for the calculation of certain thermodynamic reaction properties. The selected values have been taken from Konings et al. (2006):

$S_m°(Pa, cr, 298.15\ K) = (51.6 \pm 0.8)\ J \cdot K^{-1} \cdot mol^{-1}$

$C_{p,m}°(Pa, cr, 298.15\ K) = (28.2 \pm 0.4)\ J \cdot K^{-1} \cdot mol^{-1}$

22.3 Protactinium(IV)

22.3.1 Protactinium(IV) aqua ion

Protactinium(IV) exists as the Pa^{4+} cation in very acid aqueous solutions. The selected thermodynamic values for Pa^{4+} are taken from Konings et al. (2006):

$\Delta_f H_m°(Pa^{4+}, 298.15\ K) = -(621.4 \pm 14.3)\ kJ \cdot mol^{-1}$

$S_m°(Pa^{4+}, 298.15\ K) = -(397 \pm 40)\ J \cdot K^{-1} \cdot mol^{-1}$

Konings et al. (2006) remark that their selected $\Delta_f H_m°(Pa^{4+}, 298.15\ K)$ value refers to 1 M HCl, and that $S_m°(Pa^{4+}, 298.15\ K)$ is an estimated value. The Gibbs energy of formation calculated from the above values, $S_m°(Pa, cr, 298.15\ K)$ (see Section 22.2) and the CODATA value $S_m°(H_2, g, 298.15\ K) = (130.680 \pm 0.003)\ J \cdot K^{-1} \cdot mol^{-1}$ (Grenthe et al. 1992) according to the Gibbs-Helmholtz equation

$\Delta_f G_m°(Pa^{4+}, 298.15\ K) = \Delta_f H_m°(Pa^{4+}, 298.15\ K) - T° \cdot \Delta_f S_m°(Pa^{4+}, 298.15\ K)$

$\Delta_f S_m°(Pa^{4+}, 298.15\ K) = S_m°(Pa^{4+}, 298.15\ K) - S_m°(Pa, cr, 298.15\ K) + 2\ S_m°(H_2, g, 298.15\ K)$

$\Delta_f G_m°(Pa^{4+}, 298.15\ K) = -(565.6 \pm 18.6)\ kJ \cdot mol^{-1}$

These values are included in TDB 2020 as well as the estimates

$\varepsilon(Pa^{4+}, ClO_4^-) = (0.8 \pm 0.1)\ kg \cdot mol^{-1}$

$\varepsilon(Pa^{4+}, Cl^-) = (0.35 \pm 0.10)\ kg \cdot mol^{-1}$

Using $\Delta_f G_m°(Pa^{4+}, 298.15\ K)$ the redox equilibrium

$$Pa(cr) + 4H^+ \rightleftharpoons Pa^{4+} + 2H_2g$$

or

$$Pa(cr) \rightleftharpoons Pa^{4+} + 4e^-$$

is calculated as

$$\log_{10}K°(298.15\ K) = 99.09 \pm 3.26$$

22.3.2 Protactinium(IV) (hydr)oxide compounds and complexes

22.3.2.1 Protactinium(IV) hydroxide complexes

Only two studies seem to have been published concerning Pa(IV) hydrolysis (Guillaumont 1968, Lundqvist 1974).

In studying the complexation of Pa(IV) with acetylacetone, Lundqvist (1974) found that acetylacetone is complexed by a doubly charged Pa(IV) ion in the pH range 1 – 3. He concluded "the doubly charged positive aqueous Pa(IV) ion has hitherto been denoted M^{2+} as its formula is not evident. Neglecting the coordination of water molecules, one may propose the formula PaO^{2+} or $Pa(OH)_2^{2+}$. The formula $Pa(OH)_2^{2+}$ is preferred by some authors. However, the rather large stability range of M^{2+} (over more than two pH-units) favours the species PaO^{2+} rather than $Pa(OH)_2^{2+}$; the latter may be regarded as an intermediary between $Pa(OH)^{3+}$ and $Pa(OH)_3^+$, neither of which was indicated to exist in this investigation. However, a species like PaO^{2+} has not been observed for Zr(IV), Hf(IV) or the actinides."

By contrast, Guillaumont (1968) found in a similar solvent extraction study the hydrolysis products $Pa(OH)^{3+}$, $Pa(OH)_2^{2+}$ and $Pa(OH)_3^+$ as the pH increased from -0.5 – 3 in 3M $LiClO_4$:

$$Pa^{4+} + H_2O(l) \rightleftharpoons PaOH^{3+} + H^+$$

$$\log_{10}{}^*\beta_1\ (298.15\ K) = -0.14$$

$$Pa^{4+} + 2H_2O(l) \rightleftharpoons Pa(OH)_2^{2+} + 2H^+$$

$$\log_{10}{}^*\beta_2\ (298.15\ K) = -0.52$$

$$Pa^{4+} + 3H_2O(l) \rightleftharpoons Pa(OH)_3^+ + 3H^+$$

$$\log_{10}{}^*\beta_3\ (298.15\ K) = -1.77$$

In addition, Guillaumont (1968) gives in his Tab. V the values $\log_{10}{}^*\beta_3$ (298.15 K) = -2.00 and $\log_{10}{}^*\beta_4$ (298.15 K) = -5.32 with the remark "values obtained by using the method of Sillen", without any explanation what the "method of Sillen" actually means.

Baes & Mesmer (1986) discuss some problems of the solvent extraction method and conclude that "the possible complications just mentioned are not expected to alter Guillaumont's conclusion that Pa^{4+} appears in solution above 1 M acid or seriously affect his estimates", but further state that "the conversion of $Pa(OH)_2^{2+}$ to $Pa(OH)_3^{+}$, however, is probably not appreciable below pH 3". The latter statement would account for the findings of Lundqvist (1974) but contradict the results of Guillaumont (1968) at pH > 1.

Brown & Ekberg (2016) discuss the same two studies (Guillaumont 1968, Lundqvist 1974) but conclude "given that there are no supporting data for either of these interpretations, no data are retained for protactinium(IV)."

Despite these contradictions, this review decided to include Guillaumont's data into TDB 2020 as a reminder of the strong hydrolysis of Pa(IV), but as supplemental data to indicate the above discussed unresolved problems.

The values of Guillaumont (1968) have been transformed into stepwise stability constants and extrapolated to zero ionic strength using the estimated SIT coefficients given in Tab. 22-2, resulting in $\Delta\varepsilon = -(0.06 \pm 0.14)$ kg · mol^{-1} for all equilibria:

$$Pa^{4+} + H_2O(l) \rightleftharpoons PaOH^{3+} + H^+$$

$$log_{10}{}^*K_1^\circ(298.15\ K) = 1.3 \pm 0.5$$

$$PaOH^{3+} + H_2O(l) \rightleftharpoons Pa(OH)_2^{2+} + H^+$$

$$log_{10}{}^*K_2^\circ(298.15\ K) = 0.6 \pm 0.5$$

$$Pa(OH)_2^{2+} + H_2O(l) \rightleftharpoons Pa(OH)_3^{+} + H^+$$

$$log_{10}{}^*K_3^\circ(298.15\ K) = -1.0 \pm 0.5$$

These stepwise stability constants indicate that the first as well as the second hydrolysis equilibrium is established at pH < 0 and the third equilibrium is expected in the pH range 0.5 – 1.5.

The cumulative stability constants

$$log_{10}{}^*\beta_1^\circ(298.15\ K) = 1.3 \pm 0.5$$

$$log_{10}{}^*\beta_2^\circ(298.15\ K) = 1.9 \pm 0.5$$

$$log_{10}{}^*\beta_3^\circ(298.15\ K) = 0.9 \pm 0.5$$

are included in TDB 2020 as supplemental data as well as the estimates

$$\varepsilon(PaOH^{3+}, ClO_4^-) = (0.6 \pm 0.1)\ kg \cdot mol^{-1}$$

$$\varepsilon(PaOH^{3+}, Cl^-) = (0.25 \pm 0.10)\ kg \cdot mol^{-1}$$

$$\varepsilon(Pa(OH)_2^{2+}, ClO_4^-) = (0.4 \pm 0.1)\ kg \cdot mol^{-1}$$

$\varepsilon(Pa(OH)_2^{2+}, Cl^-) = (0.15 \pm 0.10)$ kg · mol^{-1}

$\varepsilon(Pa(OH)_3^{+}, ClO_4^-) = (0.2 \pm 0.1)$ kg · mol^{-1}

$\varepsilon(Pa(OH)_3^{+}, Cl^-) = (0.05 \pm 0.10)$ kg · mol^{-1}

22.3.2.2 Protactinium(V) (hydr)oxide compounds

Baes & Mesmer (1986) estimated the solubility of PaO_2(cr) from "an interpolation of the estimated values of K_{s0} for ThO_2 and UO_2":

$PaO_2(cr) + 4H^+ \rightleftharpoons Pa^{4+} + 2H_2O(l)$

$\log_{10}{}^*K_{s0}^\circ$ (cr, 298.15 K) = 0.6 ± 1.0

Could this guess by Baes & Mesmer (1986) at least serve as a rough estimate for calculating the solubility and hydrolysis behaviour of Pa(IV) in environmental systems? Given that there is no experimental data concerning the solubility of PaO_2(s), and no experimental data are available at pH > 3, not even a vague guess can be made about the stability of the species $Pa(OH)_4$(aq), which would accompany the above estimate of the solubility product of PaO_2(s).

Consequently, using the above guess of the solubility product of PaO_2(cr) in speciation calculations for strongly reducing conditions and pH > 3 will inevitably lead to grossly wrong results, underestimating the solubility of Pa(IV) by orders of magnitude.

Hence, this value is not included in TDB 2020.

22.4 Protactinium(V)

22.4.1 Protactinium(V) aqua ion

As discussed by Myasoedov et al. (2006), the least hydrolysed cation of Pa(V) in acid solutions (10^{-5} M < $[H^+]$ < 3 M) is $PaO(OH)^{2+}$. Only at $[H^+] \geq 3$ M the existence of PaO^{3+} has been suggested.

Hence, reliable thermodynamic data for the protactinium(V) aqua ion refer to $PaO(OH)^{2+}$.

The selected thermodynamic values for $PaO(OH)^{2+}$ are taken from Konings et al. (2006):

$\Delta_f H_m^\circ(PaO(OH)^{2+}, 298.15\ K) = -(1'115 \pm 21)$ kJ · mol^{-1}

$S_m^\circ(PaO(OH)^{2+}, 298.15\ K) = -(21 \pm 21)$ J · K^{-1} · mol^{-1}

The Gibbs energy of formation calculated from the above values, S_m°(Pa, cr, 298.15 K) (see Section 22.2) and the CODATA values $S_m^\circ(H_2, g, 298.15\ K) = (130.680 \pm 0.003)$ J · K^{-1} · mol^{-1}

and $S_m°(O_2, g, 298.15\ K) = (205.152 \pm 0.005)\ J \cdot K^{-1} \cdot mol^{-1}$ (Grenthe et al. 1992) according to the Gibbs-Helmholtz equation

$$\Delta_f G_m°(PaO(OH)^{2+}, 298.15\ K) = \Delta_f H_m°(PaO(OH)^{2+}, 298.15\ K) - T° \cdot \Delta_f S_m°(PaO(OH)^{2+}, 298.15\ K)$$

$$\Delta_f S_m°(PaO(OH)^{2+}, 298.15\ K) = S_m°(PaO(OH)^{2+}, 298.15\ K) - S_m°(Pa, cr, 298.15\ K) + (1/2)\ S_m°(H_2, g, 298.15\ K) - S_m°(O_2, g, 298.15\ K)$$

$$\Delta_f G_m°(PaO(OH)^{2+}, 298.15\ K) = -(1'051.7 \pm 21.9)\ kJ \cdot mol^{-1}$$

Using this value the redox equilibrium is calculated as

$$Pa(cr) + 2H^+ + O_2g \rightleftharpoons PaO(OH)^{2+} + ½H_2g$$

$$\log_{10}K°(298.15\ K) = 184.25 \pm 3.84$$

or, using the CODATA value $\Delta_f G_m°(H_2O, l, 298.15\ K) = -(237.140 \pm 0.041)\ kJ \cdot mol^{-1}$ (Grenthe et al. 1992), as

$$Pa(cr) + 2H_2O(l) \rightleftharpoons PaO(OH)^{2+} + 3H^+ + 5e^-$$

$$\log_{10}K°(298.15\ K) = 101.16 \pm 3.84$$

Taking these redox equilibria and combining them with the redox equilibria derived for Pa(IV) (see Section 22.3.1) this review calculates

$$Pa^{4+} + 2H_2O(l) \rightleftharpoons PaO(OH)^{2+} + 3H^+ + e^-$$

$$\log_{10}K°(298.15\ K) = 2.07 \pm 3.84$$

$$Pa^{4+} + 1.5H_2g + O_2g \rightleftharpoons PaO(OH)^{2+} + 2H^+$$

$$\log_{10}K°(298.15\ K) = 85.16 \pm 3.84$$

The latter value is included in TDB 2020.

22.4.2 Protactinium(V) (hydr)oxide compounds and complexes

22.4.2.1 Protactinium(V) hydroxide complexes

Myasoedov et al. (2006) report that the hydrolysis of Pa(V) is usually studied in perchloric acid solutions, because ClO_4^- is considered to be a non-complexing anion. However, the presence of small amounts of weakly complexing anions does not affect the results. Thus, $[HNO_3] < 0.5$ M, $[HCl] < 1$ M or $[H_2SO_4] < 0.01$ M are all equivalent to $HClO_4$ of the same acidity.

Myasoedov et al. (2006) summarise that in acid solutions (10^{-5} M $< [H^+] < 3$ M), the least hydrolysed cation is $PaO(OH)^{2+}$. At $[H^+] < 1$ M, $PaO(OH)_2^+$ begins to form and becomes predominant at pH ≈ 3. At higher pH values, the neutral species, $Pa(OH)_5(aq)$ (or $PaO(OH)_3(aq)$), is formed. At pH 5 – 6, the hydrated oxide is precipitated. In alkaline solution minute concentrations of $Pa(OH)_6^-$ (or $PaO(OH)_4^-$) are formed, and at $[H^+] \geq 3$ M the existence of PaO^{3+} has been suggested.

PaO^{3+}

Brown & Ekberg (2016) report that a stability constant for the first monomeric species of Pa(V), $PaO(OH)^{2+}$, that forms according to the reaction

$$PaO^{3+} + H_2O(l) \rightleftharpoons PaO(OH)^{2+} + H^+$$

has been given by Vitorge et al. (2007), which was calculated from earlier data of Trubert et al. (2002, 2003). The magnitude of the stability constant for the species is consistent with that expected by extrapolation of the higher monomeric species (for which there are much more data) and, as such, is retained by Brown & Ekberg (2016). Their selected stability constant is

$$\log_{10}{}^*K_1^\circ\ (298.15\ \text{K}) = -0.04 \pm 0.36$$

This value is included in TDB 2020 as well as the estimates

$$\varepsilon(PaO^{3+}, ClO_4^-) = (0.6 \pm 0.1)\ \text{kg} \cdot \text{mol}^{-1}$$

$$\varepsilon(PaO^{3+}, Cl^-) = (0.25 \pm 0.10)\ \text{kg} \cdot \text{mol}^{-1}$$

$PaO(OH)_2^+$ and $PaO(OH)_3(aq)$

Brown & Ekberg (2016) evaluated the temperature dependence of the reactions

$$PaO(OH)^{2+} + H_2O(l) \rightleftharpoons PaO(OH)_2^+ + H^+$$

$$PaO(OH)_2^+ + H_2O(l) \rightleftharpoons PaO(OH)_3(aq) + H^+$$

based on values given by Trubert et al. (2002, 2003) and La Naour et al. (2003) at zero ionic strength and the temperatures 10, 25, 40 and 60 °C. Brown & Ekberg (2016) show $\log_{10}{}^{*}K_{x}°$ versus 1 / T plots with linear regression lines (their Figs. 9-1 and 9-2) and provide the values

$$\log_{10}{}^{*}K_{2}° \text{ (298.15 K)} = -1.27 \pm 0.04$$

$$\log_{10}{}^{*}K_{3}° \text{ (298.15 K)} = -4.90 \pm 0.50$$

derived from their regression analyses, but they do not give any $\Delta_r H_m°$(298.15 K) values. In their summary of thermodynamic parameters for Pa(V) (their Tab. 9-2) Brown & Ekberg (2016) give the values $\Delta_f H_m°(PaO(OH)^{2+}, 298.15\ K) = -(1'113 \pm 21)$ kJ · mol^{-1}, $\Delta_f H_m°(PaO(OH)_2{}^{+}, 298.15\ K) = -(1394 \pm 22)$ kJ · mol^{-1}, and $\Delta_f H_m°(PaO(OH)_3(aq), 298.15\ K) = -(1'631 \pm 39)$ kJ · mol^{-1}. Using these values together with the CODATA value $\Delta_f H_m°(H_2O(l), 298.15\ K) = -(285.830 \pm 0.040)$ kJ · mol^{-1} (Grenthe et al. 1992) this review calculates for the above two reactions

$$\Delta_r H_m°(298.15\ K) = (4.8 \pm 30.4) \text{ kJ} \cdot \text{mol}^{-1}$$

$$\Delta_r H_m°(298.15\ K) = (48.8 \pm 44.8) \text{ kJ} \cdot \text{mol}^{-1}$$

The calculated uncertainties, estimated by error propagation from the $\Delta_f H_m°$ values, are unrealistically large, especially in the first case. In addition, exclusion of a data point at 25 °C in the regression analysis of Brown & Ekberg (2016) seems questionable. These observations prompted the present review to re-do these analyses (Figs. 22-1 and 22-2). The results obtained are

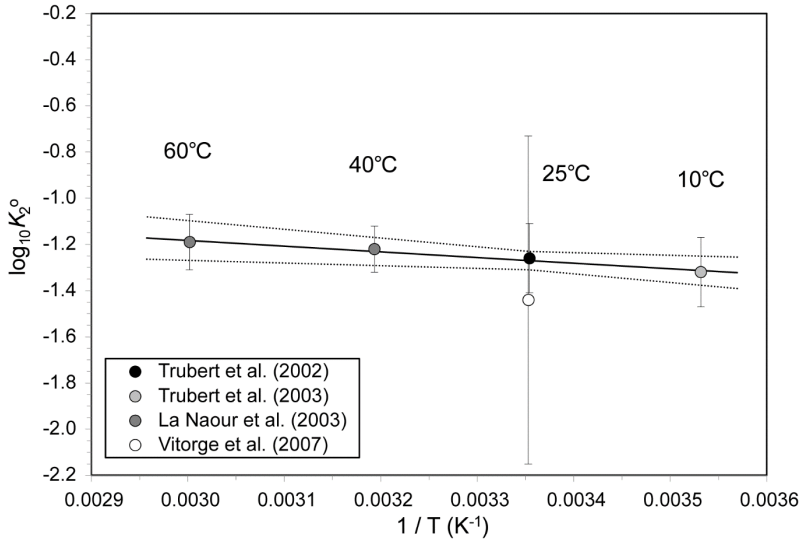

Fig. 22-1: The equilibrium constant log10∗K2° for PaO(OH)2+ + H2O(l) ⇌ PaO(OH)2+ + H+ as function of temperature in the range 10 – 60 °C

Solid line: unweighted linear regression using the data of Trubert et al. (2002, 2003) and Le Naour et al. (2003). Dotted lines: lower and upper limits using $\log_{10}{}^{*}K_{2}°$(298.15 K) = -1.27 ± 0.04 and $\Delta_r H_m°$(298.15 K) = (4.7 ± 2.5) kJ · mol^{-1} and extrapolated to lower and higher temperatures. The estimated data point of Vitorge et al. (2007) was not used in the regression analysis.

$PaO(OH)^{2+} + H_2O(l) \rightleftharpoons PaO(OH)_2^{+} + H^{+}$

$\log_{10}{}^{*}K_2°$ (298.15 K) = -1.27 ± 0.04

$\Delta_r H_m°$(298.15 K) = (4.7 ± 2.5) kJ · mol^{-1}

$PaO(OH)_2^{+} + H_2O(l) \rightleftharpoons PaO(OH)_3(aq) + H^{+}$

$\log_{10}{}^{*}K_3°$ (298.15 K) = -4.9 ± 0.5

$\Delta_r H_m°$(298.15 K) = (49 ± 14) kJ · mol^{-1}

The latter values were obtained excluding the data point at 25 °C, as Brown & Ekberg (2016) did with the argument "the stability constant at 25 °C is clearly not consistent with the values at the other three temperatures". However, this argument has no obvious chemical base as all data have been obtained by the same method by the same group of researchers. Including this data point in the regression analysis (Fig. 22-2) the following results are obtained

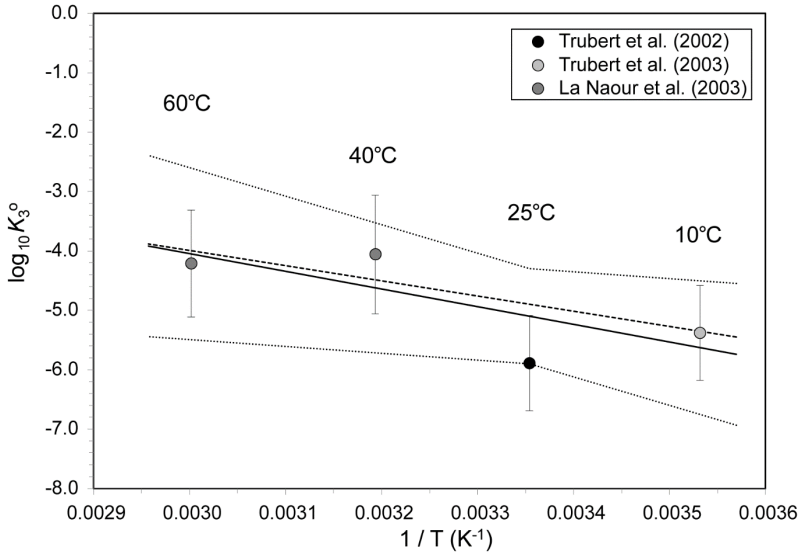

Fig. 22-2: The equilibrium constant $\log_{10}{}^{*}K_3°$ for $PaO(OH)_2^{+} + H_2O(l) \rightleftharpoons PaO(OH)_3(aq) + H^{+}$ as function of temperature in the range 10 – 60 °C

Solid line: unweighted linear regression using the data of Trubert et al. (2002, 2003) and Le Naour et al. (2003). Dotted lines: lower and upper limits using $\log_{10}{}^{*}K_2°$(298.15 K) = -5.1 ± 0.8 and $\Delta_r H_m°$(298.15 K) = (57 ± 35) kJ · mol^{-1} and extrapolated to lower and higher temperatures. Dashed line: unweighted linear regression excluding the data point at 25 °C.

$PaO(OH)_2^{+} + H_2O(l) \rightleftharpoons PaO(OH)_3(aq) + H^{+}$

$\log_{10}{}^{*}K_3°$ (298.15 K) = -5.1 ± 0.8

$\Delta_r H_m°$(298.15 K) = (57 ± 35) kJ · mol^{-1}

Considering the uncertainty estimates, there is no reason to exclude the 25 °C data point. In summary, the values

$PaO(OH)^{2+} + H_2O(l) \rightleftharpoons PaO(OH)_2^{+} + H^{+}$

$\Delta_r H_m°(298.15\ K) = (4.7 \pm 2.5)\ kJ \cdot mol^{-1}$

$PaO(OH)_2^{+} + H_2O(l) \rightleftharpoons PaO(OH)_3(aq) + H^{+}$

$\Delta_r H_m°(298.15\ K) = (57 \pm 35)\ kJ \cdot mol^{-1}$

are included in TDB 2020.

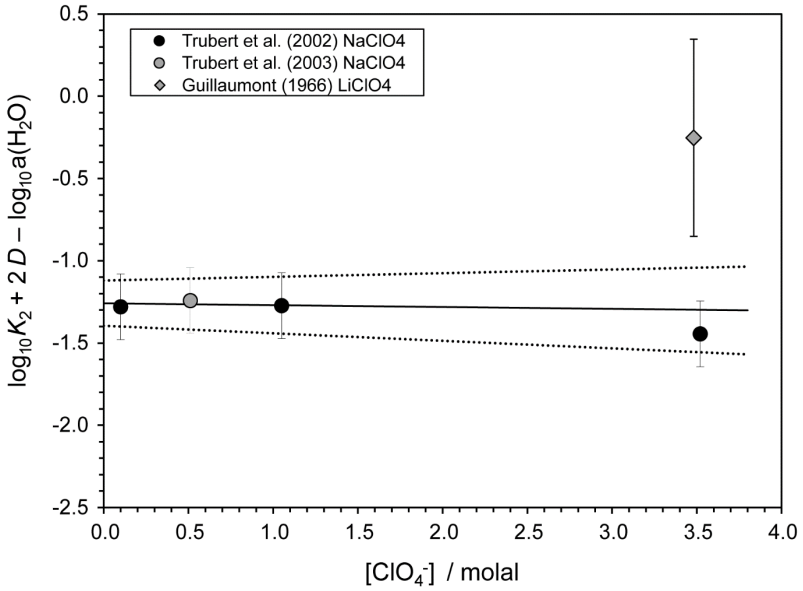

Fig. 22-3: Dependence of the equilibrium $PaO(OH)^{2+} + H_2O(l) \rightleftharpoons PaO(OH)_2^{+} + H^{+}$ on ionic strength in perchlorate media

The solid line is obtained using the derived SIT interaction coefficient and stability constant at zero ionic strength. Dotted lines represent the 95% uncertainty range extrapolated from I = 0 to higher perchlorate concentrations.

Brown & Ekberg (2016) evaluated the ionic strength dependence of the above two reactions (their Figs. 9-3 and 9-4) using $\Delta\varepsilon = \Delta\varepsilon_1 + \Delta\varepsilon_2 \cdot \log_{10} I_m$ in their extended SIT analysis. As this extended two-parameter version is incompatible with the one-parameter SIT analysis used in the NEA TDB project and TDB 2020, this review repeated the SIT analyses using the standard linear SIT procedure (Figs. 22-3 and 22-4).

Trubert et al. (2002) write that their results can compared with the only existing data available, in a thesis by Guillaumont (1966) who determined values of $\log_{10}{}^{*}K_2$ and $\log_{10}{}^{*}K_3°$, respectively, of -1.05 and -4.5 for I = 3 M. However, Guillaumont (1966) took into account neither the variation of the partition coefficient of thenoyltrifluoroacetone (TTA) as function of C_{TTA}, nor the molality of TTA in the aqueous phase. Since all the raw data of this work were available, Trubert et al. (2002) re-evaluated these values and report $\log_{10}{}^{*}K_2 = -0.9 \pm 0.4$ and $\log_{10}{}^{*}K_3 = -3.9 \pm 0.5$.

These values have been included in the present SIT analyses, together with a value $\log_{10}{}^{*}K_3 = -4.73 \pm 0.30$ at 5 M $NaClO_4$ which Trubert et al. (2002) did not seem to be aware of, but which is cited by Brown & Ekberg (2016).

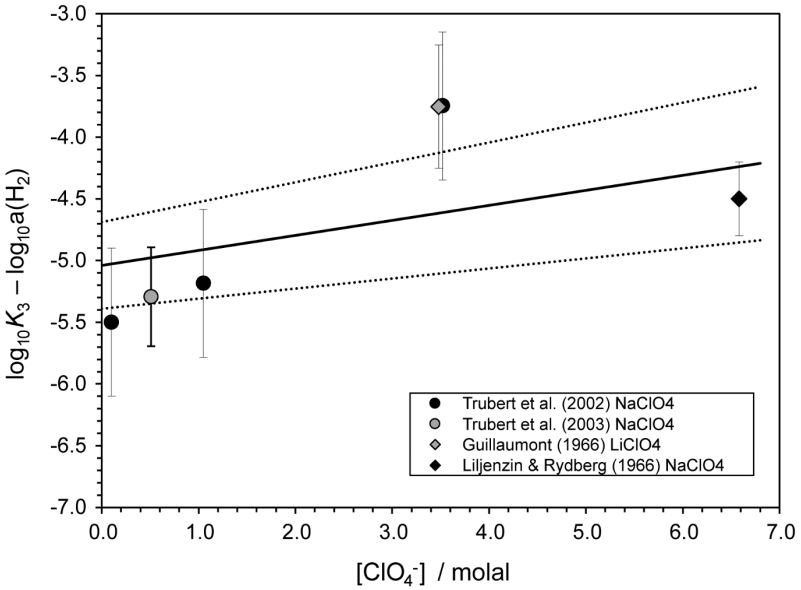

Fig. 22-4: Dependence of the equilibrium $PaO(OH)_2^+ + H_2O(l) \rightleftharpoons PaO(OH)_3(aq) + H^+$ on ionic strength in perchlorate media

The solid line is obtained using the derived SIT interaction coefficient and stability constant at zero ionic strength. The dotted lines represent the 95% uncertainty range extrapolated from zero ionic strength to higher perchlorate concentrations.

The results of the SIT regressions (Figs. 22-3 and 22-4) are

$PaO(OH)^{2+} + H_2O(l) \rightleftharpoons PaO(OH)_2^+ + H^+$

$\log_{10}{}^{*}K_2° \text{ (298.15 K)} = -1.26 \pm 0.14$

$\Delta\varepsilon = (0.01 \pm 0.06)\ kg \cdot mol^{-1}$

$PaO(OH)_2^+ + H_2O(l) \rightleftharpoons PaO(OH)_3(aq) + H^+$

$\log_{10}{}^{*}K_3° \text{ (298.15 K)} = -5.04 \pm 0.35$

$\Delta\varepsilon = -(0.12 \pm 0.08)\ kg \cdot mol^{-1}$

These values are included in TDB 2020.

Considering $\varepsilon(H^+, ClO_4^-) = (0.14 \pm 0.02)\ kg \cdot mol^{-1}$ (Lemire et al. 2013), and using the estimation method (described in Section 1.5.3) for $\varepsilon(PaO(OH)_3(aq), NaClO_4) = (0.0 \pm 0.1)\ kg \cdot mol^{-1}$ (Tab. 22-2), this review derives from the experimental $\Delta\varepsilon$ values

$\varepsilon(PaO(OH)_2^+, ClO_4^-) = (0.26 \pm 0.13)$ kg · mol^{-1}

$\varepsilon(PaO(OH)^{2+}, ClO_4^-) = (0.39 \pm 0.14)$ kg · mol^{-1}

These values are included in TDB 2020 as well as the estimates

$\varepsilon(PaO(OH)^{2+}, Cl^-) = (0.15 \pm 0.10)$ kg · mol^{-1}

$\varepsilon(PaO(OH)_2^+, Cl^-) = (0.05 \pm 0.10)$ kg · mol^{-1}

$\varepsilon(PaO(OH)_3(aq), NaCl) = (0.0 \pm 0.1)$ kg · mol^{-1}

$PaO(OH)_4^-$

Fourest et al. (2004) studied the hydrolysis of Pa(V) by capillary diffusion. They proposed the formation of $Pa(OH)_6^-$ (or $PaO(OH)_4^-$) in alkaline solutions. The stability constant obtained at 25 °C and in 0.5 M $NaClO_4$ is reported as

$PaO(OH)_3(aq) + H_2O(l) \rightleftharpoons PaO(OH)_4^- + H^+$

$\log_{10}{}^*K_4$ (298.15 K) = -9.13 ± 0.1

Note that the value -9.03 ± 0.1 given in the abstract of Fourest et al. (2004) and cited by Brown & Ekberg (2016) most probably is a typo error. The value -9.13 ± 0.1 is given in Tab. IV and in the text of Fourest et al. (2004), and is taken in this review.

Considering $\varepsilon(H^+, ClO_4^-) = (0.14 \pm 0.02)$ kg · mol^{-1} (Lemire et al. 2013) and using the estimation method (described in Section 1.5.3) for $\varepsilon(PaO(OH)_3(aq), NaClO_4) = (0.0 \pm 0.1)$ kg · mol^{-1} and $\varepsilon(PaO(OH)_4^-, Na^+) = -(0.05 \pm 0.1)$ kg · mol^{-1} (Tab. 22-2), the value $\log_{10}{}^*K_4$ (298.15 K) = -9.13 ± 0.1 has been extrapolated to I = 0

$\log_{10}{}^*K_4°$ (298.15 K) = -9.4 ± 0.2

The uncertainty has been doubled to represent 95% probability. This value is included in TDB 2020.

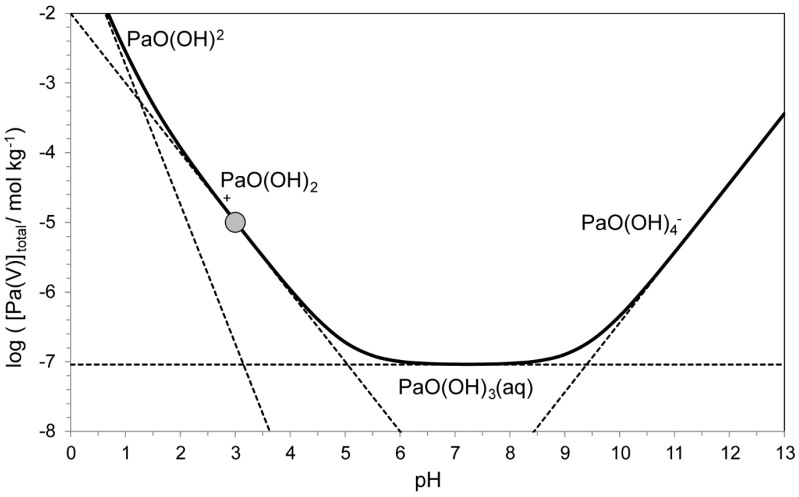

Fig. 22-5: Dependence of total Pa(V) solubility versus pH at zero ionic strength (solid line)

The dotted lines represent the concentrations of the indicated hydrolysis species, calculated using the selected hydrolysis stability constants and the estimated solubility product of Baes & Mesmer (1986). The symbol represents the maximum value of this estimate.

22.4.2.2 Protactinium(V) (hydr)oxide compounds

The solubility of Pa(V) (hydr)oxide has never been measured. The only indications about the order of magnitude of Pa(V) solubility can be derived from the review of protactinium chemistry by Guillaumont et al. (1968). They report that for [Pa(V)] < 10^{-5} M irreversible hydrolysis is far advanced in 15 hours at pH 3 or in only 1 hour at pH 5. They further note that below pH 3 the solubility of Pa(V) in perchlorate appears to be about 10^{-5} M.

Baes & Mesmer (1986) concluded that, if the solid phase is an active Pa_2O_5(act), then they could use the latter information to estimate the upper limit of the solubility product

$$½\ Pa_2O_5(act) + H^+ \rightleftharpoons PaO_2^+ + ½\ H_2O(l)$$

which is equivalent to

$$½\ Pa_2O_5(act) + H^+ + ½\ H_2O(l) \rightleftharpoons PaO(OH)_2^+$$

$$log_{10}{}^*K_s\ (298.15\ K) \leq -2$$

This value is included in TDB 2020 as supplemental datum.

Using the hydrolysis constants selected in Section 4.2.1 and the estimated upper limit of the solubility product, the total solubility of Pa(V) versus pH exhibits the typical "bathtub" shape (Fig. 22-5). However, while the form of this "bathtub" is fairly well established by the hydrolysis constants, its position on the log$[Pa(V)]_{total}$ scale is "fixed" by just one point, the estimate by Baes & Mesmer (1986), represented by the symbol in Fig. 22-5. There are no quantitative solubility data to corroborate this estimate.

22.4.3 Protactinium(V) fluoride complexes

Myasoedov et al. (2006) report that a great many complexes have been proposed to explain the behaviour of Pa(V) in aqueous HF.

Bukhsh et al. (1966) report that ion-exchange and conductometric titration experiments suggest the existence of the PaF_8^{3-} anion. Using an electrochemical method, at 25 °C and 1.0 M perchlorate, a preliminary set of values for the successive complexing constants $\log_{10}K_{1\text{-}8}$ for the protactinium fluoro complexes has been obtained: $\log_{10}K_1 = 5.4 \pm 0.5$, $\log_{10}K_2 = 5.0 \pm 0.5$, $\log_{10}K_3 = 4.9 \pm 0.4$, $\log_{10}K_4 = 4.8 \pm 0.3$, $\log_{10}K_5 = 4.5 \pm 0.2$, $\log_{10}K_6 = 4.4 \pm 0.2$, $\log_{10}K_7 = 3.7 \pm 0.2$, $\log_{10}K_8 = 1.7 \pm 0.5$.

However, reaction stoichiometries for these complexes are not given and hence, the meaning of the above values remains unclear. Bukhsh et al. (1966) only remark that measurements at different acidities justified the assumption that hydroxo complexes are not important, at least for coordination numbers ≥ 3.

Guillaumont (1966) obtained from his solvent extraction studies, at 25 °C and 3.0 M $LiClO_4$, for $[H^+] = 1 – 3$ M and $[F^-] < 10^{-6}$ M

$$PaO(OH)^{2+} + HF(aq) \rightleftharpoons PaOF^{2+} + H_2O(l)$$

$$\log_{10}\beta_1\ (298.15\ K) = 3.56$$

$$PaO(OH)^{2+} + 2HF(aq) \rightleftharpoons PaOF_2^{+} + H^+ + H_2O(l)$$

$$\log_{10}\beta_2\ (298.15\ K) = 7.65$$

$$PaO(OH)^{2+} + 3HF(aq) \rightleftharpoons PaOF_3(aq) + 2H^+ + H_2O(l)$$

$$\log_{10}\beta_3\ (298.15\ K) = 10.91$$

Considering $\varepsilon(H^+, ClO_4^-) = (0.14 \pm 0.02)$ kg · mol^{-1} (Lemire et al. 2013) and $\varepsilon(PaO(OH)^{2+}, ClO_4^-) = (0.39 \pm 0.14)$ kg · mol^{-1} (see Section 22.4.2.1) and using the estimation method (described in Section 1.5.3) for $\varepsilon(HF(aq), LiClO_4) = (0.0 \pm 0.1)$ kg · mol^{-1}, $\varepsilon(PaOF_3(aq), LiClO_4) = (0.0 \pm 0.1)$ kg · mol^{-1}, $\varepsilon(PaOF_2^+, ClO_4^-) = (0.2 \pm 0.1)$ kg · mol^{-1}, and $\varepsilon(PaOF^{2+}, ClO_4^-) = (0.4 \pm 0.1)$ kg · mol^{-1}, (Tab. 22-2), the values of Guillaumont (1966) have been extrapolated to I = 0

$$\log_{10}\beta_1^\circ\ (298.15\ K) = 3.6 \pm 0.7$$

$$\Delta\varepsilon = (0.01 \pm 0.20)\ \text{kg} \cdot \text{mol}^{-1}$$

$$\log_{10}\beta_2^\circ\ (298.15\ K) = 8.0 \pm 0.8$$

$$\Delta\varepsilon = -(0.05 \pm 0.22)\ \text{kg} \cdot \text{mol}^{-1}$$

$$\log_{10}\beta_3^\circ\ (298.15\ K) = 11.0 \pm 0.9$$

$$\Delta\varepsilon = -(0.11 \pm 0.25)\ \text{kg} \cdot \text{mol}^{-1}$$

where the uncertainties are estimated solely as the effect of extrapolating the values from $I_m = 3.48$ mol · kg^{-1} to zero, i.e., as $(\pm\Delta\varepsilon) \cdot I_m$.

Kolarich et al. (1967) also used a solvent extraction method at 25 °C and an ionic strength and acidity of 1.0 M $HClO_4$. They report:

$Pa^{5+} + HF(aq) \rightleftharpoons PaF^{4+} + H^+$

$\log_{10}K_1$ (298.15 K) = 3.95

$PaF^{4+} + HF(aq) \rightleftharpoons PaF_2^{3+} + H^+$

$\log_{10}K_2$ (298.15 K) = 3.48

$PaF_2^{3+} + HF(aq) \rightleftharpoons PaF_3^{2+} + H^+$

$\log_{10}K_3$ (298.15 K) = 3.04

We certainly do not have Pa^{5+} at 1.0 M $HClO_4$, but assuming a more realistic reaction stoichiometry involving $PaO(OH)^{2+}$, and $PaOF_x$ species, as Guillaumont (1966) proposed, the values reported by Kolarich et al. (1967), extrapolated to zero ionic strength,

$\log_{10}\beta_1^\circ$ (298.15 K) = 4.0 ± 0.2

$\log_{10}\beta_2^\circ$ (298.15 K) = 7.8 ± 0.2

$\log_{10}\beta_3^\circ$ (298.15 K) = 10.8 ± 0.3

are at variance from Guillaumont (1966) only by 0.2 – 0.4 log-units.

Hence, the averages of the values reported by Guillaumont (1966) and Kolarich et al. (1967)

$\log_{10}\beta_1^\circ$ (298.15 K) = 3.8 ± 0.5

$\log_{10}\beta_2^\circ$ (298.15 K) = 7.9 ± 0.5

$\log_{10}\beta_3^\circ$ (298.15 K) = 10.9 ± 0.5

are included in TDB 2020 as supplemental data, with uncertainties estimated in this review, as well as the estimates

$\varepsilon(PaOF^{2+}, Cl^-) = (0.15 \pm 0.10)$ kg · mol^{-1}

$\varepsilon(PaOF_2^{+}, Cl^-) = (0.05 \pm 0.10)$ kg · mol^{-1}

$\varepsilon(PaOF_3(aq), NaCl) = (0.0 \pm 0.1)$ kg · mol^{-1}

$\varepsilon(PaOF_3(aq), NaClO_4) = (0.0 \pm 0.1)$ kg · mol^{-1}

22.4.4 Protactinium(V) chloride complexes

Myasoedov et al. (2006) report that solutions of Pa(V) in hydrochloric acid are generally unstable with respect to precipitation of hydroxide when [Pa] ≥ 10^{-3} M, although complete precipitation may take as long as several weeks. If the freshly precipitated hydroxide is dissolved in 12 M HCl and then diluted to [Pa] ≤ 10^{-4} M and 1 M < [HCl] < 3 M, the solution is reasonably stable and will then contain a mixture of monomeric chloro complexes in thermodynamic equilibrium.

Myasoedov et al. (2006) further state that it is generally agreed that, for [HCl] < 1 M and [Pa] < 10^{-5} M, the species present are the same as those described above (see Section 22.4.2.1) for perchloric acid media, i.e., Pa(V) hydrolysis species, while, for [HCl] ≈ 3 M, the predominant species is $PaOOHCl^+$. Many complexes have been proposed to explain the solvent extraction and ion-exchange behaviour of Pa(V) at higher acidities.

In summary, under environmental conditions, pH > 0 and [Pa] < 10^{-5} M, Pa(V) chloro complexes are completely unimportant and none have been included in TDB 2020.

22.4.5 Protactinium(V) phosphate complexes

Le Cloarec et al. (1973) and Le Cloarec & Muxart (1973) studied the complexation of Pa(V) with phosphate and sulphate by solvent extraction at 25 ± 0.1 °C, 1 M $LiClO_4$ and [H_3PO_4] ≤ 0.5 M. They interpreted their experimental data with phosphate in terms of the species $PaO(OH)(H_2PO_4)^+$, $PaO(H_3PO_4)(H_2PO_4)^{2+}$, $PaO(H_2PO_4)_2^+$ and $PaO(H_2PO_4)_3(aq)$ and obtained

$$PaO(OH)^{2+} + H_3PO_4(aq) \rightleftharpoons PaO(OH)(H_2PO_4)^+ + H^+$$

$\log_{10}K$ (298.15 K) = 1.75

$$PaO(OH)^{2+} + 2H_3PO_4(aq) \rightleftharpoons PaO(H_3PO_4)(H_2PO_4)^{2+} + H_2O(l)$$

$\log_{10}K$ (298.15 K) = 3.04

$$PaO(OH)^{2+} + 2H_3PO_4(aq) \rightleftharpoons PaO(H_2PO_4)_2^+ + H_2O(l) + H^+$$

$\log_{10}K$ (298.15 K) = 1.91

$$PaO(OH)^{2+} + 3H_3PO_4(aq) \rightleftharpoons PaO(H_2PO_4)_3(aq) + 2H_2O(l) + 2H^+$$

$\log_{10}K$ (298.15 K) = 4.07

However, according to Fig. 3 in Le Cloarec et al. (1973), all these complexes contribute to the Pa(V) speciation at [H^+] = 1 M only at [H_3PO_4] > 10^{-3} M, while at [H^+] = 0.1 M the species $PaO(OH)(H_2PO_4)^+$ predominates at [H_3PO_4] = 10^{-2} M and $PaO(H_2PO_4)_3(aq)$ at [H_3PO_4] > 0.1 M.

Hence, at the low phosphate concentrations encountered in environmental systems none of the above proposed complexes may play any role in Pa(V) speciation. Furthermore, no independent information is available supporting the results of Le Cloarec et al. (1973) and Le Cloarec & Muxart (1973), which consequently are not included in TDB 2020.

22.4.6 Protactinium(V) sulphate complexes

Di Giandomenico et al. (2007) investigated protactinium complexation with sulphate ions with the element at trace scale (ca. 10^{-12} M) using a solvent extraction technique. Extraction experiments were conducted using the chelating agent thenoyltrifluoroacetone (TTA) in toluene. The temperature was maintained at 25 °C, while the ionic strength was varying from 0.8 – 2.9 mol · kg^{-1} $NaClO_4$.

As discussed above (see Section 22.4.2.1) in non-complexing medium, Pa(V) exists under the forms $PaO(OH)^{2+}$ and $PaO(OH)_2^{+}$, depending upon pH values. Concerning sulphate/sulphuric media three successive complexes are reported in the literature depending upon the sulphate concentration: $PaOSO_4^{+}$, $PaO(SO_4)_2^{-}$ and $PaO(SO_4)_3^{3-}$ (Le Cloarec et al. 1973).

In a recent work (Le Naour et al. 2005), it has been demonstrated through XAS measurements that the mono-oxo bond is still present in the complex $PaO(SO_4)_3^{3-}$ contrary to other formulations in the literature. Thus, Di Giandomenico et al. (2007) formulated chemical equilibria according to:

$$PaO(OH)^{2+} + SO_4^{2-} + H^{+} \rightleftharpoons PaOSO_4^{+} + H_2O(l)$$

$$PaO(OH)^{2+} + 2SO_4^{2-} + H^{+} \rightleftharpoons PaO(SO_4)_2^{-} + H_2O(l)$$

$$PaO(OH)^{2+} + 3SO_4^{2-} + H^{+} \rightleftharpoons PaO(SO_4)_3^{3-} + H_2O(l)$$

From analyses of their experimental data Di Giandomenico et al. (2007) obtained

$$\log_{10}\beta_1^{\circ}\ (298.15\ K) = 3.89 \pm 0.18$$

$$\Delta\varepsilon = (0.18 \pm 0.15)\ kg \cdot mol^{-1}$$

$$\log_{10}\beta_2^{\circ}\ (298.15\ K) = 7.00 \pm 0.20$$

$$\Delta\varepsilon = -(0.07 \pm 0.09)\ kg \cdot mol^{-1}$$

$$\log_{10}\beta_3^{\circ}\ (298.15\ K) = 8.59 \pm 0.23$$

$$\Delta\varepsilon = -(0.14 \pm 0.09)\ kg \cdot mol^{-1}$$

In the above equations the unknown quantities are $\varepsilon(PaOSO_4^{+}, ClO_4^{-})$, $\varepsilon(PaO(SO_4)_2^{-}, Na^{+})$ and $\varepsilon(PaO(SO_4)_3^{3-}, Na^{+})$. Using $\varepsilon(SO_4^{2-}, Na^{+}) = -(0.12 \pm 0.06)$ kg · mol^{-1} and $\varepsilon(H^{+}, ClO_4^{-}) = (0.14 \pm 0.02)$ kg · mol^{-1} (Lemire et al. 2013), and $\varepsilon(PaO(OH)^{2+}, ClO_4^{-}) = (0.39 \pm 0.14)$ kg · mol^{-1} derived in this review (see Section 22.4.2.1) the following set of values is obtained:

$$\varepsilon(PaOSO_4^{+}, ClO_4^{-}) = (0.59 \pm 0.21)\ kg \cdot mol^{-1}$$

$$\varepsilon(PaO(SO_4)_2^{-}, Na^{+}) = (0.22 \pm 0.19)\ kg \cdot mol^{-1}$$

$$\varepsilon(PaO(SO_4)_3^{3-}, Na^{+}) = (0.03 \pm 0.20)\ kg \cdot mol^{-1}$$

All these values are included in TDB 2020 as well as the estimate

$$\varepsilon(PaOSO_4^+, Cl^-) = (0.05 \pm 0.10)\ kg \cdot mol^{-1}$$

22.5 Selected protactinium data

Tab. 22-1: Selected protactinium data

Supplemental data are in italics.

Name	**$\Delta_f G_m°$** [kJ · mol^{-1}]	**$\Delta_f H_m°$** [kJ · mol^{-1}]	**$S_m°$** [J · K^{-1} · mol^{-1}]	**$C_{p,m}°$** [J · K^{-1} · mol^{-1}]	**Species**
Pa(cr)	0.0	0.0	51.6 ± 0.8	28.2 ± 0.4	Pa(cr)
Pa+4	-565.6 ± 18.6	-621.4 ± 14.3	-397 ± 40		Pa^{4+}
PaO(OH)+2	-1'051.7 ± 21.9	-1'115 ± 21	-21 ± 21		$PaO(OH)^{2+}$

Name	**Redox**	**$\log_{10}\beta°$**	**$\Delta\varepsilon$** [kg · mol^{-1}]	**$\Delta_r H_m°$** [kJ · mol^{-1}]	**T-range** [°C]	**Reaction**
PaOH+3	IV	*1.3 ± 0.5*	-	-		*$Pa^{4+} + H_2O(l) \rightleftharpoons PaOH^{3+} + H^+$*
Pa(OH)2+2	IV	*1.9 ± 0.5*	-	-		*$Pa^{4+} + 2H_2O(l) \rightleftharpoons Pa(OH)_2^{2+} + 2H^+$*
Pa(OH)3+	IV	*0.9 ± 0.5*	-	-		*$Pa^{4+} + 3H_2O(l) \rightleftharpoons Pa(OH)_3^{+} + 3H^+$*
PaO(OH)+2	IV/V	85.16 ± 3.84	-	-		$Pa^{4+} + 1.5H_2g + O_2g \rightleftharpoons PaO(OH)^{2+} + 2H^+$
PaO+3	V	0.04 ± 0.36	-	-		$PaO(OH)^{2+} + H^+ \rightleftharpoons PaO^{3+} + H_2O(l)$
PaO(OH)2+	V	-1.26 ± 0.14	0.01 ± 0.06	4.7 ± 2.5	10 – 60	$PaO(OH)^{2+} + H_2O(l) \rightleftharpoons PaO(OH)_2^{+} + H^+$
PaO(OH)3(aq)	V	-5.04 ± 0.35	-0.12 ± 0.08	57 ± 35	10 – 60	$PaO(OH)_2^{+} + H_2O(l) \rightleftharpoons PaO(OH)_3(aq) + H^+$
PaO(OH)4-	V	-9.4 ± 0.2	-	-		$PaO(OH)_3(aq) + H_2O(l) \rightleftharpoons PaO(OH)_4^{-} + H^+$
PaOF+2	V	*3.8 ± 0.5*	-	-		*$PaO(OH)^{2+} + HF(aq) \rightleftharpoons PaOF^{2+} + H_2O(l)$*
PaOF2+	V	*7.9 ± 0.5*	-	-		*$PaO(OH)^{2+} + 2HF(aq) \rightleftharpoons PaOF_2^{+} + H^+ + H_2O(l)$*
PaOF3(aq)	V	*10.9 ± 0.5*	-	-		*$PaO(OH)^{2+} + 3HF(aq) \rightleftharpoons PaOF_3(aq) + 2H^+ + H_2O(l)$*
PaOSO4+	V	3.89 ± 0.18	0.18 ± 0.15	-		$PaO(OH)^{2+} + SO_4^{2-} + H^+ \rightleftharpoons PaOSO_4^{+} + H_2O(l)$
PaO(SO4)2-	V	7.00 ± 0.20	-0.07 ± 0.09	-		$PaO(OH)^{2+} + 2SO_4^{2-} + H^+ \rightleftharpoons PaO(SO_4)_2^{-} + H_2O(l)$
PaO(SO4)3-3	V	8.59 ± 0.23	-0.14 ± 0.09	-		$PaO(OH)^{2+} + 3SO_4^{2-} + H^+ \rightleftharpoons PaO(SO_4)_3^{3-} + H_2O(l)$

Name	**$\log_{10}K_{s,0}°$**	**$\Delta_r H_m°$** [kJ · mol^{-1}]	**Reaction**
Pa2O5(act)	*≤ -2*	-	*$½\ Pa_2O_5(act) + H^+ + ½\ H_2O(l) \rightleftharpoons PaO(OH)_2^{+}$*

Tab. 22-2: Selected SIT ion interaction coefficients $\varepsilon_{j,k}$ [kg · mol^{-1}] for protactinium species

Data in bold face are taken from Lemire et al. (2013). Data in normal face are derived or estimated in this review. Data estimated according to charge correlations and taken from Tab. 1-7 are shaded Supplemental data are in italics.

j k → ↓	**Cl^-** $\varepsilon_{j,k}$ [kg · mol^{-1}]	**ClO_4^-** $\varepsilon_{j,k}$ [kg · mol^{-1}]	**Na^+** $\varepsilon_{j,k}$ [kg · mol^{-1}]	**$Na^+ + Cl^-$** $\varepsilon_{j,k}$ [kg · mol^{-1}]	**$Na^+ + ClO_4^-$** $\varepsilon_{j,k}$ [kg · mol^{-1}]
H+	**0.12 ± 0.01**	**0.14 ± 0.02**	0	0	0
HF(aq)	0	0	0	0.0 ± 0.1	0.0 ± 0.1
SO4-2	0	0	**-0.12 ± 0.06**	0	0
Pa+4	0.35 ± 0.1	0.8 ± 0.1	0	0	0
PaOH+3	*0.25 ± 0.1*	*0.6 ± 0.1*	*0*	*0*	*0*
Pa(OH)2+2	*0.15 ± 0.1*	*0.4 ± 0.1*	*0*	*0*	*0*
Pa(OH)3+	*0.05 ± 0.1*	*0.2 ± 0.1*	*0*	*0*	*0*
PaO+3	0.25 ± 0.1	0.6 ± 0.1	0	0	0
PaO(OH)+2	0.15 ± 0.1	0.39 ± 0.14	0	0	0
PaO(OH)2+	0.05 ± 0.1	0.26 ± 0.13	0	0	0
PaO(OH)3(aq)	0	0	0	0.0 ± 0.1	0.0 ± 0.1
PaO(OH)4-	0	0	-0.05 ± 0.1	0	0
PaOF+2	0.15 ± 0.1	*0.4 ± 0.1*	*0*	*0*	*0*
PaOF2+	0.05 ± 0.1	*0.2 ± 0.1*	*0*	*0*	*0*
PaOF3(aq)	*0*	*0*	*0*	*0.0 ± 0.1*	*0.0 ± 0.1*
PaOSO4+	0.05 ± 0.1	0.59 ± 0.21	0	0	0
PaO(SO4)2-	0	0	0.22 ± 0.19	0	0
PaO(SO4)3-3	0	0	0.03 ± 0.20	0	0

22.6 References

Baes, Jr., C.F. & Mesmer, R.E. (1986): The Hydrolysis of Cations. Reprint Edition, Krieger Publishing Company, Malabar, Florida, 490 pp.

Brown, P.L. & Ekberg, C. (2016): Hydrolysis of Metal Ions. Wiley-VCH Verlag GmbH & Co. KGaA, Weinheim, Germany, 917 pp.

Bukhsh, M.N., Flegenheimer, J., Hall, F.M., Maddock, A.G., & Ferreira De Miranda, C. (1966): The chemistry of protactinium – VII. The fluoro-complexes. J. Inorg. Nucl. Chem., 28, 421-431.

Di Giandomenico, M.V., Trubert, D. & Le Naour, C. (2007): Sulphate complexation of protactinium(V) at 25 °C. Radiochim. Acta, 95, 617-623.

Fourest, B., Perrone, J., Tarapcik, P. & Giffaut, E. (2004): The hydrolysis of protactinium(V) studied by capillary diffusion. J. Sol. Chem., 33, 957-973.

Grenthe, I., Fuger, J., Konings, R.J.M., Lemire, R.J., Muller, A.B., Nguyen-Trung, C. & Wanner, H. (1992): Chemical Thermodynamics of Uranium. Chemical Thermodynamics, Vol. 1. North-Holland, Amsterdam, 715 pp.

Guillaumont, R. (1966): Contribution à l'étude des espèces ioniques du protactinium en solution aqueuse. Ph.D. Thesis, Faculté des sciences, Université de Paris, France, No. 5528 (as cited by Trubert et al. 2002).

Guillaumont, R. (1968): Étude des espèces ioniques du protactinium en solution aqueuse V. Hydrolyse et polymerisation du protactinium tétravalent. Bull. Soc. Chim. France, 162-168.

Guillaumont, R., Bouissières, G. & Muxart, R. (1968): Chimie du protactinium. I. Solutions aqueuses de protactinium penta- et tétravalent. Actinides Reviews, 1, 135-163.

Kolarich, R.T., Ryan, V.A. & Schuman, R.P. (1967): Association constants of anionic-protactinium (V) complexes. J. Inorg. Nucl. Chem., 29, 783-797.

Konings, R.J.M., Morss, L.R. & Fuger, J. (2006): Thermodynamic Properties of Actinides and Actinide Compounds. *In:* Morss, L.R., Edelstein, N.M., Fuger, J. & Katz, J.J. (Eds.): The Chemistry of the Actinide and Transactinide Elements, Volume 4, 3$^{r\,d}$ Edition, Springer, The Netherlands, p. 2113-2224.

Le Cloarec, M.F., Guillomont, R., Miranda, C.F. & Franck, J.C. (1973): Etude des complexes de protactinium pentavalent en milieu sulfurique, phosphorique et sulfophosphorique. Radiochim. Acta, 20, 1-6.

Le Cloarec, M.F. & Muxart, R. (1973): Spectres d'absorption du protactinium pentavalent en solution phosphorique. Radiochim. Acta, 20, 7-10.

Lemire, R.J., Berner, U., Musikas, C., Palmer, D.A., Taylor, P. & Tochiyama, O. (2013): Chemical Thermodynamics of Iron, Part 1. Chemical Thermodynamics, Vol. 13a. OECD Publications, Paris, France, 1082 pp.

Le Naour, C., Trubert, D. & Jaussaud, C. (2003): Hydrolysis of protactinium(V). II. Equilibrium constants at 40 and 60 °C: A solvent extraction study with TTA in the aqueous system Pa(V) / H_2O / H^+ / ClO_4^-. J. Sol. Chem., 32, 489-504.

Le Naour, C., Trubert, D., Di Giandomenico, M.V., Fillaux, C., Den Auwer, C., Moisy, P. & Hennig, C. (2005): First structural characterization of a protactinium(V) single oxo bond in aqueous media. Inorg. Chem., 44, 9542-9546.

Liljenzin, J.O. & Rydberg, J. (1966): Complex formation between protactinium and acetylacetone. In: Physicochemie du protactinium, Orsay, 255-271 (as cited by Brown & Ekberg 2016).

Lundqvist, R. (1974): Aqueous chemistry of protactinium(IV). I. Stability constants for Pa(IV) – acetylacetone complexes. Acta Chem. Scand. A, 28, 243-247.

Myasoedov, B.F., Kirby, H.W. & Tananaev, I.G. (2006): Protactinium. *In:* Morss, L.R., Edelstein, N.M., Fuger, J. & Katz, J.J. (Eds.): The Chemistry of the Actinide and Transactinide Elements, Volume 1, 3rd Edition, Springer, The Netherlands, p. 161-252.

Trubert, D., La Naour, C. & Jaussaud, C. (2002): Hydrolysis of protactinium(V). I. Equilibrium constants at 25 °C: A solvent extraction study with TTA in the aqueous system Pa(V) / H_2O / H^+ / ClO_4^-. J. Sol. Chem., 31, 261-277.

Trubert, D., La Naour, C., Jaussaud, C. & Mrad, O. (2003): Hydrolysis of protactinium(V). III. Determination of standard thermodynamic data. J. Sol. Chem., 32, 505-517.

Vitorge, P., Phrommavanh, V., Siboulet, B., You, D., Vercouter, T., Descostes, M., Marsden, C.J., Beaucaire, C. & Gaudet, J.P. (2007): Estimating the stabilities of actinide aqueous species. Influence of sulfoxy-anions on uranium(IV) geochemistry and discussion of Pa(V) first hydrolysis. C. R. Chimie, 10, 978-993.

23 Rare earth elements

23.1 Samarium

23.1.1 Introduction

Sm has numerous isotopes, ranging from ^{128}Sm to ^{165}Sm (Audi et al. 2003), of which five are stable: ^{144}Sm, ^{149}Sm, ^{150}Sm, ^{152}Sm, and ^{154}Sm. Five radioactive isotopes of Sm are of concern for the planned deep underground repositories for radioactive waste in Switzerland, ^{145}Sm (activation and spallation product, half-life: 340 ± 3 days), ^{146}Sm (activation and spallation product, half-life: $1.00 \pm 0.08 \cdot 10^8$ years), ^{147}Sm (fission product, half-life: $1.06 \pm 0.02 \cdot 10^{11}$ years), ^{148}Sm (fission product, half-life: $8 \pm 2 \cdot 10^{15}$ years), and ^{151}Sm (fission product, half-life: 90 ± 6 years) (Hummel 2018). Of these Sm isotopes, only ^{151}Sm, contained in SF and HLW, is dose-relevant (Hummel 2018).

Sm has not been included in the precursors of TDB 2020 (Nagra/PSI TDB 05/92: Pearson & Berner 1991, Pearson et al. 1992; PSI/Nagra TDB 01/01: Hummel et al. 2002; PSI/Nagra TDB 12/07: Thoenen et al. 2014) and is therefore a new addition to the database.

The thermodynamic data for Sm selected in this review for TDB 2020 are listed in Tab. 23.1.10-1.

NEA chose the specific ion interaction theory (SIT) for the extrapolation of experimental data to zero ionic strength, see, e.g., Grenthe et al. (1997), an approach which is also adopted for TDB 2020 (as has been for all its predecessors). When referring to ion interaction coefficients recommended by NEA, we took those from Tab. B.3 in Lemire et al. (2013).

Due to a lack of experimental data, many ion interaction coefficients for cationic Sm species with ClO_4^- and Cl^-, and for anionic Sm species with Na^+ are unknown. We filled these gaps by applying the estimation method described in Section 1.5.3, which is based on a statistical analysis of published SIT ion interaction coefficients, and which allows the estimation of such coefficients for the interaction of cations with Cl^- and ClO_4^-, and for the interaction of anions with Na^+ from the charge of the considered cations or anions. Ion interaction coefficients of neutral samarium species with background electrolytes were assumed to be zero.

The ion interaction coefficients for samarium species selected for TDB 2020 are listed in Tab. 23.1.10-2.

23.1.1.1 Previous reviews of low-temperature thermodynamic data for rare earth elements

Wood (1990) reviewed the available low-temperature thermodynamic data for inorganic complexes of the REE and yttrium, considering hydroxide, fluoride, chloride, sulphate, nitrate, phosphate, and carbonate as ligands. Since the trivalent REE ions are classified as Pearson hard acids, they form complexes preferentially with hard ligands containing highly electronegative donor atoms such as oxygen and fluorine, e.g. OH^-, F^-, SO_4^{2-}, PO_4^{3-}, and CO_3^{2-}, while complexes with borderline ligands, such as Cl^- or NO_3^- are very weak, and complexes with the very soft HS^- or CN^- ligands extremely weak or unknown in aqueous solution (Wood 1990). For Sm(III), Wood (1990) could only recommend stability constants for $SmOH^+$, SmF^{2+}, and $SmCl^{2+}$. Based on a broader dataset for Eu(III), he calculated the europium species distribution as a function of pH

for several model groundwaters with varying amounts of fluoride, sulphate, phosphate, and carbonate. The general picture emerging from these calculations was that in all cases $EuCO_3^+$ turned out to be the most important species at pH between about 6.5 and 9.5, while $Eu(CO_3)_2^-$ became more important at pH above about 9.5. Fluoride, sulphate, and phosphate species were only important at pH < 7. Eu hydroxides were in all cases only minor species, but Wood (1990) pointed out that, at that time, the hydrolysis constants for Eu (and all other REE elements) were only poorly known.

Millero (1992) compiled stability constants for REE complexes with hydroxide, fluoride, chloride, sulphate, phosphate, and carbonate determined in $NaClO_4$ at room temperature and various ionic strengths and extrapolated the conditional stability constants to infinite dilution using the Pitzer interaction model. In the case of samarium, he provided stability constants for $SmOH^{2+}$, SmF^{2+}, $SmCl^{2+}$, $SmSO_4^+$, $SmNO_3^{2+}$, $SmHPO_4^+$, SmH_2PO4^{2+}, $Sm(HPO4)_2^-$, $SmCO_3^+$, $SmHCO_3^{2+}$, and $Sm(CO_3)_2^-$. Since Millero (1992) reported only a part of the original data and only graphically in figures, it is not possible to re-analyse his data in terms of the SIT.

Haas et al. (1995) compiled stability constants for REE complexes with hydroxide, fluoride, chloride, sulphate, nitrate, phosphate, and carbonate at 25 °C and 1 bar. They used estimation methods to derive missing stability constants of higher-order hydroxide, fluoride, and chloride complexes and applied correlation algorithms for estimating HKF parameters for the extrapolation of standard partial molal properties of REE complexes (and thus their stability constants) to elevated temperatures (0 – 1'000 °C) and pressures (1 – 5'000 bars). With respect to Sm, they provided standard partial molal properties and HKF parameters for $SmOH^{2+}$, SmO^+ (or $Sm(OH)_2^+$), $SmO_2H(aq)$ (or $Sm(OH)_3(aq)$), SmO_2^- (or $Sm(OH)_4^-$), SmF^{2+}, SmF_2^+, $SmF_3(aq)$, SmF_4^-, $SmCl^{2+}$, $SmCl_2^+$, $SmCl_3(aq)$, $SmCl_4^-$, $SmSO_4^+$, $SmNO_3^{2+}$, $SmH_2PO_4^{2+}$, $SmHCO_3^{2+}$, and $SmCO_3^+$. Based on their data, Haas et al. (1995) carried out speciation calculations of idealized 1 molal chloride solutions with minor amounts of fluoride, sulphate, and carbonate at elevated temperature and pressure (300, 500, and 700 °C and P_{sat}) and observed that in general REE chloride complexes are predominant under acidic conditions, fluoride complexes under neutral conditions, and hydroxide complexes under basic conditions. Under these conditions, sulphate and carbonate complexes are insignificant, but may account for much larger fractions of REE in solution at lower temperatures and pressures and may even become predominant in some cases.

Migdisov et al. (2016) reviewed experimental data of REE aqueous species obtained under hydrothermal conditions and derived standard partial molal properties and HKF equation of state parameters of REE complexes with fluoride and chloride. Due to the limited data available for hydroxide and sulphate complexes, which would not allow the derivation of HKF parameters, Migdisov et al. (2016) carried out provisional fits of the available data to the Bryzgalin-Ryzhenko equation of state. Since no hydrothermal data were available for carbonate and phosphate complexes, Migdisov et al. (2016) were not able to provide a preferred dataset for these species. Thus, in the case of samarium, these authors presented HKF parameters for SmF^{2+}, $SmCl^{2+}$, and $SmCl_2^+$, as well as Bryzgalin-Ryzhenko parameters for $SmSO_4^+$, and $Sm(SO_4)_2^-$, but none for any Sm hydroxide complexes.

Migdisov et al. (2016) also reviewed calorimetric and solubility data of solid REE oxides, hydroxides, fluorides, chlorides, phosphates, and fluorocarbonates applicable to elevated temperatures and pressures and selected data for the following Sm(III) solids: $Sm_2O_3(cr)$, $SmF_3(cr)$, $SmCl_3(cr)$, and $SmPO_4(cr)$.

23.1.2 Elemental samarium

Elemental samarium does not occur in nature as a mineral. For the calculation of certain reaction properties of samarium species, however, values for $S_m°$(Sm, cr, 298.15 K) and $C_{p,m}°$(Sm, cr, 298.15 K) are required. The most recent reviews on the thermodynamic properties of the lanthanide metals are by Konings & Beneš (2010) and Arblaster (2013). Both reviews relied on the low-temperature heat capacity measurements by Jennings et al. (1959), leading to

$$C_{p,m}°(\text{Sm, cr, 298.15 K}) = 29.53\ \text{J} \cdot \text{K}^{-1} \cdot \text{mol}^{-1}$$

which is included in TDB 2020. Small differences in interpretation of these heat capacity measurements led to slightly different values for $S_m°$(Sm, cr, 298.15 K). While Konings & Beneš (2010) obtained a value of 69.60 $\text{J} \cdot \text{K}^{-1} \cdot \text{mol}^{-1}$, Arblaster (2013) derived

$$S_m°(\text{Sm, cr, 298.15 K}) = 69.64\ \text{J} \cdot \text{K}^{-1} \cdot \text{mol}^{-1}$$

which is included in TDB 2020.

23.1.3 Samarium aquo ions

The lanthanides occur in nature as Ln(III) species only, with the exception of Ce, which also exists as Ce(IV) under oxidizing conditions, and Sm, Eu, and Yb, which also exist as Sm(II), Eu(II), and Yb(II) under extremely reducing conditions (Wood 1990). Since it is extremely unlikely that Sm(II) can exist under environmental conditions and since there are barely any thermodynamic data for reactions with Sm^{2+}, Sm(II) is not further considered.

Rard (2016) carried out an extensive review and critical evaluation of the standard molar entropies, heat capacities, enthalpies of formation and Gibbs energies of formation of the aqueous trivalent rare earth ions.

The standard molar entropy for $S_m°(Sm^{3+}, 298.15\ \text{K})$ was derived by Rard (2016) from calorimetric investigations of the dissolution of $SmCl_3 \cdot 6\ H_2O$(cr) in aqueous solution according to the reaction

$$SmCl_3 \cdot 6H_2O(\text{cr}) \rightleftharpoons Sm^{3+} + 3\ Cl^- + 6\ H_2O(\text{l})$$

The standard molar entropy of solution is given by

$$\Delta_{r,sol}S_m°(298.15\ \text{K}) = S_m°(Sm^{3+}, 298.15\ \text{K}) + 3\ S_m°(Cl^-, 298.15\ \text{K}) + 6\ S_m°(H_2O, \text{l}, 298.15\ \text{K}) - S_m°(SmCl_3 \cdot 6H_2O, \text{cr}, 298.15\ \text{K})$$

from which $S_m°(Sm^{3+}, 298.15\ \text{K})$ can be calculated if $S_m°(Cl^-, 298.15\ \text{K})$, $S_m°(H_2O, \text{l}, 298.15\ \text{K})$, $S_m°(SmCl_3 \cdot 6\ H_2O, \text{cr}, 298.15\ \text{K})$, and $\Delta_{r,sol}S_m°(298.15\ \text{K})$ are known. Rard (2016) took $S_m°(Cl^-, 298.15\ \text{K}) = (56.60 \pm 0.20)\ \text{J} \cdot \text{K}^{-1} \cdot \text{mol}^{-1}$ and $S_m°(H_2O, \text{l}, 298.15\ \text{K}) = (69.95 \pm 0.03)\ \text{J} \cdot \text{K}^{-1} \cdot \text{mol}^{-1}$ from the CODATA review (Cox et al. 1989) and selected $S_m°(SmCl_3 \cdot 6H_2O, \text{cr}, 298.15\ \text{K}) = (412 \pm 3)\ \text{J} \cdot \text{K}^{-1} \cdot \text{mol}^{-1}$ based on the value of 414 $\text{J} \cdot \text{K}^{-1} \cdot \text{mol}^{-1}$ by Wagman et al. (1982), which

he corrected for occluded solution (leading to water excess in the crystal) and errors resulting from heat capacity extrapolations to higher temperatures (note that he considered the corrected value to be an estimate). Finally, he derived $\Delta_{r,sol}S_m°$(298.15 K) from $\Delta_{r,sol}G_m°$(298.15 K) and $\Delta_{r,sol}H_m°$(298.15 K) according to

$$\Delta_{r,sol}G_m° = \Delta_{r,sol}H_m° - T\,\Delta_{r,sol}S_m°$$

The standard molar Gibbs energy of solution can be calculated from

$$\Delta_{r,sol}G_m° = -R\,T\,\ln(27\,m_{sat}^4\,\gamma_{\pm,sat}^4\,a(H_2O, l)_{sat}^6)$$

if m_{sat}, the concentration of dissolved $SmCl_3{\cdot}6H_2O$(cr) at saturation, is known from solubility experiments, as well as $\gamma_{\pm,sat}$, the mean activity coefficient of $SmCl_3$ at saturation and $a(H_2O, l)_{sat}$, the activity of water for the saturated solution, which can both be obtained from isopiestic measurements of saturated solutions. Rard (2016) derived $\Delta_{r,sol}G_m°(298.15\ K) = -(26.55 \pm 0.10)$ kJ $\cdot$ mol^{-1} from $m_{sat} = (3.641 \pm 0.002)$ mol $\cdot$ kg^{-1}, as reported by Mioduski et al. (2009), and from $\gamma_{\pm,sat} = 5.140 \pm 0.051$ and $a(H_2O, l)_{sat} = 0.4881 \pm 0.0006$, both from He & Rard (2015). By combining the value for $\Delta_{r,sol}G_m°(298.15\ K)$ with $\Delta_{r,sol}H_m°(298.15\ K) = -(36.04 \pm 0.06)$ kJ $\cdot$ mol^{-1} (Spedding et al. 1977), Rard (2016) then obtained $\Delta_{r,sol}S_m°(298.15\ K) = -(31.83 \pm 0.39)$ kJ $\cdot$ mol^{-1}, and finally the recommended

$$S_m°(Sm^{3+}, 298.15\ K) = -(209.3 \pm 3.1)\ J \cdot K^{-1} \cdot mol^{-1}$$

which is also included in TDB 2020.

The molar entropy of formation for Sm^{3+}, $\Delta_f S_m°(Sm^{3+}, 298.15)$, can be calculated from

$$\Delta_f S_m°(Sm^{3+}, 298.15) = S_m°(Sm^{3+}, 298.15) + 3\,S_m°(e^-, 298.15) - S_m°(Sm, cr, 298.15)$$

Using his recommended value for $S_m°(Sm^{3+}, 298.15\ K)$ together with $S_m°(Sm, cr, 298.15) = (69.60 \pm 0.30)$ kJ $\cdot$ mol^{-1} (Konings & Beneš 2010)[59] and $S_m°(e^-, 298.15) = 1/2\ S_m°(H_2, g, 298.15) = (65.340 \pm 0.0015)$ J $\cdot$ K^{-1} $\cdot$ mol^{-1} (CODATA, Cox et al. 1989), Rard (2016) derived

$$\Delta_f S_m°(Sm^{3+}, 298.15\ K) = -(82.9 \pm 3.1)\ J \cdot K^{-1} \cdot mol^{-1}$$

From the critical evaluation of the enthalpies of formation of the lanthanide ions by Cordfunke & Konings (2001), Rard (2016) adopted his recommended

$$\Delta_f H_m°(Sm^{3+}, 298.15\ K) = -(690.0 \pm 2.0)\ kJ \cdot mol^{-1}$$

---

[59] Note that this value for $S_m°$(Sm, cr, 298.15 K) by Konings & Beneš (2010), which was recommended by Rard (2016), is slightly different from the value by Arblaster (2013), 69.64 J $\cdot$ K^{-1} $\cdot$ mol^{-1}, which was selected for TDB 2020 in Section 23.1.2. This small difference, however, has no influence on the value of $\Delta_f G_m°(Sm^{3+}, 298.15\ K)$.

which is also included in TDB 2020. From $\Delta_f G_m°(Sm^{3+}, T) = \Delta_f H_m°(Sm^{3+}, T) - T\ \Delta_f S_m°(Sm^{3+}, T)$ then follows

$$\Delta_f G_m°(Sm^{3+}, 298.15\ K) = -(665.3 \pm 2.2)\ kJ \cdot mol^{-1}$$

which is also included in TDB 2020.

For selecting the standard molar heat capacity of Sm^{3+}, Rard (2016) accepted $C_{p,m}°(Sm^{3+}, 298.15\ K) = -110.0\ J \cdot K^{-1} \cdot mol^{-1}$ and $C_{p,m}°(Sm^{3+}, 298.15\ K) = -81.8\ J \cdot K^{-1} \cdot mol^{-1}$, based on flow microcalorimetry measurements of aqueous $Sm(ClO_4)_3 + HClO_4$ (Hakin et al. 2003) and $SmCl_3 + HCl$ (Hakin et al. 2003) solutions, respectively. Taking the average of both values and assigning an estimated uncertainty, Rard (2016) recommended

$$C_{p,m}°(Sm^{3+}, 298.15\ K) = -(95.9 \pm 20)\ J \cdot K^{-1} \cdot mol^{-1}$$

which is included in TDB 2020.

According to the specific ion interaction theory (SIT), the specific ion interaction coefficient ε(j, k), where j is a cation with zj positive charges and k an anion with zk negative charges, can be calculated from mean activity coefficient ($\gamma_\pm$) data for $j_{zk}k_{zj}$(aq) using the following equation (Ciavatta 1980)

$$\varepsilon(j, k) = [\log_{10}(\gamma_\pm) + zj\ zk\ D]\ [zj + zk]^2 / (4\ I_m)$$

where D is the Debye-Hückel term

$$D = 0.509\ I_m^{1/2} / (1 + 1.5\ I_m^{1/2})$$

Rearranging the equation for ε(j, k) leads to

$$1/4\ [zj + zk]^2 \log_{10}(\gamma_\pm) + 1/4\ zj\ zk\ [zj + zk]^2\ D = \varepsilon(j, k)\ I_m$$

or, for a 1:3 electrolyte jk_3(aq), such as $SmCl_3$(aq), $Sm(ClO_4)_3$(aq) or $Sm(NO_3)_3$(aq), to

$$4 \log_{10}(\gamma_\pm) + 12\ D = \varepsilon(j, k)\ I_m$$

In a plot of $4 \log_{10}(\gamma_\pm) + 12\ D$ vs. I_m, ε(j, k) is the slope of a straight line passing through the origin.

He & Rard (2015) published revised mean activity coefficients of the aqueous trivalent rare earth chlorides, based on the isopiestic determinations by Spedding et al. (1976) and Rard & Spedding (1982). The mean activity coefficients for $SmCl_3$(aq) by He & Rard (2015) are shown in Fig. 23.1.3-1 along with the linear least squares fit (with the restriction that the straight line passes through the origin). From the fit to the full set of data (0.1 – 3.641 $mol \cdot kg^{-1}$ $SmCl_3$, corresponding to ionic strengths between 0.6 and 21.85 $mol \cdot kg^{-1}$ follows $\varepsilon(Sm^{3+}, Cl^-) = (0.288 \pm 0.002)\ kg \cdot mol^{-1}$. Since the application range of TDB 2020 is restricted to low ionic strengths, we

also carried out a fit limited to the data at low ionic strengths (0.1 – 1.0 mol · kg^{-1} $SmCl_3$, corresponding to ionic strengths between 0.6 and 6.0 mol · kg^{-1}), resulting in $\varepsilon(Sm^{3+}, Cl^-)$ = (0.247 ± 0.004) kg · mol^{-1}, which we selected (after rounding and increasing the uncertainty) for TDB 2020:

$$\varepsilon(Sm^{3+}, Cl^-) = (0.25 \pm 0.01) \text{ kg} \cdot \text{mol}^{-1}$$

Rard et al. (1977) carried out isopiestic measurements of the osmotic coefficients of rare earth perchlorates from 0.1 m up to saturation, from which they determined mean molal activity coefficients. These are shown for $Sm(ClO_4)_3$(aq) in Fig. 23.1.3-2. From the linear least-squares fit to the full set of data (0.1 – 4.6621 mol · kg^{-1} $Sm(ClO_4)_3$(aq), which corresponds to ionic strengths between 0.6 and 27.97 mol · kg^{-1}), follows $\varepsilon(Sm^{3+}, ClO_4^-)$ = (0.539 ± 0.004) kg · mol^{-1}, and from the set of data restricted to $I_m \leq 6$ mol · kg^{-1} follows $\varepsilon(Sm^{3+}, ClO_4^-)$ = (0.466 ± 0.010) kg · mol^{-1}, which is (after rounding) included in TDB 2020:

$$\varepsilon(Sm^{3+}, ClO_4^-) = (0.47 \pm 0.01) \text{ kg} \cdot \text{mol}^{-1}$$

Chatterjee et al. (2015) determined the osmotic coefficients of lanthanide nitrate solutions by a combination of water activity and vapor pressure osmometry measurements. They calculated mean activity coefficients from the osmotic coefficients. The mean activity data they obtained for $Sm(NO_3)_3$(aq) are shown in Fig. 23.1.3-3.

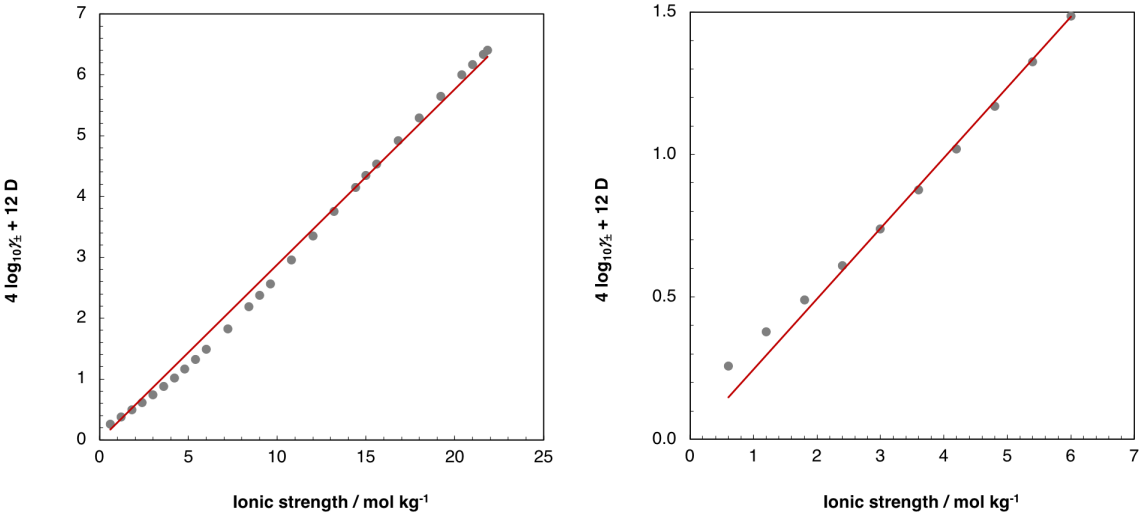

Fig. 23.1.3-1: SIT-analysis of the mean activity coefficient ($\gamma_\pm$) of $SmCl_3$(aq) as a function of ionic strength at 25 °C

Experimental data by He & Rard (2015). From the linear least-squares fit to the full set of data (left) follows $\varepsilon(Sm^{3+}, Cl^-)$ = (0.288 ± 0.002) kg · mol^{-1}, and from the set of data restricted to $I_m \leq 6$ mol · kg^{-1} (right) follows $\varepsilon(Sm^{3+}, Cl^-)$ = (0.247 ± 0.004) kg · mol^{-1}.

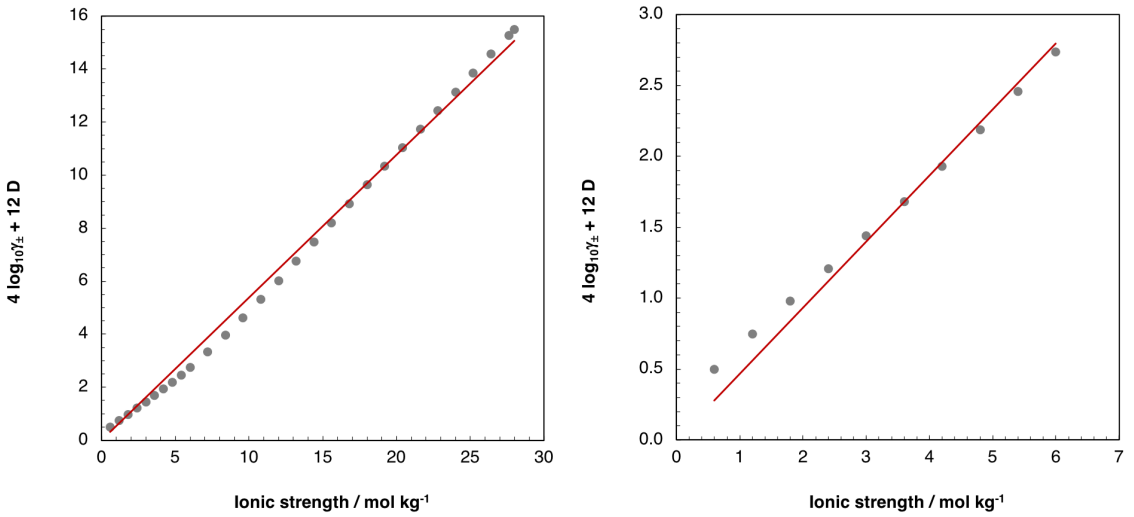

Fig. 23.1.3-2: SIT-analysis of the mean activity coefficient ($\gamma_{\pm}$) of $Sm(ClO_4)_3(aq)$ as a function of ionic strength at 25 °C

Experimental data by Rard et al. (1977). From the linear least-squares fit to the full set of data (left) follows $\varepsilon(Sm^{3+}, ClO_4^-) = (0.539 \pm 0.004)$ kg · mol^{-1}, and from the set of data restricted to $I_m \leq 6$ mol · kg^{-1} (right) follows $\varepsilon(Sm^{3+}, ClO_4^-) = (0.466 \pm 0.010)$ kg · mol^{-1}.

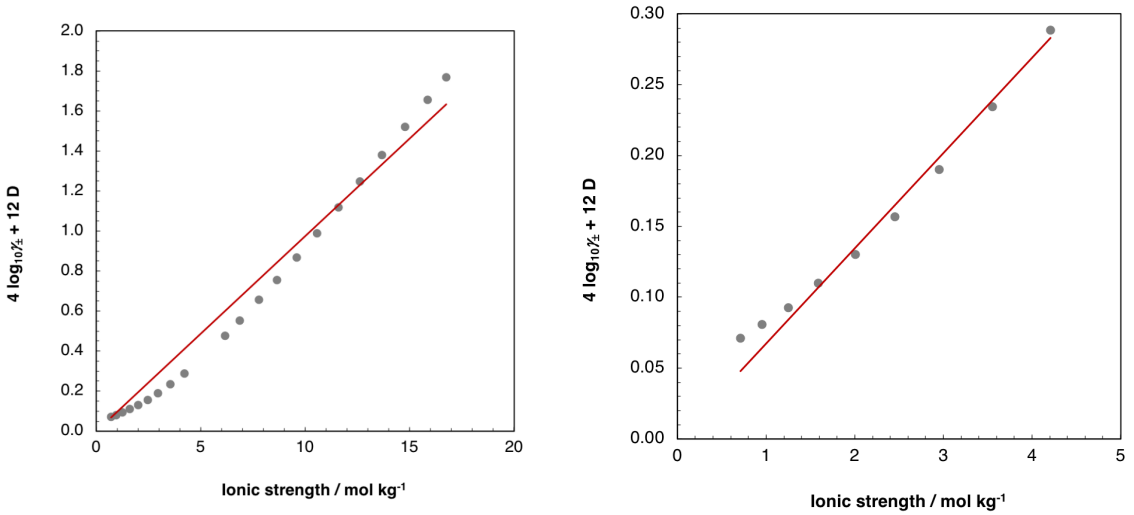

Fig. 23.1.3-3: SIT-analysis of the mean activity coefficient ($\gamma_{\pm}$) of $Sm(NO_3)_3(aq)$ as a function of ionic strength at 25 °C

Experimental data by Chatterjee et al. (2015). From the linear least-squares fit to the full set of data (left) follows $\varepsilon(Sm^{3+}, NO_3^-) = (0.098 \pm 0.002)$ kg · mol^{-1}, and from the set of data restricted to $I_m < 5$ mol · kg^{-1} (right) follows $\varepsilon(Sm^{3+}, NO_3^-) = (0.067 \pm 0.002)$ kg · mol^{-1}.

From the linear least-squares fit to the full set of data (0.118 – 2.792 mol · kg^{-1} $Sm(NO_3)_3$(aq), which corresponds to ionic strengths from 0.708 to 16.752 mol · kg^{-1}) follows $\varepsilon(Sm^{3+}, NO_3^-)$ = (0.098 ± 0.002) kg · mol^{-1}, and from the set of data restricted to I_m < 5 mol · kg^{-1} follows $\varepsilon(Sm^{3+}, NO_3^-)$ = (0.067 ± 0.002) kg · mol^{-1}, which is (after rounding and increasing the uncertainty) included in TDB 2020:

$$\varepsilon(Sm^{3+}, NO_3^-) = (0.07 \pm 0.01) \text{ kg} \cdot \text{mol}^{-1}$$

23.1.4 Samarium oxygen and hydrogen compounds and complexes

This chapter is largely based on the review of the hydrolysis of samarium by Brown & Ekberg (2016).

23.1.4.1 Aqueous samarium hydroxide complexes

Brown & Ekberg (2016) compiled experimental data on the formation of $SmOH^{2+}$

$$Sm^{3+} + H_2O(l) \rightleftharpoons SmOH^{2+} + H^+$$

in $NaClO_4$ by Frolova et al. (1966), Guillaumont et al. (1971), Nair et al. (1982), Ciavatta et al. (1999), who carried out the experiments in $LiClO_4$, Klungness & Byrne (2000), and Bentouhami et al. (2004). These data are listed in Tab. 23.1.4-1 and shown in Fig. 23.1.4-1. As shown in Fig. 23.1.4-1, the data scatter considerably, especially at very low ionic strength. Brown & Ekberg (2016) did not accept the data by Guillaumont et al. (1971), Nair et al. (1982), and Bentouhami et al. (2004), because "it is clear from the data listed in Tab. 8.31 that some of the reported data are erroneous". Brown & Ekberg (2016) carried out a non-linear SIT analysis of the accepted data by using the two-parameter equation $\Delta\varepsilon = \Delta\varepsilon_1 + \Delta\varepsilon_2 \log_{10} I_m$, see Fig. 23.1.4-2. As we do not advocate non-linear SIT-analyses (see, e.g., Chapters 5 or 12) we re-analysed the data with a standard linear SIT-fit, see Fig. 23.1.4-2. A linear SIT-fit including the data point by Ciavatta et al. (1999) at I_m = 3 mol · kg^{-1} would lead to a negative slope of the fitted line which is at variance with the trend of the datapoints at ionic strengths I_m < 1 mol · kg^{-1}. For this reason, we discarded the datapoint by Ciavatta et al. (1999) in our SIT-analysis and obtained

$$\log_{10}{}^*\beta_1^\circ(298.15 \text{ K}) = -(7.76 \pm 0.09)$$

$$\Delta\varepsilon = -(0.53 \pm 0.21) \text{ kg} \cdot \text{mol}^{-1}$$

From $\Delta\varepsilon$, $\varepsilon(H^+,ClO_4^-)$ = (0.14 ± 0.02) kg · mol^{-1} recommended by NEA, and the selected $\varepsilon(Sm^{3+},ClO_4^-)$ = (0.47 ± 0.01) kg · mol^{-1} (see Section 23.1.3) follows

$$\varepsilon(SmOH^{2+},ClO_4^-) = -(0.20 \pm 0.21) \text{ kg} \cdot \text{mol}^{-1}$$

which is included in TDB 2020 as well as

$$\varepsilon(SmOH^{2+},Cl^-) \approx (0.15 \pm 0.10) \text{ kg} \cdot \text{mol}^{-1}$$

as estimated according to the method described in Section 1.5.3.

Brown & Ekberg (2016) recommended $\log_{10}{}^*\beta_1°(298.15\ K) = -(7.84 \pm 0.11)$ based on their non-linear SIT fit of the data (see Fig. 23.1.4-2), which compares well with that selected for TDB 2020, as both values are included in each other's uncertainty range.

Klungness & Byrne (2000) measured $\log_{10}{}^*\beta_1$ in 0.7 M $NaClO_4$ at 25, 40 and 55 °C and obtained $\Delta_r H_m(298.15\ K, 0.7\ M\ NaClO_4) = (10.2 \pm 1.3)\ kcal \cdot mol^{-1} = (42.7 \pm 5.4)\ kJ \cdot mol^{-1}$ from a van't Hoff fit to the data. As it is not possible to extrapolate this value to zero ionic strength without further data, we accepted

$$\Delta_r H_m°(298.15\ K) = (42.7 \pm 5.4)\ kJ \cdot mol^{-1}$$

$$\Delta_r C_{p,m}°(298.15\ K) = 0$$

as supplemental data for TDB 2020.

According to Brown & Ekberg (2016), there are only three studies reporting stability constant data for polymeric Sm hydroxide species. Kragten & Decnop-Weever (1979) proposed the formation of $Sm_3(OH)_4^{5+}$, Ciavatta et al. (1999) the formation of $Sm_2(OH)_2^{4+}$ and $Sm_3(OH)_5^{4+}$ (both at 25 and 60 °C), and of $Sm_5(OH)_9^{6+}$ (only at 25 °C), while Bentouhami et al. (2004) claimed to have observed $Sm_2(OH)_3^{3+}$. Brown & Ekberg (2016) accepted only the data for $Sm_2(OH)_2^{4+}$ and $Sm_3(OH)_5^{4+}$, based on the conclusion by Baes & Mesmer (1976) that $Ln_2(OH)_2^{4+}$ and $Ln_3(OH)_5^{4+}$ are the most likely polymeric lanthanide hydroxide species. Brown & Ekberg (2016) extrapolated the stability constant $\log_{10}{}^*\beta_{2,2}°(298.15\ K, 3.0\ m\ LiClO_4) = -(14.75 \pm 0.20)$ (uncertainty increased from 0.02 to 0.20) by Ciavatta et al. (1999) to zero ionic strength by noting that, since $\Delta z^2 = 0$ for the reaction

$$2\ Sm^{3+} + 2\ H_2O(l) \rightleftharpoons Sm_2(OH)_2^{4+} + 2\ H^+$$

the dependence of the stability constant on ionic strength is rather weak, probably within the assigned uncertainty of the measured constant. Thus, they assumed $\log_{10}{}^*\beta_{2,2}°(298.15\ K) \approx \log_{10}{}^*\beta_{2,2}(298.15\ K, 3.0\ m\ LiClO_4) = -(14.75 \pm 0.20)$. This assumption, however, can only be justified if the corresponding $\Delta\varepsilon$ is small, but this does not follow at all from the fact that $\Delta z^2 = 0$. Brown & Ekberg (2016) derived $\Delta\varepsilon = (0.05 \pm 0.12)\ kg \cdot mol^{-1}$ for the analogous formation reaction of the scandium polymer $Sc_2(OH)_2^{4+}$ in perchlorate media, which is sufficiently small for such an assumption. We assumed that $\Delta\varepsilon = (0.05 \pm 0.12)\ kg \cdot mol^{-1}$ for scandium is also valid for samarium and used this value to extrapolate $\log_{10}{}^*\beta_{2,2}(298.15\ K, 3.0\ m\ LiClO_4) = -(14.75 \pm 0.20)$ for $Sm_2(OH)_2^{4+}$ to zero ionic strength and obtained

$$\log_{10}{}^*\beta_{2,2}°(298.15\ K) = -(14.5 \pm 0.4)$$

In the case of $Sm_3(OH)_5^{4+}$, Brown & Ekberg (2016) used the estimate $\Delta\varepsilon \approx -(0.23 \pm 0.13)\ kg \cdot mol^{-1}$ (taken from an SIT analysis of the formation reaction of $Sc_3(OH)_5^{4+}$) to extrapolate $\log_{10}{}^*\beta_{3,5}(298.15\ K, 3.0\ m\ LiClO_4) = -(34.9 \pm 0.3)$ by Ciavatta et al. (1999) for the reaction

$$3\ Sm^{3+} + 5\ H_2O(l) \rightleftharpoons Sm_3(OH)_5^{4+} + 5\ H^+$$

to zero ionic strength and obtained the selected

$$\log_{10}{}^*\beta_{3,5}^\circ(298.15\ \mathrm{K}) = -(33.9 \pm 0.3)$$

We included the stability constants for these two polymeric samarium species in TDB 2020, even though it is not very likely that they are ever formed at trace concentrations of Sm (see Fig. 23.1.4-3).

From the estimated $\Delta\varepsilon \approx (0.05 \pm 0.12)$ kg · mol^{-1} and $\Delta\varepsilon \approx -(0.23 \pm 0.13)$ kg · mol^{-1} for the formation reactions of $Sm_2(OH)_2^{4+}$ and $Sm_3(OH)_5^{4+}$, resp., and the selected $\varepsilon(H^+,ClO_4^-)$ and $\varepsilon(Sm^{3+},ClO_4^-)$ follow

Tab. 23.1.4-1: Data for the stability constant $\log_{10}{}^*\beta_1$ of $Sm^{3+} + H_2O(l) \rightleftharpoons SmOH^{2+} + H^+$ at 25 °C compiled and accepted by Brown & Ekberg (2016)

The accepted values for $\log_{10}{}^*\beta_1$ were recalculated by Brown & Ekberg (2016) from the molar to the molal scale, if necessary. Missing uncertainties were estimated, and reported uncertainties in some cases increased for further analysis of the data. Values of $\log_{10}{}^*\beta_1$ accepted for our own SIT analysis are bold. Abbreviations: pot: potentiometry, sp: spectrophotometry, gl: glass electrode, ext: solvent extraction.

Method	**Medium**	***I*** **reported**	***I*** [mol · kg^{-1}]	**$\log_{10}{}^*\beta_1$ (reported)**	**$\log_{10}{}^*\beta_1$ (accepted)**	**Reference**
pot, sp	$NaClO_4$	0 M	0	-7.84	**-7.84 ± 0.20**	Klungness & Byrne (2000)
pot, sp	$NaClO_4$	0.1 M	0.101	-8.05 ± 0.05	**-8.05 ± 0.10**	Klungness & Byrne (2000)
ext	$NaClO_4$	0.1 M	0.101	-4.4	-	Guillaumont et al. (1971)
gl	$NaClO_4$	0.1 M	0.101	-6.27 ± 0.06	-	Bentouhami et al. (2004)
pot	$NaClO_4$	0.3 M	0.304	-8.34 ± 0.02	**-8.33 ± 0.10**	Frolova et al. (1966)
pot, sp	$NaClO_4$	0.7 M	0.725	-8.15 ± 0.08	**-8.13 ± 0.10**	Klungness & Byrne (2000)
gl	$NaClO_4$	1.0 M	1.05	-8.84 ± 0.02	-	Nair et al. (1982)
pot	$NaClO_4$	3.0 m	3.0	-9.05 ± 0.02	-9.05 ± 0.10	Ciavatta et al. (1999)

$$\varepsilon(Sm_2(OH)_2^{4+},ClO_4^-) \approx (0.71 \pm 0.13)\ \mathrm{kg \cdot mol^{-1}}$$

$$\varepsilon(Sm_3(OH)_5^{4+},ClO_4^-) \approx (0.48 \pm 0.17)\ \mathrm{kg \cdot mol^{-1}}$$

which are included in TDB 2020 as well as the estimates (according to Section 1.5.3)

$$\varepsilon(Sm_2(OH)_2^{4+},Cl^-) \approx (0.35 \pm 0.10)\ \mathrm{kg \cdot mol^{-1}}$$

$$\varepsilon(Sm_3(OH)_5^{4+},Cl^-) \approx (0.35 \pm 0.10)\ \mathrm{kg \cdot mol^{-1}}$$

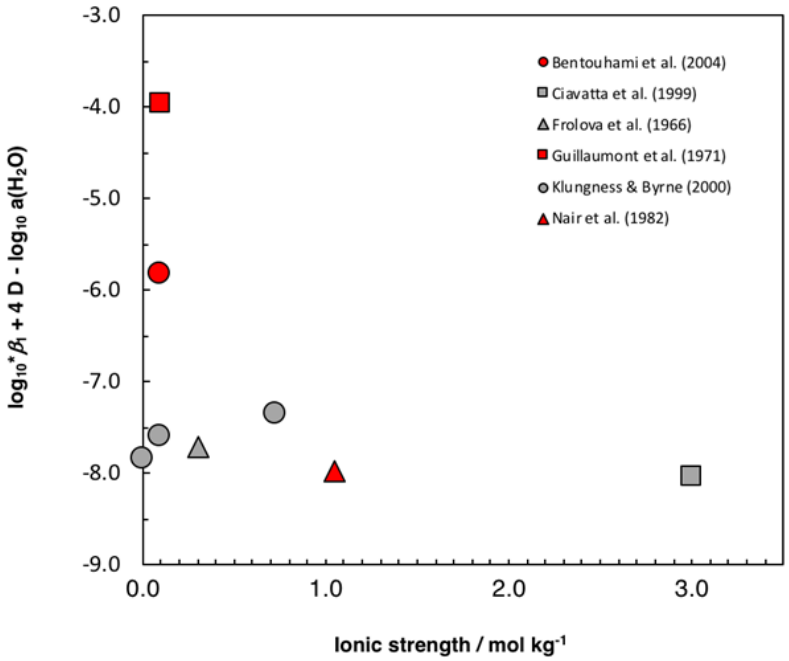

Fig. 23.1.4-1: SIT-plot of the stability constants $\log_{10}{}^*\beta_1$ for the reaction $Sm^{3+} + H_2O(l) \rightleftharpoons SmOH^{2+} + H^+$ at 25 °C compiled by Brown & Ekberg (2016)

Red symbols represent the data by Guillaumont et al. (1971), Nair et al. (1982), and Bentouhami et al. (2004), which were not accepted by Brown & Ekberg (2016).

Brown & Ekberg (2016) mentioned several papers reporting stability constant data for $Sm(OH)_2^+$ and $Sm(OH)_3(aq)$ (Kragten & Decnop-Weever 1979, Nair et al. 1982, Fatin-Rouge & Bünzli 1999, Bentouhami et al. 2004), but they came to the conclusion that the stability constants derived from these studies were not consistent with $\log_{10}{}^*\beta_1°(298.15\ K)$ selected by Brown & Ekberg (2016), since one or more of the subsequent stepwise hydrolysis constants would be more stable than the first, "which is not acceptable for the lanthanide ions".

Neglecting $Sm(OH)_3(aq)$, however, may have serious consequences when calculating solubilities of samarium in aqueous solutions. By analogy, the solubility curve of $Eu(OH)_3(cr)$ discussed by Hummel et al. (2002) may serve as an example: Bernkopf (1984) measured the solubility of $Eu(OH)_3(cr)$ in carbonate free 0.1 M $NaClO_4$. In a diagram of log $[Eu]_{tot}$ vs. pH, the data are characterized by a wide region of constant low solubility (from pH 9 – 12) on the order of around $10^{-8.8}$ M. Towards lower pH, solubility increases sharply to a value around 10^{-4} M at pH 7. The negative slope of the solubility curve in this region is mainly due to the species Eu^{3+}, $Eu(OH)^{2+}$, and $Eu(OH)_2^+$. Towards higher pH (> 12) solubility increases only slightly, which was explained by Bernkopf (1984) with the formation of $Eu(OH)_4^-$. Neglecting $Eu(OH)_3(aq)$ in solubility calculations would lead to unrealistically low values at high pH, on the order of 10^{-12} M at pH 12. Thus, by analogy, it is not reasonable to ignore $Sm(OH)_3(aq)$ as Brown & Ekberg (2016) have done.

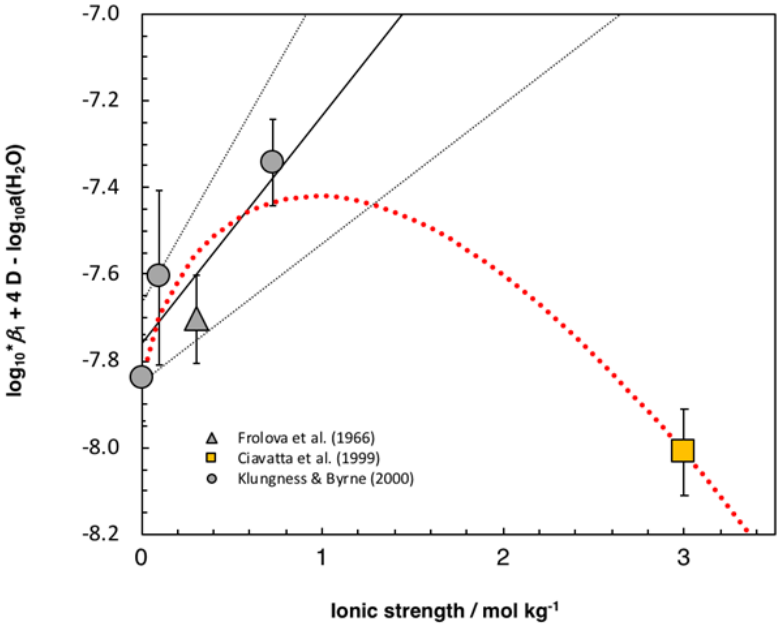

Fig. 23.1.4-2: SIT-plot of the equilibrium $Sm^{3+} + H_2O(l) \rightleftharpoons SmOH^{2+} + H^+$ in $NaClO_4$ using the experimental data by Frolova et al. (1966) and Klungness & Byrne (2000)

The solid line is obtained by using the derived SIT interaction coefficient, $\Delta\varepsilon = -(0.53 \pm 0.21)$ kg · mol^{-1}, and the stability constant at zero ionic strength, $\log_{10}{}^*\beta_1°(298.15\ K) = -(7.76 \pm 0.09)$. The dotted lines represent the associated 95% uncertainty range extrapolated from zero ionic strength to higher $NaClO_4$ concentrations. The dotted red line represents the non-linear SIT-fit obtained by Brown & Ekberg (2016), including the datapoint by Ciavatta et al. (1999) in $LiClO_4$.

Kragten & Decnop-Weever (1979) measured the solubility of fresh $Sm(OH)_3$(pr) as a function of pH in a 1 M perchlorate medium. The solubility curve showed a similar form as that of $Eu(OH)_3$(cr), but a much higher solubility in the plateau region (about $10^{-5.2}$ M). Kragten & Decnop-Weever (1979) interpreted their solubility curve in terms of the species Sm^{3+}, $SmOH^{2+}$, $Sm(OH)_2^+$, $Sm(OH)_3$(aq) and $Sm_3(OH)_4^{5+}$ and obtained the following conditional constants: $\log_{10}{}^*\beta_1(298.15\ K) = -7.5$, $\log_{10}{}^*\beta_2(298.15\ K) = -15.0$, $\log_{10}{}^*\beta_3(298.15\ K) = -22.7$, $\log_{10}{}^*\beta_{4,3}(298.15\ K) = -19.5$ and $\log_{10}{}^*K_{s,0}(298.15\ K) = 17.5$.

Since these data cannot be extrapolated to zero ionic strength without additional information, and a fresh precipitate results in unrealistically high solubilities, we decided to estimate the missing formation constants for $Sm(OH)_2^+$, $Sm(OH)_3$(aq), and $Sm(OH)_4^-$ based on the stability constants of the corresponding Eu hydroxide complexes derived by Hummel et al. (2002) from the experimental solubility measurements by Bernkopf (1984). We proceeded as follows: Hummel et al. (2002) selected $\log_{10}{}^*\beta_1°(298.15\ K, EuOH^{2+}) = -(7.64 \pm 0.04)$, $\log_{10}{}^*\beta_2°(298.15\ K, Eu(OH)_2^+) = -(15.1 \pm 0.2)$, $\log_{10}{}^*\beta_3°(298.15\ K, Eu(OH)_3(aq)) = -(23.7 \pm 0.1)$, and $\log_{10}{}^*\beta_4°(298.15\ K, Eu(OH)_4^-) = -(36.2 \pm 0.5)$. Therefore, the stepwise stability constants are $\log_{10}{}^*K_2°(298.15\ K) = -7.46$, $\log_{10}{}^*K_3°(298.15\ K) = -8.6$, and $\log_{10}{}^*K_4°(298.15\ K) = -12.5$. Based on $\log_{10}{}^*\beta_1°(298.15\ K, SmOH^{2+}) = -(7.76 \pm 0.09)$ selected for TDB 2020 and assuming that these stepwise stability constants are valid as approximations for those of the corresponding Sm hydroxide complexes, the following estimates are obtained:

$Sm^{3+} + 2\ H_2O(l) \rightleftharpoons Sm(OH)_2^+ + 2\ H^+$

$log_{10}{}^*\beta_2^\circ(298.15\ K) = -(15.22 \pm 0.3)$

$Sm^{3+} + 3\ H_2O(l) \rightleftharpoons Sm(OH)_3(aq) + 3\ H^+$

$log_{10}{}^*\beta_3^\circ(298.15\ K) = -(23.82 \pm 0.3)$

$Sm^{3+} + 4\ H_2O(l) \rightleftharpoons Sm(OH)_4^- + 4\ H^+$

$log_{10}{}^*\beta_4^\circ(298.15\ K) = -(36.32 \pm 0.3)$

These estimates are included in TDB 2020 as supplemental data, together with the SIT coefficients estimated according to the method described in Section 1.5.3.

$\varepsilon(Sm(OH)_2^+, Cl^-) \approx (0.05 \pm 0.10)\ kg \cdot mol^{-1}$

$\varepsilon(Sm(OH)_2^+, ClO_4^-) \approx (0.2 \pm 0.1)\ kg \cdot mol^{-1}$

$\varepsilon(Sm(OH)_3(aq), NaCl) = \varepsilon(Sm(OH)_3(aq), NaClO_4) \approx 0$

$\varepsilon(Sm(OH)_4^-, Na^+) \approx -(0.05 \pm 0.10)\ kg \cdot mol^{-1}$

23.1.4.2 Samarium hydroxide solids

As discussed in the previous section, Kragten & Decnop-Weever (1979) measured the solubility of fresh $Sm(OH)_3$(pr) as a function of pH in a 1 M perchlorate medium. The solubility curve showed a similar form as that of $Eu(OH)_3$(cr), but a much higher solubility in the plateau region (about $10^{-5.2}$ M). It is unrealistic to assume that a fresh precipitate with such a high solubility can survive for timeframes relevant to the long-time disposal of radioactive waste without recrystallization. As we are not aware of any solubility measurements of crystalline $Sm(OH)_3$, we approximated the solubility of $Sm(OH)_3$(cr) in the plateau region with that of $Eu(OH)_3$(cr), which amounts to about $10^{-8.8}$ M. Thus, $\log_{10}[Sm(OH)_3(aq)] \approx -8.8$ M.

Since $\log_{10}[Sm(OH)_3(aq)] = \log_{10}{}^*\beta_3^\circ + \log_{10}{}^*K_{s,0}^\circ$ (if the activity coefficient of $Sm(OH)_3$(aq) is neglected), an estimate for the solubility product of $Sm(OH)_3$(cr) is given by $\log_{10}{}^*K_{s,0}^\circ(298.15\ K) = \log_{10}{}^*\beta_3^\circ(298.15\ K) - 8.8$. From the selected $\log_{10}{}^*\beta_1^\circ(298.15\ K) = -(7.76 \pm 0.09)$ then follows

$Sm(OH)_3(cr) + 3\ H^+ \rightleftharpoons Sm^{3+} + 3\ H_2O(l)$

$log_{10}{}^*K_{s,0}^\circ(298.15\ K) = 15 \pm 1$

with a generous uncertainty. This estimated solubility product is included in TDB 2020 as supplemental datum.

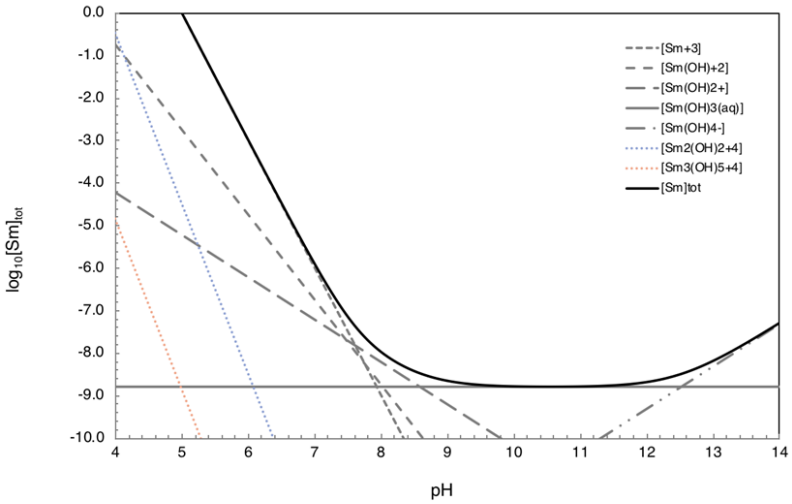

Fig. 23.1.4-3: Solubility of $Sm(OH)_3(cr)$ as a function of pH calculated with the selected data for TDB 2020

Activity coefficients have not been considered in the calculation of this diagram. It is obvious, that the polymers $Sm_2(OH)_2^{4+}$ and $Sm_3(OH)_5^{4+}$ have a negligible influence on the solubility.

23.1.5 Samarium fluoride compounds and complexes

23.1.5.1 Aqueous samarium fluoride complexes

23.1.5.1.1 SmF2+

Walker & Choppin (1967) used potentiometric titrations and solvent extraction in 1 M $NaClO_4$ at 25 °C for measuring the stability constants of 1:1 REE fluoride complexes, including SmF^{2+}. In addition, they also used calorimetric titrations for the determination of the reaction enthalpies of the complexation reactions.

Menon et al. (1988) measured the stability constants of the 1:1 and 1:2 complexes of Sm and Gd in 0.5 M NH_4NO_3 at 25 °C using a fluoride selective ion electrode. This work was extended by Menon & James (1989a, 1989b) to all REE (save promethium).

Schijf & Byrne (1999) measured stability constants of the 1:1 and 1:2 fluoride complexes of yttrium and the rare earth elements at 25 °C in 0.025 M HNO_3 solutions using the cation-exchange resin technique.

Luo & Byrne (2000) measured stability constants for the 1:1 fluoride complexes of yttrium and the rare earth elements at 25 °C in 0.15 to 6.0 molar $NaClO_4$ solutions using a fluoride ion selective electrode. They corrected these data in a later study (Luo & Byrne 2007), stating that the stability constants by Luo & Byrne (2000) were erroneously reported in molar units.

Luo & Byrne (2001) measured stability constants for the 1:1 fluoride complexes of yttrium and the rare earth elements at 25 °C in 0.7 and 3.0 molar NaCl solutions using a fluoride ion selective electrode.

Luo & Byrne (2007) measured stability constants for 1:1 fluoride complexes of yttrium and the rare earth elements at 25 °C across a range of ionic strengths in NaCl (0.7 – 5.0 m) and $NaNO_3$ (0.015 to 6.0 m) media using a fluoride ion selective combination electrode.

The conditional stability constants for the reaction

$$Sm^{3+} + F^- \rightleftharpoons SmF^{2+}$$

measured in NaCl by Luo & Byrne (2001, 2007), see Tab. 23.1.5-1, were used for the SIT analysis shown in Fig. 23.1.5-1, which resulted in

$$\log_{10}\beta_1°(298.15\ K) = (4.17 \pm 0.07)$$

$$\Delta\varepsilon = -(0.12 \pm 0.02)\ kg \cdot mol^{-1}$$

Tab. 23.1.5-1: Data for the stability constant $\log_{10}\beta_1$ of $Sm^{3+} + F^- \rightleftharpoons SmF^{2+}$ at 25 °C in NaCl

The accepted values for $\log_{10}\beta_1$ were recalculated from the molar to the molal scale, if necessary. Reported uncertainties were increased. Values of $\log_{10}\beta_1$ accepted for the SIT analysis shown in Fig. 23.1.5-1 are bold. Abbreviation: sel: ion-selective electrode.

Method	**Medium**	***I*** **reported**	I_m [mol · kg^{-1}]	**$\log_{10}\beta_1$ (reported)**	**$\log_{10}\beta_1$ (accepted)**	**Reference**
sel	NaCl	0.7 m	0.7	3.11 ± 0.03	**3.11 ± 0.10**	Luo & Byrne (2007)
sel	NaCl	0.7 M	0.711	3.12	**3.11 ± 0.10**	Luo & Byrne (2001)
sel	NaCl	1.5 m	1.5	3.07 ± 0.03	**3.07 ± 0.10**	Luo & Byrne (2007)
sel	NaCl	3.0 m	3.0	3.06 ± 0.03	**3.06 ± 0.10**	Luo & Byrne (2007)
sel	NaCl	3.0 M	3.2	3.09	**3.06 ± 0.10**	Luo & Byrne (2001)
sel	NaCl	4.0 m	4.0	3.16 ± 0.03	**3.16 ± 0.10**	Luo & Byrne (2007)
sel	NaCl	5.0 m	5.0	3.22 ± 0.04	**3.22 ± 0.10**	Luo & Byrne (2007)

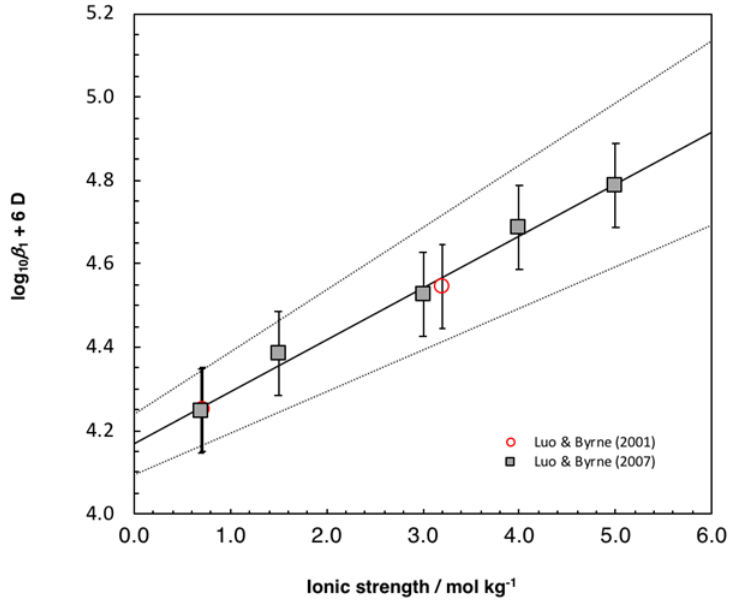

Fig. 23.1.5-1: SIT-plot of the equilibrium $Sm^{3+} + F^- \rightleftharpoons SmF^{2+}$ in NaCl using the experimental data by Luo & Byrne (2001, 2007)

The solid line is obtained by using the derived SIT interaction coefficient, $\Delta\varepsilon = -(0.12 \pm 0.02)$ kg · mol^{-1}, and the stability constant at zero ionic strength, $\log_{10}\beta_1°(298.15\ K) = (4.17 \pm 0.07)$. The dotted lines represent the associated 95% uncertainty range extrapolated from zero ionic strength to higher NaCl concentrations.

Tab. 23.1.5-2: Data for the stability constant $\log_{10}\beta_1$ of $Sm^{3+} + F^- \rightleftharpoons SmF^{2+}$ at 25 °C in $NaClO_4$

The accepted values for $\log_{10}\beta_1$ were recalculated from the molar to the molal scale, if necessary. Reported uncertainties were increased. Values of $\log_{10}\beta_1$ accepted for the SIT analysis shown in Fig. 23.1.5-2 are bold. Abbreviations: pot: potentiometry, sel: ion selective electrode.

Method	**Medium**	***I*** **reported**	I_m [mol · kg^{-1}]	**$\log_{10}\beta_1$ (reported)**	**$\log_{10}\beta_1$ (accepted)**	**Reference**
sel	$NaClO_4$	0.015 m	0.015	3.91 ± 0.03	**3.91 ± 0.10**	Luo & Byrne (2007)
sel	$NaClO_4$	0.1 m	0.1	3.50 ± 0.03	**3.50 ± 0.10**	Luo & Byrne (2007)
sel	$NaClO_4$	0.4 m	0.4	3.28 ± 0.03	**3.28 ± 0.10**	Luo & Byrne (2007)
sel	$NaClO_4$	0.7 m	0.7	3.21 ± 0.03	**3.21 ± 0.10**	Luo & Byrne (2007)
pot	$NaClO_4$	1 M	1.051	3.12 ± 0.01 [a]	**3.10 ± 0.10**	Walker & Choppin (1967)
sel	$NaClO_4$	1.5 m	1.5	3.21 ± 0.03	**3.21 ±0.10**	Luo & Byrne (2007)
sel	$NaClO_4$	3.0 m	3.0	3.25 ± 0.03	**3.25 ± 0.10**	Luo & Byrne (2007)
sel	$NaClO_4$	4.0 m	4.0	3.41 ± 0.03	**3.41 ± 0.10**	Luo & Byrne (2007)
sel	$NaClO_4$	5.0 m	5.0	3.48 ± 0.04	**3.48 ± 0.10**	Luo & Byrne (2007)
sel	$NaClO_4$	5.0 m	6.0	3.60 ± 0.04	**3.60 ± 0.10**	Luo & Byrne (2007)

[a] Calculated from $\beta_1 = 1'310 \pm 40$.

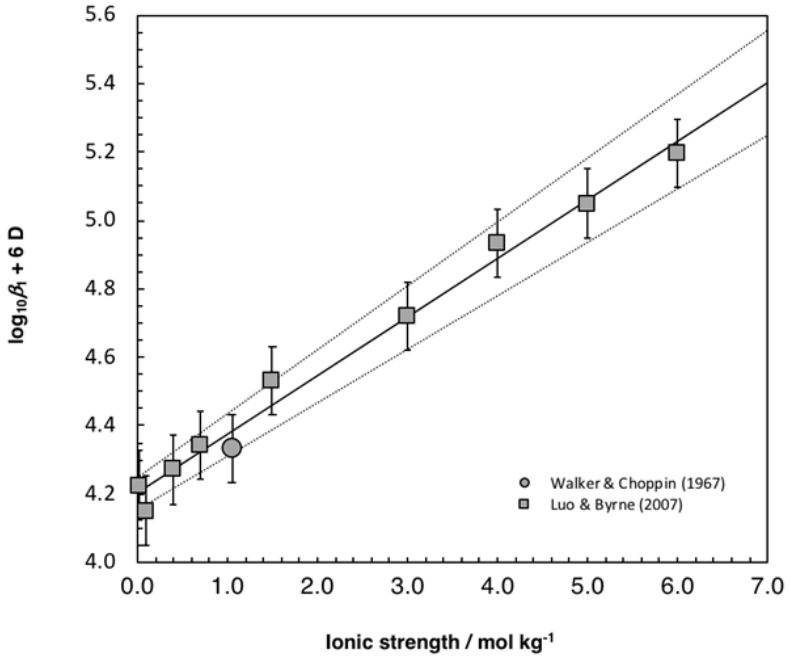

Fig. 23.1.5-2: SIT-plot of the equilibrium Sm3+ + F- ⇌ SmF2+ in NaClO4 using the experimental data by Walker & Choppin (1967) and Luo & Byrne (2007)

The solid line is obtained by using the derived SIT interaction coefficient, $\Delta\varepsilon$ = -(0.17 ± 0.02) kg · mol^{-1}, and the stability constant at zero ionic strength, $\log_{10}\beta_1°$(298.15 K) = (4.20 ± 0.05). The dotted lines represent the associated 95% uncertainty range extrapolated from zero ionic strength to higher $NaClO_4$ concentrations.

From $\Delta\varepsilon$, the NEA-selected $\varepsilon(F^-, Na+)$ = (0.02 ± 0.02) kg · mol^{-1}, and $\varepsilon(Sm^{3+}, Cl^-)$ = (0.25 ± 0.01) kg · mol^{-1} (see Section 23.1.3) then follows

$$\varepsilon(SmF^{2+}, Cl^-) = (0.15 \pm 0.03) \text{ kg} \cdot \text{mol}^{-1}$$

The values for $\log_{10}\beta_1$ measured by Walker & Choppin (1967) and Luo & Byrne (2007) in $NaClO_4$ (see Tab. 23.1.5-2) were used for the SIT-analysis shown in Fig. 23.1.5-2, which led to

$$\log_{10}\beta_1°(298.15 \text{ K}) = (4.20 \pm 0.05)$$

$$\Delta\varepsilon = -(0.17 \pm 0.02) \text{ kg} \cdot \text{mol}^{-1}$$

From $\Delta\varepsilon$, the NEA-selected $\varepsilon(F^-, Na+)$, and $\varepsilon(Sm^{3+}, ClO_4^-)$ = (0.47 ± 0.01) kg · mol^{-1} (see Section 23.1.3) then follows

$$\varepsilon(SmF^{2+}, ClO_4^-) = (0.32 \pm 0.03) \text{ kg} \cdot \text{mol}^{-1}$$

Tab. 23.1.5-3: Data for the stability constant $\log_{10}\beta_1$ of $Sm^{3+} + F^- \rightleftharpoons SmF^{2+}$ at 25 °C in nitrate media

The accepted values for $\log_{10}\beta_1$ were recalculated from the molar to the molal scale, if necessary. Reported uncertainties were increased. Values of $\log_{10}\beta_1$ accepted for the SIT analysis shown in Fig. 23.1.5-3 are bold. Abbreviations: cat: cation exchange, sel: ion-selective electrode.

Method	**Medium**	***I*** **reported**	I_m [mol · kg^{-1}]	**$\log_{10}\beta_1$ (reported)**	**$\log_{10}\beta_1$ (accepted)**	**Reference**
cat	HNO_3	0.025 M		3.59 ± 0.05		Schijf & Byrne (1999)
cat	HNO_3	0.025 M		3.61 ± 0.01		Luo & Millero (2004)
sel	NH_4NO_3	0.5 M		3.03 ± 0.01 [a]		Menon et al. (1988)
sel	NH_4NO_3	0.5 M		3.15 ± 0.01 [b]		Menon & James (1989a, 1989b)
sel	$NaNO_3$	0.7 m	0.7	3.14 ± 0.03	**3.14 ± 0.10**	Luo & Byrne (2007)
sel	$NaNO_3$	1.5 m	1.5	3.08 ± 0.03	**3.08 ± 0.10**	Luo & Byrne (2007)
sel	$NaNO_3$	3.0 m	3.0	3.16 ± 0.03	**3.16 ± 0.10**	Luo & Byrne (2007)
sel	$NaNO_3$	4.0 m	4.0	3.25 ± 0.03	**3.25 ± 0.10**	Luo & Byrne (2007)
sel	$NaNO_3$	5.0 m	5.0	3.43 ± 0.04	**3.43 ± 0.10**	Luo & Byrne (2007)

[a] Calculated from $\beta_1 = 1'076 \pm 14$.
[b] Calculated from $\beta_1 = 1'416 \pm 41$.

From an SIT-analysis of the values of $\log_{10}\beta_1$ measured by Luo & Byrne (2007) in $NaNO_3$ (see Tab. 23.1.5-3) follows

$$\log_{10}\beta_1°(298.15\ K) = (4.15 \pm 0.09)$$

$$\Delta\varepsilon = -(0.09 \pm 0.03)\ kg \cdot mol^{-1}$$

Using $\Delta\varepsilon$, the NEA-selected $\varepsilon(F^-, Na+)$, and $\varepsilon(Sm^{3+}, NO_3^-) = (0.07 \pm 0.01)\ kg \cdot mol^{-1}$ (see Section 23.1.3) leads to

$$\varepsilon(SmF^{2+}, NO_3^-) = (0.00 \pm 0.04)\ kg \cdot mol^{-1}$$

The values for $\log_{10}\beta_1°(298.15\ K)$ derived from experimental data measured in NaCl (4.17 ± 0.07), $NaClO_4$ (4.20 ± 0.05), and $NaNO_3$ (4.15 ± 0.09) all overlap within their uncertainties. For inclusion in TDB 2020 we selected the value derived from the NaCl data since it corresponds nearly to the mean of the three values and since NaCl is the background electrolyte of greater relevance to natural environments than $NaClO_4$ or $NaNO_3$. Thus

$$\log_{10}\beta_1°(298.15\ K) = (4.17 \pm 0.07)$$

is included in TDB 2020, together with

$\varepsilon(SmF^{2+}, Cl^-) = (0.15 \pm 0.03)$ kg · mol^{-1}

$\varepsilon(SmF^{2+}, ClO_4^-) = (0.32 \pm 0.03)$ kg · mol^{-1}

$\varepsilon(SmF^{2+}, NO_3^-) = (0.00 \pm 0.04)$ kg · mol^{-1}

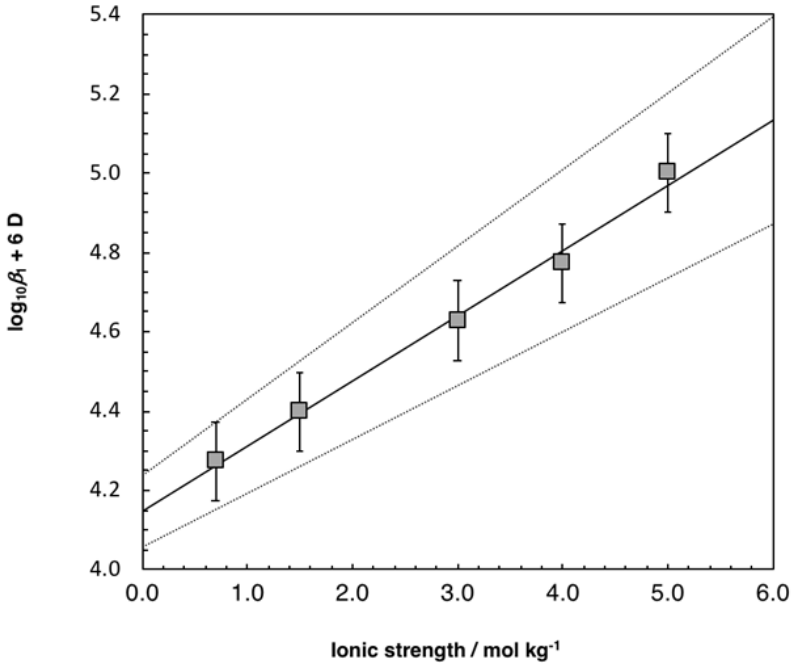

Fig. 23.1.5-3: SIT-plot of the equilibrium $Sm^{3+} + F^- \rightleftharpoons SmF^{2+}$ in $NaNO_3$ using the experimental data by Luo & Byrne (2007)

The solid line is obtained by using the derived SIT interaction coefficient, $\Delta\varepsilon = -(0.09 \pm 0.03)$ kg · mol^{-1}, and the stability constant at zero ionic strength, $\log_{10}\beta_1°(298.15\ K) = (4.15 \pm 0.09)$. The dotted lines represent the associated 95% uncertainty range extrapolated from zero ionic strength to higher NaCl concentrations.

Tab. 23.1.5-4: Stability constants $\log_{10}\beta_1$ of $Sm^{3+} + F^- \rightleftharpoons SmF^{2+}$ and $\log_{10}\beta_2$ of $Sm^{3+} + 2\ F^- \rightleftharpoons SmF_2^+$ measured by Luo & Millero (2004) in 0.025 M HNO_3 between 5.2 and 44.5 °C

	5.2 °C	**15.1 °C**	**25.0 °C**	**34.7 °C**	**44.5 °C**
$\log_{10}\beta_1$	3.53 ± 0.01	3.56 ± 0.01	3.61 ± 0.01	3.67 ± 0.01	3.71 ± 0.01
$\log_{10}\beta_2$	5.76 ± 0.02	5.90 ± 0.03	5.99 ± 0.04	6.12 ± 0.03	6.19 ± 0.04

Luo & Millero (2004) investigated the temperature dependence of the 1:1 and 1:2 fluoride complexes of yttrium and the rare earth elements by an ion-exchange method (cation resin) in dilute HNO_3 solutions (0.025 mol/L) between 5.2 and 44.5 °C (see Tab. 23.1.5-4 and Fig. 23.1.5-4). For SmF^{2+}, there is a linear relationship between stability constants and reciprocal

temperature. Fro the linear fit to the data follow $\log_{10}\beta_1 = (3.62 \pm 0.03)$, $\Delta_r H_m(298.15\ K) = (8.07 \pm 1.23)$ kJ · mol^{-1} and $\Delta_r C_{p,m}°(298.15\ K) = 0$. Since there are no data on the dependence of $\Delta_r H_m$ on ionic strength, the value for 0.025 mol/L HNO_3 is used as an approximation for zero ionic strength. Thus,

$$\Delta_r H_m°(298.15\ K) \approx (8.07 \pm 1.23)\ kJ \cdot mol^{-1}$$

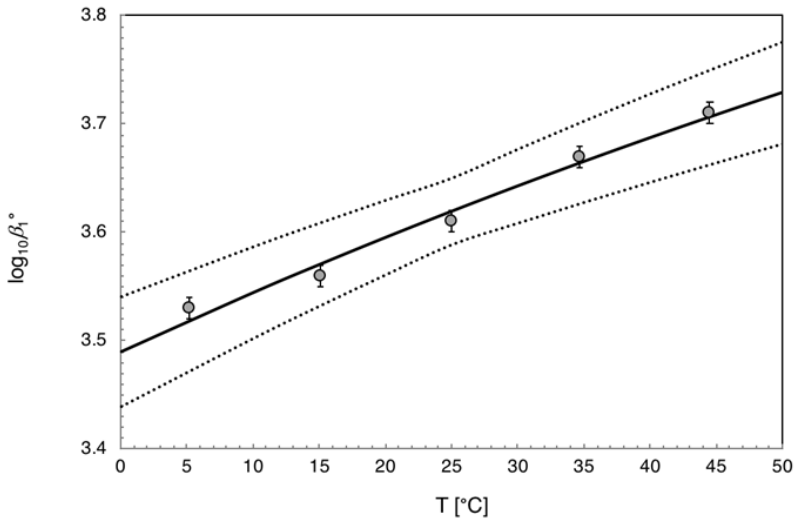

Fig. 23.1.5-4: Stability constants $\log_{10}\beta_1$ of $Sm^{3+} + F^- \rightleftharpoons SmF^{2+}$ measured by Luo & Millero (2004) in 0.025 M HNO_3

An unweighted linear regression of these data as a function of 1/T resulted in $\log_{10}\beta_1°(298.15\ K) = (3.62 \pm 0.03)$, $\Delta_r H_m(298.15\ K) = (8.07 \pm 1.23)$ kJ · mol^{-1} and $\Delta_r C_{p,m}°(298.15\ K) = 0$. Solid line: Corresponding extrapolation of $\log_{10}\beta_1°$ to lower and higher temperatures with uncertainties indicated by the dotted lines.

23.1.5.1.2 SmF2+

Quantitative data on the formation of SmF_2^+ is scarce (see Tab. 23.1.5-5). Menon et al. (1988) and Menon & James (1989a, 1989b) provided conditional stability constants $\log_{10}\beta_2(298.15\ K)$ for the reaction $Sm^{3+} + 2\ F^- \rightleftharpoons SmF_2^+$ measured in 0.5 M NH_4NO_3, whereas the values reported by Schijf & Byrne (1999) and Luo & Millero (2004) were measured in 0.025 M HNO_3. Since these data cannot be extrapolated to zero ionic strength with SIT (measurements were made at only two ionic strengths, with a different background electrolyte for each) we extrapolated the data by Schijf & Byrne (1999) and Luo & Millero (2004) using the Debye-Hückel term as used in the SIT, assuming that the specific ion interactions are negligible at the very low concentration of the background electrolyte. Thus,

$$\log_{10}\beta_2°(298.15\ K) = \log_{10}\beta_2(298.15\ K) - \Delta z^2 D$$

where

$$D = 0.509\ I_m^{0.5}/(1 + 1.5\ I_m^{0.5})$$

From the mean of the conditional constants by Schijf & Byrne (1999) and Luo & Millero (2004), $\log_{10}\beta_2(298.15\ K) = 6.05$, $\Delta z^2 = -10$ for the reaction $Sm^{3+} + 2\ F^- \rightleftharpoons SmF_2^+$, and $D = 0.065$ at $I_m \approx I_c = 0.025\ kg \cdot mol^{-1}$ follows

Tab. 23.1.5-5: Data for the stability constant $\log_{10}\beta_2$ of $Sm^{3+} + 2\ F^- \rightleftharpoons SmF_2^+$ at 25 °C in nitrate media

Values of $\log_{10}\beta_2$ accepted for extrapolation to zero ionic strength are bold. Abbreviations: cat: cation exchange, sel: ion-selective electrode.

Method	Medium	I reported	I_m [mol · kg^{-1}]	$\log_{10}\beta_2$ (reported)	$\log_{10}\beta_2$ (accepted)	Reference
cat	HNO_3	0.025 M	≈ 0.025 m	6.10 ± 0.09	**6.10 ± 0.10**	Schijf & Byrne (1999)
cat	HNO_3	0.025 M	≈ 0.025 m	5.99 ± 0.04	**5.99 ± 0.10**	Luo & Millero (2004)
sel	NH_4NO_3	0.5 M		6.06 ± 1.21 [a]		Menon et al. (1988)
sel	NH_4NO_3	0.5 M		6.95 ± 0.23 [b]		Menon & James (1989a, 1989b)

[a] Calculated from $\beta_2 = (1.14 \pm 1.07) \times 10^6$.
[b] Calculated from $\beta_2 = (9.0 \pm 3.7) \times 10^6$.

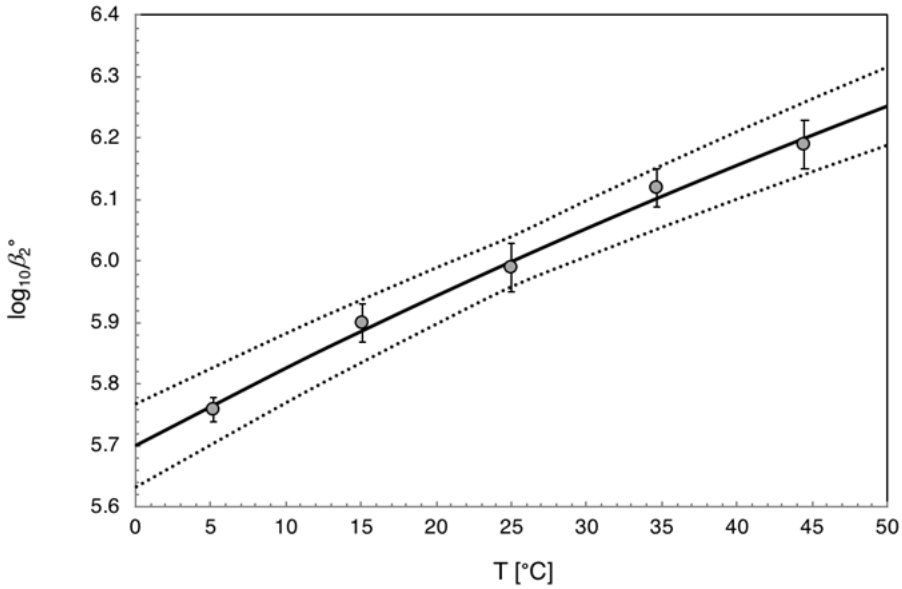

Fig. 23.1.5-5: Stability constants $\log_{10}\beta_2$ of $Sm^{3+} + 2\ F^- \rightleftharpoons SmF_2^+$ measured by Luo & Millero (2004) in 0.025 M HNO_3

An unweighted linear regression of these data as a function of 1/T resulted in $\log_{10}\beta_2°(298.15\ K) = (6.00 \pm 0.04)$, $\Delta_r H_m(298.15\ K) = (18.7 \pm 1.7)\ kJ \cdot mol^{-1}$ and $\Delta_r C_{p,m}°(298.15\ K) = 0$. Solid line: Corresponding extrapolation of $\log_{10}\beta_2°$ to lower and higher temperatures with uncertainties indicated by the dotted lines.

$$Sm^{3+} + 2\ F^- \rightleftharpoons SmF_2^+$$

$$log_{10}\beta_2°(298.15\ K) = (6.7 \pm 0.3)$$

where the uncertainty has been estimated. This value is included in TDB 2020 as supplemental datum, together with

$$\varepsilon(SmF_2^+, Cl^-) \approx (0.05 \pm 0.10)\ kg \cdot mol^{-1}$$

and

$$\varepsilon(SmF_2^+, ClO_4^-) \approx (0.2 \pm 0.1)\ kg \cdot mol^{-1}$$

as estimated according to the method described in Section 1.5.3.

The stability constants of SmF_2^+ measured by Luo & Millero (2004) in 0.025 M HNO_3 solutions between 5.2 and 44.5 °C (see Tab. 23.1.5-4 and Fig. 23.1.5-5) are characterized by a linear relationship with reciprocal temperature. From the linear fit to the data follow $\log_{10}\beta_2 =$ (6.00 ± 0.04), $\Delta_r H_m(298.15\ K) = (18.7 \pm 1.7)$ kJ · mol^{-1} and $\Delta_r C_{p,m}°(298.15\ K) = 0$. Since there are no data on the dependence of $\Delta_r H_m$ on ionic strength, the value for 0.025 mol/L HNO_3 is used as an approximation for zero ionic strength. Thus,

$$\Delta_r H_m°(298.15\ K) \approx (18.7 \pm 1.7)\ kJ \cdot mol^{-1}$$

$$\Delta_r C_{p,m}°(298.15\ K) = 0$$

are included in TDB 2020 as supplemental data.

23.1.5.2 Samarium fluoride solids

There appear to be only a few experimental determinations of the solubility of samarium fluoride solids.

Fraústo da Silva & Queimado (1973) determined the solubility products of REE fluorides from oversaturation in 0.1 M $NaNO_3$ at 25 °C using a fluoride ion-selective electrode. Precipitates were produced by adding an excess of a 0.035 M solution of REE nitrate to a 0.035 M solution of sodium fluoride, adding distilled water to adjust the total volume and an appropriate amount of $NaNO_3$ to set the ionic strength to 0.1 M. The precipitates that formed were left to age in the solution under occasional stirring and the potential was measured at regular intervals until a constant value was obtained, which was usually attained after 4 – 10 days and pH was found to be around 5. Composition, hydration, as well as crystallinity and structure of the precipitates were not characterized. The conditional solubility products were extrapolated to zero ionic strength using the Davies equation without consideration of potential complex formation. For SmF_3(pr) Fraústo da Silva & Queimado (1973) obtained $\log_{10}K_{s,0}°(298.15\ K) = -19.3$.

Itoh et al. (1984) measured the solubility products of REE fluoride powders in pure water from undersaturation at 25 °C using a fluoride ion-selective electrode. In order to prevent the formation of HF in acidic solutions, the experimental solutions were kept at pH 5 using a buffer. No information was given by these authors on the duration of the experiments and on the grain size of the powders. The solids were not examined after the experiment either. Due to the low concentrations of the solutes, the activity coefficients of the REE cations and of fluoride were assumed to be one and no complexes were considered. For SmF_3(s) Itoh et al. (1984) obtained $\log_{10}K_{s,0}°$(298.15 K) = -19.0. Itoh et al. (1984) also tried to determine the solubility product of a lanthanum fluoride single crystal but failed to obtain saturated solutions even after three months of continuous stirring.

Menon et al. (1988) used conductometry, potentiometry and radiometry to determine the solubility products of Sm and Gd fluorides in water at 25 °C. The REE fluoride precipitates were prepared by mixing hot solutions of REE chlorides with HF. For the radiometric procedure, the REE chloride solutions were mixed with an appropriate amount of the respective radioactive REE. The precipitates were washed several times with doubly distilled water and dried. Menon et al. (1988) referred to the precipitates as ($LnF_3 \cdot 0.5H_2O$), but there are no indications that they analysed the precipitates for composition or structure before and after the experiments. Small batches of the dried precipitates were agitated with doubly distilled water for at least 7 h in order to reach saturation, which was tested by repeated measurements of the conductance of the solutions. The pH of the solutions was in the range of 5.2-6.3 and the calculated ionic strength was smaller than 1.5×10^{-4} M. From the measured solubilities of samarium fluoride, Menon et al. (1988) calculated the solubility products, taking into account the formation of SmF^{2+}, $SmOH^{2+}$, and HF. They obtained $\log_{10}K_{s,0}°$(298.15 K) = -17.8 from radiometry, $\log_{10}K_{s,0}°$(298.15 K) = -16.1 from conductometry, and $\log_{10}K_{s,0}°$(298.15 K) = -16.0 from potentiometry. Menon et al. (1988) also measured the solubilities at higher temperatures (up to 60 °C), these are discussed below.

Menon & James (1989b) used similar methods as Menon et al. (1988) for the determination of the solubility products of all REE fluorides (except Pm). For Sm fluorides, they retained the values obtained in their previous work.

Migdisov et al. (2009) measured the solubilities of all REE fluoride solids (except Pm) in fluoride- and chloride-bearing aqueous solutions at 150, 200, and 250 °C and saturated water vapor pressure. They extrapolated their solubility products to 25 °C using the $C_p°$ and $S°$ values recommended by Konings & Kovács (2003) and obtained for SmF_3(cr) $\log_{10}K_{s,0}°$(298.15 K) = -19.83. Migdisov et al. (2009) also calculated a solubility product for SmF_3(cr) entirely from calorimetric data recommended by Konings & Kovács (2003) and obtained $\log_{10}K_{s,0}°$(298.15 K) = -19.81.

The values for the solubility product $\log_{10}K_{s,0}°$(298.15 K) of SmF_3(cr) by Fraústo da Silva & Queimado (1973), Itoh et al. (1984) and Migdisov et al. (2009) vary between -19.0 and -19.83, while the values obtained by Menon et al. (1988) and Menon & James (1989b) are significantly lower (spanning the range between -16.0 and -17.8), see Tab. 23.1.5-6. We are not able to resolve this discrepancy. However, Migdisov et al. (2009) argued that, since the good agreement between the experimental solubility products by Fraústo da Silva & Queimado (1973) and Itoh et al. (1984) covers the entire range of REE fluorides and is therefore systematic, they are likely the most reliable ones at 25 °C. We share this view and have therefore selected the average of the values (with an estimated uncertainty) determined by Fraústo da Silva & Queimado (1973) and Itoh et al. (1984) for TDB 2020:

$SmF_3(cr) \rightleftharpoons Sm^{3+} + 3\ F^-$

$\log_{10}K_{s,0}°(298.15\ K) = 19.2 \pm 0.4$

Menon et al. (1988) also measured the solubilities of their Sm fluoride precipitates at higher temperatures (up to 60 °C, see Tab. 23.1.5-7). We took the average of the solubility products $K_{s,0}°$ determined by potentiometry and conductometry at each temperature. The averaged solubility products are linear in a $\log_{10}K_{s,0}°$ vs. 1/T plot, an unweighted linear regression resulted in $\log_{10}K_{s,0}°(298.15\ K) = -(16.1 \pm 1.2)$, $\Delta_rH_m°(298.15\ K) = (73.2 \pm 39.5)\ kJ \cdot mol^{-1}$ and $\Delta_rC_{p,m}°(298.15\ K) = 0$, see Fig. 23.1.5-6. Although the value of $\log_{10}K_{s,0}°(298.15\ K)$ is two orders of magnitude larger than the value selected for TDB 2020, we include

$$\Delta_rH_m°(298.15\ K) = (73 \pm 40)\ kJ \cdot mol^{-1}$$

and

$$\Delta_rC_{p,m}°(298.15\ K) = 0$$

as supplemental data in TDB 2020.

Tab. 23.1.5-6: Reported solubility products $\log_{10}K_{s,0}°$ of $SmF_3(cr) \rightleftharpoons Sm^{3+} + 3\ F^-$ at 25 °C

Abbreviations: cat: cation exchange, sel: ion-selective electrode, pot: potentiometry, con: conductometry, rad: radiometry, calc: calculated.

Method	**Medium**	***I* reported**	**$\log_{10}K_{s,0}°$**	**Reference**
sel	$NaNO_3$	0.1 M	-19.3	Fráusto da Silva & Queimado (1973)
sel		dilute	-19.0	Itoh et al. (1984)
pot		dilute	-16.0	Menon et al. (1988), Menon & James (1989b)
con		dilute	-16.1	Menon et al. (1988), Menon & James (1989b)
rad		dilute	-17.8	Menon et al. (1988), Menon & James (1989b)
calc			-19.81	Migdisov et al. (2009) [a]
calc			-19.83	Migdisov et al. (2009) [b]

[a] Calculated from calorimetric data recommended by Konings & Kovács (2003).

[b] Extrapolated from their experimental data at elevated temperatures using the $C_p°$ and S° values recommended by Konings & Kovács (2003).

Tab. 23.1.5-7: Solubility products $K_{s,0}°$ of $SmF_3(cr) \rightleftharpoons Sm^{3+} + 3\ F^-$ measured by Menon et al. (1988) between 26 and 60 °C by conductometry (cond) and potentiometry (pot)

T [K]	**T** [°C]	$K_{s,0}°$ **cond**	$\log_{10}K_{s,0}°$ **cond**	$K_{s,0}°$ **pot**	$\log_{10}K_{s,0}°$ **pot**	$K_{s,0}°$ **average**	$\log_{10}K_{s,0}°$ **average**
299	26	9.50×10^{-17}	-16.02	6.40×10^{-17}	-16.19	7.95×10^{-17}	-16.10
304	31	1.41×10^{-16}	-15.85	1.63×10^{-16}	-15.79	1.52×10^{-16}	-15.82
309	36	2.11×10^{-16}	-15.68	2.05×10^{-16}	-15.69	2.08×10^{-16}	-15.68
314	41	2.25×10^{-16}	-15.65	2.90×10^{-16}	-15.54	2.58×10^{-16}	-15.59
319	46	3.42×10^{-16}	-15.47	3.53×10^{-16}	-15.45	3.48×10^{-16}	-15.46
324	51	6.59×10^{-16}	-15.18	4.80×10^{-16}	-15.32	5.7×10^{-16}	-15.24
329	56	1.29×10^{-15}	-14.89	9.31×10^{-16}	-15.03	1.11×10^{-15}	-14.95
333	60	3.07×10^{-15}	-14.51	1.50×10^{-15}	-14.82	2.29×10^{-15}	-14.64

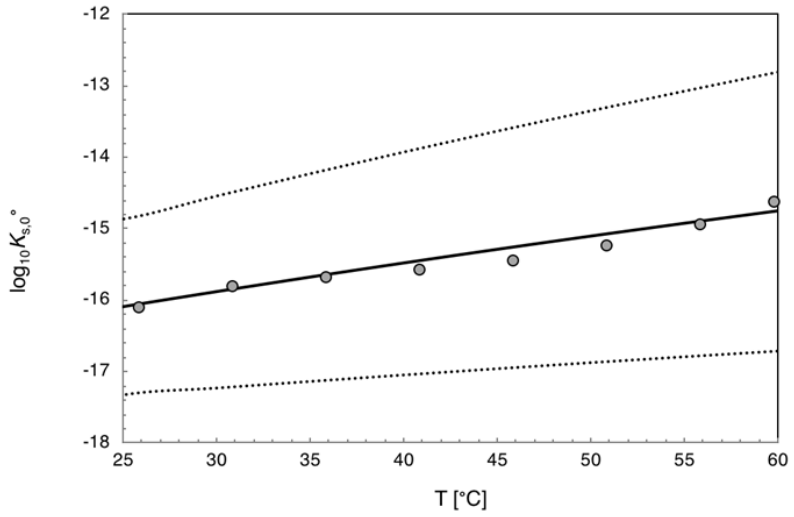

Fig. 23.1.5-6: Solubility products $\log_{10}K_{s,0}°$ of $SmF_3(cr) \rightleftharpoons Sm^{3+} + 3\ F^-$ measured by Menon et al. (1988), see Tab. 23.1.5-7.

An unweighted linear regression of these data as a function of 1/T resulted in $\log_{10}K_{s,0}°(298.15\ K) = -(16.1 \pm 1.2)$, $\Delta_r H_m°(298.15\ K) = (73.2 \pm 39.5)\ kJ \cdot mol^{-1}$ and $\Delta_r C_{p,m}°(298.15\ K) = 0$. Solid line: Corresponding extrapolation of $\log_{10}K_{s,0}°$ to higher temperatures with uncertainties indicated by the dotted lines.

23.1.6 Samarium chloride compounds and complexes

23.1.6.1 Aqueous samarium chloride complexes

Chloride complexes with Sm(III) are very weak, and high chloride concentrations are needed to form such complexes. This implies that very large amounts of perchlorate ions in the background electrolyte need to be replaced by chloride ions. Thus, changes in activity coefficients due to such large compositional changes in the background electrolyte must be accounted for, which can be done using the method described by Spahiu & Puigdomènech (1998). Jordan (in prep.) reviewed numerous experimental studies (mainly employing solvent extraction and cation exchange) on the complexation of Eu(III) with chloride and came to the conclusion that the changes in activity coefficients due to the replacement of the background electrolyte anion by chloride have a much larger impact than complexation with chloride and for this reason the experimental data can be reproduced without invoking any complexation with chloride. It is reasonable to assume that Sm(III) behaves similarly and that there is no significant Sm(III) chloride complexation at low chloride concentrations.

This is corroborated by several spectroscopic studies of trivalent actinides and lanthanides.

Fanghänel et al. (1995) investigated the formation of Cm(III) chloride complexes with time-resolved laser fluorescence spectroscopy (TRLFS) at 25 °C and chloride concentrations from 0 to about 20 mol · kg^{-1} in $CaCl_2$ solutions at acidic pH. They identified Cm^{3+}, $CmCl^{2+}$, and $CmCl_2^{+}$, but noted that at low chloride concentrations (< 3 mol · kg^{-1}) at most 5% of curium is found as chloride complexes.

Allen et al. (2000) used extended X-ray absorption fine structure (EXAFS) experiments to study the inner sphere coordination of trivalent lanthanide and actinide ions in aqueous LiCl solutions as a function of increasing chloride concentration. For Cm^{3+}, these authors were not able to observe any chloride complexes at 7.0 M LiCl, only at 8.7 M LiCl they observed an average coordination number of 1.2 ± 0.33 for all the inner sphere chloro complexes in solution. They argued that these data suggest little inner sphere complex formation for Cm^{3+} at LiCl concentrations < about 5 M and that the trivalent lanthanide ions – which show chloro complexation at higher LiCl concentrations – also lack significant chloride complex formation at LiCl concentrations < about 5 M if one assumes that they are like Cm^{3+}.

In an EXAFS study carried out by Skerencak-Frech et al. (2014) at 25, 90 and 200 °C and Am^{3+} and Cl^- concentrations of 10^{-3} and 3 mol · kg^{-1}, resp., no Am^{3+} chloride complexes were found at temperatures below 90 °C.

Koke et al. (2019) used TRLFS for the study of Cm^{3+} complexation with chloride in LiCl, NaCl, $MgCl_2$, and $CaCl_2$ at temperatures in the range of 25-200 °C. No appreciable complex formation was detected at 25 °C and chloride concentrations < 3 mol · kg^{-1}.

It is reasonable to assume that these spectroscopic findings also apply to Sm^{3+} chloride complexes.

In summary, there is no evidence from chemical and spectroscopic studies that appreciable amounts of Sm^{3+} chloride complexes can be expected to form at chloride concentrations < 3 mol · kg^{-1} and temperatures below about 90 °C.

Thus, no stability constants for Sm^{3+} chloride complexes are selected for TDB 2020. The specific ion interaction coefficient $\varepsilon(Sm^{3+}, Cl^-)$ derived in Section 23.1.3 from mean activity coefficient data of aqueous $SmCl_3$ solutions should be sufficient to describe the interaction between Sm^{3+} and Cl^- in the application range of TDB 2020.

23.1.6.2 Samarium chloride solids

Mioduski et al. (2009) reviewed and reported the results of several solubility experiments of $SmCl_3$(cr) in water. The solubility at 25 °C is on the order of 3.6 mol · kg^{-1} and the equilibrium solid is $SmCl_3 \cdot 6H_2O$(cr). Obviously, samarium chloride is highly soluble and is not considered in TDB 2020.

23.1.7 Samarium sulphate compounds and complexes

23.1.7.1 Aqueous samarium sulphate complexes

Due to a lack of reliable data for Sm sulphate complexes, we used the data for the corresponding europium sulphate complexes selected by Hummel et al. (2002) as estimates. Thus

$$Sm^{3+} + SO_4^{2-} \rightleftharpoons SmSO_4^+$$

$$\log_{10}\beta_1^\circ(298.15\ K) = (3.95 \pm 0.08)$$

$$\varepsilon(SmSO_4^+, ClO_4^-) = (0.27 \pm 0.09)\ kg \cdot mol^{-1}$$

$$Sm^{3+} + 2\ SO_4^{2-} \rightleftharpoons Sm(SO_4)_2^-$$

$$\log_{10}\beta_2^\circ(298.15\ K) = (5.7 \pm 0.2)$$

$$\varepsilon(Sm(SO_4)_2^-, Na^+) = (0.22 \pm 0.20)\ kg \cdot mol^{-1}$$

are included in TDB 2020 as supplemental data, together with the estimate (based on the estimation method (described in Section 1.5.3)

$$\varepsilon(SmSO_4^+, Cl^-) \approx (0.05 \pm 0.10)\ kg \cdot mol^{-1}$$

23.1.7.2 Samarium sulphate solids

REE form in general soluble sulphates. For $Eu_2(SO_4)_3 \cdot 8H_2O$(cr), e.g., Rard (1988) determined solubilities of around 0.032 mol kg^{-1} at 25 °C and Marshall & Slusher (1975) solubilities of 0.03252 and 0.03276 mol kg^{-1} for $Sm_2(SO_4)_3 \cdot 8H_2O$(cr) at the same temperature. As REE also form comparatively insoluble hydroxides and carbonates, it is very unlikely that REE sulphates will play any role in limiting the solubility of REE in natural environments. Therefore, no data for $Sm_2(SO_4)_3 \cdot 8H_2O$(cr) are included in TDB 2020.

23.1.8 Samarium carbonate compounds and complexes

23.1.8.1 Aqueous samarium carbonate complexes

Due to a lack of reliable data for Sm sulphate complexes Due to a lack of reliable data for Sm carbonate complexes, we used the data for the corresponding europium carbonate complexes selected by Hummel et al. (2002) as estimates. Thus

$$Sm^{3+} + CO_3^{2-} \rightleftharpoons SmCO_3^+$$

$$\log_{10}\beta_1°(298.15\ K) = (8.1 \pm 0.2)$$

$$\varepsilon(SmCO_3^+, ClO_4^-) = (0.15 \pm 0.18)\ kg \cdot mol^{-1}$$ [60]

$$Sm^{3+} + 2\ CO_3^{2-} \rightleftharpoons Sm(CO_3)_2^-$$

$$\log_{10}\beta_2°(298.15\ K) = (12.1 \pm 0.3)$$

$$\varepsilon(Sm(CO_3)_2^-, Na^+) = -(1.17 \pm 0.32)\ kg \cdot mol^{-1}$$ [61]

are included in TDB 2020 as supplemental data, together with the estimate (based on the estimation method (described in Section 1.5.3)

$$\varepsilon(SmCO_3^+, Cl^-) \approx (0.05 \pm 0.10)\ kg \cdot mol^{-1}$$

23.1.8.2 Samarium carbonate solids

Due to a lack of reliable data for Sm carbonate solids, we used the data for the corresponding europium carbonate solids selected by Hummel et al. (2002) as crude estimates with increased uncertainties. Therefore, we selected

$$Sm_2(CO_3)_3(cr) \rightleftharpoons 2\ Sm^{3+} + 3\ CO_3^{2-}$$

$$\log_{10}K_{s,0}°(298.15\ K) = -(35 \pm 2)$$

and

$$SmOHCO_3(cr) \rightleftharpoons Sm^{3+} + OH^- + CO_3^{2-}$$

$$\log_{10}K_{s,0}°(298.15\ K) = -(21.7 \pm 2.0)$$

as supplemental data for TDB 2020.

---

[60] This value follows from $\Delta\varepsilon = -(0.24 \pm 0.18)$ kg · mol^{-1} reported by Hummel et al. (2002), $\varepsilon(Eu^{3+}, ClO_4^-) = (0.47 \pm 0.01)$ kg · mol^{-1} selected by Thoenen (2019), and $\varepsilon(CO_3^{2-}, Na^+) = -(0.08 \pm 0.03)$ kg · mol^{-1} selected by NEA (Lemire et al. 2013).

[61] This value follows from $\Delta\varepsilon = -(1.48 \pm 0.31)$ kg · mol^{-1} reported by Hummel et al. (2002), $\varepsilon(Eu^{3+}, ClO_4^-) = (0.47 \pm 0.01)$ kg · mol^{-1} selected by Thoenen (2019), and $\varepsilon(CO_3^{2-}, Na^+) = -(0.08 \pm 0.03)$ kg · mol^{-1} selected by NEA (Lemire et al. 2013).

23.1.9 Samarium phosphate compounds and complexes

23.1.9.1 Aqueous phosphate carbonate complexes

There appear to be no data on the complexation of Sm(III) with phosphate. For this reason we took recourse to the corresponding data for Eu(III) which were obtained by Jordan et al. (2018) using laser-induced luminescence spectroscopy (see Section 23.2.9.1). The data selected for $EuH_2PO_4^{2+}$ are used as estimates for $SmH_2PO_4^{2+}$ and are included in TDB 2020 as supplemental data:

$$Sm^{3+} + H_3PO_4(aq) \rightleftharpoons SmH_2PO_4^{2+} + H^+$$

$$log_{10}\beta_1°(298.15\ K) = (0.89 \pm 0.13)$$

$$\Delta_r H_m°(298.15\ K) = (14.7)\ kJ \cdot mol^{-1}$$

$$\Delta_r C_{p,m}°(298.15\ K) = 0$$

$$\varepsilon(SmH_2PO_4^{2+}, ClO_4^-) = (0.18 \pm 0.08)\ kg \cdot mol^{-1}$$

$$\varepsilon(SmH_2PO_4^{2+}, Cl^-) \approx (0.15 \pm 0.10)\ kg \cdot mol^{-1}$$

23.1.9.2 Samarium phosphate solids

According to Gausse et al. (2016), rare-earth phosphates $LnPO_4 \cdot nH_2O(s)$ exhibit a variety of crystal structures: Monazite, xenotime, rhabdophane and churchite. Monazite and xenotime are both anhydrous and crystallize in the monoclinic and trigonal crystal systems, respectively. The hydrous phosphates rhabdophane, $LnPO_4 \cdot 0.667H_2O(s)$, and churchite, $LnPO_4 \cdot 2H_2O(s)$, crystallize in the monoclinic system. For the light REE from La to Eu the monazite structure has been identified, while the middle range REE from Gd to Dy can be found in both the monazite and xenotime structure. The heavy REE from Ho to Lu and Y are found in the xenotime structure. Both light and middle range REE (from La to Dy) can also be found in the rhabdophane structure. Finally, the middle range and heavy REE (from Gd to Lu and Y) can also be found in the churchite structure. Thus Sm is found either in the monazite ($SmPO_4$) or rhabdophane structure ($SmPO_4 \cdot 0.667H_2O$).

Firsching & Brune (1991) determined the solubilities of REE (except Ce and Pm) and Y phosphates in aqueous solution at 25 °C. The REE phosphates were prepared by precipitation from homogeneous solutions of REE in mixtures of phosphoric and perchloric acid using the hydrolysis of urea. Urea was added to the solutions; heating of the solutions induced the hydrolysis of urea, thereby increasing the pH and leading to the precipitation of the REE phosphates. A second method was also used that took advantage of the decreasing solubility of REE phosphates with temperature. Saturated solutions of REE in mixtures of phosphoric and perchloric acid were heated to 100 °C, leading to the precipitation of the REE phosphates. Both types of crystals were used in the solubility studies, but they were not further analysed, neither with respect to structure, nor to composition. The crystals were placed in dilute solutions of $HClO_4$ (0.0697 and 0.0910 M) and kept in contact with the solutions for more than 3 months (equilibrium from undersaturation was reached after about 80 days). Firsching & Brune (1991) noted that "undoubtedly, the surfaces of the solid phase had achieved a thermodynamically stable hydrate

form". However, composition and structure of these hydrated surfaces were not determined. Sm^{3+} and $H_3PO_4(aq)$ were found to be the only significant samarium and phosphate species under the low pH of the experiments (< 1.2) and their concentrations indicated congruent dissolution. The following stepwise dissociation constants of phosphoric acid were used by Firsching & Brune (1991) for the calculation of the solubility product: $K_1°(298.15\ K) = 7.11 \times 10^{-3}$, $K_2°(298.15\ K) = 6.34 \times 10^{-8}$, and $K_3°(298.15\ K) = 4.17 \times 10^{-13}$, which correspond to $\log_{10}K_1°(298.15\ K) = -2.15$, $\log_{10}K_2°(298.15\ K) = -7.20$, and $\log_{10}K_3°(298.15\ K) = -12.38$.

For the reaction

$$SmPO_4(s) \rightleftharpoons Sm^{3+} + PO_4^{3-}$$

they obtained $\log_{10}K_{s,0}°(298.15\ K) = -(25.99 \pm 0.05)$, which corresponds to $\log_{10}K_s°(298.15\ K) = -(4.26 \pm 0.05)$ for the reaction

$$SmPO_4(s) + 3\ H^+ \rightleftharpoons Sm^{3+} + H_3PO_4(aq)$$

Liu & Byrne (1997) measured the solubilities of REE (except Pm) and Y phosphates in aqueous solution at 25 °C. The phosphate solids were prepared in three different ways. (1) REE oxides (Ce and Tb were used as chlorides) were combined with NaH_2PO_4 to produce equimolar solutions of total phosphate and REE. 0.4 μm filters were used to separate the precipitates from the solution. (2) Precipitates from procedure 1 were aged for two months in the solution at 25 °C before filtration. Precipitates from both procedures were rinsed in deionized water until the phosphate concentrations dropped below the spectrophotometric detection limits. The precipitates were then rinsed with dilute acid followed by deionized water until the pH of the rinse solutions remained near neutral. (3) Precipitates were produced following the urea method by Firsching & Brune (1991) discussed above and finally washed with dilute acid and deionized water. Prior to being used in the solubility experiments the precipitates were analysed by X-ray diffraction. Precipitates of the light REE obtained from procedure 1 were X-ray amorphous and those of the heavy REE showed only hints of crystallinity. Precipitates from procedures 2 and 3 were well crystallized and generally conformed to the rhabdophane structure. Solubilities were measured from undersaturation in dissolution experiments in 0.1 molar perchloric acid. Sample bottles were kept at 25 °C and vigorously shaken for up to five months. For analysis, the solutions were passed through 0.2 μm filters. Total phosphate concentrations 10% below the final values were often obtained after only two weeks. As in the experiments by Firsching & Brune (1991), dissolution of the REE phosphates was congruent. The solubility products for the Sm phosphates were calculated from the solubility data by using the following stepwise dissociation constants for phosphoric acid, $\log_{10}K_1°(298.15\ K) = -1.943$, $\log_{10}K_2°(298.15\ K) = -6.8920$, and $\log_{10}K_3°(298.15\ K) = -11.887$, together with the estimated formation constants for Sm phosphate complexes $\log_{10}\beta°(SmHPO_4^+, 298.15\ K) = 4.719$ and $\log_{10}\beta°(SmH_2PO_4^{2+}, 298.15\ K) = 2.156$ (Byrne et al. 1991)[62] and the activity coefficients $\gamma(Sm^{3+}) = 0.134$ and $\gamma(PO_4^{3-}) = 0.189$. For the precipitates from procedure 2 and 3, Liu & Byrne (1997) obtained $\log_{10}K_{s,0}°(298.15\ K) = -26.18$ (100 days of equilibration) and $\log_{10}K_{s,0}°(298.15\ K) = -26.19$ (30 days of equilibration), respectively. From these two values they derived their recommended value $\log_{10}K_{s,0}°(298.15\ K)$

[62] Byrne et al. (1991) extrapolated their experimentally determined stability constants for $CmHPO_4^+$ and $GdHPO_4^+$, and $CmH_2PO_4^{2+}$ and $GdH_2PO_4^{2+}$, resp., to the other REE phosphate complexes using a linear free energy relationship.

= -(26.19 ± 0.01), which corresponds to $\log_{10}K_s°(298.15\ K)$ = -(5.47 ± 0.01) for the reaction in terms of $H_3PO_4(aq)$. The solubility of precipitates from procedure 1 is significantly higher, with $\log_{10}K_{s,0}°(298.15\ K) \approx -25.55$ after 150 days. In the discussion of their experimental results, Liu & Byrne (1997) pointed out that in natural environments Y and REE do not each form their own discrete phosphate phases but rather form solid solutions by coprecipitation.

Cetiner et al. (2005) carried out solubility experiments of La, Nd, Sm, and Y phosphates at 23 and 50 °C and pH from 0 – 2 in NaCl-HCl and $NaClO_4$-$HClO_4$ solutions with ionic strengths of 0.1, 0.5, 1.0, and 5.0 mol · kg^{-1}. Commercially available phosphates in powder form were used. All samples were characterized by X-ray diffraction (XRD) and scanning electron microscopy (SEM) both before and after experiments. According to the XRD spectra, no other components were present in the powders. The La and Nd phosphates had the monazite structure, the Sm phosphates the rhabdophane structure, and the Y phosphates the xenotime structure. XRD spectra were virtually identical before and after the experiments. The REE phosphate powders were put in the experimental solutions and kept at room temperature (23 °C) on a shaking table. Experiments at 50 °C were carried out in a constant temperature, shaking heat bath. Solutions were passed through 0.20 μm filters for analysis. Approach to equilibrium was from undersaturation, solution concentrations at 23 °C remained constant after about 15-20 days. Cetiner et al. (2005) did not try to attain equilibrium from supersaturation because of the possibility that precipitated solids would not have the same structural and hydration state as the solids used in the dissolution experiments. Cetiner et al. (2005) noted that, while the solids used in the dissolution experiments were stoichiometric within analytical uncertainty in the case of the La, Nd and Y phosphates and somewhat less so in the case of Sm phosphate, the equilibrium solutions showed an excess of P with respect to the corresponding REE, in some cases by more than an order of magnitude. Cetiner et al. (2005) considered two explanations: (1) Incongruent dissolution of the REE phosphate, resulting in a less soluble REE phase, such as an oxide, hydroxide, carbonate or hydroxycarbonate, and (2) impurity of initial REE phosphate with a phosphate that is more soluble than the REE phosphate. They concluded from several lines of evidence that the second explanation is probably more reasonable than the first. The conditional stability constants determined by Cetiner et al. (2005) in NaCl solutions are shown in Tab. 9-1. These authors used an empirical extrapolation of the data to zero ionic strength, based on the expression $\log_{10}K_s(I) = \log_{10}K_s° + A\ \Delta z^2\ I^{0.5}/(1 + I^{0.5}) + C\ I + D\ I^2 + \cdots$, where $\log_{10}K_s°$ and C, D, ··· were found by a regression analysis of the data. Thus, Cetiner et al. (2005) obtained $\log_{10}K_s°(296.15\ K)$ = -2.86 and $\log_{10}K_{s,0}°(296.15\ K)$ = -24.6. We used SIT to extrapolate the data in Tab. 9-1 to zero ionic strength, see Fig. 23.1.9-1, resulting in $\log_{10}K_s°(296.15\ K)$ = -(3.19 ± 0.13), and $\Delta\varepsilon$ = -(0.17 ± 0.05) kg · mol^{-1}. From $\Delta\varepsilon$, the NEA selected $\varepsilon(H^+, Cl^-)$ = (0.14 ± 0.01) kg · mol^{-1}, and assuming that $\varepsilon(H_3PO_4, NaCl) = 0$ then follows $\varepsilon(Sm^{3+}, Cl^-)$ = (0.25 ± 0.05) kg · mol^{-1}, which is in agreement with $\varepsilon(Sm^{3+}, Cl^-)$ = (0.25 ± 0.01) kg · mol^{-1} selected in Section 23.1.3.

Tab. 23.1.9-1: Data for the conditional solubility product $\log_{10}K_s$(298.15 K) of $SmPO_3$(cr) + 3 H^+ ⇌ Sm^{3+} + H_3PO_4(aq) measured by Cetiner et al. (2005) at 23 °C in NaCl

Uncertainties are estimated. Values of $\log_{10}K_s$ accepted for the SIT analysis shown in Fig. 23.1.9-1 are bold. Abbreviations: sol: solubility study.

Method	**Medium**	I_m [mol · kg^{-1}]	**$\log_{10}K_s$ (reported)**	**$\log_{10}K_s$ (accepted)**	**Reference**
sol	NaCl	0.1	-2.16	**-2.16 ± 0.20**	Cetiner et al. (2005)
sol	NaCl	0.5	-2.22	**-2.22 ± 0.20**	Cetiner et al. (2005)
sel	NaCl	1.0	-2.07	**-2.07 ± 0.20**	Cetiner et al. (2005)
sel	NaCl	5.0	-0.73	**-0.73 ± 0.20**	Cetiner et al. (2005)

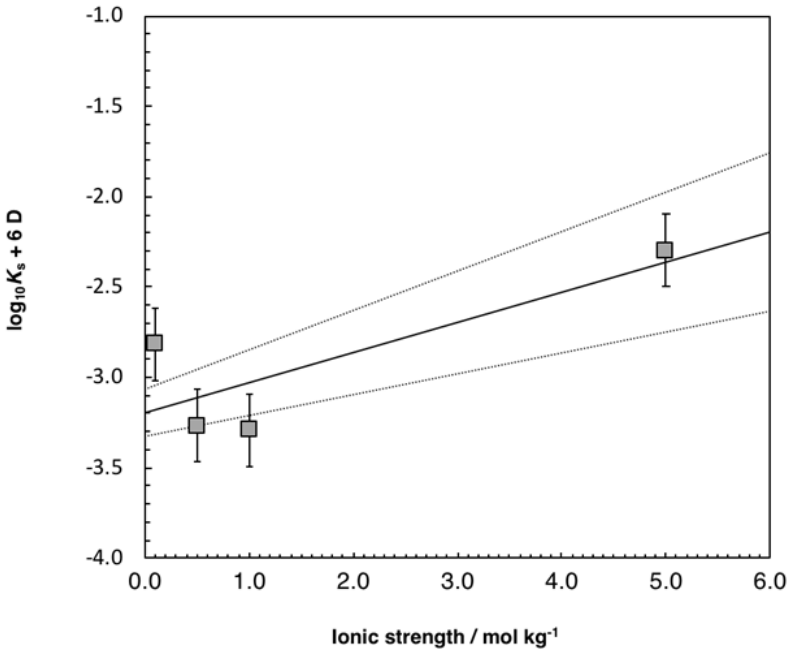

Fig. 23.1.9-1: SIT-plot of the equilibrium $SmPO_3$(cr) + 3 H^+ ⇌ Sm^{3+} + H_3PO_4(aq) in NaCl using the experimental data by Cetiner et al. (2005)

The solid line is obtained by using the derived SIT interaction coefficient, $\Delta\varepsilon$ = -(0.17 ± 0.05) kg · mol^{-1}, and the solubility product at zero ionic strength, $\log_{10}K_s°$(298.15 K) = -(3.19 ± 0.13). The dotted lines represent the associated 95% uncertainty range extrapolated from zero ionic strength to higher NaCl concentrations.

Gausse et al. (2016) determined the solubility of REE rhabdophanes $LnPO_4 \cdot 0.667H_2O$(cr), with Ln = La to Dy (without Pm) from both under- and supersaturation at 25, 60, 70, and 90 °C. For the dissolution experiments (equilibrium from undersaturation), rhabdophane samples were prepared by mixing $LnCl_3$ and H_3PO_4 solutions and keeping them for 14 d at 90 °C. The precipitates were separated from the solution by centrifugation and dried at 90 °C in air overnight. The resulting powders were analysed by powder X-ray diffraction (PXRD) and inspected by environmental scanning electron microscopy (ESEM). The dissolution experiments were carried

out by contacting the rhabdophane powders with 0.1 M HCl solutions and kept in a heating orbital stirrer at 25 ± 5 and 70 ± 5 °C. Dissolution was congruent and solution compositions remained unchanged after approximately 10 d. The remaining precipitates were again characterized by PXRD and ESEM and the rhabdophane structure was confirmed. No additional phases were detected. Gausse et al. (2016) used SIT to extrapolate the conditional solubility constants to zero ionic strength and used the integrated van't Hoff equation to derive $\Delta_r H_m°$ from the solubility constants determined at different temperatures. For samarium rhabdophane, $SmPO_4 \cdot 0.667H_2O$(cr), Gausse et al. (2016) obtained $\log_{10}K_{s,0}°(298.15\ K) = -(25.2 \pm 1.3)$, $\Delta_r H_m°(298.15\ K) = -(22 \pm 8)$ kJ · mol^{-1}, and $\Delta_r C_{p,m}°(298.15\ K) = 0$.

Gysi et al. (2018) presented solubility data for the $CePO_4$, $SmPO_4$ and $GdPO_4$ monazite endmembers measured at 100, 150, 200, and 250 °C. They prepared mm-sized crystals of these solids using a melt flux method and approached equilibrium from undersaturation in perchloric and phosphoric acid solutions at pH around 2 at the specified temperatures and at saturation water vapor pressure. The experiments were run for up to 21 days and the solutions analysed after quenching. 3- and 4-term temperature functions were fit to the data for the samarium monazite and extrapolation to 25 °C resulted in values for $\log_{10}K_{s,0}°(298.15\ K)$ between -27.56 and -27.77.

Tab. 23.1.9-2: Reported solubility products $\log_{10}K_s°(298.15\ K)$ of $SmPO_3(s) + 3\ H^+ \rightleftharpoons Sm^{3+} + H_3PO_4(aq)$ and $\log_{10}K_{s,0}°(298.15\ K)$ of $SmPO_4(s) \rightleftharpoons Sm^{3+} + PO_4^{3-}$

Structure	**$\log_{10}K_s°(298.15\ K)$**	**$\log_{10}K_{s,0}°(298.15\ K)$**	**Reference**
Not determined	-4.26 ± 0.05 [a]	-25.99 ± 0.05	Firsching & Brune (1991)
Rhabdophane	-5.47 ± 0.01 [a]	-26.19 ± 0.01	Liu & Byrne (1997)
Rhabdophane	-2.86	-24.6	Cetiner et al. (2005)
Rhabdophane	-3.19 ± 0.13		this work, based on Cetiner et al. (2005)
Rhabdophane		-25.2 ± 1.3 [b]	Gausse et al. (2016)
Monazite		-27.56, -27.67, -27.77	Gysi et al. (2018)

[a] Calculated from $\log_{10}K_{s,0}°(298.15\ K)$ and the dissociation constants for phosphoric acid used by the authors.

[b] This constant was reported by Gausse et al. (2016) for the reaction $SmPO_4 \cdot 0.667H_2O(cr) \rightleftharpoons Sm^{3+} + PO_4^{3-} + 0.667\ H_2O(l)$.

For TDB 2020, we selected the thermodynamic data determined by Gausse et al. (2016) for samarium rhabdophane because equilibrium was attained from under- and supersaturation and the solids were well characterized both before and after the experiments.

Thus, the following data were included in TDB 2020 for Sm-rhabdophane:

$$SmPO_4 \cdot 0.667H_2O(cr) \rightleftharpoons Sm^{3+} + PO_4^{3-} + 0.667\ H_2O(l)$$

$$\log_{10}K_{s,0}°(298.15\ K) = -(25.2 \pm 1.3)$$

$$\Delta_r H_m°(298.15\ K) = -(22 \pm 8)\ \text{kJ} \cdot \text{mol}^{-1}$$

$$\Delta_r C_{p,m}°(298.15\ K) = 0$$

23.1.10 Selected samarium data

Tab. 23.1.10-1: Selected samarium data (1 bar, 298.15 K) for TDB 2020

T-range refers to the experimental temperature range at which equilibrium constants, $\Delta_r H_m$, and $\Delta_r C_{p,m}°$ were determined. Supplemental data are in italics.

Name	**Redox**	**TDB 2020**				
		$\Delta_f G_m°$ [kJ · mol^{-1}]	**$\Delta_f H_m°$** [kJ · mol^{-1}]	**$S_m°$** [J · K^{-1} · mol^{-1}]	**$C_{p,m}°$** [J · K^{-1} · mol^{-1}]	**Species**
Sm(cr)	0	0	0	69.64	29.53	Sm(cr)
Sm+3	III	-665.3 ± 2.2	-690.0 ± 2.0	-209.3 ± 3.1	-95.9 ± 20	Sm^{3+}

Name	**TDB 2020**				
	$\log_{10}\beta°$	**$\Delta_r H_m°$** [kJ · mol^{-1}]	**$\Delta_r C_{p,m}°$** [J · K^{-1} · mol^{-1}]	**T-range** [°C]	**Reaction**
SmOH+2	-7.76 ± 0.09	*42.7 ± 5.4*	*0*	25 – 55	$Sm^{3+} + H_2O(l) \rightleftharpoons SmOH^{2+} + H^+$
Sm(OH)2+	*-15.22 ± 0.3*	-	-	-	$Sm^{3+} + 2\ H_2O(l) \rightleftharpoons Sm(OH)_2^{+} + 2\ H^+$
Sm(OH)3(aq)	*-23.82 ± 0.3*	-	-	-	$Sm^{3+} + 3\ H_2O(l) \rightleftharpoons Sm(OH)_3(aq) + 3\ H^+$
Sm(OH)4-	*-36.32 ± 0.3*	-	-	-	$Sm^{3+} + 4\ H_2O(l) \rightleftharpoons Sm(OH)_4^{-} + 4\ H^+$
Sm2(OH)2+4	-14.5 ± 0.4	-	-	-	$2\ Sm^{3+} + 2\ H_2O(l) \rightleftharpoons Sm_2(OH)_2^{4+} + 2\ H^+$
Sm3(OH)5+4	-33.9 ± 0.3	-	-	-	$3\ Sm^{3+} + 5\ H_2O(l) \rightleftharpoons Sm_3(OH)_5^{4+} + 5\ H^+$
SmF+2	4.17 ± 0.07	*8.07 ± 1.23*	*0*	5 – 45	$Sm^{3+} + F^- \rightleftharpoons SmF^{2+}$
SmF2+	*6.7 ± 0.3*	*18.7 ± 1.7*	*0*	*5 – 45*	$Sm^{3+} + 2\ F^- \rightleftharpoons SmF_2^{+}$
SmSO4+	*3.95 ± 0.08*	-	-	-	$Sm^{3+} + SO_4^{2-} \rightleftharpoons SmSO_4^{+}$
Sm(SO4)2-	*5.7 ± 0.2*	-	-	-	$Sm^{3+} + 2\ SO_4^{2-} \rightleftharpoons Sm(SO_4)_2^{-}$
SmCO3+	*8.1 ± 0.2*	-	-	-	$Sm^{3+} + CO_3^{2-} \rightleftharpoons SmCO_3^{+}$
Sm(CO3)2-	*12.1 ± 0.3*	-	-	-	$Sm^{3+} + 2\ CO_3^{2-} \rightleftharpoons Sm(CO_3)_2^{-}$
SmH2PO4+2	*0.89 ± 0.13*	*14.7*	*0*	*25 – 80*	$Sm^{3+} + H_3PO_4(aq) \rightleftharpoons SmH_2PO_4^{2+} + H^+$

Tab. 23.1.10-1: Cont.

Name	**TDB 2020**				
	$\log_{10}K_{s,0}°$	**$\Delta_r H_m°$** [kJ · mol^{-1}]	**$\Delta_r C_{p,m}°$** [J · K^{-1} · mol^{-1}]	**T-range** [°C]	**Reaction**
Sm(OH)3(cr)	*15 ± 1*	-	-	-	*$Sm(OH)_3(cr) + 3\ H^+ \rightleftharpoons Sm^{3+} + 3\ H_2O(l)$*
SmF3(cr)	19.2 ± 0.4	*73 ± 40*	*0*	*25 – 60*	$SmF_3(cr) \rightleftharpoons Sm^{3+} + 3\ F^-$
Sm2(CO3)3(cr)	*-35 ± 2*	-	-	-	*$Sm_2(CO_3)_3(cr) \rightleftharpoons 2\ Sm^{3+} + 3\ CO_3^{2-}$*
SmOHCO3(cr)	*-21.7 ± 2.0*	-	-	-	*$SmOHCO_3(cr) \rightleftharpoons Sm^{3+} + OH^- + CO_3^{2-}$*
Sm-rhabdophane	-25.2 ± 1.3	-22 ± 8	0	25 – *90*	$SmPO_4{\cdot}0.667H_2O(cr) \rightleftharpoons Sm^{3+} + PO_4^{3-} + 0.667\ H_2O(l)$

Tab. 23.1.10-2: Selected SIT ion interaction coefficients $\varepsilon_{j,k}$ [kg · mol^{-1}] for samarium species

Data estimated according to charge correlations and taken from Tab. 1-7 are shaded. Supplemental data are in italics.

j k → ↓	**Cl^-** $\varepsilon_{j,k}$ [kg · mol^{-1}]	**ClO_4^-** $\varepsilon_{j,k}$ [kg · mol^{-1}]	**NO_3^-** $\varepsilon_{j,k}$ [kg · mol^{-1}]	**Na^+** $\varepsilon_{j,k}$ [kg · mol^{-1}]	**$Na^+ + Cl^-$** $\varepsilon_{j,k}$ [kg · mol^{-1}]
Sm+3	0.25 ± 0.01	0.47 ± 0.01	0.07 ± 0.01	0	0
SmOH+2	0.15 ± 0.10	-0.20 ± 0.21	-	0	0
Sm(OH)2+	*0.05 ± 0.10*	*0.2 ± 0.1*	-	*0*	*0*
Sm(OH)3(aq)	*0*	*0*	*0*	*0*	*0*
Sm(OH)4-	*0*	*0*	*0*	*-0.05 ± 0.10*	*0*
Sm2(OH)2+4	0.35 ± 0.10	0.71 ± 0.13	-	0	0
Sm3(OH)5+4	0.35 ± 0.10	0.48 ± 0.17	-	0	0
SmF+2	0.15 ± 0.03	0.32 ± 0.03	0.00 ± 0.04	0	0
SmF2+	*0.05 ± 0.10*	*0.2 ± 0.1*	-	*0*	*0*
SmSO4+	*0.05 ± 0.10*	0.27 ± 0.09	-	*0*	*0*
Sm(SO4)2-	*0*	*0*	*0*	*0.22 ± 0.20*	*0*
SmCO3+	*0.05 ± 0.10*	*0.15 ± 0.18*	-	*0*	*0*
Sm(CO3)2-	*0*	*0*	*0*	*-1.17 ± 0.32*	*0*
SmH2PO4+2	*0.15 ± 0.10*	*0.18 ± 0.08*	-	*0*	*0*

23.1.11 References

Allen, P.G., Bucher, J.J., Shuh, D.K., Edelstein, N.M. & Craig, I. (2000): Coordination chemistry of trivalent lanthanide and actinide ions in dilute and concentrated chloride solutions. Inorganic Chemistry, 39, 595-601.

Arblaster, J.W. (2013): Selected values of the thermodynamic properties of scandium, yttrium, and the lanthanide elements. Handbook on the Physics and Chemistry of Rare Earths, 43, 321-565.

Audi, G., Bersillon, O., Blachot, J. & Wapstra, A.H. (2003): The NUBASE evaluation of nuclear and decay properties. Nuclear Physics, A 729, 3-128.

Baes, C.F. & Mesmer, R.E. (1976): The hydrolysis of cations. Wiley, New York, 490 pp.

Bentouhami, E., Bouet, G.M., Meullemeestre, J., Vierling, F. & Khan, M.A. (2004): Physicochemical study of the hydrolysis of rare-earth elements (III) and thorium (IV). Comptes Rendus Chimie, 7, 537-545.

Bernkopf, M.F. (1984): Hydrolysereaktionen und Karbonatkomplexierung von dreiwertigem Americium im natürlichen aquatischen System. Ph.D. thesis, Institut für Radiochemie, Technische Universität München, Germany, 200 p.

Brown, P.L. & Ekberg, C. (2016): Hydrolysis of Metal Ions. Vol. 1, Wiley-VCH, Weinheim.

Byrne, R.H., Lee, J.H. & Bingler, L.S. (1991): Rare earth element complexation by PO_4^{3-} ions in aqueous solution. Geochimica et Cosmochimica Acta, 55, 2729-2735.

Cetiner, Z.S., Wood, S.A. & Gammons, C.H. (2005): The aqueous geochemistry of the rare earth elements. Part XIV. The solubility of rare earth element phosphates from 23 to 150 °C. Chemical Geology 217, 147-169.

Chatterjee, S., Campbell, E.L., Neiner, D., Pence, N.K., Robinson, T.A. & Levitskaia, T.G. (2015): Aqueous binary lanthanide(III) nitrate $Ln(NO_3)_3$ electrolytes revisited: Extended Pitzer and Bromley treatments. Journal of Chemical and Engineering Data, 60, 2974-2988.

Ciavatta, L. (1980): The specific interaction theory in evaluating ionic equilibria. Annali di Chimica, 70, 551-567.

Ciavatta, L., Iuliano, M. & Porto, R. (1999): Temperature effect on the speciation of samarium(III) hydrolytic complexes. Annali di Chimica, 89, 881-890.

Cordfunke, E.H.P. & Konings, R.J.M. (2001): The enthalpies of formation of lanthanide compounds II. Ln^{3+}(aq). Thermochimica Acta, 375, 51-64.

Cox, J.D., Wagman, D.D. & Medvedev, V.A. (1989): CODATA Key Values for Thermodynamics. New York, Hemisphere, 271p.

Fanghänel, T., Kim, J.I., Klenze, R. & Kato, Y. (1995): Formation of Cm(III) chloride complexes in $CaCl_2$ solutions. Journal of Alloys and Compounds, 225, 308-311.

Fatin-Rouge, N. & Bünzli J.-C.G. (1999): Thermodynamic and structural study of inclusion complexes between trivalent lanthanide ions and native cyclodextrins. Inorganica Chimica Acta, 293, 53-60.

Firsching, F.H. & Brune, S.N. (1991): Solubility products of the trivalent rare-earth phosphates. Journal of Chemical and Engineering Data, 36, 93-95.

Fraústo da Silva, J.J.R. & Queimado, M.M. (1973): Solubility products of lanthanide fluorides. Revista Portuguesa de Química, 15, 29-34.

Frolova, U.K., Kumok, V.N. & Serebrennikov, V.V. (1966): Hydrolysis of ions of the rare earth elements and yttrium in aqueous solutions. Izvestiya Vysshikh Uchebnykh Zavedenii, Khimiya i Khimicheskaya Tekhnologiya, 9(2), 176-179. Chemical Abstracts, 65, 9816c.

Gausse, C., Szenknect, S., Qin, D.W., Mesbah, A., Clavier, N., Neumeier, S., Bosbach, D. & Dacheux, N. (2016): Determination of the solubility of rhabdophanes $LnPO_4 \cdot 0.667H_2O$ (Ln = La to Dy). European Journal of Inorganic Chemistry, 28, 4615-4630.

Grenthe, I., Plyasunov, A.V. & Spahiu, K. (1997): Estimations of medium effects on thermodynamic data. In: Grenthe, I. & Puigdomènech, I. (eds.): Modelling in Aquatic Chemistry. OECD NEA, Paris, France, 325-426.

Guillaumont, R., Désiré, B. & Galin, M. (1971): Première constante d'hydrolyse des lanthanides. Radiochemical and Radioanalytical Letters 8, 189-198.

Gysi, A.P., Harlov, D. & Miron, G.D. (2018): The solubility of monazite ($CePO_4$), $SmPO_4$, and $GdPO_4$ in aqueous solutions from 100 to 250 °C. Geochimica et Cosmochimica Acta, 242, 143-164.

Haas, J.R., Shock, E.L. & Sassani, D.C. (1995): Rare earth elements in hydrothermal systems: Estimates of standard partial molal thermodynamic properties of aqueous complexes of the rare earth elements at high pressures and temperatures. Geochimica et Cosmochimica Acta, 59, 4329-4350.

Hakin, A.W., Lukacs, M.J., Liu, J.L., Erickson, K. & Madhavji, A. (2003): The volumetric and thermochemical properties of $Y(ClO_4)_3(aq)$, $Yb(ClO_4)_3(aq)$, $Dy(ClO_4)_3(aq)$, and $Sm(ClO_4)_3(aq)$ at T = (288.15, 298.15, 313.15, and 328.15) K and p = 0.1 MPa. Journal of Chemical Thermodynamics, 35, 775-802.

He, M. & Rard, J.A. (2015): Revision of the osmotic coefficients, water activities and mean activity coefficients of the aqueous trivalent rare earth chlorides at T = 298.15 K. Journal of Solution Chemistry, 44, 2208-2221.

Hummel, W. (2018): Radioactive waste inventories for geochemists. PSI Internal Report, TM-44-18-03, Paul Scherrer Institut, Villigen, Switzerland, 55 pp.

Hummel, W., Berner, U., Curti, E., Pearson, F.J. & Thoenen, T. (2002): Nagra/PSI Chemical Thermodynamic Data Base 01/01. Nagra NTB 02-16, Nagra. Also published by Universal Publishers/upublish.com, Parkland, USA, 565 pp.

Itoh, H., Hachiya, H., Suzuki, Y. & Asano, Y. (1984): Determination of solubility products of rare earth fluorides by fluoride ion-selective electrode. Bulletin of the Chemical Society of Japan, 57, 1698-1690.

Jennings, L.D., Hill, E.D. & Spedding, F.H. (1959): Heat capacity of samarium from 13 to 350°K. Journal of Chemical Physics, 31, 1240-1243.

Jordan, N. (in prep.): Europium: Review of thermodynamic data for Eu(III) complexation with inorganic ligands.

Jordan, N., Demnitz, M., Lösch, H., Starke, S., Brendler, V. & Huittinen, N. (2018): Complexation of trivalent lanthanides (Eu) and actinides (Cm) with aqueous phosphates at elevated temperatures. Inorganic Chemistry, 57, 7015-7024.

Klungness, G.D. & Byrne, R.H. (2000): Comparative hydrolysis behavior of the rare earths and yttrium: the influence of temperature and ionic strength. Polyhedron, 19, 99-107.

Koke, C., Skerencak-Frech, A. & Panak, P.J. (2019): Thermodynamics of the complexation of curium(III) with chloride in alkali and alkali earth metal solutions at elevated temperatures. Journal of Chemical Thermodynamics, 131, 219-224.

Konings, R.J.M. & Beneš, O. (2010): The thermodynamic properties of the f-elements and their compounds. I. The lanthanide and actinide metals. Journal of Physical and Chemical Reference Data, 39, 043102-1–043102-48.

Konings, R.J.M. & Kovács, A. (2003): Thermodynamic properties of the lanthanide(III) halides. Handbook on the Physics and Chemistry of Rare Earths, 33, 147-247.

Kragten, J. & Decnop-Weever, L.G. (1979): Hydroxide complexes of lanthanides – II Samarium(III) in perchlorate medium. Talanta, 26, 1105-1109.

Lemire, R.J., Berner, U., Musikas, C., Palmer, D.A., Taylor, P. & Tochiyama, O. (2013): Chemical Thermodynamics of Iron, Part 1. Chemical Thermodynamics, Vol. 13a. OECD Publications, Paris, France, 1082 pp.

Liu, X. & Byrne, R.H. (1997): Rare earth and yttrium phosphate solubilities in aqueous solution. Geochimica et Cosmochimica Acta, 61, 1625-1633.

Luo, Y. & Millero F.J. (2004): Effects of temperature and ionic strength on the stabilities of the first and second fluoride complexes of yttrium and the rare earth elements. Geochimica et Cosmochimica Acta, 68, 4301-4308.

Luo, Y.-R. & Byrne, R.H. (2000): The ionic strength dependence of rare earth and yttrium fluoride complexation at 25 °C. Journal of Solution Chemistry, 29, 1089-1099.

Luo, Y.-R. & Byrne, R.H. (2001): Yttrium and rare earth element complexation by chloride ions at 25 °C. Journal of Solution Chemistry, 30, 837-845.

Luo, Y.-R. & Byrne, R.H. (2007): The influence of ionic strength on yttrium and rare earth element complexation by fluoride ions in $NaClO_4$, $NaNO_3$ and NaCl Solutions at 25 °C. Journal of Solution Chemistry, 36, 673-689.

Marshall, W.L. & Slusher, R. (1975): Solubility and thermodynamic functions for a 3-2 salt, samarium sulfate, in water and sulfuric acid solutions at temperatures to 350 °C. Journal of Inorganic and Nuclear Chemistry, 37, 2171-2176.

Menon, M. P. & James, J. (1989a): Stability constant for the lanthanide fluoride complexes in aqueous solution at 25 °C. Journal of Solution Chemistry, 18, 735-742.

Menon, M. P. & James, J. (1989b): Solubilities, solubility products and solution chemistry of lanthanon trifluoride–water systems. Journal of the Chemical Society, Faraday Transactions, 85, 2683-2694.

Menon, M.P., James, J. & Hill, T.L. (1988): Solubility products and other parameters for the samarium and gadolinium fluoride-water systems by radiometric and other methods. International Journal of Radiation Applications and Instrumentation. Part A. Applied Radiation and Isotopes, 39, 949-955.

Migdisov, A., Williams-Jones, A.E., Brugger, J. & Caporuscio, F.A. (2016): Hydrothermal transport, deposition, and fractionation of the REE: Experimental data and thermodynamic calculations. Chemical Geology 439, 13-42.

Migdisov, A.A., Williams-Jones, A.E. & Wagner, T. (2009): An experimental study of the solubility and speciation of the Rare Earth Elements (III) in fluoride- and chloride-bearing aqueous solutions at temperatures up to 300 °C. Geochimica et Cosmochimica Acta, 73, 7087-7109.

Millero, F.J. (1992): Stability constants for the formation of rare earth-inorganic complexes as a function of ionic strength. Geochimica et Cosmochimica Acta, 56, 3123-3132.

Mioduski, T., Gumiński, C. & Zeng, D. (2009): IUPAC-NIST solubility data series. 87. Rare earth metal chlorides in water and aqueous systems. Part 2. Light lanthanides (Ce–Eu). Journal of Physical and Chemical Reference Data, 38, 441-562.

Nair, G.M., Chander, K. & Joshi, J.K. (1982): Hydrolysis constants of plutonium(lll) and americium(lll). Radiochimica Acta 30, 37-40.

Pearson, F.J. & Berner, U. (1991): Nagra Thermochemical Data Base I. Core Data. Nagra Technical Report NTB 91-17.

Pearson, F.J., Jr., Berner, U. & Hummel, W. (1992): Nagra Thermochemical Data Base II. Supplemental Data 05/92. Nagra Technical Report NTB 91-18.

Rard, J.A. (1988): Aqueous solubilities of praseodymium, europium, and lutetium sulfates. Journal of Solution Chemistry, 17, 499-517.

Rard, J.A. (2016): Critical evaluation of the standard molar entropies, enthalpies of formation, Gibbs energies of formation and heat capacities of the aqueous trivalent rare earth ions, and the corresponding standard molar entropies, enthalpies of formation and Gibbs energies of formation of the thermodynamically stable $RECl_3 \cdot 7H_2O$(cr) and $RECl_3 \cdot 6H_2O$(cr). Journal of Solution Chemistry, 45, 1332-1376.

Rard, J.A. & Spedding, F.H. (1982): Isopiestic determination of the activity coefficients of some aqueous rare-earth electrolyte solutions at 25 °C. 6. $Eu(NO_3)_3$, $Y(NO_3)_3$, and YCl_3. Journal of Chemical and Engineering Data, 27, 454-461.

Rard, J.A., Weber, H.O. & Spedding, F.H. (1977): Isopiestic determination of the activity coefficients of some aqueous rare earth electrolyte solutions at 25 °C. 2. The rare earth perchlorates. Journal of Chemical and Engineering Data, 22, 187-201.

Schijf, J. & Byrne, R.H. (1999): Determination of stability constants for the mono- and difluoro-complexes of Y and the REE, using a cation-exchange resin and ICP-MS. Polyhedron, 18, 2839-2844.

Skerencak-Frech, A., Fröhlich, D.R., Rothe, J., Dardenne, K. & Panak, P.J. (2014): Combined time-resolved laser fluorescence spectroscopy and extended X-ray absorption fine structure spectroscopy study on the complexation of trivalent actinides with chloride at T = 25 – 200 °C. Inorganic Chemistry, 53, 1062-1069.

Spahiu, K. & Puigdomènech, I. (1998): On weak complex formation: Re-interpretation of literature data on the Np and Pu nitrate complexation. Radiochimica Acta, 82, 413-419.

Spedding, F.H., DeKock, C.W., Pepple, G.W. & Habenschuss, A. (1977): Heats of dilution of some aqueous rare earth electrolyte solutions at 25 °C. 3. Rare earth chlorides. Journal of Chemical and Engineering Data, 22, 58-70.

Spedding, F.H., Weber, H.O., Saeger, V.W., Petheram, H.H., Rard, J.A. & Habenschuss, A. (1976): Isopiestic determination of the activity coefficients of some aqueous rare earth electrolyte solutions at 25 °C. 1. The rare earth chlorides. Journal of Chemical and Engineering Data, 21, 341-360.

Thoenen, T., Hummel, W., Berner, U. & Curti, E. (2014): The PSI/Nagra Chemical Thermodynamic Database 12/07. Technical Report, PSI Bericht Nr. 14-04, Paul Scherrer Institut, Villigen, Switzerland, 416 pp.

Wagman, D.D., Evans, W.H., Parker, V.B., Schumm, R.H., Halow, I., Bailey, S.M., Churney, K.L. & Nuttall, R.L. (1982): The NBS tables of chemical thermodynamic properties: Selected values for inorganic and C1 and C2 organic substances in SI units. Journal of Physical and Chemical Reference Data, 11, Supplement No. 2, 1-392.

Walker, J.B. & Choppin, G.R. (1967): Thermodynamic parameters of fluoride complexes of the lanthanides. In: Fields P.R. & Moeller, T. (eds.): Lanthanide/Actinide Chemistry. Advances in Chemistry Vol 71. American Chemical Society, Washington, D.C, 127-140.

Wood, S. A. (1990): The aqueous geochemistry of the rare-earth elements and yttrium 1. Review of available low-temperature data for inorganic complexes and the inorganic REE speciation of natural waters. Chemical Geology, 82, 159-186.

23.2 Europium

23.2.1 Introduction

Thermodynamic data for Eu were reviewed in the PSI/Nagra Chemical Thermodynamic Database 01/01 (TDB 01/01, Hummel et al. 2002). In the meantime, ^{154}Eu is no more considered as a dose-relevant radionuclide for the planned deep underground repositories for radioactive waste in Switzerland (Hummel 2018). Despite this fact, the thermodynamic data for Eu were still reviewed and revised for the PSI Chemical Thermodynamic Database 2020 because Eu is one of the best studied rare earth elements in terms of thermodynamic data, and it is expected that thermodynamic data for Eu aid in evaluating the corresponding data for Sm and Ho – whose isotopes ^{151}Sm and ^{166m}Ho are dose-relevant – and in closing potential data gaps.

The thermodynamic data for Eu selected in this review for TDB 2020 are listed in Tab. 23.10-1.

NEA chose the specific ion interaction theory (SIT) for the extrapolation of experimental data to zero ionic strength, see, e.g., Grenthe et al. (1997), an approach which is also adopted for TDB 2020 (as has been for all its predecessors). When referring to ion interaction coefficients recommended by NEA, we took those from Tab. B.3 in Lemire et al. (2013).

Due to a lack of experimental data, many ion interaction coefficients for cationic Eu species with ClO_4^- and Cl^-, and for anionic Eu species with Na^+ are unknown. We filled these gaps by applying the estimation method described in Section 1.5.3, which is based on a statistical analysis of published SIT ion interaction coefficients, and which allows the estimation of such coefficients for the interaction of cations with Cl^- and ClO_4^-, and for the interaction of anions with Na^+ from the charge of the considered cations or anions. Ion interaction coefficients of neutral europium species with background electrolytes were assumed to be zero.

The ion interaction coefficients for europium species selected for TDB 2020 are listed in Tab. 23.10-2.

23.2.2 Elemental europium

Elemental europium does not occur in nature as a mineral. For the calculation of certain reaction properties of europium species, however, values for $S_m°$(Eu, cr, 298.15 K) and $C_{p,m}°$(Eu, cr, 298.15 K) are required. The most recent reviews on the thermodynamic properties of the lanthanide metals are by Konings & Beneš (2010) and Arblaster (2013). Both reviews relied on the low-temperature heat capacity measurements by Gerstein et al. (1967), resulting in

$$S_m°(\text{Eu, cr, 298.15 K}) = 77.8 \text{ J} \cdot \text{K}^{-1} \cdot \text{mol}^{-1}$$

and

$$C_{p,m}°(\text{Eu, cr, 298.15 K}) = 27.65 \text{ J} \cdot \text{K}^{-1} \cdot \text{mol}^{-1}$$

Both of these values are included in TDB 2020.

23.2.3 Europium aquo ions

The lanthanides occur in nature as Ln(III) species only, with the exception of Ce, which also exists as Ce(IV) under oxidizing conditions, and Sm, Eu, and Yb, which also exist as Sm(II), Eu(II), and Yb(II) under extremely reducing conditions (Wood 1990). Thermodynamic data on Eu(II) complexes are practically non-existent and therefore only data on the free aqueous Eu^{2+} were included in the Nagra/PSI TDB 01/01 (Hummel et al. 2002). Hummel et al. (2002) noted that Eu^{2+} has a relatively large ionic radius (0.117 nm in octahedral coordination, according to Shannon 1976) which is practically identical to that of Sr^{2+} (0.118 nm). Hummel et al. (2002) then argued that since lanthanides and alkali-earth elements have similar chemical properties, it is reasonable to assume that Eu^{2+} will have a large chemical similarity to Sr^{2+}. Sr hydrolysis is very weak and starts at very high pH as is obvious from its $\log_{10}{}^*\beta_{1,1}^\circ$(298.15 K) = -13.29. Sr complexation with common inorganic ligands like carbonate, sulphate, and chloride is also rather weak. Therefore, Hummel et al. (2002) concluded that in most groundwaters, the speciation of divalent europium is dominated by the free Eu^{2+} cation. According to Migdisov et al. (2016), Eu(II) is stable at room temperature only at pH values above neutral and under highly reducing conditions (fH$_2$g close to 1 bar). Liu et al. (2017) carried out XANES spectra of aqueous $EuCl_3$ solutions at temperatures between 35 and 400 °C, and observed that with increasing temperature a peak indicative of Eu(II) appears at 300 °C and is more intense than the peak of Eu(III) at 400 °C. They concluded that Eu(III) species become more stable with increasing temperature and are predominant at 400 °C.

Thus, it is not to be expected that Eu(II) plays any significant role in the application range of TDB 2020. For this reason, Eu^{2+} is no more considered in TDB 2020 and only Eu(III) species and compounds are reviewed in the present report.

Rard (2016) carried out an extensive review and critical evaluation of the standard molar entropies, heat capacities, enthalpies of formation and Gibbs energies of formation of the aqueous trivalent rare earth ions.

The standard molar entropy for $S_m^\circ(Eu^{3+}, 298.15\ K)$ was derived by Rard (2016) from calorimetric investigations of the dissolution of $EuCl_3{\cdot}6\ H_2O$(cr) in aqueous solution according to the reaction

$$EuCl_3{\cdot}6H_2O(cr) \rightleftharpoons Eu^{3+} + 3\ Cl^- + 6\ H_2O(l)$$

The standard molar entropy of solution is given by

$$\Delta_{r,sol}S_m^\circ(298.15\ K) = S_m^\circ(Eu^{3+}, 298.15\ K) + 3\ S_m^\circ(Cl^-, 298.15\ K) + 6\ S_m^\circ(H_2O, l, 298.15\ K) - S_m^\circ(EuCl_3{\cdot}6H_2O, cr, 298.15\ K)$$

from which $S_m^\circ(Eu^{3+}, 298.15\ K)$ can be calculated if $S_m^\circ(Cl^-, 298.15\ K)$, $S_m^\circ(H_2O, l, 298.15\ K)$, $S_m^\circ(EuCl_3{\cdot}6\ H_2O, cr, 298.15\ K)$, and $\Delta_{r,sol}S_m^\circ(298.15\ K)$ are known. Rard (2016) took $S_m^\circ(Cl^-, 298.15\ K) = (56.60 \pm 0.20)\ J \cdot K^{-1} \cdot mol^{-1}$ and $S_m^\circ(H_2O, l, 298.15\ K) = (69.95 \pm 0.03)\ J \cdot K^{-1} \cdot mol^{-1}$ from the CODATA review (Cox et al. 1989) and selected $S_m^\circ(EuCl_3{\cdot}6H_2O, cr, 298.15\ K) = (405 \pm 3)\ J \cdot K^{-1} \cdot mol^{-1}$ based on the value of 407.1 $J \cdot K^{-1} \cdot mol^{-1}$ by Wagman et al. (1982), which he corrected for occluded solution (leading to water excess in the crystal) and errors resulting from heat capacity extrapolations to higher temperatures (note that he considered the corrected value to be an estimate). Finally, he derived $\Delta_{r,sol}S_m^\circ(298.15\ K)$ from $\Delta_{r,sol}G_m^\circ(298.15\ K)$ and $\Delta_{r,sol}H_m^\circ(298.15\ K)$ according to

$$\Delta_{r,sol}G_m^\circ = \Delta_{r,sol}H_m^\circ - T\,\Delta_{r,sol}S_m^\circ$$

The standard molar Gibbs energy of solution can be calculated from

$$\Delta_{r,sol}G_m^\circ = -R\,T\,\ln(27\,m_{sat}^4\,\gamma_{\pm,sat}^4\,a(H_2O, l)_{sat}^6)$$

if m_{sat}, the concentration of dissolved $EuCl_3{\cdot}6H_2O(cr)$ at saturation, is known from solubility experiments, as well as $\gamma_{\pm,sat}$, the mean activity coefficient of $EuCl_3$ at saturation and $a(H_2O, l)_{sat}$, the activity of water for the saturated solution, which can both be obtained from isopiestic measurements of saturated solutions. Rard (2016) derived $\Delta_{r,sol}G_m^\circ(298.15\ K) = -(26.87 \pm 0.10)$ kJ $\cdot$ mol^{-1} from $m_{sat} = (3.587 \pm 0.005)$ mol $\cdot$ kg^{-1}, as reported by Mioduski et al. (2009), and from $\gamma_{\pm,sat} = 5.315 \pm 0.053$ and $a(H_2O, l)_{sat} = 0.4926 \pm 0.0006$, both from He & Rard (2015). By combining the value for $\Delta_{r,sol}G_m^\circ(298.15\ K)$ with $\Delta_{r,sol}H_m^\circ(298.15\ K) = -(36.62 \pm 0.20)$ kJ $\cdot$ mol^{-1}, based on data by Hinchey & Cobble (1970) and Spedding et al. (1977), Rard (2016) then obtained $\Delta_{r,sol}S_m^\circ(298.15\ K) = -(32.70 \pm 0.75)$ kJ $\cdot$ mol^{-1}, and finally the recommended

$$S_m^\circ(Eu^{3+}, 298.15\ K) = -(217.2 \pm 3.2)\ J \cdot K^{-1} \cdot mol^{-1}$$

which is also included in TDB 2020.

The molar entropy of formation for Eu^{3+}, $\Delta_f S_m^\circ(Eu^{3+}, 298.15)$, can be calculated from

$$\Delta_f S_m^\circ(Eu^{3+}, 298.15) = S_m^\circ(Eu^{3+}, 298.15) + 3\,S_m^\circ(e^-, 298.15) - S_m^\circ(Eu, cr, 298.15)$$

Using his recommended value for $S_m^\circ(Eu^{3+}, 298.15\ K)$ together with $S_m^\circ(Eu, cr, 298.15) = (77.81 \pm 0.16)\ J \cdot K^{-1} \cdot mol^{-1}$ (Konings & Beneš 2010) and $S_m^\circ(e^-, 298.15) = 1/2\ S_m^\circ(H_2, g, 298.15) = (65.340 \pm 0.0015)\ J \cdot K^{-1} \cdot mol^{-1}$ (CODATA, Cox et al. 1989), Rard (2016) derived

$$\Delta_f S_m^\circ(Eu^{3+}, 298.15\ K) = -(99.0 \pm 3.2)\ J \cdot K^{-1} \cdot mol^{-1}$$

From the critical evaluation of the enthalpies of formation of the lanthanide ions by Cordfunke & Konings (2001), Rard (2016) adopted his recommended

$$\Delta_f H_m^\circ(Eu^{3+}, 298.15\ K) = -(605.4 \pm 4.0)\ kJ \cdot mol^{-1}$$

which is also included in TDB 2020. From $\Delta_f G_m^\circ(Eu^{3+}, T) = \Delta_f H_m^\circ(Eu^{3+}, T) - T\,\Delta_f S_m^\circ(Eu^{3+}, T)$ then follows

$$\Delta_f G_m^\circ(Eu^{3+}, 298.15\ K) = -(575.9 \pm 4.1)\ kJ \cdot mol^{-1}$$

which is also included in TDB 2020.

Based on the flow microcalorimetric investigations of aqueous $Eu(ClO_4)_3$ solutions by Xiao & Tremaine (1997), Rard (2016) recommended

$$C_{p,m}°(Eu^{3+}, 298.15\ K) = -(80.6 \pm 20)\ J \cdot K^{-1} \cdot mol^{-1}$$

which is included in TDB 2020.

According to the specific ion interaction theory (SIT), the specific ion interaction coefficient $\varepsilon(j,k)$, where j is a cation with zj positive charges and k an anion with zk negative charges, can be calculated from mean activity coefficient ($\gamma_\pm$) data for $j_{zk}k_{zj}(aq)$ using the following equation (Ciavatta 1980)

$$\varepsilon(j, k) = [\log_{10}(\gamma_\pm) + zj\ zk\ D]\ [zj + zk]^2 / (4\ I_m)$$

where D is the Debye-Hückel term

$$D = 0.509\ I_m^{1/2} / (1 + 1.5\ I_m^{1/2})$$

Rearranging the equation for $\varepsilon(j, k)$ leads to

$$1/4\ [zj + zk]^2 \log_{10}(\gamma_\pm) + 1/4\ zj\ zk\ [zj + zk]^2\ D = \varepsilon(j, k)\ I_m$$

or, for a 1:3 electrolyte $jk_3(aq)$, such as $EuCl_3(aq)$, $Eu(ClO_4)_3(aq)$ or $Eu(NO_3)_3(aq)$, to

$$4 \log_{10}(\gamma_\pm) + 12\ D = \varepsilon(j, k)\ I_m$$

In a plot of $4 \log_{10}(\gamma_\pm) + 12\ D$ vs. I_m, $\varepsilon(j, k)$ is the slope of a straight line passing through the origin.

He & Rard (2015) published revised mean activity coefficients of the aqueous trivalent rare earth chlorides, based on the isopiestic determinations by Spedding et al. (1976) and Rard & Spedding (1982). The mean activity coefficients for $EuCl_3(aq)$ by He & Rard (2015) are shown in Fig. 23.2.3-1 along with the linear least squares fit (with the restriction that the straight line passes through the origin). From the fit to the full set of data (0.1 – 3.587 $mol \cdot kg^{-1}$ $EuCl_3$, corresponding to ionic strengths between 0.6 and 21.52 $mol \cdot kg^{-1}$ follows $\varepsilon(Eu^{3+}, Cl^-) = (0.295 \pm 0.002)\ kg \cdot mol^{-1}$. Since the application range of TDB 2020 is restricted to low ionic strengths, we also carried out a fit limited to the data at low ionic strengths (0.1 – 1.0 $mol \cdot kg^{-1}$ $EuCl_3$, corresponding to ionic strengths between 0.6 and 6.0 $mol \cdot kg^{-1}$), which resulted in the value selected for TDB 2020

$$\varepsilon(Eu^{3+}, Cl^-) = (0.260 \pm 0.005)\ kg \cdot mol^{-1}$$

Chatterjee et al. (2015) determined the osmotic coefficients of lanthanide nitrate solutions by a combination of water activity and vapor pressure osmometry measurements. They calculated mean activity coefficients from the osmotic coefficients. The mean activity data they obtained for $Eu(NO_3)_3(aq)$ are shown in Fig. 23.2.3-2.

From the linear least-squares fit to the full set of data (0.131 to 2.830 mol · kg^{-1} $Eu(NO_3)_3$(aq), which corresponds to ionic strengths from 0.786 to 16.98 mol · kg^{-1}) follows $\varepsilon(Eu^{3+}, NO_3^-) = (0.100 \pm 0.002)$ kg · mol^{-1}, and from the set of data restricted to $I_m \leq 6$ mol · kg^{-1} follows

$$\varepsilon(Eu^{3+}, NO_3^-) = (0.080 \pm 0.001) \text{ kg} \cdot \text{mol}^{-1}$$

which is included in TDB 2020.

Surprisingly, there appear to be no mean activity or osmotic coefficient data for $Eu(ClO_4)_3$. Therefore, no value for $\varepsilon(Eu^{3+}, ClO_4^-)$ could be derived and we adopted the corresponding value for $\varepsilon(Sm^{3+}, ClO_3^-)$ as an estimate:

$$\varepsilon(Eu^{3+}, ClO_4^-) \approx \varepsilon(Sm^{3+}, ClO_4^-) = (0.47 \pm 0.01) \text{ kg} \cdot \text{mol}^{-1}$$

This estimate is included in TDB 2020.

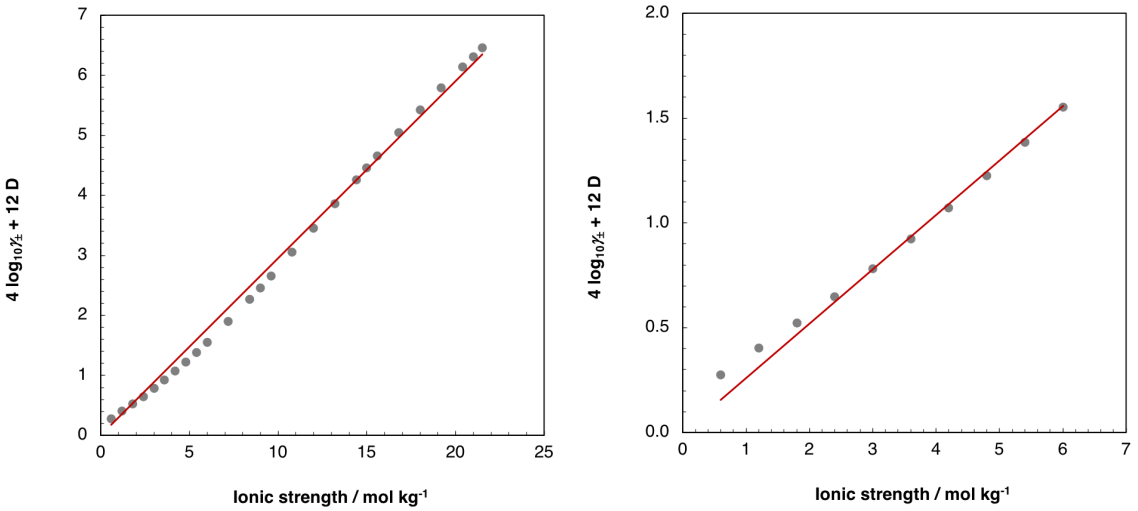

Fig. 23.2.3-1: SIT-analysis of the mean activity coefficient ($\gamma_\pm$) of $EuCl_3$(aq) as a function of ionic strength at 25 °C

Experimental data by He & Rard (2015). From the linear least-squares fit to the full set of data (left) follows $\varepsilon(Eu^{3+}, Cl^-) = (0.295 \pm 0.002)$ kg · mol^{-1}, and from the set of data restricted to $I_m \leq 6$ mol · kg^{-1} (right) follows $\varepsilon(Eu^{3+}, Cl^-) = (0.260 \pm 0.005)$ kg · mol^{-1}.

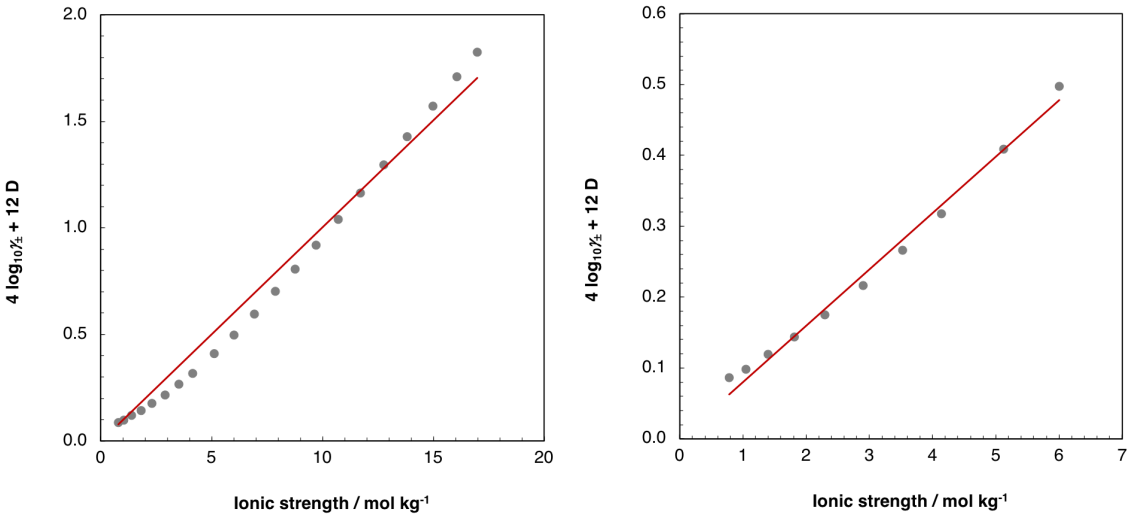

Fig. 23.2.3-2: SIT-analysis of the mean activity coefficient ($\gamma_{\pm}$) of $Eu(NO_3)_3(aq)$ as a function of ionic strength at 25 °C

Experimental data by Chatterjee et al. (2015). From the linear least-squares fit to the full set of data (left) follows $\varepsilon(Eu^{3+}, NO_3^-) = (0.100 \pm 0.002)$ kg · mol^{-1}, and from the set of data restricted to $I_m \leq 6$ mol · kg^{-1} (right) follows $\varepsilon(Eu^{3+}, NO_3^-) = (0.080 \pm 0.001)$ kg · mol^{-1}.

23.2.4 Europium hydroxide compounds and complexes

Trivalent lanthanides hydrolyse only slightly below pH 7, while in basic solutions very insoluble hydroxides precipitate. This situation makes it difficult to study the hydrolysis of lanthanides, due to the low concentrations involved and the possible competition with other strong ligands (e.g. carbonate).

23.2.4.1 Aqueous europium hydroxide complexes

The data selected by Hummel et al. (2002) for $EuOH^{2+}$, $Eu(OH)_2^+$, $Eu(OH)_3(aq)$, and $Eu(OH)_4^-$ are retained.

23.2.4.2 Europium hydroxide solids

The data selected by Hummel et al. (2002) for $Eu(OH)_3(cr)$ and $Eu(OH)_3(am)$ are retained.

23.2.5 Europium fluoride compounds and complexes

23.2.5.1 Aqueous europium fluoride complexes

The values for the stability constants of the europium fluoride complexes EuF^{2+} and EuF_2^{+} selected by Hummel et al. (2002) for TDB 01/01 were based on experimental determinations by Lee & Byrne (1993) in 0.68 M $NaClO_4$. Several experimental investigations have been carried out in the meantime, covering a larger number of background electrolytes with a larger variation of ionic strengths. Therefore, the values selected in TDB 01/01 needed an update.

23.2.5.1.1 EuF^{2+}

Walker & Choppin (1967) used potentiometric titrations and solvent extraction in 1 M $NaClO_4$ at 25 °C for measuring the stability constants of 1:1 REE fluoride complexes, including EuF^{2+}. In addition, they also used calorimetric titrations for the determination of the reaction enthalpies of the complexation reactions.

Menon & James (1989a) measured the stability constants of the 1:1 and 1:2 complexes of the rare earth elements in 0.5 M NH_4NO_3 at 25 °C using a fluoride selective ion electrode. These data were also reported by Menon & James (1989b).

Schijf & Byrne (1999) measured stability constants of the 1:1 and 1:2 fluoride complexes of yttrium and the rare earth elements at 25 °C in 0.025 M HNO_3 solutions using the cation-exchange resin technique.

Luo & Byrne (2000) measured stability constants for the 1:1 fluoride complexes of yttrium and the rare earth elements at 25 °C in 0.15 to 6.0 molar $NaClO_4$ solutions using a fluoride ion selective electrode. They corrected these data in a later study (Luo & Byrne 2007), stating that the stability constants by Luo & Byrne (2000) were erroneously reported in molar units.

Luo & Byrne (2001) measured stability constants for the 1:1 fluoride complexes of yttrium and the rare earth elements at 25 °C in 0.7 and 3.0 molar NaCl solutions using a fluoride ion selective electrode.

Luo & Byrne (2007) measured stability constants for 1:1 fluoride complexes of yttrium and the rare earth elements at 25 °C across a range of ionic strengths in NaCl (0.7 – 5.0 m) and $NaNO_3$ (0.015 to 6.0 m) media using a fluoride ion selective combination electrode.

Tab. 23.2.5-1: Data for the stability constant $\log_{10}\beta_1$ of $Eu^{3+} + F^- \rightleftharpoons EuF^{2+}$ at 25 °C in NaCl

The accepted values for $\log_{10}\beta_1$ were recalculated from the molar to the molal scale, if necessary. Reported uncertainties were increased. Values of $\log_{10}\beta_1$ accepted for the SIT analysis shown in Fig. 23.2.5-1 are bold. Abbreviation: sel: ion-selective electrode.

Method	**Medium**	***I* reported**	I_m [mol · kg^{-1}]	**$\log_{10}\beta_1$ (reported)**	**$\log_{10}\beta_1$ (accepted)**	**Reference**
sel	NaCl	0.7 m	0.7	3.22 ± 0.03	**3.22 ± 0.10**	Luo & Byrne (2007)
sel	NaCl	0.7 M	0.711	3.23	**3.22 ± 0.10**	Luo & Byrne (2001)
sel	NaCl	1.5 m	1.5	3.19 ± 0.03	**3.19 ± 0.10**	Luo & Byrne (2007)
sel	NaCl	3.0 m	3.0	3.19 ± 0.03	**3.19 ± 0.10**	Luo & Byrne (2007)
sel	NaCl	3.0 M	3.2	3.22	**3.22 ± 0.10**	Luo & Byrne (2001)
sel	NaCl	4.0 m	4.0	3.27 ± 0.03	**3.27 ± 0.10**	Luo & Byrne (2007)
sel	NaCl	5.0 m	5.0	3.35 ± 0.04	**3.35 ± 0.10**	Luo & Byrne (2007)

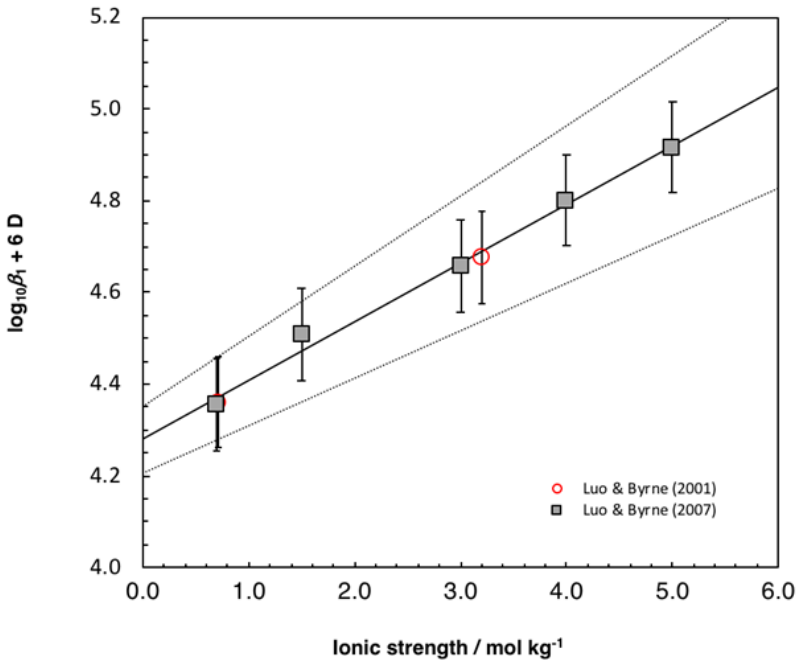

Fig. 23.2.5-1: SIT-plot of the equilibrium $Eu^{3+} + F^- \rightleftharpoons EuF^{2+}$ in NaCl using the experimental data by Luo & Byrne (2001, 2007)

The solid line is obtained by using the derived SIT interaction coefficient, $\Delta\varepsilon = -(0.13 \pm 0.02)$ kg · mol^{-1}, and the stability constant at zero ionic strength, $\log_{10}\beta_1°(298.15\ K) = (4.28 \pm 0.07)$. The dotted lines represent the associated 95% uncertainty range extrapolated from zero ionic strength to higher NaCl concentrations.

The conditional stability constants for the reaction

$$Eu^{3+} + F^- \rightleftharpoons EuF^{2+}$$

measured in NaCl by Luo & Byrne (2001, 2007), see Tab. 23.2.5-1, were used for the SIT analysis shown in Fig. 23.2.5-1, which resulted in

$$\log_{10}\beta_1°(298.15\ K) = (4.28 \pm 0.07)$$

$$\Delta\varepsilon = -(0.13 \pm 0.02)\ kg \cdot mol^{-1}$$

From $\Delta\varepsilon$, the NEA-selected $\varepsilon(F^-, Na+) = (0.02 \pm 0.02)\ kg \cdot mol^{-1}$, and $\varepsilon(Eu^{3+}, Cl^-) = (0.260 \pm 0.005)\ kg \cdot mol^{-1}$ (see Chapter 3) then follows

$$\varepsilon(EuF^{2+}, Cl^-) = (0.15 \pm 0.03)\ kg \cdot mol^{-1}$$

Tab. 23.2.5-2: Data for the stability constant $\log_{10}\beta_1$ of $Eu^{3+} + F^- \rightleftharpoons EuF^{2+}$ at 25 °C in $NaClO_4$

The accepted values for $\log_{10}\beta_1$ were recalculated from the molar to the molal scale, if necessary. Reported uncertainties were increased. Values of $\log_{10}\beta_1$ accepted for the SIT analysis shown in Fig. 23.2.5-2 are bold. Abbreviations: pot: potentiometry, sel: ion selective electrode, ext: solvent extraction.

Method	**Medium**	***I*** **reported**	I_m [mol · kg^{-1}]	**$\log_{10}\beta_1$ (reported)**	**$\log_{10}\beta_1$ (accepted)**	**Reference**
sel	$NaClO_4$	0.015 m	0.015	4.04 ± 0.03	**4.04 ± 0.10**	Luo & Byrne (2007)
sel	$NaClO_4$	0.1 m	0.1	3.58 ± 0.03	**3.58 ± 0.10**	Luo & Byrne (2007)
sel	$NaClO_4$	0.4 m	0.4	3.40 ± 0.03	**3.40 ± 0.10**	Luo & Byrne (2007)
sel	$NaClO_4$	0.7 m	0.7	3.34 ± 0.03	**3.34 ± 0.10**	Luo & Byrne (2007)
pot	$NaClO_4$	1 M	1.051	3.19 ± 0.01 [a]	**3.17 ± 0.20**	Walker & Choppin (1967)
ext	$NaClO_4$	1 M	1.051	3.20 ± 0.06 [b]	**3.18 ± 0.20**	Walker & Choppin (1967)
sel	$NaClO_4$	1.5 m	1.5	3.33 ± 0.03	**3.33 ± 0.10**	Luo & Byrne (2007)
sel	$NaClO_4$	3.0 m	3.0	3.38 ± 0.03	**3.38 ± 0.10**	Luo & Byrne (2007)
sel	$NaClO_4$	4.0 m	4.0	3.53 ± 0.03	**3.53 ± 0.10**	Luo & Byrne (2007)
sel	$NaClO_4$	5.0 m	5.0	3.60± 0.04	**3.60 ± 0.10**	Luo & Byrne (2007)
sel	$NaClO_4$	5.0 m	6.0	3.72 ± 0.04	**3.72 ± 0.10**	Luo & Byrne (2007)

[a] Calculated from $\beta_1 = 1'540 \pm 50$.
[b] Calculated from $\beta_1 = 1'593 \pm 198$.

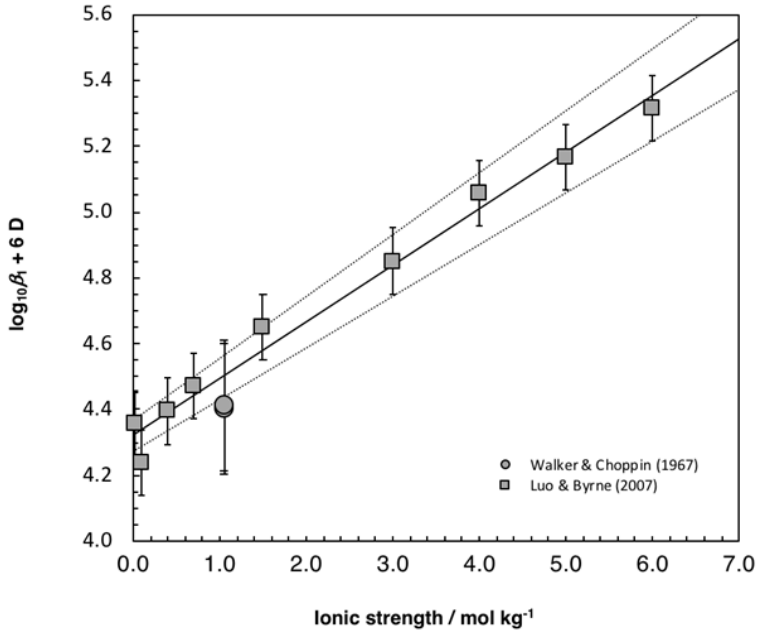

Fig. 23.2.5-2: SIT-plot of the equilibrium $Eu^{3+} + F^- \rightleftharpoons EuF^{2+}$ in $NaClO_4$ using the experimental data by Walker & Choppin (1967) and Luo & Byrne (2007)

The solid line is obtained by using the derived SIT interaction coefficient, $\Delta\varepsilon = -(0.17 \pm 0.02)$ kg · mol^{-1}, and the stability constant at zero ionic strength, $\log_{10}\beta_1°(298.15\ K) = (4.32 \pm 0.05)$. The dotted lines represent the associated 95% uncertainty range extrapolated from zero ionic strength to higher $NaClO_4$ concentrations.

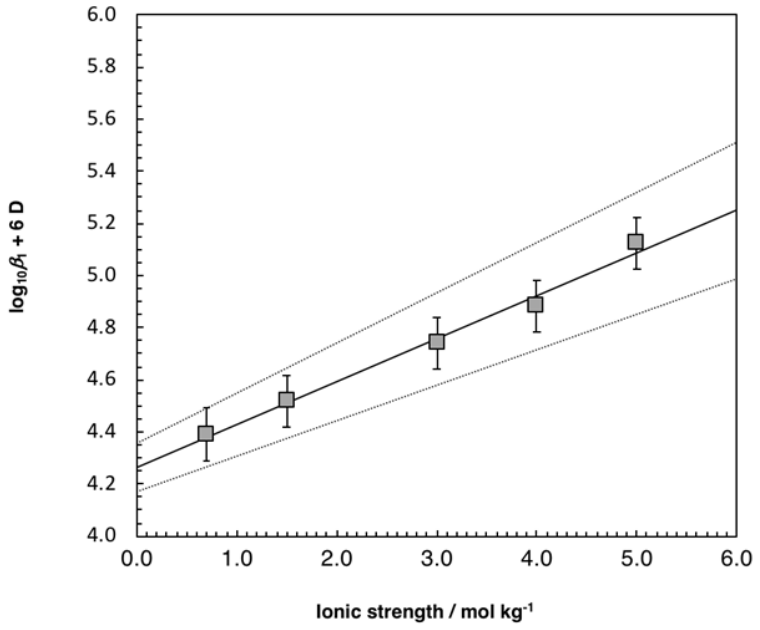

Fig. 23.2.5-3: SIT-plot of the equilibrium $Eu^{3+} + F^- \rightleftharpoons EuF^{2+}$ in $NaNO_3$ using the experimental data by Luo & Byrne (2007)

The solid line is obtained by using the derived SIT interaction coefficient, $\Delta\varepsilon = -(0.16 \pm 0.03)$ kg · mol^{-1}, and the stability constant at zero ionic strength, $\log_{10}\beta_1°(298.15\ K) = (4.26 \pm 0.09)$. The dotted lines represent the associated 95% uncertainty range extrapolated from zero ionic strength to higher NaCl concentrations.

Tab. 23.2.5-3: Data for the stability constant $\log_{10}\beta_1$ of $Eu^{3+} + F^- \rightleftharpoons EuF^{2+}$ at 25 °C in nitrate media

The accepted values for $\log_{10}\beta_1$ were recalculated from the molar to the molal scale, if necessary. Reported uncertainties were increased. Values of $\log_{10}\beta_1$ accepted for the SIT analysis shown in Fig. 23.2.5-3 are bold. Abbreviations: cat: cation exchange, sel: ion-selective electrode.

Method	**Medium**	***I*** **reported**	I_m [mol · kg^{-1}]	**$\log_{10}\beta_1$ (reported)**	**$\log_{10}\beta_1$ (accepted)**	**Reference**
cat	HNO_3	0.025 M		3.70 ± 0.05		Schijf & Byrne (1999)
cat	HNO_3	0.025 M		3.72 ± 0.01		Luo & Millero (2004)
sel	NH_4NO_3	0.5 M		3.07 ± 0.02 [a]		Menon & James (1989a, 1989b)
sel	NH_4NO_3	0.5 M		3.01 [b]		Menon & James (1989a, 1989b)
sel	$NaNO_3$	0.7 m	0.7	3.26 ± 0.03	**3.26 ± 0.10**	Luo & Byrne (2007)
sel	$NaNO_3$	1.5 m	1.5	3.20 ± 0.03	**3.20 ± 0.10**	Luo & Byrne (2007)
sel	$NaNO_3$	3.0 m	3.0	3.27 ± 0.03	**3.27 ± 0.10**	Luo & Byrne (2007)
sel	$NaNO_3$	4.0 m	4.0	3.36 ± 0.03	**3.36 ± 0.10**	Luo & Byrne (2007)
sel	$NaNO_3$	5.0 m	5.0	3.55 ± 0.04	**3.55 ± 0.10**	Luo & Byrne (2007)

[a] Calculated from $\beta_1 = 1'172 \pm 54 \pm x$.
[b] Calculated from $\beta_1 = 1'025$.

The values for $\log_{10}\beta_1$ measured by Walker & Choppin (1967) and Luo & Byrne (2007) in $NaClO_4$ (see Tab. 23.2.5-2) were used for the SIT-analysis shown in Fig. 23.2.5-2, which led to

$$\log_{10}\beta_1°(298.15\ K) = (4.32 \pm 0.05)$$
$$\Delta\varepsilon = -(0.17 \pm 0.02)\ kg \cdot mol^{-1},$$

From $\Delta\varepsilon$, the NEA-selected $\varepsilon(F^-, Na+)$, and $\varepsilon(Eu^{3+}, ClO_4^-) = (0.47 \pm 0.01)\ kg \cdot mol^{-1}$ (see Chapter 3) then follows

$$\varepsilon(EuF^{2+}, ClO_4^-) = (0.32 \pm 0.03)\ kg \cdot mol^{-1}$$

From an SIT-analysis of the values of $\log_{10}\beta_1$ measured by Luo & Byrne (2007) in $NaNO_3$ (see Tab. 23.2.5-3) follows

$$\log_{10}\beta_1°(298.15\ K) = (4.26 \pm 0.09)$$
$$\Delta\varepsilon = -(0.16 \pm 0.03)\ kg \cdot mol^{-1}$$

Using $\Delta\varepsilon$, the NEA-selected $\varepsilon(F^-, Na+)$, and $\varepsilon(Eu^{3+}, NO_3^-)$ = (0.080 ± 0.001) kg · mol^{-1} (see Chapter 3) leads to

$$\varepsilon(EuF^{2+}, NO_3^-) = (0.01 \pm 0.03)\ kg \cdot mol^{-1}$$

Tab. 23.2.5-4: Stability constants $\log_{10}\beta_1$ of $Eu^{3+} + F^- \rightleftharpoons EuF^{2+}$ and $\log_{10}\beta_2$ of $Eu^{3+} + 2\ F^- \rightleftharpoons EuF_2^+$ measured by Luo & Millero (2004) in 0.025 M HNO_3 at various temperatures

	5.2 °C	**15.1 °C**	**25.0 °C**	**34.7 °C**	**44.5 °C**
$\log_{10}\beta_1$	3.63 ± 0.02	3.67 ± 0.01	3.72 ± 0.01	3.78 ± 0.01	3.81 ± 0.01
$\log_{10}\beta_2$	5.89 ± 0.08	6.00 ± 0.02	6.11 ± 0.04	6.25 ± 0.03	6.30 ± 0.02

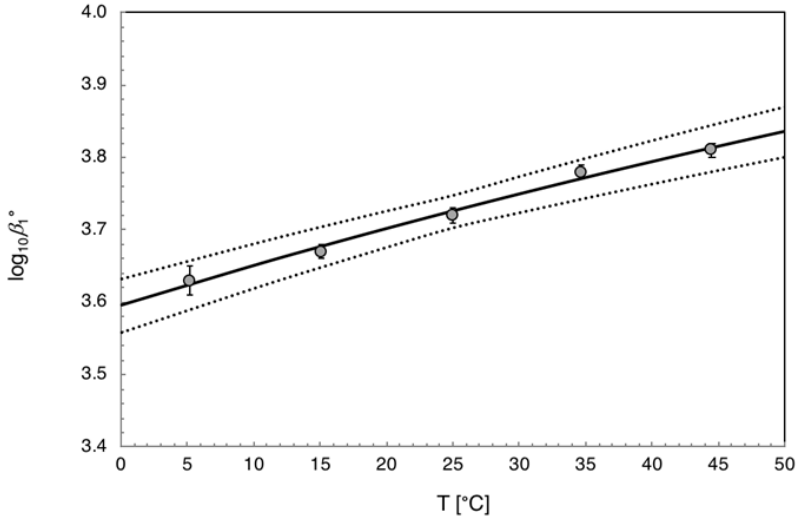

Fig. 23.2.5-4: Stability constants $\log_{10}\beta_1$ of $Eu^{3+} + F^- \rightleftharpoons EuF^{2+}$ measured by Luo & Millero (2004) in 0.025 M HNO_3 at various temperatures

An unweighted linear regression of these data as a function of 1/T resulted in $\log_{10}\beta_1°(298.15\ K)$ = (3.73 ± 0.02), $\Delta_r H_m(298.15\ K)$ = (8.10 ± 0.91) kJ · mol^{-1} and $\Delta_r C_{p,m}°(298.15\ K) = 0$. Solid line: Corresponding extrapolation of $\log_{10}\beta_1°$ to lower and higher temperatures with uncertainties indicated by the dotted lines.

The values for $\log_{10}\beta_1°(298.15\ K)$ derived from experimental data measured in NaCl (4.28 ± 0.07), $NaClO_4$ (4.32 ± 0.05), and $NaNO_3$ (4.26 ± 0.09) all overlap within their uncertainties. For inclusion in TDB 2020 we selected the value derived from the NaCl data since NaCl is the background electrolyte of greater relevance to natural environments than $NaClO_4$ or $NaNO_3$. Thus

$$\log_{10}\beta_1°(298.15\ K) = (4.28 \pm 0.07)$$

is included in TDB 2020, together with

$\varepsilon(EuF^{2+}, Cl^-) = (0.15 \pm 0.03)$ kg · mol^{-1}

$\varepsilon(EuF^{2+}, ClO_4^-) = (0.32 \pm 0.03)$ kg · mol^{-1}

$\varepsilon(EuF^{2+}, NO_3^-) = (0.01 \pm 0.03)$ kg · mol^{-1}

Luo & Millero (2004) investigated the temperature dependence of the 1:1 and 1:2 fluoride complexes of yttrium and the rare earth elements by an ion-exchange method (cation resin) in dilute HNO_3 solutions (0.025 mol/L) between 5.2 and 44.5 °C (see Tab. 23.2.5-4 and Fig. 23.2.5-4). For HF^{2+}, there is a linear relationship between stability constants and reciprocal temperature. From the linear fit to the data follow $\log_{10}\beta_1 = (3.73 \pm 0.02)$, $\Delta_r H_m(298.15\ K) = (8.10 \pm 0.91)$ kJ · mol^{-1} and $\Delta_r C_{p,m}°(298.15\ K) = 0$. Since there are no data on the dependence of $\Delta_r H_m$ on ionic strength, the value for 0.025 mol/L HNO_3 is used as an approximation for zero ionic strength. Thus,

$\Delta_r H_m°(298.15\ K) \approx (8.10 \pm 0.91)\ kJ \cdot mol^{-1}$

$\Delta_r C_{p,m}°(298.15\ K) = 0$

are included in TDB 2020 as supplemental data.

23.2.5.1.2 EuF_2^+

Quantitative data on the formation of EuF_2^+ is scarce (see Tab. 23.2.5-5). Menon & James (1989a, 1989b) provided conditional stability constants $\log_{10}\beta_2(298.15\ K)$ for the reaction $Eu^{3+} + 2\ F^- \rightleftharpoons EuF_2^+$ measured in 0.5 M NH_4NO_3, whereas the values reported by Schijf & Byrne (1999) and Luo & Millero (2004) were measured in 0.025 M HNO_3. Since these data cannot be extrapolated to zero ionic strength with SIT (measurements were made at only two ionic strengths, with a different background electrolyte for each) we extrapolated the data by Schijf & Byrne (1999) and Luo & Millero (2004) using the Debye-Hückel term as used in the SIT, assuming that the specific ion interactions are negligible at the very low concentration of the background electrolyte. Thus,

$\log_{10}\beta_2°(298.15\ K) = \log_{10}\beta_2(298.15\ K) - \Delta z^2 D$

where

$D = 0.509\ I_m^{0.5}/(1 + 1.5\ I_m^{0.5})$

From the mean of the conditional constants by Schijf & Byrne (1999) and Luo & Millero (2004), $\log_{10}\beta_2(298.15\ K) = 6.16$, $\Delta z^2 = -10$ for the reaction $Eu^{3+} + 2\ F^- \rightleftharpoons EuF_2^+$, and $D = 0.065$ at $I_m \approx I_c = 0.025$ kg · mol^{-1} follows

$Eu^{3+} + 2\ F^- \rightleftharpoons EuF_2^+$

$\log_{10}\beta_2°(298.15\ K) = (6.81 \pm 0.30)$

where the uncertainty has been estimated. This value is included in TDB 2020 as supplemental datum, together with

$$\varepsilon(EuF_2^+, Cl^-) \approx (0.05 \pm 0.10)\ kg \cdot mol^{-1}$$

and

$$\varepsilon(EuF_2^+, ClO_4^-) \approx (0.2 \pm 0.1)\ kg \cdot mol^{-1}$$

as estimated according to the method described in Section 1.5.3.

Tab. 23.2.5-5: Data for the stability constant $\log_{10}\beta_2$ of $Eu^{3+} + 2\ F^- \rightleftharpoons EuF_2^+$ at 25 °C in nitrate media

Values of $\log_{10}\beta_2$ accepted for extrapolation to zero ionic strength are bold Abbreviations: cat: cation exchange, sel: ion-selective electrode.

Method	**Medium**	***I*** **reported**	I_m [mol · kg^{-1}]	**$\log_{10}\beta_2$ (reported)**	**$\log_{10}\beta_2$ (accepted)**	**Reference**
cat	HNO_3	0.025 M	≈ 0.025 m	6.21 ± 0.09	**6.21 ± 0.10**	Schijf & Byrne (1999)
cat	HNO_3	0.025 M	≈ 0.025 m	6.11 ± 0.04	**6.11 ± 0.10**	Luo & Millero (2004)
sel	NH_4NO_3	0.5 M		6.28 ± 0.16 [a]		Menon & James (1989a, 1989b)
sel	NH_4NO_3	0.5 M		6.38 [b]		Menon & James (1989a, 1989b)

[a] Calculated from $\beta_2 = (1.9 \pm 0.6) \times 10^6$.
[b] Calculated from $\beta_2 = 2.38 \times 10^6$.

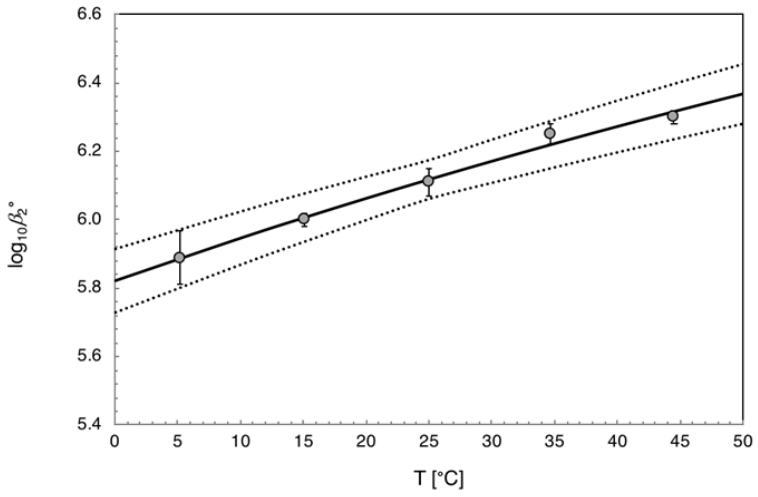

Fig. 23.2.5-5: Stability constants $\log_{10}\beta_2$ of $Eu^{3+} + 2\ F^- \rightleftharpoons EuF_2^+$ measured by Luo & Millero (2004) in 0.025 M HNO_3 at various temperatures

An unweighted linear regression of these data as a function of 1/T resulted in $\log_{10}\beta_2°(298.15\ K) = (6.12 \pm 0.06)$, $\Delta_r H_m(298.15\ K) = (18.5 \pm 2.3)$ kJ · mol^{-1} and $\Delta_r C_{p,m}°(298.15\ K) = 0$. Solid line: Corresponding extrapolation of $\log_{10}\beta_2°$ to lower and higher temperatures with uncertainties indicated by the dotted lines.

The stability constants of EuF_2^+ measured by Luo & Millero (2004) in 0.025 M HNO_3 solutions between 5.2 and 44.5 °C (see Tab. 23.2.5-4 and Fig. 23.2.5-5) are characterized by a linear relationship with reciprocal temperature. From the linear fit to the data follow $\log_{10}\beta_2 =$ (6.12 ± 0.06), $\Delta_r H_m(298.15\ K) = (18.5 \pm 2.3)\ kJ \cdot mol^{-1}$ and $\Delta_r C_{p,m}°(298.15\ K) = 0$. Since there are no data on the dependence of $\Delta_r H_m$ on ionic strength, the value for 0.025 mol/L HNO_3 is used as an approximation for zero ionic strength. Thus,

$$\Delta_r H_m°(298.15\ K) \approx (18.5 \pm 2.3)\ kJ \cdot mol^{-1}$$

$$\Delta_r C_{p,m}°(298.15\ K) = 0$$

are included in TDB 2020 as supplemental data.

23.2.5.2 Europium fluoride solids

There appear to be only a few experimental determinations of the solubility of europium fluoride solids.

Fraústo da Silva & Queimado (1973) determined the solubility products of REE fluorides from oversaturation in 0.1 M $NaNO_3$ at 25 °C using a fluoride ion-selective electrode. Precipitates were produced by adding an excess of a 0.035 M solution of REE nitrate to a 0.035 M solution of sodium fluoride, adding distilled water to adjust the total volume and an appropriate amount of $NaNO_3$ to set the ionic strength to 0.1 M. The precipitates that formed were left to age in the solution under occasional stirring and the potential was measured at regular intervals until a constant value was obtained, which was usually attained after 4 – 10 days and pH was found to be around 5. Composition, hydration, as well as crystallinity and structure of the precipitates were not characterized. The conditional solubility products were extrapolated to zero ionic strength using the Davies equation without consideration of potential complex formation. For EuF_3(pr) Fraústo da Silva & Queimado (1973) obtained $\log_{10}K_{s,0}°(298.15\ K) = -18.5$.

Itoh et al. (1984) measured the solubility products of REE fluoride powders in pure water from undersaturation at 25 °C using a fluoride ion-selective electrode. To prevent the formation of HF in acidic solutions, the experimental solutions were kept at pH 5 using a buffer. No information was given by these authors on the duration of the experiments and on the grain size of the powders. The solids were not examined after the experiment either. Due to the low concentrations of the solutes, the activity coefficients of the REE cations and of fluoride were assumed to be one and no complexes were considered. For EuF_3(s) Itoh et al. (1984) obtained $\log_{10}K_{s,0}°(298.15\ K) = -18.9$. Itoh et al. (1984) also tried to determine the solubility product of a lanthanum fluoride single crystal but failed to obtain saturated solutions even after three months of continuous stirring.

Menon & James (1989b) used conductometry, potentiometry and radiometry to determine the solubility products of all REE fluorides (except Pm) in water at 25 °C. The REE fluoride precipitates were prepared by mixing hot solutions of REE chlorides with HF. The precipitates were washed several times with doubly distilled water and dried in the oven at 110 °C. Menon & James (1989b) referred to the precipitates as ($LnF_3 \cdot 0.5H_2O$), but there are no indications that they analysed the precipitates for composition or structure before and after the experiments. Small batches of the dried precipitates were agitated with doubly distilled water for at least 48 h to reach saturation, which was tested by repeated measurements of the conductance of the solutions. The pH of the solutions was in the range of 5.0-6.0 and the calculated ionic strength was smaller than 10^{-3} M. From the measured solubilities of holmium fluoride, Menon & James (1989b) calculated

the solubility products, considering the formation of EuF^{2+}, $EuOH^{2+}$, and HF. They obtained $\log_{10}K_{s,0}°$(298.15 K) = -15.6 from radiometry, $\log_{10}K_{s,0}°$(298.15 K) = -13.7 from conductometry, and $\log_{10}K_{s,0}°$(298.15 K) = -13.1 from potentiometry.

Migdisov et al. (2009) measured the solubilities of all REE fluoride solids (except Pm) in fluoride- and chloride-bearing aqueous solutions at 150, 200, and 250 °C and saturated water vapor pressure. They extrapolated their solubility products to 25 °C using the $C_p°$ and $S°$ values recommended by Konings & Kovács (2003) and obtained for EuF_3(cr) $\log_{10}K_{s,0}°$(298.15 K) = -19.28. Migdisov et al. (2009) also calculated a solubility product for EuF_3(cr) entirely from calorimetric data recommended by Konings & Kovács (2003) and obtained $\log_{10}K_{s,0}°$(298.15 K) = -19.40.

The values for the solubility product $\log_{10}K_{s,0}°$(298.15 K) of EuF_3(cr) by Fraústo da Silva & Queimado (1973), Itoh et al. (1984) and Migdisov et al. (2009) vary between -18.5 and -19.40, while the values obtained by Menon & James (1989b) are significantly lower (-13.1 to -15.6), see Tab. 23.2.5-6. We are not able to resolve this discrepancy. However, Migdisov et al. (2009) argued that, since the good agreement between the experimental solubility products by Fraústo da Silva & Queimado (1973) and Itoh et al. (1984) covers the entire range of REE fluorides and is therefore systematic, they are likely the most reliable ones at 25 °C. We share this view and have therefore selected the average of the values (with an estimated uncertainty) determined by Fraústo da Silva & Queimado (1973) and Itoh et al. (1984) for TDB 2020:

$$EuF_3(cr) \rightleftharpoons Eu^{3+} + 3\ F^-$$

$$\log_{10}K_{s,0}°(298.15\ K) = -18.7 \pm 0.4$$

Tab. 23.2.5-6: Reported solubility products $\log_{10}K_{s,0}°$ of $EuF_3(cr) \rightleftharpoons Eu^{3+} + 3\ F^-$ at 25 °C

Abbreviations: cat: cation exchange, sel: ion-selective electrode, pot: potentiometry, con: conductometry, rad: radiometric, calc: calculated.

Method	**Medium**	***I* reported**	**$\log_{10}K_{s,0}°$**	**Reference**
sel	$NaNO_3$	0.1 M	-18.5	Fráusto da Silva & Queimado (1973)
sel		dilute	-18.9	Itoh et al. (1984)
pot		dilute	-13.1	Menon & James (1989b)
con		dilute	-13.7	Menon & James (1989b)
rad		dilute	-15.6	Menon & James (1989b)
calc			-19.40	Migdisov et al. (2009) [a]
calc			-19.28	Migdisov et al. (2009) [b]

[a] Calculated from calorimetric data recommended by Konings & Kovács (2003).

[b] Extrapolated from their experimental data at elevated temperatures using the $C_p°$ and S° values recommended by Konings & Kovács (2003).

23.2.6 Europium chloride compounds and complexes

23.2.6.1 Aqueous europium chloride complexes

Chloride complexes with Eu(III) are very weak, and high chloride concentrations are needed to form such complexes. This implies that very large amounts of perchlorate ions in the background electrolyte need to be replaced by chloride ions. Thus, changes in activity coefficients due to such large compositional changes in the background electrolyte must be accounted for, which can be done using the method described by Spahiu & Puigdomènech (1998). Jordan (in prep.) reviewed numerous experimental studies (mainly employing solvent extraction and cation exchange) on the complexation of Eu(III) with chloride and came to the conclusion that the changes in activity coefficients due to the replacement of the background electrolyte anion by chloride have a much larger impact than complexation with chloride and for this reason the experimental data can be reproduced without invoking any complexation with chloride. This also concerns all the studies that were used by Hummel et al. (2002) to derive stability constants of $EuCl^{2+}$ and $EuCl_2^+$ for the Nagra/PSI TDB 01/01.

The absence of significant Eu(III) chloride complexation at low chloride concentrations is corroborated by several spectroscopic studies of trivalent actinides and lanthanides.

Fanghänel et al. (1995) investigated the formation of Cm(III) chloride complexes with time-resolved laser fluorescence spectroscopy (TRLFS) at 25 °C and chloride concentrations from 0 to about 20 mol · kg^{-1} in $CaCl_2$ solutions at acidic pH. They identified Cm^{3+}, $CmCl^{2+}$, and $CmCl_2^+$, but noted that at low chloride concentrations (< 3 mol · kg^{-1}) at most 5% of curium is found as chloride complexes.

Allen et al. (2000) used extended X-ray absorption fine structure (EXAFS) experiments to study the inner sphere coordination of trivalent lanthanide and actinide ions in aqueous LiCl solutions as a function of increasing chloride concentration. For Cm^{3+}, these authors were not able to observe any chloride complexes at 7.0 M LiCl, only at 8.7 M LiCl they observed an average coordination number of 1.2 ± 0.33 for all the inner sphere chloro complexes in solution. They argued that these data suggest little inner sphere complex formation for Cm^{3+} at LiCl concentrations < about 5 M and that the trivalent lanthanide ions – which show chloro complexation at higher LiCl concentrations – also lack significant chloride complex formation at LiCl concentrations < about 5 M if one assumes that they are similar to Cm^{3+}.

In an EXAFS study carried out by Skerencak-Frech et al. (2014) at 25, 90 and 200 °C and Am^{3+} and Cl^- concentrations of 10^{-3} and 3 mol · kg^{-1}, resp., no Am^{3+} chloride complexes were found at temperatures below 90 °C.

Koke et al. (2019) used TRLFS for the study of Cm^{3+} complexation with chloride in LiCl, NaCl, $MgCl_2$, and $CaCl_2$ at temperatures in the range of 25 – 200 °C. No appreciable complex formation was detected at 25 °C and chloride concentrations < 3 mol · kg^{-1}.

It is reasonable to assume that these spectroscopic findings also apply to Eu^{3+} chloride complexes.

In summary, there is no evidence from chemical and spectroscopic studies that appreciable amounts of Eu^{3+} chloride complexes can be expected to form at chloride concentrations < 3 mol · kg^{-1} and temperatures below about 90 °C.

Thus, the stability constants for $EuCl^{2+}$ and $EuCl_2^+$ recommended by Hummel et al. (2002) for the Nagra/PSI TDB 01/01 (see Tab. 23.2.10-1) are not retained for TDB 2020 and no europium chloride complexes are included. The specific ion interaction coefficient $\varepsilon(Eu^{3+}, Cl^-)$ derived in Chapter 3 from mean activity coefficient data of aqueous $EuCl_3$ solutions should be sufficient to describe the interaction between Eu^{3+} and Cl^- in the application range of TDB 2020.

23.2.6.2 Europium chloride solids

Mioduski et al. (2009) reviewed and reported the results of several solubility experiments of $EuCl_3$(cr) in water. The solubility at 25 °C is on the order of 3.6 mol · kg^{-1} and the equilibrium solid is $EuCl_3 \cdot 6H_2O$(cr). Obviously, europium chloride is highly soluble and is not considered in TDB 2020.

23.2.7 Europium sulphate compounds and complexes

23.2.7.1 Aqueous europium sulphate complexes

The data for the europium sulphate complexes $EuSO_4^+$ and $Eu(SO_4)_2^-$ selected by Hummel et al. (2002) are retained.

23.2.7.2 Europium sulphate solids

REE form in general soluble sulphates. For $Eu_2(SO_4)_3 \cdot 8H_2O$(cr), e.g., Rard (1988) determined solubilities of around 0.032 mol kg^{-1} at 25 °C. As REE also form comparatively insoluble hydroxides and carbonates, it is very unlikely that REE sulphates will play any role in limiting the solubility of REE in natural environments. Therefore, no data for $Eu_2(SO_4)_3 \cdot 8H_2O$(cr) are included in TDB 2020.

23.2.8 Europium carbonate compounds and complexes

23.2.8.1 Aqueous europium carbonate complexes

The data for the europium carbonate complexes $EuCO_3^+$ and $Eu(CO_3)_2^-$ selected by Hummel et al. (2002) are retained.

23.2.8.2 Europium carbonate solids

The data for the europium carbonate solids $Eu_2(CO_3)_3$(cr) and $EuOHCO_3$(cr) selected by Hummel et al. (2002) are retained.

23.2.9 Europium phosphate compounds and complexes

23.2.9.1 Aqueous europium phosphate complexes

As discussed by Jordan et al. (2018), information on the complexation of europium with phosphate is largely missing. In fact, prior to Jordan et al. (2018), there was not a single experimental determination of any stability constant of Eu(III) phosphate complexes, and all the existing data was based Ce(III) and Gd(III) data by Byrne et al. (1991), which was extrapolated to other REE phosphate complexes using a linear free energy relationship. This unsatisfactory situation prompted Jordan et al. (2018) to carry out an experimental investigation of Eu(III) and Cm(III) complexation with phosphate at temperatures between 25 and 80 °C using laser-induced luminescence spectroscopy. Based on the spectra, the Eu(III) complex was identified as $EuH_2PO_4^{2+}$. Stability constants for the reaction

$$Eu^{3+} + H_3PO_4(aq) \rightleftharpoons EuH_2PO_4^{2+} + H^+$$

were determined at 25 °C in $NaClO_4$ with ionic strengths ranging from 0.6 – 3.1 mol · L^{-1}. Analysis of the conditional stability constants at different ionic strengths (0.6, 1.1, 2.1, and 3.1 mol · L^{-1}) using SIT resulted in

$$\log_{10}\beta_1°(298.15\ K) = (0.89 \pm 0.13)$$

$$\Delta\varepsilon = (0.15 \pm 0.07)\ kg \cdot mol^{-1}$$

Using $\Delta\varepsilon$, the NEA-selected $\varepsilon(H^+, ClO_4^-)$ = (0.14 ± 0.02), and $\varepsilon(Eu^{3+}, ClO_4^-)$ = (0.47 ± 0.001) kg · mol^{-1} (see Chapter 3) leads to

$$\varepsilon(EuH_2PO_4^{2+}, ClO_4^-) = (0.18 \pm 0.08)\ kg \cdot mol^{-1}$$

which is included in TDB 2020 together with $\log_{10}\beta_1°(298.15\ K) = (0.89 \pm 0.13)$ and the estimate (based on the estimation method described in Section 1.5.3.

$$\varepsilon(EuH_2PO_4^{2+}, Cl^-) \approx (0.15 \pm 0.10)\ kg \cdot mol^{-1}$$

Jordan et al. (2018) also measured the temperature dependence of the stability constant at I = 1.1 mol · L^{-1} and 25, 40, 50, 60, and 80 °C. They extrapolated the conditional stability constants to zero ionic strength by assuming that $\Delta\varepsilon$ is independent of temperature and by using the appropriate values of the temperature-dependent A-parameter in the Debye-Hückel term. The resulting stability constants turned out to be linear in a van't Hoff plot and could therefore be described with the integrated van't Hoff equation with

$$\Delta_r H_m°(298.15\ K) = (14.7)\ kJ \cdot mol^{-1}$$

$$\Delta_r C_{p,m}°(298.15\ K) = 0$$

These values are also included in TDB 2020.

23.2.9.2 Europium phosphate solids

According to Gausse et al. (2016), rare-earth phosphates $LnPO_4 \cdot nH_2O$(s) exhibit a variety of crystal structures: Monazite, xenotime, rhabdophane and churchite. Monazite and xenotime are both anhydrous and crystallize in the monoclinic and trigonal crystal systems, respectively. The hydrous phosphates rhabdophane, $LnPO_4 \cdot 0.667H_2O$(s), and churchite, $LnPO_4 \cdot 2H_2O$(s), crystallize in the monoclinic system. For the light REE from La to Eu the monazite structure has been identified, while the middle range REE from Gd to Dy can be found in both the monazite and xenotime structure. The heavy REE from Ho to Lu and Y are found in the xenotime structure. Both light and middle range REE (from La to Dy) can also be found in the rhabdophane structure. Finally, the middle range and heavy REE (from Gd to Lu and Y) can also be found in the churchite structure. Thus Eu can be found either in the monazite ($EuPO_4$) or rhabdophane structure ($EuPO_4 \cdot 0.667H_2O$).

Firsching & Brune (1991) determined the solubilities of REE (except Ce and Pm) and Y phosphates in aqueous solution at 25 °C. The REE phosphates were prepared by precipitation from homogeneous solutions of REE in mixtures of phosphoric and perchloric acid using the hydrolysis of urea. Urea was added to the solutions; heating of the solutions induced the hydrolysis of urea, thereby increasing the pH and leading to the precipitation of the REE phosphates. A second method was also used that took advantage of the decreasing solubility of REE phosphates with temperature. Saturated solutions of REE in mixtures of phosphoric and perchloric acid were heated to 100 °C, leading to the precipitation of the REE phosphates. Both types of crystals were used in the solubility studies, but they were not further analysed, neither with respect to structure, nor to composition. The crystals were placed in dilute solutions of $HClO_4$ (0.0697 and 0.0910 M) and kept in contact with the solutions for more than 3 months (equilibrium from undersaturation was reached after about 80 days). Firsching & Brune (1991) noted that "undoubtedly, the surfaces of the solid phase had achieved a thermodynamically stable hydrate form". However, composition and structure of these hydrated surfaces were not determined. Eu^{3+} and H_3PO_4(aq) were found to be the only significant europium and phosphate species under the low pH of the experiments (< 1.2) and their concentrations indicated congruent dissolution. The following stepwise dissociation constants of phosphoric acid were used by Firsching & Brune (1991) for the calculation of the solubility product: K_1°(298.15 K) = 7.11×10^{-3}, K_2°(298.15 K) = 6.34×10^{-8}, and K_3°(298.15 K) = 4.17×10^{-13}, which correspond to $\log_{10}K_1$°(298.15 K) = -2.15, $\log_{10}K_2$°(298.15 K) = -7.20, and $\log_{10}K_3$°(298.15 K) = -12.38.

For the reaction

$$EuPO_4(s) \rightleftharpoons Eu^{3+} + PO_4^{3-}$$

they obtained $\log_{10}K_{s,0}$°(298.15 K) = -(25.75 ± 0.27), which corresponds to $\log_{10}K_s$°(298.15 K) = -(4.02 ± 0.27) for the reaction

$$EuPO_4(s) + 3\ H^+ \rightleftharpoons Eu^{3+} + H_3PO_4(aq)$$

Liu & Byrne (1997) measured the solubilities of REE (except Pm) and Y phosphates in aqueous solution at 25 °C. The phosphate solids were prepared in three different ways. (1) REE oxides (Ce and Tb were used as chlorides) were combined with NaH_2PO_4 to produce equimolar solutions of total phosphate and REE. 0.4 μm filters were used to separate the precipitates from the solution. (2) Precipitates from procedure 1 were aged for two months in the solution at 25 °C before

filtration. Precipitates from both procedures were rinsed in deionized water until the phosphate concentrations dropped below the spectrophotometric detection limits. The precipitates were then rinsed with dilute acid followed by deionized water until the pH of the rinse solutions remained near neutral. (3) Precipitates were produced following the urea method by Firsching & Brune (1991) discussed above and finally washed with dilute acid and deionized water. Prior to being used in the solubility experiments the precipitates were analysed by X-ray diffraction. Precipitates of the light REE obtained from procedure 1 were X-ray amorphous and those of the heavy REE showed only hints of crystallinity. Precipitates from procedures 2 and 3 were well crystallized and generally conformed to the rhabdophane structure. Solubilities were measured from undersaturation in dissolution experiments in 0.1 molar perchloric acid. Sample bottles were kept at 25 °C and vigorously shaken for up to five months. For analysis, the solutions were passed through 0.2 μm filters. Total phosphate concentrations 10% below the final values were often obtained after only two weeks. As in the experiments by Firsching & Brune (1991), dissolution of the REE phosphates was congruent. The solubility products for the Eu phosphates were calculated from the solubility data by using the following stepwise dissociation constants for phosphoric acid, $\log_{10}K_1°$(298.15 K) = -1.943, $\log_{10}K_2°$(298.15 K) = -6.8920, and $\log_{10}K_3°$(298.15 K) = -11.887, together with the estimated formation constants for Eu phosphate complexes $\log_{10}\beta°(EuHPO_4^+$, 298.15 K) = 4.775 and $\log_{10}\beta°(EuH_2PO_4^{2+}$, 298.15 K) = 2.191 (Byrne et al. 1991)[63] and the activity coefficients $\gamma(Eu^{3+})$ = 0.134 and $\gamma(PO_4^{3-})$ = 0.189. For the precipitates from procedure 2 and 3, Liu & Byrne (1997) obtained $\log_{10}K_{s,0}°$(298.15 K) = -25.92 (100 days of equilibration) and $\log_{10}K_{s,0}°$(298.15 K) = -25.99 (30 days of equilibration), respectively. From these two values they derived their recommended value $\log_{10}K_{s,0}°$(298.15 K) = -(25.96 ± 0.03), which corresponds to $\log_{10}K_s°$(298.15 K) = -(5.24 ± 0.03) for the reaction in terms of H_3PO_4(aq). The solubility of precipitates from procedure 1 is significantly higher, with $\log_{10}K_{s,0}°$(298.15 K) ≈ -25.3 after 150 days. In the discussion of their experimental results, Liu & Byrne (1997) pointed out that in natural environments Y and REE do not each form their own discrete phosphate phases but rather form solid solutions by coprecipitation.

Gausse et al. (2016) determined the solubility of REE rhabdophanes $LnPO_4·0.667H_2O$(cr), with Ln = La to Dy (without Pm) from both under- and supersaturation at 25, 60, 70,and 90 °C. For the dissolution experiments (equilibrium from undersaturation), rhabdophane samples were prepared by mixing $LnCl_3$ and H_3PO_4 solutions and keeping them for 14 d at 90 °C. The precipitates were separated from the solution by centrifugation and dried at 90 °C in air overnight. The resulting powders were analysed by powder X-ray diffraction (PXRD) and inspected by environmental scanning electron microscopy (ESEM). The dissolution experiments were carried out by contacting the rhabdophane powders with 0.1 M HCl solutions and kept in a heating orbital stirrer at 25 ± 5 and 70 ± 5 °C. Dissolution was congruent and solution compositions remained unchanged after approximately 10 d. The remaining precipitates were again characterized by PXRD and ESEM and the rhabdophane structure was confirmed. No additional phases were detected. Gausse et al. (2016) used SIT to extrapolate the conditional solubility constants to zero ionic strength and used the integrated van't Hoff equation to derive $\Delta_r H_m°$ from the solubility constants determined at different temperatures. For europium rhabdophane, Gausse et al. (2016) obtained

[63] Byrne et al. (1991) extrapolated their experimentally determined stability constants for $CmHPO_4^+$ and $GdHPO_4^+$, and $CmH_2PO_4^{2+}$ and $GdH_2PO_4^{2+}$, resp., to the other REE phosphate complexes using a linear free energy relationship.

Tab. 23.2.9-1: Reported solubility products $\log_{10}K_s°$(298.15 K) of $EuPO_3(s) + 3\ H^+ \rightleftharpoons Eu^{3+} + H_3PO_4(aq)$ and $\log_{10}K_{s,0}°$(298.15 K) of $EuPO_4(s) \rightleftharpoons Sm^{3+} + PO_4^{3-}$

Structure	**$\log_{10}K_s°$(298.15 K)**	**$\log_{10}K_{s,0}°$(298.15 K)**	**Reference**
Not determined	-4.02 ± 0.27 [a]	-25.75 ± 0.27	Firsching & Brune (1991)
Rhabdophane	-5.24 ± 0.03 [a]	-25.96 ± 0.03	Liu & Byrne (1997)
Rhabdophane		-24.9 ± 1.7 [b]	Gausse et al. (2016)

[a] Calculated from $\log_{10}K_{s,0}°$(298.15 K) and the dissociation constants for phosphoric acid used by the authors.

[b] This constant was reported by Gausse et al. (2016) for the reaction $EuPO_4{\cdot}0.667H_2O(cr) \rightleftharpoons Eu^{3+} + PO_4^{3-} + 0.667\ H_2O(l)$.

$$EuPO_4{\cdot}0.667H_2O(cr) \rightleftharpoons Eu^{3+} + PO_4^{3-} + 0.667\ H_2O(l)$$

$$\log_{10}K_{s,0}°(298.15\ K) = -(24.9 \pm 1.7)$$

$$\Delta_r H_m°(298.15\ K) = -(17 \pm 7)\ kJ \cdot mol^{-1}$$

$$\Delta_r C_{p,m}°(298.15\ K) = 0$$

These data are included in TDB 2020 because in the experiments by Gausse et al. (2016) equilibrium was attained from under- and supersaturation and the solids were well characterized both before and after the experiments.

23.2.10 Selected europium data

Tab. 23.2.10-1: Selected europium data (1 bar, 298.15 K) for TDB 2020

New or changed data with respect to TDB Version 12/07 (Thoenen et al. 2014) are shaded. T-range refers to the experimental temperature range at which equilibrium constants, $\Delta_r H_m$, and $\Delta_r C_{p,m}°$ were determined.

Name	Redox	TDB Version 12/07				TDB 2020				
		$\Delta_f G_m°$ [kJ · mol^{-1}]	$\Delta_f H_m°$ [kJ · mol^{-1}]	$S_m°$ [J · K^{-1} · mol^{-1}]	$C_{p,m}°$ [J · K^{-1} · mol^{-1}]	$\Delta_f G_m°$ [kJ · mol^{-1}]	$\Delta_f H_m°$ [kJ · mol^{-1}]	$S_m°$ [J · K^{-1} · mol^{-1}]	$C_{p,m}°$ [J · K^{-1} · mol^{-1}]	Species
Eu(cr)	0	0.0	0.0	77.78	-	0	0	77.8	27.65	Eu(cr)
Eu+3	III	-555.1 ± 13.6	-586.0 ± 13.6	-222.0	-	-575.9 ± 4.1	-605.4 ± 4.0	-217.2 ± 3.2	-80.6 ± 20	Eu^{3+}
Eu+2	II	-521.3 ± 13.9	-507.9	-8.0	-	-	-	-	-	Eu^{2+}

Name	Redox	TDB Version 12/07		TDB 2020				
		$\log_{10}\beta°$	$\Delta_r H_m°$ [kJ · mol^{-1}]	$\log_{10}\beta°$	$\Delta_r H_m°$ [kJ · mol^{-1}]	$\Delta_r C_{p,m}°$ [J · K^{-1} · mol^{-1}]	T-range [°C]	Reaction
EuOH+2	III	-7.64 ± 0.04	-	-7.64 ± 0.04	-	-	-	Eu^{3+} + H_2O(l) ⇌ $EuOH^{2+}$ + H^+
Eu(OH)2+	III	-15.1 ± 0.2	-	-15.1 ± 0.2	-	-	-	Eu^{3+} + 2 H_2O(l) ⇌ $Eu(OH)_2^+$ + 2 H^+
Eu(OH)3	III	-23.7 ± 0.1	-	-23.7 ± 0.1	-	-	-	Eu^{3+} + 3 H_2O(l) ⇌ $Eu(OH)_3$(aq) + 3 H^+
Eu(OH)4-	III	-36.2 ± 0.5	-	-36.2 ± 0.5	-	-	-	Eu^{3+} + 4 H_2O(l) ⇌ $Eu(OH)_4^-$ + 4 H^+
EuF+2	III	3.8 ± 0.2	-	4.28 ± 0.07	*8.10 ± 0.91*	*0*	5-45	Eu^{3+} + F^- ⇌ EuF^{2+}
EuF2+	III	6.5 ± 0.5	-	*6.81 ± 0.3*	*18.5 ± 2.3*	*0*	5-45	Eu^{3+} + 2 F^- ⇌ EuF_2^+
EuCl+2	III	1.1 ± 0.2	-	-	-	-	-	Eu^{3+} + Cl^- ⇌ $EuCl^{2+}$
EuCl2+	III	1.5 ± 0.5	-	-	-	-	-	Eu^{3+} + 2 Cl^- ⇌ $EuCl_2^+$
EuSO4+	III	3.95 ± 0.08	-	3.95 ± 0.08	-	-	-	Eu^{3+} + SO_4^{2-} ⇌ $EuSO_4^+$
Eu(SO4)2-	III	5.7 ± 0.2	-	5.7 ± 0.2	-	-	-	Eu^{3+} + 2 SO_4^{2-} ⇌ $Eu(SO_4)_2^-$
EuCO3+	III	8.1 ± 0.2	-	8.1 ± 0.2	-	-	-	Eu^{3+} + CO_3^{2-} ⇌ $EuCO_3^+$
Eu(CO3)2-	III	12.1 ± 0.3	-	12.1 ± 0.3	-	-	-	Eu^{3+} + 2 CO_3^{2-} ⇌ $Eu(CO_3)_2^-$
EuH2PO4+2	III	-	-	0.89 ± 0.13	14.7	0	25-80	Eu^{3+} + H_3PO_4(aq) ⇌ $EuH_2PO_4^{2+}$ + H^+
Eu+2	III/II	-5.92	-	-	-	-	-	Eu^{3+} + e^- ⇌ Eu^{2+}

[a] Calculated from $\Delta_f G_m°$.

Tab. 23.2.10-1: Cont.

Name	Redox	TDB Version 12/07		TDB 2020				
		$\log_{10}K_{s,0}°$	$\Delta_r H_m°$ [kJ · mol^{-1}]	$\log_{10}K_{s,0}°$	$\Delta_r H_m°$ [kJ · mol^{-1}]	$\Delta_r C_{p,m}°$ [J · K^{-1} · mol^{-1}]	T-range [°C]	Reaction
Eu(OH)3(cr)	III	14.9 ± 0.3	124.39 [a]	14.9 ± 0.3	124.39 [a]	-	25	$Eu(OH)_3(cr) + 3\ H^+ \rightleftharpoons Eu^{3+} + 3\ H_2O(l)$
Eu(OH)3(am)	III	17.6 ± 0.8	-	17.6 ± 0.8	-	-	-	$Eu(OH)_3(am) + 3\ H^+ \rightleftharpoons Eu^{3+} + 3\ H_2O(l)$
EuF3(cr)	III	-17.4 ± 0.5	-	-18.7 ± 0.4	-	-	-	$EuF_3(cr) \rightleftharpoons Eu^{3+} + 3\ F^-$
Eu2(CO3)3(cr)	III	-35.0 ± 0.3	-	-35.0 ± 0.3	-	-	-	$Eu_2(CO_3)_3(cr) \rightleftharpoons 2\ Eu^{3+} + 3\ CO_3^{2-}$
EuOHCO3(cr)	III	-21.7 ± 0.1	-	-21.7 ± 0.1	-	-	-	$EuOHCO_3(cr) \rightleftharpoons Eu^{3+} + OH^- + CO_3^{2-}$
Eu-rhabdophane	III	-	-	-24.9 ± 1.7	-17 ± 7	0	25-90	$EuPO_4{\cdot}0.667H_2O(cr) \rightleftharpoons Eu^{3+} + PO_4^{3-} + 0.667\ H_2O(l)$

[a] Clculated from $\Delta_f H_m° = -1'319.1$ kJ · mol^{-1}.

Tab. 23.2.10-2: Selected SIT ion interaction coefficients $\varepsilon_{j,k}$ [kg · mol^{-1}] for europium species

Data estimated according to charge correlations and taken from Tab. 1-7 are shaded. Supplemental data are in italics.

j k → ↓	Cl^- $\varepsilon_{j,k}$ [kg · mol^{-1}]	ClO_4^- $\varepsilon_{j,k}$ [kg · mol^{-1}]	NO_3^- $\varepsilon_{j,k}$ [kg · mol^{-1}]	Na^+ $\varepsilon_{j,k}$ [kg · mol^{-1}]	$Na^+ + Cl^-$ $\varepsilon_{j,k}$ [kg · mol^{-1}]
Eu+3	0.260 ± 0.005	0.47 ± 0.01	0.080 ± 0.001	0	0
EuOH+2	0.15 ± 0.10	0.4 ± 0.1	-	0	0
Eu(OH)2+	0.05 ± 0.10	0.2 ± 0.1	-	0	0
Eu(OH)3(aq)	0	0	0	0	0
Eu(OH)4-	0	0	0	-0.05 ± 0.10	0
EuF+2	0.15 ± 0.03	0.32 ± 0.03	0.01 ± 0.03	0	0
EuF2+	*0.05 ± 0.10*	*0.2 ± 0.1*	-	0	0
EuSO4+	0.05 ± 0.10	0.27 ± 0.09	-	0	0
Eu(SO4)2-	0	0	0	0.22 ± 0.20	0
EuCO3+	0.05 ± 0.10	0.15 ± 0.18 [a]	-	0	0
Eu(CO3)2-	0	0	0	-1.17 ± 0.32 [b]	0
EuH2PO4+2	0.15 ± 0.10	0.18 ± 0.08	-	0	0

[a] This value follows from $\Delta\varepsilon = -(0.24 \pm 0.18)$ kg · mol^{-1} reported by Hummel et al. (2002), $\varepsilon(Eu^{3+}, ClO_4^-) = (0.47 \pm 0.01)$ kg · mol^{-1} (Section 23.2.3), and $\varepsilon(CO_3^{2-}, Na^+) = -(0.08 \pm 0.03)$ kg · mol^{-1} selected by NEA (Lemire et al. 2013).

[b] This value follows from $\Delta\varepsilon = -(1.48 \pm 0.31)$ kg · mol^{-1} reported by Hummel et al. (2002), $\varepsilon(Eu^{3+}, ClO_4^-) = (0.47 \pm 0.01)$ kg · mol^{-1} (Section 23.2.3), and $\varepsilon(CO_3^{2-}, Na^+) = -(0.08 \pm 0.03)$ kg · mol^{-1} selected by NEA (Lemire et al. 2013).

23.2.11 References

Allen, P.G., Bucher, J.J., Shuh, D.K., Edelstein, N.M. & Craig, I. (2000): Coordination chemistry of trivalent lanthanide and actinide ions in dilute and concentrated chloride solutions. Inorganic Chemistry, 39, 595-601.

Arblaster, J.W. (2013): Selected values of the thermodynamic properties of scandium, yttrium, and the lanthanide elements. Handbook on the Physics and Chemistry of Rare Earths, 43, 321-565.

Byrne, R.H., Lee, J.H. & Bingler, L.S. (1991): Rare earth element complexation by PO_4^{3-} ions in aqueous solution. Geochimica et Cosmochimica Acta, 55, 2729-2735.

Chatterjee, S., Campbell, E.L., Neiner, D., Pence, N.K., Robinson, T.A. & Levitskaia, T.G. (2015): Aqueous binary lanthanide(III) nitrate $Ln(NO_3)_3$ electrolytes revisited: Extended Pitzer and Bromley treatments. Journal of Chemical and Engineering Data, 60, 2974-2988.

Ciavatta, L. (1980): The specific interaction theory in evaluating ionic equilibria. Annali di Chimica, 70, 551-567.

Cordfunke, E.H.P. & Konings, R.J.M. (2001): The enthalpies of formation of lanthanide compounds II. Ln^{3+}(aq). Thermochimica Acta, 375, 51-64.

Cox, J.D., Wagman, D.D. & Medvedev, V.A. (1989): CODATA Key Values for Thermodynamics. New York, Hemisphere, 271p.

Fanghänel, T., Kim, J.I., Klenze, R. & Kato, Y. (1995): Formation of Cm(III) chloride complexes in $CaCl_2$ solutions. Journal of Alloys and Compounds, 225, 308-311.

Firsching, F.H. & Brune, S.N. (1991): Solubility products of the trivalent rare-earth phosphates. Journal of Chemical and Engineering Data, 36, 93-95.

Fraústo da Silva, J.J.R. & Queimado, M.M. (1973): Solubility products of lanthanide fluorides. Revista Portuguesa de Química, 15, 29-34.

Gausse, C., Szenknect, S., Qin, D.W., Mesbah, A., Clavier, N., Neumeier, S., Bosbach, D. & Dacheux, N. (2016): Determination of the solubility of rhabdophanes $LnPO_4 \cdot 0.667H_2O$ (Ln = La to Dy). European Journal of Inorganic Chemistry, 28, 4615-4630.

Gerstein, B.C., Jelinek, F.J., Mullaly, J.R., Shickell, W.D. & Spedding, F.H. (1967): Heat capacity of europium from 5°-300°K. Journal of Chemical Physics, 47, 5194-5201.

Grenthe, I., Plyasunov, A.V. & Spahiu, K. (1997): Estimations of medium effects on thermodynamic data. In: Grenthe, I. & Puigdomènech, I. (eds.): Modelling in Aquatic Chemistry. OECD NEA, Paris, France, 325-426.

He, M. & Rard, J.A. (2015): Revision of the osmotic coefficients, water activities and mean activity coefficients of the aqueous trivalent rare earth chlorides at T = 298.15 K. Journal of Solution Chemistry, 44, 2208-2221.

Hinchey, R.J. & Cobble, J.W. (1970): Standard-state entropies for the aqueous trivalent lanthanide and yttrium ions. Inorganic Chemistry, 9, 917-921.

Hummel, W. (2018): Radioactive waste inventories for geochemists. PSI Internal Report, TM-44-18-03, Paul Scherrer Institut, Villigen, Switzerland, 55 pp.

Hummel, W., Berner, U., Curti, E., Pearson, F.J. & Thoenen, T. (2002): Nagra/PSI Chemical Thermodynamic Data Base 01/01. Nagra NTB 02-16, Nagra. Also published by Universal Publishers/upublish.com, Parkland, USA, 565 pp.

Itoh, H., Hachiya, H., Suzuki, Y. & Asano, Y. (1984): Determination of solubility products of rare earth fluorides by fluoride ion-selective electrode. Bulletin of the Chemical Society of Japan, 57, 1698-1690.

Jordan, N. (in prep.): Europium: Review of thermodynamic data for Eu(III) complexation with inorganic ligands.

Jordan, N., Demnitz, M., Lösch, H., Starke, S., Brendler, V. & Huittinen, N. (2018): Complexation of trivalent lanthanides (Eu) and actinides (Cm) with aqueous phosphates at elevated temperatures. Inorganic Chemistry, 57, 7015-7024.

Koke, C., Skerencak-Frech, A. & Panak, P.J. (2019): Thermodynamics of the complexation of curium(III) with chloride in alkali and alkali earth metal solutions at elevated temperatures. Journal of Chemical Thermodynamics, 131, 219-224.

Konings, R.J.M. & Beneš, O. (2010): The thermodynamic properties of the f-elements and their compounds. I. The lanthanide and actinide metals. Journal of Physical and Chemical Reference Data, 39, 043102-1–043102-48.

Konings, R.J.M. & Kovács, A. (2003): Thermodynamic properties of the lanthanide(III) halides. Handbook on the Physics and Chemistry of Rare Earths, 33, 147-247.

Lee, J.H. & Byrne, R.H. (1993): Rare earth element complexation by fluoride ions in aqueous solution. Journal of Solution Chemistry, 22, 751-766.

Lemire, R.J., Berner, U., Musikas, C., Palmer, D.A., Taylor, P. & Tochiyama, O. (2013): Chemical Thermodynamics of Iron, Part 1. Chemical Thermodynamics, Vol. 13a. OECD Publications, Paris, France, 1082 pp.

Liu, W., Etschmann, B., Migdisov, A., Boukhalfa, H., Testemale, D., Müller, H., Hazemann, J.-L. & Brugger, J. (2017): Revisiting the hydrothermal geochemistry of europium(II/III) in light of new in-situ XAS spectroscopy results. Chemical Geology, 459, 61-74.

Liu, X. & Byrne, R.H. (1997): Rare earth and yttrium phosphate solubilities in aqueous solution. Geochimica et Cosmochimica Acta, 61, 1625-1633.

Luo, Y. & Millero, F.J. (2004): Effects of temperature and ionic strength on the stabilities of the first and second fluoride complexes of yttrium and the rare earth elements. Geochimica et Cosmochimica Acta, 68, 4301-4308.

Luo, Y.-R. & Byrne, R.H. (2000): The ionic strength dependence of rare earth and yttrium fluoride complexation at 25 °C. Journal of Solution Chemistry, 29, 1089-1099.

Luo, Y.-R. & Byrne, R.H. (2001): Yttrium and rare earth element complexation by chloride ions at 25 °C. Journal of Solution Chemistry, 30, 837-845.

Luo, Y.-R. & Byrne, R.H. (2007): The influence of ionic strength on yttrium and rare earth element complexation by fluoride ions in $NaClO_4$, $NaNO_3$ and NaCl Solutions at 25 °C. Journal of Solution Chemistry, 36, 673-689.

Menon, M. P. & James, J. (1989a): Stability constant for the lanthanide fluoride complexes in aqueous solution at 25 °C. Journal of Solution Chemistry, 18, 735-742.

Menon, M. P. & James, J. (1989b): Solubilities, solubility products and solution chemistry of lanthanon trifluoride–water systems. Journal of the Chemical Society, Faraday Transactions, 85, 2683-2694.

Migdisov, A., Williams-Jones, A.E., Brugger, J. & Caporuscio, F.A. (2016): Hydrothermal transport, deposition, and fractionation of the REE: Experimental data and thermodynamic calculations. Chemical Geology 439, 13-42.

Migdisov, A.A., Williams-Jones, A.E. & Wagner, T. (2009): An experimental study of the solubility and speciation of the Rare Earth Elements (III) in fluoride- and chloride-bearing aqueous solutions at temperatures up to 300 °C. Geochimica et Cosmochimica Acta, 73, 7087-7109.

Mioduski, T., Gumiński, C. & Zeng, D. (2009): IUPAC-NIST solubility data series. 87. Rare earth metal chlorides in water and aqueous systems. Part 2. Light lanthanides (Ce–Eu). Journal of Physical and Chemical Reference Data, 38, 441-562.

Rard, J.A. (1988): Aqueous solubilities of praseodymium, europium, and lutetium sulfates. Journal of Solution Chemistry, 17, 499-517.

Rard, J.A. (2016): Critical evaluation of the standard molar entropies, enthalpies of formation, Gibbs energies of formation and heat capacities of the aqueous trivalent rare earth ions, and the corresponding standard molar entropies, enthalpies of formation and Gibbs energies of formation of the thermodynamically stable $RECl_3 \cdot 7H_2O$(cr) and $RECl_3 \cdot 6H_2O$(cr). Journal of Solution Chemistry, 45, 1332-1376.

Rard, J.A. & Spedding, F.H. (1982): Isopiestic determination of the activity coefficients of some aqueous rare-earth electrolyte solutions at 25 °C. 6. $Eu(NO_3)_3$, $Y(NO_3)_3$, and YCl_3. Journal of Chemical and Engineering Data, 27, 454-461.

Schijf, J. & Byrne, R.H. (1999): Determination of stability constants for the mono- and difluoro-complexes of Y and the REE, using a cation-exchange resin and ICP-MS. Polyhedron, 18, 2839-2844.

Shannon, R.D. (1976): Revised effective ionic radii and systematic studies of interatomic distances in halides and chalcogenides. Acta Crystallographica, A32, 751-767.

Skerencak-Frech, A., Fröhlich, D.R., Rothe, J., Dardenne, K. & Panak, P.J. (2014): Combined time-resolved laser fluorescence spectroscopy and extended X-ray absorption fine structure spectroscopy study on the complexation of trivalent actinides with chloride at T = 25 – 200 °C. Inorganic Chemistry, 53, 1062-1069.

Spahiu, K. & Puigdomènech, I. (1998): On weak complex formation: Re-interpretation of literature data on the Np and Pu nitrate complexation. Radiochimica Acta, 82, 413-419.

Spedding, F.H., DeKock, C.W., Pepple, G.W. & Habenschuss, A. (1977): Heats of dilution of some aqueous rare earth electrolyte solutions at 25 °C. 3. Rare earth chlorides. Journal of Chemical and Engineering Data, 22, 58-70.

Spedding, F.H., Weber, H.O., Saeger, V.W., Petheram, H.H., Rard, J.A. & Habenschuss, A. (1976): Isopiestic determination of the activity coefficients of some aqueous rare earth electrolyte solutions at 25 °C. 1. The rare earth chlorides. Journal of Chemical and Engineering Data, 21, 341-360.

Thoenen, T., Hummel, W., Berner, U. & Curti, E. (2014): The PSI/Nagra Chemical Thermodynamic Database 12/07. Technical Report, PSI Bericht Nr. 14-04, Paul Scherrer Institut, Villigen, Switzerland, 416 pp.

Wagman, D.D., Evans, W.H., Parker, V.B., Schumm, R.H., Halow, I., Bailey, S.M., Churney, K.L. & Nuttall, R.L. (1982): The NBS tables of chemical thermodynamic properties: Selected values for inorganic and C1 and C2 organic substances in SI units. Journal of Physical and Chemical Reference Data, 11, Supplement No. 2, 1-392.

Walker, J.B. & Choppin, G.R. (1967): Thermodynamic parameters of fluoride complexes of the lanthanides. In: Fields P.R. & Moeller, T. (eds.): Lanthanide/Actinide Chemistry. Advances in Chemistry Vol. 71. American Chemical Society, Washington, D.C, 127-140.

Wood, S. A. (1990): The aqueous geochemistry of the rare-earth elements and yttrium 1. Review of available low-temperature data for inorganic complexes and the inorganic REE speciation of natural waters. Chemical Geology, 82, 159-186.

Xiao, C. & Tremaine, P.R. (1997): The thermodynamics of aqueous trivalent rare earth elements. Apparent molar heat capacities and volumes of $Nd(ClO_4)_3(aq)$, $Eu(ClO_4)_3(aq)$, $Er(ClO_4)_3(aq)$, and $Yb(ClO_4)_3(aq)$ from the temperatures 283 K to 328 K. Journal of Chemical Thermodynamics, 29, 827-852.

23.3 Holmium

23.3.1 Introduction

Ho has numerous isotopes, ranging from ^{140}Ho to ^{175}Ho (Audi et al. 2003). There is only one stable isotope, ^{165}Ho. Two radioactive isotopes of Ho are of concern for the planned deep underground repositories for radioactive waste in Switzerland, ^{163}Ho and ^{166m}Ho (Hummel 2018). ^{163}Ho has a half-life of $(4.57 \pm 0.02) \cdot 10^3$ years and occurs as activation product in wastes from nuclear power plants and as spallation product in targets of spallation sources used in research. ^{166m}Ho is a fission product with a half-life of $(1.2 \pm 0.2) \cdot 10^3$ years and is found in SF, HLW, and L/ILW. Only ^{166m}Ho is considered as dose-relevant radionuclide (Hummel 2018). Ho has not been included in the precursors of TDB 2020 (Nagra/PSI TDB 05/92: Pearson & Berner 1991, Pearson et al. 1992; PSI/Nagra TDB 01/01: Hummel et al. 2002; PSI/Nagra TDB 12/07: Thoenen et al. 2014) and is therefore a new addition to the database.

The thermodynamic data for Ho selected in this review for TDB 2020 are listed in Tab. 23.3.10-1.

NEA chose the specific ion interaction theory (SIT) for the extrapolation of experimental data to zero ionic strength, see, e.g., Grenthe et al. (1997), an approach which is also adopted for TDB 2020 (as has been for all its predecessors). When referring to ion interaction coefficients recommended by NEA, we took those from Tab. B.3 in Lemire et al. (2013).

Due to a lack of experimental data, many ion interaction coefficients for cationic Ho species with ClO_4^- and Cl^-, and for anionic Ho species with Na^+ are unknown. We filled these gaps by applying the estimation method described in Section 1.5.3, which is based on a statistical analysis of published SIT ion interaction coefficients and which allows the estimation of such coefficients for the interaction of cations with Cl^- and ClO_4^-, and for the interaction of anions with Na^+ from the charge of the considered cations or anions. Ion interaction coefficients of neutral niobium species with background electrolytes were assumed to be zero.

The ion interaction coefficients for holmium species selected for TDB 2020 are listed in Tab. 23.3.10-2.

23.3.1.1 Previous reviews of low-temperature thermodynamic data for rare-earth elements

Wood (1990) reviewed the available low-temperature thermodynamic data for inorganic complexes of the REE and yttrium, considering hydroxide, fluoride, chloride, sulphate, nitrate, phosphate, and carbonate as ligands. Since the trivalent REE ions are classified as Pearson hard acids, they form complexes preferentially with hard ligands containing highly electronegative donor atoms such as oxygen and fluorine, e.g. OH^-, F^-, SO_4^{2-}, PO_4^{3-}, and CO_3^{2-}, while complexes with borderline ligands, such as Cl^- or NO_3^- are very weak, and complexes with the very soft HS^- or CN^- ligands extremely weak or unknown in aqueous solution (Wood 1990). For Ho(III), Wood (1990) could only recommend stability constants for HoF^{2+}, $HoCl^{2+}$, $HoSO_4^+$, and $Ho(SO_4)_2^-$. Based on a broader dataset for Eu(III), he calculated the europium species distribution as a function of pH for several model groundwaters with varying amounts of fluoride, sulphate, phosphate, and carbonate. The general picture emerging from these calculations was that in all cases $EuCO_3^+$ turned out to be the most important species at pH between about 6.5 and 9.5, while $Eu(CO_3)_2^-$ became more important at pH above about 9.5. Fluoride, sulphate, and phosphate

species were only important at pH < 7. Eu hydroxides were in all cases only minor species, but Wood (1990) pointed out that, at that time, the hydrolysis constants for Eu (and all other REE elements) were only poorly known.

Millero (1992) compiled stability constants for REE complexes with hydroxide, fluoride, chloride, sulphate, phosphate, and carbonate determined in $NaClO_4$ at room temperature and various ionic strengths and extrapolated the conditional stability constants to infinite dilution using the Pitzer interaction model. In the case of holmium, he provided stability constants for $HoOH^{2+}$, HoF^{2+}, $HoCl^{2+}$, $HoSO_4^{+}$, $HoNO_3^{2+}$, $HoHPO_4^{+}$, HoH_2PO4^{2+}, $Ho(HPO4)_2^{-}$, $HoCO_3^{+}$, $HoHCO_3^{2+}$, and $Ho(CO_3)_2^{-}$. Since Millero (1992) reported only a part of the original data and only graphically inures, it is not possible to re-analyse his data in terms of the SIT.

Haas et al. (1995) compiled stability constants for REE complexes with hydroxide, fluoride, chloride, sulphate, nitrate, phosphate, and carbonate at 25 °C and 1 bar. They used estimation methods to derive missing stability constants of higher-order hydroxide, fluoride, and chloride complexes and applied correlation algorithms for estimating HKF parameters for the extrapolation of standard partial molal properties of REE complexes (and thus their stability constants) to elevated temperatures (0 – 1'000 °C) and pressures (1 – 5'000 bars). With respect to Ho, they provided standard partial molal properties and HKF parameters for $HoOH^{2+}$, HoO^{+} (or $Ho(OH)_2^{+}$), $HoO_2H(aq)$ (or $Ho(OH)_3(aq)$), HoO_2^{-} (or $Ho(OH)_4^{-}$), HoF^{2+}, HoF_2^{+}, $HoF_3(aq)$, HoF_4^{-}, $HoCl^{2+}$, $HoCl_2^{+}$, $HoCl_3(aq)$, $HoCl_4^{-}$, $HoSO_4^{+}$, $HoNO_3^{2+}$, $HoH_2PO_4^{2+}$, $HoHCO_3^{2+}$, and $HoCO_3^{+}$. Based on their data, Haas et al. (1995) carried out speciation calculations of idealized 1 molal chloride solutions with minor amounts of fluoride, sulphate, and carbonate at elevated temperature and pressure (300, 500, and 700 °C and P_{sat}) and observed that in general REE chloride complexes are predominant under acidic conditions, fluoride complexes under neutral conditions, and hydroxide complexes under basic conditions. Under these conditions, sulphate and carbonate complexes are insignificant, but may account for much larger fractions of REE in solution at lower temperatures and pressures and may even become predominant in some cases.

Migdisov et al. (2016) reviewed experimental data of REE aqueous species obtained under hydrothermal conditions and derived standard partial molal properties and HKF equation of state parameters of REE complexes with fluoride and chloride. Due to the limited data available for hydroxide and sulphate complexes, which would not allow the derivation of HKF parameters, Migdisov et al. (2016) carried out provisional fits of the available data to the Bryzgalin-Ryzhenko equation of state. Since no hydrothermal data were available for carbonate and phosphate complexes, Migdisov et al. (2016) were not able to provide a preferred dataset for these species. Thus, in the case of holmium, these authors presented HKF parameters for HoF^{2+}, $HoCl^{2+}$, and $HoCl_2^{+}$, as well as Bryzgalin-Ryzhenko parameters for $HoSO_4^{+}$ and $Ho(SO_4)_2^{-}$, but none for any Ho hydroxide complexes.

Migdisov et al. (2016) also reviewed calorimetric and solubility data of solid REE oxides, hydroxides, fluorides, chlorides, phosphates, and fluorocarbonates applicable to elevated temperatures and pressures and selected data for the following Ho(III) solids: $Ho_2O_3(cr)$, $Ho(OH)_3(cr)$, $HoF_3(cr)$, $HoCl_3(cr)$, and $HoPO_4(cr)$.

23.3.2 Elemental holmium

Elemental holmium does not occur in nature as a mineral. For the calculation of certain reaction properties of holmium species, however, values for $S_m°$(Ho, cr, 298.15 K) and $C_{p,m}°$(Ho, cr, 298.15 K) are required. The most recent reviews on the thermodynamic properties of the lanthanide metals are by Konings & Beneš (2010) and Arblaster (2013). Both reviews relied on the low-temperature heat capacity measurements by Gerstein et al. (1957), leading to

$$C_{p,m}°(\text{Ho, cr, 298.15 K}) = 27.15\ \text{J} \cdot \text{K}^{-1} \cdot \text{mol}^{-1}$$

which is included in TDB 2020. Based on the same measurements by Gerstein et al. (1957), Konings & Beneš (2010) obtained $S_m°$(Ho, cr, 298.15 K) = 75.19 J · K^{-1} · mol^{-1}, while Arblaster (2013) additionally considered the heat capacity data by Jayasuriya et al. (1985) resulting in

$$S_m°(\text{Ho, cr, 298.15 K}) = 75.76\ \text{J} \cdot \text{K}^{-1} \cdot \text{mol}^{-1}$$

which is also included in TDB 2020.

23.3.3 Holmium aquo ions

The lanthanides occur in nature as Ln(III) species only, with the exception of Ce, which also exists as Ce(IV) under oxidizing conditions, and Sm, Eu, and Yb, which also exist as Sm(II), Eu(II), and Yb(II) under extremely reducing conditions (Wood 1990). Rard (2016) carried out an extensive review and critical evaluation of the standard molar entropies, heat capacities, enthalpies of formation and Gibbs energies of formation of the aqueous trivalent rare earth ions.

The standard molar entropy for $S_m°(Ho^{3+}, 298.15\ K)$ was derived by Rard (2016) from calorimetric investigations of the dissolution of $HoCl_3 \cdot 6\ H_2O$(cr) in aqueous solution according to the reaction

$$HoCl_3 \cdot 6H_2O(cr) \rightleftharpoons Ho^{3+} + 3\ Cl^- + 6\ H_2O(l)$$

The standard molar entropy of solution is given by

$$\Delta_{r,sol}S_m°(298.15\ K) = S_m°(Ho^{3+}, 298.15\ K) + 3\ S_m°(Cl^-, 298.15\ K) + 6\ S_m°(H_2O, l, 298.15\ K) - S_m°(HoCl_3 \cdot 6H_2O, cr, 298.15\ K)$$

from which $S_m°(Ho^{3+}, 298.15\ K)$ can be calculated if $S_m°(Cl^-, 298.15\ K)$, $S_m°(H_2O, l, 298.15\ K)$, $S_m°(HoCl_3 \cdot 6\ H_2O, cr, 298.15\ K)$, and $\Delta_{r,sol}S_m°(298.15\ K)$ are known. Rard (2016) took $S_m°(Cl^-, 298.15\ K) = (56.60 \pm 0.20)\ J \cdot K^{-1} \cdot mol^{-1}$ and $S_m°(H_2O, l, 298.15\ K) = (69.95 \pm 0.03)\ J \cdot K^{-1} \cdot mol^{-1}$ from the CODATA review (Cox et al. 1989) and selected $S_m°(HoCl_3 \cdot 6H_2O, cr, 298.15\ K) = (403.5 \pm 0.5)\ J \cdot K^{-1} \cdot mol^{-1}$ based on the value of 403.51 J · K^{-1} · mol^{-1} by Spedding et al. (1972). Finally, he derived $\Delta_{r,sol}S_m°(298.15\ K)$ from $\Delta_{r,sol}G_m°(298.15\ K)$ and $\Delta_{r,sol}H_m°(298.15\ K)$ according to

$$\Delta_{r,sol}G_m° = \Delta_{r,sol}H_m° - T\ \Delta_{r,sol}S_m°$$

The standard molar Gibbs energy of solution can be calculated from

$$\Delta_{r,sol}G_m° = - R\ T\ \ln(27\ m_{sat}^4\ \gamma_{\pm,sat}^4\ a(H_2O, l)_{sat}^6)$$

if m_{sat}, the concentration of dissolved $HoCl_3 \cdot 6H_2O(cr)$ at saturation, is known from solubility experiments, as well as $\gamma_{\pm,sat}$, the mean activity coefficient of $HoCl_3$ at saturation and $a(H_2O, l)_{sat}$, the activity of water for the saturated solution, which can both be obtained from isopiestic measurements of saturated solutions. Rard (2016) derived $\Delta_{r,sol}G_m°(298.15\ K) = -(30.85 \pm 0.10)$ kJ $\cdot$ mol^{-1} from $m_{sat} = (3.696 \pm 0.004)$ mol $\cdot$ kg^{-1}, as estimated by him on the basis of reports from the Ames Laboratory, and from $\gamma_{\pm,sat} = 8.837 \pm 0.088$ and $a(H_2O, l)_{sat} = 0.4495 \pm 0.0006$, both from He & Rard (2015). By combining the value for $\Delta_{r,sol}G_m°(298.15\ K)$ with $\Delta_{r,sol}H_m°(298.15\ K) = -(43.58 \pm 0.13)$ kJ $\cdot$ mol^{-1} (Spedding et al. 1977), Rard (2016) then obtained $\Delta_{r,sol}S_m°(298.15\ K) = -(42.70 \pm 0.55)$ kJ $\cdot$ mol^{-1}, and finally the recommended

$$S_m°(Ho^{3+}, 298.15\ K) = -(228.7 \pm 1.0)\ J \cdot K^{-1} \cdot mol^{-1}$$

which is also included in TDB 2020.

The molar entropy of formation for Ho^{3+}, $\Delta_f S_m°(Ho^{3+}, 298.15)$, can be calculated from

$$\Delta_f S_m°(Ho^{3+}, 298.15) = S_m°(Ho^{3+}, 298.15) + 3\ S_m°(e^-, 298.15) - S_m°(Ho, cr, 298.15)$$

Using his recommended value for $S_m°(Ho^{3+}, 298.15\ K)$ together with $S_m°(Ho, cr, 298.15) = (75.19 \pm 0.60)$ kJ $\cdot$ mol^{-1} (Konings & Beneš 2010)[64] and $S_m°(e^-, 298.15) = 1/2\ S_m°(H_2, g, 298.15) = (65.340 \pm 0.0015)\ J \cdot K^{-1} \cdot mol^{-1}$ (CODATA, Cox et al. 1989), Rard (2016) derived

$$\Delta_f S_m°(Ho^{3+}, 298.15\ K) = -(107.8 \pm 1.2)\ J \cdot K^{-1} \cdot mol^{-1}$$

Rard (2016) adopted his recommended

$$\Delta_f H_m°(Ho^{3+}, 298.15\ K) = -(707.7 \pm 3.0)\ kJ \cdot mol^{-1}$$

from Morss (1976). This value is also included in TDB 2020. From $\Delta_f G_m°(Ho^{3+}, T) = \Delta_f H_m°(Ho^{3+}, T) - T\ \Delta_f S_m°(Ho^{3+}, T)$ then follows

$$\Delta_f G_m°(Ho^{3+}, 298.15\ K) = -(675.6 \pm 3.0)\ kJ \cdot mol^{-1}$$

which is also included in TDB 2020.

---

[64] Note that this value for $S_m°(Ho, cr, 298.15\ K)$ by Konings & Beneš (2010), which was recommended by Rard (2016), is slightly different from the value by Arblaster (2013), 75.76 J $\cdot$ K^{-1} $\cdot$ mol^{-1}, which was selected for TDB 2020 in Section 23.3.2. This small difference, however, has a negligible influence on the value of $\Delta_f G_m°(Ho^{3+}, 298.15\ K)$: using the former value leads to $\Delta_f G_m°(Ho^{3+}, 298.15\ K) = -675.6$ kJ $\cdot$ mol^{-1}, while using the latter leads to $\Delta_f G_m°(Ho^{3+}, 298.15\ K) = -675.4$ kJ $\cdot$ mol^{-1}, which is well within the uncertainty of $\pm$ 3.0 kJ $\cdot$ mol^{-1}.

For selecting the standard molar heat capacity of Ho^{3+}, Rard (2016) accepted $C_{p,m}°(Ho^{3+}, 298.15\ K) = -49.9\ J \cdot K^{-1} \cdot mol^{-1}$ and $C_{p,m}°(Ho^{3+}, 298.15\ K) = -47.5\ J \cdot K^{-1} \cdot mol^{-1}$, based on flow microcalorimetry measurements of aqueous $Ho(ClO_4)_3 + HClO_4$ (Hakin et al. 2004) and $Ho(NO_3)_3 + HNO_3$ (Hakin et al. 2005) solutions, respectively. Taking the average of both values and assigning an estimated uncertainty, Rard (2016) recommended

$$C_{p,m}°(Ho^{3+}, 298.15\ K) = -(48.7 \pm 10)\ J \cdot K^{-1} \cdot mol^{-1}$$

which is included in TDB 2020.

According to the specific ion interaction theory (SIT), the specific ion interaction coefficient $\varepsilon(j, k)$, where j is a cation with zj positive charges and k an anion with zk negative charges, can be calculated from mean activity coefficient ($\gamma_\pm$) data for $j_{zk}k_{zj}(aq)$ using the following equation (Ciavatta 1980)

$$\varepsilon(j, k) = [\log_{10}(\gamma_\pm) + zj\ zk\ D]\ [zj + zk]^2 / (4\ I_m)$$

where D is the Debye-Hückel term

$$D = 0.509\ I_m^{1/2} / (1 + 1.5\ I_m^{1/2})$$

Rearranging the equation for $\varepsilon(j, k)$ leads to

$$1/4\ [zj + zk]^2 \log_{10}(\gamma_\pm) + 1/4\ zj\ zk\ [zj + zk]^2\ D = \varepsilon(j, k)\ I_m$$

or, for a 1:3 electrolyte $jk_3(aq)$, such as $HoCl_3(aq)$, $Ho(ClO_4)_3(aq)$ or $Ho(NO_3)_3(aq)$, to

$$4 \log_{10}(\gamma_\pm) + 12\ D = \varepsilon(j, k)\ I_m$$

In a plot of $4 \log_{10}(\gamma_\pm) + 12\ D$ vs. I_m, $\varepsilon(j, k)$ is the slope of a straight line passing through the origin.

He & Rard (2015) published revised mean activity coefficients of the aqueous trivalent rare earth chlorides, based on the isopiestic determinations by Spedding et al. (1976) and Rard & Spedding (1982). The mean activity coefficients for $HoCl_3(aq)$ by He & Rard (2015) are shown in Fig. 23.3.3-1 along with the linear least squares fit (with the restriction that the straight line passes through the origin). From the fit to the full set of data (0.1 – 3.696 $mol \cdot kg^{-1}$ $HoCl_3$, corresponding to ionic strengths between 0.6 and 22.18 $mol \cdot kg^{-1}$ follows $\varepsilon(Ho^{3+}, Cl^-) = (0.326 \pm 0.002)\ kg \cdot mol^{-1}$. Since the application range of TDB 2020 is restricted to low ionic strengths, we also carried out a fit limited to the data at low ionic strengths (0.1 – 1.0 $mol \cdot kg^{-1}$ $HoCl_3$, corresponding to ionic strengths between 0.6 and 6.0 $mol \cdot kg^{-1}$), resulting in $\varepsilon(Ho^{3+}, Cl^-) = (0.292 \pm 0.007)\ kg \cdot mol^{-1}$, which we selected (after rounding) for TDB 2020:

$$\varepsilon(Ho^{3+}, Cl^-) = (0.29 \pm 0.01)\ kg \cdot mol^{-1}$$

Rard et al. (1977) carried out isopiestic measurements of the osmotic coefficients of rare earth perchlorates from 0.1 m up to saturation, from which they determined mean molal activity coefficients. These are shown for $Ho(ClO_4)_3(aq)$ in Fig. 23.3.3-2. From the linear least-squares fit to the full set of data (0.1 – 4.7 mol · kg^{-1} $Ho(ClO_4)_3(aq)$, which corresponds to ionic strengths between 0.6 and 28.2 mol · kg^{-1}), follows $\varepsilon(Ho^{3+}, ClO_4^-) = (0.568 \pm 0.004)$ kg · mol^{-1}, and from the set of data restricted to $I_m \leq 6$ mol · kg^{-1} follows $\varepsilon(Ho^{3+}, ClO_4^-) = (0.493 \pm 0.010)$ kg · mol^{-1}, which we selected (after rounding) for TDB 2020:

$$\varepsilon(Ho^{3+}, ClO_4^-) = (0.49 \pm 0.01) \text{ kg} \cdot \text{mol}^{-1}$$

Chatterjee et al. (2015) determined the osmotic coefficients of lanthanide nitrate solutions by a combination of water activity and vapor pressure osmometry measurements. They calculated mean activity coefficients from the osmotic coefficients. The mean activity data they obtained for $Ho(NO_3)_3(aq)$ are shown in Fig. 23.3.3-3.

From the linear least-squares fit to the full set of data (0.219 to 2.274 mol · kg^{-1} $Ho(NO_3)_3(aq)$, which corresponds to ionic strengths from 1.31 to 13.64 mol · kg^{-1}) follows $\varepsilon(Ho^{3+}, NO_3^-) = (0.151 \pm 0.001)$ kg · mol^{-1}, and from the set of data restricted to $I_m < 8.1$ mol · kg^{-1} follows $\varepsilon(Ho^{3+}, NO_3^-) = (0.155 \pm 0.002)$ kg · mol^{-1}, which we selected (after rounding and increasing the uncertainty) for TDB 2020:

$$\varepsilon(Ho^{3+}, NO_3^-) = (0.16 \pm 0.01) \text{ kg} \cdot \text{mol}^{-1}$$

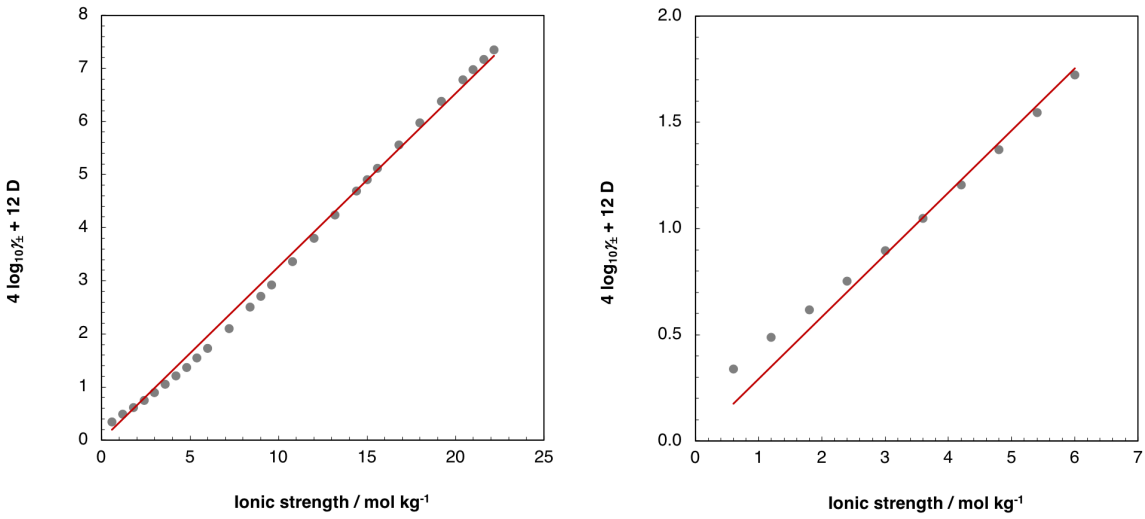

Fig. 23.3.3-1: SIT-analysis of the mean activity coefficient ($\gamma_\pm$) of $HoCl_3(aq)$ as a function of ionic strength at 25 °C

Experimental data by He & Rard (2015). From the linear least-squares fit to the full set of data (left) follows $\varepsilon(Ho^{3+}, Cl^-) = (0.326 \pm 0.002)$ kg · mol^{-1}, and from the set of data restricted to $I_m \leq 6$ mol · kg^{-1} (right) follows $\varepsilon(Ho^{3+}, Cl^-) = (0.292 \pm 0.007)$ kg · mol^{-1}.

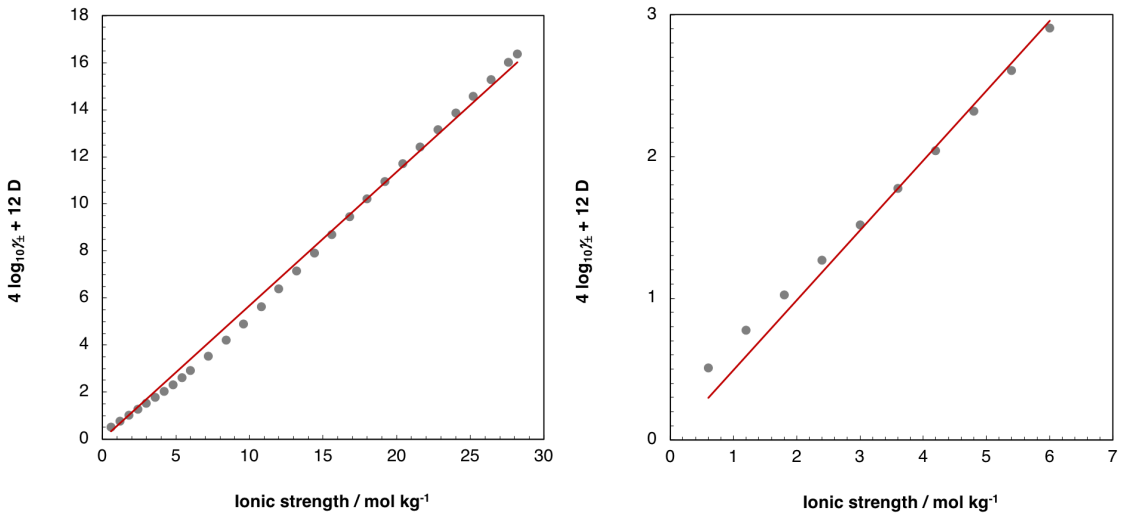

Fig. 23.3.3-2 SIT-analysis of the mean activity coefficient ($\gamma_{\pm}$) of $Ho(ClO_4)_3(aq)$ as a function of ionic strength at 25 °C

Experimental data by Rard et al. (1977). From the linear least-squares fit to the full set of data (left) follows $\varepsilon(Ho^{3+}, ClO_4^-) = (0.568 \pm 0.004)$ kg · mol^{-1}, and from the set of data restricted to $I_m \leq 6$ mol · kg^{-1} (right) follows $\varepsilon(Ho^{3+}, ClO_4^-) = (0.493 \pm 0.010)$ kg · mol^{-1}.

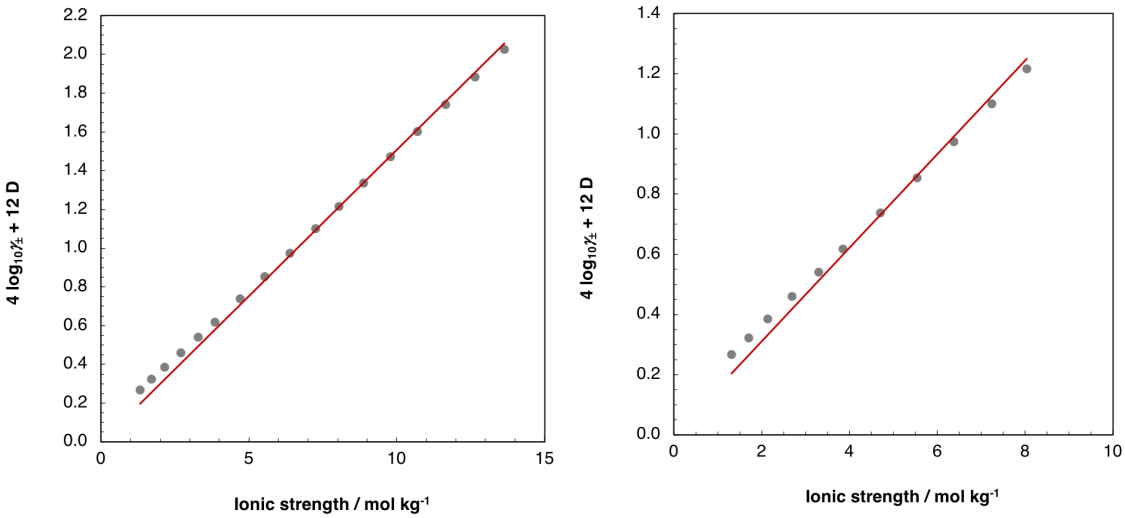

Fig. 23.3.3-3: SIT-analysis of the mean activity coefficient ($\gamma_{\pm}$) of $Ho(NO_3)_3(aq)$ as a function of ionic strength at 25 °C

Experimental data by Chatterjee et al. (2015). From the linear least-squares fit to the full set of data (left) follows $\varepsilon(Ho^{3+}, NO_3^-) = (0.151 \pm 0.001)$ kg · mol^{-1}, and from the set of data restricted to $I_m \leq 8.1$ mol · kg^{-1} (right) follows $\varepsilon(Ho^{3+}, NO_3^-) = (0.155 \pm 0.002)$ kg · mol^{-1}.

23.3.4 Holmium oxygen and hydrogen compounds and complexes

This chapter is largely based on the review of the hydrolysis of holmium by Brown & Ekberg (2016).

23.3.4.1 Aqueous holmium hydroxide complexes

Brown & Ekberg (2016) compiled experimental data on the formation of $HoOH^{2+}$

$$Ho^{3+} + H_2O(l) \rightleftharpoons HoOH^{2+} + H^+$$

by Frolova et al. (1966), Klungness & Byrne (2000), Stepanchikova & Biteikina (2006), and Chirkst et al. (2011), see Tab. 23.3.4-1. They only accepted the data acquired by Frolova et al. (1966) and Klungness & Byrne (2000) in $NaClO_4$. Brown & Ekberg (2016) carried out a non-linear SIT analysis of the accepted data by using the two-parameter equation $\Delta\varepsilon = \Delta\varepsilon_1 + \Delta\varepsilon_2 \log_{10} I_m$, see Fig. 23.3.4-1. As we do not advocate non-linear SIT-analyses (see, e.g., Chapters 5 or 12) we re-analysed the data with a standard linear SIT-fit. As is clearly seen from Fig. 23.3.4-1, the linear fit across the entire experimental range does not represent the data very well. We therefore restricted the linear fit to $I \leq 1$ M, see Fig. 23.3.4-2, and obtained

$$\log_{10}{}^*\beta_1^\circ(298.15\ K) = -(7.41 \pm 0.07)$$

$$\Delta\varepsilon = -(0.40 \pm 0.12)\ kg \cdot mol^{-1}$$

From $\Delta\varepsilon$, $\varepsilon(H^+,ClO_4^-) = (0.14 \pm 0.02)\ kg \cdot mol^{-1}$ recommended by NEA, and the selected $\varepsilon(Ho^{3+},ClO_4^-) = (0.49 \pm 0.01)\ kg \cdot mol^{-1}$ (see Section 23.3.3) follows

Tab. 23.3.4-1: Data for the stability constant $\log_{10}{}^*\beta_1$ of $Ho^{3+} + H_2O(l) \rightleftharpoons HoOH^{2+} + H^+$ at 25 °C compiled and accepted by Brown & Ekberg (2016)

The accepted values for $\log_{10}{}^*\beta_1$ were recalculated by Brown & Ekberg (2016) from the molar to the molal scale, if necessary. Missing uncertainties were estimated, and reported uncertainties in some cases increased for further analysis of the data. Values of $\log_{10}{}^*\beta_1$ accepted for our own SIT analysis are bold. Abbreviations: pot: potentiometry, sp: spectrophotometry, con: conductometry.

Method	**Medium**	***I*** **(reported)**	I_m [mol · kg^{-1}]	**$\log_{10}{}^*\beta_1$ (reported)**	**$\log_{10}{}^*\beta_1$ (accepted)**	**Reference**
pot, sp	$NaClO_4$	0 M	0	-7.56	**-7.56 ± 0.20**	Klungness & Byrne (2000)
sp	-	0 M	0	-8.14	-	Stepanchikova & Biteikina (2006)
con, pot	-	0 M	0	-7.85	-	Chirkst et al. (2011)
pot, sp	$NaClO_4$	0.1 M	0.101	-7.76 ± 0.02	**-7.76 ± 0.10**	Klungness & Byrne (2000)
pot, sp	$NaClO_4$	0.2 M	0.202	-7.80	**-7.79 ± 0.10**	Klungness & Byrne (2000)
pot	$NaClO_4$	0.3 M	0.304	-8.04 ± 0.02	**-8.03 ± 0.10**	Frolova et al. (1966)
pot, sp	$NaClO_4$	0.7 M	0.725	-7.87 ± 0.05	**-7.85 ± 0.10**	Klungness & Byrne (2000)
pot, sp	$NaClO_4$	1.0 M	1.05	-7.86	**-7.84 ± 0.10**	Klungness & Byrne (2000)
pot, sp	$NaClO_4$	1.9 M	2.09	-7.91	-7.87 ± 0.10	Klungness & Byrne (2000)
pot, sp	$NaClO_4$	2.8 M	3.25	-7.91	-7.85 ± 0.10	Klungness & Byrne (2000)
pot, sp	$NaClO_4$	3.7 M	4.48	-7.88	-7.80 ± 0.10	Klungness & Byrne (2000)
pot, sp	$NaClO_4$	4.6 M	5.80	-7.90	-7.80 ± 0.10	Klungness & Byrne (2000)
pot, sp	$NaClO_4$	5.5 M	7.23	-7.93	-7.81 ± 0.10	Klungness & Byrne (2000)

$$\varepsilon(HoOH^{2+},ClO_4^-) = -(0.05 \pm 0.12)\ kg \cdot mol^{-1}$$

which is included in TDB 2020 as well as

$$\varepsilon(HoOH^{2+},Cl^-) \approx (0.15 \pm 0.10)\ kg \cdot mol^{-1}$$

which was estimated according to the method described in Section 1.5.3.

$$\Delta_r C_{p,m}^\circ(298.15\ K) = 0$$

Brown & Ekberg (2016) recommended $\log_{10}{}^*\beta_1^\circ(298.15\ K) = -(7.43 \pm 0.05)$ based on their non-linear SIT fit of the data (see Fig. 23.3.4-2), which is practically identical to the value selected for TDB 2020. Klungness & Byrne (2000) measured $\log_{10}{}^*\beta_1$ in 0.7 M $NaClO_4$ at 25, 40 and 55 °C and obtained $\Delta_r H_m(298.15\ K, 0.7\ M\ NaClO_4) = (11.7 \pm 0.7)\ kcal \cdot mol^{-1} = (49.0 \pm 2.9)\ kJ \cdot mol^{-1}$ from a van't Hoff fit to the data. As it is not possible to extrapolate this value to zero ionic strength without further data, we accepted

$$\Delta_r H_m^\circ(298.15\ K) = (49.0 \pm 2.9)\ kJ \cdot mol^{-1}$$

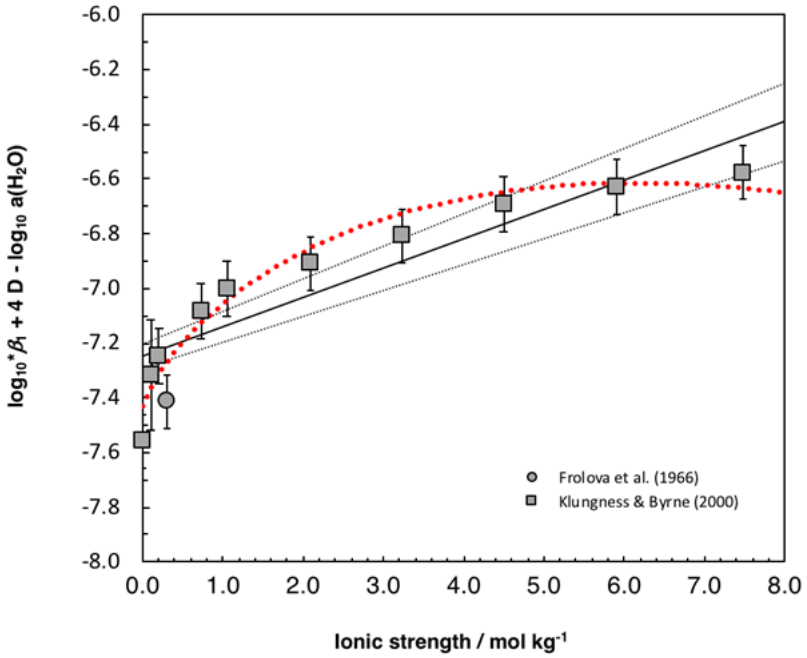

Fig. 23.3.4-1: SIT-plot of the equilibrium $Ho^{3+} + H_2O(l) \rightleftharpoons HoOH^{2+} + H^+$ in $NaClO_4$ using the experimental data by Frolova et al. (1966) and Klungness & Byrne (2000)

The solid line is obtained by using the derived SIT interaction coefficient, $\Delta\varepsilon = -(0.11 \pm 0.01)$ kg · mol^{-1}, and the stability constant at zero ionic strength, $\log_{10}{}^*\beta_1^\circ(298.15\ K) = -(7.25 \pm 0.04)$. The dotted lines represent the associated 95% uncertainty range extrapolated from zero ionic strength to higher $NaClO_4$ concentrations. The dotted red line represents the non-linear SIT-fit obtained by Brown & Ekberg (2016).

as supplemental data for TDB 2020.

Brown & Ekberg (2016) found only two studies concerned with the higher monomeric holmium hydroxide species. Fatin-Rouge & Bünzli (1999) provided a stability constant for $Ho(OH)_3(aq)$ in 0.1 M NaCl, which Brown & Ekberg (2016) deemed inconsistent with their own selected $\log_{10}{}^*\beta_1^\circ$, since "the stability constant given for $\log_1{}^*\beta_3$ indicates that it is greater than 3 $\log_{10}{}^*\beta_1$. As indicated previously, this is considered unlikely". Consequently, Brown & Ekberg (2016) did not accept the value.

Stepanchikova & Biteikina (2006) reported stability constants for $HoOH^{2+}$ (estimated), $Ho(OH)_2^+$, $Ho(OH)_3(aq)$, and $Ho(OH)_4^-$ at zero ionic strength, which were also not accepted by Brown & Ekberg (2016) because these constants "lead to stabilities for the four species which are too small".

Neglecting $Ho(OH)_3(aq)$, however, may have serious consequences when calculating solubilities of holmium in aqueous solutions. By analogy, the solubility curve of $Eu(OH)_3(cr)$ discussed by Hummel et al. (2002) may serve as an example: Bernkopf (1984) measured the solubility of $Eu(OH)_3(cr)$ in carbonate free 0.1 M $NaClO_4$. In a diagram of log $[Eu]_{tot}$ vs. pH, the data are characterized by a wide region of constant low solubility (from pH 9 – 12) on the order of around $10^{-8.8}$ M. Towards lower pH, solubility increases sharply to a value around 10^{-4} M at pH 7. The negative slope of the solubility curve in this region is mainly due to the species Eu^{3+}, $Eu(OH)^{2+}$, and $Eu(OH)_2^+$. Towards higher pH (> 12) solubility increases only slightly, which was explained by Bernkopf (1984) with the formation of $Eu(OH)_4^-$. Neglecting $Eu(OH)_3(aq)$ in solubility

calculations would lead to unrealistically low values at high pH, on the order of 10^{-12} M at pH 12. Thus, by analogy, it is not reasonable to ignore $Ho(OH)_3(aq)$ as Brown & Ekberg (2016) have done.

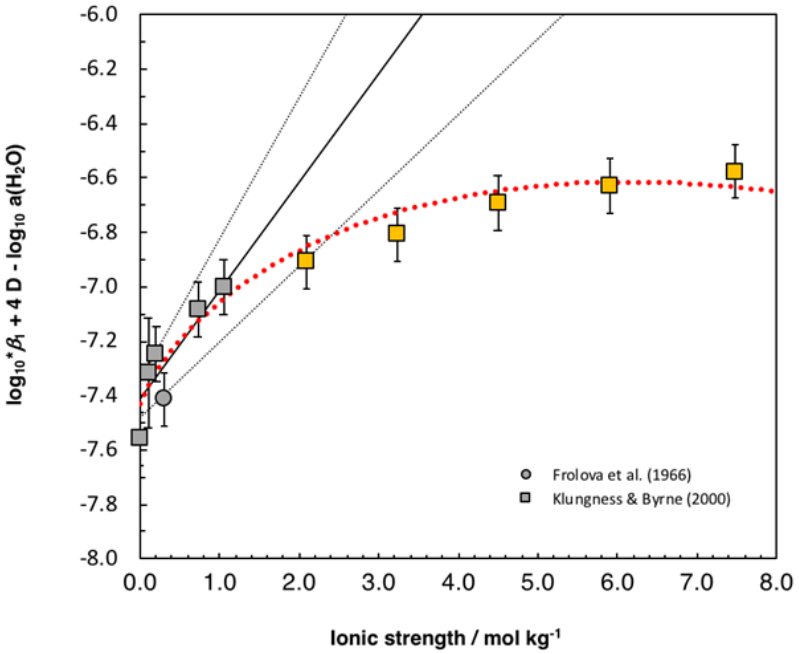

Fig. 23.3.4-2: SIT-plot of the equilibrium $Ho^{3+} + H_2O(l) \rightleftharpoons HoOH^{2+} + H^+$ in $NaClO_4$ using the experimental data at $I \leq 1$ M by Frolova et al. (1966) and Klungness & Byrne (2000).

Orange squares represent the data not included in the linear SIT fit. The solid line is obtained by using the derived SIT interaction coefficient, $\Delta\varepsilon = -(0.40 \pm 0.12)$ kg · mol^{-1}, and the stability constant at zero ionic strength, $\log_{10}{}^*\beta_1^\circ(298.15\ K) = -(7.41 \pm 0.07)$. The dotted lines represent the associated 95% uncertainty range extrapolated from zero ionic strength to higher $NaClO_4$ concentrations. The dotted red line represents the non-linear SIT-fit obtained by Brown & Ekberg (2016) with the full dataset.

Therefore, we estimated the missing formation constant $Ho(OH)_3(aq)$, and those of $Ho(OH)_2^+$ and $Ho(OH)_4^-$, based on the stability constants of the corresponding Eu hydroxide complexes derived by Hummel et al. (2002) from the experimental solubility measurements by Bernkopf (1984).

We proceeded as follows: Hummel et al. (2002) selected $\log_{10}{}^*\beta_1^\circ(298.15\ K, EuOH^{2+}) = -(7.64 \pm 0.04)$, $\log_{10}{}^*\beta_2^\circ(298.15\ K, Eu(OH)_2^+) = -(15.1 \pm 0.2)$, $\log_{10}{}^*\beta_3^\circ(298.15\ K, Eu(OH)_3(aq)) = -(23.7 \pm 0.1)$, and $\log_{10}{}^*\beta_4^\circ(298.15\ K, Eu(OH)_4^-) = -(36.2 \pm 0.5)$. Therefore, the stepwise stability constants are $\log_{10}{}^*K_2^\circ(298.15\ K) = -7.46$, $\log_{10}{}^*K_3^\circ(298.15\ K) = -8.6$, and $\log_{10}{}^*K_4^\circ(298.15\ K) = -12.5$. Based on $\log_{10}{}^*\beta_1^\circ(298.15\ K, HoOH^{2+}) = -(7.41 \pm 0.07)$ selected for TDB 2020 and assuming that these stepwise stability constants are valid as approximations for those of the corresponding Ho hydroxide complexes, the following estimates are obtained:

$Ho^{3+} + 2\ H_2O(l) \rightleftharpoons Ho(OH)_2^{+} + 2\ H^{+}$

$log_{10}{}^*\beta_2°(298.15\ K) = -(14.87 \pm 0.30)$

$Ho^{3+} + 3\ H_2O(l) \rightleftharpoons Ho(OH)_3(aq) + 3\ H^{+}$

$log_{10}{}^*\beta_3°(298.15\ K) = -(23.47 \pm 0.30)$

$Ho^{3+} + 4\ H_2O(l) \rightleftharpoons Ho(OH)_4^{-} + 4\ H^{+}$

$log_{10}{}^*\beta_4°(298.15\ K) = -(35.97 \pm 0.30)$

These estimates are included in TDB 2020 as supplemental data, together with the SIT coefficients estimated according to the method described in Section 1.5.3:

$\varepsilon(Ho(OH)_2^{+}, Cl^{-}) \approx (0.05 \pm 0.10)\ kg \cdot mol^{-1}$

$\varepsilon(Ho(OH)_2^{+}, ClO_4^{-}) \approx (0.2 \pm 0.1)\ kg \cdot mol^{-1}$

$\varepsilon(Ho(OH)_3(aq), NaCl) = \varepsilon(Ho(OH)_3(aq), NaClO_4) \approx 0$

$\varepsilon(Ho(OH)_4^{-}, Na^{+}) \approx -(0.05 \pm 0.10)\ kg \cdot mol^{-1}$

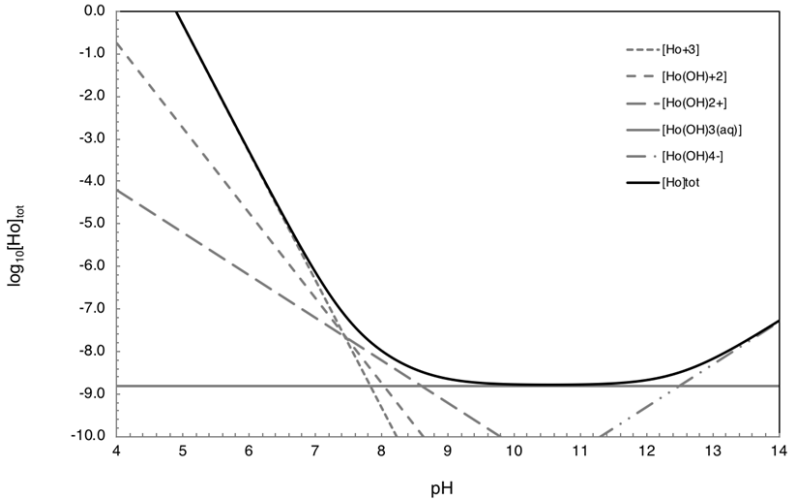

Fig. 23.3.4-3: Solubility of $Ho(OH)_3$(cr) as a function of pH calculated with the selected data for TDB 2020

Activity coefficients have not been considered in the calculation of this diagram.

According to Brown & Ekberg (2016), there appear to be no reported stability constants for polymeric holmium hydroxide species.

23.3.4.2 Holmium hydroxide solids

As we are not aware of any solubility measurements of crystalline $Ho(OH)_3$, we approximated the solubility of $Ho(OH)_3$(cr) in the plateau region with that of $Eu(OH)_3$(cr), which amounts to about $10^{-8.8}$ M. Thus, $\log_{10}$[$Ho(OH)_3$(aq)] ≈ -8.8 M. Since $\log_{10}$[$Ho(OH)_3$(aq)] = $\log_{10}{}^*\beta_3^\circ$ + $\log_{10}{}^*K_{s,0}^\circ$ (if the activity coefficient of $Ho(OH)_3$(aq) is neglected), an estimate for the solubility product of $Ho(OH)_3$(cr) is given by $\log_{10}{}^*K_{s,0}^\circ$(298.15 K) = $\log_{10}{}^*\beta_3^\circ$(298.15 K) - 8.8. From the selected $\log_{10}{}^*\beta_1^\circ$(298.15 K) = -(7.41 ± 0.07) then follows

$$Sm(OH)_3(cr) + 3\ H^+ \rightleftharpoons Sm^{3+} + 3\ H_2O(l)$$

$$log_{10}{}^*K_{s,0}^\circ(298.15\ K) = 14.7 \pm 1.0$$

with a generous uncertainty. This estimated solubility product is included in TDB 2020 as supplemental datum.

23.3.5 Holmium fluoride compounds and complexes

23.3.5.1 Aqueous holmium fluoride complexes

23.3.5.1.1 HoF2+

Walker & Choppin (1967) used potentiometric titrations and solvent extraction in 1 M $NaClO_4$ at 25 °C for measuring the stability constants of 1:1 REE fluoride complexes, including HoF^{2+}. In addition, they also used calorimetric titrations for the determination of the reaction enthalpies of the complexation reactions.

Menon & James (1989a) measured the stability constants of the 1:1 and 1:2 complexes of the rare earth elements in 0.5 M NH_4NO_3 at 25 °C using a fluoride selective ion electrode. These data were also reported by Menon & James (1989b).

Schijf & Byrne (1999) measured stability constants of the 1:1 and 1:2 fluoride complexes of yttrium and the rare earth elements at 25 °C in 0.025 M HNO_3 solutions using the cation-exchange resin technique.

Luo & Byrne (2000) measured stability constants for the 1:1 fluoride complexes of yttrium and the rare earth elements at 25 °C in 0.15 to 6.0 molar $NaClO_4$ solutions using a fluoride ion selective electrode. They corrected these data in a later study (Luo & Byrne 2007), stating that the stability constants by Luo & Byrne (2000) were erroneously reported in molar units.

Luo & Byrne (2001) measured stability constants for the 1:1 fluoride complexes of yttrium and the rare earth elements at 25 °C in 0.7 and 3.0 molar NaCl solutions using a fluoride ion selective electrode.

Luo & Byrne (2007) measured stability constants for 1:1 fluoride complexes of yttrium and the rare earth elements at 25 °C across a range of ionic strengths in NaCl (0.7 – 5.0 m) and $NaNO_3$ (0.015 to 6.0 m) media using a fluoride ion selective combination electrode.

Tab. 23.3.5-1: Data for the stability constant $\log_{10}\beta_1$ of $Ho^{3+} + F^- \rightleftharpoons HoF^{2+}$ at 25 °C in NaCl

The accepted values for $\log_{10}\beta_1$ were recalculated from the molar to the molal scale, if necessary. Reported uncertainties were increased. Values of $\log_{10}\beta_1$ accepted for the SIT analysis shown in Fig. 23.3.5-1 are bold. Abbreviation: sel: ion-selective electrode.

Method	**Medium**	***I*** **(reported)**	I_m [mol · kg^{-1}]	**$\log_{10}{}^*\beta_1$ (reported)**	**$\log_{10}{}^*\beta_1$ (accepted)**	**Reference**
sel	NaCl	0.7 m	0.7	3.23 ± 0.03	**3.23 ± 0.10**	Luo & Byrne (2007)
sel	NaCl	0.7 M	0.711	3.24	**3.23 ± 0.10**	Luo & Byrne (2001)
sel	NaCl	1.5 m	1.5	3.20 ± 0.03	**3.20 ± 0.10**	Luo & Byrne (2007)
sel	NaCl	3.0 m	3.0	3.20 ± 0.03	**3.20 ± 0.10**	Luo & Byrne (2007)
sel	NaCl	3.0 M	3.2	3.23	**3.20 ± 0.10**	Luo & Byrne (2001)
sel	NaCl	4.0 m	4.0	3.30 ± 0.03	**3.30 ± 0.10**	Luo & Byrne (2007)
sel	NaCl	5.0 m	5.0	3.36 ± 0.04	**3.36 ± 0.10**	Luo & Byrne (2007)

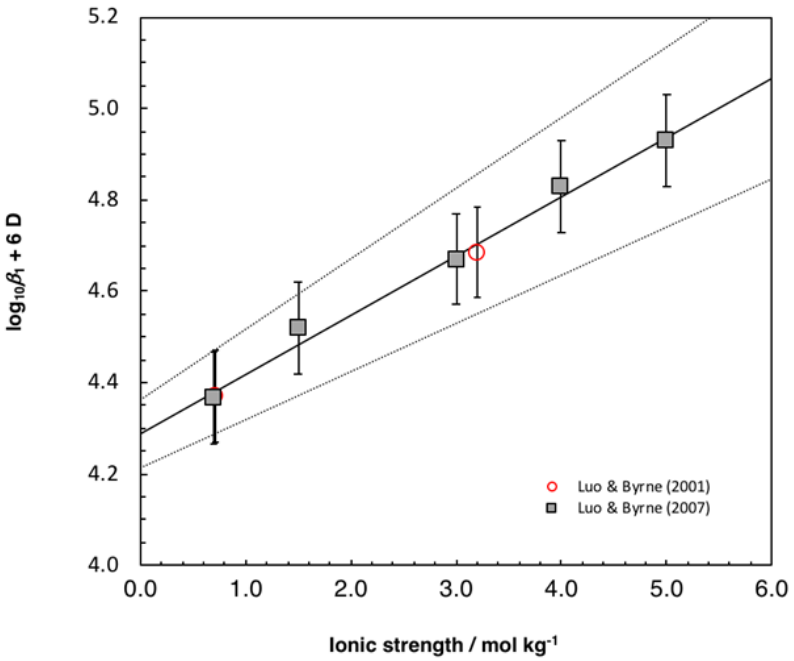

Fig. 23.3.5-1: SIT-plot of the equilibrium $Ho^{3+} + F^- \rightleftharpoons HoF^{2+}$ in NaCl using the experimental data by Luo & Byrne (2001, 2007)

The solid line is obtained by using the derived SIT interaction coefficient, $\Delta\varepsilon = -(0.13 \pm 0.02)$ kg · mol^{-1}, and the stability constant at zero ionic strength, $\log_{10}\beta_1°(298.15\ K) = (4.29 \pm 0.07)$. The dotted lines represent the associated 95% uncertainty range extrapolated from zero ionic strength to higher NaCl concentrations.

The conditional stability constants for the reaction

$$Ho^{3+} + F^- \rightleftharpoons HoF^{2+}$$

measured in NaCl by Luo & Byrne (2001, 2007), see Tab. 23.3.5-1, were used for the SIT analysis shown in Fig. 23.3.5-1, which resulted in

$$\log_{10}\beta_1°(298.15\ K) = (4.29 \pm 0.07)$$

$$\Delta\varepsilon = -(0.13 \pm 0.02)\ kg \cdot mol^{-1}$$

From $\Delta\varepsilon$, the NEA-selected $\varepsilon(F^-, Na+) = (0.02 \pm 0.02)\ kg \cdot mol^{-1}$, and $\varepsilon(Ho^{3+}, Cl^-) = (0.29 \pm 0.01)\ kg \cdot mol^{-1}$ (see Section 23.3.3) then follows

$$\varepsilon(HoF^{2+}, Cl^-) = (0.18 \pm 0.03)\ kg \cdot mol^{-1}$$

The values for $\log_{10}\beta_1$ measured by Walker & Choppin (1967) and Luo & Byrne (2007) in $NaClO_4$ (see Tab. 23.3.5-2) were used for the SIT-analysis shown in Fig. 23.3.5-2, which led to

$$\log_{10}\beta_1°(298.15\ K) = (4.34 \pm 0.05)$$

$$\Delta\varepsilon = -(0.17 \pm 0.02)\ kg \cdot mol^{-1}$$

From $\Delta\varepsilon$, the NEA-selected $\varepsilon(F^-, Na+)$, and $\varepsilon(Ho^{3+}, ClO_4^-) = (0.49 \pm 0.01)\ kg \cdot mol^{-1}$ (see Section 23.3.3) then follows

$$\varepsilon(HoF^{2+}, ClO_4^-) = (0.34 \pm 0.03)\ kg \cdot mol^{-1}$$

Tab. 23.3.5-2: Data for the stability constant $\log_{10}\beta_1$ of $Ho^{3+} + F^- \rightleftharpoons HoF^{2+}$ at 25 °C in $NaClO_4$

The accepted values for $\log_{10}\beta_1$ were recalculated from the molar to the molal scale, if necessary. Reported uncertainties were increased. Values of $\log_{10}\beta_1$ accepted for the SIT analysis shown in Fig. 23.3.5-2 are bold. Abbreviations: pot: potentiometry, sel: ion selective electrode.

Method	**Medium**	***I*** **(reported)**	I_m [mol · kg^{-1}]	**$\log_{10}{}^*\beta_1$ (reported)**	**$\log_{10}{}^*\beta_1$ (accepted)**	**Reference**
sel	$NaClO_4$	0.015 m	0.015	4.01 ± 0.03	**4.01 ± 0.10**	Luo & Byrne (2007)
sel	$NaClO_4$	0.1 m	0.1	3.61 ± 0.03	**3.61 ± 0.10**	Luo & Byrne (2007)
sel	$NaClO_4$	0.4 m	0.4	3.42 ± 0.03	**3.42 ± 0.10**	Luo & Byrne (2007)
sel	$NaClO_4$	0.7 m	0.7	3.34 ± 0.03	**3.34 ± 0.10**	Luo & Byrne (2007)
pot	$NaClO_4$	1 M	1.051	3.52 ± 0.02 [a]	**3.50 ± 0.20**	Walker & Choppin (1967)
sel	$NaClO_4$	1.5 m	1.5	3.34 ± 0.03	**3.34 ± 0.10**	Luo & Byrne (2007)
sel	$NaClO_4$	3.0 m	3.0	3.42 ± 0.03	**3.42 ± 0.10**	Luo & Byrne (2007)
sel	$NaClO_4$	4.0 m	4.0	3.54 ± 0.03	**3.54 ± 0.10**	Luo & Byrne (2007)
sel	$NaClO_4$	5.0 m	5.0	3.64 ± 0.04	**3.64 ± 0.10**	Luo & Byrne (2007)
sel	$NaClO_4$	5.0 m	6.0	3.73 ± 0.04	**3.73 ± 0.10**	Luo & Byrne (2007)

[a] Calculated from $\beta_1 = 3'320 \pm 130$.

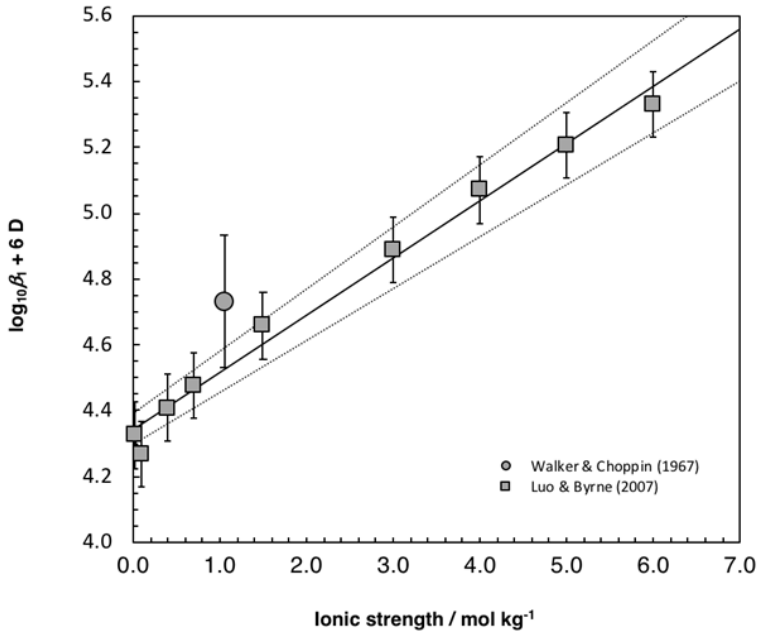

Fig. 23.3.5-2: SIT-plot of the equilibrium $Ho^{3+} + F^- \rightleftharpoons HoF^{2+}$ in $NaClO_4$ using the experimental data by Walker & Choppin (1967) and Luo & Byrne (2007)

The solid line is obtained by using the derived SIT interaction coefficient, $\Delta\varepsilon = -(0.17 \pm 0.02)$ kg · mol^{-1}, and the stability constant at zero ionic strength, $\log_{10}\beta_1°(298.15\ K) = (4.34 \pm 0.05)$. The dotted lines represent the associated 95% uncertainty range extrapolated from zero ionic strength to higher $NaClO_4$ concentrations.

From an SIT-analysis of the values of $\log_{10}\beta_1$ measured by Luo & Byrne (2007) in $NaNO_3$ (see Tab. 23.3.5-3) follows

$$\log_{10}\beta_1°(298.15\ K) = (4.30 \pm 0.09)$$

$$\Delta\varepsilon = -(0.15 \pm 0.03)\ kg \cdot mol^{-1}$$

Using $\Delta\varepsilon$, the NEA-selected $\varepsilon(F^-, Na+)$, and $\varepsilon(Ho^{3+}, NO_3^-) = (0.16 \pm 0.01)\ kg \cdot mol^{-1}$ (see Section 23.3.3) leads to

$$\varepsilon(HoF^{2+}, NO_3^-) = (0.09 \pm 0.04)\ kg \cdot mol^{-1}$$

The values for $\log_{10}\beta_1°(298.15\ K)$ derived from experimental data measured in NaCl (4.29 ± 0.07), $NaClO_4$ (4.34 ± 0.05), and $NaNO_3$ (4.30 ± 0.09) all overlap within their uncertainties. For inclusion in TDB 2020 we selected the value derived from the NaCl data since NaCl is the background electrolyte of greater relevance to natural environments than $NaClO_4$ or $NaNO_3$. Thus

$$\log_{10}\beta_1°(298.15\ K) = (4.29 \pm 0.07)$$

is included in TDB 2020, together with

Tab. 23.3.5-3: Data for the stability constant $\log_{10}\beta_1$ of $Ho^{3+} + F^- \rightleftharpoons HoF^{2+}$ at 25 °C in nitrate media

The accepted values for $\log_{10}\beta_1$ were recalculated from the molar to the molal scale, if necessary. Reported uncertainties were increased. Values of $\log_{10}\beta_1$ accepted for the SIT analysis shown in Fig. 23.3.5-3 are bold. Abbreviations: cat: cation exchange, sel: ion-selective electrode.

Method	**Medium**	***I* reported**	I_m [mol · kg^{-1}]	**$\log_{10}\beta_1$ (reported)**	**$\log_{10}\beta_1$ (accepted)**	**Reference**
cat	HNO_3	0.025 M		3.74 ± 0.02		Schijf & Byrne (1999)
cat	HNO_3	0.025 M		3.78 ± 0.01		Luo & Millero (2004)
sel	$NH4NO_3$	0.5 M		3.31 ± 0.02 [a]		Menon & James (1989a, 1989b)
sel	$NH4NO_3$	0.5 M		3.28 [b]		Menon & James (1989a, 1989b)
sel	$NH4NO_3$	0.5 M		3.10 ± 0.01 [c]		Menon & James (1989b)
sel	$NaNO_3$	0.7 m	0.7	3.26 ± 0.03	**3.26 ± 0.10**	Luo & Byrne (2007)
sel	$NaNO_3$	1.5 m	1.5	3.24 ± 0.03	**3.24 ± 0.10**	Luo & Byrne (2007)
sel	$NaNO_3$	3.0 m	3.0	3.28 ± 0.03	**3.28 ± 0.10**	Luo & Byrne (2007)
sel	$NaNO_3$	4.0 m	4.0	3.35 ± 0.03	**3.35 ± 0.10**	Luo & Byrne (2007)
sel	$NaNO_3$	5.0 m	5.0	3.53 ± 0.04	**3.53 ± 0.10**	Luo & Byrne (2007)

[a] Calculated from β_1 = 2'028 ± 74.
[b] Calculated from β_1 = 1'911.
[c] Calculated from β_1 = 1'269 ± 41.

Tab. 23.3.5-4: Stability constants $\log_{10}\beta_1$ of $Ho^{3+} + F^- \rightleftharpoons HoF^{2+}$ and $\log_{10}\beta_2$ of $Ho^{3+} + 2\ F^- \rightleftharpoons HoF_2^+$ measured by Luo & Millero (2004) in 0.025 M HNO_3 at various temperatures

	5.2 °C	**15.1 °C**	**25.0 °C**	**34.7 °C**	**44.5 °C**
$\log_{10}\beta_1$	3.66 ± 0.01	3.71 ± 0.01	3.78 ± 0.01	3.84 ± 0.01	3.88 ± 0.01
$\log_{10}\beta_2$	5.71 ± 0.02	5.82 ± 0.04	5.98 ± 0.04	6.06 ± 0.03	6.19 ± 0.03

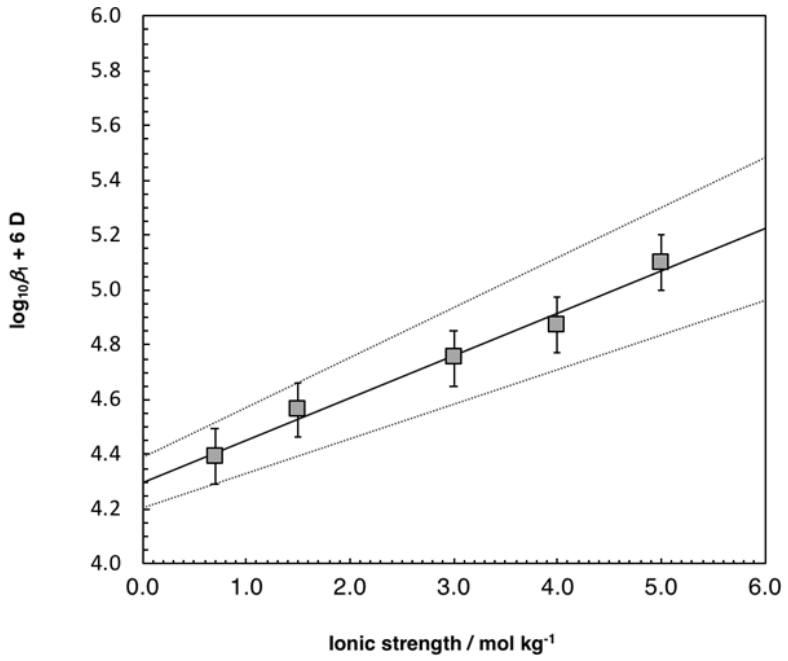

Fig. 23.3.5-3: SIT-plot of the equilibrium $Ho^{3+} + F^- \rightleftharpoons HoF^{2+}$ in $NaNO_3$ using the experimental data by Luo & Byrne (2007)

The solid line is obtained by using the derived SIT interaction coefficient, $\Delta\varepsilon = -(0.15 \pm 0.03)$ kg · mol^{-1}, and the stability constant at zero ionic strength, $\log_{10}\beta_1°(298.15\ K) = (4.30 \pm 0.09)$. The dotted lines represent the associated 95% uncertainty range extrapolated from zero ionic strength to higher NaCl concentrations.

$\varepsilon(HoF^{2+}, Cl^-) = (0.18 \pm 0.03)$ kg · mol^{-1}

$\varepsilon(HoF^{2+}, ClO_4^-) = (0.34 \pm 0.03)$ kg · mol^{-1}

$\varepsilon(HoF^{2+}, NO_3^-) = (0.09 \pm 0.04)$ kg · mol^{-1}

Luo & Millero (2004) investigated the temperature dependence of the 1:1 and 1:2 fluoride complexes of yttrium and the rare earth elements by an ion-exchange method (cation resin) in dilute HNO_3 solutions (0.025 mol/L) between 5.2 and 44.5 °C (see Tab. 23.3.5-4 and Fig. 23.3.5-4). For HF^{2+}, there is a linear relationship between stability constants and reciprocal temperature. From the linear fit to the data follow $\log_{10}\beta_1 = (3.78 \pm 0.02)$, $\Delta_r H_m(298.15\ K) =$

(9.83 ± 0.83) kJ · mol^{-1} and $\Delta_r C_{p,m}°(298.15\ K) = 0$. Since there are no data on the dependence of $\Delta_r H_m$ on ionic strength, the value for 0.025 mol/L HNO_3 is used as an approximation for zero ionic strength. Thus,

$$\Delta_r H_m°(298.15\ K) \approx (9.83 \pm 0.83)\ kJ \cdot mol^{-1}$$

$$\Delta_r C_{p,m}°(298.15\ K) = 0$$

are included in TDB 2020 as supplemental data.

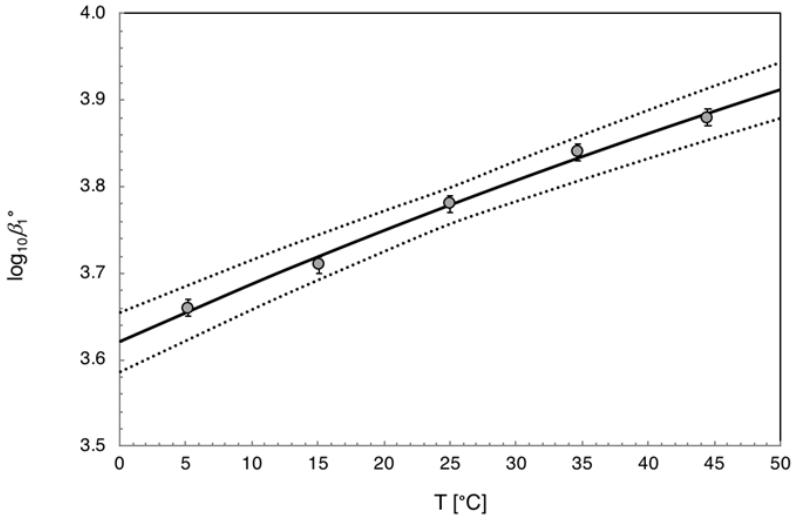

Fig. 23.3.5-4: Stability constants $\log_{10}\beta_1$ of $Ho^{3+} + F^- \rightleftharpoons HoF^{2+}$ measured by Luo & Millero (2004) in 0.025 M HNO_3 at various temperatures

An unweighted linear regression of these data as a function of 1/T resulted in $\log_{10}\beta_1°(298.15\ K) = (3.78 \pm 0.02)$, $\Delta_r H_m(298.15\ K) = (9.83 \pm 0.83)$ kJ · mol^{-1} and $\Delta_r C_{p,m}°(298.15\ K) = 0$. Solid line: Corresponding extrapolation of $\log_{10}\beta_1°$ to lower and higher temperatures with uncertainties indicated by the dotted lines.

23.3.5.1.2 HoF2+

Quantitative data on the formation of HoF_2^+ is scarce (see Tab. 23.3.5-5). Menon & James (1989a, 1989b) provided conditional stability constants $\log_{10}\beta_2(298.15\ K)$ for the reaction $Ho^{3+} + 2\ F^- \rightleftharpoons HoF_2^+$ measured in 0.5 M NH_4NO_3, whereas the values reported by Schijf & Byrne (1999) and Luo & Millero (2004) were measured in 0.025 M HNO_3. Since these data cannot be extrapolated to zero ionic strength with SIT (measurements were made at only two ionic strengths, with a different background electrolyte for each) we extrapolated the data by Schijf & Byrne (1999) and Luo & Millero (2004) using the Debye-Hückel term as used in the SIT, assuming that the specific ion interactions are negligible at the very low concentration of the background electrolyte. Thus,

$$\log_{10}\beta_2°(298.15\ \text{K}) = \log_{10}\beta_2(298.15\ \text{K}) - \Delta z^2 D$$

where

$$D = 0.509\ I_m^{0.5}/(1 + 1.5\ I_m^{0.5})$$

From the mean of the conditional constants by Schijf & Byrne (1999) and Luo & Millero (2004), $\log_{10}\beta_2(298.15\ \text{K}) = 6.08$, $\Delta z^2 = -10$ for the reaction $Ho^{3+} + 2\ F^- \rightleftharpoons HoF_2^+$, and $D = 0.065$ at $I_m \approx I_c = 0.025\ \text{kg} \cdot \text{mol}^{-1}$ follows

$$Ho^{3+} + 2\ F^- \rightleftharpoons HoF_2^+$$

$$\log_{10}\beta_2°(298.15\ K) = (6.73 \pm 0.3)$$

Tab. 23.3.5-5: Data for the stability constant $\log_{10}\beta_2$ of $Ho^{3+} + 2\ F^- \rightleftharpoons HoF_2^+$ at 25 °C in nitrate media

Values of $\log_{10}\beta_2$ accepted for extrapolation to zero ionic strength are bold Abbreviations: cat: cation exchange, sel: ion-selective electrode.

Method	**Medium**	***I* reported**	I_m [mol · kg^{-1}]	**$\log_{10}\beta_2$ (reported)**	**$\log_{10}\beta_2$ (accepted)**	**Reference**
cat	HNO_3	0.025 M	≈ 0.025 m	6.28 ± 0.04	**6.28 ± 0.10**	Schijf & Byrne (1999)
cat	HNO_3	0.025 M	≈ 0.025 m	5.98 ± 0.04	**5.98 ± 0.10**	Luo & Millero (2004)
sel	NH_4NO_3	0.5 M		6.81 ± 0.07 [a]		Menon & James (1989a, 1989b)
sel	NH_4NO_3	0.5 M		6.82 [b]		Menon & James (1989a, 1989b)
sel	NH_4NO_3	0.5 M		6.63 ± 0.19 [c]		Menon & James (1989b)

[a] Calculated from $\beta_2 = (6.4 \pm 1.0) \times 10^6$
[b] Calculated from $\beta_2 = 6.6 \times 10^6$
[c] Calculated from $\beta_2 = (4.3 \pm 1.5) \times 10^6$

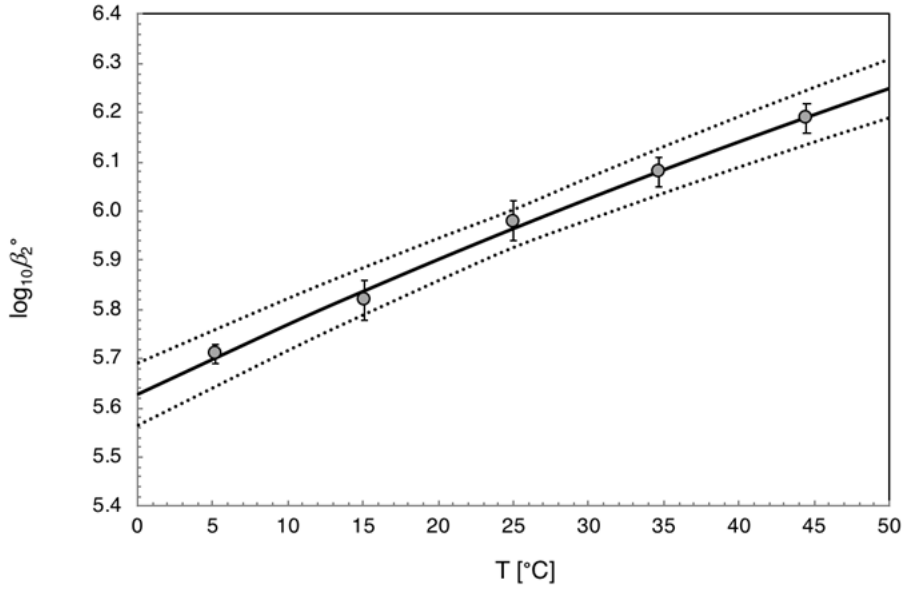

Fig. 23.3.5-5: Stability constants $\log_{10}\beta_2$ of $Ho^{3+} + 2\ F^- \rightleftharpoons HoF_2^+$ measured by Luo & Millero (2004) in 0.025 M HNO_3 at various temperatures

An unweighted linear regression of these data as a function of 1/T resulted in $\log_{10}\beta_2°(298.15\ K) = (5.96 \pm 0.04)$, $\Delta_r H_m(298.15\ K) = (21.0 \pm 1.6)$ kJ · mol^{-1} and $\Delta_r C_{p,m}°(298.15\ K) = 0$. Solid line: Corresponding extrapolation of $\log_{10}\beta_2°$ to lower and higher temperatures with uncertainties indicated by the dotted lines.

where the uncertainty has been estimated. This value is included in TDB 2020 as supplemental datum, together with

$$\varepsilon(HoF_2^+, Cl^-) \approx (0.05 \pm 0.10)\ kg \cdot mol^{-1}$$

and

$$\varepsilon(HoF_2^+, ClO_4^-) \approx (0.2 \pm 0.1)\ kg \cdot mol^{-1}$$

as estimated according to the method described in Section 1.5.3.

The stability constants of HoF_2^+ measured by Luo & Millero (2004) in 0.025 M HNO_3 solutions between 5.2 and 44.5 °C (see Tab. 23.3.5-4 and Fig. 23.3.5-5) are characterized by a linear relationship with reciprocal temperature. From the linear fit to the data follow $\log_{10}\beta_2 = (5.96 \pm 0.04)$, $\Delta_r H_m(298.15\ K) = (21.0 \pm 1.6)$ kJ · mol^{-1} and $\Delta_r C_{p,m}°(298.15\ K) = 0$. Since there are no data on the dependence of $\Delta_r H_m$ on ionic strength, the value for 0.025 mol/L HNO_3 is used as an approximation for zero ionic strength. Thus,

$$\Delta_r H_m°(298.15\ K \approx (21.0 \pm 1.6)\ kJ \cdot mol^{-1}$$

$$\Delta_r C_{p,m}°(298.15\ K) = 0$$

are included in TDB 2020 as supplemental data.

23.3.5.2 Holmium fluoride solids

There appear to be only a few experimental determinations of the solubility of holmium fluoride solids.

Fraústo da Silva & Queimado (1973) determined the solubility products of REE fluorides from oversaturation in 0.1 M $NaNO_3$ at 25 °C using a fluoride ion-selective electrode. Precipitates were produced by adding an excess of a 0.035 M solution of REE nitrate to a 0.035 M solution of sodium fluoride, adding distilled water to adjust the total volume and an appropriate amount of $NaNO_3$ to set the ionic strength to 0.1 M. The precipitates that formed were left to age in the solution under occasional stirring and the potential was measured at regular intervals until a constant value was obtained, which was usually attained after 4 – 10 days and pH was found to be around 5. Composition, hydration, as well as crystallinity and structure of the precipitates were not characterized. The conditional solubility products were extrapolated to zero ionic strength using the Davies equation without consideration of potential complex formation. For HoF_3(pr) Fraústo da Silva & Queimado (1973) obtained $\log_{10}K_{s,0}°$(298.15 K) = -17.2.

Itoh et al. (1984) measured the solubility products of REE fluoride powders in pure water from undersaturation at 25 °C using a fluoride ion-selective electrode. In order to prevent the formation of HF in acidic solutions, the experimental solutions were kept at pH 5 using a buffer. No information was given by these authors on the duration of the experiments and on the grain size of the powders. The solids were not examined after the experiment either. Due to the low concentrations of the solutes, the activity coefficients of the REE cations and of fluoride were assumed to be one and no complexes were considered. For HoF_3(s) Itoh et al. (1984) obtained $\log_{10}K_{s,0}°$(298.15 K) = -18.0. Itoh et al. (1984) also tried to determine the solubility product of a lanthanum fluoride single crystal but failed to obtain saturated solutions even after three months of continuous stirring.

Menon & James (1989b) used conductometry, potentiometry and radiometry to determine the solubility products of all REE fluorides (except Pm) in water at 25 °C. The REE fluoride precipitates were prepared by mixing hot solutions of REE chlorides with HF. The precipitates were washed several times with doubly distilled water and dried in the oven at 110 °C. Menon & James (1989b) referred to the precipitates as ($LnF_3 \cdot 0.5H_2O$), but there are no indications that they analysed the precipitates for composition or structure before and after the experiments. Small batches of the dried precipitates were agitated with doubly distilled water for at least 48 h in order to reach saturation, which was tested by repeated measurements of the conductance of the solutions. The pH of the solutions was in the range of 5.0-6.0 and the calculated ionic strength was smaller than 10^{-3} M. From the measured solubilities of holmium fluoride, Menon & James (1989b) calculated the solubility products, taking into account the formation of HoF^{2+}, $HoOH^{2+}$, and HF. They obtained $\log_{10}K_{s,0}°$(298.15 K) = -13.9 from conductometry and $\log_{10}K_{s,0}°$(298.15 K) = -14.1 from potentiometry (no radiometric measurements were made in the case of holmium fluoride).

Migdisov et al. (2009) measured the solubilities of all REE fluoride solids (except Pm) in fluoride- and chloride-bearing aqueous solutions at 150, 200, and 250 °C and saturated water vapor pressure. They extrapolated their solubility products to 25 °C using the $C_p°$ and $S°$ values recommended by Konings & Kovács (2003) and obtained for HoF_3(cr) $\log_{10}K_{s,0}°$(298.15 K) = -17.87. Migdisov et al. (2009) also calculated a solubility product for HoF_3(cr) entirely from calorimetric data recommended by Konings & Kovács (2003) and obtained $\log_{10}K_{s,0}°$(298.15 K) = -17.52.

Tab. 23.3.5-6: Reported solubility products $\log_{10}K_{s,0}°$ of $HoF_3(cr) \rightleftharpoons Ho^{3+} + 3\ F^-$ at 25 °C

Abbreviations: cat: cation exchange, sel: ion-selective electrode, pot: potentiometry, con: conductometry, calc: calculated

Method	**Medium**	***I* reported**	**$\log_{10}K_{s,0}°$**	**Reference**
sel	$NaNO_3$	0.1 M	-17.2	Fráusto da Silva & Queimado (1973)
sel		dilute	-18.0	Itoh et al. (1984)
pot		dilute	-14.1	Menon & James (1989b)
con		dilute	-13.9	Menon & James (1989b)
calc			-17.52	Migdisov et al. (2009) [a]
calc			-17.87	Migdisov et al. (2009) [b]

[a] Calculated from calorimetric data recommended by Konings & Kovács (2003).

[b] Extrapolated from their experimental data at elevated temperatures using the $C_p°$ and S° values recommended by Konings & Kovács (2003).

The values for the solubility product $\log_{10}K_{s,0}°(298.15\ K)$ of $HoF_3(cr)$ by Fraústo da Silva & Queimado (1973), Itoh et al. (1984) and Migdisov et al. (2009) vary between -17.2 and -18.0, while the values obtained by Menon & James (1989b) are significantly lower (-13.9 and -14.1), see Tab. 23.3.5-6. We are not able to resolve this discrepancy. However, Migdisov et al. (2009) argued that, since the good agreement between the experimental solubility products by Fraústo da Silva & Queimado (1973) and Itoh et al. (1984) covers the entire range of REE fluorides and is therefore systematic, they are likely the most reliable ones at 25 °C. We share this view and have therefore selected the average of the values (with an estimated uncertainty) determined by Fraústo da Silva & Queimado (1973) and Itoh et al. (1984) for TDB 2020:

$$HoF_3(cr) \rightleftharpoons Ho^{3+} + 3\ F^-$$

$$\log_{10}K_{s,0}°(298.15\ K) = -17.6 \pm 0.4$$

23.3.6 Holmium chloride compounds and complexes

23.3.6.1 Aqueous holmium chloride complexes

Chloride complexes with Ho(III) are very weak, and high chloride concentrations are needed to form such complexes. This implies that very large amounts of perchlorate ions in the background electrolyte need to be replaced by chloride ions. Thus, changes in activity coefficients due to such large compositional changes in the background electrolyte must be accounted for, which can be done using the method described by Spahiu & Puigdomènech (1998). Jordan (in prep.) reviewed numerous experimental studies (mainly employing solvent extraction and cation exchange) on the complexation of Eu(III) with chloride and came to the conclusion that the changes in activity coefficients due to the replacement of the background electrolyte anion by chloride have a much larger impact than complexation with chloride and for this reason the experimental data can be

reproduced without invoking any complexation with chloride. It is reasonable to assume that Ho(III) behaves similarly and that there is no significant Ho(III) chloride complexation at low chloride concentrations.

This is corroborated by several spectroscopic studies of trivalent actinides and lanthanides.

Fanghänel et al. (1995) investigated the formation of Cm(III) chloride complexes with time-resolved laser fluorescence spectroscopy (TRLFS) at 25 °C and chloride concentrations from 0 to about 20 mol · kg^{-1} in $CaCl_2$ solutions at acidic pH. They identified Cm^{3+}, $CmCl^{2+}$, and $CmCl_2^{+}$, but noted that at low chloride concentrations (< 3 mol · kg^{-1}) at most 5% of curium is found as chloride complexes.

Allen et al. (2000) used extended X-ray absorption fine structure (EXAFS) experiments to study the inner sphere coordination of trivalent lanthanide and actinide ions in aqueous LiCl solutions as a function of increasing chloride concentration . For Cm^{3+}, these authors were not able to observe any chloride complexes at 7.0 M LiCl, only at 8.7 M LiCl they observed an average coordination number of 1.2 ± 0.33 for all the inner sphere chloro complexes in solution. They argued that these data suggest little inner sphere complex formation for Cm^{3+} at LiCl concentrations < about 5 M and that the trivalent lanthanide ions – which show chloro complexation at higher LiCl concentrations – also lack significant chloride complex formation at LiCl concentrations < about 5 M if one assumes that they are like Cm^{3+}.

In an EXAFS study carried out by Skerencak-Frech et al. (2014) at 25, 90 and 200 °C and Am^{3+} and Cl^- concentrations of 10^{-3} and 3 mol · kg^{-1}, resp., no Am^{3+} chloride complexes were found at temperatures below 90 °C.

Koke et al. (2019) used TRLFS for the study of Cm^{3+} complexation with chloride in LiCl, NaCl, $MgCl_2$, and $CaCl_2$ at temperatures in the range of 25 – 200 °C. No appreciable complex formation was detected at 25 °C and chloride concentrations < 3 mol · kg^{-1}.

It is reasonable to assume that these spectroscopic findings also apply to Ho^{3+} chloride complexes.

In summary, there is no evidence from chemical and spectroscopic studies that appreciable amounts of Ho^{3+} chloride complexes can be expected to form at chloride concentrations < 3 mol · kg^{-1} and temperatures below about 90 °C.

Thus, no stability constants for Ho^{3+} chloride complexes are selected for TDB 2020. The specific ion interaction coefficient $\varepsilon(Ho^{3+}, Cl^-)$ derived in Section 23.3.3 from mean activity coefficient data of aqueous $HoCl_3$ solutions should be sufficient to describe the interaction between Ho^{3+} and Cl^- in the application range of TDB 2020.

23.3.6.2 Holmium chloride solids

Mioduski et al. (2009) reviewed and reported the results of several solubility experiments of $HoCl_3$(cr) in water. The solubility at 25 °C is on the order of 3.8 mol · kg^{-1} and the equilibrium solid is $HoCl_3 \cdot 6H_2O$(cr). Obviously, holmium chloride is highly soluble and is not considered in TDB 2020.

23.3.7 Holmium sulphate compounds and complexes

23.3.7.1 Aqueous holmium sulphate complexes

Due to a lack of reliable data for Ho sulphate complexes, we used the data for the corresponding europium sulphate complexes selected by Hummel et al. (2002) as estimates. Thus

$$Ho^{3+} + SO_4^{2-} \rightleftharpoons HoSO_4^{+}$$

$$\log_{10}\beta_1^\circ(298.15\ K) = (3.95 \pm 0.08)$$

$$\varepsilon(HoSO_4^{+}, ClO_4^{-}) = (0.27 \pm 0.09)\ kg \cdot mol^{-1}$$

$$Ho^{3+} + 2\ SO_4^{2-} \rightleftharpoons Ho(SO_4)_2^{-}$$

$$\log_{10}\beta_2^\circ(298.15\ K) = (5.7 \pm 0.2)$$

$$\varepsilon(Ho(SO_4)_2^{-}, Na^{+}) = (0.22 \pm 0.20)\ kg \cdot mol^{-1}$$

are included in TDB 2020 as supplemental data, together with the estimate (based on the estimation method described in Section 1.5.3)

$$\varepsilon(HoSO_4^{+}, Cl^{-}) \approx (0.05 \pm 0.10)\ kg \cdot mol^{-1}$$

23.3.7.2 Holmium sulphate solids

REE form in general soluble sulphates. For $Eu_2(SO_4)_3 \cdot 8H_2O(cr)$, e.g., Rard (1988) determined solubilities of around 0.032 $mol \cdot kg^{-1}$ at 25 °C. As REE also form comparatively insoluble hydroxides and carbonates, it is very unlikely that REE sulphates will play any role in limiting the solubility of REE in natural environments. Therefore, no data for $Ho_2(SO_4)_3 \cdot 8H_2O(cr)$ are included in TDB 2020.

23.3.8 Holmium carbonate compounds and complexes

23.3.8.1 Aqueous holmium carbonate complexes

Due to a lack of reliable data for Ho carbonate complexes, we used the data for the corresponding europium carbonate complexes selected by Hummel et al. (2002) as estimates. Thus

$$Ho^{3+} + CO_3^{2-} \rightleftharpoons HoCO_3^+$$

$$\log_{10}\beta_1°(298.15\ K) = (8.1 \pm 0.2)$$

$$\varepsilon(HoCO_3^+, ClO_4^-) = (0.15 \pm 0.18)\ kg \cdot mol^{-1}$$ [65]

$$Ho^{3+} + 2\ CO_3^{2-} \rightleftharpoons Ho(CO_3)_2^-$$

$$\log_{10}\beta_2°(298.15\ K) = (12.1 \pm 0.3)$$

$$\varepsilon(Ho(CO_3)_2^-, Na^+) = -(1.17 \pm 0.32)\ kg \cdot mol^{-1}$$ [66]

are included in TDB 2020 as supplemental data, together with the estimate (based on the estimation method described in Section 1.5.3)

$$\varepsilon(HoCO_3^+, Cl^-) \approx (0.05 \pm 0.10)\ kg \cdot mol^{-1}$$

23.3.8.2 Holmium carbonate solids

Due to a lack of reliable data for Ho carbonate solids, we used the data for the corresponding europium carbonate solids selected by Hummel et al. (2002) as crude estimates with increased uncertainties. Therefore, we selected

$$Ho_2(CO_3)_3(cr) \rightleftharpoons 2\ Ho^{3+} + 3\ CO_3^{2-}$$

$$\log_{10}K_{s,0}°(298.15\ K) = -(35 \pm 2)$$

and

$$SmOHCO_3(cr) \rightleftharpoons Sm^{3+} + OH^- + CO_3^{2-}$$

$$\log_{10}K_{s,0}°(298.15\ K) = -(21.7 \pm 2.0)$$

as supplemental data for TDB 2020.

---

[65] This value follows from $\Delta\varepsilon = -(0.24 \pm 0.18)$ kg · mol^{-1} reported by Hummel et al. (2002), $\varepsilon(Eu^{3+}, ClO_4^-) = (0.47 \pm 0.01)$ kg · mol^{-1} selected by Thoenen (2019), and $\varepsilon(CO_3^{2-}, Na^+) = -(0.08 \pm 0.03)$ kg · mol^{-1} selected by NEA (Lemire et al. 2013).

[66] This value follows from $\Delta\varepsilon = -(1.48 \pm 0.31)$ kg · mol^{-1} reported by Hummel et al. (2002), $\varepsilon(Eu^{3+}, ClO_4^-) = (0.47 \pm 0.01)$ kg · mol^{-1} selected by Thoenen (2019), and $\varepsilon(CO_3^{2-}, Na^+) = -(0.08 \pm 0.03)$ kg · mol^{-1} selected by NEA (Lemire et al. 2013).

23.3.9 Holmium phosphate compounds and complexes

23.3.9.1 Aqueous holmium phosphate complexes

There appear to be no data on the complexation of Ho(III) with phosphate. For this reason we took recourse to the corresponding data for Eu(III) which were obtained by Jordan et al. (2018) using laser-induced luminescence spectroscopy (see Section 23.2.9.1). The data selected for $EuH_2PO_4^{2+}$ are used as estimates for $HoH_2PO_4^{2+}$ and are included in TDB 2020 as supplemental data:

$$Ho^{3+} + H_3PO_4(aq) \rightleftharpoons HoH_2PO_4^{2+} + H^+$$

$$\log_{10}\beta_1^\circ(298.15\ K) = (0.89 \pm 0.13)$$

$$\Delta_r H_m^\circ(298.15\ K) = (14.7)\ kJ \cdot mol^{-1}$$

$$\Delta_r C_{p,m}^\circ(298.15\ K) = 0$$

$$\varepsilon(HoH_2PO_4^{2+}, ClO_4^-) = (0.18 \pm 0.08)\ kg \cdot mol^{-1}$$

$$\varepsilon(HoH_2PO_4^{2+}, Cl^-) \approx (0.15 \pm 0.10)\ kg \cdot mol^{-1}$$

23.3.9.2 Holmium phosphate solids

According to Gausse et al. (2016), rare-earth phosphates $LnPO_4 \cdot nH_2O(s)$ exhibit a variety of crystal structures: Monazite, xenotime, rhabdophane and churchite. Monazite and xenotime are both anhydrous and crystallize in the monoclinic and trigonal crystal systems, respectively. The hydrous phosphates rhabdophane, $LnPO_4 \cdot 0.667H_2O(s)$, and churchite, $LnPO_4 \cdot 2H_2O(s)$, crystallize in the monoclinic system. For the light REE from La to Eu the monazite structure has been identified, while the middle range REE from Gd to Dy can be found in both the monazite and xenotime structure. The heavy REE from Ho to Lu and Y are found in the xenotime structure. Both light and middle range REE (from La to Dy) can also be found in the rhabdophane structure. Finally, the middle range and heavy REE (from Gd to Lu and Y) can also be found in the churchite structure. Thus Ho is found in the xenotime ($HoPO_4$) and in the churchite structure ($HoPO_4 \cdot 2H_2O$).

We found only two studies devoted to the solubility of holmium phosphates, Firsching & Brune (1991) and Liu & Byrne (1997).

Firsching & Brune (1991) determined the solubilities of REE (except Ce and Pm) and Y phosphates in aqueous solution at 25 °C. The REE phosphates were prepared by precipitation from homogeneous solutions of REE in mixtures of phosphoric and perchloric acid using the hydrolysis of urea. Urea was added to the solutions; heating of the solutions induced the hydrolysis of urea, thereby increasing the pH and leading to the precipitation of the REE phosphates. A second method was also used that took advantage of the decreasing solubility of REE phosphates with temperature. Saturated solutions of REE in mixtures of phosphoric and perchloric acid were heated to 100 °C, leading to the precipitation of the REE phosphates. Both types of crystals were used in the solubility studies, but they were not further analysed, neither with respect to structure, nor to composition. The crystals were placed in dilute solutions of $HClO_4$

(0.0697 and 0.0910 M) and kept in contact with the solutions for more than 3 months (equilibrium from undersaturation was reached after about 80 days). Firsching & Brune (1991) noted that "undoubtedly, the surfaces of the solid phase had achieved a thermodynamically stable hydrate form". However, composition and structure of these hydrated surfaces were not determined. Ho^{3+} and $H_3PO_4(aq)$ were found to be the only significant holmium and phosphate species under the low pH of the experiments (< 1.2) and their concentrations indicated congruent dissolution. The following stepwise dissociation constants of phosphoric acid were used by Firsching & Brune (1991) for the calculation of the solubility product: $K_1°(298.15\ K) = 7.11 \times 10^{-3}$, $K_2°(298.15\ K) = 6.34 \times 10^{-8}$, and $K_3°(298.15\ K) = 4.17 \times 10^{-13}$, which correspond to $\log_{10}K_1°(298.15\ K) = -2.15$, $\log_{10}K_2°(298.15\ K) = -7.20$, and $\log_{10}K_3°(298.15\ K) = -12.38$.

For the reaction

$$HoPO_4(s) \rightleftharpoons Ho^{3+} + PO_4^{3-}$$

they obtained $\log_{10}K_{s,0}°(298.15\ K) = -(25.57 \pm 0.46)$, which corresponds to $\log_{10}K_s°(298.15\ K) = -(3.84 \pm 0.46)$ for the reaction

$$HoPO_4(s) + 3\ H^+ \rightleftharpoons Ho^{3+} + H_3PO_4(aq)$$

Liu & Byrne (1997) measured the solubilities of REE (except Pm) and Y phosphates in aqueous solution at 25 °C. The phosphate solids were prepared in three different ways. (1) REE oxides (Ce and Tb were used as chlorides) were combined with NaH_2PO_4 to produce equimolar solutions of total phosphate and REE. 0.4 μm filters were used to separate the precipitates from the solution. (2) Precipitates from procedure 1 were aged for two months in the solution at 25 °C before filtration. Precipitates from both procedures were rinsed in deionized water until the phosphate concentrations dropped below the spectrophotometric detection limits. The precipitates were then rinsed with dilute acid followed by deionized water until the pH of the rinse solutions remained near neutral. (3) Precipitates were produced following the urea method by Firsching & Brune (1991) discussed above and finally washed with dilute acid and deionized water. Prior to being used in the solubility experiments the precipitates were analysed by X-ray diffraction. Precipitates of the light REE obtained from procedure 1 were X-ray amorphous and those of the heavy REE showed only hints of crystallinity. Precipitates from procedures 2 and 3 were well crystallized and generally conformed to the rhabdophane structure. Liu & Byrne (1997), however, did not report explicitly the structure of $HoPO_4(cr)$ and it is doubtful whether it can actually occur in the rhabdophane structure. Solubilities were measured from undersaturation in dissolution experiments in 0.1 molar perchloric acid. Sample bottles were kept at 25 °C and vigorously shaken for up to five months. For analysis, the solutions were passed through 0.2 μm filters. Total phosphate concentrations 10% below the final values were often obtained after only two weeks. As in the experiments by Firsching & Brune (1991), dissolution of the REE phosphates was congruent. The solubility products for the Ho phosphates were calculated from the solubility data by using the following stepwise dissociation constants for phosphoric acid, $\log_{10}K_1°(298.15\ K) = -1.943$, $\log_{10}K_2°(298.15\ K) = -6.8920$, and $\log_{10}K_3°(298.15\ K) = -11.87$, together with the estimated formation constants for Ho phosphate complexes $\log_{10}\beta°(HoHPO_4^+, 298.15\ K) = 4.841$ and $\log_{10}\beta°(HoH_2PO_4^{2+}, 298.15\ K) = 2.119$ (Byrne et al. 1991)[67] and the activity coefficients

[67] Byrne et al. (1991) extrapolated their experimentally determined stability constants for $CmHPO_4^+$ and $GdHPO_4^+$, and $CmH_2PO_4^{2+}$ and $GdH_2PO_4^{2+}$, resp., to the other REE phosphate complexes using a linear free energy relationship.

$\gamma(Ho^{3+})$ = 0.134 and $\gamma(PO_4^{3-})$ = 0.189. For the precipitates from procedure 2 and 3, Liu & Byrne (1997) obtained $\log_{10}K_{s,0}°$(298.15 K) = -25.19 (100 days of equilibration) and $\log_{10}K_{s,0}°$(298.15 K) = -24.94 (30 days of equilibration), respectively. From these two values they derived their recommended value $\log_{10}K_{s,0}°$(298.15 K) = -(25.07 ± 0.13), which corresponds to $\log_{10}K_{s}°$(298.15 K) = -(4.35 ± 0.13) for the reaction in terms of H_3PO_4(aq). For precipitates obtained by procedure 1, $\log_{10}K_{s,0}°$(298.15 K) ≈ -25.07 after 150 days. In the discussion of their experimental results, Liu & Byrne (1997) pointed out that in natural environments Y and REE do not each form their own discrete phosphate phases but rather form solid solutions by coprecipitation.

For TDB 2020, the solubility constants recommended by Firsching & Brune (1991), $\log_{10}K_{s,0}°$(298.15 K) = -(25.57 ± 0.46), and by Liu & Byrne (1997), $\log_{10}K_{s,0}°$(298.15 K) = -(25.07 ± 0.13), were both accepted. Taking the average of these values and increasing the uncertainty to ± 0.6 (accounting for the fact that equilibrium was approached from undersaturation) leads to

$$HoPO_4(s) \rightleftharpoons Ho^{3+} + PO_4^{3-}$$

$$\log_{10}K_{s,0}°(298.15\ K) = -(25.3 \pm 0.6)$$

which is included in TDB 2020.

Tab. 23.3.9-1: Reported solubility products $\log_{10}K_{s}°$(298.15 K) of $HoPO_3(s) + 3\ H^+ \rightleftharpoons Ho^{3+} + H_3PO_4(aq)$ and $\log_{10}K_{s,0}°$(298.15 K) of $HoPO_4(s) \rightleftharpoons Ho^{3+} + PO_4^{3-}$

Structure	**$\log_{10}K_{s}°$(298.15 K)**	**$\log_{10}K_{s,0}°$(298.15 K)**	**Reference**
Not determined	-3.84 ± 0.46 [a]	-25.57 ± 0.46	Firsching & Brune (1991)
Not indicated	-4.35 ± 0.13 [a]	-25.07 ± 0.13	Liu & Byrne (1997)

[a] Calculated from $\log_{10}K_{s,0}°$(298.15 K) and the dissociation constants for phosphoric acid used by the authors.

23.3.10 Selected holmium data

Tab. 23.3.10-1: Selected holmium data (1 bar, 298.15 K) for TDB 2020

T-range refers to the experimental temperature range at which equilibrium constants, $\Delta_r H_m$, and $\Delta_r C_{p,m}°$ were determined. Supplemental data are in italics.

Name	**Redox**	**TDB 2020**				
		$\Delta_f G_m°$ [kJ · mol^{-1}]	$\Delta_f H_m°$ [kJ · mol^{-1}]	$S_m°$ [J · K^{-1} · mol^{-1}]	$C_{p,m}°$ [J · K^{-1} · mol^{-1}]	**Species**
Ho(cr)	0	0	0	75.76	27.15	Ho(cr)
Ho+3	III	-675.6 ± 3.0	-707.70 ± 3.0	-228.7 ± 1.0	-48.7 ± 10	Ho^{3+}

Name	**TDB 2020**				
	$\log_{10}\beta°$	$\Delta_r H_m°$ [kJ · mol^{-1}]	$\Delta_r C_{p,m}°$ [J · K^{-1} · mol^{-1}]	**T-range** [°C]	**Reaction**
HoOH+2	-7.41 ± 0.07	*49.0 ± 2.9*	*0*	25 – 55	$Ho^{3+} + H_2O(l) \rightleftharpoons HoOH^{2+} + H^+$
Ho(OH)2+	*-14.87 ± 0.30*	-	-	-	*$Ho^{3+} + 2\ H_2O(l) \rightleftharpoons Ho(OH)_2^+ + 2\ H^+$*
Ho(OH)3(aq)	*-23.47 ± 0.30*	-	-	-	*$Ho^{3+} + 3\ H_2O(l) \rightleftharpoons Ho(OH)_3(aq) + 3\ H^+$*
Ho(OH)4-	*-35.97 ± 0.30*	-	-	-	*$Ho^{3+} + 4\ H_2O(l) \rightleftharpoons Ho(OH)_4^- + 4\ H^+$*
HoF+2	4.29 ± 0.07	*9.83 ± 0.83*	*0*	5 – 45	$Ho^{3+} + F^- \rightleftharpoons HoF^{2+}$
HoF2+	*6.73 ± 0.3*	*21.0 ± 1.6*	*0*	*5 – 45*	*$Ho^{3+} + 2\ F^- \rightleftharpoons HoF_2^+$*
HoSO4+	*3.95 ± 0.08*	-	-	-	*$Ho^{3+} + SO_4^{2-} \rightleftharpoons HoSO_4^+$*
Ho(SO4)2-	*5.7 ± 0.2*	-	-	-	*$Ho^{3+} + 2\ SO_4^{2-} \rightleftharpoons Ho(SO_4)_2^-$*
HoCO3+	*8.1 ± 0.2*	-	-	-	*$Ho^{3+} + CO_3^{2-} \rightleftharpoons HoCO_3^+$*
Ho(CO3)2-	*12.1 ± 0.3*	-	-	-	*$Ho^{3+} + 2\ CO_3^{2-} \rightleftharpoons Ho(CO_3)_2^-$*
HoH2PO4+2	*0.89 ± 0.13*	*14.7*	*0*	*25 – 80*	*$Ho^{3+} + H_3PO_4(aq) \rightleftharpoons HoH_2PO_4^{2+} + H^+$*

Name	**TDB 2020**		
	$\log_{10}K_{s,0}°$	$\Delta_r H_m°$ [kJ · mol^{-1}]	**Reaction**
Ho(OH)3(cr)	*14.7 ± 1.0*	-	*$Ho(OH)_3(cr) + 3\ H^+ \rightleftharpoons Ho^{3+} + 3\ H_2O(l)$*
HoF3(cr)	-17.6 ± 0.4	-	$HoF_3(cr) \rightleftharpoons Ho^{3+} + 3\ F^-$
Ho2(CO3)3(cr)	*-35 ± 2*	-	*$Ho_2(CO_3)_3(cr) \rightleftharpoons 2\ Ho^{3+} + 3\ CO_3^{2-}$*
HoOHCO3(cr)	*-21.7 ± 2.0*	-	*$HoOHCO_3(cr) \rightleftharpoons Ho^{3+} + OH^- + CO_3^{2-}$*
HoPO4(s)	-25.3 ± 0.6	-	$HoPO_4(s) \rightleftharpoons Ho^{3+} + PO_4^{3-}$

Tab. 23.3.10-2: Selected SIT ion interaction coefficients $\varepsilon_{j,k}$ [kg · mol^{-1}] for holmium species

Data estimated according to charge correlations and taken from Tab. 1-7 are shaded. Supplemental data are in italics.

j k → ↓	**Cl^-** $\varepsilon_{j,k}$ [kg · mol^{-1}]	**ClO_4^-** $\varepsilon_{j,k}$ [kg · mol^{-1}]	**NO_3^-** $\varepsilon_{j,k}$ [kg · mol^{-1}]	**Na^+** $\varepsilon_{j,k}$ [kg · mol^{-1}]	**$Na^+ + Cl^-$** $\varepsilon_{j,k}$ [kg · mol^{-1}]
Ho+3	0.29 ± 0.01	0.49 ± 0.01	0.16 ± 0.01	0	0
HoOH+2	0.15 ± 0.10	-0.05 ± 0.12	-	0	0
Ho(OH)2+	*0.05 ± 0.10*	*0.2 ± 0.1*	-	*0*	*0*
Ho(OH)3(aq)	*0*	*0*	*0*	*0*	*0*
Ho(OH)4-	*0*	*0*	*0*	*-0.05 ± 0.10*	*0*
HoF+2	0.18 ± 0.03	0.34 ± 0.03	0.09 ± 0.04	0	0
HoF2+	*0.05 ± 0.10*	*0.2 ± 0.1*	-	*0*	*0*
HoSO4+	*0.05 ± 0.10*	0.27 ± 0.09	-	*0*	*0*
Ho(SO4)2-	*0*	*0*	*0*	*0.22 ± 0.20*	*0*
HoCO3+	*0.05 ± 0.10*	*0.15 ± 0.18*	-	*0*	*0*
Ho(CO3)2-	*0*	*0*	*0*	*-1.17 ± 0.32*	*0*
HoH2PO4+2	*0.15 ± 0.10*	*0.18 ± 0.08*	-	*0*	*0*

23.3.11 References

Allen, P.G., Bucher, J.J., Shuh, D.K., Edelstein, N.M. & Craig, I. (2000): Coordination chemistry of trivalent lanthanide and actinide ions in dilute and concentrated chloride solutions. Inorganic Chemistry, 39, 595-601.

Arblaster, J.W. (2013): Selected values of the thermodynamic properties of scandium, yttrium, and the lanthanide elements. Handbook on the Physics and Chemistry of Rare Earths, 43, 321-565.

Audi, G., Bersillon, O., Blachot, J. & Wapstra, A.H. (2003): The NUBASE evaluation of nuclear and decay properties. Nuclear Physics, A 729, 3-128.

Bernkopf, M.F. (1984): Hydrolysereaktionen und Karbonatkomplexierung von dreiwertigem Americium im natürlichen aquatischen System. Ph.D. thesis, Institut für Radiochemie, Technische Universität München, Germany, 200 p.

Brown, P.L. & Ekberg, C. (2016): Hydrolysis of Metal Ions. Vol. 1, Wiley-VCH, Weinheim.

Byrne, R.H., Lee, J.H. & Bingler, L.S. (1991): Rare earth element complexation by PO_4^{3-} ions in aqueous solution. Geochimica et Cosmochimica Acta, 55, 2729-2735.

Chatterjee, S., Campbell, E.L., Neiner, D., Pence, N.K., Robinson, T.A. & Levitskaia, T.G. (2015): Aqueous binary lanthanide(III) nitrate $Ln(NO_3)_3$ electrolytes revisited: Extended Pitzer and Bromley treatments. Journal of Chemical and Engineering Data, 60, 2974-2988.

Chirkst, D.E., Lobacheva, O.L. & Dzhevaga, N.V. (2011): Thermodynamic properties of lanthanum(III) and holmium(III) hydroxo compounds. Russian Journal of Physical Chemistry, 85, 1872-1875.

Ciavatta, L. (1980): The specific interaction theory in evaluating ionic equilibria. Annali di Chimica, 70, 551-567.

Cox, J.D., Wagman, D.D. & Medvedev, V.A. (1989): CODATA Key Values for Thermodynamics. New York, Hemisphere, 271p.

Fanghänel, T., Kim, J.I., Klenze, R. & Kato, Y. (1995): Formation of Cm(III) chloride complexes in $CaCl_2$ solutions. Journal of Alloys and Compounds, 225, 308-311.

Fatin-Rouge, N. & Bünzli J.-C.G. (1999): Thermodynamic and structural study of inclusion complexes between trivalent lanthanide ions and native cyclodextrins. Inorganica Chimica Acta, 293, 53-60.

Firsching, F.H. & Brune, S.N. (1991): Solubility products of the trivalent rare-earth phosphates. Journal of Chemical and Engineering Data, 36, 93-95.

Fraústo da Silva, J.J.R. & Queimado, M.M. (1973): Solubility products of lanthanide fluorides. Revista Portuguesa de Química, 15, 29-34.

Frolova, U.K., Kumok, V.N. & Serebrennikov, V.V. (1966): Hydrolysis of ions of the rare earth elements and yttrium in aqueous solutions. Izvestiya Vysshikh Uchebnykh Zavedenii, Khimiya i Khimicheskaya Tekhnologiya, 9(2), 176-179. Chemical Abstracts, 65, 9816c.

Gausse, C., Szenknect, S., Qin, D.W., Mesbah, A., Clavier, N., Neumeier, S., Bosbach, D. & Dacheux, N. (2016): Determination of the solubility of rhabdophanes $LnPO_4 \cdot 0.667H_2O$ (Ln = La to Dy). European Journal of Inorganic Chemistry, 28, 4615-4630.

Gerstein, B.C., Griffel, M., Jennings, L.D., Miller, R.E., Skochdopole, R.E. & Spedding, F.H. (1957): Heat capacity of holmium from 15 to 300°K. Journal of Chemical Physics, 27, 394-399.

Grenthe, I., Plyasunov, A.V. & Spahiu, K. (1997): Estimations of medium effects on thermodynamic data. In: Grenthe, I. & Puigdomènech, I. (eds.): Modelling in Aquatic Chemistry. OECD NEA, Paris, France, 325-426.

Haas, J.R., Shock, E.L. & Sassani, D.C. (1995): Rare earth elements in hydrothermal systems: Estimates of standard partial molal thermodynamic properties of aqueous complexes of the rare earth elements at high pressures and temperatures. Geochimica et Cosmochimica Acta, 59, 4329-4350.

Hakin, A.W., Lian Liu, J., Erickson, K. & Munoz J.-V. (2004): Apparent molar heat capacities and apparent molar volumes of $Pr(ClO_4)_3(aq)$, $Gd(ClO_4)_3(aq)$, $Ho(ClO_4)_3(aq)$, and $Tm(ClO_4)_3(aq)$ at T=(288.15, 298.15, 313.15, and 328.15) K and p=0.1 MPa. Journal of Chemical Thermodynamics, 36, 773-786.

Hakin, A.W., Liu, J.L., Erickson, K., Munoz J.-V. & Rard, J.A. (2005): Apparent molar volumes and apparent molar heat capacities of $Pr(NO_3)_3(aq)$, $Gd(NO_3)_3(aq)$, $Ho(NO_3)_3(aq)$, and $Y(NO_3)_3(aq)$ at T = (288.15, 298.15, 313.15, and 328.15) K and p = 0.1 MPa. Journal of Chemical Thermodynamics, 37, 153-167.

He, M. & Rard, J.A. (2015): Revision of the osmotic coefficients, water activities and mean activity coefficients of the aqueous trivalent rare earth chlorides at T = 298.15 K. Journal of Solution Chemistry, 44, 2208-2221.

Hummel, W. (2018): Radioactive waste inventories for geochemists. PSI Internal Report, TM-44-18-03, Paul Scherrer Institut, Villigen, Switzerland, 55 pp.

Hummel, W., Berner, U., Curti, E., Pearson, F.J. & Thoenen, T. (2002): Nagra/PSI Chemical Thermodynamic Data Base 01/01. Nagra NTB 02-16. Also published by Universal Publishers/upublish.com, Parkland, USA, 565 pp.

Itoh, H., Hachiya, H., Suzuki, Y. & Asano, Y. (1984): Determination of solubility products of rare earth fluorides by fluoride ion-selective electrode. Bulletin of the Chemical Society of Japan, 57, 1698-1690.

Jayasuriya, K.D., Campbell, S.J. & Stewart, A.M. (1985) Specific heat study of a holmium single crystal. Journal of Physics F: Metal Physics, 15, 225-239.

Jordan, N. (in prep.): Europium: Review of thermodynamic data for Eu(III) complexation with inorganic ligands.

Jordan, N., Demnitz, M., Lösch, H., Starke, S., Brendler, V. & Huittinen, N. (2018): Complexation of trivalent lanthanides (Eu) and actinides (Cm) with aqueous phosphates at elevated temperatures. Inorganic Chemistry, 57, 7015-7024.

Klungness, G.D. & Byrne, R.H. (2000): Comparative hydrolysis behavior of the rare earths and yttrium: the influence of temperature and ionic strength. Polyhedron, 19, 99-107.

Koke, C., Skerencak-Frech, A. & Panak, P.J. (2019): Thermodynamics of the complexation of curium(III) with chloride in alkali and alkali earth metal solutions at elevated temperatures. Journal of Chemical Thermodynamics, 131, 219-224.

Konings, R.J.M. & Beneš, O. (2010): The thermodynamic properties of the f-elements and their compounds. I. The lanthanide and actinide metals. Journal of Physical and Chemical Reference Data, 39, 043102-1–043102-48.

Konings, R.J.M. & Kovács, A. (2003): Thermodynamic properties of the lanthanide(III) halides. Handbook on the Physics and Chemistry of Rare Earths, 33, 147-247.

Lemire, R.J., Berner, U., Musikas, C., Palmer, D.A., Taylor, P. & Tochiyama, O. (2013): Chemical Thermodynamics of Iron, Part 1. Chemical Thermodynamics, Vol. 13a. OECD Publications, Paris, France, 1082 pp.

Liu, X. & Byrne, R.H. (1997): Rare earth and yttrium phosphate solubilities in aqueous solution. Geochimica et Cosmochimica Acta, 61, 1625-1633.

Luo, Y. & Millero, F.J. (2004): Effects of temperature and ionic strength on the stabilities of the first and second fluoride complexes of yttrium and the rare earth elements. Geochimica et Cosmochimica Acta, 68, 4301-4308.

Luo, Y.-R. & Byrne, R.H. (2000): The ionic strength dependence of rare earth and yttrium fluoride complexation at 25 °C. Journal of Solution Chemistry, 29, 1089-1099.

Luo, Y.-R. & Byrne, R.H. (2001): Yttrium and rare earth element complexation by chloride ions at 25 °C. Journal of Solution Chemistry, 30, 837-845.

Luo, Y.-R. & Byrne, R.H. (2007): The influence of ionic strength on yttrium and rare earth element complexation by fluoride ions in $NaClO_4$, $NaNO_3$ and NaCl Solutions at 25 °C. Journal of Solution Chemistry, 36, 673-689.

Menon, M. P. & James, J. (1989a): Stability constant for the lanthanide fluoride complexes in aqueous solution at 25 °C. Journal of Solution Chemistry, 18, 735-742.

Menon, M. P. & James, J. (1989b): Solubilities, solubility products and solution chemistry of lanthanon trifluoride–water systems. Journal of the Chemical Society, Faraday Transactions, 85, 2683-2694.

Migdisov, A., Williams-Jones, A.E., Brugger, J. & Caporuscio, F.A. (2016): Hydrothermal transport, deposition, and fractionation of the REE: Experimental data and thermodynamic calculations. Chemical Geology 439, 13-42.

Migdisov, A.A., Williams-Jones, A.E. & Wagner, T. (2009): An experimental study of the solubility and speciation of the Rare Earth Elements (III) in fluoride- and chloride-bearing aqueous solutions at temperatures up to 300 °C. Geochimica et Cosmochimica Acta, 73, 7087-7109.

Millero, F.J. (1992): Stability constants for the formation of rare earth-inorganic complexes as a function of ionic strength. Geochimica et Cosmochimica Acta, 56, 3123-3132.

Mioduski, T., Gumiński, C. & Zeng, D. (2009): IUPAC-NIST solubility data series. 87. Rare earth metal chlorides in water and aqueous systems. Part 3. Heavy lanthanides (Gd–Lu). Journal of Physical and Chemical Reference Data, 38, 925-1011.

Morss, L.R. (1976): Thermochemical properties of yttrium, lanthanum, and the lanthanide elements and ions. Chemical Reviews, 76, 827-841.

Pearson, F.J. & Berner, U. (1991): Nagra Thermochemical Data Base I. Core Data. Nagra Technical Report NTB 91-17.

Pearson, F.J., Jr., Berner, U. & Hummel, W. (1992): Nagra Thermochemical Data Base II. Supplemental Data 05/92. Nagra Technical Report NTB 91-18.

Rard, J.A. (1988): Aqueous solubilities of praseodymium, europium, and lutetium sulfates. Journal of Solution Chemistry, 17, 499-517.

Rard, J.A. (2016): Critical evaluation of the standard molar entropies, enthalpies of formation, Gibbs energies of formation and heat capacities of the aqueous trivalent rare earth ions, and the corresponding standard molar entropies, enthalpies of formation and Gibbs energies of formation of the thermodynamically stable $RECl_3 \cdot 7H_2O$(cr) and $RECl_3 \cdot 6H_2O$(cr). Journal of Solution Chemistry, 45, 1332-1376.

Rard, J.A. & Spedding, F.H. (1982): Isopiestic determination of the activity coefficients of some aqueous rare-earth electrolyte solutions at 25 °C. 6. $Eu(NO_3)_3$, $Y(NO_3)_3$, and YCl_3. Journal of Chemical and Engineering Data, 27, 454-461.

Rard, J.A., Weber, H.O. & Spedding, F.H. (1977): Isopiestic determination of the activity coefficients of some aqueous rare earth electrolyte solutions at 25 °C. 2. The rare earth perchlorates. Journal of Chemical and Engineering Data, 22, 187-201.

Schijf, J. & Byrne, R.H. (1999): Determination of stability constants for the mono- and difluoro-complexes of Y and the REE, using a cation-exchange resin and ICP-MS. Polyhedron, 18, 2839-2844.

Skerencak-Frech, A., Fröhlich, D.R., Rothe, J., Dardenne, K. & Panak, P.J. (2014): Combined time-resolved laser fluorescence spectroscopy and extended X-ray absorption fine structure spectroscopy study on the complexation of trivalent actinides with chloride at T = 25 – 200 °C. Inorganic Chemistry, 53, 1062-1069.

Spahiu, K. & Puigdomènech, I. (1998): On weak complex formation: Re-interpretation of literature data on the Np and Pu nitrate complexation. Radiochimica Acta, 82, 413-419.

Spedding, F.H., DeKock, C.W., Pepple, G.W. & Habenschuss, A. (1977): Heats of dilution of some aqueous rare earth electrolyte solutions at 25 °C. 3. Rare earth chlorides. Journal of Chemical and Engineering Data, 22, 58-70.

Spedding, F.H., Rulf, D.C. & Gerstein, B.C. (1972): Thermal study of entropies and crystal field splittings in heavy rare earth trichloride hexahydrates. Heat capacities from 5 – 300 °K. Journal of Chemical Physics, 56, 1498-1506.

Spedding, F.H., Weber, H.O., Saeger, V.W., Petheram, H.H., Rard, J.A. & Habenschuss, A. (1976): Isopiestic determination of the activity coefficients of some aqueous rare earth electrolyte solutions at 25 °C. 1. The rare earth chlorides. Journal of Chemical and Engineering Data, 21, 341-360.

Stepanchikova, S.A. & Biteikina, R.P. (2006): Spectrophotometric study of holmium complexation in KOH solutions at 25 °C. Russian Journal of Inorganic Chemistry, 51, 1315-1319.

Thoenen, T., Hummel, W., Berner, U. & Curti, E. (2014): The PSI/Nagra Chemical Thermodynamic Database 12/07. Technical Report, PSI Bericht Nr. 14-04, Paul Scherrer Institut, Villigen, Switzerland, 416 pp.

Walker, J.B. & Choppin, G.R. (1967): Thermodynamic parameters of fluoride complexes of the lanthanides. In: Fields P.R. & Moeller, T. (eds.): Lanthanide/Actinide Chemistry. Advances in Chemistry Vol. 71. American Chemical Society, Washington, D.C, 127-140.

Wood, S. A. (1990): The aqueous geochemistry of the rare-earth elements and yttrium 1. Review of available low-temperature data for inorganic complexes and the inorganic REE speciation of natural waters. Chemical Geology, 82, 159-186.

24 Selenium

24.1 Introduction

Selenium has been reviewed in detail by Olin et al. (2005) and the results of this NEA TDB review have been included already in TDB 12/07 (Thoenen et al. 2014). However, a more recent solubility study of selenium (Iida et al. 2010) was not reviewed by Thoenen et al. (2014). Furthermore, the solubility of zero-valent selenium, Se(aq), has not been considered so far. These gaps are closed here.

Hagemann et al. (2012) provide Pitzer coefficients for binary and ternary selenite and selenate systems, and solubility products of some selenite and selenate compounds from own experimental data in highly saline solutions. The highly soluble Na, K, and Mg selenate salts, and the highly soluble Na selenite salts discussed by Hagemann et al. (2012) have not been considered in TDB 12/07 (Thoenen et al. 2014). The solubility products reported by Hagemann et al. (2012) for $CaSeO_3$ and $MgSeO_3.H_2O$ are within the uncertainty ranges of the values selected in TDB 12/07 (Thoenen et al. 2014).

24.2 Polyselenides

Iida et al. (2010) measured the solubility of selenium, Se(cr), in the pH range 4 – 13 under anoxic conditions at the ionic strengths 0.1, 1.0 and 2.0 M NaCl. The solubility experiments were done both from oversaturation and undersaturation and lasted 40 days. Plots of data from oversaturation and undersaturation do not show any systematic differences (Figs. 24-1a to 24-1c), confirming that equilibrium was attained during the experimental periods.

As discussed by Hummel (2017), above pH 9 the results of Iida et al. (2010) are fairly consistent with the dataset of Olin et al. (2005). However, below pH 9 Iida et al. (2010) measured significantly higher total dissolved selenium concentrations than predicted with the dataset of Olin et al. (2005).

In order to explain these higher total dissolved selenium concentrations Iida et al. (2010) postulated a phase transition from Se(cr) to an amorphous selenium phase Se(am) with a higher solubility than Se(cr) below pH 9, although they found Se(cr) by X-ray powder diffraction in all cases.

In addition Iida et al. (2010) slightly adjusted the thermodynamic constant for the tetraselenide Se_4^{2-}. The latter adjustment is no problem as the stability constants of the polyselenides selected by Olin et al. (2005) are based on experiments in 0.5 – 2 M KOH solutions at pH > 13 and thus, the stability region of Se_4^{2-} might be underestimated.

However, there is no independent evidence for the formation of an amorphous selenium phase below pH 9 and the presence of Se(cr) in all experiments of Iida et al. (2010) contradicts this model assumption. A re-interpretation of the experimental data of Iida et al. (2010) by this review suggests that they actually measured the protonation of a polyselenide, presumably

$$Se_4^{2-} + H^+ \rightleftharpoons HSe_4^-$$

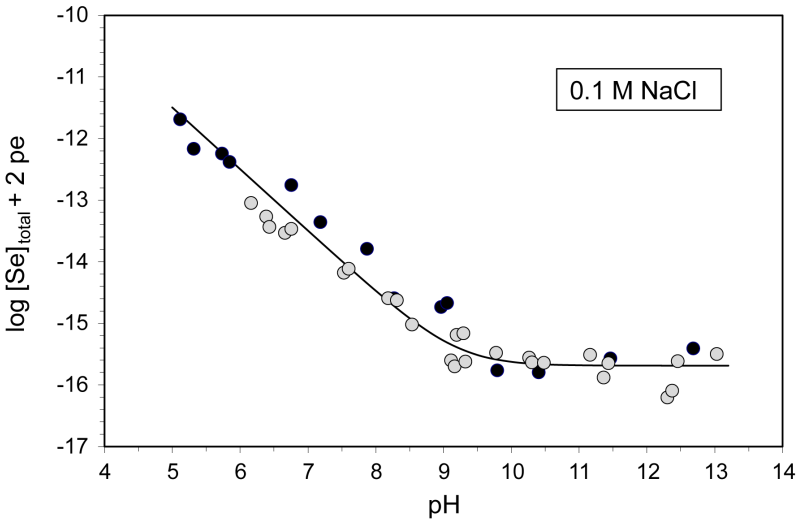

Fig. 24-1a: Plot of (log [total selenium concentration] + 2 pe) versus pH

Data taken from Tab. 1-1 of Iida et al. (2010). The black circles represent data from undersaturation, the grey circles from oversaturation experiments. The curve is calculated using equilibrium constants derived by this review (Tab. 24-1).

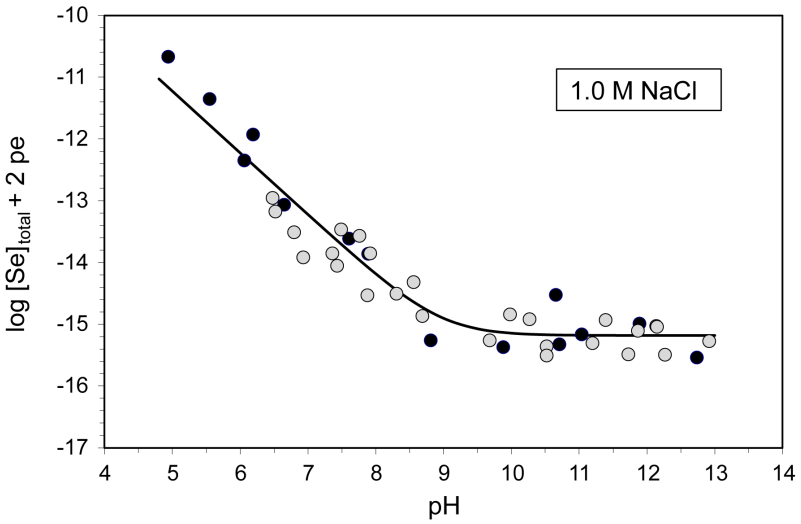

Fig. 24-1b: Plot of (log [total selenium concentration] + 2 pe) versus pH

Data taken from Tab. 1-2 of Iida et al. (2010). The black circles represent data from undersaturation, the grey circles from oversaturation experiments. The curve is calculated using equilibrium constants derived by this review (Tab. 24-1).

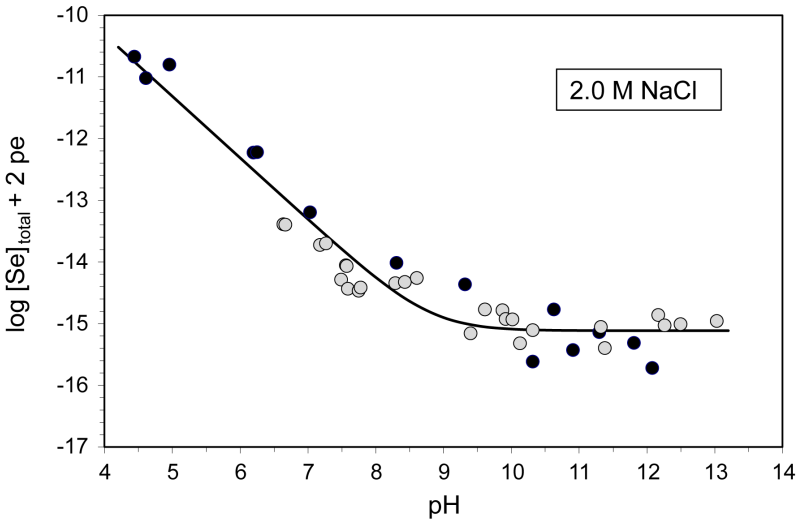

Fig. 24-1c: Plot of (log [total selenium concentration] + 2 pe) versus pH

Data taken from Tab. 1-2 of Iida et al. (2010). The black circles represent data from undersaturation, the grey circles from oversaturation experiments. The curve is calculated using equilibrium constants derived by this review (Tab. 24-1).

This review used the experimental data reported in Tab. 1-1 and 1-2 of Iida et al. (2010) and assumed that at pH > 9.5 the equilibrium

$$4\ Se(cr) + 2\ e^- \rightleftharpoons Se_4^{2-}$$

predominated, while at pH < 9.0 the predominating equilibrium was

$$4\ Se(cr) + H^+ + 2\ e^- \rightleftharpoons HSe_4^-$$

Least squares fits of all data in the respective pH regions for different ionic strengths resulted in equilibrium constants shown in Tab. 24-1.

Tab. 24-1: Conditional equilibrium constants derived by this review from the experimental solubility data of Iida et al. (2010)

Uncertainties refer to 2σ. Constants reported by Iida et al. (2010) are given in parentheses.

Ionic strength [NaCl] (mol · dm^{-3})	**4 Se(cr) + 2 e$^-$ ⇌ Se$_4^{2-}$ log$_{10}K_s$**	**4 Se(cr) + H$^+$ + 2 e$^-$ ⇌ HSe$_4^-$ log$_{10}$*K_s**
0.1	-16.29 ± 0.11 (-16.24 ± 0.09)	-7.10 ± 0.16
1.0	-15.79 ± 0.12 (-15.79 ± 0.12)	-6.84 ± 0.16
2.0	-15.72 ± 0.13 (-15.68 ± 0.10)	-6.92 ± 0.17

Note that the $\log_{10}K_s$ values reported by Iida et al. (2010) are essentially the same as the ones derived by this review (Tab. 24-1). The small differences most probably are due to an extended data range used by Iida et al. (2010) for their least squares fits. While this review used data at pH > 9.5, Iida et al. (2010) seem to have used data at pH > 9.0. Although this is not explicitly mentioned in their paper, this review could exactly reproduce the values of Iida et al. (2010) using data in the range pH > 9.0.

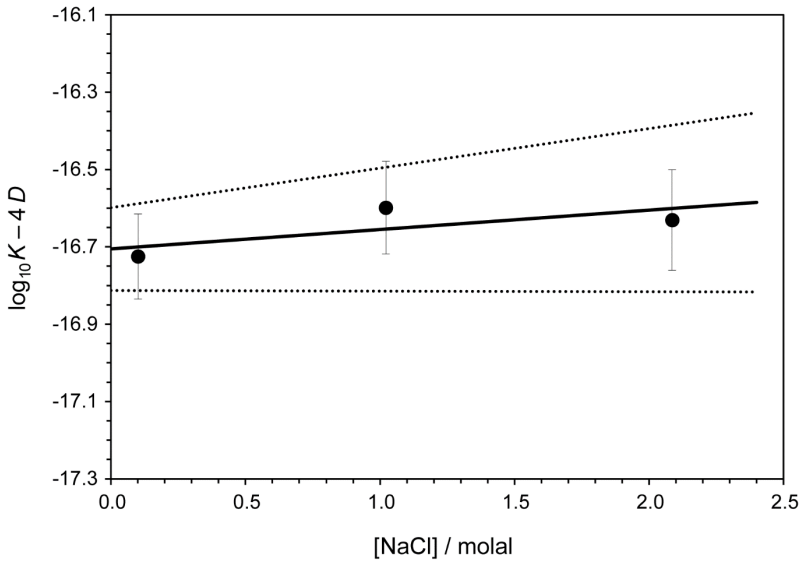

Fig. 24-2: Dependence of the equilibrium 4 Se(cr) + 2 e^- ⇌ Se_4^{2-} on ionic strength in NaCl using constants derived by this review (Tab. 24-1)

The solid line is obtained using the derived SIT interaction coefficient and stability constant at zero ionic strength. Dotted lines represent the 95% uncertainty range extrapolated from I = 0 to higher NaCl concentrations.

The equilibrium constants derived by this review (Tab. 24-1) have been extrapolated to zero ionic strength using SIT. Note that not only the formal activity of the electron, a_{e^-}, is involved in these equilibria, but also the hydrogen activity, a_{H^+}, because Iida et al. (2010) report in their Tab. 1-1 and Tab. 1-2 pH values on the activity scale, converted from the concentration scale to the activity scale using SIT:

$$4\ Se(cr) + 2\ e^- \rightleftharpoons Se_4^{2-}$$

$$K_s = [Se_4^{2-}] \cdot (a_{e^-})^{-2}$$

$$4\ Se(cr) + H^+ + 2\ e^- \rightleftharpoons HSe_4^-$$

$$^*K_s = [HSe_4^-] \cdot (a_{H^+})^{-1} \cdot (a_{e^-})^{-2}$$

where (a_M) is the activity of species M for which no activity coefficient needs to be considered. Hence, the actual SIT equations are

$$\log_{10}K_s - 4D = \log_{10}K_s^\circ - \varepsilon(Na^+, Se_4^{2-}) \cdot I_m$$

$$\log_{10}{}^*K_s - D = \log_{10}{}^*K_s^\circ - \varepsilon(Na^+, HSe_4^-) \cdot I_m$$

The results of the SIT analyses are (Figs. 24-2 and 24-3):

$4\ Se(cr) + 2\ e^- \rightleftharpoons Se_4^{2-}$

$\log_{10}K_s°(298.15\ K) = -16.71 \pm 0.11$

$\varepsilon(Na^+, Se_4^{2-}) = -(0.05 \pm 0.09)\ kg \cdot mol^{-1}$

$4\ Se(cr) + H^+ + 2\ e^- \rightleftharpoons HSe_4^-$

$\log_{10}{}^*K_s°(298.15\ K) = -7.16 \pm 0.15$

$\varepsilon(Na^+, HSe_4^-) = -(0.03 \pm 0.12)\ kg \cdot mol^{-1}$

These values have been included in TDB 2020.

Note that the values $\log_{10}K_s°(298.15\ K) = -16.67 \pm 0.03$ and $\varepsilon(Na^+, SeO_4^{2-}) = -(0.03 \pm 0.02)\ kg \cdot mol^{-1}$ reported by Iida et al. (2010) from their SIT analysis are essentially the same as the ones derived by this review. However, the values of Iida et al. (2010) are associated with probably unrealistically small uncertainties.

The value $\log_{10}K_s°(298.15\ K) = -16.71 \pm 0.11$ derived by this review from the data of Iida et al. (2010) is slightly higher than the value $\log_{10}K_s°(298.15\ K) = -17.1 \pm 0.6$, as calculated from the reaction data selected by Olin et al. (2005), $Se(cr) + 2\ e^- \rightleftharpoons Se^{2-}$, $\log_{10}K°(298.15\ K) = -22.530 \pm 0.526$, and $4\ Se^{2-} \rightleftharpoons Se_4^{2-} + 6\ e^-$, $\log_{10}K°(298.15\ K) = 73.023 \pm 0.333$. The consequence of this change is a slight increase the Se_4^{2-} predominance field in an Eh – pH diagram, compared with calculations done with the original Olin et al. (2005) data.

Combining $\log_{10}K_s°(298.15\ K)$ and $\log_{10}{}^*K_s°(298.15\ K)$ derived by this review results in

$Se_4^{2-} + H^+ \rightleftharpoons HSe_4^-$

$\log_{10}{}^*K°(298.15\ K) = 9.55 \pm 0.19$

indicating that the protonation of the tetraselenide Se_4^{2-} occurs around pH 9.

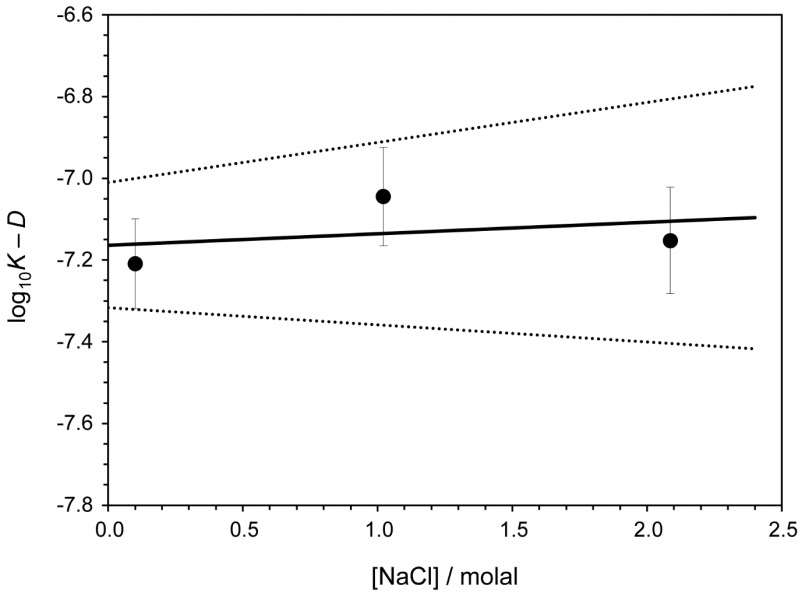

Fig. 24-3: Dependence of the equilibrium 4 Se(cr) + H^+ + 2 e^- ⇌ HSe_4^- on ionic strength in NaCl using constants derived by this review (Tab. 24-1)

The solid line is obtained using the derived SIT interaction coefficient and stability constant at zero ionic strength. Dotted lines represent the 95% uncertainty range extrapolated from I = 0 to higher NaCl concentrations.

24.3 Selenium(0) solubility

While the solubility of zero-valent sulphur, S(cr) ⇌ S(aq), $\log_{10}K°(298.15\ K) = -6.65 \pm 0.09$, is well known, and even its strong temperature dependence, ranging from $5 \cdot 10^{-8}$ mol · kg^{-1} at 4 °C to $4 \cdot 10^{-6}$ mol · kg^{-1} at 80 °C, has been studied (see Section 27.3), no published information could be found by this review concerning the solubility of zero-valent selenium, Se(aq).

The only experimental study concerning the solubility of Se(cr) in the pH range 4 – 13 has been published by Iida et al. (2010). A re-interpretation of their data by this review suggests that they explored for the first time the protonation equilibrium $Se_4^{2-} + H^+ ⇌ HSe_4^-$ (see Section 24.2). The solubility data of Iida et al. (2010) from undersaturation experiments in the pH range 5 – 9, which range from $[Se]_{total} = 10^{-5} – 10^{-6}$ mol · dm^{-3} and which were used to derive the protonation equilibrium constant, indicate an upper limit for the solubility of Se(cr) ⇌ Se(aq) of Se(aq) < 10^{-5} mol · dm^{-3}.

Preliminary but unpublished solubility measurements of Se(cr) in this laboratory (Tits, personal communication) indicate a value of Se(aq) ≈ $8 \cdot 10^{-6}$ mol · dm^{-3}. This value is only slightly below the upper limit estimated from the data of Iida et al. (2010) but needs confirmation by a more extended solubility study.

Hence, this review can only provide a very rough estimate with a large uncertainty encompassing the solubility of the well-known chemical analogue sulphur on the one hand, and the upper limit derived from the solubility data of Iida et al. (2010) on the other hand:

$$Se(cr) \rightleftharpoons Se(aq)$$

$$\log_{10}K^{\circ}(298.15\ K) = -(6 \pm 1)$$

This value has been included in TDB 2020 as supplemental datum, together with the estimate

$$\varepsilon(Se(aq), NaCl) = \varepsilon(Se(aq), NaClO_4) = (0.0 \pm 0.1)\ kg \cdot mol^{-1}$$

24.4 Selected selenium data

Tab. 24-2: Selected selenium data

Supplemental data are in italics.

Name	**$\log_{10}\beta°$**	**$\Delta_r H_m°$** [kJ · mol^{-1}]	**$\Delta_r C_{p,m}°$** [J · K^{-1} · mol^{-1}]	**Reaction**
Se4-2	-16.71 ± 0.11			4 Se(cr) + 2 e^- ⇌ Se_4^{2-}
HSe4-	-7.16 ± 0.15			4 Se(cr) + H^+ + 2 e^- ⇌ HSe_4^-
Se(aq)	*-6 ± 1*			*Se(cr) ⇌ Se(aq)*

Tab. 24-3: Selected SIT ion interaction coefficients $\varepsilon_{j,k}$ [kg · mol^{-1}] for selenium species

Data in normal face are derived in this review. Data estimated according to charge correlations and taken from Tab. 1-7 are shaded. Supplemental data are in italics.

j k → ↓	**Cl^-** $\varepsilon_{j,k}$ [kg · mol^{-1}]	**ClO_4^-** $\varepsilon_{j,k}$ [kg · mol^{-1}]	**Na^+** $\varepsilon_{j,k}$ [kg · mol^{-1}]	**$Na^+ + Cl^-$** $\varepsilon_{j,k}$ [kg · mol^{-1}]	**$Na^+ + ClO_4^-$** $\varepsilon_{j,k}$ [kg · mol^{-1}]
Se4-2	0	0	-0.05 ± 0.09	0	0
HSe4-	0	0	-0.03 ± 0.12	0	0
Se(aq)	*0*	*0*	*0*	*0.0 ± 0.1*	*0.0 ± 0.1*

24.5 References

Hagemann, S., Moog, H.C., Herbert, H.J., Erich, A. (2012): Rückhaltung und thermodynamische Modellierung von Iod und Selen in hochsalinaren Lösungen - Gewinnung von Daten für Selenit, Selenat und Iodid für Belange der Langzeitsicherheitsanalyse des Nahfelds eines Endlagers für gefährliche Abfälle, GRS-Report 245, GRS, Braunschweig, Germany, 176 pp.

Hummel, W. (2017): Chemistry of selected dose-relevant radionuclides. Nagra Technical Report NTB 17-05.

Iida, Y., Yamaguchi, T., Tanaka, T. & Nakayama, S. (2010): Solubility of selenium at high ionic strength under anoxic conditions. Journal of Nuclear Science and Technology, 47, 431-438.

Olin, Å., Noläng, B., Öhman, L.-O., Osadchii, E.G. & Rosén, E. (2005): Chemical Thermodynamics of Selenium. Chemical Thermodynamics, Vol. 7. Elsevier, Amsterdam, 851p.

Thoenen, T., Hummel, W., Berner, U. & Curti, E. (2014): The PSI/Nagra Chemical Thermodynamic Database 12/07. Technical Report, PSI Bericht Nr. 14-04, Paul Scherrer Institut, Villigen, Switzerland, 416 pp.

25 Silicon and silicates

25.1 Elemental silicon

Silicon metal and gas are not relevant under environmental conditions. Hence, the gas phase Sig is not included in the data base. For the same reason SiF_4g, selected by Grenthe et al. (1992), is also not included in the data base. The absolute entropy and heat capacity of Si(cr) are included as they are used for the calculation of certain thermodynamic reaction properties. The selected values are taken from CODATA (Cox et al. 1989).

$$S_m°(\text{Si, cr, 298.15 K}) = (18.810 \pm 0.080)\ \text{J} \cdot \text{K}^{-1} \cdot \text{mol}^{-1}$$

$$C_{p,m}°(\text{Si, cr, 298.15 K}) = (19.789 \pm 0.030)\ \text{J} \cdot \text{K}^{-1} \cdot \text{mol}^{-1}$$

25.2 Silica (quartz)

The selected values for SiO_2(cr), quartz, are taken from CODATA (Cox et al. 1989).

$$\Delta_f H_m°(\text{SiO}_2\text{, cr, 298.15 K}) = -(910.700 \pm 1.000)\ \text{kJ} \cdot \text{mol}^{-1}$$

$$S_m°(\text{SiO}_2\text{, cr, 298.15 K}) = (41.460 \pm 0.200)\ \text{J} \cdot \text{K}^{-1} \cdot \text{mol}^{-1}$$

$$C_{p,m}°(\text{SiO}_2\text{, cr, 298.15 K}) = (44.602 \pm 0.300)\ \text{J} \cdot \text{K}^{-1} \cdot \text{mol}^{-1}$$

and the Gibbs energy of formation calculated from the above values and $S_m°$(Si, cr, 298.15 K)

$$\Delta_f G_m°(\text{SiO}_2\text{, cr, 298.15 K}) = -(856.287 \pm 1.002)\ \text{kJ} \cdot \text{mol}^{-1}$$

25.3 Silica compounds and aqueous species

25.3.1 Silica compounds

Dissolution of silica in water in the pH range where $Si(OH)_4$(aq) is the dominant aqueous silica species can be expressed by the reaction

$$\text{SiO}_2\text{(s)} + 2\ \text{H}_2\text{O(l)} \rightleftharpoons \text{Si(OH)}_4\text{(aq)}$$

Taking the activity of the solid phase and water to be 1, as well as the activity coefficient of $Si(OH)_4$(aq), leads to

$$K_s = m_{\text{Si(dissolved)}}$$

where m is the measured concentration of dissolved silica in moles / kg H_2O.

Nordstrom et al. (1990) selected $\log_{10}K_s°$ and $\Delta_r H_m°$ values for quartz, chalcedony and amorphous silica as given by Fournier (1985):

$\log_{10}K_s°$(Quartz, cr, 298.15 K) = -3.98

$\Delta_r H_m°$(Quartz, cr, 298.15 K) = 5.99 kcal · mol^{-1} = 25.09 kJ · mol^{-1}

$\log_{10}m_{Si(dissolved)}$ = 0.41 – 1'309 / T

$\log_{10}K_s°$(Chalcedony, s, 298.15 K) = -3.55

$\Delta_r H_m°$(Chalcedony, s, 298.15 K) = 4.72 kcal · mol^{-1} = 19.75 kJ · mol^{-1}

$\log_{10}m_{Si(dissolved)}$ = -0.09 – 1'032 / T

$\log_{10}K_s°$(Silica, am, 298.15 K) = -2.71

$\Delta_r H_m°$(Silica, am, 298.15 K) = 3.34 kcal · mol^{-1} = 13.97 kJ · mol^{-1}

$\log_{10}m_{Si(dissolved)}$ = -0.26 – 731 / T

The poorly defined solid phase "chalcedony" has been introduced in geochemical modelling as kind of a trick (see discussion below) to circumvent the problem that almost all groundwaters appear to be oversaturated in $Si(OH)_4(aq)$ with respect to quartz(old) (Fig. 25-1), while they appear to be saturated or slightly undersaturated with respect to "chalcedony" (Fig. 25-1).

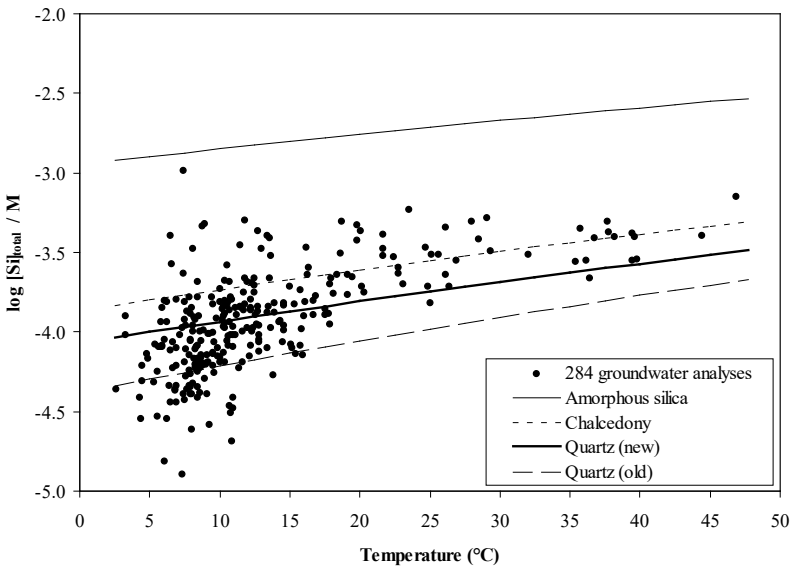

Fig. 25-1: Temperature dependence of total dissolved silica in Swiss groundwaters

The solubility of amorphous silica and quartz (new) is calculated with the integrated van't Hoff equation using $\log_{10}K_s°$ and $\Delta_r H_m°$ selected in this review. Note that the four term temperature functions of Gunnarsson & Arnorsson (2000) give identical results in this temperature range. The solubility of chalcedony and quartz (old) is calculated with the temperature function given by Nordstrom et al. (1990).

New solubility data for quartz at 21, 50, 75 and 96 °C have been reported by Rimstidt (1997). Note, that the duration of his solubility experiments at 21 °C lasted for more than 13 years! These solubility data show excellent internal consistency and fit a straight line (Rimstidt 1997):

$$\log_{10} m_{Si(dissolved)} = -0.076 - 1'093.711 / T$$

This means that in the temperature range 21 – 96 °C a two-term approximation of temperature dependence is sufficient, i.e. the integrated van't Hoff equation including only $\log_{10} K_s°$ and $\Delta_r H_m°$:

$$\log_{10} K_s°(\text{Quartz, cr, 298.15 K}) = -3.744$$

$$\Delta_r H_m°(\text{Quartz, cr, 298.15 K}) = 20.939 \text{ kJ} \cdot \text{mol}^{-1}$$

Rimstidt (1997) critically evaluated all the quartz solubility data from the literature and fitted all reliable literature data up to 300 °C together with his own results to the van't Hoff equation:

$$\log_{10} m_{Si(dissolved)} = -(0.0254 \pm 0.0247) - (1'107.12 \pm 10.77) / T$$

This function predicts that the solubility of quartz at 25 °C is 11.0 ± 1.1 ppm "SiO_2". Note that all uncertainties given by Rimstidt (1997) are expressed as ± 1 standard deviation. This results in:

$$\log_{10} K_s°(\text{Quartz, cr, 298.15 K}) = -(3.739 \pm 0.087)$$

$$\Delta_r H_m°(\text{Quartz, cr, 298.15 K}) = (21.196 \pm 0.41) \text{ kJ} \cdot \text{mol}^{-1}$$

where the uncertainties are now expressed as 2 standard deviations (95% confidence level).

Gunnarsson & Arnorsson (2000) discussed and simultaneously fitted the new data of Rimstidt (1997), their own experiments on amorphous silica, and all reliable published solubility data of quartz and amorphous silica in pure water in the temperature range 0 – 350 °C at 1 bar below 100 °C and at P_{sat} at higher temperatures. Their results are:

$$\log_{10} K_s \text{ (Quartz, cr)} = -34.188 + 197.47 / T - 5.851 \cdot 10^{-6} T^2 + 12.245 \log_{10} T$$

$$\log_{10} K_s \text{ (Silica, am)} = -8.476 - 485.24 / T - 2.268 \cdot 10^{-6} T^2 + 3.068 \log_{10} T$$

which results in:

$$\log_{10} K_s°(\text{Quartz, cr, 298.15 K}) = -(3.746 \pm 0.087)$$

$$\log_{10} K_s°(\text{Silica, am, 298.15 K}) = -(2.714 \pm 0.044)$$

$$\Delta_r H_m°(\text{Quartz, cr, 298.15 K}) = (20.637 \pm 0.41) \text{ kJ} \cdot \text{mol}^{-1}$$

$$\Delta_r H_m°(\text{Silica, am, 298.15 K}) = (14.594 \pm 0.21) \text{ kJ} \cdot \text{mol}^{-1}$$

$\Delta_r C_{p,m}°$(Quartz, cr, 298.15 K) = (42.066 ± 2.0) J · K^{-1} · mol^{-1}

$\Delta_r C_{p,m}°$(Silica, am, 298.15 K) = (2.350 ± 1.0) J · K^{-1} · mol^{-1}

These values have been included in TDB 2020.

No uncertainty estimates are given by Gunnarsson & Arnorsson (2000) except the information that the residuals of the data points used for the regressions are all within 500 J / mole for amorphous silica whereas the quartz residuals are within 1'000 J / mole. As the quartz data fitted by Gunnarsson & Arnorsson (2000) are essentially the same as the ones used by Rimstidt (1997) we used the uncertainty estimates of Rimstidt (1997) for the quartz parameters and half the quartz uncertainties as uncertainty estimates for amorphous silica parameters. The uncertainty of $\Delta_r C_{p,m}°$ (Quartz, cr, 298.15) is assumed to be similar to the uncertainty of $\Delta_r S_m°$(Quartz, cr, 298.15 K) = ($\Delta_r H_m°$(Quartz, cr, 298.15 K) – $\Delta_r G_m°$(Quartz, cr, 298.15 K)) / T° · 1'000 = -(2.5071 ± 2.1672) J · K^{-1} · mol^{-1} (see Section 25.3.2).

The solubility of amorphous silica has not changed at T < 200 °C compared with earlier results. However, the solubility of quartz is significantly higher than given in most previous compilations, e.g. by Nordstrom et al. (1990). The old quartz solubility constant at 25 °C was based on rather dubious data not in accord with most data measured at other temperatures (Rimstidt 1997).

Based on the old quartz solubility almost all groundwaters had been calculated to be significantly supersaturated with respect to quartz (Figs. 25-1 and 25-2). In an attempt to remedy this disturbing situation the solubility of chalcedony has been widely used in speciation calculations. However, the chalcedony data are based on measurements of a few ill-defined samples, as discussed by Rimstidt (1997). Using the new quartz solubility in speciation calculations the situation has changed, most groundwaters are now saturated or only slightly supersaturated with respect to quartz (Figs. 25-1 and 25-2). Hence, the dubious value of chalcedony solubility has already been removed from TDB 01/01 (Hummel et al. 2002).

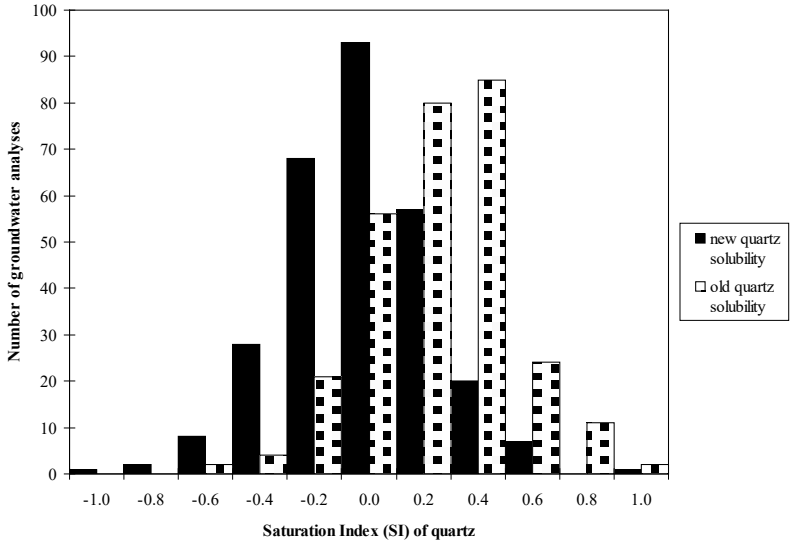

Fig. 25-2: Histogram of quartz saturation indices calculated for 284 Swiss groundwater analyses shown in Fig. 25-1

25.3.2 Aqueous silica species

$Si(OH)_4(aq)$

In aqueous media, silicon exists exclusively in the +IV oxidation state. The relevant species in solutions at pH < 9 is $Si(OH)_4(aq)$.

The thermodynamic properties of this species are based on

- CODATA (Cox et al. 1989) values for Si(cr) (see Section 25.1), SiO_2(cr) (see Section 25.2), H_2O(l), O_2g, H_2g with their given uncertainties
- and the temperature dependent solubility of quartz, $SiO_2(cr) + 2\ H_2O(l) \rightleftharpoons Si(OH)_4(aq)$, expressed as $\log_{10}K_s(T) = A + B / T - C \cdot T^2 + D \cdot \log_{10}T$ with uncertainty estimates as discussed above (see Section 25.3.1)

They are calculated as follows ($R = 8.314510\ J \cdot K^{-1} \cdot mol^{-1}$ and $T^o = 298.15\ K$):

$$\log_{10}K_s(T°) = -(3.74634 \pm 0.08715)$$

$$\Delta_r G_m° = -R \cdot T^o \cdot \ln(10) \cdot \log_{10}K_s(T^o) = (21.3843 \pm 0.4975)\ kJ \cdot mol^{-1}$$

$$\Delta_r H_m° = R \cdot (T^o)^2 \cdot \ln(10) \cdot \partial\log_{10}K_s(T)/\partial T$$
$$= R \cdot (-\ln(10) \cdot B + 2 \cdot \ln(10) \cdot C \cdot (T^o)^3 + D \cdot T^o) = (20.6368 \pm 0.4124)\ kJ \cdot mol^{-1}$$

$$\Delta_r S_m° = (\Delta_r H_m° - \Delta_r G_m°) / T^o \cdot 1'000 = -(2.5071 \pm 2.1672)\ J \cdot K^{-1} \cdot mol^{-1}$$

$$\Delta_r C_{p,m}° = \partial\Delta_r H_m(T)/\partial T = R\ (6 \cdot \ln(10) \cdot C \cdot (T^o)^2 + D) \cdot 1'000 = (42.0659 \pm 2.0)\ J \cdot K^{-1} \cdot mol^{-1}$$

$$\Delta_f G_m°(Si(OH)_4(aq)) = \Delta_r G_m° + \Delta_f G_m°(Quartz) + 2 \cdot \Delta_f G_m°(H_2O(l))$$
$$= (21.384 \pm 0.498) - (856.287 \pm 1.002) - 2 \cdot (237.140 \pm 0.041) = -(1'309.183 \pm 1.120)\ kJ \cdot mol^{-1}$$

$$\Delta_f H_m°(Si(OH)_4(aq)) = \Delta_r H_m° + \Delta_f H_m°(Quartz) + 2 \cdot \Delta_f H_m°(H_2O(l))$$
$$= (20.637 \pm 0.412) - (910.700 \pm 1.000) - 2 \cdot (285.830 \pm 0.040) = -(1'461.723 \pm 1.082)\ kJ \cdot mol^{-1}$$

$$\Delta_f S_m°(Si(OH)_4(aq)) = \Delta_r S_m° + \Delta_f S_m°(Quartz) + 2 \cdot \Delta_f S_m°(H_2O(l))$$
$$= -(2.507 \pm 2.167) - (182.502 \pm 0.200) - 2 \cdot (163.307 \pm 0.030) = -(511.623 \pm 2.177)\ J \cdot K^{-1} \cdot mol^{-1}$$

$$S_m°(Si(OH)_4(aq)) = \Delta_f S_m°(Si(OH)_4(aq)) + S_m°(Si(cr)) + 2 \cdot S_m°(O_2g) + 2 \cdot S_m°(H_2g)$$
$$= -(511.623 \pm 2.177) + (18.810 \pm 0.080) + 2 \cdot (205.152 \pm 0.005) + 2 \cdot (130.680 \pm 0.003)$$
$$= (178.851 \pm 2.178)\ J \cdot K^{-1} \cdot mol^{-1}$$

$$\Delta_f C_{p,m}°(Si(OH)_4(aq)) = \Delta_r C_{p,m}° + \Delta_f C_{p,m}°(Quartz) + 2 \cdot \Delta_f C_{p,m}°(H_2O(l))$$
$$= (42.0659 \pm 2.0) - (4.565 \pm 0.300) + 2 \cdot (31.826 \pm 0.080) = (101.153 \pm 2.024)\ J \cdot K^{-1} \cdot mol^{-1}$$

$$C_{p,m}°(Si(OH)_4(aq)) = \Delta_f C_{p,m}°(Si(OH)_4(aq)) + C_{p,m}°(Si(cr)) + 2 \cdot C_{p,m}°(O_2g) + 2 \cdot C_{p,m}°(H_2g)$$
$$= (101.153 \pm 2.024) + (19.789 \pm 0.030) + 2 \cdot (29.378 \pm 0.003) + 2 \cdot (28.836 \pm 0.002)$$
$$= (237.370 \pm 2.024)\ J \cdot K^{-1} \cdot mol^{-1}$$

Hence, the following values have been included in TDB 2020:

$\Delta_f G_m°(Si(OH)_4(aq)) = -(1'309.183 \pm 1.120)$ kJ · mol^{-1}

$\Delta_f H_m°(Si(OH)_4(aq)) = -(1'461.723 \pm 1.082)$ kJ · mol^{-1}

$S_m°(Si(OH)_4(aq)) = (178.851 \pm 2.178)$ J · K^{-1} · mol^{-1}

$C_{p,m}°(Si(OH)_4(aq)) = (237.370 \pm 2.024)$ J · K^{-1} · mol^{-1}

$SiO(OH)_3^-$ and $SiO_2(OH)_2^{2-}$

In ordinary groundwater the species $Si(OH)_4(aq)$ predominates. In alkaline waters a deprotonated species gains importance and at very high pH a second deprotonation step is observed. The thermodynamic data are taken from NEA auxiliary data (Grenthe et al. 1992):

$Si(OH)_4(aq) \rightleftharpoons SiO(OH)_3^- + H^+$

$\log_{10}\beta_1° = -9.81 \pm 0.02$

$\Delta_r H_m° = 25.6 \pm 2.0$ kJ · mol^{-1}

$Si(OH)_4(aq) \rightleftharpoons SiO_2(OH)_2^{2-} + 2\ H^+$

$\log_{10}\beta_2° = -23.14 \pm 0.09$

$\Delta_r H_m° = 75 \pm 15$ kJ · mol^{-1}

These values have been included in TDB 2020.

Note that in both cases the experimental temperature data are compatible with the van't Hoff equation, i.e. $\Delta_r C_{p,m}° = 0$ for 0 – 300 °C and 60 – 200 °C, respectively.

Both $\log_{10}\beta°$ values result from extrapolations to $I = 0$ of experimental data in NaCl media using SIT. From the slopes of these extrapolations Grenthe et al. (1992) obtained $\Delta\varepsilon = 0.04 \pm 0.03$ kg · mol^{-1} and 0.14 ± 0.07 kg · mol^{-1}, respectively. Assuming $\varepsilon(Si(OH)_4(aq), NaCl) = 0$, Grenthe et al. (1992) derived $\varepsilon(SiO(OH)_3^-, Na^+) = -0.08 \pm 0.03$ kg · mol^{-1} and $\varepsilon(SiO_2(OH)_2^{2-}, Na^+) = -0.10 \pm 0.07$ kg · mol^{-1} and commented the results as follows: "The first value is more negative than would be expected from comparison with other ion interaction coefficients for species of the same charge and similar size."

For the reaction

$SiO_2(am) + 2\ H_2O(l) \rightleftharpoons Si(OH)_4(aq)$

the solubility data of Zarubin & Nemkina (1990) were used to evaluate the SIT interaction coefficient of $Si(OH)_4(aq)$ according to the equation

$\log_{10}K_s - 2\ \log_{10}a_{H2O} = \log_{10}K_s° - \Delta\varepsilon \cdot I$ (m)

The values of $\log_{10}K_s$ (M) in 1 and 3 M NaCl were estimated from total dissolved silica measured at pH 8.5 (Zarubin & Nemkina 1990) assuming that about 10% of dissolved silica is $SiO(OH)_3^-$ in that pH range. The values given in Tab. 25-1 are numerically identical with $[Si(OH)_4(aq)]$ values calculated at pH < 7 by extrapolating a polynomial fit of experimental data in the range 8.3 < pH < 10.2 given by Zarubin & Nemkina (1990).

Tab. 25-1: Data for the reaction $SiO_2(am) + 2\ H_2O(l) \rightleftharpoons Si(OH)_4(aq)$ in NaCl media

I [M]	I_m [m]	$\log_{10}K_s$ [M]	± (est.)	$\log_{10}K_s$ [m]	$\log_{10}K_s$ (m) – 2 $\log_{10}a_{H2O}$	Reference
0	0	-2.714	0.044	-2.714	-2.714	Gunnarsson & Arnorsson (2000)
1	1.02	-2.88	0.10	-2.871	-2.841	Zarubin & Nemkina (1990)
3	3.20	-3.05	0.10	-3.022	-2.916	Zarubin & Nemkina (1990)

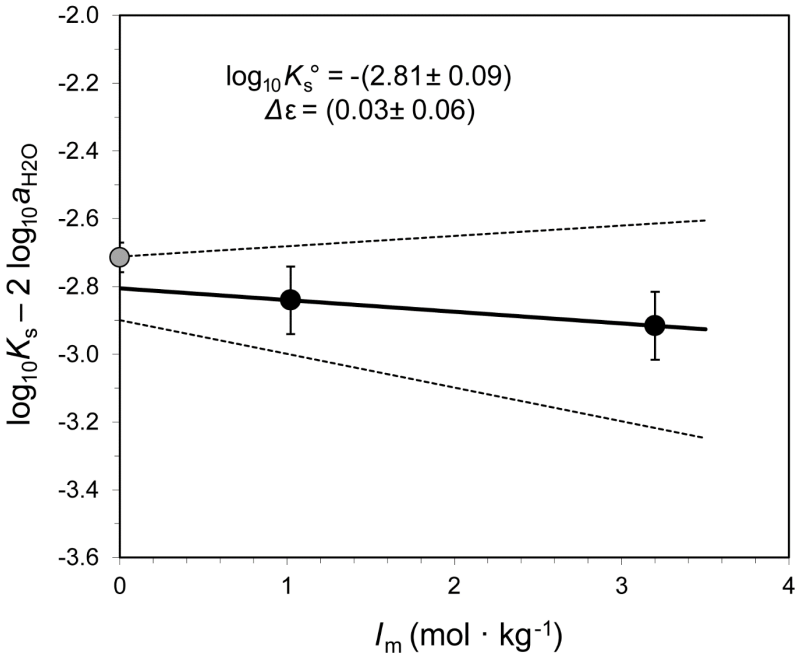

Fig. 25-3: Evaluation of the ion interaction coefficient of $Si(OH)_4(aq)$ in NaCl media

Using solubility data of amorphous silica of Zarubin & Nemkina (1990) (1 and 3 M NaCl). The value of Gunnarsson & Arnorsson (2000) at $I = 0$ is shown for comparison.

Using the data of Zarubin & Nemkina (1990) with assigned uncertainties of ±0.1 $\log_{10}$-units for an SIT analysis (Fig. 25-3), this review obtained

$$\log_{10}K_s^\circ\ (298.15\ K) = -(2.81 \pm 0.09)$$

$$\Delta\varepsilon = \varepsilon(Si(OH)_4(aq), NaCl) = 0.03 \pm 0.06\ kg \cdot mol^{-1}$$

The value $\log_{10}K_s^\circ$ (298.15 K) = -(2.81 ± 0.09) is, within its assigned uncertainty, compatible with $\log_{10}K_s^\circ$(Silica, am, 298.15 K) = -(2.714 ± 0.044) selected by this review (Fig. 25-3).

The value $\varepsilon(Si(OH)_4(aq), NaCl) = 0.03 \pm 0.06$ kg · mol^{-1} is, as expected, close to zero. In fact, considering its assigned uncertainty, statistically it cannot be distinguished from zero. Nevertheless, it is assumed that the same value can be applied in $NaClO_4$ media, and it has been used to re-evaluate the values for $SiO(OH)_3^-$ and $SiO_2(OH)_2^{2-}$ resulting in:

$$\varepsilon(Si(OH)_4(aq), NaClO_4) \approx \varepsilon(Si(OH)_4(aq), NaCl) = 0.03 \pm 0.06 \text{ kg} \cdot \text{mol}^{-1}$$

$$\varepsilon(SiO(OH)_3^-, Na^+) = -0.05 \pm 0.07 \text{ kg} \cdot \text{mol}^{-1}$$

$$\varepsilon(SiO_2(OH)_2^{2-}, Na^+) = -0.07 \pm 0.09 \text{ kg} \cdot \text{mol}^{-1}$$

These values have been included in TDB 2020.

$Si_4O_8(OH)_4^{4-}$

In the pH range above 10.5, and 10 millimolar and higher concentrations of dissolved silica, polymeric silicate species predominate.

In the first reliable potentiometric study of this system published more than half a century ago (Lagerström 1959) the results were interpreted in terms of dimeric and tetrameric silicate species, where $Si_4O_8(OH)_4^{4-}$ was the dominating species at pH > 11.

Stability constants for six polymeric species, i.e two dimers, two trimers, and two tetramers have been reported and accepted by NEA as auxiliary data (Grenthe et al. 1992). The NEA data selection is based on the seminal paper of Sjöberg et al. (1985) who did a combined potentiometric and ^{29}Si NMR study. Sjöberg et al. (1985) conclude that "within the concentration ranges studied, the main polysilicate complex is tetrameric." In the pH range 11.0 – 12.2 "the prevailing species are the tetramer and the monomer $SiO(OH)_3^-$."

Hence, the two equilibrium constants reported for the reaction

$$4\ Si(OH)_4(aq) \rightleftharpoons Si_4O_8(OH)_4^{4-} + 4\ H^+ + 4\ H_2O(l)$$

in 3 m (molal) $NaClO_4$, $\log_{10}\beta = -32.48$ (Lagerström 1959) and in 0.6 M NaCl, $\log_{10}\beta = -32.81$ (Sjöberg et al. 1985) were extrapolated to $I = 0$ using SIT with uncertainties of ±0.2 $\log_{10}$-units assigned in the present review (Fig. 25-4). Note that the resulting stability constant

$$\log_{10}\beta^\circ = -(36.28 \pm 0.16)$$

is the same as the one selected by Grenthe et al. (1992).

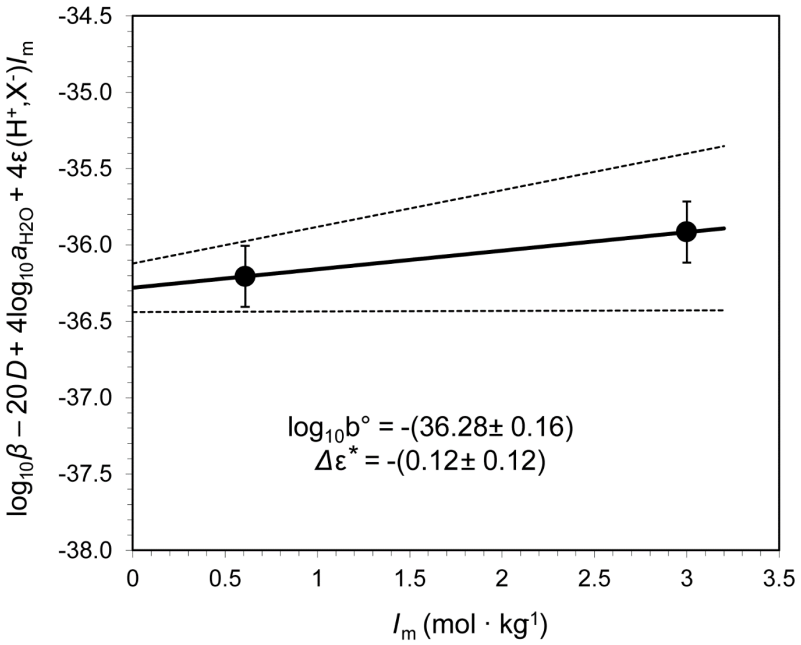

Fig. 25-4: Extrapolation to I = 0 of experimental data for the formation of $Si_4O_8(OH)_4^{4-}$ using SIT

The data are taken from Lagerström (1959) (3 m $NaClO_4$) and Sjöberg et al. (1985) (0.6 M NaCl).

From the slope $\Delta\varepsilon^* = \Delta\varepsilon + 4\ \varepsilon(H^+, X^-) = \varepsilon(Si_4O_8(OH)_4^{4-}, Na^+) - 4\ \varepsilon(Si(OH)_4(aq), NaCl) = -(0.12 \pm 0.12)$ kg · mol^{-1} the SIT interaction coefficient for the tetramer was obtained assuming that $\varepsilon(Si(OH)_4(aq), NaCl) = \varepsilon(Si(OH)_4(aq), NaClO_4) = 0.03 \pm 0.06$ kg · mol^{-1}:

$$\varepsilon(Si_4O_8(OH)_4^{4-}, Na^+) = 0.00 \pm 0.13 \text{ kg} \cdot \text{mol}^{-1}$$

These values have been included in TDB 2020.

Using a very simple model comprising only the monomeric species $Si(OH)_4(aq)$ and $SiO(OH)_3^-$ and the tetramer $Si_4O_8(OH)_4^{4-}$ with stability constants and SIT interaction coefficients derived in this review the solubility of SiO_2(am) in NaCl media (Zarubin & Nemkina 1990) is reproduced sufficiently well (Fig. 25-5). Note that a re-adjustment of the stability constant of the tetramer to $\log_{10}\beta^\circ = -37$ would result in an almost perfect fit of the data of Zarubin & Nemkina (1990), but this would lead to an inconsistency with the value selected by this review (Fig. 25-4).

Adding the other polymeric species selected by Grenthe et al. (1992) to the model with SIT interaction coefficients adjusted in analogy to the new evaluations discussed above does not significantly change the overall picture shown in Fig. 25-5. Depending on the choice of the estimated SIT interaction coefficients the measured silica solubilities are slightly to significantly overestimated. However, as already discussed by Sjöberg et al. (1985) all these other polymers were found to remain minor species in the entire range of experimental studies indicated in Fig. 25-5.

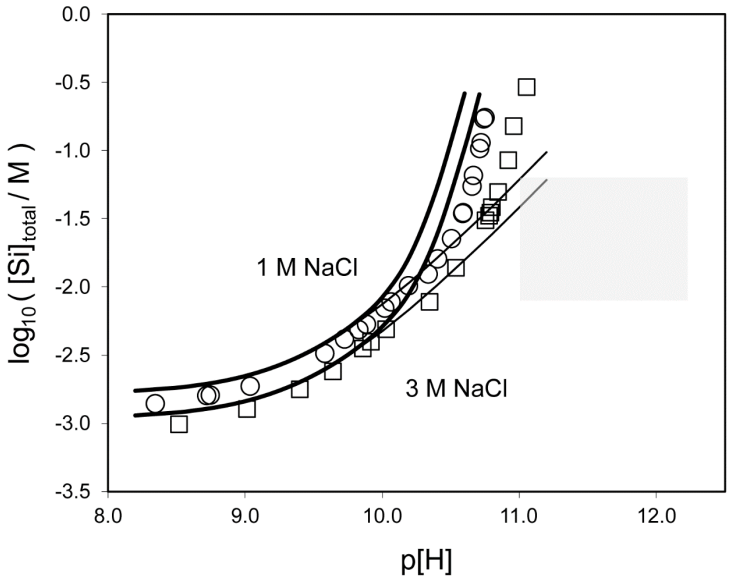

Fig. 25-5: Solubility of SiO_2(am) in NaCl media

Experimental data taken from Zarubin & Nemkina (1990), 1 M NaCl: circles, 3 M NaCl: squares. Thin solid lines: Calculated solubility using only the monomeric species $Si(OH)_4$(aq) and $SiO(OH)_3^-$ with stability constants and SIT parameters selected here. Thick solid lines: The tetrameric species $Si_4O_8(OH)_4^{4-}$ is added. White rectangle: Range of experimental study of Lagerström (1959). Grey rectangle: Range of experimental study of Sjöberg et al. (1985).

A more recent paper proposing an aqueous thermodynamic model for polymerised silica species (Felmy et al. 2001) includes nine polymeric silicate species, i.e. two dimers, two trimers, four tetramers and one hexamer. The reasoning for the selection of this set of species is based on new ^{29}Si NMR data, whereas the actual stability constants were fitted to the SiO_2(am) solubility data of Zarubin & Nemkina (1990) using the Pitzer formalism for ionic strength effects. A good fit is reported for the 3 M NaCl data, whereas the model calculations for 1 M NaCl deviate from experimental data at pH > 10.5, increasingly underestimating the measured solubilities with increasing pH.

The effect of the highly charged polymeric silica species on the speciation model strongly depends on the chosen ionic strength correction model and the estimated SIT or Pitzer parameters. On the other hand, dissolved silica concentrations in natural waters seldom exceed 0.1 mol even when contacted with highly basic solutions, because of the precipitation of calcium or other silicate-containing solid phases. Hence, the very simple model used in this review, including only one polymeric species, $Si_4O_8(OH)_4^{4-}$, besides the monomeric species $Si(OH)_4$(aq), $SiO(OH)_3^-$ and $SiO_2(OH)_2^{2-}$ seems to be sufficient for all practical purposes of environmental modelling.

However, this simple model may lead to spurios results if used for systems where the concentration of dissolved silica exceeds 0.5 mol · kg^{-1}.

25.4 Metal silicate compounds and complexes

25.4.1 Calcium and magnesium

25.4.1.1 Aqueous Ca and Mg silicates

The results of potentiometric titrations of $Si(OH)_4(aq)$ in the presence of Ca^{2+} and Mg^{2+} in 1 M $NaClO_4$ up to pH 9 are reported by Santschi & Schindler (1974). In order to avoid the formation of polymeric silicate species as well as the precipitation of amorphous silica, the total ligand concentration did not exceed $2.3 \cdot 10^{-3}$ M. In preliminary experiments it was found that the complexes formed are rather weak. Comparatively high concentrations of both the reacting metal ions and the inert salt were therefore required.

The results of this experimental study are not unambiguous in terms of the speciation model. Two limiting situations are discussed by Santschi & Schindler (1974). Based on chemical arguments, the most probable interpretation of the experimental data could be done in terms of two equilibria:

$$M^{2+} + SiO(OH)_3^- \rightleftharpoons MSiO(OH)_3^+ \quad \text{(a)}$$

$$M^{2+} + SiO_2(OH)_2^{2-} \rightleftharpoons MSiO_2(OH)_2(aq) \quad \text{(b)}$$

Values for the stability constants are extrapolated from 1 M $NaClO_4$ to zero ionic strength by the SIT formalism using $\varepsilon(Ca^{2+}, ClO_4^-) = 0.27 \pm 0.03$ kg · mol^{-1} and $\varepsilon(Mg^{2+}, ClO_4^-) = 0.33 \pm 0.03$ kg · mol^{-1} (Lemire et al. 2013), and $\varepsilon(SiO(OH)_3^-, Na^+) = -0.05 \pm 0.07$ kg · mol^{-1} and $\varepsilon(SiO_2(OH)_2^{2-}, Na^+) = -0.07 \pm 0.09$ kg · mol^{-1} derived in this review, and the estimates for $\varepsilon(MSiO(OH)_3^+, ClO_4^-) = 0.2 \pm 0.1$ kg · mol^{-1} and $\varepsilon(MSiO_2(OH)_2(aq), NaClO_4) = 0.0 \pm 0.1$ kg · mol^{-1}:

Ca $\log_{10}K°$(eq. a) = 1.17 ± 0.13 $\log_{10}K°$(eq. b) = 4.50 ± 0.15

Mg $\log_{10}K°$(eq. a) = 1.36 ± 0.14 $\log_{10}K°$(eq. b) = 5.52 ± 0.16

Although the stoichiometry of these complexes and their stability constants have not been explored by other studies we decided to include them in our data base. If these complexes are found to be of crucial importance in some systems, additional experimental studies are recommended.

25.4.1.2 Solid Ca and Mg silicates

Thermodynamic data for the Mg silicate solids chrysotile, sepiolite, and kerolite have been selected by Nordstrom et al. (1990). We did not explore the thermodynamics of these sheet silicates and decided not to include them in the data base.

Calcium silicate hydrates (CSH) and calcium aluminium silicate hydrates (CASH) are important solid phases in cementitious systems. However, these phases form solid solutions (Kulik & Kersten 2001) and their appropriate thermodynamic representation is the subject of the CEMDATA project (Lothenbach et al. 2008, Lothenbach et al. 2019; www.empa.ch/cemdata/).

25.4.2 Nickel

25.4.2.1 Aqueous nickel silicates

The complexation behaviour of Ni^{2+} with $Si(OH)_4(aq)$ has been studied as a function of ionic strength from 0.20 to 1.00 M ($NaClO_4$) at pH 4.55 and 25 °C by a solvent extraction technique (Pathak & Choppin 2006a). The authors concluded that Ni^{2+} forms a 1:1 complex, $NiSiO(OH)_3^+$, as the predominant species and interpreted their data in terms of the equilibrium

$$Ni^{2+} + SiO(OH)_3^- \rightleftharpoons NiSiO(OH)_3^+$$

The equilibrium constants $\log_{10}\beta$ derived at different ionic strengths have been fitted by Pathak & Choppin (2006a) with an extended Debye-Hückel expression like the SIT formalism and the authors obtained a value of $\log_{10}\beta^\circ = 6.34 \pm 0.03$ at zero ionic strength.

An analogous complexation study of Co^{2+} with $Si(OH)_4(aq)$ using the same method under the same conditions (Pathak & Choppin 2006b) resulted in $\log_{10}\beta^\circ = 5.61 \pm 0.03$ for $CoSiO(OH)_3^+$.

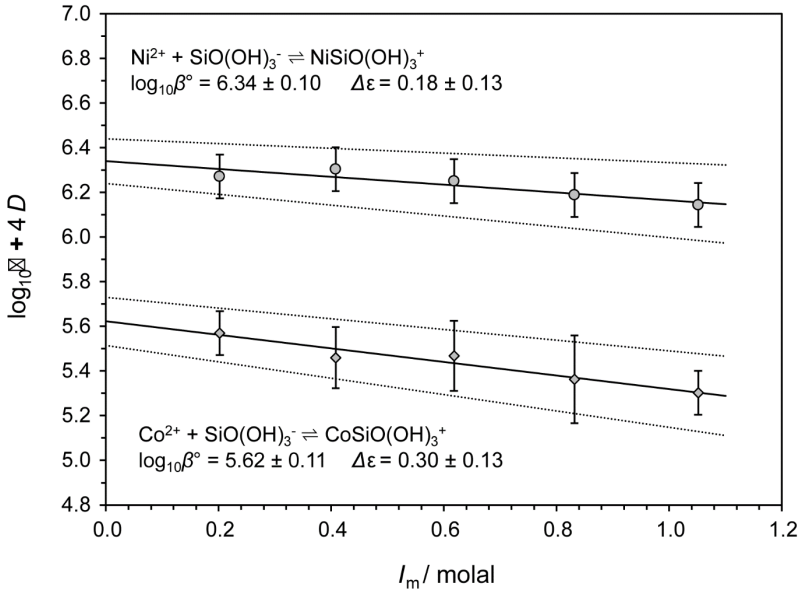

Fig. 25-6: Extrapolation to $I = 0$ of experimental data for the formation of $NiSiO(OH)_3^+$ and $CoSiO(OH)_3^+$ using SIT

The data are taken from Pathak & Choppin (2006a, 2006b).

Re-analyses of the experimental data published by Pathak & Choppin (2006a, 2006b) in the present review using the SIT formalism (Fig. 25-6) resulted in:

$\log_{10}\beta^\circ = 6.34 \pm 0.10$ and $\Delta\varepsilon = 0.18 \pm 0.13$ kg · mol^{-1} for $NiSiO(OH)_3^+$

$\log_{10}\beta^\circ = 5.62 \pm 0.11$ and $\Delta\varepsilon = 0.30 \pm 0.13$ kg · mol^{-1} for $CoSiO(OH)_3^+$

Using $\varepsilon(Ni^{2+}, ClO_4^-) = 0.37 \pm 0.03$ kg · mol^{-1} and $\varepsilon(Co^{2+}, ClO_4^-) = 0.34 \pm 0.03$ kg · mol^{-1} (Lemire et al. 2013), and $\varepsilon(SiO(OH)_3^-, Na^+) = -0.05 \pm 0.07$ kg · mol^{-1} derived in this review we calculate

$$\varepsilon(NiSiO(OH)_3^+, ClO_4^-) = 0.50 \pm 0.16 \text{ kg} \cdot \text{mol}^{-1}$$

$$\varepsilon(CoSiO(OH)_3^+, ClO_4^-) = 0.59 \pm 0.15 \text{ kg} \cdot \text{mol}^{-1}$$

However, the equilibrium constants reported by Pathak & Choppin (2006a, 2006b) might be substantially overestimated due to the presence of polymeric silica species in the experiments, the same effect as discussed for Eu(III) and Cm(III) silicate complexation measured by the same authors using the same experimental set-up (Pathak & Choppin 2006c), see Section 25.4.5. Hence, the values derived by this review from the data reported by Pathak & Choppin (2006a)

$$Ni^{2+} + SiO(OH)_3^- \rightleftharpoons NiSiO(OH)_3^+$$

$$log_{10}\beta^\circ \approx 6.3$$

$$\varepsilon(NiSiO(OH)_3^+, ClO_4^-) = 0.50 \pm 0.16 \text{ kg} \cdot \text{mol}^{-1}$$

have been included in TDB 2020 as supplemental data.

25.4.2.2 Solid nickel silicates

Thermodynamic data for Ni_2SiO_4(cr) have been selected by Gamsjäger et al. (2005). The thermodynamic data have been derived from heat capacity measurements in the temperature range from 270 to 1'570 K and from solution calorimetry in a molten oxide solvent at 965 K. There is no indication that Ni_2SiO_4(cr) forms at ambient conditions and consequently, no solution study in aqueous media is known.

Liebenbergite (Ni_2SiO_4) is an endmember of a complex solid-solution system known as the olivine group of minerals of the general formula X_2SiO_4, where X is a divalent metal cation (Mg, Fe, Mn, Ni, Ca and Co). The pure nickel olivine does not occur naturally; only liebenbergite of an approximate formula $Ni_{1.5}Mg_{0.5}SiO_4$ has been reported (Gamsjäger et al. 2005).

We conclude that liebenbergite is of no importance for thermodynamic models at ambient conditions and thus, the thermodynamic data for Ni_2SiO_4(cr) are not included in our data base.

25.4.3 Aluminium

25.4.3.1 Aqueous aluminium silicates

Several studies have been published reporting experimental data on Al silicate complexation.

Browne & Driscoll (1992) applied a fluorescent probe technique to study trace level concentrations of Al(III) (0.3-10 μM) with $[Si(OH)_4]_{tot}$ varying between 0.10 and 0.27 mM at pH 4.0 – 5.5 and 0.01 M ionic strength. At pH 4 – 5 the data were interpreted in terms of the following mononuclear reaction:

$Al^{3+} + Si(OH)_4(aq) \rightleftharpoons AlSiO(OH)_3^{2+} + H^+$

They reported $\log_{10}K° = -(1.07 \pm 0.06)$ at infinite dilution. At pH 5.5 the authors inferred in addition two dinuclear Al-Si stoichiometries from the experimental data.

Farmer & Lumsdon (1994) measured the shift in $\log[H^+]$ in Al(III) solutions with and without added silicic acid in 0.1 M $NaClO_4$. In this study, more concentrated solutions were used ($[Al]_{tot}$ = 0.5 – 2.0 mM and $[Si(OH)_4]_{tot}$ =1.33 mM) and the pH range was quite narrow (pH 3.75 – 4.11). They reported $\log_{10}K° = -(2.50 \pm 0.05)$ at infinite dilution, a value more than one magnitude lower than the one published by Browne & Driscoll (1992).

Pokrovski et al. (1996) studied the formation of $AlSiO(OH)_3^{2+}$ by measuring the pH variation of a 0.005 M silicic acid solution as a slightly acidic Al^{3+} solution was added. This allowed a wider concentration range in Al(III) to be studied (3 points with $[Al]_{tot}$ = 0.023, 0.0100 and 0.0160 M). Again a limited pH range was studied (pH = 3.710 – 3.448) in 0.1 M KCl medium. The reported stability constant at $I = 0$ is $\log_{10}K° = -(2.38 \pm 0.10)$.

Spadini et al. (2005) studied the Al – Si complexation by potentiometric titrations in 0.6 M NaCl using a hydrogen electrode with OH^- ions being generated coulometrically. The total concentrations were varied within the limits $0.3 < [Si]_{tot} < 2.5$ mM, $0.5 < [Al]_{tot} < 2.6$ mM and $2 \leq -\log[H^+] \leq 4.2$. A complex formation constant $\log_{10}K = -(2.75 \pm 0.1)$ was reported for $I = 0.6$ M NaCl and 25.0 °C.

Using $\varepsilon(Al^{3+}, Cl^-) = 0.33 \pm 0.02$ kg · mol^{-1} and $\varepsilon(H^+, Cl^-) = 0.12 \pm 0.01$ kg · mol^{-1} (Lemire et al. 2013), $\varepsilon(Si(OH)_4(aq), NaCl) = 0.03 \pm 0.06$ kg · mol^{-1} derived in this review, and the estimate $\varepsilon(AlSiO(OH)_3^{2+}, Cl^-) = 0.15 \pm 0.10$ kg · mol^{-1} this review extrapolated the value reported by Spadini et al. (2005) to $\log_{10}K° = -(2.07 \pm 0.12)$.

The data of Farmer & Lumsdon (1994) $\log_{10}K° = -(2.50 \pm 0.10)$, Pokrovski et al. (1996) $\log_{10}K° = -(2.38 \pm 0.20)$ and Spadini et al. (2005) $\log_{10}K° = -(2.07 \pm 0.21)$ seem to be consistent while the data of Browne & Driscoll (1992) $\log_{10}K° = -(1.07 \pm 0.06)$ is far away of all the others and hence, has not been considered in the final analysis. The unweighted average of the data of Farmer & Lumsdon (1994), Pokrovski et al. (1996) and Spadini et al. (2005) is

$Al^{3+} + Si(OH)_4(aq) \rightleftharpoons AlSiO(OH)_3^{2+} + H^+$

$\log_{10}K° = -(2.32 \pm 0.22)$

This value has been included in TDB 2020.

Using $\log_{10}\beta_1° = -9.81 \pm 0.02$ selected by this review for the equilibrium $Si(OH)_4(aq) \rightleftharpoons SiO(OH)_3^- + H^+$ this review calculates from the above result

$Al^{3+} + SiO(OH)_3^- \rightleftharpoons AlSiO(OH)_3^{2+}$

$\log_{10}\beta° = 7.49 \pm 0.22$

Pokrovski et al. (1996) studied in addition the temperature dependence of the equilibrium Al^{3+} + $Si(OH)_4(aq) \rightleftharpoons AlSiO(OH)_3^{2+} + H^+$ at 25, 90 and 150 °C and found a linear dependence of $\log_{10}K$ on reciprocal temperature, $\log_{10}K$ = -3473 / T + 9.25, which results in $\Delta_r H_m° = 66.6 \pm 3.0$ kJ · mol^{-1}.

This value was later confirmed by measurements at 300 °C (Salvi et al. 1998).

Hence, this review accepted the value reported by Pokrovski et al. (1996).

$$Al^{3+} + Si(OH)_4(aq) \rightleftharpoons AlSiO(OH)_3^{2+} + H^+$$

$$\Delta_r H_m°(298.15\ K) = 66.6 \pm 3.0\ kJ \cdot mol^{-1}$$

$$\Delta_r C_{p,m}°(298.15\ K) = 0\ J \cdot K^{-1} \cdot mol^{-1}$$

These values have been included in TDB 2020.

All the studies discussed so far have been carried out in the acidic pH range 3.5 < pH < 5.5.

The first study of aluminium silicate complexation by potentiometric titrations in the alkaline region, 9 < pH < 13, at 25 and 75 °C was mentioned by Pokrovski et al. (1998). In this extended abstract the authors claimed to be able to interpret their (not yet published) experimental data in terms of the equilibrium

$$Al(OH)_4^- + Si(OH)_4(aq) \rightleftharpoons Al(OH)_3SiO(OH)_3^- + H_2O(l)$$

$$\log_{10}K° = 3.64 \pm 0.20$$

The same group also claimed to have found this complex to be the dominating aqueous aluminium-silicate species in the neutral to basic pH region at 300 °C (Salvi et al. 1998).

This complex was included in TDB 01/01 (Hummel et al. 2002) as supplemental datum.

To the best of our knowledge, the potentiometric data and their interpretation mentioned in the extended abstract (Pokrovski et al. 1998) have never been published as a full paper.

However, shortly after the finalisation of TDB 01/01 (Hummel et al. 2002) the same group published a Raman spectroscopic study of aluminium-silicate complexes at 20 °C in basic solutions, 12.4 < pH < 14.3 (Gout et al. 2000).

The measurements in "ultra basic solutions" at pH about 14 were interpreted by Gout et al. (2000) in terms of the equilibrium

$$Al(OH)_4^- + SiO_2(OH)_2^{2-} \rightleftharpoons AlSiO_3(OH)_4^{3-} + H_2O(l)$$

The value of the apparent equilibrium constant for this reaction (for I = 1.2 M) was calculated by the authors as K = 3.4 ± 0.2.

Using $\varepsilon(SiO_2(OH)_2^{2-}, Na^+) = -0.07 \pm 0.09$ kg · mol^{-1}, derived by this review (see Section 25.3.2), and the estimates $\varepsilon(Al(OH)_4^-, Na^+) = -(0.05 \pm 0.10)$ kg · mol^{-1} and $\varepsilon(AlSiO_3(OH)_4^{3-}, Na^+) = -(0.15 \pm 0.10)$ kg · mol^{-1} the value $K = 3.4 \pm 0.2$ has been extrapolated to zero ionic strength as

$$log_{10}K = -0.4 \pm 0.2$$

This value has been included in TDB 2020 as supplemental datum.

In their section "basic pH (≈ 12.5)" Gout et al. (2000) wrote that "calculations using the equilibrium constant of the reaction derived above imply that the complex $SiAlO_3(OH)_4^{3-}$ is minor in these solutions and, therefore, cannot account for the observed amounts of complexes Al and Si. Thus, the important quantities of complexed Al and Si at pH 12.5 are due to the formation of other complexes, between $SiO(OH)_3^-$ and $SiO_2(OH)_2^{2-}$ and $Al(OH)_4^-$. However, it was impossible to derive the stoichiometry and charge of these complexes from our measurements because the amount of complexed and free Al and Si do not show any regular dependence on component concentrations. This strongly suggests the formation of several, likely polymerized, Al – Si species. This conclusion is also in agreement with our potentiometric and NMR measurements which demonstrated the existence of different polynuclear Al – Si complexes at $m_{(Al,Si)} > 0.006$ m (Pokrovski et al. 1998). Complementary studies are necessary to determine the nature of these complexes and their stabilities."

Although Gout et al. (2000) never mentioned it explicitly, in their statement cited above they implicitly retracted the complex $Al(OH)_3SiO(OH)_3^-$ and its associated stability constant $\log_{10}K° = 3.64 \pm 0.20$ published in their extended abstract (Pokrovski et al. 1998). Consequently, we removed this complex and its stability constant from our data base.

We are left with some sobering statements concerning Al – Si complexation: The complex $AlSiO(OH)_3^{2+}$ is fairly well established in acidic solutions, but as it predominates at pH < 5 it is of little importance for groundwater modelling. The complex $SiAlO_3(OH)_4^{3-}$ was identified in "ultra basic solutions" at pH about 14; it may hardly be of any importance in environmental modelling. In neutral to basic solutions there is qualitative evidence of polynuclear Al – Si complexes but no quantitative data are available.

25.4.3.2 Solid aluminium silicates: Solubility data for clay minerals

Friedrich Lippmann discussed in a seminal paper (Lippmann 1982) the thermodynamic status of clay minerals. He started with the observations that (1) illites, montmorillonites and related interstratifications show solid solution to an extent which is unusual at ordinary temperature, and (2) that they do not grow into coarser crystals through dissolution-precipitation cycles (Ostwald ripening). Solid solution systems in petrology generally are characterised by an upper critical point (UCP) in temperature. Above the UCP total miscibility is observed, while below the UCP a miscibility gap opens up increasing toward room temperature. For the wide range of solid solutions of illites and smectites to represent thermodynamically stable phases, one might consider a solubility diagram characterized by a lower critical point (LCP) as known for binary systems of certain organic compounds with water, e.g. triethylamine-water (Fig. 25-11, left). For a LCP to exist, chemical thermodynamics requires that the mixing be exothermic; but in all solid solutions for which the heat of mixing is known, the sign is endothermic. The crucial point for determining the heat of mixing of clay minerals is the knowledge of their heat of hydration. However, experimental heat of hydration values always contains the heat evolved by water adsorption on the external surface of the nano-crystals, and models based on assumptions are

needed to separate the different effects. Although hydration explains why expandable minerals form at all, hydration appears not to be sufficient to render the mixing outright exothermic and to lead to a distinct increase of equilibrium miscibility toward low temperature. Lippmann (1982) concluded that virtually all clay minerals are more or less metastable or even completely unstable. From the fine grain size, he concluded that they precipitate at considerable super-saturation. Then they persist through geological times but never reach stable or metastable thermodynamic equilibrium.

Essene & Peacor (1995) criticised the use of clay minerals as thermometers (e.g., illite and chlorite crystallinity, chlorite thermometry based on correlations between natural chlorite compositions with temperature). They supported the conclusions by Lippmann (1982) and noted that TEM studies of pelitic rocks commonly reveal the presence of heterogeneous detrital clay minerals that coexist with diagenetic clay minerals. Such mineral associations violate the phase rule and equilibrium would require phase homogeneity. They further argued that the ubiquitous presence of local composition variation, stacking disorder and other features observed by TEM are inconsistent with the requirements of homogeneity. In addition, they remarked that the prograde evolution of clay minerals from diagenesis to low grade metamorphism is characterised by increasing homogeneity. This suggests that homogenization compatible with equilibrium is kinetically hindered at low temperatures.

25.4.3.2.1 Solubility of kaolinite

In the case of kaolinite, equilibrium solubility data have been published (Kittrick 1970, May et al. 1986). As is obvious from the experimental data by May et al. (1986) shown in Fig. 25-7, equilibrium had been attained both from under- and oversaturation. In addition to solubility data, kinetic data for dissolution and precipitation are available, e.g., Marty et al. (2015) or http://www.thermochimie-tdb.com/pages/kinetic_models.php. Last but not least, calorimetric data provide evidence that kaolinite is the stable phase and the polymorph dickite is metastable (Fialips et al. 2003). Hence, stable chemical equilibrium of kaolinite in aqueous solutions is well established.

Nordstrom et al. (1990) selected thermodynamic data for kaolinite, $Al_2Si_2O_5(OH)_4$(cr),

$$Al_2Si_2O_5(OH)_4(cr) + 6\ H^+ \rightleftharpoons 2\ Al^{3+} + 2\ Si(OH)_4(aq) + H_2O(l)$$

$$\log_{10}{}^{*}K_{s,0}^{\circ}\ (\text{Kaolinite, cr, 298.15 K}) = 7.435$$

$$\Delta_r H_m^{\circ}(\text{Kaolinite, cr, 298.15 K}) = -35.3\ \text{kcal} \cdot \text{mol}^{-1} = -147.7\ \text{kJ} \cdot \text{mol}^{-1}$$

reporting Robie et al. (1979) as reference for these data.

Robie et al. (1979) actually give $\Delta_f G_m^{\circ} = -3799.364 \pm 4.017\ \text{kJ} \cdot \text{mol}^{-1}$ and $\Delta_f H_m^{\circ} = -4120.114 \pm 3.975\ \text{kJ} \cdot \text{mol}^{-1}$ for $Al_2Si_2O_5(OH)_4$(cr). Using auxiliary data given by Robie et al. (1979) this review calculated $\log_{10}{}^{*}K_{s,0}^{\circ}$ (Kaolinite, cr, 298.15 K) = 5.707 ± 0.80 and $\Delta_r H_m^{\circ}$(Kaolinite, cr, 298.15 K) = -149.5 ± 5.9 kJ · mol^{-1}.

While $\Delta_r H_m^{\circ}$(Kaolinite, cr, 298.15 K) selected by Nordstrom et al. (1990) might originate from Robie et al. (1979), calculated using slightly different auxiliary data, $\log_{10}{}^{*}K_{s,0}^{\circ}$ (Kaolinite, cr, 298.15 K) selected by Nordstrom et al. (1990) certainly has been taken from a different source.

Actually May et al. (1986) report from their solubility study (Fig. 25-7) an equilibrium constant ${}^{*}K_{s,0}°$ (Kaolinite, cr, 298.15 K) = (2.72 ± 0.35) · 10^{7} which gives $\log_{10}{}^{*}K_{s,0}°$ (Kaolinite, cr, 298.15 K) = 7.435 ± 0.057. Hence, Nordstrom et al. (1990) actually selected the value reported by May et al. (1986). This review agrees with this selection and includes the following value in TDB 2020:

$$\log_{10}{}^{*}K_{s,0}° \text{ (Kaolinite, cr, 298.15 K)} = 7.44 \pm 0.06$$

Fialips et al. (2001) synthesized six kaolinite samples under different conditions of temperature, pressure and pH from two different starting materials. The enthalpy of formation of these kaolinites at 25 °C was investigated by drop solution calorimetry into molten lead borate at 700 °C. All data were corrected for impurities. Fialips et al. (2001) found that whatever the synthesis conditions and the kaolinite properties, the standard enthalpy of formation values from the elements at 25 °C are constant: $\Delta_f H_m° = -4'115.3 \pm 4.1$ kJ · mol^{-1}.

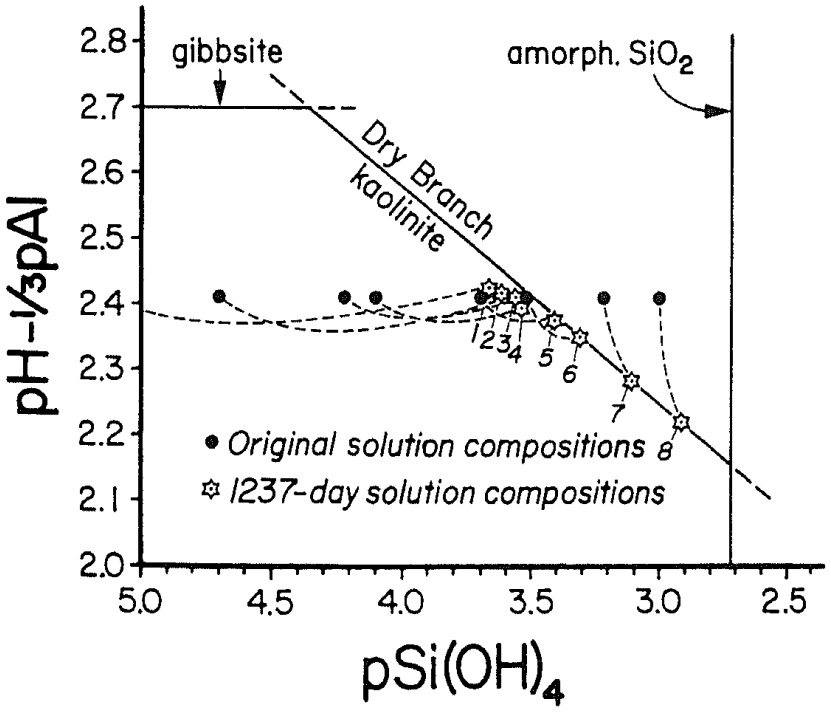

Fig. 25-7: Approach to equilibrium solubility for 5% suspensions of Dry Branch kaolinite, from over- and undersaturation

Dashed lines connecting points of initial and final solution composition show general compositional trends and are curved in some instances to avoid unintended intersection with unrelated points. Undersaturated conditions are at the left of the kaolinite saturation line, oversaturated conditions at the right. Taken from May et al. (1986).

Using $\Delta_f H_m°$ = -1461.723 ± 1.082 kJ · mol^{-1} for Si(OH)$_4$(aq) and $\Delta_f H_m°$ = -539.4 ± 2.7 kJ · mol^{-1} for Al^{3+}, both selected by this review, and the CODATA value $\Delta_f H_m°$ = -285.83 ± 0.04 kJ · mol^{-1} for H_2O(l) (Cox et al. 1989) this review calculates

$$\Delta_r H_m°(\text{Kaolinite, cr, 298.15 K}) = -172.8 \pm 5.0 \text{ kJ} \cdot \text{mol}^{-1}$$

This value is included in TDB 2020.

25.4.3.2.2 Solubility of illite

Perhaps motivated by the initial success of the kaolinite precipitation study (Kittrick 1970) Kittrick and Rosenberg of the Washington State University, Pullman, Washington, ran a long-term project that they later termed "The Illite Project" (e.g. Kittrick 1984, Sass et al. 1987, Aja et al. 1991b, Yates & Rosenberg 1996). In all these equilibrium studies natural illites were used. No changes in solid phases were detected by X-ray powder diffraction in samples before and after the long-term experiments. Hence, interpretation of the experiments relied on aqueous chemistry only. In all theses and publications related to the "illite project" the authors tried to fit phase boundaries to their specific data. However, synopses of all data measured at a certain temperature (Figs. 25-8 – 25-10) are largely featureless. Hence, the tremendous efforts of the "illite project" do not give any evidence of (meta)stable chemical equilibria in aqueous solutions.

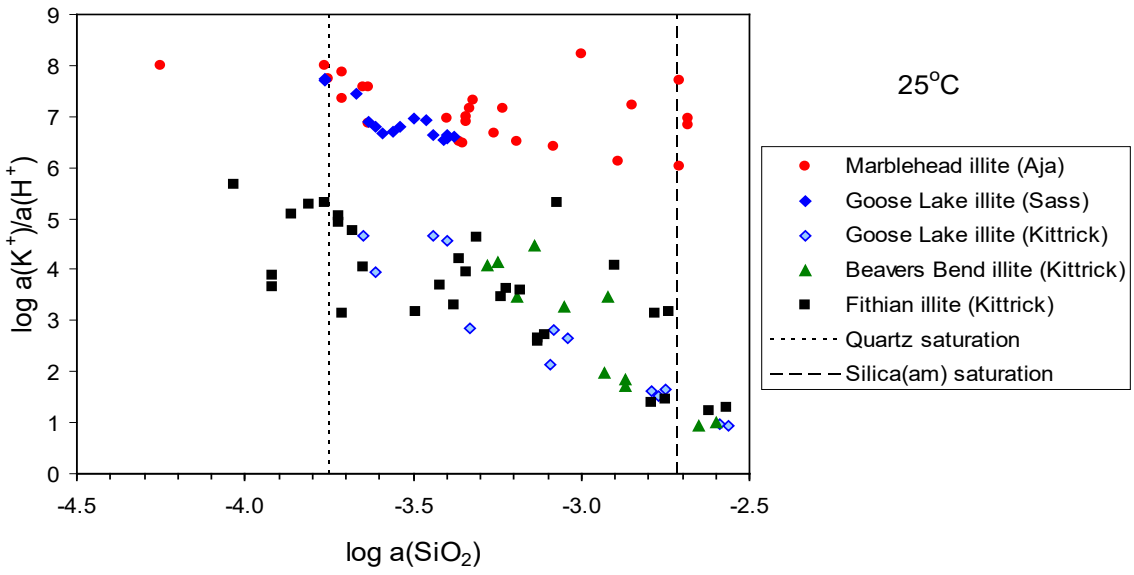

Fig. 25-8: Synopsis of experimental data for illite at 25 °C

Data from to Tab. A-1 in Aja et al. (1991b), Tab. in Appendix A in Sass et al. (1987), and Tab. 1 in Kittrick (1984). The symbol "a( )" denotes the activity of the species in brackets.

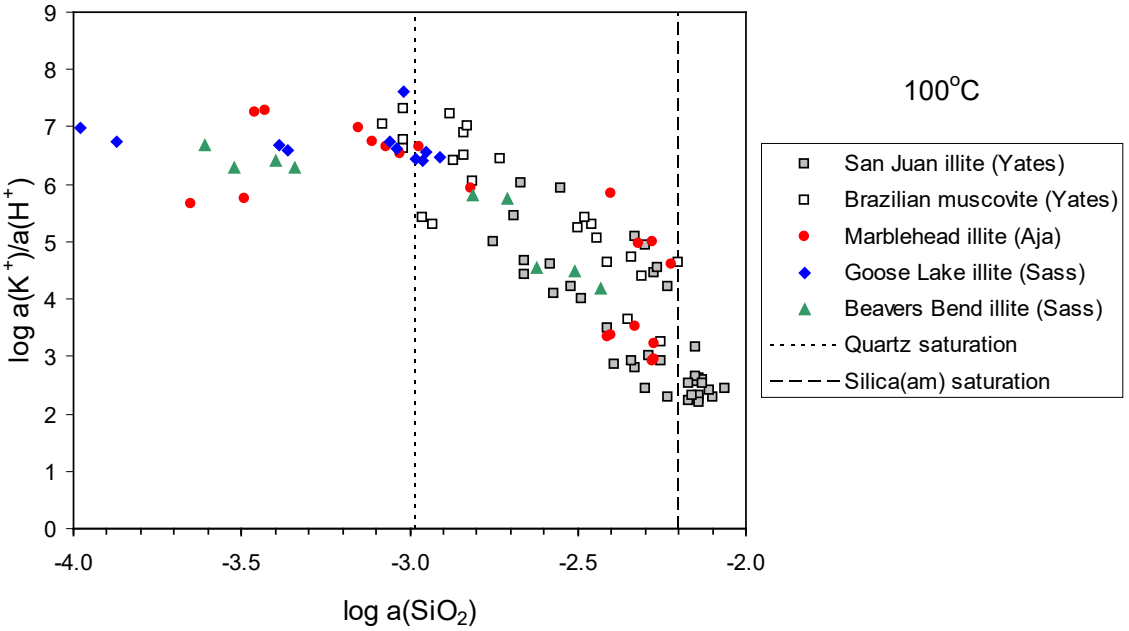

Fig. 25-9: Synopsis of experimental data for illite at 100 °C

Data from Tab. B1 in Yates & Rosenberg (1996), Tab. A-1 in Aja et al. (1991b), and Tab. in Appendix A (90 °C) in Sass et al. (1987). The symbol "a( )" denotes the activity of the species in brackets.

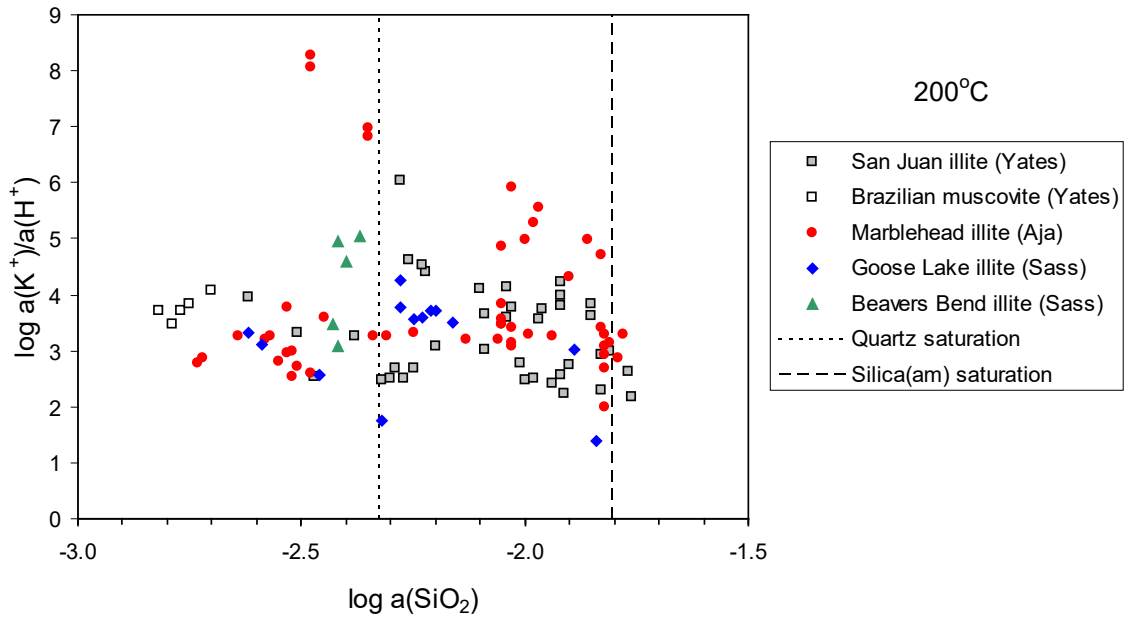

Fig. 25-10: Synopsis of experimental data for illite at 200 °C

Data from to Tab. B1 in Yates & Rosenberg (1996), Tab. A-1 in Aja et al. (1991b), and Tab. in Appendix A in Sass et al. (1987). The symbol "a( )" denotes the activity of the species in brackets.

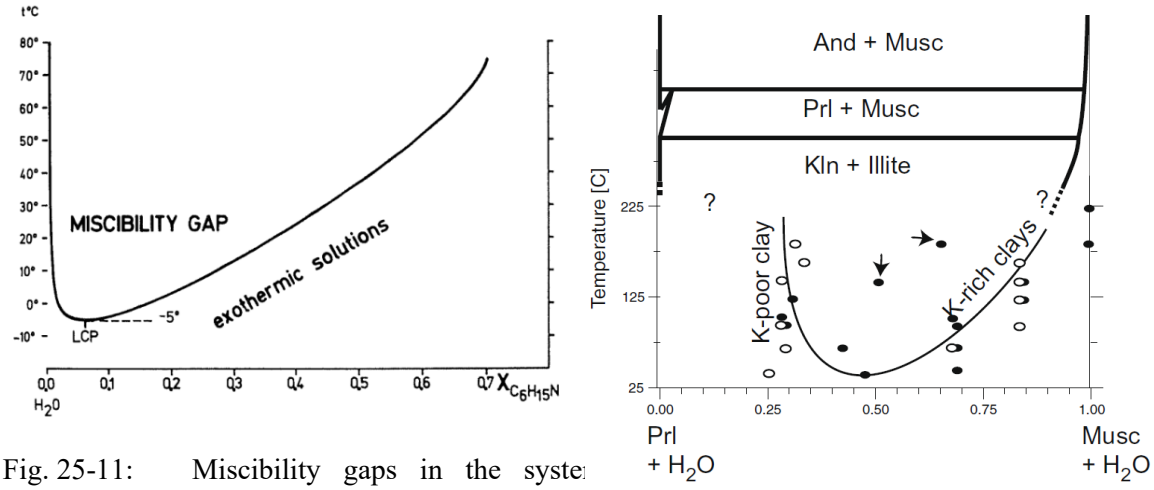

Fig. 25-11: Miscibility gaps in the syste K_2O-Al_2O_3-SiO_2-H_2O

Left: The system triethylamine–water showing a miscibility gap characterised by a lower critical point (LCP). In a system of this type, the mixing process is exothermic. Taken from Lippmann (1982). Right: Phase relations in the system K_2O–Al_2O_3–SiO_2–H_2O proposed at high temperature by Loucks (1991) (thick lines, no quantitative scale) and interpreted at low temperature (thin line) from the composition of clay (circles) inferred from the experiments of Rosenberg et al. (1990) and Aja et al. (1991a) (compilation from Aja et al. 1991a). The arrows indicate the composition of possible illite/smectite phases. Taken from Vidal & Dubacq (2009).

In a more recent modelling effort Vidal & Dubacq (2009) re-invented Lippmann's hypothetic LCP phase diagram (Fig. 25-11, left) based on (selected?) experimental data from the "illite project" (Fig. 25-11, right). These seem to be the only experimental data they found to support their various calculated LCP phase diagrams (Fig. 25-12). This is shaky ground.

25.4.3.2.3 Solubility of smectites

There are only a few publications known to us that have dealt with the experimental determination of the solubility of smectite minerals, all of them were carried out at room temperature.

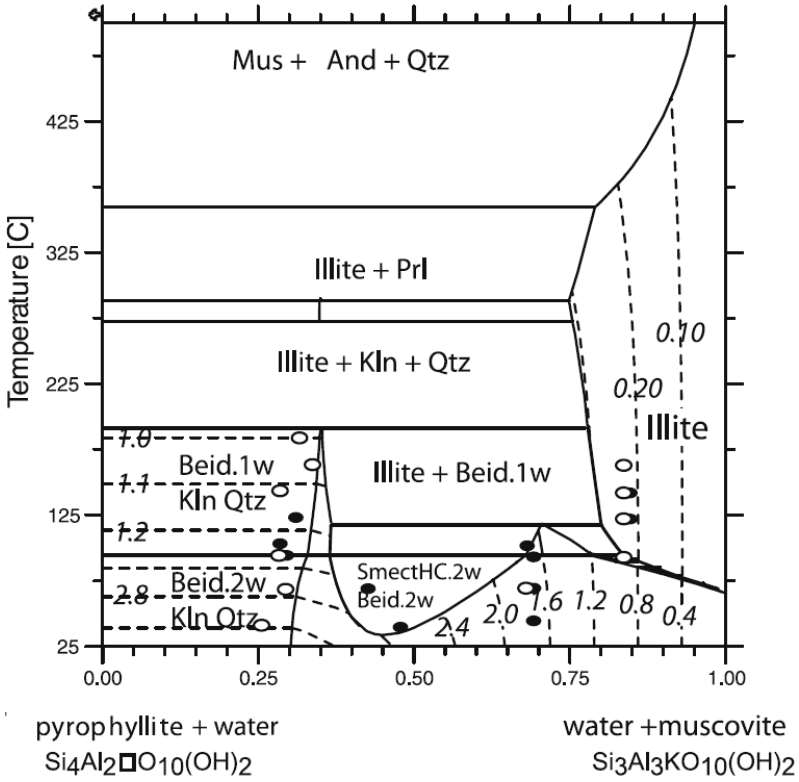

Fig. 25-12: Composition-temperature phase diagram calculated along the pyrophyllite–muscovite binary

The continuous lines show the limits of the stability fields, and the dashed lines show the interlayer water content (the numbers of moles H_2O per $O_{10}(OH)_2$ are in italics). High-charge smectite (SmectHc), andalusite (And), beidellite (Beid), kaolinite (Kln), muscovite (Mus), pyrophyllite (Prl), quartz (Qtz). The circles show the composition of clay inferred from the experiments of Aja (1991) and Aja et al. (1991a) (see Fig. 25-11). Taken from Vidal & Dubacq (2009).

In a study concerned with the solubilities of high-alumina and clay minerals, Reesman & Keller (1968) also investigated the solubilities of Cheto and Clay Spur montmorillonites (see Tab. 25-2 for their compositions). Clay suspensions were shaken in distilled water from 3 – 1'000 days. The authors argued that their experiments had reached equilibrium since they observed very high initial solubilities which declined for a period of time, but declined too rapidly, according to the authors, to have dissolved all of the clay particles that were structurally disordered during the grinding process. They interpreted the rapid decline in solubility as caused "by restoration, or rehealing", of disrupted crystal edges and faces, and further interpret[ed] this effect to mean that saturation-equilibrium had been reached between clay crystals and liquid". In the case of their montmorillonites, Reesman & Keller (1968) remarked that "the montmorillonites used in this

study seem to be rather unstable with respect to kaolinite and quartz," and that "apparent instability of these montmorillonites may result from inferior analytical values because of incomplete removal of ultra-fine colloidal material from solution".

Kittrick (1971a) determined the solubilities of Belle Fourche and Clay Spur montmorillonites and in a later study (Kittrick 1971b) the solubility of Panther Creek (Aberdeen) montmorillonite (see Tab 25.2 for the compositions of these montmorillonites). The experiments were carried out at pH < 3.48. It was later shown by Churchman & Jackson (1976) and May et al. (1986), see below, that montmorillonites do not reach an equilibrium state with such acid solutions.

Huang & Keller (1973) performed dissolution experiments with Cheto and Clay Spur montmorillonites (see Tab. 25-2 for their compositions) in distilled water and reported that solution compositions approached nearly constants values after 102 days, deriving "apparent" solubilities from the data.

Churchman & Jackson (1976) showed that in dissolution experiments with three montmorillonites (see Tab. 25-2 for their compositions) carried out for up to 432 days in acid aqueous solutions over the pH range of 1.5 – 4.2 (these conditions were chosen to ensure that Al^{3+} is not hydrolysed) montmorillonite is not in a unique state of equilibrium. Rather, a secondary unidentified solid phase, enriched in Si relative to montmorillonite controls the activities of solutes, as well as another unidentified secondary, Al-enriched phase. This was deduced from the lack of congruency in the dissolution of montmorillonite and by the dependence of the concentrations of some, but not all, constituents of montmorillonite upon each other. Churchman & Jackson (1976) explicitly mentioned that the experiments by Kittrick (1971a, 1971b) suffered from the same shortcoming.

In their study demonstrating equilibrium of kaolinite with aqueous solutions from both under- and oversaturation (see Section 25.4.3.2.1), May et al. (1986) also investigated the solubility of five different smectites (see Tab. 25-2 for their compositions) in the pH range of 5 – 8. After running the experiments for up to 419 days, there were no signs that equilibrium had been attained by any of the smectites. Most of the Upton and Panther Creek smectite suspensions evolved towards aqueous compositions suggesting the control of Al solubility by gibbsite, while the suspensions involving the soil clays from Hawaii evolved towards aqueous compositions suggesting Al control by amorphous $Al(OH)_3$.

According to Peryea & Kittrick (1986), two conventions can be used to represent the composition of smectites with exchangeable cations in the interlayer for the interpretation of solubility experiments. The first convention includes interlayer cations as part of the smectite phase (monophase model). The second convention treats the interlayer cations and the structurally charged smectite structure as two separate phases (charged structure model). Kittrick & Peryea (1989) considered the former as a solid solution with variable composition on the timescale of laboratory experiments, and the latter as a solid solution of fixed composition on that timescale. In order to investigate which of the two models is supported by experimental data, Peryea & Kittrick (1986) carried out solubility experiments with Belle Fourche montmorillonite (see Tab. 25-2 for composition). After pre-treatment of montmorillonite with KCl solutions, mixtures of montmorillonite, kaolinite, goethite, and magnesite were brought in contact with 0.01, 0.1, and 1.0 M KCl solutions for up to 54 days at low solution/solid ratios and pH = 8.7 to ascertain the structural integrity of montmorillonite. Addition of kaolinite and goethite served to constrain the activities of Al^{3+} and Fe^{3+}, resp., since their concentrations were too low for accurate measurement. Magnesite of known solubility served as an internal equilibrium monitor, assuming that equilibrium with respect to magnesite indicated system-wide meta-equilibrium. Montmorillonite dissolution and precipitation were assumed to be congruent. Peryea & Kittrick

(1986) acknowledged that true chemical equilibrium cannot be attained, citing Lippmann (1982) but assumed that the investigated mineral system could attain a metastable equilibrium state that is reproducible and characteristic of the system. Direct validation of this assumption was not obtained. Constancy of the calculated Gibbs free energies of formation for montmorillonite over 24 solubility determinations was interpreted as an indication that a characteristic metastable equilibrium had been attained. The results, however, did not permit to validate either the monophase or the charged structure model based on precision. Peryea & Kittrick (1986) concluded that alternative criteria must be found for selecting the more appropriate model. Based on a re-evaluation of the experimental data by Peryea & Kittrick (1986), ascertaining that the montmorillonite was actually saturated with K^+, Kittrick & Peryea (1988) favoured the monophase model. Kittrick & Peryea (1989) performed additional solubility experiments. This time, gibbsite and goethite were added to the Belle Fourche montmorillonite pre-treated with $MgCl_2$ (see Tab. 25-2 for composition) and 36 samples put in contact with $MgCl_2$ solutions with pH varying from 2.08 to 7.55. After equilibration, pH varied from 3.26 to 8.16.

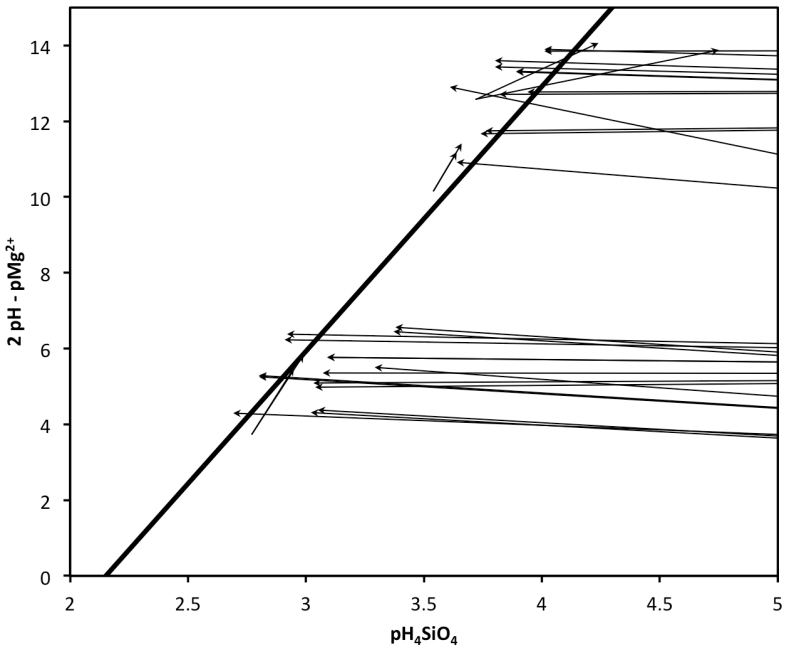

Fig. 25-13: Mg-saturated Belle Fourche montmorillonite equilibrated with gibbsite and goethite. Data from Kittrick & Peryea (1989)

The line represents equilibrium of the reaction montmorillonite + 2.16 H^+ + 17.56 H_2O(aq) = 3.6 gibbsite + 0.28 goethite + 1.08 Mg^{2+} + 7.55 H_4SiO_4(aq). Gibbsite: $Al(OH)_3$, montmorillonite: $Mg_{0.47}(Si_{7.55}Al_{0.45})(Al_{3.15}Mg_{0.61}Fe_{0.28})O_{20}(OH)_4$, goethite: FeOOH. Arrows connect points of initial and final solution. Undersaturated conditions are to the right of the equilibrium curve. The slope of the equilibrium curve is given by the reaction stoichiometry, the position was fitted by Kitrick & Peryea (1989) to the final solution compositions.

Kittrick & Peryea (1989) claimed that their solubility experiments had reached equilibrium, since "during the course of equilibration some individual samples increased and some decreased with regard to the $pSI(OH)_4°$, pH, pMg^{2+}, and $2pH\text{-}pMg^{2+}$ of initial solutions. Thus, equilibrations from both undersaturation and supersaturation were well presented". A look at Fig. 25-13 reveals, however, that this bold assertion is not at all backed by their experimental data.

To summarise, there does not appear to be a single experimental solubility experiment with smectites that has convincingly shown that equilibrium was attained.

25.4.3.2.4 Calorimetric data for smectites

In a series of calorimetric studies, Gailhanou and coworkers produced thermodynamic data for several clay minerals (see Tab. 25-3 for their compositions). Low temperature adiabatic calorimetry and differential scanning calorimetry were used for deriving standard entropies, heat contents, and heat capacity functions for montmorillonite MX-80, illite IMt-2, and illite-smectite mixed-layer ISCz-1 (Gailhanou et al. 2007), chlorite CCa-2 (Gailhanou et al. 2009), and smectite MX-80, illite IMt-2, and beidellite SBId-1 (Gailhanou et al. 2012). These thermodynamic parameters for montmorillonite MX-80, illite IMt-2, and beidellite were complemented by Gailhanou et al. (2012) with standard enthalpies of formation derived from solution-reaction calorimetry at 298.15 K, permitting the calculation of standard Gibbs free energies of formation and of equilibrium constants, and thus providing a complete thermodynamic parameter set. Similarly, Blanc et al. (2014) performed complementary solution-reaction calorimetry for chlorite CCa-2. In addition, they also determined the complete set of thermodynamic parameters for berthierine ISGS. Gailhanou et al. (2013), finally, obtained the complete thermodynamic parameter set for saponite Sap-Ca-1, nontronite NAu-1, and Santa Olalla vermiculite.

The energetics of hydration/dehydration of montmorillonite MX-80 were determined by Tajeddine et al. (2015) by measuring dehydration enthalpies using thermogravimetric and differential thermal analysis. Gailhanou et al. (2017) developed a methodology for extracting the thermodynamic hydration properties of clay minerals from water adsorption isotherms by removing the contribution of non-interlayer water (capillary and multilayer water) and considering only the contribution of the cation hydration in the interlayer. This removal was done by suitable adaptation of a solid solution model for clay water.

Tab. 25-2: Compositions of smectites used in solubility experiments

Types, origins and compositions as taken from references. Abbreviations: beid beidellite, mont montmorillonite, nont nontronite, AZ Arizona, CO Colorado, HI Hawaii, MS Mississippi, SD, South Dakota, WY Wyoming.

Reference	**Type**	**Origin**	**Composition**
Reesman & Keller (1968)	Mont	Bentonite, Cheto, AZ	Not indicated, but see Huang & Keller (1973) below
Reesman & Keller (1968)	Mont	Bentonite, Clay Spur, WY	Not indicated, but see Huang & Keller (1973) below
Kittrick (1971a)	Mont	Bentonite, Belle Fourche, SD	$M_{0.56}(Si_{7.87}Al_{0.13})(Al_{3.03}Mg_{0.58}Fe_{0.45})O_{20}(OH)_4$
Kittrick (1971a)	Mont	Bentonite, Clay Spur, WY	not indicated, „essentially identical to Belle Fourche"
Kittrick (1971b)	Mont	Bentonite, Panther Creek (Aberdeen), MS	$M_{0.83}(Si_{7.64}Al_{0.36})(Al_{2.58}Fe_{0.67}Mg_{0.89})O_{20}(OH)_4$
Huang & Keller (1973)	Mont	Bentonite, Cheto, AZ	$(Ca_{0.38}Na_{0.04}K_{0.04})(Al_{3.04}Fe_{0.28}Mg0._{66})(Si_{7.86}Al_{0.14})O_{20}(OH)_4$
Huang & Keller (1973)	Mont	Bentonite, Clay Spur, WY	$(Na_{0.54}Ca_{0.20}K_{0.04})(Al_{3.04}Fe_{0.38}Mg0._{44})(Si_{7.88}Al_{0.12})O_{20}(OH)_4$
Churchman & Jackson (1976)	Mont	Bentonite, Colony, WY	$M_{0.80}(Si_{7.60}Al_{0.40})(Al_{3.16}Fe_{0.40}Mg_{0.52})O_{20}(OH)_4$
Churchman & Jackson (1976)	Mont	Bentonite, Castle Rock, CO	$M_{0.48}(Si_{7.36}Al_{0.64})(Al_{3.04}Fe_{0.42}Mg_{0.92})O_{20}(OH)_4$
Churchman & Jackson (1976)	Mont	Bentonite, Panther Creek, MS	$M_{0.83}(Si_{7.64}Al_{0.36})(Al_{2.58}Fe_{0.67}Mg_{0.89})O_{20}(OH)_4$
May et al. (1986)	Beid	Bentonite, Upton, WY	$Mg_{0.36}(Si_{7.10}Al_{0.90})(Al_{3.36}Fe_{0.34}Mg_{0.54})O_{20}(OH)_4$
May et al. (1986)	Mont	Bentonite, Panther Creek, MS	$Mg_{0.415}(Si_{7.64}Al_{0.36})(Al_{2.58}Fe_{0.67}Mg_{0.89})O_{20}(OH)_4$
May et al. (1986)	Mont	Soil clay, Lualualei, HI	$Mg_{0.61}(Si_{7.64}Al_{0.36})(Al_{2.20}Fe_{1.20}Mg_{0.47})O_{20}(OH)_4$
May et al. (1986)	Beid	Soil clay, St. Louis Heights, HI	$Mg_{0.42}(Si_{7.12}Al_{0.88})(Al_{2.44}Fe_{1.44}Mg_{0.20})O_{20}(OH)_4$
May et al. (1986)	Nont	Soil clay, Kokokahi, HI	$Mg_{0.39}(Si_{6.78}Al_{1.22})(Al_{1.80}Fe_{2.26}Mg_{0.13})O_{20}(OH)_4$
Peryea & Kittrick (1986)	Mont	Bentonite, Belle Fourche, SD	$K_xMg_{(0.92-x)/2}(Si_{7.57}Al_{0.43})(Al_{3.15}Mg_{0.61}Fe_{0.28})O_{20}(OH)_4$
Kittrick & Peryea (1988)	Mont	Bentonite, Belle Fourche, SD	$K_{0.92}(Si_{7.57}Al_{0.43})(Al_{3.15}Mg_{0.61}Fe_{0.28})O_{20}(OH)_4$
Kittrick & Peryea (1989)	Mont	Bentonite, Belle Fourche, SD	$Mg_{0.47}(Si_{7.55}Al_{0.45})(Al_{3.15}Mg_{0.61}Fe_{0.28})O_{20}(OH)_4$

Tab. 25-3: Compositions of clay minerals used in calorimetry

Reference	Type	Composition
Gailhanou et al. (2007)	Montmorillonite MX-80	$Na_{0.435}K_{0.026}Ca_{0.010}(Si_{3.612}Al_{0.388})(Al_{1.593}Fe^{3+}_{0.184}Mg_{0.228}Fe^{2+}_{0.038}Ti_{0.011})O_{10}(OH)_2$
Gailhanou et al. (2007), Gailhanou et al. (2012)	Illite imt-2	$Na_{0.044}K_{0.762}(Si_{3.387}Al_{0.613})(Al_{1.427}Fe^{3+}_{0.292}Mg_{0.241}Fe^{2+}_{0.084})O_{10}(OH)_2$
Gailhanou et al. (2007)	Mixed-layer iscz-1	$Na_{0.135}K_{0.530}(Si_{3.565}Al_{0.435})(Al_{1.709}Fe^{3+}_{0.051}Mg_{0.218}Fe^{2+}_{0.017}Ti_{0.005})O_{10}(OH)_2$
Gailhanou et al. (2009), Blanc et al. (2014)	Chlorite cca-2	$(Si_{2.633}Al_{1.367})(Al_{1.116}Fe^{3+}_{0.215}Mg_{2.952}Fe^{2+}_{1.712}Mn_{0.012}Ca_{0.011})O_{10}(OH)_8$
Gailhanou et al. (2012), Tajeddine et al. (2015)	Smectite MX-80	$Na_{0.409}K_{0.024}Ca_{0.009}(Si_{3.7.38}Al_{0.262})(Al_{1.598}Fe^{3+}_{0.173}Mg_{0.214}Fe^{2+}_{0.035})O_{10}(OH)_2$
Gailhanou et al. (2012)	Beidelite sbid-1	$Ca_{0.185}K_{0.104}(Si_{3.574}Al_{0.426})(Al_{1.812}Fe^{3+}_{0.112}Mg_{0.09})O_{10}(OH)_2$
Gailhanou et al. (2013)	Saponite Sap-Ca-1	$Na_{0.394}K_{0.021}Ca_{0.038}(Si_{3.569}Al_{0.397}Fe^{3+}_{0.034})(Mg_{2.948}Fe^{2+}_{0.021}Mn_{0.001})O_{10}(OH)_2$
Gailhanou et al. (2013)	Nontronite nau-1	$K_{0.020}Ca_{0.247}(Si_{3.458}Al_{0.542})(Al_{0.268}Fe^{3+}_{1.688}Mg_{0.066}Ti_{0.007})O_{10}(OH)_2$
Gailhanou et al. (2013)	Vermiculite, Santa Olalla	$Ca_{0.445}(Si_{2.778}Al_{1.222})(Al_{0.192}Fe^{3+}_{0.226}Mg_{2.468}Fe^{2+}_{0.028}Ti_{0.018}Mn_{0.007})O_{10}(OH)_2$
Blanc et al. (2014)	Berthierine, ISGS	$(Si_{1.332}Al_{0.668})(Al_{0.975}Fe^{3+}_{0.182}Mg_{0.157}Fe^{2+}_{1.422}Li_{0.035}Mn_{0.002})O_{10}(OH)_2$

25.4.3.2.5 Estimation methods for thermodynamic data for smectites

Many methods for estimating thermodynamic properties for minerals have been developed and only a small number of these can be discussed here. A widely used method is based on the assumption that the thermodynamic properties of silicate minerals can be modelled as the linear combination of the contributions of coordination polyhedra building up the structural framework of minerals, see, e.g. Chermak & Rimstidt (1989, 1990) who estimated Gibbs free energies and enthalpies of formation for a wide variety of silicate minerals at 25 °C and higher temperatures, and Van Hinsberg et al. (2005a, 2005b), who extended the polyhedral method and provided enthalpies of formation, entropies, molar volumes, heat capacities, compressibilities and thermal expansions for 35 different types of polyhedra to be used in the estimation of corresponding thermodynamic parameters for silicate minerals and some double oxides.

A number of other methods were specifically developed for estimating thermodynamic properties of phyllosilicates, or clay minerals in particular. Tardy & Garrels (1974) estimated Gibbs free energies of formation of montmorillonites, illites, chlorites, and micas by assuming that such silicates can be represented by oxide and hydroxide components in the silicate structure with fixed Gibbs free energies of formation that may differ from those of the components as separate phases. Noting that this estimation method for phyllosilicates could not be applied to other silicates or to hydroxides, Tardy & Garrels (1976, 1977) found an empirical parameter, ΔO^{2-} that could be used for correlations with the Gibbs free energies of formation of other types of silicates and hydroxides. ΔO^{2-} is defined as the difference between the Gibbs free energy of formation from

the elements of a crystalline oxide and the Gibbs free energy of formation from the elements of its cation in aqueous solution (per O^{2-} in the oxide), which is a function of the electronegativity of the cation. For silicates, the Gibbs free energies of formation from the oxides were shown to be linear functions of ΔO^{2-} of their constituent cations. These linear functions can then be used to estimate the Gibbs free energies of formation for silicates.

Tardy & Fritz (1981) refined this method by directly correlating solubility products of phyllosilicates with the ΔO^{2-} parameter. This correlation was used to estimate solubility products for 36 ideal clay mineral endmembers which can be used to estimate the solubility product of a clay mineral with a specific composition by combining appropriate endmembers into an ideal solid solution.

Tardy & Duplay (1992) devised a method for estimating the Gibbs free energies of hydrated and dehydrated clay minerals based on the ideal solution model by Tardy & Fritz (1981), estimates of the Gibbs free energies of formation of the clay mineral endmembers based on the ΔO^{2-} parameter and assuming that hydration energies of clay minerals are proportional to the layer charge and, for a specific layer charge and a specific interlayer cation, also proportional to ΔO^{2-}.

Vieillard (1994a, 1994b) estimated enthalpies of formation based on ΔO^{2-} parameters and refined crystal structures for a multitude of silicate minerals.

Vieillard (2000, 2002) improved the Gibbs free energy estimation methods for phyllosilicate based on ΔO^{2-} parameters by considering ΔO^{2-} for a specific cation to be different in interlayer, octahedral, and tetrahedral sites.

Several more recent studies estimated thermodynamic data of montmorillonites with different cation occupancies and/or different degrees of hydration (Marty et al. 2001, Vieillard et al. 2011, Tajeddine et al. 2015). The different mono-cationic occupancies as well as different hydration states can be seen as solid solution endmembers. Such a solid solution can then describe any montmorillonite with a given sheet structure, following the approach of Tardy & Fritz (1981). A solid solution with constant degree of hydration was successfully applied in a reactive transport simulation (Berner et al. 2013), where GEMS predicted the phase equilibria including the solid solution.

Blanc et al. (2015a), finally, presented a generalised model for estimating the enthalpies of formation, the entropies, the heat capacities and the volumes of dehydrated phyllosilicates. Entropies and heat capacities were estimated using the polyhedral method, and enthalpies of formation were estimated based on the method developed by Vieillard (1994a, 1994b).

To complement the ThermoChimie database with thermodynamic data for clay minerals, Blanc et al. (2015b) used such estimation methods to extend the results of calorimetric measurements to other compositions.

25.4.3.2.6 Conclusions

Besides the principal objection put forth by Lippmann (1982) that clay minerals are most probably not equilibrium phases and that the results of solubility experiments are not representative of thermodynamic equilibrium, there are numerous experimental problems that impede the straightforward interpretation of solubility experiments with clay minerals:

- In the ideal case, equilibrium must be attained from over- and undersaturation. Equilibrium from oversaturation, however, can often not be reached, since nucleation of a mineral phase is characterised by an activation energy barrier which is difficult to overcome at room temperature (Blanc et al. 2013).
- Equilibration times may oftentimes exceed reasonable experimental timescales. The quartz solubility experiment by Rimstidt (1997), e.g., lasted for more than 13 years.
- Smectites commonly show incongruent dissolution behaviour, however, the nature and crystallinity of the secondary minerals controlling the solubility of Al and Si are usually not known (Tardy & Fritz 1981).
- Even purified clays are in fact mixtures of several phases with different size or compositions, reacting as different phases and dissolving at different rates (Tardy & Fritz 1981)
- Kittrick & Peryea (1989) identified the most difficult aspect of their solubility experiments as the requirement for an exact correspondence between the bulk composition of the montmorillonite sample (which is all that can be analysed) and the composition that actually controls the solubility. Also, impurities such as other smectite phases may be difficult to detect. Kittrick & Peryea (1989) declared that, with respect to their experiments, "in retrospect, it appears that obtaining a sample with the required composition correspondence was a matter of good fortune".

In their review on the thermodynamics of clay minerals, Blanc et al. (2013) make an important statement: "In spite of the large number of studies aiming to determine the solubility of clay minerals by solution equilibrium experiments, these types of data are not often used in geochemical calculations. The reason lies in the uncertainty concerning equilibrium attainment. One way to overcome this problem would be to assess equilibrium experiments by calorimetric measurements performed on the same clay mineral, since calorimetry is independent of any equilibrium in aqueous solution". It is certainly true that calorimetry is independent of any equilibrium in solution, but that does not mean that thermodynamic data obtained with calorimetry for a structurally and compositionally heterogeneous smectite is in any way useful for true equilibrium calculations. Similar considerations hold for estimated thermodynamic data. However, they may well be used in combination with kinetic data for modelling the dissolution of a specific smectite.

In summary, Lippmann's conclusions have not been falsified yet. What are the consequences in the case of illites and smectites? Calorimetric data may indicate the chemical driving force towards dissolution or precipitation of a clay phase in a certain aqueous system. But actual equilibrium reactions are kinetically inhibited. We can use kinetic data to model dissolution. We cannot model precipitation.

Having said all that, this review decided to include the calorimetric data $\Delta_f H_m°$, $S_m°$ and $C_{p,m}°$ as measured and estimated by Blanc et al. (2015a, 2015b) (Tab. 25-4 – 25-7).

The $\Delta_f G_m°$ values in Tab. 25-4 and 25.6 have been calculated by this review according to the Gibbs-Helmholtz equation:

$$\Delta_f G_m° = \Delta_f H_m° - T° \cdot \Delta_f S_m°$$

where $\Delta_f S_m°$ [$J \cdot K^{-1} \cdot mol^{-1}$] is the standard molar entropy of formation of the solid, which in turn is calculated from the elements according to the reaction

$$\Delta_f S_m° = \Sigma\, S_m°(\text{elements}) - S_m°$$

Values for $S_m°$(elements) have been taken as selected by this review.

The "equilibrium parameters" $\log_{10} K_s°$ and $\Delta_r H_m°$ (Tab. 25-5 and 25-7) have been calculated by this review using $\Delta_f G_m°$ and $\Delta_f H_m°$ from Tab. 25-4 and 25-6 and $\Delta_f G_m°$ and $\Delta_f H_m°$ values for the aqueous species as selected by this review in order to provide a complete data set formally consistent with TDB 2020.

All these values have been included in TDB 2020 as supplemental data.

Tab. 25-4: Predicted values for thermodynamic properties of clay mineral endmembers according to Blanc et al. (2015a)

Mineral		**Formula**	$\Delta_f G_m°$ [kJ · mol^{-1}]	$\Delta_f H_m°$ [kJ · mol^{-1}]	$S_m°$ [J · mol^{-1} · K^{-1}]	$C_{p,m}°$ [J · mol^{-1} · K^{-1}]	$V°$ [cm^3 · mol^{-1}]
Montmorillonite *(Low-charge)*	(MgK)	$K_{0.34}Mg_{0.34}Al_{1.66}Si_4O_{10}(OH)_2$	-5'332.65	-5'703.51	273.04	311.33	134.69
	(MgNa)	$Na_{0.34}Mg_{0.34}Al_{1.66}Si_4O_{10}(OH)_2$	-5'322.35	-5'690.41	277.88	310.60	133.96
	(MgCa)	$Ca_{0.17}Mg_{0.34}Al_{1.66}Si_4O_{10}(OH)_2$	-5'322.63	-5'690.29	268.85	305.88	135.58
	(MgMg)	$Mg_{0.17}Mg_{0.34}Al_{1.66}Si_4O_{10}(OH)_2$	-5'309.00	-5'676.01	269.52	304.71	131.58
Montmorillonite *(High-charge)*	(HcK)	$K_{0.6}Mg_{0.6}Al_{1.4}Si_4O_{10}(OH)_2$	-5'388.47	-5'757.74	296.34	319.96	138.75
	(HcNa)	$Na_{0.6}Mg_{0.6}Al_{1.4}Si_4O_{10}(OH)_2$	-5'370.31	-5'734.63	304.90	318.67	137.47
	(HcCa)	$Ca_{0.3}Mg_{0.6}Al_{1.4}Si_4O_{10}(OH)_2$	-5'370.80	-5'734.42	288.96	310.34	140.32
	(HcMg)	$Mg_{0.3}Mg_{0.6}Al_{1.4}Si_4O_{10}(OH)_2$	-5'346.75	-5'709.22	290.13	308.29	133.27
Saponite	(K)	$K_{0.34}Mg_3Al_{0.34}Si_{3.66}O_{10}(OH)_2$	-5'632.90	-6'010.39	293.96	334.54	141.69
	(Na)	$Na_{0.34}Mg_3Al_{0.34}Si_{3.66}O_{10}(OH)_2$	-5'623.07	-5'997.76	298.8	333.81	140.96
	(Ca)	$Ca_{0.17}Mg_3Al_{0.34}Si_{3.66}O_{10}(OH)_2$	-5'624.15	-5'998.44	289.78	329.09	142.57
	(Mg)	$Mg_{0.17}Mg_3Al_{0.34}Si_{3.66}O_{10}(OH)_2$	-5'610.70	-5'984.34	290.44	327.93	138.58
Saponite-Fe	(FeK)	$K_{0.34}Mg_2Fe^{II}Al_{0.34}Si_{3.66}O_{10}(OH)_2$	-5'284.04	-5'645.53	342.04	344.95	144.27
	(FeNa)	$Na_{0.34}Mg_2Fe^{II}Al_{0.34}Si_{3.66}O_{10}(OH)_2$	-5'275.20	-5'633.89	346.87	344.23	143.54
	(FeCa)	$Ca_{0.17}Mg_2Fe^{II}Al_{0.34}Si_{3.66}O_{10}(OH)_2$	-5'275.28	-5'633.57	337.85	339.50	145.15
	(FeMg)	$Mg_{0.17}Mg_2Fe^{II}Al_{0.34}Si_{3.66}O_{10}(OH)_2$	-5'261.84	-5'619.48	338.52	338.33	141.16
Nontronite	(K)	$K_{0.34}Fe^{III}_{1.67}Al_{0.67}Si_{3.66}O_{10}(OH)_2$	-4'638.59	-4'994.27	323.66	334.23	132.85
	(Na)	$Na_{0.34}Fe^{III}_{1.67}Al_{0.67}Si_{3.66}O_{10}(OH)_2$	-4'628.76	-4'981.64	328.49	333.50	132.12
	(Ca)	$Ca_{0.17}Fe^{III}_{1.67}Al_{0.67}Si_{3.66}O_{10}(OH)_2$	-4'629.84	-4'982.32	319.47	328.78	133.74
	(Mg)	$Mg_{0.17}Fe^{III}_{1.67}Al_{0.67}Si_{3.66}O_{10}(OH)_2$	-4'616.39	-4'968.22	320.14	327.62	129.74
Beidellite	(K)	$K_{0.34}Al_{2.34}Si_{3.66}O_{10}(OH)_2$	-5'376.58	-5'749.86	266.65	310.35	133.22
	(Na)	$Na_{0.34}Al_{2.34}Si_{3.66}O_{10}(OH)_2$	-5'376.75	-5'747.23	271.49	309.62	132.49
	(Ca)	$Ca_{0.17}Al_{2.34}Si_{3.66}O_{10}(OH)_2$	-5'367.83	-5'737.91	262.47	304.90	134.10
	(Mg)	$Mg_{0.17}Al_{2.34}Si_{3.66}O_{10}(OH)_2$	-5'354.38	-5'723.81	263.13	303.74	130.11
Illite	(Mg)	$K_{0.85}Mg_{0.25}Al_{2.35}Si_{3.4}O_{10}(OH)_2$	-5'509.03	-5'881.39	306.28	326.41	140.06
	(FeII)	$K_{0.85}Fe^{II}_{0.25}Al_{2.35}Si_{3.4}O_{10}(OH)_2$	-5'426.71	-5'796.29	314.23	329.00	140.67
	(FeIII)	$K_{0.85}Fe^{III}_{0.25}Al_{2.6}Si_{3.15}O_{10}(OH)_2$	-5'423.28	-5'795.39	308.1	329.28	138.92
	(Al)	$K_{0.85}Al_{2.85}Si_{3.15}O_{10}(OH)_2$	-5'537.36	-5'913.65	294.41	325.70	138.98
Vermiculite	(K)	$K_{0.86}Mg_3Al_{0.86}Si_{3.14}O_{10}(OH)_2$	-5'792.89	-6'173.41	322.36	350.19	147.56
	(Na)	$Na_{0.86}Mg_3Al_{0.86}Si_{3.14}O_{10}(OH)_2$	-5'769.82	-6'143.26	334.60	348.34	145.71
	(Ca)	$Ca_{0.43}Mg_3Al_{0.86}Si_{3.14}O_{10}(OH)_2$	-5'775.64	-6'148.06	311.78	336.40	149.80
	(Mg)	$Mga_{0.43}Mg_3Al_{0.86}Si_{3.14}O_{10}(OH)_2$	-5'742.33	-6'113.11	313.46	333.46	139.69
Berthierine(FeIII)		$(Fe^{II}_{2.34}Fe^{III}_{0.33}Al_{0.33})(Si_{1.34}Al_{0.66})O_5(OH)_4$	-3'153.29	-3'458.03	287.97	297.41	103.27
Berthierine(FeII)		$(Fe^{II}_2Al)(SiAl)O_5(OH)_4$	-3'454.11	-3'770.46	253.07	283.50	103.86
Cronstedtite		$(Fe^{II}_2Fe^{III})(SiFe^{III})O_5(OH)_4$	-2'616.84	-2'914.55	313.16	257.02	76.80
Glauconite		$K_{0.75}(Mg_{0.25}Fe^{II}_{0.25}Fe^{III}_{1.25}Al_{0.25})(Al_{0.25}Si_{3.75})O_{10}(OH)_2$	-4'800.21	-5'151.13	366.58	344.54	139.76

Tab. 25-5: Solubility products and reaction enthalpies of clay minerals calculated from estimated data (see Tab. 25-4) for clay minerals and selected data for aqueous species

Reaction	**$\log_{10}K_s°$**	**$\Delta_r H_m°$** [kJ · mol^{-1}]
Montmorillonite(MgK) + 4 H_2O(l) + 6 H^+ ⇌ 0.34 K^+ + 0.34 Mg^{2+} + 1.66 Al^{3+} + 4 $Si(OH)_4$(aq)	2.65	-139.97
Montmorillonite(MgNa) + 4 H_2O(l) + 6 H^+ ⇌ 0.34 Na^+ + 0.34 Mg^{2+} + 1.66 Al^{3+} + 4 $Si(OH)_4$(aq)	3.24	-149.06
Montmorillonite(MgCa) + 4 H_2O(l) + 6 H^+ ⇌ 0.17 Ca^{2+} + 0.34 Mg^{2+} + 1.66 Al^{3+} + 4 $Si(OH)_4$(aq)	4.05	-159.78
Montmorillonite(MgMg) + 4 H_2O(l) + 6 H^+ ⇌ 0.51 Mg^{2+} + 1.66 Al^{3+} + 4 $Si(OH)_4$(aq)	3.53	-161.14
Montmorillonite(HcK) + 4 H_2O(l) + 6 H^+ ⇌ 0.6 K^+ + 0.6 Mg^{2+} + 1.4 Al^{3+} + 4 $Si(OH)_4$(aq)	4.29	-132.48
Montmorillonite(HcNa) + 4 H_2O(l) + 6 H^+ ⇌ 0.6 Na^+ + 0.6 Mg^{2+} + 1.4 Al^{3+} + 4 $Si(OH)_4$(aq)	5.32	-148.51
Montmorillonite(HcCa) + 4 H_2O(l) + 6 H^+ ⇌ 0.3 Ca^{2+} + 0.6 Mg^{2+} + 1.4 Al^{3+} + 4 $Si(OH)_4$(aq)	6.75	-167.41
Montmorillonite(HcMg) + 4 H_2O(l) + 6 H^+ ⇌ 0.9 Mg^{2+} + 1.4 Al^{3+} + 4 $Si(OH)_4$(aq)	5.84	-169.81
Saponite(K) + 2.64 H_2O(l) + 7.36 H^+ ⇌ 0.34 K^+ + 3 Mg^{2+} + 0.34 Al^{3+} + 3.66 $Si(OH)_4$(aq)	28.12	-255.05
Saponite(Na) + 2.64 H_2O(l) + 7.36 H^+ ⇌ 0.34 Na^+ + 3 Mg^{2+} + 0.34 Al^{3+} + 3.66 $Si(OH)_4$(aq)	28.61	-263.67
Saponite(Ca) + 2.64 H_2O(l) + 7.36 H^+ ⇌ 0.17 Ca^{2+} + 3 Mg^{2+} + 0.34 Al^{3+} + 3.66 $Si(OH)_4$(aq)	29.28	-273.58
Saponite(Mg) + 2.64 H_2O(l) + 7.36 H^+ ⇌ 3.17 Mg^{2+} + 0.34 Al^{3+} + 3.66 $Si(OH)_4$(aq)	28.74	-274.76
Saponite(FeK) + 2.64 H_2O(l) + 7.36 H^+ ⇌ 0.34 K^+ + 2 Mg^{2+} + Fe^{2+} + 0.34 Al^{3+} + 3.66 $Si(OH)_4$(aq)	25.35	-243.20
Saponite(FeNa) + 2.64 H_2O(l) + 7.36 H^+ ⇌ 0.34 Na^+ + 2 Mg^{2+} + Fe^{2+} + 0.34 Al^{3+} + 3.66 $Si(OH)_4$(aq)	25.67	-250.83
Saponite(FeCa) + 2.64 H_2O(l) + 7.36 H^+ ⇌ 0.17 Ca^{2+} + 2 Mg^{2+} + Fe^{2+} + 0.34 Al^{3+} + 3.66 $Si(OH)_4$(aq)	26.52	-261.75
Saponite(FeMg) + 2.64 H_2O(l) + 7.36 H^+ ⇌ 2.17 Mg^{2+} + Fe^{2+} + 0.34 Al^{3+} + 3.66 $Si(OH)_4$(aq)	25.97	-262.92
Nontronite(K) + 2.64 H_2O(l) + 7.36 H^+ ⇌ 0.34 K^+ + 1.67 Fe^{3+} + 0.67 Al^{3+} + 3.66 $Si(OH)_4$(aq)	-4.11	-131.76
Nontronite(Na) + 2.64 H_2O(l) + 7.36 H^+ ⇌ 0.34 Na^+ + 1.67 Fe^{3+} + 0.67 Al^{3+} + 3.66 $Si(OH)_4$(aq)	-3.61	-140.38
Nontronite(Ca) + 2.64 H_2O(l) + 7.36 H^+ ⇌ 0.17 Ca^{2+} + 1.67 Fe^{3+} + 0.67 Al^{3+} + 3.66 $Si(OH)_4$(aq)	-2.94	-150.30
Nontronite(Mg) + 2.64 H_2O(l) + 7.36 H^+ ⇌ 0.17 Mg^{2+} + 1.67 Fe^{3+} + 0.67 Al^{3+} + 3.66 $Si(OH)_4$(aq)	-3.49	-151.48
Beidellite(K) + 2.64 H_2O(l) + 7.36 H^+ ⇌ 0.34 K^+ + 2.34 Al^{3+} + 3.66 $Si(OH)_4$(aq)	4.39	-193.38
Beidellite(Na) + 2.64 H_2O(l) + 7.36 H^+ ⇌ 0.34 Na^+ + 2.34 Al^{3+} + 3.66 $Si(OH)_4$(aq)	3.14	-192.00
Beidellite(Ca) + 2.64 H_2O(l) + 7.36 H^+ ⇌ 0.17 Ca^{2+} + 2.34 Al^{3+} + 3.66 $Si(OH)_4$(aq)	5.56	-211.91
Beidellite(Mg) + 2.64 H_2O(l) + 7.36 H^+ ⇌ 0.17 Mg^{2+} + 2.34 Al^{3+} + 3.66 $Si(OH)_4$(aq)	5.02	-213.09
Illite(Mg) + 1.6 H_2O(l) + 8.4 H^+ ⇌ 0.85 K^+ + 0.25 Mg^{2+} + 2.35 Al^{3+} + 3.4 $Si(OH)_4$(aq)	10.80	-229.80
Illite(FeII) + 1.6 H_2O(l) + 8.4 H^+ ⇌ 0.85 K^+ + 0.25 Fe^{2+} + 2.35 Al^{3+} + 3.4 $Si(OH)_4$(aq)	9.25	-220.72
Illite(FeIII) + 0.6 H_2O(l) + 9.4 H^+ ⇌ 0.85 K^+ + 0.25 Fe^{3+} + 2.6 Al^{3+} + 3.15 $Si(OH)_4$(aq)	12.14	-266.81
Illite(Al) + 0.6 H_2O(l) + 9.4 H^+ ⇌ 0.85 K^+ + 2.85 Al^{3+} + 3.15 $Si(OH)_4$(aq)	12.78	-270.89
Vermiculite(K) + 0.56 H_2O(l) + 9.44 H^+ ⇌ 0.86 K^+ + 3 Mg^{2+} + 0.86 Al^{3+} + 3.14 $Si(OH)_4$(aq)	37.35	-338.06
Vermiculite(Na) + 0.56 H_2O(l) + 9.44 H^+ ⇌ 0.86 Na^+ + 3 Mg^{2+} + 0.86 Al^{3+} + 3.14 $Si(OH)_4$(aq)	38.30	-358.06
Vermiculite(Ca) + 0.56 H_2O(l) + 9.44 H^+ ⇌ 0.43 Ca^{2+} + 3 Mg^{2+} + 0.86 Al^{3+} + 3.14 $Si(OH)_4$(aq)	39.46	-380.06
Vermiculite(Mg) + 0.56 H_2O(l) + 9.44 H^+ ⇌ 3.43 Mg^{2+} + 0.86 Al^{3+} + 3.14 $Si(OH)_4$(aq)	37.95	-382.33
Berthierine(FeIII) + 8.64 H^+ ⇌ 2.34 Fe^{2+} + 0.33 Fe^{3+} + 0.99 Al^{3+} + 1.34 $Si(OH)_4$(aq) + 3.64 H_2O(l)	28.76	-302.91
Berthierine(FeII) + 10 H^+ ⇌ 2 Fe^{2+} + 2 Al^{3+} + $Si(OH)_4$(aq) + 5 H_2O(l)	34.45	-379.80
Cronstedtite + 10 H^+ ⇌ 2 Fe^{2+} + 2 Fe^{3+} + $Si(OH)_4$(aq) + 5 H_2O(l	16.11	-257.03
Glauconite + 3 H_2O(l) + 7 H^+ ⇌ 0.75 K^+ + 0.25 Mg^{2+} + 0.25 Fe^{2+} + 1.25 Fe^{3+} + 0.5 Al^{3+} + 3.75 $Si(OH)_4$(aq)	1.77	-133.54

Tab. 25-6: Thermodynamic properties of clay minerals measured by calorimetry according to Blanc et al. (2015b).

Mineral	**Formula**	$\Delta_f G_m°$ [kJ · mol^{-1}]	$\Delta_f H_m°$ [kJ · mol^{-1}]	$S_m°$ [J · mol^{-1} · K^{-1}]	$C_{p,m}°$ [J · mol^{-1} · K^{-1}]	$V°$ [cm^3 · mol^{-1}]
Smectite MX80	$(Na_{0.409}K_{0.024}Ca_{0.009})(Si_{3.738}Al_{0.262})(Al_{1.598}Mg_{0.214}Fe^{III}_{0.173}Fe^{II}_{0.035})O_{10}(OH)_2$	-5'293.18 ± 5.4	-5'656.37 ± 5.4	301.92 ± 0.2	322.74	134.92
Saponite SapCa-2	$(Na_{0.394}K_{0.021}Ca_{0.038})(Si_{3.569}Al_{0.397})(Mg_{2.949}Fe^{III}_{0.034}Fe^{II}_{0.021})O_{10}(OH)_2$	-5'622.45 ± 5.0	-5'994.06 ± 4.9	314.55 ± 1.6	346.87	141.66
Nontronite Nau-1	$(Ca_{0.247}K_{0.020})(Si_{3.458}Al_{0.542})(Fe^{III}_{1.688}Al_{0.276}Mg_{0.068})O_{10}(OH)_2$	-4'684.90 ± 6.5	-5'035.69 ± 5.3	332.75 ± 7.0	335.15	136.38
Beidellite SBld-1	$(Ca_{0.185}K_{0.104})(Si_{3.574}Al_{0.426})(Al_{1.812}Mg_{0.090}Fe^{III}_{0.112})O_{10}(OH)_2$	-5'357.24 ± 6.5	-5'720.69 ± 6.5	293.53 ± 0.4	318.58	137.98
Illite IMt-2	$(K_{0.762}Na_{0.044})(Si_{3.387}Al_{0.613})(Al_{1.427}Fe^{III}_{0.292}Mg_{0.241}Fe^{II}_{0.084})O_{10}(OH)_2$	-5'325.87 ± 8.5	-5'711.25 ± 8.5	324.92 ± 0.2	328.21	139.18
Vermiculite SO	$Ca_{0.445}(Si_{2.778}Al_{1.222})(Al_{0.192}Mg_{2.468}Fe^{III}_{0.226}Fe^{II}_{0.028}Ti_{0.018}Mn_{0.007})O_{10}(OH)_2$	-5'671.20 ± 5.7	-6'034.41 ± 5.7	325.77 ± 0.5	346.39	148.36
Ripidolite Cca-2	$(Si_{2.633}Al_{1.367})(Al_{1.116}Fe^{III}_{0.215}Mg_{2.952}Fe^{II}_{1.712}Mn_{0.012})(Ca_{0.011})O_{10}(OH)_8$	-7'593.46 ± 8.7	-8'240.14 ± 8.6	469.40 ± 2.9	547.02	211.83
Berthierine ISGS	$(Si_{1.332}Al_{0.668})(Al_{0.976}Fe^{III}_{0.182}Fe^{II}_{1.44}Mg_{0.157})O_5(OH)_4$	-3'461.94 ± 7.3	-3'774.46 ± 6.3	257.00 ± 6.7	263.57	101.16

Tab. 25-7: Solubility products and reaction enthalpies of clay minerals calculated from calorimetric data (see Tab. 25-6) for clay minerals and selected data for aqueous species

Reaction	$\log_{10} K_s°$	$\Delta_r H_m°$ [kJ · mol^{-1}]
Smectite MX80 + 2.952 H_2O(l) + 7.048 H^+ ⇌ 0.024 K^+ + 0.409 Na^+ + 0.009 Ca^{2+} + 0.214 Mg^{2+} + 0.035 Fe^{2+} + 0.173 Fe^3 + 1.860 Al^{3+} + 3.738 $Si(OH)_4$(aq)	5.09 ± 1.2	-188.06 ± 6.9
Saponite SapCa-2 + 2.276 H_2O(l) + 7.724 H^+ ⇌ 0.021 K^+ + 0.394 Na^+ + 0.038 Ca^{2+} + 2.949 Mg^{2+} + 0.021 Fe^{2+} + 0.034 Fe^3 + 0.397 Al^{3+} + 3.569 $Si(OH)_4$(aq)	31.40 ± 1.1	-287.83 ± 5.6
Nontronite Nau-1 + 1.832 H_2O(l) + 8.168 H^+ ⇌ 0.020 K^+ + 0.247 Ca^{2+} + 0.068 Mg^{2+} + 1.688 Fe^3 + 0.818 Al^{3+} + 3.458 $Si(OH)_4$(aq)	1.21 ± 1.3	-191.95 ± 6.3
Beidellite SBld-1 + 2.296 H_2O(l) + 7.704 H^+ ⇌ 0.104 K^+ + 0.185 Ca^{2+} + 0.090 Mg^{2+} + 0.112 Fe^3 + 2.238 Al^{3+} + 3.574 $Si(OH)_4$(aq)	7.38 ± 1.3	-228.73 ± 7.9
Illite IMt-2 + 1.548 H_2O(l) + 8.452 H^+ ⇌ 0.762 K^+ + 0.044 Na^+ + 0.241 Mg^{2+} + 0.084 Fe^{2+} + 0.292 Fe^{3+} + 2.040 Al^{3+} + 3.387 $Si(OH)_4$(aq)	15.13 ± 1.6	-234.97 ± 9.6
Vermiculite SO + 10.852 H^+ ⇌ 0.445 Ca^{2+} + 2.468 Mg^{2+} + 0.007 Mn^{2+} + 0.028 Fe^{2+} + 0.226 Fe^3 + 1.414 Al^{3+} + 0.018 TiO^{2+} + 2.778 $Si(OH)_4$(aq) + 0.870 H_2O(l)	43.62 ± 1.2	-457.48 ± 7.0
Ripidolite Cca-2 + 17.468 H^+ ⇌ 0.011 Ca^{2+} + 2.952 Mg^{2+} + 0.012 Mn^{2+} + 1.712 Fe^{2+} + 0.215 Fe^3 + 2.483 Al^{3+} + 2.633 $Si(OH)_4$(aq) + 7.468 H_2O(l)	-174.86 ± 1.7	743.55 ± 9.8
Berthierine ISGS + 8.672 H^+ ⇌ 0.157 Mg^{2+} + 1.440 Fe^{2+} + 0.182 Fe^3 + 1.644 Al^{3+} + 1.332 $Si(OH)_4$(aq) + 3.672 H_2O(l)	27.80 ± 1.4	-321.35 ± 7.3

25.4.3.3 Solid aluminium silicates: Solubility data for zeolites

In a late stage of the review work for TDB 2020 two important papers (Ma & Lothenbach 2020a, 2020b) became available concerning the solubility of zeolites.

Ma & Lothenbach (2020a) state that "zeolites are crystalline aluminosilicates with three-dimensional framework structures that can form in alkali activated cements, Roman cements, and the interaction zone of cements and clays. However, their stability domains are uncertain due to their high structural variability and the lack of experimental solubility data. Thermodynamic data were here determined for selected Na-based zeolites built from six different secondary building units that could possibly form in the interaction zones of cement/clay. The zeolites were synthesized by hydrothermal methods and full-scale characterized with respect to framework structures, extra-framework cations, Si/Al ratios, and water contents."

Ma & Lothenbach (2020a) investigated the solubility of these zeolites from under-saturation at 20, 50, 60, and 80 °C and compared their data where possible with literature values. Based on these solubility measurements $\log_{10}K_{sp}$ and $\Delta_f G_m°$ values at different temperatures could be calculated using GEMS. Completing these data with measured or calculated data for the heat capacity, $C_{p,m}°$, and entropy, $S_m°$, allowed to compute the solubility of the zeolites at 25 °C and its changes with temperature.

Ma & Lothenbach (2020a) found that "in general, the zeolites synthesized in this study have a higher solubility than natural zeolites. Such differences between natural and synthetic zeolites could be related to the presence of minor elements that can stabilize the natural zeolites, to different crystallinity of the zeolites, and/or to smaller crystal sizes of synthetic zeolites."

Ma & Lothenbach (2020a) finally conclude that the experimentally derived thermodynamic data provide insights on the early stage of the zeolite ageing and allow predicting zeolite stability domains during cementitious material hydration.

As GEMS combined with our database has been used to derive the standard thermodynamic data of Na-based zeolites at 25 °C (Tab. 8), these data have been included in TDB 2020 as reported by Ma & Lothenbach (2020a).

In their second publication, Ma & Lothenbach (2020b) state that "alteration of widespread interfaces between cements and clays in geological time scales is essential to the safety assessment of radioactive waste repositories but not well understood partly due to the low reliability of thermodynamic data for zeolites. Here, we collected and full-scale characterized Ca-based zeolites with six types of frameworks that could possibly form in the interfaces."

By using hydrothermal cation exchange methods, Ca-based zeolites with framework types of chabazite, gismondine and mordenite were synthesised. Natural zeolites of scolecite, stilbite, heulandite, and clinoptilolite were also collected for the thermodynamic study. Their framework structures, ratios between extra-framework cations, Si, and Al, water contents, and low-frequency bonding vibrations were characterized by XRD, EDS, TGA, and FT-IR, respectively. All the solid characterisation results indicated that the target zeolites with high purity and homogeneous particle size distribution were synthesised successfully. By carrying out geochemical modelling with GEMS, thermodynamic data of $\Delta_f G_m°$, $\Delta_f H_m°$, and $S_m°$ for each zeolite was generated based on the experimental solubility products at 20, 50, 60, and 80 °C.

Tab. 25-8: Standard thermodynamic data of Na-based zeolites at 25 °C according to Ma & Lothenbach (2020a)

Zeolite	**Formula**	$\Delta_f G_m°$ [kJ · mol^{-1}]	$\Delta_f H_m°$ [kJ · mol^{-1}]	$S_m°$ [J · mol^{-1} · K^{-1}]	$C_{p,m}°$ [J · mol^{-1} · K^{-1}]	$V°$ [cm^3 · mol^{-1}]
Analcime	$Na_2Al_2Si_4O_{12}·2H_2O$	-6'139.70	-6'575.84	469	425	194.84
Low-silica P-Na	$Na_2Al_2Si_2O_8·3.8H_2O$	-4'858.72	-5'314.82	374	384	153.49
Phillipsite-Na	$Na_{2.5}Al_{2.5}Si_{5.5}O_{16}·5H_2O$	-8'717.83	-9'438.72	692	620	304.74
Phillipsite-NaK	$Na_{1.5}KAl_{2.5}Si_{5.5}O_{16}·5H_2O$	-8'741.26	-9'461.67	707	626	304.74
Linda type A	$Na_{1.98}Al_{1.98}Si_{2.02}O_8·5.31H_2O$	-5'203.75	-5'701.89	584	513	186.95
Molecular sieve 4Å	$Na_2Al_2Si_2O_8·4.5H_2O$	-5'029.88	-5'486.36	536	475	187.00
Hydrosodalite	$Na_8Al_6Si_6O_{24}(OH)_2 · 2H_2O$	-13'221.4	-14'120.1	943	895	424.74
Sodalite	$Na_8Al_6Si_6O_{24}Cl_2$	-12'719.1	-13'473.4	848	812	421.53
Cancrinite-NO_3	$Na_8Al_6Si_6O_{24}(NO_3)_2 · 4H_2O$	-13'600.8	-14'717.6	1'149	1'119	435.96
Chabazite-Na	$Na_2Al_2Si_4O_{12}·6H_2O$	-7'117.55	-7'808.31	548	578	249.95
Faujasite-X	$Na_2Al_2Si_{2.5}O_9·6.2H_2O$	-5'857.79	-6'456.94	566	586	195.80
Faujasite-Y	$Na_2Al_2Si_4O_{12}·8H_2O$	-7'578.22	-8'352.62	734	739	282.94
Natrolite	$Na_2Al_2Si_3O_{10}·2H_2O$	-5'305.15	-5'707.02	360	359	169.36
Mordenite-Na	$Na_{0.72}Al_{0.72}Si_{5.28}O_{12}·2.71H_2O$	-5'955.95	-6'442.40	388	405	210.59

Tab. 25.9: Standard thermodynamic data of Ca-based zeolites at 25 °C according to Ma & Lothenbach (2020b).

Zeolite	**Formula**	$\Delta_f G_m°$ [kJ · mol^{-1}]	$\Delta_f H_m°$ [kJ · mol^{-1}]	$S_m°$ [J · mol^{-1} · K^{-1}]	$C_{p,m}°$ [J · mol^{-1} · K^{-1}]	$V°$ [cm^3 · mol^{-1}]
Chabazite-Ca	$CaAl_2Si_4O_{12}·6H_2O$	-7'144.01	-7'806.74	581	617	247.61
Low-silica P-Ca	$CaAl_2Si_2O_8·4.5H_2O$	-5'076.03	-5'527.74	491	435	157.58
Mordenite-Ca	$Ca_{0.34}Al_{0.68}Si_{5.32}O_{12}·2.9H_2O$	-5'995.73	-6'489.11	386	404	209.72
Scolecite	$CaAl_2Si_3O_{10}·3H_2O$	-5'560.52	-6'011.65	367	383	172.42
Stilbite	$Ca_{1.11}Al_{2.22}Si_{6.78}O_{18}·6.8H_2O$	-9'944.75	-1'0815.6	748	782	327.43
Heulandite_1	$Ca_{1.07}Al_{2.14}Si_{6.86}O_{18}·4.4H_2O$	-9'353.66	-1'0118.6	541	611	317.88
Heulandite_2	$Ca_{1.07}Al_{2.14}Si_{6.86}O_{18}·4.5H_2O$	-9'371.26	-1'0131.2	581	619	317.88
Clinoptilolite	$Ca_{0.52}Al_{1.04}Si_{4.96}O_{12}·3.1H_2O$	-6'151.94	-6'642.18	454	449	210.91

As GEMS combined with our database has also been used to derive the standard thermodynamic data of Ca-based zeolites at 25 °C (Tab. 25-9), these data have been included in TDB 2020 as reported by Ma & Lothenbach (2020b).

25.4.4 Iron

Four studies have been published reporting experimental data on Fe(III) silicate complexation in $NaClO_4$ media for the equilibrium

$$Fe^{3+} + Si(OH)_4(aq) \rightleftharpoons FeSiO(OH)_3^{2+} + H^+$$

i.e. measurements with a spectrophotometer at $I = 0.1$ M (Weber & Stumm 1965, Porter & Weber 1971), spectrophotometric analyses at $I = 0.1$ M and polarography at $I = 0.15$ M (Olson & O'Melia 1973), and UV absorbance spectroscopy at 0.1, 0.3 and 0.7 M (Patten & Byrne 2017).

The reported values are given in Tab. 10 with uncertainties estimated by this review. These data have been used for an SIT analysis (Fig. 25-14) and this review obtained

$$\log_{10}K^\circ = -0.12 \pm 0.06$$

$$\Delta\varepsilon = -0.58 \pm 0.13 \text{ kg} \cdot \text{mol}^{-1}$$

Note that only using the data reported by Patten & Byrne (2017) this review obtained almost identical values: $\log_{10}K^\circ = -0.12 \pm 0.06$ and $\Delta\varepsilon = -0.57 \pm 0.14$ kg · mol^{-1}. Patten & Byrne (2017) obtained from their SIT analysis the same results, $\log_{10}K^\circ = -0.12 \pm 0.04$ and $\Delta\varepsilon = -0.57 \pm 0.10$ kg · mol^{-1} with slightly smaller uncertainties.

Using $\varepsilon(Fe^{3+}, ClO_4^-) = 0.73 \pm 0.04$ kg · mol^{-1} and $\varepsilon(H^+, ClO_4^-) = 0.14 \pm 0.032$kg · mol^{-1} (Lemire et al. 2013), and $\varepsilon(Si(OH)_4(aq), NaClO_4) = 0.03 \pm 0.06$ kg · mol^{-1} derived in this review we calculate

$$\varepsilon(FeSiO(OH)_3^{2+}, ClO_4^-) = 0.04 \pm 0.15 \text{ kg} \cdot \text{mol}^{-1}$$

Using $\log_{10}\beta_1^\circ = -9.81 \pm 0.02$ selected by this review for the equilibrium $Si(OH)_4(aq) \rightleftharpoons SiO(OH)_3^- + H^+$ this review calculates from the above result

$$Fe^{3+} + SiO(OH)_3^- \rightleftharpoons FeSiO(OH)_3^{2+}$$

$$\log_{10}\beta^\circ = 9.69 \pm 0.06$$

This value has been included in TDB 2020. Reardon (1979) measured the solubility of amorphous silica in acidified ferric nitrate solutions at $0.01 \leq I < 0.08$ M and obtained an average value from six measurements of $\log_{10}\beta = 9.8 \pm 0.2$, a value compatible with the value selected by this review.

The same papers have been considered by Lemire et al. (2020) in their NEA TDB review, published after this review had been finished.

Tab. 25-10: Data for the reaction $Fe^{3+} + Si(OH)_4(aq) \rightleftharpoons FeSiO(OH)_3^{2+} + H^+$ in $NaClO_4$ media

I [M]	I_m [m]	K [M]	$\log_{10}K$ [m]	± (95%)	Reference
0.1	0.101	0.57	-0.244	0.2	Weber & Stumm (1965)
0.1	0.101	0.18	-0.745	0.2	Porter & Weber (1971)
0.1	0.101	0.25	-0.602	0.2	Olson & O'Melia (1973) spectroscopy
0.15	0.151	0.34	-0.469	0.2	Olson & O'Melia (1973) polarography
0.1	0.101	0.297 ± 0.06	-0.527	0.09	Patten & Byrne (2017)
0.1	0.101	0.301 ± 0.06	-0.521	0.09	Patten & Byrne (2017)
0.3	0.304	0.298 ± 0.04	-0.526	0.09	Patten & Byrne (2017)
0.3	0.304	0.294 ± 0.04	-0.532	0.09	Patten & Byrne (2017)
0.7	0.727	0.273 ± 0.01	-0.526	0.10	Patten & Byrne (2017)
0.7	0.727	0.382 ± 0.01	-0.418	0.08	Patten & Byrne (2017)

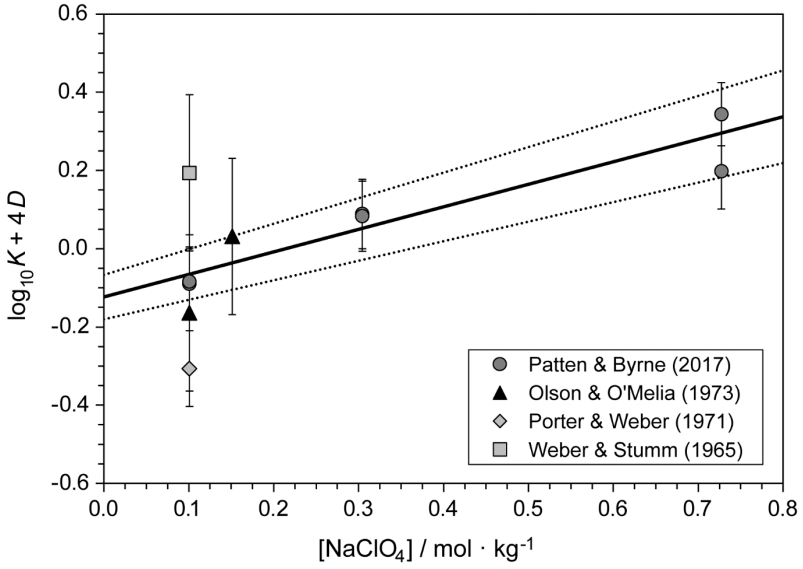

Fig. 25-14: Dependence of the equilibrium $Fe^{3+} + Si(OH)_4(aq) \rightleftharpoons FeSiO(OH)_3^{2+} + H^+$ on ionic strength

The solid line is obtained using the derived SIT interaction coefficient and stability constant at zero ionic strength. Dotted lines represent the 95% uncertainty range extrapolated from I = 0 to higher $NaClO_4$ concentrations.

Lemire et al. (2020) used the values K = 0.57 (Weber & Stumm 1965) and K = 0.25 and 0.34 (Olson & O'Melia 1973), ignored that the latter refers to 0.15 M ionic strength, and calculated an unweighted average K = 0.39 ± 0.32 (2σ). This value corresponds to $\log_{10}K$ = -0.41 ± 0.36 (2σ). Lemire et al. (2020) extrapolated this value from 0.1 M ionic strength to zero using Δε = -0.568 ± 0.098 kg · mol^{-1} from Patten & Byrne (2017) and obtained $\log_{10}K°$ = -0.03 ± 0.04 (2σ).

Recalculation by this review showed that the value itself is correct, but the assigned uncertainty is one order of magnitude too small, it should be ± 0.36.

Furthermore, Lemire et al. (2020) state that "no complexation constants were reported" by Porter & Weber (1971), which is not true. Porter & Weber (1971) reported $K = 0.18$, see Tab. 25-10.

Lemire et al. (2020) used $\log_{10}K° = -0.03 \pm 0.04$ (2σ) together with $\log_{10}K° = -0.12 \pm 0.04$ (2σ) as reported by Patten & Byrne (2017), and $\log_{10}K° = -0.02 \pm 0.45$ (2σ) derived from the data of Reardon (1979), and state that "a weighted average of these values results in $\log_{10}K° = -0.08 \pm 0.15$ (2σ) which is not selected but is provided for informational purposes only".

Recalculation by this review showed that this value is wrong. Using the values with the erroneous uncertainty assigned by Lemire et al. (2020) to the first value, the weighted average would be $\log_{10}K° = -0.08 \pm 0.03$ (2σ). Using ± 0.36 as the correct uncertainty of the first value, the weighted average is $\log_{10}K° = -0.12 \pm 0.04$ (2σ), the same value as obtained by this review but with a slightly lower uncertainty.

Note that all studies considered here have been carried out at pH < 4. No conclusions can be drawn from these investigations whether bidentate Fe(III) complexes with $SiO_2(OH)_2^{2-}$ form at high pH in analogy with Ca and Mg complexation, or whether polymerised species are formed in analogy with Al. The latter possibility is discussed by Olson & O'Melia (1973), who assume that their spectrophotometric data at pH above 3 indicate that polymeric species were formed.

No thermodynamic data concerning Fe(II) silicate complexation have been found in the literature.

25.4.5 Europium, Americium and Curium

Silicate complexation of europium, americium and curium sometimes has been studied by the same groups using the same experimental methods, or the data of one element have been used as an approximation for the other elements and hence, they are discussed together in this section.

Jensen & Choppin (1996) studied the interaction of Eu(III) with silicic acid in aqueous solutions of 0.1 M ionic strength by solvent extraction. The authors interpreted the results of their solvent extraction study in terms of 1:1 and 1:2 complexes according to the equilibrium

$$Eu^{3+} + n\ SiO(OH)_3^- \rightleftharpoons Eu(SiO(OH)_3)_n^{3-n}$$

The following constants are reported (Tab. 1 in Jensen & Choppin 1996):

$$\log_{10}\beta_1 = 7.16 \pm 0.34$$

derived from the distribution of Eu(III) between a 0.1 M aqueous NaCl solution and an organic phase (HDEHP in toluene) at 25 °C in the pH range 4.05 – 4.63, and

$$\log_{10}\beta_1 = 7.25 \pm 0.13 \text{ and } \log_{10}\beta_2 = 11.7 \pm 0.4$$

derived from extractions of Eu(III) from 0.1 M $NaClO_4$ solutions obtained using HDBM and TOPO in n-heptane at 25 °C in the pH range 8.48 – 9.15.

Patten & Byrne (2017) re-analysed the experimental data of Jensen & Choppin (1996). As Jensen & Choppin (1996) did not provide numerical data or detailed figures that could be used for reinterpretation of their results, Patten & Byrne (2017) digitised figures provided in sufficient size and detail in Jensen's PhD thesis, which is the basis of the paper by Jensen & Choppin (1996).

Patten & Byrne (2017) show that the solvent extraction data in 0.1 M aqueous NaCl solution and HDEHP at pH 4.05 and 4.63 have too much scatter and cannot be used for accurate characterisation of $\log_{10}\beta_1$.

From their re-analysis of extraction data obtained from 0.1 M $NaClO_4$ solutions and HDBM / TOPO in the pH range 8.48 – 9.15 Patten & Byrne (2017) conclude that useful $\log_{10}\beta_1$ values cannot be derived, but that $\log_{10}\beta_2$ values were relatively well defined. The average result obtained by Patten & Byrne (2017) from their least squares analyses is

$$\log_{10}\beta_2 = 11.73 \pm 0.10$$

However, the existence of the complex $Eu(SiO(OH)_3)_2^+$ at pH 9 could not be confirmed by other studies carried out in the neutral and basic pH range for Cm(III) (Steinle et al. 1997, Panak et al. 2005, Wang et al. 2005), see discussions below.

In summary, the present review decided not to consider the results of Jensen & Choppin (1996), neither the values for $\log_{10}\beta_1$, which cannot be derived from this study as shown by Patten & Byrne (2017), nor the "relatively well defined" $\log_{10}\beta_2$ value, which refers to undefined, polymeric or colloidal species.

Steinle et al. (1997) studied the interaction of Cm(III) with orthosilicic acid in aqueous solutions of ionic strength 0.1 M $NaClO_4$ at room temperature by time-resolved laser fluorescence spectroscopy (TRLFS). Data obtained in the pH range 5.0 – 5.5 were interpreted in terms of

$$Cm^{3+} + SiO(OH)_3^- \rightleftharpoons CmSiO(OH)_3^{2+}$$

$$\log_{10}\beta_1 = 7.4 \pm 0.2$$

Above pH 5.5 a further Cm species was detected which the authors interpreted as probably due to sorption of Cm to a polymeric silicate species.

Wadsak et al. (2000) reported experimental data on Am(III) silicate complexation. The authors interpreted the results of their solvent extraction study, carried out at pH 3.0 – 3.8 in 0.2 M $NaClO_4$ solutions, in terms of a 1:1 complex according to the equilibrium

$$Am^{3+} + SiO(OH)_4(aq) \rightleftharpoons AmSiO(OH)_3^{2+} + H^+$$

$$\log_{10}K_1 = -2.16 \pm 0.04 \ (1\ \sigma).$$

Guillaumont et al. (2003) extrapolated the above value to zero ionic strength, and increased the uncertainty to the 1.96 σ level, and obtained $\log_{10}K^\circ = -1.61 \pm 0.08$ Guillaumont et al. (2003) also recalculated and extrapolated the value reported by Steinle et al. (1997) to $\log_{10}K^\circ = -1.76 \pm 0.10$, and selected the unweighted average of both values as a common parameter for Am and Cm:

$\log_{10}K° = -1.68 \pm 0.18$

Using $\log_{10}\beta_1° = -9.81 \pm 0.02$ for the equilibrium $Si(OH)_4(aq) \rightleftharpoons SiO(OH)_3^- + H^+$ this results in

$(Am, Cm)^{3+} + SiO(OH)_3^- \rightleftharpoons (Am, Cm)SiO(OH)_3^{2+}$

$\log_{10}\beta_1° = 8.13 \pm 0.18$

Wang et al. (2005) studied the complexation of Cm(III) and Eu(III) with dissolved silica by solubility measurement and time-resolved laser fluorescence spectroscopy (TRLFS) in basic solutions (pH 7.5 – 12) over a range of total silica concentrations at different electrolyte ($NaNO_3$) concentrations. The authors conclude: "The increase in solubility of the $Eu(OH)_3$ / silica precipitates at high pH values indicated the possible formation of strong Eu-silicate aqueous complexes. The presence of these strong complexes was confirmed by TRLFS measurements of both Eu(III) and Cm(III) silicate solutions. The complexes present at the high pH values appeared to be fully coordinated with silicates and possibly nitrates in concentrated $NaNO_3$. The changes in fluorescence lifetime, fluorescence intensity and the concentrations of the monomeric and polymeric silicates suggested that the Cm(III) complex(es) in basic solution mostly involve polysilicates."

Wang et al. (2005) do not provide information on the composition of the species formed, or on equilibrium constants.

Panak et al. (2005) investigated the complexation of Cm(III) with aqueous silicic acid in the pH range 1.5 – 9.0 in 0.03 M NaCl by time-resolved laser fluorescence spectroscopy (TRLFS). The silicate concentration was varied from under- to over-saturation with respect to the solubility of amorphous silica. Three different complexation products were observed: Cm-silicate(I), Cm-silicate(II) and Cm-silicate(III).

Cm-silicate(I) appears in both, under- and over-saturation of silicic acid only as a minor fraction at pH 4 – 7 and could be interpreted in terms of the equilibrium

$Cm^{3+} + SiO(OH)_3^- \rightleftharpoons CmSiO(OH)_3^{2+}$

$\log_{10}\beta_1 = 7.32 \pm 0.08$

This value has been extrapolated by Panak et al. (2005) to zero ionic strength:

$\log_{10}\beta_1° = 7.74 \pm 0.08$

Cm-silicate(II) and Cm-silicate(III) were found to be colloidal. Cm-silicate(II) shows spectroscopic characteristics varying with the experimental conditions, whereas Cm-silicate(III), which formed exclusively with polysilicic acid, remained consistent and stable. The existence of a species $Cm(SiO(OH)_3)_2^+$, in analogy to the species $Eu(SiO(OH)_3)_2^+$ proposed by Jensen & Choppin (1996), could not be confirmed.

Pathak & Choppin (2006c) measured the complex formation of silicate with U(VI), Cm(III) and Eu(III) in the temperature range 5 – 45 °C in an aqueous medium of 0.20 M ($NaClO_4$) ionic strength and pH ≈ 3.5 by solvent extraction. Enthalpies of reaction were derived from the temperature variation of the obtained stability constants.

The stability constants at 25 °C and 0.2 M $NaClO_4$ reported for the equilibria

$$Cm^{3+} + SiO(OH)_3^- \rightleftharpoons CmSiO(OH)_3^{2+}$$

$$Eu^{3+} + SiO(OH)_3^- \rightleftharpoons EuSiO(OH)_3^{2+}$$

are $\log_{10}\beta_1 = 7.83 \pm 0.02$ and 7.79 ± 0.01, respectively (Tab. 1 in Pathak & Choppin 2006c). A re-evaluation in the present review of the experimental data given in graphical form in Figs. 2 and 3 of Pathak & Choppin (2006c) resulted in $\log_{10}\beta_1 = 7.82 \pm 0.02$ and 7.79 ± 0.02 (1 σ), respectively. Considering the errors induced by digitising graphical data the results are identical with the values published by Pathak & Choppin (2006c).

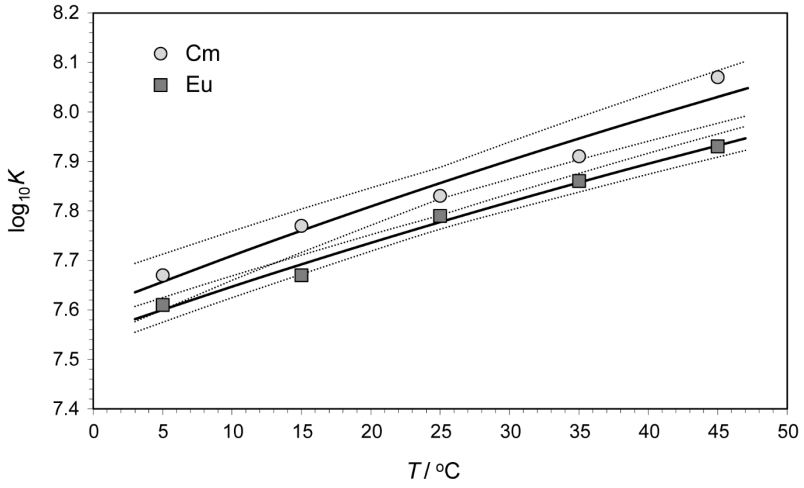

Fig. 25-15: Temperature dependence of the stability constant for the equilibrium (Cm, $Eu)^{3+} + SiO(OH)_3^- \rightleftharpoons$ (Cm, Eu)$SiO(OH)_3^{2+}$

Data taken from Tab. 1 in Pathak & Choppin (2006c). An unweighted least squares fit gives: $\log_{10}\beta_1$ (25 °C) = 7.86 ± 0.02 kJ · mol^{-1} and $\Delta_r H_m = 15.8 \pm 1.9$ kJ · mol^{-1} (1 σ), for Cm(III) and $\log_{10}\beta_1$ (25 °C) = 7.78 ± 0.01 and $\Delta_r H_m = 14.1 \pm 0.8$ kJ · mol^{-1} (1 σ) for Eu(III). The dotted lines are the 1 σ standard deviations extrapolated from 25 °C to lower and higher temperatures.

In their Tab. 2 Pathak & Choppin (2006c) reported enthalpies of reaction for Cm(III) and Eu(III) as $\Delta_r H_m = 15.8 \pm 2.0$ and 14.5 ± 1.0 kJ · mol^{-1}, respectively. A re-evaluation in the present review by least squares fits of the experimental data given in Tab. 1 of Pathak & Choppin (2006c) resulted in $\log_{10}\beta_1$ (25 °C) = 7.86 ± 0.02 kJ · mol^{-1} and $\Delta_r H_m = 15.8 \pm 1.9$ kJ · mol^{-1} (1 σ), for Cm(III) and $\log_{10}\beta_1$ (25 °C) = 7.78 ± 0.01 and $\Delta_r H_m = 14.1 \pm 0.8$ kJ · mol^{-1} (1 σ) for Eu(III) (Fig. 25-15).

Within the statistical uncertainties these re-evaluated values are identical with the values published by Pathak & Choppin (2006c). Hence, the values

$\Delta_r H_m = 15.8 \pm 4.0\ kJ \cdot mol^{-1}$ (2 σ) for Cm(III)

$\Delta_r H_m = 14.5 \pm 2.0\ kJ \cdot mol^{-1}$ (2 σ) for Eu(III)

have been included as supplemental data in TDB 2020.

In addition, an estimate

$\Delta_r H_m \approx 15\ kJ \cdot mol^{-1}$ for Am(III), Pu(III) and Np(III)

has been added as supplemental data to TDB 2020.

Thakur et al. (2007) measured the complex formation of silicate with Am(III), Cm(III) and Eu(III) at pH 3.5 and in ionic strengths of 0.20 – 1.00 M ($NaClO_4$) by solvent extraction. Hence, they used the same experimental set-up as Pathak & Choppin (2006c) in order to study the same equilibria. Instead of temperature variation at constant ionic strength (Pathak & Choppin 2006c) now the ionic strength was varied at constant temperature.

The authors reported for I = 0.20 M $\log_{10}\beta_1 = 8.02 \pm 0.10$, 7.78 ± 0.08 and 7.81 ± 0.11 for Am(III), Cm(III) and Eu(III), respectively. While the values reported for Cm(III) and Eu(III) are virtually the same as the values reported by Pathak & Choppin (2006c), the stability constant of Am(III) is higher than the others.

Experimental solvent extraction data for I = 0.20 M are given in graphical form in Fig. 3 of Thakur et al. (2007). These data were digitised, and the stability constants re-evaluated in the present review. The results are: $\log_{10}\beta_1 = 7.77 \pm 0.06$, 7.79 ± 0.03 and 7.83 ± 0.03 for Am(III), Cm(III) and Eu(III), respectively. Considering their assigned uncertainties all these values are the same, especially the stability constants of Am(III) and Cm(III) are undistinguishable. However, while the values for Cm(III) and Eu(III) re-evaluated in this review are the same as reported by Thakur et al. (2007), the value for Am(III) is at variance. Assuming that the experimental data shown in Fig. 3 of Thakur et al. (2007) are correct, the $\log_{10}\beta_1$ value for Am(III) given in Tab. 1 of Thakur et al. (2007) is incorrect.

Unfortunately, experimental solvent extraction data are published only for I = 0.20 M (Fig. 3 in Thakur et al. (2007) but no experimental data are published for I = 0.50, 0.75 and 1.00 M. Hence, the $\log_{10}\beta_1$ values given for these higher ionic strengths in Tab. 1 of Thakur et al. (2007) cannot be checked for correctness by re-evaluating the original experimental data. Inspecting Tab. 1 of Thakur et al. (2007) one recognises that the $\log_{10}\beta_1$ values for Cm(III) and Eu(III) are very similar at all ionic strengths, differing by not more than 0.03 log units, while the Am(III) values are all systemically higher, differing from the Cm(III) data by 0.24 - 0.30 log units. This review assumed that all $\log_{10}\beta_1$ values reported for Am(III) in Tab. 1 are affected by the same systematic error in data evaluation and tentatively "corrected" them by -0.25 log units, as determined from the re-evaluation of the 0.2 M data.

A tentative common SIT analysis of Eu, Cm and the "corrected" Am data of Thakur et al. (2007) resulted in (Fig. 25-16):

$$\log_{10}\beta_1^\circ = 8.61 \pm 0.04$$

$$\Delta\varepsilon = 0.00 \pm 0.06 \text{ kg} \cdot \text{mol}^{-1}$$

Using $\varepsilon(Eu^{3+}, ClO_4^-) = 0.47 \pm 0.01$ kg · mol^{-1} (see Section 23.2.2) and $\varepsilon(SiO(OH)_3^-, Na^+) = -0.05 \pm 0.07$ kg · mol^{-1} derived in this review we calculate

$$\varepsilon(Eu, Am, CmSiO(OH)_3^{2+}, ClO_4^-) = 0.42 \pm 0.10 \text{ kg} \cdot \text{mol}^{-1}$$

The latter value compares favourably with the expected value $\varepsilon(X^{2+}, ClO_4^-) = 0.40 \pm 0.10$ kg · mol^{-1} for divalent metal cations and complexes (Section 1.5.3).

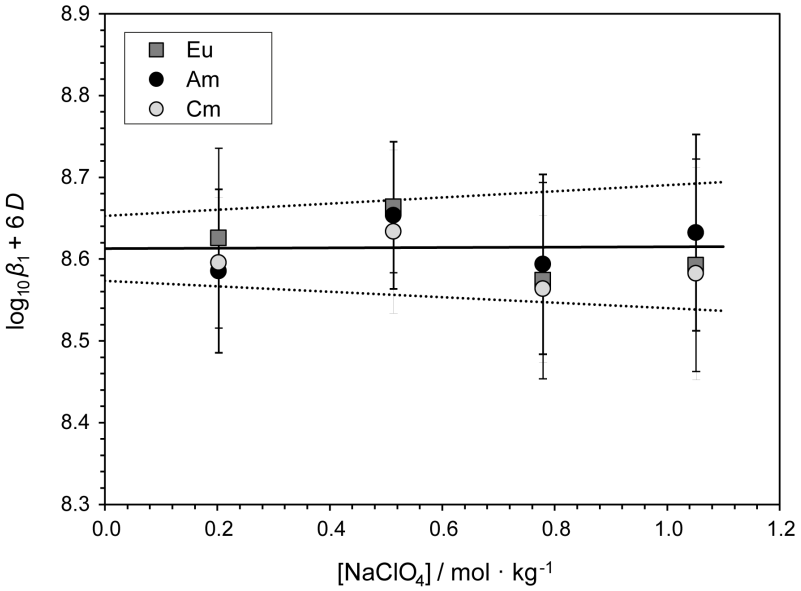

Fig. 25-16: Extrapolation to $I = 0$ of experimental data for the formation of $(Eu, Am, Cm)^{3+} + SiO(OH)_3^- \rightleftharpoons (Eu, Am, Cm)SiO(OH)_3^{2+}$ using SIT

The Eu and Cm data are directly taken from Tab. 1 of Thakur et al. (2007), while the Am data have been tentatively "corrected" by -0.25 log units in this review (see text).

Thakur et al. (2007) corrected their stability constants to zero ionic strength using the extended Debye-Hückel expression. However, the $\log_{10}\beta_1^\circ$ values they report, i.e. 8.23 ± 0.09, 7.94 ± 0.06 and 8.04 ± 0.08 for Am(III), Cm(III) and Eu(III), respectively, are incorrect. Probably the authors neglected the term Δz^2 in the extended Debye-Hückel expression and thus effectively used $\Delta z^2 = -1$ instead of the correct value $\Delta z^2 = -6$. By chance, these incorrectly extrapolated values "agree well with the reported values at $I = 0.00$" for Am(III), 8.20 ± 0.04 (Wadsak et al. 2000), for Cm(III), 7.74 ± 0.08 (Panak et al. 2005), and Eu(III), 7.98 ± 0.06 (Jensen & Choppin 1996), as reported by Thakur et al. (2007) and the error went unnoticed.

Patten & Byrne (2017), who re-analysed the data published by Jensen & Choppin (1996) and concluded that no value for $\log_{10}\beta_1$ can be derived from this study, also criticised the study of Thakur et al. (2007), carried out in the same laboratory using the same experimental set-up as Jensen & Choppin (1996). Patten & Byrne (2017) regard the assertion of Thakur et al. (2007) that complexation of Eu(III) with polymeric silicic acid is unimportant under their experimental conditions as "unsubstantiated and unlikely". Patten & Byrne (2017) conclude that the presence of polymeric silica species in the experiments of Thakur et al. (2007) resulted in substantially overestimated $\log_{10}\beta_1$ values.

Grenthe et al. (2020) extrapolated the values given by Thakur et al. (2007) for 0.20 M $NaClO_4$ to zero ionic strength, i.e. 8.84 ± 0.10, 8.60 ± 0.08 and 8.63 ± 0.08 for Am(III), Cm(III) and Eu(III), respectively.

However, Grenthe et al. (2020) only used the values for Cm and Eu, ignoring the Am value without explanation, further considered the value reported by Panak et al. (2005) for zero ionic strength, i.e. 7.74 ± 0.08 for Cm, as well as a value of Jensen & Choppin (1996), extrapolated to zero ionic strength by Panak et al. (2005), i.e. 7.93 ± 0.20 for Eu, and calculated the unweighted average of these four values as

$$\log_{10}\beta_1^\circ = 8.2 \pm 0.4$$

Grenthe et al. (2020) then state that this value is consistent with $\log_{10}\beta_1^\circ = 8.13 \pm 0.20$, selected by Guillaumont et al. (2003), and decided to retain the latter value as their selected one.

This review does not agree with the data selection of Grenthe et al. (2020), first of all because Grenthe et al. (2020) did not consider or comment on the re-analyses of criticisms by Patten & Byrne (2017) of the results reported by Jensen & Choppin (1996) and Thakur et al. (2007), but more importantly because Grenthe et al. (2020) ignored the recent paper of Soli & Byrne (2017) reporting experimental results concerning the formation of $EuSiO(OH)_3^{2+}$.

Soli & Byrne (2017) report direct experimental observations of equilibrium constants for $EuSiO(OH)_3^{2+}$ formation based on potentiometric analyses at 25 °C and 0.7 M $NaClO_4$ solutions. Low silicate concentrations were used in these analyses to preclude significant complexation by silicate polymers. Soli & Byrne (2017) conclude from the raw data and the calculated values of β_1 for each of 16 data sets, where the total silica and total Eu(III) concentrations were varied, that within the statistical uncertainties, there appears to be no concentration dependence. So, all 16 data sets were averaged to yield an overall value of $\beta_1 = 1.51 \cdot 10^6$ (RSD = 34%). The best-estimate europium silicate complexation constant at 25 °C and 0.7 M ionic strength is given by Soli & Byrne (2017) as

$$\log_{10}\beta_1 = 6.18 \pm 0.18$$

This review concludes that, in qualitative terms, the results of Pathak & Choppin (2006c) and Thakur et al. (2007) clearly show that the complexation effects of Eu(III), Am(III) and Cm(III) with silicate are statistically indistinguishable. Likewise, the temperature (Pathak & Choppin 2006c) and ionic strength effects (Thakur et al. 2007) of these complexation reactions seem to be statistically indistinguishable.

However, the absolute values of the stability constants reported by Pathak & Choppin (2006c) and Thakur et al. (2007) might be significantly overestimated and useful $\log_{10}\beta_1$ values cannot be derived from the study of Jensen & Choppin (1996), as discussed by Patten & Byrne (2017). Hence, the $\log_{10}\beta_1$ values reported by Jensen & Choppin (1996), Pathak & Choppin (2006c) and Thakur et al. (2007) have been rejected by this review.

The $\Delta_r H_m$ values reported by Pathak & Choppin (2006c) are considered by this review as useful guesses and are included as supplemental data in TDB 2020.

Likewise the value $\varepsilon(Eu, Am, CmSiO(OH)_3^{2+}, ClO_4^-) = 0.42 \pm 0.10$ kg · mol^{-1} derived above from the experimental data by Thakur et al. (2007) is included in TDB 2020 as a useful guess.

Tab. 25-11: Data for the reaction $(Eu,Am, Cm)^{3+} + Si(OH)_4(aq) \rightleftharpoons (Eu, Am, Cm)SiO(OH)_3^{2+} + H^+$ in NaCl and $NaClO_4$ media

	Medium	***I*** [M]	I_m	**$\log_{10}K$** [M]	**$\log_{10}K$** [m]	**$\log_{10}K°$**	**± (95%)**	**Reference**
$Am^{3+} + Si(OH)_4(aq) \rightleftharpoons AmSiO(OH)_3^{2+} + H^+$								
Am	$NaClO_4$	0.2	0.203	-2.16	-2.160	-1.605	0.08	Wadsak et al. (2000)
$(Eu,Am, Cm)^{3+} + SiO(OH)_3^- \rightleftharpoons (Eu, Am, Cm)SiO(OH)_3^{2+}$								
Am	$NaClO_4$					8.21	0.09	Wadsak et al. (2000)
Cm	$NaClO_4$	0.1	0.101	7.4	7.397	8.05	0.20	Steinle et al. (1997)
Cm	NaCl	0.03	0.030	7.32	7.320	7.74	0.08	Panak et al. (2005)
Eu	$NaClO_4$	0.7	0.725	6.18	6.165	7.31	0.20	Soli & Byrne (2017)

Using $\varepsilon(Cm^{3+}, ClO_4^-) = \varepsilon(Am^{3+}, ClO_4^-) = 0.49 \pm 0.03$ kg · mol^{-1} (Lemire et al. 2013), $\varepsilon(Eu^{3+}, ClO_4^-) = 0.47 \pm 0.01$ kg · mol^{-1} (see Section 23.2.2), and $\varepsilon(SiO(OH)_3^-, Na^+) = -0.05 \pm 0.07$ kg · mol^{-1}, $\varepsilon(CmSiO(OH)_3^{2+}, ClO_4^-) = \varepsilon(AmSiO(OH)_3^{2+}, ClO_4^-) = \varepsilon(EuSiO(OH)_3^{2+}, ClO_4^-) = 0.42 \pm 0.10$ kg · mol^{-1} derived in this review, the values reported by Soli & Byrne (2017) for Eu, Panak et al. (2005) for Cm, Wadsak et al. (2000) for Am and Steinle et al. (1997) for Cm have been extrapolated to zero ionic strength (Tab. 11). The unweighted average of these four values (with increased uncertainty to account for the variation of these values of almost one order of magnitue) is:

$$\log_{10}\beta_1° = 7.8 \pm 0.5$$

This value has been included in TDB 2020 for Eu(III), Am(III) and Cm(III), and as an estimate (supplemental data) for Pu(III) and Np(III).

25.4.6 Zirconium

No information about aqueous zirconium silicate complexes could be found in the literature during the present review.

Thermodynamic data for twelve zirconium silicate compounds have been selected in the NEA review of zirconium (Brown et al. 2005). However, none of these data are included in our data base (see Tab. 25-13) for reasons discussed in Section 12.8.2 of Thoenen et al. (2014).

25.4.7 Thorium

Rai et al. (2008) studied the solubility of ThO_2(am) in alkaline silica solutions, pH 10 – 13.3, at room temperature (22 ± 2 °C) in a controlled atmosphere chamber containing an inert gas. Freshly precipitated ThO_2(am) was washed and the precipitate then suspended in appropriate Na_2SiO_3 solutions. Either the sodium silicate concentration was varied at constant pH or the pH was varied at constant sodium silicate concentration. The solubility experiments from undersaturation lasted from 7 – 487 days. The maximum Na concentration measured in these experiments was 0.4 M.

The experimental data were interpreted by Rai et al. (2008) in terms of the equilibrium

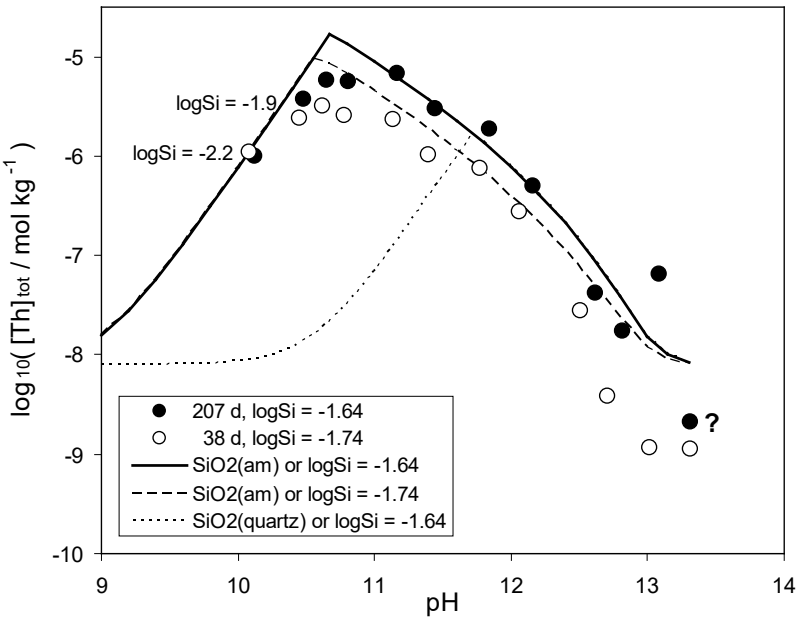

Fig. 25-17: Solubility of ThO_2(am) as a function of pH and time

At fixed aqueous Na_2SiO_3 concentration of approximately 0.018 mol · dm^{-3} (38 days reaction time) or 0.023 mol · dm^{-3} (207 days reaction time), except where shown explicitly otherwise. Data points taken from Tab. 11 in Rai et al. (2008). Data point with question mark refers to log[Th] given as < -8.677. Lines calculated in the present review with a simplified speciation model discussed in the text.

$$ThO_2(am) + 3\ Si(OH)_4(aq) + H_2O \rightleftharpoons Th(OH)_3(SiO(OH)_3)_3^{2-} + 2\ H^+$$

$$\log_{10}{}^*K_s^\circ = -(18.5 \pm 0.7)$$

Note that the solubility product $\log_{10}K_{s,0}° = -46.7$ is numerically identical with the solubility product $\log_{10}{}^{*}K_{s,0}° = 9.3 \pm 0.9$ for ThO_2(am, hyd, fr) + 4 H^+ ⇌ Th^{4+} + 2 H_2O selected by Rand et al. (2008) and included in our data base.

In the present review the solubility products given above were used together with equilibrium constants for $SiO(OH)_3^-$, $SiO_2(OH)_2^{2-}$ and $Th(OH)_4$(aq), and the solubility of SiO_2(am) as included in our data base in order to calculate the solubility of ThO_2(am) (Figs. 25-17 and 25-18). The tetramer $Si_4O_8(OH)_4^{4-}$ was not included in this simplified speciation model as Fig. 6 in Rai et al. (2008) shows that polymeric silica species contribute less than 10% to the total silica speciation at these low total silica concentrations. The agreement between measured data points and calculated Th concentration is good in Fig. 25-17 and poor in Fig. 25-18.

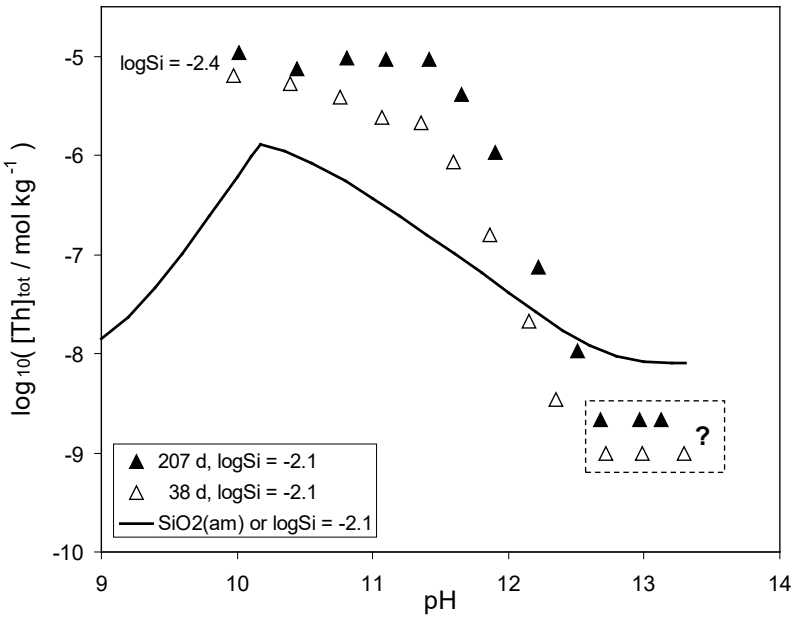

Fig. 25-18: Solubility of ThO_2(am) as a function of pH and time

At fixed aqueous Na_2SiO_3 concentration of approximately 0.008 mol · dm^{-3}, except where shown explicitly otherwise. Data points taken from Tab. 12 in Rai et al. (2008). Data points in the dashed box with question mark refers to log[Th] given as < -8.667 and < -9.000. Lines calculated in the present review with a simplified speciation model discussed in the text.

Rai et al. (2008) assumed $\log_{10}K_{s,0}° = -46.7$ for the solubility product ThO_2(am) + 2 H_2O ⇌ Th^{4+} + 4 OH^- and obtained for

$$Th^{4+} + 3\ Si(OH)_4(aq) + 3\ H_2O \rightleftharpoons Th(OH)_3(SiO(OH)_3)_3^{2-} + 6\ H^+$$

$$\log_{10}K° = -(27.8 \pm 0.7)$$

The data points with question marks in Figs. 25-17 and 25-18 refer to the unresolved question of detection limits. Rai et al. (2008) state that their detection limit for measured Th concentrations is $10^{-9.67}$, and indeed in their Tab. 9 (Set II) several numbers log[Th] < -9.67 appear. On the other hand, in Tab. 8 (Set I) log[Th] goes a low as -10.363. No detection limits in Set I? In Tab. 11

(Set III) we find one number log[Th] < -8.677 (question mark in Fig. 25-17). Does this indicate a detection limit one order of magnitude higher than stated in the text? In Tab. 12 (Set IV) we find three numbers log[Th] < -8.667 and three numbers log[Th] < -9.000 (dashed box with question mark in Fig. 25-18). Yet other detection limits? All these data should perhaps not be included in thermodynamic modelling.

The thermodynamic interpretation of experimental data by Rai et al. (2008) has several further shortcomings.

First of all, measurements at generally low ionic strength (the maximum Na concentration was 0.4 M) were interpreted in terms of both, the Pitzer and SIT formalism. The authors were aware of the fact that the results of the speciation calculations are insensitive to the Pitzer or SIT coefficients used. Nevertheless, they give Pitzer and SIT coefficients for $Th(OH)_3(SiO(OH)_3)_3^{2-}$ which are mere guesses. The SIT coefficient is not included in our data base.

Secondly, the authors claim to have included the solubility of quartz in their speciation model (Tab. 4 in Rai et al. (2008)). This cannot be correct. Using the solubility of quartz in our simplified speciation model results in calculated total silica incompatible with measurements and totally wrong Th solubility at pH < 11 (dotted line in Fig. 25-17).

Thirdly, the calculated Th concentration show in Fig. 6 of Rai et al. (2008) could be reproduced in the present review only in the pH range 11.5 – 13. Below pH 11.5 the calculated curve of Rai et al. (2008) exhibits a parabolic shape which is incompatible with the effect of SiO_2(am) solubility which leads to the sharp edge in Fig 25.17 and a solubility limited total Si concentration at pH < 10.7. The measured log[Si] numbers shown in Fig. 25-17 are in perfect agreement with concentrations calculated with our simplified speciation model. This is not mentioned and was probably not recognised by Rai et al. (2008).

Finally, there is a discrepancy of measured and calculated Th concentrations in data set IV (Fig. 25-18) and Rai et al. (2008) comment "it was surprising to find disagreement in this set, and exact reasons for this are not known". A closer look at Fig. 25-18 here and Fig. 11 in Rai et al. (2008) reveals even stranger disagreements. In Fig. 11 again the parabolic line appears, with a maximum Th concentration at pH 10.5 about one order of magnitude lower than calculated with our simplified speciation model (Fig. 25-18). The only difference between calculations shown in Fig. 25-17 and Fig. 25-18 is the total concentration of dissolved silica. Hence, it is unclear why we calculated something totally different than Rai et al. (2008) in this case, whereas the calculated curves in the first case (Fig. 25-17) agree well, at least at pH > 11.5. But the data shown in Fig. 25-18 may hide some more fundamental problems than differences in speciation calculations. The long-term solubility experiments (207 days) result in almost the same dissolved Th concentrations as the data shown in Fig. 25-17 although the total dissolved silica concentration differs by a factor of four. Furthermore, although the measured silica concentration at pH 10 (log[Si] = -2.4) agrees well with the one calculated as a result of solubility limitation by SiO_2(am), the total dissolved Th concentration is not lower than the other values at higher pH, in contrast to the effects seen in Fig. 25-17. Both effects cannot be explained by the formation of a single thorium silicate complex.

In summary, the experimental data of Rai et al. (2008) show strong thorium silicate complex formation in alkaline solutions, and their thermodynamic interpretation is not unreasonable. We included their equilibrium constant in TDB 2020, as well as the estimate $\varepsilon(Th(OH)_3(SiO(OH)_3)_3^{2-}, Na^+) = -(0.10 \pm 0.10)$ kg · mol^{-1}, but because of the shortcomings discussed above, as supplemental datum only:

$Th^{4+} + 3\ Si(OH)_4(aq) + 3\ H_2O(l) \rightleftharpoons Th(OH)_3(SiO(OH)_3)_3^{2-} + 6\ H^+$

$log_{10}K° = -(27.8 \pm 0.7)$

Rand et al. (2008) selected in their NEA review of thorium standard molar enthalpies of formation for the minerals $ThSiO_4$(huttonite) and $ThSiO_4$(thorite). Neither solubility products nor standard molar Gibbs free energies of formation are known for these solids and Rand et al. (2008) concluded that both compounds are metastable towards quartz and thorium dioxide under standard conditions. Therefore, they are not included in TDB 2020 (see Tab. 25-13).

25.4.8 Uranium

25.4.8.1 Aqueous uranium silicates

Seven papers have been published until 2019 reporting experimental data on U(VI) silicate complexation (Tab. 25-12). Five of these papers, i.e. Porter & Weber (1971), Satoh & Choppin (1992), Jensen & Choppin (1998), Moll et al. (1998) and Hrnecek & Irlweck (1999) have been discussed in detail and some data re-evaluated by Guillaumont et al. (2003). The experimental data in these papers have been interpreted in terms of the equilibrium

$UO_2^{2+} + Si(OH)_4(aq) \rightleftharpoons UO_2SiO(OH)_3^+ + H^+$

Tab. 25-12: Equilibrium constants for the reaction $UO_2^{2+} + Si(OH)_4(aq) \rightleftharpoons UO_2SiO(OH)_3^+ + H^+$.

Values re-evaluated by Grenthe et al. (2020) are shaded.

Reference	**Ionic medium $NaClO_4$**	**T (°C)**	**$log_{10}{}^*K$**	**$log_{10}{}^*K°$**
Porter & Weber (1971)	0.2 M	25	-(1.98 ± 0.13)	-(1.71 ± 0.13)
Satoh & Choppin (1992)	0.2 M	25	-(2.01 ± 0.09)	-(1.74 ± 0.09)
Jensen & Choppin (1998)	0.1 M	25	-(2.92 ± 0.06)	-(2.65 ± 0.06)
Moll et al. (1998)	0.3 M	20	-(1.74 ± 0.30)	-(1.48 ± 0.30)
Hrnecek & Irlweck (1999)	0.2 M	25	-(2.21 ± 0.40)	-(1.96 ± 0.40)
Yusov & Fedoseev (2005)	0.2 M	23	-(2.39 ± 0.40)	-(2.18 ± 0.40)
Pathak & Choppin (2006c)	0.2 M	25	-(2.69 ± 0.50)	-(2.43 ± 0.50)

Guillaumont et al. (2003) gave no credit to the results of Jensen & Choppin (1998), and selected from the remaining four studies

$log_{10}{}^*K° = -(1.84 \pm 0.10)$

Grenthe et al. (2020) did not give credit to the results of Porter & Weber (1971) and Satoh & Choppin (1992) "because the silicic acid concentration employed in these studies exceeded 0.010 M, resulting in formation of oligomers, which most likely dominated the silica speciation". In addition, Grenthe et al. (2020) agreed with Guillaumont et al. (2003) not giving credit to the results of Jensen & Choppin (1998). Grenthe et al. (2020) recalculated the $\log_{10}{}^{*}K$ values derived from the new studies of Yusov & Fedoseev (2005) and Pathak & Choppin (2006c), increased the uncertainties of the values obtained from Moll et al. (1998), Hrnecek & Irlweck (1999), Yusov & Fedoseev (2005) and Pathak & Choppin (2006c), extrapolated these values to zero ionic strength, and selected the weigthed average of the four selected studies (Tab. 25-12):

$$\log_{10}{}^{*}K^{\circ} = -(1.88 \pm 0.19)$$

Grenthe et al. (2020) remark that the close agreement with the selected avalue in Guillaumont et al. (2003) may be fortuitous.

Using $\log_{10}\beta^{\circ} = -(9.81 \pm 0.02)$ for $Si(OH)_4(aq) \rightleftharpoons SiO(OH)_3^- + H^+$ this review calculated for the equilibrium

$$UO_2^{2+} + SiO(OH)_3^- \rightleftharpoons UO_2SiO(OH)_3^+$$

$$\log_{10}\beta^{\circ} = 7.93 \pm 0.19$$

This value has been included in TDB 2020, as well as the estimates (Guillaumont et al. 2003)

$$\varepsilon(UO_2SiO(OH)_3^+, Cl^-) \approx \varepsilon(UO_2SiO(OH)_3^+, ClO_4^-) = 0.3 \pm 0.1 \text{ kg} \cdot \text{mol}^{-1}$$

Based on the temperature dependence of equilibrium constants in the range 5 – 45 °C and 0.2 M $NaClO_4$ Pathak & Choppin (2006c) obtained for the above reaction

$$\Delta_r H_m = 8.3 \pm 0.7 \text{ kJ} \cdot \text{mol}^{-1}$$

where the error limit corresponds to one standard deviation. Grenthe et al. (2020) then extrapolated this value to zero ionic strength

$$\Delta_r H_m^{\circ} = 9.9 \pm 3 \text{ kJ} \cdot \text{mol}^{-1}$$

where the uncertainty is estimated.

This value has been included in TDB 2020.

25.4.8.2 Solid uranium silicates

25.4.8.2.1 Solid uranium(VI) silicates

Guillaumont et al. (2003) discuss solubility data for a number of solid U(VI) silicates, i.e. $(UO_2)_2SiO_4 \cdot 2H_2O$ (soddyite), $Ca(UO_2)_2(SiO_3OH)_2 \cdot 5H_2O$ (uranophane), $Na(UO_2)(SiO_3OH) \cdot H_2O$ (sodium boltwoodite) and $Na_2(UO_2)_2(Si_2O_5)_3 \cdot 4H_2O$ (sodium weeksite).

In all cases, no solubility constant was included in their tables of selected values.

Grenthe et al. (2020) re-interpretated old data and evaluated new data published after the review of Guillaumont et al. (2003).

Soddyite, $(UO_2)_2SiO_4 \cdot 2H_2O$

Grenthe et al. (2020) state that soddyite, $(UO_2)_2SiO_4 \cdot 2H_2O$, has the simplest chemical composition of the uranyl silicates and is a common uranyl mineral in nature and an alteration product of spent nuclear fuel under oxidising conditions. The solubility of soddyite was investigated in a number of studies, and based on these studies Grenthe et al. (2020) selected a weighted average

$$(UO_2)_2SiO_4 \cdot 2H_2O(cr) + 4\ H^+ \rightleftharpoons 2\ UO_2^{2+} + Si(OH)_4(aq) + 2\ H_2O(l)$$

$$\log_{10}{}^*K_s^\circ = 5.75 \pm 0.26$$

This value has been included in TDB 2020.

Although enthalpy of formation values for soddyite have been published for soddyite, Grenthe et al. (2020) consider them as unreliable and do not recommend any value, not even for "scoping calculations".

Boltwoodite, $K(UO_2)(SiO_3OH) \cdot H_2O$, sodium boltwoodite, $Na(UO_2)(SiO_3OH) \cdot H_2O$

Grenthe et al. (2020) state that boltwoodite, a layer-mineral with an idealised formula $K(UO_2)(SiO_3OH) \cdot nH_2O$, is formed at oxidation and alteration of spent nuclear fuel or primary uranium ores under moist oxidising conditions. Its structure is composed of two-dimensional sheets containing uranyl polyhedra and silicate tetrahedra, while K and H_2O occupy sites in the interlayer. The flexibility of the boltwoodite structure permits the substitution of K by various monovalent cations, from Na to Cs in natural samples and also variable water content.

Grenthe et al. (2020) found that most studies were made for sodium boltwoodite, $Na(UO_2)(SiO_3OH) \cdot H_2O$, and, after scrutinising these studies, they finally calculated the weighted average of two selected $\log_{10}{}^*K_s^\circ$ values for the reaction

$$Na(UO_2)(SiO_3OH) \cdot H_2O(cr) + 3\ H^+ \rightleftharpoons Na^+ + UO_2^{2+} + Si(OH)_4(aq) + H_2O(l)$$

$$\log_{10}{}^*K_s^\circ = 5.81 \pm 0.44$$

This value has been included in TDB 2020.

Grenthe et al. (2020) discuss in detail a recent solubility study of synthetic boltwoodite, and select based on their recalculations a value

$$K(UO_2)(SiO_3OH)\cdot H_2O(cr) + 3\ H^+ \rightleftharpoons K^+ + UO_2^{2+} + Si(OH)_4(aq) + H_2O(l)$$

$$\log_{10}{}^*K_s^\circ = 4.48 \pm 1.17$$

This value has been included in TDB 2020.

Grenthe et al. (2020) evaluated calorimetric data to obtain values of S_m° and $\Delta_f H_m^\circ$ for boltwoodite and sodium boltwoodite. In the case of boltwoodite they selected an experimental value of S_m° to derive

$$\Delta_f H_m^\circ(K(UO_2)(SiO_3OH)\cdot H_2O, cr, 298.15\ K) = -(2991.0 \pm 7.8)\ kJ \cdot mol^{-1}$$

whereas in the case of sodium boltwoodite Grenthe et al. (2020) estimated value of S_m° to derive

$$\Delta_f H_m^\circ(Na(UO_2)(SiO_3OH)\cdot H_2O, cr, 298.15\ K) = -(2962.1 \pm 5.5)\ kJ \cdot mol^{-1}$$

Note that the latter value is not included in the list of selected values of Grenthe et al. (2020).

Using $\Delta_f H_m^\circ$ values selected by this review for the aqueous species, this review calculated

$$K(UO_2)(SiO_3OH)\cdot H_2O(cr) + 3\ H^+ \rightleftharpoons K^+ + UO_2^{2+} + Si(OH)_4(aq) + H_2O(l)$$

$$\Delta_r H_m^\circ = -(27.7 \pm 8.0)\ kJ \cdot mol^{-1}$$

$$Na(UO_2)(SiO_3OH)\cdot H_2O(cr) + 3\ H^+ \rightleftharpoons Na^+ + UO_2^{2+} + Si(OH)_4(aq) + H_2O(l)$$

$$\Delta_r H_m^\circ = -(44.8 \pm 5.8)\ kJ \cdot mol^{-1}$$

These values have been included in TDB 2020, the latter value as supplemental datum only.

Uranophane, $Ca(UO_2)_2(SiO_3OH)_2\cdot 5H_2O$

Grenthe et al. (2020) state that uranophane is a U-bearing layer-mineral of the formula $Ca(UO_2)_2(SiO_3OH)_2\cdot 5H_2O(cr)$. It belongs to the most common U(VI) minerals and forms at oxidation and alteration of spent nuclear fuel or primary uranium ores under moist oxidising conditions.

The aqueous solubility of uranophane was investigated in a number of studies with the aim to evaluate $\log_{10}{}^*K_s^\circ$ for the reaction

$$Ca(UO_2)_2(SiO_3OH)_2\cdot 5H_2O(cr) + 6\ H^+ \rightleftharpoons Ca^{2+} + 2\ UO_2^{2+} + 2\ Si(OH)_4(aq) + 5\ H_2O(l)$$

However, Grenthe et al. (2020) found that in several studies the test solutions were oversaturated with respect to soddyite, $(UO_2)_2SiO_4 \cdot 2H_2O$(cr) and for this reason the reported $\log_{10}{}^*K_s^\circ$ values were not accepted. Grenthe et al. (2020) finally calculated a weighted average from two studies were uranophane was the thermodynamically stable phase

$$\log_{10}{}^*K_s^\circ = 11.52 \pm 0.16$$

This value has been included in TDB 2020.

Grenthe et al. (2020) derived from a calorimetric study $\Delta_f H_m^\circ$ of uranphane as

$$\Delta_f H_m^\circ(Ca(UO_2)_2(SiO_3OH)_2 \cdot 5H_2O, cr, 298.15\ K) = -(6848 \pm 16)\ kJ \cdot mol^{-1}$$

but state that, unfortunately, the exact elemental composition of the studied sample of synthetic uranophane was not reported, although deviations from the exact stoichiometric composition may represent a very large and difficult-to-account-for contribution to the error in the $\Delta_f H_m^\circ$ value and for this reason the thermodynamic data are given for information only.

Using $\Delta_f H_m^\circ$ values selected by this review for the aqueous species, this review calculated

$$\Delta_r H_m^\circ = -(86 \pm 16)\ kJ \cdot mol^{-1}$$

This value has been included in TDB 2020 as supplemental datum.

Sodium weeksite, $Na_2(UO_2)2(Si_2O_5)_3 \cdot 4H_2O$

Grenthe et al. (2020) discuss one study concerning the solubility of a synthetic sodium weeksite, $Na_2(UO_2)_2(Si_2O_5)_3 \cdot 4H_2O$(cr). They found that the solution was oversaturated with respect to soddyite, $(UO_2)_2SiO_4 \cdot 2H_2O$(cr), and no solubility constant was therefore selected by Grenthe et al. (2020).

25.4.8.2.2 Solid uranium(IV) silicates

Coffinite, $USiO_4$

Grenthe et al. (2020) state that coffinite, $USiO_4$, is found in nature in igneous and metamorphic rocks and uranium sedimentary deposits. This mineral is expected to be an important alteration product of spent nuclear fuel in contact with silica-bearing aqueous solutions under reducing conditions. In nature coffinite forms fine-grained crystals almost always associated with other minerals, often uraninite, UO_2(cr), quartz and organic matter. Hence, the determination of experimental data from natural samples is questionable. The synthesis of coffinite, either by reaction oxides at high temperatures or by precipitating from aqueous solutions, is faced with several difficulties, presumably because this phase is thermodynamically metastable with respect to quartz and uraninite.

Grenthe et al. (2020) discuss experimental values which have recently been published and conclude that the problem of precise determination of thermodynamic properties of coffinite is not yet resolved. They state that all indirect results point to the fact that coffinite is metastable with respect to a mixture of oxides. Grenthe et al. (2020) provide the thermodynamic values

$\Delta_f G_m°(USiO_4, cr, 298.15\ K) = -1'864.6\ kJ \cdot mol^{-1}$

$\Delta_f H_m°(USiO_4, cr, 298.15\ K) = -2'974\ kJ \cdot mol^{-1}$

but state that "these values are given for information only". No values of thermodynamic properties for coffinite are selected by Grenthe et al. (2020).

Using $\Delta_f G_m°$ and $\Delta_f H_m°$ values selected by this review for the aqueous species, this review calculated for the reaction

$$USiO_4(cr) + 4\ H^+ \rightleftharpoons U^{4+} + Si(OH)_4(aq)$$

$$log_{10}{}^*K_s° = -4.5$$

$$\Delta_r H_m° = -79\ kJ \cdot mol^{-1}$$

These values have been included in TDB 2020 as supplemental data.

25.4.9 Neptunium and Plutonium

Silicate complextion of neptunium and plutonium often has been studied using the same experimental methods by the same groups and hence, they are discussed together in this section.

25.4.9.1 Neptunium(III) and plutonium(III)

No information about aqueous Np(III) and Pu(III) silicate complexes could be found in the literature during the present review. On the other hand, silicate complexation with Eu(III), Am(III) and Cm(III) is well established (see Section 4.5) and these elements are considered as reasonably good chemical analogues for Pu(III) and Np(III). Therefore, we included the estimates

$$log_{10}\beta_1° = 7.8 \pm 0.5$$

$$\Delta_r H_m° \approx 15\ kJ \cdot mol^{-1}$$

$$\varepsilon(NpSiO(OH)_3^{2+}, ClO_4^-) = \varepsilon(PuSiO(OH)_3^{2+}, ClO_4^-) = 0.4 \pm 0.1\ kg \cdot mol^{-1}$$

$$\varepsilon(NpSiO(OH)_3^{2+}, Cl^-) = \varepsilon(PuSiO(OH)_3^{2+}, Cl^-) = 0.15 \pm 0.10\ kg \cdot mol^{-1}$$

as supplemental data in TDB 2020 for the equilibria

$$Np^{3+} + SiO(OH)_3^- \rightleftharpoons NpSiO(OH)_3^{2+}$$

$$Pu^{3+} + SiO(OH)_3^- \rightleftharpoons PuSiO(OH)_3^{2+}$$

25.4.9.2 Neptunium(IV) and plutonium(IV)

The first paper reporting experimental data on Pu(IV) silicate complexation was published by Pazukhin et al. (1990). The system Pu(IV) nitrate – sodium silicate was studied by potentiometric and spectrophotometric methods. Addition of sodium silicate to a Pu(IV) solution is proposed to form a complex in which the mole ratio Pu:silicate is 1:8 at pH 1.36. The authors report a value $K = 5$. However, the equilibrium this value refers to and the stoichiometry of the complex are not defined in the paper. Shilov & Fedoseev (2003) later comment on this paper: "we think that the authors dealt with colloid solutions in which Pu(IV) was sorbed on polysilicic acid particles". The study of Pazukhin et al. (1990) is not considered further in this review.

Yusov et al. (2004) studied the hydrolysis and interaction of Np(IV) and Pu(IV) with orthosilicic acid, $Si(OH)_4(aq)$, in 0.1 – 1.0 M $(H,Na)ClO_4$ solutions. Spectrophotometry was used to study the reactions at about 10^{-4} M Np(IV) and Pu(IV) concentrations. Formation of the complexes $NpSiO(OH)_3^{3+}$ and $PuSiO(OH)_3^{3+}$ is demonstrated in the presence of 0.005 – 0.016 M $Si(OH)_4(aq)$ in the $p[H^+]$ range 1.0 – 2.2 and 0.3 – 1.4, respectively. Equilibrium constants at different ionic strengths are given in Tab. 2 of Yusov et al. (2004).

Grenthe et al. (2020) discuss the paper of Yusov et al. (2004) in detail, but due to concerns associated with the Np(IV) and Pu(IV) hydrolysis constants, they cannot recommend the data reported in Yusov et al. (2004) and no thermodynamic data are selected by Grenthe et al. (2020).

This review decided to use the data reported by Yusov et al. (2004) for tentative SIT analyses (Fig. 25-19) and obtained

$$Np^{4+} + Si(OH)_4(aq) \rightleftharpoons NpSiO(OH)_3^{3+} + H^+$$

$$\log_{10}K^\circ = 1.34 \pm 0.18$$

$$\Delta\varepsilon = -(0.29 \pm 0.29)\ kg \cdot mol^{-1}$$

$$Pu^{4+} + Si(OH)_4(aq) \rightleftharpoons PuSiO(OH)_3^{3+} + H^+$$

$$\log_{10}K^\circ = 2.07 \pm 0.18$$

$$\Delta\varepsilon = -(0.16 \pm 0.27)\ kg \cdot mol^{-1}$$

Using $\varepsilon(Np^{4+}, ClO_4^-) = 0.84 \pm 0.06\ kg \cdot mol^{-1}$, $\varepsilon(Pu^{4+}, ClO_4^-) = 0.82 \pm 0.07\ kg \cdot mol^{-1}$ and $\varepsilon(H^+, ClO_4^-) = 0.14 \pm 0.02\ kg \cdot mol^{-1}$ (Lemire et al. 2013), and $\varepsilon(SiO(OH)_4(aq), NaClO_4) = \varepsilon(SiO(OH)_4(aq), NaCl) = 0.03 \pm 0.06\ g \cdot mol^{-1}$ derived in this review we calculate

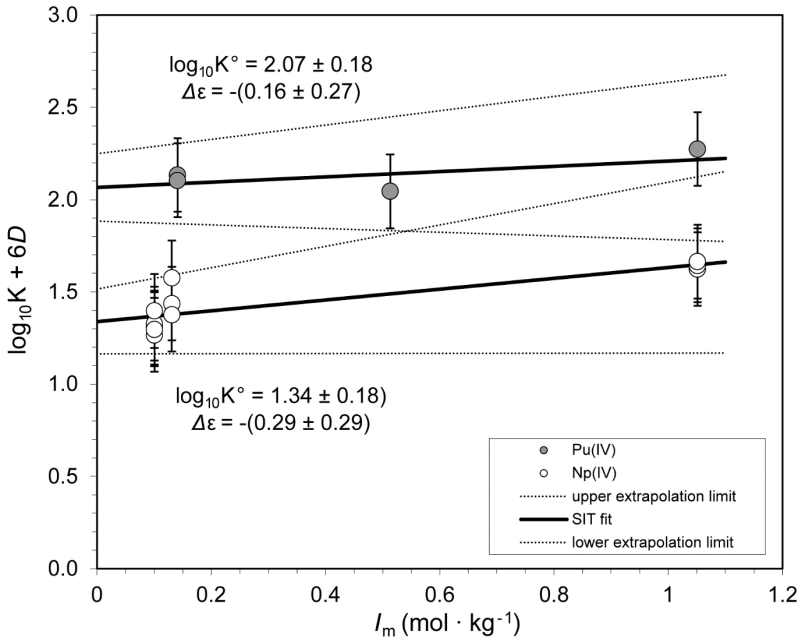

Fig. 25-19: SIT analysis of the equilibrium $An^{4+} + Si(OH)_4(aq) \rightleftharpoons AnSiO(OH)_3^{3+} + H^+$ where An is Np(IV) or Pu(IV)

The experimental data are taken from Yusov et al. (2004).

$$\varepsilon(NpSiO(OH)_3^{3+}, ClO_4^-) = 0.44 \pm 0.30 \text{ kg} \cdot \text{mol}^{-1}$$

$$\varepsilon(PuSiO(OH)_3^{3+}, ClO_4^-) = 0.55 \pm 0.28 \text{ kg} \cdot \text{mol}^{-1}$$

Using $\log_{10}\beta^\circ = -(9.81 \pm 0.02)$ for $Si(OH)_4(aq) \rightleftharpoons SiO(OH)_3^- + H^+$ this review calculated

$$Np^{4+} + SiO(OH)_3^- \rightleftharpoons NpSiO(OH)_3^{3+}$$

$$\log_{10}\beta_1^\circ = 11.15 \pm 0.18$$

$$Pu^{4+} + SiO(OH)_3^- \rightleftharpoons PuSiO(OH)_3^{3+}$$

$$\log_{10}\beta_1^\circ = 11.88 \pm 0.18$$

The values estimated by Yusov et al. (2004), $\log_{10}\beta_1^\circ = 11.2$ for Np(IV) and $\log_{10}\beta_1^\circ = 11.8$ for Pu(IV), are consistent with the SIT analyses in this review.

However, this review agrees with the concerns of Grenthe et al. (2020) and included the above values in TDB 2020 as supplemental data only.

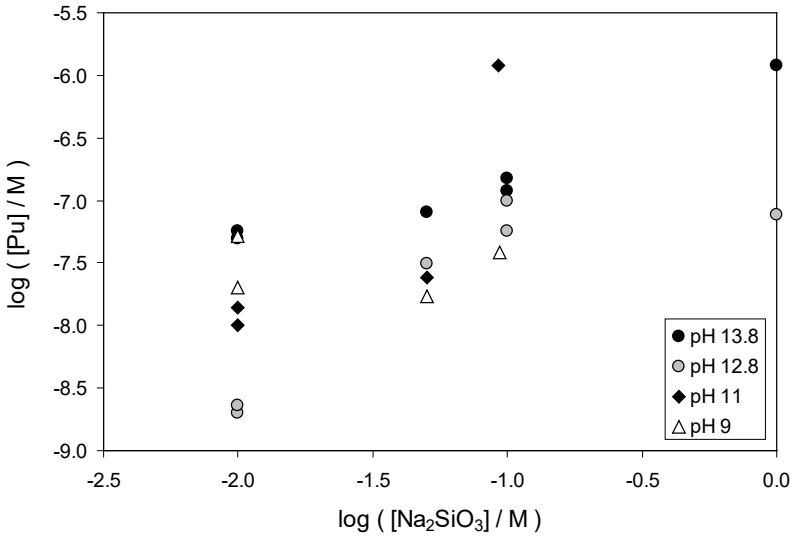

Fig. 25-20: Plutonium(IV) concentration in Na_2SiO_3 solution after filtration at different pH values

Data taken from Tab. 2 of Shilov & Fedoseev (2003).

Shilov & Fedoseev (2003) studied radiometrically the solubility of hydrated Pu(IV) oxide in 0.09 – 0.9 M NaOH containing 0.01 – 1 M Na_2SiO_3 and in 0.1 – 0.2 M $NaClO_4$ containing 0.01-0.09 M Na_2SiO_3 (pH 11 and 9). They stated that the experimental log-log dependence of the Pu(IV) solubility in 0.90 and 0.09 M NaOH (pH 13.8 an 12.8) on the silicate concentration "is almost linear" and interpreted these data in terms of the equilibrium

$$Pu(IV) + n\ SiO_3^{2-} \rightleftharpoons Pu^{IV}(SiO_3^{2-})_n$$

with n = 0.7 and 1.2, respectively. They further stated that "although the plutonium solubility at pH 11 also increased with increasing Na_2SiO_3 concentration, strong scattering of the experimental points was observed. At pH 9, the solubility was almost independent of the Na_2SiO_3 concentration".

A plot of all experimental data published in Tab. 2 (after filtration) of Shilov & Fedoseev (2003) shows (Fig. 25-20) that "almost linear" in the cases pH 13.8 and 12.8 and "almost independent" at pH 9 are euphemisms.

The data at 0.01 M Na_2SiO_3 concentration do not show any systematic pH dependence, and the log mean value of the measured Pu(IV) concentrations is -7.8 ± 0.5. This is the same value as measured without addition of Na_2SiO_3 (-7.9 ± 0.5, derived from Tab. 1 in Shilov & Fedoseev 2003). With increasing Na_2SiO_3 concentration there seems to be a systematic increase in measured Pu concentrations, which could be due to Pu silicate complex formation. However, the scatter and some erratic data points (Fig. 25-20) prevent any meaningful interpretation of these data in terms of a simple thermodynamic equilibrium.

25.4.9.3 Neptunium(V) and plutonium(V)

As discussed by Grenthe et al. (2020), Yusov et al. (2005a) investigated the hydrolysis of Np(V) and its complexation with silicate under weakly alkaline conditions (pH 8 – 10) using a spectrophotometric approach. Ionic strength was kept constant at I = 0.1 M $NaClO_4$. The concentration of Np(V) ranged between $5 \cdot 10^{-5}$ M and $1 \cdot 10^{-4}$ M. The total concentration of silicate ranged between 0.004 and 0.002 M. Most of the samples evaluated were supersaturated with respect to amorphous silica, resulting in the formation of significant amounts of polymeric Si species (up to 80% of $[Si]_{tot}$, as quantified by the molybdate method). Yusov et al. (2005a) calculated

$$NpO_2^+ + SiO(OH)_3^- \rightleftharpoons NpO_2SiO(OH)_3(aq)$$

$$\log_{10}\beta_1 \text{ (0.1 M } NaClO_4) = 2.1 \pm 0.3$$

as average of 16 independent measurements at different concentrations $[Np]_{tot}$, $[Si]_{tot}$ and $-\log_{10}[H^+]$. Grenthe et al. (2020) remark that the presence of polymeric Si species was not accounted for in the calculations, resulting in a likely overestimation of $[OSi(OH)_3^-]$ and consequent underestimation of $\log_{10}\beta_1$ (0.1 M $NaClO_4$).

Hence, the equilibrium constant reported by Yusov et al. (2005a) is not selected by Grenthe et al. (2020), but

$$\log_{10}\beta_1 \text{ (0.1 M } NaClO_4) = 2.3$$

determined in Yusov et al. (2005a) at the lowest silicate concentration ([Si]tot = 0.004 M) is reported for information.

Using $\varepsilon(NpO_2^+, ClO_4^-) = 0.25 \pm 0.05$ kg · mol^{-1} (Lemire et al. 2013) and $\varepsilon(SiO(OH)_3^-, Na^+) = -0.05 \pm 0.07$ kg · mol^{-1} derived in this review, and the estimate $\varepsilon(NpO_2SiO(OH)_3(aq), NaClO_4) = 0.0 \pm 0.1$ kg · mol^{-1} the above value has been extrapolated to zero ionic strength

$$\textit{log}_{10}\beta_1^\circ = \textit{2.5} \pm \textit{0.3}$$

This value is included in TDB 2020 as supplemental datum.

Pathak & Choppin (2007) studied the complexation behaviour of NpO_2^+ with silicic acid using solvent extraction at ionic strengths varying from 0.10 to 1.00 M $NaClO_4$ at $p[H^+]$ 3.68 ± 0.08 and 25 °C. The stability constant value for the 1:1 complex

$$NpO_2^+ + SiO(OH)_3^- \rightleftharpoons NpO_2SiO(OH)_3(aq)$$

was found to decrease with increase in ionic strength. The values have been extrapolated to zero ionic strength by Pathak & Choppin (2007) using SIT and the authors obtained

$$\log_{10}\beta_1^\circ = 7.04 \pm 0.02$$

This value is significantly larger than the value reported by Yusov et al. (2005a).

As discussed by Grenthe et al. (2020), different solvents, extraction ligands and ligand concentrations were evaluated for the analysis of the extraction data by Pathak & Choppin (2007). In most cases, both the uncomplexed metal ion and the Np(V)-silicate complex were extracted into the organic phase, preventing the use of these data for the evaluation of the equilibrium constants. The conditions finally chosen relied on a dilute solution (10^{-3} M) of HDEHP in *n*-heptane, which was the only system showing a decrease of the extraction coefficient of neptunium (D_{Np}) in the presence of silicic acid. Pathak & Choppin (2007) observed only minor changes in D_{Np} with increasing $[Si]_{tot}$, which were interpreted as a result of the formation of the complex $NpO_2OSi(OH)_3(aq)$ according with the above reaction. The largest variation in D_{Np} observed in the presence of silicate accounted for ~ 4.5 % ($[(D_0/D) - 1] \leq 0.045$, Fig. 3 in their paper), which casts severe doubts on the accuracy of the measurements, especially considering that the uncertainty reported by Pathak & Choppin (2007) in the mass-balance of the extraction process is 5 %.

Grenthe et al. (2020) do not accept the data in Pathak & Choppin (2007), and this review agrees with the decision of Grenthe et al. (2020).

No information about aqueous Pu(V) silicate complexes could be found in the literature during the present review. Hence, the supplemental datum selected for Np(V) has been used as an estimate for Pu(V) and has been included in TDB 2020 as supplemental datum.

25.4.9.4 Neptunium(VI) and plutonium(VI)

Yusov & Fedoseev (2003) studied the reaction of Pu(VI) with orthosilicic acid (at concentrations 0.004 – 0.025 mol · dm^{-3}) in a 0.2 M $NaClO_4$ solution at pH 3 – 8 by spectrophotometry.

Data in the pH range 4.5 – 5.5 were interpreted by the authors in terms of the equilibrium

$$PuO_2^{2+} + Si(OH)_4(aq) \rightleftharpoons PuO_2SiO(OH)_3^{+} + H^{+}$$

$$\log_{10}K_1 = -(3.91 \pm 0.17)$$

Grenthe et al. (2020) remark that the direct quantification of $PuO_2SiO(OH)_3^{+}$ by spectra deconvolution is problematic and due to the uncertainties associated with the experiment and data analysis, they do not select the reported $\log_{10}K_1$ value, and report it for information only.

Yusov & Fedoseev (2003) further report that "for comparison with the spectrophotometric data, we performed the experiment on estimation of the stability constant of the Pu(VI) complex with $OSi(OH)_3^-$ by the potentiometric method like Pokrovski et al. (1996) studied the Al(III) complexes with $OSi(OH)_3^-$." They obtained $\log_{10}K_1$ = -3.53 and -3.71 in two experiments in a 0.207 M $NaClO_4$ solution and state "though these values somewhat exceed the values of the constants obtained from spectrophotometric data, they show reasonable agreement with them." (which gives $\log_{10}\beta_1° = 6.55$ and 6.37, respectively).

Using $\varepsilon(PuO_2^{2+}, ClO_4^-) = 0.46 \pm 0.05$ kg · mol^{-1} and, $\varepsilon(H^+, ClO_4^-) = 0.14 \pm 0.02$ kg · mol^{-1} (Lemire et al. 2013), and $\varepsilon(Si(OH)_4(aq), NaClO_4) = \varepsilon(Si(OH)_4(aq), NaCl) = 0.03 \pm 0.06$ g · mol^{-1} derived in this review, and the estimate $\varepsilon(NpO_2SiO(OH)_3^+, ClO_4^-) = 0.2 \pm 0.1$ kg · mol^{-1} the above values have been extrapolated to zero ionic strength as $\log_{10}K_1° = -3.29$ and -3.47.

Using $\log_{10}\beta^\circ$ = -(9.81 ± 0.02) for $Si(OH)_4(aq) \rightleftharpoons SiO(OH)_3^- + H^+$ this review calculated the unweighted average of the above two values as

$$PuO_2^{2+} + SiO(OH)_3^- \rightleftharpoons PuO_2SiO(OH)_3^+$$

$$\log_{10}\beta_1^\circ \approx 6.4$$

This value has been included in TDB 2020 as supplemental datum.

At pH > 5.5 Yusov & Fedoseev (2003) interpreted their spectrophotometric data in terms of the formation of either $PuO_2SiO_2(OH)_2(aq)$ or $PuO_2(OH)SiO(OH)_3(aq)$. Since the formation of these complexes differs just by the absence or presence of one water molecule and hence, the equilibrium constant should be the same, it is unclear why Yusov & Fedoseev (2003) report $\log_{10}\beta_2 \approx 12.6$ for

$$PuO_2^{2+} + SiO_2(OH)_2^{2-} \rightleftharpoons PuO_2SiO_2(OH)_2(aq)$$

but $\log_{10}\beta_2 \approx 13$ for

$$PuO_2^{2+} + SiO_2(OH)_2^{2-} + H_2O \rightleftharpoons PuO_2(OH)SiO(OH)_3(aq)$$

Due to the lack of information on the ligand and reaction stoichiometry and the increasing polymerisation of the silicic acid at high pH, the proposed formation constants for the second Pu(VI) silicate complex are not recommended by Grenthe et al. (2020).

This review agrees with the conclusions of Grenthe et al. (2020), especially considering the contradicting results of Yusov et al. (2005b) for $NpO_2SiO_2(OH)_2(aq)$ (see below).

Shilov et al. (2004) studied the complexation of Np(VI) in silicate solutions in the presence of carbonate at pH 10.5 – 12.0 by spectrophotometry. The authors conclude from optical density data the occurrence of a fast competition reaction between carbonate and silicate

$$NpO_2(CO_3)_3^{4-} + SiO_3^{2-} \rightleftharpoons NpO_2SiO_3(aq) + 3\ CO_3^{2-}$$

and reported $\log_{10}\beta$ = 16.5 at pH 10.13 in 0.1 M $NaClO_4$ solution for the equilibrium

$$NpO_2^{2+} + SiO_3^{2-} \rightleftharpoons NpO_2SiO_3(aq)$$

In order to obtain this value they used $\log_{10}\beta_3$ = 20.41 (I = 0.1) for the equilibrium $NpO_2^{2+} + CO_3^{2-} \rightleftharpoons NpO_2(CO_3)_3^{4-}$, which is one order of magnitude at variance with the value selected in our database ($\log_{10}\beta_3$ = 19.04 at I = 0.1). In addition, while their dissociation constants of carbonic acid are almost identical with our values, the cumulative dissociation constant of "metasilicic acid" taken from a Russian "Chemist's Handbook", $\log_{10}\beta_2^\circ$ = -21.45, is two orders of magnitude different from our established value $\log_{10}\beta_2^\circ$ = -23.14 ± 0.09. It is not clear what "dissociation constants of metasilicic acid" means, as Shilov et al. (2004) write in the introductory part of their

paper about "silicate solutions in which both metasilicate SiO_3^{2-} and orthosilicate SiO_4^{4-} ions (and protonated species of the latter) can exist."

However, even assuming that Shilov et al. (2004) actually meant

$$NpO_2(CO_3)_3^{4-} + SiO_2(OH)_3^{2-} \rightleftharpoons NpO_2SiO_2(OH)_2(aq) + 3\ CO_3^{2-}$$

as Grenthe et al. (2020) assumed, does not really help. Grenthe et al. (2020) discussed experimental shortcomings in some detail and concluded that the stoichiometry of the the complex proposed in Shilov et al. (2004) is considered speculative due to the lack of a systematic variation of carbonate concentration in the experiments and hence, no thermodynamic data are recommended from this study.

This review agrees with the conclusions of Grenthe et al. (2020).

In the last paper of this series, Yusov et al. (2005b) studied the complexation of Np(VI) in silicate solutions in the acid and neutral pH range by spectrophotometry. The interaction at pH < 4.5 is described by the equilibrium

$$NpO_2^{2+} + Si(OH)_4(aq) \rightleftharpoons NpO_2SiO(OH)_3^{+} + H^{+}$$

with $\log_{10}K_1 = -(2.88 \pm 0.12)$ at ionic strength $I = 0.1 - 0.2$ and $\log_{10}K_1^\circ = -(2.61 \pm 0.12)$, recalculated to $I = 0$ by Yusov et al. (2005b).

Grenthe et al. (2020) discuss this study in detail and remark that all experiments were performed in test solutions over-saturated with respect to amorphous silica, and the presence of dimeric, trimeric and tetrameric Si species was experimentally confirmed in all samples. Grenthe et al. (2020) thus do not accept the $\log_{10}K_1$ value reported by Yusov et al. (2005b) as it has been obtained under non-equilibrium conditions, although

$$\log_{10}K_1\ (0.1\ M\ NaClO_4) = -2.8$$

calculated from the experiments with the lowest silicate concentration ($[Si]_{tot} = 0.022$ M) is probably the best estimate available and can be considered in scoping calculations.

Using $\varepsilon(NpO_2^{2+}, ClO_4^-) = 0.46 \pm 0.05$ kg · mol^{-1} and $\varepsilon(H^+, ClO_4^-) = 0.14 \pm 0.02$ kg · mol^{-1} (Lemire et al. 2013) and $\varepsilon(Si(OH)_4(aq), NaClO_4) = \varepsilon(Si(OH)_4(aq), NaCl) = 0.03 \pm 0.06$ g · mol^{-1} derived in this review, and the estimate $\varepsilon(NpO_2SiO(OH)_3^+, ClO_4^-) = 0.2 \pm 0.1$ kg · mol^{-1} the above value has been extrapolated to zero ionic strength

$$\log_{10}K_1^\circ = -2.60$$

Using $\log_{10}\beta^\circ = -(9.81 \pm 0.02)$ for $Si(OH)_4(aq) \rightleftharpoons SiO(OH)_3^- + H^+$ this review calculated

$$NpO_2^{2+} + SiO(OH)_3^- \rightleftharpoons NpO_2SiO(OH)_3^+$$

$$\log_{10}\beta_1^\circ \approx 7.2$$

This value has been included in TDB 2020 as supplemental datum.

Yusov et al. (2005b) further write: "We attempted to reveal the neutral complex with monomeric silicic acid, $NpO_2SiO_2(OH)_2(aq)$. However, in the solution containing 4.5×10^{-4} M Np(VI) and 0.002 M $Si(OH)_4$ [at such concentration, $Si(OH)_4$ does not polymerize] and pH ≈ 7.5, we failed to detect the complexation because of the strong effect of the hydrolysis." This result sheds doubts on results reported earlier by the same group (Yusov & Fedoseev 2003) for $PuO_2SiO_2(OH)_2(aq)$ at pH > 5.5 using the same experimental set-up (see above). The hydrolysis effects of Np(VI) and Pu(VI) are rather similar, and the stability constants reported for Np(VI) – silicate complexes are even higher than for Pu(VI). So why should hydrolysis prevent the detection of a $NpO_2SiO_2(OH)_2(aq)$ complex, while under very similar conditions a stability constant for the (perhaps weaker?) $PuO_2SiO_2(OH)_2(aq)$ complex was reported?

The discussion in Yusov et al. (2005b) becomes even stranger in the section "Regular trends in interaction of actinide ions with silicate ions in the series U(VI) – Np(VI) – Pu(VI)": "As we reported (Shilov et al. 2004), at pH > 10 Np(VI) forms the silicate complex $NpO_2SiO_3(aq)$ with the stability constant $\log_{10}\beta = 16.5$ ($I = 0.1$). … Similar experiments with Pu(VI) gave an appreciably lower value: $\log_{10}\beta = 14.4$, which is close to the stability constant of the Pu(VI) complex with another double-charged anion, $SiO_2(OH)_2^{2-}$, arising at pH ≈ 7: $\log_{10}\beta = 12.6$ ($I = 0.2$) (Yusov & Fedoseev 2003)."

The value $\log_{10}\beta = 14.4$ for a complex $PuO_2SiO_3(aq)$ appears here out of the blue, without any further comment or reference. And the authors seem to be convinced that SiO_3^{2-} and $SiO_2(OH)_2^{2-}$ are structurally different anions really existing in silicate solutions and forming metal – silicate complexes with rather different stabilities. However, there is no indication of a ligand SiO_3^{2-} existing in aqueous solution where silicon is coordinated to just three oxygen atoms (like in CO_3^{2-}) instead of four as in $SiO_2(OH)_2^{2-}$. Sometimes in the chemical thermodynamic literature SiO_3^{2-} is used as an alternative expression to $SiO_2(OH)_2^{2-}$ where formally one H_2O is "subtracted". The stability constants for equilibria formulated with these alternative expressions are the same, only $\Delta_f G_m$ values derived therefrom are different because of the inclusion or exclusion of the formal H_2O. Hence, the value $\log_{10}\beta = 14.4$ referring to "$PuO_2SiO_3(aq)$" is not considered further by this review.

25.5 Selected silicon and silicate data

Tab. 25-13: Silicon and silicate data selected by NEA (Grenthe et al. 1992, Brown et al. 2005, Gamsjäger et al. 2005, Rand et al. 2008) but not included in TDB 2020

For explanations see text.

Gases	Sig, SiF_4g
Solids	$Ni_2SiO_4(cr)$, $ZrSiO_4(cr)$, $Ca_2ZrSi_3O_{12}(cr)$, $Ca_3ZrSi_2O_9(cr)$, $Sr_6ZrSi_5O_{18}(cr)$, $SrZrSi_2O_7(cr)$, $Na_2ZrSiO_5(cr)$, $Na_2ZrSi_2O_7(cr)$, $Na_4Zr_2Si_3O_{12}(cr)$, $Na_2ZrSi_3O_9{\cdot}2H_2O(cr)$, $Na_2ZrSi_4O_{11}(cr)$, $Na_2ZrSi_6O_{15}{\cdot}3H_2O(cr)$, $Cs_2ZrSi_2O_7(cr)$, $ThSiO_4$(huttonite), $ThSiO_4$(thorite),
Aqueous species	$Si_2O_3(OH)_4^{2-}$, $Si_2O_2(OH)_5^{-}$, $Si_3O_6(OH)_3^{3-}$, $Si_3O_5(OH)_5^{3-}$, $Si_4O_7(OH)_5^{3-}$

Tab. 25-14: Selected silicon and silicate data

Core data are bold and supplemental data in italics.

Name	**$\Delta_f G_m°$** [kJ · mol^{-1}]	**$\Delta_f H_m°$** [kJ · mol^{-1}]	**$S_m°$** [J · K^{-1} · mol^{-1}]	**$C_{p,m}°$** [J · K^{-1} · mol^{-1}]	**Formula**
Si(cr)	0.0	0.0	**18.810 ± 0.080**	**19.789 ± 0.030**	Si(cr)
Si(OH)4(aq)	-1'309.183 ± 1.120	-1'461.723 ± 1.082	178.851 ± 2.178	237.370 ± 2.024	$Si(OH)_4(aq)$
Quartz	**-856.287 ± 1.002**	**-910.700 ± 1.000**	**41.460 ± 0.200**	**44.602 ± 0.300**	$SiO_2(cr)$
Smectite MX80	*-5'293.18 ± 5.4*	*-5656.37 ± 5.4*	*301.92 ± 0.2*	*322.74*	$(Na_{0.409}K_{0.024}Ca_{0.009})(Si_{3.738}Al_{0.262})(Al_{1.598}Mg_{0.214}Fe^{III}_{0.173}Fe^{II}_{0.035})O_{10}(OH)_2$
Saponite SapCa-2	*-5'622.45 ± 5.0*	*-5994.06 ± 4.9*	*314.55 ± 1.6*	*346.87*	$(Na_{0.394}K_{0.021}Ca_{0.038})(Si_{3.569}Al_{0.397})(Mg_{2.949}Fe^{III}_{0.034}Fe^{II}_{0.021})O_{10}(OH)_2$
Nontronite Nau-1	*-4'684.90 ± 6.5*	*-5035.69 ± 5.3*	*332.75 ± 7.0*	*335.15*	$(Ca_{0.247}K_{0.020})(Si_{3.458}Al_{0.542})(Fe^{III}_{1.688}Al_{0.276}Mg_{0.068})O_{10}(OH)_2$
Beidellite SBld-1	*-5'357.24 ± 6.5*	*-5720.69 ± 6.5*	*293.53 ± 0.4*	*318.58*	$(Ca_{0.185}K_{0.104})(Si_{3.574}Al_{0.426})(Al_{1.812}Mg_{0.090}Fe^{III}_{0.112})O_{10}(OH)_2$
Illite IMt-2	*-5'325.87 ± 8.5*	*-5711.25 ± 8.5*	*324.92 ± 0.2*	*328.21*	$(K_{0.762}Na_{0.044})(Si_{3.387}Al_{0.613})(Al_{1.427}Fe^{III}_{0.292}Mg_{0.241}Fe^{II}_{0.084})O_{10}(OH)_2$
Vermiculite SO	*-5'671.20 ± 5.7*	*-6034.41 ± 5.7*	*325.77 ± 0.5*	*346.39*	$Ca_{0.445}(Si_{2.778}Al_{1.222})(Al_{0.192}Mg_{2.468}Fe^{III}_{0.226}Fe^{II}_{0.028}Ti_{0.018}Mn_{0.007})O_{10}(OH)_2$
Ripidolite Cca-2	*-7'593.46 ± 8.7*	*-8240.14 ± 8.6*	*469.40 ± 2.9*	*547.02*	$(Si_{2.633}Al_{1.367})(Al_{1.116}Fe^{III}_{0.215}Mg_{2.952}Fe^{II}_{1.712}Mn_{0.012})(Ca_{0.011})O_{10}(OH)_8$
Berthierine ISGS	*-3'461.94 ± 7.3*	*-3774.46 ± 6.3*	*257.00 ± 6.7*	*263.57*	$(Si_{1.332}Al_{0.668})(Al_{0.976}Fe^{III}_{0.182}Fe^{II}_{1.44}Mg_{0.157})O_5(OH)_4$
Montmorillonite(MgK)	*-5'332.65*	*-5'703.51*	*273.04*	*311.33*	$K_{0.34}Mg_{0.34}Al_{1.66}Si_4O_{10}(OH)_2$
Montmorillonite(MgNa)	*-5'322.35*	*-5'690.41*	*277.88*	*310.60*	$Na_{0.34}Mg_{0.34}Al_{1.66}Si_4O_{10}(OH)_2$
Montmorillonite(MgCa)	*-5'322.63*	*-5'690.29*	*268.85*	*305.88*	$Ca_{0.17}Mg_{0.34}Al_{1.66}Si_4O_{10}(OH)_2$
Montmorillonite(MgMg)	*-5'309.00*	*-5'676.01*	*269.52*	*304.71*	$Mg_{0.17}Mg_{0.34}Al_{1.66}Si_4O_{10}(OH)_2$
Montmorillonite(HcK)	*-5'388.47*	*-5'757.74*	*296.34*	*319.96*	$K_{0.6}Mg_{0.6}Al_{1.4}Si_4O_{10}(OH)_2$
Montmorillonite(HcNa)	*-5'370.31*	*-5'734.63*	*304.90*	*318.67*	$Na_{0.6}Mg_{0.6}Al_{1.4}Si_4O_{10}(OH)_2$
Montmorillonite(HcCa)	*-5'370.80*	*-5'734.42*	*288.96*	*310.34*	$Ca_{0.3}Mg_{0.6}Al_{1.4}Si_4O_{10}(OH)_2$
Montmorillonite(HcMg)	*-5'346.75*	*-5'709.22*	*290.13*	*308.29*	$Mg_{0.3}Mg_{0.6}Al_{1.4}Si_4O_{10}(OH)_2$
Saponite(K)	*-5'632.90*	*-6'010.39*	*293.96*	*334.54*	$K_{0.34}Mg_3Al_{0.34}Si_{3.66}O_{10}(OH)_2$
Saponite(Na)	*-5'623.07*	*-5'997.76*	*298.80*	*333.81*	$Na_{0.34}Mg_3Al_{0.34}Si_{3.66}O_{10}(OH)_2$
Saponite(Ca)	*-5'624.15*	*-5'998.44*	*289.78*	*329.09*	$Ca_{0.17}Mg_3Al_{0.34}Si_{3.66}O_{10}(OH)_2$
Saponite(Mg)	*-5'610.70*	*-5'984.34*	*290.44*	*327.93*	$Mg_{0.17}Mg_3Al_{0.34}Si_{3.66}O_{10}(OH)_2$
Saponite(FeK)	*-5'284.04*	*-5'645.53*	*342.04*	*344.95*	$K_{0.34}Mg_2Fe^{II}Al_{0.34}Si_{3.66}O_{10}(OH)_2$
Saponite(FeNa)	*-5'275.20*	*-5'633.89*	*346.87*	*344.23*	$Na_{0.34}Mg_2Fe^{II}Al_{0.34}Si_{3.66}O_{10}(OH)_2$
Saponite(FeCa)	*-5'275.28*	*-5'633.57*	*337.85*	*339.50*	$Ca_{0.17}Mg_2Fe^{II}Al_{0.34}Si_{3.66}O_{10}(OH)_2$
Saponite(FeMg)	*-5'261.84*	*-5'619.48*	*338.52*	*338.33*	$Mg_{0.17}Mg_2Fe^{II}Al_{0.34}Si_{3.66}O_{10}(OH)_2$
Nontronite(K)	*-4'638.59*	*-4'994.27*	*323.66*	*334.23*	$K_{0.34}Fe^{III}_{1.67}Al_{0.67}Si_{3.66}O_{10}(OH)_2$
Nontronite(Na)	*-4'628.76*	*-4'981.64*	*328.49*	*333.50*	$Na_{0.34}Fe^{III}_{1.67}Al_{0.67}Si_{3.66}O_{10}(OH)_2$
Nontronite(Ca)	*-4'629.84*	*-4'982.32*	*319.47*	*328.78*	$Ca_{0.17}Fe^{III}_{1.67}Al_{0.67}Si_{3.66}O_{10}(OH)_2$
Nontronite(Mg)	*-4'616.39*	*-4'968.22*	*320.14*	*327.62*	$Mg_{0.17}Fe^{III}_{1.67}Al_{0.67}Si_{3.66}O_{10}(OH)_2$
Beidellite(K)	*-5'376.58*	*-5'749.86*	*266.65*	*310.35*	$K_{0.34}Mg_{0.34}Al_{1.66}Si_4O_{10}(OH)_2$
Beidellite(Na)	*-5'376.75*	*-5'747.23*	*271.49*	*309.62*	$Na_{0.34}Mg_{0.34}Al_{1.66}Si_4O_{10}(OH)_2$

Tab. 25-14: Cont.

Name	**$\Delta_f G_m°$** [kJ · mol^{-1}]	**$\Delta_f H_m°$** [kJ · mol^{-1}]	**$S_m°$** [J · K^{-1} · mol^{-1}]	**$C_{p,m}°$** [J · K^{-1} · mol^{-1}]	**Formula**
Beidellite(Ca)	*-5'367.83*	*-5'737.91*	*262.47*	*304.90*	$Ca_{0.17}Mg_{0.34}Al_{1.66}Si_4O_{10}(OH)_2$
Beidellite(Mg)	*-5'354.38*	*-5'723.81*	*263.13*	*303.74*	$Mg_{0.17}Mg_{0.34}Al_{1.66}Si_4O_{10}(OH)_2$
Illite(Mg)	*-5'509.03*	*-5'881.39*	*306.28*	*326.41*	$K_{0.6}Mg_{0.6}Al_{1.4}Si_4O_{10}(OH)_2$
Illite(FeII)	*-5'426.71*	*-5'796.29*	*314.23*	*329.00*	$Na_{0.6}Mg_{0.6}Al_{1.4}Si_4O_{10}(OH)_2$
Illite(FeIII)	*-5'423.28*	*-5'795.39*	*308.10*	*329.28*	$Ca_{0.3}Mg_{0.6}Al_{1.4}Si_4O_{10}(OH)_2$
Illite(Al)	*-5'537.36*	*-5'913.65*	*294.41*	*325.70*	$Mg_{0.3}Mg_{0.6}Al_{1.4}Si_4O_{10}(OH)_2$
Vermiculite(K)	*-5'792.89*	*-6'173.41*	*322.36*	*350.19*	$K_{0.34}Mg_3Al_{0.34}Si_{3.66}O_{10}(OH)_2$
Vermiculite(Na)	*-5'769.82*	*-6'143.26*	*334.60*	*348.34*	$Na_{0.34}Mg_3Al_{0.34}Si_{3.66}O_{10}(OH)_2$
Vermiculite(Ca)	*-5'775.64*	*-6'148.06*	*311.78*	*336.40*	$Ca_{0.17}Mg_3Al_{0.34}Si_{3.66}O_{10}(OH)_2$
Vermiculite(Mg)	*-5'742.33*	*-6'113.11*	*313.46*	*333.46*	$Mg_{0.17}Mg_3Al_{0.34}Si_{3.66}O_{10}(OH)_2$
Berthierine(FeIII)	*-3'153.29*	*-3'458.03*	*287.97*	*297.41*	$K_{0.34}Mg_2Fe^{II}Al_{0.34}Si_{3.66}O_{10}(OH)_2$
Berthierine(FeII)	*-3'454.11*	*-3'770.46*	*253.07*	*283.50*	$Na_{0.34}Mg_2Fe^{II}Al_{0.34}Si_{3.66}O_{10}(OH)_2$
Cronstedtite	*-2'616.84*	*-2'914.55*	*313.16*	*257.02*	$Ca_{0.17}Mg_2Fe^{II}Al_{0.34}Si_{3.66}O_{10}(OH)_2$
Glauconite	*-4'800.21*	*-5'151.13*	*366.58*	*344.54*	$Mg_{0.17}Mg_2Fe^{II}Al_{0.34}Si_{3.66}O_{10}(OH)_2$
Analcime	-6'139.70	-6'575.84	469	425	$Na_2Al_2Si_4O_{12}·2H_2O$
Low-silica P-Na	-4'858.72	-5'314.82	374	384	$Na_2Al_2Si_2O_8·3.8H_2O$
Phillipsite-Na	-8'717.83	-9'438.72	692	620	$Na_{2.5}Al_{2.5}Si_{5.5}O_{16}·5H_2O$
Phillipsite-NaK	-8'741.26	-9'461.67	707	626	$Na_{1.5}KAl_{2.5}Si_{5.5}O_{16}·5H_2O$
Linda type A	-5'203.75	-5'701.89	584	513	$Na_{1.98}Al_{1.98}Si_{2.02}O_8·5.31H_2O$
Molecular sieve 4A	-5'029.88	-5'486.36	536	475	$Na_2Al_2Si_2O_8·4.5H_2O$
Hydrosodalite	-13'221.4	-14'120.1	943	895	$Na_8Al_6Si_6O_{24}(OH)_2 · 2H_2O$
Sodalite	-12'719.1	-13'473.4	848	812	$Na_8Al_6Si_6O_{24}Cl_2$
Cancrinite-NO3	-13'600.8	-14'717.6	1'149	1'119	$Na_8Al_6Si_6O_{24}(NO_3)_2 · 4H_2O$
Chabazite-Na	-7'117.55	-7'808.31	548	578	$Na_2Al_2Si_4O_{12}·6H_2O$
Faujasite-X	-5'857.79	-6'456.94	566	586	$Na_2Al_2Si_{2.5}O_9·6.2H_2O$
Faujasite-Y	-7'578.22	-8'352.62	734	739	$Na_2Al_2Si_4O_{12}·8H_2O$
Natrolite	-5'305.15	-5'707.02	360	359	$Na_2Al_2Si_3O_{10}·2H_2O$
Mordenite-Na	-5'955.95	-6'442.40	388	405	$Na_{0.72}Al_{0.72}Si_{5.28}O_{12}·2.71H_2O$
Chabazite-Ca	-7'144.01	-7'806.74	581	617	$CaAl_2Si_4O_{12}·6H_2O$
Low-silica P-Ca	-5'076.03	-5'527.74	491	435	$CaAl_2Si_2O_8·4.5H_2O$
Mordenite-Ca	-5'995.73	-6489.11	386	404	$Ca_{0.34}Al_{0.68}Si_{5.32}O_{12}·2.9H_2O$
Scolecite	-5'560.52	-6011.65	367	383	$CaAl_2Si_3O_{10}·3H_2O$
Stilbite	-9'944.75	-10'815.6	748	782	$Ca_{1.11}Al_{2.22}Si_{6.78}O_{18}·6.8H_2O$
Heulandite_1	-9'353.66	-10'118.6	541	611	$Ca_{1.07}Al_{2.14}Si_{6.86}O_{18}·4.4H_2O$
Heulandite_2	-9'371.26	-10'131.2	581	619	$Ca_{1.07}Al_{2.14}Si_{6.86}O_{18}·4.5H_2O$
Clinoptilolite	-6'151.94	-6'642.18	454	454	$Ca_{0.52}Al_{1.04}Si_{4.96}O_{12}·3.1H_2O$

Tab. 25-14: Cont.

Name	**$\log_{10}\beta°$**	**$\Delta_r H_m°$** [kJ · mol^{-1}]	**$\Delta_r C_{p,m}°$** [J · K^{-1} mol^{-1}]	**T-range** [°C]	**Reaction**
SiO(OH)3-	-9.81 ± 0.02	25.6 ± 2.0	0	0 – 300	$Si(OH)_4(aq) \rightleftharpoons SiO(OH)_3^- + H^+$
SiO2(OH)2-2	-23.14 ± 0.09	75 ± 15	0	60 – 200	$Si(OH)_4(aq) \rightleftharpoons SiO_2(OH)_2^{2-} + 2\ H^+$
Si4O8(OH)4-4	-36.28 ± 0.16				$4Si(OH)_4(aq) \rightleftharpoons Si_4O_8(OH)_4^{4-} + 4H^+ + 4H_2O(l)$
CaSiO(OH)3+	1.17 ± 0.13				$Ca^{2+} + SiO(OH)_3^- \rightleftharpoons CaSiO(OH)_3^+$
$CaSiO_2(OH)_2$(aq)	4.50 ± 0.15				$Ca^{2+} + SiO_2(OH)_2^{2-} \rightleftharpoons CaSiO_2(OH)_2(aq)$
MgSiO(OH)3+	1.36 ± 0.14				$Mg^{2+} + SiO(OH)_3^- \rightleftharpoons MgSiO(OH)_3^+$
MgSiO2(OH)2(aq)	5.52 ± 0.16				$Mg^{2+} + SiO_2(OH)_2^{2-} \rightleftharpoons MgSiO_2(OH)_2(aq)$
NiSiO(OH)3+	*≈ 6.3*				*$Ni^{2+} + SiO(OH)_3^- \rightleftharpoons NiSiO(OH)_3^+$*
AlSiO(OH)3+2	-2.32 ± 0.22	66.6 ± 3.0	0	25 – 300	$Al^{3+} + Si(OH)_4(aq) \rightleftharpoons AlSiO(OH)_3^{2+} + H^+$
AlSiO3(OH)4-3	*-0.4 ± 0.2*				*$Al(OH)_4^- + SiO_2(OH)_2^{2-} \rightleftharpoons AlSiO_3(OH)_4^{3-} + H_2O(l)$*
FeSiO(OH)3+2	9.69 ± 0.06				$Fe^{3+} + SiO(OH)_3^- \rightleftharpoons FeSiO(OH)_3^{2+}$
EuSiO(OH)3+2	7.8 ± 0.5	*14.5 ± 2.0*	0	5 – 45	$Eu^{3+} + SiO(OH)_3^- \rightleftharpoons EuSiO(OH)_3^{2+}$
AmSiO(OH)3+2	7.8 ± 0.5	*≈ 15*			$Am^{3+} + SiO(OH)_3^- \rightleftharpoons AmSiO(OH)_3^{2+}$
CmSiO(OH)3+2	7.8 ± 0.5	*15.8 ± 4.0*	0	5 – 45	$Cm^{3+} + SiO(OH)_3^- \rightleftharpoons CmSiO(OH)_3^{2+}$
Th(OH)3(SiO(OH)3)3-2	*-27.8 ± 0.7*				*$Th^{4+} + 3Si(OH)_4(aq) + 3H_2O(l) \rightleftharpoons Th(OH)_3(SiO(OH)_3)_3^{2-} + 6H^+$*
UO2SiO(OH)3+	7.93 ± 0.19	9.9 ± 3	0	5 – 45	$UO_2^{2+} + SiO(OH)_3^- \rightleftharpoons UO_2SiO(OH)_3^+$
NpSiO(OH)3+2	*7.8 ± 0.5*	*≈ 15*			*$Np^{3+} + SiO(OH)_3^- \rightleftharpoons NpSiO(OH)_3^{2+}$*
PuSiO(OH)3+2	*7.8 ± 0.5*	*≈ 15*			*$Pu^{3+} + SiO(OH)_3^- \rightleftharpoons PuSiO(OH)_3^{2+}$*
NpSiO(OH)3+3	*11.15 ± 0.18*				*$Np^{4+} + SiO(OH)_3^- \rightleftharpoons NpSiO(OH)_3^{3+}$*
PuSiO(OH)3+3	11.88 ± 0.18				*$Pu^{4+} + SiO(OH)_3^- \rightleftharpoons PuSiO(OH)_3^{3+}$*
NpO2SiO(OH)3(aq)	2.5 ± 0.3				*$NpO_2^+ + SiO(OH)_3^- \rightleftharpoons NpO_2SiO(OH)_3(aq)$*
PuO2SiO(OH)3(aq)	2.5 ± 0.3				*$PuO_2^+ + SiO(OH)_3^- \rightleftharpoons PuO_2SiO(OH)_3(aq)$*
NpO2SiO(OH)3+	≈ 7.2				*$NpO_2^{2+} + SiO(OH)_3^- \rightleftharpoons NpO_2SiO(OH)_3^+$*
PuO2SiO(OH)3+	≈ 6.4				*$PuO_2^{2+} + SiO(OH)_3^- \rightleftharpoons PuO_2SiO(OH)_3^+$*

Tab. 25-14: Cont.

Name	**$\log_{10}K_{s,0}°$**	**$\Delta_r H_m°$** [kJ · mol^{-1}]	**$\Delta_r C_{p,m}°$** [J · K^{-1} · mol^{-1}]	**T-range** [°C]	**Reaction**
Quartz	-3.746 ± 0.087	20.637 ± 0.41	42.066 ± 2.0	0 – 350	SiO_2(cr) + 2 H_2O(l) ⇌ $Si(OH)_4$(aq)
Silica(am)	-2.714 ± 0.044	14.594 ± 0.21	2.350 ± 1.0	0 – 350	SiO_2(am) + 2 H_2O(l) ⇌ $Si(OH)_4$(aq)
Kaolinite	7.44 ± 0.06	-172.8 ± 5.0			$Al_2Si_2O_5(OH)_4$(cr) + 6H^+ ⇌ 2Al^{3+} + 2$Si(OH)_4$(aq) + H_2O(l)
Smectite MX80	*5.09 ± 1.2*	*-188.06 ± 6.9*			Smectite MX80 + 2.952 H_2O(l) + 7.048 H^+ ⇌ 0.024 K^+ + 0.409 Na^+ + 0.009 Ca^{2+} + 0.214 Mg^{2+} + 0.035 Fe^{2+} + 0.173 Fe^3 + 1.860 Al^{3+} + 3.738 $Si(OH)_4$(aq)
Saponite SapCa-2	*31.40 ± 1.1*	*-287.83 ± 5.6*			Saponite SapCa-2 + 2.276 H_2O(l) + 7.724 H^+ ⇌ 0.021 K^+ + 0.394 Na^+ + 0.038 Ca^{2+} + 2.949 Mg^{2+} + 0.021 Fe^{2+} + 0.034 Fe^3 + 0.397 Al^{3+} + 3.569 $Si(OH)_4$(aq)
Nontronite Nau-1	*1.21 ± 1.3*	*-191.95 ± 6.3*			Nontronite Nau-1 + 1.832 H_2O(l) + 8.168 H^+ ⇌ 0.020 K^+ + 0.247 Ca^{2+} + 0.068 Mg^{2+} + 1.688 Fe^3 + 0.818 Al^{3+} + 3.458 $Si(OH)_4$(aq)
Beidellite SBld-1	*7.38 ± 1.3*	*-228.73 ± 7.9*			Beidellite SBld-1 + 2.296 H_2O(l) + 7.704 H^+ ⇌ 0.104 K^+ + 0.185 Ca^{2+} + 0.090 Mg^{2+} + 0.112 Fe^3 + 2.238 Al^{3+} + 3.574 $Si(OH)_4$(aq)
Illite IMt-2	*15.13 ± 1.6*	*-234.97 ± 9.6*			Illite IMt-2 + 1.548 H_2O(l) + 8.452 H^+ ⇌ 0.762 K^+ + 0.044 Na^+ + 0.241 Mg^{2+} + 0.084 Fe^{2+} + 0.292 Fe^3+ 2.040 Al^{3+} + 3.387 $Si(OH)_4$(aq)
Vermiculite SO	*43.62 ± 1.2*	*-457.48 ± 7.0*			Vermiculite SO + 10.852 H^+ ⇌ 0.445 Ca^{2+} + 2.468 Mg^{2+} + 0.007 Mn^{2+} + 0.028 Fe^{2+} + 0.226 Fe^3 + 1.414 Al^{3+} + 0.018 TiO^{2+} + 2.778 $Si(OH)_4$(aq) + 0.870 H_2O(l)
Ripidolite Cca-2	*-174.86 ± 1.7*	*743.55 ± 9.8*			Ripidolite Cca-2 + 17.468 H^+ ⇌ 0.011 Ca^{2+} + 2.952 Mg^{2+} + 0.012 Mn^{2+} + 1.712 Fe^{2+} + 0.215 Fe^3 + 2.483 Al^{3+} + 2.633 $Si(OH)_4$(aq) + 7.468 H_2O(l)
Berthierine ISGS	*27.80 ± 1.4*	*-321.35 ± 7.3*			Berthierine ISGS + 8.672 H^+ ⇌ 0.157 Mg^{2+} + 1.440 Fe^{2+} + 0.182 Fe^3 + 1.644 Al^{3+} + 1.332 $Si(OH)_4$(aq) + 3.672 H_2O(l)
Montmorillonite(MgK)	*2.65*	*-139.97*			Montmorillonite(MgK) + 4 H_2O(l) + 6 H^+ ⇌ 0.34 K^+ + 0.34 Mg^{2+} + 1.66 Al^{3+} + 4 $Si(OH)_4$(aq)
Montmorillonite(MgNa)	*3.24*	*-149.06*			Montmorillonite(MgNa) + 4 H_2O(l) + 6 H^+ ⇌ 0.34 Na^+ + 0.34 Mg^{2+} + 1.66 Al^{3+} + 4 $Si(OH)_4$(aq)
Montmorillonite(MgCa)	*4.05*	*-159.78*			Montmorillonite(MgCa) + 4 H_2O(l) + 6 H^+ ⇌ 0.17 Ca^{2+} + 0.34 Mg^{2+} + 1.66 Al^{3+} + 4 $Si(OH)_4$(aq)
Montmorillonite(MgMg)	*3.53*	*-161.14*			Montmorillonite(MgMg) + 4 H_2O(l) + 6 H^+ ⇌ 0.51 Mg^{2+} + 1.66 Al^{3+} + 4 $Si(OH)_4$(aq)

Tab. 25-14: Cont.

Name	**$\log_{10}K_{s,0}°$**	**$\Delta_r H_m°$** [kJ · mol^{-1}]	**$\Delta_r C_{p,m}°$** [J · K^{-1} · mol^{-1}]	**T-range** [°C]	**Reaction**
Montmorillonite(HcK)	*4.29*	*-132.48*			Montmorillonite(HcK) + 4 H_2O(l) + 6 H^+ ⇌ 0.6 K^+ + 0.6 Mg^{2+} + 1.4 Al^{3+} + 4 $Si(OH)_4$(aq)
Montmorillonite(HcNa)	*5.32*	*-148.51*			Montmorillonite(HcNa) + 4 H_2O(l) + 6 H^+ ⇌ 0.6 Na^+ + 0.6 Mg^{2+} + 1.4 Al^{3+} + 4 $Si(OH)_4$(aq)
Montmorillonite(HcCa)	*6.75*	*-167.41*			Montmorillonite(HcCa) + 4 H_2O(l) + 6 H^+ ⇌ 0.3 Ca^{2+} + 0.6 Mg^{2+} + 1.4 Al^{3+} + 4 $Si(OH)_4$(aq)
Montmorillonite(HcMg)	*5.84*	*-169.81*			Montmorillonite(HcMg) + 4 H_2O(l) + 6 H^+ ⇌ 0.9 Mg^{2+} + 1.4 Al^{3+} + 4 $Si(OH)_4$(aq)
Saponite(K)	*28.12*	*-255.05*			Saponite(K) + 2.64 H_2O(l) + 7.36 H^+ ⇌ 0.34 K^+ + 3 Mg^{2+} + 0.34 Al^{3+} + 3.66 $Si(OH)_4$(aq)
Saponite(Na)	*28.61*	*-263.67*			Saponite(Na) + 2.64 H_2O(l) + 7.36 H^+ ⇌ 0.34 Na^+ + 3 Mg^{2+} + 0.34 Al^{3+} + 3.66 $Si(OH)_4$(aq)
Saponite(Ca)	*29.28*	*-273.58*			Saponite(Ca) + 2.64 H_2O(l) + 7.36 H^+ ⇌ 0.17 Ca^{2+} + 3 Mg^{2+} + 0.34 Al^{3+} + 3.66 $Si(OH)_4$(aq)
Saponite(Mg)	*28.74*	*-274.76*			Saponite(Mg) + 2.64 H_2O(l) + 7.36 H^+ ⇌ 3.17 Mg^{2+} + 0.34 Al^{3+} + 3.66 $Si(OH)_4$(aq)
Saponite(FeK)	*25.35*	*-243.20*			Saponite(FeK) + 2.64 H_2O(l) + 7.36 H^+ ⇌ 0.34 K^+ + 2 Mg^{2+} + Fe^{2+} + 0.34 Al^{3+} + 3.66 $Si(OH)_4$(aq)
Saponite(FeNa)	*25.67*	*-250.83*			Saponite(FeNa) + 2.64 H_2O(l) + 7.36 H^+ ⇌ 0.34 Na^+ + 2 Mg^{2+} + Fe^{2+} + 0.34 Al^{3+} + 3.66 $Si(OH)_4$(aq)
Saponite(FeCa)	*26.52*	*-261.75*			Saponite(FeCa) + 2.64 H_2O(l) + 7.36 H^+ ⇌ 0.17 Ca^{2+} + 2 Mg^{2+} + Fe^{2+} + 0.34 Al^{3+} + 3.66 $Si(OH)_4$(aq)
Saponite(FeMg)	*25.97*	*-262.92*			Saponite(FeMg) + 2.64 H_2O(l) + 7.36 H^+ ⇌ 2.17 Mg^{2+} + Fe^{2+} + 0.34 Al^{3+} + 3.66 $Si(OH)_4$(aq)
Nontronite(K)	*-4.11*	*-131.76*			Nontronite(K) + 2.64 H_2O(l) + 7.36 H^+ ⇌ 0.34 K^+ + 1.67 Fe^{3+} + 0.67 Al^{3+} + 3.66 $Si(OH)_4$(aq)
Nontronite(Na)	*-3.61*	*-140.38*			Nontronite(Na) + 2.64 H_2O(l) + 7.36 H^+ ⇌ 0.34 Na^+ + 1.67 Fe^{3+} + 0.67 Al^{3+} + 3.66 $Si(OH)_4$(aq)
Nontronite(Ca)	*-2.94*	*-150.30*			Nontronite(Ca) + 2.64 H_2O(l) + 7.36 H^+ ⇌ 0.17 Ca^{2+} + 1.67 Fe^{3+} + 0.67 Al^{3+} + 3.66 $Si(OH)_4$(aq)
Nontronite(Mg)	*-3.49*	*-151.48*			Nontronite(Mg) + 2.64 H_2O(l) + 7.36 H^+ ⇌ 0.17 Mg^{2+} + 1.67 Fe^{3+} + 0.67 Al^{3+} + 3.66 $Si(OH)_4$(aq)
Beidellite(K)	*4.39*	*-193.38*			Beidellite(K) + 2.64 H_2O(l) + 7.36 H^+ ⇌ 0.34 K^+ + 2.34 Al^{3+} + 3.66 $Si(OH)_4$(aq)

Tab. 25-14: Cont.

Name	**$\log_{10}K_{s,0}°$**	**$\Delta_r H_m°$** [kJ · mol^{-1}]	**$\Delta_r C_{p,m}°$** [J · K^{-1} · mol^{-1}]	**T-range** [°C]	**Reaction**
Beidellite(Na)	*3.14*	*-192.00*			Beidellite(Na) + 2.64 H_2O(l) + 7.36 H^+ ⇌ 0.34 Na^+ + 2.34 Al^{3+} + 3.66 $Si(OH)_4$(aq)
Beidellite(Ca)	*5.56*	*-211.91*			Beidellite(Ca) + 2.64 H_2O(l) + 7.36 H^+ ⇌ 0.17 Ca^{2+} + 2.34 Al^{3+} + 3.66 $Si(OH)_4$(aq)
Beidellite(Mg)	*5.02*	*-213.09*			Beidellite(Mg) + 2.64 H_2O(l) + 7.36 H^+ ⇌ 0.17 Mg^{2+} + 2.34 Al^{3+} + 3.66 $Si(OH)_4$(aq)
Illite(Mg)	*10.80*	*-229.80*			Illite(Mg) + 1.6 H_2O(l) + 8.4 H^+ ⇌ 0.85 K^+ + 0.25 Mg^{2+} + 2.35 Al^{3+} + 3.4 $Si(OH)_4$(aq)
Illite(FeII)	*9.25*	*-220.72*			Illite(FeII) + 1.6 H_2O(l) + 8.4 H^+ ⇌ 0.85 K^+ + 0.25 Fe^{2+} + 2.35 Al^{3+} + 3.4 $Si(OH)_4$(aq)
Illite(FeIII)	*12.14*	*-266.81*			Illite(FeIII) + 0.6 H_2O(l) + 9.4 H^+ ⇌ 0.85 K^+ + 0.25 Fe^{3+} + 2.6 Al^{3+} + 3.15 $Si(OH)_4$(aq)
Illite(Al)	*12.78*	*-270.89*			Illite(Al) + 0.6 H_2O(l) + 9.4 H^+ ⇌ 0.85 K^+ + 2.85 Al^{3+} + 3.15 $Si(OH)_4$(aq)
Vermiculite(K)	*37.35*	*-338.06*			Vermiculite(K) + 0.56 H_2O(l) + 9.44 H^+ ⇌ 0.86 K^+ + 3 Mg^{2+} + 0.86 Al^{3+} + 3.14 $Si(OH)_4$(aq)
Vermiculite(Na)	*38.30*	*-358.06*			Vermiculite(Na) + 0.56 H_2O(l) + 9.44 H^+ ⇌ 0.86 Na^+ + 3 Mg^{2+} + 0.86 Al^{3+} + 3.14 $Si(OH)_4$(aq)
Vermiculite(Ca)	*39.46*	*-380.06*			Vermiculite(Ca) + 0.56 H_2O(l) + 9.44 H^+ ⇌ 0.43 Ca^{2+} + 3 Mg^{2+} + 0.86 Al^{3+} + 3.14 $Si(OH)_4$(aq)
Vermiculite(Mg)	*37.95*	*-382.33*			Vermiculite(Mg) + 0.56 H_2O(l) + 9.44 H^+ ⇌ 3.43 Mg^{2+} + 0.86 Al^{3+} + 3.14 $Si(OH)_4$(aq)
Berthierine(FeIII)	*28.76*	*-302.91*			Berthierine(FeIII) + 8.64 H^+ ⇌ 2.34 Fe^{2+} + 0.33 Fe^{3+} + 0.99 Al^{3+} + 1.34 $Si(OH)_4$(aq) + 3.64 H_2O(l)
Berthierine(FeII)	*34.45*	*-379.80*			Berthierine(FeII) + 10 H^+ ⇌ 2 Fe^{2+} + 2 Al^{3+} + $Si(OH)_4$(aq) + 5 H_2O(l)
Cronstedtite	*16.11*	*-257.03*			Cronstedtite + 10 H^+ ⇌ 2 Fe^{2+} + 2 Fe^{3+} + $Si(OH)_4$(aq) + 5 H_2O(l
Glauconite	*1.77*	*-133.54*			Glauconite + 3 H_2O(l) + 7 H^+ ⇌ 0.75 K^+ + 0.25 Mg^{2+} + 0.25 Fe^{2+} + 1.25 Fe^{3+} + 0.5 Al^{3+} + 3.75 $Si(OH)_4$(aq)
Soddyite	5.75 ± 0.26				$(UO_2)_2SiO_4 \cdot 2H_2O$(cr) + $4H^+$ ⇌ $2UO_2^{2+}$ + $Si(OH)_4$(aq) + $2H_2O$(l)
Sodium boltwoodite	5.81 ± 0.44	*-44.8 ± 5.8*			$Na(UO_2)(SiO_3OH) \cdot H_2O$(cr) + $3H^+$ ⇌ Na^+ + UO_2^{2+} + $Si(OH)_4$(aq) + H_2O(l)
Boltwoodite	4.48 ± 1.17	-27.7 ± 8.0			$K(UO_2)(SiO_3OH) \cdot H_2O$(cr) + $3H^+$ ⇌ K^+ + UO_2^{2+} + $Si(OH)_4$(aq) + H_2O(l)

Tab. 25-14: Cont.

Name	**$\log_{10}K_{s,0}°$**	**$\Delta_r H_m°$** [kJ · mol^{-1}]	**$\Delta_r C_{p,m}°$** [J · K^{-1} · mol^{-1}]	**T-range** [°C]	**Reaction**
Uranophane	11.52 ± 0.16	*-86 ± 16*			$Ca(UO_2)_2(SiO_3OH)_2{\cdot}5H_2O(cr) + 6H^+ \rightleftharpoons Ca^{2+} + 2UO_2^{2+} + 2Si(OH)_4(aq) + 5H_2O(l)$
Coffinite	*-4.5*	*-79*			*$USiO_4(cr) + 4\,H^+ \rightleftharpoons U^{4+} + Si(OH)_4(aq)$*

Tab. 25-15: Selected SIT ion interaction coefficients $\varepsilon_{j,k}$ [kg · mol^{-1}] for silicate species

Data in bold face are taken from Lemire et al. (2013). Data in normal face are derived or estimated in this review. Data estimated according to charge correlations and taken from Tab. 1-7 are shaded. Supplemental data are in italics.

j k → ↓	**Cl^-** $\varepsilon_{j,k}$	**ClO_4^-** $\varepsilon_{j,k}$	**Na^+** $\varepsilon_{j,k}$	**NaCl** $\varepsilon_{j,k}$	**$NaClO_4$** $\varepsilon_{j,k}$
H+	**0.12 ± 0.01**	**0.14 ± 0.02**	0	0	0
Mg+2	**0.19 ± 0.02**	**0.33 ± 0.03**	0	0	0
Ca+2	**0.14 ± 0.01**	**0.27 ± 0.03**	0	0	0
Ni+2	0.37 ± 0.03 [a]	**0.37 ± 0.03**	0	0	0
Al+3	**0.33 ± 0.02**		0	0	0
Fe+3	**0.76 ± 0.03**	**0.73 ± 0.04**	0	0	0
Eu+3	0.47 ± 0.01 [a]	0.47 ± 0.01 [b]	0	0	0
Am+3	0.49 ± 0.03 [a]	**0.49 ± 0.03**	0	0	0
Cm+3	0.49 ± 0.03 [a]	**0.49 ± 0.03**	0	0	0
Np+4	0.84 ± 0.06 [a]	**0.84 ± 0.06**	0	0	0
Pu+4	0.82 ± 0.07 [a]	**0.82 ± 0.07**	0	0	0
NpO2+	**0.09 ± 0.05**	**0.25 ± 0.05**	0	0	0
NpO2+2	0.46 ± 0.05 [a]	**0.46 ± 0.05**	0	0	0
PuO2+2	0.46 ± 0.05 [a]	**0.46 ± 0.05**	0	0	0
Si(OH)4(aq)	0	0	0	0.03 ± 0.06	0.03 ± 0.06 [c]
SiO(OH)3-	0	0	-0.05 ± 0.07	0	0
SiO_2(OH)2-2	0	0	-0.07 ± 0.09	0	0
Si_4O_8(OH)4-4	0	0	0.00 ± 0.13	0	0
CaSiO(OH)3+	0.05 ± 0.10	0.2 ± 0.1	0	0	0
CaSiO2(OH)2(aq)	0	0	0	0.0 ± 0.1	0.0 ± 0.1
MgSiO(OH)3+	0.05 ± 0.10	0.2 ± 0.1	0	0	0
MgSiO2(OH)2$_{(}$aq)	0	0	0	0.0 ± 0.1	0.0 ± 0.1
NiSiO(OH)3+	*0.50 ± 0.16* [a]	*0.50 ± 0.16*	*0*	*0*	*0*
AlSiO(OH)3+2	0.15 ± 0.10	0.4 ± 0.1	0	0	0
AlSiO3(OH)4-3	*0*	*0*	*-0.15 ± 0.10*	*0*	*0*
FeSiO(OH)3+2	0.04 ± 0.15 [a]	0.04 ± 0.15	0	0	0

Tab. 25-15: Selected SIT ion interaction coefficients $\varepsilon_{j,k}$ [kg · mol^{-1}] for silicate species

j k → ↓	**Cl^-** $\varepsilon_{j,k}$	**ClO_4^-** $\varepsilon_{j,k}$	**Na^+** $\varepsilon_{j,k}$	**NaCl** $\varepsilon_{j,k}$	**$NaClO_4$** $\varepsilon_{j,k}$
EuSiO(OH)3+2	0.42 ± 0.10 [a]	0.42 ± 0.10	0	0	0
AmSiO(OH)3+2	0.42 ± 0.10 [a]	0.42 ± 0.10	0	0	0
CmSiO(OH)3+2	0.42 ± 0.10 [a]	0.42 ± 0.10	0	0	0
*Th(OH)3(SiO(OH)3*3-2	*0*	*0*	*-0.10 ± 0.10*	*0*	*0*
UO2SiO(OH)3+	0.3 ± 0.1 [a]	0.3 ± 0.1	0	0	0
NpSiO(OH)3+2	*0.15 ± 0.10*	*0.4 ± 0.1*	*0*	*0*	*0*
PuSiO(OH)3+2	*0.15 ± 0.10*	*0.4 ± 0.1*	*0*	*0*	*0*
NpSiO(OH)3+3	*0.44 ± 0.30* [a]	*0.44 ± 0.30*	*0*	*0*	*0*
PuSiO(OH)3+3	*0.55 ± 0.28* [a]	*0.55 ± 0.28*	*0*	*0*	*0*
NpO2SiO2(OH)2(aq)	*0*	*0*	*0*	*0.0 ± 0.1*	*0.0 ± 0.1*
PuO2SiO2(OH)2(aq)	*0*	*0*	*0*	*0.0 ± 0.1*	*0.0 ± 0.1*
NpO2SiO(OH)3+	*0.2 ± 0.1* [a]	*0.2 ± 0.1*	*0*	*0*	*0*
PuO2SiO(OH)3+	*0.2 ± 0.1* [a]	*0.2 ± 0.1*	*0*	*0*	*0*

[a] Assumed to be equal to the corresponding ion interaction coefficient with ClO_4^-.
[b] See Section 23.2.2.
[c] Assumed to be equal to the corresponding ion interaction coefficient with Cl^-.

25.6 References

Aja, S.U. (1991): Illite equilibria in solutions: III. A re-interpretation of the data of Sass et al. (1987). Geochim. Geochimica et Cosmochimica Acta 55, 3431-3435.

Aja, S.U., Rosenberg, P.E. & Kittrick J.A. (1991a): Illite equilibria in solutions: I. Phase relationships in the system K_2O-Al_2O_3-SiO_2-H_2O between 25 and 250 °C. Geochimica et Cosmochimica Acta 55, 1353-1364.

Aja, S.U., Rosenberg, P.E., & Kittrick J.A. (1991b): Illite equilibria in solutions: II. Phase relationships in the system K_2O-MgO-Al_2O_3-SiO_2-H_2O. Geochimica et Cosmochimica Acta 55, 1365-1374.

Blanc, P., Vieillard, P., Gailhanou, H. & Gaboreau, S. (2013): Thermodynamics of Clay Minerals. In: Developments in Clay Science, Vol. 5A, Elsevier, 173-210.

Blanc, P., Gailhanou, H., Rogez, J., Mikaelian, G., Kawaji, H., Warmont, F., Gaboreau, S., Grangeon, S., Greneche, J.-M., Vieillard, P., Fialips, C.I., Giffaut, E., Gaucher, E.C. & Claret, F. (2014): Thermodynamic properties of chlorite and berthierine derived from calorimetric measurements. Physics and Chemistry of Minerals 41, 603-615.

Blanc, P., Vieillard, P., Gailhanou, H., Gaboreau, S., Gaucher, E., Fialips, C.I., Madé, B. & Giffaut, E. (2015a): A generalized model for predicting the thermodynamic properties of clay minerals. American Journal of Science 315, 734-780.

Blanc, P., Vieillard, P., Gailhanou, H., Gaboreau, S., Marty, N., Claret, F., Madé, B. & Giffaut, E. (2015b): ThermoChimie database developments in the framework of cement/clay interactions. Applied Geochemistry 55, 95-107.

Berner, U., Kulik, D.A. & Kosakowski, G. (2013): Geochemical impact of a low-pH cement liner on the near field of a repository for spent fuel and high-level radioactive waste. Physics and Chemistry of the Earth 64, 46-56.

Brown, P.L, Curti, E. & Grambow, B. (2005): Chemical Thermodynamics of Zirconium. Chemical Thermodynamics, Vol. 8. Elsevier, Amsterdam, 512 p.

Browne, B.A. & Driscoll, C.T. (1992): Soluble aluminum silicates: stoichiometry, stability, and implications for environmental geochemistry. Science, 256, 1667-1670.

Churchman, G.J. & Jackson, M.L. (1976): Reaction of montmorillonite with acid aqueous solutions: solute activity control by a secondary phase. Geochimica et Cosmochimica Acta 40, 1251-1259.

Chermak, J.A. & Rimstidt, J.D. (1989): Estimating the thermodynamic properties (ΔG_f° and ΔH_f°) of silicate minerals at 298 K from the sum of polyhedral contributions. American Mineralogist 74, 1023-1031.

Chermak, J.A. & Rimstidt, J.D. (1990): Estimating the free energy of formation of silicate minerals at high temperatures from the sum of polyhedral contributions. American Mineralogist 75, 1376-1380.

Cox, J.D., Wagman, D.D. & Medvedev, V.A. (1989): CODATA Key Values for Thermodynamics. New York, Hemisphere Publishing, 271p.

Essene, E.J. & Peacor, D.R. (1995): Clay Mineral Thermometry – A Critical Perspective. Clays and Clay Minerals 43, 540-553.

Farmer, V.C. & Lumsdon, D.G. (1994): An assessment of complex formation between aluminium and silicic acid in acidic solutions. Geochim. Cosmochim. Acta, 58, 3331-3334.

Felmy, A.R., Cho, H., Rustad, J.R. & Mason, M.J. (2001): An aqueous thermodynamic model for polymerized silica species to high ionic strength. J. Sol. Chem., 30, 509-525.

Fialips, C.I., Majzlan, J., Beaufort, D. & Navrotsky A. (2003): New thermochemical evidence on the stability of dickite vs. kaolinite. American Mineralogist, 88, 837-845.

Fialips, C.I., Navrotsky, A. & Petit, S. (2001): Crystal properties and energetics of synthetic kaolinite. American Mineralogist, 86, 304-311.

Fournier, R.O (1985): The behavior of silica in hydrothermal solutions. In: Geology and Geochemistry of Epithermal Systems. Berger, B.R. & Bethke, P.M. (Eds.) Reviews in Economic Geology, Vol. 2, Society of Economic Geologists, 45-61.

Gailhanou, H., van Miltenburg, J.C., Rogez, J., Olives, J., Amouric, A., Gaucher, E.C. & Blanc, P. (2007): Thermodynamic properties of anhydrous smectite MX-80, illite IMt-2, and mixed-layer illite-smectite ISCz-1 as determined by calorimetric methods: Part I. Heat capacities, heat contents and entropies. Geochim. Cosmochim. Acta, 71, 5463-5473.

Gailhanou, H., Rogez, J., van Miltenburg, J.C., van Genderen, A.C.G., Grenèche, J.M., Gilles, C., Jalabert, D., Michau, N., Gaucher, E.C. & Blanc, P. (2009): Thermodynamic properties of chlorite CCa-2. Heat capacities, heat contents and entropies. Geochim. Cosmochim. Acta, 73, 4738-4749.

Gailhanou, H., Blanc, P., Rogez, J., Mikaelian, G., Kawaji, H., Olives, J., Amouric, M., Denoyel, R., Bourelly, S., Montouillout, V., and others (2012): Thermodynamic properties of illite, smectite and beidellite by calorimetric methods: enthalpies of formation, heat capacities, entropies and Gibbs free energies of formation. Geochim. Cosmochim. Acta, 89, 279-301.

Gailhanou, H., Blanc, P., Rogez, J., Mikaelian, G., Horiuchi, K., Yamamura, Y., Saito, K., Kawaji, H., Warmont, F., Grenèche, J.M., Vieillard, P., Fialips, C.I., Giffaut, E. & Gaucher, E.C. (2013): Thermodynamic properties of saponite, nontronite, and vermiculite derived from calorimetric measurements 98, 1834-1847.

Gailhanou, H., Vieillard, P., Blanc, P., Lassin, A., Denoyel, R., Bloch, E., De Weireld, G., Gaboreau, S., Fialips, C.I., Madé, B. & Giffaut, E. (2017): Methodology for determining the thermodynamic properties of smectite hydration. Applied Geochemistry 82, 146-163.

Gamsjäger, H., Bugajski, J., Gajda, T., Lemire, R.J. & Preis, W. (2005): Chemical Thermodynamics of Nickel. Chemical Thermodynamics, Vol. 6. Elsevier, Amsterdam, 617 p.

Gout, R., Pokrovski, G.S., Schott, J. & Zwick, A. (2000): Raman Spectroscopic Study of Aluminum Silicate Complexes at 20 °C in Basic Solutions. J. Solution Chem., 29, 1173-1185.

Grenthe, I., Gaona, X., Plyasunov, A.V., Rao, L., Runde, W.H., Grambow, B., Konings, R.J.M., Smith, A.L. & Moore, E.E. (2020): Second Update on the Chemical Thermodynamics of Uranium, Neptunium, Plutonium, Americium and Technetium. Chemical Thermodynamics, Vol. 14. OECD Publications, Paris, France, 1503 p.

Grenthe, I., Fuger, J., Konings, R.J.M., Lemire, R.J., Muller, A.B., Nguyen-Trung, C. & Wanner, H. (1992): Chemical Thermodynamics of Uranium. Chemical Thermodynamics, Vol. 1. Elsevier, Amsterdam, 715p.

Guillaumont, R., Fanghänel, T., Fuger, J., Grenthe, I., Neck, V., Palmer, D.A. & Rand, M.H. (2003): Update on the Chemical Thermodynamics of Uranium, Neptunium, Plutonium, Americium and Technetium. Chemical Thermodynamics, Vol. 5. Elsevier, Amsterdam, 919p.

Gunnarsson, I. & Arnorsson, S. (2000): Amorphous silica solubility and the thermodynamic properties of $H_4SiO_4^o$ in the range of 0º to 350 °C at P_{sat}. Geochim. Cosmochim. Acta, 64, 2295-2307.

Hrnecek, F. & Irlweck, K. (1999): Formation of Uranium(VI) Complexes with Monomeric and Polymeric Species of Silicic Acid. Radiochim. Acta, 87, 29-35.

Huang, W.H. & Keller, W.D. (1973): Gibbs free energies of formation calculated from dissolution data using specific mineral analyses III. Clay minerals. American Mineralogist 58, 1023-1028.

Hummel, W., Berner, U., Curti, E., Pearson, F.J. & Thoenen, T. (2002): Nagra/PSI Chemical Thermodynamic Data Base 01/01. Nagra Technical Report NTB 02-16. Also published by Universal Publishers/uPublish.com, Parkland, Florida, USA.

Jensen, M.P. & Choppin, G.R. (1996): Complexation of Europium(III) by Aqueous Orthosilicic Acid. Radiochim. Acta, 72, 143-150.

Jensen, M.P. & Choppin, G.R. (1998): Complexation of Uranyl(VI) by Aqueous Orthosilicic Acid. Radiochim. Acta, 82, 83-88.

Kittrick, J.A. (1970): Precipitation of kaolinite at 25 °C and 1 atm. Clays and Clay Minerals 18, 261-267.

Kittrick, J.A. (1971a): Stability of montmorillonites: I. Belle Fourche and Clay Spur montmorillonites. Soil Science Society of America Journal 35, 140-145.

Kittrick, J.A. (1971b): Stability of montmorillonites: II. Aberdeen montmorillonite. Soil Science Society of America Journal 35, 820-823.

Kittrick, J.A. (1984): Solubility measurements of phases in three illites. Clays and Clay Minerals 32, 115-124.

Kittrick, J.A. & Peryea, F.J. (1988): Experimental validation of the monophase structure model for montmorillonite solubility. Soil Science Society of America Journal 52, 1199-1201.

Kittrick, J.A. & Peryea, F.J. (1989): The monophase model for magnesium-saturated montmorillonite. Soil Science Society of America Journal 53, 292-295.

Kulik, D.A. & Kersten, M. (2001): Aqueous Solubility Diagrams for Cementitious Waste Stabilization Systems: II, End-Member Stoichiometries of Ideal Calcium Silicate Hydrate Solid Solutions. J. Amer. Ceram. Soc., 84, 3017-3026.

Lagerström, G. (1959): Equilibrium Studies of Polyanions III. Silicate Ions in NaClO4 Medium. Acta Chem. Scand., 13, 722-736.

Lemire, R.J., Berner, U., Musikas, C., Palmer, D.A., Taylor, P. & Tochiyama, O. (2013): Chemical Thermodynamics of Iron, Part 1. Chemical Thermodynamics, Vol. 13a. OECD Publications, Paris, France, 1082 pp.

Lemire, R.J., Palmer, D.A., Taylor, P. & Schlenz, H. (2020): Chemical Thermodynamics of Iron, Part 2. Chemical Thermodynamics, Vol. 13b. OECD Publications, Paris, France, 921 pp.

Lippmann, F. (1982): The thermodynamic status of clay minerals. In: Developments in Sedimentology 35, International Clay Conference 1981 (H. van Olphen & F. Veniale eds.) Elsevier, Amsterdam, 475-485.

Lothenbach, B., Kulik, D.A., Matschei, T., Balonis, M., Baquerizo, L., Dilnesa, B., Miron, G.D. & Myers, J. (2019): Cemdata18: A chemical thermodynamics database for hydrated Portland cements and alkali-activated materials. Cement and Concrete Research 115, 472-506.

Lothenbach, B., Matschei, T., Möschner, G. & Glasser, F. (2008): Thermodynamic modelling of the effect of temperature on the hydration and porosity of Portland cement. Cement and Concrete Research 38, 1-18.

Loucks, R.R. (1991): The bound interlayer H_2O content of potassic white micas: muscovite-hydromuscovite–hydropyrophyllite solutions. American Mineralogist 76, 1563-1579.

Ma, B. & Lothenbach, B. (2020a): Synthesis, characterization, and thermodynamic study of selected Na-based zeolites. Cement and Concrete Research 135, 106111.

Ma, B. & Lothenbach, B. (2020b): Thermodynamic study of cement/rock interactions using experimentally generated solubility data of zeolites. Cement and Concrete Research 135, 106149.

Marty, N.C.M., Cama, J., Sato, T., Chino, D., Villiéras, F., Razafitianamaharavo, A., Brendlé, J., Giffaut, E., Soler, J.M., Gaucher, E.C. & Tournassat, C. (2011): Dissolution kinetics of synthetic Na-smectite. An integrated experimental approach. Geochimica et Cosmochimica Acta 75, 5849-5864.

Marty, N.C.M., Claret, F., Lassin, A., Tremosa, J., Blanc, P., Madé, B., Giffaut, E., Cochepin, B. & Tournassat, C. (2015): A database of dissolution and precipitation rates for clay-rocks minerals. Applied Geochemistry 55, 108-118.

May, H.M., Kinniburgh, D.G., Helmke, P.A. & Jackson, M.L. (1986): Aqueous dissolution, solubilities and thermodynamic stabilities of common aluminosilicate clay minerals: Kaolinite and smectites. Geochim. Cosmochim. Acta, 50, 1667-1677.

Moll, H., Geipel, G., Brendler, V., Bernhard, G. & Nitsche, H. (1998): Interaction of uranium(VI) with silicic acid in aqueous solutions studied by time-resolved laser-induced fluorescence spectroscopy (TRLFS). Journal of Alloys and Compounds, 271-273, 765-768.

Nordstrom, D.K., Plummer, L.N., Langmuir, D., Busenberg, E., May, H.M., Jones, B.F. & Parkhurst, D.L. (1990): Revised Chemical Equilibrium Data for Major Water-Mineral Reactions and Their Limitations. In: Melchior, D. C. & Basset, R. L. (eds.): Chemical Modeling of Aqueous Systems II. Washington, D.C., American Chemical Society, ACS Symposium Series 416, 398-413.

Olson, L.L. & O'Melia, C.R. (1973): The interaction of Fe(III) with $Si(OH)_4$. J. Inorg. Nucl. Chem., 35, 1977-1985.

Panak, P.J., Kim, M.A., Klenze, R., Kim, J.I. & Fanghänel. Th. (2005): Complexation of Cm(III) with aqueous silicic acid. Radiochim. Acta, 93, 133-139.

Pathak, P.N. & Choppin, G.R. (2006a): Complexation / speciation studies of Ni^{2+} ion with ortho silicic acid in perchlorate media. J. Radioanal. Nucl. Chem. 267, 309-314.

Pathak, P.N. & Choppin, G.R. (2006b): Complexation studies of Co^{2+} ion with orthosilicic acid. J. Radioanal. Nucl. Chem. 267, 175-182.

Pathak, P.N. & Choppin, G.R. (2006c): Thermodynamic study of metal silicate complexation in perchlorate media. Radiochim. Acta, 94, 81-86.

Pathak, P.N. & Choppin, G.R. (2007): Silicate complexation of NpO_2^+ ion in perchlorate media. J. Radioanal. Nucl. Chem. 274, 3-7.

Patten, J.T. & Byrne, R.H. (2017): Assessment of Fe(III) and Eu(III) complexation by silicate in aqueous solutions. Geochim. Cosmochim. Acta, 202, 361-373.

Pazukhin, E.M., Krivokhatskii, A.S. & Kudryavtsev, E.G. (1990): Possible formation of Pu(IV) complexes with silicic acid. Soviet Radiochemistry, 32, 325-330 (translated from Radiokhimiya, 32 (1990) 26-32).

Peryea, F.J. & Kittrick, J.A. (1986): Experimental evaluation of two operational standard states for montmorillonite in metastable hydrolysis reactions. Soil Science Society of America Journal 50, 1613-1617.

Pokrovski, G.S., Schott, J., Harrichoury, J.-C. & Sergeyev, A. S. (1996): The stability of aluminum silicate complexes in acidic solutions from 25 to 150 °C. Geochim. Cosmochim. Acta, 60, 2495-2501.

Pokrovski, G.S., Schott, J., Salvi, S., Gout, R. & Kubicki, J.D. (1998): Structure and stability of aluminum-silica complexes in neutral to basic solutions. Experimental study and molecular orbital calculations. Mineralogical Magazine, 62A, 1194-1195.

Porter, R.A. & Weber, W.J. (1971): The interaction of silicic acid with iron(III) and uranyl ions in dilute aqueous solution. J. Inorg. Nucl. Chem., 33, 2443-2449.

Rai, D., Yui, M., Moore, D.A., Lumetta, G.J., Rosso, K.M., Xia, Y., Felmy, A.R. & Skomurski, F. N. (2008): Thermodynamic Model for ThO_2(am) Solubility in Alkaline Silica Solutions. J. Solution Chem., 37, 1725-1746.

Rand, M., Fuger, J., Grenthe, I., Neck, V. & Rai, D. (2008): Chemical Thermodynamics of Thorium. Chemical Thermodynamics, Vol. 11. OECD Publishing, Paris, 900p.

Reardon, E.J. (1979): Complexing of silica by iron(III) in natural waters. Chem. Geol., 25, 339-345.

Reesman, A.L. & Keller, W.D. (1968): Aqueous solubility studies of high-alumina and clay minerals. American Mineralogist 53, 929-942.

Rimstidt, J.D. (1997): Quartz solubility at low temperatures. Geochim. Cosmochim. Acta, 61, 2553-2558.

Robie, R.A., Hemingway, B.S. & Fisher, J.R. (1979): Thermodynamic Properties of Minerals and Related Substances at 298.15 K and 1 Bar (10^5 Pascals) Pressure and at Higher Temperatures. United States Geological Survey Bulletin, 1452, Reprinted with corrections, 464 pp.

Rosenberg, P. E., Kittrick, J.A. & Aja, S.U. (1990): Mixed-layer illite/smectite, a multiphase model. American Mineralogist 75, 1182-1185.

Salvi, S., Pokrovski, G.S. & Schott, J. (1998): Experimental investigation of aluminum-silica aqueous complexing at 300 °C. Chemical Geology, 151, 51-67.

Santschi, P.H. & Schindler, P.W. (1974): Complex formation in the ternary systems Ca^{II}-H_4SiO_4-H_2O and Mg^{II}-H_4SiO_4-H_2O. J. Chem. Soc. Dalton Transactions, 181-184.

Sass, B.M., Rosenberg, P.E. & Kittrick, J.A. (1987): The stability of illite/smectite during diagenesis: An experimental study. Geochimica et Cosmochimica Acta 51, 2103-2115.

Satoh, I. & Choppin, G.R. (1992): Interaction of Uranyl(VI) with Silicic Acid. Radiochim. Acta, 56, 85-87.

Shilov, V.P. & Fedoseev, A.M. (2003): Solubility of Pu(IV) in Weakly Alkaline Solutions (pH 9-14) Containing Silicate Anions. Radiochemistry, 45, 491-494 (translated from Radiokhimiya, 45 (2003) 441-444).

Shilov, V.P., Fedoseev, A.M., Yusov, A.B. & Delegard, C.H. (2004): Behavior of Np(VII, VI, V) in Silicate Solutions. Radiochemistry, 46, 574-577 (translated from Radiokhimiya, 46 (2004) 527-530).

Soli, A.L., & Byrne, R.H. (2017): Europium silicate complexation at 25 °C and 0.7 molar ionic strength. Marine Chemistry, 195, 138-142.

Sjöberg, S., Öhman, L.O. & Ingri, N. (1985): Equilibrium and Structural Studies of Silicon(IV) and Aluminium(III) in Aqueous Solution. 11. Polysilicate Formation in Alkaline Aqueous Solution. A Combined Potentiometric and ^{29}Si NMR Study. Acta Chem. Scand., A39, 93-107.

Spadini, L., Schindler. P.W. & Sjöberg, S. (2005): On the Stability of the $AlOSi(OH)_3^{2+}$ Complex in Aqueous Solution. Aquatic Geochemistry, 11, 21-31.

Steinle, E., Fanghänel, Th. & Klenze, R. (1997): Komplexierung von Cm(III) mit Monokieselsäure. In: Forschungszentrum Karlsruhe, Technik und Umwelt, Wissenschaftliche Berichte FZKA 6036, 143-152. Forschungszentrum Karlsruhe FZKA 6036. Sammlung der Vorträge anlässlich des internen INE-Mitarbeiterseminars am 3. – 4. Juli 1997.

Tajeddine, L., Gailhanou, H., Blanc, P., Lassin, A., Gaboreau, S. & Vieillard, P. (2015): Hydration-dehydration behavior and thermodynamics of MX-80 montmorillonite studied using thermal analysis. Thermochimica Acta 604, 83-93.

Tardy, Y. & Duplay, J. (1992): A method of estimateng the Gibbs free energies of formation of hydrated and dehydrated clay minerals. Geochimica et Cosmochimica Acta 56, 3007-3029.

Tardy, Y. & Fritz, B. (1981): An ideal solid-solution model for calculating solubility of clay-minerals. Clay Minerals 16, 361-373.

Tardy, Y. & Garrels, K.M. (1974): A method of estimating the Gibbs energies of formation of layer silicates. Geochimica et Cosmochimica Acta 38, 1101-1116.

Tardy, Y. & Garrels, K.M. (1976): Prediction of Gibbs energies of formation – I. Relationships among Gibbs energies of formation of hydroxides, oxides and aqueous ions. Geochimica et Cosmochimica Acta 40, 1051-1056.

Tardy, Y. & Garrels, K.M. (1977): Prediction of Gibbs energies of formation of compounds from the elements – II. Monovalent and divalent metal silicates. Geochimica et Cosmochimica Acta 41, 87-92.

Thakur, P., Singh, D.K., & Choppin, G.R. (2007): Polymerization study of *o*-$Si(OH)_4$ and complexation with Am(III), Eu(III) and Cm(III). Inorg. Chimica Acta, 360, 3705-3711.

Thoenen, T., Hummel, W., Berner, U. & Curti, E. (2014): The PSI/Nagra Chemical Thermodynamic Database 12/07. Technical Report, PSI Bericht Nr. 14-04, Paul Scherrer Institut, Villigen, Switzerland, 416 pp.

Van Hinsberg, V.J., Vriend, S.P. & Schumacher, J. C. (2005a): A new method to calculate end-member thermodynamic properties of minerals from their constituent polyhedra I: enthalpy, entropy and molar volume. Journal of Metamorphic Geology 23, 165-179.

Van Hinsberg, V.J., Vriend, S.P. & Schumacher, J. C. (2005b): A new method to calculate end-member thermodynamic properties of minerals from their constituent polyhedra II: heat capacity, compressibility and thermal expansion. Journal of Metamorphic Geology 23, 681-693.

Vidal, O. & Dubacq, B. (2009): Thermodynamic modelling of clay dehydration, stability and compositional evolution with temperature, pressure and H_2O activity. Geochimica et Cosmochimica Acta 73, 6544-6564.

Vieillard, P. (1994a): Prediction of enthalpy of formation based on refined crystal structures of multisite compounds: Part 1. Theories and examples. Geochimica et Cosmochimica Acta 58, 4049-4063.

Vieillard, P. (1994b): Prediction of enthalpy of formation based on refined crystal structures of multisite compounds: Part 2. Application to minerals belonging to the system Li_2O-Na_2O-K_2O-BeO-MgO-CaO-MnO-FeO-Fe_2O_3-Al_2O_3-SiO_2-H_2O. Results and discussion. Geochimica et Cosmochimica Acta 58, 4065-4107.

Vieillard, P. (2000): A new method for the prediction of Gibbs free energies of formation of hydrated clay minerals based on the electronegativity scale. Clays and Clay Minerals 48, 459-473.

Vieillard, P. (2002): A new method for the prediction of Gibbs free energies of formation of phyllosilicates (10Å and 14Å) based on the electronegativity scale. Clays and Clay Minerals 50, 352-363.

Vieillard, P., Blanc, P., Fialips, C.I., Gailhanou, H. & Gaboreau, S. (2011): Hydration thermodynamics of the swy-1 montmorillonite saturated with alkali and alkaline-earth cations: A predictive model. Geochimica et Cosmochimica Acta 75, 5664-5685.

Wadsak, W., Hrnecek, E. & Irlweck, K. (2000): Formation of americium(III) complexes with aqueous silicic acid. Radiochim. Acta, 88, 61-64.

Wang, Z., Felmy, A.R., Xia, Y.X., Qafoku, O., Yantassee, W. & Cho, H. (2005): Complexation of Cm(III)/Eu(III) with silicates in basic solutions. Radiochim. Acta, 93, 741-748.

Weber, W.J. & Stumm, W. (1965): Formation of a silicato-iron(III) complex in dilute aqueous solution. J. Inorg. Nucl. Chem., 27, 237-239.

Yates, D.M. & Rosenberg, P.E. (1996): Formation and stability of endmember illite: I. Solution equilibration experiments at 100-200 °C and $P_{v,soln}$. Geochimica et Cosmochimica Acta 60, 1873-1883.

Yusov, A.B. & Fedoseev, A. M. (2003): Reaction of Plutonium(VI) with Orthosilicic Acid $Si(OH)_4$. Russian Journal of Coordination Chemistry, 29. 582-590 (translated from Koordinatsionnaya Khimiya, 29 (2003) 623-634).

Yusov, A.B. & Fedoseev, A. M. (2005): A Spectrophotometric Study of the Interaction of Uranyl Ions with Orthosilicic Acid and Polymeric Silicic Acids in Aqueous Solutions. Radiochemistry, 47, 345-351 (translated from Radiokhimiya, 47 315-321).

Yusov, A.B., Fedoseev, A. M. & Delegard, C.H. (2004): Hydrolysis of Np(IV) and Pu(IV) and their complexation by aqueous $Si(OH)_4$. Radiochim. Acta, 92, 869-881.

Yusov, A.B., Fedoseev, A. M., Isakova, O.V. & Delegard, C.H. (2005a): Complexation of Np(V) with silicate ions. Radiochemistry, 47, 39-44 (translated from Radiokhimiya, 47 (2005) 39-43).

Yusov, A.B., Shilov, V.P., Fedoseev, A.M., Astafurova, L.N. & Delegard, C.H. (2005b): A Spectrophotometric Study of the Interaction of Np(VI) with Orthosilicic Acid and Polymeric Silicic Acids in Aqueous Solutions. Radiochemistry, 47, 352-357 (translated from Radiokhimiya, 47 (2005) 322-327).

Zarubin, D.P. & Nemkina, N.V. (1990): The solubility of amorphous silica in an alkaline aqeous medium at constant ionic strength. Russ. J. Inorg. Chem., 35, 16-21.

26 Silver

26.1 Introduction

Silver has two stable isotopes, ^{107}Ag and ^{109}Ag, with natural abundances of 51.839% and 48.161%, respectively, one long-lived radioactive isotope, ^{108m}Ag, with a half-life of 437.7 ± 8.8 years, and two short-lived radioactive isotopes, ^{110m}Ag and ^{105}Ag with half-lives of 249.83 ± 0.04 and 41.29 ± 0.07 days, respectively. All other radioactive silver isotopes have half-lives less than nine days. In a nuclear reactor ^{108m}Ag and ^{110m}Ag are produced by neutron capture of the stable nuclides ^{107}Ag and ^{109}Ag, respectively. The short-lived ^{110m}Ag mainly decays in interim storage, but the long-lived ^{108m}Ag is a dose-relevant nuclide in radioactive waste (Hummel 2017). The latter fact triggered the inclusion of silver into the PSI Chemical Thermodynamic Database 2020 (TDB 2020).

In aqueous solution, silver occurs in two oxidation states: Ag(0) and Ag(I). Eh-pH diagrams indicate that the Eh-pH space of aqueous solutions is dominated by a very large field of native silver, Ag(cr). Under reducing conditions, Ag_2S(cr) occupies a major part of the Eh-pH space as well (if sulphide is present). At high Eh, i.e., Eh > 0 V, Ag(0) oxidises to Ag(I) (Brookins 1988).

As discussed by Hummel (2017), native silver, Ag(cr), and acanthite, Ag_2S(cr), are the main minerals from which silver is extracted by mining activities. A minor silver mineral is chlorargyrite, AgCl(cr), which is found in the oxidation zone of silver mineral deposits. Rare silver minerals are naumannite, α-Ag_2Se(cr) and iodargyrite, β-AgI(cr). The latter one is found in the same geochemical environment as chlorargyrite, AgCl(cr). In summary, sparingly soluble pure solid phases of silver, also found in nature as minerals, are: Ag(cr), AgCl(cr), AgI(cr), Ag_2S(cr) and Ag_2Se(cr).

Ag^+ forms strong complexes with Cl^-, Br^-, I^-, HS^-, HSe^- and CN^-, and rather weak complexes with OH^-, F^-, CO_3^{2-} and SO_4^{2-}.

The thermodynamic data included into the PSI TDB 2020 have been taken from

- CODATA key values (Cox et al. 1989)
- the recent review of the hydrolysis of metal ions (Brown & Ekberg 2016)
- the NEA review on selenium (Olin et al. 2005)
- and own reviews of experimental data

The selected thermodynamic data for silver compounds and complexes are presented in Tab. 26-1.

IUPAC, as well as NEA (see, e.g., Grenthe et al. 1992) used the specific ion interaction theory (SIT) for making ionic strength corrections to the experimental data, an approach which is also adopted for TDB 2020 (as has been for all its predecessors). The interaction of Ag^+ with Cl^- is very strong and the formation of silver chloride complexes is explicitly considered. Therefore, ion interaction coefficients ε for cationic silver species with Cl^- are missing. They can be approximated by the corresponding interaction coefficients with ClO_4^-. Thus, e.g., $\varepsilon(Ag^+, Cl^-) \approx \varepsilon(Ag^+, ClO_4^-) = (0.00 \pm 0.01)$ kg · mol^{-1}.

In many cases, the ion interaction coefficients of silver species were not available. We approximated these with the estimation method described in Section 1.5.3, which draws on a statistical analysis of published SIT ion interaction coefficients, and which allows the estimation of missing coefficients for the interaction of cations with Cl^- and ClO_4^-, and for the interaction of anions with Na^+, from the charge of the cations or anions of interest.

The selected SIT ion interaction coefficients for silver species are presented in Tab. 26-2.

26.2 Silver(0)

26.2.1 Elemental silver

Elemental silver has, in the absence of sulphide, a very large stability field in the Eh – pH range of water (e.g., Brookins 1988) and hence, native silver, Ag(cr), is an environmentally important substance at Eh < 0 V. On the other hand, the gas phase Agg is not important in aqueous systems and is not included in TDB 2020.

The selected values for Ag(cr) are taken from CODATA (Cox et al. 1989):

$$S_m°(\text{Ag, cr, 298.15 K}) = (42.550 \pm 0.200)\ \text{J} \cdot \text{K}^{-1} \cdot \text{mol}^{-1}$$

$$C_{p,m}°(\text{Ag, cr, 298.15 K}) = (25.350 \pm 0.100)\ \text{J} \cdot \text{K}^{-1} \cdot \text{mol}^{-1}$$

26.2.2 Silver(0) solubility

If the speciation and solubility of silver are calculated under reducing conditions with data usually found in thermodynamic databases, unusual results are obtained. With decreasing redox potential metallic silver, Ag(cr), becomes the thermodynamically stable solid phase and the calculated solubility of silver in water drops to improbably low values. The reason for these strange results is the ignorance of dissolved silver in redox state zero, Ag(aq), in all thermodynamic data bases (Hummel 2017).

In the chemically similar system of the heavy metal mercury, metallic mercury, Hg(l), becomes the stable phase under reducing conditions. Here, we find that the existence of the species Hg(aq) and the solubility of mercury,

$$\text{Hg(l)} \rightleftharpoons \text{Hg(aq)}$$

$$\log_{10}K°(\text{298.15 K}) = -6.53 \pm 0.03$$

as well as its temperature dependence are well established (Clever et al. 1985) and are now included in TDB 2020 (see Section 14.2.2).

By contrast, the experimental determination of the solubility of metallic silver,

$$\text{Ag(cr)} \rightleftharpoons \text{Ag(aq)}$$

at 200 and 280 °C by Kozlov & Khodakovskiy (1983)

$$\log_{10}K°(473.15\ \text{K}) = -(4.47 \pm 0.03)$$

$$\log_{10}K°(553.15\ \text{K}) = -(3.55 \pm 0.15)$$

and at 20 °C by Dobrowolski & Oglaza (1963)

$$\log_{10}K°(293.15\ \text{K}) = -6.50$$

went unnoticed. Also, the possible influence of Ag(aq) on the speciation in the Ag(I) – sulphide system has never been considered (see Section 26.3.7.2).

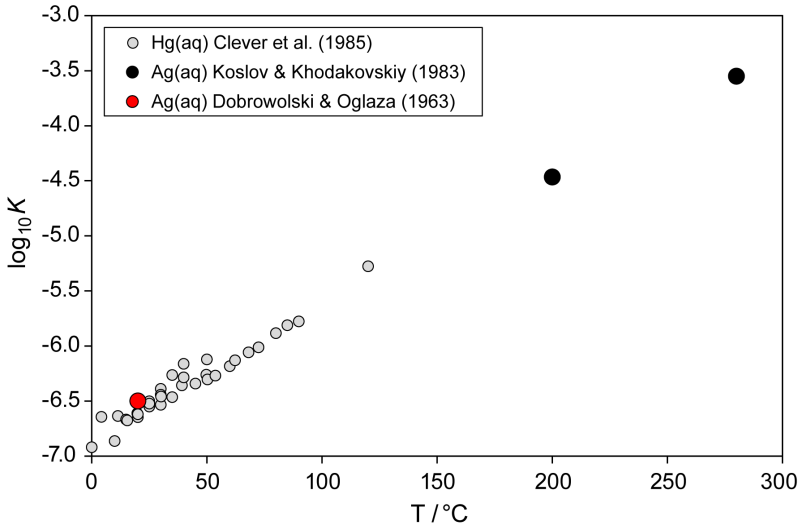

Fig. 26-1: Temperature dependence of $\log_{10}K°(T)$ for Hg(l) ⇌ Hg(aq) and Ag(cr) ⇌ Ag(aq)

The very similar values for the solubility of Hg(aq) and Ag(aq) at 25 °C and the also similar temperature dependence (Fig. 26-1) might be just coincidences. The linear dependence of $\log_{10}K°(T)$ versus temperature (Fig. 26-1) suggests a non-linear dependence versus 1 / T (Tab. 26-2)

Note that no uncertainty and no comment to their measured datum are given by Dobrowolski & Oglaza (1963), just a number in a table. Furthermore, the uncertainties given by Kozlov & Khodakovskiy (1983) seem to be too optimistic, especially for the value obtained at 200 °C.

A three-parameter fit, i.e., calculating $\log_{10}K°(298.15\ \text{K})$, $\Delta_r H_m°(298.15\ \text{K})$ and $\Delta C_{p,m}°(298.15\ \text{K})$ using three data points of unknown and underestimated uncertainty was therefore rejected by this review. An unweighted linear regression of $\log_{10}K°(T)$ versus 1 / T resulted in

$\log_{10}K°(298.15\ K) = -(6.4 \pm 0.5)$

$\Delta_r H_m°(298.15\ K) = (33.7 \pm 8.5)\ kJ \cdot mol^{-1}$

$\Delta C_{p,m}°(298.15\ K) = 0\ J \cdot K^{-1} \cdot mol^{-1}$

These values are included in TDB 2020.

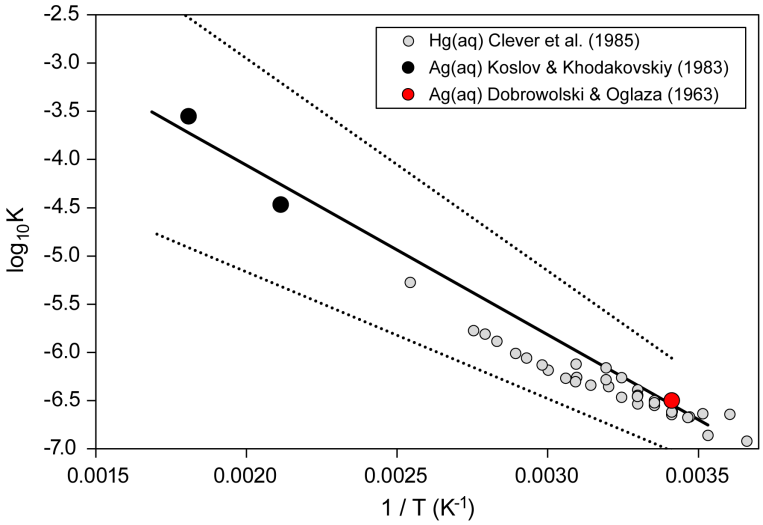

Fig. 26-2: Log10K°(T) for Hg(l) ⇌ Hg(aq) and Ag(cr) ⇌ Ag(aq) versus the inverse of the absolute temperature

Solid line: Result of an unweighted linear regression using the data of Dobrowolski & Oglaza (1963) and Kozlov & Khodakovskiy (1983). Dotted lines: extrapolation of the uncertainties from 25 °C to higher temperatures.

The specific ion interaction coefficients for Ag(aq) are estimated to be zero (see Tab. 1-7):

$\varepsilon(Ag(aq), NaCl) = \varepsilon(Ag(aq), NaClO_4) = (0.0 \pm 0.1)\ kg \cdot mol^{-1}$

26.3 Silver(I)

26.3.1 Silver(I) aqua ion

Silver(I) exists as the Ag^+ cation in aqueous solutions. The selected thermodynamic values for Ag^+ are taken from CODATA (Cox et al. 1989):

$$\Delta_f G_m°(Ag^+, 298.15\ K) = (77.096 \pm 0.156)\ kJ \cdot mol^{-1}$$

$$\Delta_f H_m°(Ag^+, 298.15\ K) = (105.790 \pm 0.080)\ kJ \cdot mol^{-1}$$

$$S_m°(Ag^+, 298.15\ K) = (73.450 \pm 0.400)\ J \cdot K^{-1} \cdot mol^{-1}$$

Using the selected CODATA $\Delta_f G_m°(Ag^+, 298.15\ K)$, the redox equilibrium

$$Ag(cr) \rightleftharpoons Ag^+ + e^-$$

is calculated as

$$\log_{10} K°(298.15\ K) = -13.507 \pm 0.027$$

The specific ion interaction coefficient selected by NEA (Grenthe et al. 1992, Lemire et al. 2013), is also adopted for TDB 2020:

$$\varepsilon(Ag^+, ClO_4^-) = (0.00 \pm 0.01)\ kg \cdot mol^{-1}$$

Since this report explicitly considers the formation of silver(I) chloride complexation, $\varepsilon(Ag^+, Cl^-)$ must be approximated by using the corresponding ion interaction coefficient with perchlorate (Lemire et al. 2013):

$$\varepsilon(Ag^+, Cl^-) \approx \varepsilon(Ag^+, ClO_4^-) = (0.00 \pm 0.01)\ kg \cdot mol^{-1}$$

26.3.2 Silver(I) oxide compounds and complexes

26.3.2.1 Silver(I) oxide compounds

Ag_2O(am)

Brown & Ekberg (2016) report that there have been quite several measurements of the solubility of amorphous (active) silver(I) oxide, Ag_2O(am); however, all of the studies have utilised a temperature in the range of 15 – 25 °C. The solubility constants for the reaction

$$0.5\ Ag_2O(am) + 0.5\ H_2O \rightleftharpoons Ag^+ + OH^-$$

that have been reported within this temperature range relate to zero ionic strength and are in reasonable agreement. Using these data Brown & Ekberg (2016) derived the relationship between the solubility constant and temperature as

$$\log_{10}K_{s0}(T) = -(0.77 \pm 2.32) - (2070 \pm 686) / T$$

From this relationship, the solubility constant at 25 °C is found to be

$$\log_{10}K_{s0}°(298.15\ K) = -7.72 \pm 0.05$$

$$\Delta_r H_m°(298.15\ K) = (40 \pm 13)\ kJ \cdot mol^{-1}$$

Note that the above enthalpy of reaction is erroneously assigned to the reaction 0.5 Ag_2O(am) + $H^+ \rightleftharpoons Ag^+ + 0.5\ H_2O$ in Brown & Ekberg (2016).

Combining this value with the protolysis constant of water (zero ionic strength) leads to

$$0.5\ Ag_2O(am) + H^+ \rightleftharpoons Ag^+ + 0.5\ H_2O(l)$$

$$\log_{10}{}^*K_{s0}°(298.15\ K) = 6.27 \pm 0.05$$

$$\Delta_r H_m°(298.15\ K) = -(16 \pm 13)\ kJ \cdot mol^{-1}$$

Brown & Ekberg (2016) remark that the large uncertainty in $\Delta_r H_m°$ is not surprising given the small temperature range over which solubility constants have been measured.

Brown & Ekberg (2016) report that the solubility of crystalline silver oxide (black) has been studied as a function of ionic strength in $NaClO_4$ media in a number of investigations (Antikainen et al. (1960), Näsänen & Meriläinen (1960), Hietanen & Sillén (1970)). Brown & Ekberg (2016) further state that "the solubility constants derived in these studies are in quite good agreement. Moreover, a study conducted by Maya (1983) on the solubility of amorphous (brown) silver oxide in 3.0 mol l^{-1} $NaClO_4$ derived a solubility constant which differed in magnitude from studies conducted using the same conditions on black silver oxide by the same amount as the difference found by Kozlov et al. (1983) for the two silver oxides at zero ionic strength."

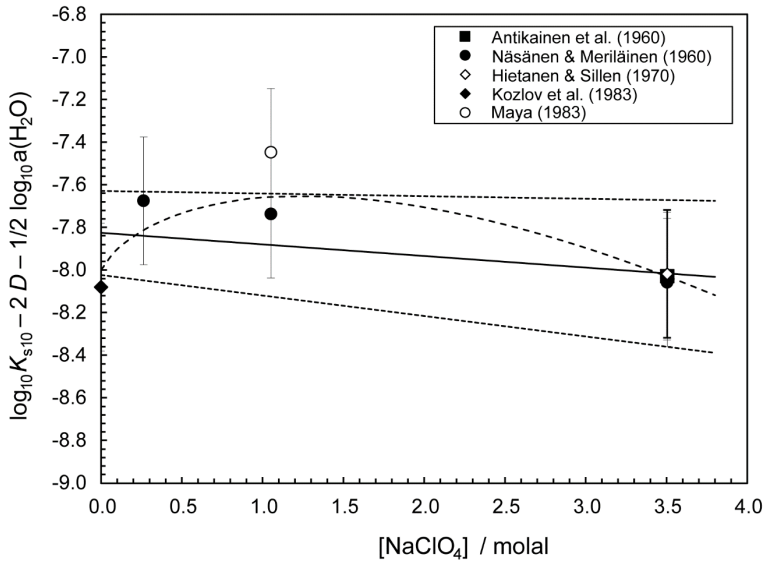

Fig. 26-3: The equilibrium 0.5 $Ag_2O(s) + 0.5\ H_2O(l) \rightleftharpoons Ag^+ + OH^-$

Dashed curve: extended SIT analysis of Brown & Ekberg (2016), for details see text. Solid line and dotted lines: SIT regression by this review. The data of Maya (1983) has been excluded from the SIT analyses.

Brown & Ekberg (2016) assigned the data of Antikainen et al. (1960), Näsänen & Meriläinen (1960), Hietanen & Sillén (1970) and Kozlov et al. (1983) an uncertainty of ± 0.1 log units and did an extended SIT analysis resulting in

$$\Delta\varepsilon = \Delta\varepsilon_1 + \Delta\varepsilon_2 \cdot \log_{10} I_m = -(0.34 \pm 0.51)\ kg \cdot mol^{-1} + (0.64 \pm 0.24)\ kg \cdot mol^{-1} \cdot \log_{10} I_m$$

The results are shown in Fig. 26-3 as dashed curve.

However, the data of Maya (1983) are not measured in 3 M $NaClO_4$, as stated in Brown & Ekberg (2016), but in 1.0 M $NaClO_4$, as shown in Fig. 26-3.

This review assigned the data of Antikainen et al. (1960), Näsänen & Meriläinen (1960), Hietanen & Sillén (1970) and Kozlov et al. (1983) an uncertainty of ± 0.3 log units and did a linear SIT regression resulting in

$$\log_{10} K_{s0}^\circ(298.15\ K) = -7.83 \pm 0.20$$

$$\Delta\varepsilon = (0.05 \pm 0.08)\ kg \cdot mol^{-1}$$

The Δε value is in excellent agreement with the expected value

$$\Delta\varepsilon = \varepsilon(Ag^+, ClO_4^-) + \varepsilon(Na^+, OH^-) = (0.00 \pm 0.01) + (0.04 \pm 0.01) = (0.04 \pm 0.01)\ kg \cdot mol^{-1}$$

The $\log_{10} K_{s0}^\circ$ value is, within uncertainty limits, in agreement with the value derived by Brown & Ekberg (2016) for amorphous (active) silver(I) oxide, $\log_{10} K_{s0}^\circ = -7.72 \pm 0.05$.

What is the implication of that finding?

Kozlov et al. (1983) were not convinced that in any of the above-mentioned studies the solid was actually crystalline silver(I) oxide, $Ag_2O(cr)$, but merely a more or less "active" and probably not pure $Ag_2O(s)$, considering the method of preparation of the solid and the short equilibrium times in the experiments. Kozlov et al. (1983) obtained in their own study $\log_{10}K_{s0}° = -7.71 \pm 0.03$ from their experiments with short equilibrium times of a few days. Only in their experiments running up to 55 days they found reproducible results relating to $Ag_2O(cr)$, as discussed below.

The data of Maya (1983) refer to a fresh precipitate (see Section 26.3.4.2) with even higher solubility than the "active" solids aged for several days.

Considering all these ambiguities and the fact that Brown & Ekberg (2016) ignored the data measured by Näsänen & Meriläinen (1960) in KNO_3 media, this review decided to re-evaluate all available data.

Assigning the data in $NaClO_4$ media of Antikainen et al. (1960), Näsänen & Meriläinen (1960) and Hietanen & Sillén (1970) an uncertainty of ± 0.1 log units, in agreement with Brown & Ekberg (2016), a linear SIT regression (Fig. 26-4) resulted in:

$$\log_{10}K_{s0}°(298.15\ K) = -7.63 \pm 0.09$$

$$\Delta\varepsilon = (0.06 \pm 0.03)\ kg \cdot mol^{-1}$$

The $\Delta\varepsilon$ value is in excellent agreement with the expected value

$$\Delta\varepsilon = \varepsilon(Ag^+, ClO_4^-) + \varepsilon(Na^+, OH^-) = (0.00 \pm 0.01) + (0.04 \pm 0.01) = (0.04 \pm 0.01)\ kg \cdot mol^{-1}$$

Using the data of Näsänen & Meriläinen (1960) in KNO_3 media, with uncertainties of ± 0.1 log units, a linear SIT regression (Fig. 26-4) resulted in:

$$\log_{10}K_{s0}°(298.15\ K) = -7.68 \pm 0.06$$

$$\Delta\varepsilon = -(0.07 \pm 0.05)\ kg \cdot mol^{-1}$$

The $\Delta\varepsilon$ value is, within uncertainty limits, in good agreement with the expected value

$$\Delta\varepsilon = \varepsilon(Ag^+, NO_3^-) + \varepsilon(K^+, OH^-) = -(0.12 \pm 0.03) + (0.09 \pm 0.01) = -(0.03 \pm 0.03)\ kg \cdot mol^{-1}$$

(the values for $\varepsilon(Ag^+, NO_3^-)$ and $\varepsilon(K^+, OH^-)$ were taken from Lemire et al. 2013).

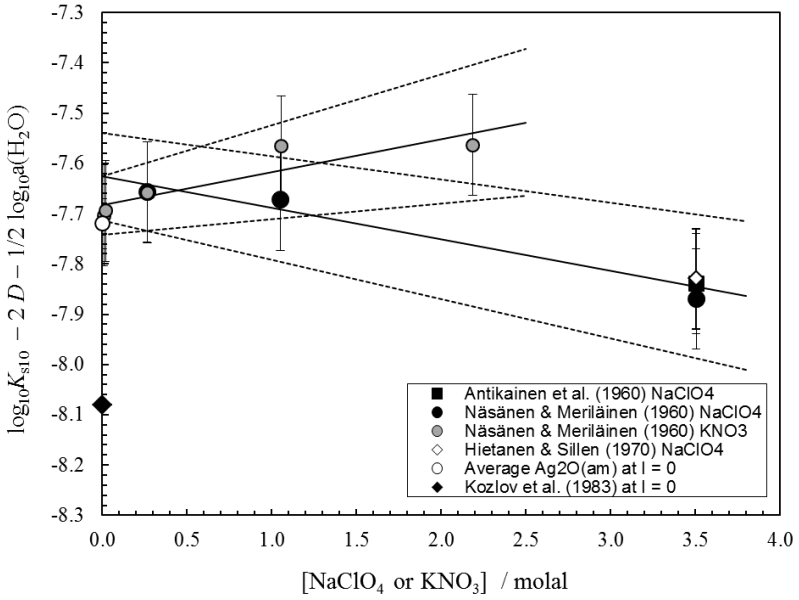

Fig. 26-4: The equilibrium 0.5 $Ag_2O(s) + 0.5\ H_2O(l) \rightleftharpoons Ag^+ + OH^-$

Solid line and dotted lines: SIT regression analyses by this review for data obtained in $NaClO_4$ and KNO_3 media, respectively. The data of Kozlov et al. (1983) and the average Ag_2O(am) at $I_m = 0$ value have been excluded from the SIT analyses.

Considering that data measured in different media ($NaClO_4$ and KNO_3), and extrapolated to zero ionic strength by SIT in this review, and the data in dilute solutions, as evaluated by Brown & Ekberg (2016), are consistent within their derived uncertainties, this review calculated a weighted mean from the three values, i.e. -7.72 ± 0.05, -7.63 ± 0.09 and -7.68 ± 0.06, and obtained

$$\log_{10}K_{s0}°(Ag_2O(am), 298.15\ K) = -7.69 \pm 0.04$$

Combining this value with the protolysis constant of water leads to

$$0.5\ Ag_2O(am) + H^+ \rightleftharpoons Ag^+ + 0.5\ H_2O(l)$$

$$\log_{10}{}^*K_{s0}°(298.15\ K) = 6.31 \pm 0.04$$

This value is included in TDB 2020, together with the enthalpy value derived by Brown & Ekberg (2016) in the temperature range 15 – 25 °C, assuming $\Delta C_{p,m}°(298.15\ K) = 0\ J \cdot K^{-1} \cdot mol^{-1}$:

$$\Delta_r H_m°(298.15\ K) = -(16 \pm 13)\ kJ \cdot mol^{-1}$$

Ag_2O(cr)

Kozlov et al. (1983) measured the equilibrium

$$AgCl(cr) + OH^- \rightleftharpoons 0.5\ Ag_2O(cr) + 0.5\ H_2O(l) + Cl^-$$

in experiments running up to 55 days at 25 and 60 °C and obtained

$$\log_{10}K°(298.15\ K) = -1.66 \pm 0.03$$

$$\log_{10}K°(333.15\ K) = -1.12 \pm 0.03$$

This review estimated from these two values

$$\Delta_r H_m°(298.15\ K) = (29.3 \pm 3.3)\ kJ \cdot mol^{-1}$$

Using the value $\log_{10}K_{s0}°(298.15\ K) = -9.75 \pm 0.02$ for the reaction $AgCl(cr) \rightleftharpoons Ag^+ + Cl^-$, in perfect agreement with the value selected by this review, Kozlov et al. (1983) obtained for

$$0.5\ Ag_2O(cr) + 0.5\ H_2O(l) \rightleftharpoons Ag^+ + OH^-$$

$$\log_{10}K_{s0}°(298.15\ K) = -8.08 \pm 0.02$$

which was accepted by Brown & Ekberg (2016) with an increased uncertainty:

$$\log_{10}K_{s0}°(298.15\ K) = -8.08 \pm 0.10$$

Using the value $\Delta_r H_m°(298.15\ K) = (65.72 \pm 0.14)\ kJ \cdot mol^{-1}$ for the reaction $AgCl(cr) \rightleftharpoons Ag^+ + Cl^-$, selected by this review (see Section 26.3.3.2.1), yields

$$\Delta_r H_m°(298.15\ K) = (36.4 \pm 3.3)\ kJ \cdot mol^{-1}$$

Combining these values with the corresponding values for the protolysis of water leads to

$$0.5\ Ag_2O(cr) + H^+ \rightleftharpoons Ag^+ + 0.5\ H_2O(l)$$

$$\log_{10}{}^*K_{s0}°(298.15\ K) = 5.91 \pm 0.10$$

$$\Delta_r H_m°(98.15\ K) = -(19.4 \pm 3.3)\ kJ \cdot mol^{-1}$$

$$\Delta C_{p,m}°(298.15\ K) = 0\ J \cdot K^{-1} \cdot mol^{-1}$$

These values are included in TDB 2020.

Note that the $\Delta_r H_m°$ value obtained here for Ag_2O(cr) in the temperature range 25 – 60 °C is in good agreement with the value $\Delta_r H_m°(Ag_2O(am), 298.15\ K) = -(16 \pm 13)\ kJ \cdot mol^{-1}$ derived by Brown & Ekberg (2016) in the temperature range 15 – 25 °C.

26.3.2.2 Silver(I) hydroxide complexes

As discussed by Brown & Ekberg (2016), for the reactions

$$0.5\ Ag_2O(cr) + 0.5\ H_2O(l) \rightleftharpoons AgOH(aq)$$

$$0.5\ Ag_2O(cr) + 0.5\ H_2O(l) + OH^- \rightleftharpoons Ag(OH)_2^-$$

Kozlov et al. (1983) determined solubility constants at 25, 60 and 90 °C. The authors found that the solubility constants were linearly dependent on the inverse of absolute temperature. The relationships found were

$$\log_{10}K_{s1}(T) = -3.41 - 701.1 / T$$

$$\log_{10}K_{s2}(T) = -0.29 - 1'209 / T$$

From these relationships, Kozlov et al. (1983) determined solubility constants and reaction enthalpies at 25 °C of

$$\log_{10}K_{s1}°(298.15\ K) = -5.76 \pm 0.10$$

$$\Delta_r H_m°(298.15\ K) = (13.42 \pm 3.3)\ kJ \cdot mol^{-1}$$

$$\log_{10}K_{s2}°(298.15\ K) = -4.35 \pm 0.10$$

$$\Delta_r H_m°(298.15\ K) = (23.15 \pm 3.3)\ kJ \cdot mol^{-1}$$

with an uncertainty of ± 0.10 assigned to $\log_{10}K°$ by Brown & Ekberg (2016) and ± 3.3 assigned to $\Delta_r H_m°$ by this review in analogy to the uncertainty for the solubility product (see Section 26.3.2.1). Coupled with the selected solubility constant $\log_{10}K_{s0}°(298.15\ K) = -8.08 \pm 0.10$ for crystalline silver oxide, these values were used to derive stability constants for the reactions

$$Ag^+ + OH^- \rightleftharpoons AgOH(aq)$$

$$\log_{10}\beta_1°(298.15\ K) = 2.24 \pm 0.14$$

$$\Delta_r H_m°(298.15\ K) = (23.00 \pm 4.7)\ kJ \cdot mol^{-1}$$

$$Ag^+ + 2\ OH^- \rightleftharpoons Ag(OH)_2^-$$

$\log_{10}\beta_2°(298.15\ K) = 3.65 \pm 0.14$

$\Delta_r H_m°(298.15\ K) = (13.27 \pm 4.7)\ kJ \cdot mol^{-1}$

As discussed by Brown & Ekberg (2016), these values are in reasonable to excellent agreement with the results of earlier studies, and hence, Brown & Ekberg (2016) retained these values in their review. Coupling these values with the protolysis values of water for 25 °C leads to the following two accepted stability constants and reaction enthalpies:

$Ag^+ + H_2O(l) \rightleftharpoons AgOH(aq) + H^+$

$\log_{10}{}^*\beta_1°(298.15\ K) = -11.75 \pm 0.14$

$\Delta_r H_m°(298.15\ K) = (78.8 \pm 4.7)\ kJ \cdot mol^{-1}$

$\Delta C_{p,m}°(298.15\ K) = 0\ J \cdot K^{-1} \cdot mol^{-1}$

$Ag^+ + 2\ H_2O(l) \rightleftharpoons Ag(OH)_2^- + 2\ H^+$

$\log_{10}{}^*\beta_2°(298.15\ K) = -24.34 \pm 0.14$

$\Delta_r H_m°(298.15\ K) = (69.1 \pm 4.7)\ kJ \cdot mol^{-1}$

$\Delta C_{p,m}°(298.15\ K) = 0\ J \cdot K^{-1} \cdot mol^{-1}$

These values are included in TDB 2020, together with estimated SIT interaction coefficients (see Tab. 1-7)

$\varepsilon(AgOH(aq), NaCl) = \varepsilon(AgOH(aq), NaClO_4) = (0.0 \pm 0.1)\ kg \cdot mol^{-1}$

$\varepsilon(Ag(OH)_2^-, Na^+) = -(0.05 \pm 0.10)\ kg \cdot mol^{-1}$

26.3.3 Silver(I) halogenide compounds and complexes

26.3.3.1 Silver(I) fluoride compounds and complexes

26.3.3.1.1 Silver(I) fluoride compounds

AgF(s) is a highly soluble salt, with a solubility of about 1.8 kg/L at 25 °C. It is not expected that this highly soluble salt will be of any significance in environmental aqueous systems and hence, no attempt was made to derive thermodynamic data for AgF(s).

26.3.3.1.2 Silver(I) fluoride complexes

Leden & Marthén (1952) studied the complexation of Ag^+ with F^- by emf measurements using silver – silver chloride electrodes at an ionic strength of 1.0 M $NaClO_4$ and 25 °C. They report 12 experimental data measured in the ranges 0.003 to 0.1 M Ag^+ and 0.1 – 0.4 M F^-. For the reaction

$$Ag^+ + F^- \rightleftharpoons AgF(aq)$$

they obtained

$$K_1 \text{ (1.0 M } NaClO_4\text{, 298.15 K)} = 0.48 \pm 0.03$$

where the uncertainty represents the 95% confidence interval of the experimental data as calculated by this review.

Their work was extended to other temperatures but at an ionic strength of 0.50 M $NaClO_4$ by Connick & Paul (1961). The measurements were made potentiometrically on the silver – silver ion couple. Connick & Paul (1961) report K_1 = 0.77, 0.68 and 0.56 at 15, 25 and 25 °C, respectively. No uncertainties for these values are given by Connick & Paul (1961). From the temperature dependence of K_1 Connick & Paul (1961) calculated $\Delta_r H_m$(298.15 K) = -(2.8 ± 1.0) kcal · mol^{-1}, where they estimated the uncertainty by assuming an error of 0.1 mV in the potential. This value is recalculated to

$$\Delta_r H_m(0.5 \text{ M } NaClO_4, 298.15 \text{ K}) = -(11.7 \pm 4.2) \text{ kJ} \cdot \text{mol}^{-1}$$

This value is included in TDB 2020 assuming $\Delta_r H_m°(298.15 \text{ K}) \approx \Delta_r H_m(0.5 \text{ M } NaClO_4, 298.15 \text{ K})$, as well as assuming $\Delta C_{p,m}°(298.15 \text{ K}) = 0 \text{ J} \cdot \text{K}^{-1} \cdot \text{mol}^{-1}$.

Using

$$\Delta\varepsilon = \varepsilon(AgF(aq), NaClO_4) - \varepsilon(F^-, Na^+) - \varepsilon(Ag^+, ClO_4^-)$$

$$= (\textit{0.0} \pm \textit{0.1}) - (0.02 \pm 0.02) - (0.00 \pm 0.01)$$

$$= -(0.02 \pm 0.10) \text{ kg} \cdot \text{mol}^{-1}$$

the K_1 values at 25 °C reported by Leden & Marthén (1952) and Connick & Paul (1961) were extrapolated to zero ionic strength and the average calculated by this review as

$$\log_{10}K_1^\circ\ (298.15\ \text{K}) = 0.11 \pm 0.10$$

This value is included in TDB 2020, together with estimated SIT interaction coefficients (see Tab. 1-7)

$$\varepsilon(\text{AgF(aq)}, \text{NaCl}) = \varepsilon(\text{AgF(aq)}, \text{NaClO}_4) = (0.0 \pm 0.1)\ \text{kg} \cdot \text{mol}^{-1}$$

26.3.3.2 Silver(I) chloride compounds and complexes

26.3.3.2.1 Silver(I) chloride compounds

The thermodynamic parameters of AgCl(cr) belong to the most precisely known values in chemical thermodynamics of aqueous solutions due to extensive measurements with the Ag – AgCl electrode. The selected thermodynamic values for AgCl(cr) are taken from CODATA (Cox et al. 1989):

$$\Delta_f G_m^\circ(\text{AgCl, cr, 298.15 K}) = -(109.765 \pm 0.098)\ \text{kJ} \cdot \text{mol}^{-1}$$

$$\Delta_f H_m^\circ(\text{AgCl, cr, 298.15 K}) = -(127.010 \pm 0.050)\ \text{kJ} \cdot \text{mol}^{-1}$$

$$S_m^\circ(\text{AgCl, cr, 298.15 K}) = (96.250 \pm 0.20)\ \text{J} \cdot \text{K}^{-1} \cdot \text{mol}^{-1}$$

Using the selected CODATA values $\Delta_f G_m^\circ$(AgCl, cr, 298.15 K), $\Delta_f G_m^\circ(Ag^+, 298.15\ \text{K}) = (77.096 \pm 0.156)\ \text{kJ} \cdot \text{mol}^{-1}$ (see Section 26.3.1) and $\Delta_f G_m^\circ(Cl^-, 298.15\ \text{K}) = -(131.217 \pm 0.117)\ \text{kJ} \cdot \text{mol}^{-1}$ (Cox et al. 1989) the solubility product

$$\text{AgCl(cr)} \rightleftharpoons Ag^+ + Cl^-$$

is calculated as

$$\log_{10}K_{s0}^\circ(298.15\ \text{K}) = -9.748 \pm 0.038$$

Using the selected CODATA values $\Delta_f H_m^\circ$(AgCl, cr, 298.15 K), $\Delta_f H_m^\circ(Ag^+, 298.15\ \text{K}) = (105.790 \pm 0.080)\ \text{kJ} \cdot \text{mol}^{-1}$ (see Section 26.3.1) and $\Delta_f H_m^\circ(Cl^-, 298.15\ \text{K}) = -(167.080 \pm 0.100)\ \text{kJ} \cdot \text{mol}^{-1}$ (Cox et al. 1989) gives

$$\Delta_r H_m^\circ(298.15\ \text{K}) = (65.72 \pm 0.14)\ \text{kJ} \cdot \text{mol}^{-1}$$

$$\Delta C_{p,m}^\circ(298.15\ \text{K}) = 0\ \text{J} \cdot \text{K}^{-1} \cdot \text{mol}^{-1}$$

In their very careful study of the standard electrode potential of silver Owen & Brinkley (1938) measured the solubility product of AgCl(cr) at 5 – 45 °C using a potentiometric method. They report $\log_{10}K_{s0}° = -9.7492$ and $\Delta_r H_m°(298.15\ K) = 15.653$ kcal · mol^{-1} (= 65.49 kJ · mol^{-1}) at 25 °C, no uncertainty estimate given.

Using the $\log_{10}K_{s0}°$ values reported by Owen & Brinkley (1938) for 5, 15, 25, 35, and 45 °C for a linear regression analysis this review obtained $\log_{10}K_{s0}°(298.15\ K) = -9.758 \pm 0.013$ and $\Delta_r H_m°(298.15\ K) = (65.73 \pm 1.60)$ kJ · mol^{-1}. The uncertainties represent 95% confidence intervals.

Gledhill & Malan (1954) reported values for the solubility of silver chloride in water at 10° intervals between 5 and 55 °C, determined by the conductimetric method using "ultra-pure" water. Their value at 25 °C, $K_{s0}° = (1.780 \pm 0.010) \cdot 10^{-10}$, results in $\log_{10}K_{s0}° = -9.7496 \pm 0.0024$.

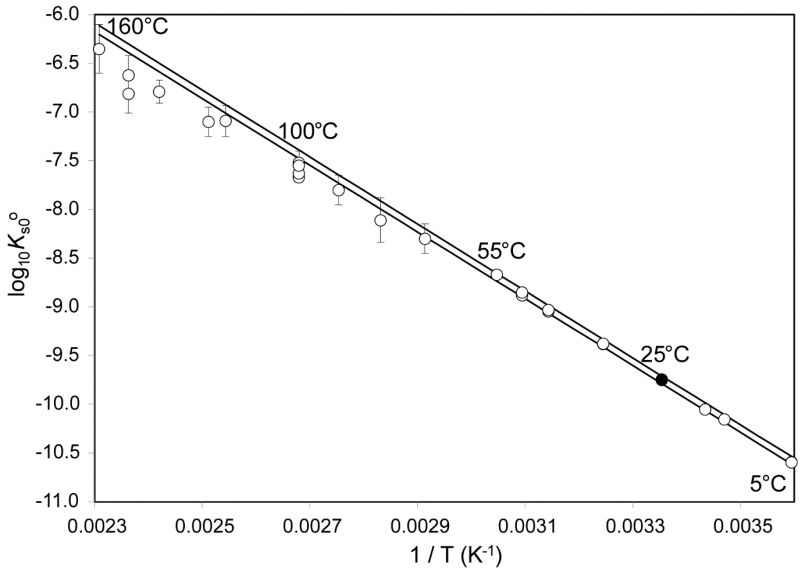

Fig. 26-5: The equilibrium constant $\log_{10}K_{s0}°$ for AgCl(cr) ⇌ $Ag^+ + Cl^-$ as function of temperature

Circles: data taken from the compilation of Zotov et al. (1986a), including the data of Owen & Brinkley (1938) at 5 – 45 °C, Gledhill & Malan (1954) at 5 – 55 °C and Lieser (1957) at 18 °C. Filled circle: data at 25 °C. Lines: lower and upper limits calculated using $\log_{10}K_{s0}°(298.15\ K) = -9.748 \pm 0.038$, $\Delta_r H_m°(298.15\ K) = (65.72 \pm 0.14)$ kJ · mol^{-1}, calculated from CODATA vales, and assuming $\Delta_r C_{p,m}° = 0$.

Using the $\log_{10}K_{s0}°$ values reported by Gledhill & Malan (1954) for 5, 15, 25, 35, 45 and 55 °C for a linear regression analysis this review obtained $\log_{10}K_{s0}°(298.15\ K) = -9.752 \pm 0.011$ and $\Delta_r H_m°(298.15\ K) = (66.78 \pm 1.10)$ kJ · mol^{-1}. The uncertainties represent 95% confidence intervals.

Lieser (1957) measured the solubility of AgCl(cr) very precisely by radiometric methods using the isotopes ^{110}Ag and ^{111}Ag. He obtained $\log_{10}K_{s0}° = -10.055 \pm 0.009$ at 18 °C.

Zotov et al. (1986a) measured the solubility of AgCl(cr) at 250 and 300 °C. In their careful analysis of previously published data, they compiled the most reliable $\log_{10}K_{s0}°$ values (Tab. 3 in Zotov et al. 1986a).

Fig. 26-5 shows these data in the temperature range 5 – 160 °C together with the lower and upper limits calculated from the selected CODATA values. As can be seen in Fig. 26-5, the CODATA values $\log_{10}K_{s0}°(298.15\ K) = -9.748 \pm 0.038$, $\Delta_r H_m°(298.15\ K) = (65.72 \pm 0.14)\ kJ \cdot mol^{-1}$, and implicitly, $\Delta_r C_{p,m}° = 0$, perfectly fit the experimental data in the range 5 – 55 °C and are a good approximation up to 160 °C.

Gammons & Yu (1997) compiled data for the temperature range 25 – 300 °C and recommend $\log_{10}K_{s0}°(298.15\ K) = -9.76$, $\Delta_r H_m°(298.15\ K) = 67.530\ kJ \cdot mol^{-1}$ and $\Delta_r C_{p,m}° = 854.39 - 4.533 \cdot T\ 0.004959533 \cdot T^2\ J \cdot mol^{-1}$, based on the data from Owen & Brinkley (1938) and Zotov et al. (1986a). The $\Delta_r C_{p,m}°$ function describes the curvature of $\log_{10}K_{s0}°$ vs. 1/T above 100 °C and is given here for information only.

26.3.3.2.2 Silver(I) chloride complexes

Silver(I) forms up to four consecutive chloride complexes in aqueous solution:

$$Ag^+ + Cl^- \rightleftharpoons AgCl(aq)$$

$$Ag^+ + 2\ Cl^- \rightleftharpoons AgCl_2^-$$

$$Ag^+ + 3\ Cl^- \rightleftharpoons AgCl_3^{2-}$$

$$Ag^+ + 4\ Cl^- \rightleftharpoons AgCl_4^{3-}$$

Lieser (1957) measured the solubility of AgCl(cr) in 10^{-4} – 2 M NaCl solutions at 18 °C and determined the complexation of Ag^+ with Cl^- by radiometric methods using the isotopes ^{110}Ag and ^{111}Ag. He obtained the stability constants $\log_{10}\beta_1°(291.15\ K) = 3.41$ (AgCl(aq) dominating in 10^{-4} – 10^{-2} M NaCl solution), $\log_{10}\beta_2°(291.15\ K) = 5.28$ ($AgCl_2^-$ dominating in 10^{-2} – 0.2 M NaCl), and $\log_{10}\beta_3°(291.15\ K) = 5.24$ ($AgCl_3^{2-}$ dominating above 0.2 M NaCl).

The review by Fritz (1985) "used all numerical results available for monovalent chlorides up to 6.5 M and 160 °C. The measurements had been made by chemical and radiochemical analysis of saturated solutions. Most were carried out at the ionic strength produced by the host solutions used; some were maintained at constant ionic strength by use of suitable amounts of perchlorate. There were 469 data points in all, about half at 25 °C. Over half of the measurements were made in NaCl, the reminder in aqueous solutions of HCl, KCl, LiCl and NH_4Cl. About one third of the measurements were made at concentrations of host chloride less than 0.1 M (as low as $5 \cdot 10^{-4}$ M). In addition, there is a set of 28 potentiometric measurements of the activity of Ag^+ in 5 M NaCl – $NaClO_4$ mixtures at 25 °C."

Fritz (1985) analysed these data using the virial model of activity coefficients developed by Pitzer to obtain the best values of the stability constants and heats of formation at 25 °C and zero ionic strength, together with the Pitzer parameters necessary to describe their behaviour at chloride concentrations up to 5 M. The results by Fritz (1985) are:

$$\log_{10}\beta_1°(298.15\ K) = 3.23 \pm 0.11$$

$$\log_{10}\beta_2°(298.15\ K) = 5.15 \pm 0.11$$

$\log_{10}\beta_3°(298.15\ K) = 5.04 \pm 0.08$

$\log_{10}\beta_4°(298.15\ K) = 3.64 \pm 0.11$

$\Delta_r H_{m1}°(298.15\ K) = -(27.6 \pm 4.2)\ kJ \cdot mol^{-1}$

$\Delta_r H_{m2}°(298.15\ K) = -(21.3 \pm 1.3)\ kJ \cdot mol^{-1}$

$\Delta_r H_{m3}°(298.15\ K) = -(41.8 \pm 2.1)\ kJ \cdot mol^{-1}$

$\Delta_r H_{m4}°(298.15\ K) = -(69.9 \pm 4.2)\ kJ \cdot mol^{-1}$

$\Delta C_{p,m1,2,3,4}°(298.15\ K) = 0\ J \cdot K^{-1} \cdot mol^{-1}$

The Pitzer coefficients $\beta^{(0)}$, $\beta^{(1)}$ and C for all ion pairs are given in Tab. II of Fritz (1985).

Gammons & Yu (1997) report solubility experiments for AgBr at 200° and 300 °C and for AgI at 150°, 200° and 300 °C. They combined the results of their high-temperature experiments with existing data to compile a complete set of equilibrium constants for AgCl, AgBr and AgI at 25 – 300 °C.

For the solubility product of AgCl(cr) Gammons & Yu (1997) recommend a temperature dependent $\Delta_r C_{p,m}°$ function (see Section 26.3.3.2.1).

For the reactions

$AgCl(cr) \rightleftharpoons AgCl(aq)$

$AgCl(cr) + Cl^- \rightleftharpoons AgCl_2^-$

Gammons & Yu (1997) report that "values of $\log_{10}K$ may be calculated in the complete temperature range 25 – 350 °C from the data of Seward (1976) and Zotov et al. (1986b). These two studies are in excellent agreement and need no further comment." Gammons & Yu (1997) found that $\Delta_r C_{p,m}° = 0$, i.e., $\Delta_r H_m°(298.15\ K)$ = constant. This is no surprise as both reactions are isocoulombic.

For the reaction

$AgCl(cr) + 2\ Cl^- \rightleftharpoons AgCl_3^{2-}$

Gammons & Yu (1997) report that "estimates of $\log_{10}K$ at 25 – 300 °C were obtained by Seward (1976), Zotov et al. (1986b), and Levin (1992). We adopted the values of Levin (1992), as this author took into account all previous work, as well as his own experimental results at very high Cl concentrations." Gammons & Yu (1997) recommend a temperature dependent $\Delta_r C_{p,m}°$ function.

Combining the data of the above reactions with the data of the solubility product, Gammons & Yu (1997) recommend $\log_{10}\beta_1°(298.15\ K) = 3.28$, $\log_{10}\beta_2°(298.15\ K) = 5.21$, $\log_{10}\beta_3°(298.15\ K) = 5.10$, $\Delta_r H_{m1}°(298.15\ K) = -21.7\ kJ \cdot mol^{-1}$, $\Delta_r H_{m2}°(298.15\ K) = -20.3\ kJ \cdot mol^{-1}$, $\Delta_r H_{m3}°(298.15\ K) = -35.5\ kJ \cdot mol^{-1}$.

The $\log_{10}\beta_x°$ values of Gammons & Yu (1997) are all within the error limits of the values recommended by of Fritz (1985).

The $\Delta_r H_{mx}°$ values of Gammons & Yu (1997) are in reasonable agreement with the values recommended by of Fritz (1985), considering that Gammons & Yu (1997) fitted a much larger temperature range with temperature dependent $\Delta_r C_{p,m}°$ functions for the solubility product and $AgCl(cr) + 2\ Cl^- \rightleftharpoons AgCl_3^{2-}$.

Hence, the $\log_{10}\beta_x°$ and $\Delta_r H_{mx}°$ values, as well as $\Delta C_{p,m}°(298.15\ K) = 0$, valid in the temperature range 5 – 160 °C, recommended by Fritz (1985) are included in TDB 2020, together with the estimated SIT interaction coefficients (see Tab. 1-7)

$$\varepsilon(AgCl(aq), NaCl) = \varepsilon(AgCl(aq), NaClO_4) = (0.0 \pm 0.1)\ kg \cdot mol^{-1}$$

$$\varepsilon(AgCl_2^-, Na^+) = -(0.05 \pm 0.10)\ kg \cdot mol^{-1}$$

$$\varepsilon(AgCl_3^-, Na^+) = -(0.10 \pm 0.10)\ kg \cdot mol^{-1}$$

$$\varepsilon(AgCl_4^-, Na^+) = -(0.15 \pm 0.10)\ kg \cdot mol^{-1}$$

26.3.3.3 Silver(I) bromide compounds and complexes

26.3.3.3.1 Silver(I) bromide compounds

The solubility product of AgBr(cr) according to the reaction

$$AgBr(cr) \rightleftharpoons Ag^+ + Br^-$$

has been very precisely measured.

In their very careful study of the standard electrode potential of silver Owen & Brinkley (1938) measured the solubility product of AgBr(cr) at 5 – 45 °C using a potentiometric method. They report $\log_{10}K_{s0}° = -12.3026$ and $\Delta_r H_m°(298.15\ K) = 20.150\ kcal \cdot mol^{-1}$ (= $84.31\ kJ \cdot mol^{-1}$) at 25 °C, no uncertainty estimate given. Using the $\log_{10}K_{s0}°$ values reported by Owen & Brinkley (1938) for 5, 15, 25, 35, and 45 °C for a linear regression analysis this review obtained $\log_{10}K_{s0}°(298.15\ K) = -12.312 \pm 0.015$ and $\Delta_r H_m°(298.15\ K) = (84.47 \pm 1.80)\ kJ \cdot mol^{-1}$. The uncertainties represent 95% confidence intervals.

Gledhill & Malan (1954) reported values for the solubility of silver bromide in water at 10 °C intervals between 5 and 55 °C, determined by the conductimetric method using "ultra-pure" water. Their value at 25 °C, $K_{s0}° = (5.20 \pm 0.40) \cdot 10^{-13}$ results in $\log_{10}K_{s0}° = -12.283 \pm 0.033$. Using the $\log_{10}K_{s0}°$ values reported by Gledhill & Malan (1954) for 5, 15, 25, 35, 45 and 55 °C for a linear regression analysis this review obtained $\log_{10}K_{s0}°(298.15\ K) = -12.279 \pm 0.027$ and $\Delta_r H_m°(298.15\ K) = (85.6 \pm 2.7)\ kJ \cdot mol^{-1}$. The uncertainties represent 95% confidence intervals.

Lieser (1957) measured the solubility of AgBr(cr) very precisely by radiometric methods using the isotopes ^{110}Ag and ^{111}Ag. He obtained $\log_{10}K_{s0}° = -11.676 \pm 0.009$ at 18 °C.

Using the $\log_{10}K_{s0}°$ values reported by Owen & Brinkley (1938), Gledhill & Malan (1954) and Lieser (1957) for a common linear regression analysis (Fig. 26-6) this review obtained

$$\log_{10}K_{s0}°(298.15\ K) = -12.30 \pm 0.04$$

$$\Delta_r H_m°(298.15\ K) = (85.5 \pm 1.8)\ kJ \cdot mol^{-1}$$

$$\Delta C_{p,m}°(298.15\ K) = 0\ J \cdot K^{-1} \cdot mol^{-1}$$

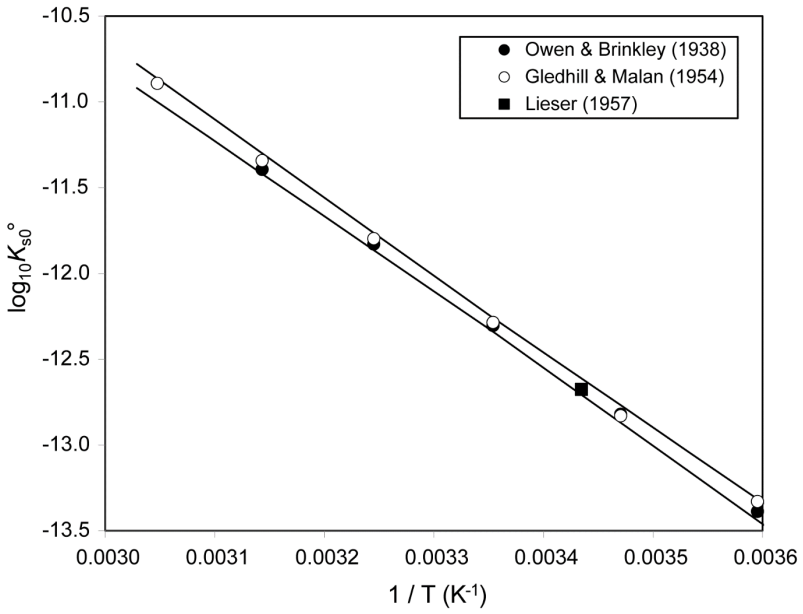

Fig. 26-6: The equilibrium constant $\log_{10}K_{s0}°$ for AgBr(cr) ⇌ $Ag^+ + Br^-$ as function of temperature in the range 5 – 55 °C

Lines: lower and upper limits calculated using $\log_{10}K_{s0}°(298.15\ K) = -12.30 \pm 0.04$ and $\Delta_r H_m°(298.15\ K) = (85.5 \pm 1.8)\ kJ \cdot mol^{-1}$.

These values are included in TDB 2020.

Gammons & Yu (1997) accepted $\log_{10}K_{s0}° = -12.31$ at 25 °C from Owen & Brinkley (1938). This value agrees perfectly with the result obtained by this review by re-analysing the data of Owen & Brinkley (1938).

Gammons & Yu (1997) further used $\Delta_r H_m°$(298.15 K) "recommended by Owen & Brinkley (1938)", together with the temperature dependent $\Delta_r C_{p,m}°$ function they derived for AgCl(cr) as an estimate in order to extrapolate the AgBr(cr) solubility product to temperatures above 50 °C.

26.3.3.3.2 Silver(I) bromide complexes

Silver(I) forms up to four consecutive bromide complexes in aqueous solution:

$$Ag^+ + Br^- \rightleftharpoons AgBr(aq)$$

$$Ag^+ + 2\ Br^- \rightleftharpoons AgBr_2^-$$

$$Ag^+ + 3\ Br^- \rightleftharpoons AgBr_3^{2-}$$

$$Ag^+ + 4\ Br^- \rightleftharpoons AgBr_4^{3-}$$

Lieser (1957) measured the solubility of AgBr(cr) in $5 \cdot 10^{-6}$ – 2 M NaBr solutions at 18 °C and determined the complexation of Ag^+ with Br^- by radiometric methods. He obtained the stability constants $\log_{10}\beta_1°$(291.15 K) = 4.68 (AgBr(aq) dominating in 10^{-5} – 10^{-3} M NaBr solution), $\log_{10}\beta_2°$(291.15 K) = 7.66 ($AgBr_2^-$ dominating in 10^{-3} – $5 \cdot 10^{-2}$ M NaBr), $\log_{10}\beta_3°$(291.15 K) = 8.51 ($AgBr_3^{2-}$ dominating in 0.1 – 2 M NaBr) and $\log_{10}\beta_4°$(291.15 K) ≈ 7.2 ($AgBr_4^{3-}$ dominating above 2 M NaBr).

Gammons & Yu (1997) report solubility experiments for AgBr(cr) at 200° and 300 °C for the reactions

$$AgBr(cr) \rightleftharpoons AgBr(aq)$$

$$AgBr(cr) + Br^- \rightleftharpoons AgBr_2^-$$

which they combined with the results reported by Lieser (1957) at 18° and finally obtained $\log_{10}\beta_1°$(298.15 K) = 4.54, $\log_{10}\beta_2°$(298.15 K) = 7.48, $\Delta_r H_{m1}°$(298.15 K) = -32.9 kJ · mol^{-1}, $\Delta_r H_{m2}°$(298.15 K) = -48.0 kJ · mol^{-1}. Using these values, we obtain $\log_{10}\beta_1°$(291.15 K) = 4.68 and $\log_{10}\beta_2°$(291.15 K) = 7.68, in agreement with the values reported by Lieser (1957) at 18 °C.

For the reaction

$$AgBr(cr) + 2\ Br^- \rightleftharpoons AgBr_3^{2-}$$

Gammons & Yu (1997) used data reported in the range 20 – 70 °C by Pouradier et al. (1954) and obtained $\log_{10}\beta_3°$(298.15 K) = 8.86 and $\Delta_r H_{m3}°$(298.15 K) = -64.5 kJ · mol^{-1}. Using these values this review calculated $\log_{10}\beta_3°$(291.15 K) = 9.13, at variance with the value $\log_{10}\beta_3°$(291.15 K) = 8.51 reported by Lieser (1957) at 18 °C.

Pouradier et al. (1954) interpreted their experimental data assuming that the complexes $AgBr_3^{2-}$ and $AgBr_5^{4-}$ are formed, and found for both equilibria linear dependences versus 1 / T. The complex $AgBr_5^{4-}$ has not been confirmed by any other study. On the other hand, Pouradier et al.

(1954) did not consider the formation of $AgBr_4^{3-}$ or $AgBr_2^-$ which could be the reason for the offset of their stability constants for $AgBr_3^{2-}$ of about 0.6 log units compared with the value of Lieser (1957). Hence, this review does not accept the absolute values of the stability constants reported by Pouradier et al. (1954) for $AgBr_3^{2-}$ but considered their 1 / T dependence as an estimate for $\Delta_r H_{m3}°(298.15\ K) = -12.6\ kcal \cdot mol^{-1} = -52.7\ kJ \cdot mol^{-1}$.

This value has been used to extrapolate the value of Lieser (1957) from 18 °C to 25 °C, i.e., $\log_{10}\beta_3°(291.15\ K) = 8.5$ recalculated as $\log_{10}\beta_3°(298.15\ K) = 8.3$. In summary, this review obtained

$\log_{10}\beta_1°(298.15\ K) = 4.54 \pm 0.10$

$\log_{10}\beta_2°(298.15\ K) = 7.48 \pm 0.10$

$\log_{10}\beta_3°(298.15\ K) = 8.3 \pm 0.2$

$\Delta_r H_{m1}°(298.15\ K) = -(32.9 \pm 4.0)\ kJ \cdot mol^{-1}$

$\Delta_r H_{m2}°(298.15\ K) = -(48.0 \pm 4.0)\ kJ \cdot mol^{-1}$

$\Delta C_{p,m1,2}°(298.15\ K) = 0\ J \cdot K^{-1} \cdot mol^{-1}$

with uncertainties assigned by this review. These values are included in TDB 2020.

$\Delta_r H_{m3}°(298.15\ K) \approx -52.7\ kJ \cdot mol^{-1}$

$\log_{10}\beta_4°(298.15\ K) \approx 7.2$

These values are included in TDB 2020 as supplemental data, together with the estimated SIT interaction coefficients (see Tab. 1-7)

$\varepsilon(AgBr(aq), NaCl) = \varepsilon(AgBr(aq), NaClO_4) = (0.0 \pm 0.1)\ kg \cdot mol^{-1}$

$\varepsilon(AgBr_2^-, Na^+) = -(0.05 \pm 0.10)\ kg \cdot mol^{-1}$

$\varepsilon(AgBr_3^-, Na^+) = -(0.10 \pm 0.10)\ kg \cdot mol^{-1}$

$\varepsilon(AgBr_4^-, Na^+) = -(0.15 \pm 0.10)\ kg \cdot mol^{-1}$

26.3.3.4 Silver(I) iodide compounds and complexes

26.3.3.4.1 Silver(I) iodide compounds

The solubility product of AgI(cr) according to the reaction

$$AgI(cr) \rightleftharpoons Ag^{+} + I^{-}$$

has been very precisely measured.

In their very careful study of the standard electrode potential of silver Owen & Brinkley (1938) measured the solubility product of AgI(cr) at 5 – 45 °C using a potentiometric method. They report $\log_{10}K_{s0}° = -16.0813$ and $\Delta_r H_m°(298.15\ K) = 26.473$ kcal · mol^{-1} (= 110.76 kJ · mol^{-1}) at 25 °C, no uncertainty estimate given. Using the $\log_{10}K_{s0}°$ values reported by Owen & Brinkley (1938) for 5, 15, 25, 35, and 45 °C for a linear regression analysis this review obtained $\log_{10}K_{s0}°(298.15\ K) = -16.091 \pm 0.015$ and $\Delta_r H_m°(298.15\ K) = (110.90 \pm 1.76)$ kJ · mol^{-1}. The uncertainties represent 95% confidence intervals.

Lieser (1957) measured the solubility of AgI(cr) very precisely by radiometric methods. He obtained $\log_{10}K_{s0}° = -16.500 \pm 0.009$ at 18 °C.

Using the $\log_{10}K_{s0}°$ values reported by Owen & Brinkley (1938) and Lieser (1957) for a common linear regression analysis (Fig. 26-7) this review obtained

$$\log_{10}K_{s0}°(298.15\ K) = -16.08 \pm 0.03$$

$$\Delta_r H_m°(298.15\ K) = (110.4 \pm 4.0)\ kJ \cdot mol^{-1}$$

$$\Delta C_{p,m}°(298.15\ K) = 0\ J \cdot K^{-1} \cdot mol^{-1}$$

These values are included in TDB 2020.

Gammons & Yu (1997) accepted $\log_{10}K_{s0}° = -16.09$ at 25 °C from Owen & Brinkley (1938). This value agrees perfectly with the result obtained by this review by re-analysing the data of Owen & Brinkley (1938).

Gammons & Yu (1997) further used $\Delta_r H_m°(298.15\ K)$ "recommended by Owen & Brinkley (1938)", together with the temperature dependent $\Delta_r C_{p,m}°$ function they derived for AgCl(cr) as an estimate in order to extrapolate the AgI(cr) solubility product to temperatures above 50 °C.

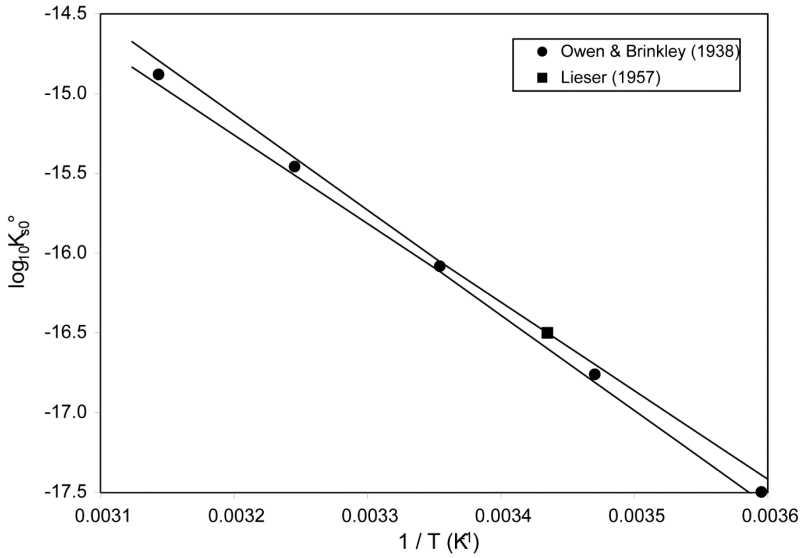

Fig. 26-7: The equilibrium constant $\log_{10}K_{s0}°$ for AgI(cr) ⇌ Ag^+ + I^- as function of temperature in the range 5 – 45 °C

Lines: lower and upper limits calculated using $\log_{10}K_{s0}°(298.15\ K) = -16.08 \pm 0.03$ and $\Delta_r H_m°(298.15\ K) = (110.4 \pm 4.0)\ kJ \cdot mol^{-1}$.

26.3.3.4.2 Silver(I) iodide complexes

Silver(I) forms up to four consecutive iodide complexes in aqueous solution:

$$Ag^+ + I^- \rightleftharpoons AgI(aq)$$

$$Ag^+ + 2\ I^- \rightleftharpoons AgI_2^-$$

$$Ag^+ + 3\ I^- \rightleftharpoons AgI_3^{2-}$$

$$Ag^+ + 4\ I^- \rightleftharpoons AgI_4^{3-}$$

Lieser (1957) measured the solubility of AgI(cr) in 10^{-7} – 2 M NaI solutions at 18 °C and determined the complexation of Ag^+ with I^- by radiometric methods. He obtained the stability constants $\log_{10}\beta_1°(291.15\ K) = 6.58$ (AgI(aq) dominating in 10^{-7} – 10^{-5} M NaI solution), $\log_{10}\beta_2°(291.15\ K) = 11.74$ (AgI_2^- dominating in 10^{-5} – 10^{-3} M NaI), $\log_{10}\beta_3°(291.15\ K) = 13.68$ (AgI_3^{2-} dominating in $5 \cdot 10^{-3}$ – 0.2 M NaI) and $\log_{10}\beta_4°(291.15\ K) \approx 13.1$ (AgI_4^{3-} dominating above 0.52 M NaI).

Gammons & Yu (1997) used the value reported by Lieser (1957) at 18° and the constant $\Delta_r H_m°(298.15\ K)$ value they obtained for AgCl(cr) ⇌ AgCl(aq) to extrapolate the reaction

$$AgI(cr) \rightleftharpoons AgI(aq)$$

to higher temperatures as an estimate. Furthermore, Gammons & Yu (1997) report solubility experiments for AgI at 150°, 200° and 250 °C for the reactions

$$AgI(cr) + I^- \rightleftharpoons AgI_2^-$$

$$AgI(cr) + 2\ I^- \rightleftharpoons AgI_3^{2-}$$

which they combined with the results reported by Lieser (1957) at 18° and finally obtained $\log_{10}\beta_1°(298.15\ K) = 6.41$, $\log_{10}\beta_2°(298.15\ K) = 11.54$, $\log_{10}\beta_3°(298.15\ K) = 13.36$, $\Delta_r H_{m1}°(298.15\ K) = -68.3\ kJ \cdot mol^{-1}$, $\Delta_r H_{m2}°(298.15\ K) = -80.0\ kJ \cdot mol^{-1}$ and $\Delta_r H_{m3}°(298.15\ K) = -101.4\ kJ \cdot mol^{-1}$.

Using these values, we obtain $\log_{10}\beta_1°(291.15\ K) = 6.70$, $\log_{10}\beta_2°(291.15\ K) = 11.88$ and $\log_{10}\beta_3°(291.15\ K) = 13.79$. There is a constant shift of about +0.12 in all these values compared with the values reported by Lieser (1957) at 18 °C. This is obviously the result of a typo error somewhere in the data of Gammons & Yu (1997) because they used $\log_{10}\beta_1°(291.15\ K)$ of Lieser (1957), together with the AgI solubility product of Owen & Brinkley (1938) as "anchor point" for the temperature estimation of the reaction AgI(cr) ⇌ AgI(aq) and hence, we should obtain exactly the value of Lieser (1957) at 18 °C.

Hence, this review decided to use the $\Delta_r H_{mx}°(298.15\ K)$ values derived by Gammons & Yu (1997) to extrapolate the $\log_{10}\beta_x°(291.15\ K)$ values of Lieser (1957) from 18 °C to 25 °C:

$$\log_{10}\beta_1°(298.15\ K) = 6.29 \pm 0.10$$

$$\log_{10}\beta_2°(298.15\ K) = 11.42 \pm 0.10$$

$$\log_{10}\beta_3°(298.15\ K) = 13.24 \pm 0.10$$

$$\Delta_r H_{m1}°(298.15\ K) = -(68.3 \pm 4.0)\ kJ \cdot mol^{-1}$$

$$\Delta_r H_{m2}°(298.15\ K) = -(80.0 \pm 4.0)\ kJ \cdot mol^{-1}$$

$$\Delta_r H_{m3}°(298.15\ K) = -(101.4 \pm 4.0)\ kJ \cdot mol^{-1}$$

$$\Delta C_{p,m1,2,3}°(298.15\ K) = 0\ J \cdot K^{-1} \cdot mol^{-1}$$

with uncertainties assigned by this review. These values are included in TDB 2020.

$$\log_{10}\beta_4°(298.15\ K) \approx 13.1$$

This value is included in TDB 2020 as supplemental datum, together with the estimated SIT interaction coefficients (see Tab. 1-7)

$\varepsilon(AgI(aq), NaCl) = \varepsilon(AgI(aq), NaClO_4) = (0.0 \pm 0.1)$ kg · mol^{-1}

$\varepsilon(AgI_2^-, Na^+) = -(0.05 \pm 0.10)$ kg · mol^{-1}

$\varepsilon(AgI_3^-, Na^+) = -(0.10 \pm 0.10)$ kg · mol^{-1}

$\varepsilon(AgI_4^-, Na^+) = -(0.15 \pm 0.10)$ kg · mol^{-1}

26.3.4 Silver(I) carbonate compounds and complexes

26.3.4.1 Silver(I) carbonate compounds

Silver carbonate, Ag_2CO_3(cr), is characterised in the chemical literature as "poorly soluble in water" with a solubility of about 0.03 g/L at 25 °C. No natural occurrence of silver carbonate as a mineral is reported so far.

It seems that the solubility product of Ag_2CO_3(cr) has been determined only once, as reported in the study of Walker et al. (1927) almost a century ago. Despite of (or because of) its age, the study of Walker et al. (1927) is of high quality and the obtained results are reliable.

Walker et al. (1927) made measurements with a silver – silver carbonate electrode for which they needed good macroscopic crystals of Ag_2CO_3(cr). As they report "to get good crystals of a sparingly soluble substance, it is necessary to precipitate it quite slowly, which can be achieved only if at any moment the concentrations of the pair of precipitating ions are maintained very slightly in excess of the solubility product; also, it is convenient to have a reservoir which will furnish the ions as fast as they are used. In the preparation of silver carbonate these conditions were fulfilled by passing a slow stream of carbon dioxide through a filtered solution of the silver – ammonia complex, made by addition of ammonia to 0.3 *N* silver nitrate solution until the precipitate had just disappeared. This process yields glistening crystals of silver carbonate, which can readily be made in any desired quality, though some of the silver in the solution remains unprecipitated in accordance with the equilibrium conditions. The crystals obtained in this way proved by analysis (both by thermal decomposition and by precipitation as chloride) to be pure silver carbonate. They are a beautiful sulfur yellow color but darken upon even a brief exposure to bright light. They have high indices of refraction, above 1.88, and show parallel extinction and pleochroism; interference patterns indicate that they are biaxial."

Using these crystals in their silver – silver carbonate electrode Walker et al. (1927) determined very precisely the normal potential of carbonate, CO_3^{2-}, as

$E\,°C_{O3\text{-}2} = -(0.4716 \pm 0.0003)$ V

The solubility product of Ag_2CO_3(cr) according to reaction

$Ag_2CO_3(cr) \rightleftharpoons 2\ Ag^+ + CO_3^{2-}$

can now be derived from the normal potential, $E\,°C_{O3\text{-}2}$, of the silver – silver carbonate electrode, combined with $E°_{Ag^+}$, the normal potential of silver. As Walker et al. (1927) state, the silver – silver carbonate electrode is reversible with respect to both silver and carbonate ions, and thus

$$RT / (2F) \cdot \ln(10) \cdot \log_{10}K_{s0}° = E°_{Ag^+} - E\,°C_{O3\text{-}2}$$

Walker et al. (1927) used $RT / (2F) \cdot \ln(10) = 0.02957$ and $E°_{Ag^+} = -0.7995$ V together with their own value $E\,°C_{O3\text{-}2} = -0.4716$ and calculated $K_{s0}° = 8.2 \cdot 10^{-12}$, which is $\log_{10}K_{s0}° = -11.09$.

Using F = 96485.309 C · mol^{-1} and R = 8.31451 J · K^{-1} · mol^{-1} (Grenthe et al. 1992), T = 298.15 K and ln(10) = 2.302585 this review calculated $RT / (2F) \cdot \ln(10) = 0.02958$.

The standard potential of Ag^+ can be calculated from the selected CODATA value $\Delta_f G_m°(Ag^+, 298.15\ K) = (77.096 \pm 0.156)$ kJ · mol^{-1} = $\Delta_r G_m°(Ag(cr) \rightleftharpoons Ag^+ + e^-, 298.15\ K)$ (see Section 26.3.1) as $E°_{Ag^+} = -\Delta_r G_m° / F = -(0.79904 \pm 0.0004)$ V. The uncertainty is taken from Walker et al. (1927) who state "we may recall the fact that there is still a difference of 0.4 millivolt between the two best values of the silver-silver chloride electrode". This leads to the recommended value

$$\log_{10}K_{s0}° = -11.07 \pm 0.04$$

where the uncertainty, derived from the mentioned 0.4 millivolt difference, has been doubled to represent a 95% confidence interval. This value is included in TDB 2020.

26.3.4.2 Silver(I) carbonate complexes

Maya (1983) found that reports in the literature regarding the interaction between carbonate and silver ions in aqueous solutions are limited to the determination of the solubility product of crystalline Ag_2CO_3 (Walker et al. 1927). Hence, potentiometric titrations were conducted by Maya (1983) using a silver-ion-sensitive electrode at 25 ± 0.1 °C using $NaClO_4$ as the background electrolyte to provide a medium of 1.0 M ionic strength.

Titrations were performed by addition of Na_2CO_3 to silver ion solutions. A graphical display of the results in the form of $\log[Ag^+]$ *versus* $\log[CO_3^{2-}]$ (Fig.1 in Maya 1983) revealed a series of almost horizontal lines that extend to an apparent boundary at which $[Ag^+]$ drops more rapidly. This behaviour suggested the formation of a solid phase. The relative flatness of the horizontal portion indicated a weak interaction between silver and carbonate ions.

The solid phase formed at higher pH values is $Ag_2O(s)$. This is concluded by Maya (1983) on the basis of the pH dependence of the solubility which conforms to the equilibrium

$$½\ Ag2O(s) + ½\ H_2O \rightleftharpoons Ag^+ + OH^-$$

At the higher silver concentrations, the solid can be seen as a fine suspension of a brownish black precipitate which is the same colour as $Ag_2O(s)$. The formation of $Ag_2CO_3(cr)$ in carbonate media could have been a possibility but this solid was not observed ($Ag_2CO_3(cr)$ forms bright yellow

crystals). Thermodynamic considerations also favour formation of $Ag_2O(s)$ over $Ag_2CO_3(cr)$ under the conditions examined. The solubility product $[Ag^+] \cdot [OH^-]$ calculated from the titration data is

$$\log_{10}K_s = -7.0$$

The formation of an $AgCO_3^-$ species according to the reaction

$$Ag^+ + CO_3^{2-} \rightleftharpoons AgCO_3^-$$

can be deduced from the titration data. The complex is relatively weak and accounts at most for 10% of the total silver under the most favourable conditions, those just prior to the formation of $Ag_2O(s)$ in the low silver concentration area. Maya (1983) could only use three experimental data from which stability constants $K_1 = 36$, 33 and 32 could be calculated. The average of these three values is $\log_{10}K_1 = 1.50$. This is considered by Maya (1983) as an upper limit in view of the limitations of the system. Given the relative weakness of the complex, the difference in the electrode potentials at low carbonate concentrations are within the uncertainty of the electrode response while larger carbonate concentrations bring about the formation of $Ag_2O(s)$.

Hence, in 1 M $NaClO_4$ Maya (1983) obtained:

$$\log_{10}K_1 \text{ (298.15 K)} < 1.5$$

Using

$$\Delta\varepsilon = \varepsilon(AgCO_3^-, Na^+) - \varepsilon(CO_3^{2-}, Na^+) - \varepsilon(Ag^+, ClO_4^-)$$

$$= -(0.05 \pm 0.1) + (0.08 \pm 0.05) - (0.00 \pm 0.01)$$

$$= (0.03 \pm 0.11) \text{ kg} \cdot \text{mol}^{-1}$$

$\log_{10}K_1$ was extrapolated to zero ionic strength by this review:

$$\log_{10}K_1^\circ \text{ (298.15 K)} < 2.4$$

This value is included in TDB 2020 as supplemental datum, together with the estimated SIT interaction coefficient (see Tab. 1-7)

$$\varepsilon(AgCO_3^-, Na^+) = -(0.05 \pm 0.10) \text{ kg} \cdot \text{mol}^{-1}$$

26.3.5 Silver(I) phosphate compounds and complexes

26.3.5.1 Silver(I) phosphate compounds

Silver phosphate, $Ag_3PO_4(s)$, is characterised in the chemical literature as a "water-insoluble chemical compound" with a solubility of about 0.006 g/L at 25 °C. No natural occurrence of silver phosphate as a mineral is reported so far.

The solubility of $Ag_3PO_4(s)$ has been studied by Baldwin (1970) at 25 °C in 3 M $Na(ClO_4)$ using glass and silver – silver phosphate electrodes (to measure $[H^+]$ and $[Ag^+]$) in the range $2 \leq pH \leq 7.5$. The X-ray photographs did not indicate the presence of a solid phase other than $Ag_3PO_4(s)$, nor of any variation in composition. The silver electrode came to equilibrium rapidly and maintained a constant potential for at least 12 hours. For the reaction

$$Ag_3PO_4(s) + H^+ \rightleftharpoons 3\ Ag^+ + HPO_4^{2-}$$

Baldwin (1970) obtained in 3 M $Na(ClO_4)$:

$$\log_{10}K_{s0} = -6.73 \pm 0.04$$

Using

$$\Delta\varepsilon = 3 \cdot \varepsilon(Ag^+, ClO_4^-) + \varepsilon(HPO_4^{2-}, Na^+) - \varepsilon(H^+, ClO_4^-)$$

$$= 3 \cdot (0.00 \pm 0.01) - (0.15 \pm 0.06) - (0.14 \pm 0.02)$$

$$= -(0.29 \pm 0.07)\ kg \cdot mol^{-1}$$

$\log_{10}K_{s0}$ was extrapolated to zero ionic strength by this review:

$$\log_{10}K_{s0}^\circ = -9.05 \pm 0.08$$

This value is included in TDB 2020.

26.3.5.2 Silver(I) phosphate complexes

In his study of $Ag_3PO_4(s)$ solubility Baldwin (1970) (see Section 26.3.5.1) found a systematic increase of the apparent solubility product K_s with increasing pH (Fig. 1 in Baldwin 1970). He concluded that carbonate contamination and the resultant formation of silver – carbonate complexes or precipitates would lead to the opposite effect, i.e., to a decrease of K_s with increasing pH. He considered a second possibility: silver – phosphate complexation according to the reaction

$$Ag^+ + HPO_4^{2-} \rightleftharpoons AgHPO_4^-$$

By fitting linear equations to his data Baldwin (1970) obtained at 3 M $NaClO_4$ the solubility product $K_{s0} = (1.88 \pm 0.03) \cdot 10^{-7}$ (resulting in $\log_{10}K_{s0} = -6.73 \pm 0.04$, with increased uncertainty, see Section 26.3.5.1) and the complexation constant $K_1 = (1.46 \pm 0.27) \cdot 10^3$. As Baldwin (1970) states: "The existence of this complex with the indicated stability constant would account for, under the most favorable conditions of the titrations, a maximum of 5 % of the total phosphate present in the mixture. However, some preliminary experiments using a variant of the solubility measurements have indicated that rather less silver is complexed than expected assuming $AgHPO_4^-$ with $K = 1.5 \times 10^3$. Using these preliminary measurements, K was estimated as 1.3×10^2." Hence, Baldwin (1970) considered his K_1 value 1.5×10^3 representing only an upper limit:

$$\log_{10}K_1 \text{ (298.15 K)} < 3.18$$

Using

$$\Delta\varepsilon = \varepsilon(AgHPO_4^-, Na^+) - \varepsilon(HPO_4^{2-}, Na^+) - \varepsilon(Ag^+, ClO_4^-)$$

$$= -(0.05 \pm 0.1) + (0.15 \pm 0.06) - (0.00 \pm 0.01)$$

$$= (0.10 \pm 0.12) \text{ kg} \cdot \text{mol}^{-1}$$

$\log_{10}K_1$ was extrapolated to zero ionic strength by this review:

$$log_{10}K_1^\circ (298.15\ K) < 4.5$$

This value is included in TDB 2020 as supplemental datum, together with the estimated SIT interaction coefficient (see Tab. 1-7)

$$\varepsilon(AgHPO_4^-, Na^+) = -(0.05 \pm 0.10)\ kg \cdot mol^{-1}$$

26.3.6 Silver(I) sulphate compounds and complexes

26.3.6.1 Silver(I) sulphate complexes

Experimental data concerning the formation of $AgSO_4^-$ according to the reaction

$$Ag^+ + SO_4^{2-} \rightleftharpoons AgSO_4^-$$

are sparse and consists only of the conductance measurements of Righellato & Davies (1930) and the potentiometric studies of Leden (1952) at high ionic strength.

Righellato & Davies (1930) report $\log_{10}K_1$ (298.15 K) = 0.983 at 0.0025 m Ag_2SO_4 ($I_m = 0.0073$) and $\log_{10}K_1$ (298.15 K) = 1.022 at 0.005 m Ag_2SO_4 ($I_m = 0.01409$).

Extrapolating these values to zero ionic strength using solely the Debye-Hückel term of the SIT equation (i.e., assuming $\Delta\varepsilon = 0$) results in $\log_{10}K_1°$ (298.15 K) = 1.137 and 1.227, respectively.

Leden (1952) could fit his potentiometric titration data obtained in a medium $NaClO_4$ + Na_2SO_4 of 3 M total ionic strength, where the total sulphate concentration increased up to 0.6 M, with two constants $\beta_1 = (1.7 \pm 0.05)$ and $\beta_2 = (1.9 \pm 0.1)$. A second series of potentiometric titration data in a medium of 3 M constant Na^+ concentration, where the total ionic strength increased from 3.0 – 3.6, could be fitted with the two constants $\beta_1 = (1.7 \pm 0.05)$ and $\beta_2 = (1.0 \pm 0.1)$.

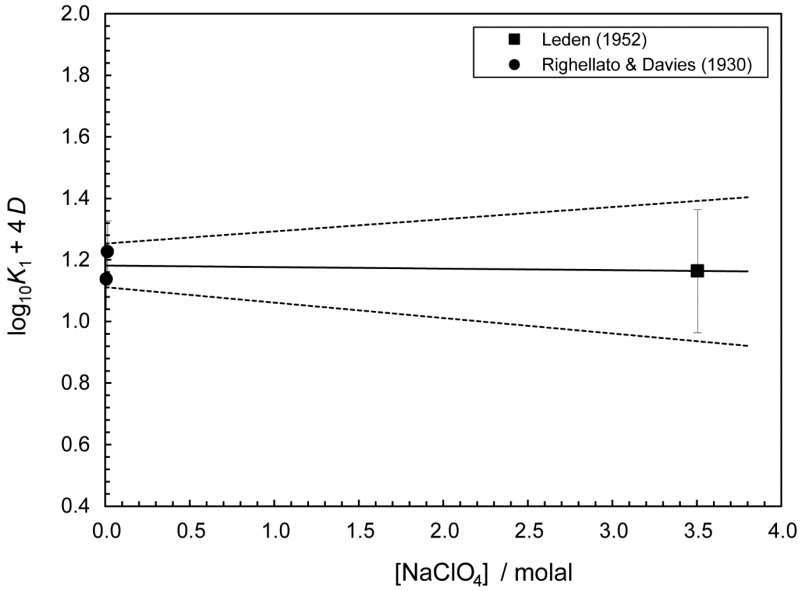

Fig. 26-8: Dependence of the equilibrium $Ag^+ + SO_4^{2-} \rightleftharpoons AgSO_4^-$ on ionic strength in $NaClO_4$

The solid line is obtained using the derived SIT interaction coefficient and stability constant at zero ionic strength. The dotted lines represent the 95% uncertainty range extrapolated from zero ionic strength to higher perchlorate concentrations.

This review considers the two different β_2 values as medium effects, accounting for the varying ClO_4^-/SO_4^{2-} ratios. Only the consistent β_1 values are retained, representing the above equilibrium in 3 M $NaClO_4$, and $\log_{10}K_1$ (298.15 K) = 0.23 with an estimated uncertainty of ± 0.2 was used in an SIT plot together with the data of Righellato & Davies (1930) with estimated uncertainties of ± 0.1 (Fig. 26-8). The results are

$$\log_{10}K_1° \text{ (298.15 K)} = 1.18 \pm 0.07$$

$$\Delta\varepsilon = 0.01 \pm 0.06$$

Using $\varepsilon(Ag^+, ClO_4^-) = 0.00 \pm 0.01$ and $\varepsilon(Na^+, SO_4^{2-}) = -(0.12 \pm 0.06)$ a new value

$$\varepsilon(Na^+, AgSO_4^-) = -(0.11 \pm 0.09)$$

is calculated. This value is within its uncertainty limits in the range expected for $\varepsilon(Na^+, X^-)$.

Note that the constant $\varepsilon(Na^+, SO_4^{2-}) = -(0.12 \pm 0.06)$ is an approximation, and could be calculated more precisely as $\varepsilon(Na^+, SO_4^{2-}) = \varepsilon_1 + \varepsilon_2 \cdot \log_{10}(I_m) = -0.184 + 0.139 \cdot \log_{10}(I_m)$ (Lemire et al. 2013). For I_m= 3.503 we get $\varepsilon(Na^+, SO_4^{2-}) = -0.108$, which is in good agreement with the constant approximation for the single experimental point at high ionic strength.

Hence, the above approximation $\varepsilon(Na^+, AgSO_4^-) = -(0.11 \pm 0.09)$ together with $\log_{10}K_1° (298.15\ K) = 1.18 \pm 0.07$ and $\Delta_r H_m°(298.15\ K) = (6.3 \pm 1.3)\ kJ \cdot mol^{-1}$ (see Section 26.3.6.2) are included in TDB 2020.

26.3.6.2 Silver(I) sulphate compounds

Silver sulphate, $Ag_2SO_4(s)$, is characterised in the chemical literature as "poorly soluble in water" with a solubility of 8.3 g/L at 25 °C. No natural occurrence of silver sulphate as a mineral is reported so far.

The solubility of $Ag_2SO_4(s)$ in pure water at 25 °C has been determined many times: Drucker (1901) reports 0.0257 moles per litre, Harkins (1911) measured 0.02676 moles per litre and cites an unpublished "Chemistry Thesis" by Swan (1899) who obtained 0.02699 moles per litre, Davis et al. (1939) determined 0.02684 moles per litre, and Vosburgh & McClure (1943) found 0.02683 moles per kg H_2O. It might be more than a pure coincidence that the re-calculated average of these values, 8.30 g/L, agrees perfectly with the solubility value established in the chemical literature.

In addition, the solubility of $Ag_2SO_4(s)$ at 25 °C has been measured in many supporting electrolytes: in KNO_3, $Mg(NO_3)_2$, $AgNO_3$, K_2SO_4, $MgSO_4$ (Harkins 1911), in HNO_3, H_2SO_4, $KHSO_4$, K_2SO_4 (Swan 1899, cited by Harkins 1911), in K_2SO_4 (Vosburgh & McClure 1943), in KNO_3, HNO_3, K_2SO_4, H_2SO_4, $MgSO_4$ up to 200 °C (Stoughton & Lietzke 1960) and in $La_2(SO_4)_3$ up to 100 °C (Lietzke & Hall 1967).

Using the solubility data of Harkins (1911), measured in K_2SO_4, and their own data obtained in the same medium, Vosburgh & McClure (1943) obtained a straight line for the equation

$$2 \log [Ag^+] + \log [SO_4^{2-}] - 3 \sqrt{I_m} / (1 + \sqrt{I_m}) = -4.8035 + 0.360\ I_m$$

in the range $0.8 < I_m < 0.4$ (Fig. 1 in Vosburgh & McClure (1943)). Thus, for the equilibrium

$$Ag_2SO_4(s) \rightleftharpoons 2\ Ag^+ + SO_4^{2-}$$

they obtained $\log_{10}K_{s0}° = -4.8035$ (no uncertainty given).

Stoughton & Lietzke (1960) used a similar extended Debye-Hückel expression to extrapolate their data measured in different salt solutions to zero ionic strength. Values of $\log_{10}K_{s0}°$ at 25 °C were averaged for H_2SO_4, HNO_3 and $MgSO_4$ media, resulting in $\log_{10}K_{s0}° = -4.835 \pm 0.006$. The average $\log_{10}K_{s0}°$ values were fitted between 25 and 200 °C to a quadratic equation by Stoughton & Lietzke (1960), resulting in $\Delta_r H_m°(298.15\ K) = 4.47\ kcal \cdot mol^{-1}$, with $\Delta_r H_m°$ as a function of temperature.

Finally, Lietzke & Hall (1967) obtained $\log_{10}K_{s0}° = -4.81$ (no uncertainty given) from their data measured in $La_2(SO_4)_3$.

All the above results are quite consistent but, as discussed by Hopkins & Wulff (1965), they all ignored the complex $AgSO_4^-$, whose dissociation is also called the "second ionization step". The discussion in Hopkins & Wulff (1965) is as follows:

"In their tabulation of the activity product of silver sulfate, Stoughton & Lietzke (1960) did not include their results utilizing KNO_3 as supporting medium. This latter value they report to be low by 0.103 pK unit – 140 cal / mole. This is perhaps the only electrolyte in which the solubility of silver sulfate is uncomplicated by the medium. The value of $\Delta_r G_m°$, in KNO_3, is then 6'595 + 140 = 6'737 cal / mole.

An independent evaluation of $\Delta_r G_m°$ is reported by Pan & Lin (1959) from their thorough study of the electromotive force of the $Ag(s)/Ag_2SO_4(s)$ electrode. Their value for the standard free energy of solution is 6707 cal / mole and is independent of any assumption about the strength of the second ionization step.

Righellato & Davies (1930) report the extent of the second ionization step at only two concentrations of silver sulphate. If the concentration dependence of this quantity (but not its numerical value) is assumed to be the same as that for Tl_2SO_4 and K_2SO_4, the degree of the second ionization in the saturated solution is 0.77. This datum leads to a silver concentration of 0.047 m and a sulphate ion concentration of 0.021 m. The saturated solution is still sufficiently dilute to permit estimation of the activity coefficients by $-\log \gamma = 0.505 z^2 \cdot \sqrt{I_m} / (1 + \sqrt{I_m})$, as $\gamma_{Ag^+} = 0.785$ and $\gamma_{SO4-2} = 0.382$. The standard free energy of solution corresponding to these data is $\Delta_r G_m° = -RT \ln (0.047)^2(0.782)^2(0.021) \cdot (0.0382) = 6770$ cal / mole.

The average of the last three values cited for $\Delta_r G_m°$, 6740 ± 24 cal / mole, may tentatively be taken as representing the standard free energy of solution for silver sulphate on the assumption of a "weak" second ionization step."

Recalculation of the latter value, and increasing its uncertainty by a factor of two to represent a 95% confidence interval, results in

$$\log_{10} K_{s0}° = -4.94 \pm 0.04$$

Finally, Hopkins & Wulff (1965) calorimetrically determined the enthalpy of solution at different concentrations of silver sulphate and obtained $\Delta_r H_m° = 4140 \pm 50$ cal/mole for the solubility product and $\Delta_r H_m° = -1.5 \pm 0.3$ kcal/mole for the "second ionization step".

Converting these values in kJ / mol, and increasing their uncertainties by a factor of two to represent a 95% confidence interval, results in

$$\Delta_r H_m°(298.15\ K) = (17.3 \pm 0.4)\ kJ \cdot mol^{-1}$$

for the solubility reaction $Ag_2SO_4(s) \rightleftharpoons 2\ Ag^+ + SO_4^{2-}$, and

$$\Delta_r H_m°(298.15\ K) = (6.3 \pm 1.3)\ kJ \cdot mol^{-1}$$

for the complexation equilibrium $Ag^+ + SO_4^{2-} \rightleftharpoons AgSO_4^-$.

All these values are included in TDB 2020.

26.3.7 Silver(I) sulphide compounds and complexes

26.3.7.1 Silver(I) sulphide compounds

Rickard & Luther (2006) and Rickard (2012) presented extensive reviews on the chemistry of aqueous metal-sulphide complexes and clusters. Concerning silver, they reported that the black precipitate that occurs through the reaction between S(-II) and Ag salts in aqueous solution at room temperature is monoclinic Ag_2S, acanthite. Above 177 °C this transforms rapidly and reversibly to the isomorphic polymorph, argentite. It is claimed that that Ag_2S is the least soluble of all known silver compounds. However, it was known as long ago as 1949 that the solubility is pH independent in acid solutions but increases markedly with pH in alkaline systems.

Schwarzenbach & Widmer (1966) (based on the Ph.D. thesis of Widmer 1962)) measured the solubility of Ag_2S in aqueous sulphide solutions at constant ionic strength of 1.0 M $NaClO_4$ at 20 °C. In order to determine the solubility product

$$0.5\ Ag_2S(s) + H^+ \rightleftharpoons Ag^+ + 0.5\ H_2S(aq)$$

Widmer (1962) determined the concentration of the free Ag ion, $\log_{10}[Ag^+]$, from the potentials of the silver electrode,

$$E_{Ag} = E_0 + 0.05816 \cdot \log_{10}[Ag^+],\ E_0 = 0.5735\ V$$

measured at different pH values. A re-evaluation by this review of the experimental data given by Widmer (1962) in the pH ranges 0.00 – 5.6 and 8.2 – 13.9, and $[S]_{tot}$ = 0.02 M resulted in

$$\log_{10}{}^*K_s\ (1.0\ M\ NaClO_4,\ 293.15\ K) = -14.50 \pm 0.05$$

in perfect agreement with the value -14.51, obtained by Widmer (1962) from the average of the best fit of two lines in the pH ranges 0 – 5 and 9 – 12.

Note that actually, Widmer (1962) reported $\log_{10}K_s$ = -49.7 referring to the reaction $Ag_2S(s) \rightleftharpoons 2\ Ag^+ + S^{2-}$, which, considering the pK_1 and pK_2 values he used to obtain his value, translates back to the above constant.

Mehra (1968) used similar experimental methods as Widmer (1962) and obtained $\log_{10}K_s$ = -49.03 ± 0.20 (1σ) in 1.0 M $NaClO_4$ at 25 °C. Considering the pK_1 and pK_2 values Mehra (1968) used to obtain his value, this translates back to

$$\log_{10}{}^*K_s\ (1.0\ M\ NaClO_4,\ 298.15\ K) = -14.33 \pm 0.20$$

Extrapolation of the stability constant of this isocoulombic reaction to zero ionic strength involves the recalculation of the stability constant from molar to molal scale

$\log_{10}{}^{*}K_s$ (1.05 m $NaClO_4$, 293.15 K) = -14.49 ± 0.05

$\log_{10}{}^{*}K_s$ (1.05 m $NaClO_4$, 298.15 K) = -14.32 ± 0.20

and using

$\Delta\varepsilon = \varepsilon(Ag^+, ClO_4^-) + 0.5 \cdot \varepsilon(H_2S(aq), NaClO_4) - \varepsilon(H^+, ClO_4^-)$

$= (0.00 \pm 0.01) + 0.5 \cdot (0.055 \pm 0.004) + (0.14 \pm 0.02)$

$= -(0.113 \pm 0.02)$ kg · mol^{-1}

to obtain the results

$\log_{10}{}^{*}K_s°$(293.15 K) = -14.61 ± 0.05

$\log_{10}{}^{*}K_s°$(298.15 K) = -14.44 ± 0.20

Stefánsson & Seward (2003) estimated the solubility product from tabulated thermodynamic properties of the aqueous species and the mineral and report the temperature function

$\log_{10}{}^{*}K_s°(T) = 3.62418 - 5408.9 / T$

which they applied in the temperature range 25 – 350 °C.

Using the above temperature function this review calculated

$\log_{10}{}^{*}K_s°$(298.15 K) = -14.52

$\Delta_r H_m°$(298.15 K) = 103.5 kJ · mol^{-1}

No uncertainty estimate is given by Stefánsson & Seward (2003). Using $\Delta_r H_m°$ to extrapolate the solubility product of Widmer (1962) from 20 to 25 °C gives:

$\log_{10}{}^{*}K_s°$(298.15 K) = -14.30 ± 0.05

An unweighted mean of the values from Widmer (1962), Mehra (1968) and Stefánsson & Seward (2003) at 25 °C and zero ionic strength gives

$\log_{10}{}^{*}K_s°$(298.15 K) = -14.42 ± 0.20

with the uncertainty assigned by this review. This value is included in TDB 2020.

In addition, $\Delta_r H_m°$ reported by Stefánsson & Seward (2003) is included in TDB 2020 with an uncertainty assigned by this review:

$\Delta_r H_m°(298.15\ K) = (103.5 \pm 2.0)\ kJ \cdot mol^{-1}$

$\Delta C_{p,m}°(298.15\ K) = 0\ J \cdot K^{-1} \cdot mol^{-1}$

26.3.7.2 Silver(I) sulphide complexes

Rickard & Luther (2006) and Rickard (2012) reported a variety of complexes proposed in the literature: AgHS(aq), $Ag(HS)_2^-$, AgS^-, $Ag_2S(HS)_2^{2-}$, $Ag_2S(aq)$, and some complexes involving polysulphides. Most of them were used to interpret Ag_2S solubility experiments (AgHS(aq), $Ag(HS)_2^-$, $Ag_2S(HS)_2^{2-}$, complexes involving polysulphides), some have been used to explain sulphide titration experiments (AgHS(aq), $Ag(HS)_2^-$, AgS^-, $Ag_2S(aq)$). None of these complexes has been confirmed by spectroscopic studies so far.

Three solubility studies

Schwarzenbach & Widmer (1966) (based on the Ph.D. thesis of Widmer (1962)) measured the solubility of Ag_2S in aqueous sulphide solutions at constant ionic strength of 1.0 M $NaClO_4$ at 20 °C using ^{110}Ag to determine radiometrically the total concentration of dissolved silver. They interpreted their results with respect to AgHS(aq), $Ag(HS)_2^-$ and $Ag_2S(HS)_2^{2-}$ complexes dominating successively with increasing pH and obtained:

$0.5\ Ag_2S(s) + 0.5\ H_2S(aq) \rightleftharpoons AgHS(aq)$

$\log_{10}K_{s11}$ (1.0 M $NaClO_4$, 293.15 K) = -7.89

$0.5\ Ag_2S(s) + 0.5\ H_2S(aq) + HS^- \rightleftharpoons Ag(HS)_2^-$

$\log_{10}K_{s12}$ (1.0 M $NaClO_4$, 293.15 K) = -4.02

$Ag_2S(s) + 2\ HS^- \rightleftharpoons Ag_2S(HS)_2^{2-}$

$\log_{10}K_{s23}$ (1.0 M $NaClO_4$, 293.15 K) = -4.82

Stefánsson & Seward (2003) studied the solubility of crystalline Ag_2S between 25 – 400 °C and treated the data with a non-linear least squares fitting routine which considered all the hitherto proposed complexes. They found that the data were consistent with AgHS(aq), $Ag(HS)_2^-$ and $Ag_2S(HS)_2^{2-}$ being the dominant species and obtained

$\log_{10}K_{s11}°(298.15) = -5.62 \pm 0.04$

$\log_{10}K_{s12}°(298.15) = -3.97 \pm 0.04$

$\log_{10}K_{s23}°(298.15) = -4.78 \pm 0.04$

The uncertainties are 1σ. In their discussion Stefánsson & Seward (2003) remark that "Schwarzenbach & Widmer (1966) obtained much lower solubilities in acidic solutions compared to the present results. The reason for this is unclear". This discrepancy remained unresolved and was puzzling for Stefánsson & Seward (2003), considering that "with respect to the $Ag(HS)_2^-$ complex, the equilibrium solubility constants obtained at 20 °C of $\log_{10}K_{s12}° = -4.05$ in the present study is practically the same as the one obtained by Schwarzenbach & Widmer (1966) of -4.02 at zero ionic strength. The same is true for the solubility constant with respect to $Ag_2S(HS)_2^{2-}$ of $\log_{10}K_{s23}° = -4.79$ obtained in the present study at 20 °C compared to -4.82 by Schwarzenbach & Widmer (1966) at zero ionic strength".

Note that contrary to the statements of Stefánsson & Seward (2003), the $\log_{10}K_s$ values reported by Schwarzenbach & Widmer (1966) refer to 1.0 M $NaClO_4$, and not to zero ionic strength. However, $\log_{10}K_{s11}$ and $\log_{10}K_{s12}$ refer to isocoulombic reactions whose dependence on ionic strength is negligible, and the fact remains, that the $\log_{10}K_{s11}$ values reported by Schwarzenbach & Widmer (1966) and Stefánsson & Seward (2003) differ by more than two orders of magnitude, while their $\log_{10}K_{s12}$ values are practically the same.

Several years after Widmer's pioneering work (Widmer 1962), Mehra (1968) used similar experimental methods in his extensive solubility studies of metal selenites, sulphides and selenides in 1M $NaClO_4$ at 25 °C. Most results of his Ph.D. thesis have never been published in journals, and hence the study of Ag_2S solubility went unnoticed until the present author re-discovered it in the Ph.D. thesis, almost half a century after its publication.

Mehra (1968) studied the solubility of $Ag_2S(s)$ at different sulphide concentrations (S_{tot}) in the pH range 0.3 – 13.2. He found that "the solubility data indicate that the Ag_2S solubility initially remains constant (pH 1 – 4), then it increases in the close vicinity of pK_1 of H_2S, and finally in alkaline medium (pH 10 – 13) it attains the same value as in the acidic region. The system has therefore two distinct features: a when the solubility is independent of the experimental variables pH and S_{tot}, and b when the solubility exhibits characteristic slopes both as a function of pH and S_{tot} in the neutral medium. In the first case, comparison of experimental data with the theoretical possibility at once confirms the formation of the thio-complex $Ag_2(HS)(OH)$, since this is the only species that remains unaffected with change in pH or S_{tot}. In the second case the solubility slopes measured from the curve of the highest S_{tot} give a value of +1 and -0.5 before and after pK_1 of H_2S. The slope as a function of S_{tot} at constant pH remains consistently at -1.5. The only complex that corresponds to these characteristic slopes is the species $Ag(HS)_2^-$, which is thus identified".

$Ag(HS)_2^-$

This review agrees with the interpretation of the "second case" of Mehra (1968) that in the pH range 5 – 9 the species $Ag(HS)_2^-$ predominates. Here, not only the data of Schwarzenbach & Widmer (1966) agree with the data of Stefánsson & Seward (2003), as mentioned above, also the data of Mehra (1968), measured at different $[S]_{total}$ concentrations, perfectly fit with the first two datasets (Fig. 26-9). Or, in terms of the equilibrium

$$Ag^+ + 2\ HS^- \rightleftharpoons Ag(HS)_2^-$$

Schwarzenbach & Widmer (1966) obtained

$$\log_{10}\beta_2(1\ M\ NaClO_4, 293.15\ K) = 17.17$$

while Mehra (1968) reported

$\log_{10}\beta_2$(1 M $NaClO_4$, 298.15 K) = 16.97

Using the $\log_{10}K_{s,12}°(T)$ values reported by Stefánsson & Seward (2003) for the temperature range 25 – 250 °C, exhibiting a linear dependence on 1 / T, this review calculated

$\log_{10}K_{s,12}°(298.15) = -4.01 \pm 0.10$

$\Delta_r H_m°(298.15\ K) = (20.1 \pm 2.1)\ kJ \cdot mol^{-1}$

The ionic strength effect for this isocoulombic reaction seems to be very close to zero, considering the data of Schwarzenbach & Widmer (1966) and Mehra (1968). Hence, assuming

$\Delta\varepsilon = \varepsilon(Ag(HS)_2^-, Na^+) - 0.5 \cdot \varepsilon(H_2S(aq), NaClO_4) - \varepsilon(HS^-, Na^+) \approx 0$

and using $\varepsilon(H_2S(aq), NaClO_4) = 0.055 \pm 0.004$ and $\varepsilon(HS^-, Na^+) = 0.08 \pm 0.01$, this review estimates

$\varepsilon(Ag(HS)_2^-, Na^+) \approx 0.1$

This value is included in TDAB 2020 as supplemental datum.

Combined with the selected solubility product of Ag_2S(s) (see Section 26.3.7.1) this review obtained

$Ag^+ + H_2S(aq) + HS^- \rightleftharpoons Ag(HS)_2^- + H^+$

$\log_{10}K°(298.15) = 10.41 \pm 0.22$

$\Delta_r H_m°(298.15\ K) = -(83.4 \pm 2.9)\ kJ \cdot mol^{-1}$

Combined with the selected first dissociation constant of H_2S(aq) (Hummel et al. 2002)

$H_2S(aq) \rightleftharpoons HS^- + H^+$

$\log_{10}K°(298.15) = -6.99 \pm 0.17$

$\Delta_r H_m°(298.15\ K) = -(22.3 \pm 2.1)\ kJ \cdot mol^{-1}$

this review selected

$Ag^+ + 2\ HS^- \rightleftharpoons Ag(HS)_2^-$

$\log_{10}\beta_2°(298.15\ K) = 17.40 \pm 0.28$

$\Delta_r H_m°(298.15\ K) = -(61.1 \pm 3.6)\ kJ \cdot mol^{-1}$

$\Delta C_{p,m}°(298.15\ K) = 0\ J \cdot K^{-1} \cdot mol^{-1}$

valid in the temperature range 25 – 350 °C. These values are included in TDB 2020.

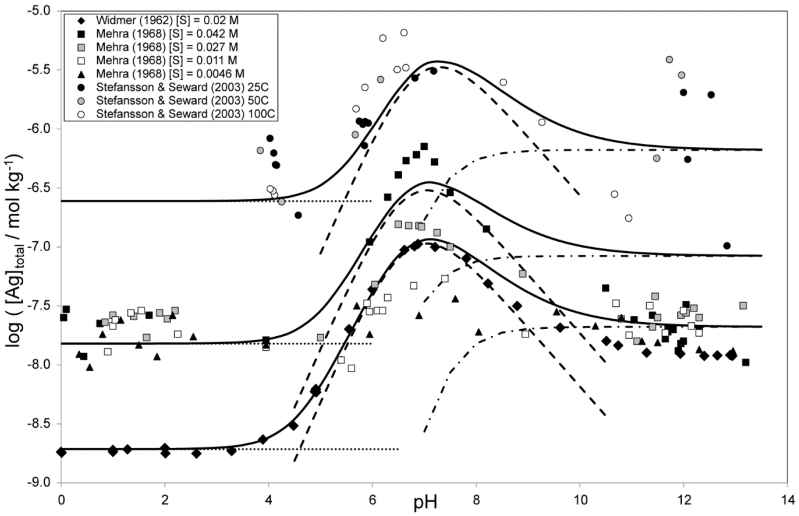

Fig. 26-9: Solubility of $Ag_2S(s)$ in water as a function of pH at different total dissolved sulphide concentrations, $[S]_{total}$

Different symbols: experimental data of Widmer (1962), Mehra (1968) and Stefánsson & Seward (2003). Solid lines: solubility model according to this review, with $[S]_{total}$ = 0.02, 0.04 and 0.2 M for Widmer (1962), Mehra (1968) and Stefánsson & Seward (2003), respectively. Dotted lines: Ag(aq) with P_{H2} values calculated by this review. Dashed lines: $Ag(HS)_2^-$. Dot-dashed lines: $Ag_2S(HS)_2^{2-}$.

Note that the selected parameters $\log_{10}\beta_2°(298.15\ K)$, $\Delta_r H_m°(298.15\ K)$ and $\varepsilon(Ag(HS)_2^-, Na^+)$, based on the data of Stefánsson & Seward (2003), lead to $\log_{10}\beta_2$(1 M $NaClO_4$, 298.15 K) = 17.07 and $\log_{10}\beta_2$(1 M $NaClO_4$, 293.15 K) = 17.27, in excellent agreement with the values derived by Mehra (1968) and Schwarzenbach & Widmer (1966), respectively. In summary, the stoichiometry and the thermodynamic parameters of $Ag(HS)_2^-$ are well established by the three solubility studies.

Ag(aq) ?

The most interesting feature of Fig. 26-9, however, is the observation that the solubility data of Mehra (1968) in the pH range 0 – 5 are not only independent of $[S]_{total}$ concentrations but are located in between the data of Widmer (1962) and Stefánsson & Seward (2003). Also, the solubility data of Mehra (1968) in the pH range 10 – 13 are located in between the data of Widmer (1962) and Stefánsson & Seward (2003). But more importantly, they are independent of $[S]_{total}$ concentrations, in contradiction to Widmer (1962) and Stefánsson & Seward (2003) who interpreted their data in terms of the reaction $Ag_2S(s) + 2\ HS^- \rightleftharpoons Ag_2S(HS)_2^{2-}$.

However, the interpretation of the solubility data in both regions, pH 0 – 5 and 10 – 13, in terms of the reaction $Ag_2S(s) + H_2O \rightleftharpoons Ag_2(HS)(OH)(aq)$ by Mehra (1968) is also questionable. The formation of a mixed silver(I) sulphide – hydroxide complex in the acidic region down to pH 0 is rather improbable, considering that silver(I) hydrolysis is weak and starts at pH > 11 (see Section 26.3.2.2).

Also, the alternative reaction $Ag_2S(s) \rightleftharpoons Ag_2S(aq)$ is questionable. Why should a dimer $Ag_2S(aq)$ predominate at pH 0 – 5 and 10 – 13, while in between the complex $Ag(HS)_2^-$ increases the solubility of $Ag_2S(s)$.

Moreover, both alternative stoichiometries do not explain the variations in measured solubilities of two orders of magnitude in pH range 0 – 5 which puzzled Stefánsson & Seward (2003).

A possible solution to this riddle involves the consideration of Ag(aq) in the speciation model. A solubility equilibrium between $Ag_2S(s)$ and Ag(aq) can be formulated as

$$0.5\ Ag_2S(s) + 0.5\ H_2g \rightleftharpoons Ag(aq) + 0.5\ H_2S(aq)$$

If this equilibrium predominates, the measured Ag solubility is pH independent at constant partial pressure of hydrogen. To test whether the hypothesis works that Ag(aq) could have been the predominating species in the studies of Widmer (1962), Mehra (1968) and Stefánsson & Seward (2003) at pH < 5, the partial pressure of hydrogen, P_{H2}, has been calculated for each experimental datum (Fig. 26-10).

The basic equilibria for these calculations are

$$H_2g \rightleftharpoons 2\ e^- + 2\ H^+$$

with $\log_{10}K(H_2g) = 0$ (per definition),

$$Ag^+ + e^- \rightleftharpoons Ag(aq)$$

derived from the selected values $\log_{10}K°(298.15\ K) = -6.4 \pm 0.5$ for $Ag(cr) \rightleftharpoons Ag(aq)$ (see Section 26.2.2) and $\log_{10}K°(298.15\ K) = -13.507 \pm 0.02$ for $Ag(cr) \rightleftharpoons Ag^+ + e^-$ (see Section 26.3.1) as

$$\log_{10}K°(298.15\ K) = 7.11 \pm 0.5$$

and extrapolated to 1 M $NaClO_4$ using $\varepsilon(Ag^+, ClO_4^-) = 0.00 \pm 0.01\ kg \cdot mol^{-1}$ and $\varepsilon(Ag(aq), NaClO_4) = 0.0 \pm 0.1\ kg \cdot mol^{-1}$ (Tab. 26-2), leading to

$$\log_{10}K(1M\ NaClO_4, 298.15\ K) = 6.70 \pm 0.5$$

and the solubility product

$$0.5\ Ag_2S(s) + H^+ \rightleftharpoons Ag^+ + 0.5\ H_2S(aq)$$

as selected in this review for zero ionic strength (see Section 26.3.7.1)

$\log_{10}{}^{*}K_s°(298.15\ K) = -14.42 \pm 0.20$

and extrapolated to 1 M $NaClO_4$

$\log_{10}{}^{*}K_s\ (1.0\ M\ NaClO_4, 298.15\ K) = -14.50 \pm 0.05$

Combining $\log_{10}K(H_2g)$, and $\log_{10}K°$ and $\log_{10}{}^{*}K_s°$, or $\log_{10}K$ and $\log_{10}{}^{*}K_s$, results in

$\log_{10}K_s°\ (298.15\ K) = -7.31 \pm 0.5$ and

$\log_{10}K_s\ (1.0\ M\ NaClO_4, 298.15\ K) = -7.62 \pm 0.5$ for

$0.5\ Ag_2S(s) + 0.5\ H_2g \rightleftharpoons Ag(aq) + 0.5\ H_2S(aq)$

At pH < 6 the total dissolved sulphur is $H_2S(aq)$, $[H_2S(aq)] = [S]_{total}$, and we assume that the total dissolved silver is Ag(aq), $[Ag]_{total} = [Ag(aq)]$.

In Fig. 26-10 $[Ag]_{total}$ and $[S]_{total}$ values for individual measurements from Schwarzenbach & Widmer (1966), Mehra (1968) and Stefánsson & Seward (2003) were used to calculate $[H_2g]$, and Eh values have been calculated therefrom for the given pH values.

The average partial pressure of hydrogen, $[H_2g]$ or P_{H2}, using the data at pH < 5, is

Schwarzenbach & Widmer (1966)	$P_{H2} = (1.3 \pm 0.2) \cdot 10^{-4}$ bar
Mehra (1968)	$P_{H2} = (1.6 \pm 0.6) \cdot 10^{-2}$ bar
Stefánsson & Seward (2003)	$P_{H2} = (5 \pm 4)$ bar

These results suggest that Ag(aq) could have been the dominating dissolved silver species at pH < 5 in the experiments of Schwarzenbach & Widmer (1966), Mehra (1968) and Stefánsson & Seward (2003). The average partial hydrogen pressure increases by a factor about 100 in the sequence of the mentioned solubility studies, concomitantly with an increase of dissolved silver by a factor of about 10, or one log-unit (Fig. 26-9). It seems that efforts towards more reducing conditions in the experiments have been made in the mentioned sequence of studies, leading towards higher silver concentrations at pH < 5.

Note that the above equilibrium predicts that at constant partial hydrogen pressure the total dissolved silver concentration decreases with increasing $H_2S(aq)$ concentration, in contrast to an increase if AgHS(aq) would be the dominating mercury species. However, P_{H2} was neither controlled nor measured in the above-mentioned experiments, and it is not unreasonable that P_{H2} increases with increasing dissolved sulphide concentration, leading to roughly constant Ag(aq) concentrations. Dedicated experiments are needed to finally resolve this question.

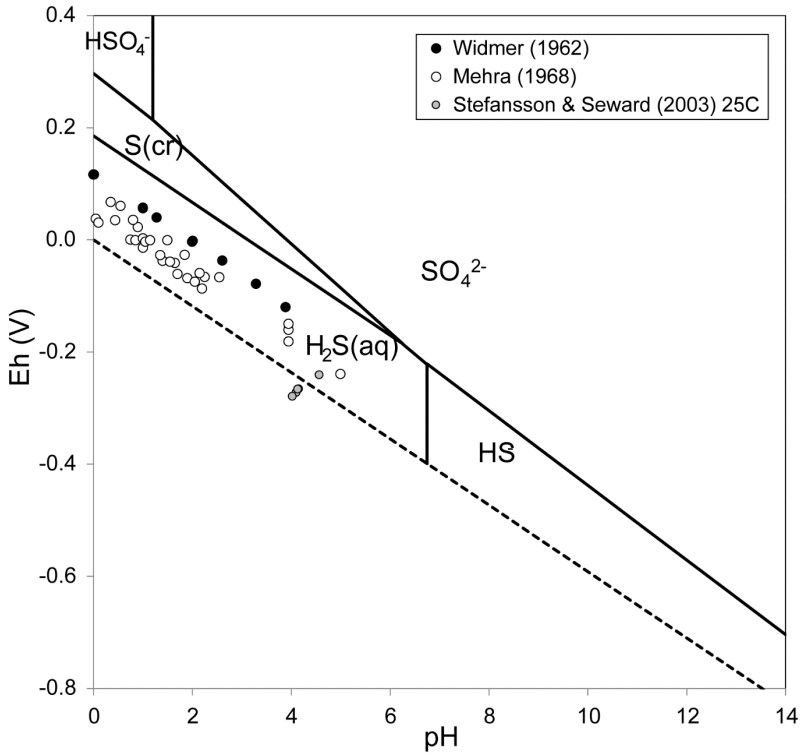

Fig. 26-10: Eh – pH diagram for part of the S – O – H system at 1 M $NaClO_4$ and $[S]_{total}$ = 0.02 M

The dashed line represents the lower stability limit of water where P_{H2} = 1 bar. Symbols: Experimental $Ag_2S(s)$ solubility data assuming Ag(aq) as the predominating aqueous silver species (see text).

AgHS(aq) ?

It seems that the species AgHS(aq) did not predominate at pH < 5 in any of the above discussed solubility studies. If there was any influence of AgHS(aq) on the results, the most probable candidate is the study of Schwarzenbach & Widmer (1966), carried out at the presumably least reducing conditions. Hence, the value derived by Schwarzenbach & Widmer (1966) could serve as an estimation of the upper limit for the stability constant of the equilibrium

$$0.5\ Ag_2S(s) + 0.5\ H_2S(aq) \rightleftharpoons AgHS(aq)$$

$$\log_{10}K_{s,11}\ (1.0\ M\ NaClO_4) \approx \log_{10}K_{s,11}^{\circ} < -7.9$$

It is assumed that the ionic strength dependence of this isocoulombic reaction is negligible, i.e.

$$\varepsilon(AgHS(aq), NaClO_4) \approx 0$$

Combined with the selected solubility product of $Ag_2S(s)$ (see Section 26.3.7.1) and the selected first dissociation constant of $H_2S(aq)$ (Hummel et al. 2002), this review obtained

$$Ag^+ + HS^- \rightleftharpoons AgHS(aq)$$

$$\log_{10}\beta_1^\circ(298.15\ K) < 13.5$$

This value is included in TDB 2020 as supplemental datum.

Note that Rickard & Luther (2006) report conditional stability constants determined by sulphide titration in seawater (I = 0.7 M) from different studies as $\log_{10}\beta_1 \geq 9.5$, $\log_{10}\beta_1 = 10.8$, and $\log_{10}\beta_1 = 11.6$ (Tab. 17 in Rickard & Luther 2006). Extrapolation of these values to zero ionic strength with the above estimated SIT coefficient yield: $\log_{10}\beta_1^\circ \geq 9.8$, $\log_{10}\beta_1^\circ = 11.1$, and $\log_{10}\beta_1^\circ = 11.9$. Hence, the above estimated upper limit for $Ag^+ + HS^- \rightleftharpoons AgHS(aq)$ is not unreasonable. The actual value might be one to two orders of magnitude lower.

$Ag_2S(HS)_2^{2-}$?

The almost perfect agreement of $\log_{10}K_{s,23}$ (1.0 M $NaClO_4$, 293.15 K) = -4.82 of Schwarzenbach & Widmer (1966) and $\log_{10}K_{s,23}^\circ(298.15) = -4.78 \pm 0.04$ of Stefánsson & Seward (2003) seems to be a coincidence. The equilibrium

$$Ag_2S(s) + 2\ HS^- \rightleftharpoons Ag_2S(HS)_2^{2-}$$

is not isocoulombic and thus not independent of ionic strength. Extrapolating the value of Schwarzenbach & Widmer (1966) to zero ionic strength applying the vague guess

$$\varepsilon(Ag_2S(HS)_2^{2-}, Na^+) \approx \varepsilon(Ag(HS)_2^-, Na^+) \approx 0.1$$

results in

$$\log_{10}K_{s,23}^\circ(293.15) = -5.32$$

This is more than half a log-unit at variance with the result of Stefánsson & Seward (2003).

Moreover, the solubilities measured by Mehra (1968) at pH > 10 do not show any dependence on the total sulphide concentration (Fig. 26-9), as they should if $Ag_2S(HS)_2^{2-}$ is the dominating species in this pH range. Considering the scatter in the data of Mehra (1968) one could even assume that the data of Mehra (1968) and Schwarzenbach & Widmer (1966), at pH > 10, belong to a common data cluster showing no dependence on the total sulphide concentration (Fig. 26-9).

On the other hand, interpreting these data in terms of the mixed complex $Ag_2(HS)(OH)$, as Mehra (1968) proposed, is questionable, as silver(I) hydrolysis is weak and starts at pH > 11 (see Section 26.3.2.2).

The problem of the Ag – sulphide speciation at pH > 10 remains unresolved, but just including the complex $Ag(HS)_2^-$ in the database but neither $Ag_2(HS)(OH)$ nor $Ag_2S(HS)_2^{2-}$ will inevitably lead to much too low solubility values in any calculation concerning the solubility of silver in the presence of sulphide at pH > 10.

Hence, this review decided to consider the equilibrium

$$Ag_2S(s) + 2\ HS^- \rightleftharpoons Ag_2S(HS)_2^{2-}$$

as a "placeholder" in the database. Using the value derived by Stefánsson & Seward (2003)

$$\log_{10}K_{s,23}°(298.15) \approx -4.78$$

and combining this value with the selected solubility product of $Ag_2S(s)$ (see Section 26.3.7.1) and the selected first dissociation constant of $H_2S(aq)$ (Hummel et al. 2002) this review obtained

$$2\ Ag^+ + 3\ HS^- \rightleftharpoons Ag_2S(HS)_2^{2-} + H^+$$

$$\log_{10}K°(298.15\ K) \approx 31.1$$

This value is included in TDB 2020 as supplemental datum.

26.3.8 Silver(I) selenium compounds and complexes

26.3.8.1 Silver(I) selenate compounds and complexes

26.3.8.1.1 Silver(I) selenate compounds

Olin et al. (2005) report that four observations of the solubility of $Ag_2SeO_4(cr)$ in water are available. Based on these observations Olin et al. (2005) estimated that the solubility of $Ag_2SeO_4(cr)$ is situated in the interval $(1.2 – 2.4) \cdot 10^{-3}$ mol · kg^{-1}.

Olin et al. (2005) identified two sets of published solubility data which allow to calculate the solubility product

$$Ag_2SeO_4(cr) \rightleftharpoons 2\ Ag^+ + SeO_4^{2-}$$

The results obtained from these two studies are $\log_{10}K_{s0}° = -8.26 \pm 0.15$ and -7.46 ± 0.03. As there is no obvious ground for rejecting one of the values, Olin et al. (2005) selected the mean of the two solubility products with a large uncertainty:

$$\log_{10}K_{s0}° = -7.86 \pm 0.50$$

Based on a calorimetric study of the reaction between a silver nitrate and a selenic acid solution with formation of Ag_2SeO_4(cr) Olin et al. (2005) selected

$$\Delta_f H_m°(Ag_2SeO_4, cr, 298.15\ K) = -(422.51 \pm 2.12)\ kJ \cdot mol^{-1}$$

These values are included in TDB 2020.

26.3.8.1.2 Silver(I) selenate complexes

No published data concerning silver(I) – selenate complexation have been found by Olin et al. (2005). Hence, this review estimated for the reaction

$$Ag^+ + SeO_4^{2-} \rightleftharpoons AgSeO_4^-$$

a value, based on the chemically analogous reaction $Ag^+ + SO_4^{2-} \rightleftharpoons AgSO_4^-$ (see Section 26.3.6.1), as

$$log_{10}\beta_1° (298.15\ K) = 1 \pm 0.5$$

with increased uncertainty. This value is included in TDB 2020 as supplemental datum, together with the estimated SIT interaction coefficient (see Tab. 1-7)

$$\varepsilon(AgSeO_4^-, Na^+) = -(0.05 \pm 0.10)\ kg \cdot mol^{-1}$$

and

$$\varepsilon(SeO_4^{2-}, Na^+) = -(0.12 \pm 0.06)\ kg \cdot mol^{-1}$$

The latter interaction coefficient as estimated by Olin et al. (2005) in analogy with $\varepsilon(SO_4^{2-}, Na^+)$.

26.3.8.2 Silver(I) selenite compounds and complexes

26.3.8.2.1 Silver(I) selenite compounds

Olin et al. (2005) accepted experimental determinations of the solubility product of silver(I) selenite defined by the equilibrium:

$$Ag_2SeO_3(cr) \rightleftharpoons 2\ Ag^+ + SeO_3^{2-}$$

from five published studies. Olin et al. (2005) calculated the average of four $\log_{10}K_{s0}°$ values obtained in low ionic strength media, excluding the value of Mehra (1968) determined in 1 M $NaClO_4$, and selected:

$$\log_{10}K_{s0}° = -15.80 \pm 0.30$$

Based on a calorimetric experiment measuring the enthalpy change when crystalline silver(I) selenite was formed from $AgNO_3$(cr) and a solution of sodium selenite, Olin et al. (2005) selected

$$\Delta_f H_m°(Ag_2SeO_3, cr, 298.15\ K) = -(363.44 \pm 1.02)\ kJ \cdot mol^{-1}$$

These values are included in TDB 2020.

26.3.8.2.2 Silver(I) selenite complexes

Mehra (1968) made extensive measurements of the solubility of Ag_2SeO_3(cr) in aqueous solutions at 298.15 K as a function of pH and total selenite concentration. Olin et al. (2005) evaluated these measurements and accepted (Appendix A in Olin et al. 2005) the stability constant of the reaction:

$$Ag^+ + SeO_3^{2-} \rightleftharpoons AgSeO_3^-$$

$$\log_{10}\beta_1(1\ M\ NaClO_4, 298.15\ K) = 2.30 \pm 0.25$$

No attempt was made by Olin et al. (2005) to extrapolate this value to zero ionic strength, and it is not in their list of selected values.

Using the estimated $\varepsilon(SeO_3^{2-}, Na^+) \approx \varepsilon(SO_3^{2-}, Na^+) = -(0.08 \pm 0.05)\ kg \cdot mol^{-1}$ and $\varepsilon(AgSeO_3^-, Na^+) = -(0.05 \pm 0.10)\ kg \cdot mol^{-1}$ this review obtained

$$\Delta\varepsilon = \varepsilon(Ag^+, ClO_4^-) + \varepsilon(SeO_3^{2-}, Na^+) - \varepsilon(AgSeO_3^-, Na^+)$$

$$= (0.00 \pm 0.01) - \textit{(0.08 ± 0.10)} + \textit{(0.05 ± 0.10)}$$

$$= \textit{-(0.03 ± 0.12)}\ kg \cdot mol^{-1}$$

and extrapolated $\log_{10}\beta_1(1\ M\ NaClO_4, 298.15\ K)$ to zero ionic strength by SIT:

$$\textit{log}_{10}\beta_1° = \textit{3.1 ± 0.3}$$

This value is included in TDB 2020 as supplemental datum, together with the estimated SIT interaction coefficients

$$\textit{ε(SeO}_3^{2-}\textit{, Na}^+\textit{) = -(0.08 ± 0.10) kg · mol}^{-1}$$

$$\textit{ε(AgSeO}_3^-\textit{, Na}^+\textit{)= -(0.05 ± 0.10) kg · mol}^{-1}$$

26.3.8.3 Silver(I) selenide compounds and complexes

26.3.8.3.1 Silver(I) selenide compounds

Ag_2Se(cr) exists in two polymorphs, α and β. The α form is stable below 406 K (133 °C). Olin et al. (2005) evaluated heat capacity measurements of α-Ag_2Se and selected a weighted mean of the heat capacity values:

$$C_{p,m}°(Ag_2Se, \alpha, 298.15\ K) = (81.15 \pm 0.90)\ J \cdot K^{-1} \cdot mol^{-1}$$

Furthermore, Olin et al. (2005) scrutinised entropy determinations from low temperature heat capacity measurements and values obtained from electrochemical measurements and selected:

$$S_m°(Ag_2Se, \alpha, 298.15\ K) = (149.9 \pm 0.5)\ J \cdot K^{-1} \cdot mol^{-1}$$

These values are included in TDB 2020.

Mehra (1968) studied the solubility of Ag_2Se(s) in aqueous solutions at 298.15 K as a function of pH and total selenide concentration. Olin et al. (2005) evaluated these measurements. From the data in the pH range of 4.4 – 10.0, as reported in Mehra (1968), Olin et al. (2005) calculated the equilibrium constant of the reaction

$$Ag_2Se(s) + H^+ \rightleftharpoons 2\ Ag^+ + HSe^-$$

$$\log_{10}K(1\ M\ NaClO_4, 298.15\ K) = -42.2 \pm 0.4$$

Olin et al. (2005) extrapolated this value to zero ionic strength with SIT and $\Delta\varepsilon = -0.09\ kg \cdot mol^{-1}$

$$\log_{10}K° = -42.7 \pm 0.4$$

From the measurement in the pH range of 1.3 – 2.2, Olin et al. (2005) calculated the equilibrium constant of the reaction

$$Ag_2Se(s) + 2\ H^+ \rightleftharpoons 2\ Ag^+ + H_2Se(aq)$$

$$\log_{10}K(1\ M\ NaClO_4, 298.15\ K) = -38.8 \pm 0.4$$

Olin et al. (2005) extrapolated this value to zero ionic strength with SIT and $\Delta\varepsilon = -0.14\ kg \cdot mol^{-1}$

$$\log_{10}K° = -38.95 \pm 0.40$$

Combining these values with the accepted protonation constants of Se^{2-} and HSe^{-}, Olin et al. (2005) calculated $\log_{10}K_{s0}° = -57.6 \pm 0.4$ and $\log_{10}K_{s0}° = -57.7 \pm 0.4$, respectively, for the reaction

$$Ag_2Se(s) \rightleftharpoons 2\ Ag^{+} + Se^{2-}$$

The two estimates of the solubility product thus agree with a mean value of

$$\log_{10}K_{s0}° = -57.65 \pm 0.50$$

Combined with the CODATA values for Ag^{+} and the selected data for Se^{2-} this corresponds to

$$\Delta_f G_m°(Ag_2Se, s, 298.15\ K) = -(46.3 \pm 4.1)\ kJ \cdot mol^{-1}$$

Olin et al. (2005) further state that the $\Delta_f G_m°(Ag_2Se, s, 298.15\ K)$ from the high temperature measurements and from solution measurements agree within uncertainty limits, and hence, these data were combined (α-Ag_2Se is assumed to be present in the solubility measurement) with the weights 2:1 to the selected value:

$$\Delta_f G_m°(Ag_2Se, \alpha, 298.15\ K) = -(46.9 \pm 1.3)\ kJ \cdot mol^{-1}$$

The selected standard enthalpy of formation is calculated with the selected entropy to be:

$$\Delta_f H_m°(Ag_2Se, \alpha, 298.15\ K) = -(40.129 \pm 1.32)\ kJ \cdot mol^{-1}$$

These values are included in TDB 2020.

The estimate of the solubility product from the Gibbs energy of formation of α-Ag_2Se is

$$\log_{10}K_{s0}° = -57.76 \pm 0.50$$

or for the equilibrium

$$Ag_2Se(\alpha) + H^{+} \rightleftharpoons 2\ Ag^{+} + HSe^{-}$$

$$\log_{10}K° = -42.85 \pm 0.50$$

which overlaps the values from experimental measurements.

26.3.8.3.2 Silver(I) selenide complexes

Olin et al. (2005) report that in the measurements performed by Mehra (1968), the solubility measurements conducted with radioactively labelled silver showed a "constant dissolved" silver selenide concentration of about $6 \cdot 10^{-8} – 8 \cdot 10^{-9}$ M at pH < 10 (Fig. 26-11). The solubility was independent of the total Se(-II) concentration in the test solutions. From this finding Mehra (1968) concluded that a species of the formula $Ag_2(HSe)(OH)(aq)$ was formed and evaluated its stability from the data. The composition of this complex is formally equivalent to the composition $Ag_2Se(aq)$ and therefore not unique. The observed constant solubility would then correspond to an intrinsic solubility of $Ag_2Se(s)$ according to

$$Ag_2Se(s) \rightleftharpoons Ag_2Se(aq)$$

and the data in Mehra (1968) have been recalculated by Olin et al. (2005) to yield

$$\log_{10}K(1\ M\ NaClO_4, 298.15\ K) = -7.66 \pm 0.48$$

However, Olin et al. (2005) did not accept this species and the resulting stability constant.

As in the case of $Ag_2S(s)$ (see Section 26.3.7.2) a possible solution could be the consideration of Ag(aq) in the speciation model. A solubility equilibrium between $Ag_2Se(s)$ and Ag(aq) can be formulated as

$$0.5\ Ag_2Se(s) + 0.5\ H_2g \rightleftharpoons Ag(aq) + 0.5\ H_2Se(aq)$$

Combining the solubility product derived at 1 M $NaClO_4$ (see Section 26.3.8.3.1) and auxiliary data (see Section 26.3.7.2) this review calculated

$$\log_{10}K_s\ (1.0\ M\ NaClO_4, 298.15\ K) = -12.7 \pm 0.6$$

If this equilibrium predominates, the measured Ag solubility is pH independent at constant partial pressure of hydrogen. In order to test whether the hypothesis works that Ag(aq) could have been the predominating species in the study of Mehra (1968) at pH < 4, the partial pressure of hydrogen, P_{H2}, has been calculated. The calculations yielded absurdly high values in the range of 10^8 bar. Hence, Ag(aq) does not play any role in the solubility of $Ag_2Se(s)$.

On the other hand, just including the solubility product of α-Ag_2Se (see Section 26.3.8.3.1) in the database but no aqueous complexes at all will inevitably lead to grossly wrong solubility values in any calculation concerning the solubility of silver in the presence of selenium.

Hence, this review decided to consider the equilibrium

$$Ag_2Se(\alpha) \rightleftharpoons Ag_2Se(aq)$$

$$\log_{10}K°(298.15\ K) = \log_{10}K(1\ M\ NaClO_4, 298.15\ K) = -7.66 \pm 0.5$$

$$\Delta\varepsilon = \varepsilon(Ag_2Se(aq), NaClO_4) = (0.0 \pm 0.1)\ kg \cdot mol^{-1}$$

in order to reproduce the measured solubility of $Ag_2Se(s)$ in the pH range 0 – 11 (Fig. 26-11).

These values have been included in TDB 2020 as supplemental data.

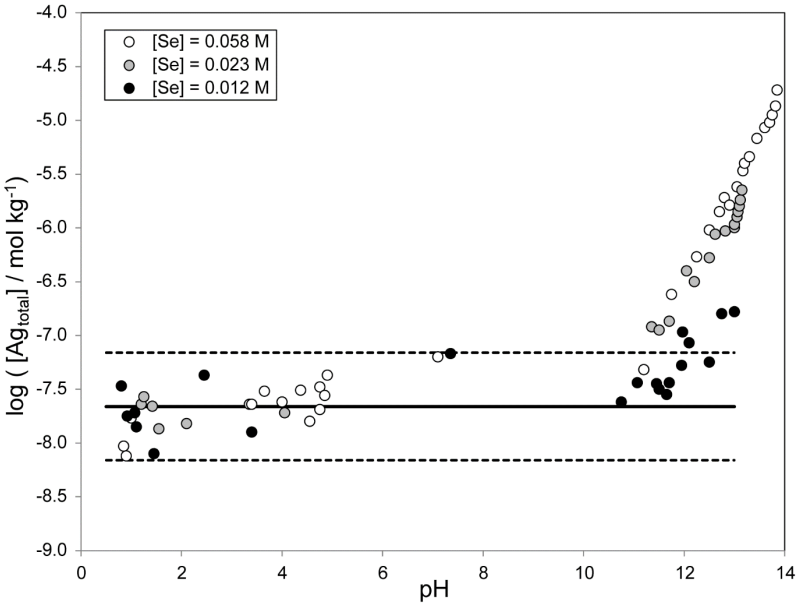

Fig. 26-11: Solubility of $Ag_2Se(s)$ in water as a function of pH at different total dissolved selenide concentrations, $[Se]_{total}$

Different symbols: experimental data of Mehra (1968). Solid line: solubility model according to $Ag_2Se(s) \rightleftharpoons Ag_2Se(aq)$, $log_{10}K°(298.15\ K) = -7.66$. Dashed lines: upper and lower limits ($\pm\ 0.5$).

At pH values well above 11, the data show an increase in the Ag(I) concentration with pH and $[Se]_{total}$. The formation of the species $Ag(Se)_2(OH)^{4-}$ was suggested by Mehra (1968). As Olin et al. (2005) state, the stoichiometry of this species is unlikely since Ag(I) is well known to prefer a linear coordination. Moreover, the derivation of its stoichiometry assumed that Se^{2-} predominates in the experimental pH range, which is not correct. The composition of the complex and its formation constant are thus refuted by Olin et al. (2005), although soluble Ag(I)-species of unknown stoichiometry apparently form at increasing selenide concentration and high pH. No attempt was made by Olin et al. (2005) to re-evaluate the data of Mehra (1968).

This review agrees with the rejection of the species $Ag(Se)_2(OH)^{4-}$ as an explanation of the observed $Ag_2Se(s)$ solubility at pH > 11. With the inclusion of the species $Ag_2Se(aq)$ in TDB 2020, constant solubility values will be calculated even at pH > 11. However, the measured increase of $Ag_2Se(s)$ solubility above pH 11 strongly depends on the total selenium concentration, $[Se]_{total}$ (Fig. 26-11). It is expected that at $[Se]_{total} < 0.01$ M this effect will be negligible and the approximation $Ag_2Se(s) \rightleftharpoons Ag_2Se(aq)$ will be sufficient for environmental system with low total selenium concentrations.

26.3.9 Silver(I) cyanide compounds and complexes

As discussed by Hummel (2004), Prussian Blue, $Fe^{III}_4[Fe^{II}(CN)_6]_3$, and structurally related transition metal compounds are used as caesium ion exchangers in decontamination procedures of liquid radioactive waste. The used ion exchangers are conditioned as a cementitious waste form for interim storage and finally will become part of the radioactive waste in geological repositories. The problem is the long-term behaviour of the ion exchangers in planned geological repositories. The worst-case scenario is the instantaneous and complete dissolution and decomposition of the ion exchangers in the cementitious environment and the release of free cyanide. Strong complexation and extensive cyanide leaching is found for Ni, Co, Pd, Ag (Hummel 2004). Hence, silver(I) cyanide compounds and complexes have been reviewed here.

26.3.9.1 Silver(I) cyanide compounds

Silver(I) cyanide is a white solid which forms in the lab upon treatment of solutions containing Ag^+ with sodium cyanide. This precipitation step is used in some schemes to recover silver from solution. The solubility of AgCN(s) at 20 °C is given in the chemical literature as $2.6 \cdot 10^{-6}$ g/L.

The solubility product of

$$AgCN(s) \rightleftharpoons Ag^+ + CN^-$$

has been determined by Kolthoff & Stock (1956) at 22 – 24 °C and $I \approx 0.1$ M $NaClO_4$ as $K_{so} = (2.5 \pm 1) \cdot 10^{-16}$ which is $\log_{10}K_{so} = -15.64 \pm 0.20$.

Gübeli & Côté (1972) determined the same solubility product at 25 °C and 1 M $NaClO_4$ as $\log_{10}K_{so} = -15.54 \pm 0.06$ (1σ) which is accepted by this review as $\log_{10}K_{so} = -15.54 \pm 0.12$ (2σ).

Using $\Delta\varepsilon = \varepsilon(Ag^+, ClO_4^-) + \varepsilon(CN^-, Na^+) = (0.00 \pm 0.01) + (0.07 \pm 0.03) = 0.03 \pm 0.12$ kg · mol^{-1} both values have been extrapolated to zero ionic strength, yielding $\log_{10}K_{so}° = -15.85 \pm 0.20$ and $\log_{10}K_{so}° = -15.83 \pm 0.12$, respectively. The average

$$\log_{10}K_{s0}° = 15.84 \pm 0.20$$

is included in TDB 2020.

26.3.9.2 Silver(I) cyanide complexes

In his critical survey of stability constants of cyano complexes Beck (1987) states that, although many papers have been published on the stability constants of different cyano complexes of silver(I), only a few studies meet the requirements for obtaining reliable constants. Potentiometrically obtained values are regarded as the most reliable ones for the reactions

$$Ag^+ + 2\ CN^- \rightleftharpoons Ag(CN)_2^-$$

$$Ag^+ + 3\ CN^- \rightleftharpoons Ag(CN)_3^{2-}$$

Hancock et al. (1972) obtained at 25 °C and 0.025 M KCN $\log_{10}\beta_2 = 20.9 \pm 0.1$ and $\log_{10}\beta_3 = 21.8 \pm 0.1$, Beck (1987) recommends these values and corroborates with two additional papers not available to this review: at 20.5 °C and $I = 0$, $\log_{10}\beta_2 = 20.85$ and $\log_{10}\beta_3 = 21.8$, and at 21 °C and 3.25 M $NaClO_4$ $\log_{10}\beta_2 = 20.23 \pm 0.06$.

This review accepted these values but assigned uncertainties of ± 0.3. In addition, the value $\log_{10}\beta_2 = 20.14 \pm 0.05$ (1σ) obtained by Gübeli & Côté (1972) was accepted by this review with an increased uncertainty of ± 0.4, considering the good agreement of the solubility product determined by the same authors with the value of Kolthoff & Stock (1956) (see Section 26.3.9.1).

A SIT regression analysis (Fig. 26-12) using all accepted $\log_{10}\beta_2$ values resulted in

$$\log_{10}\beta_2^\circ(298.15\ \text{K}) = 20.88 \pm 0.20$$

$$\Delta\varepsilon = (0.09 \pm 0.10)\ \text{kg} \cdot \text{mol}^{-1}$$

$$\varepsilon(Na^+, Ag(CN)_2^-) = \Delta\varepsilon + \varepsilon(Ag^+, ClO_4^-) + 2 \cdot \varepsilon(CN^-, Na^+)$$

$$= (0.09 \pm 0.10) + (0.00 \pm 0.01) + 2 \cdot (0.07 \pm 0.03)$$

$$= (0.23 \pm 0.10)\ \text{kg} \cdot \text{mol}^{-1}$$

These values are included in TDB 2020.

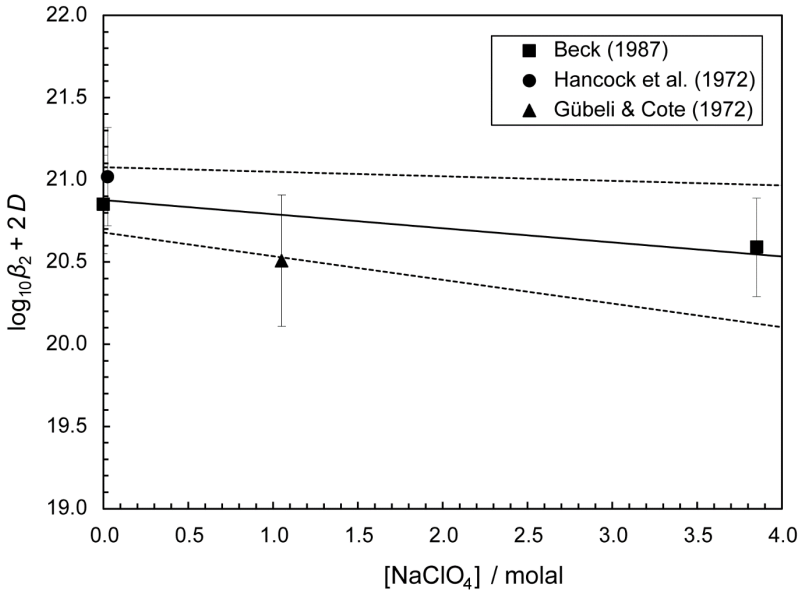

Fig. 26-12: Dependence of the equilibrium $Ag^+ + 2\ CN^- \rightleftharpoons Ag(CN)_2^-$ on ionic strength in $NaClO_4$

The solid line is obtained using the derived SIT interaction coefficient and stability constant at zero ionic strength. The dotted lines represent the 95% uncertainty range extrapolated from zero ionic strength to higher perchlorate concentrations.

Note that the seemingly high value $\varepsilon(Na^+, Ag(CN)_2^-) = (0.23 \pm 0.10)$ kg · mol^{-1} is in line with previously obtained SIT interaction coefficients for cyanide complexes: $\varepsilon(Na^+, Ni(CN)_4^{2-}) = (0.185 \pm 0.08)$ kg · mol^{-1} and $\varepsilon(Na^+, Ni(CN)_5^{3-}) = (0.25 \pm 0.14)$ kg · mol^{-1} (Lemire et al. 2013).

As mentioned, for the reaction

$$Ag^+ + 3\ CN^- \rightleftharpoons Ag(CN)_3^{2-}$$

Hancock et al. (1972) obtained $\log_{10}\beta_3 = 21.8 \pm 0.1$ at 25 °C and 0.025 M KCN, and Beck (1987) reports in addition: $\log_{10}\beta_3 = 21.8$ at 20.5 °C and $I = 0$. The Debye-Hückel term for the above reaction vanishes as $\Delta z^2 = 0$. Hence, this review selected

$$\log_{10}\beta_3°(298.15\ K) = 21.8 \pm 0.2$$

with increased uncertainty. This value is included in TDB 2020.

If we assume the same ionic strength effect as obtained for the reaction $Ag^+ + 2\ CN^- \rightleftharpoons Ag(CN)_2^-$, $\Delta\varepsilon = (0.09 \pm 0.20)$ kg · mol^{-1}, we obtain

$$\varepsilon(Na^+, Ag(CN)_3^{2-}) = (0.30 \pm 0.20)\ kg \cdot mol^{-1}$$

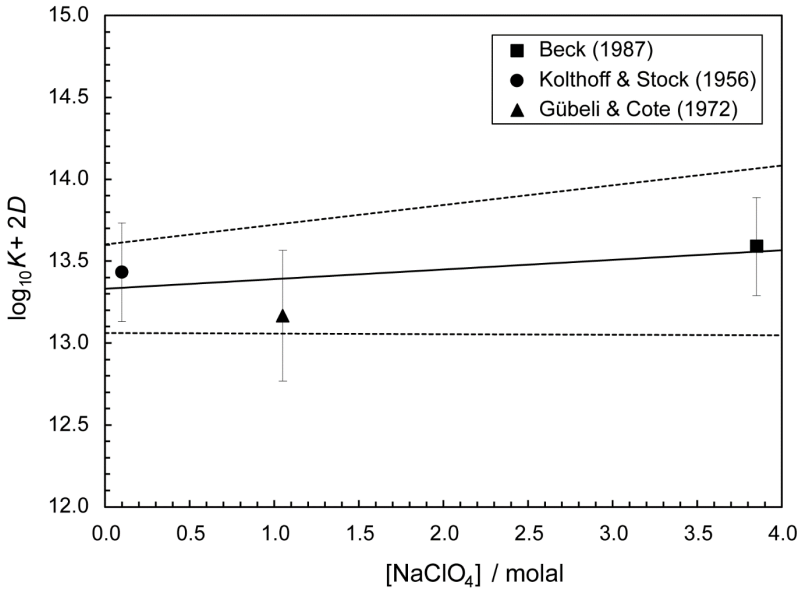

Fig. 26-13: Dependence of the equilibrium $Ag^+ + OH^- + CN^- \rightleftharpoons Ag(OH)CN^-$ on ionic strength in $NaClO_4$

The solid line is obtained using the derived SIT interaction coefficient and stability constant at zero ionic strength. The dotted lines represent the 95% uncertainty range extrapolated from zero ionic strength to higher perchlorate concentrations.

This value is included in TDB 2020 as supplemental datum.

For the reaction

$$Ag^+ + OH^- + CN^- \rightleftharpoons Ag(OH)CN^-$$

Beck (1987) reported that the overall stability constant of this mixed ligand complex was determined amperometrically by Kolthoff & Stock (1956) (at 22 – 24 °C and $I \approx 0.1$ M $NaClO_4$ as $1/K = 6 \cdot 10^{-14}$ which is $\log_{10}K = 13.22$) and in a paper not available to this review pH metrically (at 21 °C and 3.25 M $NaClO_4$ $\log_{10}K = 13.23$).

This review accepted these values but assigned uncertainties of ± 0.3. In addition, the value $\log_{10}K = 12.80 \pm 0.08$ (1σ) obtained by Gübeli & Côté (1972) was accepted by this review with an increased uncertainty of ± 0.4, considering the good agreement of the solubility product determined by the same authors with the value of Kolthoff & Stock (1956) (see Section 26.3.9.1).

A SIT regression analysis (Fig. 26-13) using all accepted $\log_{10}K$ values resulted in

$$\log_{10}K°(298.15\ K) = 13.3 \pm 0.3$$

$$\Delta\varepsilon = -(0.06 \pm 0.11)\ kg \cdot mol^{-1}$$

$$\varepsilon(Na^+, Ag(OH)CN^-) = \Delta\varepsilon + \varepsilon(Ag^+, ClO_4^-) + \varepsilon(CN^-, Na^+) + \varepsilon(OH^-, Na^+)$$

$$= -(0.06 \pm 0.11) + (0.00 \pm 0.01) + (0.07 \pm 0.03) + (0.04 \pm 0.01)$$

$$= (0.05 \pm 0.12)\ kg \cdot mol^{-1}$$

These values are included in TDB 2020.

26.3.10 Silver(I) selenocyanate compounds and complexes

The selenocyanate ion, $SeCN^-$, is an ambidentate ion which may coordinate to metal ions via either the nitrogen atom (to "hard" metal ions) or the selenium atom (to "soft" metal ions). Hence, in the case of Ag^+, as a "soft" metal ion, the coordination is via the selenium atom.

Olin et al. (2005) state that a salt of low solubility is formed with Ag(I) according to the reaction

$$AgSeCN(cr) \rightleftharpoons Ag^+ + SeCN^-$$

and selected

$$\log_{10}K_{s0}°(298.15\ K) = -14.0 \pm 0.5$$

Furthermore, Olin et al. (2005) found that the formation of aqueous silver(I) – selenocyanate complexes has been characterised in two restricted studies, both reporting ion-selective (Ag^+/Ag) electrode data for the dominating reaction

$$Ag^+ + 3\ SeCN^- \rightleftharpoons Ag(SeCN)_3^{2-}$$

Olin et al. (2005) selected the average of the two values reported and assigned it an uncertainty of ± 0.3 logarithmic units for the extrapolation to standard conditions:

$$\log_{10}\beta_3°(298.15\ K) = 13.85 \pm 0.30$$

In order to re-calculate the above values in terms of

$$CN^- + HSe^- \rightleftharpoons SeCN^- + H^+ + 2\ e^-$$

This review used the values $\Delta_f G_m°(SeCN^-, 298.15\ K) = (136.051 \pm 3.8)\ kJ \cdot mol^{-1}$, $\Delta_f G_m°(CN^-, 298.15\ K) = (166.939 \pm 2.5)\ kJ \cdot mol^{-1}$, and $\Delta_f G_m°(HSe^{2-}, 298.15\ K) = (43.471 \pm 2.0)\ kJ \cdot mol^{-1}$, all selected by Olin et al. (2005), and $\Delta_f G_m°(e^-, 298.15\ K) = 0$ (by definition) and $\Delta_f G_m°(H^+, 298.15\ K) = 0$ (per definition) to calculate

$$\log_{10}K°(298.15\ K) = 13.03 \pm 0.5$$

Using the above equilibrium constant this review calculates

$$AgSeCN(cr) + H^+ + 2\ e^- \rightleftharpoons Ag^+ + CN^- + HSe^-$$

$$\log_{10}K°(298.15\ K) = -27.03 \pm 0.7$$

$$Ag^+ + 3\ CN^- + 3\ HSe^- \rightleftharpoons Ag(SeCN)_3^{2-} + 3\ H^+ + 6\ e^-$$

$$\log_{10}K°(298.15\ K) = 52.94 \pm 0.6$$

These values are included in TDB 2020 as well as the estimate

$$\varepsilon(Na^+, Ag(SeCN)_3^{2-}) = -(0.10 \pm 0.10)\ kg \cdot mol^{-1}$$

26.4 Selected silver data

Tab. 26-1: Selected silver data

Core data are bold and supplemental data in italics. T-range refers to the experimental range of temperatures at which equilibrium constants, $\Delta_r H_m°$ and $\Delta_r C_{p,m}°$ were determined.

Name	**$\Delta_f G_m°$** [kJ · mol^{-1}]	**$\Delta_f H_m°$** [kJ · mol^{-1}]	**$S_m°$** [J · K^{-1} · mol^{-1}]	**$C_{p,m}°$** [J · K^{-1} · mol^{-1}]	**Species**
Ag(cr)	0.0	0.0	**42.550 ± 0.200**	**25.350 ± 0.100**	Ag(cr)
Ag+	**77.096 ± 0.156**	**105.790 ± 0.080**	**73.450 ± 0.400**		Ag^+
AgCl(cr)	**-109.765 ± 0.098**	**-127.010 ± 0.050**	**96.250 ± 0.200**		AgCl(cr)
Ag2SeO4(cr)		-422.51 ± 2.12			Ag_2SeO_4(cr)
Ag2SeO3(cr)		-363.44 ± 1.02			Ag_2SeO_3(cr)
α-Ag2Se	-46.9 ± 1.3	-40.129 ± 1.32	149.9 ± 0.5	81.15 ± 0.90	α-Ag_2Se

Name	**$\log_{10}\beta°$**	**$\Delta_r H_m°$** [kJ · mol^{-1}]	**$\Delta_r C_{p,m}°$** [J · K^{-1} · mol^{-1}]	**T-range** [°C]	**Reaction**
Ag(aq)	-6.4 ± 0.5	33.7 ± 8.5	0	20 – 280	Ag(cr) ⇌ Ag(aq)
AgOH(aq)	-11.75 ± 0.14	78.8 ± 4.7	0	25 – 90	$Ag^+ + H_2O(l) \rightleftharpoons AgOH(aq) + H^+$
Ag(OH)2-	-24.34 ± 0.14	69.1 ± 4.7	0	25 – 90	$Ag^+ + 2\ H_2O(l) \rightleftharpoons Ag(OH)_2^- + 2\ H^+$
AgF(aq)	0.11 ± 0.10	-11.7 ± 4.2	0	15 – 25	$Ag^+ + F^- \rightleftharpoons AgF(aq)$
AgCl(aq)	3.23 ± 0.11	-27.6 ± 4.2	0	5 – 160	$Ag^+ + Cl^- \rightleftharpoons AgCl(aq)$
AgCl2-	5.15 ± 0.11	-21.3 ± 1.3	0	5 – 160	$Ag^+ + 2\ Cl^- \rightleftharpoons AgCl_2^-$
AgCl3-2	5.04 ± 0.08	-41.8 ± 2.1	0	5 – 160	$Ag^+ + 3\ Cl^- \rightleftharpoons AgCl_3^{2-}$
AgCl4-3	3.64 ± 0.11	-69.9 ± 4.2	0	5 – 160	$Ag^+ + 4\ Cl^- \rightleftharpoons AgCl_4^{3-}$
AgBr(aq)	4.54 ± 0.10	-32.9 ± 4.0	0	18 – 300	$Ag^+ + Br^- \rightleftharpoons AgBr(aq)$
AgBr2-	7.48 ± 0.10	-48.0 ± 4.0	0	18 – 300	$Ag^+ + 2\ Br^- \rightleftharpoons AgBr_2^-$
AgBr3-2	8.3 ± 0.2	*≈ -52.7*	-	20 – 70	$Ag^+ + 3\ Br^- \rightleftharpoons AgBr_3^{2-}$
AgBr4-3	*≈ 7.2*	-	-		*$Ag^+ + 4\ Br^- \rightleftharpoons AgBr_4^{3-}$*
AgI(aq)	6.29 ± 0.10	-68.3 ± 4.0	0	18 – 250	$Ag^+ + I^- \rightleftharpoons AgI(aq)$
AgI2-	11.42 ± 0.10	-80.0 ± 4.0	0	18 – 250	$Ag^+ + 2\ I^- \rightleftharpoons AgI_2^-$
AgI3-2	13.24 ± 0.10	-101.4 ± 4.0	0	18 – 250	$Ag^+ + 3\ I^- \rightleftharpoons AgI_3^{2-}$
AgI4-3	*≈ 13.1*	-	-		*$Ag^+ + 4\ I^- \rightleftharpoons AgI_4^{3-}$*
AgCO3-	*< 2.4*	-	-		*$Ag^+ + CO_3^{2-} \rightleftharpoons AgCO_3^-$*
AgHPO4-	*< 4.5*	-	-		*$Ag^+ + HPO_4^{2-} \rightleftharpoons AgHPO_4^-$*
AgSO4-	1.18 ± 0.07	6.3 ± 1.3	-		$Ag^+ + SO_4^{2-} \rightleftharpoons AgSO_4^-$
AgHS(aq)	*< 13.5*	-	-		*$Ag^+ + HS^- \rightleftharpoons AgHS(aq)$*
Ag(HS)2-	17.40 ± 0.28	-61.1 ± 3.6	0	25 – 350	$Ag^+ + 2\ HS^- \rightleftharpoons Ag(HS)_2^-$
Ag2S(HS)2-2	*≈ 31.1*	-	-		*$2\ Ag^+ + 3\ HS^- \rightleftharpoons Ag_2S(HS)_2^{2-} + H^+$*
AgSeO4-	*1 ± 0.5*	-	-		*$Ag^+ + SeO_4^{2-} \rightleftharpoons AgSeO_4^-$*

Tab. 26-1: Cont.

Name	**$\log_{10}\beta°$**	**$\Delta_r H_m°$** [kJ · mol^{-1}]	**$\Delta_r C_{p,m}°$** [J · K^{-1} · mol^{-1}]	**T-range** [°C]	**Reaction**
AgSeO3-	*3.1 ± 0.3*	-	-		*$Ag^+ + SeO_3^{2-} \rightleftharpoons AgSeO_3^-$*
$Ag_2Se(aq)$	*-7.66 ± 0.5*	-	-		*$Ag_2Se(\alpha) \rightleftharpoons Ag_2Se(aq)$*
Ag(CN)2-	20.88 ± 0.20	-	-		$Ag^+ + 2\ CN^- \rightleftharpoons Ag(CN)_2^-$
Ag(CN)3-2	21.8 ± 0.2	-	-		$Ag^+ + 3\ CN^- \rightleftharpoons Ag(CN)_3^{2-}$
Ag(OH)CN-	13.3 ± 0.3	-	-		$Ag^+ + OH^- + CN^- \rightleftharpoons Ag(OH)CN^-$
Ag(SeCN)3-2	52.94 ± 0.6	-	-		$Ag^+ + 3\ CN^- + 3\ HSe^- \rightleftharpoons Ag(SeCN)_3^{2-} + 3\ H^+ + 6\ e^-$

Name	**$\log_{10}K_{s,0}°$**	**$\Delta_r H_m°$** [kJ · mol^{-1}]	**$\Delta_r C_{p,m}°$** [J · K^{-1} · mol^{-1}]	**T-range** [°C]	**Reaction**
Ag2O(am)	6.31 ± 0.04	-16 ± 13	0	15 – 25	$0.5\ Ag_2O(am) + H^+ \rightleftharpoons Ag^+ + 0.5\ H_2O(l)$
Ag2O(cr)	5.91 ± 0.10	-19.4 ± 3.3	0	25 – 60	$0.5\ Ag_2O(cr) + H^+ \rightleftharpoons Ag^+ + 0.5\ H_2O(l)$
AgCl(cr)	**-9.748 ± 0.038**	**65.72 ± 0.14**	0	5 – 160	$AgCl(cr) \rightleftharpoons Ag^+ + Cl^-$
AgBr(cr)	-12.30 ± 0.04	85.5 ± 1.8	0	5 – 55	$AgBr(cr) \rightleftharpoons Ag^+ + Br^-$
AgI(cr)	-16.08 ± 0.03	110.4 ± 4.0	0	5 – 45	$AgI(cr) \rightleftharpoons Ag^+ + I^-$
Ag2CO3(cr)	-11.07 ± 0.04	-	-		$Ag_2CO_3(cr) \rightleftharpoons 2\ Ag^+ + CO_3^{2-}$
Ag3PO4(s)	-9.05 ± 0.08	-	-		$Ag_3PO_4(s) + H^+ \rightleftharpoons 3\ Ag^+ + HPO_4^{2-}$
Ag2SO4(s)	-4.94 ± 0.04	17.3 ± 0.4			$Ag_2SO_4(s) \rightleftharpoons 2\ Ag^+ + SO_4^{2-}$
Ag2S(cr)	-14.42 ± 0.20	103.5 ± 2.0	0	25 – 350	$0.5\ Ag_2S(s) + H^+ \rightleftharpoons Ag^+ + 0.5\ H_2S(aq)$
Ag2SeO4(cr)	-7.86 ± 0.50	-	-		$Ag_2SeO_4(cr) \rightleftharpoons 2\ Ag^+ + SeO_4^{2-}$
Ag2SeO3(cr)	-15.80 ± 0.30	-	-		$Ag_2SeO_3(cr) \rightleftharpoons 2\ Ag^+ + SeO_3^{2-}$
Ag2Se(α)	-42.85 ± 0.50				$Ag_2Se(\alpha) + H^+ \rightleftharpoons 2\ Ag^+ + HSe^-$
AgCN(s)	-15.84 ± 0.20	-	-		$AgCN(s) \rightleftharpoons Ag^+ + CN^-$
AgSeCN(cr)	-27.03 ± 0.7	-	-		$AgSeCN(cr) + H^+ + 2\ e^- \rightleftharpoons Ag^+ + CN^- + HSe^-$

Tab. 26-2: Selected SIT ion interaction coefficients $\varepsilon_{j,k}$ [kg · mol^{-1}] for silver species

Data in bold face are taken from Lemire et al. (2013). Data in normal face are derived or estimated in this review. Data estimated according to charge correlations and taken from Tab. 1-7 are shaded. Supplemental data are in italics.

j k → ↓	**Cl^-** $\varepsilon_{j,k}$ [kg · mol^{-1}]	**ClO_4^-** $\varepsilon_{j,k}$ [kg · mol^{-1}]	**Na^+** $\varepsilon_{j,k}$ [kg · mol^{-1}]	**$Na^+ + Cl^-$** $\varepsilon_{j,k}$ [kg · mol^{-1}]	**$Na^+ + ClO_4^-$** $\varepsilon_{j,k}$ [kg · mol^{-1}]
SO4-2	0	0	**-0.12 ± 0.06**	0	0
SeO4-2	0	0	-0.12 ± 0.06	0	0
SO3-2	0	0	**-0.08 ± 0.05**	0	0
SeO3-2	*0*	*0*	-0.08 ± 0.10	*0*	*0*
H2S(aq)	0	0	0	(0.055 ± 0.004) [b]	(0.055 ± 0.004) [c]
H2Se(aq)	0	0	0	0.06 ± 0.10	0.06 ± 0.10
HS-	0	0	(0.08 ± 0.01) [b]	0	0
HSe-	0	0	0.08 ± 0.10	0	0
CN-	0	0	**0.07 ± 0.03**	0	0
Ag(aq)	0	0	0	0.0 ± 0.1	0.0 ± 0.1
Ag+	(0.00 ± 0.01) [a]	**0.00 ± 0.01**	0	0	0
AgOH(aq)	0	0	0	0.0 ± 0.1	0.0 ± 0.1
Ag(OH)2-	0	0	-0.05 ± 0.10	0	0
AgF(aq)	0	0	0	0.0 ± 0.1	0.0 ± 0.1
AgCl(aq)	0	0	0	0.0 ± 0.1	0.0 ± 0.1
AgCl2-	0	0	-0.05 ± 0.10	0	0
AgCl3-2	0	0	-0.10 ± 0.10	0	0
AgCl4-3	0	0	-0.15 ± 0.10	0	0
AgBr(aq)	0	0	0	0.0 ± 0.1	0.0 ± 0.1
AgBr2-	0	0	-0.05 ± 0.10	0	0
AgBr3-2	0	0	-0.10 ± 0.10	0	0
AgBr4-3	0	0	-0.15 ± 0.10	*0*	*0*
AgI(aq)	0	0	0	0.0 ± 0.1	0.0 ± 0.1
AgI2-	0	0	-0.05 ± 0.10	0	0
AgI3-2	0	0	-0.10 ± 0.10	0	0
AgI4-3	0	0	-0.15 ± 0.10	*0*	*0*
AgCO3-	*0*	*0*	*-0.05 ± 0.10*	*0*	*0*
AgHPO4-	*0*	*0*	*-0.05 ± 0.10*	*0*	*0*
AgSO4-	0	0	-0.11 ± 0.09	0	0
AgHS(aq)	*0*	*0*	*0*	*≈ 0* [a]	*≈ 0*
Ag(HS)2-	*0*	*0*	*≈ 0.1*	*0*	*0*
Ag2S(HS)2-2	*0*	*0*	*≈ 0.1*	*0*	*0*
AgSeO4-	*0*	*0*	*-0.05 ± 0.10*	*0*	*0*
AgSeO3-	*0*	*0*	*-0.05 ± 0.10*	*0*	*0*
Ag2Se(aq)	*0*	*0*	*0*	*0.0 ± 0.1* [a]	*0.0 ± 0.1*

Tab. 26-2: Cont.

j k → ↓	**Cl^-** $\varepsilon_{j,k}$ [kg · mol^{-1}]	**ClO_4^-** $\varepsilon_{j,k}$ [kg · mol^{-1}]	**Na^+** $\varepsilon_{j,k}$ [kg · mol^{-1}]	**$Na^+ + Cl^-$** $\varepsilon_{j,k}$ [kg · mol^{-1}]	**$Na^+ + ClO_4^-$** $\varepsilon_{j,k}$ [kg · mol^{-1}]
Ag(CN)2-	0	0	0.23 ± 0.10	0	0
Ag(CN)3-2	0	0	*0.30 ± 0.20*	0	0
Ag(OH)CN-	0	0	0.05 ± 0.12	0	0
Ag(SeCN)3-2	0	0	-0.10 ± 0.10	0	0

[a] Assumed to be equal to the corresponding ion interaction coefficient with ClO_4^-, see Section 26.1 for explanation.
[b] Hummel et al. (2002)
[c] Assumed to be equal to the corresponding ion interaction coefficient with NaCl.

26.5 References

Antikainen, P.J., Hietanen, S. & Sillén, L.G. (1960): Studies on the hydrolysis of metal ions. 27. Potentiometric study of the argentate(I) complex in alkaline solution. Acta Chemica Scandinavica, 14, 95-101.

Baldwin, W.G. (1970): Some pholsphate equilibria. II. Studies on the silver-phosphate electrode. ARKIV FÖR KEMI Band 31 nr 32.

Beck, M.T. (1987): Critical survey of stability constants of cyano complexes. Pure & Appl. Chem., 59, 1703-1720.

Brookins, D.G. (1988): Eh-pH Diagrams for Geochemistry. Springer-Verlag Berlin Heidelberg, Germany, 184 pp.

Brown, P.L. & Ekberg, C. (2016): Hydrolysis of Metal Ions. Wiley-VCH Verlag GmbH & Co. KGaA, Weinheim, Germany, 917 pp.

Clever, H.L., Johnson, S.A. & Derrick, M.E. (1985): The Solubility of Mercury and Some Sparingly Soluble Mercury Salts in Water and Aqueous Electrolyte Solutions. J. Phys. Chem. Ref. Data, 14, 631-680.

Connick, R.E. & Paul, A.D. (1961): The fluoride complexes of silver and stannous ions in aqueous solution. J. Phys. Chem., 65, 1216-1220.

Cox, J.D., Wagman, D.D., Medvedev, V.A. (1989): CODATA Key Values for Thermodynamics. New York, Hemisphere Publishing, 271 pp.

Davis, T.W., Ricci, J.E. & Sauter, C.G. (1939): Solubilities of salts in dioxane – water solvents. J. Amer. Chem. Soc., 61, 3274-3284.

Dobrowolski, J. & Oglaza J. (1963) Zastoswanie izotopu ^{110}Ag do badania rozpuszczalnosci srebra metalicznego i chlorku srebra w roztworach wodnych siarczanu cynku [use of the isotope ^{110}Ag in studying the solubility of silver metal and silver chloride in aqueous solutions of zinc sulphide]. Nucleonika 8, 79-81 (in Polish).

Drucker, K. (1901): Über die Löslickeitsverhältnisse des Silbersulfats und des Merkurosulfats. Z. anorg. Chem., 28, 361-363.

Fritz, J.J. (1985): Thermodynamic properties of chloro-complexes of silver chloride in aqueous solution. Journal of Solution Chemistry, 14, 865-879.

Gammons, C.H. & Yu, Y. (1997): The stability of aqueous silver bromide and iodide complexes at 25 – 300 °C: Experiments, theory and geologic applications. Chemical Geology, 137, 155-173.

Gledhill, J.A. & Malan, G.M. (1954): The solubilities of sparingly soluble salts in water. Part 3. – The solubilities of silver chloride and silver bromide from 5° to 55 °C. Trans. Faraday Soc., 50, 126-128.

Grenthe, I., Fuger, J., Konings, R.J.M., Lemire, R.J., Muller, A.B., Nguyen-Trung, C. & Wanner, H. (1992): Chemical Thermodynamics of Uranium. Chemical Thermodynamics, Vol. 1. North-Holland, Amsterdam, 715 pp.

Gübeli, A.O. & Côté, P.A. (1972): Constants de stabilité de cyano-complexes d'argent at produit de solubilité de AgCN. Canadian J. Chem., 50,1144-1148.

Hancock, R.D., Finkelstein, N.P. & Evers, A. (1972): Stabilities of the cyanide complexes of the monovalent group IB metal ions in aqueous solution. J. inorg. nucl. Chem., 34, 3747-3751.

Harkins, W.D. (1911): The effect of salts upon the solubility of other salts, V. The solubility of unibivalent salts in solutions of salts of different types. J. Amer. Chem. Soc., 33, 1807-1827.

Hietanen, S. & Sillén, L.G. (1970): On silver – borate equilibria in aqueous solution. Arkiv för Kemi, 32, 111-120.

Hopkins, Jr., H.P. & Wulff, C.A. (1965): The solution thermochemistry of polyvalent electrolytes. II. Silver sulfate. J. Phys. Chem., 69, 9-11.

Hummel, W. (2004): The influence of cyanide complexation on the speciation and solubility of radionuclides in a geological repository. Environmental Geology, 45, 633-646.

Hummel, W. (2017): Chemistry of selected dose-relevant radionuclides. Nagra Technical Report NTB 17-05.

Hummel, W., Berner, U., Curti, E., Pearson, F.J. & Thoenen, T. (2002): Nagra/PSI Chemical Thermodynamic Data Base 01/01. Nagra Technical Report NTB 02-16 and Universal Publishers, Parkland, Florida, 565 pp.

Kolthoff, I.M. & Stock, J.T. (1956): Equilibria in alkaline argentocyanide solutions. J. Amer. Chem. Soc., 78, 2081-2085.

Kozlov, V.K. & Khodakovskiy, I.L. (1983): The thermodynamic parameters of atomic silver in aqueous solution at 25 – 280 °C. Geochemistry International, 20, 118-131 (translated from Geokhimiya 6 (1983) 836-848).

Kozlov, V.K., Kuznetsov, V.N. & Khodakovskiy, I.L. (1983): The thermodynamic parameters of Ag_2O_c and silver(I) hydroxyl complexes in aqueous solution at elevated temperatures. Geochemistry International, 20, 137-149 (translated from Geokhimiya 6 (1983) 215-227).

Leden, I. (1952): On the complexity of cadmium and silver sulphate. Acta Chemica Scandinavica, 6, 971-987.

Leden, I. & Marthén, L.-E. (1952): The dissociation constant of silver fluoride. Acta Chemica Scandinavica, 6, 1125.

Lemire, R.J., Berner, U., Musikas, C., Palmer, D.A., Taylor, P. & Tochiyama, O. (2013): Chemical Thermodynamics of Iron, Part 1. Chemical Thermodynamics, Vol. 13a. OECD Publications, Paris, France, 1082 pp.

Levin, K.A. (1992): An experimental and thermodynamic study of the stabilities of silver chloride complexes in KCl and NaCl solutions up to 7 m at 300 °C. Geochemistry International, 29, 103-108 (translated from Geokhimiya 10 (1991) 1463-1468).

Lieser, K.H. (1957): Radiochemische Messung der Löslichkeit von Silberhalogeniden in Wasser und in Natriumhalogenidlösungen und die Komplexbildung der Silberhalogenide mit Halogenionen. Z. anorg. allg. Chem., 292, 97-113.

Lietzke, M.H. & Hall, J.O. (1967): The thermodynamics of aqueous silver sulphate – lanthanum sulphate solutions. J. inorg. nucl. Chem., 29, 1249-1253.

Maya, L. (1983): Silver(I) Ion Compexation by Carbonate and Oxalate at 25 °C. Journal of the Less-Common Metals, 90 (1983) 137-142.

Mehra, M.C. (1968): Studies on the stabilities of some metal selenite, sulphide, and selenide complexes in solution. Ph.D. thesis, Laval University, Quebec, 191 pp.

Näsänen, R. & Meriläinen, P. (1960): Potentiometric determination of the solubility product of silver(I) oxide in potassium nitrate and sodium perchlorate solutions. Suomen Kemistilehti B, 33, 197-199.

Olin, Å., Noläng, B., Osadchii, E.G., Öhman, L.O. & Rosén, E. (2005): Chemical Thermodynamics of Selenium. Chemical Thermodynamics, Vol. 7. Elsevier, Amsterdam, 851 pp.

Owen, B.B. & Brinkley, Jr., S.R. (1938): The elimination of liquid junction potentials. II. The standard electrode potential of silver from 5 to 45°, and related thermodynamic quantities. J. Amer. Chem. Soc. 60, 2233-2239.

Pan, K. & Lin, J.-L. (1959): The thermodynamics of silver sulfate from e.m.f. measurements. J. Chinese Chem. Soc. (Taiwan), 6, 1-11.

Pouradier, J., Venet, A.M. & Chateau, H. (1954): Influence de la température sur la stabilité des complexes bromo-argentiques. J. Chim. Phys., 51, 375-384.

Rickard, D. & Luther III, G.W. (2006): Metal sulfide complexes and clusters. Reviews in Mineralogy & Geochemistry, 61, 421-504.

Rickard, D. (2012): Aqueous metal-sulfide chemistry: Complexes, clusters and nanoparticles. Developments in Sedimentology, 65, 121-194.

Righellato, E.C. & Davies, C.W. (1930): The extent of dissociation of salts in water. Part II. Uni-bivalent salts. Trans. Faraday Soc., 26, 592-600.

Schwarzenbach, G. & Widmer, M. (1966): Die Löslichkeit von Metallsulfiden II. Silbersulfid. Helvetica Chimica Acta, 49, 111-123.

Seward, T.M. (1976): The stability of chloride complexes of silver in hydrothermal solutions up to 350 °C. Geochim. Cosmochim. Acta, 40, 1329-1341.

Stefánsson, A. & Seward, T.M. (2003): Experimental determination of the stability and stoichiometry of sulphide complexes of silver(I) in hydrothermal solutions to 400 °C. Geochim. Cosmochim. Acta, 67, 1395-1413.

Stoughton, R.W. & Lietzke, M.H. (1960): The solubility of silver sulfate in electrolyte solutions. Part 6. Heats and entropies of solution vs. temperature. Species present in HNO_3 and H_2SO_4 media. J. Phys. Chem., 64, 133-136.

Swan, C.M. (1899) Chemistry Thesis, Massachusetts Institute of Technology (as cited by Harkins 1911).

Vosburgh, W.C. & McClure, R. (1943): Complex Ions. IV. Monammine-silver Ion. Contribution from the Department of Chemistry of Duke University.

Walker, A.C., Bray U.B. & Johnston J. (1927): Equilibrium in solutions of alkali carbonates. J. Amer. Chem. Soc., 49, 1235-1256.

Widmer, M. (1962): Über die Löslichkeit des schwarzen Quecksilbersulfids und Silbersulfids. Ph.D. thesis, ETH Zurich, Zürich, Switzerland, 104 pp.

Zotov, A.V., Levin, K.A., Khodakovskiy, I.L & Kozlov, V.K. (1986a): Thermodynamic parameters of Ag^+ in aqueous solution at 273-573 °K. Geochemistry International 23, 23-33 (translated from Geokhimiya 9 (1985) 1300-1310).

Zotov, A.V., Levin, K.A., Khodakovskiy, I.L & Kozlov, V.K. (1986b): Thermodynamic parameters of Ag(I) chloride complexes in aqueous solution at 273-623 K. Geochemistry International, 23, 103-116 (translated from Geokhimiya 5 (1986) 690-702).

27 Sulphur

27.1 Introduction

Elemental sulphur and aqueous species containing sulphur as sulphide (HS^-) or sulphate (SO_4^{2-}) are included in TDB 2020 and all its predecessors. However, the solubility of zero-valent sulphur, S(aq), has not been considered so far. This gap is closed here.

While sulphate, S(VI), is stable under oxidising conditions and sulphide, S(-II) under reducing conditions, and zero-valent sulphur, S(0), has a small range of stability under intermediate conditions, various other species including sulphites, SO_3^{2-}, S(IV), and thiosulphates, $S_2O_3^{2-}$, S(II), are metastable. The species SO_3^{2-}, HSO_3^-, and $S_2O_3^{2-}$, are added to the supplemental data. However, no metal complexation data involving these metastable species are included in TDB 2020.

Note that this contrasts with the selenium system, where selenite, SeO_3^{2-}, Se(IV), is stable under mildly oxidising conditions, and metal selenite species and compounds are included in TDB 2020 (Chapter 24).

27.2 Elemental sulphur

The thermodynamically stable form of elemental sulphur is orthorhombic α-sulphur consisting of cycloocta-S molecules (S_8 rings).

The selected values for S(cr)(orthorhombic) are taken from CODATA (Cox et al. 1989):

$$S_m°(\text{S, cr, orthorhombic, 298.15 K}) = (32.054 \pm 0.050)\ \text{J} \cdot \text{K}^{-1} \cdot \text{mol}^{-1}$$

$$C_{p,m}°(\text{S, cr, orthorhombic, 298.15 K}) = (22.750 \pm 0.050)\ \text{J} \cdot \text{K}^{-1} \cdot \text{mol}^{-1}$$

27.3 Sulphur(0) solubility

Boulegue (1978) measured the solubility of elemental orthorhombic sulphur in deionised water at 298 K. Three experiments were carried out in the dark with different time intervals (1, 2 and 3 months). At the end of the equilibration, the water was filtered on 0.01 μm Millipore filters. Then the dissolved sulphur was extracted with chloroform or trichloroethylene, and UV absorption spectra of sulphur were measured. Boulegue (1978) report that the solubility of orthorhombic sulphur in water is $(1.9 \pm 0.6) \cdot 10^{-8}$ mol $S_8 \cdot \text{kg}^{-1}$.

Boulegue (1978) state that in organic solvents the molecular form of dissolved sulphur is cyclooctasulphur and that it is highly probable that the molecular form of dissolved orthorhombic sulphur in water is also cyclooctasulphur. This assumption is reasonable but to the knowledge of the present authors it has never been verified by spectroscopic measurements. However, the molecular form of dissolved zero-valent sulphur is of no relevance for pure thermodynamic considerations and hence, this review multiplied the solubility value of Boulegue (1978) by 8 and obtained

$S(cr) \rightleftharpoons S(aq)$

$K°$ (298.15 K) = (1.52 ± 0.48) · 10^{-7} mol · kg^{-1}

$\log_{10}K°$ (298.15 K) = -6.82 ± 0.28 (2σ)

Wang & Tessier (2009) also measured the solubility of orthorhombic sulphur. The experiments were done in a glovebox under N_2 at 25 ± 0.2 °C using Milli-Q water. At predetermined times samples were taken and dissolved zero-valent sulphur was analysed by square wave cathodic stripping voltammetry. Wang & Tessier (2009) report that S(aq) concentrations in the presence of orthorhombic sulphur rapidly increased between 0 and 2 days, remained stable between 6 and 28 days, and did not vary with membrane pore size (0.2 and 0.001 μm). From the plateau between 6- and 28-days, Wang & Tessier (2009) calculate $K°$ (298.15 K) = (2.10 ± 0.03) · 10^{-7} mol · kg^{-1}. This review assumed that the overall uncertainty of this solubility value might actually be ten times higher and obtained

$\log_{10}K°$ (298.15 K) = -6.68 ± 0.12 (2σ)

Kamyshny (2009) measured the solubility of cyclooctasulphur in water with an experimental set-up similar to Wang & Tessier (2009) but at various temperatures in the range between 4 and 80 °C. Samples were taken after 45 to 94 days and the results showed that equilibrium was reached in all cases after 45 days. Kamyshny (2009) reports equilibrium constants for the different temperatures without error estimates (Tab. 2 in Kamyshny 2009) and used these values for an unweighted linear regression with the integrated van't Hoff equation

$$\log_{10}K°(T) = \log_{10}K°(T°) + \Delta_r H_m°(T°) / (R \cdot \ln(10)) \cdot (1 / T° - 1 / T)$$

with T° = 298.15 K and R = 8.31451 J · K^{-1} · mol^{-1}. He obtained $\Delta_r H_m°$(298.15 K) = (47.4 ± 3.6) kJ · mol^{-1} (1σ) and $K°$ (298.15 K) = (3.01 ± 1.04) · 10^{-8} mol S_8 · kg^{-1} (1σ). These results could be reproduced by this review.

An unweighted regression, multiplying the solubility values of Kamyshny (2009) by 8, and including the data of Boulegue (1978) and Wang & Tessier (2009), shown above, results in:

$\log_{10}K°$(298.15 K) = -6.65 ± 0.09

$\Delta_r H_m°$(298.15 K) = (48.4 ± 7.1) kJ · mol^{-1}

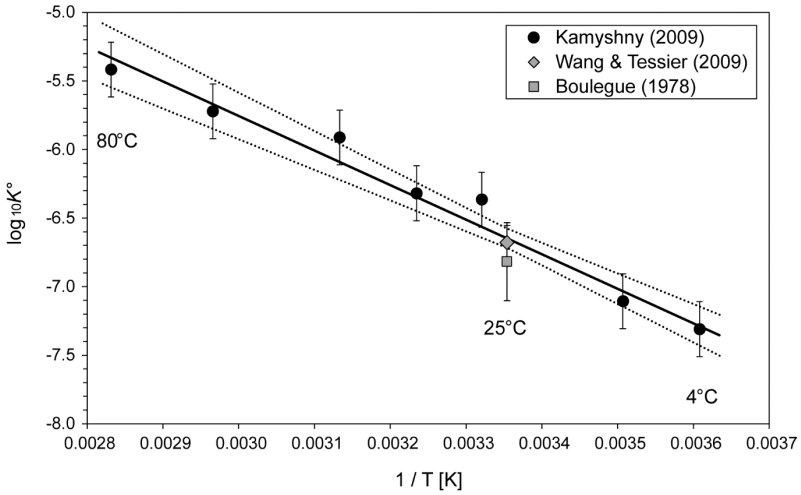

Fig. 27-1: Temperature dependence of S(cr) ⇌ S(aq)

Solid line: weighted linear regression of all data with the integrated van't Hoff equation. Dotted lines: 95% uncertainty range extrapolated from 25 °C to higher and lower temperatures.

Finally, this review assigned an uncertainty of ± 0.2 to the $\log_{10}K°$ values of Kamyshny (2009) for a weighted regression of all data. The results (Fig. 27-1) are):

$$\log_{10}K°(298.15\ \text{K}) = -6.65 \pm 0.07$$

$$\Delta_r H_m°(298.15\ \text{K}) = (48.2 \pm 5.4)\ \text{kJ} \cdot \text{mol}^{-1}$$

$$\Delta_r C_{p,m}°(298.15\ \text{K}) = 0\ \ \text{J} \cdot \text{K}^{-1} \cdot \text{mol}^{-1}$$

These values are included in TDB 2020.

The specific ion interaction coefficients for S(aq) are estimated to be zero (see Section 1.5.3):

$$\varepsilon(\text{S(aq)}, \text{NaCl}) = \varepsilon(\text{S(aq)}, \text{NaClO}_4) = (0.0 \pm 0.1)\ \text{kg} \cdot \text{mol}^{-1}$$

Using the above selected values for S(aq) together with the CODATA values for S(cr)(ortho-rhombic) this review calculated

$$\Delta_f G_m°(\text{S, aq, 298.15 K}) = (37.96 \pm 0.40)\ \text{kJ} \cdot \text{mol}^{-1}$$

$$\Delta_f H_m°(\text{S, aq, 298.15 K}) = (48.2 \pm 5.4)\ \text{kJ} \cdot \text{mol}^{-1}$$

$$S_m°(\text{S, aq, 298.15 K}) = (66.4 \pm 18.2)\ \text{J} \cdot \text{K}^{-1} \cdot \text{mol}^{-1}$$

$$C_{p,m}°(\text{S, aq, 298.15 K}) = (22.75 \pm 20.0)\ \text{J} \cdot \text{K}^{-1} \cdot \text{mol}^{-1}$$

The uncertainty of $C_{p,m}°$(S, aq, 298.15 K) is assumed to be of the same order of magnitude as the uncertainty derived for $S_m°$(S, aq, 298.15 K).

27.4 Selected sulphur data

Tab. 27-1: Selected sulphur data

Core data are bold.

Name	**$\Delta_f G_m°$** [kJ · mol^{-1}]	**$\Delta_f H_m°$** [kJ · mol^{-1}]	**$S_m°$** [J · K^{-1} · mol^{-1}]	**$C_{p,m}°$** [J · K^{-1} · mol^{-1}]	**Species**
S(cr)	**0.0**	**0.0**	**32.054 ± 0.050**	**22.750 ± 0.050**	S(cr)(orthorhombic)
S(aq)	37.96 ± 0.40	48.2 ± 5.4	66.4 ± 18.2	22.75 ± 20.0	S(aq)

Name	**$\log_{10}\beta°$**	**$\Delta_r H_m°$** [kJ · mol^{-1}]	**$\Delta_r C_{p,m}°$** [J · K^{-1} · mol^{-1}]	**T-range** [°C]	**Reaction**
S(aq)	-6.65 ± 0.07	48.2 ± 5.4	0	4 – 80	S(cr) ⇌ S(aq)

27.5 References

Boulegue, J. (1978): Solubility of elemental sulfur in water at 298 K. Phosphorus and Sulfur, 5, 127-128.

Cox, J.D., Wagman, D.D. & Medvedev, V.A. (1989): CODATA Key Values for Thermodynamics. New York, Hemisphere Publishing, 271 pp.

Kamyshny, A. (2009): Solubility of cyclooctasulfur in pure water and sea water at diferent temperatures. Geochim. Cosmochim. Acta, 73, 6022-6028.

Wang., F. & Tessier, A. (2009): Zero-valent sulfur and metal speciation in sediment porewaters of freshwater lakes. Environ. Sci. Technol., 43, 7252-7257.

28 Technetium

In a late state of the review work for TDB 2020 the NEA TDB Second Update on the Chemical Thermodynamics of Uranium, Neptunium, Plutonium, Americium and Technetium (Grenthe et al. 2020) became available to the reviewers. In the following, only changes with respect to previous TDB versions are shortly discussed. For a detailed discussion of the previous technetium chemical thermodynamic data the reader is referred to Thoenen et al. (2014) and Hummel et al. (2002).

Grenthe et al. (2020) discuss simple aqueous technetium ions of different oxidation states, technetium oxide and hydroxide compounds and complexes, and aqueous technetium chlorides.

28.1 Simple aqueous technetium ions of different oxidation states

Grenthe et al. (2020) report that Rard et al. (1999) recommended a standard potential, E° = (0.745 ± 0.012) V for the TCO_4^- / $TcO_2 \cdot 1.6H_2O$(s) couple that refers to a reasonably well characterised solid phase, which translates into the equilibrium:

$$TcO_2 \cdot 1.6H_2O(s) + 0.4\ H_2O(l) \rightleftharpoons TcO_4^- + 4\ H^+ + 3\ e^-$$

$$\log_{10}K_s^\circ = -(37.83 \pm 0.61)$$

Grenthe et al. (2020) state that this value is supported by many experimental observations, but the hydration number of the precipitated solid phases used as electrodes change with time. Hence, Grenthe et al. (2020) accept the value of E° recommended by Rard et al. (1999) but as referring to an electrode made from a freshly formed solid TcO_2(am, hyd, fresh) of undefined state of hydration:

$$TcO_2(am, hyd, fresh) + 2\ H_2O(l) \rightleftharpoons TcO_4^- + 4\ H^+ + 3\ e^-$$

$$\log_{10}K_s^\circ = -(37.83 \pm 0.61)$$

Grenthe et al. (2020) retain the value of $\Delta_f G_m^\circ(TcO_4^-)$ selected by Rard et al. (1999) and calculate from the above equilibrium a new value for $\Delta_f G_m^\circ(TcO_2$, am, hyd, fresh).

Grenthe et al. (2020) in addition report that seven-day data (three to four days equilibration + three-day ageing) from Hess et al. (2004) result in

$$TcO_2(am, hyd, fresh) + H_2O(l) \rightleftharpoons TcO(OH)_2(aq)$$

$$\log_{10}K_s^\circ = -(7.66 \pm 1.22)$$

Note that this value has been selected in the text of Grenthe et al. (2020) but is not included in their Tab. 7-2: Selected thermodynamic data for reactions involving technetium compounds and complexes. Nevertheless, this value is included in TDB 2020.

Using their calculated value for $\Delta_f G_m°(TcO_2, am, hyd, fresh)$ and the above selected $\log_{10}K_s° = -(7.66 \pm 1.22)$ Grenthe et al. (2020) calculate a new Gibbs energy of formation for $TcO(OH)_2(aq)$:

$$\Delta_f G_m°(TcO(OH)_2, aq) = -(572.47 \pm 10.89)\ kJ \cdot mol^{-1}$$

This value is included in TDB 2020.

Combining the above two solubility equilibria for TcO_2(am, hyd, fresh) results in

$$TcO(OH)_2(aq) + H_2O(l) \rightleftharpoons TcO_4^- + 4\ H^+ + 3\ e^-$$

$$\log_{10}K° = -(30.17 \pm 1.36)$$

Note that this equation is reported in the text of Grenthe et al. (2020) and was also included in an early version of their Tab. 7-2 but is missing in the final version of Tab. 7-2. Nevertheless, this value is included in TDB 2020.

Grenthe et al. (2020) report that there are indications that Tc^{3+} is the dominant species of Tc(III) at pH values below 3, and calculated, using the available data and their hydrolysis scheme of Tc(IV):

$$\Delta_f G_m°(Tc^{3+}) = (71.2 \pm 11.2)\ kJ \cdot mol^{-1}$$

There is conflicting evidence about the validity of this value but Grenthe et al. (2020) state that it can nevertheless be used for scoping calculations of the stability domain of Tc^{3+}.

Hence, this value is included in TDB 2020 as supplemental datum, together with SIT estimates (Tab. 28-2) based on charge correlations (see Section 1.5.3).

28.2 Technetium oxygen and hydrogen compounds and complexes

Grenthe et al. (2020) discuss the available evidence for the existence of TcO^{2+} and conclude that in all experimental studies polymeric Tc(IV) species seem to be dominant in the low pH regime. Although it can of course not be excluded, that at much lower concentrations than those employed experimentally, monomer species exist also in the non-complexing low pH regime, Grenthe et al. (2020) do not recommend thermodynamic data for TcO^{2+}.

Hence, the limiting value selected by Rard et al. (1999), and included in TDB Version 12/07, is not retained in TDB 2020.

Grenthe et al. (2020) state that the existence of $TcO(OH)^+$ was inferred principally from slope analyses of solubility data at pH < 3 of $TcO_2 \cdot nH_2O$(am). However, scrutinising all available studies, Grenthe et al. (2020) conclude that no coherent model can be obtained, and no thermodynamic data are recommended for $TcO(OH)^+$.

Hence, the stability constant selected by Rard et al. (1999), and included in TDB Version 12/07, is not retained in TDB 2020.

Grenthe et al. (2020) accept the presence of $TcO(OH)_3^-$ and obtain from an SIT plot comprising data of three experimental studies:

$$TcO(OH)_2(aq) + H_2O(l) \rightleftharpoons TcO(OH)_3^- + H^+$$

$$\log_{10}K^\circ = -(10.92 \pm 0.17)$$

$$\varepsilon(TcO(OH)_3^-, Na^+) = -(0.08 \pm 0.04)\ kg \cdot mol^{-1}$$

These values have been included in TDB 2020.

Grenthe et al. (2020) state that more recent spectroscopic observations of Tc(IV) solutions in acid media demonstrate the predominance of polymer formation in chloride, sulphate and non-complexing media. This observed predominance of cationic polymeric hydrolysis species of Tc(IV) in the low pH range is inconsistent with the model of Rard et al. (1999). Hence, a reinterpretation of the entire set of solubility data for $TcO_2 \cdot nH_2O(am)$ and the associated hydrolysis model for Tc(IV) was necessary. In conclusion, Grenthe et al. (2020) recommend the use of the stoichiometry of a +2-charged dimer as the reference hydrolysis species in non-complexing solutions at low pH and selected $Tc_2O_2(OH)_2^{2+}$ formed by the reaction

$$2\ TcO(OH)_2(aq) + 2\ H^+ \rightleftharpoons Tc_2O_2(OH)_2^{2+} + 2\ H_2O(l)$$

Grenthe et al. (2020) obtain from an SIT plot including data of four experimental studies:

$$\log_{10}K^\circ = (12.99 \pm 0.41)$$

$$\varepsilon(Tc_2O_2(OH)_2^{2-}, Cl^-) = -(0.43 \pm 0.11)\ kg \cdot mol^{-1}$$

These values have been included in TDB 2020.

Finally, Grenthe et al. (2020) obtain a "long term value" considering the time dependence of solubility data for $TcO_2(am)$ from Hess et al. (2004) and others:

$$TcO_2(am, hyd, aged) + H_2O(l) \rightleftharpoons TcO(OH)_2(aq)$$

$$\log_{10}K_s^\circ = -(8.72 \pm 0.40)$$

This value is included in TDB 2020.

28.3 Technetium chloride complexes

Grenthe et al. (2020) report that $TcCl_6^{2-}$ can easily be produced by dissolution of K_2TcCl_6 in concentrated HCl solutions and is well characterised spectroscopically and stable between 3 and 12 M HCl, and that $TcCl_5^-$ can be produced quickly by photochemical reaction of $TcCl_6^{2-}$. However, monomeric Tc(IV) chloride complexes are only stable at rather low Tc concentrations, and at pH ≤ 0. At Tc concentrations higher than about 10^{-4} m, and/or higher pH, the monomeric chloride complexes are dimerised to give $Tc_2OCl_{10}^{4-}$. Grenthe et al. (2020) further report that it has been shown that none of the monomeric or polymeric chloride complexes of Tc(IV) stays stable at pH > 1.5. In this pH range only species of the type $Tc_2O_2(OH)_2^{2+}$ are stable.

Grenthe et al. (2020) finally select

$$TcCl_5^- + Cl^- \rightleftharpoons TcCl_6^{2-}$$

$$\log_{10}K° = -(2.08 \pm 1.29)$$

$$Tc_2OCl_{10}^{4-} + 2\ H^+ \rightleftharpoons 2\ TcCl_5^- + H_2O(l)$$

$$\log_{10}K° = -(3.53 \pm 1.29)$$

$$Tc_2O_2(OH)_2^{2+} + 10\ Cl^- + 4\ H^+ \rightleftharpoons Tc_2OCl_{10}^{4-} + 3\ H_2O(l)$$

$$\log_{10}K° = -(0.4 \pm 1.1)$$

$$\varepsilon(Tc_2OCl_{10}^{4-}, Na^+) = (0.89 \pm 0.40)\ kg \cdot mol^{-1}$$

Note that the latter equilibrium is important as it links the formation of Tc(IV) chloride complexes to the Tc(IV) hydrolysis.

These values have been included in TDB 2020, together with SIT estimates for $TcCl_5^-$ and $TcCl_6^{2-}$ (Tab. 28-2) based on charge correlations (see Section 1.5.3).

28.4 Selected technetium data

Tab. 28-1: Selected technetium data

All data included in TDB 2020 are taken from Rard et al. (1999), which are identical with the data by Guillaumont et al. (2003), and Grenthe et al. (2020). Supplemental data are in italics. New or changed data with respect to TDB Version 12/07 (Thoenen et al. 2014) are shaded.

Name	Redox	TDB Version 12/07				TDB 2020				
		$\Delta_f G_m°$ [kJ · mol^{-1}]	$\Delta_f H_m°$ [kJ · mol^{-1}]	$S_m°$ [J · K^{-1} · mol^{-1}]	$C_{p,m}°$ [J · K^{-1} · mol^{-1}]	$\Delta_f G_m°$ [kJ · mol^{-1}]	$\Delta_f H_m°$ [kJ · mol^{-1}]	$S_m°$ [J · K^{-1} · mol^{-1}]	$C_{p,m}°$ [J · K^{-1} · mol^{-1}]	Species
Tc(cr)	0	0	0	32.5 ± 0.7	24.9 ± 1.0	0	0	32.5 ± 0.7	24.9 ± 1.0	Tc(cr)
Tc+3	III	-	-	-	-	*71.2 ± 11.2*	-	-	-	*Tc^{3+}*
TcO(OH)2	IV	-568.2 ± 8.8	-	-	-	-572.47 ± 10.89	-	-	-	$TcO(OH)_2$(aq)
TcO4-	VII	-637.4 ± 7.6	-729.4 ± 7.6	199.6 ± 1.5	-15 ± 8	-637.4 ± 7.6	-729.4 ± 7.6	199.6 ± 1.5	-15 ± 8	TcO_4^-

Name	Redox	TDB Version 12/07		TDB 2020		
		$\log_{10}\beta°$	$\Delta_r H_m°$ [kJ · mol^{-1}]	$\log_{10}\beta°$	$\Delta_r H_m°$ [kJ · mol^{-1}]	Reaction
TcO+2	IV	< 4	-	-	-	$TcO(OH)_2$(aq) + 2 H^+ ⇌ TcO^{2+} + 2 H_2O(l)
TcO(OH)+	IV	2.5 ± 0.3	-	-	-	$TcO(OH)_2$(aq) + H^+ ⇌ $TcO(OH)^+$ + H_2O(l)
TcO(OH)3-	IV	-10.9 ± 0.4	-	-10.92 ± 0.17	-	$TcO(OH)_2$(aq) + H_2O(l) ⇌ $TcO(OH)_3^-$ + H^+
Tc2O2(OH)2+2	IV	-	-	12.99 ± 0.41	-	2 $TcO(OH)_2$(aq) + 2 H^+ ⇌ $Tc_2O_2(OH)_2^{2+}$ + 2 H_2O(l)
TcCO3(OH)2(aq)	IV	19.3 ± 0.3	-	19.3 ± 0.3	-	$TcO(OH)_2$(aq) + CO_3^{2-} + 2H^+ ⇌ $TcCO_3(OH)_2$(aq) + H_2O(l)
TcCl6-2	IV	-	-	-2.08 ± 1.29	-	$TcCl_5^-$ + Cl^- ⇌ $TcCl_6^{2-}$
TcCl5-	IV	-	-	-3.53 ± 1.29	-	$Tc_2OCl_{10}^{4-}$ + 2 H^+ ⇌ 2 $TcCl_5^-$ + H_2O(l)
Tc2OCl10-4	IV	-	-	-0.4 ± 1.1	-	$Tc_2O_2(OH)_2^{2+}$ + 10 Cl^- + 4 H^+ ⇌ $Tc_2OCl_{10}^{4-}$ + 3 H_2O(l)
TcCO3(OH)3-	IV	11.0 ± 0.6	-	11.0 ± 0.6	-	$TcO(OH)_2$(aq) + CO_3^{2-} + H^+ ⇌ $TcCO_3(OH)_3^-$
TcO4-	VII	-29.4 ± 0.8	-	-30.17 ± 1.36	-	$TcO(OH)_2$(aq) + H_2O(l) ⇌ TcO_4^- + 4 H^+ + 3 e^-

Name	Redox	TDB Version 12/07		TDB 2020		
		$\log_{10}K_{s,0}°$	$\Delta_r H_m°$ [kJ · mol^{-1}]	$\log_{10}K_{s,0}°$	$\Delta_r H_m°$ [kJ · mol^{-1}]	Reaction
TcO2:1.6H2O	IV	-8.4 ± 0.5	-	-	-	TcO_2·1.6H_2O(s) ⇌ $TcO(OH)_2$(aq) + 0.6 H_2O(l)
TcO2(am, hyd, fresh)	IV	-	-	-7.66 ± 1.22	-	TcO_2(am, hyd, fresh) + H_2O(l) ⇌ $TcO(OH)_2$(aq)
TcO2(am, hyd, aged)	IV	-	-	-8.72 ± 0.40	-	TcO_2(am, hyd, aged) + H_2O(l) ⇌ $TcO(OH)_2$(aq)

Tab. 28-2: Selected SIT ion interaction coefficients $\varepsilon_{j,k}$ [kg · mol^{-1}] for technetium species.

Data included in TDB 2020 are taken from Grenthe et al. (2020). Own data estimates based on charge correlations (see Section 1.5.3) are shaded. Supplemental data are in italics.

j k → ↓	**Cl^-** $\varepsilon_{j,k}$ [kg · mol^{-1}]	**ClO_4^-** $\varepsilon_{j,k}$ [kg · mol^{-1}]	**NO_3^-** $\varepsilon_{j,k}$ [kg · mol^{-1}]	**Li^+** $\varepsilon_{j,k}$ [kg · mol^{-1}]	**Na^+** $\varepsilon_{j,k}$ [kg · mol^{-1}]	**K^+** $\varepsilon_{j,k}$ [kg · mol^{-1}]
Tc+3	*0.25 ± 0.10*	*0.6 ± 0.1*	-	*0*	*0*	*0*
TcO(OH)2(aq)	0	0	0	0	0	0
TcO(OH)3-	0	0	0	-	-0.08 ± 0.04	-
Tc2O2(OH)2+2	-0.43 ± 0.11	0.4 ± 0.1	-	0	0	0
TcCl6-2	0	0	0	-	-0.10 ± 0.10	-
TcCl5-	0	0	0	-	-0.05 ± 0.10	-
Tc2OCl10-4	0	0	0	-	0.89 ± 0.40	-
TcCO3(OH)2	0	0	0	0	0	0
TcCO3(OH)3-	0	0	0	-	-0.05 ± 0.1	-
TcO4-	0	0	0	-	-0.05 ± 0.1	-

28.5 References

Grenthe, I., Gaona, X., Plyasunov, A.V., Rao, L., Runde, W.H., Grambow, B., Konings, R.J.M., Smith, A.L. & Moore, E.E. (2020): Second Update on the Chemical Thermodynamics of Uranium, Neptunium, Plutonium, Americium and Technetium. Chemical Thermodynamics, Vol. 14. OECD Publications, Paris, France, 1503 pp.

Guillaumont, R., Fanghänel, T., Fuger, J., Grenthe, I., Neck, V., Palmer, D.A. & Rand, M.H. (2003): Update on the Chemical Thermodynamics of Uranium, Neptunium, Plutonium, Americium and Technetium. Chemical Thermodynamics, Vol. 5. Elsevier, Amsterdam, 919 pp.

Hess, N.J., Xia, Y., Rai, D. & Conradson, S.D. (2004): Thermodynamic model for the solubility of $TcO_2 \cdot xH_2O$(am) in the aqueous Tc(IV)-Na^+-Cl^--H^+-OH^--H_2O system. J. Solution Chem., 33, 199-226.

Hummel, W., Berner, U., Curti, E., Pearson, F.J. & Thoenen, T. (2002): Nagra/PSI Chemical Thermodynamic Data Base 01/01. Nagra Technical Report NTB 02-16. Also published by Universal Publishers/uPublish.com, Parkland, Florida, USA.

Rard, J.A., Rand, M.H., Anderegg, G. & Wanner, H. (1999): Chemical Thermodynamics of Technetium. Chemical Thermodynamics, Vol. 3. Elsevier, Amsterdam, 542 pp.

Thoenen, T., Hummel, W., Berner, U. & Curti, E. (2014): The PSI/Nagra Chemical Thermodynamic Database 12/07. Technical Report, PSI Bericht Nr. 14-04, Paul Scherrer Institut, Villigen, Switzerland, 416 pp.

29 Tin

29.1 Introduction

The chemical thermodynamic data for tin selected by Pearson et al. (1992) for their Nagra Thermochemical Data Base 05/92 (TDB 05/92) were taken as a block of data from the HATCHES 3.0 database (Cross & Ewart 1991). These data were discarded by Hummel et al. (2002) for the Nagra/PSI Chemical Thermodynamic Data Base 01/01 (TDB 01/01) and replaced with data from an own review that was based on the review by Lothenbach et al. (1999). Thoenen et al. (2014) accepted these data for the PSI/Nagra Chemical Thermodynamic Data Base 12/07 (TDB 12/07) and no new data were evaluated in anticipation of OECD NEA's review "Chemical Thermodynamics of Tin" (Gamsjäger et al. 2012) which was published after the cut-off date for inclusion into TDB 12/07. This NEA volume now serves as an excellent basis for a review of the tin data to be included in the PSI Chemical Thermodynamic Database 2020 (TDB 2020).

Note that not all values recommended by Gamsjäger et al. (2012) were considered for our database since the NEA reviews (unlike our database) are not restricted to data relevant for radioactive waste management or even environmental modelling in general. We tried to exclude from our database all phases and complexes which most probably will never be relevant in low-temperature and low-salinity environmental systems. The excluded data are listed in Tab. 29.9-1 and the selected data in Tab. 29.9-2.

The notation of formulae and symbols used in this text follows the NEA recommendations.

29.1.1 SIT

NEA chose the specific ion interaction theory (SIT) for the extrapolation of experimental data to zero ionic strength, see, e.g., Grenthe et al. (1997), an approach which is also adopted for TDB 2020 (as has been for all its predecessors). When referring to ion interaction coefficients recommended by NEA, we took those from Tab. B.3 in Lemire et al. (2013). Gamsjäger et al. (2012) explicitly considered the formation of chloride complexes with Sn^{2+} and Sn^{4+}. If equilibrium constants of reactions with tin species are determined in solutions with chloride salts as background electrolytes, the equilibrium constants must be corrected for the formation of the tin chloride complexes. The ion interaction coefficients for cationic Sn species with Cl^- can then be approximated by the corresponding interaction coefficients with ClO_4^- (see Hummel et al. 2005, Chapter V.4.). Likewise, if ion interaction coefficients for cationic Sn species with Cl^- are not known, they can be approximated by equating them to the corresponding interaction coefficients with ClO_4^-.

Due to a lack of experimental data, several ion interaction coefficients for cationic Sn species with ClO_4^- and for anionic Sn species with Na^+ are unknown. We filled these gaps by applying the estimation method described in Section 1.5.3, which is based on a statistical analysis of published SIT ion interaction coefficients and which allows the estimation of such coefficients for the interaction of cations with Cl^- and ClO_4^-, and for the interaction of anions with Na^+ from the charge of the considered cations or anions.

Ion interaction coefficients of neutral tin species with background electrolytes were assumed to be zero.

The ion interaction coefficients for tin species selected for TDB 2020 are listed in Tab. 29.9-3.

As noted, e.g., by Grenthe et al. (2013), the specific ion interaction coefficients are not strictly constant. They may vary slightly as a function of ionic strength. The variation depends on the charge and is often negligible, as is usually the case for 1:1, 1:2, and 2:1 electrolytes for molalities lower than 3.5 mol · kg^{-1} (Grenthe et al. 2013). To cope with variations of ε with ionic strength, Ciavatta (1980) proposed the use of

$$\varepsilon = \varepsilon_1 + \varepsilon_2 \log_{10} I_m$$

in a footnote to a table without any further explanation or theoretical justification. He applied this expression in all cases where the uncertainties in the specific interaction coefficients exceeded ± 0.03 kg · mol^{-1}. This expression was also used in several cases in NEA reviews, see, e.g., Lemire et al. (2013)[68], but Grenthe et al. (2020) remarked that "even if the value of ε calculated in this way describes the variation with ionic strength slightly better than a constant value, this equation has no theoretical basis; ε is a fitting parameter and the term $\varepsilon_2 \log_{10} I_m$ goes to minus infinity at the limiting value $I_m = 0$. This expression for the composition dependence of ε should be avoided, even though the term $\varepsilon \cdot m = (\varepsilon = \varepsilon_1 + \varepsilon_2 \log_{10} I_m) \cdot m$ (in the calculation of activity coefficients) is zero at $I_m = 0$. There may be cases where reviewers may still want to use [$\varepsilon = \varepsilon_1 + \varepsilon_2 \log_{10} I_m$] to describe ionic strength variation of the interaction parameters, but the rationale behind this should then be described". For these reasons, we did not use this equation in TDB 2020.

As an alternative, Grenthe et al. (2013), suggested the use of

$$\varepsilon = \varepsilon_1 + \varepsilon_{1.5} I_m^{1/2}$$

with the well-behaved property that $\varepsilon \rightarrow \varepsilon_1$ as $I_m \rightarrow 0$. This expression is the consequence of a virial expansion of the mean-activity coefficient $\gamma_\pm$ (in this case for a binary electrolyte with charge z_+ and z_-), see Grenthe et al. (1997, p. 347), truncated after the term with $I_m^{3/2}$ (the classical SIT equation is truncated one term earlier)

$$\log_{10} \gamma_\pm = -(A|z_+ z_-|I_m^{0.5}) / (1 + 1.5\, I_m^{0.5}) + \varepsilon_1 I_m + \varepsilon_{1.5} I_m^{1.5}$$

where the last two terms can be written as $\varepsilon I_m = (\varepsilon_1 + \varepsilon_{1.5} I_m^{0.5}) I_m$. We also did not use this equation in TDB 2020.

29.2 Elemental tin (β-tin or white tin)

Solid tin is found in two forms. White tin or β-tin, the allotrope stable at standard state conditions (298.15 K and 1 bar), is a metal with a tetragonal crystal structure. At lower temperatures it is transformed to the cubic grey tin or α-tin, which is not a metal but a semiconductor (Cornelius et al. 2017). The transition temperature is around 13 °C, but the transformation is sluggish and white tin can persist to temperatures as low as -30 to -40 °C, where the transformation rate reaches a maximum (Cornelius et al. 2017). The transformation from white to grey tin is accompanied by a 27% volume increase, the grey tin product is structurally weak and readily decomposes into a

[68] $\varepsilon = \varepsilon_1 + \varepsilon_2 \log_{10} I_m$ was used by Lemire et al. (2013), e.g., in the determination of $\varepsilon(Fe^{3+}, Cl^-)$, $\varepsilon(Fe^{3+}, ClO_4^-)$, $\varepsilon(FeOH^{2+}, ClO_4^-)$, $\varepsilon(FeCl^{2+}, Cl^-)$, and $\varepsilon(FeCl^{2+}, ClO_4^-)$.

powder, referred to as tin pest (Cornelius et al. 2017). Gamsjäger et al. (2012) selected thermodynamic data for grey tin, which we chose not to include in TDB 2020, since grey tin is not relevant for the modelling of geochemical processes taking place at room temperature and above.

For white tin Gamsjäger et al. (2012) selected

$$S_m°(\text{Sn, } \beta, 298.15\ \text{K}) = (51.18 \pm 0.08)\ \text{J} \cdot \text{K}^{-1} \cdot \text{mol}^{-1}$$

taken from CODATA (Cox et al. 1989) and

$$C_{p,m}°(\text{Sn, } \beta, 298.15\ \text{K}) = (27.11 \pm 0.08)\ \text{J} \cdot \text{K}^{-1} \cdot \text{mol}^{-1}$$

which are both included in TDB 2020.

Gamsjäger et al. (2012) also selected the heat capacity function

$$C_{p,m}°(\text{Sn, } \beta, 298.15\ \text{K} - 505\ \text{K})/\text{J} \cdot \text{K}^{-1} \cdot \text{mol}^{-1} =$$

$$34.297 - 2.9957 \times 10^{-2}\ T/\text{K} + 5.0794 \times 10^{-5}\ (\text{T/K})^2 - 2.461 \times 10^{5}\ (\text{T/K})^{-2}$$

This function is not included in TDB 2020 and is reported here for information only.

29.3 Tin aquo ions

Tin has two main oxidation states in aqueous solution, Sn^{2+} and Sn^{4+}, but the redox equilibrium between these two simple tin aquo ions is not very well known. For this reason, Sn^{2+} and Sn^{4+} were considered as redox decoupled in TDB 01/01 and TDB 12/07 and no thermodynamic data were selected for the redox reaction linking Sn^{2+} with Sn^{4+}. During their review, Gamsjäger et al. (2012) also recognized that the existing thermodynamic data on this redox couple were far from reliable and even carried out their own experiments to fill this critical data gap (Gajda et al. 2009).

29.3.1 Sn^{2+}

CODATA (Cox et al. 1989) recommended $\Delta_f H_m°(Sn^{2+}, 298.15\ \text{K}) = -(8.9 \pm 1.0)\ \text{kJ} \cdot \text{mol}^{-1}$ and $S_m°(Sn^{2+}, 298.15\ \text{K}) = -(16.7 \pm 4.0)\ \text{J} \cdot \text{K}^{-1} \cdot \text{mol}^{-1}$ as key values for Sn^{2+}, where the latter was calculated from their selected $\Delta_f G_m°(Sn^{2+}, 298.15\ \text{K}) = -(27.60 \pm 0.40)\ \text{kJ} \cdot \text{mol}^{-1}$ and their selected $\Delta_f H_m°(Sn^{2+}, 298.15\ \text{K})$. Gamsjäger et al. (2012) decided to carry out their own evaluation.

They selected

$$\Delta_f G_m°(Sn^{2+}, 298.15\ \text{K}) = -(27.39 \pm 0.30)\ \text{kJ} \cdot \text{mol}^{-1}$$

based on 3 studies that determined the standard potential of the reaction $Sn^{2+} + H_2g \rightleftharpoons Sn(\beta) + 2\ H^+$, and a study each that determined the equilibrium constant of the reaction $Sn(\beta) + Pb^{2+} \rightleftharpoons Pb(cr) + Sn^{2+}$ or the standard half-cell potential of the reaction $Sn^{2+} + 2\ e^- \rightleftharpoons Sn(\beta)$. Gamsjäger et al. (2012) selected the weighted average of $-(27.39 \pm 0.08)$ kJ · mol^{-1} but increased the uncertainty to ± 0.30 kJ · mol^{-1}. This value overlaps with the value selected by CODATA.

For the enthalpy of formation of Sn^{2+}, Gamsjäger et al. (2012) relied on two calorimetric measurements and selected the weighted mean

$$\Delta_f H_m°(Sn^{2+}, 298.15\ K) = -(9.42 \pm 1.24)\ kJ \cdot mol^{-1}$$

which also overlaps with the corresponding CODATA value. From the selected $\Delta_f G_m°(Sn^{2+}, 298.15\ K)$ and $\Delta_f H_m°(Sn^{2+}, 298.15\ K)$ then follows (keeping in mind that G = H - TS) $\Delta_f S_m°(Sn^{2+}, 298.15\ K)$. $S_m°(Sn^{2+}, 298.15\ K)$, finally, can be calculated from

$$S_m°(Sn^{2+}, 298.15\ K) = \Delta_f S_m°(Sn^{2+}, 298.15\ K) - S_m°(H_2, g, 298.15\ K) + S_m°(Sn, \beta, 298.15\ K)$$

with $S_m°(Sn, \beta, 298.15\ K)$ selected above and the NEA-selected $S_m°(H_2, g, 298.15\ K) = (130.680 \pm 0.003)\ J \cdot K^{-1} \cdot mol^{-1}$. Hence

$$S_m°(Sn^{2+}, 298.15\ K) = -(19.2 \pm 4.3)\ J \cdot K^{-1} \cdot mol^{-1}$$

The values for $\Delta_f G_m°(Sn^{2+}, 298.15\ K)$, $\Delta_f H_m°(Sn^{2+}, 298.15\ K)$, and $S_m°(Sn^{2+}, 298.15\ K)$ selected by Gamsjäger et al. (2012) are included in TDB 2020.

Gamsjäger et al. (2012) used SIT for the determination of $\Delta\varepsilon$ for the reaction

$$Sn^{2+} + H_2g \rightleftharpoons Sn(\beta) + 2\ H^+$$

from standard potential measurements reported by a study at 15, 25, and 35 °C in 1.0, 2.0, 3.0, and 4.0 M $NaClO_4$. At 25 °C they obtained $\Delta\varepsilon = (0.094 \pm 0.006)$ kg · mol^{-1}, which leads, together with $\varepsilon(H^+, ClO_4^-) = (0.14 \pm 0.02)$ kg · mol^{-1}, to

$$\varepsilon(Sn^{2+}, ClO_4^-) = (0.19 \pm 0.04)\ kg \cdot mol^{-1}$$

This value is included in TDB 2020.

Gamsjäger et al. (2012) also used SIT for a "manually controlled" refinement of formation constants for $SnCl^+$, $SnCl_2(aq)$, and $SnCl_3^-$ – including the simultaneous evaluation of the corresponding values for $\Delta\varepsilon$ and of $\varepsilon(Sn^{2+}, Cl^-)$ – determined from measured potential changes of $Sn^{2+} + 2\ e^- \rightleftharpoons Sn(\beta)$ as a function of chloride concentration (Prytz 1928)[69]. They obtained the following parameters: $\log_{10}\beta_1°(298.15\ K) = 1.34$, ($\Delta\varepsilon(KCl) = -0.10$ kg · mol^{-1}), $\log_{10}\beta_2°$

[69] Gamsjäger et al. (2012) gave no information on how this "manually controlled" refinement was achieved.

(298.15 K) = 2.13, ($\Delta\varepsilon$(KCl) = -0.14 kg · mol^{-1}), $\log_{10}\beta_3°$(298.15 K) = 1.99, ($\Delta\varepsilon$(KCl) = -0.19 kg · mol^{-1}), and ε(Sn^{2+}, Cl^-) = 0.14 kg · mol^{-1}. Considering the difficulties in refining the experimental data (Prytz 1928 used a mixture of electrolytes, HCl and KCl, to increase the chloride concentrations and only few experimental data were available), Gamsjäger et al. (2012) assigned an uncertainty of ± 0.10 to ε(Sn^{2+}, Cl^-) and selected

$$\varepsilon(Sn^{2+}, Cl^-) = (0.14 \pm 0.10) \text{ kg} \cdot \text{mol}^{-1}$$

This value is also included in TDB 2020. Note, that it overlaps within the uncertainty with the selected value ε(Sn^{2+}, ClO_4^-) = (0.19 ± 0.04) kg · mol^{-1}. This observation provides some support to the approximation $\varepsilon(M^{n+}, Cl^-) \approx \varepsilon(M^{n+}, ClO_4^-)$ recommended in Section 29.1.1. The values for $\log_{10}\beta_1°$(298.15 K), $\log_{10}\beta_2°$(298.15 K), and $\log_{10}\beta_3°$(298.15 K) are within the uncertainties of the values selected by Gamsjäger et al. (2012), see Section 29.5.1.2.1.

The equilibrium constant for the redox reaction

$$Sn(\beta) \rightleftharpoons Sn^{2+} + 2\ e^-$$

$$\log_{10}K_s°(298.15\text{ K}) = (4.80 \pm 0.05)$$

follows from the selected $\Delta_f G_m°$(Sn^{2+}, 298.15 K) = -(27.39 ± 0.30) kJ · mol^{-1} and from $\Delta_f G_m°$(Sn, β, 298.15 K) = $\Delta_f G_m°$(e^-, 298.15 K) = 0.

29.3.2 Sn^{4+}

The determination of thermodynamic data for Sn^{4+} is hampered by the fact that Sn^{4+} in aqueous solution has a very large tendency to hydrolyse. According to Fatouros et al. (1978), the complete suppression of Sn(IV) hydrolysis can only be achieved in at least about 5 M $HClO_4$. For this reason, Sn^{4+} cannot be expected to be present in common natural waters in measurable quantities.

Gamsjäger et al. (2012) could find only one study (Prytz 1934) that determined $\Delta_f G_m°$(Sn^{4+}) directly by the potentiometric investigation of the reaction

$$Sn^{4+} + 2\ H_2g \rightleftharpoons Sn(\beta) + 4\ H^+$$

Gamsjäger et al. (2012) did not accept the results of this study, because the molality of $HClO_4$ used in the experiment (0.5 – 1.0 mol · kg^{-1}) was too low to suppress any hydrolysis of Sn(IV) and also because in the chosen experimental setup, spontaneous oxidation of Sn(β) to Sn^{2+} by Sn^{4+} is to be expected.

During the preparation of their review, Gamsjäger et al. (2012) found only four potentiometric studies that investigated the reaction

$$Sn^{4+} + H_2g \rightleftharpoons Sn^{2+} + 2\ H^+$$

and concluded that all studies suffered from major deficiencies: Forbes & Bartlett (1914) measured in the acidity range from 0.5 – 5.4 mol · kg^{-1} HCl. At least in the lower part of this range Sn(IV) hydroxide complexes are stable, making it impossible to correctly estimate the molality of Sn^{4+}. In addition, Forbes & Bartlett (1914) assumed that Sn(II) and Sn(IV) chloride complexes vanish as the concentration of chloride goes to zero. According to Gamsjäger et al. (2012), however, they do so in a highly non-linear way, which was not considered by Forbes & Bartlett (1914).

The measurements by Huey & Tartar (1934) in 0.10 to 2.02 M HCl were also not accepted by Gamsjäger et al. (2012), however, no specific reasons were given except for an entry in their Tab. VI-6, "Sn(IV), Sn(II) chlorido and hydroxido complexes ?".

Despic et al. (1972) obtained their measurements in either 4 M HCl or 1 M Na_2SO_4 + 1 M H_2SO_4. The results were not accepted by Gamsjäger et al. (2012) because the ionic strength was not constant during the experiments, Na_2SO_4 + H_2SO_4 cannot be considered an inert electrolyte, and the stability constants of the chloride complexes were derived in a doubtful manner.

Vasil'ev et al. (1979) carried out experiments in 2 – 4 M $HClO_4$ solutions containing $SnCl_2$ and $SnCl_4$. They neglected the formation of Sn(II) and Sn(IV) complexes, since in previous experiments (Vasil'ev & Glavina 1976 and 1977) they had shown that $SnCl_4$ and $(NH_4)_2SnCl_6$ appeared to dissociate completely in 0.6 – 2.0 m $HClO_4$. This conclusion is in contradiction to the findings of Fatouros et al. (1978), who studied the formation of Sn(IV) complexes in 5 M $HClO_4$, where the hydrolysis of Sn^{4+} can be expected to be completely suppressed, and found the entire sequence of chloride complexes from $SnCl^{3+}$ to $SnCl_6^{2}$. Gamsjäger et al. (2012) argued that these contradictory findings can be explained by the inability of the cells used by Vasil'ev & Glavina (1976, 1977) to distinguish between hydrolysis (which certainly takes place in the concentration range 0.6 – 2.0 m $HClO_4$) and dissociation.

Because of these deficiencies, none of the studies by Forbes & Bartlett (1914), Huey & Tartar (1934), Despic et al. (1972), and Vasil'ev et al. (1979) were trusted by Gamsjäger et al. (2012). This prompted a part of the NEA review team (Gajda et al. 2009) to carry out their own electrochemical measurements in strongly acidic solutions. The experiments were performed in mixed HCl/$HClO_4$ solutions of the composition (I - 1) M $HClO_4$ + 1 M HCl, with I = 4, 5, 6 M, to which were added $SnCl_2$ and $SnCl_4$. In order to evaluate the experimental data (i.e., to determine the concentrations of free Sn^{2+} and free Sn^{4+}), the conditional stability constants for the Sn(II) and Sn(IV) chloride complexes at the given ionic strengths were required. Since a mixed background electrolyte was used, the true conditional stability constants had to be approximated with known constants in pure background electrolytes. For Sn(II), the dataset (stability constants and ion interaction coefficients) selected by Gamsjäger et al. (2012) for $NaClO_4$ (see Section 29.5.1.2.1) was used. For Sn(IV), Gajda et al. (2009) carried out their own experiments in $HClO_4$ to determine the required stability constants and ion interaction coefficients (see Section 29.5.1.2.2). In order to evaluate the measured potential values as a function of $\log_{10}([Sn^{4+}{}_{free}]/[Sn^{2+}{}_{free}])$, Gajda et al. (2009) also needed to determine $\log_{10}\gamma(H^+)$ as a function of the concentration of ClO_4^-. The isopiestic and partial vapor measurements by Haase et al. (1965) on $HClO_4$ solutions were evaluated by Gajda et al. (2009) using SIT. Since at $I_m > 3$, the activity coefficients derived from the linear SIT equation

$$\log_{10}\gamma(H^+) = -D + \varepsilon(H^+, ClO_4^-)\, m(ClO_4^-)$$

deviate from the experimental values, Gajda et al. (2009) used the non-linear SIT formulation (see Section 29.1.1)

$$\log_{10}\gamma(H^+) = -D + \varepsilon_1(H^+, ClO_4^-)\, m(ClO_4^-) + \varepsilon_{1.5}(H^+, ClO_4^-)\, m(ClO_4^-)^{1.5}$$

From the analysis of their data, Gajda et al. (2009) finally obtained

$$E°(Sn^{4+}, Sn^{2+}, 298.15\ K) = (0.384 \pm 0.020)\ V$$

which was selected by Gamsjäger et al. (2012). This is equivalent to

$$Sn^{2+} + 2\ H^+ \rightleftharpoons Sn^{4+} + H_2g$$

$$\log_{10}K°(298.15\ K) = -12.98 \pm 0.68$$

which is included in TDB 2020. From this value and the selected $\Delta_f G_m°(Sn^{2+}, 298.15\ K) = -(27.39 \pm 0.30)\ kJ \cdot mol^{-1}$ then follows the selected

$$\Delta_f G_m°(Sn^{4+}, 298.15\ K) = -(46.7 \pm 3.9)\ kJ \cdot mol^{-1}$$

which is included in TDB 2020.

Due to the experimental limitations of high ionic strength (leading to a long extrapolation to zero ionic strength) and mixed background electrolytes, Gamsjäger et al. (2012) were only able to provide a rough estimate for the ion interaction coefficient

$$\varepsilon(Sn^{4+}, ClO_4^-) = (0.7 \pm 0.2)\ kg \cdot mol^{-1}$$

which is included in TDB 2020 as well as the estimate (see Section 29.1.1)

$$\varepsilon(Sn^{4+}, Cl^-) \approx \varepsilon(Sn^{4+}, ClO_4^-) = (0.7 \pm 0.2)\ kg \cdot mol^{-1}$$

Based on a modified Powell-Latimer linear correlation between ionic entropies and characteristic parameters (combining crystallographic radii, molar masses and electrical charges) for 33 monatomic cations, Gamsjäger et al. (2012) estimated

$$S_m°(Sn^{4+}, 298.15\ K) = -(472.5 \pm 20.5)\ J \cdot K^{-1} \cdot mol^{-1}$$

from the crystallographic radius, molar mass and electrical charge of Sn^{4+}. Gamsjäger et al. (2012) did not select this value (since according to the NEA guidelines only experimentally determined values can be selected). We include this estimate as supplemental datum into TDB 2020, as well as

$$\Delta_f H_m°(Sn^{4+}, 298.15\ K) = -(31.5 \pm 7.3)\ kJ \cdot mol^{-1}$$

calculated from the selected $\Delta_f G_m°(Sn^{4+}, 298.15\ K)$ and $\Delta_f S_m°(Sn^{4+}, 298.15\ K) = -(262.3 \pm 20.5)\ J \cdot K^{-1} \cdot mol^{-1}$ which itself can be calculated from the selected $S_m°(Sn^{4+}, 298.15\ K)$, $S_m°(H_2, g, 298.15\ K) = (130.680 \pm 0.003)\ J \cdot K^{-1} \cdot mol^{-1}$, and $S_m°(Sn, \beta, 298.15\ K) = (51.18 \pm 0.08)\ J \cdot K^{-1} \cdot mol^{-1}$, by virtue of $\Delta_f S_m°(Sn^{4+}) = S_m°(Sn^{4+}) + 2\ S_m°(H_2, g) - S_m°(Sn, \beta)$.

29.4 Tin oxygen and hydrogen compounds and complexes

29.4.1 Aqueous tin hydroxide complexes

29.4.1.1 Aqueous tin(II) hydroxide complex

Sn(II) has a strong tendency to hydrolyse and forms several hydroxide complexes, depending on the pH and the tin ion concentration. According to the review by Gamsjäger et al. (2012), there are only a few reports available on the equilibrium properties of Sn(II) hydroxide complexes, probably due to the relative ease of Sn(II) oxidation and to precipitation at a low degree of hydrolysis. There are some discrepancies among various authors concerning the nature of the Sn(II) hydroxide complexes forming under acidic conditions. $SnOH^+$ was identified in 8 from 9 studies. At total dissolved Sn(II) concentrations > 0.1 mM, $Sn_3(OH)_4^{2+}$ is the dominating species. Two studies also reported the formation of $Sn_2(OH)_2^{2+}$, however, Gamsjäger et al. (2012) considered this as unjustified because this species made up at most a few percent of the total dissolved Sn(II) concentrations. In the neutral pH range, $Sn(OH)_2(aq)$ is the dominating species at a very low solubility. Under alkaline conditions, $Sn(OH)_3^-$ dominates.

According to Gamsjäger et al. (2012), the formation constants reported for $SnOH^+$ at I = 3 M $NaClO_4$ are remarkably consistent. For lower ionic strengths, however, only the data from one study (Pettine et al. 1981) can be used to determine the dependence of $\log_{10}{}^*\beta_{1,1}$ on ionic strength and the results of three other studies were rejected. The formation constants by Pettine et al. (1981) were determined by differential pulse anodic stripping voltammetry in $NaNO_3$. Nitrate forms weak complexes with Sn(II), see Section 29.7.1.1, and their formation cannot be ruled out. Since the experimental data by Pettine et al. (1981) were only reported graphically, they could not be re-evaluated by Gamsjäger et al. (2012), and a correct allowance for potential nitrate complexes was not possible. They were therefore neglected, but their potential presence was accounted for by increasing the uncertainties of the recalculated formation constants of $SnOH^+$. From an SIT analysis of the data at 0.1, 0.5, and 1.0 M $NaNO_3$, Gamsjäger et al. (2012) obtained the selected

$$Sn^{2+} + H_2O(l) \rightleftharpoons SnOH^+ + H^+$$

$$\log_{10}{}^*\beta_{1,1}°(298.15\ K) = -(3.53 \pm 0.40)$$

assuming negligible variation between 20 (experimental temperature) and 25 °C. The resulting $\Delta\varepsilon = -(0.13 \pm 0.60)\ kg \cdot mol^{-1}$ in $NaNO_3$ cannot be used to derive $\varepsilon(SnOH^+, NO_3^-)$ since the value for $\varepsilon(Sn^{2+}, NO_3^-)$ is not known. However, Gamsjäger et al. (2012) used the selected value for $\log_{10}{}^*\beta_{1,1}°(298.15\ K)$ and the accepted values for $\log_{10}{}^*\beta_{1,1}$ in 3 M $NaClO_4$ (-3.68 ± 0.10, -3.63 ± 0.10, -3.70 ± 0.20) to derive $\Delta\varepsilon = -(0.12 \pm 0.12)\ kg \cdot mol^{-1}$ in $NaClO_4$ media , from which follows

$$\varepsilon(SnOH^+, ClO_4^-) = -(0.07 \pm 0.13)\ kg \cdot mol^{-1}$$

using the selected values for $\varepsilon(Sn^{2+}, ClO_4^-)$ and $\varepsilon(H^+, ClO_4^-)$, see Tab. 29.9-3 and 29.9-5, respectively. Estimating $\varepsilon(SnOH^+, Cl^-)$ with $\varepsilon(SnOH^+, ClO_4^-)$, see Section 29.1.1, results in

$$\varepsilon(SnOH^+, Cl^-) \approx \varepsilon(SnOH^+, ClO_4^-) = -(0.07 \pm 0.13)\ kg \cdot mol^{-1}$$

These values for $\log_{10}{}^*\beta_{1,1}°(298.15\ K)$, $\varepsilon(SnOH^+, ClO_4^-)$, and $\varepsilon(SnOH^+, Cl^-)$ are included in TDB 2020.

There appears to be only one reliable experimental study on the formation of $Sn(OH)_2(aq)$. Gamsjäger et al. (2012) accepted the formation constants obtained by Pettine et al. (1981) in 0.1, 0.5, and 1.0 M $NaNO_3$. As in the case of $SnOH^+$, Gamsjäger et al. (2012) used SIT to extrapolate the constants to $I = 0$, neglecting the potential formation of nitrate complexes and assuming that the temperature correction from 20 to 25 °C is negligible. This resulted in the selected

$$Sn^{2+} + 2\ H_2O(l) \rightleftharpoons Sn(OH)_2(aq) + 2\ H^+$$

$$\log_{10}{}^*\beta_{2,1}°(298.15\ K) = -(7.68 \pm 0.40)$$

with $\Delta\varepsilon = -(0.31 \pm 0.60)\ kg \cdot mol^{-1}$, which cannot be used for deriving $\varepsilon(Sn(OH)_2(aq), NaNO_3(aq))$ since the value for $\varepsilon(Sn^{2+}, NO_3^-)$ is not known. We estimated

$$\varepsilon(Sn(OH)_2(aq), NaCl(aq)) \approx \varepsilon(Sn(OH)_2(aq), NaClO_4(aq)) \approx (0.0 \pm 0.1)\ kg \cdot mol^{-1}$$

see Section 29.1.1 and 1.5.3. These values for $\log_{10}{}^*\beta_{2,1}°(298.15\ K)$, $\varepsilon(Sn(OH)_2(aq), NaClO_4(aq))$, and $\varepsilon(Sn(OH)_2(aq), NaCl(aq))$ are included in TDB 2020.

For selecting the formation constant of $Sn(OH)_3^-$, Gamsjäger et al. (2012) relied on solubility experiments on the one hand, and on experiments using potentiometry or ion-sensitive electrodes on the other hand. Garrett & Heiks (1941) investigated the solubility of SnO(s) in acid (HCl) near neutral (H_2O) and alkaline (NaOH) solutions. At near neutral conditions, the solubility of SnO(s) can be expressed in terms of

$$SnO(s) + H_2O(l) \rightleftharpoons Sn(OH)_2(aq)$$

Since equilibrium constants for this reaction are nearly independent of ionic strength (assuming negligible interactions of $Sn(OH)_2(aq)$ with any cations or anions) the mean value of five solubility determinations in water, resulting in $\log_{10}(m_{Sn(II)}/mol \cdot kg^{-1}) = -5.30 \pm 0.13$, directly translates into

$$\log_{10}K_{s,2}°(298.15\ K) = -(5.30 \pm 0.13)$$

In alkaline solutions, SnO(s) dissolves according to

$$SnO(s) + OH^- + H_2O(l) \rightleftharpoons Sn(OH)_3^-$$

Gamsjäger et al. (2012) re-evaluated the experimental data by Garrett & Heiks (1941) using SIT and obtained

$$\log_{10}K_{s,3}°(298.15\ K) = -(0.84 \pm 0.02)$$

with $\Delta\varepsilon = (0.16 \pm 0.04)$ kg · mol^{-1}[70]. Combining this value with that selected for $\varepsilon(OH^-, Na^+) = (0.04 \pm 0.01)$ kg · mol^{-1}, see Tab. 29.9-5, results in $\varepsilon(Sn(OH)_3^-, Na^+) = (0.20 \pm 0.04)$ kg · mol^{-1}[71]. Gamsjäger et al. (2012) then combined $\log_{10}K_{s,2}°(298.15\ K)$ and $\log_{10}K_{s,3}°(298.15\ K)$, leading to

$$Sn(OH)_2(aq) + OH^- \rightleftharpoons Sn(OH)_3^-$$

$$\log_{10}K_3°(298.15\ K) = (4.46 \pm 0.13)$$[72]

Finally, Gamsjäger et al. (2012) combined this value with $\log_{10}{}^*\beta_{2,1}°(298.15\ K) = -(7.68 \pm 0.40)$, see above, and $pK_w°(298.15\ K) = 14.00$, resulting in

$$Sn^{2+} + 3\ H_2O(l) \rightleftharpoons Sn(OH)_3^- + 3\ H^+$$

$$\log_{10}{}^*\beta_{3,1}°(298.15\ K) = -(17.22 \pm 0.42)$$[73,74]

Gamsjäger et al. (2012) accepted this value as well as a value extrapolated to $I = 0$ with the Pitzer formalism from potentiometric measurements in 0.5 – 5.47 m NaOH and two values measured with ion sensitive electrodes in 3 M $NaClO_4$. From an SIT analysis of these values, Gamsjäger et al. (2012) obtained the selected

$$\log_{10}{}^*\beta_{3,1}°(298.15\ K) = -(17.00 \pm 0.60)$$[75]

(also included in TDB 2020) with

$$\Delta\varepsilon = (0.21 \pm 0.08)\ kg \cdot mol^{-1}$$

which corresponds to $\varepsilon(Sn(OH)_3^-, Na^+) = -(0.01 \pm 0.10)$ kg · mol^{-1} if the selected values for $\varepsilon(Sn^{2+}, ClO_4^-)$ and $\varepsilon(H^+, ClO_4^-)$, see Tab. 29.9-3 and 29.9-5, resp., are considered. Gamsjäger et al. (2012), however, selected

---

[70] Note that this value for $\Delta\varepsilon$ is reported by Gamsjäger et al. (2012) on p. 281, while on p. 283 it is reported as (0.190 ± 0.038) kg · mol^{-1}.

[71] With $\Delta\varepsilon = (0.190 \pm 0.038)$ kg · mol^{-1}, see the previous footnote, $\varepsilon(Sn(OH)_3^-, Na^+)$ would be 0.23 ± 0.04 kg · mol^{-1}.

[72] The uncertainty reported by Gamsjäger et al. (2012) is ± 0.01 on p.111 and ± 0.13 on p. 281.

[73] The uncertainty reported by Gamsjäger et al. (2012) is ± 0.40.

[74] Note that the explanations given by Gamsjäger et al. (2012) for how they arrived at $\log_{10}{}^*\beta_{3,1}°(298.15\ K)$ are rather obscure and the account given here is our own interpretation.

[75] The uncertainty of ± 0.24 was increased by Gamsjäger et al. (2012) to ± 0.60 in order to accommodate $\log_{10}{}^*\beta_{3,1}°(298.15\ K) = -(17.56 \pm 0.40)$ which they derived by a SIT analysis of re-evaluated stability constants determined by Pettine et al. (1981) in $NaNO_3$ media.

$\varepsilon(Sn(OH)_3^-, Na^+) = (0.22 \pm 0.03)$ kg · mol^{-1}

which they derived from $\Delta\varepsilon$ of the above-mentioned re-evaluation and SIT analysis of the experimental data by Garrett & Heiks (1941). Gamsjäger et al. (2012) considered this $\Delta\varepsilon$ more reliable than that obtained from their SIT analysis of the reaction $Sn^{2+} + 3\ H_2O(l) \rightleftharpoons Sn(OH)_3^- + 3\ H^+$. We also accept this value for inclusion in TDB 2020, despite the small discrepancies with $\varepsilon(Sn(OH)_3^-, Na^+) = (0.20 \pm 0.04)$ kg · mol^{-1} derived above and $\varepsilon(Sn(OH)_3^-, Na^+) = (0.23 \pm 0.04)$ kg · mol^{-1} derived in footnote *71*.

For the trinuclear complex $Sn_3(OH)_4^{2+}$, Gamsjäger et al. (2012) accepted three stability constants (from three publications) measured in 3 M $NaClO_4$ and one constant (from an additional publication) measured at 0.5 M $NaClO_4$. The SIT extrapolation resulted in the selected

$$3\ Sn^{2+} + 4\ H_2O(l) \rightleftharpoons Sn_3(OH)_4^{2+} + 4\ H^+$$

$$\log_{10}{}^*\beta_{4,3}^\circ(298.15\ K) = -(5.60 \pm 0.47)$$

with

$$\Delta\varepsilon = -(0.06 \pm 0.14)\ kg \cdot mol^{-1}$$

From this value, together with those selected for $\varepsilon(Sn^{2+}, ClO_4^-)$ and $\varepsilon(H^+, ClO_4^-)$, see Tab. 29.9-3 and 29.9-5, resp., then follows

$$\varepsilon(Sn_3(OH)_4^{2+}, ClO_4^-) = -(0.02 \pm 0.16)\ kg \cdot mol^{-1}$$

which leads to the estimate (see Section 29.1.1)

$$\varepsilon(Sn_3(OH)_4^{2+}, Cl^-) \approx \varepsilon(Sn_3(OH)_4^{2+}, ClO_4^-) = -(0.02 \pm 0.16)\ kg \cdot mol^{-1}$$

These values for $\log_{10}{}^*\beta_{4,3}^\circ(298.15\ K)$, $\varepsilon(Sn_3(OH)_4^{2+}, ClO_4^-)$, and $\varepsilon(Sn_3(OH)_4^{2+}, Cl^-)$ are included in TDB 2020.

29.4.1.2 Mixed tin(II) hydroxide complexes

The values for the stability constant of $SnOH^+$ determined in NaCl media are considerably higher than those determined in $NaNO_3$ and $NaClO_4$ (see Gamsjäger et al. 2012 and references therein). This may be explained by the possible formation of Sn(OH)Cl(aq). The stability constant ${}^*\beta_{1,1,Cl}$ for the reaction

$$Sn^{2+} + H_2O(l) + Cl^- \rightleftharpoons Sn(OH)Cl(aq) + H^+$$

is related to the stability constants of $SnOH^+$ measured in NaCl, ${}^*\beta_{1,1}(NaCl)$, and measured in $NaNO_3$ or $NaClO_4$, ${}^*\beta_{1,1}(NaNO_3/NaClO_4)$, by

$$*\beta_{1,1}(NaCl) = *\beta_{1,1}(NaNO_3/NaClO_4) + *\beta_{1,1,Cl}(NaCl)$$

(Pettine et al. 1981). Using this relationship, Gamsjäger et al. (2012) derived values for $\log_{10}*\beta_{1,1,Cl}$ based on the experimental data by Pettine et al. (1981) in 0.5 M NaCl and in 0.5 M $NaNO_3$ and by Djurdjević et al. (1995) in 3 M NaCl and in 3 M $NaNO_3$ and obtained $\log_{10}*\beta_{1,1,Cl}$(0.5 M NaCl) ≈ -3.2 and $\log_{10}*\beta_{1,1,Cl}$(3 M NaCl) ≈ -2.2. Gamsjäger et al. (2012) did not select any values for $*\beta_{1,1,Cl}$ since "the high uncertainty of the constants reported in [1995DJU/JEL] . . . does not allow to estimate reliably the thermodynamic equilibrium constant for [the above reaction]".

Hummel et al. (2002) selected for TDB 01/01

$$\log_{10}*\beta_{1,1,Cl}°(298.15\ K) = -(3.1 \pm 0.2)^{76}$$

which they derived from the experimental data obtained by Vanderzee & Rhodes (1952) in 3 M $NaClO_4$. Gamsjäger et al. (2012), however, did not accept the data by Vanderzee & Rhodes (1952) for Sn(OH)Cl(aq) and $SnOH^+$ (in contrast to those of the chloride complexes) and regarded them as tentative.

Since the experimental data by Vanderzee & Rhodes (1952) and Djurdjević et al. (1995) are uncertain, one is left with the experimental data by Pettine et al. (1981) who used differential pulse anodic stripping voltammetry to investigate the hydrolysis of Sn(II) in several ionic media ($NaNO_3$, NaCl, and artificial seawater) at 20 °C. These authors reported $\log_{10}*\beta_{1,1}$(0.5 M NaCl) = -(3.1 ± 0.2) and $\log_{10}*\beta_{1,1}$(0.5 M $NaNO_3$) = -(3.8 ± 0.2) which lead to $\log_{10}*\beta_{1,1,Cl}$(0.5 M NaCl) = -(3.2 ± 0.2). Pettine et al. (1981) remarked that this value "must only be considered to be a reasonable estimate" since "our measurements were not made over a wide range of Cl^- concentrations". We extrapolated $\log_{10}*\beta_{1,1,Cl}$(0.5 M NaCl) = -(3.2 ± 0.2) to $I = 0$ using SIT with $\Delta\varepsilon$ = -(0.10 ± 0.11) kg · mol^{-1} calculated from $\varepsilon(Sn^{2+}, Cl^-) \approx \varepsilon(Sn^{2+}, ClO_4^-)^{77}$ = (0.19 ± 0.04) kg · mol^{-1}, $\varepsilon(Cl^-, Na^+)$ = (0.03 ± 0.01) kg · mol^{-1}, $\varepsilon(H^+, Cl^-)$ = (0.12 ± 0.01) kg · mol^{-1}, and assuming ε(Sn(OH)Cl(aq), NaCl(aq)) ≈ (0.0 ± 0.1) kg · mol^{-1}. With ρ = 1.01177 dm^3 · kg^{-1} (conversion of molarity to molality, Grenthe & Puigdomènech 1997, Tab. II.4, p. 55), I_m = 0.505885 mol · kg^{-1}, a(H_2O) = 0.9833 (Gamsjäger et al. 2012, Tab. B-1, p. 441), Δz^2 = -4, and D = 0.509 $I_m^{-1/2}$ / (1 + 1.5 $I_m^{-1/2}$) = 0.17516, we obtained from

Note that this value reported by HUMMEL et al. (2002) is incorrect. They extrapolated $\log_{10}*\beta_{1,1,Cl}$(298.15 K, 3 M $NaClO_4$) = -(2.76 ± 0.11) to $I = 0$ with SIT using $\Delta\varepsilon$ = -(0.11 ± 0.06) kg · mol^{-1}. We tried to reproduce this extrapolation using the same $\Delta\varepsilon$, as well as ρ = 1.16776 dm^3 · kg^{-1} (conversion of molarity to molality, Grenthe & Puigdomènech 1997, Table II.4, p. 55)

---

76 Note that this value reported by HUMMEL et al. (2002) is incorrect. They extrapolated $\log_{10}*\beta_{1,1,Cl}$(298.15 K, 3 M $NaClO_4$) = -(2.76 ± 0.11) to $I = 0$ with SIT using $\Delta\varepsilon$ = -(0.11 ± 0.06) kg · mol^{-1}. We tried to reproduce this extrapolation using the same $\Delta\varepsilon$, as well as ρ = 1.16776 dm^3 · kg^{-1} (conversion of molarity to molality, Grenthe & Puigdomènech 1997, Table II.4, p. 55) and a(H_2O) = 0.8840 (GAMSJÄGER et al. 2012, Table B-1, p. 441). Thus, we obtained $\log_{10}*\beta_{1,1,Cl}°$(298.15 K) = -2.09 from $\log_{10}*\beta_{1,1,Cl}° = \log_{10}*\beta_{1,1,Cl} - \Delta z^2\ D - \log a(H_2O) + \Delta\varepsilon\ I_m$, where Δz^2 = -4 and D = 0.509 $I_m^{-1/2}$ / (1 + 1.5 $I_m^{-1/2}$) = 0.2502, with I_m = 3.50328 mol · kg^{-1}. Assuming a(H_2O) = 1 and neglecting the conversion from molarity to molality has practically no influence on the extrapolation and leads to $\log_{10}*\beta_{1,1,Cl}°$(298.15 K) = -2.11. Thus, the value of -3.1 ± 0.2 for $\log_{10}*\beta_{1,1,Cl}°$(298.15 K) should be replaced by -2.1 ± 0.2.

77 Note that this assumption is made because the formation of Sn(II) chloride complexes was explicitly taken into account by Pettine et al. (1981).

and a(H_2O) = 0.8840 (Gamsjäger et al. 2012, Table B-1, p. 441). Thus, we obtained $\log_{10}{}^*\beta_{1,1,Cl}^\circ$(298.15 K) = -2.09 from $\log_{10}{}^*\beta_{1,1,Cl}^\circ = \log_{10}{}^*\beta_{1,1,Cl} - \Delta z^2\, D - \log a(H_2O) + \Delta\varepsilon\, I_m$, where Δz^2 = -4 and $D = 0.509\, I_m^{-1/2} / (1 + 1.5\, I_m^{-1/2}) = 0.2502$, with I_m = 3.50328 mol · kg^{-1}. Assuming a(H_2O) = 1 and neglecting the conversion from molarity to molality has practically no influence on the extrapolation and leads to $\log_{10}{}^*\beta_{1,1,Cl}^\circ$(298.15 K) = -2.11. Thus, the value of -3.1 ± 0.2 for $\log_{10}{}^*\beta_{1,1,Cl}^\circ$(298.15 K) should be replaced by -2.1 ± 0.2.

$$\log_{10}{}^*\beta_{1,1,Cl}^\circ = \log_{10}{}^*\beta_{1,1,Cl} - \Delta z^2\, D - \log a(H_2O) + \Delta\varepsilon\, I_m$$

a value of -2.5 ± 0.3 for $\log_{10}{}^*\beta_{1,1,Cl}^\circ$(298.15 K), where the uncertainty is increased to account for the assumptions made in the extrapolation and the fact that the experimental data were obtained at 20 °C. Due to these assumptions and the fact that Pettine et al. (1981) qualified their data for Sn(OH)Cl(aq) as "reasonable estimates" we include

$$Sn^{2+} + H_2O(l) + Cl^- \rightleftharpoons Sn(OH)Cl(aq) + H^+$$

$$\log_{10}{}^*\beta_{1,1,Cl}^\circ(298.15\ K) = -(2.5 \pm 0.3)$$

in TDB 2020 as supplemental datum, in addition to the estimated

$$\varepsilon(Sn(OH)Cl(aq), NaCl(aq)) \approx \varepsilon(Sn(OH)Cl(aq), NaClO_4(aq)) \approx (0.0 \pm 0.1)\ kg \cdot mol^{-1}$$

see Section 29.1.1 and estimation method described in Section 1.5.3.

29.4.1.3 Aqueous tin(IV) hydroxide complexes

In their review of aqueous Sn(IV) hydroxide complexes, Gamsjäger et al. (2012) remarked that only a single study is available for the hydrolysis of Sn(IV) under acidic conditions. According to this spectrophotometric study, Sn(IV) hydrolyses strongly, even at pH values as low as 1.2. Due to several questionable experimental details, Gamsjäger et al. (2012) did not select the reported stability constants for $SnOH^{3+}$, $Sn(OH)_2^{2+}$, and $Sn(OH)_3^+$.

Stability constants for $Sn(OH)_4$(aq), $Sn(OH)_5^-$, and $Sn(OH)_6^{2-}$ were derived from 5 studies investigating the solubility of crystalline and amorphous SnO_2(s) under alkaline conditions. The solubilities of SnO_2(cassiterite) and SnO_2(am) were found to be constant in the pH range between 1.9 and 8 (and increase at higher pH, see below). This is consistent with the formation of $Sn(OH)_4$(aq). Based on two radiometric studies using ^{113}Sn and ICP-MS (inductively coupled plasma mass-spectrometry), Gamsjäger et al. (2012) selected

$$SnO_2(cassiterite) + 2\ H_2O(l) \rightleftharpoons Sn(OH)_4(aq)$$

$$\log_{10}K_{s,4}^\circ(298.15\ K) = -(8.06 \pm 0.11)$$

for crystalline and

$SnO_2(am) + 2\ H_2O(l) \rightleftharpoons Sn(OH)_4(aq)$

$\log_{10}K_{s,4}°(298.15\ K) = -(7.22 \pm 0.08)$[78]

for amorphous SnO_2. These solubility products are included in TDB 2020.

Note that these two reactions introduce three new tin substances, SnO_2(cassiterite), SnO_2(am), and $Sn(OH)_4$(aq). Thus, given both solubility products and the selected $\Delta_f G_m°(H_2O, l, 298.15\ K) = -(237.140 \pm 0.041)\ kJ \cdot mol^{-1}$, only two of the three unknown values for $\Delta_f G_m°(SnO_2$, cassiterite, 298.15 K), $\Delta_f G_m°(SnO_2$, am, 298.15 K), and $\Delta_f G_m°(Sn(OH)_4$, aq, 298.15 K) can be calculated. As discussed in Section 29.4.2.1.2, Gamsjäger et al. (2012) used calorimetric data to derive $\Delta_f G_m°(SnO_2$, cassiterite, 298.15 K) $= -(516.64 \pm 0.21)\ kJ \cdot mol^{-1}$. From this value, together with $\log_{10}K_{s,4}°(SnO_2$, cassiterite, 298.15 K) and $\Delta_f G_m°(H_2O$, l, 298.15 K), then follows $\Delta_f G_m°(Sn(OH)_4$, aq, 298.15 K) $= -(944.914 \pm 0.666)\ kJ \cdot mol^{-1}$. Using this value, together with the selected $\Delta_f G_m°(Sn^{4+}$, 298.15 K) $= (46.711 \pm 3.871)\ kJ \cdot mol^{-1}$ and the selected $\Delta_f G_m°(H_2O$, l, 298.15 K) leads to

$Sn^{4+} + 4\ H_2O(l) \rightleftharpoons Sn(OH)_4(aq) + 4\ H^+$

$\log_{10}{}^*\beta_{4,1}°(298.15\ K) = (7.54 \pm 0.69)$

which is included in TDB 2020. The magnitude of this formation constant makes it very improbable that the aforementioned lower monomeric Sn(IV) hydroxide species $SnOH^{3+}$, $Sn(OH)_2^{2+}$, and $Sn(OH)_3^+$ occur in measurable amounts in aqueous solution.

The solubilities of both SnO_2(cassiterite) and SnO_2(am) increase at pH > 8 which is explained by the formation of $Sn(OH)_5^-$ and $Sn(OH)_6^{2-}$. Again, based on the two radiometric studies, Gamsjäger et al. (2012) derived the selected

$Sn(OH)_4(aq) + H_2O(l) \rightleftharpoons Sn(OH)_5^- + H^+$

$\log_{10}K_{5,1}°(298.15\ K) = -(8.60 \pm 0.40)$

and

$Sn(OH)_4(aq) + 2\ H_2O(l) \rightleftharpoons Sn(OH)_6^{2-} + 2\ H^+$

$\log_{10}{}^*K_{6,1}°(298.15\ K) = -(18.67 \pm 0.30)$

by using SIT to extrapolate the experimental data ($I \approx 0.1$ M $NaClO_4$) to $I = 0$, assuming that $\Delta\varepsilon$ of both reactions is equal to 0 (i.e., assuming that at such low ionic strength the specific ion interactions are negligible and therefore considering only the Debye-Hückel term). Both stability constants are included in TDB 2020.

---

[78] Note that, although selected by Gamsjäger et al. (2012), this reaction and its solubility product are not listed in Table III-2 of selected thermodynamic data for reactions in Gamsjäger et al. (2012).

We estimated the missing ion interaction coefficients according to estimation method described in Section 1.5.3 and obtained for inclusion in TDB 2020

$$\varepsilon(Sn(OH)_4(aq), NaCl(aq)) \approx \varepsilon(Sn(OH)_4(aq), NaClO_4(aq)) \approx (0.0 \pm 0.1)\ kg \cdot mol^{-1}$$

$$\varepsilon(Sn(OH)_5^-, Na^+) \approx -(0.05 \pm 0.10)\ kg \cdot mol^{-1}$$

$$\varepsilon(Sn(OH)_6^{2-}, Na^+) \approx -(0.10 \pm 0.10)\ kg \cdot mol^{-1}$$

29.4.1.4 Mixed tin(IV) hydroxide complexes

According to Gamsjäger et al. (2012), there is spectroscopic evidence for $SnCl_5OH^{2-}$, $SnCl_4(OH)_2^{2-}$, $SnCl_3(OH)_3^{2-}$, $SnCl_2(OH)_4^{2-}$, and SnF_5OH^{2-}. Equilibrium constants have been reported for the reactions $SnF_5(H_2O)^- + F^- \rightleftharpoons SnF_6^{2-} + H_2O(l)$, $SnF_6^{2-} + X^- \rightleftharpoons SnF_5X^{2-}$ (where $X^- = Cl^-, F^-, OH^-$), $SnO_2(s) + HF(aq) + H_2O(l) \rightleftharpoons Sn(OH)_3F(aq)$, $SnO_2(s) + 2\ HF(aq) \rightleftharpoons Sn(OH)_2F_2(aq)$, $SnO_2(s) + F^- + 2\ H_2O(l) \rightleftharpoons Sn(OH)_4F^-$, and $SnO_2(s) + 2\ F^- + 2\ H_2O(l) \rightleftharpoons Sn(OH)_4F_2^{2-}$. These constants were not selected by Gamsjäger et al. (2012) due to deficiencies in the experimental investigations and are therefore not included in TDB 2020 as well.

29.4.2 Tin oxide and hydroxide solids

29.4.2.1 Tin oxide solids

29.4.2.1.1 Tin(II) oxide solids

Romarchite, SnO(cr), is an alteration product of tin and is found in veins containing native tin, or on surfaces of tin or pewter objects.

As seen in Section 29.4.1.1, Gamsjäger et al. (2012) combined the solubility products for $SnO(s) + H_2O(l) \rightleftharpoons Sn(OH)_2(aq)$ and $SnO(s) + OH^- + H_2O(l) \rightleftharpoons Sn(OH)_3^-$ in order to get the stepwise stability constant $\log_{10}K_3°(298.15\ K)$ for the reaction $Sn(OH)_2(aq) + OH^- \rightleftharpoons Sn(OH)_3^-$. This stability constant is independent of the solubility of SnO(s) as long as the tin oxide solids (or their reacting surfaces) in the employed solubility reactions are equivalent, i.e., have the same $\Delta_f G_m°(298.15\ K)$. Thus, any solubility product involving SnO(s) would be compatible with this choice of $\log_{10}K_3°(298.15\ K)$. Gamsjäger et al. (2012) did not explicitly select one of the solubility products used to derive $\log_{10}K_3°(298.15\ K)$, but $\log_{10}K_{s,3}°(298.15\ K) = -(0.84 \pm 0.02)$ for

$$SnO(s) + OH^- + H_2O(l) \rightleftharpoons Sn(OH)_3^-$$

which they obtained from a re-evaluation of the experimental data by Garrett & Heiks (1941), see Section 29.4.1.1, and used to derive $\log_{10}K_3°(298.15\ K)$, tacitly appears in their Tab. III-2 of selected thermodynamic data for reactions involving tin compounds and complexes. Combining this $\log_{10}K_{s,3}°(298.15\ K)$ with the selected $\log_{10}{}^*\beta_{3,1}°(298.15\ K) = -(17.00 \pm 0.60)$ for $Sn^{2+} + 3\ H_2O(l) \rightleftharpoons Sn(OH)_3^- + 3\ H^+$ and with $pK_w°(298.15\ K) = 14.00$

$$SnO(s) + 2\ H^+ \rightleftharpoons Sn^{2+} + H_2O(l)$$

$$\log_{10}K_{s,0}°(298.15\ K) = (2.16 \pm 0.60)$$

However, Gamsjäger et al. (2012) also derived and selected a value for $\Delta_f G_m°$(SnO, s, 298.15 K) based on additional experimental data. They selected

$$S_m°(SnO, romarchite, 298.15\ K) = (57.18 \pm 0.22)\ J \cdot K^{-1} \cdot mol^{-1}$$

$$C_{p,m}°(SnO, romarchite, 298.15\ K) = (47.76 \pm 0.08)\ J \cdot K^{-1} \cdot mol^{-1}$$

from low temperature heat capacity measurements (4.281 to 310.70 K). From this value for $S_m°$ and the selected $S_m°$(Sn, β, 298.15 K) = (51.18 ± 0.08) J · K^{-1} · mol^{-1} and $S_m°$(O_2, g, 298.15 K) = (205.152 ± 0.005) J · K^{-1} · mol^{-1}, follows

$$\Delta_f S_m°(SnO, romarchite, 298.15\ K) = -(96.58 \pm 0.23)$$

which was used by Gamsjäger et al. (2012) to calculate $\Delta_f G_m°$(SnO, s, 298.15 K) from measured $\Delta_f H_m°$(SnO, s, 298.15 K) or vice versa. They accepted two values for $\Delta_f G_m°$(SnO, s, 298.15 K) derived from three solubility studies and two values from galvanic cell potential measurements using different galvanic cells. In addition, they accepted a value for $\Delta_f H_m°$(SnO, romarchite, 298.15 K) from combustion calorimetry. Taking the weighted average of this value and the four values derived from the four accepted values for $\Delta_f G_m°$(SnO, s, 298.15 K), Gamsjäger et al. (2012) obtained

$$\Delta_f H_m°(SnO, s, 298.15\ K) = -(284.24 \pm 0.76)\ kJ \cdot mol^{-1}$$

which finally leads to the selected

$$\Delta_f G_m°(SnO, s, 298.15\ K) = -(255.44 \pm 0.76)\ kJ \cdot mol^{-1}$$

This value and the selected $\Delta_f G_m°$(Sn^{2+}, 298.15 K) = -(27.39 ± 0.30) kJ · mol^{-1} and $\Delta_f G_m°$(H_2O, l, 298.15 K) = -(237.140 ± 0.041) kJ · mol^{-1} lead to

$$SnO(s) + 2\ H^+ \rightleftharpoons Sn^{2+} + H_2O(l)$$

$$\log_{10}K_{s,0}°(298.15\ K) = (1.59 \pm 0.14)$$

By comparing this $\log_{10}K_{s,0}°$(298.15 K) with that derived above from $\log_{10}K_{s,3}°$(298.15 K), i.e. $\log_{10}K_{s,0}°$(298.15 K) = (2.16 ± 0.60), it is obvious, that Gamsjäger et al. (2012) ran into a contradiction by selecting a value for $\Delta_f G_m°$(SnO, s, 298.15 K) based on different experimental data than the selected $\log_{10}K_{s,3}°$(298.15 K).

For TDB 2020 we decided to consider $\log_{10}K_{s,0}°$(298.15 K) = (1.59 ± 0.14), since it is based on more experimental data, including all those from which $\log_{10}K_{s,3}°$(298.15 K) itself was derived.

We increased the uncertainty because in two of the considered solubility studies, SnO(s) had not been very well characterized and, according to Gamsjäger et al. (2012) "the identity of the actually investigated phase has not yet been unambiguously ascertained". Thus, we include

$$SnO(s) + 2\ H^+ \rightleftharpoons Sn^{2+} + H_2O(l)$$

$$\log_{10}K_{s,0}°(298.15\ K) = (1.6 \pm 0.3)$$

in TDB 2020.

29.4.2.1.2 Tin(IV) oxide solids

As discussed in Section 29.4.1.3, the solubility products for the Sn(IV) oxide solids SnO_2(cassiterite) and SnO_2(am) selected by Gamsjäger et al. (2012) and included in TDB 2020 are expressed in terms of $Sn(OH)_4$(aq). For a complete thermodynamic description of these equilibria, another piece of thermodynamic information is needed in addition to the two solubility products, i.e. one of $\Delta_f G_m°(SnO_2$, cassiterite, 298.15 K), $\Delta_f G_m°(SnO_2$, am, 298.15 K), or $\Delta_f G_m°(Sn(OH)_4$, aq, 298.15 K) must be determined independently. Gamsjäger et al. (2012) reviewed calorimetric data for SnO_2(cassiterite) and selected "based on the reviews of all data"

$$S_m°(SnO_2, \text{cassiterite}, 298.15\ K) = (51.77 \pm 0.14)\ J \cdot K^{-1} \cdot mol^{-1}$$

$$C_{p,m}°(SnO_2, \text{cassiterite}, 298.15\ K) = (55.26 \pm 0.09)\ J \cdot K^{-1} \cdot mol^{-1}$$

$$\Delta_f H_m°(SnO_2, \text{cassiterite}, 298.15\ K) = -(577.63 \pm 0.20)\ kJ \cdot mol^{-1}$$

This choice of values for $S_m°$ and $\Delta_f H_m°$, in combination with the selected values $S_m°$(Sn, β, 298.15 K) = (51.18 ± 0.08) J · K^{-1} · mol^{-1} and $S_m°(O_2$, g, 298.15 K) = (205.152 ± 0.005) J · K^{-1} · mol^{-1}, leads to the selected

$$\Delta_f G_m°(SnO_2, \text{cassiterite}, 298.15\ K) = -(516.64 \pm 0.21)\ kJ \cdot mol^{-1}$$

The value for $\Delta_f H_m°(SnO_2$, cassiterite, 298.15 K) selected by Gamsjäger et al. (2012) was taken from the critical review by CODATA. The four values for $S_m°(SnO_2$, cassiterite, 298.15 K) reported by Gamsjäger et al. (2012) cover the range from (49.01 ± 0.10) to (51.82 ± 0.07) J · K^{-1} · mol^{-1}. However, Gamsjäger et al. (2012) did not explain how they derived their selected value from these.

This value for $\Delta_f G_m°(SnO_2$, cassiterite, 298.15 K) is implicitly included in TDB 2020, as it was used in Section 29.4.1.3 in the derivation of $\log_{10}{}^*\beta_{4,1}°$(298.15 K) for the reaction $Sn^{4+} + 4\ H_2O(l) \rightleftharpoons Sn(OH)_4(aq) + 4\ H^+$.

29.4.2.2 Tin hydroxide solids

Lothenbach et al. (2000) studied the solubility of Sn(IV) in cementitious systems. In the presence of Ca^{2+} at concentrations typical for cementitious environments, concentrations of dissolved Sn(IV) are about four to six orders of magnitude lower than in alkaline but Ca-free systems and the solubility is controlled by the precipitation of $CaSn(OH)_6$(pr). Lothenbach et al. (2000) determined the solubility from undersaturation with well-crystallized synthetic $CaSn(OH)_6$(burtite) and from oversaturation with the corresponding precipitate. These experiments were discussed and analysed by Hummel et al. (2002) who obtained the following solubility products from SIT regressions:

$$CaSn(OH)_6(burtite) \rightleftharpoons Ca^{2+} + Sn(OH)_6^{2-}$$

$$\log_{10}K_{s,6}°(298.15\ K) = -(10.8 \pm 0.1)$$

and

$$CaSn(OH)_6(pr) \rightleftharpoons Ca^{2+} + Sn(OH)_6^{2-}$$

$$\log_{10}K_{s,6}°(298.15\ K) = -(9.7 \pm 0.1)$$

Hummel et al. (2002) selected the solubility product of the latter equilibrium for inclusion in TDB 01/01 and it is also included in TDB 2020. The corresponding reaction can also be expressed in terms of $Sn(OH)_4$(aq) by using $\log_{10}{}^*\beta_{6,1}°(298.15\ K) = -(18.67 \pm 0.30)$ for $Sn(OH)_4(aq) + 2\ H_2O(l) \rightleftharpoons Sn(OH)_6^{2-} + 2\ H^+$ (see Section 29.4.1.3). This leads to

$$CaSn(OH)_6(pr) + 2\ H^+ \rightleftharpoons Sn(OH)_4(aq) + Ca^{2+} + 2\ H_2O(l)$$

$$\log_{10}{}^*K_{s,4}° = (8.97 \pm 0.3)$$

In their Appendix A (Discussion of selected references), Gamsjäger et al. (2012) discussed the experimental data by Lothenbach et al. (2000) and made no comments on potential shortcomings of the data. However, these solids and their data do not appear anywhere in the main text by Gamsjäger et al. (2012) and are also not included in the tables of selected data.

29.4.3 Gaseous tin hydrides

Gamsjäger et al. (2012) selected calorimetric data for stannane, SnH_4g, which is a gas under ambient conditions with an atmospheric boiling point of 221.4 K. At room temperature, SnH_4g slowly decomposes into Sn(β) and H_2g (Greenwood & Earnshaw 1997). For this reason, SnH_4g is very unlikely to have any importance for the purposes of TDB 2020 and is therefore not considered.

29.5 Group 17 halogen compounds and complexes

29.5.1 Aqueous tin halide complexes

29.5.1.1 Aqueous tin fluoride complexes

29.5.1.1.1 Aqueous tin(II) fluoride complexes

Sn(II) fluoride complexes are rather stable. According to Gamsjäger et al. (2012), the mononuclear complexes SnF^+, $SnF_2(aq)$, and SnF_3^- are formed, but higher order complexes have not been observed, even in experiments with a 4000-fold excess of fluoride over Sn(II).

For SnF^+, Gamsjäger et al. (2012) accepted 5 conditional stability constants determined by 3 potentiometric studies in 0.1, 0.5, 1, and 3.0 M $NaClO_4$. From their SIT analysis, Gamsjäger et al. (2012) obtained

$$Sn^{2+} + F^- \rightleftharpoons SnF^+$$

$$\log_{10}\beta_1°(298.15\ K) = (5.25 \pm 0.19)$$

with

$$\Delta\varepsilon = -(0.08 \pm 0.09)\ kg \cdot mol^{-1}$$

from which they derived

$$\varepsilon(SnF^+, ClO_4^-) = (0.14 \pm 0.10)\ kg \cdot mol^{-1}$$

by using the selected $\varepsilon(Sn^{2+}, ClO_4^-) = (0.19 \pm 0.04)\ kg \cdot mol^{-1}$ and $\varepsilon(F^-, Na^+) = (0.02 \pm 0.02)\ kg \cdot mol^{-1}$, see Tab. 29.9-3 and 29.9-5.

We used $\varepsilon(SnF^+, ClO_4^-)$ as an estimate for $\varepsilon(SnF^+, Cl^-)$, see Section 29.1.1. Thus

$$\varepsilon(SnF^+, Cl^-) \approx \varepsilon(SnF^+, ClO_4^-) = (0.14 \pm 0.10)\ kg \cdot mol^{-1}$$

These values for SnF^+ are included in TDB 2020.

For $SnF_2(aq)$, Gamsjäger et al. (2012) accepted 5 conditional stability constants from 4 studies, four of the constants were determined potentiometrically in 0.1, 0.5, 1.0, and 3 M $NaClO_4$ (2 studies), and one was determined by polarography in 0.8 M $NaNO_3$. SIT analysis of the $NaClO_4$ data resulted in

$Sn^{2+} + 2\ F^- \rightleftharpoons SnF_2(aq)$

$\log_{10}\beta_2°(298.15\ K) = (8.89 \pm 0.21)$

with

$\Delta\varepsilon = -(0.23 \pm 0.09)\ kg \cdot mol^{-1}$

from which Gamsjäger et al. (2012) calculated

$\varepsilon(SnF_2(aq), NaClO_4(aq)) = (0.01 \pm 0.10)\ kg \cdot mol^{-1}$

by using the selected $\varepsilon(Sn^{2+}, ClO_4^-)$ and $\varepsilon(F^-, Na^+)$, see Tab. 29.9-3 and 29.9-5.

Using $\varepsilon(SnF_2(aq), NaClO_4(aq))$ as an estimate for $\varepsilon(SnF_2(aq), NaCl(aq))$, see Section 29.1.1, leads to

$\varepsilon(SnF_2(aq), NaCl(aq)) \approx \varepsilon(SnF_2(aq), NaClO_4(aq)) = (0.01 \pm 0.10)\ kg \cdot mol^{-1}$

These values for $SnF_2(aq)$ are included in TDB 2020.

For SnF_3^-, finally, Gamsjäger et al. (2012) accepted 7 conditional stability constants from 4 studies: Schaap et al. (1954), polarography in 0.8 M $NaNO_3$ and 2.5 M KNO_3, Bond & Taylor (1970), potentiometry with a fluoride-sensitive electrode in 1 M $NaClO_4$, Djokić-Konstantinovska & Zmbova (1985), potentiometry with a fluoride-sensitive electrode in 0.1, 0.5, and 1.0 M $NaClO_4$, and Schwartz & Cronau (1975), potentiometry with a fluoride-sensitive electrode in 3 M $NaClO_4$. Gamsjäger et al. (2012) remarked that "although there is no doubt concerning the formation of the trifluoro species, the $\log_{10}\beta_3$ values reported in [1970BON/TAY] and [1985DJO/ZMB] for $NaClO_4$ media are rather scattered (Fig. VIII-18). Since the experiments of the above papers seem to be equally reliable, the inherent uncertainties of the reported/ re-evaluated constants were considerably increased (see Appendix A)". Gamsjäger et al. (2012) performed an SIT analysis of the 5 data points in $NaClO_4$ media and got $\log_{10}\beta_3°(298.15\ K) = (11.5 \pm 1.0)$ for the reaction

$Sn^{2+} + 3\ F^- \rightleftharpoons SnF_3^-$

Since Gamsjäger et al. (2012) did not provide a value for $\Delta\varepsilon$ of this reaction, we did our own SIT analysis using the data reported by Gamsjäger et al. (2012) in their Tab. VIII-7 and obtained $\log_{10}\beta_3°(298.15\ K) = (10.04 \pm 0.42)$ and $\Delta\varepsilon = -(0.73 \pm 0.14)\ kg \cdot mol^{-1}$, see Fig. 29.5-1. Wondering about the discrepancy between these two stability constants, we noticed that in the SIT analysis illustrated in Fig. VIII-18 by Gamsjäger et al. (2012), a larger uncertainty (± 1.0) was used for the conditional stability constant by Bond & Taylor (1970) than reported in Tab. VIII-7 by Gamsjäger et al. (2012) (± 0.30). We recalculated the SIT analysis with the larger uncertainty (see Fig. 29.5-2) and found $\log_{10}\beta_3°(298.15\ K) = (11.45 \pm 0.99)$, virtually identical to the value by Gamsjäger et al. (2012), with $\Delta\varepsilon = -(0.33 \pm 0.29)\ kg \cdot mol^{-1}$. In addition, we also carried out an SIT analysis of the same data points with unenlarged uncertainties (see Fig. 29.5-3), as assigned by Gamsjäger et al. (2012) in the discussion (in their Appendix A) of the experimental data by

Djokić-Konstantinovska & Zmbova (1985) and Bond & Taylor (1970), see Tab. 29.5-1. This analysis resulted in $\log_{10}\beta_3°(298.15\ K) = (11.47 \pm 0.30)$ with $\Delta\varepsilon = -(0.30 \pm 0.11)\ kg \cdot mol^{-1}$. These values are very similar to those obtained in the previous analysis, albeit with much smaller uncertainties.

For inclusion in TDB 2020 we chose the rounded results of the SIT analysis with enlarged uncertainties (Fig. 29.5-2). Thus,

$$\log_{10}\beta_3°(298.15\ K) = (11.5 \pm 1.0)$$

identical to the value selected by Gamsjäger et al. (2012), and

$$\Delta\varepsilon = -(0.3 \pm 0.3)\ kg \cdot mol^{-1}$$

from which follows

$$\varepsilon(SnF_3^-, Na^+) = -(0.05 \pm 0.31)\ kg \cdot mol^{-1}$$

by using the selected $\varepsilon(Sn^{2+}, ClO_4^-)$ and $\varepsilon(F^-, Na^+)$, see Tab. 29.9-3 and 29.9-5, respectively.

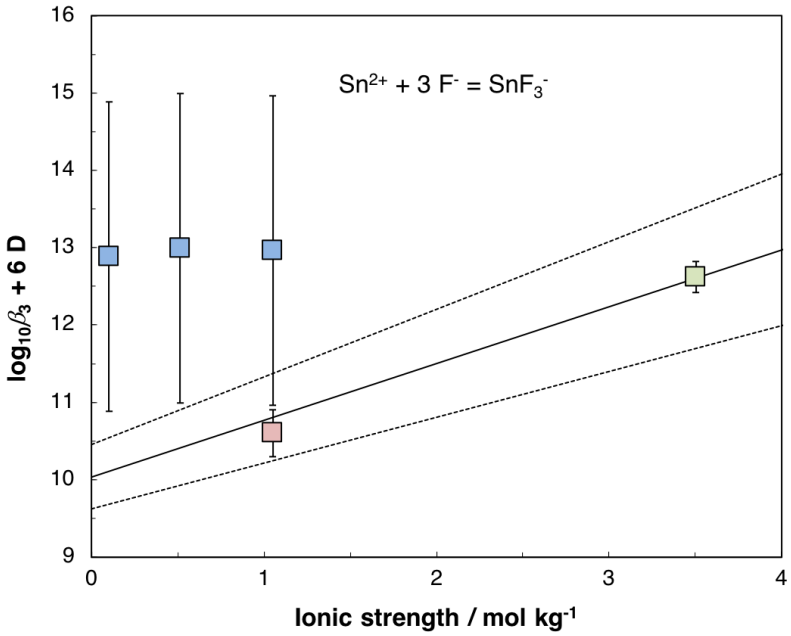

Fig. 29.5-1: Extrapolation to $I = 0$ of experimental data

(blue: Djokić-Konstantinovska & Zmbova 1985, red: Bond & Taylor 1970, green: Schwartz & Cronau 1975) for $Sn^{2+} + 3\ F^- \rightleftharpoons SnF_3^-$ using SIT. Uncertainties of experimental data according to Tab. VIII-7 by Gamsjäger et al. (2012). $\log_{10}\beta_3°(298.15\ K) = (10.04 \pm 0.42)$, $\Delta\varepsilon = -(0.73 \pm 0.14)\ kg \cdot mol^{-1}$, $\varepsilon(SnF_3^-, Na^+) = -(0.48 \pm 0.16)\ kg \cdot mol^{-1}$

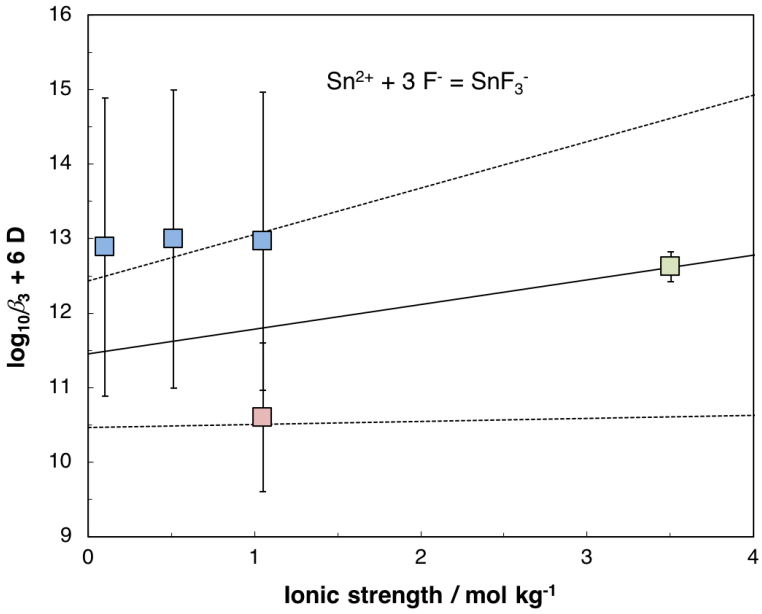

Fig. 29.5-2: Extrapolation to $I = 0$ of experimental data

(blue: Djokić-Konstantinovska & Zmbova 1985, red: Bond & Taylor 1970, green: Schwartz & Cronau 1975) for $Sn^{2+} + 3\ F^- \rightleftharpoons SnF_3^-$ using SIT. Uncertainties of experimental data according to Fig. VIII-18 by Gamsjäger et al. (2012), differing from Fig. 29.5-1 above only in the increased uncertainty of the red data point (± 1.0 vs. ± 0.30). $\log_{10}\beta_3°(298.15\ K) = (11.45 \pm 0.99)$, $\Delta\varepsilon = -(0.33 \pm 0.29)$ kg · mol^{-1}, $\varepsilon(SnF_3^-, Na^+) = -(0.08 \pm 0.30)$ kg · mol^{-1}

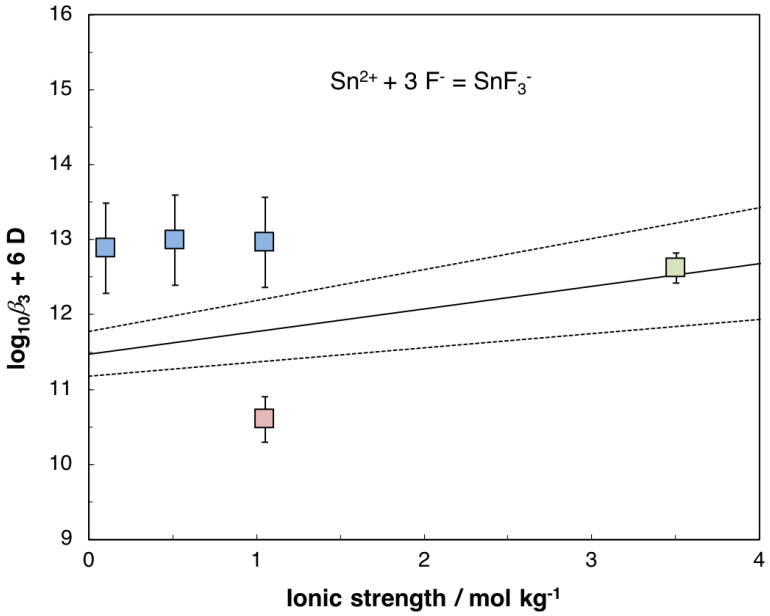

Fig. 29.5-3: Extrapolation to $I = 0$ of experimental data

(blue: Djokić-Konstantinovska & Zmbova 1985, red: Bond & Taylor 1970, green: Schwartz & Cronau 1975) for $Sn^{2+} + 3\ F^- \rightleftharpoons SnF_3^-$ using SIT. Uncertainties as assigned by Gamsjäger et al. (2012) in their assessments of the experimental data in their Appendix A. $\log_{10}\beta_3°(298.15\ K) = (11.47 \pm 0.30)$, $\Delta\varepsilon = -(0.30 \pm 0.11)$ kg · mol^{-1}, $\varepsilon(SnF_3^-, Na^+) = -(0.05 \pm 0.13)$ kg · mol^{-1}

Tab. 29.5-1: Conditional stability constants and their uncertainties for the reaction Sn^{2+} + 3 F^- ⇌ SnF_3^- as used in the SIT analyses shown in Figs. 29.5-1, 29.5-2, and 29.5-3

Increased uncertainties are marked in bold. [1970BON/TAY]: Bond & Taylor (1970), [1975SCH/CRO]: Schwartz & Cronau 1975, [1985DJO/ZMB]: Djokić-Konstantinovska & Zmbova (1985).

Ionic medium	**$\log_{10}\beta_3$**	**$\log_{10}\beta_3$**	**$\log_{10}\beta_3$**	**Reference**
	Fig. 29.5-1	**Fig. 29.5-2**	**Fig. 29.5-3**	
0.1 M $NaClO_4$	12.23 ± **2.00**	12.23 ± **2.00**	12.23 ± 0.60	[1985DJO/ZMB]
0.5 M $NaClO_4$	11.94 ± **2.00**	11.94 ± **2.00**	11.94 ± 0.60	[1985DJO/ZMB]
1.0 M $NaClO_4$	11.73 ± **2.00**	11.73 ± **2.00**	11.73 ± 0.60	[1985DJO/ZMB]
1.0 M $NaClO_4$	9.37 ± 0.30	9.37 ± **1.00**	9.37 ± 0.30	[1970BON/TAY]
3 M $NaClO_4$	11.12 ± 0.20	11.12 ± 0.20	11.12 ± 0.20	[1975SCH/CRO]

29.5.1.1.2 Aqueous tin(IV) fluoride complexes

According to Gamsjäger et al. (2012), Sn(IV) forms strong complexes with the fluoride anion. However, Gamsjäger et al. (2012) found only three studies concerned with these complexes, but none of the studies were of sufficient quality to allow the derivation of selected values. For the reaction

$$Sn^{4+} + 6\ F^- \rightleftharpoons SnF_6^{2-}$$

they provided the rough estimate

$$\log_{10}\beta_6^\circ(298.15\ K) \approx 25$$

based on a polarographic study (I = 0.1 – 0.2 M, with 0.1 M KF and 0 – 0.1M HF).

This estimate is included in TDB 2020 as supplemental datum together with

$$\varepsilon(SnF_6^{2-}, Na^+) \approx -(0.10 \pm 0.10)\ kg \cdot mol^{-1}$$

estimated according to estimation method described in Section 1.5.3.

29.5.1.2 Aqueous tin chloride complexes

29.5.1.2.1 Aqueous tin(II) chloride complexes

The formation of Sn(II) chloride complexes has been studied by a variety of experimental techniques. Gamsjäger et al. (2012) mention the use of solubility, spectrophotometric, polarographic, voltammetric, kinetic, electrophoretic and potentiometric methods. They evaluated stability constants for $SnCl^+$, $SnCl_2(aq)$, $SnCl_3^-$, and $SnCl_4^{2-}$ from the accepted experimental data at 25 °C listed in Tab. 29.5-2 by using SIT for the extrapolation of the conditional stability constants to $I = 0$. Although they also accepted the stability constants obtained by Müller & Seward (2001) at temperatures between 25 and 300 °C, Gamsjäger et al. (2012) did not use these for extracting values of $\Delta_r H_m°$(298.15 K) and $\Delta_r C_{p,m}°$(298.15 K) that would allow to extrapolate stability constants to higher temperatures, but rather relied on calorimetric determinations of $\Delta_r H_m°$(298.15 K) for the formation reactions of $SnCl^+$ and $SnCl_2(aq)$. Gamsjäger et al. (2012) argued that "the temperature variation of the $\log_{10}\beta_q$ values is comparable with, or even smaller than, their uncertainties". These very large uncertainties, however, were assigned by Gamsjäger et al. (2012) themselves, since "the extended Debye-Hückel equation used by the authors to calculate the individual ion activity coefficients is not strictly identical with that applied in the SIT, [...] an uncertainty of ± 0.3 has been assigned to the $\log_{10}\beta_q°$ values reported for 25 °C". The uncertainties assigned by Gamsjäger et al. (2012) are ± 0.3 for $\log_{10}\beta_q°$ at 25 and 50 °C, ± 0.4 for $\log_{10}\beta_q°$ at 100, 150, and 200 °C, and ± 0.5 for $\log_{10}\beta_q°$ at 250 and 300 °C. We do not agree with this assessment and regard the assigned uncertainties as overly conservative. We also believe that it is reasonable to assume that the temperature trends of $\log_{10}\beta_q°$ observed by Müller & Seward (2001) are not an artifact of the chosen method to extrapolate the measured $\log_{10}\beta_q$ to zero ionic strength. Therefore, we accepted the data by Müller & Seward (2001) and used them for deriving values for $\log_{10}\beta_q°$(298.15 K) (q = 1-4) and the related $\Delta_r H_m°$(298.15 K) and $\Delta_r C_{p,m}°$(298.15 K). As mentioned above, Gamsjäger et al. (2012) rather relied on calorimetric determinations of $\Delta_r H_m°$(298.15 K) for the formation reactions of $SnCl^+$ and $SnCl_2(aq)$, which are, even if they appear to be of very good quality and were even measured at various ionic strengths, either not sufficient to extrapolate $\log_{10}\beta°$ to higher temperatures, as in the case of $SnCl_2(aq)$, which requires a three term equation for temperature extrapolation, instead of the two term van 't Hoff equation (see Fig. 29.5-5), or are clearly discordant to the values of $\log_{10}\beta°$ measured at various temperatures, as is the case for $SnCl^+$ (see Fig. 29.5-4). For $SnCl_3^-$, Gamsjäger et al. (2012) only provided a tentative $\Delta_r H_m°$(298.15 K) value. For these reasons, we did not adopt the values

$$\Delta_r H_m°(Sn^{2+} + Cl^- \rightleftharpoons SnCl^+, 298.15\ K) = (12.7 \pm 2.3)\ kJ \cdot mol^{-1}$$

$$\Delta_r H_m°(Sn^{2+} + 2\ Cl^- \rightleftharpoons SnCl_2(aq), 298.15\ K) = (19.7 \pm 4.5)\ kJ \cdot mol^{-1}$$

$$\Delta_r H_m°(Sn^{2+} + 3\ Cl^- \rightleftharpoons SnCl_3^-, 298.15\ K) = (17.4 \pm 8.0)\ kJ \cdot mol^{-1}$$

selected by Gamsjäger et al. (2012) but chose to base our selection of enthalpy and heat capacity data for TDB 2020 on the formation constants for $SnCl^+$, $SnCl_2(aq)$, $SnCl_3^-$, and $SnCl_4^{2-}$ determined by Müller & Seward (2001) using UV spectrophotometry at saturated vapor pressure and temperatures between 25 and 300 °C, see Tab. 29.5-3. The investigated solutions contained Sn(II) (1.0×10^{-4} – 5.0×10^{-4} m), 0.01 m HCl and NaCl from 0 – 2.936 m. The results were interpreted in terms of Sn^{2+}, $SnCl^+$, $SnCl_2(aq)$, $SnCl_3^-$, and $SnCl_4^{2-}$. All these species could be reliably identified, and their formation constants determined between 25 and 150 °C, in the case of $SnCl_2(aq)$ and $SnCl_3^-$ even to 300 °C. $SnCl_4^{2-}$, however, was not detected above 150 °C and the

determination of stability constants for $SnCl^+$ above 200 °C was fraught with large uncertainties. Müller & Seward (2001) fitted the stepwise formation constants as a function of temperature with the equation

$$\ln K°(T) = A + B\,T + C\,T^2$$

We preferred to use

$$\log_{10}\beta°(T) = a + b/T + c\,\ln T$$

which can be directly related to $\Delta_r H_m°(298.15\ K)$ and $\Delta_r C_{p,m}°(298.15\ K)$, see Hummel et al. (2002).

For the reaction

$$Sn^{2+} + Cl^- \rightleftharpoons SnCl^+$$

the experimental data at 25, 50, 100, 150 and 200 °C can be represented by an equation linear in $1/T$

$$\log_{10}\beta_1°(T) = 1.800 - 117.6/T$$

(see Fig. 29.5-4) from which follows

$$\log_{10}\beta_1°(298.15\ K) = (1.41 \pm 0.20)$$

with increased uncertainty and

$$\Delta_r H_m°(298.15\ K) = 2.25\ kJ \cdot mol^{-1}$$

$$\Delta_r C_{p,m}°(298.15\ K) = 0$$

For

$$Sn^{2+} + 2\,Cl^- \rightleftharpoons SnCl_2(aq)$$

the experimental data at 25, 50, 100, 150, 200, 250, and 300 °C lead to the three term equation

$$\log_{10}\beta_2°(T) = -63.92 + 3158/T + 9.749\,\ln T$$

(see Fig. 29.5-5) and consequently to

$$\log_{10}\beta_2°(298.15\ K) = (2.22 \pm 0.20)$$

with increased uncertainty and

$\Delta_r H_m°(298.15\ K) = -4.81\ kJ \cdot mol^{-1}$

$\Delta_r C_{p,m}°(298.15\ K) = 187\ J \cdot K^{-1} \cdot mol^{-1}$

The experimental data at 25, 50, 100, 150, 200, 250, and 300 °C for the reaction

$Sn^{2+} + 3\ Cl^- \rightleftharpoons SnCl_3^-$

can also be expressed in terms of a three term equation (see Fig. 29.5-6)

$\log_{10}\beta_3°(T) = -143.4 + 7243/T + 21.32\ \ln T$

resulting in

$\log_{10}\beta_3°(298.15\ K) = (2.37 \pm 0.20)$

again, with increased uncertainty and

$\Delta_r H_m°(298.15\ K) = -17.0\ kJ \cdot mol^{-1}$

$\Delta_r C_{p,m}°(298.15\ K) = 408\ J \cdot K^{-1} \cdot mol^{-1}$

For the reaction

$Sn^{2+} + 4\ Cl^- \rightleftharpoons SnCl_4^{2-}$

finally, the data at 25, 50, 100, and 150 °C can be represented by

$\log_{10}\beta_4°(T) = 1.809 + 60.49/T$

As is obvious from Fig. 29.5-7, the slope of this linear inverse temperature function is indistinguishable from zero within the experimental uncertainties, thus the value determined by Müller & Seward (2001) at 25 °C

$\log_{10}\beta_4°(298.15\ K) = 2.03 \pm 0.20$

(with increased uncertainty) can be well used across the entire range of experimental temperatures (25 – 150 °C). Therefore

$\Delta_r H_m°(298.15\ K) = 0$

and

$$\Delta_r C_{p,m}°(298.15\ K) = 0$$

These data for the Sn(II) chloride complexes, derived from the experimental data by Müller & Seward (2001) are all included in TDB 2020.

In order to derive SIT coefficients for $SnCl^+$, $SnCl_2(aq)$, and $SnCl_3^-$, we relied on all the data accepted by Gamsjäger et al. (2012) (see Tab. 29.5-2), except for those at $I = 0$ which were not included, and carried out constrained SIT extrapolations with the formation constants $\log_{10}\beta°(298.15\ K)$ held constant at the values obtained from our analyses of the experimental data by Müller & Seward (2001). Before performing the constrained extrapolations, we tried to reproduce the unconstrained ones by Gamsjäger et al. (2012), since these authors did report values for I_c of the experimental data, but not for I_m as used in SIT (we did the conversions from molarity to molality, see Tab. 29.5-2, using the appropriate conversion factors listed by Grenthe & Puigdomènech 1997). In doing so, we noticed that in our plot for $SnCl^+$ (Fig. 29.5-8), the plotting positions of the data by Duke & Courtney (1950) and Duke & Pinkerton (1951) were shifted towards lower values of $\log_{10}\beta_1 + 4$ D compared to Gamsjäger et al. (2012) (their Fig. VIII-19). In the plots for $SnCl^+$ (Fig. 29.5-8), $SnCl_2(aq)$(Fig. 29.5-9), and $SnCl_3^-$ (Fig. 29.5-10), the plotting positions of the data by Fedorov et al. (1975) at $I_c = 6$ M were shifted to lower values of I_m compared to Fig. VIII-19, Fig. VIII-20, and Fig. VIII-21, resp., by Gamsjäger et al. (2012). Despite these differences, the resulting $\log_{10}\beta°(298.15\ K)$ and $\Delta\varepsilon$ values (see Tab. 29.5-4 and 29.5.5) are quite similar.

From the constrained extrapolations shown in Figs. 29.5-8, 29.5-9, and 29.5-10, we obtained

$$\Delta\varepsilon(Sn^{2+} + Cl^- \rightleftharpoons SnCl^+) = -(0.18 \pm 0.03)\ kg \cdot mol^{-1}$$

$$\Delta\varepsilon(Sn^{2+} + 2\ Cl^- \rightleftharpoons SnCl_2(aq)) = -(0.25 \pm 0.04)\ kg \cdot mol^{-1}$$

$$\Delta\varepsilon(Sn^{2+} + 3\ Cl^- \rightleftharpoons SnCl_3^-) = -(0.21 \pm 0.04)\ kg \cdot mol^{-1}$$

From these values and the selected $\varepsilon(Sn^{2+}, ClO_4^-) = (0.19 \pm 0.04)\ kg \cdot mol^{-1}$ and $\varepsilon(Cl^-, Na+) = (0.03 \pm 0.01)$ follow

$$\varepsilon(SnCl^+, ClO_4^-) = (0.04 \pm 0.05)\ kg \cdot mol^{-1}$$

$$\varepsilon(SnCl_2(aq), NaClO_4) = (0.00 \pm 0.06)\ kg \cdot mol^{-1}$$

$$\varepsilon(SnCl_3^-, Na^+) = (0.07 \pm 0.06)\ kg \cdot mol^{-1}$$

which are included in TDB 2020, as well as the estimates (see Section 29.1.1)

$$\varepsilon(SnCl^+, Cl^-) \approx \varepsilon(SnCl^+, ClO_4^-) = (0.04 \pm 0.05)\ kg \cdot mol^{-1}$$

and

$$\varepsilon(SnCl_2(aq), NaCl\ (aq)) \approx \varepsilon(SnCl_2(aq), NaClO_4(aq)) = (0.00 \pm 0.06)\ kg \cdot mol^{-1}$$

Finally, $\varepsilon(SnCl_4^{2-}, Na^+)$ also needed an estimate, and following estimation method described in Section 1.5.3 we included

$$\varepsilon(SnCl_4^{2-}, Na^+) = -(0.10 \pm 0.10)\ kg \cdot mol^{-1}$$

in TDB 2020.

Tab. 29.5-2: Experimental data accepted by Gamsjäger et al. (2012) for the formation constants of Sn(II) chloride complexes at 25 °C

Ionic medium	I_c [mol · dm^{-3}]	**ρ = m/c** [a]	I_m [b] [mol · kg^{-1}]	**log$_{10}\beta$** [298.15 K]	**Reference**
$Sn^{2+} + Cl^- \rightleftharpoons SnCl^+$					
(H/K)Cl	0	1	0.00	1.34 ± 0.50	Prytz (1928)
NaCl	0	1	0.00	(1.25 ± 0.50) [c]	Pettine et al. (1981)
(H/Na)Cl	0	1	0.00	1.42 ± 0.30	Müller & Seward (2001)
$HClO_4$	2.03	1.10189	2.24	1.03 ± 0.40	Duke & Courtney (1950)
$HClO_4$	2.03	1.10189	2.24	1.07 ± 0.50	Duke & Pinkerton (1951)
(H/Na)ClO_4	3	1.16776 [d]	3.50	1.05 ± 0.30	Vanderzee & Rhodes (1952)
(H/Na)ClO_4	3	1.16776 [d]	3.50	1.11 ± 0.20	Tobias & Hugus (1961)
$NaClO_4$	0.5	1.02646	0.51	1.08 ± 0.40	Fedorov et al. (1975)
$NaClO_4$	1.0	1.05148	1.05	1.00 ± 0.40	Fedorov et al. (1975)
$NaClO_4$	3.0	1.16776	3.50	1.11 ± 0.40	Fedorov et al. (1975)
$NaClO_4$	4.0	1.23743	4.95	1.25 ± 0.40	Fedorov et al. (1975)
$NaClO_4$	6	1.40774	8.45	1.63 ± 0.40	Fedorov et al. (1975)
$Sn^{2+} + 2\ Cl^- \rightleftharpoons SnCl_2(aq)$					
(H/K)Cl	0	1	0.00	2.13 ± 0.50	Prytz (1928)
NaCl	0	1	0.00	(1.99 ± 0.50) [c]	Pettine et al. (1981)
(H/Na)Cl		1	0.00	2.18 ± 0.30	Müller & Seward (2001)
(H/Na)ClO_4	3	1.16776 [d]	3.50	1.54 ± 0.30	Vanderzee & Rhodes (1952)
(H/Na)ClO_4	3	1.16776 [d]	3.50	1.61 ± 0.20	Tobias & Hugus (1961)
$NaClO_4$	0.5	1.02646	0.51	1.34 ± 0.40	Fedorov et al. (1975)
$NaClO_4$	1.0	1.05148	1.05	1.09 ± 0.40	Fedorov et al. (1975)
$NaClO_4$	3.0	1.16776	3.50	1.65 ± 0.40	Fedorov et al. (1975)

Tab. 29.5-2: Cont.

Ionic medium	I_c [mol · dm^{-3}]	**ρ = m/c** [a]	I_m [b] [mol · kg^{-1}]	**log$_{10}\beta$** [298.15 K]	**Reference**
$NaClO_4$	4.0	1.23743	4.95	1.93 ± 0.40	Fedorov et al. (1975)
$NaClO_4$	6	1.40774	8.45	2.70 ± 0.40	Fedorov et al. (1975)
$Sn^{2+} + 3\ Cl^- \rightleftharpoons SnCl_3^-$					
(H/K)Cl	0	1	0.00	1.99 ± 0.50	Prytz (1928)
NaCl	0	1	0.00	(1.94 ± 0.50) [c]	Pettine et al. (1981)
(H/Na)Cl	0	1	0.00	2.33 ± 0.30	Müller & Seward (2001)
(H/Na)ClO_4	3	1.16776 [d]	3.50	1.39 ± 0.30	Vanderzee & Rhodes (1952)
(H/Na)ClO_4	3	1.16776 [d]	3.50	1.48 ± 0.20	Tobias & Hugus (1961)
$NaClO_4$	3.0	1.16776	3.50	1.45 ± 0.40	Fedorov et al. (1975)
$NaClO_4$	4.0	1.23743	4.95	1.84 ± 0.40	Fedorov et al. (1975)
$NaClO_4$	6	1.40774	8.45	2.78 ± 0.40	Fedorov et al. (1975)
$Sn^{2+} + 4\ Cl^- \rightleftharpoons SnCl_4^{2-}$					
(H/Na)Cl	0	1	0.00	2.03 ± 0.30	Müller & Seward (2001)

[a] Data from Tab. II.4 (p. 55) by Grenthe & Puigdomènech (1997).
[b] Calculated from I_c and ρ, as values for I_m were not explicitly reported by Gamsjäger et al. (2012).
[c] 20 °C
[d] Calculated with ρ for $NaClO_4$.

Tab. 29.5-3: Experimental data by Müller & Seward (2001) for the formation constants of Sn(II) chloride complexes obtained at various temperatures and saturated vapor pressure

The 1σ uncertainties reported by Müller & Seward (2001) were increased to 2σ.

T [°C]	**log$_{10}\beta_1$°** $Sn^{2+} + Cl^- \rightleftharpoons SnCl^+$	**log$_{10}\beta_2$°** $Sn^{2+} + 2\ Cl^- \rightleftharpoons SnCl_2(aq)$	**log$_{10}\beta_3$°** $Sn^{2+} + 3\ Cl^- \rightleftharpoons SnCl_3^-$	**log$_{10}\beta_4$°** $Sn^{2+} + 4\ Cl^- \rightleftharpoons SnCl_4^{2-}$
25	1.42 ± 0.10	2.18 ± 0.06	2.33 ± 0.08	2.03 ± 0.04
50	1.45 ± 0.16	2.25 ± 0.16	2.21 ± 0.18	1.98 ± 0.20
100	1.43 ± 0.20	2.25 ± 0.16	2.39 ± 0.12	1.95 ± 0.20
150	1.52 ± 0.08	2.52 ± 0.18	2.59 ± 0.20	1.97 ± 0.28
200	1.58 ± 0.14	2.83 ± 0.12	3.13 ± 0.08	-
250	-	3.06 ± 0.10	3.96 ± 0.08	-
300	-	3.56 ± 0.10	4.66 ± 0.06	-

Tab. 29.5-4: Comparison of formation constants of Sn(II) chloride complexes, selected by Gamsjäger et al. (2012), derived in this work, and selected for TDB 2020

Species	**$\log_{10}\beta°$(298.15 K)** Gamsjäger et al. (2012)	**$\log_{10}\beta°$(298.15 K)** This work, from unconstrained SIT analysis	**$\log_{10}\beta°$(298.15 K)** This work, from temperature function, assigned uncertainty	**$\log_{10}\beta°$(298.15 K)** TDB 2020
$SnCl^+$	1.52 ± 0.20	1.53 ± 0.16	1.41 ± 0.20	1.41 ± 0.20
$SnCl_2(aq)$	2.17 ± 0.17	2.15 ± 0.17	2.22 ± 0.20	2.22 ± 0.20
$SnCl_3^-$	2.13 ± 0.19	2.11 ± 0.20	2.37 ± 0.20	2.37 ± 0.20
$SnCl_4^{2-}$	2.03 ± 0.40	-	2.01 ± 0.20	2.03 ± 0.20

Tab. 29.5-5: Comparison of $\Delta\varepsilon$ values of the formation reactions of Sn(II) chloride complexes obtained from unconstrained SIT extrapolations by Gamsjäger et al. (2012) and this work, and from constrained extrapolations by this work

Species	**$\Delta\varepsilon$** $[kg \cdot mol^{-1}]$ Gamsjäger et al. (2012)	**$\Delta\varepsilon$** $[kg \cdot mol^{-1}]$ This work, from unconstrained SIT analysis	**$\Delta\varepsilon$** $[kg \cdot mol^{-1}]$ TDB 2020, from constrained SIT analysis
$SnCl^+$	-(0.15 ± 0.05)	-(0.16 ± 0.05)	-(0.18 ± 0.03)
$SnCl_2(aq)$	-(0.26 ± 0.05)	-(0.27 ± 0.05)	-(0.25 ± 0.04)
$SnCl_3^-$	-(0.25 ± 0.05)	-(0.26 ± 0.05)	-(0.21 ± 0.04)

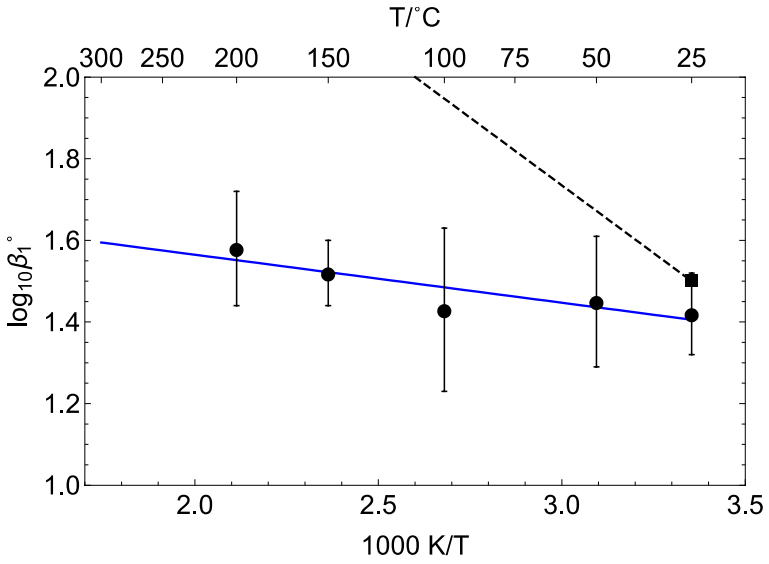

Fig. 29.5-4: Temperature dependence of $\log_{10}\beta_1°$ for $Sn^{2+} + Cl^- \rightleftharpoons SnCl^+$

According to the experimental data (filled circles) by Müller & Seward (2001), see Tab. 29.5-3. The data can be represented by the linear equation (blue line)

$\log_{10}\beta_1°(T) = 1.800 - 117.6/T$

For comparison, $\log_{10}\beta_1°(298.15)$ selected by Gamsjäger et al. (2012) (filled square) is shown together with the extrapolation to higher temperatures (dashed line) based on the calorimetric value for $\Delta_r H_m°$ selected by Gamsjäger et al. (2012).

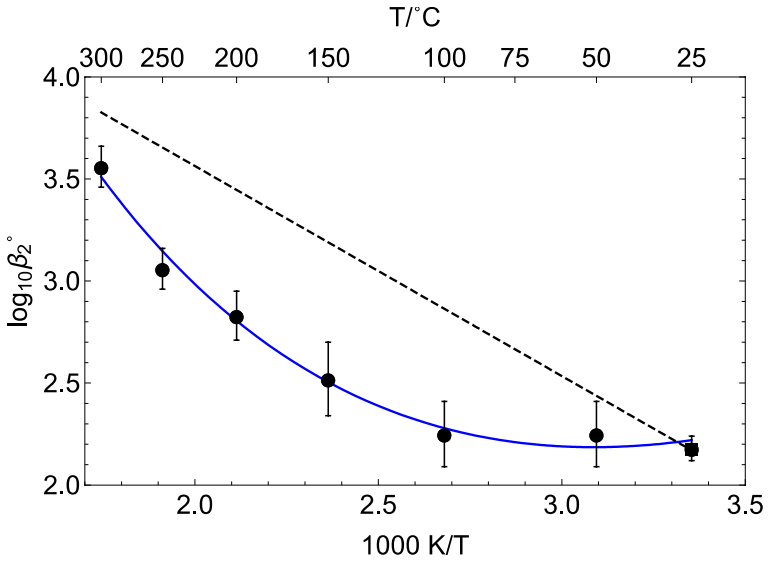

Fig. 29.5-5: Temperature dependence of $\log_{10}\beta_2°$ for $Sn^{2+} + 2\ Cl^- \rightleftharpoons SnCl_2(aq)$

According to the experimental data (filled circles) by Müller & Seward (2001), see Tab. 29.5-3. The data can be represented by the three term equation (blue line)

$\log_{10}\beta_2°(T) = -63.92 + 3158/T + 9.749\ \ln T$

For comparison, $\log_{10}\beta_2°(298.15)$ selected by Gamsjäger et al. (2012) (filled square) is shown together with the extrapolation to higher temperatures (dashed line) based on the calorimetric value for $\Delta_r H_m°$ selected by Gamsjäger et al. (2012).

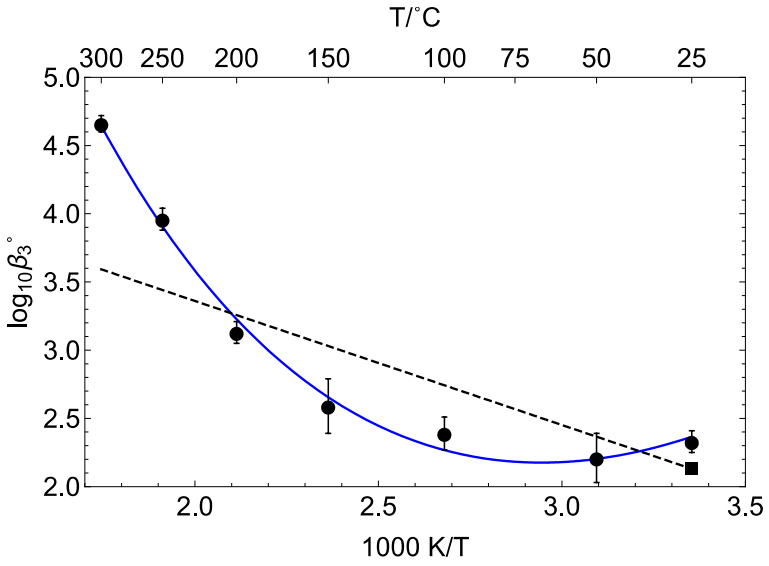

Fig. 29.5-6: Temperature dependence of $\log_{10}\beta_3°$ for $Sn^{2+} + 3\ Cl^- \rightleftharpoons SnCl_3^-$

According to the experimental data (filled circles) by Müller & Seward (2001), see Tab. 29.5-3. The data can be represented by the three term equation (blue line)

$\log_{10}\beta_3°(T) = -143.4 + 7243/T + 21.32\ \ln T$

For comparison, $\log_{10}\beta_3°(298.15)$ selected by Gamsjäger et al. (2012) (filled square) is shown together with the extrapolation to higher temperatures (dashed line) based on the calorimetric value for $\Delta_r H_m°$ reported by Gamsjäger et al. (2012) as tentative.

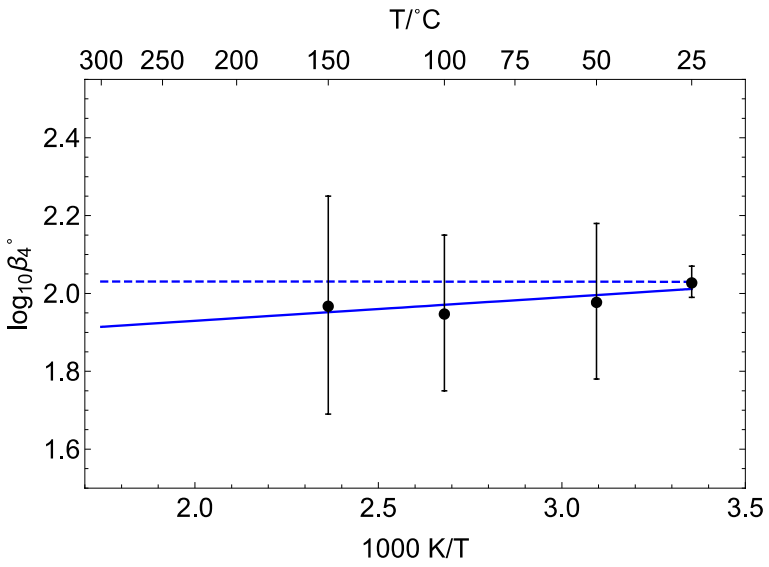

Fig. 29.5-7: Temperature dependence of $\log_{10}\beta_4°$ for $Sn^{2+} + 4\ Cl^- \rightleftharpoons SnCl_4^{2-}$

According to the experimental data (filled circles) by Müller & Seward (2001), see Tab. 29.5-3. The data can be represented by the linear equation (continuous line)

$\log_{10}\beta_4°(T) = 1.809 + 60.49/T$

Since the slope of this line is indistinguishable from zero within the experimental uncertainties, $\log_{10}\beta_4°(298.15) = 2.03 \pm 0.20$ (with increased uncertainty) can well be used within the entire experimental range of temperatures.

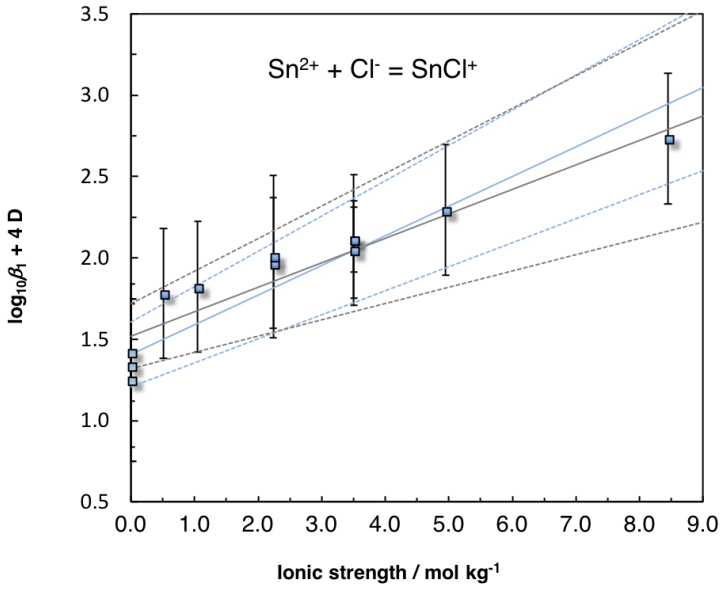

Fig. 29.5-8: Constrained extrapolation (blue lines) with fixed $\log_{10}\beta_1°$(298.15 K) to $I = 0$ of experimental data (see Tab. 29.5-2) for $Sn^{2+} + Cl^- \rightleftharpoons SnCl^+$

Using SIT (blue lines): $\log_{10}\beta_1°(298.15\ K) = (1.41 \pm 0.20)$, $\Delta\varepsilon = -(0.18 \pm 0.03)$ kg · mol^{-1}. The value fixed for $\log_{10}\beta_1°$(298.15 K) was calculated from the temperature function shown in Fig. 29.5-4. For comparison, the unconstrained extrapolation by Gamsjäger et al. (2012) is shown as light grey lines. The three data points at $I = 0$ were only used in the unconstrained extrapolation.

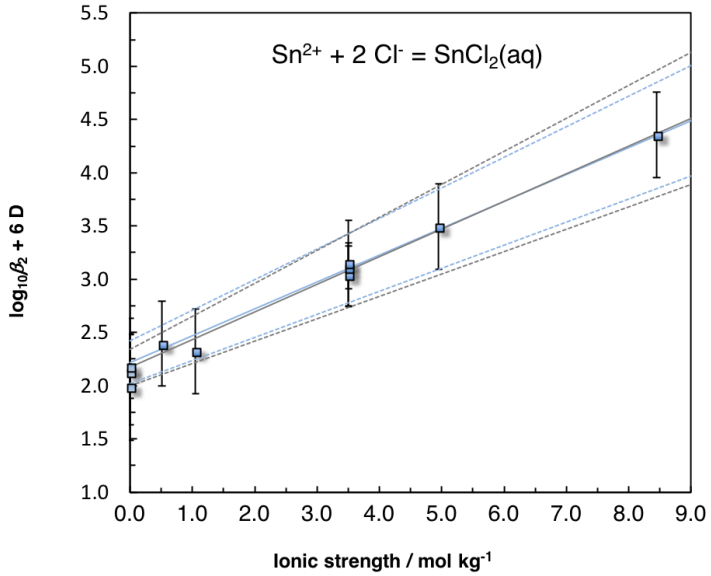

Fig. 29.5-9: Constrained extrapolation (blue lines) with fixed $\log_{10}\beta_1°$(298.15 K) to $I = 0$ of experimental data (see Tab. 29.5-2) for $Sn^{2+} + 2\ Cl^- \rightleftharpoons SnCl_2(aq)$

Using SIT (blue lines): $\log_{10}\beta_2°(298.15\ K) = (2.22 \pm 0.20)$, $\Delta\varepsilon = -(0.25 \pm 0.04)$ kg · mol^{-1}. The value fixed for $\log_{10}\beta_2°$(298.15 K) was calculated from the temperature function shown in Fig. 29.5-5. For comparison, the unconstrained extrapolation by Gamsjäger et al. (2012) is shown as light grey lines. The three data points at $I = 0$ were only used in the unconstrained extrapolation.

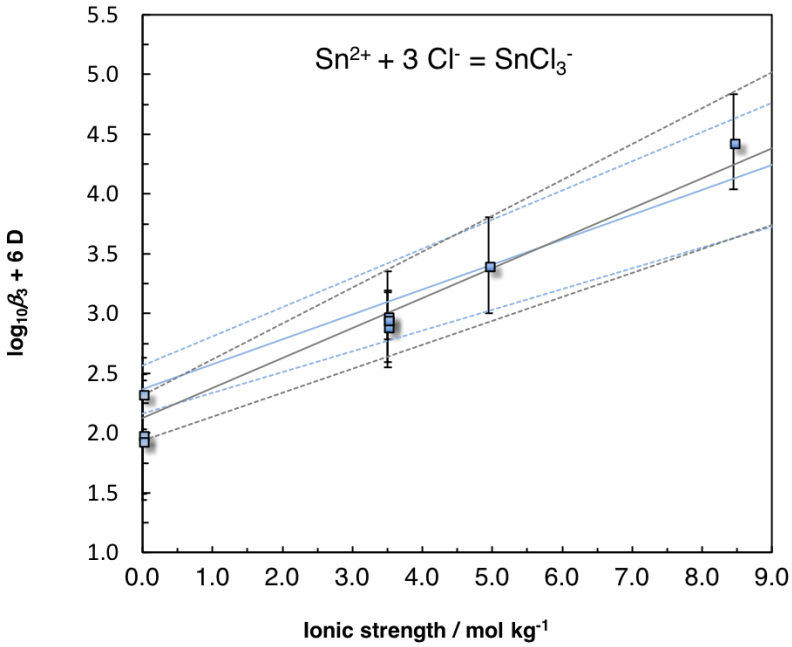

Fig. 29.5-10: Constrained extrapolation to I = 0 of experimental data (see Tab. 29.5-2) for $Sn^{2+} + 3\ Cl^- \rightleftharpoons SnCl_3^-$

Using SIT (blue lines): $\log_{10}\beta_3°(298.15\ K) = (2.37 \pm 0.20)$, $\Delta\varepsilon = -(0.21 \pm 0.04)\ kg \cdot mol^{-1}$. The value fixed for $\log_{10}\beta_3°(298.15\ K)$ was calculated from the temperature function shown in Fig. 29.5-6. For comparison, the unconstrained extrapolation by Gamsjäger et al. (2012) is shown as light grey lines. The three data points at I = 0 were only used in the unconstrained extrapolation.

Tab. 29.5-6: Comparison of ε values of Sn(II) chloride complexes obtained from the $\Delta\varepsilon$ values listed in Tab. 29.5-5

	Gamsjäger et al. (2012)	**This work, from unconstrained SIT analysis**	**TDB 2020, from constrained SIT analysis**
$\varepsilon(SnCl^+, ClO_4^-)$	0.08 ± 0.07	0.06 ± 0.06	0.04 ± 0.05
$\varepsilon(SnCl_2, NaClO_4)$	0.00 ± 0.07	-0.02 ± 0.07	0.00 ± 0.06
$\varepsilon(SnCl_3^-, Na^+)$	0.04 ± 0.07	0.02 ± 0.07	0.07 ± 0.06

29.5.1.2.2 Aqueous tin(IV) chloride complexes

According to Gamsjäger et al. (2012) there are only very few experimental data available for equilibria of Sn(IV) chloride complexes, and some of the data concerning $\log_{10}\beta_q$ values for the reaction $Sn^{4+} + q\ Cl^- \rightleftharpoons SnCl_q^{4-q}$ differ by enormous margins. In the case of $\log_{10}\beta_6$, e.g., reported values vary from 1.6 – 12.4. Gamsjäger et al. (2012) argued that the reason for such large discrepancies is probably due to the very large tendency of Sn(IV) to hydrolysis: In moderately acidic solutions, hydrolysis leads to reactions of the type

$$Sn(OH)_x^{4-x} + Cl^- \rightleftharpoons SnCl_q(OH)_y^{4-y-q} + (x - y)\ OH^-$$

whose equilibrium constants are obviously much smaller than those for the corresponding unhydrolyzed Sn(IV) chloride complexes. Gamsjäger et al. (2012) cite a Mössbauer spectroscopic study showing that the main species in a 1 M HCl solution of Sn(IV) are $SnCl_4(OH)_2^{2-}$ and $SnCl_3(OH)_3^{2-}$. The complete suppression of Sn(IV) hydrolysis can only be achieved in at least about 5 M $HClO_4$ (Fatouros et al. 1978). Because of this and the lack of reliable data for Sn(IV) hydrolysis under acidic conditions (see Section 29.4.1.3), Gamsjäger et al. (2012) only considered experimental determinations of stability constants for $SnCl_q^{4-q}$ (q = 1 – 6) carried out in at least 4.5 M $HClO_4$, i.e. the potentiometric measurements by Fatouros et al. (1978) in 5.0 M $HClO_4$ and the spectrophotometric determinations by Gajda et al. (2009) at five different $HClO_4$ concentrations (4.5 – 8.0 M). The latter measurements were made in connection with the determination of the standard electrode potential for the redox couple Sn^{4+}/Sn^{2+} (see Section 29.3). Comparing the results by Fatouros et al. (1978) and Gajda et al. (2009), Gamsjäger et al. (2012) concluded that both studies confirmed the expected high stability of Sn(IV) chloride complexes, but noted that the succession of the stepwise conditional stability constants reported by Fatouros et al. (1978), $\log_{10}K_3 = 2.32$, $\log_{10}K_4 = 0.7$, and $\log_{10}K_5 = 1.75$, is non-regular and not steadily decreasing, as one would expect from the observed octahedral geometry (indicated by ^{119}Sn NMR chemical shifts) of all Sn(IV) chloride complexes. In contrast, $\log_{10}K_4 < < \log_{10}K_5$ would suggest a change in the coordination geometry during the reaction $SnCl_3^+ + Cl^- \rightleftharpoons SnCl_4(aq)$. Furthermore, Gamsjäger et al. (2012) remarked that a "surprising consequence of these data [by Fatouros et al. (1978)] is that $SnCl_4(aq)$ is only a minor species (max. 10%) in the proposed speciation scheme". For these reasons, Gamsjäger et al. (2012) relied only on the experimental data by Gajda et al. (2009) for deriving stability constants for the Sn(IV) chloride complexes. The latter authors used UV spectroscopy to observe the spectral changes of Sn(IV) perchlorate solutions induced by the addition of chloride. With increased chloride concentrations, spectral changes were observed that reflected changes in the coordination sphere of Sn(IV). The spectral changes were best explained with the formation of $SnCl^{3+}$, $SnCl_2^{2+}$, $SnCl_4(aq)$, $SnCl_5^-$, and $SnCl_6^{2-}$. $SnCl_3^+$, however, was not detected. Gamsjäger et al. (2012) explained this as follows: "Since ^{119}Sn NMR spectra of concentrated $SnCl_4$ solution seem to prove the existence of this species [...], the former observation is probably due to the high similarity of the individual spectrum of $SnCl_3^+$ and $SnCl_4(aq)$, which prevents their differentiation by the method used". Despite this shortcoming, Gamsjäger et al. (2012) accepted the data and the SIT analyses by Gajda et al. (2009) and selected their stability constants and $\Delta\varepsilon$ values, writing on p. 184: "Since the data published in [2009 GAJ/SIP] are more complete (the $\log_{10}\beta_q$ values are reported for five different ionic strengths) the selection in this review is based on the latter publication", and on p. 185: "The above listed selected thermodynamic formation constants correspond to [...]". However, neither the "selected" formation constants, nor any SIT coefficients derivable from the $\Delta\varepsilon$ values are listed in the tables of selected tin data or in the tables of selected ion interaction coefficients. Since Gamsjäger et al. (2012) only presented plots of the SIT extrapolation of the experimental data to zero ionic strength for $SnCl^{3+}$ and $SnCl_6^{2-}$ we redid the SIT analyses and obtained essentially the same values for the

stability constants and $\Delta\varepsilon$ as Gajda et al. (2009)[79]. For comparison, we added the data by Fatouros et al. (1978) in the SIT plots shown in Figs. 29.5-11 to 29.5-15. We include the data obtained by Gajda et al. (2009) and "selected" by Gamsjäger et al. (2012) as supplemental data only in TDB 2020 because $SnCl_3^+$ and $SnCl_4(aq)$ could not be distinguished with UV spectroscopy and because the unhydrolyzed Sn(IV) chloride complexes $SnCl_q^{4-q}$ observable only in extremely acid $HClO_4$ solutions (at least about 4.5 M $HClO_4$) are irrelevant for the purposes of TDB 2020. Thus, the following supplemental data are included in TDB 2020:

$$Sn^{4+} + Cl^- \rightleftharpoons SnCl^{3+}$$

$$\log_{10}\beta_1°(298.15\ K) = (3.19 \pm 0.50)$$

$$\Delta\varepsilon = -(0.26 \pm 0.06)\ kg \cdot mol^{-1}$$

$$Sn^{4+} + 2\ Cl^- \rightleftharpoons SnCl_2^{2+}$$

$$\log_{10}\beta_2°(298.15\ K) = (5.95 \pm 0.36)$$

$$\Delta\varepsilon = -(0.45 \pm 0.04)\ kg \cdot mol^{-1}$$

$$Sn^{4+} + 4\ Cl^- \rightleftharpoons SnCl_4(aq)$$

$$\log_{10}\beta_4°(298.15\ K) = (9.57 \pm 0.32)$$

$$\Delta\varepsilon = -(0.64 \pm 0.03)\ kg \cdot mol^{-1}$$

$$Sn^{4+} + 5\ Cl^- \rightleftharpoons SnCl_5^-$$

$$\log_{10}\beta_5°(298.15\ K) = (10.93 \pm 0.41)$$

$$\Delta\varepsilon = -(0.60 \pm 0.04)\ kg \cdot mol^{-1}$$

$$Sn^{4+} + 6\ Cl^- \rightleftharpoons SnCl_6^{2-}$$

$$\log_{10}\beta_6°(298.15\ K) = (9.83 \pm 0.49)$$

$$\Delta\varepsilon = -(0.67 \pm 0.05)\ kg \cdot mol^{-1}$$

From the selected values for $\Delta\varepsilon$ and the selected $\varepsilon(Sn^{4+}, ClO_4^-) = (0.7 \pm 0.2)$ kg · mol^{-1} and $\varepsilon(Cl^-, H^+) = (0.12 \pm 0.01)$ kg · mol^{-1} follow

$$\varepsilon(SnCl^{3+}, ClO_4^-) = (0.56 \pm 0.21)\ kg \cdot mol^{-1}$$

$$\varepsilon(SnCl_2^{2+}, ClO_4^-) = (0.49 \pm 0.20)\ kg \cdot mol^{-1}$$

$$\varepsilon(SnCl_4(aq), HClO_4(aq)) = (0.54 \pm 0.21)\ kg \cdot mol^{-1}$$

$$\varepsilon(SnCl_5^-, H^+) = (0.70 \pm 0.21)\ kg \cdot mol^{-1}$$

$$\varepsilon(SnCl_6^{2-}, H^+) = (0.75 \pm 0.21)\ kg \cdot mol^{-1}$$

---

[79] The sole exceptions are negligible differences in $\log_{10}\beta_4°$(298.15 K), where we obtained 9.58 ± 0.32 instead of 9.57 ± 0.32 by Gajda et al. (2009), in $\log_{10}\beta_5°$(298.15 K), where we obtained 10.94 ± 0.41 instead of 10.94 ± 0.41, and in $\log_{10}\beta_6°$(298.15 K), where we obtained 9.84 ± 0.49 instead of 9.83 ± 0.49.

These data are also included in TDB 2020, as well as the estimates, following the estimation method described in Section 1.5.3,

$\varepsilon(SnCl_4(aq), NaCl\ (aq)) \approx \varepsilon(SnCl_4(aq), NaClO_4(aq)) \approx (0.0 \pm 0.1)\ kg \cdot mol^{-1}$

$\varepsilon(SnCl_5^-, Na^+) = -(0.05 \pm 0.10)\ kg \cdot mol^{-1}$

$\varepsilon(SnCl_6^{2-}, Na^+) = -(0.10 \pm 0.101)\ kg \cdot mol^{-1}$

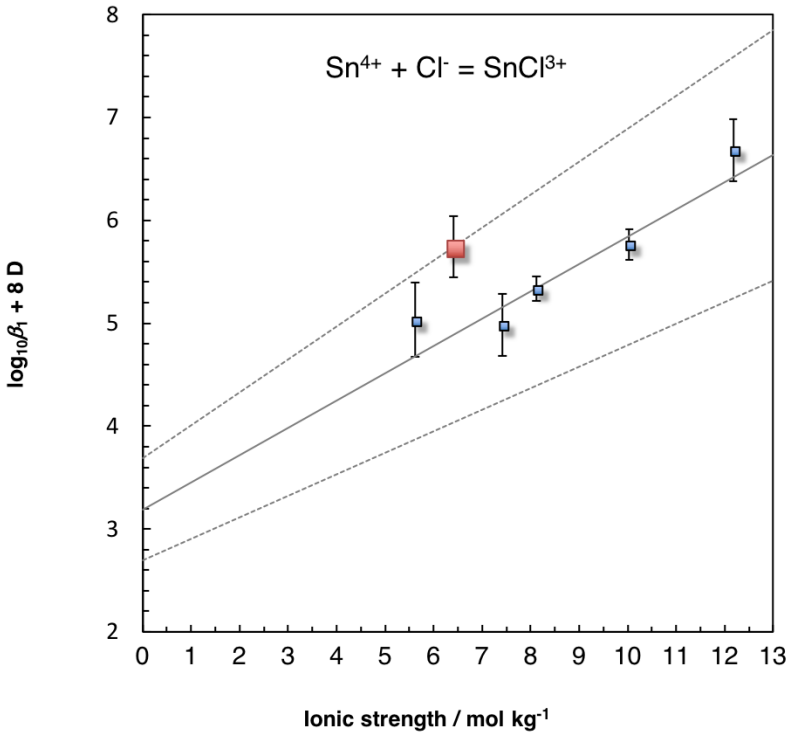

Fig. 29.5-11: Extrapolation to $I = 0$ of experimental data (blue: Gajda et al. 2009, see Tab. A-77 in Gamsjäger et al. 2012) for $Sn^{4+} + Cl^- \rightleftharpoons SnCl^{3+}$ using SIT

The red data point (Fatouros et al. 1978) was not used for the extrapolation. $log_{10}\beta_1°(298.15\ K) = (3.19 \pm 0.50)$. $\Delta\varepsilon = -(0.26 \pm 0.06)\ kg \cdot mol^{-1}$

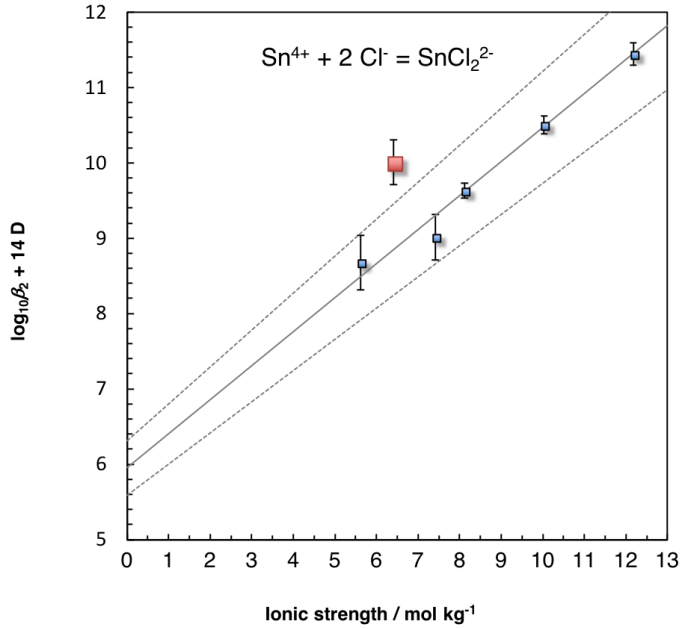

Fig. 29.5-12: Extrapolation to $I = 0$ of experimental data (blue: Gajda et al. 2009, see Tab. A-77 in Gamsjäger et al. 2012) for $Sn^{4+} + 2\ Cl^- \rightleftharpoons SnCl_2^{2+}$ using SIT

The red data point (Fatouros et al. 1978) was not used for the extrapolation. $log_{10}\beta_2°(298.15\ K) = (5.95 \pm 0.36)$, $\Delta\varepsilon = -(0.45 \pm 0.04)\ kg \cdot mol^{-1}$

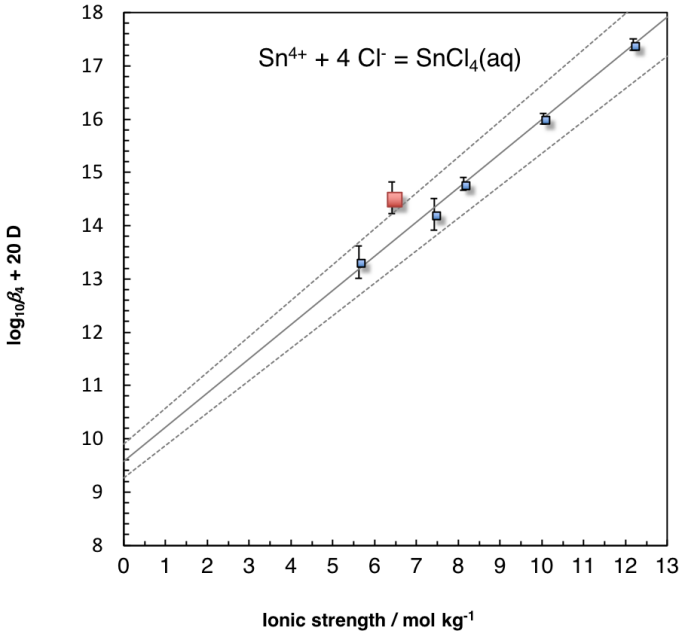

Fig. 29.5-13: Extrapolation to $I = 0$ of experimental data (blue: Gajda et al. 2009, see Tab. A 77 in Gamsjäger et al. 2012) for $Sn^{4+} + 4\ Cl^- \rightleftharpoons SnCl_4(aq)$ using SIT

The red data point (Fatouros et al. 1978) was not used for the extrapolation. $log_{10}\beta_4°(298.15\ K) = (9.58 \pm 0.32)$, $\Delta\varepsilon = -(0.64 \pm 0.03)\ kg \cdot mol^{-1}$. There is a negligible difference between this value for $\log_{10}\beta_4°(298.15\ K)$ and that of 9.57 ± 0.32 obtained by Gamsjäger et al. 2012).

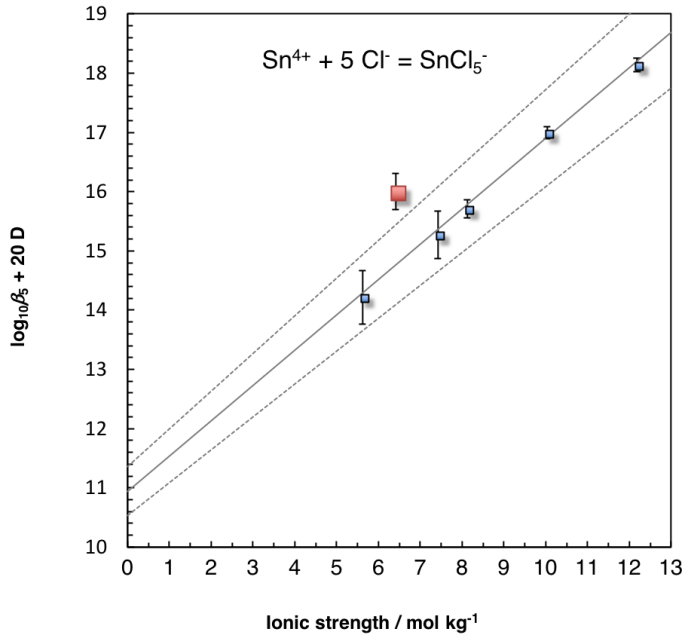

Fig. 29.5-14: Extrapolation to $I = 0$ of experimental data (blue: Gajda et al. 2009, see Tab. A-77 in Gamsjäger et al. 2012) for $Sn^{4+} + 5\ Cl^- \rightleftharpoons SnCl_5^-$ using SIT

The red data point (Fatouros et al. 1978) was not used for the extrapolation. *$log_{10}\beta_5°(298.15\ K) = (10.94 \pm 0.41)$, $\Delta\varepsilon = -(0.60 \pm 0.04)\ kg \cdot mol^{-1}$*. There is a negligible difference between this value for $\log_{10}\beta_5°(298.15\ K)$ and that of 10.93 ± 0.41 obtained by Gamsjäger et al. 2012).

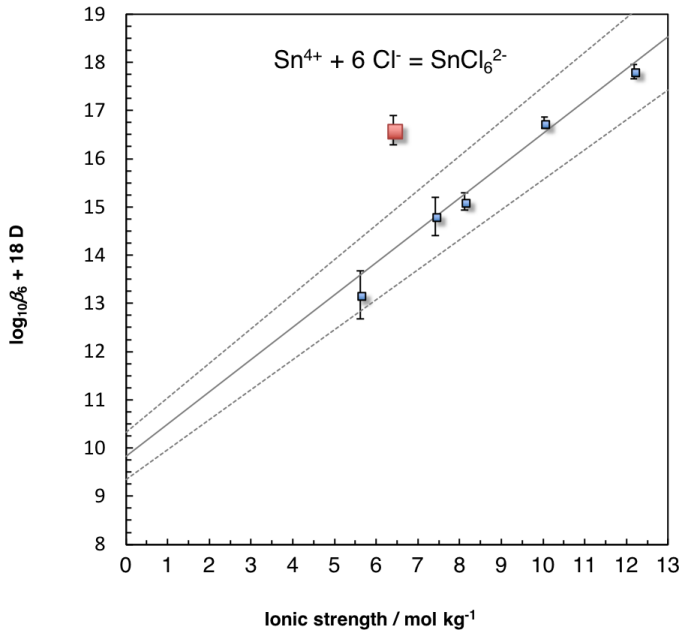

Fig. 29.5-15: Extrapolation to $I = 0$ of experimental data (blue: Gajda et al. 2009, see Tab. A 77 in Gamsjäger et al. 2012) for $Sn^{4+} + 6\ Cl^- \rightleftharpoons SnCl_6^{2-}$ using SIT

The red data point (Fatouros et al. 1978) was not used for the extrapolation. *$log_{10}\beta_6°(298.15\ K) = (9.84 \pm 0.49)$, $\Delta\varepsilon = -(0.67 \pm 0.05)\ kg \cdot mol^{-1}$*. There is a negligible difference between this value for $\log_{10}\beta_6°(298.15\ K)$ and that of 9.83 ± 0.49 obtained by Gamsjäger et al. 2012).

and the estimates (see Section 29.1.1)

$$\varepsilon(SnCl^{3+}, Cl^-) \approx \varepsilon(SnCl^{3+}, ClO_4^-) = (0.56 \pm 0.21)\ kg \cdot mol^{-1}$$

$$\varepsilon(SnCl_2^{2+}, Cl^-) \approx \varepsilon(SnCl_2^{2+}, ClO_4^-) = (0.49 \pm 0.20)\ kg \cdot mol^{-1}$$

29.5.1.3 Aqueous tin bromide complexes

29.5.1.3.1 Aqueous tin(II) bromide complexes

Gamsjäger et al. (2012) compiled formation constants for the Sn(II) bromide complexes $SnBr^+$, $SnBr_2(aq)$, $SnBr_3^-$, $SnBr_4^{2-}$, $SnBr_5^{3-}$, and $SnBr_6^{4-}$ but only accepted data for $SnBr^+$, $SnBr_2(aq)$, and $SnBr_3^-$. The higher complexes $SnBr_5^{3-}$, and $SnBr_6^{4-}$ were found in a potentiometric study in $NaClO_4$ only at I = 8.0 M with a very high excess of bromide over tin, while experimental data up to I = 4.0 M could be well represented by $SnBr^+$, $SnBr_2(aq)$, and $SnBr_3^-$, without taking $SnBr_4^{2-}$ into account.

For the formation of $SnBr^+$, Gamsjäger et al. (2012) accepted 10 data points from 6 studies (one using kinetics, one voltammetry, and the others potentiometry) in the range from 0 – 6.0 $NaClO_4$. Extrapolation of the data to I = 0 using SIT resulted in

$$Sn^{2+} + Br^- \rightleftharpoons SnBr^+$$

$$\log_{10}\beta_1^\circ(298.15\ K) = (1.33 \pm 0.18)$$

$$\Delta\varepsilon = -(0.10 \pm 0.05)\ kg \cdot mol^{-1}$$

From $\Delta\varepsilon$ and the selected $\varepsilon(Sn^{2+}, ClO_4^-) = (0.19 \pm 0.04)\ kg \cdot mol^{-1}$ and $\varepsilon(Br^-, Na^+) = (0.05 \pm 0.01)\ kg \cdot mol^{-1}$, see Tab. 29.9-3 and 29.9-5, Gamsjäger et al. (2012) obtained

$$\varepsilon(SnBr^+, ClO_4^-) = (0.15 \pm 0.07)\ kg \cdot mol^{-1}$$

which also serves as an estimate for $\varepsilon(SnBr^+, Cl^-)$, see Section 29.1.1. Thus,

$$\varepsilon(SnBr^+, Cl^-) \approx \varepsilon(SnBr^+, ClO_4^-) = (0.15 \pm 0.07)\ kg \cdot mol^{-1}$$

For the 1:2 complex, Gamsjäger et al. (2012) accepted 8 data points from 5 studies (one using voltammetry, the others potentiometry) in the range from 0 – 6.0 $NaClO_4$. An SIT analysis resulted in

$$Sn^{2+} + 2\ Br^- \rightleftharpoons SnBr_2(aq)$$

$$\log_{10}\beta_2^\circ(298.15\ K) = (1.97 \pm 0.21)$$

$$\Delta\varepsilon = -(0.16 \pm 0.05)\ kg \cdot mol^{-1}$$

with

$\varepsilon(SnBr_2(aq), NaClO_4(aq)) = (0.14 \pm 0.07)$

calculated from $\Delta\varepsilon$ and the selected $\varepsilon(Sn^{2+}, ClO_4^-)$ and $\varepsilon(Br^-, Na^+)$, see Tab. 29.9-3 and 29.9-5. Using $\varepsilon(SnBr_2(aq), NaClO_4(aq))$ as an estimate for $\varepsilon(SnBr_2(aq), NaCl(aq))$, see Section 29.1.1, leads to

$\varepsilon(SnBr_2(aq), NaCl(aq)) \approx \varepsilon(SnBr_2(aq), NaClO_4(aq)) = (0.14 \pm 0.07)$

For the 1:3 complex, finally, Gamsjäger et al. (2012) accepted 6 data points from 4 studies (one using voltammetry, the others potentiometry) in the range from 0 – 6.0 $NaClO_4$. From an SIT analysis of the data, Gamsjäger et al. (2012) obtained

$Sn^{2+} + 3\ Br^- \rightleftharpoons SnBr_3^-$

$\log_{10}\beta_3°(298.15\ K) = (1.93 \pm 0.27)$

$\Delta\varepsilon = -(0.18 \pm 0.06)\ kg \cdot mol^{-1}$

with

$\varepsilon(SnBr_3^-, Na^+) = (0.16 \pm 0.08)\ kg \cdot mol^{-1}$

calculated from $\Delta\varepsilon$ and the selected $\varepsilon(Sn^{2+}, ClO_4^-)$ and $\varepsilon(Br^-, Na^+)$, see Tab. 29.9-3 and 29.9-5.

These data for $SnBr^+$, $SnBr_2(aq)$, and $SnBr_3^-$ are all included in TDB 2020.

Gamsjäger et al. (2012) also derived reaction enthalpies from stability constants measured in a study by potentiometry in 3.0 M $NaClO_4$ at 0, 25, 35, and 45 °C. Since it is reasonable to assume that these reaction enthalpies are dependent on ionic strength, as is the case for the reaction enthalpies of $SnCl^+$ and $SnCl_2(aq)$, see Section 29.5.1.2.1, Gamsjäger et al. (2012) did not select them but suggested that they can be used as estimates for the standard reaction enthalpies. Hence, the following estimates are included in TDB 2020 as supplemental data:

$\Delta_r H_m°(Sn^{2+} + Br^- \rightleftharpoons SnBr^+, 298.15\ K) \approx$

$\Delta_r H_m(Sn^{2+} + Br^- \rightleftharpoons SnBr^+, 3.0\ M\ NaClO_4) = (5.1 \pm 2.0)\ kJ \cdot mol^{-1}$

$\Delta_r H_m°(Sn^{2+} + 2\ Br^- \rightleftharpoons SnBr_2(aq), 298.15\ K) \approx$

$\Delta_r H_m(Sn^{2+} + 2\ Br^- \rightleftharpoons SnBr_2(aq), 3.0\ M\ NaClO_4) = (12.9 \pm 2.0)\ kJ \cdot mol^{-1}$

$\Delta_r H_m°(Sn^{2+} + 3\ Br^- \rightleftharpoons SnBr_3^-, 298.15\ K) \approx$

$\Delta_r H_m(Sn^{2+} + 3\ Br^- \rightleftharpoons SnBr_3^-, 3.0\ M\ NaClO_4) = (7.2 \pm 4.0)\ kJ \cdot mol^{-1}$

These reaction enthalpies were derived from linear van't Hoff plots. This implies that the corresponding heat capacities of reaction are zero. Thus

$$\Delta_r C_{p,m}°(Sn^{2+} + Br^- \rightleftharpoons SnBr^+, 298.15\ K) \approx \Delta_r C_{p,m}(Sn^{2+} + Br^- \rightleftharpoons SnBr^+, 3.0\ M\ NaClO_4) = 0$$

$$\Delta_r C_{p,m}°(Sn^{2+} + 2\ Br^- \rightleftharpoons SnBr_2(aq), 298.15\ K) \approx$$

$$\Delta_r C_{p,m}(Sn^{2+} + 2\ Br^- \rightleftharpoons SnBr_2(aq), 3.0\ M\ NaClO_4) = 0$$

$$\Delta_r C_{p,m}°(Sn^{2+} + 3\ Br^- \rightleftharpoons SnBr_3^-, 298.15\ K) \approx$$

$$\Delta_r C_{p,m}(Sn^{2+} + 3\ Br^- \rightleftharpoons SnBr_3^-, 3.0\ M\ NaClO_4) = 0$$

are also included in TDB 2020 as supplemental data.

29.5.1.3.2 Aqueous tin(IV) bromide complexes

Gamsjäger et al. (2012) discussed a spectroscopic study of Sn(IV) bromide complexes, but did not accept the results, since the proposed speciation scheme did not involve any partially hydrolysed bromide complexes, which are to be expected due to the strong hydrolysis of Sn(IV), see also Section 29.5.1.2.2.

29.5.1.4 Aqueous tin iodide complexes

Formation constants for Sn(II) iodide complexes were reported by two studies. The only reliable constants for the complexes SnI^+, $SnI_2(aq)$, SnI_3^-, SnI_4^{2-}, SnI_6^{4-}, and SnI_8^{6-} were obtained at I = 4.0 M in $NaClO_4$ (with substantial replacement of the background electrolyte by NaI). Without additional data, these conditional formation constants cannot be extrapolated to zero ionic strength and were therefore not selected by Gamsjäger et al. (2012).

According to Gamsjäger et al. (2012), there are apparently no thermodynamic data available for any Sn(IV) iodide complexes.

29.5.1.5 Mixed aqueous tin halogen and thiocyanate complexes

Gamsjäger et al. (2012) reported conditional formation constants for the mixed aqueous tin(II) halogen and thiocyanate complexes SnClBr(aq), $SnCl_2Br^-$, $SnClBr_2^-$, SnCl(SCN)(aq), $SnCl_2(SCN)^-$, and $SnCl(SCN)_2^-$ obtained in two studies in 0.5 – 6.0 M $NaClO_4$. The $NaClO_4$ media in these experiments were completely replaced during measurement of the ternary complexes, causing considerable changes in the activity coefficients. Therefore, Gamsjäger et al. (2012) were not able to derive any selected values.

Gamsjäger et al. (2012) also reported conditional formation constants for the mixed aqueous tin(IV) halogen complexes $SnClF_5^{2-}$, $SnCl_2F_4^{2-}$, and $SnBrF_5^{2-}$. NMR spectroscopy of these complexes was carried out in 1.2 M $(NH_4)_2SnF_6$ + 3 M (H, NH_4)Cl. Unable to extrapolate the data to zero ionic strength, Gamsjäger et al. (2012) did not select any of them.

29.5.2 Solid tin halides

29.5.2.1 Solid tin fluorides

Gamsjäger et al. (2012) selected calorimetric data for SnF_2(cr) and the ternary fluorides $PbSnF_4$(cr), $BaSnF_4$(cr) and $SrSnF_4$(cr). Since SnF_2(cr) is highly soluble and the thermodynamic data for the ternary fluorides only comprise $S_m°$(298.15 K), $C_{p,m}°$(298.15 K) and $C_{p,m}°(T)$, these solids are not included in TDB 2020. Gamsjäger et al. (2012) also discussed solubility experiments of SnF_2(cr) but did not select any solubility products. They also mentioned SnF_4(s) and SnO(OH)F(s) but did not select any data.

29.5.2.2 Solid tin chlorides

$SnCl_2$(cr) and $SnCl_2·2H_2O$(cr) are very soluble. The calorimetric data selected by Gamsjäger et al. (2012) are therefore not included in TDB 2020. Gamsjäger et al. (2012) also discussed the solubility of $SnCl_2$(s) but did not select any data. They also mentioned $SnCl_2·SnF_2$(s), $SnCl_2·3SnF_2$(s), $Sn(OH)Cl_3·3H_2O$(s), $Sn(OH)_2Cl_2$(s), and $Sn(OH)_3Cl·H_2O$(s) but, again, selected no data.

According to Gamsjäger et al. (2012), white or colourless solids precipitate when concentrated aqueous Sn(II) chloride solutions are diluted or alkalized. Numerous stoichiometries of such basic Sn(II) chloride solids have been proposed. Gamsjäger et al. (2012), however, concluded that all these stoichiometries refer to mixtures of abhurite, $Sn_{21}Cl_{16}(OH)_{14}O_6$(cr), and a Sn(II) chloride oxide formed as an artefact during synthesis and isolation of the solid. Abhurite was originally described as an alteration product of tin ingots found in a shipwreck in the Red Sea (see Edwards et al. 1992 and references therein). It was observed in blisters on the surface of the corroding ingots where the pH of the enclosed solution was around 1. Edwards et al. (1992) calculated stability field diagrams (pH vs. log $a(Cl^-)$) for the system SnO-HCl-H_2O at 298.15 K and 10^5 Pa. According to this diagram, romarchite, SnO(cr), is more stable than abhurite across the whole pH range at low salinities. In order for abhurite to be stable at pH = 3, log $a(Cl^-)$ would need to be larger than 0. Thus, the stability of abhurite lies clearly outside the application range of TDB 2020 and the solubility product of abhurite selected by Gamsjäger et al. (2012) is not included.

29.5.2.3 Solid tin bromides

Gamsjäger et al. (2012) selected calorimetric data for $SnBr_2$(cr) and $SnBr_4$(cr). Since both of these solids are soluble in water, they are not included in TDB 2020. Gamsjäger et al. (2012) also discussed the solubility of $SnBr_2$(s), but did not give any quantitative data. They also mentioned the existence of SnBrF(s), Sn_3BrF_5(s), $SnBr_4·4H_2O$(s), $SnBr_4·8H_2O$(s), and $Sn(OH)Br_3·3H_2O$(s), but did not select any data.

29.5.2.4 Solid tin iodides

Gamsjäger et al. (2012) selected calorimetric data for SnI_2(cr) and SnI_4(cr) and also discussed solubility data for SnI_2(cr) but did not select a solubility product. Both solids do not occur in nature (i.e., they are not minerals). SnI_2(cr) is slightly soluble in water: In pure water, Young (1897) measured solubilities of 1.03 g/100 g solution at 20.8 °C and 0.96 g/100 g solution at 19.8 °C. This corresponds roughly to a 0.03 molar solution of SnI_2, making it very improbable for SnI_2(cr) to limit the solubility of either Sn(II) or iodide in repository systems. Hence, SnI_2(cr) is not included in TDB 2020. SnI_4(cr) is not stable in the presence of water, when brought in contact with a limited amount of pure water it hydrolyses to form a gel-like precipitate of Sn(IV) hydroxide which dissolves when the amount of water is increased (Hickling 1990). Therefore, SnI_4(cr) is not included in TDB 2020 as well.

29.5.3 Gaseous tin halides

Gamsjäger et al. (2012) selected thermodynamic data for the gaseous halides SnF_2g, $SnCl_2$g, $SnCl_4$g, $SnBr_2$g, $SnBr_4$g, SnI_2g, and SnI_4g. As gaseous halides are hardly of any relevance to the purposes of TDB 2020, they are not included.

29.5.4 Liquid tin halides

According to Gamsjäger et al. (2012), $SnCl_4$(cr) melts at 239.05 K. Thus, $SnCl_4$(l) is stable above -34.1 °C. Since $SnCl_4$(l) is hardly of any relevance to the purposes of TDB 2020, the data selected by Gamsjäger et al. (2012) for this liquid are not considered for TDB 2020.

29.6 Sulphur compounds and complexes

29.6.1 Aqueous tin sulphide complexes

Data on the formation of aqueous Sn(II) and Sn(IV) sulphide complexes are exceedingly rare. Gamsjäger et al. (2012) only reported the results of two studies (Babko & Lisetskaya 1956, Hseu & Rechnitz 1968) concerning the formation of the thiostannate ion (SnS_3^{2-}) from SnS_2(s) according to the reaction $SnS_2(s) + S^{2-} \rightleftharpoons SnS_3^{2-}$. Gamsjäger et al. (2012) recalculated the equilibrium constants from these studies by using the first protonation constant for the sulphide ion of $\log_{10}K_1°(S^{2-} + H^+ \rightleftharpoons HS^-$, 298.15 K) = (19.0 ± 2.0) instead of 14.92 used by Babko & Lisetskaya (1956) and 14.44 used by Hseu & Rechnitz (1968).

Since the value of the first protonation constant of S^{2-} is highly uncertain (see, e.g., Section 5.19.1.3 in Hummel et al. 2002), Gamsjäger et al. (2012) preferred to consider the reaction $SnS_2(s) + HS^- \rightleftharpoons SnS_3^{2-} + H^+$ which is thermodynamically better constrained. According to Gamsjäger et al. (2012), only Babko & Lisetskaya (1956) provided sufficient data for deriving an equilibrium constant for this reaction. However, Gamsjäger et al. (2012) reported several shortcomings of the experimental data presented by Babko & Lisetskaya (1956) and Hseu & Rechnitz (1968): Babko & Lisetskaya (1956) did not describe the method used for the determination of the concentrations in the colloidal SnS_2 suspensions and the ionic strength was probably not controlled, as the solutions contained an unknown amount of acetate-ammonium buffer. Hseu & Rechnitz (1968) used a newly developed Ag_2S based membrane electrode for the determination of the sulphide

ion concentration in aqueous solution. While the electrode showed excellent sensitivity, the calibration of the electrode is questionable, due to the high uncertainty of the first protonation constant of S^{2-}.

For these reasons, Gamsjäger et al. (2012) did not select the recalculated equilibrium constants[80] but provided them as provisional data "until more data will be published on this system".

There appear to be no other data on tin sulphide complexes. In the comprehensive critical review of inorganic tin species by Séby et al. (2001), e.g., only stability constants for the reaction SnS(s) $\rightleftharpoons Sn^{2+} + S^{2-}$ are reported.

Rickard & Luther (2006) carried out an extensive review on metal sulphide complexes and clusters. They also reported no stability constants for Sn sulphide complexes and concluded that tin "does have a significant sulphide chemistry. SnS may be prepared by reaction of S(-II) with Sn(II) salts. Sn_2S_3 with Sn(III) is also known. However, very little appears to be known about Sn sulphide complexes. The main interest has been in polynuclear Sn sulphide clusters, which display complex structures". Rickard & Luther (2006) mentioned $(Sn_5S_{12}^{4-})_\infty$ in Cs salts, $(Sn_3S_7^{2-})_\infty$ in Rb salts and the $Sn_2S_6^{4-}$ anion and finally stated that "Séby [sic] et al. (2001) reviewed all published inorganic thermodynamic data on Sn sulfides and only noted various measurements of the solubility of SnS to produce the $Sn(II)_{aq}$ ion and free S(-II). No data on Sn sulphide complexes were reported. It appears that it is possible that a significant inorganic Sn sulphide complex chemistry exists which has not been widely investigated as yet".

29.6.2 Tin sulphide solids

Gamsjäger et al. (2012) selected calorimetric data for the tin sulphide solids SnS(α) (herzenbergite), Sn_2S_3(cr) (ottemannite), and SnS_2(cr) (berndtite), and for the ternary sulfides Cu_8SnS_6(cr), Cu_4SnS_4(cr), Cu_2SnS_3(cr) (mohite), and $Cu_2Sn_4S_9$(cr). Of these solids, the tin sulphide minerals herzenbergite, ottemannite, and berndtite, are rather rare and have never been found in mineable quantities (Clark 1972). The ternary sulphide mohite is also rare and was first described in 1982 (Fleischer & Pabst 1983). Herzenbergite and mohite are of hydrothermal origin, while ottemannite and berndtite were first described by Moh & Berndt (1964) as secondary minerals in a zone of secondary enrichment or oxidation of a tin orebody (Cerro de Potosí, Bolivia).

Without selecting any data, Gamsjäger et al. (2012) also mentioned $Cu_4Sn_3S_8$(cr), as well as Sn_3S_4(cr), which is most likely a mixture of SnS(cr) and Sn_2S_3(cr), and Sn_4S_5(cr), which is most likely a mixture of 2 SnS(cr) and Sn_2S_3(cr).

Gamsjäger et al. (2012) also discussed several solubility studies involving SnS(cr) and SnS_2(cr), without selection of data (since they preferred the calorimetric data mentioned above).

We chose to exclude all the data selected by Gamsjäger et al. (2012) for tin sulphide solids from TDB 2020 because no stability constants of tin sulphide complexes are known – besides the uncertain formation constant of SnS_3^{2-} from SnS_2(s) – and this may lead to a severe underestimation of tin solubility in sulfidic systems, especially under alkaline conditions.

---

[80] $\log_{10}K(SnS_2(s) + S^{2-} \rightleftharpoons SnS_3^{2-}, 293.15\ K) = (9.1 \pm 2.0)$, recalculated from Babko & Lisetskaya (1956), $\log_{10}K(SnS_2(s) + S^{2-} \rightleftharpoons SnS_3^{2-}, 298.15\ K) = (9.2 \pm 2.0)$, recalculated from Hseu & Rechnitz (1968), $\log_{10}K(SnS_2(s) + HS^- \rightleftharpoons SnS_3^{2-} + H^+, 293.15\ K) = (-9.9 \pm 1.0)$, recalculated from Babko & Lisetskaya (1956)

29.6.3 Aqueous tin sulphate complexes

29.6.3.1 Aqueous tin(II) sulphate complexes

There appear to be only two studies concerning the stability of Sn(II) sulphate complexes. Gamsjäger et al. (2012) accepted the data by Wada & Ito (1975) based on potentiometric titrations in 0.037 to 1 M (H, Na)ClO_4 at 25 °C. Wada & Ito (1975) considered the formation of both $SnSO_4$(aq) and $SnHSO_4^+$. Gamsjäger et al. (2012) carried out an SIT analysis of the data which resulted in an unrealistically high $\Delta\varepsilon$ value (0.85 kg · mol^{-1}) for the reaction $Sn^{2+} + HSO_4^- \rightleftharpoons SnHSO_4^+$. For this reason, Gamsjäger et al. (2012) decided to neglect $SnHSO_4^+$ and reevaluated the data only in terms of $SnSO_4$(aq). From SIT they obtained

$$Sn^{2+} + SO_4^{2-} \rightleftharpoons SnSO_4(aq)$$

$$\log_{10}\beta_1°(298.15\ K) = (3.43 \pm 0.25)$$

with

$$\Delta\varepsilon = (0.11 \pm 0.33)\ kg \cdot mol^{-1}$$

from which they calculated

$$\varepsilon(SnSO_4(aq), NaClO_4(aq)) = (0.19 \pm 0.35)\ kg \cdot mol^{-1}$$

using the selected $\varepsilon(Sn^{2+}, ClO_4^-) = (0.19 \pm 0.04)$ kg · mol^{-1} and $\varepsilon(SO_4^{2-}, Na^+) = -(0.12 \pm 0.06)$ kg · mol^{-1}, see Tab. 29.9-3 and 29.9-5. Using $\varepsilon(SnSO_4(aq), NaClO_4(aq))$ as an estimate for $\varepsilon(SnSO_4(aq), NaCl(aq))$, see Section 29.1.1, results in

$$\varepsilon(SnSO_4(aq), NaCl(aq)) \approx \varepsilon(SnSO_4(aq), NaClO_4(aq)) = (0.19 \pm 0.35)\ kg \cdot mol^{-1}$$

These values for $SnSO_4$(aq) are all included in TDB 2020.

Wada & Ito (1975) also measured $\log_{10}\beta_1$ at I = 0.5 M for four different temperatures between 15 and 45 °C. They derived $\Delta_r H_m°(298.15\ K)$[81] = 4.05 kcal · mol^{-1} from the almost perfect linear trend of $\log_{10}\beta_1$ vs. 1/T. According to their Fig. 5, the $\log_{10}\beta_1$ values increase from about 1.75 at 15 °C to about 2 at 45 °C, in clear contradiction to the values of $\log_{10}\beta_1(298.15\ K)$ listed in their Tab. 1, which are > 3 for all ionic strengths (0.037-1.0 M). Since the paper by Wada & Ito (1975) is in Japanese, we cannot resolve this issue and the value for $\Delta_r H_m°(298.15\ K)$ by Wada & Ito (1975) is not included in TDB 2020. Gamsjäger et al. (2012) reported the value and stated that it "can be used as tentative value".

---

[81] We assume that this value refers to I = 0.

The voltammetric study by Pettine et al. (1981) reported formation constants for $SnSO_4(aq)$ and $Sn(SO4)_2^{2-}$. Measurements were carried out in 1.5 M $NaNO_3$ or in a self-medium with increasing concentrations of Na_2SO_4. According to Gamsjäger et al. (2012), the limited number of data did not allow a correct SIT extrapolation and the data were therefore not accepted.

29.6.3.2 Aqueous tin(IV) sulphate complexes

Gamsjäger et al. (2012) reported the results of three publications by the same author concerning the formation of $SnSO_4^{2+}$ and $Sn(SO_4)_2(aq)$. Gamsjäger et al. (2012) did not dispute the existence of Sn(IV) sulphate complexes. However, due to deficiencies in the derivation of the stability constants (neglect of Sn(IV) hydroxide complexes, of possible mixed hydroxide-sulphate complexes, and of complexes with HSO_4^-), Gamsjäger et al. (2012) did not select these data.

29.6.4 Tin sulphate solids

$SnSO_4(cr)$ is very soluble and does not occur as mineral in nature. Gamsjäger et al. (2012) discussed some solubility data but made no selection.

According to Edwards et al. (1996), the basic Sn(II) sulphate $Sn_3(OH)_2OSO_4(cr)$ is a rare corrosion product found on the surfaces of certain tin alloys and is even less common than the basic Sn(II) chloride abhurite (see Section 29.5.2.2). Using tin amalgam and sulphate ion selective electrodes, Edwards et al. (1996) determined a solubility product for this solid, which was not selected by Gamsjäger et al. (2012) due to deficiencies in the description of the experimental procedures (note, however, that this value still appears in their Tab. III-1 of selected tin compounds and complexes). Since the stability of $Sn_3(OH)_2OSO_4(cr)$ is restricted to very low pH and high sulphate concentrations (Edwards et al. 1996), it is formed under geochemical conditions clearly outside the application range of TDB 2020 and its solubility product is therefore not included in TDB 2020, not even as supplemental datum.

Gamsjäger et al. (2012) also mentioned the basic Sn(II) sulphates $SnSO_4 \cdot SnO(cr)$ and $Sn_3O_2SO_4(cr)$ for which no thermodynamic data are available.

29.7 Group 15 compounds and complexes

29.7.1 Nitrogen compounds and complexes

29.7.1.1 Aqueous tin(II) nitrate complexes

Gamsjäger et al. (2012) found only a single study which investigated the stability of Sn(II) nitrate complexes. The potentiometric measurements were carried out in $NaClO_4$ (1.0 – 8.0 M) using a capillary tin amalgam electrode and the resulting data were interpreted in terms of $SnNO_3^+$, $Sn(NO_3)_2(aq)$, $Sn(NO_3)_3^-$, and $Sn(NO_3)_4^{2-}$. Since these nitrate complexes with Sn(II) are very weak, the experimental investigations required high excesses of nitrate over tin in order to measure the stability constants (especially for the higher complexes $Sn(NO_3)_3^-$ and $Sn(NO_3)_4^{2-}$), and a large part of the background electrolyte needed to be replaced by $NaNO_3$ to ensure constancy of the ionic strength. Gamsjäger et al. (2012) argued that under these circumstances it is not at all obvious how to differentiate between complex formation and medium effects. Therefore, they only accepted data points for which the total concentration of NO_3^- was ≤ 0.6 M (maximum 20% replacement of the background electrolyte). This limited dataset could be well represented in terms of the formation of $SnNO_3^+$ and $Sn(NO_3)_2(aq)$ and Gamsjäger et al. (2012) extrapolated the accepted conditional stability constants (at 1.0, 2.0, 3.0, 4.0, and 6.0 M $NaClO_4$ for the 1:1 complex, and at 3.0, 4.0, and 6.0 M $NaClO_4$ for the 1:2 complex) to zero ionic strength using SIT. Thus Gamsjäger et al. (2012) obtained

$$Sn^{2+} + NO_3^- \rightleftharpoons SnNO_3^+$$

$$\log_{10}\beta_1°(298.15\ K) = (1.27 \pm 0.31)$$

$$\Delta\varepsilon = (0.02 \pm 0.07)\ kg \cdot mol^{-1}$$

and

$$Sn^{2+} + 2\ NO_3^- \rightleftharpoons Sn(NO_3)_2(aq)$$

$$\log_{10}\beta_2°(298.15\ K) = (1.39 \pm 0.53)$$

$$\Delta\varepsilon = (0.01 \pm 0.09)\ kg \cdot mol^{-1}$$

From the respective values of $\Delta\varepsilon$ and the selected $\varepsilon(Sn^{2+}, ClO_4^-) = (0.19 \pm 0.04)\ kg \cdot mol^{-1}$ and $\varepsilon(NO_3^-, Na^+) = -(0.04 \pm 0.03)\ kg \cdot mol^{-1}$, see Tab. 29.9-3 and 29.9-5, they obtained

$$\varepsilon(SnNO_3^+, ClO_4^-) = (0.17 \pm 0.09)\ kg \cdot mol^{-1}$$

and

$$\varepsilon(Sn(NO_3)_2(aq), NaClO_4(aq)) = (0.130 \pm 0.111)\ kg \cdot mol^{-1}$$

Using $\varepsilon(SnNO_3^+, ClO_4^-)$ and $\varepsilon(Sn(NO_3)_2(aq), NaClO_4(aq))$ as estimates for the corresponding ion interaction coefficients with Cl^- and NaCl(aq), see Section 29.1.1, leads to

$$\varepsilon(SnNO_3^+, Cl^-) \approx \varepsilon(SnNO_3^+, ClO_4^-) = (0.17 \pm 0.09)\ kg \cdot mol^{-1}$$

$$\varepsilon(Sn(NO_3)_2(aq), NaCl(aq)) \approx \varepsilon(Sn(NO_3)_2(aq), NaClO_4(aq)) = (0.130 \pm 0.111)$$

All these data for $SnNO_3^+$ and $Sn(NO_3)_2(aq)$ are included in TDB 2020.

29.7.2 Phosphorus compounds and complexes

29.7.2.1 Aqueous tin(II) phosphate complexes

Only two reports were found by Gamsjäger et al. (2012) concerning the formation of Sn(II) phosphate (synonymous with orthophosphate) complexes. They did not accept the stability constants by Duffield et al. (1991) which are based on solubility measurements at constant pH and provide therefore no information on the protonation state of the phosphate ligand. In contrast, Gamsjäger et al. (2012) accepted the data by Ciavatta & Iuliano (2000) who studied complexation equilibria of tin(II) with differently protonated phosphate ions ($H_2PO_4^-$, HPO_4^{2-}, and PO_4^{3-}) in 3 M $NaClO_4$ using potentiometric titrations with tin amalgam and glass electrodes at 25 °C. Concentrations of the metal and the ligand varied from $2.5 \cdot 10^{-4} – 2.5 \cdot 10^{-5}$ M and from 0.01 to 0.3 M, respectively. Ciavatta & Iuliano (2000) interpreted the results in terms of the complexes $SnH_2PO_4^+$, $Sn(H_2PO_4)_2(aq)$, $SnH_2PO_4HPO_4^-$, $SnHPO_4(aq)$, $Sn(HPO_4)_2^{2-}$, $Sn(HPO_4)_3^{4-}$, and $SnPO_4^-$ and reported conditional formation constants $\log_{10}{}^*\beta_c$ (in the molar scale, see Tab. 29.7-1) for their formation reactions according to

$$Sn^{2+} + m\ H_2PO_4^- \rightleftharpoons SnH_{-n}(H_2PO_4)_m^{2-n-m} + n\ H^+$$

Ciavatta & Iuliano (2000) transformed the values for $\log_{10}{}^*\beta_c$ into values for $\log_{10}{}^*\beta_m$ in the molal scale without giving results. We reproduced these calculations using the relation (as given by Grenthe & Puigdomènech 1997)

$$\log_{10}K_m = \log_{10}K_c + \sum\nu_B \log_{10}\rho$$

where $\sum\nu_B$ is the sum (over the substances B) of the stoichiometric coefficients ν_B of the substances taking part in the reaction (with $\nu_B < 0$ for reactants and $\nu_B > 0$ for products) and $\rho = m_B/c_B$, the factor for the conversion of molarity (c_B) to molality (m_B) of a substance B in a specific electrolyte. For 3 M $NaClO_4$, ρ = 1.16776 dm^3 of solution per kg of $H_2O(l)$, see Grenthe & Puigdomènech (1997), Tab. II.4. The resulting values for $\log_{10}{}^*\beta_m$ are listed in Tab. 29.7-1. Ciavatta & Iuliano (2000) then corrected these conditional stability constants to zero ionic strength using SIT with estimated specific ion interaction coefficients for the phosphate complexes. For the estimation methods they referred to Ciavatta (1990). In the case of $Sn(HPO_4)_3^{4-}$, they explicitly stated that they set

$$\varepsilon(Sn(HPO_4)_3^{4-}, Na^+) \approx 3/2\,\varepsilon(HPO_4^{2-}, Na^+)$$

Ciavatta & Iuliano (2000) did not report the values of the estimated coefficients, nor did they report the results of the extrapolations. We tried to reproduce the extrapolations to zero ionic strength by assuming that Ciavatta & Iuliano (2000) used the estimate

$$\varepsilon(ML, XY) \approx 1/2\ [\varepsilon(M, Y) + \varepsilon(L, X)$$

(Ciavatta 1990) for the 1:1 complexes $SnH_2PO_4^+$, $SnHPO_4(aq)$, and $SnPO_4^-$, and the estimate

$$\varepsilon(ML_2, XY) \approx 1/3\ [\varepsilon(M, Y) + 2\ \varepsilon(L, X)$$

(Ciavatta 1990) for the 1:2 complexes $Sn(H_2PO_4)_2(aq)$ and $Sn(HPO_4)_2^{2-}$. For $\varepsilon(SnH_2PO_4HPO_4^-, Na^+)$ we assumed that Ciavatta & Iuliano (2000) made the estimate

$$\varepsilon(SnH_2PO_4HPO_4^-, Na^+) \approx 1/3\ [\varepsilon(Sn^{2+}, ClO_4^-) + \varepsilon(H_2PO_4^-, Na^+) + \varepsilon(HPO_4^{2-}, Na^+)]$$

Using $\varepsilon(Sn^{2+}, ClO_4^-) = 0.3$ kg · mol^{-1} (Ciavatta & Iuliano 2000), $\varepsilon(H_2PO_4^-, Na^+) = -0.11$ kg · mol^{-1} (Ciavatta 1980), $\varepsilon(HPO_4^{2-}, Na^+) = -0.19$ kg · mol^{-1} (Ciavatta 1980), $\varepsilon(PO_4^{3-}, Na^+) = -0.29$ kg · mol^{-1} (Ciavatta 1980), for the above mentioned estimations (resulting values are listed in Tab. 29.7-3), and $\varepsilon(H^+, ClO_4^-) = 0.14$ kg · mol^{-1} (Ciavatta 1980) we calculated the stability constants $\log_{10}{}^*\beta_m^\circ$ listed in Tab. 29.7-1 and converted them, where necessary, into values for $\log_{10}\beta_m^\circ$ of the formation reactions written in terms of the actual ligands (HPO_4^{2-} and PO_4^{3-}, instead of $H_2PO_4^-$) using $\log_{10}{}^*K^\circ(298.15) = -7.198$ for $H_2PO_4^- \rightleftharpoons HPO_4^{2-} + H^+$ and $\log_{10}{}^*K^\circ(298.15) = -12.35$ for $HPO_4^{2-} \rightleftharpoons PO_4^{3-} + H^+$, as did Ciavatta & Iuliano (2000). The resulting values for $\log_{10}\beta_m^\circ$ are listed in Tab. 29.7-2 where they can be compared with those reported by Ciavatta & Iuliano (2000). The recalculated values for $SnH_2PO_4^+$, $SnHPO_4(aq)$, and $SnPO_4^-$ are identical to those by Ciavatta & Iuliano (2000), the value for $Sn(H_2PO_4)_2(aq)$ is 0.1 logarithmic units higher, those for $SnH_2PO_4HPO_4^-$ and $Sn(HPO_3)_3^{4-}$ are 0.2 logarithmic units higher, and that for $Sn(HPO_4)_2^{2-}$ is 0.3 logarithmic units higher.

Tab. 29.7-1: Stability constants for Sn(II) phosphate complexes based on the experimental data by Ciavatta & Iuliano (2000), see text for discussion

(a) Original conditional stability constants (3 M $NaClO_4$) by Ciavatta & Iuliano (2000) on the molar concentration scale. (b) Recalculated conditional stability constants on the molal scale. (c) – (f) Stability constants extrapolated to $I = 0$ using measured or estimated SIT coefficients according to (c) Ciavatta (1980, 1990), see Tab. 29.7-3, column (a), (d) Gamsjäger et al. (2012), see Tab. 29.7-3, column (b), (e) Gamsjäger et al. (2012), as reproduced in this work, see Tab. 29.7-3, column (c), (f) this work using the estimation method described in Section 1.5.3, see Tab. 29.7-3, column (d).

	(a)	**(b)**	**(c)**	**(d)**	**(e)**	**(f)**
	$\log_{10}{}^*\beta_c$	$\log_{10}{}^*\beta_m$	$\log_{10}{}^*\beta_m^\circ$	$\log_{10}{}^*\beta_m^\circ$	$\log_{10}{}^*\beta_m^\circ$	$\log_{10}{}^*\beta_m^\circ$
	Ciavatta & Iuliano (2000)	Re-calculated	Ciavatta	NEA	NEA a	This work
$Sn^{2+} + H_2PO_4^- \rightleftharpoons SnH_2PO_4^+$	2.17 ± 0.03	2.10	2.77	3.10	2.91	3.42
$Sn^{2+} + 2\ H_2PO_4^- \rightleftharpoons Sn(H_2PO_4)_2(aq)$	4.816 ± 0.007	4.68	6.00	6.25	6.11	6.08
$Sn^{2+} + 2\ H_2PO_4^- \rightleftharpoons SnH_2PO_4HPO_4^- + H^+$	2.17 ± 0.04	2.10	3.31	3.03	3.44	3.31
$Sn^{2+} + H_2PO_4^- \rightleftharpoons SnHPO_4(aq) + H^+$	1.287 ± 0.006	1.29	2.31	2.67	2.46	2.39
$Sn^{2+} + 2\ H_2PO_4^- \rightleftharpoons Sn(HPO_4)_2^{2-} + 2\ H^+$	-1.32 ± 0.03	-1.32	-0.71	-0.44	-0.57	-0.79
$Sn^{2+} + H_2PO_4^- \rightleftharpoons Sn(HPO_4)_3^{4-} + 3\ H^+$	-6.10 ± 0.01	-6.10	-8.52	-8.26	-8.24	-8.16
$Sn^{2+} + H_2PO_4^- \rightleftharpoons SnPO_4^- + 2\ H^+$	-2.41 ± 0.01	-2.34	-1.51	-1.14	-1.35	-1.42

Tab. 29.7-2: Stability constants of reformulated complexation reactions based on the stability constants listed in Tab. 29.7-1 and auxiliary data

(a) – (d) Stability constants based on those listed in columns (c) – (f) of Tab. 29.7-1. (e) Stability constants reported by Ciavatta & Iuliano (2000) based on their experimental data listed in column a of Tab. 29.7-1.

	(a)	**(b)**	**(c)**	**(d)**	**(e)**
	$\log_{10}\beta_m^\circ$	$\log_{10}\beta_m^\circ$	$\log_{10}\beta_m^\circ$	$\log_{10}\beta_m^\circ$	$\log_{10}\beta_m^\circ$
	Ciavatta	NEA	NEA a	This work	Ciavatta & Iuliano (2000)
Auxiliary data					
$PO_4^{3-} + H^+ \rightleftharpoons HPO_4^{2-}$	12.35	12.35	12.35	12.35	12.35
$HPO_4^{2-} + H^+ \rightleftharpoons H_2PO_4^-$	7.198	7.212	7.212	7.212	7.198
Reformulated complexation reactions					
$Sn^{2+} + H_2PO_4^- \rightleftharpoons SnH_2PO_4^+$	2.77	3.10	2.91	3.42	2.8 ± 0.2
$Sn^{2+} + 2\ H_2PO_4^- \rightleftharpoons Sn(H_2PO_4)_2(aq)$	6.00	6.25	6.11	6.08	5.9 ± 0.2
$Sn^{2+} + H_2PO_4^- + HPO_4^{2-} \rightleftharpoons SnH_2PO_4HPO_4^-$	10.51	10.25	10.65	10.53	10.3 ± 0.2
$Sn^{2+} + HPO_4^{2-} \rightleftharpoons SnHPO_4(aq)$	9.50	9.89	9.68	9.60	9.5 ± 0.2
$Sn^{2+} + 2\ HPO_4^{2-} \rightleftharpoons Sn(HPO_4)_2^{2-}$	13.68	13.98	13.85	13.63	13.4 ± 0.2
$Sn^{2+} + 3\ HPO_4^{2-} \rightleftharpoons Sn(HPO_4)_3^{4-}$	13.07	13.37	13.39	13.48	12.9 ± 0.2
$Sn^{2+} + PO_4^{3-} \rightleftharpoons SnPO_4^-$	18.04	18.42	18.21	18.14	18.0 ± 0.2

Tab. 29.7-3: Measured or estimated SIT coefficients (see text for discussion)

According to (a) Ciavatta (1980, 1990). (b) Gamsjäger et al. (2012). (c) Gamsjäger et al. (2012), as reproduced in this work, d this work using the estimation method described in Section 1.5.3.

	(a)	(b)	(c)	(d)
	Ciavatta	NEA	NEA a	This work
Auxiliary data				
$\varepsilon(H_2PO_4^-, Na^+)$	-0.11	-0.08	-0.08	-0.08
$\varepsilon(HPO_4^{2-}, Na^+)$	-0.19	Not used	-0.15	Not used
$\varepsilon(PO_4^{3-}, Na^+)$	-0.29	Not used	-0.25	Not used
$\varepsilon(Sn^{2+}, ClO_4^-)$	0.3	0.19	0.19	0.19
$\varepsilon(H^+, ClO_4^-)$	0.14	0.14	0.14	0.14
Estimated data				
$\varepsilon(SnH_2PO_4^+, ClO_4$-)	0.095	0.11	0.055	0.2
$\varepsilon(Sn(H_2PO_4)_2, NaClO_4)$	0.027	0.05	0.01	0.0
$\varepsilon(SnH_2PO_4HPO_4^-, Na^+)$	0.000	-0.13	-0.013	-0.05
$\varepsilon(SnHPO_4, NaClO_4)$	0.055	0.08	0.02	0.0
$\varepsilon(Sn(HPO_4)_2^{2-}, Na^+)$	-0.027	0.00	-0.037	-0.10
$\varepsilon(Sn(HPO_4)_3^{4-}, Na^+)$	-0.285	-0.23	-0.225	-0.20
$\varepsilon(SnPO_4^-, Na^+)$	0.005	0.03	-0.03	-0.05

In the discussion of the work by Ciavatta & Iuliano (2000), Gamsjäger et al. (2012) came to the conclusion that "the experimental work was done carefully, but the validity of the estimated ion interaction coefficients is uncertain. Therefore the reported thermodynamic formation constants are only useful estimates". They write that "the equilibrium constants determined for $I = 3$ M were extrapolated to $I = 0$, using the ion interaction coefficients listed in Appendix B (Tab. B-3 and B-4 ($\varepsilon(H^+, ClO_4^-)$, $\varepsilon(Na^+, HPO_4^{2-})$, $\varepsilon(Na^+, PO_4^{3-})$), as well as estimated values ($\varepsilon(Sn^{2+}, ClO_4^-)$ = 0.19 mol · kg^{-1} [sic!], $\varepsilon(H_3PO_4, NaClO_4)$ = 0.05 mol · kg^{-1} [sic!], $\varepsilon(SnH_2PO_4^+, ClO_4^-)$ = 0.11 mol · kg^{-1} [sic!], $\varepsilon(Sn(H_2PO_4)_2, NaClO_4)$ = 0.05 mol · kg^{-1} [sic!], $\varepsilon(Sn(H_2PO_4)(HPO_4)^-)$ = -0.13 mol · kg^{-1} [sic!], $\varepsilon(SnHPO_4, NaClO_4)$ = 0.08 mol · kg^{-1} [sic!], $\varepsilon(Na^+, Sn(HPO_4)_2^{2-})$ = 0.00 mol · kg^{-1} [sic!], $\varepsilon(Na^+, Sn(HPO_4)_3^{4-})$ = -0.23 mol · kg^{-1} [sic!], $\varepsilon(Na^+, SnPO_4^-)$ = 0.03 mol · kg^{-1} [sic!]). The estimation of the ion interaction coefficients of the complex species were based on Eqs. B.22 and B.23 (Appendix B)". Since these equations cannot be found at the specified place (or elsewhere) in Gamsjäger et al. (2012), we tried to reproduce the estimates by assuming that the two equations are identical to those by Ciavatta (1990) referred to above. As seen in Tab. 29.7-3, the reproduced estimates do not match those reported by Gamsjäger et al. (2012). Nevertheless, we used both sets of estimates to perform the extrapolation of the conditional formation constants to $I_m = 0$, the results of which can be seen in Tab. 29.7-1 and 29.7-2.

Finally, we used the estimation method described in Section 1.5.3 to produce the specific ion interaction coefficients listed in Tab. 29.7-3 that lead to the stability constants shown in Tab. 29.7-1 and 29.7-2. These estimated values together with the corresponding stability constants in Tab. 29.7-2 (rounded to one decimal place and uncertainties set to ± 0.2) are included in TDB 2020 as supplemental data:

$Sn^{2+} + H_2PO_4^- \rightleftharpoons SnH_2PO_4^+$

$log_{10}\beta°(298.15\ K) = (3.4 \pm 0.2)$

$\varepsilon(SnH_2PO_4^+, ClO_4^-) = (0.2 \pm 0.1)\ kg \cdot mol^{-1}$

$Sn^{2+} + 2\ H_2PO_4^- \rightleftharpoons Sn(H_2PO_4)_2(aq)$

$log_{10}\beta°(298.15\ K) = (6.1 \pm 0.2)$

$\varepsilon(Sn(H_2PO_4)_2(aq), NaClO_4(aq)) = (0.0 \pm 0.1)\ kg \cdot mol^{-1}$

$Sn^{2+} + H_2PO_4^- + HPO_4^{2-} \rightleftharpoons SnH_2PO_4HPO_4^-$

$log_{10}\beta°(298.15\ K) = (10.5 \pm 0.2)$

$\varepsilon(SnH_2PO_4HPO_4^-, Na^+) = -(0.05 \pm 0.10)\ kg \cdot mol^{-1}$

$Sn^{2+} + HPO_4^{2-} \rightleftharpoons SnHPO_4(aq)$

$log_{10}\beta°(298.15\ K) = (9.6 \pm 0.2)$

$\varepsilon(SnHPO_4(aq), NaClO_4(aq)) = (0.0 \pm 0.1)\ kg \cdot mol^{-1}$

$Sn^{2+} + 2\ HPO_4^{2-} \rightleftharpoons Sn(HPO_4)_2^{2-}$

$log_{10}\beta°(298.15\ K) = (13.6 \pm 0.2)$

$\varepsilon(Sn(HPO_4)_2^{2-}, Na^+) = -(0.10 \pm 0.10)\ kg \cdot mol^{-1}$

$Sn^{2+} + 3\ HPO_4^{2-} \rightleftharpoons Sn(HPO_4)_3^{4-}$

$log_{10}\beta°(298.15\ K) = (13.5 \pm 0.2)$

$\varepsilon(Sn(HPO_4)_3^{4-}, Na^+) = -(0.20 \pm 0.30)\ kg \cdot mol^{-1}$

$Sn^{2+} + PO_4^{3-} \rightleftharpoons SnPO_4^-$

$log_{10}\beta°(298.15\ K) = (18.1 \pm 0.2)$

$\varepsilon(SnPO_4^-, Na^+) = -(0.05 \pm 0.10)\ kg \cdot mol^{-1}$

Using $\varepsilon(SnH_2PO_4^+, ClO_4^-)$, $\varepsilon(Sn(H_2PO_4)_2(aq), NaClO_4(aq))$, and $\varepsilon(SnHPO_4(aq), NaClO_4(aq))$ as estimates for the corresponding ion interaction coefficients with Cl^- and NaCl(aq), see Section 29.1.1, results in

$\varepsilon(SnH_2PO_4^+, Cl^-) \approx \varepsilon(SnH_2PO_4^+, ClO_4^-) = (0.2 \pm 0.1)\ kg \cdot mol^{-1}$

$\varepsilon(Sn(H_2PO_4)_2(aq), NaCl(aq)) \approx \varepsilon(Sn(H_2PO_4)_2(aq), NaClO_4(aq)) = (0.0 \pm 0.1)\ kg \cdot mol^{-1}$

$\varepsilon(SnHPO_4(aq), NaCl(aq)) \approx \varepsilon(SnHPO_4(aq), NaClO_4(aq)) = (0.0 \pm 0.1)\ kg \cdot mol^{-1}$

These estimates are also included in TDB 2020 as supplemental data.

29.7.2.2 Aqueous tin(II) pyrophosphate complexes

Pyrophosphate ($P_2O_7^{4-}$, also called diphosphate) forms very stable complexes with Sn(II). Gamsjäger et al. (2012) reported conditional stability constants for $SnH_2P_2O_7(aq)$, $SnHP_2O_7^-$, $SnP_2O_7^{2-}$, $SnP_2O_7OH^{3-}$, $SnP_2O_7(OH)_2^{4-}$, $SnH_4(P_2O_7)_2^{2-}$, $SnH_3(P_2O_7)_2^{3-}$, $SnH_2(P_2O_7)_2^{4-}$, $SnH(P_2O_7)_2^{5-}$, $Sn(P_2O_7)_2^{6-}$, $Sn(P_2O_7)_2OH^{7-}$, and $Sn(P_2O_7)_3^{10-}$ that were determined in seven studies using potentiometry, polarography, spectrophotometry, and solubility measurements. Gamsjäger et al. (2012) did not accept any of these data and made no selections mainly because of the following reason: It is known that alkali metals (supplied in these experiments by the background electrolyte) form relatively stable complexes with pyrophosphate, especially at pH > 8 where the pyrophosphate ion is dominant. Such alkali metal pyrophosphate complexes must be taken into account when extracting stability constants for Sn(II) pyrophosphate complexes from the experimental data. All of the studies neglected the alkali metal pyrophosphate complexes and only one of them was carried out at relatively low concentrations of the background electrolyte, but still not sufficiently low enough.

29.7.2.3 Aqueous tin(IV) pyrophosphate complexes

According to Gamsjäger et al. (2012), the highly charged pyrophosphate anion, $P_2O_7^{4-}$, forms very strong complexes with Sn(IV) such that the formation of SnO_2(cassiterite) is suppressed in the whole pH range. Gamsjäger et al. (2012) discussed the experimental study by Duffield et al. (1991) that reported stability constants for $SnHP_2O_7^+$, $SnP_2O_7(aq)$, $SnH(P_2O_7)_2^{3-}$, $Sn(P_2O_7)_2^{4-}$, and $SnP_2O_7(OH)_2^{6-}$ found by pH-potentiometry over the pH range from 1 – 8. Gamsjäger et al. (2012) did not accept these data by pointing to the fact that Sn(IV) hydrolyses very strongly and arguing that Duffield et al. (1991) "considered only the formation of $SnOH^{3+}$ and $Sn(OH)_6^{2-}$, disregarding e.g. the complex $Sn(OH)_5^-$" in the derivation of stability constants for the Sn(IV) pyrophosphate complexes from their experimental data. That the hydrolysis model employed by Duffield et al. (1991) is inadequate is also corroborated by the statement made by Brown & Ekberg (2016) that, based on the value of the stability constant of $Sn(OH)_4(aq)$, lower monomeric Sn(VI) hydroxide species, such as $SnOH^{3+}$, $Sn(OH)_2^{2+}$, and $Sn(OH)_3^+$ would not occur.

29.7.2.4 Solid tin phosphides

Gamsjäger et al. (2012) selected calorimetrically determined thermodynamic data for $Ag_6Sn_4P_{12}Ge_6$(cr). It is very unlikely that this solid (not known from natural occurrences) may play any role for the purposes of TDB 2020 and its data are therefore not included.

29.7.3 Arsenic compounds

Gamsjäger et al. (2012) selected calorimetrically determined thermodynamic data for the tin arsenide solids SnAs(cr) and Sn_4As_3(cr) of which no natural occurrences are known. These solids are hardly of any relevance to the purposes of TDB 2020 and their data are therefore not included in TDB 2020.

29.8 Thiocyanate complexes

Gamsjäger et al. (2012) reported formation constants for the Sn(II) thiocyanate complexes $SnSCN^+$, $Sn(SCN)_2(aq)$, and $Sn(SCN)_3^-$ from three publications. All constants were measured potentiometrically with Sn-amalgam electrodes. Gamsjäger et al. (2012) accepted only four constants, three for $SnSCN^+$ (1.0, 2.2, and 3.0 M $NaClO_4$) and one for $Sn(SCN)_2(aq)$ (2.2 M $NaClO_4$). The SIT analysis of the three formation constants resulted in the selected constant

$$Sn^{2+} + SCN^- \rightleftharpoons SnSCN^+$$

$$\log_{10}\beta_1°(298.15\ K) = (1.5 \pm 0.7)$$

with

$$\Delta\varepsilon = -(0.07 \pm 0.29)\ kg \cdot mol^{-1}$$

From this value for $\Delta\varepsilon$ and the selected $\varepsilon(Sn^{2+}, ClO_4^-)$ and $\varepsilon(SCN^-, Na^+)$, see Tab. 29.9-3 and 29.9-5, follows the selected

$$\varepsilon(SnSCN^+, ClO_4^-) = (0.17 \pm 0.29)\ kg \cdot mol^{-1}$$

which was used for the estimate

$$\varepsilon(SnSCN^+, Cl^-) \approx \varepsilon(SnSCN^+, ClO_4^-) = (0.17 \pm 0.29)\ kg \cdot mol^{-1}$$

see Section 29.1.1.

All these data for $SnSCN^+$ are included in TDB 2020.

The formation constant for $Sn(SCN)_2(aq)$ measured in 2.2 M $NaClO_4$ was not selected by Gamsjäger et al. (2012) as it cannot be extrapolated to zero ionic strength without additional data.

29.9 Selected tin data

Tab. 29.9-1: Tin bearing solids, liquids, and gases for which NEA selected thermodynamic data (Gamsjäger et al. 2012, Tab. III-1 and III-2) but are not included in TDB 2020

See text for explanations. All aqueous species for which Gamsjäger et al. (2012) selected

Solids	α-Sn [a], SnF_2(cr) [b,d], $BaSnF_4$(cr) [b], $PbSnF_4$(cr) [b], $SrSnF_4$(cr) [b], $SnCl_2$(cr) [a,d], $SnCl_2 \cdot 2H_2O$(cr) [a], $Sn_{21}Cl_{16}(OH)_{14}O_6$(cr) [a,c], $SnBr_2$(cr) [a,d], $SnBr_4$(cr) [a,d], SnI_2(cr) [a,d], SnI_4(cr) [a,d], SnS(cr) [a], Sn_2S_3(cr) [a], SnS_2(cr) [a], $Cu_2Sn_4S_9$(cr) [a], Cu_2SnS_3(cr) [a], Cu_4SnS_4(cr) [a], Cu_8SnS_6(cr) [b], $Sn_3(OH)_2OSO_4$(cr) [a,e], $Ag_6Sn_4P_{12}Ge_6$(cr) [a], Sn_4As_3(cr) [b], SnAs(cr) [a]
Liquids	$SnCl_4$(l) [b,d],
Gases	SnH_4g [a], SnF_2g [a,d], $SnCl_2$g [a,d], $SnCl_4$g [a,d], $SnBr_2$g [a,d], $SnBr_4$g [a,d], SnI_2g [a,d], SnI_4g [a,d],

[a] Single species data including $\Delta_f G_m°$
[b] Single species data excluding $\Delta_f G_m°$
[c] Reaction data including $\log_{10} K°$
[d] Reaction data excluding $\log_{10} K°$
[e] Data for $Sn_3(OH)_2OSO_4$(cr) were not selected by Gamsjäger et al. (2012) but appear erroneously in their Tab. III-1.

Tab. 29.9-2: Selected tin data (1 bar, 298.15 K) for TDB 2020

All data are taken from the data selected by Gamsjäger et al. (2012) with the exception of those marked with an asterisk (*). Values taken from CODATA are bold (Cox et al. 1989). Supplemental data are in italics. New or changed data with respect to TDB Version 12/07 (Thoenen et al. 2014) are shaded. T-range refers to the experimental range of temperatures at which equilibrium constants, $\Delta_r H_m°$ and $\Delta_r C_{p,m}°$ were determined.

Name	Redox	TDB Version 12/07				TDB 2020				
		$\Delta_f G_m°$ [kJ · mol^{-1}]	$\Delta_f H_m°$ [kJ · mol^{-1}]	$S_m°$ [J · K^{-1} · mol^{-1}]	$C_{p,m}°$ [J · K^{-1} · mol^{-1}]	$\Delta_f G_m°$ [kJ · mol^{-1}]	$\Delta_f H_m°$ [kJ · mol^{-1}]	$S_m°$ [J · K^{-1} · mol^{-1}]	$C_{p,m}°$ [J · K^{-1} · mol^{-1}]	Species
Sn(β)	0	0.0	0.0	51.18 ± 0.08	-	0.0	0.0	**51.18 ± 0.08**	27.11 ± 0.08	Sn(cr)
Sn+2	II	-26.43 ± 0.46	-7.7 ± 1.3	-16.7 ± 4.0	-	-27.39 ± 0.30	-9.42 ± 1.24	-19.2 ± 4.3	-	Sn^{2+}
Sn+4	IV	-	-	-	-	(46.7 ± 3.9) [a]	*(-31.5 ± 7.3)* [b]	*(-472.5 ± 20.5)** [c]	-	Sn^{4+}

[a] Calculated from reaction data.
[b] Calculated using $\Delta_r G_m° = \Delta_r H_m° - T\Delta_r S_m°$.
[c] Value reported, but not selected, by Gamsjäger et al. (2012).

Name	Redox	TDB Version 12/07		TDB 2020				
		$\log_{10}\beta°$	$\Delta_r H_m°$ [kJ · mol^{-1}]	$\log_{10}\beta°$	$\Delta_r H_m°$ [kJ · mol^{-1}]	$\Delta_r C_{p,m}°$ [J · K^{-1} · mol^{-1}]	T-range [°C]	Reaction
SnOH+	II	-3.8 ± 0.2	-	-3.53 ± 0.40	-	-	-	$Sn^{2+} + H_2O(l) \rightleftharpoons SnOH^+ + H^+$
Sn(OH)2(aq)	II	-7.7 ± 0.2	-	-7.68 ± 0.40	-	-	-	$Sn^{2+} + 2\ H_2O(l) \rightleftharpoons Sn(OH)_2(aq) + 2\ H^+$
Sn(OH)3-	II	-17.5 ± 0.2	-	-17.00 ± 0.60	-	-	-	$Sn^{2+} + 3\ H_2O(l) \rightleftharpoons Sn(OH)_3^- + 3\ H^+$
Sn3(OH)4+2	II	-5.6 ± 1.6	-	-5.60 ± 0.47	-	-	-	$3\ Sn^{2+} + 4\ H_2O(l) \rightleftharpoons Sn_3(OH)_4^{2+} + 4\ H^+$

Tab. 29.9-2: Cont.

Name	Redox	TDB Version 12/07		TDB 2020				
		$\log_{10}\beta°$	$\Delta_r H_m°$ [kJ · mol^{-1}]	$\log_{10}\beta°$	$\Delta_r H_m°$ [kJ · mol^{-1}]	$\Delta_r C_{p,m}°$ [J · K^{-1} · mol^{-1}]	T-range [°C]	Reaction
Sn(OH)Cl(aq)	II	(-3.1 ± 0.2) [a]	-	*(-2.5 ± 0.3)**	-	-	-	*Sn^{2+} + $H_2O(l)$ + Cl^- ⇌ Sn(OH)Cl(aq) + H^+*
SnF+	II	5.0 ± 0.3	-	5.25 ± 0.19	-	-	-	$Sn^{2+} + F^- ⇌ SnF^+$
SnF2(aq)	II	-	-	8.89 ± 0.21	-	-	-	$Sn^{2+} + 2\ F^- ⇌ SnF_2(aq)$
SnF3-	II	-	-	11.5 ± 1.0	-	-	-	$Sn^{2+} + 3\ F^- ⇌ SnF_3^-$
SnCl+	II	1.70 ± 0.11	-	(1.41 ± 0.20) *	(2.25) *	(0)*	25 – 200	$Sn^{2+} + Cl^- ⇌ SnCl^+$
SnCl2(aq)	II	2.36 ± 0.23	-	(2.22 ± 0.20) *	(-4.81) *	(187)*	25 – 300	$Sn^{2+} + 2\ Cl^- ⇌ SnCl_2(aq)$
SnCl3-	II	2.1 ± 0.4	-	(2.37 ± 0.20) *	(-17.0) *	(408)*	25 – 300	$Sn^{2+} + 3\ Cl^- ⇌ SnCl_3^-$
SnCl4-2	II	-	-	(2.03 ± 0.20) *	(0)*	(0)*	25 – 150	$Sn^{2+} + 4\ Cl^- ⇌ SnCl_4^{2-}$
SnBr+	II	-	-	1.33 ± 0.18	*5.1 ± 2.0*	*(0)**	*0 – 45*	$Sn^{2+} + Br^- ⇌ SnBr^+$
SnBr2(aq)	II	-	-	1.97 ± 0.21	*12.9 ± 2.0*	*(0)**	*0 – 45*	$Sn^{2+} + 2\ Br^- ⇌ SnBr_2(aq)$
SnBr3-	II	-	-	1.93 ± 0.27	*7.2 ± 4.0*	*(0)**	*0 – 45*	$Sn^{2+} + 3\ Br^- ⇌ SnBr_3^-$
SnSO4(aq)	II	2.6 ± 0.3	-	3.43 ± 0.25	-	-	-	$Sn^{2+} + SO_4^{2-} ⇌ SnSO_4(aq)$
SnNO3+	II	-	-	1.27 ± 0.31	-	-	-	$Sn^{2+} + NO_3^- ⇌ SnNO_3^+$
Sn(NO3)2(aq)	II	-	-	1.39 ± 0.53	-	-	-	$Sn^{2+} + 2\ NO_3^- ⇌ Sn(NO_3)_2(aq)$
SnH2PO4+	II	-	-	*(3.4 ± 0.2)**	-	-	-	*$Sn^{2+} + H_2PO_4^- ⇌ SnH_2PO_4^+$*
Sn(H2PO4)2(aq)	II	-	-	*(6.1 ± 0.2) **	-	-	-	*$Sn^{2+} + 2\ H_2PO_4^- ⇌ Sn(H_2PO_4)_2(aq)$*
SnH2PO4HPO4-	II	-	-	*(10.5 ± 0.2 **	-	-	-	*$Sn^{2+} + H_2PO_4^- + HPO_4^{2-} ⇌ SnH_2PO_4HPO_4^-$*
SnHPO4(aq)	II	-	-	*(9.6 ± 0.2) **	-	-	-	*$Sn^{2+} + HPO_4^{2-} ⇌ SnHPO_4(aq)$*
Sn(HPO4)2-2	II	-	-	*(13.6 ± 0.2 **	-	-	-	*$Sn^{2+} + 2\ HPO_4^{2-} ⇌ Sn(HPO_4)_2^{2-}$*
Sn(HPO4)3-4	II	-	-	*(13.5 ± 0.2 **	-	-	-	*$Sn^{2+} + 3\ HPO_4^{2-} ⇌ Sn(HPO_4)_3^{4-}$*
SnPO4-	II	-	-	*(18.1 ± 0.2 **	-	-	-	*$Sn^{2+} + PO_4^{3-} ⇌ SnPO_4^-$*
SnSCN+	II	-	-	1.5 ± 0.7	-	-	-	$Sn^{2+} + SCN^- ⇌ SnSCN^+$
Sn^{4+}	II/IV	-	-	-12.98 ± 0.68	-	-	-	$Sn^{2+} + 2\ H^+ ⇌ Sn^{4+} + H_2g$
Sn(OH)4(aq)	IV	-	-	(7.54 ± 0.69) [b]	-	-	-	$Sn^{4+} + 4\ H_2O(l) ⇌ Sn(OH)_4(aq) + 4\ H^+$
Sn(OH)5-	IV	-8.0 ± 0.3	-	-8.60 ± 0.40	-	-	-	$Sn(OH)_4(aq) + H_2O(l) ⇌ Sn(OH)_5^- + H^+$
Sn(OH)6-2	IV	-18.4 ± 0.3	-	-18.67 ± 0.30	-	-	-	$Sn(OH)_4(aq) + 2\ H_2O(l) ⇌ Sn(OH)_6^{2-} + 2\ H^+$
SnF6-2	IV	-	-	*≈ 25*	-	-	-	*$Sn^{4+} + 6\ F^- ⇌ SnF_6^{2-}$*
SnCl+3	IV	-	-	*(3.19 ± 0.50) ** [c]	-	-	-	*$Sn^{4+} + Cl^- ⇌ SnCl^{3+}$*
SnCl2+2	IV	-	-	*(5.95 ± 0.36) ** [c]	-	-	-	*$Sn^{4+} + 2\ Cl^- ⇌ SnCl_2^{2+}$*
SnCl4(aq)	IV	-	-	*(9.57 ± 0.32) ** [c]	-	-	-	*$Sn^{4+} + 4\ Cl^- ⇌ SnCl_4(aq)$*

Tab. 29.9-2: Cont.

Name	Redox	TDB Version 12/07		TDB 2020				
		$\log_{10}\beta°$	$\Delta_r H_m°$ [kJ · mol^{-1}]	$\log_{10}\beta°$	$\Delta_r H_m°$ [kJ · mol^{-1}]	$\Delta_r C_{p,m}°$ [J · K^{-1} · mol^{-1}]	T-range [°C]	Reaction
SnCl5-	IV	-	-	*(10.93 ± 0.41)* [*c]	-	-	-	*Sn^{4+} + 5 Cl^- ⇌ $SnCl_5^-$*
SnCl6-2	IV	-	-	*(9.83 ± 0.49)* [*c]	-	-	-	*Sn^{4+} + 6 Cl^- ⇌ $SnCl_6^{2-}$*

[a] Note that this value originally reported in TDB01/01 (Hummel et al. 2002) is incorrect and should be replaced by -2.1, see Section 29.4.1.2 for explanations.
[b] Calculated from $\Delta_f G_m°$(Sn(OH)$_4$, aq, 298.15 K), which follows from the values selected by Gamsjäger et al. (2012) for $\log_{10} K_{s,4}°$(SnO_2(cassiterite) + 2 H_2O(l) ⇌ Sn(OH)$_4$(aq), 298.15 K) and $\Delta_f G_m°$(SnO_2, cassiterite, 298.15 K), see Section 29.4.1.3 for explanations.
[c] Data reported by Gamsjäger et al. (2012) as selected, but not appearing in the list of selected data.

Name	TDB Version 12/07		TDB 2020				
	$\log_{10} K_{s,0}°$	$\Delta_r H_m°$ [kJ · mol^{-1}]	$\log_{10} K_s°$	$\Delta_r H_m°$ [kJ · mol^{-1}]	$\Delta_r C_{p,m}°$ [J · K^{-1} · mol^{-1}]	T-range [°C]	Reaction
Sn(β)	4.63 ± 0.08	-	4.80 ± 0.05	-	-	-	Sn(cr) ⇌ Sn^{2+} + 2 e^-
SnO(s)	2.5 ± 0.5	-	(1.6 ± 0.3) [*a]	-	-	-	SnO(s) +2 H^+ ⇌ Sn^{2+} + H_2O(l)
SnO2(cassiterite)	-8.0 ± 0.2	-	-8.06 ± 0.11	-	-	-	SnO_2(cr) + 2 H_2O(l) ⇌ Sn(OH)$_4$(aq)
SnO2(am)	-7.3 ± 0.3	-	-7.22 ± 0.08	-	-	-	SnO_2(am) + 2 H_2O(l) ⇌ Sn(OH)$_4$(aq)
CaSn(OH)6(pr)	-9.7 ± 0.1	-	(-9.7 ± 0.1) [*b]	-	-	-	CaSn(OH)$_6$(pr) ⇌ Sn(OH)$_6^{2-}$ + Ca^{2+}

[a] Gamsjäger et al. (2012) selected conflicting data for SnO(s), see Sections 29.4.1.1 and 29. 4.2.1.1.
[b] This corresponds to $\log_{10}{}^*K_{s,4}° = (8.97 \pm 0.3)$ for the reaction CaSn(OH)$_6$(pr) + 2 H^+ ⇌ Sn(OH)$_4$(aq) + Ca^{2+} + 2 H_2O(l).

Tab. 29.9-3: Selected SIT ion interaction coefficients $\varepsilon_{j,k}$ [kg · mol^{-1}] for tin species

All data included in TDB 2020 are taken from Gamsjäger et al. (2012) unless indicated otherwise. Data estimated according to charge correlations and taken from Tab. 1-7 are shaded. Supplemental data are in italics.

j k → ↓	**Cl^-** $\varepsilon_{j,k}$ [kg · mol^{-1}]	**ClO_4^-** $\varepsilon_{j,k}$ [kg · mol^{-1}]	**NO_3^-** $\varepsilon_{j,k}$ [kg · mol^{-1}]	**Li^+** $\varepsilon_{j,k}$ [kg · mol^{-1}]	**Na^+** $\varepsilon_{j,k}$ [kg · mol^{-1}]	**K^+** $\varepsilon_{j,k}$ [kg · mol^{-1}]	**H^+** $\varepsilon_{j,k}$ [kg · mol^{-1}]
Sn+2	0.14 ± 0.10	0.19 ± 0.04	-	0	0	0	0
SnOH+	-0.07 ± 0.13 [a]	-0.07 ± 0.13	-	0	0	0	0
Sn(OH)3-	0	0	0	-	0.22 ± 0.03	-	-
Sn3(OH)4+2	-0.02 ± 0.16 [a]	-0.02 ± 0.16	-	0	0	0	0
SnF+	0.14 ± 0.10 [a]	0.14 ± 0.10	-	0	0	0	0
SnF3-	0	0	0	-	-0.05 ± 0.31 [b]	-	-
SnCl+	0.04 ± 0.05 [a]	0.04 ± 0.05 [b]	-	0	0	0	0
SnCl3-	0	0	0	-	0.07 ± 0.06 [b]	-	-
SnCl4-2	0	0	0	-	-0.10 ± 0.10	-	-
SnBr+	(0.15 ± 0.07) [a]	0.15 ± 0.07	-	0	0	0	0
SnBr3-	0	0	0	-	0.16 ± 0.08	-	-
SnNO3+	(0.17 ± 0.09) [a]	0.17 ± 0.09	-	0	0	0	0
SnH2PO4+	(*0.2 ± 0.1*) [a]	*0.2 ± 0.1*	-	*0*	*0*	*0*	*0*
SnH2PO4HPO4-	*0*	*0*	*0*	-	*-0.05 ± 0.10*	-	-
Sn(HPO4)2-2	*0*	*0*	*0*	-	*-0.10 ± 0.10*	-	-
Sn(HPO4)3-4	*0*	*0*	*0*	-	*-0.20 ± 0.30*	-	-
SnPO4-	*0*	*0*	*0*	-	*-0.05 ± 0.10*	-	-
SnSCN+	(-0.17 ± 0.29) [a]	-0.17 ± 0.29	-	0	0	0	0
Sn+4	(0.7 ± 0.2) [a]	0.7 ± 0.2	-	0	0	0	0
Sn(OH)5-	0	0	0	-	-0.05 ± 0.10	-	-
Sn(OH)6-2	0	0	0	-	-0.10 ± 0.10	-	-
SnF6-2	*0*	*0*	*0*	-	*-0.10 ± 0.10*	-	-
SnCl+3	(*0.56 ± 0.21*) [a]	(*0.56 ± 0.21*) [c]	-	*0*	*0*	*0*	*0*
SnCl2+2	(*0.49 ± 0.20*) [a]	(*0.49 ± 0.20*) [c]	-	*0*	*0*	*0*	*0*
SnCl5-	*0*	*0*	*0*	-	*-0.05 ± 0.10*	-	(*0.70 ± 0.21*) [c]
SnCl6-2	*0*	*0*	*0*	-	*-0.10 ± 0.10*	-	(*0.75 ± 0.21*) [c]

[a] Assumed to be equal to the corresponding ion interaction coefficient with ClO_4^-, see Section 29.1.1 for explanation.
[b] This work
[c] This work, calculated from $\Delta\varepsilon$ values reported but not selected by Gamsjäger et al. (2012), see Section 29.5.1.2.2 for discussion.

Tab. 29.9-4: SIT ion interaction coefficients $\varepsilon_{j,k}$ [kg · mol^{-1}] with neutral tin species selected for TDB 2020

All data included in TDB 2020 are taken from Gamsjäger et al. (2012) unless indicated otherwise. Data estimated according to charge correlations and taken from Tab. 1-7 are shaded. Supplemental data are in italics.

Redox	**j k →** ↓	**$Na^+ + Cl^-$** $\varepsilon_{j,k}$ [kg · mol^{-1}]	**$Na^+ + ClO_4^-$** $\varepsilon_{j,k}$ [kg · mol^{-1}]	**$H^+ + ClO_4^-$** $\varepsilon_{j,k}$ [kg · mol^{-1}]
II	Sn(OH)2(aq)	(0.0 ± 0.1)	(0.0 ± 0.1)	-
II	*Sn(OH)C(aq)l*	(*0.0 ± 0.1*)	(*0.0 ± 0.1*)	-
II	SnF2(aq)	(0.01 ± 0.10) [a]	0.01 ± 0.10	-
II	SnCl2(aq)	(0.00 ± 0.06) [a]	0.00 ± 0.06 [b]	-
II	SnBr2(aq)	(0.14 ± 0.07) [a]	0.14 ± 0.07	-
II	SnSO4(aq)	(0.19 ± 0.35) [a]	0.19 ± 0.35	
II	Sn(NO3)2(aq)	(0.130 ± 0.111) [a]	0.130 ± 0.111	-
II	*Sn(H2PO4)2(aq)*	(*0.0 ± 0.1*)	(*0.0 ± 0.1*)	-
II	*SnHPO4(aq)*	(*0.0 ± 0.1*)	(*0.0 ± 0.1*)	-
IV	Sn(OH)4(aq)	(0.0 ± 0.1)	(0.0 ± 0.1)	-
IV	*SnCl4(aq)*	*(0.0 ± 0.1)*	*(0.0 ± 0.1)*	(*0.54 ± 0.21*) [c]

[a] Assumed to be equal to the corresponding ion interaction coefficient with ClO_4^-, see Section 29.1.1 for explanation.
[b] This work
[c] This work, calculated from $\Delta\varepsilon$ values derived by Gamsjäger et al. (2012), see Section 29.5.1.2.2 for a discussion.

Tab. 29.9-5: Selected SIT ion interaction coefficients $\varepsilon_{j,k}$ [kg · mol^{-1}] used for calculating specific ion interaction coefficients for tin species from $\Delta\varepsilon$ values

All data are taken from Lemire et al. (2013) unless indicated otherwise.

j k → ↓	**Cl^-** $\varepsilon_{j,k}$ [kg · mol^{-1}]	**ClO_4^-** $\varepsilon_{j,k}$ [kg · mol^{-1}]	**Na^+** $\varepsilon_{j,k}$ [kg · mol^{-1}]
H^+	0.12 ± 0.01	0.14 ± 0.02	0
OH^-	0	0	0.04 ± 0.01
F-	0	0	0.02 ± 0.02
Cl-	0	0	0.03 ± 0.01
Br-	0	0	0.05 ± 0.01
SO4-2	0	0	-0.12 ± 0.06
NO3-	0	0	-0.04 ± 0.03
H2PO4-	0	0	-0.08 ± 0.04
SCN-	0	0	0.05 ± 0.01

29.10 References

Babko, A.K. & Lisetskaya, G.S. (1956): Equilibrium in reactions of formation of thiosalts of tin, antimony, and arsenic in solution. Journal of Inorganic Chemistry, USSR, 1, 95-107. English translation of original article in Zhurnal Neorganicheskoi Khimii, 1, 969-980.

Bond, A.M. & Taylor, R.J. (1970): Polarographic studies of the fluoride complexes of tin(II) in neutral and acid media. Electroanalytical Chemistry and Interfacial Electrochemistry, 28, 207-215.

Brown, P.L. & Ekberg, C. (2016): Hydrolysis of Metal Ions. Vol. 2, Wiley-VCH, Weinheim.

Ciavatta, L. (1980): The specific interaction theory in evaluating ionic equilibria. Annali di Chimica, 70, 551-567.

Ciavatta, L. (1990): The specific interaction theory in equilibrium analysis. Some empirical rules for estimating interaction coefficients of metal ion complexes. Annali di Chimica, 80, 255-263.

Ciavatta, L. & Iuliano, M. (2000): Formation equilibria of tin(II) orthophosphate complexes. Polyhedron, 19, 2403-2407.

Clark, A.H. (1972): On the natural occurrence of tin sulphides (berndtite). Naturwissenschaften, 59, 361-361.

Cornelius, B., Treivish, S., Rosenthal, Y. & Pecht, M. (2017): The phenomenon of tin pest: A review. Microelectronics Reliability, 79, 175-192.

Cox, J.D., Wagman, D.D. & Medvedev, V.A. (1989): CODATA Key Values for Thermodynamics. New York, Hemisphere, 271p.

Cross, J.E. & Ewart, F.T. (1991): HATCHES - a thermodynamic database and management system. Radiochimica Acta, 52/53, 421-422.

Despic, A.R., Jovanovic, D.R., Rakic, T.B. & Baljkovic, N.A. (1972): Potentiometric study of the tin(II)-tin(IV) redox equilibrium in chloride solution. Bull. Soc. Chim. Beograd, 37, 349-362, in Serbian (as cited by Gamsjäger et al. 2012).

Djokić-Konstantinovska, D. & Zmbova, B. (1985): Investigation of the formation of tin(II)-fluoride complex by potentiometric titration. The International Journal of Applied Radiation and Isotopes, 36, 669-671.

Djurdjević, P., Jelić, R., Djokić, D. & Veselinović, D. (1995): Hydrolysis of tin(II) ion in sodium chloride medium. Journal of the Serbian Chemical Society, 60, 785-795.

Duffield, J.R., Williams, D.R. & Kron, I. (1991): Speciation studies of the solubility and aqueous solution chemistry of tin(II)- and tin(IV)-pyrophosphate complexes. Polyhedron, 10, 377-387.

Duke, F.R. & Courtney, W.G. (1950): The stannous chloride equilibrium. Iowa State Journal of Science, 24, 397-403 (as cited by Gamsjäger et al. 2012).

Duke, F.R. & Pinkerton, R.C. (1951): The Role of halide ions in the ferric-stannous reaction. Journal of the American Chemical Society, 73, 3045-3049.

Edwards, R., Gillard, R.D. & Williams, P.A. (1992): The stabilities of secondary tin minerals: abhurite and its relationships to Sn(II) and Sn(IV) oxides and oxyhydroxides. Mineralogical Magazine, 56, 221-226.

Edwards, R., Gillard, R.D. & Williams, P.A. (1996): The stabilities of secondary tin minerals. Part 2: The hydrolysis of tin(II) sulphate and the stability of $Sn_3O(OH)_2SO4$. Mineralogical Magazine, 60, 427-432.

Fatouros, N., Rouelle, F. & Chemla, M. (1978): Influence de la formation de complexes chlorure sur la réduction électrochimique de Sn^{IV} en milieu perchlorique acide. Journal de Chimie Physique, 75, 476-483.

Fedorov, V.A., Bol'shakova, I.M. & Moskalenko, T.G. (1975): Formation of mixed bromo(chloro)-complexes of tin(II) in aqueous solutions. Russian Journal of Inorganic Chemistry, 20, 859-861 (as cited by Gamsjäger et al. 2012).

Fleischer, M. & Pabst, A. (1983): New mineral names. American Mineralogist, 68, 280-283.

Forbes, G.S. & Bartlett, E.P. (1914): The measurement of oxidation potentials at mercury electrodes. I. The stannic-stannous potential. Journal of the American Chemical Society, 36, 2030-2040.

Gajda, T., Sipos, P. & Gamsjäger, H. (2009): The standard electrode potential of the Sn^{4+}/Sn^{2+} couple revisited. Monatshefte für Chemie, 140, 1293-1303.

Gamsjäger, H., Gajda, T., Sangster, J., Saxena, S.K. & Voigt, W. (2012): Chemical Thermodynamics of Tin. Chemical Thermodynamics Series, Vol. 12, OECD NEA, Issy-les-Moulineaux, France, 609 pp.

Garrett, A.B. & Heiks, R.E. (1941): Equilibria in the stannous oxide-sodium hydroxide and in the stannous oxide-hydrochloric acid systems at 25°. Analysis of dilute solutions of stannous tin. Journal of the American Chemical Society, 63, 562-567.

Greenwood, N.N. & Earnshaw, A. (1997): Chemistry of the Elements (Second Edition). Butterworth-Heinemann, Oxford. 1341 pp.

Grenthe, I., Gaona, X., Plyasunov, A.V., Rao, L., Runde, W.H., Grambow, B., Konings, R.J.M., Smith, A.L. & Moore, E.E. (2020): Second Update on the Chemical Thermodynamics of Uranium, Neptunium, Plutonium, Americium and Technetium. Chemical Thermodynamics, Vol. 14. OECD Publications, Paris, France, 1503 pp.

Grenthe, I. & Puigdomènech, I. (1997): Symbols, standards, and conventions. In: Grenthe, I. & Puigdomènech, I. (eds.): Modelling in Aquatic Chemistry. OECD NEA, Paris, France, 35-67.

Grenthe, I., Mompean, F., Spahiu, K. & Wanner, H. (2013): TDB-2 Guidelines for the extrapolation to zero ionic strength (Version of 18 June 2013). OECD NEA, Data Bank, Issy-les-Moulineaux, France, 78 pp.

Grenthe, I., Plyasunov, A.V. & Spahiu, K. (1997): Estimations of medium effects on thermodynamic data. In: Grenthe, I. & Puigdomènech, I. (eds.): Modelling in Aquatic Chemistry. OECD NEA, Paris, France, 325-426.

Haase, R., Dücker, K.-H. & Küppers, H.A. (1965): Aktivitätskoeffizienten und Dissoziationskonstanten wässriger Salpetersäure und Überchlorsäure. Berichte der Bunsen-Gesellschaft, 69, 97-109.

Hickling, G.G. (1990): Gravimetric analysis: The synthesis of tin iodide. Journal of Chemical Education, 67, 702-703.

Hseu, T.-M. & Rechnitz, G.A. (1968): Analytical study of a sulfide ion-selective membrane electrode in alkaline solution. Analytical Chemistry 40, 1054-1060.

Huey, C.S. & Tartar, H.V. (1934): The stannous–stannic oxidation–reduction potential. Journal of the American Chemical Society, 56, 2585-2588.

Hummel, W., Anderegg G., Puigdomènech, I., Rao, L. & Tochiyama, O. (2005): Chemical Thermodynamics of Compounds and Complexes of U, Np, Pu, Am, Tc, Se, Ni and Zr with Selected Organic Ligands. Chemical Thermodynamics Series, Vol. 9, OECD NEA, Paris, 1088 pp.

Hummel, W., Berner, U., Curti, E., Pearson, F.J. & Thoenen, T. (2002): Nagra/PSI Chemical Thermodynamic Data Base 01/01. Nagra Technical Report NTB 02-16. Also published by Universal Publishers/upublish.com, Parkland, USA, 565 pp.

Lemire, R.J., Berner, U., Musikas, C., Palmer, D.A., Taylor, P. & Tochiyama, O. (2013): Chemical Thermodynamics of Iron, Part 1. Chemical Thermodynamics, Vol. 13a. OECD Publications, Paris, France, 1082 pp.

Lothenbach, B., Ochs, M. & Hager, D. (2000): Thermodynamic data for the solubility of tin(IV) in aqueous cementitious environments. Radiochimica Acta, 88, 521-526.

Lothenbach, B., Ochs, M., Wanner, H. & Yui, M. (1999): Thermodynamic Data for the Speciation and Solubility of Pd, Pb, Sn, Sb, Nb and Bi in Aqueous Solution. Japan Nuclear Cycle Development Institute (JNC), TN8400 99-011.

Moh, G.H. & Berndt, F. (1964): Two new natural tin sulfides Sn_2S_3 and SnS_2. Neues Jahrbuch für Mineralogie, Monatshefte, 94-95.

Müller, B. & Seward, T.M. (2001): Spectrophotometric determination of the stability of tin(II) chloride complexes in aqueous solution up to 300 °C. Geochimica et Cosmochimica Acta, 65, 4187-4199.

Pearson, F.J., Jr., Berner, U. & Hummel W. (1992): Nagra Thermochemical Data Base II. Supplemental Data 05/92. Nagra Technical Report NTB 91-18.

Pettine, M., Millero, F.J. & Macchi, G. (1981): Hydrolysis of tin(II) in aqueous solutions. Analytical Chemistry, 53, 1039-1043.

Prytz, M. (1928): Komplexbildung in Stannochlorid- und Stannobromidlösungen. Zeitschrift für anorganische und allgemeine Chemie, 172, 147-166.

Prytz, M. (1934): Potentialmessungen in Zinnchloridlösungen. Zeitschrift für anorganische und allgemeine Chemie, 219, 89-96.

Rickard, D. & Luther III, G.W. (2006): Metal sulfide complexes and clusters. Reviews in Mineralogy & Geochemistry, 61, 421-504.

Schaap, W.B., Davis, J.A. & Nebergall, W.H. (1954): Polarographic study of the complex ions of tin in fluoride solutions. Journal of the American Chemical Society, 76, 5226-5229.

Schwartz, E.P. & Cronau, T.C. (1975): Study of the fluoride complexes of tin(II) using a fluoride ion specific electrode. Proceedings of the Indiana Academy of Science, 85, 140-145.

Séby, F., Potin-Gautier, M., Giffaut, E. & Donard, O.F.X. (2001): A critical review of thermodynamic data for inorganic tin species. Geochimica et Cosmochimica Acta, 65, 3041-3053.

Thoenen, T., Hummel, W., Berner, U. & Curti, E. (2014): The PSI/Nagra Chemical Thermodynamic Database 12/07. Technical Report, PSI Bericht Nr. 14-04, Paul Scherrer Institut, Villigen, Switzerland, 416 pp.

Tobias, R.S. & Hugus, Z.Z. Jr. (1961) Least squares computer calculations of chloride complexing of tin(II), the hydrolysis of tin(II), and the validity of the ionic medium method. J. Physical Chemistry, 65, 2165-2169.

Vanderzee, C.E. & Rhodes, D.E. (1952): Thermodynamic data on the stannous chloride complexes from electromotive force measurements. Journal of the American Chemical Society, 74, 3552-3555.

Vasil'ev, V.P. & Glavina, S.R. (1976): Effect of the ionic strength on the potential of a silver chloride electrode and the activity coefficients of HCl in the presence of $HClO_4$. Russian Journal of Electrochemistry, 12, 745-749 (as cited by Gamsjäger et al. 2012).

Vasil'ev, V.P. & Glavina, S.R. (1977): State of tin tetrachloride and diammonium hexachlorostannate in perchloric acid solutions. Russian Journal of General Chemistry, 47, 1325-1327 (as cited by Gamsjäger et al. 2012).

Vasil'ev, V.P., Glavina, S.R. & Shorokhova, V.I. (1979): Potentiometric determination of normal Gibbs' energy of formation of tin(IV) ion in an aqueous solution. Izv. Vyssh. Uchebn. Zaved., Khim. Khim. Tekhnol., 22, 1082-1085, [in Russian] (as cited by Gamsjäger et al. 2012).

Wada, S. & Ito, T. (1975): Determination of ion association constant of tin(ll) sulfate in aqueous solutions by electro motive force measurements. Nippon Kagaku Kaishi, 1975, 611-616 [in Japanese].

Young, S.W. (1897): The solubility of stannous iodide in water and in solutions of hydriodic acid. Journal of the American Chemical Society, 19, 845-851.

30 Titanium

30.1 Introduction

^{44}Ti with a half-life of 60.0 ± 1.1 years is produced in spallation induced neutron sources (e.g. SINQ at PSI) and contributes in dose-relevant quantities to the inventory of L/ILW waste coming from research facilities like PSI (Hummel 2018). For this reason, titanium, previously not considered in the PSI/Nagra Chemical Thermodynamic Database 12/07 (TDB 12/07, Thoenen et al. 2014) and its predecessors, is included in the PSI Chemical Thermodynamic Database 2020 (TDB 2020).

The titanium data selected for TDB 2020 are listed in Tab. 30.5-1.

The notation of formulae and symbols used in this text largely follows the NEA recommendations.

30.1.1 SIT

Due to a lack of experimental data, practically none of the ion interaction coefficients for cationic titanium species with ClO_4^- and Cl^-, and for anionic titanium species with Na^+ are known. We filled these gaps by applying the estimation method described in Section 1.5.3, which is based on a statistical analysis of published SIT ion interaction coefficients, and which allows the estimation of such coefficients for the interaction of cations with Cl^- and ClO_4^-, and for the interaction of anions with Na^+ from the charge of the considered cations or anions. Ion interaction coefficients of neutral titanium species with background electrolytes were assumed to be zero.

The ion interaction coefficients for titanium species selected for TDB 2020 are listed in Tab. 30.5-2.

30.2 Elemental titanium

Native titanium occurs very rarely (see below) in nature and is not relevant under environmental conditions. However, in search for alternative canister materials, Nagra is also considering the coating of carbon-steel canisters with copper, nickel, or titanium. For this reason, Ti(cr) is included in TDB 2020. The value

$$S_m°(\text{Ti}, \alpha, 298.15\ \text{K}) = (30.29 \pm 0.10)\ \text{J} \cdot \text{K}^{-1} \cdot \text{mol}^{-1}$$

was taken from CODATA (Cox et al. 1989) and applies to Ti(α) with a hexagonal close packed structure which is transformed at 882 °C into Ti(β) with a body centred cubic structure. There appears to be no data on the heat capacity of Ti(α). Native Ti(α) was found in granite from the Bezymyannyy pluton, eastern Yakutia, Russia (Jambor & Vanko 1991 and reference therein) and native Ti(β) as inclusion in garnet from a coesite-bearing eclogite in an ultrahigh-pressure metamorphic complex near Yingshan County, Dabieshan, China (Chen et al. 2000, as cited by Jambor & Roberts 2001). Native Ti was also reported as a component of cosmic dust (Jambor & Puziewicz 1990 and reference therein).

30.3 Titanium aquo ions

Titanium exists in various oxidation states (from -II to IV), in aqueous solution, however, only trivalent Ti^{3+} and tetravalent TiO^{2+} are stable (Brown & Ekberg 2016).

30.3.1 TiO^{2+}

Ti^{4+} has a high charge and a relatively small ionic radius (0.605 Å for octahedral coordination, Shannon 1976). It therefore qualifies as a Pearson hard acid, bonding preferably by electrostatic forces and forming strong complexes with strong, hard ligands such as O^{2-}, OH^-, and F^-, and somewhat weaker ones with weak, hard ligands such as carbonate, sulphate, and phosphate (see Wood 2005 in his discussion of Nb^{5+}). Due to its strong hydrolysis, Ti^{4+} exists in even very acid aqueous solutions as the titanyl oxocation TiO^{2+}, According to Brown & Ekberg (2016) and references therein, the presence of the oxocation rather than Ti^{4+} has been verified by kinetics, dialysis, and by solubility studies, where the slope of the logarithm of Ti solubility versus pH turned out to be -2 rather than -4. Spectroscopic evidence for the presence of the titanyl oxocation in acid solutions was presented by Graetzel & Rotzinger (1985) who observed the Ti = O bond using Raman spectroscopy. Further evidence was provided by means of EXAFS, FTIR and NMR (see Brown & Ekberg 2016 and references therein). Despite the spectroscopic evidence for the existence of the titanyl oxocation, some authors (e.g., Sugimoto et al. 2002) have instead used the stoichiometric formula $Ti(OH)_2^{2+}$ which differs from TiO^{2+} by one H_2O. Both formulations are thermodynamically equivalent as chemical experiments (such as solubility measurements) can generally not distinguish between aqueous species with different amounts of H_2O in the stoichiometric formula and the stability constants of formation reactions of complexes with such different stoichiometries are identical. Therefore, if two stoichiometric formulations of an aqueous species differ by n H_2O, their Gibbs free energies of formation differ by n $\Delta_f G_m°(H_2O, l, 298.15\ K)$. In what follows, we use the formulations of Ti(IV) hydroxide complexes based on the titanyl oxocation and present alternative formulations for information only.

The value

$$\Delta_f G_m°(TiO^{2+}, 298.15\ K) = -(577.4 \pm 2.5)\ kJ \cdot mol^{-1}$$

selected for TDB 2020 was taken from James & Johnson in Bard et al. (1985) with our estimate of the uncertainty.

As no specific ion interaction coefficients are known for TiO^{2+}, we estimated

$$\varepsilon(TiO^{2+}, Cl^-) \approx (0.15 \pm 0.10)\ kg \cdot mol^{-1}$$

$$\varepsilon(TiO^{2+}, ClO_4^-) \approx (0.4 \pm 0.1)\ kg \cdot mol^{-1}$$

according to Section 1.5.3. These values are included in TDB 2020.

The redox equilibrium between Ti(α) and TiO^{2+}

$$Ti(\alpha) + H_2O(l) \rightleftharpoons TiO^{2+} + 2\ H^+ + 4\ e^-$$

can be calculated from the selected $\Delta_f G_m°(TiO^{2+}, 298.15\ K)$ and $\Delta_f G_m°(H_2O, l, 298.15\ K) = -(237.140 \pm 0.041)\ kJ \cdot mol^{-1}$, keeping in mind that $\Delta_f G_m°(Ti, \alpha, 298.15\ K) = \Delta_f G_m°(H^+, 298.15\ K) = \Delta_f G_m°(e^-, 298.15\ K) = 0$. Thus

$$\log_{10} {}^{*}K_{s,0}°(298.15\ K) = (59.6 \pm 0.4)$$

which is included in TDB 2020.

30.3.2 Ti^{3+}

The value

$$\Delta_f G_m°(Ti^{3+}, 298.15\ K) = -(350 \pm 5)\ kJ \cdot mol^{-1}$$

selected for TDB 2020 was taken from James & Johnson (1985) in Bard et al. (1985) with the uncertainty estimated by Brown & Ekberg (2016).

As no specific ion interaction coefficients are known for Ti^{3+}, we estimated

$$\varepsilon(Ti^{3+}, Cl^-) \approx (0.25 \pm 0.10)\ kg \cdot mol^{-1}$$

$$\varepsilon(Ti^{3+}, ClO_4^-) \approx (0.6 \pm 0.1)\ kg \cdot mol^{-1}$$

according to Section 1.5.3. These values are included in TDB 2020.

From the selected $\Delta_f G_m°(Ti^{3+}, 298.15\ K)$, $\Delta_f G_m°(TiO^{2+}, 298.15\ K)$ and $\Delta_f G_m°(H_2O, l, 298.15\ K) = -(237.140 \pm 0.041)\ kJ \cdot mol^{-1}$, keeping in mind that $\Delta_f G_m°(H^+, 298.15\ K) = \Delta_f G_m°(e^-, 298.15\ K) = 0$, follows

$$TiO^{2+} + 2\ H^+ + e^- \rightleftharpoons Ti^{3+} + H_2O(l)$$

$$\log_{10} K°(298.15\ K) = (1.7 \pm 1.0)$$

which is included in TDB 2020.

30.4 Titanium oxygen and hydrogen compounds and complexes

This chapter is partially based on the critical review of the hydrolysis of metal ions by Brown & Ekberg (2016).

30.4.1 Aqueous titanium hydroxide complexes

30.4.1.1 Aqueous titanium(IV) hydroxide complexes

Brown & Ekberg (2016) discussed and selected stability constants for the Ti(IV) hydroxide complexes $TiO(OH)^+$, $TiO(OH)_2(aq)$, and $TiO(OH)_3^-$ based on various experimental solubility studies.

The solubility of a Ti(IV) oxide/hydroxide precipitate was reported by Babko et al. (1962), Liberti et al. (1963), Nabivanets & Lukachina (1964) and Sugimoto et al. (2002) (the first three studies were also discussed by Brown & Ekberg 2016). The precipitate was referred to by Babko et al. (1962), Liberti et al. (1963), and Brown & Ekberg (2016) as $TiO(OH)_2(am)$, while Sugimoto et al. (2002) called it $Ti(OH)_4(am)$, based on thermogravimetry and differential thermal analysis.

Babko et al. (1962) determined the solubility of the precipitate in the acid region between pH 1.3 and 2.3 at 25 °C in 0.1 M (H,Na)Cl and interpreted the results in the formation of TiO^{2+}. Liberti et al. (1963) measured partition data for titanium between very dilute aqueous solutions of Ti ($< 10^{-4}$ M) and organic solvents with various ligands in the pH range 0.5-3 and derived stability constants for $Ti(OH)_2^{2+}$, $Ti(OH)_3^+$, and $Ti(OH)_4(aq)$, the least hydrolysed species being $Ti(OH)^{3+}$. They also measured the solubility of a titanium hydroxide precipitate at pH 1.856, 2.192, and 2.401, in a 0.1 M perchlorate medium at 25 °C. The solubility determinations by Nabivanets & Lukachina (1964) were carried out at 18 °C in 0.1 M in either chloride or perchlorate media (we cannot tell which, since we had no access to this paper) in the pH-range 3-7. Sugimoto et al. (2002), finally, measured the solubility of a titanium hydroxide precipitate at 25 °C in 0.1 M $NaClO_4$ with pH ranging between 1 and 12. They interpreted the observed solubilities in terms of $Ti(OH)_2^{2+}$, $Ti(OH)_3^+$, and $Ti(OH)_4(aq)$.

As seen from Fig. 30.4-1 which combines all these solubility determinations, the concentration of Ti(IV) remains nearly constant (at around $10^{-5.3}$ M) in the broad pH range between about 3 and 12, indicative of the predominance of a neutral Ti(IV) hydroxide complex. The concentrations measured by Sugimoto et al. (2002) are not entirely constant in this range. Sugimoto et al. (2002) noted that in their experimental data "one may find a pH range from 3 – 8 where the experimental data are a little higher than the average solubility level", and that "on the other hand, the measured solubilities above pH 10 appear to be lower than the average level". They explained this variation in the concentration of $Ti(OH)_4(aq)$ in equilibrium with the precipitate that its "rigidity, or degree of hydrogen bonding, may depend on pH to some extent".

Brown & Ekberg (2016) did not rely on any of these solubility studies because "more recent solubility studies, on either rutile or anatase ($TiO_2(s)$), have shown that these phases are much less soluble than the amorphous titanium hydroxide phase". Their selected solubility constant for crystalline TiO_2 leads to solubilities about three orders of magnitude smaller than with the solubility product for the precipitate.

Instead, Brown & Ekberg (2016) based their selected solubility product for TiO_2(cr) and their selected stability constants for $TiO(OH)^+$, $TiO(OH)_2$(aq), and $TiO(OH)_3^-$ on the solubility studies by Ziemniak et al. (1993), Knauss et al. (2001), and Schmidt & Vogelsberger (2009).

Ziemniak et al. (1993) performed hydrothermal solubility studies on rutile, TiO_2(cr), in sodium hydroxide and ammonium hydroxide solutions between 17 and 288 °C in the pH range (measured at 25 °C) between 9.33 and 11.88. Pressure values were not reported, but Ziemniak et al. (1993) mention that in their evaluation of the experimental data, K_w was corrected to a pressure of 8.97 MPa (89.7 bar). Rutile was prepared from reagent grade titanic oxide powder which was fired for four hours at 1'400 °C in a flowing oxygen atmosphere and slowly cooled to room temperature. Particles reached dimensions of 1.3 – 2.5 mm. Aqueous Ti concentrations were measured by atomic absorption spectrophotometry.

The hydrothermal solubility study by Knauss et al. (2001) on rutile covered a wider pH range (1 – 13) and was carried out between 100 and 300 °C at 200 bar. Rutile samples were prepared by crushing parts of a single crystal laser window quality rutile. After sieving and cleaning, the grains were annealed at > 300 °C in the buffer solutions used for the experiments. Aqueous Ti concentrations were measured by ICP-MS.

Schmidt & Vogelsberger (2009) studied the solubility of commercially available titania nanoparticles (anatase and rutile) at 25 °C in NaCl solutions in the pH range 1-13 using adsorptive stripping voltammetry.

Brown & Ekberg (2016) selected the solubility product

$$TiO_2(cr) + 2\ H^+ \rightleftharpoons TiO^{2+} + H_2O(l)$$

$$\log_{10}{}^*K_{s,0}^\circ(298.15\ K) = -(3.56 \pm 0.10)$$

determined by Schmidt & Vogelsberger (2009), and also accepted

$$TiO_2(cr) + H^+ \rightleftharpoons TiOOH^+$$

$$\log_{10}{}^*K_{s,1}^\circ(298.15\ K) = -(6.04 \pm 0.14)$$

and

$$TiO_2(cr) + H_2O(l) \rightleftharpoons TiO(OH)_2(aq)$$

$$\log_{10}K_{s,2}^\circ(298.15\ K) = -(9.05 \pm 0.10)$$

by the same authors. In all cases, the uncertainties were assigned by Brown & Ekberg (2016).

By combining $\log_{10}{}^*K_{s,0}^\circ$ with $\log_{10}{}^*K_{s,1}^\circ$, Brown & Ekberg (2016) obtained the selected

$$TiO^{2+} + H_2O(l) \rightleftharpoons TiOOH^+ + H^+$$

$$\log_{10}{}^*\beta_1^\circ(298.15\ K) = -(2.48 \pm 0.10)$$

and by combining $\log_{10}{}^*K_{s,0}^\circ$ with $\log_{10}{}^*K_{s,2}^\circ$ the selected

$$TiO^{2+} + 2\ H_2O(l) \rightleftharpoons TiO(OH)_2(aq) + 2\ H^+$$

$$\log_{10}{}^*\beta_2^\circ(298.15\ K) = -(5.49 \pm 0.14)$$

Brown & Ekberg (2016) also determined the temperature dependence of $\log_{10}{}^*K_{s,1}^\circ$, $\log_{10}K_{s,2}^\circ$, and $\log_{10}{}^*K_3^\circ$. Using the $\log_{10}{}^*K_{s,1}^\circ$ data reported by Schmidt & Vogelsberger (2009) at 25 °C and by Knauss et al. (2001) at 100, 150, 200, 250, and 300 °C, Brown & Ekberg (2016) derived a linear relationship with respect to 1/T resulting in $\log_{10}{}^*K_{s,1}^\circ(298.15\ K) = -(6.06 \pm 0.30)$, which is consistent with the selected value $\log_{10}{}^*K_{s,1}^\circ(298.15\ K) = -(6.04 \pm 0.14)$, and in $\Delta_r H_m^\circ(298.15\ K) = (14.5 \pm 2.5)\ kJ{\cdot}mol^{-1}$.

Based on the $\log_{10}K_{s,2}^\circ$ values determined by Schmidt & Vogelsberger (2009) at 25 °C and by Ziemniak et al. (1993) at 17, 25, 50, 75, 100, 150, 200, 250, and 288 °C, the linear relationship with respect to 1/T leads to $\log_{10}K_{s,2}^\circ(298.15\ K) = -(9.02 \pm 0.02)$, again consistent with the selected value $\log_{10}K_{s,2}^\circ(298.15\ K) = -(9.05 \pm 0.10)$, and to $\Delta_r H_m^\circ(298.15\ K) = (1.3 \pm 1.0)\ kJ{\cdot}mol^{-1}$.

Finally, Brown & Ekberg (2016) calculated the stepwise stability constants $\log_{10}{}^*K_3^\circ$ for the reaction

$$TiO(OH)_2(aq) + H_2O(l) \rightleftharpoons TiO(OH)_3^- + H^+$$

from the $\log_{10}K_{s,2}^\circ$ and $\log_{10}{}^*K_{s,3}^\circ$ data by Schmidt & Vogelsberger (2009) at 25 °C, by Ziemniak et al. (1993) at 25, 100, 150, 200, 250, and 288 °C, and by Knauss et al. (2001) at 25, 100, 150, 200, 250, and 300 °C. The linear relationship with respect to 1/T resulted in

$$\log_{10}{}^*K_3^\circ(298.15\ K) = -(11.9 \pm 0.5)$$

$$\Delta_r H_m^\circ(298.15\ K) = (55.7 \pm 1.8)\ kJ{\cdot}mol^{-1}$$

Combining this accepted value for $\log_{10}{}^*K_3^\circ(298.15\ K)$ with the selected value $\log_{10}{}^*\beta_2^\circ(298.15\ K) = -(5.49 \pm 0.10)$, Brown & Ekberg (2016) obtained the selected

$$\log_{10}{}^*\beta_3^\circ(298.15\ K) = -(17.4 \pm 0.5)$$

for the reaction

$$TiO^{2+} + 3\ H_2O(l) \rightleftharpoons TiO(OH)_3^- + 3\ H^+$$

For inclusion into TDB 2020, we accepted $\log_{10}{}^*\beta_1^\circ(298.15\ K) = -(2.48 \pm 0.14)$, $\log_{10}{}^*\beta_2^\circ(298.15\ K) = -(5.49 \pm 0.10)$, and $\log_{10}{}^*\beta_3^\circ(298.15\ K) = -(17.4 \pm 0.5)$ selected by Brown & Ekberg (2016) but did not accept crystalline TiO_2 as potential solubility limiting solid. We chose to prefer a solubility product derived from the solubility measurements by Nabivanets & Lukachina (1964) and Sugimoto et al. (2002) of the precipitated Ti(IV) solid in the pH range

5 – 12, where the Ti concentration is nearly constant due to the predominance of the neutral hydroxide complex (see Fig. 30.4-1) at $10^{-5.3 \pm 0.4}$ mol/l, where the uncertainty was chosen such that it encloses all measured values.

Since the precipitates were not structurally analysed and the degree of hydration was not measured (and might vary as a function of time and experimental conditions), their stoichiometry can be represented, e.g., by TiO_2(am, hyd), $TiO(OH)_2$(am, hyd), or $Ti(OH)_4$(am, hyd), where the total amount of hydration is not explicitly accounted for. One may note, however, that formally $TiO(OH)_2$(am, hyd) differs from TiO_2(am, hyd) by one H_2O, while $Ti(OH)_4$(am, hyd) differs from TiO_2(am, hyd) by two H_2O. The solubility in the near-horizontal region can thus be expressed by either one of the following equilibria

$$TiO_2(am, hyd) + H_2O(l) \rightleftharpoons TiO(OH)_2(aq)$$

$$TiO(OH)_2(am, hyd) \rightleftharpoons TiO(OH)_2(aq)$$

$$Ti(OH)_4(am, hyd) \rightleftharpoons TiO(OH)_2(aq) + H_2O(l)$$

Assuming that the activities of the solids and of water are equal to one and that the activity of the aqueous species can be approximated by its concentration, the solubility constant of any of the three equilibria is given by

$$\log_{10} K_{s,2}^\circ = \log_{10} m(TiO(OH)_2(aq))$$

By the same token, the neutral Ti(IV)-hydroxide complex can be written as $Ti(OH)_4$(aq), $TiO(OH)_2$(aq), or TiO_2(aq), each leading to the same value for $\log_{10} K_{s,2}^\circ$ in combination with any of the three solid stoichiometries.

With $\log_{10} m(TiO(OH)_2(aq)) = -(5.3 \pm 0.4)$ mol/l, one obtains

$$TiO_2(am, hyd) + H_2O(l) \rightleftharpoons TiO(OH)_2(aq)$$

$$\log_{10} K_{s,2}^\circ = -(5.3 \pm 0.4)$$

Combining this with the selected $\log_{10} {}^*\beta_2^\circ(298.15\ K) = -(5.49 \pm 0.10)$ results in

$$TiO_2(am, hyd) + 2\ H^+ \rightleftharpoons TiO^{2+} + H_2O(l)$$

$$\log_{10} {}^*K_{s,0}^\circ(298.15\ K) = (0.19 \pm 0.42)$$

which is included in TDB 2020 together with the previously discussed

$$TiO^{2+} + H_2O(l) \rightleftharpoons TiOOH^+ + H^+$$

$$\log_{10} {}^*\beta_1^\circ(298.15\ K) = -(2.48 \pm 0.10)$$

$$TiO^{2+} + 2\ H_2O(l) \rightleftharpoons TiO(OH)_2(aq) + 2\ H^+$$

$\log_{10}{}^*\beta_2°(298.15\ K) = -(5.49 \pm 0.14)$

$TiO^{2+} + 3\ H_2O(l) \rightleftharpoons TiO(OH)_3^- + 3\ H^+$

$\log_{10}{}^*\beta_3°(298.15\ K) = -(17.4 \pm 0.5)$

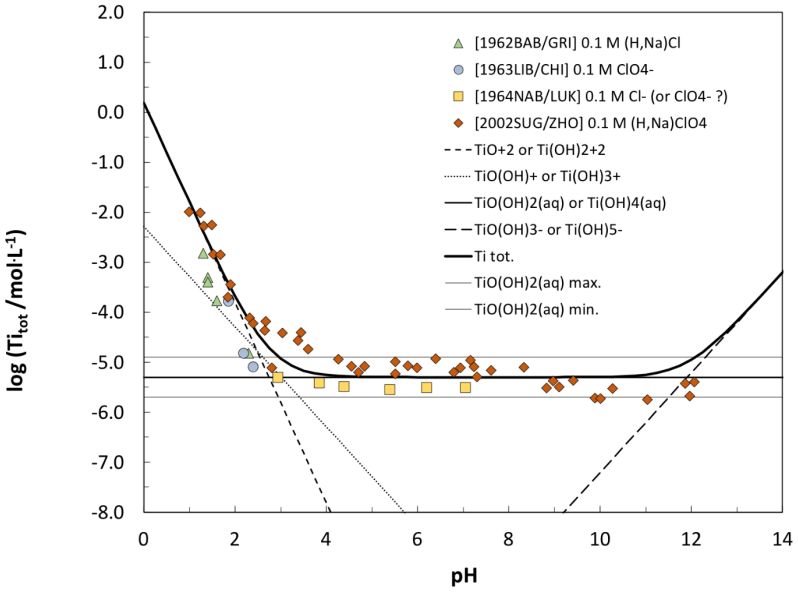

Fig. 30.4-1: Solubility of TiO_2(am, hyd) as a function of pH as determined by Babko et al. (1962), Liberti et al. (1963), Nabivanets & Lukachina (1964), and Sugimoto et al. (2002)

The straight lines were calculated with the selected solubility product for TiO_2(am, hyd) in terms of TiO^{2+}, or $Ti(OH)_2^{2+}$, and the selected stability constants for $TiO(OH)^+$, $TiO(OH)_2$(aq), and $TiO(OH)_3^-$, or in alternative formulation $Ti(OH)_3^+$, $Ti(OH)_4$(aq), and $Ti(OH)_5^-$, respectively.

In the absence of any data for specific ion interaction coefficients we selected

$\varepsilon(TiOOH^+, Cl^-) \approx (0.05 \pm 0.10)\ kg \cdot mol^{-1}$

$\varepsilon(TiOOH^+, ClO_4^-) \approx (0.2 \pm 0.1)\ kg \cdot mol^{-1}$

$\varepsilon(TiO(OH)_2(aq), NaCl(aq)) \approx (0.0 \pm 0.1)\ kg \cdot mol^{-1}$

$\varepsilon(TiO(OH)_3^-, Na^+) \approx -(0.05 \pm 0.10)\ kg \cdot mol^{-1}$

for TDB 2020, based on the estimation method (described in Section 1.5.3).

30.4.1.2 Aqueous titanium(III) hydroxide complexes

Brown & Ekberg (2016) discussed stability constants for $TiOH^{2+}$ and $Ti_2(OH)_2^{4+}$ measured by Pecsok & Fletcher (1962), Pâris & Gregoire (1968), Krentzien & Brito (1970), Pócsi & Fabian (1988), Turiyan & Maluka (1982), Bakač et al. (1977), Shuvalov et al. (1978), and Nabivanets et al. (1981), but only accepted those by Pâris & Gregoire (1968), Krentzien & Brito (1970), Pócsi & Fabian (1988), and Bakač et al. (1977), see Tab. 30.4-1.

Pâris & Gregoire (1968) used coulometry to determine the stability constants of $TiOH^{2+}$ ($\log_{10}{}^{*}\beta_1$(298.15 K) = -2.55) and $Ti_2(OH)_2^{4+}$ ($\log_{10}{}^{*}\beta_{2,2}$(298.15 K) = -3.30) at 25 °C in 3.0 M KBr. The potentiometric study by Krentzien & Brito (1970) in 3.0 M (K,H)Cl at 25 °C resulted in $\log_{10}{}^{*}\beta_1$(298.15 K) = -(2.77 ± 0.08) and $\log_{10}{}^{*}\beta_{2,2}$(298.15 K) = -(3.91 ± 0.17). Pócsi & Fabian (1988) determined $\log_{10}{}^{*}\beta_1$(298.15 K) = -(2.59 ± 0.03) and $\log_{10}{}^{*}\beta_{2,2}$(298.15 K) = -(3.03 ± 0.04) from pH-titrations in 1.0 M KCl at 25 °C. Brown & Ekberg (2016) noted that "these data appear to be in good agreement and are retained". The stability constant $\log_{10}{}^{*}\beta_1$(298.15 K) = -(2.42 ± 0.03) obtained by Bakač et al. (1977) at 25 °C in 1.0 M NaCl was also accepted by Brown & Ekberg (2016) since it is very close to the constant determined by Pócsi & Fabian (1988).

Pecsok & Fletcher (1962) measured the first hydrolysis constant of Ti(III) (formation of $TiOH^{2+}$) in KBr and KI media at ionic strengths between 0.25 and 1.5 M in the temperature range of 15 – 35 °C using potentiometry. Brown & Ekberg (2016) did not accept these data since the stability of $TiOH^{2+}$ according to their accepted data is about an order of magnitude lower.

The stability constant for $TiOH^{2+}$ determined by Turiyan & Maluka (1982) in 1.0 M $NaClO_4$ at 25 °C, $\log_{10}{}^{*}\beta_1$(298.15 K) = -2.14 is also significantly larger than those accepted by Brown & Ekberg (2016). These authors argued that at the titanium concentration[82] used in the experiments by Turiyan & Maluka (1982) the dimer $Ti_2(OH)_2^{4+}$ should be stable. Turiyan & Maluka (1982) did not consider the dimer in their calculations, which would explain the undue stability increase of the monomer. For this reason, Brown & Ekberg (2016) rejected the constant by Turiyan & Maluka (1982).

The stability constants measured by Shuvalov et al. (1978) in 0.06-0.12 M KCl and 1.0 M KBr at 0 – 60 °C result in a stability of $TiOH^{2+}$ an order of magnitude less than when obtained with the constants accepted by Brown & Ekberg (2016) and were therefore rejected.

Finally, Nabivanets et al. (1981) determined $\log_{10}{}^{*}\beta_1$ and $\log_{10}{}^{*}\beta_{2,2}$ in 1.0 M HCl at 18 °C. These constants were rejected by Brown & Ekberg (2016) on the grounds that "the constants given are marginally more stable than those given at 25 °C in other studies. Thus, these constants are not accepted, since at the lower temperature it would be expected that the stability constants should indicate a lower stability".

Brown & Ekberg (2016) used the three conditional stability constants for $TiOH^{2+}$ determined by Krentzien & Brito (1970), Pócsi & Fabian (1988), and Bakač et al. (1977) in chloride media, see Tab. 30.4-1., for a linear SIT extrapolation and obtained

[82] No value was given by Brown & Ekberg (2016) and we had no access to the paper by Turiyan & Maluka (1982).

$Ti^{3+} + H_2O(l) \rightleftharpoons TiOH^{2+} + H^+$

$\log_{10}{}^{*}\beta_1°(298.15\ K) = -(1.65 \pm 0.11)$

$\Delta\varepsilon = (0.01 \pm 0.05)\ kg \cdot mol^{-1}$

From this value for $\Delta\varepsilon$ and the selected values $\varepsilon(H^+, Cl^-) = (0.12 \pm 0.01)\ kg \cdot mol^{-1}$ (NEA: Lemire et al. 2013), and $\varepsilon(Ti^{3+}, Cl^-) \approx (0.25 \pm 0.10)\ kg \cdot mol^{-1}$ follows

$\varepsilon(TiOH^{2+}, Cl^-) = (0.14 \pm 0.11)\ kg \cdot mol^{-1}$

In the absence of experimental data for perchlorate media we estimated

$\varepsilon(TiOH^{2+}, ClO_4^-) \approx (0.4 \pm 0.1)\ kg \cdot mol^{-1}$

according to Section 1.5.3. All these data for $TiOH^{2+}$ are included in TDB 2020.

According to Brown & Ekberg (2016), there are no data for other monomeric Ti-hydroxide complexes but in light of other trivalent metals in the first transition series, the formation of $Ti(OH)_4^-$ can be expected.

From an SIT regression of the two conditional stability constants for $Ti_2(OH)_2^{4+}$ measured by Krentzien & Brito (1970) and Pócsi & Fabian (1988) in chloride media, Brown & Ekberg (2016) obtained

$2\ Ti^{3+} + 2\ H_2O(l) \rightleftharpoons Ti_2(OH)_2^{4+} + 2\ H^+$

$\log_{10}{}^{*}\beta_{2,2}°(298.15\ K) = -(2.64 \pm 0.10)$

$\Delta\varepsilon = (0.34 \pm 0.10)\ kg \cdot mol^{-1}$

with estimated uncertainties, since only two data points were considered.

From the value for $\Delta\varepsilon$ and those selected for $\varepsilon(H^+, Cl^-)$ and $\varepsilon(Ti^{3+}, Cl^-)$, see above, then follows

$\varepsilon(Ti_2(OH)_2^{4+}, Cl^-) = (0.60 \pm 0.30)\ kg \cdot mol^{-1}$

In the absence of any data for perchlorate media, we estimated

$\varepsilon(Ti_2(OH)_2^{4+}, ClO_4^-) \approx (0.8 \pm 0.1)\ kg \cdot mol^{-1}$

according to Section 1.5.3. All these data for $Ti_2(OH)_2^{4+}$ are included in TDB 2020.

Tab. 30.4-1: Experimental stability constants for titanium hydroxide complexes accepted by Brown & Ekberg (2016)

(cou.: coulometry, pot.: potentiometry, tit.: pH-titration, kin: reaction kinetics)

$\log_{10}{}^{*}\beta_1$	$\log_{10}{}^{*}\beta_{2,2}$	T [°C]	I [M]	Medium	Method	Reference
-2.55	-3.30	25	3.0	KBr	cou.	Pâris & Gregoire (1968)
-2.77 ±0.08	-3.91 ± 0.17	25	3.0	(K,H)Cl	pot.	Krentzien & Brito (1970)
-2.59 ± 0.03	-3.03 ± 0.04	25	1.0	KCl	tit.	Pócsi & Fabian (1988)
-2.42 ± 0.03	-	25	1.0	NaCl	kin.	Bakač et al. (1977)

30.4.2 Titanium oxide and hydroxide solids

30.4.2.1 Titanium(IV) oxide and hydroxide solids

Rutile, TiO_2(cr), is the most common simple Ti(IV) oxide and is found as an accessory mineral in high-temperature and high-pressure igneous and metamorphic rocks. Its polymorphs anatase and brookite are of secondary nature and are most commonly found in alpine veins, derived by hydrothermal solutions from the enclosing gneisses and schists. All three minerals are not formed under surficial conditions in aqueous environments.

Brown & Ekberg (2016) reviewed solubility data for TiO_2(cr), anatase and rutile, which they used to derive stability constants for aqueous Ti(IV)-hydroxide complexes and a solubility product for TiO_2(cr). As discussed in Section 30.4.1.1, we preferred to select a solubility product for TiO_2(am, hyd) derived from the measured solubilities of Ti(IV) precipitates by Nabivanets & Lukachina (1964) and Sugimoto et al. (2002). Precipitates are much more likely to form under surficial conditions than crystalline rutile, anatase or brookite. We selected

$$TiO_2(am, hyd) + 2\ H^+ \rightleftharpoons TiO^{2+} + H_2O(l)$$

$$\log_{10}{}^{*}K_{s,0}^{\circ}(298.15\ K) = (0.19 \pm 0.42)$$

30.4.2.2 Titanium(III) oxide solids

There exist only two titanium(III) minerals in nature, tistarite (Ti_2O_3) and grossmanite ($CaTiAlSiO_6$).

Both minerals were found as refractory minerals in the Allende meteorite and were first described by Ma & Rossman (2009a) and Ma & Rossman (2009b), respectively. They were interpreted as condensate minerals which were formed under highly reduced conditions at the earliest stage of the solar system. During an exploration campaign for diamond, sapphire and other gem minerals, the first terrestrial occurrence of tistarite was discovered by Griffin et al. (2016) in highly reduced mineral assemblages, crystallized from high temperature melts derived from the upper mantle and trapped in corundum aggregates ejected from Cretaceous volcanoes in Israel.

Brown & Ekberg (2016) determined a solubility constant

$$TiO_{1.5}(cr) + 3\ H^+ \rightleftharpoons Ti^{3+} + 1.5\ H_2O(l)$$

$$\log_{10}K_{s0}°(298.15\ K) = -(1.96 \pm 0.50)$$

for Ti_2O_3(cr) from $\Delta_f G_m°(Ti_2O_3, s, 298.15\ K) = -(1'433.9 \pm 8.4)\ kJ \cdot mol^{-1}$ by Robie & Hemingway (1995), $\Delta_f G_m°(Ti^{3+}, 298.15\ K) = -350\ kJ \cdot mol^{-1}$ by Bard et al. (1985), and their $\Delta_f G_m°(H_2O, l, 298.15\ K) = -(237.17 \pm 0.04)\ kJ \cdot mol^{-1}$ derived from the standard oxidation potential for the oxygen-water couple. Brown & Ekberg (2016) claimed that "solubility data are available for the trivalent oxide phase of titanium(III), Ti_2O_3(s)". However, they did not report any solubility data for this solid and none of the known stability constants for Ti(III) hydroxide were derived from solubility measurements of Ti_2O_3(s).

Since solubility data for this solid are missing and only one terrestrial occurrence is known, it is not reasonable to assume that it may limit the solubility of Ti(III) in repository environments by precipitation under any circumstances. Therefore, it is not included in TDB 2020.

30.5 Selected titanium data

Tab. 30.5-1: Selected titanium data (1 bar, 298.15 K) for TDB 2020

Values taken from CODATA are bold (Cox et al. 1989).

Name	**Redox**	**TDB 2020**				
		$\Delta_f G_m°$ [kJ · mol^{-1}]	$\Delta_f H_m°$ [kJ · mol^{-1}]	$S_m°$ [J · K^{-1} · mol^{-1}]	$C_{p,m}°$ [J · K^{-1} · mol^{-1}]	**Species**
Ti(cr)	0	0.0	0.0	**30.72 ± 0.10**	-	Ti(cr)
Ti+3	III	-350 ± 5	-	-	-	Ti^{3+}
TiO+2	IV	-577.4 ± 2.5	-	-	-	TiO^{2+}

Name	**Redox**	**TDB 2020**			
		$\log_{10}\beta°$	$\Delta_r H_m°$ [kJ · mol^{-1}]	$\Delta_r C_{p,m}°$ [J · K^{-1} · mol^{-1}]	**Reaction**
TiOOH+	IV	-2.48 ± 0.10	-	-	$TiO^{2+} + H_2O(l) \rightleftharpoons TiOOH^+ + H^+$
TiO(OH)2(aq)	IV	-5.49 ± 0.14	-	-	$TiO^{2+} + 2\ H_2O(l) \rightleftharpoons TiO(OH)_2(aq) + 2\ H^+$
TiO(OH)3-	IV	-17.4 ± 0.5	-	-	$TiO^{2+} + 3\ H_2O(l) \rightleftharpoons TiO(OH)_3^- + 3\ H^+$
Ti+3	IV/III	1.7 ± 1.0	-	-	$TiO^{2+} + 2\ H^+ + e^- \rightleftharpoons Ti^{3+} + H_2O(l)$
TiOH+2	III	-1.65 ± 0.11	-	-	$Ti^{3+} + H_2O(l) \rightleftharpoons TiOH^{2+} + H^+$
Ti2(OH)2+4	III	-2.64 ± 0.10	-	-	$2\ Ti^{3+} + 2\ H_2O(l) \rightleftharpoons Ti_2(OH)_2^{4+} + 2\ H^+$

Name	**TDB 2020**			
	$\log_{10}K_{s,0}°$	$\Delta_r H_m°$ [kJ · mol^{-1}]	$\Delta_r C_{p,m}°$ [J · K^{-1} · mol^{-1}]	**Reaction**
Ti(α)	59.6 ± 0.4	-	-	$Ti(\alpha) + H_2O(l) \rightleftharpoons TiO^{2+} + 2\ H^+ + 4\ e^-$
TiO2(am, hyd)	0.19 ± 0.42	-	-	$TiO_2(am, hyd) + 2\ H^+ \rightleftharpoons TiO^{2+} + H_2O(l)$

Tab. 30.5-2: Selected SIT ion interaction coefficients $\varepsilon_{j,k}$ [kg · mol^{-1}] for titanium species

Data estimated according to charge correlations and taken from Tab. 1-7 are shaded.

j k → ↓	**Cl^-** $\varepsilon_{j,k}$ [kg · mol^{-1}]	**ClO_4^-** $\varepsilon_{j,k}$ [kg · mol^{-1}]	**Na^+** $\varepsilon_{j,k}$ [kg · mol^{-1}]	**$Na^+ + Cl^-$** $\varepsilon_{j,k}$ [kg · mol^{-1}]
TiO+2	0.15 ± 0.10	0.4 ± 0.1	0	0
TiOOH+	0.05 ± 0.10	0.2 ± 0.1	0	0
TiO(OH)2(aq)	0	0	0	0.0 ± 0.1
TiO(OH)3-	0	0	-0.05 ± 0.10	
Ti+3	0.25 ± 0.10	0.6 ± 0.1	0	0
TiOH+2	0.14 ± 0.11	0.4 ± 0.1	0	0
Ti2(OH)2+4	0.60 ± 0.30	0.8 ± 0.1	0	0

30.6 References

Babko, A.K., Gridchina, G.I. & Nabivanets, B.I. (1962): Study of titanium(IV) in hydrochloric acid by dialysis and ion-exchange chromatography. Russian Journal of Inorganic Chemistry, 7, 66-70.

Bakač, A., Marčec, R. & Orhanović, M. (1977): Titanium(III) reduction of the tris(1,10-phenanthroline)cobalt(III) and bis(2,2':6',2"-terpyridine)cobalt(III) ions. Inorganic Chemistry, 16, 3133-3135.

Bard, A.J., Parsons, R. & Jordan, J. (1985): Standard Potentials in Aqueous Solution, Marcel Dekker Inc., New York, 834 pp.

Brown, P.L. & Ekberg, C. (2016): Hydrolysis of Metal Ions. Vol. 2, Wiley-VCH, Weinheim.

Chen, J., Lee, J. & Wu, J. (2000): Native titanium inclusions in the coesite eclogites from Dabieshan, China. Earth and Planetary Science Letters, 177, 237-240.

Cox, J.D., Wagman, D.D. & Medvedev, V.A. (1989): CODATA Key Values for Thermodynamics. Hemisphere, New York, 271 pp.

Graetzel, M. & Rotzinger, F.P. (1985): Raman spectroscopic evidence for the existence of titanyl (TiO^{2+}) in acidic aqueous solutions. Inorganic Chemistry, 24, 2320-2321.

Griffin, W.L., Gain, S.E.M., Adams, D. T., Huang, J.-X., Saunders, M., Toledo, V., Pearson, N.J. & O'Reilly, S.Y. (2016): First terrestrial occurrence of tistarite (Ti2O3): Ultra-low oxygen fugacity in the upper mantle beneath Mount Carmel, Israel. Geology, 44, 815-818.

Hummel, W. (2018): Radioactive waste inventories for geochemists. PSI Internal Report, TM-44-18-03, Paul Scherrer Institut, Villigen, Switzerland, 55 pp.

Jambor, J.L. & Puziewicz, J. (1990): New mineral names. American Mineralogist, 75, 1209-1216.

Jambor, J.L. & Roberts, A.C. (2001): New mineral names. American Mineralogist, 86, 197-201.

Jambor, J.L. & Vanko, D.A. (1991): New mineral names. American Mineralogist, 76, 1434-1440.

James, W.J., Johnson, J.W. & Truck, D.G. (1985): Titanium, zirconium, and hafnium. In: Bard, A.J., Parsons, R. & Jordan, J. (eds.): Standard Potentials in Aqueous Solution. Marcel Dekker, Inc., New York and Basel, 539-553.

Knauss, K.G., Dibley, M.J., Bourcier, W.L. & Shaw, H.F. (2001): Ti(IV) hydrolysis constants derived from rutile solubility measurements made from 100 to 300 °C. Applied Geochemistry 16, 1115-1128.

Krentzien, H. & Brito, F. (1970): Contribución al estudio de la hidrólisis del titanio (III). Ion 30, 1-3.

Lemire, R.J., Berner, U., Musikas, C., Palmer, D.A., Taylor, P. & Tochiyama, O. (2013): Chemical Thermodynamics of Iron, Part 1. Chemical Thermodynamics, Vol. 13a. OECD Publications, Paris, France, 1082 pp.

Liberti, A., Chiantella, V. & Corigliano, F. (1963): Mononuclear hydrolysis of titanium (IV) from partition equilibria. Journal of Inorganic and Nuclear Chemistry, 25, 415-427.

Ma, C. & Rossman, G.R. (2009a): Tistarite, Ti_2O_3, a new refractory mineral from the Allende meteorite. American Mineralogist, 94, 841-844.

Ma, C. & Rossman, G.R. (2009b): Grossmanite, $CaTi^{3+}AlSiO_6$, a new pyroxene from the Allende meteorite. American Mineralogist, 94, 1491-1494.

Nabivanets, B.I. & Lukachina, V.V. (1964): Hydroxo-complexes of titanium(IV). Ukrainskii Khimicheskii Zhurnal, 30, 1123-1128 (as cited by Brown & Ekberg 2016).

Nabivanets, B.I., Matyashev, V.G. & Chernaya, N. V. (1981): Properties in solution and analytical-chemical properties of polyvalent metals in lower degrees of oxidation. Hydrolysis and polynuclear forms of titanium(III). Journal of Analytical Chemistry of the USSR, 36, 182-185.

Pâris, M.R. & Gregoire, C. (1968): Application de la coulometrie à l'etude des complexes. II. Complexation du titane(III) par les ions hydroxyde et l'acide picolique. Analytica Chimica Acta, 42, 439-444.

Pecsok, R.L. & Fletcher, A.N. (1962): Hydrolysis of titanium(III). Inorganic Chemistry, 1, 155-159.

Pócsi, I. & Fábián, I. (1988): Complex equilibria in aqueous solutions of Ti^{3+}-glycine and -malonic acid. Journal of the Chemical Society, Dalton Transactions 8, 2231-2233.

Robie, R.A. & Hemingway, B.S. (1995): Thermodynamic properties of minerals and related substances at 298.15 K and 1 bar (10^5 Pascals) pressure and at higher temperatures. United States Geological Survey Bulletin, 2131, 453.

Schmidt, J. & Vogelsberger, W. (2009): Aqueous long-term solubility of titania nanoparticles and titanium(IV) hydrolysis in a sodium chloride system studied by adsorptive stripping voltammetry. Journal of Solution Chemistry, 38, 1267-1282.

Shannon, R.D. (1976): Revised effective ionic radii and systematic studies of interatomic distances in halides and chalcogenides. Acta Crystallographica, Section A, 32, 751-767.

Shuvalov, V.F., Solovev, S.L. & Lebedev, Y.S. (1978): ESR investigation of the hydrolysis of titanium(III) in aqueous hydrochloric acid solutions. Russian Chemical Bulletin, 27, 5-9.

Sugimoto, T., Zhou, X. & Muramatsu, A. (2002): Synthesis of uniform anatase TiO_2 nanoparticles by gel–sol method: 1. Solution chemistry of $Ti(OH)_n^{(4-n)+}$ complexes. Journal of Colloid and Interface Science, 252, 339-346.

Thoenen, T., Hummel, W., Berner, U. & Curti, E. (2014): The PSI/Nagra Chemical Thermodynamic Database 12/07. Technical Report, PSI Bericht Nr. 14-04, Paul Scherrer Institut, Villigen, Switzerland, 416 pp.

Turiyan, Y.I. & Maluka, L.M. (1982): Polarographic study of the mechanism and kinetics of the electro-oxidation and equilibrium of Ti(III) hydrolysis. Zh. Obshch. Khim., 51, 260-265 (as cited by Brown & Ekberg 2016).

Wood, S.A. (2005): The aqueous geochemistry of zirconium, hafnium, niobium, and tantalum. In: Linnen, R.L. & Samson, I.M. (eds.): Rare-element geochemistry and mineral deposits. Geological Association of Canada, GAC Short Course Notes, 17, 217-268.

Ziemniak, S.E., Jones, M.E. & Combs, K.E.S. (1993): Solubility behavior of titanium(IV) oxide in alkaline media at elevated temperatures. Journal of Solution Chemistry, 22, 601-623.

31 Uranium

In a late state of the review work for TDB 2020 the NEA TDB Second Update on the Chemical Thermodynamics of Uranium, Neptunium, Plutonium, Americium and Technetium (Grenthe et al. 2020) became available to the reviewers. In the following, only changes with respect to previous TDB versions are shortly discussed. For a detailed discussion of the previous uranium chemical thermodynamic data the reader is referred to Thoenen et al. (2014) and Hummel et al. (2002).

31.1 Uranium oxygen and hydrogen compounds and complexes

The stability constants of the U(VI) hydrolysis complexes have not been changed by Grenthe et al. (2020). However, based on a new calorimetric study by Crea et al. (2004), Grenthe et al. (2020) selected $\Delta_r H_m°$ values for several U(VI) hydrolysis complexes:

$UO_2^{2+} + H_2O(l) \rightleftharpoons UO_2OH^+ + H^+$

$\Delta_r H_m° = (43.3 \pm 2.3)$ kJ · mol^{-1}

$2\ UO_2^{2+} + 2\ H_2O(l) \rightleftharpoons (UO_2)_2(OH)_2^{2+} + 2\ H^+$

$\Delta_r H_m° = (47.8 \pm 0.5)$ kJ · mol^{-1}

$3\ UO_2^{2+} + 4\ H_2O(l) \rightleftharpoons (UO_2)_3(OH)_4^{2+} + 4\ H^+$

$\Delta_r H_m° = (99.2 \pm 0.5)$ kJ · mol^{-1}

$3\ UO_2^{2+} + 5\ H_2O(l) \rightleftharpoons (UO_2)_3(OH)_5^{+} + 5\ H^+$

$\Delta_r H_m° = (120.7 \pm 0.6)$ kJ · mol^{-1}

In addition, Grenthe et al. (2020) increased the uncertainty of the stability constant of the $(UO_2)_2(OH)_2^{2+}$ complex from ± 0.04 to ± 0.08.

All these values have been included in TDB 2020.

Concerning the stability constants of the U(IV) hydrolysis complexes, Grenthe et al. (2020) selected new values for $U(OH)_2^{2+}$ and $U(OH)_3^{+}$, based on a new experimental study by Fujiwara et al. (2003) and in good agreement with earlier estimates:

$U^{4+} + 2\ H_2O(l) \rightleftharpoons U(OH)_2^{2+} + 2\ H^+$

$\log_{10}{}^*\beta_2° = -(1.9 \pm 0.2)$

$U^{4+} + 3\ H_2O(l) \rightleftharpoons U(OH)_3^{+} + 3\ H^+$

$\log_{10}{}^*\beta_3° = -(5.2 \pm 0.4)$

These values have been included in TDB 2020.

Grenthe et al. (2020) considered the solubility study of Altmaier et al. (2017) as the most reliable and accurate study published so far and have therefore based their selected solubility constant for metaschoepite, $UO_3 \cdot 2H_2O$(cr), on this paper alone. Likewise, Grenthe et al. (2020) accepted the solubility constant for $Na_2U_2O_7 \cdot H_2O$(cr) as reported by Altmaier et al. (2017):

$$UO_3 \cdot 2H_2O(cr) + 2\ H^+ \rightleftharpoons UO_2^{2+} + 3\ H_2O(l)$$

$$\log_{10}{}^*K_s^\circ = 5.35 \pm 0.13$$

$$\tfrac{1}{2}\ Na_2U_2O_7 \cdot H_2O(cr) + 3\ H^+ \rightleftharpoons Na^+ + UO_2^{2+} + 2\ H_2O(l)$$

$$\log_{10}{}^*K_s^\circ = 12.2 \pm 0.2$$

These values have been included in TDB 2020.

Grenthe et al. (2020) discuss some U(VI) peroxide complexes and compounds. They report equilibrium constants and enthalpy of reactions for the ternary complexes $[UO_2(O_2)(OH)]^-$ and $[(UO_2)_2(O_2)_2(OH)]^-$ "for information only". Furthermore, Grenthe et al. (2020) select, based on the experimental study by Hughes Kubatkoet al. (2003), a solubility constant and a standard enthalpy of formation of studtite, $(UO_2)O_2(H_2O)_4$(cr). Using the only auxiliary datum for peroxide available in the NEA TDB data base, the enthalpy of formation of H_2O_2(aq), Grenthe et al. (2020) calculated $\Delta_r H_m^\circ$ and $\Delta_r S_m^\circ$ of studtite. However, due to the lack of a $\Delta_f G_m^\circ$ value for H_2O_2(aq), or, more general, the total lack of reaction data for the formation of H_2O_2(aq) and HO_2^-, the above data, selected or "for information only", cannot be used in speciation calculations. Hence, none of these data is included in TDB 2020.

31.2 Uranium halogen compounds and complexes

The stability constants of the uranium halogen complexes have not been changed by Grenthe et al. (2020). However, based on a new microcalorimetric study by Tian & Rao (2009), Grenthe et al. (2020) revised the selected $\Delta_r H_m^\circ$ values for the U(VI) fluoride complexes:

$$UO_2^{2+} + F^- \rightleftharpoons UO_2F^+$$

$$\Delta_r H_m^\circ = -(0.54 \pm 0.26)\ kJ \cdot mol^{-1}$$

$$UO_2^{2+} + 2\ F^- \rightleftharpoons UO_2F_2(aq)$$

$$\Delta_r H_m^\circ = -(1.34 \pm 0.18)\ kJ \cdot mol^{-1}$$

$$UO_2^{2+} + 3\ F^- \rightleftharpoons UO_2F_3^-$$

$$\Delta_r H_m^\circ = -(1.18 \pm 0.30)\ kJ \cdot mol^{-1}$$

$$UO_2^{2+} + 4\ F^- \rightleftharpoons UO_2F_4^{2-}$$

$$\Delta_r H_m^\circ = -(2.12 \pm 0.47)\ kJ \cdot mol^{-1}$$

Note that the values previously selected by Guillaumont et al. (2003) and included in TDB Version 12/07 (Thoenen et al. 2014) refer to 1.00 M $NaClO_4$, while the new selected values have been extrapolated to zero ionic strength by Grenthe et al. (2020).

Finally, Grenthe et al. (2020) selected an equilibrium constant for uranyl periodate, $UO_2IO_4^+$. There are no NEA auxiliary data for periodate, IO_4^-, and periodate is not considered in TDB 2020. Hence, $UO_2IO_4^+$ is not included in TDB 2020.

31.3 Uranium sulphur and selenium compounds and complexes

31.3.1 Uranium sulphur compounds and complexes

The stability constants of the uranium sulphate complexes have not been changed by Grenthe et al. (2020). They only increased the uncertainties of the equilibrium constants for $UO_2SO_4(aq)$ and $UO_2(SO_4)_2^{2-}$ from ± 0.02 to ± 0.10 and from ± 0.07 to ± 0.15, respectively. These changes have been included in TDB 2020.

Based on new calorimetric studies using dissolution calorimetry and adiabatic low-temperature calorimetry in the range 7 – 300 K, Grenthe et al. (2020) selected values for the standard enthalpy of formation, the molar entropy and the molar heat capacity of $M[UO_2(SO_4)_2] \cdot 5H_2O(cr)$, M = Mn, Fe, Co, Ni, Cu, Zn. However, none of these compounds is known as a mineral, presumably due to their high solubility. Also, no measured solubility data for these compounds could be found by this review. Hence, the selected calorimetric data have not been included in TDB 2020.

31.3.2 Uranium selenium compounds and complexes

Grenthe et al. (2020) selected equilibrium constants for uranyl selenite and selenate complexes. In the case of selenate complexes, Grenthe et al. (2020) also selected enthalpies of reaction determined from the temperature dependence of the equilibrium constants in the range 15 – 55 °C:

$$UO_2^{2+} + HSeO_3^- \rightleftharpoons UO_2HSeO_3^+$$

$$\log_{10}\beta_1^\circ = (3.27 \pm 0.15)$$

$$UO_2^{2+} + 2\ HSeO_3^- \rightleftharpoons UO_2(HSeO_3)_2(aq)$$

$$\log_{10}\beta_2^\circ = (5.51 \pm 0.11)$$

$$UO_2^{2+} + SeO_4^{2-} \rightleftharpoons UO_2SeO_4(aq)$$

$$\log_{10}\beta_1^\circ = (2.93 \pm 0.04)$$

$$\Delta_r H_m^\circ = (20 \pm 2)\ kJ \cdot mol^{-1}$$

$$UO_2^{2+} + 2\ SeO_4^{2-} \rightleftharpoons UO_2(SeO_4)_2^{2-}$$

$$\log_{10}\beta_2^\circ = (4.03 \pm 0.09)$$

$$\Delta_r H_m^\circ = (31 \pm 4)\ kJ \cdot mol^{-1}$$

All these values have been included in TDB 2020.

31.4 Uranium nitrate, phosphate and arsenate compounds and complexes

31.4.1 Uranium nitrate complexes

Based on a new spectrophotometric study by Suleimenov et al. (2007) in the aqueous U(VI)-nitrate system at different temperatures Grenthe et al. (2020) revised the equilibrium constant for $UO_2NO_3^+$ and selected a new enthalpy of reaction value:

$$UO_2^{2+} + NO_3^- \rightleftharpoons UO_2NO_3^+$$

$$\log_{10}\beta_1^\circ = -(0.19 \pm 0.15)$$

$$\Delta_r H_m^\circ = (20.9 \pm 3.5)\ \text{kJ} \cdot \text{mol}^{-1}$$

These values have been included in TDB 2020.

31.4.2 Uranium phosphate compounds and complexes

Based on a new solubility study of $(UO_2)_3(PO_4)_2 \cdot 4H_2O$(cr) by Rai et al. (2005) over a wide range of pH (2.5 – 10.5) Grenthe et al. (2020) revised the equilibrium constant for $UO_2PO_4^-$:

$$UO_2^{2+} + PO_4^{3-} \rightleftharpoons UO_2PO_4^-$$

$$\log_{10}\beta_1^\circ = (11.01 \pm 0.48)$$

This value has been included in TDB 2020.

Note that the solubility product for $(UO_2)_3(PO_4)_2 \cdot 4H_2O$(cr) has not been changed.

Grenthe et al. (2020) selected a new equilibrium constant for $UH_2PO_4^{3+}$ based on a time-resolved laser fluorescence spectroscopy (TRLFS) study by Lehmann et al. (2010) on the complex formation between U(IV) and phosphate at pH below 2:

$$U^{4+} + H_2PO_4^- \rightleftharpoons UH_2PO_4^{3+}$$

$$\log_{10}\beta_1^\circ = (6.8 \pm 0.7)$$

This value has been included in TDB 2020.

Grenthe et al. (2020) retained the previously selected solubility constant for chernikovite, $UO_2HPO_4 \cdot 4H_2O$(cr), but selected heat capacity and entropy values of this phase from a new low-temperature calorimetry study:

$$S_m^\circ(UO_2HPO_4 \cdot 4H_2O, \text{cr}, 298.15\ \text{K}) = (328 \pm 10)\ \text{J} \cdot \text{K}^{-1} \cdot \text{mol}^{-1}$$

$$C_{p,m}^\circ(UO_2HPO_4 \cdot 4H_2O, \text{cr}, 298.15\ \text{K}) = (317 \pm 10)\ \text{J} \cdot \text{K}^{-1} \cdot \text{mol}^{-1}$$

These values have been included in TDB 2020.

Grenthe et al. (2020) selected new solubility constants for $M[(UO_2)(PO_4)] \cdot xH_2O(cr)$, where M = Li, Na, K, Rb, Cs, NH_4, and state that all these phases belong to the autunite mineral group. The selected solubility constants of all these phases have been included in TDB 2020, with the exception of the Rb phase, as Rb is not part of TDB 2020:

$$Li(UO_2)(PO_4) \cdot 4H_2O(cr) \rightleftharpoons UO_2^{2+} + Li^+ + PO_4^{3-} + 4\ H_2O(l)$$

$$\log_{10}K_s^\circ = -(25.5 \pm 1.0)$$

$$Na(UO_2)(PO_4) \cdot 3H_2O(cr) \rightleftharpoons UO_2^{2+} + Na^+ + PO_4^{3-} + 3\ H_2O(l)$$

$$\log_{10}K_s^\circ = -(24.3 \pm 1.0)$$

$$K(UO_2)(PO_4) \cdot 3H_2O(cr) \rightleftharpoons UO_2^{2+} + K^+ + PO_4^{3-} + 3\ H_2O(l)$$

$$\log_{10}K_s^\circ = -(25.5 \pm 1.0)$$

$$Cs(UO_2)(PO_4) \cdot 2.5H_2O(cr) \rightleftharpoons UO_2^{2+} + Cs^+ + PO_4^{3-} + 2.5\ H_2O(l)$$

$$\log_{10}K_s^\circ = -(25.9 \pm 1.0)$$

$$NH_4(UO_2)(PO_4) \cdot 3H_2O(cr) \rightleftharpoons UO_2^{2+} + NH_4^+ + PO_4^{3-} + 3\ H_2O(l)$$

$$\log_{10}K_s^\circ = -(26.1 \pm 1.0)$$

Grenthe et al. (2020) discuss experimentally determined and estimated heat capacity and entropy values for these alkali metal uranyl phosphates, but finally report entropy values which they considered most reliable "for information only":

$$S_m^\circ(Li(UO_2)(PO_4) \cdot 4H_2O, cr, 298.15\ K) = (336 \pm 20)\ J \cdot K^{-1} \cdot mol^{-1}$$

$$S_m^\circ(Na(UO_2)(PO_4) \cdot 3H_2O, cr, 298.15\ K) = (323 \pm 20)\ J \cdot K^{-1} \cdot mol^{-1}$$

$$S_m^\circ(K(UO_2)(PO_4) \cdot 3H_2O, cr, 298.15\ K) = (343 \pm 15)\ J \cdot K^{-1} \cdot mol^{-1}$$

$$S_m^\circ(Cs(UO_2)(PO_4) \cdot 2.5H_2O, cr, 298.15\ K) = (338 \pm 15)\ J \cdot K^{-1} \cdot mol^{-1}$$

$$S_m^\circ(NH_4(UO_2)(PO_4) \cdot 3H_2O, cr, 298.15\ K) = (350 \pm 20)\ J \cdot K^{-1} \cdot mol^{-1}$$

These values have been included in TDB 2020 as supplemental data.

Grenthe et al. (2020) discuss new solubility constants for $M[(UO_2)(PO_4)]_2 \cdot xH_2O(cr)$, where M = Mg, Ca, Sr, Ba. These phases belong to the autunite mineral group, the name autunite itself designates the hydrated calcium uranyl phosphate of the general formula $Ca[(UO_2)(PO_4)]_2 \cdot 10 - 12H_2O(cr)$, which at dehydration transforms into meta-autunite $Ca[(UO_2)(PO_4)]_2 \cdot 2 - 6H_2O(cr)$. Grenthe et al. (2020) state that "in these phases there is a large variation of the degree of hydration that is still compatible with the autunite structure, and it is not clear which hydrate is stable in water at ambient conditions. Most probably, the difference in the thermodynamic stability of various hydrates is small". They finally selected solubility constants for the meta-phases, i.e., for meta-saleite $Mg[(UO_2)(PO_4)]_2 \cdot 8H_2O(cr)$, meta-autunite

$Ca[(UO_2)(PO_4)]_2 \cdot 6H_2O$(cr), $Sr[(UO_2)(PO_4)]_2 \cdot 6H_2O$(cr) and meta-uranocircite II $Ba[(UO_2)(PO_4)]_2 \cdot 6H_2O$(cr).

$$Mg[(UO_2)(PO_4)]_2 \cdot 8H_2O(cr) \rightleftharpoons 2\ UO_2^{2+} + Mg^{2+} + 2\ PO_4^{3-} + 8\ H_2O(l)$$

$$\log_{10}K_s^\circ = -(49.2 \pm 1.2)$$

$$Ca[(UO_2)(PO_4)]_2 \cdot 6H_2O(cr) \rightleftharpoons 2\ UO_2^{2+} + Ca^{2+} + 2\ PO_4^{3-} + 6\ H_2O(l)$$

$$\log_{10}K_s^\circ = -(50.0 \pm 1.0)$$

$$Sr[(UO_2)(PO_4)]_2 \cdot 6H_2O(cr) \rightleftharpoons 2\ UO_2^{2+} + Sr^{2+} + 2\ PO_4^{3-} + 6\ H_2O(l)$$

$$\log_{10}K_s^\circ = -(51.3 \pm 1.0)$$

$$Ba[(UO_2)(PO_4)]_2 \cdot 6H_2O(cr) \rightleftharpoons 2\ UO_2^{2+} + Ba^{2+} + 2\ PO_4^{3-} + 6\ H_2O(l)$$

$$\log_{10}K_s^\circ = -(52.2 \pm 1.0)$$

These values have been included in TDB 2020.

Grenthe et al. (2020) discuss experimentally determined and estimated heat capacity and entropy values for these alkaline earth metal uranyl phosphates, and finally prefer entropy values estimated by the Latimer method but with the caveat "these data are reported for information only, but might be used for scoping calculations":

$$S_m^\circ(Mg[(UO_2)(PO_4)]_2 \cdot 8H_2O, cr, 298.15\ K) = (704 \pm 40)\ J \cdot K^{-1} \cdot mol^{-1}$$

$$S_m^\circ(Ca[(UO_2)(PO_4)]_2 \cdot 6H_2O, cr, 298.15\ K) = (622 \pm 40)\ J \cdot K^{-1} \cdot mol^{-1}$$

$$S_m^\circ(Sr[(UO_2)(PO_4)]_2 \cdot 6H_2O, cr, 298.15\ K) = (633 \pm 20)\ J \cdot K^{-1} \cdot mol^{-1}$$

$$S_m^\circ(Ba[(UO_2)(PO_4)]_2 \cdot 6H_2O, cr, 298.15\ K) = (641 \pm 40)\ J \cdot K^{-1} \cdot mol^{-1}$$

These values have been included in TDB 2020 as supplemental data.

Grenthe et al. (2020) discuss experimental, mostly solubility data, that have been reported for several transition metal uranyl phosphates, which all belong to the autunite mineral group. They finally selected solubility constants for $M[(UO_2)(PO_4)]_2 \cdot xH_2O$(cr), where M = Cu, Zn, Co, Ni. As in the case of alkaline earth uranyl phosphates Grenthe et al. (2020) have assumed that the solubility of the various hydrates is similar and that data can be averaged, ignoring the difference in the amount of water of crystallization. Hence, their basic selection are the octahydrates $M[(UO_2)(PO_4)]_2 \cdot 8H_2O$(cr), but they also selected solubility constants for $Zn[(UO_2)(PO_4)]_2 \cdot 0H_2O$(cr), $Co[(UO_2)(PO_4)]_2 \cdot 7H_2O$(cr) and $Ni[(UO_2)(PO_4)]_2 \cdot 10H_2O$(cr) with numerically identical values as selected for the respective octahydrates. Grenthe et al. (2020) state that the latter phases were included in their list of selected values "in order to make a direct comparison between experimental thermodynamic data of these phases … for which S_m° and $\Delta_f H_m^\circ$ are reported in the literature".

However, dealing in a speciation code with two solid phases with identical solubility constants, differing only in the amount of water of crystallization, may cause unnecessary numerical problems and thus, $Zn[(UO_2)(PO_4)]_2 \cdot 10H_2O(cr)$ and $Ni[(UO_2)(PO_4)]_2 \cdot 10H_2O(cr)$ are not included in TDB 2020.

In addition, $Co[(UO_2)(PO_4)]_2 \cdot 8H_2O(cr)$ and $Co[(UO_2)(PO_4)]_2 \cdot 7H_2O(cr)$ are not included in TDB 2020 as Co is not part of TDB 2020.

$$Cu[(UO_2)(PO_4)]_2 \cdot 8H_2O(cr) \rightleftharpoons 2\ UO_2^{2+} + Cu^{2+} + 2\ PO_4^{3-} + 8\ H_2O(l)$$

$$\log_{10}K_s^\circ = -(52.8 \pm 0.3)$$

$$Zn[(UO_2)(PO_4)]_2 \cdot 8H_2O(cr) \rightleftharpoons 2\ UO_2^{2+} + Zn^{2+} + 2\ PO_4^{3-} + 8\ H_2O(l)$$

$$\log_{10}K_s^\circ = -(49.8 \pm 1.0)$$

$$Ni[(UO_2)(PO_4)]_2 \cdot 8H_2O(cr) \rightleftharpoons 2\ UO_2^{2+} + Ni^{2+} + 2\ PO_4^{3-} + 8\ H_2O(l)$$

$$\log_{10}K_s^\circ = -(49.9 \pm 1.0)$$

Grenthe et al. (2020) report that experimentally determined S_m° values are available only for the Cu- and Ni-phases, but the results are considered semi-quantitative. Grenthe et al. (2020) decided to accept the same value for all octahydrates, which is given for information only. Hence, the following values are included in TDB 2020 as supplemental data:

$$S_m^\circ(Cu[(UO_2)(PO_4)]_2 \cdot 8H_2O, cr, 298.15\ K) = (686 \pm 30)\ J \cdot K^{-1} \cdot mol^{-1}$$

$$S_m^\circ(Zn[(UO_2)(PO_4)]_2 \cdot 8H_2O, cr, 298.15\ K) = (686 \pm 30)\ J \cdot K^{-1} \cdot mol^{-1}$$

$$S_m^\circ(Ni[(UO_2)(PO_4)]_2 \cdot 8H_2O, cr, 298.15\ K) = (686 \pm 30)\ J \cdot K^{-1} \cdot mol^{-1}$$

Grenthe et al. (2020) report that experimental solubility results are available for a few additional uranyl phosphates. However, data for these compounds were not selected by Grenthe et al. (2020) because the results in each case were obtained from a single study without the possibility for an independent verification. Still, the published results can be used for scoping calculations. Hence, the following values have been included in TDB 2020 as supplemental data:

$$Mn[(UO_2)(PO_4)]_2 \cdot 10H_2O(cr) \rightleftharpoons 2\ UO_2^{2+} + Mn^{2+} + 2\ PO_4^{3-} + 10\ H_2O(l)$$

$$\log_{10}K_s^\circ = -(50.22 \pm 0.40)$$

$$Cd[(UO_2)(PO_4)]_2 \cdot 10H_2O(cr) \rightleftharpoons 2\ UO_2^{2+} + Cd^{2+} + 2\ PO_4^{3-} + 10\ H_2O(l)$$

$$\log_{10}K_s^\circ = -(50.34 \pm 0.30)$$

$$Pb[(UO_2)(PO_4)]_2 \cdot 8H_2O(cr) \rightleftharpoons 2\ UO_2^{2+} + Pb^{2+} + 2\ PO_4^{3-} + 8\ H_2O(l)$$

$$\log_{10}K_s^\circ = -(49.85 \pm 0.50)$$

$$Pb_2(UO_2)(PO_4)_2 \cdot 2H_2O(cr)\ (parsonite) \rightleftharpoons UO_2^{2+} + 2\ Pb^{2+} + 2\ PO_4^{3-} + 2\ H_2O(l)$$

$$\log_{10}K_s^\circ = -(52.2 \pm 0.8)$$

$HAl[(UO_2)(PO_4)]_4 \cdot 16H_2O(cr)$ (sabugalite) + $7H^+ \rightleftharpoons 4\ UO_2^{2+} + Al^{3+} + 4\ H_2PO_4^- + 16\ H_2O(l)$

$log_{10}{}^*K_s° = -(13.1 \pm 1.2)$

31.4.3 Uranium arsenate compounds and complexes

Grenthe et al. (2020) state that there are no new studies reporting thermodynamic properties of U(VI) arsenate complexes.

Concerning solid uranium arsenate compounds Grenthe et al. (2020) report that available solubility and structure data demonstrate a strong similarity between phosphate and arsenate U(VI) compounds, although uranyl arsenates typically have higher solubility compared to the corresponding phosphate phase.

Grenthe et al. (2020) report that according to a recent study of the uranyl arsenate system, $(UO_2)_3(AsO_4)_2 \cdot 4H_2O(cr)$, the analogue of the corresponding phosphate phase $(UO_2)_3(PO_4)_2 \cdot 4H_2O(cr)$, has a very narrow field of existence, between pH 1.8 – 2.0, in aqueous solution at 25 °C, and transforms at pH > 2 into trögerite, $(UO_2)_3(AsO_4)_2 \cdot 12H_2O(cr)$. Grenthe et al. (2020) conclude that this system is not sufficiently well studied, and it is not clear if the tetrahydrate is a stable phase, or if its formation is kinetically driven. In any case, the solubility products of both phases must be practically identical, and Grenthe et al. (2020) select a solubility product only for trögerite:

$(UO_2)_3(AsO_4)_2 \cdot 12H_2O(cr) \rightleftharpoons 3\ UO_2^{2+} + 2\ AsO_4^{3-} + 12\ H_2O(l)$

$\log_{10}K_s° = -(45.33 \pm 1.00)$

This value has been included in TDB 2020.

Grenthe et al. (2020) report that the phase with the composition $UO_2HAsO_4 \cdot 4H_2O(cr)$ is called hydrogen uranospinite in the mineralogical literature and is the As analogue of the well-studied chernikovite, $UO_2HPO_4 \cdot 4H_2O(cr)$, see Section 31.4.2. Based on three experimental solubility studies, which were found to be in good agreement, and on low-temperature heat capacity measurements, Grenthe et al. (2020) selected

$UO_2HAsO_4 \cdot 4H_2O(cr) \rightleftharpoons UO_2^{2+} + H^+ + AsO_4^{3-} + 4\ H_2O(l)$

$\log_{10}K_s° = -(23.0 \pm 0.3)$

$S_m°(UO_2HAsO_4 \cdot 4H_2O, cr, 298.15\ K) = (349 \pm 10)\ J \cdot K^{-1} \cdot mol^{-1}$

$C_{p,m}°(UO_2HAsO_4 \cdot 4H_2O, cr, 298.15\ K) = (326 \pm 10)\ J \cdot K^{-1} \cdot mol^{-1}$

These values have been included in TDB 2020.

Grenthe et al. (2020) selected new solubility constants for $M[(UO_2)(AsO_4)] \cdot xH_2O(cr)$, where M = Li, Na, K, Rb, Cs, NH_4. The selected solubility constants of all these phases have been included in TDB 2020, except for the Rb phase, as Rb is not part of TDB 2020:

$$Li(UO_2)(AsO_4) \cdot 4H_2O(cr) \rightleftharpoons UO_2^{2+} + Li^+ + AsO_4^{3-} + 4\ H_2O(l)$$

$$\log_{10}K_s^\circ = -(20.4 \pm 1.0)$$

$$Na(UO_2)(AsO_4) \cdot 3H_2O(cr) \rightleftharpoons UO_2^{2+} + Na^+ + AsO_4^{3-} + 3\ H_2O(l)$$

$$\log_{10}K_s^\circ = -(22.8 \pm 1.0)$$

$$K(UO_2)(AsO_4) \cdot 3H_2O(cr) \rightleftharpoons UO_2^{2+} + K^+ + AsO_4^{3-} + 3\ H_2O(l)$$

$$\log_{10}K_s^\circ = -(23.3 \pm 1.0)$$

$$Cs(UO_2)(AsO_4) \cdot 2.5H_2O(cr) \rightleftharpoons UO_2^{2+} + Cs^+ + AsO_4^{3-} + 2.5\ H_2O(l)$$

$$\log_{10}K_s^\circ = -(25.2 \pm 1.0)$$

$$NH_4(UO_2)(AsO_4) \cdot 3H_2O(cr) \rightleftharpoons UO_2^{2+} + NH_4^+ + AsO_4^{3-} + 3\ H_2O(l)$$

$$\log_{10}K_s^\circ = -(24.7 \pm 1.0)$$

Grenthe et al. (2020) discuss experimentally determined and estimated heat capacity and entropy values for these alkali metal uranyl arsenates, but finally report entropy values estimated by the Latimer method, which they considered most reliable, "for information only, but might be used for scoping calculations":

$$S_m^\circ(Li(UO_2)(AsO_4) \cdot 4H_2O, cr, 298.15\ K) = (367 \pm 25)\ J \cdot K^{-1} \cdot mol^{-1}$$

$$S_m^\circ(Na(UO_2)(AsO_4) \cdot 3H_2O, cr, 298.15\ K) = (339 \pm 19)\ J \cdot K^{-1} \cdot mol^{-1}$$

$$S_m^\circ(K(UO_2)(AsO_4) \cdot 3H_2O, cr, 298.15\ K) = (346 \pm 19)\ J \cdot K^{-1} \cdot mol^{-1}$$

$$S_m^\circ(Cs(UO_2)(AsO_4) \cdot 2.5H_2O, cr, 298.15\ K) = (342 \pm 17)\ J \cdot K^{-1} \cdot mol^{-1}$$

$$S_m^\circ(NH_4(UO_2)(AsO_4) \cdot 3H_2O, cr, 298.15\ K) = (366 \pm 19)\ J \cdot K^{-1} \cdot mol^{-1}$$

These values have been included in TDB 2020 as supplemental data.

Grenthe et al. (2020) discuss new solubility constants for $M[(UO_2)(AsO_4)]_2 \cdot xH_2O(cr)$, where M = Mg, Ca, Sr, Ba and state "as was the case for the corresponding phosphate analogues, we assume that phases differing in the amount of water of hydration have practically identical solubility products". They finally selected:

$$Mg[(UO_2)(AsO_4)]_2 \cdot 10H_2O(cr) \rightleftharpoons 2\ UO_2^{2+} + Mg^{2+} + 2\ AsO_4^{3-} + 10\ H_2O(l)$$

$$\log_{10}K_s^\circ = -(44.6 \pm 0.5)$$

$$Ca[(UO_2)(AsO_4)]_2 \cdot 10H_2O(cr) \rightleftharpoons 2\ UO_2^{2+} + Ca^{2+} + 2\ AsO_4^{3-} + 10\ H_2O(l)$$

$$\log_{10}K_s^\circ = -(45.1 \pm 1.0)$$

$Sr[(UO_2)(AsO_4)]_2 \cdot 8H_2O(cr) \rightleftharpoons 2\ UO_2^{2+} + Sr^{2+} + 2\ AsO_4^{3-} + 8\ H_2O(l)$

$\log_{10}K_s° = -(45.1 \pm 1.0)$

$Ba[(UO_2)(AsO_4)]_2 \cdot 7H_2O(cr) \rightleftharpoons 2\ UO_2^{2+} + Ba^{2+} + 2\ AsO_4^{3-} + 7\ H_2O(l)$

$\log_{10}K_s° = -(44.7 \pm 1.0)$

These values have been included in TDB 2020.

For unknown reasons, Grenthe et al. (2020) list in their Tab. 9-57 two compounds, $Cu[(UO_2)(AsO_4)]_2 \cdot 10H_2O(cr)$ and $Cu[(UO_2)(AsO_4)]_2 \cdot 6H_2O(cr)$, with numerically identical solubility constants. For the latter compound neither solubility data nor experimentally determined $S_m°$ data seem to be available and thus, $Cu[(UO_2)(AsO_4)]_2 \cdot 6H_2O(cr)$ is not included in TDB 2020.

Grenthe et al. (2020) discuss experimentally determined and estimated entropy values for these alkaline earth metal uranyl arsenates, and finally prefer experimentally determined entropy values but with the caveat "these data are reported for information only":

$S_m°(Mg[(UO_2)(AsO_4)]_2 \cdot 10H_2O, cr, 298.15\ K) = (859 \pm 40)\ J \cdot K^{-1} \cdot mol^{-1}$

$S_m°(Ca[(UO_2)(AsO_4)]_2 \cdot 10H_2O, cr, 298.15\ K) = (874 \pm 30)\ J \cdot K^{-1} \cdot mol^{-1}$

$S_m°(Sr[(UO_2)(AsO_4)]_2 \cdot 8H_2O, cr, 298.15\ K) = (758 \pm 20)\ J \cdot K^{-1} \cdot mol^{-1}$

$S_m°(Ba[(UO_2)(AsO_4)]_2 \cdot 7H_2O, cr, 298.15\ K) = (738 \pm 30)\ J \cdot K^{-1} \cdot mol^{-1}$

These values have been included in TDB 2020 as supplemental data.

Grenthe et al. (2020) discuss experimental, mostly solubility data, that have been reported for several transition metal uranyl arsenates. As in the case of the alkaline earth uranyl phosphate hydrates, they have assumed that the solubility of various hydrates is similar and that data for phases with different amounts of water of crystallization can be averaged. Grenthe et al. (2020) have in general used the stoichiometry corresponding to less hydrated meta-phases, known as the minerals metazeunerite, $Cu[(UO_2)(AsO_4)]_2 \cdot 8H_2O(cr)$, metakirchheimerite, $Co[(UO_2)(AsO_4)]_2 \cdot 8H_2O(cr)$, metakahlerite, $Fe[(UO_2)(AsO_4)]_2 \cdot 8H_2O(cr)$. The Ni phase $Ni[(UO_2)(AsO_4)]_2 \cdot 10H_2O(cr)$, is known as the mineral rauchite.

$Cu[(UO_2)(AsO_4)]_2 \cdot 8H_2O(cr) \rightleftharpoons 2\ UO_2^{2+} + Cu^{2+} + 2\ AsO_4^{3-} + 8\ H_2O(l)$

$\log_{10}K_s° = -(45.7 \pm 1.0)$

$Ni[(UO_2)(AsO_4)]_2 \cdot 10H_2O(cr) \rightleftharpoons 2\ UO_2^{2+} + Ni^{2+} + 2\ AsO_4^{3-} + 10\ H_2O(l)$

$\log_{10}K_s° = -(45.9 \pm 1.0)$

$Fe[(UO_2)(AsO_4)]_2 \cdot 8H_2O(cr) \rightleftharpoons 2\ UO_2^{2+} + Fe^{2+} + 2\ AsO_4^{3-} + 8\ H_2O(l)$

$\log_{10}K_s° = -(46.1 \pm 2.2)$

$Mn[(UO_2)(AsO_4)]_2 \cdot 8H_2O(cr) \rightleftharpoons 2\ UO_2^{2+} + Mn^{2+} + 2\ AsO_4^{3-} + 8\ H_2O(l)$

$\log_{10}K_s° = -(44.4 \pm 1.0)$

$Zn[(UO_2)(AsO_4)]_2 \cdot 8H_2O(cr) \rightleftharpoons 2\ UO_2^{2+} + Zn^{2+} + 2\ AsO_4^{3-} + 8\ H_2O(l)$

$\log_{10}K_s° = -(45.1 \pm 1.0)$

$Cd[(UO_2)(AsO_4)]_2 \cdot 8H_2O(cr) \rightleftharpoons 2\ UO_2^{2+} + Cd^{2+} + 2\ AsO_4^{3-} + 8\ H_2O(l)$

$\log_{10}K_s° = -(45.4 \pm 1.0)$

$Pb[(UO_2)(AsO_4)]_2 \cdot 10H_2O(cr) \rightleftharpoons 2\ UO_2^{2+} + Pb^{2+} + 2\ AsO_4^{3-} + 10\ H_2O(l)$

$\log_{10}K_s° = -(46.3 \pm 1.0)$

These values have been included in TDB 2020.

Note that, $Co[(UO_2)(AsO_4)]_2 \cdot 8H_2O(cr)$, metakirchheimerite, is not included in TDB 2020 as Co is not part of TDB 2020.

Grenthe et al. (2020) report that experimentally determined $S_m°$ values are available only for the Cu- and Ni-phases. Thus, Grenthe et al. (2020) have used the experimental value for $Ni[(UO_2)(AsO_4)]_2 \cdot 10H_2O(cr)$, $S_m° = (783 \pm 30)\ J \cdot K^{-1} \cdot mol^{-1}$, as an anchor, and based the estimated $S_m°$ for other phases on this value, using the Latimer method to evaluate the $S_m°$ changes between the Ni- and other uranyl arsenate phases. These values are given for information only:

$S_m°(Cu[(UO_2)(AsO_4)]_2 \cdot 8H_2O, cr, 298.15\ K) = (695 \pm 30)\ J \cdot K^{-1} \cdot mol^{-1}$

$S_m°(Ni[(UO_2)(AsO_4)]_2 \cdot 10H_2O, cr, 298.15\ K) = (783 \pm 30)\ J \cdot K^{-1} \cdot mol^{-1}$

$S_m°(Fe[(UO_2)(AsO_4)]_2 \cdot 8H_2O, cr, 298.15\ K) = (693 \pm 30)\ J \cdot K^{-1} \cdot mol^{-1}$

$S_m°(Mn[(UO_2)(AsO_4)]_2 \cdot 8\ H_2O, cr, 298.15\ K) = (693 \pm 30)\ J \cdot K^{-1} \cdot mol^{-1}$

$S_m°(Zn[(UO_2)(AsO_4)]_2 \cdot 8\ H_2O, cr, 298.15\ K) = (695 \pm 30)\ J \cdot K^{-1} \cdot mol^{-1}$

$S_m°(Cd[(UO_2)(AsO_4)]_2 \cdot 8H_2O, cr, 298.15\ K) = (710 \pm 30)\ J \cdot K^{-1} \cdot mol^{-1}$

$S_m°(Pb[(UO_2)(AsO_4)]_2 \cdot 10H_2O, cr, 298.15\ K) = (804 \pm 30)\ J \cdot K^{-1} \cdot mol^{-1}$

These values have been included in TDB 2020 as supplemental data.

31.5 Uranium carbonate and silicate compounds and complexes

31.5.1 Uranium carbonate compounds and complexes

The complex formation in the Ca(II)-U(VI)-carbonate system was discussed by Guillaumont et al. (2003), but the reported equilibrium constants were not accepted. Since then, new studies appeared and Grenthe et al. (2020) selected equilibrium constants for Mg, Ca, Sr and Ba complexes. In addition, based on a calorimetric study by Endrizzi & Rao (2014), Grenthe et al. (2020) selected enthalpies of reaction for the Ca complexes:

$Mg^{2+} + UO_2^{2+} + 3\ CO_3^{2-} \rightleftharpoons MgUO_2(CO_3)_3^{2-}$

$\log_{10}\beta_1° = (26.2 \pm 0.2)$

$2\ Mg^{2+} + UO_2^{2+} + 3\ CO_3^{2-} \rightleftharpoons Mg_2UO_2(CO_3)_3(aq)$

$\log_{10}\beta_2° = (27.1 \pm 0.6)$

$Ca^{2+} + UO_2^{2+} + 3\ CO_3^{2-} \rightleftharpoons CaUO_2(CO_3)_3^{2-}$

$\log_{10}\beta_1° = (27.0 \pm 0.2)$

$\Delta_r H_m° = -(47 \pm 6)\ kJ \cdot mol^{-1}$

$2\ Ca^{2+} + UO_2^{2+} + 3\ CO_3^{2-} \rightleftharpoons Ca_2UO_2(CO_3)_3(aq)$

$\log_{10}\beta_2° = (30.8 \pm 0.4)$

$\Delta_r H_m° = -(47 \pm 7)\ kJ \cdot mol^{-1}$

$Sr^{2+} + UO_2^{2+} + 3\ CO_3^{2-} \rightleftharpoons SrUO_2(CO_3)_3^{2-}$

$\log_{10}\beta_1° = (25.9 \pm 0.2)$

$2\ Sr^{2+} + UO_2^{2+} + 3\ CO_3^{2-} \rightleftharpoons Sr_2UO_2(CO_3)_3(aq)$

$\log_{10}\beta_2° = (29.7 \pm 0.5)$

$Ba^{2+} + UO_2^{2+} + 3\ CO_3^{2-} \rightleftharpoons BaUO_2(CO_3)_3^{2-}$

$\log_{10}\beta_1° = (25.6 \pm 0.3)$

These values have been included in TDB 2020.

Note that Grenthe et al. (2020) have not selected an equilibrium constant for the formation of $Ba_2UO_2(CO_3)_3(aq)$, but they state that the value 29.75 proposed in one study "is consistent with the ones from Ca and Sr". Hence, this value, selected as supplemental datum by Thoenen et al. (2014), is retained in TDB 2020.

Grenthe et al. (2020) selected Gibbs energies, enthalpies, entropies and heat capacities for $Na_4[UO_2(CO_3)_3](cr)$, $K_4[UO_2(CO_3)_3](cr)$ and $NaK_3[UO_2(CO_3)_3](cr)$ based on reaction calorimetry data and a thermodynamic cycle involving only solids. No solubility studies for these compounds are available and it remains unclear whether these anhydrous solids are stable in water. Hence, these solids have not been included in TDB 2020.

Based on dissolution calorimetry data Grenthe et al. (2020) selected enthalpies of formation for the compounds

$Li_4[UO_2(CO_3)_3] \cdot 5H_2O(cr)$

$(NH_4)_4[UO_2(CO_3)_3](cr)$

$Mg_2[UO_2(CO_3)_3](cr)$

$Mg_2[UO_2(CO_3)_3] \cdot 18H_2O(cr)$

$Ca_2[UO_2(CO_3)_3](cr)$

$Ca_2[UO_2(CO_3)_3] \cdot 10H_2O(cr)$

$Sr_2[UO_2(CO_3)_3](cr)$

$Sr_2[UO_2(CO_3)_3] \cdot 8H_2O(cr)$

$Ba_2[UO_2(CO_3)_3](cr)$

$Ba_2[UO_2(CO_3)_3] \cdot 6H_2O(cr)$

As enthalpies of formation alone are useless in speciation calculations, these compounds have not been included in TDB 2020.

31.5.2 Uranium silicate compounds and complexes

Uranium silicate compounds and complexes are discussed in Section 25.8.

31.6 Boron compounds and complexes

No data for uranium borate complex formation have been reported by Grenthe et al. (2020).

Concerning boron compounds Grenthe et al. (2020) report that the thermodynamics of uranyl borate and uranyl metaborate compounds have been studied by Russian groups at Niyhny Novgorod State University with N.K. Chernorukov and N.V. Karyakin as lead authors. These studies include both extensive structure characterisation of the compounds using X-ray diffraction, elemental analysis, but rarely the water content, IR spectroscopy and thermal TGA and DTA analyses. The thermodynamic data are based on solubility data to obtain Gibbs energies of formation, dissolution reaction calorimetry to obtain enthalpies of formation and low temperature calorimetry to obtain molar heat capacity and molar entropy of the compounds studied. Many of these compounds form hydrates and this requires a careful analysis of their water content, data that are not always available in the publications.

Solubility measurements have been reported for the compounds $M[UO_2(BO_3)] \cdot xH_2O(cr)$, where M = Li, Na, K, Rb, Cs, and Grenthe et al. (2020) selected solubility constants only for these hydrated alkali uranyl borates. The selected solubility constants have been included in TDB 2020, except for the Rb phase, as Rb is not part of TDB 2020:

$$Li(UO_2)(BO_3) \cdot 1.5H_2O(cr) + 2\ H^+ \rightleftharpoons 0.5\ (UO_2)_2(OH)_2^{2+} + Li^+ + B(OH)_3(aq) + 0.5\ H_2O(l)$$

$$\log_{10}K_s^\circ = (4.58 \pm 0.20)$$

$$Na(UO_2)(BO_3) \cdot H_2O(cr) + 2\ H^+ \rightleftharpoons 0.5\ (UO_2)_2(OH)_2^{2+} + Na^+ + B(OH)_3(aq)$$

$$\log_{10}K_s^\circ = (4.47 \pm 0.20)$$

$$K(UO_2)(BO_3) \cdot H_2O(cr) + 2\ H^+ \rightleftharpoons 0.5\ (UO_2)_2(OH)_2^{2+} + K^+ + B(OH)_3(aq)$$

$$\log_{10}K_s^\circ = (3.90 \pm 0.20)$$

$$Cs(UO_2)(BO_3) \cdot H_2O(cr) + 2\ H^+ \rightleftharpoons 0.5\ (UO_2)_2(OH)_2^{2+} + Cs^+ + B(OH)_3(aq)$$

$$\log_{10}K_s^\circ = (3.92 \pm 0.20)$$

Grenthe et al. (2020) selected heat capacity and entropy values for $Na(UO_2)(BO_3) \cdot H_2O(cr)$ derived from low-temperature calorimetry

$$S_m^\circ(Na(UO_2)(BO_3) \cdot H_2O, cr, 298.15\ K) = (183.8 \pm 3.0)\ J \cdot K^{-1} \cdot mol^{-1}$$

$$C_{p,m}^\circ(Na(UO_2)(BO_3) \cdot H_2O, cr, 298.15\ K) = (159.0 \pm 1.0)\ J \cdot K^{-1} \cdot mol^{-1}$$

and calculated entropy values from reported enthalpies of formation based on dissolution calorimetry for $Li(UO_2)(BO_3) \cdot 1.5H_2O(cr)$, $K(UO_2)(BO_3) \cdot H_2O(cr)$ and $Cs(UO_2)(BO_3) \cdot H_2O(cr)$

$$S_m^\circ(Li(UO_2)(BO_3) \cdot 1.5H_2O, cr, 298.15\ K) = (194 \pm 14)\ J \cdot K^{-1} \cdot mol^{-1}$$

$$S_m^\circ(K(UO_2)(BO_3) \cdot H_2O, cr, 298.15\ K) = (174 \pm 14)\ J \cdot K^{-1} \cdot mol^{-1}$$

$$S_m^\circ(Cs(UO_2)(BO_3) \cdot H_2O, cr, 298.15\ K) = (267 \pm 15)\ J \cdot K^{-1} \cdot mol^{-1}$$

All these values have also been included in TDB 2020.

Grenthe et al. (2020) selected Gibbs energies, enthalpies, entropies and heat capacities for

$Li(UO_2)(BO_3)(cr)$

$Na(UO_2)(BO_3)(cr)$

$K(UO_2)(BO_3)(cr)$

$Rb(UO_2)(BO_3)(cr)$

$Cs(UO_2)(BO_3)(cr)$

based on dissolution calorimetry and low-temperature calorimetry data. No solubility studies for these compounds are available and it remains unclear whether these anhydrous solids are stable in water. Hence, these solids have not been included in TDB 2020.

Grenthe et al. (2020) selected enthalpies of formation, based on dissolution calorimetry data, for

$Li(UO_2)(BO_3) \cdot H_2O(cr)$

$Li(UO_2)(BO_3) \cdot 0.5H_2O(cr)$

$Na(UO_2)(BO_3) \cdot 0.5H_2O(cr)$

$K(UO_2)(BO_3) \cdot 0.2H_2O(cr)$

$Rb(UO_2)(BO_3) \cdot H_2O(cr)$

$Rb(UO_2)(BO_3) \cdot 0.25H_2O(cr)$

$Cs(UO_2)(BO_3) \cdot 0.5H_2O(cr)$

As enthalpies of formation alone are useless in speciation calculations, these compounds have not been included in TDB 2020.

Grenthe et al. (2020) selected Gibbs energies, enthalpies, entropies and heat capacities for

$Mg[(UO_2)(BO_3)]_2(cr)$

$Ca[(UO_2)(BO_3)]_2(cr)$

$Sr[(UO_2)(BO_3)]_2(\alpha,cr)$

$Sr[(UO_2)(BO_3)]_2(\beta,cr)$

$Ba[(UO_2)(BO_3)]_2(\alpha,cr)$

$Ba[(UO_2)(BO_3)]_2(\beta,cr)$

based on dissolution calorimetry and low-temperature calorimetry data. No solubility studies for these compounds are available and it remains unclear whether these anhydrous solids are stable in water. Hence, these solids have not been included in TDB 2020.

Grenthe et al. (2020) discuss experimental solubility measurements which have been used to determine the Gibbs energy of formation of

$Mg[(UO_2)(BO_3)]_2 \cdot 4H_2O(cr)$

$Ca[(UO_2)(BO_3)]_2 \cdot H_2O(cr)$

$Sr[(UO_2)(BO_3)]_2 \cdot 2H_2O(cr)$

$Ba[(UO_2)(BO_3)]_2) \cdot 2H_2O(cr)$

and conclude that these values differ significantly from Gibbs energy of formation values calculated from calorimetric data. Hence, the solubility data were not selected. Instead, Grenthe et al. (2020) selected Gibbs energy, enthalpy, entropy and heat capacity for

$Mg[(UO_2)(BO_3)]_2 \cdot 4H_2O(cr)$

based on dissolution calorimetry and low-temperature calorimetry data, entropies, and heat capacities for

$Sr[(UO_2)(BO_3)]_2 \cdot 2H_2O(cr)$

$Ba[(UO_2)(BO_3)]_2) \cdot 2H_2O(cr)$

based on low-temperature calorimetry data. These data, based on calorimetry but at variance with solubility data, have not been included in TDB 2020.

Finally, Grenthe et al. (2020) selected Gibbs energy, enthalpy, entropy and heat capacity for uranyl metaborate, $UO_2(BO_2)_2(cr)$, based on dissolution calorimetry and low-temperature calorimetry data. No solubility study for this compound is available and it remains unclear whether the anhydrous solid is stable in water. Hence, this solid has not been included in TDB 2020.

31.7 Vanadium compounds

Grenthe et al. (2020) selected thermodynamic data for a considerable number of uranyl vanadate compounds. However, vanadium is not part of TDB 2020 and thus, none of these compounds is included in TDB 2020.

31.8 Uranium molybdate compounds

Grenthe et al. (2020) selected Gibbs energy, enthalpy, entropy and heat capacity for uranyl molybdate, $UO_2MoO_4(cr)$, based on dissolution calorimetry in 10 M HF and low-temperature calorimetry data. No solubility study for this compound is available and it remains unclear whether the anhydrous solid is stable in water. Hence, this solid has not been included in TDB 2020.

31.9 Selected uranium data

Tab. 31-1: Uranium data selected by NEA (Grenthe et al. 2020) but not included in TDB 2020

For explanations see text.

Gases	
Solids	$(UO_2)O_2(H_2O)_4$(cr) (studtite), $M[UO_2(SO_4)_2] \cdot 5H_2O$(cr), M = Mn, Fe, Co, Ni, Cu, Zn, $Rb[(UO_2)(PO_4)] \cdot 3H_2O$(cr), $Zn[(UO_2)(PO_4)]_2 \cdot 10H_2O$(cr), $Co[(UO_2)(PO_4)]_2 \cdot 7H_2O$(cr), $Co[(UO_2)(PO_4)]_2 \cdot 8H_2O$(cr), $Ni[(UO_2)(PO_4)]_2 \cdot 10H_2O$(cr), $Rb(UO_2)(AsO_4) \cdot 3H_2O$(cr), $Cu[(UO_2)(AsO_4)]_2 \cdot 6H_2O$(cr), $Co[(UO_2)(AsO_4)]_2 \cdot 8H_2O$(cr), $Na_4[UO_2(CO_3)_3]$(cr), $K_4[UO_2(CO_3)_3]$(cr), $NaK_3[UO_2(CO_3)_3]$(cr), $Li_4[UO_2(CO_3)_3] \cdot 5H_2O$(cr), $(NH_4)_4[UO_2(CO_3)_3]$(cr), $Mg_2[UO_2(CO_3)_3]$(cr), $Mg_2[UO_2(CO_3)_3] \cdot 18H_2O$(cr), $Ca_2[UO_2(CO_3)_3]$(cr), $Ca_2[UO_2(CO_3)_3] \cdot 10H_2O$(cr), $Sr_2[UO_2(CO_3)_3]$(cr), $Sr_2[UO_2(CO_3)_3] \cdot 8H_2O$(cr), $Ba_2[UO_2(CO_3)_3]$(cr), $Ba_2[UO_2(CO_3)_3] \cdot 6H_2O$(cr), $Rb(UO_2)(BO_3) \cdot H_2O$(cr), $Li(UO_2)(BO_3)$(cr), $Na(UO_2)(BO_3)$(cr), $K(UO_2)(BO_3)$(cr), $Rb(UO_2)(BO_3)$(cr), $Cs(UO_2)(BO_3)$(cr), $Li(UO_2)(BO_3) \cdot H_2O$(cr), $Li(UO_2)(BO_3) \cdot 0.5H_2O$(cr), $Na(UO_2)(BO_3) \cdot 0.5H_2O$(cr), $K(UO_2)(BO_3) \cdot 0.2H_2O$(cr), $Rb(UO_2)(BO_3) \cdot H_2O$(cr), $Rb(UO_2)(BO_3) \cdot 0.25H_2O$(cr), $Cs(UO_2)(BO_3) \cdot 0.5H_2O$(cr), $Mg[(UO_2)(BO_3)]_2$(cr), $Ca[(UO_2)(BO_3)]_2$(cr), $Sr[(UO_2)(BO_3)]_2$(α,cr), $Sr[(UO_2)(BO_3)]_2$(β,cr), $Ba[(UO_2)(BO_3)]_2$(α,cr), $Ba[(UO_2)(BO_3)]_2$(β,cr), $Mg[(UO_2)(BO_3)]_2 \cdot 4H_2O$(cr), $Sr[(UO_2)(BO_3)]_2 \cdot 2H_2O$(cr), $Ba[(UO_2)(BO_3)]_2) \cdot 2H_2O$(cr), $UO_2(BO_2)_2$(cr), UO_2MoO_4(cr)
Aqueous species	$UO_2IO_4^+$

Tab. 31-2: Selected uranium data

All data included in TDB 2020 are taken from Grenthe et al. (1992), Grenthe et al. (1995), Guillaumont et al. (2003) and Grenthe et al. (2020), except where marked with an asterisk (*). The latter data were taken unchanged from Thoenen et al. (2014). Core data are bold and supplemental data are in italics. New or changed data with respect to TDB Version 12/07 (Thoenen et al. 2014) are shaded.

Name	**Redox**	**TDB Version 12/07**				**TDB 2020**				
		$\Delta_f G_m°$ [kJ · mol^{-1}]	**$\Delta_f H_m°$** [kJ · mol^{-1}]	**$S_m°$** [J · K^{-1} · mol^{-1}]	**$C_{p,m}°$** [J · K^{-1} · mol^{-1}]	**$\Delta_f G_m°$** [kJ · mol^{-1}]	**$\Delta_f H_m°$** [kJ · mol^{-1}]	**$S_m°$** [J · K^{-1} · mol^{-1}]	**$C_{p,m}°$** [J · K^{-1} · mol^{-1}]	**Species**
U(cr)	0	0.0	0.0	50.2 ± 0.20	27.66 ± 0.05	0.0	0.0	50.2 ± 0.20	27.66 ± 0.05	U(cr)
U+4	IV	-529.9 ± 1.8	-591.2 ± 3.3	(-416.9 ± 12.6) [a]	-220 ± 50	-529.9 ± 1.8	-591.2 ± 3.3	(-416.9 ± 12.6) [a]	-220 ± 50	U^{4+}
UO2+	V	-961.0 ± 1.8	-(1'025.1 ± 3.0) [a]	-25 ± 8	-	-961.0 ± 1.8	-(1'025.1 ± 3.0) [a]	-25 ± 8	-	UO_2^+
UO2+2	VI	**(-952.55 ± 1.75)** [a]	**-1'019.0 ± 1.5**	**-98.2 ± 3.0**	**42.4 ± 3.0**	**(-952.55 ± 1.75)** [a]	**-1'019.0 ± 1.5**	**-98.2 ± 3.0**	**42.4 ± 3.0**	UO_2^{2+}

[a] Calculated value

Name	**Redox**	**TDB Version 12/07**				**TDB 2020**			
		$\log_{10}\beta°$	**$\Delta_r H_m°$** [kJ · mol^{-1}]	**$\Delta_r S_m°$** [J · K^{-1} · mol^{-1}]	**$S_m°$** [J · K^{-1} · mol^{-1}]	**$\log_{10}\beta°$**	**$\Delta_r H_m°$** [kJ · mol^{-1}]	**$\Delta_r S_m°$** [J · K^{-1} · mol^{-1}]	**Reaction**
UO2OH+	VI	-5.25 ± 0.24	-	-	17 ± 50	-5.25 ± 0.24	43.3 ± 2.3	-	$UO_2^{2+} + H_2O(l) \rightleftharpoons UO_2OH^+ + H^+$
UO2(OH)2(aq)	VI	-12.15 ± 0.07	-	-	-	-12.15 ± 0.07	-	-	$UO_2^{2+} + 2\ H_2O(l) \rightleftharpoons UO_2(OH)_2(aq) + 2\ H^+$
UO2(OH)3-	VI	-20.25 ± 0.42	-	-	-	-20.25 ± 0.42	-	-	$UO_2^{2+} + 3\ H_2O(l) \rightleftharpoons UO_2(OH)_3^- + 3\ H^+$
UO2(OH)4-2	VI	-32.40 ± 0.68	-	-	-	-32.40 ± 0.68	-	-	$UO_2^{2+} + 4\ H_2O(l) \rightleftharpoons UO_2(OH)_4^{2-} + 4\ H^+$
(UO2)2OH+3	VI	-2.7 ± 1.0	-	-	-	-2.7 ± 1.0	-	-	$2\ UO_2^{2+} + H_2O(l) \rightleftharpoons (UO_2)_2OH^{3+} + H^+$
(UO2)2(OH)2+2	VI	-5.62 ± 0.04	-	-	-38 ± 15	-5.62 ± 0.08	47.8 ± 0.5	-	$2\ UO_2^{2+} + 2\ H_2O(l) \rightleftharpoons (UO_2)_2(OH)_2^{2+} + 2\ H^+$
(UO2)3(OH)4+2	VI	-11.9 ± 0.3	-	-	-	-11.9 ± 0.3	99.2 ± 0.5	-	$3\ UO_2^{2+} + 4\ H_2O(l) \rightleftharpoons (UO_2)_3(OH)_4^{2+} + 4\ H^+$
(UO2)3(OH)5+	VI	-15.55 ± 0.12	-	-	83 ± 30	-15.55 ± 0.12	120.7 ± 0.6	-	$3\ UO_2^{2+} + 5\ H_2O(l) \rightleftharpoons (UO_2)_3(OH)_5^+ + 5\ H^+$
(UO2)3(OH)7-	VI	-32.2 ± 0.8	-	-	-	-32.2 ± 0.8	-	-	$3\ UO_2^{2+} + 7\ H_2O(l) \rightleftharpoons (UO_2)_3(OH)_7^- + 7\ H^+$
(UO2)4(OH)7+	VI	-21.9 ± 1.0	-	-	-	-21.9 ± 1.0	-	-	$4\ UO_2^{2+} + 7\ H_2O(l) \rightleftharpoons (UO_2)_4(OH)_7^+ + 7\ H^+$
UO2F+	VI	5.16 ± 0.06	1.70 ± 0.08	-	-	5.16 ± 0.06	-0.54 ± 0.26	-	$UO_2^{2+} + F^- \rightleftharpoons UO_2F^+$
UO2F2(aq)	VI	8.83 ± 0.08	2.10 ± 0.19	-	-	8.83 ± 0.08	-1.34 ± 0.18	-	$UO_2^{2+} + 2\ F^- \rightleftharpoons UO_2F_2(aq)$
UO2F3-	VI	10.90 ± 0.10	2.35 ± 0.31	-	-	10.90 ± 0.10	-1.18 ± 0.30	-	$UO_2^{2+} + 3\ F^- \rightleftharpoons UO_2F_3^-$
UO2F4-2	VI	11.84 ± 0.11	0.29 ± 0.47	-	-	11.84 ± 0.11	-2.12 ± 0.47	-	$UO_2^{2+} + 4\ F^- \rightleftharpoons UO_2F_4^{2-}$
UO2Cl+	VI	0.17 ± 0.02	8 ± 2	-	-	0.17 ± 0.02	8 ± 2	-	$UO_2^{2+} + Cl^- \rightleftharpoons UO_2Cl^+$
UO2Cl2(aq)	VI	-1.1 ± 0.4	15 ± 6	-	-	-1.1 ± 0.4	15 ± 6	-	$UO_2^{2+} + 2\ Cl^- \rightleftharpoons UO_2Cl_2(aq)$
UO2IO3+	VI	2.00 ± 0.02	-	-	-	2.00 ± 0.02	-	-	$UO_2^{2+} + IO_3^- \rightleftharpoons UO_2IO_3^+$
UO2(IO3)2(aq)	VI	3.59 ± 0.15	-	-	-	3.59 ± 0.15	-	-	$UO_2^{2+} + 2\ IO_3^- \rightleftharpoons UO_2(IO_3)_2(aq)$
UO2SO4(aq)	VI	3.15 ± 0.02	19.5 ± 1.6	-	-	3.15 ± 0.10	19.5 ± 1.6	-	$UO_2^{2+} + SO_4^{2-} \rightleftharpoons UO_2SO_4(aq)$
UO2(SO4)2-2	VI	4.14 ± 0.07	35.1 ± 1.0	-	-	4.14 ± 0.15	35.1 ± 1.0	-	$UO_2^{2+} + 2\ SO_4^{2-} \rightleftharpoons UO_2(SO_4)_2^{2-}$
UO2(SO4)3-4	VI	3.02 ± 0.38	-	-	-	3.02 ± 0.38	-	-	$UO_2^{2+} + 3\ SO_4^{2-} \rightleftharpoons UO_2(SO_4)_3^{4-}$
UO2HSeO3+	VI	-	-	-	-	3.27 ± 0.15	-	-	$UO_2^{2+} + HSeO_3^- \rightleftharpoons UO_2HSeO_3^+$
UO2(HSeO3)2(aq)	VI	-	-	-	-	5.51 ± 0.11	-	-	$UO_2^{2+} + 2\ HSeO_3^- \rightleftharpoons UO_2(HSeO_3)_2(aq)$
UO2SeO4(aq)	VI	2.74 ± 0.25	-	-	-	2.93 ± 0.04	20 ± 2	-	$UO_2^{2+} + SeO_4^{2-} \rightleftharpoons UO_2SeO_4(aq)$
UO2(SeO4)2-2	VI	*3.10 ± 0.50*	-	-	-	4.03 ± 0.09	31 ± 4	-	$UO_2^{2+} + 2\ SeO_4^{2-} \rightleftharpoons UO_2(SeO_4)_2^{2-}$
UO2NO3+	VI	0.30 ± 0.15	-	-	-	-0.19 ± 0.15	20.9 ± 3.5	-	$UO_2^{2+} + NO_3^- \rightleftharpoons UO_2NO_3^+$
UO2PO4-	VI	13.23 ± 0.15	-	-	-	11.01 ± 0.48	-	-	$UO_2^{2+} + PO_4^{3-} \rightleftharpoons UO_2PO_4^-$
UO2HPO4(aq)	VI	7.24 ± 0.26	-	-	-	7.24 ± 0.26	-	-	$UO_2^{2+} + HPO_4^{2-} \rightleftharpoons UO_2HPO_4(aq)$
UO2H2PO4+	VI	1.12 ± 0.06	-	-	-	1.12 ± 0.06	-	-	$UO_2^{2+} + H_3PO_4(aq) \rightleftharpoons UO_2H_2PO_4^+ + H^+$
UO2H3PO4+2	VI	0.76 ± 0.15	-	-	-	0.76 ± 0.15	-	-	$UO_2^{2+} + H_3PO_4(aq) \rightleftharpoons UO_2H_3PO_4^{2+}$

Tab. 31-2: Cont.

Name	Redox	TDB Version 12/07				TDB 2020			
		$\log_{10}\beta°$	$\Delta_r H_m°$ [kJ · mol^{-1}]	$\Delta_r S_m°$ [J · K^{-1} · mol^{-1}]	$S_m°$ [J · K^{-1} · mol^{-1}]	$\log_{10}\beta°$	$\Delta_r H_m°$ [kJ · mol^{-1}]	$\Delta_r S_m°$ [J · K^{-1} · mol^{-1}]	Reaction
UO2(H2PO4)2	VI	0.64 ± 0.11	-	-	-	0.64 ± 0.11	-	-	UO_2^{2+} + 2 H_3PO_4(aq) ⇌ $UO_2(H_2PO_4)_2$(aq) + 2 H^+
UO2(H2PO4)(H3PO4)+	VI	1.65 ± 0.11	-	-	-	1.65 ± 0.11	-	-	UO_2^{2+} + 2 H_3PO_4(aq) ⇌ $UO_2(H_2PO_4)(H_3PO_4)^+$ + H^+
UO2HAsO4(aq)	VI	7.16 ± 0.37	-	-	-	7.16 ± 0.37	-	-	UO_2^{2+} + $HAsO_4^{2-}$ ⇌ UO_2HAsO_4(aq)
UO2H2AsO4+	VI	1.34 ± 0.42	-	-	-	1.34 ± 0.42	-	-	UO_2^{2+} + H_3AsO_4(aq) ⇌ $UO_2H_2AsO_4^+$ + H^+
UO2(H2AsO4)2	VI	0.29 ± 0.53	-	-	-	0.29 ± 0.53	-	-	UO_2^{2+} + 2 H_3AsO_4(aq) ⇌ $UO_2(H_2AsO_4)_2$(aq) + 2 H^+
UO2CO3(aq)	VI	9.94 ± 0.03	5 ± 2	-	-	9.94 ± 0.03	5 ± 2	-	UO_2^{2+} + CO_3^{2-} ⇌ UO_2CO_3(aq)
UO2(CO3)2-2	VI	16.61 ± 0.09	18.5 ± 4.0	-	-	16.61 ± 0.09	18.5 ± 4.0	-	UO_2^{2+} + 2 CO_3^{2-} ⇌ $UO_2(CO_3)_2^{2-}$
UO2(CO3)3-4	VI	21.84 ± 0.04	-39.2 ± 4.1	-	-	21.84 ± 0.04	-39.2 ± 4.1	-	UO_2^{2+} + 3 CO_3^{2-} ⇌ $UO_2(CO_3)_3^{4-}$
(UO2)3(CO3)6-6	VI	54.0 ± 1.0	-62.7 ± 2.4	-	-	54.0 ± 1.0	-62.7 ± 2.4	-	3 UO_2^{2+} + 6 CO_3^{2-} ⇌ $(UO_2)_3(CO_3)_6^{6-}$
(UO2)2CO3(OH)3-	VI	-0.86 ± 0.50	-	-	-	-0.86 ± 0.50	-	-	2 UO_2^{2+} + CO_3^{2-} + 3 H_2O(l) ⇌ $(UO_2)_2CO_3(OH)_3^-$ + 3 H^+
(UO2)3O(OH)2(HCO3)+	VI	0.66 ± 0.50	-	-	-	0.66 ± 0.50	-	-	3 UO_2^{2+} + CO_3^{2-} + 3 H_2O(l) ⇌ $(UO_2)_3O(OH)_2(HCO_3)^+$ + 3 H^+
UO2CO3F-	VI	13.75 ± 0.09	-	-	-	13.75 ± 0.09	-	-	UO_2^{2+} + CO_3^{2-} + F^- ⇌ $UO_2CO_3F^-$
UO2CO3F2-2	VI	15.57 ± 0.14	-	-	-	15.57 ± 0.14	-	-	UO_2^{2+} + CO_3^{2-} + 2 F^- ⇔ $UO_2CO_3F_2^{2-}$
UO2CO3F3-3	VI	16.38 ± 0.11	-	-	-	16.38 ± 0.11	-	-	UO_2^{2+} + CO_3^{2-} + 3 F^- ⇌ $UO_2CO_3F_3^{3-}$
MgUO2(CO3)3-2	VI	*(26.11 ± 0.50)**	-	-	-	26.2 ± 0.2	-	-	Mg^{2+} + UO_2^{2+} + 3 CO_3^{2-} ⇌ $MgUO_2(CO_3)_3^{2-}$
Mg2UO2(CO3)3(aq)	VI	-	-	-	-	27.1 ± 0.6	-	-	2 Mg^{2+} + UO_2^{2+} + 3 CO_3^{2-} ⇌ $Mg_2UO_2(CO_3)_3$(aq)
CaUO2(CO3)3-2	VI	*(27.18 ± 0.50)**	-	-	-	27.0 ± 0.2	-47 ± 6	-	Ca^{2+} + UO_2^{2+} + 3 CO_3^{2-} ⇌ $CaUO_2(CO_3)_3^{2-}$
Ca2UO2(CO3)3(aq)	VI	*(29.22 ± 0.25)**[b]	-	-	-	30.8 ± 0.4	-47 ± 7	-	2 Ca^{2+} + UO_2^{2+} + 3 CO_3^{2-} ⇌ $Ca_2UO_2(CO_3)_3$(aq)
SrUO2(CO3)3-2	VI	*(26.86 ± 0.50)**	-	-	-	25.9 ± 0.2	-	-	Sr^{2+} + UO_2^{2+} + 3 CO_3^{2-} ⇌ $SrUO_2(CO_3)_3^{2-}$
Sr2UO2(CO3)3(aq)	VI	-	-	-	-	29.7 ± 0.5	-	-	2 Sr^{2+} + UO_2^{2+} + 3 CO_3^{2-} ⇌ $Sr_2UO_2(CO_3)_3$(aq)
BaUO2(CO3)3-2	VI	*(26.68 ± 0.50)**	-	-	-	25.6 ± 0.3	-	-	Ba^{2+} + UO_2^{2+} + 3 CO_3^{2-} ⇌ $BaUO_2(CO_3)_3^{2-}$
Ba2UO2(CO3)3(aq)	VI	*(29.75 ± 0.50)**	-	-	-	*29.75 ± 0.50*	-	-	*2 Ba^{2+} + UO_2^{2+} + 3 CO_3^{2-} ⇌ $Ba_2UO_2(CO_3)_3$(aq)*
UO2SCN+	VI	1.40 ± 0.23	3.22 ± 0.06	-	-	1.40 ± 0.23	3.22 ± 0.06	-	UO_2^{2+} + SCN^- ⇌ UO_2SCN^+
UO2(SCN)2(aq)	VI	1.24 ± 0.55	8.9 ± 0.6	-	-	1.24 ± 0.55	8.9 ± 0.6	-	UO_2^{2+} + 2 SCN^- ⇌ $UO_2(SCN)_2$(aq)
UO2(SCN)3-	VI	2.1 ± 0.5	6.0 ± 1.2	-	-	2.1 ± 0.5	6.0 ± 1.2	-	UO_2^{2+} + 3 SCN^- ⇌ $UO_2(SCN)_3^-$
UO2+	VI/V	1.484 ± 0.022	-	-	-	1.484 ± 0.022	-	-	UO_2^{2+} + e^- ⇌ UO_2^+
UO2(CO3)3-5	V	(7.19 ± 0.36)*	-	-	-	(7.19 ± 0.36)*	-	-	UO_2^+ + 3 CO_3^{2-} ⇌ $UO_2(CO_3)_3^{5-}$
U+4	VI/IV	9.038 ± 0.041	-	-	-	9.038 ± 0.041	-	-	UO_2^{2+} + 4H^+ + 2e^- ⇌ U^{4+} + 2H_2O(l)
UOH+3	IV	-0.54 ± 0.06	(46.91)[a]	147 ± 30	-	-0.54 ± 0.06	(46.91)[a]	147 ± 30	U^{4+} + H_2O(l) ⇌ UOH^{3+} + H^+
U(OH)2+2	IV	*(-1.1 ± 1.0)**	-	-	-	-1.9 ± 0.2	-	-	U^{4+} + 2 H_2O(l) ⇌ $U(OH)_2^{2+}$ + 2 H^+
U(OH)3+	IV	*(-4.7 ± 1.0)**	-	-	-	-5.2 ± 0.4	-	-	U^{4+} + 3 H_2O(l) ⇌ $U(OH)_3^+$ + 3 H^+
U(OH)4(aq)	IV	-10.0 ± 1.4	-	-	-	-10.0 ± 1.4	-	-	U^{4+} + 4 H_2O(l) ⇌ $U(OH)_4$(aq) + 4 H^+
UF+3	IV	9.42 ± 0.51	-5.6 ± 0.5	-	-	9.42 ± 0.51	-5.6 ± 0.5	-	U^{4+} + F^- ⇌ UF^{3+}
UF2+2	IV	16.56 ± 0.71	-3.5 ± 0.6	-	-	16.56 ± 0.71	-3.5 ± 0.6	-	U^{4+} + 2 F^- ⇌ UF_2^{2+}
UF3+	IV	21.89 ± 0.83	0.5 ± 4.0	-	-	21.89 ± 0.83	0.5 ± 4.0	-	U^{4+} + 3 F^- ⇌ UF_3^+
UF4(aq)	IV	26.34 ± 0.96	-	476 ± 17	-	26.34 ± 0.96	-	476 ± 17	U^{4+} + 4 F^- ⇌ UF_4(aq)
UF5-	IV	27.73 ± 0.74	-	-	-	27.73 ± 0.74	-	-	U^{4+} + 5 F^- ⇌ UF_5^-
UF6-2	IV	29.80 ± 0.70	-	-	-	29.80 ± 0.70	-	-	U^{4+} + 6 F^- ⇌ UF_6^{2-}
UCl+3	IV	1.72 ± 0.13	-19 ± 9	-	-	1.72 ± 0.13	-19 ± 9	-	U^{4+} + Cl^- ⇌ UCl^{3+}
UI+3	IV	1.25 ± 0.30	-	-	-	1.25 ± 0.30	-	-	U^{4+} + I^- ⇌ UI^{3+}
USO4+2	IV	6.58 ± 0.19	8.0 ± 2.7	-	-	6.58 ± 0.19	8.0 ± 2.7	-	U^{4+} + SO_4^{2-} ⇌ USO_4^{2+}
U(SO4)2	IV	10.51 ± 0.20	32.7 ± 2.8	-	-	10.51 ± 0.20	32.7 ± 2.8	-	U^{4+} + 2 SO_4^{2-} ⇌ $U(SO_4)_2$(aq)

Tab. 31-2: Cont.

Name	Redox	TDB Version 12/07				TDB 2020			
		$\log_{10}\beta°$	$\Delta_r H_m°$ [kJ · mol^{-1}]	$\Delta_r S_m°$ [J · K^{-1} · mol^{-1}]	$S_m°$ [J · K^{-1} · mol^{-1}]	$\log_{10}\beta°$	$\Delta_r H_m°$ [kJ · mol^{-1}]	$\Delta_r S_m°$ [J · K^{-1} · mol^{-1}]	Reaction
UNO3+3	IV	1.47 ± 0.13	-	-	-	1.47 ± 0.13	-	-	$U^{4+} + NO_3^- \rightleftharpoons UNO_3^{3+}$
U(NO3)2+2	IV	2.30 ± 0.35	-	-	-	2.30 ± 0.35	-	-	$U^{4+} + 2\ NO_3^- \rightleftharpoons U(NO_3)_2^{2+}$
UH2PO4+3	IV	-	-	-	-	6.8 ± 0.7	-	-	$U^{4+} + H_2PO_4^- \rightleftharpoons UH_2PO_4^{3+}$
U(CO3)4-4	IV	35.22 ± 1.03	-	-	-	35.22 ± 1.03	-	-	$U^{4+} + 4\ CO_3^{2-} \rightleftharpoons U(CO_3)_4^{4-}$
U(CO3)5-6	IV	33.9 ± 1.0	-20 ± 4	-	-	33.9 ± 1.0	-20 ± 4	-	$U^{4+} + 5\ CO_3^{2-} \rightleftharpoons U(CO_3)_5^{6-}$
UCO3(OH)3-	IV	*(4)**	-	-	-	*(4)**	-	-	$U^{4+} + CO_3^{2-} + 3\ H_2O(l) \rightleftharpoons UCO_3(OH)_3^- + 3\ H^+$
USCN+3	IV	(2.83 ± 0.15)*	-27 ± 8	-	-	(2.83 ± 0.15)*	-27 ± 8	-	$U^{4+} + SCN^- \rightleftharpoons USCN^{3+}$
U(SCN)2+2	IV	4.26 ± 0.18	-18 ± 4	-	-	4.26 ± 0.18	-18 ± 4		$U^{4+} + 2\ SCN^- \rightleftharpoons U(SCN)_2^{2+}$

[a] Calculated value
[b] Value not selected but supplied by Guillaumont et al. (2003) for guidance or for scoping calculations

Name	Redox	TDB Version 12/07			TDB 2020			
		$\log_{10}K_{s,0}°$	$S_m°$ [J · K^{-1} · mol^{-1}]	$C_{p,m}°$ [J · K^{-1} · mol^{-1}]	$\log_{10}K_{s,0}°$	$S_m°$ [J · K^{-1} · mol^{-1}]	$C_{p,m}°$ [J · K^{-1} · mol^{-1}]	Reaction
UO2(am, hyd)	IV	1.5 ± 1.0	-	-	1.5 ± 1.0	-	-	UO_2(am, hyd) + 4 $H^+ \rightleftharpoons U^{4+}$ + 2 H_2O(l)
Metaschoepite[a]	VI	5.96 ± 0.18*	188.54 ± 0.38	172.07 ± 0.34	5.35 ± 0.13	188.54 ± 0.38	172.07 ± 0.34	$UO_3 \cdot 2H_2O$(cr) + 2 $H^+ \rightleftharpoons UO_2^{2+}$ + 3 H_2O(l)
UF4:2.5H2O(cr)	IV	-30.12 ± 0.70*	263.5 ± 15.0	263.7 ± 15.0	-30.12 ± 0.70*	263.5 ± 15.0	263.7 ± 15.0	$UF_4 \cdot 2.5H_2O$(cr) $\rightleftharpoons U^{4+}$ + 4 F^- + 2.5 H_2O(l)
U(OH)2SO4(cr)	IV	-3.17 ± 0.50	-	-	-3.17 ± 0.50	-	-	$U(OH)_2SO_4$(cr) + 2 $H^+ \rightleftharpoons U^{4+}$ + SO_4^{2-} + 2 H_2O(l)
Rutherfordine	VI	-14.76 ± 0.02	144.2 ± 0.3	20.1 ± 0.1	-14.76 ± 0.02	144.2 ± 0.3	20.1 ± 0.1	UO_2CO_3(cr) $\rightleftharpoons UO_2^{2+}$ + CO_3^{2-}
(UO2)3(PO4)2:4H2O(cr)	VI	-5.96 ± 0.30	-	-	-5.96 ± 0.30	-	-	$(UO_2)_3(PO_4)_2 \cdot 4H_2O$(cr) + 6$H^+ \rightleftharpoons$ 3UO_2^{2+} + 2H_3PO_4(aq) + 4H_2O(l)
Chernikovite	VI	-2.50 ± 0.09	-	-	-2.50 ± 0.09	328 ± 10	317 ± 10	$UO_2HPO_4 \cdot 4H_2O$(cr) + 2$H^+ \rightleftharpoons UO_2^{2+}$ + H_3PO_4(aq) + 4H_2O(l)
Meta-saleite	VI	-	-	-	-49.2 ± 1.2	*704 ± 40*	-	$Mg[(UO_2)(PO_4)]_2 \cdot 8H_2O$(cr) $\rightleftharpoons$ 2UO_2^{2+} + Mg^{2+} + 2PO_4^{3-} + 8H_2O(l)
Becquerelite	VI	40.5 ± 1.6	-	-	40.5 ± 1.6	-	-	$CaU_6O_{19} \cdot 11H_2O$(cr) + 14$H^+ \rightleftharpoons Ca^{2+}$ + 6UO_2^{2+} + 18H_2O(l)
Meta-autunite	VI	-	-	-	-50.0 ± 1.0	*622 ± 40*	-	$Ca[(UO_2)(PO_4)]_2 \cdot 6H_2O$(cr) $\rightleftharpoons$ 2UO_2^{2+} + Ca^{2+} + 2PO_4^{3-} + 6H_2O(l)
Sr[(UO2)(PO4)]2:6H2O(cr)	VI	-	-	-	-51.3 ± 1.0	*633 ± 20*	-	$Sr[(UO_2)(PO_4)]_2 \cdot 6H_2O$(cr) $\rightleftharpoons$ 2UO_2^{2+} + Sr^{2+} + 2PO_4^{3-} + 6H_2O(l)
Meta-uranocircite II	VI	-	-	-	-52.2 ± 1.0	*641 ± 40*	-	$Ba[(UO_2)(PO_4)]_2 \cdot 6H_2O$(cr) $\rightleftharpoons$ 2UO_2^{2+} + Ba^{2+} + 2PO_4^{3-} + 6H_2O(l)
Li(UO2)(PO4):4H2O(cr)	VI	-	-	-	-25.5 ± 1.0	*336 ± 20*	-	$Li(UO_2)(PO_4) \cdot 4H_2O$(cr) $\rightleftharpoons UO_2^{2+}$ + Li^+ + PO_4^{3-} + 4H_2O(l)
Na2U2O7:H2O(cr)	VI	-	-	-	12.2 ± 0.2	-	-	0.5 $Na_2U_2O_7 \cdot H_2O$(cr) + 3 $H^+ \rightleftharpoons Na^+$ + UO_2^{2+} + 2 H_2O(l)
Na(UO2)(PO4):3H2O(cr)	VI	-	-	-	-24.3 ± 1.0	*323 ± 20*	-	$Na(UO_2)(PO_4) \cdot 3H_2O$(cr) $\rightleftharpoons UO_2^{2+}$ + Na^+ + PO_4^{3-} + 3H_2O(l)
Compreignacite	VI	37.1 ± 0.5	-	-	37.10 ± 0.54	-	-	$K_2U_6O_{19} \cdot 11H_2O$(cr) + 14$H^+ \Leftrightarrow$ 2K^+ + 6UO_2^{2+} + 18H_2O(l)
K(UO2)(PO4):3H2O(cr)	VI	-	-	-	-25.5 ± 1.0	*343 ± 15*	-	$K(UO_2)(PO_4) \cdot 3H_2O$(cr) $\rightleftharpoons UO_2^{2+}$ + K^+ + PO_4^{3-} + 3H_2O(l)
Cs(UO2)(PO4):2.5H2O(cr)	VI	-	-	-	-25.9 ± 1.0	*338 ± 15*	-	$Cs(UO_2)(PO_4) \cdot 2.5H_2O$(cr) $\rightleftharpoons UO_2^{2+}$ + Cs^+ + PO_4^{3-} + 2.5H_2O(l)
NH4(UO2)(PO4):3H2O(cr)	VI	-	-	-	-26.1 ± 1.0	*350 ± 20*	-	$NH_4(UO_2)(PO_4) \cdot 3H_2O$(cr) $\rightleftharpoons UO_2^{2+}$ + NH_4^+ + PO_4^{3-} + 3H_2O(l)
Cu[(UO2)(PO4)]2:8H2O(cr)	VI	-	-	-	-52.8 ± 0.3	*686 ± 30*	-	$Cu[(UO_2)(PO_4)]_2 \cdot 8H_2O$(cr) $\rightleftharpoons$ 2UO_2^{2+} + Cu^{2+} + 2PO_4^{3-} + 8H_2O(l)
Zn[(UO2)(PO4)]2:8H2O(cr)	VI	-	-	-	-49.8 ± 1.0	*686 ± 30*	-	$Zn[(UO_2)(PO_4)]_2 \cdot 8H_2O$(cr) $\rightleftharpoons$ 2UO_2^{2+} + Zn^{2+} + 2PO_4^{3-} + 8H_2O(l)
Ni[(UO2)(PO4)]2:8H2O(cr)	VI	-	-	-	-49.9 ± 1.0	*686 ± 30*	-	$Ni[(UO_2)(PO_4)]_2 \cdot 8H_2O$(cr) $\rightleftharpoons$ 2UO_2^{2+} + Ni^{2+} + 2PO_4^{3-} + 8H_2O(l)
Mn[(UO2)(PO4)]2:10H2O(cr)	VI	-	-	-	*-50.22 ± 0.40*	-	-	*$Mn[(UO_2)(PO_4)]_2 \cdot 10H_2O$(cr) $\rightleftharpoons$ 2UO_2^{2+} + Mn^{2+} + 2PO_4^{3-} + 10H_2O(l)*

Tab. 31-2: Cont.

Name	Redox	TDB Version 12/07			TDB 2020			
		$\log_{10}K_{s,0}°$	$S_m°$ [J · K^{-1} · mol^{-1}]	$C_{p,m}°$ [J · K^{-1} · mol^{-1}]	$\log_{10}K_{s,0}°$	$S_m°$ [J · K^{-1} · mol^{-1}]	$C_{p,m}°$ [J · K^{-1} · mol^{-1}]	Reaction
Cd[(UO2)(PO4)]2:10H2O(cr)	VI	-	-	-	*-50.34 ±0.30*	-	-	*$Cd[(UO_2)(PO_4)]_2 \cdot 10H_2O(cr) \rightleftarrows 2UO_2^{2+} + Cd^{2+} + 2PO_4^{3-} + 10H_2O(l)$*
Pb[(UO2)(PO4)]2:8H2O(cr)	VI	-	-	-	*-49.85 ±0.50*	-	-	*$Pb[(UO_2)(PO_4)]_2 \cdot 8H_2O(cr) \rightleftarrows 2UO_2^{2+} + Pb^{2+} + 2PO_4^{3-} + 8H_2O(l)$*
Parsonite	VI	-	-	-	*-52.2 ±0.8*	-	-	*$Pb_2(UO_2)(PO_4)_2 \cdot 2H_2O(cr) \rightleftarrows UO_2^{2+} + 2Pb^{2+} + 2PO_4^{3-} + 2H_2O(l)$*
Sabugalite	VI	-	-	-	*-13.1 ± 1.2*	-	-	*$HAl[(UO_2)(PO_4)]_4 \cdot 16H_2O(cr) + 7H^+ \rightleftarrows 4UO_2^{2+} + Al^{3+} + 4H_2PO_4^- + 16H_2O(l)$*
Trögerite	VI	-	-	-	-45.33 ± 1.00	-	-	$(UO_2)_3(AsO_4)_2 \cdot 12H_2O(cr) \rightleftarrows 3UO_2^{2+} + 2AsO_4^{3-} + 12H_2O(l)$
Hydrogen uranospinite	VI	-	-	-	-23.0 ± 0.3	349 ± 10	326 ± 10	$UO_2HAsO_4 \cdot 4H_2O(cr) \rightleftarrows UO_2^{2+} + H^+ + AsO_4^{3-} + 4H_2O(l)$
Li(UO2)(AsO4):4H2O(cr)	VI	-	-	-	-20.4 ± 1.0	*367 ±25*	-	$Li(UO_2)(AsO_4) \cdot 4H_2O(cr) \rightleftarrows UO_2^{2+} + Li^+ + AsO_4^{3-} + 4H_2O(l)$
$Na(UO_2)(AsO_4):3H_2O(cr)$	VI	-	-	-	-22.8 ± 1.0	*339 ± 19*	-	$Na(UO_2)(AsO_4) \cdot 3H_2O(cr) \rightleftarrows UO_2^{2+} + Na^+ + AsO_4^{3-} + 3H_2O(l)$
K(UO2)(AsO4):3H2O(cr)	VI	-	-	-	-23.3 ± 1.0	*346 ± 19*	-	$K(UO_2)(AsO_4) \cdot 3H_2O(cr) \rightleftarrows UO_2^{2+} + K^+ + AsO_4^{3-} + 3H_2O(l)$
Cs(UO2)(AsO4):2.5H2O(cr)	VI	-	-	-	-25.2 ± 1.0	*342 ± 17*	-	$Cs(UO_2)(AsO_4) \cdot 2.5H_2O(cr) \rightleftarrows UO_2^{2+} + Cs^+ + AsO_4^{3-} + 2.5H_2O(l)$
NH4(UO2)(AsO4):3H2O(cr)	VI	-	-	-	-24.7 ± 1.0	*366 ± 19*	-	$NH_4(UO_2)(AsO_4) \cdot 3H_2O(cr) \rightleftarrows UO_2^{2+} + NH_4^+ + AsO_4^{3-} + 3H_2O(l)$
Mg[(UO2)(AsO4)]2:10H2O(cr)	VI	-	-	-	-44.6 ± 0.5	*859 ±40*	-	$Mg[(UO_2)(AsO_4)]_2 \cdot 10H_2O(cr) \rightleftarrows 2UO_2^{2+} + Mg^{2+} + 2AsO_4^{3-} + 10H_2O(l)$
Ca[(UO2)(AsO4)]2:10H2O(cr)	VI	-	-	-	-45.1 ± 1.0	*874 ±30*	-	$Ca[(UO_2)(AsO_4)]_2 \cdot 10H_2O(cr) \rightleftarrows 2UO_2^{2+} + Ca^{2+} + 2AsO_4^{3-} + 10H_2O(l)$
Sr[(UO2)(AsO4)]2:8H2O(cr)	VI	-	-	-	-45.1 ± 1.0	*758 ±20*	-	$Sr[(UO_2)(AsO_4)]_2 \cdot 8H_2O(cr) \rightleftarrows 2UO_2^{2+} + Sr^{2+} + 2AsO_4^{3-} + 8H_2O(l)$
Ba[(UO2)(AsO4)]2:7H2O(cr)	VI	-	-	-	-44.7 ± 1.0	*738 ±30*	-	$Ba[(UO_2)(AsO_4)]_2 \cdot 7H_2O(cr) \rightleftarrows 2UO_2^{2+} + Ba^{2+} + 2AsO_4^{3-} + 7H_2O(l)$
Metazeunerite	VI	-	-	-	-45.7 ± 1.0	*695 ±30*	-	$Cu[(UO_2)(AsO_4)]_2 \cdot 8H_2O(cr) \rightleftarrows 2UO_2^{2+} + Cu^{2+} + 2AsO_4^{3-} + 8H_2O(l)$
Rauchite	VI	-	-	-	-45.9 ± 1.0	*783 ±30*	-	$Ni[(UO_2)(AsO_4)]_2 \cdot 10H_2O(cr) \rightleftarrows 2UO_2^{2+} + Ni^{2+} + 2AsO_4^{3-} + 10H_2O(l)$
Metakahlerite	VI	-	-	-	-46.1 ± 2.2	*693 ±30*	-	$Fe[(UO_2)(AsO_4)]_2 \cdot 8H_2O(cr) \rightleftarrows 2UO_2^{2+} + Fe^{2+} + 2AsO_4^{3-} + 8H_2O(l)$
Mn[(UO2)(AsO4)]2:8H2O(cr)	VI	-	-	-	-44.4 ± 1.0	*693 ±30*	-	$Mn[(UO_2)(AsO_4)]_2 \cdot 8H_2O(cr) \rightleftarrows 2UO_2^{2+} + Mn^{2+} + 2AsO_4^{3-} + 8H_2O(l)$
Zn[(UO2)(AsO4)]2:8H2O(cr)	VI	-	-	-	-45.1 ± 1.0	*695 ±30*	-	$Zn[(UO_2)(AsO_4)]_2 \cdot 8H_2O(cr) \rightleftarrows 2UO_2^{2+} + Zn^{2+} + 2AsO_4^{3-} + 8H_2O(l)$
Cd[(UO2)(AsO4)]2:8H2O(cr)	VI	-	-	-	-45.4 ± 1.0	*710 ±30*	-	$Cd[(UO_2)(AsO_4)]_2 \cdot 8H_2O(cr) \rightleftarrows 2UO_2^{2+} + Cd^{2+} + 2AsO_4^{3-} + 8H_2O(l)$
Pb[(UO2)(AsO4)]2:10H2O(cr)	VI	-	-	-	-46.3 ± 1.0	*804 ±30*	-	$Pb[(UO_2)(AsO_4)]_2 \cdot 10H_2O(cr) \rightleftarrows 2UO_2^{2+} + Pb^{2+} + 2AsO_4^{3-} + 10H_2O(l)$
Li(UO2)(BO3):1.5H2O(cr)	VI	-	-	-	4.58 ± 0.20	194 ± 14	-	$Li(UO_2)(BO_3) \cdot 1.5H_2O(cr) + 2H^+ \rightleftarrows 0.5(UO_2)_2(OH)_2^{2+} + Li^+ + B(OH)_3(aq) + 0.5H_2O(l)$
Na(UO2)(BO3):H2O(cr)	VI	-	-	-	4.47 ± 0.20	183.8 ± 3.0	159.0 ± 1.0	$Na(UO_2)(BO_3) \cdot H_2O(cr) + 2H^+ \rightleftarrows 0.5(UO_2)_2(OH)_2^{2+} + Na^+ + B(OH)_3(aq)$
K(UO2)(BO3):H2O(cr)	VI	-	-	-	3.90 ± 0.20	174 ± 14	-	$K(UO_2)(BO_3) \cdot H_2O(cr) + 2H^+ \rightleftarrows 0.5(UO_2)_2(OH)_2^{2+} + K^+ + B(OH)_3(aq)$
Cs(UO2)(BO3):H2O(cr)	VI	-	-	-	3.92 ± 0.20	267 ± 15	-	$Cs(UO_2)(BO_3) \cdot H_2O(cr) + 2H^+ \rightleftarrows 0.5(UO_2)_2(OH)_2^{2+} + Cs^+ + B(OH)_3(aq)$

[a] Previously referred to as schoepite by Grenthe et al. (1992) and Hummel et al. (2002)

Tab. 31-3: Selected SIT ion interaction coefficients $\varepsilon_{j,k}$ [kg · mol^{-1}] for uranium species

All data included in TDB 2020 are taken from Grenthe et al. (1992), Guillaumont et al. (2003) and Grenthe et al. (2020), unless indicated otherwise. Own data estimates based on charge correlations (see Section 1.5.3) are shaded. Supplemental data are in italics.

j k → ↓	**Cl^-** $\varepsilon_{j,k}$	**ClO_4^-** $\varepsilon_{j,k}$	**NO_3^-** $\varepsilon_{j,k}$	**Li^+** $\varepsilon_{j,k}$	**Na^+** $\varepsilon_{j,k}$	**K^+** $\varepsilon_{j,k}$
UO2+2	(0.21 ± 0.02) [a]	0.46 ± 0.03	(0.24 ± 0.03) [a]	0	0	0
UO2OH+	0.05 ± 0.10	-0.06 ± 0.40	0.51 ± 1.40	0	0	0
UO2(OH)3-	0	0	0	-	-0.24 ± 0.09	-
UO2(OH)4-2	0	0	0	-	0.01 ± 0.04	-
(UO2)2OH+3	0.25 ± 0.10	0.6 ± 0.1	-	0	0	0
(UO2)2(OH)2+2	0.69 ± 0.07	0.57 ± 0.07	0.49 ± 0.09	0	0	0
(UO2)3(OH)4+2	0.50 ± 0.18	0.89 ± 0.23	0.72 ± 1.00	0	0	0
(UO2)3(OH)5+	0.81 ± 0.17	0.45 ± 0.15	0.41 ± 0.22	0	0	0
(UO2)3(OH)7-	0	0	0	-	-0.05 ± 0.10	-
(UO2)4(OH)7+	0.05 ± 0.10	0.2 ± 0.1	-	0	0	0
UO2F+	(0.05 ± 0.10) [b]	0.28 ± 0.04	-	0	0	0
UO2F3-	0	0	0	-	-0.14 ± 0.05	-
UO2F4-2	0	0	0	-	-0.30 ± 0.06	-
UO2Cl+	(0.33 ± 0.04) [c]	0.33 ± 0.04	-	0	0	0
UO2Cl2	0	0	0	0	0	0
UO2IO3+	0.05 ± 0.10	0.33 ± 0.04	-	0	0	0
UO2(SO4)2-2	0	0	0	-	-0.12 ± 0.06	-
UO2(SO4)3-4	0	0	0	-	(-0.26 ± 0.05) [d]	-
UO2HSeO3+	0.05 ± 0.10	0.2 ± 0.1	-	0	0	0
UO2(SeO4)2-2	0	0	0	-	-0.10 ± 0.10	-
UO2NO3+	0.05 ± 0.10	0.33 ± 0.04	-	0	0	0
UO2PO4-	0	0	0	-	(-0.09 ± 0.05) [e]	-
UO2H2PO4+	0.05 ± 0.10	0.2 ± 0.1	-	0	0	0
UO2H3PO4+2	0.15 ± 0.10	0.4 ± 0.1	-	0	0	0
UO2H2PO4H3PO4+	0.05 ± 0.10	0.2 ± 0.1	-	0	0	0
UO2HAsO4	0	0	0	0	0	0
UO2H2AsO4+	0.05 ± 0.10	0.2 ± 0.1	-	0	0	0
UO2(CO3)2-2	0	0	0	-	(-0.15 ± 0.08) [f]	-
UO2(CO3)3-4	0	0	0	-	-0.01 ± 0.11	-
(UO2)3(CO3)6-6	0	0	0	-	0.37 ± 0.11	-
(UO2)2CO3(OH)3-	0	0	0	-	0.00 ± 0.05	-
(UO2)3O(OH)2HCO3+	0.05 ± 0.10	(0.0 ± 0.1) [g]	-	0	0	0
UO2CO3F-	0	0	0	-	(0.00 ± 0.05) [h]	-
UO2CO3F2-2	0	0	0	-	(-0.02 ± 0.09) [h]	-
UO2CO3F3-3	0	0	0	-	(-0.25 ± 0.05) [h]	-

Tab. 31-3: Cont.

j k → ↓	Cl^- $\varepsilon_{j,k}$	ClO_4^- $\varepsilon_{j,k}$	NO_3^- $\varepsilon_{j,k}$	Li^+ $\varepsilon_{j,k}$	Na^+ $\varepsilon_{j,k}$	K^+ $\varepsilon_{j,k}$
MgUO2(CO3)3-2	*0*	*0*	*0*	-	*-0.10 ± 0.10*	-
CaUO2(CO3)3-2	*0*	*0*	*0*	-	*-0.10 ± 0.10*	-
SrUO2(CO3)3-2	*0*	*0*	*0*	-	*-0.10 ± 0.10*	-
BaUO2(CO3)3-2	*0*	*0*	*0*	-	*-0.10 ± 0.10*	-
UO2SCN+	0.05 ± 0.10	(0.26 ± 0.04) [i]	-	0	0	0
UO2(SCN)3-	0	0	0	-	(0.00 ± 0.05) [j]	-
UO2+	0.05 ± 0.10	0.26 ± 0.03	-	0	0	0
UO2(CO3)3-5	0	0	0	-	(-0.92 ± 0.23) [k]	-
U+4	0.35 ± 0.10	0.76 ± 0.06	-	0	0	0
UOH+3	0.25 ± 0.10	0.48 ± 0.08	-	0	0	0
U(OH)2+2	*0.15 ± 0.10*	*0.4 ± 0.1*	-	*0*	*0*	*0*
U(OH)3+	*0.05 ± 0.10*	*0.2 ± 0.1*	-	*0*	*0*	*0*
UF+3	0.25 ± 0.10	0.48 ± 0.08	-	0	0	0
UF2+2	(0.3 ± 0.1) [l]	0.3 ± 0.1	-	0	0	0
UF3+	0.1 ± 0.1	0.1 ± 0.1	-	0	0	0
UF5-	0	0	0	-	-0.05 ± 0.10	-
UF6-2	0	0	0	-	-0.10 ± 0.10	-
UCl+3	(0.59 ± 0.10)[p]	(0.59 ± 0.10)[m]	-	0	0	0
UI+3	0.25 ± 0.10	0.55 ± 0.10	-	0	0	0
USO4+2	0.15 ± 0.10	0.3 ± 0.1	-	0	0	0
U(SO4)2(aq)	0	0	0	0	0	0
UNO3+3	0.25 ± 0.10	0.62 ± 0.08	-	0	0	0
U(NO3)2+2	0.15 ± 0.10	0.49 ± 0.14	-	0	0	0
UH2PO4+3	0.25 ± 0.10	0.6 ± 0.1	0	0	0	0
U(CO3)4-4	0	0	0	-	-0.09 ± 0.10	-
U(CO3)5-6	0	0	0	-	-0.30 ± 0.15	-0.70 ± 0.31
UCO3(OH)3-	*0*	*0*	*0*	-	*-0.05 ± 0.10*	-
USCN+3	0.25 ± 0.10	(0.52± 0.10)[n]	-	0	0	0
U(SCN)2+2	0.15 ± 0.10	(0.3 ± 0.1)[o]	-	0	0	0

Tab. 31-3: Cont.

[a] This value by Ciavatta (1980) was not used by Grenthe et al. (1992), since Ciavatta (1980) did not explicitly consider the formation of complexes of the metal cations with the background electrolyte anions. Grenthe et al. (1992) did explicitly consider the weak complexation of UO_2^{2+} with chloride and nitrate (if these anions were part of the background electrolyte), using $\varepsilon(UO_2^{2+}, Cl^-) = \varepsilon(UO_2^{2+}, NO_3^-) = \varepsilon(UO_2^{2+}, ClO_4^-) = (0.46 \pm 0.03)$ kg · mol^{-1}.

[b] Instead of the value (0.04 ± 0.07) kg · mol^{-1} by Grenthe et al. (1992), whose origins are unknown, see Thoenen et al. (2014) for discussion.

[c] Thoenen et al. (2014), in combination with $\varepsilon(UO_2^{2+}, Cl^-) = \varepsilon(UO_2^{2+}, ClO_4^-) = (0.46 \pm 0.03)$ kg · mol^{-1}.

[d] Neither Grenthe et al. (1992) nor Guillaumont et al. (2003) selected a value. This value is estimated from $\varepsilon(P_2O_7^{4-}, Na^+) = -0.26 \pm 0.05)$ kg · mol^{-1}, see Thoenen et al. (2014) for discussion.

[e] Sandino (1991)

[f] Thoenen et al. (2014)

[g] Not included by Grenthe et al. (1992) in their list of selected ion interactions coefficients, but used by them (see their p. 646).

[h] Not included by Guillaumont et al. (2003) in their list of selected ion interaction coefficients, but used by them (see their p. 568).

[i] The value (0.22 ± 0.04) kg · mol^{-1} selected by Grenthe et al. (1992) is incorrect, see Thoenen et al. (2014) for discussion.

[j] Not included by Grenthe et al. (1992) in their list of selected ion interactions coefficients, but used by them (see their p. 331).

[k] Thoenen et al. (2014), instead of $-(0.62 \pm 0.15)$ kg · mol^{-1} selected by Grenthe et al. (1995) and retained by Guillaumont et al. (2003).

[l] Not included by Grenthe et al. (1992) in their list of selected ion interaction coefficients, but used by them (see their p. 630).

[m] This value by Grenthe et al. (1992) was replaced by Guillaumont et al. (2003) by (0.50 ± 0.10) kg · mol^{-1}. For reasons discussed in Thoenen et al. (2014), we retained the value by Grenthe et al. (1992).

[n] Thoenen et al. (2014)

[o] Not included by Grenthe et al. (1992) in their list of selected ion interaction coefficients, but used by them (see their p. 332).

[p] Thoenen et al. (2014), in combination with $\varepsilon(U^{4+}, Cl^-) = \varepsilon(U^{4+}, ClO_4^-) = (0.76 \pm 0.06)$ kg · mol^{-1}.

Tab. 31-4: Selected SIT ion interaction coefficients $\varepsilon_{j,k}$ [kg · mol^{-1}] for neutral uranium species

All data were derived by Thoenen et al. (2014) and this work. Own data estimates based on charge correlations (see Section 1.5.3) are shaded.

J k → ↓	**$Na^+ + ClO_4^-$** $\varepsilon_{j,k}$
UO2(OH)2(aq)	0.00 ± 0.10
UO2F2(aq)	0.13 ± 0.05
UO2(IO3)2(aq)	0.00 ± 0.10
UO2SO4(aq)	0.00 ± 0.10
UO2(HSeO3)2(aq)	0.00 ± 0.10
UO2SeO4(aq)	0.00 ± 0.10
UO2HPO4(aq)	0.00 ± 0.10
UO2(H2PO4)2(aq)	0.00 ± 0.10
UO2(H2AsO4)2(aq)	0.00 ± 0.10
UO2CO3(aq)	0.15 ± 0.06
Mg2UO2(CO3)3(aq)	*0.00 ± 0.10*
Ca2UO2(CO3)3(aq)	*0.00 ± 0.10*
Sr2UO2(CO3)3(aq)	*0.00 ± 0.10*
Ba2UO2(CO3)3(aq)	*0.00 ± 0.10*
UO2(SCN)2(aq)	0.00 ± 0.10
U(OH)4(aq)	0.00 ± 0.10
UF4(aq)	0.00 ± 0.10
U(SO4)2(aq)	0.00 ± 0.10

31.10 References

Altmaier, M., Yalçintaş, E., Gaona, X., Neck, V., Muller, R., Schlieker, M. & Fanghänel, T. (2017): Solubility of U(VI) in chloride solutions. I. The stable oxides/hydroxides in NaCl systems, solubility products, hydrolysis constants and SIT coefficients. J. Chem. Thermodyn., 114, 2-13.

Ciavatta, L. (1980): The specific interaction theory in evaluating ionic equilibria. Ann. Chim. (Rome), 70, 551-567.

Crea, F., de Stefano, C., Pettignano, A. & Sammartano, S. (2004): Hydrolysis of dioxouranium(VI): a calorimetric study in NaCl(aq) and $NaClO_4$(aq), at 25 °C. Thermochim. Acta, 414, 185-189.

Endrizzi, F. & Rao, L. (2014): Chemical speciation of uranium(VI) in marine environments: complexation of calcium and magnesium ions with $[(UO_2)(CO_3)_3]^{4-}$] and the effect on the extraction of uranium from seawater. Chem. Eur. J., 20, 14499-14506.

Fujiwara, K., Yamana, H., Fujii, T. & Moriyama, H. (2003): Determination of uranium(IV) hydrolysis constants and solubility product of $UO_2 \cdot xH_2O$. Radiochim. Acta, 91, 345-350.

Grenthe, I., Gaona, X., Plyasunov, A.V., Rao, L., Runde, W.H., Grambow, B., Konings, R.J.M., Smith, A.L. & Moore, E.E. (2020): Second Update on the Chemical Thermodynamics of Uranium, Neptunium, Plutonium, Americium and Technetium. Chemical Thermodynamics, Vol. 14. OECD Publications, Paris, France, 1503 pp.

Grenthe, I., Puigdomènech, I., Sandino, M.C.A. & Rand, M.H. (1995): corrections to theUranium NEA-TDB review. In: Silva, R.J., Bidoglio, G., Rand, M.H., Robouch, P.B., Wanner, H. & Puigdomènech, I. (1995): Chemical Thermodynamics of Americium. Chemical Thermodynamics, Vol. 2. Elsevier, Amsterdam, Appendix D, 347-374.

Grenthe, I., Fuger, J., Konings, R.J.M., Lemire, R.J., Muller, A.B., Nguyen-Trung, C. & Wanner, H. (1992): Chemical Thermodynamics of Uranium. Chemical Thermodynamics, Vol. 1. Elsevier, Amsterdam, 715 pp.

Guillaumont, R., Fanghänel, T., Fuger, J., Grenthe, I., Neck, V., Palmer, D.A. & Rand, M.H. (2003): Update on the Chemical Thermodynamics of Uranium, Neptunium, Plutonium, Americium and Technetium. Chemical Thermodynamics, Vol. 5. Elsevier, Amsterdam, 919 pp.

Hughes Kubatko, K.-A., Helean, K.B., Navrotsky, A. & Burns, P.C. (2003): Stability of peroxide-containing uranyl minerals. Science, 302, 1191-1193.

Hummel, W., Berner, U., Curti, E., Pearson, F.J. & Thoenen, T. (2002): Nagra/PSI Chemical Thermodynamic Data Base 01/01. Nagra Technical Report NTB 02-16. Also published by Universal Publishers/uPublish.com, Parkland, Florida, USA.

Lehmann, S., Geipel, G., Grambole, G. & Bernhard, G. (2010): Complexation of aqueous uranium(IV) with phosphate investigated using time-resolved laser-induced fluorescence spectroscopy. J. Radioanal. Nucl. Chem., 283, 395-401.

Rai, D., Xia, Y., Rao, L., Hess, N.J., Felmy, A.R., Moore, D.A. & McCready, D.E. (2005): Solubility of $(UO_2)_3(PO_4)_2 \cdot 4H_2O$ in H^+-Na^+-OH^--$H_2PO_4^-$-HPO_4^{2-}-PO_4^{3-}-H2O and its comparison to the analogous PuO_2^{2+} system. J. Solution Chem., 34, 469-498.

Sandino, M.C.A. (1991): Processes affecting the mobility of uranium in natural waters. Ph.D. thesis in inorganic chemistry. The Royal Institute of Technology, Stockholm, Sweden.

Suleimenov, O.M., Seward, T.M., & Hovey, J.K. (2007): A spectrophotometric study on uranyl nitrate complexation to 150 °C. J. Solution Chem., 36, 1093-1102

Tian, G. & Rao, L. (2009): Effect of temperature on the complexation of uranium(IV) with fluoride in aqueous solutions. Inorg. Chem., 48, 6748-6754.

Thoenen, T., Hummel, W., Berner, U. & Curti, E. (2014): The PSI/Nagra Chemical Thermodynamic Database 12/07. Technical Report, PSI Bericht Nr. 14-04, Paul Scherrer Institut, Villigen, Switzerland, 416 pp.

32 Zinc

32.1 Introduction

Many zinc compounds and complexes are toxic and thus, zinc is an environmentally significant heavy metal. In addition, zinc is used as a representative of divalent transition metals in experimental sorption studies, and for interpreting and using the experimental data reliable information about zinc speciation is needed (Bradbury & Baeyens 1997, 1999, Soltermann et al. 2014). The latter fact triggered the inclusion of zinc into the PSI Chemical Thermodynamic Database 2020 (TDB 2020), besides its relevance as a chemically toxic substance.

The only stable oxidation state of zinc in aqueous solution is Zn(II).

The thermodynamic data included into the TDB 2020 have been taken from

- CODATA key values (Cox et al. 1989)
- an IUPAC review of Zn^{2+} + OH^-, Cl^-, CO_3^{2-}, SO_4^{2-} and PO_4^{3-} aqueous systems (Powell et al. 2013)
- the recent review of the hydrolysis of metal ions (Brown & Ekberg 2016)
- and own reviews of experimental data concerning the ZnS(cr) – H_2S – water system

The selected thermodynamic data for zinc compounds and complexes are presented in Tab. 32-2.

Hagemann (2012) provides complexation constants of Zn hydrolysis and carbonate species from own experimental data in highly saline solutions. All these species are also considered in TDB 2020 and their selected values are in good agreement with the data of Hagemann (2012). Hagemann (2012) also reports solubility products for ZnO (zinkite), $Zn(OH)_2$ (wülfingite), $ZnCO_3$ (smithsonite) and $Zn_5(OH)_6(CO_3)_2$ (hydrozinkite). These solid compounds are also considered in TDB 2020 and their selected values are in good agreement with the data of Hagemann (2012). In addition, Hagemann (2012) provides solubility products of more soluble Zn hydroxide-chloride and -sulphate salts which are not included in TDB 2020.

IUPAC, as well as NEA (see, e.g., Grenthe et al. 1992) used the specific ion interaction theory (SIT) for making ionic strength corrections to the experimental data, an approach which is also adopted for TDB 2020 (as has been for all its predecessors). Powell et al. (2013) only evaluated experiments in perchlorate media and explicitly considered the formation of zinc chloride complexes. Therefore, ion interaction coefficients ε for cationic zinc species with Cl^- are missing. They can be approximated by the corresponding interaction coefficients with ClO_4^-, e.g. $\varepsilon(Zn^{2+}, Cl^-) \approx \varepsilon(Zn^{2+}, ClO_4^-) = (0.35 \pm 0.01)$ kg · mol^{-1}.

In some cases, the ion interaction coefficients of zinc species were not available. We approximated these with the estimation method described in Section 1.5.3, which draws on a statistical analysis of published SIT ion interaction coefficients and which allows the estimation of missing coefficients for the interaction of cations with Cl^- and ClO_4^-, and for the interaction of anions with Na^+, from the charge of the cations or anions of interest.

The selected SIT ion interaction coefficients for zinc species are presented in Tab. 32-3.

32.2 Elemental zinc

Zinc metal and gas are not relevant under environmental conditions. Hence, the gas phase Zng is not included in the data base. The absolute entropy and heat capacity of Zn(cr) are included as they are used for the calculation of certain thermodynamic reaction properties.

The selected values for Zn(cr) are taken from CODATA (Cox et al. 1989):

$S_m°(Zn, cr, 298.15\ K) = (41.630 \pm 0.150)\ J \cdot K^{-1} \cdot mol^{-1}$

$C_{p,m}°(Zn, cr, 298.15\ K) = (25.390 \pm 0.040)\ J \cdot K^{-1} \cdot mol^{-1}$

32.3 Zinc(II)

32.3.1 Zinc(II) aqua ion

Zinc(II) exists as the Zn^{2+} cation in aqueous solutions. The selected thermodynamic values for Zn^{2+} are taken from CODATA (Cox et al. 1989):

$\Delta_f G_m°(Zn^{2+}, 298.15\ K) = -(147.203 \pm 0.254)\ kJ \cdot mol^{-1}$

$\Delta_f H_m°(Zn^{2+}, 298.15\ K) = -(153.390 \pm 0.200)\ kJ \cdot mol^{-1}$

$S_m°(Zn^{2+}, 298.15\ K) = -(109.800 \pm 0.500)\ J \cdot K^{-1} \cdot mol^{-1}$

Using the selected CODATA $\Delta_f G_m°(Zn^{2+})$ and $\Delta_f H_m°(Zn^{2+})$, the redox equilibrium

$$Zn(cr) \rightleftharpoons Zn^{2+} + 2e^-$$

is calculated as

$\log_{10} K°(298.15\ K) = 25.79 \pm 0.04$

$\Delta_r H_m°(298.15\ K) = -(153.39 \pm 0.2)\ kJ \cdot mol^{-1}$

Powell et al. (2013) determined from mean activity and osmotic coefficients the SIT interaction parameters $\varepsilon(Zn^{2+}, ClO_4^-) = (0.351 \pm 0.005)$ and $\varepsilon(Zn^{2+}, ClO_4^-) = (0.351 \pm 0.010)\ kg \cdot mol^{-1}$, respectively. These values are in good agreement with $\varepsilon(Zn^{2+}, ClO_4^-) = (0.33 \pm 0.03)\ kg \cdot mol^{-1}$ (Grenthe et al. 1992), most probably derived from the same experimental data. This review selects

$\varepsilon(Zn^{2+}, ClO_4^-) = (0.35 \pm 0.01)\ kg \cdot mol^{-1}$

and estimated

$\varepsilon(Zn^{2+}, Cl^-) \approx \varepsilon(Zn^{2+}, ClO_4^-) = (0.35 \pm 0.01)$ kg · mol^{-1}

32.3.2 Zinc(II) (hydr)oxide compounds and complexes

32.3.2.1 Zinc(II) hydroxide complexes

Powell et al. (2013) report that the hydrolysis of Zn^{2+} has been studied at low ionic strength (with data extrapolated or corrected to I = 0) for a wide range of temperatures, enabling stability constants at zero ionic strength and 25 °C to be determined with a high degree of certainty.

However, less certain is the behaviour of the system Zn^{2+} – OH^- with changes in ionic strength, because of the paucity of accepted data over a range of fixed ionic strengths. Thus, the SIT ion interaction coefficients determined by Powell et al. (2013) should be viewed, at best, as provisional. In summary, Powell et al. (2013) report

$Zn^{2+} + H_2O(l) \rightleftharpoons ZnOH^+ + H^+$

$\log_{10}{}^*\beta_1° (298.15\ K) = -8.96 \pm 0.05$

$\Delta\varepsilon(1) = (0.03 \pm 0.02)$ kg · mol^{-1}

$\Delta_r H_m°(298.15\ K) = (56.8 \pm 0.9)$ kJ · mol^{-1}

$Zn^{2+} + 2H_2O(l) \rightleftharpoons Zn(OH)_2(aq) + 2H^+$

$\log_{10}{}^*\beta_2° (298.15\ K) = -17.82 \pm 0.08$

$\Delta\varepsilon(2) = (0.18 \pm 0.04)$ kg · mol^{-1}

$\Delta_r H_m°(298.15\ K) = (109 \pm 4)$ kJ · mol^{-1}

$Zn^{2+} + 3H_2O(l) \rightleftharpoons Zn(OH)_3^- + 3H^+$

$\log_{10}{}^*\beta_3° (298.15\ K) = -28.05 \pm 0.05$

$\Delta\varepsilon(3) = (0.19 \pm 0.06)$ kg · mol^{-1}

$\Delta_r H_m°(298.15\ K) = (151 \pm 3)$ kJ · mol^{-1}

$Zn^{2+} + 4H_2O(l) \rightleftharpoons Zn(OH)_4^{2-} + 4H^+$

$\log_{10}{}^*\beta_4° (298.15\ K) = -40.41 \pm 0.12$

$\Delta\varepsilon(4) = (0.46 \pm 0.04)$ kg · mol^{-1}

$\Delta_r H_m°(298.15\ K) = (188 \pm 6)$ kJ · mol^{-1}

Powell et al. (2013) state that all $\log_{10}{}^*\beta_x°$ and $\Delta_r H_m°$ values have been determined at 25 °C from the temperature dependence of the respective equilibrium and they are all recommended.

Concerning $\Delta_r H_m°$ values Powell et al. (2013) state that only $\log_{10}{}^*\beta_1$ "was found to have a linear dependence on T^{-1}. In this case, the van't Hoff equation could be used to determine the standard enthalpy change (from the slope of the regression line) and the entropy change (from the intercept). For the other three species, the enthalpy change has been determined from the gradient at T = 298.15 K of the temperature dependence of the respective stability constant."

Powell et al. (2013) do not reveal what kind of non-linear function they fitted to the data (their Figs. A4-3, A4-4 and A4-6) and how the gradient at 25 °C was determined. Furthermore, no argument is provided why they did not directly fit $\Delta_r H_m°$ and $\Delta C_{p,m}°$ values in these cases.

The SIT interaction parameters $\Delta\varepsilon(1)$, $\Delta\varepsilon(3)$ and $\Delta\varepsilon(4)$ have been determined by Powell et al. (2013) from SIT analyses where the values for $\log_{10}{}^*\beta_x°$ were fixed at the values derived from the temperature dependence and additional 3 values at 2 and 4 M $NaClO_4$ for $\Delta\varepsilon(1)$, and 2 values at 3 M $NaClO_4$ for $\Delta\varepsilon(3)$ and $\Delta\varepsilon(4)$. All these $\Delta\varepsilon(x)$ values are considered "provisional".

In the absence of reliable experimental values at I > 0, a value for $\Delta\varepsilon(2)$ in $NaClO_4$ medium has been estimated by Powell et al. (2013) by assuming that the interaction coefficient $\varepsilon(Zn(OH)_2(aq), NaClO_4) = (0.25 \pm 0.03)$, is "the average of the values found for $\varepsilon(ZnCO_3(aq), NaClO_4)$ and $\varepsilon(ZnCl_2(aq), NaClO_4)$, where the uncertainty is chosen to span the range in the two values". Using $\Delta\varepsilon$ values reported by Powell et al. (2013) this review calculated: $\varepsilon(ZnCl_2(aq), NaClO_4) = (0.21 \pm 0.04)$ (see Section 3.3.1), close to the above estimate, but in total contradiction to $\varepsilon(ZnCO_3(aq), NaClO_4) = (0.08 \pm 0.58)$ (see Section 32.3.4.1). Hence, the estimate of $\Delta\varepsilon(2)$ is rejected by this review.

Brown & Ekberg (2016) scrutinised the same data sets as Powell et al. (2013) and report

$Zn^{2+} + H_2O(l) \rightleftharpoons ZnOH^+ + H^+$

$\log_{10}{}^*\beta_1° (298.15\ K) = -8.94 \pm 0.06$

$\Delta\varepsilon(1) = -(0.02 \pm 0.01)\ kg \cdot mol^{-1}$

$\Delta_r H_m°(298.15\ K) = (56.7 \pm 0.7)\ kJ \cdot mol^{-1}$

$Zn^{2+} + 2H_2O(l) \rightleftharpoons Zn(OH)_2(aq) + 2H^+$

$\log_{10}{}^*\beta_2° (298.15\ K) = -17.89 \pm 0.15$

$\Delta_r H_m°(298.15\ K) = (107.1 \pm 3.1)\ kJ \cdot mol^{-1}$

$\Delta_r C_{p,m}°(298.15\ K) = -(65 \pm 27)\ J \cdot K^{-1} \cdot mol^{-1}$

$Zn^{2+} + 3H_2O(l) \rightleftharpoons Zn(OH)_3^- + 3H^+$

$\log_{10}{}^*\beta_3° (298.15\ K) = -27.98 \pm 0.10$

$\Delta\varepsilon(3) = (0.14 \pm 0.05)\ kg \cdot mol^{-1}$

$\Delta_r H_m°(298.15\ K) = (143.5 \pm 2.5)\ kJ \cdot mol^{-1}$

$\Delta_r C_{p,m}°(298.15\ K) = -(196 \pm 23)\ J \cdot K^{-1} \cdot mol^{-1}$

$Zn^{2+} + 4H_2O(l) \rightleftharpoons Zn(OH)_4^{2-} + 4H^+$

$\log_{10}{}^*\beta_4^\circ$ (298.15 K) = -40.35 ± 0.22

$\Delta\varepsilon(4) = (0.19 \pm 0.09)$ kg · mol^{-1}

$\Delta_r H_m^\circ(298.15\ K) = (178.3 \pm 5.8)$ kJ · mol^{-1}

$\Delta_r C_{p,m}^\circ(298.15\ K) = -(348 \pm 56)$ J · K^{-1} · mol^{-1}

All $\log_{10}{}^*\beta_x^\circ$ values reported by Brown & Ekberg (2016) are in excellent agreement with the results of Powell et al. (2013), considering their assigned uncertainties. Also, the $\Delta_r H_m^\circ$ values for the first hydrolysis reaction (the "linear dependence on T^{-1}" in the temperature range 15 – 350 °C) are in perfect agreement. Of course, the "gradient" $\Delta_r H_m^\circ$ values of Powell et al. (2013) disagree with the full set of $\Delta_r H_m^\circ$ plus $\Delta C_{p,m}^\circ$ values of Brown & Ekberg (2016) in the other three cases, determined in the temperature ranges 20 – 350 °C, 12 – 350 °C and 12 – 350 °C, respectively.

For consistency reasons, especially with the derived SIT interaction parameters (see below), the entire set of $\log_{10}{}^*\beta_x^\circ$, $\Delta_r H_m^\circ$ and $\Delta C_{p,m}^\circ$ values reported by Brown & Ekberg (2016) is included in TDB 2020.

Considering the $\Delta\varepsilon(1)$ and $\Delta\varepsilon(3)$ values, determined by Brown & Ekberg (2016) by the same procedure as Powell et al. (2013) (see above), and using the reported values $\varepsilon(Zn^{2+}, ClO_4^-) = (0.35 \pm 0.01)$ kg · mol^{-1} and $\varepsilon(H^+, ClO_4^-) = (0.14 \pm 0.02)$ kg · mol^{-1} (Tab. 32-3) this review calculated the new values

$\varepsilon(ZnOH^+, ClO_4^-) = (0.19 \pm 0.02)$ kg · mol^{-1}

$\varepsilon(Na^+, Zn(OH)_3^-) = (0.07 \pm 0.06)$ kg · mol^{-1}

and estimated

$\varepsilon(ZnOH^+, Cl^-) \approx \varepsilon(ZnOH^+, ClO_4^-) = (0.19 \pm 0.02)$ kg · mol^{-1}

$\varepsilon(Zn(OH)_2(aq), NaCl) \approx \varepsilon(Zn(OH)_2(aq), NaClO_4) = (0.0 \pm 0.1)$ kg · mol^{-1}

The discrepant $\Delta\varepsilon(4)$ values determined by Brown & Ekberg (2016) and by Powell et al. (2013) are both wrong. Brown & Ekberg (2016) erroneously used $\Delta z^2 = 2$ for reaction

$Zn^{2+} + 4H_2O(l) \rightleftharpoons Zn(OH)_4^{2-} + 4H^+$

leading to the term $-2D$ in their calculations (Fig. 11.96 in Brown & Ekberg 2016). Using the correct value $\Delta z^2 = 4$, leading to the term $-4D$, this review calculated from the data given by Brown & Ekberg (2016)

$\Delta\varepsilon(4) = (0.34 \pm 0.07)$ kg · mol^{-1}

$\varepsilon(Na^+, Zn(OH)_4^{2-}) = (0.13 \pm 0.08)$ kg · mol^{-1}

Using the data given by Powell et al. (2013) this review calculated $\Delta\varepsilon(4) = (0.30 \pm 0.04)$ kg · mol^{-1}. The reason for the erroneous value given by Powell et al. (2013) (their Fig. A4-7) is unclear, perhaps they used $+4\log_{10} a_W$ instead of $-4\log_{10} a_W$ in their calculations.

For the formation of the dimeric hydrolysis species of zinc(II)

$$2Zn^{2+} + H_2O(l) \rightleftharpoons Zn_2OH^{3+} + H^+$$

Powell et al. (2013) and Brown & Ekberg (2016) used the same data and the same procedure to derive stability constants and SIT interaction coefficients: Three values measured in 2 and 3 M NaCl/KCl media were used for SIT regression analyses resulting in $\log_{10}{}^*\beta_{2,1}^\circ$ (298.15 K) = -7.9 ± 0.3 and $\log_{10}{}^*\beta_{2,1}^\circ$ (298.15 K) = -7.89 ± 0.31, and $\Delta\varepsilon \approx 0$ and $\Delta\varepsilon = (0.02 \pm 0.01)$, respectively. The zero ionic strength stability constant has been used, in turn, with three values measured in 3 M $NaClO_4$/LiClO4 media, to determine the ion interaction coefficient for the interaction with perchloride media: $\Delta\varepsilon = (0.3 \pm 0.1)$ and $\Delta\varepsilon = (0.35 \pm 0.10)$, respectively. The values

$$\log_{10}{}^*\beta_{2,1}^\circ \text{ (298.15 K)} = -7.9 \pm 0.3$$

$$\Delta\varepsilon = (0.3 \pm 0.1) \text{ kg} \cdot \text{mol}^{-1}$$

are included in TDB 2020.

Using the reported values $\varepsilon(Zn^{2+}, ClO_4^-) = (0.35 \pm 0.01)$ kg · mol^{-1} and $\varepsilon(H^+, ClO_4^-) = (0.14 \pm 0.02)$ kg mol^{-1} (Tab. 32-3) this review calculated the new value

$$\varepsilon(Zn_2OH^{3+}, ClO_4^-) = (0.86 \pm 0.10) \text{ kg} \cdot \text{mol}^{-1}$$

and estimated

$$\varepsilon(Zn_2OH^{3+}, Cl^-) \approx \varepsilon(Zn_2OH^{3+}, ClO_4^-) = (0.86 \pm 0.10) \text{ kg} \cdot \text{mol}^{-1}$$

32.3.2.2 Zinc(II) (hydr)oxide compounds

Powell et al. (2013) report that there are several different phases of zinc oxide and hydroxide. These include ZnO(s), α-$Zn(OH)_2$(s), β_1-$Zn(OH)_2$(s), β_2-$Zn(OH)_2$(s), γ-$Zn(OH)_2$(s), δ-$Zn(OH)_2$(s), and ε-$Zn(OH)_2$(s). The solubility of each hydroxide phase as well as active and inactive ZnO(s) and amorphous $Zn(OH)_2$ has been determined. However, many solubility studies have been performed where the solid phase was not characterised; results from such studies were not accepted by Powell et al. (2013).

Powell et al. (2013) state that solubility constant data have been reported for the acid dissolution reaction of ZnO(s), zincite,

$$ZnO(s) + 2H^+ \rightleftharpoons Zn^{2+} + H_2O(l)$$

over a wide range of temperature. The majority of these data were determined in dilute solutions, or over a range of ionic strengths using a non-complexing medium and were corrected by the original authors to I = 0. The data from different sources join smoothly across the whole experimental temperature range (25 – 300 °C) and show a linear dependence on T^{-1}. From these data Powell et al. (2013) determined

$$\log_{10}{}^{*}K_{s0}^{\circ}\ (298.15\ \mathrm{K}) = 11.12 \pm 0.05$$

$$\Delta_r H_m^{\circ}(298.15\ \mathrm{K}) = -(86.7 \pm 1.7)\ \mathrm{kJ \cdot mol^{-1}}$$

Brown & Ekberg (2016) scrutinised the same data and report $\log_{10}{}^{*}K_{s0}^{\circ}$ (298.15 K) = 11.11 ± 0.10 and $\Delta_r H_m^{\circ}$(298.15 K) = -(86.7 ± 1.0) kJ · mol^{-1}, in perfect agreement with Powell et al. (2013).

CODATA (Cox et al. 1989) report for ZnO(cr) the values

$$\Delta_f G_m^{\circ}(\mathrm{ZnO, cr}, 298.15\ \mathrm{K}) = -(320.479 \pm 0.299)\ \mathrm{kJ \cdot mol^{-1}}$$

$$\Delta_f H_m^{\circ}(\mathrm{ZnO, cr}, 298.15\ \mathrm{K}) = -(350.460 \pm 0.270)\ \mathrm{kJ \cdot mol^{-1}}$$

$$S_m^{\circ}(\mathrm{ZnO, cr}, 298.15\ \mathrm{K}) = (43.65 \pm 0.400)\ \mathrm{J \cdot K^{-1} \cdot mol^{-1}}$$

Using the CODATA values $\Delta_f G_m^{\circ}(H_2O, l, 298.15\ K) = -(237.140 \pm 0.041)$ kJ · mol^{-1} and $\Delta_f G_m^{\circ}(Zn^{2+}, 298.15\ K)$ (see Section 3.1) this review calculates

$$\log_{10}{}^{*}K_{s0}^{\circ}\ (298.15\ \mathrm{K}) = 11.19 \pm 0.07$$

in good agreement with the values reported by Powell et al. (2013) and Brown & Ekberg (2016).

Using the CODATA values $\Delta_f H_m^{\circ}(H_2O, l, 298.15\ K) = -(285.830 \pm 0.040)$ kJ · mol^{-1} and $\Delta_f H_m^{\circ}(Zn^{2+}, 298.15\ K)$ (see Section 3.1) this review calculates

$$\Delta_r H_m^{\circ}(298.15\ \mathrm{K}) = -(88.76 \pm 0.34)\ \mathrm{kJ \cdot mol^{-1}}$$

in fair agreement with the values reported by Powell et al. (2013) and Brown & Ekberg (2016).

The temperature dependent data, from which Powell et al. (2013) and Brown & Ekberg (2016) derived their $\log_{10}{}^{*}K_{s0}^{\circ}$ and $\Delta_r H_m^{\circ}$ values, have been published after the CODATA team finished their project. However, simply replacing the CODATA values for ZnO(cr) with these new values would lead to internal inconsistencies, because the CODATA value for $\Delta_f H_m^{\circ}(Zn^{2+}, 298.15\ K)$ has been calculated from measurements of the enthalpy of solution of ZnO(cr) in aqueous $HClO_4$, which in turn was used to determine $\Delta_f H_m^{\circ}$(ZnO, cr, 298.15 K).

On the other hand, the difference in calculated stability constants as a function of temperature, $\log_{10}{}^{*}K_{s0}^{\circ}$(CODATA) – $\log_{10}{}^{*}K_{s0}^{\circ}$(Powell et al. 2013) decreases from 0.07 at 25 °C to 0.00 at 100 °C, then leading to -0.06 at 200 °C, and finally to -0.10 at 300 °C.

Hence, this review decided to retain the CODATA values for ZnO(cr), which reproduce, within experimental uncertainties, very well the new data in the temperature range 25 – 300 °C.

The acid dissolution of ε-$Zn(OH)_2$(s), wülfingite,

$$\varepsilon\text{-}Zn(OH)_2(s) + 2H^+ \rightleftharpoons Zn^{2+} + 2\ H_2O(l)$$

has also been studied over a wide range of temperature, although not as wide as that for ZnO(s). The data from different sources join smoothly across the whole experimental temperature range (12.5 – 75 °C) and show a linear dependence on T^{-1}. From these data Powell et al. (2013) determined

$$\log_{10}{}^*K_{s0}^\circ\ (298.15\ K) = 11.38 \pm 0.20$$

$$\Delta_r H_m^\circ(298.15\ K) = -(100 \pm 11)\ kJ \cdot mol^{-1}$$

which are both classified as "provisional" values and have been included in TDB 2020.

Brown & Ekberg (2016) scrutinised the same data and report $\log_{10}{}^*K_{s0}^\circ$ (298.15 K) = 11.38 ± 0.20 and $\Delta_r H_m^\circ$(298.15 K) = -(99.0 ± 3.7) kJ · mol^{-1}, in excellent agreement with Powell et al. (2013).

Powell et al. (2013) recommend further solubility constants for β$_1$-$Zn(OH)_2$(s), β$_2$-$Zn(OH)_2$(s), γ-$Zn(OH)_2$(s) and δ-$Zn(OH)_2$(s), in the range of $\log_{10}{}^*K_{s0}^\circ$ (298.15 K) = (11.70 – 11.81) ± 0.04). As all these hydroxide phases are slightly more soluble than ε-$Zn(OH)_2$(s) they are not included in TDB 2020.

32.3.3 Zinc(II) chloride compounds and complexes

32.3.3.1 Zinc(II) chloride complexes

Zinc(II) appears to form up to four consecutive chloride complexes in aqueous solution:

$$Zn^{2+} + Cl^- \rightleftharpoons ZnCl^+$$

$$Zn^{2+} + 2Cl^- \rightleftharpoons ZnCl_2(aq)$$

$$Zn^{2+} + 3Cl^- \rightleftharpoons ZnCl_3^-$$

$$Zn^{2+} + 4Cl^- \rightleftharpoons ZnCl_4^{2-}$$

For the first three complexes Powell et al. (2013) recommend stability constants and SIT interaction parameters, derived from weighted linear SIT regression analyses of data in $NaClO_4$ or $LiClO_4$ media in the first two cases, and from data in $NaClO_4$ media alone in the third case.

$$\log_{10}K_1^\circ\ (298.15\ K) = 0.40 \pm 0.09$$

$$\Delta\varepsilon = -(0.14 \pm 0.02)\ kg \cdot mol^{-1}$$

$\log_{10}\beta_2°$ (298.15 K) = 0.69 ± 0.15

$\Delta\varepsilon$ = -(0.20 ± 0.04) kg · mol^{-1}

$\log_{10}\beta_3°$ (298.15 K) = 0.48 ± 0.54

$\Delta\varepsilon$ = -(0.27 ± 0.13) kg · mol^{-1}

These values have been included in TDB 2020.

The $\Delta\varepsilon$ values derived by Powell et al. (2013), together with the reported values $\varepsilon(Zn^{2+}, ClO_4^-)$ = (0.35 ± 0.01) kg · mol^{-1} and $\varepsilon(Cl^-, Na^+)$ = (0.03 ± 0.01) kg · mol^{-1} (Tab. 32-3) were used to calculate the new values

$\varepsilon(ZnCl^+, ClO_4^-)$ = (0.24 ± 0.02) kg · mol^{-1}

$\varepsilon(ZnCl_2(aq), NaClO_4)$ = (0.21 ± 0.04) kg · mol^{-1}

$\varepsilon(Na^+, ZnCl_3^-)$ = (0.17 ± 0.13) kg · mol^{-1}

as well as the estimates

$\varepsilon(ZnCl^+, Cl^-) \approx \varepsilon(ZnCl^+, ClO_4^-)$ = (0.24 ± 0.02) kg · mol^{-1}

$\varepsilon(ZnCl_2(aq), NaCl) \approx \varepsilon(ZnCl_2(aq), NaClO_4)$ = (0.21 ± 0.04) kg · mol^{-1}

Powell et al. (2013) state that "some authors have reported stability constants for the 1:4 complex based on their evaluations of emf data. However, the data are too scattered to be evaluated with confidence. It is therefore not possible to give even an indicative value for the formation constant of $ZnCl_4^{2-}$."

For at least a rough estimate, this review has chosen the data set reported by Fedorov et al. (1978). Their stability constants for the 1:1, 1:2 and 1:3 complexes, measured at 3 and 4 M $NaClO_4$, have been included by Powell et al. (2013) in their SIT analyses, showing an average deviation of -0.2 $\log_{10}$-units from their linear regression lines. Using the value reported by Fedorov et al. (1978) for the 1:4 complex at 3 and 4 M $NaClO_4$, extrapolated to zero ionic strength with SIT interaction coefficients given in Tab. 32-3, results in $\log_{10}\beta_4°$ (298.15 K) = -2.0 ± 0.4 and -2.4 ± 0.5, respectively. Hence, the estimate

$\log_{10}\beta_4°(298.15\ K) = \approx -2$

is included in TDB 2020 as supplemental datum, as well as the estimate

$\varepsilon(Na^+, ZnCl_4^{2-}) = -(0.10 \pm 0.10)$ kg · mol^{-1}

32.3.3.2 Zinc(II) chloride compounds

The chemical literature reports that five hydrates of zinc chloride are known: $ZnCl_2 \cdot nH_2O(s)$ with n = 1, 1.5, 2.5, 3 and 4. The tetrahydrate $ZnCl_2 \cdot 4H_2O(s)$ precipitates from aqueous solutions of zinc chloride. They are all highly soluble in water. Anhydrous $ZnCl_2(s)$ itself is hygroscopic and even deliquescent.

None of these highly soluble salts is included in TDB 2020.

32.3.4 Zinc(II) carbonate compounds and complexes

32.3.4.1 Zinc(II) carbonate complexes

Powell et al. (2013) state that the only experimental values for the formation of $ZnCO_3(aq)$ are those obtained by Bilinski et al. (1976) using 0.101 mol · kg^{-1} KNO_3 as the supporting electrolyte and Stanley & Byrne (1990) using a synthetic seawater medium consisting of a NaCl – $NaClO_4$ mixture at $[Cl^-]_{total}$ = 0.55 mol · kg^{-1} and I_m = 0.68 mol · kg^{-1}. A SIT analysis by Powell et al. (2013) using the two values provided the following formation constant estimate and ion interaction coefficient:

$$Zn^{2+} + CO_3^{2-} \rightleftharpoons ZnCO_3(aq)$$

$$\log_{10}K_1^\circ\ (298.15\ K) = 4.76 \pm 0.35$$

$$\Delta\varepsilon = -(0.19 \pm 0.58)\ kg \cdot mol^{-1}$$

Powell et al. (2013) further used the observation of Stanley & Byrne (1990) that their $\log_{10}K_1^\circ$ value for $ZnCO_3(aq)$ was 2.06 smaller than that for $CuCO_3(aq)$ to estimate $\log_{10}K_1^\circ = 4.69 \pm 0.09$.

Powell et al. (2013) used a similar observation of Bilinski et al. (1976) of a 0.4 difference in their $\log_{10}K_1$ values for $CdCO_3(aq)$ and $ZnCO_3(aq)$ to estimate $\log_{10}K_1^\circ = 4.8 \pm 0.2$ for $ZnCO_3(aq)$.

An unweighted average of the above estimates calculated by Powell et al. (2013) gives a "provisional" value of

$$\log_{10}K_1^\circ\ (298.15\ K) = 4.75 \pm 0.06$$

where the listed uncertainty reflects the range of the three values.

This value is included in TDB 2020, as well as the estimate

$$\varepsilon(ZnCO_3(aq), NaCl) \approx \varepsilon(ZnCO_3(aq), NaClO_4) = (0.0 \pm 0.1)\ kg \cdot mol^{-1}$$

Note that the value $\log_{10}K_1^\circ = 4.75 \pm 0.05$ is given by Powell et al. (2013) in their Tab. 32-3, somewhat inconsistent with the above statement about ranges.

The $\Delta\varepsilon$ value is poorly defined but nevertheless can serve as an indicative estimate of $\varepsilon(ZnCO_3(aq), NaCl, NaClO_4)$, calculated using the reported values $\varepsilon(Zn^{2+}, ClO_4^-) = (0.35 \pm 0.01)$ kg · mol^{-1} and $\varepsilon(CO_3^{2-}, Na^+) = -(0.08 \pm 0.05)$ kg · mol^{-1} (Tab. 32-3) as $\varepsilon(ZnCO_3(aq), NaCl) \approx \varepsilon(ZnCO_3(aq), NaClO_4) = (0.08 \pm 0.58)$ kg · mol^{-1}. Due to its large uncertainty, this value is compatible with the assumption of zero for uncharged species and thus, this review prefers the estimate

$$\varepsilon(ZnCO_3(aq), NaCl) \approx \varepsilon(ZnCO_3(aq), NaClO_4) = (0.0 \pm 0.1) \text{ kg} \cdot \text{mol}^{-1}$$

For the formation of $Zn(CO_3)_2^{2-}$ according to the reaction

$$Zn^{2+} + 2CO_3^{2-} \rightleftharpoons Zn(CO_3)_2^{2-}$$

Powell et al. (2013) accepted the value $\log_{10}\beta_2$ (298.15 K) = 5.4 ± 0.6 derived from Stanley & Byrne (1990) data, but state that it was poorly defined due to the very small extent of $Zn(CO_3)_2^{2-}$ formation in their "synthetic seawater" solutions at $I_m = 0.68$ mol · kg^{-1}. Combining this $\log_{10}\beta_2$ with $\log_{10}K_1$ from Stanley & Byrne (1990) results in an estimate for the isocoulombic reaction

$$ZnCO_3(aq) + CO_3^{2-} \rightleftharpoons Zn(CO_3)_2^{2-}$$

$$\log_{10}K_2 \text{ (298.15 K)} = 2.0 \pm 0.6$$

Considering the estimated $\Delta\varepsilon = -(0.02 \pm 0.15)$, derived from values in Tab. 32-3, this review obtained

$$\log_{10}K_2^\circ \text{ (298.15 K)} = 2.0 \pm 0.6$$

$$\log_{10}\beta_2^\circ \text{ (298.15 K)} = 6.75 \pm 0.6$$

The latter value is included in TDB 2020, as well as the estimate

$$\varepsilon(Na^+, Zn(CO_3)_2^{2-}) = -(0.10 \pm 0.10) \text{ kg} \cdot \text{mol}^{-1}$$

Powell et al. (2013) report that three investigations (Ryan & Bauman 1978, Ferri et al. 1985, Stanley & Byrne 1990) have provided results which they used for a SIT analysis in order to obtain the following formation constant estimate and ion interaction coefficient:

$$Zn^{2+} + HCO_3^- \rightleftharpoons ZnHCO_3^+$$

$$\log_{10}K \text{ (298.15 K)} = 1.62 \pm 0.10$$

$$\Delta\varepsilon = (0.10 \pm 0.04) \text{ kg} \cdot \text{mol}^{-1}$$

These values are included in TDB 2020.

Using $\Delta\varepsilon$ and the reported values $\varepsilon(Zn^{2+}, ClO_4^-) = (0.35 \pm 0.01)$ kg · mol^{-1} and $\varepsilon(Na^+, HCO_3^-) = (0.00 \pm 0.02)$ kg · mol^{-1}, this review obtained the new values

$$\varepsilon(ZnHCO_3^+, Cl^-) \approx \varepsilon(ZnHCO_3^+, ClO_4^-) = (0.45 \pm 0.05) \text{ kg} \cdot \text{mol}^{-1}$$

Powell et al. (2013) provide a value for the formation constant for the reaction

$$2Zn^{2+} + CO_3^{2-} \rightleftharpoons Zn_2CO_3^{2+}$$

$$\log_{10}\beta_{2,1} \text{ (298.15 K)} = 4.04 \pm 0.20$$

based on an experimental study by Ferri et al. (1985) at $I_m = 3.503$ mol · kg^{-1}. However, Powell et al. (2013) did not include this constant in their summary Tab. 32-3, although they discuss it in the text.

Using the reported values $\varepsilon(Zn^{2+}, ClO_4^-) = (0.35 \pm 0.01)$ kg · mol^{-1}, $\varepsilon(CO_3^{2-}, Na^+) = -(0.08 \pm 0.05)$ kg · mol^{-1} and the estimate $\varepsilon(Zn_2CO_3^{2+}, ClO_4^-) = (0.4 \pm 0.1)$ kg · mol^{-1} (Tab. 32-3) this review calculated $\Delta\varepsilon = -(0.22 \pm 0.11)$ kg · mol^{-1}, which was used to extrapolate $\log_{10}\beta_{2,1}$ to $I = 0$:

$$\log_{10}\beta_{2,1}^\circ \text{ (298.15 K)} = 5.3 \pm 0.4$$

This value is included in TDB 2020, as well as the estimate

$$\varepsilon(Zn_2CO_3^{2+}, Cl^-) \approx \varepsilon(Zn_2CO_3^{2+}, ClO_4^-) = (0.4 \pm 0.1) \text{ kg} \cdot \text{mol}^{-1}$$

32.3.4.2 Zinc(II) carbonate compounds

$ZnCO_3$(s) (smithsonite)

Solubility constants have been reported for the acid dissolution of $ZnCO_3$(s) (smithsonite) over a range of ionic strengths in $NaClO_4$ at 25 °C by Schindler et al. (1969), at $I_m = 0.202$ mol · kg^{-1}, and Preis et al. (2000), at $I_m = 1.0$, 2.0 and 3.0 mol · kg^{-1}, which are broadly consistent. Powell et al. (2013) used only the highly coherent data of Preis et al. (2000) for an SIT analysis and obtained

$$ZnCO_3(s) + 2H^+ \rightleftharpoons Zn^{2+} + H_2O(l) + CO_2g$$

$$\log_{10}K_{ps0}^\circ = 7.21 \pm 0.04$$

$$\Delta\varepsilon = (0.09 \pm 0.02) \text{ kg} \cdot \text{mol}^{-1}$$

Powell et al. (2013) regarded these data as "provisional" and included both of them in their summary Tab. 32-3.

Note that $\Delta\varepsilon$ is in excellent agreement with $\Delta\varepsilon = (0.07 \pm 0.03)$ kg · mol^{-1} calculated from the reported values $\varepsilon(Zn^{2+}, ClO_4^-) = (0.35 \pm 0.01)$ kg · mol^{-1} and $\varepsilon(H^+, ClO_4^-) = (0.14 \pm 0.02)$ kg · mol^{-1} (Tab. 32-3).

The temperature dependence of the above equilibrium was examined by Preis et al. (2000) between 15 and 65 °C at I_m = 1.0 mol · kg^{-1} $NaClO_4$. Powell et al. (2013) used these data in a linear $\log_{10}K$ vs $1/T$ regression analysis (their Fig. A4-18) and obtained a "provisional" value of

$$\Delta_r H_m°(298.15\ K) = -(8.2 \pm 1.3)\ kJ \cdot mol^{-1}$$

For unknown reasons Powell et al. (2013) did not include this value in their summary Tab. 32-3.

Combining the above solubility constant $\log_{10}K_{ps0}°$ and $\Delta_r H_m°$ with the CODATA values for the equilibrium $CO_2g + H_2O(l) \rightleftharpoons 2H^+ + CO_3^{2-}$ ($\log_{10}K° = -18.152 \pm 0.073$, $\Delta_r H_m° = -4.11 \pm 0.28$) this review obtained

$$ZnCO_3(s) \rightleftharpoons Zn^{2+} + CO_3^{2-}$$

$$\log_{10}K_{s0}° = -10.94 \pm 0.08$$

$$\Delta_r H_m°(298.15\ K) = -(4.1 \pm 1.3)\ kJ \cdot mol^{-1}$$

These values are included in TDB 2020.

$Zn_5(OH)_6(CO_3)_2(s)$ (hydrozincite)

Solubility constants have been reported for the acid dissolution of $Zn_5(OH)_6(CO_3)_2(s)$ (hydrozincite) over a range of ionic strengths in $NaClO_4$ by Schindler et al. (1969) and Preis & Gamsjäger (2001). Powell et al. (2013) used these data for an SIT analysis and obtained

$$0.2Zn_5(OH)_6(CO_3)_2(s) + 2H^+ \rightleftharpoons Zn^{2+} + 1.6H_2O(l) + 0.4CO_2g$$

$$\log_{10}K_{ps0}° = 9.07 \pm 0.09$$

$$\Delta\varepsilon = (0.12 \pm 0.05)\ kg \cdot mol^{-1}$$

Powell et al. (2013) regarded only $\log_{10}K_{ps0}°$ (but not $\Delta\varepsilon$) as "provisional" and included it in their summary Tab. 32-3.

Note that $\Delta\varepsilon$ is in good agreement with $\Delta\varepsilon = (0.07 \pm 0.03)$ kg · mol^{-1} calculated from the reported values $\varepsilon(Zn^{2+}, ClO_4^-) = (0.35 \pm 0.01)$ kg · mol^{-1} and $\varepsilon(H^+, ClO_4^-) = (0.14 \pm 0.02)$ kg · mol^{-1} (Tab. 32-3).

The temperature dependence of the above equilibrium was examined by Preis & Gamsjäger (2001) between 15 and 65 °C at I_m = 1.0 mol · kg^{-1} $NaClO_4$ who obtained a value of (Tab. 4 in Preis & Gamsjäger 2001)

$\Delta_r H_m° = -51.3 \text{ kJ} \cdot \text{mol}^{-1}$

This value is regarded as "provisional" by Powell et al. (2013). However, for unknown reasons Powell et al. (2013) did not include this value in their summary Tab. 32-3.

Combining the above solubility constant $\log_{10}K_{ps0}°$ and $\Delta_r H_m°$ with the CODATA values for the equilibrium $CO_2g + H_2O(l) \rightleftharpoons 2H^+ + CO_3^{2-}$ ($\log_{10}K° = -18.152 \pm 0.073$, $\Delta_r H_m° = -4.11 \pm 0.28$) this review obtained

$Zn_5(OH)_6(CO_3)_2(s) + 6H^+ \rightleftharpoons 5Zn^{2+} + 2CO_3^{2-} + 6H_2O(l)$

$\log_{10}{}^*K_{s0}° = 9.05 \pm 0.10$

$\Delta_r H_m°(298.15 \text{ K}) = -(248 \pm 15) \text{ kJ} \cdot \text{mol}^{-1}$

The uncertainty of $\Delta_r H_m°$ has been assigned by this review considering the discussion by Preis & Gamsjäger (2001) about the appropriate uncertainty of their derived value $\Delta_f H_m°$ for hydrozincite.

These values are included in TDB 2020.

32.3.5 Zinc(II) phosphate compounds and complexes

32.3.5.1 Zinc(II) phosphate complexes

Powell et al. (2013) state that the composition of the identified Zn(II) phosphate complexes strongly depends on the pH range, the total concentrations, and their ratios $[Zn(II)]_{total}:[PO_4^{3-}]_{total}$. As a consequence, the formation of eight differently protonated mono- and bis-complexes: $ZnH_2PO_4^+$, $Zn(H_2PO_4)_2(aq)$, $Zn(H_2PO_4)(HPO_4)^-$, $ZnHPO_4(aq)$, $Zn(HPO_4)_2^{2-}$, $Zn(HPO_4)_3^{4-}$, $Zn(HPO_4)(PO_4)^{3-}$ and $Zn(OH)_2(HPO_4)^{2-}$ have been proposed.

Powell et al. (2013) conclude that the diverse set of experimental conditions and speciation models adopted by different authors, allows the assignment of only one recommended value

$Zn^{2+} + HPO_4^{2-} \rightleftharpoons ZnHPO_4(aq)$

$\log_{10}K = 2.47 \pm 0.20$

at 25 °C and $I_m = 0.1$ mol kg^{-1}. Note that for unknown reasons the value $\log_{10}K = 2.44 \pm 0.20$ is given in the summary Tab. 5 of Powell et al. (2013).

This review obtained $\Delta\varepsilon = -(0.2 \pm 0.1)$ kg · mol^{-1}, assuming $\varepsilon(ZnHPO_4(aq), NaClO_4) = (0.0 \pm 0.1)$ kg · mol^{-1}, and using the reported values $\varepsilon(Zn^{2+}, ClO_4^-) = (0.35 \pm 0.01)$ kg · mol^{-1} and $\varepsilon(Na^+, HPO_4^{2-}) = -(0.15 \pm 0.06)$ kg · mol^{-1} (Tab. 32-3) for extrapolating the above $\log_{10}K$ to $I = 0$:

$\log_{10}K° \text{ (298.15 K)} = 3.3 \pm 0.2$

This value is included in TDB 2020, as well as the estimate

$$\varepsilon(ZnHPO_4(aq), NaCl) \approx \varepsilon(ZnHPO_4(aq), NaClO_4) = (0.0 \pm 0.1)\ kg \cdot mol^{-1}$$

The stability constants listed in Tab. A-3-12 of Powell et al. (2013) for the formation of other phosphate complexes can, in the absence of independent confirmation, only considered as "indicative" and hence, these values have been included in TDB 2020 as "supplemental data":

$$Zn^{2+} + H_2PO_4^- \rightleftharpoons ZnH_2PO_4^+$$
$$log_{10}K°\ (298.15\ K) = 0.9 \pm 0.2$$

$$Zn^{2+} + 2\ H_2PO_4^- \rightleftharpoons Zn(H_2PO_4)_2(aq)$$
$$log_{10}K°\ (298.15\ K) = 2.0 \pm 0.2$$

$$Zn^{2+} + H_2PO_4^- + HPO_4^{2-} \rightleftharpoons Zn(H_2PO_4)(HPO_4)^-$$
$$log_{10}K°\ (298.15\ K) = 4.0 \pm 0.5$$

$$Zn^{2+} + 2\ HPO_4^{2-} \rightleftharpoons Zn(HPO_4)_2^{2-}$$
$$log_{10}K°\ (298.15\ K) = 7.1 \pm 0.2$$

$$Zn^{2+} + 3\ HPO_4^{2-} \rightleftharpoons Zn(HPO_4)_3^{4-}$$
$$log_{10}K°\ (298.15\ K) = 7.4 \pm 0.2$$

$$Zn^{2+} + HPO_4^{2-} + PO_4^{3-} \rightleftharpoons Zn(HPO_4)(PO_4)^{3-}$$
$$log_{10}K°\ (298.15\ K) = 12.5 \pm 0.2$$

$$Zn(OH)_2(aq) + HPO_4^{2-} \rightleftharpoons Zn(OH)_2HPO_4^{2-}$$
$$log_{10}K°\ (298.15\ K) = 0.9 \pm 0.25$$

together with the estimates

$$\varepsilon(ZnH_2PO_4^+, Cl^-) \approx \varepsilon(ZnH_2PO_4^+, ClO_4^-) = (0.2 \pm 0.1)\ kg \cdot mol^{-1}$$

$$\varepsilon(Zn(H_2PO_4)_2(aq), NaCl) \approx \varepsilon(Zn(H_2PO_4)_2(aq), NaClO_4) = (0.0 \pm 0.1)\ kg \cdot mol^{-1}$$

$$\varepsilon(Na^+, Zn(H_2PO_4)(HPO_4)^-) = -(0.05 \pm 0.10)\ kg \cdot mol^{-1}$$

$$\varepsilon(Na^+, Zn(HPO_4)_2^{2-}) = -(0.10 \pm 0.10)\ kg \cdot mol^{-1}$$

$$\varepsilon(Na^+, Zn(HPO_4)_3^{4-}) = -(0.20 \pm 0.10)\ kg \cdot mol^{-1}$$

$$\varepsilon(Na^+, Zn(HPO_4)(PO_4)^{3-}) = -(0.15 \pm 0.10)\ kg \cdot mol^{-1}$$

$$\varepsilon(Na^+, Zn(OH)_2HPO_4^{2-}) = -(0.10 \pm 0.10)\ kg \cdot mol^{-1}$$

The equilibrium $Zn(OH)_2(aq) + HPO_4^{2-} \rightleftharpoons Zn(OH)_2HPO_4^{2-}$ has been combined with the selected value $\log_{10}{}^*\beta_2^\circ$ (298.15 K) = -17.89 ± 0.15 for the equilibrium $Zn^{2+} + 2H_2O(l) \rightleftharpoons Zn(OH)_2(aq) + 2H^+$ (see Section 3.2.1) in order to obtain:

$$Zn^{2+} + 2H_2O(l) + HPO_4^{2-} \rightleftharpoons Zn(OH)_2HPO_4^{2-} + 2H^+$$

$$\log_{10}K^\circ\ (298.15\ K) = -17.0 \pm 0.3$$

32.3.5.2 Zinc(II) phosphate compounds

Powell et al. (2013) state that the formation of insoluble phosphates, $Zn_3(PO_4)_2{\cdot}nH_2O$, may influence both the availability of Zn in soil and the Zn levels in natural water systems. The only reliable data for the solubility constant of $Zn_3(PO_4)_2{\cdot}4H_2O(s)$, hopeite (orthorhombic) or parahopeite (triclinic),

$$Zn_3(PO_4)_2 \cdot 4H_2O(s) \rightleftharpoons 3Zn^{2+} + 2PO_4^{3-} + 4H_2O(l)$$

$$\log_{10}K_{s0}^\circ\ (298.15\ K) = -35.3 \pm 0.1$$

were determined from solubility measurements in dilute phosphoric acid (pH = 3.4 – 4.6) at 25C. These indicated a low solubility for this solid. The resultant solubility constant is accepted by Powell et al. (2013) as "provisional". However, for unknown reasons Powell et al. (2013) did not include this value in their summary Tab. 5.

This value is included in TDB 2020.

32.3.6 Zinc(II) sulphate compounds and complexes

32.3.6.1 Zinc(II) sulphate complexes

Powell et al. (2013) state that at low ionic strengths, an exceptional number of determinations (19 in all) have been accepted, and the association constant for $ZnSO_4(aq)$ at $I_m = 0$ has been determined as the weighted average of these 19 accepted values:

$$Zn^{2+} + SO_4^{2-} \rightleftharpoons ZnSO_4(aq)$$

$$\log_{10}K_1^\circ\ (298.15\ K) = 2.30 \pm 0.04$$

Powell et al. (2013) further remark that in contrast to the plethora of results at infinite dilution, there are few data for the above equilibrium at finite ionic strength. An SIT regression of the accepted results in LiClO4 media, with $\log_{10}K_1^\circ$ fixed at the above recommended value, gives

$$\Delta\varepsilon = -(0.05 \pm 0.03)\ kg \cdot mol^{-1}$$

Using Δε and the reported values ε(Zn^{2+}, ClO_4^-) = (0.35 ± 0.01) kg · mol^{-1} (Tab. 32-3) and ε(Li^+, SO_4^{2-}) = -(0.03 ± 0.04) kg · mol^{-1} (Lemire et al. 2013) this review calculated the new value

$$\varepsilon(ZnSO_4(aq), LiClO_4) = (0.27 \pm 0.05) \text{ kg} \cdot \text{mol}^{-1}$$

and estimated

$$\varepsilon(ZnSO_4(aq), NaCl) \approx \varepsilon(ZnSO_4(aq), NaClO_4) \approx \varepsilon(ZnSO_4(aq), LiClO_4) = (0.27 \pm 0.05) \text{ kg} \cdot \text{mol}^{-1}$$

Powell et al. (2013) report that the enthalpy change associated with the formation of $ZnSO_4(aq)$ has been extensively studied using a range of techniques. At infinite dilution (I = 0), there is excellent agreement amongst many of the publications reporting enthalpy data, which enabled Powell et al. (2013) to make a stringent selection. They accepted seven enthalpy results and obtained an unweighted average of

$$\Delta_r H_m^\circ(298.15 \text{ K}) = (6.04 \pm 0.54) \text{ kJ} \cdot \text{mol}^{-1}$$

which is recommended by Powell et al. (2013).

These values are included in TDB 2020.

Concerning the complex $Zn(SO_4)_2^{2-}$ Powell et al. (2013) state that as for some other $M^{2+} + SO_4^{2-}$ systems, the apparent "observation" of $Zn(SO_4)_2^{2-}$ may simply reflect changes in activity coefficients when there is significant replacement of the medium anion (typically ClO_4^-). Accordingly, pending further investigation, all the published results are considered "indicative" only by Powell et al. (2013).

An SIT regression of the data in $LiClO_4$ media yielded

$$Zn^{2+} + 2SO_4^{2-} \rightleftharpoons Zn(SO_4)_2^{2-}$$

$$log_{10}\beta_2^\circ(298.15 \text{ K}) = 3.2 \pm 0.2$$

$$\Delta\varepsilon = (0.09 \pm 0.08) \text{ kg} \cdot \text{mol}^{-1}$$

Using Δε and the reported values ε(Zn^{2+}, ClO_4^-) = (0.35 ± 0.01) kg · mol^{-1} (Tab. 32-3) and ε(Li^+, SO_4^{2-}) = -(0.03 ± 0.04) kg · mol^{-1} (Lemire et al. 2013) this review calculated the new value

$$\varepsilon(Li^+, Pb(SO_4)_2^{2-}) = (0.38 \pm 0.10) \text{ kg} \cdot \text{mol}^{-1}$$

and estimated

$$\varepsilon(Na^+, Pb(SO_4)_2^{2-}) \approx \varepsilon(Li^+, Pb(SO_4)_2^{2-}) = (0.38 \pm 0.10) \text{ kg} \cdot \text{mol}^{-1}$$

Powell et al. (2013) remark that all of the available enthalpy values for the formation of $Zn(SO_4)_2^{2-}$ have been derived from potentiometric $K(T)$ data in the temperature range 15 – 65 °C and reported graphically in a single publication. The value

$$\Delta_r H_m°(298.15\ K) = (10 \pm 5)\ kJ \cdot mol^{-1}$$

should therefore be regarded as "indicative" only.

These values have been included in TDB 2020 as "supplemental data".

32.3.6.2 Zinc(II) sulphate compounds

Powell et al. (2013) report that under conditions typically encountered in the natural environment, the equilibrium form of the solid Zn(II) sulphate will be the heptahydrate, $ZnSO_4 \cdot 7H_2O(s)$ (goslarite). The solubility of this salt is high (> 3 $mol \cdot dm^{-3}$ at 25 °C in water) and increases rapidly with temperature up to ≈ 50 °C before becoming retrograde. It will not therefore have a significant influence on Zn(II) speciation in natural waters. No thermodynamic data for $ZnSO_4 \cdot 7H_2O(s)$ (goslarite) are in included in TDB 2020.

32.3.7 Zinc(II) sulphide compounds and complexes

Solubility data of zinc(II) sulphide have been published by Gubeli & Ste-Marie (1967), Hayashi et al. (1990), Daskalakis & Helz (1993), Tagirov et al. (2007), and Tagirov & Seward (2010). As discussed in the following, the final selection of equilibrium constants by this review is based on the experimental data of Tagirov et al. (2007) and Tagirov & Seward (2010) because of shortcomings and ambiguities encountered in the other above-mentioned studies.

Gubeli & Ste-Marie (1967) measured the solubility of a ZnS(s) precipitate after 7 – 10 days equilibration time in 1 M $NaClO_4$ medium at 25 °C in the pH range 0.75 – 13.4, varying the total dissolved sulphide concentration from $4 \cdot 10^{-4}$ – 0.01 M and using Zn-65 as radiotracer. The experiments were done from oversaturation only with ZnS precipitates of unknown crystallinity.

As can be seen in Fig. 32-1 the measured total Zn concentration varies systematically below pH 3 as a function of total dissolved sulphide, with a slope of -2. Above pH 3 the data do not show any pH dependence and no dependence on total dissolved sulphide concentration.

Data at pH < 3 were interpreted by Gubeli & Ste-Marie (1967) in terms of the equilibrium

$$ZnS(s) + 2\ H^+ \rightleftharpoons Zn^{2+} + H_2S(aq)$$

$$\log_{10}{}^*K_s\ (298.15\ K,\ 1\ M\ NaClO_4) = -3.99 \pm 0.24$$

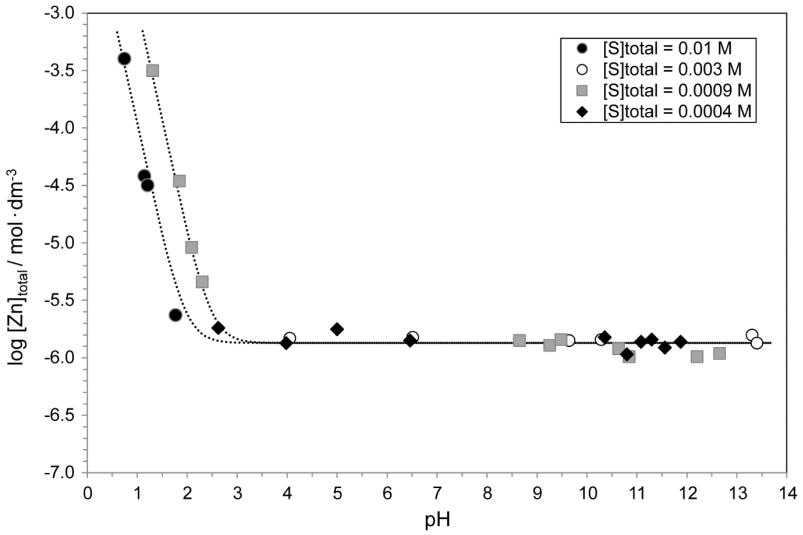

Fig. 32-1: Solubility data of Gubeli & Ste-Marie (1967) for ZnS(s) in water as a function of pH at different total dissolved sulphide concentrations, $[S]_{total}$, at 25 °C in 1 M $NaClO_4$

Dotted lines: calculated total dissolved concentration of zinc, $[Zn]_{total}$, with equilibrium constants derived by Gubeli & Ste-Marie (1967).

This review obtained an almost identical value, $\log_{10}{}^*K_s$ (298.15 K, 1 M $NaClO_4$) = -3.98 ± 0.25 (2σ), using the data given in Tab. II of Gubeli & Ste-Marie (1967). Using $\varepsilon(H^+, ClO_4^-)$ = 0.14 ± 0.02, $\varepsilon(Zn^{2+}, ClO_4^-)$ = 0.35 ± 0.01, and $\varepsilon(H_2S(aq), NaClO_4)$ = 0.055 ± 0.004 (Tab. 32-3) this value has been extrapolated to zero ionic strength: $\log_{10}{}^*K_s^\circ$ (298.15 K) = -4.26 ± 0.25. It suggests that the precipitate of unknown crystallinity used by Gubeli & Ste-Marie (1967) would be more than half an order of magnitude less soluble than well-characterised sphalerite, ZnS(cr), used by Daskalakis & Helz (1993), $\log_{10}{}^*K_s^\circ$ (298.15 K) = -3.68 ± 0.18, and Tagirov & Seward (2010), $\log_{10}{}^*K_s^\circ$ (298.15 K) = -3.68 ± 0.05 (see below). Moreover, the solubility of a CdS(s) precipitate, reported from a similar study by Ste-Marie et al. (1964), turned out to be more than two orders of magnitude more soluble than well-characterised CdS(cr) (see Section 8.3.7.2). This casts severe doubts on the data set of Gubeli & Ste-Marie (1967).

Data at pH > 3 were interpreted by Gubeli & Ste-Marie (1967) in terms of the equilibrium

$$ZnS(s) + H_2O(l) \rightleftharpoons Zn(OH)(HS)(aq)$$

$\log_{10}K$ (298.15 K, 1 M $NaClO_4$) = -5.87

where the value is just the average of all solubility data at pH > 3. This review obtained an identical value, $\log_{10}K$ (298.15 K, 1 M $NaClO_4$) = -5.87 ± 0.12 (2σ), using the data given in Tab. II of Gubeli & Ste-Marie (1967). Note that Zn(OH)(HS)(aq) could also be written as ZnS(aq). There is no way to distinguish between the two complexes by fitting solubility data.

However, the pH and concentration independence of data at pH > 3 is contradicted by all later studies (Hayashi et al. 1990, Daskalakis & Helz 1993, Tagirov et al. 2007, Tagirov & Seward 2010). It is also in contradiction with the companion solubility study of a CdS(s) precipitate (Ste-Marie et al. 1964), where at pH > 3 similar behaviour was found as reported for ZnS(cr) in the above-mentioned studies (see Section 8.3.7.2).

In summary, the data set published by Gubeli & Ste-Marie (1967) appears self-consistent but it is contradicted in all aspects by all later studies. The reason for these discrepancies remains unclear. Hence, the data of Gubeli & Ste-Marie (1967) were rejected by this review.

Hayashi et al. (1990) measured the solubility of sphalerite, ZnS(cr), in NaOH-H_2S solutions of 0.5 – 3.0 m total sulphide concentrations in the pH range 3 – 11 at temperatures of 25 to 240 °C. Sphalerite used in the solubility experiments was synthetized from elemental zinc and sulphur, and solubility experiments were carried out both from undersaturation and oversaturation.

Hayashi et al. (1990) interpreted their experimental data in terms of the complexes $Zn(HS)_2(aq)$, $Zn(HS)_3^-$, $Zn(HS)_4^{2-}$, $Zn(OH)(HS)_2^-$ (or $ZnS(HS)^-$) and $Zn(OH)(HS)_3^{2-}$ (or $ZnS(HS)_2^{2-}$). The latter complex is always a minor species in their model, even at the highest sulphide concentrations.

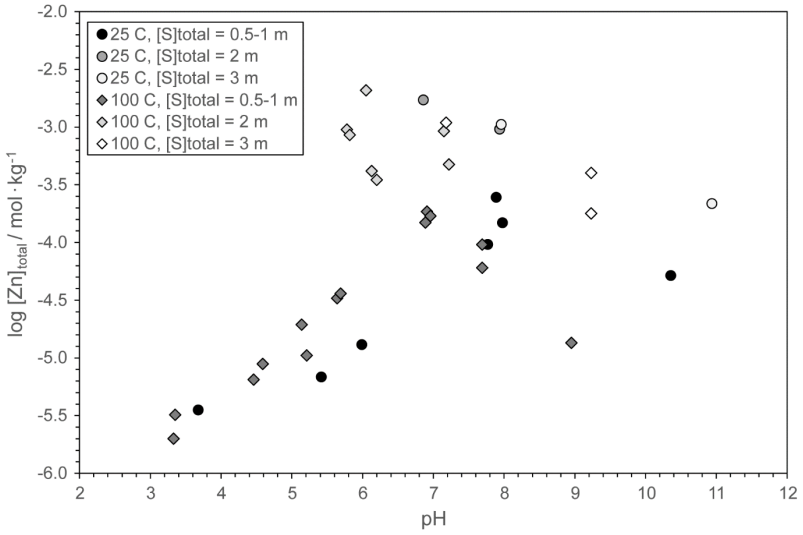

Fig. 32-2: Solubility data of Hayashi et al. (1990) for ZnS(cr) in NaOH-H_2S solutions of 0.5 – 3.0 m total sulphide concentrations in the pH range 3 – 11 at temperatures of 25 and 100 °C

In qualitative terms, the dependence of the measured total Zn concentration on pH and total sulphur concentration (Fig. 32-2) is the same as found by Tagirov et al. (2007) and Tagirov & Seward (2010) (Figs. 32.4 – 32-7).

However, in quantitative terms, there are significant inconsistencies between the results obtained by Hayashi et al. (1990) and Tagirov & Seward (2010). While the maximum solubility around pH 7 is described in both models by the same value for $ZnS(cr) + H_2S(aq) + 2HS^- \rightleftharpoons Zn(HS)_4^{2-}$ (at 25 °C), the value reported by Hayashi et al. (1990) for $ZnS(cr) + H_2S(aq) + HS^- \rightleftharpoons Zn(HS)_3^-$ (at 25 °C) is one order of magnitude higher than the one reported by Tagirov & Seward (2010).

In the acidic and alkaline regions, where lower solubilities are measured, Hayashi et al. (1990) report equilibrium constants three orders of magnitude higher than Tagirov & Seward (2010) for $ZnS(cr) + H_2S(aq) \rightleftharpoons Zn(HS)_2(aq)$ and $ZnS(cr) + HS^- \rightleftharpoons ZnS(HS)^-$ (at 25 °C).

Interestingly, the largest discrepancies between the results of Hayashi et al. (1990) and Tagirov & Seward (2010) are encountered for isocoulombic reactions where the effect of varying ionic strength should be smaller than for $ZnS(cr) + H_2S(aq) + 2HS^- \rightleftharpoons Zn(HS)_4^{2-}$. Hayashi et al. (1990) did not use an electrolyte medium like $NaClO_4$ to control the ionic strength, but varying amounts of NaHS causing the ionic strength varying from 0.0002 to 2.98 m. Nevertheless, ionic strength effects on isocoulombic reactions involving only neutral and negatively charged species should not cause differences by three orders of magnitude on equilibrium constants extrapolated to zero ionic strength.

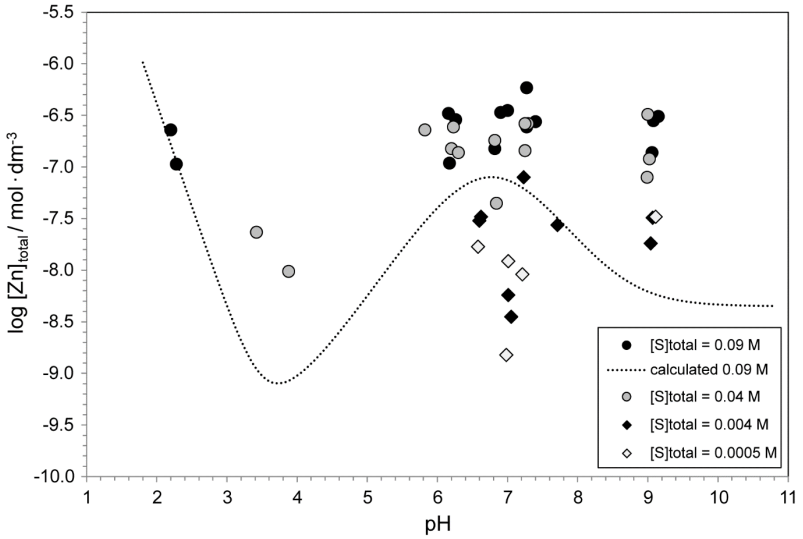

Fig. 32-3: Solubility of ZnS(cr) in water as a function of pH at different total dissolved sulphide concentrations, $[S]_{total}$, at 25 °C and ionic strength 0.1 – 0.2 M

Symbols: experimental data of Daskalakis & Helz (1993). Line: calculated total dissolved concentration of zinc, $[Zn]_{total}$, with equilibrium constants derived by this review (Tab. 32-1).

It seems that in solutions of 0.5 – 3 m total sulphide concentrations other effects may influence sphalerite solubility, for example complexation with polysulphides or formation of colloids. Considering these unresolved ambiguities, this review did not retain the data of Hayashi et al. (1990).

Daskalakis & Helz (1993) measured the solubility of both synthetic and natural sphalerite, ZnS(cr), in solutions of $0.1 – 4 \cdot 10^{-4}$ M total sulphide concentrations in the pH range 2 – 9 at 25 °C. Most experiments were done at an ionic strength of about 0.1 – 0.2 M (Fig. 32-3) but also some at higher ionic strengths. Sphalerite used in the solubility experiments was either natural, low-iron sphalerite or sphalerite synthetized from elemental zinc and sulphur. Solubility experiments were carried out from undersaturation, with run durations of several months.

Daskalakis & Helz (1993) fitted their experimental data to several models comprising three to five complexes and conclude that three complexes are essential to model the data adequately: $Zn(HS)_4^{2-}$, $ZnS(HS)^-$ and $ZnS(HS)_2^{2-}$. They further state that additional complexes improve the fit marginally, but they do not show any plots comparing their experimental data with their model fits.

Fig. 32-3 indicates why Daskalakis & Helz (1993) did not report any such plots: The experimental solubility data show a large scatter up to one order of magnitude for a certain pH and total dissolved sulphide concentration. Although the data do not contradict the model derived by this review based on the data of Tagirov et al. (2007) and Tagirov & Seward (2010), they are hardly suitable to derive any reliable speciation model. This can also be seen from the reported sums of the squared residuals for the different model fits (Tab. 2 of Daskalakis & Helz 1993): They are all essentially the same, indicating that all model fits are equally good (or bad).

Two data points at pH ≈ 2 (Fig. 32-3) can be interpreted in terms of the equilibrium

$$ZnS(s) + 2\ H^+ \rightleftharpoons Zn^{2+} + H_2S(aq)$$

$$\log_{10}{}^*K_s\ (298.15\ K,\ I = 0.21\ M) = -3.44 \pm 0.18$$

Extrapolating this value to zero ionic strength results in $\log_{10}{}^*K_s^\circ$ (298.15 K) = -3.68 ± 0.18, which is the same value as derived from the data of Tagirov & Seward (2010), i.e. $\log_{10}{}^*K_s^\circ$ (298.15 K) = -3.68 ± 0.05 (see below). However, this could be a coincidence.

Considering their large scatter, this review did not retain the data of Daskalakis & Helz (1993).

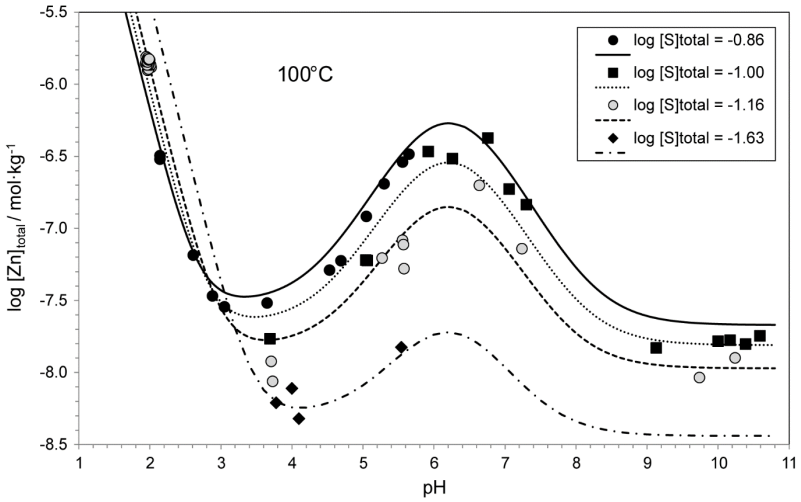

Fig. 32-4: Solubility of ZnS(cr) in water as a function of pH at different total dissolved sulphide concentrations, $[S]_{total}$, at 100 °C

Symbols: experimental data of Tagirov et al. (2007). Lines: calculated total dissolved concentration of zinc, $[Zn]_{total}$, with equilibrium constants derived by this review (Tab. 32-1).

Tagirov et al. (2007) measured the solubility of synthetic sphalerite, ZnS(cr), in solutions of 0.15 to 0.02 M total sulphide concentrations in the pH range 2 – 11 at 100 °C and 150 bars. Sphalerite used in the solubility experiments was commercial ZnS recrystallised by the authors to get a coarser-grained (≈ 0.1 mm) product. The XRD pattern of this product corresponded to pure sphalerite. Prior to the experiments, a long-term in situ conditioning of the solid phase was performed to attain reproducible Zn solubilities (Fig. 32-4).

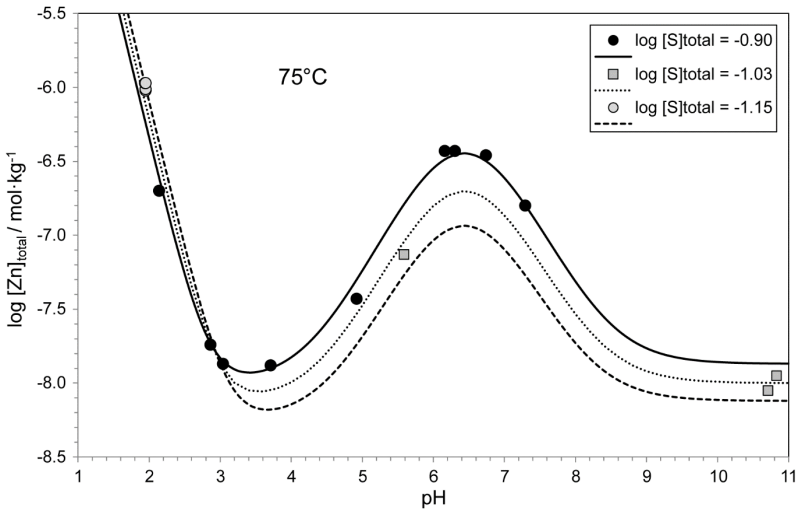

Fig. 32-5: Solubility of ZnS(cr) in water as a function of pH at different total dissolved sulphide concentrations, $[S]_{total}$, at 75 °C

Symbols: experimental data of Tagirov & Seward (2010). Lines: calculated total dissolved concentration of zinc, $[Zn]_{total}$, with equilibrium constants derived by this review (Tab. 32-1).

Tagirov et al. (2007) interpreted their experimental data in terms of the complexes $Zn(HS)_2(aq)$, $Zn(HS)_3^-$ and $ZnS(HS)^-$. Tagirov et al. (2007) state that as some of the auxiliary thermodynamic constants are available only for water at vapour saturated pressure (P_{sat}), all thermodynamic values used were for P_{sat}, and the pressure during thermodynamic calculations was set at P_{sat}. This procedure was also followed by this review.

The solubility study of Tagirov et al. (2007) was extended by Tagirov & Seward (2010) who measured the solubility of synthetic sphalerite, ZnS(cr), in solutions of 0.15 to 0.015 M total sulphide concentrations in the range 25 – 250 °C and 150 bars. In addition to the synthetic ZnS(cr), prepared by Tagirov et al. (2007), Tagirov & Seward (2010) also used a large crystal of sphalerite (clear, glassy, weakly orange-yellow colour) from "Santander" (i.e. from Aliva, Picos de Europa, Cantabria, Spain).

The solubility studies of Tagirov et al. (2007) and Tagirov & Seward (2010) finally became part of an extended review and modelling study aiming at a thermodynamic model of zinc in hydrothermal systems up to 350 °C, including hydroxide, chloride, and hydrosulphide complexes (Akinfiev & Tagirov 2014). This is far outside the scope of TDB 2020 and hence, the results of Akinfiev & Tagirov (2014) have not been considered by this review.

Tab. 32-1: Equilibrium constants for the Zn – S system derived by this review from experimental data of Tagirov et al. (2007) and Tagirov & Seward (2010)

Values in italics are extrapolated using the temperature parameters derived by this review.

Temperature	$\log_{10}K_s°$	$\log_{10}\beta_2°$	$\log_{10}\beta_3°$	$\log_{10}K°$
25 °C	-3.69 ± 0.04	*9.3*	13.30 ± 0.10	*3.4*
50 °C	-3.41 ± 0.04	9.10 ± 0.10	12.60 ± 0.10	*2.8*
75 °C	-3.25 ± 0.04	9.00 ± 0.10	12.05 ± 0.10	2.71 ± 0.10
100 °C	-3.05 ± 0.04	8.80 ± 0.10	11.50 ± 0.10	2.45 ± 0.10

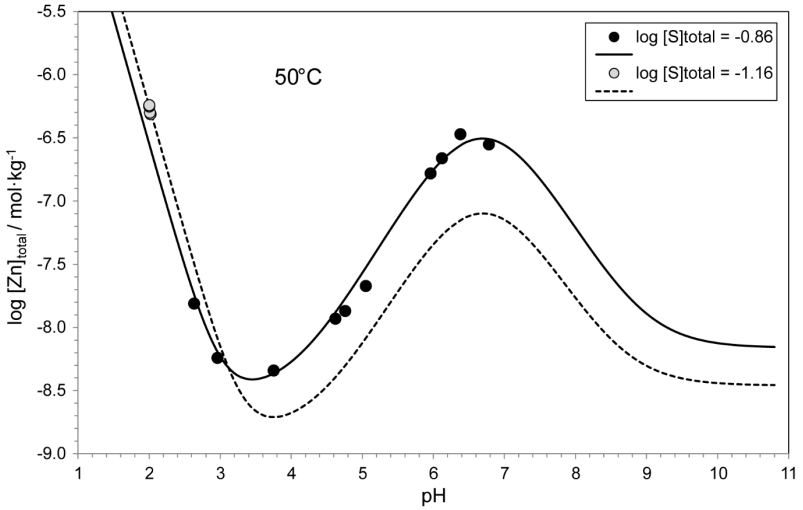

Fig. 32-6: Solubility of ZnS(cr) in water as a function of pH at different total dissolved sulphide concentrations, $[S]_{total}$, at 50 °C

Symbols: experimental data of Tagirov & Seward (2010). Lines: calculated total dissolved concentration of zinc, $[Zn]_{total}$, with equilibrium constants derived by this review (Tab. 32-1).

Tagirov & Seward (2010) interpreted their experimental data in terms of the complexes $Zn(HS)_2(aq)$, $Zn(HS)_3^-$, $Zn(HS)_4^{2-}$ and $ZnS(HS)^-$. They state that "initially, we did not include the formation of $Zn(HS)_4^{2-}$ in the speciation model, however, at temperatures from 25 to 75 °C, a systematic deviation of calculated from measured concentrations was observed in weakly acidic to weakly alkaline solutions (pH = 5.5-8)". This deviation is marginal, and could not be reproduced by this review. In addition, it remains unclear why $Zn(HS)_4^{2-}$ should be important at 25 °C but is supposed to not play any role anymore at temperatures above 75 °C. Hence, this review re-interpreted the data of Tagirov et al. (2007) and Tagirov & Seward (2010) in terms of the complexes $Zn(HS)_2(aq)$, $Zn(HS)_3^-$ and $ZnS(HS)^-$ only (Tab. 32-1, Figs. 32-4 – 32-7). Note that the data available for 25 °C only allowed a fit of $\log_{10}K_s°$ and $\log_{10}\beta_3°$ (Fig. 32-7) while the data available for 50 °C allowed a fit of $\log_{10}K_s°$, $\log_{10}\beta_2°$ and $\log_{10}\beta_3°$ but not of $\log_{10}K°$ (Fig. 32-6).

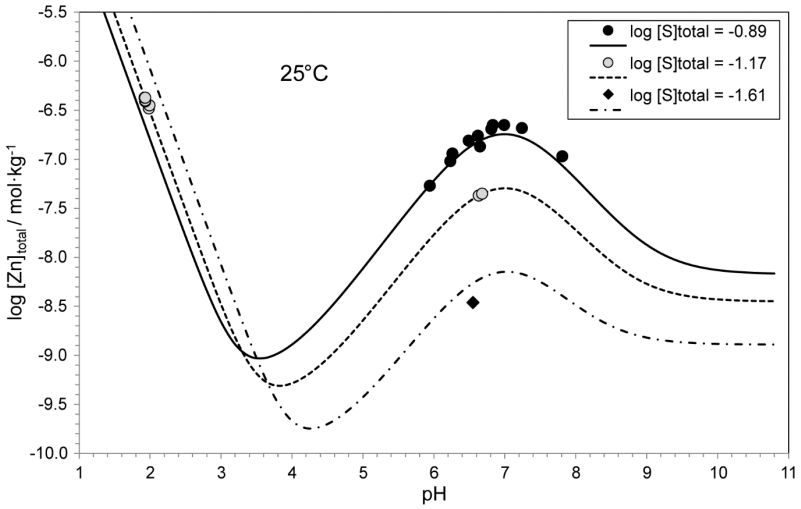

Fig. 32-7: Solubility of ZnS(cr) in water as a function of pH at different total dissolved sulphide concentrations, $[S]_{total}$, at 25 °C

Symbols: experimental data of Tagirov & Seward (2010). Lines: calculated total dissolved concentration of zinc, $[Zn]_{total}$, with equilibrium constants derived by this review (Tab. 32-1).

The equilibrium constants obtained by this review at 25 °C are almost identical with the values reported by Tagirov & Seward (2010). However, with increasing temperature increasing differences between the equilibrium constants reported by Tagirov & Seward (2010) and those obtained by this review are observed for the complexes ($\log_{10}\beta_2°$, $\log_{10}\beta_3°$, $\log_{10}K°$).

The reason for these increasing discrepancies is that Tagirov & Seward (2010) used a slightly different temperature function than that selected by this review for the basic equilibrium $H_2S(aq) \rightleftharpoons 2H^+ + HS^-$. While the solubility product $ZnS(cr) + 2H^+ \rightleftharpoons Zn^{2+} + H_2S(aq)$ is derived assuming that $[H_2S(aq)]$ is equal to the total sulphide concentration at pH ≈ 2, and hence does not show an increasing discrepancy with increasing temperature, the equilibrium constants of the complexes involve $[HS^-]$ which is calculated from the total sulphide concentration as a function of pH via the equilibrium $H_2S(aq) \rightleftharpoons 2H^+ + HS^-$. The equilibrium constants obtained by this review are internally consistent and are in good agreement with the experimental data in the temperature range 25 – 100 °C (Figs. 32.4 – 32.6).

Tagirov & Seward (2010) fitted temperature functions in the range 25 – 250 °C including $\Delta_r C_{p,m}°(298.15\ K) = \text{const}$. Inspecting Fig. 3 of Tagirov & Seward (2010) reveals that the fairly large $\Delta_r C_{p,m}°(298.15\ K)$ values mainly account for the temperature behaviour above 100 °C, involving very few experimental data and a number of model assumptions. This review decided to limit the assessment of the temperature behaviour to the range 25 – 100 °C. Then, in all cases $\Delta_r C_{p,m}°(298.15\ K) = 0$ is a very good approximation (Figs. 32-8 – 32-10).

The results from unweighted linear regressions of the equilibrium constants shown in Tab. 32-1 versus the reciprocal of absolute temperature are (Figs. 32-8 – 32-10):

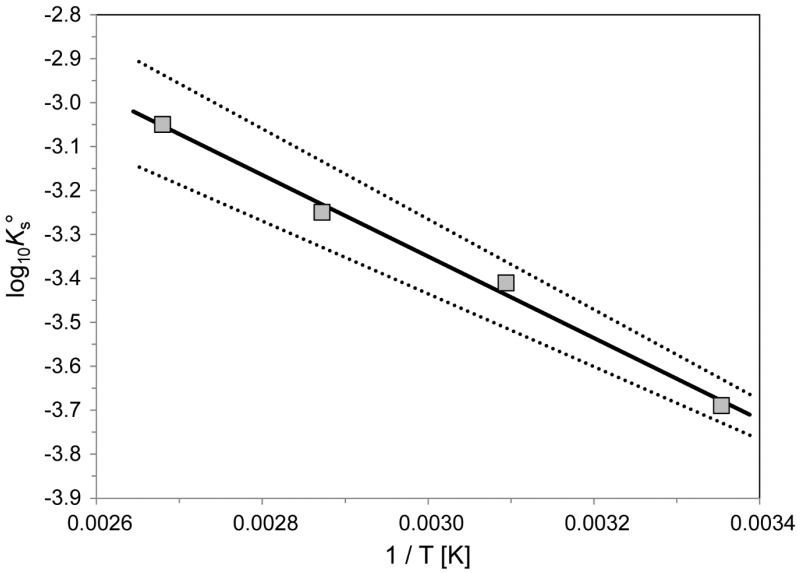

Fig. 32-8: The equilibrium constant $\log_{10}K_s°$ for ZnS(cr) + 2 H^+ ⇌ Zn^{2+} + H_2S(aq) as function of temperature in the range 25 – 100 °C

Symbols: equilibrium constants as derived by this review (Tab. 32-1). Solid line: unweighted linear regression. Dotted lines: lower and upper limits using $\log_{10}K_s°$ (298.15 K) = -3.68 ± 0.05 and $\Delta_rH_m°$ (298.15 K) = (17.8 ± 1.9) kJ · mol^{-1} and extrapolated to higher temperatures.

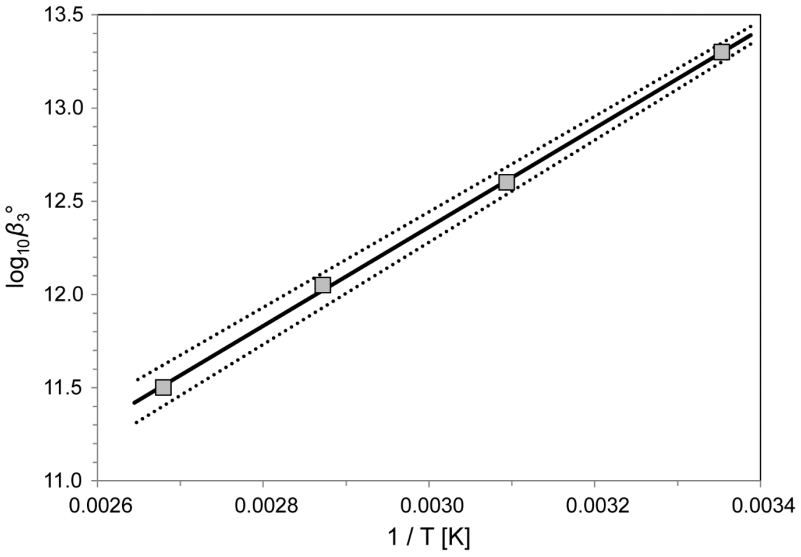

Fig. 32-9: The equilibrium constant $\log_{10}\beta_3°$ for Zn^{2+} + 3 HS^- ⇌ $Zn(HS)_3^-$ as function of temperature in the range 25 – 100 °C

Symbols: equilibrium constants as derived by this review (Tab. 32-1). Solid line: unweighted linear regression. Dotted lines: lower and upper limits using $\log_{10}\beta_3°$ (298.15 K) = 13.30 ± 0.05 and $\Delta_rH_m°$ (298.15 K) = -(50.7 ± 1.7) kJ · mol^{-1} and extrapolated to higher temperatures.

$ZnS(cr) + 2H^+ \rightleftharpoons Zn^{2+} + H_2S(aq)$

$\log_{10}K_s°$ (298.15 K) = -3.68 ± 0.05

$\Delta_rH_m°$ (298.15 K) = 17.8 ± 1.9 kJ · mol^{-1}

$\Delta_rC_{p,m}°$(298.15 K) = 0 J · K^{-1} · mol^{-1}

$Zn^{2+} + 2\ HS^- \rightleftharpoons Zn(HS)_2(aq)$

$\log_{10}\beta_2°$ (298.15 K) = 9.30 ± 0.17

$\Delta_rH_m°$ (298.15 K) = -13.7 ± 3.2 kJ · mol^{-1}

$\Delta_rC_{p,m}°$(298.15 K) = 0 J · K^{-1} · mol^{-1}

$Zn^{2+} + 3\ HS^- \rightleftharpoons Zn(HS)_3^-$

$\log_{10}\beta_3°$ (298.15 K) = 13.30 ± 0.05

$\Delta_rH_m°$ (298.15 K) = -50.7 ± 1.7 kJ · mol^{-1}

$\Delta_rC_{p,m}°$(298.15 K) = 0 J · K^{-1} · mol^{-1}

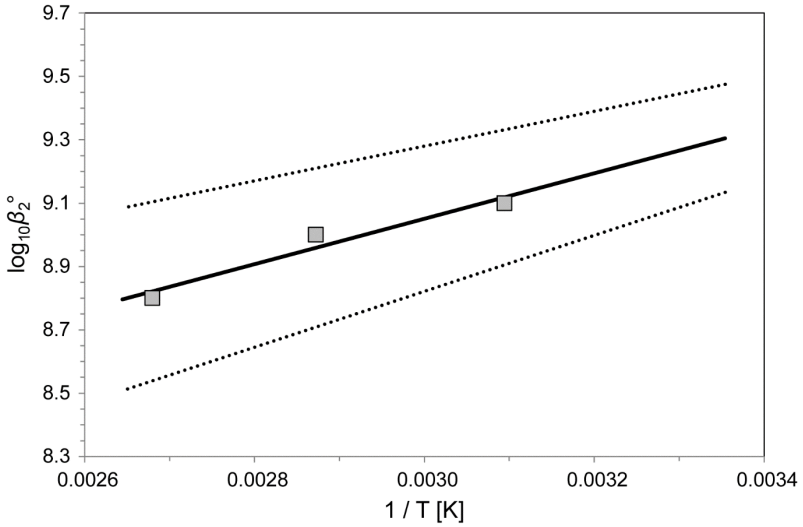

Fig. 32-10: The equilibrium constant $\log_{10}\beta_2°$ for $Zn^{2+} + 2\ HS^- \rightleftharpoons Zn(HS)_2(aq)$ as function of temperature in the range 50 – 100 °C

Symbols: equilibrium constants as derived by this review (Tab. 32-1). Solid line: unweighted linear regression. Dotted lines: lower and upper limits using $\log_{10}\beta_2°$ (298.15 K) = 9.30 ± 0.17 and $\Delta_rH_m°$ (298.15 K) = -(13.7 ± 3.2) kJ · mol^{-1} and extrapolated to higher temperatures.

$Zn^{2+} + 2\ HS^- \rightleftharpoons ZnS(HS)^- + H^+$

$\log_{10}K°$ (298.15 K) = 3.36 ± 0.20

$\Delta_r H_m°$ (298.15 K) = -25.9 ± 3.0 kJ · mol^{-1}

$\Delta_r C_{p,m}°$(298.15 K) = 0 J · K^{-1} · mol^{-1}

These values are included in TDB 2020, as well as the estimates

$\varepsilon(Zn(HS)_2(aq), NaCl) \approx \varepsilon(Zn(HS)_2(aq), NaClO_4)$ = (0.0 ± 0.1) kg · mol^{-1}

$\varepsilon(Na^+, Zn(HS)_3^-)$ = -(0.05 ± 0.10) kg · mol^{-1}

$\varepsilon(Na^+, ZnS(HS)^-)$ = -(0.05 ± 0.10) kg · mol^{-1}

32.4 Selected zinc data

Tab. 32-2: Selected zinc data

Core data are bold and supplemental data in italics.

Name	**$\Delta_f G_m°$** [kJ · mol^{-1}]	**$\Delta_f H_m°$** [kJ · mol^{-1}]	**$S_m°$** [J · K^{-1} · mol^{-1}]	**$C_{p,m}°$** [J · K^{-1} · mol^{-1}]	**Species**
Zn(cr)	0.0	0.0	**41.630 ± 0.150**	**25.390 ± 0.040**	Zn(cr)
Zn+2	**-147.203 ± 0.254**	**-153.390 ± 0.200**	**-109.800 ± 0.500**		Zn^{2+}
ZnO(cr)	**-320.479 ± 0.299**	**-350.460 ± 0.270**	**43.650 ± 0.400**		ZnO(cr)

Name	**$\log_{10}\beta°$**	**$\Delta\varepsilon$** [kg · mol^{-1}]	**$\Delta_r H_m°$** [kJ · mol^{-1}]	**$\Delta_r C_{p,m}°$** [J · K^{-1} · mol^{-1}]	**T-range** [°C]	**Reaction**
Zn+2	25.79 ± 0.04		-153.39 ± 0.2			$Zn(cr) \rightleftharpoons Zn^{2+} + 2e^-$
ZnOH+	-8.94 ± 0.06	-0.02 ± 0.01	56.7 ± 0.7	0	15 – 350	$Zn^{2+} + H_2O(l) \rightleftharpoons ZnOH^+ + H^+$
Zn(OH)2(aq)	-17.89 ± 0.15		107.1 ± 3.1	-65 ± 27	20 – 350	$Zn^{2+} + 2\ H_2O(l) \rightleftharpoons Zn(OH)_2(aq) + 2\ H^+$
Zn(OH)3-	-27.98 ± 0.10	0.14 ± 0.05	143.5 ± 2.5	-196 ± 23	12 – 350	$Zn^{2+} + 3\ H_2O(l) \rightleftharpoons Zn(OH)_3^- + 3\ H^+$
Zn(OH)4-2	-40.35 ± 0.22	0.34 ± 0.07	178.3 ± 5.8	-348 ± 56	12 – 350	$Zn^{2+} + 4\ H_2O(l) \rightleftharpoons Zn(OH)_3^{2-} + 4\ H^+$
Zn2OH+3	-7.9 ± 0.3	0.3 ± 0.1	-	-		$2\ Zn^{2+} + H_2O(l) \rightleftharpoons Zn_2OH^{3+} + H^+$
ZnCl+	0.40 ± 0.09	-0.14 ± 0.02	-	-		$Zn^{2+} + Cl^- \rightleftharpoons ZnCl^+$
ZnCl2(aq)	0.69 ± 0.15	-0.20 ± 0.04	-	-		$Zn^{2+} + 2\ Cl^- \rightleftharpoons ZnCl_2(aq)$
ZnCl3-	0.48 ± 0.54	-0.27 ± 0.13	-	-		$Zn^{2+} + 3\ Cl^- \rightleftharpoons ZnCl_3^-$
ZnCl4-2	*≈ -2*		-	-		*$Zn^{2+} + 4\ Cl^- \rightleftharpoons ZnCl_4^{2-}$*
ZnCO3(aq)	4.75 ± 0.06		-	-		$Zn^{2+} + CO_3^{2-} \rightleftharpoons ZnCO_3(aq)$
Zn(CO3)2-2	6.75 ± 0.6		-	-		$Zn^{2+} + 2\ CO_3^{2-} \rightleftharpoons Zn(CO_3)_2^{2-}$
ZnHCO3+	1.62 ± 0.10	0.10 ± 0.04	-	-		$Zn^{2+} + HCO_3^- \rightleftharpoons ZnHCO_3^+$
Zn2CO3+2	5.3 ± 0.4		-	-		$2\ Zn^{2+} + CO_3^{2-} \rightleftharpoons Zn_2CO_3^{2+}$
ZnH2PO4+	*0.9 ± 0.2*		-	-		*$Zn^{2+} + H_2PO_4^- \rightleftharpoons ZnH_2PO_4^+$*
Zn(H2PO4)2(aq)	*2.0 ± 0.2*		-	-		*$Zn^{2+} + 2\ H_2PO_4^- \rightleftharpoons Zn(H_2PO_4)_2(aq)$*
Zn(H2PO4)(HPO4)-	*4.0 ± 0.5*		-	-		*$Zn^{2+} + H_2PO_4^- + HPO_4^{2-} \rightleftharpoons Zn(H_2PO_4)(HPO_4)^-$*
ZnHPO4(aq)	3.3 ± 0.2		-	-		$Zn^{2+} + HPO_4^{2-} \rightleftharpoons ZnHPO_4(aq)$
Zn(HPO4)2-2	*7.1 ± 0.2*		-	-		*$Zn^{2+} + 2\ HPO_4^{2-} \rightleftharpoons Zn(HPO_4)_2^{2-}$*
Zn(HPO4)3-4	*7.4 ± 0.2*		-	-		*$Zn^{2+} + 3\ HPO_4^{2-} \rightleftharpoons Zn(HPO_4)_3^{4-}$*
Zn(HPO4)(PO4)-3	*12.5 ± 0.2*		-	-		*$Zn^{2+} + HPO_4^{2-} + PO_4^{3-} \rightleftharpoons Zn(HPO_4)(PO_4)^{3-}$*
Zn(OH)2HPO4-2	*-17.0 ± 0.3*		-	-		*$Zn^{2+} + 2H_2O(l) + HPO_4^{2-} \rightleftharpoons Zn(OH)_2HPO_4^{2-} + 2H^+$*

Tab. 32-2: Cont.

Name	**$\log_{10}\beta°$**	**$\Delta\varepsilon$** [kg · mol^{-1}]	**$\Delta_r H_m°$** [kJ · mol^{-1}]	**$\Delta_r C_{p,m}°$** [J · K^{-1} · mol^{-1}]	**T-range** [°C]	**Reaction**
ZnSO4(aq)	2.30 ± 0.04	-0.05 ± 0.03	6.04 ± 0.54	-		$Zn^{2+} + SO_4^{2-} \rightleftharpoons ZnSO_4(aq)$
Zn(SO4)2-2	*3.2 ± 0.2*	*0.09 ± 0.08*	*10 ± 5*	-	*15 – 65*	*$Zn^{2+} + 2\ SO_4^{2-} \rightleftharpoons Zn(SO_4)_2^{2-}$*
Zn(HS)2(aq)	9.30 ± 0.17		-13.7 ± 3.2	0	50 – 100	$Zn^{2+} + 2\ HS^- \rightleftharpoons Zn(HS)_2(aq)$
Zn(HS)3-	13.30 ± 0.05		-50.7 ± 1.7	0	25 – 100	$Zn^{2+} + 3\ HS^- \rightleftharpoons Zn(HS)_3^-$
ZnS(HS)-	3.36 ± 0.20		25.9 ± 3.0	0	75 – 100	$Zn^{2+} + 2\ HS^- \rightleftharpoons ZnS(HS)^- + H^+$

Name	**$\log_{10} K_{s,0}°$**	**$\Delta_r H_m°$** [kJ · mol^{-1}]	**$\Delta_r C_{p,m}°$** [J · K^{-1} · mol^{-1}]	**T-range** [°C]	**Reaction**
Zincite	11.19 ± 0.07	-88.76 ± 0.34	0	25 – 300	$ZnO(cr) + 2\ H^+ \rightleftharpoons Zn^{2+} + H_2O(l)$
Wülfingite	11.38 ± 0.20	-100 ± 11	0	12.5 – 75	$\varepsilon\text{-}Zn(OH)_2(s) + 2H^+ \rightleftharpoons Zn^{2+} + 2\ H_2O(l)$
Smithsonite	-10.94 ± 0.08	-4.1 ± 1.3	0	15 – 65	$ZnCO_3(s) \rightleftharpoons Zn^{2+} + CO_3^{2-}$
Hydrozincite	9.05 ± 0.10	-248 ± 15	0	15 – 65	$Zn_5(OH)_6(CO_3)_2(s) + 6H^+ \rightleftharpoons 5Zn^{2+} + 2CO_3^{2-} + 6H_2O(l)$
Zn3(PO4)2:4H2O(s)	-35.3 ± 0.1	-	-		$Zn_3(PO_4)_2 \cdot 4H_2O(s) \rightleftharpoons 3Zn^{2+} + 2PO_4^{3-} + 4H_2O(l)$
Sphalerite	-3.68 ± 0.05	17.8 ± 1.9	0	25 – 100	$ZnS(cr) + 2\ H^+ \rightleftharpoons Zn^{2+} + H_2S(aq)$

Tab. 32-3: Selected SIT ion interaction coefficients $\varepsilon_{j,k}$ [kg · mol^{-1}] for zinc species

Data in bold face are taken from Lemire et al. (2013). Data in normal face are derived or estimated in this review. Data estimated according to charge correlations and taken from Tab. 1-7 are shaded Supplemental data are in italics.

j k → ↓	**Cl^-** $\varepsilon_{j,k}$ [kg · mol^{-1}]	**ClO_4^-** $\varepsilon_{j,k}$ [kg · mol^{-1}]	**Na^+** $\varepsilon_{j,k}$ [kg · mol^{-1}]	**$Na^+ + Cl^-$** $\varepsilon_{j,k}$ [kg · mol^{-1}]	**$Na^+ + ClO_4^-$** $\varepsilon_{j,k}$ [kg · mol^{-1}]
H2S(aq)	0	0	0	(0.055 ± 0.004) [b]	(0.055 ± 0.004) [c]
HS-	0	0	(0.08 ± 0.01) [b]	0	0
Zn+2	(0.35 ± 0.01) [a]	0.35 ± 0.01	0	0	0
ZnOH+	(0.19 ± 0.02) [a]	0.19 ± 0.02	0	0	0
Zn(OH)2(aq)	0	0	0	0.0 ± 0.1 [a]	0.0 ± 0.1
Zn(OH)3-	0	0	0.07 ± 0.06	0	0
Zn(OH)4-2	0	0	0.13 ± 0.08	0	0
Zn2(OH)+3	(0.86 ± 0.10) [a]	0.86 ± 0.10	0	0	0
ZnCl+	(0.24 ± 0.02) [a]	0.24 ± 0.02	0	0	0
ZnCl2(aq)	0	0	0	0.21 ± 0.04) [a]	0.21 ± 0.04
ZnCl3-	0	0	0.17 ± 0.13	0	0
ZnCl4-2	*0*	*0*	*-0.10 ± 0.10*	*0*	*0*
ZnCO3(aq)	0	0	0	0.0 ± 0.1 [a]	0.0 ± 0.1
Zn(CO3)2-2	0	0	-0.10 ± 0.10	0	0
ZnHCO3+	(0.45 ± 0.05) [a]	0.45 ± 0.05	0	0	0
Zn2CO3+2	0.4 ± 0.1 [a]	0.4 ± 0.1	0	0	0
ZnH2PO4+	*0.2 ± 0.1* [a]	*0.2 ± 0.1*	*0*	*0*	*0*
Zn(H2PO4)2(aq)	*0*	*0*	*0*	*0.0 ± 0.1* [a]	*0.0 ± 0.1*
Zn(H2PO4)(HPO4)-	*0*	*0*	*-0.05 ± 0.10*	*0*	*0*
ZnHPO4(aq)	0	0	0	0.0 ± 0.1 [a]	0.0 ± 0.1
Zn(HPO4)2-2	*0*	*0*	*-0.10 ± 0.10*	*0*	*0*
Zn(HPO4)3-4	*0*	*0*	*-0.20 ± 0.10*	*0*	*0*
Zn(HPO4)(PO4)-3	*0*	*0*	*-0.15 ± 0.10*	*0*	*0*
Zn(OH)2HPO4-2	*0*	*0*	*-0.10 ± 0.10*	*0*	*0*
$ZnSO_4$(aq)	0	0	0	(0.27 ± 0.05) [a]	0.27 ± 0.05
Zn(SO4)2-2	*0*	*0*	*0.38 ± 0.10*	*0*	*0*
Zn(HS)2(aq)	0	0	0	0.0 ± 0.1	0.0 ± 0.1
Zn(HS)3-	0	0	-0.05 ± 0.10	0	0
ZnS(HS)-	0	0	-0.05 ± 0.10	0	0

[a] Assumed to be equal to the corresponding ion interaction coefficient with ClO_4^-, see Section 32.1 for explanation
[b] Hummel et al. (2002)
[c] Assumed to be equal to the corresponding ion interaction coefficient with NaCl

32.5 References

Akinfiev, N.N. & Tagirov, B.R. (2014): Zn in hydrothermal systems: Thermodynamic description of hydroxide, chloride, and hydrosulfide complexes. Geochemistry International, 52, 197-214 (translated from: Geokhimiya, 52 (2014), 214-232).

Bilinski, H., Huston, R. & Stumm, W. (1976): Determination of the stability constants of some hydroxo and carbonato complexes of Pb(II), Cu(II), Cd(II) and Zn(II) in dilute solutions by anodic stripping voltammetry and differential pulse polarography. Analytica Chimica Acta, 84, 157-164.

Bradbury, M.H. & Baeyens, B. (1997): A mechanistic description of Ni and Zn sorption on Na-montmorillonite. Part II: Modelling. Journal of Contaminant Hydrology 27, 223-248.

Bradbury M.H. & Baeyens B. (1999): Modelling the sorption of Zn and Ni on Ca-montmorillonite. Geochimica et Cosmochimica Acta 63, 325-336.

Brown, P.L. & Ekberg, C. (2016): Hydrolysis of Metal Ions. Wiley-VCH Verlag GmbH & Co. KGaA, Weinheim, Germany, 917 pp.

Cox, J.D., Wagman, D.D. & Medvedev, V.A. (1989): CODATA Key Values for Thermodynamics. New York, Hemisphere Publishing, 271 pp.

Daskalakis, K. & Helz, G.R. (1993): The solubility of sphalerite (ZnS) in sulfidic solutions at 25 °C and 1 atm pressure. Geochim. Cosmochim. Acta, 57, 4923-4931.

Fedorov, V.A., Kuznechikhina, M.A., Kanarsh, I.V., Kirnyuk, G.M. & Chernikova, G.E. (1978): Formation of mixed zinc halide complexes in aqueous solutions. Soviet Journal of Coordination Chemistry, 4, 33-38 (Translated from Koordinatsionnaya Khimiya, 4, 1978, 48-59).

Ferri, D., Grenthe, I., Hietanen, S., Néher-Neumann, E. & Salvatore, F. (1985): Studies on metal carbonate equilibria. 12. Zinc(II) carbonate complexes in acid solutions. Acta Chemica Scandinavica, A 39, 347-353.

Grenthe, I., Fuger, J., Konings, R.J.M., Lemire, R.J., Muller, A.B., Nguyen-Trung, C. & Wanner, H. (1992): Chemical Thermodynamics of Uranium. Chemical Thermodynamics, Vol. 1. North-Holland, Amsterdam, 715 pp.

Gubeli, A.O. & Ste-Marie, J. (1967): Constantes de stabilité de thiocomplexes et produits de solubilité de sulfures de métaux. II. Sulfure de zinc. Canadian Journal of Chemistry, 45, 2101-2108.

Hagemann, S. (2012): Entwicklung eines thermodynamischen Modells für Zink, Blei und Cadmium in salinaren Lösungen, GRS-Report 219, GRS, Braunschweig, Germany, 494 pp.

Hayashi, K., Sugaki, A. & Kitakaze, A. (1990): Solubility of sphalerite in aqueous sulphide solutions at temperatures between 25 and 240 °C. Geochim. Cosmochim. Acta, 54, 715-725.

Hummel, W., Berner, U., Curti, E., Pearson, F.J. & Thoenen, T. (2002): Nagra/PSI Chemical Thermodynamic Data Base 01/01. Nagra Technical Report NTB 02-16 and Universal Publishers, Parkland, Florida, 565 pp.

Lemire, R.J., Berner, U., Musikas, C., Palmer, D.A., Taylor, P. & Tochiyama, O. (2013): Chemical Thermodynamics of Iron, Part 1. Chemical Thermodynamics, Vol. 13a. OECD Publications, Paris, France, 1082 pp.

Powell, K.J., Brown, P.L., Byrne, R.H., Gajda, T., Hefter, G., Leuz, A.-K., Sjöberg, S. & Wanner, H. (2013): Chemical speciation of environmentally significant metals with inorganic ligands. Part 5: The Zn^{2+} + OH^-, Cl^-, CO_3^{2-}, SO_4^{2-}, and PO_4^{3-} systems. Pure Appl. Chem., 85, 2249-2311.

Preis, W. & Gamsjäger, H. (2001): (Solid + solute) phase equilibria in aqueous solution. XIII. Thermodynamic properties of hydrozincite and predominance diagrams for (Zn^{2+} + H_2O + CO_2). Journal of Chemical Thermodynamics, 33, 803-819.

Preis, W., Königsberger, E. & Gamsjäger, H. (2000): Solid-solute phase equilibria in aqueous solution. XII. Solubility and thermal decomposition of smithsonite. Journal of Solution Chemistry, 29, 605-618.

Ryan, M.P. & Bauman, Jr., J.E. (1978): Thermodynamics of the zinc bicarbonate ion pair. Inorganic Chemistry, 17, 3329-3331.

Schindler, P., Reinert, M. & Gamsjäger, H. (1969): Zur Thermodynamik der Metallcarbonate. 3. Mitteilung. Löslichkeitskonstanten und freie Bildungsenthalpien von $ZnCO_3$ und $Zn_5(OH)_6(CO_3)_2$ bei 25°. Helvetica Chimica Acta, 52, 2327-2332.

Soltermann, D., Marques Fernandes, M., Baeyens, B., Miehé-Brendlé, J. & Dähn, R. (2014): Competitive Fe(II)-Zn(II) uptake on a synthetic montmorillonite. Environmental Science & Technology 48, 190-198.

Stanley, Jr., J.K. & Byrne, R.H. (1990): Inorganic complexation of zinc(II) in seawater. Geochim. Cosmochim. Acta, 54, 753-760.

Ste-Marie, J., Torma, A.E. & Gübeli, A.O. (1964): The stability of thiocomplexes and solubility products of metal sulphides I. Cadmium sulphide. Canadian Journal of Chemistry, 42, 662-668.

Tagirov, B.R. & Seward, T.M. (2010): Hydrosulfide/sulfide complexes of zinc 250 °C and the thermodynamic properties of sphalerite. Chemical Geology, 269, 301-311.

Tagirov, B.R., Suleimenov, O.M. & Seward, T.M. (2007): Zinc complexation in aqueous sulfide solutions: Determination of the stoichiometry and stability of complexes via ZnS(cr) solubility measurements at 100 °C and 150 bars. Geochim. Cosmochim. Acta, 71, 4942-4953.

Acknowledgments

Special thanks go to Dr. Dan Miron who created all the scripts for entering the thermodynamic data of TDB 2020 with ThermoMatch into ThermoHub and for exporting/importing them into GEMS. Dan also prepared the export scripts for creating the tables of the selected thermodynamic data in the Appendix.

The entire manuscript of this report has undergone a peer review by an independent reviewer, according to Nagra's QA procedures. The peer review records may be obtained on request from Nagra. The peer reviewer was Prof. Dr, Vinzenz Brendler, Helmholtz-Zentrum Dresden-Rossendorf (HZDR), Dresden, Germany. His contributions are gratefully acknowledged.

Appendix: Tables of selected thermodynamic data

All tables of selected thermodynamic data were created with ThermoMatch (https://thermohub.org/thermomatch/thermomatch/), with minor manual editing. ThermoMatch is a graphical user interface (GUI) module for thermodynamic database management and consistency improvement, which was used to build and maintain all thermodynamic datasets and database records for TDB 2020 in the graph database ThermoHub (https://thermohub.org/thermohub/thermohub/).

For each aqueous species, liquid, gas, and solid, thermodynamic data were either entered into ThermoMatch for the substance itself, or for its formation reaction. This is reflected in the content of the following tables.

The selected standard state thermodynamic properties refer to pure solids, liquids, and gases, and to aqueous species at infinite dilution (I = 0), at the reference temperature of 298.15 K (25 °C) and the reference pressure of 0.1 MPa (1 bar).

Derived thermodynamic properties calculated by ThermoMatch from the entered "primary" data are followed by an asterisk (*).

The uncertainties represent the 95 % confidence level.

Explanations to Tab. A-1 to A3

Thermodynamic data of individual entities (elements, aqueous species, liquids, gases and solids) are tabulated as standard state properties of formation from the elements in their reference state:

$\Delta_f G_m°$	the standard molar Gibbs free energy of formation	(kJ · mol^{-1})
$\Delta_f H_m°$	the standard molar enthalpy of formation	(kJ · mol^{-1})

or as absolute quantities:

$S_m°$	the standard molar entropy	(J · K^{-1} · mol^{-1})
$C_{p,m}°$	the standard molar heat capacity	(J · K^{-1} · mol^{-1})

Tab. A-1 comprises thermodynamic data of elements.

Tab. A-2 comprises thermodynamic data of aqueous species, liquids and gases for which no reaction data were entered.

Tab. A-3 comprises thermodynamic data of solids for which no reaction data were entered.

Explanations to Tab. A-4 and A5:

Thermodynamic parameters of reactions include:

$\log_{10}K°$	the equilibrium constant of the reaction (logarithmic)	
$\Delta_r G_m°$	the standard molar Gibbs free energy of reaction	($kJ \cdot mol^{-1}$)
$\Delta_r H_m°$	the standard molar enthalpy of reaction	($kJ \cdot mol^{-1}$)
$\Delta_r S_m°$	the standard molar entropy of reaction	($J \cdot K^{-1} \cdot mol^{-1}$)
$\Delta_r C_{p,m}°$	the standard molar heat capacity of reaction	($J \cdot K^{-1} \cdot mol^{-1}$)

Tab. A-4 comprises thermodynamic data for the formation reactions of aqueous species and gases.

Tab. A-5 comprises thermodynamic data for the formation reactions of solids.

Notation of names of solids

In the following tables, H_2O given explicitly in a mineral name is represented by w. Thus, e.g., (UO2)3(PO4)2:4H2O(cr) is written as (UO2)3(PO4)2w4(cr).

Redox states: In some cases, in **Tab. A-3**, the redox state of an element in a mineral composition is indicated between two bars, as, e.g., in Hg|+2|Hg|0|Cl2.

Tab. A-1: Thermodynamic data of elements

Name	$\Delta_f G_m^o$ [kJ · mol^{-1}]	$\Delta_f H_m^o$ [kJ · mol^{-1}]	S_{um}^o [J · K^{-1} · mol^{-1}]	±	$C_{p,m}^o$ [J · K^{-1} · mol^{-1}]	±
Elements						
Ac	0	0	61.9	0.8	26	2
Ag	0	0	42.55	0.20	25.35	0.10
Al	0	0	28.3	0.10	24.20	0.07
Am	0	0	55.4	1.5		
As	0	0	35.1	0.6	24.64	0.5
B	0	0	5.90	0.08	11.087	0.10
Ba	0	0	62.42	0.84		
Br	0	0	76.105	0.30	37.845	
C	0	0	5.74	0.10	8.517	0.08
Ca	0	0	41.59	0.4	25.929	0.3
Cd	0	0	51.80	0.15	26.02	0.04
Cf	0	0	81	5		
Cl	0	0	111.540	0.010	16.974	0.002
Cm	0	0	70.8	3.0		
Cs	0	0	85.23	0.4	32.21	0.20
Cu	0	0	33.15	0.08	24.44	0.05
Eu	0	0	77.8		27.65	
F	0	0	101.395	0.005	15.652	0.002
Fe	0	0	27.085	0.16	25.084	0.5
H	0	0	65.340	0.003	14.418	0.002
Hg	0	0	75.90	0.12		
Ho	0	0	75.76		27.15	
I	0	0	58.07	0.30	27.219	
K	0	0	64.68	0.20	29.60	0.10
Li	0	0	29.12	0.20	24.86	0.20
Mg	0	0	32.67	0.10	24.869	0.02
Mn	0	0	32.01	0.08	26.32	
Mo	0	0	28.581	0.05	24.06	
N	0	0	95.805	0.004	14.562	0.001
Na	0	0	51.3	0.20	28.23	0.20
Nb	0	0	36.4		24.6	
Ni	0	0	29.87	0.20	26.07	0.10
Np	0	0	50.46	0.8	29.62	0.8
O	0	0	102.576	0.005	14.689	0.003
P	0	0	41.09	0.25	23.824	0.20
Pa	0	0	51.6	0.8	28.2	0.4

Tab. A-1: Cont.

Name	$\Delta_f G_m^o$ [kJ · mol^{-1}]	$\Delta_f H_m^o$ [kJ · mol^{-1}]	S_{um}^o [J · K^{-1} · mol^{-1}]	±	$C_{p,m}^o$ [J · K^{-1} · mol^{-1}]	±
Pb	0	0	64.8	0.3	26.65	0.10
Pd	0	0	37.8	0.4	25.9	0.3
Po	0	0	62.8			
Pu	0	0	54.46	0.8	31.49	0.4
Ra	0	0	71	5		
S	0	0	32.054	0.05	22.75	0.05
Se	0	0	42.09	0.33	25.09	0.30
Si	0	0	18.81	0.08	19.789	0.03
Sm	0	0	69.64		29.53	
Sn	0	0	51.18	0.08	27.11	0.08
Sr	0	0	55.7	0.21		
Tc	0	0	32.5	0.7	24.9	1.0
Th	0	0	52.64	0.5	26.23	0.5
Ti	0	0	30.72	0.10		
U	0	0	50.20	0.20	27.66	0.05
Zn	0	0	41.63	0.15	25.39	0.04
Zr	0	0	39.08	0.10	26.08	0.05

Tab. A-2: Thermodynamic data of aqueous species, liquids and gases

Name	$\Delta_f G_m^\circ$ [kJ · mol^{-1}]	±	$\Delta_f H_m^\circ$ [kJ · mol^{-1}]	±	S_m° [J · K^{-1} · mol^{-1}]	±	$C_{p,m}^\circ$ [J · K^{-1} · mol^{-1}]	±
Aqueous species								
Ac+3	-639.3	25.5	-653	25	-180	17		
Ag+	77.096	0.156	105.79	0.08	73.45	0.4		
Al+3	-487.2	2.3	-539.4	2.7	-342.8	5	-96	30
Am+3	-598.7	4.8	-616.7	1.5	-201	15		
AmO2+	-732.4	6.3	-804.3	5.4	-45.9	10.7		
B(OH)3(aq)	-969.268	0.82	-1'072.8	0.8	162.4	0.6		
Ba+2	-557.656	2.582	-534.8	2.5	8.4	2		
Br-	-103.85	0.167	-121.41	0.15	82.55	0.2		
Ca+2	-552.806	1.05	-543	1	-56.2	1		
Cd+2	-77.733	0.75	-75.92	0.6	-72.8	1.5		
Cf+3	-552.6	7.3	-577	5	-197	17		
Cit-3	-1'162.26	2.014	-1'198.165*		75.587	1.855		
Cl-	-131.217	0.117	-167.08	0.1	56.6	0.2		
ClO4-	-8.53536		-129.327		182.004		-24.0032	
Cm+3	-595.4	6.8	-615	6	-191	10		
Cs+	-291.456	0.535	-258	0.5	132.1	0.5		
Cu+	48.96	0.8						
Cu+2	65.04	1.56	64.9	1	-98	4		
e-	0		0		65.34	0.0015	14.418	0.001
Edta-4	0		-1'704.8	3.751	-5'456.6*			
Eu+3	-575.9	4.1	-605.4	4	-217.2	3.2	-80.6	20
F-	-281.523	0.692	-335.35	0.65	-13.8	0.8		
Fe+2	-90.72	0.64	-90.29	0.52	-102.17	2.78	-23	10
Fe+3	-16.23	0.65	-50.06	0.97	-282.4	3.93	-108	20
H+	0		0		0		0	
H2O(l)	-237.14	0.041	-285.83	0.04	69.95	0.03	75.351	0.08
H2Po(aq)	206.5							
H2Se(aq)	21.5	2	14.3	2	148.6	1		
H3Isa-	0							
HAsO4-2	-714.592	4.008	-906.34	4	-1.7	0.6		
HCO3-	-586.875		-690.215		98.4			
Hg+2	164.667	0.31	170.21	0.2	-36.19	0.8		
Hg2+2	153.567	0.56	166.87	0.5	65.74	0.8		
Ho+3	-675.6	3	-707.7	3	-228.7	1	-48.7	10
HPo-	209.3							
HPO4-2	-1'095.99	1.567	-1'299	1.5	-33.5	1.5		

Tab. A-2: Cont.

Name	$\Delta_f G_m^o$ [kJ · mol^{-1}]	±	$\Delta_f H_m^o$ [kJ · mol^{-1}]	±	S_m^o [J · K^{-1} · mol^{-1}]	±	$C_{p,m}^o$ [J · K^{-1} · mol^{-1}]	±
HSeO4-	-449.5	1.3	-582.7	4.7	136.2	16.4		
I-	-51.724	0.112	-56.78	0.05	106.45	0.3		
K+	-282.51	0.116	-252.14	0.08	101.2	0.2		
Li+	-292.918	0.109	-278.47	0.08	12.24	0.15		
Mg+2	-455.375	1.335	-467	0.6	-137	4		
Mn+2	-228.27	0.58	-220.8	0.5	-73.6	1		
Mn+3	-83	0.5	-113	2	-264.6*			
MoO4-2	-836.542	0.881	-996.807	0.826	32.03	4.05		
Na+	-261.953	0.096	-240.34	0.06	58.45	0.15		
Nb(OH)4+	-1'196		-1'375		42.4		179	
Ni+2	-45.77	0.77	-55.01	0.88	-131.8	1.4	-46.1	7.5
NO3-	-110.794	0.417	-206.85	0.4	146.7	0.4		
Np+3	-512.9	5.7	-527.2	2.1	-193.6	20.3		
Np+4	-491.8	5.6	-556	4.2	-426.4	12.4		
NpO2+	-907.8	5.6	-978.2	4.6	-45.9	10.7	-4	25
NpO2+2	-795.9	5.6	-860.7	4.7	-92.4	10.5		
Ox-2	-680.134	1.83	-704.905*		47.597	3.02		
Pa+4	-565.6	18.6	-621.4	14.3	-397	40		
PaO(OH)+2	-1'051.7	21.9	-1'115	21	-21	21		
Pb+2	-24.238	0.399	0.92	0.25	18.5	1		
Pd+2	175.4	2.6	176.8	2.6	-88.3	0.3		
Po-2	274							
Po+2	124.1							
Po+4	276.5							
PoCl4-2	-443.9							
PoCl6-2	-555.3							
PoSO4(aq)	-626.3							
Pu+3	-579	2.7	-591.8	2	-184.5	6.2		
Pu+4	-478	2.7	-539.9	3.1	-414.5	10.2		
PuO2+	-852.6	2.9	-910.2*		1	30		
PuO2+2	-762.4	2.8	-822	6.6	-71.2	22.1		
Ra+2	-561.5	2.9	-527.6	2	54	5		
SeO3-2	-362.39	1.76	-504.13*		5.1	7		
Si(OH)4(aq)	-1'309.18	1.12	-1'461.72	1.082	178.851	2.178	237.37	2.024
Sm+3	-665.3	2.2	-690	2	-209.3	3.1	-95.9	20
Sn+2	-27.39	0.3	-9.42	1.24	-19.2	4.3		
Sn+4	46.7	3.9	-31.5	7.3	-472.5	20.5		

Tab. A-2: Cont.

Name	$\Delta_f G_m^o$ [kJ · mol^{-1}]	±	$\Delta_f H_m^o$ [kJ · mol^{-1}]	±	S_m^o [J · K^{-1} · mol^{-1}]	±	$C_{p,m}^o$ [J · K^{-1} · mol^{-1}]	±
SO4-2	-744.004	0.418	-909.34	0.4	18.5	0.4		
Sr+2	-563.864	0.781	-550.9	0.5	-31.5	2		
Tc+3	71.2	11.2						
TcO(OH)2(aq)	-572.47	10.89						
TcO4-	-637.4	7.6	-729.4	7.6	199.6	1.5	-15	8
Th+4	-704.783	5.298	-768.7	2.3	-423.1	16	-224	15
Ti+3	-350	5						
TiO+2	-577.4	2.5						
U+4	-529.9	1.8	-591.2	3.3	-416.9	12.6	-220	50
UO2+	-961	1.8	-1'025.1	3	-25	8		
UO2+2	-952.55	1.75	-1'019	1.5	-98.2	3	42.4	3
Zn+2	-147.203	0.254	-153.39	0.2	-109.8	0.5		
Zr+4	-528.5	9.2	-608.5	5	-491	35.2		
Liquid								
Hg(l)	0		0		75.9	0.12		
Gas								
Hgg	31.842	0.054	61.38	0.04	174.971	0.005	20.786	0.001

Tab. A-3: Thermodynamic data of solids

Name	**Composition**	$\Delta_f G_m^\circ$ [kJ · mol^{-1}]	±	$\Delta_f H_m^\circ$ [kJ · mol^{-1}]	±	S_m° [J · K^{-1} · mol^{-1}]	±	$C_{p,m}^\circ$ [J · K^{-1} · mol^{-1}]	±
Ag(cr)	Ag|0|	0		0		42.55	0.2	25.35	0.1
Ag2Se(alpha)	Ag2Se|-2|	-46.9	1.3	-40.129	1.32	149.9	0.5	81.15	0.9
Analcime	Na2Al2Si4O12(H2O)2	-6'139.7		-6'575.84		469		425	
Beidellite_SBld-1	(Ca0.185K0.104)(Si3.574Al0.426)(Al1.812Mg0.090Fe|+3|0.112)O10(OH)2	-5'357.24	6.5	-5'720.69	6.5	293.53	0.4	318.58	
Beidellite(Ca)	Ca0.17Al2.34Si3.66O10(OH)2	-5'367.83		-5'737.91		262.47		304.9	
Beidellite(K)	K0.34Al2.34Si3.66O10(OH)2	-5'376.58		-5'749.86		266.65		310.35	
Beidellite(Mg)	Mg0.17Al2.34Si3.66O10(OH)2	-5'354.38		-5723.81		263.13		303.74	
Beidellite(Na)	Na0.34Al2.34Si3.66O10(OH)2	-5'376.75		-5'747.23		271.49		309.62	
Berthierine_ISGS	(Si1.332Al0.668)(Al0.976Fe|+3|0.182Fe|+2|1.44Mg0.157)O5(OH)4	- 3'461.94	7.3	-3'774.46	6.3	257	6.7	263.57	
Berthierine(FeII)	(Fe|+2|2Al)(SiAl)O5(OH)4	-3'454.11		-3'770.46		253.07		283.5	
Berthierine(FeIII)	(Fe|+2|2.34Fe|+3|0.33Al0.33)(Si1.34Al0.66)O5(OH)4	-3'153.29		-3'458.03		287.97		297.41	
CaMg(CO3)2(cr)	CaMg(CO3)2	-2'161.69	1.1	-2'324.47*		155.18	0.42	157.53	0.42
Cancrinite-NO3	Na8Al6Si6O24(NO3)2(H2O)4	-13'600.8		-14'717.6		1149		1119	
Chabazite-Ca	CaAl2Si4O12(H2O)6	-7'144.01		-7'806.74		581		617	
Chabazite-Na	Na2Al2Si4O12(H2O)6	-7'117.55		-7'808.31		548		578	
Clinoptilolite	Ca0.52Al1.04Si4.96O12(H2O)3.1	-6'151.94		-6'642.18		454		449	
Cronstedtite	(Fe|+2|2Fe|+3|)(SiFe|+3|)O5(OH)4	-2'616.84		-2'914.55		313.16		257.02	
Faujasite-X	Na2Al2Si2.5O9(H2O)6.2	-5'857.79		-6'456.94		566		586	
Faujasite-Y	Na2Al2Si4O12(H2O)8	-7'578.22		-8'352.62		734		739	
Fe(alpha)	Fe|0|	0		0		27.085	0.16	25.084	0.5
Glauconite	K0.75(Mg0.25Fe|+2|0.25Fe|+3|1.25Al0.25)(Al0.25Si3.75)O10(OH)2	-4'800.21		-5'151.13		366.58		344.54	
Heulandite_1	Ca1.07Al2.14Si6.86O18(H2O)4.4	-9'353.66		-10'118.6		541		611	
Heulandite_2	Ca1.07Al2.14Si6.86O18(H2O)4.5	-9'371.26		-10'131.2		581		619	
Hg2Cl2(cr)	Hg|+2|Hg|0|Cl2	-210.725	0.47	-265.37	0.4	191.6	0.8		

Tab. A-3: Cont.

Name	**Composition**	$\Delta_f G_m^\circ$ [kJ · mol^{-1}]	±	$\Delta_f H_m^\circ$ [kJ · mol^{-1}]	±	S_m° [J · K^{-1} · mol^{-1}]	±	$C_{p,m}^\circ$ [J · K^{-1} · mol^{-1}]	±
HgO(cr)	HgO	-58.523	0.15	-90.79	0.12	70.25	0.3		
Hydrosodalite	Na8Al6Si6O24 (OH)2(H2O)2	-13'221.4		-14'120.1		943		895	
Illite_IMt-2	(K0.762Na0.044) (Si3.387Al0.613) (Al1.427 Fe|+3|0.292Mg0.241 Fe|+2|0.084)O10 (OH)2	-5'325.87	8.5	-5'691.91*		324.92	0.2	328.21	
Illite(Al)	K0.85Al2.85Si3.15O10(OH)2	-5'537.36		-5'913.65		294.41		325.7	
Illite(FeII)	K0.85Fe|+2|0.25Al2.35Si3.4O10 (OH)2	-5'426.71		-5'796.29		314.23		329	
Illite(FeIII)	K0.85Fe|+3|0.25Al2.6Si3.15O10 (OH)2	-5'423.28		-5'795.39		308.1		329.28	
Illite(Mg)	K0.85Mg0.25Al2.35Si3.4O10(OH)2	-5'509.03		-5'881.39		306.28		326.41	
Linda_type_A	Na1.98Al1.98Si2.02O8(H2O)5.31	-5'203.75		-5'701.89		584		513	
Low-silica_P-Ca	CaAl2Si2O8 (H2O)4.5	-5'076.03		-5'527.74		491		435	
Low-silica_P-Na	Na2Al2Si2O8 (H2O)3.8	-4'858.72		-5'314.82		374		384	
Mn2O3(cr)	Mn|+3|2O3	-882.1	1	-959	1	113.7	0.2		
Mn3O4(cr)	Mn|+2|Mn|+3|2O4	-1'282.5	1.4	-1'384.5	1.5	164.1	0.2		
MnCO3(cr)	MnCO3	-818.13	0.55	-891.91	0.52	98.03	0.1		
MnO(cr)	MnO	-362.9	0.5	-385.22	0.5	59.71	0.4		
MnO2(cr)	Mn|+4|O2	-465	0.7	-520	0.7	52.8	0.1		
Molecular_sieve_4Å	Na2Al2Si2O8 (H2O)4.5	-5'029.88		-5'486.36		536		475	
Montmorillonite(HcCa)	Ca0.3Mg0.6Al1.4Si4O10(OH)2	-5'370.8		-5'734.42		288.96		310.34	
Montmorillonite(HcK)	K0.6Mg0.6Al1.4Si4O10(OH)2	-5'388.47		-5'757.74		296.34		319.96	
Montmorillonite(HcMg)	Mg0.3Mg0.6Al1.4Si4O10(OH)2	-5'346.75		-5'709.22		290.13		308.29	
Montmorillonite(HcNa)	Na0.6Mg0.6Al1.4Si4O10(OH)2	-5'370.31		-5'734.63		304.9		318.67	
Montmorillonite(MgCa)	Ca0.17Mg0.34Al1.66Si4O10(OH)2	-5'322.63		-5'690.29		268.85		305.88	
Montmorillonite(MgK)	K0.34Mg0.34Al1.66Si4O10(OH)2	-5'332.65		-5'703.51		273.04		311.33	
Montmorillonite(MgMg)	Mg0.17Mg0.34Al1.66Si4O10(OH)2	-5'309		-5'676.01		269.52		304.71	
Montmorillonite(MgNa)	Na0.34Mg0.34Al1.66Si4O10(OH)2	-5'322.35		-5'690.41		277.88		310.6	
MoO2(cr)	Mo|+4|O2	-533.053	2.51	-587.85	2.09	50.02	0.3		
MoO3(cr)	MoO3	-667.49	0.52	-744.6	0.5	77.66	0.5		

Tab. A-3: Cont.

Name	**Composition**	$\Delta_f G_m^\circ$ [kJ · mol^{-1}]	±	$\Delta_f H_m^\circ$ [kJ · mol^{-1}]	±	S_m° [J · K^{-1} · mol^{-1}]	±	$C_{p,m}^\circ$ [J · K^{-1} · mol^{-1}]	±
Mordenite-Ca	Ca0.34Al0.68Si5.32O12(H2O)2.9	-5'995.73		-6'489.11		386		404	
Mordenite-Na	Na0.72Al0.72Si5.28O12(H2O)2.71	-5'955.95		-6'442.4		388		405	
Natrolite	Na2Al2Si3O10(H2O)2	-5'305.15		-5'707.02		360		359	
Nontronite_Nau-1	(Ca0.247K0.020)(Si3.458Al0.542)(Fe|+3|1.688Al0.276Mg0.068)O10(OH)2	- 4'684.9	6.5	-5'035.69	5.3	332.75	7	335.15	
Nontronite(Ca)	Ca0.17Fe|+3|1.67Al0.67Si3.66O10(OH)2	-4'629.84		- 4'982.32		319.47		328.78	
Nontronite(K)	K0.34Fe|+3|1.67Al0.67Si3.66O10(OH)2	-4'638.59		-4'994.27		323.66		334.23	
Nontronite(Mg)	Mg0.17Fe|+3|1.67Al0.67Si3.66O10(OH)2	-4'616.39		-4'968.22		320.14		327.62	
Nontronite(Na)	Na0.34Fe|+3|1.67Al0.67Si3.66O10(OH)2	-4'628.76		-4'981.64		328.49		333.5	
Pb(cr)	Pb|0|	0	0	0	0	64.8	0.3	26.65	0.1
PbSO4(cr)	PbSO4	-813.036	0.447	-919.97	0.4	148.5	0.6		
Pd(cr)	Pd|0|	0		0		37.8	0.4	25.9	0.3
PdO(cr)	PdO	-82.68	0.35	-112.69	0.32	39.58	0.15	38.61	0.1
Phillipsite-Na	Na2.5Al2.5Si5.5O16(H2O)5	-8'717.83		-9'438.72		692		620	
Phillipsite-NaK	Na1.5KAl2.5Si5.5O16(H2O)5	-8'741.26		-9'461.67		707		626	
Po(cr)	Po|0|	0		0		62.8			
PoO2(s)	PoO2	-192.1							
Ripidolite_Cca-2	(Si2.633Al1.367)(Al1.116Fe|+3|0.215Mg2.952Fe|+2|1.712Mn0.012)(Ca0.011)O10(OH)8	-7'593.46	8.7	-8'240.14	8.6	469.4	2.9	547.02	
S(orth)	S|0|	0		0		32.054	1.6	22.75	
Saponite_SapCa-2	(Na0.394K0.021Ca0.038)(Si3.569Al0.397)(Mg2.949Fe|+3|0.034Fe|+2|0.021)O10(OH)2	-5'622.45		-5'994.06	4.9	314.55	1.6	346.87	
Saponite(Ca)	Ca0.17Mg3Al0.34Si3.66O10(OH)2	-5'624.15		-5'998.44		289.78		329.09	
Saponite(FeCa)	Ca0.17Mg2Fe|+2|Al0.34Si3.66O10(OH)2	-5'275.28		-5'633.57		337.85		339.5	
Saponite(FeK)	K0.34Mg2Fe|+2|Al0.34Si3.66O10(OH)2	-5'284.04		-5'645.53		342.04		344.95	

Tab. A-3: Cont.

Name	**Composition**	$\Delta_f G_m^\circ$ [kJ · mol^{-1}]	±	$\Delta_f H_m^\circ$ [kJ · mol^{-1}]	±	S_m° [J · K^{-1} · mol^{-1}]	±	$C_{p,m}^\circ$ [J · K^{-1} · mol^{-1}]	±
Saponite(FeMg)	Mg0.17Mg2Fe|+2|Al0.34Si3.66O10(OH)2	-5'261.84		-5'619.48		338.52		338.33	
Saponite(FeNa)	Na0.34Mg2Fe|+2|Al0.34Si3.66O10(OH)2	-5'275.2		-5'633.89		346.87		344.23	
Saponite(K)	K0.34Mg3Al0.34Si3.66O10(OH)2	-5'632.9		-6'010.39		293.96		334.54	
Saponite(Mg)	Mg0.17Mg3Al0.34Si3.66O10(OH)2	-5'610.7		-5'984.34		290.44		327.93	
Saponite(Na)	Na0.34Mg3Al0.34Si3.66O10(OH)2	-5'623.07		-5'997.76		298.8		333.81	
Scolecite	CaAl2Si3O10(H2O)3	-5'560.52		-6'011.65		367		383	
Se(cr)	Se|0|	0		0		42.09	0.33	25.09	0.3
SiO2(cr)	SiO2	-856.29	1.002	-910.7	1	41.46	0.2	44.602	0.3
Smectite_MX80	(Na0.409K0.024Ca0.009)(Si3.738Al0.262)(Al1.598Mg0.214Fe|+3|0.173Fe|+2|0.035)O10(OH)2	-5'293.18	5.4	-5'656.37	5.4	301.92	0.2	322.74	
Sn(beta)	Sn|0|	0		0		51.18	0.08	27.11	0.08
Sodalite	Na8Al6Si6O24Cl2	-12'719.1		-13'473.4		848		812	
Stilbite	Ca1.11Al2.22Si6.78O18(H2O)6.8	-9'944.75		-10'815.6		748		782	
Vermiculite_SO	Ca0.445(Si2.778Al1.222)(Al0.192Mg2.468 Fe|+3|0.226Fe|+2|0.028Ti0.018Mn0.007)O10(OH)2	-5'671.2	5.7	-6'039.4*		325.77	0.5	346.39	
Vermiculite(Ca)	Ca0.43Mg3Al0.86Si3.14O10(OH)2	-5'775.64		-6'148.06		311.78		336.4	
Vermiculite(K)	K0.86Mg3Al0.86Si3.14O10(OH)2	-5'792.89		-6'173.41		322.36		350.19	
Vermiculite(Mg)	Mg0.43Mg3Al0.86Si3.14O10(OH)2	-5'742.33		-6'113.11		313.46		333.46	
Vermiculite(Na)	Na0.86Mg3Al0.86Si3.14O10(OH)2	-5'769.82		-6'143.26		334.6		348.34	

Tab. A-4: Thermodynamic data for formation reactions of aqueous species and gases

Name	**Reaction**	**$\log_{10}K^{o}$**	±	$\Delta_r G_m^o$ [kJ · mol^{-1}]	$\Delta_r H_m^o$ [kJ · mol^{-1}]	±	$\Delta_r S_m^o$ [J · K^{-1} · mol^{-1}]	$\Delta_r C_{p,m}^o$ [J · K^{-1} · mol^{-1}]	±
Aqueous species									
(NpO2)2(OH)2+2	2NpO2+2 + 2H2O(l) -2H+ = (NpO2)2(OH)2+2	-6.27	0.21	35.789*					
(NpO2)2CO3(OH)3-	2NpO2+2 + 1CO3-2 + 3H2O(l) -3H+ = (NpO2)2CO3(OH)3-	-1.81	1.66	10.332*					
(NpO2)3(CO3)6-6	3NpO2+2 + 6CO3-2 = (NpO2)3(CO3)6-6	51.43	1.69	-293.565*					
(NpO2)3(OH)5+	3NpO2+2 + 5H2O(l) -5H+ = (NpO2)3(OH)5+	-17.12	0.22	97.722*					
(PuO2)2(OH)2+2	2PuO2+2 + 2H2O(l) -2H+ = (PuO2)2(OH)2+2	-7.5	1	42.81*	65.4	1	75.766*		
(PuO2)3(CO3)6-6	3PuO2+2 + 6CO3-2 = (PuO2)3(CO3)6-6	48.6	2.5	-277.411*					
(UEdtaOH)2-2	2UEdtaOH- = (UEdtaOH)2-2	2.7		-15.412*					
(UO2)2(OH)2+2	2UO2+2 + 2H2O(l) -2H+ = (UO2)2(OH)2+2	-5.62	0.08	32.079*	47.8	0.5	52.728*		
(UO2)2CO3(OH)3-	2UO2+2 + 1CO3-2 + 3H2O(l) -3H+ = (UO2)2CO3(OH)3-	-0.86	0.5	4.909*					
(UO2)2Edta(aq)	2UO2+2 + 1Edta-4 = (UO2)2Edta(aq)	20.6	0.4	-117.586*					
(UO2)2NpO2(CO3)6-6	2UO2+2 + 1NpO2+2 + 6CO3-2 = (UO2)2NpO2(CO3)6-6	53.59	2.7	-305.894*					
(UO2)2OH+3	2UO2+2 + 1H2O(l) -1H+ = (UO2)2OH+3	-2.7	1	15.412*					
(UO2)2PuO2(CO3)6-6	2UO2+2 + 1PuO2+2 + 6CO3-2 = (UO2)2PuO2(CO3)6-6	53.5	1.4	-305.38*					
(UO2)3(CO3)6-6	3UO2+2 + 6CO3-2 = (UO2)3(CO3)6-6	54	1	-308.234*	-62.7	2.4	823.526*		
(UO2)3(OH)4+2	3UO2+2 + 4H2O(l) -4H+ = (UO2)3(OH)4+2	-11.9	0.3	67.926*	99.2	0.5	104.895*		
(UO2)3(OH)5+	3UO2+2 + 5H2O(l) -5H+ = (UO2)3(OH)5+	-15.55	0.12	88.76*	120.7	0.6	107.127*		
(UO2)3(OH)7-	3UO2+2 + 7H2O(l) -7H+ = (UO2)3(OH)7-	-32.2	0.8	183.799*					
(UO2)3O(OH)2(HCO3)+	3UO2+2 + 1CO3-2 + 3H2O(l) -3H+ = (UO2)3O(OH)2(HCO3)+	0.66	0.5	-3.767*					
(UO2)4(OH)7+	4UO2+2 + 7H2O(l) -7H+ = (UO2)4(OH)7+	-21.9	1	125.006*					
(UO2Cit)2-2	2UO2+2 + 2Cit-3 = (UO2Cit)2-2	21.3	0.5	-121.581*					
Ac(Cit)(aq)	1Ac+3 + 1Cit-3 = Ac(Cit)(aq)	8.9	0.5	-50.802*					
Ac(Edta)-	1Ac+3 + 1Edta-4 = Ac(Edta)-	16.8	0.5	-95.895*					
Ac(OH)3(aq)	1Ac+3 + 3H2O(l) -3H+ = Ac(OH)3(aq)	-31.2	0.2	178.091*					
Ac(Ox)+	1Ac+3 + 1Ox-2 = Ac(Ox)+	5.9	0.6	-33.677*					

Tab. A-4: Cont.

Name	Reaction	$\log_{10}K^{\circ}$	±	$\Delta_r G_m^{\circ}$ [kJ · mol^{-1}]	$\Delta_r H_m^{\circ}$ [kJ · mol^{-1}]	±	$\Delta_r S_m^{\circ}$ [J · K^{-1} · mol^{-1}]	$\Delta_r C_{p,m}^{\circ}$ [J · K^{-1} · mol^{-1}]	±
Ac(Ox)2-	1Ac+3 + 2Ox-2 = Ac(Ox)2-	9.6	1.2	-54.797*					
AcCl+2	1Ac+3 + 1Cl- = AcCl+2	0.6	0.5	-3.425*					
AcF+2	1Ac+3 + 1F- = AcF+2	3.61	0.2	-20.606*					
AcF2+	1Ac+3 + 2F- = AcF2+	6.73	0.2	-38.415*					
AcF3(aq)	1Ac+3 + 3F- = AcF3(aq)	9.75		-55.653*					
AcH2PO4+2	1Ac+3 + 1H2PO4- = AcH2PO4+2	2.7	0.2	-15.412*					
AcHEdta(aq)	1Ac(Edta)- + 1H+ = AcHEdta(aq)	2.6	0.8	-14.841*					
AcOH+2	1Ac+3 + 1H2O(l) -1H+ = AcOH+2	-8.6	0.2	49.089*					
AcSCN+2	1Ac+3 + 1SCN- = AcSCN+2	1	0.5	-5.708*					
AcSO4+	1Ac+3 + 1SO4-2 = AcSO4+	3.5	0.2	-19.978*					
Ag(aq)	1Ag(cr) = Ag(aq)	-6.4	0.5	36.531*	33.7	8.5	-9.497*	0	
Ag(CN)2-	1Ag+ + 2CN- = Ag(CN)2-	20.88	0.2	-119.184*					
Ag(CN)3-2	1Ag+ + 3CN- = Ag(CN)3-2	21.8	0.2	-124.435*					
Ag(HS)2-	1Ag+ + 2HS- = Ag(HS)2-	17.4	0.28	-99.32*	-61.1	3.6	128.19*	0	
Ag(OH)2-	1Ag+ + 2H2O(l) -2H+ = Ag(OH)2-	-24.34	0.14	138.934*	69.1	4.7	-234.224*	0	
Ag(OH)CN-	1Ag+ + 1OH- + 1CN- = Ag(OH)CN-	13.3	0.3	-75.917*					
Ag(SeCN)3-2	1Ag+ + 3CN- + 3HSe- - 3H-6e- = Ag(SeCN)3-2	52.94	0.6	-302.184*					
Ag2S(HS)2-2	2Ag+ + 3HS- -1H+ = Ag2S(HS)2-2	31.1		-177.52*					
Ag2Se(aq)	1Ag2Se(alpha) = Ag2Se(aq)	-7.66	0.5	43.724*					
AgBr(aq)	1Ag+ + 1Br- = AgBr(aq)	4.54	0.1	-25.915*	-32.9	4	-23.429*	0	
AgBr2-	1Ag+ + 2Br- = AgBr2-	7.48	0.1	-42.696*	-48	4	-17.789*	0	
AgBr3-2	1Ag+ + 3Br- = AgBr3-2	8.3	0.2	-47.377*	-52.7		-17.854*		
AgBr4-3	1Ag+ + 4Br- = AgBr4-3	7.2		-41.098*					
AgCl(aq)	1Ag+ + 1Cl- = AgCl(aq)	3.23	0.11	-18.437*	-27.6	4.2	-30.733*	0	
AgCl2-	1Ag+ + 2Cl- = AgCl2-	5.15	0.11	-29.396*	-21.3	1.3	27.156*	0	
AgCl3-2	1Ag+ + 3Cl- = AgCl3-2	5.04	0.08	-28.769*	-41.8	2.1	-43.708*	0	
AgCl4-3	1Ag+ + 4Cl- = AgCl4-3	3.64	0.11	-20.777*	-69.9	4.2	-164.758*	0	
AgCO3-	1Ag+ + 1CO3-2 = AgCO3-	2.4		-13.699*					
AgF(aq)	1Ag+ + 1F- = AgF(aq)	0.11	0.1	-0.628*	-11.7	4.2	-37.136*	0	
AgHPO4-	1Ag+ + 1HPO4-2 = AgHPO4-	4.5		-25.686*					
AgHS(aq)	1Ag+ + 1HS- = AgHS(aq)	13.5		-77.059*					
AgI(aq)	1Ag+ + 1I- = AgI(aq)	6.29	0.1	-35.904*	-68.3	4	-108.658*	0	
AgI2-	1Ag+ + 2I- = AgI2-	11.42	0.1	-65.186*	-80	4	-49.687*	0	

Tab. A-4: Cont.

Name	**Reaction**	**$\log_{10}K^{o}$**	±	$\Delta_r G_m^{o}$ [kJ · mol^{-1}]	$\Delta_r H_m^{o}$ [kJ · mol^{-1}]	±	$\Delta_r S_m^{o}$ [J · K^{-1} · mol^{-1}]	$\Delta_r C_{p,m}^{o}$ [J · K^{-1} · mol^{-1}]	±
AgI3-2	1Ag+ + 3I- = AgI3-2	13.24	0.1	-75.574*	-101.4	4	-86.619*	0	
AgI4-3	1Ag+ + 4I- = AgI4-3	13.1		-74.775*					
AgOH(aq)	1Ag+ + 1H2O(l) -1H+ = AgOH(aq)	-11.75	0.14	67.069*	78.8	4.7	39.344*	0	
AgSeO3-	1Ag+ + 1SeO3-2 = AgSeO3-	3.1	0.3	-17.695*					
AgSeO4-	1Ag+ + 1SeO4-2 = AgSeO4-	1	0.5	-5.708*					
AgSO4-	1Ag+ + 1SO4-2 = AgSO4-	1.18	0.07	-6.735*	6.3	1.3	43.721*		
Al(OH)2+	1Al+3 + 2H2O(l) -2H+ = Al(OH)2+	-10.63	0.02	60.676*	110.8	0.8	168.115*	0	
Al(OH)2F(aq)	1Al(OH)4- + 1HF(aq) -1OH- -1H2O(l) = Al(OH)2F(aq)	1.41	0.15	-8.048*	-14.7	3	-22.31*	-201	27
Al(OH)2F2-	1Al(OH)4- + 2F- -2OH- = Al(OH)2F2-	-7.26	0.15	41.44*	75.2	2.8	113.23*	-216	22
Al(OH)3(aq)	1Al+3 + 3H2O(l) -3H+ = Al(OH)3(aq)	-15.99	0.23	91.272*	135.2	2.1	147.337*	0	
Al(OH)4-	1Al+3 + 4H2O(l) -4H+ = Al(OH)4-	-22.91	0.1	130.771*	190.4	2.5	199.996*	-182	27
Al(SO4)2-	1AlSO4+ + 1SO4-2 = Al(SO4)2-	1.89	0.2	-10.788*	-12.8	5	-6.748*	1'100	200
Al13(OH)32+7	13Al+3 + 32H2O(l) -32H+ = Al13(OH)32+7	-100.03	0.09	570.975*	1255.8	9.7	2296.913*	0	
Al2(OH)2+4	2Al+3 + 2H2O(l) -2H+ = Al2(OH)2+4	-7.62	0.11	43.495*	83.6	4.9	134.512*	0	
Al3(OH)4+5	3Al+3 + 4H2O(l) -4H+ = Al3(OH)4+5	-13.9	0.12	79.342*	146.3	4.5	224.579*	0	
AlF+2	1Al+3 + 1F- = AlF+2	7.08	0.07	-40.413*	4.81	0.2	151.678*		
AlF2+	1AlF+2 + 1F- = AlF2+	5.65	0.08	-32.25*	3.26	0.4	119.103*		
AlF3(aq)	1AlF2+ + 1F- = AlF3(aq)	4.05	0.11	-23.118*	0.79	0.4	80.186*		
AlF4-	1AlF3(aq) + 1F- = AlF4-	2.51	0.14	-14.327*	1.17	0.4	51.978*		
AlF5-2	1AlF4- + 1F- = AlF5-2	1	0.2	-5.708*	-3.14	0.4	8.613*		
AlF6-3	1AlF5-2 + 1F- = AlF6-3	0	0.3	0*	-6.5	0.8	-21.801*		
AlOH+2	1Al+3 + 1H2O(l) -1H+ = AlOH+2	-4.98	0.02	28.426*	56	0.5	92.483*	0	
AlOHF2(aq)	1Al(OH)4- + 2HF(aq) -1OH- -2H2O(l) = AlOHF2(aq)	2.63	0.15	-15.012*	-8.4	2.9	22.177*	-192	27
AlSiO(OH)3+2	1Al+3 + 1Si(OH)4(aq) -1H+ = AlSiO(OH)3+2	-2.32	0.22	13.243*	66.6	3	178.961*	0	
AlSO4+	1Al+3 + 1SO4-2 = AlSO4+	3.56	0.2	-20.321*	-10.7	5	32.268*	1'180	200
Am(Cit)(aq)	1Am+3 + 1Cit-3 = Am(Cit)(aq)	8.55	0.2	-48.804*					
Am(Cit)2-3	1Am+3 + 2Cit-3 = Am(Cit)2-3	13.9	1	-79.342*					
Am(CO3)2-	1Am+3 + 2CO3-2 = Am(CO3)2-	12.9	0.4	-73.634*					
Am(CO3)3-3	1Am+3 + 3CO3-2 = Am(CO3)3-3	15	0.5	-85.621*					

Tab. A-4: Cont.

Name	**Reaction**	**$\log_{10}K^{o}$**	±	$\Delta_r G_m^o$ [kJ · mol^{-1}]	$\Delta_r H_m^o$ [kJ · mol^{-1}]	±	$\Delta_r S_m^o$ [J · K^{-1} · mol^{-1}]	$\Delta_r C_{p,m}^o$ [J · K^{-1} · mol^{-1}]	±
Am(Edta)-	1Am+3 + 1Edta-4 = Am(Edta)-	19.67	0.11	-112.277*	-10.6	2	341.027*		
Am(Edta)OH-2	1Am(Edta)- + 1OH- = Am(Edta)OH-2	2.66	0.19	-15.183*					
Am(HCit)+	1Am+3 + 1HCit-2 = Am(HCit)+	6.5	1	-37.102*					
Am(HCit)2-	1Am+3 + 2HCit-2 = Am(HCit)2-	10.8	1	-61.647*					
Am(HEdta)(aq)	1Am(Edta)- + 1H+ = Am(HEdta)(aq)	2.17	0.25	-12.386*					
Am(Isa)-	1Am+3 + 1H3Isa- -3H+ = Am(Isa)-	22.2	1	-126.719*					
Am(NO3)2+	1Am+3 + 2NO3- = Am(NO3)2+	0.88	0.11	-5.023*	10.8	2.2	53.071*	0	
Am(OH)2+	1Am+3 + 2H2O(l) -2H+ = Am(OH)2+	-15.1	0.7	86.191*					
Am(OH)3(aq)	1Am+3 + 3H2O(l) -3H+ = Am(OH)3(aq)	-26.2	0.5	149.551*					
Am(Ox)+	1Am+3 + 1Ox-2 = Am(Ox)+	6.51	0.15	-37.159*					
Am(Ox)2-	1Am+3 + 2Ox-2 = Am(Ox)2-	10.71	0.2	-61.133*					
Am(Ox)3-3	1Am+3 + 3Ox-2 = Am(Ox)3-3	13	1	-74.205*					
Am(SO4)2-	1Am+3 + 2SO4-2 = Am(SO4)2-	5	1	-28.54*	70	7	330.505*	0	
AmCl+2	1Am+3 + 1Cl- = AmCl+2	0.24	0.35	-1.37*					
AmCl2+	1Am+3 + 2Cl- = AmCl2+	-0.81	0.35	4.624*	54.9	4.5	168.628*	0	
AmCO3+	1Am+3 + 1CO3-2 = AmCO3+	8	0.4	-45.664*					
AmF+2	1Am+3 + 1F- = AmF+2	3.4	0.3	-19.407*	12.1	2.2	105.676*	0	
AmF2+	1Am+3 + 2F- = AmF2+	5.8	0.2	-33.107*	45.1	14.5	262.306*	0	
AmH2PO4+2	1Am+3 + 1H2PO4- = AmH2PO4+2	2.46	0.13	-14.042*					
AmHCO3+2	1Am+3 + 1HCO3- = AmHCO3+2	3.1	0.3	-17.695*					
AmHPO4+	1Am+3 + 1HPO4-2 = AmHPO4+	6.2	0.8	-35.39*					
AmNO3+2	1Am+3 + 1NO3- = AmNO3+2	1.28	0.05	-7.306*	1.8	1	30.543*	0	
AmO2(CO3)2-3	1AmO2+ + 2CO3-2 = AmO2(CO3)2-3	6.7	0.8	-38.244*					
AmO2(CO3)3-5	1AmO2+ + 3CO3-2 = AmO2(CO3)3-5	5.1	1	-29.111*					
AmO2(OH)2-	1AmO2+ + 2H2O(l) -2H+ = AmO2(OH)2-	-23.6	0.5	134.71*					
AmO2CO3-	1AmO2+ + 1CO3-2 = AmO2CO3-	5.1	0.5	-29.111*					
AmO2OH(aq)	1AmO2+ + 1H2O(l) -1H+ = AmO2OH(aq)	-11.3	0.7	64.501*					

Tab. A-4: Cont.

Name	**Reaction**	**$\log_{10}K^{o}$**	±	$\Delta_r G_m^o$ [kJ · mol^{-1}]	$\Delta_r H_m^o$ [kJ · mol^{-1}]	±	$\Delta_r S_m^o$ [J · K^{-1} · mol^{-1}]	$\Delta_r C_{p,m}^o$ [J · K^{-1} · mol^{-1}]	±
AmOH+2	1Am+3 + 1H2O(l) -1H+ = AmOH+2	-7.2	0.5	41.098*					
AmSCN+2	1Am+3 + 1SCN- = AmSCN+2	1.3	0.3	-7.42*					
AmSiO(OH)3+2	1Am+3 + 1SiO(OH)3- = AmSiO(OH)3+2	7.8	0.5	-44.523*	15		199.64*		
AmSO4+	1Am+3 + 1SO4-2 = AmSO4+	3.5	0.3	-19.978*	40	4	201.168*	0	
As(OH)3(aq)	1HAsO4-2 + 4H+ + 2e- = 1H2O(l) + As(OH)3(aq)	28.441		-162.342*	-121.693		136.339*	31.827	
As(OH)4-	1As(OH)3(aq) + 1H2O(l) -1H+ = As(OH)4-	-9.232		52.697*	27.343		-85.037*		
AsO4-3	1HAsO4-2 -1H+ = AsO4-3	-11.603		66.23*	18.2		-161.095*		
B(OH)4-	1B(OH)3(aq) + 1H2O(l) -1H+ = B(OH)4-	-9.235		52.714*	14.053		-129.669*	-196.602	
Ba2UO2(CO3)3(aq)	2Ba+2 + 1UO2+2 + 3CO3-2 = Ba2UO2(CO3)3(aq)	29.75	0.5	-169.814*					
BaCO3(aq)	1Ba+2 + 1CO3-2 = BaCO3(aq)	2.68	0.05	-15.298*	12.6	1	93.569*	286	53
BaF+	1Ba+2 + 1F- = BaF+	0.67	0.21	-3.824*	11.7	3.4	52.069*	0	
BaH2PO4+	1Ba+2 + 1H2PO4- = BaH2PO4+	0.6	0.3	-3.425*					
BaHCO3+	1Ba+2 + 1HCO3- = BaHCO3+	0.99	0.05	-5.651*	22	2.8	92.742*	266	13
BaHPO4(aq)	1Ba+2 + 1HPO4-2 = BaHPO4(aq)	2.25	0.2	-12.843*					
BaOH+	1Ba+2 + 1H2O(l) -1H+ = BaOH+	-13.32	0.07	76.031*	60.9	10.5	-50.75*	0	
BaPO4-	1Ba+2 + 1PO4-3 = BaPO4-	4.7	0.3	-26.828*					
BaSO4(aq)	1Ba+2 + 1SO4-2 = BaSO4(aq)	2.27	0.04	-12.957*	3.2	0.6	54.192*	0	
BaUO2(CO3)3-2	1Ba+2 + 1UO2+2 + 3CO3-2 = BaUO2(CO3)3-2	25.6	0.3	-146.126*					
Ca(Cit)-	1Ca+2 + 1Cit-3 = Ca(Cit)-	4.8	0.03	-27.399*	0	6	91.895*	0	
Ca(Edta)-2	1Ca+2 + 1Edta-4 = Ca(Edta)-2	12.69	0.06	-72.435*	-22.2	0.4	168.489*		
Ca(H2Cit)+	1Ca+2 + 1H2Cit- = Ca(H2Cit)+	1.53	0.16	-8.733*					
Ca(H2Isa)(aq)	1Ca+2 + 1H3Isa- -1H+ = Ca(H2Isa)(aq)	-10.4	0.5	59.364*					
Ca(H3Isa)+	1Ca+2 + 1H3Isa- = Ca(H3Isa)+	1.7	0.3	-9.704*					
Ca(HCit)(aq)	1Ca+2 + 1HCit-2 = Ca(HCit)(aq)	2.92	0.07	-16.667*					
Ca(HEdta)-	1Ca(Edta)-2 + 1H+ = Ca(HEdta)-	3.54	0.09	-20.206*					
Ca(Ox)(aq)	1Ca+2 + 1Ox-2 = Ca(Ox)(aq)	3.19	0.06	-18.209*					

Tab. A-4: Cont.

Name	**Reaction**	**$\log_{10}K^{o}$**	±	$\Delta_r G_m^o$ [kJ · mol^{-1}]	$\Delta_r H_m^o$ [kJ · mol^{-1}]	±	$\Delta_r S_m^o$ [J · K^{-1} · mol^{-1}]	$\Delta_r C_{p,m}^o$ [J · K^{-1} · mol^{-1}]	±
Ca(Ox)2-2	1Ca+2 + 2Ox-2 = Ca(Ox)2-2	4.02	0.19	-22.946*					
Ca2Am(OH)4+3	2Ca+2 + 1Am+3 + 4H2O(l) -4H+ = Ca2Am(OH)4+3	-37.2	0.6	212.339*					
Ca2Cm(OH)4+3	2Ca+2 + 1Cm+3 + 4H2O(l) -4H+ =Ca2Cm(OH)4+3	-37.2	0.6	212.339*					
Ca2UO2(CO3)3(aq)	2Ca+2 + 1UO2+2 + 3CO3-2 = Ca2UO2(CO3)3(aq)	30.8	0.4	-175.808*	-47	6	432.023*		
Ca2Zr(OH)6+2	2Ca+2 + 1Zr+4 + 6H2O(l) -6H+ = Ca2Zr(OH)6+2	-22.6	0.3	129.002*					
Ca3Am(OH)6+3	3Ca+2 + 1Am+3 + 6H2O(l) -6H+ = Ca3Am(OH)6+3	-60.7	0.5	346.478*					
Ca3Cm(OH)6+3	3Ca+2 + 1Cm+3 + 6H2O(l) -6H+ = Ca3Cm(OH)6+3	-60.7	0.5	346.478*					
Ca3NpO2(OH)5+2	1NpO2+ + 3Ca+2 + 5H2O(l) -5H+ =Ca3NpO2(OH)5+2	-54.8	0.3	312.801*					
Ca3Zr(OH)6+4	3Ca+2 + 1Zr+4 + 6H2O(l) -6H+ = Ca3Zr(OH)6+4	-23.2	0.3	132.427*					
Ca4Np(OH)8+4	4Ca+2 + 1Np+4 + 8H2O(l) -8H+ = Ca4Np(OH)8+4	-56.1	0.8	320.221*					
Ca4Pu(OH)8+4	4Ca+2 + 1Pu+4 + 8H2O(l) -8H+ = Ca4Pu(OH)8+4	-56.2	0.6	320.792*					
Ca4Th(OH)8+4	4Ca+2 + 1Th+4 + 8H2O(l) -8H+ = Ca4Th(OH)8+4	-62.4	0.6	356.182*					
CaAm(OH)3+2	1Ca+2 + 1Am+3 + 3H2O(l) -3H+ = CaAm(OH)3+2	-26.3	0.5	150.122*					
CaCm(OH)3+2	1Ca+2 + 1Cm+3 + 3H2O(l) -3H+ = CaCm(OH)3+2	-26.3	0.5	150.122*					
CaCO3(aq)	1Ca+2 + 1CO3-2 = CaCO3(aq)	3.23	0.14	-18.437*	13.9	2.2	108.459*	447	130
CaF+	1Ca+2 + 1F- = CaF+	1.33	0.04	-7.592*	12.8	1	68.394*	0	
CaH2PO4+	1Ca+2 + 1H2PO4- = CaH2PO4+	0.99	0.09	-5.651*	3	13	29.015*	0	
CaHCO3+	1Ca+2 + 1HCO3- = CaHCO3+	1.07	0.07	-6.108*	8.7	2.5	49.665*	0	
CaHPO4(aq)	1Ca+2 + 1HPO4-2 = CaHPO4(aq)	2.58	0.05	-14.727*	13.1	6.3	93.331*	0	
CaMoO4(aq)	1Ca+2 + 1MoO4-2 = CaMoO4(aq)	2.5	0.5	-14.27*	7		71.34*		
CaNpO2(OH)2+	1NpO2+ + 1Ca+2 + 2H2O(l) -2H+ = CaNpO2(OH)2+	-20.6	0.2	117.586*					
CaOH+	1Ca+2 + 1H2O(l) -1H+ = CaOH+	-12.57	0.03	71.75*	53.9	1.4	-59.869*	-446.8	39.3

Tab. A-4: Cont.

Name	**Reaction**	**$\log_{10}K^{o}$**	±	$\Delta_r G_m^{o}$ [kJ · mol^{-1}]	$\Delta_r H_m^{o}$ [kJ · mol^{-1}]	±	$\Delta_r S_m^{o}$ [J · K^{-1} · mol^{-1}]	$\Delta_r C_{p,m}^{o}$ [J · K^{-1} · mol^{-1}]	±
CaPO4-	1Ca+2 + 1PO4-3 = CaPO4-	6.46	0.11	-36.874*	-1	18	120.322*	0	
CaSeO4(aq)	1Ca+2 + 1SeO4-2 = CaSeO4(aq)	2	0.1	-11.416*					
CaSiO(OH)3+	1Ca+2 + 1SiO(OH)3- = CaSiO(OH)3+	1.17	0.13	-6.678*					
CaSiO2(OH)2(aq)	1Ca+2 + 1SiO2(OH)2-2 = CaSiO2(OH)2(aq)	4.5	0.15	-25.686*					
CaSO4(aq)	1Ca+2 + 1SO4-2 = CaSO4(aq)	2.31	0.04	-13.186*	6.9	1.7	67.367*	0	
CaUO2(CO3)3-2	1Ca+2 + 1UO2+2 + 3CO3-2 = CaUO2(CO3)3-2	27	0.2	-154.117*	-47	6	359.273*		
CaZr(OH)6(aq)	1Ca+2 + 1Zr+4 + 6H2O(l) -6H+ = CaZr(OH)6(aq)	-24.6	0.3	140.418*					
Cd(CO3)2-2	1Cd+2 + 2CO3-2 = Cd(CO3)2-2	6.2		-35.39*					
Cd(HS)2(aq)	1Cd+2 + 2HS- = Cd(HS)2(aq)	14.43	0.05	-82.367*					
Cd(HS)3-	1Cd+2 + 3HS- = Cd(HS)3-	16.3	0.6	-93.041*					
Cd(HS)4-2	1Cd+2 + 4HS- = Cd(HS)4-2	18.43	0.05	-105.199*					
Cd(OH)2(aq)	1Cd+2 + 2H2O(l) -2H+ = Cd(OH)2(aq)	-20.19	0.13	115.245*					
Cd(OH)3-	1Cd+2 + 3H2O(l) -3H+ = Cd(OH)3-	-33.5	0.5	191.219*					
Cd(OH)4-2	1Cd+2 + 4H2O(l) -4H+ = Cd(OH)4-2	-47.28	0.15	269.876*					
Cd(SO4)2-2	1Cd+2 + 2SO4-2 = Cd(SO4)2-2	3.32	0.15	-18.951*	5.7	2.5	82.679*		
Cd2OH+3	2Cd+2 + 1H2O(l) -1H+ = Cd2OH+3	-8.74	0.1	49.888*	45.6	2	-14.383*		
CdCl+	1Cd+2 + 1Cl- = CdCl+	1.98	0.06	-11.302*	3.3	0.6	48.975*		
CdCl2(aq)	1Cd+2 + 2Cl- = CdCl2(aq)	2.64	0.09	-15.069*	7.9	1.4	77.039*		
CdCl3-	1Cd+2 + 3Cl- = CdCl3-	2.3	0.21	-13.128*					
CdCl4-2	1Cd+2 + 4Cl- = CdCl4-2	1.7		-9.704*					
CdCO3(aq)	1Cd+2 + 1CO3-2 = CdCO3(aq)	4.4	0.2	-25.115*					
CdH2PO4+	1Cd+2 + 1H2PO4- = CdH2PO4+	1.9	0.4	-10.845*					
CdHCO3+	1Cd+2 + 1HCO3- = CdHCO3+	1.7	0.4	-9.704*					
CdHPO4(aq)	1Cd+2 + 1HPO4-2 = CdHPO4(aq)	3.72	0.2	-21.234*					
CdHS+	1Cd+2 + 1HS- = CdHS+	7.4	0.7	-42.24*					
CdOH+	1Cd+2 + 1H2O(l) -1H+ = CdOH+	-9.8	0.1	55.939*	54.8	2	-3.82*		
CdS(HS)-	1Cd+2 + 2HS- -1H+ = CdS(HS)-	6.8	0.2	-38.815*					

Tab. A-4: Cont.

Name	**Reaction**	**$\log_{10}K^{o}$**	±	$\Delta_r G_m^{o}$ [kJ · mol^{-1}]	$\Delta_r H_m^{o}$ [kJ · mol^{-1}]	±	$\Delta_r S_m^{o}$ [J · K^{-1} · mol^{-1}]	$\Delta_r C_{p,m}^{o}$ [J · K^{-1} · mol^{-1}]	±
CdSO4(aq)	1Cd+2 + 1SO4-2 = CdSO4(aq)	2.36	0.04	-13.471*	8.3	0.5	73.02*		
CfF+2	1Cf+3 + +1F- = CfF+2	4	0.4	-22.832*	11.8	1.6	116.157*		
CfSCN+2	1Cf+3 + +1SCN- = CfSCN+2	1.5	0.3	-8.562*					
CfSO4+	1Cf+3 + +1SO4-2 = CfSO4+	3.6	0.4	-20.549*	18.1	3.1	129.629*		
CH4(aq)	1HCO3- + 9H+ + 8e- = 3H2O(l) + CH4(aq)	27.849		-158.963*	-255.882		-325.067*	429.061	
Cm(CO3)2-	1Cm+3 + 2CO3-2 = Cm(CO3)2-	12.9	0.4	-73.634*					
Cm(CO3)3-3	1Cm+3 + 3CO3-2 = Cm(CO3)3-3	15	0.5	-85.621*					
Cm(NO3)2+	1Cm+3 + 2NO3- = Cm(NO3)2+	0.88	0.11	-5.023*	10.8	2.2	53.071*	0	
Cm(OH)2+	1Cm+3 + 2H2O(l) -2H+ = Cm(OH)2+	-15.1	0.7	86.191*					
Cm(OH)3(aq)	1Cm+3 + 3H2O(l) -3H+ = Cm(OH)3(aq)	-26.2	0.5	149.551*					
Cm(SO4)2-	1Cm+3 + 2SO4-2 = Cm(SO4)2-	5	1	-28.54*	70	7	330.505*	0	
CmCl+2	1Cm+3 + 1Cl- = CmCl+2	0.24	0.35	-1.37*					
CmCl2+	1Cm+3 + 2Cl- = CmCl2+	-0.81	0.35	4.624*	54.9	4.5	168.628*	0	
CmCO3+	1Cm+3 + 1CO3-2 = CmCO3+	8	0.4	-45.664*					
CmF+2	1Cm+3 + 1F- = CmF+2	3.4	0.3	-19.407*	12.1	2.2	105.676*	0	
CmF2+	1Cm+3 + 2F- = CmF2+	5.8	0.2	-33.107*	45.1	14.5	262.306*	0	
CmH2PO4+2	1Cm+3 + 1H2PO4- = CmH2PO4+2	2.46	0.13	-14.042*					
CmHCO3+2	1Cm+3 + 1HCO3- = CmHCO3+2	3.1	0.3	-17.695*					
CmHPO4+	1Cm+3 + 1HPO4-2 = CmHPO4+	6.2	0.8	-35.39*					
CmNO3+2	1Cm+3 + 1NO3- = CmNO3+2	1.28	0.05	-7.306*	1.8	1	30.543*	0	
CmOH+2	1Cm+3 + 1H2O(l) -1H+ = CmOH+2	-7.2	0.5	41.098*					
CmSCN+2	1Cm+3 + 1SCN- = CmSCN+2	1.3	0.3	-7.42*					
CmSiO(OH)3+2	1Cm+3 + 1SiO(OH)3- = CmSiO(OH)3+2	7.8	0.5	-44.523*	15.8	4	202.323*	0	
CmSO4+	1Cm+3 + 1SO4-2 = CmSO4+	3.5	0.3	-19.978*	40	4	201.168*	0	
CN-	1HCN(aq) -1H+ = CN-	-9.21		52.571*	43.6		-30.089*		
CO2(aq)	1H+ -1H2O(l) + 1HCO3- = CO2(aq)	6.352		-36.257*	-9.109		91.056*	366.658	
CO3-2	-1H+ + 1HCO3- = CO3-2	-10.329		58.958*	14.901		-147.769*	-290.513	
Cu(CO3)2-2	1Cu+2 + 2HCO3- -2H+ = Cu(CO3)2-2	-10.3	0.1	58.793*					

Tab. A-4: Cont.

Name	**Reaction**	**$\log_{10}K^{o}$**	±	$\Delta_r G_m^{o}$ [kJ · mol^{-1}]	$\Delta_r H_m^{o}$ [kJ · mol^{-1}]	±	$\Delta_r S_m^{o}$ [J · K^{-1} · mol^{-1}]	$\Delta_r C_{p,m}^{o}$ [J · K^{-1} · mol^{-1}]	±
Cu(CO3)OH-	1Cu+2 + 1CO3-2 + 1OH- = Cu(CO3)OH-	11.21	0.3	-63.987*					
Cu(H2PO4)(HPO4)-	1Cu+2 + 1H2PO4- + 1HPO4-2 = Cu(H2PO4)(HPO4)-	5.4	0.2	-30.823*					
Cu(H2PO4)(HPO4)-2	1Cu+ + 2H2PO4- -1H+ = Cu(H2PO4)(HPO4)-2	-3	0.2	17.124*					
Cu(H2PO4)2-	1Cu+ + 2H2PO4- = Cu(H2PO4)2-	1.8	0.2	-10.274*					
Cu(H2PO4)2(aq)	1Cu+2 + 2H2PO4- = Cu(H2PO4)2(aq)	1.9	0.2	-10.845*					
Cu(HPO4)2-2	1Cu+2 + 2HPO4-2 = Cu(HPO4)2-2	7.4	0.2	-42.24*					
Cu(HS)2-	1Cu+ + 2HS- = Cu(HS)2-	17.18	0.13	-98.064*	-102	7	-13.201*	800	300
Cu(OH)2-	1Cu+ + 2H2O(l) -2H+ = Cu(OH)2-	-18.64	0.6	106.398*	61	12	-152.265*	-277	98
Cu(OH)2(aq)	1Cu+2 + 2H2O(l) -2H+ = Cu(OH)2(aq)	-16.2	0.2	92.47*	89.9	0.7	-8.621*	1'174	6
Cu(OH)3-	1Cu+2 + 3H2O(l) -3H+ = Cu(OH)3-	-26.6	0.09	151.834*					
Cu(OH)4-2	1Cu+2 + 4H2O(l) -4H+ = Cu(OH)4-2	-39.74	0.18	226.838*	167	5.7	-200.696*	864	57
Cu2(OH)2+2	2Cu+2 + 2H2O(l) -2H+ = Cu2(OH)2+2	-10.43	0.07	59.535*	71.4	5	39.796*	0	
Cu2Cl4-2	2Cu+ + 4Cl- = Cu2Cl4-2	10.32	0.5	-58.907*					
Cu2OH+3	2Cu+2 + 1H2O(l) -1H+ = Cu2OH+3	-6.4	0.12	36.531*					
Cu2S(HS)2-2	2Cu+ + 3HS- -1H+ = Cu2S(HS)2-2	29.87	0.13	-170.499*					
Cu3(OH)4+2	3Cu+2 + 4H2O(l) -4H+ = Cu3(OH)4+2	-21.1	0.2	120.44*					
CuCl(aq)	1Cu+ + 1Cl- = CuCl(aq)	3.3	0.25	-18.837*					
CuCl+	1Cu+2 + 1Cl- = CuCl+	0.83	0.09	-4.738*					
CuCl2-	1Cu+ + 2Cl- = CuCl2-	5.48	0.25	-31.28*					
CuCl2(aq)	1Cu+2 + 2Cl- = CuCl2(aq)	0.6	0.3	-3.425*					
CuCl3-2	1Cu+ + 3Cl- = CuCl3-2	4.81	0.25	-27.456*					
CuCO3(aq)	1Cu+2 + 1HCO3- -1H+ = CuCO3(aq)	-3.56	0.03	20.321*					
CuH2PO4(aq)	1Cu+ + 1H2PO4- = CuH2PO4(aq)	0.87	0.3	-4.966*					
CuH2PO4+	1Cu+2 + 1H2PO4- = CuH2PO4+	1.14	0.15	-6.507*					
CuHCO3+	1Cu+2 + 1HCO3- = CuHCO3+	1.84	0.1	-10.503*					
CuHPO4(aq)	1Cu+2 + 1HPO4-2 = CuHPO4(aq)	4.11	0.3	-23.46*					
CuHS(aq)	1Cu+ + 1HS- = CuHS(aq)	13		-74.205*					
CuOH(aq)	1Cu+ + 1H2O(l) -1H+ = CuOH(aq)	-7.85	0.41	44.808*	41.3	4.4	-11.766*	-848	123

Tab. A-4: Cont.

Name	**Reaction**	**$\log_{10}K^{o}$**	±	$\Delta_r G_m^{o}$ [kJ · mol^{-1}]	$\Delta_r H_m^{o}$ [kJ · mol^{-1}]	±	$\Delta_r S_m^{o}$ [J · K^{-1} · mol^{-1}]	$\Delta_r C_{p,m}^{o}$ [J · K^{-1} · mol^{-1}]	±
CuOH+	1Cu+2 + 1H2O(l) -1H+ = CuOH+	-7.95	0.16	45.379*	66	2.8	69.163*	1'008	23
CuSO4(aq)	1Cu+2 + 1SO4-2 = CuSO4(aq)	2.35	0.05	-13.414*	7.3	1.5	69.475*		
Eu(CO3)2-	1Eu+3 + 2CO3-2 = Eu(CO3)2-	12.1	0.3	-69.067*					
Eu(OH)2+	1Eu+3 + 2H2O(l) -2H+ = Eu(OH)2+	-15.1	0.2	86.191*					
Eu(OH)3(aq)	1Eu+3 + 3H2O(l) -3H+ = Eu(OH)3(aq)	-23.7	0.1	135.281*					
Eu(OH)4-	1Eu+3 + 4H2O(l) -4H+ = Eu(OH)4-	-36.2	0.5	206.631*					
Eu(SO4)2-	1Eu+3 + 2SO4-2 = Eu(SO4)2-	5.7	0.2	-32.536*					
EuCO3+	1Eu+3 + 1CO3-2 = EuCO3+	8.1	0.2	-46.235*					
EuF+2	1Eu+3 + 1F- = EuF+2	4.28	0.07	-24.43*	8.1	0.91	109.108*	0	
EuF2+	1Eu+3 + 2F- = EuF2+	6.81	0.3	-38.872*	18.5	2.3	192.426*	0	
EuH2PO4+2	1Eu+3 + 1H3PO4(aq) - 1H+ = EuH2PO4+2	0.89	0.13	-5.08*	14.7		66.343*	0	
EuOH+2	1Eu+3 + 1H2O(l) -1H+ = EuOH+2	-7.64	0.04	43.609*					
EuSiO(OH)3+2	1Eu+3 + 1SiO(OH)3- = EuSiO(OH)3+2	7.8	0.5	-44.523*	14.5	2	197.963*	0	
EuSO4+	1Eu+3 + 1SO4-2 = EuSO4+	3.95	0.08	-22.547*					
Fe(CN)6-3	1Fe+3 + 6CN- = Fe(CN)6-3	47.39	5.12	-270.504*	286.9	32.8	1'869.543*		
Fe(CN)6-4	1Fe+2 + 6CN- = Fe(CN)6-4	40.41	4.57	-230.662*	-358.9	30.1	-430.112*		
Fe(CO3)2-2	1Fe+2 + 2HCO3- -2H+ = Fe(CO3)2-2	-13.33	0.29	76.088*					
Fe(CO3)3-3	1Fe+3 + 3CO3-2 = Fe(CO3)3-3	24	2	-136.993*					
Fe(H2PO4)3(aq)	1Fe+3 + 3H3PO4(aq) - 3H+ = Fe(H2PO4)3(aq)	3.5	1	-19.978*					
Fe(HSeO4)2(aq)	1Fe+2 + 2HSeO4- = Fe(HSeO4)2(aq)	5.7	1	-32.536*					
Fe(OH)2(aq)	1Fe+2 + 2H2O(l) -2H+ = Fe(OH)2(aq)	-20.52	0.08	117.129*	115.4	1	-5.799*	0	
Fe(OH)2+	1Fe+3 + 2H2O(l) -2H+ = Fe(OH)2+	-5.71	0.1	32.593*					
Fe(OH)3-	1Fe+2 + 3H2O(l) -3H+ = Fe(OH)3-	-32.68	0.15	186.539*	140.3	2.2	-155.086*	0	
Fe(OH)3(aq)	1Fe+3 + 3H2O(l) -3H+ = Fe(OH)3(aq)	-12.26	0.26	69.981*	146.3	4.8	255.977*	-150	43
Fe(OH)4-	1Fe+3 + 4H2O(l) -4H+ = Fe(OH)4-	-21.6	0.23	123.294*	146.8	1.8	78.84*	0	
Fe(OH)CO3(aq)	1Fe+3 + 1CO3-2 + 1H2O(l) -1H+ = Fe(OH)CO3(aq)	10.7	2	-61.076*					

Tab. A-4: Cont.

Name	**Reaction**	**$\log_{10}K^{o}$**	±	$\Delta_r G_m^{o}$ [kJ · mol^{-1}]	$\Delta_r H_m^{o}$ [kJ · mol^{-1}]	±	$\Delta_r S_m^{o}$ [J · K^{-1} · mol^{-1}]	$\Delta_r C_{p,m}^{o}$ [J · K^{-1} · mol^{-1}]	±
Fe(SCN)2+	1FeSCN+2 + 1SCN- = Fe(SCN)2+	2.23	0.5	-12.729*					
Fe(SO4)2-	1Fe+3 + 2SO4-2 = Fe(SO4)2-	6.22	0.16	-35.504*					
Fe(SO4)2-2	1Fe+2 + 2SO4-2 = Fe(SO4)2-2	2	0.4	-11.416*					
Fe2(OH)2+4	2Fe+3 + 2H2O(l) -2H+ = Fe2(OH)2+4	-2.91	0.07	16.61*	30.1	9.5	45.244*	0	
Fe3(OH)4+5	3Fe+3 + 4H2O(l) -4H+ = Fe3(OH)4+5	-6.3		35.961*	59.8		79.958*		
FeCl+	1Fe+2 + 1Cl- = FeCl+	-1	0.8	5.708*	21.55	1.77	53.134*	0	
FeCl+2	1Fe+3 + 1Cl- = FeCl+2	1.52	0.1	-8.676*	22.48	4.6	104.498*	0	
FeCl2+	1Fe+3 + 2Cl- = FeCl2+	2.2	0.2	-12.558*					
FeCl3(aq)	1Fe+3 + 3Cl- = FeCl3(aq)	1	0.3	-5.708*					
FeCl4-	1Fe+3 + 4Cl- = FeCl4-	-1	0.8	5.708*					
FeCO3(aq)	1Fe+2 + 1HCO3- -1H+ = FeCO3(aq)	-4.77	0.27	27.227*					
FeF+	1Fe+2 + 1F- = FeF+	1.7	0.2	-9.704*					
FeF+2	1Fe+3 + 1F- = FeF+2	6.09	0.04	-34.762*	12.8	7.4	159.524*	0	
FeF2+	1Fe+3 + 2F- = FeF2+	10.41	0.33	-59.421*	22	14	273.086*	0	
FeH2PO4+	1Fe+2 + 1H2PO4- = FeH2PO4+	2.7	1	-15.412*					
FeHPO4(aq)	1Fe+2 + 1HPO4-2 = FeHPO4(aq)	3.6	1	-20.549*					
FeHSeO3(H2SeO3)+	1Fe+2 + 1HSeO3- + 1H2SeO3(aq) = FeHSeO3(H2SeO3)+	7	1	-39.956*					
FeHSeO3+	1Fe+2 + 1HSeO3- = FeHSeO3+	3.7	1.05	-21.12*					
FeHSO4+	1Fe+2 + 1SO4-2 + 1H+ = FeHSO4+	3.068		-17.512*					
FeHSO4+2	1Fe+3 + 1HSO4- = FeHSO4+2	1.73	0.76	-9.875*					
FeOH+	1Fe+2 + 1H2O(l) -1H+ = FeOH+	-9.43	0.1	53.827*	54.6	0.9	2.593*	0	
FeOH+2	1Fe+3 + 1H2O(l) -1H+ = FeOH+2	-2.2	0.02	12.558*	43.3	0.6	103.11*	0	
FePO4(aq)	1Fe+3 + 1H3PO4(aq) -3H+ = FePO4(aq)	0.7	1	-3.996*					
FeS(aq)	1Fe+2 + 1H2S(aq) -2H+ = FeS(aq)	-8.8	1.1	50.231*					
FeSCN+2	1Fe+3 + 1SCN- = FeSCN+2	3.06	0.05	-17.467*					
FeSeO3+	1Fe+3 + 1H2SeO3(aq) -2H+ = FeSeO3+	0.9	0.5	-5.137*					
FeSiO(OH)3+2	1Fe+3 + 1SiO(OH)3- = FeSiO(OH)3+2	9.69	0.06	-55.311*					
FeSO4(aq)	1Fe+2 + 1SO4-2 = FeSO4(aq)	2.44	0.03	-13.928*	8.4	6.2	74.887*	0	

Tab. A-4: Cont.

Name	**Reaction**	**$\log_{10}K^{o}$**	±	$\Delta_r G_m^{o}$ [kJ · mol^{-1}]	$\Delta_r H_m^{o}$ [kJ · mol^{-1}]	±	$\Delta_r S_m^{o}$ [J · K^{-1} · mol^{-1}]	$\Delta_r C_{p,m}^{o}$ [J · K^{-1} · mol^{-1}]	±
FeSO4+	1Fe+3 + 1SO4-2 = FeSO4+	4.25	0.1	-24.259*					
H2(aq)	2H+ + 2e- = H2(aq)	-3.105		17.723*	-4.039		-72.992*	144.187	
H2AsO4-	1HAsO4-2 + 1H+ = H2AsO4-	6.764		-38.609*	-3.22		118.696*		
H2Cit-	1HCit-2 + 1H+ = H2Cit-	4.78	0.01	-27.284*	-2.4	0.3	83.463*	167	8
H2Edta-2	1HEdta-3 + 1H+ = H2Edta-2	6.8	0.02	-38.815*	-15.2	0.4	79.204*		
H2Fe(CN)6-2	1HFe(CN)6-3 + 1H+ = H2Fe(CN)6-2	2.4	0.3	-13.699*					
H2MoO4(aq)	2H+ + 1MoO4-2 = H2MoO4(aq)	8.1	0.1	-46.235*	-35.02	5.1	37.616*	0	
H2Nb6O19-6	1Nb6O19-8 + 2H+ = H2Nb6O19-6	27	0.4	-154.117*					
H2Ox(aq)	1HOx- + 1H+ = H2Ox(aq)	1.4	0.03	-7.991*	3.3	0.5	37.871*		
H2PO4-	1HPO4-2 + 1H+ = H2PO4-	7.212		-41.166*	-3.6		125.998*		
H2S(aq)	1HS- + 1H+ = H2S(aq)	6.99		-39.899*	-22.3		59.028*		
H2SeO3(aq)	1HSeO3- + 1H+ = H2SeO3(aq)	2.64	0.14	-15.069*					
H3AsO4(aq)	1HAsO4-2 + 2H+ = H3AsO4(aq)	9.027		-51.526*	3.84		185.7*		
H3Cit(aq)	1H2Cit- + 1H+ = H3Cit(aq)	3.13	0.01	-17.866*	-4.5	0.3	44.83*	116	6
H3Edta-	1H2Edta-2 + 1H+ = H3Edta-	3.15	0.02	-17.98*	7.1	0.4	84.12*		
H3Nb6O19-5	6Nb(OH)5(aq) -5H+ -11H2O(l) = H3Nb6O19-5	-20.6	0.8	117.586*					
H3PO4(aq)	1HPO4-2 + 2H+ = H3PO4(aq)	9.352		-53.382*	4.88		195.41*		
H4Edta(aq)	1H3Edta- + 1H+ = H4Edta(aq)	2.23	0.05	-12.729*	1.9	1.5	49.066*		
H4Isa(aq)	1H3Isa- + 1H+ = H4Isa(aq)	4	0.5	-22.832*					
H5Edta+	1H4Edta(aq) + 1H+ = H5Edta+	1.3	0.1	-7.42*					
H6Edta+2	1H5Edta+ + 1H+ = H6Edta+2	-0.5	0.2	2.854*					
HCit-2	1Cit-3 + 1H+ = HCit-2	6.36	0.02	-36.303*	3.3	0.3	132.83*	222	14
HCN(aq)	13H+ + 1CO3-2 + 1NO3- + 10e- -6H2O(l) = HCN(aq)	117.336		-669.759*	-729.066		-198.917*		
HEdta-3	1Edta-4 + 1H+ = HEdta-3	11.24	0.03	-64.158*	-19.8	0.5	148.779*		
HF(aq)	1H+ + 1F- = HF(aq)	3.176		-18.129*	13.307		105.436*	144.356	
HF2-	1H+ + 2F- = HF2-	3.62		-20.663*	15.2		120.285*	273.6	
HFe(CN)6-3	1Fe(CN)6-4 + 1H+ = HFe(CN)6-3	4.28	0.1	-24.43*	2.1	3	88.983*		
Hg(aq)	1Hg(l) = Hg(aq)	-6.53	0.03	37.274*	23	2.2	-47.874*	0	

Tab. A-4: Cont.

Name	**Reaction**	**$\log_{10}K^{o}$**	±	$\Delta_r G_m^{o}$ [kJ · mol^{-1}]	$\Delta_r H_m^{o}$ [kJ · mol^{-1}]	±	$\Delta_r S_m^{o}$ [J · K^{-1} · mol^{-1}]	$\Delta_r C_{p,m}^{o}$ [J · K^{-1} · mol^{-1}]	±
Hg(HS)2(aq)	1Hg+2 + 2HS- = Hg(HS)2(aq)	37.8		-215.764*					
Hg(OH)2(aq)	1Hg+2 + 2H2O(l) -2H+ = Hg(OH)2(aq)	-5.98	0.06	34.134*	51	1.8	56.569*		
Hg(OH)3-	1Hg+2 + 3H2O(l) -3H+ = Hg(OH)3-	-21.1	0.3	120.44*					
Hg(SO4)2-2	1Hg+2 + 2SO4-2 = Hg(SO4)2-2	3.8		-21.691*					
Hg2OH+	1Hg2+2 + 1H2O(l) -1H+ = Hg2OH+	-4.6	0.5	26.257*					
HgCl+	1Hg+2 + 1Cl- = HgCl+	7.31	0.04	-41.726*	-21.3	0.7	68.508*		
HgCl2(aq)	1Hg+2 + 2Cl- = HgCl2(aq)	14	0.07	-79.913*	-49.1	1	103.346*		
HgCl3-	1HgCl2(aq) + 1Cl- = HgCl3-	0.925	0.09	-5.28*	0.5	2.5	19.386*		
HgCl4-2	1HgCl3- + 1Cl- = HgCl4-2	0.61	0.12	-3.482*	-10.5	2.5	-23.539*		
HgCO3(aq)	1Hg(OH)2(aq) + 1CO2g -1H2O(l) = HgCO3(aq)	-0.7	0.2	3.996*					
HgHCO3+	1Hg(OH)2(aq) + 1CO2g + 1H+ -1H2O(l) = HgHCO3+	3.63	0.1	-20.72*					
HgHPO4(aq)	1Hg+2 + 1HPO4-2 = HgHPO4(aq)	10.9	0.6	-62.218*					
HgOH+	1Hg+2 + 1H2O(l) -1H+ = HgOH+	-3.4	0.08	19.407*					
HgOHCl(aq)	1Hg+2 + 1Cl- + 1H2O(l) -1H+ = HgOHCl(aq)	4.27	0.35	-24.373*					
HgOHCO3-	1Hg(OH)2(aq) + 1HCO3- -1H2O(l) = HgOHCO3-	0.98	0.1	-5.594*					
HgPO4-	1Hg+2 + 1HPO4-2 -1H+ = HgPO4-	5.3	0.6	-30.253*					
HgS(HS)-	1Hg+2 + 2HS- -1H+ = HgS(HS)-	31.5	0.2	-179.803*					
HgS2-2	1Hg+2 + 2HS- -2H+ = HgS2-2	22.3	0.2	-127.289*					
HgSO4(aq)	1Hg+2 + 1SO4-2 = HgSO4(aq)	2.8	0.2	-15.983*					
HIO3(aq)	1H+ + 1IO3- = HIO3(aq)	0.788		-4.498*					
HMoO4-	1H+ + 1MoO4-2 = HMoO4-	4.1	0.05	-23.403*	15.67	1.98	131.051*	0	
HNb6O19-7	1Nb6O19-8 + 1H+ = HNb6O19-7	14	0.4	-79.913*					
Ho(CO3)2-	1Ho+3 + 2CO3-2 = Ho(CO3)2-	12.1	0.3	-69.067*					
Ho(OH)2+	1Ho+3 + 2H2O(l) -2H+ = Ho(OH)2+	-14.87	0.3	84.879*					
Ho(OH)3(aq)	1Ho+3 + 3H2O(l) -3H+ = Ho(OH)3(aq)	-23.47	0.3	133.968*					
Ho(OH)4-	1Ho+3 + 4H2O(l) -4H+ = Ho(OH)4-	-35.97	0.3	205.318*					

Tab. A-4: Cont.

Name	**Reaction**	**$\log_{10}K^{o}$**	±	$\Delta_r G_m^o$ [kJ · mol^{-1}]	$\Delta_r H_m^o$ [kJ · mol^{-1}]	±	$\Delta_r S_m^o$ [J · K^{-1} · mol^{-1}]	$\Delta_r C_{p,m}^o$ [J · K^{-1} · mol^{-1}]	±
Ho(SO4)2-	1Ho+3 + 2SO4-2 = Ho(SO4)2-	5.7	0.2	-32.536*					
HoCO3+	1Ho+3 + 1CO3-2 = HoCO3+	8.1	0.2	-46.235*					
HoF+2	1Ho+3 + 1F- = HoF+2	4.29	0.07	-24.488*	9.83	0.83	115.101*	0	
HoF2+	1Ho+3 + 2F- = HoF2+	6.73	0.3	-38.415*	21	1.6	199.279*	0	
HoH2PO4+2	1Ho+3 + 1H3PO4(aq) -1H+ = HoH2PO4+2	0.89	0.13	-5.08*	14.7		66.343*	0	
HoOH+2	1Ho+3 + 1H2O(l) -1H+ = HoOH+2	-7.41	0.07	42.297*	49	2.9	22.483*	0	
HoSO4+	1Ho+3 + 1SO4-2 = HoSO4+	3.95	0.08	-22.547*					
HOx-	1Ox-2 + 1H+ = HOx-	4.25	0.01	-24.259*	7.3	0.1	105.85*		
HP2O7-3	2HPO4-2 + 1H+ -1H2O(l) = HP2O7-3	6.01		-34.305*					
HS-	1SO4-2 + 9H+ + 8e- -4H2O(l) = HS-	33.69		-192.304*	-250.28		-194.453*		
HSe-	1H2Se(aq) -1H+ = HSe-	-3.85	0.05	21.976*					
HSe4-	4Se(cr) + 1H+ + 2e- = HSe4-	-7.16	0.15	40.87*					
HSeO3-	1SeO3-2 + 1H+ = HSeO3-	8.36	0.23	-47.719*					
HSO3-	1H+ + 1SO3-2 = HSO3-	7.22		-41.212*	120.95		543.894*		
HSO4-	1H+ + 1SO4-2 = HSO4-	1.988		-11.348*	16.128		92.154*	239.237	
I2(aq)	2I- -2e- = I2(aq)	-20.95		119.583*					
I3-	1I- + 1I2(aq) = I3-	2.87		-16.382*					
IO3-	0.5I2(aq) + 3H2O(l) -6H+ -5e- = IO3-	-101.09		577.026*					
KCO3-	1K+ + 1CO3-2 = KCO3-	0.9	0.5	-5.137*	18.6	5	79.615*		
KEdta-3	1K+ + 1Edta-4 = KEdta-3	1.8	0.3	-10.274*					
KFe(CN)6-2	1Fe(CN)6-3 + 1K+ = KFe(CN)6-2	1.46	0.05	-8.334*	2.1	1.3	34.995*		
KFe(CN)6-3	1Fe(CN)6-4 + 1K+ = KFe(CN)6-3	2.35	0.05	-13.414*	3.6	1	57.065*		
KH2PO4(aq)	1K+ + 1H2PO4- = KH2PO4(aq)	0.29	0.16	-1.655*	5	8	22.322*	0	
KHCO3(aq)	1K+ + 1HCO3- = KHCO3(aq)	-0.34	0.5	1.941*	12.5	5	35.416*		
KHPO4-	1K+ + 1HPO4-2 = KHPO4-	0.88	0.07	-5.023*	18	15	77.22*	0	
KOH(aq)	1K+ + 1H2O(l) -1H+ = KOH(aq)	-14.5	0.4	82.767*	59	1.9	-79.714*	0	
KPO4-2	1K+ + 1PO4-3 = KPO4-2	1.46	0.16	-8.334*	6	8	48.076*	0	
KSO4-	1K+ + 1SO4-2 = KSO4-	0.84	0.05	-4.795*	12.9	1.7	59.349*	0	
LiF(aq)	1Li+ + 1F- = LiF(aq)	0.23	0.11	-1.313*	6	1.2	24.527*	0	
LiH2PO4(aq)	1Li+ + 1H2PO4- = LiH2PO4(aq)	0.6	0.4	-3.425*					

Tab. A-4: Cont.

Name	**Reaction**	**$\log_{10}K^{o}$**	±	$\Delta_r G_m^{o}$ [kJ · mol^{-1}]	$\Delta_r H_m^{o}$ [kJ · mol^{-1}]	±	$\Delta_r S_m^{o}$ [J · K^{-1} · mol^{-1}]	$\Delta_r C_{p,m}^{o}$ [J · K^{-1} · mol^{-1}]	±
LiHPO4-	1Li+ + 1HPO4-2 = LiHPO4-	1.28	0.12	-7.306*	20	12	91.586*	0	
LiOH(aq)	1Li+ + 1H2O(l) -1H+ = LiOH(aq)	-13.84	0.14	78.999*	55.3	3.7	-79.488*	-64.1	34.6
LiPO4-2	1Li+ + 1PO4-3 = LiPO4-2	1.8	0.3	-10.274*					
LiSO4-	1Li+ + 1SO4-2 = LiSO4-	0.9	0.3	-5.137*	0		17.23*		
Mg(Cit)-	1Mg+2 + 1Cit-3 = Mg(Cit)-	4.81	0.03	-27.456*					
Mg(Edta)-2	1Mg+2 + 1Edta-4 = Mg(Edta)-2	10.9	0.1	-62.218*	19.8	0.4	275.089*		
Mg(H2Cit)+	1Mg+2 + 1H2Cit- = Mg(H2Cit)+	1.31	0.16	-7.478*					
Mg(HCit)(aq)	1Mg+2 + 1HCit-2 = Mg(HCit)(aq)	2.6	0.07	-14.841*					
Mg(HEdta)-	1Mg(Edta)-2 + 1H+ = Mg(HEdta)-	4.5	0.2	-25.686*					
Mg(Ox)(aq)	1Mg+2 + 1Ox-2 = Mg(Ox)(aq)	3.56	0.04	-20.321*					
Mg(Ox)2-2	1Mg+2 + 2Ox-2 = Mg(Ox)2-2	5.17	0.08	-29.511*					
Mg2UO2(CO3)3(aq)	2Mg+2 + 1UO2+2 + 3CO3-2 = Mg2UO2(CO3)3(aq)	27.1	0.6	-154.688*					
MgCO3(aq)	1Mg+2 + 1CO3-2 = MgCO3(aq)	2.98	0.03	-17.01*	11	1.1	93.946*	90	44
MgF+	1Mg+2 + 1F- = MgF+	1.88	0.05	-10.731*	10.5	1	71.21*	-30.5	7.3
MgH2PO4+	1Mg+2 + 1H2PO4- = MgH2PO4+	1.11	0.2	-6.336*					
MgHCO3+	1Mg+2 + 1HCO3- = MgHCO3+	1.07	0.03	-6.108*	3.25	0.22	31.386*	175.7	8.8
MgHPO4(aq)	1Mg+2 + 1HPO4-2 = MgHPO4(aq)	2.73	0.06	-15.583*	13.3	7.4	96.874*	0	
MgOH+	1Mg+2 + 1H2O(l) -1H+ = MgOH+	-11.7	0.04	66.784*	70.8	0.7	13.469*	0	
MgPO4-	1Mg+2 + 1PO4-3 = MgPO4-	4.9	0.5	-27.969*					
MgSeO4(aq)	1Mg+2 + 1SeO4-2 = MgSeO4(aq)	2.2	0.2	-12.558*					
MgSiO(OH)3+	1Mg+2 + 1SiO(OH)3- = MgSiO(OH)3+	1.36	0.14	-7.763*					
MgSiO2(OH)2(aq)	1Mg+2 + 1SiO2(OH)2-2 = MgSiO2(OH)2(aq)	5.52	0.16	-31.508*					
MgSO4(aq)	1Mg+2 + 1SO4-2 = MgSO4(aq)	2.25	0.05	-12.843*	20.3	2	111.162*	0	
MgUO2(CO3)3-2	1Mg+2 + 1UO2+2 + 3CO3-2 = MgUO2(CO3)3-2	26.2	0.2	-149.551*					
Mn(OH)2(aq)	1Mn+2 + 2H2O(l) -2H+ = Mn(OH)2(aq)	-22.18	0.2	126.604*	117.4	2.6	-30.872*	0	
Mn(OH)2+	1Mn+3 + 2H2O(l) -2H+ = Mn(OH)2+	1.5	0.5	-8.562*					

Tab. A-4: Cont.

Name	**Reaction**	**$\log_{10}K^{o}$**	±	$\Delta_r G_m^{o}$ [kJ · mol^{-1}]	$\Delta_r H_m^{o}$ [kJ · mol^{-1}]	±	$\Delta_r S_m^{o}$ [J · K^{-1} · mol^{-1}]	$\Delta_r C_{p,m}^{o}$ [J · K^{-1} · mol^{-1}]	±
Mn(OH)3-	1Mn+2 + 3H2O(l) -3H+ = Mn(OH)3-	-34.34	0.45	196.014*	171.9	3.1	-80.879*	0	
Mn(OH)4-2	1Mn+2 + 4H2O(l) -4H+ = Mn(OH)4-2	-48.28	0.4	275.584*	256.4	5.2	-64.344*	0	
MnCl+	1Mn+2 + 1Cl- = MnCl+	0.1	0.5	-0.571*	11.5	3.5	40.486*	323	40
MnCl+2	1Mn+3 + 1Cl- = MnCl+2	0.8	0.5	-4.566*	22.5	10	90.781*		
MnCO3(aq)	1Mn+2 + 1CO3-2 = MnCO3(aq)	4.6	0.17	-26.257*	16	6	141.731*		
MnF+	1Mn+2 + 1F- = MnF+	1.35	0.18	-7.706*	15.1	1.6	76.491*		
MnF+2	1Mn+3 + 1F- = MnF+2	6.6	0.5	-37.673*	4.8	1	142.455*		
MnF2+	1Mn+3 + 2F- = MnF2+	11.9	0.5	-67.926*	8.1	1	254.991*		
MnF3(aq)	1Mn+3 + 3F- = MnF3(aq)	15.3	0.6	-87.333*	8.9	1	322.767*		
MnHCO3+	1Mn+2 + 1HCO3- = MnHCO3+	1.27	0.05	-7.249*	4.2	1.4	38.401*	231	90
MnOH+	1Mn+2 + 1H2O(l) -1H+ = MnOH+	-10.58	0.04	60.391*	57.3	1.1	-10.368*	0	
MnOH+2	1Mn+3 + 1H2O(l) -1H+ = MnOH+2	1.2	0.4	-6.85*	22.9	5.5	99.781*	0	
MnOHF+	1Mn+3 + 1F- + 1H2O(l) -1H+ = MnOHF+	7.3	0.5	-41.669*					
MnSeO4(aq)	1Mn+2 + 1SeO4-2 = MnSeO4(aq)	2.43	0.05	-13.871*					
MnSO4(aq)	1Mn+2 + 1SO4-2 = MnSO4(aq)	2.23	0.05	-12.729*	12.7	1.1	85.289*	180	23
N2(aq)	2NO3- + 12H+ + 10e- - 6H2O(l) = N2(aq)	207.263		-1183.066*	-1311.717		-431.498*	689.398	
Na(Edta)-3	1Na+ + 1Edta-4 = Na(Edta)-3	2.8	0.2	-15.983*	-4	3	40.19*		
NaCO3-	1Na+ + 1CO3-2 = NaCO3-	1.01	0.2	-5.765*	18	4	79.709*	0	
NaF(aq)	1Na+ + 1F- = NaF(aq)	-0.28	0.13	1.598*	13.6	2.2	40.254*	0	
NaH2PO4(aq)	1Na+ + 1H2PO4- = NaH2PO4(aq)	0.3	0.17	-1.712*	17	8	62.762*	0	
NaHCO3(aq)	1Na+ + 1HCO3- = NaHCO3(aq)	-0.18	0.25	1.027*	11.6	4	35.461*	0	
NaHPO4-	1Na+ + 1HPO4-2 = NaHPO4-	1.03	0.07	-5.879*	23	15	96.862*	0	
NaOH(aq)	1Na+ + 1H2O(l) -1H+ = NaOH(aq)	-14.4	0.2	82.196*	51.9	1.8	-101.613*	0	
NaPO4-2	1Na+ + 1PO4-3 = NaPO4-2	1.56	0.17	-8.905*	7	8	53.344*	0	
NaSO4-	1Na+ + 1SO4-2 = NaSO4-	0.71	0.05	-4.053*	4.7	3.3	29.357*		
Nb(OH)5(aq)	1Nb(OH)4+ + 1H2O(l) -1H+ = Nb(OH)5(aq)	-1.89	0.12	10.788*	9	4	-5.998*	0	
Nb(OH)6-	1Nb(OH)4+ + 2H2O(l) -2H+ = Nb(OH)6-	-6.69	0.14	38.187*	26	9	-40.875*	0	
Nb(OH)7-2	1Nb(OH)4+ + 3H2O(l) -3H+ = Nb(OH)7-2	-16.09	0.34	91.842*	63	22	-96.738*	0	

Tab. A-4: Cont.

Name	**Reaction**	**$\log_{10}K^{o}$**	±	$\Delta_r G_m^{o}$ [kJ · mol^{-1}]	$\Delta_r H_m^{o}$ [kJ · mol^{-1}]	±	$\Delta_r S_m^{o}$ [J · K^{-1} · mol^{-1}]	$\Delta_r C_{p,m}^{o}$ [J · K^{-1} · mol^{-1}]	±
Nb6O19-8	1H3Nb6O19-5 -3H+ = Nb6O19-8	-38.6	0.5	220.33*					
NH3(aq)	1NH4+ -1H+ = NH3(aq)	-9.237		52.725*	52.09		-2.13*		
NH4+	1NO3- + 10H+ + 8e- - 3H2O(l) = NH4+	119.134		-680.022*	-783.9		-348.409*	277.178	
Ni(Cit)-	1Ni+2 + 1Cit-3 = Ni(Cit)-	6.76	0.08	-38.586*					
Ni(Cit)2-4	1Ni+2 + 2Cit-3 = Ni(Cit)2-4	8.5	0.4	-48.518*					
Ni(CN)4-2	1Ni+2 + 4CN- = Ni(CN)4-2	30.2	0.12	-172.383*	-180.7	4	-27.896*		
Ni(CN)5-3	1Ni+2 + 5CN- = Ni(CN)5-3	28.5	0.5	-162.679*	-191.1	8	-95.324*		
Ni(CO3)2-2	1Ni+2 + 2CO3-2 = Ni(CO3)2-2	6		-34.248*					
Ni(Edta)-2	1Ni+2 + 1Edta-4 = Ni(Edta)-2	20.54	0.13	-117.243*	-26.1	0.4	305.696*		
Ni(H2Cit)+	1Ni+2 + 1H2Cit- = Ni(H2Cit)+	2.05	0.25	-11.701*					
Ni(H3Isa)+	1Ni+2 + 1H3Isa- = Ni(H3Isa)+	2.4		-13.699*					
Ni(HCit)(aq)	1Ni+2 + 1HCit-2 = Ni(HCit)(aq)	4.16	0.1	-23.745*					
Ni(HEdta)-	1Ni(Edta)-2 + 1H+ = Ni(HEdta)-	3.66	0.16	-20.891*	-7.5	1.3	44.915*		
Ni(HS)2(aq)	1Ni+2 + 2HS- = Ni(HS)2(aq)	11.1	0.1	-63.359*					
Ni(NH3)2+2	1Ni+2 + 2NH3(aq) = Ni(NH3)2+2	4.9		-27.969*					
Ni(NH3)3+2	1Ni+2 + 3NH3(aq) = Ni(NH3)3+2	6.5		-37.102*					
Ni(NH3)4+2	1Ni+2 + 4NH3(aq) = Ni(NH3)4+2	7.6		-43.381*					
Ni(NH3)5+2	1Ni+2 + 5NH3(aq) = Ni(NH3)5+2	8.3		-47.377*					
Ni(NH3)6+2	1Ni+2 + 6NH3(aq) = Ni(NH3)6+2	8.2		-46.806*					
Ni(OH)2(aq)	1Ni+2 + 2H2O(l) -2H+ = Ni(OH)2(aq)	-18		102.745*	90		-42.746*	0	
Ni(OH)3-	1Ni+2 + 3H2O(l) -3H+ = Ni(OH)3-	-29.2	1.7	166.675*	121.2	6.5	-152.523*	0	
Ni(Ox)(aq)	1Ni+2 + 1Ox-2 = Ni(Ox)(aq)	5.19	0.04	-29.625*	0	0.3	99.362*		
Ni(Ox)2-2	1Ni+2 + 2Ox-2 = Ni(Ox)2-2	7.64	0.07	-43.609*	-7.8	0.3	120.105*		
Ni(SCN)2(aq)	1Ni+2 + 2SCN- = Ni(SCN)2(aq)	2.69	0.07	-15.355*	-21	8	-18.935*	0	
Ni(SCN)3-	1Ni+2 + 3SCN- = Ni(SCN)3-	3.02	0.18	-17.238*	-29	10	-39.449*		
Ni(SeCN)2(aq)	1Ni+2 + 2SeCN- = Ni(SeCN)2(aq)	2.24	0.14	-12.786*	-25	4	-40.966*		

Tab. A-4: Cont.

Name	**Reaction**	**$\log_{10}K^{o}$**	±	$\Delta_r G_m^o$ [kJ · mol^{-1}]	$\Delta_r H_m^o$ [kJ · mol^{-1}]	±	$\Delta_r S_m^o$ [J · K^{-1} · mol^{-1}]	$\Delta_r C_{p,m}^o$ [J · K^{-1} · mol^{-1}]	±
Ni2OH+3	2Ni+2 + 1H2O(l) -1H+ = Ni2OH+3	-10.6	1	60.505*	45.9	6	-48.986*		
Ni4(OH)4+4	4Ni+2 + 4H2O(l) -4H+ = Ni4(OH)4+4	-27.52	0.15	157.085*	190	10	110.396*		
NiCl+	1Ni+2 + 1Cl- = NiCl+	0.08	0.6	-0.457*					
NiCO3(aq)	1Ni+2 + 1CO3-2 = NiCO3(aq)	4.2	0.4	-23.974*					
NiF+	1Ni+2 + 1F- = NiF+	1.43	0.08	-8.163*	9.5	3	59.24*		
NiHAsO4(aq)	1Ni+2 + 1HAsO4-2 = NiHAsO4(aq)	2.9	0.3	-16.553*					
NiHCO3+	1Ni+2 + 1HCO3- = NiHCO3+	1		-5.708*					
NiHP2O7-	1Ni+2 + 1HP2O7-3 = NiHP2O7-	5.14	0.25	-29.339*	47.9	15	259.062*	0	
NiHPO4(aq)	1Ni+2 + 1HPO4-2 = NiHPO4(aq)	3.05	0.09	-17.41*					
NiHS+	1Ni+2 + 1HS- = NiHS+	5.5	0.2	-31.394*					
NiNH3+2	1Ni+2 + 1NH3(aq) = NiNH3+2	2.7		-15.412*					
NiNO3+	1Ni+2 + 1NO3- = NiNO3+	0.5	1	-2.854*					
NiOH+	1Ni+2 + 1H2O(l) -1H+ = NiOH+	-9.54	0.14	54.455*	53.8	1.7	-2.196*	0	
NiP2O7-2	1Ni+2 + 1P2O7-4 = NiP2O7-2	8.73	0.25	-49.831*	30.6	10	269.768*	0	
NiSCN+	1Ni+2 + 1SCN- = NiSCN+	1.81	0.04	-10.332*	-11.8	5	-4.925*	0	
NiSeCN+	1Ni+2 + 1SeCN- = NiSeCN+	1.77	0.06	-10.103*	-12.8	0.4	-9.045*		
NiSeO4(aq)	1Ni+2 + 1SeO4-2 = NiSeO4(aq)	2.67	0.05	-15.24*					
NiSiO(OH)3+	1Ni+2 + 1SiO(OH)3- = NiSiO(OH)3+	6.3		-35.961*					
NiSO4(aq)	1Ni+2 + 1SO4-2 = NiSO4(aq)	2.35	0.03	-13.414*	5.66	0.81	63.974*	0	
Np(CO3)2-	1Np+3 + 2CO3-2 = Np(CO3)2-	12.9		-73.634*					
Np(CO3)3-3	1Np+3 + 3CO3-2 = Np(CO3)3-3	15		-85.621*					
Np(CO3)4-4	1Np+4 + 4CO3-2 = Np(CO3)4-4	38.9	0.5	-222.043*					
Np(CO3)5-6	1Np+4 + 5CO3-2 = Np(CO3)5-6	37.8	0.6	-215.764*					
Np(Edta)(aq)	1Np+4 + 1Edta-4 = Np(Edta)(aq)	31.2	0.6	-178.091*					
Np(OH)2(CO3)2-2	1Np+4 + 2H2O(l) + 2HCO3- -4H+ = Np(OH)2(CO3)2-2	-2.2	0.5	12.558*					
Np(OH)2+	1Np+3 + 2H2O(l) -2H+ = Np(OH)2+	-14.7		83.908*					

Tab. A-4: Cont.

Name	**Reaction**	**$\log_{10}K^{o}$**	±	$\Delta_r G_m^{o}$ [kJ · mol^{-1}]	$\Delta_r H_m^{o}$ [kJ · mol^{-1}]	±	$\Delta_r S_m^{o}$ [J · K^{-1} · mol^{-1}]	$\Delta_r C_{p,m}^{o}$ [J · K^{-1} · mol^{-1}]	±
Np(OH)2+2	1Np+4 + 2H2O(l) -2H+ = Np(OH)2+2	0.35	0.3	-1.998*					
Np(OH)3(aq)	1Np+3 + 3H2O(l) -3H+ = Np(OH)3(aq)	-25.8		147.267*					
Np(OH)3(H3Isa)(aq)	1Np+4 + 3OH- + 1H3Isa- = Np(OH)3(H3Isa)(aq)	43.5		-248.3*					
Np(OH)3(H3Isa)2-	1Np(OH)3(H3Isa)(aq) + 1H3Isa- = Np(OH)3(H3Isa)2-	2.1		-11.987*					
Np(OH)3+	1Np+4 + 3H2O(l) -3H+ = Np(OH)3+	-2.8	1	15.983*					
Np(OH)4(aq)	1Np+4 + 4H2O(l) -4H+ = Np(OH)4(aq)	-8.3	1.1	47.377*					
Np(OH)4(H3Isa)-	1Np+4 + 4OH- + 1H3Isa- = Np(OH)4(H3Isa)-	50.1		-285.973*					
Np(OH)4(H3Isa)2-2	1Np(OH)4(H3Isa)- + 1H3Isa- = Np(OH)4(H3Isa)2-2	1.9		-10.845*					
Np(OH)4CO3-2	1Np+4 + 4H2O(l) + 1CO3-2 -4H+ = Np(OH)4CO3-2	-5.5	0.5	31.394*					
Np(Ox)+2	1Np+4 + 1H2Ox(aq) -2H+ = Np(Ox)+2	6.5		-37.102*					
Np(Ox)2(aq)	1Np+4 + 2H2Ox(aq) -4H+ = Np(Ox)2(aq)	7.5		-42.81*					
Np(Ox)3-2	1Np+4 + 3H2Ox(aq) -6H+ = Np(Ox)3-2	8		-45.664*					
Np(SCN)2+2	1Np+4 + 2SCN- = Np(SCN)2+2	4.1	0.5	-23.403*	-9	9	48.308*		
Np(SCN)3+	1Np+4 + 3SCN- = Np(SCN)3+	4.8	0.5	-27.399*	-13	9	48.293*		
Np(SO4)2-	1Np+3 + 2SO4-2 = Np(SO4)2-	3.7		-21.12*					
Np(SO4)2(aq)	1Np+4 + 2SO4-2 = Np(SO4)2(aq)	11.05	0.27	-63.074*	55.4	3.9	397.363*		
NpCl+2	1Np+3 + 1Cl- = NpCl+2	0.24		-1.37*					
NpCl+3	1Np+4 + 1Cl- = NpCl+3	1.5	0.3	-8.562*					
NpCl2+	1Np+3 + 2Cl- = NpCl2+	-0.74		4.224*					
NpCO3+	1Np+3 + 1CO3-2 = NpCO3+	8		-45.664*					
NpF+2	1Np+3 + 1F- = NpF+2	3.4		-19.407*					
NpF+3	1Np+4 + 1F- = NpF+3	8.96	0.14	-51.144*	1.5	2	176.569*		
NpF2+	1Np+3 + 2F- = NpF2+	5.8		-33.107*					
NpF2+2	1Np+4 + 2F- = NpF2+2	15.7	0.3	-89.616*					
NpI+3	1Np+4 + 1I- = NpI+3	1.5	0.4	-8.562*					
NpNO3+3	1Np+4 + 1NO3- = NpNO3+3	1.9	0.15	-10.845*					
NpO2(CO3)2-2	1NpO2+2 + 2CO3-2 = NpO2(CO3)2-2	15		-85.621*					

Tab. A-4: Cont.

Name	**Reaction**	**$\log_{10}K^{o}$**	±	$\Delta_r G_m^o$ [kJ · mol^{-1}]	$\Delta_r H_m^o$ [kJ · mol^{-1}]	±	$\Delta_r S_m^o$ [J · K^{-1} · mol^{-1}]	$\Delta_r C_{p,m}^o$ [J · K^{-1} · mol^{-1}]	±
NpO2(CO3)2-3	1NpO2+ + 2CO3-2 = NpO2(CO3)2-3	6.53	0.1	-37.274*					
NpO2(CO3)2OH-4	1NpO2+ + 2CO3-2 + 1H2O(l) -1H+ = NpO2(CO3)2OH-4	-5.3	1.17	30.253*					
NpO2(CO3)3-4	1NpO2+2 + 3CO3-2 = NpO2(CO3)3-4	19.9	0.5	-113.59*	-41.9	4.1	240.45*		
NpO2(CO3)3-5	1NpO2+ + 3CO3-2 = NpO2(CO3)3-5	5.5	0.15	-31.394*	-13.3	5.1	60.688*		
NpO2(H2Edta)-	1NpO2+ + 1H2Edta-2 = NpO2(H2Edta)-	4.47	0.14	-25.515*					
NpO2(HEdta)-2	1NpO2+ + 1HEdta-3 = NpO2(HEdta)-2	5.82	0.11	-33.221*					
NpO2(HPO4)2-2	1NpO2+2 + 2HPO4-2 = NpO2(HPO4)2-2	9.5	1	-54.226*					
NpO2(OH)(aq)	1NpO2+ + 1H2O(l) -1H+ = NpO2(OH)(aq)	-11.3	0.7	64.501*	64.784		0.95*		
NpO2(OH)2-	1NpO2+ + 2H2O(l) -2H+ = NpO2(OH)2-	-23.6	0.5	134.71*	118.61		-53.999*		
NpO2(OH)2(aq)	1NpO2+2 + 2H2O(l) -2H+ = NpO2(OH)2(aq)	-12.2		69.638*					
NpO2(OH)3-	1NpO2+2 + 3H2O(l) -3H+ = NpO2(OH)3-	-21.2	1.1	121.01*					
NpO2(OH)4-2	1NpO2+2 + 4H2O(l) -4H+ = NpO2(OH)4-2	-33	1.1	188.365*					
NpO2(Ox)2-3	1NpO2+ + 2Ox-2 = NpO2(Ox)2-3	5.8	0.2	-33.107*					
NpO2(SO4)2-2	1NpO2+2 + 2SO4-2 = NpO2(SO4)2-2	4.7	0.1	-26.828*	26	1.2	177.185*		
NpO2Cit-2	1NpO2+ + 1Cit-3 = NpO2Cit-2	3.68	0.05	-21.006*					
NpO2Cl+	1NpO2+2 + 1Cl- = NpO2Cl+	0.4	0.17	-2.283*					
NpO2CO3-	1NpO2+ + 1CO3-2 = NpO2CO3-	4.96	0.06	-28.312*					
NpO2CO3(aq)	1NpO2+2 + 1CO3-2 = NpO2CO3(aq)	9.86	0.1	-56.281*					
NpO2CO3(OH)2-3	1NpO2+ + 1CO3-2 + 2H2O(l) -2H+ = NpO2CO3(OH)2-3	-20.34	0.15	116.102*					
NpO2CO3OH-2	1NpO2+ + 1CO3-2 + 1H2O(l) -1H+ = NpO2CO3OH-2	-7	0.3	39.956*					
NpO2Edta-3	1NpO2+ + 1Edta-4 = NpO2Edta-3	9.23	0.13	-52.685*					
NpO2EdtaOH-4	1NpO2Edta-3 + 1H2O(l) -1H+ = NpO2EdtaOH-4	-12.4		70.78*					
NpO2F(aq)	1NpO2+ + 1F- = NpO2F(aq)	1.4	0.3	-7.991*					
NpO2F+	1NpO2+2 + 1F- = NpO2F+	4.57	0.07	-26.086*					

Tab. A-4: Cont.

Name	**Reaction**	**$\log_{10}K^{o}$**	±	$\Delta_r G_m^{o}$ [kJ · mol^{-1}]	$\Delta_r H_m^{o}$ [kJ · mol^{-1}]	±	$\Delta_r S_m^{o}$ [J · K^{-1} · mol^{-1}]	$\Delta_r C_{p,m}^{o}$ [J · K^{-1} · mol^{-1}]	±
NpO2F2-	1NpO2+ + 2F- = NpO2F2-	1.9	0.4	-10.845*					
NpO2F2(aq)	1NpO2+2 + 2F- = NpO2F2(aq)	7.6	0.08	-43.381*					
NpO2H2PO4(aq)	1NpO2+ + 1H2PO4- = NpO2H2PO4(aq)	1.4	0.2	-7.991*					
NpO2H2PO4+	1NpO2+2 + 1H2PO4- = NpO2H2PO4+	3.32	0.5	-18.951*					
NpO2HPO4-	1NpO2+ + 1HPO4-2 = NpO2HPO4-	2.95	0.1	-16.839*	-11	11	19.583*	0	
NpO2HPO4(aq)	1NpO2+2 + 1HPO4-2 = NpO2HPO4(aq)	6.2	0.7	-35.39*					
NpO2IO3(aq)	1NpO2+ + 1IO3- = NpO2IO3(aq)	0.5	0.3	-2.854*					
NpO2IO3+	1NpO2+2 + 1IO3- = NpO2IO3+	1.2	0.3	-6.85*					
NpO2OH+	1NpO2+2 + 1H2O(l) -1H+ = NpO2OH+	-5.1	0.4	29.111*					
NpO2Ox-	1NpO2+ + 1Ox-2 = NpO2Ox-	3.9	0.1	-22.261*					
NpO2SCN(aq)	1NpO2+ + 1SCN- = NpO2SCN(aq)	0.08	0.3	-0.457*					
NpO2SiO(OH)3(aq)	1NpO2+ + 1SiO(OH)3- = NpO2SiO(OH)3(aq)	2.5	0.3	-14.27*					
NpO2SiO(OH)3+	1NpO2+2 + 1SiO(OH)3- = NpO2SiO(OH)3+	7.2		-41.098*					
NpO2SO4-	1NpO2+ + 1SO4-2 = NpO2SO4-	1.3	0.2	-7.42*	22	7	98.677*		
NpO2SO4(aq)	1NpO2+2 + 1SO4-2 = NpO2SO4(aq)	3.28	0.06	-18.722*	16.7	0.5	118.807*		
NpOH+2	1Np+3 + 1H2O(l) -1H+ = NpOH+2	-6.8	0.3	38.815*					
NpOH+3	1Np+4 + 1H2O(l) -1H+ = NpOH+3	0.55	0.2	-3.139*					
NpSCN+3	1Np+4 + 1SCN- = NpSCN+3	3	0.3	-17.124*	-7	3	33.956*		
NpSiO(OH)3+2	1Np+3 + 1SiO(OH)3- = NpSiO(OH)3+2	7.8	0.5	-44.523*	15		199.64*		
NpSiO(OH)3+3	1Np+4 + 1SiO(OH)3- = NpSiO(OH)3+3	11.15	0.18	-63.645*					
NpSO4+	1Np+3 + 1SO4-2 = NpSO4+	3.3		-18.837*					
NpSO4+2	1Np+4 + 1SO4-2 = NpSO4+2	6.85	0.16	-39.1*	29.8	8.9	231.092*		
O2(aq)	2H2O(l) -4H+ -4e- = O2(aq)	-85.984		490.8*	559.601		230.759*	136.132	
OH-	1H2O(l) -1H+ = OH-	-14		79.913*	55.906		-80.518*	-210.948	
P2O7-4	2HPO4-2 -1H2O(l) = P2O7-4	-3.39		19.35*					
Pa(OH)2+2	1Pa+4 + 2H2O(l) -2H+ = Pa(OH)2+2	1.9	0.5	-10.845*					

Tab. A-4: Cont.

Name	**Reaction**	**$\log_{10}K^{o}$**	±	$\Delta_r G_m^{o}$ [kJ · mol^{-1}]	$\Delta_r H_m^{o}$ [kJ · mol^{-1}]	±	$\Delta_r S_m^{o}$ [J · K^{-1} · mol^{-1}]	$\Delta_r C_{p,m}^{o}$ [J · K^{-1} · mol^{-1}]	±
Pa(OH)3+	1Pa+4 + 3H2O(l) -3H+ = Pa(OH)3+	0.9	0.5	-5.137*					
PaO(OH)2+	1PaO(OH)+2 + 1H2O(l) -1H+ = PaO(OH)2+	-1.26	0.14	7.192*	4.7	2.5	-8.359*		
PaO(OH)3(aq)	1PaO(OH)2+ + 1H2O(l) -1H+ = PaO(OH)3(aq)	-5.04	0.35	28.769*	57	35	94.689*		
PaO(OH)4-	1PaO(OH)3(aq) + 1H2O(l) -1H+ = PaO(OH)4-	-9.4	0.2	53.656*					
PaO(SO4)2-	1PaO(OH)+2 + 2SO4-2 + 1H+ -1H2O(l) = PaO(SO4)2-	7	0.2	-39.956*					
PaO(SO4)3-3	1PaO(OH)+2 + 3SO4-2 + 1H+ -1H2O(l) = PaO(SO4)3-3	8.59	0.23	-49.032*					
PaO+3	1PaO(OH)+2 + 1H+ -1H2O(l) = PaO+3	0.04	0.36	-0.228*					
PaOF+2	1PaO(OH)+2 + 1HF(aq) -1H2O(l) = PaOF+2	3.8	0.5	-21.691*					
PaOF2+	1PaO(OH)+2 + 2HF(aq) -1H+ -1H2O(l) = PaOF2+	7.9	0.5	-45.094*					
PaOF3(aq)	1PaO(OH)+2 + 3HF(aq) -2H+ -1H2O(l) = PaOF3(aq)	10.9	0.5	-62.218*					
PaOH+3	1Pa+4 + 1H2O(l) -1H+ = PaOH+3	1.3	0.5	-7.42*					
PaOSO4+	1PaO(OH)+2 + 1SO4-2 + 1H+ -1H2O(l) = PaOSO4+	3.89	0.18	-22.204*					
Pb(aq)	1Pb(cr) = Pb(aq)	-7.3		41.669*					
Pb(CO3)2-2	1Pb+2 + 2CO3-2 = Pb(CO3)2-2	10.13	0.24	-57.822*					
Pb(CO3)Cl-	1Pb+2 + 1CO3-2 + 1Cl- = Pb(CO3)Cl-	6.47	0.16	-36.931*					
Pb(CO3)OH-	1Pb+2 + 1CO3-2 + 1OH- = Pb(CO3)OH-	10.9	0.2	-62.218*					
Pb(HPO4)2-2	1Pb+2 + 2HPO4-2 = Pb(HPO4)2-2	6.5		-37.102*					
Pb(HS)2(aq)	1Pb+2 + 2HS- = Pb(HS)2(aq)	12.5		-71.351*					
Pb(OH)2(aq)	1Pb+2 + 2H2O(l) -2H+ = Pb(OH)2(aq)	-16.94	0.09	96.694*	90	0.9	-22.453*	0	
Pb(OH)3-	1Pb+2 + 3H2O(l) -3H+ = Pb(OH)3-	-28.03	0.06	159.996*	135.8	3	-81.155*	251	36
Pb(SO4)2-2	1Pb+2 + 2SO4-2 = Pb(SO4)2-2	3.15	0.5	-17.98*	18.4	1	122.02*		
Pb2OH+3	2Pb+2 + 1H2O(l) -1H+ = Pb2OH+3	-6.73	0.31	38.415*					
Pb3(OH)4+2	3Pb+2 + 4H2O(l) -4H+ = Pb3(OH)4+2	-23.01	0.07	131.342*	111.4	5.6	-66.886*		
Pb4(OH)4+4	4Pb+2 + 4H2O(l) -4H+ = Pb4(OH)4+4	-20.57	0.06	117.414*	85	2	-108.719*		
Pb6(OH)8+4	6Pb+2 + 8H2O(l) -8H+ = Pb6(OH)8+4	-42.89	0.07	244.818*	210.9	7.1	-113.761*		

Tab. A-4: Cont.

Name	**Reaction**	**$\log_{10}K^{o}$**	±	$\Delta_r G_m^{o}$ [kJ · mol^{-1}]	$\Delta_r H_m^{o}$ [kJ · mol^{-1}]	±	$\Delta_r S_m^{o}$ [J · K^{-1} · mol^{-1}]	$\Delta_r C_{p,m}^{o}$ [J · K^{-1} · mol^{-1}]	±
PbCl+	1Pb+2 + 1Cl- = PbCl+	1.5	0.03	-8.562*	10.3	1.5	63.264*	0	
PbCl2(aq)	1Pb+2 + 2Cl- = PbCl2(aq)	2.1	0.05	-11.987*	17	0.6	97.223*	0	
PbCl3-	1Pb+2 + 3Cl- = PbCl3-	2	0.1	-11.416*	14.7	1	87.594*	0	
PbCl4-2	1Pb+2 + 4Cl- = PbCl4-2	1.46	0.1	-8.334*	14	5	74.908*		
PbCO3(aq)	1Pb+2 + 1CO3-2 = PbCO3(aq)	6.45	0.7	-36.817*					
PbH2PO4+	1Pb+2 + 1H2PO4- = PbH2PO4+	2.8		-15.983*					
PbHCO3+	1Pb+2 + 1HCO3- = PbHCO3+	3	0.4	-17.124*					
PbHPO4(aq)	1Pb+2 + 1HPO4-2 = PbHPO4(aq)	4.2	0.2	-23.974*					
PbOH+	1Pb+2 + 1H2O(l) -1H+ = PbOH+	-7.46	0.06	42.582*	56	1.5	45.004*	0	
PbS(HS)-	1Pb+2 + 2HS- -1H+ = PbS(HS)-	6.1		-34.819*					
PbSO4(aq)	1Pb+2 + 1SO4-2 = PbSO4(aq)	2.72	0.05	-15.526*	9.2	0.5	82.931*		
Pd(aq)	1Pd(cr) = Pd(aq)	-9.5	0.5	54.226*					
Pd(NH3)2+2	1Pd+2 + 2NH3(aq) = Pd(NH3)2+2	18.5	0.2	-105.599*					
Pd(NH3)3+2	1Pd+2 + 3NH3(aq) = Pd(NH3)3+2	26	0.2	-148.409*					
Pd(NH3)4+2	1Pd+2 + 4NH3(aq) = Pd(NH3)4+2	32.8	0.2	-187.224*					
Pd(OH)2(aq)	1Pd+2 + 2H2O(l) -2H+ = Pd(OH)2(aq)	-4.6		26.257*					
Pd(OH)3-	1Pd+2 + 3H2O(l) -3H+ = Pd(OH)3-	-16.6		94.753*					
PdCl+	1Pd+2 + 1Cl- = PdCl+	5.02	0.04	-28.654*	-18.6	0.8	33.723*	121	21
PdCl2(aq)	1PdCl+ + 1Cl- = PdCl2(aq)	3.45	0.06	-19.693*	-10.9	1.2	29.491*	124	32
PdCl3-	1PdCl2(aq) + 1Cl- = PdCl3-	2.1	0.06	-11.987*	-3.5	1.1	28.465*	30	32
PdCl4-2	1PdCl3- + 1Cl- = PdCl4-2	0.88	0.09	-5.023*	-13.6	1.9	-28.767*	113	52
PdNH3+2	1Pd+2 + 1NH3(aq) = PdNH3+2	9.6	0.2	-54.797*					
PdOH+	1Pd+2 + 1H2O(l) -1H+ = PdOH+	-2		11.416*					
Po(aq)	1Po(cr) = Po(aq)	-7		39.956*					
Po(NO3)2+2	1Po+4 + 2NO3- = Po(NO3)2+2	3.7	0.4	-21.12*					
Po(NO3)3+	1Po+4 + 3NO3- = Po(NO3)3+	4.4	0.5	-25.115*					
Po(OH)2+2	1PoO2(s) + 2H+ = Po(OH)2+2	-0.5		2.854*					
Po(OH)3+	1PoO2(s) + 1H2O(l) + 1H+ = Po(OH)3+	-3		17.124*					

Tab. A-4: Cont.

Name	**Reaction**	**$\log_{10}K^{o}$**	±	$\Delta_r G_m^o$ [kJ · mol^{-1}]	$\Delta_r H_m^o$ [kJ · mol^{-1}]	±	$\Delta_r S_m^o$ [J · K^{-1} · mol^{-1}]	$\Delta_r C_{p,m}^o$ [J · K^{-1} · mol^{-1}]	±
Po(OH)4(aq)	1PoO2(s) + 2H2O(l) = Po(OH)4(aq)	-7.5		42.81*					
Po(OH)6-2	1PoO2(s) + 4H2O(l) -2H+ = Po(OH)6-2	-32.43	0.05	185.112*					
Po(OH)Cl4-	1PoCl6-2 + 1H2O(l) -1H+ -2Cl- = Po(OH)Cl4-	-2.16		12.329*					
Po(SO4)2(aq)	1Po+4 + 2SO4-2 = Po(SO4)2(aq)	9.1	0.7	-51.943*					
Po(SO4)3-2	1Po(SO4)2(aq) + 1SO4-2 = Po(SO4)3-2	2.2		-12.558*					
PO4-3	1HPO4-2 -1H+ = PO4-3	-12.35		70.494*	14.6		-187.47*		
PoCl+	1Po+2 + 1Cl- = PoCl+	3.75		-21.405*					
PoCl2(aq)	1Po+2 + 2Cl- = PoCl2(aq)	6.13		-34.99*					
PoCl3-	1Po+2 + 3Cl- = PoCl3-	7.02		-40.07*					
PoNO3+3	1Po+4 + 1NO3- = PoNO3+3	2	0.9	-11.416*					
PoOH+3	1PoO2(s) + 3H+ = PoOH+3 + +H2O(l)	0.5		-2.854*					
PoSO4+2	1Po+4 + 1SO4-2 = PoSO4+2	5.2	0.6	-29.682*					
Pu(Cit)(aq)	1Pu+3 + 1Cit-3 = Pu(Cit)(aq)	8.7		-49.66*					
Pu(CO3)2-	1Pu+3 + 2CO3-2 = Pu(CO3)2-	12.9		-73.634*					
Pu(CO3)3-3	1Pu+3 + 3CO3-2 = Pu(CO3)3-3	15		-85.621*					
Pu(CO3)4-4	1Pu+4 + 4CO3-2 = Pu(CO3)4-4	37	1.1	-211.198*					
Pu(CO3)5-6	1Pu+4 + 5CO3-2 = Pu(CO3)5-6	35.65	1.13	-203.492*					
Pu(Edta)-	1Pu+3 + 1Edta-4 = Pu(Edta)-	20.18	0.37	-115.188*	-8.7	1.2	357.163*		
Pu(Edta)(aq)	1Pu+4 + 1Edta-4 = Pu(Edta)(aq)	31.6	1	-180.374*					
Pu(Edta)(OH)2-2	1Pu(Edta)OH- + 1OH- = Pu(Edta)(OH)2-2	6.9		-39.385*					
Pu(Edta)OH-	1Pu(Edta)(aq) + 1OH- = Pu(Edta)OH-	9.3		-53.085*					
Pu(HCit)+	1Pu+3 + 1HCit-2 = Pu(HCit)+	6.1		-34.819*					
Pu(HEdta)(aq)	1Pu(Edta)- + 1H+ = Pu(HEdta)(aq)	1.84	0.26	-10.503*					
Pu(OH)2+	1Pu+3 + 2H2O(l) -2H+ = Pu(OH)2+	-14.8		84.479*					
Pu(OH)2+2	1Pu+4 + 2H2O(l) -2H+ = Pu(OH)2+2	-1.2	0.6	6.85*					
Pu(OH)3(aq)	1Pu+3 + 3H2O(l) -3H+ = Pu(OH)3(aq)	-25.9		147.838*					
Pu(OH)3+	1Pu+4 + 3H2O(l) -3H+ = Pu(OH)3+	-3.1	0.9	17.695*					

Tab. A-4: Cont.

Name	**Reaction**	**$\log_{10}K^{o}$**	±	$\Delta_r G_m^{o}$ [kJ · mol^{-1}]	$\Delta_r H_m^{o}$ [kJ · mol^{-1}]	±	$\Delta_r S_m^{o}$ [J · K^{-1} · mol^{-1}]	$\Delta_r C_{p,m}^{o}$ [J · K^{-1} · mol^{-1}]	±
Pu(OH)4(aq)	1Pu+4 + 4H2O(l) -4H+ = Pu(OH)4(aq)	-9.3	0.5	53.085*					
Pu(Ox)+	1Pu+3 + 1Ox-2 = Pu(Ox)+	8.5		-48.518*					
Pu(Ox)+2	1Pu+4 + 1H2Ox(aq) -2H+ = Pu(Ox)+2	7.3		-41.669*					
Pu(Ox)2-	1Pu+3 + 2Ox-2 = Pu(Ox)2-	12.7		-72.492*					
Pu(Ox)2(aq)	1Pu(Ox)+2 + 1H2Ox(aq) -2H+ = Pu(Ox)2(aq)	3.3		-18.837*					
Pu(Ox)3-2	1Pu(Ox)2(aq) + 1H2Ox(aq) -2H+ =Pu(Ox)3-2	0.3		-1.712*					
Pu(Ox)3-3	1Pu+3 + 3Ox-2 = Pu(Ox)3-3	12.1		-69.067*					
Pu(SO4)2-	1Pu+3 + 2SO4-2 = Pu(SO4)2-	5.7	0.8	-32.536*	12	16	149.374*		
Pu(SO4)2(aq)	1Pu+4 + 2SO4-2 = Pu(SO4)2(aq)	11.14	0.34	-63.588*					
PuCl+2	1Pu+3 + 1Cl- = PuCl+2	1.2	0.2	-6.85*					
PuCl+3	1Pu+4 + 1Cl- = PuCl+3	1.8	0.3	-10.274*					
PuCO3(OH)3-	1Pu+4 + 1CO3-2 + 3H2O(l) -3H+ = PuCO3(OH)3-	6		-34.248*					
PuCO3+	1Pu+3 + 1CO3-2 = PuCO3+	8		-45.664*					
PuF+2	1Pu+3 + 1F- = PuF+2	3.4		-19.407*					
PuF+3	1Pu+4 + 1F- = PuF+3	8.84	0.1	-50.459*	9.1	2.2	199.762*		
PuF2+	1Pu+3 + 2F- = PuF2+	5.8		-33.107*					
PuF2+2	1Pu+4 + 2F- = PuF2+2	15.7	0.2	-89.616*	11	5	337.469*		
PuH2PO4+2	1Pu+3 + 1H2PO4- = PuH2PO4+2	2.2	0.6	-12.558*					
PuH3PO4+4	1Pu+4 + 1H3PO4(aq) = PuH3PO4+4	2.4	0.3	-13.699*					
PuNO3+3	1Pu+4 + 1NO3- = PuNO3+3	1.95	0.15	-11.131*					
PuO2(CO3)2-2	1PuO2+2 + 2CO3-2 = PuO2(CO3)2-2	14.7	0.5	-83.908*	-27	4	190.871*		
PuO2(CO3)2-3	1PuO2+ + 2CO3-2 = PuO2(CO3)2-3	6.34	0.2	-36.189*					
PuO2(CO3)3-4	1PuO2+2 + 3CO3-2 = PuO2(CO3)3-4	18	0.5	-102.745*	-38.6	2	215.143*		
PuO2(CO3)3-5	1PuO2+ + 3CO3-2 = PuO2(CO3)3-5	5.61	0.24	-32.022*	-19.11	8.5	43.307*		
PuO2(H2PO4)2(aq)	1PuO2+2 + 2H2PO4- = PuO2(H2PO4)2(aq)	4.92		-28.084*					
PuO2(OH)2(aq)	1PuO2+2 + 2H2O(l) -2H+ = PuO2(OH)2(aq)	-13.2	1.5	75.346*					
PuO2(OH)3-	1PuO2+2 + 3H2O(l) -3H+ = PuO2(OH)3-	-24	1.6	136.993*					

Tab. A-4: Cont.

Name	**Reaction**	**$\log_{10}K^{o}$**	±	$\Delta_r G_m^{o}$ [kJ · mol^{-1}]	$\Delta_r H_m^{o}$ [kJ · mol^{-1}]	±	$\Delta_r S_m^{o}$ [J · K^{-1} · mol^{-1}]	$\Delta_r C_{p,m}^{o}$ [J · K^{-1} · mol^{-1}]	±
PuO2(SO4)2-2	1PuO2+2 + 2SO4-2 = PuO2(SO4)2-2	4.4	0.2	-25.115*	43	9	228.46*		
PuO2Cl+	1PuO2+2 + 1Cl- = PuO2Cl+	0.23	0.03	-1.313*					
PuO2Cl2(aq)	1PuO2+2 + 2Cl- = PuO2Cl2(aq)	-1.15	0.3	6.564*					
PuO2CO3-	1PuO2+ + 1CO3-2 = PuO2CO3-	5.03	0.12	-28.711*					
PuO2CO3(aq)	1PuO2+2 + 1CO3-2 = PuO2CO3(aq)	9.5	0.5	-54.226*					
PuO2F+	1PuO2+2 + 1F- = PuO2F+	4.56	0.2	-26.029*					
PuO2F2(aq)	1PuO2+2 + 2F- = PuO2F2(aq)	7.25	0.45	-41.383*					
PuO2H2PO4+	1PuO2+2 + 1H2PO4- = PuO2H2PO4+	3.26		-18.608*					
PuO2HPO4(aq)	1PuO2+2 + 1HPO4-2 = PuO2HPO4(aq)	7.24		-41.326*					
PuO2OH(aq)	1PuO2+ + 1H2O(l) -1H+ = PuO2OH(aq)	-9.73		55.539*					
PuO2OH+	1PuO2+2 + 1H2O(l) -1H+ = PuO2OH+	-5.5	0.5	31.394*	28	15	-11.384*		
PuO2PO4-	1PuO2+2 + 1PO4-3 = PuO2PO4-	11.76	0.7	-67.127*					
PuO2SiO(OH)3(aq)	1PuO2+ + 1SiO(OH)3- = PuO2SiO(OH)3(aq)	2.5	0.3	-14.27*					
PuO2SiO(OH)3+	1PuO2+2 + 1SiO(OH)3- = PuO2SiO(OH)3+	6.4		-36.531*					
PuO2SO4-	1PuO2+ + 1SO4-2 = PuO2SO4-	1.26	0.12	-7.192*					
PuO2SO4(aq)	1PuO2+2 + 1SO4-2 = PuO2SO4(aq)	3.38	0.2	-19.293*	16.1	0.6	118.709*		
PuOH+2	1Pu+3 + 1H2O(l) -1H+ = PuOH+2	-6.9	0.3	39.385*					
PuOH+3	1Pu+4 + 1H2O(l) -1H+ = PuOH+3	0	0.2	0*					
PuSCN+2	1Pu+3 + 1SCN- = PuSCN+2	1.3	4	-7.42*					
PuSiO(OH)3+2	1Pu+3 + 1SiO(OH)3- = PuSiO(OH)3+2	7.8	0.5	-44.523*	15		199.64*		
PuSiO(OH)3+3	1Pu+4 + 1SiO(OH)3- = PuSiO(OH)3+3	11.88	0.18	-67.812*					
PuSO4+	1Pu+3 + 1SO4-2 = PuSO4+	3.9	0.6	-22.261*	17.2	2.3	132.354*		
PuSO4+2	1Pu+4 + 1SO4-2 = PuSO4+2	6.89	0.23	-39.328*					
RaCO3(aq)	1Ra+2 + 1CO3-2 = RaCO3(aq)	2.67	0.09	-15.24*	13	7	94.719*		
RaF+	1Ra+2 + 1F- = RaF+	0.48	0.13	-2.74*	11.6	2.6	48.096*		
RaHCO3+	1Ra+2 + 1HCO3- = RaHCO3+	1.08	0.16	-6.165*	27	12	111.235*		

Tab. A-4: Cont.

Name	**Reaction**	**$\log_{10}K^{o}$**	±	$\Delta_r G_m^{o}$ [kJ · mol^{-1}]	$\Delta_r H_m^{o}$ [kJ · mol^{-1}]	±	$\Delta_r S_m^{o}$ [J · K^{-1} · mol^{-1}]	$\Delta_r C_{p,m}^{o}$ [J · K^{-1} · mol^{-1}]	±
RaOH+	1Ra+2 + 1H2O(l) -1H+ = RaOH+	-13.7	0.4	78.2*	62	14	-54.336*		
RaSO4(aq)	1Ra+2 + 1SO4-2 = RaSO4(aq)	2.28	0.05	-13.014*	1.4	4.4	48.346*		
S(aq)	1S(orth) = S(aq)	-6.65	0.07	37.958*	48.2	5.4	34.350*	0	
S-2	1HS- -1H+ = S-2	-19		108.453*					
S2O3-2	2SO4-2 + 10H+ + 8e- -5H2O(l) = S2O3-2	38.014		-216.986*	-258.97		-140.817*		
SCN-	1HCN(aq) + 1HS- -2e- -2H+ = SCN-	5.941		-33.911*	-11.05		76.678*		
Se-2	1HSe- -1H+ = Se-2	-14.91	0.2	85.107*					
Se(aq)	1Se(cr) = Se(aq)	-6	1	34.248*					
Se2-2	2Se-2 -2e- = Se2-2	25.32	0.33	-144.528*					
Se3-2	3Se-2 -4e- = Se3-2	49.97	0.68	-285.231*					
Se4-2	4Se(cr) + 2e- = Se4-2	-16.71	0.11	95.381*					
SeCN-	1HCN(aq) + 1SeO3-2 + 5H+ + 4e- -3H2O(l) = SeCN-	57.3	0.6	-327.071*					
SeO4-2	1HSeO4- -1H+ = SeO4-2	-1.75	0.1	9.989*	-20.8	3.2	-103.267*	0	
Si4O8(OH)4-4	4Si(OH)4(aq) -4H+ -4H2O(l) = Si4O8(OH)4-4	-36.28	0.16	207.088*					
SiAlO3(OH)4-3	1Al(OH)4- + 1SiO2(OH)2-2 -1H2O(l) = SiAlO3(OH)4-3	-0.4	0.2	2.283*					
SiO(OH)3-	1Si(OH)4(aq) -1H+ = SiO(OH)3-	-9.81	0.02	55.996*	25.6	2	-101.948*	0	
SiO2(OH)2-2	1Si(OH)4(aq) -2H+ = SiO2(OH)2-2	-23.14	0.09	132.084*	75	15	-191.461*	0	
Sm(CO3)2-	1Sm+3 + 2CO3-2 = Sm(CO3)2-	12.1	0.3	-69.067*					
Sm(OH)2+	1Sm+3 + 2H2O(l) -2H+ = Sm(OH)2+	-15.22	0.3	86.876*					
Sm(OH)3(aq)	1Sm+3 + 3H2O(l) -3H+ = Sm(OH)3(aq)	-23.82	0.3	135.966*					
Sm(OH)4-	1Sm+3 + 4H2O(l) -4H+ = Sm(OH)4-	-36.32	0.3	207.316*					
Sm(SO4)2-	1Sm+3 + 2SO4-2 = Sm(SO4)2-	5.7	0.2	-32.536*					
Sm2(OH)2+4	2Sm+3 + 2H2O(l) -2H+ = Sm2(OH)2+4	-14.5	0.4	82.767*					
Sm3(OH)5+4	3Sm+3 + 5H2O(l) -5H+ = Sm3(OH)5+4	-33.9	0.3	193.503*					
SmCO3+	1Sm+3 + 1CO3-2 = SmCO3+	8.1	0.2	-46.235*					
SmF+2	1Sm+3 + 1F- = SmF+2	4.17	0.07	-23.803*	8.07	1.23	106.901*	0	
SmF2+	1Sm+3 + 2F- = SmF2+	6.7	0.3	-38.244*	18.7	1.7	190.991*	0	
SmH2PO4+2	1Sm+3 + 1H3PO4(aq) -1H+ = SmH2PO4+2	0.89	0.13	-5.08*	14.7		66.343*	0	

Tab. A-4: Cont.

Name	**Reaction**	**$\log_{10}K^{o}$**	±	$\Delta_r G_m^o$ [kJ · mol^{-1}]	$\Delta_r H_m^o$ [kJ · mol^{-1}]	±	$\Delta_r S_m^o$ [J · K^{-1} · mol^{-1}]	$\Delta_r C_{p,m}^o$ [J · K^{-1} · mol^{-1}]	±
SmOH+2	1Sm+3 + 1H2O(l) -1H+ = SmOH+2	-7.76	0.09	44.294*	42.7	5.4	-5.348*	0	
SmSO4+	1Sm+3 + 1SO4-2 = SmSO4+	3.95	0.08	-22.547*					
Sn(H2PO4)2(aq)	1Sn+2 + 2H2PO4- = Sn(H2PO4)2(aq)	6.1	0.2	-34.819*					
Sn(HPO4)2-2	1Sn+2 + 2HPO4-2 = Sn(HPO4)2-2	13.6	0.2	-77.629*					
Sn(HPO4)3-4	1Sn+2 + 3HPO4-2 = Sn(HPO4)3-4	13.5	0.2	-77.059*					
Sn(NO3)2(aq)	1Sn+2 + 2NO3- = Sn(NO3)2(aq)	1.39	0.53	-7.934*					
Sn(OH)2(aq)	1Sn+2 + 2H2O(l) -2H+ = Sn(OH)2(aq)	-7.68	0.4	43.838*					
Sn(OH)3-	1Sn+2 + 3H2O(l) -3H+ = Sn(OH)3-	-17	0.6	97.037*					
Sn(OH)4(aq)	1Sn+4 + 4H2O(l) -4H+ = Sn(OH)4(aq)	7.54	0.69	-43.039*					
Sn(OH)5-	1Sn(OH)4(aq) + 1H2O(l) -1H+ = Sn(OH)5-	-8.6	0.4	49.089*					
Sn(OH)6-2	1Sn(OH)4(aq) + 2H2O(l) -2H+ = Sn(OH)6-2	-18.67	0.3	106.569*					
Sn(OH)Cl(aq)	1Sn+2 + 1H2O(l) + 1Cl- -1H+ = Sn(OH)Cl(aq)	-2.5	0.3	14.27*					
Sn3(OH)4+2	3Sn+2 + 4H2O(l) -4H+ = Sn3(OH)4+2	-5.6	0.47	31.965*					
SnBr+	1Sn+2 + 1Br- = SnBr+	1.33	0.18	-7.592*	5.1	2	42.568*	0	
SnBr2(aq)	1Sn+2 + 2Br- = SnBr2(aq)	1.97	0.21	-11.245*	12.9	2	80.982*	0	
SnBr3-	1Sn+2 + 3Br- = SnBr3-	1.93	0.27	-11.017*	7.2	4	61.099*	0	
SnCl+	1Sn+2 + 1Cl- = SnCl+	1.41	0.2	-8.048*	2.25		34.541*	0	
SnCl+3	1Sn+4 + 1Cl- = SnCl+3	3.19	0.5	-18.209*					
SnCl2(aq)	1Sn+2 + 2Cl- = SnCl2(aq)	2.22	0.2	-12.672*	-4.81		26.369*	187	
SnCl2+2	1Sn+4 + 2Cl- = SnCl2+2	5.95	0.36	-33.963*					
SnCl3-	1Sn+2 + 3Cl- = SnCl3-	2.37	0.2	-13.528*	-17		-11.645*	408	
SnCl4-2	1Sn+2 + 4Cl- = SnCl4-2	2.03	0.2	-11.587*	0		38.864*	0	
SnCl4(aq)	1Sn+4 + 4Cl- = SnCl4(aq)	9.57	0.32	-54.626*					
SnCl5-	1Sn+4 + 5Cl- = SnCl5-	10.93	0.41	-62.389*					
SnCl6-2	1Sn+4 + 6Cl- = SnCl6-2	9.83	0.49	-56.11*					
SnF+	1Sn+2 + 1F- = SnF+	5.25	0.19	-29.967*					
SnF2(aq)	1Sn+2 + 2F- = SnF2(aq)	8.89	0.21	-50.744*					
SnF3-	1Sn+2 + 3F- = SnF3-	11.5	1	-65.642*					
SnF6-2	1Sn+4 + 6F- = SnF6-2	25		-142.701*					
SnH2PO4+	1Sn+2 + 1H2PO4- = SnH2PO4+	3.4	0.2	-19.407*					
SnH2PO4HPO4-	1Sn+2 + 1H2PO4- + 1HPO4-2 = SnH2PO4HPO4-	10.5	0.2	-59.934*					

Tab. A-4: Cont.

Name	**Reaction**	**$\log_{10}K^{o}$**	±	$\Delta_r G_m^{o}$ [kJ · mol^{-1}]	$\Delta_r H_m^{o}$ [kJ · mol^{-1}]	±	$\Delta_r S_m^{o}$ [J · K^{-1} · mol^{-1}]	$\Delta_r C_{p,m}^{o}$ [J · K^{-1} · mol^{-1}]	±
SnHPO4(aq)	1Sn+2 + 1HPO4-2 = SnHPO4(aq)	9.6	0.2	-54.797*					
SnNO3+	1Sn+2 + 1NO3- = SnNO3+	1.27	0.31	-7.249*					
SnOH+	1Sn+2 + 1H2O(l) -1H+ = SnOH+	-3.53	0.4	20.149*					
SnPO4-	1Sn+2 + 1PO4-3 = SnPO4-	18.1	0.2	-103.316*					
SnSCN+	1Sn+2 + 1SCN- = SnSCN+	1.5	0.7	-8.562*					
SnSO4(aq)	1Sn+2 + 1SO4-2 = SnSO4(aq)	3.43	0.25	-19.579*					
SO3-2	1SO4-2 + 2H+ + 2e- - 1H2O(l) = SO3-2	-3.397		19.39*	-11.99		-105.25*		
Sr2UO2(CO3)3(aq)	2Sr+2 + 1UO2+2 + 3CO3-2 = Sr2UO2(CO3)3(aq)	29.7	0.5	-169.529*					
SrCO3(aq)	1Sr+2 + 1CO3-2 = SrCO3(aq)	2.79	0.05	-15.925*	20.6	1.9	122.507*	241	100
SrF+	1Sr+2 + 1F- = SrF+	0.92	0.15	-5.251*	10.9	3.7	54.172*	0	
SrH2PO4+	1Sr+2 + 1H2PO4- = SrH2PO4+	0.69	0.2	-3.939*					
SrHCO3+	1Sr+2 + 1HCO3- = SrHCO3+	1.18	0.04	-6.735*	25	1.5	106.441*	226	90
SrHPO4(aq)	1Sr+2 + 1HPO4-2 = SrHPO4(aq)	2.35	0.12	-13.414*	9	15	75.177*	0	
SrOH+	1Sr+2 + 1H2O(l) -1H+ = SrOH+	-13.15	0.05	75.061*	61.6	10.5	-45.148*	0	
SrPO4-	1Sr+2 + 1PO4-3 = SrPO4-	5.62	0.2	-32.079*					
SrSO4(aq)	1Sr+2 + 1SO4-2 = SrSO4(aq)	2.29	0.04	-13.071*	8.7	2	73.022*	0	
SrUO2(CO3)3-2	1Sr+2 + 1UO2+2 + 3CO3-2 = SrUO2(CO3)3-2	25.9	0.2	-147.838*					
Tc2O2(OH)2+2	2TcO(OH)2(aq) + 2H+ - 2H2O(l) = Tc2O2(OH)2+2	12.99	0.41	-74.147*					
Tc2OCl10-4	1Tc2O2(OH)2+2 + 10Cl- + +4H+ -3H2O(l) = Tc2OCl10-4	-0.4	1.1	2.283*					
TcCl5-	0.5Tc2OCl10-4 + 1H+ - 0.5H2O(l) = TcCl5-	-1.765	0.645	10.075*					
TcCl6-2	1TcCl5- + 1Cl- = TcCl6-2	-2.08	1.29	11.873*					
TcCO3(OH)2(aq)	1TcO(OH)2(aq) + 1CO3-2 + 2H+ -1H2O(l) = TcCO3(OH)2(aq)	19.3	0.3	-110.165*					
TcCO3(OH)3-	1TcO(OH)2(aq) + 1CO3-2 + 1H+ = TcCO3(OH)3-	11	0.6	-62.788*					
TcO(OH)3-	1TcO(OH)2(aq) + 1H2O(l) -1H+ = TcO(OH)3-	-10.92	0.17	62.332*					

Tab. A-4: Cont.

Name	**Reaction**	**$\log_{10}K^{o}$**	±	$\Delta_r G_m^o$ [kJ · mol^{-1}]	$\Delta_r H_m^o$ [kJ · mol^{-1}]	±	$\Delta_r S_m^o$ [J · K^{-1} · mol^{-1}]	$\Delta_r C_{p,m}^o$ [J · K^{-1} · mol^{-1}]	±
Th(CO3)5-6	1Th+4 + 5CO3-2 = Th(CO3)5-6	31	0.7	-176.949*					
Th(H2PO4)2+2	1Th+4 + 2H3PO4(aq) - 2H+ = Th(H2PO4)2+2	6.2	0.32	-35.39*					
Th(H3PO4)(H2PO4)+3	1Th+4 + 2H3PO4(aq) - 1H+ = Th(H3PO4)(H2PO4)+3	5.42	0.32	-30.938*					
Th(IO3)2+2	1Th+4 + 2IO3- = Th(IO3)2+2	6.97	0.12	-39.785*					
Th(IO3)3+	1Th+4 + 3IO3- = Th(IO3)3+	9.87	0.11	-56.338*					
Th(NO3)2+2	1Th+4 + 2NO3- = Th(NO3)2+2	2.3	0.4	-13.128*					
Th(OH)2(CO3)2-2	1Th+4 + 2OH- + 2CO3-2 = Th(OH)2(CO3)2-2	36.8	0.5	-210.056*					
Th(OH)2+2	1Th+4 + 2H2O(l) -2H+ = Th(OH)2+2	-6.2	0.5	35.39*	85.7	41.4	168.741*	0	
Th(OH)2CO3(aq)	1Th+4 + 2OH- + 1CO3-2 = Th(OH)2CO3(aq)	30.5	0.6	-174.095*					
Th(OH)3(SiO(OH)3)3-2	1Th+4 + 3Si(OH)4(aq) + 3H2O(l) -6H+ = Th(OH)3(SiO(OH)3)3-2	-27.8	0.7	158.684*					
Th(OH)3CO3-	1Th+4 + 3OH- + 1CO3-2 = Th(OH)3CO3-	38.3	0.7	-218.618*					
Th(OH)4(aq)	1Th+4 + 4H2O(l) -4H+ = Th(OH)4(aq)	-17.4	0.7	99.32*					
Th(OH)4CO3-2	1Th+4 + 4OH- + 1CO3-2 = Th(OH)4CO3-2	40.4	0.6	-230.605*					
Th(SCN)2+2	1Th+4 + 2SCN- = Th(SCN)2+2	3.4	0.8	-19.407*					
Th(SO4)2(aq)	1Th+4 + 2SO4-2 = Th(SO4)2(aq)	9.69	0.27	-55.311*	40.38	1.08	320.949*		
Th(SO4)3-2	1Th+4 + 3SO4-2 = Th(SO4)3-2	10.748	0.076	-61.35*					
Th2(OH)2+6	2Th+4 + 2H2O(l) -2H+ = Th2(OH)2+6	-5.9	0.5	33.677*	58.3	5.7	82.584*	0	
Th2(OH)3+5	2Th+4 + 3H2O(l) -3H+ = Th2(OH)3+5	-6.8	0.2	38.815*					
Th4(OH)12+4	4Th+4 + 12H2O(l) -12H+ = Th4(OH)12+4	-26.6	0.2	151.834*					
Th4(OH)8+8	4Th+4 + 8H2O(l) -8H+ = Th4(OH)8+8	-20.4	0.4	116.444*	243	21.3	424.471*	0	
Th6(OH)14+10	6Th+4 + 14H2O(l) -14H+ = Th6(OH)14+10	-36.8	1.2	210.056*					
Th6(OH)15+9	6Th+4 + 15H2O(l) -15H+ = Th6(OH)15+9	-36.8	1.5	210.056*	472.8	22	881.248*	0	
ThCl+3	1Th+4 + 1Cl- = ThCl+3	1.7	0.1	-9.704*					
ThF+3	1Th+4 + 1F- = ThF+3	8.87	0.15	-50.63*	-0.4	2	168.473*		
ThF2+2	1Th+4 + 2F- = ThF2+2	15.63	0.23	-89.217*	-3.3	0.4	288.166*		
ThF3+	1Th+4 + 3F- = ThF3+	20.67	0.16	-117.985*					

Tab. A-4: Cont.

Name	**Reaction**	**$\log_{10}K^{o}$**	±	$\Delta_r G_m^o$ [kJ · mol^{-1}]	$\Delta_r H_m^o$ [kJ · mol^{-1}]	±	$\Delta_r S_m^o$ [J · K^{-1} · mol^{-1}]	$\Delta_r C_{p,m}^o$ [J · K^{-1} · mol^{-1}]	±
ThF4(aq)	1Th+4 + 4F- = ThF4(aq)	25.58	0.18	-146.012*					
ThF6-2	1Th+4 + 6F- = ThF6-2	29.23	0.62	-166.846*					
ThH2PO4+3	1Th+4 + 1H3PO4(aq) - 1H+ = ThH2PO4+3	3.45	0.32	-19.693*					
ThH3PO4+4	1Th+4 + 1H3PO4(aq) = ThH3PO4+4	1.89	0.31	-10.788*					
ThIO3+3	1Th+4 + 1IO3- = ThIO3+3	4.14	0.1	-23.631*					
ThNO3+3	1Th+4 + 1NO3- = ThNO3+3	1.3	0.2	-7.42*					
ThOH(CO3)4-5	1Th+4 + 1OH- + 4CO3-2 = ThOH(CO3)4-5	35.6	0.5	-203.206*					
ThOH+3	1Th+4 + 1H2O(l) -1H+ = ThOH+3	-2.5	0.5	14.27*	44.2	6.3	100.385*	0	
ThSCN+3	1Th+4 + 1SCN- = ThSCN+3	2	0.5	-11.416*					
ThSO4+2	1Th+4 + 1SO4-2 = ThSO4+2	6.17	0.32	-35.219*	20.92	0.74	188.29*		
Ti2(OH)2+4	2Ti+3 + 2H2O(l) -2H+ = Ti2(OH)2+4	-2.64	0.1	15.069*					
TiO(OH)2(aq)	1TiO+2 + 2H2O(l) -2H+ = TiO(OH)2(aq)	-5.49	0.14	31.337*					
TiO(OH)3-	1TiO+2 + 3H2O(l) -3H+ = TiO(OH)3-	-17.4	0.5	99.32*					
TiOH+2	1Ti+3 + 1H2O(l) -1H+ = TiOH+2	-1.65	0.11	9.418*					
TiOOH+	1TiO+2 + 1H2O(l) -1H+ = TiOOH+	-2.48	0.1	14.156*					
U(CO3)4-4	1U+4 + 4CO3-2 = U(CO3)4-4	35.22	1.03	-201.037*					
U(CO3)5-6	1U+4 + 5CO3-2 = U(CO3)5-6	33.9	1	-193.503*	-20	4	581.931*		
U(NO3)2+2	1U+4 + 2NO3- = U(NO3)2+2	2.3	0.35	-13.128*					
U(OH)2+2	1U+4 + 2H2O(l) -2H+ = U(OH)2+2	-1.9	0.2	10.845*					
U(OH)3+	1U+4 + 3H2O(l) -3H+ = U(OH)3+	-5.2	0.4	29.682*					
U(OH)4(aq)	1U+4 + 4H2O(l) -4H+ = U(OH)4(aq)	-10	1.4	57.08*					
U(Ox)2(aq)	1UOx+2 + 1Ox-2 = U(Ox)2(aq)	8		-45.664*					
U(Ox)3-2	1U(Ox)2(aq) + 1Ox-2 = U(Ox)3-2	5		-28.54*					
U(Ox)4-4	1U(Ox)3-2 + 1Ox-2 = U(Ox)4-4	3		-17.124*					
U(SCN)2+2	1U+4 + 2SCN- = U(SCN)2+2	4.26	0.18	-24.316*	-18	4	21.185*		
U(SO4)2(aq)	1U+4 + 2SO4-2 = U(SO4)2(aq)	10.51	0.2	-59.992*	32.7	2.8	310.889*		

Tab. A-4: Cont.

Name	Reaction	$\log_{10}K^{o}$	±	$\Delta_r G_m^{o}$ [kJ · mol^{-1}]	$\Delta_r H_m^{o}$ [kJ · mol^{-1}]	±	$\Delta_r S_m^{o}$ [J · K^{-1} · mol^{-1}]	$\Delta_r C_{p,m}^{o}$ [J · K^{-1} · mol^{-1}]	±
UCl+3	1U+4 + 1Cl- = UCl+3	1.72	0.13	-9.818*	-19	9	-30.797*		
UCO3(OH)3-	1U+4 + 1CO3-2 + 3H2O(l) -3H+ = UCO3(OH)3-	4		-22.832*					
UEdta(aq)	1U+4 + 1Edta-4 = UEdta(aq)	29.5	0.2	-168.387*					
UEdta(OH)2-2	1UEdtaOH- + 1OH- = UEdta(OH)2-2	5.9		-33.677*					
UEdtaOH-	1UEdta(aq) + 1OH- = UEdtaOH-	9.1		-51.943*					
UF+3	1U+4 + 1F- = UF+3	9.42	0.51	-53.77*	-5.6	0.5	161.562*		
UF2+2	1U+4 + 2F- = UF2+2	16.56	0.71	-94.525*	-3.5	0.6	305.3*		
UF3+	1U+4 + 3F- = UF3+	21.89	0.83	-124.949*	0.5	4	420.758*		
UF4(aq)	1U+4 + 4F- = UF4(aq)	26.34	0.96	-150.35*	-8.43		476.001*		
UF5-	1U+4 + 5F- = UF5-	27.73	0.74	-158.284*					
UF6-2	1U+4 + 6F- = UF6-2	29.8	0.7	-170.1*					
UH2PO4+3	1U+4 + 1H2PO4- = UH2PO4+3	6.8	0.7	-38.815*					
UI+3	1U+4 + 1I- = UI+3	1.25	0.3	-7.135*					
UNO3+3	1U+4 + 1NO3- = UNO3+3	1.47	0.13	-8.391*					
UO2(CO3)2-2	1UO2+2 + 2CO3-2 = UO2(CO3)2-2	16.61	0.09	-94.811*	18.5	4	380.046*		
UO2(CO3)3-4	1UO2+2 + 3CO3-2 = UO2(CO3)3-4	21.84	0.04	-124.664*	-39.2	4.1	286.646*		
UO2(CO3)3-5	1UO2+ + 3CO3-2 = UO2(CO3)3-5	7.19	0.36	-41.041*					
UO2(H2AsO4)2(aq)	1UO2+2 + 2H3AsO4(aq) -2H+ = UO2(H2AsO4)2(aq)	0.29	0.53	-1.655*					
UO2(H2PO4)(H3PO4)+	1UO2+2 + 2H3PO4(aq) - 1H+ = UO2(H2PO4)(H3PO4)+	1.65	0.11	-9.418*					
UO2(H2PO4)2(aq)	1UO2+2 + 2H3PO4(aq) - 2H+ = UO2(H2PO4)2(aq)	0.64	0.11	-3.653*					
UO2(H3Isa)+	1UO2+2 + 1H3Isa- = UO2(H3Isa)+	3.5	0.2	-19.978*	-1	1	63.653*		
UO2(H3Isa)2(aq)	1UO2+2 + 2H3Isa- = UO2(H3Isa)2(aq)	6.2	0.2	-35.39*	1.4	1.8	123.394*		
UO2(H3Isa)3-	1UO2+2 + 3H3Isa- = UO2(H3Isa)3-	8	0.2	-45.664*	-6.2	3	132.364*		
UO2(HCit)(aq)	1UO2+2 + 1HCit-2 = UO2(HCit)(aq)	5	1	-28.54*					
UO2(HEdta)-	1UO2+2 + 1HEdta-3 = UO2(HEdta)-	8.37	0.1	-47.776*					
UO2(HSeO3)2(aq)	1UO2+2 + 2HSeO3- = UO2(HSeO3)2(aq)	5.51	0.11	-31.451*					
UO2(IO3)2(aq)	1UO2+2 + 2IO3- = UO2(IO3)2(aq)	3.59	0.15	-20.492*					

Tab. A-4: Cont.

Name	**Reaction**	**$\log_{10}K^{o}$**	±	$\Delta_r G_m^{o}$ [kJ · mol^{-1}]	$\Delta_r H_m^{o}$ [kJ · mol^{-1}]	±	$\Delta_r S_m^{o}$ [J · K^{-1} · mol^{-1}]	$\Delta_r C_{p,m}^{o}$ [J · K^{-1} · mol^{-1}]	±
UO2(OH)2(aq)	1UO2+2 + 2H2O(l) -2H+ = UO2(OH)2(aq)	-12.15	0.07	69.353*					
UO2(OH)3-	1UO2+2 + 3H2O(l) -3H+ = UO2(OH)3-	-20.25	0.42	115.588*					
UO2(OH)4-2	1UO2+2 + 4H2O(l) -4H+ = UO2(OH)4-2	-32.4	0.68	184.941*					
UO2(Ox)2-2	1UO2+2 + 2Ox-2 = UO2(Ox)2-2	11.65	0.15	-66.499*					
UO2(Ox)3-4	1UO2+2 + 3Ox-2 = UO2(Ox)3-4	13.8	1.5	-78.771*					
UO2(SCN)2(aq)	1UO2+2 + 2SCN- = UO2(SCN)2(aq)	1.24	0.55	-7.078*	8.9	0.6	53.59*		
UO2(SCN)3-	1UO2+2 + 3SCN- = UO2(SCN)3-	2.1	0.5	-11.987*	6	1.2	60.328*		
UO2(SeO4)2-2	1UO2+2 + 2SeO4-2 = UO2(SeO4)2-2	4.03	0.09	-23.003*	31	4	181.128*		
UO2(SO4)2-2	1UO2+2 + 2SO4-2 = UO2(SO4)2-2	4.14	0.15	-23.631*	35.1	1	196.986*		
UO2(SO4)3-4	1UO2+2 + 3SO4-2 = UO2(SO4)3-4	3.02	0.38	-17.238*					
UO2Cit-	1UO2+2 + 1Cit-3 = UO2Cit-	8.96	0.17	-51.144*					
UO2Cl+	1UO2+2 + 1Cl- = UO2Cl+	0.17	0.02	-0.97*	8	2	30.087*		
UO2Cl2(aq)	1UO2+2 + 2Cl- = UO2Cl2(aq)	-1.1	0.4	6.279*	15	6	29.251*		
UO2CO3(aq)	1UO2+2 + 1CO3-2 = UO2CO3(aq)	9.94	0.03	-56.738*	5	2	207.07*		
UO2CO3F-	1UO2+2 + 1CO3-2 + 1F- = UO2CO3F-	13.75	0.09	-78.486*					
UO2CO3F2-2	1UO2+2 + 1CO3-2 + 2F- = UO2CO3F2-2	15.57	0.14	-88.874*					
UO2CO3F3-3	1UO2+2 + 1CO3-2 + 3F- = UO2CO3F3-3	16.38	0.11	-93.498*					
UO2Edta-2	1UO2+2 + 1Edta-4 = UO2Edta-2	13.7	0.2	-78.2*					
UO2F+	1UO2+2 + 1F- = UO2F+	5.16	0.06	-29.453*	-0.54	0.26	96.976*		
UO2F2(aq)	1UO2+2 + 2F- = UO2F2(aq)	8.83	0.08	-50.402*	-1.34	0.18	164.555*		
UO2F3-	1UO2+2 + 3F- = UO2F3-	10.9	0.1	-62.218*	-1.18	0.3	204.721*		
UO2F4-2	1UO2+2 + 4F- = UO2F4-2	11.84	0.11	-67.583*	-2.12	0.47	219.565*		
UO2H2AsO4+	1UO2+2 + 1H3AsO4(aq) -1H+ = UO2H2AsO4+	1.34	0.42	-7.649*					
UO2H2PO4+	1UO2+2 + 1H3PO4(aq) -1H+ = UO2H2PO4+	1.12	0.06	-6.393*					
UO2H3PO4+2	1UO2+2 + 1H3PO4(aq) = UO2H3PO4+2	0.76	0.15	-4.338*					
UO2HAsO4(aq)	1UO2+2 + 1HAsO4-2 = UO2HAsO4(aq)	7.16	0.37	-40.87*					

Tab. A-4: Cont.

Name	**Reaction**	**$\log_{10}K^{o}$**	±	$\Delta_r G_m^o$ [kJ · mol^{-1}]	$\Delta_r H_m^o$ [kJ · mol^{-1}]	±	$\Delta_r S_m^o$ [J · K^{-1} · mol^{-1}]	$\Delta_r C_{p,m}^o$ [J · K^{-1} · mol^{-1}]	±
UO2HPO4(aq)	1UO2+2 + 1HPO4-2 = UO2HPO4(aq)	7.24	0.26	-41.326*					
UO2HSeO3+	1UO2+2 + 1HSeO3- = UO2HSeO3+	3.27	0.15	-18.665*					
UO2IO3+	1UO2+2 + 1IO3- = UO2IO3+	2	0.02	-11.416*					
UO2NO3+	1UO2+2 + 1NO3- = UO2NO3+	-0.19	0.15	1.085*	20.9	3.5	66.461*		
UO2OH+	1UO2+2 + 1H2O(l) -1H+ = UO2OH+	-5.25	0.24	29.967*	43.3	2.3	44.718*		
UO2Ox(aq)	1UO2+2 + 1Ox-2 = UO2Ox(aq)	7.13	0.16	-40.698*	25.4	18.4	221.695*		
UO2PO4-	1UO2+2 + 1PO4-3 = UO2PO4-	11.01	0.48	-62.846*					
UO2SCN+	1UO2+2 + 1SCN- = UO2SCN+	1.4	0.23	-7.991*	3.22	0.06	37.603*		
UO2SeO4(aq)	1UO2+2 + 1SeO4-2 = UO2SeO4(aq)	2.93	0.04	-16.725*	20	2	123.175*		
UO2SiO(OH)3+	1UO2+2 + 1SiO(OH)3- = UO2SiO(OH)3+	7.93	0.19	-45.265*	9.9	3	185.024*	0	
UO2SO4(aq)	1UO2+2 + 1SO4-2 = UO2SO4(aq)	3.15	0.1	-17.98*	19.5	1.6	125.71*		
UOH+3	1U+4 + 1H2O(l) -1H+ = UOH+3	-0.54	0.06	3.082*	46.91		146.999*		
UOx+2	1U+4 + 1Ox-2 = UOx+2	11		-62.788*					
USCN+3	1U+4 + 1SCN- = USCN+3	2.83	0.15	-16.154*	-27	8	-36.378*		
USO4+2	1U+4 + 1SO4-2 = USO4+2	6.58	0.19	-37.559*	8	2.7	152.805*		
Zn(CO3)2-2	1Zn+2 + 2CO3-2 = Zn(CO3)2-2	6.75	0.6	-38.529*					
Zn(H2PO4)(HPO4)-	1Zn+2 + 1H2PO4- + 1HPO4-2 = Zn(H2PO4)(HPO4)-	4	0.5	-22.832*					
Zn(H2PO4)2(aq)	1Zn+2 + 2H2PO4- = Zn(H2PO4)2(aq)	2	0.2	-11.416*					
Zn(HPO4)(PO4)-3	1Zn+2 + 1HPO4-2 + 1PO4-3 = Zn(HPO4)(PO4)-3	12.5	0.2	-71.351*					
Zn(HPO4)2-2	1Zn+2 + 2HPO4-2 = Zn(HPO4)2-2	7.1	0.2	-40.527*					
Zn(HPO4)3-4	1Zn+2 + 3HPO4-2 = Zn(HPO4)3-4	7.4	0.2	-42.24*					
Zn(HS)2(aq)	1Zn+2 + 2HS- = Zn(HS)2(aq)	9.3	0.17	-53.085*	-13.7	3.2	132.097*	0	
Zn(HS)3-	1Zn+2 + 3HS- = Zn(HS)3-	13.3	0.05	-75.917*	-50.7	1.7	84.578*	0	
Zn(OH)2(aq)	1Zn+2 + 2H2O(l) -2H+ = Zn(OH)2(aq)	-17.89	0.15	102.117*	107.1	3.1	16.713*	-65	27
Zn(OH)2HPO4-2	1Zn+2 + 2H2O(l) + 1HPO4-2 -2H+ = Zn(OH)2HPO4-2	-17	0.3	97.037*					

Tab. A-4: Cont.

Name	**Reaction**	**$\log_{10}K^{o}$**	±	$\Delta_r G_m^{o}$ [kJ · mol^{-1}]	$\Delta_r H_m^{o}$ [kJ · mol^{-1}]	±	$\Delta_r S_m^{o}$ [J · K^{-1} · mol^{-1}]	$\Delta_r C_{p,m}^{o}$ [J · K^{-1} · mol^{-1}]	±
Zn(OH)3-	1Zn+2 + 3H2O(l) -3H+ = Zn(OH)3-	-27.98	0.1	159.711*	143.5	2.5	-54.372*	-196	23
Zn(OH)4-2	1Zn+2 + 4H2O(l) -4H+ = Zn(OH)4-2	-40.35	0.22	230.319*	178.3	5.8	-174.474*	-348	56
Zn(SO4)2-2	1Zn+2 + 2SO4-2 = Zn(SO4)2-2	3.2	0.2	-18.266*	10	5	94.804*		
Zn2CO3+2	2Zn+2 + 1CO3-2 = Zn2CO3+2	5.3	0.4	-30.253*					
Zn2OH+3	2Zn+2 + 1H2O(l) -1H+ = Zn2OH+3	-7.9	0.3	45.094*					
ZnCl+	1Zn+2 + 1Cl- = ZnCl+	0.4	0.09	-2.283*					
ZnCl2(aq)	1Zn+2 + 2Cl- = ZnCl2(aq)	0.69	0.15	-3.939*					
ZnCl3-	1Zn+2 + 3Cl- = ZnCl3-	0.48	0.54	-2.74*					
ZnCl4-2	1Zn+2 + 4Cl- = ZnCl4-2	-2		11.416*					
ZnCO3(aq)	1Zn+2 + 1CO3-2 = ZnCO3(aq)	4.75	0.06	-27.113*					
ZnH2PO4+	1Zn+2 + 1H2PO4- = ZnH2PO4+	0.9	0.2	-5.137*					
ZnHCO3+	1Zn+2 + 1HCO3- = ZnHCO3+	1.62	0.1	-9.247*					
ZnHPO4(aq)	1Zn+2 + 1HPO4-2 = ZnHPO4(aq)	3.3	0.2	-18.837*					
ZnOH+	1Zn+2 + 1H2O(l) -1H+ = ZnOH+	-8.94	0.06	51.03*	56.7	0.7	19.018*	0	
ZnS(HS)-	1Zn+2 + 2HS- -1H+ = ZnS(HS)-	3.36	0.2	-19.179*	25.9	3	151.196*	0	
ZnSO4(aq)	1Zn+2 + 1SO4-2 = ZnSO4(aq)	2.3	0.04	-13.128*	6.04	0.54	64.291*		
Zr(CO3)4-4	1Zr+4 + 4CO3-2 = Zr(CO3)4-4	42.9	1	-244.875*					
Zr(NO3)2+2	1Zr+4 + 2NO3- = Zr(NO3)2+2	2.64	0.17	-15.069*					
Zr(OH)2+2	1Zr+4 + 2H2O(l) -2H+ = Zr(OH)2+2	0.98	1.06	-5.594*					
Zr(OH)4(aq)	1Zr+4 + 4H2O(l) -4H+ = Zr(OH)4(aq)	-2.19	1.7	12.501*					
Zr(OH)6-2	1Zr+4 + 6H2O(l) -6H+ = Zr(OH)6-2	-29	0.7	165.533*					
Zr(SO4)2(aq)	1Zr+4 + 2SO4-2 = Zr(SO4)2(aq)	11.54	0.21	-65.871*	67.38	7.258	446.925*		
Zr(SO4)3-2	1Zr+4 + 3SO4-2 = Zr(SO4)3-2	14.3	0.5	-81.625*					
Zr3(OH)4+8	3Zr+4 + 4H2O(l) -4H+ = Zr3(OH)4+8	0.4	0.3	-2.283*	-1.98	18.028	1.017*		
Zr3(OH)9+3	3Zr+4 + 9H2O(l) -9H+ = Zr3(OH)9+3	12.19	0.08	-69.581*					
Zr4(OH)15+	4Zr+4 + 15H2O(l) - 15H+ = Zr4(OH)15+	12.58	0.24	-71.807*					
Zr4(OH)16(aq)	4Zr+4 + 16H2O(l) - 16H+ = Zr4(OH)16(aq)	8.39	0.8	-47.89*	301.12	21.266	1170.587*		

Tab. A-4: Cont.

Name	**Reaction**	**$\log_{10}K^{o}$**	**±**	**$\Delta_r G_m^{o}$** [kJ · mol^{-1}]	**$\Delta_r H_m^{o}$** [kJ · mol^{-1}]	**±**	**$\Delta_r S_m^{o}$** [J · K^{-1} · mol^{-1}]	**$\Delta_r C_{p,m}^{o}$** [J · K^{-1} · mol^{-1}]	**±**
Zr4(OH)8+8	4Zr+4 + 8H2O(l) -8H+ = Zr4(OH)8+8	6.52	0.65	-37.216*					
ZrCl+3	1Zr+4 + 1Cl- = ZrCl+3	1.59	0.06	-9.076*					
ZrCl2+2	1Zr+4 + 2Cl- = ZrCl2+2	2.17	0.24	-12.386*					
ZrF+3	1Zr+4 + 1F- = ZrF+3	10.12	0.07	-57.765*	-5.3	0.8	175.97*		
ZrF2+2	1Zr+4 + 2F- = ZrF2+2	18.55	0.31	-105.884*	-9.9	1.3	321.933*		
ZrF3+	1Zr+4 + 3F- = ZrF3+	24.72	0.38	-141.103*	-8.9	2.1	443.41*		
ZrF4(aq)	1Zr+4 + 4F- = ZrF4(aq)	30.11	0.4	-171.869*	-18.7	3.4	513.732*		
ZrF5-	1Zr+4 + 5F- = ZrF5-	34.6	0.42	-197.498*					
ZrF6-2	1Zr+4 + 6F- = ZrF6-2	38.11	0.43	-217.533*					
ZrNO3+3	1Zr+4 + 1NO3- = ZrNO3+3	1.59	0.08	-9.076*					
ZrOH+3	1Zr+4 + 1H2O(l) -1H+ = ZrOH+3	0.32	0.22	-1.827*					
ZrSO4+2	1Zr+4 + 1SO4-2 = ZrSO4+2	7.04	0.09	-40.185*	36.94	7.153	258.677*		
Gases									
CH4g	1CH4(aq) = CH4g	2.856		-16.302*	13.797		100.953*	-207.47	
CO2g	1H+ -1H2O(l) + 1HCO3- = CO2g	7.82		-44.637*	10.875		186.188*	188.054	
H2g	1H2(aq) = H2g	3.106		-17.729*	4.04		73.014*	-144.19	
H2Sg	1HS- + 1H+ = H2Sg	8.01		-45.721*	-4.3		138.928*		
H2Seg	1H2Se(aq) = H2Seg	1.1	0.01	-6.279*	-29	2.02	-76.207*		
N2g	1N2(aq) = N2g	3.186		-18.186*	10.438		96.005*	-221.073	
O2g	1O2(aq) = O2g	2.894		-16.519*	12.06		95.855*	-199.788	

Tab. A-5: Thermodynamic data for formation reactions of solids

Name	**Reaction**	**$\log_{10}K^{o}$**	±	$\Delta_r G_m^{o}$ [kJ · mol^{-1}]	$\Delta_r H_m^{o}$ [kJ · mol^{-1}]	±	$\Delta_r S_m^{o}$ [J · K^{-1} · mol^{-1}]	$\Delta_r C_{p,m}^{o}$ [J · K^{-1} · mol^{-1}]	±
Solids									
(HgOH)3PO4(s)	3Hg+2 + 1HPO4-2 + 3H2O(l) -4H+ = (HgOH)3PO4(s)	14	1.1	-79.913*					
(NH4)4NpO2(CO3)3(s)	4NH4+ + 1NpO2+2 + 3CO3-2 = (NH4)4NpO2(CO3)3(s)	27.34	0.58	-156.058*					
(PuO2)3(PO4)2w4(am)	3PuO2+2 + 2PO4-3 + 4H2O(l) = (PuO2)3(PO4)2w4(am)	48.97	0.69	-279.523*					
(UO2)2SiO4w2(cr)	2UO2+2 + 1Si(OH)4(aq) + 2H2O(l) -4H+ = (UO2)2SiO4w2(cr)	-5.75	0.26	32.821*					
(UO2)3(AsO4)2w12(cr)	3UO2+2 + 2AsO4-3 + 12H2O(l) = (UO2)3(AsO4)2w12(cr)	45.33	1	-258.746*					
(UO2)3(PO4)2w4(cr)	3UO2+2 + 2H3PO4(aq) + 4H2O(l) -6H+ = (UO2)3(PO4)2w4(cr)	5.96	0.3	-34.02*					
Ac(OH)3(ag)	1Ac+3 + 3H2O(l) - 3H+ = Ac(OH)3(ag)	-21.1	0.2	120.44*					
Ac(OH)3(fr)	1Ac+3 + 3H2O(l) - 3H+ = Ac(OH)3(fr)	-23.3	0.2	132.997*					
Ac2(Ox)3(s)	2Ac+3 + 3Ox-2 = Ac2(Ox)3(s)	25.7	0.6	-146.697*					
Ag2CO3(cr)	2Ag+ + 1CO3-2 = Ag2CO3(cr)	11.07	0.04	-63.188*					
Ag2O(am)	2Ag+ + 1H2O(l) -2H+ = Ag2O(am)	-12.62	0.08	72.035*	32	26	-134.28*	0	
Ag2O(cr)	2Ag+ + 1H2O(l) -2H+ = Ag2O(cr)	-11.82	0.2	67.469*	38.8	6.6	-96.156*	0	
Ag2S(cr)	2Ag+ + 1H2S(aq) - 2H+ = Ag2S(cr)	28.84	0.4	-164.62*	-207	4	-142.143*	0	
Ag2SeO3(cr)	2Ag+ + 1SeO3-2 = Ag2SeO3(cr)	15.8	0.3	-90.187*	-67.82	1.51	75.02*		
Ag2SeO4(cr)	2Ag+ + 1SeO4-2 = Ag2SeO4(cr)	7.86	0.5	-44.865*	-30.59	4.1	47.879*		
Ag2SO4(s)	2Ag+ + 1SO4-2 = Ag2SO4(s)	4.94	0.04	-28.198*	-17.3	0.4	36.551*		
Ag3PO4(s)	3Ag+ + 1HPO4-2 - 1H+ = Ag3PO4(s)	9.05	0.08	-51.658*					
AgBr(cr)	1Ag+ + 1Br- = AgBr(cr)	12.3	0.04	-70.209*	-85.5	1.8	-51.287*	0	
AgCl(cr)	1Ag+ + 1Cl- = AgCl(cr)	9.748	0.038	-55.642*	-65.72	0.14	-33.802*	0	
AgCN(s)	1Ag+ + 1CN- = AgCN(s)	15.84	0.2	-90.415*					
AgI(cr)	1Ag+ + 1I- = AgI(cr)	16.08	0.03	-91.785*	-110.4	4	-62.434*	0	
AgSeCN(cr)	1Ag+ + 1CN- + 1HSe- - 1H+ -2e- = AgSeCN(cr)	27.03	0.7	-154.288*					
Al(OH)3(cr)	1Al+3 + 3H2O(l) -3H+ = Al(OH)3(cr)	-7.75	0.08	44.237*	104.3	2.3	201.451*	0	
Al2Si2O5(OH)4(cr)	2Al+3 + 2Si(OH)4(aq) + 1H2O(l) -6H+ = Al2Si2O5(OH)4(cr)	-7.44	0.06	42.468*	172.8	5	437.136*		

Tab. A-5: Cont.

Name	**Reaction**	**$\log_{10}K^{o}$**	±	$\Delta_r G_m^o$ [kJ · mol^{-1}]	$\Delta_r H_m^o$ [kJ · mol^{-1}]	±	$\Delta_r S_m^o$ [J · K^{-1} · mol^{-1}]	$\Delta_r C_{p,m}^o$ [J · K^{-1} · mol^{-1}]	±
AlOOH(cr)	1Al+3 + 2H2O(l) -3H+ = AlOOH(cr)	-9.4	0.4	53.656*	148.5	8.3	318.11*	0	
Am(OH)3(am)	1Am+3 + 3H2O(l) - 3H+ = Am(OH)3(am)	-16.9	0.8	96.466*					
Am(OH)3(cr)	1Am+3 + 3H2O(l) - 3H+ = Am(OH)3(cr)	-15.6	0.6	89.045*					
Am2(CO3)3(am_hyd)	2Am+3 + 3CO3-2 = Am2(CO3)3(am_hyd)	33.4	2.2	-190.649*					
AmO2OH(am)	1AmO2+ + 1H2O(l) - 1H+ = AmO2OH(am)	-5.3	0.5	30.253*					
AmOHCO3(am_hyd)	1Am+3 + 1OH- + 1CO3-2 = AmOHCO3(am_hyd)	20.2	1	-115.302*					
AmOHCO3w0.5(cr)	1Am+3 + 1OH- + 1CO3-2 + 0.5H2O(l) = AmOHCO3w0.5(cr)	22.4	0.5	-127.86*					
As(cr)	1HAsO4-2 + 7H+ + 5e- - 4H2O(l) = As(cr)	40.989		-233.967*	-236.98		-10.106*		
Ba[(UO2)(AsO4)]2w7(cr)	2UO2+2 + 1Ba+2 + 2AsO4-3 + 7H2O(l) = Ba[(UO2)(AsO4)]2w7 (cr)	44.7	1	-255.149*	-27.977		761.94*		
Ba[(UO2)(PO4)]2w(cr)	2UO2+2 + 1Ba+2 + 2PO4-3 + 6H2O(l) = Ba[(UO2)(PO4)]2w(cr)	52.2	1	-297.96*	-44.162		851.242*		
Ba3(PO4)2(s)	3Ba+2 + 2PO4-3 = Ba3(PO4)2(s)	29	0.5	-165.533*					
BaCO3(cr)	1Ba+2 + +CO3-2 = BaCO3(cr)	8.57	0.03	-48.918*	-3.3	0.4	153.003*	508	10
BaHPO4(cr)	1Ba+2 + 1HPO4-2 = BaHPO4(cr)	7.2	0.3	-41.098*					
BaSeO3(cr)	1Ba+2 + 1SeO3-2 = BaSeO3(cr)	6.5	0.25	-37.102*	5.3	3.98	142.218*		
BaSeO4(cr)	1Ba+2 + 1SeO4-2 = BaSeO4(cr)	7.25	0.11	-41.383*	-5.7	6.6	119.682*		
BaSO4(cr)	1Ba+2 + +SO4-2 = BaSO4(cr)	9.96	0.07	-56.852*	-26.1	0.4	103.143*	422.5	2.9
C(cr)	1HCO3- + 5H+ + 4e- - 3H2O(l) = C(cr)	21.819		-124.544*	-167.275		-143.321*		
Ca(H3Isa)2(cr)	1Ca+2 + 2H3Isa- = Ca(H3Isa)2(cr)	6.4	0.2	-36.531*					
Ca(OH)2(cr)	1Ca+2 + 2H2O(l) -2H+ = Ca(OH)2(cr)	-22.75	0.02	129.858*	122.8	0.6	-23.673*	-104.5	6.5
Ca(Ox)w1(cr)	1Ca+2 + 1Ox-2 + 1H2O(l) = Ca(Ox)w1(cr)	8.73	0.06	-49.831*	-21.5	0.5	95.023*	0	
Ca(Ox)w2(cr)	1Ca+2 + 1Ox-2 + 2H2O(l) = Ca(Ox)w2(cr)	8.3	0.06	-47.377*	-25.2	1.1	74.381*	0	
Ca(Ox)w3(cr)	1Ca+2 + 1Ox-2 + 3H2O(l) = Ca(Ox)w3(cr)	8.19	0.04	-46.749*	-29.7	1.3	57.182*	0	
Ca(UO2)2(SiO3OH)2w5(cr)	1Ca+2 + 2UO2+2 + 2Si(OH)4(aq) + 5H2O(l) -6H+ = Ca(UO2)2(SiO3OH)2w5 (cr)	-11.52	0.16	65.757*	86	16	67.897*		

Tab. A-5: Cont.

Name	**Reaction**	**$\log_{10}K^{o}$**	±	$\Delta_r G_m^{o}$ [kJ · mol^{-1}]	$\Delta_r H_m^{o}$ [kJ · mol^{-1}]	±	$\Delta_r S_m^{o}$ [J · K^{-1} · mol^{-1}]	$\Delta_r C_{p,m}^{o}$ [J · K^{-1} · mol^{-1}]	±
Ca[(UO2)(AsO4)]2w10(cr)	2UO2+2 + 1Ca+2 + 2AsO4-3 + 10H2O(l) = Ca[(UO2)(AsO4)]2w10 (cr)	45.1	1	-257.433*	-33.018		752.691*		
Ca[(UO2)(PO4)]2w6(cr)	2UO2+2 + 1Ca+2 + 2PO4-3 + 6H2O(l) = Ca[(UO2)(PO4)]2w6(cr)	50	1	-285.402*	-18.009		896.841*		
Ca0.5NpO2(OH)2w1.3(cr)	1NpO2+ + 0.5Ca+2 + 3.3H2O(l) -2H+ = Ca0.5NpO2(OH)2w1.3 (cr)	-12.3	0.07	70.209*					
Ca3(Cit)2w4(cr)	3Ca+2 + 2Cit-3 + 4H2O(l) = Ca3(Cit)2w4(cr)	17.9	0.1	-102.174*					
Ca3(PO4)2(cr)	3Ca+2 + 2PO4-3 = Ca3(PO4)2(cr)	28.9	0.1	-164.962*	81.2	5	825.633*	5'620	100
Ca4H(PO4)3w2.5(s)	4Ca+2 + 3PO4-3 + 1H+ + 2.5H2O(l) = Ca4H(PO4)3w2.5(s)	48.48	0.16	-276.726*	21	19	998.577*	0	
Ca5(PO4)3Cl(cr)	5Ca+2 + 3PO4-3 + 1Cl- = Ca5(PO4)3Cl(cr)	46	5	-262.57*	120	41	1283.146*	1'920	100
Ca5(PO4)3F(cr)	5Ca+2 + 3PO4-3 + 1F- = Ca5(PO4)3F(cr)	59.63	0.2	-340.371*	61	15	1346.203*	1'887	50
Ca5(PO4)3OH(cr)	5Ca+2 + 3PO4-3 + 1OH- = Ca5(PO4)3OH(cr)	58.29	0.15	-332.722*	68	15	1344.027*	1'938	50
CaCO3(aragonite)	1Ca+2 + 1CO3-2 = CaCO3(aragonite)	8.32	0.05	-47.491*	10.9	0.3	195.844*	366	19
CaCO3(calcite)	1Ca+2 + 1CO3-2 = CaCO3(calcite)	8.45	0.07	-48.233*	10.2	0.4	195.985*	404	2.6
CaCO3(vaterite)	1Ca+2 + 1CO3-2 = CaCO3(vaterite)	7.91	0.05	-45.151*	15.4	0.8	203.088*	321	36
CaF2(cr)	1Ca+2 + 2F- = CaF2(cr)	10.46	0.09	-59.706*	-7.8	1.9	174.094*	170	15
CaHK3(PO4)2(cr)	1Ca+2 + 1H+ + 3K+ + 2PO4-3 = CaHK3(PO4)2(cr)	22.4	0.8	-127.86*					
CaHPO4(cr)	1Ca+2 + 1HPO4-2 = CaHPO4(cr)	6.86	0.02	-39.157*	18.8	0.7	194.389*	345	20
CaHPO4w2(cr)	1Ca+2 + 1HPO4-2 + 2H2O(l) = CaHPO4w2(cr)	6.59	0.02	-37.616*	5.4	1.3	144.276*	282	20
CaMoO4(cr)	1Ca+2 + 1MoO4-2 = CaMoO4(cr)	8.46	0.31	-48.29*	-4.79	1.66	145.9*	0	
CaNpO2(OH)2.6Cl0.4w2(cr)	1NpO2+ + 1Ca+2 + 4.6H2O(l) + 0.4Cl- - 2.6H+ = CaNpO2(OH)2.6Cl0.4w 2(cr)	-19.9	0.1	113.59*					
CaSeO3w1(cr)	1Ca+2 + 1SeO3-2 + 1H2O(l) = CaSeO3w1(cr)	6.4	0.25	-36.531*					
CaSn(OH)6(pr)	1Sn(OH)6-2 + 1Ca+2 = CaSn(OH)6(pr)	9.7	0.1	-55.368*					
CaSO4(cr)	1Ca+2 + 1SO4-2 = CaSO4(cr)	4.21	0.17	-24.031*	17.7	1	139.966*	396.9	2.9

Tab. A-5: Cont.

Name	**Reaction**	**$\log_{10}K^{o}$**	±	$\Delta_r G_m^{o}$ [kJ · mol^{-1}]	$\Delta_r H_m^{o}$ [kJ · mol^{-1}]	±	$\Delta_r S_m^{o}$ [J · K^{-1} · mol^{-1}]	$\Delta_r C_{p,m}^{o}$ [J · K^{-1} · mol^{-1}]	±
CaSO4w2(cr)	1Ca+2 + 1SO4-2 + 2H2O(l) = CaSO4w2(cr)	4.58	0.05	-26.143*	0.46	0.04	89.226*	208.4	3
CaU6O19w11(cr)	1Ca+2 + 6UO2+2 + 18H2O(l) -14H+ = CaU6O19w11(cr)	-40.5	1.6	231.176*					
Cd(OH)2(s)	1Cd+2 + 2H2O(l) - 2H+ = Cd(OH)2(s)	-13.72	0.12	78.314*	-206.2	5	-954.266*		
Cd[(UO2)(AsO4)]2w8(cr)	2UO2+2 + 1Cd+2 + 2AsO4-3 + 8H2O(l) = Cd[(UO2)(AsO4)]2w8 (cr)	45.4	1	-259.145*	-36.967		745.189*		
Cd[(UO2)(PO4)]2w10(cr)	2UO2+2 + 1Cd+2 + 2PO4-3 + 10H2O(l) = Cd[(UO2)(PO4)]2w10 (cr)	50.34	0.3	-287.343*					
Cd3(PO4)2(s)	3Cd+2 + 2PO4-3 = Cd3(PO4)2(s)	36.9	0.4	-210.627*					
Cd5H2(PO4)4w4(s)	5Cd+2 + 4HPO4-2 + 4H2O(l) -2H+ = Cd5H2(PO4)4w4(s)	31.8	1	-181.516*					
CdCO3(cr)	1Cd+2 + 1CO3-2 = CdCO3(cr)	12.06	0.04	-68.839*	-8		204.055*	0	
CdS(s)	1Cd+2 + 1HS- -1H+ = CdS(s)	14.1	0.3	-80.483*					
Cs(UO2)(AsO4)w2.5(cr)	1UO2+2 + 1Cs+ + 1AsO4-3 + 2.5H2O(l) = Cs(UO2)(AsO4)w2.5(cr)	25.2	1	-143.843*	-55.584		296.021*		
Cs(UO2)(BO3)w1(cr)	0.5(UO2)2(OH)2+2 + 1Cs+ + 1B(OH)3(aq) - 2H+ = Cs(UO2)(BO3)w1(cr)	-3.92	0.2	22.376*	14.739		-25.613*		
Cs(UO2)(PO4)w2.5(cr)	1UO2+2 + 1Cs+ + 1PO4-3 + 2.5H2O(l) = Cs(UO2)(PO4)w2.5(cr)	25.9	1	-147.838*	-43.428		350.194*		
Cu(cr)	1Cu+2 + 2e- = Cu(cr)	11.39	0.27	-65.015*	-64.9	1	0.384*		
Cu(OH)2(s)	1Cu+2 + 2H2O(l) -2H+ = Cu(OH)2(s)	-8.67	0.05	49.489*					
Cu[(UO2)(AsO4)]2w8(cr)	2UO2+2 + 1Cu+2 + 2AsO4-3 + 8H2O(l) = Cu[(UO2)(AsO4)]2w8 (cr)	45.7	1	-260.858*	-35.638		755.39*		
Cu[(UO2)(PO4)]2w8(cr)	2UO2+2 + 1Cu+2 + 2PO4-3 + 8H2O(l) = Cu[(UO2)(PO4)]2w8(cr)	52.8	0.3	-301.385*	-44.158		862.742*		
Cu2CO3(OH)2(cr)	2Cu+2 + 1CO3-2 + 2OH- = Cu2CO3(OH)2(cr)	33.16	0.08	-189.279*					
Cu2O(cr)	2Cu+ + 1H2O(l) -2H+ = Cu2O(cr)	0.5	0.24	-2.854*	-17.2	3.8	-48.117*	0	
Cu2S(cr)	2Cu+ + 1HS- -1H+ = Cu2S(cr)	34.62	0.13	-197.612*					
Cu3(CO3)2(OH)2(cr)	3Cu+2 + 2CO3-2 + 2OH- = Cu3(CO3)2(OH)2(cr)	44.9	0.2	-256.291*					
CuCl(s)	1Cu+ + 1Cl- = CuCl(s)	6.7	0.2	-38.244*					
CuO(cr)	1Cu+2 + 1H2O(l) - 2H+ = CuO(cr)	-7.64	0.06	43.609*	61.7	1.5	60.676*	1'175	13

Tab. A-5: Cont.

Name	**Reaction**	**$\log_{10}K^{o}$**	±	$\Delta_r G_m^{o}$ [kJ · mol^{-1}]	$\Delta_r H_m^{o}$ [kJ · mol^{-1}]	±	$\Delta_r S_m^{o}$ [J · K^{-1} · mol^{-1}]	$\Delta_r C_{p,m}^{o}$ [J · K^{-1} · mol^{-1}]	±
CuS(cr)	1Cu+2 + 1HS- -1H+ = CuS(cr)	22.05	0.16	-125.862*					
Eu(OH)3(am)	1Eu+3 + 3H2O(l) -3H+ = Eu(OH)3(am)	-17.6	0.8	100.462*					
Eu(OH)3(cr)	1Eu+3 + 3H2O(l) -3H+ = Eu(OH)3(cr)	-14.9	0.3	85.05*	-124.39		-702.465*		
Eu2(CO3)3(cr)	2Eu+3 + 3CO3-2 = Eu2(CO3)3(cr)	35	0.3	-199.781*					
EuF3(cr)	1Eu+3 + 3F- = EuF3(cr)	18.7	0.4	-106.74*					
EuOHCO3(cr)	1Eu+3 + 1OH- + 1CO3-2 = EuOHCO3(cr)	21.7	0.1	-123.865*					
EuPO4w0.667(cr)	1Eu+3 + 1PO4-3 + 0.667H2O(l) = EuPO4w0.667(cr)	24.9	1.7	-142.13*	17	7	533.725*	0	
Fe(OH)2(s)	1Fe+2 + 2H2O(l) -2H+ = Fe(OH)2(s)	-12.26	0.88	69.981*					
Fe(OH)3(mic)	1Fe+3 + 3H2O(l) -3H+ = Fe(OH)3(mic)	-3.5	0.4	19.978*					
Fe[(UO2)(AsO4)]2w8(cr)	2UO2+2 + 1Fe+2 + 2AsO4-3 + 8H2O(l) = Fe[(UO2)(AsO4)]2w8 (cr)	46.1	2.2	-263.141*	-37.274		757.561*		
Fe0.875S(cr)	0.625Fe+2 + 0.25Fe+3 + 1H2S(aq) -2H+ = Fe0.875S(cr)	1.51	0.52	-8.619*	12.02	2.53	69.224*		
Fe0.875Se(cr)	0.625Fe+2 + 0.25Fe+3 + 1H2Se(aq) -2H+ = Fe0.875Se(cr)	5.1	0.93	-29.111*	-10.48	5.28	62.489*		
Fe0.9S(cr)	0.7Fe+2 + 0.2Fe+3 + 1H2S(aq) -2H+ = Fe0.9S(cr)	0.61	0.54	-3.482*	15.93	2.72	65.108*		
Fe1.042Se(cr)	1.042Fe+2 + 1H2Se(aq) + 0.084e- -2H+ = Fe1.042Se(cr)	0.39	0.79	-2.226*	5.08	4.5	24.505*		
Fe2(SeO3)3w3(cr)	2Fe+3 + 3H2SeO3(aq) + 3H2O(l) -6H+ = Fe2(SeO3)3w3(cr)	11.3	0.6	-64.501*					
Fe2Cl(OH)3(beta)	2Fe+2 + 1Cl- + 3H2O(l) -3H+ = Fe2Cl(OH)3(beta)	-17.2	0.2	98.178*					
Fe2O3(alpha)	2Fe+3 + 3H2O(l) -6H+ = Fe2O3(alpha)	-0.72	0.8	4.11*	136.6	3.8	444.374*	0	
Fe2O3(gamma)	2Fe+3 + 3H2O(l) -6H+ = Fe2O3(gamma)	-3.22	1.22	18.38*					
Fe3(PO4)2w8(cr)	3Fe+2 + 2HPO4-2 + 8H2O(l) -2H+ = Fe3(PO4)2w8(cr)	11.3	0.4	-64.501*					
Fe3O4(cr)	3Fe+2 + 4H2O(l) -6H+ -1H2g = Fe3O4(cr)	-35.31	0.66	201.551*	268.2	14.1	223.542*	0	126
Fe3S4(cr)	1Fe+2 + 2Fe+3 + 4H2S(aq) -8H+ = Fe3S4(cr)	13.18	2.31	-75.232*					
Fe3Se4(gamma)	1Fe+2 + 2Fe+3 + 4H2Se(aq) -8H+ = Fe3Se4(gamma)	38.51	3.79	-219.817*	-114.8	21.6	352.228*		

Tab. A-5: Cont.

Name	**Reaction**	**$\log_{10}K^{o}$**	±	$\Delta_r G_m^{o}$ [kJ · mol^{-1}]	$\Delta_r H_m^{o}$ [kJ · mol^{-1}]	±	$\Delta_r S_m^{o}$ [J · K^{-1} · mol^{-1}]	$\Delta_r C_{p,m}^{o}$ [J · K^{-1} · mol^{-1}]	±
Fe4(OH)8Clwn(s)	4Fe+2 + 1Cl- + 8H2O(l) -7H+ -0.5H2g = Fe4(OH)8Clwn(s)	-39.7	3.5	226.609*					
Fe6(OH)12CO3wn(s)	6Fe+2 + 1CO3-2 + 12H2O(l) -10H+ - 1H2g = Fe6(OH)12CO3wn(s)	-52.4	5.3	299.101*					
Fe6(OH)12SO4wn(s)	6Fe+2 + 1SO4-2 + 12H2O(l) -10H+ - 1H2g = Fe6(OH)12SO4wn(s)	-55.2	5.3	315.084*					
FeCO3(cr)	1Fe+2 + 1CO3-2 = FeCO3(cr)	10.9		-62.218*	15.654		261.183*	405.855	
FeOOH(alpha)	1Fe+3 + 2H2O(l) -3H+ = FeOOH(alpha)	-0.33	0.1	1.884*	65.5	2.3	213.37*	0	
FeOOH(gamma)	1Fe+3 + 2H2O(l) -3H+ = FeOOH(gamma)	-1.86	0.37	10.617*	72.5	2.2	207.557*		
FePO4(cr)	1Fe+3 + 1H2PO4- -2H+ = FePO4(cr)	1.39	0.39	-7.934*	85.1	2.2	312.038*		
FePO4w2(s)	1Fe+3 + 1H2PO4- + 2H2O(l) -2H+ = FePO4w2(s)	8.1	1	-46.235*					
FeS(mackinawite)	1Fe+2 + 1H2S(aq) - 2H+ = FeS(mackinawite)	-3.8	0.4	21.691*					
FeS(troilite)	1Fe+2 + 1H2S(aq) - 2H+ = FeS(troilite)	-3	0.52	17.124*	27.98	2.55	36.411*		
FeS2(marcasite)	1Fe+2 + 2H2S(aq) -4H+ -2e- = FeS2(marcasite)	2.16	0.86	-12.329*	-1.94	3.86	34.846*		
FeS2(pyrite)	1Fe+2 + 2H2S(aq) -4H+ -2e- = FeS2(pyrite)	2.84	0.86	-16.211*	-6.14	3.85	33.778*		
FeSe2(cr)	1Fe+2 + 2H2Se(aq) - 4H+ -2e- = FeSe2(cr)	11.21	1.73	-63.987*	-58.31	9.86	19.041*		
H4Edta(cr)	1H4Edta(aq) = H4Edta(cr)	3.8	0.19	-21.691*	-29	3	-24.516*		
HAl[(UO2)(PO4)]4w16(cr)	4UO2+2 + 1Al+3 + 4H2PO4- + 16H2O(l) - 7H+ = HAl[(UO2)(PO4)]4w16 (cr)	13.1	1.2	-74.775*					
Hg3(PO4)2(s)	3Hg+2 + 2HPO4-2 - 2H+ = Hg3(PO4)2(s)	30	0.9	-171.241*					
HgCO3(HgO)2(s)	3Hg(OH)2(aq) + 1CO2g -3H2O(l) = HgCO3(HgO)2(s)	11.27	0.35	-64.33*					
HgHPO4(s)	1Hg+2 + 1HPO4-2 = HgHPO4(s)	15.2	0.3	-86.762*					
HgS(s)	1Hg+2 + 1HS- -1H+ = HgS(s)	36.77	0.18	-209.885*					
Ho(OH)3(cr)	1Ho+3 + 3H2O(l) - 3H+ = Ho(OH)3(cr)	-14.7	1	83.908*					
Ho2(CO3)3(cr)	2Ho+3 + 3CO3-2 = Ho2(CO3)3(cr)	35	2	-199.781*					
HoF3(cr)	1Ho+3 + 3F- = HoF3(cr)	17.6	0.4	-100.462*					
HoOHCO3(cr)	1Ho+3 + 1OH- + 1CO3-2 = HoOHCO3(cr)	21.7	2	-123.865*					

Tab. A-5: Cont.

Name	**Reaction**	**$\log_{10}K^{o}$**	±	$\Delta_r G_m^o$ [kJ · mol^{-1}]	$\Delta_r H_m^o$ [kJ · mol^{-1}]	±	$\Delta_r S_m^o$ [J · K^{-1} · mol^{-1}]	$\Delta_r C_{p,m}^o$ [J · K^{-1} · mol^{-1}]	±
HoPO4(s)	1Ho+3 + 1PO4-3 = HoPO4(s)	25.3	0.6	-144.413*					
K(UO2)(AsO4)w3(cr)	1UO2+2 + 1K+ + 1AsO4-3 + 3H2O(l) = K(UO2)(AsO4)w3(cr)	23.3	1	-132.997*	-44.761		295.946*		
K(UO2)(BO3)w1(cr)	0.5(UO2)2(OH)2+2 + 1K+ + 1B(OH)3(aq) - 2H+ = K(UO2)(BO3)w1(cr)	-3.9	0.2	22.261*	-3.891		-87.715*		
K(UO2)(PO4)w3(cr)	1UO2+2 + 1K+ + 1PO4-3 + 3H2O(l) = K(UO2)(PO4)w3(cr)	25.5	1	-145.555*	-40.869		351.119*		
K(UO2)(SiO3OH)w1(cr)	1K+ + 1UO2+2 + 1Si(OH)4(aq) + 1H2O(l) -3H+ = K(UO2)(SiO3OH)w1(cr)	-4.48	1.17	25.572*	27.7	8	7.137*		
K2U6O19w11(cr)	2K+ + 6UO2+2 + 18H2O(l) -14H+ = K2U6O19w11(cr)	-37.1	0.54	211.768*					
K3NpO2(CO3)2(s)	3K+ + 1NpO2+ + 2CO3-2 = K3NpO2(CO3)2(s)	15.46	0.16	-88.246*					
K4NpO2(CO3)3(s)	4K+ + 1NpO2+2 + 3CO3-2 =K4NpO2(CO3)3(s)	26.93	1	-153.718*					
KNpO2CO3(s)	1K+ + 1NpO2+ + 1CO3-2 = KNpO2CO3(s)	13.15	0.19	-75.061*					
Li(UO2)(AsO4)w4(cr)	1UO2+2 + 1Li+ + 1AsO4-3 + 4H2O(l) = Li(UO2)(AsO4)w4(cr)	20.4	1	-116.444*	-16.279		335.955*		
Li(UO2)(BO3)w1.5(cr)	0.5(UO2)2(OH)2+2 + 1Li+ + 1B(OH)3(aq) + 0.5H2O(l) -2H+ = Li(UO2)(BO3)w1.5(cr)	-4.58	0.2	26.143*	22.05		-13.727*		
Li(UO2)(PO4)w4(cr)	1UO2+2 + 1Li+ + 1PO4-3 + 4H2O(l) = Li(UO2)(PO4)w4(cr)	25.5	1	-145.555*	-37.288		363.13*		
Mg(OH)2(s)	1Mg+2 + 2H2O(l) -2H+ = Mg(OH)2(s)	-17.11	0.04	97.665*	111.5	0.7	46.404*	0	
Mg(Ox)w2(cr)	1Mg+2 + 1Ox-2 + 2H2O(l) = Mg(Ox)w2(cr)	6.4	0.2	-36.531*					
Mg[(UO2)(AsO4)]2w10(cr)	2UO2+2 + 1Mg+2 + 2AsO4-3 + 10H2O(l) = Mg[(UO2)(AsO4)]2w10 (cr)	44.6	0.5	-254.579*	-10.546		818.49*		
Mg[(UO2)(PO4)]2w8(cr)	2UO2+2 + 1Mg+2 + 2PO4-3 + 8H2O(l) = Mg[(UO2)(PO4)]2w8(cr)	49.2	1.2	-280.836*	-6.615		919.741*		
Mg2KH(PO4)2w15(cr)	2Mg+2 + 1K+ + 1H+ + 2PO4-3 + 15H2O(l) = Mg2KH(PO4)2w15(cr)	28.67	0.6	-163.65*	-58.9		351.332*	690	
Mg3(PO4)2(cr)	3Mg+2 + 2PO4-3 = Mg3(PO4)2(cr)	22.41	0.3	-127.917*	184.3		1047.182*	1'316	
Mg3(PO4)2w22(cr)	3Mg+2 + 2PO4-3 + 22H2O(l) = Mg3(PO4)2w22(cr)	23.03	0.56	-131.456*	-22.4		365.776*	449	

Tab. A-5: Cont.

Name	Reaction	$\log_{10}K^{o}$	±	$\Delta_r G_m^{o}$ [kJ · mol^{-1}]	$\Delta_r H_m^{o}$ [kJ · mol^{-1}]	±	$\Delta_r S_m^{o}$ [J · K^{-1} · mol^{-1}]	$\Delta_r C_{p,m}^{o}$ [J · K^{-1} · mol^{-1}]	±
Mg3(PO4)2w4(cr)	3Mg+2 + 2PO4-3 + 4H2O(l) = Mg3(PO4)2w4(cr)	23.5	1.8	-134.139*	232		1228.036*	1'175	
Mg3(PO4)2w8(cr)	3Mg+2 + 2PO4-3 + 8H2O(l) = Mg3(PO4)2w8(cr)	25.3	1	-144.413*	183.9		1101.169*	1'034	
MgCO3(s)	1Mg+2 + 1CO3-2 = MgCO3(s)	7.66	0.34	-43.724*	35.9	1.9	267.059*	387.7	9.6
MgHPO4w3(cr)	1Mg+2 + 1H+ + 1PO4-3 + 3H2O(l) = MgHPO4w3(cr)	17.93	0.23	-102.345*	0.8		345.951*	497	
MgHPO4w7(cr)	1Mg+2 + 1H+ + 1PO4-3 + 7H2O(l) = MgHPO4w7(cr)	17.01	0.25	-97.094*	27.9		419.231*	356	
MgKPO4w1(cr)	1Mg+2 + 1K+ + 1PO4-3 + 1H2O(l) = MgKPO4w1(cr)	10.95	1.5	-62.503*	35.9		330.045*	581	
MgKPO4w6(cr)	1Mg+2 + 1K+ + 1PO4-3 + 6H2O(l) = MgKPO4w6(cr)	10.96	0.31	-62.56*	-6.2		189.033*	405	
MgSeO3w6(cr)	1Mg+2 + 1SeO3-2 + 6H2O(l) = MgSeO3w6(cr)	5.82	0.25	-33.221*	-18.03	1.82	50.95*		
Mn(OH)2(cr)	1Mn+2 + 2H2O(l) - 2H+ = Mn(OH)2(cr)	-15.19	0.1	86.705*	123	17	121.733*		
Mn[(UO2)(AsO4)]2w8(cr)	2UO2+2 + 1Mn+2 + 2AsO4-3 + 8H2O(l) = Mn[(UO2)(AsO4)]2w8(cr)	44.4	1	-253.437*	-36.089		728.989*		
Mn[(UO2)(PO4)]2w10(cr)	2UO2+2 + 1Mn+2 + 2PO4-3 + 10H2O(l) = Mn[(UO2)(PO4)]2w10(cr)	50.22	0.4	-286.658*					
MnOOH(cr)	1Mn+3 + 2H2O(l) -3H+ = MnOOH(cr)	0.08	0.3	-0.457*	64	5.3	216.189*		
MnSeO3w2(cr)	1Mn+2 + 1SeO3-2 + 2H2O(l) = MnSeO3w2(cr)	7.6	1	-43.381*					
Na(UO2)(AsO4)w3(cr)	1UO2+2 + 1Na+ + 1AsO4-3 + 3H2O(l) = Na(UO2)(AsO4)w3(cr)	22.8	1	-130.143*	-31.249		331.693*		
Na(UO2)(BO3)w1(cr)	0.5(UO2)2(OH)2+2 + 1Na+ + 1B(OH)3(aq) - 2H+ = Na(UO2)(BO3)w1(cr)	-4.47	0.2	25.515*	15.031		-35.163*		
Na(UO2)(PO4)w3(cr)	1UO2+2 + 1Na+ + 1PO4-3 + 3H2O(l) = Na(UO2)(PO4)w3(cr)	24.3	1	-138.705*	-27.236		373.87*		
Na(UO2)(SiO3OH)w1(cr)	1Na+ + 1UO2+2 + 1Si(OH)4(aq) + 1H2O(l) -3H+ = Na(UO2)(SiO3OH)w1(cr)	-5.81	0.44	33.164*	44.8	5.8	39.028*		
Na2Np2O7w0.1(cr)	2Na+ + 2NpO2+2 + 3.1H2O(l) -6H+ = Na2Np2O7w0.1(cr)	-25.2	2.2	143.843*					
Na2U2O7w1(cr)	2Na+ + 2UO2+2 + 4H2O(l) -6H+ = Na2U2O7w1(cr)	-24.4	0.4	139.276*					

Tab. A-5: Cont.

Name	**Reaction**	**$\log_{10}K^{o}$**	±	$\Delta_r G_m^o$ [kJ · mol^{-1}]	$\Delta_r H_m^o$ [kJ · mol^{-1}]	±	$\Delta_r S_m^o$ [J · K^{-1} · mol^{-1}]	$\Delta_r C_{p,m}^o$ [J · K^{-1} · mol^{-1}]	±
Na3NpO2(CO3)2(cr)	3Na+ + 1NpO2+ + 2CO3-2 = Na3NpO2(CO3)2(cr)	14.22	0.5	-81.168*					
Na6Th(CO3)5w12(cr)	6Na+ + 1Th+4 + 5CO3-2 + 12H2O(l) = Na6Th(CO3)5w12(cr)	42.2	0.8	-240.879*					
Na7HNb6O19w15(cr)	7Na+ + 1HNb6O19-7 + 15H2O(l) = Na7HNb6O19w15(cr)	11.6		-66.213*					
NaAlCO3(OH)2(cr)	1Al+3 + 1HCO3- + 1Na+ + 2H2O(l) -3H+ = NaAlCO3(OH)2(cr)	-5.02	0.3	28.654*	93.4	7	217.158*	3.5	30
NaAm(CO3)2w5(cr)	1Na+ + 1Am+3 + 2CO3-2 + 5H2O(l) = NaAm(CO3)2w5(cr)	21	0.5	-119.869*					
NaAmO2CO3(s)	1Na+ + 1AmO2+ + 1CO3-2 = NaAmO2CO3(s)	10.9	0.4	-62.218*					
NaNpO2CO3w3.5(cr)	1Na+ + 1NpO2+ + 1CO3-2 + 3.5H2O(l) = NaNpO2CO3w3.5(cr)	11	0.24	-62.788*					
Nb2O5(pr)	2Nb(OH)5(aq) -5H2O(l) = Nb2O5(pr)	16	0.5	-91.329*					
NH4(UO2)(AsO4)w3(cr)	1UO2+2 + 1NH4+ + 1AsO4-3 + 3H2O(l) = NH4(UO2)(AsO4)w3(cr)	24.7	1	-140.989*	-49.76		305.982*		
NH4(UO2)(PO4)w3(cr)	1UO2+2 + 1NH4+ + 1PO4-3 + 3H2O(l) = NH4(UO2)(PO4)w3(cr)	26.1	1	-148.98*	-45.176		348.16*		
Ni(OH)2(cr)	1Ni+2 + 2H2O(l) -2H+ = Ni(OH)2(cr)	-11.02	0.2	62.903*	84.34		71.901*	-22.602	
Ni(Ox)w2(cr)	1Ni+2 + 1Ox-2 + 2H2O(l) = Ni(Ox)w2(cr)	-9.96		56.852*					
Ni[(UO2)(AsO4)]2w10(cr)	2UO2+2 + 1Ni+2 + 2AsO4-3 + 10H2O(l) = Ni[(UO2)(AsO4)]2w10 (cr)	45.9	1	-261.999*	-42.176		737.29*		
Ni[(UO2)(PO4)]2w8(cr)	2UO2+2 + 1Ni+2 + 2PO4-3 + 8H2O(l) = Ni[(UO2)(PO4)]2w8(cr)	49.9	1	-284.831*	-17.528		896.54*		
Ni3(AsO3)2(s)	3Ni+2 + 2As(OH)3(aq) -6H+ = Ni3(AsO3)2(s)	-28.7	0.7	163.821*					
Ni3(AsO4)2w8(s)	3Ni+2 + 2AsO4-3 + 8H2O(l) = Ni3(AsO4)2w8(s)	28.1	0.5	-160.396*	48.962		702.19*		
NiCO3(cr)	1Ni+2 + 1CO3-2 = NiCO3(cr)	11	0.18	-62.788*	16.689		266.569*		
NiCO3w5.5(s)	1Ni+2 + 1CO3-2 + 5.5H2O(l) = NiCO3w5.5(s)	7.53	0.1	-42.982*	-10.917		107.545*		
NiO(cr)	1Ni+2 + 1H2O(l) -2H+ = NiO(cr)	-12.48	0.15	71.236*	61.83		-31.549*	-30.951	
NiSeO3w2(cr)	1Ni+2 + 1SeO3-2 + 2H2O(l) = NiSeO3w2(cr)	5.8	1	-33.107*					

Tab. A-5: Cont.

Name	**Reaction**	**$\log_{10}K^o$**	±	$\Delta_r G_m^o$ [kJ · mol^{-1}]	$\Delta_r H_m^o$ [kJ · mol^{-1}]	±	$\Delta_r S_m^o$ [J · K^{-1} · mol^{-1}]	$\Delta_r C_{p,m}^o$ [J · K^{-1} · mol^{-1}]	±
Np(Ox)2w6(cr)	1Np+4 + 2H2Ox(aq) + 6H2O(l) -4H+ = Np(Ox)2w6(cr)	12.7	1	-72.492*					
NpO2(am_hyd)	1Np+4 + 2H2O(l) -4H+ = NpO2(am_hyd)	0.7	0.5	-3.996*					
NpO2(OH)2w1(cr_hex)	1NpO2+2 + 3H2O(l) -2H+ = NpO2(OH)2w1(cr_hex)	-5.47	0.4	31.223*					
NpO2CO3(cr)	1NpO2+2 + 1CO3-2 = NpO2CO3(cr)	14.83	0.23	-84.65*					
NpO2OH(am)	1NpO2+ + 1H2O(l) -1H+ = NpO2OH(am)	-5.3	0.2	30.253*	41.1	3	36.382*		
Pa2O5(act)	2PaO(OH)2+ -2H+ -1H2O(l) = Pa2O5(act)	4		-22.832*					
Pb[(UO2)(AsO4)]2w10(cr)	2UO2+2 + 1Pb+2 + 2AsO4-3 + 10H2O(l) = Pb[(UO2)(AsO4)]2w10 (cr)	46.3	1	-264.282*	-83.01		607.99*		
Pb[(UO2)(PO4)]2w8(cr)	2UO2+2 + 1Pb+2 + 2PO4-3 + 8H2O(l) = Pb[(UO2)(PO4)]2w8(cr)	49.85	0.5	-284.546*					
Pb2(CO3)Cl2(s)	2Pb+2 + 1CO3-2 + 2Cl- = Pb2(CO3)Cl2(s)	19.86	0.16	-113.362*					
Pb2(UO2)(PO4)2w2(cr)	1UO2+2 + 2Pb+2 + 2PO4-3 + 2H2O(l) = Pb2(UO2)(PO4)2w2(cr)	52.2	0.8	-297.96*					
Pb3(PO4)2(s)	3Pb+2 + 2PO4-3 = Pb3(PO4)2(s)	44.4	1	-253.437*					
Pb5(PO4)3Cl(s)	5Pb+2 + 3PO4-3 + 1Cl- = Pb5(PO4)3Cl(s)	84.4	2	-481.759*					
PbClOH(s)	1Pb+2 + 1Cl- + 1OH- = PbClOH(s)	13.27		-75.746*					
PbCO3(s)	1Pb+2 + 1CO3-2 = PbCO3(s)	13.18	0.07	-75.232*					
PbHPO4(s)	1Pb+2 + 1HPO4-2 = PbHPO4(s)	11.4	0.3	-65.072*					
PbO(s_red)	1Pb+2 + 1H2O(l) -2H+ = PbO(s_red)	-12.62	0.07	72.035*	66.1	0.7	-19.908*	0	
PbO(s_yellow)	1Pb+2 + 1H2O(l) -2H+ = PbO(s_yellow)	-12.9	0.08	73.634*					
PbS(s)	1Pb+2 + 1HS- -1H+ = PbS(s)	12.28	0.1	-70.095*					
Po(SO4)2w1(s)	1Po(SO4)3-2 + 1H+ + 1H2O(l) -1HSO4- = Po(SO4)2w1(s)	6.33	0.04	-36.132*					
PoSO4(s)	1Po+2 + 1SO4-2 = PoSO4(s)	8.91		-50.859*					
Pu(HPO4)2(am_hyd)	1Pu+4 + 2HPO4-2 = Pu(HPO4)2(am_hyd)	30.45	0.51	-173.81*					
Pu(OH)3(am)	1Pu+3 + 3H2O(l) -3H+ = Pu(OH)3(am)	-14.58	0.75	83.223*					
Pu(Ox)2w6(cr)	1Pu(Ox)2(aq) + 6H2O(l) = Pu(Ox)2w6(cr)	4.6	0.2	-26.257*					

Tab. A-5: Cont.

Name	**Reaction**	**$\log_{10}K^{o}$**	±	$\Delta_r G_m^{o}$ [kJ · mol^{-1}]	$\Delta_r H_m^{o}$ [kJ · mol^{-1}]	±	$\Delta_r S_m^{o}$ [J · K^{-1} · mol^{-1}]	$\Delta_r C_{p,m}^{o}$ [J · K^{-1} · mol^{-1}]	±
Pu2(Ox)3w10(cr)	2Pu+3 + 3H2Ox(aq) + 10H2O(l) -6H+ = Pu2(Ox)3w10(cr)	7.5		-42.81*					
PuO2(am_hyd)	1Pu+4 + 2H2O(l) -4H+ = PuO2(am_hyd)	2.33	0.52	-13.3*					
PuO2(OH)2(am_hyd)	1PuO2+2 + 2H2O(l) -2H+ = PuO2(OH)2(am_hyd)	-5.17	0.65	29.511*					
PuO2CO3(cr)	1PuO2+2 + 1CO3-2 = PuO2CO3(cr)	14.82	0.12	-84.593*					
PuO2OH(am)	1PuO2+ + 1H2O(l) -1H+ = PuO2OH(am)	-5	0.5	28.54*					
PuPO4(am_hyd)	1Pu+3 + 1PO4-3 = PuPO4(am_hyd)	24.44	0.55	-139.505*					
RaCO3(cr)	1Ra+2 + 1CO3-2 = RaCO3(cr)	7.57	0.7	-43.21*	-3.4	1	133.523*	430.8	5
RaSO4(cr)	1Ra+2 + 1SO4-2 = RaSO4(cr)	10.26	0.3	-58.565*	-38.8	1	66.29*	428.3	3.8
SiO2(am)	1Si(OH)4(aq) -2H2O(l) = SiO2(am)	2.714	0.044	-15.492*	-14.594	0.21	3.011*	-2.35	1
Sm(OH)3(cr)	1Sm+3 + 3H2O(l) -3H+ = Sm(OH)3(cr)	-15	1	85.621*					
Sm2(CO3)3(cr)	2Sm+3 + 3CO3-2 = Sm2(CO3)3(cr)	35	2	-199.781*					
SmF3(cr)	1Sm+3 + 3F- = SmF3(cr)	-19.2	0.4	109.594*	-73	40	-612.425*	0	
SmOHCO3(cr)	1Sm+3 + 1OH- + 1CO3-2 = SmOHCO3(cr)	21.7	2	-123.865*					
SmPO4w0.667(cr)	1Sm+3 + 1PO4-3 + 0.667H2O(l) = SmPO4w0.667(cr)	25.2	1.3	-143.843*	22	8	556.239*	0	
SnO(s)	1Sn+2 + 1H2O(l) -2H+ = SnO(s)	-1.6	0.3	9.133*					
SnO2(am)	1Sn(OH)4(aq) -2H2O(l) = SnO2(am)	7.22	0.08	-41.212*					
SnO2(cr)	1Sn(OH)4(aq) -2H2O(l) = SnO2(cr)	8.06	0.11	-46.007*					
Sr[(UO2)(AsO4)]2w8(cr)	2UO2+2 + 1Sr+2 + 2AsO4-3 + 8H2O(l) = Sr[(UO2)(AsO4)]2w8(cr)	45.1	1	-257.433*	-33.257		751.889*		
Sr[(UO2)(PO4)]2w6(cr)	2UO2+2 + 1Sr+2 + 2PO4-3 + 6H2O(l) = Sr[(UO2)(PO4)]2w6(cr)	51.3	1	-292.823*	-29.514		883.141*		
Sr3(PO4)2(s)	3Sr+2 + 2PO4-3 = Sr3(PO4)2(s)	28.8	0.4	-164.392*					
SrCO3(cr)	1Sr+2 + +CO3-2 = SrCO3(cr)	9.27	0.03	-52.914*	1.6	0.6	182.839*	471	28
SrHPO4(beta)	1Sr+2 + 1HPO4-2 = SrHPO4(beta)	6.94	0.07	-39.614*	19.3	3.9	197.598*	345	50
SrSeO3(cr)	1Sr+2 + 1SeO3-2 = SrSeO3(cr)	6.3	0.5	-35.961*	6.2	2.96	141.408*		
SrSO4(cr)	1Sr+2 + +SO4-2 = SrSO4(cr)	6.58	0.1	-37.559*	1.3	0.6	130.333*	413.5	2.9

Tab. A-5: Cont.

Name	**Reaction**	**$\log_{10}K^{o}$**	±	$\Delta_r G_m^{o}$ [kJ · mol^{-1}]	$\Delta_r H_m^{o}$ [kJ · mol^{-1}]	±	$\Delta_r S_m^{o}$ [J · K^{-1} · mol^{-1}]	$\Delta_r C_{p,m}^{o}$ [J · K^{-1} · mol^{-1}]	±
TcO2(am_hyd_ag)	1TcO(OH)2(aq) - 1H2O(l) = TcO2(am_hyd_ag)	8.72	0.4	-49.774*					
TcO2(am_hyd_fr)	1TcO(OH)2(aq) - 1H2O(l) = TcO2(am_hyd_fr)	7.66	1.22	-43.724*					
Th3(PO4)4(s)	3Th+4 + 4PO4-3 = Th3(PO4)4(s)	112	2.1	-639.301*					
ThF4(cr_hyd)	1Th+4 + 4F- = ThF4(cr_hyd)	31.8	0.4	-181.516*					
ThO2(am_hyd_ag)	1Th+4 + 2H2O(l) -4H+ = ThO2(am_hyd_ag)	-8.5	0.9	48.518*					
ThO2(am_hyd_fr)	1Th+4 + 2H2O(l) -4H+ = ThO2(am_hyd_fr)	-9.3	0.9	53.085*					
Ti(alpha)	1TiO+2 + 2H+ + 4e- - 1H2O(l) = Ti(alpha)	-59.6	0.4	340.199*					
TiO2(am_hyd)	1TiO+2 + 1H2O(l) - 2H+ = TiO2(am_hyd)	-0.19	0.42	1.085*					
U(OH)2SO4(cr)	1U+4 + 1SO4-2 + 2H2O(l) -2H+ = U(OH)2SO4(cr)	3.17	0.5	-18.094*					
U(Ox)2w6(cr)	1U(Ox)2(aq) + 6H2O(l) = U(Ox)2w6(cr)	4.82	0.2	-27.513*	-10.4	1	57.396*	-513	41
UF4w2.5(cr)	1U+4 + 4F- + 2.5H2O(l) = UF4w2.5(cr)	30.12	0.7	-171.926*	-4.746		560.725*		
UO2(am_hyd)	1U+4 + 2H2O(l) -4H+ = UO2(am_hyd)	-1.5	1	8.562*					
UO2CO3(cr)	1UO2+2 + 1CO3-2 = UO2CO3(cr)	14.76	0.02	-84.251*	2.74		291.768*		
UO2HAsO4w4(cr)	1UO2+2 + 1H+ + 1AsO4-3 + 4H2O(l) = UO2HAsO4w4(cr)	23	0.3	-131.285*	-32.837		330.196*		
UO2HPO4w4(cr)	1UO2+2 + 1H3PO4(aq) + 4H2O(l) -2H+ = UO2HPO4w4(cr)	2.5	0.09	-14.27*	-18.895		-15.512*		
UO2Oxw3(cr)	1UO2Ox(aq) + 3H2O(l) = UO2Oxw3(cr)	1.8	0.27	-10.274*	-20.2	3.5	-33.29*	0	
UO3w2(cr)	1UO2+2 + 3H2O(l) - 2H+ = UO3w2(cr)	-5.35	0.13	30.538*	53.463		76.891*	-96.383	
USiO4(cr)	1U+4 + 1Si(OH)4(aq) - 4H+ = USiO4(cr)	4.5		-25.686*	79		351.119*		
Zn(OH)2(s)	1Zn+2 + 2H2O(l) -2H+ = Zn(OH)2(s)	-11.38	0.2	64.958*	100	11	117.533*	0	
Zn[(UO2)(AsO4)]2w8(cr)	2UO2+2 + 1Zn+2 + 2AsO4-3 + 8H2O(l) = Zn[(UO2)(AsO4)]2w8 (cr)	45.1	1	-257.433*	-28.695		767.19*		
Zn[(UO2)(PO4)]2w8(cr)	2UO2+2 + 1Zn+2 + 2PO4-3 + 8H2O(l) = Zn[(UO2)(PO4)]2w8(cr)	49.8	1	-284.26*	-23.516		874.541*		
Zn3(PO4)2w4(s)	3Zn+2 + 2PO4-3 + 4H2O(l) = Zn3(PO4)2w4(s)	35.3	0.1	-201.494*					

Zn5(OH)6(CO3)2(s)	5Zn+2 + 2CO3-2 + 6H2O(l) -6H+ = Zn5(OH)6(CO3)2(s)	-9.05	0.1	51.658*	248	15	658.535*	0	
ZnCO3(s)	1Zn+2 + 1CO3-2 = ZnCO3(s)	10.94	0.08	-62.446*	4.1	1.3	223.196*	0	
ZnO(cr)	1Zn+2 + 1H2O(l) -2H+ = ZnO(cr)	-11.19	0.07	63.873*	88.76	0.34	83.471*	0	
ZnS(cr)	1Zn+2 + 1H2S(aq) -2H+ = ZnS(cr)	3.68	0.05	-21.006*	-17.8	1.9	10.752*	0	
Zr(HPO4)2w(cr)	1Zr+4 + 2H3PO4(aq) + 1H2O(l) -4H+ = Zr(HPO4)2w(cr)	22.8	3.1	-130.143*	16.47	6.17	491.744*		
Zr(OH)4(am_fr)	1Zr+4 + 4H2O(l) -4H+ = Zr(OH)4(am_fr)	3.24	0.1	-18.494*					
ZrO2(cr)	1Zr+4 + 2H2O(l) -4H+ = ZrO2(cr)	7	1.6	-39.956*	79.56	5.17	400.86*		

Tab. A-6: SIT ion interaction coefficients $\varepsilon_{j,k}$ [kg · mol^{-1}] for aqueous species in NaCl medium

The uncertainties represent the 95 % confidence level. SIT coefficients for neutral species M(aq) have arbitrarily been divided into Na^+ and Cl^- parts according to ε(M(aq), Na^+) = ε (M(aq), Cl^-) = ½ ε (M(aq), $Na^+ + Cl^-$), as described in Section 1.5.1.

j	***k***	***ε(j,k)***	±
(NpO2)2(OH)2+2	Cl-	0.15	0.1
(NpO2)2CO3(OH)3-	Na+	0	0.05
(NpO2)3(CO3)6-6	Na+	-0.46	0.73
(NpO2)3(OH)5+	Cl-	0.05	0.1
(PuO2)2(OH)2+2	Cl-	0.15	0.1
(PuO2)3(CO3)6-6	Na+	0.37	0.11
(UEdtaOH)2-2	Na+	-0.1	0.1
(UO2)2(OH)2+2	Cl-	0.69	0.07
(UO2)2CO3(OH)3-	Na+	0	0.05
(UO2)2Edta(aq)	Cl-	0	0.05
(UO2)2Edta(aq)	Na+	0	0.05
(UO2)2NpO2(CO3)6-6	Na+	0.09	0.71
(UO2)2OH+3	Cl-	0.25	0.1
(UO2)2PuO2(CO3)6-6	Na+	0.37	0.11
(UO2)3(CO3)6-6	Na+	0.37	0.11
(UO2)3(OH)4+2	Cl-	0.5	0.18
(UO2)3(OH)5+	Cl-	0.81	0.17
(UO2)3(OH)7-	Na+	-0.05	0.1
(UO2)3O(OH)2(HCO3)+	Cl-	0.05	0.1
(UO2)4(OH)7+	Cl-	0.05	0.1
(UO2Cit)2-2	Na+	-0.1	0.1
Ac(Cit)(aq)	Cl-	0	0.025
Ac(Cit)(aq)	Na+	0	0.025
Ac(Edta)-	Na+	0.01	0.16
Ac(OH)3(aq)	Cl-	0	0.05
Ac(OH)3(aq)	Na+	0	0.05
Ac(Ox)+	Cl-	0.08	0.1
Ac(Ox)2-	Na+	0.21	0.08
Ac+3	Cl-	0.6	0.1
AcCl+2	Cl-	0.4	0.1

Tab. A-6: Cont.

j	*k*	*ε(j,k)*	±
AcF+2	Cl-	0.4	0.1
AcF2+	Cl-	0.2	0.1
AcF3(aq)	Cl-	0	0.05
AcF3(aq)	Na+	0	0.05
AcH2PO4+2	Cl-	0.4	0.1
AcHEdta(aq)	Cl-	0	0.05
AcHEdta(aq)	Na+	0	0.05
AcOH+2	Cl-	0.4	0.1
AcSCN+2	Cl-	0.4	0.1
AcSO4+	Cl-	0.2	0.1
Ag(aq)	Cl-	0	0.05
Ag(aq)	Na+	0	0.05
Ag(CN)2-	Na+	0.23	0.1
Ag(CN)3-2	Na+	0.3	0.2
Ag(OH)2-	Na+	-0.05	0.1
Ag(OH)CN-	Na+	0.05	0.12
Ag(SeCN)3-2	Na+	-0.1	0.1
Ag+	Cl-	0	0.01
Ag2Se(aq)	Cl-	0	0.05
Ag2Se(aq)	Na+	0	0.05
AgBr(aq)	Cl-	0	0.05
AgBr(aq)	Na+	0	0.05
AgBr2-	Na+	-0.05	0.1
AgBr3-2	Na+	-0.1	0.1
AgBr4-3	Na+	-0.15	0.1
AgCl(aq)	Cl-	0	0.05
AgCl(aq)	Na+	0	0.05
AgCl2-	Na+	-0.05	0.1
AgCl3-2	Na+	-0.1	0.1
AgCl4-3	Na+	-0.15	0.1
AgCO3-	Na+	-0.05	0.1
AgF(aq)	Cl-	0	0.05
AgF(aq)	Na+	0	0.05

Tab. A-6: Cont.

j	*k*	*ε(j,k)*	±
AgHPO4-	Na+	-0.05	0.1
AgHS(aq)	Cl-	0	0.05
AgHS(aq)	Na+	0	0.05
AgI(aq)	Cl-	0	0.05
AgI(aq)	Na+	0	0.05
AgI2-	Na+	-0.05	0.1
AgI3-2	Na+	-0.1	0.1
AgI4-3	Na+	-0.15	0.1
AgOH(aq)	Cl-	0	0.05
AgOH(aq)	Na+	0	0.05
AgSeO3-	Na+	-0.05	0.1
AgSeO4-	Na+	-0.05	0.1
AgSO4-	Na+	-0.11	0.09
Al(OH)2+	Cl-	0.05	0.1
Al(OH)2F(aq)	Cl-	0	0.05
Al(OH)2F(aq)	Na+	0	0.05
Al(OH)2F2-	Na+	-0.05	0.1
Al(OH)3(aq)	Cl-	0	0.05
Al(OH)3(aq)	Na+	0	0.05
Al(OH)4-	Na+	-0.05	0.1
Al(SO4)2-	Na+	-0.05	0.1
Al+3	Cl-	0.33	0.02
Al13(OH)32+7	Cl-	1.21	0.08
Al2(OH)2+4	Cl-	0.36	0.08
Al3(OH)4+5	Cl-	0.51	0.07
AlF+2	Cl-	0.15	0.1
AlF2+	Cl-	0.05	0.1
AlF3(aq)	Cl-	0	0.05
AlF3(aq)	Na+	0	0.05
AlF4-	Na+	-0.05	0.1
AlF5-2	Na+	-0.1	0.1
AlF6-3	Na+	-0.15	0.1
AlOH+2	Cl-	0.15	0.1

Tab. A-6: Cont.

j	*k*	*ε(j,k)*	±
AlOHF2(aq)	Cl-	0	0.05
AlOHF2(aq)	Na+	0	0.05
AlSiO(OH)3+2	Cl-	0.15	0.1
AlSO4+	Cl-	0.05	0.2
Am(Cit)(aq)	Cl-	0	0.025
Am(Cit)(aq)	Na+	0	0.025
Am(Cit)2-3	Na+	-0.15	0.1
Am(CO3)2-	Na+	-0.14	0.06
Am(CO3)3-3	Na+	-0.23	0.07
Am(Edta)-	Na+	0.01	0.16
Am(Edta)OH-2	Na+	-0.1	0.1
Am(HCit)+	Cl-	0.2	0.1
Am(HCit)2-	Na+	-0.05	0.1
Am(HEdta)(aq)	Cl-	0	0.05
Am(HEdta)(aq)	Na+	0	0.05
Am(Isa)-	Na+	-0.05	0.1
Am(NO3)2+	Cl-	0.05	0.1
Am(OH)2+	Cl-	-0.27	0.2
Am(OH)3(aq)	Cl-	0	0.05
Am(OH)3(aq)	Na+	0	0.05
Am(Ox)+	Cl-	0.08	0.05
Am(Ox)2-	Na+	-0.21	0.08
Am(Ox)3-3	Na+	-0.23	0.1
Am(SO4)2-	Na+	-0.05	0.05
Am+3	Cl-	0.23	0.02
AmCl+2	Cl-	0.15	0.1
AmCl2+	Cl-	0.05	0.1
AmCO3+	Cl-	0.01	0.05
AmF+2	Cl-	0.15	0.1
AmF2+	Cl-	0.05	0.1
AmH2PO4+2	Cl-	0.15	0.1
AmHCO3+2	Cl-	0.16	0.1
AmHPO4+	Cl-	0.05	0.1

Tab. A-6: Cont.

j	*k*	*ε(j,k)*	±
AmNO3+2	Cl-	0.15	0.1
AmO2(CO3)2-3	Na+	-0.33	0.17
AmO2(CO3)3-5	Na+	-0.53	0.19
AmO2(OH)2-	Na+	-0.01	0.07
AmO2+	Cl-	0.09	0.05
AmO2CO3-	Na+	-0.18	0.15
AmO2OH(aq)	Cl-	0	0.05
AmO2OH(aq)	Na+	0	0.05
AmOH+2	Cl-	-0.04	0.07
AmSCN+2	Cl-	0.15	0.1
AmSiO(OH)3+2	Cl-	0.42	0.1
AmSO4+	Cl-	0.05	0.1
As(OH)3(aq)	Cl-	0	0.05
As(OH)3(aq)	Na+	0	0.05
As(OH)4-	Na+	-0.05	0.1
AsO4-3	Na+	-0.15	0.2
B(OH)3(aq)	Cl-	0	0.05
B(OH)3(aq)	Na+	0	0.05
B(OH)4-	Na+	-0.07	0.05
Ba+2	Cl-	0.07	0.01
Ba2UO2(CO3)3(aq)	Cl-	0	0.05
Ba2UO2(CO3)3(aq)	Na+	0	0.05
BaCO3(aq)	Cl-	0	0.05
BaCO3(aq)	Na+	0	0.05
BaF+	Cl-	0.05	0.1
BaH2PO4+	Cl-	0.05	0.1
BaHCO3+	Cl-	0.05	0.1
BaHPO4(aq)	Cl-	0	0.05
BaHPO4(aq)	Na+	0	0.05
BaOH+	Cl-	0.05	0.1
BaPO4-	Na+	-0.05	0.1
BaSO4(aq)	Cl-	0	0.05
BaSO4(aq)	Na+	0	0.05

Tab. A-6: Cont.

j	*k*	*ε(j,k)*	±
BaUO2(CO3)3-2	Na+	-0.1	0.1
Br-	Na+	0.05	0.01
Ca(Cit)-	Na+	0.03	0.03
Ca(Edta)-2	Na+	-0.01	0.15
Ca(H2Cit)+	Cl-	0.05	0.1
Ca(H2Isa)(aq)	Cl-	0	0.05
Ca(H2Isa)(aq)	Na+	0	0.05
Ca(H3Isa)+	Cl-	0.05	0.1
Ca(HCit)(aq)	Cl-	0.01	0.025
Ca(HCit)(aq)	Na+	0.01	0.025
Ca(HEdta)-	Na+	0.11	0.2
Ca(Ox)(aq)	Cl-	0	0.015
Ca(Ox)(aq)	Na+	0	0.015
Ca(Ox)2-2	Na+	-0.15	0.03
Ca+2	Cl-	0.14	0.01
Ca2Am(OH)4+3	Cl-	0.29	0.07
Ca2Cm(OH)4+3	Cl-	0.29	0.07
Ca2UO2(CO3)3(aq)	Cl-	0	0.05
Ca2UO2(CO3)3(aq)	Na+	0	0.05
Ca2Zr(OH)6+2	Cl-	0.1	0.1
Ca3Am(OH)6+3	Cl-	0	0.06
Ca3Cm(OH)6+3	Cl-	0	0.06
Ca3NpO2(OH)5+2	Cl-	-0.2	0.11
Ca3Zr(OH)6+4	Cl-	0.4	0.07
Ca4Np(OH)8+4	Cl-	-0.01	0.1
Ca4Pu(OH)8+4	Cl-	-0.01	0.1
Ca4Th(OH)8+4	Cl-	-0.01	0.1
CaAm(OH)3+2	Cl-	0.05	0.04
CaCm(OH)3+2	Cl-	0.05	0.04
CaCO3(aq)	Cl-	0	0.05
CaCO3(aq)	Na+	0	0.05
CaF+	Cl-	0.1	0.06
CaH2PO4+	Cl-	0.05	0.1

Tab. A-6: Cont.

j	*k*	*ε(j,k)*	±
CaHCO3+	Cl-	0.05	0.1
CaHPO4(aq)	Cl-	0	0.05
CaHPO4(aq)	Na+	0	0.05
CaMoO4(aq)	Cl-	0	0.05
CaMoO4(aq)	Na+	0	0.05
CaNpO2(OH)2+	Cl-	-0.07	0.08
CaOH+	Cl-	0.05	0.1
CaPO4-	Na+	-0.05	0.1
CaSeO4(aq)	Cl-	0	0.05
CaSeO4(aq)	Na+	0	0.05
CaSiO(OH)3+	Cl-	0.05	0.1
CaSiO2(OH)2(aq)	Cl-	0	0.05
CaSiO2(OH)2(aq)	Na+	0	0.05
CaSO4(aq)	Cl-	0	0.05
CaSO4(aq)	Na+	0	0.05
CaUO2(CO3)3-2	Na+	-0.1	0.1
CaZr(OH)6(aq)	Cl-	0	0.05
CaZr(OH)6(aq)	Na+	0	0.05
Cd(CO3)2-2	Na+	-0.1	0.1
Cd(HS)2(aq)	Cl-	0	0.05
Cd(HS)2(aq)	Na+	0	0.05
Cd(HS)3-	Na+	-0.05	0.1
Cd(HS)4-2	Na+	-0.1	0.1
Cd(OH)2(aq)	Cl-	-0.005	0.02
Cd(OH)2(aq)	Na+	-0.005	0.02
Cd(OH)3-	Na+	-0.05	0.1
Cd(OH)4-2	Na+	0.2	0.05
Cd(SO4)2-2	Na+	0.1	0.11
Cd+2	Cl-	0.23	0.04
Cd2OH+3	Cl-	0.56	0.07
CdCl+	Cl-	0.12	0.05
CdCl2(aq)	Cl-	0.01	0.025
CdCl2(aq)	Na+	0.01	0.025

Tab. A-6: Cont.

j	*k*	*ε(j,k)*	±
CdCl3-	Na+	-0.08	0.08
CdCl4-2	Na+	-0.1	0.1
CdCO3(aq)	Cl-	0	0.05
CdCO3(aq)	Na+	0	0.05
CdH2PO4+	Cl-	0.2	0.1
CdHCO3+	Cl-	0.2	0.1
CdHPO4(aq)	Cl-	0	0.05
CdHPO4(aq)	Na+	0	0.05
CdHS+	Cl-	0.2	0.1
CdOH+	Cl-	0.04	0.06
CdS(HS)-	Na+	-0.05	0.1
CdSO4(aq)	Cl-	0.01	0.035
CdSO4(aq)	Na+	0.01	0.035
Cf+3	Cl-	0.25	0.1
CfF+2	Cl-	0.15	0.1
CfSCN+2	Cl-	0.15	0.1
CfSO4+	Cl-	0.05	0.1
CH4(aq)	Cl-	0	0.05
CH4(aq)	Na+	0	0.05
Cit-3	Na+	-0.076	0.03
Cm(CO3)2-	Na+	-0.14	0.06
Cm(CO3)3-3	Na+	-0.23	0.07
Cm(NO3)2+	Cl-	0.05	0.1
Cm(OH)2+	Cl-	-0.27	0.2
Cm(OH)3(aq)	Cl-	0	0.05
Cm(OH)3(aq)	Na+	0	0.05
Cm(SO4)2-	Na+	-0.05	0.05
Cm+3	Cl-	0.23	0.02
CmCl+2	Cl-	0.15	0.1
CmCl2+	Cl-	0.05	0.1
CmCO3+	Cl-	0.01	0.05
CmF+2	Cl-	0.15	0.1
CmF2+	Cl-	0.05	0.1

Tab. A-6: Cont.

j	*k*	*ε(j,k)*	±
CmH2PO4+2	Cl-	0.15	0.1
CmHCO3+2	Cl-	0.16	0.1
CmHPO4+	Cl-	0.05	0.1
CmNO3+2	Cl-	0.15	0.1
CmOH+2	Cl-	-0.04	0.07
CmSCN+2	Cl-	0.15	0.1
CmSiO(OH)3+2	Cl-	0.42	0.1
CmSO4+	Cl-	0.05	0.1
CN-	Na+	0.07	0.03
CO2(aq)	Cl-	0	0.05
CO2(aq)	Na+	0	0.05
CO3-2	Na+	-0.08	0.03
Cs+	Cl-	0.05	0.1
Cu(CO3)2-2	Na+	0.34	0.21
Cu(CO3)OH-	Na+	0.1	0.05
Cu(HS)2-	Na+	-0.05	0.1
Cu(OH)2(aq)	Cl-	0.09	0.18
Cu(OH)2(aq)	Na+	0.09	0.18
Cu(OH)2-	Na+	-0.05	0.1
Cu(OH)3-	Na+	0.4	0.09
Cu(OH)4-2	Na+	0.19	0.1
Cu+	Cl-	0.11	0.01
Cu+2	Cl-	0.32	0.02
Cu2(OH)2+2	Cl-	0.29	0.12
Cu2Cl4-2	Na+	-0.1	0.1
Cu2OH+3	Cl-	0.54	0.06
Cu2S(HS)2-2	Na+	-0.1	0.1
Cu3(OH)4+2	Cl-	0.33	0.11
CuCl(aq)	Cl-	0	0.05
CuCl(aq)	Na+	0	0.05
CuCl+	Cl-	0.3	0.05
CuCl2(aq)	Cl-	0.14	0.035
CuCl2(aq)	Na+	0.14	0.035

Tab. A-6: Cont.

j	*k*	*ε(j,k)*	±
CuCl2-	Na+	-0.05	0.1
CuCl3-2	Na+	-0.1	0.1
CuCO3(aq)	Cl-	-0.005	0.05
CuCO3(aq)	Na+	-0.005	0.05
CuH2PO4(aq)	Cl-	0	0.05
CuH2PO4(aq)	Na+	0	0.05
CuHCO3+	Cl-	0.46	0.15
CuHPO4(aq)	Cl-	0	0.05
CuHPO4(aq)	Na+	0	0.05
CuHS(aq)	Cl-	0	0.05
CuHS(aq)	Na+	0	0.05
CuOH(aq)	Cl-	0	0.05
CuOH(aq)	Na+	0	0.05
CuOH+	Cl-	-0.15	0.08
CuSO4(aq)	Cl-	0.075	0.035
CuSO4(aq)	Na+	0.075	0.035
Edta-4	Na+	0.32	0.14
Eu(CO3)2-	Na+	-1.17	0.32
Eu(OH)2+	Cl-	0.05	0.1
Eu(OH)3(aq)	Cl-	0	0.05
Eu(OH)3(aq)	Na+	0	0.05
Eu(OH)4-	Na+	-0.05	0.1
Eu(SO4)2-	Na+	0.22	0.2
Eu+3	Cl-	0.26	0.005
EuCO3+	Cl-	0.05	0.1
EuF+2	Cl-	0.15	0.03
EuF2+	Cl-	0.05	0.1
EuH2PO4+2	Cl-	0.15	0.1
EuOH+2	Cl-	0.15	0.1
EuSiO(OH)3+2	Cl-	0.42	0.1
EuSO4+	Cl-	0.05	0.1
F-	Na+	0.02	0.02
Fe(CN)6-3	Na+	-0.15	0.2

Tab. A-6: Cont.

j	*k*	*ε(j,k)*	±
Fe(CN)6-4	Na+	-0.2	0.3
Fe(CO3)2-2	Na+	-0.05	0.05
Fe(CO3)3-3	Na+	-0.23	0.07
Fe(H2PO4)3(aq)	Cl-	0	0.05
Fe(H2PO4)3(aq)	Na+	0	0.05
Fe(HSeO4)2(aq)	Cl-	0	0.05
Fe(HSeO4)2(aq)	Na+	0	0.05
Fe(OH)2(aq)	Cl-	0	0.05
Fe(OH)2(aq)	Na+	0	0.05
Fe(OH)2+	Cl-	0.43	0.1
Fe(OH)3(aq)	Cl-	0	0.05
Fe(OH)3(aq)	Na+	0	0.05
Fe(OH)3-	Na+	-0.05	0.1
Fe(OH)4-	Na+	-0.05	0.1
Fe(OH)CO3(aq)	Cl-	0	0.05
Fe(OH)CO3(aq)	Na+	0	0.05
Fe(SCN)2+	Cl-	0.2	0.1
Fe(SO4)2-	Na+	0.24	0.14
Fe(SO4)2-2	Na+	-0.1	0.1
Fe+2	Cl-	0.17	0.01
Fe+3	Cl-	0.76	0.03
Fe2(OH)2+4	Cl-	1	0.1
Fe3(OH)4+5	Cl-	1	0.2
FeCl+	Cl-	0.16	0.01
FeCl+2	Cl-	0.64	0.06
FeCl2+	Cl-	0.52	0.05
FeCl3(aq)	Cl-	0	0.05
FeCl3(aq)	Na+	0	0.05
FeCl4-	Na+	-0.05	0.1
FeCO3(aq)	Cl-	0	0.05
FeCO3(aq)	Na+	0	0.05
FeF+	Cl-	0.05	0.1
FeF+2	Cl-	0.46	0.08

Tab. A-6: Cont.

j	*k*	*ε(j,k)*	±
FeF2+	Cl-	0.1	0.3
FeH2PO4+	Cl-	0.05	0.1
FeHPO4(aq)	Cl-	0	0.05
FeHPO4(aq)	Na+	0	0.05
FeHSeO3(H2SeO3)+	Cl-	0.05	0.1
FeHSeO3+	Cl-	0.05	0.1
FeHSO4+	Cl-	0.05	0.1
FeHSO4+2	Cl-	0.58	0.13
FeOH+	Cl-	0.05	0.1
FeOH+2	Cl-	0.27	0.05
FePO4(aq)	Cl-	0	0.05
FePO4(aq)	Na+	0	0.05
FeS(aq)	Cl-	0	0.05
FeS(aq)	Na+	0	0.05
FeSCN+2	Cl-	0.49	0.05
FeSeO3+	Cl-	0.2	0.1
FeSiO(OH)3+2	Cl-	0.04	0.15
FeSO4(aq)	Cl-	0	0.05
FeSO4(aq)	Na+	0	0.05
FeSO4+	Cl-	0.4	0.1
H+	Cl-	0.12	0.01
H2(aq)	Cl-	0	0.05
H2(aq)	Na+	0	0.05
H2AsO4-	Na+	-0.01	0.01
H2Cit-	Na+	-0.05	0.01
H2Edta-2	Na+	-0.37	0.14
H2Fe(CN)6-2	Na+	-0.1	0.1
H2MoO4(aq)	Cl-	0	0.05
H2MoO4(aq)	Na+	0	0.05
H2Nb6O19-6	Na+	0.3	0.5
H2Ox(aq)	Cl-	0	0.005
H2Ox(aq)	Na+	0	0.005
H2Po(aq)	Cl-	0	0.05

Tab. A-6: Cont.

j	*k*	*ε(j,k)*	±
H2Po(aq)	Na+	0	0.05
H2PO4-	Na+	-0.08	0.04
H2S(aq)	Cl-	0.0275	0.002
H2S(aq)	Na+	0.0275	0.002
H2Se(aq)	Cl-	0	0.05
H2Se(aq)	Na+	0	0.05
H2SeO3(aq)	Cl-	0	0.05
H2SeO3(aq)	Na+	0	0.05
H3AsO4(aq)	Cl-	0	0.05
H3AsO4(aq)	Na+	0	0.05
H3Cit(aq)	Cl-	0	0.005
H3Cit(aq)	Na+	0	0.005
H3Edta-	Na+	-0.33	0.14
H3Isa-	Na+	-0.05	0.1
H3Nb6O19-5	Na+	0.25	0.4
H3PO4(aq)	Cl-	0	0.05
H3PO4(aq)	Na+	0	0.05
H4Edta(aq)	Cl-	-0.145	0.07
H4Edta(aq)	Na+	-0.145	0.07
H4Isa(aq)	Cl-	0	0.05
H4Isa(aq)	Na+	0	0.05
H5Edta+	Cl-	-0.23	0.15
H6Edta+2	Cl-	-0.2	0.16
HAsO4-2	Na+	-0.1	0.1
HCit-2	Na+	-0.04	0.02
HCN(aq)	Cl-	0	0.05
HCN(aq)	Na+	0	0.05
HCO3-	Na+	0	0.02
HEdta-3	Na+	-0.1	0.14
HF(aq)	Cl-	0	0.05
HF(aq)	Na+	0	0.05
HF2-	Na+	-0.11	0.06
HFe(CN)6-3	Na+	-0.15	0.2

Tab. A-6: Cont.

j	*k*	*ε(j,k)*	±
Hg(aq)	Cl-	0	0.05
Hg(aq)	Na+	0	0.05
Hg(HS)2(aq)	Cl-	0.0275	0.05
Hg(HS)2(aq)	Na+	0.0275	0.05
Hg(OH)2(aq)	Cl-	-0.04	0.025
Hg(OH)2(aq)	Na+	-0.04	0.025
Hg(OH)3-	Na+	-0.05	0.1
Hg(SO4)2-2	Na+	-0.1	0.1
Hg+2	Cl-	0.34	0.03
Hg2+2	Cl-	0.09	0.02
Hg2OH+	Cl-	-0.13	0.16
HgCl+	Cl-	0.15	0.05
HgCl2(aq)	Cl-	0.005	0.02
HgCl2(aq)	Na+	0.005	0.02
HgCl3-	Na+	0.05	0.06
HgCl4-2	Na+	0.08	0.09
HgCO3(aq)	Cl-	0	0.05
HgCO3(aq)	Na+	0	0.05
HgHCO3+	Cl-	0.2	0.1
HgHPO4(aq)	Cl-	0	0.05
HgHPO4(aq)	Na+	0	0.05
HgOH+	Cl-	0.06	0.05
HgOHCl(aq)	Cl-	-0.005	0.045
HgOHCl(aq)	Na+	-0.005	0.045
HgOHCO3-	Na+	-0.05	0.1
HgPO4-	Na+	-0.05	0.1
HgS(HS)-	Na+	0.08	0.1
HgS2-2	Na+	-0.1	0.1
HgSO4(aq)	Cl-	0	0.05
HgSO4(aq)	Na+	0	0.05
HIO3(aq)	Cl-	0	0.05
HIO3(aq)	Na+	0	0.05
HMoO4-	Na+	-0.05	0.1

Tab. A-6: Cont.

j	*k*	*ε(j,k)*	±
HNb6O19-7	Na+	0.35	0.6
Ho(CO3)2-	Na+	-1.17	0.32
Ho(OH)2+	Cl-	0.05	0.1
Ho(OH)3(aq)	Cl-	0	0.05
Ho(OH)3(aq)	Na+	0	0.05
Ho(OH)4-	Na+	-0.05	0.1
Ho(SO4)2-	Na+	0.22	0.2
Ho+3	Cl-	0.29	0.01
HoCO3+	Cl-	0.05	0.1
HoF+2	Cl-	0.18	0.03
HoF2+	Cl-	0.05	0.1
HoH2PO4+2	Cl-	0.15	0.1
HoOH+2	Cl-	0.15	0.1
HoSO4+	Cl-	0.05	0.1
HOx-	Na+	-0.07	0.01
HP2O7-3	Na+	-0.15	0.2
HPo-	Na+	-0.05	0.1
HPO4-2	Na+	-0.15	0.06
HS-	Na+	0.08	0.01
HSe-	Na+	-0.05	0.1
HSe4-	Na+	-0.03	0.12
HSeO3-	Na+	-0.05	0.1
HSeO4-	Na+	-0.01	0.02
HSO3-	Na+	-0.05	0.1
HSO4-	Na+	-0.01	0.02
I-	Na+	0.08	0.02
I2(aq)	Cl-	0	0.05
I2(aq)	Na+	0	0.05
I3-	Na+	-0.05	0.1
IO3-	Na+	-0.06	0.02
K+	Cl-	0	0.01
KCO3-	Na+	-0.05	0.1
KEdta-3	Na+	-0.15	0.1

Tab. A-6: Cont.

j	*k*	*ε(j,k)*	±
KFe(CN)6-2	Na+	-0.1	0.1
KFe(CN)6-3	Na+	-0.15	0.2
KH2PO4(aq)	Cl-	0	0.05
KH2PO4(aq)	Na+	0	0.05
KHCO3(aq)	Cl-	0	0.05
KHCO3(aq)	Na+	0	0.05
KHPO4-	Na+	-0.05	0.1
KOH(aq)	Cl-	0	0.05
KOH(aq)	Na+	0	0.05
KPO4-2	Na+	-0.1	0.1
KSO4-	Na+	-0.05	0.1
Li+	Cl-	0.1	0.01
LiF(aq)	Cl-	0	0.05
LiF(aq)	Na+	0	0.05
LiH2PO4(aq)	Cl-	0	0.05
LiH2PO4(aq)	Na+	0	0.05
LiHPO4-	Na+	-0.05	0.1
LiOH(aq)	Cl-	0	0.05
LiOH(aq)	Na+	0	0.05
LiPO4-2	Na+	-0.1	0.1
LiSO4-	Na+	-0.05	0.1
Mg(Cit)-	Na+	0.03	0.03
Mg(Edta)-2	Na+	-0.01	0.15
Mg(H2Cit)+	Cl-	0.05	0.1
Mg(HCit)(aq)	Cl-	0.01	0.025
Mg(HCit)(aq)	Na+	0.01	0.025
Mg(HEdta)-	Na+	0.11	0.2
Mg(Ox)(aq)	Cl-	0	0.015
Mg(Ox)(aq)	Na+	0	0.015
Mg(Ox)2-2	Na+	-0.15	0.03
Mg+2	Cl-	0.19	0.02
Mg2UO2(CO3)3(aq)	Cl-	0	0.05
Mg2UO2(CO3)3(aq)	Na+	0	0.05

Tab. A-6: Cont.

j	*k*	*ε(j,k)*	±
MgCO3(aq)	Cl-	0	0.05
MgCO3(aq)	Na+	0	0.05
MgF+	Cl-	-0.02	0.06
MgH2PO4+	Cl-	0.05	0.1
MgHCO3+	Cl-	0.05	0.1
MgHPO4(aq)	Cl-	0	0.05
MgHPO4(aq)	Na+	0	0.05
MgOH+	Cl-	0.05	0.1
MgPO4-	Na+	-0.05	0.1
MgSeO4(aq)	Cl-	0	0.05
MgSeO4(aq)	Na+	0	0.05
MgSiO(OH)3+	Cl-	0.05	0.1
MgSiO2(OH)2(aq)	Cl-	0	0.05
MgSiO2(OH)2(aq)	Na+	0	0.05
MgSO4(aq)	Cl-	0	0.05
MgSO4(aq)	Na+	0	0.05
MgUO2(CO3)3-2	Na+	-0.1	0.1
Mn(OH)2(aq)	Cl-	0	0.05
Mn(OH)2(aq)	Na+	0	0.05
Mn(OH)2+	Cl-	0.2	0.1
Mn(OH)3-	Na+	-0.05	0.1
Mn(OH)4-2	Na+	-0.1	0.1
Mn+2	Cl-	0.38	0.02
Mn+3	Cl-	0.6	0.1
MnCl+	Cl-	0.4	0.03
MnCl+2	Cl-	0.4	0.1
MnCO3(aq)	Cl-	0	0.05
MnCO3(aq)	Na+	0	0.05
MnF+	Cl-	0.23	0.09
MnF+2	Cl-	0.4	0.1
MnF2+	Cl-	0.2	0.1
MnF3(aq)	Cl-	0	0.05
MnF3(aq)	Na+	0	0.05

Tab. A-6: Cont.

j	*k*	*ε(j,k)*	±
MnHCO3+	Cl-	0.2	0.1
MnOH+	Cl-	0.2	0.1
MnOH+2	Cl-	0.4	0.13
MnOHF+	Cl-	0.2	0.1
MnSeO4(aq)	Cl-	0	0.05
MnSeO4(aq)	Na+	0	0.05
MnSO4(aq)	Cl-	0	0.05
MnSO4(aq)	Na+	0	0.05
MoO4-2	Na+	0.04	0.1
N2(aq)	Cl-	0	0.05
N2(aq)	Na+	0	0.05
Na(Edta)-3	Na+	-0.15	0.1
NaCO3-	Na+	-0.05	0.1
NaF(aq)	Cl-	0	0.05
NaF(aq)	Na+	0	0.05
NaH2PO4(aq)	Cl-	0	0.05
NaH2PO4(aq)	Na+	0	0.05
NaHCO3(aq)	Cl-	0	0.05
NaHCO3(aq)	Na+	0	0.05
NaHPO4-	Na+	-0.05	0.1
NaOH(aq)	Cl-	0	0.05
NaOH(aq)	Na+	0	0.05
NaPO4-2	Na+	-0.1	0.1
NaSO4-	Na+	-0.05	0.1
Nb(OH)4+	Cl-	0.05	0.1
Nb(OH)5(aq)	Cl-	-0.035	0.01
Nb(OH)5(aq)	Na+	-0.035	0.01
Nb(OH)6-	Na+	1.57	0.26
Nb(OH)7-2	Na+	1.98	0.64
Nb6O19-8	Na+	0.4	0.7
NH3(aq)	Cl-	0	0.05
NH3(aq)	Na+	0	0.05
NH4+	Cl-	-0.01	0.01

Tab. A-6: Cont.

j	*k*	*ε(j,k)*	±
Ni(Cit)-	Na+	0.22	0.5
Ni(Cit)2-4	Na+	-0.2	0.1
Ni(CN)4-2	Na+	0.185	0.081
Ni(CN)5-3	Na+	0.25	0.14
Ni(CO3)2-2	Na+	-0.1	0.1
Ni(Edta)-2	Na+	-0.1	0.1
Ni(H2Cit)+	Cl-	0.12	0.5
Ni(H3Isa)+	Cl-	0.2	0.1
Ni(HCit)(aq)	Cl-	-0.035	0.25
Ni(HCit)(aq)	Na+	-0.035	0.25
Ni(HEdta)-	Na+	-0.05	0.1
Ni(HS)2(aq)	Cl-	0	0.05
Ni(HS)2(aq)	Na+	0	0.05
Ni(NH3)2+2	Cl-	0.15	0.1
Ni(NH3)3+2	Cl-	0.15	0.1
Ni(NH3)4+2	Cl-	0.15	0.1
Ni(NH3)5+2	Cl-	0.15	0.1
Ni(NH3)6+2	Cl-	0.15	0.1
Ni(OH)2(aq)	Cl-	0	0.05
Ni(OH)2(aq)	Na+	0	0.05
Ni(OH)3-	Na+	-0.05	0.1
Ni(Ox)(aq)	Cl-	-0.035	0.015
Ni(Ox)(aq)	Na+	-0.035	0.015
Ni(Ox)2-2	Na+	-0.26	0.03
Ni(SCN)2(aq)	Cl-	0.19	0.04
Ni(SCN)2(aq)	Na+	0.19	0.04
Ni(SCN)3-	Na+	0.66	0.13
Ni(SeCN)2(aq)	Cl-	0	0.05
Ni(SeCN)2(aq)	Na+	0	0.05
Ni+2	Cl-	0.17	0.02
Ni2OH+3	Cl-	0.25	0.1
Ni4(OH)4+4	Cl-	0.43	0.08
NiCl+	Cl-	0.47	0.06

Tab. A-6: Cont.

j	*k*	*ε(j,k)*	±
NiCO3(aq)	Cl-	0	0.05
NiCO3(aq)	Na+	0	0.05
NiF+	Cl-	0.05	0.1
NiHAsO4(aq)	Cl-	0	0.05
NiHAsO4(aq)	Na+	0	0.05
NiHCO3+	Cl-	0.05	0.1
NiHP2O7-	Na+	-0.05	0.1
NiHPO4(aq)	Cl-	0	0.05
NiHPO4(aq)	Na+	0	0.05
NiHS+	Cl-	0.05	0.1
NiNH3+2	Cl-	0.15	0.1
NiNO3+	Cl-	0.05	0.1
NiOH+	Cl-	-0.01	0.07
NiP2O7-2	Na+	-0.1	0.1
NiSCN+	Cl-	0.05	0.1
NiSeCN+	Cl-	0.05	0.1
NiSeO4(aq)	Cl-	0	0.05
NiSeO4(aq)	Na+	0	0.05
NiSiO(OH)3+	Cl-	0.5	0.16
NiSO4(aq)	Cl-	0	0.05
NiSO4(aq)	Na+	0	0.05
NO3-	Na+	-0.04	0.03
Np(CO3)2-	Na+	-0.14	0.06
Np(CO3)3-3	Na+	-0.23	0.07
Np(CO3)4-4	Na+	-0.2	0.3
Np(CO3)5-6	Na+	-0.3	0.5
Np(Edta)(aq)	Cl-	-0.095	0.095
Np(Edta)(aq)	Na+	-0.095	0.095
Np(OH)2(CO3)2-2	Na+	-0.3	0.2
Np(OH)2+	Cl-	0.05	0.1
Np(OH)2+2	Cl-	0.15	0.1
Np(OH)3(aq)	Cl-	0	0.05
Np(OH)3(aq)	Na+	0	0.05

Tab. A-6: Cont.

j	*k*	*ε(j,k)*	±
Np(OH)3(H3Isa)(aq)	Cl-	0	0.05
Np(OH)3(H3Isa)(aq)	Na+	0	0.05
Np(OH)3(H3Isa)2-	Na+	-0.05	0.1
Np(OH)3+	Cl-	0.05	0.1
Np(OH)4(aq)	Cl-	0	0.05
Np(OH)4(aq)	Na+	0	0.05
Np(OH)4(H3Isa)-	Na+	-0.05	0.1
Np(OH)4(H3Isa)2-2	Na+	-0.1	0.1
Np(OH)4CO3-2	Na+	0	0.3
Np(Ox)+2	Cl-	0.4	0.1
Np(Ox)2(aq)	Cl-	0	0.05
Np(Ox)2(aq)	Na+	0	0.05
Np(Ox)3-2	Na+	-0.1	0.1
Np(SCN)2+2	Cl-	0.15	0.1
Np(SCN)3+	Cl-	0.05	0.1
Np(SO4)2(aq)	Cl-	0	0.05
Np(SO4)2(aq)	Na+	0	0.05
Np(SO4)2-	Na+	-0.05	0.1
Np+3	Cl-	0.25	0.1
Np+4	Cl-	0.35	0.1
NpCl+2	Cl-	0.15	0.1
NpCl+3	Cl-	0.25	0.1
NpCl2+	Cl-	0.05	0.1
NpCO3+	Cl-	0.01	0.05
NpF+2	Cl-	0.15	0.1
NpF+3	Cl-	0.25	0.1
NpF2+	Cl-	0.05	0.1
NpF2+2	Cl-	0.15	0.1
NpI+3	Cl-	0.25	0.1
NpNO3+3	Cl-	0.25	0.1
NpO2(CO3)2-2	Na+	-0.02	0.14
NpO2(CO3)2-3	Na+	-0.33	0.17
NpO2(CO3)2OH-4	Na+	-0.4	0.19

Tab. A-6: Cont.

j	*k*	*ε(j,k)*	±
NpO2(CO3)3-4	Na+	-0.4	0.19
NpO2(CO3)3-5	Na+	-0.53	0.19
NpO2(H2Edta)-	Na+	-0.18	0.16
NpO2(HEdta)-2	Na+	0.07	0.16
NpO2(HPO4)2-2	Na+	-0.1	0.1
NpO2(OH)(aq)	Cl-	0	0.05
NpO2(OH)(aq)	Na+	0	0.05
NpO2(OH)2(aq)	Cl-	0	0.05
NpO2(OH)2(aq)	Na+	0	0.05
NpO2(OH)2-	Na+	-0.01	0.07
NpO2(OH)3-	Na+	-0.2	0.02
NpO2(OH)4-2	Na+	-0.12	0.04
NpO2(Ox)2-3	Na+	-0.3	0.2
NpO2(SO4)2-2	Na+	-0.1	0.1
NpO2+	Cl-	0.09	0.05
NpO2+2	Cl-	0.15	0.1
NpO2Cit-2	Na+	-0.06	0.03
NpO2Cl+	Cl-	0.05	0.1
NpO2CO3(aq)	Cl-	0	0.05
NpO2CO3(aq)	Na+	0	0.05
NpO2CO3(OH)2-3	Na+	-0.15	0.1
NpO2CO3-	Na+	-0.18	0.15
NpO2CO3OH-2	Na+	-0.1	0.1
NpO2Edta-3	Na+	0.2	0.16
NpO2EdtaOH-4	Na+	0.32	0.14
NpO2F(aq)	Cl-	0	0.05
NpO2F(aq)	Na+	0	0.05
NpO2F+	Cl-	0.05	0.1
NpO2F2(aq)	Cl-	0	0.05
NpO2F2(aq)	Na+	0	0.05
NpO2F2-	Na+	-0.01	0.07
NpO2H2PO4(aq)	Cl-	0	0.05
NpO2H2PO4(aq)	Na+	0	0.05

Tab. A-6: Cont.

j	*k*	*ε(j,k)*	±
NpO2H2PO4+	Cl-	0.05	0.1
NpO2HPO4(aq)	Cl-	0	0.05
NpO2HPO4(aq)	Na+	0	0.05
NpO2HPO4-	Na+	-0.05	0.11
NpO2IO3(aq)	Cl-	0	0.05
NpO2IO3(aq)	Na+	0	0.05
NpO2IO3+	Cl-	0.05	0.1
NpO2OH+	Cl-	0.05	0.1
NpO2Ox-	Na+	-0.4	0.1
NpO2SCN(aq)	Cl-	0	0.05
NpO2SCN(aq)	Na+	0	0.05
NpO2SiO(OH)3(aq)	Cl-	0	0.05
NpO2SiO(OH)3(aq)	Na+	0	0.05
NpO2SiO(OH)3+	Cl-	0.2	0.1
NpO2SO4(aq)	Cl-	0	0.05
NpO2SO4(aq)	Na+	0	0.05
NpO2SO4-	Na+	0.07	0.13
NpOH+2	Cl-	0.15	0.1
NpOH+3	Cl-	0.25	0.1
NpSCN+3	Cl-	0.25	0.1
NpSiO(OH)3+2	Cl-	0.15	0.1
NpSiO(OH)3+3	Cl-	0.44	0.3
NpSO4+	Cl-	0.05	0.1
NpSO4+2	Cl-	0.15	0.1
O2(aq)	Cl-	0	0.05
O2(aq)	Na+	0	0.05
OH-	Na+	0.04	0.01
Ox-2	Na+	-0.08	0.01
P2O7-4	Na+	-0.26	0.05
Pa(OH)2+2	Cl-	0.15	0.1
Pa(OH)3+	Cl-	0.05	0.1
Pa+4	Cl-	0.35	0.1
PaO(OH)+2	Cl-	0.15	0.1

Tab. A-6: Cont.

j	*k*	*ε(j,k)*	±
PaO(OH)2+	Cl-	0.05	0.1
PaO(OH)3(aq)	Cl-	0	0.05
PaO(OH)3(aq)	Na+	0	0.05
PaO(OH)4-	Na+	-0.05	0.1
PaO(SO4)2-	Na+	0.22	0.19
PaO(SO4)3-3	Na+	0.03	0.2
PaO+3	Cl-	0.25	0.1
PaOF+2	Cl-	0.15	0.1
PaOF2+	Cl-	0.05	0.1
PaOF3(aq)	Cl-	0	0.05
PaOF3(aq)	Na+	0	0.05
PaOH+3	Cl-	0.25	0.1
PaOSO4+	Cl-	0.05	0.1
Pb(aq)	Cl-	0	0.05
Pb(aq)	Na+	0	0.05
Pb(CO3)2-2	Na+	-0.2	0.12
Pb(CO3)Cl-	Na+	-0.05	0.1
Pb(CO3)OH-	Na+	-0.05	0.1
Pb(HPO4)2-2	Na+	-0.1	0.1
Pb(HS)2(aq)	Cl-	0.0275	0.05
Pb(HS)2(aq)	Na+	0.0275	0.05
Pb(OH)2(aq)	Cl-	-0.13	0.025
Pb(OH)2(aq)	Na+	-0.13	0.025
Pb(OH)3-	Na+	-0.01	0.06
Pb(SO4)2-2	Na+	-0.11	0.2
Pb+2	Cl-	0.15	0.02
Pb2OH+3	Cl-	0.34	0.1
Pb3(OH)4+2	Cl-	-0.5	0.06
Pb4(OH)4+4	Cl-	-0.15	0.06
Pb6(OH)8+4	Cl-	-0.63	0.08
PbCl+	Cl-	0.04	0.02
PbCl2(aq)	Cl-	-0.025	0.015
PbCl2(aq)	Na+	-0.025	0.015

Tab. A-6: Cont.

j	*k*	*ε(j,k)*	±
PbCl3-	Na+	-0.08	0.04
PbCl4-2	Na+	-0.1	0.1
PbCO3(aq)	Cl-	0	0.05
PbCO3(aq)	Na+	0	0.05
PbH2PO4+	Cl-	0.2	0.1
PbHCO3+	Cl-	0.2	0.1
PbHPO4(aq)	Cl-	0	0.05
PbHPO4(aq)	Na+	0	0.05
PbOH+	Cl-	-0.05	0.05
PbS(HS)-	Na+	0.08	0.1
PbSO4(aq)	Cl-	0.025	0.035
PbSO4(aq)	Na+	0.025	0.035
Pd(aq)	Cl-	0	0.05
Pd(aq)	Na+	0	0.05
Pd(NH3)2+2	Cl-	0.82	0.13
Pd(NH3)3+2	Cl-	0.82	0.13
Pd(NH3)4+2	Cl-	0.82	0.13
Pd(OH)2(aq)	Cl-	0	0.05
Pd(OH)2(aq)	Na+	0	0.05
Pd(OH)3-	Na+	-0.05	0.1
Pd+2	Cl-	0.82	0.13
PdCl+	Cl-	0.2	0.1
PdCl2(aq)	Cl-	0	0.05
PdCl2(aq)	Na+	0	0.05
PdCl3-	Na+	-0.02	0.1
PdCl4-2	Na+	-0.1	0.1
PdNH3+2	Cl-	0.82	0.13
PdOH+	Cl-	0.2	0.1
Po(aq)	Cl-	0	0.05
Po(aq)	Na+	0	0.05
Po(NO3)2+2	Cl-	0.7	0.3
Po(NO3)3+	Cl-	0.5	0.4
Po(OH)2+2	Cl-	0.4	0.1

Tab. A-6: Cont.

j	*k*	*ε(j,k)*	±
Po(OH)3+	Cl-	0.2	0.1
Po(OH)4(aq)	Cl-	0	0.05
Po(OH)4(aq)	Na+	0	0.05
Po(OH)6-2	Na+	-0.1	0.1
Po(OH)Cl4-	Na+	-0.05	0.1
Po(SO4)2(aq)	Cl-	0	0.05
Po(SO4)2(aq)	Na+	0	0.05
Po(SO4)3-2	Na+	-0.1	0.1
Po+2	Cl-	0.4	0.1
Po+4	Cl-	0.8	0.1
Po-2	Na+	-0.1	0.1
PO4-3	Na+	-0.25	0.03
PoCl+	Cl-	0.2	0.1
PoCl2(aq)	Cl-	0	0.05
PoCl2(aq)	Na+	0	0.05
PoCl3-	Na+	-0.05	0.1
PoCl4-2	Na+	-0.1	0.1
PoCl6-2	Na+	-0.1	0.1
PoNO3+3	Cl-	0.7	0.6
PoOH+3	Cl-	0.6	0.1
PoSO4(aq)	Cl-	0	0.05
PoSO4(aq)	Na+	0	0.05
PoSO4+2	Cl-	0.4	0.1
Pu(Cit)(aq)	Cl-	0	0.05
Pu(Cit)(aq)	Na+	0	0.05
Pu(CO3)2-	Na+	-0.1	0.1
Pu(CO3)3-3	Na+	-0.15	0.2
Pu(CO3)4-4	Na+	-0.2	0.3
Pu(CO3)5-6	Na+	-0.3	0.5
Pu(Edta)(aq)	Cl-	-0.095	0.095
Pu(Edta)(aq)	Na+	-0.095	0.095
Pu(Edta)(OH)2-2	Na+	-0.1	0.1
Pu(Edta)-	Na+	0.01	0.16

Tab. A-6: Cont.

j	*k*	*ε(j,k)*	±
Pu(Edta)OH-	Na+	-0.05	0.1
Pu(HCit)+	Cl-	0.05	0.1
Pu(HEdta)(aq)	Cl-	0	0.05
Pu(HEdta)(aq)	Na+	0	0.05
Pu(OH)2+	Cl-	0.05	0.1
Pu(OH)2+2	Cl-	0.1	0.1
Pu(OH)3(aq)	Cl-	0	0.05
Pu(OH)3(aq)	Na+	0	0.05
Pu(OH)3+	Cl-	0.05	0.1
Pu(OH)4(aq)	Cl-	0	0.05
Pu(OH)4(aq)	Na+	0	0.05
Pu(Ox)+	Cl-	0.05	0.1
Pu(Ox)+2	Cl-	0.4	0.1
Pu(Ox)2(aq)	Cl-	0	0.05
Pu(Ox)2(aq)	Na+	0	0.05
Pu(Ox)2-	Na+	-0.05	0.1
Pu(Ox)3-2	Na+	-0.1	0.1
Pu(Ox)3-3	Na+	-0.15	0.1
Pu(SO4)2(aq)	Cl-	0	0.05
Pu(SO4)2(aq)	Na+	0	0.05
Pu(SO4)2-	Na+	-0.05	0.1
Pu+3	Cl-	0.23	0.02
Pu+4	Cl-	0.37	0.1
PuCl+2	Cl-	0.39	0.16
PuCl+3	Cl-	0.85	0.09
PuCO3(OH)3-	Na+	-0.05	0.1
PuCO3+	Cl-	0.05	0.1
PuF+2	Cl-	0.15	0.1
PuF+3	Cl-	0.25	0.1
PuF2+	Cl-	0.05	0.1
PuF2+2	Cl-	0.15	0.1
PuH2PO4+2	Cl-	0.15	0.1
PuH3PO4+4	Cl-	0.35	0.1

Tab. A-6: Cont.

j	*k*	*ε(j,k)*	±
PuNO3+3	Cl-	0.25	0.1
PuO2(CO3)2-2	Na+	-0.1	0.1
PuO2(CO3)2-3	Na+	-0.15	0.2
PuO2(CO3)3-4	Na+	-0.2	0.3
PuO2(CO3)3-5	Na+	-0.25	0.4
PuO2(H2PO4)2(aq)	Cl-	0	0.05
PuO2(H2PO4)2(aq)	Na+	0	0.05
PuO2(OH)2(aq)	Cl-	0	0.05
PuO2(OH)2(aq)	Na+	0	0.05
PuO2(OH)3-	Na+	-0.05	0.1
PuO2(SO4)2-2	Na+	-0.1	0.1
PuO2+	Cl-	0.05	0.1
PuO2+2	Cl-	0.19	0.09
PuO2Cl+	Cl-	0.36	0.06
PuO2Cl2(aq)	Cl-	0	0.05
PuO2Cl2(aq)	Na+	0	0.05
PuO2CO3(aq)	Cl-	0	0.05
PuO2CO3(aq)	Na+	0	0.05
PuO2CO3-	Na+	-0.18	0.18
PuO2F+	Cl-	0.05	0.1
PuO2F2(aq)	Cl-	0	0.05
PuO2F2(aq)	Na+	0	0.05
PuO2H2PO4+	Cl-	0.05	0.1
PuO2HPO4(aq)	Cl-	0	0.05
PuO2HPO4(aq)	Na+	0	0.05
PuO2OH(aq)	Cl-	0	0.05
PuO2OH(aq)	Na+	0	0.05
PuO2OH+	Cl-	0.05	0.1
PuO2PO4-	Na+	-0.05	0.1
PuO2SiO(OH)3(aq)	Cl-	0	0.05
PuO2SiO(OH)3(aq)	Na+	0	0.05
PuO2SiO(OH)3+	Cl-	0.2	0.1
PuO2SO4(aq)	Cl-	0	0.05

Tab. A-6: Cont.

j	*k*	*ε(j,k)*	±
PuO2SO4(aq)	Na+	0	0.05
PuO2SO4-	Na+	0.07	0.13
PuOH+2	Cl-	0.15	0.1
PuOH+3	Cl-	0.2	0.1
PuSCN+2	Cl-	0.15	0.1
PuSiO(OH)3+2	Cl-	0.15	0.1
PuSiO(OH)3+3	Cl-	0.55	0.28
PuSO4+	Cl-	0.05	0.1
PuSO4+2	Cl-	0.15	0.1
Ra+2	Cl-	0.06	0.02
RaCO3(aq)	Cl-	0	0.05
RaCO3(aq)	Na+	0	0.05
RaF+	Cl-	0.05	0.1
RaHCO3+	Cl-	0.05	0.1
RaOH+	Cl-	0.05	0.1
RaSO4(aq)	Cl-	0	0.05
RaSO4(aq)	Na+	0	0.05
S-2	Na+	-0.1	0.1
S2O3-2	Na+	-0.08	0.05
SCN-	Na+	0.05	0.01
Se(aq)	Cl-	0	0.05
Se(aq)	Na+	0	0.05
Se-2	Na+	-0.1	0.1
Se2-2	Na+	-0.1	0.1
Se3-2	Na+	-0.1	0.1
Se4-2	Na+	-0.05	0.09
SeCN-	Na+	0.05	0.01
SeO3-2	Na+	-0.1	0.1
SeO4-2	Na+	-0.12	0.06
Si(OH)4(aq)	Cl-	0.015	0.03
Si(OH)4(aq)	Na+	0.015	0.03
Si4O8(OH)4-4	Na+	0	0.13
SiAlO3(OH)4-3	Na+	-0.15	0.1

Tab. A-6: Cont.

j	*k*	*ε(j,k)*	±
SiO(OH)3-	Na+	-0.05	0.07
SiO2(OH)2-2	Na+	-0.07	0.09
Sm(CO3)2-	Na+	-1.17	0.32
Sm(OH)2+	Cl-	0.05	0.1
Sm(OH)3(aq)	Cl-	0	0.05
Sm(OH)3(aq)	Na+	0	0.05
Sm(OH)4-	Na+	-0.05	0.1
Sm(SO4)2-	Na+	0.22	0.2
Sm+3	Cl-	0.25	0.01
Sm2(OH)2+4	Cl-	0.35	0.1
Sm3(OH)5+4	Cl-	0.35	0.1
SmCO3+	Cl-	0.05	0.1
SmF+2	Cl-	0.15	0.03
SmF2+	Cl-	0.05	0.1
SmH2PO4+2	Cl-	0.15	0.1
SmOH+2	Cl-	0.15	0.1
SmSO4+	Cl-	0.05	0.1
Sn(H2PO4)2(aq)	Cl-	0	0.05
Sn(H2PO4)2(aq)	Na+	0	0.05
Sn(HPO4)2-2	Na+	-0.1	0.1
Sn(HPO4)3-4	Na+	-0.2	0.3
Sn(NO3)2(aq)	Cl-	0.065	0.0555
Sn(NO3)2(aq)	Na+	0.065	0.0555
Sn(OH)2(aq)	Cl-	0	0.05
Sn(OH)2(aq)	Na+	0	0.05
Sn(OH)3-	Na+	0.22	0.03
Sn(OH)4(aq)	Cl-	0	0.05
Sn(OH)4(aq)	Na+	0	0.05
Sn(OH)5-	Na+	-0.05	0.1
Sn(OH)6-2	Na+	-0.1	0.1
Sn(OH)Cl(aq)	Cl-	0	0.05
Sn(OH)Cl(aq)	Na+	0	0.05
Sn+2	Cl-	0.14	0.1

Tab. A-6: Cont.

j	*k*	*ε(j,k)*	±
Sn+4	Cl-	0.7	0.2
Sn3(OH)4+2	Cl-	-0.02	0.16
SnBr+	Cl-	0.15	0.07
SnBr2(aq)	Cl-	0.07	0.035
SnBr2(aq)	Na+	0.07	0.035
SnBr3-	Na+	0.16	0.08
SnCl+	Cl-	0.04	0.05
SnCl+3	Cl-	0.56	0.21
SnCl2(aq)	Cl-	0	0.03
SnCl2(aq)	Na+	0	0.03
SnCl2+2	Cl-	0.49	0.2
SnCl3-	Na+	0.07	0.06
SnCl4(aq)	Cl-	0	0.05
SnCl4(aq)	Na+	0	0.05
SnCl4-2	Na+	-0.1	0.1
SnCl5-	Na+	-0.05	0.1
SnCl6-2	Na+	-0.1	0.1
SnF+	Cl-	0.14	0.1
SnF2(aq)	Cl-	0.005	0.05
SnF2(aq)	Na+	0.005	0.05
SnF3-	Na+	-0.05	0.31
SnF6-2	Na+	-0.1	0.1
SnH2PO4+	Cl-	0.2	0.1
SnH2PO4HPO4-	Na+	-0.05	0.1
SnHPO4(aq)	Cl-	0	0.05
SnHPO4(aq)	Na+	0	0.05
SnNO3+	Cl-	0.17	0.09
SnOH+	Cl-	-0.07	0.13
SnPO4-	Na+	-0.05	0.1
SnSCN+	Cl-	-0.17	0.29
SnSO4(aq)	Cl-	0.095	0.175
SnSO4(aq)	Na+	0.095	0.175
SO3-2	Na+	-0.08	0.05

Tab. A-6: Cont.

j	*k*	*ε(j,k)*	±
SO4-2	Na+	-0.12	0.06
Sr+2	Cl-	0.12	0.01
Sr2UO2(CO3)3(aq)	Cl-	0	0.05
Sr2UO2(CO3)3(aq)	Na+	0	0.05
SrCO3(aq)	Cl-	0	0.05
SrCO3(aq)	Na+	0	0.05
SrF+	Cl-	0.05	0.1
SrH2PO4+	Cl-	0.05	0.1
SrHCO3+	Cl-	0.05	0.1
SrHPO4(aq)	Cl-	0	0.05
SrHPO4(aq)	Na+	0	0.05
SrOH+	Cl-	0.05	0.1
SrPO4-	Na+	-0.05	0.1
SrSO4(aq)	Cl-	0	0.05
SrSO4(aq)	Na+	0	0.05
SrUO2(CO3)3-2	Na+	-0.1	0.1
Tc+3	Cl-	0.25	0.1
Tc2O2(OH)2+2	Cl-	-0.43	0.11
Tc2OCl10-4	Na+	0.89	0.4
TcCl5-	Na+	-0.05	0.1
TcCl6-2	Na+	-0.1	0.1
TcCO3(OH)2(aq)	Cl-	0	0.05
TcCO3(OH)2(aq)	Na+	0	0.05
TcCO3(OH)3-	Na+	-0.05	0.1
TcO(OH)2(aq)	Cl-	0	0.05
TcO(OH)2(aq)	Na+	0	0.05
TcO(OH)3-	Na+	-0.08	0.04
TcO4-	Na+	-0.05	0.1
Th(CO3)5-6	Na+	-0.3	0.15
Th(H2PO4)2+2	Cl-	0.15	0.1
Th(H3PO4)(H2PO4)+3	Cl-	0.25	0.1
Th(IO3)2+2	Cl-	0.15	0.1
Th(IO3)3+	Cl-	0.05	0.1

Tab. A-6: Cont.

j	*k*	*ε(j,k)*	±
Th(NO3)2+2	Cl-	0.15	0.1
Th(OH)2(CO3)2-2	Na+	-0.1	0.2
Th(OH)2+2	Cl-	0.13	0.05
Th(OH)2CO3(aq)	Cl-	0	0.05
Th(OH)2CO3(aq)	Na+	0	0.05
Th(OH)3(SiO(OH)3)3-2	Na+	-0.1	0.1
Th(OH)3CO3-	Na+	-0.05	0.2
Th(OH)4(aq)	Cl-	0	0.05
Th(OH)4(aq)	Na+	0	0.05
Th(OH)4CO3-2	Na+	-0.1	0.2
Th(SCN)2+2	Cl-	0.15	0.1
Th(SO4)2(aq)	Cl-	0	0.05
Th(SO4)2(aq)	Na+	0	0.05
Th(SO4)3-2	Na+	-0.091	0.038
Th+4	Cl-	0.25	0.03
Th2(OH)2+6	Cl-	0.4	0.16
Th2(OH)3+5	Cl-	0.29	0.09
Th4(OH)12+4	Cl-	0.25	0.2
Th4(OH)8+8	Cl-	0.7	0.2
Th6(OH)14+10	Cl-	0.83	0.3
Th6(OH)15+9	Cl-	0.72	0.3
ThCl+3	Cl-	0.62	0.11
ThF+3	Cl-	0.25	0.1
ThF2+2	Cl-	0.15	0.1
ThF3+	Cl-	0.05	0.1
ThF4(aq)	Cl-	0	0.05
ThF4(aq)	Na+	0	0.05
ThF6-2	Na+	-0.3	0.06
ThH2PO4+3	Cl-	0.25	0.1
ThH3PO4+4	Cl-	0.35	0.1
ThIO3+3	Cl-	0.25	0.1
ThNO3+3	Cl-	0.25	0.1
ThOH(CO3)4-5	Na+	-0.22	0.13

Tab. A-6: Cont.

j	*k*	*ε(j,k)*	±
ThOH+3	Cl-	0.19	0.05
ThSCN+3	Cl-	0.25	0.1
ThSO4+2	Cl-	0.14	0.15
Ti+3	Cl-	0.25	0.1
Ti2(OH)2+4	Cl-	0.6	0.3
TiO(OH)2(aq)	Cl-	0	0.05
TiO(OH)2(aq)	Na+	0	0.05
TiO(OH)3-	Na+	-0.05	0.1
TiO+2	Cl-	0.15	0.1
TiOH+2	Cl-	0.14	0.11
TiOOH+	Cl-	0.05	0.1
U(CO3)4-4	Na+	-0.09	0.1
U(CO3)5-6	Na+	-0.3	0.15
U(NO3)2+2	Cl-	0.15	0.1
U(OH)2+2	Cl-	0.15	0.1
U(OH)3+	Cl-	0.05	0.1
U(OH)4(aq)	Cl-	0	0.05
U(OH)4(aq)	Na+	0	0.05
U(Ox)2(aq)	Cl-	0	0.05
U(Ox)2(aq)	Na+	0	0.05
U(Ox)3-2	Na+	-0.1	0.1
U(Ox)4-4	Na+	-0.2	0.1
U(SCN)2+2	Cl-	0.15	0.1
U(SO4)2(aq)	Cl-	0	0.05
U(SO4)2(aq)	Na+	0	0.05
U+4	Cl-	0.35	0.1
UCl+3	Cl-	0.59	0.1
UCO3(OH)3-	Na+	-0.05	0.1
UEdta(aq)	Cl-	-0.095	0.095
UEdta(aq)	Na+	-0.095	0.095
UEdta(OH)2-2	Na+	-0.1	0.1
UEdtaOH-	Na+	-0.05	0.1
UF+3	Cl-	0.25	0.1

Tab. A-6: Cont.

j	*k*	*ε(j,k)*	±
UF2+2	Cl-	0.3	0.1
UF3+	Cl-	0.1	0.1
UF4(aq)	Cl-	0	0.05
UF4(aq)	Na+	0	0.05
UF5-	Na+	-0.05	0.1
UF6-2	Na+	-0.1	0.1
UH2PO4+3	Cl-	0.25	0.1
UI+3	Cl-	0.25	0.1
UNO3+3	Cl-	0.25	0.1
UO2(CO3)2-2	Na+	-0.15	0.08
UO2(CO3)3-4	Na+	-0.01	0.11
UO2(CO3)3-5	Na+	-0.92	0.23
UO2(H2AsO4)2(aq)	Cl-	0	0.05
UO2(H2AsO4)2(aq)	Na+	0	0.05
UO2(H2PO4)(H3PO4)+	Cl-	0.05	0.1
UO2(H2PO4)2(aq)	Cl-	0	0.05
UO2(H2PO4)2(aq)	Na+	0	0.05
UO2(H3Isa)+	Cl-	0.2	0.1
UO2(H3Isa)2(aq)	Cl-	0	0.05
UO2(H3Isa)2(aq)	Na+	0	0.05
UO2(H3Isa)3-	Na+	-0.05	0.1
UO2(HCit)(aq)	Cl-	0	0.05
UO2(HCit)(aq)	Na+	0	0.05
UO2(HEdta)-	Na+	-0.18	0.16
UO2(HSeO3)2(aq)	Cl-	0	0.05
UO2(HSeO3)2(aq)	Na+	0	0.05
UO2(IO3)2(aq)	Cl-	0	0.05
UO2(IO3)2(aq)	Na+	0	0.05
UO2(OH)2(aq)	Cl-	0	0.05
UO2(OH)2(aq)	Na+	0	0.05
UO2(OH)3-	Na+	-0.24	0.09
UO2(OH)4-2	Na+	0.01	0.04
UO2(Ox)2-2	Na+	-0.18	0.07

Tab. A-6: Cont.

j	*k*	*ε(j,k)*	±
UO2(Ox)3-4	Na+	-0.01	0.11
UO2(SCN)2(aq)	Cl-	0	0.05
UO2(SCN)2(aq)	Na+	0	0.05
UO2(SCN)3-	Na+	0	0.05
UO2(SeO4)2-2	Na+	-0.1	0.1
UO2(SO4)2-2	Na+	-0.12	0.06
UO2(SO4)3-4	Na+	-0.26	0.05
UO2+	Cl-	0.05	0.1
UO2+2	Cl-	0.21	0.02
UO2Cit-	Na+	-0.11	0.09
UO2Cl+	Cl-	0.33	0.04
UO2Cl2(aq)	Cl-	0	0.05
UO2Cl2(aq)	Na+	0	0.05
UO2CO3(aq)	Cl-	0.075	0.03
UO2CO3(aq)	Na+	0.075	0.03
UO2CO3F-	Na+	0	0.05
UO2CO3F2-2	Na+	-0.02	0.09
UO2CO3F3-3	Na+	-0.25	0.05
UO2Edta-2	Na+	-0.22	0.18
UO2F+	Cl-	0.05	0.1
UO2F2(aq)	Cl-	0.065	0.025
UO2F2(aq)	Na+	0.065	0.025
UO2F3-	Na+	-0.14	0.05
UO2F4-2	Na+	-0.3	0.06
UO2H2AsO4+	Cl-	0.05	0.1
UO2H2PO4+	Cl-	0.05	0.1
UO2H3PO4+2	Cl-	0.15	0.1
UO2HAsO4(aq)	Cl-	0	0.05
UO2HAsO4(aq)	Na+	0	0.05
UO2HPO4(aq)	Cl-	0	0.05
UO2HPO4(aq)	Na+	0	0.05
UO2HSeO3+	Cl-	0.05	0.1
UO2IO3+	Cl-	0.05	0.1

Tab. A-6: Cont.

j	*k*	*ε(j,k)*	±
UO2NO3+	Cl-	0.05	0.1
UO2OH+	Cl-	0.05	0.1
UO2Ox(aq)	Cl-	-0.025	0.03
UO2Ox(aq)	Na+	-0.025	0.03
UO2PO4-	Na+	-0.09	0.05
UO2SCN+	Cl-	0.05	0.1
UO2SeO4(aq)	Cl-	0	0.05
UO2SeO4(aq)	Na+	0	0.05
UO2SiO(OH)3+	Cl-	0.3	0.1
UO2SO4(aq)	Cl-	0	0.05
UO2SO4(aq)	Na+	0	0.05
UOH+3	Cl-	0.25	0.1
UOx+2	Cl-	0.4	0.1
USCN+3	Cl-	0.25	0.1
USO4+2	Cl-	0.15	0.1
Zn(CO3)2-2	Na+	-0.1	0.1
Zn(H2PO4)(HPO4)-	Na+	-0.05	0.1
Zn(H2PO4)2(aq)	Cl-	0	0.05
Zn(H2PO4)2(aq)	Na+	0	0.05
Zn(HPO4)(PO4)-3	Na+	-0.15	0.1
Zn(HPO4)2-2	Na+	-0.1	0.1
Zn(HPO4)3-4	Na+	-0.2	0.1
Zn(HS)2(aq)	Cl-	0	0.05
Zn(HS)2(aq)	Na+	0	0.05
Zn(HS)3-	Na+	-0.05	0.1
Zn(OH)2(aq)	Cl-	0	0.05
Zn(OH)2(aq)	Na+	0	0.05
Zn(OH)2HPO4-2	Na+	-0.1	0.1
Zn(OH)3-	Na+	0.07	0.06
Zn(OH)4-2	Na+	0.13	0.08
Zn(SO4)2-2	Na+	0.38	0.1
Zn+2	Cl-	0.35	0.01
Zn2CO3+2	Cl-	0.4	0.1

Tab. A-6: Cont.

j	*k*	*ε(j,k)*	±
Zn2OH+3	Cl-	0.86	0.1
ZnCl+	Cl-	0.24	0.02
ZnCl2(aq)	Cl-	0.105	0.02
ZnCl2(aq)	Na+	0.105	0.02
ZnCl3-	Na+	0.17	0.13
ZnCl4-2	Na+	-0.1	0.1
ZnCO3(aq)	Cl-	0	0.05
ZnCO3(aq)	Na+	0	0.05
ZnH2PO4+	Cl-	0.2	0.1
ZnHCO3+	Cl-	0.45	0.05
ZnHPO4(aq)	Cl-	0	0.05
ZnHPO4(aq)	Na+	0	0.05
ZnOH+	Cl-	0.19	0.02
ZnS(HS)-	Na+	-0.05	0.1
ZnSO4(aq)	Cl-	0.135	0.025
ZnSO4(aq)	Na+	0.135	0.025
Zr(CO3)4-4	Na+	-0.09	0.2
Zr(NO3)2+2	Cl-	0.15	0.1
Zr(OH)2+2	Cl-	0.15	0.1
Zr(OH)4(aq)	Cl-	0	0.05
Zr(OH)4(aq)	Na+	0	0.05
Zr(OH)6-2	Na+	-0.1	0.1
Zr(SO4)2(aq)	Cl-	0	0.05
Zr(SO4)2(aq)	Na+	0	0.05
Zr(SO4)3-2	Na+	-0.1	0.1
Zr+4	Cl-	0.33	0.09
Zr3(OH)4+8	Cl-	0.33	0.28
Zr3(OH)9+3	Cl-	0.25	0.1
Zr4(OH)15+	Cl-	0.05	0.1
Zr4(OH)16(aq)	Cl-	0	0.05
Zr4(OH)16(aq)	Na+	0	0.05
Zr4(OH)8+8	Cl-	0.75	0.5
ZrCl+3	Cl-	0.87	0.1

Tab. A-6: Cont.

j	*k*	*ε(j,k)*	±
ZrCl2+2	Cl-	0.84	0.11
ZrF+3	Cl-	0.25	0.1
ZrF2+2	Cl-	0.15	0.1
ZrF3+	Cl-	0.05	0.1
ZrF4(aq)	Cl-	0	0.05
ZrF4(aq)	Na+	0	0.05
ZrF5-	Na+	-0.14	0.03
ZrF6-2	Na+	-0.15	0.06
ZrNO3+3	Cl-	0.25	0.1
ZrOH+3	Cl-	0.25	0.1
ZrSO4+2	Cl-	0.15	0.1